SCIENCE ABSTRACTS, SERIES A

Physics Abstracts

U. of ILL. LIBRARY
MAY 21 1969
CHICAGO CIRCLE

1968 Subject Index Number
Part II (July – December)

An INSPEC Publication
The Institution of Electrical Engineers

SUBJECT INDEX-PART II

INTRODUCTION

The entries in this index refer to the abstracts by their serial number, not by the page number. The entries are grouped under headings (printed in bold type, e.g. "**Abrasion**") which represent, in the main, general categories or concepts rather than specific names. If a heading for a particular subject does not appear, a more general heading should be consulted; for example, "Zone plates" would be listed under "**Diffraction/light**"; "Barkhausen discontinuities" under "**Magnetization process**". There are numerous cross-references directing attention to related headings in other parts of the index.

Many of the headings are subdivided by the use of subheadings, which are indented (i.e. printed slightly to the right) and commence with a small letter (for example, see the subheadings under "**Absorption**").

ARRANGEMENT OF HEADINGS AND SUBHEADINGS

The headings are arranged throughout the index in alphabetical order according to British Standard 1749:1951 (the "word by word" system, not "reading right through"). The subheadings, with a few exceptions, are themselves arranged in alphabetical order under their respective headings. The exceptions (for example, see the subheadings under "**Spectra**", "**Crystal structure, atomic**") are cases where a more logical order is preferable to a purely alphabetical one.

ARRANGEMENTS OF ENTRIES UNDER HEADINGS

Entries are arranged in two alphabetical groups as follows. First group: generalities and named substances (in words); second group: named substances (chemical formulae). If a search is being made for a particular substance, both the first and second alphabetical groups should be inspected since, for example, alumina may also be listed as Al_2O_3.

COLLECTED LIST OF SUBJECT HEADINGS

The alphabetical arrangement of the headings is the most convenient for locating a known heading quickly, but there may be other related headings elsewhere in the index of which the reader is unaware, and which he would only come across by accident. To assist the reader to discover all the headings appropriate to his subject, a collected list of the headings is given on pages S540 to S554, which follow this page; they should be consulted as a matter of routine each time a search is made. In this list, the headings are not arranged in alphabetical order, but are grouped into sections by subject on the same basis as the arrangement of the abstracts in the monthly issues of Physics Abstracts. By using this list, the reader can quickly determine which are the headings appropriate to his subject, and they are then easily found in the main index in their alphabetical position.

HEADINGS WITH NO ENTRIES

Because physics is a developing subject, it is not possible to maintain the list of headings unchanged from year to year; it is subject to a continuous process of revision, with the introduction of new headings and subheadings, and the alteration and elimination of old ones. This process is a gradual one, however, and the great majority of the headings are the same as those of the previous year. To assist in maintaining the continuity of the index, all the headings in current use in a given year are printed, even those for which there are no abstracts to be recorded. The latter are followed by the announcement "No entries"; this supplies confirmation that these headings have not been dropped from the index, and entries may reappear under them in the next issue of the index.

ELEMENTS, COMPOUNDS AND OTHER SUBSTANCES

The names of elements, their compounds, a few compounds of special interest (e.g. "**Ruby**", "**Water**") and a few common materials (e.g. "**Wood**", "**Paper**") are included as headings or subheadings (e.g. "**barium titanate**" under "**Barium compounds**"). Under these, as well as under the appropriate "subject" headings, are listed any abstracts which contain significant physical information about the element, compound or substance named; except however, that abstracts listed under headings referring to nuclear properties, including radioactivity, are not necessarily also listed under the substance name. The entries under these headings are themselves arranged in alphabetical order of substance or nuclide names, so that a given substance can be readily located.

Inorganic compounds of the elements are listed under the first element in the chemical formula, and all the compounds of a given element are grouped under a single heading (e.g. "**Sodium compounds**"). Alloys are listed under compounds of the base or first-named constituent, e.g. Au–Ag alloys under "**Gold compounds**". There are also four special headings for the common alloys: "**Aluminium alloys**", "**Copper alloys**", "**Iron alloys**", "**Nickel alloys**". Organic compounds are grouped under "**Organic compounds**", "**Polymers**", "**Plastics**" and under special substance headings such as "**Paper**", "**Proteins**", etc.; all the latter are listed in the collected list of headings at the end of the index.

BEFORE USING INDEX, CONSULT LIST OF SUBJECT HEADINGS ON PAGES S540-S554 WHICH FOLLOW THIS PAGE

LIST OF SUBJECT INDEX HEADINGS

The headings used in the Alphabetical Index are listed below. The headings are grouped into sections on the same basis as the arrangement of the abstracts in the monthly issues of Physics Abstracts. Each section lists the headings which concern its subject and it follows that many of the headings are listed in several places.

An introduction to the Subject Index will be found on page S539.

GENERAL

- Bibliographies
- Biographies
- Books
- Collections of physical data
- Conferences
- History
- Laboratories
- Laboratory apparatus and technique
- Nomenclature and symbols
- Physics
- Physics fundamentals
- Reviews

EDUCATION

- Biographies
- Books
- History
- Laboratories
- Laboratory apparatus and technique
- Physics
- Physics fundamentals
- Reviews
- Teaching
    - demonstrations

UNITS · MEASUREMENT · METROLOGY

- Acceleration measurement
- Alignment
- Anemometers
- Angle measurement
- Angular velocity measurement
- Area measurement
- Balances
- Constants
- Density measurement
- Dimensions
- Dynamometers
- Force measurement
- Instruments
- Interferometry
- Length measurement
- Manometers
- Measurement
    - errors
- Mechanical measurement
- Micrometry
- Nomenclature and symbols
- Particle size
- Pressure measurement
- Recording
- Standards
- Strain gauges
- Stroboscopes
- Surface measurement
- Thickness measurement
- Time interval measurement
- Time measurement
- Units
- Vapour pressure measurement
- Velocity measurement
- Volume measurement

MATHEMATICAL PHYSICS

- Algebra
- Differential equations
- Equations
- Field theory, classical
- Fluctuations
- Fourier analysis
- Functions
- Geometry
- Group theory
- Hysteresis
- Information theory
- Integral equations
- Integrals
- Mathematics
- Matrices
- Probability
- Radiation
- Relaxation
- Series
- Statistical analysis
    - applications
- Tensors
- Transformations, mathematical
- Vectors
- Waves

MATHEMATICAL METHODS COMPUTATION

- Calculating apparatus
    - analogue apparatus
    - digital computers
    - digital computer programmes
- Calculation
- Graphs
- Nomograms
- Sliderules
- Statistical analysis
    - applications
- Tables, mathematical

MECHANICS

- Ballistics
- Centrifuges
- Dynamics
- Friction
- Gravitation
- Gyroscopes
- Impact
- Kinematics
- Mechanics
- Pendulums
- Pressure
- Rockets
- Rotating bodies
- Torsion
- Velocity

Elasticity · Plasticity

- Bending
- Compressibility
- Damping
- Deformation
- Elastic deformation
- Elasticity
- Photoelasticity
- Plastic deformation
- Plasticity
- Relaxation
- Rheology
- Stress analysis
- Stresses, internal
- Thermoelasticity
- Viscoelasticity

GRAVITATION · RELATIVITY

- Gravitation
- Relativity
    - general
    - special
    - unified field theories

STATISTICAL PHYSICS

- Bosons
- Brownian movement
- Electron gas
- Fermions
- Fluctuations
- Hysteresis
- Information theory
- Kinetic theory
- Probability
- Quantum theory
    - many-particle systems
- Random processes
- Relaxation
- Statistical analysis
    - applications
- Statistical mechanics
- Thermodynamics

Thermodynamics

- Entropy
    - properties of substances
- Equations of state
    - gases
    - liquids
    - solids
- Joule—Thomson effect
- Thermodynamic properties
- Thermodynamics
    - applications

TRANSPORT PROCESSES

- Diffusion
- Radiation
- Radiative transfer
- Transport processes

VIBRATIONS · WAVES · ACOUSTICS

- Oscillations
- Vibrations
- Waves

VIBRATIONS · ELASTIC WAVES

- Damping
- Elastic waves
- Membranes
- Oscillations
- Piezoelectric oscillations
- Relaxation
- Resonators
- Seismic waves
- Shock waves
  - effects
- Vibrating bodies
- Vibrations
  - excitation
  - measurement
- Waves

SHOCK WAVES

- Detonation
- Explosions
  - nuclear
- Schlieren systems
- Shock tubes
- Shock waves
  - effects
- Supersonic flow

ACOUSTICS

- Absorption/
  - acoustic waves
  - acoustic waves, ultrasonic
- Acoustic analysis
- Acoustic generators
- Acoustic impedance
- Acoustic radiators
- Acoustic receivers
- Acoustic resonators
- Acoustic streaming
- Acoustic transducers
- Acoustic wave propagation
  - ultrasonic
- Acoustic waves
  - effects
- Acoustical laboratories
- Acoustical measurement
- Acoustics
  - musical
- Acoustoelectric effects
- Architectural acoustics
- Atmospheric acoustics
- Biological effects of radiations
- Chemical effects of radiations/
  - acoustic waves
- Diffraction/
  - acoustic waves
  - acoustic waves, ultrasonic
- Diffusion/
  - acoustic waves
- Dispersion, acoustic
  - ultrasonic
- Doppler effect
- Echo
- Helium/
  - liquid, sound propagation
- Holography
- Intensity measurement/
  - acoustics
- Interference/
  - acoustic waves
- Interferometers/
  - acoustic waves
- Interferometry/
  - acoustic waves
- Magnetoacoustic effects
- Microphones
- Musical instruments
- Noise/
  - acoustic
- Noise abatement
- Physical effects of radiations
- Radiation pressure
- Reflection/
  - acoustic waves
  - acoustic waves, ultrasonic
- Refraction/
  - acoustic waves
  - acoustic waves, ultrasonic
- Reverberation
- Scattering/
  - acoustic waves
  - acoustic waves, ultrasonic
- Schlieren systems
- Sound ranging
- Sound recording
- Sound reproduction
- Speech
- Stroboscopes
- Transmission/
  - acoustic waves
  - acoustic waves, ultrasonic
- Ultrasonics
- Velocity/
  - acoustic waves
  - acoustic waves, ultrasonic
- Velocity measurement/
  - acoustic waves
  - acoustic waves, ultrasonic

Hearing · Speech

- Ear
- Hearing
- Noise/
  - acoustic
- Speech

HEAT

- Bolometers
- Calorimeters
- Calorimetry
- Combustion
- Conductivity, thermal
- Convection
- Cooling
- Cryostats
- Emissivity
- Flames
- Heat
- Heat conduction
- Heat transfer
- Heat treatment
- Heating
- High-temperature production [and effects
- Latent heat
- Pyrometers
- Radiation
  - heat
- Radiation detectors
- Radiation pressure
- Radiative transfer
- Specific heat
- Temperature
- Temperature distribution
- Temperature measurement
  - spectral methods
- Thermal expansion
- Thermal measurement
- Thermocouples
- Thermometers
  - resistance
- Thermostats

LOW-TEMPERATURE PHYSICS

- Cryostats
- Joule-Thomson effect
- Liquefaction, gases
- Low-temperature phenomena
- Low-temperature production
- Low-temperature technique
- Magnetic cooling
- Quantum theory/
  - many-particle systems
- Superconductivity

Liquid and Solid Helium

- Helium/
  - liquid
  - liquid, sound propagation
  - solid
- Superfluidity

ELECTRICITY AND MAGNETISM

Electricity
Electromagnetism
Magnetism

ELECTRICAL MEASUREMENTS AND CIRCUITS

- Amplifiers
- Circuits
- Counting circuits
- Dielectric measurement
- Electrical measurement
- Fluctuations/
  - electrical
- High-voltage production
- Image convertors and amplifiers
- Plasma/
  - measurement technique

ELECTROSTATICS · DIELECTRICS

- Breakdown, electric
- Contact potential
- Dielectric devices
- Dielectric phenomena
- Electrets
- Electric charge
- Electric fields
  - effects
- Electric strength
- Electroluminescence
- Electrostatics
- Electrostriction
- Ferroelectric phenomena
- High-voltage production
- Hysteresis
- Piezoelectric oscillations
- Piezoelectricity
- Pyroelectricity
- Relaxation
- Space charge
- Triboelectricity

CURRENT ELECTRICITY

- Acoustoelectric effects
- Conduction, electrical
- Conductivity, electrical
  - measurement
- Contact potential
- Contact resistance
- Current, electrical
- Eddy-currents
- Electric charge
- Electrical properties of substs.
- Electrokinetic effects
- Electromotive force
- Electron gas
- Electrons
- Electro-optical effects
- Electrophoresis
- Fluctuations/
  - electrical
- Hall effect
- Inductance
- Magnetoelectric effects
- Magnetoresistance
- Photoconductivity
- Photoelectricity
- Photoelectromagnetic effects
- Photovoltaic effects
- Piezoresistance
- Rectifiers
- Resistance, electrical
- Semiconductors
- Skin effect
- Space charge
- Superconductivity
- Thermocouples
- Thermoelectricity

Direct Conversion

- Electricity/
  - direct conversion
- Magnetohydrodynamics

MAGNETISM

- Antiferromagnetism
- Compasses
- de Haas—van Alphen effect
- Diamagnetism
- Ferrimagnetism
- Ferromagnetism
  - spin-wave theory
- Gyromagnetic effect
- Gyromagnetic ratio
- Hall effect
- Magnetic devices
- Magnetic field measurement
- Magnetic fields
  - effects
- Magnetic films
- Magnetic measurement
- Magnetic resonance and relaxation
- Magnetism
- Magnetization process
- Magnetization state
- Magnetoacoustic effects
- Magnetoelectric effects
- Magnetomechanical effects
- Magneto-optical effects
- Magnetoresistance
- Magnetostriction
- Magnetothermal effects
- Magnets
- Paramagnetism

ELECTROMAGNETISM

Eddy-currents
Electromagnetism
Electromagnetic fields
Electromotive force
Inductance

ELECTRODYNAMICS · PARTICLE OPTICS

- Electrodynamics
- Particle optics
- Particle range
- Particle velocity analysis

ELECTRON BEAMS
ELECTRON OPTICS AND TUBES

- Electron beams
  - effects
- Electron diffraction
- Electron gas
- Electron lenses
  - electrostatic
  - magnetic
- Electron microscopes
- Electron microscopy
- Electron optics
- Electron tubes
- Electrons
  - absorption
  - ionization
  - radiation
  - scattering
- Fluctuations/
  - electrical
- Gas-discharge tubes
- Image convertors and amplifiers
- Photomultipliers
- Space charge

ION BEAMS
ION OPTICS AND SOURCES

- Bremsstrahlung
- Ion beams
  - effects
- Ion microscopes
- Ion optics
- Ion sources
- Ion velocity
- Ions
  - recombination
  - scattering
- Sputtering

MAGNETOHYDRODYNAMICS
MAGNETOGASDYNAMICS

- Electricity/
  - direct conversion
- Magnetohydrodynamics
- Plasma/
  - magnetohydrodynamics
- Shock waves
  - effects

ELECTROMAGNETIC WAVES AND OSCILLATIONS

- Electromagnetic oscillations
- Electromagnetic waves
- Light/
  - electromagnetic theory
- Radiation

GENERATION AND PROPAGATION

- Absorption/
  - electromagnetic waves
- Amplifiers
- Diffraction/
  - electromagnetic waves
- Diffusion/
  - electromagnetic waves
- Doppler effect
- Electromagnetic oscillations
- Electromagnetic wave
  - atmosphere [propagation
  - ionosphere
  - guided waves
- Electromagnetic waves
  - radiators
- Interference/
  - electromagnetic waves
- Interferometers/
  - electromagnetic waves
- Interferometry/
  - electromagnetic waves
- Plasma/
  - electromagnetic wave propagation
- Reflection/
  - electromagnetic waves
- Refraction/
  - electromagnetic waves
- Scattering/
  - electromagnetic waves

RADIOFREQUENCY SPECTROSCOPY
MAGNETIC RESONANCES

- Antiferromagnetic resonance
- Cyclotron resonance
- Ferrimagnetic resonance
- Ferromagnetic relaxation
- Ferromagnetic resonance
- Magnetic resonance and
  - [relaxation
- Nuclear magnetic resonance and
  - measurement [relaxation
- Nuclear quadrupole resonance
- Paramagnetic resonance and
  - measurement [relaxation
- Spectra
- Spectrometers, radiofrequency
- Spectroscopy, radiofrequency

MASERS

- Amplifiers
- Masers
- Optical pumping

Lasers

- Amplifiers
- Holography
- Lasers
  - gaseous
  - solid
- Light
  - coherence
- Optical pumping

OPTICS

- Doppler effect
- Electro-optical effects
- Light
  - coherence
  - e.m. theory
- Light sources
- Optics
- Photons
- Photophoresis
- Radiation
- Radiation pressure
- Velocity/
  - light
- Velocity measurement/
  - light

PHOTOMETRY · COLORIMETRY

- Bolometers
- Brightness
- Colorimetry
- Colour
- Densitometry
- Emissivity
- Illumination
- Photometers
- Photometry
  - light sources
- Pyrometers
- Radiation detectors

GEOMETRICAL OPTICS

- Aberrations, optical
- Dispersion, optical
- Lenses
  - aspherical
  - photographic
- Mirrors
- Optical images
- Optical systems
- Optics/
  - geometrical
- Prisms, optical
- Reflection/
  - light
- Refraction/
  - light
- Refractive index/
  - light
- Resolving power, optics
- Schlieren systems
- Stereoscopy

INSTRUMENTAL OPTICS

- Aberrations, optical
- Dispersion, optical
- Filters, optical
- Glass
- Image convertors and
- Lasers [amplifiers
  - gaseous
  - solid
- Lenses
  - aspherical
  - photographic
- Light sources
- Luminescent devices
- Microscopes
- Microscopy
- Mirrors
- Optical constants
- Optical films
- Optical images
- Optical instrument testing
- Optical instruments
- Optical materials
- Optical systems
- Prisms, optical
- Projectors, optical
- Quartz
- Reflection/
  - light
- Refraction/
  - light
- Refractive index/
  - light
- Refractive index measurement
- Refractometers
- Resolving power, optics
- Schlieren systems
- Stereoscopy
- Stroboscopes
- Telescopes

Spectroscopy

- Astronomical spectra
- Atmospheric spectra
- Monochromators
- Spectral line breadth
- Spectrochemical analysis
- Spectrometers
  - accessories
- Spectrophotometers
- Spectrophotometry
- Spectroscopy
  - light sources
- Stark effect
- Temperature measurement/
  - spectral methods
- Zeeman effect

PHYSICAL OPTICS

- Absorption/
  - light
- Diffraction/
  - light
- Diffraction gratings
- Diffusion/
  - light
- Dispersion, optical
- Doppler effect
- Double refraction
  - flow
  - mechanical
- Electro-optical effects
- Filters, optical
- Holography
- Interference/
  - light
- Interferometers/
  - light
- Interferometry/
  - light
- Magneto-optical effects
- Optical constants
- Optical films
- Optical pumping
- Optical rotation
- Photoelasticity
- Pleochroism
- Polarimeters
- Polarized light
- Reflection/
  - light
- Reflectivity
- Refraction/
  - light
- Refractive index/
  - light
- Scattering/
  - light
- Transmission/
  - light
- Transparency

PHOTOGRAPHY

- Cameras
- Cinematography
- Densitometry
- Lenses/
    - photographic
- Light sources
- Nuclear track emulsions
- Photographic materials
    - sensitivity
- Photographic process
    - development
- Photography
    - applications
    - colour
    - high-speed
- Radiography

VISION

- Eye
- Colour vision
- Stereoscopy
- Vision

X-RAYS · TUBES AND TECHNIQUES

- Dosimetry
- High-voltage production
- Radiation monitoring
- Radiation protection
- Radiography
- X-ray absorption
- X-ray diffraction
- X-ray examination of materials
- X-ray measurement
- X-ray monochromators
- X-ray reflection
- X-ray scattering
- X-ray spectra
    - absorption
    - emission
- X-ray spectrometers
- X-ray spectroscopy
- X-ray tubes
- X-rays
    - effects

QUANTUM THEORY

- Collision processes
- Dispersion relations
- Indeterminacy
- Parity
- Quantum electrodynamics
- Quantum theory
    - application methods
    - many-particle systems
    - quantization
    - wave equations
- Scattering

QUANTUM FIELD THEORY

- Current algebra
- Dispersion relations
- Field theory, quantum
    - interactions
    - interactions, strong
    - interactions, weak
    - meson field
    - quantization
- Nuclear forces
- Parity
- Quantum electrodynamics
- Quantum theory
    - application methods
    - many-particle systems
    - quantization
    - wave equations
- S-matrix theory
- Scattering

ELEMENTARY PARTICLE AND NUCLEAR MEASUREMENTS

APPARATUS · PARTICLE DETECTORS

- Alpha-ray spectrometers
- Beta-ray spectrometers
- Counters
    - accessories
    - Cherenkov
    - crystal
    - Geiger
    - operation technique
    - proportional
    - scintillation
    - semiconductor
    - spark
    - statistical analysis
- Dosimetry
- Gamma-ray spectrometers
- Ionization chambers
- Neutron spectrometers
- Nuclear bombardment targets
- Particle accelerators
- Particle detectors
- Particle optics
- Particle spectrometers
- Particle velocity analysis
- Photomultipliers
- Radioactivity measurement/
    - apparatus

Counting Circuits

- Amplifiers
- Counting circuits

Track Visualization

- Bubble chambers
- Cloud chambers
- Luminescence chambers
- Nuclear track emulsions
- Particle range
- Particle tracks
- Particle track visualization
- Spark chambers

PARTICLE ACCELERATORS

- High-voltage production
- Ion sources
- Particle accelerators
    - linear
    - orbital
    - orbital, cyclotrons

ELEMENTARY PARTICLES

- Bosons
- Elementary particles
- Fermions
- Parity
- Particle range
- Particle velocity analysis
- Quarks
- Scattering, particles
- Strange particles

Elementary Particle Theory

- Bosons
- Collision processes
- Current algebra
- Dispersion relations
- Elementary particles
- Fermions
- Field theory, quantum
    - interactions
    - interactions, strong
    - interactions, weak
    - meson field
    - quantization
- Nuclear forces
- Parity
- S-matrix theory
- Scattering, particles
- Strange particles

Photons · Gamma-rays · X-rays

- Bremsstrahlung
- Cherenkov radiation
- Compton effect
- Gamma-ray spectrometers
- Gamma-rays
    - absorption
    - angular distribution
    - detection, measurement
    - effects
    - scattering
- Mössbauer effect
- Photons
    - interactions
    - polarization
    - scattering
- X-ray absorption
- X-ray diffraction
- X-ray measurement
- X-ray reflection
- X-ray scattering
- X-rays
    - effects

Leptons

- Leptons

Neutrinos

- Neutrinos and antineutrinos

Electrons

- Beta-ray spectra
    - conversion electrons
- Beta-ray spectrometers
- Beta-rays
    - absorption
    - angular distribution
    - detection, measurement
    - effects
    - polarization
    - scattering
- Electron pairs
    - annihilation
    - production
- Electron theory
- Electrons
    - absorption
    - ionization
    - radiation
    - scattering
    - scattering, electron-proton
- Positronium
- Positrons

Muons

- Muons
    - capture
    - decay
    - detection, measurement
    - interactions
    - production
    - scattering
- Muonium

Hadrons

- Hadrons
- Quarks

Mesons

- Mesons
    - absorption
    - capture
    - decay
    - decay observations
    - detection, measurement
    - effects
    - interactions
    - magnetic moment
    - mass
    - production
    - scattering
    - spin and parity
- Pions
    - decay
    - interactions
    - interactions, pion—nucleon
    - interactions, pion—pion
    - interactions, pion—proton
    - production
    - scattering
    - scattering, pion—nucleon
    - scattering, pion—pion
    - scattering, pion—proton
- Strange particles

Meson Resonances

- Mesons
    - resonances

Baryons

- Baryons

Nucleons

- Nuclear forces
- Nucleons and antinucleons
    - antinucleons
    - interactions
    - interactions, nucleon—nucleon
    - scattering
    - scattering, nucleon—nucleon

Protons

- Proton spectra
- Protons and antiprotons
    - absorption
    - angular distribution
    - antiprotons
    - detection, measurement
    - effects
    - interactions
    - interactions, proton—proton
    - magnetic moment
    - polarization
    - production
    - scattering
    - scattering, proton—deuteron
    - scattering, proton—proton

Neutrons

- Neutron diffraction
- Neutron spectra
- Neutron spectrometers
- Neutrons and antineutrons
    - absorption
    - angular distribution
    - detection, measurement
    - diffusion
    - effects
    - interactions
    - moderation
    - polarization
    - production
    - reflection
    - scattering
    - scattering, proton-neutron

Hyperons

- Hypernuclei
- Hyperons
    - absorption
    - capture
    - decay
    - decay observations
    - detection, measurement
    - effects
    - interactions
    - magnetic moment
    - mass
    - production
    - resonances
    - scattering
    - spin and parity
- Strange particles

Baryon Resonances

- Baryons
    - resonances
- Hyperons
    - resonances
- Nucleons

Deuterons

- Deuterons
    - effects
    - interactions
    - photodisintegration
    - polarization
    - scattering

Tritons

- Tritons

Alpha-particles, He Nuclei

- Alpha-particles and He nuclei
- Alpha-ray spectrometers
- Alpha-rays
    - absorption
    - angular distribution
    - detection, measurement
    - effects
    - scattering

COSMIC RAYS

- Cosmic rays
  - absorption
  - apparatus
  - composition
    - alpha-particles
    - deuterons
    - electrons
    - mesons
    - muons
    - neutrons
    - photons
    - protons
  - effects and interactions
  - origin
  - primary
  - showers and bursts
  - variation

NUCLEAR PHYSICS

Nuclear physics

NUCLEUS. ENERGY LEVELS

- Beta-ray spectra
  - conversion electrons
- Gamma-ray spectra
- Gamma-rays
  - angular distribution
  - internal conversion
- Gyromagnetic ratio
- Hypernuclei
- Mössbauer effect
- Nuclear excitation
- Nuclear forces
- Nuclear isomerism
- Nuclear magnetic resonance and relaxation measurement
- Nuclear orientation
- Nucleus
  - electric moment
  - energy levels
  - magnetic moment
  - models
  - size
  - spin and parity
  - theory

NUCLEAR DECAY. RADIOACTIVITY

- Alpha-particles and He nuclei
- Alpha-ray spectra
- Alpha-ray spectrometers
- Alpha-rays
  - absorption
  - angular distribution
  - detection, measurement
  - effects
  - scattering
- Beta-decay theory
- Beta-ray spectra
  - conversion electrons
- Beta-ray spectrometers
- Beta-rays
  - absorption
  - angular distribution
  - detection, measurement
  - effects
  - polarization
  - scattering
- Biological effects of radiations
- Chemical effects of radiations/
  - ionizing radiations
- Dosimetry
- Fallout
- Gamma-ray spectra
- Gamma-ray spectrometers
- Gamma-rays
  - absorption
  - angular distribution
  - detection, measurement
  - effects
  - internal conversion
  - scattering
- Nuclear decay theory
- Nuclear bombardment targets
- Physical effects of radiations
- Radiation monitoring
- Radiation protection
- Radioactive dating
- Radioactive tracers
- Radioactivity
  - decay periods
  - decay schemes
  - electron capture
- Radioactivity measurement
  - apparatus
- Radiochemistry

NUCLEAR REACTIONS

- Alpha-rays/
  - scattering
- Chemical analysis/
  - by nuclear reactions
- Collision processes
- Deuterons/
  - scattering
- Electrons/
  - scattering
- Gamma-rays/
  - scattering
- Hyperons/
  - scattering
- Mesons/
  - scattering
- Muons/
  - scattering
- Neutrinos and antineutrinos
- Neutrons and antineutrons/
  - scattering
- Nuclear bombardment targets
- Nuclear excitation
- Nuclear forces
- Nuclear reactions
  - chemical effects
- Nuclear reactions due to/
  - alpha-rays
  - cosmic rays
  - deuterons
  - electrons
  - helium-3
  - mesons
  - muons
  - neutrinos
  - neutrons
  - nuclei of $Z > 2$
  - photons
  - protons
  - tritons
- Nuclear spallation
- Nucleons and antinucleons/
  - scattering
- Photons/
  - scattering
- Pions/
  - scattering
- Protons and antiprotons/
  - scattering
- Radiation monitoring
- Radiation protection
- Scattering, particles

Nuclear Fission

- Explosions/
  - nuclear
- Nucleons
- Nuclear fission
  - products
  - uranium

Thermonuclear Reactions
Nuclear Fusion

- Explosions/
  - nuclear
- Nuclear fusion
- Plasma
- Thermonuclear reactions

NUCLEAR POWER STUDIES

- Biological effects of radiations
- Chemical analysis/
  - by nuclear reactions
- Chemical effects of radiations/
  - ionizing radiations
- Dosimetry
- Neutrons
  - absorption
  - angular distribution
  - detection, measurement
  - diffusion
  - effects
  - interactions
  - moderation
  - polarization
  - production
  - reflection
  - scattering
- Nuclear fission
  - products
  - uranium
- Nuclear fusion
- Nuclear reactions
  - chemical effects
- Nuclear reactors, fission
  - materials
  - operation
  - theory
- Nuclear reactors, fusion
- Physical effects of radiations
- Plasma
  - devices
- Radiation monitoring
- Radiation protection
- Radiochemistry
- Thermonuclear reactions

ATOMIC AND MOLECULAR PHYSICS

- Collision processes
- Orbital calculation methods
- Quantum theory

MASS SPECTROMETERS

- Mass spectra
- Mass spectrometers
    - accessories
    - applications

ATOMS

- Atomic beams
- Atomic mass and weight
- Atoms
    - electron scattering
    - excitation
    - magnetic moment
    - structure
- Collision processes
- Electron emission/
    - photoelectric
- Elements
    - origin
    - relative abundances
- Gyromagnetic ratio
- Ionization potential
- Luminescence
    - gases
- Optical pumping
- Orbital calculation methods
- Periodic system
- Spectra
    - atoms
- Spectral line breadth
- Stark effect
- X-ray spectra
    - absorption
    - emission
- Zeeman effect

Isotopes

- Isotope effects
- Isotope exchanges
- Isotope separation
- Isotopes
    - detection
    - relative abundances
- Mass spectra
- Mass spectrometers/
    - applications
- Radioactive dating
- Radioactive tracers
- Radiochemistry
- Tracers

Mesic and Muonic Atoms

- Atoms, mesic and muonic

MOLECULES

- Molecules

Structure · Internal Mechanics

Spectra

- Bonds
- Chemical structure
- Isomerism
- Luminescence
    - gases
- Molecular weight
- Molecules
    - configuration and dimensions
        - inorganic
        - organic
    - excitation
    - internal mechanics
    - electronic structure
    - electronic structure, inorganic
    - electronic structure, organic
    - nuclear coupling
    - rotation
    - vibration
    - moments
- Optical pumping
- Orbital calculation methods
- Raman spectra
    - inorganic
    - organic
- Spectra
    - inorganic molecules
        - diatomic
        - diatomic, radiofrequency
        - polyatomic
        - polyatomic, radiofrequency
    - inorganic liquids and solutions
    - inorganic solids
        - radiofrequency
    - organic molecules and substances
        - infrared
        - radiofrequency
- Spectral line breadth
- Stark effect
- Valency
- Zeeman effect

Magnetic Resonances

- Magnetic resonance and relaxation
- Molecules/
    - nuclear coupling
    - relaxation
- Nuclear magnetic resonance and relaxation
- Nuclear quadrupole resonance
- Paramagnetic resonance and relaxation

Dissociation · Free Radicals

- Association
    - gases
- Free radicals
- Heat of dissociation
- Molecules/
    - dissociation
    - dissociation energies

Intermolecular Mechanics

- Collision processes
- Molecular beams
- Molecules/
    - intermolecular mechanics

Macromolecules · Polymers

- Association
- Heat of formation
- Isomerism
- Macromolecules
- Molecules/
    - configuration and dimensions, macromolecules
- Polymers
- Proteins

Mesic and Muonic Molecules

- Molecules, mesic and muonic

ELECTRIC DISCHARGES

- Arcs, electric
- Breakdown, electric
    - gases
- Corona, electric discharge
- Discharges, electric
    - glows
    - high-frequency
- Gas-discharge tubes
- Lightning
- Sparks, electric
- Sputtering

IONIZATION

- Dissociation
- Ion velocity
- Ionization
    - gases
- Ionization potential
- Ionization, surface
- Ions
    - recombination
    - scattering
- Shock waves/
    - effects
- Space charge

PLASMA

- Discharges, electric
    - glows
    - high-frequency
- Electron gas
- Ionization
    - gases
- Nuclear fusion
- Nuclear reactors, fusion
- Plasma
    - electromagnetic wave propagation
    - magnetohydrodynamics
    - measurement techniques
- Shock waves/
    - effects
- Space charge
- Thermonuclear reactions

Plasma Confinement

- Plasma/
    - confinement

Plasma Oscillations and Stability

- Plasma/
    - magnetohydrodynamics
    - oscillations
    - stability

Plasma Devices

- Nuclear reactors, fusion
- Plasma/
    - devices

FLUIDS

- Flow
- Fluids
- Hydrodynamics
- Hydrostatics
- Oscillations
- Turbulence
- Viscosity
- Vortices
- Waves

MECHANICS OF GASES

- Acoustic streaming
- Aerodynamics
- Anemometers
- Compressibility/
  - gases
- Condensation
- Density/
  - gases
- Diffusion in gases
  - thermal
- Flow/
  - gases
- Flowmeters
- Gases
- Humidity
- Hygrometers
- Jets
- Manometers
- Moisture
- Pressure
- Pumps
- Radiation pressure
- Supersonic flow
- Turbulence
- Viscometers
- Viscosity/
  - gases
- Vortices
- Waves

GASEOUS STATE

- Absorption/
  - acoustic waves
  - acoustic waves, ultrasonic
  - electromagnetic waves
  - light
- Association/
  - gases
- Breakdown, electric/
  - gases
- Conductivity, electrical/
  - gases
  - measurement
- Conductivity, thermal/
  - gases
  - measurement
- Dielectric properties of substances/
  - gases
- Diffraction/
  - acoustic waves
  - acoustic waves, ultrasonic
  - electromagnetic waves
  - light
- Diffusion/
  - acoustic waves
  - electromagnetic waves
  - light
- Electrical properties of substances
- Electroluminescence
- Equations of state/
  - gases
- Gases
- Helium/
  - gas
- Interference/
  - acoustic waves
- Joule—Thomson effect
- Kinetic theory/
  - gases
- Lasers/
  - gaseous
- Luminescence/
  - gases
- Magnetic resonance and relaxation
- Molecules/
  - intermolecular mechanics
- Nuclear magnetic resonance and relaxation
- Nuclear quadrupole resonance
- Optical properties of substances
- Paramagnetic resonance and relaxation
- Reflection/
  - acoustic waves
  - acoustic waves, ultrasonic
  - electromagnetic waves
  - light
- Refraction/
  - acoustic waves
  - acoustic waves, ultrasonic
  - electromagnetic waves
  - light
- Scattering/
  - acoustic waves
  - acoustic waves, ultrasonic
  - electromagnetic waves
  - light
- Sorption
- Specific heat/
  - gases
- Spectra
- Statistical mechanics
- Thermoluminescence
- Transmission/
  - acoustic waves
  - acoustic waves, ultrasonic
  - light
- Velocity/
  - acoustic waves
  - acoustic waves, ultrasonic

Viscosity · Diffusion

- Diffusion in gases
  - thermal
- Transport processes
- Viscosity/
  - gases

VACUUM PHYSICS

- Glass—metal seals
- Leak detection
- Manometers
- Sputtering
- Vacuum apparatus
- Vacuum gauges
- Vacuum pumps
- Vacuum technique

MECHANICS OF LIQUIDS

- Acoustic streaming
- Bubbles
- Capillarity
- Cavitation
- Compressibility/
    - liquids
- Density/
    - liquids
- Diffusion in liquids
    - thermal
- Double refraction/
    - flow
- Drops
- Elasticity/
    - liquids
- Emulsions
- Films/
    - liquid
- Filters
- Flow/
    - liquids
- Flowmeters
- Foams
- Hydrodynamics
- Hydrostatics
- Jets
- Liquid oscillations
- Liquid waves
    - surface
- Lubrication
- Moisture
- Pressure
- Pumps
- Radiation pressure
- Rheology
- Schlieren systems
- Sprays
- Surface energy
- Surface tension
- Surface tension measurement
- Thixotropy
- Turbulence
- Viscometers
- Viscosity/
    - liquids
- Vortices
- Wetting

LIQUID STATE

Liquids

Theory and Structure of Liquids Solutions

- Association/
    - liquids
- Electron diffraction examination of materials
- Equations of state/
    - liquids
- Films/
    - liquid
- Heat of solution
- Liquid crystals
- Liquids
    - structure
    - theory
- Neutron diffraction examination of materials
- Neutrons/
    - scattering
- Polymers
- Solubility
- Solutions
- X-ray examination of materials/
    - liquids

Viscosity · Surface Tension · Diffusion

- Diffusion in liquids
    - thermal
- Filters
- Membranes
- Osmosis
- Sorption
- Surface tension
- Surface tension measurement
- Transport processes
- Viscosity/
    - liquids

Optical Properties of Liquids

- Absorption/
    - electromagnetic waves
    - light
- Diffraction/
    - electromagnetic waves
    - light
- Diffusion/
    - electromagnetic waves
    - light
- Double refraction
    - flow
- Electroluminescence
- Luminescence/
    - liquids and solutions
- Optical pumping
- Optical properties of substs.
- Raman spectra
    - inorganic
    - organic
- Reflection/
    - electromagnetic waves
    - light
- Refraction/
    - electromagnetic waves
    - light
- Scattering/
    - electromagnetic waves
    - light
- Spectra/
    - inorganic liquids and solutions
- Thermoluminescence
- Transmission/
    - light

Thermal Properties of Liquids

- Conductivity, thermal/
    - liquids
    - measurement
- Heat of solution
- Specific heat/
    - liquids
- Thermal expansion
- Thermodynamic properties

Acoustical Properties of Liquids

- Absorption/
    - acoustic waves
    - acoustic waves, ultrasonic
- Acoustic wave propagation
    - ultrasonic
- Diffraction/
    - acoustic waves
    - acoustic waves, ultrasonic
- Diffusion/
    - acoustic waves
- Interference/
    - acoustic waves
- Reflection/
    - acoustic waves
    - acoustic waves, ultrasonic
- Refraction/
    - acoustic waves
    - acoustic waves, ultrasonic
- Scattering/
    - acoustic waves
    - acoustic waves, ultrasonic
- Transmission/
    - acoustic waves
    - acoustic waves, ultrasonic
- Velocity/
    - acoustic waves
    - acoustic waves, ultrasonic

Electrical and Magnetic Properties of Liquids

- Absorption/
    - electromagnetic waves
- Breakdown, electric/
    - liquids
- Conductivity, electrical/
    - liquids
    - liquids, electrolytic
    - measurement
- Dielectric properties of substs./
    - liquids and solutions
- Electrical properties of substs.
- Ionization, liquids
- Magnetic properties of substs.
- Magnetic resonance and relaxation
- Metals
- Nuclear magnetic resonance and relaxation
- Nuclear quadrupole resonance
- Paramagnetic resonance and relaxation
- Semiconducting materials
- Semiconductors

DISPERSIONS · COLLOIDS

- Aerosols
- Centrifuges
- Colloids
- Disperse systems
- Electrophoresis
- Emulsions
- Filters
- Foams
- Gels
- Heat of solution
- Membranes
- Osmosis
- Particle size
- Precipitation
- Sedimentation
- Sols
- Solubility
- Solutions
- Surface phenomena
- Suspensions
- Thixotropy

CHANGE OF STATE

- Boiling
- Boiling point
- Condensation
- Critical constants, thermal
- Distillation
- Drying
- Equations of state
    - gases
    - liquids
    - solids
- Evaporation
- Freezing
- Heat of fusion
- Heat of sublimation
- Heat of transformation
- Heat of vaporization
- Humidity
- Liquefaction, gases
- Melting
- Melting point
- Phase equilibrium
- Phase transformations
- Sublimation
- Supercooling
- Vapour pressure
- Vapour pressure measurement
- Vaporization

SOLID-STATE PHYSICS

- Bonds
- Crystals
    - internal fields
- Crystal properties
- Equations of state/
    - solids
- Metals
    - theory
- Mössbauer effect
- Nuclear orientation
- Orbital calculation methods
- Solids
    - structure
    - theory

STRUCTURE OF SOLIDS · ALLOYS

- Alloys
- Crystal structure
- Density/
    - solids
- Fibres
- Filters
- Granular structure
- Heat treatment
    - alloys
- Membranes
- Particle size
- Permeability, mechanical
- Polymorphism
- Porous materials
- Powders
- Sintering
- Solids
    - structure
- Solid solutions
- Solubility

Solid-State Phase Transformations

- Heat treatment
    - alloys
- Phase equilibrium
- Phase transformations/
    - solid-state
- Polymorphism
- Precipitation

Surfaces

- Surface energy
- Surface measurement
- Surface phenomena
- Surface texture

Films

- Evaporation
- Films/
    - solid
- Magnetic films
- Optical films
- Sputtering
- Sublimation

Adsorption

- Adsorbed layers
- Adsorption
- Heat of adsorption
- Sorption

NON-CRYSTALLINE STATE

- Amorphous state
- Glass
- Plastics
- Polymers
- Rubber
- Vitreous state
- Waxes

CRYSTALLOGRAPHY

- Crystal chemistry
- Crystal properties
- Crystal structure
- Crystallization
- Crystallography
- Crystals
    - etching
    - faces
    - growth
    - orientation
    - twinning
    - whiskers
- Minerals
- Polymorphism
- Precipitation
- Solids/
    - structure
- Surface texture
- Zone melting and refining

MICROSTRUCTURE OF SOLIDS

- Amorphous state
- Crystal structure/
    - microstructure
- Electron diffraction examination [of materials
- Electron microscope examination [of materials
- Electron microscopy
- Fibres
- Granular structure
- Ion microscopes
- Metallurgy
- Microscopy
- Neutron diffr. exam. of materials
- Particle size
- Porous materials
- Powders
- Radiography
- Surface texture
- X-ray examination of materials/
    - microstructure
    - molecular structure

CRYSTAL LATTICE STRUCTURES

- Crystal structure, atomic
    - elements
    - alloys
    - inorganic compounds
    - organic compounds
- Electron diffraction crystallography
- Electron diffraction examination [of materials
- Electron microscope examination [of materials
- Neutron diffraction crystallography
- Neutron diffraction examination [of materials
- Polymers
- X-ray absorption
- X-ray crystallography
    - apparatus
    - calculation apparatus
    - calculation methods
    - technique
- X-ray diffraction
- X-ray examination of materials/
    - molecular structure
- X-ray measurement
- X-ray monochromators
- X-ray reflection
- X-ray scattering
- X-ray tubes

LATTICE MECHANICS

- Crystals/
    - lattice mechanics
- Mössbauer effect

ACOUSTICAL PROPERTIES OF SOLIDS

- Absorption/
    - acoustic waves
    - acoustic waves, ultrasonic
- Acoustic wave propagation
    - ultrasonic
- Acoustoelectric effects
- Diffraction/
    - acoustic waves
    - acoustic waves, ultrasonic
- Dispersion, acoustic
    - ultrasonic
- Magnetoacoustic effects
- Reflection/
    - acoustic waves
    - acoustic waves, ultrasonic
- Refraction/
    - acoustic waves
    - acoustic waves, ultrasonic
- Scattering/
    - acoustic waves
    - acoustic waves, ultrasonic
- Transmission/
    - acoustic waves
    - acoustic waves, ultrasonic
- Velocity/
    - acoustic waves
    - acoustic waves, ultrasonic

THERMAL PROPERTIES OF SOLIDS

- Conductivity, thermal/
    - measurement
    - solids
- Equations of state/
    - solids
- Heat conduction
- Specific heat/
    - solids
- Thermal expansion
- Thermodynamic properties

DIFFUSION IN SOLIDS

- Diffusion in solids
- Permeability, mechanical

DEFECT PROPERTIES OF SOLIDS

- Cold working
- Creep
- Crystal imperfections
    - dislocations
    - interstitials
    - vacancies
- Crystal structure
- Crystals
    - etching
    - twinning
- Deformation
- Elastic deformation
- Electron diffraction examination [of materials
- Electron microscope examination [of materials
- Heat treatment
    - alloys
- Internal friction
- Neutron diffraction examination [of materials
- Plastic deformation
- Plastic flow
- Slip
- Stresses, internal
- Work hardening
- X-ray examination of materials/
    - microstructure

Colour Centres

- Absorption/
    - light
- Colour centres
- X-rays/
    - effects

RADIATION EFFECTS IN SOLIDS

- Acoustic waves/
    - effects
- Alpha-rays/
    - effects
- Beta-rays/
    - effects
- Deuterons/
    - effects
- Electron beams/
    - effects
- Gamma-rays/
    - effects
- Hyperons/
    - effects
- Ion beams/
    - effects
- Mesons/
    - effects
- Neutrons and antineutrons/
    - effects
- Physical effects of radiations
- Protons and antiprotons/
    - effects
- Sputtering
- X-rays/
    - effects

MECHANICAL PROPERTIES OF SOLIDS

- Abrasion
- Adhesion
- Bending
- Brittleness
- Cold working
- Compressibility
- Corrosion
- Cracks
- Creep
- Deformation
- Density/
    - solids
- Elastic constants
    - measurement
- Elastic deformation
- Elastic fatigue
- Elastic limit
- Elastic relaxation
- Elasticity
- Fracture
- Friction
- Hardness
- Heat treatment
    - alloys
- High-pressure phenomena [and effects
- Hysteresis
- Impact
- Internal friction
- Lubrication
- Magnetomechanical effects
- Mechanical properties of substs.
- Mechanical strength
    - compressive
    - shear
    - tensile
- Photoelasticity
- Physical effects of radiations
- Plastic deformation
- Plastic flow
- Plasticity
- Rheology
- Slip
- Strain gauges
- Stress analysis
- Stress effects
- Stress/strain relations
- Stresses, internal
- Thermoelasticity
- Thixotropy
- Torsion
- Viscoelasticity
- Wear
- Work hardening

ELECTRON STATES IN SOLIDS

- Crystal electron states
    - band structure
    - excitons
    - Fermi level
    - Fermi surface
    - plasma
    - polarons
    - surface
- Crystal properties
- Cyclotron resonance
- Electron beams/
    - effects
- Electron gas
- Electron pairs/
    - annihilation
- Electrons
    - absorption
    - radiation
    - scattering
- Hall effect
- Magnetoacoustic effects
- Metals
    - theory
- Piezoresistance
- Solids
    - theory
- Surface phenomena

ELECTRICAL PROPERTIES OF SOLIDS

- Acoustoelectric effects
- Conduction, electrical
- Conductivity, electrical/
    - measurement
    - solids
- Contact potential
- Contact resistance
- Crystal electron states
- Eddy-currents
- Electrical properties of substs.
- Electron gas

Metals · Conductors

- Electron gas
- Hall effect
- Magnetoelectric effects
- Magnetoresistance
- Metals
    - theory
- Piezoresistance
- Skin effect

Superconductivity

- Superconductivity

Superconducting Materials and Devices

- Superconducting materials and devices

Semiconductors

- Acoustoelectric effects
- Contact potential
- Contact resistance
- Electron gas
- Electro-optical effects
- Fluctuations/
    - electrical
- Hall effect
- Magnetoelectric effects
- Magnetoresistance
- Magnetothermal effects
- Piezoelectricity
- Piezoresistance
- Semiconductors
- Space charge

Semiconducting Materials

- Semiconducting materials
    - gallium arsenide
    - germanium
    - indium antimonide
    - silicon

Semiconducting Devices

- Counters/
    - semiconductor
- Semiconducting devices
    - diodes
    - p–n junctions
    - transistors
    - tunnel diodes
- Rectifiers

- Electro-optical effects
- Fluctuations/
    - electrical
- Hall effect
- Magnetoelectric effects
- Magnetoresistance
- Magnetothermal effects
- Piezoelectricity
- Piezoresistance
- Resistance, electrical
- Space charge

Dielectrics

- Breakdown, electric/
    - solids
- Contact potential
- Dielectric devices
- Dielectric materials
- Dielectric measurement
- Dielectric phenomena
- Dielectric properties of substs./
    - solids
- Electrets
- Electric charge
- Electric fields
- Electric strength
- Electrostriction
- Ferroelectric materials
    - barium titanate
- Ferroelectric phenomena
- Hysteresis
- Piezoelectric oscillations
- Piezoelectricity
- Pyroelectricity
- Relaxation
- Rochelle salt
- Space charge
- Triboelectricity

THERMOELECTRIC PROPERTIES OF SOLIDS

- Thermocouples
- Thermoelectricity

PHOTOCONDUCTIVITY · PHOTOVOLTAIC EFFECTS

- Photoconductivity
- Photoelectricity
- Photoelectromagnetic effects
- Photovoltaic effects

ELECTRON AND ION EMISSION BY SOLIDS

- Cathodes
    - oxide
- Electron emission
    - field emission
    - photoelectric
    - secondary
    - thermionic
- Ion emission
    - secondary
    - thermionic
- Ionization/
    - solids
- Ionization, surface
- Work function

MAGNETIC PROPERTIES OF SOLIDS

- Antiferromagnetism
- de Haas—van Alphen effect
- Diamagnetism
- Electron diffraction examination [of materials
- Electron microscope examination [of materials
- Ferrimagnetism
- Ferrites
- Ferromagnetism
  - spin-wave theory
- Gyromagnetic ratio
- Hall effect
- Hysteresis
- Magnetic devices
- Magnetic fields/
  - effects
- Magnetic films
- Magnetic materials
- Magnetic properties of substs.
  - antiferromagnetic
  - diamagnetic
  - ferrimagnetic
  - ferromagnetic
  - paramagnetic
  - transitions
- Magnetism
- Magnetization process
- Magnetization state
  - domains
- Magnetoacoustic effects
- Magnetoelectric effects
- Magneto-optical effects
- Magnetoresistance
- Magnetostriction
- Magnetothermal effects
- Neutron diffraction examination [of materials
- Paramagnetism
- Zeeman effect

Paramagnetic Properties

- Magnetic properties of substances/
  - paramagnetic
- Paramagnetism

Ferromagnetic Properties

- Ferromagnetism
  - spin-wave theory
- Hysteresis
- Magnetic devices
- Magnetic films
- Magnetic properties of substances/
  - ferromagnetic
- Magnetization process
- Magnetization state
  - domains

Ferrimagnetic Properties · Ferrites

- Ferrimagnetism
- Ferrites
- Hysteresis
- Magnetic devices
- Magnetic films
- Magnetic properties of substs./
  - ferrimagnetic

Antiferromagnetic Properties

- Antiferromagnetism
- Magnetic properties of substs./
  - antiferromagnetic

MAGNETIC RESONANCES IN SOLIDS

- Antiferromagnetic resonance
- Cyclotron resonance
- Ferrimagnetic resonance
- Ferromagnetic relaxation
- Ferromagnetic resonance
- Gyromagnetic ratio
- Magnetic resonance and relaxation
- Magnetomechanical effects
- Nuclear magnetic resonance and
  - measurement [relaxation
- Nuclear quadrupole resonance
- Optical pumping
- Paramagnetic resonance and
  - measurement [relaxatio

OPTICAL PROPERTIES OF SOLIDS

- Absorption/
  - electromagnetic waves
  - light
- Diffraction/
  - electromagnetic waves
  - light
- Diffusion/
  - electromagnetic waves
  - light
- Dispersion, optical
- Double refraction
  - mechanical
- Electromag. wave propagation
- Electro-optical effects
- Emissivity
- Interference/
  - light
- Lasers/
  - solid
- Magneto-optical effects
- Optical constants
- Optical films
- Optical materials
- Optical properties of substances
- Optical pumping
- Optical rotation
- Photoelasticity
- Pleochroism
- Polarized light
- Raman spectra
  - inorganic
  - organic
- Reflection/
  - electromagnetic waves
  - light
- Reflectivity
- Refraction/
  - electromagnetic waves
  - light
- Refractive index/
  - light
- Scattering/
  - electromagnetic waves
  - light
- Spectra/
  - inorganic solids
    - radiofrequency
  - organic molecules and
    - infrared [substances
    - radiofrequency
- Spectral line breadth
- Stark effect
- Transmission/
  - light
- Transparency
- Velocity/
  - light
- X-ray spectra
  - absorption
  - emission
- Zeeman effect

Luminescence of Solids

- Colour centres
- Counters,scintillation
- Electroluminescence
- Luminescence/
  - solids, inorganic
  - solids, organic
- Luminescent devices
- Thermoluminescence

PHYSICAL CHEMISTRY

- Atomic mass and weight
- Balances
- Bonds
- Centrifuges
- Chemical structure
- Chemical technology
- Distillation
- Elements
  - origin
  - relative abundances
- Filters
- Isomerism

THERMOCHEMISTRY · REACTIONS

- Association
  - gases
  - liquids
- Catalysis
- Chemical reactions
- Combustion
- Corrosion
- Crystal chemistry
- Detonation
- Dissociation
- Exchanges, chemical
- Explosions
- Flames
- Heat of adsorption
- Heat of combustion
- Heat of dissociation
- Heat of formation
- Heat of reaction
- Isotope exchanges
- Oxidation
- Phase equilibrium
- Phase transformations
- Polymerization
- Polymers
- Reaction kinetics
- Sorption

ELECTROCHEMISTRY

- Conductivity, electrical/
  - liquids, electrolytic
- Dissociation/
  - electrolytic
- Electrochemistry
  - electrodes
- Electrokinetic effects
- Electrolysis
- Electrolytic deposition
- Electrophoresis
- Ion velocity/
  - electrolytic
- Ions, electrolytic

- Laboratory app. and technique
- Macromolecules
- Molecular weight
- Molecular weight determn.
- Periodic system
- Physical chemistry
- Precipitation
- Pumps
- Quantum chemistry
- Sedimentation
- Valency

PHOTOCHEMISTRY
RADIATION CHEMISTRY
RADIOCHEMISTRY

- Chemical effects of radiations
  - acoustic waves
  - ionizing radiations
- Nuclear reactions/
  - chemical effects
- Photochemistry
- Radiochemistry

PHYSICAL METHODS OF CHEMICAL ANALYSIS

- Chemical analysis
  - adsorption
  - by mass spectrometry
  - by nuclear reactions
  - electrochemical
  - radioactive
  - X-ray
- Chromatography
- Radioactive tracers
- Spectrochemical analysis
- Tracers

GEOPHYSICS

- Earth
  - age
  - composition
  - electricity
  - heat
  - rotation
- Geodesy
- Geophysical prospecting
- Geophysics
- Glaciers
- Gravity
- Minerals
- Oceanography
- Radioactive dating
- Radioactivity
- Seawater
- Seismic waves
- Seismology
- Soil

ATMOSPHERE

- Anemometers
- Atmosphere
  - composition
  - humidity
  - movements
  - precipitation
  - radioactivity
  - structure
  - temperature
  - thermodynamics
- Atmospheric acoustics
- Atmospheric electricity
- Atmospheric optics
- Atmospheric pressure and density
- Atmospheric spectra
- Atmospherics
- Clouds
- Condensation
- Electromagnetic wave propagation
  - atmosphere
- Evaporation
- Fallout
- Fog
- Humidity
- Hygrometers
- Ice
- Lightning
- Meteorological instruments
- Meteorology
- Rain
- Rockets
- Satellites, artificial
- Sky brightness
- Snow
- Sunlight
- Thunderstorms
- Twilight
- Wind

UPPER ATMOSPHERE

- Airglow
- Atmosphere
  - composition
  - movements
  - radiation belts
  - radioactivity
  - structure
  - temperature
  - thermodynamics
  - upper
- Atmospheric electricity
- Atmospheric optics
- Atmospheric pressure and density
- Atmospheric spectra
- Atmospherics
- Aurora
- Fallout
- Ionization, atmosphere
- Meteors
- Rockets
- Satellites, artificial
- Sky brightness
- Sunlight
- Twilight
- Zodiacal light

Ionosphere

- Atmospherics
- Aurora
- Electromag. wave propagation
  - ionosphere
- Ionization, atmosphere
- Ionosphere
  - D-region
  - E-region
  - F-region
- Ionosphere meas. apparatus

SPACE RESEARCH TECHNIQUES

- Rockets
- Satellites, artificial
- Space research
- Space vehicles
  - instrumentation

GEOMAGNETISM

- Compasses
- Earth/
  - magnetic field
  - magnetic field, variations
- Magnetic storms
- Rock magnetism

ASTROPHYSICS

- Astronomical instruments
- Astronomical observations
- Astronomical spectra
- Astronomy and astrophysics
- Celestial mechanics
- Cosmic rays
- Cosmology
- Elements/
  - origin
  - relative abundances
- Gravitation
- Interstellar matter
- Telescopes/
  - astronomical

STARS · GALAXIES

- Cosmic radiations,r.f.
- Galaxies
  - the Galaxy
- Interstellar matter
- Magnetohydrodynamics
- Nebulae
- Novae
- Quasars
- Stars
  - composition
  - evolution
  - magnetism
  - radiation
  - spectra
  - structure
- Thermonuclear reactions

SOLAR SYSTEM · SUN

- Comets
- Cosmic rays
- Earth
  - rotation
- Gravitation
- Interplanetary magnetic field
- Interplanetary matter
- Meteorites
- Meteors
- Moon
- Planets
- Solar system
- Sun
  - corona
  - eclipses
  - flares
  - magnetism
  - prominences
  - radiation
  - radiation, corpuscular
  - radiation, r.f.
  - spectra
- Sunspots
- Zodiacal light

RADIOASTRONOMY TECHNIQUES

- Cosmic radiations, r.f.
- Radioastronomy

BIOPHYSICS

- Biological effects of radiations
- Biological technique and instruments
- Biology
- Biophysics
- Blood
- Dosimetry
- Medical science
- Physiology
- Proteins
- Radiation protection
- Radiography
- Zoology

TECHNIQUE · MATERIALS

- Biological technique and instruments
- Chemical technology
- Heat treatment
  - alloys
- Laboratory apparatus and technique
- Leak detection
- Low-temperature technique
- Materials
- Metallurgy
- Vacuum technique
- Zone melting and refining

HIGH-PRESSURE TECHNIQUES

- High-pressure phenomena and effects

SUBSTANCES

Chemical elements and inorganic compounds

All the chemical elements are listed by name, followed by their compounds, e.g. "Cadmium", "Cadmium compounds".

"Hydrogen" is subdivided by the subheadings "neutral atoms", "neutral molecules", and "ions". "Deuterium" and "Tritium" are independent headings. "Hydrogen compounds" is supplemented by "Ice", "Steam", and "Water".

"Oxygen" is supplemented by "Ozone", and "Carbon" is supplemented by "Diamonds" and "Graphite".

The following inorganic compounds are further subdivided by subheadings as shown:-

- Barium compounds
  - barium titanate*
- Cadmium compounds
  - cadmium sulphide
- Calcium compounds
  - calcium fluoride
- Gallium compounds
  - gallium arsenide**
- Indium compounds
  - indium antimonide**
- Lithium compounds
  - lithium fluoride
- Nitrogen compounds
  - ammonia
  - ammonium compounds
- Potassium compounds
  - potassium bromide
  - potassium chloride
- Sodium compounds
  - sodium chloride
- Zinc compounds
  - zinc sulphide

* Ferroelectric properties are listed under "Ferroelectric materials/barium titanate"

** Semiconducting properties are listed under the corresponding subheadings of "Semiconducting materials"

Organic compounds

Organic compounds are grouped under headings "Organic compounds", "Polymers", "Plastics", "Proteins". "Rochelle salt" is an independent heading.

Substance groups

In addition there are the following headings for groups of elements, compounds or substances:-

- Actinides
- Actinide compounds
- Alkali metals
- Alkali-metal compounds
  - halides
- Alkaline-earth metals
- Alkaline-earth compounds
- Ferrites
- Ferroelectric materials
  - barium titanate*
- Garnets
- Halogens
- Inert gases
- Metals
- Minerals
- Rare-earth metals
- Rare-earth compounds
- Semiconductors
- Semiconducting materials
  - gallium arsenide**
  - germanium**
  - indium antimonide**
  - silicon**
- Transition metals
- Transition-metal compounds

* Used for ferroelectric properties only

** Used for semiconducting properties only

Alloys

General papers on alloys are indexed under "Alloys". Alloys of specified composition are listed under, either

(i) special alloy headings (there are five of them: "Aluminium alloys", "Copper alloys", "Iron alloys", "Nickel alloys", "Steel"), e.g. Al–Ni alloys under "Aluminium alloys", or

(ii) compounds of the base or first-named element, e.g. Mn–Zn alloys under "Manganese compounds", and silicon-iron under "Iron alloys".

Special substances and materials

There are also the following special headings for certain common substances:-

- Air
- Blood
- Ceramics
- Clay
- Coal
- Concrete
- Fibres
- Gelatin
- Glass
- Mica
- Optical materials
- Paper
- Porous materials
- Powders
- Quartz
- Rubber
- Ruby
- Sand
- Seawater
- Soil
- Waxes
- Wood

ADP (ammonium dihydrogen phosphate). See Nitrogen compounds/ammonium compounds.
Abacs. See Nomograms.
Aberrations, optical
See also Electron lenses; Ion optics; Optical instrument testing; Optics/geometrical; Particle optics.
aperture, annular, with spherical and coma, irradiance distrib. in diffr. patterns 8=42169
aperture, of 3rd order of stigmatic quadrupolar systems 8=28727
aspherical surfaces, calc. method 8=24363
astigmatic difference, sign estimation 8=24364
astigmatism in Mach-Zehnder interferometer 8=28863-5
astigmatism, lens correction in Czerny-Turner spectrograph 8=46664
chromatic, of two-dimensional quadrupole e.s. lens 8=37421
coma in Czerny-Turner spectrographs, compensation 8=28730
correction, optimal conditions, and optimal position of image plane 8=42162
diffraction gratings, concave, approx. formulae 8=24415
dome-shaped lens for signal lights, formula for computation 8=42156
electron beam two-dimensional deflection 8=46407
electron lens, spherical correction in two-sections 8=24144
electrostatic focusing systems 8=41963
eye, lens astigmatism in accommodation 8=37726
Gaussian type (F/1.8) lens, in direct and reversed system, comparison 8=33245
image distortion, new theory 8=37638
lens, mag., probe-forming, spherical obs. and calc. 8=33086
on and off-axis, correction by insertion of aspherical surfaces 8=46663
precision meas. 8=28752
quadrupole lenses, spherical, compensation by octupole 8=33071
spectrometer, focal isolation, using lens chromatic aberration 8=28797
spherical, coeff., for stigmatic quadrupole doublet 8=33070
spherical, in optical system, quality 8=28739
spherical, partially coherent light, imaging of straight edge 8=37694
third order coeffs., paraxial ray trace procedure for 8=28753
third-order region, computerized design of cemented two-lens objectives 8=42163
transfer function, meas. and use 8=28736
transmission through aberrated and misaligned lenses, effect of redirectors refocusers and mode filters 8=46662
wave aberration, depend. of Strehl ratio on magnitude of variance 8=28731
wave aberration, evaluation of variance, direct approach 8=37640
wave function, variance evaluation 8=42254
wave optics calc. of light distrib. in image plane of photographic objective 8=46764
in wide angle lenses, asymmetrical, rel. to image forming props. 8=28910
Abrasion
See also Hardness; Wear.
alkali halide crystals in org. liquids, rel. to interfacial energy calcs. 8=30724
alumina ceramics, resistance, rel. to densification and grinding 8=48987
crystals, effects on X-ray absorpt. spectra during crystal processing to cylinder or sphere 8=41038
diamond grains, frictional coeffs. between metal and grains 8=31184
diamond, spark-erosion shaping 8=35662
grinding process dynamics, theoretical anal. 8=40120
metal surfaces, rel. to contact area 8=26775
solid fuels, radiochemical method 8=35645
Al_2O_3 grains, frictional coeffs. between metal and grains 8=31184
Cu-Au solid solution alloys, rel. to surface hardness, friction and wear 8=40149
Cu-Zn alloys, rel. to surface and subsurface structure 8=26294
SiC grains, frictional coeffs. between metal and grains 8=31184
Absorption
See also subheadings of Alpha-rays; Beta-rays; Cosmic rays; Electrons; Gamma-rays; Hyperons; Mesons; Neutrons and antineutrons; Protons and antiprotons; and also Sorption; X-ray absorption.
crystals, of isomorphous impurities rel. to compounds of different solubilities 8=26612
electrolytic, Debye-Hückel limiting law Gibb's equation 8=36591
electron beam, diffracting, abnormal, by plasmon 8=44662
electron probe X-ray microanalysis, and atomic no. corrections 8=41311
exciton spectra, low temp., theory 8=40258
gas, in packed columns, correlation of gravitational force 8=50003

Absorption—contd
gases and evolution in chemical reactions, automatic constant pressure apparatus 8=30270
interstellar bands, diffuse, origin 8=28062
Michelson interferometers, and for spectroscopy and refractometry 8=33272
monoethanolamine, absorpt. of CO_2, optical study of interfacial turbulance 8=32093
multicomponent systems, curved operating lines 8=48248
Planck and Rosseland mean absorpt. coeffs. for optically thin and thick gases 8=25822
radiant heating of an absorbing and scattering slab 8=46228
radiative transfer, grey absorpt. coeffs. 8=32862
relativistic Doppler eqns. for attenuated waves and drag effect 8=46470
steel, porous castings, hydrogenated, rel. to defects 8=30663
water jets, turbulent, absorpt. of CO_2 and H_2 8=30425
wedge crystals, effect on multi-beam intensity profiles 8=45150
zinnwaldite, mica, Mossbauer effect spectroscopy investigations 8=43960
in Fe aerosols, spectral, of excited mols. 8=34950
Fe particles dispersed in N, Ar or H gas, spectra including carrier gas contrib. 8=25968
GaAs, coeff. at microwave and mm. freqs. 8=27568
Hg electrode, adsorpt. energy of ions 8=36600
KI, due to U-centres and F-centres, far i.r. 8=44480
NaF:OH^-, u.v. and i.r. 8=45208
O, solid at 4°K, in range $(15-33) \times 10^3 cm^{-1}$, rel. to simultaneous transitions 8=32019
Si, adsorpt. of Au, Sb and O_2, rel. to elec. props. 8=27134
Zn electrodes, adsorpt. of org. materials, pot. vars. 8=36601
Zn K-absorpt. edge in Zn-Al alloys, fine structure investigation 8=41155
acoustic waves
See also Noise abatement; Transmission/acoustic waves.
acoustic paramag. resonance, 1-200 Mc/s, methods for study 8=49592
antiferromagnets, uniaxial, anomalous attenuation near spin-flop transition point 8=26580
attenuation due to magnon-phonon interaction 8=35401
attenuation near magnetic critical points 8=30939
azoxybenzenes, liq. cryst. 8=25882
crystals with quasi-local states, theoretical analysis 8=35399
decaying sound field diffusion, reverberation room obs. 8=23961
in dielectrics with high permittivity, elec. field effects, theory 8=40560
ferrite plate, parametric excitation rel. to spin oscill. instability 8=40833
filter, time-varying as equivalent of moving target 8=32910
fourth sound, in plano-parallel capillary. depend. on width and temp. 8=37264
gas, interaction with external radiation applied instantaneously at boundary 8=43692
liquid mixture, damping and dispersion near critical point 8=30465
metal thin sheet, simple and constrained damping layers, loss factor obs. 8=35612
monatomic gas, using relaxation theory 8=30297
multiple panels, loss in random incidence field 8=37265
n.m.r., Bloch-type equations 8=33150
non-thermal, by thermal X-ray source, model 8=45770
partition walls, investigation of theory using model 8=32921
piezoelectric semiconductor with traps, amplification theory 8=35404
piston array, reception and refl. calc. 8=46182
quartz, anomalous phenomenon near λ pt. in $\alpha \rightarrow \beta$ transition 8=26584
Rochelle salt, mechanism in vibration damping near phase transition 8=39899
ruby: (Cr^{3+} and Al^{27}), electron and nuclear paramag. acoustic obs. at 4.2°K 8=40914
steels, carbon and stainless, attenuation, 20-800°C 8=30945
superconductors, h.f. attenuation 8=44309
suspensions and marine sediments 8=25961-2
in two-zone type II superconductors, of longitudinal waves 8=35400
CO_2-H_2O vapour, pressure, temp. effects 8=30298
KH_2PO_4-type ferroelectric, attenuation and thermal conduction, critical anomaly 8=48716
O, in applied mag. field 8=39210
O_2 containing H_2, CO_2 or H_2O impurity, obs. 8=39211
$RbMnF_3$: F^{19}, nuclear acoustic resonance, dispersion mode saturation 8=41000
Si, phonon conductivity and attenuation 8=44324
YFe garnets, attenuation due to magnon-phonon interaction 8=35401
acoustic waves, ultrasonic
attenuation near magnetic critical point 8=39885
in binary liquid mixtures 8=25998
o-chlorophenol binary liq. mixtures, excess absorpt. 8=34842

Absorption—contd
- **acoustic waves, ultrasonic**—contd
  - dielectric crystals, predominance of Akhiezer effect 8=35402
  - ethanol-ethyl halide mixtures. relax 8=30471
  - ferromagnetic metallic film, magnetoelastic waves, boundary-value-problems 8=40797
  - gas mixture, with molecular masses largely different 8=43690
  - glycerol and water at 0. 6 MHz formation of a complex 8=34840
  - glycerol, press. depend. 8=34841
  - glycine, diglycine and triglycine in aq. solns. 8=48142
  - insulating crystals, imperfection, temp. depend 8=48715
  - lanthanide sulphates, rates of complex formation in solutions 8=48141
  - liquid, h. p., meas. method and error analysis 8=48137
  - in liquid, non-linear, parametric amplification 8=43801
  - nitrobenzene-n-hexane mixtures near critical region 8=25912
  - nuclear acoustic resonance, research summary 8=37539
  - organic liquids at 1 GHz, relaxation 8=25910
  - phonon-paramagnon interactions, effect on attenuation 8=48714
  - piezoelectric semiconductors, amplification wave amplitude dependence 8=44315
  - polypeptide solns., and helix-coil transition 8=48145
  - polystyrene solns. in benzene 8=43807
  - quartz, hypersonic phonon lifetime meas. by two successive light pulses 8=44323
  - quartz unirrad., and neutron irrad., attenuation 8=39897
  - rotational relax. time, origin of temp. depend. 8=39209
  - semiconductors attenuation and amplification by Mott excitons 8=44311
  - semiconductors, by Mott excitons 8=39888
  - superconductors, pure strong-coupling, longit. attenuation 8=44310
  - urea-urease mixture, relax. obs. 8=48144
  - Al, supercond., rel. to min. energy gap 8=40367
  - Au, attenuation meas. at low temps. rel. to dislocation motion effects 8=39894
  - CaF$_2$:U^{4+}, paramag. resonance rel. to multiple phonon interactions 8=31853
  - CCl$_4$, vibr. relax 8=39360
  - CdS, hypersound, low temp. 8=35411
  - CdS, nonelectronic attenuation meas. 8=48719
  - CdS$_x$Se$_{1-x}$, and amplification rel. to e-phonon interaction 8=35410
  - C$_6$H$_{12}$ vapours, propag. for large freq. /press. 8=43691
  - Cr, field-cooled, quantum oscillations in attenuation 8=39891
  - Ga, cyclotron resonance, Doppler-shifted 8=48720
  - Gd, at Curie temp. 8=35416
  - CdS, piezoelectric semiconductors, amplification wave amplitude dependence 8=44315
  - CoO, rel. to elastic and mag. props. 8=44560
  - GeCl$_4$, vibr. relax 8=39360
  - He-Ar mixtures, effect of diffusion rel. to press. and temp. 8=43689
  - HgTe, phonon viscosity attenuation 8=30946
  - InSb, amplification rel. to microwave emission stimulation 8=49249
  - K, attenuation meas., 2. 5-77°K rel. to dislocation motion effects 8=39894
  - KBr:Li$^+$, attenuation and velocity, stress and temp. dependence, 1. 6-77°K 8=35417
  - KCl, effect of Li$^+$ and CN$^-$ doping 8=44316
  - KCl:OH, acoustical paraelec. resonance 8=27246
  - KCl:Li$^+$, attenuation and velocity, stress and temp. dependence, 1. 6-77°K 8=35417
  - KMgF$_3$:M^{2+}(M=Ni, Fe, Co), paramag. resonance, rel. to 3d impurity ion magnetoelastic coeffs. 8=31871
  - KTaO$_3$, by nuclear spins 8=45126
  - LiNbO$_3$:Cr^{3+}, acoustic paramag. reson., 4. 2°K 8=44318
  - LiNbO$_3$:Cr^{3+}, polydomain crystal, paramagnetic, by Cr^{3+} 8=31873
  - MgAl$_2$O$_4$, microwave phonon attenuation 8=39895
  - MgO, microwave attenuation 8=30948
  - MgO: Cr^{2+} dynamic lattice coupling determ. 8=35053
  - MnF$_2$, attenuation meas. near Néel point 8=48720
  - MnF$_2$, attenuation near and above spin-flop transition, mag. field dependence 8=44319
  - NaCl, n. m. r. rel. to plastic deformation 8=44320
  - Nb, attenuation near Hc$_2$ 8=30949
  - Pb, normal-state, low temp. amplitude-independent longit. attenuation 8=44321
  - Pb, superconducting, low-temp. amplitude-independent longit. attenuation 8=44322
  - Si, attenuation freq. dependence 8=48725
  - SiCl$_4$, vibr. relax 8=39360
  - SnCl$_4$, vibr. relax 8=39360
  - TiCl$_4$, vibr. relax 8=39360
  - UO$_2$, attenuation temp. dependence rel. to elastic constants 4. 2-300°K 8=39898
  - YFe garnet, microwave phonon attenuation 8=26585
- **electromagnetic waves**
  - See also Spectra (radiofrequency subheadings).
  - in accelerators with static and h.f. mag. fields, rel. to injected plasma density 8=25749

Absorption—contd
- **electromagnetic waves**—contd
  - atmosphere, affecting solar 10 cm. obs. 8=37054
  - ionosphere, initial height determ. method 8=36824
  - atmospheric, 35 GHz solar radiation 8=27902
  - energy dissipated in absorbing plane parallel plate 8=33131
  - ferrites, imaginary refractive index 8=46473
  - films, thin, after excitation of plasmons by e.m. waves 8=40272
  - ionized gas in magnetic field near cyclotron frequencies 8=39020
  - in ionosphere, v.l.f. in range 3 kc/s, theory 8=36832
  - plasma columns, anomalous attenuation of surface waves 8=20263
  - plasma columns, anomalous attenuation of surface waves 8=39097
  - plasma, plane layer, magneto-active, obliquely incident plane wave 8=25748
  - by polarizable particle system, calc. 8=24215
  - resonant ferrite isolator in plane-parallel waveguide with dielectric 8=28620
  - screen, thin black for diffraction meas. 8=46483
  - trapezoidal grooves 8=23987
  - n-Ge, at low temp. by hopping 8=49723
  - KI, doped, far i.r. 8=49734
  - N$_2$O, spectral transmission in near i.r. bands, calc. 8=25506
  - n-Si, at low temp., by hopping 8=49723
- **light**
  - See also Atmospheric optics; Densitometry; Filters, optical; Optical constants; Optical films; Pleochroism; Transmission/light; Spectra.
  - absorptance meas., by cyclic incident radiation 8=27566
  - acetylene in solution, i. r. band widths 8=34867
  - alkali halides, extreme u.v. 8=41060
  - alkali halides, paraelastic electron-vacancy centres 8=49706
  - alkali halides, U centre isotopic effects rel. to electron-phonon interaction 8=27557
  - alkali metal, u. v. absorbing power, plasmon contrib. 8=31962
  - amplification of weak pulse by absorber saturated with simultaneous strong pulse 8=37593
  - anthracene derivatives, thin layers 8=49144
  - anthracene, rel. to exciton-phonon interact. and band struct 8=41161
  - anthracene, two-photon, cryst. and molecule 8=45237
  - aromatic hydrocarbon crysts., triplet factor group states 8=27622
  - atomic attenuation cross-section 8=38684
  - beam self-trapping in molecular fluids for saturation of non-linear refractive index 8=30478
  - Beckman photometer type DK, combined luminesc. and absorpt. meas. 8=33243
  - benzene, higher excimer states 8=34872
  - benzene, polyalkyl substitutes of, electronic u.v. spectra 8=41162
  - benzene with Na atoms, spectrum at 55-100°K 8=49769
  - n-bromophenylsulphonyl chloride, i.r. spectra in polarized light 8=41169
  - butadiene acidic and basic copolymers mixtures, rel. to H-bonds mech. lability, i.r. obs. 8=48507
  - calcite, and effect of impurity addition on absorpt. 8=26194
  - coefficient due to interband transitions in case of resonance scattering 8=45148
  - colour centres, aligned, obs. of electro-optical effects and differences between ground and excited states 8=44471
  - crystal, mol., i. r. vibr. line breadth rel. to reorientation 8=36292
  - crystals, co-operative, donor-acceptor mechanisms 8=31942
  - crystals, phonon processes in bound e. transitions 8=49678
  - crystals, rel. to Urbach's rule 8=36295
  - crystals of square planar complexes, origin of colour 8=27535
  - cyanoanthracene solns., vitreous, temp. dependence rel. to dimer and crystallite formation 8=43823
  - diamond, interband, rel. to band structure 8=40233
  - diffuse interstellar bands, origin 8=28099
  - dust grains, effect on spectral line formation 8=50337
  - dyes, Q-switch, for Nd lasers 8=42112
  - ethers of aliphatic and aromatic acids, optical parameters 8=30493
  - F-centre, three-body model, 0- and 1-phonon spectrum 8=44472
  - far i.r. in disordered mats, correl functions 8=49681
  - fluorenon in soln., absorpt. bands, elec. field effects 8=34328
  - fluorite, irradiated, change, and elec. cond. change 8=26946
  - Franz-Keldysh effect, high-freq. 8=31950
  - gaseous, transmittance rel. to average absorpt., weak-line and strong-line 8=34666
  - glass, emerald green, u.v. absorbing, colour characts. 8=49720
  - glass, hot, i. r., and heat radiation 8=44371
  - glass, soft, far i.r., rel. to inherent disorder 8=49681
  - glass, special effect of As$_2$O$_3$ 8=41097
  - guanidine chromium sulphate hexahydrate, dilution splitting of Cr^{3+} lines 8=41164

Absorption—contd
- **light**—contd
  - holographic measurement 8=24410
  - hydrogen plasma, neutral atom density determ. 8=43545
  - hyperchromism, two-band model 8=39365
  - ice, alkaline, spectrum of trapped dielectrons 8=45194
  - ice, far i.r. rel. to Bjerrum type defects 8=49681
  - ice, u.v. spectra, vacuum 8=31998
  - impurity states in crystals, line broadening by resonant phonon interactions 8=41027
  - integral intensity meas. using Jogansen's function, applied in organic liquids 8=34865
  - interstellar, in M17 direction 8=32482
  - ionic crystals, i.r., charged defect induced 8=41026
  - ionic crystals, i.r. in range of local impurity lattice vibrs. 8=41024
  - iron-group ionic crystals, colour dependence on structure 8=27534
  - i.r. by local vibrations at multiple and combination freqs. 8=31939
  - i.r. due to impurities, reln. bet. resonant mode and vib. of defect mol. 8=49680
  - laser beam attenuation and polarization rotation meas. through rocket plumes 8=50234
  - leucosapphire grown from tungstate melts 8=39648
  - liquid-air interfaces, surface wave attenuation meas. 8=24412
  - luminescent solids spectra 8=36449
  - magnetic crystals, theories 8=36297
  - magnetic mats., far-i.r. spectroscopy, techniques, mag. ion spectra and magnon absorpt. in antiferromagnets 8=36294
  - Magnus'-type salts, origin of colour 8=27535
  - manganese arsenic borate glasses, γ-ray induced, rel. to dosimeter characts. 8=44500
  - metal iodides with layer structures, spectra 8=45176
  - methane, and deuterated, gaseous, collision induced in far i.r. 8=47657
  - minerals, absorbing anisotropic, coeff. and refractive index 8=41061
  - montmorillonite with adsorbed cations, rel. to particle size 8=34943
  - naphalene vapour, spectrum rel. to e transitions, 30 000-53 000 cm^{-1} 8=38900
  - optical density determ., correction factor 8=37681
  - ozone, mean coeffs rel. to Dobson spectrometric atmos. obs., 8=47973
  - γ-phenyl-pyridene derivatives, u. v. absorpt. spectrum 8=29797
  - phosphate glass, Mo^{3+} doped 8=31879
  - plasma, optically dense, and emission coeffs., radial distribs. 8=30078
  - plastic with increased transparency for scintillation counters 8=46882
  - polar liquid films, i.r. absorpt. rel. to orientation by cell surface elec. fields 8=39302
  - polar mols. in liq. state, charact. in far i. r. 8=34859
  - polaron excitation 8=49679
  - by polarons, rel. to excitation modes 8=27530
  - polyacrylonitrile films, obs. 8=39605
  - polypeptides, helical, theory 8=25680
  - quartz : Co-doped, spectrum and changes on X-ray exposure 8=48556
  - quartz, fused, far i.r., rel. to inherent disorder 8=49681
  - ruby, grown from tungstate melts 8=39648
  - rutile (TiO_2) crystals, doped, by polarons 8=36418
  - sapphire, blue, charge transfer band 8=27603
  - semiconductor, electron-hole complexes form. 8=31941
  - semiconductor, electron-optical-phonon system at zero temp. 8=27532
  - semiconductor, inhomogeneously inverted, nonlinear negative absorpt. 8=31943
  - semiconductors, electro-absorpt., excitonic effects 8=31297
  - semiconductors, magnetic, mag. and thermal induced edge shifts rel. to strain 8=36299
  - semiconductors, magnetooptic interband, effect of spatial dispersion of optical phonons 8=45160
  - semiconductors with spheroidal conduction band, due to donor electrons 8=36293
  - solid solutions, Davydov's splitting of bands 8=35547
  - solids, impurity bands, method of moments 8=41028
  - solids and liquids rel. to mol. Einstein coeffs. 8=39367
  - solids, two-photon spectroscopy, theory 8=41025
  - spatial spectral radiation props. of materials as fn. of temp. 8=49677
  - spectrophotofluorometer 8=46694
  - spectrum calc., net interval requirement 8=28794
  - spheres, $m \simeq 1$, obs. 8=24420
  - spiral galaxies, polarization obs. 8=28116
  - steady-state probability calc. 8=24409
  - stilbene derivatives, 8=49145
  - stratosphere, u. v. absorpt., satellite meas. 8=27911
  - tetramethyl-2, 2, 6, 6, -piperidinol-4-oxyl-1, free radical in crystal, i. r. at low temps. 8=25654
  - toluene, higher excimer states 8=34872
  - triglycine-sulphate ferroelec. group, temp.-induced changes in the 575 cm^{-1} band at phase transition 8=36438

Absorption—contd
- **light**—contd
  - triglycine sulphate, fundamental edge temp. dependence, room temp. -62°K 8=41172
  - trimethylene sulphide, $(CH_2)_3S$, crystals, i.r. spectra and Raman scatt. 8=41171
  - tryptophan solns., photo-induced trapped electron behaviour at 77°K 8=25935
  - turbid medium illuminated by narrow beam, field 8=24421
  - II-VI crystals, scattering of polaritons by phonons, contrib. 8=27533
  - two-photon, polarization dependence 8=45149
  - Urbach's rule for impurity centres 8=35548
  - Wannier-Mott exciton band profile, optical phonons effects 8=36285
  - water, far i.r., rel. to rotational transitions 8=49681
  - water, liquid, u. v. spectra, vacuum 8=31998
  - water, supersaturated vapour, i. r. 8=25477
  - water vapour in atmosphere 8=36749
  - water vapour, 6943. 8 Å laser beam 8=39218
  - $A_VB_{VI}C_{VII}$-type semiconductors, rel. to phase transforms. 8=27077
  - Ag, 50-340Å, and calc. of partial oscillator sums 8=31981
  - Ag colloid in gelatin, effect of particle shape 8=39460
  - Ag film, absorbent and anisotropic, abnormal charact. band 8=49707
  - Ag films, abnormalities from meas. in vacuum and Ar atmos. 8=45168
  - Ag particles, elongated, in glass selective polarization 8=41051
  - Ag, surface plasmon excitation 8=49700
  - Ag, thin films, effect of mean free path of conduction electrons 8=36315
  - AgBr containing iodide, mirror-like, and luminesc. 8=41050
  - AgBr, spectra pressure dependence up to 50 kbar 8=41053
  - AgBr:I^-, multiphonon structures in spectra 8=31956
  - AgCl, spectra pressure dependence up to 50 kbar 8=41053
  - AgCl:I^-, multiphonon structures in spectra 8=31956
  - AgCl:V, meas. on V ions 8=35523
  - AgIn molecule, system B of u. v. bands 8=25443
  - Al, infrared at 4. 2°K 8=27551
  - AlN crystal, coeff. rel. to band gap determ. 8=31958
  - Al_2O_3, reflectance and transmittance 8=41057
  - Al_2O_3:Cr, Ti, V, rel. to exchange coupled transitions, intraband vibr. and crystal field splitting 8=49701
  - Ar:H(D), solid, isotopic effects rel. to electron-phonon interaction 8=27557
  - Ar, u. v. cross sections, bandwidth depend. 8=25356
  - Au, 50-340Å, and calc. of partial oscillator sums 8=31981
  - Au film, absorbent and anisotropic, abnormal charact. band 8=49707
  - β-B, 0. 7-25μ and forbidden band-with temp. coeff, 160-400°C 8=41065
  - Ba films 8=27560
  - BaF_2 : Co^{2+}, spectra temp. dependences 8=41076
  - $Ba(N_3)_2$, cryst. 8=27485
  - Bi, 50-340Å, and calc. of partial oscillator sums 8=31981
  - BiSCl, and photocond. 8=32028
  - C films, evaporated, i. r. edge 8=36335
  - CaF_2, synthetic, photoconduction 8=36338
  - CaF_2 : $Co^{2+}(Ni^{2+})$, spectra temp. dependences 8=41076
  - CaF_2: H interstitial atoms, i.r. spectrum rel. to localized vibrations of H 8=41072
  - CaF_2/Na, synthetic photoconduction 8=36338
  - CaF_2:Ho^{3+}, two-photon, on laser illumination 8=45180
  - $CdCr_2Se_4$, ferromagnetic, i.r. spectrum 8=41078
  - CdF_2 : $Co^{2+}(Ni^{2+})$, spectra temp. dependences 8=41076
  - CdS, e-beam excited, saturation 8=31973
  - CdS films, vapour-deposited, colour changes rel. to interstitials 8=26114
  - CdS particles in glass, with a.c. elect. field modulation, obs. 8=40267
  - CdS, two-photon spectrum, anisotropy 8=45181
  - CdSe, effect of uniaxial stress 8=36342
  - CdSe films, nonlinear 8=36340
  - CdSe semiconductor lasers, two-photon absorpt. anisotropy in the optical excitation 8=36341
  - CdSe:Cu, fundamental edge impurity conc. dependence 8=36349
  - CdSe:Cu, i. r. spectrum rel. to Cu impurity conc. 8=36345
  - CdTe:Fe, selective abs. changes under influence of high elec. fields 8=36339
  - Co acetate tetrahydrate, spectrum obs. 8=32046
  - Co^{2+} in fluoride salts, transitions, mag.-ordering dependence 8=36350
  - CO_2, intensities of 12-18μ bands 8=25462
  - CO_2-H_2O vapour, pressure, temp. effects 8=30298
  - CO_2-N_2 mixture, 9.6μ laser beam 8=39218
  - Cr ions in Ag halogens 8=41052
  - Cu acetate monohydrate, rel. to anomalous mag. behaviour 8=36434
  - Cu, infrared at 4. 2°K 8=27551
  - Cu, 50-340Å, and calc. of partial oscillator sums 8=31981
  - Cu^{2+} ion in blue proteins 9=49782
  - Cu-Au alloys, spectrum, electron transitions mechanisms 8=41082
  - CuCl film, obs. 8=31982
  - Cu_2O, exciton quadrupole transition in elec. and mag. fields 8=31984

Absorption—contd

light—contd

Cu_2O, spectrum rel. to annealing prod. stoichiometric defects, obs. 8=41083

Cu_2O, stressed, exciton lines,polarization effect 8=45185

$DyAlO_3$, spectroscopy rel. to mag. props. 8=36356

$DyFeO_3$, spectroscopy rel. to mag. props. 8=36356

Eu^{2+} in alkaline-earth fluorides, multiplet structure in spectra 8=31986

F-absorption band, temp. range 8=31111

Fe bulk, determ. from Fe thin film exam. 8=41085

Fe glazes, shade rel. to FeO content 8=49717

Fe, thin films, in vacuum 8=36359

GaAs, absorpt. edge fuzziness when fast n-irrad., model 8=27569

n-GaAs, modulation at intrinsic edge by acoustoelectric domains 8=27570

GaAs:Li, i. r. peak, rel. to localized vib. modes of impurities 8=44298

GaP, band gap meas., 0.900°K 8=45188

GaP, exciton absorpt. profile, 77-673°K 8=41087

n-GaP, i.r., impurity photoionization 8=41091

n-GaP, i.r., scattering mechanism 8=41090

GaSb, i.r. spectra, rel. to wavelength for various impurity concs. 8=41089

GaSe(S), 2.5-200μ rel. to one- and two-phonon absorpt. 8=27571

$GdVO_4:Eu^{3+}$, determ. of phenomenological parameters of crystal field Hamiltonian 8=31992

Ge, amorphous, rel. to band struct. 8=44791

n-Ge, and dispersion in Q-band 8=27572

Ge film thickness meas., i. r. laser method 8=35173

GeO, molecule, u.v. band spectrum 8=43301

GeSe, and photoelectric props., in energy range 0.5-1.5eV 8=49727

$GeSe_{0.75}Te_{0.25}$ 8=31994

GeTe, and elec. meas. rel. to band structure determ. 8=49726

HDO in H_2O, i.r. absorpt. at high press. and temp. 8=25930

HgS_xSe_{1-x}, $0 \leq x \leq 0.4$, rel. to e effective mass, 7-10μ 8=40319

$HoFeO_3$, spectroscopy rel. to mag. props. 8=36356

In_2O_3 sputtered films, intrinsic, electrical props. 8=40469

InSb, photon absorpt, with phonon creation and excitation of electronic impurity state 8=40665

n-InSe, and reflection spectra, optical transitions 8=45196

n-InSe, fundamental spectra and optical transitions 8=41100

K film, for photons 3.96 to 9.69 eV 8=49731

KBr, of, excitons, longit. and transverse 8=41107

KBr:Ag, Greek bands 8=36323

KCl and RbCl, mixed, coloured, L_1 band forbidden transition 8=31118

KCl, F-center ground state transition to L-bands 8=48877

KCl, rel. to F-aggregate centres 8=44478

KCl, far u. v. obs. 8=27592

KCl, of, excitons, longit. and transverse 8=41107

KCl, rel. to colloidal dentres 8=44477

KCl, X-irradiated, i.r. spectra 8=41104

KCl: Cd, uncoloured and coloured. 8=48876

$KCl:Eu^{2+}$ 8=36379

KCl:I, rel. to ICl^- Vκ centre. 8=48875

KCl–KI solid solutions, spectra 8=49736

KCl:RbCl, L_1 band, new Mollwo-Ivey law 8=36375

K_2CoF_4, spectrum compared to $KCoF_3$ 8=45197

KI:Ag, Greek bands 8=36323

KI:Cl^-, (Br^-), i. r. lattice vibration absorpt. by gap and resonance modes, theory 8=27576

$KMnF_3$, spectra of Mn^{2+} 8=41109

K_2NiF_4, electronic spectrum 8=41110

KNO_3, I-II phases, i. r. spectra rel. to internal interaction 8=27597

K_2O-RO-B_2O_3 glasses, R=(Ca, Sr, Ba), u. v. absorpt. of Cr(VI) 8=36325

$KTaO_3$, elec. field depend. polarization-induced band structure changes 8=32004

LiF, band, after irradiation at 81°K 8=49738

LiF, e-irradiated, rel. to colouring process 8=40062

$Li^{6,7}F$, isotope-induced acoustic band far i. r. absorpt., 7°K 8=36396

LiF: Mg, effects of pre-irrad. isothermal annealing 8=45280

LiH-LiD mixed crystals, i. r. freq. rel. to lattice dynamics 8=45202

$MgAl_2O_4$:Cr, spectra, visible and u. v. 8=45210

MgO, bands rel. to colour centres after neutron irrad. 8=35589

MgO, F band, temp. depend. 8=45209

MgO, irradiated, phonon-assisted 8=41049

MgO, n-irradiated at 80°K, colour centres, zero-phonon lines and phonon-coupling 8=27588

MgO:Fe^{2+}, far i. r. spectra at low temps. 8=27589

$MnCO_3$, spectrum at 4.2°K rel. to magnon side bands 8=32010

$MnCO_3$, vis. and u.v. spectra 8=32008

$MnCO_2O_4$, far i. r., ferrimagnetic spiral 8=45204

MnF_2, stressed, magnon sideband shapes rel. to exciton dispersion and exciton-magnon interactions 8=36389

MoO_3, film and cryst., temp. depend. of absorpt. edge 8=32013

Absorption—contd

light—contd

NH_4I and $NH_4I(Tl)$, spectra 8=32014

N_2, dissociating in shock tube, vac. u. v. 8=25651

NaCl, F-centres 8=35591

NaCl, far u. v. obs. 8=27592

$NaCl^{35,37}$ isotope-induced acoustic band far i.r. absorpt., 7°K 8=36396

NaCl:$CdCl_2$, associated with colour centres induced by X-irradiation 8=31113

NaCl: Cu, new broad band after period of storage 8=49741

NaF : Co^{2+}, spectrum 8=49743

NaF, O_2^-, and e.s.r. studies 8=45097

$Na_2O.2MnO.2SiO_2$, spectra rel. to Mn^{2+} bands changes on temp. decrease 8=41119

Na_2SO_4, X-irradiated, single crystal colour centre obs. 8=44483

Ni glyoximates, origin of colour 8=27535

Ni, infrared at 4.2°K 8=27551

α-O_2, rel. to temp. and impurity conc. 8=49745

O_3, i.r. 8=34278

Pb, infrared at 4.2°K 8=27551

PbO, yellow, forbidden band width, determ. 8=32022

Pt dithizonate in CCl_4, nonlinear abs., positive and negative saturation effects 8=34856

RO-B_2O_3 glasses, R=(Ca, Sr, Ba), u. v. absorpt. of Cr(VI) 8=36325

R_2O-B_2O_3 glass, (R=K, Na, Li), absorpt. of Co(II), reln. to basicity of glass 8=36324

$R_2{}^{I}O$-$R_2{}^{II}O$-B_2O_3 glasses, R^I, R^{II}=(K, Li, Na), u. v. absorpt. of Cr(VI) 8=36325

RbCl, K-absorption, stress-induced effects 8=41132

$RbMnF_3$, spectra of Mn^{2+} 8=41109

S_2^- centre in alkali halides, bands rel. to paraelastic behaviour 8=45173

SbSeI, and photocond. 8=32028

Se films, thin, and reflecting power, in fundamental absorpt. region 8=27605

Se, granular, phenomenological quantitative description rel. to permittivity of bulk mat. 8=41135

Se, trigonal, edge 8=27604

$SeOCl_2:Nd^{+3}$, cross section for Nd^{+3} laser transition 8=46624

Si, edge, interband Faraday rotation and ellipticity obs. 8=36404

Si, one-electron spectrum, high-resolution exam. 8=45218

SiC, higher absorpt. edges 8=49752

α-SiC, spectra of exciton-impurity complexes 8=36406

Si_3N_4 films on Si, i.r., obs. 8=40545

SiO 8=41145

SiO_2, glassy, i.r. absorpt. peaks 8=49754

Sm, trivalent, in oxide glasses 8=36412

Sn, 50-340Å, and calc. of partial oscillator sums 8=31981

SnO_2 crystals, i. r. spectra rel. to optical lattice-vibration modes 8=45222

n-SnO_2:Sb, rel. to e.mobilities 8=49270

n-SnO_2:Sb, rel. to e-mobility 8=27135

$SnSe_2$, coeff., and refractive index 8=45220

SnTe, and elec. meas. rel. to band structure determ. 8=49726

$SrF_2 : Co^{2+}$, spectra temp. dependences 8=41076

$SrTiO_3$, coeff. near absorpt. edge 8=27609

$TbAlO_3$, spectra rel. to mag. interactions 8=45066

Ti ions in Ag halogens 8=41052

α- and β-$TiCl_3$, spectra 8=36417

TiO_2, i.r., small polarons 8=40498

TiO_2-Sb_2O_3-NiO system. comp., structure and colour 8=26039

$UO_2{}^{2+}$, photo-induced absorpt. in glass, solns., and in spinel 8=27610

VO_2, in semiconducting and metallic states 8=49760

Xe, crystalline, kinematic resonances in spectrum 8=27611

Xe and Xe_2, photo-attenuation cross section, 1050-1550Å 8=43206

YFe garnet, hydrothermal and flux-grown, rel. to OH groups and Fe valence 8=35206

YGdAl:Nd^{3+} laser characts. 8=39692

YVO_4, high temp., under 3650Å excitation 8=45229

YVO_4 :Eu, high temp., under 3650Å excitation 8=45229

ZnO:Co^{2+}, and photoconduction 8=36029

ZnS, exciton complexes spectrum 8=36430

ZnS: Cu, Al(Ag, Al), i.r., due to donor states 8=41156

ZnSe, photoelectronic props. in p-type-Cu-activated and n-type-self-activated 8=45296

ZnSe, photo-induced i.r. 8=41153

$ZnSnAs_2$, edge absorption spectrum 8=45231

$ZnSnP_2$ platelets, optical band gap meas. 8=26267

Abundance ratio. See Elements/relative abundances; Isotopes/relative abundances.

Acceleration. See Dynamics; Kinematics.

Acceleration measurement

See also Velocity measurement.

accelerometer l. f. calibrator 8=32641

falling sphere for atm. density meas. 8=41620

vertical gravity gradient in motion, determ. with group of accelerometers 8=50005

Accelerators. See Particle accelerators.

Accommodation coefficient. See Gases; Kinetic theory/gases; Surface phenomena.

Acids, inorganic. See Individual compounds, and Hydrogen compounds.
Acids, organic. See Organic compounds.
Acoustic amplification in solids. See Acoustoelectric effects.
Acoustic analysis
acoustic imaging by diffracted light, two-dimensional interaction 8=37272
creeping-wave of scatt. of acoustic wave off cylinder 8=32911
discharge of IG-3 generator, oscillation spectrum 8=29875
field of multispan plate 8=41838
holographic acoustic imaging 8=37273
noise, impulsive deep-sea, resembling whale sounds 8=50100
piezoelectric resonators, coupled system 8=32896
plate, multispan, sound field 8=41838
steel, during crack propagation 8=35415
Acoustic field. See Acoustic radiators; Acoustics; Intensity measurement/acoustics.
Acoustic generators
See also Musical instruments.
aerodynamic generation by rotating cylinder 8=37259
bottlenose dolphin, sonic burst count matching 8=37258
electromechanical piston of infrasound, use in calibrating infrasonic sensors 8=32916
liquid cavitation, subharmonic generation 8=30370
point source in strongly focussing medium, modal solution 8=23808
sphere, deformable axisymmetric pulse prod. 8=23953
Acoustic impedance
absorbents, calc. for plane wave refl. 8=46189
cavity, gas-filled, heat cond. effects. 8=46186
conduit, cylindrical, calc. 8=46185
cylindrical shell finite, sound transmission effect 8=23958/9
cylindrical vibrator, relationship to far field 8=37257
electrostatic transducers resistance due to viscous losses in air gap 8=23955
elastic waves, isotropic medium, impedance effect 8=28365
metallic plate surface impedance, singularities due to excitation by e.m. waves 8=41839
piston in nonrigid baffle 8=23921
Acoustic paramagnetic resonance. See Paramagnetic resonance and relaxation.
Acoustic radiators
See also Doppler effect.
point source at boundary of plane semi-infinite impedance system 8=32913
pure-tone sources, power determ. in reverberation chamber 8=23965
transducer radiation impedance at air-water interface, effect of compliant-tube arrays 8=37271
Acoustic receivers
See also Microphones.
calibration, by comparison, in diffuse sound field 8=32917
condenser-earphone, distortion compensating for physiological studies 8=32926
hydrophone arrays, effect of phase errors 8=27862
piston array, reception and refl. calc. 8=46182
sector-coverage of linear array 8=23957
Acoustic resonators
cavity containing rotating fluid, normal modes 8=39359
cavity, gas-filled, heat cond. effects 8=46186
Fitzgerald resonances, rel. to particle-wave theory 8=46176
forced oscs. and standing waves of sound, with virtual mass source 8=41842
Ni film, stripe domain, ultrasound prod. 8=31682
Acoustic streaming
magnetoacoustic, in elec. cond. fluid in mag. field 8=41845
Acoustic transducers
See also Acoustic generators; Acoustic receivers; Microphones; Sound reproduction.
ceramic sensors, thermal grad. and temp. effects, rel. to cosmic dust expts. 8=41576
earphone, audiometric, pressure generated in ear 8=46204
electrostatic 8=23954
electrostatic, resistance due to air gap viscous losses 8=23955
elemental sonar unit 8=46178
flush-mounted, response to turbulent boundary-layer field 8=37261
free-flooding cylindrical array, behaviour computation 8=46179
freq. response functions generation, computer programme 8=23952
intensity fluctuations due to photon-phonon interactions 8=46638
piezoelectric efficiency, effect of intermediate coupling layers 8=44903
piezoelectric film on delay rod, efficiency 8=23956
piezoelectric slab, excitation of elastic waves 8=46157
pressure oscill. meas. 8=45963
rectangular, optical probing of Fresnel and Fraunhofer regions 8=37262
sonar system, blanket dome noise filtering 8=46180
sonic, power limitations, audio frequency and ultrasonic ranges 8=46181
Acoustic transducers—contd
thin-film, insertion and coupling factors 8=49380-1
u.s. magnetostrictive with clamped ferrite core 8=41840
u.s. probes using shear wave crystals, principles 8=46195
ZnO film on delay rod, efficiency 8=23956
Acoustic wave propagation
See also Absorption/acoustic waves; Dispersion/acoustic; Doppler effect; Helium/liquid, sound propagation; Shock waves; Velocity/acoustic waves.
in aerosols, attenuation and dispersion rel. to relax. processes 8=43889
in atmosphere with variable viscosity 8=32258
cavitation, radiation-induced, apparatus and results 8=48032
conduit, cylindrical, impedance calc. 8=46185
crystal, liq. nematic, weak waves 8=48133
electrical discharge produced 8=38981
ferroelectrics, displacive-type, coupled mode of sound with soft mode 8=39881
fluid lineberg lense, theory 8=30466
fluid, viscous, transient sound, theory 8=46183
in fluids and elastic solids, spherical waves boundary conditions 8=44307
gas circuits, h.p. corrections 8=23960
gas, interaction with external radiation applied instantaneously at boundary 8=43692
in gas/solid particle suspension, vel. and damping coeff. 8=39455
ionosphere up to 120 km at 0.01 and 10 Hz, model 8=45534
lamellar composite materials 8=40100
liquid, cavitation refraction wave onset and development 8=43730
liquid sphere within a fluid of different acoustic props. 8=30467
liquid, viscous, in flexible viscoelastic tube 8=48136
in ocean SOFAR layer rel. to Love wave propag. along interface 8=32895
ocean, 2-700 miles, periodic var. obs. 8=27863
plasma, coupled e.m. and e acoustic waves 8=30053
in plasma, energy density 8=47878
plasma, highly ionized, correl. obs. 8=43570
plasma, ion-acoustic waves 8=47879
plasma, low press. 8=25746
quartz, generation by electrostrictive mixing of two light waves 8=45162
quartz, in stimulated Mandel'shtam-Brillouin scatt., elastic nonlinearity effects 8=41036
rotating fluid, normal modes of containing cavity 8=39359
sapphire, generation by electrostrictive mixing of two light waves 8=45162
sector coverage of linear array of sources 8=23957
shallow-water c.w. phase characts. 8=50111
shock wave, N-shaped from spark, directional depend. 8=32901
in solids, first and second sound interacts, attenuation and temp. depend. 8=39882
solids, surface waves confined to boundary curvature 8=44308
sound generation, aerodynamic in pipe 8=39186
steel, sonic and ultrasonic pulses during crack propagation 8=35415
in stimulated Mandel'shtam-Brillovin scatt., elastic nonlinearity effects 8=41036
transition zone refl. and transmission, theory 8=46184
in tube, transient states 8=41844
in two-phase condensing medium, alternation and dispersion rel. to freq. 8=43688
underwater, convergence obs. 8=27864
underwater duct with pseudorandom bottom, ray optics 8=41329
underwater, horizontal, fluctuation over short depth increments 8=36698
underwater sonar, pressure and displacement sensors used simultaneously 8=41330
water, 150 kHz finite-amplitude distortion 8=48139
Ca–Bi–V–Fe garnet excitation of acoustic waves 8=40838
CdS, sound wave coupling mode at current saturation 8=35413
CO_2-H_2O vapour, optical-acoustic radiation, press. temp. effect 8=30298
He^3, liquid, impedance 8=46310
KCl, emission rel. to microscopic deform., model 8=26582
LiF, emission and related dislocation displacements 8=44317
LiF, emission, rel. to microscopic deform model 8=26582
Si, phonon conductivity and attenuation 8=44324
$SrTiO_3$, generation by electrostrictive mixing of two light waves 8=45162
TiO_2, generation by electrostrictive mixing of two light waves 8=45162
ZnO, shear waves in cryst. under high elec. field, Brillouin scattering 8=44325
ultrasonic
in diffusion cell, freezing of standing waves 8=48135
EDTA, Ba chelate form. study 8=25914
elastic constants, third-order, meas., theory 8=40089

Acoustic wave propagation—contd
- **ultrasonic**—contd
  - elastic materials, deformed isotropic, acoustical birefringence 8=46187
  - field of focusing spherical source in water, at finite amps. 8=43804
  - in gas, rarified, viscous 8=34602
  - liquid and saturated vapours near critical point, vel. curve intersection 8=43802
  - in metals, quantum theory 8=35407
  - 3-methyl 2, 4-heptanediol, u.s. relaxation 8=48189
  - plasma, gaseous, amplification 8=39111
  - quartz crystal, vibration analysis by X-ray topography 8=48722
  - quartz, method of exciting 10 GHz phonons 8=48723
  - quartz, second-harmonic generation of microwave phonons 8=30950
  - sapphire second-harmonic generation of microwave phonons 8=30950
  - in semiconductors with high dielec. const., theory of amplification 8=35405
  - shear wave crystals, principles 8=46195
  - steel, ultrasonic and sonic pulses during crack propag. 8=35415
  - Al crystal, rel. to plastic deform. 8=31191
  - Al, third harmonic generation due to dislocation anharmonicity 8=44442
  - CdS, parametric amplification 8=39890
  - Cu, third harmonic of initially u.s. wave 8=26581
  - InSb, waves amplification under d.c. operating conditions and transverse mag. field 8=39893
  - NaCl crystal, rel. to plastic deform. 8=31191
  - Pu, temp. var. 8=44632
  - Si, velocity variation rel. to temp. 8=39896

Acoustic waves
- See also Diffraction; Interference, etc.; Elastic waves; Shock waves; Ultrasonics.
- balloon burst, deviation from theoretical N waveform 8=37260
- caustics, ratio of amplitudes on and away from smooth curve 8=32908
- crystal with planar defect, vibrational spectrum 8=30930
- electron conc. after excitation in ionized plasma by microwaves 8=43526
- equations, two sided Cauchy problem, solution for m-dimensional acoustic system 8=46188
- fourth sound absorpt. in plano-parallel capillary, depend. on width and temp. 8=37264
- frequency analyzing power of human ear 8=23980
- frequency, intrinsic and energy conservation 8=23807
- generation in crystals under forced phonon induction conditions 8=35398
- hypersonic, transformation in piezoelectric crystals 8=35987
- Josephson tunnel current in sound field 8=44708
- Luneberg lens theory 8=30466
- microwave, interaction of spin waves in ferromagnetic crystals 8=49508
- in plasma, excitation on conducting cylinder 8=47834
- plasma, ion-atom collision effect on propag. and damping 8=34487
- pure-tone sources, power radiated determ. in reverberation chamber 8=23965
- stagnant, particle motion in field, rel. to density, radius and rate of sound distrib. 8=23819
- surface, instrument for visualization on TV screen 8=37274
- with virtual mass source and force densities, in resonator 8=41842
- **effects**
  - See also Chemical effects of radiations/acoustic waves.
  - acoustic imaging by diffracted light, two-dimensional interaction 8=37272
  - cavitation voids, pulsations, describing eqns. 8=43729
  - diffusion at liquid-solid interface, ultrasound effects 8=34814
  - front, in coupled thermoelasticity problem for half-space 8=46068
  - holography, 3-D information storage 8=46752
  - lattice of ultrasonic waves, analysis of light reflection 8=36290
  - low freq., thermal and subthermal n scatt. 8=24959
  - middle ear muscles, stimulation 8=28377
  - plasma ionic 10^4Hz, nonlinear interaction with travelling wave 10^9Hz 8=30047
  - plate stiffeners, induced strains 8=32871
  - on standing striations in pos. column of glow discharge 8=47747
  - ultrasonic modulation of Gaussian light beam 8=37630
  - ultrasonic, on Gaussian light beam 8=24417
  - water, u.s. induced cavitation bubbles, models ad damaging mechanism 8=43733
  - LiF, ultrasonically irradiated, dislocation behaviour 8=26688
  - NaCl, ultrasonically irradiated, dislocation behaviour 8=26688

Acoustical laboratories
- diffuse sound field, statistical characteristics, calcs. and experimental confirmation 8=32917

Acoustical measurement
- See also Interferometry/acoustic waves; and under separate subjects e.g. Intensity measurement/acoustics.
- of aerosol particle size and conc. 8=30563
- angle of arrival from two plane-wave sources 8=37280
- Doppler shift 8=32909
- fundamental frequency meas. using higher harmonics 8=23974
- hypersonic wide-band, sample holder and tuning technique 8=28376
- hydrophones, simple method of calibrating 8=33695
- infrasonic sensors, Moire variometer, electromechanical piston for calibrating 8=32916
- intensity, cardioid microphone method 8=46190
- liquid-solid boundary, u.s. reflection goniometry 8=48134
- liquid u.s. absorpt. at h.p., error analysis 8=48137
- mechanical loss meas. at low temp. 8=35614
- power, pressure squaring and integrating device 8=32915
- power radiated by pure-tone sources, determ. in reverberation chamber 8=23965
- pulse-echo instrumentation, 0.2-2.0 GHz 8=32914
- Rayleigh disc method, improvements 8=28375
- reflection coeff., cardioid microphone method 8=46190
- sonic boom, instrumentation requirements 8=32902
- subjective sound intensity analyser 8=46196
- supernormal hearing, threshold assessment 8=46215
- ultrasonic pulse-echo apparatus, tests 8=37281
- wave vectors due to sea storms limitation on determ. of wave vectors 8=36666

Acoustics
- See also Acoustic resonators; Architectural acoustics; Atmospheric acoustics; Hearing; Noise/acoustic; Sound reproduction; Speech; Ultrasonics; Vibrations.
- characteristics of bullet shock wave, survey 8=46163
- computer retrieval of papers (1955-67) 8=37254
- geometrical, problems in one-dimensional nonstationary and 2-dimensional stationary flows 8=30205
- geometrics, energy invariant, in moving medium 8=46177
- holography 8=46480
- holography, electronic simulation of variable inclination reference via u.s. camera 8=37275
- laser acoustic techniques for variable time compression, expansion and reversal of r.f. signals 8=28721
- response function for T-burner with high-heat loss 8=32972
- reverberant field, statistical props. 8=37256
- sound distribution at low freq. in rectangular enclosure 8=23951
- temperature scale compared with Pt resistance and gas scales 8=46262
- underwater pressure in oceans, calc. 8=50101
- underwater sound research before 1939 8=36696
- **musical**
  - See also Musical instruments.
  - No entries

Acoustoelectric effects
- in crystals, amplification with strong current-striction and elasto-cond. effects 8=35406
- delay line, continuously variable, at 720 MHz, obtained by Brillouin effect 8=28609
- electroacoustic electrostatic transducers 8=23954
- in dielectrics, theory 8=40560
- Heisenberg ferro- and antiferromagnetic with uniaxial anisotropy, anomalous behaviour of sound near int. pt. 8=39883
- large signal, rel. to energy losses by hot electrons 8=48717
- piezoelectric mats., acoustic wave interact. with cyclotron and helicon waves 8=27296
- piezoelectric semiconductors, propagating high-field domain, simple analysis 8=40423
- piezosemiconductors and dielectrics, sound generation rel. to elastic oscills. instability in alternating field 8=30940
- quartz, laser-stimulated, hypersound parametric amplification, (Brillouin effects) 8=26583
- quartz, resonance frequency, modification, various cuts, particle irrad. 8=35418
- semiconductors, amplification of hypersound by Mott excitons 8=39888
- semiconductors, piezoelectric, photoelectroacoustic effect and resonance phenomena 8=35871
- semiconductors, piezoelectric, u.s. wave amplification and current saturation, non-linear theory 8=44312
- semiconductors, ultrasound amplification 8=39887
- semimetals in crossed elec. and mag. fields, u.s. amplification 8=35408
- 10 GHz phonons, method of excitation in quartz 8=48723
- triglycine sulphate, polarization process, ultrasound effects under static conditions 8=35986
- n-type, acoustic amplification of 9GHZ waves due to application of elect. field 8=39892
- CdS, alternating field dependence on sound intensity and conductivity 8=35412
- CdS, amplification with space- and time-varying parameters 8=30941
- CdS, amplifying, freq. spectrum time and field dependences revealed by Brillouin scatt. meas. 8=48718
- CdS, current-oscillating, microwave transmission meas. 8=27087

Acoustoelectric effects—contd
CdS, inhomogeneities using optical probe 8=44313
CdS, microwave cond. rel. to relax. of excess phonons 8=49234
CdS, nonlinearity of u.s. wave interaction with conduction electrons 8=35409
CdS, sound generation and velocity field dependence 8=35414
CdS, sound vel. rel. to drift field intensity, obs. 8=39889
CdS, stationary wave instability in strong drift fields 8=30943
CdS_xSe_{1-x}, rel. to e-phonon interaction 8=35410
CdSe, acoustic noise and current saturation 8=30942
CdSe, alternating field dependence on sound intensity and conductivity 8=35412
n-GaAs, explanation for current saturation 8=49238
n-GaAs, UHF emission rel. to acoustoelectric domain 8=27095
p-GaSb, optical modulation by acoustoelect. domains 8=31991
n-Ge-W point contact, rel. to oscillatory back-current 8=40503
n-InSb, amplification of acoustic wave by interact. with drifting electrons 8=27116
InSb, by acoustic wave packets injected from CdS, phenomena 8=27112
InSb, domains, helicon diagnostics 8=49256
KCl:OH, acoustical paraelec. resonance 8=27246
ZnO, vapour-phase grown, relative u.s. amplification 8=26586
Acoustomagnetic effects. See Magnetoacoustic effects.
Actinides
complex, octahedral, free and in crystals, vibronic level Zeeman splitting 8=43964
transuranic elements and element 104, Dubna heavy-ion expts. review 8=38521
Actinide compounds
electrical and magnetic props. 9=49348
electrical and thermal props. 8=27233
electrical and thermal props., 8=49336
magnetic and elec. meas. rel. to mag. ordering 8=27234
Actinium
Ac^{227} fuelled thermionic generator, heat source optimization 8=28492
Actinium compounds
No entries
Actinometry. See Photometry.
Activation analysis. See Chemical analysis/by nuclear reactions.
Active nitrogen. See Nitrogen.
Active oxygen. See Oxygen.
Adhesion
alkali halide crystals in org. liquids, rel. to interfacial energy calcs. 8=30724
bonded joints, capacitive stress/strain meas. 8=35639
contact with incremental loading, self-similar solns. 8=28270-1
fluid films, disjoining pressure 8=30195
fluid to wall, formulation of conditions 8=43638
ice-plastic bond strengths at −12°C, correl. with phys. and chem. props. 8=31215
joints, time depend. of strength, effect of relaxation processes 8=48967
mechanism, from rolling-friction meas. 8=31186
metals, with high polymers, effect of elec. field appl. during bonding on strength 8=31185
methacrylate, mounting for X-ray crystallography 8=31233
n-alkanes, adhesive energy calc. 8=43779
to sapphire, adherence of Ni, Ni-Ti alloys 8=43744
spherical solid particles, effect of capillary liq. 8=39451-4
strain gauges, effect on sensitivity 8=48981
Au-Ag bonds, ultrasonically joined, purple-plague formation 8=48771
In(liq.) to Al 8=39336
Se surface, of insulating polymer particles, force rel. to triboelec. charge 8=49045
on SiO_2, thermal of photoresists. rel. to surface constitution, obs. 8=44601
Sn sheet, bound by Araldite or Cemendine 3000, hardness 8=40121
W, chemisorbed gases effects 8=49061
in ZnS phosphor powders using resin binders to enhance electroluminescence 8=41217
Adiabatic demagnetization. See Magnetic cooling.
Adion. See Adsorption.
Adsorbed layers
grisan derivatives in monolayers 8=39611
methanol and methanol-d_3 on porous glass, proton relaxation times 8=47699
monooctadecyl phosphate monolayer desorpt. from air/water interface, kinetics 8=30442
myristic acid gaseous monolayer at air/water interface, mol. dipole moment obs. 8=30438
palmitic acid gaseous monolayer at air/water interface, mol. dipole moment obs. 8=30438
octadecanol monolayers, retention of solvent 8=39613
poly benzyl-l-glutamate, conformation determ. by reflect. spectroscopy 8=39612
polymer on TiO_2, thickness determ. 8=39620
Adsorbed layers—contd
stearic acid, reaction with Ca^{2+} ions at air/water interface 8=41264
He, mobile monolayers 8=37336
$C_{16,18,20,22}$-OH monomol. films surface viscosity rel. to phase transitions, 15–30°C 8=30428
H_2O on protein, proton relaxation of H_2O 8=49649
H_2O on zeolite, translational diffusion, model 8=39619
Li on O covered W, surface reconstruction, electron diffraction examination 8=39593
NH_3 on W (100) surface, LEED obs. of electron impact effects 8=26140
Na on Ni(110), one dimens. incoherent struct., obs. 8=39579
S on Cu, structure and formation conditions 8=48490
Adsorption
See also Chemical analysis/adsorption; Chromatography; Films; Heat of adsorption; Sorption.
Aerosil, of benzene, i. r. spectra 8=44076
air, on activated charcoal, liquid-N_2-cooled, vacuum prod. 8=43710
n-alkane mixture, at liquid/vapour, water, solid interfaces 8=48102
benzene-hexane mixtures, equilib. isotherms 8=30782
benzene-hexane system, rates of adsorpt. 8=30783
at binary hydrocarbon liq-vapour interface isotherms 8=48041
of binary liquid mixtures on solids 8=48477
carbons, of liquids, H^1 and F^{19} n. m. r. lineshift study 8=30766
β-carotene, effect of adsorbed gases on semicond. 8=31397
carotene films, effect of gas adsorpt. on absorpt. spectra 8=49773
chemical reactions in adsorbed gases 8=41268
chemisorbed molecules, reactivity in semiconductor 8=41267
corundum, of water, in hydrothermal crystallization kinetics 8=26230
at crack, of ambient gas, rel. to fatigue crack propagation 8=31183
crystal faces, rel. to growth 8=44106
crystals, growing, of impurities rel. to impurity distribution anisotropy 8=26207
desorption of thin films on solid surfaces 8=39609
DPPH on SiO_2-Al_2O_3 catalysts. 8=27736
first-order transitions in adsorpt. phase 8=44067
Frenkel eqn., significance of oscill. time and bond strength 8=26132
gas monolayer, homogeneous and heterogeneous solid surfaces 8=44069
gas-solid interface, thermal accommodation coeff. 8=44066
gases, multilayer model for surface flow 8=48476
gases on solids, rel. to vacuum technology 8=30323
glass, porous, adsorpt. of HCN, i.r. spectrum surface reaction and polymerization 8=48491
glass, porous Vycor, surface conduction current rel. to water vapour adsorpt. 8=27252
graphite, adsorpt. of CCl_4 8=48473
graphite, anisotropy in energy calcs. 8=48299
graphite, of impurities and effect on growth, scanning-e-microscope obs. 8=26236
graphitized, of hydrocarbons, in 'lying-down' position 8=44069
heterogeneous surfaces, computation 8=30774
Hill eqn. for adsorpt. on uniform surfaces 8=48473
ice, adsorpt. isotherms for N_2, rel. to surface struct. 8=30769
isotherms, analytical representation 8=35191
kaolin, homoionic, from aqueous solns. of surfactants, effect on physicochem. props. 8=44071
kinetics, isotherm evaluation from mol. flow experiments 8=35190
lattice gases, computer simulation 8=30763
liquid-liquid interface, kinetics 8=43792
at liquid-solid interface, i.r. spectra of adsorbed mols 8=48474
macromolecules, flexible, theory 8=39614
metal surface, adsorpt. of Cs rel. to vapour press and temp. 8=31466
metals, desorpt. energies of electroneg. adsorbates O and halogens 8=35193
methyl and deuteromethyl radicals on Si gel, tumbling, e. s. r. obs. 8=25660
moisture diffusion coeff. in colloidal capillary-porous mats. rel. to moisture content 8=30662
non-metallic solids, effect on indentation deform 8=44524
orientation of molecules adsorbed on solid surfaces, n.m.r. obs. 8=39615
polystyrenesulfonic acid membranes, of H_2O rel. to dielec. props. 8=49357
porous solid in liq. N_2 bath, temp. determ. 8=48352
potential parameters from thick-order gas-solid interactions 8=48472
pump for low temp. serial mass spectrometer evacuation 8=38608
pyrex, adsorpt. of Xe+Kr 8=30774
quartz, of water in hydrothermal crystallization kinetics 8=26230

Adsorption—contd
rayon fibres, n. m. r. of adsorbed H_2O 8=27508
refractory metals, field electron microscopy of Cs layers 8=39624
rutile defined surfaces, of ethanol, n-octanol and n-dodecanol 8=35196
silica CaB–O–Sil, of aniline from CCl_4 soln, i.r. spectra 8=48474
silica gel of O_3 rel. to annealing temp., –80°C 8=30786
silicate minerals, surface area by Xe adsorb. 8=48426
solids, of H_2O, rel. to changes in dielectric props. of H_2O below 0°C 8=39402
from solution, on free liq. surface and on solid 8=44068
sucrose, of impurities rel. to growth and habit 8=26266
surface, patchwise heterogeneous, math. anal. of step-function approximation to local isotherm 8=30761
of tetrahydronaphthalene with acetone, diethylether or ethylbromide on solids 8=48477
TlI, of organic mols., surface charge-transfer groups form., obs. 8=36028
water on Pt, effect on propane chemisorption 8=27738
water vapour in evaporated Au and Cu films 8=35194
wool, equilib. adsorpt. isotherms of Na hexadecyl sulphate 8=30781
wool, equilib. adsorpt. of Na dodecyl sulphate at 40° and 60°C 8=30780
zeolites, i. r. spectra of adsorbed NO, N_2O and NO_2 8=27553
zeolites, surface area determ. 8=48432
zinkite, of water, in hydrothermal crystallization kinetics 8=26230
Ag, of O_2 and reaction with co-adsorbed H_2 8=39616
Ag(111), of O_2, surface rearrangement study by LEED 8=26133
Al (100) face, of oxygen, LEED obs. 8=44072
Al_2O_3, of Br_2 and I_2, refl. spectra 8=48479
α-Al_2O_3, of Na dodecyl sulfonate ions from soln., rel. to heat of immersion 8=49854
Ar, solid, of noble gases on (100) face, Van der Waals interactions 8=39617
Ar solid, of noble gases on (111) face, Van der Waals interactions 8=39618
Au, heated in air, impurity adsorption and surface energy 8=26095
Bi, adsorpt. of O_2 rel. to reactivity of surfaces 8=26106
CO desorption from W 8=48496
CO on hot W, dissociative chemisorption 8=49893
CO, on transition metal surface, nature of bond 8=48298
of CO on Pt films, effect on electrical resistance change 8=49169
CO_2, on molecular sieve, thermodynamic and rate behaviour 8=48481
on CO_2 solid of H, amorphous and granular structure below 100°K 8=30765
$CaCO_3$, adsorpt. of Cs sulfonate, cryst. struct. effects rel. to oil sol form 8=30767
CaF_2, of surface-active ions or mols rel. to Rebinder effects occurrence and mechanism 8=40136
CaO, of Br_2, and I_2, refl. spectra 8=48479
CdS powders, adsorpt. of gases H_xA and O_2, effects on cond. 8=26135
CdS {0001} surfaces, of O_2, and structure study, by LEED 8=30719
CdTe, of gases, effect on photovoltaic effect 8=44924
Cs form of zeolite, n. m. r. investigation 8=27510
Cu, adsorpt. of O_2, and resulting surface structs., LEED studies 8=26136
Cu spherical crysts., surface structs. after O_2 adsorpt. 8=26099
Cu, of Sr, Ba and alkaline atoms, ionization probab. and bonds, quantum calc. 8=35199
Fe-3% Si, of O_2, rel. to surface and grain boundary energies 8=26102
$Fe(OH)_3$, adsorpt. and coprecipitation of Ag 8=48478
GaAs surface, of Ga and As_2 from vapour in layer growth kinetic mechanism, mol. beams, in meas. 8=48449
Ge, adsorption-desorption mechanism rel. to electrophysical parameters of surface 8=48484
Ge, p-type powder, mechanism of chemisorption of H_2O 8=35192
Ge, of H_2O, from surface exam. by total internal reflection spectroscopy 8=35895-6
Ge, of O_2, effects on surface conductivity 8=48421
H from H_2-Ar solns., 87-120°K 8=25898
He rel. to heat transfer Kapitza effect, 1.5-4°K 8=34652
$He^{3,4}$ on Cu sponge at 4°K 8=24056
Hg/sulpholane interface, specific adsorpt. rel. to elec. double layer 8=30396
H_2O molecules adsorbed on zeolite, translational diffusion, model 8=39619
Li form of zeolite, n. m. r. investigation 8=27510
MgO, of Br_2 and I_2, refl. spectra 8=48479
Mo, adsorpt. and desorpt. energies of O_2, thermionic meas. 8=31469
Mo films, of Ba, O_2 and BaO, effect on resistance and work function 8=40322
Mo films, sticking probabilities of N_2 8=30771
Mo(111), faceting from CO adsorpt. 8=48486
Mo, of CO_2 on (001) and (110) faces, monolayer struct. and work function obs. 8=41269
Mo, of K ions, 960-1200°K 8=30770
Mo, of N_2 and N on (001) and (110) faces, monolayer struct. and work function obs. 8=41269
Mo, of O_2 on (100) face 8=35195
Mo, of O_2 on (001) and (110) faces, monolayer struct., and work function, obs. 8=41269
Na form of zeolite, n. m. r. investigation 8=27510
on Na halides, of Br_2 and I_2, refl. spectroscopy 8=48480
NH_3 on Si, vibrations obs., rel. to bonding strength 8=25508
Ni films, adsorpt. and interact. of N_2 8=26138
Ni, of CO 8=48487
O, on CdS, effect on spectral distrib. fine structure of CdS photocond. 8=44917
of O_2 on W, (110) and (113) faces 8=39622
OH surface groups, effect of adsorbed benzene on n.m.r. 8=38923
Pd films, adsorpt. and interact. of N_2 8=26138
Pd, of CO, effect of surface annealing changes 8=48424
Pd-Au alloys, adsorpt. of H, electron-donation model 8=26139
Pt films on W, of Cs, characts. cf. Cs-W system 8=35178
Pt, Si-supported, i. r. absorpt. of adsorbed CO 8=30773
Pt, Si-supported, i.r. spectrum of adsorbed CO 8=48488/9
Re, adsorpt. and desorpt. energies of O_2, thermionic meas. 8=31469
Sb, adsorpt. of O_2 rel. to reactivity of surfaces 8=26106
Si, gettering process rel. to lattice disorders 8=44077
Si, of O_2, effects on surface conductivity 8=48421
SiO_2 gel, adsorpt. of mols., n.m.r. signal shifts 8=39462
SiO_2 gel, proton spin relax. of adsorbed C_6H_6 8=29814
SiO_2-Al_2O_3, n. m. r. of combined H_2O 8=45123
ThO_2, porous and nonporous, adsorpt. of H_2O 8=48492
Ti films, of Ba, O_2 and BaO, effect on resistance and work function 8=40322
Ti films, sticking probabilities of N_2 8=30771
Ti from W in strong electric field 8=35197
TiO_2, of surface-active substances and polymers 8=48494
W, adsorbed CO, electron bombard. effect 8=30776
W, adsorpt. and desorpt. energies of O_2, thermionic meas. 8=31469
W, desorption of CO by electron bombard. 8=48495
W, of chloromethane, rel. to whisker formation using field-emission micro 8=26272
W, of Ba, search for substrate rearrangement 8=30777
W, of CO on (100) and (211) faces, work function 8=35200
W, of CsF 8=48498
W, of N_2 on (110) and (112) planes 8=39621
W, of NH_3 and decomp, field-emission meas. 8=27734
W, of O_2, and effects associated with thermal desorpt. 8=39626
W, of O_2 on (110), (211), (111) and (100) planes, field emission study 8=30778
W, of O_2, thermal rearrangement of surface 8=31464
W, of Sr, Ba and alkaline atoms, ionization probab. and bonds, quantum calc. 8=35199
W, of Zr, and nucleation, α and β phases, obs. 8=39625
W(110), adsorpt. of CO 8=39627
W, (112) face, adsorpt. of O_2, and oxidation structs. 8=26107
Xe solid, of noble gases on (100) face, Van der Waals interactions 8=39617
Xe, solid, of noble gases on (111) face, Van der Waals interactions 8=39618
Zn, stepwise isotherms of Kr, effect of chemisorbed O_2 8=48500
ZnO, e.s.r. of adsorbed NO_2 8=48499
Aerials. See Electromagnetic waves/radiators.
Aerodynamics
See also Flow/gases; Jets; Shock waves; Supersonic flow; Turbulence.
acoustic generation by rotating cylinder 8=37259
atmosphere, stably-stratified, with considerable wind-shear, excitation of internal waves 8=30262
aviation and aerodynamics, conference 8=30265
blunt body flows in superorbital re-entry, effects of non-grey self-absorpt. and energy loss 8=41488
compression shocks at low pressure, calc. method 8=39183
finned surface, cooling flow calc. 8=24001
binary gas mixture, structure of normal shock waves 8=30261
convection near stagnation point on parabolic cylinder and paraboloid 8=43637
delta-wing leading-edge separation calc., vortex-sheet model 8=34627
delta wing with forced antisymmetry 8=34626
entropy layer developed around a blunt cone, asymptotic behaviour 8=30267
flow noise, spoiler generated, obs. 8=32919
friction meas. on wall/plane tangential jet, using Preston tube and balance 8=30268
gas, gravitating, with homogeneous deform. and transverse vel. compts., exact solns. of eqns. of motion 8=34628
hypersonic flow, cone-cylinders in pressure distrib. calc. 8=34631
hypersonic rarefied gas flow over blunt body 8=25814
hypersonic rarefied gas flow past sharp leading edge of flat plate 8=25815

Aerodynamics—contd
- hypersonic shock layer, radiative heat loss effect on subsonic region 8=34636
- hypersonic sphere wake, density fluctuations 8=30264
- hypersonic sphere wakes, meas. of convection vel., comparison of two methods 8=39188
- hypersonic 3D flow around blunt bodies 8=25816
- hypersonic wakes 8=25820
- inviscid flow with surface injection 8=43669
- jet-engine nacelle treatment to reduce noise 8=32918
- laminar boundary-layer eqns., with mass transfer, approx. soln. 8=25813
- laminar free mixing, method of integral relations 8=25819
- of loose (falling) layer, conc. and heat transfer to wall 8=28396
- luminous flow region ahead of cylinder in flow generated by elec. shock tube 8=47943
- in Newtonian impact theory, relns for three-dimens. config. and any attitude 8=32704
- noise depend. on mean shear 8=43671
- nozzle boundary layer and heat transfer meas., effect of uncooled inlet length and convergence angle 8=30252
- potential flow about arbitrary bodies 8=34581
- re-entry models, simulated, time-resolved spectra from shock cap and wake 8=41485
- reentry simulation, use of i.r. rad. to calc. temps. of wakes 8=41484
- satellite perturbation rel. to resistance 8=32386
- shock propag., spherically symmetric exponential atmosphere 8=43670
- shock wave, plane, at Mach number interface, irregular refraction 8=30260
- skin friction, fluctuating, in air meas. with heated thin-film gauges 8=39236
- skin friction, incompressible transpired turbulent layers 8=30263
- sonic boom, comments and reply on Farfeld spectrum 8=25817-18
- sound generation in pipe 8=39186
- sphere in turbulent air jet, heat transfer rel. to flow regime 8=39205
- stationary compressible flow as a limit of a non-stationary flow, numerical solution 8=34624
- supersonic flow, rarefied, density disturbance ahead of sphere 8=43672
- supersonic flow, unsteady, around blunt bodies, theoretical investigation 8=47944
- wind tunnel instantaneous temp. sensor 8=46264
- wind-tunnel model incidence meas., optical methods 8=28733
- wind tunnel, spurious pressure fluctuations 8=34622
- Ar and He gas mixture, structure of normal shock waves 8=30261

Aeronomy. See Atmosphere; Meteorology.

Aerosols
- See also Foams.
- aspiration theory, large Stokes' numbers 8=34945
- aspirator, dry, clock-driven 8=37095
- atmosphere, effect on radiation density var. in sun's vertical 8=27901
- atmosphere, rel. to solar aureole spectral radiance 8=50149
- atomization of liq. by rotating disc, and 'secondary' break-up of droplets 8=30389
- charging in an electric field, theory 8=25969
- content of air, obs. from freq. spectrum of laser echoes from atmos. constituents 8=45442
- dust in atmos., vertical distrib. at 30 km 8=36717-8
- earth's atmosphere, transmitted and reflected radiance by Monte Carlo calc. 8=45466
- entry into sampling tubes and heads 8=43887
- ionization meas., spectro-ionometer 8=25709
- La Mer generator, particle size control 8=34947
- loose layer, aerodynamics, conc., and heat transfer 8=28396
- mean particle size and conc., meas. by attenuation and dispersion of sound 8=30563
- mesospheric distrib. and particle sizes, rel. to noctilucent clouds 8=36738
- microstructure continuous meas. by small angle method, halo apparatus 8=34946
- optical counting, spurious consts. prod. by high sub-size particle concs. 8=30560
- particle motion in rotating potential flow, stabilizing and inertia deviations 8=30551
- particle-size distrib. determ. using Fraunhofer holograms 8=24429
- particle size distribution of radioactive aerosols in selected areas at AERE 8=50159
- photodiffusiophoresis 8=30561
- polystyrene sub-micron particles, electrical mobility 8=43888
- production for use in atomic absorption spectroscopy 8=48239
- in rectangular jets, collection of particles by impaction, efficiency 8=48240
- scattering, multiple, coherent light, lab. meas. for nonabsorbing case 8=42258
- self-preserving, dynamic equilib. 8=39458
- smoke, chain aggregate, charging and mobility, obs. 8=30562

Aerosols—contd
- smokes, backward scattering of laser radiation optical thickness dependence 8=34949
- sooty flames, dispersion of absorpt. coeff. 8=32975
- sound attenuation and dispersion, rel. to particulate relax. processes 8=43889
- in stratosphere, layer meas. via diffuse skylight as function of height 8=36716
- stratosphere, u. v. absorpt., satellite meas. 8=27911
- surface meas., laser technique 8=34948
- turbid layer, conc., effect on polarization of sky-light 8=36743
- u.s. nebulization in at. absorpt. spectroscopy 8=46689
- water, evaporation kinetics in optical radiation field 8=30564
- water droplets, evaporation rate meas. by optical scatter 8=39484
- water, supercooled, crystallization processes 8=25985
- Fe, spectral absorpt. of excited molecules 8=34950
- MgO flame, dispersion of absorpt. coeff. 8=32975
- N_2, with oleic acid particles, sound attenuation and dispersion 8=43889
- NaCl solns., homogeneous nucleation 8=34973
- Pt, submicron particles, evaporation in shock tube 8=39493

Afterglow. See Discharges, electric.

Ageing. See Alloys; Metallurgy; Phase transformations/solid-state.

Air
- See also Atmosphere.
- aerosol content, obs. from freq. spectrum of laser echoes from atmos. constituents 8=45442
- afterglow, mechanism 8=32274
- ageing effects on insulators 8=40556
- arc, unipolar, Sn-Bi alloy substance entering 8=47777
- atmospheric density, space averages by dispersion for refractive correction of e. m. range meas. 8=36722
- bearing support for pendulum 8=37122
- breakdown between spherical electrodes, calc. 8=34423
- breakdown, laser-induced and spark emission, mag. field effects, 210 kG 8=29925
- breakdown threshold rel. to wavelength of laser radiation 8=34425
- bubbles, bursting, time exposure obs. 8=25856
- composition and props. in system with temp. gradient 8=47947
- compressibility effect in impact of flat body on free surface 8=41648
- condensation in hypersonic wind tunnel 8=30599
- condensation nuclei production by radiolysis 8=25992
- consumption per syllable in whispered speech, obs. 8=37285
- corona discharge, rectifying action rel. to electrode temp. 8=34430
- couette and boundary-layer flow, hypervelocity with radiative transfer 8=39207
- density variation, day-to-night, contraction effect on satellite orbit 8=28023
- discharge, high press. vortex 8=29894
- discharge, hollow cathode in longit. mag. field, cathode surface current distribution 8=29896
- discharge, r. f. nonequilibrium 8=29893
- dry, positive-ion mobility obs. 8=39027
- dry, Rayleigh-Cabannes scatt. and depolarization 8=30301
- dry, vapour pressure at 34°-64°K 8=35004
- electrical conditioning, combination with illum. systems 8=41928
- electrical conditioning, improvement of illum. in combined plant 8=41929
- equilibrium stagnation point heat transfer calcs using variable heat of dissociation model 8=39206
- flow in annuli with small cores, heat and momentum transfer, and max. pts of vel. profiles 8=34647
- flow in inlet region of tube, heat transfer rel. to initial turbulence 8=39203
- flow meas., ionic flowmeter 8=34610
- glow discharge, acoustic wave effects on pos. column 8=47747
- group refractive index 8=47967
- heat transfer from vib. surface by free convection 8=34646
- heat transfer in turbulent pipe flow, effect of prandtl number on temp. profile 8=30367
- hydrocarbon fuel/air mixture, ignition in laminar supersonic boundary layer 8=32969
- injection, Mach 10, numerical results 8=25838
- ion mobility, time-of-flight meas. 8=43474
- ions, mobility spectra, law and medium A 8=39043
- jet, meas of velocity and temp. fields, and osc. intensity 8=39190
- kinetic props. at high temp. 8=30273
- liquid, elec. conduction in diode cell 8=48200
- metallic screen insulation in air 8=48755
- microwave breakdown at 9 GHz 8=47768
- negative-impulse breakdown in compressed air 8=47764
- in nozzle operation, effects of convergence angle and uncooled inlet length on heat transfer and boundary layer 8=30252
- nuclei, N, π interaction models for e. a. s. calc. 8=38217

Air—contd
- plasma, radiated power at high temp. 8=34509
- plasma, shock ionized, cold electrode I-V characts. 8=30029
- shock-wave ionization, e temp. meas. 8=39221
- shock wave soln, normal, radiation coupled chemical nonequilib. 8=39182
- skin friction, fluctuating, meas. with heated thin-film gauges 8=39236
- spark discharge at atmos. press., superradiant laser action obs. 8=24301
- spark formation relationships 8=34427
- spark, laser-induced, shock wave theory 8=28369
- spark, laser-prod., expansion mechanism, obs. 8=34432
- spectral radiation intensity, shock-tube heated 8=24399
- stopping cross section for $6 \leq Z \leq 24$ 8=47976
- supersonic rarefied flow, study using wedge shaped Fabry-Perot interferom. 8=30243
- thermodynamic props. up to 1000°C and 1000 bars 8=34654
- turbulent natural convection along vertical plate, temp. profiles 8=34648
- velocity distribution in room due to ceiling fan 8=47941
- viscosity, dynamic, meas. to 500°C, and statistical mech correl. 8=43704
- water-air, horiz. annular flow, heat transfer and pressure drop 8=43653
- water droplets falling in, supercooling and freezing 8=25984
- Ar-air mixtures, equilib. props. behind incident and refl. shock waves 8=34625
- Li$^+$ ion beam, charge equilib. 8=28584
- Rn decay products, mean free paths and diffusion coeffs. 8=38441

Airglow
- See also Atmospheric spectra; Aurora; Sky brightness; Twilight; Zodiacal light.
- dayglow, emission features, obs., interpret. and meas. techs. 8=32275
- dayglow, photoelec. Fabry–Perot, magnetostriction scanned for 6300 Å 8=32272
- far u.v., daytime obs. 8=45497
- i. r. night sky rad. 8=36792
- meas. u.v., dayglow, with x-15 aircraft 8=36791
- night continuum and 5577 Å line of oxygen 8=41392
- night emission, midlatitude 8=32277
- night, [OI] 5577Å emission and continuum at 5300 Å 8=45499
- night, S. America, photometric obs. 8=45498
- night sky spectral radiance rel. to cloud cover, 0.5-1.1μ 8=27913
- nightglow arcs at 5577 and 6300Å, equatorial region 8=36801
- nightglow, emission heights profiles of O 6300Å line rel. to geographic position 8=36800
- night-glow, hydroxyl emission, intensity and rotational temp. variations 8=50168
- nightglow photography by Gemini spacecraft, edge-on max altitude 8=36802
- nightglow, reln. with presence of sporadic E and spread-F 8=32278
- photometry, extreme u.v. detector 8=41393
- simulation by standard source 8=46678
- u. v., obs. for night meas. of mesospheric O_3 8=36760
- H_β radiation in night sky spectrum 8=41354
- He nightglow, 304- and 584-Å, upper limits 8=27951
- He twilight emission at 10 830Å (2^3P-2^3S) 8=32287
- NaI 5890-96Å, nocturnal intensity, diurnal, seasonal and solar cycle vars. 8=32276
- O_2 in dayglow, altitude profile in i. r. atmos. system 8=36797
- OI 5577 and 6300 Å, nocturnal intensity, diurnal, seasonal and solar cycle vars 8=32275
- OI λ5577 line at night, variations in width 8=27950
- [01] 6300Å nightglow and ionospheric electron content 8=36827

Albedo. See Cosmic rays; Earth; Nuclear reactors, fission.

Alfvén waves. See Magnetohydrodynamics; Plasma/oscillations.

Algebra
- algebraic geometry, fibre bundles and sheaves applied to axioms in quantum field theory 8=33360
- C*-, and Mackey's axioms 8=32830
- C*, Borel structure, rel. to probability theory 8=32655
- calculus of four-spinors 8=24594
- edge of the wedge theorem, generalized for boundary on an analytic curve 8=32648
- field operator, mass renormalization automorphism 8=37856
- group transformations of O(2, 1), representations in continuous basis 8=24593
- Hilbert space, critical point theory 8=45989
- Hilbert spaces, nuclear operators 8=47196
- lectures on modern algebra, book 8=23796
- Lie groups and Lie algebras, representation theory methods and results 8=45992
- Lie, Poisson bracket realization by analytic functions of generators 8=28231
- Lie representations, multiplicities 8=45993
- Lie, unitary, inhomogeneous, compact number of invariants for two types computed 8=32651
- logic, in spectrochemical analysis 8=41303
- Macaulay rings, extensions 8=45972

Algebra—contd
- Neumann, and translation group unitary reprentation Araki theorem, proof 8=33361
- polynomial coeffs., appl. to e. p. r. spectra 8=34367
- Racah, possible extension of L_3 8=28235
- unitary, compact, inhomogeneous, invariants and scalars 8=32650
- von Neumann, struct. for free systems 8=32853
- W*-algebra, non-abelian, sequential convergence 8=32654

Algol. See Calculating apparatus/digital computer programmes.

Algorithms. See Calculation.

Alignment
- goniometer for single crystals 8=35210
- Weissenberg camera, photographic method, shutter 8=35305

Aliphatic compounds. See Organic compounds.

Alkali metals
- See also the individual metals.
- atom, influence of core electrons 8=47464
- atom oscillator strengths 8=47500
- atomic oscillator strength calc. 8=34136
- atomic spectra, theory of satellite bands prod. by foreign gases 8=47532
- atoms, elec. dipole moment, upper limit determ. 8=43177
- atoms, ionization by slow electrons 8=43477
- atoms, van der Waal's const. with inert-gas atoms 8=25388
- boiling pressure drop, prediction method 8=48281
- elec. dipole moment meas. 8=29614
- electrical resistivity effect of dissociating and thermally stable gaseous impurities 8=48203
- electron-phonon interactions, scatt. and transport coeffs. 8=44631
- electron photoemission into anthracene rel. to its band structure determ. 8=31283-4-5
- inert gas collisions, interatomic pot. 8=47541
- lattice-dynamic calc. 8=30931
- lattice mechanics 8=35380
- liquid, heat transfer from in short vertical tubes with natural convection 8=30460
- liquid, surface tension, ultra high vac. obs. 8=25897
- magnetoplasma modes due to Fermi liquid interactions 8=40271
- magnetoplasma modes, Fermi liquid effects 8=35798
- photoelectric emission into anthracene, rel. to Fermi level 8=31472
- plasma, variable ionization equilib. 8=30004
- plasma, volume recomb. coeffs. from atomic flux emergence meas. 8=47849
- pseudopotential form factors, local, calcs, errors on omitting conduction-electron exchange potential 8=44630
- solutions in amines, origin of 660 mμ band 8=34868
- solutions in fused alkali metal salts, spectra 8=39374
- strained lattices, phonon spectra 8=44296
- surface ionization on porous substrate, analysis 8=49449
- ultra-violet absorbing power, plasmon contrib. 8=31962
- vapour, atomic, absorpt. oscillator strength, and photoionization continua 8=29603
- vapour elec. cond., semicond model 8=43696
- Rb^{87} atom, light shift due to virtual transitions 8=38708

Alkali metal compounds
- See also the compounds of the individual metals.
- alkali-AlH_4, i. r. spectra, obs. 8=31959
- alkali-aromatic radical ion pairs in soln., n.m.r. 8=34919
- alkali-chlorozirconate cpds. in alkali-chloride melts, activities 8=34780
- alkali metal-NH_3 solns., internal reflection spectra 8=30490
- alloys, ht. of mixing calcs. 8=43796
- azides, radiation phys. and chem. effects 8=31140
- binary alloys, knight shift 8=43876
- bromates, n-irrad. crysts., Br^{82g} recoils 8=27769
- carbonates, radiation phys. and chem. effects 8=31140
- chlorosulphate solns. in HSO_3Cl, elec. cond. 8=48194
- chlorosulphates, i.r. spectra and preparation 8=49705
- feldspars, O mobility, mech. of autodiffusion and alkali atom exchanges 8=35477
- hydride mol., interactomic potl. calc. 8=43281
- ion motion in soln., i.r. bands 8=25931
- methyl alkali halides, new mol. type, i. r. spectra 8=47656
- nitrates, fused, enthalpies of mixing in ternary systems 8=48080
- nitrates, fused, high-press. elec. cond. 8=39410
- nitrates, molten, electromigration of $Na^{22,24}$ ions 8=43782
- nitrates, molten, i.r. spectra and struct. 8=39378
- nitrates, molten, u. v. spectra of NO_3^- 8=30489
- nitrates, radiation phys. and chem. effects 8=31140
- nitrates, spectra and interactions in aq. solns. 8=34869
- separation on org. resin ion exchangers, effect of temp. 8=32145
- NaCl-type, Anderson-Gruneisen parameter 8=48939
- R_2O-B_2O_3 glass, optical absorpt. of Co(II), reln. to basicity 8=36324
- halides
  - See also the compounds of the individual metals.
  - absorption, extreme u.v. 8=41060
  - additively coloured, polarization capacity with blocking electrode 8=49073
  - box model theory, validity test by binding energy, compressibility and thermal props. calc. 8=35315

Alkali metal compounds—contd
halides—contd
compressibility, isothermal, meas. by capacitance method 8=49031
crystal growth technique for high purity 8=39665
crystal, plastic yield stress pressure dependence 8=44550
Debye-Waller factors temp. dependence, calcs. 0-900°K 8=39869
dielectric constant, low frequency meas. and review of other meas. 8=40567
dipole moments, by molec. beam elec. reson. 8=34232
edge dislocations, thermal equilib. charge 8=44444
electron emission, thermostimulated 8=40697
exciton theory in crystals with complex band structure 8=49112
external X-ray photo-effect, quantum yield obs. 8=36005
F-centre electron distrib. 8=31122
F-centre production, effect of impurities 8=35582
crystallization from supersaturated aq. soln., relaxation times 8=26217
crystals, e-beam energy losses rel. to band structure and plasmon energy determ. 8=26937
crystals, etch-pit star formation rel. to dislocation mobility 8=26682
crystals, M centre, triplet state lifetime 8=26718
crystals with NaCl structure, vacancies, computer calcs. 8=35532
crystals, X-centre formation mode 8=35583
defects, quantitative evaluation using ultra-microscopy 8=35530
dislocation mobility dependence on electrostatic field 8=26667
electron-vacancy centres, paraelastic 8=49706
heat of fusion, melting pt., electronic polarizability and ionic radius ratio, relationship 8=39474
i. r. spectra of BH$_4^-$ doped crysts. 8=36327
lattice dynamics of imperfect crysts. 8=48701
lattice modes anharmonicity 8=48702
lattice vibration local modes due to U-centres 8=39866
luminescence relax. processes, effect of crystal lattice microdefects 8=36472
microdyn. model of solns. from nucl. mag. relax. 8=25953
migration of gas inclusions(cavities), effect of elec. field 8=39966
molecular beam elec. reson. spectra 8=25670
molecular mechanics calc., improved potential function 8=43323
molecular parameter calc. from Wasastjerna potential function 8=43324
molecule, interatomic potl. calc. 8=43281
n. m. r. chemical shifts of monovalent substitutional ions 8=45113
optical properties, in u. v. 8=27556
and organic insulators, charge transfer by friction 8=27223
phase transitions, Born treatment using new van der Waals coeffs. 8=48246
phosphors, F centers interaction with microdefects in crystal lattice 8=31123
photoluminesc. rel. to lattice structure 8=36470
point defects, interactions 8=31030
scattering of lattice waves by dislocations 8=30933
Schottky defects, their creation, interaction, and migration 8=44407
second-harmonic generation of light obs. 8=27555
spectra, molec. beam elec. reson. 8=25405
Stark effect in colour centres 8=31112
surface distortion calc. 8=30725
surface, elec. field gradient 8=30717
surface ionization on metals of Pt group, e. g. Ir 8=27365
thin crystals, pre-melting and pre-freezing, dislocation arrays 8=43902
tribo-electron emisssion and luminescence 8=31462
X-irradiated, lattice disorder at room temp. 8=44198
Z$_1$ centres, vacancy-centred models, props. calc. 8=44473
F$_2^+$ colour centre, ground and extited states, allowing for polarization 8=35581
H$^-$ defects, multiphonon absorption 8=48703
NaCl-type, Anderson-Grüneison parameter for Born-Mayer potential 8=39906
NaCl-type, elastic constants and tensile strength 8=49036
O$_2^-$ center, electronic structure from paramagnetic resonance and optical spectra 8=49703
O$_2^-$ centers, electronic structure 8=49704
O$_2^-$ impurity reorientation 8=48822
S$_2^-$ centre, paraelastic behaviour 8=45173
Alkaline earth metals
See also the individual metals.
alkaline bromides, stability constants of Pb complexes 8=48148
photoelectric emission into anthracene, rel. to Fermi level 8=31472
Alkaline earth compounds
See also the compounds of the individual metals.
aluminates:Eu^{2+}, luminesc. mechanisms, obs. 8=45253
carbonates, C-isotope effects on i. r. spectra 8=31966
chalcogenides, ionic radii 8=43966
chlorosulphate solns. in HSO$_3$Cl, elec. cond. 8=48194
chlorosulphates, i.r. spectra and preparation 8=49705
F-centre e. s. r. g shift values, theory 8=40057
Alkaline earth compounds —contd
fluorides, bond energies from mass spectra 8=38934
fluorides, H- and F-bands, Mollwo-Ivey relation 8=48873
germanates and silicates, crystallochemical similarities 8=26167
halide solns., microdyn. model from nucl. mag. relax. 8=25953
nitrates, radiation phys. and chem. effects 8=31140
oxides, lattice luminesc. 8=36504
oxides, thermal dissoc. in high vacuum 8=30605
stearate isotope separator targets for CERN ISOLDE 8=38768
(BaSrCa)O, electrical cond., thermoelectric power and work function, effect of Ba vapour 8=26945
Eu^{2+} activated, luminescence, 390-520 nm 8=45254
Allotropes. See Phase transformations; Polymorphism.
Alloys
See also Crystal structure, atomic/alloys; Heat treatment/alloys; Solid solutions; Steel; and under alloys or compounds of the base of the first-named element. Alloys such as Au$_3$Cu, Au-Cu, Au-Cu-Zn are indexed under compounds of the first-named element, i. e. Gold compounds in these examples.
of alkalis in alkalis, thermoelectric powers 8=27305
binary alloy-mixtures, effective thermal and elec. conds., reln. 8=39937
binary, diffusion of vacancies, correlation factors 8=31039
binary eutectic system, freezing with time depend. surface temp, heat transfer anal. 8=34967
binary, planar interface stability during melting 8=30582
binary, spherical model and Clapp-Moss eqns. rel. to Ising model 8=39527
7-3 brass, heavily rolled, annealing texture 8=40151
β-brass-type ordered, diffusion theory rel. to vacancy conc. and migration energy 8=26613
cellular reaction, Cahn and Turnbull theories, exam. and appl. to Pb-Sn 8=30670
chemical potential generation by phase diagram analysis 8=49836
critical resolved shear stress calc. 8=40105
critical resolved shear stress. calc., due to particles 8=40106
crystallization after immersion of small plate 8=39660
dilute, disordered, electron state model 8=26890
dilute, electric field gradients created around impurities, direct meas. 8=48313
dilute, electronic correlation effect on props., variational treatment 8=26892
dilute, impurity transport meas. using e-microprobe 8=44380
dilute, Kondo effect, Takano-Ogawa theory exam. and mag. susceptibility calc. 8=44956
dilute, mag. impurities electronic scattering problem 8=31271
dilute, magnetic impurities, electronic structure 8=31270
dilute, mag. impurities, Kondo effect 8=31272
dilute mag., Kondo effect, Green's function theory 8=31263
dilute magnetic, low-temp. exchange-interactions uniquely defined by logarithmic accuracy 8=31492
dilute, with short range-order, theory of vibrations 8=48705
disordered binary, correlation functions 8=43972-3
disordered, e-scattering, dynamic theory 8=35596
disordered, self-consistent-field approxs. 8=44294
electron cell model appl. to Cu-Ag-Au liq. ternary alloy 8=26002
electron theory, rel. to soft X-ray spectrometry 8=49687
eutectoid decomposition theory assuming local equilib. and boundary diffusion 8=26051
evaporation in a vacuum 8=34998
f.c.c., disordered, Zener relax., time and jump freq. reln. 8=31188
f.c.c., internal friction rel. to dislocation viscous movement 8=35615
f.c.c., ordered, diffusion rel. to vacancy conc. and migration energy 8=26614
ferromagnetic binary, vapour pressure temp. dependence rel. to mag. and structural transitions 8=35014
Flow in explosive cladding and welding 8=39262
Hastelloy neutron irrad. effects on stress rupture and creep 8=47400
heat-resistant, creep and fracture in creep, physical parameters, high-temp. and high stresses 8=26760
heat-resistant, thermal conductivity 8=39943
Heusler, order rel. to mag. and chem. order in Pd$_2$MnAl 8=31700
high-strength, fatigue toughness microstructure dependence 8=49011
ignition temp., min, rel. to O$_2$ press. and surface deform. 8=36578
kinetic properties, effect of phonon drag 8=35817
Kondo scatt., influence on de Haas-van Alphen oscillations 8=31490
liquid, Knight shift comment on WBF theory 8=39421
liquid, quenching by torsion-catapult method 8=43746
magnetic, dilute, enhanced effective exchange interaction due to localized spins 8=31594

Alloys—contd
- magnetic, dil., with spin-½ impurities, s-d scatt. theory 8=44980
- magnetization distrib. in diluted systems 8=31486
- mechanical props at low temp., review 8=26738
- metal binary systems, liq., diffusion coeff. meas. using conc. cell 8=43784
- metallic, particle size distrib. in dispersed phases 8=26295
- metallic, thermionic emission props., review 8=36047
- microstruct. deformation and recryst., microscope for high-temp. study 8=42183
- molten, activities determ. by Touch instant e.m.f. method 8=36592
- noble metal, α and β phase stability 8=26055
- noble-metal-rare-earth, dil. Kondo effect rel. to impurity mag. effects 8=31316
- noble metal–rare earth, e.p.r. and susceptibility meas. rel. to local moments 8=31882
- noble metal, Tefel slope rel. to cathodic reduction kinetics 8=45380
- nuclear indirect exchange and pseudodipolar interactions by spin echoes 8=36068
- ordered, elastic interaction of atoms near an antiphase boundary 8=35058
- ordered, of AuCu-type, dislocation damping mechanism 8=40031
- ordered phase structures, phenomenological theory 8=30671
- ordering, rel. to pressure, including volume depend, on degree of long-range order 8=30673
- ordering, steep gradients in degree of order, meas. 8=30669
- ordering structures, theory rel. to alloys with several transition pts. 8=30672
- oxidation, linear, comp. changes 8=32092
- phonon conductivity calc. 8=30928
- radioactive, C, O, N, H determ. 8=36629
- resistance, electrical, rel. to phonon drag, at low temp. 8=26959
- resistor, thin film, material and characts., 8=44675
- self-diffusion mechanism rel. to defect densities 8=26615
- solvent Knight shifts, origin 8=30528
- stacking fault energy rel. to density of electron states 8=26698
- steel, EI 702, segregation kinetics 8=35054
- strain excitation from exo-emission meas. rel. to defect props. 8=44938
- superconducting, dil. mag., behaviour in applied mag. field 8=27004
- superconductor, with paramag. impurities, nonstationary generalization of Ginzburg-Landau thoery 8=40341
- superdislocations with thresholds in $L1_2$ superstructure braking 8=26655
- superplastic, microstructure 8=30872
- ternary, dilute, solidification, solid-liquid interface stability 8=43910
- ternary, disordered, linear approx. 8=30652
- thermal analysis, contactless, 20-2800°C 8=28411
- thermal conductivity, cryostat for meas. of lattice component 8=48758
- ticonal-type, oriented modulated structure 8=35056
- transition metal, dilute, intra-atomic Coulomb interactions and local exchange-enhancement 8=35433
- transition metal, n.m.r. for local susceptibilities exam. 8=49657
- work hardening of alloys containing hard particles, model 8=35640
- X-ray spectrometry, soft-, rel. to e. theory 8=49687
- Ag-Au, short range order kinetics, rel. to diffusion 8=35059
- β-Cu-Sn alloy, quenched, structure and decomposition products 8=39528
- Fe-rich solid soln., with non-transition elements, saturation magnetization 8=49519
- Fe–1.35Si, fibre-reinforced, mag. and mech. props. 8=31209
- Fe–50Si, fibre-reinforced, mag. and mech. props. 8=31209
- Hg, liquid, Knight shift 8=39438
- Mg–Zr, fine grain effect through Zr 8=48343
- Pb–Ag eutectic alloy, structure during solidification 8=26037
- Pd:Ni dilute, low-temp. specific heat and ferromag., localized exchange enhancement model 8=35432
- Pu, phase diagrams 8=35080
- Tl-Te, liquid, n-type, elect. props. 8=34897
- α W–β W–WO_2 mixture, quantitative X-ray anal., calibration problems 8=35288
- WC-TiC-TaC-10% Co, properties rel. to C content 8=30657

Alnico alloys. See Nickel alloys.

Alpha decay. See Nuclear decay theory; Radioactivity/decay periods; Radioactivity/decay schemes.

Alpha-particle model. See Nucleus/models.

Alpha-particles and helium nuclei

See also Alpha-rays.
- α slowing down in H plasma, optical emission 8=43542
- atmospheric pressure gauge appl, 8=45964
- $d + He^3 \to \alpha + p$, single-level resonance formula 8=25007

Alpha-particles and helium nuclei—contd
- e-He^4 scatt., implications of a new approach to Q.E.D. 8=24723
- energy spectrum from $t(d, He^3)2n$ 8=43005
- ionization by p bomb, cross-sect. calc. 8=34452
- neutron scatt., $E_n = 1.01/2.44$ MeV, obs. 8=24956
- n-He interaction, neutron ang. distrib., $E_n = 0.2$-7.0 MeV, obs. 8=24957
- optical potentials 8=47338
- optical potential calc. 8=25052
- photodisintegration cross section 8=38451
- photodisintegration cross-section calc. using short-range correls. 8=25013
- photodisintegration, elec. quadrupole contrib. to mean square radius 8=42830
- three-nucleon bound state 8=33844
- virtual state in p-T scatt., 300-990 KeV suggested 8=29185
- C^{12} three-α model, ground-state energy calc. 8=42836
- He binding energy, variation calc. using two-body central velocity-dependent potential 8=42824
- p-He scatt., angular distrib. rel. to nucleus struct., 1 GeV 8=33845
- π-He scatt., Coulomb interference corrections 8=29389
- π^+-He, scatt., double charge exchange obs. 8=33681
- π-He^4 double charge exchange, cross section calc. 8=33674
- He^3-α scatt., 3-11 MeV, cross-section obs. 8=24937
- He^3 and H^3, e.m. and binding energy difference, rel. to charge asymmetry in n-n and p-p interacts. 8=24950
- He^3, axial-vector sum rule 8=25017
- He^3, binding energy and charge radii 8=33893
- He^3, d capture, γ spectra obs. 8=29227
- He^3, elec. moment meas. with supercond mag. shield 8=29000
- He^3, Faddeev eqns. and Coulomb effects 8=42829
- He^3 particles and He nuclei 8=42825
- He^3 photodisint., two-body, calc. 8=25018
- He^3, photodisintegration at high energy obs. 8=29226
- He^3, p scatt. at 30 MeV, polarization obs. 8=29192
- He^3 recoil from D(d, n), mag. analyser-detector 8=47179
- He^3 three-body photodisintegration 8=29223
- $He^3 + C^{12}$, polarization and spin-orbital optical potential 8=38104
- He^3-d elastic scatt. obs., 239-630 MeV 8=25007
- He^3-H^3 scatt., 3-11 MeV, cross-section obs. 8=24937
- He^3-He^3 scatt., cross-section obs. 8=24937
- He^3-He^3, two-channel calc., elastic 8=34041
- $He^3(He^3, t)3p$ at 44 MeV, t spectra obs. 8=25019
- $^3He(^3He, 2p)^4He$, final-state interactions 8=25020
- $He^3(n, p)H^3$, resonance parameters from p-T scatt., 300-990 KeV 8=29185
- $He^3[n, p(n)]$ T, He^3, diff. cross section extrema due to excited state of He^4, Feymann diag. 8=24914
- $_\Lambda He^4 \to$ all e^-, β-decay rate calc. 8=29351
- He^4, 42.2 MeV fission of $Ir^{191,193}$, cross section obs. 8=43119
- $He^4(\gamma, p)$ photodisint. cross-section calc. 8=47304
- $He^4(\gamma, p)T$, diff. cross section extrema due to excited state of He^4, Feymann diag. 8=24914
- He^4, ground state, single-particle model calc. 8=29228
- He^4, level with excitation energy of 20.5 MeV 8=25007
- He^4, μ^- capture rate obs. 8=38460
- He^4, μ^- total capture rate 8=29229
- $He^4(n, p)H^4$, H^4 excited levels and bound states, obs. 8=34007
- He^4, one-particle level calc., using real N-N interaction 8=42827
- He^4, p elastic scatt. rel. to diffr. approx., 600 MeV 8=33746
- He^4, spallation, p-induced 8=29436
- He^4, ternary fission of U^{238}, evidence 8=43118
- $He^4 \to He^3 + p + \pi^-$ decay, final state interactions and excited states, obs. 8=33949
- He^4, N scatt. < 20 MeV, optical model 8=29231
- $He^5 \to He^4 + P + \pi^-$ decay, final state interactions and excited states, obs. 8=33949
- He^5, 19 MeV excitation energy obs. in d-H^3 scatt., 3-11 MeV 8=24937
- He^6 ang. distrib. from Li^7, $B^{10,11} + Li^7$ reaction at 3.0, 3.5, 3.8 MeV obs. 8=43099
- He^6, excited bound states, deformed orbits calc. 8=25093
- He^6, three body decay, 1.71 MeV(2^+) state 8=25021
- He^7 excited levels rel. to γ transitions 8=33947
- He^8, 13% of hammer tracks prod. by K^- in nuclear emulsions 8=25022
- He^8 prod. in π^- capture in C, N and O 8=25257
- Ne^{22} (He^3, He^3) Ne^{22} ambigiuties in optical-model 10 MeV 8=38514
- $Ni^{58}(He^3, He^{3\prime})$, optical model analysis, 51.3 MeV 8=43076
- Po^{210} source, neutral excitation of superfluid He 8=24045
- $T(^3He, np)^4He$, final-state interactions 8=25020
- $Ti^{48}(He^3, He^3)$, quasi-elastic, 25 MeV 8=38518

Alpha-ray spectra

See also Nuclear decay theory.
- element 102, decay, review 8=29381
- in fission, ternary, and angular correl. and emission probab. 8=29535
- $Ac^{224} \xrightarrow{\alpha} Fr^{220}$ 8=47299
- $Ac^{223,224} \to Fr^{219,220} \to At^{215,216}$ rel. to Fr and At energy levels, obs. 8=33943

Alpha-ray spectra—contd
- Am^{243} decay obs. 8=42975
- Be^{9}(Li^{6}, α) rel. to α- and d-cluster transfer, 26 MeV 8=38524
- C^{12}(Li^{6}, α) rel. to α- and d-cluster transfer, 26 MeV 8=38524
- Li^{6,7}(Li^{6}, α) rel. to α- and d-cluster transfer, 26 MeV 8=38524
- Pa^{231}, new α-decay lines with energies, 5631, 5027, 5009 KeV 8=38412
- Po$^{197-203}$ and isomenic states, obs. 8=38440
- Sm^{148}, highly excited states 8=33929
- Tb^{159}(n, α)Eu^{156}, 14.2 MeV, inadequency of evaporation theory 8=25251
- Te^{122}(n, α)Sn^{119}, 14.2 MeV, inadequacy of evaporation theory 8=25251
- Tm^{169}(n, α)Ho^{166}, 14.2 MeV, indequacy of evaporation theory 8=25251
- U^{235}, tripartition, meas. of low energy part 8=43126

Alpha-ray spectrometers
- stratospheric fallout, analysis of transuranium elements 8=27928

Alpha-rays
- See also Alpha-particles; Cosmic rays/alpha-particles; Radioactivity.
- α-α optical pot. at high energies, rel. to existence of low-energy repulsive core 8=25015
- energy dissipation in finite cavity 8=47350
- isotopic spin zero from p-T scatt. obs. 8=29185
- π^-, s-orbit, absorpt. 8=24813
- Cu-Au alloys, stopping power of 0.5 to 3.5 particles 8=44497
- Pt, channeling rel to radiographic obs. of defects. 8=48830
- Z > 50 and N < 126 emitters, decay schemes and periods, tables 8=38413
- **absorption**
  - Ag, of 54.4 MeV α, energy loss and dispersion obs. 8=48919
  - Au, of 54.4 MeV α, energy loss and dispersion obs. 8=48919
  - in BeO crysts., channelling, 5.15 MeV 8=31144
  - Cu, of 54.4 MeV α, energy loss and dispersion obs. 8=48919
  - Tb, of 54.4 MeV α, energy loss and dispersion obs. 8=48919
  - Tm, of 54.4 MeV α, energy loss and dispersion obs. 8=48919
- **angular distribution**
  - in fission, ternary, angular correl. and spectrum 8=29535
  - B^{10}(d, α)Be^{8}, 0.5-2.0 MeV, obs. 8=25266
  - B^{11} (p, α_0) Be^{8}, direct reaction analysis 8=33990
  - Be^{9}(Li^{6}, α) rel. to α- and d-cluster transfer, 26 MeV 8)38524
  - C^{12}(α, α_0), E$_{\alpha}$ = 6.6-8.5 MeV, obs. 8=29295
  - C^{12}(Li^{6}, α) rel. to α- and d-cluster transfer, 26 MeV 8=38524
  - F^{19}(p, α)O^{16} ground-state analysis 8=38472
  - Li^{6,7}(Li^{6}, α) rel. to α- and d-cluster transfer, 26 MeV 8=38524
  - Ra^{223} decay, α-γ angular correl. rel. to Rn^{219} levels, 270 keV 8=33942
  - Rn^{219} decay, α-γ correls. rel. to Po^{215} levels, 272 and 402 keV 8=33942
  - rel. to Rn^{219} levels, α-γ angular correl. obs. 8=29346
  - Si^{28}(n$_0$, α)Mg^{25}, E$_n$=21.3 MeV. obs. 8=29467
  - Sn isotopes, 116, 117, 118, 119, 120, scattering, 34.4 MeV 8=47352
  - U^{233} aligned nuclei, low-temp. obs. 8=30634
  - U^{235} fission, prompt α-rays anisotropy rel. to fragments energy, obs. 8=29537
  - in U^{238} ternary fission, 14 MeV n induced 8=29536
- **detection, measurement**
  - See also Alpha-ray spectrometers; Dosimetry; Particle detectors; Radioactivity measurement.
  - α channelling to study crystal faults 8=48578
  - aurora, moderate storm, >50 keV rocket obs. 8=32283
  - channel e multiplier appl. 8=47178
  - internal amplification detector 8=29225
  - telescope, meas. from fast n-reaction 8=29456
  - rel. to ultra-n deficient nuclei identification 8=38424
  - Si: Li detector response 8=38103
- **effects**
  - See also Nuclear reactions due to/alpha-rays.
  - acoustic cavitation, α-induced, apparatus and results 8=48032
  - anthracene, α-radiation damage studied by etching in benzene. 8=48826
  - anthracene, electron and hole generation 8=40595
  - anthracene 7.5 MeV, excitation of scintillation pulses, direction and temp. depend. 8=36526
  - anthracene scintillator excitation, decay obs. 8=49832
  - Ar radioluminescence obs. 8=47521
  - CdS, self-diffusion, radiation-stimulated coeff. determ. 8=35482
  - Cu annealing stage I after α-irrad., influence of defect conc. 8=48926
  - He gas, high-pressure, recombination luminescence in induced scintillation 8=29642
  - Np^{237} resistivity, low-temp., self-irrad. damage effects. obs. 8=31322
  - Pa resistivity, low-temp., self-irrad. damage effects. obs. 8=31322
  - U^{233} resistivity, low-temp., self-irrad. damage effects. obs. 8=31322

Alpha-rays—contd
- **effects**—contd
  - Xe, liquid, luminescence in electric field 8=25937
  - ZnO, Ga scintillation, obs. 8=37789
  - ZnS(Ag) based crystals, scintillation output rel. to α-radiation of surface 8=27662
- **scattering**
  - α-α, low energy, Yukawa attraction and pot. wall 8=37752
  - α-α, one-boson-exchange pot. calc. 8=25016
  - elastic on light nuclei, differential cross sections, E$_{\alpha}$ = 104 MeV 8=38513
  - Honda-Kudo-Ui theory, applic. to C^{12} 8=43073
  - inelastic, rel. to γ deexcitation pattern outside reaction plane 8=38512
  - metals, backscatt. from thick backings, Z depend., obs. 8=43071
  - optical model, back-scatt., E$_{\alpha}$ = 18-50 MeV 8=33974
  - optical potential calc. 8=25052
  - rare-earth for nuclei shapes obs., 50-MeV, review 8=33860
  - Rutherford, appl. to foil target thickness meas. 8=46850
  - Rutherford, student expts. with annular target 8=42669
  - A, ang. distrib. analysed in Akhieser-Pomeranchuk-Blair model 8=25263
  - Ag^{107,109} core excitation at E$_{\alpha}$ = 42 MeV, obs. 8=43077
  - C, ang. distrib. analysed in Akhieser-Pomeranchuk-Blair model 8=25263
  - C^{12}(α, α)C^{12} ang. distrib. rel. to O^{16} levels 8=38357
  - C^{12}, (α, α_0), E$_{\alpha}$ = 6.6-8.5 MeV, obs. 8=29295
  - by C^{12}, ang. distrib. anal. by direct interact. and diffraction scatt. theories 8=34038
  - C^{12}, Honda-Kudo-Ui theory 8=43073
  - C^{12}, 24 MeV, elastic obs., compound mechanism 8=43072
  - C^{12}, 2.8-6.6 MeV, levels of O^{16} deduced 8=25270
  - C^{13}, cross-sections obs., 3.5-6.5 MeV rel. to O^{17} energy levels 8=25103
  - Ca^{40}, E$_{\alpha}$ = 12-18 MeV, optical-model analysis 8=43075
  - F^{19}, angular distribution and cross sections obs. 20-23 MeV 8=47351
  - H^{3}-α, 3-11 MeV excitation function obs. 8=24937
  - He^{3}-α, 3-11 MeV, cross-section obs. 8=24937
  - He^{3} on C^{12}, 3.7-15 MeV, optical model analysis 8=29511
  - He^{3}-He^{3}, two-channel calc., elastic 8=34041
  - π^--He^{4}, 8 BeV/c, cross-section 8=29230
  - d-He^{4}, elastic, rel. to N exchange, Ed = 0.2-10.3 MeV 8=43052
  - $\pi^{\pm}$He^{4}, elastic scatt., 610 MeV/c obs. 8=24794
  - e-He^{4}, implication of new approach to Q.E.D. 8=24723
  - π-He^{4}, impulse model theory 8=33679
  - πHe^{4}, 129, 140, 150 MeV/c cross-section obs., π charge radius calc. 8=33664
  - π-He^{4}, 139 MeV/c rel. to final state interaction effects in $_{\Lambda}$H^{4} $\rightarrow \pi^-$ + He^{4} 8=25168
  - e-He^{4} 150-400 MeV, 20 MeV O^{+} level obs. 8=24724
  - p-He^{4}, nucleons released at 660 MeV 8=25227
  - p-He^{4}, 1.7 BeV/c, cross-section calc. 8=29230
  - t-He^{4}, polarization meas. on He^{4} 8=38102
  - In^{113,115} core excitation at E$_{\alpha}$ = 42 MeV, obs. 8=43077
  - K^{39}, E$_{\alpha}$ = 42 MeV, inelastic, obs. 8=43074
  - N, ang. distrib. analysed in Akhieser-Pomeranchuk-Blair model 8=25263
  - O, ang. distrib. analysed in Akhieser-Pomeranchuk-Blair model 8=26263
  - by O, elastic, differential cross-sections, and backward scatt., 20.2 to 23.4 MeV 8=34039
  - O^{18}(α, α)O^{18}, and (α, nγ), (α, γ_0), rel. to Ne^{22} excited levels, E$_{\alpha}$ = 2.5-5 MeV 8=42845
  - Ru^{98,100,102,104} Coulomb excited states obs. 8=38375
  - S-wave scatt., vacuum polarization effects 8=33748
  - Sb^{121,123} core excitation at E$_{\alpha}$ = 42 MeV, obs. 8=43077
  - Sn isotopes, 116, 117, 118, 119, 120, angular distrib. 8=47352
  - V^{51}, E$_{\alpha}$ = 42 MeV, inelastic, obs. 8=43074

Altimeters. See Length measurement.

Aluminium
- abundance in solar photosphere 8=28172
- absorption, infra-red, at 4.2°K 8=27551
- addition to Fe-Cr alloys, influence on anodic passivation 8=36602
- adhesion of liq. In 8=39336
- adsorption of oxygen on (100) face, LEED obs. 8=44072
- annealed, deformation waves, small-plastic, exptl. data 8=40126
- annealing, grain refining rel. to heating speed and dispersion 8=39714
- annealing twin boundaries 8=44161
- anodic oxide films on Al, growth mechanism by electron microscope obs. 8=44032
- atom, inelastic e scatt., E$_e$=200, 400 keV, cross-section 8=38719
- auger electron emission, chemical effect 8=43227
- blistering on p-irradiation, 10-200 KeV 8=40070
- bremsstrahlung production in thick targets on 0.5-2.8 MeV e.-irradiation 8=40071
- brightening and anodizing, surface structure appearance 8=48417
- chemisorption of diphite molecules 8=49899
- coatings on U, ion-plated, parametric study rel. to max. corrosion protection 8=49844
- combustion of droplets in air and O$_2$-Ar mixture 8=49885

Aluminium—contd
- corrosion in alkaline soln., inhibition 8=45322
- corrosion in NaCl, transient charge fluctuations, obs. 8=45368
- corrosivity of natural fresh waters, eqn. 8=41240
- creep, cyclic, of tubes rel. to second-order strain increments amplification obs. 8=44541
- crystal, strained, substructure changes on heating 8=44162
- crystal, 50 keV Al$^+$, Cu$^+$ bombard., damage obs. 8=48910
- crystals, external photoelec. effect rel. to Fermi surface anisotropy 8=40704
- cutting at 100–700 m/s, force meas. 8=35655
- deformation, critical, and structure during thermo-mechanical treatment 8=35672
- depth dose distrib. prop. by electron irrad., energy losses and ionization 8=31143
- diffusion in Au, purple plague formation 8=48771
- diffusion in Sb_2S_3 films 8=35505
- diffusion of Cu, coefficient determ, step annealing procedure 8=48773
- diffusion of Pd, Ag, Cd, In and Sn, due to near surface effect 8=39964
- diffusion of V, coeffs. 8=35476
- direct current size effect meas. rel. to Fermi surface dimensions 8=26899
- dislocation drag coeff. meas. by strain rate method 8=44441
- on dislocation-surface interactions, effect of oxide film 8=26094
- dislocations, elec. resistivity, temp. depend. 8=35821
- dislocations, glide, and vacancy aggregates, interaction, from density determ. 8=31070
- doped with Mg and Zn, electric field gradients 8=30625
- dry cell with Al anode 8=33031
- ductile-brittle transition in presence of Hg-3%Zn or Sn–10%Zn liq. 8=35656
- ductile-brittle transition temp., in liq. metals, strain-rate depend. 8=35657
- elastic field, effect of spherical inclusions 8=48938
- electron absorption coeff. and stopping distance at 50 and 1200 keV 8=44494
- electron beam energy loss distrib. obs. 8=31142
- electron energy losses, charact. on low-energy reflection 8=48905
- electron irradiated, elec. resist. recovery rel. to lattice defects 8=31147
- electron momenta from X-ray meas. 8=44647
- electron scatt., energy loss spectra, quantitative comparison with dielectric theory 8=26727
- equation of state, from determ. of Debye temp. as function of press., 0 to 135 kbars 8=43946
- exoelectron emission, photostimulated, external elec. field effects, obs. 8=36041
- exoelectron emission, photostimulated, in plastic deform., obs. 8=36039
- exoelectronic emission during friction 8=44939
- exploding foil, fast circuit switching appl. 8=32906
- extrusion temp. meas. using BACO radiation pyrometer 8=32982
- fatigue behaviour, effect of residual gas composition 8=44540
- fatigue damage from Au nucleation exam. rel. to fatiguing environments 8=26778
- Fermi momentum pressure dependence, 0-100 kbar, using positron annihilation 8=44635
- film, electron energy loss spectra 8=48904
- film, epitaxial growth on NaCl crystal 8=30745
- film on BK7 glass, X-ray refl. obs. 8=31961
- film on glass, light refl. phase retardation meas. 8=32960
- film, photocurrent induced by synchrotron radiation 8=27550
- film, size effects in magnetoresist., intepret. using two-band model 8=44683
- film struct. from evaporation, localized growths and elec. props. 8=44040
- film, transmission and reflection of synchrotron radiation near plasma wavelength 8=27549
- film, very thin, unique superconducting energy gap obs. 8=35845
- films, intrinsic resistivity and e. mean free path 8=49153
- films, orientation after deposition on NaCl 8=44085
- films, Righi–Leduc effect, size effects 8=40308
- films, thermal Hall effect, size effects 8=40308
- films, transparency thickness depend. oscills. rel. to e quantization, 4.2°K 8=31957
- films, vacuum-condensed, elastic anisotropy rel. to structure 8=44545
- films, vacuum-deposited, temp. coeff. of resistance 8=35819
- fluorescence under ion bombard. 100-200keV 8=49788
- foils, 100 to 800 μ thick, energy losses of electrons, initially 0.6 to 1.2 MeV 8=48908
- fracture analysis by acoustic emission 8=48996
- gamma-ray cross sections, analysis 8=26728
- grain size in forming rel. to sheet ribbing 8=39713
- ground level h.f.s. Stark effect obs. 8=29602
- hardening effect, of electron irradiation, rel. to point defect props. 8=31141
- helicon-wave resonances in Hall coeff. determ. rel. to surface-mode loss 8=44682

Aluminium—contd
- high-strength, fracture toughness dependence on thickness, work-hardening exponent effect 8=26766
- impurity capture during synthetic quartz growth, effect of supersaturation and temp. 8=44424
- internal friction, amplitude-dependent, at high deformation amplitudes 8=26776
- interstitials and solute additions, interaction 8=31050
- ions, doping of Si by implantation 8=40485
- Knight shift and pseudopotentials 8=45129
- liquid, coordination number transforms., viscosity obs. 8=25866
- liquid, neutron scatt. and relaxation phenomena 8=39305
- liquid, radial distrib. function from Percus-Yevick and convolution hypernetted-chain eqns. at high densities 8=48058
- low temp. deformation, stored energy rel. to strain and orientation 8=49000
- magnetoresistance in terms of mag. breakdown 8=49462
- mass spectrographic analysis, using ion beam chopper 8=27779
- m.i.m., with ferromag. metal electrodes or impurities at barrier electrode interface, tunnel current flow 8=44899
- mirror, front surface reflectivity rel. to high dose irrad. 8=28742
- modulus effect after low temp. electron irrad. 8=48907
- neutron crystal spectrometer results 8=33827
- neutron irrad., defects and lattice distortion, subthermal n scatt. obs. 8=44203
- occurrence of brass texture, after cold rolling cast strip 8=35264
- (100) face, secondary emission rel. to low and medium energy e-diffr. 8=27356
- oxide films, sputtering in plasma anodization 8=39587
- pair interaction, phase change 8=35027
- particle combustion, system morphology and mechanism 8=32112
- passivation by chromate solns., 8=45379
- photoelectric cross sections in 1-150 keV range, calcs. 8=44912
- photoelectric γ cross-section determ. 50-208 keV 8=36004
- pitting corrosion of hollow-wave by acidic gelatinous materials 8=45327
- plasma, laser-induced, ion energy and abundances 8=36051
- plasma resonance in reflection spectrum of thin films 8=30746
- plastic deform. of macrocrysts., grain boundary props., EPMA-Kossel obs. 8=30856
- plastic deformation during very high speed cutting 8=44539
- plastically deformed, exoelectron emission, effect of u.v. and electron bombardment pre-stimulation 8=44942
- plastically deformed, exoelectron emission, photo-stimulated, temp. effect 8=44943
- polycrystal, secondary ionization by 40keV Ar$^+$, mass spectrum 8=49448
- polycrystals, thermal diffuse X-ray scatt. time dependence 8=48632
- porous plugs with different internal structs and voids, combustion with O_2 throughput 8=36580
- positron annihilation angular distribs. rel. to single-particle positron wave functions 8=44669
- powder briquets for spectrochem. anal., techs for preparation 8=32158
- powder, nuclear spin-lattice and spin-spin relax. times rel. to press. 8=45110
- powdered, Al^{27} resonance, line narrowing expts. 8=49630
- pressure switch for shock-wave arrival timing 8=32904
- proton accelerator target, residual radiation dose rate 8=33402
- pure, substructure from cold rolling 8=26781
- qualification by X-ray fluorescent spectrum line shift 8=41059
- radiation from tangential surface plasmons 8=40281
- recovery, models and stage III mobile defects nature 8=39991
- refining by three-layer electrolysis, study using radio-active tracers 8=36607
- reflectivity changes during laser pulse 8=45169
- refraction of polarized light obs. 8=36319
- resistivity elec. due to vacancies and impurities rel. to band structure effects in defect scatt. in polyvalent metals 8=49154
- Righi-Leduc effect in high mag. fields 8=40727
- second-order strain accumulation, reverse cyclic torsion, devated temps. 8=40125
- secondary emission angular dependence, fine structure origin 8=40711
- seeding in propane-O_2 flame, effect on heat transfer characts. 8=32973
- self-diffusion, activation vol. and press. depend., 0-10kbar, 400-610°C 8=39967
- self-diffusion and quenching studies, analysis 8=35479
- self-diffusion coeff. from annealing kinetics of voids 8=35478
- sequence Fe^{+13} to Al, configuration mixing, oscillator strengths 8=34137

Aluminium—contd
shade etchings, orientation dependency 8=35222
shock deformation microstructures 8=44399
sheet, work softening rel. to previous cold work and struct. 8=44543
single crystal, u.s. propag. rel. to plastic deform. 8=31191
slabs, grain size and orientation 8=48589
slip band continuity across grain boundaries 8=31090
slurry in H_2SO_4, heat transfer by forced convection, rel. to Bingham plastics 8=39266
spectral lines in u.v., relative intensities, photoelec. meas. compared with photographic 8=42219
spectrochemical determ. in white cast iron, hollow-cathode discharge method 8=36642
sputtering, by 1 to 5 keV Ar^+ 8=40069
sputtering pattern structure between 100 and 560°K 8=48906
stacking-fault energies, and surface energies 8=31072
in steel, analysis for C using vacuum spectrometer, interference effects 8=32155
stored energy measurement after plastic deformation, rel. to temp. 8=26784
strain field interaction between vacancies 8=26641
strain rate effects during reversed loading 8=40128
strengthening by low temp. deformation due to mosaic block misalignment 8=35653
strips, basic theory of rolling 8=48994
substrate for Si_3N_4 films, diffusion coeff. and activation energy temp. dependence 8=31001
superconducting amorphous film, tunnelling obs. 8=40368
superconducting film, diffusion of impaired electrons obs. 8=40212
superconducting films, granular, prep. and enhanced T_c value 8=27013
superconducting, quasiparticle recomb. time, temp. depend. obs. 8=35847
superconductivity predictions from phonon spectrum and e.-phonon interactions 8=44719
superconductor, u.s. absorpt. rel. to min. energy gap 8=40367
surface, Kikuchi line interpret. rel. to 2 dimensional lattice 8=44202
thermal conductivity, anisotropic 8=48750
thermal conductivity below 1°K, rel. to supercond. energy gap 8=30988
thermal expansion coeff. of film, e diffr. meas., 20-420°C 8=35446
thermoelectric power phonon-drag and e.-diff. components 8=44904
thin film, resistance monitoring and nonadhesion effects 8=30743
thin films, plasma resonance in reflection spectrum 8=30746
thin films, use of anodisation for measurement 8=35158
thin plates, electrical resistance, temp. dependence 8=40306
third harmonic generation due to dislocation anharmonicity u.s. study 8=44442
tunnel diode, barrier decrease on oxidation, cancellation by n-type zone narrowing 8=31459
ultramicrotome-cut foils, deformation 8=48850
vacancy activation energies, temp. depend. 8=44408
vacancy and impurity solute atom, interaction energies 8=31043
vacancy-impurity pairs, binding entropy, and validity of nearest-neighbour interaction model 8=31037
valence electron distrib., investigation 8=44648
vapour deposition by e beam bombard. 8=30744
visible radiation produced by electron bombardment 8=36317
winding for injector-synchrotron and storage ring 8=33410
wire, grain size orientation-dependence rel. to texture development 8=26290
wire ohmic contact on p-Si crystal 8=40483
X-ray band spectra, intensity distrib. interpretation 8=45171
X-ray band spectra, interpret. from effective potentials determ. 8=45172
zone melting, effect of third component on impurities behaviour 8=35235
zone-refined, mechanical props. changes during recrystallisation after low-temp. deform. 8=35660
Ag^{110} diffusion coeff., 450-630°C 8=44381
Al^{27} resonance in powdered Al, line narrowing expts. 8=49630
Al^{27}: ruby nuclear paramag. acoustic absorption at 4.2°K 8=40914
Al^{27} n.m.r. in $CaAl_2Si_2O_8$, anorthite, obs. 8=40972
Al^{27}, zero field resonances, in Al containing Zn impurity 8=49631
Al-polypropylene glycol suspensions, thermal cond. meas. 8=43883
Al(III) coordination no. in aq. solns. determ. by p.m.r. 8=39431
Al 99.5, microstruct., texture and annealing depend. on deform. 8=35266
Al-Al_2O_3-metal structures, I-V characts. 8=27240
Al-Al_2O_3-Al, current transmission asymmetry, theory 8=27239
Al-Al_2O_3-Al struct., e energy loss obs. 8=27316
Al-Al_2O_3-Au sandwich, electroluminescence, correlation with electron emission 8=40700
Al-Al_2O_3-Au tunnel cathode, e emission fluctuations 8=44935
Al-H_2O n slowing down anisotropy, obs. in plate lattices 8=38576
Al-H_2O, n slowing down anisotropy in slab systems, Monte Carlo calcs 8=38577
Al-Si_3N_4-Si MNS diodes characts. and prep., obs. 8=40545
Al:Cr, impurity ion effect on crystal structure 8=26642
D^+, 5-80 keV, range obs. 8=48912
Fe, in melts, u.s. dispersion, 740-800°C 8=39442
with Fe and Si impurities, precipitation effect on cold or rolling texture 8=35267
Gd ion sputtering, ang. distrib. obs. 8=48909
Kr ion sputtering, ang. distrib. obs. 8=48909
Mg ion sputtering, ang. distrib. obs. 8=48909
O content determ. by $O^{16}(n,\gamma)N^{16}$ 8=32167
Sb^{124} diffusion coeff., 450-630°C 8=44381
in SiC particle varistor, effect on voltage nonlinearity 8=31404
on SiO_2, reactivity, moisture effects, obs. 8=45328
Ti, in melts, u.s. dispersion, 740-800°C 8=39442

Aluminium alloys
See also Aluminium compounds.
aged, struct. and props., influence of small Ag additions 8=48590
Alni alloy, chem. comp. and magnetization ageing dependence, Mössbauer exam. 8=49514
Alni alloys, coercive force and structural changes 8=35090
alnico, Ti determination 8=49984
annealing characts rel. to precipitate interact. with dislocations 8=48849
antifriction props. 8=44544
corrosion in NaCl, transient charge fluctuations obs. 8=45268
crude, production by reduction of aluminous ores: thermal props. of bauxites 8=30956
crude, production by reduction of aluminous ores: thermal props. of Japanese colloidal earth 8=30955
diffusion of dilute impurities, e microprobe obs. 8=31003
dilute, de Haas-van Alphen effect 8=31494
dilute, thermoelectric power phonon-drag and e.-diff. components 8=44904
dislocations, ratio of true density to apparent density determ. by e-transmission microscopy 8=26665
duralumin, reflectivity changes during laser pulse 8=45169
fatigue crack growth rate in thin sheets, local plastic deformation effects 8=35652
fatigue props, long-life, controlling factors 8=48995
fracture toughness, effect of specimen type and crack orientation 8=48989
hardening curves similarities from elec. resistivity meas. on ageing up to 100°C 8=35654
oxidation-vacancy production 8=26640
resistance, electrical, new theory, optical diffraction phenomena analogy 8=40307
SAP, (sintered Al/Al_2O_3 alloy), lattice defects, behaviour on cold working, resistometric exam., 8=48817
SAP, (sintered Al/Al_2O_3 alloy), lattice defects, behaviour quenching, resistometric exam., 8=48816
serrated yielding, dislocation model of temp. and strain rate depend. 8=44548
splat-cooled, effect of cooling rate on dendrite spacing 8=26232
strips, basic theory of rolling 8=48994
for telescope mirrors 8=46677
2024-T3, fatigue due to broad and narrow-band random loading 8=44547
yield surfaces, prestraining effect, exptl. study 8=40127
Ag-Al, massive and martensitic transformation, microstructure 8=48370
Al-Ag alloy, Ag conc. from Guinier-Preston zone exam., 8=49996
Al-Ag, cellular reaction, growth kinetics, influence of precipitation 8=39540
Al-Al_2O_3, ball-milled, phys. and mech. props. 8=26782
Al-Al_2O_3, influence of grain size on high-temp. ductility 8=26779
Al-An-Mg, fatigue-crack propag. rel. to struct. and cycle freq. 8=44542
Al-Be 0.1%, clustering 8=44425
Al-Cu alloy, columnar to equiaxed, effect of mech. stirring in melt 8=48372
Al-Cu, chill zone in ingot solidification 8=43912
Al-Cu, columnar to equiaxed transition, effect of mech. stirring 8=48372
Al-Cu, grain boundary precip. 8=26708
Al-4% Cu, grain boundary precipitate growth, interfacial diffusion 8=39715
Al-Cu, crit. shear stress and yield strength rel. to orientation 8=48991
A-Cu, liquid, coordination number transforms., viscosity obs. 8=25866
Al-Cu, viscosity-conc. curves rel. to phase relns in solid state 8=34799

Aluminium alloys—contd

- Al-4%Cu, $\theta' \rightarrow \theta$ transform., effect of plastic deform. 8=48371
- Al-Cu: MgSi, increase in ageing rate due to two impurity assoc. 8=35089
- Al-Cu-Cd, θ-precip., vacancy cluster mechanism 8=35085
- Al-Cu-Mn, rapidly solidified, supersaturated solid soln. formation, comp. and decomposition kinetics 8=35084
- Al-Fe, precip. processes, morphology and kinetics 8=30677
- Al-Fe, Fe precip. Mossbauer study 8=30678
- Al-Fe-Si, precip. processes, morphology and kinetics 8=30677
- Al-Ge, atom distribution in liquid eutectic 8=39298
- Al-Ge solid solns., stacking faults in precip. particles and elastic stresses 8=31096
- Al-In, dilute, electron-microscope observations 8=35265
- Al-Mg, dynamic recovery, dislocation networks, vacancy annihilation 8=48992
- Al-Mg, liquid, coordination number transforms., viscosity obs. 8=25866
- Al-Mg, plasmon losses 8=44666
- Al-Mg, prismatic dislocation loop diam. and density, yield stress dependence 8=40033
- Al-5% Mg, sheet work softening rel. to previous cold work and struct. 8=44543
- Al-Mg single crystals, flow stress 8=40123
- Al-Mg, superconducting, energy gap anistropy and specific heat 8=48734
- Al-5 wt.%Mg, thin foils from quenched specimens, vacancy lifetimes 8=31042
- Al-Mg, viscosity-conc. curves rel. to phase relns in solid state 8=34799
- Al-Mg-Si, ageing mechanism 8=35088
- Al-Mg-Zn, mech. props. rel. to precip.-free zone effects 8=26785
- Al- Mg-Zn, new rupture pattern obs. by replica tech. 8=35658
- Al-Mn 1.04% alloy, deform. structures and recrystallization behaviour 8=48803
- Al-NbAl$_3$ dispersion phase, prep. and mech. props., obs. 8=44546
- Al-Ni, electronic structure of Ni atoms 8=49744
- Al-0.04 wt % Fe, recryst. and recovery rel. to Fe precip., obs. 8=39664
- Al-Si eutectic, microstructure and growth obs. 8=35234
- Al-Si, liquid, coordination number transforms., viscosity obs. 8=25866
- Al-Si, modification 8=43975
- Al-Si, viscosity-conc. curves rel. to phase relns in solid state 8=34799
- Al-Ta dilute, resistivity, temp. depend. 8=35822
- Al-U-Zr, phase equilib. near region of Al-uAl$_2$-ZrAl$_2$ 8=35086
- Al-V, plasma-jet spray-quenching in dispersion hardening 8=26780
- Al-60-78% Zn, α^1-phase decomposition 8=35091
- Al-Zn, clustering kinetics rel. to quenched-in vacancies 8=48807
- Al-Zn cold-worked at −195°C, resist. recovery 8=40305
- Al-Zn, decomposition 8=30679/80
- Al-35% Zn, dislocation activation lengths, effects of attractive precipitate particles 8=48851
- Al-20%Zn, effect of temp. on fracture characts 8=48993
- Al-8.7 at. % Zn, internal strain field X-ray determ. 8=26786
- Al-10% Zn, point defects existing Zn clustering, nature 8=48802
- Al-25 wt.%Zn precip., effect of quenching conditions 8=26058
- Al 78 wt. % Zn, superplastic deform. and dislocation climb. 8=44538
- Al-60Zn, superplasticity, struct. depend. 8=48990
- Al-Zn, viscosity-conc. curves rel. to phase relns in solid state 8=34799
- Al-Zn, Young's mod., temp. depend., rel. to phase diagram 8=48988
- Al-Zn-Mg, hardness changes associated with fatigue-crack propag. 8=26783
- Al-Zn-Mg, precipitation process 8=35087
- in NaCl, hot, corrosion rate and films tan δ rel. to cation impurities 8=44864

Aluminium compounds

- See also Aluminium alloys; Ruby.
- alumina ceramics, grinding, densification and abrasion resistance 8=48987
- alumina ceramics, surface resistivity, cleaning and humidity effects 8=49337
- alumina-chromia alloys, twist boundaries 8=44463
- alumina, commercial ceramics, loss tangent and permittivity, 20-400°C 8=27238
- alumina fibres for plastic resin reinforcement 8=26857
- alumina inclusions group, initial O content in liquid Fe as formation factor 8=35651
- alumina insulating ceramics, vol. resistivity at high temps. 8=49334
- alumina, l.f. grain-boundary relax. 8=44549
- alumina mats, commercial, loss tangent and permittivity meas. at 9368 MHz and 20-400°C 8=49339

Aluminium compounds—contd

- alumina (96%) rods, thermally conditioned, residual stress and flexural strength 8=35659
- alumina, plasma-sprayed, structural changes on reheating 8=48354
- γ-alumina with adsorbed methane, radiolysis at 77°K 8=41290
- aluminoalkalisilicate glasses, Al^{27}n.m.r. 8=40971
- aluminosilicates, X-irradiated, e.p.r. and luminescence 8=40936
- alums, α and β, morphological difference 8=26173
- alums, Ti^{3+} substituted, crystal-field origin 8=43935
- anodic films, high field kinetic processes 8=36603-4
- bayerite, structure from n.-diffr. exam. 8=39804
- blue, visible charge transfer band 8=27603
- corundum bed, fluidized by vibs. or gas flow, comparison of heat transfer coeffs. 8=39448
- corundum, Cr^{3+} and Ti^{3+} doped, catalytic hydration of C_2H_5 8=32122
- corundum, crystal form on evaporation at high temps. and low pressures 8=39643
- corundum, dislocation structure obs. by reverse decoration technique 8=26664
- corundum, exchange-coupled Cr ion pairs, spectra 8=36322
- corundum, heat-treated, surface defects, e-diffr. exam. 8=31054
- corundum, hydrothermal crystallization kinetics 8=26230
- corundum, synthetic, structure defects distribution 8=35554
- corundum, transparent sintered, prep. and props. 8=45940
- felspars, X-irradiated, structure defect exam. by e.p.r. and thermoluminescence 8=26710
- leucosapphire, growth from tungstate melts, morphology and optical props. 8=39648
- leucosapphire optical props., effect of γ-radiation 8=41054
- leucosapphire, substructure from x-ray exam. 8=30812
- methyl-ammonium alum, low-temp. sp. ht. anomalies meas. by continuous heating calorimetry 8=46299
- muscovites, harmonic, epitaxic power temp. dependence 8=26279
- oxide films on anodized Al, pore struct. and barrier layer, obs. 8=44038
- ruby, electron cross relax. and nuclear polarization 8=40905
- ruby, luminescence, two-photon excitation 8=45259
- sapphire, acoustic wave generation by electrostrictive mixing of light waves 8=45162
- sapphire, adherence and wettability of Ni, Ni-Cr and Ni-Ti alloys 8=43744
- sapphire, birefringence, 1500 to 3000 Å 8=41056
- sapphire, colourless crystals, optical inhomogeneity 8=41055
- sapphire, crystals, conductivity, 20-850°C 8=27236
- sapphire crystals, elec. conductivity 8=49338
- sapphire, czochralski crystals, interface growth morphology 8=44117
- sapphire, deposition of thin Si films in u.h.v. 8=44056
- sapphire insulating ceramics, vol. resistivity at high temps. 8=49334
- sapphire, microwave phonons, second-harmonic generation 8=30950
- sapphire, principle dielectric consts., meas. by mech. action method, comments 8=40569
- sapphire substrate for Si film, crystallog. orientation relations 8=44058
- sapphire, substrate for Si perfect single cryst. film growth 8=39595
- sapphire substrate prep. for Si epitaxial deposition 8=39699
- sapphire surfaces in contact, ht. resistance, 1·5-300°K 8=48749
- sapphire whiskers, Young's modulus 8=35661
- sapphire, TiO$_2$ doping, reduction of laser prod. damage 8=33198
- specific heat and enthalpies of change of phase; meas. 8=46286
- trimethyl Al trail in upper atmos., for meas. of wind, temp. press. and density 8=36769
- zeolites, i.r. spectra of adsorbed NO, N_2O and NO_2 8=27553
- zeolites, i.r. spectra rel. to chem. struct. 8=27552
- Al borohydride, flash photolysis 8=25444
- Al^{27} n.m.r. structures under dynamic nuclear polarization 8=45111
- Al(III) ions, hydration, O^{17} n.m.r. 8=30540
- $AlBr_3$, crit. temp. and coexistence curve 8=43894
- $AlBr_3$, molten, vapour press. to crit. pt. 8=43895
- $AlCl_3$ aqueous solution, proton transfer between hydration and solvent H_2O, n.m.r. studies 8=34931
- $AlCl_3$ in aq. solvent mixtures, proton magnetic resonance coordination number study 8=25954
- $AlCl_3.6H_2O$, crystal structure, from n.- and X-ray diffr. meas. 8=39766
- $AlCl_3$-NaCl-KCl eutectic, fused, electrochem, of Zn, Cd and Hg ions 8=49917
- Al_2Cl_6 and methyl derivatives, Coriolis coupling coeffs. 8=43348
- Al-Cu-Si alloy, dislocation sources, obs. 8=48848
- AlF_3 layer formation on quartz during 3½ yrs. ageing after HF treatment. 8=49900

Aluminium compounds—contd
AlF_3, vapour press., ht. of sublimation 8=30607
AlF_3: Cr^{3+}, e.p.r. 8=36236
16 AlFe Vacodur 16 permeability, n irrad. effects, 6 × 10^{19} n/cm², > 1 MeV 8=29553
$Al_xGa_{1-x}P$, preparation and photoluminescence 8=26233
AlH, absorpt. spectrum 8=25444
AlH, emission lines in χ Cygni near minimum light 8=45662
AlH_3, pyrolysis, flash spectra 8=32110
Al-MeO, dispersion strengthened, devated temps. 8=40124
AlMn, annealing, grain refining rel. to heating speed and dispersion 8=39714
Al_3Mg_2, brittleness, temp. threshold, alloying additions effects 8=35671
AlN crystal, absorpt. coeff. rel. to band gap determ. 8=31958
AlN, energy structure exam. by ultrasoft X-ray spectroscopy 8=36320
AlN films, current-voltage characts. 8=44900
AlN, films prep. by chem. transport 8=30742
$Al(NO_3)_3$, hydration no. determ. by n.m.r. 8=48215
AlO, uniqueness of vibronic transition moment expression 8=43283
$Al(OH)_3$ gel, struct. 8=25971
AlOOH crystals, preferential orientation 8=26183
Al_2O_3 abrasive grains, frictional coeffs. with metals 8=31184
Al_2O_3, absorption, transmittance and reflectance 8=41057
Al_2O_3, addition to $BaTiO_3$ to promote conduction 8=49228
Al_2O_3, adsorpt. of binary, org., liq. mixtures 8=48477
Al_2O_3, ads. of Br_2 and I_2, refl. spectra 8=48479
Al_2O_3, Al K_α line shift rel. to e microprobe analysis, obs. 8=27804
Al_2O_3 ceramics of high purity, production 8=35071
Al_2O_3, chemisorption effects on electronic props. 8=44866
α-Al_2O_3 crystals, dislocations rel. to growth method 8=26663
α-Al_2O_3, diffusion of inert gas, high resolution meas. 8=39965
α-Al_2O_3, diffusion of Pu^{239} and Am^{241}, meas. by α-absorpt. method 8=35480
Al_2O_3, diffusion rate in molten Fe_2O_3 8=39343
Al_2O_3 dispersions, scatt. and absorpt. rel. to reflectance of clouds 8=39447
Al_2O_3, energy structure exam. by ultrasoft X-ray spectroscopy 8=36320
Al_2O_3, films, elec. conductivity 8=44894
Al_2O_3 films, luminescent brightness waves rel. to electrode mat. effects 8=45260
Al_2O_3 films on W, electron field emission rel. to thickness, and Fowler-Nordheim lines 8=27341
α-Al_2O_3, heat of immersion in aqueous Na dodecyl sulfonate, rel. to adsorpt. of detergent ions 8=49854
Al_2O_3, inert gas depth distrib., sputtering obs. 8=48923
Al_2O_3 in melts, u.s. dispersion 740-800°C 8=39442
Al_2O_3, in Al melts, u.s. dispersion, 740-800°C 8=39442
Al_2O_3, irradiated, e.s.r. of triplet state trapped hole pairs 8=40903
Al_2O_3, lattice vibrations in thin film, electron diffraction obs. 8=35387
Al_2O_3 layers, dielectric constant rel. to temp. 8=44865
Al_2O_3, macroscopic and lattice growth under n irrad. 8=26234
Al_2O_3 molten particle cloud, spectral emissivity from extinction and absorpt. meas. 8=34939
Al_2O_3 neutron dosimeters 8=47162
Al_2O_3, n-induced damage and macroscopie props. changes, review 8=44496
α-Al_2O_3, n-induced macroscopic growth and damage effect of annealing 8=26666
Al_2O_3 ortho-positronium form. and annihilation 8=49130
Al_2O_3 particle size in two-phase nozzle flow, effect of liq. surface tension 8=34634
Al_2O_3, particulate, replication for e. microscope exam. 8=44160
Al_2O_3, polycryst., n-irrad. effects on length, thermal cond., lattice and macroscopic parameters 8=26366
Al_2O_3-polypropylene glycol suspensions, thermal cond. meas. 8=43883
Al_2O_3 powder, ortho-positronium form. and annihilation 8=49130
Al_2O_3 powder, positronium diffusion constant and annihilation spectra mean length 8=44378
α-Al_2O_3, Raman active lattice modes temp-dependence 8=39868
Al_2O_3 reactions with Curium cpds. det. from Cm^{244} fission fragments 8=36649
α-Al_2O_3, retention of additives 8=39693
Al_2O_3, secondary emission, shot noise fluctuations 8=44949
Al_2O_3, spectral reflectance 8=41128
Al_2O_3 substrates coated with VO_2, rel. to device fabrication 8=30758
γ-Al_2O_3, surface radiational defects, adsorpt. exam. methods 8=44024
γ-Al_2O_3, surface radiational defects, exo-emission exam methods 8=44025

Aluminium compounds—contd
Al_2O_3 thermal cond., low-temp., rel. to radiation damage 8=26722
Al_2O_3 trichites, rupture constraint rel. to structural state 8=26777
α-Al_2O_3, Voigt-Reuss-Hill approx. rel. to meas. of elastic moduli 8=40188
Al_2O_3, X-ray spectra and zone structure 8=49702
Al_2O_3:Cr, Ti, V, exchange coupled transitions, intraband vibr. and crystal field splitting 8=49701
α-Al_2O_3: Fe^{3+}, e.p.r. spectra, effect of applied elec. field 8=45070
Al_2O_3:Fe^{57}, ht. treatment effects on Mössbauer effect rel. to cation valence states 8=43943
α-Al_2O_3:Mn, growth by hydrolysis of vapour 8=44118
Al_2O_3-Si cermets, reaction formed, microstructure 8=39712
α-Al_2O_3; V^{2+}, Cr^{3+} and Mn^{4+}, interact. with lattice from press. effects on e.p.r. spectra 8=45076
α-Al_2O_3: V^{2+}(Cr^{3+}), (Mn^{4+}), trigonal splitting, stress dependence 8=43929
Al_2O_3: V^{3+}, Jahn–Teller effect in $^3T_{2g}$ state, Zeeman study 8=43965
Al_2O_3 : V^{3+}, mag. anisotropy meas., 1.5-5.0°K 8=44965
Al_2O_3 : V^{3+}, resonance at mm. wavelength and in intense field 8=49599
$2Al_2O_3 . 5WO_3$, linear thermal expansion 8=35448
AlP, synthesis in soln. of excess Al, increased yield from stirring motion 8=44116
AlP, yield and cryst. size in two-temp. synthesis 8=44115
AlSb, elastically deformed, elec. field gradient at nuclei from n.m.r. obs. 8=31909
Al-Si catalysate, water-induced p centres obs. 8=36318
AlSb, dislocation structure and mech. props. 8=44443
$Al_2SiO_4F_2$: Fe^{+3} isotropic and dipolar contribs. to shfs tensor 8=36244
$AlTbO_3$, magneto-electric effect 8=36217
AlX_3(X=Cl, Br)-diethylether and -$(CH_3CD_2)_2O$ coordination compounds, i. r. spectra 8=25569
KAl $(SO_4)_2$ $12H_2O$ crystal growth and dissolution rates 8=48537
Nb-Al_2O_3 powder between Nb slabs, cermet seal for thermionic diode 8=28499

Americium
phase diagram, compressibility, resistance, rel. to pressure 8=39541
Am^{241}, diffusion in α-Al_2O_3, meas. by α-absorpt. method 8=35480
Am^{2+}, zero-field splitting in CaF_2 8=30622

Americium compounds
$Am(OH)_3$, crystal structure 8=39767

Ammonia. See Nitrogen compounds/ammonia.

Ammonium compounds. See Nitrogen compounds/ammonium compounds.
halides, new defect centre, motional effects 8=48879
NH_4 halides, F-centre, e. p. r. studies 8=26721

Amorphous state
See also Vitreous state.
coordination no. determ. without knowledge of density rel. to ZrO_2 structure 8=26141
crystallite models, calc. of upper bounds to small-angle X-ray scattering 8=26142
galactose, sp. ht. and enthalpy, 15-45°C, rel. to mol. structure 8=30966
glucose, sp. ht. and enthalpy, 15-45°C, rel. to mol. structure 8=30966
halloysite, water mol. arrangement 8=26143
mannose, sp. ht. and enthalpy, 15-45°C, rel. to mol. structure 8=30966
mixtures, X-ray or neutron scatt. data anal. 8=39628
paracrystals, theory 8=30799
polymers, anomalous cond. in glass transition region 8=26949
range of penetrating projectile, calc. 8=48896
random-layer line profile, Fourier-transform methods 8=26308
silica, fused, microcrystal orientation in ordered isotopic structure 8=26150
sputtering efficiency calc. 8=48895
thermal cond. of amorphous solids at low-temp. 8=30975
vapour-deposition effect on replication in electron microscopy 8=39707
As_2Se_3, band structure from ultrasoft X-ray spectroscopy 8=26901
B, layers, switching and negative resistance 8=27079
$CdGeP_2$, short-range order and crystal structure refinement 8=26373
$CdGeP_2$, structure exam. 8=26144
Ge, structure obtained by Ar ion bombardment of crystalline form. 8=39723
H adsorbed on solid CO_2 at 20.4°K 8=30765
Pb–Bi system, superconducting transition temp. 8=35844
Pd–20 at.% Si alloy, amorphization on irradiation with U^{235} fission products 8=31154
Si, ion-bombard., temp. and channelling effects 8=48931
ZrO_2, structure analysis using method of coordination no. determ. without density meas. 8=26141

Amplifiers
buffer, for pen recorder drive 8=41908

Amplifiers—contd
  coherent, 30 Hz-20 kHz 8=28458
  connecting, decoupling and grounding problems 8=46929
  distributed FET amplifiers 8=40541
  e. m. waves, electron system with anisotropic impulse distribution 8=42006
  fast electrometer type 8=33016
  klystron, high power radio frequency source for accelerators 8=24546
  laser, chain, high-gain, optical isolation technique 8=46600
  light pulse in nonlinear medium 8=46646
  light pulse, weak, by absorber saturated with strong light pulse simultaneously 8=37593
  light signal, modulated, by gas lasers 8=24269
  lock-in, galvanometer as l.f. bandpass filter 8=33011
  logarithmic, 9-decade temp. compensated 8=46938
  low noise at high impedance for far i.r. detectors 8=41853
  low-noise f.e.t., for InSb i.r. detector 8=41856
  low-noise u. h. f. preamplifier for ultrasonics 8=41909
  magnetron-type microwave amplifiers, ways of increasing gain 8=24202
  masers, USSR, review 8=33157
  microwave horn gain meas. with revised proximity corrections 8=24207
  microwave monotron oscillator with superconducting cavity, freq. stability 8=27012
  optical heterodyne receivers broadband matching 8=28774
  optical, linear, wide-band, by stagger tuning 8=28654
  optical, multi-path cell, 15 dB gain, 9-11μ 8=24374
  optical parametric, second-harmonic generation, coherence functions 8=24358
  optical quantum, gas mixture 8=24299
  parametric, supercond., for d. c. voltage meas. 8=31347
  parametric, USSR today 8=33241
  parametric, with self-polarized junction, parameter dependence on diode I-V characteristic 8=28460
  plasma, parametric 8=30144
  plasma waveguide, by use of gap coupling, theory and expt. 8=42024
  pulse, d. c. -coupled, base-line stabilization 8=24529
  pulse, 6 nsec output rise time, using transistors 8=46332
  quantum electronics, effect on technology 8=28655
  r. f. for heavily loaded beam of linear accelerator 8=24560
  r. f., low distortion using switch tube 8=24548
  r. f. system for proton accelerator 8=24558
  ruby maser preamplifier for e. p. r. spectrometer 8=33146
  selective, particle detector time constant determ. 8=33365
  servoamplifier for ion current ratio recording in mass spectrometer 8=38610
  stereophonic system, stability 8=41841
  time-sampling, with logic programme 8=33381
  two-quantum amplification of short light pulse 8=46546
  UHF power tubes e. g. klystrons, computation methods for design 8=24547
  of ultrasound, theory for semiconds. with high dielec. const. 8=35405
  U.S., construction, operation and relative gain using vapour phase grown ZnO cryst. 8=26586
  CdS, acoustic, with space- and time-varying parameters 8=30941
  CdS, light demodulator with u. s. amplification 8=27216
  GaAs lasers 8=33219
  n-InSb, of u. h. f. acoustic waves, by piezoelec. interact. with drifting electrons 8=27116
  Nd glass, nonlinear amp. of light pulses, saturation energy 8=41126
Analogue computers. See Calculating apparatus/analogue apparatus.
Analysis. See Chemical analysis; Statistical analysis.
Anechoic rooms. See Acoustical laboratories.
Anelasticity. See Internal friction.
Anemometers
  anemometry with fine hot wires, calcs. 8=30258
  hot thermistor, meas. of sheer stress exerted by fluid on surface bounding the flow 8=45449
  hot-wire, signal/noise ratio analysis 8=30238
  single hot wire, for Reynolds stress meas. 8=47926
  turbulence, wall pressure, orifice hot-wire probe 8=28225
Angle measurement
  See also Alignment.
  displacements, very small, using open circuit voltage of symmetric photodiode 8=41618
  glass, comparative reflection method 8=32637
  goniometer attachment, for quicker readings 8=23790
  goniometer, u. s. for liq.-solid boundary reflectivity meas. 8=48134
  instrument, specifications and technical data 8=41616
  (n, γ) reactions, device for Cauchois spectrometer 8=25236
  Russian instruments 8=23791
  solid angle subtended by one circular disc at another, FORTRAN prog. for calc. 8=32639
  using laser light 8=45950
  X-ray film goniometer for crystallography 8=30816
Angular distribution. See Gamma-rays/angular distribution; Neutrons and antineutrons/angular distribution; Protons and antiprotons/angular distribution.
Angular velocity measurement
  See also Stroboscopes.
Angular velocity measurement—contd
  basic means for reproduction and meas. 8=45960
  photoelectric tachometer 8=28220
Annealing. See Heat treatment.
Annihilation of electrons. See Electron pairs.
Anodic films. See Electrochemistry; Films/solid.
Antennae. See Electromagnetic waves/radiators.
Antiferroelectric materials. See Ferroelectric materials.
Antiferromagnetic resonance
  Ising spin systems, spin-cluster resonance 8=31836
  spin cluster, in Ising spin system 8=27450
  $CoBr_2.6H_2O$, and mag. susceptibility 8=36204
  $CoCl_2$, field-dependent modes 8=31837
  $CoCl_2.2H_2O$, spin-cluster resonance 8=31836
  $CoCl_2.6H_2O$, higher harmonic 8=36229
  FeF_3 twinned crystals, 4.2–400°K 8=31838
  MnF_2, and u. s. attenuation expts. 8=44319
  MnI_2 insulating spiral, freq. and temp. dependence 8=31831
  $NaNiF_3$, orthorhombic weak ferromagnet, rel. to canting 8=31839
  $RbMnF_3$, nucl. and electronic spin wave excitation by parallel pumping 8=31835
  Tm orthoferrites, modes in spin reorientation region 8=27456
  $ZnCr_2S(Se)_4$ insulating spiral, freq. and temp. dependence 8=31831
Antiferromagnetism
  See also Magnetic properties/antiferromagnetic.
  absence in one and two dimensions in many-band model for interacting electrons in a metal 8=44993
  cubic cryst., zero-point and excited state energies 8=36199
  d^3 ions, exchange interaction, night-angle nearest-neighbour, systematics 8=31748
  dynamical critical exponent in isotropic system near transition temp. 8=31553
  energy-band theory 8=31545
  excitation spectra of rings, biperiodicity 8=45050
  ground state in mag. field of arbitrary direction 8=45045
  Heisenberg antiferromagnet, anisotropic, low temp. behaviour near mag. phase boundaries 8=27440
  Heisenberg antiferromagnets, spin impurity effects 8=31750
  Heisenberg antiferromagnet with impurities, diffuse elastic n. cross section 8=31752
  Heisenberg linear chains, alternating, eigenvalue spectrum and thermodynamic props. 8=31751
  Heisenberg magnet, free surface effects 8=45048
  Heisenberg magnets, ordering fluctuations 8=31747
  Heisenberg, principal susceptibilities, spin-wave theory 8=31783
  Heisenberg ring, excitation spectrum 8=45049
  Heisenberg systems, two-dimensional, expt. verification of spin-wave predictions 8=36088
  indirect exchange theory, impurity influence 8=36066
  Ising ferro- and antiferromagnet, spin pair correlation function 8=40779
  magnetostatic oscill. spectrum of spheroid with easy anisotropy axis 8=45046
  magnon-sidebands 8=36298
  many-spin systems, dynamical spin correlations rel. to sublattice orderings 8=36091
  metallic, rel. to band structure 8=36201
  model, Cr-like, itinerant-electron 8=31753
  Mössbauer absorpt. spectra rel. to spin relax. 8=43940
  in narrow band materials, electron correlations for normal and mag. state 8=27439
  neutrons critical mag. scatt., theory 8=36096
  s-d exchange interaction and singlet ground states coupled to localized spin 8=40223
  s-d exchange interaction, bound state magnetic field depend. of conduction electrons system 8=49569
  s-d interaction, exactly soluble model 8=27441
  s-f, dynamic effects 8=45051
  spin-correlation function, time-dependent 8=36090
  spin density wave antiferromagnetic transition, pressure effect in Cr. alloys. 8=31767
  spin-$\frac{1}{2}$ Heisenberg antiferromagnet, Green function theory 8=40854
  spin wave nonlinear excitation 8=44985
  spin wave spectrum in strong mag. fields 8=40853
  spin wave spectrum, wave vector k dependence 8=40852
  spin-wave stimulated second-order Raman scattering 8=31944
  spin-waves, nonlinear, in presence of ext. mag. field 8=40856
  superexchange and direct interactions, model calcs. 8=31749
  superexchange in binary mixtures with one mag. component statistical effects 8=27438
  superexchange interactions, orbital degeneracy effects 8=49568
  MnF_2, Fe^{2+} impurity, critical-point magnetization 8=31787
Antimony
  adsorption on Si, influence of elec. props. 8=27134
  carrier density change under hydrostatic compression 8=49088
  carrier density pressure dependence 8=40313
  chemical separation from $SiHCl_3$ and $SiCl_4$ 8=49998
  crystal, laser-produced dislocations and twins 8=40043

Antimony—contd
- crystalline structure changes at high pressures, investigation 8=44010
- dislocation multiplication mechanisms 8=26668
- epitaxial film production on disordered substrates 8=26124
- etching, chem. and thermal, and growth from melt, obs. 8=35223
- films, evaporated, thermoelec. motive force, thickness depend 8=49391
- freezing temp. standard, apparatus 8=30585
- freezing temp. standard, measurements 8=30586
- galvanomagnetic effects, 50-300°K rel. to band model 8=40330
- galvanomagnetic props. in transverse fields up to 100kOe at 4. 2, 20. 4 and 77°K 8=49170
- γ-quanta, annihilative, obtained by positron annihilation, ang. distrib. 8=49128
- grain boundary self-diffusion meas. 8=48788
- impurities in cooled Ge bolometer, depend. of parameters on conc. 8=41855
- liquid, x-ray scatt. 8=34765
- magnetothermal oscs. meas., rel. to Fermi surface 8=44686
- metastable atoms, from flash photolysis 8=29646
- phonon drag effects on Nernst-Ettingshausen effect and thermoelec. power 8=40219
- photoeffect, I-V characts. on X-irradiation and at 6000 V 8=27325
- photoelectron emission on X-ray excitation, energy distrib. 8=40707
- photomechanical effect, wavelength dependence 8=36368
- shock-induced polymorphic phase transforms., dynamic obs. 8=39562
- solid-liquid boundary, Peltier coeff. meas. rel. to impurity 8=44909
- surface structure and reactivity, study by LEED and O adsorpt. 8=26106
- vacuum distillation, apparatus and spectrochemical meas. 8=28204
- vapour from PtSb evaporation at 900°C, nature of species from at. absorpt. 8=30608
- x-ray scatt. by liquid 8=34765
- K-Sb-Cs photocathodes 8=36023
- Sb^{121}, Sb^{123}, thermal neutron capture cross section 8=29478
- Sb^{124} diffusion in Al, 450–630°C 8=44381
- Sb: Sn, Fermi surface and level shift 8=49090
- Sb: Te, Fermi surface and level shift 8=49090

Antimony compounds
- antimonates, Nb^{5+}-activated, fluoresc. 8=41207
- antimonides with D8$_8$ and Hf$_5$Sn$_3$Cu structure types 8=26440
- halides, trivalent, isomer shifts of Mossbauer γ line 8=43956
- isostructural oxide, crystal structure 8=48676
- oxides, in silicate glasses, vibr. spectra 8=31964
- Sb sulpho-iodide, dielectric behaviour with elec. field freq. up to microwave range 8=35983
- Sb–Au system, form. of metastable simple cubic π phases 8=48402
- Sb$_x$Bi$_{1-x}$SJ and SbS$_x$Se$_{1-x}$J, electrical, optical and photoelectric props. 8=40670
- p-(Sb, Bi)$_2$Te$_3$, n-irradiated, thermo-emf, elec. and thermal conductivity 8=27136
- SbBr$_3$ molecules normal oscillations, dynamic and reduced coeffs. 8=34283
- SbCl$_3$-acetophenone complexes in CCl$_4$, i. r. spectra 8=34866
- 2SbCl$_3$. dibenzyl, mol. complex. structure 8=35353
- 4SbCl$_3$. dibenzyl, mol. complex. structure 8=35353
- 4:1SbCl$_3$. stilbene, mol. complex. structure 8=35353
- SbCs$_3$ films, quantum yield, thickness depend. 8=36054
- SbF$_3$ normal oscillation freq. calc. 8=34283
- SbF$_5$. SO$_2$, cryst. and molec. struct. 8=39820
- SbI$_3$ crystals, external photoeffect 8=44947
- Sb–Ni system, form. of metastable simple cubic π phases 8=48402
- Sb–Pd system, form. of metastable simple cubic π phases 8=48402
- Sb$_2$S$_3$ crystals, dielectric constant determ. at high freqs. 8=40585
- Sb$_x$S$_3$ film, energy bandgap, reflectance and refractive index 8=31963
- Sb$_2$S$_3$ films, diffusion of Al 8=35505
- Sb$_2$S$_3$ films, optical parameters, meas. for diff. thicknesses 8=49748
- Sb$_2$S$_3$ reflection in photon energy range 1. 5-3. 0eV 8=49749
- p-Sb$_2$S$_3$, trap depths from thermally stimulated and dark conductivities 8=44807
- Sb$_2$S$_3$. X-ray illuminated photocurrent distribution and X-ray absorpt. spectra 8=49422
- Sb$_2$S$_3$–Bi$_2$Te$_3$ solid solns., morphotropy 8=48672
- Sb$_2$Se$_3$ detectors in X-ray defectmeter 8=39989
- Sb$_2$Se$_3$, energy spectrum of traps from thermally stimulated depolarization meas. 8=40251
- Sb$_2$Se$_3$ melts, doping effects on conductivity and thermo-power temp. dependence, 1300-1400°K 8=34899
- Sb$_2$Se$_3$, thermal conductivity, 650°K–1300°K 8=30991
- SbSeI grown from gaseous phase, volatile component vapour pressure effect on elec. props. 8=35989

Antimony compounds—contd
- SbSeI, optical absorpt. and photocond. 8=32028
- SbSeI, prep. and photoelec. properties 8=44932
- SbSi, elect. and photoelect. properties 8=49269
- SbSI crystal growth, hydrothermal 8=39684
- SbSI, dielectric props., press depend. 8=49374
- SbSI, ferroelectric, far i.r. spectra 8=41134
- SbSI grown from gaseous phase, volatile component vapour pressure effect on elec. props. 8=36026
- SbSI, phase transition 8=31436
- SbSI, photodielectric effect 8=40669
- SbSI, photoferroelectric, anomalous props. 8=49373
- Sb–Te system, phase analysis 8=48398
- Sb$_2$Te$_3$, elec. and thermal props rel. to complex valence band structure 8=44808
- TiO$_2$–Sb$_2$O$_3$–NiO system, comp., structure and colour 8=26039

Antineutrinos. See Neutrinos and antineutrinos.

Antineutrons. See Neutrons and antineutrons.

Antinucleons. See Nucleons and antinucleons.

Antiparticles. See under corresponding particle.

Antiphase domains. See Alloys; Crystal structure/microstructure; Solids/structure.

Antiprotons. See Protons and antiprotons.

Antireflection coatings. See Optical films.

Apodization. See Optical images.

Apparatus. See Cosmic rays/apparatus; Instruments; Ionosphere measuring apparatus; Laboratory apparatus and technique; Radioactivity measurement/apparatus; Vacuum apparatus; X-ray crystallography/apparatus. Further entries describing apparatus for specific purposes are included under the headings of the appropriate subjects.

Appearance potential. See Ionization potential.

Architectural acoustics
- See also Echo; Noise abatement; Reverberation; Transmission/acoustic waves.
- auditorium design, Madras university sound-reinforcement 8=23968
- doors and windows, sound transmission loss 8=23966
- footstep noise on floors, assessment 8=23967
- insulation, problems of partition design 8=32920
- lecture hall design 8=23969
- noise propagation in buildings, indirect paths 8=41848
- partition walls, investigation of theory using model 8=32921
- u.s. airborne wave visualization, effect of hall shape on reflection time distributions 8=23970

Arcs, electric
- a. c. in plasmatron, dynamic characts. 8=29940
- air, unipolar, Sn-Bi alloy substance entering 8=47777
- alkali-vapour anode-spot oscills., 8=43461
- anode spots obs. by high speed camera 8=29931
- cathode surface, pulse discharge behaviour 8=34435
- cathode temperature field and current density in cathode spot 8=43462
- current chopping, low press., magnetically induced 8=34434
- cylindrically symmetrical, Abel integral eqn. soln. 8=25702
- dipped-cathode light souce for spectroscopy 8=28840
- displacement without meas. transfer 8=29932
- gaps, short gaseous, low voltage 8=43465
- heavy current, in transverse mag. field, temp. and cross section obs. 8=29933
- hollow cathode, cathode diameter, gas flow rate 8=47772
- hollow-cathode, gas fed, rot. and plasma waves 8=29926
- inert gas, low-voltage modes, pressure and impurity effects 8=47773
- impulse, electrophysical principles of theory 8=43463
- jet current, transistor regulation system 8=33020
- lightning, pressure pulse from triggered lab. stroke 8=36752
- magnetic field effect 8=38983
- moving in transverse magnetic fields, correlation of experimental data 8=47775
- moving, ionization in cathode-fall region 8=29938
- nonstationary, time constants 8=29928
- oxide-containing graphite electrodes, thermochem. mechanism 8=34436
- plasma, e beam fluctuation propag. 8=39009
- plasma diodes low voltage mode, Monte-carlo simulation 8=43607
- plasma discharge, p beam anomalous deceleration 8=39006
- plasma rays formation during separation of contacts, avoidance 8=29935
- plasma torch, projecting device for obs. of phenomena near cathode 8=39144
- power, gas temperatures and electrode metal densities, spectroscopic study 8=47776
- simultaneous multipolar discharge 8=29937
- spectra of elements, maximum sensitivity 8=29578
- spectrographic, thermochemistry of samples in carbon electrode 8=41237
- stationary, analytic eqns., solns. for thermal and elec. cond. 8=29929
- turbulent heat transfer in a cross-flow 8=29939
- universal arc-pulse generator UBI 1 for spectrochemical analysis 8=43464
- vacuum, high-current, theory of cathode spots 8=25704
- Voigt contours of spectral lines, atom temp. and e concs. obs. 8=29936

Arcs, electric—contd
- wall-stabilized d.c. in air, column recovery 8=29934
- wall-stabilized, with transverse mag. field, adjustable characts. 8=39008
- wall-stabilized, with transverse mag. field, field flow theory 8=39007
- Ar at. beam from arc source, elec. props. 8=47545
- Ar, energy balance with axial gas flow 8=43466
- Ar, excitation and ionization equilib. rel. to plasma disturbances 8=29942
- Ar, gas, for determ. of electron mobility and elec. cond. 8=39231
- Ar plasma-beam discharge stimulated emission, 4545–5145Å 8=28673
- Ar plasma source, channel, temp. distribution with axial flow of working body, spectral obs. 8=29941
- Ar II magnetoplasmadynamic, electron temp. 8=43525
- Ar-Cs discharge, plasma ionization instability in crossed elec. and mag. fields, obs. 8=34556
- C, as standard source and electrode temp. determ. 8=29927
- C, magnetized, l.f. oscills 8=25779
- C, spectral emissivity of anode 8=36333
- Ca atoms in arc discharge, spectral line broadening 8=34437
- Cs, low voltage, theory 8=39010
- Cs, plasma params. and wall ion current rel. to ionization 0.03-0.3 torr 8=25714
- Cs vapour, low-voltage, with non-isothermal cathode 8=25703
- Cu atoms in arc discharge, spectral line broadening 8=34437
- DC-arc emission spectrography, Li cpd buffers 8=27792
- Fe line intensity rel. to gas pressure reduction 8=34433
- H arc in axial parallel mag. field 8=43467-8
- H_2, pulsed high current, characts. 8=29943
- He, unipolar, Sn-Bi alloy substance entering 8=47777
- He-Ne discharge, low-voltage, rel. to cw laser oscillations 8=24315
- He-Ne laser, comparison with h.f. discharge 8=43456
- Hg plasma, i. r. bremsstrahlung calc. 8=30069
- Hg-vapour green-band emission 8=29944
- Li, plasma exam. by emission spectrum 8=47778
- N, d.c. wall-stabilized, static and recovery characts. 8=39011
- N, thermal cond. and total emission coeffs., high-temp., expt. and theory 8=47955
- Ne, low-voltage mode in plasma diode, predominant ionization and loss mechanisms 8=47779
- Pb, spectrum 8=38678
- SF_6 plasma, transport props. from temp. meas. 8=39012
- Ti atomic spectra lines press. broadening in Ar atm. 8=34153
- Xe, high press., in stationary and flashed modes, spectral emission and abs. obs. 8=29945
- Xe, pulsed, energy balance and transfer in arc plasma 8=39090
- Zn atoms in arc discharge, spectral line broadening 8=34437

Area measurement
- No entries

Area measurement, porous substances. See Surface measurement.

Argon
- absorbed, effect on props. of thin Cu films 8=49158
- in achondrites, U and Ca rich, anal. 8=28160
- afterglow, ion conversion 8=43452
- afterglow plasma, conversion rates and ion velocity 8=43480
- arc, energy balance with axial gas flow 8=43466
- arc plasma excitation and ionization rel. to equilib. disturbance 8=29942
- arc plasma source channel, temp. distribution with axial flow of working body, spectral obs. 8=29941
- atom, charge exchange with He^+ and Ne^+, 2-250 eV 8=38758
- atom collisions on Cu surface 8=29661
- atom, e scatt., E_e = 20eV-150 keV, relativistic effects 8=38720
- atom, e scatt., transport cross section calc. 8=25383
- atom, low-energy e scatt., data analysis 8=25385
- atom, polarizability in solid Ar 8=35051
- atomic beam from arc source, elec. props. 8=47545
- atomic jet excitation for u. v. source 8=38660
- beam, reflection at Pt surface at different temps. 8=25668
- breakdown, laser-induced, influence of freon-12 impurity 8=39000
- breakdown rel. to laser appl. 8=29910
- burner, h. f., temp. distribution in plasma torch 8=30179
- charge transfer from p and H atom, cross-sections 8=38737
- in chemiluminescent reactions involving atomic N, and H_2, CH_4, and N_2 8=41245
- coexistence curve shape near critical state from refractive index meas. 8=30590
- compressed, absorpt. and emission of impurity lines with trace of graphite powder 8=34138
- conductivity, thermal, high temp. change 8=34653
- cooling effect in high-vel. streams, on injection into reacting or non-reacting boundary layer 8=32958

Argon—contd
- density measurement, solid and liq. 8=28219
- diffusion in CaF_2 and U doped CaF_2 8=26618
- diffusion in UO_2, UC and U doped CaF_2 8=34107
- discharge, h. f. induction stationary, temp. 8=29900
- discharge, high press. vortex 8=29894
- discharge, low press., induction interaction of currents, obs. 8=43451
- discharge, r. f. nonequilibrium 8=29893
- discharges, microwave and h. f., energy distrib. of electrons and positive ions in plasma 8=25692
- discharges, Tonks, Dattner resonances damping rel. to microwave field 8=43443
- electron-atom scattering, mobility max. 8=43229
- electron energy loss, charact., on transmission 8=34449
- energy widths of X-ray levels 8=29649
- equation of state 8=39193
- ethane-Ar mixtures, u.s. vel. dispersion interferometry 8=47966
- excited states, cross sections for stepwise excitation and quenching process parameters 8=47489
- explosive ionization light source 8=28768
- fluid, correlation function, direct, and equation of state 8=34756
- gas, elec. cond. and electron mobility using laser interferometry of transient arc 8=39231
- gas, Fe particles dispersed, absorpt. spectra including carrier gas contrib. 8=25968
- gas, intermol. pot. from X-ray scatt. 8=30274
- gas, laser-irradiation and resulting light emission 8=29906
- gas-liquid coexistence curve shape near critical state from refractive index meas. 8=30590
- gas, shock wave of Z-pinch discharge, dynamics 8=34410
- gaseous, absorption spectrum, 1070-1135 Å region 8=25355
- gaseous, dense, three body forces contribution to thermodynamic properties 8=37198
- hydrates, dielec. props. 8=49343
- incorporation in solidifying enstatite melts 8=34972
- interatomic pot. from second virial coeffs. 8=30282-3
- ion laser, 4880, 4765, 5145 Å intensification, saturation 8=24303
- ion refl. from Cu single crystal 8=48918
- ionic sorption pumping 8=39245
- ionization coeffs. and sparking voltages 8=25701
- ionized flows at high-temps., e. attachment on SF_6 injection 8=43478
- ionized, struct. of supersonic stream moving in alt. mag. field by plotting induced e.m.f. 8=41992
- ions, 10-20keV, scattering effect of lattice thermal oscillations 8=46440
- laser, anomalous competition between transitions 8=37575
- laser, continuous, saturation obs. 8=28677
- laser, ion c.w., excitation processes 8=28675
- laser, ion, extension of range of oscillation 8=46573
- laser, ionised gas, construction and theory 8=42085
- laser, pulsed, ion, saturation of power output in very high current regions 8=28676
- laser, pulsed ion, with axial mag. field, improved performance 8=24304
- laser, pulsed, output power characteristics 8=42083
- lasers, applics. 8=42080
- liquid and solid, thermodynamic props calc. from modified cell model 8=25865
- liquid, bubbles due to zero-point motion of positronium atoms 8=30388
- liquid, coherent neutron scattering theory, convolution approx. 8=43758
- liquid, correl. and intermolec. pot. functions, determ. from X-ray diffraction 8=25877
- liquid, dielec. permeability from meas. on N_2, O_2 and Ar at about. –190°C 8=30512
- liquid, dielec. permeability meas. at ca. –190°C rel. to liq. air permeability calc. 8=30512
- liquid, neutron scatt. and relaxation phenomena 8=39305
- liquid, radial distrib. and distrib. functions, X-ray study 8=43759
- liquid, semiempirical model 8=43747
- liquid, supercooled, prod. of crysts. on ions as nuclei 8=39656
- liquid, thermodynamic props., calc. from Lennard-Jones parameters by Monte Carlo method 8=25907
- liquid, u. s. velocity at high press. 8=48138
- liquified, ion mobility and liq. motion 8=48193
- low-energy e stopping cross sections 8=47977
- melting at high temp. 8=43904
- microwave breakdown at 9 GHz 8=47768
- number density, with He, in thermosphere, rel. to altitude of turbopause 8=36775
- pair and non-pair potential 8=43924
- Percus-Yevick isotherm for exp-6 potential 8=34390
- photoabsorption of K_α X-rays, double e ejection 8=38714
- pinch shock tube current sheet 8=34448
- plasma-beam discharge stimulated emission, 4545-5145Å 8=28673
- plasma column, ion temp., charge exchange and coulomb collision 8=39077
- plasma, dense, weakly ionized kinetic energy exchange 8=47805

Argon—contd
  plasma, density decay by three-body electron-ion recombination 8=47882
  plasma, disintegrating, in impulse discharge, e-densities 8=43458
  plasma, elec. props. calc. from shock tube obs. 8=34485
  plasma flows, radiating, relax. 8=25741
  plasma in e.m. shock tube, origin of 2 regions 8=25744
  plasma, interferometric meas. in 8mm band 8=38989
  plasma, ionization waves, characteristic pots. rel. to press. and current for three types 8=25742
  plasma jet at atmos. press. , test of local thermodynamic equilib. 8=39146
  plasma jet, distrib. meas. by BN particles 8=30181
  plasma jet, electron density from Thomson scatt. of laser beam 8=34517
  plasma jet, underexpanded, continuum and line rad. rel. to temp. 8=43612
  plasma, r.f. local thermodynamic equilib. obs. using emission spectroscopy 8=43508
  plasma sheath, reflection of ion-acoustic waves 8=47876
  plasma, shock-prod, skin-depth effect of microwave reflection and transmission 8=25743
  plasma source, r.f., for m.h.d. expts, ballistic and spectroscopic study 8=43610
  plasma with K, electron temp. meas. by line reversal method 8=39075
  positive column discharge, collision-induced pumping obs. 8=38987
  positive column, e density and collision freq. meas. 8=30052
  precursor radiation in explosive-driven shock tube 8=25830
  primordial, diffusion in Fayetheville meteorite 8=37024
  radiogenic in ultramafic inclusions, Hawaii 8=50073
  rarefied, stationary between concentric cylinders, wire probe temp. meas. 8=34655
  Rayleigh light depolarisation, 15-1500 bar 8=39217
  refractive index and Lorentz-Lorenz function, gas, liq. and crit. state 8=47968
  resonance rel. to transfer shock precursor radiation 8=34441
  Rutherford scatt. of H and H^+ 8=38754
  seeding in Cs plasma, ion species present, relative abundance and ion signals 8=29987
  shock front propag., e. m. excited, for press. 0. 1 to 20 mm Hg 8=34635
  shock ionized in mag. field, microwave signal attenuation 8=29960
  shock-wave ionization, e temp. meas. 8=39221
  solid, adsorpt. of noble gases on (100) face, Van der Waals interactions 8=39617
  solid, adsorpt. of noble gases on (111) face, Van der Walls interactions 8=39618
  solid and liquid, charge transport 8=26943
  solid, compression up to 20 kbar at 38 and 77°K 8=26836
  solid, H_2 dissolved in, induced i. r. fund. band obs. 8=36326
  solid, H(D)-doped, isotope effects in absorpt. bands rel. to e-phonon interaction 8=27557
  solid, electric breakdown, conductivity 8=35951
  solid, metastable-stable transition rel. to N_2 soln. 8=39567
  solid, model potentials and sound vel. calcs. 8=35389
  solid, pair pot. calc. 8=30615
  solidification 8=43909
  solubility of water in compressed Ar 8=30302
  spark, laser-prod., expansion mechanism, obs. 8=34432
  spectral line widths and transition probabilities in plasma torch 8=43181
  spectral radiation intensity, shock-tube heated 8=24399
  supersonic beam, low-temp. viscosity cross-sections 8=30311
  surface tension rel. to mol.-statistical theory, 87-140°K 8=25898
  thermal cond., in hot-wire diffusion column 8=43683
  thermal cond., Langmuir calc. for incandescent lamps 8=42210
  thermal cond., 90°-300°K., obs. 8=43682
  ultrasonic vel., temp. and pressure dependence 8=25828
  ultraviolet absorpt. cross sections, bandwidth depend. 8=25356
  viscosity, low-temp. 8=39237
  Ar-air mixtures, equilib. props. behind incident and refl. shock waves 8=34625
  Ar-air, thermodynamic and transport props., 50° to 3500°K 8=25838
  Ar-methane system, solid-liquid equilib. diagram 8=25978
  Ar-propylene system, liq.-vapour phase equilib., and solubility 8=39479
  Ar I solar isoelectronic sequence, spectral resonance line strength 8=45871
  Ar I, $3p^m-3p^{m-1}3d$ transitions 8=43178
  Ar I, transition probabilities and relative level populations calc. from spectra 8=47490
  ArII laser, pulse, mag. field, effects on quenching an enhancement of output 8=28674
  Ar II laser, transition probabilities in lower states 8=46580
  Ar II, line profiles, obs. in plasma torch jet 8=43180

Argon—contd
  Ar II lines, Stark shifts 8=25354
  Ar II magnetoplasmadynamic arc, electron temp. 8=43525
  ArII multiplets, Stark broadening, temp. depend. 8=39028
  ArII, spectral line shift in plasma 8=34507
  Ar II transition probabilities and continuous spectra meas. 8=43179
  Ar^+ charge transfer dissociative reaction with propylene 8=34445
  Ar^+ ion bombardment of metal surfaces, X-ray production 8=31130
  Ar^+, resonance radiation trapping in pulsed ion laser 8=42084
  Ar^+ laser light scattering by He reflex discharge rel. to e-density and -temp. meas. 8=38991
  Ar^+ lasers, high power, parameters affecting power output 8=37572
  Ar^+, 1- to 5-keV, sputtering expts. on Mg, Zn, Zr, Cd 8=40076
  Ar^+, 1 to 5 keV, sputtering of Al, Cu, Au 8=40069
  Ar^+, sputtering of metals and alloys, mechanism 8=35606
  $Ar^+ + D_2$ and $Ar^+ + H_2$, reaction kinetics 8=45323
  Ar^{36}, isotope separation by thermal diffusion 8=47548
  Ar^{37} diff. in neutron irrad. CaO 8=39969
  Ar^{41}, low conc. meas. device 8=49997
  Ar-CH_4 mixture, ionization coefficient and sparking voltage 8=43479
  Ar-C_2H_6 mixture, ionization coeffs. and sparking voltages 8=25701
  Ar-C_3H_8 mixture, ionization coefficient and sparking voltage 8=43479
  Ar-CO_2 mixtures, thermal diffusion 8=47987
  ArI, $3p^54s-3p^55p$ configs., optical transition probabilities 8=38690
  Ar-N_2 liq. mixtures, surface tension statistical-mech. calc. 8=48107-8
  Au foil bombard., lattice defect penetration 8=48815
  Br^- ions collision with atoms, detached electrons energy obs. 8=29972
  Cl^- ions collision with atoms, detached electrons energy obs. 8=29972
  Cu foil bombard, lattice defect penetration 8=48815
  Cu sputtering, ion channelling obs. 8=48921
  and He gas mixture, structure of normal shock waves 8=30261
  I^- ions collision with atoms, detached electrons energy obs. 8=29972
  K seeded, in subsonic m. h. d. generator, core flow 8=41933
  $N_2^* + Ar$ collisions, ionization cross section enhancement, obs. 8=34454
  with NH_3, SO_2 or H_2S, thermal cond., 273-1173°K 8=47962
  Ni sputtering by Ar^+, [110] and [100] close-packed directions yields, 25-600 eV 8=40078
  O_2 and O, density in lower thermosphere above Sardinia, mass spectrometric determ. 8=27939
  Ti lines, press. broadening and shift by Ar 8=43204
  Zn 3075.9 Å, perturbation of resonance line 8=47512
  Zn-Ar plasma, in local thermodynamic equilib., 4000 to 50 000°K, composition 8=47809
Argon compounds
  H_2Ar, bound states, i. r. absorpt. 8=25472
Aromatic compounds. See Organic compounds.
Arsenic
  Azbel'-Kaner cyclotron resonance, expt. and theory 8=44684
  bands, galvanomagnetic investigation 8=26902
  carrier density change under hydrostatic compression 8=49088
  chemical separation from $SiHCl_3$ and $SiCl_4$ 8=49998
  diffusion from GaAs of As into Ge substrate 8=35494
  diffusion in Ge, dislocation formation 8=35568
  dislocation etch pits, 8=48852
  galvanomagnetic effects and Fermi surface, correlation 8=40232
  growth from vapour, and etch pit studies 8=44119
  implanted in Si, impurity distrib. determ. 8=27131
  interband transitions from infrared magnetoreflectivity obs. 8=26900
  ions implanted in Si, distrib. 8=49266
  metastable atoms, from flash photolysis 8=29646
  vaporization 8=39497
  As_2 spectral bands in $D \rightarrow X$ system 8=43284
  $As(4^2D)$, cross-sections for deactivation 8=34160
  As^+, type conversion and p-n junction production in n-CdTe by ion implantation 8=35882
  As^{75} quadrupole interaction in KH_2AsO_4 ferroelectric cryst., crit. temp. behaviour 8=45137
  As: Ge, de Haas-van Alphen effect 8=49091
Arsenic compounds
  oxides, in silicate glasses, vibr. spectra 8=31964
  AsD_3, flash photolysis, AsD_2 $^2A_1-^2B_1$ band spectra 8=29713
  AsF_6^- anion in non-aq. solns., spin-lattice relax. 8=34928
  AsH_3, flash photolysis, AsH_2 $^2A_1-^2B_1$ band spectra 8=29713
  AsH_3, K-type doubling in ν_3 band 8=25445
  AsI_3 crystals, external photoeffect 8=44947
  AsI_3, far i. r. cryst. spectra 8=45223
  As_2O_3, special effect on the optical absorption of glasses 8=41097
  $As_2O_5 \cdot 5/3H_2O$, crystal structure 8=39768
  $(As_xSb_{1-x})_2Se_3$ film, energy bandgap, reflectance and refractive index 8=31963

Arsenic compounds—contd
- As_2Se_3, electron emission, thermostimulated 8=40697
- As_2Se_3 film, energy bandgap, reflectance and refractive index 8=31963
- As_2Se_3, n.q.r. 8=31926
- As_2Se_3, thermal cond., Ge and Ag impurities effect 8=44360
- $AsSe_3$, amorphous band structure from ultrasoft X-ray spectroscopy 8=26901
- $2H_3AsO_4 . H_2O$, crystal structure 8=44204

Assistors. See Semiconducting devices; Resistance, electrical.

Association
- heavy nuclei, rel. to density 8=25068
- ionic system, chem. relax. timing by pressure shock technique 8=45360
- pyridinyl diradicals, stable, intramolec. assoc. 8=43424
- radical recombination obs. by e. s. r., n. m. r. methods 8=38939
- $CaCl_2$ in NaCl 8=48390
- O atom recomb. rates, direct shock tube meas. 8=29666
- **gases**
  - reaction kinetics, effect of dead space 8=49841
  - H_2O supersaturated vapour 8=25477
  - $Ne^+ \rightarrow Ne_2^+$ reaction rate obs. 300°K 8=39049
- **liquids**
  - See also Colloids.
  - butanone-2-oxime in various solvents 8=43763
  - formamide 8=39306
  - macromolecules in soln., effect of dielec. consts. of solvent 8=30418
  - methyl-heptanols, pressure depend. from dielec. props. 8=39394
  - octanols, pressure depend. from dielec. props. 8=39394
  - octyl alcohols, isomeric 8=30508-9
  - octyl alcohols, isomeric, press. depend., dielec. determ. 8=48182
  - tetraethylammonium perchlorate in valeronitrile 8=48197
  - tributylphosphate and H_2O 8=34775
  - H_2O, self-association in dichloroethane 8=34874
  - Li Br solns., elec. cond., association const. calc. 8=48198

Astatine
- in epitaxial crystallization mechanism 8=39698

Astatine compounds
- No entries

Asteroids. See Planets; Solar system.

Astigmatism. See Aberrations, optical.

Astronautics. See Space research.

Astronomical instruments
- See also Radioastronomy; Telescopes/astronomical.
- astrophotometer, differential, for relative determ. of stellar magnitudes 8=36933
- balloon-borne spark chamber for γ-ray astron. 8=45798
- balloon borne spark chamber for γ-ray astronomy 8=45795
- cascade intensifier, use in Coudé spectroscopy 8=28773
- Cherenkov detector of 10^{11}-10^{12} eV region for obs. on earth's surface 8=42679
- clear-sky detector 8=50146
- coleosat for catania observatory 8=28163
- coronograph, light scatt. in objective, laboratory meas. 8=45921
- for galactic emission regions meas., multi-lens Perot-Fabry assembly 8=32414
- γ-ray detector vidicon spark chamber, for balloons and satellites 8=45610
- γ-ray scintillation counter for balloon borne obs. 8=38112
- heliostat, simply-aligned 8=32416
- high speed stellar polarimeter, electronic circuitry 8=50270
- integrating photometers 8=36974
- interferometer, Fabry-Perot improvements 8=32415
- interferometer, Michelson variant, converged beams coincident 8=33276
- interferometer, Mock, telescope mounted, visible and near i.r. 8=32412
- interferometer, photoelec. Fabry-Perot, magnetostriction scanned for solar and dayglow meas. 8=32272
- interferometers, Fabry-Perot, for rocket appls., 1700-5500 Å 8=32411
- Lyot-coronagraph with 53 cm objective, description 8=28187
- mirrors, supports for minimum deflection 8=42182
- photodiodes, p. i. n., for astrophotometry 8=42135
- photography using different filters, of Venus 8=50422
- photometer, double beam photoelec. filter photometer, for astronomy 8=41497
- radiometer, three-channel, polarization of cosmic radiation at 210 Mc/s, obs. 8=41543
- solar magnetograph, Locarno, errors 8=50439
- solar magnetograph using a subtracting double-dispersion optical system 8=41581
- for solar monochromatic images, Fabry-Perot etalon appls. 8=45857
- spark chamber, vidicon for γ-ray balloon astronomy 8=45796
- spectrometer, Fourier, 4300-8000 cm^{-1} 8=32413
- spectrophotometer, Fabry-Perot, use with telescope, non-uniform illum. effects 8=32410

Astronomical instruments—contd
- spectropolarimeter, three-channel photoelec. 8=36921
- star tracker photomultiplier tubes, electron induced noise 8=28577
- stellar interferometer at Narrabi, description and obs. procedure 8=28073
- stellar interferometer, precision meas. 8=28752
- stellar spectrograph, high speed, for gratings to 128 mm and dispersions 80 to 20Å/mm 8=36946
- telescope, high resolution photography of solar chromosphere 8=45917
- for zodiacal light and twilight, press. scanned Fabry-Perot 8=32568

Astronomical observations
- See also Radioastronomy.
- astrolabe., corrections for planets phase and flattening 8=36925
- astrometry, colour effects 8=28063
- atmosphere seeing, effect on photospheric vel. meas. 8=41591
- atmospheric H_2O absorpt. effects, 50 μ-1 mm 8=41499
- atmospheric refraction obs. at the Pic-du-Midi observatory 8=36922
- comet 1963b, obs. 8=32557
- comet 1964h, obs. 8=32556
- comets, 1963i, 1964h, obs. 8=32555
- γ-ray astronomy, review 8=45798
- i.r. coronagraph, balloon borne 8=45609
- light of night sky, diffuse galactic light extraction 8=50272
- lunar effects on vertical deduced from obs. 8=36924
- observable quantities in anisotropic and homogeneous universe, theoretical relations 8=50263
- photometric error analysis, Reiger's theory of scintillation, confirmation 8=41498
- photometry in region 8–14 μ, using liq. He cooled photo-cond. cell 8=36920
- planets, minor, astrograph obs. 8=32540
- planets, minor, photographic 8=32537
- pulsars, at 11 cm. 8=45765
- radio sources, southern, accurate R. A. meas. 8=32512
- radio sources, 2. 8 cm variable 8=45766
- radio-star visibility fades in Alaska near solar minimum 8=41437
- radio-star visibility fades, phase variance and autocorrelation obs. 8=41436
- Rosette nebula, radial velocity, Fabry-Pérot obs. 8=32486
- satellites, artificial; visual, radio, radar and optical methods 8=50238
- soft X-rays, extragalactic objects 8= 36923
- solar photosphere, magnetograph obs. method 8=45890
- star declination, absolute meas. with instrums. without precise graduated circles 8=45613
- strip-chart photometry, reading error analysis 8=42139
- techniques, general review 8=32417

Astronomical spectra
- See also Atmospheric spectra; Cosmic radiations, radio-frequency; Stars/spectra; Sun/spectra; and other individual astronomical bodies.
- Fourier rapid scanning spectroscopy, visible and i. r. 8=28791
- Fourier transform spectroscopy, advances 8=50273
- Fourier transform spectroscopy for line profiles obs. 8=42217
- Fraunhofer lines calc. by wt. function theory 8=36908
- galaxies, NGC 1672, 5236, 7552, 1808, 2997; spectra of peculiar nuclei 8=50358
- γ-ray astronomy, use of Cherenkov detectors 8=33847
- γ-ray, balloon borne obs. in MeV region 8=38112
- γ-ray, Cherenkov system for directional determ. 8=45797
- γ-ray detector vidicon spark chamber, for balloons and satellites 8=45610
- γ-ray obs. balloon-borne, rel. to matter-antimatter model for quasars 8=45789
- γ-ray obs. with balloon borne spark chamber of various sources 8=45795
- γ-ray sources, Cherenkov detector, on earth's surface, 10^{11}-10^{12} eV 8=42679
- γ-ray sources obs. on Cyg A, Cas A, the Crab 8=45799
- γ -ray sources, search with balloon mounted odicon-spark chamber, $E > 100$ MeV 8=45796
- γ-ray spectra from sun, earth and sky, above 50 MeV obs. by spacecraft 8=45794
- line formation, effect of continuous absorption by dust grains 8=50337
- Martian transmission in 2μ region, interpret. rel. to surface press. 8=37011
- Milky Way, u.v. radiation, high level winter obs. 8=36966
- planetary atmos., absorpt. lines in scatt. radiation 8=37006
- pulsating object, spectral shift of light rays 8=28033
- quasars, reinterpretation with quark losses 8=45781
- shock wave structure, radiative effects 8=37253
- X-radiation spectrum relation with optical spectrum for Cas A and Vir A 8=45775
- X-ray background radiation evidence on number of electrons in space from cosmic γ-rays 8=41493
- X-rays, optimum drilled scintillation collimators 8=50269

Astronomical spectra—contd
Zeeman triplets, shape of line profile and line intensity compared 8=50310
Astronomical telescopes. See Radioastronomy; Telescopes/astronomical.
Astronomy and astrophysics
See also Cosmology; Radioastronomy.
daytime astrometry, limitations arising from scatt. light and mirrors 8=50271
high energy nuclear reactions in astrophysics, Pennsylvania University, Jan. 1967 8=28029
journals, historical review (1823-1968) 8=36907
planets, minor, astrograph obs. technique 8=32539
radiation diffusion in presence of elongated dispersion indicatrix 8=50246
radiation flow, polarized in free electron atmosphere 8=28341
supraluminous plasma wave phenomena 8=41529
synchrotron radiation, electron density calc. for laser-like action 8=33636
time scales, astronomical 8=45955
X-ray meas., instrumental background effects 8=45611
Atmosphere
See also Air; Electromagnetic wave propagation/atmosphere; Ionosphere.
aeronomics, convective phenomena, contrib. to theory 8=50017
ageing effects on insulators 8=40556
auroral v.l.f. chorus rel. to microbursts 8=32281
charged particle conc. below 80 km, meas. of day and night profiles 8=27875
cloudless sky detector 8=50146
by cosmic ray nucleons, n and isotope prod. 8=29254
density meas. by optical radar 8=45440
density variations affecting e.a.s. intensity, obs. 8=38222
downward i.r. radiative fluxes averaged over large territories 8=50145
dust influx of microparticles during meteor showers 8=41346
dust particle influx, from anal. of exposure plates on LUSTER 1966. and Gemini 9 and 12 8=41371
dust particle number densities and chem. anal. from exposed surfaces of Luster 1966 and Gemini 9 and 12 8=41371
earth-atmos. system, distrib. of albedo, emitted thermal rad. and rad. balance 8=41316
energy balance of layer near mesopause 8=50128
energy inflow in region 100 to 500 km, from studies of electron, ion, and neutral gas characts. 8=41378
escape thermal, extension of kinetic theory 8=37008
explosion, strong, shock wave propag. upward 8=28371
exponential, spatial diffusion of small particles 8=41345
freezing nuclei conc., meas. by improved Millipore filter tech. 8=36737
gravity waves, internal, in hydrostatic compressible fluid with vertical wind shear 8=50137
internal rad. field on monodirectional illumination of lower surface 8=37004
i.r. radiative transfer, coupling between temp. field and self-emission spectrum 8=41363
local seeing conds. rel. to short-period oscs. in solar spectra 8=41583
longwave radiative influx in cloudy atmos. 8=50147
lower, radio refractive index, variation with angle of incidence of e. m. wave 8=27926
mesosphere, aerosol distrib. and particle sizes rel. to noctilucent clouds 8=36738
mesosphere, struct. and quasi-biennial osc. 8=36714
mesospheric-stratospheric coupling relationships 8=36700
optical props, new method for study 8=32244
particle size average, 70 to 450 km, from 5300Å brightness obs. 8=36793
planetary, diffuse reflection and transmission of rays 8=41560
planetary diffuse reflection and transmission of time-dependent parallel rays 8=41561
radiation field, two dimens., Duhamel's principle applied 8=50404
radiation in spectral region 8-12μ, surface meas. 8=32175
Rayleigh scatt. Chandrasekhar's scatt. matrix new formulation 8=50119
with reflecting bottom surface, diffuse reflection and transmission 8=37005
scale height profiles above 150 km, at sunspot min. 8=36765
scanning effect on photospheric vel. meas. 8=41591
space research conference, London (1967) 8=28020
stratosphere and mesosphere, southern hemisphere, wind and temp. obs. 8=50135
stratosphere, annual behaviour, similarities with ionosphere D and E layers 8=50117
stratosphere circulation, vertical motions rel. to dynamo elec. current system 8=41368
stratosphere, struct. and quasi-biennial osc. 8=36714
stratosphere, u. v. absorpt., satellite obs. 8=27911
troposphere, gravity wave fading of signals from geostationary satellites 8=41434
"triptosphere", suggested term 8=36701
turbulence profile, clear air, optical remote sensing 8=50121
two-layered medium, magnetic field of vertical dipole 8=50120
Atmosphere—contd
ultralong waves, behaviour 8=50148
unidirectional optical heterodyne system over 2.6 km atmos. path, design and output 8=27915
v.l.f. hiss decrease rel. to sudden commencement 3 Sept., 1966 8=32305
whistlers, micropulsation, propag. in poss. evanescence region of magnetosphere 8=32268
composition
above 100 km, neutral comp. in mass number range 1-4 and 12-48 amu 8=36771
aerosol content of air, obs. from freq. spectrum of laser echoes from atmos. constituents 8=45442
air and H_2O vapour densities, space averages by dispersion for refractive correction of e. m. range meas. 8=36722
ammonium particles size distribution obs. 8=50129
charged particle conc., 10-60 km, interpret. of density-distrib. profiles 8=36715
chloride particles size distribution obs. 8=50129
desert basin in south-central New Mexico, dust anal. 8=41349
dust, vertical distrib. to 30 km 8=36717-8
heliosphere radius, and interplanetary neutral H 8=41573
magnetosphere, electron density profiles, obs. with high altitude rocket 8=50166
mesopause, sampling of particle content in presence and absence of noctilucent clouds 8=36799
mesosphere, ozone density distrib. in Japan, meas. by u. v. photometers 8=36719
mesosphere, var. in O and Ozone content during auroral events 8=27938
mesospheric electron. concs., governing ion chemistry 8=27880
negative ion-neutral molecule reaction obs. 8=41347
neutral constituents, N_2, O_2, O and Ar in lower thermosphere above Sardinia, mass spectrometric determ. 8=27939
neutral constituents in upper atmos., height distrib. dynamic effects, model between 70 and 500km 8=41377
neutral gas and electron densities and temps, and ion prod., 100 to 500 km 8=41378
nitrogen in, fixation by transition metal hydride complexes 8=25521
ozone distrib. on isobaric surfaces, May 3, 4th (1963), rel. to aviation 8=36720
ozone in stratosphere and mesosphere, quasi-biennial osc. 8=36714
ozone, mean absorpt. coeffs. rel. to Dobson spectrometer 8=47973
ozone planetary distrib., latitude depend., from u. v. spectra of reflected solar rad. 8=36721
ozone. transmission meas., appl. of new random model 8=38780
ozone vars. rel. to upper air peturbations 8=41348
particle clusters, large-scale dispersion 8=36728
particles, water soluble, size distribution obs. 8=50129
quark content, cyclic reflection mechanism 8=24741
radon conc., urban and rural Washington D. C. obs. 8=27881
small ions in atmos., struct. 8=50133
stratosphere, aerosol layer, determ. from diffuse skylight rel. to height 8=36716
sulphate particles size distribution obs. 8=50129
suspensoid concentration and distribution, from spectral radiance of solar aureole 8=50149
thermosphere, and mean molec. weight, diurnal and latitude effects 8=36770
thermosphere, number densities of N_2, O_2 and O_1 at high latitudes 8=36761
upper, in Arctic, neutral gas and predominant ions 8=36772
variations in region of 200 km 8=45443
water vapour distribution in stratosphere and high troposphere 8=32202
water vapour, spectral absorption meas. 8=27908
CH_4, deuterium and tritium content 8=27883
CO_2 absorption spectra in artificial atmosphere 8=27907
CO_2 at 500 and 700 mb. concentration 8=50131
CO_2 direct mass spectrometry 8=36631
CO_2 effect on radiative flux divergence 8=41342
H, neutral, number density variation with altitude 8=36777
HNO_3 and NO_2 in lower stratosphere from absorption spectra 8=27877
H_4 and C_3H_6, tritium content 8=27879
He, neutral, number density rel. to altitude and latitude 8=36777
He, winter diurnal bulge, characts. 8=36776
Kr diffusion in scintillation counter plastic 8=35499
N_2 density and temp. altitute profiles to 300 km 8=41339
N_2 density and temp. in thermosphere, diurnal 8=36774
N_2, tritium and deuterium isotopic content, 1958 to 1963 obs. 8=27882
O_2 absorption meas. in lower atmos. 8=36748
O_2, meas. from Ariel III 8=41438
O_3. absorption coefficient, Dobson spectrophotometer obs. 8=45465
O_3 content during ring Sun eclipse, 20 May 1966 8=50130
O_3 content, Jan.-Mar. 1967 obs. 8=50132
O_3, 40 years research at Oxford, history 8=36723
O_3, in Arctic and Antarctic stratospheres, seasonal changes 8=45441

Atmosphere—contd
- **humidity**
  - See also Humidity.
  - freezing nuclei conc., improved Millipore filter tech. for meas. 8=36737
  - isotopes for meas. 8=43245
  - mass of H_2O vapour in column, rel. to total vertical absorpt. on $\lambda = 1.3$ cm 8=32204
  - microsensor 8=43644
  - radio wave absorpt. meas. near $\lambda = 1.35$ cm 8=32205
  - troposphere, fine scale struct. and refr. index meas. 8=32201
- **ionization**. See Atmospheric electricity; Ionization, atmosphere; Ionosphere.
- **movements**
  - See also Wind.
  - air parcels in stable atmos., adiabatic ascent 8=32207
  - air-sea waves excited by volcano Krakatoa, pulse propagation 8=27829
  - Arabian Sea summer monsoon, air-mass dynamics or subsidence processes? 8=45446
  - balloon flight meas., super press., GHOST program from New Zealand 8=36707
  - baratropic divergent model, numerical integration 8=41352
  - below turbopause, statification of turbulent processes 8=36839
  - biennial oscillation, propagation 8=45451
  - biographic disturbances, rel. to mountain height, lee waves, vortices etc. 8=27888
  - boundary layer adjustment as initial value problem 8=32210
  - breeze in stable stratified atmos., non-stationary nonlinear soln. 8=32206
  - cirrus canopy formation in relation to mass of air flow in typhoons 8=32215
  - cold air mass motion over ridges, use of long-wave method of calc. 8=27887
  - diffusion for point-type continuous source, analysis 8=41797
  - diurnal S-N wind components, seasonal and latitudinal variations 8=36733
  - rel. to earths rotation vel., calc. methods evaluation 8=45827
  - eddy cond. to eddy viscosity ratio in lapse conditions 8=41340
  - equatorial upper atmos winds, components and diurnal variations 8=36778
  - frontal waves, instability 8=32198
  - front ogenesis, quasi-geostrophic equation solution 8=32209
  - global monsoons and circulations, soln. of two diff. eqns. arising in theory 8=36726
  - gravity waves, transient, calc. 8=27886
  - hurricane, lab. model, incorporating analogue to release of latent heat 8=32208
  - hurricane vortex, evidence of existence of Rossby-like waves 8=36734
  - ionosphere wind profiles, anal. rel. to seasonal and time differences 8=36842
  - ionospheric drift obs., analysis method 8=45535
  - island wake eddies, energy dissipation obs. 8=36730
  - large scale processes, boundary layer influence rel. to forecasting 8=32197
  - lunar tidal winds, semi-diurnal surface, American obs. 8=50139
  - mean meridional circulations, prod. mechanisms and props. 8=45444
  - mountain wind, velocity fluctuations 8=45450
  - ozone vars. rel. to upper air perturbations 8=41348
  - particle clusters, large-scale dispersion 8=36728
  - planetary equatorial waves 8=50103
  - planetary waves, geostrophic scale analysis 8=50136
  - plumes flow, similarity and outer boundary conditions 8=41351
  - quasi-biennial oscillation, diagnostic numerical model 8=32212
  - quasilinear eqns., group invariance soln. 8=27890
  - rel. to radioactivity variations 8=50161
  - relative dispersion of particles in stratified rotating atmos. 8=45447
  - return flow of air and H_2O vapour to stratosphere, using tritium tracer 8=36725
  - Rusby wave vels., calc. 8=41350
  - shallow-layer thermal convection, eqns. based on Boussinesq approx. 8=36727
  - to 60 km, wind meas. by rocket-grenade method from Indonesia 8=36712
  - stably-stratified, with considerable wind-shear, excitation of internal waves 8=30262
  - storms, conditions for occurrence 8=41355
  - stratosphere circulation in N and S hemispheres, from meas. of temp. distribs. 8=36711
  - stratosphere over Minicoy Island, turbulence obs. 8=45445
  - stratospheric oscillation, quasi-biennial, rel. to sunspot cycle 8=27884
  - stratospheric-tropospheric exchange based on radioactivity O_3 and potential vorticity 8=45448
  - supercooled aerosol flow, ice formation, density and struct. 8=27899

Atmosphere—contd
- **movements**—contd
  - thermosphere, neutral, wave struct. characts, probably gravity waves 8=36764
  - 30 to 100 km region, diurnal, long-term and longit. variations of wind 8=36731
  - thunderstorms split into anticyclonic and cyclonic storms, motion from numerical model expts. 8=45452
  - tidal theory, application 8=27892
  - tritium fallout from 1961/2 nuclear tests 8=32256
  - troposphere (upper) and stratosphere (lower), meridional circulation and eddy diffusion in tracer transport 8=50163
  - tropospheric mesometeorological solitary waves 8=27891
  - upper, F-region apparent rotation 8=41379
  - upper, general circulation equations 8=50164
  - waves, mesoscale, seasonal, troposphere to stratosphere 8=27885
  - waves, planetary, structure and motion 8=50134
  - waves produced by marine storms, limitations on meas. 8=36666
  - wind interaction with severely convective clouds 8=27893
  - zonal flow stability rel. to eddy viscosity and heat conductivity 8=27889
  - zonal winds, excitation and propagation in atmos. with Newtonian cooling 8=32213
  - zonal wind zonal oscillation, 26-month, in lower stratosphere of southern hemisphere 8=32211
  - Kr^{85} diffusion monitoring by multiparameter analyser 8=36729
- **precipitation**
  - See also Ice; Rain; Snow.
  - aurora, riometer obs. 8=45502
  - cloud and fog drops, elect. charged by diffusion 8=36740
  - cloud nuclei, altitude distribution 8=36739
  - concentrations of Cs^{137}, Ce^{144}, Zr^{95}(Nb^{95}) and Ru^{106} (RG^{106}) over Bucharest, winters 1964-6 rel. to 1962-4 8=45479
  - cosmic ray-produced radio nuclides as tracers of precipitation processes 8=50142
  - dry and moist convection including rain stage, numerical expt. 8=45455
  - formation in mountainous coast region 8=41357
  - freely falling waterdrops, structure of ventilation coeffs., physical interpretation 8=25854
  - hailstones, spongy, growth criteria, microstructs. 8=45461
  - hailstones, spongy, growth criteria, orientation fabrics 8=45460
  - hailstones, spongy, growth mechanism 8=45459
  - hydrometers, numerically determ. collision efficiencies 8=36735
  - ice, habit and charge of crystals, modification by vapour contamination 8=32220
  - ice nucleation by AgI, nature of nucleating site 8=32216
  - micron size stratosphere, cosmic dust 8=41359
  - nuclei in air initially free of aerosols, formation and evolution 8=50141
  - rain showers, radar anal. 8=41358
  - stratus consisting of drops and crystals, numerical integration of equation system describing processes 8=32218
  - subcloud level, fallout of diversion products 8=27929
  - SW monsoon in India, meteorology and vorticity considerations 8=36708
- **radiation belts**
  - electron intensity ($E > 100$ keV), time variation rel. to radial diffusion 8=36817
  - electron and photon flux obs. with satellite mounted Cherenkov counter 8=29236
  - inner, proton solar-cycle changes 8=27960
  - inner protons origin rel. to cosmic-ray albedo flux, $\leqslant 20$ MeV 8=33857
  - inner zone, electrons, model distribs. for intensities 8=36816
  - magnetic field confinement by beam of ions 8=36822/3
  - magnetospheric, and tail plasma sheet 8=45495
  - magnetospheric protons radial diffusion coeffs. for Pc 1, 2 and 3 hydromag. waves 8=41411
  - outer belt, electrons ($E > 100$ keV) intensity, time variations rel. to diffusion 8=36817
  - proton beam penetrating cold electrons, scattering rel. to Akasofu's hypothesis 8=41409
  - radial diffusion coeff. for electrons at low L values 8=27961
  - South Atlantic anomaly, evidence of nonfission electrons 8=36820
  - storm-time, growth during magnetospheric substorm 8=50172
  - temporary radiation zones caused by geomag. storms 8=45564
  - westward drift of ring current rel. mag. field DS, low latit. rot. 8=50212
  - H and charged particles interaction, consequent Ly-α emission 8=36818-19
- **radioactivity**
  - See also Fallout.
  - in the Dagestan, thermal current generation of particles 8=45480
  - fission products, Finland, Dec. 1966 obs. 8=27927
  - γ-ray background, by means of NaI(Tl) scintillation counter 8=50157
  - hard γ radiation 8=45477

Atmosphere—contd

radioactivity—contd

hard γ-radiation at sea level, vertical intensity 8=45478

radioactive products in the organs of animals and men after inhalation 8=45927

stratospheric tropospheric exchange based on radioactivity, O_3 and potential vorticity 8=45448

variations, rel. with atmos. motions 8=50161

$Ce^{141,144}$, concs. in ground-level air after nuclear explosion of 9-5-66 8=36757

Cs^{137}, Ce^{144}, $Zr^{95}(Nb^{95})$, and $Ru^{106}(Rh^{106})$, conc-over Bucharest, winters 1964-6 rel. to 1962-4 8=45479

Rn, conc. and diurnal variations of exhalation 8=50160

Rn^{222}, degree of equilib. with daughters, obs. by α-pulse spectroscopy 8=32255

structure

model based on isentropic surfaces 8=27873

troposphere, refractive index variations, relation with meteorological conditions 8=50154

troposphere, refractive index variations, spectral charact. 8=50155

troposphere, rel. to transmission beyond horizon 8=45476

temperature

above 90 km, from obs. of shock waves in luminous trimethyl Al trail 8=36769

annual and semi-annual oscillations over sea surface 8=50127

apparent sky temp. and tropospheric absorption on solar radiation at 7 GHz 8=45877

earth-atmos. system, global rad. balance from data of Nimbus 8=41316

earth horizon radiance profiles, 14-16μ 8=45422

eddy cond. to eddy viscosity ratio in lapse conditions 8=41340

field inhomogeneities, determ. from light propag. expts. on turbulence 8=36710

inferred from inversion of outgoing radiances, effects of cloud amounts 8=41361

lower, profile definition 8=27874

Martian, radiation equilibrium temp. distribution 8=37013

measurement by microwave radiometry 8=41344

mesosphere and stratosphere, southern hemisphere 8=50135

near water surface layer, daily variations 8=27868

periodic oscs., amplitude and phase angles, tropical regions at 25 to 50 km 8=36713

radiative heat budget, effect of CO_2 8=41342

to 60 km, meas. by rocket-grenade method from Indonesia 8=36712

stratopause, diurnal var. estimation from horizon radiance satellite obs. 8=36709

stratosphere and mesosphere, quasi-biennial osc. 8=36714

stratosphere, Arctic and Antarctic, seasonal changes 8=45441

stratosphere, horiz. patterns in N and S hemispheres, from Nimbus II 8=36711

stratosphere warming (1967-8) 8=50126

stratospheric heating rel. to ionospheric geomag. obs. 8=27982

thermal sounding problem soln. 8=27876

thermosphere, calc. from altitude rate of change of ratios of pairs of constituents 8=36770

thermosphere, 100 to 200 km, from density profiles, vib. rot. spectra and vel. of sound 8=36763

30 to 100 km region, review of results and comparison with CIRA (1965) 8=36731

troposphere, fine scale struct. and refr. index meas. 8=32201

troposphere, lower acoustic sounding 8=41374

upper, heating during geomag. disturbances 8=27931

upper, response to changes in solar EUV rad. and geomag. activity 8=27934

N_2, altitude profiles from ground to 300 km, diural variations 8=41339

thermodynamics

adiabatic ascent of air parcels in stable atmos. 8=32207

air-sea transfer coeffs., depend. on bulk stability 8=32200

atmospheric available energy concept 8=41343

expansion, gas sphere in rarified air, spherical and cylindrical flow 8=34601

planetary thermal escape, transition domain in spherical geometry 8=37008

upper

above 200 km, characts, new results and comparison with CIRA (1965), review 8=36762

Alfven waves and magnetopause—solar wind interaction rel. to pc-3 and pc-4 pulsations 8=50217

in Arctic, neutral gas composition 8=36772

auroral brightness vars., power spectral densities 8=41396

auroral zone, 129 to 212 km daytime, temp. profile from N_2^+ rocket spectra 8=45483

backscattering optical radar detection 8=36814

bow shock plasma wave emission 8=41389

bow shock temp. jumps, gasdynamic prediction rel. to Vela 3 obs. 8=41388

circulation, general equations 8=50164

composition below 3000 km from ion and proton whistlers 8=36773

Atmosphere—contd

upper—contd

conjugate regions, auroral electron precipitation 8=41395

cosmic rays, low energy, magnetospheric tail arrival 8=38160

densities and scale heights above 150 km, Soviet data, anal. at sunspot min. 8=36765

density and temp. at 1000 km, early effects of increasing solar activity 8=41386

density at 191 km. height, obs. (1966-7) 8=41376

density var. at 480 km, semiannual, obs. 8=27935

density variations, correl. with X-rays and solar flux 8=36766

diurnal elec. struct., dynamo elec. current system 8=41368

80 to 110 km, wind components, of different periods, from meteoritic radar 8=36780

electrojet over Thumba, India, quiet day obs. 8=41406

electrojet rel. to polar mag. substorms in conjugate areas 8=41462

electron and ion temp. and composition 8=45513

electron density profiles above Antarctica, during solar event of Jan. 28, (1967) 8=36768

electron fluxes, low-energy, in polar regions, universal-time control 8=41408

electrons, energetic, geomag. equator at 6. 6 Re intensity fluctuations 8=41382

electrons, energetic terrestrial upstream in solar wind beyond bow shock 8=32587

equatorial electrojet, simple model 8=50171

equatorial jet, elec. current, origin of associated small-scale inhomogeneities 8=45506

equatorial, winds, zonal comp. 100 to 170 km, diurnal variation 8=36778

exosphere, charged-particle temps. and conc. 8=36783

F-region apparent rotation 8=41379

geomag. harmonic series evaluation for 1100 km height 8=36880

geomagnetotail sudden impulses 8=36887

heating during geomag. disturbances 8=27931

inospheric heating, presunrise at Arecibo due to conjugate point photoelectrons 8=41421

lower thermosphere, air densities from jet radii 8=36759

mag. field confinement by ion beam 8=32366-7

magnetically conjugate photoelectron flux heating, low latitude effects 8=41410

magnetopause current layer, rot. and tangential discontinuities from Explorer 12 obs. 8=41387

magnetopause hydromag. disturbances, 3 to 15 minutes period, rel. to bow shock spikes 8=32266

magnetopause position and cosmic ray intensity changes 8=45494

magnetosheath, direction distrib. rel. to polar mag. disturbances 8=41466

magnetosphere, Alfven wave formation in magnet force tubes 8=41470

magnetosphere, Alfven wave velocity distribs. 8=27944

magnetosphere boundary, depend-on nonidiple part of geomag. field 8=45487

magnetosphere boundary, hydromag. stability 8=41385

magnetosphere boundary rel. to solar wind, synthetic model 8=32265

magnetosphere, Cherenkov radiation from proton flux as cause of geomag. PP pulsations 8=41469

magnetosphere, convective elect. field rel. to solar wind speed 8=36786

magnetosphere, ducted whistler-mode propagation, half-gyrofreq. upper intensity cutoff and associated wave growth phenomena 8=36789

magnetosphere, electron conc. vertical distribution from whistler data 8=36782

magnetosphere, electron density profiles, obs. with high altitude rocket 8=50166

magnetosphere e, ion and neutral particle temp., rocket and satellite obs. review 8=32297

magnetosphere, e. m. wave guidance along inhomogeneous field aligned plasma stratum 8=32262

magnetosphere expts., suggestions for satellite obs. 8=32260

magnetosphere field and plasma, Pioneer 7 obs. 8=32267

magnetosphere, forbidden zone size and config. rel. to continuous spectrum of injected particles 8=27943

magnetosphere, geomag. micropulsation diagnostics review 8=45486

magnetosphere, hydromag. wave instabilities in non-neutral plasma-beam system 8=27942

magnetosphere, large-scale elec. field systems, origin, distrib. and effects 8=32269

magnetosphere, low-energy electrons in evening sector, survey by OGO 1 and OGO 3 8=36787

magnetosphere, micropulsation whistlers propag. in poss. region of evanescence 8=32268

magnetosphere, outer, and boundary mag. field obs. 8=36878

magnetosphere, particle flux turbulence 8=36784

magnetosphere, particle injection and auroral substorms 8=36805

magnetosphere particle meas. by satellite detectors 8=27946

magnetosphere, pc 1 micropulsations, longit. spread 8=27945

Atmosphere—contd
- upper—contd
  - magnetosphere, plasma and e. m. wave generation 8=36784
  - magnetosphere plasma convection rel. to D_p2 geomag. fluctuations 8=41479
  - magnetosphere plasma density, determ. by use of long-period geomag. micropulsations 8=50167
  - magnetosphere, plasma, flux, energy distrib. and conc. of ions and electrons 8=36781
  - magnetosphere plasmapause 8=41383
  - magnetosphere, proton and electron fluxes, rapid increases 8=36790
  - magnetosphere, protons, low-energy, pitch angle diffusion due to gyroresonant interaction with hydromag. waves 8=41380
  - magnetosphere, radio noise obs. from satellites 8=45496
  - magnetosphere, rapid intensity variations of energetic electrons 8=45489
  - magnetosphere, ray paths of Pc 1 waves 8=45490
  - magnetosphere ring current rel. to auroral oval 8=32289
  - magnetosphere ring current rel. to storm time whistler cutoff 8=41407
  - magnetosphere, satellite obs. of v. l. f. phenom, inc. whistlers, review 8=32263
  - magnetosphere shock interact. with solar blast wave, dynamics 8=41391
  - magnetosphere substorm, concept and rel. to electron precipitation and micropulsations, review 8=41399
  - magnetosphere, substorm growth and decay, and auroral substorm 8=36806
  - magnetosphere, tail appearance of energetic electrons, associated inospheric effects 8=45510
  - magnetosphere tail as hydromagnetic waveguide 8=32270
  - magnetosphere tail flapping 8=32261
  - magnetosphere transition region with ionosphere, electron density 8=36829
  - magnetosphere, variations of spectrum and intensity of electrons on morning and day sides 8=45488
  - magnetosphere, zone of corpuscular precip. 8=45493
  - mesopause, sampling of particle content in presence and absence of noctilucent clouds 8=36799
  - metal vapour artificial clouds, expansion 8=32259
  - micropulsation diagnostics of magnetosphere plasma pause, e. conc. exam., 8=45491
  - neutral comp. above 100 km, for mass number ranges 1-4 and 12-48 amu 8=36771
  - neutral constituents, dynamic effects on height distrib. model between 70 and 500 km 8=41377
  - neutral, structure review 8=45481
  - neutrons, epithermal albedo, flux determ. from activity obs. 8=41384
  - noctilucent clouds form., study via OH emissions 8=36794
  - noctilucent clouds, geographical distribution 8=27896
  - noctilucent clouds, spatial and temporal border visibility 8=27897
  - plasma, low press. in mag. field, convection when heated underneath (model) 8=39087
  - plasma prod. by h.f. discharge, feasibility 8=38978
  - plasmapause, e. conc. exam., 8=45491
  - plasmapause, whistler rate and v. l. f. noise variations, abrupt changes, Alouette 1 and 2 obs. 8=36788
  - plasmasphere, contraction during geomag. disturbed periods 8=27947
  - plasmasphere, thermal ion struct. 8=45492
  - polar electron density and temp., 2000 to 3000 km, satellite obs. 8=36826
  - pressure meas., α-ray gauge for balloons 8=45964
  - proton gyrofrequency band emisssions obs. from OGO2 8=36821
  - quadruprobe for d.c. field meas. 8=41381
  - radial diffusion coeffs. for electrons of 50-100 keV from L=4 to L=7, empirical evaluation 8=36785
  - scalar mag. field at 1100 km, mid and low latits. 8=36881
  - sounding techniques 8=36705
  - spectroscopy, Fabry–Perot spectrometer appls. 8=32271
  - structure determ. by obs. of trimethyl Al trails and grenades 8=36769
  - thermosphere, Ar and He number densities rel. to altitude of turbopause 8=36775
  - thermosphere, diffusion coeffs., temp. and densities from growth of chemiluminous clouds 8=36795
  - thermosphere, diurnal variation of electron temp. 8=50175
  - thermosphere, lower, number densities of N_2, O_2 and O_1 above Fort Churchill and Sardinia 8=36761
  - thermosphere, lower, long-term variation in density rel. to solar cycle 8=41375
  - thermosphere, neutral, characts. of wave propag. 8=36764
  - thermosphere, N_2 density and temp. meas, diurnal 8=36774
  - thermosphere, 100 to 200 km, density, temp., neutral composition and minor constituents 8=36763
  - thermosphere, semi-annual density variation 8=27936
  - turbopause altitude, from Ar and He number densities in thermosphere 8=36775
  - v. l. f. meas. by satellite, receiver parameters 8=32264
  - VLF phase anomaly induced by nuclear explosion 8=27959
  - whistler precursor generation 8=32249
  - wind shears in 80-100 km region, from meas. of meteor drifts 8=36779
  - winds above 80 km, evidence for strong nonlinearity of horiz. flow 8=27941

Atmosphere—contd
- upper—contd
  - H and He number densities, rel. to altitude and latitude 8=36777
  - He bulge in winter, rel. to altitude, solar and geomag. activity, and semi-annual variation 8=36776
  - He nightglow, 304- and 584-Å, upper limits 8=27951
  - He$^+$ reactions with N_2, O_2 8=27937
  - He^{++} in magnetosphere conc. allowing for thermal diffusion 8=50165
  - NO, vertical motions and distribution in upper mesosphere 8=45485
  - OH emissions, behaviour rel. to form. of noctilucent clouds 8=36794
  - O$^+$ and O^{++} in magnetosphere, conc. allowing for thermal diffusion 8=50165
  - O$^+(^4S)$ + H(1s) low-energy collisions, charge transfer cross-section 8=27940

Atmospheric acoustics
- infrasound radiation into atmos. by ocean waves 8=32227
- noise pulses, statistical characts of time intervals 8=27924
- radio terrestrial noise and v. l. f. rads, meas. from Ariel III 8=41438
- sonic boom, comments and reply on Farfeld spectrum 8=25817-18
- sound propag., vertical, for variable viscosity 8=32258
- troposphere, lower, acoustic sounding 8=41374
- wave effect on antenna impedance 8=24243

Atmospheric disturbances. See Atmosphere/movements; Thunderstorms.

Atmospheric duct. See Electromagnetic wave propagation.

Atmospheric electricity
- See also Atmosphere/radioactivity; Atmospherics; Aurora; Electromagnetic wave propagation/atmosphere; Ionization, atmosphere; Ionosphere; Lightning; Thunderstorms.
- aurora, e flux and luminosity, simultaneous obs. 8=32286
- ball lightning within metal aircraft 8=45472
- charged particle motion in geomag. dipole field, under action of e. m. pulses 8=36815
- current moments at e. l. f. of lightning discharges associated with mature tropical hurricane 8=32251
- discharges, vortex-stabilized, threshold conditions 8=32248
- dynamo elec. current system, modified by stratospheric circulation and making of D and E regions 8=41368
- electrojet, equatorial, rel. to general ionospheric current system 8=45569
- electrojet over Thumba, India, quiet day obs. 8=41406
- electron flux, low energy, poleward of auroral zone, satellite obs. 8=45501
- equatorial jet, elec. current, origin of associated small-scale inhomogeneities 8=45506
- ionosphere conductivities rel. to Sq 8=50178
- ionospheric current systems, daily automatic calc. 8=50180
- ionospheric current systems due to Sun and Moon 8=50179
- ionospheric currents, N and D hemispheres, comparison 8=45569
- potential gradient, balloon obs. 8=32247
- proton beam penetrating cold electrons, scattering rel. to Akasofu's hypothesis 8=41409
- quadruprobe for d.c. field meas. 8=41381
- Q-type e. l. f. burst in Schumann resonance freq. range, worldwide simultaneity of occurrence 8=32245
- space elec. field, detect. and meas. 8=27958
- sparks, temp. meas. from spectrum 8=39004
- Sq ionospheric midlatitude current system, vector obs. 8=41416
- universal aspects 8=32246
- VLF phase anomaly induced by nuclear explosion 8=27959

Atmospheric optics
- See also Airglow; Sky brightness; Sunlight; Twilight.
- backscattering optical radar detection 8=36814
- Chapman function for linear temp. gradient 8=50158
- chemiluminous clouds, growth rate meas. rel. to diffusion coeffs, temp. and densities in thermosphere 8=36795
- cloud and dust layers, diffuse refl., transmission and absorpt. 8=41362
- clouds, light, reflected and transmitted, effect of particle size distribution 8=41367
- Colorado central, meas. in connection with long range oblique photography 8=36746
- Curtis-Godson approx. and radiation transmission through inhomogeneous atmos., analysis 8=32234
- directional fluctuations, rel. to turbulence 8=27912
- dust and smoke clouds, plane-parallel, reflectance 8=39447
- image of distant source in lens focus, random displacements due to refractive index vats. 8=24369
- imaging through randomly inhomogeneous medium by wavefront reconstruction 8=28889
- integral transmission function for cloudy conditions 8=32232
- i.r. visibility, temp. fluctuation noise effects 8=45468
- laser and conventional light scatt. 8=32243
- laser backscatter, correlation with turbulent region 8=27917

Atmospheric optics—contd
laser beam attenuation and polarization rotation meas. through rocket plumes 8=50234
laser echoes from atmos. constituents, freq. spectrum. aerosol content of air obs. 8=45442
light refl. and transmission by clouds, depend. on single scatt. albedo 8=32230
light scatt. from clouds, Monte Carlo calcs. 8=36741
light scatter in surface layer, phase function 8=32241
light transmission, 92 km air-surface path 8=50150
of mesospheric aerosols, rel. to appearance of noctilucent clouds 8=36738
multiple scatt., equivalence of isotropic and mono-directional source problems 8=36744
new method for study 8=32244
noctilucent clouds, spatial and temporal border visibility 8=27897
path radiance for downward path of sight, from ground-based or low-altitude obs. 8=32237
phenomena, unusual or neglected 8=27906
propagation of coherence function through random media 8=28715
radiance of sea and sky in i. r. window 800-1200 cm^{-1} 8=36689
radiance, transmitted and reflected, Monte Carlo, calc. 8=45466
radiant intensity of light scatt. from clouds 8=32226
rainbows in science and the arts 8=32238
ray optics in turbulent atmos., validity 8=32239
refraction obs. at the Pic-du-Midi observatory 8=36922
saturation of irradiance fluctuations due to turbulent atmos. 8=32240
scattering function at small angle distances from sun, spectral studies 8=50152
sky components due to clear blue sky for vertical rectangular aperture, precise values 8=50151
sky radiance, 8-13 μ, effect of cirrus 8=41366
skylight neutral points over smooth water 8=50118
skylight polarization, effect of conc. turbid layer 8=36743
softening of radiation by multiple Compton scatt. 8=37231
solar aureole, intensity correl. with weather conds. 8=37041
solar aureole spectral radiance 8=50149
solar u.v. rad., scatt. and absorpt. 8=41360
specular reflection at ground, effect on light scatt. from Rayleigh atmos. 8=32242
stratosphere, u. v. absorpt., satellite meas. 8=27911
stratospheric i. r. sky radiance 8=32233
sun's image on airborne ice crystals 8=36745
surface diffusive radiation flux under cloudy conditions 8=27903
surface layer transmission of laser rad. 8=27918
transmission, 8-13μ region (middle i. r.), obs. from 1600 m altitude in Pyrenees 8=27914
turbulence profile, clear air, remote sensing 8=50121
visibility phase meas. by interferometer in presence of atmos. seeing, technique 8=28857
wavefront distortion compensation, holographic simulation 8=37708
H_2O absorpt. rel. to astronomical obs., 50 μ-1 mm 8=41499
H_2O, optical back scatt. from single droplets 8=27916

Atmospheric pressure and density
above 90 km, from obs. of shock waves in luminous trimethyl Al trail 8=36769
annual and semi-annual oscillations over sea surface 8=50127
barometric effect for cosmic ray photons at sea level 8=29257
Chapman function for linear temp. gradient 8=50158
density above 150 km, anal. of meas. at sunspot min., Soviet data 8=36765
density at 191 km. height, obs. (1966-7) 8=41376
density at 480 km., satellite obs. 8=45484
density scale height at sunspot max. and min. 8=27933
die press. depend. of cosmic ray neutron intensity 8=33850
diurnal var. obs. from satellite drag 8=27932
EOLE balloon flights at 400, 300 and 200 mb levels 8=36706
falling sphere accelerometer for density meas. 8=41620
high-altitude balloon α-ray gauge 8=45964
lower thermosphere, air densities from jet radii 8=36759
mesosphere density, long-term variation rel. to solar cycle 8=41375
microfluctuations of press. in atmos. surface layer 8=32199
neutral particle density from orbital behaviour of grid-sphere satellite 8=28024
in 150 to 180 km range, density correl. with geomag. activity solar flux and seasons 8=36767
periodic oscs. of density, amplitude and phase angles, in tropical regions 8=36713
planetary, atmospheres, absorpt. integral and press. var. 8=41564
problems and successes in soviet metreology 8=45962
shock-wave effects of earth's rotation 8=36724
surface, and wind components, sea level, relation 8=36692
surface, meas. with satellite laser 8=45439
thermosphere density, long-term variation rel. to solar cycle 8=41375

Atmospheric pressure and density—contd
thermosphere, neutral, local density variations rel. to gravity wave propag. 8=36764
thermosphere, number densities of N_2, O_2 and O, 8=36761
thermosphere, 100 to 200 km, density from ionization meas. and satellite drag 8=36763
thermosphere, semi-annual density variation 8=27936
upper, density variations, correl. with X-rays 8=36766
variations affecting e. a. s. intensity, obs. 8=38222
variations with thunder, obs. Saskatoon, Canada (1962-63) 8=27894
Ar and He number densities in thermosphere rel. to altitude of turbopause 8=36775
N_2 density, altitude profiles to 300 km, and diural variation 8=41339
N_2 density in thermosphere diurnal 8=36774

Atmospheric spectra
See also Atmospheric optics.
absorption calc., net interval requirement 8=28794
absorption obs., 2mm-300μm, 1957-Dec. 1967 8=27948
absorption of rad. from weakly heated black body by horiz. layer, method, app. and result 8=32228
absorption of selective radiation 8=32235
absorption spectra of atmos. gases in vac. u.v. region 8=43196
dayglow, photoelec. Fabry-Perot, magnetostriction scanned for 6300Å 8=32272
Doppler-Lorentz line absorpt. calc. 8=45467
downward i. r. radiative fluxes, computation in partial cloudness conditions 8=32225
8-13μ region (middle i. r.), obs. from 1600 m altitude in Pyrenees 8=27914
in 4. 5μ region, theoretical interpret. rel. to inversion expts. 8=36747
hydroxyl emission in night-glow. intensity and rotational temp. variations 8=50168
integral transmission function for cloudy conditions 8=32232
i.r., 8. 5 to 16 μ over desert, aircraft obs. at different heights 8=45464
i. r. night sky rad. 8=36792
i. r. rad. from earth to space, angular and spectral distrib. 8=36657
i.r. radiative transfer, inverse problem rel. to vertical thermal struct. 8=41363
molecular band transmission, gen. line shape for new random model 8=38780
nightglow arcs at 5577 and 6300Å, equatorial region 8=36801
night sky spectral radiance rel. to cloud cover, 0. 5-1. 1μ 8=27913
radiation in 8-12μ region, surface meas. 8=32175
rainbows in science and the arts 8=32238
skyshine, Monte Carlo calc. 8=36758
solar cell Langley plots, anomalies associated with tropopause 8=32231
tropical daylight, typical spectral distributions and colour 8=27900
twilight N_2^+ emission, tropospheric scatt. model 8=41365
twilight, press, scanned Fabry-Perot 8=32568
upper atm., Fabry-Perot spectrometer appls. 8=32271
u.v. radiation, scatt. and absorpt., rel. to distrib. of ozone, and optical thickness 8=41360
water vapour luminesc. under laser irradiation 8=38824
water vapour, meas. of spectral absorpt. in bands 8=27908
zenith sky brightness and colour during total eclipse of 12-11-66, Bolivia 8=36742
CO_2 absorpt. in artificial atmos., meas. 8=27907
CO_2, earth's horizon profile spatial energy distrib., 15μ 8=27910
HNO_3 and NO_2, absorption in lower stratosphere 8=27877
H_2O vapour, selective radiation obs. near 2.7μ 8=36749
N_2 luminesc. rel. to detection of cosmic ray showers 8=42680
He emissions in auroral zone, search 8=36796
He twilight emission at 10 830Å (2^3P-2^3S) 8=32287
O emission, red at λ6300Å, rel. to geomag. activity 8=36750
O, 6300, 5577 Å line profiles during twilight and night 8=27949
O_2 abs. 1. 3 to 0. 23μ, and role of short-living 8=32236
OH emissions at 70-90 km, rel. to noctilucent cloud nature 8=36794

Atmospherics
computations of shapes 8=45471
current moments at e. l. f. of lightning discharges associated with mature tropical hurricane 8=32251
e. l. f., antenna-coil, highly sensitive 8=42030
in magnetosphere, whistlers freq.-time characts, and discrete emissions and hiss 8=32263
lightning 27 kHz, Durban, earth-ionosphere multiple reflection propag. 8=27920
noise pulses, distrib. of probabilities of intervals between 8=27924
planetary, radiation, molec., continuum and line type. expt. and theory study 8=43287
Q-type e. l. f. burst in Schumann resonance freq. range, worldwide simultaneity of occurrence 8=32245
radio noise survey, Aerial III equipment 8=28026
source and propag. phenom., sub-ionosphere, survey 8=32250

Atmospherics—contd
  transients in freq. band 1 to 100 kHz, digital data collection system 8=32253
  whistler cutoff, storm time, rel. to magnetosphere ring current 8=41407
  whistler determ. magnetospheric vertical electron distribution 8=36782
  whistlers, ions and proton, below 3000 km, use for composition derivation 8=36773
  whistlers, obs. rel. to electron density gradient in ionosphere 8=36844
  whistler precursors, obs. 8=32249
  whistlers, solar wind ion cyclotron growth and damping 8=41584
  whistlers, v.l.f., ion effects 8=41425
Atomic beams
  See also Particle velocity analysis.
  calibration in crossed beam expts. method 8=43242
  inert gas, e scatt. 40-150 eV spin polarization obs. 8=34175
  inert gases, scatt. from Ag surface 8=39575
  metastable, thermal energy, produced by gas e-irradiation 8=29668
  microwave discharge source 8=43241
  pyroelectric ceramic detector 8=47544
  scattered from specular surfaces, ang. distrib. 8=39574
  Zeeman quenching method for determ. of energies and lifetimes of autoionizing states 8=43243
  Ar, from arc source, elec. props. 8=47545
  Ar, supersonic, low-temp. viscosity cross-sections 8=30311
  Cs, atomic clocks, systems analysis 8=41621
  H, neutral atoms, sensitivity of stripping analyzer in energy range 50 to 300 eV 8=43236
  H, polarized in metastable $2S_{1/2}$ state 8=38763
  He, fast metastable atoms in electron-loss collisions 8=38764
  He^4 atom 2^3P_1-2^3P_2 fine structure meas. technique 8=38651
  K and Cs, crossed, interaction in spin change collisions 8=47534
  K cathode sputtering source for 0.2-45eV 8=43240
  K, scatt. on CO_2 molec beam, time-of-flight anal. 8=38952
  K, Rb and Cs reactions with Cl_2 in crossed beams 8=49875
  Li, glory scatt. by diatomic mols. 8=38959
  Rb, reactive scatt. with oriented CH_3I 8=47728
Atomic clocks. See Time measurement.
Atomic frequency standards. See Time measurement.
Atomic mass and weight
  See also Isotopes; Mass spectra.
  No entries
Atomic orbitals. See Atoms/structure; Orbital calculation methods.
Atomic scattering factors. See Crystal structure, atomic; X-ray crystallography; X-ray scattering.
Atomic spectra. See Spectra/atoms.
Atoms
  See also Atoms, mesic; Elements; Nucleus; Positronium.
  alkali and inert-gas, van der Waal's const. calc. 8=25388
  alkali, elec. dipole moment, upper limit from mag. res. expts 8=43177
  alloy, ordered, near anitphase boundary, elastic interaction of atoms 8=35058
  chemisorbed, long-range forces 8=47533
  collision with diatomic mol., distorted wave expansion 8=29833
  collisions, impact parameter treatment 8=38741
  collisions, interf. expts., high resolution 8=29665
  dipole-quadrupole dispersion forces 8=38745
  electric dipole moment, calc. for open electron shells 8=34127
  electric dipole moment contribution of electron electric dipole moment 8=38612
  electric dipole moment, implications of parity and time reversal invariance 8=38611
  electron affinity, validity of Hartree-Fock approximation 8=38618
  electron capture cross-sections, high energy 8=38744
  electron capture into excited states, impulse approx. 8=38743
  electron capture of fast protons in gases 8=34172
  electron collision, conditions for bound states 8=47535
  electric quadrupolar moments in excited states, meas. 8=43271
  electron subshell binding energies, H to Zn 8=43156
  element 102, chemical properties, review 8=29381
  energy levels, X-ray, effect of pressure 8=47497
  exchange interactions between atoms and mols., perturbation theory 8=38738
  in field of plane travelling monochromatic wave, behaviour in model of strong interacts. 8=38613
  Firsov's interaction potential, anal. form 8=38635
  force constants and equilibrium distance determin., from united-atom model 8=47459
  Hartree-Fock approx. applied to harmonic oscillator 8=25329
Atoms—contd
  highly excited, near metallic surface, ionization probability calc. 8=25707
  hydrogen-like, 2s state two-photon decay, analytic soln. 8=38647
  interaction energy, third-order 8=29656
  ion collisions, boundary condition for theoretical treatment 8=29655
  ionization by colliding with excited atom, formula without rotating-atom approx. 8=25706
  ions, octahedrally co-ordinated, in E-type orbital state, interaction with lattice 8=48339
  level-crossing meas., optical pumping effects 8=25342
  lifetime of excited states, meas. method 8=38706
  long-range forces, error bounds 8=38739
  mechanics, algebraic struct., reformulation of axiomatic basis 8=33324
  multilevel, resonance line problems and radiative transitions 8=38627
  multilevel, transfer of line rad., effects of coupling mechs. and stimulated emission 8=38628
  multi-photon ionization, effect of Coulomb interact. 8=39017
  neutral, binding energy of electrons 8=34439
  perturbation theory of self-consistent field 8=34123
  Rayleigh scatt. and e.m. susceptibility 8=25375
  relativistic related operators at resonance 8=38616
  photoelectric absorpt. curves, resonance processes rel. to polarisability of atomic residue 8=38713
  quenching cross-sections, meas. and true 8=38748
  radiation in absorbing medium, effects of conversion to non-wave zone heat 8=38629
  scattering, large-angle, perturbation calc. 8=29569
  scattering, multiple turning-point, semiclassical calc. 8=28945
  scattering of energetic atoms in gas, energy distrib. 8=36626
  short-range interactions, perturbation theory 8=34176
  spin filter for polarized ion source 8=34124
  statistical model, Gaussian approximation for quantum corrections 8=41766
  superconductivity appl. 8=34113
  temperature, and e concs., obs. according to Voigt contours of spectral lines under arc discharge conditions 8=29936
  thermalization by elastic collisions 8=34177
  van der Waal's forces, atomistic derivation of macroscopic forces 8=43234
  Al sequence to Fe^{+13}, config. mixing and transitions from ground state 8=34137
  $B^{10,11}$, 2p-1s pionic X-ray transition obs. 8=29674
  Eu II spectrum obs. 8=47495
  H, chemisorbed, long-range forces 8=47533
  H, electric dipole moment contribution of electron electric dipole moment 8=38612
  H, Lamb shift, hadronic contrib. 8=37944
  H, latent symmetry 8=47481
  H, nonrelativistic, Runge-Lenz vector, physical interpret. 8=38649
  H, recombination rate 8=36563
  H, transport mechanism in chem. reactions 8=41252
  H, two-dimensional, Schrödinger equation appl. 8=34131
  H, 2s state two-photon decay, analytic soln. 8=38647
  H_3-system, interaction energy 8=29738
  H_3-system, nuclear motion 8=29739
  H+D and D+D, hyperfine splitting of interaction energy 8=38751
  $H + F^-$ collisions, electron detachment 8=34451
  H, O_4 symmetry, from factorization of eqns. from ladder operators 8=34129
  H, SO_4 algebra as symmetry group, and use of point rotor 8=34128
  He, incoherent-scatt. function and pair prod. length 8=43174
  He, metastable and cascading, in plasma, effect of electron temp. determ. from spectral lines 8=34468
  He, van der Waals energy between two or three, calc. 8=38757
  He-He interaction potential 8=34181
  Hg, in ^3P, state, inelastic collisions of second kind with electrons 8=43230
  Li, quadrupolar birefringence in excited states 8=43271
  Li, Schrödinger wave eqn., numerical soln. 8=29579
  N, photoionization cross-sections 8=39044
  Na, quadrupolar birefringence in excited states 8=43271
  Na-Hg collisions, meas. 8=29665
  Ne levels by g value meas. in Zeeman laser 8=43198
  O, radiative combination by inverse dissoc. 8=38932
  O, recombination rates, direct shock tube meas. 8=29666
  Th I energy levels 8=47509
  W, binding energy on W cryst. 8=30775
 electron scattering
  adiabatic exchange approx., orthogonality 8=25381
  collision theory and calc. methods 8=29660
  two electron atomic systems, calc. of ground state energy 8=47460
  excited states, mechanical demonstration 8=29652
  extended polarization potential 8=25390
  impact ionization, Z=41-98 8=39013
  impact radiation, polarization rel. to spin magnetism 8=25382

Atoms—contd

- **electron scattering**—contd
  - inelastic, semi-empirical calc. 8=34169
  - inert gas at. beam, e spin polarization 40-150 eV obs. 8=34175
  - inert gases, metastable excitation total cross sections 8=25377
  - ion linewidths, formulae for predicting 8=38718
  - ionization, quantum theory 8=43470
  - Lin theory confirmed in obs. on Hg 8=34171
  - long-range forces and threshold cross-sections 8=38716-17
  - mobility max in rare-gas liquids 8=43229
  - optical model of pot. scatt., energy depend. of pot. 8=34167
  - particle exchange collision theory appl. 8=29659
  - phase scatt. of 5-waves, Kohn's principle, calc. 8=29650
  - plasma, multiple scatt., Molière's theory 8=39076
  - polarization of radiation, anomalous energy depend. 8=34170
  - polarization of threshold-excited radiation 8=34168
  - threshold electron impact excitation 8=25402
  - Al, inelastic, E_e=200, 400 keV, cross-section 8=38719
  - Ar, analysis of exptl. data 8=25385
  - Ar, E_e=20 eV-150 keV, relativistic effects 8=38720
  - Ar plasma, calc. from shock tube obs. 8=34485
  - Ar, transport cross section calc. 8=25383
  - Au, inelastic, E_e=200, 400 keV, cross-section 8=38719
  - Be$^+$, of slow e, elastic process 8=43231
  - C, low-energy, polarization calc. 8=47527
  - C II, line broadening calc. 8=47507
  - Ca$^+$, close coupling approx. autoionizing states, 4s → 4p, 4s → 3d transitions 8=43232
  - Cu, inelastic, E_e=200, 400 keV, cross-section 8=38719
  - H, collisional cross-section for excitation of various states 8=38721
  - H, diffr. theory 8=29653
  - H, elastic scatt. phase shift calc. 8=38723
  - H, excitation of n = 2 states 8=29640
  - H, integral eqn. approach collision processes 8=38724
  - H, optical-potential calc. 8=38725
  - H, positron scatt., resonance mechanism 8=38722
  - He, analysis of exptl. data 8=25385
  - He, Born cross-section for excitation of 2^1S and 3^1S states 8=38695
  - He, collision with H_2^+, Born cross-section calc. 8=38951
  - He-e collision, excitation cross section calcs. 8=38703
  - by He correlation importance in Born cross sections evaluation 8=38728
  - He, elastic scattering 8=38730
  - He, elastic scatt. cross-sections, Born approximation tests 8=38731
  - He, elastic scatt., energy distrib. functions 8=47975
  - He, excitation, effect of electron exchange 8=38701
  - He, excitation of 2^3S state, ang. depend. 8=38696
  - He, fast electrons, excitation calc. 8=38700
  - He, fast electrons, excitation to 2^1P state 8=38699
  - He$^-$ free-free absorpt. coefficient 8=47484
  - He ($I'S \rightarrow 2^3S$) transition, inapplicability of Born approx. 8=34173
  - He, low energy, excitation of forbidden transitions 8=25384
  - He, n=2 states, differential excitation functions 8=38729
  - He$^+$, position and width of $2p^2\ ^1D$ resonance by configuration interaction method 8=38756
  - He, resonances, exchange and product wave function 8=38726-7
  - He, short-lived compound excited states 8=47528
  - He , 6-8 Torr, 20-40 keV electron beams, spectrum 8=29651
  - He, transport cross section calc. 8=25383
  - Hg, elastic, cross-section and Mott asymm. function calc. 8=34174
  - Hg, excitation of 6^1P_1, $6^3P_{0.1.2}$ states 8=38705
  - Hg, Mott, influence of screening, obs. rel. to Lin theory 8=34171
  - I, E_e=20 eV-150 keV, relativistic effects 8=38720
  - K, elastic spin-exchange, expt. and close-coupling calc. 8=47538
  - K, generalized oscil. strengths and absolute differential cross-sections 8=43242
  - Kr, E_e=20 eV-150 keV, relativistic effects 8=38720
  - Li, of slow e, elastic process, 8=43231
  - Mg II, line broadening calc. 8=47507
  - Mg$^+$, close coupling approx. autoionizing states, 3s → 3p, 3s → 3d transitions 8=43232
  - N, low-energy, polarization calc. 8=47527
  - N^{14}, inelastic scatt., 8.5-11.5 MeV excitation obs. 8=29654
  - Na, meas. method for free electron spin and cyclotron resonances 8=42040
  - Ne, analysis of exptl. data 8=25385
  - O$^+$, auto-ionizing e energy spectra 8=39050
  - Si, 50-625 keV, obs. 8=33638
  - S II/III, line broadening calc. 8=47507
  - Si II/III, line broadening calc. 8=47507
  - Sn, inelastic, E_e=200, 400 keV, cross-section 8=38719
  - Xe, elastic scatt. 8=47529
- **excitation**
  - absorption analysis, critical review 8=46692
  - Auger effect in multiple ionization 8=39019
  - diagonalization method for calc. reson. 8=43220
  - by electron beam, radiation, anomalous energy depend. of polarization 8=34170

Atoms—contd

- **excitation**—contd
  - electron collision cross-section calc. 8=34169
  - electron correlation for excited and ground state configurations 8=43167
  - electron impact, theory and expt. 8=25369
  - electron-induced, effective Born cross-section 8=43208
  - electron shake-off, SCF wave function calc. 8=38688
  - elastic scattering and inelastic collisions 8=25387
  - electron hole formation after effects, h.f. interactions 8=47271
  - electron impact, threshold excitation 8=25402
  - by electrons, quantum heat and level crossing expts 8=43215
  - energies, semiempirical calc., isoelectronic 8=47478
  - excited state mixing, during optical pumping 8=29631
  - experimental equipment and evaluation methods 8=29636
  - fluorescence excited by molec. dissoc. 8=38687
  - fluorescence, sensitized, conservation of r.f. coherence 8=38733
  - gas mixtures, spectral analysis 8=34159
  - graphite, Auger spectra with low energy electrons 8=44656
  - halogens, electronically excited, spin orbit relax. 8=25373
  - inert gases, by e impact, total cross sections 8=25377
  - influence of gas laser on fluoresc. emitted by gas in magnetic field 8=47515
  - intermediate states role, by electron impact 8=43213
  - ions, e collision cross-section, theory and appl. to line-broadening 8=43210
  - ions, positive, collisions and inter-level transitions 8=43209
  - level population in stationary nonthermal plasma 8=39069
  - lifetime of excited states, apparatus for precise obs. 8=29582
  - line radiation effect on precursor ionization 8=39015
  - linear response to an external field 8=47463
  - Lorentzian line shapes, averaging products over thermal velocities 8=43214
  - metastable, review of unusual props. 8=29591
  - multiply charged ions, metastable states 8=43217
  - neon-like, ions, X-ray satellite intensities 8=25372
  - oscillator strengths, transitions s^2-sp, and ss-sp 8=43211
  - photoeffect, K-shell, relativistic, soln. with Laplace integrals 8=47526
  - by radiation point source, reson. radiation transfer 8=29635
  - Raman effect induced by optical pumping 8=43207
  - resonance fluorescence at level crossings for energy and nuclear magnetic moment determ. 8=38683
  - resonance radiation transfer in semi-infinite medium 8=25368
  - resonant and auto-ionizing states, energy calcs. 8=43307
  - r.f. emission in optical resonance 8=38689
  - r.f. transitions, single and double, in excited state 8=47519
  - stepwise, cross-section estimation, choice of method 8=25344
  - stimulated emission when emission wave beats with second-order scattered wave 8=33173
  - threshold 4 impact, polarization of radiation 8=34168
  - transfer process by collision, theory 8=43233
  - transitions coupled through upper state 8=25337
  - two atom excitation by single photon 8=29633
  - two-level, interactions with coherent radiation, quantitative classical analogy 8=25371
  - Ar arc plasma rel. to equilib. disturbance 8=29942
  - Ar, cross sections for stepwise excitation and quenching process parameters 8=47489
  - Ar energy widths of X-ray levels 8=29649
  - Ar ion laser, c.w., processes 8=28675
  - Ar, luminescence due to α, obs. 8=47521
  - ArI, $3p^54s$-$3p^55p$ configs., optical transition probabilities 8=38690
  - As, metastable from flash photolysis 8=29646
  - As(4^2D). cross-sections for deactivation 8=34160
  - Au I resonance doublets, absolute line strengths, quantum-mechanical calcs. 8=43216
  - Ba, lowest $^1P_1$ and $^3P_1$ states, g_J factor obs. 8=38691
  - Be, photo-ionization cross-section near threshold calc. 8=39029
  - C v triplet to singlet excitation, relative intensities 8=38662
  - Ca, lifetime of $4\ ^1F^\circ$ term, determ. 8=34164
  - CaF_2:Dy^{2+}, forbidden and allowed radiative transitions 8=47522
  - Cd, direct and stepwise of single levels, by electron collision 8=34157
  - Cd ionization by e impact, direct and stepwise cross-sections 8=29961
  - Cd isotopes, optical, polarization of radiation (2288 Å) emitted 8=25359
  - Cd 5^3P_1 level double resonance, by modulated light 8=38685
  - Cd, 6^3S_1 level, lifetime and depolarisation cross section for N_2 and inert gas collisions, obs. 8=38692
  - CdI series, intercombinational transition probabilities 8=38711
  - Cr I, II, u.v. lines, gf shock tube meas. 8=29638
  - Cs, atomic lifetimes, direct obs. 8=29612

Atoms—contd
excitation—contd
Cs-inert-gas collision, $6^2P_{1/2} \rightleftharpoons 6^2P_{3/2}$ transfer cross-section calc. 8=47543
Cs, lifetime of $6^2P_{3/2}$ and $7^2P_{3/2}$ states 8=34162
Cs, resonance transfer and de-excitation in collisions with anols. N_2, H_2, HD, D_2 8=38957
Fe I u.v. lines. gf shock tube meas. 8=29638
H, beam-foil-excited, elec. field and multi-foil effects 8=25376
H maser freq. shifts, due to coherently excited $\Delta m_F = \pm 1$ transitions between $F = 1$ levels of ground state 8=25350
H, of $n = 2$ states, by electron impact 8=29640
H, 1s-2s, by slow electrons, theoretical and numerical study 8=38694
pH(1S) → pH 2s), 1-500 keV, invalidity of peaking approx. method 8=43218
H, $2l_0$-$3l$, electron collision cross sections 8=38721
He, autoionizing $2p^2\ {}^1D$ state calc. of position and width 8=38756
He, by electrons and protons, cross-sections and polarization of radiation 8=38702
He, by electron impact, effect of electron exchange 8=38701
He, by fast electrons, calc. 8=38700
He, by fast electrons to 2^1P state 8=38699
He, by fast protons, calc. 8=38698
He, by H^+ and H_2^+-impact, polarization of 4^1D-2^1P transition 8=38697
He, by low-energy electrons, forbidden transitions 8=25384
He. collision excitation transfer cross-section calc. 8=47540
He, doubly excited states, R_4 invariants 8=25352
He, e impact light, polarization obs. 8=29641
He, in e-collision, cross section calcs. 8=38703
He in hollow cathode discharge, mechanism for higher singlet and triplet levels 8=25353
He, metastable, lifetime rel. to population inversion in He-Ne lasers 8=24312
He, n=2 states, differential excitation functions 8=38729
He, n^1P, 3^1D, 4^1D and 3^3D levels, apparent lifetimes and energy transfer 8=43219
He, resonances and wave function in electron scattering 8=38726-7
He, slow e scatt., short-lived compound states 8=47528
He3^1P_1 state lifetime determ. 8=29597
He, 2^3S by e impact, ang. depend. approximation 8=38696
He 2^1S, 3^1S states, Born cross sections for electron impact excitation 8=38695
He^3, radiooptical resonance 8=47517
He–Ne laser freq. rel. to at. freq. 8=28688
Hg, by $N_2(A^3\Sigma_u^+)$ 8=34163
Hg, coeffs. for internal conversion for K, L and M shell e. m. transitions 8=38670
Hg, double-resonance broadening, 6^3P_1 state 8=38732
Hg, metastable $6s6p^3P_2$ state, elec. dipole polarizabilities, E-H gradient-balance meas. 8=38704
Hg vapour, associative ionization cross section 8=25716
Hg, 6^1P_1 level lifetime, coherence scattering of light 8=47498
Hg 6^1P_1, $6^3P_{0,1,2}$ states, by electron 8=38705
Hg, 6^3P_2 lifetime obs. 8=29616
Hg, 7^3S_1 state, lifetime and depopulation rate 8=38706
Hg^{201}, on optical pumping and in pulsating e.m. field 8=43222
HgI series, intercombinational transition probabilities 8=38711
K, magnetically oriented 4^2p atoms, collisional depolarization 8=47520
K-shell electrons, inelastic interactions with γ rays 8=43226
Mg. lifetime of $4\ {}^1D$ term. determ. 8=34164
Mo, successive onsets rel. to excitation pot. 8=29643
N^{14}, 8.5-11.5 MeV, by inelastic e scatt., obs. 8=29654
N, multiply ionized, beam-foil excitation 8=29644
N_2^+ ions, by electrons, at near threshold energies 8=47523
Na, atomic lifetimes, direct obs. 8=29612
Na^{23}, h.f.s. in $3^2P_{3/2}$ state, level crossing investigation 8=34145
Ne, auto-ionizing levels, by ion impact 8=39048
Ne, double resonance in He-Ne laser operating at 6328 Å π transitions 8=47502
Ne energy widths of X-ray levels 8=29649
Ne, optically pumped, $3S_2$ level relax. rel. to theory of multiple coherent scattering 8=43224
Ne, ${}^3P^0$ and ${}^1P^0$ populations time dependence during post-luminescence under c. m. wave pulses 8=38686
Ne, $2p_4$, $3S_2$ in discharge, collisional disalignment 8=34183
Ne, $2p^6$, $2p^53s$, $2p^53p$, $2p^54s$ states, wave functions 8=29624
Ne, $3P_4$ level lifetime in laser 8=34184
Ne I, 3p level, lifetime meas. using ion beam 8=29645
O VII by electron impacts, theoretical rates 8=25378
$O({}^1D)$, deactivation by O_2 8=47542
O_2^+ cross-sections by crossing beams 8=47518
P, metastable from flash photolysis 8=29646
PbIII series, intercombinational transition probabilities 8=38711
Pb, ${}^3P_1{}^0$ state, lifetime and oscillator strength 8=38707
Pd, first ${}^3P_1$ state, h.f.s. and lifetime obs. 8=25379
Pu^{240} Auger effect, L_2-subshell yield obs. 8=38715

Atoms—contd
excitation—contd
Rb. in flames. quenching of excited 5^2P atoms 8=34150
Rb-inert-gas collision, $5^2P_{1/2} \rightleftharpoons 5^2P_{3/2}$ transfer cross-section calc. 8=47543
Rb, resonance, quenching by gases 8=29626
Rb, spin states, time dependence of quantum-state amplitudes 8=38710
$Rb^{85,87}$ $8^2P_{3/2}$ state hyperfine structure and lifetime 8=34149
Sb, metastable from flash photolysis 8=29646
Sn, ${}^3P_1{}^0$ state, lifetime and oscillator strength 8=38707
Tl, coeffs. for internal conversion for K, L and M shell e. m. transitions 8=38670
$U^{234\ 236}$ Auger effect, L_2-subshell yield obs. 8=38715
Xe, by electron collision, cross-sections of spectral line excitation 8=34165
ZnI series, intercombinational transition probabilities 8=38711
magnetic moment
See also Gyromagnetic ratio.
adiabatic inversion with light pulses 8=47437
relaxation rate meas. using laser oscillator 8=29588
transition metals, ferro- and antiferromag., rel. to localized d electrons 8=35047
F, wave function calc. 8=47531
structure
See also Nucleus; Spectra/atoms.
alkali, influence of core electrons 8=47464
alkaline earth chalcogenides, ionic radii 8=43966
bound states, Green's function phase-integral approx. in momentum space 8=29586
bounds on polarizabilities, Rebane, and Kohn 8=25324
core-electron binding energies, chem. effects 8=38620
core electrons effects, simulation by pseudo-potential 8=47464
correlated wavefunctions, using limited Gaussian basis sets 8=29571
diamagnetic susceptibility of ions with ${}^1S_0$ terms 8=38644
dipole hyperpolariziabilities, atoms in first two rows 8=25334
distinguishable electron method for struct. calc. 8=34118
effective operators and spectrosc. props. 8=34115
electron affinity, theory and exptl. determ. 8=25338
two-electron atoms, perturbation theory of extended Hartree-Fock approx. 8=47469
electron binding energies, next inner subshell, $5 \leqslant Z \leqslant 30$, calc. 8=25357
electron correlation for excited and ground state configurations 8=43167
electron density calc. with oscillatory correction in Thomas-Fermi model 8=43162
electron gas, new formulation of ground state energy 8=28340
electron system collective oscillations, plasma concepts 8=34125
electronic wave functions, correl. coeffs. 8=47462
energy calc. with oscillatory correction in Thomas-Fermi model 8=43163
energy states with parallel spin, correction for nuclear mass. 8=29584
extended Hartree-Fock calcs. 8=47483
extended Hartree-Fock wavefunctions 8=25330
extended method of struct. calc. 8=47470
Fermi–Dirac function, tabulated for integer indices, series expansion 8=33329
Feynman diagrams of 1st and 2nd orders of some states 8=47472
Feynman diags. for first and second orders for some states of light atoms 8=38657-8
forbidden transitions, variational principle for intensity 8=47443
Hamiltonians, model 8=38622
harmonic oscillator methods 8=38597
Hartree-Fock energies for helium-like ions 8=38652
Hartree-Fock eqns., l-averaged exchange term 8=38640
Hartree-Fock exchange potential for electrons 8=38617
Hartree-Fock integro-differential eqns. 8=29587
Hartree-Fock perturbation theory, non-orthogonal formulation 8=25331
Hartree product wavefunctions, projected 8=29572
hemoproteins, fine, of Fe ions 8=35044
integrals containing $r_{23}{}^{\lambda} r_{31}{}^{\mu} r_{12}{}^{\nu}$ 8=29583
integrals, one centre and two centre, double zeta function 8=43159
isoelectronic, semiempirical calc. of excitation and ionization energies 8=47478
magnetic interactions for f electrons 8=38669
magnetic polarizability of closed shell 8=25343
many-electron atoms, spin-orbit coupling 8=38666
many-electron systems, GF wavefunctions 8=47439
modified Green function calc. 8=43155
multiple moments, magnetic and elect. of levels, meas. with laser oscillator in mag. field 8=29588
orbitals and classical motion 8=25346
ordering of crossing levels from resonance scattering 8=38683
oscillatory correction to electron density in Thomas-Fermi model 8=43162

- **Atoms**—contd
  - **structure**—contd
    - oscillatory correction to energy in Thomas-Fermi model 8=43163
    - pair eqns., numerical soln. 8=47438
    - perturbation theory, appl. of separable pots. 8=47477
    - relative transition probabilities determ. by Faraday effect 8=38676
    - relativistic wave functions, screening constant calc. 8=38630
    - r.f. transitions, spectroscopic methods 8=38596
    - Rydberg levels, correl. with molec. levels 8=29746
    - satellite X-ray lines due to transitions involving double ionization of inner shells 8=43228
    - screening parameters, determ. 8=38626
    - Slater-Condon integrals calc. from Hartree-Fock function for atoms from He to Ar 8=34133
    - Slater-type orbitals, multicentre integrals of r_{12}^{-1} 8=38600-2
    - spin density in quantum chem. 8=27672
    - spin-forbidden electronic transition probabilities, correct operator 8=25327
    - spin-orbit consts. calc. with scaled Thomas-Fermi potential 8=38634
    - spin-orbit interaction energy for open shell, matrix elements 8=47468
    - spin-other-orbit interaction in many-electron atoms 8=25335
    - spin-spin contact Hamiltonian, symmetry props. 8=38632
    - spin-spin interaction in many-electron atoms 8=25336
    - spin-spin matrix elements for f^3 e config. 8=38637
    - statistical method successfully applied to H 8=29595
    - statistical model, Brachman relations 8=38642
    - statistical model, Maxwell relations 8=38643
    - g-tensor, perturbation corrections 8=43160
    - term energies, anal. 8=47474
    - tetrahedrally localized orbitals, correl. 8=34117
    - thermodynamic functions on Thomas-Fermi-Dirac theories 8=38641
    - Thomas-Fermi atoms, electron eigenfunctions 8=29592
    - Thomas-Fermi energy, upper and lower bounds 8=38636
    - Thomas-Fermi screening function, anal. form 8=38635
    - three-electron, Euler-angle reduction of Schrődinger eqn. 8=47461
    - transition ions, orbit-orbit interactions 8=38656
    - transition probabilities for excited states of two-electron atoms 8=25332
    - translawrencium elements, SCF calcs. 8=47513
    - two-electron, effective charge radial dependence 8=38621
    - two-photon bound state-bound state transitions in Coulomb field 8=29648
    - wavefunctions and correl. energies for 2-, 3- and 4-electron atoms 8=25333
    - wavefunctions and diamag. susceptibilities 8=47466
    - wavefunctions calc., computer programme 8=38633
    - $Z > 118$, electronic config. predictions from Periodic System 8=47458
    - Ar, polarizability in solid Ar 8=35051
    - Ar I, $3p^m$-$3p^{m-1}3d$ spectra 8=43178
    - B^{++}, new type of wave function 8=38672
    - Ba, lowest $^1P_1$ and $^3P_1$ states, g_J factor obs. 8=38691
    - Ba, two-electron transitions 8=43184
    - Be, ground state, pair correl. calc. 8=29604
    - Be, ground state energy, biorbitals calc. 8=47491
    - Be, ground state, wave function, configuration-interaction method 8=25358
    - Be, Hartree-Fock calc. refr. index, dynamic polarizability and Verdet coeffs. 8=47485
    - Be-like systems, augmented separated-pair expansion 8=38625
    - Be-like systems, electron correl. and separated-pair approx. 8=38623
    - Be 2-matrix, energy props. 8=38598
    - Be^+, new type of wave function 8=38672
    - Bi^{209}, hyperfine in $6p^2(^3P_0)7s\,^4P_{1/2}$ state 8=43183
    - C, bond participation of inner electrons 8=47627
    - Ca, two-electron transitions 8=43184
    - Cd I, dipole transitions from ground state, peculiar behaviour HF solns. for excited odd configurations 8=43186
    - CdI series, intercombinational transition probabilities 8=38711
    - Cl I, $3p^m$-$3p^{m-1}3d$ spectra 8=43178
    - Cr positive ions, spin-orbit coupling 8=38665
    - Dy^{3+}, energy levels in LaF_3 8=31985
    - Eu, core-electron binding energies, chem. effects 8=38620
    - Eu and Eu^{++}, hyperfine, polarization effect calcs. 8=29615
    - Fe positive ions, spin-orbit coupling 8=38665
    - H, construction of generators of SO(4, 1) group 8=43171
    - H, excited states, charge exchange into in $H^+ + Li^+ \rightarrow H(n) + Li^{++}$ 8=25392
    - H, Green's function calculations 8=34130
    - H, polarized in $2S_{1/2}$ metastable state 8=38763
    - H, relativistic partial group-theory treatment 8=29593
    - H to Ne, model Hamiltonians 8=38622
    - He, annihilation of slow positrons 8=38740
    - He^-, autoionization of $1s2s2p\,^4P_{5/2}$ state 8=39041
    - He, ground state calc. using 3-body problem solution 8=33315
    - He ground state, extended Hartree-Fock calcs. 8=47483
    - He, Hartree-Fock calc. refr. index, dynamic polarizability and Verdet coeffs. 8=47485
    - He isoelectronic series, 3^1D and 3^3D states, variational calc. 8=46802
    - He-like ions, Hartree-Fock energies 8=38652
    - He, numerical soln. of S-limit Schrodinger eqn. 8=29596
    - He, pair function calc. 8=47438
    - He I, probability of 2γ decay from 2^3S_1 metastable level 8=43175
    - He^4, 2^3P_1-2^3P_2 fine structure obs. 8=38651
    - He, S-type wavefunctions, natural occupation amplitudes 8=38655
    - Hg, atomic levels by optical methods 8=43191
    - Hg, polarizability of $6s6p\,^3P_2$ state meas. 8=38704
    - HgI series, intercombinational transition probabilities 8=38711
    - Hg, 6^3P_2 metastable state, Zeeman sublevel decay constant using pulse technique 8=34142
    - I, core-electron binding energies, chem. effects 8=38620
    - K, autoionizing states, metastable, identified 8=43244
    - Li, autoionization of $1s2s2p\,^4P_{5/2}$ state 8=39041
    - Li, dipole spectrum 8=34143
    - Li, new type of wave function 8=38672
    - Li^+, numerical soln. of S-limit Schrodinger eqn. 8=29596
    - Li, ^2S ground state, Hylleraas wave function calc. 8=38671
    - Li-F, Rydberg orbitals calc. 8=29620
    - Mn positive ions, spin-orbit coupling 8=38665
    - Nd^{3+}, approx. analytical wavefunctions 8=38674
    - Ne, Hartree-Fock calc. refr. index, dynamic polarizability and Verdet coeffs. 8=47485
    - Ne, radiative transition probabilities 8=34146
    - NeI, relative transition probabilities determ. by Faraday effect 8=38676
    - Ni, in solid solutions 8=49744
    - O, hyperfine, many-body calc. 8=43199
    - PbIII series, intercombinational transition probabilities 8=38711
    - Pr^{3+}, energy levels in hydrated crysts. 8=45215
    - Pr^{3+} in LaF_3, spontaneous emission probabilities for excited states 8=49805
    - Pu, configuration, interaction integrals 8=38679
    - $Rb^{85,87}$ of $^2P_{3/2}$ state, hyperfine splitting meas. by optical double resonance 8=34151
    - S, inner-electron binding energy and chem. bonding 8=29627
    - S, nonempirical SCF calc. 8=47596
    - S, satellite X-ray lines due to transitions involving double ionization of inner shells 8=43228
    - SCF calcs., correction to exchange pot. 8=38615
    - Ti V, $3p^6$-$3p^5 4d$ spectra 8=43178
    - ZnI series, intercombinational transition probabilities 8=38711
- **Atoms, mesic and muonic**
  - e.s.r. rates close to splitting freqs., rel. to μ^+-meson depolarization, muonium mech. 8=38773
  - even-even nuclei isomer shift 8=42809
  - isomer shifts, magnetic coupling 8=47551
  - K-mesic atoms, review 8=34193
  - light elements, μ^- depolarization obs. 8=29673
  - μ-mesic, spectra h.f.s. and isotope shifts rel. to nucleus struct. 8=29260
  - muonic, effect of extranuclear electron 8=34188
  - muonic with heavily deformed nuclei, x-ray spectra rel. to nuclear dynamics 8=34192
  - π-mesic, $4 \leqslant Z \leqslant 28$, $2p \rightarrow 1S$ and $3d \rightarrow 2p$ transitions, obs. 8=34190
  - π-mesic, spectra h.f.s. and isotope shifts rel. to nucleus struct. 8=29260
  - X-ray spectra, different phys. and chem. targets, intensity obs. 8=25396
  - X-ray transitions for determ. of nuclear O^+-O^+ vibrational excitation 8=38344
  - Be^9, 2p-1s pionic X-ray transition obs. 8=29674
  - Bi^{209}, muonic, hyperfine interactions obs. 8=38772
  - C^{12}, 2p-1s pionic X-ray transition obs. 8=29674
  - $Eu^{151,153}$, muonic x-rays spectra rel. to nuclear charge distrib., obs. 8=34194
  - μ-Ho^{165}, dynamic quadrupole interaction, K and L x-rays obs. 8=34191
  - K^- capture by nucleus, approx. calc. 8=47333
  - $Li^{6,7}$, 2p-1s pionic X-ray transition obs. 8=29674
  - μ-$O^{16,18}$, $2p \rightarrow 1s$ transitions and atomic radius, obs. 8=34190
  - Pb^{206-8}, muonic, hyperfine interactions obs. 8=38772
  - μ-Sm^{152}, nuclear γ-ray energy rel. to isomer shift, obs. 8=29332
  - μ-Tb^{159}, dynamic quadrupole interaction, K and L x-rays obs. 8=34191
  - μ-Ti^{48}, x-ray Lyman and Balmer line energies, obs. 8=34189
- **Attenuation.** See Absorption.
- **Auger effect.** See Atoms/excitation; Atoms, mesic; Radioactivity.

Auger showers. See Cosmic rays/showers and bursts.

Aurora

See also Airglow; Atmospheric spectra.
absorption events, meas. of bremsstrahlung X-ray spectra in range 1 to 10 keV 8=36808
α particles >50 keV moderate storm, rocket obs. 8=32283
ancient, use in tracing secular variation of geomag. field 8=50211
arc, red, electron heating mechanism 8=27995
band at local geomag. noon, 1QSY boundary changes 8=35803
borealis, dark segment 8=32284
brightness vars., power spectral densities 8=41396
charge precipitation and electron content, simultaneous ground, aircraft and satellite obs. 8=32282
charged particle meas. instrument 8=50169
conjugate regions, electron precipitation 8=41395
cycles and climatic var. from 2260 B.C. 8=50228
daylit day-time type, spectra and luminosity-height data 8=36809
daytime, 129 to 212 km, temp. profile from N_2^+ rocket spectra 8=45483
electrojet and precipitated electrons, mutual effect 8=41404
electron density and temp. profile calc. 8=27953
electron energy spectra, differential, 180 to 250 km obs. 8=32290
electron flux, near monoenergetic ~4 keV rocket obs. 8=32291
electron microburst and rel. to X-rays, obs. 8=32280-81
electron precipitation, average props. determined by satellite obs. 8=27955
electron spectra, differential, double-peaked at energies ≃ 80 keV 8=36811
electron spectrum, effects on O and Ozone density below 80 km 8=27938
electrons, atmospherically scattered, and transfer to conjugate region via lines of force 8=41394
excitation by electrons, protons or m.h.d. waves, charact. props. 8=32288
far-u.v. radiation, rocket studies 8=36812
geomagnetic activity 27 day period, 1963 8=28008
green line, excitation by dissociative recombination of O_2^+ ion, rocket expt. 8=41401
interferometry of 5577 Å emission temp. 8=41400
ionization, e flux and luminosity, simultaneous obs. 8=32286
ionospheric E layer, elect. field estimates 8=27991
magnetic Pg micropulsations at conjugate points, high lats. (1963 and 1964) 8=41477
magnetospheric substorm, concept and rel. to electron precipitation and micropulsations, review 8=41399
magnetospheric substorm, energetic electron precipitation, modulated 8=41397
magnetospheric substorm, micropulsations rel. to electron precipitation 8=41398
magnetospheric substorms, energetic electron effects at 6.6 Re equator and auroral subzone, correl. 8=41405
microbursts, high-intensity, temporal features 8=36804
oval, and ring current in magnetosphere, in I GY and IQSY 8=32289
particle fluxes, rapid variations 8=27954
primaries and substorms, rel. to tail reconnection, theoretical review 8=36807
protons >50 keV, moderate storm rocket obs. 8=32283
radio absorption obs. at conjugate points, correlation 8=41402
radio, irregularities due to ion-acoustic waves 8=27957
radiowave absorption in Alaska sector, morphology 8=41403
rocket obs., review 8=45500
satellite scintillation at Kiruna, rel. to time and mag. activity 8=32284
spectral meas. of particles 8=36813
and spread-F and radio-star scintillations 8=32355
stable red arcs, excitation in low latitudes 8=45503
substorm, accel. mechanism search 8=32292
substorm growth and decay, rel. to magnetospheric substorm 8=36806
substorms, rel. to particle injection into magnetosphere 8=36805
substorm, rel. to polar "hiss" and "chorus" in magnetosphere 8=41390
thicknesses of structures in mag. zenith, meas. using image orthicon television system 8=27952
v.h.f. radio star refraction by visible forms 8=50170
v.l.f. chorus rel. to microbursts 8=32281
v.l.f. emissions, stations close to auroral zone 8=45505
visible, three, low-energy electron spectra 8=36810
X-rays during slowly varying ionospheric absorption events, simultaneous obs. 8=27956
X-rays interrupted by sudden geomag. impulse, persisting 24 sec periodicity 8=45504
X-rays microburst and rel. to electron parent burst 8=32279-80
X-rays, their association with rapidly changing auroral forms, expt. methods 8=41430
He emissions in auroral zone, search 8=36796
He twilight emission at 10 830Å (2^3P-2^3S) 8=32287

Austenite. See Iron alloys; Steel.
Avogadro's number. See Constants.
Axicons. See Lenses.

BCS theory. See Nucleus/theory; Superconductivity.
Backscattering. See Scattering, particles; and under "scattering" subheadings of the appropriate particles.
Backward wave oscillations. See Electromagnetic oscillations; Electron tubes.

Balances

lever equal-arm, testing and adjusting method 8=45953
microbalance, convection increasing high temp. 8=46252
microbalance, elec. for mag. torque meas. 8=37381
quartz crystal microbalance, direct gravimetric calibration 8=23793
quartz crystal microbalance for oil diffusion pump backstreaming 8=39243
quartz-crystal microbalance technique for prep. of alkali-antimonide photocathodes 8=40683
semimicroanalytic, fast, OVM-20 type 8=45952
thermal, for cryst. vapour phase growth transport meas. 8=35230
thermobalance, 0.1 mg sensitivity, ≤ 1,150°C 8=23792

Ballistics

See also Impact.
circular sattelite orbit stability in planet's gravitational field, allowing for dipole mag. field 8=50236
projectile, impacted, free surface vel. meas. by optical Doppler method 8=41622
satellite, magnetized equatorial, motion about own centre of mass 8=45579
simulated reentry conds, time-resolved spectra of wake and shock cap of models 8=41485
teaching demonstration 8=41646
in Ar, r.f. plasma source, rel. to use in m.h.d. expts 8=43610

Band theory of solids. See Crystal electron states/band structure; Solids/theory.
Bardeen–Cooper–Schrieffer theory. See Nucleus/theory; Superconductivity.

Barium

adsorption by Mo and Ti films, effect on resistance and work function 8=40322
atom, lowest $^1P_1$ and $^3P_1$ states, g_3 factor obs. 8=38691
atom, metastable 6s5d levels and g_J obs. 8=34140
atom, two-electron transitions 8=43184
diffusion from soda-potash-baria glass into refractories 8=48780
distribution between potassium feldspar and plagioclase simultaneously crystallized at 600℃ 8=36627
ferrite, Bitter patterns rel. to changes in width and domain shape 8=31557
film deposited on Ni, nature and thermionic emission 8=27347
films, absorpt. props. 8=27560
isotope exchange rate, zeolith A and aq. soln., 100-180°C 8=45313
plasma, in Q-machine, self-luminosity 8=34522
$Ba^{135,137}$, h.f.s. of $6s6p^3P_1$ level, obs. 8=34139
W, adsorption, search for substrate rearrangement 8=30777

Barium compounds

barite ($BaSO_4$) crystals, low angle grain boundaries 8=39717
chelate form. in EDTA, ultrasonic study 8=25914
ferrites mag. props. rel. to magnets for transport appls. 8=24114
ferrites, pure, lo and Ti substituted, chem. comp. on micron range scale 8=31720
methacrylate dihydrate, X-ray polymerization 8=27741
orthorhombic and rhombohedral phases, e.s.r. of Gd^{3+} 8=31852
Ba tetraoxometalates, i.r. spectra 8=31965
$BaAl_2O_4$, cryst. struct. 8=35318
$Ba(BrO_3)_2$, anhydrous, crystal forms 8=30808
$Ba_{0.15}Ca_{0.85}MnO_3$, at. mag. structure from n.-diffr. exam. 8=04859
$Ba_{1-x}Ca_xMnO_3$, solid solns., structure and mag. phase transitions 8=27377
$BaCl_2$, heat capacity, enthalpy and entropy 8=44339
$BaCl_2.2H_2O$ crystal growth, effect of bivalent cation addition to soln. before crystallization 8=44120
$Ba(ClO_3).H_2O$, cryst. struct., neutron-diffr. refinement 8=30886
$BaC^{14}O_3$ powder, radioactivity meas. when insoluble in liquid scintillator counter 8=47278
$BaCo_2Fe_{16}O_{27}$, mag. rotatory hysteresis losses and anisotropy 8=45037
BaF_2, exoelectron emission, X-ray and thermo-stimulated, obs. 8=36040
BaF_2, formation energies of anion and cation point defects Born-model calc. 8=35540
BaF_2, F-vacancy cond. and mobility 8=49340
BaF_2, Grüneisen parameter, low-temp. limit, calc. on Axe's shell model 8=48748
BaF_2, intenstitial cond. and mobility 8=49341
BaF_2, n-irradiated, self-trapped holes, e.s.r. exam. 8=31854
BaF_2, reflectivity spectra from (111)-cleavage plane, 78°K 8=45175

Barium compounds—contd
BaF_2, third-order elastic constants from acoustic meas. 8=26787
BaF_2, unipolar dielectric, conduction mechanism from solid-state electrolysis 8=40579
BaF_2, u.v. reflectivity spectra 8=36374
$BaF_2:Co^{2+}$, absorpt. spectra temp. dependences 8=41076
$BaF_2:Gd^{3+}$, e.p.r. spectral cubic splitting temp. dependence, 77-950°K 8=40909
$Ba_2(FeMo)O_6$, mag. and elec. props. 8=36195
$BaFe_{12}O_{19}$, as permanent magnet material 8=36184
$BaFe_{12}O_{19}$ flexible magnets, anisotropic, prep. and props. 8=24110
$BaFe_{12}O_{19}$, mag. rotatory hysteresis losses and anisotropy 8=45037
$BaF_2:U^{3+}$, magneto-optical rot. and struct. of U^{3+} centre 8=36336
BaI_2, heat capacity, enthalpy and entropy 8=44339
BaI_2, luminesc. for X-ray and photo. extinction 8=41182
$BaLiD_3$, cryst. struct. by neutron diffr. 8=48639
$BaLiH_3$, cryst. struct. by neutron diffr. 8=48639
$BaMg(CO_3)_2$, crystal structure rel. to $CaMg(CO_3)_2$ 8=48637
$Ba(N_3)_2$, u.v. irrad. cryst. e.s.r. of N_2^- 8=27485
$Ba_2NaNb_5O_{15}$ in continuous 0.532μ solid-state source 8=33253
$Ba_2NaNb_5O_{15}$, continuous optical parametric oscillation 8=36328
$Ba_2NaNb_5O_{15}$, linear and quadratic electro-optic coeffs., relationship based on spontaneous polarization obs. 8=27583
$Ba_2NaNb_5O_{15}$ low threshold optical parametric oscillator 8=46612
$BaNb_2O_6$, structural comparison with other Anb_2O_6 and ATa_2O_6 type phases 8=48636
$Ba(NO_3)_2$ structure rel. to NO_3 config., n-diffr. exam. 8=39773
BaO, adsorption by Mo and Ti films, effect on resistance and work function 8=40322
BaO_2 for ionization enhancement in m.h.d. channel 8=30043
BaO glasses, heat capacity as function of composition and temp. 8=44333
BaO stream over SrO and CaO, emission props. 8=27349
Ba-O system, vapour species 8=30606
BaO, x-irrad., thermoluminescence 8=41184
$BaO-B_2O_3$ glass sytem, n.m.r. studies rel. to struct. 8=27499
$BaO:Gd^{3+}$, e.p.r. 8=45078
$BaO-Li_2O-SiO_2$ system, calc. of silica activities and metastable immiscibility 8=30413
$BaO:Mn^{2+}$, vibrational reson. mode and temp. depend. of hyperfine coupling 8=45079
$BaO-SiO_2$ system, phase separation, liquid-liquid immiscibility 8=39318
BaO, $2Ta_2O_5$ tungsten bronze, crystal structure 8=26369
$BaO-TiO_2$ system, new compound 8=48363
$BaO-TiO_2-SiO_2$ glasses, structural states of TiO_2 8=44078
$BaO-TiO_2-SiO_2$ systems, glass formation 8=44079
$(Ba-Pb)TiO_4$ mixtures, prep. with dielec. const. approx. 500 8=27286
Ba. $Sc^{3+}_{1\cdot 8}$ $Fe^{3+}_{10\cdot 2}$ O_{19}(M), antiphase spin ordering 8=36183
$BaSiO_3-BaGeO_3$ phase equilib. diag. 8=35092
$BaSO_4$, crystals growth by chemically reacted flux method 8=44121
$BaSO_4$ solubility in sea water 8=34783
$BaSO_4$ suspension in nonpolar media, electrokinetic pot. and stability, H_2O effects, obs. 8=30550
$(Ba_xSr_yCa_z)MgSi_2O_8:Eu$, equilibria in subsolidus phases rel. to luminescence 8=49789
(BaSrCa)O, electrical cond., thermoelectric power and work function, effect of Ba vapour 8=26945
$Ba_{0.27}Sr_{0.75}Nb_2O_{5.78}$, ferroelec., cryst. struct. 8=48638
$(Ba-Sr)TiO_4$ mixtures, prep. with dielec. const. approx. 500 8=27286
$BaTa_2O_6$, hexagonal, tunnel struct. in a.c. direction, rel. to dielec. props. 8=35959
$BaTiO_3$, electro-optical props. near phase transitions 8=27637
$Ba_6Ti_2Nb_8O_{30}$, bronze-type tetragonal ferroelec. crystal structure re-exam. 8=39774
$BaTi_3O_7$, dielec. props. 8=40571
$BaTi_4O_9$, dielec. props. 8=40571
$Ba_2Zn_2Fe_{12}O_{22}$ ferromag. resonance 8=40885
$Ba_4Zn_2Fe_{36}O_{60}$, mag. props. 8=31719
Na_2CO_3 soln., acid differentiation, rel. to hydrothermal crystal growth 8=26213
barium titanate
See also Ferroelectric materials/barium titanate.
absorption edge rel. to TiO_6^{-8} units, MO calcs. 8=45225
atomic displacements rel. to real structure determ. 8=3088
crystals grown from KF flux, chemical comp. and doping 8=26163
films, ferroelec., sputtering prep. 8=35161
fine, -grained, x-ray diffraction line shifts 8=39716
hydrogen reduction process in crystal grown from KI flux 8=27695
linear disorder on (001) face on heating in u.h. vacuum 8=39649
Raman scatt. resonant interference between one and two phonon states 8=41066

Barium compounds—contd
barium titanate—contd
Raman spectra in tetragonal form, rel. to long-wavelength phonons 8=27559
refractive index, temp. depend. 8=49708
semiconducting, ionic-relax. polarization 8=35974
semiconducting ceramic, I-V characts. rel. to current channeling model 8=40438
semiconducting props. in plates with c-domains, thermodynamic equilib. 8=27081
substituting sites of rare earth ions from F centre obs. 8=48818
surface domain structure and topography from e.-mirror photomicrographs 8=39576
X-ray scattering, anomalous 8=36329
$(Ba_{0.05}Sr_{0.95})TiO_3$, press. depend. of dielec. consts. at low temp. 8=27283
$BaTiO_3-BiFeO_3$ solid solns., e.p.r. rel. to dielec. and mag. transitions 8=27488
$BaTiO_3$:1 at % La, cond., thermo-e.m.f. and i.r. refl., polaron model and —198-300°C 8=35878
$BaTiO_3$:La, oxide impurity effect on elec. resistivity 8=49229
$BaTiO_3$:La, resistivity dependence on oxide impurities 8=27080
$BaTi_{0.75}Sn_{0.25}O_3$, Mössbauer effect and dielec. const., —200 -20°C 8=30639
Ti^{3+} electronic transition theory 8=39362
Barkhausen effect. See Magnetization process.
Barnett effect. See Gyromagnetic effect.
Baryons
See also Hyperons; Nucleons and antinucleons.
Aleph, part in very high energy (cosmic ray) nuclear interactions 8=42734
baryon-antibaryon interactions, strangeness-exchange, quark model 8=33659
baryon-antibaryon model for pion decay of mesons 8=24754
baryon-baryon collisions, polarization and reson. decay rel. to transversity amplitudes 8=33736
baryon-meson coupling constants, sum rules derived 8=24625
baryon-meson supermultiplet symmetry from spinor currents 8=42483
baryon-meson, $U(6) \otimes U(6)$ scheme SU(6) mixing 8=25001
baryon-meson vertex in SL(6, C) 8=47098
boson model, mass formulae 8=33548
decay into spin-$^3/_2$ particle and pseudoscalar meson or vector boson 8=37863
decay, leptonic, and exchange current, in quark model 8=47126
decay, non-leptonic, amplitudes rel. to current divergence 8=33529
decay, nonleptonic, systematic and steady phenomenological approach 8=37860
exchange reactions $0^- + {}^1/_2 \rightarrow 0^- + {}^1/_2$, kinematic singularities and Macdowell symm. 8=29047
interactions baryon-meson interaction lagrangian, SU(3) × SU(3) 8=47127
interactions, data compilation review 8=24863
lepton-baryon interactions with neutrino production 8=47075
lepton decay spectrum, including weak Q-depend. of form factors 8=33734
mass eigenvalue, nonlinear spinor theory 8=24862
mass-splitting, N/D calc. in broken $U_{6,6}$ symm. 8=29179
meson-baryon composite, structure of high-spin spectrum 8=29178
meson-baryon coupling consts. in broken SU(6) static model 8=24749
meson-baryon interaction in derivative coupling model, sum rules in coupling constants 8=37958
meson-baryon interactions, prod. of neutral vector and pseudoscalar mesons, quark model 8=37957
meson-baryon interactions, strangeness-exchange, quark model 8=33659
meson-baryon peripheral collisions, multichannel approach 8=42504
meson-baryon scatt., dispersion relations and backward amplitudes 8=29116
meson-baryon scatt. off shell method 8=42376
meson-baryon scatt., quark model calcs. 8=24765
meson-baryon scatt., s-wave, incorportion of SU(6) invariance 8=33660
meson-baryon, scatt., threshold relations 8=42505
meson-baryon scattering, vector dominance sum-rules 8=24761
and mesons, pseudoscalar, coupling consts., dispersion sum rules 8=37959
models, rel. to s-wave non-leptonic hyperon decay 8=24987
nucleon isobars in $\pi^- n \rightarrow \{p\pi^-\}\pi^-\pi^0$, at 5 GeV/c 8=33675
octet, chiral dynamics 8=42619
octet, in quark model, mag. moment calc. 8=38048
passing state, existence checked in cosmic ray shower obs. at Tien Shan 8=42616
π-baryon ($^1/_2{}^+$) scatt., in formation on Regge exchanges 8=42543
polarization correl. with μ, prod. in ν-N interactions 8=29091

Baryons—contd
- quark model, d-wave q-q forces, energy spectrum obtained 8=38046
- quark model of higher baryons, decay widths 8=33735
- quark model, s-wave 8=25000
- quarks-on-springs model 8=33733
- radiative β decay, e.m. T-od correl. calc. 8=47176
- resonance D-wave decays, SU(6) $\times$ O(3) quark model 8=29215
- resonance, N(eé)N* form factors model dependent 8=38056
- resonances, spin density matrix for prod. mechanisms 8=42592
- scale factor in algebra of factorized Regge residues 8=42440
- scattering, baryon-baryon, in S(U(3) $\otimes$ U(3)) model 8=38049
- scattering by mesons, effective range formulae, extrapolated below threshold 8=37962
- scattering, meson-baryon, superconvergent sum rule for factorized amplitudes 8=37960
- spectrum, spontaneous symmetry-breaking model 8=47125
- sum rules for mixing angles, SU(3) $\otimes$ SU(3) chiral algebra infinite momentum 8=38047
- weak BBπ vertex, current algebra and PCAC appl. 8=42618
- N* resonance photoproduction rel. to cross sections and photon energy dependence 8=47123
- N$\pi\pi$ enhancements in $\pi^-n \rightarrow p\pi^-\pi^-\pi^\circ$ at 5 GeV/c 8=33676
- SU(6) bootstrap model, e. m. mass differences 8=42617
- SU(6) bound-state model, e. m. mass differences 8=47128
- Yo(1520) $\rightarrow \Lambda\pi\pi$, triangular diagram contribution rel. to π scatt. length 8=38097
- Z_0, Z_1, aleph-particle, strange spin formalism for supermultiplet 8=42487
- **resonances**
  - Breit-Wigner formula and Wigner conditions 8=29214
  - Byers-Fenster method for spin-parity determ. 8=29037
  - coefficients, angular distribution and polarization 8=29214
  - decay calc., U(6) $\otimes$ U(6) scheme for baryon-meson interactions 8=25001
  - decuplet, $^5\!/_2{}^+$ 8=42660
  - electroexcitation, belonging to two main Regge trajectories, relations between form factors 8=42661
  - e.m. transitions in three-triplet model 8=38095
  - Δ(1236) in pion photoprod partial-wave amplitude calc. 8=33840
  - Δ(1238) prod. in πp, Kp, $\bar{p}$p, Regge pole analysis 8=29217
  - Δ_{33} isobar in πd scatt. at 200 MeV 8=42544
  - Δ_{33} rescatt. in $C^{12}(\pi^-, \pi^-n)C^{11}$ 8=25256
  - Δ in pp $\rightarrow K^+\Sigma^+n$, 5 GeV/c 8=24913
  - Δ prod. in $\pi + N \rightarrow V + \Delta$, conspiracy relations 8=24846
  - Δ^{++} prod. in pp $\rightarrow \Delta^{++}p\pi^-$ 8=24912
  - Δ^{++} (1236) isobar mag. moment in $\pi^+p \rightarrow \pi^+p\gamma$ meas. 8=24809
  - γNN* form factor obtained 8=29216
  - in π photoprod. and N Compton scatt. 8=29162
  - $\bar{\Lambda}$N system, evidence for mass enhancement 8=24991
  - level density parameters calc. 8=25075
  - N isobar series for the group of [SU(2) $\otimes$ SU(3)] $\times$ T_{24} use of contraction on SU(9) 8=29034
  - N* contrib. to pionic disintegration of d 8=33843
  - N* electroproduction and form factors 8=47097
  - N*(1400) daughter pole hypothesis and P_{11} π-N scatt. phase shift analysis 8=47113
  - $N_{1/2}$*(1525), π° photoproduction from neutrons 8=47108
  - $N^*_{1/2}$ (1688), coupling consts. to meson and nucleons 8=42662
  - N*, general method for deriving ang. correls. 8=24687
  - N* $\rightarrow$ Nγ rel. to quark charge-commutation relations 8=29108
  - N^{*+} N^{*-} $\rightarrow \pi^- p\pi^+$ from $\pi^-p \rightarrow \pi^{*-}\pi^-$ 8=37980
  - $N^{*++}(1236)\rho^\circ$ decays obs. 8=42664
  - N* in p-p at 6 GeV/c obs. 8=29187
  - N* in quark model for ep $\rightarrow$ eN* 8=33631
  - $N^{*\circ}$ in $\pi^-p \rightarrow \gamma n$, e. m. couplings 8=37916
  - N*, from $\pi p \rightarrow \rho N^*$, $\pi p \rightarrow \rho N^*$, energy- and momentum-transfer dependence of cross-sections 8=37981
  - N* in $\pi + N \rightarrow p + N^* \rightarrow N + 3\pi$, Regge-pole model 8=24780
  - N* in πN charge exchange scatt. 8=24779
  - N*$\pi \rightarrow n\rho$, superconvergent sum rules 8=24786
  - N^{*++}(1238) prod. in $\gamma p \rightarrow$ multipion 4. 8-6. 0 BeV 8=33669
  - $N^*_{1238} \rightarrow p\pi^+$ rel. to pp $\rightarrow nN^*_{1238}$, 2. 8–10 GeV/c, one pion exchange model 8=38096
  - N* prod. by neutrinos rel. to quark charge-commutation relations 8=29108
  - N* prod. in $\pi + N \rightarrow \rho + N^*$, ang, decay correls at 8 GeV 8=24781
  - N^{*-} prod. in $\pi^- + p \rightarrow \pi^+ + \pi^- + n$, ang. distrib., diagram 8=24782
  - $N_{3/2}$*, $N_{1/2}$* prod. in π^-p scatt, 2. 4-3. 8, 6, 10 GeV/c obs. 8=29160
  - $N^*_{3/2}$ (1236) prod. in p-p collisions, 6. 92 BeV/c final states 8=24916
  - N*(1236)$\bar{K}$ prod. in $K^-p \rightarrow \bar{K}N\pi$, 1. 33 GeV/c 8=33706
  - N*(1236), prod. mech. in π^+-p interacts. at 900 MeV 8=42539
  - N_{11}* parameters, self-consistent - calc. 8=29218
  - N*(1400), SU_3 mixing 8=42663
  - $pp\bar{p}$(3755) obs. in $\pi^+p \rightarrow \pi^+pp\bar{p}$, 8.4 BeV/c 8=24789
  - quark model, s-wave 8=25000

Baryons—contd
- **resonances**—contd
  - reactions, use of Rarita-Schwinger wave functions 8=42662
  - Roper, assignment to octet state 8=47124
  - Roper, composite in field theory 8=24480
  - SO(4) symmetry in πN scatt., applications 8=42550
  - $SU(3)^{11}$ excitation predictions 8=25002
  - U_6 composite model for quarks 8=47100
  - Ξ^* (1817) $\rightarrow \Lambda + \bar{K}$, analysis from K^-p at 17–2.7 BeV/c 8=24997
  - Y_0^*, breaking of couplings in $\bar{K}N$ system 8=42585
  - $Y^{*\circ}$ in $K^-p \rightarrow \gamma\Lambda$, e. m. coupling 8=37916
  - Y_0^* (1815), coupling consts. to meson and nucleons 8=42662
  - Y_1^*(1910), $J^P = {}^5\!/_2{}^+$ in $K^-N \rightarrow \Lambda\pi$, 1900-2, 215 MeV 8=33841
  - $Y^{*+}(1385)K^+$ decays, obs. 8=42664
  - Y_1^*(1660, 1695) in K^-p collisions, obs. 8=25005
  - Y* prod. in K^-p, 10 GeV/c 8=33834
  - Y_1^*(1385) state, prod. in K^-d interacts at 2. 24 BeV/c 8=42666
  - Y_0^* and Y_1^*, prod. in $K^-n \rightarrow \Sigma^-\pi^+\pi^-$ reaction, 1660 to 1900 MeV 8=42665
  - Y_1^*, Y_0^* obs. in $K^\pm + p$, $K^\pm d$ scatt., 0. 6-2. 65 GeV/c 8=29159

Barysphere. See Earth.

Bauschinger effect. See Deformation.

Bayard–Alpert gauges. See Vacuum gauges.

Bays. See Earth/magnetic field; Magnetic storms.

Bells. See Musical instruments.

Bending

See also Stress analysis; Torsion.
- annular slab supported on columns of outer edge 8=32737
- bar, flexible, subject to arbitrary discrete loads and boundary conditions 8=46052
- bars, thick, straight, theory 8=41664
- beam, compressed, oscillation freq. calc. 8=46140
- beam, impact of mass . 8=37132
- beam on elastic foundation with moving load, nonlinear effects 8=41652
- beam, simply supported, min. dynamic response 8=28267
- beam, stress distribution round hole in web 8=23826
- beams, indeterminate, elastoplastic analysis under reverse loadings 8=37135
- beams, min. weight design with inequality constraints on stress and deflection 8=23828
- beams. perfectly plastic, class of complete soln. 8=41726
- beams with concentrated loads, nonlinear 8=37125
- brittle solids, high-temp. rapid testing apparatus 8=44532
- circular plate. example of linearized theory of viscoplasticity 8=41722
- circular ring, radially constrained, buckling under distributed loading 8=32731
- cosserat plate, stress singularities around crack 8=41698
- cylindrical shell, orthotropic, stability to axial compression, external press. and bending moment 8=32752
- cylindrical shell roofs, self-supporting, critical loads 8=37143
- elastic plates, theory, contribution to Reissnerian algorithm 8=41669
- epitaxial films on mica and NaCl substrates, stresses causing film curling 8=35157
- ferroelectric film, on polarization 8=40608
- fibres, three-point bend tester 8=31172
- flexure of dielectric rectangle reinforced with inextensible cords, anal. 8=23843
- frame, two-member, non-linear buckling and snap-over 8=41655
- glass-reinforced plastics, creep 8=31241
- metals alternatingly, thermal activation energy determ. 8=35613
- notched bars, rigid/plastic, calcs. 8=37126
- ovaloid rigid core in beam subjected to bending, problem solns. 8=32742
- plastic square bar, work-hardening, combined bending and torsion, numerical anal. 8=23836
- plate, conforming finite element 8=41656
- plate on elastic half-space, due to moving line load 8=23830
- plate stability problem solution without preliminary determination of initial stress state 8=46031
- plate, triangular equilib. model · 8=41660
- plates, circular, of hardening material 8=41727
- plates, fibre-reinforced, under rotationally symmetric conditions, plastic anal. 8=37157
- of plates, intense, solvability of eqns. 8=37151
- plates, thick, with circular hole 8=37134
- rectangular plates, inherent instability anal. for various transverse cross-sections 8=37138
- rings, thin circular, buckling under uniform pressure 8=41654
- shell, circular and cylindrical, var. wall thickness 8=46046
- shells, cylindrical, buckling under axial compression, testing machine effects 8=32728
- shells, cylindrical, creep buckling under axial compression 8=32739
- shells, shallow spherical, and membrane stresses 8=37141
- shells with +ve curvature under concentrated load 8=41662
- singularity for pt. load at plate edge 8=32729
- steel beam, applic. of stress/strain law 8=44571
- strip and sheet, large deform. exceeding elasticity interval 8=23842

Bending—contd
  thermal deflection of non-homogeneous rectangular plate 8=41872
  transverse isotropic bodies, finite strain cal. 8=41649
  viscoplastic cylindrical shell, buckling due to impulsive load 8=32770
  BaTiO$_3$ film, on polarization 8=40608
  Cu$_5$Si, rel. to gaseous impurity segregation 8=35673
  Fe-Si alloys, two, in opposite directions, rel. to slip bands 8=48863
  Ni$_3$Ge, rel. to gaseous impurity segregation 8=35673
  Ni$_3$Sn$_2$, rel. to gaseous impurity segregation 8=35673
  Pb-0.5%Sb, reversed cycling and fatigue band development 8=35714
Berkelium
  No entries
Beryllium
  atom, energy props. of Be 2-matrix 8=38598
  atom, ground state energy, biorbitals calc. 8=47491
  atom, ground state pair correl. calc. 8=29604
  atom, ground state wave function calc. configuration-interaction method 8=25358
  atom, Hartree-Fock calc. refr. index, dynamic polarizability and Verdet coeffs. 8=47485
  atom, photo-ionization cross-section near threshold, calc. 8=39029
  atoms, Rydberg orbitals, calc. 8=29620
  in cosmic rays, galactic, p-fragmentation prod. rel. to dating 8=38176
  crystal preparation and microstrain props 8=44554
  crystal, slip rel. to temp., dislocation identification 8=44555
  density of states calc. from theoretical partition function 8=35765
  depth dose distrib. prop. by electron irrad., energy losses and ionization 8=31143
  electron momenta from X-ray meas. 8=44647
  fracture analysis by acoustic emission 8=48996
  h.c.p. polycrystals, ductile-brittle behaviour theory 8=26757
  Ion, III, IV, emission spectra obs. 8=29605
  i.r. absorpt. spectra 8=36330
  Knight shift, rel. to Fermi surface 8=27500
  magnetothermal oscs, showing mag. interacts 8=44686
  neutron wave propag., theory 8=33774
  oriented sheets, angular variation of charact. energy losses of 30 kV electrons 8=26936
  origin, in solar system, big bang and solar spallation theory 8=36990
  planes studied for neutron diffraction 8=48640
  reduced density matrices, and natural orbital and geminal expansions 8=43182
  reflectance in far u.v., rel. to $1/\epsilon$ resonance 8=49709
  resistance oscills. rel. to mag. breakdown, 45-80 kOe 8=26962
  self-diffusion coeff., 650-1200°C 8=35481
  specimen preparation and microscopic examination 8=39718
  spectral emissivity, normal, correl. with struct. anisotropy 8=36332
  stars, envelope support, hypotheses 8=28041
  Be(II) coordination no. in aq. solns. determ. by p.m.r. 8=39431
  Be III, vacuum u.v. spectrum, high energy satellites 8=47492
  Be^{7,9} in solar cosmic rays, flux, calc. 8=37057
  Be^9 in stars and interstellar medium, obs. 8=36927
  Be^9 ion beams, lifetimes and excited states for multiply charged ions 8=43217
  Be^9 ion paths in NIKFI-Ya$_2$, photoemulsions 8=46984
  Be$^+$ ion, new type of wave function 8=38672
  Be$^+$, slow electron scatt., elastic 8=43231
  in n-SiC, diffusion, 1700-2250°C, mechanisms and anisotropy 8=35506
Beryllium compounds
  beryl, l.f. vibrs. of H$_2$O mols. 8=48704
  fluoroberyllate complexes in soln., n.m.r. 8=48209
  halides, i.r. spectra 8=25449
  metal beryllides, magnetism investigations at low temps. 8=45009
  phosphate glass, struct., i.r. spectroscopy of NaBeF$_3$-NaPO$_3$ system 8=30791
  Be-4.4 wt%Cu alloy, slip rel. to temp., dislocation identification 8=44555
  Be-4.37%Cu, crystal preparation and microstrain props. 8=44554
  Be-5.2 wt.% Ni alloy, slip rel. to temp., dislocation identification 8=44555
  Be-5.24%Ni, crystal preparation and microstrain props 8=44554
  BeAl$_2$O$_4$, chrysoberyl, n-irrad., crystal growth obs. 8=31145
  BeBr, emission spectrum obs. 8=25452
  BeBr excited in presence of argon, emission spectrum 8=38810
  Be-Ca alloys, specimen preparation and microscopic examination 8=39718
  Be-Cu alloy, hardness anisotropy rel. to slip resist., Cu conc. effects, obs. 8=44552
  Be-Cu foil, thermal conductivity, electrical resistivity 8=39947
Beryllium compounds—contd
  BeF, ground state reduced potential curves 8=29717
  BeF$_2$, glassy, atomic radial distrib. from X-ray diffr. meas. 8=26148
  BeF$_2$, molten, viscosity temp. depend. 8=25892
  BeF$_2$, vitreous, vibrational spectra 8=35392
  BeH$_2$, diatomics-in-mols. calc. 8=25450
  BeH$_2$, pyrolysis and combustion, flash spectra 8=32110
  BeH$_2$, total energy of molecule 8=25451
  BeH$^+$, valence-only correl. calc. 8=34254
  BeO, Be diffusion rate rel. to radiation damage 8=26722
  BeO ceramics, extended, residual stress and grain deform. 8=44556
  BeO crysts., α-particle channelling, 5.15 MeV 8=31144
  BeO, elec. conductivity, activation energy, polarization effects 8=27241
  BeO, exciton line splitting, phonon induction, obs. 8=36331
  BeO-graphite in reactor, compatability, 1500°C, Li^6 distribution 8=34100
  BeO, hydrothermal growth 8=48538
  BeO, macroscopic and lattice growth under n-irrad. 8=26234
  BeO, molten particle cloud, spectral emissivity from extinction and absorpt. meas. 8=34939
  BeO, n-induced damage and macroscopic props. changes, review 8=44496
  BeO, neutron irrad., X-ray scattering, random defect distribution 8=40016
  BeO, optical phonons, reflection and Raman spectra meas. 8=27561
  BeO polycrystals, grains, subgrains and stress analyses 8=26291
  BeO, rupture mod., effect of strain rate, environment and surface cond. 8=26788
  BeO, self-diffusion and creep activation energies correl 8=44553
  BeO, thermal diffusion, accuracy of pulsed n meas. 8=25308
  BeO, thermal diffusion, pulsed n obs. 8=25307
  BeO/Al$_2$O$_3$ binary, elec. conductivity, activation energy, polarization effects 8=27241
  BeO/Fe$_2$O$_3$ binary, elec. conductivity, activation energy, plarization effects 8=27241
  BeO + BeF$_2$ system at high temp., mass spectra 8=35012
  Be$_4$O(CH$_3$.COO)$_6$, optical constants in 600-1800 cm^{-1} range 8=45239
  BeSO$_4$.4H$_2$O and BeSO$_4$.4D$_2$O, vibr. freqs. of metal-hydrate complexes 8=35381
  CrBe$_{12}$, paramagnetic and ferromagnetic state, NMR meas. of hyperfine fields 8=45115
Bessel functions. See Functions.
Beta-decay theory
  See also Nuclear decay theory.
  baryon, radiative, e.m. T-odd correl. calc. 8=47176
  Cabibbo theory status 8=38009
  double, superweak interaction with G ~ 10^{-9} 8=29356
  Fermi decay, $\Delta T = 0, 1$ ft rel. to isospin and $\Delta T = 2$ transitions in medium A nuclei 8=38410
  Fermi ft values rel. to isospin mixing in ground state 8=25076
  Fermi nuclear matrix elements, mesonic exchange effects 8=25174
  Fermi theory, invariance principles and nature of neutrinos 8=25173
  Gamow-Teller decays retardation, collective effects, model 8=38409
  $i \rightarrow f + e^- + \bar{\nu}$, order-$\alpha$ radiative corrections proved finite 8=33630
  internal bremsstrahlung, forbidden 8=42938
  L$_1$/K orbital electron capture ratio for allowed transitions Hartree-Fock calc., low-z elements 8=38408
  magic nuclei far from stability, $\beta^{\pm}$ decay 8=38328
  muon capture systemmatics in independent shell model 8=33983
  PT invariance, tests for violation, in nuclei 8=38407
  radiative corrections, including strong interaction effects 8=37967
  shapes of β spectra, survey of exptl. data 8=42936
  vector coupling constant calc. 8=42937
  Al^{26}, T = 2 component in Mg^{26} ground state 8=47282
  As^{74}, pairing-model calc. of nuclear matrix 8=42946
  Bi^{210}, β^- auto-ionization 8=29373
  $C^{14} \rightarrow N^{14}$, calc. 8=25100
  Ca^{50}, anomaly resolved 8=42943
  Ce^{146}, γ spectrum and transitions obs. 8=42959
  Dy^{165}, new γ transitions 8=47296
  Er^{119}, β^- auto-ionization 8=29373
  Lu^{177}, Nilsson model rel. to 386 keV β-113 keV γ directional correl. obs. 8=29375
  Ni^{57,65}, β-γ (CP) correlation measurements, deduced Coulomb matrix elements 8=42944
  O^{14}, purity violation 8=47280
  Yb^{175}, Nilsson model rel. to 352 keV β-114 keV γ directional correl. obs. 8=29375
Beta-ray spectra
  See also Nuclear decay theory.
  average energy, tables 8=29357
  helicity meas. methods 8=24718

Beta-ray spectra—contd
satellite scintillation instrument for relativistic e 8=50243
shapes, survey of exptl. data 8=42936
2-forbidden β transitions, spectrum calc. 8=25172
Au^{198}, transitions to first excited level, shape rel. to struct. models, obs. 8=29378
Ce^{145,146} rel. to decay schemes, and total β-decay energy, obs. 8=38430
Cl^{38}, β, γ-transitions obs. 8=29359
Co^{60}, end-point energy obs. 8=29363
Cs^{137} double forbidden 8=47292
Cs^{137}, end-point energy obs. 8=29363
I^{123}, upper limit to positron decay 8=42955
K^{38}, β^{+} and half-life, obs. 8=29361
K^{38m}, β^{+} and half-life, obs. 8=29361
Lu^{168}, β^{+}, rel. to Yb^{168} levels, obs. 8=29339
Lu^{177}, shape factor, 386 keV 8=29375
Nb^{94}-Mo^{94} at 473 keV, transition 8=47285
Nd^{147} → Pm^{147} 8=29369
O^{15} → N^{15}, β^{+} decay 8=29294
Pr^{141,143}, transition multipolarities obs. 8=29330
Rb^{86}, transitions to first excited level, shape rel. to struct. models, obs. 8=29378
Rb$^{90-96}$ 8=29367
Rb^{91} obs. 8=25181
Ru^{95}, and γ- spectra and decay scheme, obs. 8=42952
Re$^{186, 188}$ $1^{-} \rightarrow 2^{+}$ transitions, non-statistical shape, obs. 8=38437
Se^{83m}(69 sec), and γ-spectrum, rel. to to decay scheme, obs. 8=38420
Sm^{155} → Eu^{155} and level scheme, obs. 8=29334
Te^{133} decay, Q_{β} meas. 8=25186
Th^{233} → Pa^{233} 8=29380
Tl^{204}, end-point energy obs. 8=29363
Tm^{170} transitions to first excited level, shape rel. to struct. models, obs. 8=29378
V^{52} and half-life, obs. 8=29361
Yb^{175}, shape factor, 352 keV 8=29375
conversion electrons
α-recoil atoms, spectra deform. in elec. field 8=29287
coefficient meas. with Si(Li) and Ge(Li) detectors for obs. of electrons and γ-rays 8=42970
coefficient of mixed transition, odd-mass deformed nuclei 8=47217
internal conversion coeffs., Rose's, Sliv and Band's tables compared 8=47223
isomers, millisec, formed in p reactions, study with 'ketron' β-spectrometer 8=38346
pair formation rel. to nuclear multipolarity transitions 8=25086
rare-earth E2 transition particle parameters 8=47257
Ac^{227} ground state odd parity obs. 8=42926
Am^{241} α-disintegration obs. 8=25198
As^{75}, K-coeff. for 280 keV level 8=25133
Au^{193} decay, $E_{e} = 0.8$-700 keV obs. 8=25193
in Au^{197} α-bombard. rel. to Au^{197}(α, pn)Hg^{199}, 25 MeV 8=29361
Bi^{207}, conversion ratio for 570 and 1064 KeV transition obs. 8=33967
Co^{58M}, for 25 KeV isomeric transition 8=33966
Eu^{144}, rel. to Sm^{144} 1659 and 2481 KeV levels population in (p, p^{1}), obs. 8=38435
Eu^{151}(n, γ)Eu^{152}, coincidence obs. 8=47255
Ga^{65} decay to Zn^{65}, obs. 8=25178
Gd^{152,154} E2 transition particle parameters 8=47257
Gd^{157,158}(n, γ), surface barrier detect. in thermal n counter 8=33813
Ir fraction of p irrad. Au, 660 MeV 8=29342
Ir^{192m}, for isomeric transitions 8=33966
Lu^{175}, of dipole trans. 8=33932
Nb^{96}, coeffs. obtained 8=25183
Os$^{180, 181}$ decay, conversion coeffs. obs., transition multipolarities calc. 8=38438
Pa^{231} 58.5 KeV transition obs. of L subshell fluorescence 8=43200
Po^{210}, K-conversion coeffs. 8=25195
Pt^{195}, directional correl. meas. with conversion electrons 8=38392
Re^{178} decay, conversion coeffs. obs., transition multipolarities calc. 8=38438
Ru^{219} rel. to energy levels, obs. 8=29346
Se^{75} → As^{75} decay conversion electrons, energy and intensity obs. 8=25179
Sm^{150} excited levels, e-γ coincidence obs. 8=29333
Sm^{152} E2 transition particle parameters 8=47257
Sm^{155}(β^{-})Eu^{155}, spectrum 8=47293
Sm^{150,152,154}(α, Xn)Gd$^{150-156}$, conversion electrons rel. to reaction mechanism and nuclear model 8=47258
Th^{233} → Pa^{233}, spectrum 8=42979
Tm^{165} → Er^{165} decay scheme, e–e coincidence obs. 8=29374
Tm^{168} decay, internal conversion coeffs. determ. 8=25191
Tm^{169}, rel. to chem. environment 8=29336
Tm^{170}, transverse polarization meas. 8=47297
Xe^{127m} rel. to 125 and 175 keV γ transitions assignments, obs. 8=38427
Zn^{69m} decay, conversion coeff. and K-fluoresc. yield obs. 8=38418
Beta-ray spectrometers
crossed-beam using electrostatic vel. analysers 8=43242
Beta-ray spectrometers—contd
double-focusing, mag. field optics, computation and expt. 8=37940
e-γ coincidence spectrometer 8=29333
fallout meas., instrument with 2 Li-drifted Si semicond. detectors in stack assembly 8=46851
focusing props., computation and expt. 8=37413
4$\pi\beta$ with Li-Si counters 8=24730
'ketron', use with p accelerator for study of isomers in nuclear reactions 8=38346
magnetic, appl. of var. field distrib. lenses 8=24731
magnetic field stabilizer 8=47096
magnetic, UMB-type, resolving power 8=37939
photoelectron spectroscopic system 8=36050
stabilization and meas. of field up to 350 Oe, 10^{3}Oe sensitivity, instrument for βs spectrometers 8=47096
toroid-sector type, resolution and transmission improvement 8=33641
12-channel semiconductor counter system for electron scattering 8=47095
winding mag. field, higher-order calc. 8=24732
Beta-rays
See also Electrons.
double decay and superweak interaction with $G \sim 10^{-9}$ 8=29356
emitter identification, by comparing pulse rates of unknown and standard emitters 8=33951
emitter standardization by efficiency tracing 8=29352
absorption
See also Electrons/absorption.
emitter standardization by efficiency tracing 8=29352
angular distribution
Au^{198}, β-γ directional correls. rel. to struct. models, obs. 8=29378
Lu^{177}, 386 keV β-113 keV γ directional correl. rel. to Nilsson model 8=29375
Pt^{192}, e–γ directional correlation meas. 8=33935
Rb^{86}, β-γ directional correls. rel. to struct. models, obs. 8=29378
Tm^{170}, β-γ directional correls. rel. to struct. models, obs. 8=29378
Yb^{175}, 352 KeV β–114 keV γ directional correl. rel. to Nilsson model 8=29375
detection, measurement
See also Beta-ray spectrometers; Dosimetry; Particle detectors; Radioactivity measurement.
anthracene scintillation counter, response to low energy electrons 8=24728
apparatus for meas. electron scatt. at 180° 8=24725
calorimeter for energies of accelerated electrons 8=47091
Cherenkov radiation method for β-emitters 8=29353
electron capture detector cleaning 8=33640
electron, low energy, employing channel electron multipliers 8=47093
4$\pi\beta$-γ coincidence, correction 8=24727
in coincidence with γ, Ge pin diode 8=46894
polyethylene, Hg lamp excitation of fluorescence 8=24729
position meas. using surface barrier diode 8=47094
PW 4127 assembly, automatic sample changer 8=42476
satellite mag. analyser for 100keV-1MeV 8=50242
scintillation counter with low background count 8=33639
semiconductor detector telescope for satellite, calibration 8=28025
solid-state, for electron measurements on orbiting geophysical observatory 8=47092
CsI(Tl) scintillator for low energy 8=46877
H^{3} in H$_2$O by ethane gas counting, and counter shielding 8=42474
H^{3} in H$_2$O, toluene-Triton-water emulsion scintillator optimum comp. 8=42473
H^{3} in H$_2$O, water vapour filled counter 8=42475
PbF$_2$ Cherenkov counter for e$^{\pm}$ 8=46885
Si drifted detectors, pulse time spread 8=29097
Si, measured and calculated response function for electrons 8=46916
effects
See also Electron beams/effects; Nuclear reactions due to/electrons.
electronic components, transient effects 8=31126
γ quanta production by Compon effect with relativistic electrons colliding with laser beam photons 8=47045
polarization
D atoms, ionization, ejected e spin polarization obs. 8=29662
Tm^{170}, L-conversion electrons 8=47297
scattering
See also Electrons/scattering.
backscattering radiation intensity calc. 8=47088
energy maxima target number dependence 8=47309
Betatrons. See Particle accelerators/orbital.
Bethe–Salpeter equation. See Field theory, quantum.
Bethe–Uhlenbeck equations. See Statistical mechanics.
Bevatron. See Particle accelerators/orbital.
Bibliographies
atomic collisions in stellar atmospheres 8=36939
British radioastronomical obs. 1963-66 8=32608
computer modelling and simulation 8=28246
dislocation kinks affecting internal friction 8=26743

Bibliographies—contd
  e.m. wave scattering and diffraction, two-dimensional 8=46464
  energy-momentum tensor in polarized media 8=32841
  exchange reactions, high and low energy, peripheral model 8=29384
  experimental studies of forces on model structures by wind and blast waves 8=46170
  fast-acting e. m. isotope separators 8=38765
  heat transfer 8=32950
  heat transfer, Japanese works (1966-67) 8=28387
  heat transfer, review of 1965, 66 literature 8=28388
  heat transfer, Russian works (1964-66) 8=37304
  holography and related topics (655 refs) 8=37709
  inert-gas crystal lattice props. 8=35390
  internal friction and fatigue in b. c. c. metals 8=26813
  laser devices, July to December (1967) 8=33161
  lasers, 4357 original refs. 8=33171-2
  masers, theory and expt. in USSR 8=28644
  mass-flow meas. by heat transfer 8=34591
  measurement standards, length, time, freq. (1918-1968) 8=28209
  medical instrumentation (1918-68) 8=41604
  microwave applications of ferrites 8=24203
  non-linear optics and coherent freq. conversion in USSR 8=28719
  normal-superconducting thin films, proximity effect 8=27006
  nuclear fission 8=29526
  nuclear instruments (1918-1968) 8=28967
  nuclear spallation cross-sections 8=29436
  optics and spectroscopy, USSR (1917-67) 8=33234
  oxygen isotopes (O^{15}, O^{17} and O^{18}), uses in research 1963-66 8=34185
  plasma, refractive methods in diagnostics 8=34516
  Raman effect in gases (1950-1966) 8=29694
  relativity, general, teaching resource letter 8=32805
  ultrasonic holography for image visualisation in opaque media 8=28374
  vacuum u.v. spectroscopy 8=24384
  viscoplasticity, fundamental problems 8=28274
Binary stars. See Stars.
Binding energy, solid state. See Bonds; Solids.
Bingham plastics and solids. See Rheology.
Biographies
  No entries
Biological effects of radiations
  conference, Boston Mass. USA, November 1967 8=32626
  cortical pot. rel. to tone burst duration and rise time 8=46211
  DNA, diamine bound 8=48903
  Gemini XI S4 blood experiment 8=50466
  hexane ionization chamber, quality factor 8=37787
  interactions above 10 GeV, classification 8=42720
  noise, acoustic, temporary threshold shift models 8=28378
  π^- beams, on ascites tumor cells 8=50465
  π^- beams, on mammalian cells in vivo 8=50464
  retind photocoagulation with ruby laser 8=28912
  solar flares, dose rel. to shielding 8=41595
  thermal spike effect in heavy ion tracks, mathematical model particle tracks 8=41292
  ultraviolet, safe limits of illum. 8=45925
  Cs-137 in humans, meas. in 1958-67 8=41605
Biological technique and instruments
  acidity meas., glass microelectrode 8=37092
  arterial flowmeter, e.m. eqn., soln. for cylindrical geometries 8=43727
  counter, liq. scintillation, whole-body 8=32627
  differential microcalorimeter for biochemical reaction studies 8=27687
  double-beam vibrating mirrors flying spot scanning-integrating microspectrophotometer for animal cell study 8=24394
  electron micrography, reconstruction of the tail of the bacteriophage 8=35260
  electron-mirror microscopy for meas. of electrical and topological features of biol. mat. 8=41603
  heavy ion irrad. of mammalian cells in vitro 8=50463
  isotope scanning of small animals 8=50467
  K content of new tissue growth, spectrographic meas. 8=27787
  medical instrumentation, 1918-68, bibliography 8=41604
  microscope, visual u.v., employing M-9 electro-optical converter 8=42214
  pulmonary ventilation recording 8=37094
  scintillomicroscope for radioactive tracer detection in biological specimens 8=32623
  solution permittivity meas. below 1 MHz 8=28452
  structure models, ball-drilling methods 8=32631
  whole-body 4π liq. -scintillation counter 8=28978
  whole-body n. m. r. spectrometer 8=32618
  X-ray diffraction and electron microscopy applic. 8=32624
  for $C^{14}O_2$ continuous monitoring, large animal metabolism chamber 8=45928
  I radioactivity meas., samples prep. 8=42339
Biology
  See also Medical science; Physiology; Zoology.
  availability of surfactants rel. to adsorpt. by kaolin 8=44071
Biology—contd
  diffusion at liquid-solid interface, ultrasound effects 8=34814
  use of low angle electron diffraction camera, techs 8=24149
  noise neoplasms n therapy, B^{10} dose and thermal flux effects 8=45926
  registration of charged particles in solids, fission alternative to autoradiography 8=32622
  Ca distrib. in leaves, autoradiography and chem. analysis obs. 8=45929
Biophysics
  biological membranes, active transport of K and Na ions 8=50461
  butterfly (Morpho) wing, spectral reflectance 8=46656
  collagen and bone, transmission and attenuated total, refl. i.r. spectra 8=32041
  cortical pot. rel. to tone burst duration and rise time 8=46211
  data collection in medical γ spectroscopy 8=50462
  DNA pairon condensation, double-stranded 8=32620
  ferricytochrome c, beef-heart, e.s.r. 8=31865
  gramicidine S in soln., molecular structure from n. m. r. obs. 8=34332
  localization, theory 8=42454
  low energy radiation from thorax of human male, comparison of predicted and obs. 8=28199
  mammalian tissue, geometrical efficiency of solid state radio-activity detector 8=32621
  minimum conc. rel. to non-combustion region in diving atmospheres 8=49884
  plant canopy interaction with light 8=46735
  rabbit lens (crystalline), refractive index distribution model 8=46779
  radioactive material assay by γ spectrometer 8=47065
  relative permeabilities for constant field eq., expt. determ. 8=48122
  rem meas. method for mixed γ-neutron radiation fields 8=46923
  sense organs as transducers of the environment 8=32625
  soft tissues, discrete viscoelastic models 8=45924
  vision, human, direction of movement and contour orientation mechanisms, selectivities 8=46774
  whole-body liquid scintillation counters, safety and economy 8=33373
  whole-body liquid scintillation counter, safety and economy 8=33374
  Cs^{137} in human infants, 4π plastic scintillation counter 8=42934
  K^{40} in human infants, 4π plastic scintillation counter 8=42934
Biot-Savart law. See Electromagnetism.
Birefringence. See Double refraction.
Bismuth
  absorption in 50-340Å range, calc. of partial oscillator sums 8=31981
  Alfvén wave propag., second harmonic generation obs. 8=40282
  atom, spectra obs. on each side of resonance line 8=29600
  band structure, pseudopotential approach 8=26903
  carrier density pressure dependence 8=40313
  charge-carrier density from galvanomag. data at 4.2°K 8=26963
  de Haas-van Alphen effect beats rel. to e energy spectrum 8=27376
  diffusion of charged carriers through shock wave front 8=35826
  diffusion of ions in KCl cryst. 8=48781
  dislocation multiplication mechanisms 8=26668
  electrical conductivity of films in elec. field, quantum size effect oscills., 10^3 v/cm 8=40312
  Fermi surface tilt. 8=49100
  films, evaporated, thermoelec. motive force, thickness depend. 8=49391
  films, thickness depend. of elec. props. and quantum effects 8=27082
  films, thin, transition to semiconducting state 8=27083
  fission by electrons 8=38534
  hyperfine structure 8=27562
  liquid, structure factor 8=48062
  liquid, supercooled, u.s. vibs effect on nucleation 8=48261
  magneto plasma waves, cyclotron damping due to mode mixing 8=31308
  magneto plasma waves, u.h.f., propag. vel. 8=49124
  magnetoresistance, anomalous longit., rel. to impurity of sample 8=40728
  magnetoresistance, boundary surface influence 77 and 4.2°K 8=49155
  magnetothermal oscs. meas., rel. to Fermi surface 8=44686
  phase changes under high pressure 8=35093
  plasma, mobile, self-induction 8=26928
  reluctance anisotropy mag. field dependence at 77°K 8=40729
  spectrochemical determ. in white cast iron, hollow-cathode discharge method 8=36642
  superconducting amorphous film, tunnelling obs. 8=40368
  supercooling, nucleation behaviour 8=48257

Bismuth—contd
- surface structure and reactivity, study by LEED and O adsorpt. 8=26106
- thermoelec. Ukehr effect at 80°K 8=27307
- voltage, transverse, in longit. mag. field 8=35825
- Bi^{209} hyperfine structure in $6p^2(^3P_0)7s^4P_{1/2}$ state 8=43183
- Bi^{209}, muonic, hyperfine interactions obs. 8=38772
- Bi: Te, helicon propag., second harmonic generation obs. 8=40282
- La_2O_3(Bi) phosphor, excitation and emission spectra 8=45279
- O content determ. by $O^{16}(n,\gamma)N^{16}$ 8=32167

Bismuth compounds
- bismuthyl halides, i.r. absorpt. spectra rel. to vibr. modes 8=38812
- BVC garnets, two-magnon-one-phonon confluence process 8=40837
- eutectic alloys, metastable, superconductivity 8=44722
- perovskites, phase rel. to ferro- and antiferroelec. transitions 8=26063
- titanate, ferroelectricity, thermodynamic analysis 8=44887
- trihalides, phase diagrams, high-press. 8=39468
- Bi–Au system, form of simple cubic π phase at –190°C 8=48402
- Bi-Bi halide, molten solns., viscosity 8=43772
- Bi + $BiBr_3$ solutions, thermoelect. power 8=25947
- $Bi_{3-2x}Ca_{2x}Fe_{5-x}V_xO_{12}$, two-sublattice cpd., first magnetocrystalline anisotropy constant temp. dependence 8=45042
- $BiCl_3$, far i. r. cryst. spectra 8=45223
- $BiCl_3$-Pb molten mixtures, interact. study by absorpt. spectra 440-1000 mμ 8=34878
- BiF molecule, rotational structure of 2650-2850 Å system 8=38813
- $BiFeO_3$, e-microdiffr. exam. 8=26430
- $BiFeO_3$ and solid solns., mag. and ferroelec. transitions 8=27285
- $BiFeO_3$, spontaneous polarization, elec. field and field gradient calcs. 8=27269
- $BiFeO_3$-$Pb(Fe_{0.5}Nb_{0.5})O_3$ solid soln. system, phase transitions 8=39543
- $BiFeO_3$-$PrFeO_3$ system, structural transitions rel. to ferroelec. and mag. props. 8=26064
- $(1-x)BiFeO_3-xSr(Sn_{1/2}Mn_{2/3})O_3$, solid solns., transitions from Mossbauer studies 8=27442
- BiI_3 crystals, external photoeffect 8=44947
- Bi-Ga, liq., critical opalescence, temp. depend. 8=48149
- $Bi_{12}GeO_{20}$, photo-induced carriers, transport processes 8=27318
- $Bi_{1-x}La_x(Fe_{0.98}Mn_{0.02})O_3$ solid solns., phase transforms. 8=39542
- $Bi_2M_3''(NO_3)_{12}.24H_2O$: Gd, (M″=Zn or Mg), e.p.r. angular spectra, anomalous 8=45080
- Bi-O system, tetragonal phase, e diffr. obs. 8=30888
- Bi_2O_3, dielectric props. 8=49335
- $3Bi_2O_3.17Nb_2O_5$, projection of structure on [001] plane 8=26367
- Bi–Sb alloys, extrinsic, magneto-seebeck effect 8=44905
- Bi-Sb-Pb alloys, de Haas-van Alphen effect 8=31496
- p-$Bi_{0.5}Sb_{1.5}Te_{3+x}$, thermoelec. props. growth conditions and Te phase effects 8=49392
- BiSCl, optical absorpt. and photocond. 8=32028
- Bi-Se system cryst and amorphous, ionic and neutral species in vapour 8=35007
- Bi_2Se_3, electrical and heat conduction mechanism 8=30514
- Bi_2Se_3-Bi_2S_3, phase diagram, lattice constants 8=35094
- n-$Bi_2Se_{0.45}Te_{3+x}$, thermoelec. props, growth conditions and Te phase effects 8=49392
- Bi-Sn alloy, high pressure phase transforms. by n-diffractometry 8=26361
- Bi-Sn alloys, liquid, diffusion coeff. rel. to composition 8=39344
- Bi-Sn-Te alloys, thermoelec. and magnetothermoelec. props. 8=35996
- Bi-Te alloyed luminescent diodes, spectra at 78 and 300°K, I-V characts. at 300°K 8=36538
- Bi-Te, galvanomag., thermoelect. and thermomag. props. 8=31312
- Bi_2Te_3, Ag thermal diffusion and ht. of transport calc. 8=39968
- Bi_2Te_3, electrical and heat conduction mechanism 8=30514
- Bi_2Te_3II, high-temp. and pressure polymorph, lattice parameters 8=30681
- Bi_2Te_3 + 20 mol.% Bi_2Se_3, thermoelectric props. rel. to supercooling conditions 8=44906
- Bi_2Te_3-Sb_2Te_3-Sb_2Se_3 pseudoternary alloy, thermoelec. props. growth-rate dependence 8=44907
- n-Bi_2Te_3, specific ht. from 1.3 to 90°K 8=39910
- n-Bi_2Te_{3+x}, thermoelec. props. growth conditions and Te phase effects 8=49392
- n-$Bi_2(Te,Se)_3$, n-irradiated, thermo-emf, elec. and thermal conductivity 8=27136
- n and p-Bi_2Te_3, conductivity, Hall coeff., carrier lifetime 8=40439
- Bi-Te-Se(Sb) system, γ-irrad. effects on elec. and thermal conductivities and thermoelec. force 8=44763
- Bi-Te-Se semicond., scatt. mechanism 8=40440
- $Bi_4Ti_3O_{12}$ crystals, dielec. props. 8=27270

Bismuth compounds—contd
- $Bi_4Ti_3O_{12}$ crystals, electrical-optical behaviour 8=27271
- $Bi_8Te_7S_5$, very thin crystal, electrical conductivity 8=40314
- Bi-Zn, liq., critical opalescence, temp. depend. 8=48149
- Sb_2S_3–Bi_2Te_3 solid solns., morphotropy 8=48672

Bitter patterns. See Magnetization state/domains.

Bitumen. See Materials.

Bloch walls. See Ferromagnetism; Magnetization state/domains.

Blood
- convective diffusion of O_2, CO_2 and inert gases, rel. to artificial lung app. 8=43793
- Gemini XI S4 experiment 8=50466
- haemoglobin crystallization, procedures for human and horse types 8=26210
- plasma, Mg spectrochem. anal. using improved plasma jet equipped with inexpensive analyzer 8=47894
- Co, spectrochem. determ. of nanogram amounts, using Cu-spark method 8=49987

Boiling
- See also Distillation.
- alkali metals, pressure drop, prediction method 8=48281
- bubble growth in binary systems adhering to solid surfaces 8=34995
- bubble type, heat transfer coeff. rel. to evaporation and liq. mixing 8=39489
- bubble type, temp.-transition at fluid-vapour interface 8=39490
- composite conductors, stability, effect of nucleate to film boiling transition 8=44706
- flash boiling systems, effect of u. s. field on heat transfer 8=25994
- flow crisis, boundary layer analysis 8=43917
- Freon-22-dibutylphthalate soln, on horiz. tube, heat transfer 8=34999
- heat fluxes, peak and min., effects of geometry and gravity 8=34997
- heater size effects on critical heat loads. liquid with free convection 8=48280
- nucleate, in pure liqs. and binary mixtures, theory 8=25997
- nucleate, surface, in pure liqs. and binary mixtures, theory and expt. 8=25998
- nucleate, transition and film, transfer functions, evaluation and development 8=48282
- nucleation rate, in rel. to superheat 8=25999
- organic liqs. heat transfer rel. to state of heating surface 8=35001
- pool boiling heat transfer to cryogenic liquids 8=48127-9
- pool, incipient, in Na 8=48279
- refrigerant-22, subcooled, average void fractions 8=35000
- structure of liquids and solns. in above-critical region, theory 8=25995
- subcooled, volumetric vapor conc., effects of various parameters 8=35000
- transient, bubbles growth rate in transient boiling 8=48049
- in transition pool, heat transfer stability, and anal. and ex. pt. methods 8=35002
- vapour bubble growth in H_2O and organic liquids 8=34996
- Hg corrosion in steel boilers, Ti, Zr inhibition 8=47426
- N_2, cooling in X-ray cryatallography 8=32992

Boiling point
- No entries

Bolometers
- far i.r., pre-amp. with low noise performance at high impedance 8=41853
- metal layers, absorptive, for long-wave i.r. 8=23994
- operating points for max. sensitivity 8=37300
- superconducting film, for radiant-energy detection, microwave-near i.r. 8=37299
- voltage/current meas. in GHz range 8=24058
- C resistance, for far i. r. spectroscopy 8=32939
- Ge, cooled, depend. of parameters on conc. of Sb and Ga impurities 8=41855
- Ge doped, for far i.r. spectroscopy 8=32939
- Ge, i.r. detector 8=41854
- InSb, rolling free-carrier, heterodyne detection at mm wavelengths 8=23995

Boltzmann equation. See Transport processes.

Bonding of materials. See Adhesion.

Bonds
- See also Molecules.
- acetic acid-sulphuric acid, 1:1 addition cpds., H bonding rel. to crystal structure 8=26527
- acetylene, monosubstituted, solns., intermol. H-band form. rel. to C ≡ C group absorpt. band intensity 8=34301
- alkyl phosphonates, P=O-group valence oscillation calc. 8=30618
- ammonium formate, H bonding rel. to crystal structure 8=26528
- aromatic non-planar hydrocarbons, CH-bond moments 8=34344
- aromatic planar hydrocarbons, CH-bond moments 8=34343
- aryl phosphates, P=O-group valence oscillation calc. 8=30618
- benzene and deuterobenzenes, new force consts. 8=38871
- binaphthyl, distances and crystal structure 8=26470
- α,α'-bipyridil conjugation in cryst. and liquid states, Raman obs. 8=34355

Bonds—contd
- γ,γ'-bipyridil conjugations in cryst. and liquid states, Raman obs. 8=34355
- 5-bromouridine, and dimethylsuphoxide 1:1 complex bond lengths and angles 8=26471
- butadiene-acidic and basic copolymers mixtures, H-bonding rel. to elastic props., obs. 8=48506
- butadiene acidic and basic copolymers mixtures, H-bonds mech. lability, obs. 8=48507
- butadiene copolymer mixtures, ionic bonds, obs. 8=48508
- butadiene copolymers, ionic bonds mech. lability, obs. 8=48509
- butadiene-lithium methylacrylate copolymers, ionic bonds, obs. 8=48508
- butadiene-methacrylic acid copolymers, H-bonding rel. to elastic props., obs. 8=48506
- butadiene-2-methyl-5-vinylpyridine copolymers, H-bonding rel. to elastic props., obs. 8=48506
- butadiene-methyl (2-methyl-5-vinyl-pyridinium iodide copolymer, ionic bonds, obs. 8=48508
- n-butylamine and N-deutero derivative, H and D bridge bonds investigation from spectra 8=27620
- carbonyl, dipole-moment derivative 8=38875
- carboxylic acids, H-bonding, i.r. data 8=25554
- cations in aq. soln., coordination numbers 8=34779
- chemical, high-pressure effects, Raman spectra data 8=41031
- chlorophyll-ligand interactions, from n. m. r. 8=29850
- complexes, bond-length compression effects in solvents 8=34864
- conjugated mols., bond index and bond length relation 8=43272
- core-electron binding energies, chem. effects 8=38620
- covalent, effect on optical phonons, empirical relation 8=30924
- in crystals, covalent, anisotropy and quadrupole moments 8=30612
- crystals covalent, elements of structural theory 8=26004
- in crystals, covalent, lattice deformation energy calcs. 8=30613
- in crystals, covalent, partially ionic binding effects 8=30611
- cyanocobalamin monoacid deriv., by n diffraction 8=25676
- cyclic alkanes, fragmentation of skeletal bonds in mass spectra 8=29824
- dialkylamido-transition metal cpds., metal-N_2 i. r. stretching frequencies 8=29712
- diamond, valence-bonding rel. to at. vibration spectrum, review 8=43922
- diatomic mols., bond strength calc. 8=25426
- diatomic mols, bond strength calc. 8=25595
- Diels-Alder quinone adducts, C-C double bonds, study by i. r. spectra 8=25924
- 8, 8′-dimethyl binaphthyl, distances and crystal structure 8=26470
- dimethylammonium chloride, H bonding rel. to crystal structure 8=26525
- dissociation energies from equilibrium studies 8=47702
- donor-acceptor complexes 8=29768
- electron binding energies, next inner subshell, $5 \leqslant Z \leqslant 30$, calc. 8=25357
- energies, semiempirical quantum-mech. eqns. 8=49851
- ethylamine and N-deutero derivative, H and D bridge bonds investigation from spectra 8=27620
- f.c.c. crystals, surface, rel. to force-constant changes 8=26567
- formation in terms of molec. charge distrib. 8=34221
- gelatin, rigidity and bond energy 8=25972
- glasses. covalency estimate from effective mag. field at Mn^{2+} nuclei 8=48304
- grinding, formation of free radicals 8=25656
- hexachlorocyclohexane, bond mag. anisotropies 8=31515
- h. c. p. metals, elastically strained, binding energy rel. to inner-displacement tensor 8=26406
- homonuclear diatomic molecule, bond strength, FEMO model 8=47577
- hybridization, atomic orbital calc. 8=43265
- hydrazides. substituted. C–Br bond 8=49780
- hydrazidones, substituted. C–Br bond 8=49780
- hydrocarbons (isobutane, pentanes, hexanes), case of rupture of C-H bonds, e. s. r. obs. of radicals formed by ionizing radiations 8=25659
- hydrogen, slow n. scattering by protons, double potential well model rel. to solids study 8=35017
- hydropholic, formation in binary complexes, fluoresc. data 8=43850
- ionic crysts., polarizabilities, covalency contrib. 8=36390
- lanthanides, compressed polymorphs and intra-alloys, 4f contrib. rel. to crystal structures 8=26178
- lysozyme crystals, crosslinking rel. to stabilization 8=26008
- interfacial cohesion, practical implications of breakdown, review 8=39499
- length and force constant relationship for diatom 8=38802
- length and freq., empirical relation 8=38783
- macromolecular crystals, chemical 8=43923
- metastable, in binary glasses 8=30620
- methane I^{129} derivatives, Mössbauer effect 8=48332
- methanes, substituted, bond strength calc. 8=25595

Bonds—contd
- methyl alkali halides, new mol. type 8=47656
- methyl silane, isomeric derivs., bonding of halogen to Si or C, differences 8=43925
- molecular, double, π-electrons, one and two centre electron repulsion integrals 8=34218
- molecule properties, review 8=38803
- molecules, organic, two photon sensitized breaking of bonds, mech., at 77°K 8=29704
- nickelous nitrate–MgO aq. cements 8=26010
- n-propylamine and N-deutero derivative, H and D bridge bonds investigation from spectra 8=27620
- pair pot. for Ne, Ar, Kr, Xe 8=30615
- Pauling's energy equation, accuracy 8=49834
- pentaerythritol, deuterated, H bonds, structural investigations by n. m. r. 8=43926
- periodic bond chains and thermal vibrations in crystal 8=26005
- β perylene, distances and crystal structure 8=26470
- polar molecules, double, metastably bound, lifetime 8=34217
- polarizable, quantitative discription 8=43274-6
- polymer, under mechanical stress, i.r. spectroscopy 8=43437
- potassium hydrogen diformate, crystal structure rel. to H bonding 8=39837
- resonance valence state, alternative definition 8=25433
- Rochelle salt, of Cu^{2+}, e.p.r. obs. 8=36243
- semiconductor compounds, chemical bonding and structure 8=30614
- σ, localized orbitals 8=47578
- solids with paramagnetic ions, axial-field-splitting, covalency effects 8=35046
- sulphurised polymer carbons, rel. to spin centres, thermal stability etc. 8=35016
- tetrachlorohydroquinone, H bonding system from crystal structure analysis 8=30619
- tetrahedron, trigonally distorted, collective coordinates 8=48311
- tetramethyl-2, 2, 6, 6, -piperidinol-4-oxyl-1, free radical in crystal, and structure 8=25654
- s-tetrazine, lengths in ^1A_g and $\tilde{A}\,^1B_{3u}$ states, from 5515Å transition 8=25627
- III-V cpds. dipole moments rel. to second-order optical susceptibility 8=36314
- tobacco mosaic virus, binding of Xe 8=25974
- transition metal hydride complexes, covalent metal-hydrogen bonds 8=25521
- transition metal impurity covalent complexes, covalency 8=35018
- transition metal polynuclear complexes 8=27595
- transition metals, cohesion and surface tension by tight binding method 8=43928
- triglycine sulphate, of Cu^{2+}, e.p.r. obs. 8=36243
- trimethylammonium chloride, H bonding rel. to crystal structure 8=26526
- two-electron bonds, nature 8=29742
- urethanes, substituted, C–Br bond 8=49780
- urotropin-halogen in Br and I complexes. from vibr. spectra, 4000-350cm^{-1} 8=49781
- water, H bonding, mol. orbital treatment 8=43313
- XCO free radicals 8=47713
- X-H stretching vibr. intensities in gas to CCl_4 solns. transition, obs. 8=34298
- Ag, cohesive energy and isotropic band effective mass 8=48303
- AgBr. e. distribs. from X-ray structural analysis 8=48302
- AgCNO, ionic and covalent bonding rel. to stability 8=26006
- B compounds, i.r. evidence for single H bridges 8=38808
- C-atom inner electrons, bond participation 8=47627
- C-C double bond, reactions with ethylenimine 8=32097
- C–C, C = C, and C–H, electron densities 8=26009
- CF_3COOH-HCOOH, H-bond, microwave rotation spectra 8=25577
- C-H in methyl halides, electron cloud distrib. rel. to i.r. absorpt. intensity 8=43373
- C-H, C-C, C=C, electron densities 8=26009
- $(CH_3)_3X\text{-}C{\equiv}C\text{-}Cl$ (X=C, Si, Ge, Sn), n. q.r., bonding props. 8=38912
- C-N rupture in semicarbazide hydrochloride γ-irrad. crysts. 8=49604
- [C-N] valence reflectivity obs. 8=47622
- C-N, in F_2CN 8=38946
- Co to transition metal surface, nature 8=48298
- $Cr(CO)_6$, semiempirical MO model 8=47594
- $Cr(CO)_6$, Cr-C bond length from electron structure exam. 8=38821
- CrH, hexagonal, conversion to metallic Cr 8=48376
- CrH_x, $(x < 1)$, H orbital expansion effects on d-electron exchange rel. to mag. props. 8=49480
- in $CsBr_3$, bond lengths for Br_3^- ion 8=44247
- Cu, cohesive energy and isotropic band effective mass 8=48303
- Cu, of adsorbed Sr, Ba and alkaline atoms, quantum calc. 8=35199
- Cu II-Na-chlorophyllin chem. bonding from e. s. r. h. f. s. 8=34368

Bonds—contd
Cu_2O, exciton bond energy, change under uniaxial deform. 8=35790
Eu(II), spectrochem. and nephelauxetic parameters 8=43927
$Fe(CO)_5$, semiempirical MO model 8=47594
Ge-I, Mossbauer determ. 8=39520
H, bent O-H---O in crysts. 8=48300
H bonding in alcohols 8=48059
H-bonds, strong, n.m.r. and i.r. study 8=48301
H halides, correl. between mean amplitude quantities and bond covalency 8=34228
H, in pyrrole-dimethyl sulphoxide 8=25644
H, internal, in rel. to NH bands in porphin type compounds 8=34353
H, of phenol to vinyl derivatives thermodynamics 8=43379
H, steric effects in n. m. r. and i. r. spectra 8=25639
H, two-dimens. double-minimum model 8=47602
H-bond, MO calc. for dimeric H_2O 8=38828
H-bonded systems, infrared spectra, review 8=38887
H-bonded systems, theory of i. r. spectra 8=38787
H-bonds in cryst. KH_2PO_4, i.r. absorpt. by H-bonds in cryst. 8=27598
H-bonds, neutron scatt. 8=24963
H-bonds, n.m.r. study, review 8=48219
H_3^+, multicentre bonds 8=29742
He_3^+, binding energy 8=34249
$Hg(CNO)_2$, covalent bonding rel. to stability 8=26006
Hg-X, regularity rel. to structure of mercury-organic crystals, R-Hg-X 8=30616
$H_2SO_4 . H_2O$, H bonding rel. to crystal structure 8=26400
IBr, ICl, I_2Cl_6, from Mössbauer effect in I^{129} 8=35040
$I^{129}CN$, Mossbauer determ. 8=30643
ICN charge-transfer complexes, C-I and C-N polarizabilities 8=48163
KCNO, ionic bonding rel. to stability 8=26006
KH bisphenylacetate, H bonding and crystal structure 8=26514
$La_4Re_6O_{19}$, metal-metal bonding 8=48305
Li_2, binding energies calc. using quantum defect method 8=25489
$LiTaO_3$, ferroelec., Ta bond 8=40987
MgO, effective atomic charges by X-ray method 8=26169
Mn^{3+} in α-Mn_2O_3-type structures, from dislocations exam. 8=39501
MnO, covalency parameters 8=30617
α-MnS, covalency parameters 8=30617
MoO_2, distorted rutile, metal-metal bonding 8=48305
N cpds., charge distribution molecular spectroscopy 8=47604
NaCl, effective atomic charges by X-ray method 8=26169
NaCNO, ionic bonding rel. to stability 8=26006
NH_3 adsorbed on Si, vibrations obs. 8=25508
NH. . . H intramolec. H bonds 8=25609
[N-H] valence reflectivity obs. 8=47622
$Ni(CO)_4$, semiempirical MO model 8=47594
NiO, covalency parameters 8=30617
Ni-Si alloys, from viscosity temp. dependence 8=34796
in PBr_7, bond lengths for Br_3^- ion 8=44247
P–O, intetrahderal cryst. 8=44213
Pt-ammine complexes, nature of co-ordination bonds 8=43330
Pt-SCN in ethylene diamine complexes 8=43329
α-ReO_2, distorted rutile, metal-metal bonding 8=48305
S, inner-electron binding energy 8=29627
Si-I, Mossbauer determ. 8=39520
Si-O, force constants rel. to nature of substituents at Si and O 8=38784
Sm(II), spectrochem. and nephelauxetic parameters 8=43927
TlCNO, ionic bonding rel. to stability 8=26006
TiH_x, ($x < 2$), H orbital expansion effects on d-electron exchange rel. to mag. props. 8=49480
V–O, intetrahedral cryst. 8=44213
W, binding energy on W cryst. 8=30775
W, cohesive energy of surface atoms, field evaporation obs. 8=39503
W, of adsorbed Sr, Ba and alkaline atoms, quantum calc. 8=35199
WO_2, distorted rutile, metal-metal bonding 8=48305
Xe chlorides, Xe^{129} Mossbauer studies 8=30645
Yb(II), spectrochem. and nephelauxetic parameters 8=43927
Zn-Cn-NH_3 complex in aqueous soln, mixed ligands raman study 8=43842
ZnS and similar lattices, chem. rel. to luminescence props. 8=36522
Bone. See Materials.
Books
aeronautical science, progress 8=34614
algebra, modern, lectures 8=23796
atomic collisions 8=38747
computer modelling and simulation 8=28246
cosmic rays and problems of space physics 8=38110
cosmic rays, radiation belts, e. a. s. 8=25023
dictionary of nuclear physics and technology, English-German-French-Russian 8=38291
dictionary of semiconductor physics and electronics, English-German; German-English 8=41609
direct energy conversion, introduction 8=41932
Books—contd
electricity and magnetism, physics of 8=28448
electromagnetic fields 8=28538
electron microscopy and specimen preparation, advances 8=37422
field theory, advanced, introduction 8=33349
field theory and dispersion relations, introduction 8=28951
general physics, mechanics and molecular physics 8=37102
homology and Feynman integrals 8=33338
hydromagnetic stability of a plasma 8=25780
ion bombardment of solids 8=48886
lattice defects and their interactions 8=31022
light, colour and vision 8=42293
liquid metals 8=34753
magnetic props. of materials 8=49459
magnetism and magnetic materials 8=49460
mathematical assistance in physics 8=32686
mathematical models for e. m. field evaluation 8=33054
mathematics for physics students 8=41631
measurement and control of noise 8=37282
Modern Physics: an introductory survey 8=32636
nuclear radiation accidents and effects 8=38586
organic coatings 8=32628
organic semiconductors 8=27140
paleomagnetism 8=45574
particle kinetics of plasmas 8=25721
plasma diagnostic techniques 8=30092
quantum field theory, lectures 8=28952
quantum liquids, Fermi 8=30397
quantum mechanics, advanced 8=33312
quantum optics fundamentals 8=24352
radiation damage in semiconducting devices 8=31399
relativity, principle and application 8=28286
Russian-English scientific dictionary for students and research workers 8=37101
semiconductor physics, devices and circuits 8=49284
spectral analysis and its applications 8=45977
statistical mechanics 8=28324
superconductivity, introduction to the theory 8=26981
thermal props. of prismatic elements 8=35441
thermodynamics 8=37222
transmutations of nuclei 8=33950
vacuum technique, physical principles 8=30323
Ge-Si solid solutions, electronic props. 8=49225
Si, surface props. rel. to device technology 8=49267
Bootstrap theory. See Elementary particles; Field theory; Quantum.
Bordoni effect. See Acoustic wave propagation/ultrasonic; Damping; Internal friction.
Boron
amorphous layers, switching and neg. resistance 8=27079
amorphous, optical transitions 8=45174
atom-ionization, e affinity calc. 8=38661
atoms, Rydberg orbitals calc. 8=29620
in cosmic rays, galactic, p-fragmentation prod. rel. to dating 8=38176
detector, enriched, for thermal n dose rate meas. 8=38081
diffusion in Si, effect on Sn diffusion 8=48791
diffusion in Si, rel. to Si-B phase surface layer control 8=49264
electrical properties 8=35823
electrical properties of different modifications 8=35824
electron momenta from X-ray meas. 8=44647
fibres, internal friction and shear modulus, amplitude dependence · 8=40131
implanted in Si, impurity distrib. determ. 8=27131
ion bombardment of SiO_2, distrib. and range 8=35604
ions implanted in Si, distrib. 8=49266
neutron therapy of noise neoplasms, B^{10} dose effects 8=45926
non-crystalline, atomic radial distrib. function, from X-ray diff. studies 8=26043
optical absorption, 0. 7-25μ and forbidden band-width temp. coeff, –160 to 400°C 8=41065
origin, in solar system, big bang and solar spallation theory 8=36990.
particulate, surface burning in air, gas-phase chem. kinetics 8=36581
polycrystals, etched by H_2SO_4 and photomicrographs 8=39651
powder, ultra-fine, ignition temp. in air, N_2, CO_2, and N_2–CO_2 mixtures 8=32113
redistribution in Si with SiO_x damping 8=48793
β-rhomohedral, growth process conditions 8=26235
β-rhombohedral, reflection coeff. anisotropy 8=41064
spectrochemical determ. in white cast iron, hollow-cathode discharge method 8=36642
zone-melted beta-rhombohedral, with low C content, photoconductivity and photo-induced e.p.r. 8=40908
B^{++} new type of wave function 8=38672
B^8 solar ν flux, reduction by core spin-down 8=45887
$B^{10,11}$ separation by BF_3 distillation, pressure effect 8=25394
B^{11} ion beams, lifetimes and excited states for multiply charged ions 8=43217
B^{11} ion paths in NIKFI-YaZ photoemulsions 8=46984
in Cu-0. 01 wt.% B^{10}, n irrad., dislocation loop spheres surrounding B particles, obs. 8=35564
in U alloys, α-phase grain refinement by B addition, obs. 8=44171

Boron compounds
borate mineral systematology 8=48511
borates with dolomite structure, refinement of oxygen positions 8=48635
boroxine, aromaticity 8=47644
carborane and derivs. gas e diff. study 8=25553
diborane, liq. vapour press., thermal props, surface tension, in significant struct. theory 8=43755
halides, F^{19} chem. shifts 8=43406
i.r. evidence for single H bridges 8=38808
methyldiboranes, characteristic i.r. freqs. 8=34335
1-methylpentaborane, microwave spectrum 8=25600
1-methylpentaborane(9), microwave spectrum and molec. consts. 8=29791
polymeric, C and H microdeterm. 8=36628
proton-bonded, collapse of spin multiplets in n.m.r. 8=34372
tetrafluoroborate salts, ion motion and n.m.r. 8=31905
trihalide complexes with organic bases, variable-temp. n.m.r. 8=38916
trimethylamino borontrichloride, crystal and mol. structure 8=44264
B complex, bis(dimethylamine) boron chloride, crystal structure 8=39771
B complex, bis(dimethylamine)boronium chloride, crystal structure 8=26368
B-C, mag. props. and resonances 8=31520
B-C, paramag. centre comp. dependence 8=45077
BBr, radiative lifetimes 8=38807
BBr_3, electron-beam excited, u.v. emission 8=38807
BBr_3, ionization potential 8=34450
B_4C, ht. of formation 8=49856
BCl, absolute u.v. transition probabilities 8=34230
BCl_3, ionization potential 8=34450
BCl_3 saturating filter, for CO_2-N_2-He laser Q-switching 8=46588
B_2Cl_4, internal rotation from gas e-diffr. temp. dependence meas. 8=25446
BF, absolute u.v. transition probabilities 8=34230
BF, molecule, mag. props. calc. 8=25447
BF_3, anal. of ν_2 and molec. geometry 8=29715
BF_3-dimethyl selenide and sulphide complexes, i.r. spectra 8=38806
BF_3, distillation for $B^{10,11}$ separation, pressure effect 8=25394
BF_3, F exchange with tetrabutylammonium hexafluorophosphate in CH_2Cl_2 soln., n.m.r. obs. 8=25960
BF_3, ionization potential 8=34450
BF_3 n monitor, portable, for pulsed fields, 1–3000 mrem/hr 8=33815
BF_3, proportional counters, wall effect 8=24508
BF_3 short counter with spherical moderator for neutrons in γ background 8=33792
BF_3, $2\nu_3$ bands, ζ_{33} determ. 8=34233
$BF_3S(CH_3)_2$ Raman and i.r. spectra 8=25541
BH, molecule, mag. props. calc. 8=25447
BH_3 complexes with organic bases, variable-temp. n.m.r. 8=38916
BH_4^-, i.r. spectra in alkali halide crysts. 8=36327
B_2H_6, electronic density distrib. 8=43285
BN, band struct. calc. 8=49098-9
BN, dense modifications by high pressures and shear stresses 8=48374
BN, F-centres, e.p.r. spectra confirmation 8=35584
BN film, prep. and props. 8=48445
BN, hexagonal and cubic X-ray spectra investigation 8=41063
BN, hexagonal, irreversible transformation by shock compression 8=26062
BN particle appl. in Ar plasma jet vel. distrib. meas. 8=30181
BN, pyrolytic, structural anisotropy correl. with normal spectral emissivity 8=36332
BO, dissociation energy, mass spectrometric determ. 8=29825
BO_4 group complexes, i.r. spectra rel. to asymmetric stretching vibrations 8=29714
B_2O_3, cryst. struct. 8=48634
B_2O_3 crystallites, crystal structure 8=44206
B_2O_3 high-pressure form, crystal structure 8=39772
B_2O_3, molec. struct. 8=38809
B_2O_3, mol., valency electron X-ray emission bands of B 8=29716
B_2O_3, viscous relaxation and non-Arrhenious behaviour 8=34802
B_2O_3-PbO-Al_2O glass, spinodal decomposition from X-ray diffr. studies 8=26061
BP, energy band structure from ultrasoft X-ray spectroscopy 8=41062
B_6P, crysts. growth from soln., theory 8=35232
BS, blue-green spectrum 8=25448
Borrmann effect. See X-ray diffraction.
Bose gas. See Bosons.
Bosons
See also Elementary particles; Quantum theory/many-particle systems.
avalanche, superradiation 8=23895
background for dilute fermion system 8=28334
baryon-antibaryon model, mass formulae 8=33548

Bosons—contd
Bethe-Salpeter eqn. with Feynman propagations, cancellation of spurious corrections 8=33561
Bose condensation of electric modes, strongly excited longit. 8=23893
Bose-Einstein gas, hard-core models 8=28344
Bose-Einstein system, nonideal, corrections to modified formulation of problem 8=37206
Bose-Einstein systems, weakly nonideal, temp. Green's functions 8=37205
boson-fermion reactions, kinematic singularities and Macdowell symm. 8=29047
boson-lepton pair couplings and μ anomalous magnetic moment 8=29102
composite, condition that renormalization constant is zero 8=37833
decay into vector boson and pseudoscalar meson, for parity conservation 8=37863
field identified with current operators, for e.m. corrections for hadrons, leptons 8=29106
fields with nonlinear selfinteraction in two dimensions 8=24482
gas, Bose-Einstein condensation 8=37211
gas, condensation, resolution of paradoxes 8=32845
gas, ideal, Bose-Einstein condensation 8=32846
$I = {}^1/_2, 1$ assignment to O(4, 2) group, mass spectrum obtained 8=24768
impact parametrization and daughter trajectories 8=37908
integral representation of Bose functions 8=28333
intermediate, strong-interaction possibility 8=24643
intermediate vector, model for $K_1^\circ \sim K_2^\circ$ mass difference calc. 8=24824
intermediate W, e.m. interaction 8=47024
ladder series convergence and Bethe-Salpeter equation 8=37884
Lee-Yang theory of charged spin-one, radiative correction to photon propagator 8=37836
liquid, elementary excitations rel. to He II 8=28331
mass calc. in higher new Tamm-Dancoff approx. 8=29036
mass spectrum formula 8=29114
N/D eqns., singular, with vector boson exchange inelasticity, soln. 8=24673
neutral vector, of mass O(30 GeV), evidence for existence 8=42361
octets, coupling constants, sum rules 8=24624
photons and gravitons, low-energy scatt. theorems 8=29080
pion decay in baryon-antibaryon model 8=24754
resonances of any spin in $\gamma\pi$-$\pi\pi$ and $\gamma\pi$-π 8=47119
resonances prod., in quark model 8=37951
resonances, with sequential decay modes, determ. of spin and parity 8=33715
R, S, T, U mesons classification, adopting spin-orbit and spin-spin forces 8=42593
scattering, three-body problem, partial wave function method 8=29060
self-conjugate, field operators and commutation relations 8=37913
spin and parity determ. applying symm. props. to its decay 8=38021
spin one and Bargmann-Wigner eqns. 8=37946
$SU_3 \otimes SU_3$ symmetry rel. to existence of 27-plet 8=33533
superfluid system, eqn. of motion of condensate wave function, excitation spectrum gap 8=37212
system, Bijl-Feynman formula for elementary excitation, H variance 8=41776
system, critical current of foreign particles, calc. 8=37208
system, degenerate fluids, cluster expansion at finite temp. 8=37209
system, density-density correlation and one-particle Green's function connection, 0°K 8=46098
system, effect of low-conc. outside particles, kinetic eqns. 8=37207
system, equilib. props. at low temp., rel. to Bose-Einstein transition and restricted geometry 8=41777
system, ideal, condensation in finite geometry 8=46117
system, modifed pairing treatment, hyperspin formulation 8=37210
system, ordering of 2 and n identical particles, dynamical theory of Pauli princ. 8=33519
system, single-particle condensate and pair theory 8=32847
system, 2-dimensional, superfluidity 8=46116
systems, Bogoliubov approx., asymptotic exactness 8=23894
systems, Bogoliubov approximation 8=28332
system Fermi-Bose, mixed, dispersion relation for eigenfrequencies of low-lying states 8=23891
systems, two dimensional, low temp. transition 8=23892
27-plet in unitary-symmetry model, SU_3 and SU_6 8=29033
vector, intermediate, and charged, consequences for stellar evolution 8=29161
vector, Pauli approximation 8=24640
vector, resonances rel. to N e.m. form factors 8=29165
W-boson prod. in e beam collisions 8=24720
W-bosons, Yang-Mills, and CP violation 8=24845
W electroproduction 8=24648
W has pair strong interactions consistent with CP nonconservation 8=37837

Bosons—contd
W, scatt., Bjarken's asymptotic formula validity in perturbation theory 8=29050
W theory for interaction of hadrons with neutral lepton currents 8=29110
Boundary layer flow. See Flow.
Bragg reflection. See X-ray crystallography.
Brass. See Copper alloys.
Bravais lattice. See Crystal structure, atomic.
Breakdown, electric
See also Discharges, electric; Electric strength.
dielectric, response to applied d.c. voltages 8=40549
insulator test, allowance for nonsustained breakdown 8=37368
insulators, partial discharge resistance testing 8=24060
oil-paper insulation, space-charge effects 8=40559
partial discharge by insulating surfaces, mechanism 8=24061
partial discharge, power dissipation calorimetry 8=24059
polymethyl methacrylate, dielectric, laser-induced 8=40566
semiconductor detector, protection by leakage current monitor and voltage divider 8=37775
spark-discharge counters, distinguishing readout for 8=46863
transformer insulation, diagnosis by envolved-gas analysis 8=22617
in vacuum, between Cu electrodes, plane-parallel electrode temp. effects. 8=38996
vacuum gap between electrodes, capture and identification of particles 8=25699
vacuum-gap, Cu anode erosion obs. 8=34424
vacuum gap, effect of cooling Nb electrodes to 4.2°K 8=29909
vacuum-gap, Mo cathode erosion obs. 8=34424
vacuum, Mo electrodes, effect of conditioning processes 8=34426
vacuum, prebreakdown currents 8=25698
vacuum, steadying of breakdown voltage with repetition 8=38998
Ge p-n junction, in microwave elec. field, exptl. investigation 8=27158
n-Ge, uniaxial stress rel. to critical field 8=27104
He, liq., voltage dispersion, external ionization source effects 8=41890
KBr, dielectric, laser-induced 8=40566
KCl, dielectric, laser-induced 8=40566
KI, dielectric, laser-induced 8=40566
Mo electrodes in vacuum, effect of conditioning processes 8=34426
NaCl, dielectric, laser-induced 8=40566
Ni electrodes in vacuo 8=47763
gases
air, between spherical electrodes, calc. 8=34423
air, compressed, negative-impulse breakdown 8=47764
air, laser-induced in mag. field, threshold reduction, 210 kG 8=29925
air, long gaps, humidity effect obs. 8=29902
air microwave at 9 GHz 8=47768
air, nonuniform gaps, influence of water vapour on impulse flashover 8=34428
air, spark form. relationships 8=34427
air, threshold rel. to wavelength of laser radiation 8=34425
capacitive discharge, h.f., conditions for fast electrons at low pressures 8=29907
electron avalanche, space-time evolution at mean or high pressures 8=38999
high-freq., nonuniform gases; in spatially varying fields 8=29908
laser-induced, subnanosecond Schlieren photography 8=29901
under laser irradiation, light emission obs. 8=29906
molecular, obs. rel. to laser appl. 8=29904
optical, one to intense laser pulse, theory of mechanism 8=29952
plasma and electrode at negative potential 8=47762
rare gases, hot alkali-metal-seeded, voltage 8=47759
streamers, field criterion for sustained propagation 8=43460
streamers in positive point-to-plane gap, propagation sequences 8=29913
striation phenomena in prebreakdown 8=38997
thermionic diodes, Xe-filled, irradiated in nuclear reactor core 8=46417
vacuum, current between Cu electrodes in presence of microdischarges, pre-breakdown 8=43459
Ar: freon-12, laser-induced, threshold behaviour 8=39000
Ar, microwave at 9 GHz 8=47768
Ar, rel. to laser application 8=29910
CF$_4$, growth of ionization currents 8=29983
C$_2$F$_6$, growth of ionization currents 8=29983
Cs vapour under laser irradiation, light emission obs. 8=29906
H$_2$, cylindrical positive corona discharges 8=47765
H$_2$, formative time in strong crossed fields 8=29903
He, by laser beam, threshold parameter meas. 8=47761
He free-electron gas, negative point-to-plane 8=39001
He, microwave at 9 GHz 8=47768
He, rel. to laser application 8=29910

Breakdown, electric—contd
gases—contd
Hg, at low pressure, current limitation and gas clean-up 8=47767
Hg vapour, by laser beam, threshold values 8=47766
Hg vapour, mechanisms 8=43484
N$_2$, under high pressure, a.c. induced, statistical time lags effect 8=47760
Ne, ionization growth times analysis 8=29912
Ne, microwave at 9 GHz 8=47768
liquids
dielectric, effect of liq. motion 8=39393
n-hexane, high density plasma production 8=39383
oil film, a.c. voltage 8=48178
oil, insulating, formation of partial discharges on points 8=30504
oil-solid systems, polarization mechanism 8=34891
water, computer calc. of process 8=30522
water-solid systems, polarization mechanism 8=34891
He, by laser beam threshold parameter meas. 8=47761
He, destruction of electrodes 8=46303
solids
dielectric surface, sliding discharge in vacuum 8=27224
glass subject to ionizing radiations, optimal thickness calc. 8=31417
ionizing radiations, optimal thickness calc. 8=31417
p-n junctions, localization, effects of transverse and longit. mag. fields 8=27153
polymer films, dielectric 8=40564
polystyrene subject to ionizing radiations, optimal thickness calc. 8=31417
polythene, laminated, voids obs. 8=40591
porcelain subject to ionizing radiations, optimal thickness calc. 8=31417
quartz subject to ionizing radiations, optimal thickness calc. 8=31417
rocksalt, films, anode surface and material effects on strength 8=40578
semiconductors, impact ionization of impurity atoms, in strong elec. fields 8=35864
time-to-breakdown curves for insulators under action of partial discharge statistical determ. 8=44861
transparent dielectric mats., charged-particle emission on ruby laser irradiation without physical damage 8=40703
Ar, conduction 8=35951
n-GaAs, epitaxial, impact ionization breakdown at liq. He temps. 8=27098
Ge, extra-pure, at 10°K 8=35894
InSb, transverse, Hall voltage caused by instability 8=40468
KBr, e avalanche, obs. 8=31421
NaCl, directional, due to e bombard. 8=48925
Si p-n junction, development 8=40518
Si p-n$^+$ junction, surface breakdown 8=35923
Si p-n junctions, effective carrier ionization coeff. at breakdown 8=27163
Si p-n junctions, effects on voltage of multiply-charged Au impurity 8=27161
Si, p-n junctions, temp. coeff. of breakdown voltage 8=27162
SiO film, pulse breakdown obs. 8=40586
Breaking strength. See Mechanical strength.
Breeders. See Nuclear reactors, fission.
Bremsstrahlung
See also Electrons/radiation: Gamma-ray spectra; Gamma-rays; X-ray spectra/emission; X-rays.
coincidence spectrum, solid structure effects 8=41037
cosmic ray cross-section calc. 8=29387
cross-section calcs. using p-p interact., e.m. pot. and strictly nuclear pot. 8=24899
crystal, thin, high-energy calc. and meas. methods 8=42460
electron-electron scatt. at 2 × 160 MeV, obs. 8=47085
electron synchrotron radiation in accelerator with megagauss fields 8=46987
emission from e.a.s., atm. elec. field source 8=38205
generation of short pulses in 140 MeV Braunschweig sunchrotron 8=47072
internal, following K-electron capture, probability calc. 8=29354
measurement by coincidence expts. 8=37929
e, Mork-Olsen radiative correction and pair, prod. cross-sections obs. 8=24706
muon, cross-section rel. to nuclear and at. form factors 8=38256
in N-N interacts, calc. rel. to off-energy-shell props. of a potential 8=24871
N-N, soft-photon theory 8=42625
n-p at 208 MeV, obs. 8=24953
p-d scatt. at 197 MeV 8=29182
plasma, slightly ionized, calc. 8=30069
polarized, production 8=47081
p-p collisions, bremsstrahlungs model taking phase space into account 8=24758
p-p, coplanar and non-coplanar, potential model calc. 8=24907
in p-p interacts, at energies between 1 and 10 MeV, prod. rel. to $^1S_0$ state 8=24908
in p-p interacts, matrix element calc. from initial and final scatt. wave functions 8=24900
p-p obs. at 52.3 MeV 8=42633

Bremsstrahlung—contd
- p-p at 10.5 MeV, obs. 8=24906
- p-p at 20 MeV, 35°, obs. 8=24903
- p-p at 20 MeV, 35°, theory 8=24904
- p-p scatt., scross section in terms of quasi phases of off shell matrix 8=24930
- $p + p \rightarrow p + p + \gamma, E_p = 61.7$ MeV, obs. 8=24905
- production in p-p interacts at 61.8 MeV 8=24898
- prod. radiative corrections 8=29075
- thick-target spectra, absolute, meas. 8=33621
- wide angle, virtual proton Compton effect 8=42458
- Al, 500 MeV e scatt. followed by pair, triplet prod. 8=29411
- Al nucleus interaction, secondary photon energy spectra 8=29400
- in Al thick targets, production on 0.5-2.8 MeV e.-irradiation 8=40071
- Be, 500 MeV e scatt. followed by pair, triplet prod. 8=29411
- Be nucleus interaction, secondary photon energy spectra 8=29400
- C nucleus interaction, secondary photon energy spectra 8=29400
- Cr^{51}, β-decay 8=29362
- Cu nucleus interaction, secondary photon energy spectra 8=29400
- in Fe thick targets, production on 0.5-2.8 MeV e.-irradiation 8=40071
- in K halides, energy losses rel. to beam collimation and crystal thickness 8=31310
- Ne discharge, positive column 8=29898
- Pt, 500 MeV e scatt. followed by pair, triplet prod. 8=29411
- Sb^{119}, polarized, parity nonconservation by inner bremsstrahlung, obs. 8=33962

Brightness
- See also Illumination.
- focon reflecting system 8=42124
- galaxies in rich clusters, luminosity distrib. model 8=45746
- laser beam, increase with aspherical lens 8=28728

Brillouin scattering. See Scattering/light

Brillouin zones. See Crystal electron states.

Brittleness
- See also Breaking strength.
- dunite and gabbro, transition to ductile 8=48976
- ferritic steel, at bonded part of welded joint with austenitic strainless steel electrodes 8=31210
- h.c.p. polycrystals, ductile-brittle behaviour theory 8=26757
- limestone, transition to ductile 8=48976
- porous brittle material, biaxial fracture criterion 8=48974
- quasi-brittle fracture conditions 8=44530
- rapid bend testing, high-temp. apparatus 8=44532
- sheet materials for reactors tendency to fracture 8=29558
- solids, controlled fracture, rel. to interruption of elec. current 8=35632
- steel, austenitic stainless, He embrittlement, 540-760°C 8=31213
- steel, neutron irradiated, depend. on uncombined N conc. 8=47405
- steel, reversible temper brittleness development rel. to C content changes in grain-boundary regions 8=35683
- steel, stainless as reactor material, due to He prod. in (n, α) reaction 8=47406
- Al, ductile-brittle transition in presence of Hg−3% Zn or Sn−10% Zn liq. 8=35656
- Al, ductile-brittle transition temp., in liq. metals, strain-rate depend. 8=35657
- Al_3Mg_2, temp. threshold, alloying additions effects 8=35671
- Be, h.c.p. polycrystals, ductile-brittle behaviour theory 8=26757
- Cr, brittle-ductile transition temp., effects of N conc. and Cv_2N precipitates 8=44561
- Cu_xSi, (x = 3, 5), temp. threshold, alloying additions effects 8=35671
- Fe-27% Cr, annealed, rel. to Guinier-Preston zones form., 475°C 8=35273
- Ge, brittle deformation mode, anomalous X-ray transmission exam. 8=26648
- Ir crystals, fracture, scanning e-microscope obs. 8=26825
- W, sintered, fracture nucleation at low temp. 8=44608

Bromine
- active to passive gravitational mass ratio, comp. with F 8=41743
- adsorption on oxides, refl. spectra 8=48479
- determination in brines, X-ray fluorescence obs. 8=27815
- gas, ads. on Na halides, refl. spectroscopy 8=48480
- ions, Br^- collisions with He, Ne, Ar and Kr atoms, detached electrons energy obs. 8=29972
- photochemistry, using ruby laser 8=41287
- Br^{79} ion beams in mylar, stopping powers 8=44508
- Br_2, vibr-relax. in Ar 8=47726
- Ni surface morphology, effects of reaction 8=30726

Bromine compounds
- thermal degradation of polyolefins at 400°C 8=36583
- BrCl, visible absorption spectrum 8=29718

Bromine compounds—contd
- $BrO_{1,2}$, γ-absorpt. from oxybromine cpd. radiolysis 8=27768

Brownian movement
- acetonitrile, rotatory motion, rel. to dipole-dipole intermol. forces in vibr. 8=43827
- benzonitrile, rotary motion rel. to dipole-dipole intermol. forces in vibr. 8=43827
- branching process of restricted Brownian particles, averaging process asymptotic behaviour 8=46097
- crystallites on cleavage planes 8=44022
- in flow, anal. 8=47922
- fluctuation-dissipation theorem, connection with many body theories 8=28313
- fluid moving with temp. gradient, theory 8=46096
- functional integrals appl. to theory 8=37182
- irregular objects, Stokes resistance calc. for imperfect sphere 8=32827
- rotating particles, kinetic theory using Fokker-Planck equation 8=32828
- systems with frozen rot. motion, nonradiative energy transfer 8=34883
- useful energy theorem appl. 8=28314
- Au crystallites on KCl cleavage planes 8=44022

Brush discharges. See Corona, electric discharge.

Bubble chambers
- Algol procedure for bubble chamber photographs 8=46957
- Argonne and Brookhaven, stabilized superconducting strip 8=42349
- data evaluation 8=24539
- K^- interaction with propane, freon, Σ°, π° prod. obs. 8=25254
- liquid hydrogen, 55 × 35 × 30 cm volume 8=46959
- momentum and angle of tracks, nonuniform magnetic field 8=33388
- particle separation at high energies, electrostatic 8=28999
- photograph analysis, flying image digitizer 8=46960
- pulse magnet, 60 kOe 8=46958
- Scotchlite sheeting reflectivity in liq. H_2, obs. 8=36312
- stereocameras, adjustment 8=46767
- stereocameras, requirements of optical heads 8=46955
- superconducting magnet for ANL 12-ft. hydrogen bubble chamber 8=37802
- telecentric camera lens for photography 8=46956
- H_2 liquid, particle movement, algorithm applic. to computer programme 8=46961

Bubbles
- See also Foams.
- acoustic cavitation refraction wave onset and development 8=43730
- air, bursting, time exposure obs. 8=25856
- cavitation rectified diffusion, frequency depend of threshold 8=34735
- electron, in liq. He, vibration freq. estimate 8=37346
- formation in constant gas flow, non-viscous liq. 8=34737
- gas, in liquids, formation under influence of elec. fields 8=25855
- gas in solids, stress induction, obs. 8=31108
- gas, passing through liq. interfaces, mass transfer expts. 8=43743
- gas, unmovable spherical bulb growth in spherical liq. volume, Rayleigh eqn. 8=30382
- generation and increase in liquids after pressure decrease 8=48046
- growth in binary systems adhering to solid surfaces 8=34995
- growth rate in transient boiling 8=48049
- hemispherical asymptotic growth rate on surface in non-linear conc. fields 8=34734
- mass transfer to bubbles at high Reynolds no. 8=30387
- "microtome" for sampling liq. surface 8=30380
- moving in liqs. with pressure gradient, dynamics 8=39285
- in nitrogen liquid, motion study 8=34739
- in nucleate boiling, departure radius 8=25997
- in nucleate surface boiling in pure liqs. and binary mixtures 8=25998
- organic liquid, growth rel. to Jakob number 8=34996
- packed columns, with liq. moving downwards, performance when fitted with Raschig rings 8=25858
- size in gas fluidized beds with photocell 8=48230
- spherical, behaviour near solid wall 8=34743
- surface tension determ. from profile dimens. 8=39337
- tetrachloroethylene, cavitation bubble dynamics 8=25850
- toroidal, gas in water, motion 8=30383
- trajectories and equilibrium levels in liquid columns 8=34742
- tribonucleation 8=48044
- in water, cavitation, u.s. induced models and damaging mechanism 8=43733
- water growth rel. to Jakob number 8=34996
- in Ag, during solidification 8=30587
- Ar, liquid, due to zero-point motion of positronium atoms 8=30388
- H_2, liquid, due to zero-point motion of positronium atoms 8=30388
- He, liquid, due to zero-point motion of positronium atoms 8=30388
- in N, liq., growth and collapse, rel. to superheating, and decreasing press 8=34738

Bubbles—contd
Ne, liquid, due to zero-point motion of positronium atoms 8=30388
Burgers vector. See Crystal imperfections/dislocations.

CPT (charge, parity, time) conservation. See Field theory, quantum ⁄ interactions; Parity.
Cadmium
anodic behaviour in alkali 8=32132
atom, excitation of single levels, direct and stepwise, effective cross-sections 8=34157
atom, 3261Å line collision broadening by Ar gas, pressure and temp. dependence 8=38750
atomic, photoionization cross section meas. 8=29949
atomic spectrum obs. in discharge tube with high voltage pulses 8=29630
atoms ionization by e impact, direct and stepwise cross-sections 8=29961
atoms, 6^3S_1 level lifetime and depolarisation cross section for N_2 and inert gas collisions, obs. 8=38692
colour centres induced in NaCl by doping and X-rays 8=31113
compressive internal stress during electrodeposition, role of hydrogen 8=31167
crystal face, cylindrical, pitting and hopper growth obs. 8=26195
crystal growth surface, LEED exam. 8=26196
crystallization, grain size, vibr. effects, obs. 8=35269
diffusion in Al, due to near surface effect 8=39964
diffusion in n-GaSb(Te) rel. to p-n junction formation 8=31005
electrodeposition from non-aqueous solns., review and prelim. studies 8=45393
electron reflection, 600 to 1200 keV 8=44197
field peak excitation under cyclotron reson. in mag. field normal to surface 8=44668
5 $^3P_1$ level, double resonance excited by modulated light 8=38685
h. c. p., anisotropic, stress fields around edge multipole and multipole arrays 8=26795
ions CD^{++}, polarographic investigation in $LiNO_3$-$NaNO_3$-KNO_3 melt 8=45414
ions, electrochem. in fused $AlCl_3$-NaCl-KCl 8=49917
isotope, optical resonance, polarization of radiation (2288 Å) emitted 8=25359
Knight shift, temp. depend. 8=41002
oscillatory size-dependent magnetoresistance, appl. to mag. field meas. 8=28517
preferred orientation during recrystallization 8=35213
seeding in Cs plasma diode, rel. to performance 8=28475
single crystal, nature of oxide layers on surface 8=35167
single crystals, optical const. from reflectance ratios 8=45164
stopping power for 3.75–5.5 MeV próton, using (p, n) obs. 8=43030
sputtering by 1- to 5-keV Ar^+, rel. to orientation dependence 8=40076
vapour photoionization curves up to 19 eV 8=39031
Cd, halide complex with azines, prep. and infra-red study 8=36432
Cd halide complex with azines, prep. 8=36432
Cd^+ in rare gas matrix at 4°K, e.s.r. 8=40202
Cd I, Hartree-Fock solns. for excited odd configurations 8=43186
CdI series, intercombinational transition probabilities 8=38711
Cd(II) electrode in $NaNO_3$-KNO_3 eutectic, linear sweep voltammetry 8=27750
Cd^{111} in Ni, hyperfine fields at solute 8=40992
$Cd^{111,114}$ polarization of light emitted by optical resonance of 2288Å radiation 8=34158
Cd-Ar(Ne) low pressure, discharges, 2288Å and 3261Å radiation intensities 8=38990
Cd-Xe atom collision cross section calc. 8=34180
Sn^{119m} isomer shift 8=26015
Cadmium compounds
bisthiourea $Cd(NO_3)_2$ atomic crystal structure 8=35324
chalcogenide films, mono- and multilayer, epitaxially grown, structure and photoelec. props. 8=26115
chalcogenides, hexagonal or cubic phases formation rel. to stoichiometry effects 8=44082
electron-beam excited, photocurrent, luminescence and absorption saturation 8=31973
electron microscopy of surface changes rel. to photoconductivity on ht. treatment, 100–600°C 8=35268
CaF_2:U^{4+}, u.s. paramag. resonance rel. to multiple phonon interactions 8=31853
Cd arsenide, thermomagnetic effects, 65-300°K 8=40731
Cd complex, diethyldithiocarbamate crystal and mol. structure 8=26376
Cd complex, diquinolium-tetrachloro-cadmate, crystal structure 8=26374
Cd complex, L-α-glycerophosphorylcholine cadmium chloride trihydrate structure 8=35325
Cd diethyldithiocarbamate, crystal and mol. structure 8=26375
Cd-Ag-Cu-Zn system, univarient equilibria formation by decomposition 8=30675

Cadmium compounds—contd
Cd_3As_2, crystal structure 8=44212
Cd_3As_2, evaporated Hall elements, props. 8=27088
Cd_3As_2 films, high mobility, prep-by evap. method 8=48447
Cd_3As_2 high-press. polymorph., crystal struct. and metallic props. 8=26066
$Cd_xCa_{1-x}O$, elec. and optical props. 8=49137
Cd-$CdCl_2$ liq. system, vol. change on mixing 8=30414
$Cd(CH_3)_2$, indirect nucl. spin coupling consts. 8=43408
$CdCl_2$-alkali chloride liquid systems, surface tension 8=30439
$CdCl_2$. $2HCONH_2$, crystal structure 8=26377
$CdCl_2$: Ni^{2+} e.s.r. spectra at 9 and 35 GHz 8=27468
$CdCr_2S_4$, n.m.r. of Cr^{53} at 4.2°K 8=31896
$CdCr_2Se_4$, distant-neighbour interaction analysis 8=31596
$CdCr_2Se_4$, ferromagnetic, i.r. absorption spectrum and Faraday rotation 8=41078
$CdCr_2Se_4$, growth and properties 8=48541
$CdCr_2Se_4$, magnetization and n.m.r. 8=31895
$CdCr_2Se_4$, n.m.r. of Cr^{53} and $Se.^{77}$ at 4.2°K 8=31896
$CdCr_2Se_4$, spin-wave relax., 4.3°K to near T_c (≈130°K) 8=31812
CdF_2, carrier mobility and photoelectric props. 8=36011
CdF_2:iron group ions, e.p.r. spectra 8=31857
CdF_2, polaron effects and transitions 8=44765
CdF_2 : Co^{2+}(Ni^{2+}), absorpt. spectra temp. dependences 8=41076
CdF_2: Eu, transformation of Eu^{3+} to Eu^{2+}, e.s.r. 8=27473
CdF_2 : Gd^{3+}, trigonal spectra obs. from E.P.R. 8=49609
CdF_2:Ni^{2+}, vis. and near i. r. absorpt. spectra, at room temp. and 4.2°K 8=31967
CdF_2:Sm, Nd, relax. flow teeth obs. 8=26794
$CdGeAs_2$, amorphous and polycryst., reflectivity in 0.6-5.5eV region 8=49712
$CdGeP_2$, amorphous structure exam. 8=26144
$CdGeP_2$ crystal structure refinement and ordering in amorphous state 8=26373
$CdGeP_2$, recombination radiation, electric props. 8=49791
$Cd_{0.23}Hg_{0.77}Te$ alloy, quantum yield of internal photoelectric effect 8=35879
$Cd_x Hg_{1-x}$ Te : Mn^{2+}, e.p.r. 8=40934
$Cd_{0.11}Hg_{0.89}Te$, semi-metal → semiconductor transition induced by hydrostatic press. 8=27086
CdI_2, growth spirals on (0001) face 8=44124
CdI_2 polytypism, dislocation theory 8=26180
CdI_2, polytypoism as high-order transformation 8=44012
CdI_2 polytypism, dislocation theory 8=26180
CdI_2 rhombohedral polytype 12R 8=39644
Cd-In alloyed luminescent diodes, spectra at 78 and 300°K, I-V characts. at 300°K 8=36538
Cd-Mn alloy, mag. ordering 8=31760
Cd-Pb system, electrotransfer inversion, and scatt. of impurity atoms 8=40315
$CdMoO_4$, Czochralski growth 8=30824
CdO, crystal growth by sublimation 8=26244
CdO, lattice distortion rel. to particle size by X-ray reflex broadening 8=48591
CdO, powdered, phosphorescent excitation spectra recording 8=36484
CdO, struct. exam. 8=48592
CdO, APW method for energy band structure 8=49101
CdO: Ga_2O_3, mixtures, order-disorder 8=39549
CdO-TiO_2-SiO_2 systems, glass formation 8=44079
CdSb crystal growth from melt rel. to segregation of Se, S, Tl and Fe 8=26242
CdSb, p- and n-type, electroconductivity, anisotropy, 5-500°K 8=35881
p-CdSb, negative magnetoresistance, rel. to impurity band conduction 8=35880
CdSb, thermopower anisotropy in intrinsic conduction region 8=40639
CdSb, Ag doped resistivity and Hall-effect at low-temp. 8=44773
CdSb : (Mn, Fe, Ni and La), mag. susceptibility, temp. depend. 8=49464
$Cd[S_2CN(C_2H_5)_2]_2$ crystal and mol. struct. 8=35323
CdSe, acoustic noise and current saturation 8=30942
CdSe, acoustoelectric field, alternating, dependence on sound intensity and conductivity 8=35412
CdSe, anticrossing of dispersion curves due to spatial dispersion 8=36346
CdSe, coherent emission of free excitons 8=31972
CdSe, coherent radiation of free excitons 8=36343
CdSe crystal, 0.93μ luminescence rel. to photoconductivity 8=36482
CdSe crystals, photocurrent instability after ion bombardment obs. 8=49415
CdSe, defect structure from X-ray topography 8=39994
CdSe, elec. domain formation due to Joule heating 8=44767
CdSe evaporated films, photoelectronic props. 8=44922
CdSe film, as base for photocells with p-n heterotransition 8=40647
CdSe film utilization for transistors if vapour deposited 8=31414
CdSe films, nonlinear optical absorption 8=36340
CdSe films, photocurrent saturation 8=44923
CdSe films, photosensitive, field effect effective mobility freq. and temp. dependence 8=36016

Cadmium compounds—contd
CdSe films, resistance 8=44772
CdSe, growth by temp. gradient solution zoning 8=48540
CdSe, i.r. luminescence ($\lambda_m = 1.2\mu$) mechanism rel. to photoconductivity 8=45266
CdSe laser resonator, pumped by Ga(AsP) junction, photon output energy rel. to bandgap 8=33215
CdSe, optical props., effect of uniaxial stress 8=36342
CdSe, optically quenched, electronic fluctuation spectra 8=40659
CdSe, photoconductivity, influence of doped surface on spectral dependence 8=49417
CdSe, photocond., sonde characts 8=49412
n-CdSe, prepared under N pressure, elec. props. 8=49230
CdSe semiconductor lasers, two-photon absorpt. anisotropy in the optical excitation 8=36341
CdSe, shallow donor ground states 8=31278
CdSe, stress induced splitting of exciton lines 8=26920
CdSe thin films transistor, instability and stabilization techniques 8=44848
CdSe, transient analysis of piezoelectric oscills. 8=27295
CdSe, wurtzite, photoemission study of electronic structure 8=31287
CdSe, X-ray illumination effect on current characts. 8=40656
CdSe:Cu, fundamental absorpt. edge impurity conc. dependence 8=36349
CdSe:Cu, i. r. absorpt. spectrum, rel. to Cu impurity conc. 8=36345
CdSe-Sb_2S_3 targets in vidicon-type tube, characts. 8=46419
CdSe-SiO_2 thin film transistors, effects of instability on l. f. characts. 8=27198
$CdSe_x(CdTe)_{1-x}$ alloys, forbidden band width comp. dependence 8=36344
Cd(SeS), semiconductor thin-platelets, optically pumped, laser emission 8=46613
CdSe(Te), X-ray photoconductivity, electron-hole generation energy 8=49418
n-$CdSnAs_2$, elec. props. rel. to temp. and impurity concs. 8=31370
$CdSO_4$ single crystal layers 8=44041
$CdSO_4.H_2O$, crystallographic study 8=44211
CdS_xSe_{1-x} crystals, electron effective mass 8=35768
CdS_xSe_{1-x} monocrystal, component conc. calc. by dispersion 8=30803
$Cd_xSr_{1-x}O$, elec. and optical props. 8=49137
CdTe, band structure, including spin-orbit effects 8=44825
CdTe, by screened single-particle e excitations, obs. 8=36363
CdTe diodes, electroluminesc., temp. depend. 8=49790
CdTe, electric instability 8=40445
CdTe, energy bands, spin-orbit splittings 8=44826
CdTe films, photovoltaic effect, gas adsorption effects 8=44924
CdTe films, preparation by ion bombardment method 8=30750
CdTe, growth process rel. to stoichiometry 8=26243
CdTe, luminescence emission at 77°K 8=49795
p-CdTe, photomagnetoelectric effect obs. rel. to orientation 8=44915
CdTe p-n counters for γ-ray spectrometry 8=33618
CdTe, p-n junction, electroluminesc. 8=36521
CdTe, polaron effect enhancement in magnetophonon resist. oscillations 8=44661
CdTe, polaron mass change, magnetic field effect 8=31302
CdTe, pure and In doped, i. r. reflection 20 to 200μ and Reststrahlen band 8=31974
CdTe, recombination radiation, evidence for super-radiance 8=31971
CdTe, semi-insulating, transient currents charact. of deep traps 8=40441
CdTe, stoichiometric variations and impurity levels 8=30804
CdTe surface barrier detectors for γ-ray spectroscopy 8=47069
CdTe surface barrier detectors, high energy resolution for γ-rays 8=46900
CdTe surface barrier detectors, transient response, trapping and detrapping model 8=46901
n-CdTe, thermal n irrad., Cd vacancies, Hall and cond. obs. 8=35533
n-CdTe, type conversion and p-n junctions produced by As^+ implantation 8=35882
CdTe:Fe, selective abs. changes under influence of high elec. fields 8=36339
CdTe-ZnTe alloys, p-n junction, electroluminesc. 8=36521
$CdTiO_3$, perovskite modification, phase and dielec. transitions, 20-1000°C 8=27242
$Cd_2V_2O_7:Mn^{2+}$, e.p.r. obs. 8=31856
$CdWO_4:Cr^{3+}$, e.p.r. rel. to elec. field effects 8=45084
$CdWO_4:Gd^{3+}$, e.p.r. at 24GHz 8=45083
$CdWO_4:Mn^{2+}$ and Fe^{3+}, e.p.r. lines splitting by elec. field, 320 kv/cm 8=40929
Cd-Zn, electrotransport mechanism 8=34900
$Cd_2Zn(PO_4)_2$, cryst. struct. 8=35322
$CdZn_2(PO_4)_2$, cryst. struct. 8=35322
CO_2-air, thermodynamic and transport props., 50° to 3500°K 8=25838
KdTe, pure, production and elec. props. 8=26239
$PbS + CdO \rightarrow PbO + CdS$, solid state, reaction kinetics and diff. mech. 8=49839-40

Cadmium compounds—contd
Tl-Cd liquid alloy, thermodynamic props. 8=30455
cadmium sulphide
absorption spectrum, two-photon, anisotropy 8=45181
acoustic amplification with space- and time-varying parameters 8=30941
acoustic wave packets from CdS injected into InSb, acoustoelectric phenomena 8=27112
acoustoelectric field, alternating, dependence on sound intensity and conductivity 8=35412
acousto-electric inhomogeneities, using optical probe 8=44313
acoustoelectric interaction nonlinearity 8=35409
amplifying, acoustic freq. spectrum time and field dependences revealed by Brillouin scatt. meas., 8=48718
anticrossing of dispersion curves due to spatial dispersion 8=36346
brittle crystals, microhardness rel. to dislocation mobility 8=26796
cathodoluminescence, high density bombard. obs 8=41187
current noise, excited, in non-ohmic region 8=31371
current-oscillating, microwave transmission meas. 8=27087
dielectric loss meas. to study lattice defects 8=44867
diffusion of Li 8=44383
diodes, thin-film, heat treating in various ambients 8=27176
domains, stationary anode-adjacent high-field, electron density depend. 8=44769
domains, stationary high-field, in neg. differential conductivity range 8=44770
donor-acceptor pairs from luminescence of pure and doped samples at 77 and 4.2°K 8=27643
electrical cond. of n-type, 1.8 to 294°K 8=31369
electro-optical effect, Stark effect of exciton levels 8=36348
electroluminescence mechanism at 77°K 8=45264
electron radiation damage, photoelectronic evaluation 8=40654
emission bands in 2.0eV region 8=49792
e.p.r. of Cu^{2+} ion impurities, microstructure, calc. 8=39779
e.s.r., excitation and quenching dependence rel. to trapped electrons 8=27467
evaporated thin films, conductivity rel. to thickness 8=49233
film, electrical processes and vacancy transport 8=40442
film, electromech. coupling coeffs. determ. from admittance meas. 8=40626
film, epitaxial growth and polymorphic transforms. 8=26113
film, epitaxial growth on CdS and ZnS platelets, dislocations and cryst. orientation 8=35165
film, thin, deposition study 8=48446
film utilization for transistors if spray deposited 8=31414
films, epitaxy and crystal growth 8=26114
films, evaporated by e bombard., props. 8=35166
films, Faraday effect near fundamental absorpt. edge, at 300°K 8=36347
films, forbidden band width film-thickness dependence 8=26904
films, photoeffect, electrically induced, props. 8=27319
films, whisker-formation and structural changes during crystal growth 8=26270
green edge emission, a.c. modulated 8=49794
growth by transport in vapour phase 8=26240
growth of crystals and determ. of some characts. 8=26241
hypersound absorption, low temp. 8=35411
illuminated, thermoelectric power 8=35997
implanted with high energy P^+, change to p type conductivity on implanted surface 8=40443
intrinsic photoconductivity under unipolar injection conditions, agreement with calc. 8=44919
lattice luminesc. props. 8=36522
layers, chem. deposited, elec. and photocond. props. 8=44918
layers, photoresistors, prep. and props. 8=49433
light scattering by light, obs. with freq. changes 8=49711
local centre formation in presence of free electrons and holes 8=36015
luminescence, low-temp., ion bombard. effects rel. to vacancies creation 8=36483
luminophor emission spectra 8=45295
microwave cond. and relax. of excess phonons 8=49234
monocrystals with blocking cathode current flow characts. and mechanism 8=49231
MOS diode, electroluminescence at low-voltage, high-current and 77°K 8=27644
movement of high field domains, anode-cathode direction 8=40573
neutron irradiation effects on dark resistivity and Hall mobility 8=49235
{0001} surfaces, structure study and O_2 adsorption by LEED 8=30719
optical demodulator with u.s. amplification 8=27216
optically quenched, electronic fluctuation spectra 8=40659
parameters of slow recombination centres affected by heat treatment 8=40655
particles in glass, light absorption with a.c. elect. field modulation, obs. 8=40267
phonon-assisted free exciton recombination 8=44760

- **Cadmium compounds**—contd
  - **cadmium sulphide**—contd
    - photoconductive, rel. to piezoelectric oscillations 8=27297
    - photoconductivity, behaviour of holes and electrons, revealed by laser excitation 8=36012
    - photoconductivity, induced impurity, spectral distrib. effect of i.r. quenching 8=44921
    - photoconductivity, oscillatory depend. on photon energy 8=31452
    - photoconductivity, spectral distrib. fine structure, effect of O adsorption 8=44917
    - photoconductor, l.f. oscillations induced by i.r. quenching 8=44934
    - photoconductors, temp. depend. 8=27337
    - photoconducting, transient currents 8=40653
    - photoconductivity, microwave meas. 8=49426
    - photoconductivity, sonde characts 8=49412
    - photocurrent props. under unipolar injection conditions 8=44920
    - photomagnetic effect, influence of surface 8=31453
    - photomechanical effect, negative 8=40137
    - photoreflectance at fundamental absorption edge 8=45183
    - photosensitive tunneling and superconductivity 8=35848
    - piezoelectric semiconductor, sound amplification wave amplitude dependence 8=44315
    - platelets, growth, structural properties 8=40034
    - p-n heterojunctions, photoelectric props., convertor preparation 8=36013
    - p-n junctions, props., and construction of photoelectron transducers 8=49291
    - polycrystalline, recrystallization and photoelec. props., effect of press. 8=48539
    - powders, adsorpt. of gases H_xA and O_2, effects on cond. 8=26135
    - Raman scatt. cross section at 293°K in crystalline powder 8=45189
    - rare earth doped, injection luminesc. of heterojunctions 8=45265
    - recombination kinetics of luminescence and photoconductivity 8=27645
    - refractive index rel. to temp. 8=45182
    - self-diffusion radiation stimulated on α- and γ-ray bombardment, coeff. determ. 8=35482
    - self-scanning image sensor using high field domains 8=27317
    - semiconducting, piezoelectric, current oscillation, nonlinear theory 8=31372
    - shallow donor ground states 8=31278
    - sintering kinetics, 780°-820°C 8=39534
    - solar cells, performance after micrometeoroid exposure 8=24093
    - sound generation and velocity field dependence 8=35414
    - sound wave coupling mode, at crit. elec. field of current saturation 8=35413
    - sound vel. rel. to drift field intensity, obs. 8=39889
    - space-charge-limited diode, limiting noise 8=27177
    - stationary wave instability in strong drift fields 8=30943
    - surface, {0001}, potential temp. dependence 8=44766
    - thick films, chemical deposition, props. 8=39589
    - surface photoconductivity, oxygen chemisorption and desorption influence 8=49413
    - thin films, amorphous to crystalline transition 8=43993
    - trapping level disposition 8=49793
    - n-type, elect. cond., 1.8 to 294°K 8=31369
    - p type high conductivity, Hall effect and carrier lifetime 8=40444
    - u.s. attenuation, nonelectronic 8=48719
    - u.s. wave delay time meas. at h.f. by phase comparison method 8=44314
    - u.s. waves, parametric amplification 8=39890
    - wurtzite-type crysts., optically active lattice vibrs. 8=35394
    - CdS active oscillator, focusing of laser beam 8=28882
    - CdS, chemisorption states of oxygen 8=32118
    - CdS, electron-phonon interaction 8=49085
    - CdS-metal barriers from photo-voltage meas. 8=40511
    - CdS, oscillatory exciton emission 8=41077
    - CdS, plastic deformation, influence of light 8=35670
    - CdS, sputtered, long-range oriented crystallization 8=30809
    - CdS, stress induced splitting of exciton lines 8=26920
    - CdS, surface photoconductivity, effect of self-purification and polarity 8=40658
    - CdS-Cu_2S film system, photovoltaic effect rel. to thickness and prep. 8=40652
    - CdS-In contact region, dark current relax. obs. 8=44916
    - CdS-SiO_2-Al structure, field-effect conductance temp. dependence 8=40544
    - CdS : Au, precipitate growth and dislocation generation rel. to annealing 8=48375
    - CdS:Co^{2+}, Co^{2+} absorpt. and emission rel. to ion centre levels, 3500 cm^{-1} 8=27613
    - CdS : Cu precipitate growth and dislocation generation rel. to annealing 8=48375
    - CdS:P, photocond., i.r. quenching band, 2.15 eV 8=40657
    - CdS: P, photocurrent excitation spectra 8=31454
    - CdS:Te as scintillation counter material 8=46864
    - CdS+Te, small inertia photoresistors 8=36014

- **Cadmium compounds**—contd
  - **cadmium sulphide**—contd
    - CdS/ZnS mixture, e.p.r. of Mn^{2+} exchange-coupled pairs 8=45105
    - CdS_xSe_{1-x}, acoustoelec. effect and ultrasound absorpt. and amplification 8=35410
    - In-CdS-In system in constant elec. field, non-stationary processes 8=35990
- **Caesium**
    - adsorption on Pt films on W 8=35178
    - adsorption on W and Mo, theory comp. with expt. for work functions 8=31466
    - arc, low voltage, theory 8=39010
    - atom, collisions with N_2, H_2, HD, D_2 cross-sections obs. 8=38957
    - atom, elec. dipole moment meas. 8=29614
    - atom, elec. dipole moment, upper limit determ. 8=43177
    - atom, emission spectra, satellite bands 8=25360
    - atom, ground state, differential polarizability of Zeeman substates, atomic-beam resonance obs. 8=38667
    - atom reactions with Cl_2 in crossed beams 8=49875
    - atom scatt. on Ar, total scattering cross sections 8=34178
    - atom, spin-exchange cross-sections for Cs^{133} atoms 8=43239
    - atomic beam, crossed with K atomic beam, spin change collisions 8=47534
    - atomic lifetimes, direct obs. 8=29612
    - atomic spectrum, frequency standard obs. 8=28210
    - atoms lifetime of $6^2P_{3/2}$ and $7^2P_{3/2}$ states 8=34162
    - contents in components of adsorpt. Cs reservoir converter, after life test 8=28503
    - desorption from W on interaction with low energy electrons 8=39623
    - diode, thermionic, optimum added noble gas pressure 8=41974
    - discharge, electron-atom collision momentum transfer cross sections from drift velocity meas. 8=29911
    - discharge plasma params. rel. to ionization, 0.03-0.3 torr 8=25714
    - discharge plasma, recomb., radiative-energy loss and level populations 8=34494
    - distribution between potassium feldspar and plagioclase simultaneously crystallized at 600°C 8=36627
    - equation of state, theory, and calc. of thermal parameters 8=30973
    - fluorescence, quenching cross-sections, determ. by flame tech. 8=29617
    - inert-gas collision excitation transfer cross-section calc. 8=47543
    - isotope distrib. in p-reactions on U, Th, Ta 8=34001
    - Knight shift and pseudopotentials 8=45129
    - layers on refractory metals, work function 8=39624
    - melting curve, and elec. resistance of melt., to 30 × 10^3 kg/cm^2 press. 8=39473
    - metal, indirect nuclear interactions, theory 8=43937
    - MHD arc jet, operating 4-12 kW at 1000G mag. field strengths 8=39147
    - optical pumping in N_2, enhancement by quenching 8=47514
    - optical pumping rel. to absorpt. line width and Ne buffer press., obs. 8=25374
    - optimum seeding of non-equilibrium He plasma 8=29997
    - oxidation in flames 8=49877
    - plasma confinement lifetime in Q-device 8=47871
    - plasma diode, influence of seeding with Cd and Hg 8=28475
    - plasma e. density meas. by Langmuir probe 8=30099
    - plasma in thermionic converter, anal. of distrib. 8=28495
    - plasma, ion-sound oscills. and e heating in h.f. elec. field, obs. 8=30008
    - plasma, seeded with Ar, ion species present, relative abundance and ion signals 8=29987
    - saturated vapour press., obs. 8=30604
    - thermionic converter, effect of O additions, use of Cs oxide reservoir 8=28479
    - thermoreflectance spectrum in visible and near u.v. region 8=41101
    - trace, in He plasma, phys. props. of plasma 8=47818
    - vapour, arc, low voltage short gap 8=43465
    - vapour, diffusion of Cs ions, time-of-flight analysis rel. to conduction studies 8=43705
    - vapour, hyperfine optical pumping with mag. filter 8=38693
    - vapour, hyperfine relax., rel. to diffusion coeff. and cross section meas. 8=47537
    - vapour, laser-irradiation and resulting light emission 8=29906
    - vapour, low voltage arc with non-isothermal cathode 8=25703
    - vapour, photoionization absorpt. continua 8=29973
    - vapour, spectral profile of r.f. modulated light beam in optical pumping expt. 8=29613
    - vapour, transport coeffs. calc. 8=30306
    - vapour viscosity, 1000 to 10 000°K and 10^{-5} to 10 atm. 8=30312
    - vapour, viscosity in range 1000° to 2400°K, effect of partial ionization 8=30310
    - vapours, P, V, T relationship evaluation 8=48296
    - wetting of Re, W, Mo, Ta and Nb rel. to bare work function of metal 8=35168
    - Cs^+ field desorption, theory 8=44953
    - Cs vapour of Cs_2^+, diff. coeff., time-of-flight obs. 8=30314

Caesium—contd
Cs_2, 6250Å band system 8=29733
Cu, sputtering, 77°K 8=31150
K-Sb-Cs photocathodes 8=36023
on W, effect on thermal rad. during thermionic emission 8=31465

Caesium compounds
amalgam, conc., electron work function and surface tension 8=49435
Cs^{137} as fission product in coated fuel particles, determination 8=47404
Cs^+ emission from 50-75μ diam. hole in W(110) face 8=49446
Cs-graphite absorpt. reservoir system for heat-pipe converter 8=28490
Cs-graphite lamellar cpds rel. to Cs vapour press. and temp. 8=35011
Cs oxides, reservoir in thermionic converter, as possible source of both O and Cs 8=28479
$CsBeF_3$, crystal structure 8=39783
CsBr, adiabatic elastic consts. rel. to press. and temp. 8=44562
CsBr, colour centre photochemical reactions 8=27758
CsBr in rock salt structure, reflectivity spectra 8=45184
CsBr, lattice dynamics and sp. ht. 8=39871
CsBr, luminescence after shock compression 8=49806
CsBr, neutron irrad., Xe diffusion 8=39970
CsBr-RbBr system, phase diagrams from X-ray diff. and thermal anal. 8=35096
$CsBr_3$, cryst. struct. and bonding for Br_3^- ion, compared with PBr_7 8=44247
CsC_{10}, inserted in graphite, cryst. structure 8=35320
CsCl allotropic type crystals, phase transformations 8=48377
CsCl, lattice dynamics and sp. ht. 8=39871
CsCl: K^+, Rb^+, Br^-, ionic conductivity 8=31419
CsCl-RbCl system, phase diagrams from X-ray diff. and thermal anal. 8=35096
$CsCl_2$, phase transforms. 8=26067
Cs_2CO_3, evaporation products, mass-spectrometer obs. 8=48294
Cs_3CoCl_5, magnetic, optical and e.p.r. props. 8=31501
$Cs_5Cu_3(NO_2)_{11}$, crystal structure 8=39786
CsF, adsorption on W 8=48498
CsF beam state selection and focusing 8=38964
CsF, neutron irrad., Xe diffusion 8=39970
CsF in thermionic converter 8=24083
CsF, second-order, Raman spectrum rel. to lattice dynamics 8=31980
$Cs^{133}F^{19}$, hyperfine struct. of J=1 rot. state and vib. states 0, 1, and 2 8=43298
CsH_2AsO_4, n.q.r. spectra, rel. to temp. 8=41009
CsI, adiabatic elastic consts. rel. to press. and temp. 8=44562
CsI, charged dislocations produced on deformation 8=26669
CsI crystals, mech. behaviour and tensile strength 8=40139
CsI, energy band calc., mixed basis method 8=44641
CsI films, X-irradiated, e.-emission-event statistics 8=44950
CsI in rock salt structure, reflectivity spectra 8=45184
CsI, lattice dynamics and sp. ht. 8=39871
CsI, neutron irrad., Xe diffusion 8=39970
CsI and CsI: Ba^{2+}, Sr^{2+}, impurities effect on ionic transport 8=40574
CsI(Tl), long-lived phosphoresc. components in cryst. 8=27657
CsI(Tl) on plastic layer as scintillator for p, e, det. protons/det. meas. 8=46877
CsI(Tl) scintillation characteristics, vacuum deposited 8=46875
$CsMnCl_3 . 2H_2O$, NMR and antiferromag. props. 8=36275
CS_2 photon interactions, 3000-1100Å, spectral range, u.v. cross section obs. 8=43315
$Cs_2MnCl_4 . 2H_2O$, NMR and antiferromag. props. 8=36275
Cs_2NaTF_6, (T = Yb, Er, Ho, Y, Tb and Sm), crystal structure 8=44250
$CsNO_3$, far i.r. absorpt., solid and fused 8=49742
$CsNO_3$ molten, optical determ. of thermal cond. 8=39355
$CsNO_3$ molten, vib. freqs. by i. r. emission spectroscopy near 600°C 8=38842
Cs–O system evaporation products, mass spectrometric obs. 8=32096
CsOH, unstable mol., microwave spectrum 8=25468
Cs_2PtCl_6, luminesc. 8=36505
Cs-Sb films, photoelectron attenuation length determ. 8=31455
Cs_3Sb films on MnO, e.- and X-ray diffr. exam. 8=39591
Cs_3Sb, i. r. photoemission 8=40705
Cs_2SO_4, vibr. spectra 8=35382
$Cs_3ZnBr_5 : Co^{2+}$, exchange interactions in pairs of coupled Co^{2+} ions 8=49606
$Cs_3ZnCl_5 : Co^{2+}$, exchange interactions in pairs of coupled Co^{2+} ions 8=49606
Cs_3ZnCl_5: Co^{2+}, magnetic, optical and e.p.r. props. 8=31501

Calcium
atom autoionization broadening fitted to Shore parameters 8=43185
atom, lifetime of 4 $^1F°$ term, determ. 8=34164

Calcium—contd
atom, oscillator strengths and matrix elements, calc. 8=29607
atom, two-electron transitions 8=43184
atomic, photoionization cross section meas. 8=29949
electrodes, vacuum breakdown temp. effects 8=38996
fractionation trends in plagioclases, comp. with Sr 8=50074
ions, Ca XV and XVI spectra in laser prod. plasma, 120-240 Å 8=29608
K-type stars, abundance by photometric meas. 8=45633
in leaves, distrib., autoradiography and chem. analysis obs. 8=45929
metallic, X-ray K-absorption spectrum 8=27565
spectral line breadth with Na as impurity in arc discharge 8=34437
spectrochemical detect. in Ta 8=45416
Ca^{43}, 0.13% in CaF_2, double resonance detection 8=37536
$Ca^{43.48}$, determ. by neutron time-of-flight 8=36648
Ca^+, electron scatt., autoionization states, excitation of 4s → 4p, 4s → 3d transitions 8=43232
Ca II in sunspots, K-line spectra and origin of emission 8=28178
Ca II, K-line in sunspots 8=50453
Ca II lines in stellar spectra, Wilson-Bappu effect 8=28070
Ca II solar line, centre-limb var. of $K_{2,3}$ components calc. 8=45878
Ca II stellar H and K lines equivalent widths 8=41525
Ca^{++} in $CaSO_4$ and hydrides, X-ray K edge fine structure 8=27564
Ca^{2+} ions in NaCl, aggregation study by ionic, dielec. and bulk density methods 8=35965
Ca_2 molecule, orange bands, $^1\Sigma$-$^1\Sigma$ system, rotatory quantum analysis 8=43296
in Na, influence on V-10wt.% Ti alloy corrosion 8=27723

Calcium compounds
acetate, in gelatin, decomposition on drying of gelatin with acetic acid loss, mechanism 8=25793
calcic amphiboles, unit-cell volume and packing density, isotypic replacement effects 8=26372
calcite crystals, Bauschinger effect in twinning 8=35669
calcite crystal growth control by regulated chemical reaction 8=39671
calcite, elastic constants 8=40132
calcite, elastic constants pressure dependence to 6kbar at 25°C 8=48998
calcite, elastic constants temp.-dependence, 25-375°C 8=44558
calcite, e.s.r. of Y^{3+}-stabilized CO_3^{3-} mol.-ion 8=49620
calcite : Mn^{2+}, e.s.r. 8=40932
calcite, multiplication of twinning dislocations 8=26686
calcite, synthetic, morphology and optical props. 8=26194
calcite, third-order elastic constants at 0°C 8=48999
calcite, twinning and dislocation growth during twin layer expansion under stress 8=31104
calcite, X-irrad., e.p.r. of CO_3^- 8=49600
chemical and polymorphic equilibria under hydrostatic press., X-ray obs. 8=43901
gypsum, spherically bent cryst., soft X-ray spectroscopy 3 to 30Å 8=32033
halide phosphates, thermolum. obs. 8=36480
hydroxyapatite, n.m.r. 8=40981
mangates mag. props. rel. to comp. and lattice geometries 8=31757
Ca complex, $CaBr_2 . 10H_2O . 2(CH_2)_6N_4$, crystal and mol. structure 8=26370
Ca halophosphate (As, Mn), luminescence decay obs. 8=27642
$Ca_3Al_2(O_4D_4)_3$, neutron and X-ray diffr. 8=39777
$Ca_6[Al(OH)_6]_2(SO_4)_3 . 26H_2O$, ettringtie, cryst. struct. 8=44210
$CaAl_2Si_2O_8$, n.m.r. of Al^{27}, obs. 8=40972
$(Ca_zBa_xSr_y)MgSi_2O_8$, equilibria in subsolidus phases rel. to luminescence 8=49789
Ca–Bi–V–Fe garnet, excitation of magnetostatic, magnetoelastic and acoustic waves 8=40838
$Ca[B(OH)_4]_2 . 2H_2O$, OD-disordered modification, structure determ. 8=26379
CaBr, discharge-excited mol., u.v. emission spectrum 8=43295
CaC_2, phase diagram, comment 8=39465
$CaCl_2$, precipitation and association in NaCl crystals 8=48390
$CaCO_3$ as neutron monochromator structure factors 8=42651
$CaCO_3$ cryst., stimulated Raman scatt., additional anti-Stokes components, obs. 8=41073
$CaCO_3$, cryst. struct. effects in Ca sulfonate adsorpt., rel. to form. of oil sols 8=30767
$CaCO_3$, phase transformations and decomposition, effect of impurities 8=30682
$CaCO_3$, rel. to oversaturation of seawater 8=50097
$CaC^{14}O_3$ powder, radioactivity meas. when insoluble in liquid scintillator counter 8=47278
$CaCO_3$:Gd^{3+}, e.p.r. absorpt. spectrum at 77°K 8=45087
$CaCrO_3$ perovskite, synthesis, struct. and band antiferromagnetism 8=49570
CaF_2 crysts and U doped, Ar, Kr and Xe diffusion 8=26618
CaF_2, inert gas diffusion mechanism 8=26619
CaF_2/Na, synthetic, absorption, photoconduction 8=36338

Calcium compounds—contd
- CaF_2 : Nd^{3+} ions in sites of tetragonal symmetry direct one-phonon spin-lattice relaxation times 8=40938
- CaF_2: U^{3+} ions in sites of tetragonal symmetry direct one-phonon spin-lattice relaxation times 8=40938
- CaF_2: U^{3+}, spin-lattice interactions in uniaxially stressed crystal, e.s.r. obs. 8=40939
- CaF_2, V_K centre, influence of Y and O on formation 8=40060
- $Ca_2(FeMo)O_6$, mag. and elec. props. 8=36195
- Ca_2FeAlO_5, mag. props. and spin orientation 8=31758
- $Ca_2Fe_2O_5$, magnetic structure 8=31759
- CaF_2: Nd^{3+}, spin-lattice interactions in uniaxially stressed crystal, e.s.r. obs. 8=40939
- CaF_2:Yb^{3+}, ENDOR meas. rel. to crystal field splitting of Yb^{3+} in cubic sites 8=27501
- CaF_2, Yb^{3+} and Tm^{2+} transferred hyperfine interactions, F^{19} ENDOR obs. 8=36266
- CaH and CaD, u. v. absorpt. spectra 8=38820
- $CaHAsO_4.H_2O$, haidingerites, cry. struct. 8=48641
- $Ca_3H_2(CO_3/SO_4)SiO_4.13H_2O$, thaumasite, thermal decomposition, i. r. study 8=26065
- $CaHPO_4$, crysts. hydrothermal growth in SnO and unsaturated fatty acids presence, obs. 8=35237
- $(Ca, Mg)_5Al_5BSi_3O_{20}$, space group, cell dimensions 8=48644
- $CaMg(CO_3)_2$, crystal structure rel. to $BaMg(CO_3)_2$ 8=48637
- $CaMnSi_2O_6$, johannsenite, struct. and cryst. chem. 8=44248
- $CaMoO_4$, elastic consts. 8=40133
- $CaMoO_4$, i. r. spectra 8=45179
- $CaMoO_4$, lattice perturbations 8=26572
- $CaMoO_4$, laser-induced Raman spectra 8=31969
- $CaMoO_4$, powellite, crystal structure 8=39778
- α-Ca_3N_2, crystal structure 8=26371
- $CaNb_2O_6$, crysts. prep. by Cl chem. transport, and lattice struct., obs. 8=35238
- CaO, ads. of Br_2 and I_2, refl. spectra 8=48479
- CaO, colour centre bands, Faraday rot. anal. 8=35588
- CaO, emission props. in BaO stream 8=27349
- CaO, Faraday rotation of F band and 3557 Å zero-phonon peak 8=45178
- CaO, i.r. bands 8=34237
- CaO, i.r. dielectric response rel. to lattice vibrations 8=41075
- CaO, luminescence, radical-recombination mechanism on excitation with H 8=41177
- CaO, neutron irrad., Ar^{37} diff. 8=39969
- CaO, n-irradiated, colour centres 8=31115
- CaO, phosphoresc. decay rel. to trap depths distrib. 8=41186
- CaO, struct. exam. 8=48592
- CaO transformation to CaS, 1400° to 1650°C 8=45324
- CaO, x-irrad., thermoluminescence 8=41184
- $CaO.6Al_2O_3$, crystal structure 8=48642
- CaO-B_2O_3-V_2O_5 glasses, compared with phosphate, role of network former in elec. props. 8=27085
- CaO: Cu^{2+}, e.p.r., tunneling effect at 1.2°K 8=40916
- CaO, Fe group impurities, uniaxial stress meas., strain coeffs. 8=40134
- $Ca(OH)_2$ and $Ca(OD)_2$, vibr. spectra, coord. anal. 8=31970
- CaO-P_2O_3-V_2O_5 glasses, compared with phosphate, role of network former in elec. props. 8=27085
- $Ca_3(PO_4)_2$ activated by Hg-like ions, luminesc. 8=36479
- $Ca_5(PO_4)_3F$:Nd^{3+}, laser characts. 8=37620
- $Ca_3(PO_4)_2.H_2O$, and mineral whitlockites, crystal chemistry 8=39639
- $CaRuO_3$, antiferromagnetic props. 8=36177
- CaS: Ce, phosphor decay and thermoluminesc. obs. 8=45305
- Ca_2SiO_4 phase diagram, comments 8=39464-5
- $CaSO_4$, crystallization from H_3PO_4, nucleation and growth rates 8=35239
- $CaSO_4$. photo-effect, influence of electric field 8=36337
- $CaSO_4.2H_2O$, i.r. combination vibr. spectrum, 10,000-1,200 cm^{-1} 8=41074
- $CaSO_4.H_2O$ system, thermally dehydrated, precise forms of products, by i. r. spectroscopy 8=49858
- CaS: Zr, phosphor thermoluminesc. obs. 8=45306
- CaS : Zr phosphors, mag. susceptibility rel. to Zr conc. 8=44967
- $CaWO_4$, defect sites identification from correlation of e. s. r. and thermoluminesc. meas. 8=31028
- $CaWO_4$, e.p.r. and thermoluminescence meas. 8=49602
- $CaWO_4$, i. r. spectra 8=45179
- $CaWO_4$, laser-induced Raman spectra 8=31969
- $CaWO_4$, lattice perturbations 8=26572
- $CaWO_4$, luminescence props., effect of electron irradiation 8=36481
- $CaWO_4$ luminophor, pulse-excited, decay rel. to temp. 8=4529C
- $CaWO_4$, oxygen vacancies prod. by fast reactor neutrons, direct obs. 8=31047
- $CaWO_6$: Ce^{3+}, Yb^{3+}, spin-lattice relax., contrib. processes 8=40911
- $CaWO_3$: Er^{3+} (Tb^{3+}) EPR and spin lattice relax times, 1.5 to 30°K 8=36238
- $CaWO_4$: Er, Ce(Mn), electron-spin-echo phase memory limited by lattice relax processes 8=27466
- $CaWO_4$:Gd^{3+}, ^6P Stark levels and line polarization 8=31993
- $CaWO_4$:Nb^{3+}, coherent radiation from optical, effect of parameters of pumping light source and discharge regime on output 8=24330

Calcium compounds—contd
- $CaWO_4$:V, e.p.r. and charge compensation 8=31855
- $CaWO_4$:V, e.s.r. rel. to site occupances and charge compensation 8=45082
- $CaWO_4$: Yb^{3+}, microwave-optical double reson. using circularly polarized light 8=41070
- CdS laser, electron pumped, far field patterns 8=33202
- $Cs(OH)_2$, i. r. spectra 8=27563
- GaSb, elastically deformed, elec. field gradient at nuclei form n.m.r. obs. 8=31909

calcium fluoride
- charge compensation of Ce^{3+}, Nd^{3+} and Sn^{3+} by interstitial H^- or D^- ions 8=49601
- crystal chemistry of CaF_2 with TbF_3, Tb_4O_7 and TbOF admixtures 8=26168
- crystal-field splitting of rare-earth ions 8=35025
- crystal infrared emissivity 8=32006
- defect energies, Born model calc. 8=40004
- electron irrad., production of colloidal calcium 8=40074
- electronics structure study by photoemission 8=31287
- elastic constants temp. dependence, room temp. –420°C 8=35667
- F-centres, X-ray induced, formation and bleaching 8=40059
- fracture surface as function of crystallographic direction and treatment method 8=44593
- γ-irradiated at 77°K, thermoluminescence, activation energies and emission spectra 8=36477
- hydrolysis kinetics, 1000-1120°C 8=49859
- hyperfine coupling of S-state Eu^{2+} in crystals, temp. depend. 8=27465
- fluorite, irradiated, elec. cond. and optical absorpt. changes 8=26946
- formation energies of anion and cation point defects Born-model calc. 8=35540
- Grüneisen parameter, low-temp. limit, calc. on Axe's shell model 8=48748
- n-irradiated, self-trapped holes, e.s.r. exam. 8=31854
- neutron-irradiated liq. N_2 temps., induced colour centre obs. 8=26719
- with paramagnetic impurities, n.m. r. of F^{19}, temp. and impurity conc. dpendence 8=40974
- photo-effect, influence of electric field 8=36337
- Rebinder effects, occurrence and mechanism 8=40136
- synthetic, absorption, photoconduction 8=36338
- synthetic γ-irradiated. thermoluminescent spectra and transition kinetics 8=45262
- u. v. reflectivity spectra 8=36374
- Zeeman and dipolar nucl. relax., Ce impurity 8=45119
- Ca^{43}, 0.13%, double resonance detection 8=37536
- CaF_2 to correct u.v. wavelength 8=37724
- CaF_2:(Am^{2+}. Cm^{3+}). zero-field splittings 8=30622
- CaF_2:Ce^{3+} line splitting in electric field 8=36308
- CaF_2: Ce^{3+}, f-d transitions, relative intensities calc. 8=36476
- CaF_2:Ce^{4+}, 4f ↔ 5d transitions from thermoluminescence and optical spectra 8=45263
- CaF_2:CeO_2, M centres rel. to photochromic colouration 8=44474
- CaF_2 : Co^{2+}(Ni^{2+}), absorpt. spectra temp. dependences 8=41076
- CaF_2:Dy^{2+}, excitation of forbidden and allowed radiative transitions 8=47522
- CaF_2:Dy^{2+}, laser emission mechanism 8=37610
- CaF_2 : Er^{3+}(Nd^{4+}), spin-lattice relaxation, effect of quasi-local vibrations 8=40910
- CaF_2-ErF_3: Ho^{3+}, luminesc. and excitation energy transfer $Er^{3+} \rightarrow Ho^{3+}$ 8=41185
- CaF_2-ErF_3: Tm^{3+} luminesc. and excitation energy transfer $Er^{3+} \rightarrow Tm^{3+}$ 8=41185
- CaF_2:Eu^{2+}, optical spectrum and Zeeman effect 8=45177
- CaF_2 : Eu^{2+} relaxation time meas. using optical Faraday rotation technique 8=49479
- CaF_2 : F^{19} longitudinal nuclear mag. relaxation, field dependence 8=49634
- CaF_2 : Gd^{3+}, e.p.r. spectral cubic splitting temp. dependence, 77-950°K 8=40909
- CaF_2:GdF_3, volume and density changes due to pt. defects 8=44559
- CaF_2: Ho^{2+}, g-factor stress dependence 8=31510
- CaF_2:Ho^{3+}, two-photon absorpt. on laser illumination 8=45180
- CaF_2:Mn, read-out, u. v. induced thermoluminesc. rel. to irrad. dose, obs. 8=45261
- CaF_2 : Mn, thermoluminescence rel. to doping and dosimetric props. 8=49807
- CaF_2 : Mn^{2+}, F^{19} nuclear spin-lattice relaxation 8=49633
- CaF_2: Nd^{3+}, (U^{3+}) spin-lattice interactions in uniaxially stressed crystals 8=40912
- CaF_2:Ni^{2+}, vis. and near i. r. absorpt. spectra, at room temp. and 4.2°K 8=31967
- CaF_2:$Pu^{3+,4+}$, optical spectrum 8=31968
- CaF_2: Sm^{2+} crystal generation, spectrum-time studies for ruby laser excitation 8=41071
- CaF_2:Sm^{2+}, oxygen penetration 8=44382
- CaF_2-Tb_2O_3($Tb(OF)_3$)(TbF_3) solid solns., crystal chemistry 8=39640
- CaF_2 Tm^{2+}, 12% nuclear polarization using optical pumping 8=30633
- CaF_2:U^{3+}, magneto-optical rot. and struct. of U^{3+} centre 8=36336

Calcium compounds—contd
  calcium fluoride—contd
    CaF_2: U^{4+}, u.s. paramagnetic resonance, absorption, freq. dependence 8=40946
    CaF_2: Yb + Nd, multiple sensitization effects 8=41183
    CaF_2: Y, X-irradiated, polarized luminescence and structure of luminesc. centres 8=36478
    with H interstitial atoms, localized H vibrations 8=41072
    Mn^{2+}, hyperfine coupling temp. depend. 8=31876
    Sm, Nd impurities, relax. flow teeth obs. 8=26794
    UO_2, UC or U doped, diffusion of inert gases 8=34107
Calculating apparatus
      See also Fourier analysis; X-ray crystallography/calculation apparatus.
    b.c.c. and f.c.c. crystals, computer simulation of spherical surfaces, dislocation loops and dipoles. 8=26652
    computer generated spatial filters for coherent opt. data processing 8=28764
    computer simulation of Si:Au diode, charge distrib. and recomb. rate 8=27182
    data streams, interacting, processing efficiency calc. 8=32689
    digital or analog readout for automatic refractometer 8=28750
    digital data collection system for v.l.f. transient waveforms, appl. to atmospherics 8=32253
    meteorological data processing 8=36704
    satellite plasma data processor 8=32564
    spectroscopy, Fourier transform real time synthesizer 8=28832
  analogue apparatus
      See also Nomograms; Sliderules.
    A/D convertor for chart records 8=28244
    analogue-digital conversion, acceleration by auto-equalization 8=24528
    computer soln. of convection transport eqns. of axi-symm. flow 8=34822
    computers for e. m. field evaluation by models, book 8=33054
    control system dynamics, analog simulation 8=28459
    device solving Cauchy problem for Laplace eqn. 8=45984
    digitizer, wide range, for direct coupled analogue signals 8=32690
    electrolytic tank, automated, for cyclotron injection 8=24587
    electrolytic tank for two-port network analysis 8=46005
    electron trajectory recording 8=46406
    Fourier transform computer IFTAC for spectroscopy 8=28827
    Fourier transform computer, optical 8=28828
    heat generation by frictional contact, simulation 8=37319
    heat transfer boundary-problem soln. 8=41863
    interference microphotometer for Fabry-Perot ring photographs, reduction 8=28833
    magnetic film storage elements, controlled easy-axis distrib. 8=49511
    magnetic shield simulator, (for space vehicles), meas. of forbidden volume 8=41481
    optical rangefinder stadimetric slide rule calculator 8=37661
    plasma model, 2 dimens., correl time and r,m.s. E field meas. 8=34466
    pulse devices for logarithmic and power functions and mult. and division of power fns. 8=45985
  digital computers
    analogue-digital converter, added-step differential linearization 8=23814
    beam-addressable memory device, low temp. with EuO film 8=36123
    betatron oscillation control appl. 8=33466
    Bevatron inflection system control 8=33495
    for celestial mechanics analytical development Colloquium, Prague August 1967 8=50266
    communication-line data transmission to computer 8=46004
    control wiring recording appl. 8=37808
    in crystal diffractometer system 8=26337
    data acquisition control system 8=37120
    data collection in medical γ spectroscopy 8=50462
    data terminal network system 8=37774
    diatomic mol. vibr.-rot. spectrum analysis, line rot. quantum numbers calc. 8=29684
    diffraction pattern calc. by Fourier transform of aperture elec. field 8=28871
    electron gun simulation 8=46408
    evaluation of e. m. fields by models, book 8=33054
    ferromagnetic films, strain-sensitive for sonic film memory 8=36125
    gas, fissioning, pressure wave generation, method of characteristics analysis 8=39170
    glass containers prod. system appls. 8=50471
    grain section, dimension distrib. rel. to grain size distrib. 8=43986
    growth curve construction from equiv. line breadth 8=28776
    information searching with addressed memory system, for multichannel analysers 8=46942
    ionosphere N(h) profile calc., assigning reference elements for memory 8=36831
    for light scatt modeling in spherical nebulae 8=36962

Calculating apparatus—contd
  digital computers—contd
    liquid scintillation counting automation 8=46867
    liquid-solid suspension, simulation of thermal conductivity 8=43883
    Los Alamos linear accelerator control 8=33428
    low-density crossed-field electron beams, computer experiments 8=28558
    magnetic films, coupled, device for associative memories 8=36121
    for minimizing errors prod. by coherent averaging of interferograms 8=28862
    modelling and simulation appl., book 8=28246
    molecular vibr.-rot. spectra, analysis, wavelength calc. 8=29680
    neutron cross section evaluation, curve fitting technique 8=33789
    nuclear data acquisition counting schemes 8=47194
    phonemic symbols, transcription standard 8=46202
    plasma model, charact. magnitudes numerical investigation 8=39072
    readout, magneto-optic, amplitude-modulated 8=36122
    research nuclear reactor control 8=47396
    sharp film NDRO bit organized memory 8=36124
    simulation of lunar craters 8=45816
    spectrum analysis, separation of branches 8=29681
    Standford linear accelerator beam switchyard control 8=33423
    synchrotron, alternating-gradient, control and analysis appl. 8=33447
    for thermionic converter plasma transport eqns soln 8=28494
    tune profile prep. for orbital accelerator 8=33449
    x-y charts reading into computer for processing 8=23813
    X-ray intensity, conversion to, and plotting of pole figures 8=48584
    MnBi film memory 8=49531
  digital computer programmes
    Abel inversion, electronic analogue 8=30070
    accelerator tubes, sectional, with oblique fields, ALGOL design programme 8=46988
    adsorption of lattice gases, simulation 8=30763
    Algol procedure for bubble chamber photographs 8=46957
    algorithm applic. for particle moving in liquid H_2 chamber 8=46961
    alkali halides with NaCl structure, for vacancies study 8=35532
    amino acid structure determ. by computer-controlled diffractometer 8=35362
    atomic spectra, theoretical calc. 8=38631
    atomic wavefunctions 8=38633
    complex spectrum decomp. 8=28245
    Compton γ polarimeter asymmetry ratio calc. 8=33615
    crystal diffractometer, real-time controlled 8=26362
    in crystal diffractometer system, programme variety 8=26339
    for crystal diffractometer system with low angle X-ray meas. 8=26340
    crystal struct. X-ray and n powder diffr. pattern indexing 8=44188
    crystal structure analysis, computer formulae representation in parametrical form 8=26310
    crystal structure calculation 8=39744
    for crystallographic indexing of powder patterns of unknown structures 8=26311
    crystallographic least squares refinement 8=39753
    crystallographic rotation-function high-speed programme and appl. 8=26312
    crystallography, stereographic projections, construction 8=48623
    crystallography, unit cell parameter refinement 8=39747
    for cyclotrons, precalc. of control settings 8=42358
    diffractometer, computer-controlled, for structure determ. of aliphatic amino acids 8=35362
    discriminating interfering seismic waves, optimal algorithm 8=50059
    double coincidence circuits, calc. of statistical parameters 8=28988
    elastic-plastic torsion 8=41710
    electroacoustic transducer freq. response function generation 8=23952
    electromagnetic problems, rel. to numerical soln. 8=46391
    electron diffraction intensities from crystals 8=30848
    electron probe microanalysis, quantitative 8=27803
    energy level determination equations, invariant imbedding and band theory of solids 8=49096
    Fermi surface cross-section from empty-lattice model 8=40222
    field-ion micrograph indexing, in FORTRAN IV 8=44174
    filter for pulse-height distrib. 8=33382
    fluorocarbon reactions at high temp. 8=41247
    FORTRAN IV ATTOW two dimensional programme for reactor shielding 8=47392
    Fortran, momentum and angle of bubble chamber tracks 8=33388
    free radicals, polyoriented, e. p. r. spectrum interpretation 8=34378
    for frequencies and nodal patterns of flexural vibs. of circular plates with rotatory inertia 8=41808

Calculating apparatus—contd
digital computer programmes—contd
γ-γ directional correl., acquisition, reduction and analysis 8=24703
GASPAN, code for analyzing γ-ray spectra 8=46846
heat eqn., continuous approximation method for solutions 8=32934
Heisenberg model, magnetization and pair correlation functions 8=31550
hologram synthesis, binary computer generated, 3 dim. images showing grey scale 8=46749
integration of molec. wave eqn. 8=25415
inviscid flow problems, comparison of fine algorithms rel. to ease of coding, and execution time 8=34632
i. r. spectrometers 8=24401
metallic systems, pattern recognition of binary phase diagrams 8=48364
for minimum weight design of beams with state variable inequality constraints 8=23828
molecular packing arrangements in crystals 8=26453
molecular spectra, anal. of bands 8=25412
molecules, Coriolis resonances 8=25416
molecules, internal rotation 8=25423
for MOS transistors, large signal equiv. circuit for predicting behaviour in pulsed rad. 8=27206
MUFT for neutron slowing down in reactors, inclusion of Doppler broadening 8=43132
n.m.r. moments, direct computation from broad-line spectra varying temps. 8=46524
for n. m. r. spectra, high resolution, line assignment and matrix element calc. 8=42046
nuclear data acquisition system 8=47193
nuclear emuslsion experimental data processing 8=46985
for nuclear spectroscopy data handling 8=37776
OLDMAN computer-controlled diffractometer 8=26338
on-line systems for nuclear physics 8=47195
optical constants determ. from intensity meas. at normal incidence 8=36289
for optical design, adaptive correction tech. 8=28748
optical systems design by refinement in Newton's method 8=42170
plasma ion-saturation currents in 2-dims. geom. of uniform density 8=47828
pole figure recording and analysis by computer 8=48580
polymer chain freq. 8=38975
for radiation damage prediction in semiconductor junctions 8=27146
rotation of diatomic mols., calc. 8=38790
seismograms, calc. from distant explosion sources in layered crustal structs. 8=50038
seismograms for point-sources in layered media, two ALGOL programmes 8=32176
solar cell irrad. degradation and equiv. 1 MeV e flux 8=24085
for solid angle subtended by one circular disc at another 8=32639
spectral band contours 8=25594
spectrometry, Fabry-Perot photoelec., h.f.s. calc. 8=28829
sputtering simulation in mechanism investigation 8=48902
for surface wave signal extraction from seismic data 8=50033
tandem accelerator beam tube optics 8=37817
transistor response to pulse of ionizing rad. 8=27190
UHF power tube design 8=24547
for X-ray pole figure plotting, using terminal printer as output device 8=48583
GaAs bulk oscillators, random one-dimensional doping fluctuations effect 8=49308
Si solar cells in-flight performance prediction 8=24086

Calculation
See also Graphs; Nomograms.
algorithm for discriminating interfering seismic waves 8=50059
atmosphere model eqns., numerical integration 8=41352
data fitting by least-squares method 8=28241
deconvolution of physical data 8=23785
dispersive non-linear eqn. model 8=46003
frequency response from transient response, paractical method 8=41638
ionic solns., equilib. props., integral eqn. methods 8=34782
mathematical methods for physics and engineering, book 8=32686
matrix element, off-diagonal, square of modulus, variational method 8=32685
nonlinear boundary-value problems, expansion method 8=23812
plotting of component parameters to build or modify normal-mode pulsed systems 8=46554
SU_3 Clebsch-Gordan coeffs. explicit computation 8=37850
X-ray diffraction data, continuous averaging with multichannel analyser 8=28242

Calculus. See Differential equations; Integrals; Mathematics.

Californium
alpha, long range, props of neutrons emitted from Cf^{252} 8=38541
Cf^{252} response of double-scintillator detectors 8=37790

Californium compounds
No entries

Calorimeters
adiabatic, for ht. capacity 50°-400°C 8=30961
adiabatic, for internal energy of water 8=28424
adiabatic for thermal analysis 8=24028
coaxial, for r.f. power meas. 8=33007
collector, for meas. of energies of accelerated electrons 8=47091
conduction, adaption to study of fast phenomena 8=37326
differential, compensated power, −196 —400°C 8=24029
differential, for heat of soln. and mixing 8=32989
differential, for heat of soln. at high dilution 8=41879
differential microcalorimeter for biochemical reaction studies 8=27687
eddy current heated microcal., for high temp. sp. hts and enthalpies 8=46286
electronic, for heat capacities of gaseous and subliming subs. 8=37327
isoperibol, two-body model 8=46285
isothermal titration apparatus 8=46282
liquids, enthalpy mixing 8=39348
low-temperature, automatic regulation of adiabatic region 8=46283
sample holders for solution calorimetry 8=34831
steady state and adiabatic for meas. of radiation heating in a reactor 8=47434

Calorimetry
See also Heat of adsorption, etc; Specific heat.
calorotor, simple heat engine to obs. molecular motion 8=34196
combustion radiation and convection determ. 8=32987
continuous heating method for low-temp. sp. ht. meas. 8=46299
dosimetry, gamma rays, above 5 rad/sec. 8=24688
electrical calibration 8=46284
guard-heater automatic control 8=32988
heater circuits, resistance stabilization 8=28423
hydrate binary systems, analysis under pressure 8=28413
large heat flux meas. methods 8=37325
martensite ageing in carbon-steels, microcalorimetric exam. 8=35105
power dissipation in partial discharges 8=24059
solar devices, high-temp. 8=41864
solid state phase transition energies meas. 8=30674
Pu^{241}, average β energy determ. 8=25197

Cameras
aerial mapping, specifications 8=42285
amateur, featuring automatic exposure controls 8=42284
catadoptric objective system 8=46667
dielectric tape, limiting resolution and S/N 8=42287
electron diffraction EVR-1, use of scintillation counter 8=42346
electronic shutter for holographic applics. 8=46753
high-speed motion picture, with optical compensation, applic. for meas. of colour temps. of self-luminous objects 8=46265
image-tube framing, time dispersion effects 8=37433
pinhole, general transfer function 8=28908
stereocameras for bubble chamber photographs, adjustment 8=46767
stereocameras for bubble chambers, requirements for optical heads 8=46955
stereophotogrammetric, specifications and technical data 8=42286
telecentric lens for bubble chamber photography 8=46956
Weissenberg, shutter for photographic alignment 8=35305
X-ray back refl. for single crystal areas 8=30842
for X-ray diffraction topography 8=26331

Candoluminescence. See Luminescence.

Capillarity
See also Bubbles; Drops; Films/liquid; Foams; Surface tension.
effect on adhesion of spherical solid particles 8=39451-4
flow into capillaries and slits 8=39283
immiscible liquids in cracked porous medium 8=34714
instability of liquid jet 8=43740
interfacial ripples, propagation theory 8=39284
mass transfer pots. in various meas. scales, interconnection 8=39282
moisture transfer eqn. inc. final vel. of capillary motion, particlar soln. 8=30378
penetration between dissimilar solids 8=34733
radius of draining film beneath drop approaching plane interface 8=30381
slug stimulus and laminar dispersion coeff. 8=30379
He II, capillary wave modes 8=37350

Capture cross-sections. See Nuclear reactions and subheadings.

Carathéodory's principle. See Thermodynamics.

Carbon
See also Diamonds; Graphite.
ablation chars, emittance and reflectance, visible and near i. r., 2200 to 3500°K 8=36334
abundance in solar photosphere 8=28171
adsorption of liquids, H^1 and F^{19} n. m. r. lineshift study 8=30766
Allen-Bradley thermometers, $\frac{1}{4}$ W, 100 Ω, magnetoresistance meas. 8=24020

Carbon—contd
- amorphous powders, elec. discharge sintering and graphitization 8=30667
- arc, as standard source and electrode temp. determ. 8=29927
- arc, magnetized, l.f. oscillations 8=25779
- arc, spectral emissivity of anode 8=36333
- artefacts, dynamic Young's mod., from −196°C to 1000°C 8=26790
- articles, monolithic, semi-isostatic forming 8=45933
- atom, bond participation of inner electrons 8=47627
- atom, low-energy e scatt., polarization calc. 8=47527
- atoms, Rydberg orbitals calc. 8=29620
- in austenite, thermodynamic props., electrochem. study 8=44327
- austenitic Fe base alloys, statistical thermodynamics 8=39903
- BD + 10° 2179 He star, C content 8=28066
- black, suitability as load-bearing high temp. insulating mat. 8=35456
- black suspension in nonpolar media, electrokinetic pot. and stability, H_2O effects, obs. 8=30550
- blacks, atomic radial density curves, anal. of termination effects 8=35321
- carbon black, struct. determ. by light scatt. 8=43885
- catalytic graphitization, kinetic study 8=27740
- charcoal, activated, adsorpt. of binary, org., liq. mixtures 8=48477
- charcoal adsorbent cooled with liq. N_2, for obtaining limiting vacuum 8=43710
- coal-tar pitch, carbonized, mesophase microstruct. 8=30576
- conference, Buffalo, New York (USA), 1967 8=43971
- creep rate tensile stress dependence 8=26792
- diffusion in iron-based alloys at 350°C, preliminary cold plastic deformation effects 8=35490
- diffusion in Hf, coeff. temp. dependence, 1120-2130°C 8=35495
- diffusion in $NbC_{0\cdot 64}$, temp. dependence 8=31018
- diffusion in $TaC_{0\cdot 66}$, temp. dependence 8=31018
- diffusion in TiC, coeff. comp. -dependence, 1450-2280°C 8=39985
- diffusion in W and Mo, mobility determ. from low-temp. internal friction peaks 8=35513
- diffusion in $ZrC_{0\cdot 56}$, temp. dependence 8=31018
- dimensional changes due to neutron irrad., influence of crystallite size 8=35600
- dissolved in Ni, lattice dilation effect 8=44243
- electron interference on charged film edge, obs. 8=37419
- on electron microprobe samples, gas jet decontamination 8=27808
- electron stopping power, oscillating behaviour 8=48894
- fibre reinforcement of polymers, effect on friction and wear 8=40192
- fibres, recrystallization, Ni stimulated 8=35236
- film, evaporated, i. r. absorpt. edge 8=36335
- films, condensed, structure from e.-diffr. and microscope exam. 8=35162
- films, evaporated, electron energy loss spectra 8=48913
- films, low-temp. non-linear resistance 8=31318
- foil, stable, $2 mg/cm^2$, preparation 8=35163
- glassy, disruption in K vapour 8=49888
- glassy, mag. susceptibility, field strength, ht. treatment, and deform. dependence 8=44966
- graphite crystal growth mechanism in Fe-C-Si 8=39670
- graphitized, lattice distortion of elementary layers, and rate of interstitial atoms 8=35553
- graphon, chemisorpt. of O_2, kinetics, 450-675°C 8=45362
- high-pressure bands in CO discharge, isotope shift obs. 8=34161
- interstitial solute trapping in quenched and irrad. Fe 8=44420
- Ion, C I, II, III, IV, emission spectra obs. 8=29605
- ions, low energy, resonance charge exchange 8=47536
- isotope fractionation in CO_2-gas-CO_2 in soln., and HCO_3–CO_2 in soln. systems 8=47547
- isotopic composition var. in cave concretion 8=50096
- layer on Ag foil, e energy loss spectra obs. 8=35808
- in liquid steel, activity rel. to Co, Mo, Ni, V, W conc 8=30458
- microdetermination in B, Si polymeric cpds. 8=36628
- molecules C_2, higher rot. levels 8=29724
- petroleum-coke, graphitized, absolute crystallite size and lattice distortion determ. 8=26293
- photon activation analysis in liq. Na 8=32148
- porous and dense, emittance and reflectance, visible and near i. r., 2200 to 3500°K 8=36334
- pregraphitic carbons., detection of interstitial atoms 8=26639
- in propane diffusion flame, particles size and temp. distrib., i. r. obs. 8=46257
- proton accelerator target, residual radiation dose rate 8=33402
- pyrocarbon structures of varying porosity for fission product recoil behaviour exam. 8=43127
- pyrocarbons, B-doped, electronic props. rel. to B content 8=27084
- pyrocarbons compressed at high temps., prep. and props. 8=45941
- pyrolytic, model for dimensional changes during n-irrad. 8=31148

Carbon—contd
- pyrolytic, preferred orientation rel. to thermal expansion coeff. 8=30971
- resistance far i. r. bolometer appl. 8=32939
- resonance lamp, line width and band identification 8=43288
- self-supporting low-temp. resistance thermometers 8=32983
- solubility in Ni anc Co, metastable extension, splat-quenching effects 8=30656
- soot dispersions, scatt. and absorpt. rel. to reflectance of clouds 8=39447
- stars, evolution, neutrino loss effect 8=32433
- stars, thermal stability rel. to ν losses, models 8=45636
- in steel, analysis using vacuum spectrometer, interference of Al 8=32155
- stellar spectrograms, comparison with M stars 8=28067
- stopping cross-section meas. using recoil ions from radioactive decay 8=29658
- vitreous, internal friction and elastic modulus, 4-570°K 8=44557
- X-ray spectra from carbonaceous gases 8=47652
- X-ray spectra from chloromethanes 8=47653
- C^-, laser photodetachment, ang. depend 8=25713
- C^-, prod and extraction from h.f. source 8=46431
- C I $2p^2$-$2p3s$ arrays, line strengths and transition probabilities 8=45915
- CI, vac. u. v. spectrum 8=33264
- C II, e impact line broadening calc. 8=47507
- C IV hydrogenic transition rel. to excitation temp. of Wolf-Rayet stars 8=45661
- C^{13} data from proton spectra by double irradiation method 8=37537
- C^{13} Knight shift in uranium and thorium carbides 8=41004
- C^{13} ion beams, lifetimes and excited states for multiply charged ions 8=43217
- C^{14} counting in liq. scintillators, by u. s. dispension 8=33372
- C^{14} from 1961-62 tests by U.S.A. and U.S.S.R., time and space distribution 8=27930
- C^{14} labelled materials, scintillation counting with Triton X-100 8=46880
- C^{14}, natural β scintillation counting 8=47279
- C^{21} ion paths in NIKFI-YaZ photoemulsions 8=46984
- C, tartan film by superimposing two evaporations 8=35164
- C v triplet to singlet excitation, relative intensities 8=38662
- C_2 molecule, dissoc. through rot. 8=29826
- C_2 mol., new $c'\,{}^3\Pi_g$-$b\,{}^1\Pi_u$ band syst. 8=29725
- C_2 mols. high-press. bands excitation in CCl_4-Na, K flames, mechanism, obs. 8=38816
- C_2, population inversion in $A^3\Pi g$ state by chem. reaction 8=29727
- C_2 radical in comets, forbidden intercombination transition 8=28154
- α-Fe, cold-deformed, solid solubility, normal and in stacking faults 8=35543
- in α-Fe solid solution, internal friction, effect of osc. modes on quantitative anal. 8=35695
- in Si, effects on lattice parameter 8=48674
- in SiC, C X-rays absorption, extended Philibert's correction 8=27798
- in TaC, diffusivity rel. to comp., 2100-2650°C 8=44392
- in Ta_2C, diffusivity, 2100-2650°C 8=44392
- in Th, effect on mech. strength and flow stress 8=44603

Carbon compounds
- See also Organic compounds.
- carbonaceous mats., opt. and e. microscopy 8=44164
- composite sintered materials containing excess silica, temp. depend. of resistivity 8=44687
- electro-graphite, diffusion and chemisorption of O_2 8=41266
- IV—A group metal carbides, solubility in Mo 8=48344
- gaseous, X-ray spectra, carbon emission 8=47652
- graphite nitrates, phase transforms, resistivity and thermo-elec. power 8=35827
- methane, atmospheric, deuterium and tritium content 8=27883
- Al films on Ta(110), interaction of CO 8=35159
- Ca_3N_2, vapour press. and ht. of sublimation 8=48295
- CCl_4 raman spectra asymm., due to time depend. mol. reorientation 8=43830
- CCl_4, Raman spectra, teaching demonstration 8=29696
- CCl_2F_2 atm., ageing of insulators 8=40556
- CF, absolute u.v. transition probabilities 8=34230
- CF_2, adsorpt. spectrum 8=25453
- CF_2, matrix-isolated, i. r. spectra 8=29723
- CF_3, matrix-isolated, i. r. spectra 8=29723
- C_3F_8, rate of ionization by electron attachment, two-body process 8=43471
- C_7F_{14}, rate of ionization by electron attachment, two-body process 8=43471
- CH_4 or CD_4 added to H_2 or D_2, θ pinch at 0. 8 mTorr filling press. 8=34417
- CH_4 and C_2H_6, atmosphere, tritium content 8=27879
- $CHClF_2$ atm., ageing of insulators 8=40556
- CN^- in KCN, hindered rotation above 168°K 8=26030
- CN^-, polarization, perturbation point charge calc. 8=25454
- CN^-, rel. to bright Cu electrodeposition from $CuSO_4$ solns. 8=45395
- CN^-, SCF minimal basis set calc. 8=29719

Carbon compounds—contd
CN, $B^2\Sigma \to A^2\Pi i$ bands 8=29721
CN, electronic transition probabilities 8=47591
CN, excitation in active N_2 8=27699
CN, extension of red and violet bands 8=29726
CN, in solar spectrum, red system vibr. band oscill. strengths 8=45867
CN lasers, far i.r., pulsed output, mode pattern and polarization characts. 8=46582
CN, reactions e absorpt spectroscopy 8=27700
CN, σ-states, electronic configs. and N^{14} quadrupole coupling 8=47710
CN, stimulated emission, optical detection at 20 cm wavelength 8=38819
CNFN, matrix-isolated i. r. spectra 8=47712
$CNNF_2$, matrix-isolated i. r. spectra 8=47712
C_2N_2 (cyanogen) condensed in solid N_2 and Ar, luminescence 8=25455
C_2N_2/O_2 mixtures, detonation limits 8=45357
C_3N_{12}, cryst., vibr. spectrum 8=25456
C_3N_{12}, vibr. spectra 8=31976
CO, absolute u.v. transition probabilities 8=34230
CO, adsorbed on Pt, i.r. spectrum 8=48488/9
CO, adsorbed on Si-supported Pt, i. r. absorpt. 8=30773
CO adsorbed on transition metal surface, nature of bond 8=48298
CO adsorbed on W, electron bombard. effect 8=30776
CO, adsorption and oxidation on Ni 8=48487
CO, adsorpt. on Mo(111), faceting 8=48486
CO, adsorption on Pd, effect of surface annealing changes 8=48424
CO, adsorption on W(110) 8=39627
CO, adsorpt. on W (100) and (211) faces, work function 8=35200
CO, absorpt. spectrum in extreme u. v. 8=25458
CO, Asundi bands excitation 8=38994
CO, charge transfer from p and H atom, cross-sections 8=38737
CO, chemiluminesc. from flames 8=27698
CO, chemisorption on TaC 8=49903
CO desorption from W by electron bombard. 8=48495
CO desorption from W 8=48496
CO, dissociative chemisorption on hot W 8=49893
CO, e beam dissoc., O^- prod. cross-section obs. 8=47703
CO, electronic transition moment integrals for ionization 8=25460
CO, electronic transition probabilities 8=47591
CO, energy relax. for thermal e 8=38818
CO, fourth positive system in solar u. v. spectra 8=45870
CO gas, γ-radiolysis, detection of O atoms 8=36623
CO, ground and ionized states, potential energy calc. 8=25492
CO, high resolution interferometric spectra of Venus atmosphere 8=50420
CO, influence on CO_2 laser plasmas 8=33181
CO, i.r. spectra, absorpt. coeffs. 8=34236
CO, line-strengths at low press. 8=42218
CO luminesc. during u.v. photolysis 8=34266
CO, metastable state 8=25459
CO, molecular constants 8=47589
CO, molecular line absorpt. in late-type stellar atm. 8=45666
CO molecule, distortion in intense elec. fields 8=43291
CO mols. trapped in rare gas matrix, e transitions perturbation 8=39523
CO, pulse radiolysis 8=45405
CO, solid, kinetics of order-disorder transition 8=39546
CO spectra by double-beam, two-beam interferometry far i.r. 8=28818
CO, spectral radiance scale model rocket exhaust 8=38815
CO, vibr. relax. in nozzle flow 8=47586
CO, Xe-sensitized fluoresc. 8=25457
CO, Cl, NO_2, reactions at 381-473°C, kinetic eqn. setup 8=49857
$CO-N_2$ laser, line selection, amplification and vibrational population 8=28681
$CO + O_2 + M$, vac. u.v. flash photolysis 8=45398
CO^+, absolute u.v. transition probabilities 8=34230
CO^+ and CO excitation, lifetimes and decay cross-sections 8=34261
CO^+, electronic transition moment integrals 8=25460
CO_2^- state e spectra, obs. 8=34224
CO_2, absorpt. band Q-branch transmission calc. 8=43294
CO_2, absorpt. by monoethanolamine, optical study of interfacial turbulence 8=32093
CO_2, absorpt. into turbulent jets of water 8=30425
CO_2, adsorption on MgO, i.r. study 8=47974
CO_2, adsorpt. on Mo (001) and (110) faces, monolayer struct., obs. 8=41269
CO_2, anharmonic force consts. 8=43292
CO_2, band and total emissivities 8=43280
CO_2, bands at 4.3μ 8=29730
CO_2, charge transfer from p and H atom, cross-sections 8=38737
CO_2, collisional relax. in 10°0 state 8=47715
CO_2, convective diffusion in blood, rel. to membrane-type artificial lungs 8=43793
CO_2, coupled rad. conduction and convection in entrance

Carbon compounds—contd
CO_2 cryodeposits on 77°K surface, refractive index from Bragg interference meas. 8=41068
CO_2, desorption from water in packed bubble column 8=25858
CO_2, diffusion and wall-de-excitation of (00°1) state 8=38817
CO_2 dilute soln in cyanogen, vib. spectra 8=45236
CO_2, dissociative ionization 8=29976
CO_2, earth's horizon profile spatial energy distrib., 15μ 8=27910
CO_2 effect on radiative flux divergence in atmosphere 8=41342
CO_2, eqn. of state, 273-4000°K for pressures up to $1000 \times 10^5 N/m^2$ 8=39466
CO_2 escape from cave concretions 8=50096
CO_2, 4.3μ transient laser oscill. 8=28680
CO_2 gas laser, vibration-rotation transitions, sequential Q-switching 8=24308
CO_2, in critical region, free-convection heat transfer from Pt wire 8=34823
CO_2 impurity in O_2, effect on acoustic absorpt. 8=39211
CO_2 in atmosphere at 500 and 700 mb, concentration 8=50131
CO_2-inert gas mixtures, thermal diffusion 8=34679
CO_2 in Martian atm., 1.05μ spectrometry 8=45828
CO_2 in mesosphere, role in governing electron conc. 8=27880
CO_2, in seawater under Arctic ice 8=41327
CO_2, integrated intensity meas., 2.0-, 1.6-and 1.43-μ regions 8=34235
CO_2, intensities of 12-18 μ bands 8=25462
CO_2, intensity of 1.6μ bands 8=34234
CO_2 ionizing collisions and electron mean free paths obs. at 10^{-4} torr 8=34458
CO_2, i. r. abs., 1-1.25μ 8=29728
CO_2 laser applics. 8=42080
CO_2 laser, c. w. high power, generation and appl. as heat source in welding 8=28678
CO_2 laser, heterodyne detection of beat freq. with $Pb_{0.88}Sn_{0.12}Te$ diode laser 8=42098
CO_2 laser, high-power, sealed-off, theory and design 8=4208
CO_2 laser induced fast photocond. in Te 8=40676
CO_2 laser, mode locking using GaAs intracavity acousto-optic loss modulator 8=24305
CO_2 laser output timing by selective intracavity absorpt., 8=46586
CO_2 laser, passive Q switching by vinyl chloride 8=28679
CO_2 laser plasmas, influence of Xe 8=33181
CO_2 laser, production of multijoule pulses 8=33180
CO_2 laser, Q-switching and pulse sharpening, analysis 8=33162
CO_2 laser, Q-switching, technique to provide h. f. output pulse repetition rate 8=33185
CO_2 laser, repetitive pulsing by means of CO_2 gas and other absorbers 8=24306
CO_2-laser, sealed-off, gas comp. rel. to water vapour and hydrogen effects 8=24307
CO_2 laser, sealed-off, influence of Xe as gas additive 8=33184
CO_2 laser-system, sealed-off, effect of H and O on gas composition 8=46584
CO_2 laser, vibr. levels population, 9-11μ 8=24374
CO_2 laser welding of quartz component 8=33179
CO_2 laser with near confocal optical resonator obs. 8=4207
CO_2 lasers, high power, parameters affecting power output 8=37572
CO_2 line parameters using CO_2-N_2-He laser 8=29720
CO_2, liq., self-diffusion 8=34812
CO_2, low alloy steels corrosion and excrescence form. mechanisms, ≤ 550°C 8=32098
CO_2, low conc. in N_2, mass spectrometric determ. 8=32153
CO_2 luminesc. during u.v. photolysis 8=34266
CO_2, mixed-gas adsorption and vacuum desorption on mol. sieve, thermodynamic and rate behaviour 8=48481
CO_2 molec. beam, scatt. of K at. beam, time-of-flight anal. 8=38952
CO_2 mols., charge exchange with He^+ and Ne^+, 2-250 eV 8=38758
CO_2, near crit. point anomalous shear viscosity and thermal cond. rel. to density fluctuations 8=30291
CO_2, new i.r. bands in Venus spectra 8=28153
CO_2, 9.4 and 10.4μ bands, strengths and widths 8=43289
CO_2, population inversion, thermal production 8=37578
CO_2, Rayleigh scattering, depolarized, as new probe of intermolecular forces 8=39212
CO_2, 667 cm^{-1} band strength determ. 8=25461
CO_2 solid, adsorption of H, amorphous and granular structure below 100°K 8=30765
CO_2, solid, Brillouin linewidths near critical point 8=41069
CO_2, spectral absorpt. in artificial atmos. 8=27907
CO_2, spectral radiance scale model rocket exhaust 8=38815
CO_2 spectral transmission functions 8=30300
CO_2, temp. field in volume of gas 8=47959
CO_2, 10 μ band, temp. depend. of total intensity 8=25463
CO_2, thermal diffusivity in crit. region 8=39241
CO_2, transmittance, 4590-5346 cm^{-1}, eqns. 8=43293
CO_2, viscosity, dynamic meas. to 500°C, and statistical mech. correls. 8=43704

Carbon compounds—contd
CO_2, viscosity 8=25835
CO_2^+, absolute u.v. transition probabilities 8=34230
CO_2^+ band excitation by e-impact (80–1500 eV) 8=25490
CO_2-Ar mixtures, thermal diffusion 8=47987
CO_2-He mixture, 43.7 MeV p-irradiated, energy deposited freq. distrib. 8=29663
CO_2-He-N_2, laser composition and power output, gas flow dependence 8=46585
CO_2 + He + Ne system, thermal diffusion 8=30320
CO_2-H_2O mixture, 80-230°K obs. rel. to composition of Martian icecaps 8=32547
CO_2-H_2O vapour mixture, optical-acoustic radiative power, absorpt., press. temp. effects 8=30298
CO_2-Kr and CO_2-Xe thermal diffusion, 330°-600°K, Chapman-Enskog theory 8=43707
CO_2:NO_2 and I_2, gaseous, stimulated thermal Rayleigh scatt., obs. 8=34665
CO_2-N_2 mixture, shock tube meas. of rad. in range 7000-16 000°K 8=43287
CO_2-N_2-He laser gain distribution, population densities and rotational temperature for rotation-vibration transition 8=33183
CO_2-N_2-He laser, output power rel. to pump current and length 8=42086
CO_2-N_2-He laser, passive mode locking 8=37579
CO_2-N_2-He lasers, increased efficiency through addition of Xe 8=46583
CO_2-N_2-He mixture, increasing output of laser 8=37577
CO_2 + N_2O, near-resonant energy transfer between i.r.-active vibrs. 8=47725
CO_3^- in calcite, X-irradiated, paramag. resonance 8=49600
CO_3^{3-}, Y^{3+}-stabilized mol. ion in calcite 8=49620
CO_3, production, i.r. spectrum and struct. 8=25464
CO_4 group complexes, i.r. spectra rel. to asymmetric stretching vibrations 8=29714
C_3O_2, gas electron diffr., temp. effects 8=25466
C_3O_2, vac. u.v. absorpt. spectrum 8=25467
C_3O_2, vibr. amplitudes and shrinkage effects 8=25465
$C^{12,13}O_2^{16}$, rotational constants D_{eff} numerical values determ. 8=47592
$^{12}C^{16}O_2$, molecular vibrational analysis 8=47590
COS, quadrupole moment, from microwave spectral broadening 8=29729
CS, ground state reduced potential curves 8=29717
CS, Zeeman effect from millimeter interferometry 8=38814
CS_2, cryst. struct. and molec. motion in solid 8=39776
CS_2, dielect. const. rel. to pressure and temp. 8=39396
Cs_2, 4-photon amplification of quartz stimulated M-B scatt. components, obs. 8=43822
CS_2, light scatt. by fluctuations of anisotropy 8=25920
CS_2, non-linear dielec. susceptibility obs. 8=34888
CS_2, raman spectra 8=43835
CS_2 Raman spectra, teaching demonstration 8=29696
CS_2, refractive index meas. using interferrometric arrangement 8=42246
CS_2, stimulated Brillouin scattering, anti-Stokes components origin 8=25922
CS_2, viscosity, gaseous state 8=25835
CS_2-O_2 chem. laser, analysis showing new lines and selective excitation 8=46569
C_3S_2, vibr. and shrinkage, mean amplitude rel. to temp. 8=43290
$M_{23}C_6$ carbide, growth on grain boundaries of stainless steel 8=39668
N^{15} content, determ. by recording spectrometer 8=28817
NH_2CN, microwave spectrum, N^{14}-quadrupole coupling 8=43297
Carbon tetrachloride (CCl_4). See Organic compounds.
Carcinotrons. See Electromagnetic oscillations; Electron tubes.
Carrier mobility. See Crystal electron states; Semiconducting materials; Semiconductors.
Carrier scattering. See Crystal electron states; Semiconducting materials; Semiconductors.
Catalysis
See also Reaction kinetics.
carbons, kinetic study of graphitization with CuO 8=27740
combined action of metal and semiconductor 8=49906
effect of intraparticle temp. grads. on activity expt. study 8=32121
hydrogenation, liq.-phase, catalyst potential displacement rel. to activation energy 8=36553
germane, thermal decomp., accel. by Pt-Ge contacts 8=32123
kinetic theory, in cylinder 8=48109
negative temp. coefficients for surface diffusion 8=49898
steel, stainless, in H_2SO_4, corrosion inhibition by $Na_3PMo_{12}O_{40}$, mechanism, 8=45370
surface reaction, props of laminar boundary layers 8=36587
transition metal hydride complexes as catalysts 8=25521
Cr^{3+} doped corundum, ethylene hydration 8=32122
Cu-Ni alloys, activity toward isotopic exchange of H_2 8=49911
Fe in H_2SO_4 corrosion inhibition by dissolved ring-substituted anilines 8=45377-8
Mo, synthesis of NH_3 8=49909
Catalysis—contd
Mo, H_2 + D_2 $\rightleftarrows$ 2HD reaction 8=49907
Mo, N_2^{28} + N_2^{30} $\rightleftarrows$ N_2^{29} reaction 8=49908
NH_3 decomp. on W, field-emission meas. 8=27734
Ni catalyst beds, Q meas. 8=32120
O atom decay in catalytic cylinder 8=49910
Ti^{3+} doped corundum, ethylene hydration 8=32122
Cataphoresis. See Electrophoresis.
Cathode-ray oscillographs. See Electrical measurement.
Cathode-ray tubes. See Electron tubes.
Cathode rays. See Electron beams.
Cathodes
See also Electron emission.
bar, indirectly heated, construction 8=36035
cold, electron source, brightness obs. 8=47744
cold, opto-electronic, for cathode ray tubes 8=44937
convertor, thermionic, e cooling, 1400°–1800°C obs. 8=33037
cooling effects of thermal autoelectronic emission and evaporation, (4 to 8) × 10^3°K 8=40698
craters, in high-current vacuum arc, theory 8=25704
damage caused by oxide cathode Hg vapour discharges 8=36042
electric arc, temperature field and current density in cathode spot 8=43462
electrode destruction in breakdown of liquid He 8=46303
electrodes in spark discharges, erosion characts. 8=29915
electrodes in vacuum systems, capture and identification of particles in gap 8=25699
for electron interferometer with mag. lenses 8=41952
field emission for coherent illumination of e. biprism 8=41953
field-emission, thin-film, structure, fabrication, performance and e.-micrography 8=40696
hollow, temp. regime obs. 8=27344
hot, new development 8=36044
non-isothermal, Cs vapour low voltage arc. 8=25703
Penning discharge, power dissipation 8=43445
photocathode formation from alkali-antimonide films, chem. comp. meas. using crystal-quartz microbalance 8=40683
photomultiplier, rel. sensitivity distrib., wavelength depend. 8=33094
plasma air stream containing K, work 8=29946
plasma-arc torch, obs. projection system 8=39144
sandwich, with mica layer, e emission 8=44941
shielded, discharge current density, radial distrib. 8=25691
Ag-O-Cs photo cathode, origin of photoelectrons 8=49440
Ar ion laser, high-current continuous-action 8=46579
Cs-Sb film in photocathode formation, chem. comp. meas. using crystal-quartz microbalance 8=40683
Cs_3Sb, on MnO, e.- and X-ray-diffr. exam. 8=39591
K-Sb film in photocathode formation, chem. comp. meas. using crystal-quartz microbalance 8=40683
LaB_6, emission characts. 8=27348
LaB_6, rod cathode for high-brightness electron gun 8=28555
Mo, vacuum-gap discharge erosion obs. 8=34424
oxide
emission layer application, development 8=36045
impregnated aluminate on W, Mo or Re base, limiting emission current 8=27345
structure of emitting coating 8=36043
well-activated, thermionic emission and work function, temp. range 500 to 1100°K 8=27346
Cathodoluminescence. See Luminescence.
Causality. See Physics fundamentals.
Cavitation
See also Vortices.
acoustic. threshold obs. of subharmonic generation 8=30370
alchohol, u.s. dispersion of insoluble particles, obs. 8=39442
breeder reactor, Na-cooled 8=29560
bubble diffusion, frequency depend. of threshold 8=34735
hydrodynamic, light emission from 8=43813
liquid, refraction wave onset and development 8=43730
radiation-induced acoustic cavitation, apparatus and results 8=48032
sonoluminescence produced in liqs. under cavitation, thermal and elec. hypotheses 8=48167
tetrachlorethylene, degassed, elucidation of bubble motion 8=25850
tetrachloroethylene, u.s. cavitation using pulsed n source 8=25849
ultrasonic, relaxation phenomena appl. 8=37278
u.s. irradiation cell for liquids 8=34722
voids, pulsation in u.s. field, solns. of describing eqns. 8=43729
vorticity induced at smooth flat wall 8=30369
water, u.s. dispersion of insoluble particles, obs. 8=39442
in water, u.s. induced bubbles, models and damaging mechanism 8=43733
Al melts, u.s. dispersion of Al_2O_3, Fe and Ti, 740-800°C 8=39442
Na liquid cooled breeder reactor 8=29560
Cavity resonators. See Acoustic resonators; Electromagnetic oscillations.
Celestial mechanics
adiabatic radial motions of uniformly dense spheres, time-dependent internal solns. in general relativity 8=41495

Celestial mechanics—contd
- binary systems, viscous tidal lag 8=32460
- Computers for analytical development, Colloquium, Prague August 1967 8=50266
- deformable bodies, precession and nutation 8=32402
- earth satellite, torque in non-inverse square gravitational field 8=32388
- fundamental proper motions, deriv. and comparison of four systems 8=32499
- Galactic disc stars near sun, kinematic models 8=36970
- gravitational field of rotating body, e.g. star, sources for Kerr soln. 8=23867
- Keppler motion, general perturbed two body problem 8=46007
- Lagrangian 3-body problem as test for equiv. of gravitational and inertial mass 8=32817
- moon capture by earth 8=50401
- moon, capture hypothesis 8=36993
- moon libration in longitude, approx. soln. 8=28138
- nearly periodic Hamiltonian systems, invariant calc. 8=28251
- orbit, intermed. from generalized problem of two fixed centres, comparison with others 8=36918
- orbit, Newtonian, in pulsating Universe 8=8=46082
- periodic orbits, symmetric, distribution in three body problem 8=32406
- plane elliptical restraint problem, regularization 8=32705
- plane n-body problem, quasi-periodic first kind solns. 8=32401
- Pluto, mass determ. 8=32549
- product of two rotations 8=28247
- relativistic stellar dynamics 8=45606
- resonant periodic orbits in galactic models 8=41643
- Roche-Riemann ellipsoids, equilib. and stability 8=45607
- statistical mechanics, nonequilibrium applied to inhomogeneous systems 8=32405
- stellar dynamics, collective effects, one-dimensional model, 8=50287
- stellar dynamics tensor virial-equation 8=45621
- systems with 2 degrees of freedom invariant surfaces 8=45604
- third integral of the Galaxy 8=32496
- three-body problem 8=45605
- three-body problem, restricted, orbits through L_1 8=32403
- three-body problem, restricted, periodic orbits rel. to gaps in asteroid belt 8=32404

Cell model. See Liquids, theory.

Centrifuges
- solid particle motion in rotating potential flow, stabilization 8=30551
- ultracentrifugation determ. of polymer mol. wt. 8=38967-8
- ultracentrifuges, rotor deceleration formula 8=30542

Ceramics
- actinide cpds, elec. and thermal props. 8=27233
- alumina, commercial, dielec. props., 20-400°C 8=27238
- alumina, grinding, densification and abrasion resistance 8=48987
- alumina, insulating, vol. resistivity meas. problems at high temps., 8=49334
- alumina, plasma-sprayed, structural changes on reheating 8=48354
- alumina, surface resistivity cleaning and humidity effects 8=49337
- alumina, surface resistivity dependence on ambient humidity and cleanness 8=27237
- cermets, as thin film resistors, characts., 8=44675
- cermets, structure rel. to geometry and phase distrib., effects on props. 8=35263
- coatings of archaelogical specimens, e-micrographs 8=43970
- conference, American Ceramic Society 70th annual meeting, Chicago (USA), 1968 8=40085
- corundum, transparent sintered, prep. and props. 8=45940
- damage by fast neutrons, isothermal irrad. assembly 8=35597
- dielectric, review 8=49333
- dielectric, sintered in reducing atmos. for high-quality capacitor production 8=27220
- dielectric, sintered in reducing atmos., prep. constitution and elec. props., 8=49332
- electroceramics of cordierite structure, production 8=30666
- electroceramics with cordierite structure, development rel. to comp. and firing 8=48355
- forsterite lapping characts. using diamond abrasives 8=48949
- glass containers prod. system, computers appls. 8=50471
- insulating, volume resistivity meas. at high temps. 8=27219
- insulating, vol. resistivity meas. problems at high temps., 8=49334
- in klystrons, props. and behaviour 8=28602
- lapping charactieries, with ordinary abrasives 8=48948
- magnesia spinel, reactive, prep. and props. 8=43989
- mass spectrometer appl. 8=29575
- nuclear reactor materials, radiation damage and defect cluster growth 8=31129
- pellitized packings, thermal cond. meas. in region 100-1600°C, and formula deriv. 8=30978

Ceramics—contd
- piezoelectric cube, resonant props. 8=32897
- point defects, study techs., relns. with mass transport, interpret. of rad. damage, review 8=35519
- polycrystalline, creep rate rel. to porosity 8=35625
- polycrystals, appl. of Von Mises criterion to fracture 8=31180
- pyroelectric, detector for at. beams 8=47544
- radiation damage rel. to physical props. 8=26722
- refractory oxide solid solutions, with fluorite, pyrochlore and perovskite structures, anionic conduction 8=27232
- relaxation polarization, rel. to discloations 8=49322
- SAP, (sintered Al/Al_2O_3 alloy), lattice defects, behaviour on cold working, resistometric exam., 8=48817
- SAP, (sintered Al/Al_2O_3 alloy), lattice defects, behaviour on quenching, resistometric exam., 8=48816
- sapphire, insulating, vol. resistivity meas. problems at high temps. 8=49334
- single crystal, fracture mech., rel. to crack nucleation and plastic deform. 8=31180
- strengthening methods 8=48968
- structural properties, relation to firing temp. 8=48356
- talc, structural changes on heating 8=30699
- vacuum chamber for p synchrotron 8=34696
- Al_2O_3, of high purity, production 8=35071
- BeO, extruded, residual stress and grain deform. 8=44556
- Cm^{244} presence det. from fission fragment tracks `=36649
- $Li_2Al_2O_4$-SiO_2 system, titania and zirconia nucleated for casting mirror blanks 8=41137
- MgO, isostatically hot-pressed, fabrication and characterization 8=26045
- Ni-Zn ferrites, hot-pressed, fine-grained, hf and microwave props. 8=49562
- $Pb(Mg_{1/3}Nb_{2/3})O_3$-$PbTiO_3$-$PbZrO_3$, with Ba and Sr substitutions, piezoelectric props. and phase relations 8=31442
- $PbTiO_3$, piezoelec. coupling factors and aging rates 8=49384
- $PbZrO_3$-$PbTiO_3$, by hot-pressing and elec. props. 8=39535
- $PbZrO_3$-TiO_3, PbO deficiency on vaporization rel. to piezoelectric props. 8=35010
- $Pb(Zr_{0\cdot65}Ti_{0\cdot35})O_3$, cold-pressed vaporization in vacuo, 690-1130°C 8=35009
- $Pb(ZrTi)O_3$, mechanical quality and microstruct. 8=44597
- $Pb(Zr_{0\cdot65}Ti_{0\cdot35})O_3$, vaporization of hot pressed pellets of near theoretical density 8=43919
- PuP, thermal conductivity and ht. capacity 8=44368
- PuS, thermal conductivity and ht. capacity 8=44368
- SiC, sintered, heater elements, oxidation ageing rel. to elec. resistivity changes 8=31231
- SiO_2 with W inclusions network, 2000°C 8=48092
- TaN-TiB_2, hot-pressed, densification and wear resistance 8=49053
- $(Zn_{0\cdot65}Mg_{0\cdot35})_2SiO_4$, high-temp. mech. props. 8=35725

Cerenkov radiation. See Cherenkov radiation.

Cerium
- α, β, susceptibility above magnetic ordering temp., temp. depend. 8=40750
- doping of CaS phosphor, effect on thermoluminesc. and decay, obs. 8=45305
- in fluorite crystals, magneto-optical rotation of impurity centres 8=49718
- plasma, Ce, density perturbations, propag., 8=43594
- in CaF_2 as paramag. impurity, nucl. relax. 8=45119
- α-Ce, heat capacity at 11 kbar pressure between 0.3 and 6°K 8=39911
- γ-Ce, slow-cooled, crystal structure temp. dependence, 300-100°K 8=30891
- Ce^{144} as fission product in coated fuel particles, determination 8=47404
- Ce^{3+}, in hexagonal cryst. field, electronic Raman scatt. tensor 8=31975
- Ce^{3+} in CaF_2 line splitting in electric field 8=36308
- Ce^{3+} in $LaCl_3$, i.r. Zeeman effect at 77 and 27°K 8=36383
- in In, solid solns., superconductivity, resistivity and thermoelec. power rel. to localized moments 8=31339
- in Sn, solid solns., superconductivity, resistivity and thermoelec. power rel. to localized moments 8=31339

Cerium compounds
- cerium magnesium nitrate low temp. scale, evidence from critical magnetic field curve of superconducting W 8=37331
- cerium magnesium nitrate, specific heat obs. rel. to low temp. thermometry 8=30962
- cerium magnesium nitrate thermometry, applic. to liquid helium 8=37332
- cerous magnesium nitrate, high field magnetization anomaly obs. 8=44968
- mischmetal-Co alloy powders, coercivity milling dependence 8=31597
- monochalcogenides, antiferromag props., 4-1300°K 8=31761
- oxide solid solns., X-ray absorpt. spectra indicating tri- and tetra-valent ions 8=39638
- spin lattice relaxation of Dy^{3+} and Yb^{3+} 8=36222
- Ce(III) complex, $K_2Ce(CH_3COO)_5 . H_2O$, crystal structure 8=26378

Cerium compounds—contd
- Ce-alkali metal tungstates, hydrothermal synthesis and morphology 8=26259
- CeAs, magnetic props. from neutron scattering data 8=45052
- $CeCl_3$, interaction constants determ. 8=36239
- $CeCl_3 . 7H_2O$, sp. ht. meas. between 1.1 and 3.3°K 8=30963
- CeF_4, solid, chemical shift anisotropy 8=40980
- CeMg nitrate, spin-lattice relax. mag.-field dependence by resonant two-phonon process 8=31858
- CeO ceramic, elec. conduction 300 to 1000°C, rel. to O_2 partial press. 8=44868
- CeO_2, rare-earth impurity ion doping in melt-grown crystals 8=26645
- CeO_2, spectral reflectance 8=41128
- CeO_3:Cm^{3+}, e. s. r. at 10 Gc/sec and liq. He temps. 8=27490
- CeO_2: Dy^{3+}, e.s.r. spectra 8=40918
- CeSb, magnetic props. from neutron scattering data 8=45052
- CeSb, magnetic state phase diagram 8=49465
- $CeSn_3$, Mõssbauer study of Sn^{119}, phases at 4.2°K 8=43944
- $Ce_2W_2O_9$, structure and hydrothermal synthesis, obs. 8=39636

Cermets. See Ceramics; Metals.

Change of state. See Boiling; Condensation; Freezing; Melting; Phase transformations; Sublimation; Vaporization.

Characteristic temperature. See Specific heat.

Charcoal. See Carbon.

Charge. See Electric charge.

Charge carriers. See Crystal electron states; Semiconducting materials; Semiconductors.

Charge exchange. See Collision processes; Ionization/gases.

Chelates. See Molecules; Organic compounds.

Chemical analysis
- See also Spectrochemical analysis.
- alnico, Ti determination, gravimetric 8=49984
- ferro-titanium, Ti determination, gravimetric 8=49984
- gas, in vacuum apparatus, equipment and limitations 8=43715
- gas sampling tube for separation of condensables 8=49982
- gases, differential thermal cond. analyser, theory and design 8=27774
- glass, silicate, acceleration by SiO_2 precip. into $H2Si_2O_5$ 8=45413
- katharometer, thermistor sensor, sensitivity 8=43679
- metals, microanalysis, ion optics appl. 8=27777
- microscopy of field and domain structs. 8=48577
- nitrogen conc. determ. by interferometry in gaseous mixtures 8=49988
- oxygen conc. determ. by interferometry in gaseous mixtures 8=49988
- potassium feldspar and plagioclase, simultaneously crystallized at 600°C, distrib. of trace elements 8=36627
- powder mixture, photosensitive transformer bridge method 8=43984
- rare-earth, methods of trace analysis 8=49983
- residual gas, in vacuum apparatus 8=41297
- 2, 4, 6-trinitrotoluene, isomer determ. by n. m. r. 8=30534
- water-organic mixtures, thermometric method 8=27771
- C in liq. Na, photon activation method 8=32148
- C in polymeric B, Si cpds., microdeterm. 8=36628
- Fe, passive layer, detect. of H in outer layer 8=35171
- H in polymeric B, Si cpds., microdeterm. 8=36628
- U^{233}, amine extraction from irrad. ThO_2 8=36634
- **adsorption**
  - See also Chromatography.
  - gas, with molecular sieve 8=27772
- electrochemical
  - polarographic electrode, metallized membrane type, atm. O_2 monitoring and other appl. 8=27775
  - polarography in molten $LiNO_3$-$NaNO_3$-KNO_3 8=45414
  - Co in Ni, cathode ray polarographic microdeterm. 8=27776
  - H_2O vapour traces in gases, meas. with solid electrolyte cells 8=41298
  - H_2O_2 on Pt microelectrode, polarographic behaviour on periodic renewal of diffusion layer 8=41275
  - $LiNO_3$-$NaNO_3$-KNO_3 melt, polarographic investigation of Tl^+, Cd^{++}, Pb^{++}, Zn^{++}, Ni^{++} 8=45414
  - Ni in Co, cathode ray polarographic micro determination 8=27776
  - Ni_2P in Ni, as-plated electroless, from dissilution kinetics 8=45383
  - O_2 traces in gases, meas. with solid electrolyte cells 8=41298
- **by mass spectrometry**
  - See also Mass Spectrometers/applications.
  - amino acids on photoionization 8=41299
  - aromatic diterpenes 8=32152
  - coal, laser heated in source of time-of-flight spectrometer 8=27780
  - glass, surface composition, spark source mass spectrometer 8=41300
  - interface mol. separator, polar chemisorpt. deactivation 8=32150
  - mass spectra deciphering for high temp. thermodynamic reactions 8=38609
  - oxygen 8=36633
  - pyrolytic fibre products, gaseous and volatile 8=36632

Chemical analysis—contd
- **by mass spectrometry**—contd
  - standard mixture problem, math. soln. 8=32151
  - steel, using ion beam chopper, reproducibility of results 8=27779
  - ultra-high vacuum system, omegatron and ionic sorption pump appl. to residual gas 8=36630
  - Al, using ion beam chopper, reproducibility of results 8=27779
  - CO_2, atm., direct determ. 8=36631
  - CO_2, low conc. in N_2, determ. 8=32153
  - Cs–O system, evaporation products obs. 8=32096
  - $N + CH_3CHO \rightarrow HCN + H_2 + HCO$ reaction study 8=27710
- **by nuclear reactions**
  - neutron activation analysis 8=50002
  - neutron-capture γ-ray activation anal. 8=32168
  - rocks, determ. of Si content by n activation analysis 8=50062
  - steel, B content determ. from neutron flux depression 8=37100
  - $Ca^{43,48}$, determ. by neutron time-of-flight 8=36648
  - CoO, volume diffusion of O, by proton activation of O^{18} 8=35483
  - Fe-Cr alloy, activation anal. of Cr contents in inclusions 8=36652
  - Hf, anal. of O content by He^3 irrad. 8=27818
  - LiF solid, oxide doped, neutron activation anal. 8=36593
  - Mo, anal. of O content by He^3 irrad. 8=27818
  - $O^{16}(n, \gamma)N^{16}$ as means of meas. the O content of metals 8=32167
  - O^{18} in gases, isotopic determ. by n time-of-flight spectrometry 8=32149
  - Si, to determine Cu, Zn, Mn, P, S, Cl, Fe and Co content 8=50000
  - $SiCl_4$, $SiHCl_3$, neutron activation anal. for trace contaminants 8=49998
  - SiO_2 in marine sediments, by 14 MeV neutron activation 8=41314
  - $U^{235,238}$ isotopic ratio, activation analysis by γ spectrometry 8=47546
  - W, anal. of O content by He^3 irrad. 8=27818
  - ZnS phosphor, trace metal determ. by n. activation 8=50001
  - Zr, anal. of O content by He^3 irrad. 8=27818
- **radioactive**
  - See also Radiochemistry.
  - alloys, radioactive, C, O, N, H determ. 8=36629
  - β-active gases, low conc., meas. device 8=49997
  - γ-spectra, pulse height analysis 8=47043
  - minerals, gamma spectrometry applic., 20-610 KeV 8=36651
  - power metallurgy, use of isotopes 8=43987
  - reservoir water contamination detector 8=38403
  - tritium, assay of solns. 8=49999
  - C^{14} conc. in organic liquids, using internal filling counters 8=27817
  - C^{14} labelled materials, Triton X-100 scintillant 8=46880
  - Cm^{244} det. using fission tracks 8=36649
  - Pu^{239} in irrad. samples, non-destructive assay, Pb spectrometer 8=36650
  - $SiHCl_3$, neutron activation anal. for trace contaminants 8=49998
  - U^{235} in irrad. samples, non-destructive assay, Pb spectrometer 8=36650
- **X-ray**
  - See also X-ray examination of materials.
  - brass standard, Midwest Probe Users Group report 8=30851
  - electron microprobe absorpt. corrections rel. to target Z 8=27796
  - electron microprobe absorpt. correction functions, evaluation 8=27797
  - electron microprobe, automatic scanning and data analysis 8=27807
  - electron microprobe calibration, transport eqn. calc. 8=28560
  - electron microprobe correction factors, calc. methods evaluation 8=27801
  - electron microprobe, fluoresc. corrections errors 8=27800
  - e microprobe, impurities diffusion coeffs., obs. 8=30998
  - electron microscope/microanalyser and appls. 8=27805
  - electron microscope/microanalyser EMMA, appls. 8=27806
  - electron microprobes optical signals detect. 8=36461
  - electron microprobe, quantitative, computer programme 8=27803
  - electron microprobe sample contamination by C and O, gas jet cleaning 8=27808
  - electron microprobe, target absorpt. correction 8=27799
  - electron probe microanalysis, absorpt. and atomic no. corrections 8=41311
  - electron probe micro-analysis, absorpt. correction functions 8=41309
  - electron probe microanalysis, basic principles and performance 8=36646
  - electron probe microanalysis, electron penetration and atomic no. correction 8=41312
  - electron probe microanalysis quantitative, accuracy exam. 8=41310
  - electron probe microanalysis X-ray mass absorpt. coeffs. meas. 8=41048

Chemical analysis—contd
- **X-ray**—contd
    - electron probes quantitative meas. by shadow projection method 8=33081
    - for electron probe, scanning single channel pulse height analyser, and lines identification tables 8=24530
    - electron triple backscattering 8=49995
    - fluorescence anal., compressed powders 8=32163
    - fluorescence anal., solid and liq. solns., matrix effect 8=32164
    - fluorescence determ. of metals, Polish applications 8=41306
    - fluorescence, effect of sample grain size 8=45419
    - K and L X-ray lines, relative intensities rel. to electron-
    - light elements, absorption, extended Philibert's correction extension 8=27798
    - light elements, cryst. spectrometry and pulse-height analysis comparison 8=27812
    - mass absorption coeffs., determ. 8=41048
    - metal oxides, electron probe microanalysis: comparison of correction methods 8=45420
    - metal oxides, e probe microanalysis standards 8=41307
    - meteorite alloys, constituent determ., e-probe microanalysis 8=39722
    - microanalysis, e probe current stability 8=28553
    - microanalyzer, neutralizing insulating targets by low-energy electrons 8=45421
    - oxides, e microanalysis with oxide standards, correction factors 8=27810
    - particle analysis, e microscope-microprobe for particles 0.1-10μ 8=34935
    - particle identification by electron microprobe 8=30557
    - phospho-silicon films on Si substrates, P non-destructive determ. 8=49994
    - powder crystallography, peak intensity errors rel. to grain size and crystalline structure 8=26285
    - proportional counter and low-activity source applications 8=41313
    - scans integration, photographic, optical and electronic, evaluation 8=30840
    - sensitivity optima, equipment and operating conditions 8=27795
    - silicate minerals, quantitative, and absorption corrections, obs. 8=27809
    - silicates, e microanalysis with oxide standards, correction factors 8=27810
    - solid solns., diffr. and fluoresc. spectrometry 8=27814
    - spectrometer attachment for e microscope Phillips EM-200 8=24451
    - steel particles by e microprobe 2.8-30μ 8=30557
    - steel, segregation study by fluorescence technique 8=30860
    - steel, stainless, oxide fluoroscopy 8=41304
    - vacuum spectrometer 8=41305
    - Ag in Sn/Pb solder, by X-ray spectrometry 8=27816
    - Ag dental alloys, fluoresc. anal. 8=32165
    - Al-Ag alloy, Ag conc. from Guinier-Preston zone exam.. 8=49996
    - Al_2O_3 by e microprobe, Al K_α line shift effects, obs. 8=27804
    - Au in Sn/Pb solder, by X-ray spectrometry 8=27816
    - $AuAg_3Te_2$, phase transforms during e microprobe analysis, obs. 8=30857
    - Au-Cu alloys, absorpt., fluoresc. and 2 corrections 8=27802
    - Ba ferrites, Co and Ti substituted, comp. on micron range scale 8=31720
    - Br in brines, X-ray fluorescence obs. 8=27815
    - CoO by e microprobe, Co K_α line shift effects, obs. 8=27804
    - Cu, quantitative, cryst. imperfections effects. obs. 8=41308
    - Cu in Sn/Pb solder, by X-ray spectrometry 8=27816
    - Cu 55%- Zn 45% α and β phases, comp. and location rel. to grain struct., obs. 8=30688
    - Fe, 2MnO. SiO_2 inclusions identification, obs. 8=27802
    - Fe-Al alloys, absorpt., fluoresc. and 2 corrections 8=27802
    - Fe-C standard, Midwest Probe Users Group report 8=30851
    - Fe-Cr standard, New York Metropolitan Probe Users Group report 8=27813
    - Fe-Ni standard, New York Metropolitan Probe Users Group report 8=27813
    - Fe-Ni standard, Midwest Probe Users Group report 8=30851
    - Fe_2O_3 by e microprobe, Fe K_α line shift effects, obs. 8=27804
    - Ni-Co-Cr superalloy sulphidation corrosion layers comp., obs. 8=30806
    - Pu-Fe alloys, electron-probe micro-analysis of Fe 8=36647
    - Pu-Ga alloys, electron-probe micro-analysis of Ga 8=36647
    - SiC, C radiation absorption, extended Philibert's correction 8=27798
    - TiO_2 by e microprobe Ti K_α line shift effects, obs. 8=27804
    - $ZrSiO_4$, Pb, U and Th traces, e microprobe meas. 8=27811

Chemical effects of radiations
- See also Nuclear reactions/chemical effects; Photochemistry.

Chemical effects of radiations—contd
- acrylamide, γ-irradiated aq. solns, 77°K, e. s. r. 8=30524
- diamond, reactions induced by p and d bombard 8=45406
- hexafluoropropylene copolymer, γ-irradiated, photoinduced and thermal radical conversions 8=49953
- molecular crystals, of ion implantation 8=45404
- organic cpds, γ-irrad., short-life free radical formation and stabilization by nitroso scavengers 8=49980
- oxybromine cpds., $BrO_{1\ 2}$ γ-absorpt. spectra 8=27768
- polymerization, low-temp., obs. and theory 8=27742
- radiochemical cross sections for p and π^-, 50-400 MeV, calc. 8=45400
- steel, Cr-Ni/Nb stainless CO_2 oxidation n-irrad. 580°-840°C obs. 8=27705
- tetrafluoroethylene copolymer, γ-irradiated, photoinduced and thermal radical conversions 8=49953
- Ge crystal, IIIA-VA ion bombard., substitutional impurities 8=48922
- NaOBr, γ-radiolysis, radical yields 8=27767
- **acoustic waves**
    - cavitation, ultrasonic, relaxation appl. 8=37278
- **ionizing radiations**
    - alcohols, liq., reactions of electrons during radiolysis 8=49964
    - alkali azides, carbonates, nitrates, radiolytic decomp. 8=31140
    - alkali metal bromates, n-irrad. crysts., Br^{82g} recoils 8=27769
    - alkaline earth nitrates, radiolytic decomp. 8=31140
    - α-amino acids, γ or X irrad., dissociative electron capture 8=36621
    - aniline, nanosec. pulse radiolysis 8=49978
    - anthracene in cyclohexane, nanosec. pulse radiolysis 8=32141
    - aqueous solns., γ-radiolysis at high press., reaction of hydrated electron 8=32143
    - benzene, nanosec. pulse radiolysis 8=49979
    - benzene, pulse radiolysis, higher excimer states 8=34872
    - biphenyl in cyclohexane, nanosec. pulse radiolysis 8=32141
    - dielectric liquids, radiolysis 8=32139-40
    - dithiodiglycolic acid, irrad. at 4.2°K, ion formation 8=40917
    - DNA, diamine bound 8=48903
    - ethylene-silica gel system, γ-polymerization, e.p.r. obs. 8=32127
    - fluorescein, aq. soln., pulse radiolysis 8=49969
    - formamide, struct. of radical formed 8=32138
    - hydrocarbon glasses, trapped electrons, optical and e.s.r. spectra 8=45401
    - hydrocarbons, liq. radiolysis, scavenging mechanism 8=27765
    - hydroxyurea, struct. of radical formed 8=32138
    - isobutene-silica gel system, γ-polymerizatin, e.p.r. obs. 8=32127
    - liquids, ionic processes 8=45403
    - metal halides, sulphates, permanganates, radiolytic decomp. 8=31140
    - methane adsorbed on γ-alumina, radiolysis at 77°K 8=41290
    - methanol-d_1, isotopic comp. of H prod. 8=32136
    - methyl oleate, γ-induced oxidation 8=41293-4
    - methylclopentane, liq. radiolysis 8=45407
    - 3-methylpentane glass, γ-irrad., e.s.r. of trapped electrons 8=27483
    - olefins, liq., radiolysis 8=27766
    - oxyhalides, radiolytic decomp. 8=31140
    - particle studies of very high linear energy transfer 8=41289
    - n-pentane, H formation in radiolysis 8=41291
    - n-pentane, radiolysis of liq. 8=49971
    - meta-terphenyl, e radiolysis, temp., intensity and post irrad. effects, 1.35 MeV 8=36624
    - thermal spike effect in heavy ion tracks, mathematical model particle tracks 8=41292
    - toluene, nanosec. pulse radiolysis 8=49979
    - toluene, pulse radiolysis, higher excimer states 8=34872
    - transient free-radicals prod. by pulse radiolysis, e.p.r. 8=49970
    - water, reactions of electrons during radiolysis 8=49964
    - CO gas, γ-radiolysis, O atom detection 8=36623
    - CO, pulse radiolysis 8=45405
    - D_2O, primary radical yields 8=49972
    - D_2S solns., in ethers, ionic reactions in γ-radiolysis 8=45402
    - HBr, gas-phase radiolysis 8=49977
    - HBr, radiolysis mechanism 8=32142
    - HCl, gaseous, gamma-radiolysis, effect of applied elec. field 8=36622
    - HCl, gaseous, mechanism of H formation 8=27764
    - H_2O vapour irrad. with 1 MeV He^+, e.s.r. 8=49968
    - $LiNO_3$, molten, γ-radiolysis 8=49973
    - $LiNO_3$, neutron radiolysis 8=49974
    - $NaHCO_3$, aqueous soln, (plus glucose or isopropanol), γ-radiolysis 8=36625
    - Na_2SO_4 single crystal, X-irradiated, SO_3^-, SO_2^- and colloidal S colour centre obs. 8=44483
    - O_2, pulse radiolysis, vibr. excited O_3 8=36620

Chemical equilibrium. See Chemical reactions.

Chemical exchanges. See Exchanges, chemical.

Chemical kinetics. See Reaction kinetics.

Chemical reactions

See also Exchanges, chemical; Heat of formation; Heat of reaction; Oxidation; Photochemistry; Polymerization; Reaction kinetics.

- acetylene, and acetylene-methane mixtures, ion-mol. reactions 8=49852
- acid treatments on pre-heated mica rel. to interstratified structure formation 8=36572
- aggregate of particles and gas, ignition during surface reaction 8=32970
- anisol-nitrobenzene system, complex formation from spectral analysis 8=45347
- anthracene photo-oxide decomp., temp dependence 8=27694
- atmospheric negative ion reaction obs. 8=41347
- biochemical systems, differential microcalorimeter 8=27687
- biphenylene, thermal fragmentation 8=39058
- in boundary layers, effect of mass transfer cooling of H, He, N and Ar 8=32958
- calcined ferric oxides, dissolution behaviour rel. to calcining temp. 8=45337
- in carbonate solns., acid differentiation, rel. to hydrothermal crystal growth 8=26213
- cellulose I and II acetylation reactivities, viscosity and X-ray diffr. obs. 8=45325
- cellulose, $KHCO_3$ contaminated, pyrolysis compared with pure sample 8=32095
- cellulose ethers, etherification from i.r. absorpts. obs. 8=27728
- chain reaction kinetics, $A + B \rightarrow C, C + D \rightarrow E$ syst. 8=49843
- chemiluminescent involving atomic N_2 and H_2, CH_4, N_2 and Ar 8=41245
- chemisorption of N and NH_3 synthesis of Fe purified in ultra vacuum 8=41265
- chloroplasts, phosphorylation, e. flow and p.-translocation 8=49860
- complex mixtures, comp. equilib., calc. by generalized free energy method 8=36542
- complex systems of 1st order reactions cont. irreversible steps, struct. and anal. 8=32085
- Curium oxide with Al_2O_3 det. from Cm^{244} fission fragments 8=36649
- in diamonds, due to proton and deuteron bombardment 8=45406
- diethyl methylphosphanite, hydrolysis n.m.r. study 8=27727
- 2, 5-dimethoxysemiquinone anion radical solvation by protic and aprotic solvants 8=45358
- diphenylamine-nitrobenzene system, complex formation from spectral analysis 8=45347
- electrons, chemical properties 8=25322
- ethylene, thermal gas phase bromination at room temp., kinetics 8=49863
- ethylenimine, reactivity to C–C double bonds 8=32097
- ethyl free radical with SO_2, 28-75°C 8=49848
- gas absorp. and evolution in, automatic constant pressure apparatus 8=30270
- gas mixtures, non-ideal, equilib. comp. and thermodynamic props. 8=32088
- in gas mixtures, and relaxed flow calcs. 8=36547
- gas phase, obs. with shock tube coupled to molec. beam mass. spectrometer 8=45321
- gas reacting with substance in porous plate, transport processes in boundary layer 8=30308
- gaseous association, effects of dead space 8=49841
- gaseous, fast at high temp., shock wave technique 8=45315
- gelatin, drying, decomposition of introduced calcium acetate with acetic acid loss, mechanism 8=25973
- graphite, intercalation isotherm of $FeCl_3$ vapour 8=27697
- heterogeneous, at stagnation point, dynamics 8=25812
- hexamethylenetramine-water, solvent-solute interactions 8=41254
- hexanitroethane, thermal decomposition in gaseous phase 8=49879
- homogeneous (gaseous, liq. or equilib) systems, with components undergoing reactions, themodynamics 8=27681
- hydrates, cryst., thermal dehydration, obs. 8=27689
- hydrocarbons with electron donating solvents, molecular 8=36550
- hydrocarbons, ion impact, proton transfer 8=29984
- hydrogenation, liquid-phase, activation energy rel. to displacement of catalyst potential 8=36553
- at infinite surface to which reactant diffuses from point source 8=36549
- ion-molecule, elevated press, investigation by modified time-of-flight spectrometer 8=29843
- ion-molecule mechanisms, cyclotron double resonance exam. 8=47554
- ion-polar mol. reactions, preferred dipole orientation 8=34444
- long-lived complexes in crossed molec. beams 8=25669
- mass spectra deciphering for high temp. thermodynamic reactions 8=38609
- methyl free radicals with SO_2, 25-164°C 8=49847
- methyl radicals with alkali halides 8=47656

Chemical reactions—contd

- methylene, with C_2H_5Cl in gas phase 8=45345
- methylurea-water, solvent-solute interactions 8=41254
- molecular beams, use in 8=27683
- with molecular scatt., appl. of R-matrix theory 8=43427
- muscovite dehydration, mechanism 8=49876
- naphthoquinone photodimer ions, loss of CO_2 in mass spectrometer 8=38607
- in non-ideal flow reactor vessel, effects of changing viscosity on transient response 8=32087
- organic coatings, book 8=32628
- Pauling's bond energy equation 8=49834
- phenol-nitrobenzene system, complex formation from spectral analysis 8=45347
- polymers solid of secondary free radicals during mech. damage 8=45361
- polymethylene, pyrolysis, intramol. radical transfer, obs. 8=45344
- proline with chloranil in buffered 50% (V/V) aqueous ethanol, complex form. 8=36571
- propane, self-inhibited pyrolysis 8=36570
- propylene, $+ Ar^+$, Kr^+ or CH_4^+, charge transfer dissociative reaction 8=34445
- propylene, ion-mol. reactions 8=43492
- pyrolytic, study by molec. interact. with hot W filament 8=36577
- quartz: Al impurity + HF, AlF_3 formation on surface during ageing (3½ yrs) 8=49900
- radicals, organic solns., from e.s.r. 8=32117
- reactor, continuous flow stirred tank, limit cycle behaviour analysis 8=32081
- silane $+ N_2$ in r.f. discharge. prep. of Si_3N_4 film 8=35183
- soap films, solvation forces 8=27686
- solid state, analysis by thermogravity, thermal analysis and i.r. absorpt. 8=27688
- in solution, optical stopped-flow apparatus 8=32084
- spectrographic samples in carbon arc 8=41237
- steel in CO_2, carburisation and oxidation rel. to transport in porous scales 8=48777
- surface catalysis, props of laminar boundary layers 8=36587
- surface reactions effect on interphase mass and energy transfer 8=34829
- tetranitromethane, thermal decomposition in gaseous phase 8=49879
- thermal decomposition, growth of Cu crystals from gaseous cupric fluorides 8=44127
- in tubular reactors, influence of mixing on performance, three models 8=32082
- in turbulent flow reactors, effect of diffusion on reaction rate 8=36548
- unimolecular reacts. in thermal systems 8=25647
- Ag-molten $BiCl_3$ solns., metal-molten salts reaction, study by elec. cond. 8=39409
- Al reactivity on SiO_2 moisture effects, obs. 8=45328
- AlH_3, flash pyrolysis, kinetic spectra 8=32110
- BeH_2, flash pyrolysis, kinetic spectra 8=32110
- CCl_4 matrix reaction with Li atoms 8=29775
- CCl_4 matrix reaction with Li atoms 8=29831
- $CD_3^+ + CD_4 \rightarrow C_2D_5^+ + D_2$, kinematics 8=38963
- $CD_4^+ + CD_4 \rightarrow CD_5^+ + CD_3$, kinematics 8=38962
- CO, Cl, NO_2 reactions at 381-473°C, kinetic eqn. setup 8=49857
- CaF_2 hydrolysis kinetics, 1000-1120°C 8=49859
- CaO transformation to CaS, 1400°to 1650°C 8=45324
- $CaSO_4 . H_2O$ system, thermally dehydrated, precise forms of products, by i. r. spectroscopy 8=49858
- between Cs and graphite, compound formed rel. to Cs vapour press and graphite temp. 8=35011
- Cu tough pitch wire bar, water vapour determ. by Al reduction technique 8=45330
- Cu(II) basic halides, thermal decomp. under air, obs. 8=27701
- F, atoms and mols, with C atoms 8=29723
- F_2 and F with NCN, matrix-isolation 8=47712
- Fe:Na_2O. $2SiO_2$ systems, kinetics of interfacial reaction 8=26621
- Fe_3S_4, magnetic, synthesis 8=41248
- $Gd_3Fe_5O_{12}$ + fused quartz. 8=41251
- Ge-As-Cu system, complex formation 8=49871
- H-atom transport mechanism 8=41252
- H atoms, from elec. discharge, with liquids 8=32101
- H with graphite at high temp. and press. 8=47422
- H $+ O_3$, i.r. chemiluminesc. 8=32099
- HCN, adsorbed on glass, surface reaction 8=48491
- H^3He^+ ions with gaseous methane and ethane 8=45341
- H_2 formation in dehydration of single hydroxide crystals 8=36554
- $H_2 + D_2 \rightleftarrows 2HD$, catalyzed by Mo 8=49907
- $H_2 + O_2$ on Ag 8=39616
- H_2O, proton affinity 8=32100
- H_2S, proton affinity 8=32100
- H_3^+ with propane or butane, struct. of alkyl ions 8=39057
- He^+ with N_2, O_2 in upper atmosphere, loss of He from earth's atm. 8=27937
- Hg halide complex with azines, prep. 8=36432
- Hg-Tl eutectic, interfacial reactions with metals, dielectrics and polymers 8=49873
- I vapour with 8 metals, effects of Co^{60} γ-irrad. on rate 8=36555

Chemical reactions—contd
  KCl, doped, crystals, with H_2 rel. to dislocation decoration mechanism 8=31081
  Mg-Cu-F, high-temp. gaseous equilibria 8=34375
  $N + CH_3CHO \rightarrow HCN + H_2 + HCO$, mass spectrometric study 8=27710
  N_2 active, chemilumminesc. reaction with anhydrous $Na_2 50_4$ 8=41255
  $N_2^{28} + N_2^{30} \rightleftarrows 2N_2^{29}$ catalyzed by Mo 8=49908
  $N_2^+ + N_2 \rightarrow NO^+ + NO$, as possible source of NO in D- and E-regions 8=41442
  $N_2O_4 \rightleftharpoons 2NO_2$, effect on diffusion of Kr 8=34681
  $NaMF_3$, ($M=Mg^{2+}, Co^{2+}, Ni^{2+}, Zn^{2+}$), synthesis and structural data 8=26258
  NaN_3, thermal decomposition, crystal size effects, topochemistry and gas analysis 8=39701
  Na_2O activities in Na_2SO_4 and Na silicate melts 8=34826
  $NdWO_4Cl$ thermal decomp. in air, obs. 8=39815
  NiO, decomposition on photo-absorption 8=36567
  NiO-MgO solid solns., formation on thermal decomp. of mixed hydroxides 8=39532
  O transfer from CO_2 to metal surface, kinetics 8=27735
  OCN^- formation in gas phase ion-mol. reactions 8=41259
  OH chemiluminesc. in $H_2 + O_2$ reaction in shock tube 8=49889
  $O_2 + H_2$ mixtures, detonation, influence of molec. mass on limits 8=32115
  in Pb-$BiCl_3$ molten mixtures, study with absorpt. spectra 440-1000 $m\mu$ 8=34878
  $PbS + CdO \rightarrow PbO + CdS$, solid state, kinetics and diff. mech. 8=49839-40
  $PbTiO_3$, formation mechanism 8=36569
  $PdO-Ln_2O_3$, phase relations in air 8=35123
  Pt surface, appearance of Na, K oxides at 20-1100°C 8=35549
  S^{35} amino acid synthesis, high-temp. attempt. 8=41261
  Si and Ti carbides, formation by chemical vapour deposition discussion 8=45348
  Ti, interact. of NH_3, H_2 and N_2 8=32103
  UN, prep. from $UCl_4 + Al + N_2$, two-step reactions 8=36574
  UO_2 powders, oxidation and O chemisorpt. rel. to pyropharic process 8=45349
  UO_2-TaB_2 fuel, heated in steam, reactions 8=27717
  UO_2-WB_2 fuel, heated in steam, reactions 8=27717
  V-C system, diffusion and phase equilibria above 1900°C 8=36575
  $VO_{2\cdot5}$, molten thermal dissoc., thermogravimetric obs. 8=27724
  Zn halide complex with azines, prep. 8=36432
  Zn^{65} drop extraction, between liq. metals and fused salts 8=27725
  W, surface chemisorption of water, investigation 8=27739
  W surfaces, appearance of Na, K oxides at 20-700°C 8=35549
Chemical structure
    See also Bonds.
  atomic, bonding and valency, use of 3-dimens. models in teaching 8=45309
  hydrazides, substituted, C-Br bond 8=49780
  hydrazidones, substituted, C-Br bond 8=49780
  interstratified structure formed by acid treatments on pre-heated mica 8=36572
  organic liqs., correl. with positronium annihilation 8=30406
  α-oxalic acid dihydrate, d.m.r. and molec. struct. 8=49638
  pyrrol ring, substitution of H atoms by groups of CH_3, $C_3O_2H_5$, COH 8=34353
  urethanes, substituted, C-Br bond 8=49780
  villamaninite, and cry. structure analyses 8=48646
  wustite($Fe_{1-y}O$), stoichiometry deviations from composition-oxygen partial pressure diag., thermo-gravimetric determ. 8=36540
  zeolite, synthetic, surface state evolution from r.f. spectrometry during dehydration 8=39581
  zeolites, i.r. spectra data 8=27552
  zeolites, synthesis 8=36541
  Al atom, auger electron emission, chemical effect 8=43227
  Ba ferrites, Co and Ti substituted, comp. and micron range scale 8=31720
  Cu formate tetrahydrate, d.m.r. and molec. struct. 8=49638
  $Cu_{0.5}Fe_{2.5}O_4$, constitution from elec. props. meas. 8=48341
  Fe compounds, Mossbauer spectra 8=39514
  GaM, (M = Sb, As, P), quadrupole relax. time and chemical shift rel. to covalence 8=31928
  InM, (M = Sb, As, P), quadrupole relax. time and chemical shift rel. to covalence 8=31928
  $LiD_3(SeO_3)_2$, d.m.r. and molec. struct. 8=49638
  Mg, basic sulphate, composition determ. by thermogravimetry, thermal anal, and i.r. absorpt. spectriphotometry 8=27671
  $NaD_3(SeO_3)_2$, d.m.r. and molec. struct. 8=49638
  Ni-Fe-Ni strip, rel. to gas emission in vacuum apparatus 8=39254
  S atom, auger electron emission, chemical effect 8=43227
Chemical structure—contd
  Si atom, auger electron emission, chemical effect 8=43227
  SnX_4, (X = Cl, Br, I, H, Li, Na), at. radius of X rel. to Sn^{119} isomeric shift 8=30637
  U oxides, phase limits 8=48292
Chemical technology
  acidity biochemistry, glass microelectrode 8=37092
  acidity sensor, h.p., for oceanography 8=45436
  alkali metals, separation on org. resin ion exchangers, effect of temp. 8=32145
  binary batch distillation, time-optimal reflux policy 8=32080
  etching of minerals to make U fission tracks visible 8=32185
  extraction efficiency flow distrib. and droplet boundary-layer behaviour dependences 8=48123
  extraction separation of trace contaminants in silicochloro derivatives 8=49998
  flow reaction vessels, effect of changing viscosity on transient response 8=32087
  osmometry, high-speed, appl. of diffusible polymers 8=34819
  packed liquid extraction column, dynamic behaviour 8=49833
  thermobalance for h.p. reactions 8=45316
  tubular reactors, influence of mixing, three models considered 8=32082
  turbulent flow reactors, effect of diffusion on rate of reaction 8=36548
  HF fractionation column 8=41608
Chemiluminescence. See Chemical reactions; Luminescence.
Chemisorption. See Chemical reactions; Sorption.
Cherenkov radiation
    See also Counters/Cherenkov; Electrons/radiation.
  detectors for e.a.s. obs. at 5200m altitude 8=38259
  e.a.s., flash fluct. rel. to primary cosmic ray comp. 8=38190
  e.a.s., search for point sources 8=38157
  electrodynamics of moving media, appl. 8=33060
  electron beam monitors for electron linear accelerator 8=33077
  imaging system for e.a.s. optical emission 8=38195
  interference-like phenomenon 8=24707
  magnetospheric proton flux, cause of geomag. PP pulsations 8=41469
  point charge moving perpendicularly to a conducting barrier 8=47073
  production in night sky and by cosmic rays 8=33847
  resonance props., at longitudinal waves 8=37930
  space charge systems, extended, calc. method 8=42000
  Vavilov-Cherenkov radiation, integral expression for component of reaction force 8=31952
  Vavilov-Cherenkov 2-photonic effect, condition for frequencies 8=37937
Chirality. See Elementary particles; Field theory, quantum.
Chlorine
  atom, absorpt. series and ionization potential 8=38663
  gas, ads. on Na halides, refl. spectroscopy 8=48480
  graphite oxidation inhibition 8=27696
  ion channeling in NaCl and KCl lattices, computer analysis 8=40075
  ions, Cl^- collisions with He, Ne, Ar and Kr atoms, detached electrons energy obs. 8=29972
  molecular beams, reactions with K, Rb and Cl atoms 8=49875
  n.q.r. description of an autodyne 8=37545
  solid, cryst. struct. and intermolec. forces 8=48648
  X-ray spectra from chloromethanes 8=47653
  Cl I-lines in u.v., absorpt. oscill. strengths meas. 8=29609
  Cl I, $3p^m$-$3p^{m-1}3d$ transitions 8=43178
  ClI and II, vac. u.v. spectrum 8=33264
  Cl^{35} in ammonium hydrogen monochloroacetate n.q.r. 8=49668
  Cl^{35}, n.m.r. in solution of paramagnetic ions 8=48214
  Cl^{35} ion beams in mylar, stopping powers 8=44508
  Cl^{35}, n.m.r. in HCl aq. solns. of Co(II) 8=30541
  Cl, CO, NO_2, reactions at 381-473°C, kinetic eqn. setup 8=49857
  $Cl + H_2 \rightleftarrows HCl + H$, reaction kinetics, e.s.r. study 8=49861
  Cl + Hg atom combination 8=49960
Chlorine compounds
  chloride, atmosphere, particle size distribution obs. 8=50129
  ClCO radical, potential functions and bonding 8=47713
  $(ClO)_2$, i.r. spectrum 8=29731
  $ClSi(NCO)_3$, vibr. spectra 8=29732
  Cl_2SiNCO, vibr. spectra 8=29732
  Cl_3SiNCS, vibr. spectra 8=29732
  $ClWO_4Cl$, hydrothermal synthesis and struct., obs. 8=39815
  $HClO_4$-$DClO_4$-H_2O-D_2O system, p.m.r. 8=34920
Chondrites. See Meteorites.
Chromatic aberration. See Aberrations, optical.
Chromatography
    See also Adsorption; Chemical analysis/adsorption.
  alkali metals, separation on org. ion exchangers, effect of temp. 8=32145
  gas absorption in packed columns, correlation of gravitational force 8=50003

Chromatography—contd
gas, temp. independ. retention 8=45412
gas, thermal cond. microdetector 8=27773
polymers, gel permeation chromatography stochastic model 8=45415
radioactive gases, sorption and steady-state conc. distrib. along column 8=32144
thin layer, for separation of radioelements 8=32146
thin-layer, solvent vapour in sandwich chambers 8=32147
$Ce^{145,146,147}$ separation by column partition chromatography, obs. 8=38430
UF_6, gas, -10°C-40°C 8=49981
Chromium
antiferromagnetic, elec. resist. 8=40316
antiferromagnetic high-pressure changes by neutron-diffractometry 8=26361
attenuation of transverse u.s. waves 8=39891
brittle-ductile transition, effects of N conc., heat treatment and Cr_2N precipitates 8=44561
chemisorption of alcohols, aldehydes, keetones and ocides, surface species formed, i.r. spectra 8=45363
cleavage cracks on surface due to spark machining 8=39577
electrodes, measured conductance rel. to measured capacitance and Faradaic current 8=49929
deformation under hydrostatic press., struct. rel. to plasticity, <18 kbar 8=35562
diffusion coating on hyper eutectoid carbon steels 8=39973
distribution, nonuniform, in synthetic ruby, causes 8=40011
effect on Cu solubility in austenitic steel 8=30655
electrolytic deposition, internal tension rel. to current density 8=36609
electrolytically deposited, Cr black coatings, props. 8=45394
films, prep. by oblique incidence of mol. beam and optical anisotropy 8=31977
films, prep., elec. and mag. props. 8=39590
films, vacuum-deposited, effect of dielectric coating on resist. 8=26964
films, vacuum-deposited, structure and substructure from e.-diffr. exam. rel. to deposition temps. 8=35169
Hall coeff. temp. dependence 77-330°K rel. to "mag. cooling" effects 8=45054
in inclusions in Fe-Cr alloys, activation anal. of contents 8=36652
ion pairs, exchange-coupled in corundum, spectra 8=36322
ion-pairs in ruby, exchange-coupled, e.p.r. in excited optical states 8=31859
ions, Cr^{3+} doped corundum, catalytic C_2H_5 hydration 8=32122
ions, Cr^{3+} in $LiNbO_3$, acoustic paramag. reson., 4.2°K 8=44318
layers under Au film, grain boundary diffusion effects 8=26112
magnetic props., pressure and mag. field, dependence, n-diffr. exam. 8=31766
magnetic props. of sinusoidal spin-density waves, band model 8=36206
metal, conversion of hexagonal CrH, crystallography and bonding relationships 8=48376
microsegregation in directionally solidified steel 8=39552
Néel temp., effect of plastic deform. 8=45055
neutron scattering, critical, near Neel temp. rel. to itinerant e. -model of mag. props. 8=31764
optical absorption and ionic conductivity in silver halogens 8=41052
optical properties in the far. u. v. 8=31978
polycrystalline, optical consts. from reflectance ratios 8=45164
positive ions, spin-orbit coupling 8=38665
in ruby cryst., $>1\%$, e.s.r. 8=49598
in ruby, distribution effect on spin-lattice interaction 8=49621
in rutile, e. s. r., crystal orientation 8=26184
spin-density-wave distribs. 8=31765
spin density waves from self-consistent HF method 8=36205
tensile internal stress during electrodeposition, role of hydrogen 8=31167
AlF_3: Cr^{3+}, e.p.r. 8=36236
Cr I, gf for 41 lines 8=29611
Cr I, II u.v. lines, of shock tube meas. 8=29638
Cr II, gf for 2 lines 8=29611
Cr(VI) in alkali and alkaline earth oxide glasses, u. v. absorpt. 8=36325
Cr^+, e.s.r. in rare gas matrix 8=40202
Cr^{2+} in MgO, dynamic lattice couplings, from microwave u.s. and thermal-conductivity studies 8=35053
Cr_2WO_6, linear thermal expansion 8=35448
Cr^{3+}, diffusion in MgO, luminesc. determ. 8=31010
Cr^{3+} in α-Al_2O_3, trigonal splittings stress dependence 8=43929
Cr^{3+} in ruby, relaxation time, influence of impurities 8=40915
Cr^{3+}: ruby, electron paramag. acoustic absorption at 4.2°K 8=40914
Cr^{3+}, $^2E \leftrightarrow {}^4A_2$ transition in $K_3CO(CN)_6$:Cr^{3+} 8=31979
Cr^{3+} in MgO, ENDOR 8=40977
Chromium—contd
Cr^{3+} in TiO_2, structure determ. by e.s.r. 8=39823
Cr^{3+}, optical spectra in spinels 8=49715
Cr^{3+} pairs in ruby, mag. resonance, elec. field effects 8=40904
Cr^{3+} sites in glasses, effect of high press. 8=39632
Cr^{53} in $CoCr_2S_4$, n.m.r. obs. 8=36262
Cr/SiO mixed films, structural and elec. props. 8=48448
in GaAs, activation energies 8=40238
H liberation, electrolytic, with different crystal structures 8=49943
Zr oxidation prevention by Cr coating, $\leqslant 650$ °C 8=32107
Chromium compounds
alloys, spin-density-wave distribs. 8=31765
alloys spin density wave to antiferromagnetic transition pressure effect 8=31767
alloys, spin-density-wave periodicity conc. dependence 8=36207
alloys spin density waves from self-consistent HF method 8=36205
carbonyl complex, $(CO)_5CrCO.CH_3$ 8=26446
steel, high-C, marensite crystal domain structure from e-microscope exam. 8=40805
tris(dihydroxobis(diethylamine)chromium)chromium (III) sulphate decahydrate, suscept. 8=40860
Cr binuclear complex cpds., biquidratic exchange interaction 8=49467
Cr chalcogenide spinels, exchange interaction, night-angle nearest-neighbour 8=31748
Cr(III) compounds, luminescence spectra 8=49796
Cr-Cs alum crystal, paramag. cross relax. 660Hz-1MHz 8=27486
Cr-Mn alloys, antiferromagnetic specific heat 8=48735
Cr-Mo alloys, absolute thermoelectric power between 100 and 600°K 8=49393
Cr-Mo(W) alloys, antiferromag. props. from resisitivy meas. 4-325°K 8=31763
Cr-Ni (Fe), pitting corrosion critical potentials 8=49928
Cr-Ni-Fe solid solns., lattice type and phase forms on prolonged crystallization 8=26246
$CrBe_{12}$, ferromagnetism at low temps. 8=45009
$CrBe_{12}$, paramagnetic and ferromagnetic state, NMR meas. of hyperfine fields 8=45115
$CrBr_3$, paramagnetic, n-scattering energy distrib. 8=31521
$Cr(CO)_6$, semiempirical MO model 8=47594
$Cr(CO)_6$, Cr-C bond length from electron structure exam. 8=38821
$[Cr\ urea_6][Cr(CN)_6]$. $3H_2O$, excitation energy transfer Cr-Cr 8=41188
CrF_3, paramagnetic, n. scattering energy distrib. 8=31521
CrFe alloys, 3d-electron redistrib. from X-ray spectra 8=35780
$(CrFe)_{23}C_6$, austenitization influence in Cr contents and Curie point 8=30684
$Cr_{11}Ge_{19}$, crystal structure 8=39782
CrH, hexagonal, conversion to metallic Cr, crystallography and bonding relationships 8=48376
CrH_x, $(x < 1)$, H orbital expansion effects on d-electron exchange rel. to mag. props. 8=49480
$Cr_{1-x}Mn_xO_2$ $(0 \leqslant x \leqslant 0.7)$, mixed mag. oxides crystallizing in rutile structure 8=31603
Cr_2N precipitates in Cr, effects on brittle-ductile transitions temp. 8=44561
$CrOF_5^{2-}$ ions, X- and Q-band e.s.r. spectra, comparison 8=38911
CrO_2, decomposition to Cr_2O_3 from 800° to 1580°C and 15 to 65 kb, in 'belt' apparatus 8=26281
CrO_2-Cr_2O_3 system, phase equilibrium up to 35 kbar and 1400°C 8=43996
CrO_4K_2, γ- and n-irradiated, e.s.r. 8=49605
$CrO_4(NH_4)_2$, γ- and n-irradiated, e.s.r. 8=49605
Cr_2O_3, elec. conductivity temp.-depend., 500-1300°C 8=49138
Cr_2O_3, gyrotropic birefringence 8=45155
Cr_2O_3 inclusion in steel, thermal expansion and reln. to tessellated stresses 8=44350
Cr_2O_3, Neel temp. pressure dependence up to 13.3 kbar 8=27443
Cr_2O_3 powder, Néel temp. depend. on particle size 8=40861
Cr_2O_3, reduction sintering, shrinkage and cavitation 8=35072
Cr_2O_3, S diffusion at 1000°C 8=44384
Cr_2O_3, sublattice magnetization, susceptibility 8=40862
Cr_2O_3, X-ray spectra and zone structure 8=49702
Cr_2O_3-Fe_2O_3 solid solutions, helical spin ordering, development of theory 8=31309
Cr_2O_3-Fe_2O_3 system, mag. structure 8=27444
CrS_x, oxidation at 1050°C 8=36558
CrS_x-coated Cr, oxidation at 1050°C 8=36558
CrSb, dilute solutions in superconducting PdSb 8=27029
CrTe, spin relaxation of Fe^{57} below Curie point 8=49532
$CrTe_{1-x}Sb_x$ alloys, resistivity and Hall effect comp. and temp. dependence 8=35883
Cr_2TeO_6, magnetic structure by neutron diffraction 8=40863
Cr_2WO_6, magnetic structure by neutron diffraction 8=40863
Cu-Ni alloys, electronic structure of Ni atoms 8=49744
W-Cr solid soln., decomposition from X-ray diffr. study 8=26086

- **Chromosphere**. See Sun.
- **Chronographs**. See Time measurement.
- **Cinematography**
  - See also Cameras.
  - holographic interferrogram recording for time-dependent deform. 8=46760
  - movie projectors, 8 mm, useful light fluxes 8=42282
- **Circuits**
  - See also Amplifiers; Counting circuits.
  - a.c. generator excitation 8=46327
  - amplifier, coherent 30 Hz-20 kHz 8=28458
  - arc jet current regulation by transistor 8=33020
  - autodyne used in Cl n.q.r. 8=37545
  - capacitance, temp. coeff., new meas. methods 8=24063
  - carcinotron modulation 8=46421
  - comparison, high speed 8=46336
  - connecting, decoupling and grounding problems 8=46929
  - control for strain-gauge gas-pressure transducer 8=28223
  - control system dynamics, meas. using describing function method 8=28459
  - corona discharge tube for high-voltage stabilization 8=41921
  - cryoelectric arrays, dynamic fault tolerance 8=40408
  - current integrator to measure neutron target wear grade 8=47142
  - current pulse generator, short rise time, high current for semicond. laser. 8=46333
  - d.c.-d.c. convertor, 1-1.5kV, regulated 8=46341
  - d.c. regulator for magnet supply 8=47005
  - delay time interval multiplier for shock tube meas. 8=4633
  - digital correlator, freq.-swept one-bit, for plasma studies 8=47854
  - dynamic logic circuits for solid state reactor safety system 8=25321
  - electrometer needle, parametric resonance obs. 8=37360
  - electronic for cloudless sky detector 8=50146
  - electronic grey matter using superconducting tunnel junction 8=40407
  - electronics of high speed stellar polarimeter 8=50270
  - filter, time-dependent, for pulse shaping in nuclear spectroscopy 8=46339
  - frequency synthesizer digital control 8=33014
  - generator of sinusoidal oscillations, 0.01 to 100 Hz range 8=41912
  - graph-signal convertor 8=46316
  - for heat regulation 8=28420
  - heating for calorimetry, resistance stabilization 8=28423
  - high-voltage supply for solid-state particle detectors 8=37364
  - impedance comparator as fast-balancing a.c. bridge 8=24065
  - integrated, and arrays, appl. of III-V compound semiconds. 8=44856
  - integrated, use of Mo thin-film resistors 8=44693
  - integrator for 15-2 spectrogram 8=46328
  - inverter, megawatt, solid state, for synchrotrons 8=33487
  - inverter, single phase bridge, commutation 8=28461
  - i.r. pulse generator 8=28770
  - keyed stabilizing system for single-channel γ-spectrometer 8=29085
  - linear microsecond-pulse gate 8=46337
  - linear ramp generator, solid-state, for epitaxial growth temp. control 8=41919
  - linear staircase generator for synchronized pulse display 8=46330
  - linear sweep, for current-regulated magnet power supplies 8=24069
  - log. multiplier, XY plotting of cross sections 8=29657
  - magnetic films pulse switching, noise subtraction circuit for gated oscillograph c.r.o. 8=31575
  - magnetic pulsing of neutron beam, rel. to time-of-flight meas. of inelastic scattering 8=35314
  - marker generator for n.m.r. spectrometer 8=41916
  - microwave, integrated, planar Gunn oscillator 8=44857
  - modulator, freq. for orbital accelerator resonator 8=29004
  - modulator, of immersed, compact for driving Klystron 8=28994
  - multipole network, unconditionally stable, optimum performance conditions 8=37362
  - nonlinear-resistance harmonic generators, anal. rel. to conversion efficiency 8=24071
  - nonlinear two-terminal, with neg. resistance, props. 8=24070
  - optical heterodyne receivers broadband matching 8=28774
  - oscillator, marginal, e.f. band pass. 8=41910
  - oscillator, marginal, h.f. band pass. 8=41911
  - oscillator with v.h.f. stability using superconducting cavity 8=46466
  - parallel diodes, or thyristors with current sharing transformers, current distribution calc. 8=31405
  - periodic heat flow through brick wall, elec. analogue 8=46248
  - phase plane ellipse generator 8=33015
  - power supply system for stable Xe arc lamp operation 8=24073
  - power supply, thyristor controlled, for synchrotron beam-line magnet 8=47003
  - pulse amplifier, d.c.-coupled, base-line stabilization 8=24529
- **Circuits**—contd
  - for pulse counting systems 8=46329
  - pulse generator, explosive, driven magnetic-field compression 8=24072
  - pulse generator for betatron electromagnet 8=24586
  - pulse generator, ramp-controlled for repetitive data collection 8=41913
  - pulse generator, sliding, electronic chopper and shaper 8=33019
  - pulse generator with controllable thyratrons 8=46335
  - pulse generators, r.f. for plasma confinement 8=34523
  - pulse, low-impedance 2.5ns risetime stripline 8=33018
  - pulse shaper for scintillation detectors 8=46928
  - pulse-width control in pulse-transformer ccts. 8=46334
  - pulsed LCR, with skin impedance, anal. of transients 8=41927
  - pulsed power supply for electrolum. display 8=46340
  - register, direct readout, for spark chamber 8=46964
  - regulator-modulator for a.c./d.c. 8=41922
  - repetitive nanosec impulse technology, appls. of suppressed elec. discharges in gases 8=25693
  - r.f. pulse generator 8=46331
  - scintillation spectrometer with pulse-height analyser, stabilization with light-flash peak 8=46852
  - SCR preregulator for magnet power supply 8=24068
  - square-wave generator, bidirectional, for mag. resonance spectrometers 8=33141
  - subnanosecond pulse generation by two circuits utilizing bulk n-GaAs 8=27094
  - switch, synchronous for high current 8=28462
  - thyristors subjected to high-current gradient, performance improvement process 8=37361
  - time-to-amplitude converters for short interval meas. 8=23794
  - timer for integrating digital voltmeter 8=41920
  - transducer for liq. conductivity meas. 8=30521
  - transistorized meter for field strength meas. of medium wave transmitter 8=28634
  - transistorized time amplitude convertor 8=45954
  - tunnelling cryotron flip-flop 8=40406
  - two-channel data logger 8=37359
  - two-port network problems, electrolytic tank as analogue computer 8=46005
  - variable limit sweep generator 8=24067
  - v.h.f. square wave generator, type T-402 8=33017
  - voltage-freq. converter for integrating digital voltmeter 8=41918
  - voltage, plug-in shunt regulator 8=28464
  - voltage stabilizers, transistor, efficiency increase 8=33022
  - voltmeter, integrating digital, use of reversible decimal pulse counter 8=41915
  - Nb_3Sn high-Q r.f. coils for 15°K 8=31359
- **Clathrates**. See Molecules; Organic compounds.
- **Clay**
  - aqueous suspensions, Newton's cooling coeffs. 8=25963
  - electrical potential meas. 8=26947
  - halloysite, water mol. arrangement 8=26143
  - illite group, water permeability, porosity and effective specific surface 8=30661
  - kaolin-dimethylsulphoxide complexes, i.r. spectra 8=27554
  - kaolin, homoionic, surfactant adsorpt., effect on physicochem. props. 8=44071
  - kaolinite group, water permeability, porosity and effective specific surface 8=30661
  - kaolinite, H_2 formation in dehydration of single crystals 8=36554
  - microstructure and drying shrinkage, effect of graphite 8=39709
  - moisture extraction 8=45935
  - montmorillonite group, water permeability, porosity and effective specific surface 8=30661
  - montmorillonite suspensions, tactoid rearrangement and optical density 8=39450
  - organo-clays, sorption, swelling and intracryst. porosity 8=30779
  - sintering kinetics, thermal analysis, meas. 8=30665
  - solution, flow in pipe with permeable walls, hydraulic resistance 8=48023
  - X-ray studies rel. to contact metamorphism 8=39571
- **Cleavage**. See Crystals/faces; Fracture.
- **Clebsch-Gordan coefficients**. See Field theory, quantum; Nucleus/theory; Quantum theory.
- **Climatology**. See Meteorology.
- **Clock paradox**. See Relativity.
- **Clocks**. See Time measurement.
- **Cloud chambers**
  - condensation of water 8=30595
  - Wilson, minimum critical expansion ratio for supersaturated vaps. in prsence of air, rel. to nucleate boiling theory 8=25998
- **Clouds**
  - albedo of striated medium of isotropically scatt. particles 8=45462
  - anomalous cloud lines, comments 8=32221
  - artificial, release height determined photographically 8=50143
  - band orientation in wind shear direction 8=36736
  - chemiluminous and fluoresc., growth rate rel. to diffusion coeffs., temp. and densities in thermosphere 8=36795

Clouds—contd
cirrus canopy formation in relation to mass of air flow in typhoons 8=32215
cirrus, effect on 8-13μ sky radiance 8=41366
clear-sky detector 8=50146
condensation nuclei in free atmosphere, altitude distribution 8=36739
convective, interaction with wind 8=27893
cumulus evolution, model developing under influence of artificial heat source 8=32222
cumulus, initiation and development over mountains, effects of ambient winds 8=45457
cumulus, modelling 8=45456
distribution effects on earths i.r. rad. into space 8=36657
drops, electrically charged by diffusion 8=36740
dry and moist convection including rain stage, numerical expt. 8=45455
electrification, disintegration of pairs of drops raised to equal and opposite potentials 8=25852
evaporation, expansion effects 8=48273
evaporation in radiation field 8=27898
freezing, radar refl. obs. 8=32224
hydrometers, numerically determ. collision efficiencies 8=36735
ice multiplication in atmos. possibilities 8=45454
integral transmission function for cloudy conditions 8=32232
intermass cumuli development, possibility of stimulation 8=50144
inversion problem of temp. inferred from outgoing radiances effect of height and coverage 8=41361
layers, diffuse refl. and transmission, appl. of probability distrib. of photon paths. 8=41362
light refl. and transmission, depend. on single scatt. albedo 8=32230
light, reflected and transmitted, effect of particle size distribution 8=41367
light scatt. from., Monte Carlo calcs. 8=36741
longwave radiative influx in cloudy atmos. 8=50147
metal vapour in upper atm., expansion 8=32259
microstructure continuous meas. by small angle method, halo apparatus 8=34946
noctilucent, abundance, rel. to spring transition of wind in mesosphere 8=41356
noctilucent, geographical distribution 8=27896
noctilucent and nacreous, antartic sightings 8=27895
noctilucent, nature study by OH emissions in 70-90 km range 8=36794
noctilucent, rel. to mesospheric aerosol distribs. and particle sizes 8=36738
noctilucent, sampling of particle content, rel. to altitude 8=36799
noctilucent, spatial and temporal border visibility 8=27897
partial cloudness conditions, computation of downward i.r. radiative fluxes 8=32225
radiant intensity of scatt. light 8=32226
satellite study 8=45438
solar radiation reflection, angular distrib., TIROS IV radiometer obs. 8=32229
solar 10 cm. radiation absorpt. 8=37054
stratus consisting of drops and crystals, numerical integration of equation system describing processes 8=32218
supercooled layer clouds, questions of action 8=32223
suspended waterdrops, freezing and fragmentation, influence of environmental parameters 8=25853
water and ice spheres, i.r. optical properties; radiative transfer application 8=50140
H in Galaxy, intermediate-velocity cloudlets 8=45732
H_2O drops charging in ion stream rel. to electrification by selective ion-capture, obs. 8=30517
H_2O vapour to ice conversion by AgI 8=45458
Clusius-Dickel columns. See Isotope separation.
Coal
abrasiveness meas., radiochemical method 8=35645
American; magnetic susceptibility obs. 8=49478
coal-I batteries, props. rel. to charge-transfer complexes, obs. 8=45369
dielectric constant and loss meas., temp. and freq. dependence 8=40572
diffusion of sat. hydrocarbons, meas. 8=48775
pyrolysis, laser induced, in time-of-flight spectrometer source 8=27780
Cobalt
crystals, domain structure, tensile elastic strain effects 8=36173
crystals, floating zone-melting-grown, effect of molten zone travel speed on orientation 8=26222
crystals tensile strain effects on domain structure 8=36173
diffusion in α and δ Fe 8=44388
dislocation arrangement rel. to deform. and plasticity 8=48853
dispersion-strengthened, mag. props. dispersoid effects 8=31620
electrolytic deposition, crystal growth 8=26245
f.c.c., surface and boundary energies, diffusion coefficient 8=44026
ferromagnetic films, planar Hall effect, thickness (100-1500Å) and temp. (77-293°K) dependence 8=31687

Cobalt—contd
ferromagnetic, thermal neutrons, critical scattering 8=31626
film, hexagonal, spin-wave reson. 8=40886
film, high-coercivity, domain magneto-optic obs. 8=36134
film, hysteresis loops from transverse Kerr effect, azimuthal variation effect 8=40786
film, magneto-optic and mag. props. 8=32018
films, domains and coercive force in supercritical transition, obs. 8=31629
films, domains and mag. fine structures form., e microscope obs. 8=31640
films, electroless, nucleation and microstruct., obs. 8=44165
films, epitaxial, anisotropy constant 8=31631
films, galvanomagnetic effects and domain struct. rel. to thickness, 200-2000Å 8=31598
films, n.m.r. 8=40976
films, transverse Kerr effect and application to hysteresis loop plotter 8=45007
films, transverse Kerr effect, and application to hysteresis loop plotter 8=49516
floating zone method, effect of molten zone travel speed on orientation 8=26222
Kerr effect in dielec. permeability tensor freq. dependence determ. 8=31696
liquid, atomic structure from X-ray diffr. exam. 8=25874
in liquid steel, conc. rel. to C activity 8=30458
magnetic after-effect 8=45008
magnetic after-effect 8=49515
magnetic domains, 20° to 400°C 8=31498
magnetic form factor anisotropy rel. to band structure 8=31600
nanogram amounts in blood, spectrochem. anal. using Cu-spark method 8=49987
nuclear mag. resonance in $CuCo_2S_4$ and Co_3S_4 8=31901
oxidation, 750° to 1000°C using inert Au spheroidal markers 8=49862
plasma, ion acoustic waves amplitude oscills., obs. 8=34543
polycrystal, secondary ionization by 40keV Ar$^+$, mass spectrum 8=49448
single domain, nuclear spin-lattice relax. rate 8=31897
solid solution with P, magnetic moment rel. to P content 8=45006
spin waves 8=31627
stress-strain curves, slip rel. to dislocation struct., single crysts., 78-573°K 8=40138
β-Co, superparamagnetism obs. by Mössbauer effect 8=49521
Co I, spectra, in excited configs., theory 8=43187
Co(II) in alkali borate glasses, optical absorpt. and reln. to glass basicity 8=36324
Co^{2+} hyperfine field in tetrahedral site from NMR of Co^{59} in $CoCr_2O_4$ 8=27502
Co^{2+} in fluoride salts, optical-absorpt. transitions, mag.-ordering dependence 8=36350
Co^{2+} ion in octahedral $MnF_2$and $ZnWO_4$, i.r. absorpt. spectra 8=32011
Co^{2+} ions in fluorite-type lattices, absorpt. spectra temp. dependences 8=41076
Co^{2+} in Cs_3ZnBr_5, exchange interactions in pairs of coupled Co^{2+} ions 8=49606
Co^{2+} in Cs_3ZnCl_5, exchange interactions in pairs of coupled Co^{2+} ions 8=49606
Co^{2+} in $KMgF_3$, magnetoelastic coeffs. from acoustic paramag. resonance 8=31817
Co^{2+} in TiO_2, ENDOR 8=41007
Co^{2+} in ZnS, CdS, ZnSe and ZnS-CdS, absorpt. and emission rel. to impurity levels, 3500 cm^{-1} 8=27613
Co^{56,59} in solar cosmic rays, flux, calc. 8=37057
Co^{59} low levels, h. f. s. and nuclear quadrupole moment 8=38664
Co^{60} heat source, for reactor, encapsulation 8=47421
20°K, electron bombardment, elec. resistivity rel. to point defects 8=48914
on LiF, films, single-cryst., epitaxial growth 8=35170
on MgO, films, single-cryst., epitaxial growth 8=35170
in Ni, cathode ray polarographic microdeterm. 8=27776
Cobalt compounds
alloy films on MgO, ferromag., epitaxial growth 8=35170
alloys with dil. impurities of 4d and 5d elements of group VIII 8=49642
borides, electronic sp. heat meas. 8=35426
carbonyl complexes, crystal structure 8=26380
ferrite, magnetostriction by X-ray differential photometry 8=26323
fluoride salts:Co^{2+}, optical-absorpt. transitions, mag.-ordering dependence 8=36350
Malcalloy, (Co-Al), magnetic alloy, effect of Mn additions 8=36071
Malcolloy (Co-Al) magnetic alloys, effect of Ti additions on props. 8=40803
Malcalloy, (Co-Al), magnetic alloy, effect of W additions 8=36070
Malcalloy, magnetic alloy, (in Co-Al system), Cr additions rel. to props. 8=31602
Mössbauer spectra, charged states of Fe from Co^{57} decay 8=35034

Cobalt compounds—contd
rare-earth-cobalt, R_xCo_y, mag. behaviours 8=31506
ticonal alloy, 3-d structure modification 8=35270
vicalloy, domain structure in various structural states strained in tension 8=40804
vicalloy strip, mag. props., thermomechanical treatment effects 8=36135
Co^{57} Mössbauer effect sources mag., r. f. mag. fields effects 8=43945
Co acetate tetrahydrate, absorpt. spectrum 8=32046
Co-akermanite system, high-temp. substitution, phase transform 8=35095
alloy films on LiF, ferromag., epitaxial growth 8=35170
Co ammonium metaphosphates, rhombohedral form, crystal structure 8=44245
Co(II) aq. HCl solns., O^{17} and Cl^{35} n. m. r. 8=30541
Co complex, ammonium diethiocyanate-bis-dimethylglyoximatecobaltiate, structure 8=26381
Co(III) complex, aquopentammine Co perchlorate complex ion rotation 8=26384
Co complex, bispyridinocobalt(II)dichloride, structural isomers, intermolecular interaction by Mössbauer spectroscopic study 8=29837
Co(II) di-n-alkylphosphinates, single crystal studies and polymeric structures 8=30797
Co complex, decammine μ-peroxo dicobalt monosulphate tris(bisulphate), structure 8=26385
Co(III) complex, dichloro-bis-phenanthroline-Co(III)-chloride trihydrate, structure 8=26387
trans-$[Co\,en_2(NO_2)_2]NO_3$ annealing of interstitials formed by Szilard–Chalmers recoil, crystal size effect 8=31049
Co complex, nitropentamminocobalt(III) bromide crystal and mol. structure 8=26386
Co^{2+} complexes, electron spin density attenuation 8=47593
Co molybdate hydrates, non-stoichiometric, structures for two phases, and vacancies 8=30916
Co_5(rare-earth) high-coercive force mat., domain-boundary model 8=31500
Co-C, metastable extension of C solubility, splat-quenching effects 8=30656
Co-Ni, films, domains and mag. fine structures form., e microscope obs. 8=31640
$Co_2BaFe_{16-x}In_xO_7$, mag. props. comp. dependence 8=45038
$Co_2BaFe_{16}O_{27}$ crystals, energy anisotropy constants and temp. dependence, 20-500°C 8=40732
Co(II) Br in water, methanol and ethanol, bonding, interacts and ion form. 8=43764
$CoBr_2$ in alkali halide soln., absorpt. spectra 8=48159
$CoBr_2.6H_2O$, mag. props. 8=36204
$CoBr_2 \cdot 6H_2O$, spin-flopping 8=45053
Co(II) Cl in water, methanol and ethanol, bonding, interacts and ion form. 8=43764
$CoCl_2$, aqueous soln, dielec. consts. and loss factors 8=34887
$CoCl_2$ in alkali halide soln., absorpt. spectra 8=48159
$CoCl_2$, antiferromag. resonance, field-dependent modes 8=31837
$CoCl_2$, far i.r. absorption in ferro-, ferri and antiferromag. phases 8=31813
$CoCl_2$, $4CH_2OH$ addition cpd., crystal structure 8=26383
$CoCl_2.2H_2O$ and Mn-doped, mag. resonances 8=31836
$CoCl_2.6H_2O$, antiferromag., higher harmonic reson. 8=36229
$CoCl_2.2H_2O$, antiferromagnet, nuclear spin-lattice relax., 1.3° to 12°K 8=31898
$CoCl_2.6H_2O$, n.m.r. of Cl^-, para-and anti- ferromagnetic state 8=36261
$CoCl_2.6H_2O$ crystals, thermal expansion coeffs., 1.5–4.2°K 8=35442
$CoCl_4$-$ZnCl_4^{2-}$ mixed crysts., spectra at 4°K 8=27590
$Co(CO)_3NO$, laser Raman spectrum 8=48161
Co-CoO films, magnetic after effect of ferro-antiferro magnetic coupling 8=49517
Co-CoO multilayer films, mag. coupling 8=36133
$CoCr_2O_4$ insulating spirals, ferrimagnetic resonance freq. and temp. dependence 8=31831
$CoCr_2O_4$, mag. structure determ. from n.-diffr. 8=31721
$CoCr_2O_4$, NMR of Co^{59} rel. to hyperfine field of Co^{2+} in tetrahedral site 8=27502
$CoCr_2O_4$, spin-structure determ. from magnetization and resonance 8=31731
$CoCr_2S_4$, n.m.r. of Cr^{53}, temp. and d.c. mag. field depend. of reson. freq. 8=36262
$CoCr_2S_4$, NiAs-type structure, magnetization, 1.5°K to room temp., 8=45064
$CoCs_2(SO_4)_2.6H_2O$, relaxation 8=40913
CoF_2, antiferromagnet, behaviour in high mag. field normal to c axis 8=36230
CoF_2, mag. and phonon excitation obs. 8=39870
CoF_2, magnetic excitations near Neel pt. from n. scattering meas. 8=31762
Co-Fe-Au alloys, low-magnetostrictive, coercive force rel. to cold working and ageing 8=31599
$CoFe_2O_4$, cation distrib. 8=39780
$CoFe_2O_4$, ferrimag. spinel, cation distrib. in octahedral and tetrahedral sites, Mössbauer determ. 8=35035
$CoMn_2O_4$, mag. structure from low-temp. n.-diffr. 8=31722

Cobalt compounds—contd
Co_2MnSn, Heuser alloy, Mössbauer effect 8=35033
$Co(NCS)_4Hg$, crystal structure 8=39781
$[Co(NH_3)_6](NO_3)_3$ annealing of interstitials formed by Szilard–Chalmers recoil, crystal size effect 8=31049
$CoNH_4PO_4.H_2O$, cryst. struct., unit cell and space group 8=35326
Co-Ni, Co^{59} resonance satellite lines rel. to mag. disturbance by solute Ni atoms 8=31899
Co-Ni-Fe films, critical thickness and coercivity 8=27400
Co–Ni–Fe films, stress, production parameter dependence 8=31192
$Co_xNi_{1-x}S_2$, pyrite solid solutions, prep. and lattice parameters 8=48342
CoO, anomalous elastic props. and internal friction 8=44560
CoO, containing Fe, multiple charge states 8=39521
CoO, volume diffusion of O, meas. by proton activation of O^{18} 8=35483
CoO, Co K_α line shift rel. to e microprobe analysis, obs. 8=27804
CoO(I) and (II), hyperfine Mössbauer spectra of Fe^{57} below Neel temp. 8=26018
CoO(I) and (II), valency states and Neel temps. 8=26017
Co-P films, Mag. coercivity rel. to substructure 8=27402
Co–Pb–Te system, constitution of stable pseudobinary section 8=43995
$CoPt_3$ ferromagnetic alloy, spin wave dispersion law 8=31649
Co-Rh alloys, n.m.r. relaxation rates, and enhanced susceptibilities 8=31499
CoS_2 powder mag. resonance 8=49603
CoS_2 pyrite, ferromagnetic props. 8=31493
CoS_2 pyrites, mag. props. 8=36078
CoS_2, pyrites struct., growth by Cl_2 transport 8=26249
Co_3S_4, nuclear mag. resonance of Co 8=31901
$Co(S_xSe_{1-x})_2$ pyrite, mag. props. rel. to composition 8=31493
$CoSb_2O_6$, neutron and X-ray diffraction studies 8=48614
Co_5Sm–Cu_5Sm, mag. props., use as permanent magnet material 8=40801
$CoTa_2O_6$, neutron and X-ray diffraction studies 8=48614
Co–Ti alloys, dil., Zener disaccommodation rel. to solute atom motion 8=27401
Co–Ti system, antiferromagnetic Laves phase 8=49571
Co-V alloys, X-ray investigation of σ-phase 8=49713
Co-W ferromagnetic high-temp. structural alloy, development 8=31601
$(PO_3)_3CoNH_4$, orthorhombic crystal structure 8=26382
$RbNi_{1-x}Co_xF_3$, mag. and optical props. 8=49555
Cochlea. See Ear.
Coherence. See Electromagnetic waves; Lasers; Light/coherence; Masers.
Cohesive energy. See Bonds; Solids.
Coincidence circuits. See Counting circuits.
Cold working
See also Plastic deformation; Slip; Work hardening.
brass, 70/30, machine cutting process and prod. of deformed layers 8=35555
f. c. c. metals, fatigue mechanisms rel. to stress magnitude, ductility and texture 8=26772
graphite, grinding rel. to mag. prop. change by creating rhombohedral sequences 8=31497
metals, f. c. c., rel. to internal friction 8=26742
metals, pear-shaped method of cold-welding, deformation state 8=37099
nylon 66, spherulite deform. in cold drawing, 20°C 8=44097
SAP, (sintered Al+Al_2O_2 alloy), lattice defect behaviour, resistometric exam., 8=48817
steel, mild annealed rimmed, ductility rel. to prior cold reduction 8=26817
steel, transformer, in cubic texture perfection rel. to mag. props. 8=36140
vicalloy, cold-rolled, domain structure on straining in tension 8=40804
Ag, cold drawing, internal friction 8=48986
Al, pure, heavy rolling, substructure produced 8=26781
Al sheet, extent rel. to subsequent secondary work softening 8=44543
Al strips and alloys, basic theory of rolling 8=48994
Al–Zn alloys, at −195°C, resist. recovery 8=40305
Co-Fe-Au alloys, low-magnetostrictive, effect on coercive force 8=31599
Cu, fatigue softening by cyclic loading 8=44565
Cu, rolling texture and orientation distrib. function 8=48593
Cu sheet, cold rolled, recrystallization texture 8=44125
Cu-Al alloys, fatigue softening by cyclic loading 8=44565
Cu-Al, second-phase deformations after cold rolling 8=49001
Cu-Sn, second-phase deformations after cold rolling 8=49001
Cu-Zn, second-phase deformations after cold rolling 8=49001
α-Fe, damping peak 8=31204/5
Fe, rolling textures rel. to deformation mechanism and sample orientation 8=26820

Cold working—contd
- Mo permalloy tapes, rolled 4-79, process variables effect on magnetostriction and coercivity 8=31658
- Ni-10 at. %W, rel. to local at. arrangements 8=44244
- Ni-SOCo alloy, induced mag. anisotropy on cold-rolling 8=31661
- Sn-Sb, second-phase deformations after cold rolling 8=49001

Collections of physical data
- Only comprehensive works of reference are listed here
- atmosphere, O_3 content, Jan.-Mar. 1967 obs. 8=50132
- D source, colorimetry tables 8=46655
- ionospheric observations, May 1968, Belgium 8=50174
- ionospheric observations (Nov. 1967) 8=50173
- ionospheric observations, October 1967 8=27963
- ionospheric observations, September 1967 8=27962
- mass spectrometry instruments and applics. 8=47455
- optical indices of internal strains, glasses in optical glass catalogues 8=41096
- optical systems, classification, for automatic retrieval of available designs 8=42166
- organic liquids, relaxation at 1 GHz 8=25910
- Stark effect constants for 13 elements 8=47467
- stars, space-velocity vectors (1962), criticism 8=45615-6
- radionuclide precipitations over Bucharest, winters 1964-6 rel. to 1962-4 8=45479
- solar photosphere, 2000Å-100μ radiation 8=50448
- thermal conductivity of solid, U.S. National bureau of standards 8=30979
- transport property tables of dilute gases, appl. to real gases 8=34672
- Victoria Magnetic Observatory, observations 1966 8=45557
- Wolf-R a yet stars, catalogue 8=50314

Collision processes
- See also Atoms/electron scattering; Elementary particles; Field theory, quantum/interactions; Ionization; Nuclear forces; Nuclear reactions; Scattering, particles; and under the individual particles.
- air, stopping cross section for 6 ⩽ Z ⩽ 24 8=47976
- alkali-inert gas interatomic pot. from scatt. data 8=47541
- alkali metal atoms with foreign gases, theory of satellite bands 8=47532
- alkaline vapour mixture, spin exchange relax., obs. 8=38749
- anharmonic oscillators, vibr. relax. 8=29839
- atom with excited atom, ionization formula without rotating-atom approx. 8=25706
- atom-atom, dispersion forces 8=38745
- atom-diatomic mol., distorted wave expansion 8=29833
- atom-electron, conditions for bound states 8=47535
- atomic collisions in crystals 8=48887
- atomic, particle exchange, theory 8=29659
- atomic, quantal description by eikonal method 8=38742
- atomic systems, time correl. function formalism 8=29386
- atoms, excitation transfer theory 8=43233
- atoms, excited ^3P, state, inelastic collisions of second kind with electrons 8=43230
- atoms, impact parameter treatment 8=38741
- atoms, interf. expts., high resolution 8=29665
- Auger mechanism of energy losses 8=39019
- Chapman-Enskog method in chem. kinetics 8=49849
- charge exchange controlled ion motion, steady state in elect. field. 8=25712
- chemically activated radicals, vibr. energy transfer 8=49846
- dense gases, nuclear spin relax. and collision freq. 8=34669
- diatomic gases, nuclear mag. relax. 8=38913
- discharge plasmas, high-pressure, excited in diatomic gases, energy exchange 8=47742
- electron-atom, ionization quantum theory 8=43470
- electron—atom, theory and calc. methods 8=29660
- energy transfer in thermal unimolec. systems 8=27682
- ethyl iodide mols. e scatt., spin polarization calc. 300-400 eV 8=34214-5
- excitation expts., equipment and evaluation methods 8=29636
- focusing in sputtering, model 8=48900
- gas-discharge tube, transport pumping force 8=38986
- gas, reduction of photon echo intensity 8=39213
- gases, dense neutral, atom-atom, ionization cross section calc. from Thomson's theory 8=29951
- Gryzinskis classical method for electron-impact ionization, extension 8=43483
- hadron-nucleus, semiclassical theory 8=42491
- of heavy systems, bound on inelastic cross-sections 8=43149
- inelastic, quantum mechanics 8=37743-4
- inert gas ions with atoms and mols., 1-100 eV charge transfer cross-section obs. 8=38735
- inert gas mixture, collision-induced translational absorpt. theory 8=34384
- integrals for high-temp. gases 8=34670
- intracollisional dipole correl. function 8=38746
- ion-atom, boundary condition for theoretical treatment 8=29655
- ion-atom, charge exchange orthogonal channel projections 8=25389
- ion-molecule reaction mechanisms, cyclotron double resonance exam. 8=47554
- ion-molecule reaction rates in drift tubes 8=29835

Collision processes—contd
- ion-molecule reactions, elevated press, investigation by modified time-of-flight spectrometer 8=29843
- in ionized gases, Fokker-Planck operator and photon scatt. by electrons 8=43475
- ionosphere, D-region, electron energy loss factor 8=27990
- in ionosphere F-region, of elections, freq. 8=50195
- ions He^+ and Ne^+ with Ar, Kr, N_2, O_2 and CO_2, at 2-250 eV, charge exchange 8=38758
- ions, positive, excitation and inter-level transitions 8=43209
- Larmor radius and collisional effects on combined Taylor and Kelvin instabilities in composite medium 8=43596
- low-energy matrix, unitary model 8=29388
- magnetoplasma, Maxwellian and non-Maxwellian, effective parameters 8=39066
- metastable double mol. and double mol. ions, formation 8=29834
- molecular beam with hot filament, appl. to pyrolytic reactions 8=36577
- molecular non-reactive, distorted-wave Magnus approximation 8=43426
- molecular scatt. data used to obtain Lennard-Jones pot. 8=39192
- molecular scatt. reactive and elastic, appl. of R-matrix theory 8=43427
- molecule-electron, inelastic scatt., theory 8=43279
- molecules, diagrammatic methods for cross-sections 8=29838
- molecules, long-lived complexes in crossed beams 8=25669
- molecules, lower bounds of adiabatic phase shifts 8=29842
- molecules, nuclear spin and statistics effects 8=47723
- molecules, transfer of rotational energy 8=25662
- molecules, transport collision integrals 8=29848
- molecules, vibr. transition probabilities, WKB calc. 8=38953
- mosaic virus, southern bean, interparticle interactions, small-angle X-ray scattering studies 8=25967
- nuclear resonance widths and spacings, matrix calc. 8=42986
- nuclear, unitary resonance matrix for elastic scatt. 8=42985
- oscillator with particle, vibr. energy transfer 8=47721
- pairs in low-density Fermi gas 8=32852
- physics of atomic collisions, book 8=38747
- plasma Coulomb collisions, equilibrium states, statistical considerations 8=30021
- plasma, effect on ionization equilib. 8=25722
- plasma, effect on wave motions 8=34551
- plasma, electron collisions and critical drift 8=30148
- plasma, freq. calc. from r.f. cond. meas. 8=43546
- plasma, weakly ionized, inelastic effect on elec. field 8=47821
- polar mols. scatt. by nonpolar gases, comment on $1/r^6$ pot. 8=29853
- pressure-induced i. r. spectra, intercollisional interf. effects 8=34385
- $pD(1S) \rightarrow H(1S; 2S)D^+$ cross-section calc., 20KeV-100MeV 8=43237
- proton-gas charge transfer cross-sections, obs. 8=38737
- p-H atom, Sturmian coupled-state calc. 8=38736
- p-H, impact parameter representation 8=46821
- $pH(1S) \rightarrow pH(2s)$, 1-500 keV, invalidity of peaking approx. method 8=43218
- p-H scatt. with variable effective charge, cross sections calc. 25 keV 8=38752
- $pHe(1S^2) \rightarrow H(1S)He^+(1S)$, cross-section calc., 0.1-100 MeV 8=43237
- rearrangement, coupled channel method 8=25205
- rearrangement, in unified theory of nuclear reactions 8=33975
- rotationally degenerate gases, thermal cond. 8=47958
- spectral broadening, in combination with Doppler effect 8=43235
- stellar atm., spectral evidence 8=36939
- stellar, 2-dimensional theory of quasars 8=45619
- in suspended particle motion in rectilinear channel, rel. to acceleration 8=30544
- theory, method of moments 8=46820
- thermalization by elastic collisions 8=34177
- three-body, Lippmann-Schwinger eqns. applied to e-H 8=38724
- 2-body relativistic, kinematic broadening 8=47028
- two atom excitation by single photon 8=29633
- van der Waals interactions, calc. from oscill. strength sums 8=43429
- vibrational transition probabilities WKB evaluation 8=47442
- XY plotting of cross sections using log multiplier circuit 8=29657
- Ar, low-energy e stopping cross sections 8=47977
- Ar, Rutherford scatt. of H and H^+ 8=38754
- $As(4^2D)$, cross-sections for deactivation 8=34160
- Br^- ions with He, Ne, Ar and Kr atoms, detached electrons energy obs. 8=29972
- C ions, low energy, resonance charge exchange 8=47536
- C, stopping cross-section meas. using recoil ions from radioactive decay 8=29658
- CO_2, population inversion by collision with N_2 8=37578
- Cd, 3261A line broadening by Ar gas, pressure and temp. dependence 8=38750

Collision processes—contd

- Cd 6^3S_1 atoms with inert gases, depolarisation cross sections, obs. 8=38692
- Cd 6^3S_1 atoms with N_2, depolarisation cross section, obs. 8=38692
- Cd-Xe in positive column, effective cross section calc. 8=34180
- Cl^- ions with He, Ne, Ar and Kr atoms, detached electrons energy obs. 8=29972
- Cs^{133} atoms, spin-exchange cross-sections, meas. 8=43239
- Cs discharge, electron-atom, rel. to momentum transfer cross sections from drift velocity meas. 8=29911
- Cs^0, e bombardment, source for polarized Cs^+, Cs^{2+} and Cs^{3+} 8=24160
- Cs-inert-gas, excitation transfer cross-section calc. 8=47543
- Cs vapour, hyperfine relax. and diffusion coeff. and cross section meas. 8=47537
- Cs-Ar, total scattering cross sections 8=34178
- Cs-Kr, total scattering cross sections 8=34178
- Cs-N_2, H_2, HD, D_2, resonant state transfer and de-excitation obs. 8=38957
- Cu surface, Ar and Cu atoms 8=29661
- D atoms, ionization, ejected e spin polarization obs. 8=29662
- D_2^+ in H_2, charge-transfer cross-section obs. 8=47539
- H atom-gas charge transfer cross-sections, obs. 8=38737
- H atom, 1s-2s excitation by slow electrons, theoretical and numerical study 8=38694
- H, neutral atoms, sensitivity of stripping analyzer in energy range 50 to 300 eV 8=43236
- H_α profile, effects 8=38645
- H with inert gases, Lyman-α excitation cross-sections 8=38760
- H with inert gases, Lyman-α polarization 8=38759
- H^+ cooling in He gas 8=43681
- $H^+ + H$, high-energy electron capture cross-sections 8=38744
- H^+, H° and H^- interaction with Xe atom, charge state changes, investigation by coincidence method 8=43238
- $H^+ + H(1s)$, impulse approx. 8=38743
- $H^+ + (H(1s) \rightarrow H(2s)) + H^+$ cross-section for metastable 2s state 8=38753
- $H^+ + Li^+ \rightarrow H(n) + Li^{++}$, e capture cross section 8=25392
- $H^- + F$ and $H + F^-$, electron detachment 8=34451
- $HH^- \rightarrow H^-H$ charge transfer, restrictions on complex pot. energy 8=43308
- $H + H^- \rightarrow H_2{}^* + e$, associative detachment 8=25391
- H_2, impact of p and H atom, vacuum u.v. emission 8=38834
- H_2 Maxwellian beam scattered by room temp. H_2 and He, total cross-sections 8=47729
- H_2, para and ortho, with He, rotational excitation 8=47720
- H_2^+ in H_2, D_2, Ar, charge-transfer cross-section obs. 8=47539
- H_2^+-He, Born cross-section calc. from e scatt. data 8=38951
- H_2O-H_2O, vibr. transition probabilities 8=34389
- in He, α particles 10-300° K, protons 1-600°K, mobilities obs. 8=38836
- He atom, with N_2 mol., rotational excitation 8=25666
- He atoms, excitation transfer cross-section calc. 8=47540
- He-e, excitation cross section calcs. 8=38703
- He flowing afterglow, atom-e spin exchange 8=43221
- He Maxwellian beam scattered by room temp. H_2 and He, total cross-sections 8=47729
- 2^3s He metastable with Ne rel. to afterglow of He-Ne plasma 8=30080
- He, Rutherford scatt. of H and H^+ 8=38754
- He, 2, 3-atom nonretarded van der Waals coeffs., Padé approximant calc. 8=38757
- He, weakly ionized, and radiative mechanisms 8=29969
- He-CO_2 mixture, energy loss freq. distrib. of 43.7 MeV protons 8=29663
- He-H_2, high-velocity scatt. 8=25667
- He^+-H, H_2, Lyman-α emission cross sections and polarization obs. 8=38755
- $He^{2+} + H(1s)$, impulse approx. 8=38743
- $He^+ \rightarrow He_2^+$ in afterglow plasma, obs. of rate 8=43449
- He^+ in He; mobility and total, charge-transfer, diffusion and viscosity cross sections obs. 8=38835
- Hg atoms, metastable and ground state, depolarization cross section calc. 8=34142
- Hg^{198} atoms, with inert gases, relax. cross sections, temp. effect 20°-600°C 8=29664
- Hg vapour jet, charge exchange of polarized ions from positive into negative 8=39039
- I^- ions, with He, Ne, Ar and Kr atoms, detached electrons energy obs. 8=29972
- I_2 mols. e scatt., spin polarization calc., 300-400 eV 8=34214-5
- K atom beam scatt. on CO_2 molec. beam, time-of-flight anal. 8=38952
- K^{39} atoms, spin-exchange cross-sections, meas. 8=43239
- K atoms with N_2, H_2, HD and D_2, mixing and quenching 8=29836
- K, magnetically oriented 4^2p atoms, collisional depolarization 8=47520
- K vapour, proton charge exchange, $E_p = 2.5$-22 keV 8=38761

Collision processes—contd

- K and Cs crossed atomic beams, spin exchange 8=47534
- Kr^+-Kr, sudden change in number of electrons at 25 keV 8=39018
- Li^0, e bombardment, source for polarized Li^+ and Li^{2+} 8=24160
- Li-Li^+, charge transfer, oscills. in total cross-section 8=38762
- N ions, low energy, resonance charge exchange 8=47536
- N_2, low-energy e stopping cross sections 8=47977
- N_2 with atomic ions, rot. and vib. energy transfer to form N_2^+ $(B^2\Sigma_u^+)$ 8=39046
- N_2, with He atoms, rotational excitation 8=25666
- N_2^+ ions, excitation by electrons, at near threshold energies 8=47523
- Na vapour and inert gases, rel. to energy transfer and Na fluoresc. 8=34182
- Na-Ar, total scattering cross sections 8=34178
- Na-Hg, interf. expts., high resolution 8=29665
- Na-Kr, total scattering cross sections 8=34178
- Ne auto-ionization excitation by ion impact 8=39048
- Ne, collisional disalignment 8=34183
- Ne, Rutherford scatt. of H and H^+ 8=38754
- Ne-Kr mixture, excited by a discharge 8=29882
- Ne-Ne, Ne^+-Ne, Ne^{++}-Ne, ratio of prod. of fast electrons 8=39018
- O mols, cross-section reson. in crossed mag. fields, obs. 8=34660
- $O^{16} + O^{16}$ scatt. nuclear molecular potentials cross sections, angular distribution obs 8-30 MeV 8=43098
- $O^+(^4S) + H(1s)$ low-energy collisions, charge transfer cross-section 8=27940
- Pb^{206} 103 keV recoil particles in pure and binary gases, ionization and range 8=29950
- Rb-inert-gas, excitation transfer cross-section calc. 8=47543
- Rb-Kr, total scattering cross sections 8=34178
- SF_6 mols., laser excited, with SF_6, He, Ne and H, relax., photon echo obs. 8=34282
- Ti, press. broadening and shift of lines by Ar 8=43204

Colloids

- See also Electrophoresis; Emulsions; Gels; Sols; Thixotropy.
- aqueous colloidal electrolytes, light scatt. 8=43890
- arrays of spheres, light diffr. 8=48237
- chasov yar clay, moisture diffusion coeff. and thermograd. coeff. rel. to moisture content 8=30662
- chrysotile asbestos suspensions, surface charge stabilization 8=48242
- coagulation of compounds in chemical reaction 8=48238
- colloid-surface interact, small conc. determ. on planar inorg. subs. rel. to removal 8=30568
- colloidal Ca product, electron irrad. CaF_2 8=40074
- fluctuating phenomena, physical study 8=43886
- latexes, light diffr. 8=48237
- loams, moisture diffusion coeff. and thermograd, coeff. rel. to moisture content 8=30662
- micellar diffusion coeffs., polarographic determ. 8=34941
- nitrosylruthenium, sorption on $Fe(OH)_2$, obs. 8=44073
- nonionic detergent in aq. soln., micellar props., temp. effect by light scatt. 8=30559
- optical nonlinearities 8=34951
- polydisperse spheres, number determ. by light scattering 8=34940
- potential, field and surface charge in diffuse layer round particle, local thermodynamic calc. 8=30565
- ruthenium, sorption on $Fe(OH)_2$, obs. 8=44073
- Ag in gelatin, effect of particle shape on spectral absorpt. 8=39460
- AgBr, complex refr. index, near-u. v. 8=43891

Colorimeters. See Colorimetry.

Colorimetry

- See also Spectrochemical analysis; Spectrophotometry.
- butterfly wing spectral reflection characteristics 8=46656
- D source, colarimetry tables 8=46655
- fluorescent light viewing of Melde expt. 8=28724
- interocular brightness matching, pupil diameters and retinal illuminances 8=33297
- photoelectric, design for clinical laboratories 8=42140
- standardization of measurements 8=46657
- Fe, high-purity, plastically deformed, on heating to 600°C 8=35677
- MgO flame colour temp. determ. 8=37312

Colour

- See also Photography/colour.
- chromatic strengths of colours, Munsell system 8=28925
- crystals of square planar complexes, origin 8=27535
- dichromatism as homomorphism of trichromatism 8=37635
- filter glasses, luminous transmittance and chromaticity in CIE 1964 colour space 8=37664
- glass, effect on emissivity and cooling rate 8=44331
- glass emerald green, u.v. absorbing, characts. 8=49720
- iron-group ionic crystals, dependence on structure 8=27534
- optical aspects, introduction 8=42141
- optical aspects, light source effects 8=42143
- optical aspects, metamerism 8=42145
- optical aspects, numerical description 8=42142

Colour—contd
  optical aspects, perception and description 8=42144
  photographic objectives, "amber coating" 8=42289
  standardization of measurement 8=46657
  trichromatism, dichromatism and monochromatism 8=37634
  Co-akermanite system, high-temp. substitution, phase transform 8=35095
  Cu^{2+} ion in blue proteins 8=49782
  Fe glazes, shade rel. to FeO content 8=49717
  TiO_2-Sb_2O_3-NiO system, rel. to comp. and structure 8=26039
Colour centres
  absorption of light difference between ground and excited states obs. 8=44471
  aggregate, e struct. and stress effects, zero-phonon line obs. 8=40056
  alkali halide crystal phosphors, F centers interaction with microdefects in crystal lattice 8=31123
  alkali halide crystals, M centre, triplet state lifetime 8=26718
  alkali halide crystals, X-centre formation mode 8=35583
  alkali halides, F-centre electron distrib. 8=31122
  alkali halides, F-centre production, effect of impurities 8=35582
  alkali halides, F_2^+ centre, ground and excited states, allowing for polarization 8=35581
  alkali halides, paraelastic electron-vacancy centres 8=49706
  alkali halides, Stark effect 8=31112
  alkali halides, U-centres, cause of lattice-vibration local modes 8=39866
  alkali halides, Z_1-centre models, vacancy-centred, props. calc. 8=44473
  alkaline earth fluorides, H- and F-bands, Mollwo-Ivey relation 8=48873
  crystal phosphors, effective recombination cross-section of charged centres 8=26715
  electrolytic colouration, influence of dislocations 8=44469
  electron-excess, polaron model, appl. to U_1 centre 8=40061
  F-absorption band, temp. range 8=31111
  F-centre e.s.r. g shift values in divalent cpds., theory 8=40057
  F-centres, chemical determ. in Co^{60} γ-irradiated crystals of NaCl 8=48884
  F-centres, shallow, in ionic cryst. 8=44470
  F-formation by electron excitation from sub-system 8=35517
  F, e.p.r. optical saturation 8=49586
  F, in ionic crystals, semi-continuum polaron models 8=31110
  F, three-body model, 0- and 1-phonon absorpt. spectrum 8=44472
  glass, photochromic, production by Ag^+ exchange 8=41140
  glasses, Ag atom impurity stabilization and atomic centres production by X-rays 8=31114
  in interstellar grains, 8=50349
  ionic crystals, rare-gas centres, possibility 8=26716
  polar solvents, mixed, photo-induced trapped electron rel. to photobleaching study 77°K 8=36446
  potassium halide crystals, U centre phonon scatt., thermal conductivity meas. and theory 8=44301
  quartz, coloured varieties, growth 8=26264
  quartz, crystalline, E_1^1 electron spin-echo obs. 8=44486
  quartz, ε-centre formation mechanism and kinetics 8=48885
  Ag halide particles in glass, bleaching process 8=41094
  BN, F-centres, e.p.r. spectra confirmation 8=35584
  BaF_2, n-irradiated, self-trapped hole formation, e.s.r. exam. 8=31854
  BaF_2:U^{3+}, struct. of U^{3+} centre from magneto-optical rotation 8=36336
  $BaTiO_3$: rare earth ions, F-centres, e.s.r. obs of substituting sites 8=48818
  CaF_2, F-centres, X-ray induced, formation and bleaching 8=40059
  CaF_2, n-irradiated at liq. N_2 temps., obs. 8=26719
  CaF_2, n-irradiated, self-trapped hole formation, e.s.r. exam. 8=31854
  CaF_2, V_K centre, influence of Y and O on formation 8=40060
  CaF_2:CeO_2, M centres rel. to photochromic colouration 8=44474
  CaF_2:$Pu^{3+,4+}$ 8=31968
  CaF_2:U^{3+}, struct. of U^{3+} centre from magneto-optical rotation 8=36336
  CaO, F-band and 3557 Å zero-phonon peak, Faraday rotation 8=45178
  CaO, Faraday rot. anal. of bands 8=35588
  in CaO, n-irradiated 8=31115
  CdS crystals, local centre formation in presence of free electrons and holes 8=36015
  CsBr, F- and X-centres, photochemical reactions 8=27758
  Fe centres in amethyst 8=31116
  KBr, F-aggregate bands, optical and thermal stability, half-widths and oscillator strengths 8=49732
  KBr(I), F-centre form. by u.v. irrad. 8=44479
  KBr, M-centre luminescence 8=41199
  KBr, plastically deformed, F-centre thermal stability rel. to dislocation density 8=35586
  KBr, U → F and U → α transforms. rel. to volume expansion, photoelastic meas. 8=26826
Colour centres—contd
  KBr: Tl, F and A scintills., recombination luminescence 8=36493
  KCl, additively coloured, F_n centres 8=26717
  KCl, cationic vacancy displacement during coloration on divalent impurity addition, from conductivity meas. 8=35535
  KCl, colloidal centres, optical, e.s.r. and elec. exam. 8=44477
  KCl, coloured additively, photochemical reaction and photocond., at low temp. 8=31457
  KCl crystals, deformed, colour centre—dislocation interaction from photoconduction 8=44928
  KCl, deformation effects, on colourability, room temp. 8=31119
  KCl, F-aggregate centres, optical, e.s.r. and elec. exam. 8=44478
  KCl, F-centre density effect on dislocation mobility and microhardness 8=26690
  KCl, F-center, light absorpt. calc. for transition to L bands 8=48877
  KCl, f-centres, dependence of luminescence on conc. 8=36491
  KCl, F-centres, endor 8=36272
  KCl, F centres, simultaneous production and bleaching 8=26720
  KCl(I), F-centre form. and ICl^- V_K centre due to u.v. irrad. 8=44479
  KCl, hardening by F_A centres 8=44583
  KCl, M-centre luminescence 8=41199
  KCl, plastically deformed, F-centre thermal stability rel. to dislocation density 8=35586
  KCl, R-centre transitions from mag. circular dichroism. 8=48874
  KCl whiskers, X-irradiated, F-centre accumulation 8=35585
  KCl:Cd, optical, elec. and e.s.r. exam., 8=48876
  KCl:H^- interstitial ion, U_1 centre, electron-excess centre polaron model appl. 8=40061
  KCl:In, F and A scintills., luminesc. kinetics 8=36492
  KCl:I, ICl^- V_K, optical and e.s.r. exam., 8=48875
  KCl-KBr solid soln., p-irradiation, F-centre production, comp. dependence 8=31117
  KCl:Pb, F and A scintills., luminesc. kinetics 8=36492
  KCl and RbCl, mixed, F-centre, L_1 band forbidden transition 8=31118
  KCl:Sr, Z_2 centre, photocond. 8=44929
  KCl: Tl, F and A scintills., recombination luminescence 8=36493
  KI, absorption, far i.r., due to U-centres and F-centres 8=44480
  KI, α-centre, polarization of luminescence 8=27654
  KI crystal, e beam pulse effect 8=44475
  KI, F-centre form. by u.v. irrad. 8=44479
  KI, V band preferential bleaching 8=44476
  KI: Tl F and A scintills., recombination luminescence 8=36493
  La_2O_3:Bi^{3+}, configuration curves calc. rel. to band widths and phonon emission 8=40058
  LiF, e-irradiated, formation process from absorpt. and luminescence 8=40062
  LiF, excitation for stimulation of thermoluminescence 8=41200
  LiF, F-centres, effect of X-rays, concentration 8=35603
  LiF, F-centre, hyperfine interaction constants, temp. dependence 8=35587
  LiF, F_3^+-conversion and R-centres destruction on R light bleach 8=44482
  LiF, F_3^+, linear Stark effect 8=31120
  LiF, linear Stark effect on zero-phonon absorpt. lines, obs. 8=27581
  LiF, n/e-irradiated, aggregate defect centres, Mollwo-Ivey relation 8=31032
  LiF, R′ centre, Jahn-Teller vibronic structure 8=44481
  LiF, R′centre, magnetic circular dichroism 8=48878
  LiF, X-irradiated, dislocations effect on F-centre thermal stability, e-emission exam. 8=35570
  MgO, effect of low dose n irrad. on conc. 8=26829
  MgO, F band rel. to F centre, temp. depend. 8=45209
  MgO, Faraday rot. anal. of bands 8=35588
  MgO, heavily neutron irrad., study by optical absorpt. bands 8=35589
  MgO, irradiated, phonon-assisted optical absorpt. 8=41049
  MgO, n/e-irradiated, aggregate defect centres, Mollwo-Ivey relation 8=31032
  MgO, n-irradiated at 80°K 8=27588
  MgO, V^1 centre thermal decay temp. dependence, 18°-50°C 8=31121
  NH_4 halides, F-centre, e.p.r. studies 8=26721
  NH_4 halides, new defect centre, motional effects 8=48879
  NaCl additively discoloured, effect of laser irrad. 8=44485
  NaCl, Co^{60} γ-irradiated crystal, F-centres, chemical determ. 8=48884
  NaCl crystal, e beam pulse effect 8=44475
  NaCl, F-centre density effect on dislocation mobility and microhardness 8=26690
  NaCl, F-centre thermal destruction rel. to dielec. losses 8=44484

Colour centres—contd
NaCl, F-centres, optical absorption 8=35591
NaCl, F-centres, photothermal stability, effect of plastic deformation 8=35590
NaCl, F-colouring dependence, at room temp., on quenching 300-710 °C 8=48882
NaCl, M centre, lifetime of first excited state 8=40063
NaCl, plastically deformed, F-centre thermal stability rel. to dislocation density 8=35586
NaCl, surface F-centres formation in γ-irrad. rel. to Au nucleation 8=44152
NaCl:$CdCl_2$, absorpt. bands, X-ray induced F-centres 8=31113
NaCl-Tl, -Ag, phosphers, F, photothermal destruction, efficiency of recombination luminescence 8=48881
NaF crystals, R_N and N, thermal annealing after p.-irrad. at liq. N_2 temp. 8=48883
NaF, electron irrad., obs. with oven cryostat 8=48880
NaF, F_3^+, linear Stark effect 8=31120
NaF, M-centre delayed luminescence in F-to-M conversion 8=41203
Na_2SO_4, X-irradiated, single crystal absorpt. peaks obs. 8=44483
Nb centres in irrad. Nb glasses, e.s.r. 8=40937
PH_4I, e.p.r. of I_2^- centres 8=31124
Pb halides, γ-irrad., prod. by electron and hole trapping, e.s.r. and optical meas. 8=36249
RbF, electron irrad., obs. with oven cryostat 4=48880
RbI, F-centre form. by u.v. irrad. 8=44479
Si, n-irradiated, A-centre production 8=44416
SiO_2 rel. to radiation damage 8=26722
ZnS, accumulation during bombardment with fast neutrons 8=31125
Colour photography. See Photography/colour.
Colour vision
chromatic strengths of colours, Munsell system 8=28925
colour names of very small fields varying in duration and luminance 8=33299
hue perception, luminance requirements 8=24447
land effect rules, temporal reversal 8=37731
LGN cells, responses analysis 8=28926
light, colour and vision, book 8=42293
man and animals 8=46778
opponent-response functions related to measured cone photo pigments 8=28927
perception and description of colour 8=42144
photopic mechanisms of early dark adaption 8=28923
red-green discrimination, residual in dichromats, obs. 8=46777
retina, struct. model relating obs. trichromatic and opponent-colour responses 8=28924
rhesus monkey, increment-threshold spectral sensitivity rel. to background spectrum 8=24448
yellow blur, role in human eye 8=46771
Columbium. See Niobium.
Coma. See Aberrations, optical.
Combustion
See also Explosions; Flames; Heat of combustion; Reaction kinetics.
acetylene, in shock waves, source of schlieren signals 8=49886
calorimeter for radiation and convection determ. 8=32987
explosives, burning and thermal decomposition 8=32114
extinction conditions, solid, prediction 8=25812
of flames, open turbulent, rate rel. to noise emission 8=32108
in fuel bed, temp. distrib. rel. to temp. differences between gas and mat. 8=37313
gas flow, electrical control 8=25710
gases, ignition by hot surfaces prod. by friction, obs. of temp. prod. during oblique impact 8=32981
heat and mass transfer in system of plane turbulent layers in presence of diffusion combustion 8=43666
ignition and extinction, in forced convection systems 8=32971
ignition of monodispersed aggregate of particles in gas oxidiser during reaction 8=32970
ignition regime of hydrocarbon fuel in air, in supersonic boundary layer of plate 8=32969
instability, acoustic—nonacoustic relationship 8=24012
live, role of free electrons 8=32974
methane, thermodynamic props, of products, computer calcs. 8=27730
nonpremixed systems near equilibrium, chemical kinetic effects analysis by matched asymptotic expansions 8=36579
polyolefins, Br cpd. effects on thermal degradation at 400 °C 8=36583
propane-O_2 flames, effect of Al on heat transfer characts. 8=32973
pyrolysis using hot W filament 8=36577
rocket exhaust plume, i.r. radiant heating to base of vehicle 8=41482
in rocket motor chambers, spectral meas. of gas and particle temps. 8=32977
steel, minimum ignition temp. rel. to O_2 press., and surface deform. 8=36578
Combustion—contd
super alloys, minimum ignition temp. rel. to O_2 press., and surface deform. 8=36578
thermal ignition in hollow circular cylinder heated on inner face 8=32976
Al droplets in air and O_2-Ar mixture 8=49885
Al particles, system morphology rel. to mechanism 8=32112
Al porous plug with O_2 throughput, with different internal structs and void contents 8=36580
B, particulate, surface burning in air, gas phase chem. kinetics 8=36581
B, ultra-fine powder, ignition temp. in air N_2, CO_2 and N_2-CO_2 mixtures 8=32113
BeH_2, mechanism 8=32110
H, liquid, burning, diffusion theory 8=32111
H_2-O_2 in shcok waves, kinetics 8=32109
H_2 + O_2, luminous emission and combustion peninsula 8=45354
H_2S flame, rarefied, stages in burning 8=36582
N_2-O_2 and He-O_2 diving atmospheres, non-combustion region 8=49884
NH_3-O_2 mixtures, ignition by shock waves 8=27729
Pu and alloys, ignition behaviour 8=45353
T-burner with high heat loss, acoustic response function, rel. to lower sonic vel. 8=32972
Comets
coma region, struct. of tailrays 8=32554
consisting of anti-matter, possibility 8=32559
Copernicus crater, cometary impact origin 8=32526
infrared continuum, grain emission obs. 8=45837
Ikeya-Seki, obs. near sun 8=45840
Iyeka-Seki (1965f), Na velocity fields 8=45841
Ikeya-Seki (1965f), spectrum 8=37016
Iyeka-Seki, tail photography 8=32560
major-axes distrib., long-period 8=45838
Morehouse 1908 III, number of rays 8=37017
1961 V (Wilson-Hubbard), orbit 8=32558
1962-III, optical pumping and D-line ratio 8=37018
1963, obs. 8=32555
1963b, obs. 8=32557
1964h, obs. 8=32556
1964h, obs. 8=32555
orbits, nongravitational acceleration obs. 8=45839
photographic obs. 8=32553
photographic obs. (1957) 8=45836
radicals and ions production, photochemical effects 8=50425
tails, type I; structure and kinematics 8=50426
C_2 radical, forbidden intercommunication transition 8=28154
C_3 spectra, resonance-fluorescence mechanism; synthetic profile computed, 4050Å 8=50424
Compasses
No entries
Complimentarity. See Physics fundamentals; Quantum theory.
Compressibility
See also High-pressure phenomena and effects.
air effect in impact of flat body on free surface 8=41648
alkali halides, calcs. for validity test of box model 8=35315
alkali halides, compressibility, isothermal, meas. by capacitance method 8=49031
axial compression of slightly-curved panels, buckling behaviour including shear deformability effect 8=41657
critical density determ., effects of sample config. in earth's field 8=30574
Gruneisen solid, h.p., thermodynamic calc. 8=30972
homogeneous subs., isothermal, rel. to density mean fluctuation, and small angle X-ray scatt. 8=25879
ice VII, H_2O and D_2O 8=49026
isothermal, meas. by capacitance method 8=49031
plane strain extrusion, upper bound solns. 8=35618
plastic layer between parallel plates 8=23852
in relativistic m.h.d., and shock waves 8=28587
sediment, electrolytically flocculated rel. to particle size 8=30556
slip-line fields geometric props. 8=40112
water into ice VII phase transf. by shock compression 8=48262
Am, rel. to pressure 8=39541
Cs, calc. from eq. of state 8=30973
Cu-Ni alloys 8=26807
Fe, compared with Pb, under impact press. 31 to 34 m bars 8=40108
Fe-Ni alloys, isothermal compression up to 300 kb, crystallographic obs. 8=49006
GaP, calc. from u.s. phase-comparison meas. of elastic constants 8=49021
GaSb, compression to 80kbar and elastic moduli pressure dependence 8=49022
Gd, anomalous, and Curie temp. variation with hydrostatic press. 8=36149
He^3, solid, obs. 8=37358
K, calc. from eq. of state 8=30973
KCl, isothermal, meas. by capacitance method 8=49031
Kr, solid, meas. rel. to thermodynamic props. 8=48745
MgO, rel. to creep curve shape 8=31221
MnSb 8=26407
Pb, compared with Fe, under impact press. 31 to 34 m bars 8=40108

Compressibility—contd
Pb cylinders, strain-time, strain-rate and dynamic force-time characts. 8=35711
Pd–Ni alloys 8=35715
Rb, calc. from eq. of state 8=30973
gases
adiabatic, thermodynamic upper bounds 8=37225
displacement meas. for up to 10 000 atm 8=34600
escape, unsteady, in constant gravity field 8=47936
ethane 8=34643
iron phosphate glasses, electronic carriers thermally activated diffusion 8=49079
methane 8=34643
Ar, adiabatic, from u.s. vel. meas. 8=25828
CH_4 and CD_4 8=30588-9
N, displacement meas., $\leq$10 000 atm and 400°C 8=34600
liquids
aniline solns., adiabatic 8=30469
benzene + n-heptane system, excess isothermal 8=43794
critical state study using gravitational waves 8=48055
isothermal. temp. dependence. calcs. 8=43766
silica, molten, adiabatic, and speed of ultrasound 8=48140
Ar, meas. and computation 8=28219
CCl_4, shock-compressed, brightness temp. meas. and P-T curves 8=48089
CCl_4-C_6H_6, shock-compressed, brightness temp. meas. and P-T curves 8=48089
CH_4 and CD_4 8=30588-9
Li-NH_3 soln., from u.s. vel. data 8=30468
Compressive strength. See Mechanical strength/compressive.
Compton effect
background in NaI(Tl) counter, suppression 8=46914
deuteron scatt., cross-section sum rules for magnetic moment 8=42622
double and triple cross-sections meas. for 0. 662 MeV photons 8=24697
e anomalous magnetic moment, sixth order contrib. 8=29094
electron scatt., 1 GeV, near 180°, obs. 8=42459
γP Compton scatt., < 150 MeV, expt. and calc. 8=24696
γ quanta production by Compton effect with relativistic electrons colliding with laser beam photons 8=47045
γ-ray, scatt., freq. and direction, centre-of-mass calc. 8=42452
gauge-noninvariant part of amplitude, Feynman diagram analysis 8=37918
hadron, kinematic singularity structure of helicity amplitude 8=29079
inverse, rel. to quasar optical spectrum 8=45780
inverse, stimulated term rel. to distance of quasars 8=28134
isovector photons with nucleons, forward scatt. amplitude, phenomenological Lagrangian method 8=37920
lepton pair photoprod., compton diagram 8=33623
multiple scatt., softening of radiation 8=37231
nucleon at low energy 8=47129
nucleon scatt., cross-section sum rules for magnetic moment 8=42622
photon scatt., E_γ = 662 keV, polarization effect obs. 8=33607
π, low-energy theorems 8=33606
plasma, e-photon interactions rel. to radiation distrib. 8=39067
quantum theory of incoherent scattering, exchange contrib. for assoc. Compton band 8=43278
in radio sources, stimulated inverse scattering 8=36978
sum rules, off stable particles 8=24695
in stars, variable, inverse effect rel. to continuous emission 8=32458
virtual π scatt., use of Weinberg sum rules 8=42545
Al, e. -momentum densities determ., 8=44647
B, e. -momentum densities determ., 8=44647
Be, e. -momentum densities determ., 8=44647
Fe, profile 8=31989
H_2O, scattering profile 8=48066
Li, e. -momentum densities determ., 8=44647
LiF, e. -momentum densities determ., 8=44647
Mg, e. -momentum densities determ., 8=44647
N, finite energy sum rules for Pomeranchuk trajectories 8=24694
N, low-energy theorems 8=33606
N, rel. to calc. of $\pi^{\circ} \to 2\gamma, \eta^{\circ} \to 2\gamma$ decay rates 8=33663
Na, e. -momentum densities determ., 8=44647
V, anomalies 8=41149
Computation. See Calculation.
Computer memories. See Calculating apparatus/digital computers; Magnetic devices; Magnetic films; Superconducting materials and devices.
Computers. See Calculating apparatus.
Concrete
attenuation of X and γ rays 8=48891
conventional, radiation damage under neutron bombardment 8=26730
creep characts, stress anal. inc. viscoelastic response 8=44536
heat-resistant high-alumina-cement thermal cond., 200-1500°C 8=48756
microcrack distrib. 8=40135
Concrete—contd
shielding for D-T neutrons 8=29199
slabs, reinforced, large plastic deformations 8=41728
Condensation
See also Drops; Fog.
air in hypersonic wind tunnel 8=30599
Bose–Einstein of Bose gas 8=37211
Bose gas, ideal, in finite geometry 8=46117
cloud nuclei, altitude distribution in free atmosphere 8=36739
critical saturation during aqueous vapour condensation 8=48277
droplets, nucleation from vapour, surface tension rel. to radius 8=43781
dropwise, effects of local venting on meas. of steam-to-surface temp. difference 8=34986
and evaporation, system with 2 interphase surfaces and arbitrary condensation coeffs. 8=34976
film, on vertical tubes, enhancement by longitudinal fins 8=48276
Freon-113, inside vertical tube, effect of elec. field on condensing heat transfer 8=34990
heat transfer, effect of molecular-kinetic resistance 8=25990
homogeneous nucleation, statistical thermodynamics 8=30594
ice, habit and charge of crystals, modification by vapour contamination 8=32220
irreversible, translation-rotation paradox 8=30597
kinetics, expansion chamber study by high-speed photography 8=39483
laminar film, on surface normal to body or inertial forces, flow rel. to hydrostatic press 8=34989
Mayer's theory, reformulation 8=25991
metal vapour, coeff. meas., improvement on Knudsen's method 8=34988
metal vapours, drop formation mechanism 8=34992
nebulae, ionized, thermal instability mechanism 8=45716
nucleation, conc. of clusters and classical phase integral 8=34987
nucleation in condensed media 8=48274
nucleation kinetics, generalized theory 8=48251/2
nucleation theory, equilib. distrib. of droplets 8=39485
nucleation theory, translation-rotation paradox 8=48275
nuclei in air initially free of aerosols, formation and evolution 8=50141
nuclei production by radiolysis of gaseous impurities in air 8=25992
steam, dropwise on Cu, heat transfer rel. to presence of non-condensable gases 8=34993
stream of vapour on plane parallel fluid jet 8=30598
of supersaturated binary vap. mixtures, rel. to nucleate boiling theory 8=25998
two-phase medium with mass transfer, sound attenuation and dispersion 8=43688
vapour, critical supersaturation for homogeneous nucleation 8=39482
vapor-deposition effect in amorphous mats. on replication in electron microscopy 8=39707
vapour, in shock tubes, electrostatic effects 8=23943
vapour on rectangular fin, temp. distrib. and heat transfer coeffs. 8=34991
vapour pumping with coded condensers, formula for pumping speed. 8=47994
water, homogeneous nucleation theory 8=30596
water in cloud chamber 8=30595
water, maximum rates 8=43915
CCl_4, maximum rates 8=43915
CO_2-H_2O mixture, 80-230°K obs. rel. to composition of Martian icecaps 8=32547
H and D, condensation pumping on to liq-He-cooled surface 8=30593
H_2O vapour, in conversion to ice by AgI 8=45458
K vapour, in preserved Ar or He as non-condensable gases, effect on heat transfer 8=25993
N_2 in hypersonic wind tunnel 8=30599
Na, intensity of heat transfer in film condensation of pure vapour 8=48132
Condensation of gases. See Liquefaction, gases.
Conduction, electrical
See also Conductivity, electrical; Contact resistance; Current, electrical; Photoconductivity; Resistance, electrical; Semiconductors; Skin effect; Superconductivity.
band electron, non-linear second-order conductivity 8=26885
composite materials, transport coeffs. 8=26939
dielectric, unipolar conduction mechanism from solid-state electrolysis 8=40579
film-covered symmetric contacts, tunnel and thermionic currents 8=40628
impedance of two-layer semicond. structs, anal. of spiral-shaped curves 8=35917
ion electrotransport temp. dependence, 1000-1400°C 8=39980
ionosphere D region, low field cond. in presence of high field signal 8=45540
Kondo problem, Suhl's approach 8=49078

Conduction, electrical—contd
in magnetic field, quantum theory 8=44674
mechanism study using org. struct. of π-electron chain of C atoms with bridging struct. at each end 8=26893
m.i.m. system, processes, transition from electrode-limited to bulk-limited 8=27303
nonlinear, electrodynamics of continuous media, hodograph method 8=46351
organic semiconds., dark cond., energy gap and pre-exponential factor 8=26891
organic semiconductors, electron-phonon system 8=40425
physical aspects, book 8=28448
plasma, K-seeded non-equilibrium, effect of bulk gas on elect. cond. 8=25732
polaronic impurity hopping conduction 8=49119
poly(N-vinyl carbazole)-I complex, rel. to charge-transfer state 8=27462
refractory oxide solid solns. with fluorite, pyrochlore and perovskite, anionic contrib. 8=49920
refractory oxide solid solutions, with fluorite, pyrochlore and perovskite structures, anionic mechanism 8=27232
rutile, h.f. 8=49331
semiconductor, piezoelectric, transport eqns. for electrons and phonons 8=27061
space-charge, in insulators 8=49327
space-charge limited, semiconductors with donors 8=35870
strip conductor with sectional cracks 8=26953
Wiedemann-Franz and Mott equations, degree of universality 8=39905
Ag, thin films, mean free path of conduction electrons rel. to optical absorption 8=36315
BaF_2, unipolar mechanism from solid-state electrolysis 8=40579
Bi, carrier density pressure dependence meas. 8=40313
Ca stearate Langmuir films, mechanism, obs. 8=44902
Cd-Zn, electrotransport mechanism 8=34900
CdS film, anode blocking contact and carrier injection process rel. to vacancy transport mechanism 8=40442
CeO ceramic, 300 to 1000°C, rel to O_2 partial press. 8=44868
Cs_2^+ in Cs vapour, time-of-flight analysis rel. to conduction mechanism 8=43705
Cu-Cr alloys, Kondo effect by electron scattering 8=44688
$CuCr_{1+x}Rh_{1-x}Se_4$, and magnetic properties 8=31609
$CuCr_{1+x}Ti_{1-x}S_4$, and magnetic properties 8=31609
n-Ge, impurity hop cond., mag. induced spin-reversal transitions 8=31380
Na silicate glasses, ionic transport vacancy model appl. to high-temp. internal friction data 8=40176
NaCl, unipolar mechanism from solid-state electrolysis 8=40579
Ni, pure, ion electrotransport temp. dependence, 1000-1400°C 8=39980
Sb, carrier density pressure dependence meas. 8=40313
Si films, 1-2μ thick, epitaxially grown on sapphire, carrier transport 8=40489
Si_3N_4 films, pyrolytic on quartz and Si substrates 8=49352
Sn-Zn alloys, electrotransport at 500°C 8=34901
Su, liquid, electrotransfer of Ag impurities 8=39408
UO_2 powder, n-irradiated, electronic props. from e.m.f. meas. 8=40290
$V_2O_5-P_2O_5-WO_3$ system glasses, mechanism studied by e.s.r. 8=40291
Xe, conversion to metal-like state on shock compression 8=43851
$ZnNi_xMn_{2-x}O_4$, comp. dependence 8=40745
ZnO: Li, high-resistivity, electronic drift mobilities and SCL currents 8=40588
Conduction, heat. See Heat conduction.
Conduction bands. See Crystal electron states.
Conduction electron scattering. See Crystal electron states.
Conductivity, electrical
See also Resistance, electrical; Semiconducting materials; Semiconductors; Skin effect; Superconducting materials and devices; Superconductivity.
arc., stationary, analytic eqns. 8=29929
auroral E-region, Hall and Pedersen currents, exptl. evidence for existence 8=36861
Faraday space of d.c. discharge, absorpt. meas. 8=47740
plasma, at low freq. 8=30030
plasma in induced elect. field, m.h.d. generator model 8=30026
plasma, longit. rel. to enhanced transverse diffusion 8=30028
plasma, Lorentzian, inhomogeneous, and diffusion tensors, non-linear terms calc. 8=30025
plasma, microwave, in mag. field, particle-orbit theory 8=39083
of plasma, partially ionized, high-freq. 8=34478
plasma, scalar cond. calc. at low ionized, accuracy 8=34476
plasma, turbulent, d.c. 8=30031
of plasma with arbitrary ionization ratio in mag. field 8=34479
polyethylene, I-doped, enhancement 8=40596
pyrolytic aromatic polyimide, rel. to unpaired spin conc. and struct. 8=26976
resistivity meas. without elec. contacts, method 8=49136

Conductivity, electrical—contd
sediments from Bering Sea 8=50108
semiconductors, ion bombard. induced 8=26861
semimetals, carrier density pressure dependence, determ. method 8=40313
small rapid change meas. 8=28456
superconducting current carrying filament, no mag. field, calc. 8=27045
Ar plasma, calc. from shock tube obs. 8=34485
Ge-Si alloys: Au, Hall coeff., donor level 8=40460
H plasma, meas. 8=43518
Li ferrites, heat treatment effects 8=35962
MgO at high temp., impurity effects 8=26950
Ne plasma, negative 8=25733
Si web crystal, homogeneity 8=31389
gases
alkali metal vapour, semicond. model 8=43696
dust-laden, photoelectric enhancement 8=25831
ionized (weakly) in mag. field, components 8=47783
Lorentz model, a.c. cond 8=25735
propane-O_2-N_2 detonation products, at cm. wavelengths 8=27731
Ar-air mixtures, behind shock waves 8=34625
Ar, meas., using laser interferometry of transient arc 8=39231
He, partially ionized, from convergence of approxs. of transport coeffs. 8=29968
Na vapour, above 10 torr, effect of molecular association 8=39220
liquids
activation energy in capillaries 8=34895
air, in diode cells 8=48200
aqueous solns., electronic cond. 8=27749
benzene, effect of H_2O impurity 8=30523
dielectric, effect of liq. motion 8=39393
disordered systems, localized electronic states 8=40205
gelatine gels, melting mechanism 8=34962
of low dielec. const., effects of space charge on photocurrent response 8=43861
measurement by freq. transducer using tunnel diode oscillator 8=30521
melt, method of meas. up to 1600° C 8=34902
mesitylene-benzonitrile mixture, conductance showing charge-transfer interacts. 8=30515
nitrobenzene 8=34898
pyridine-benzonitrile mixture, conductance showing charge-transfer interacts. 8=30515
pyridine-trinitrotoluene mixture, conductance showing charge-transfer interacts. 8=30515
salts, molten, critical-temp. cell meas. 8=34894
seawater, effect. of freq. 8=48202
shock-compressed, optimum-geometric meas. 8=34903
tetraethylammonium perchlorate in valeronitrile 8=48197
2-dodecylaminoethanol salts, study of micellar props., effect of counterions 8=39289
water, supercritical, high at high temps. and pressures 8=43862
Ag-molten $BiCl_3$ solutions, rel. to study of metal-molten salts reaction 8=39409
AgI, molten 8=35810
Au-Co, resistivity, and ferromagnetism 8=43871
Au-Ni, resistivity, and ferromagnetism 8=43871
Bi chalcogenides, charge transport mechanism 8=30514
$CaO-FeO-Fe_2O_3-SiO_2$ melts, ion and electron cond. 8=25946
Cd-Zn, rel. to electrotransport mechanism 8=34900
Cs, resistance, press. depend. to 30 × 10^3 kg/cm^2 8=39473
Hg alloys, invalidity of Mott model 8=25948
Hg, and equation of state, at 0-2000°C and 200-5000 atm. pressure 8=25945
Li, effect of dissociating and thermally stable gaseous impurities at 300°C 8=48203
Li Br solns., association constant calc. 8=48198
Mg, rel. to electronic props. and lattice dynamics 8=48707
N, in diode cells 8=48200
Na, effect of dissociation and thermally stable gaseous impurities at 350°C 8=48203
Ni-Si alloys, resistance-temp. dependence, 750°C to m.p. 8=44694
(Na-Rb) NO_3 molten 8=43865
Sn-Co, resistivity, and ferromagnetism 8=43871
Sn-Ni, resistivity, and ferromagnetism 8=43871
Sn-Zn alloys, rel. to electrotransport at 500°C 8=34901
Tl $MeSO_4$ (Me=alkali metal). 700-1150°C 8=39411
$TlNO_3$, molten 8=39331
(Tl-Rb) NO_3 molten 8=43865
Tl_2SO_4, 700-1150°C 8=39411
Tl-Te alloys, n-type 8=34897
liquids, electrolytic
See also Chemical analysis/electrochemical; Ion velocity/electrolytic.
alkali-metal nitrates, fused, high press., activation vols. 8=39410
aqueous solns. in Pt-in-glass cells, conductance meas., experimental requirements 8=49926
compressed, viscosity meas. with remote control 8=34793
polystyrene-diphenylmethane soln., rel. to conc., temp. and field 8=39412
$AgNO_3$, fused, effect of inert gas press. and solubility 8=25949

liquids, electrolytic
See also Chemical analysis/electrochemical; Ion velocity/electrolytic.
HBr aq. solns., 0°-800°C, to 4000 bar 8=43864
HSO_3Cl solns. of simple bases 8=48194
KCl in H_2O-alcohol solns., high press. 8=39407
KOH and KOH-ZnO, 36 to -66°C 8=45372
KOH-ZnO solns., 10-55°C 8=45373
NaBr aq. solns., 0°-800°C and to 4000 bars 8=48195
$NaClO_3$-$NaNO_3$ molten system 8=48088
n-ZnO, current flow on dissolution in acid, 8=49918
solids
acridizinium cpds 8=49273
actinide cpds 8=49336
actinide cpds, and thermal props. 8=27233
actinide cpds, at low temps. 8=49348
actinide cpds, resistivity meas. 8=27234
alloy, binary ordered, effect of phonon drag 8=35817
alloys, rel. to phonon drag, at low temp. 8=26959
alumina ceramics, surface resistivity, cleaning and humidity effects 8=49337
alumina ceramics, surface resistivity dependence on ambient humidity and cleanness 8=27237
alumina insulating ceramic, volume resistivity at high temps., 8=49334
amorphous polymers, in glass transition region, anomalous rel. to T_g 8=26949
anisotropic crystal, tensor component expt. determ., theory 8=26940
anthracene derivatives, thin layers 8=49144
binary alloy-mixtures, connection with effective thermal cond. 8=39937
bis(tetrahydroindenyl)Fe:tetracyanoethylene, d. c. resistivity rel. to press. and elec. field 8=27078
changes with elect. field, expt. using stationary high-field domain analysis 8=31368
cobaltocene:tetracyanoethylene, d. c. resistivity rel. to press. and elec. field 8=27078
N, N'-diphenyl-p-phenylenodiamine, influence of impurities 8=40333
elasto-conductivity effects, rel. to sound amplification 8=35406
electrolytic, of polar crystals with divalent cation and anion admixtures 8=49921
film resistance decrease on annealing 8=49135
films, negative cond. in transverse mag. field, mechanism 8=40300
fluorite, irradiated, change, and optical absorpt. change 8=26946
glass, porous Vycor, surface conduction current rel. to water vapour adsorpt. 8=27252
glasses, alkali silicate 8=44676
glasses, Tl silicate 8=44676
graphite nitrates, resistivity rel. to ordering 8=35827
graphite, resistivity and Hall effect, allowing for trigonal warping of bands 8=35767
graphitic mats. hot-worked with dispersed liq. carbide 8=44361
insulators, nonlinearities in response 8=35595
Kondo behaviour of resistivity due to impurity 8=40299
Kondo Hamiltonian, equivalence of Nagaoka and Suhl treatments 8=35750
metal electrodes in ionized gas flow, voltamp characts. 8=26952
metal layers, resistances, stability conds. 8=35818
metal, refractory, above 1000°C, absolute meas. and obs. 8=31314
metal resistivity, eddy-current decay meas., analysis 8=46326
metal thin films, rel. to e transport 8=26954
metals, Bi-type, temp. dependence, 80-300°K 8=40301
metals, ferromagnetic, electron-phonon scattering rel. to freq. depend. of expression 8=31949
metals in mag. field, hydrodynamic mechanism 8=49150
metals, low-temp. dimensional effects 8=26951
metals, plated by plasmic method, compared with uncoated sample 8=35815
metals, resistivity due to impurities rel. to impurity diffusion 8=30996
metals, transverse 8=49148
methane, solid, 20-80°K 8=30990
mixed alkali silicate glasses, resistivity peaks 8=27235
moon 8=37002
MOS capacitors, radiation effects, determ. from conductance obs. 8=27204
non-crystalline disordered systems, localized electronic states 8=40205
non-crystalline systems, metal-insulator transition in random array of centres 8=40206
Nylon 66, doubly oriented, rel. to direction, 23-150°C, anisotropic 8=27257
p-phenylenediamine:tetracyanoethylene, d. c. resistivity rel. to press. and elec. field 8=27078
polyacenequinones, specific resistivities rel. to substitution of heterocyclic acenes 8=27141
polyacrylonitrile films, resistivity and trap depth, obs. 8=39605
polyethylene, γ-irradiation effect 8=40084
polymers, activation energy 8=35831

Conductivity, electrical—contd
solids—contd
polymers, carrier mobility theory 8=40593
polymers, H-bonded 8=40295
polymers, ionic, weak-electrolyte theory 8=40590
poly(N-vinyl carbazole)I complex, resistivity rel. to existence of charge-transfer state 8=27462
pyrene-iodine complex, a.c. behaviour rel. to temp 8=44700
pyrocarbons, B-doped, resistivity rel. to electron states and Fermi level 8=27084
pyrocarbons compressed at high temps., anisotropy 8=45941
pyrolytic aromatic polyimide, development rel. to unpaired spin conc. and struct. 8=26976
rare earth cpds, at low temps. 8=49348
rare earth cpds, resistivity meas. 8=27234
refractory oxide solid solns with fluorite, pyrochlore and perovskite, anionic contrib. 8=49920
resistivity anomaly due to mag. impurities, effect of scattering 8=44673
resistor, thin film, mats. and characts., 8=44675
ruby crystals, temp. dependence, 20-850°C 8=49338
ruby, 20-850°C and Seebeck coeff., 500-850°C 8=27236
sapphire crystals, temp. dependence, 20-850°C, 8=49338
sapphire insulating ceramic, volume resistivity at high temps., 8=49334
sapphire, 20-850°C 8=27236
selenospinels, binary, rel. to misibility studies 8=30653
semiconductor thin films, specific conductivity, meas. 8=40424
semiconductor wafer in mag. field, resistance calc. 8=44829
semiconductors based on GeTe:(Bi, Cu), effect of n and γ irrad. 8=40637
semiconductors in strong elec. field, calc. 8=27075
steel, transformer, hot-rolled, changes on internal oxidation zone formation 8=36562
stilbene derivatives 8=49145
superconductors, high-field type II, resistive states 8=26995
tectosilicates, method and exptl. results 8=40289
thin conducting films in longit. mag. field 8=26955
thin films, temp. coeff. of resistance, effect of expansion mismatch 8=31315
thin films, temp. dependence 8=40296
transverse dielectric and ohmic, influence on corona discharge in solid dielectric 8=44862
triethylammonium:tetracyanoquinodimethan complex 8=27139
triglycine sulphate, effect of atmospheric humidity 8=35985
triglycine sulphate, resistivity determ. 8=40618
trinitroluene, transition conduction zone behind shock wave front, time interval 8=49058
US, near Curie temp., and thermoelec. power 8=44677
Wiedemann-Franz law, deviations at low temp. 8=26960
Ag films, 4.2 to 295°K 8=26944
Ag films, p-bombardment effects on resistance, —13 to —158°C 8=40302
Ag films, vacuum-deposited, resistance behaviour rel. to structural formation 8=26110
Ag films, vacuum-deposited, and temp. coeff. of resistance 8=35819
Ag-41.8 wt. % Pt alloy, resistivity recovery stages and mechanisms 8=40303-4
Ag, in range 0.3-1.2°K, electron-electron scattering c.f. Pt 8=30987
Ag pastes hardened at 20-150°C 8=35820
Ag thin films, ion-bombardment induced changes 8=49151
AgI 8=35810
AgI, to 100 kbar 8=31311
β-Ag_2S film, obs. 8=49152
Al alloys, resistance, new theory, optical diffraction phenomena analogy 8=40307
Al alloys, resistivity meas. on ageing up to 100°C rel. to hardening curve similarities 8=35654
Al, dislocation resistivity, temp. depend. 8=35821
Al, due to vacancies and impurities rel. to band structure effects in defect scatt. in polyvalent metals 8=49154
Al, electron irradiated, recovery rel. to lattice defects 8=31147
Al films, intrinsic resistivity and e. mean free path 8=49153
Al films, rel. to struct. and stress conds. 8=44040
Al films, vacuum-deposited, and temp. coeff. of resistance 8=35819
Al, n irrad., resist. rel. to defects, obs. 8=44203
Al thin plates, resistance, temp. dependence 8=40306
Al_2O_3 films 8=44894
Al-Ta dilute alloy, resistivity, temp. depend. 8=35822
Al-Zn alloys, cold-worked at —195°C, resist. recovery 8=40305
Ar, electric breakdown 8=35951
Au, cold-worked, resistivity 8=40130
Au films on amorphous substrate, grain-boundary effects on residual resistivity 8=44551
Au films, triode-sputtered 8=40309
Au-rare-earth alloys, resistivity temp. dependences 1.3 - 20°K 8=31317

Conductivity, electrical—contd
solids—contd
Au-rare earth (Gd, Tb, Ho) alloys, resistivity meas., 1.3-20°K 8=40311
Au thin films, ion-bombardment induced changes 8=49151
Au, vacancy resistivity rel. to temp. 8=44409
Au-Co disordered alloys, resistivity rel. to temp.. 8=44685
Au_3Cu, resistivity changes on ordering after quenching 8=26059
B modifications, and other elec. props. 8=35824
B, temp. dependence 8=35823
BaF_2, interstitial cond. 8=49341
BaF_2, F-vacancy cond. 8=49340
(BaSrCa)O, and thermoelectric power and work function, effect of Ba vapour 8=26945
$BaTiO_3$:1 at %La, semicond., polaron model and −198-300°C 8=35878
Be-Cu foil, resistivity 8=39947
BeO, activation energy and polarization effects 8=27241
BeO binaries with Al and Fe, activation energy and polarization effects 8=27241
Bi films in elec. field, quantum size effect oscills., 10^3 v/cm 8=40312
Bi films, resistivity thickness depend. and quantum effects 8=27082
n and p-Bi_2Te_3, Hall coeffs., carrier lifetime 8=40439
$Bi_8Te_7S_5$, very thin crystal 8=40314
C compositer sintered materials containing excess silica, temp. depend. of resistivity 8=44687
C films, low-temp. non-linearity 8=31318
$Cd_xCa_{1-x}O$, and Hall effect and optical props. 8=49137
CdS evaporated thin film, rel. to thickness 8=49233
n-CdS, 1.8 to 294°K 8=31369
CdSb, p- and n-type, anisotropy of electrocond., 5-500°K 8=35881
$Cd_xSr_{1-x}O$, and Hall effect and optical props. 8=49137
CdTe, low temp. 8=44771
n-CdTe, thermal n irrad., rel. to Cd vacancies, obs. 8=3 5533
CeO ceramic, rel. to O partial press., 300° to 1000°C 8=44868
Co, effect of bombard., point defects at 20°K 8=48914
Cr, antiferromag., resistivity 8=40316
Cr films, resistivity anomaly rel. to antiferro-paramag. transition 8=39590
Cr films, vacuum-deposited, effect of dielectric coating 8=26964
Cr, ionic, in Ag halogens 8=41052
Cr-Mo(W) alloys, resistivity meas, 4-325°K, rel. to antiferromag. props. 8=31763
Cr_2O_3, temp. dependence, 500-1300°C 8=49138
Cr/SiO mixed films, temp. and field dependences 8=48448
CsCl: K^+, Rb^+, Br^-, ionic 8=31419
CsI and CsI: Ba^{2+}, Sr^{2+}, impurities effect on ionic transport 8=40574
Cu alloys, high conductivity improvement 8=40144
Cu alloys, resistance, new theory, optical diffraction phenomena analogy 8=40307
Cu, electron-irradiated, recovery rel. to lattice defects interactions 8=31146
Cu films, effect of absorbed Ar 8=49158
Cu foil, effect of heat treatment 8=49161
Cu, resistivity rel. to shear modulus on cyclic stressing 8=40317
Cu ternary chalcogenides, correl. with Seebeck coeff. 8=31448
Cu wire microwave impedance effect of high current density pulse 8=42002
CuAu alloy, and thermoelectric power 8=26967
Cu-16.7% Pd, resistivity rel. to diffuse X-ray scattering 8=36354
Cu_2S-Ag_2S system, changes on phase transformations 8=48378
$Cu_{2-x}S$ ($0 \leqslant x \leqslant 0.2$) 8=49156
$^{151}Eu_3S_4$, rel. to electron hopping 8=30638
Fe, Armco sample, −195 to +1380°C 8=48761
Fe, thin films, in vacuum 8=36359
Fe-Al alloys, residual resistivity, effect of K-state 8=49525
Fe-Al alloys, resistivity decrease due to growth of ordered domains 8=48597
Fe in Ir, Os-Ir and Ir-Pt alloys, temp. dependence 8=40318
Fe-N solid solns, resistivity mag. field dependence at 4.2°K 8=31319
FePd alloys, resistive anomaly near Curie point 8=49163
Fe-Ru alloys, resistivity for mag. props. 8=49481
β-$FeSi_2$:Co, Al, mechanism 8=35885
n-GaAs, differential neg. cond., microwave meas. 8=31375
GaAs, Hall effect, current instability 8=44779
GaAs, resistivity rel. to impurity conc. 8=40452
p-GaSb, mobility in impurity band 8=44780
Gd-Y alloys, spin-disorder resistivity meas., comments 8=49165
Ge crystals, e. irrad., rel. to primary electron interactions 8=44951

Conductivity, electrical—contd
solids—contd
Ge, on dislocation lines, accepted e cond., obs. 8=35900
Ge, epitaxially grown layer, sheet resistivity 8=40465
p-Ge, anisotropy in d.c. elec. field 8=35914
p-Ge, impurity a.c. cond. and phonon-induced hopping, calc., 10^2-10^5 cps 8=35888
Ge, resistivity rel. to impurity conc. 8=40452
Ge-Al_2O_3-ZnO films, I-V characts. 8=40488
$Ge_{1-x}Mn_xTe$, $0.01 < x < 0.1$, resist. rel. to s-d scatt., 4.2-400°K 8=40456
Ge: Sb, 300°-1000°K obs. 8=49086
Ge-Si alloys, hot-pressed, resistivity, 300-1300°K 8=35893
Hf diborides, rel. to conduction e-parameter calcs. based on single zone model 8=35830
HgS_xSe_{1-x}, $0 \leqslant x \leqslant 0.4$, temp. depend., 25−300°K 8=40319
I_2, single cryst, anisotropy, a.c. and d.c. meas. 8=27107
p-InAs, and Hall coefficient and magnetoresist. 8=27114
n-InSb microwave conductivity in high elec. field 8=49251
p-InSb, X-ray induced changes 8=40471
n-$InAs_xSb_{1-x}$ alloys, high-temp. obs. 8=40475
In-Ce solid solns., resistivity impurity (Ce) conc.-dependence rel. to localized moments 8=31339
α-In_2Se_3, h.f. 8=27244
InSb: Mn, rel. to temp., Mn behaviour 8=44799
Ir complexes, anisotropic, temp. dependence 8=40320
K, resistance 8=49167
KBr, impure, rel. to vacancy migrations 8=40576
KBr, pure and doped, ionic, temp. dependence 8=27248
KCl, changes on coloration by divalent cation-replacing impurities 8=35535
KCl, impure, rel. to vacancy migrations 8=40576
KCl, impurity anion doping effect 8=40570
KCl, pure, doped and irradiated, ionic, temp. dependence 8=27248
KCl, rel. to colloidal centres 8=44477
KCl, rel. to F-aggregate centres 8=44478
KCl, Teltow 4-defect theory examined 8=27225
KCl: Cd, uncoloured and coloured. 8=48876
KCl-KBr solid soln., p-irradiated, rel. to carrier conc. and F-centre comp. dependence 8=31117
KI, impure, rel. to vacancy migrations 8=40576
LaF_3, temp. depend., rel. to Schottky defects and diffusion of F ions 8=31048
LaSb, temp. dependence rel. to semi-metal charact., 8=39948
LiF, X-rays effects 8=35603
LiH, solid 8=49139
$LiNbO_3$ up to 1400°K 8=27276
Mg, rel. to electronic props. and lattice dynamics 8=48707
Mg-Cd alloys, effect of ordering on residual resistivity 8=40321
MgO: Cr^{2+} dynamic lattice coupling determ. 8=35053
Mn ferrites, Fe-rich, at low temps. 8=49140
MnO, resistivity, 1100°C 8=40477
MnO: Li, resistivity 8=44801
MnTe, antiferromagnetic semiconductor, freq. and i.r. spectrum interpret. using magnon drag 8=32009
p-MnTe: Ag, obs. 300°-1000°K 8=44908
Mo film, effect of Ba, O_2 and BaO adsorpt. 8=40322
Na, resistance 8=49167
NaCl, anomalous high temp. conductance 8=40323
NaCl, divalent impurity doped, temp. and comp. dependence, rel. to vacancy behaviour 8=44423
NaCl, pure and doped, ionic, temp. dependence 8=27248
$NaNO_3$ single crystal, rel. to interstial defects 8=35964
Nb, supercond., resistivity, n-irrad. effects, obs. 8=40373
Nb, superconducting obs. of magnetic field effect 8=44724
Nb and V, superconducting, in mixed state, nonlinear resistivity and dissipation 8=27027
NbC-graphite composites, thin rods 8=49040
Nd-H system 8=49141
Ni alloys, residual resistivity 8=49168
Ni films, vacuum-deposited, and temp. coeff. of resistance 8=35819
Ni-34.5 at. % Cr alloy, rel. to ordering from e. diffr. exam. 8=35064
Ni-Au alloys, resistivity investigations 8=44802
Ni-Cr alloy films, vacuum-deposited, and temp. coeff. of resistance 8=35819
Ni-Cr layers, resistances, stability conds. 8=35818
Ni-Cu alloy film, temp. (20−600°C) and comp. dependence 8=40235
Ni-Cu and Ni, var. in mag. field 8=45022
Ni-Fe thin films, and magnetoresist. 8=44695
Ni-Mo alloys, resistivity anomaly rel. to ordering 8=40326
Ni_4Mo-Ni_4W solid soln., resistivity rel. to ordering 8=39530
Ni-Si alloys, resistance-temp. dependence, m.p. to 1700°C 8=44694
NiO, high frequency 8=31384
NiS, metallic-semiconducting transition 8=31788
Np^{237} resistivity, low-temp., α self-irrad. damage effects obs. 8=31322
Pa resistivity, low-temp., α self-irrad. damage effects obs. 8=31322
Pb, supercond., complex cond., strong-coupling calc. 8=35854
Pb-Bi alloys, rel. to examination of structure 8=35152

Conductivity, electrical—contd
solids—contd
$Pb_{85}In_{15}$, exptl. demonstration, superconductivity 8=35855
n-PbS, rel. to conduction band structure, 77-300°K 8=27119
PbSe:Gd, doping effects 8=44805
PbTe, 77-450°K, valence band, effective mass 8=44804
PbTe:Sb, and Hall effect 8=40478
$PbTe_xSe_{1-x}$, rel. to forbidden band width temp. dependence 8=40247
Pd, and thermal cond., e-e and phonon scatt. Lorenz numbers, 4-20°K 8=35462
Pd, resistance at high pressures of gaseous H at room temp. 8=44697
Pd–x at. % Ni alloys ($x \geqslant 0$), low temp. resistivity rel. to s-electron-paramagnon scattering 8=31323/4
Pd-Ag alloys with Gd and Nd impurities, resistance anomaly 8=31326
Pd_x–Ag_y: Cd(Nd), resistance anomalies rel. to matrix. comp. 8=31325
Pd–D alloys, 4°-300°K obs. 8=40329
Pd–H alloys, 4°-300°K obs. 8=40329
Pt film, resistance change due to CO adsorption 8=49169
Pt films, resistivity and temp. coeff., thermal treatment effects 8=44698
Pt, in range 0.3–1.2°K, electron–electron scattering c.f. Ag 8=30987
Pt, 100 to 900°C 8=48763
Pt, resistivity change rel. to quenching medium 8=48813
PtO_2, synthesis and properties 8=35205
$RbAg_4I_5$ solid-electrolyte, rel. to Ag diffusion 8=48787
Rh, h.f., wavelength depend. rel. to cryst. e states, 0.4–11μm 8=32026
RhO_2, synthesis and properties 8=35205
Ru-Rh-Pd-Ag: Fe, 1.5-40°K 8=31328
SAP, (sintered Al/Al_2O_3 alloy), lattice defects, behaviour on cold working, resistometric exam., 8=48817
SAP, (sintered Al/Al_2O_3 alloy), lattice defects, behaviour on quenching, resistometric exam.. 8=48816
Sb, phonon drag obs. 8=40219
SbSI grown from gaseous phase, volatile component saturation vapour pressure effects 8=36026
Sb_2Te_3, temp. dependence rel. to complex valence band structure 8=44808
Se, hexagonal, and photocond., effect of reactor irradiation 8=44809
Se, temp. dependence, thermoelectric power in phase transition region 8=40481
p-Si, anisotropy in d.c. elec. field 8=35914
Si, rel. to carrier density after ion irradiation 8=44814
Si, resistivity by four probes method 8=49252
Si, resistivity rel. to impurity conc. 8=40452
SiC films, noncrystalline, rel. to annealing 8=48467
SiC heater elements, sintered, rel. to oxidation ageing 8=49349
Si(Ge)-ZnO films, I-V characts. 8=40488
SiP_2 and $SiAs_2$ resistivity, room temp. 8=40484
Si : Te, resistivity distribution 8=44817
Sn, supercond., complex cond., strong-coupling calc. 8=35854
Sn films, resistance rel. to impurity conc. 8=35828
Sn-Ce solid solns., resistivity impurity (Ce) conc.-dependence rel. to localized moments 8=31339
$SrTi_{1-x}Fe_xO_{3-x/2}\phi_{x/2}$, ϕ = oxygen vacancies, resistivities 8=35252
Ta anodic film activation energies of conduction 8=49924
Ta–W alloys, resistivity, 300 to 2400°K 8=26973
TaC_x, resistivity comp. and temp. dependence 8=26972
Te films, e-irradiated, decrease due to CO_2 desorpt. 8=35829
Te, single crystal, effect of reactor irradiation 8=31393
Ti diborides, rel. to conduction e-parameter calcs. based on single zone model 8=35830
Ti film, effect of Ba, O_2 and BaO adsorpt. 8=40322
Ti, ionic, in Ag halogens 8=41052
Ti thin films, ion-bombardment induced changes 8=49151
TiC, and thermoelec. power, 20-2000°C 8=27310
TiO_2, and work function, changes in response to chemisorpt. of O 8=40691
TiO_2 single crystals, time-dependent conduction 8=27250
TiO_2, small polaron 8=40498
TiO_{2-x}, resist. rel. to stoichiometric defects, 20-1000°C 8=39999
Ti_2O_3, resistivity and mag. order 8=31313
Tl_5Te_3, γ-phase in Tl–Te system, resistivity meas., 4.2–500°K 8=40390
U, changes on thermal n.-irrad. at 4.6°K 8=48933
U^{233} resistivity, low-temp., α self-irrad. damage effects obs. 8=31322
V alloys with transition metals, anomalies 8=44699
VO thin film single crystals, resistivity rel. to temp. 8=48470
VO_2, and mag. props. 8=40293
VO_2 crystal, resistivity anisotropy 8=40292
VO_2, crystal, semiconductor-metal transition rel. to reflection spectra 8=41150
VO_2 sputtered films, in metal-semiconductor range 8=27138
V_2O_5-P_4O_{10} glasses, effects of n and γ irrad. 8=27137

Conductivity, electrical—contd
solids—contd
W-on-glass films, ultra-high-vacuum-evaporated, temp. effects 8=40332
W, recovery from electron irradiation 8=48934
W, residual resistivity, varying C content 8=26974
W thin films, ion-bombardment induced changes 8=49151
ZnS, doped, thermally stimulated, correl. with thermoluminesc. 8=49817
ZnS films, stimulated cond. and electroluminesc. 8=32060
ZnSb, anisotropy 8=44910
$ZnSnP_2$ platelets, p-type, meas. 190-400°K 8=26267
Zr diborides, rel. to conduction e-parameter calcs. based on single zone model 8=35830
Zr polycrystals, e-irradiated, low-temp. resistivity recovery 8=31158
ZrC, and thermoelec. power, 20-2000°C 8=27310
measurement
cell for oxide powders, wide temp. range 8=44866
dielectric, surface resistivity 8=28454
electrodeless falling sample method, source coupling corrections 8=33012
films, thin, 4-point Hg contact probe 8=41907
insulating ceramics, volume resistivity, at high temps. 8=27219
insulating ceramics, volume resistivity meas. problems at high temp., 8=49334
in insulator range, apparatus 8=24064
low temp., difficulties rel. to thin films 8=26954
metal resistivity, eddy-current decay method analysis 8=46326
plasma, circuit methods, role of capacitance between coil and plasma 8=47822
plasma, r.f. cond., for density and collision freq. clac. 8=43546
polymers, difficulties 8=40592
resistivity, eddy-current decay meas. method, analysis 8=46326
resistivity meas. in megagauss fields, method 8=24066
salts, molten, critical-temp. cell meas. 8=34894
seeded flame plasmas 8=47853
semiconductor, distrib. from β cond. response 8=35877
semiconductor, resistivity ratio, automatic apparatus 8=33013
semiconductors, remote meas. apparatus 8=49220
shock-compressed liquids 8=34903
toroidal discharge, Thomson scatt. obs. 8=29878

Conductivity, thermal
See also Heat conduction.
arc., stationary, analytic eqns. 8=29929
of anisotropic medium within cylindrical tube, unsteady-state problem 8=28400
bodies of complex config., method for estimating heat resistance 8=28398
contact between solid and liq, local study of temp. field 8=26601
Fermi liquid calc. 8=41778
granular insulations, CO_2 gas pressure dependence 8=26600
Heisenberg chain, $O \ll T \ll \infty$ 8=39938
liquid-solid two-phase suspensions, digital simulation and expt. data 8=43883
model rate eqn. for gases, liquids and solids 8=28399
one-dimens. lattices, numerical study of equilib. props. 8=32825
plasmas produced by O-pinch conical discharge, and temp. 8=43506-7
porous medium, three-phase 8=37301
power fluid on plate of variable temp., boundary layer and temp. profile 8=39357
statistical mixtures 8=37309
H plasma, meas. 8=43518
LiF crystals, plastically deformed and annealed 8=30989
gases
critical, anomalous transport 8=47963
measurement methods 8=43678
mixtures, rarefied nonreacting, temp. dependence 8=30286
near critical point, anomalous due to large density fluctuation 8=30291
plasma, effects of electron interaction 8=43505
polar organic, obs. 38°-200°C 8=34657
rotationally degenerate gases, steady-state 8=47958
thermistor katharometer, sensitivity 8=43679
transfer of heat to cooled plate, temp. slip coeff. dependence on model 8=43684
in transition regime heat transfer, approx. method 8=23999
Ar, determ. in hot-wire diffusion column 8=43683
Ar, Langmuir calc. for incandescent lamps 8=42210
Ar, 90°-300°K, obs. 8=43682
Ar_2, high temp. change 8=34653
CH_3Cl pure and with Ar, C_2H_5Cl and Ne, CH_3Br-C_2H_5Cl, 273-1173°K 8=47962
H-He mixtures 8=47957
H_2S and H_2S_4-Ar, 273-1173°K 8=47962
He^3 and He^4, rel. to low temp. transport props. mutual consistency 8=34671
K vapour, 841 to 1241°K, 0.022 to 0.94 kg/cm² 8=47964

Conductivity, thermal—contd
  gases—contd
    K vapour 550-820°C, 0.005 to 1.3 atm., meas. by coaxial cylinder method 8=47965
    Kr, Langmuir calc. for incandescent lamps 8=42210
    N, coeff., and total emission coeff., high-temp., expt. and theory 8=47955
    NH_3-methylamine mixtures 8=34644
    NH_3, NH_3-Ar and NH_3-Ne, 273-1173°K 8=47962
    Na vapour, 670-900°C, 0.008 to 0.82 atm., meas. by coaxial cylinder method 8=47965
    Na vapour, 886 to 1264°K, 0.034 to 0.69 Kg/cm² 8=47964
    Ne, using hot-wire thermal diffusion 8=47956
    O_2, mag. field gradient depend., obs. 8=39199
    O rel. to mols. collision cross-section reson. in crossed mag. fields, obs. 8=34660
    SO_2 and SO_2-Ar, 273-1173°K 8=47962
    Xe, Langmuir calc. for incandescent lamps 8=42210
  liquids
    alkyl-(aryl)-chlorosilanes, expt. determ. 8=48131
    ethyl alcohol, press. oscills. during heat transfer in tubes 8=34832
    Freons 22, 113 and 142, use of regular regime and cylindrical bicalorimeter 8=34824
    haline convection induced by sea water freezing 8=41332
    heat transfer mechanism in spray column heat exchanger 8=46232
    liquid metal heat transfer, effect of internal source. 8=48021
    metal, heat transfer 8=39353
    nematic liq. crysts., interfacial and elec. field effects 8=34833
    Oseksuat oils of narrow-boiling range, temp. depend 8=30461
    research at Moscow Univ., expt. methods, results, and appl. of theory 8=30462
    sample holders for solution calorimetry 8=34831
    solutions, theoretical calc. rel. to reln of molecular component sizes 8=39354
    sulphide melt, radial heat flow apparatus 8=43800
    telluride melt, radial heat flow apparatus 8=43800
    transfer alkali earth metals in short vertical tubes with natural convection, heat transfer from 8=30460
    Ar, 90°-300°K. obs. 8=43682
    Bi chalcogenides, heat transport mechanism 8=30514
    $CsNO_3$ molten, optical determ. 8=39355
    Ga, and Lorenz number determ, 283°K to m.p., 8=39945
    Hg, 350°K-500°K 8=48130
    $LiNO_3$ molten, optical determ. 8=39355
    $NaNO_3$, in phase transition 8=48391
    $RbNO_3$ molten, optical determ. 8=39355
    Sb_2Se_3, 650°K-1300°K 8=30991
    Sn-Zn alloys, heat conductance 8=39351
  solids
    actinide cpds. and elec. conductivity 8=49336
    actinide cpds, and elec. props. 8=27233
    alloy binary ordered, effect of phonon drag 8=35817
    alloys, heat-resistant 8=39943
    amorphous solids, low-temp. 8=30975
    austenitic steel, temp. cond. at 0° to 1000°C 8=39944
    bed (reactor) of coated fuel particles 8=47410
    binary alloy-mixtures connection with effective elec. cond. 8=39937
    capillary-porous mats., effects of moisture at temps. above and below 0°C 8=30985
    ceramic packings, pellitized, in region 100-1600°C and formula deriv. 8=30978
    concrete, heat-resistant high-alumina-cement, 200-1500°C 8=48756
    of crystal lattices, formulae in Debye approx. using π theorem 8=26599
    crystal plate, rel. to plane temp. field and thermal stresses 8=44355
    crystals, rel. to edge dislocations, elevated temp. 8=30980
    crystallizing metal crust, on cooled Cu wall, heat transfer with liq. metal 8=30974
    crystals, nonlinear effects, at low temps. 8=48936
    data, U.S. national bureau of standards 8=30979
    dielectric, finite size sample, theory 8=39939
    in dielectrics with high permittivity, elec. field effects, theory 8=40560
    diffusivity meas. by laser flash method 8=39950
    electric insulation testing 8=48752
    fibre systems of irregular struct., effective cond. calc. 8=35452
    finite dielec., phonon-phonon interaction effects 8=35454
    glass, rel. to oxide dilution 8=44579
    glasses, at low temp., rel. to vib. density of states 8=35455
    graphite, highly oriented, effect of crystallite boundaries 8=35457
    graphitic mats. hot-worked with dispersed liq. carbide 8=44361
    magnetic structures, complex, with dislocation 8=39936
    metal, deposited layers 8=35453
    metallic foil insulation in high pressure gas 8=26602
    metallic screen insulation in air and helium 8=48755
    metals and alloys, cryostat for meas. of lattice component 8=48758

Conductivity, thermal—contd
  solids—contd
    metals, plated by plasmic method, compared with uncoated sample 8=35815
    metals, transport props. in e.m. field 8=35451
    microinhomogeneous, macroscopic coeff., eqn. 8=48741
    nylon, 1.2-20°K rel. to ht. transport mechanism 8=44362
    phonon, limitation by edge-disloc. dipoles, isolated dislocations and normal processes 8=48754
    polyethylene, 1.2-20°K rel. to ht. transport mechanism 8=44362
    polymer coatings, thermophysical props. rel. to internal stresses 8=30759
    polystyrene, radiation induced cross-links at low temp., effects 8=26606
    porous mats., in different gases, effects of mixing powders 8=30984
    porous systems, exptl. data analysis 8=39941
    potassium halides, rel. to phonon scatt. by U centres 8=44301
    pyrocarbons compressed at high temps., anisotropy 8=45941
    sapphire surfaces in contact, ht. resistance, 15-300°K 8=48749
    seignette salt, temp. dependence near Curie temp. 8=44358
    semiconductors, photothermal effect in sinusoidal state 8=30981
    semiconductors, 100-400°K 8=44357
    structurally disordered 8=35449
    superconductor, intermediate state 8=44354
    temperature depend., variational princ. for general heat conduction 8=30982
    two-layer composite samples, and diffusivity meas. by flash method 8=48751
    with variable heat-transfer coeffs, calc. of temp. field 8=28415
    walls, outer characts. determ. by non-stationary methods 8=41862
    Wiedemann-Franz and Mott equations, degree of universality 8=39905
    Wiedemann-Franz law, deviations at low temp. 8=26960
    Ag, in range 0.3-1.2°K, electron-electron scattering c.f. Pt 8=30987
    AgCl, point-defect aggregates effect rel. to phonon scattering 8=30986
    Al, anisotropic 8=48750
    Al, below 1°K, rel. to supercond. energy gap 8=30988
    Al_2O_3, low-temp., rel. to radiation damage 8=26722
    Al_2O_3, polycryst., resistivity change due to fast n irrad. 8=26366
    As_2Se_3, influence of Ge and Ag impurities 8=44360
    Au-Pt alloys, annealed and quenched, vacancy effects 8=48759
    $BaTiO_3$, near ferroelectric transition point 8=48760
    Be-Cu foil 8=39947
    Bi_2Te_3, thermal diffusion of Ag and ht. of transport calc. 8=39968
    Bi_2Te_3 + 20 mol% Bi_2Se_3, rel. to supercooling conditions 8=44906
    n-$Bi_2(Te, Se)_3$, n-irradiated, and elec. parameters 8=27136
    Bi-Te-Se(Sb) system, γ-irrad. effects 8=44763
    Cd arsenide, magnetothermal effects, 65-300°K 8=40731
    Cu ferrite, diffusivity meas. by laser flash method 8=39950
    Dy, temp. dependence, 5-300°K rel. to mag. transition 8=35458
    Er, temp. dependence, 5-300°K rel. to mag. transition 8=35458
    Fe, Armco sample, -160 to +640°C 8=48761
    Fe, temp. cond. at 0° to 1000°C 8=39944
    Ga, and Lorenz number determ, up to 673°K 8=39945
    Ga, thermal magnetoresist. rel. to heat switch appls., 1-10°K 8=35459
    n-Ge, diffusivity by temp. waves meas, 20°C 8=39953
    He^4 calc. using self-consistent phonon approx. 8=39940
    Hf diborides, rel. to conduction e-parameter calcs. based on single zone model 8=35830
    InBi film with Mn on each side, obs. in superconducting and normal states rel. to proximity effect 8=40372
    $In_{1-x}Ga_xSb$ solid solutions, temp. dependence 8=44363
    In-Pb alloys, type II superconductors, comparison with Caroli-Cyrot theory 8=39946
    InSe, 100 to 600°K 8=44364
    KH_2PO_4-type ferroelectric, and sound attenuation, critical anomaly 8=48716
    $KTaO_3$, temp. and field dependence (up to 55 kV/cm) rel. to Cochran modes 8=26605
    LaSb, temp. dependence rel. to semi-metal charact., 8=39948
    $LiNbO_3$, 77-500°K 8=44341
    Lu, temp. dependence, 5-300°K 8=35458
    n-Mg_2Sn, from 4.2 to 300°K 8=26603
    n-Mg_2Sn, 4.2 to 300°K 8=44365
    p-MnTe: Ag, obs. 300°-1000°K 8=44908
    Nb, mixed state anisotropy 8=26604
    Nb-Mo alloys, conc. depend. rel. to changes in density of states N(O) 8=31292
    Nb-Ti, rel. to temp. 8=44367
    Ne, calc. using self-consistent phonon approx. 8=39940
    NH_3, 28-114°K 8=35460
    Ni, by Jain and Krishnan method, 1150-1400°K 8=39949

Conductivity, thermal—contd
solids—contd
Ni, diffusivity meas. by laser flash method 8=39950
Ni–Cu and Ni, var. in mag. field 8=45022
$PbTe_xSe_{1-x}$, rel. to forbidden band width temp. dependence 8=40247
$PbTe_{0\cdot5}Se_{0\cdot5}$, I^+ doping effects, 100-400 °K 8=35461
PbTe(Se)(S), lattice and electronic components, separate meas. 3-100°K 8=39951
$Pb(Zr_{0\cdot52}-Ti_{0\cdot48})O_3$, diffusivity meas. by laser flash method 8=39950
Pd, and elec. cond., e-e and phonon scatt. Lorenz numbers, 4-20°K 8=35462
Pt, in range 0.3–1.2°K, electron–electron scattering c.f. Ag 8=30987
Pt, 100 to 900°C 8=48763
PuP, cold-pressed, sintered, up to 650°C 8=44368
PuS, cold-pressed, sintered, up to 650°C 8=44368
RbCl, rel. to phonon scatt. by U centres 8=44301
Re, below 1°K, rel. to supercond. energy gap 8=30988
p-$(Sb, Bi)_2Te_3$, n-irradiated, and elec. parameters 8=27136
Sb_2Se_3, 650°K–1300°K 8=30991
Sb_2Te_3, temp dependence rel. to complex valence band structure 8=44808
β-SiC, porous, n-irrad. induced changes 8=26735
SnS, calc, from experimental parameters 8=48764
SnTe, 100–450°K 8=30992
$SrTiO_3$, temp. and field dependence (up to 55 kV/cm) rel. to Cochran modes 8=26605
Ta, below 1°K, rel. to supecond. energy gap 8=30988
Ti diborides, rel. to conduction e-parameter calcs. based on single zone model 8=35830
UO_2, rel. to temp. gradient and thermal stress depend., obs. 8=44369
UO_2, sintered, high temp. 8=44370
$(U, Pu)O_{2-x}$, and thermal diffusivity, rel. to comp., 50–2000°C 8=35464
Y-C system, thermal analysis, phase diagram proposal 8=39569
$Zn_xHg_{1-x}Te$ solid solutions 8=44372
Zr diborides, rel. to conduction e-parameter calcs. based on single zone model 8=35830
measurement
contact-surface temps. for determination of thermal props. 8=46247
differential analyser, theory and design 8=27774
ferrite-metal interface, transient technique 8=48757
flash method for two-layer composite mats. 8=48751
gases, by hot-wire thermal diffusion column 8=47956
gases, steady and unsteady state methods 8=43678
heat flow in right circular cylinder with internal heat generation, applic. 8=46246
high temp. method, periodic excitation of test bar 8=39944
insulating materials, thermoelectric probe 8=30983
k-meter applic. to electrical insulation testing 8=48752
liquid surface temp., thermistor apparatus 8=37318
liquids and gases, at various press. and temp, app. for meas. by regular regime method 8=34824
low temperature, a.c. bridge, 0.25% accuracy, 1-4°K 8=28426
microdetector, response in gases of low thermal cond. 8=27773
new methods at Moscow Univ., for liqs, brief review with results 8=30462
pulse method for very small specimens 8=30977
semiconductors by bridge method 8=39942
solids, diffusivity by temp. waves meas. 8=39953
sulphide melt, radial heat flow apparatus 8=43800
telluride melt, radial heat flow appratus 8=43800
$CsNO_3$ molten, optical determ. with plane source technique 8=39355
GaAs laser structures, thermal impedance 8=33223
$LiNO_3$ molten, optical determ. with plane source technique 8=39355
PuO_2, from diffusivity measurements 8=35463
$RbNO_3$ molten, optical determ. with plane source technique 8=39355
Conferences
advanced propulsion, Polo Alto, (1965) 8=41480
American Ceramic Society 70th annual meeting, Chicago (USA), 1968 8=40085
applied superconductivity, U.S.A. (1967) 8=31338
aviation and aerodynamics, Israel (1968) 8=30265
calibration of vacuum gauges and related problems, Teddington, England (1967) 8=30336
carbon, Buffalo, New York (USA), 1967 8=43971
collection and processing of field data, Canberra, Australia (1966) 8=45437
Computers for analytical developments in celestial mechanics, Colloquium, Prague August 1967 8=50266
continental drift, secular motion of pole and earth rotation, Conference, Stresa, Italy 1967 8=32196
cosmic rays, 10th international, Alberta, Canada, June 1967 8=38109
electric insulation and dielectric phenomena USA (1967) 8=31418
electronic components, Washington U.S.A. (1968) 8=31416
e.m. wave theory Delft, Netherlands, Sept. 1966 8=28606
Conferences—contd
heavy-water power reactors, Vienna (1967) 8=25301
high energy nuclear reactions in astrophysics, Pennsylvania University, Jan. 1967 8=28029
high pressure engineering, London, England 1967 8=32634
IEEE Region 3 convention, USA (1968) 8=29991
information storage and retrieval, mechanized systems, Cranfield, England (1967) 8=41610
ion beam penetration obs., Chalk River (1967) 8=44491
Liperi Summer School in Theoretical Physics, Finland, 1967 8=24598
macromolecular chemistry, Prague, Aug.-Sept. 1965 8=34392
on magnetism, in Boston, Sept. 1967, review 8=49454
magnetism, USA (1967) 8=27368
medicine and biology, Boston Mass. USA, November 1967 8=32626
molecular forces, Vatican City, April 1966 8=38960
N-N interaction, 1967, state of knowledge and summary of contribs. 8=24870
Nuclear Science symposium, Los Angeles, Oct-Nov 1967 8=28968
nuclear spectroscopy and nuclear structure, Khar'kov 1967 8=38294
1967 NEREM records, Boston USA 8=24279
organic scintillations, Argonne National Laboratory (USA), 1966 8=45250
particle physics, Hawaii tropical conference, August 1967 8=29027
Pisa, 1964, on particle symmetries, field theory and measurement 8=24609
planetary nebulae, Czechoslovakia (1967) 8=45711
point defects in non-metallic solids, Brighton (England), 1966 8=31029
polymer cyrstallinity, Arizona, USA 18 Jan 1966 8=35204
precision e.m. measurement, Boulder (1968) 8=41906
radiation effects, Ashevill, North Carolina, USA Sept. 1965 8=35593
radiative energy transfer, Philadelphia (USA), 1966. 8=23909
radio communication in Arctic, Finse, Norway, April 1967 8=32313
scintillation and semiconductor counters, Washington D.C Feb-March 1968 8=46895
semiconductor detectors in radiation protection and radiation meas., Germany (1967) 8=33377
solar active regions, struct. and development, Budapest (1967) 8=45900
space research, London (1967) 8=28020
structure of quiet photosphere and low chromosphere, Arnhem, Holland, April 1967 8=32592
20th Annual Southwestern IEEE, USA (1968) 8=28645
II–VI semiconducting cpds., USA (1967) 8=31362
vacuum technique colloquium, Warsaw, June 1966 8=47991
X-ray spectroscopy, USSR July 1966 8=45163
TiNi and associated cpds., Maryland, USA (1967) 8=30868
Confinement of plasma. See Plasma/confinement.
Constants
atomic, metrological implications of secular change 8=41613
Brans-Dicke coupling, necessarily positive 8=45589
G, possible var. evidence from solar structure 8=45861
G, universal gravitational, meas. with pendulums 8=32780
Newman-Penrose, rel. to invariant transformations 8=24474
physical, determination, survey of work 8=45944
Contact potential
difference induced by gravit. field, rel. to surface-stress concept 8=44679
meas. using controlled atmosphere Langmuir trough 8=34805
vibrating capacitor meas. with electrostatic drive 8=28450
Hg monolayer obs. 8=48061
p-Si crystal, ohmic contact with Al wire 8=40483
Contact resistance
Gunn elements, ohmic 8=49282
between rough flat surfaces, considering surface roughness 8=48412
surface roughness effects on tarnished contacts 8=48413
thermal, short signal method of meas. 8=24006
p-GaAs, Ag-Mn evaporated ohmic contacts 8=49237
Continuous creation hypothesis. See Cosmology.
Convection
air, natural and turbulent, along vertical heated plate 8=34648
axisymmetric flow in rotating annulus 8=39350
axi-symmetric flow uniform, analogue computer soln. of eqns. 8=34822
axisymmetric free, boundary layer flow past slender body 8=41868
Bénard pt. of soln., and thermal diffusion 8=34818
Bernard, steady laminar between conducting plates 8=43641
in box, three-dimens., preferred wave-number depend. on Rayleigh number 8=47919
cloud interaction with wind 8=27893
combined free and forced turbulent, in vertical cylinder with vol. heat sources 8=24010
between concentric spheres, for low Rayleigh numbers 8=32966
convective diffusion in capillaries 8=30447

Convection—contd
near cooled disk, infinite, rotating at same ang. vel. as its environment 8=32967
cooling of substrates containing multiple heat sources 8=48727
in cylindrical tube, temp. and heat flux calc. by Bubnov-Galerkin method 8=37311
dry and moist, including rain stage, numerical expt. 8=45455
from fin, downward projecting, immersed in fluid, laminar 8=32964
flow past vertical porous plate, effect of periodic suction 8=34583
flow stability of fluids heated from below in gravitational field 8=46251
fluid between horiz. plates heated from below, effect of side walls on natural convection 8=25909
fluid, compressible, shallow-layer thermal convection eqns. 8=36727
fluid with time depend. temp. profile, onset rel. to boundary conditions 8=34593
fluids, confined, thermal stability, Hilbert spaces analysis 8=25786
forced, cylinder in flow at low Reynolds numbers 8=30231
forced flow over flat plate cont. heat source, transient heat transfer 8=24003
forced laminar convective heat transfer in heated horiz. tubes, theory 8=24007
forced systems, ignition and extinction problems 8=32971
forced, to Bingham plastic in laminar tube flow with internal heat generation 8=39266
forced, turbulene heat transfer in rotating pipe 8=41858
free, about plates, vert. and horiz., at small Grashof numbers 8=32968
free, along vertical plate for small Grashov numbers, non-soln. of zero-order problem 8=41870
free field round heated body, interferometric obs. 8=23009
free, from heated inclined plate, study of stability of boundary layer 8=30222
free, from vertical plate, turbulent heat transfer 8=41869
free laminar, around isothermal vertical plate, anal. 8=34658
free, patterns adjacent to horiz. heated surface 8=41867
in gas cross-flow over right-angled wedge 8=28405
in gas, laminar flow region near heated plate, rel. to absorpt. and emission props. 8=43685
in gases, convection-radiation interacts, role of optically thick aprox. 8=25825
instabilities in fully developed quasi-incompressible flow 8=34580
instability problems, application of Galerkin method 8=47920
laminar forced convection in eccentric annuli 8=46249
laminar free flow, and heat transfer, about inclined isothermal plate 8=28404
liquid, elastoviscous, thermal oscillating 8=43771
liquid flow patterns due to temp. grads. in horiz. cryst. growth 8=26212
in liquids, circulation in closed vertical circular ducts or slots 8=30464
liquids ideal and viscous analogue computer soln. to transport eqns. 8=34822
microbalance, increasing high temp. 8=46252
motion of fluid between two vertical planes, spectrum of perturbations. and stability 8=46250
planetary interors, explicit equations 8=45821
planetary mantles 8=45822
plasma, in mag. field, low press. and heated underneath 8=39087
Rayleigh-Jeffreys problem with boundary slab of finite conductivity 8=30187
scalar field, turbulent straining of small-spatial-scale amplitude vars. 8=30232
sea water, induced by freezing 8=41332
spherical shell with no rotation 8=41871
near stagnation point on parabolic cylinder and paraboloid 8=43637
from surfaces with heated side down, for two flow regions 8=39202
thermal, around cylinders, by pulsed flow 8=34656
thermal, in horizontal fluid layers 8=43614
use of transcendental profile function approx. 8=28403
during turbulent flow of elec. cond. liq. in channel, alt. mag. field effect 8=41994
turbulent, from vertical surface, mean temp. distribs. and mean vel. in boundary layer 8=32965
velocity in hypersonic sphere wakes, meas. and decay 8=39188
vibrating plane surface, heat transfer to air, appl. of Danckwerts-Mickley model 8=34646
in viscous fluid, classical cellular, with spatial heat source 8=30189
in water at 4°C, heat transfer coeffs. and immersed plate temp. 8=34838
in water below 277°K, min. effect for temp. differences <16° 8=34837
water layer formed by melting ice from below 8=34827
CO$_2$, in crit. region, free-convection heat transfer from Pt wire 8=34823

Convection—contd
He, high flux heat transfer correls 8=24008
Hg liq., superimposed in turbulent flow, rel. to temp. profiles 8=34836
in Na liq., forced-convection heat transfer from a sphere 8=34839
NaK eutectic, superimposed in turbulent flow, rel. to temp. profiles 8=34836

Conversion electrons. See Beta-ray spectra/conversion electrons; Gamma-rays/internal conversion.

Cooling
See also Joule-Thomson effect; Low-temperature production; Magnetic cooling; Supercooling.
cathode, thermionic convertor, 1400°-1800°C e coding obs. 8=33037
cathodes, in (4-8)×10^3 °K range, by thermal autoelectronic emission and evaporation 8=40698
clay, aqueous suspensions, Newton's coeffs. 8=25963
convection and conduction, of substrates containing multiple heat sources 8=48727
energy converter staging, thermoelectric-thermomagnetic 8=46238
evaporative, effect of depth of surface 8=41861
evaporation, heat and mass transfer equation 8=48290
finned surface, aerodynamic calc. 8=24001
glass, emissivity rel. to coloration 8=44331
liquid, new method for magnet coils 8=33048
by mass transfer of H, He, N$_2$ and Ar, in reacting and non-reacting boundary layers 8=32958
nuclear reactors, gas moisture detection, dewpoint device 8=47932
optical Dewar and photomultiplier cooler 8=46291
optical, of solids by transfer of laser radiation into atomic vibrations 8=39900
plate, with thermal characts depend on temp., soln by Kantorovich's method 8=24004
of plate, transient, by combined convection and radiation 8=28402
of porous mat, steady state temp. field for transpiration cooling 8=28416
porous metals under vacuum, rate of water evaporation 8=30602
porous surface, by transpiration, transient temp. response in forced convection 8=35450
reactor fuel elements, finned surface geometry 8=24000
reactor fuel elements, herringbone fin designs 8=24002
space vehicle, heat carrier choice 8=32389
spheres, transient, via thermal rad. at bounding surface 8=41859
in supersonic flow round cone, effects with roughness on boundary-layer transition 8=39189
transpiration, from capillary-porous mat., heat and mass transfer 8=39488
wall, semi-infinite, 2nd order approximate soln. 8=32952
water, equipment protection 8=32986
water, of ion beam targets 8=33397
X-ray crystallography, N$_2$ boiling technique 8=32992
CaWO$_4$:Nd laser, air cooling system 8=28705
H$^+$ ions, by elastic collisions in He gas 8=43681
H$_2$ liquid target, mechanical refrigeration 8=46849
H$_2$O drops on metal plate, cooling rate and freezing temp. interdependence 8=48263
He^3/He^4 dilution refrigerator for low-temp. Mössbauer expt. 8=41880
Ne glow discharge, effects on ionization waves 8=47757

Copper
absolute thermopower of α-brass, change during plastic deform. 8=31447
absorptance and emittance, 1 nil polished sample, by cyclic incident radiation 8=27566
absorption, infra-red, at 4.2°K 8=27551
absorption in 50-340Å range, calc. of partial oscillator sums 8=31981
adsorption layers of S, structure and formation conditions 8=48490
adsorption of alkaline atoms, heat, bonds and ionization probab., quantum calc. 8=35199
α-ray absorpt. at 54.4 MeV, obs. 8=48919
annealing stage I after α-irrad., influence of defect conc. 8=48926
atom, inelastic e scatt., E_e=200, 400 keV, cross-section 8=38719
band structure, self-consistent, augmented-plane-wave calcs., 8=44643
Bevatron, Cu-tape-wound, edge-cooled solenoid for preinjector 8=33052
cavity distrib. during creep 8=44401
cementation with Fe, kinetics, and activation enthalpy 8=43898
chemical separation from SiHCl, and SiCl 8=49998
cohesive energy and isotropic band effective mass 8=48303
cold-worked, ang. distrib. of scatt. neutrons rel. to defects 8=26355
concentration in acetylene flame, linear absorpt. method 8=27790
continuous casting, heat dissipation problems 8=28207
corrosion inhibition in K persulphate soln., 8=45332

Copper—contd
- creep-extended at 1000 °C, dislocation structure 8=35565
- creep rate at low pressure rel. to annealing in air effect 8=26803
- creep recovery of commercially pure variety 8=26805
- crystal, Ar^+, He^+, Ne^+ refl. obs. 8=48918
- crystal defect structure on n.-irradiation at 400°C 8=48804
- crystal, n-irradiated, radiation hardened, critical shear stress temp. and strain rate dependence 8=31196-7
- crystal surface layer, dislocation distrib. after tensile deform. 8=48856
- crystals and whiskers, diffusion of Zn, mechanism 8=35487
- crystals, deformed, dislocation density determ. from X-ray diffr. profiles 8=26673
- crystals, n-irradiated, third-order elastic constants from u. s. meas. of non-linearity parameters 8=26800
- crystals, nearly perfect, fast neutron radiation damage obs. by X-ray diffraction 8=26732
- Debye temp. determ. by one-temp. X-ray method 8=48736
- Debye-Waller factor of Fe, mössbauer meas., 8=39873
- deformation mode, ductile, anomalous X-ray transmission exam. 8=26648
- deformed crystals, flow stress gradient between surface and centre 8=26804
- deformed, dislocation arrangement in work hardening curve, X-ray topography study 8=44445-6
- depth dose distrib. prop. by electron irrad., energy losses and ionization 8=31143
- diffusion in Al, coefficient determ, step annealing procedure 8=48773
- diffusion in GaAs, complex formation influence 8=35492
- diffusion in n-GaAs, rel. to transducer prep. 8=35491
- diffusion in InAs rel. to effect on elec. props. 8=40473
- direct recovery from white metal 8=41281
- dislocation line resonant vibrations 8=35563
- dislocations arrangement on deformation at 4.2, 78 and 293°K 8=48854
- drawn, Young's and shear moduli, annealing temp. dependence 8=31195
- dropwise condensation of steam on surface, heat transfer coeffs. 8=34993
- elastic field, effect of spherical inclusions 8=48938
- electrode in HF (anhydrous), anodization to Cu/CuF_2(s) couple and its reversible behaviour 8=49930
- electrodeposition from $CuSO_4$ solns. containing CN^-, bright Cu, obs. 8=45395
- electrodes, in 3% NaCl aqueous soln., effect of dissolved O on stability of Cu_2O surface film 8=41279
- electrodes, pre-breakdown (vacuum) current in presence of microdischarges 8=43459
- electron beam energy loss distrib. obs. 8=31142
- electron energy loss spectra rel. to plasmon states, 30–350 eV 8=35809
- electron energy losses, charact. on low-energy reflection 8=48905
- electron-irradiated, lattice defects interactions 8=31146
- electronic emission, current density coeff. and other characts. 8=40698
- energy band structures 8=44642
- epitaxy of single crystal film on sapphire 8=30751
- evaporated film, water vapour adsorption 8=35194
- extraction from InSb 8=44582
- fatigue softening after cyclic loading 8=44565
- fatigued, dislocation structure associated with fracture surface 8=40143
- f.c.c., crossslip of screw dislocations 8=48855
- Fermi surface, effect of alloying 8=40234
- Fermi surface, effect of lattice parameters change 8=40237
- Fermi surface, hydrostatic pressure effect, expt. determ. 8=40235
- film coating on single crystals, surface damage rel. to strengthening effects 8=40150
- film, epitaxial growth on NaCl crystal 8=30745
- film on glass, light refl. phase retardation meas. 8=31960
- film on Pb, proximity effects in supercond. 8=27015
- film, polycrystalline thin, photoelec. emissivity obs. 8=27353
- films, thin, effect of absorbed Ar on props. 8=49158
- films, vacuum-condensed, elastic anisotropy rel. to structure 8=44545
- fine structure meas., energy angular distrib. of secondary electrons 8=40713
- flow stress, effect of impurity and forest dislocations 8=31199
- foil, Ar ion bombard., lattice defect penetration 8=48815
- foil, elec. conductivity ht. treatment dependence 8=49161
- foils for nuclear resonance obs., texture parameters 8=49663
- fractional order peaks in diffracted LEED beams, surface asymmetry mech. 8=26100
- fracture, activation energy, temp. effect 8=26797
- gamma-ray cross sections, analysis 8=26728
- grain boundary cavity stability during annealing 8=26802

Copper—contd
- grain growth, u.s. enhancement 8=26247
- growth of crystals by thermal decomposition of gaseous cupric fluorides 8=44127
- Hall coeff. and magnetoresistance, mag. field, temp and crystal orientation dependence 8=49157
- internal fields, nuclear and electronic adiabatic demag. meas. 8=39507
- interstitials and solute additions, interaction 8=31050
- ion penetration, chem. film technique 8=48920
- ions, Cu^{2+} bonding in Rochelle salt and triglycine sulphate e.p.r. obs. 8=36243
- n-irradiated, active crystal length in yield region under deform. 8=40054
- n-irradiated, strengthening mechanism after mild annealing 8=31198
- isochromat at 10kV 8=49714
- Knight shift in $CuCr_2Se_4$ and $CuCr_2Te_4$ 8=31901
- layer on NiFeCo film, effect on mag. props. 8=40822
- liquid, atomic structure from X-ray diffr. exam. 8=25874
- liquid solvent, Knight shifts in alloys, origin 8=30528
- low temp. deformation, stored energy rel. to strain and orientation 8=49000
- mean inner potential calc. method 8=30629
- mean inner pot. meas. by electron diffr. 8=30628
- mechanical strength, reduction by presence of thin epitaxial Ni overgrowth 8=40146
- neutron irradiated, cyclic deformation 8=26801
- nuclear spin-lattice relax. time at temps. below 2×10^{-2}°K 8=31902
- optical constants, uniaxial and hydrostatic strain dependence rel. to interband transitions 8=49724
- orientation dependence of dislocation damping, elastic wave propagation mode 8=44563
- oxidation of (111) rel. to diffusion in Cu_2O films struct. defects, obs. 8=44042
- photoelectric effect rel. to temp. 8=36008
- photoelectric γ cross-section determ. 50-208 keV 8=36004
- plasma, laser-induced, ion energy and abundances 8=36051
- plastic deformation during alternating torsion, macroscopic localization 8=44567
- polycrystalline, dislocation loss in thin film electron microscopy 8=26671
- polycrystalline, explosively shocked, dislocation damping 8=26672
- polycrystals, thermal diffuse X-ray scatt. time dependence 8=48632
- pore formation during creep, temp. and stress effects 8=35524
- proton accelerator target, residual radiation dose rate 8=33402
- recovery of mech. props., laws 8=35709
- reflectivity changes during laser pulse 8=45169
- resistivity, elec., rel. to shear modulus on cyclic stressing 8=40317
- resistivity with magnetic impurity a function of concentration 8=26966
- rolling texture and orientation distrib. junction 8=48593
- scattering of lattice waves by dislocations 8=30933
- secondary emission angular dependence, fine structure origin 8=40711
- self-diffusion, activation vol. and press. depend., 0-10 kbar, 700-990 °C 8=39967
- shade etchings, orientation dependency 8=35222
- sheet, recrystallization textures and cold rolling 8=44125
- single crystals, dislocations, persistent slip bands 8=40140
- single crystals, flow stress, temp. dependence 8=40142
- single crystals, u. s. reflectivity and surface wave phenomena 8=30944
- slip distrib. rel. to initial dislocation substract., and stress-strain curves 8=44459
- solubility in austenite steel, effect of Cr 8=30655
- specific heat, cryostat obs. 1°-30°K 8=24033
- specific heat, 40-920°C 8=30964
- specific heat in pure samples, below 3°K 8=39912
- specific ht. and ht. of melting 8=35424
- spectral line breadth with Na as impurity in arc discharge 8=34437
- spectrum in plasma jet, pulsation of intensity 8=36353
- spherical crysts., LEED study, spot patterns and behaviour rel. to reciprocal lattice of bulk 8=26098
- spherical crysts., surface structs. after O_2 adsorpt. 8=26099
- sputtered atoms, energy distrib. analysis by mechanical spectrometer 8=48915
- sputtering, by 1 to 5 keV Ar^+ 8=40069
- sputtering, energy spectrum of ejected atoms 8=48917
- sputtering of Cs-ions, 77 °K 8=31150
- sputtering intensity in directions of dense packing rel. to incidence angle of ions 8=26731
- square diaphragm, plastic deform. and failure 8 =37155
- stacking fault energies 8=31097
- stacking-fault energies, dislocations, and surface energies 8=31072
- stage III recovery rel. to dislocation pinning during continuous α-irrad. 8=39995
- strain excitationfrom exo-emission meas. rel. to defect props. 8=44938
- strain field interaction between vacancies 8=26641

- **Copper**—contd
  - structural defects in slip-lines during fatigue 8=48827
  - substitutional impurity in GaAs, charact. recomb. times 8=27089
  - in supply waters, mechanism of pitting corrosion 8=45331
  - surface, collisions with Ar atoms 8=29661
  - surface hardening, preferential, in early stage II 8=40145
  - surface, promoted with dioctadecyl disulphide, meas. of heat transfer in steam condensation 8=34986
  - surface struct. due to adsorpt. and interact. of O_2, LEED studies 8=26136
  - surfaces, energy anal. of back-scattered electrons rel. to structs. 8=30730
  - tensile internal stress during electrodeposition, role of hydrogen 8=31167
  - tensile props., Hg addition effects 8=31203
  - thermal expansion coeff. temp. depend., theory and obs. 8=26594
  - thermoelectric power due to electron-phonon interaction 8=49394
  - third harmonic of initially u.s. wave 8=26581
  - tough pitch wire bar, water vapour determ. by Al reduction technique 8=45330
  - ultramicrotome-cut foils, deformation 8=48850
  - vacuum-gap anode erosion by discharge 8=34424
  - valence state in $CuMn_2O_4$ spinel determ. by X-ray absorpt. edge meas. 8=30801
  - vapour lasers, high power, parameters affecting power output 8=37572
  - weight increase of cryst. on heating in Zn vapour, rel. to thickness and orientation 8=35485
  - whiskers, deformation behaviour 8=44566
  - whiskers, plastic behaviour, thickness depend. 8=40148
  - whiskers, structural features on deformation by torsion 8=35254
  - wire, effect of pulse of high current density 8=42002
  - wire, heavily drawn, annealing spectrum 8=26808
  - wires, exploding discharges, restrike mechanisms 8=40288
  - X-ray absorpt. spectra at K edge 8=27567
  - X-ray K-absorpt., fine structure at 300°, 77°, 4.2°K. obs. 8=41124
  - X-ray L spectrum, sample self absorpt. effects 8=36355
  - X-ray microanalysis, Kα emission rel. to cryst. imperfections, obs. 8=41308
  - X-ray spectra, band structure calc. 8=36352
  - X-rays, primary, depth distrib. in anticathode, 17-35 kV 8=36420
  - yield surfaces, effects of plastic deform. and neutron irrad. 8=44564
  - Al-base, neutron irrad., precipitation 8=48379
  - Ar^+ sputtering, channelling obs. 8=48921
  - Cu(II) electrode in $NaNO_3$-KNO_3 eutectic, linear sweep voltammetry 8=27750
  - Cu III, spectra, in excited configs., theory 8=43187
  - Cu(100) surface, purity and structure from Auger spectroscopy and LEED 8=27355
  - Cu^{2+}, effect on n.m.r. relax. of F^{19} in aq. solns. 8=48222
  - Cu^{2+}, e.p.r. in CaO, tunneling effect at 1.2°K 8=40916
  - Cu^{2+}, e.p.r. in MgO at 1.2°K, Jahn-Teller effect 8=27470
  - Cu^{2+} in blue proteins, noncovalent model 8=49782
  - Cu^{2+} ions in tetrahedral cryst. fields, linear elec. field effect on e.p.r. spectrum 8=49585
  - Cu^{2+} in AgCl, Se(S) codopants, e.s.r. 8=36235
  - $Cu^{63,65}$ in $CuCr_2S_4$, n.m.r. obs. 8=36262
  - Cu-CuO, liquid, miscibility gap 8=48075
  - Cu : Fe^{57}, f number and isomer shift pressure dependence 8=48321
  - Cu: Fe, Mössbauer effect rel. to spin compensated state 8=35036
  - Cu:Fe, n.m.f. rel. to singlet ground state of Fe 8=31900
  - Cu : Mn, e.s.r. meas. of s-d admixture 8=40935
  - Cu–Mn interdiffusion kinetics, e microprobe obs., 640–820°C 8=31002
  - Cu-Nb_3Sn-stainless steel composite superconductors mech. and elec. props. 8=27014
  - Cu-Ni film thermocouple for mag. film substrates meas. 8=31676
  - Cu–Ni system, Cu diffusion on Ni side 8=31013
  - Cu-O, liquid phase diagrams 8=48074
  - Cu:T (T = Ti, Mn, Ni), conduction-electron spin relax., interpretation 8=31863
  - Kr bombard., thermal desorption obs. 8=48483
  - in Si, precipitation kinetics near room temp. 8=30705
  - Sn^{119m} isomer shift 8=26015
  - in Sn/Pb solder, X-ray spectrometric analysis 8=27816
  - Xe bombard., thermal desorption obs. 8=48483
  - Xe^+ bombard., thermal desorption obs. 8=48482
- **Copper alloys**
  - See also Copper compounds.
  - α-brass, absolute thermopower, change during plastic deform. 8=31447
  - α-brass, discontinuous yielding and stretcher strains rel. to grain size and strain ageing temp., obs. 8=40141
  - α-brass, grain size, influence of Fe and P additions 8=48594
  - α-brass, incubation period at start of flow obs. 8=32100
  - α-brass, single and bi-crystals, stress-corrosion cracking 8=26799
- **Copper alloys**—contd
  - α-brass, stress relax., 78–295°K rel. to dislocation behaviour 8=31193
  - α-brass, surface hardening, preferential, in early stage II 8=40145
  - α-brass, vacancy formation, activation energy depend. on Zn content 8=48808
  - α-brass, wire texture variation with stacking fault energy 8=40048
  - β-brass, B2 superlattice antiphase domain growth kinetics 8=30689
  - β-brass, B2 superlattice, interact. of defects at antiphase boundaries 8=44448
  - β-brass, order-disorder critical temp., pressure dependence 8=39547
  - β-brass, quenching effects, on microstructure and defect structure 8=48595
  - β_1-brass, metastable, phase transformations 8=35081
  - brass/Cu pressed contacts as heat switch, heat transfer at low temp 8=23997
  - brass, Debye temp. determ. by one-temp. X-ray method 8=48736
  - brass diaphragm, square, plastic deform. and failure 8=37155
  - 7-3 brass, heavily rolled, annealing texture 8=40151
  - brass rods, Young's and shear moduli, annealing temp. dependence 8=31195
  - brass, 70/30, deformation layers prod. by machining 8=35555
  - brass, stress-corrosion cracking, mechanism 8=26798
  - brass, tube, radial expansion by explosive gas 8=31202
  - brass, X-ray microanalysis of standard, Midwest Probe Users Group report 8=30851
  - diffusion of dilute impurities, e microprobe obs. 8=31003
  - dilute mag., NMR meas. rel. to ground-state of mag. impurity problem 8=45116
  - dilute, thermally activated dislocation depinning 8=26670
  - Hall constant changes on plastic deform. rel. to order and stacking fault energy 8=44689
  - magnetic, dil., solute Knight shifts rel. to rigid band theory 8=45117
  - resistance, electrical, new theory, optical diffraction phenomena analogy 8=40307
  - strength, conductivity and hardness improvement by increasing Pb content 8=40144
  - thermal expansion at high temp. X-ray determ. 8=26593
  - wires, exploding discharges, restrike mechanisms 8=40288
  - Cu-Al, β-phase, transform. during continuous cooling 8=26069
  - Cu–Al, dispersion hardening by internal oxidation 8=35649
  - Cu–Ag–Au liq. ternary, Ag vapour pressure rel. to electron cell model 8=26002
  - Cu-Ag-Zn, Hume-Rothery type, zeta-phase stability 8=30687
  - Cu-Al, β' martensite, stacking fault probabilities 8=48867
  - Cu-Al, fatigue softening after cyclic loading 8=44565
  - Cu-Al, Fermi surfaces by positron annihilation 8=31288
  - Cu-Al lattice wave scattering by dislocations 8=26573
  - Cu-Al, magnetic susceptibility of dilute solutions of Fe 8=27403
  - Cu-Al, second-phase deformations after cold rolling 8=49001
  - Cu-Al solid solutions, stacking-fault energy, annealing and irrad. effects 8=26702
  - Cu-Al, solute atom segregation on stacking faults 8=26643
  - Cu-15 at.% Al, stacking fault energy rel. to short range order and temp. 8=35575
  - 4% Cu–Al, strength rel. to time and temp. 8=31201
  - Cu-Al, stress induced stacking faults 8=48868
  - Cu–Al–Fe solid solutions, hardening action of short range order 8=26806
  - Cu–Al–Ni solid solutions, hardening action of short range order 8=26806
  - Cu-Au alloys with Fe, mag. ordering rel. to spin compensation of Fe from Kondo temp. meas. 8=27404
  - CuAu, electrical resistivity and thermoelectric power 8=26967
  - Cu–Au films, vol. and surface diffusion 8=35486
  - Cu-Au, optical props., 8=41082
  - Cu-Au, stopping power of 0.5 to 3.5 MeV α-particles 8=44497
  - Cu-Au, surface roughening during electrolytic dissolution 8=49938
  - Cu-Au system, friction, wear and surface hardness in abrasion 8=40149
  - CuAuII, long period ordered, lattice modulation, by X-ray diffraction 8=30893
  - Cu_3Au order-disorder, diffusion of Au rel. to vacancy rôle 8=39971
  - Cu_3Au, sp. ht. below 3°K, effect of ordering 8=35427
  - $Cu_{0 \cdot 907}Au_{0 \cdot 093}$, theory of vibrations 8=48705
  - $Cu_xAu_{51-x}Zn_{49}$, low-temp β-phase stability 8=48368
  - Cu–2 wt.% Be, ageing characts. with or without additional elements 8=35674

Copper alloys—contd
Cu-2%Be, ageing, nucleated precip. phase space lattice, obs. 8=25271
Cu-Be, ageing rel. to thermodynamic props. 8=35098
Cu-2%Be, diffuse striations obs. at 200°C rel. to strain-contrast effect 8=30859
Cu 1.79 wt.%Be, discontinous precipitation of γ-phase, and oreintation 8=43997
Cu-Be, dispersion hardening by internal oxidation 8=35649
Cu-Co alloy, n.m.r. of Co^{59} 8=40978
Cu-Co, dilute, thermoelect. power in mag. field 8=31449
Cu-Co, radiation-induced coherency loss 8=26036
Cu-Cr, electron scattering, Kondo effect 8=44688
Cu-Cr, grain-boundary cavity formation, stress limitation 8=48871
Cu-Fe, dil, low temp. susceptibility rel. to spin compensation 8=31604
Cu-Fe, Kondo, specific heat down to 2×10^{-3} T_K 8=44334
Cu-Fe, mag. props. s-d exchange model analysis 8=31608
Cu-Fe, Mossbauer line spectra 8=39512
Cu-Ga, feathery structure formation in massive transform 8=30690
Cu-Ga, massive phase, duplex nature and dislocation structure 8=30685
Cu-10.5 at.% Ge, resistance recovery following quenching 8=49160
Cu-12.5 wt.%Ge, solid soln., f.c.c. → h.c.p. transform. 8=26068
ζ-CuGe stacking fault probab., X-ray obs. 8=26704
Cu-Ge, ultramicrotome-cut foils, deformation 8=48850
Cu-16.8%In, structure and orientation of equilib. phase, δ-Cu_9In_4 8=39548
Cu-In system, cell growth, calc. of limiting boundary diffusivities 8=48533
Cu-Mn, dil, low temp. susceptibility rel. to spin compensation 8=31604
Cu-Mn, mag. props. s-d exchange model analysis 8=31608
Cu-Mn, transmission spin resonance of conduction-electron-local-moment obs. 8=31860
Cu-Mn(Cr), dilute, magnetoresistance calc. by S-matrix theory 8=26965
Cu-Ni, affected volume and temp. rise in discontinuous slip 8=40147
Cu-Ni, catalytic activity toward isotopic exchange of H, 8=49911
Cu-Ni, compressibility 8=26807
Cu-Ni, diffusion phenomena omnidirectional pressure effects 8=35488
Cu-Ni, dilute, thermoelect. power in mag. field 8=31449
Cu-Ni, oblique impact with steel plate, temp. developed 8=32981
Cu-Ni system, Debye temp. conc. depend. rel. to ferromag. ordering, obs. 8=39913
Cu-Ni, work hardening rel. to internal strains from plastic deformation 8=31194
CuNi, X-ray small angle scatt. obs. of clustering 8=30892
Cu-Ni, Cu rich, virtual bound state model of band structure 8=40236
Cu-Ni-Fe, Mössbauer line spectra 8=39512
Cu-Ni-Mn system, diffusion rel. to thermodynamic activities, obs. 8=31004
Cu-0.01 wt.%B^{10}, n irrad., dislocation loop spheres surrounding B particles, obs. 8=35564
Cu-Pb, superconducting, magnetization meas. rel. to microstructure 8=44723
Cu-16.7% Pd diffuse X-ray scattering rel. to elec. resistivity and short-range-order 8=36354
α-CuSi, chem. interdiffusion coeff. 8=44385
Cu_3Si phase, diffusion 8=44386
Cu-Si-Mn, stress relax. anomalies, 200-400°C 8=35668
Cu-Sn, γ and δ phases, self-diffusion coeffs. and energies 8=35484
β-Cu-Sn, quenched, structure and decomposition products 8=39528
Cu-Sn, second-phase deformations after cold rolling 8=49001
Cu-Zn, abraded, surface and subsurface structure 8=26294
Cu 55% - Zn 45% α and β phases, comp. and location rel. to grain struct., obs. 8=30688
Cu-Zn, electronic specific ht. 8=44335
Cu-38% Zn, polycrystalline, alternating micro-deformation 8=35644
Cu-Zn, second-phase deformations after cold rolling 8=49001
Cu-Zn, selective corrosion in H_2SO_4 8=45381
Cu-Zn system, max. stacking fault energy 8=48869
Cu-Zn, X-ray absorption spectra, K edges 8=41080

Copper compounds
See also Copper alloys.
brass-NH_3 system, stress-corrosion cracking mechanism 8=35675
calcite, growth shape rel. to twinning 8=26238
complex, e.s.r., saturation and spectral diffusion 8=49607
copper chromium halochalcogenides, spinel structure, magnetic props. 8=40806

Copper compounds—contd
cupric amine complexes, e.p.r. and optical spectra 8=31861
exciton band splitting in light and dark blue series by unidirectional pressure 8=35791
glasses, X-ray absorpt. spectroscopy 8=27567
halides, crystals grown from melt, luminescence 8=36485
halides, photoluminesc. rel. to lattice structure 8=36470
oxides, phase fields and thermal expansion 8=30686
oxides, thermodynamic props. by e.m.f. meas. 8=48729
pyridine Cu(II) chlorobenzoates, mag. props. 8=36072
villamaninite, chem. and structural analyses 8=48646
Cu(I) complex, cupritetramine di-[catena-di-μ-thiosulphato-cuprate(I)], structure 8=26392
Cu(II) alkanoates, structure by X-ray analysis 8=26463
Cu(II) basic halides, thermal decomp. under air, obs. 8=27701
Cu-(II)-chelate complexes of N', N'-dimethyl-thioformohydrazide, crystallography 8=48689
Cu(II) complex, tricycloquinazoline copper chloride, crystal structures 8=26486
Cu(II) complex, bis-trimethylbenzylammonium tetrachlorocuprate (II) structure 8=26394
Cu II-Na-chlorophyllin chem. bonding from e.s.r. h.f.s. 8=34368
Cu(II)2,2'-dipyridine aq. solns., n.m.r. and e.p.r. 8=34926
Cu complex, Cu-bis-N-ethylsalicylaldimine, crystal structure 8=26390
Cu complex, bis(ethylenediamine) copper (II) fluoroborate, crystal structure 8=39785
Cu complex, bis-N-phenylethyl-salicyl-aldiminato-copper II, crystal structure 8=26391
Cu complex, $Cu_2(SCN)_3(NH_3)_3$, crystal structure 8=26395
Cu complex, diacetate tetramethyl distannoxane 8=26368
Cu complex, tris-(2-dimethylaminoethyl)amine copper (II) bromide, crystal structure 8=26418
Cu complexes, N-substituted salicylaldimine, structure regularities 8=26421
Cu diethyldithiocarbamate, paramagnetism 8=49485
Cu ferrite, thermal diffusivity meas. by laser flash method 8=39950
Cu formate tetrahydrate, antiferroelec., deuteron n.m.r. 8=44269
Cu hexamethylene-dithiocarbamate, struct., X-ray obs. 8=30919
Cu phthalocyanine, field effect on photocarriers 8=36018
Cu ternary chalcogenides, elec. and thermal cond., Seebeck coeff. and microhardness 8=31448
Cu tutton slats, spin-lattice relaxation, field dependence 8=40954
Cu-containing perovskites, phase transforms. from high temp. X-ray exam. and dielec. meas. 8=27243
Cu^{2+}, Jahn-Teller effect in $Sr_2(Cu_xZn_{1-x}Me)O_6$, ($Me = W^{6+}$, Te^{6+}) 8=41081
$Cu_2Al[AsO_4](OH)_4 . 4H_2O$, liroconite, crystal structure 8=39787
$Cu_3(AsO_4)_2$, cryst. struct. 8=35327
$CuAu_3$, calc. of n-beam electron diffraction intensities 8=48627
Cu_3Au, ordered and disordered, low temp. dislocation mechanisms 8=31076
CuBr, phase diag. up to 40 kbar 8=48253
CuCl crystal prep. for optical purposes, process conditions 8=26248
CuCl, etching and regrowth 8=44101
CuCl, excitonic molecule 8=31300
CuCl film, optical props. 8=31982
CuCl in molten salts, absorpt. of O_2, and oxidation kinetics 8=32102
CuCl, luminescence, laser excited 8=32053
CuCl, phase diag. up to 40 kbar 8=48253
CuCl, photoconductivity, oscillatory depend. on photon energy 8=31452
CuCl, Zeeman effect, 4.2°K 8=36351
$CuCl_2$, aqueous soln., dielec. consts. and loss factors 8=34887
$CuCl_2 . 2H_2O$, antiferromagnetic, proton relaxation 8=49635
$CuCl_2 . 2H_2O$-d_x, deuteration effects on PMR and antiferromagnetism 8=36264
$CuCo_2S_4$, nuclear mag. resonance of Co 8=31901
$CuCr_{1+x}Rh_{1-x}Se_4$, magnetic properties and electrical conduction 8=31609
$CuCrS(Se)_2$, crystal structure and mag. props., 8=39810
$CuCr_2S_4$, n.m.r. of Cr^{53}, $Cu^{63, 65}$ temp. and d.c. mag. field depend. of reson. freq. 8=36262
$CuCr_2SeBr$, ferromag. props. from n. diffr. exam 8=31606
$CuCr_2Se_xS_{4-x}$ solid solution, mag. props. 8=40733
$CuCr_2Te_4$, hyperfine field of Te^{125} determ. by NMR at 1.4°K 8=27503
$CuCr_{1+x}Ti_{1-x}S_4$, magnetic properties and electrical conduction 8=31609
$CuCr_2X_4$, (X = S, Se, Te), cation-anion distances rel to monovalent Cu 8=48645
$CuCr_2X_3Y$, ($X = Se^{2-}$, Te^{2-}; $Y = Cl^-$, Br^-, I^-) 8=31605/6
$CuCs_2(SO_4)_2 . 6H_2O$, spin-lattice ht. transfer in pulsed mag. fields 8=31862

Copper compounds—contd
  CuF^+ complex, lifetime 8=48222
  CuF, dissoc. energy 8=34375
  $Cu_2[Fe(CN)_6]$ membranes, H_2O transport kinetics 8=48121
  $Cu_{0.5}Fe_{2.5}O_4$, constitution from elec. props. meas. 8=48341
  $CuFe_2S_3$, antiferromag. ordering from Mőssbauer spectroscopy 8=40864
  Cu_5FeS_4, stability of phases 8=35097
  $Cu(HCO_2)_2.4H_2O$, thermal expansion in antiferroelectric transition region −170°C to 30°C 8=44346
  $CuHgO(NO_3)_2.3H_2O$, crystal structure 8=26393
  CuI(Br), nuclear resonance 8=49636
  δ-Cu_9In_4, equilib. phase inCu-16.8% In alloy, structure and orientation 8=39548
  $Cu_2In_2O_5$, crystal structure 8=26389
  CuI, phase diag. up to 40 kbar 8=48253
  $CuK_2Cl_4.2H_2O$, mag. props., spin-wave theory analysis 8=31607
  Cu-La double nitrate, heat capacity below 1°K 8=44336
  $Cu_{1-x}M_xFe_2O_4$, (M = Cu, Zn, Cd), Fe^{57} Mossbauer resonance, 4.2–1000°K 8=31907
  Cu_2MnAl, ordering temp. 8=45010
  $Cu_{0.09}Mn_{0.61}Fe_{2.3}O_4$, ferrite, magnetic anisotropy rel. to temp. 8=31723
  $Cu_{0.5}Mn_xFe_{2.5-x}O_{4+\gamma}$ spinels, compensated tetragonal deformation, and O nonstoichiometry 8=48380
  $CuMn_2O_4$, spinel, Cu valence state determ. by X-ray absorpt. edge meas. 8=30801
  Cu–Mn–Sb system, magnetic, phase equilibrium 8=45056
  $CuMoO_4$, paramag., cryst. struct. 8=35329
  $CuMoO_4$, single crystals, growth from melt, powder photograph, space group 8=44126
  $Cu(NH_4)_2Br_4.2H_2O$, spin–spin relaxation 8=31845
  $Cu(NH_3)_4SO_4.H_2O$, antiferromag. order from PMR 8=36263
  $Cu(NH_3)_4SO_4.H_2O$, proton double resonance and temp. of electron spins, liq. He temp. 8=40979
  $Cu_{1-x}Ni_xCr_2O_4$, cooperative Jahn-Teller distortions 8=35052
  $Cu_xNi_{1-x}S_2$, pyrite solid solutions, prep. and lattice parameters 8=48342
  $Cu(NO_3)_2.2.5H_2O$, ht. capacity, 0.5–4.2°K, rel. to antiferromagnetic props. 8=35428
  $Cu(NO_3)_2.3H_2O$, antiferromag. ordering from PMR 8=36263
  CuO catalyst in kinetic study of hard carbon graphitization 8=27740
  CuO, dissociation, near equilibrium kinetics 8=41246
  CuO, epitaxial growth by ion bombardment 8=26116
  CuO, X-ray absorpt. spectra 8=27567
  Cu_2O, absorpt. spectrum rel. to annealing prod. stoichiometric defects, obs. 8=41083
  Cu_2O, compensated, non-linear photoconductivity 8=40660
  Cu_2O crystal defects, energy spectra 8=31055
  Cu_2O, electrolum. rel. to injection-chem. effect 8=45267
  Cu_2O, electroreflectance spectrum 8=49159
  Cu_2O, exciton bond energy, change under uniaxial deform. 8=35790
  Cu_2O, exciton luminescence at 77 and 4.2°K 8=49797
  Cu_2O, exciton quadrupole transition in elec. and mag. fields 8=3 1984
  Cu_2O films on Cu(111), diffusion in struct. defects. rel. to oxidation, obs. 8=44042
  Cu_2O, lattice fundamental vibrs., optical and dielec. consts. 290°K 8=39873
  Cu_2O, long duration photoconductivity 8=36017
  Cu_2O, luminescence due to electron bombardment 8=41189
  Cu_2O n.q.r. obs. 8=3 1927
  Cu_2O, stressed, absorpt. exciton lines, polarization effect 8=45185
  Cu_2O surface film on Cu electrode in 3% NaCl aqueous soln., effect of dissolved O on stability 8=41279
  Cu_2O, thin films, optical and transport props. 8=31983
  Cu_2S-Ag_2S system, phase transformations rel. to elec. resistivity changes 8=48378
  Cu_2S–CdS photovoltaic cells, spectral response 8=40684
  $CuUO_4$, crystal structure 8=39784
  β-$Cu_2P_2O_7$, cryst. struct. 8=35328
  Cu-S films, phase transform kinetics by new e-diffr. procedure 8=26082
  $Cu_{2-x}S(0 \leqslant x \leqslant 0.2)$, electrical and optical props. 8=49156
  Cu_2S, anodic dissolution 8=41281
  Cu_2S, nuclear resonance 8=49636
  $CuSeO_4.5H_2O$, proton magnetic resonance down to 0.3°K 8=49637
  Cu_5Si, gaseous impurity segregation 8=35673
  Cu_xSi, (x = 3, 5), brittleness, temp. threshold, alloying additions effects 8=35671
  $CuSiF_6.4H_2O$, e.p.r. at 300° and 90°K, obs. 8=45085
  $CuSnF_6.4H_2O$, e.p.r. at 300° and 90°K, obs. 8=45085
  $CuSO_4-H_2O$, phase boundaries below 500°C 8=48366
  $CuSO_4.3H_2O$, structure rel. to crystal chemistry of salt hydrates 8=26388
  $CuSO_4.5H_2O$, D/H ratio during dehydration 8=30802
  $CuSO_4.5H_2O$, ht. capacity at 0.4°–4.2°K in mag. fields 8=39915
  $CuSO_4.5H_2O$, ht. capacity below 4°K in mag. fields 8=39914
  $CuSO_4.5H_2O$, proton magnetic resonance down to 0.3°K 8=49637
  Cu–Zn–Cd–Ag system, univarient equilibria formation by decomposition 8=30675

Copper compounds—contd
  ϵ Cu-Zn: Fe, local moment formation from susceptibility 8=31617
  Cu–Zu–Sn solid solutions, ternary diffusion 8=39972
Corbino effect. See Current, electrical.
Coriolis forces. See Dynamics.
Cornea. See Eye.
Corona, electric discharge
    See also Breakdown, electric.
  air, rectifying action rel. to electrode temp. 8=34430
  cylindrical positive, breakdown voltage in H_2 8=47765
  electrode, mechanical forces exerted through internal friction 8=39003
  gas absorption in liquids in wetted-wall columns, acceleration by discharge 8=32119
  high-voltage stabilizing circuit application 8=41921
  impulse type in rod/plane gap, elec. field and current density meas. 8=29923
  insulating materials corona resistance 8=29914
  peak-reading voltage meas. and recording 8=24062
  sheath radius obs. in H-filled SC1 tubes 8=47769
  streamers in positive point-to-plane gap, propagation sequences 8=29913
  SF_6, relevance of electron detachment in swarm conds 8=29978
Corona, solar. See Sun/corona.
Coronagraphs. See Sun/corona.
Corpuscular streams. See Cosmic rays; Sun/radiation, corpuscular.
Correspondence principle. See Quantum theory.
Corrosion
  α-brass, single and bi-crystals, rel. to stress cracking 8=26799
  brass-NH_3 system, stress-corrosion cracking mechanism 8=35675
  brass, stress-corrosion cracking, mechanism 8=26798
  Chromium molybdeunum steels, CO_2 oxidation resistance effects of chem. comp., mech. treatment and remelting 8=45339
  glass, optical, durability 8=41241
  kovar, stress-corrosion cracking prevention by Ni plating 8=31211
  metals, stress susceptibility rel. to ambient press. 8=49034
  mild steel, by H_2S 8=35691
  stainless steel, electrolytic and thermal, effect of Si content 8=45334
  stainless steel, pitting critical potentials 8=49928
  steel, austenitic stainless, stress cracking study by internal friction meas. 8=40159
  steel, effect of Mn 8=49866
  steel, 18/8 stainless, intergranular and power formation 8=43983
  steel, high-tensile, stress-corrosion cracking 8=31212
  steel, mild, grain boundary, and stress-corrosion cracking, effect of structure 8=44569
  steel, mild, in NaCl solns., transient charge fluctuations, obs. 8=45368
  steel pipe with water flow, mass transfer model and isothermal correl. 8=36560
  steel, stainless, in H_2SO_4, inhibition by $Na_3PMo_{12}O_{40}$, mechanism, 8=45370
  steels, austenitic stainless, in nitric environment, influence of Mo 8=49867
  Steel, stressed and unstressed, in nitrate soln. 8=45335
  steels, low alloy, in CO_2, oxidation and excrescence form. mechanisms, ⩽ 550°C 8=32098
  stress cracking by wedge force loading 8=48977
  Zircaloy-2, in water and steam, effect of surface prep. and fluorine contamination 8=45352
  Zircaloy-2 rel. to internal stresses and deformation 8=26852
  Ag liners of autoclaves for hydrothermal crystal growth 8=49855
  Ag-Sn amalgam, studies 8=45326
  Al alloys in hot NaCl, rate and films tan δ rel. to cation impurities 8=44864
  Al alloys in NaCl solns., transient charge fluctuations, obs. 8=45368
  Al, by natural fresh waters, eqn. 8=41240
  Al coatings on U, ion-plated, parametric study rel. to max. protection 8=49844
  Al hollow-wave, effect of acidic gelatinous materials on pitting 8=45327
  Al, inhibition in alkaline soln. 8=45322
  Al_2 in NaCl solns., transient charge fluctuations, obs. 8=45368
  Al-$NbAl_3$ dispersion phase alloy, terphenyl resist., 420°C 8=44546
  Au liners of autoclaves for hydrothermal crystal growth 8=49855
  Cr black coating, electrolytically deposited, corrosion resistance 8=45394
  Cr-Fe alloy, catrastrophic grain boundary corrosion 8=45329
  Cr-Ni(Fe) alloys, pitting critical potentials 8=49928
  Cu in K persulphate soln., inhibition 8=45332
  Cu in supply waters, mechanism of pitting 8=45331
  Cu-Zn in H_2SO_4, selective, using disc. electrode 8=45381

Corrosion—contd
  Fe-16 Cr alloy, pitting in solns. of Cl^- 8=44102
  Fe in H_2SO_4, inhibition by dissolved ring-substituted anilines 8=45377-8
  Fe in dilute LiOH, rel. to Fe_3O_4 films growth mechanism, obs. 8=44043
  Fe, pure, surface, influence of reactor irrad. 8=30720
  Ge lenses, resistance 8=40162
  Hg liquid in steel boilers inhibited by Zr and Ti 8=47426
  Mg in NaCl solns., transient charge fluctuations, obs. 8=45368
  Ni, pitting critical potentials 8=49928
  Ni-Co-Cr superalloy sulphidation layers comp. and struct., obs. 8=30806
  Pt, liners of autoclaves for hydrothermal crystal growth 8=49855
  Ta by liquid Pu alloys, effect of O, N impurities 8=47412
  Ti alloys, stress cracking 8=27716
  Ti, in methanol vapour, stress-corrosion cracking 8=40184
  Ti-8Al-Mo-V, in methanol vapour stress-corrosion cracking 8=40184
  V-10 wt. % Ti alloy, influence of Ca content in Na 8=27723
  Va-Ti alloys as reactor fuel jackets for Na 8=47430
  Zn in NaCl solns., transient charge fluctuations, obs. 8=45368
  Zr, breakaway region, inelastic behaviour of metal and oxide 8=36576
  Zr, rel. to internal stresses and deformation 8=26852
Cosmic dust. See Interplanetary matter; Interstellar matter; Meteorites.
Cosmic noise. See Cosmic radiations, radiofrequency.
Cosmic radiations, radiofrequency
    See also Quasars; Radioastronomy; Sun/radiation, r.f.
  Cas A, rel. to optical spectrum 8=45775
  CAS flux density obs. at 38.0, 81.5 and 152.0 MHz 8=36981
  Coma cluster obs. differences from other results 8=45776
  cosmic ray photon emission, 10^{13}eV from local sources 8=32400
  CP 0950, impulsive emission 8=50314
  CPO950 and CP 1133, pulsed sources, accurate positions 8=50381
  CP1919, Parkes period confirm. 8=45754
  CP 1919, search for optical flashes 8=41542
  Crab nebula, Cygnus XR-1 and several unknown sources obs. by balloon 8=45720
  Crab nebula, radiobrightness distrib. at 535 MHz 8=32483
  Cyg A flux density obs. at 38.0, 81.5 and 152.0 MHz 8=36981
  Cyg X-1 obs. 8=45776
  Cygnus X region, NGC 7000 emission contours, 610.5, 750 and 1414 MHz 8=50354
  Cygnus X region II, obs. at 610.5 MHz 8=41544
  Cygnus XR-1 obs. 8=45720
  discrete sources, with reabsorpt., energy of relativistic particles and mag. fields 8=32511
  dissipative force in rad. flux, rel. to accn. of charged particles 8=32515
  from EAS, 520 MHz, obs. 8=25035
  ejected source assocs. and parent galaxies atruct. obs. 8=45772
  e.m. band emission between 500 and 1000 Hz, simultaneous ground and satellite recordings 8=50382
  emission from e.a.s., atm. elec. field source 8=38205
  4C 50.11/NRAO 150, radio spectrum 8=28129
  galactic background emission and energy spectrum of electrons in interstellar space 8=32500
  Galactic centre obs. 8=45738
  galactic OH emission, 1665-7 MHz, obs. 8=45768
  galaxies in Perseus cluster 8=50359
  galaxies, spiral emission rel. to nuclei type and optical activity 8=28108
  galaxies, spiral, single satellite sources, obs. 8=45773
  Galaxy, polarized emission at $\lambda = 1.25$m 8=28102
  German obs. 8=32612
  identification as variable star BL Lac 8=41547
  Jupiter 21 cm. obs., magnetic axis determ. 8=28149
  mercury emission phase depend. rel. to surface layer props., 0.8 cm 8=45824
  metagalactic black-body background, sources model 8=45586
  metre wavelength, distrib., hypotheses 8=32607
  microwave background at $\lambda = 3.3$mm, thermodynamic temp. 2.46°K 8=45597
  microwave background interpretation 8=28034
  microwave background radiation and galaxy formation 8=36977
  microwave of 3°K as real black body radiation rel. to Jordan's gravitational theory 8=32795-6
  noise absorption in ionosphere F region, electron temp. calc. 8=27996
  Nova Delphini 1967, upper limit to emission 8=41518
  pulsar CP 1919, meas. between 85 and 2,700 MHz 8=45759
  pulsar Io effect 8=45764
  pulsars, estimate of gravitational radiation reaching the earth 8=45782
  pulsars, obs. at 11 cm. 8=45765
  pulsars, preliminary obs. 8=45754
Cosmic radiations, radiofrequency—contd
  pulsars, proper motion search 8=50379
  pulsars, submillicecond radio intensity variations 8=45758
  pulsating, amplitude variations 8=50383
  pulsed, model including pulse structure and polarization 8=36979
  pulsed, spaced receiver observations 8=45757
  pulses, interpretation based on plasma oscills. in magnetosphere of neutron star 8=45763
  quasars, and Seyfert's galaxy NGC 1275, flux densities at λ 5.2 cm 8=41552
  radio galaxies as evolved quasars or plasma clouds ejected from galaxies 8=32521
  radio star fadeouts and scintillations due to ionosphere irregularities 8=32516
  radio-star scintillations and spread-F, in auroral zone 8=32355
  radiometer, three-channel, polarization obs. at 210 Mc/s 8=41543
  red-shift law for quasars and radio galaxies 8=45793
  scintillations, broadband, of Cassiopeia A, correl. with occurrence of spread-F 8=32332
  Sco X-1, effect on X-ray background uniformity obs. 8=45602
  Sco X-1 obs. 8=45776
  Scorpio X-1, detection of emission 8=41551
  self-absorbed sources, relativistic electron spectra relaxation 8=50384
  Sgr XR-1 vicinity obs. 8=45738
  source, ang. structure in 0″.1-11″ range, derived from interplanetary scintillation 8=36982
  source flux densities and R.A., 100 obs., 60 MHz 8=45774
  source, optical pulsating search 8=41535
  source, pulsating, at $\alpha = 19^h19^m$, $\delta = +22°$, possible neutron star 8=36983
  source pulsating, CP 1919, detection at 13 cm wavelength 8=28125
  source, pulsating, general relativistic influence on observed freqs. if pulsars are orbiting 8=41534
  source, pulsating, Hamada-Salpeter white dwarf models, stability and radial vibr. periods 8=41545
  source, pulsating, meas. on period at 1919 + 21 8=28121
  source, pulsating, obs. at 81.5 MHz 8=28118
  source, pulsating, position optical identification as possible neutron star 8=36949
  source, pulsating rapidly, models 8=28120
  source, pulsating, rel. to new test of general relativity 8=41536
  source, pulsed, accurate position 8=28127
  source, 3C 398 (W49), spectra of components 8=32510
  source, stimulated inverse Compton scattering 8=36978
  sources at 408 and 1407 MHz, fan-beam obs. 8=50377
  sources at 2700 MHz away from galactic plane, log N to log S ratio 8=28128
  sources, counts at 2700 MHz 8=28130
  sources, discrete γ-ray emission 8=41549
  sources, extended, evolution model 8=45760
  sources, extension of number flux density relation to small flux densities 8=41541
  sources, $5C_2$ survey 8=41540
  sources, galactic, catalogue 8=41548
  sources in 3C catalogue, obs. and struct. 8=36984
  sources opposite quasars as cosmological test 8=50378
  sources, Parkes catalogue, declination +20°- +27° 8=41550
  sources, pulsating, linear polarization 8=28123
  sources, pulsating, model based on vibrational models of star 8=45777
  sources, pulsating, models 8=41538
  sources, pulsating, neutron star as model 8=41537
  sources, pulsating, obs. 8=28122
  sources, pulsating, pulse shape and spectra 8=32518
  sources, pulsating, rotating neutron stars as origin 8=41539
  sources, pulsed 8=28124
  sources, pulsed, observations 8=28126
  sources, pulsing rapidly 8=28119
  sources, redshifts distribution 8=50386
  sources spectra in 4C catalogue, 0°-20° declination range obs. 8=36980
  in steady-state universe, microwave background 8=36916-17
  supernova SN1967h, X-rays, upper limit 8=41517
  synchrotron, omnidirectional, in r.f. and X-ray regions 8=32513
  Tau A flux density obs. at 81.5 and 162.0 MHz 8=36981
  Tau X-1 obs. 8=45776
  Vir A, rel. to optical spectrum 8=45775
  VRO 42 22 01, variable source with circular polarization 8=45755
  W49, components right ascensions and dimens., 21 cm 8=45761
  white dwarfs, pulsar condition 8=50317
  white dwarfs, pulsating, rel. to pulse profiles 8=50380
  white dwarfs, rotating, pulsation periods 8=50324
  X-ray background component obs. 8=45602
  X-ray background obs. above polar atmosphere 8=45584
  X-ray diffuse spectrum up to 180KeV obs. 8=45603
  X-ray source, focusing telescope, 20-140 keV 8=45800

Cosmic radiations, radiofrequency—contd
- X-ray source in Sagittarius, celestial positions 8=50390
- X-ray sources, accreting gas model 8=45769
- X-ray sources in Sagittarius, celestial positions search 8=50391
- H gas, high-level transitions, oscillator strengths 8=41546
- H II regions, 4170 MHz obs. 8=32493

Cosmic rays
- antimatter search, upper limit to antiprotons 8=38107
- background radiation in mines 8=25027
- cascade processes, charact. functional 8=25034
- cascades, inverse problem 8=29397
- Conference 10th International, Alberta, Canada, June 1967 8=38109
- diffusion tensor for random mag. field 8=32393
- directional distribution investigated by matrix method 8=42676
- electrons, energy spectrum in interstellar space and galactic radio emission 8=32500
- energy density, ultraviolet background meas. 8=38131
- energy losses from microwaves etc., var. with age of universe 8=42672
- energy spectra obs. at mountain altitudes 8=42729
- fireballs, lifetime possibility 8=29042
- galactic, change in energy spectrum, over 11-year solar activity cycle 8=42761
- galactic nucleus as source of energetic particles 8=50368
- galactic, relativistic plasma, quasilinear resonant diffusion eqns. (model) 8=47819
- galactic, solar radial gradient in interplanetary region 8=42670
- galactic storage, disc and halo components 8=38167
- heavy singly charged particle, search rel. to SU_3 predictions 8=42674
- He spectra and solar modulation effects in new solar cycle 8=42687
- intensity gradient, and daily-variaton second harmonic, perpendicular to ecliptic 8=42766
- intensity in interplanetary space, eleven-year modulation 8=42759
- interplanetary radiation intensity, time variations analysis, obs. by Mariner 4 8=37032
- interstellar and interplanetary matter effects, allowing for He, and ionized particles 8=38172
- jets in TeV region, very low multiplicity, interpret. rel. to nucleon isobars 8=33855
- Jokipii model for propag. through interplanetary mag. field, improvements 8=42671
- laboratory, underground, near Turin (the Monte Cappucini lab.) 8=38133
- lifetime in galaxy estimated at 10^6 years 8=42702
- low rigidity. modulation and power spectrum of interplanetary magnetic field 1962-5 8=42677
- in magnetic random field, backscatter and diffusion 8=47181
- metagalactic, energy density from γ obs. 8=32395
- multiple-core events rel. to existence of neutral vector boson 8=42361
- neutrinos, solar, from B^8 decay, calc. 8=45888
- nuclear emulsion stars, connecting lines, statistical evaluation 8=38113
- propagation, effect of interplanetary magnetic field on 8=38152
- propagation in random and regular interplanetary mag. field 8=42703
- propag. of $Z \geqslant 20$ nuclei 8=42706
- propagation through interstellar space of various nuclei 8=38161
- propagation through space, path length determ. assuming He-3 and d are secondary 8=42713
- propagation through space, prod. of $Li^{6,7}$, $Be^{9,10}$, $B^{10,11}$ by nuclear spallation reactions of p with O 8=38156
- propag. through space and ratio of light to medium nuclei near the earth 8=38163
- quark search unsuccessful 8=42490
- radial gradient, obs. by Mariners 2 and 4 8=38132
- radial intensity gradients, obs. during minimum solar modulation 8=42678
- search for particle with charge $^2/_3$e 8=42489
- secondary, general properties of radiation processes and spectra 8=42722
- secondary radiation background near earth 8=38171
- solar, acceleration, and development of solar flares 8=45904
- solar, activity increase 1966-7 8=38108
- solar-flare increase of January 28, 1967 8=41598
- solar radial gradient in interplanetary region 8=42670
- at solar wind boundary, accel. by magnetic field 8=47182
- solar-wind modulation of intensity 8=42675
- and space physics problems 8=38110
- in space, trajectories due to random walk of interstellar magnetic field 8=41526
- steady state of primary and secondary in space 8=42700
- transport in interplanetary medium 8=42673
- transverse momentum distribs. in fireball model assuming Planck's momentum spectrum 8=29237
- $2 \leqslant Z \geqslant 21$ region, rigidity spectrum 8=25041

Cosmic rays—contd
- underground obs. survey 8=33848
- work of Lebedev institute 8=25023
- X-ray background, galactic and non-galactic components obs. 8=32398

absorption
- delayed shower particles 70 m. w. e. underground, obs. 8=38246
- ionization bursts underground, obs. 8=38244
- meon free paths and fragmentation parameters with $Z \geqslant 10$ 8=42721
- muon energy-range relation, exptl. determ. 8=38245
- neutrino underground meas. project 8=37931
- neutrons in paraffin and graphite for n-p scatt. cross-section 60-100 GeV 8=38248
- underground μ obs. installation 8=38247
- underground obs., data interpretation 8=38243
- Fe, nuclear-component energy flux obs. 8=29245
- NaI(Tl) crystal, Cherenkov shield 8=28981

apparatus
- See also Particle detectors.
- air shower recorder, Sydney Univ., prelim. results 8=38197
- Cherenkov detection of 10^{11}-10^{12} eV region for obs. on earth's surface 8=42679
- Cherenkov light receivers, servo systems 8=38128
- Cherenkov system for determ. of possible astronomical sources 8=45797
- counter, scintillation, plastic for primary meas 8=47186
- counter telescope for high mass resolution of low energy cosmic particles 8=38127
- counter, thin-window proportional for X-rays 8=47187
- detection of showers by N_2 luminesc. in atmos. 8=42680
- e.a.s. optical emission imaging system 8=38195
- e.m. cascades, transition effects meas. 8=38120
- emulsion chambers, influence of electron lateral spread in air slit 8=38116
- energy meas. by ionization calorimetry influence of ionization fluctuations on accuracy 8=25026
- half-wave dipole system for e.a.s. radio emission detect. 8=38242
- Harwell-Grove radio installation for e.a.s. 8=38238
- Haverah Park 500m e.a.s. array, facilities 8=38237
- Haverah Park 2km e.a.s. array, operation 8=38236
- hodoscope Geiger counter arrays, ionization chambers, night sky Cherenkov detectors, review 8=29244
- image intensifier for cosmic ray shower photography 8=33847
- instrumental effects in e.a.s. particle density meas. 8=38240
- ionization calorimeter and nuclear emulsion with time selection for interactions above 10^{12} eV 8=42682
- ionization calorimeter appl. to underground burst obs. 8=38244
- ionization calorimeter for investigation of primary particles 8=29235
- ionization chambers for recording stars 8=29233
- iron, solid magnets, for nuclear-active particles obs. 8=38123
- monitors IGY, changes of attenuation coeff. w. r. t. time 8=42699
- muon high energy horizonal flux momentum spectrum and charge ratio 8=38118
- for muon momentum spectrum, charge ratio and interaction obs. 8=38122
- muon spectrograph, bursts in iron, interpretation 8=38221
- neutron monitor airborne, latitide survey of frequency of multiple events 8=38125
- neutron monitor, IGY multiplicity meas. October-December 1966 8=38121
- neutron monitor, NM64, radiation attenuation in the atmosphere 8=42684
- NM64 neutron monitor, selected multiplicities intensity var. 8=42723
- neutron monitor, specific yield function calc. from vertically incident protons 8=42695
- neutron monitors EGY and NM64 contributions to counting rate and temp. dependence 8=42683
- neutron monitors IGY and NM64 multiplicity measurements 8=38111
- noise, correction of energy spectra 8=29232
- nuclear emulsion detector aboard Gemini satellite 8=42705
- nuclear emulsions, Fowler-Perkins parameter meas. for sensitive determ. of cosmic ray charge and energy spectra 8=42708
- for nuclear interactions obs. 10^{12}-10^{13}eV 8=38124
- photography, image intensifier, of simulated showers in large-area plastic scintillator layers 8=38119
- plastic track detectors 8=38117
- proportional counter, large areas having uniform sensitivity 8=42344
- proportional large area detectors for quarks in sea level radiation 8=38126
- for 'Proton' type satellites, spectrometer for energy and charge spectra of primary particles 8=25024
- radio detection of air showers, basic requirements 8=38239
- recording array for 10^{21} eV showers 8=38241
- review of detection apparatus 8=33847

Cosmic rays—contd
- **apparatus**—contd
  - satellite particle detector systems 8=47183
  - scintillation counter for γ-ray obs. from balloon 8=38112
  - solar p, α differential energy spectrum meas. 8=47184
  - sonic spark chamber 8=38114
  - spark calorimeter for MPP penetration obs. 8=38130
  - spark chamber for primary e flux meas. 8=33849
  - spectrograh for μ charge ratio at large zenith angles 8=38179
  - spectrograph using spark chamber technique 8=38115
  - underground μ obs. installation 8=38247
  - water Cherenkov detectors, anomalous pulse spectrum 8=38129
- **composition**
  - charge measurement between 10^{10} and 10^{14} ev 8=47185
  - charged-to-neutral ratio obs. at 3250m 8=42689
  - e.a.s., hadronic component, multiple core 8=38231
  - electron charge composition 8=38154
  - e.m. cascades, energy meas. in nuclear emulsions 8=38135
  - e.m. cascades, lateral and ang. struct. 8=38137
  - fractionally charged particles, determ. 8=24636
  - high-energy N particles in e.a.s., obs. 8=38220
  - high energy obs. aboard Gemini XI 8=42705
  - interplanetary cosmic ray gradient and electron, proton intensity 1964-65 Mariner IV obs. 8=42681
  - light, medium and heavy low-energy nuclei obs. during solar minimum 8=42711
  - light-to-medium nuclei ratio rel. to propag. thru interstellar space 8=38163
  - μ in N induced showers, 10^{12}-10^{14} eV 8=29250
  - nuclei in galaxy, energy spectrum 8=42739
  - μ prod., direct, review of evidence 8=25039
  - μ, prop. rel. to shower size obs. 8=29244
  - N interactions above 10^{13} eV 8=29252
  - neutral particles 20 m.w.e. underground, search 8=38144
  - neutrino underground meas. project 8=37931
  - neutrinos, atm., Aleph-model inferences 8=38149
  - nuclear-active particles in e.a.s., fluctuations calc. 8=38219
  - nuclear-active particles in sea-level e.a.s., distrib. calc. 8=38216
  - nuclei $Z \geqslant 2$, $Z \geqslant 5$, $Z \geqslant 15$, chemical composition and energy spectra obs., inside and outside earth's magnetic field 8=29236
  - nucleon diurnal var., anisotropies 8=38270
  - nucleonic cascade in atmosphere, Monte Carlo calc. 8=38262
  - nucleonic, time-varying, barometric coeffs. calc., by regression analysis 8=38275
  - nucleons, energy determination by absorpt. calorimeter 8=38139
  - primary analysis of Cherenkov flash fluct. 8=38190
  - primary, obs., various nuclei to Ne, 25-200 MeV/N 8=38164
  - primary, search for γ, progress report 8=38225
  - specific yield functions calc. for IGY neutron monitors from vertically incident protons 8=42695
  - Utah neutrino experiment 8=38147
  - X-ray, thin-window proportional counter 8=47187
  - $Z \geqslant 30$ region, chem. comp. and energy spectra 8=25028
  - He, C, N, O, above 30 MeV/N, B, Ne, Mg, Si above 50 MeV/N, energy spectrum obs. 8=38161
  - Li to F, energy spectrum and chemical composition obs. 8=38162
  - Li, rel. to T Tauri stars content, calc. 8=36926
  - U particles, massive, charged, possibility examined 8=42688
- **alpha-particles**
  - α to electron ratio as test for solar modulation 8=42691
  - energy spectrum differential obs. 70-240 MeV/nucleon 8=42693
  - in interplanetary space, 1-20 MeV, satellite obs. 8=38105
  - rigidity spectrum obs., 12-35 GeV 8=38174
  - source spectrum proposed 8=42710
  - He-3, secondary, used to determ. path-length 8=42713
  - $He^3/He^3 + He^4$, 70-240 MeV/N obs. 8=38145
  - He^3/He^4 isotope ratio obs., and interpreted 30-90 MeV/N 8=38138
- **deuterons**
  - secondary, used to determ. path-length 8=42713
  - H^2/He^4, 150 MeV/N obs. 8=38145
  - d/He^4 isotope ratio obs., 20-50 MeV/N 8=38138
- **electrons**
  - α to electron ratio as test for solar modulation 8=42691
  - angular distrib. in shower, arbitrary boundary conditions 8=38209
  - antiproton-positron flux ratio calc. 8=42685
  - cascade, ang. distrib. in Fe and Pb, calc. 8=38181
  - cascade showers, ang. distrib. rel. to depth 8=38208
  - charge composition 8=38154
  - e.a.s., probability distrib. functions 8=38213
  - e-γ cascades in Fe, Pb 8=29246
  - e-γ cascades prod. by 10^{13} eV N interactions 8=29252
  - e.m. cascade, distrib. equilib. function and excess calc. 8=38207
  - in e.m. cascades, lateral and angular distribs. rel. to core approx. 8=42719
  - energy distrib. obs. in showers 8=29242
  - energy flux 2-15 keV and > 15keV, 200-500 km 8=29234

Cosmic rays—contd
- **electrons**—contd
  - energy loss rate in galaxy 8=38165
  - energy, Pomeranchuk eff. 8=47180
  - energy spectrum obs., 3.5-80 BeV 8=38170
  - flux and east-west asymmetry meas. 8=33849
  - for galactic magnetic field estimation 8=41530
  - intensity and interplanetary gradient, 1964-65 Mariner IV obs. 8=42681
  - interactions with relic radiation 8=42715
  - interplanetary and solar, 3-12 MeV 8=41590
  - low-energy flux obs., regions of high intensity over S. Atlantic 8=29236
  - low-energy, rel. to heavy primaries 8=38151
  - positrons, low energy, 0-3 MeV obs. 8=38168
  - primary component, long term variations 8=42692
  - primary component obs., 13-50 GeV 8=38166
  - primary component, smooth spectrum and galactic storage 8=38167
  - primary, flux rel. to galactic origin and solar modulation, 17-63 MeV 8=33853
  - primary spectrum, 0.5-30 GeV 8=38169
  - μ to e density ratio in EAS, rel. to development fluctuations 8=29241
  - shower, mean square fluctuation of number 8=29243
  - shower, sea-level and mountain obs. 8=29244
  - in space, prod. in cosmic ray collisions, evidence from high energy γ-rays 8=41493
  - spectra of secondary radiation 8=42735
  - spectrum above 60 BeV, rel. to confinement 8=32397
  - spectrum at 2.3g/cm² atmospheric depth, 4 MeV to 6 BeV 8=42694
  - spectrum of primary, 300 MeV–4 BeV, 1964-66 8=42760
  - spectrum, 0.09-8.4 BeV, 1965, obs. 8=47188
  - storage and diffusion in the Galaxy 8=32396
- **mesons**
  - diurnal var., anisotropies 8=38270
  - e.a.s., π probability distrib. functions 8=38213
  - π collision with emulsion nuclei, incoherent multiple particle prod., 200 GeV 8=33854
  - π-to-nuclei, π-to-p ratios obs. at 3250m 8=42689
  - π prod. mechanism and props., energetic 8=38177
  - π prod. in N induced showers 10^{12}-10^{14} eV 8=29250
  - π secondary prod. 8=29255
  - π° prod. in local targets and atmosphere 8=29252
- **muons**
  - anomalous pulse spectrum in water Cherenkov detectors 8=38129
  - anomalous spectrum 8=38159
  - arrival time distrib. in e.a.s. 8=38189
  - atmospheric, Aleph-model inferences 8=38149
  - atmospheric and ν-induced, energy spectra 8=38146
  - rel. to boson neutral vector, of mass O(30 GeV), evidence for existence 8=42361
  - charge ratio at 80° to zenith, obs. 8=38179
  - charge ratio at large zenith angles, fine struct. 8=38142
  - charge ratio in e.a.s. 8=38184
  - component in centre of e.a.s., fluctuations 8=38185
  - component in centre of e.a.s., lateral distrib. 8=38187
  - component of e.a.s., fluctuation calc. 8=38218
  - density spectrum at large zenith angles 8=38140
  - directional flux and primary radiation correlation in lower atmosphere 8=38173
  - e.a.s., muon-poor, interpretation 8=38223
  - e.a.s., probability distrib. functions 8=38213
  - energy-range relation, exptl. determ. 8=38245
  - energy spectrum, sea-level, from underground obs. 8=38148
  - fluctuation spectra of e.a.s. 8=38212
  - flux meas. to 10 TeV from burst size spectrum obs. 8=38134
  - high-energy e.m. interactions in Fe 8=38250
  - high-energy, in e.a.s., obs. 8=38186
  - hypothetical particle without strong interactions 8=25029
  - interactions 5-1000 GeV, obs. 8=38258
  - large e.a.s., high-momentum excess obs. 8=38183
  - lateral distrib. function in e.a.s. 8=38188
  - lateral distrib. in e.a.s., obs. 8=38194
  - low-energy, in e.a.s. obs. 8=38182
  - momentum meas. by solid iron magnets 8=38123
  - momentum spectrum and charge excess at large zenith angles 8=38143
  - momentum spectrum, charge ratio and interactions obs., proposed apparatus 8=38122
  - μ to e density ratio in EAS, rel. to fluctuations in longit. and lateral development 8=29241
  - μ^+ scatt. by Al, momentum region 1.60 BeV/c 8=42704
  - muon high energy horizontal flux momentum spectrum and charge ratio, magnetic spectrometer obs. 8=38118
  - sea-level spectrum calc. from depth intensity obs. in underground expts. 8=33848
  - sidereal wave in the galactic plane from underground obs. of muons 8=42755
  - spectra analysed by spectrograph using spark chamber technique 8=38115
  - spectra near geomag. equator 8=38141
  - underground decay, identification 8=38150
  - underground spectrum obs. installation 8=38247
  - Al^{26} induced in terrestrial rock, search 8=41324
- **neutrons**
  - albedo, altitudinal distribution and flux obs. $< 10^5$ eV 8=42696

Cosmic rays—contd
  neutrons—contd
    albedo, flux rel. to inner radiation belt protons origin,
    in atmosphere, prod. by primary nucleons 8=29254
    barometric effect, allowance for, during bursts 8=42716
    epithermal albedo, upper atmosphere, flux determ. from activity obs. 8=41384
    fast-neutron flux variation rel. to latitude in atmosphere 8=42743
    high energy solar emission, detection, ⩾ 50 MeV 8=42697
    increase preceding Forbush effects, possible galactic origin 8=38287
    intensities between arctic and antarctic, north-south direction anisotropy 8=38269
    intensity analysis after generation during chromospheric flares 8=38153
    intensity depend-on die press., gen. regressional model 8=33850
    latitude and solar cycle variation relationship in IGY neutron-monitor mass-absorpt. coeff. 8=38261
    monitor airborne, latitude survey of frequency of multiple events 8=38125
    monitor acceptance vectors for 72 stations 8=38273
    monitors, IGY, changes of attenuation coeff. w. r. t. time 8=42699
    multiplicity intensity variations in NM64 monitor during Forbush decreases 8=42723
    multiplicty latitudinal survey using shipborne NM-64 neutron monitor 8=38136
    solar, flux at earth in 1962, meas. by BF_3 counters on OSO-1 8=32588
    spectrum epithermal atmospheric and energies obs. by resonance detector 8=42698
    temp. effect on n component obs. on Mt. Mussala 8=25040
  photons
    barometric effect at sea level, 3.8 to 183 MeV 8=29257
    Cherenkov detector of 10^{11}-10^{12} eV region for obs. on earth's surface 8=42679
    e.m. cascade, distrib. equilib. function and excess calc. 8=38207
    e-γ cascades in Fe, Pb 8=29246
    e-γ cascades prod. by 10^{13} eV N interactions 8=29252
    γ obs. from balloon 8=38112
    γ-ray intensity obs. at 2900m 8=25038
    γ ray spectrum, 10^{11}-10^{13} eV, obs. 8=42690
    γ-rays, above 50 MeV, in upper atmos., obs. rel. to discrete and diffuse sources 8=42686
    γ-rays detection 1-5 MeV 8=42697
    high energy γ obs. rel. to electrons in space and source of X-ray background 8=41493
    low-energy flux obs., regions of high intensity over S. Atlantic 8=29236
    primary origin, diffusion and $\bar{p}$ component calc. 8=42701
    secondary, general properties of radiation processes and spectra 8=42722
    shower, mean square fluctuation of number 8=29243
    solar diurnal time variation near sea level, 3.8 to 183 MeV 8=29258
    in N 10^{14} eV interactions 8=29251
    X-ray diffuse background of outer space, 1-1.5 keV 8=32399
    X-ray, thin-window proportional counter 8=47187
  protons
    antiprotons, upper limit to abundance 8=38107
    astronomical source determ. with fast Cherenkov system 8=45797
    energy spectrum differential obs. 70-240 MeV/nucleon 8=42693
    energy spectrum in region 10^{10}-10^{13} eV, from Proton satellite meas. 8=25025
    flux variation rel. to atmospheric height 8=42768
    intensity and interplanetary gradient, 1964-65 Mariner IV obs. 8=42681
    in interplanetary space, 1-20 MeV, satellite obs. 8=38105
    π-to-p ratio obs. at 3250m 8=42689
    spectra, and solar modulation effects in new solar cycle 8=42687
    spectra of secondary radiation 8=42735
  effects and interactions
    See also Nuclear reactions due to/cosmic rays.
    air nuclei, N, π effect models for e. a. s. calc. 8=38217
    albedo, epithermal neutrons, upper atmosphere, flux determ. from activity obs. 8=41384
    in atmosphere, primary nucleons, n and isotope prod. 8=29254
    atmosphere, secondary particle spectra, discrepancy 8=29253
    atmospheric and ν-induced, μ energy spectra 8=38146
    with black-body radiation, effect on spectrum 8=42714
    Cherenkov light obs. at 5200m altitude 8=38259
    e^+e^- pair prod., spark calorimeter obs. 8=38130
    electron pair prod. by μ in nuclear field 8=38257
    electron production in low ionosphere, obs. 8=50176
    electron production rate in ionosphere of bolar cap due to solar cosmic rays 8=50177
    electrons with relic radiation 8=42715
    extremely high energy obs. in emulsion chamber 8=42733
    5.10^{10}-10^{12} eV with C and Fe 8=42728
    galactic, reaction cross sections rel. to propag. 8=33852
    γ, high energy prod. in N interactions above 10^{13} eV 8=29252

Cosmic rays—contd
  effects and interactions—contd
    γ-ray intensity obs. at 2900m 8=25038
    with HI clouds, e.m. interaction rel. to source function $\alpha E^{-2.5}$ 8=42712
    high-energy μ, nuclear and e.m., obs. 8=38255
    high-energy particle studies 8=25030
    high transverse momentum events 8=33856
    hydromagnetic wave generation 8=47191
    incoherent multiple prod. of particles, 200 GeV pion collision with photographic emulsion nuclei 8=33854
    inelastic final states, use of momentum depend. phases for one particle amps. 8=29240
    inelasticity of 10^{15} eV jets 8=29248
    installations for nuclear interactions obs. 10^{12}-10^{13} eV 8=38124
    interstellar garden-hose instability, growth rate 8=45729
    iron magnets, solid, for nuclear-active particles obs. 8=38123
    jets, transverse momentum distribs. in fireball model assuming Planck's momentum spectrum 8=29237
    large-angle μ scatt. processes 8=38254
    meteorites and moon surface, nuclide prod. 8=37025
    meteorites, stony, H^3 and He^3 production 8=50428
    mica, ancient cosmic rays tracks? 8=25036
    μ bremsstrahlung cross-section, influence of nuclear and at. form factors 8=38256
    μ, high-energy e.m. interactions in Fe 8=38250
    μ-induced horizontal air showers 8=38252
    μ interactions 5-1000 GeV, obs. 8=38258
    muon prod., direct, not obs. in spectrum at zenith angle of 75° 8=25037
    nuclear interactions at 5200m altitude, obs. 8=38249
    nuclear μ interactions, photonuclear cross-section calc. 8=38253
    nucleons above 10^{14} eV, γ prod. obs. 8=29251
    100 GeV π and N on C, Pb, cross-section obs. at 2000 m 8=42727
    φ production by 10^{12} eV nuclei 8=42734
    with photons in universe, ultrahigh energy 8=33846
    π, above 100 GeV, obs. of path length and pair prod. in emulsions 8=42732
    π prod. by 10^{14} eV nucleons 8=42690
    π prod. in showers 8=29242
    π secondary prod. 8=29255
    p-p as source of d 8=38138
    radionuclide prod. on Moon's surface 8=32531
    secondary particles, anomalous interactions 8=29249
    secondary particles, multiplicity and ang. distrib. analysed rel. to fireball model 8=29238
    spectra secondary, of electrons and photons and their number ratio 8=42735
    above 10 GeV 8=42720
    10^{11}-10^{12} eV multiple production, mean characteristics of process 8=42731
    350 GeV, emission of secondaries and their fireball 8=42726
    transverse momentum and ang. distrib. for low energy transfer into soft component 8=29239
    200 GeV, asymm. shower prod. 8=42718
    200 GeV, meas. of energy transfer to neutral pions 8=42730
    ultra-high-energy, secondary transverse momentum distrib. 8=38251
    uncorrelated jet model, anal. and momentum depend. phases for one particle amps. 8=29240
    Al^{26} in terrestrial rock, induced by cosmic-ray muons, search 8=41324
    Fe, e-photon cascades investigated with ionization calorimeters 8=29246
    He^4 fragmentation as source of d and He^3 8=38138
    N, 10^{12}-10^{14} eV, energy of secondary showers obs. 8=29250
    Pb, e-photon cascades investigated with ionization calorimeters 8=29246
  jets. See Cosmic rays/showers and bursts.
  origin
    low energy, from outside solar system 8=38158
    neutron star mass in fall 8=45676
    point sources $>10^{12}$eV, search 8=38157
    primary, diffusion and $\bar{p}$ component calc. 8=42701
    quasars, escape and interaction with photons 8=42714
    source function that is power law in kinetic energy per nucleon 8=42712
    supernova explosions, review 8=38106
    He and M nuclei, source spectrum 8=42710
  primary
    antiproton-positron flux ratio calc. 8=42685
    composition, analysis of Cherenkov flash fluct. 8=38190
    composition, various nuclei to Ne obs. from satellite 8=38164
    counter, scintillation, plastic for heavy nuclei 8=47186
    e.a.s., attenuation length meas. 8=38192
    electron component obs., 13-50 GeV 8=38166
    electron component, power low representation rel. to galactic storage 8=38167
    electron energy loss rate in galaxy 8=38165
    electron flux, 2-15 keV and > 15 keV, 200-500 km 8=29234
    electron, long-term var. 8=42692
    electron spectrum 0.09-8.4 BeV, 1965 obs. 8=47188

Cosmic rays—contd
- **primary**—contd
  - electron spectrum obs. 0.5-30 GeV 8=38169
  - electrons, flux rel. to galactic origin and solar modulation, 17-63 MeV 8=33853
  - energy determ. and transfer to π° obs. at mountain top 8=29235
  - energy estimation, improved method 8=33851
  - energy $\geq 5 \times 10^{19}$ eV evidence of existence 8=47190
  - energy spectrum above 10^{14}eV, obs. 8=38155
  - energy spectrum in neighbourhood of earth examined 8=38171
  - fragmentation parameters of multiply-charged component on 'hydrogen' of nuclear emulsion 8=25031
  - galactic, nuclei p-fragmentation rel. to Be/B dating, $6 \leq Z \leq 26$ 8=38176
  - heavy nuclei, energy spectrum obs. above 10 MeV/N 8=42709
  - heavy stable fundamental particles, limit on presence 8=38159
  - high-energy particle studies 8=25030
  - integral energy spectrum of all particles in energy range 6×10^{10}-10^{14} eV, from Proton satellites 8=25025
  - light, medium and heavy low-energy nuclei obs. during solar minimum 8=42711
  - magnetospheric tail arrival, low energy 8=38160
  - metagalactic, energy density from γ obs. 8=32395
  - muon directional flux and radiation correlation in lower atmosphere 8=38173
  - nuclei in ionized source regions and interstellar medium, confinement 8=41494
  - origin, diffusion and $\bar{p}$ component calc. 8=42701
  - positrons, low energy, 0-3 MeV obs. 8=38168
  - rigidity spectra, change 8=42741
  - search for γ evidence, progress report 8=38225
  - solar, $Z \geq 15$ nuclei increase and X-ray bursts, 23-24 Feb., (1964) 8=32586
  - spectrometers for 'Proton' type satellites, energy and charge spectra 8=25024
  - spectrum rel. to p and heavy-nucleus initiated air showers 8=38235
  - X-ray and u. v. backgrounds outside atm., rel. to inter-galactic gas density, obs. 8=32490
  - X-ray diffuse background of outer space, 1-1.5 keV 8=32399
  - X-rays, diffuse flux isotropy between 20 and 80 keV 8=38175
  - X-rays, solar, $\leq$ 1038Å and $\leq$ 44Å, 200-500 km 8=29234
  - $Z \geq 3$, flux obtained from nuclear emulsions, rel. to geomag. cut-off 8=25032
  - $Z \geq 16$, charge distrib. obs. 8=42707
  - $Z \geq 20$, energy spectrum obs. 8=42706
  - $Z = 10$ - 28, charge and energy spectra 8=42708
  - $Be^{7,9}$ in solar rays, flux, calc. 8=37057
  - $Co^{56,59}$ in solar rays, flux, calc. 8=37057
  - He, C, N, O, above 30 MeV/N, B, Ne, Mg, Si above 50 MeV/N, energy spectrum obs. 8=38161
  - Li to F, energy spectrum and chemical composition obs. 8=38162
- **showers and bursts**
  - air shower cores, at sealevel and under 800g/cm² shielding, simultaneous obs. 8=38229
  - air shower cores, Monte Carlo simulation 8=38230
  - air shower cores at sea level, e. m. struct. 8=38228
  - air shower cores, fine struct. obs. 8=38226
  - asymmetric prod. obs., 200 GeV nuclear interaction of cosmic ray nucleons and pions 8=42718
  - burst-size spectrum obs. for muon flux meas. 8=38134
  - cascade e ang. distrib. in Fe and Pb, calc. 8=38181
  - cascade, e ang. distrib. rel. to depth 8=38208
  - cascade theory, birth-and-death process with immigration calc. 8=38206
  - composition survey development, counters 8=29244
  - core fine struct. obs. at 5200m altitude 8=38227
  - core struct. and high-energy events 8=38193
  - core struct., Monte Carlo simulations 8=38215
  - delayed particles 70 m. w. e. underground, obs. 8=38246
  - density spectrum of e.a.s. at 1575, 4300m, obs. 8=38180
  - detection by N_2 luminesc. in atmos. 8=42680
  - detection by radio echoes, Tokyo expt. 8=38199
  - development obs. in upper atmosphere 8=29242
  - e. a. s. arrival directions, analysis 8=38224
  - e. a. s. at aircraft altitudes, obs. 8=38196
  - e. a. s., atm. and sidereal var. obs. 8=38222
  - e. a. s. charact. sensitivity to model parameters 8=38214
  - e.a.s., Cherenkov flash fluct. rel. to primary composition 8=38190
  - e.a.s. Cherenkov radiation, search for point sources 8=38157
  - e.a.s., core multiple composition obs. 8=38233
  - e.a.s., hadronic component, multiple core 8=38231
  - e.a.s., lateral density distrib. obs. 8=38191
  - e.a.s., muon-poor, interpretation 8=38223
  - e.a.s., probability distrib. functions for e, μ, π numbers 8=38213
  - e. a. s. survey, 1952-9 8=25023
  - EAS, density spectrum parameters, maximum-likelihood determ. 8=47189
  - EAS, fluctuation in development rel. to ratio of μ to e component density 8=29241

Cosmic rays—contd
- **showers and bursts**—contd
  - EAS, particles with energy $\geq 5 \times 10^{19}$ eV, existence 8=47190
  - EAS, radio emission, 520 MHz, obs. 8=25035
  - EAS transverse momenta, derivation 8=42717
  - electron ang. distrib., arbitrary boundary conditions 8=38209
  - electron component fluctuations, calc. and expt. 8=38210
  - electrons in e. m. cascades, angular and lateral distribs. 8=42719
  - e. m. cascade, e distrib. equilib. function and excess calc. 8=38207
  - e. m. cascades in e. a. s., Monte Carlo calc. 8=38211
  - energy determ. from total number of particles 8=29246
  - energy spectra obs. 3200 m above sea level 8=42729
  - e, photon-initiated, fluctuation of e and γ numbers 8=29243
  - fifty obs., from 350 GeV primaries 8=42726
  - fluctuations in e. a. s., lateral struct. and e transition curve 8=38217
  - fluctuations in e. a. s., muon component calc. 8=38218
  - γ-prod. and development of nuclear cascades due to 10^{14} eV N obs. 8=29251
  - Haverah Park 500m array, facilities 8=38237
  - Haverah Park 2km array obs. 8=38236
  - high-energy jet, relative four-momentum between two secondary particles, new method of analysis 8=38178
  - high-energy muons in e.a.s. obs. 8=38186
  - horizontal μ-induced, obs. 8=38252
  - ionization calorimeter 8=29235
  - Isobar, Landau processes in cosmic-ray jets 8=38177
  - Kolar Gold Fields e. a. s. expt. 8=38232
  - large e.a.s., muon component, high-momentum excess obs. 8=38183
  - large e. a. s., structure of front, obs. 8=38234
  - low-energy muons in e.a.s. 8=38182
  - muon arrival time distrib. in e.a.s. 8=38189
  - muon charge ration in e.a.s. 8=38184
  - muon component fluctuations, calc. and expt. 8=38210
  - muon component in centre of e.a.s., lateral distrib. 8=38187
  - muon component in e.a.s., lateral distrib. 8=38188
  - muon component in centre of e.a.s., fluctuations 8=38185
  - muons in e.a.s., lateral distrib. obs. 8=38194
  - neutron component, allowance for barometric effect 8=42716
  - nuclear-active particle fluctuations calc. 8=38219
  - optical emission imaging system 8=38195
  - particle density meas., instrumental effects 8=38240
  - photon induced, 10^{13}eV, from local radio sources 8=32400
  - predominantly e. m., 10^{14}-10^{16} eV, obs. 8=38225
  - proton and heavy-nucleus initiated, comparison 8=38235
  - radio detection, basic requirements 8=38239
  - radio detection, Harwell-Grove installation 8=38238
  - radio emission at 22 MHz, obs. 8=38200
  - radio emission, geomag. polarization mechanism, exptl. tests 8=38204
  - radio emission detect., half-wave dipole system 8=38242
  - radio pulse coincidence long-distance expt. 8=38198
  - radio pulse correl., use of arrival directions 8=38201
  - radio pulse emission theory 8=38203
  - radio pulses from e. a. s., 32, 60 MHz obs. 8=38202
  - recording array for 10^{21} eV 8=38241
  - size spectra and fluctuations 8=38212
  - sea-level nuclear-active particle distrib. calc. 8=38216
  - spectrograph iron, bursts, interpretation 8=38221
  - "stars", recording by ionization chambers 8=29233
  - stellar diurnal vars., compensation for atmospheric effects 8=25033
  - Sydney Univ. recorder, prelim. results 8=38197
  - Tien Shan obs. rel. to existence of baryon passive state 8=42616
  - N induced, 10^{12}-10^{14} eV obs., dominant π prod. 8=29250
- **variations**
  - air showers, stellar diurnal, compensation for atmospheric effects 8=25033
  - anistropy of transient variations, daily and latitudinal 8=42745
  - anisotropy, small, 7.5 to 45 MeV cosmic rays, implications 8=38286
  - rel. to atmospheric height 8=42768
  - background count, increase during thunder-storms 8=38263
  - bursts, anisotropic, interplanetary regular mag. field estimation from 8=37038
  - coronal expansion and solar wind theory effects 8=41586
  - cutoff rigidity, effective geomag. in penumbra 8=38272
  - daily, correl. with geomag. activity 8=38289
  - daily directional measurements at 60 m. w. e. vertical depth 8=38271
  - daily, during quiet and disturbed periods 1965-6 8=38280
  - daily intensity var. 8=38276
  - daily, of second harmonic, intensity gradient, perpendicular to ecliptic 8=42766
  - distribution and acceptance vectors of detectors 8=42736
  - diurnal and interplanetary magnetic field orientation, second spherical harmonic 8=42752
  - diurnal and semidiurnal, recorded on earth, modulation 8=42738
  - diurnal anisotropy, spatial distribution and spectra obs. 8=38279
  - diurnal, difference between filtered and unfiltered data, Monte Carlo calc. 8=42749

Cosmic rays—contd
variations—contd
diurnal dynamic phenomena 8=25042
diurnal effects separated from small-state fluctuations, Oct. 1965–April 1966 8=42742
diurnal, meson and nucleon components, two anisotropies 8=38270
diurnal, possibility of two-way solar anisotropy 8=38278
diurnal 22-year revolution, assumed two perpendicular cosmic-ray streamings 8=42767
diurnal, underground variation with solar cycle obs. 8=38277
diurnal variation and Forbush decreases, solar activity cycle effect 8=42762
diurnal, variation with opposite phases in northern and southern hemispheres 8=42744
east-west asymmetry measurement for antiproton-proton flux ratio 8=38267
electron flux, east-west asymmetry meas. 8=33849
eleven year modulation, galactic in interplanetary space 8=42759
eleven year, of flux and charge composition 8=42764
11-year solar cycle, change in energy spectrum, galactic 8=42761
Forbush decrease, multiplicity intensity variations in NM64 monitor 8=42723
Forbush decrease of September 23, 1966, anisotropy of intensity obs. 8=38284
Forbush decrease on March 23, 1966, morphology 8=38274
Forbush decreases at different periods of solar cycle 8=38285
Forbush decreases, comparison of corotating and flare-initiated characteristics 8=42746
Forbush decreases, intensity, analysis 8=42757
Forbush events 1966, spectra 8=42758
Forbush, particle flux acceleration in interplanetary space 8=38283
galactic, solar modulation near solar minimum, 1965 8=42756
intensities compared simultaneously over the Antarctic and Arctic 8=38264
intensity, and interplanetary field, short period fluctuations 8=47192
intensity and magnetopause position 8=45494
and interplanetary mag. field 8=37037
interplanetary magnetic field's sector structure 8=42748
interplanetary magnetic field's sector structure 8=42750
ionizing total component obs. during cold-front perturbations 8=38260
latitude and solar cycle's relationship in IGY neutron-monitor mass-absorpt. coeff. 8=38261
latitude, geomagnetic cutoffs meas. 8=38266
latitude of fast-neutron flux measurements in atmosphere 8=42743
long-term, dependent on energy, rigidity 8=42765
Monte Carlo calculation, from measurements, of atmospheric nucleonic cascade 8=38262
neutron increase preceding Forbush effects, possible galactic origin 8=38287
neutron intensities between arctic and antarctic, north-south direction anisotropy 8=38269
neutron monitor acceptance vectors for 72 stations 8=38273
19-24 days, intensity variations 8=38281
1942, March 7, rel. to limb flare 8=37073
photons at sea level, barometric effect 8=29257
primary electron spectrum 300 MeV–4 BeV, 1964-66 8=42760
recording level of cosmic-ray station, stability, standard algorithm for verification 8=42737
rigidities, vertical cutoff, trajectory determ. by 5° by 15° world grid 8=38265
rigidity dependence and correlation with solar activity 8=42763
rigidity spectra, change 8=42741
ring current effects 8=38288
sidereal and atm. density effects, obs. 8=38222
sidereal, obs. in different directions to eliminate meteorological ansitropies 8=42754
sidereal time, two-way, confirmed from analysis of data at Christchurch and Cheltenham 1938-58 8=42753
sidereal wave in the galactic plane from underground obs. of muons 8=42755
solar daily variation at equatorial station, east/west directional measurements 8=38268
solar semidiurnal variation of intensity 70 m.w.e. underground 8=38282
solar wind modulation and hysteresis phenomena 8=42739
storm-time increase in intensity 8=42747
sudden commencement 3 Sept. 1966 rel. to v.l.f. hiss decrease 8=32305
systematic intensity grad. along earth's rot. axis, N-S asymmetry, three-dimens. model 8=29256
temp. effect on n component obs. on Mt. Mussala 8=25040
time, barometric coeffs. calc., by regression analysis 8=38275
27 day, caused by modulation regions 8=42751
rel. to zenith angles obs. 8=42740
Cosmogony. See Cosmology.

Cosmology
See also Elements, origin.
antimatter search, upper limit to antiprotons 8=38107
background γ-ray intensity over Texas 8=45798
black body radiation interaction with cosmic rays 8=42714
Brans-Dicke coupling constant, necessarily positive 8=45589
collapsing clouds, fragmentation, rotation and pressure gradients effects, 8=50256
contracting gas cloud, effect of ohmic diffusion on mag. field distrib. 8=36965
cosmic fireball theory rel. to scalar-tensor gravitation 8=23858
cosmic ray energy spectrum, universe age effect 8=42672
cosmogonic fragmentation 8=28027
density in universe, large-scale inhomogeneities 8=28031
diffuse primary X-ray background up to 180KeV 8=45603
Doppler effect and red shift in classical mechanics 8=50261
Einstein const non-zero and non-zero photon rest mass 8=37915
electric charge, proposed variation with time laboratory test 8=28212
(electron charge)^2, possible var. with the age of the universe 8=28028
electron pair prod. spontaneous in magnetic field 8=45590
Friedman universe, irregularities formation, 8=50255
Friedmann universe, observation of part of surface, calc. 8=45594
G, universal gravitational, meas. with pendulums 8=32780
galaxies development and nucleosynthesis rel. to antimatter 8=41492
galaxy formation and statistical mechanics of violent relax. 8=50374
galaxy formation, thermal instabilities in process, 8=50375
γ-ray obs. background 8=45796
gravitation, Lorentz invariant theory 8=28032
gravitational and magnetodynamic stability, applied to force-free fields 8=50257
gravitational collapse and frequency shift 8=36915
gravitational collapse in presence of mag.-field 8=50264
gravitational collapse of gaseous ellipsoid 8=32393
gravitational collapse problems, numerical methods 8=50265
gravitational collapse rel. to Schwarzschild singularity 8=32812
gravitational instability prod. system, stability rel. to density 8=28052
gravitational motions of collapse or of expansion in general relativity 8=50250
gravitational theory rel. to cosmic microwave radiation at 3°K 8=32795-6
He galactic abundance, early formation evidence 8=45641
homogeneous Euclidean models with shear 8=45583
homogeneous notating models without shear 8=50247
inhomogeneous models, conformally equivalent to classical ones 8=32391
intergalactic gas, possible thermal history 8=50345
irreversibility of time and entropy 8=50248
Jeans's criterium and dimensions of stars and galaxies 8=50280
Lemaître model, rel. to metagalactic cosmic rays 8=32395
Mach's principle, and Green's function in expanding universe 8=45587
matter distrib. models for fluid spheres in general relativity 8=46080
metagalactic black-body background, sources, model 8=45586
microwave background at $\lambda = 3.3$mm, thermodynamic temp. 2.46°K 8=45597
model perturbations and angular variations of microwave background. 8=50252
models, relativistic, with radiation and matter 8=36909
models with press. 8=36910
neutrino filled universe, new soln. 8=32392
nucleosynthesis in big and little bangs 8=36911
oscillating relativistic world model, galaxies origin 8=50370
photon ageing as explanation of red shift 8=36914
primeval fireball plasma recombination theory 8=45596
protostellar bodies, massive superdense, models rel. to stability 8=28053
pulsating model rel. to Newtonian orbit 8=46082
pulsating object, spectral shift of light rays 8=28033
and quantum electrodynamics, reln. 8=45588
quasar, obs. in opposite directions rel. to models with pole in the red shift 8=28030
radiation damping in conformally flat spaces 8=32809
radiative energy transfer, conference 8=23909
radio sources opposite quasers, as test of universe model 8=50378
red-shift law for radio galaxies and quasars 8=45793
red-shift, rederivation of formula in gen. relativity 8=41744
rel. to time direction 8=50260
relation to some fundamental laws of physics 8=50262

Cosmology—contd
- relativity, general, with cosmological const., and elementary particle theory, vacuum props. 8=28292
- relic radiation, interaction with cosmic ray electrons 8=42715
- self-gravitating gas, one dimensional, Vlasov equation 8=50251
- self-gravitating stellar system with uniform rotation, stability of density waves 8=28037
- solid hydrogen and microwave background 8=45595
- spherical collapse, non-linear eqs., numerical integration 8=50258
- stationary character of Universe, possible test 8=50259
- steady-state universe rel. to microwave background 8=36916-17
- system formation in expanding universe, clustering model 8=50253
- time reversal, significance 8=41491
- universe, anisotropic and homogeneous, theoretical relations among observable quantities 8=50263
- universe, empty singularity-free, model 8=45593
- universe, expanding, elementary particle creation 8=42362
- universe, historical review 8=50249
- universe, hot model, recombination of H 8=45592
- universe, isotropic, with cosmological const., stability investigation 8=45591
- universe models, origin of structure 8=50254
- universe, steady state, galaxy formation 8=50356
- X-ray background component obs. 8=45602
- X-ray background obs. above polar atmosphere 8=45584
- X-ray background radiation evidence on number of electrons in space from cosmic γ-rays 8=41493
- Y model, uniform axisymmetrical ultrarelativistic 8=36913
- $Z \leqslant 5$ elements prod., p spallation cross sections, obs 8=32390

Cosmotron. See Particle accelerators/orbital.

Costa Ribeiro effect. See Dielectric phenomena; Phase transformations.

Cotton–Mouton effect. See Magneto-optical effects.

Cottrell atmosphere. See Crystal imperfections/dislocations.

Couette flow. See Flow; Hydrodynamics.

Counters
- See also Ionization chambers.
- electronic 8=46843
- exoelectron, quenching-vapour detector 8=27340
- fission chamber, to provide better discrimination between alpha and fission fragments 8=47366
- reversible decimal pulse, for integrating digital voltmeter 8=41915
- solid state, merits of semicond. versus crystal, phys. processes occurring 8=24517
- X-ray detectors and counters, review 8=46842
- **Cherenkov**
  - for β-emitting nuclides 8=29353
  - in cosmic ray det., meas. 8=33847
  - fast system for astronomical source determ. 8=45797
  - light receivers, servo systems 8=38128
  - metaphosphate glass:Ag n activation dosimeter 8=33798
  - reactor power level monitor 8=47436
  - water Cherenkov detectors, anomalous pulse spectrum 8=38129
  - $P^{32}(n, p)S^{31}$ fast-n activation dosimeter 8=33798
  - PbF_2, for electrons, positrons and gamma rays 8=46885
  - $S^{32}(n, p)P^{32}$ fast-n activation dosimeter 8=33798
- **crystal**
  - No entries
- **Geiger**
  - anode current passage strength, parameter depend 8=28973
  - dead time and recovery rel. to pulse amplitude 8=28972
  - declining processes studied 8=24505
  - pulses, delayed, generation in double counter expt. by photoelectric effect 8=37773
  - for H^3 in H_2O, water vapour filled, characts. 8=42475
- **proportional**
  - afterpulse meas., time and energy distrib. 8=24509
  - end-effect elimination by field-tube pulses 8=46861
  - fluctuation errors, validity of conclusions drawn from ratemeter 8=42345
  - 4π-recoil, finite size effects 8=46859
  - gas, probable energy loss, relativistic rise 8=46860
  - internal filling, for organic liq. mixtures concs. 8=27817
  - large area, for quarks in sea level radiation 8=38126
  - large areas having uniform sensitivity 8=42344
  - multiwire, for selecting stoppage of particles in thin gas target 8=46857
  - multiwire, particle selection and localization 8=37785
  - operation mechanisms 8=28974
  - pulse height distrib., count rate depend. shifts, mechanism 8=24507
  - pulse-height spectra, nonlinear energy level representation 8=24510
  - resolving power, anode wire limitations 8=24506
  - scintillation, using Xe and Xe mixtures 8=28499
  - scintillation, using Xe and Xe mixtures 8=46878
  - space dosimetry appl. 8=46858
  - spherical, high-resolution, isotropic response 8=24511
  - thin-window, for cosmic X-ray meas. 8=47187

Counters—contd
- **proportional**—contd
  - X-ray, cosmic background reduction by risetime discrimination 8=33620
  - X-ray radiometric analysis applications 8=41313
  - BF_3 n monitor, portable, for pulsed fields, 1–3000 mrem/hr 8=33815
  - BF_3, short, with spherical moderator for neutrons in γ background 8=33792
  - BF_3, wall effect on pulse spectrum 8=24508
  - CS_2 Lyman-α photons 8=24698
- **scintillation**
  - anthracene, α, e-excited, decay obs. 8=49832
  - anthracene, response to low energy electrons 8=24728
  - anthracene, scintillation response to heavy charged particles, directional anisotropy 8=46870
  - β-activity, determ. in natural radiocarbon 8=47279
  - for β-rays, with low background count rate 8=33639
  - β -spectrometer for satellite 8=50243
  - Conference, Washington D.C Feb-March 1968 8=46895
  - decay time meas. by simulated photomultiplier pulses 8=46883
  - double layered scintillator for separating and detecting low energy protons and electrons 8=46877
  - for electron-diffraction camera EVR-1 8=42346
  - γ-ray, multilayer 8=47051
  - for γ-ray obs., balloon borne 8=38112
  - gas proportional, using Xe and Xe mixtures 8=28499
  - gas proportional, using Xe and Xe mixtures 8=46878
  - light collection by various light pipes, non-uniformities 8=46871
  - liquid, appl. to absolute standardization 8=28977
  - liquid, automation with time-shared computer 8=46867
  - liquid, efficiency determ. standard 8=33375
  - liquid, for insoluble C^{14}-labelled powders 8=47278
  - liquid, low-background meas., alternating method 8=37772
  - liquid mixes for aq. T, efficiencies and costs 8=28979
  - liquid scintillators, benzene derivatives under electron impact 8=48172
  - liquid scintillators, organic, temp. dependence of energy degradation 8=46869
  - liquid scintillators with high-speed and efficiency, excited by gamma rays 8=46866
  - liquid, u.s. dispersion of $BaCO_3$–C^{14} in SiO_2 8=33372
  - liquid, whole-body, performance 8=32627
  - liquid, whole-body, safety and economy 8=33373
  - liquid, whole-body, safety and economy 8=33374
  - luminescence in vitreous state, appl. 8=36465
  - neutron, directional meas. using anisotropy of stilbene scintillation 8=47154
  - neutron p-recoil spectrometry, organic scintillator, 0.4–18 MeV 8=33823
  - for neutron tissue dose distrib. 8=33809
  - neutrons, slow with spherical polyethylene moderator and Cd shields, 5 eV–17 MeV 8=33791
  - noble-gas, for X-rays, quantum efficiency meas. 8=37928
  - organic, for fast n, recoil p distrib. 8=24979
  - organic phosphor efficiency for n detect. 8=29208
  - organic scintillations, conference, 1966 8=45250
  - plastic for a spectroscopy 8=29205
  - plastic, for primary cosmic ray meas. 8=47186
  - plastic mixed preparation and efficiency 8=49829
  - plastic, response to electrons 8=46884
  - plastic, transient nonlinear response to electron irradiation 8=46865
  - plastic with increased transparency 8=46882
  - pulse shape discrimination parameter meas. 8=46950
  - pulse shaper for scintillation detectors 8=46928
  - radioluminescence, theory 8=36462
  - rare earth phosphors and scintillators, survey of electron- and X-ray-stimulated luminescence 8=46874
  - r.f. emission from e.a.s., atm. elec. field source 8=38205
  - scintillators, time dependence of scintillations and the effect on pulse-shape discrimination 8=46868
  - scintillomicroscope for radioactive tracer detection in biological specimens 8=32623
  - semiconductors used as scintillation phosphors, CdS:Te and ZnTe:O 8=46864
  - stilbene, for neutrons, with γ discrimination, 1–10 MeV 8=33822
  - stilbene, for n flux, 2.5 MeV 8=33817
  - three-crystal-NaI pair spectrometers, efficiency calc. 8=24515
  - time statistics of sensitive volume 8=46872
  - tritium det. meas. 8=29224
  - for tritium, effects of vial on background rates, tests on glass and polythene 8=25014
  - Triton X-100 scintillant for C^{14} labelled materials 8=46880
  - whole-body, 4π liq. 8=28978
  - X-ray astronomy, optimum drilled collimators 8=50269
  - Cd^{252} response of coincidence detectors 8=37790
  - for Cs^{137} in human infants, 4π plastic counter 8=42934
  - CsI(Tl) scintillation characteristics, vacuum deposited 8=46875
  - He, for neutrons, with sodium salicylate wavelength converter, 14 MeV 8=33825
  - for K40 in human infants, 4π plastic counter 8=42934
  - Li^6-glass, for n flux $<$2.5 MeV 8=33817
  - LiI, Eu n monitor, portable, 0.5–1000 mrem/hr 8=33815

- **Counters**—contd
  - **scintillation**—contd
    - NaI well type, photopeak efficiency determ. 8=28980
    - NaI(Tl) crystal, contribution to total linewidth of counter, Monte-Carlo calculations 8=46879
    - NaI(Tl), emission bands, excited by X-irradiation, 5-80°K 8=46856
    - NaI(Tl), energy absorpt.-dose conversion operator 8=24495
    - NaI(Tl), γ-ray background determ., absolute method 8=50157
    - NaI(Tl) monocrystals, vibration- and thermo-stable characts. 8=24514
    - NaI(Tl), primary photoelectron yield obs. 8=24516
    - NaI(Tl), pulse-height spectra, nonlinear energy level representation 8=24510
    - NaI(Tl), pulse shape rel. to Tl conc. and temp. 8=46876
    - NaI(Tl) response to ions, $Z > 5$, 1-10 MeV/amu 8=44501
    - NaI(Tl) scintillation characteristics, vacuum deposited 8=46875
    - NE213, response to neutron induced proton recoils 8=46881
    - Xe, for (n, α) reactions in multilayer target 8=46873
    - ZnO:Ga, α-excitation, output and decay time obs. 8=37789
  - **semiconductor**
    - Conference, Washington D.C. Feb-March 1968 8=46895
    - current pulses from radiation detectors 8=46887
    - detectors in radiation protection and radiation meas., conference, Germany (1967) 8=33377
    - detectors, plasma time, experimental results 8=46892
    - detectors, X-ray spectra anal. 8=46783
    - development, manufacture and operation reviewed 8=28982
    - electron avalance anal., appl of Goods theorem for branching processes 8=33376
    - Fano factor, pair-creation model 8=46889
    - γ-ray spectrometer, Ge(Li), anticoincidence-shielded, for high sensitivity counting 8=47058
    - leakage current monitor for protection 8=37775
    - n^+ and p^+ prod. by ion-implantation 8=46893
    - n-p and p-n type, with pulse shape discrimination, signal shape investigation 8=24520
    - for neutrons, fast, dosimetry 8=33787
    - operating principles, characts., prop. and appls., review 8=24519
    - p-n junctions in radiation detection instruments 8=46886
    - position sensitive, fabrication by ion implantation 8=46890
    - resolution, influence of carrier capture 8=46891
    - semiconductor telescope, for satellite, e and p calibration 8=28025
    - surface barrier detectors, window thickness and rectifying process 8=46917
    - surface-barrier, for e position sensing 8=47094
    - CdTe p-n, for γ-ray spectrometry 8=33618
    - CdTe surface barrier detectors, high energy resolution for γ-rays 8=46900
    - CdTe surface barrier detectors, transient response, trapping and detrapping model 8=46901
    - CdTe surface barrier, use as γ-ray spectrometer 8=47069
    - Ge avalanche-type and detector arrays 8=46903
    - Ge, compensation with radiation-produced structural defects 8=46904
    - Ge for γ-rays, inelastic n scatt., excitation $\leqslant$ 200 keV 8=29088
    - Ge p-i-n detectors, determination of compensated-region width by light probe 8=46899
    - Ge pin diode for coincidence recording of γ and e 8=46894
    - Ge, reverse biased junction, merits, phys. processes occurring appls. 8=24517
    - Ge(Li) coaxial detectors, characteristics through warm-up and re-drift cycles 8=46906
    - Ge(Li) coaxial, time compensation for coincidence meas. 8=37798
    - Ge(Li) detector surface protective coating 8=46913
    - Ge(Li) detectors, precipitation of Li during ion drift 8=46905
    - Ge(Li) diode, energy resolving capability rel. to space expts. 8=29087
    - Ge(Li) double-open-end coaxial γ-ray detectors, charge collection 8=46908
    - Ge, Li driftability 8=49246
    - Ge, Li drifted, ionization energy determ. 8=24522
    - Ge(Li), γ-ray detection efficiencies and operating characteristics 8=46902
    - Ge(Li), growth of Ge in hydrogen atmosphere 8=48545
    - Ge(Li), high-resolution charged particle spectroscopy applications 8=46910
    - Ge(Li), paralleling for large biological samples 8=46912
    - Ge(Li) planar detectors, relaxation phenomena 8=46907
    - Ge(Li) planar, slow rising pulse obs. 8=37791
    - Ge(Li), pulse timing by constant-fraction discriminator 8=37796
    - Ge-Li, timing circuit 8=46909
    - Li^6 sandwich type, efficiency in directional n fluxes 8=38084
    - NaI(Tl), suppression of Compton background 8=46914
    - Si damage, appl. in n exposure meas. 8=29207
    - Si diode dosimeter for fast-neutrons, $<$1-15,000 rads. 8=33788

- **Counters**—contd
  - **semiconductor**—contd
    - Si, e scatt. at 50-625 keV, obs. 8=33638
    - Si fast-n dosimeters, p-n junction 8=33790
    - Si, high-resolution timing system 8=46919
    - Si n dosimeter, surface-barrier, 2-5 MeV 8=33787
    - Si p-i-n detectors, study with travelling light probe 8=46888
    - Si p-i-n, p-n junction defects rel. to elec. props. 8=28983
    - Si, pulse height defects due to nuclear collisions 8=46896
    - Si, reverse biased junction, merits, phys. processes occurring appls. 8=24517
    - Si spectrometers Li drifted and surface barrier, p irrad. resistance, 2.3 MeV 8=28984
    - Si surface-barrier detectors, effects of damage by 0.8-5.0 MeV protons 8=46918
    - n-Si surface barrier detectors for X-ray spectroscopy 8=47071
    - Si surface barrier, p damage 8=46897
    - Si transmission detectors, response function for electrons 8=46916
    - Si, Li drifted, ionization energy determ. 8=24522
    - Si, Li-drifted, 12-channel system for electron scattering spectrometers 8=47095
    - Si(Li), response to high-energy particles 8=46898
    - n-SiC (6H): B diffusion, for strongly ionizing particles, elec. props. 8=33378
  - **spark**
    - for particle spectrometer, magnetic, inductive spark chamber detector 8=37788
    - passive readout distinguishing breakdowns 8=46863
    - sonic, with long piezoelectric microphones 8=38114
  - **accessories**
    - See also Counting circuits.
    - analogue-digital converters, differential linearity meas. 8=24497
    - β-assembly PW 4127, automatic sample changer 8=42476
    - Cherenkov, fast timing circuit 8=24537
    - collimators for scanning, single- and double-head, sensitivity depth depend. 8=42343
    - collimators, multihole focusing longit. and lateral response 8=42342
    - computer program for nuclear spectroscopy data handling 8=37776
    - computer radiation analyser system 8=37777
    - data terminal network computer system 8=37774
    - energy resolving power, spectral effects, correction 8=24513
    - leakage current monitor for protection 8=37775
    - magnetostrictive readout of spark chambers 8=37803
    - pulse height analyser, 2-dimens. and appls. 8=24532
    - ratiometer for beam fluctuation compensation 8=37779
    - time-of-flight converter for computer display 8=24499
    - time-of-flight system, on-line, digital regulation 8=24500
    - NaI(Tl), cosmic-ray Cherenkov shield 8=28981
  - **operation technique**
    - See also Counting circuits.
    - correlation counting appl. to absolute disint. rate determ. 8=25170
  - **statistical analysis**
    - cross-correlation chopper for time-of-flight meas. 8=46848
    - energy absorpt.-dose conversion operator principle 8=24495
    - low background meas., alternating counting method 8=37772
    - neutron count in short time interval, third moment 8=38082
    - noise errors rel. to charact. peaks 8=46847
    - of radiation meas. 8=46845
    - scintillation, time statistics of sensitive volume 8=46872
    - X-ray wavelengths, effect of counting errors 8=46784
- **Counting circuits**
  - A/D convertor, multichannel, for pulse height analysis 8=37793
  - address counter with parallel input and ripple-through carry of control signal 8=46952
  - amplitude meas. in noise, high resolution 8=37795
  - analogue-digital conversion, acceleration by auto-equalization 8=24528
  - binary scaler, isolated tunnel diode appl. 8=46933
  - coincidence and anticoincidence cct. with 40 MHz count rate 8=46954
  - coincidence cct. for multichannel recording system, 3.8 nsec resolving time 8=46953
  - coincidence, $4\pi\beta$-γ correction method 8=24727
  - coincidence, slow-fast for angular correls. meas. 8=28989
  - coincidence, time compensation for coaxial Ge(Li) detectors 8=37798
  - connecting, decoupling and grounding problems 8=46929
  - constant-fraction discriminator for Ge(Li) detector timing 8=37796
  - control system for high-energy expt. 8=46930
  - data output system from AI-100 analyser to recording potentiometer 8=46946
  - digital windows for γ-γ coincidence meas. 8=37799
  - digitizing system for spark chamber 8=46974
  - disperse pulse detector, efficiency on registration threshold 8=37797
  - double coincidence, statistical parameters calc. using point method, prog. and tables 8=28988
  - double-decatron on/off controller 8=28463

Counting circuits—contd
- electronic counters 8=46843
- energy absorption spectrum-radiation dose conversion operator, automation of operation 8=24535
- expander for high-resolution amplitude analysis 8=46943
- fast discriminator with zero-crossover, for pulses from photomultiplier anode 8=46949
- fast timer for Cherenkov counters 8=24537
- filter, digital for pulse-height distrib. 8=33382
- filter, time-dependent, S/N calc. 8=33386
- filtering by tapped delay lines 8=33385
- γ discriminator for n spectrometer, $E_n \geqslant 0.2$ MeV 8=33384
- γ-ray pulse height spectra, time-dependent, vector analysis 8=46945
- lifetime of excited states, apparatus for precise obs. 8=29582
- multichannel analyser, appl. to X-ray diffr. data continuous averaging 8=28242
- multichannel pulse-amplitude ratio analyser 8=46941
- multi-coincidence, alignment and calibration 8=24536
- multiparameter simultaneous pulse analyser 8=46940
- pile-up detection 8=46931
- plasma H emission 2-80 keV spectrum analyser 8=38646
- pulse-amplitude analysis, optimum processing for random interval sequence 8=24531
- pulse analysers, associative information searching with addressed memory system, design 8=46942
- pulse analyser memory data display, channel identification 8=46980
- pulse analyser, resolution degradation causes 8=46947
- pulse-height analyser and pile-up selector 8=24534
- pulse-height analyser, computer-compatible output 8=46944
- pulse-height analyser for γ spectra 8=47064
- pulse-height analyser for γ spectrometry 8=33383
- pulse height analyser, 2-dimens. and appls. 8=24532
- pulse height analysers, multichannel, recent developments 8=46948
- pulse height analysis, compensation for gain shift and zero drift 8=37794
- pulse-height analysis of radioactive mineral spectra 8=46939
- pulse shape discriminating p-i-n detector 8=46951
- pulse shape discrimination in n-p and p-n type semiconductor detectors, signal shape 8=24520
- pulse shape discrimination in n spectrometer 8=33818
- pulse shape discrimination meas. on scintillators 8=46950
- pulse-shaping for high-resolution spectroscopy 8=46937
- pulse-to-analogue convertor for photomultipliers 8=33387
- pulse transformer input and links in measuring lines with neutron detectors 8=47151
- pulse, use of ferrite cores 8=46329
- pulse width-height convertor, 0-1μsec and 0-10μsec 8=46934
- pulsed expt. automatic data plotting 8=46926
- pulsed rad. meas., appl. of information theory of discrete systems 8=46935
- reactor EBR-II, mean-square voltage channel performance 8=47157
- reversible decimal pulse counter for integrating digital voltmeter 8=41915
- scaler, adequacy for derandomization 8=33380
- scaler, inadequacy for derandomization 8=33379
- scaler-ratemeter combination, statistical props. 8=46932
- scaler, tunnel-diode/transistor binary 8=28986
- spurious counts from elec. noise, rejection 8=46927
- time-amplitude converter for e^+ lifetime meas. 8=24526
- time-amplitude converters, calibration 8=24527
- time-to-pulse-height convertor using bitripoles 8=46936
- timing for Ge(Li) detector 8=46909
- timing for Si detectors 8=46919
- v.h.f. square wave generator, type T-402 8=33017
- v.h.v. ns pulse amplitude meas. 8=28987
- X-ray pulse height spectrum display instrument 8=26284
- for X-ray wavelength scanning, single channel pulse height analyser 8=24530
- Ge(Li) detector pulse height spectral decomp. 8=24533
- Ge(Li) detector pulse timing system 8=47049
  - NaI(Tl) low-level γ counter 8=33614

Cracks
- α-brass, single and bi-crystals, stress-corrosion cracking 8=26799
- brass, stress-corrosion cracking, mechanism 8=26798
- brass-NH_3 system, stress-corrosion cracking mechanism 8=35675
- cleavage, double-cantilever, discussion on theory 8=26769
- cleavage, formation rel. structure of nucleating deformation process 8=26774
- coated particles, config. system, theory rel. to reactor mats. 8=29561
- concrete, microcrack distrib. 8=40135
- ductile metals, initiation of fracture 8=48972
- elastic brittle, propagating, stress distrib. on extension surface 8=35634
- fatigue, in railheads, microspectral analysis 8=35633
- film coating on Cu single crystal, rel. to strengthening effects 8=40150
- in columns, effect on load carrying capacity 8=44520
- cosserat plate, bent, stress singularities around crack 8=41698

Cracks—contd
- curvilinear, in bonded dissimilar mats, elastostatic problems 8=26773
- deformation, plane strain, near tip in power-law hardening material 8=41717
- disturbing uniform heat flow, extension criteria for two-dimens. and axisymmetric types 8=44535
- in elastic anisotropic medium, elliptical stress field 8=41706
- elastic medium, three-dimensional theory 8=41709
- fatigue growth and cracking under static load 8=48979
- fatigue, propagation, gas environment effects 8=31183
- fatigue propagation in metals 8=44586
- fatigue reliability under random loadings 8=35629
- flat elliptical, extension to 3-dimens. by Griffith theory of brittle fracture 8=26767
- fracture nature in relation to total potential energy 8=26768
- Griffith, two coplanar, in infinite elastic medium 8=46042
- infinite, in thin circular cylindrical shells 8=32708
- internal from cavities in elastic plates, plastic enclave sizes 8=46048
- kovar, stress-corrosion cracking prevention by Ni plating 8=31211
- longitudinal shear crack with infinitely narrow plastic zone 8=46061
- penny-shaped in infinite solid, plastic zone due to thermal stress 8=37156
- plastic deformation generation, hydrostatic pressure influence 8=35635
- plate fracture under plane stress 8=46025
- polymethylmethacrylate, laser destruction, orientation, stress effects 8=40191
- polystyrene, laser destruction, orientation, stress effects 8=40191
- porous brittle material, distribution with random orientations during fracture 8=48974
- propagation along junction of elastic material, surface waves 8=46050
- propagation, brittle fracture energy criterion 8=40115
- propagation in continuous media 8=44533
- in reactor graphite, before and after n-irrad., propag. 8=26789
- steel, acceleration by martensite transformation 8=49012
- steel, austenitic stainless, stress corrosion cracking study by internal friction meas. 8=40159
- steel, ball bearing, propag. rel. to growth, electron microfractographical studies 8=35696
- steel, fatigue propagation rel. to environment 8=49008
- steel, high-tensile, stress-corrosion cracking 8=31212
- steel, initiation and propagation, influence of notches 8=35689
- steel, mild and high strength, propag. behaviour 8=35697
- steel, mild, stress-corrosion cracking and grain boundary corrosion effect of structure 8=44569
- steel, propagation rel. to acoustic pulse analysis 8=35415
- stress concentration, effect of couple-stresses 8=40117
- stress-corrosion cracking by wedge force loading 8=48977
- stress corrosion cracking, rate controlling step. 8=44534
- tensile, in hardening material, singular behaviour at end 8=41718
- viscoelastic mats., linear, initiation rel. to loading history 8=31178
- Zircaloy-2, fatigue initiation 8=26854
- Al alloys, orientation effect on fracture toughness 8=48989
- Al sheets, fatigue, growth rate, local plastic deformation effects 8=35652
- Al-Zn-Mg alloy, hardness changes associated with fatigue-crack propag. 8=26783
- Al-Zn-Mg alloy, propag. rel. to struct. and cycle freq. 8=44542
- Cr surface, cleavage cracks due to spark machining 8=39577
- Cu steel edge cracking in oxidation, Ni prevention mechanism, obs. 8=26811
- MgO, interaction with cleavage steps 8=44591
- MgO, rel. to toughness, effect of water 8=40173
- Ni alloy, high-strength, stage I fatigue crack propag. characts. 8=26839
- Pu rods, microcracks elimination by chill casting and heat treatment 8=31228
- Si-Mn steel, fatigue, initiation and propag., previous austenitic grain size effects 8=44575
- Ti, in methanol vapour, due to stress-corrosion 8=40184
- Ti alloys, stress corrosion 8=27716
- Ti-8Al-Mo-V, in methanol vapour, due to stress-corrosion 8=40184
- WC-Co alloy system, obs. after plastic deformation 8=44606
- W-C-Co system alloys, around Vickers hardness indentation, lapping time effects 8=49063
- Zr, corrosion breakaway region, inelastic behaviour of metal and oxide 8=36576

Cranking model. See Nucleus/theory.

Creation of electron pairs. See Electron pairs.

Creep
- See also Slip.
- alloys, heat resistant, physical parameters, high temp. and high stresses 8=26760

Creep—contd
- in brittle rock, mechanism 8=40111
- carbons and graphites, tensile creep rate stress dependence 8=26792
- ceramics, polycrystalline, rate rel. to porosity 8=35625
- concrete, stress anal. inc. viscoelastic response 8=44536
- contact problems in creep theory 8=41713
- deformation rates, uniaxial testing 8=28266
- fibre reinforced composites, theoretical anal. 8=40110
- gases, rarefied, thermal flow through cylindrical tube 8=25807
- glass-reinforced plastics, in bending 8=31241
- graphite, highly-oriented, high-temp. behaviour 8=35664
- jogged screw dislocation model, used hyperbolic tangent junction 8=48842
- linear, solution by generalized thermoelasticity problems 8=41737
- measuring apparatus for 10^{-7} min^{-1} at 77°K 8=44525
- metal foils, time-to-rupture from creep tests under tensile loads of periodically varying orientation 8=35626
- metals with high stacking-fault energy, high temp. creep, mechanism 8=35622
- metals, equation describing 8=35648
- methane, crystalline, temp. effects 8=40190
- non linear, steadily creeping body, uniqueness theorem 8=46071
- plates, circular, variable thickness 8=37153
- plexiglass 8=31250
- polycarpamide unoriented cryst. film 8=40196
- polycrystalline aggregates, role of grain boundary sliding 8=35621
- polyethylene, highly anisotropic, low density 8=40197
- polyethylene, meas. of tension and torsion 8=40195
- polyethylene unoriented cryst. film 8=40196
- poly(methyl methacrylate), shear and tensile creep compliance rel. to secondary processes, −150–75°C 8=44017
- refractory metals, b. c. c., analysis 8=26759
- rotating disc, varying thickness, analysis 8=35623
- rubber vulcanizates, natural, filled with carbon black, behaviour 8=26860
- rupture characts. of metals on basis of short-term creep data 8=44526
- from seismic wave attenuation obs., transient creep calc. 8=27830
- steady state, model of screw dislocations motion 8=48843
- steel, carbon, at room temperature 8=40160
- steel, stainless, due to n irradiation, 100°C obs. 8=26833
- structural optional design, stationary creep 8=46020
- thermoplastics, torsion meas. apparatus 8=35624
- viscoelastic very early-time props. 8=32773
- Zircaloy-2, rel. to corrosion behaviour 8=26852
- Zircalloy-2, uniaxial in-reactor, rel. to pre-treatment 200–400°C 8=35729
- Zircalloy, in-reactor, rel. to dislocation climb 8=35728
- Zircalloy-2 pressure tubes, in-reactor, rel. to n flux, temp. and stress obs. 8=35733
- Ag, rate at low pressure rel. to annealing in air effect 8=26803
- Ag, void formation during creep 8=31225-6
- Al tubes in cylic torsion rel. to second-order strain increments amplification obs. 8=44541
- Al-$NbAl_3$ dispersion phase alloy, 20-450°C 8=44546
- Au, diffusion creep, abnormal at high temp., rel. to impurity adsorpt. 8=26095
- BeO, and self-diffusion, activation energies correl. 8=44553
- C–Mn steel, under cyclic stress and temp. conds. 8=26822
- 12%Cr-Mo-V-Nb creep-resisting steel, rel. to microstructure 8=44576
- Cu, activation energy of creep, temp. effect 8=26797
- Cu, at 1000°C, rel. to dislocation structure 8=35565
- Cu, commercially pure, tension and torsion creep recovery 8=26805
- Cu, flow stress, effect of impurity and forest dislocations 8=31199
- Cu, pore formation during creep, temp. and stress effects 8=35524
- Cu rate at low pressure rel. to annealing in air effect 8=26803
- Cu, OFHC, distrib. of cavities 8=44401
- Fe-24%Ni-17%Cr-2%Ti, rel. to size of γ' particles of Ni_3Ti phase 8=49002
- Fe–Si alloys, mechanisms 8=40154
- Fe–3%Si, twinned, at 600°C 8=35681
- MgO, curve rel. to compression 8=31221
- MgO(magnesia), high temp., effect of additives 8=40171
- MgO(magnesia), high temp., effect of simultaneous grain gowth 8=41070
- Mg-6 wt.% Zn-0.5 wt.% Zr alloy, diffusional, with low strain rate sensitivity 8=26830
- Mg–Zr alloys, denuded zones form. at grain boundaries 8=26831
- Mo, due to n irradiation, 100°C obs. 8=26833
- Mo, properties at 650–750°C 8=35707
- Nb-Mo alloys, rel. to temp. 8=49038
- Ni, due to n irradiation, 100°C obs. 8=26833
- Ni, near Curie pt., rel. to stacking fault energy 8=35710

Creep—contd
- Ni, void formation during creep 8=31225-6
- Ni, with recrystallization, mechanism 8=48552
- Ni alloys, due to n irradiation, 100°C obs. 8=26833
- Ni based alloys, graphical anal., prediction of relaxation 8=49042
- Pb, activation energy of creep, temp. effect 8=26797
- Pb, at high temp., secondary stages, activation energies and stress depend 8=49043
- PbS crystals, steady-state, stoichiometric defects and foreign atom addition effects 8=40179
- Pd_2MnAl, order rel. to Pd_2MnIn, Pd_2MnSn, Pd_2MnSb (Heusler alloys) 8=31700
- Ti, due to n irradition, 100°C obs. 8=26833
- Ti-8Al-1Mo-IV alloy, creep rupture props. 8=49060
- TiNi, 700-1000°C 8=26849
- Ti-Zr-O alloys, rel. to polymorphic substitution temp. 8=49059
- W, in presence of non-equilib. conc. of kinks 8=26850
- Zr alloys, in-reactor, rel. to dislocation climb 8=35728
- Zr alloys, irrad. creep, yielding creep theory appl. 8=35730
- Zr, rel. to corrosion behaviour 8=26852
- Zr–2.5 at.%Nb, in-reactor and unirrad., and mechanism, 300–400°C 8=35731
- Zr–2.5 wt.%Nb, uniaxial in-reactor, rel. to pre-treatment, 200–400°C 8=35729
- Zr-2.5 wt.%Nb pressure tubes, in-reactor, rel. to n flux, temp. and stress obs. 8=35733

Critical constants, thermal
- acetone, orthobaric data near crit. pt. 8=34956
- benzene, orthobaric data near crit. pt. 8=34956
- chloroform, orthobaric data near crit. pt. 8=34956
- critical density determ., effects of sample config. in earth's field 8=30574
- entropy, communal, influence on liq. state reappearance 8=25976
- expt. obs. 8=34980
- gas critical region, transport coeffs. 8=39229
- hydrocarbon binary mixtures, correlation 8=48250
- liquid-vapour equilib., latticed gas model including thermal expansion 8=34979
- liquid-vapor point, isochoric thermal capacity meas. 8=48266
- metals, superconducting, mixed with anthroquinone, T_c increase 8=27005
- Ornstein-Zernike theory 8=25975
- relaxation phenomena near critical point 8=28317
- transition temp., nonlinear effects 8=23904
- van der Waals gas in critical region, anomalous transport props. 8=30305
- $AlBr_3$, crit. press. 8=43895
- $AlBr_3$, crit. temp. and coexistence curve 8=43894
- Ar, coexistence curve near crit. state 8=47968
- CH_4 and CD_4 8=30588-9
- He^4, pressure-density-temp. surface near critical point 8=37342
- Xe, near-critical isotherms, interferometric determ. 8=25977

Critical mixtures. See Solutions.

Critical opalescence. See Phase transformations; Solutions.

Crowdions. See Crystal imperfections/interstitials.

Cryopumping. See Vacuum pumps; Vacuum technique.

Cryoscopy. See Freezing; Low-temperature production; Low-temperature technique.

Cryostats
- cap, connection to vacuum vessel of dewer, use of elastic vac. connector 8=48003
- continuous flow, for n scatt. expts. 8=49548
- cryopump system, fast, for ultra-high vac. 8=47992
- electrical connections, encapsulation in plastic tape 8=28429
- for electron-diffraction experiments, 300-4.2°K 8=46296
- for e. p. v. spectra at lig. He temp., effect of light 8=24259
- glass immersion, for optical meas. 8=41884
- heat capacity meas., 1°-30°K 8=24033
- high-vacuum valve 8=34689
- horizontal, for polarized p targets 8=24939
- instrumentation leakage current improvement 8=41884
- i.r. detectors, Joule-Thomson coolers 8=32944
- i.r. detectors, Joule-Thomson cooling 8=32947
- liquid He, for X-ray diffractometry 8=48622
- for magneto-optical studies 8=41881
- for Mossbauer expts., demag. cryostat., $\geqslant$ 0.025°K 8=37330
- for specific heat meas. at low temps. by continuous heating method 8=46299
- thermal conductivity, meas. of lattice component in metals and alloys 8=48758
- for paramagnetic absorpt. meas. at 4.2°K 8=24261
- for 2-300°K thermal measurements 8=24032
- He, for use in neutron diffraction studies, 3°-300°K 8=39763
- He, high-voltage coaxial connector 8=28430
- He^3 direct-access design 8=46297
- He^3/He^4 dilution refrigerator for Mössbauer's expts. at 0.03°K 8=41880

Cryotrons. See Superconducting materials and devices.

Crystal chemistry
  alkaline-earth germanates and silicates, rel. to similarities 8=26167
  alums, α and β, morphological difference 8=26173
  bitumen and components, structure and empirical formulae 8=48516
  borate mineral systematology 8=48511
  cadmium chalcogenides, stoichiometry effects on hexagonal or cubic phases formation 8=44082
  charge-transfer complexes, and solid-state spectra 8=26166
  covalent bond theory, anisotropy and quadrupole moments 8=30612
  covalent bond theory, lattice deformation energy calcs. 8=30613
  covalent bond theory, partially ionic binding effects 8=30611
  diamond, valence-bonding rel. to at. vibration spectrum, review 8=43922
  double-layer structures formation, brucite-like layer ions 8=48514
  haematite, vapour-solvent grown 8=26251
  hydrates, thermal dehydration, obs. 8=27689
  lanthanides, compressed polymorphs and intra-alloys, 4f contrib. to bonding rel. to crystal structures 8=26178
  lithium niobate, melt-grown comp. effects on refractive index and second harmonic generation 8=41114
  macromolecular crystals, chemical bonding 8=43923
  minerals, classification based on i.r. spectroscopy 8=39637
  molecular sieve, type A Linde, containing Ni^{2+} ions, spectra rel. to coordination states 8=41143
  norbormide, stereochemistry from X-ray investigations 8=26165
  orthopytoxenes, cation distribution, Mössbauer determ. 8=48324
  salt hydrates, structure of $CuSO_4.3H_2O$ 8=26388
  spinels, cation migration 8=44377
  transition metal cpds with S, Se or Te, non-stoichiometry and ordered structs. 8=26164
  whitlockites 8=39639
  wustite($Fe_{1-y}O$), stoichiometry deviations from composition-oxygen partial pressure diag., thermogravimetric determ. 8=36540
  zeolites, synthetic, containing transition metal ions, spectra rel. to coordination states 8=41143
  zinc chalcogenides, stoichiometry effects on hexagonal or cubic phases formation 8=44082
  $AgCl:Fe^{n+}$, valency state determ. of Fe impurities 8=35550
  $Al_2O_3:Fe^{57}$, cation valence states, changes on ht. treatments, from Mössbauer spectra 8=43943
  $BaO-TiO_2-SiO_2$ glasses, coordination state of TiO_2 8=44078
  $BaTiO_3$, bond-types from appl. of ionic for calc. electro-optical effects 8=41067
  $BaTiO_3$, grown from KF flux, comp. and doping 8=26163
  Bi–Au system, of simple cubic π phases 8=48402
  $CaMnSi_2O_6$, johannsenite 8=44248
  of CaF with $TbF_3.Tb_4O_7$ and TbOF admixtures 8=26168
  $CaF_2-Tb_2O_3(Tb(OF)_3)(TbF_3)$ solid solns. 8=39640
  $Ca_3(PO_4)_2.H_2O$, and mineral whitlockites 8=39639
  CdS_xSe_{1-x} monocrystal, component conc. calc. by dispersion 8=30803
  CdTe, growth process rel. to stoichiometry 8=26243
  CdTe, stoichiometric variations and impurity levels 8=30804
  Ce alkali metal tungstates, hydrothermal synthesis and morphology 8=26259
  $Cu_{0.15}Mn_xFe_{2.5-x}O_{4+\gamma}$ spinels, compensated tetragonal deformation and O nonstoichiometry 8=48380
  Ge, oxygen distrib. coeff. determ. 8=48779
  Co(II) di-n-alkylphosphinates and polymers, prep. and structural props. 8=30797
  CoO(I) and (II), stoichiometry and reactivities 8=26017
  CrO_2, stability at high press. and temp. rel. to decomp. to Cr_2O_3 8=26281
  Cu 55 %- Zn 45% α and β phases comp. and location rel. to grain struct., obs. 8=30688
  $CuMn_2O_4$ spinel, Cu valence state determ. by X-ray absorpt. edge meas. 8=30801
  $CuSO_4.3H_2O$ 8=26388
  Fe in Co cpds, valence states from Mössbauer determ. 8=35034
  $Ga_2(SO_4)_3$, hydrated, n.m.r. evidence of H_3O^+ ions 8=49643
  $K_2Mn(C_2O_4)_2.2H_2O$, data 8=48512
  Li_5GaO_4 and Li_5AlO_4 8=48513
  MgO, effective atomic charges by X-ray method 8=26169
  NaCl, effective atomic charges by X-ray method 8=26169
  NaN_3, thermal decomposition, crystal size effects, topochemistry and gas analysis 8=39701
  Nd alkali metal tungstates, hydrothermal synthesis and morphology 8=26259
  Ni-Co-Cr superalloy sulphidation corrosion layers comp., obs. 8=30806
  Ni 25%-Cr 20%-Nb 0.7% stainless steel precipitates comp. obs. 8=30805
  $PbCa_2Si_3O_9$, margarosanite 8=44248
  Pd_2MnIn, Pd_2MnSn, Pd_2MnSb (Heusler alloys), order rel. to chem. and mag. order in Pd_2MnAl 8=31700
  Pr alkali metal tungstates, hydrothermal synthesis and morphology 8=26259

Crystal chemistry—contd
  PtO_2, synthesis and properties 8=35205
  RhO_2, synthesis and properties 8=35205
  Sb–Au system, of simple cubic π phases 8=48402
  Sb–Ni system, of simple cubic π phases 8=48402
  Sb–Pd system, of simple cubic π phases 8=48402
  $[Si_2O_5]$-layer silicates 8=39641
  $SrTiO_3:Fe^{57}$, iron sites in lattice and valency rel. to oxygen vacancy behaviour, Mossbauer exam. 8=43958
  Ta, zone-refined, purity and structural perfection rel. to growth condition effects 8=35231
  Zn(II) di-n-alkylphosphinates and polymers, prep. and structural props. 8=30797
  $ZnSnP_2$ platelets, prep., stoichiometry, and melting pt. 8=26267
  YFe garnet, hydrothermal and flux-grown, OH groups and Fe valence 8=35206
Crystal classes. See Crystallography; Crystal structure, atomic
Crystal counters. See Counters, crystal.
Crystal electron states
    See also Colour centres.
  absorption and luminescence, co-operative, donor-acceptor mechanisms 8=31942
  acoustic absorption rel. to quasi-local states 8=35399
  acoustoelectric effects, large-signal, rel. to energy losses by hot electrons 8=48717
  alkali halide crystals, M centre, triplet state lifetime 8=26718
  alkali halide monocryst. with blocking electrode, polarization capacity 8=49073
  alkali halides, U centres, isotopic effects in absorpt. bands rel. to electron-phonon interaction 8=27557
  alkali metals, e-phonon interactions, scatt. and transport coeffs., 8=44631
  alkali metals, local pseudopotential form factors calcs. errors on omitting conduction-electron exchange potential 8=44630
  alkaline-silicate, glasses, irradiated, nature of hole centres 8=40218
  alloys, dilute, electronic correlation effect on props. variational treatment 8=26892
  alloys, dilute, Kondo effect, Takano-Ogawa theory exam. and mag. susceptibility calc. 8=44956
  alloy, dilute mag., Green's function theory of Kondo effect 8=31263
  alloy, dil., s-d exchange in neg. magnetoresistivity calcs. 8=40723
  alloys, phonon drag rel. to elec. resist., at low temp. 8=26959
  alloys, stacking fault energy rel. to density of electron states 8=26698
  alloys with paramag. impurities, nonlinear, nonstationary Ginzburg-Landau theory 8=40341
  anthracene, carrier generation and transport under electron bombard 8=49084
  anthracene, current carriers mobilities, temp. depend 8=31396
  anthracene:tetracene, trapping of photo-carriers 8=36030
  antiferromagnet ground state in mag. field of arbitrary direction 8=45045
  antiferromagnetic, cubic, zero-point and excited state energies 8=36199
  aromatic hydrocarbons, triplet factor group states 8=27622
  benzene, isotopic mixed crysts., trap-trap triplet energy transfer 8=36527
  β-B, carrier densities, mobilities and effective mass from elec. meas. 8=35824
  Bloch electron motion in external fields, classical and quantum dynamics 8=26875
  bound electron-neutral impurity states 8=44625
  bound state of conduction electron coupled with localized spin, diagram analysis 8=40230
  Brillouin zone, integrals of product of atomic orbitals and sums of plane waves 8=40207
  carbonyl group, assignment of lowest triplet state 8=25560
  carbonyl $n \rightarrow \pi^*$ transitions 8=27630
  carrier generation and transport in short-range order systems 8=26879
  charge carriers, mixed scatt. by lattice vibs. and ionized impurities 8=49076
  collective bound state due to s-d exchange interaction, closed-form soln. 8=26897
  condenson type in strong mag. field 8=49071
  conduction electrons, effective masses, temp. depend. 8=44637
  core polarization in $4d^n$ and $5d^n$ configs. from e. s. r. data 8=36087
  coronene in cryst. matrices, trapping sites 8=45242
  crystal phosphors, effective recombination cross-section of charged centres 8=26715
  current carrier anisotropic scattering, theory from partial waves method 8=35751
  1, 4-dibromonaphthalene, electronic Zeeman meas. 8=27629
  disordered system, energy spectrum and impurity condition 8=44621
  disordered systems, localized electronic states 8=40205
  distribution functions, steady state, calc. by exploiting stability 8=26880

Crystal electron states
See also Colour centres.
effective mass concept., classical analogy 8=35746
effective mass of f.c.c. transition metals 8=40250
electron distrib. function in strong fields 8=44626
e excitation by ion and atom bombard. 8=26861
electron phonon effective mass renormalization 8=44622
electron-phonon interaction and phonon dispersion relations using augmented-plane-wave method 8=31260
electron-phonon interaction, magnitude and superconductivity 8=35838
electron-phonon mass. correction, calc. 8=44634
electron scattering by ionized impurities, strong degeneracy 8=40216
energy spectra computation methods 8=35762
exchange interaction, magnetic-ions multiplicity effects 8=31254
g-factor of d^3 configuration 8=43962
Fermi-Dirac function, tabulated for integer indices, series expansion 8=33329
ferromagnetic Fermi liquid, phase transition 8=35803
ferromagnetism of itinerant electrons with strong correlations 8=49486
Goldstone theorem for non relativistic systems 8=44623
Goldstone's theorem for non-relativistic systems 8=40208
graphite, electronic structure, optical study 8=31279
graphite, pyrolytic, electron and hole, location from laser magnetoreflection data 8=35757
gravitationally induced elec. fields in conductors form statistical electron model 8=26876
Hall constant, quantum oscillation theory 8=31265
halogenated benzenes, triplet states 8=27625
Hartree-Fock exchange pot. for electron gas adaptation to atoms and solids 8=38617
Heisenberg chain, anisotropic, Bethe hypothesis considerations 8=26869
helical spin ordering, development of theory 8=31309
hot electrons in metal-semiconductor system, diffuse reflection from surface 8=40254
hydrocarbon glasses, electron trapping sites, saturation and removal 8=40082
impedance of thin conducting films in longit. mag. field 8=26955
imperfection model, one-band one-site, improved 8=31019
impurity centre non-adiabatic transitions within band model 8=31053
impurity, optical phonons interaction with electrons in semiconductors 8=44629
impurity pot. scatt., low-temp. anomalies due to s. d interaction 8=49082
interface-charge-limited, current, unipolar, model 8=26871
ionic, conduction electrons ground-state props. Feynman model 8=49116
ionic crysts., point imperfections, electronic processes theory 8=31259
ionic crysts., polarizabilities, covalency contrib. 8=36390
iron phosphate glasses, carriers, thermally activated diffusion 8=49079
Kondo effect, physical perspective 8=26867
laser, electron-beam-pumped, effect of inhomogeneous minority carrier distributions 8=28696
magnetic alloys, dilute, enhanced effective exchange interaction due to localized spins 8=31594
magnetic alloys, dilute, low temp. exchange interactions uniquely defined by logarithmic accuracy 8=31492
magnetic alloys, dilute, singlet-triplet formulation, s-d exchange and Anderson models 8=27369-70
magnetic alloys, dilute, superconductivity below Kondo temp., Nagaoka's model 8=26988
magnetic alloys, dil., with spin-$\frac{1}{2}$ impurities, s-d scatt. theory 8=44980
magnetic exchange interactions, orbital effects 8=31544
magnetic fields, ultra-quantum, kinetic coeffs. theory 8=35737
magnetic semiconductors, spin-disorder scattering of carriers and magnetoresistance 8=27058
magnetic space groups and their irreducible representation 8=31488
magnetic system, e-magnon scattering and polarization of scattered beam 8=35754
many-electron correl. model, quantized form 8=31258
metal, field peak excitation along chain trajectories in mag. field normal to surface 8=44668
metal-metal boundary tunnel current, structure due to electron-phonon interaction 8=26956
metal, monovalent, e-phonon interaction, screening and e. correlation effects 8=49074
metal-semiconductor system (photodiode), hot e-scattering from surface on illumination 8=35752/3
metals, effective mag. field seen by one electron 8=40722
metals, ferromagnetic, electron-phonon scattering contrib. to anomalous magneto-optical effects 8=31949
metals, ferromagnetic, energy spectrum of Fermi excitations
metals, ion bombard. excited deep holes in bounded orbitals, Auger de-excitation time 8=40718

Crystal electron states—contd
metals, localized mag. impurities 8=26865
metals, localized states, survey 8=35741
metals, local-moment-conduction-electron exchange coupling and RKKY spin densities 8=35742
metals, monovalent, interionic potentials 8=35813
metals, simple, screened interionic potential 8=40204
metals, singlet ground state of localized spin, Schrödinger equation solved 8=40223
metals, soft X-ray emission, quantum-mechanical treatment 8=27541
metals, resistivity due to impurities rel. to impurity diffusion 8=30996
metals, stacking fault energy rel. to density of electron states 8=26698
metals, ultrasonic wave propag., quantum theory 8=35407
metals with mag. impurity, ordinary scattering rel. to exchange scattering 8=26863
m. i. m. system, symmetric, tunnel current density distrib. of enery levels 8=40631
mixed disordered systems, optical model 8=39293
MO-LCAO crystal field theory, diagram method 8=43931
Mott eqns and Wiedemann-Franz degree of universality 8=39905
negatively thermally stimulated conductivity, theory and possible obs. 8=40645
noble metals, localized impurity d state splitting 8=26868
non-crystalline systems, metal-insulator transition in random array of centres 8=40206
optic transitions of bound electrons, phonon processes 8=49678
organic mixed crysts., intermolec. triplet decay of luminesc. 8=32070
organic semiconductors, electron-phonon system 8=40425
organic structs. with π-electron chains, elec. cond. mechanism 8=26893
orthodiazines, electronic states and radiationless processes 8=27667
oscillatory effects, rel. to min displacement of valleys in mag. fields 8=49070
paramagnet, spin-phonon excitations, kinematic interaction effects 8=36074
paramagnetic impurity in metal, ground state analysis 8=40200
permalloy, alloying with Mo, Cr, Si and Cu, effect on 3d-electron state 8=35775
photoconductivity due to localized excitation 8=27312
piezoelectric; nonlinear phonon interaction and effect on current saturation 8=31367
polar semiconductors, warm electron temp. and mobility 8=40214-5
polymer, carrier origins and mobilities, and polarization mechanisms 8=26878
polymeric semiconds., band conduction and fluctuations 8=27066
in polyvalent metal defect scatt., rel. to resistivity in Al due to impurities and vacancies 8=49154
positron lifetimes in metal hydrides, bound to H$^-$ unrealistic model 8=40286
positron lifetime, paramagnetic impurity effect 8=29851
pseudopotential form factors, local, in alkali metals, errors on omitting conduction-electron exchange potential 8=44630
pseudo-potentials, analytic props. 8=46788
pyrene in biphenyl, delayed excimer fluoresc. 8=32076
quartz, laser-illuminated, Brillouin scattering component separation and interferometric analysis 8=36408
quantum structure in dielectric function of metals and anomalous prop. modes. 8=31307
quantum theory rel. to structure 8=28934
random impurity vibrational props. Green's-function analysis 8=35546
rare-earth ions electric multipole interactions 8=31255
rare earth ions, magnetoelastic coupling constants, from optical data 8=31229
rare-earth metal oxides, forbidden zone, width 8=35740
rare-earth metals, enhanced effective exchange interaction due to localized spins 8=31594
rare-earth-Pt alloys, conduction-electron polarization from n. m. r. 8=36279
rare gas matrix, photo-induced transfer between impurity atoms of different species 8=40202
real spectral function of electron Green's function, distinction between conduction and core electrons 8=49072
recombination radiation in inorganic solids 8=31953
recombination waves in short-wavelength region, nonlinear theory 8=40210
relativistic and spin effects in uniform elec. and mag. fields 8=44624
ruby, exchange-coupled Cr^{3+} ion pairs, piezo spectroscopic studies 8=27646
$^8S_{7/2}$ ground state splitting, orbit-lattice interaction contrib. 8=40203
semiconducting wire, plasma eqns. soln. 8=35745
semiconductor diode, minority carrier lifetime rel. to impedance 8=33195
semiconductor diodes, charge carrier diffusion induced by X-ray irrad. 8=27164

Crystal electron states—contd
semiconductor, displacive vibronic phase transitions due to electron-phonon iteractions 8=49075
semiconductor, electron-hole complexes form. by light abosrpt. 8=31941
semiconductors, electron-phonon Umklapp process, photoconductive spectral response obs. 8=27315
semiconductors, emission by direct band-band transitions 8=36291
semiconductor, Fano factor, pair creation model 8=46889
semiconductors, homogeneous, microwave mixing by hot electrons 8=27056
semiconductors in strong elec. field, calc. of elec. cond. 8=27075
semiconductors interband transitions in mag. field and strong e.m. wave 8=31261
semiconductors, many-valley, dissipative effects disappearance 8=40427
semiconductors, many-valley, e-phonon inelastic scatt., dissipative effects loss 8=31264
semiconductors, many-valley, indirect exchange interactions 8=36085
semiconductors, microwave methods for meas. of carrier effective mass 8=26898
semiconductor, nonlinear excitation of electrons in strong a.c. field 8=49209
semiconductor, nuclei polarization on e-heating in cyclotron resonance 8=35806
semiconductor, piezoelectric, transport eqns. 8=27061
semiconductor, recombination of free carrier autooscillations 8=49077
semiconductors, SCL currents in presence of donors 8=35870
semiconductor, space-charge layer, minority carrier distrib. 8=40433
semiconductors, spin-e-phonon coupling consts., magneto-optic interband absorpt. meas. 8=27074
semiconductor, thermopower calc. in quantizing mag. field allowing for phonon drag 8=35993
semiconductor, transitions, USSR work over 20 years, development survey 8=35869
semiconductors, transport coeffs. taking into account electron-phonon scattering 8=44751
semiconductors with spheroidal conduction band, optical absorpt. due to donor electrons 8=36293
semimetals, carrier density pressure, dependence, determ. methods 8=40313
semimetals, superfluidity possibility at dielec. transition 8=44627
s-f ferromagnetism dynamic effects of conduction electrons 8=27391
shallow donor ground states in uniaxial crystals 8=31278
singly-ionized-impurity scatt. in degenerate material 8=31262
spin-flip scatt. of conduction electrons from impurities 8=49083
Stark ladder in solids 8=40201
superconductors, Bernoulli pot. var. with elec. field. depends. on band structure 8=40348
superconductors in high fields, zero bias tunnelling cond. 8=26994
superconductors, highly impure, theory 8=43051
superconductors with paramag. impurities, order parameter spatial variations 8=31332
tandem two-photon processes, polarization correl. 8=49692
thin film narrow channel transport, quantum theory 8=26874
tin, white, rel. to de Haas-van Alphen effect 8=31508
Tomonaga model, one-dimensional, ground state momentum distrib. 8=23896
transition at probe ion, vibronic spectra for lattice mechanics obs. 8=39859
transition metal alloys and cpds., transport props. dependence on e-no 8=26872
transition metal carbides, nitrides and oxides, M-M interaction effects 8=26441
transition metals and alloys, mass renormalization, spin fluctuation-induced, rel. to n.m.r. 8=31922
transition metals, ferromag., e.-magnon interaction 8=36178
transport eqns appl. to e-phonon and e.-impurity eqns., 8=49080
triethylammonium:tetracyanoquinodimethan complex, energy gap and cond. 8=27139
tunnelling electrons, interaction with collective modes of the electrodes 8=35943
valence electron model of atoms 8=31257
zero-temp. impurity resistivity, breakdown of conc. expansion 8=31306
Ag, conduction-electron spin resonance obs. 8=31860
Ag, electron–electron scattering from elec. and thermal cond. 8=30987
Ag, thin films, mean free path of conduction electrons rel. to optical absorption 8=36315
Ag halide emulsions, electron trap distribution and low temp. Herschel effect 8=35744
AgBr, photoexcited holes, diffusion rel. to temp. 8=49410
Ag–Mn alloy, conduction-electron-local-moment system, transmission resonance obs. 8=31860

Crystal electron states—contd
Al, e.-momenta from X-ray meas., 8=44647
Al, quantization, transparency thickness depend. oscills. 4.2°K 8=31957
Al, supercond., energy gap determ. from u.s. absorpt. 8=40367
Al, supercond., quasiparticle recomb. time, obs. 8=35847
Al, thermoelec. power phonon-drag and e.-diff. components 8=44904
Al alloys, thermoelec. power phonon-drag and e.-diff. components 8=44904
Al-based dilute alloys, de Haas-van Alphen effect study 8=31494
Al films, superconducting, diffusion of quasiparticles 8=40212
Ar, polarizability of an Ar atom 8=35051
Ar:H(D), solid, isotopic effects in absorpt. bands rel. to electron-phonon interaction 8=27557
As, carrier density change under hydrostatic compression 8=49088
B, e.-momenta from X-ray meas., 8=44647
Be, e.-momenta from X-ray meas., 8=44647
Bi, carrier density pressure dependence 8=40313
Bi, charge-carrier density from galvanomag. data at 4.2°K 8=26963
n and p-Bi_2Te_3, carrier lifetime, conductivity, Hall coeff. 8=40439
Bi-Te-Se semicond., scatt. mechanism 8=40440
CaO, trap depths distrib. rel. to phosphoresc. decay 8=41186
Cd-Pb system, scatt. cross-sections of impurity atoms 8=40315
CdS, carrier recombination kinetics of luminescence and photoconductivity 8=27645
CdS crystals, local centre formation in presence of free electrons and holes 8=36015
CdS, electron-phonon interaction 8=49085
CdS, free carrier conc. changes rel. to neg. photomechanical effect 8=40137
CdS_xSe_{1-x} crystals, electron effective mass 8=35768
CdS_xSe_{1-x}, e-phonon interaction rel. to acoustoelec. effect and ultrasound absorpt. and amplification 8=35410
CdSe(Te), electron-hole generation energy 8=49418
n-$CdSnAs_2$, carrier scatt. by vibs. and impurities, rel. to temp. and impurity conc. 8=31370
CdTe, recombination radiation, evidence for super-radiance 8=31971
CdTe, semi-insulating, transient currents charact. of deep traps 8=40441
CdTe surface barrier detectors, trapping and detrapping 8=46901
Ce^{3+}, in hexagonal cryst. field, electronic Raman scatt. tensor 8=31975
CrFe alloys, 3d-electron redistrib. from X-ray spectra 8=35780
Cs, indirect nuclear interactions, theory 8=43937
Cu layer on Pb, proximity effects in supercond. 8=27015
Cu alloys, dil., ground state of mag. impurity problem, rel. to NMR meas. 8=45116
Cu–Mn alloy, conduction-electron-local-moment system, transmission resonance obs. 8=31860
$Cu_{1-x}Ni_xCr_2O_4$, cooperative Jahn-Teller distortions 8=35052
Cu_2O, compensated, recombination centre cross sections from non-linear photoconductivity 8=40660
$Cu_{2-x}S(0 \leqslant x \leqslant 0.2)$, carrier mobility and conc. 8=49156
Eu^{3+} in crystals, elec.-dipole transitions, symmetry selection rules rel. to i.r. photon amplification 8=42137
Eu-chalcogenide alloys, magnetic and transport phenomena, anomalous 8=31268
$^{151}Eu_3S_4$, electron hopping obs. by Mossbauer spectroscopy 8=30638
F-containing crystals, from NMR data 8=27506
Fe, annihilation of polarized positrons 8=49129
Fe(II) octahedral complexes, $^5T_2$-'A, crossover 8=35038
FeCo alloys, 3d-electron redistrib. from X-ray spectra 8=35780
$FeCr_2O_4$, electronic and mag. props. from Mossbauer spectra 8=31726
Fe_5LiO_8, short range order 8=26866
$Fe_{1-x}Ni_xCr_2O_4$, cooperative Jahn-Teller distortions 8=35052
FeV_2O_4, electronic and mag. props. from Mossbauer spectra 8=31726
in GaAs, activation energies of Cr, Fe and Ni 8=40238
GaAs, current carrier lifetime, effect of heat treatment 8=40449
n-GaAs diodes, electron-hole generation in bulk and at anode contact 8=27180
GaAs, effect of substrate orientation, epitaxially grown crystals 8=39592
GaAs, electron distribution function, velocity-field relationship 8=40450
GaAs, electronic charge transfer 8=31266
GaAs epitaxial compensated, recombination rel. to temp., and band tailing 8=33225
GaAs, mobility rel. to impurity conc. 8=40452
GaAs:Cu, recombination centres, parameters determ. from photoconductivity 8=36020

Crystal electron states—contd
GaP, effective electron mass, anisotropy 8=31290
n-GaSb, oscillations of longitudinal magnetic resistance in degenerate electron gas 8=40466
n-Ge, hot carriers, thermoelectric force 8=40641
p-Ge, hot current carrier noise 8=40457
n-Ge, impurity hop cond., mag. induced spin-reversal transitions 8=31380
Ge, mobility rel. to impurity conc. 8=40452
Ge, n-irrad., recomb. and lifetime reduction processes, two level model 8=27126
n-Ge, phonon-induced electron transitions 8=27100
n-Ge, strained, intervalley transfer and microwave current oscills. 8=26881
Ge, transverse negative differential mobilities for hot electrons and domain formation 8=40453
$GeFe_2O_4$, electronic and mag. props. from Mossbauer spectra 8=31726
Ge, Sb-doped, mobility at high temp. 8=49086
Ge: Zn, Sb, photodielectric effect 8=27322
o-H, f. c. c., elementary excitations, spin-wave treatment 8=26908
Hf diborides, conduction e-parameters calc. based on single zone method 8=35830
HgS_xSe_{1-x}, $O \leqslant x \leqslant 0.4$, e effective mass, optical and elec. obs. 8=40319
HgTe, effective meas. of holes, density of states 8=40242
HgTe, oscillations of longitudinal magnetic resistance in degenerate electron gas 8=40466
In, second band hole surface de Haas van Alphen effect study 8=40226
n-InAs, magnetophonon oscillations in longitudinal thermoelec. power 8=27308
InAs, non-ohmic transport, non-parabolicity effects 8=27115
InAs, space-charge-induced localized state, energy and lifetimes 8=26882
InAs trap level, photocond. obs. 8=27324
InAs-GaAs alloys, impurity levels rel. to comp., photocond. obs. 8=27324
n-$InAs_xSb_{1-x}$ alloys, conduction band electrons, determ. of effective mass 8=36370
InGaAs: (Cr, Zn) trap and acceptor levels, photocond. obs. 8=27324
In_2O_3, sputtered films, electron mobility, temp. dependence 8=40469
In_2S_3, hot electron mobility investigation 8=31381
InSb, carrier waves, growth obs. 8=35908
in n-InSb, conduction, energy transfer to and from acoustic waves 8=39892
n-InSb, donor-cond. band exchange, modulated 0.8-10mm waves 8=49421
n-InSb, e-effective mass pressure dependence from magnetophonon resonance meas. 8=27110
InSb, electron effective mass, pressure effect 8=35772
p-InSb, magnetophonon oscills. in longit. magnetoresistance 8=35904
InSb, non-ohmic transport, non-parabolicity effects 8=27115
InSb type semiconductor, transport phenomena rel. to carrier scattering mechanisms 8=40467
InSb-GaSb alloys, impurity levels rel. to comp., photocond. obs. 8=27324
K, conduction-ESR, 0.5G splitting, theoretical exam. 8=27478
KBr, avalanche breakdown time obs. 8=31421
KBr, avalanche, mobility and lifetime obs. 8=31269
KCl: Ag^+, transitions of impurities, symm. assignment by two-photon-induced emission 8=36494
KCl: Li, tunneling phenomena rel. to impurity-phonon interactions exam. by sp. ht meas. 8=44628
$KMgF_3$, perovskite-type crystals, from NMR data 8=27506
LaF_3, tysonite-type crystals, from NMR data 8=27506
La_2O_3:Bi^{3+}, configuration curves calc. rel. to excitation and emission bandwidths 8=40058
La_3Se_4, rel. to superconductivity 8=27017
Li, calc. using model pot. 8=49103
Li, conduction-ESR g value meas. 8=27482
Li, e. -momenta from X-ray meas.. 8=44647
Li(Ag, Au), Li(In, Tl, Pb, Sb, Bi) system, Zinth phases, valence electron conc. 8=49102
LiF, e.-momenta from X-ray meas. 8=44647
Mg, electronic props. rel. to lattice dynamics 8=48707
Mg, e. -momenta from X-ray meas., 8=44647
Mg phthalocyanine films, barrier height rel. to photoconductivity mechanism 8=40678
MgF_2, rutile-type crystals, from NMR data 8=27506
MgO: Cr, $^{3+}$ (V^{2+}), e.s.r. of excited $^2E(3d^3)$ level 8=27484
$Mn(Mn_xV^{4+}_xV^{3+}_{2-2x})O_4$, $x < 0.68$, rel. to elec. props. and structure 8=35340
Mo bronzes, energy levels 8=40245
Mo, correlation effects in optical props. 8=36392
Na, e. -momenta from X-ray meas., 8=44647
NaCl, carrier mobility temp. dependence, 7.7-200°K, theory 8=44872
Nb–Mo alloys, density of states N(O) rel. to thermal cond. depend. on conc. 8=31292
Ni, alloying with Mo, Cr, Si and Cu, effect on 3d-electron state 8=35775

Crystal electron states—contd
Ni, annihilation of polarized positrons 8=49129
Ni, ferromag. transition temp. pressure-dependence itinerant-electron theory 8=27424
Ni: Cd^{111}, (Ru^{99}), hyperfine fields at solutes from perturbed-angular-correlation exam. above and below T 8=40992
Pb, phonon states, tunnelling and neutron-derived densities, origin of discrepancy 8=26883
PbF_2: Gd^{3+}, excited levels of Gd^{3+} from spectrum 8=36250
PbO polycrystalline, SCL currents and trap distrib. from photoconductivity 8=36024
PbTe, atomlike localized levels in forbidden gap, PbTe-Al_2O_3 junction tunnelling obs. 8=35910
PbTe, augmented-plane-wave calcs. of Knight shift 8=40995
Pd, electronic structure from $L\beta_2$ emission band 8=41129
Pd-xat.%Ni alloys ($x \geqslant O$), s-electron-paramagnon scattering rel. to low temp. elec. resistivity 8=31323-4
Pt, electron–electron scattering from elec. and thermal cond. 8=30987
Pu, cooperative electron transition at 66°K evidence 8=44632
Rb, indirect nuclear interactions, theory 8=43937
Rh:Co, Rh 5s cond. band exchange polarization, n. m. r. obs. 8=36281
Rh–Fe, magnetic impurity, ordinary scattering rel. to exchange scattering 8=26863
Sb, carrier density change under hydrostatic compression 8=49088
Sb, carrier density pressure dependence 8=40313
Sb, phonon drag effects on Nernst-Ettingshausen effect and thermoelec. power 8=40219
Se hexagonal, saturation photocurrent temp. dependence rel. to band structure 8=40673
Se, trigonal, photocurrent decay rel. to hopping recombination 8=36027
Si, carrier density rel. to conductivity after ion irradiation 8=44814
p-Si, elec. fluctuations due to hot electrons, room temp. and liq. N_2 temp. meas. 8=35759
Si films, 1-2μ thick, epitaxially grown on sapphire, carrier transport 8=40489
p-Si, helical density waves and oscillistor-effect in electron-hole-plasma 8=49127
n-Si, hot electrons absorption by surface 8=49260
p-Si inversion layers, mobility anisotropy and piezoresistance 8=27133
Si, mobility rel. to impurity conc. 8=40452
Si, n-irrad., carrier lifetime depend. on excess density 8=27125
Si, n-irrad., carrier removal and annealing, influence of impurities 8=27124
Si, n-irrad., recomb. and lifetime reduction processes, two level model 8=27126
p-Si, phonon drag rel. to magnetothermal effect meas., 100-400°K 8=35912
n-Si, phonon-induced electron transitions 8=27100
Si, radiative recomb. props. 8=36475
Si:Au, emission rates of Au acceptor level, photocurrent determ. 8=40674
Si : Te, carrier density and mobility distributions 8=44817
SiC:N, e. delocalization and e. system degeneracy from NMR 8=45134
Sm^{2+} in crystals, elec.-dipole transitions, symmetry selection rules rel. to i. r. photon amplification 8=42137
Sn, superconducting, helicon-like oscillations in intermediate state 8=44736
$SrTiO_3$, a.c. Hall obs., depend. of Hall mobility on charge-carrier density 8=31392
$SrTiO_3$, electrorefl. oscills. rel. to h. f. free-carrier mass 8=36415
Tb, exchange interactions, from inelastic n. -scattering 8=31709
Tb, exchange interactions and spin-wave spectra 8=31707
Ti diborides, conduction e-parameters calc. based on single zone method 8=35830
TiFe alloys, 3d-electron redistrib. from X-ray spectra 8=35780
Tb-10% Ho, exchange interactions, from inelastic n. -scattering 8=31709
TiNi, electronic transform rel. to phase transform, in irreversible critical range 8=30708
TiO_2-containing-glasses, as charge carrier 8=40499
Tl_2Se, carrier props. from thermoelectric power meas. 8=49396
VFe alloys, 3d-electron redistrib. from X-ray spectra 8=35780
VO, electronic phase transitions 8=26084
VO_2, electronic phase transitions 8=26084
V_2O_3, electronic phase transitions 8=26084
V_2O_5, carrier localized states from e.s.r. 8=40947
(Zn, Cd)(S, Se) :Cu phosphors rel. to photo- and electroluminesc., obs. 8=45293
ZnS, drift -mobilities of electrons and holes 8=40500
ZnS, photodepolarization currents, shallow capture levels rel. to kinetics 8=27332
ZnSb, forbidden band width and hole density 8=44910
ZnTe, hole-traps, Ge- and Pb-associated 8=26884

Crystal electron states—contd
ZnTe:Pb, impurity state, e.p.r. meas. 8=35738
ZnV_2O_4–LiV_2O_4 system, electronic props., V–V separation, i.r. spectra, connection 8=35739
Zr diborides, conduction e-parameters calc. based on single zone method 8=35830
band structure
alkali halides, from e-beam energy losses 8=26937
alloys, dil. disordered, model 8=26890
anisotropic crystals, review 8=35766
anthracene, band gap from electron photoemission threshold energies 8=44640
anthracene, determ. from e-photoemission of alkali-metals into anthracene 8=31283-4-5
anthracene, from photoemission 8=44639
antiferromagnetism relationship 8=36201
antiferromagnets, theory 8=31545
colour centres, aggregate, zero-phonon line obs. 8=40056
conduction in filled bands, correction 8=26888
conductivity, non-linear, second-order, of band electron 8=26885
correlation effect between electrons solved exactly in ID case of one band model 8=40221
determination from intraband and donor-band transitions in high electric fields 8=31281
diamond and zincblende structures, double group full-zone k. p expansions 8=44636
diamond, rel. to interband optical absorpt. 8=40233
diamond semiconductor, isotropic, total single-particle energy calcs. 8=40228
dielectric interband function in electric field 8=27226
in disordered systems 8=35763
elements K to V, "number of d-electrons", rel. to pressure 8=40241
empty lattice test, Kohn–Rostoker method 8=40229
and fermi surfaces 8=49092
ferromagnetic films 8=36117
ferromagnetic films, density of states formulae in band theory generalization 8=31592
ferromagnetic metals, wave functions symmetry in one-electron band theory 8=44990
ferromagnetism, theory, dipolar corrections to magnon energy 8=31539
ferromagnets, theory 8=31545
graphite, trigonal warping, and Hall effect 8=35767
insulator, diamond and zinc-blende structs, and form factors insulator 8=44753
invariant imbedding and band theory 8=49096
ion beams, fast, in matter electronic structure effects 8=44671
ionic and paramag. levels and internal field coupling coeffs., SO(2) algebra 8=39505
iron oxides, valency energy bands from Fe Kβ X-ray spectra 8=41084
Kominga–Kohn–Rostoker theory, extension rel. to impurity problem 8=40227
Kondo effect, truncated Green's function theory 8=31272
localized, one-dimesional model 8=31275
luminescence, solid-state, theory 8=36458
magnetic electronics, localized vs collective descriptions 8=31274
magnetic impurities in metals 8=31270
magnetic impurities in metals, Kondo effect 8=31272
magnetic impurities in metals, scattering problem 8=31271
magnetic, model calculations 8=26894
magnetic ordering, absence in one and two dimensions in many-band model for interacting electrons in a metal 8=44993
magnetized states, local, formation in degenerated bands 8=36063
metals, rel. to charact. props. of mag. moments in strong mag. fields 8=44962
metals, divalent 8=26364
metal, influence on thermal props 8=39904
metals, non-transitional, stacking fault energy correlations 8=44462
metals, paramagnetic, rel. to virtual spin-wave effects 8=31517
metal, three dimensional, periodic distortion 8=49095
metals with impurities, energy spectrum and props., theory 8=35760
M_3X type superconductor, two overlapping bands, n. m. r. study 8=40349
naphthalene, effects of H atoms 8=31291
narrow energy bands, correlation and mag. effects 8=31276
noble metals, energy 8=44642
noble metals, rel. to optical spectra 8=32036
non-closed-shell linear chain of 4n H atoms, low-lying energy levels 8=44644
nonparabolicity effects on light scattering from plasma 8=45152
organic semiconds., energy gap in dark conduction 8=26891
partition function calc., derived from Bloch density matrix 8=35765
perylene molecular crystal, electronic spectra calc. 8=40249
polypeptides 8=35777
quantum theory rel. to structure 8=28934

Crystal electron states—contd
band structure—contd
pyrene molecular crystal, electronic spectra calc. from Davydov decay 8=40248
saddle point optical transitions under crossed elec. and mag. fields 8=27543
semiconductor, diamond and zinc-blende structs, and form factors 8=44753
semiconductors and semimetals, superconducting and insulating mechanisms 8=26886
semiconductors, bandgap depend. and related features of radiation ionization energies 8=27065
semiconductors, isotropic, total single-particle energy calcs. 8=40228
semiconductors, mag., indirect exchange interactions, intervalley transitions effect 8=40768
semiconductors, rel to quantum theory of permittivity of free electrons 8=35761
semiconductors, uniaxially stressed zinc-blende-type, handover levels 8=26889
semiconductors with chalcopyrite structure, features 8=26887
semiconductor, wurtzite type, mag. levels in valence band 8=49094
sphalerite-type crysts., hole bands and dispersion law from many electron approach 8=31273
stacking fault energy correlations in non-transitonal metals 8=44462
superconducting mats., M_3X-type, rel. to spin-lattice relax 8=36257
superconductivity, explanation of occurence 8=31330
superconductor, gap, and e scatt. by paramag. impurities, calc. 8=40211
superconductor with nonmag. impurity and energy bands overlap 8=39901
superconductors, Bernoulli pot. var. with elec. field depends. on band structure 8=40348
symmetry in tight binding approx., consistent treatment 8=31282
tin, gray, Sb-doped, Γ_8^+ conduction band non-parabolicity 8=26911
tin, gray, Γ_8^+ conduction band anisotropy 8=26912
transition metals and alloys, energy spectra by various techniques 8=26913
transition metal dilute alloys, ferro- and paramag., impurity states 8=45005
transition metals, d bands structure dependence 8=44653
transition metals, rel. to ferromag. props. 8=31632
transition metals, rel. to optical spectra 8=32036
transition metals, rel. to orbital susceptibility calc. 8=31529
transition metals, surface tension and cohesion by tight binding method 8=43928
transition metals, theory 8=35781
two-photon spectroscopy theory 8=41025
ultralocalized, pseudopotential method of representation 8=40231
Wannier functions generalized and effective Hamiltonians 8=26895
wide-gap drift mobility meas., spark light source 8=42205
wide band gap, thermal activation energies 8=31277
in X-ray spectra interpretation, 8=41041
zero-slope pts. in Brillouin zone rel. to carrier mobility 8=44633
Ag, self-consistent energy bands by augmented-plane-wave method 8=49097
Ag-In alloys, dil., and interband transitions, from opt. constants 8=49699
AlN, by ultrasoft X-ray spectroscopy 8=36320
AlN, gap determ. from absorpt. coeff. 8=31958
Al_2O_3, by ultrasoft X-ray spectroscopy 8=36320
As, energy bands, galvanomagnetic investigation 8=26902
As, from Azbel'-Kaner cyclotron resonance 8=44684
As, interband transitions from infrared magnetoreflectivity 8=26900
As_2Se_3, amorphous, band structure from ultrasoft X-ray spectroscopy 8=26901
BN, band struct. calc. 8=49098-9
BN, rel. to X-ray spectra interpretation 8=41041
BP, from ultrasoft X-ray spectra 8=41062
Be, calc. from partition function derived from Bloch density matrix 8=35765
Bi, pseudopotential approach 8=26903
CdS, APW method 8=49101
n-CdS, elect. cond., 1.8 to 294°K 8=31369
CdS, trapping level disposition 8=49793
CdS, wurtzite, photoemission study 8=31287
CdSe, wurtzite, photoemission study 8=31287
$CdSe_x(CdTe)_{1-x}$ alloys, forbidden band width comp. dependence 8=36344
CdTe, energy bands, spin-orbit splittings 8=44826
CdTe, including spin-orbit effects 8=44825
CeS films, forbidden band width film-thickness dependence 8=26904
Co, rel. to mag. form factor anisotropy 8=31600
Cr, rel. to antiferromagnetism 8=36201
Cr, rel. to magnetic props. of sinusoidal spin-density waves 8=36206
Cr alloys, rel. to spin-density-wave periodicity conc. dependence 8=36207

Crystal electron states—contd
- **band structure**—contd
  - CsI, mixed-basis calc. 8=44641
  - Cu, from opt. constants uniaxial and hydrostatic strain dependence 8=49724
  - Cu, self-consistent, augmented-plane-wave calcs. 8=44643
  - Cu–Ni alloys, Cu rich, virtual bound state model 8=40236
  - Dy, from positron annihilation studies 8=26906
  - Dy, from relativistic augmented-plane-wave calcs. 8=26905
  - Er, from relativistic augmented-plane-wave calcs. 8=26905
  - Fe, electron spectrum computation using Slater-Koster interpolation method 8=35770
  - Fe, electronic transitions rel. to Fe^{57} isomer shift pressure dependence 8=43950
  - Fe, rel. to ferromag. props. 8=31632
  - Fe, tight-binding calcs. in deduction of mag. props. 8=36145
  - FeCr$_2$S$_4$-CuCr$_2$S$_4$ spinels, rel. to elec. transport props. 8=31373
  - FeSi, from elec. meas., 100–450°K 8=35769
  - GaAs carrier distribution at high temp., band shape effect 8=35749
  - p-, n-GaAs, conduction band density of states from fluorescence at 300 and 77°K 8=32054
  - n-GaAs, e-concs. and conc.-profiles from Faraday effect obs. 8=40239
  - GaAs, from electroreflectance stress dependence 8=49725
  - n-GaAs, high-field transport 8=27097
  - GaAs stimulated emission delays rel. to temp., trapping model 8=33221
  - GaAs$_{1-x}$P$_x$, effect of Te and S donor levels on direct–indirect transition 8=27093
  - GaS, layer compounds, near Fermi level 8=44774
  - n-GaSb, carrier conc. temp. dependence and conduction-band minima 8=49241
  - GaSb, from I-V characts. of tunnel diodes 8=35764
  - GaSb, i.r. absorption and reflection spectra 8=41089
  - n-GaSb:S, (Se), (Te), conduction-, from resistivity-pressure dependence to 50 kbar 8=49236
  - GaSe, layer compounds, near Fermi level 8=44774
  - Gd, from positron annihilation studies 8=26906
  - Gd, from relativistic augmented-plane-wave calcs. 8=26905
  - Ge, amorphous, from elec. and optical meas. 8=44791
  - Ge, Δ_1 conduction-band minimum from high pressure effects on p-n junctions 8=44783
  - Ge energy gap rel. to high uniaxial press. along main axes 8=27102
  - Ge films, amorphous, rel. to electron tunnelling 8=31411
  - Ge, from electroreflectance stress dependence 8=49725
  - n-Ge, rel. to elastic moduli meas. in heavily doped mat., 300–550°K 8=40163
  - p-Ge, transport properties, crystal symmetry rel. to theory 8=26907
  - GeTe, from optical and elec. meas. 8=49726
  - HgSe-βHgS mixed crystal, inverted struct. 8=31320
  - n-HgTe, from Shubnikov-de Haas effect studies 8=27106
  - HgTe–βHgS mixed crystal, inverted struct. 8=31320
  - HgTe-HgSe mixed crystal, inverted struct. 8=31320
  - Ho, from positron annihilation studies 8=26906
  - Ho–Er alloy, from positron annihilation studies 8=26906
  - n-InAs, conduction band structure from reflection spectra 8=35771
  - InAs, nonparabolicity effects on light scattering from plasma 8=45152
  - InAs, parameters at 20, 80 and 298°K 8=40240
  - InAs p-n junction, rel. to radiative recombination mechanism 8=36489
  - InSb, conduction band carrier density, theoretical investigation under carrier multiplication condns. 8=44793
  - InSb, including spin-orbit effects 8=44825
  - InSb, nonparabolicity effects on light scattering from plasma 8=45152
  - InSb, p-type, intraband transitions calc. from cyclotron resonance obs. 8=44796
  - K, magnetoresistance meas., 8=44691
  - KCl, electronic spectra 8=26909
  - KI, from ultrasoft X-ray spectra of iodine rel. to band structure 8=41105
  - KTaO$_3$, from electron-absorpt. meas. 8=32004
  - (La, Sr)CoO$_3$, localized- to collective-electron transition 8=35773
  - Li, electron transition probability from bound to excited states under e-bombardment 8=42043
  - Li, tight-binding method calc. 8=44692
  - Lu, from relativistic augmented-plane-wave calcs. 8=26905
  - Mg-Al alloys, valence electron distrib., investigation 8=44648
  - MgO, optical constants from electronic structure by pseudo-potential calc., 7-28eV 8=27587
  - MgO:Fe^{2+}, low-lying energy level from spin-relax. time meas., 4.2–13°K 8=45086
  - γ-Mn, rel. to antiferromagnetism 8=36201
  - MnO, energy gap at 1100°C 8=40477
  - NaCl, electronic spectra 8=26909

Crystal electron states—contd
- **band structure**—contd
  - NaCl, energy bands, plane wave calc. 8=40224
  - NaCl, pseudopotential calc. 8=41121
  - Nb-Mo alloys, effect on lattice dynamics 8=44303
  - NbSe$_2$, band model calcs. 8=49105
  - Ni ferromagnet, from de Haas-van Alphen effect rel. to electronic structure 8=31698
  - Ni, ferromagnetic, exchange and spin-orbit interactions rel. to mag. breakdown and de Haas-van Alphen effect 8=44649
  - Ni, ferromagnetic, 3d-band, density of states curve 8=40246
  - Ni, rel. to ferromag. props. 8=31632
  - Ni, rel. to low-energy optical transitions 8=35774
  - Ni, rel. to mag. form factor anisotropy 8=31600
  - Ni–Co alloys, f.c.c., from low temp. sp. ht. meas. 8=48739
  - NiMn, rel. to antiferromagnetism 8=36201
  - PbI$_2$, defect energy-levels from photo excitation studies 8=44650
  - Pb$_{1-x}$Sn$_x$Se, of rocksalt struct. 8=43980
  - Pb$_{1-x}$Sn$_x$Te, of rocksalt struct. 8=43980
  - n-PbS, conduction band nonparabolicity 8=35776
  - n-PbS, conduction band structure, 77-300°K 8=27119
  - n-PbSe, conduction band nonparabolicity 8=35776
  - Pb$_{1-x}$ Sn$_x$ Te, two valence band evidence and thermal energy gap 8=44651
  - PbTe, effective mass rel. to carrier density, 77-450°K 8=44804
  - PbTe$_x$Se$_{1-x}$ solid solns., forbidden band width temp. dependence 8=40247
  - Pd, alloys, electronic structure rel. to pure metals 8=31294
  - Pd, photoemission and optical studies 8=31293
  - Pt, alloys, electronic structure rel. to pure metals 8=31294
  - Rh near Fermi level from optical props., 0.4–1.0μm 8=32026
  - Rh–Pd–Ag alloys, density of states 8=35778
  - Sb, from galvanomagnetic effect meas., 50-300°K 8=40330
  - Sb$_2$Se$_3$, energy spectrum of traps from thermally stimulated depolarization meas. 8=40251
  - Sb$_2$Te$_3$, complex valence, from elec. and thermal props. 8=44808
  - Sc, Ti, Y, Zr, La, Hf, La, Ce, X-ray bremsstrahlung isochromats, conduction bandwidth 8=36405
  - Se, trigonal, from electronic spectrum 8=32030
  - Si, Brillouin zone, wave function expansion 8=26910
  - Si, deep energy levels of impurities, model, and capture processes 8=35911
  - Si energy gap rel. to high uniaxial press. along main axes 8=27102
  - Si, from electroreflectance stress dependence 8=49725
  - p-Si, interpenetrating spheroids of rot. symm. rel. to anisotropy in elec. cond. 8=35914
  - Si, LCAO energy bands, empirical third neighbour 8=49106
  - n-Si, semiconductor to metal transition 8=40252
  - Si, total single-particle energy calcs. 8=40228
  - SiC, from ultrasoft X-ray emission spectra 8=41136
  - α-SiC (6H), high-resistivity, doped accidentally 8=35779
  - Si$_3$N$_4$, from ultrasoft X-ray emission spectra 8=41136
  - Sn, dependence on mag. field and film thickness by e-tunnelling 8=27033
  - α-Sn, including spin-orbit effects 8=44825
  - SnTe, from optical and elec. meas. 8=49726
  - p-SnTe, valences, rel. to elec. and thermal props. 8=44652
  - Tb, from positron annihilation studies 8=26906
  - Te$_{70}$Cu$_{25}$Au$_5$ alloy, amorphous, from resistance and thermopower meas., 80-300°K 8=40497
  - VO$_2$, from opt. props. between 0.25 and 5 eV in semiconducting and metallic states 8=49760
  - V$_3$Si, d electrons in conduction band, rel. to absence of paramagnetic n. scattering 8=40754
  - WSe$_2$, band model calcs. 8=49105
  - Xe, and effective masses 8=44646
  - Y, from positron annihilation studies 8=26906
  - Zn$_x$Cd$_{1-x}$S, from optical and elec. props. 8=39696
  - ZnO, valence band symmetry and deform. potentials 8=35782
  - ZnS and similar lattices, rel. to luminescence props. 8=36522
  - ZnS, energy bands, spin-orbit splittings 8=44826
  - ZnSe, energy bands, spin-orbit splittings 8=44826
  - ZnSe, photoelectronic props. in p-type-Cu-activated and n-type-self-activated 8=45296
  - ZnTe, energy bands, spin-orbit splittings 8=44826
  - ZnTe–CdTe, forbidden band width rel. to composition, effective mass of holes 8=40253
- **excitons**
  - absorption spectra, low temp., theory 8=40258
  - alkali halides, theory for crystals with complex band structure 8=49112
  - Anthracene, annihilation prod. blue fluorescence, magnetic field effects 8=41223
  - anthracene, charge carrier generation, exciton–exciton versus exciton-photon interacts. 8=31298
  - anthracene, charge-transfer level, from photocond. and electroluminesc. meas. 8=27254
  - anthracene, exciton-phonon interact 8=41161

Crystal electron states—contd
excitons—contd
anthracene, photo-charge carrier generation, exciton–exciton versus exciton–photon interacts. 8=31298
anthracene, rel. to p n.m.r., anomalies using u.v. and blue light 8=40973
anthracene, singlet exciton-exciton interaction, λ=315-405 nm 8=44658
anthracene, triplet exciton phosphorescence 8=27665
anthracene, Wannier excitons 8=26918
anthracene, X-ray excited 8=27666
benzene, $^1B_{2u}$ state, 4th forbidden factor group component 8=40266
benzene cryst., interactions 8=49114
benzene, electronic and vibr. struct. 8=49115
benzene, exciton splittings 8=27628
benzene, first excited singlet states, expt. determ. 8=31299
benzene, theory of cryst. spectra 8=49772
cone scattering of fast electrons 8=35787
diamond radiative recomb. props. 8=36475
exciton-magnon, magnon-magnon interaction effects on antiferromagnetic spectra 8=40843
insulator, excitonic, mag. fields effects 8=40261
insulators, and plasmons, relation 8=35949
insulators, excitonic in one and two dimens., nonexistence 8=31295
"light excitons", scattering by impurity centres in molecular crystals 8=40265
in linear cryst., containing impurity molecules 8=40259
magneto-optical absorpt. near saddle pts., 8=49694
metal-dielectric boundary, quenching process 8=44657
metal iodide crystals, peak position rel. to lattice parameter 8=49113
molecular crysts., detailed exciton band struct. 8=26919
molecular crystals, dielectric const. and energies 8=49110
molecular crysts., , free exciton diffusion 8=35788
molecular crysts., moment theorems for vibronic exciton spectra 8=41023
Mott, hypersound amplification in semiconductors 8=39888
naphthalene, detailed exciton band struct. 8=26919
naphthalene, first excited singlet states, expt. determ. 8=31299
napththalene, theory of cryst. spectra 8=49772
non-localized of Mott, fast electron scatt. 8=35789
phenazine, singlet–triplet transition in mag. field 8=31296
p-phenylenediamine-chloranil charge-transfer complex mag. excitations 8=31880
phonon-assisted recombination in compound semiconductors 8=44760
in semiconductor electro-absorpt. 8=31297
in semiconductor, interacts., ground state energy and Bose condensation 8=40263
semiconductor photoconductivity, exciton-exciton collision contrib. 8=36000
semiconductor, rel. to magneto-optical absorpt. spectrum in elec. field 8=36305
semiconductors, Mott excitons, attenuation and amplification of hypersound 8=44311
semiconductors, theory for crystals with complex band structure 8=49112
tetracene, charge-transfer level, from photocond. and electroluminesc. meas. 8=27254
triplet excitons, mutual annihilation, mag. field effects 8=42060
triplet, polarization of transitions to mag. substates 8=31296
two-exciton states of rigid-lattice model of molec. cryst. 8=49111
in two-photon spectroscopy in solids, theory 8=41025
Wannier-Mott absorpt. band profile, optical phonons effects 8=36285
BeO dielec. response exciton line splitting, phonon induction, obs. 8=36331
CdS, oscillatory emission 8=41077
CdS particles in glass, absorption with a.c. elect. field modulation, obs. 8=40267
CdS, phonon-assisted recombination 8=44760
CdS, spectral splitting due to e-hole spin interactions 8=26920
CdS, Stark effect of levels 8=36348
CdSe, coherent emission of free excitons 8=31972
CdSe, coherent radiation 8=36343
CdSe, spectral splitting due to e-hole spin interaction 8=26920
CdTe, generation causing photoeffect 8=36010
CdTe, light scatt. by screened single-particle e excitations, obs. 8=36363
CuCl, excitonic molecule 8=31300
Cu_2O, band splitting in light and dark blue series by unidirectional pressure 8=35791
Cu_2O, bond energy change under uniaxial deform. 8=35790
Cu_2O, quadrupole transitions in elec. and mag. fields 8=31984
GaAs, generation causing photoeffect 8=36010
GaAs, light scatt. by screened single-particle e excitations, obs. 8=36363

Crystal electron states—contd
excitons—contd
GaP, exciton absorpt. profile, 77-673° K 8=41087
Ge, generation causing photoeffect 8=36010
Ge, radiative recomb. props. 8=36475
InP, light scatt. by screened single-particle e excitations, obs. 8=36363
KBr, energy loss spectrum 8=44659
KBr, longit. and transverse, optical absorpt. 8=41107
KCl, electronic structure 8=40264
KCl, longit. and transverse, optical absorpt. 8=41107
MgO dielec. response exciton line splitting, phonon induction, obs. 8=36331
RbI:Tl, exciton induced luminesc. in activator centre 8=36506
Si, molecules, binding energy determ. 8=40262
Si, n-irradiated of disordered regions formed 8=35551
α-SiC, -impurity complexes, absorpt. spectra 8=36406
SiC, radiative recomb. props. 8=36475
ZnO, edge luminescence, contrib. 8=27660
ZnO, emission rel. to temp. and uniaxial stress, 4.2°-90°K 8=31301
ZnO, phonon-assisted recombination 8=44760
ZnO, spectral splitting due to e-hole spin interactions 8=26920
ZnS, complexes, spectrum 8=36430
ZnS and similar lattices, rel. to luminescence props. 8=36522
ZnS, spectrum rel. to stacking fault probability 8=49766
Fermi level
alkali metal, photoelec. emission into anthracene 8=31472
alkaline metal, photoelec. emission into anthracene 8=31472
dyes, photosensitive, rel. to work function 8=40687
pyrocarbons, B-doped, rel. to B content and from mag. and elec. props. meas. 8=27084
semiconductors, surface, chem. control, two- and one-equiv. additives 8=35874
zeolites, synthetic, containing transition metal ions, $d^9(d^1)$ and $d^8(d^2)$ configs in D_{3h} symmetry 8=41142
InBi film, with Mn layers on each side, states available at all temp. 8=40372
Si surfaces, n-, p-type and caesiated, from photoelec. emission, 80 and 290°K 8=40495
p-Si, n-irradiated, rel. to dimensions and conductivity of disordered regions temp. dependence 8=35913
Fermi surface
from de Haas–van Alphen effect, inversion scheme 8=40225
ellipsoidal, arbitrarily oriented, e.-transport kinetic coeffs. 8=49089
empty-lattice model, cross-section computation programme 8=40222
and energy bands 8=49092
energy derivative of integral, appl. to diffusion thermoelec. power 8=40220
f.c.c. transition metals, effective mass 8=40250
nonspherical, s-d model 8=26896
planes in space, ang. distrib. determ., applic. of 8=26282
rare-earths, topology thermal deform. rel. to anomalous e props. 8=31280
Ag, effect of lattice parameters change 8=40237
Al crystals, anisotropy rel. to external photoelec. effect 8=40704
Al, direct current size effect meas. rel. to dimensions 8=26899
Al, Fermi momentum pressure dependence, 0-100 kbar, using positron annihilation 8=44635
As, and galvanomagnetic effects, correlation 8=40232
As, pure and Ge doped, de Haas-van Alphen effect 8=49091
Au, effect of lattice parameters change 8=40237
Be, rel. to Knight shift obs. 8=27500
Bi, tilt. 8=49100
Bi-Sb-Pb alloys, and e.-densities rel. to de Haas-van Alphen effect exam. 8=31496
Cr and alloys, rel. to spin density waves 8=36205
Cr alloys, rel. to spin-density-wave periodicity conc. dependence 8=36207
Cr, field-cooled, atteration at onset of antiferromagnetism 8=39891
Cr rel. to magnetic props of sinusoidal spin-density waves 8=36206
Cu, effect of alloying 8=40234
Cu, effect of lattice parameters change 8=40237
Cu, hydrostatic pressure effect, expt. determ. 8=40235
Cu–Al alloys, by positron annihilation 8=31288
Dy, from positron annihilation studies 8=26906
Dy, from relativistic augmented-plane-wave calcs. 8=26905
Er, from relativistic augmented-plane-wave calcs. 8=26905
Fe, from galvanomag. coeffs. and de Haas–van Alphen effect 8=31289
at Ge in electrolyte surface states and radicals, reln. 8=36599
Gd, from Hall effect meas. 8=44690
Gd, from positron annihilation studies 8=26906
Gd, from relativistic augmented-plane-wave calcs. 8=26905
Hg, crystalline, topology, and magnetoresistance 8=26968

Crystal electron states—contd
- **Fermi surface**—contd
  - Ho, from positron annihilation studies 8=26906
  - Ho-Er alloy from positron annihilation studies 8=26906
  - K, effect of Hartree field due to conduction electron 8=40244
  - K, meas. using r.f. size effect 8=44645
  - K, rel. to field-dependent Hall coeff. 8=26969
  - Li, and density of states, using model pot. 8=49103
  - Li, effect of Hartree field due to conduction electron 8=40244
  - Lu, from Hall effect meas. 8=44690
  - Lu, from relativistic augmented-plane-wave calcs. 8=26905
  - Mo, and correlation effects in optical props. 8=36392
  - Mo. size of electron bands 8=49104
  - Na, effect of Hartree field due to conduction electron 8=40244
  - Ni, from galvanomag. coeff. and de Haas-van Alphen effect 8=31289
  - Ni alloys. "sd" bound state occurence by residual electrical resistivity results 8=49168
  - Ni-Al alloys, and Brillouin zones rel. to colour 8=45213
  - Os, monocryst., open net of corrugated cylinders with hexagonal symmetry 8=40327
  - Pb, effective masses of holes, and anisotropy 8=40328
  - Sb: Sn(Te), changes due to level shift, de Haas van Alphen effect 8=49090
  - Sn, model rel. to magnetoresistance meas. 8=27031
  - Tb, from positron annihilation studies 8=26906
  - V_3Si, density of states effect on tetragonal-cubic low temp. transition 8=39568
  - Y, from Hall effect meas. 8=44690
  - Y, from positron annihilation studies 8=26906
  - YAg, density of states rel. to sp. ht meas. 1.3-5°K 8=48740
  - YCu, density of states rel. to sp. ht. meas. 1.3-5°K 8=48740
  - Yb, magnetoresistance 8=40744
- **plasma**
  - Alfvén and helicon waves, excitation by electron beam 8=40278
  - Alfvén wave prod. due to decay instabilities of helicons 8=40277
  - alkali halides, plasmon excitation energies from e-beam energy losses 8=26937
  - alkali metal, u.v. absorbing power, plasmon contrib. 8=31962
  - alkali metals, magnetoplasma modes due to Fermi liquid interactions 8=40271
  - alkali metals, magnetoplasma modes, Fermi liquid effects 8=35798
  - avalanche semiconductor, hole wave instabilities under mag. fields 8=35797
  - cylindrical electron-hole, behaviour in mag. field with transverse component 8=35799
  - degenerate semiconductors, strong quantum damping of helicons 8=49121
  - electron absorpt. due to plasmon excitation 8=35795
  - electron beams, diffracting, abnormal absorptions by plasmons 8=44662
  - electron-gas, almost-degenerate, corrections for Grüneisen coeff. and sp. ht., 8=39908
  - e.m. wave dispersion and amplification conditions 8=40280
  - e.m. waves excitation, negative I–V characts. 8=35800
  - exchange and dielec. screening function 8=44664
  - films, excitation by e.m. waves 8=40272
  - finite amplitude resistive drift waves 8=40274
  - fluctuations in external electric field 8=40279
  - foil, metal, optical transmission rel. to resonance 8=27531
  - graphite, anisotropy of oscillations 8=26929
  - Gunn effect, domain dynamics 8=40273
  - helicon propagation, band theory 8=35793
  - insulators, plasmons and excitons, relation 8=35949
  - in Josephson tunnel junctions, reson., obs. 8=35858
  - light scattering, band nonparabolicity effects 8=45152
  - metals, galvanomagnetic studies by heliconlike waves 8=26961
  - metals, helicon wave propag., mode struct. for resonances 8=44663
  - metals, h.f. wave propag., Fermi-liquid effects 8=49120
  - metals, zero-point energy, exchange and correl. contrib. 8=26922
  - nonequilibrium, in InSb, magnetoconductance 8=44667
  - oscillation damping due to e-phonon interaction 8=35792
  - oscillations in external elec. field 8=35801
  - oscillator effect in Ge 8=49245
  - plasmons and zeroth sound in electron gas 8=44665
  - plasmons in metal spheres, e. bombardment stimulation and radiative decay 8=45145
  - review 8=49122
  - in semiconductor detectors 8=46892
  - semiconductor, e.m.wave amplification, carrier diffusion effects for neg. I–V charact. 8=26923
  - semiconductor electron-hole, l.f. drift instability 8=40430
  - semiconductor, non-linear optical props. in elec. field 8=31930

Crystal electron states—contd
- **plasma**—contd
  - semiconductor, oscs., in stationary elec. field and induced current 8=40276
  - semiconductor, overheating instability in crossed elec. and mag. fields 8=40421
  - semiconductor, soft mode near Gunn instability 8=31365
  - semiconductors, electron-hole type, prod. and instabilities 8=27108
  - semiconductors, ion, coupled lattice, plasmic and e.m. waves 8=31304
  - semiconductors, waves, energy depend. mobility in small-signal anal. 8=26924
  - semimetals, stress modulated Alfven waves to meas. piezogalvanomagnetic effects 8=49147
  - solid drifted, oscillation freq. of transverse waves 8=20270
  - solid drifted, oscillation freq. of transverse waves 8=35796
  - solids, optical resonance., review 8=49123
  - streaming carriers in solids, collisions effects 8=26873
  - surface oscs., and inelastic electron scatt., as tool in surface exam. 8=26926
  - surface, plasma reson. emission, light or electron irrad. 8=35802
  - synchrotron instability of system of relativistic electrons 8=39133
  - tin, white, helicon propagation, mag. breakdown effects 8=26932
  - Ag films, excitation of surface oscillations 8=35804
  - Ag foil, resonance radiation peak obs. 8=26927
  - Ag. surface plasmon excitation rel. to light absorpt. 8=49700
  - Ag-In alloys, dil., oscills from opt. constants, rel. to alloying effects 8=49699
  - Al film irradiated by synchrotron radiation near plasma wavelength, effect on photocurrent 8=27550
  - Al, helicon-wave resonances in Hall coeff. determ. rel. to surface-mode loss 8=44682
  - Al, radiation from tangential surface plasmons due to 50 keV electrons 8=40281
  - Al thin films, transmission and reflection of synchrotron radiation near plasma wavelength 8=27549
  - Al-Mg, plasmon losses 8=44666
  - Be, $1/\epsilon$ resonance rel. to far u.v. reflectance 8=49709
  - Bi, Alfvén wave propag., second harmonic generation obs. 8=40282
  - Bi, magnetoplasma waves, cyclotron damping due to mode mixing 8=31308
  - Bi, magnetoplasma waves. u.h.f., propag. vel. 8=49124
  - Bi, mobile, self-induction 8=26928
  - Bi: Te, helicon propag., second harmonic generation obs. 8=40282
  - Cu rel. to e energy loss spectra, 30–350 eV 8=35809
  - GaAs, reson. on non-equilib. carriers, refl. obs., 10.6μ 8=40454
  - GaAs, soft plasma mode 8=40451
  - n-Ge, electron-hole, helical surface waves and oscillator effect 8=27103
  - Ge, reson. on non-equilib. carriers, refl. obs., 10.6μ 8=40454
  - In, helicon-wave resonances in Hall coeff. determ. rel. to surface-mode loss 8=44682
  - In, surface impedance in mag. field perp. to surface of metal 8=49125
  - InAs, light scattering, band nonparabolicity effects 8=45152
  - InSb, coherent emission prod. mag. field, obs. 8=32001
  - InSb, impact ionization rates and instabilities, effect of mag. fields 8=31303
  - InSb, input ionization, avalanche plasma prod., and instabilities 8=35794
  - InSb, l.f. instability in weak mag. fields. 8=49126
  - InSb, light scattering, band nonparabolicity effects 8=45152
  - InSb, microwave emission from nonequilib. plasmas in mag. fields 8=40476
  - InSb, microwave instabilities, theory 8=26930
  - InSb, nonequilib., prod., instabilities and decay 8=27108
  - K, helicon-wave resonances in Hall coeff. determ. rel. to surface-mode loss 8=44682
  - MgF_2, plasmon and interband transition excitation on e-bombardment 8=26931
  - Na, helicon-wave resonances in Hall coeff. determ. rel. to surface-mode loss 8=44682
  - p-Si electron-hole-plasma, helical density waves and oscillistor-effect 8=49127
  - Si, reson. on non-equilib. carriers, refl. obs., 10.6μ 8=40454
- **polarons**
  - in anisotropic energy bands 8=49118
  - colour centre with electron-excess, model, appl. to U_2 centre 8=40061
  - electronic polaron analogy, shallow impurity states, theory 8=40008
  - energy spectrum calc. in magnetic field using Onsager's method 8=31302
  - excitation on light absorption 8=27530
  - excitation on light absorpt. 8=49679
  - Feynman model evaluation 8=26921

Crystal electron states—contd
polarons—contd
Feynman model. rel. to ground-state props. of conduction electrons in ionic crystals 8=49116
impurity hopping conduction 8=49119
intermediate-coupling, ground-state energy upper and lower bounds 8=49117
jump to adjacent lattice site, high temp. probability, anal. of formula 8=40269
in lattice vibrations, effect of small radius polaron 8=39863
in magnetic field, energy spectrum 8=40268
mass change effects due to magnetic field and nonparabolicity of conduction band 8=31302
in metals, polaritons 8=44660
piezoelectric, cyclotron resonance calcs. in quantum limit 8=40283
polaritons, rel. to Raman scattering 8=41032
rutile (TiO_2) crystals, doped, rel. to optical absorpt. 8=36418
$BaTiO_3$:1 at % La, rel. to thermoelec. and i. r. refl., model 8=35878
in CdF_2, effects and transitions 8=44765
CdTe, effect enhancement in magnetophonon resist. oscillations 8=44661
CdTe, mass change effects due to magnetic field and nonparabolicity of conduction band 8=31302
F-centre in ionic crystals, semi-continuum polaron models 8=31110
GaAs, mass change effects due to magnetic field and nonparabolicity of conduction band 8=31302
InSb, effect on magneto-optics 8=49729
InSb, resonant-polaron-coupling from cyclotron resonance and magneto-optical exam. 8=40270
$SrTiO_3$, in anisotropic energy bands 8=49118
TiO_2, conductivity, i.r. absorption 8=40498
surface
additional pot., classification 8=31275
deformed crystals, by tight-binding approx. 8=40256
finite linear, nature of TAMM states 8=49107
graphite, structure by Auger spectra 8=44656
growing surface waves in semicond. in presence of transverse mag. field 8=35868
ionic bonded crystals, intrinsic and extrinsic states 8=35786
junction impurity, localized states var. determ. 8=49108
Kronig-Penney model of semi-infinite cryst. 8=49109
magnetic level transitions obs. in surface impedance meas. geom. modifications effects 8=44655
metal, radio frequency size effect for drift motion of electron 8=44638
microwave impedance, quantum spectroscopy 8=26914
mixed crysals, deformed AB-type, mol. orbital calc. 8=35784
one-dimensional Mathieu potential with arbitary termination, ionic, covalent and metallic states 8=44654
plasma oscs., and inelastic electron scatt., as tool in surface exam. 8=26926
proton channeling investigation technique 8=31286
semiconductor, band bendings rel. to photocond. 8=40646
semiconductors, chem. control, two- and one-equiv. additives 8=35874
semiconductor, generation of nonequilib. carriers rel. to impedance and field-effect theory 8=26915
semiconductors, intrinsic surface-state distribs. model 8=35785
semiconductor, narrow channel transport quantum theory 8=46874
semiconductor, recombination vel., determ. by photomag. effect 8=40434
semiconductor surface state calcs. using pseudopotential method 8=35783
surface states calc., model of crystal potential 8=40255
tunnel junction, plasmon interaction with Josephon current 8=27048
Ag, plasmon excitation rel. to light absorpt. 8=49700
Au single-crystal films, from proton channeling 8=31286
CdSe, surface enhancement by SiO_2 8=49232
n-GaAs, barrier, trap density and mobility 8=35144
GaAs, interact. with induced carriers, rel. to field effect in depletion layers 8=35867
GaAs laser, electron-beam pumped, nonradiative surface recombination 8=49226
Ge, cleaved, valency band from conductivity meas. 8=40455
Ge, electronic states, effect of metal impurities 8=40257
Ge, shallow impurity states 8=44810
NaCl-type, ionic crystal, energy loss of electron beam due to surface optical mode 8=44871
In, impedance in mag. field perp. to surface of metal 8=49125
InSb, electronic configuration 8=26916
InSb films, photoconductivity and field effect 8=27326
Si, carrier motion in surface band, $^1/f$ noise 8=40213
Si, from e.p.r. meas. of clean single-crystal cleavage faces 8=40943
p-Si, Landau levels in surface quantization capacitance obs. 8=40492
Si, n-, p-type and caesiated, rel. to Fermi level, from photoelec. emission, 80 and 290°K 8=40495

Crystal electron states—contd
surface—contd
Si, recombination rates, effects of Co^{60} γ-irrad. 8=27120
Si, shallow impurity states 8=44810
Si, thermally oxidized, majority carrier surface mobilities 8=31390
Si, transport props. of electrons in inverted surfaces 8=31388
Si-SiO_2 fast interface state meas. from MOS-C(V) curves at 77°K 8=49320
TlI, adsorbed organic mols. charge-transfer groups form., obs. 8=36028
ZnO, charge and e. multiplication 8=49354
Crystal energy. See Bonds; Crystals; Solids/structure.
Crystal fields. See Crystals/internal fields.
Crystal imperfections
See also Colour centres.
absorption and luminescence, co-operative, donor-acceptor, mechanisms 8=31942
aggregate defect centres, Mollwo-Ivey relation 8=31032
alkali halide crystal phosphors, F centers interaction with microdefects 8=31123
alkali halide crystals, influence on luminescence relaxation process 8=36472
alkali halides, dissolution of precipitates cont. impurities, and Schottky defect form. 8=35536
alkali halides, gas inclusions, migration, elec. field effect 8=39966
alkali halides, impurities, effect on F-centre production 8=35582
alkali halides, lattice dynamics of imperfect crysts. 8=48701
alkali halides, point defects, interactions 8=31030
alkali halides, reorientation time of O_2^- impurities 8=48822
alkali halides, Schottky defects, their creation, interaction and migration 8=44407
alkali halides with H^- defects, multiphonon absorption 8=48703
alloys, containing precipitates, interaction, critical resolved shear stress calc. 8=40105
alloys, rel. to strain excitation from exo-emission meas. 8=44938
alloys, self-diffusion mechanism rel. to defect densities 8=26615
alloys, stacking fault energy rel. to density of electron states 8=26698
alumina-chromia alloys, twist boundaries 8=44463
amino acids, γ-irradiated, e.s.r. and optical spectral investigation of defects 8=26634
anthracene, α-radiation damage studied by etching in benzene 8=48826
barrier hardening, dispersed, temp. depend. 8=26631
b.c.c. lattice, interstitial sites in stacking faults, solubility theory 8=35543
b.c.c. crystals, stacking faults and dislocations rel. to slip asymmetry 8=44458
b.c.c. stacking fault energies 8=31095
benzophenone, rel. to luminescence at 77°K 8=41224
α-brass, stacking fault energy rel. to wire texture variation 8=40048
β-brass, quenching effects 8=48595
calcic amphiboles, unit-cell volume and packing density, isotypic replacement effects 8=26372
calcite, e.s.r. of Y^{3+}-stabilized CO_3^{3-} mol.-ion 8=49620
cavitation-induced damage, microscope study of first stages 8=31023
ceramic reactor materials, radiation prod., and defect cluster growth 8=31129
ceramics, point defects, techs. for study and interpret., review 8=35519
channelling obs. technique 8=48578
charged-defect-induced i.r. absorpt. in ionic crystals 8=41026
corundum, heat-treated, surface defects., e-diffr. exam. 8=31054
corundum, synthetic, structure defects distribution 8=35554
defect concentrations, variation rel. to recovery spectra 8=48799
defect production and morphology rel. to growth conditions 8=39661
diamond, synthetic, nitrogen impurity effects on crystal habit 8=48521
dl-alanine, primary defects by $\bar{\gamma}$-irradiation, optical annealing investigation by e.s.r. 8=44400
cristobalite, stacking fault conc. calc. from X-ray diffr. line profiles 8=26703
defect formation by electron excitation from subsystem 8=35517
defect motion, rate formula including quantum effects 8=35516
defects symmetry props. from zero-phonon lines stress spectroscopy 8=35520
deformation twinning crystallography, theory 8=26705
diamond, damaged layer exam. on bombardment with Li^7, B^{11}, P^{31} ions, 20-120 keV 8=35601
diamond, random distribution, X-ray scattering 8=40016

Crystal imperfections—contd
- diffraction contrast, dynamical theory approximations 8=31020
- diphenyl, void formation process kinetics 8=26709
- domain structure in imperfect crystals 8=35573
- extended defects. rel. to singularities in phonon spectra, determ. by n. scattering 8=39865
- f.c.c., line defects and plane defects, energies and atomic configurations 8=31072
- f. c. c. metals, stacking fault energy determ. from anisotropic elasticity theory 8=26700
- f.c.c., stacking faults and partial dislocation, computer simulation of spherical surfaces 8=48865
- ferromagnets with plane defects, spin system spectrum and h.f. props. 8=44986
- ferrite, doublet defects, diffuse x-ray scattering 8=39996
- felspars, X-irradiated, structure defects, e. p. r. and thermoluminescence exam. 8=26710
- ferromagnet with non-magnetic impurities, local magnetization of neighbouring ions 8=36105
- ferrous oxalate and isotypic cpds, OD-structure from Guinier patterns 8=26534
- films, vacuum-deposited, structural defects and growth mechanisms 8=35156
- gas and crystal system with isotopic defects, thermodynamic equilib. 8=48293
- generation peaks, double-kink, relaxation strength 8=31062
- glasses, Ag atom impurity stabilization by X-rays, and e. p. r. spectra 8=31114
- glasses, borated, lattice defects, e.p.r. study 8=26628
- grain boundary cavities, effect on vacancy diffusion 8=44406
- grain boundary sliding, role in high temp. creep of polycryst. mats. 8=35621
- graphite, adsorbed impurity effects on growth, scanning-e-microscope obs. 8=26236
- graphite, lattice defect energies, extended Huckel theory calc. 8=31021
- graphite, 'pinning' defects after neutron irrad., rel. to shear compliance 8=35665
- grinding effects using vibro-grinder, X-ray diffr. and e-microscope exam. 8=26286
- haematite, vapour-solvent grown 8=26251
- ice, 1h and 1c, orientationally-disordered, far i. r. spectra 8=27574
- ice, submicroscopic gaseous inclusions, nuclei for Tyndall figures 8=30579
- ice, void formation during non-basal glide under tension 8=44402
- ice with HCl impurity, dielec. props. 8=31420
- impurities, ionized, mixed scatt. of charged carriers with lattice obs. 8=49076
- impurities, one-dimensional model 8=31275
- impurity atoms, location using charact. X-ray generation by channelled protons 8=40009
- impurity centre non-adiabatic transitions within band model 8=31053
- impurity centre orientation in cubic crystals, from magneto-optical rotation 8=45159
- impurity centres, e.p.r. spectra, effect of applied elec. field 8=45070
- impurity centres, two-e correlation, in model pot. approx. rel. to luminescence 8=32049
- impurity centres, Urbach's rule theory 8=35548
- impurity distribution anisotropy in growth 8=26207
- impurity-doped, nonlinear polarization 8=31948
- impurity heterogeneities from multiple-beam interferometry 8=48821
- impurity i.r. absorpt., reln between vib. of defect mol. and resonant mode 8=49680
- impurity molecules, effect on exciton states 8=40259
- impurity, paramag., e spin-lattice relax 8=31842
- impurity segregation induced by cellular convection, effect on crystal growth 8=43753
- impurity states, line broadening by resonant phonon interactions 8=41027
- inclusions, spherical in anisotropic solid, effect on elastic field 8=48938
- interaction with inhomogeneities 8=40023
- ion channelling obs. technique 8=49132
- ionic crystals, inert-gas diffusion as probe for defects 8=39992
- ionic crysts., point imperfections, electronic processes theory 8=31259
- ionic crysts., reacts. between defects 8=26633
- ionized impurities, scattering of electrons, strong degeneracy 8=40216
- lattice defects and their interactions, book 8=31022
- lattice defect energies, extended Hückel theory calc. 8=31021
- lattice with substitutional impurity, generalized Wannier and Bloch functions 8=48606
- lattices, 3-dim., line defects 8=48845
- layer-type, vapour-deposited, stacking fault obs. by e-diffr. 8=26699
- leucosapphire, effect of γ-radiation on optical props. 8=41054

Crystal imperfections—contd
- line defect, rel. to scattering of lattice waves 8=40019
- localized impurity states, Kominga-Kohn-Rostoker theory extension 8=40227
- many-impurity problems, self-consistent soln. of Dyson eqn. 8=31051
- martensite, doublet defects, diffuse x-ray scattering 8=39996
- metal mosaic block size and disorientation changes on crystallization 8=40051
- in metallic crystals, esp. impurities, methods of investigation 8=26629
- metals, impurity diffusion rel. to elec. resistivity due to impurities 8=30996
- metals, non-transitional, stacking fault energy rel. to electronic structure 8=44462
- metals, self-diffusion mechanism rel. to defect densities 8=26615
- metals stacking fault energy rel. to density of electron states 8=26698
- mica cleavage surfaces, fission-fragment tracks and dislocation-type defects 8=26693
- mica, knick-band indexing using the X-ray universal stage 8=26714
- mica sheets, thin, fission-fragment tracks, kinetics of healing 8=40055
- model, one-band one-site, improved 8=31019
- motion of concentrated defects in elastic media 8=39993
- ordered Fe$_3$Al type domains, characterization of Fe-Al alloy "K-state" 8=48597
- oxides: CdO, CaO, MnO, NiO, rel to particle size 8=48592
- paraelastic and paraelectric defect systems in solids 8=48798
- paramagnetic impurities, electron scattering, analytic structure solution 8=40748
- permalloy films, S-produced defects and annealing effects 8=31222
- phonon spectrum singularities rel. to extended defects 8=39864
- with planar defect, vibrational spectrum 8=30930
- planar defect, X-ray dynamical contrasts 8=31094
- point and line, continum theory 8=48952
- point defect interaction, allowing for spatial distrib. 8=35522
- point defect motion, linear eqns. 8=35521
- point defect scatt. of anisotropic current carriers 8=35751
- point defects, anelasticity and internal friction, thermodynamics 8=31027
- point defects, diffusion, appl. of anelasticity 8=31127
- point defects formed in Cu by α-irrad., pinning of dislocations 8=39995
- point defects, in isotropic and cubic media theory 8=48800
- point defects in metals, migration. 8=48801
- point defects in non-metallic solids, conference 8=31029
- pores, hydrostatic pressure influence 8=35635
- polyethylene, crystallized, lattice defects and crystallite size 8=39990
- polytype structure, stacking sequence determ., calc. method 8=26172
- powders, ultramicrotomed, fault structures rel. to X-ray peak profiles 8=48585
- production by mechanical pressure rel. to crystalline structure 8=26658
- quartz, γ-induced, obs. by thermoluminesc. 8=49812
- quartz, knick-band indexing using the X-ray universal stage 8=26714
- quartz, natural and synthetic, fault-surfaces from X-ray exam. 8=26707
- quartz, natural, structural defects, delineation by selective etching 8=44428
- quartz, synthetic, Al impurity capture during crystal growth, supersaturation and temp. effects 8=44424
- quasi-local states rel. to acoustic absorpt. 8=35399
- radiation field perturbation by local inhomogeneity, calcs. 8=45146
- random impurity vibrational props., Green's-function analysis 8=35546
- resonance scattering of carriers by point defects, absorption coeff. due to interband transitions 8=45148
- ruby, effect of γ-radiation on optical props. 8=41054
- ruby, influence on radiation characts. of laser 8=42105
- ruby, synthetic, Cr nonuniform distribution, causes 8=40011
- Scheelite-type: Pr^{3+} activated, charge compensation mechanisms 8=35028
- semiconductors, defects due to ion beams, annealing 8=48892
- shallow impurity states, interactions with phonons 8=40008
- silicon bronze, with low stacking fault energy, shock loading effects on lattice 8=31098
- solid solns., slow neutron scatt. cross-sections 8=35379
- solids, impurity bands, optical absorpt., method of moments 8=41028
- spin resonance line shapes, broadening by point defects 8=49589
- stacking fault, contrast on X-ray topographs 8=35574

Crystal imperfections—contd
stacking fault energy derivation from X-ray diffr. analysis, temp. effects 8=31093
stacking fault energy rel. to electronic structure in non-transitional metals 8=44462
stacking faults and partial dislocations, rel. to contrast in field-ion microscope 8=31092
stainless austenitic steel, stacking fault energies, compositional effects 8=40157
steel, high-carbon, martensite defect structure from e microscope exam. 8=35272
steel, porous castings, effect of H, compared with wrought steel 8=30663
steels, strain-aged, discontinuous yielding grain-size dependence 8=26809
strict bounds for out-of-band freqs. due to impurities and defects 8=26571
substrate defect structure effect on crystal deposition process 8=26280
superconductor with mag. impurity, appearance of local bound states 8=44710
superconducting surface nucleation fields, influence of planar defects 8=35834
superstructure, rel. to work-hardening 8=44527
surface impurity formation on narrow e-beam irradiation, mechanism 8=40010
thermal light scattering by defects 8=41034
transition metal carbides, nitrides and oxides, rel. to M-M interaction 8=26441
transition metals, stacking fault energies on $\{111\}$ in b.c.c. lattice 8=48870
triglycine sulphate defect and domain structs. in ferroelec. and paraelec. phases, obs. 8=31031
triglycine sulphate, interaction of defect and domain structures in ferro- and para-electric states 8=40620
triglycinesulphate, primary defects by γ-irradiation, optical annealing investigation by e.s.r. 8=44400
ultrasonic absorpt. depend 8=48715
ultrasonic spectroscopy determ. 8=23964
X-ray defectmeter with Sb_2Se_3 detectors, construction and appls. 8=39989
X-ray topograph, rel. to contrast 8=48618
Zircaloy-2, white spotting in oxide films, structural effect 8=35187
Ag films, thermal behaviour of stacking faults 8=40047
Ag, stacking fault energies 8=31097
Ag, void formation during creep 8=31225-6
Ag-Au-Ag layers, planar defects, dechannelling of 40 kV Au ions 8=35599
AgBr cryst, reacts between defects 8=26633
AgBr cryst/soln. phase, self defect points at cryst. surface 8=34959
AgCl, point-defect aggregates effect on thermal conductivity rel. to phonon scattering 8=30986
AgCl, structural defects in slip-lines during fatigue 8=48827
AgCl:Fe^{n+}, valency state determ. of Fe impurities 8=35550
AgCl:V, optical absorpt. and ionic cond. meas. on V ions 8=35523
ζ-AgSb, stacking fault probab., X-ray obs. 8=26704
Al, defect structure on thermomechanical treatment 8=35672
Al, electron irradiated, elec. resist. recovery rel. to lattice defects 8=31147
Al, electron irradiation hardening, rel. to point defect props. 8=31141
Al, impurities in elec. resistivity rel. to band structure effects in defect scatt. in polyvalent metals 8=49154
Al, recovery, models and stage III mobile defects nature 8=39991
Al, shock deformation, prod. of point defects 8=44399
Al, slip band continuity across grain boundaries 8=31090
Al-Be 0.1%, clustering 8=44425
Al-Cu alloy, grain boundary precip. 8=26708
Al-Cu: MgSi, increase in ageing rate due to two impurity assoc. 8=35089
Al-Ge solid solns., stacking faults in precip. particles and elastic stresses 8=31096
Al-In alloys, dilute, electron microscope observations 8=35265
Al_2O_3, n-irrad., defects. rel. to macroscopic and lattice growth 8=26234
Al_2O_3:Fe^{57}, iron clustering and cation valence states on ht. treatment, from Mössbauer spectra 8=43943
Al-Zn alloys, clustering kinetics rel. to quenched-in vacancies 8=48807
Al-Zn 10% alloy, point defects existing clustering, nature 8=48802
Al-3.5% Zn, precipitate particles, effects on dislocation activation lengths 8=48851
As, etch pit studies on cryst. grown from vapour 8=44119
Au films on amorphous substrate, grain boundary effects on elastic deform. and residual resistivity 8=44551
Au microcrystals, rel. to growth 8=39666
Au, quenched, activation energy spectrum, effect of impurity atoms 8=31052
Au, quenched, black spot defects, nature 8=44465
Au, quenched, stacking fault tetrahedra nucleation and growth, obs. 8=48866

Crystal imperfections—contd
Au, stacking fault energies 8=31097
Au, stacking fault tetrahedra, stability and growth, effect of multiple quenching 8=44464
Au-Cd alloys, hexagonal, stacking faults 8=26701
Au-Pt alloy, dil., impurity-vacancy interaction from quenching resistance 8=48805
$Ba(N_3)_2$, u.v. irrad. cryst. e.s.r. of N_2^- 8=27485
$BaTiO_3$ (001) face, linear disorder on heating in u.h. vacuum 8=39649
BeO, n-irrad., defects rel. to macroscopic and lattice growth 8=26234
BeO polycrystals, grains, subgrains and stress analyses 8=26291
BeO, random distribution, X-ray scattering 8=40016
Bi, impurity rel. to anomalous longit. magnetoresist. 8=40728
Ca-Bi-V-ferrite, from U^{235} fission fragment irrad., effect on ferromag. resonance 8=36225
CaF_2, defect energies, Born model calc. 8=40004
CaF_2, GdF_3, pt. defect production of volume and density changes 8=44559
$CaWO_4$, defect sites identification from correlation of e.s.r. and thermoluminesc. meas. 8=31028
$CaWO_4$:V, e.s.r. rel. to site occupances and charge compensation 8=45082
CdO, lattice distortion rel. to particle size by X-ray reflex broadening 8=48591
CdSe, defect structure from X-ray topography 8=39994
CdTe, impurity levels and stoichiometric variations 8=30804
CeO_2, rare-earth impurity doping in crystals grown from the melt 8=26645
Co, effect of e bombard., point defects at 20°K 8=48914
Co electroless films, lattice fault densities, obs. 8=44165
Co-Ti alloys, dil., solute atom motion from Zener disaccommodation studies 8=27401
Cr films, vacuum-deposited, in substructure from e.-diffr. exam. rel. to deposition temp. 8=35169
$CsCl_2$, Schottky defects rel. to thermal expansion 8=26067
CsI and CsI:Ba^{2+}, Sr^{2+}, impurities effect on ionic transport 8=40574
Cu, active crystal length in yield region 8=40054
Cu alloys, stacking fault energy and order rel. to Hall constant changes on plastic deform. 8=44689
Cu, defect conc. effect on annealing stage I after α-irrad. 8=48926
Cu, defect structure on n.-irradiation at 400 °C. 8=48804
Cu, electron-irradiated, lattice defects, interactions by elec. resist. recovery 8=31146
Cu, grain boundary cavity stability during annealing 8=26802
Cu, impurity concentration effect on resistivity 8=26966
Cu, OFHC, distrib. of cavities, during creep 8=44401
Cu, pore formation during creep, temp. and stress effects 8=35524
Cu, rel. to strain excitation from exo-emission meas. 8=44938
Cu, rel. to X-ray $K\alpha$ emission, obs. 8=41308
Cu, stacking fault energies 8=31097
Cu, structural defects in slip-lines during fatigue 8=48827
Cu-15 at.% Al, alloy, stacking fault energy rel. to short range order and temp. 8=35575
Cu-Al alloys, β' martensite, stacking fault probabilities 8=48867
CuAl alloys, solute atom segregation on stacking faults 8=26643
Cu-Al alloys, stress induced stacking faults 8=48868
Cu-Al solid solutions, stacking-fault energy, annealing and irrad. effects 8=26702
Cu-Cr alloys, grain-boundary cavity formation, stress limitation 8=48871
ζ-CuGe, stacking fault probab., X-ray obs. 8=26704
Cu_2O, energy spectra 8=31055
Cu_2O films on Cu(111), diffusion in struct. defects rel. to oxidation, obs. 8=44042
Cu_2O, stoichiometric defects rel. to absorpt. spectrum , obs. 8=41083
Cu_5Si, gaseous impurity segregation 8=35673
Cu-Zn system, max. stacking fault energy 8=48869
α-Fe, cold-deformed, solid solubility of C and N, normal and in stacking faults 8=35543
Fe, points defects created by strong rolling in liq. N_2 elimination 8=31024
Fe, stacking fault energies on $\{111\}$ planes in b.c.c. lattice 8=48870
Fe, twin interlayers, volumetric form 8=44467
Fe-Al alloys, characterization of "K-state", Fe_3Al type ordered domains 8=48597
Fe-Cr alloys, inclusions, activation anal. of Cr contents 8=36652
Fe-Mn alloys, stacking fault conc. rel. to Mn content, e-microscope exam. 8=35576
Fe-Si alloys, slip bands after two bendings in opposite directions 8=48863
α-Fe_2O_3 whiskers and twinned platelets, grain boundary diffusion during growth 8=44150
GaAs p-n junction, defect location rel. to elec. imperfections 8=49292
Au-Cd alloys, hexagonal, structural, from X-ray diffraction 8=44426

Crystal imperfections—contd
GaAs, rel. to growth methods, sawing and polishing, and routine handling 8=44427
InSb:Te, impurity heterogeneities from multiple-beam interferometry 8=48821
GaAs:Te, microprecipitates 8=40012
GaAs:Te, obs. 8=40013
GaAs:Zn, defect formation during Cu diffusion from photoluminescence data 8=48819
GaP, impurity effects on platelet growth 8=26205
GaP, role of vacancies and substitutional impurities in luminescence band formation 8=45274
Ge, epitaxial, packing defects rel. to annealing and plastic deform. 8=31099
Ge films, epitaxially grown, defect structure rel. to growth processes 8=26647
Ge, ion-bombarded, structural defects from e. -diffr. exam. 8=39793
Ge, n-irradiated, defect detection using anomalous X-ray transmission 8=48834
Ge layer, epitaxially grown, rel. to sheet resistivity 8=40465
Ge overgrowth defect formation in vapour deposition droplet mechanism 8=26277
Ge, surface defects after irradiation and mech. treatment rel. to exoelectron emission 8=40694
Ge, smooth surface defects, effect on breaking strength, 300°K and 4.2°K 8=40161
Ge surface, effect of metal impurities on electronic states 8=40257
Ge-GaAs epitaxial combinations, linear defects interpretation as misfit dislocations 8=31078
Ge–GaAs epitaxial combinations, linear defects interpretation as slip 8=31077
Hf, cold-worked, stacking fault probab., X-ray obs. 8=26704
HfO_2, rare-earth impurity doping in crystals grown from the melt 8=26645
Hg, glide and deformation twinning, –39°C to –196°C 8=26706
InSb, impurity incorporation during facet growth 9=48820
KBr, lattice distortion due to substitutional ion, n.m.r. meas. 8=36273
KBr, point-defects in volume expansion 8=26826
KBr, X-irradiated, Frenkel defect formation at 8°K 8=40005
KCl cryst, reacts between defects 8=26633
KCl, impurity effect on perfection and mech. and optical props. 8=26401
KCl, radiation-induced macrodefects 8=26711
KCl, X-irradiated, Frenkel defect formation at 8°K 8=40005
KCl: Ag^+, transitions, electronic, of impurities, symm. assignment by two-photon-induced emission 8=36494
KCl: Cu^+, Ag^+, impurity ion distrib. coeff. on crystallization from melt 8=39674
KCl: Li, impurity-phonon interactions exam. by sp. ht. meas., rel. to tunneling phenomena 8=44628
$KH_2Al_2(SiO_4)_3$ (muscovite) isomorphic substitution obs. by X-ray diffraction 8=35338
KI, lattice distortion due to substitutional ion, n.m.r. meas. 8=36273
KI:NO_2^-, inducement of Raman spectra 8=41106
$KTa_{0.65}Nb_{0.35}O_3$, in lamellae origin 8=48519
Li borate cpds and glasses, γ-irrad., trapped-hole centres 8=49612
Li, electrotransport of lattice defects 8=35501
LiF, impurity effect on perfection and mech. and optical props. 8=26401
LiF, n/e-irradiated, aggregate defect centres, Mollwo-Ivey relation 8=31032
LiF, pt. defect formation on plastic deform. 8=44403
LiF, radiation-induced macrodefects 8=26711
LiF, slip bands, dislocation multipoles, electron microscopy obs. 8=44460
LiF:Ni^{2+}, impurity ion clustering from small-angle X-ray scattering exam. 8=44422
$LiFe_5O_8$, from U^{235} fission fragment., irrad. effect on ferromag. resonance 8=36225
$MgAl_2O_4$ spinels, structural defects, etching investigations for visibility 8=48526
MgO, cont. < 5000 ppm Fe, rel. to low dose n irrad. 8=26829
MgO, effect of impurities on luminesc. 8=49809
MgO, n/e-irradiated, aggregate defect centres, Mollwo-Ivey relation 8=31032
MgO, irradiated, defect clusters, very small, study by neutron scattering meas. 8=35525
MgO, neutron irradiated, $(OF)^{2-}$ molecular ion as paramag. defect 8=44404
MgO, Rebinder effects, obs. 8=31083
N, N'-diphenyl-p-phenylenediamine, influence of impurities on electrical conductivity 8=40333
NaCl, divalent impurity elec. behaviour 8=44423
NaCl, grain boundary energies, rigid lattice approx. 8=40053
NaCl, impurites, effect on charged dislocations 8=40041
NaCl, impurity effect on mech. props. 8=26401
NaCl: Cu^+, Ag^+, impurity ion distrib. coeff. on crystallization from melt 8=39674
NaCl:Mn, impurity distrib. coeff. from e.p.r., 8=48823

Crystal imperfections—contd
Nb, dissolved oxygen clusters rel. to supercond. peak effect 8=49192
Nb, extended, effect on superconductivity 8=49193
Nb-Zr25 superconductor, type III, lattice defects, nature, size and distrib. and effect on high-field props. 8=48828
NH_4Cl, effect of impurities on spin-lattice relax. 8=40955
Ni alloys, binary, fundamental to Nimonic series, stacking-fault energies 8=35577
Ni electrodeposited, process conditions effect on stacking-fault, microstrain and particle size 8=26298
Ni, grain boundary damping peaks 8=48872
Ni, stacking fault energy from creep meas. near Curie pt. 8=35710
Ni, void formation during creep 8=31225-6
$NiAl_2O_4$ cryst, reacts between defects 8=26633
NiGa, structure defects, constitutional and thermal. 8=48829
Ni_3Ge, gaseous impurity segregation 8=35673
Ni_4Mo, ordered, tetragonal superstruct. and three classes of interfaces 8=26713
Ni_3Sn_2, gaseous impurity segregation 8=35673
O in metals, determ. by $O^{16}(n, \gamma)N^{16}$ 8=32167
OD-structures, of geometrically equiv: rods, systematics 8=26630
Pb, slip bands, orientation distrib. under pure shear 8=48864
Pb, zone-refined, solute-induced hardening near grain boundaries 8=26842
PbI_2, defect energy level structure from photo-excitation studies 8=44650
Pb–In alloys, stacking fault formation during deformation rel. to alloy comp. 8=35578
Pb–Sn alloys, cell boundary diffusivity calcs. from Cahn and Turnbull theories 8=30670
PbS, stoichiometric defects and foreign atom addition effects on steady-state creep 8=40179
$Pb(ZrTi)O_3$ ferroelec. ceramic, pt. defect - 90° domain wall interaction 8=44405
Pd-Ag alloys with Gd and Nd impurities, resistance anomaly 8=31326
Pt, damage rate meas., by electron irradiation 8=31155
Pt, defect production and recovery, plastic deformation and Au substitution effects. 8=39997
Pt, quenched, polyhedral voids and prismatic dislocations, e- and field-ion-microscope exam. 8=31086
Pt, radiographic obs. using channeled α-particles. 8=48830
Pt surface, Na and K impurities appearing at 20-1100°C 8=35549
Pu, microcracks elimination by chill casting and heat treatment 8=31228
Re, neutron irrad., defect cluster identification 8=40080
SAP, (sintered Al/Al_2O_3 alloy), lattice defects, behaviour on cold working, resistometric exam., 8=48817
SAP, (sintered Al/Al_2O_3 alloy), lattice defects, behaviour on quenching, resistometric exam., 8=48816
$Sc(Ni_{1-x}Co_x)_2$, impurities and vacancies effect on Sc^{45} n.m.r. 8=45133
n-, p-Si, electrically active defect introduction rates on e. -and n. -irradiation 8=39998
Si, causing anomalous etching and X-ray double images, origin and structs. 8=48835
Si epitaxial layers, stacking-fault defect nature 8=40050
Si epitaxial layers, stacking fault disappearance 8=40049
Si epitaxial layers, stacking fault transformation during P diffusion 4=48833
Si, epitaxial, shear and twin-type stacking faults 8=31100
Si films, 1-2μ thick, epitaxially grown on sapphire, rel. to carrier transport 8=40489
Si, gettering effect of metallic impurities 8=40494
Si, impurity atom effects on lattice defects, X-ray studies 8=26644
Si impurity striations, reasons for appearance, cryst. grown by Czochralski method 8=48824
Si, interaction of Li with O 8=26632
Si layers, formation by epitaxial deposition of Mg-Al 4=48832
Si, lattice disorders rel. to different gettering processes 8=44077
Si, n-irradiated, defect character from anomalously wide images using stereo e-microscopy 8=31025
Si, n-irradiated, defect detection using anomalous X-ray transmission 8=48834
p-Si, n-irradiated, disordered regions, dimensions and conductivity temp. dependences 8=35913
Si, n-irradiated, disordered regions formation from carrier mobility decrease 8=35551
Si, P^+ bombard, temp. effects 8=48831
Si slices, impurities distrib. by neutron activation 8=40014
Si, surface defects after irradiation and mech. treatment rel. to exoelectron emission 8=40694
Si, surface, during thermal treatment 8=30728
Si wafer near oxide film edge rel. to localized diffusion, X-ray micrographic obs. 8=35552
Si, X-ray Berg-Barret skew reflection tables for detection 8=35347
Si, Au and Cu impurity and dopant distribs. on pulling crystals in floating-zone technique 8=40015

Crystal imperfections—contd
β-SiC, soln.-grown, stacking faults, partial dislocations and twinning 8=31101
Si:Sb, structural defects rel. to doping conc. 8=40018
Sn, zone-refined, solute-induced hardening near grain boundaries 8=26842
Ta, impurity effects on surface superconductivity 8=44739
Th, stacking fault probability plastically deformed 8=35579
ThO$_2$, rare-earth impurity doping in crystals grown from the melt 8=26645
Ti, cold-worked, stacking fault probab., X-ray obs. 8=26704
TiBe$_{12}$, hexagonal, OD-structure 8=26442
TiO$_{2-x}$, stoichiometric defects rel. to resist. temp. depend, 20-1000°C 8=39999
α-U, stacking faults and extended dislocations in (110) and (001) planes, theory 8=31102
UN, deformation and oxidation studies by e-micros. 8=27718
UO$_2$, fission-induced, rel. to density var. during annealing, obs. 8=44605
(U$_{0\cdot85}$Pu$_{0\cdot15}$) O$_2$ reactor fuel, irrad., metallic fission-product inclusions 8=29557
W, grain boundaries rel. to partial dislocation system 8=39728
W stacking faults, ion microscope investigation 8=35580
W surface, Na and K impurities appearing at 20-700°C 8=35549
YAl garnet, inclusions rel. to growth on seed by flux technique 8=26198
YAl garnet, three planar defects, obs. by e.-microscope 8=44429
Y$_3$Fe$_5$O$_{12}$ from U^{235} fission fragment irrad., effect on ferromag. resonance 8=36225
Zn bicrystals, grain boundary sliding anisotropy rel. to dislocation climb-glide mechanism 8=31106
Zn, hexagonal, quasidipoles in basal plane 8=48862
Zn, melt-grown, substructure dependence on impurities 8=26268
Zn, stacking faults on prism planes of first kind, obs. 8=44466
Zn, zone-refined, solute-induced hardening near grain boundaries 8=26842
ZnS hexagonal crystals, stacking fault introduction rel. to photovoltaic effect changes 8=31103
ZnS, lanthanide impurity doped, crystal field effects rel. to structures 8=26646
ZnS, melt-grown under pressure, stacking faults 8=44084
ZnS platelets, type II stacking faults 8=40034
ZnS, stacking fault probability rel. to exciton spectrum 8=49766
ZnS with one dimensional stacking faults, internal optical reflection 8=45230
ZnS/ZnSe mixed-crystals, associate defects of ^{6}S-state ions obs. by e.s.r. 8=26636
ZnTe:Pb, impurity state, e.p.r. meas. 8=35738
Zr, cold-worked, stacking fault probab., X-ray obs. 8=26704
ZrO$_2$ films, point-defect population after gamma, neutron or Ne irrad. 8=35607

dislocations
alkali halides, edge, thermal equilib. charge 8=44444
alkali halides mobility dependence on electrostatic field 8=26667
alkali halides, scattering of lattice waves 8=30933
alloys, containing hard particles, rel. to work hardening 8=35640
alloys, ordered, of AuCu-type, damping mechanism 8=40031
alloys, superdislocations with thresholds in the L1$_2$ superstructure, braking 8=26655
Almotion and interacts. study by third harmonic generation 8=44442
annealing kinetics of vacancies to dislocations 8=26637
anthracene, direct obs. by X-ray topography and Burgers vectors determ. 8=31074
arrays, pre-melting and pre-freezing, thin crystals 8=43902
α-brass, rel. to stress relax., 78-295°K 8=31193
β-brass, interacts. at antiphase boundaries in B2 superlattice 8=44448
b.c.c. and f.c.c. crystals, dislocation loops and dipoles computer simulation of spherical surfaces 8=26652
b.c.c. metals, reaction energy changes 8=44439
bending at small obstacle, line tension geometry 8=31060
Berg-Barrett method for obs., expt. techniques 8=44430
Bravais rule, -energy interpretation 8=26304
calcite, growth and twinning during twin layer expansion under stress 8=31104
calcite, multiplication of twinning dislocations 8=26686
cementite 8=31075
in cleavage crack formation mechanism 8=26774
continuously distributed, dynamic theory, rel. to plasticity theory 8=46060
continuum theory for internal stresses of media with microstructure 8=44519
core structures in cubic, b.c.c. and diamond lattices 8=40020
corundum, obs. by reverse decoration technique 8=26664
crystalline solid, accumulation rel. to cleavage cracking 8=48951

Crystal imperfections—contd
dislocations—contd
damping, dynamic, by impurities 8=40032
dechanneling effect rel. to 8=31059
density meas. using e microscope 8=35559
diamond, luminesc. evidence 8=36475
diffusion in stress fields, precipitation hardening 8=39537
diffused structures, planar, propag. through strain effects, 8=48844
dynamics 8=44438
dynamics, review 8=44434
edge array, stability of arbitrary config. 8=26653
edge, rel. to conc. forces, 8=48838
edge, rel. to thermal cond., elevated temp. 8=30980
effect on line width of ferro- and antiferromagnetic resonances 8=40884
in elasto-plastic deformation classification, behaviour 8=26756
etch pits, shape at intersection with surface. 8=48837
f.c.c. alloys, viscous movement rel. to internal friction 8=35615
f.c.c., partial, and stacking faults, computer simulation of spherical surfaces 8=48865
ferrite-garnets, and effect of hydrothermal synthesis conditions rel. to dislocation formation 8=26660
ferromagnetics, anisotropy due to screw dislocations 8=40790
in ferromagnetics, interact. energies with domain boundaries 8=40784
in ferromagnetics with cubic lattice, rel. to spin waves and spin states 8=40761
ferrospinels, split dislocation structure 8=40027
film coating on Cu single crystals, density increase rel. to cracking at substrate surface 8=40149
finite length, stress tensor 8=48836
glide, interaction with vacancy aggregates, from density determ. 8=31070
graphite, geometry in characterization 8=44123
h. c. p. crystals, anisotropic, stress fields around edge multipole and multipole arrays 8=26795
h.c.p. crysts. Burgers vectors, use of Miller indices instead of Miller-Bravais notation 8=48958
hexagonal arrays forming twist boundaries, energy calcs. 8=40022
ice, effect of H disorder 8=35569
interaction allowing for spatial dispersion 8=35560
interaction with large local defects (stoppers) in real lattices 8=26659
internal friction, high-temp. theory 8=44435
ionic crystals, multiplication including perfect and twinning dislocations 8=26686
jogged screw model for creep, use of hyperbolic tangent function 8=48842
jogged screw type, diffusion controlled motion, comments 8=48841
kinetics of structures 8=31067
kinks, effects on internal friction 8=26743
lattice waves, scattering 8=30933
loops, coherency loss of growing particles by prismatic punching 8=26651
loops, finite circular-glide, properties 8=26650
loops in anisotropic media, elastic field calc. 8=31068
loops, junction reaction hardening 8=31066
in magnetic structures, complex, scattering by spin waves rel. to spin thermal conductivity 8=39935
metals, as sources and sinks for point defects 8=31071
metals, b.c.c., sessile splitting of screw dislocations 4=48847
metals, face-centred, density distrib. rel. to work hardening theories 8=35558
metals, fatigued, effect of surface-active substs. on distrib. 8=35556
metals, hexagonal, dissociation and sliding on prismatic planes 8=44440
in microstrain regions, rel. to friction stress and mechanical hysteresis 8=26744
migration polarization from motion of ions 8=49322
mobile, density and velocity, stress dependence from Lüders band front propag. velocity 8=31057
mobility theory 4=48846
movement through solid with dislocation pileups, stress required 8=40021
moving, frictional stress 8=44431-2
moving, unifying relns. 8=31065
observation by X-ray diffraction camera 8=26331
paired and triple, electron microscope image profiles 8=40030
partial, and stacking faults, rel. to contrast in field-ion microscope 8=31092
partial, consituting dynamic twins, deformation behaviour 8=48825
pearlite and spheroidite, velocity exponent from strain-rate change tests 8=35557
Peierls-barrier minima 8=26657
phonon thermal conductivity limitation by edge-disloc. dipoles, isolated dislocs. and normal processes 8=48754
pile-up break-through mechanism in deformation transmission through a crystal 8=26661

Crystal imperfections—contd
- **dislocations**—contd
  - pile-up time-dependence rel. to linear arrays and stresses 8=31073
  - pinning by pt. defects during continuous low-level α-irrad. appl. to stage III in Cu 8=39995
  - polycrystalline materials, behaviour during cleavage fracture under hydrostatic pressure 8=48978
  - prismatic defects, identification by electron microscopy 8=31061
  - quartz, brittle, mobility rel. to microhardness 8=26796
  - radioactive tracer decoration for high density meas. 8=40039
  - random distrib., rel. to internal stresses production 8=31165
  - relaxation in b.c.c. transition metals 8=31088
  - screw pile-up in infinite body containing elliptically cylindrical rigid inhomogeneity 8=40024
  - screw, piling up against circular cylindrical rigid inclusion 8=40025
  - screw type, in steady creep, state model 8=48843
  - segment bending and Franck-Read sources 8=44437
  - self-energy and energy of configurations 8=40028
  - semi-coherent precipitates, interfacial structure, electron miscroscope investigations 8=26656
  - semiconductors, distrib. rel. to heat treatment on prep. 8=26679
  - shear-stress field of simple cell, 8=44433
  - slip, incorporation in twins 8=44088
  - solid-solution, behaviour in hardening in conc. solns. 8=48964
  - spheroidite and pearlite, velocity exponent from strain-rate change tests 8=35557
  - spontaneous generation and cause of melting 8=31058
  - statistical theory rel. to plasticity 8=26654
  - steel, low C, Lüders front exam. by transmission electron microscopy 8=44449
  - in steel, stainless, surface layers in cyclic deform., obs. 8=40035
  - steel, strain-aged, rel. to discontinuous yielding grain-size dependence 8=26809
  - steels, Fe-C and Fe-Ni-C, in martensite substructure rel. to strength 8=26815
  - stress-field diffusion rel. to precip. shape change 8=26649
  - superconductivity, effect 8=40342
  - Suzuki atmosphere, X-ray determ. 8=40029
  - theory, on basis of continuum mech. 8=48840
  - theory reln. to non-Riemannian diff. geometry, K and Cartans displacement 8=44436
  - thermal and subthermal n scatt. 8=24959
  - thermal light scattering in ionic crystals 8=41034
  - tilted foil, computed e micrograph 8=40017
  - transition from lattice of one type to lattice of another type 8=40026
  - triglycine sulphate, and ferroelectric domains, interactions 8=27287
  - ultrasonic saturation of n.m.r. line, influence of motion 8=36260
  - unpinning, thermomechanical in hysteretic contrib. to internal friction. 8=48839
  - velocity, jog-dragging controlled, impurity effects 8=31063
  - yield stress of binary solid soln. crystals, depend on temp. and alloy conc. 8=26763
  - Zircalloy, in-reactor creep rel. to dislocation climb 8=35728
  - Ag foils, ultramicrotome-cut, density from transmission e.-microscopy, 8=48850
  - AgCl, plastically deformed, and strain exam. methods 8=26662
  - Ag-Sn solid solutions, extended nodes, effect of annealing 8=35561
  - Al alloys, interact. with precipitates rel. to annealing characts 8=48849
  - Al alloys, model for serrated yielding, temp. and strain rate depend. 8=44548
  - Al, density on thermomechanical treatment 8=35672
  - Al, dislocation-surface interacts., effect of oxide film 8=26094
  - Al, drag coeff. meas. by strain rate method 8=44441
  - Al, electrical resistivity, temp. depend. 8=35821
  - Al foils, ultramicrotome-cut, density from transmission e.-microscopy 8=48850
  - Al, glide, interaction with vacancy aggregates, from density determ. 8=31070
  - Al, ratio of true density to apparent density determ. by e-transmission microscopy 8=26665
  - Al-Cu-Si alloy, sources, obs. 8=48848
  - Al-Mg alloy, prismatic loop diam. and density, yield stress dependence 8=40033
  - Al-Mg alloys, networks and annihilation 8=48992
  - α-Al$_2$O$_3$, induced by n. irrad., effects of annealing 8=26666
  - α-Al$_2$O$_3$ powder, explosively shocked, from X-ray line broadening analysis 8=44168
  - γ-Al$_2$O$_3$, rel. to growth method 8=26663
  - AlSb, structure rel. to mech. props. 8=44443
  - Al-3.5% Zn, activation lengths, effects of attractive precipitate particles 8=48851

Crystal imperfections—contd
- **dislocations**—contd
  - Al 78 wt.% Zn alloy, climb in superplastic deform. 8=44538
  - As, etchpits 8=48852
  - Au, motion effects on u.s. attenuation at low temps. 8=39894
  - Be and alloys identification using transmission electron microscopy 8=44555
  - Bi, multiplication mechanisms 8=26668
  - CaF$_2$, near-surface mobility in Rebinder effects occurrence and mechanism 8=40136
  - in CdI$_2$ polytypism 8=26180
  - CdS, brittle, mobility rel. to microhardness 8=26796
  - CdS epitaxial films on CdS and ZnS platelets, obs. 8=35165
  - CdS platelets, obs. 8=40034
  - CdS: Au, rel. to annealing conds. 8=48375
  - CdS: Cu, rel. to annealing conds. 8=48375
  - Co single crysts. rel. to slip, impurity depend., 78-573°K 8=40138
  - Cr, deformed under hydrostatic press., rel. to plasticity, < 18 kbar 8=35562
  - CsI, charged dislocations produced on deformation 8=26669
  - Cu alloys, dilute, thermally activated dislocation depinning 8=26670
  - Cu, arrangement on deformation at 4.2, 78 and 293°K 8=48854
  - Cu, cold-work, ang. distrib. of scatt. neutrons 8=26355
  - Cu, creep-extended at 1000°C, structure 8=35565
  - Cu, deformed, arrangement in work hardening curve, X-ray topography study 8=44445-6
  - Cu, deformed, density determ. from X-ray diffr. profiles 8=26673
  - Cu, f.c.c. screw disloc cross-slip obs. 8=48855
  - Cu, flow stress, forest dislocations and impurity effects 8=31199
  - Cu foils, ultramicrotome-cut, density from transmission e.-microscopy, 8=48850
  - Cu, initial substruct. rel. to slip distrib. and strain hardening 8=44459
  - Cu, line resonant vibrations 8=35563
  - Cu, n-irradiated, behaviour in radiation hardening 8=31197
  - Cu, orientation dependence of damping 8=44563
  - Cu-0.01 wt.%B^{10}, n irrad., surrounding elemental B particles, obs. 8=35564
  - Co, order rel. to deform. and plasticity 8=48853
  - Cu, polycrystalline, explosively shocked, damping 8=26672
  - Cu, polycrystalline, loss in thin film electron microscopy 8=26671
  - Cu, scattering of lattice waves 8=30933
  - Cu single crystals, fatigued at low stress amplitudes 8=40140
  - Cu, structure associated with fatigue crack growth 8=40143
  - Cu, surface layer, distrib. after tensile deform. 8=48856
  - Cu-Al alloys, extension by action of stress 8=48868
  - Cu-Al alloys, lattice wave scattering by dislocations 8=26573
  - Cu-Al-Fe solid solutions, hardening action of short range order 8=26806
  - Cu-Al-Ni solid solutions, hardening action of short range order 8=26806
  - Cu$_3$Au, ordered and disordered, low temp. mechanisms 8=31076
  - Cu-Co alloys, radiation-induced coherency loss 8=26036
  - Cu-Ga alloy, massive phase, structure and duplex nature 8=30685
  - Cu-Ge alloy foils ultramicrotome-cut density from transmission e.-microscopy, 8=48850
  - Cu-Zn alloys, abraded, rel. to surface and subsurface structure 8=26294
  - Fe, b.c.c., edge disloc-impurity interaction, force-distance curve calc. rel. to hardening model 8=26674
  - Fe, density and distrib. changes rel. to local stress relax. 8=35676
  - Fe, density and disrib. rel. to growth by strain-anneal 8=26250
  - Fe, dragging by interstitial impurities rel. to internal friction peak 8=26814
  - Fe filoform microscrystals, effect on magnetization process 8=26677
  - Fe-3.14% Si, single and polycryst., velocity rel. to stress 8=26675
  - Fe polycrystalline, using etch-pit technique 8=26676
  - Fe, rel. to X-ray diffr. line intensity changes, on plastic deformation 8=44166
  - α-Fe$_2$O$_3$ whiskers and twinned platelets, diffusion during growth 8=44150
  - Fe-Si alloys, creep mechanisms 8=40154
  - Fe-Si, effect on magnetization curve and energy losses in alt. mag. fields 8=36142
  - GaAs grown from supercooling melts, rel. to growth conditions 8=26678
  - gaAsP, Zn-diffused, p-n junctions, effect on geom. irregularities 8=40512
  - GaAs: Te, 1.6 × 10^{18} carriers 1 cm^3, helical dislocations, obs. 8=40036
  - GaP, creation during spark erosion 8=40037
  - GaSb, density changes on back-melting 8=44447

Crystal imperfections—contd
  dislocations—contd
    Ge, accepted e cond. on dislocation lines, obs. 8=35900
    Ge, deformed, e-microscope exam. 8=31064
    Ge, e.-irradiated, and defects interaction 8=40038
    Ge, formation during As diffusion 8=35568
    Ge, line resonant vibrations 8=35563
    Ge, lines, space orientation determ. from topograms obtained by Borman's method 8=40040
    Ge, luminesc. evidence 8=36475
    in n-Ge, magneto-conductivity and low-field magnetoresist. 8=35890
    Ge, pure and In doped, rel. to internal friction peak in 100 to 300°K range 8=35703
    Ge, radioactive tracer decoration for high densities meas. 8=40039
    n-Ge, rel. to acceptor level position 8=35891
    n-Ge, rel. to resistivity and donor conc. 8=44784
    Ge, scattering of lattice waves 8=30933
    Ge, structure at stages of work hardening curve 8=35566
    Ge:As, prismatic loops, e-microsc. obs. on annealing 8=35567
    Ge–GaAs epitaxial combinations, misfit, in interpretation of linear defects 8=31078
    HgS epitaxial films on CdS and ZnS platelets, obs. 8=35165
    InSb, effect on elec. props. 8=49254
    n-InSb, high density, magnetoresistance and Hall effect 8=49248
    InSb-GaSb heterojunctions, generation during lattice mismatch accommodation. 8=48857
    K, motion effects on u. s. attenuation, 2.5-77°K 8=39894
    KBr, and grain boundaries, effect on Br diffusion 8=35497
    KBr, electrolytic colouration, influence 8=44469
    KBr, multiplication 8=26686
    KBr, pinning by crystal-lattice defects 8=26680
    KBr, plastically deformed, density rel. to F-centre thermal stability 8=35586
    KBr, velocity temp. and shear-stress dependence 8=26681
    KCl, coloured, deformed, —colour centres interaction from photoconduction 8=44928
    KCl, density and distrib., from X-ray scatt. 8=45198
    KCl, doped, decoration mechanism from reaction with H_2 8=31081
    KCl, mobility and microhardness dependence on F-centre density 8=26690
    KCl, motion during plastic deform. rel. to charge flow 8=35961
    KCl, multiplication 8=26686
    KCl, pinning by crystal-lattice defects 8=26680
    KCl, plastically deformed, density rel. to F-centre thermal stability 8=35586
    KCl, rel. to reciprocal and self-diffusion 8=26620
    KCl, structure formation on plastic deformation 8=31080
    KCl, velocity temp. and shear-stress dependence 8=26681
    KCl:Ba^{2+}, velocity, stress-dependence rel. to Ba^{2+} impurities 8=31079
    KCl:Eu, conc. rel. to dopant conc. 8=40001
    KH_2PO_4, and precipitates exam. by X-ray diffr. microscopy 8=26691
    KI, rel. to reciprocal and self-diffusion 8=26620
    LiF, density and distrib. from X-ray scatt. 8=45198
    LiF, distrib. rel. to loading regime 8=31082
    LiF, edge disloc-impurity interaction force-distance curve calc. rel. to hardening model 8=26674
    LiF, interaction with point defects from internal friction meas. 8=26683
    LiF, mobility pressure dependence 8=44451
    LiF, movements rel. to acoustic emission 8=44317
    LiF, multipoles in slip bands, electron microscopy obs. 8=44460
    LiF negative thread crystals, effect on growth and evaporation kinetics 8=26256
    LiF, programme-hardened, mobility 8=44449
    LiF, structure formation on plastic deformation 8=31080
    LiF, ultrasonically irradiated, origin and reactions 8=26688
    LiF, X-irradiated, effect on F-centre thermal stability, e-emission exam. 8=35570
    $LiNbO_3$, rel. to ferroelec. domain wall obs. 8=31434
    $MgAl_2O_4$ spinels, etching investigations for visibility 8=48526
    MgO, Rebinder effects, obs. 8=31083
    MgO, scattering of lattice waves 8=30933
    α-Mn_2O_3-type structures, produced by Mn^{3+} rel. to cation bonding 8=39501
    Mo, deformed under hydrostatic press., rel. to plasticity, < 18 kbar 8=35562
    Mo, velocity stress dependence at 77 and 300°K 8=26684
    MoS_2, molybdenite, non-basal 8=35526
    NaCl, charged, effect of impurities 8=40041
    NaCl, density and distrib., from X-ray scatt. 8=45198
    NaCl, dissolution kinetics at dislocation sites, rel. to solvent and poisons 8=26685
    NaCl, distrib. rel. to growth micromechanism in vacuum-condensation process 8=48551
    NaCl, due to e bombard., directional breakdown 8=48925
    NaCl, effect on vaporization rate 8=35008
    NaCl, mobility and microhardness dependence on F-centre density 8=26690

Crystal imperfections—contd
  dislocations—contd
    NaCl, multiplication 8=26686
    NaCl, pinning by crystal-lattice defects 8=26680
    NaCl, plastically deformed, density rel. to F-centre thermal stability 8=35586
    NaCl, rel. to reciprocal and self-diffusion 8=26620
    NaCl, single edge dislocation penetration through slip lines 8=26687
    NaCl, ultrasonically irradiated, origin and reactions 8=26688
    NaCl: $Pb(NO_3)_2$ density increase on heat treatment at 300°C 8=26689
    NaI, effect on F^{27} n. m. r. intensity 8=36278
    $NaNO_3$, dislocations visualization by etching 8=48858
    Nb, distribs. in vicinity of spark-machined notched, obs. from etch figures 8=40042
    Nb, velocity, stress dependence, etching meas. 8=31085
    $(NH_4)H_2PO_4$, and precipitates exam. by X-ray diffr. microscopy 8=26691
    Ni-base alloy, irradiated, haloes 8=44452
    Ni, cold-work, ang. distrib. of scatt. neutrons 8=26355
    Ni, contribution to magnetic saturation curve anisotropy 8=49536
    Ni crystals, in rate-controlling stress relax. mechanisms 8=40178
    Ni, distrib. effects on coercivity 8=31699
    Ni, e. microscope obs., 8=48859
    Ni, edge, vels. rel. to stress, activation vol. and enthalpy 8=44454
    Ni, grain boundary, large-angle, influence 8=31105
    Ni, magnetization anisotropy due to screw dislocations, calc. 8=40790
    Ni, magnetostrictive crystalline energy from anisotropy of approach to saturation 8=35571
    Ni polycrystalline, dislocations, small angle mag. scattering of sub-thermal neutrons 8=31084
    Ni, polycrystalline, small angle mag. scattering of sub-thermal neutrons 8=31084
    β^1-NiAl, prismatic loops 8=44453
    Ni_3Fe, magnetization anisotropy due to screw dislocations, calc. 8=40790
    Ni-Mo alloys, e. microscope obs., 8=48859
    Pt, quenched, prismatic, and polyhedral voids, e- and field-ion-microscope exam. 8=31086
    RbI, pinning by crystal-lattice defects 8=26680
    RbI, selective etchant 8=31087
    Sb, laser-produced, behaviour 8=40043
    Sb, multiplication mechanisms 8=26668
    in Si crystallization mechanism from Al-Si melts by zone-melting with temp. gradient 8=39686
    Si, distribs. from Laue-case diffr. expts., 8=48860
    Si epitaxial layers, generation and density during P diffusion 4=48833
    Si, e. p. r. of B rel. to density 8=45101
    Si, luminesc. evidence 8=36475
    Si, pure edge, parallel arrays, obs. on plastic deformation 8=40044
    Si, secondary, formation after diffusion of B and P 8=35572
    Si, semiconducting web-dendrites, origin and reactions 8=26692
    Si, surface dislocation sources 8=26694
    Si, vacancies at diffusion-induced dislocations, and enhanced diffusion in (001) crystals 8=26622
    SiC, luminesc. evidence 8=36475
    in SiC polytypism 8=26180
    Si-Fe, density during low cycle fatigue 8=39963
    Si-Fe, effect on magnetization process 8=26677
    Si, P diffused, obs. by X-ray and etching techs. 8=48861
    Si:P planar diffused structure, propag. through strain effects 8=48844
    α-U, and stacking faults in (110) and (001) planes, theory 8=31102
    W, rel. to stress-strain relns. 8=44455
    W, screw, field-ion microscopy 8=31089
    W–Re alloys, rel. to stress-strain relns. 8=44455
    W–3% Ta, rel. to stress-strain relns. 8=44455
    Zn, basal mobility and internal stress 8=44456
    Zn bicrystals, in climb-glide mechanism for grain boundary sliding 8=31106
    Zn, density and rate effects in twinning 8=26189
    Zn, edge, in basal slip system, vels. rel. to applied shear stress 8=44457
    Zn, multilayer vacancy disloc. loops 8=40002
    Zn, pyramidal, stress state required for movement 8=40045
    Zn, velocity shear-stress dependence 8=26695
    ZnS, brittle, mobility rel. to microhardness 8=26796
    ZnS epitaxial films on CdS and ZnS platelets, obs. 8=35165
    ZnS, twist boundary array, effect on luminescence 8=41214
    Zr alloys, in-reactor creep rel. to dislocation climb 8=35728
    Zr-O solid solns. interdiffusion zone obs. 8=30658
  interstitials
    in b.c.c. lattices, energy of interstition of impurity atoms into octahedral and tetragonal positions 8=35542
    carbon, graphitized, layer distortions rel. to interstitials 8=35553
    formed by Szilard–Chalmers recoil, crystal size effect on annealing 8=31049

Crystal imperfections—contd
- **interstitials**—contd
  - graphite, n-irradiated below 200°C, cluster size and temp. dependence 8=44419
  - metals, f.c.c., energies and atomic configurations 8=31026
  - migration energy, structure-factor approach 8=48814
  - permalloy, formed on H charging, rel. to mag. anisotropy 8=49538
  - pregraphitic carbons., detection interstitial atoms 8=26639
  - Al, and solute additions, interaction 8=31050
  - AgCl, defect conc., effect of defect interactions 8=40003
  - Au, atom clusters form. by aggregation of point defects, by Au ion bombard. 8=44418
  - Au foil, Ar ion bombard., agglomerate penetration 8=48815
  - BaF$_2$, anion and cation, formation energies, Born-model calc. 8=35540
  - BaF$_2$: GdF$_3$, F$^-$ interstitial mobility and cond. 8=49341
  - C, trapping in quenched and irrad. Fe 8=44420
  - CaF$_2$, anion and cation, formation energies, Born-model calc. 8=35540
  - CaF$_2$:H atoms, localized H vibrations 8=41072
  - CdS films, vapour-deposited, rel. to colour 8=26114
  - Cu, and solute additions, interaction 8=31050
  - Cu foil, Ar ion bombard., agglomerate penetration 8=48815
  - Fe, b.c.c. discrete-atom model for aggregates 8=35544
  - Fe, b.c.c., interstitial migration of O 8=48361
  - Fe, b.c.c. lattices, energy of interstition of impurity atoms into octahedral and tetragonal positions 8=35542
  - Fe, impurities in dislocation dragging rel. to internal friction peak 8=26814
  - KCl, X-irrad., Frenkel defect recombination on thermal annealing 8=40166
  - LiF, X-irradiated, e.s.r. of [111] defect 8=40006
  - Mo, radiation defects, thermal stability 8=40077
  - N, trapping in quenched and irrad. Fe 8=44420
  - NaNO$_3$, elec. cond. anisotropy obs. 8=35964
  - Nb, b.c.c. lattices, energy of interstition of impurity atoms into octahedral and tetragonal positions 8=35542
  - Ni, electroplated, formed on H charging, rel. to mag. anisotropy 8=49538
  - Ni, neutron-irrad., clusters 8=35538
  - NiCo–C alloys, C, rel. to mag. anisotropy 8=49526
  - NiFe–C alloys, C, rel. to mag. anisotropy 8=49526
  - Si, diffusion of implanted In and Tl from subst. to interstitial sites 8=40007
  - SiP precipitation on high-conc. P diffusion in Si, defect structure 8=39983
  - SrF$_2$, anion and cation, formation energies, Born-model calc. 8=35540
  - Ta, b.c.c. lattices, energy of interstition of impurity atoms into octahedral and tetragonal positions 8=35542
  - UO$_2$, O atoms reorientation, rel. to relax. in internal friction 8=35545
  - V b.c.c. lattices, energy of interstition of impurity atoms into octahedral and tetragonal positions 8=35542
- **vacancies**
  - alkali-halides, -centred Z$_1$-centre models, props. calc. 8=44473
  - alkali halides, with NaCl structure, computer calcs. 8=35532
  - alloys, ordered, of β-brass type, conc. and migration energy rel. to diffusion theory 8=26613
  - alloys, ordered f. c. c., conc. and migration energy rel. to diffusion study 8=26614
  - annealing kinetics, to dislocations 8=26637
  - binary alloys, diffusion, correlation factors 8=31039
  - α-brass, activation energy of formation, depend. on Zn content 8=48808
  - β-brass B2 superlattice, rel. to antiphase domain growth mechanism and kinetics 8=30689
  - cavitation fatigue mechanisms, high-temp., fractographic obs. 8=26771
  - diffusion, effect of grain boundary cavities 8=44406
  - ferrites, Co-substituted, rôle in uniaxial mag. anisotropy 8=49556
  - ferrite-spinels, two-components, formation and behaviour 8=26638
  - formation energy, temp.-dependence 8=31035
  - interaction with glide dislocations, from density determ. 8=31070
  - life-time, mean, in thermal equilib. 8=48806
  - metals, f.c.c., energies and atomic configurations 8=31026
  - metals, f.c.c., quenched, small clusters 8=31036
  - metals, migration, thermodynamics 8=35528
  - metals, quenched, excess vacancy coalescence during annealing, theory 8=35527
  - metals, vacancy-impurity pairs, binding entropy, and validity of nearest-neighbour interaction model 8=31037
  - in molecular solids, rel. to diffusion mechanism 8=35531
  - occurrence, simultaneously, of two, on introduction of trivalent impurity 8=40000
  - permalloy, formed on H charging, rel. to mag. anisotropy 8=49538
  - pre-precipitate assoc. 8=31033-4
  - rare gas solids, conc. and diffusion 8=44415
  - relaxation phenomena 8=44421

Crystal imperfections—contd
- **vacancies**—contd
  - stabilisation energies for ordered systems 8=35529
  - thermal light scattering in ionic crystals 8=41034
  - transition metal cpds with S, Se or Te, ordering and struct. 8=26635
  - Ag–Zn solid solns., in controlling atomic mobility, Zener-relax. studies 8=31040-1
  - Al, activation energies, temp. depend. 8=44408
  - Al, in elec. resistivity rel. to band structure effects in defect scatt. in polyvalent metals 8=49154
  - Al, and impurity solute atom, interaction energies 8=31043
  - Al, interaction with glide dislocations, from density determ. 8=31070
  - Al, n-irrad. lattice vol. distortion, subthermal n scatt. obs. 8=44203
  - Al, strain field interaction between 8=26641
  - Al, vacancy-impurity pairs, binding entropy, and validity of nearest-neighbour interaction model 8=31037
  - Al alloys, production by oxidation 8=26640
  - Al-Cu-Cd alloys, cluster mechanism of θ'-precip. 8=35085
  - Al–In alloys, dilute, rel. to electron-microscope observations 8=35265
  - Al-Mg alloys, annihilation 8=48992
  - Al-5 wt. %Mg, thin foils from quenched specimens, lifetimes 8=31042
  - Al-Zn alloys, effect on clustering kinetics 8=48807
  - Au, activation energies, temp. depend. 8=44408
  - Au, quenched, activation energy spectrum, effect of impurity atoms 8=31052
  - Au, quenched, annealing kinetics at elevated temps. 8=31044
  - Au, quenched, plastic deformation rel. to clustering 8=31045
  - Au, resistivity rel. to temp. 8=44409
  - Au–Ag alloy, conc. 8=31046
  - Au-Pt alloy, dil., vacancy-impurity interaction from quenching resistance 8=48805
  - Au-Pt alloys, quenched and annealed, effects on thermal conductivity 8=48759
  - BaF$_2$, anion and cation, formation energies, Born-model calc. 8=35540
  - BaF$_2$, F-vacancy cond. and mobility 8=49340
  - BaTiO$_3$ solid solns., rel. to relax. polarization 8=35975
  - CaF$_2$, anion and cation, formation energies, Born-model calc. 8=35540
  - CaWO$_4$, oxygen vacancies prod. by fast reactor neutrons, direct. obs. 8=31047
  - CdS, dielectric loss meas. study 8=44867
  - CdS film, transport phenomena rel. to anode electrical processes 8=40442
  - CdS rel. to ion bombard. effects in low-temp. luminesc. 8=36483
  - n-CdTe, thermal n irrad., Cd vacancies Hall and cond. obs. 8=35533
  - Cu, nearly perfect crystals, vacancy clusters, X-ray topograph exam. 8=35534
  - Cu, strain field interaction between 8=26641
  - Cu$_3$Au order-disorder alloy, rôle in diffusion of Au 8=39971
  - Fe, concentration during high temp. deformation 8=31038
  - Ge, Schottky defect, formation energy calc. 8=44411
  - β-In$_2$S$_3$, ordering of In vacancies and domain struct. 8=48599
  - KBr, impure, rel. to elec. conductivity 8=40576
  - KBr, Schottky defect form., from dissolution of impurity cont. precipitates 8=35536
  - KCl, cationic, displacement during coloration on divalent impurity addition, from conductivity meas. 8=35535
  - KCl, diffusion of Bi ion-vacancy complex 8=48781
  - KCl elect. cond. theory 8=27225
  - KCl, impure, rel. to elec. conductivity 8=40576
  - KCl, Schottky defect form., from dissolution of impurity cont. precipitates 8=35536
  - KCl:Eu, conc. rel. to dopant conc. 8=40001
  - KI, impure, rel. to elec. conductivity 8=40576
  - KI, Schottky defect form., from dissolution of impurity cont. precipitates 8=35536
  - Kr, solid, equilib. conc. meas. 8=48809
  - Kr, solid, equilib. conc. meas. rel. to thermodynamic props. 8=48745
  - LiF, anion and cation, diffusion rel. to ionic cond. 8=35963
  - in LiF negative thread crystal formation 8=26256
  - LiF:Fe^{3+}, field distortion, e.s.r. and n.m.r. obs. 8=48810
  - LiF: MgF$_2$, energy of motion of Li$^+$ and assoc. with Mg^{2+}, from ionic cond. 8=31423
  - MgO, Cr^{3+}-vacancy assoc. 8=31010
  - MgO, neutron irrad., negative ion vacancies 8=44412
  - MoS$_2$, molybdenite, surface point defects and non-basal dislocations 8=35526
  - Na silicate glasses, role in ionic transport and high-temp. internal friction 8=40176
  - NaCl, aggregation of Ca^{2+} ions, from ionic, dielec. and bulk density meas. 8=35965
  - NaCl, association energy of Pb^{2+}-cation vacancy 8=31011

Crystal imperfections—contd
vacancies—contd
NaCl, conc. and mobility determ. by conductivity meas. of divalent impurity doped crystals 8=44423
NaCl, Schottky defect form., from dissolution of impurity cont. precipitates 8=35536
NaCl, temp. depend of Mn-vacancy pairs 8=48811
NaCl:Mn, and pure, motion of cations and form. of Schottky pair 8=35537
Ni, clustering during quenching 8=44413
Ni, concentration during high temp. deformation 8=31038
Ni, electroplated, formed on H charging. rel. to mag. anisotropy 8=49538
Ni, neutron-irrad., clusters 8=35538
NiAs, order 8=35539
Ni-2%Cu solid soln., quenching 8=44410
Ni-Fe alloys, e-irradiated, migration during low-temp. mag. anneal rel. to remanence growth 8=36156
Pb halides, γ-irrad., trapping of electrons and holes to form colour centres 8=36249
$PbBr_2$, anion vacancies conc. and mobility 8=48812
Pt, n-irradiated, rel. to hardening 8=35716
Pt, thermal quasi-equilibrium and possible interactions 8=48813
RbI, Schottky defect form., from dissolution of impurity cont. precipitates 8=35536
Si, n-irradiated, divacancy production and annealing 8=44416
SrF_2, anion and cation, formation energies, Born-model calc. 8=35540
$SrTiO_3$:Fe^{57}, oxygen-, rel. to iron sites in lattice, from Mossbauer exam. 8=43958
Ta/Ta_2O_5 structures, annealed, exponential distrib. origin. 8=44417
Te, pulse-heated, rel. to anomalous Hall reversal at 515°K 8=31329
TiO, supercond. depend. on conc. 8=31345
Ti_5Te_8, ordering 8=35359
UC_xO_y, C- and O-deficient, lattice parameter obs. 8=35541
VC_{1-x}, nonstoichiometric, from lattice structure exam. 8=30913
Zn, multi-layer dislocation loops 8=40002

Crystal properties
acoustical activity and other first-order spacial dispersion effects 8=39884
anharmonic, thermodynamics, molec. field theory, classical and quantum, book 8=30954
anisotropic, elec. conductivity tensor component expt. determ., theory 8=26940
anisotropic, forbidden directions for elastic surface-wave propag. 8=48946
crystals, acoustical activity and other first-order special dispersion effects 8=39884
dielectric, photocarrier transport meas. apparatus 8=35747
i.r. optics, materials 8=31954
lattice thermal conductivity, formulae in Debye approx. using π theorem 8=26599
mica, synthetic, dependence on crystallization conditions 8=26193
optics, ciné-films for lectures 8=27519
organic matter, crystalline nature 8=41220
ortho-H, solid, theory of ang. mom. waves 8=35743
phonon spectrum rel. to supercond. energy gap 8=31331
polymer films, optical transmission obs. 8=45245
protonographic exam. 8=26363
pyrolytic graphite, carrier density rel. to pressure 8=35756
quartz, synthetic, homogeneity of refractive index obs. 8=35207
ruby laser, thermal deform. 8=24335
step structure, non-equilib., rel. to supersaturation 8=30813
transition metal cpds with S, Se or Te, non-stoichiometry and ordered structs. 8=26164
Al, Si^{28} nuclear resonance fluorescence anisotropy 8=30631
CaV_2O_6, microscopic props . 8=30798
$Ca_2V_2O_7$, microscopic props. 8=30798
$Ca_3V_2O_8$, microscopic props. 8=30798
Cu, mean inner potential calc. method 8=30629
Cu. mean inner pot. meas. by electron diffr. 8=30628
$CuSO_4$, $5H_2O$, D/H ratio during dehydration 8=30802
$HoCo_5$, magnetocrystalline anisotropy and mag. structure 8=40737
KBr, mean inner potential calc. method 8=30629
KBr, mean inner pot. meas. by electron diffr. 8=30628
NaCl, mean inner potential calc. method 8=30629
NaCl, mean inner pot. meas. by electron diffr. 8=30628
α-$NiSO_4.6H_2O$, internal energy 0.4-4.2°K, in mag. field 8=30968
PtO_2, and synthesis 8=35205
RhO_2, and synthesis 8=35205
Tm^{169} internal conversion, rel. to chemical environment 8=29336
U^{233} aligned nuclei, α ang. distrib., obs. 8=30634
$Zn_xCd_{1-x}S$, varying composition effect slow and abrupt 8=39696
ZnO, laser action under e.-beam pumping 8=49765

Crystal structure
See also Polymorphism.
affinity relations in impurity effect mechanism on crystallization and growth 8=30819
alums, α and β, morphological difference 8=26173
anthracene, α-radiation damage study 8=48826
bainite needles and plates in low-alloy steel, struct. and growth characts. 8=44002
bitumen and components, morphology 8=48516
bonds, covalent, elements of theory 8=26004
borate mineral systematology 8=48511
cadmium chalcogenides, hexagonal or cubic phases formation rel. to stoichiometry effects 8=44082
calcite, synthetic, morphology and optical props. 8=26194
charge-transfer complexes, and solid-state spectra 8=26166
corundum, form on evaporation at high temps. and low pressures 8=39643
diamonds, natural and synthetic, features in stable and metastable regions 8=26192
diphenyl-α, α′ dipyridyl, of single crystal from solid soln. 8=26040
double-layer, formation, brucite-like layer ions 8=48514
equilibrium forms for polyhedral crystals, theory 8=44083
families, main and subclasses and homeotypes of structure types 8=26162
grain size and recrystallization 8=30820
grain size on solidification 8=35233
graphite, on n-irrad. under restraint 8=31149
graphite, pyrolytic, anisotropy correl. with normal emissivity 8=36332
hailstones, artificial, lobe-like growth, and surface config. 8=35228
hydrothermally grown, rel. to soln. ionic or colloidal charact. 8=26223
ice, growing in supercooled water 8=26176
rel. to imperfection types produced by mechanical pressure 8=26658
iron-group containing, rel. to colour 8=27534
lanthanides, compressed polymorphs. and intra-alloys, rel. to 4f contrib. to binding 8=26178
leukosapphire, substructure from x-ray exam. 8=30812
models, ball-drilling methods 8=32631
molecular, symmetry of pot. functions 8=34391
morphology dependence periodic bond chain model 8=26191
muscovite heated in vacuum, superstructure phase, electron microscopy study 8=26190
nylon 66, spherulite deform. in cold drawing, 20°C 8=44097
organic materials with low m. p. s., apparatus for routine studies 8=26214
organic matter, crystalline nature 8=41220
organic phosphors 8=41221
paracrystalline state theory 8=30799
paradibromobenzene-paranitrochlorobenzene, of single crystal from solid soln. 8=26040
permalloy sheet obs. of texture during recrystallization 8=35282
polyethylene, extended-chain lamellae, origin 8=44094
polymer crystallinity, definition rel. to X-ray diffr. obs. 8=44092
polymer crystallinity from thermal meas. 8=44093
polytetrafluoroethylene oxide, packing and mol. configuration 8=35366
polyvinylidene fluoride, in $\alpha \rightleftharpoons \beta$ transform. on stretching in temps., 20-150° and annealing 8=26155
powders, crystalline, highly compressed, struct of boundaries 8=49325
rel. to rounded forms and plane faces 8=26170
in solid phase, morphology theory 8=26171
steel, high-carbon, of martensite, e. microscope exam. 8=35272
sucrose growth and habit rel. to adsorbed impurity effect 8=26266
sulphide ores, grain boundary movement, under annealing 8=26843
superplastic alloy 8=30872
superstructure, work hardening 8=44527
symmetry of helical structures 8=29858
tolane-diphenyl mercury, of single crystal from solid soln. 8=26040
transformer steel, change of blast furnace struct. 8=40153
transition metal chalcogenides, order of vacancies and non-stoichiometry 8=26635
twins, symmetry group generalization 8=39647
II-VI compounds, semiconducting, rel. to growth conditions 8=48561
villamaninite, chem. and structural analyses 8=48646
würtzite classification 8=35209
zinc chalcogenides, hexagonal or cubic phases formation rel. to stoichiometry effects 8=44082
Zircalloy-2 film, rel. to white spotting in oxide films 8=35187
Zircalloy-2, ZrH precip. habit planes, obs. 8=44098
Zircalloy-4, ZrH precip. habit planes, obs. 8=44098
Ag crystallizing in thin films at high evaporation rate 8=30741
Ag, during electrocrystallization initial stages 8=30822
Au epitaxial films in high vacuum 8=30747

Crystal structure—contd
Au film, vacuum deposition effects 8=35160
Au films, discontinuous, morphological changes following deposition mechanism 8=39588
3-Au-Cd alloys, martensites 8=26035
BN, pyrolytic, anisotropy correl. with normal emissivity 8=36332
$Ba(BrO_3)_2$, anhydrous, forms 8=30808
Be, anisotropy correl. with normal emissivity 8=36332
$[(C_6H_5)_3FC_4]_2$, isomerization 8=39642
$CaCO_3$, effect on adsorpt. of Ca sulfonate, rel. to oil sol form 8=30767
$CaCO_3$, interplanar distances and structure factors 8=42651
CaF_2, changes on TbF_3. Tb_4O_7 and TbOF admixtures 8=26168
CdS {0001} surfaces, study and O_2 adsorption by LEED 8=30719
$Ce_2W_2O_9$, and hydrothermal synthesis, obs. 8=39636
$ClWO_4Cl$, and hydrothermal synthesis, obs. 8=39815
CoO(I) and (II), from X-ray powder meas. 8=26017
Cu-Co alloys, coherency loss 8=26036
Cu-Zn alloys, abraded, surface and subsurface structure 8=26294
DCl, and phase transforms. by X-ray and n-diffr. 8=26073
Fe-Ni alloy, changes during isothermal compression up to 300 kb 8=49006
α-Fe_2O_3, topotaxial relations with its reduction product, Fe_3O_4 8=26072
Fe_3O_4 films grown in LiOH solns., two-phase struct., 300°C 8=44043
Fe-3% Si secondary recryst., cube textured, rel. to impurities and processing 8=26265
GaAs grown from supercooling melts, dislocation structure rel. to growth conditions 8=26678
GaP platelets, effect of impurities and crystallization conditions 8=26205
GaP, VLS grown, morphology 8=35208
p-Ge, transport properties, symmetry rel. to theory 8=26907
$2(H_2Ca_2Mg_5(SiO_3)_8)$: Mn^+, effect on e.s.r. line intensities 8=36245
HCl, and phase transforms. by X-ray and n-diffr. 8=26073
H_xWO_3, X-ray and neutron diffraction studies 8=35336
$K_4Fe(CN)_6 . 3H_2O$, polytypic transforms. rel. to ferroelec. props., 0 to −100°C 8=31432
KO_2, and phase transforms. 8=26075
$La_{3.33}Cu_2S_6$, double sulphide, data 8=30800
$La_{3.33}MnS_6$, double sulphide, data 8=30800
LiF:Ni^{2+}, struct. and comp. of stable monocryst. clusters 8=35219
$Li(Ta_{0.5}Fe_{0.5})O_2F$, and dielec props 8=31435
$MgSO_4 . 7H_2O$, left form predominance, crystallization conditions effect 8=26177
$MnAs_{0.92}P_{0.08}$, polycrystalline, and mag. props. 8=31503
Mo dendrites, morphology 8=48568
NaCl: $Pb(NO_3)_2$, changes on heat treatment at 300°C 8=26689
NaO_2, and phase transforms. 8=26075
$Nd_2W_2O_9$, and hydrothermal synthesis, obs. 8=39636
$NdWO_4Cl$, and hydrothermal synthesis, obs. 8=39815
Ni boracites, sector-growth and twinning, exam. by polarized-light microscopy 8=26188
Ni, during electrocrystallization intitial stages 8=30822
Ni-Co-Cr superalloy sulphidation corrosion, and phase distrib., obs. 8=30806
Ni_4Mo, ordered, tetragonal superstruct. and three classes of interfaces 8=26713
$Li(Nb_{0.5}Fe_{0.5})O_2F$, and dielec. props. 8=31435
OD-structures, of geometrically equiv: rods, systematics 8=26630
$Pb_2(NiW)O_6$ synthesized under high pressures, phase transitions 8=35122
PbS, artificial, morphology rel. to hydrodynamic flow theory 8=26197
$Pr_2W_2O_9$, and hydrothermal synthesis, obs. 8=39636
$PrWO_4Cl$, and hydrothermal synthesis, obs. 8=39815
RbO_2, and phase transforms. 8=26075
Sb_2S_3–Bi_2Te_3 solid solns., morphotropy 8=48672
SiC, conversion of cubic to hexagonal as fn. of temp. and press. 8=48399
Sn chalcogenides, struct. and props. 8=39600
Ta, sintered, recrystallization rel. to deformation and temp. 8=48560
Ta, zone-refined, degree of perfection rel. to growth condition effects 8=35231
TaFe lamellas in TaFe-$TaFe_2$ position and melting point 8=35220
in TiNi films in premartensitic states, formed in cooling 200-0°C 8=30710
U, change in β phase, rel. to anomalous thermal arrest. 8=35129
W(110), with double Li-O films 8=39593
YAl garnet, morphology rel. to growth on seed by flux technique 8=26198
Zn, melt-grown, substructure dependence on impurities 8=26268
ZnO, hydrothermally crystallized, effect of Li^+ 8=26201
ZnS, melt-grown under pressure 8=44084

Crystal structure—contd
ZnS, polytype formation rel. to periodic slip processes 8=44461
ZnS, (Se), (Te), semiconducting, rel. to growth conditions 8=48561
Zr compounds with Laves structure, and magnetism 8=31711
ZrB_2, of second phase precipitates, and relative orientation 8=35136
Zr–O interstitial solid solution, superstructure rel. to ordered arrangement of O 8=35289
microstructure
See also X-ray examination of materials/microstructure.
alkylacrylates-methacrylic acid copolymers later particles and films, obs. 8=26156
"alni" type alloys, 3-d modification 8=35270
alumina, grain-boundary relax., l.f. 8=44549
barite ($BaSO_4$) crystals, low angle grain boundaries 8=39717
basalt, white pattern zones of titanomagnetite grains, obs. 8=48588
brass, 70/30, deformed layers prod. by machine cutting 8=35555
α-brass, grain size, influence of Fe and P additions 8=48594
β-brass, quenching effects 8=48595
carbonized coal-tar pitch, microstruct. of coalesced mesophase 8=30576
cermets, rel. to geometry and phase distrib., effects on mech., thermal and elec. props. 8=35263
channelling to study crystal faults 8=48578
chloroprene-vulcanizate blocks, crystalline structures 8=26145
clay, effect of graphite 8=39709
domain boundary caused diffr. spots, fine structure 8=30846
explosion bonded metals, electron microscope investigation 8=44157
fabrication induced variations 8=35258
ferrites, hot-pressed, fine-grained, rel. to h.f. and microwave props. 8=27435
fine structure surrounding undiffracted beam in e diffraction, obs. 8=26288
glass, densification under cutting wheel using Zeiss interference microscope 8=39724
glass fracture surfaces, mist zone 8=30722
grain boundary diffusion meas. analysis 8=39957
grain size determ. of coarse crystals 8=30841
graphite, after thermal oxidation 8=44167
graphite, changes on creep strain at 2500°C 8=44163
graphite, highly oriented, crystallite boundaries effect on princ. thermal conds. 8=35457
graphite, rel. to field-ion microscopy 8=26292
grinding effects using vibro-grinder, X-ray diffr. and e-microscope exam. 8=26286
gumbelite, fibre crystallites 8=26174
interaction, elastic and diffusional, of pores with each other and with boundaries 8=30839
internal stresses, extension of dislocation continuum theory 8=44519
metal sheet texture determ., neutron diffraction method 8=35261
metals and alloys, high-temp., microscope for study 8=42183
metals, grain size reln. with diffusion 8=48349
metals, pure, grain-boundary migration, characts. under fatigue at elevated temps. 8=39710
meteorite alloys, sulphide inclusions, miscroscope obs. 8=39722
mica, knick-band indexing using the X-ray universal stage 8=26714
microscopy of field and domain structs. 8=48577
minerals, grain size and crystalline structure rel. to peak intensity errors in powder diags. 8=26285
nylon 4, precip. from H_2O-glycerol solns., and lattice spacings, obs. 8=44285
orientation effect, by electron microscopy, improvements 8=35262
oxide layers from reactive cathode sputtering, texture from X-ray obs. 8=39711
oxides: CdO, CaO, MnO, NiO electron microscope investigation 8=48592
petroleum-coke, graphitized, absolute crystallite size and lattice distortion determ. 8=26293
phenanthrene-biphenyl mixed crysts. 8=41159
planes in space, ang. distrib. determ. 8=26282
pole figure plotting by computer 8=48583
pole figure plotting from X-ray intensities, computer-directed 8=48584
polyalkylacrylates later particles and films, obs. 8=26156
polycrystalline mats, orientation distrib. functions 8=26181
polyethylene, chain folding, vibr. analysis 8=44305
polyethylene, crystallized, crystallite size and lattice defects 8=39990
polyethylene, lamellar, from m. p. and branching determ. 8=44096
polyethylene, linear fractions, mol. dispersed eutectic systems 8=44095
polyethylene supermol. struct., reorientation effects, X-ray obs. 8=26157

Crystal structure—contd
  microstructure—contd
    poly-L-alanine spherulites, morphology 8=35291
    polymers, oriented, intercrystallite layer density from X-ray diffr. 8=35290
    polypropylene, spherulites, light scatt. determ. 8=49783
    polystyrene, spherulites, light scatt. determ. 8=49783
    poly(theylene terephthalate) fibres, amorphous orientation and crystallite form., obs. 8=44175
    poly-2, 2′-octamethylene-5, 5′-dibenzimidozole amorphisation in annealing, obs. 8=26158
    polyvinyl alcohol, rel. to electrokinetic potential 8=26154
    quartz, knick-band indexing using the X-ray universal stage 8=26714
    quasi-mosaic effect, elastic 8=39706
    refractory metal carbides, field ion microscopy 8=26289
    rel. to Poisson's ratio anomalies, anisotropy, $\mu < 0.5$ 8=40095
    rel. to tensile brittle fracture initiation 8=31174
    silica, fused, microcrystal orientation in ordered isotopic structure 8=26150
    steel, austenitic 20% Cr/25% Ni-Nb-stabilised, surface oxides formed in CO$_2$ at high temp. 8=41238
    steel, cold-rolled, recrystallization texture, influence of phase transformations 8=39719
    steel, grain size and C content effects on discontinuous deformation 8=35682
    steel, hot-rolled, properties and process control 8=48598
    steel, low-carbon, deformation and recrystallization textures, rolling temp. dependence 8=26818
    steel, P segregation, etching determ. 8=30861
    steel, segregation study by X-ray fluorescence technique 8=30860
    steel, transformer, cubic texture perfection rel. to mag. props. 8=36140
    steel, transformer, hot-rolled, internal oxidation zone 8=36562
    steels, strain-aged, discontinuous yielding grain-size dependence 8=26809
    steels with f.c.c. lattice of solid soln., rel. to internal friction peak 8=35678
    steels, cast austenitic, grain size decrease by phase transformations on thermal cycling 8=35698
    superstructures, concentration inhomogeneites in ordered soln. 8=35057
    talc, changes during heating, thermal and X-ray analysis 8=48601
    talc, changes on heating 8=30699
    texture representation, complex, by biaxial pole figures, analytical methods 8=48576
    texture study, instruments for magnetic analysis 8=48579
    thoria, arc-melted, precip. e-microscope obs. 8=30867
    thoria gel, crystallite sizes, equivalence of X-ray and electron microscopy 8=35284
    ticonal alloy, 3-d modification 8=35270
    Ag films on CaF$_2$ and NaCl, X-ray investigation 8=44158
    Ag^{110}, grain boundary self diffusion coeff. meas. 8=39961
    Ag-Al alloys, of massive and martensitic transformation 8=48370
    AgCu alloy film, vapour-quenched, from X-ray scatt. 8=44159
    Al alloys, aged, influence of small additions of Ag 8=48590
    Al, annealing twin boundaries 8=44161
    on Al, anodic oxide films, pore struct. and barrier layer, obs. 8=44038
    Al, cast strips after cold rolling, transform. to brass-texture 8=35263
    Al, mosaic block misalignment and strengthening on low-temp. deformation 8=35653
    Al 99.5, cube or rolling texture, rel. to degree of deformation 8=35266
    Al, pure, substructure from cold rolling 8=26781
    Al, self-diffusion coeff. from annealing kinetics of voids 8=35478
    Al slabs, grain size orientation 8=48589
    Al, strained, substructure changes on heating 8=44162
    Al wire, grain size orientation-dependence rel. to texture development 8=26290
    Al-Al$_2$O$_3$, influence of grain size on high-temp. ductility 8=26779
    Al-4% Cu, grain boundary precipitate growth, interfacial diffusion 8=39715
    Al:(Fe, Si) sheet, texture form. in final anneal, influence of precipitation 8=35267
    Al-In alloys, dilute, electron microscope observations 8=35265
    α-Al$_2$O$_3$:Mn, distribution of Mn-content 8=44118
    Al$_2$O$_3$-Si cermets, reaction formed, two discrete types 8=39712
    Al-Si eutectic alloys, growth mechanisms 8=35234
    Be, specimen preparation and microscopic examination 8=39718
    Be-Ca alloys, specimen preparation and microscopic examination 8=39718
    BeO ceramics, extruded, grain deform and residual stress 8=44556
    BeO polycrystals, grains, subgrains and stress analyses 8=26291

Crystal structure—contd
  microstructure—contd
    CdS, from X-ray diffraction work, calc. 8=39779
    Co electroless films, grain size and fibre axes, obs. 8=44165
    12% Cr-Mo-V-Nb creep resisting steel, rel. to creep and creep rupture data 8=44576
    Cu, rolling texture and orientation distrib. function 8=48593
    Cu-2% Be, aged, nucleated precip. phase space lattice, obs. 8=35271
    Cu-2% Be alloy, diffuse striations obs. at 200°C rel. to strain-contrast effect 8=30859
    Cu-Ga alloy, feathery structure formation in massive transform. 8=30690
    Cu-Ni steel rel. to edge crack prevention in oxidation, obs. 8=26811
    Cu-Pb superconducting alloys, rel. to magnetization meas., 8=44723
    Cu$_2$O films on Cu(111), and diffusion in defects rel. to oxidation, obs. 8=44042
    Fe-rolling textures rel. to deformation mechanism and sample orientation 8=26820
    Fe-Al alloys, phase transformations 8=39720
    Fe-27% Cr, annealed, Guinier-Preston zones rel. to brittleness 475°C 8=35273
    Fe-N martensite, electron transmission study 8=39721
    Fe-Ni-Cr-Nb alloys, strengthening phase identification 8=44574
    Fe-Ni-Ti alloys, texture changes in $\gamma \rightarrow \alpha$ and $\gamma \rightarrow \alpha \rightarrow \gamma$ transforms. rel. to Young's modulus 8=35701
    Fe-3% Si, surface and grain boundary energies in presence of O$_2$ 8=26102
    γ-Fe$_2$O$_3$ particles, acicular, mag. props. crystallite size dependence 8=31635
    FeSi$_2$, β phase 8=30862
    Ge, amorphous, Ar ion bombardment of crystalline form. 8=39723
    β-In$_2$S$_3$, domain struct. due to ordering of In vacancies 8=48599
    Li-Zn ferrites, hot-pressed, fine-grained, rel. to h.f. and microwave props. 8=27435
    LiF, X-ray diffr., Debye-Scherrer obs. with Fe^{55} source 8=28930
    Mg-Zr alloys, form. of denuded zones at grain boundaries in diffusion creep 8=26831
    Mn(TiMn)O$_4$ 8=40872
    Na aluminosilicate glass, ion-exchange hardening, i. r. spectrum obs. 8=30864
    NaCl, doped with divalent cations, evaporation structure 8=48603
    Nb, rolled, orientation distrib, of crystallites 8=35275
    Nb$_3$Sn; ZrO$_2$ particles, influence of superconducting performance 8=44728
    Ni, angular characts. of intergranular structure by small-angle X-ray scattering 8=26297
    Ni-containing permanent magnets, extruded, texture and props. 8=33046
    Ni, electrodeposited, effects of addition agents 8=35277
    Ni, electrodeposited, process conditions rel. to particle size and microstrain formation 8=26298
    Ni, grain-boundary damping peaks 8=48872
    Ni oxide bicrystals, [001] tilt boundaries, grain boundary energies and grooving kinetics 8=35278
    Ni-2.2% Be, aged nucleated precip. phase space lattice, obs. 8=35271
    Ni$_3$Al-Ni$_3$Nb system oxide scale exam. 8=35276
    NiCr, ThO$_2$ dispersed, grain growth rel. to cold working 8=48604
    Ni-Fe films, electrolytically prepared, conditions for formation of hexagonal structure 8=26122
    Ni$_3$Nb oxide scale exam. 8=35276
    Ni, ThO$_2$ dispersed, grain growth rel. to cold working 8=48604
    Ni-Zn ferrites, hot-pressed, fine-grained, rel. to h.f. and microwave props 8=27435
    Pb alloys, grain growth dependence on low solubility additions during recrystallization 8=35280
    Pb alloys with 0.5% Sb, Te, Cu, effect of dopant rel. to alloy fatigue life 8=26841
    Pb ferrites, oxide additives effect rel. to mag. props. 8=40842
    Pb, grain size and boundaries rel. to flow under simple shear 8=35713
    Pb-Bi alloy films at low temp., by electron diffraction examination 8=35152
    PbO layers, rel. to optical filter characts. 8=28765
    PbO vapour deposited layers, preferred orientation 8=30756
    Pb(ZrTi)O$_3$ ceramics 8=44597
    Pt-Co ordered, texture rel. to mag. props. 8=36175
    α-Pu, after heat treatments at press. over 30 kbar 8=35281
    Re, irradiated, unit cell and dimensional changes 8=26737
    ReTe$_2$, synthetic, x-ray powder data, unit cell parameters 8=39726
    Si-Mn steel, austenitic grain size effects on fatique crack initiation and propagation 8=44575

- **Crystal structure**—contd
  - **microstructure**—contd
    - Si_3N_4 films, Na diffusion 8=48605
    - Ta, crystallographic analysis of oxide plate formation 8=39690
    - Ta, oxide plate formation, growth and morphology 8=39689
    - TaC, grain growth during hot-pressing 8=35283
    - Ti alloys, equiaxed $\alpha + \beta$, determ. of β grain size 8=44170
    - Ti-6% Mo alloy, quenched, study by electron microscopy 8=30869
    - Ti-22 at. %Nb/Cu composite conductors ω precip. size and distrib. 8=40419
    - TiNb33:N and O, and supercond. and workability, obs. 8=44742
    - TiNb40:N and O, and supercond. and workability, obs. 8=44742
    - U, alloys, α-phase grain refinement by B addition, obs. 8=44171
    - UC, Ar-sintered, effects of Ni 8=26299
    - UO_2, columnar grain growth under steep thermal grads 8=26301
    - UO_2, factors influencing equiaxed grain growth 8=26300
    - V steel, isothermal transformations, diffraction patterns 8=39791
    - V_6C_5, ordered compound, domain structure and superlattice 8=44172
    - W, grain boundary struct., step heights and sublattices 8=39728
    - WC-Co alloys, rel. to fracture and plastic deform. 8=26851
    - WC and W_2C, indexing of field-ion micrograph using computer 8=44174
    - Y-C system, phase diagram proposal 8=39569
    - Zn-Al alloys, influence on flow stress-strain rate behaviour 8=40187
    - Zn-Al alloy, superplastic 8=30872
    - ZnS, influence on electroluminescence 8=41215
    - Zr-Nb alloys, dispersed precips. effect on critical current density 8=35857
- **Crystal structure, atomic**
  - See also Crystal electron states; Crystals/lattice mechanics; Electron diffraction crystallography; Neutron diffraction crystallography; X-ray crystallography.
  - bent O-H---O bonds 8=48300
  - Bravais lattices, four-dimensional 8=35294
  - Bravais rule, dislocation-energy interpretation 8=26304
  - classification of substances by crystal systems and classes, Bravais lattices and space groups 8=26161
  - computer programs, DSPIN and LSQRS 8=39747
  - contact rule for rigid-sphere models 8=26303
  - deformed, surface states by tight-binding approx. 8=40256
  - disordered cryst. with nearly perfect unit cell, X-ray diffraction theory and correl. functions 8=26328
  - distorted, line shape, dynamical calc. 8=26306
  - extended fine structure, x-ray k-absorption spectra 8=39748
  - false structures from combination of structure amplitudes with arbitrary phases 8=39730
  - f.c.c., condensed sheets of interstitial atoms, X-ray scattering calcs. 8=44180-1
  - ferroelectrics, displacive, at. displacement rel. to Curie temp. and spontaneous polarization 8=44882
  - ferroelectrics (magnets), determ. using micro e.-diffr. techniques 8=39761
  - ferroelectrics, soft, spectra-struct. correl. 8=27544
  - ferromagnetic crysts., lattice uniaxial deform. rel. to magnetization curve 8=36104
  - films, vacuum deposited rel. to residual stresses, X-ray diffr. obs. 8=44537
  - h.c.p. crysts. indices of planes and dirns. Miller VS Miller-Bravais 8=48958
  - indexing e. diff. diagrams and struct. projections for arbitrary crystal orientation 8=35312
  - interchange symmetry for mols. and crysts. 8=25410
  - internal mag. fields, Shubnikov group representation 8=27375
  - lattice constant precision determs. using Kossel line technique in back reflection region 8=39738
  - lattice deformation energy calcs. from covalent bond theory 8=30613
  - lattice energy minimum search 8=26316
  - lattice thermal conductivity, formulae in Debye approx. using π theorem 8=26599
  - lattice with substitutional impurity, generalized Wannier and Block functions 8=48606
  - least-squares refinement, convergence-criteria 8=39752
  - least-squares refinement method for isomorphous replacement 8=44186
  - macromolecular, chem. bonding 8=43923
  - magnetic space groups and their irreducible representation 8=31488
  - microphotometer, Siemens, use with single crystal photographs 8=26320
  - microscopy of field and domain structs. 8=48577
  - minimization method for solving structure, analysis problems 8=26317
  - molecular, calc. method for densest distrib. of plane mols. in layers 8=30878
  - molecular centre location from morphological and unit-cell data 8=39735
  - non-cubic cell parameters, depend. of accuracy on reflection indices 8=35298
- **Crystal structure, atomic**—contd
  - non-Kramers doublets, transitions in electron paramagnetic resonance 8=49584
  - orientation distrib. calcs. in fibres and sheets 8=44178
  - orthorhombic diatomic groups, Patterson diagrams 8=26305
  - packing density and molec. struct. rel. to rotational diffusion rates 8=48767
  - phase determ. using anomalous dispersion and directly measurable parameters 8=39733
  - phase determ. using correlation-eqn. method 8=48611
  - point groups in 4-dims. 8=48609
  - positron and electron motion dependences 8=48889
  - potential distribs. in atoms, Z = 1-18, integral characts. 8=39731
  - protonographic exam. 8=26363
  - radial density curves, anal. of termination effects 8=35321
  - radiation damage investigations by liq. He field-ion microscope 8=31128
  - radii and pressure-induced phase transforms 8=26054
  - random-layer line profile, Fourier-transform methods 8=26308
  - refinement of parameter of atoms in special positions, general procedure 8=26315
  - rocksalt O_h^5-Fm3m, space group selection rules 8=39732
  - semiconductor, and bonding 8=30614
  - shock compressed lattice distortion analysis 8=26745
  - space group, theory of regular divisions 8=48608
  - sterographic projections, computer constructions 8=48623
  - substructure of single crystals by high resolution Laue diagrams 8=35300
  - symmetry in tight binding approx., consistent treatment 8=31282
  - symmorphic space groups, symmetry coords. 8=35373
  - transformations studied using composite reciprocal lattice 8=26052
  - twinning shear, theory rel. to deformation 8=35215
  - two-line Fourier analysis, influence of cut-off 8=35299
  - valence struct. from coherent scatt., Fourier difference synthesis 8=48620
  - **elements**
    - diamonds, type Ia, reciprocal lattice spikes 8=44209
    - graphite, dimensional changes due to neutron irrad., effect of crystallite size 8=35600
    - graphite, empty-channel lattice, pulsed-source obs. 8=30890
    - graphite, lattice expansion on condensable vapour intercalation rel. to friction and wear 8=44208
    - graphite, lattice fringes resolution, axial e illum., 100 kV 8=39775
    - graphite, line intensity on X-ray diagrams 8=35319
    - metal, divalent 8=26364
    - rare-earth metals, heavy, rel. to mag. structures 8=35350
    - transition metals 8=44258
    - transition metals, effect on d bands 8=44653
    - Ag, lattice parameters change, effects on Fermi surface 8=40237
    - Al, n-irrad., lattice vol. distortion, subthermal n scatt. obs. 8=44203
    - Au, lattice parameters change, effects on Fermi surface 8=40237
    - Be, planes studied for neutron diffraction 8=48640
    - C blacks, atomic radial density curves, anal. of termination effects 8=35321
    - C, dimensional changes due to neutron irrad., effect of crystallite size 8=35600
    - Cl, molec.-orbital calc. 8=48648
    - Cu, lattice parameters change, effects on Fermi surface 8=42037
    - Cu on sapphire, epitaxy of single crystal films 8=30751
    - Cu, spherical crysts., reciprocal lattice and LEED spot patterns 8=26098
    - D, 4.2 to 0.91°K, neutron diffraction obs. 8=39795
    - F, molec.-orbital calc. 8=48648
    - Fe, lattice constants rel. to temp 8=48649
    - Gd, parameters rel. to pressure 8=48669
    - Ge crystal, ion-bombarded, defective structure, e.-diffr. exam. 8=39793
    - Ge ion implantation effects, analysis by 1 MeV He^+ scatt. 8=48927
    - Ge, via transmission pseudo-Kossel lines 8=48653
    - H and para H, 4.2 to 0.91°K, neutron diffraction obs. 8=39795
    - γ-Hg 8=44220
    - In films, degree of lattice distortion effect on superconductivity 8=35849
    - Mn, at 77-300°K 8=48663
    - Mn, lattice consts. rel. to para-antiferromag. transition, −180-950°C 8=44253
    - Mo, 15° to 65°C 8=44233
    - Mo, lattice consts and densities, effect of S, Se and Te solubility 8=48664
    - Nb, lattice parameter X-ray determ. rel. to density hydrostatic determ. 8=48670
    - Ni, dilating effect on unit cell of dissolved C 8=44243
    - Ni, lattice constants rel. to temp 8=48649
    - S, unit cell parameters, rel. to calc. of pot. energy 8=39502
    - Sc, lattice consts. rel. to para-antiferromag. transition, 20-660°C 8=44253

Crystal structure, atomic—contd
- **elements—contd**
  - Si, ion implantation effects, analysis by 1 MeV He$^+$ scatt. 8=48927
  - Si, [111] planes, imaging 8=44218
  - Si surface atomic and electronic states from e.p.r meas. 8=40943
  - Te, electron microscope investigation 8=35356
  - Ti, lattice consts. rel. to para-antiferromag. transition, —180-1500°C 8=44253
  - Te lattice, temp. depend. of coordinates 8=44256
  - V, lattice consts. rel. to para-antiferromag. transition, —180-1500°C 8=44253
  - Y, study 8=26434
- **alloys**
  - alnico, high-coercivity, powder pattern exam. 8=35346
  - austenite in steel, lattice parameter changes rel. to intermediate transformation 8=35333
  - disordered binary, correlation functions 8=43972-3
  - rare earth 8=48671
  - Ag$_3$Mg, long range order, quenching temp. dependence 8=44200
  - Au–V solid solutions, lattice parameter comp. dependence, 0-10 at.%V 8=44205
  - Cr–Ni–Fe solid solns., lattice type and parameters on prolonged crystallization 8=26246
  - CuAuII, long period ordered, lattice modulation, X-ray diffraction study 8=30893
  - Fe–Mn–C steels, c/a ratio variation during martensitic transformation, —196 to 20°C 8=35334
  - Fe-Ni, parameter change due to diffusion of Au 8=39789
  - Fe W system, α-solid soln, and intermed. phases 8=30692
  - GdPd, and mag. props. 8=44216
  - Hf-X, (X = Os, Ir, Pt), rel. to phase transforms 8=30899
  - HfSb$_2$ phase, rel. to quasi-homologs 8=35360
  - InSb-GaSb heterojunction, lattice mismatch accommodation. 8=48857
  - Li$_2$MgX, f.c.c. with body-centred substructs., obs. 8=39800
  - Ni-10 at. %W, local at. arrangements rel. to heat treatment and cold deformation 8=44244
  - O and α-Ti mixed crystals, lattice struct. rel. to hydrogenation, n diffr. obs. 8=35357
  - PbTiO$_3$–PbMn$_{2/3}$W$_{1/3}$O$_3$ system, solid solns., cell parameter comp. dependence 8=40616
  - PbTiO$_3$–PbMn$_{2/3}$W$_{1/3}$O$_3$ system, solid solns., structural 8=40616
  - Pt-Mn alloys, and ferromagnetism 8=26432
  - TiFe$_x$Co$_{1-x}$, from n-diffr. meas. 8=30912
  - V$_5$Sb$_4$ phase, rel. to quasi-homologs 8=35360
  - ZrBi$_2$ phase, rel. to quasi-homologs 8=35360
  - ZrSb$_2$ phase, rel. to quasi-homologs 8=35360
- **inorganic compounds**
  - alkali halides, box model theory, test of validity 8=35315
  - alkali halides, X-irradiated, lattice disorder at room temp. 8=44198
  - alums, Ti^{3+} substituted, rel. to crystal-field origin 8=43935
  - ammonium metaphosphates, rhombohedral form 8=44245
  - antimonides with D8$_8$ and Hf$_5$Sn$_3$Cu structure types 8=26440
  - ardennite, rel. to Si$_3$O$_{10}$ group positioning 8=39808
  - bayerite, from n. -diffr. exam. 8=39804
  - borates with dolomite structure, refinement of oxygen positions 8=48635
  - botryogen, and refinement 8=39790
  - β-brass, B2 superlattice, interact. of defects at antiphase boundaries 8=44448
  - brucite, from n. - diffr. exam. 8=39804
  - calcic amphiboles, unit-cell volume and packing density, isotypic replacement effects 8=26372
  - chlorite, new polymorph and polytypes, X-ray exam. 8=26174
  - chrysotile, X-ray diffr. profiles of faulted cylindrical lattice 8=39805-6
  - corundum group crystals correlation between optical spectra and struct. 8=35024
  - diamond lattices, asymmetric aspects of atomic charge density 8=26302
  - ettringite 8=44210
  - fluoroberyllates with langbeinite structure, new 8=44207
  - in graphite, structs. of insertion compounds 8=35320
  - hydrates, H atom positions determ. by NMR 8=44219
  - kaolin-dimethylsulphoxide complexes 8=27554
  - Kröhnkite, from n.m.r. 8=48660
  - lanthanide oxidecarbides 8=39802
  - lattice parameter-precision determ. using Siemens diffractometer 8=26324
  - lead(II) hydroxide, stable state 8=44255
  - manganites of perovskite structure, lattice distortions effect on mag. behaviour 8=49534
  - metal iodide crystals, exciton peak position rel. to lattice parameter 8=49113
  - metavauxite 8=48631
  - niobates, oxidic, cryst. struct. effect on luminesc. 8=45284
  - opals, gem, packing sequences from light diffraction 8=44254
  - oxides: CdO, CaO, MnO, NiO, X-ray exam. 8=48592
  - parawollastonite 8=48643
  - petroleum-coke, graphitized, absolute crystallite size and lattice distortion determ. 8=26293

Crystal structure, atomic—contd
- **inorganic compounds—contd**
  - polyphosphate [Na$_3$H(PO$_3$)$_4$]$_x$ 8=44239
  - potassium hydrogen fumarate, X-ray analysis 8=44275
  - pyroavrite 8=39803
  - quartz, electron diffr. exam. 8=35355
  - quartz, smoky, rel. to anomalous pleochrism 8=27608
  - rare-earth borates of dolomite structure, prep. and characts. 8=44249
  - rare earth sulphates, study 8=26434
  - sapphirine 8=35352
  - silica glass, densified at very high press., quasi-crystalline atomic arrangements 8=48504
  - spherical packing in 3-dimensional space 8=39734
  - spinel ferrite lattice, cubic, local Jahn-Teller distortions rel. to phase transitions 8=26408
  - tantalates, oxidic, cryst. struct. effect on luminesc. 8=45284
  - tapiolite and synthetic trirutile substances, neutron and X-ray diffraction studies 8=48614
  - tin(II) hydroxide, stable state 8=44255
  - titanates, oxidic, cryst. struct. effect on luminesc. 8=45284
  - transition metal carbides, nitrides and oxides, rel. to M-M interaction effect 8=26441
  - transition metal oxides, centred around Nb$_2$O$_5$, non-stoichiometric mechanisms 8=26365
  - triploidite 8=48652
  - tungstates, oxidic, cryst. struct. effect on luminesc. 8=45284
  - II-VI compounds, cubic and hexagonal, non-linear polarisability tensor relations 8=27545
  - Ag complex, bis (8-hydroxyquinoline) Ag(1) pyridine solvate 8=39765
  - Ag$_2$Al, lattice parameters rel. to temp. 8=44201
  - AgCrS(Se)$_2$, and mag. props., 8=39810
  - AgI, at 3 kbar 8=35316
  - AgMnO$_4$, redetermination 8=44199
  - Al chlorite, dioctahedral, X-ray exam. 8=26174
  - AlCl$_3$. 6H$_2$O, from n. - and x-ray diffr. meas. 8=39766
  - Al:Cr, impurity ion effect from X-ray diffr. study 8=26642
  - Al$_2$O$_3$, polycryst., porous, lattice changes due to fast n irrad. 8=26366
  - Am(OH)$_3$ 8=39767
  - As$_2$O$_5$. $^5/_3$H$_2$O 8=39768
  - Au–Cu–Zn alloy, martensitic θ-struct. 8=48633
  - Au(III)-dimethyl hydroxide 8=39770
  - B complex, bis(dimethylamine) boron chloride 8=39771
  - B complex, bis(dimethylamine)boronium chloride 8=26368
  - B$_2$O$_3$ 8=48634
  - B$_2$O$_3$ crystallites by electron diffr. 8=44206
  - B$_2$O$_3$ high-pressure form. 8=39772
  - BaAl$_2$O$_4$ 8=35318
  - Ba(ClO$_3$). H$_2$O, neutron-diffr. refinement 8=30886
  - BaLiD$_3$, neutron diffr. 8=48639
  - BaLiH$_3$, neutron diffr. 8=48639
  - BaMg(CO$_3$)$_2$, rel. to CaMg(CO$_3$)$_2$ 8=48637
  - Ba(NO$_3$)$_2$, NO$_3$-groups config. from n-diffr. 8=39773
  - BaNb$_2$O$_6$, and comparison with other ANb$_2$O$_6$ and ATa$_2$O$_6$ type phases 8=48636
  - BaO, 2Ta$_2$O$_5$ tungsten bronze 8=26369
  - Ba$_{0.27}$Sr$_{0.75}$Nb$_2$O$_{5.78}$, ferroelec. 8=48638
  - BaTa$_2$O$_6$, hexagonal tunnel struct. rel. to dielec. props. 8=35959
  - Ba$_6$Ti$_2$Nb$_8$O$_{30}$, bronze-type tetragonal ferroelec., re-examination 8=39774
  - BaTiO$_3$, atomic displacements rel. to real structure determ. 8=30887
  - BiFeO$_3$, by e-microdiffr. 8=26430
  - 3Bi$_2$O$_3$. 17Nb$_2$O$_5$, [001] projection 8=26367
  - Bi$_2$Se$_3$-Bi$_2$S$_3$, lattice constants, phase diagram 8=35094
  - Bi$_2$Te$_3$II, high-temp. and pressure polymorph, lattice parameters 8=30681
  - CS$_2$, and molec. motion 8=39776
  - Ca complex, CaBr$_2$. 10H$_2$O. 2(CH$_2$)$_6$N$_4$, and mol. structure 8=26370
  - Ca$_3$Al$_2$(O$_4$D$_4$)$_3$ 8=39777
  - Ca[B(OH)$_4$]$_2$. 2H$_2$O, OD-disordered modification, determ. method and results 8=26379
  - CaF$_2$-type lattice, asymmetric aspects of atomic charge density 8=26302
  - CaHAsO$_4$. H$_2$O, haidingerites 8=48641
  - (Ca, Mg)$_5$Al$_5$BSi$_3$O$_{20}$, space group, cell dimensions 8=48644
  - CaMg(CO$_3$)$_2$, rel. to BaMg(CO$_3$)$_2$ 8=48637
  - CaMnSi$_2$O$_6$, (johannsenite) 8=44248
  - CaMoO$_4$, powellite 8=39778
  - α-Ca$_3$N$_2$ 8=26371
  - CaNb$_2$O$_6$, prep. by Cl chem. transport, obs. 8=35238
  - CaO. 6Al$_2$O$_3$ 8=48642
  - CaWO$_4$:V, charge compensation 8=31855
  - Cd complex, diethyldithiocarbamate, and mol. structure 8=26375-6
  - Cd complex, diquinolium-tetrachloro-cadmate 8=26374
  - Cd complex, L-α-glycerophosphorylcholine cadmium chloride trihydrate 8=35325
  - Cd$_3$As$_2$ 8=44212
  - Cd$_3$As$_2$ high-press. polymorph 8=26066
  - CdCl$_2$. 2HCONH$_2$ 8=26377
  - CdGeP$_2$, refinement and ordering in amorphous state 8=26373

Crystal structure, atomic—contd
  inorganic compounds—contd
    CdI_2, rhombohedral polytype 12R 8=39644
    $Cd(NO_3)_2$ bisthiourea 8=35324
    CdS thick films, lattice parameters rel. to experimental conditions 8=39589
    $Cd[S_2CN(C_2H_5)_2]_2$, X-ray analysis 8=35323
    $CdSO_4 . H_2O$ 8=44211
    $CdTiO_3$, perovskite modification, structure changes over 20-1000°C 8=27242
    $Cd_2Zn(PO_4)_2$ 8=35322
    $CdZn_2(PO_4)_2$ 8=35322
    γ-Ce, slow-cooled, lattice parameters temp. dependence, 300-100°K 8=30891
    Ce-alkali metal tungstates, rel. to hydrothermal crystallization 8=26259
    Ce(III) complex, $K_2Ce(CH_3COO)_5 . H_2O$, by X-ray analysis 8=26378
    $Ce_2W_2O_9$, and hydrothermal synthesis, obs. 8=39636
    Co carbonyl complexes 8=26380
    Co complex, ammonium diethiocyanate-bis-dimethylglyoximatecobaltiate 8=26381
    Co complex, decammine μ-peroxo dicobalt monosulphate tris(bisulphate) 8=26385
    Co complex, nitropentamminocobalt (III) bromide, and mol. structure 8=26386
    Co(II) di-n alkylphosphinates, single crystal studies, and polymeric structures 8=30797
    Co(III) complex, aquopentammine Co perchlorate, rel. to complex in rotation 8=26384
    Co(III) complex, dichloro-bis-phenanthroline-Co(III)-chloride trihydrate 8=26387
    Co molybdate hydrates, non-stoichiometric, two phases 8=30916
    $CoCl_2, 4CH_3OH$ addition cpd. 8=26383
    $CoFe_2O_4$, cation distrib. 8=39780
    $Co(NCS)_4$ Hg, and refinement 8=39781
    $CoNH_4PO_4 . H_2O$, unit cell and space group, orthorhombic 8=35326
    $Co_xNi_{1-x}S_2$, pyrite solid solns., prep. and lattice parameters 8=48342
    Cr carbonyl complex, $(CO)_5CrCOCH_3$ 8=26446
    $Cr_{11}Ge_{19}$, and refinement 8=39782
    CrH, hexagonal, conversion to metallic Cr, crystallography and bonding relationship 8=48376
    $CsBr_3$, and bond lengths for Br_3^- 8=44247
    $Cs_5Cu_3(NO_2)_{11}$ 8=39786
    Cs_2NaTF_6, (T = Yb, Er, Ho, Y, Tb and Sm) 8=44250
    Cu-bis-N-ethylsalicylaldimine 8=26390
    Cu complex, bis(ethylenediamine) copper (II) fluoroborate 8=39785
    Cu complex, bis-N-phenylethyl-salicyl-aldiminato-copper II 8=26391
    Cu complex, copper-N-N-hexamethylenedithiocarbamate 8=26368
    Cu complex, $Cu_2(SCN)_3(NH_3)_3$, by X-ray analysis 8=26395
    Cu complex, tris-(2-dimethylaminoethyl)amine copper (II) bromide 8=26418
    Cu complexes, N-substituted salicylaldimine, structure regularities 8=26421
    Cu(I) complex, cupritetramine di-[catena-di-μ-thiosulphato-cuprate (I)] 8=26392
    Cu(II) alkanoates, by X-ray analysis 8=26463
    Cu-(II)-chelate complexes of N′, N′-dimethylthioformohydrazide 8=48689
    Cu(II) complex, bis-trimethylbenzylammonium tetrachlorocuprate (II) 8=26394
    Cu(II) complex, tricycloquinazoline copper chloride 8=26486
    $Cu_2Al[AsO_4](OH)_4 . 4H_2O$, liroconite, by heavy atom technique 8=39787
    $Cu_3(AsO_4)_2$ 8=35327
    $CuAsSe_2$ semiconducting film, from e-diffr. exam. 8=39788
    $CuAu_3$, from n-beam electron diffraction intensities 8=48627
    $CuCrS(Se)_2$, and mag. props. 8=39810
    $CuCr_2X_4$, (X = S, Se, Te), cation-anion distances rel. to monovalent Cu 8=48645
    $CuHgO(NO_3)_2 . 3H_2O$ 8=26393
    δ-Cu_9In_4, equilib. phase in Cu-16.8% In alloy formed on precip. 8=39548
    $Cu_2In_2O_5$ 8=26389
    $Cu_{0.15}Mn_xFe_{2.5-x}O_{4+\gamma}$ spinels, compensated tetragonal deformation and O nonstoichiometry 8=48380
    $CuMoO_4$, paramag. 8=35329
    $CuMoO_4$, space groups, single crystal grown from melt 8=44126
    $Cu_xNi_{1-x}S_2$, pyrite solid solns., prep. and lattice parameters 8=48342
    β-$Cu_2P_2O_7$ 8=35328
    $CuSO_4 . 3H_2O$, rel. to crystal chemistry of salt hydrates 8=26388
    $CuUO_4$ 8=39784
    DBr, solid, rel. to lower phase transition 8=26396
    DCl, cubic 8=35330
    $DyAlO_3$, nuclear and magnetic structure 8=48647
    DyC_2, neutron diffr. 8=40865
    $ErPO_4$, neutron diffr. 8=44213

Crystal structure, atomic—contd
  inorganic compounds—contd
    $ErVO_4$, lattice parameters and Miller indices, using computer programmes 8=44252
    $ErVO_4$, neutron diffr. 8=44213
    $Eu_3Fe_{1.94}Ga_{3.06}O_{12}$, cation distrib. 8=30895
    $Eu(ReO_4)_3$, high-temp. modification, X-ray obs. 8=30914
    Fe carbides, similarities between phases 8=44003
    Fe carbonyl, cyclopentadienylcarbonyliron mercury tetracarbonyl cobalt 8=26398
    Fe carbonyl, $[(C_6H_5)CSFe(CO)_3]_2$ 8=26398
    Fe carbonyl complex, $C_{13}H_{12}Fe(CO)_8$ 8=26446
    Fe carbonyl complex, $Fe(en)_3Fe_2(CO)_8$ 8=26380
    $FeAl_2O_4$, cation distrib., Mossbauer and X-ray diffraction study 8=35331
    $Fe(C_{12}H_8N_2)_3Sb_2(C_4H_2O_6)_2 . 8H_2O$, and mol. structure 8=26397
    $Fe_xCo_{1-x}S_2$, pyrite solid solns., prep. and lattice parameters 8=48342
    FeF_3, cubic–rhombohedral transition, 410°C 8=44005
    FeF_3-FeF_2-MF, (M = Li, Na, K, Rb, Tl,) system, classification of phases rel. to FeF_6 octahedra 8=48651
    $FeHo_4S_7$ and certain isotypic cpds. 8=44214
    α-FeOOH, from n-diffr., —190 to 120°C 8=30894
    β–$FeSi_2$, space group symmetry, Mössbauer determ. 8=48325
    α-Fe_2O_3 fine particles, lattice dilation particle size dependence rel. to spin flip temp. shift 8=27414
    δ-Fe_2O_3 (hydrate) 8=44215
    Fe_2O_3-$3La_2O_3$-SnO_2, and formation kinetics 8=48650
    Fe_5LiO_8, short range order 8=26866
    Ga_2Te_3:Cu, lattice parameters 8=30896
    $GdFeO_3$-type 8=26399
    $GeBi_4Te_7$, e diffr. obs. 8=30898
    GeI_2, e diffr. obs. 8=30897
    $Ge_2Sb_2Te_5$, by e. -diffr. 8=39794
    $GeSb_4Te_7$, by e.-diffr. 8=39794
    $2H_3AsO_4 . H_2O$ 8=44204
    $H_2SO_4 . H_2O$, rel. to H bonding 8=26400
    $Hg(OHg)_4Br_2$, least-squares refinement 8=48654
    HgTe, lattice constant rel. to temp. 8=48744
    $In_2(MoO_4)_3$, X-ray obs. 8=30900
    In_3Te_4, and optical and photoconductive props. 8=39796
    K graphites, formation and structure 8=30904
    KBr, Br nuclei surrounding substitutional Cl ion, n. m. r. obs. of field gradients 8=26403
    KCl, effect on proton energy losses from orientation dependence 8=35598
    KCl: Pb(Ca), impurity ion effect from X-ray diffr. study 8=26642
    $K_2Cr_2O_7$, triclinic 8=35337
    $K_3[Cu(NO_2)_5]$, from vis. and i. r. absorpt. spectra 8=30901
    $K_4Fe(CN)_6$, Mössbauer radiation scattering by nucl. resonance, diffr. and interference effects 8=26025
    $KH_2Al_2(SiO_4)_3$ (muscovite) isomorphic substitution obs. by X-ray diffraction 8=35338
    $K_4Mo(CN)_8 . 2H_2O$ 8=41118
    $K_2MoO_2F_4$, e diffr. obs. 8=30903
    $KNbO_3$, atomic displacements rel. to real structure determ. 8=30887
    $KNbO_3$, by e-microdiffr. 8=26430
    K_2NbOF_5, by e-diffr. 8=26404
    $K_{0.23}NiO_{1.8}$, e diffr. obs. 8=30902
    $K_2[Pt(N)_6]$ 8=26402
    KSCN, refinement from redetermined data 8=44222
    $KSnF_3 . ½H_2O$ 8=39798
    $K_4W(CN)_8 . 2H_2O$ 8=41118
    $KY(MoO_4)_2$, x-ray diffraction study 8=48655
    $KY(WO_4)_2$ 8=39797
    La complex, ethylene diamine tetra acetic La(III) 8=44223
    $La_2Be_2O_5$, and refinement 8=39799
    $La_{2-x}Gd_xCoMnO_6$, and mag. interactions 8=27417
    $(La, Gd)_2CoMnO_6$ system, rel. to mag. interactions 8=49527
    $La_2O_3 . 3B_2O_3$, and isotypism 8=48657
    LaOOH, synthetic 8=48658
    La_3Se_4, lattice props. rel. to superconductivity 8=27017
    LaC_2, rel. to phase transform at 1060°C 8=26405
    $LaTO_3$, (T = Ho, Y, Er, Tm, Yb, Lu) 8=48656
    Li_9Al_4 8=39801
    $LiClO_4 . 3H_2O$, n diff. exam. 8=35339
    LiF, lattice constant, X-ray effect 8=35603
    LiF, lattice fringes resolution, axial e illum., 100 kV 8=39775
    LiF:Ni impurity ion effect from X-ray diffr. study 8=26642
    $Li_2SO_4 . H_2O$, neutron diffr. 8=48659
    $LiTaO_3$, high-temp. X-ray investigation 8=35978
    $LiTaO_3$, lattice consts., and Curie point 8=49371
    $Lu(ReO_4)_3$, high-temp. modification, X-ray obs. 8=30914
    $M_xV_2O_5$ bronzes, homogeneity range rel. to charge and ionic radius inserted element 8=26444
    ε-$Mg_{23}Al_{30}$, and refinement 8=44227
    MgO, changes due to low dose n irrad. 8=26829
    MgO, lattice fringes resolution, axial e illum., 100 kV 8=39775
    MgO–MnO solid solns. and with LiO_2 8=48662
    Mg_2SnO_4-$MgFe_2O_4$, X-ray diffraction study 8=40738
    Mn complex, diaquobisacetylacetonatomanganese (II), and refinement 8=44228

Crystal structure, atomic—contd
  inorganic compounds—contd
    Mn complex, phthalocyanatopyridinemanganese(III)-μ-oxo-phthalocyanatopyridine-manganese(III) dipyridinate 8=26409
    $MnAs_{0.9}P_{0.1}$, at 119°K and 298°K, X-ray powder pattern determ. 8=35341
    Mn_2GeO_4, high-pressure form, crystal structure 8=39807
    $Mn(Mn_xV^{4+}_xV^{3+}_{2-2x})O_4$, $x < 0.68$, and elec. props. 8=35340
    Mn_2N, antiferromagnetic 8=49573
    MnO, deformed, meas. 33-157°K and mag. anomaly 8=30906
    MnO. OH. H location and mag. structure 8=49533
    MnSb, high-press. effect 8=26407
    $Mn_xZn_{1-x}Fe_2O_4$, cation distribs. and lattice parameters from X-ray and n.-exams. 8=44229
    Mo complex, thiocyanate, $K_3Mo(NCS)_6H_2O.CH_3COOH$ 8=26410
    MoCoB and related $PbCl_2$-type crystals 8=39809
    Mo_3CoSi 8=35342
    $Mo_{13}Ge_{23}$, and refinement 8=39782
    $MoNb_{15}O_{40}F$, 8=44232
    MoS_2, lattice parameter meas. 8=44231
    $MoZn_{22}$ 8=44230
    $NH_4H_2PO_4$, paralec. phase e. diffr. exam., 8=39816
    NH_4I, polycrystalline, e diff. exam. 8=35343
    $(NH_4)_2[Sb_2(C_4H_2O_6)_2].5H_2O$ 8=26416
    $(NH_4)_3(VO_2F_4)$, space group, unit cell 8=35344
    $N_4P_4Cl_8$, T form 8=48665
    Na complex, sodium-N-diethyldithiocarbamate 8=26368
    $Na_8Ba_2Ti_4O_4(B_4Si_{20}O_{56})$, leucospherite, X-ray obs. 8=30907
    $Na_{0.5}Bi_{4.5}Ti_4O_{15}$, cation ordering, X-ray meas. 8=26413
    $(Na, Ca)_3(Ca, Sr, Ba, TR)_3(CO_3)_5$, berbankite, X-ray exam. 8=35345
    NaCl: Pb(Ca), impurity ion effect from X-ray diffr. study 8=26642
    NaCl, effect on proton energy losses from orientation dependence 8=35598
    $NaCrS(Se)_2$, and mag. props. 8=39810
    Na_3FeF_6, x-ray diffraction powder data 8=48666
    $Na_xFe_xTi_{2-x}O_4$, $0.90 > x > 0.75$ 8=39813
    $Na_2Ge_4O_9$, X-ray powder data 8=26412
    $[Na_3H(PO_3)_4]_x$, polyphosphate 8=44239
    $NaH_3(SeO_3)_2$ and deutero-cpd., H atom coordination from NMR study 8=27511
    $Na_2(H_2SiO_4).4H_2O$ 8=48081
    $NaIO_4$, lattice parameter temp. dependence and expansion coeffs., 8=39929
    $NaMF_3$, ($M=Mg^{2+}, Co^{2+}, Ni^{2+}, Zn^{2+}$), and synthesis 8=26258
    $Na_4Mn_4Ti_5O_{18}$ 8=44234
    $NaNb_3O_8-Nb_2W_3O_4$ solid solution, study and existence 8=43978
    Na_5Pb 8=43762
    NaSCN 8=30701
    β-$Na_2Si_2O_5$, refinement from redetermined data 8=44237
    $NaSmSiO_4$, 8=39811
    Na_3TaF_8 8=41118
    $Na_4Ti_4[Si_2O_6]_2[Si_4O_{10}]O_4.nH_2O$ 8=48667
    $Na_6V_{10}O_{28}.18H_2O$ 8=44238
    $Na_2W_4O_{13}$, data 8=44235
    $Na_2Zn_2[Si_2O_7]$ 8=39812
    Nb complex, tetrabromobis(acetonitrile)Nb(IV) 8=44241
    $Nb_2O_3.WO_3-WO_3$ system, stable phases 8=39814
    Nb_2Se_3 8=44240
    Nb_3Sn, lattice expansion on H_2 up-take 8=26414
    NbZn. μ-phase, lattice consts of unit cell 8=48392
    Nd-alkali metal tungstates, rel. to hydrothermal crystallization 8=26259
    Nd(III) complex of nitrilotriacetic acid, X-ray analysis and refinement 8=26415
    $NdWO_4Cl$, and hydrothermal synthesis, obs. 8=39815
    $Nd_2W_2O_9$, and hydrothermal synthesis, obs. 8=39636
    Ni complex, diaquobisglycinatonickel (II), refinement 8=44246
    Ni complex, diethylenediamine Ni(II) iodide, Ni $en_2I_2.H_2O$ 8=26420
    Ni complex, diethylenediamine Ni(II) nitrate, Ni $en_2(NO_2)_2$ 8=26420
    Ni complex, tris-(2-dimethylaminoethyl)amine nickel(II) bromide 8=26418
    Ni complex, tetrakis (3, 4-dimethylpyridine) nickel (II) perchlorate 8=39818
    Ni complex, bis(N, N-di-n-propyl-dithiocarbamate)Ni(II), and mol. structure 8=26419
    Ni complex, bis-(N-ethylsalicylaldiminato)nickel, and structure regularities 8=26421
    Ni complex, hydrazinecarboxylate, X-ray study 8=26427
    Ni(II) complex, bis(N-isopropyl-3-methylsalicylaldiminato) nickel(II) 8=26425
    Ni complex, Ni glyoxime, and mol. structure 8=26417
    Ni complex, bisperchloratotetrakis-(3, 5-dimethylpyridine) nickel (II) 8=39817
    Ni complex, di-(2-thioimidazolidine)nickel thiocyanate 8=26423
    Ni complex with N-β-diethylamine ethyl -5-chlorosalicylaldimine 8=26424
    Ni complexes, chloro- and nitro-thiocyanato bis (ethylenediamine) nickel 8=26426
    Ni complexes, Ni en_2NCSI and Ni $en_2NCSClO_4$ (en=ethylenediamine) 8=26422

Crystal structure, atomic—contd
  inorganic compounds—contd
    Ni complexes, thiosemicarbazides 8=26428
    Ni molybdate hydrates, non-stoichiometric two phases 8=30916
    NiAl alloy, martensitic phase 8=48668
    $NiCr_2O_4$, lattice parameters and axial ratio of phases, 92-298°K 8=26076
    $Ni[(H_2O)_6]^{2+}$, evidence for distortion from octahedral symmetry, O^{17} hyperfine coupling constants data 8=49652
    NiO, parameters rel. to pressure 8=48669
    OD-structures, generalized for n-dimens. 8=48610
    PBr_7, and bond lengths for Br_3^- 8=44247
    $(PO_3)_3CoNH_4$, orthorhombic 8=26382
    Pa bromides, obs. 8=26429
    Pb thioborate, new type 8=35349
    $PbBi_2Se_4$, electron diffraction study 8=35348
    $PbCa_2Si_3O_9$, (margarosanite) 8=44248
    α-PbN_6, neutron diffr. 8=30908
    $PbSnO_3$, perovskite 8=48554
    $Pb_{1-x}Sn_xTe$ alloys, lattice parameter values rel. to comp. 8=26077
    PbS(Te), parameters rel. to pressure 8=48669
    $PbTiO_3$, by e-microdiffr. 8=26430
    $PbTiO_3$ ferroelec., determ. using micro e.-diffr. techniques 8=39761
    Pd(II) complex, bis(N-isopropyl-3-methylsalicylaldiminato) Pd(II) 8=26425
    Pd-Sb system in thin films, electron diff. study 8=30909
    $Pd(SO_3)(NH_3)_3$, and mol. structure 8=26431
    Pr-alkali metal tungstates, rel. to hydrothermal crystallization 8=26259
    $Pr_2W_2O_9$, and hydrothermal synthesis, obs. 8=39636
    PtO_2, synthesis and properties 8=35205
    PuC_2, high temp. by X-ray diffraction 8=44196
    Pu_3Zn_{22} 8=26433
    RbH_2AsO_4, temp. depend. and thermal expansion anisotropy 8=44348
    Rb_2NaTF_6, (T = Yb, Er, Ho, Y, Tb and Sm) 8=44250
    $RbNiF_3$, pressure effect 8=48661
    Re complexes, $[Re(en)_2OOH][ClO_4]_3$, $[Re_2O_2H(CO)_8]^-$ and $ReCl_2(acac)(PPh_3)_2$ 8=26435
    $ReCl_5$ 8=39819
    Rh-acetate complexes, and refinement 8=26437
    Rh complex, triacetylacetonatorpodium(III) 8=26436
    RhO_2, synthesis and properties 8=35205
    Ru complex, diethyldithiocarbamate and nitrosyl salt, and mol. structure 8=26375
    Ru complex, tetraphenyl arsonium tetrachloro cis-diaquo ruthanate monohydrate 8=35351
    $[RuBr_2(CO)_3]_2$, and mol. structure 8=26438
    $RuNO(OH)(NO_2)_2(NH_3)_2$ 8=26439
    Sb isostructural oxide cpds 8=48676
    $2SbCl_3$. dibenzyl, mol. complex, and mol. structure 8=35353
    $4SbCl_3$. dibenzyl, mol. complex, and mol. structure 8=35353
    $4:1SbCl_3$. stilbene, mol. complex, and mol. structure 8=35353
    $SbF_5.SO_2$ 8=39820
    $Sb_2S_3-Bi_2Te_3$ solid solns., lattice parameter changes on equilib. relationship changes 8=48672
    $Sb_2Te_{3-x}Se_x$ syst. 8=48677
    $(Sc, Er)VO_4$, lattice parameters and Miller indices, using computer programmes 8=44252
    Sc_2O_3 8=48673
    $ScVO_4$, lattice parameters and Miller indices, using computer programmes 8=44252
    Se, amorphous → polycrystalline, and monoclinic → hexagonal 8=26078
    Si, lattice parameter C conc. dependence 8=48674
    SiP_2 and $SiAs_2$, verification of pyrite type structure 8=40484
    Sn complex, diacetate tetramethyl distannoxane 8=26368
    SnTe-PbTe solid soln., rel. to composition 8=43981
    $SrHAsO_4.H_2O$, haidingerites 8=48641
    $SrTi_{1-x}Fe_xO_{3-x/2}\phi_{x/2}$, ϕ = oxygen vacancies 8=35252
    Ta-O system, γ-phase, annealed, e.-diffr. exam. 8=39822
    Ta_2O_5 8=48403
    Ta_2Se_3 8=44240
    Tb complex, ethylene diamine tetra acetic Tb(III) 8=44223
    $TbAu_2$ 8=27426
    Te isostructural oxide cpds 8=48676
    ThC_2, cubic phase above 1480°C, tetragonal, 1430-1480° and C_2-type monoclinic 8=44257
    Th-ThAs system and phase diagram, obs. 8=30577
    $TiBe_{12}$, hexagonal, OD-structure 8=26442
    $TiCr_2S_4$, neutron diffraction study 8=35358
    $TiCr_2Se_4$, neutron diffraction study 8=35358
    TiO_2: Cr, e.s.r. investigation 8=39823
    Ti_2O_3, lattice parameter change in range 390-470°K 8=48678
    TiO_x $(1.1 < x \leq 1.25)$ alloys, ordering and lattice parameters 8=48679
    $TiTa_2O_7$ 8=48403
    Ti_5Te_8, unit cell parameters, and vacancy ordering 8=35359
    $U_{20}C_3Si_{16}$, refinement 8=44261
    UF_2, $2.5H_2O$, rhombic, and dehydration products, X-ray diffr. obs. 8=30870
    $UFeO_4$, neutron diffraction meas. 8=26443

Crystal structure, atomic—contd
- **inorganic compounds**—contd
  - U(NH)Cl 8=48680
  - UO_2, n-irradiated, investigation with X-ray counter diffractometer 8=44260
  - UO_2-type lattice, asymmetric aspects of atomic charge density 8=26302
  - $UO_2(OAc)_2 . 2Ph_3AsO$ and $[UO_2(OAc)_2 . Ph_3AsO]_3$; (Ac = acetate, Ph = phenyl) 8=44259
  - V_6C_5, ordered compound, superlattice and domain structure 8=44172
  - VC_{1-x} with non-stoichiometric vacancies 8=30913
  - $V_{17}Ge_{31}$, and refinement 8=39782
  - $VOSO_4 . 5H_2O$, three polymorphs 8=49759
  - V_3Si, sublattice distortion, search 8=26445
  - W carbonyl complex, $(CO)_5WCO . CH_3 . C_6H_5$ 8=26446
  - YCd_2, and refinement 8=26448
  - $YTaO_4$, M^1 phase structure, bond angle correction 8=26447
  - $Yb(ReO_4)_3$, high-temp. modification, X-ray obs. 8=30914
  - Yb_3S_4, unit cell, layers 8=26449
  - Zn complex, bis (acetylacetonato) zinc (II), and mol. structure 8=39824
  - Zn complex, di-thiourea-zinc acetate 8=26451
  - Zn complex, tris(thiourea) zinc (II) sulphate, and mol. structure 8=39825
  - Zn complex, zinc-N-N-diethyldithiocarbamate 8=26368
  - Zn molybdate hydrates, non-stoichiometric, two phases 8=30916
  - Zn(II) di-n-alkylphosphinates, single crystal studies and polymeric structures 8=30797
  - ZnF_2 phases, lattice params., ≤ 130 kbar, 25 and 300°C 8=39570
  - $ZnSeO_3 . 3H_2O$ 8=26450
  - $ZnSnP_2$ platelets, and prep. 8=26267
  - $ZnWO_4$, pseudo-rhombic, obs. 8=30915
  - $Zr_4Co_4Ge_7$ 8=48682
  - ZrO_2:Ce, baddeleyite, impurity positions 8=30917
  - Zr_2Se, and refinement, rel. to isostructures 8=26452
- **organic compounds**
  - acetic acid-sulphuric acid, 1:1 addition cpds., crystal structure rel. to H bonding 8=26527
  - acetonitrile: bromine 2:1 complex 8=39826
  - para-acetotoluidide crystals, monoclinic modification X-ray study 8=44262
  - 3β-acetoxy-17α-hydroxy-16β-bromo-5α-pregnan-11, 20-dione, and mol. structure 8=26459
  - acetylcholine and related mols. in solid state 8=26460
  - acetylene, high temp. phase 8=27618
  - aconitase substrate, potassium dihydrogen isocitrate 8=26462
  - adenosine-3′-phosphate dihydrate, and mol. structure 8=35361
  - amino acids, non-carboxylic aliphatic, by computer-controlled diffractometer 8=35362
  - 1, 2-0-aminoisopropylidene-α-D-glucopyranose, rel. to mol. conformations 8=25623
  - ammonium bis-μ-(d-tartrato)-distibate (III) 8=39848
  - ammonium formate, rel. to H bonding 8=26528
  - 9-anthraldehyde dimer 8=44263
  - anthranilic acid by X-ray diffraction 8=26464
  - antifurfuraldoxiome 8=26512
  - barium inosine-5′-phosphate 8=44265
  - p-benzoquinone, 2, 5-dihalogen derivs, comparative study 8=26466
  - bigeranyl tetrahydrochloride, triclinic, and mol. structure 8=39827
  - binaphthyl, and bond distances 8=26470
  - 4, 4′-bis(dimethylamino) diphenylamine dihydroiodide, unit-cell dimensions and space group 8=26498
  - 2, 3-bis-(cis-chloro-1-methylcyclohexyl)-trans-2-butene, and mol. structure 8=39830
  - bispiperidinium $Bi^{III}Br_5$ 8=26546
  - α-brassylic acid, 8=26478
  - p-bromo-benzoylethyleneimine, rel to amido group structure 8=26465
  - 12α-bromo-11β-hydroxyprogesterone, and mol. structure 8=39828
  - 2-bromo-2-p-tolylethyldimethylammonium bromide 8=26510
  - 1-bromotriptycene $BrC_{20}H_{13}$, and mol. structure 8=44266
  - 5-bromouridine and dimethylsulphoxide 1:1 complex 8=26471
  - bullvalene, by X-ray exam. 8=39829
  - calcium dipicolinate trihydrate 8=26473
  - calcium hexa-antipyrine perchlorate, and mol. structure rel. to other metal hexa-antipyrine perchlorates 8=44268
  - carbamide phosphate, rel. to H bonding 8=26475
  - cellobiose, confirmation 8=39838
  - 3-chloro-5-(3-dimethylaminopropylidene)-5H-dibenzo[a, d]cycloheptane 8=26487
  - 2-chlorotropene, crystal and mol. structure 8=26476
  - α-chymotrypsin, using inhibitor and heavy atom technique 8=26477
  - complicated, model soln using 2-dimens. least squares refinement 8=48607
  - copper monochloracetate 2. 5 hydrate, unit cell dimensions and density obs. 8=44270
  - corrin skeleton of vit. B_{12}, and its precorrinoid intermediate 8=26479
  - trans-1, 3-cyclobutane dicarboxylic acid, crystal structure 8=26484

Crystal structure, atomic—contd
- **organic compounds**—contd
  - cis, cis, cis, -1, 4, 7-cyclononatriene $AgNO_3$ adduct, and mol structure 8=26485
  - cyclooctane analogues, and conformational analysis 8=26483
  - cyclooctanone, of phases above and below—87°C 8=26091
  - cyclopentadienyl iron sulphide, and mol. structure 8=26537
  - π-cyclopentadienyl molybdenum tricarbonyl chloride 8=26488
  - cyclotetratriacontane, and mol. structure 8=39831
  - demissidine hydroiodide, $C_{27}H_{46}INO$, rel. to mol. config. 8=26489
  - deoxycholic acid clathrates with naphthalene, phenanthrene and benzanthracene 8=26491
  - diacids, saturated aliphatic, comparative study 8=26494
  - diazonium salts, $o-CH_3OC_6H_4N_2Cl . FeCl_3$ and $[(CH_3)_2NC_6H_4N_2Cl]_2 . ZnCl_2$ 8=26492
  - diazulenium azulene perchlorate, X-ray analysis 8=26495
  - dibenzothiophene sulphone 8=39832
  - 4, 12-di(bromomethyl) [2. 2] metacyclophane 8=26472
  - dicarboxylic acids, $COOH[CH_2]_{2n+1}$ COOH, and mol. structure 8=26478
  - 3, 6-dichloro-2, 5-diaminobenzoquinone-(1, 4), and mol. structure 8=26493
  - 2, 2-dichloro-4, 4, 6, 6, tetraphenylcyclo triphos phaza-triene, 8=26542
  - 2, 5-dichloro-1, 4-xylene and 4, 5 dichloro-1, 2-xylene crysts., and i.r. vibr. spectra 8=39833
  - 9-dicyanomethylene, -2, 4, 7-trinitrofluorene 8=26481
  - trans-15, 16-diethyl-15, 16-dihydropyrene, at −160°C 8=26552
  - diethylamine hydrate, $12(C_2H_5)_2NH . 104 H_2O$. 8=26505
  - diferrocenyl and derivs., and mol. structure 8=26497
  - difluorostilbene derivs., and mol. structure 8=26559
  - diglycine nitrate, ferro-and paraelectric phases determ. 8=48685
  - dihydrothymine 8=30918
  - 3β, 17α-dihydroxy-21-bromo-5α-pregnan-11, 20-dione, and mol. structure 8=39834
  - dihydroxyfumaric acid dihydrate 8=39835
  - dimethylammonium chloride, rel. to H bonding 8=26525
  - 8, 8′-dimethyl binaphthyl, and bond distances 8=26470
  - 2, 6-dimethyl-4-bromo-N-methyl-anti-benzaldoxime isomer 8=26512
  - 2, 6-dimethyl-4-chloro-N-methyl-anti-benzaldoxime 8=26511
  - 1, 3-dimethyl-[1, 7]-heptahydropyrimido[1, 2-a] [1, 3, 5] triazine-2-thione-4-one, 8=26553
  - 1, 3-dimethyl-2-thioxo-4-oxo-1, 2, 3, 4, 6, 7, 8 hepta-hydro-pyrimido [1, 2-a] [1, 3, 5] triazine, and mol. structure 8=48686
  - N, N′-dinitroethylenediamine, refinement 8=39836
  - N, N′-diphenyl-p-phenylenediamine iodide, 8=26543
  - disodium inosine-5′-phosphate 8=44265
  - disordered molecular crystals, X-ray and NQR investigations 8=26454
  - di(tetramethylammonium)bis(maleonitriledithialato)CuII, X-ray and e.s.r. studies 8=35364
  - dithienyls, disorder from 3D-X-ray exam. 8=26499
  - DNA of phage T2, and mol. configs. rel. to glucoside residue effect 8=26490
  - DNA, rel. to RNA and DNA-RNA hybrids and synthetic analogs 8=26556
  - erythrocruorin heavy-atom derivatives 8=26500
  - erythrocruorins, analyses at 5. 5 Å resolution 8=48684
  - ethionamide hydrochloride, antitubercular cpds 8=26502
  - ethionamide hydrobromide, antitubercular cpds. 8=26503
  - ethylenebidiguanide silver (III) nitrate 8=26501
  - ferritin, and mol. structure 8=26506
  - ferrous oxalate and isotypic cpds., OD-structure from Guinier patterns 8=26534
  - gliotoxin at -150°C, 8=26508
  - β-D-glucose, confirmation 8=39838
  - glycocyanine hydrobromide, 3 dimens. Patterson and heavy atom phased Fourier synthesis 8=44274
  - gramicidin S derivatives, and mol. structure 8=26509
  - 2-halogenoalkylammonium halides, N-substituted. 8=26510
  - 9, 10-hydroxy-borazaro-phenanthrene, 8=26540
  - 2-hydroxy-1-phenazine carboxylic acid from pseudomonas aureofaciens, and mol. structure 8=26541
  - hydroxyurea, and other hydroxylamine derivs. 8=26511
  - iso-eremolactone, and mol. structure 8=44273
  - isonitrose-acetyl, derivatives of amines, morphological, optical and X-ray study 8=26533
  - isopropyl-4-phenol, and other alkyl phenols 8=26539
  - L-cysteine, and mol. structure 8=44271
  - labdanolic acid, p-bromophenacylester, analysis rel. to configuration at C(13) in labdanolic and eperuic acids 8=39840
  - lactic dehydrogenase from dog-fish muscle 8=26515
  - β-lactoglobulin, Fourier maps from 2 different crystals 8=26516
  - lead n-butylxanthate, disordered structure 8=39855
  - lecithins, some structural studies 8=26517
  - lincomycin hydrochloride, 8=26518

Crystal structure, atomic—contd
organic compounds—contd
lysozyme crystals, crosslinking rel. to stabilization 8=26008
lysozyme forms, structural relationships 8=26520
malates, cell dimens., from X-ray powder diffr. 8=39841
mercury-organic crystals, R-HgX, rel. to Hg-X bond regularity 8=30616
metal-metal carbonyl derivatives, X-ray study 8=26474
methanesulfonianilide 8=39843
1-methyl-5-bromouracil: 9-methyladenine, and mol. structure 8=26566
methyl-α-D-glucopyranoside 8=39845
N-methyl-hydroxylammonium-chloride, and other hydroxylamine derivs 8=26511
methyl-3-isopropyl-4-phenol and other alkyl phenols 8=26539
methyl-3-isopropyl-2-phenol and other alkyl phenols 8=26539
methylzinc methoxide and t-butyl sulphide 8=26529
micrococcinic acid bis-4'-bromoanilide, and mol. structure 8=26531
molecular-crystals, determ. from potential energy-rotation angle minima 8=26455
from molecule triplet states mag. reson. spectra. 8=27449
monobromoduclauxin, and mol. structure rel. to duclauxin structure 8=44272
monomethylammonium perchlorate, 8=26522
monoselenoparaldehyde, rel. to mol. conformations 8=35365
myxin, at −160°C 8=44277
natural products, rel. to stereochemistry 8=26457
nylon 4, precip. from H_2O-glycerol solns., and morphology, obs. 8=44285
octahydroxycyclobutane 8=44267
packing arrangements of mols. 8=26453
palladium-8-mercaptochinolinates 8=39842
papain, by X-ray heavy atom method 8=26536
pentaerythritol, deuterated, H bonding from n.m.r. exam. 8=43926
pepsin, by X-ray analysis 8=26538
pepsin, isomorphous derivative prep. for x-ray exam. 8=30833
perhydrotriphenylene (PHTP) + n-hydrocarbons; + chloroform; + cyclohexane, inclusion cpds. 8=30920
β perylene, and bond distances 8=26470
1-phenyl-6-benzyl-7,7-dichlor-3,5-diaza-bicyclo-122-hepten-5-on-2, obs. 8=35363
phenyl salicylate, unit cell dimensions, growth 8=44280
phosphobenzol 8=48687
phosphoenol pyruvate, monocyclohexylammonium salt, 8=26544
phospholipids, some structural bodies 8=26517
N-phosphorylcreatine hydrate, disodium salt 8=44279
photo iso pyrocalciferyl-m-bromobenzoate 8=26469
piperazine hexahydrate 8=39846
poly-L-proline II, 8=26547
porphyrin diacids 8=44282
potassium dihydrogen isocitrate, aconitase, substrate 8=26462
potassium hydrogen diformate, rel. to H bonding 8=39837
potassium oxalate monoperhydrate, $K_2C_2O_4.H_2O_2$, rel. to monohydrate 8=26535
proteins, heavy atom location method 8=26548
proteins, by isotypic replacement, statistical tests for isotypism 8=26549
pyranthrone, rel. to flavanthone structure 8=26550
1,1-pyrene-pyromellitic dianhydride, at 110-300 °K 8=26554
pyridoxine hydrochloride, by 2 methods 8=26551
quaternary ammonium salts displaying anticholinergic activity 8=39847
rabbit psoas muscle, glycerol-extracted, filament lattice studies 8=26458
ribonuclease, bovine pancreatic, tertiary structure investigations 8=26557
ribonuclease, e-density maps obtained using multiple isomorphous replacement 8=26558
RNA, and mol. structure of double helix 8=26555
RNA, rel. to DNA and DNA-RNA hybrids and synthetic analogs 8=26556
rubidium oxalate monoperhydrate, $Rb_2C_2O_4.H_2O_2$, rel. to monohydrate 8=26535
salutaridine methiodide, space group, unit cell and ring config. 8=44276
Schiff bases, aromatic, lattice parameters and space groups 8=26456
seal myoglobin, y coordinates of heavy atoms, determ. at low resolution 8=26532
para-terphenyl 8=26560
testosterone: mercuric chloride 2:1 complex, and absolute config. 8=44283
1,2,3,4-tetrabromo-1,2,3,4-diphthaloyl-cyclobutane 8=48688
4,5,9,10-tetrachloro-2,7,11,12-tetrathia,1,3,6,6,tetra-zatricyclo dodeca-3,8-diene 8=26496
tetrachlorohydroquinone, rel. to H bonding system 8=30619

Crystal structure, atomic—contd
organic compounds—contd
tetracyanocyclobutane 8=39854
tetracyanoethylene-Pt complex 8=34322
7,7,8,8-tetracyanoquinodimethan: N,N,N',N'-tetramethyl-p-phenylenediamine 2:1 complex 8=39852
tetracyanothiophene 8=39850
2,4,4,6-tetrahalogenocyclohexa-2,5-diene-1-one, rel. to bond system 8=26482
tetrahymanone, 8=26562
tetramethyl ammonium hydroxide pentahydrate 8=26505
tetramethylbiphosphine-bis(monoborane), and mol. structure 8=39851
N,N,N',N', -tetramethyl-p-diaminobenzene-chloranil, and mol. structure 8=39849
N,N,N',N'-tetramethyl-p-diaminobenzene iodide, and mol. structure 8=26524
tetramethyl-2,2,6,6,-piperidinal-4-oxyl-1, free radical, and bonding 8=25654
tetraphenylphosphinium bis(tetracyanoquinodimethanide) 8=39853
thioacetamide-S-oxides, crystallography 8=48689
β-thiophenic acid, disorder from 3D-X-ray exam. 8=26499
thiourea and deuterated deriv., by n-diffr. above and below ferroelec. transition 8=44251
thiourea derivatives, e.s.r. data 8=31886
L-threonyl L-phenylalanine p-nitrobenzylester hydrobromide 8=26468
titanium tetramethoxide, and mol. structure 8=44284
N,N'-bis(4-tolyl)-p-phenylenediamine iodide 8=26543
tomatidine hydrobromide and related steroidal sapogenins 8=26563
tosyloxylupinane rearrangement product, structure determ. 8=26564
tricycloquinazoline, and $CuCl_2$ complex 8=26486
trimethylamino borontrichloride, and mol. structure 8=44264
trimethylammonium chloride, rel. to H bonding 8=26526
triphenylphosphine sulphide-I_2 addition complex 8=44281
triselenoparaldehyde, rel. to mol. conformations 8=35365
1,3,5-trithiane, 8=26565
tryptamine derius, preliminary X-ray data 8=39839
uracil, valence-electron density maps 8=48620
uranyl acetate/triphenylphosphine oxide complexes 8=44259
urea/thiourea inclusion cpds. gen. structural principle 8=48691
Wurster's blue iodide, and mol. structure 8=26524
vit. B_{12}, corrin skeleton and its precorrinoid intermediate 8=26479
$CH_3CN.2HCl$, by n-diffr. 8=26530
$4(CH_3)_3N.41H_2O$ 8=39844
$(C_5H_5)_2TiAl(C_2H_5)_2$, and mol. structure 8=26504
$(C_6H_5)_3Sn.Mn(CO)_5$, cell constants and space group determ. 8=26467
$C_{24}H_{10}$ 8=39856
$C_{26}H_{26}O_2$ 8=39856
Co formate, and other formates of transition metals 8=26507
$CsBeF_3$ 8=39783
Cu(II) alkanoates, by X-ray analysis 8=26463
Cu formate tetrahydrate, H_2O mols. 8=44269
Cu hexamethylene-dithiocarbamate, X-ray obs. 8=30919
Cu phthalocyanine, α and β forms 8=26545
Cu salicylate hydrate, OD-structure from X-ray investigations 8=26480
$[HgOSi(CH_3)_4]_2$ 8=48683
K phthalocyanine, 8=26545
K_2 tetranitroethide 8=26561
$K_2C_2O_4.H_2O_2$, potassium oxalate monoperhydrate, rel. to monohydrate 8=26535
KH bisphenylacetate, and H bonding, redetermination 8=26514
$Mo_3O_4(C_5H_7O_2)(C_2H_5O)_3$ 8=26461
$(NH_4)_2$ dimolybdomalate, X-ray analysis 8=26521
$OP(OCH_2)_3CCH_3$ 8=44278
$Rb_2C_2O_4.H_2O_2$, rubidium oxalate monoperhydrate, rel. to monohydrate 8=26535
Rh formate, and other formates of transition metals 8=26507
Sc formate, and other formates of transition metals 8=26507
$Sn_3(CH_3)_4Fe_4(CO)_{16}$, and mol. structure 8=26537
Ti methoxide, and mol. structure 8=26523
Zn insulin, X-ray study and prep techniques 8=26513
Crystal symmetry. See Crystallography; Crystal structure, atomic.
Crystallites. See Crystal structure/microstructure.
Crystallization
See also Crystals/growth.
andesite, synthetic, under high press. hydrous conds. 8=35227
in aqueous solutions on application of mag. field 8=34776
basalt, synthetic, under high press. hydrous conds. 8=35227
betol, kinetics rel. to active impurities and centres 8=39667
on constant temp. surface, heat and mass transfer effect 8=48529
continuous crystallizers with size-depend. growth rate 8=39658
corundum, effect of Nb_2O_5, MnO_2, ZrO_2 and Na_3AlF_6 on recrystallization 8=48536

Crystallization—contd
- crystallizers with classified product removal, steady state behaviour 8=48528
- cyananthracene solns., vitreous, crystallite formation rel. to optical absorpt. temp. dependence 8=43823
- diamond-lattice type, theory of nuclei formation 8=26204
- films, epitaxial, from mol. beams, transfer calc. 8=30737
- front stability, theoretical analysis 8=26219
- glass powder, compression under 10-65 kbar effects, on reheating 8=40164
- grain size on solidification 8=35233
- hydrothermal, hydro- and thermamechanical ratios in cylindrical vessel 8=30354
- ice, dendritic, from aq. solns 8=30835
- ice, nucleation props of mineral particles in controlled humidity 8=35229
- impurity effect mechanism on nuclei origin 8=30819
- impurity effect theory 8=26208
- on ions as nuclei, in supercooled fluids 8=39656
- martensite nucleation in Ni-Fe alloys showing disrupture transform. kinetics 8=39555
- metals, effect on mosaic block size and disorientation 8=40051
- mica, synthetic, rel. to morphology and other props. 8=26193
- from molecular beams, phenomenological theory of non-isothermic process 8=30739
- nucleation in evaporated films 8=48440
- nucleation kinetics, effect on dynamic behaviour of continuous crystallizer 8=48534
- organic materials with low m. p. s. apparatus for routine crystal studies 8=26214
- oriented, impurity distribution analysis 8=26218
- pepsin, and preparation of isomorphous derivatives 8=30833
- permalloy sheet obs. of texture during recrystallization 8=35282
- polybutene-1, isotactic, nucleation and undercooling, obs. 8=44122
- polychlorotrifluoroethylene copolymer films 8=39680
- polyethylene, linear 8=30578
- polyethylene terephthalate, X-ray studies at 140, 180, 200°C 8=26206
- polymer chains, effect of mol. wt. 8=44108
- polymers, rate temp. depend. rel. to nucleation mechanism 8=44109
- polymers, spherulite growth rate 8=39681
- polymers, two-dimens. chain-folding model 8=39663
- polyoctadecene-1, transition temps. and crystallinity 8=39635
- polypropylene, light scatt. determ. 8=49783
- polystyrene, isotactic, spherulite growth rate in benzophenone mixts., obs. 8=44146
- polystyrene, light scatt. determ. 8=49783
- poly(tetramethylene oxide), high-mol. wt., dilatometry 8=44134
- powder-grain enlargement in aqueous soln. 8=39655
- recrystallization and grain size 8=30820
- relaxation time in germination of condensed systems, appl. to alkali halide solns. 8=26217
- rubber, stretched, kinetics 8=39683
- solid solution single crystals production, rel. to component segregation on crystallization 8=39654
- steel, Al-killed low C, recrystallization and texture development 8=44129
- steel, low-carbon, deformation and recrystallization textures, rolling temp. dependence 8=26818
- two-component liquids, undercooled, nucleation theory 8=26203
- virus protein study 8=26262
- water drops, supercooled, processes 8=25985
- water-ice interface, precrystallization theory applied to surface-free energy 8=34957
- water, supercooled, basal-plane solidification, effects of impurities 8=25982
- zinkite, hydrothermal crystallization kinetics 8=26230
- Ag, electrocrystallization 8=41283
- Ag films, structure, at high evaporation rate 8=30741
- AgBr in emulsion, recrystallization effects of NH_3 and triethanolamine 8=30821
- AgBr, X-ray diffraction study 8=44114
- Ag-Cu-Zn-Cd, primary invariant equilibria 8=35083
- Al, zone-refined, mechanical props. changes during recrystallisation after low-temp. deform. 8=35660
- Al-Mn 1.04% alloy, recryst. behaviour and deform. structures 8=48803
- Bi, supercooled liq., effect of u.s. vibs on nucleation 8=48261
- C fibres, recrystallization, Ni stimulated 8=35236
- $CaSO_4$, from H_3PO_4, nucleation and growth rates 8=35239
- Cd, grain size, vibr. effects, obs. 8=35269
- Cd, recrystallization, preferred orientation reins. 8=35213
- CdS, polycrystalline, effect of press. on recrystallization 8=48539
- CdS, sputtered, long-range oriented 8=30809
- Ce-alkali metal tungstates, rel. to morphology 8=26259
- Cr–Ni–Fe solid soln., prolonged, rel. to lattice parameters and phase dimensions 8=26246
- Cu, grain growth, u.s. enhancement 8=26247

Crystallization—contd
- Cu sheet, cold rolled, recrystallization texture 8=44125
- Fe, low-C, recryst. diag. obtained by vacuum melting 8=35240
- Fe, secondary recrystallization 8=39672
- GaP, effect of conditions on platelet growth 8=26205
- GaSb, back-melting effects on dislocation density 8=44447
- Hg, electrocrystallization 8=41283
- KCl, from aqueous solution containing Pb ions, calorimetric study 8=44132
- KCl: Cu^+, Ag^+, from melt, impurity ion distrib. coeff. determ. 8=39674
- La_2O_3:Bi^{3+}, configuration curves calc. rel. to phonon emission 8=40058
- Li precip. in Si, nucleation and growth 8=44105
- Li_2O-SiO_2 glasses, kinetics, comp. and ht. treatment effects 8=44133
- Mg borides prepared under superhigh-pressure condns. 8=35245
- $MgSO_4 . 7H_2O$, effect of conditions on left form predominance 8=26177
- NaCl: Cu^+, Ag^+, from melt, impurity ion distrib. coeff. determ. 8=39674
- NaCl solns., homogeneous nucleation 8=34973
- $NaPO_3$, vitreous, on metallic condensation-nuclei with cubic lattice 8=44136
- Nd-alkali metal tungstates, rel. to morphology 8=26259
- Ni, recryst. during creep, mechanism 8=48552
- Ni, thoriated, S effect on recrystallization 8=44138
- Ni, ThO_2 dispersed, recryst. rel. to cold working 8=48604
- Ni, vacuum-fused, diag. 8=39659
- NiCr, ThO_2 dispersed, recryst. rel. to cold working 8=48604
- Pb alloys, grain growth dependence on low solubility additions during recrystallization 8=35280
- Pd, electrocrystallization 8=41283
- Se amorphous films, crystallized by electron irradiation 8=39691
- Se, effect of thermal pretreatment 8=30834
- Se thin films, vacuum-deposition illumination 8=30757
- Se, trigonal, rel. to morphology of spherulites and single-crystals 8=44100
- Si films, chemically grown epitaxial, nucleation study using molecular beam techniques 8=44144
- Si, from Al-Si melts by zone-melting method with temp. gradient, mechanism 8=39686
- SiC, effect of N_2 and P impurities 8=26208
- Si–Fe, collective recrystallization and polygonization in fatigue testing 8=48558
- SiO_2, amorphous to cristobalite 8=44011
- SiO_2 powder, by annealing at 1400°C 8=35251
- Ti, recrystallization, reorientation mechanism 8=44086
- TiO_2 films, crystallized by electron irradn. into anatase and nitrile 8=39691
- Zn, recrystallization, preferred orientation relns. 8=35213
- ZnS, particle size and morphology, effect of precipitation condns. 8=48565
- Zr nucleation on W, and adsorption, α and β phases, obs. 8=39625

Crystallography
- See also Electron diffraction crystallography; Neutron diffraction crystallography; X-ray crystallography.
- classification of substances by crystal systems and classes, Bravais lattices and space groups 8=26161
- computer programs, DSPIN and LSQRS 8=39747
- crystallites, metallic, optical refl. determ. of orientation 8=30814
- of deformation twinning 8=26705
- diffraction and diffuse scatt. of X-rays and electrons 8=26347
- false structures from combination of structure amplitudes with arbitrary phases 8=39730
- families, main and subclasses and homeotypes of structure types 8=26162
- generalized theory for all degrees of ordering 8=26160
- goniometer head for low-temp. crystal rotation 8=30815
- magnetic groups, corepresentations, theory 8=26159
- of martensite in low carbon-steel, rel. to composite nature of 225 habit, theory 8=26175
- phase determ. using anomalous dispersion and directly measurable parameters 8=39733
- of shock compression 8=26745
- spherical packing in 3-dimensional space 8=39734
- symmetry, influence on translational slip and surface flow 8=26761
- twinning shears in lattices, theory 8=35215
- Al_2O_3, polycryst., porous, macroscopic changes due to n irrad. 8=26366
- of Fe-8%Cr-1.1%C alloy bainite transformation 8=30693
- $La_{3.33}Cu_2S_6$, double sulphide, data 8=30800
- $La_{3.33}MnS_6$, double sulphide, data 8=30800
- $MnIn_xCr_{2-x}S_4$, $(0 \leq x \leq 1.0)$, rel. to mag. props. 8=36190

Crystals
- See also Liquid crystals.
- alkali halides, gas inclusions, migration, elec. field effect 8=39966
- Anderson-Gruneisen parameter 8=48939
- asymmetry in mag. second-rank tensor quantities 8=49575
- cubic, symmetry props. of defects from uniaxial stress spectroscopy 8=35520

Crystals—contd
- dispersion surface in rot. cryst. electron diffr. pattern 8=35309
- effective field eqns. of model cryst., rel. to self-consistent multiple-scatt. approach to LEED interpret. 8=26350
- Einstein approx. of intermolec pots, effects of anharmonicity 8=35049
- elasticity, relation between macroscopic and microscopic theory 8=31160
- graphite, effect of size on dimensional changes due to neutron irrad. 8=35600
- haemoglobin crysts., human and horse procedures 8=26210
- ice, long-range forces and far i. r. spectra 8=31997
- ionic, evaporation by laser irradiation, obs. 8=39494
- ionic, polarizabilities, covalency contrib. 8=36390
- ionic, quantum-statistical ab initio calcs. 8=48338
- with isomorphous impurities, doping process rel. to compounds of different solubility 8=26612
- molecular dipole interaction 8=48335
- molecular rigid-body motion analysis 8=26028
- molecular, scattering of "light excitons" by impurity centres 8=40265
- momentum transfer rel. to Schroedinger eqn. 8=35609
- surface-atom van der Waals force 8=30610
- volume determ. by X-ray crystallography, interf. point counting 8=35259
- Al 99.5, annealing depend. on degree of deform. 8=35266
- C, effect of size on dimensional changes due to neutron irrad. 8=35600
- Cu, heated in Zn vapour, weight increase due to Zn diffusion 8=35485
- GaP, synthesis and epitaxial growth by fused salt electrolysis 8=48573
- He, correlation theory 8=28446
- $KTa_{0.65}Nb_{0.35}O_3$, lamellae origin 8=48519
- LiNi piezoelectric, surface waves excitation, estimation of optimal crystal cuts and propagation directions 8=46158
- MgO rot. cryst., dispersion surface, electron diffr. pattern 8=35309
- Mo_6Fe_7 lamellae, precipitation in Mo-Fe solid soln 8=35115

electron states. See Crystal electron states.

etching
- anthracene in benzene, α-radiation damage study 8=48826
- carbonaceous mats., in microscopy sample prep. 8=44164
- cellulose nitrate, etchable track formation 8=44492
- dielectrics, etchable track formation 8=44492
- epitaxial, effect of gaseous etchants 8=30754
- graphite, in characterization 8=44123
- ice, rel. to obs. of surface features 8=35147
- Lexan polycarbonate, etchable track formation 8=44492
- mica, etchable track formation 8=44492
- phenyl salicylate rel. to growth retardation in capillary tube, obs. 8=35247
- quartz, natural, selective rel. to delineation of structural defects 8=44428
- quartz, synthetic, patterns for prism faces and fracture surfaces 8=35224
- stainless steel, electrolytic and thermal, effect of Si content 8=45334
- steel, to determ. P segregation 8=30861
- Al, shade, orientation dependency 8=35222
- As, dislocation etch pits, 8=48852
- B, by H_2SO_4 and photomicrograph results 8=39651
- $BaTiO_3$, single domain prod. 8=30817
- Cu, shade, orientation dependency 8=35222
- CuCl, and regrowth 8=44101
- Fe, polycrystalline , dislocation 8=26676
- Fe-16 Cr alloy, pitting in solns. of Cl^- 8=44102
- Fe-Si alloys, shade, orientation dependency 8=35222
- GaAs, automatic jet thinning 8=33088
- Ge epitaxial films, with gaseous HI, HBr and HCl 8=30754
- In_2O_3 grown from $PbO-B_2O_3$, pits and tubes rel. to crystal growth 8=44103
- KCl, cleavage surfaces, obs. of evaporation spirals and loops 8=48525
- $MgAl_2O_4$ spinels, stoichiometric investigations for dislocations and slip planes 8=48526
- NaCl cleavage faces, thermal, in vacuum 8=35221
- NaCl, decoration of cleavage surface through amorphous C layer 8=26200
- NaCl, dissolution at dislocation sites, rel. to solvent and conc. of poisons 8=26685
- $NaNO_3$, for dislocations visualization 8=48858
- RbI dislocations, selective etchant 8=31087
- Sb, chemical and thermal, obs. 8=35223
- Si cleaved surface, electrical-decoration by Pt and e.-microscope exam. 8=40496
- Si surfaces, by HCl selective vapour, obs. of facets 8=48523
- SiN films on Si, rate rel. to distance between subst. in prep. 8=48464
- Si_3N_4 films 8=39652
- SiO_2, thermal photoresists adherence rel. to surface constitution, obs. 8=44601
- UO_2 in HNO_3 rel. to cryst. orientation, 1-37 molar 8=30818

Crystals—contd

excitons. See Crystal electron states/excitons.

faces
- alums, α and β, morphological difference 8=26173
- corundum, heat treated, surface defects, e-diffr. exam. 8=31054
- calcite, synthetic, morphology and optical props. 8=26194
- diamond-lattice type, rel. to theory of nuclei formation 8=26204
- diamonds, natural and synthetic, features in stable and metastable regions 8=26192
- diamond, octahedral, (III) face rel. to growth mechanism involving wing trigons 8=26237
- diamond, synthetic, habit rel. to nitrogen impurity content 8=48521
- dickite, microcrystals, Au-decorated and e-diffr. exam. in growth study 8=26230
- epitaxic overgrowth rel. to habit modification 8=26273
- free surface rel. to ferromagnetic spin system 8=27389
- graphite, gold decoration and epitaxial growth 8=44099
- graphite, morphological characterization 8=44123
- haematite, vapour-solvent grown 8=26251
- ice, growing cylindrical crystal, morphological stability 8=39673
- kaolinite microcrystals, Au-decoration and e-diffr. exam. in growth study 8=26230
- leucosapphire grown from tungstate melts, morphology 8=39648
- mica, synthetic, morphology dependence on crystallization conditions 8=26193
- molybdenite, cleavage, LEED study 8=48524
- molybdenite cleavage surfaces, LEED exam. 8=26199
- morphology dependence on structure, periodic bond chain model 8=26191
- morphology and defect production rel. to growth conditions 8=39661
- muscovites, harmonic, epitaxic power temp. dependence 8=26279
- phenazine/N-oxyphenazine mixed crystals habit changes 8=48522
- plane, and rounded forms, morphology 8=26170
- quartz, synthetic, habit prism and facture surfaces, etch patterns 8=35224
- ruby, grown from tungstate melts, morphology 8=39648
- structure defects, active centres and long-range effects rel. to epitaxy 8=26274
- X-ray film goniometer 8=30816
- Ag(111), rearrangement on O_2 adsorpt., study by LEED 8=26133
- Al, rel. to work function in external photoelec. effect exam. 8=40704
- $BaTiO_3$ (001), linear disorder on heating in u.h. vacuum 8=39649
- Cd, cylindrical, pitting and hopper growth obs. 8=26195
- Cd growth surface, LEED exam. 8=26196
- GaAs, epitaxially grown on Ge, twin structure obs. 8=26276
- $H_2PO_4^-$, rel. to growth and impurity effects 8=26254
- KCl, cleavage, obs of evaporation spirals and loops 8=48525
- KH_4PO_4, (100) and (101), growth rate dependence on Al ions and pH of soln. 8=48547
- Mo dendrites, morphology 8=48568
- Mo(111), faceting from CO adsorpt. 8=48486
- NaCl, cleavage surface, decoration through amorphous C layer 8=26200
- NaCl cleavage, thermal etching in vacuum 8=35221
- NaCl, Au nucleation rel. to surface F-centre formation in γ-irrad. 8=44152
- NiO (100), heating effects from e-diffr. exam. 8=39650
- PbS, artificial, morphology rel. to hydrodynamic flow theory 8=26197
- Se, trigonal, morphology of spherulites and single-crystals rel. to crystallization process 8=44100
- Si, cleaved, electrical-decoration by Pt and e.-microscope exam. 8=40496
- Si, facets formed by HCl selective vapour etching 8=48523
- UO_2, low-energy electron diffr. 8=48430
- W, C contaminated, (110) face metastable phase, obs. 8=39583
- W, inert gas bombard., thermal desorption obs., depend. on bombarded face 8=48497
- W, (112), adsorpt. of O_2, and oxidation 8=26107
- YAl garnet, morphology rel. to growth on seed by flux technique 8=26198
- Zn, single {0001} plane decoration with metal chlorides 8=48520
- ZnO, hydrothermally crystallized, effect of Li^+ 8=26201
- ZnS, morphology, precip. conditions dependence 8=48565

growth
- See also Crystallization; Zone melting and refining.
- and adsorption 8=44106
- alkali halide, with high-purity, technique 8=39665
- p-amino salicylic acid-on-quartz, epitaxy 8=48571
- anthracene, doped with tetracene, growth from vapour 8=30823
- apophyllite crysts., mech., study by surface microstructs. 8=26211
- in autoclaves, conditions analysis 8=26221

Crystals—contd
  growth—contd
    β-boron, rhomohedral, process conditions 8=26235
    cadmium chalcogenides, of hexagonal or cubic phases rel. to stoichiometry effects 8=44082
    calcite, control by regulated chemical reaction 8=39671
    calcite, synthetic, rel. to morphology and optical props. 8=26194
    calcite, shape rel. to twinning 8=26238
    capture of solution by growing crystals 8=35226
    cine-films of various phenomena 8=26202
    copper chromium halochalcogenides, by vapour transport method, spinel structure 8=40806
    corundum, hydrothermal crystallization kinetics 8=26230
    defect production rel. to growth speeds and morphology 8=39661
    diamond-lattice type, theory of nuclei formation 8=26204
    diamond, octahedral, peculiar mechanism involving wing trigons 8=26237
    diamond, techniques for luminesc. 8=36475
    diamond seed, by vapour-deposition 8=39669
    dickite microcrystals, revealed by Au-decoration in e-diffr. exam. 8=26230
    distintegration process in evaporation under high-vacuum 8=48575
    electrochemical. and surface diffusion 8=48531
    epitaxial, from at. beams, mechanism 8=39698
    epitaxial from liq., temp. control by solid-state linear ramp generator 8=41919
    epitaxial metal films, by thermal evaporation on ionic crystals in vacuo and air 8=30738
    epitaxial overgrowths, site exchange processes 8=44151
    epitaxic overgrowth rel. to habit modification 8=26273
    epitaxy, mechanism 8=48569
    fascia technique for float zone metal crystals 8=35225
    ferrite-garnets, hydrothermal synthesis conditions rel. to dislocation formation 8=26660
    films, polycrystalline. II-VI compounds, deposition methods and physical props. 8=48444
    flux process exam. 8=26225
    foreign mat. effects 8=26216
    γ-oxygen, by vapour-condensation, and neutronographs 8=26260
    grain growth, similarities between metals and plastic crystals 8=39657
    graphite, and characterization 8=44123
    graphite, in Fe-C-Si melt, mechanism 8=39670
    graphite, rel. to adsorbed impurity effects, scanning-e-microscope obs. 8=26236
    haematite, by vapour-solvent method 8=26251
    hailstones, spongy, growth criteria, microstructs. 8=45461
    hailstones, spongy, growth criteria, orientation fabrics 8=45460
    hailstones, spongy, growth mechanism 8=45459
    heterogeneous nucleation in thick ad layers 8=44104
    hydrothermal, hydro- and thermomechanical ratios in cylindrical vessel 8=30354
    hydrothermal, in carbonate solns., acid differentiation at high temps. and pressures 8=26213
    hydrothermal, large noble metal can technique 8=44112
    hydrothermal, morphological differences rel. to soln. ionic or colloidal charact. 8=26223
    hydrothermal, noble metal autoclave liner corrosion 8=49855
    ice, basal-plane solidification of supercooled water, effects of impurities 8=25982
    ice filaments, and destruction, in elec. field 8=35244
    ice, free growth rate in supercooled aqueous solns., rel. to ice-soln. interface 8=35242
    ice, growing cylindrical crystal, morphological stability 8=39673
    ice, in supercooled water rel. to morphology 8=26176
    ice nucleation, nature of nucleating site 8=32216
    impurity distribution anisotropy 8=26207
    impurity effect mechanism 8=30819
    impurity segregation effect, induced by cellular convection 8=43753
    kaolinite microcrystals, revealed by Au-decoration in e-diffr. exam. 8=26231
    light intensity viewing port 8=42171
    liquid flow patterns from horiz. temp. grads. during horiz. growth 8=26212
    leucosapphire, from tungstate melts 8=39648
    manganic ferrites, by different methods 8=26257
    mechanism rel. to crystallization conditions rel. to periodic bond chain model of morphology 8=26191
    metal epitaxial films, elec. field effects 8=26109
    metals on glass, vacuum-condensed and orientation rel. to deposition conditions 8=26226
    mica, synthetic, rel. to morphology and other props. 8=26193
    microcrystals, from melt on foreign substrate, thermal conditions mathematically analysed 8=26275
    microscopic, rel. to impurity heterogeneities from multiple-beam interferometry 8=48821
    molecular beam crystallization, non-isothermic, phenomenological theory 8=30739
    naphthalene, temp. gradient optimization for single crystals 8=44137

Crystals—contd
  growth—contd
    nucleation kinetics, effect on dynamic behaviour of continuous crystallizer 8=48534
    organic, from vapour phase, technique 8=39662
    organic, rate retardation in capillaries 8=26261
    orientated, on base, expt. confirm. of theory 8=44111
    phenyl salicylate, from melt in capillary tube, retardation, obs. 8=35247
    phenyl salicylate, unit cell dimensions 8=44280
    polyethylene, nucleation, droplet expt. 8=44128
    polyethylene, soln. grown folded-chain crysts. 8=35248
    polypropylene lamellae grown from dil. α-chlornaphthalene solns., twinning 8=35218
    from powder-grain enlargement in aqueous soln. 8=39655
    purification by vacuum distillation 8=28204
    quartz, artificial, overgrowth of holes 8=39700
    quartz : Co-doped, and opt. props. 8=48556
    quartz, coloured varieties synthesis and pigment distribution 8=26264
    quartz, hydrothermal crystallization kinetics 8=26230
    quartz, synthetic, from (0001) and $(10\bar{1}1)$ seeds, homogeneity of refractive index obs. 8=35207
    quartz, synthetic, supersaturation and temp. conditions, effect on Al impurity capture 8=44424
    rare-earth orthoferrites, hydrothermal 8=35249
    rare-earth silicates, trivalent, synthesis by Verneuil's method 8=35250
    ruby, Cr nonuniform distribution, Verneuil method 8=40011
    ruby, from tungstate melts 8=39648
    salol, rate retardation in capillaries 8=26261
    sapphire, czochralski crystals, interface morphology 8=44117
    from saturated soln., morphological effects of successive nucleation 8=26215
    sapphire substrate prep. for Si epitaxial deposition 8=39699
    seeded from flux, slow pulling apparatus 8=44110
    semiconductors synthesis and crystallization, universal apparatus 8=48527
    in silica gel using a co-solute 8=35243
    size-dependent rate, models 8=39658
    size distribution, effect of suspension density 8=48532
    sodium arsenoaluminate, hydrated 8=26411
    solid solution single-crystal, rel. to component segregation on crystallization 8=39654
    from solution, smooth-interface growth, theory 8=35232
    stress distribution in growing process, theoretical investigation 8=26224
    sucrose, and habit rel. to adsorbed impurity effect 8=26266
    in supercooling, deep 8=25987
    temperature-alternating methods 8=44107
    tetraphenylporphin and Ag deriv., solid solns., and growth 8=26034
    thermal balance for transport meas. in vapour phase growth 8=35230
    topotaxial texture, mechanism of formation 8=48570
    transient, under non-isothermal conditions 8=48530
    transition metal niobates, and study of chem. transport 8=26209
    travelling-solvent method, zone-movement kinetics 8=26220
    triglycine sulphate, domain twins formation 8=27292
    trilaurin, from melt, mechanism and rate 8=26255
    II-VI compounds, semiconducting, and morphologies 8=48561
    vacuum condensates, mechanism and structural defects 8=35156
    zinc chalcogenides, of hexagonal or cubic phases rel. to stoichiometry effects 8=44082
    zinkite, hydrothermal crystallization kinetics 8=26230
    Ag, electrocrystallization process rel. to structure and orientation 8=30822
    Ag, epitaxial growth on NaCl crystals 8=30745
    Ag films on mica in ultra-high vacuum 8=44037
    Ag halide single, from silica gel 8=26229
    Ag, through 2-dimen. nucleus formation and mono-atomic layer spread on dislocation-free surfaces 8=44113
    Ag_3AsS_3, proustite, from melt 8=26228
    AgI single, from silica gel 8=26227
    AgN_3 habit modification for i.r. and Raman spectral exam. 8=48535
    Ag_3SbS_3, pyrargyrite, from melt 8=26228
    Al alloys, splat-cooled, dendrite spacing rel. to cooling rate 8=26232
    Al, epitaxial growth on NaCl crystals 8=30745
    Al-Ag alloys, kinetics of cellular reaction, influence of precipitation 8=39540
    Al-4% Cu, grain boundary precipitates, interfacial diffusion 8=39715
    $Al_xGa_{1-x}P$, and optical props. 8=26233
    Al_2O_3, under neutron-irradiation 8=26234
    α-Al_2O_3, n-irrad. induced macroscopic growth, and damage 8=26666
    α-Al_2O_3, process rel. to dislocations 8=26663
    α-Al_2O_3, retention of additives 8=39693
    α-Al_2O_3:Mn, vapour hydrolysis 8=44118
    AlP, in excess Al soln., increased yield rel. to stirring motion 8=44116

Crystals—contd
growth—contd
AlP, yield and cryst. size in two-temp. synthesis 8=44115
Al-Si eutectic alloys, obs. 8=35234
As, from vapour, and etch pit studies 8=44119
Au epitaxial films in high vacuum 8=30747
Au microcrystals, rel. to defect structure 8=39666
$BaCl_2.2H_2O$, effect of bivalent cation addition to soln. before crystallization 8=44120
$BaSO_4$, chemically reacted flux method 8=44121
$BaTiO_3$, from KF flux rel. to chemical comp. of different types 8=26163
$BeAl_2O_4$, chrysoberyl, n-irrad. effects 8=31145
BeO, hydrothermally 8=48538
BeO, under neutron-irradiation 8=26234
B_6P, from solution, smooth-interface growth, theory 8=35232
Ca tartrate, doped and undoped, gel growth obs. 8=35246
$CaCrO_3$ perovskite 8=49570
$CaNb_2O_6$, by Cl chem. transport, lattice struct. and thermodynamics 8=35238
$CaHPO_4$, hydrothermal, in SnO and unsaturated fatty acids presence, obs. 8=35237
Cd surface, LEED exam. 8=26196
$CdCr_2Se_4$ 8=48541
CdSe, by temp. gradient solution zoning 8=48540
GdFe garnet, growth form and solubility obs. 8=30807
CdI_2, spirals on (0001) face 8=44124
$CdMoO_4$, Czochralski 8=30824
CdO, by sublimation 8=26244
CdS, and determination of some characts. 8=26241
CdS, by transport in vapour phase 8=26240
CdS films, and epitaxy 8=26114
CdS films, epitaxial, on CdS and ZnS platelets, dislocations and cryst. orientation 8=35165
CdS films, whisker-formation and structural changes 8=26270
CdS platelets, gas transport technique 8=40034
CdSb, from melt rel. to segregation of Se, S, Tl and Fe 8=26242
n-CdSe, under 100 atm. of N 8=49230
CdTe, pure, production and elec. props. 8=26239
CdTe, rel. to stoichiometry 8=26243
Ce-alkali metal tungstates, rel. to morphology 8=26259
CeO_2, from melt rel. to rare-earth impurity doping 8=26645
$Ce_2W_2O_9$, hydrothermal synthesis and struct., obs. 8=39636
$CeWO_4Cl$, hydrothermal synthesis and struct., obs. 8=39815
Co alloys, ferromag., films epitaxial growth on LiF and MgO 8=35170
Co, electroless films nucleation and microstruct., obs. 8=44165
Co electrolytic deposition 8=26245
Co, films epitaxial growth on LiF and MgO 8=35170
CoS_2, with pyrites struct., prep. by Cl_2 transport 8=26249
Cu, epitaxial growth on NaCl crystals 8=30745
Cu halide, grown from melt, luminescence 8=36485
Cu on sapphire, epitaxy of single crystal films 8=30751
Cu, thermal decompositiin of gaseous cupric fluorides 8=44127
CuCl, for optical purposes, process conditions 8=26248
CuCl, regrowth during water rinse 8=44101
$CuMoO_4$, single crystals, structure, powder photograph, space group 8=44126
DyFe garnet, growth form and solubility obs. 8=30807
Fe alloys, ferromag., films epitaxial growth on LiF and MgO 8=35170
Fe, by strain-anneal, and dislocation density and distrib. 8=26250
Fe, films epitaxial growth on LiF and MgO 8=35170
α-Fe_2O_3, by temp.-alternating method 8=44107
α-Fe_2O_3, twinned, bladelike platelet growths on iron, selected area e.-diffr. exam. 8=48518
α-Fe_2O_3 whiskers and twinned platelets, defect diffusion rel. to gaseous oxidation 8=44150
Fe_3O_4 films in LiOH solns., two-phase struct., 300°C 8=44043
FeS_2, with pyrites struct., prep. by Cl_2 transport 8=26249
Ga chalcogenides, synthesis in Ga and In melts 8=48563
Ga, rates rel. to supercooling and dislocations 8=44130
GaAs, bulk and epitaxial, struct. defects rel. to method 8=44427
GaAs, epitaxial for high efficiency Gunn oscillator 8=49283
GaAs, epitaxially grown on Ge, twin structure obs. 8=26276
GaAs, epitaxial, surface features and twins 8=35241
GaAs, epitaxial, high electron mobility rel. to substrate orientation 8=39592
GaAs films, epitaxy on rocksalt, 25-430°C 8=35172
GaAs, from solution, smooth-interface growth, theory 8=35232
GaAs, high mobility layers, obtained by liq. phase epitaxy 8=30753
GaAs hole deposits, faceted, effect of vapour comp. on growth rates 8=48572

Crystals—contd
growth—contd
GaAs, laser diodes, orientation influence 8=33214
GaAs, single-crystal on insulating substrates 8=30826
GaAs, vapour growth on Ge 8=30752
$GaAs_{1-x}P_x$, epitaxial, vapour transport method, injection laser production 8=46617
GaP, czochralski growth under boric oxide layer 8=44131
GaP, epitaxial, on Si substrates by fused salt electrolysis 8=48573
GaP, from solution, smooth-interface growth, theory 8=35232
GaP, in bulk ingot form, by vertical Bridgman tech. 8=48542
GaP, large crysts, from stoichiometric melt 8=48543
GaP platelets, effect of impurities and crystallization conditions 8=26205
GaP_xAs_{1-x}, by soln. zone sandwich of liquidus comp. migrating thro' solid feed 8=44147
GaP-GaAs solid solns, epitaxial, departures from homogeneity 8=30838
GaP, VLS growth and morphology, obs. 8=35208
GaP : Zn(Cd), epitaxial, by $GaCl_2$ vapour transport 8=48544
n-GaSb, epitaxial on p-GaSb, from liq. phase 8=44044
Gd_2O_3, retention of additives 8=39693
Ge, by Czochralski method, crystal temp. field 8=30827/8
Ge, by Czochralski method melt temp. field 8=30829
Ge, Czochralski method, shielding conditions invest. 8=26253
Ge, dendrite mechanism 8=48567
Ge dendritic ribbons, lateral growth 8=26271
Ge epitaxial layer by close-spaced system 8=48574
Ge, in hydrogen atmosphere, use of Ge(Li) detectors 8=48545
Ge monocrystals from Sn-Pb mixtures 8=26252
Ge mosaic, epitaxial for infrared image tube 8=44844
Ge, techniques for luminesc. 8=36475
Ge, vapour crystallization droplet mechanism and overgrowth defect formation 8=26277
Ge, vapour crystallization processes 8=26278
Ge--GaAs epitaxial combinations, linear defects interpretation as misfit dislocations 8=31078
Ge—GaAs epitaxial combinations, linear defects interpretation as slip 8=21077
Ge-GaAs system, heteroepitaxy from liq. phase on contact fusion 8=48546
Ge_3N_4 amorphous films, obs. 8=44046
$H_2PO_4^-$, rel. to impurity effect and crystallization conditions 8=26254
HfO_2, from melt rel. to rare-earth impurity doping 8=26645
HgS films, epitaxial, on CdS and ZnS platelets, dislocations and cryst. orientation 8=35165
InSb, characts. and impurity incorporation during facet growth 8=48819
InS, synthesis in Ga and In melts 8=48563
InSb: Te, rel. to impurity heterogeneities from multiple-beam interferometry. 8=48821
$KAl(SO_4)_2\ 12H_2O$, growth and dissolution rates 8=48537
KCl, effect of conditions on perfection and mech. and optical props. 8=26401
KCl, with 10^{-9} mol/mol purity, technique 8=39665
$KD_3(SeO_3)_2$, phase transition and dielec. anomaly 8=30698
KH_2PO_4, (100) and (101) faces, rate dependence on Al ions and pH of soln. 8=48547
$KMgF_3$, perovskite structure 8=30830
$KMnF_3$, perovskite structure 8=30830
$K_2Mn_2(SO_4)_3$, langbeinite structure, rel. to electro-optical effect 8=39678
$K_2Ni_2(SO_4)_3$, langbeinite structure, rel. to electro-optical effect 8=39678
$KY(MoO_4)_2$, structure from growth forms and x-ray diffraction 8=48655
La_2O_3, retention of additives 8=39693
Li metagallate, Czochralski growth in Ar or CO_2 8=48548
LiF, effect of conditions on perfection and mech. and optical props. 8=26401
LiF negative thread, and evaporation kinetics 8=26256
$M_{23}C_6$ on austenitic stainless steel grain boundaries 8=39668
Mg-Al spinel, Czochralski method 8=39675
$MgAl_2O_4$, travelling isotherm technique 8=44135
MgO whiskers, spontaneous 8=35257
MgO, C arc furnace technique 8=48549
$MgSO_4.7H_2O$, rate dependence on supersaturation of soln. 8=39676
Mn ferrite: Ba, discontinuous 8=39677
Mo, vapour deposited, orientation rel. to temp. and annealing 8=35154
$(NH_4)_2Mn_2(SO_4)_3$, langbeinite structure, rel. to electro-optical effect 8=39678
NaCl, containing ⟨110⟩ oriented Na dendrites, mechanism 8=30836
NaCl, micromechanism in vacuum-condensation process 8=48551
NaCl, with 4×10^{-6} mol/mol purity, technique 8=39665
NaCl : Na_2CO_3, NaCl : NaOH, and segration coeffs. 8=48550
$NaMF_3$, ($M=Mg^{2+}, Co^{2+}, Ni^{2+}, Zn^{2+}$), chem. synthesis and structural data 8=26258
$NaMgF_3$, perovskite structure 8=30830

Crystals—contd
- **growth**—contd
  - Nd-alkali metal tungstates, rel. to morphology 8=26259
  - $Nd_2W_2O_9$, hydrothermal synthesis and struct., obs. 8=39636
  - $NdWO_4Cl$, hydrothermal synthesis and struct., obs. 8=39815
  - Ni alloys, ferromag., films epitaxial growth on LiF and MgO 8=35170
  - Ni, electrocrystallization process rel. to structure and orientation 8=30822
  - Ni ferrite, epitaxial, on MgO (111) and (110) surfaces 8=39594
  - Ni, films epitaxial growth on LiF and MgO 8=35170
  - Ni, high-purity, by e. beam float zone melting 8=48553
  - Ni on Cu, epitaxial overgrowth, reduction in mechanical strength of Cu 8=40146
  - NiS_2, with pyrites struct., prep. by Cl_2 transport 8=26249
  - P, black, plate, from vapour phase at h.p. 8=30832
  - $PbCl_2$, effect of bivalent cation addition to soln. before crystallization 8=44120
  - $Pb(NO_3)_2$, effect of methylene blue impurity 8=39679
  - $PbO-B_2O_3-PbF_2$ melts, rel. to solubility of trivalent oxides, temp. dependence, 1000-1500°C 8=39320
  - PbS, in silica gels, thioacetamide ion donor 8=48555
  - PbS on Si, mica and PbS single-crystal substrates, process rel. to substrate defect structure 8=26280
  - PbSe, by Bridgman tech. 8=44141
  - PbSe epitaxic film formation by sublimation in vacuo 8=26123
  - $PbSnO_3$, perovskite, high press. synthesis 8=48554
  - $Pb_{1-y}Sn_ySe$, by Bridgman tech. 8=44141
  - $Pb_{1-x}Sn_xTe$, by Bridgman tech. 8=44141
  - $(Pb_xSr_{1-x})TiO_3$, by traveling heater method 8=44139
  - PbTe-SnTe, by Czochralski tech. 8=44140
  - Pr-alkali metal tungstates, rel. to morphology 8=26259
  - $Pr_2W_2O_9$, hydrothermal synthesis and struct., obs. 8=39636
  - $PrWO_4Cl$, hydrothermal synthesis and struct., obs. 8=39815
  - $PtSb_2$, horizontal zone refining, Czochralski method 8=40479
  - Pu-3.3at.% Ga alloy, large crysts, modified solidification techs. 8=26263
  - RbH_2PO_4, static method, optical conditions 8=44142
  - $Rb_2Mn_2(SO_4)_3$, langbeinite structure, rel. to electro-optical effect 8=39678
  - Sb single cryst. rods from melt, and etching, obs. 8=35223
  - SbSI, hydrothermal 8=39684
  - Se, by seeding under high-pressure 8=44143
  - Se, single-crystal, 25mm. length × 10mm. diam. 8=39685
  - Se-Te alloy, single-crystal, 25 mm. length × 10 mm. diam. 8=39685
  - $Se_xTe_{1-x}Hg$ solid soln., and structure 8=26269
  - Si, by Czochralski method, impurity striations, reasons for appearance 8=48824
  - Si epitaxial deposition on sapphire, substrate prep. 8=39699
  - Si, epitaxial films on Si substrate 8=39597
  - Si epitaxial layers, by sublimation in vacuum 8=35256
  - Si epitaxial layers, crystal perfection, effect of substrate surfaces 8=39596
  - Si films on spinels, growth twins and carrier mobility 8=35181
  - Si, (111) and (100) epitaxial shallow surface depressions stability, obs. 8=44145
  - Si {311} planes, epitaxial, surface characts. 8=39582
  - Si, techniques for luminesc. 8=36475
  - Si, from Al-Si melts by zone-melting method with temp. gradient, mechanism 8=39686
  - Si, Au and Cu impurity and dopant distribs. on pulling crystals in floating-zone technique 8=44015
  - SiC, from solution, smooth-interface growth, theory 8=35232
  - β-SiC, porous, macroscopic growth induced by n-irrad. 8=26735
  - SiC, techniques for luminesc. 8=36475
  - SiO_2, anodic mechanisms 8=39687
  - Sn foils, production from melt and degrees of perfection 8=39688
  - SnTe(Se)(S), epitaxial deposition on NaCl/KBr substrates at 293-873°K 8=39599
  - $SrTi_{1-x}Fe_xO_{3-x/2}\phi_{x/2}$, ϕ = oxygen vacancies 8=35252
  - $SrTiO_3$, by flux method, with slow cooling 8=48559
  - $Sr_3Yb_2Ge_3O_{12}$, by precipitation in NaOH soln 8=48557
  - $Sr_3(Yb, Lu)_2(OH)_{12}$, by precipitation in NaOH soln. 8=48557
  - Ta, oxide plate formation, crystallographic, analysis 8=30690
  - Ta, oxide plate formation, morphology 8=39689
  - ThO_2, from melt rel. to rare-earth impurity doping 8=26645
  - $Tl_2Mn_2(SO_4)_3$, langbeinite structure, rel. to electro-optical effect 8=39678
  - Tl_2Te_3, from melt rel. to segregation of Se, S, Tl and Fe 8=26242
  - UO_2 films on UC crysts. kinetics rel. to O diffusion through film, 60-160°C 8=39604
  - VO thin film single crystals, epitaxial 8=48470
  - W, vapour deposited, orientation rel. to temp. and annealing 8=35154

Crystals—contd
- **growth**—contd
  - YAl garnet, on seed by flux technique rel. to morphology 8=26198
  - YFe garnet, growth form and solubility obs. 8=30807
  - YGa garnet: Nd, and laser oscills., obs. 8=39694
  - YGdAl garnet:Nd^{3+}, and laser characts. 8=39692
  - Y_2O_3, retention of additives 8=39693
  - Zn chalcogenides, synthesis in Ga and In melts 8=48563
  - Zn, forms, microscopic obs. 8=48562
  - $Zn_xCd_{1-x}S$, graded-band-gap type, and elec. props. 8=39696
  - $Zn_xHg_{1-x}Te$ solid soln., and structure 8=26269
  - $Zn_xHg_{1-x}Te$, by soln. zone sandwich of liquidus comp. migrating thro' solid feed 8=44147
  - ZnO, hydrothermally crystallized, effect of Li^+ rel. to facet effect and dentritic growth 8=26201
  - ZnO:Fe^{3+}, Mn^{2+}, cubic field paramater rel. to behaviour 8=45104
  - $ZnRh_2O_4$, single crystals, from PbO flux 8=39695
  - ZnS, cubic, from molten $PbCl_2$ 8=44149
  - ZnS films, epitaxial, on CdS and ZnS platelets, dislocations and cryst. orientation 8=35165
  - ZnS on Si, epitaxial, by vac. evaporation 8=30740
  - ZnS platelets, gas transport technique 8=40034
  - ZnS, polytype formation rel. to periodic slip processes 8=44461
  - ZnSe epitaxial layers, on p-Ge, and elec. characts. 8=44834
  - ZnSe-ZnTe, solid soln. in Te_2 atmosphere 8=48564
  - $ZnSnP_2$ platelets, and props. 8=26267
  - ZnS, (Se), (Te) semiconducting, and morphologies 8=48561
  - ZnTe, by temp. gradient soln. zoning 8=44148
  - ZnTe from melt in Zn atm., gradient freeze method 8=35253
  - ZnTe, from solution, smooth-interface growth, theory 8=35232
  - $ZnTe_{1-x}Se_x$, by temp. gradient soln. zoning 8=44148
- **imperfections.** See Crystal imperfections.
- **internal fields**
  - alkali halides, dislocation mobility dependence on electrostatic field 8=26667
  - alkali halides, elec. field gradient at (100) surface 8=30717
  - α-quartz crystal, rel. to refractivity interpret. 8=49756
  - alums, Ti^{3+} substituted, crystal-field energy-level splittings rel. to structure details 8=43935
  - anthracene, Davydov splittings of intense transitions 8=35048
  - axial model field, splitting of d^2 and d^8 levels 8=30647
  - benzene, site group splitting and orientational effects 8=27627
  - chalcopyrite, $CuFeS_2$, Q.S. and mag. field temp. dependence, 300-448°K from Mossbauer studies 8=2601
  - c.m. short range in metal lattice meas. method 8=35026
  - cohesive energy, cluster expansion for a quantum crystal 8=26007
  - correction matrices for d^5 config. in cubic symmetry 8=48306
  - correlation cryst. field, theory 8=35023
  - d^3 configuration g-factor, covalency and theory 8=43962
  - coupling and recoupling coeffs. and ionic and paramag. energy levels, SU(2) algebra 8=39505
  - d^3 and d^8 ions in cubic crystals, strain induced zero-field splitting, e.p.r. study 8=39504
  - dicyanodiacetylene Σ_g^+ modes 8=26031
  - electric field gradients created around impurities in dilute alloys, direct meas. 8=48313
  - energy levels for various symmetries 8=43930
  - e.s.r. line splitting by Jahn-Teller effect of ions in cubic lattice sites 8=31841
  - ferricytochrome c, beef-heart 8=31865
  - ferrihaemoglobin, and Jahn-Teller effect in g factor anisotropy 8=36234
  - field theory, MO-LCAO, diagram method 8=43931
  - GF method generalisation, inter- and intramolecular coupling 8=43961
  - giant mag. fields produced at nucleus by hole in K shell 8=48315
  - ground-state splitting, isotope effects 8=26012
  - h.c.p. lattices, non-central force model 8=30621
  - hemoproteins, fine structure of Fe ions 8=35044
  - hyperfine transient fields for implantation of ions in ferromagnetic media 8=26011
  - ionic crystals, short range order, electrostatic energy calc. 8=35020
  - isotope shift in field-splitting 8=39506
  - lanthanide impurity doped, crystal field effects rel. to structures 8=26646
  - magnetic, automatic recording for ellipsoidal specimen 8=46372
  - magnetic-field-induced quadrupole splitting 8=43939
  - magnetic ions in host lattices, isotope shift temp. dependence and phonon-induced zero-field splitting 8=49451
  - magnetic, Shubnikov group representation 8=27375
  - metals with paramag. impurity, form. of localized mag. moment 8=31519

Crystals—contd
- **internal fields**—contd
  - molecular field coeffs. from mag. saturation temp. dependence using Néel-Weiss theory 8=45033
  - naphthalene, Davydov splittings of intense transitions 8=35048
  - nuclear and electronic adiabatic demag. meas. 8=39507
  - with paramagnetic ions, axial-field-splitting, convalency effects 8=35046
  - paramagnetic reson., induced forbidden transitions ($\Delta M=2$) 8=45073
  - point lattice potential of bounded crystal, calc. 8=48312
  - rare earth cpds, low-lying crystal-field spectra 8=36296
  - rare earth h.c.p. paramagnetic effects on inelastic n scatt. 8=40749
  - S-state ion zero-field splitting 8=43933
  - Scheelite-type: Pr^{3+} activated, charge compensation mechanisms 8=35028
  - space charge wave interaction with streaming carriers, effects of collision 8=26873
  - splitting parameter and apparent temp. dependence assessed 8=43936
  - temperature-gradient instability in low-symmetry, highly conducting crystals 8=35022
  - tetrahedron, trigonally distorted, collective coordinates 8=48311
  - $A^{III}B^{V}$ crystals, elastically deformed, rel. to elec. field gradients at nucleus from n.m.r. obs. 8=31909
  - AgBr, e. distribs. from X-ray structural analysis 8=48302
  - Al, pair interaction, phase change 8=35027
  - Al:Mg, Zn, electric field gradients 8=30625
  - Al_2O_3:Cr, Ti, V, field splitting, exchange coupled transitions and intraband vibr. 8=49701
  - α-Al_2O_3:V^{2+}(Cr^{3+}), (Mn^{4+}), trigonal splitting, stress dependence 8=43929
  - AlSb, elastically deformed, elec. field gradient at nuclei from n.m.r. obs. 8=31909
  - $(C_4H_9)_2$ SnO, quadrupole doublet, ang. distrib. of resonance scatt. of γ-rays 8=39511
  - CaF_2 lattice, rare-earth ion field splitting 8=35025
  - CaF_2:(Am^{2+}, Cm^{3+}), zero-field splittings 8=30622
  - CaF_2:Yb^{3+}, ENDOR meas. rel. to crystal field splitting of Yb^{3+} in cubic sites 8=27501
  - Cu, nuclear and electronic adiabatic demag. meas. 8=39507
  - $Cu_{1-x}Ni_xCr_2O_4$, bulk strain, -Jahn-Teller ion 8=35052
  - Er ethylsulphate, ratios of odd-parity parameters 8=48307
  - Er^{3+} in ethylsulphate, Zeeman effect theory 8=36357
  - $ErCO_2$, electric effects, and first order phase transition 8=26014
  - Eu(II), spectrochem. and nephelauxetic parameters 8=43927
  - Fe, one-dimensional e.m. field, calc. methods 8=26013
  - Fe(III) porphyrin cpds., zero-field splitting 8=30623
  - Fe stilbene, mag. fld. at nucleus, Mossbauer meas. 8=30641
  - Fe—C martensite, mag. field, Q.S. and isomer shift from Mossbauer studies 8=26020
  - FeCl, mag. fld. at nucleus, Mossbauer meas. 8=30641
  - $FeCl_2.H_2O$, mag. fld at nucleus, Mossbauer meas. 8=30641
  - Fe-Co alloys, hyperfine field distrib. from Fe^{57} and Co^{57} NMR 8=45120
  - $Fe(NH_4SO_4)_2.6H_2O$, nuclear electric-field-gradient determ. 8=30626
  - $Fe(NH_4SO_4)_2.6H_2O$, orientation and symmetry from elec.-field-gradient and susceptibility axes 8=43951
  - $FeSO_4.7H_2O$, nuclear electric-field-gradient determ. 8=30626
  - $Fe(MSO_4)_2$, M=NH_4^+, K^+, Rb^+, Cs^+, field splitting from Mössbauer studies 8=26023
  - Fe-Ni single crystal, Mossbauer effect, contribution of dipolar fields 8=35037
  - $Fe_{1-x}Ni_xCr_2O_4$, bulk strain, Jahn Teller ion interaction rel. to distortions 8=35052
  - GaAs(Sb), elastically deformed, elec. field gradient at nuclei from n.m.r. obs. 8=31909
  - $Gd_{2.7}Ca_{0.3}Fe_{4.7}Sn_{0.3}O_{12}$, effective at Sn^{119} nucleus through compensation point 8=49469
  - $GdVO_4$:Eu^{3+}, crystal field Hamiltonian parameters 8=31992
  - InAs, elastically deformed, elec. field gradient at nuclei from n.m.r. obs. 8=31909
  - K, pair interaction, phase change 8=35027
  - KBr, elec. field gradients at nuclei surrounding different subst. halogen ions, n.m.r. meas. 8=48314
  - KCl:OH, dipole interaction through phonon field 8=40577
  - $K_3Fe(CN)_6$, mag. field, Mossbauer h.f.s. obs., 0.025–0.04°K 8=37330
  - KI, elec. field gradients at nuclei surrounding different subst. halogen ions, n.m.r. meas. 8=48314
  - $La_2Mg_3(NO_3)_{12}.24H_2O$:$Mn^{2+}$ zero-field splitting 8=30627
  - Li, pair interaction, phase change 8=35027
  - $LiTaO_3$, ferroelec. 8=40987
  - Na, pair interaction, phase change 8=35027
  - $NaNO_2$, charge distrib. of NO_2^- 8=48308
  - Nd^{3+} in ethyl sulphate, mag. anisotropy and field parametrization 8=43932

Crystals—contd
- **internal fields**—contd
  - PbF_2: Gd^{3+}, near Gd^{3+} ion from e.p.r. spectrum 8=36250
  - S, orthorhombic, pot. energy calc. as function of unit cell parameters 8=39502
  - Sm(II), spectrochem. and nephelauxetic parameters 8=43927
  - TiO_2 d^1 configuration, e.s.r. spectrum 8=45102
  - Tm^{169} in Fe, time-dependent hyperfine interaction 8=39524
  - Tm, salts electronic shielding examined by Mossbauer effect 8=39508
  - $TmAl_3$, cryst. stark splitting 8=48309
  - YVO_4 from Eu^{3+}, $(4f)^6$ level splittings, obs. 8=41152
  - Yb(II), spectrochem. and nephelauxetic parameters 8=43927
  - ZnO, point-charge model for thermal eqn. 8=30630
  - ZnS:Fe^{3+}, cubic field splitting of S-state ions 8=43934
  - ZnSe:Fe^{3+}, cubic field splitting of S-state ions 8=43934
  - ZnTe:Fe^{3+}, cubic field splitting of S-state ions 8=43934
  - α-$Zn_3(VO)_2$: Ni^{2+}, optical spectra rel. to crystal field theory 8=48310
- **lattice mechanics**
  - See also Mössbauer effect.
  - actinide complexes, octahedral, free and in crystals, vibronic level Zeeman splitting 8=43964
  - adamantane, solid, phonons, torsons and rotational diffusion 8=35397
  - alkali halides, Debye-Waller factors temp-dependence, calcs. 0-900°K 8=39869
  - alkali halides, imperfect crysts. 8=48701
  - alkali halides, lattice modes anharmonicity 8=48702
  - alkali halides, scattering of lattice waves by dislocations 8=30933
  - alkali halides, U centres, isotopic effects in absorpt. bands rel. to electron-phonon interaction 8=27557
  - alkali halides, vibration modes due to U-centres 8=39866
  - alkali halides with H^- defects, multiphonon absorption 8=48703
  - alkali metals, lattice-dynamic calc. 8=30931
  - alkali metals, e-phonon interactions, scatt. and transport coeffs. 8=44631
  - alkali metals, phonon spectra on extension and hydrostatic compression 8=35380
  - alkali metals, strained, phonon spectra 8=44296
  - alkaline-earth carbonates, C-isotope effects 8=31966
  - alloy, binary ordered, kinetic properties, effect of phonon drag 8=35817
  - alloys, dil., with short-range order, theory of vibrations 8=48705
  - alloys, disordered, self-consistent-field approxs. 8=44294
  - anharmonic vibrations, quantum-dissipation theory 8=48695
  - anharmonicity, low temp. and Debye-Waller factor 8=35372
  - anthracene, i.r. modes 8=49768
  - anisotropic temp. factors and screw rotation coeffs from dynamical calcs. 8=26569
  - anthracene, phonon freqs. from X-ray scatt. photographs 8=26577
  - b.c.c. metals, zero-point energy and Θ_c^{∞} 8=30932
  - benzene, energy rel. to intermolecular pot. 8=35396
  - benzene, exciton splittings 8=27628
  - benzene, lattice energy in atom-atom approx. 8=35395
  - benzene, rot. barrier heights of intermolec. rots. 8=43963
  - beryl, l.f. vibrs. of H_2O mols. 8=48704
  - bravais lattice, anharmonic freq. shift and free energy, analysis of cubic contribs 8=30952
  - charge carrier scatt. by acoustical and optical vibs. 8=49076
  - cyanamide, vibrs. 8=48710
  - diamond, at vibration spectrum studies, review 8=43922
  - diamond, vibration spectra, freq. along asymmetric dims. 8=30934
  - dielectric crystals, ideal, second sound in absence of Umklapp process 8=35957
  - dielectric crystals, one-particle densities, thermal propagation and second sound 8=26587
  - diffusion-jump processes in monatomic crystals, theory rel. to phonon system 8=44379
  - digermane force field calc. from frequencies and coriolis constants of Ge_2H_6, Ge_2D_6 8=48711
  - dynamic damping of dislocations by impurities 8=40032
  - dynamics of diatomic alternative superstructure rel. to their phonon spectra 8=30929
  - dynamics of simple lattices with 2-d defects 8=35368
  - dynamics, quantum many-body theory, collective fluctuation approx. 8=26568
  - dynamics, quantum theory 8=30922
  - e.s.r. line splitting by Jahn-Teller effect of ions in cubic lattice sites 8=31841
  - exciton-phonon interactions in recombination spectra in compound semiconductors 8=44760
  - f.c.c., surface force-constant changes rel. to atomic mean square displacements 8=26567
  - finite dielec., thermal cond. rel. to phonon-phonon interactions 8=35454
  - frequency distrib. function calc. from continued functions 8=44290
  - germania, vitreous, vibrational spectra 8=35392

Crystals—contd
- lattice mechanics—contd
  - glasses, atomic vibs. rel. to thermal props. 8=35455
  - graphite, lattice vibration 8=35383
  - h. c. p. lattices, non-central force model 8=30621
  - hydrazine, vib. anal., and force consts from i. r. spectra 8=45244
  - hydrogenous molec. solids freq. spectrum by neutron scatt. 8=39875
  - ice, cubic I and hexagonal, long-range forces and far i. r. spectrum 8=31997
  - ice, freq. distrib. from inelastic neutron scatt. 8=26574
  - ice, hexagonal, freq. spectrum from neutron scatt. 8=39875
  - ice, 1h and 1c, orientationally-disordered 8=27574
  - ice, proton dynamics from slow n. inelastic scattering 8=39303
  - imidazole, H-bond freqs. 8=41165
  - impurity, paramag., e spin-lattice relax. 8=31842
  - impurity states, resonant phonon interactions effect on line broadening 8=41027
  - impurity vibr. in ionic cryst., rel. to i.r. absorpt. 8=41024
  - inert-gas, theory and expt. 8=35390
  - interstitial atom in b. c. c. lattice, localized vibrations, theory 8=44293
  - ion semiconds, coupled system of lattice, plasmic and e.m. waves 8=31304
  - ionic cryst. slab, phonon modes 8=39858
  - ionic crystal sphere, optical modes 8=35374
  - ionic crystals, optical vibrs. 8=44287-8
  - i.r. absorption by local vibrations at multiple and combination freqs. 8=31939
  - isotopically disordered, freq. distrib. function moments calc. 8=44289
  - lanthanide complexes, octahedral, free and in crystals, vibronic level Zeeman splitting 8=43964
  - linear chain, monatomic with impurity vibr. with long-range interaction 8=23872
  - localized modes and low-freq, reson., asymptotic description 8=26570
  - magnetic ions in host lattices, phonon-induced zero-field splitting and isotope shift temp. dependence 8=49451
  - mechanical and shape equilibrium, Gibbs surface model 8=40086
  - metal-metal boundary tunnel current, structure due to electron-phonon interaction 8=26956
  - metal, monovalent, e-phonon interaction, screening and e. correlation effects 8=49074
  - metals and ionic, thermal vibration anharmonicity 8=35367
  - metals, electron-lattice interactions rel. to spin-paramagnetism 8=36077
  - metals and alloys, phonon conductivity calc. 8=30928
  - metals, melting criterion 8=34964
  - metals, model for lattice dynamics 8=30927
  - of microcrystallites 8=35371
  - mixed crystals, long-wavelength optic phonons, modified random-element-isodisplacement model 8=48696
  - molecular crysts., displacement vibrs., central force field calc. 8=30926
  - molecular crysts., group-theoretical anal. 8=39861
  - molecular crysts., vibrs. in pair potential approx. 8=30925
  - molecular vibrational modes, anharmonic interactions 8=25411
  - molecular vibrations rigid-body, Schomaker-Trueblood analysis 8=39862
  - neutron scattering from n-dimensional lattice (n = 1, 2, 3) rel. to multiphonon processes 8=31132
  - noble gas solids, model poentials 8=35389
  - non-cubic lattices, dynamical matrix Coulomb contribution 8=44295
  - Optic transitions of bound electrons, phonon processes 8=49678
  - Optical cooling by laser radiation transfer 8=39900
  - optical phonons, covalent bonding effect, empirical relation 8=30924
  - organic molec. crysts, vibronic spectra, dynamic theory 8=39860
  - oscillations of separate atoms, effective Debye freq. and Mossbauer effect 8=39509
  - phase transition of Ising spin systems, effect of lattice vibration 8=36098
  - phonon attenuation in solids measurement by Brillouin scattering 8=49686
  - phonon dispersion effects on heat-pulse shape 8=48753
  - phonon dynamics role in weak itinerant ferromagnetism 8=45032
  - phonon-magnon interaction rel. to acoustic wave velocity changes 8=30937
  - phonon-paramagnon interactions, effect on u.s. attenuation 8=48714
  - phonon-photon interactions, coherent 8=46638
  - phonon scatt. by edge-disloc. dipoles rel. to lattice thermal conductivity limitation by phonon-single disloc. interactions 8=48754
  - phonon spectrum singularities rel. to extended defects 8=39864
  - phonon transport equation 8=48693

Crystals—contd
- lattice mechanics—contd
  - phonons, coherent, generation mechanism theory 8=35398
  - phonons in multi-made crystals, long wavelength longitudinal 8=48698
  - phonons, microwaves, in metals, freq. depend. of e.m. generation 8=49087
  - piezoelectric vibrating resonators, neutron diffraction 8=35378
  - with planar defect, vibrational spectrum 8=30930
  - polarons, small-radius, effects in vibrations 8=39863
  - polyacetaldehyde, vibr. assignments from neutron scatt. 8=48712
  - polyethylene, phonon freq. from neutron scatt. 8=26579
  - polyethylene, vibrs. rel. to chain folding, calc. 8=44305
  - polyglycine, vibr. spectra 8=39880
  - poly(vinylidene fluoride), α- and β-, fundamental modes and force consts., i. r. obs. 8=44306
  - potassium halides, phonon scatt. by U centres, thermal conductivity meas. and theory 8=44301
  - pyrazine, at 4. 2°K 8=36534
  - pyrazine, spin-lattice relax. and low temp. phosphoresc. decay 8=36535
  - quadrupole interaction, two quadrupole-octupole phonon states 8=48699
  - quantum crystals, hard-core renormalization 8=48694
  - quantum crystals with hard-core potential, dispersive anharmonic effects 8=44292
  - α quartz, excitation by mercury discharge 8=49753
  - α-quartz, phonon dispersion effects on heat-pulse shape 8=48753
  - α-quartz, phonons, extraordinary optical, directional dispersion 8=45221
  - quartz, second-harmonic generation of microwave phonons 8=30950
  - random impurity vibrational props. Green's-function analysis 8=35546
  - relaxation times and normal mode freqs. 8=39857
  - resonance rel. to parametric gain, theory 8=45141
  - sapphire, second-harmonic generation of microwave phonons 8=30950
  - self-consistant polarization waves and dispersion forces in crystals 8=30921
  - semiconductors, displacive vibronic phase transitions 8=49075
  - semiconductors, slow neutron scattering study of lattice dynamics 8=44759
  - shock wave in non-ideal lattice rel. to collision of two semi-infinite crystals 8=48700
  - sidebands in vibrational spectra and pressure dependence 8=35370
  - silica, vitreous, vibrational spectra 8=35392
  - singularities in phonon spectra rel. to extended defects, determ. by n. scattering 8=39865
  - solid solns., disordered, monophonon neutron scatt. rel. to impurities 8=35379
  - solid solutions, substitutional, vibrs. and order 8=30923
  - sound velocity rel. to isotopic mass 8=35376
  - spectral gaps in vibrational systems; evaporation method applied to non-isotopically disordered lattices 8=35377
  - spectral gaps in vibrational systems, in isotropically disordered two-or three-dim. lattices 8=35376
  - spin-lattice Raman relaxation 8=39867
  - spin-lattice relax. determ. by adiabatic rapid-passage meas. 8=31804
  - spin-phonon interactions in paramagnetic ion crystals 8=49593
  - sputtering and ion-electron emission coeffs. anisotropy thermal vibration dependence 8=40685
  - strict bounds for out-of-band freqs, due to impurities and defects 8=26571
  - superconductivity predictions from phonon spectrum and e. -phonon interactions 8=44719
  - symmorphic space groups, vibr. anal. 8=35373
  - thermal lattice vibrs., effect on electron scatt. 8=48697
  - thermal oscillations, effect on scattering of Ar ions 8=46440
  - thermal oscs. interact. with elastic waves, attenuation and temp. depend. 8=39882
  - thermodynamics calc. from continued fractions 8=44291
  - tin, white, thermal vibration spectrum determ. 8=35393
  - torsional oscillations and n.m.r. linewidth transition 8=31940
  - two-phonon scatt. of X-rays in diatomic crystals, intensity calc. 8=35369
  - unit cell deform. describing second-order phase transitions 8=35079
  - vibrational energy, zero-point 8=48692
  - vibronic spectra of e transitions at probe ion 8=39859
  - waves, scattered by line defect 8=40019
  - zig-zag chains, randomly folded, vibr. freq. 8=47735
  - AgCl, phonon scattering by point-defect aggregates from thermal conductivity meas. 8=30986
  - α-Al_2O_3, Raman active lattice modes, temp. dependence 8=39868
  - Al_2O_3, thin films, by electron beam diffraction 8=35387
  - Ar:H(D), solid, isotopic effects in absorpt. bands rel. to electron-phonon interaction 8=27557

Crystals—contd
- **lattice mechanics**—contd
  - BaO:Mn^{2+}, vibrational reson. mode and temp. depend. of hyperfine coupling 8=45079
  - BaTiO$_3$, ferroelectrically active vibration mode, 200 to −60 °C 8=35984
  - BeF$_2$, vitreous, vibrational spectra 8=35392
  - BeO, optical phonons, rel. to vibrations, reflection and Raman spectra meas. 8=27561
  - BeSO$_4$.4H$_2$O and BeSO$_4$.4D$_2$O, vibr. freqs. of metal-hydrate complexes 8=35381
  - B$_2$O$_3$ crystallites, rel. to molecular fibr. contrib. 8=44206
  - C$_2$Br$_2$(Cl$_2$ and I$_2$), vib. modes from i.r. spectra 8=45236
  - CH$_2$I$_2$, and mol. vibr., n inelastic scatt. obs. 8=35385
  - CH$_3$I, and mol. vibr., n inelastic scatt. obs. 8=35385
  - CaF$_2$: Er^{3+} (Nd^{3+}), spin-lattice relaxation, effect of quasi-local vibrations 8=40910
  - CaO, rel. to i.r. dielectric response 8=41075
  - Ca(OH)$_2$, lattice vibr. 8=27563
  - Ca(OH)$_2$ and Ca(OD)$_2$, vibr. spectra, coord. anal. 8=31970
  - CaMoO$_4$, i.r. modes 8=45179
  - CaMoO$_4$, lattice perturbations 8=26572
  - CaMoO$_4$, vibr. assignment 8=31969
  - CaWO$_4$, i.r. modes 8=45179
  - CaWO$_4$, lattice perturbations 8=26572
  - CaWO$_4$, vibr. assignment 8=31969
  - CaWO$_6$: Ce^{3+}, Yb^{3+}, spin-lattice relax., contrib. processes 8=40911
  - CdS, excess phonons, relax, rel. to microwave cond. 8=49234
  - CdS, phonon-assisted free exciton recombination 8=44760
  - CdS, wurtzite-type, optically-active vibrs. 8=35394
  - CdSe, phonon-exciton transitions rel. to coherent emission 8=31972
  - CoF$_2$, mag. and phonon excitation obs. 8=39870
  - CsCl, CsBr and CsI 8=39871
  - CsF, rel. to second-order Raman spectrum 8=31980
  - Cs$_2$SO$_4$, vibr. spectra 8=35382
  - Cu, scattering of lattice waves by dislocations 8=30933
  - Cu-Al alloys, lattice wave scattering by dislocations 8=26573
  - Cu-4% Al, obs. of localized vibrations by coherent inelastic neutron scatt. 8=39872
  - Cu$_{0\cdot907}$Au$_{0\cdot093}$, theory of vibrations 8=48705
  - Cu$_2$O, fundamental vibrs., refl. obs., 290°K 8=39873
  - D$_2$, solid, rotational excitations 8=44297
  - Fe^{2+}, high-spin, electronic factors in paramag. relax. 8=40921
  - FeCl$_2$, low-temp. anharmonicity in anomalous Mössbauer fraction temp.-dependence, 10-300°K 8=48326
  - Fe in Cu and Au, model for Debye-Waller factor 8=39874
  - GaAs: Li, localized vib. modes of impurities, i.r. active 8=44298
  - Ge, scattering of lattice waves by dislocations 8=30933
  - Ge, vibration spectra, freq. along asymmetric dims. 8=30934
  - HCl, low-temp. phase, phonon freq. distrib. 8=35384
  - H$_2$O, D$_2$O, and HDO films, i.r. intensities of stretching and vibrational bands 8=36369
  - H$_3$O.NO$_3$, and mol. vibr., n inelastic scatt. obs. 8=35385
  - He, solid, phonon scatt. by isotopes 8=37355
  - He^3, exchange operator matrix elements calc. 8=28447
  - HgTe, phonon viscosity attenuation of u.s. waves 8=30946
  - IBr, ICl, I$_2$Cl$_6$, from Mössbauer effect in I^{129} 8=35041
  - n-InAs, magnetophonon oscillations in longitudinal thermoelec. power 8=27308
  - InSb, vib. curves and phonon spectra 8=26576
  - K, freq. distrib. function and sp. ht. calc. 8=44300
  - KBr:Li$^+$, resonant modes rel. to isotope shifts from far i.r. spectra 8=36393
  - KCl: Li, impurity-phonon interactions exam. by sp. ht. meas., rel. to tunneling phenomena 8=44628
  - KCl:OH, dipole interaction through phonon field 8=40577
  - KH$_2$PO$_4$ ferroelec., vibrational mode disappearance from n. time-of-flight spectra 8=44299
  - KI:Ag$^+$, resonant modes rel. to isotope shifts from far i.r. spectra 8=36393
  - KI:Cl$^-$, (Br$^-$), i.r. lattice vibration absorpt. by gap and resonance modes, theory 8=27576
  - KNiF$_3$, vibrations rel. to magnetic ordering 8=48706
  - KTaO$_3$, ferroelectric phase transitions, dynamical theory elastic and dielectric anomalies 8=27284
  - LaF$_3$, from i.r. dispersion meas. 8=45201
  - LiF, freq. distrib. of normal modes at 298°K 8=35388
  - LiF, thin films, by electron beam diffraction 8=35387
  - LiH, rel. to bonding 8=35386
  - LiH-LiD mixed crystals, from i.r. absorpt. freq. exam. 8=45202
  - Mg, rel. to elec. and electronic props., 8=48707
  - MgAl$_2$O$_4$, microwave phonon attenuation 8=39895
  - MgF$_2$, vibr. freq. determ. by n scatt. rel. to Raman scatt. 8=44302
  - MgO, n-irradiated at 80°K, zero-phonon lines and phonon-coupling 8=27588
  - MgO, scattering of lattice waves by dislocations 8=30933
  - MgO, thin films, by electron beam diffraction 8=35387
  - MgSO$_4$.7H$_2$O and MgSO$_4$.7D$_2$O, vibr. spectra 8=35382
  - NH$_3$, displacement vibrs. calc. 8=30926

Crystals—contd
- **lattice mechanics**—contd
  - NH$_4$Br, l.f. vibrs. 8=27596
  - NH$_4$Cl, l.f. vibrs. 8=27596
  - Na, freq. distrib. function and sp. ht. calc. 8=44300
  - NaCl, transverse acoustic [OhO] phonon dispersion curve from X-ray thermal diffuse scatt., 8=39876
  - NaCl: Cu$^+$, resonant bandmode stress dependent freq. shift 8=48708
  - NaCl:Cu$^+$, resonant modes rel. to isotope shifts from far i.r. spectra 8=36393
  - NaF, X-ray scattering by phonons 8=44286
  - Nb-Mo alloys, rel. to electronic structures 8=44303
  - Ne, solid, ground-state energy 8=48709
  - NaF, thin films, by electron beam diffraction 8=35387
  - NaNO$_3$, Raman data 8=41122
  - Ne, anharmonic contrib. to entropy 8=35431
  - Ni, ferromagnetic and paramagnetic, dynamics 8=35391
  - O-H$_2$ and HD solid mixtures, spin-lattice relax. time 8=27493
  - Pb, mean displacement of surface atoms 8=30935
  - PbMoO$_4$, i.r. modes 8=45179
  - PbMoO$_4$, vibr. assignment 8=31969
  - PbMoO$_4$: Ce^{3+}, Yb^{3+}, spin-lattice relax., contrib. processes 8=40911
  - PbWO$_4$, i.r. modes 8=45179
  - PbWO$_4$, vibr. assignment 8=31969
  - Pd, anomalous vibration obs. 8=26575
  - Pd, mean displacement of surface atoms 8=30935
  - Pt-ammine complexes, i.r. vibrs. 8=43330
  - RbCl, phonon scatt. by U centres, thermal conductivity meas. and theory 8=44301
  - S-triazine, energy calc. 8=26578
  - Si, phonon conductivity and acoustic attenuation 8=44324
  - Si, vibration spectra, freq. along a symmetric dims. 8=30934
  - Si, vibrations in microscopic dielectric model 8=44304
  - SnO$_2$, optical lattice-vibration modes rel. to i.r. absorpt. spectra 8=45222
  - SrNO$_3$, vibration freq. uniaxial pressure-dependence 8=39877
  - SrO, rel. to i.r. dielectric response 8=41075
  - SrTiO$_3$, ferroelectric phase transitions, dynamical theory, elastic and dielectric anomalies 8=27284
  - SrTiO$_3$, ferroelectrically active vibration mode, 77 to −173 °C 8=35984
  - V, vib. curves and phonon spectra° 8=26576
  - VH$_x$, vibr. spectra in three phases by neutron scatt. 8=39878
  - V$_3$Si, softening, rel. to phase transformations 8=31107
  - YVO$_4$, lattice vibrations rel. to Raman and i.r. spectra 8=36424
  - Zn, mean square atomic displacements thermal, variation rel. to Debye temp. evaluation 8=44395
  - ZnO, wurtzite-type, optically-active vibrs. 8=35394
  - ZnSe, phonon freq. from i.r. meas. 8=49764
  - ZnTe, phonon freq. from i.r. meas. 8=49764
  - ZrH$_2$, central force dynamical model 8=39879
- **orientation**
  - A^{III}B^{V}, determ. by light reflection 8=39645
  - cellulose films, effect on dimens. stability 8=39634
  - crystallites, metallic, optical refl. determ. of orientation 8=30814
  - fibre, distrib. calc. formulae 8=44178
  - goniometer for single-crystal alignment 8=35210
  - goniometer head for low-temp. crystal rotation 8=30815
  - goniostat, aid for orienting crystals on head 8=35211
  - graphite, high, princ. thermal conds. rel. to crystallite boundaries 8=35457
  - graphite, influence on high-temp. creep behaviour 8=35644
  - graphite, polycryst., rel. to Young's mod. and thermal expansions 8=35663
  - graphite, pyrolytic, preferred 8=39646
  - in growth on base, expt. confirm. of theory 8=44111
  - Lave photography, glancing-angle, determ. 8=26182
  - metals glass, vacuum-condensed and growth rel. to deposition conditions 8=26226
  - organic materials with low m.p.s., apparatus for crystallization and orientation 8=26214
  - polaroid adapter for Weissenberg goniometer 8=44190
  - polycrystalline mats, orientation distrib. functions 8=26181
  - polyethyleneterephthalate fibres, influence on sonic velocity and birefringence 8=44175
  - polymers crystallinity, conference, Arizona, USA, 18 Jan 1966 8=35204
  - in polyvinylidene fluoride, from X-ray exam. on heat treatment 8=26155
  - quartz, rel. to Rutherford scattering of protons 8=44504
  - rutile, Cr-doped, microwave e.s.r. method 8=26184
  - samples for n.q.r. determ. of mag. axes 8=44959
  - sheet, distrib. calc. formulae 8=44178
  - silicate-mineral inclusions, in natural diamond 8=26179
  - single crystal, orientation method 8=49587
  - substrate, effect on high electron mobility of epitaxial GaAs 8=39592
  - Ag, during electrocrystallization initial stages 8=30822
  - Ag film on NaCl and KCl 8=44085
  - Al, dependency of shade etching 8=35222

Crystals—contd
orientation—contd
Al film on NaCl 8=44085
Al-Cu alloys, aged, effect on crit. shear stress and yield strength 8=48991
AlOOH, preferential, X-ray meas. 8=26183
Au film on NaCl and KCl 8=44085
C, pyrolytic, preferred orientation rel. to thermal expansion coeff. 8=30971
Cd, preferred growth during recrystallization 8=35213
CdS epitaxial films on CdS and ZnS platelets, obs. 8=35165
CdS, sputtered, long-range oriented crystallization 8=30809
Co-floating zone-melting-grown, rel. to effect of molten zone travel speed 8=26222
Cu dependence of dislocation damping 8=44563
Cu, dependency of shade etching 8=35222
Cu, distrib, function, 3-dimens., after cold rolling 8=48593
Cu 1.79 wt.%Be, discontinuous precipitation of γ-phase 8=43997
δ-Cu_9In_4, equilib. phase in Cu-16.8% In alloy formed on precip. 8=39548
Fe-Si alloys, dependency of shade etching 8=35222
GaAs epitaxial films on rocksalt, 25-430°C 8=35172
GaAs, laser diodes, rel. to gain factor and loss 8=33214
p-Ge, elec. conductivity anisotropy effect in d.c. elec. field 8=35914
HgS epitaxial films on CdS and ZnS platelets, obs. 8=35165
InSb, determ. by light reflection 8=39645
KBr, dependence of fast protons energy loss 8=35602
KCl, proton energy loss dependence, rel. to lattice effects 8=35598
LiF, internal friction dependence under static compressive load 8=44585
Mo, from MoF_6, rel. to deposition temp. and annealing 8=35154
NaCl, proton energy loss dependence, rel. to lattice effects 8=35598
Nb in mixed state, rel. to superconducting props. 8=35852
Ni, during electrocrystallization initial stages 8=30822
Ni film on NaCl 8=44085
Pd film on NaCl 8=44085
p-Si, elec. conductivity anisotropy effect in d.c. elec. field 8=35914
Si epitaxial films on quartz 8=48465
Si film on sapphire, relns. at interface 8=44058
Ta, zone-refined, growth condition effects 8=35231
Ti, h.c.p., angular relns. between plane normals and crystallog. directions 8=33087
Ti, reorientation mechanism during recrystallization 8=44086
UO_2 rel. to HNO_3 etching, 1-37 molar 8=30818
W, from WF_6, rel. to deposition temp. and annealing 8=35154
Zn films, cold-rolled, from Hall effect and magnetoresistance anisotropy obs. 8=30810
Zn, preferred growth during recrystallization 8=35213
ZnS epitaxial films on CdS and ZnS platelets, obs. 8=35165
Zr, monoclinic, sterographic projection 8=35214
ZrB_2, of second phase precipitates 8=35136
polarons. See Crystal electron states/polarons.
twinning
annealing twins, theory of origin 8=35216
4,4'-bis(dimethylamino)diphenylamine dihydro iodide, unit-cell dimensions and space group 8=26498
calcite, and dislocation growth during twin layer expansion under stress 8=31104
calcite, Bauschinger effect in twinning 8=35669
calcite, rel. to growth shape 8=26238
deformation twinning crystallography, theory 8=26705
dynamic twins, deformation behaviour, numerical analysis of equilib. config. and stress distribs., 8=48825
graphite, in characterization 8=44123
laws, derivation 8=26185
leucosapphire grown from tungstate melts 8=39648
$\{10\bar{1}1\}$, models and prediction 8=30811
polypropylene lamellae grown from dil. α-chlornaphthalene solns. 8=35218
quartz, natural and synthetic, and other fault-surfaces from X-ray exam. 8=26707
ruby, grown from tungstate melts 8=39648
shears in lattices, theory rel. to deform. and other modes 8=35215
slip dislocation incorporation for type I and II 8=44088
spodume, effect on internal friction 8=49033
symmetry group generalization 8=39647
triglycine sulphate, domain twins in growth 8=27292
Ag foils on ultramicrotome-cutting, 8=48850
Al, annealing twin boundaries 8=44161
Al foils, on ultramicrotome-cutting, 8=48850
Au microcrystals, in growth mechanism and defect structure 8=39666
Cu foils, on ultramicrotome-cutting, 8=48850
Cu-Ge alloy foils, on ultramicrotome-cutting, 8=48850
Fe-N martensite, internal plates, electron transmission study 8=39721
Fe-Ni-C, austenite alloys, deform. at room temp. 8=44468
α-Fe_2O_3 bladelike platelet growths on iron, selected area e.-diffr. exam. 8=48518

Crystals—contd
twinning—contd
α-Fe_2O_3, twinned platelet growth, dislocation and grain boundary diffusion rel. to gaseous oxidation 8=44150
α-Fe_2O_3 whiskers 8=35255
Fe-3%Si, rel. to creep at 600°C 8=35681
in GaAs epitaxially grown on Ge 8=26276
GaAs, epitaxial surface features and twins 8=35241
in Ge overgrowth formation in vapour deposition droplet mechanism 8=26277
$H_4Fe(CN)_6$, rel. to H bonding 8=26186
Hg crystals, deformation twins, modes 8=26187
Hg, glide and deformation modes, −39°C to −196°C 8=26706
In, and alloys, cold rolled, effect of alloying additions on twinning activation energies 8=35217
Mg and alloy MA-8, contrib. to fast deform. mechanisms 8=40169
Mg-Sn alloy, and fracture along {1011} planes 8=44592
Ni boracites, and sector-growth, exam. by polarized-light microscopy 8=26188
NiMn alloy, superlattice struct. due to periodic twinning 8=26712
Sb, laser-produced, behaviour 8=40043
Si web dendrites, scanning e microscopy obs. 8=44089
α-U, deform. twinning modes in Bravais lattice, table 8=44090
Zn, by indentation at 5 kg loads 8=31056
Zn, dislocation density and rate effects 8=26189
Zn, internal friction peak at 265°K due to stress relax. at twin boundaries 8=35727
Zr, deformed, texture formation 8=44091
whiskers
metallic matrix, alignment by extruding plasticized mixture thro'slit 8=48566
sapphire, Young's modulus 8=35661
Stefan problem in evaporation, soln., 8=39697
CdS films, growth and structural changes during crystal growth 8=26270
Cu, diffusion of Zn, mechanism 8=35487
Cu, structural features on deformation by torsion 8=35254
Fe, plastic flow, 4-300°K 8=49032
α-Fe_2O_3, dislocation and grain boundary diffusion during growth rel. to gaseous oxidation 8=4 4150
α-Fe_2O_3, growth and props. 8=35255
MgO, spontaneous growth 8=35257
NiO, growth and props. 8=35255
Sn, electrolytic growth conditions 8=30837
KCl, X-irradiated, F-centre accumulation 8=35585
W or its carbide on W by chloromethane adsorption using field-emission micro 8=26272
ZnO, hydrothermally crystallized, effect of Li^+ on dendritic growth 8=26201
Curie temperature. See Ferroelectric materials; Ferroelectric phenomena; Magnetic properties of substances.
Curie–Weiss law. See Magnetic properties of substances/paramagnetic; Paramagnetism.
Curium
Cm^{3+}, zero-field splitting in CaF_2 8=30622
Curium compounds
Curium oxide reactions with Al_2O_3 det. from Cm^{244} fission fragments 8=36649
Cm_2O_3, high temp. stability rel. to Cm^{244} use as isotopic heat source 8=35425
Current, electrical
See also Conduction, electrical.
alternating, interruption by controlled fracture of brittle solids 8=35632
cryostat leakage, instrumentation, improvement 8=41885
in crystals, current-striction effects, rel. to sound amplification 8=35406
distrib. in and on porous electrodes 8=49933
distribution inside cylinder with temp. depend. conductance in const. longit. elec. field 8=41946
equal-time commutators, theory 8=24080
galvanic short-cct., monitoring 8=46352
galvanometer, ballistic, appl. to pulsed laser threshold meas. 8=33164
in ionosphere of polar caps, mean intensity rel. to planetary mag. activity 8=27964
p-n junctions, heavily doped, thermally activated, and radiation 8=27147
limit for linear proton accelerator, eqn. 8=46994
plasma, nanosecond duration, meas. with Rogovskii loop 8=47850
regulator for switched inductive loads 8=33021
synchronous switching circuit for 7kA 8=28462
vacuum, prebreakdown 8=25698
Li exploding wire, extrusion die-electrode combination 8=33028
Current algebra
chiral algebra, g_0 evaluation 8=24849
choice of canonical coordinates 8=47010
conference, Liperi Summer School, Finland, 1965 8=24598
connection with PCAC 8=47013
consistency condition for $|\Delta S| = 1$ currents 8=29043
covariant relations with no Schwinger terms, in Feynman diagram of non-relativistic q.m. 8=24610

Current algebra—contd
- current commutators in broken SU_3 used to derive mass formula for vector mesons 8=33720
- deduction of results of convential symmetry groups, appl. to elementary particles 8=42365
- densities representations 8=37839
- divergence conditions, formalism and implications for current-current equal time commutators 8=29020
- Dyson representation in calc. 8=42336
- energy-momentum tensor in terms of currents 8=42371
- η decay applic. 8=24837
- first-moment operator, general and non-trivial solns. 8=33553
- Fubine's analysis of dispersion relation sum rules, reformation involving transformation of M-function 8=37895
- Fubini-Dashen-Gell-Mann sum rules for arbitrary spin and mass 8=29038
- Fubini-Halliday-Landshoff sum rules applied in pole-dominance approx. to current x meson x meson vertices 8=33526
- Fubini operators and partial symmetry 8=37827
- γ-3π coupling const. calc. 8=42374
- generalized currents for spin in $2(2s+1)$ component formalism 8=37835
- hadron scatt. restrictions deducible from conspiracy theory 8=29136
- hadronic currents rel. to self-induced strong interactions 8=29111
- Hawaii tropical conference, August 1967 8=29027
- hyperon and K decay applic. 8=29210
- hyperon decay, nonleptonic, appl. 8=33829
- hyperon decay, s, p-wave amplitude calc. 8=24988
- hyperon decays, nonleptonic 8=42654
- $K \to l\nu\, \pi l\nu\, \pi\pi l\nu$, theory 8=37830
- $K^+ - K^0$ mass difference calc. 8=24825
- K_{e5}, decay vector form factors calc. 8=42579
- K_{13} form factor calc. 8=24818
- K_{13} form factor calc. 8=38002
- K_{13} form factor calc., new approach 8=33699
- K_{13} form factors, with subtracted dispersion relations 8=42578
- for K_{13} parameters calc. 8=38003
- K_{13}, K_{14} form factors calc. 8=33694
- $K_{\mu 4}$ decay spectrum calc. 8=24822
- $K \to 3\pi$ decay, $\Delta T = 1/2$ violation 8=24823
- local current algebras, representation theory 8=28233
- low-energy applications, from extension of minimal e.m. interact. hypothesis 8=42515
- meson radiative two-body decay applic. 8=37955
- model with nontrivial mass spectrum 8=24611
- nonlocal, coordinates for particles 8=42368
- and PCAC in calc. of form factors for K_{15} decay 8=29149
- and PCAC rel. to meson dynamics 8=38025
- perturbative approach and superconvergence relations 8=29017
- π_{e2} decay, radiative corrections 8=24770
- π-N scatt. lengths, s-wave, and $\rho + \rho'$ dominance 8=24799
- πNscatt., spin-flip amplitude sum rule 8=42549
- $\pi N \to \pi\pi N$, coupling const. relations 8=42533
- π-π scattering amplitude calc. using condition of elastic unitarity 8=29145
- π-π scatt. length, absence of Mandelstam variables 8=24802
- and pole dominance approx., form of unsubtracted dispersion relations 8=29021
- prediction for shape and magnitude of $\sigma(e^+e^- \to \pi^+\pi^-)$ 8=42607
- representations at infinite momentum completeness relation for set of spinors implying degenerate mass spectrum 8=33525
- ρ meson dominance 8=38034
- Schnitzer-Weinberg technique applied to ϕ, K decay 8=33723
- Schwinger terms directly from local currents 8=33343
- single particle representations, no-go theorem in the covariant approach 8=24597
- spin currents, field theoretical model 8=24603
- sum rule relating nucleon anomalous magnetic moment to pion photoprod. amplitude 8=42364
- sum rules from charge-charge and charge-charge-density computators 8=42369
- sum rules in Khur, representation, Fubini-Dashen-Gell-Mann inconsistencies resolved 8=29015
- sum rules saturation, role of Schwinger terms 8=24633
- superconvergence for spin-$1/2$ traget 8=42405
- $SU(3) \otimes SU(3)$ in $K\pi$ scatt, κ meson 8=29158
- SU(4), axial vector renormalization constant derivation 8=24615
- SU(4), sum rule for axial vector renormalization const. 8=33527
- SU_6 and 4π coupling constant 8=29120
- in T^1 decay, soft-pion prediction 8=42569
- tensor currents, symm., spectral representation, new sum rules 8=42367
- validity in axiomatic field theory in quasi-local terms only 8=37770
- vector and axial-vector, meson decay calc. 8=42597
- vector current, matrix element of divergence in K_{13} decay 8=42580
- Ward identities, 3- and 4-point functions 8=42373
- weak $BB\pi$ vertex, current algebra and PCAC appl. 8=42618

Current algebra—contd
- weak process, ang. mom., requirement for Kronecker delta 8=24647

Curvature measurement. See Mechanical measurement.

Cyanogen (C_2N_2). See Carbon compounds.

Cyclotron resonance
- electron cyclotron freq., Doppler effect, exptl. investigations 8=47823
- electron, free-free bremsstrahlung from plasma 8=30063
- electrons, free, meas. method using collisions with polarized atoms 8=42040
- electrons in plasma with anisotropic temp., harmonics excitation 8=43589
- heating in mag. mirror, limit of plasma temp. 8=30122
- hot electrons, theory 8=44749
- inmetals, in inclined mag. field, characts. 8=40284
- ions, solar wind, whistler growth and damping 8=41584
- nonparabolic band carriers absorption hysteresis 8=26933
- photocarrier transport meas., differential technique 8=35747
- photoelectrons, non-equilib. 8=35805
- piezoelectric polarons, calcs. in quantum limit 8=40283
- plasma, electron, anisotropic energy distribution 8=43568
- plasma, electron momentum and energy relaxation, cyclotron echo meas. 8=47824
- plasma, hot, microwave absorption 8=30064
- plasma, ion instability convective and absolute in mirror machines 8=30164
- proton freq. to free electron cyclotron freq. ratio. precision meas. 8=46520
- semiconductor, nuclei polarization on e-heating 8=35806
- in semiconductors, charact. features of obs. from static conductivity changes 8=26934
- p-type InSb. obs. of quantum of intraband transitions 8=44796
- Al, thin films, plasma resonance in reflection spectrum 8=30746
- As, Azbel'-Kaner type, rel. to band struct. 8=44684
- Bi, damping of magnetoplasma waves due to mode mixing 8=31308
- Cd, field peak excitation in mag. field normal to surface 8=44668
- Ga, acoustic, Doppler-shifted 8=48720
- Ga, line shape, mass extremum effect 8=26935
- Ge, n- and p-, at 4°K and 70 GHz, by d. c. thermoelectric current meas. 8=27099
- Ge, of hot holes 8=35807
- Ge hot carriers, line width angular dependence 8=35898
- H ions, heating and nonadiabatic trapping in mag. mirror machine 8=30120
- InSb, rel. to resonant-polaron-coupling 8=40270
- p–Si, of holes 8=44819

Cyclotrons. See Particle accelerators/orbital, cyclotrons.

Czochralski method. See Crystals, growth.

D-layer. See Ionosphere/D-region.

DNA. See Proteins.

DPPH (diphenylpicrylhydrazyl). See Free radicals; Organic compounds.

Damping
- See also Internal friction.
- composite structs, for response calcs to earthquakes 8=32885
- elastico-viscous fluid, dragon oscill. cylinder 8=47930
- fluid coupling, vibrations, quantitative analysis 8=25788
- hysteretic, effects on dynamic response of system with one-degree of freedom 8=32870
- oscillations in alternating-gradient synchrotron 8=33443
- plasma u. h. f. fields, model 8=34536
- in plastic deform., correction to critical strain amp. 8=48957
- plastic structures, free vibrations 8=28263
- recovering after plastic deform., comment on used Granato-Hikata-Lucke eqn 8=48956
- solid subject to follower loads, local stability 8=46024
- sphere in elastic solid, torsional oscills. 8=23927
- of torsional vibs. in elastic half-space subject to radial stress distrib. 8=28262
- vibrating system chatter minimization 8=23929
- He II, of cylinder pairs oscs., rel. to fluid and superfluid viscosity 8=41902

Dark space. See Discharges, electric.

Data tables. See Collections of physical data; Tables, mathematical.

Dating. See Earth/age; Radioactive dating

Daughter. See Nucleus; Radioactivity.

Dawn chorus. See Atmospherics; Ionosphere.

Dayglow. See Airglow.

Debye-Hückel theory. See Conductivity, electrical/liquids, electrolytic, Electrochemistry; Solutions.

Debye-Scherrer cameras. See Cameras; X-ray crystallography/apparatus.

Debye temperature. See Specific heat

Debye-Waller factors. See Electron diffraction crystallography; X-ray crystallography.

Decay periods. See Hyperons/decay observations; Mesons/decay observations; Pions/decay; Radioactivity/decay periods.

Decay schemes. See Hyperons/decay observations; Mesons/decay observations; Pions/decay; Radioactivity/decay schemes.
Decomposition. See Dissociation.
Decomposition, thermal. See Chemical reactions.
Decoration techniques. See Crystal imperfections/dislocations; Crystals/etching.
Defects. See Crystal imperfections.
Deformation
  See also Bending; Elastic deformation; Plastic deformation.
  alloys, in surface layer, rel. to ignition process 8=36578
  alkali metals, extension effects on phonon spectra 8=35380
  brass, 70/30, fragmented outer layer, and deformed inner layer, by machining 8=35555
  brass, tube, radial expansion by explosive gas 8=31202
  buckling behaviour in axial compression of slightly-curved panels, including shear deformability effect 8=41657
  buckling of plates and beams by Lagrangian multipliers method, incorrect results 8=41661
  calcite crystals, Bauschinger effect in twinning 8=35669
  conical film reflector under normal press. and corresponding axial forces 8=46052
  in contact of rigid cylinder on elastic layer connected to rigid base 8=37139
  continuous systs., instability and energy criterion 8=46022
  crystals of rock-salt structure, cyclic stressing 8=44518
  curvature defined using f.m. amplitude gratings 8=35616
  cyclic loading and microstrain, surface effects 8=31170
  dislocation motion, continuum theory 8=48840
  elastic, homogeneous, incompressible materials, rel. to quasi-equilibrated motion 8=37124
  fading memory of material, weak principle formulation 8=32707
  ferromagnetic cryst. lattices, uniaxial rel. to magnetization curve 8=36104
  fibres, broken, in composite materials, load transfer 8=48975
  fluids, viscous nonlinear incompressible isotropic, plane fields character 8=47899
  glass, foam, under compression, obs. 8=35647
  glass-reinforced plastics, press. distrib. in moulding 8=31240
  graphite, by n-irrad., effect of restraining mechanism 8=31149
  in hot-pressing, theory giving density eqn. 8=26755
  mechanical, interact. with elec. cond. mats 8=26752
  metal working, microphotoplasticity techniques using laser systems 8=48954
  metals and alloys, high-temp., microscopes for study of mechanisms 8=42183
  metals, meas. by Xe^{133} diff. 8=48766
  metals, state after pear-shaped method of cold-welding 8=37099
  micromachine, for metallic specimens at temps. down to 1.3°K 8=44522
  minerals, in h.f. e.m. fields, rates 8=35643
  necking in homogeneous test bar 8=32764
  non-metallic solids, indentation, effects of adsorption 8=44524
  nylon-6, α-γ phase transition by stretching 8=30715
  opaque bodies, surface deform. meas. by bonded birefringent strip 8=44521
  piezoelectric annular disc, radial, rel. to gamma ray heating and elec. voltage 8=31441
  plastic square bar, work-hardening, combined bending and torsion, numerical anal. 8=23836
  plate under edge thrust, displacement-dependent buckling resistance, stability calc. 8=41650
  polyethylene films, stretching processes, X-ray diffr. studies 8=26859
  polyethylene, orientational stretching changes in structure 8=35293
  polyethylene terephthalate, oriented, bands 8=31244
  polymers, oriented, effect of elongation on n.m.r. 8=31914
  polymers, solid, rel. to secondary free radical reactions, during mech., damage 8=45361
  polyoxypropylene, by uniaxial tension, structural transform., wide temp. range 8=35203
  prolate spheroids of mag. saturated polycryst. materials, form effect 8=40793
  prolate spheroids of saturated polycryst. materials, form effect 8=40794
  in protein secondary structure, model 8=25678
  rectangular plates, with cambered cross-sections, bending instability 8=37138
  rings, thin circular, buckling under uniform pressure 8=41654
  rods, general theory 8=37127
  rotating sphere, soln. 8=32698
  rubber in equilibrium compression 8=31251
  rubber membrane permeability, elongation dependence 8=44397
  ruby laser crystal, rel. to temp. 8=24335
  shear flow with interacting deformable substruct. 8=47901
  shear forming, buildup and diametral growth control 8=48955
Deformation—contd
  shells, cylindrical, buckling under axial compression, testing machine ffects 8=32728
  shells with positive curvature under concentrated load 8=41662
  solid solns., rel. to short-range ordering 8=26033
  stainless austenitic steel, modes, compositional effect 8=40157
  steel, discontinuous, grain size and C content effects 8=35682
  steel, in surface layer, rel. to ignition process 8=36578
  steel, 0.2%carbon, ingot, non-metallic inclusion behaviour during hot rolling 8=49020
  steel, low-carbon, and recrystallization textures, rolling temp.-dependence 8=26818
  strain, near crack-tip in power-law hardening material 8=41717
  strain, near end of crack, in hardening material 8=41718
  transmission through crystal by dislocation pile-up break-through mechanism 8=26661
  transverse isotropic bodies, finite strain calc. 8=41649
  twins, dynamic, behaviour, numerical analysis 8=48825
  understressing effects on fatigue strength, explanation 8=40114
  viscoelastic materials, mathematical description 8=41731
  viscoelastic, rapid, tensile stresses 8=30376
  Zircaloy-2, rel. to corrrosion behaviour 8=26852
  Ag foils, on ultramicrotome-cutting, 8=48850
  Al, at high amplitudes rel. to amplitude-dependent internal friction 8=26776
  Al, critical value on thermomechanical treatment 8=35672
  Al foils, on ultramicrotome-cutting, 8=48850
  Al, low temp., stored energy rel. to strain and orientation 8=49000
  Al, low-temp., strengthening due to mosaic block misalignment 8=35653
  Al 99.5, rel. to microstruct., texture and earing 8=35266
  Al, shock loaded, point defects 8=44399
  Al, strained, substructure changes on heating 8=44162
  Al-Mn 1.04% alloy, recryst. behaviour and deform. structures 8=48803
  BeO ceramics, extruded, grain deform and residual stress 8=44556
  C, glassy, effects on mag. susceptibility 8=44966
  C, pyrolytic, dimensional changes during n-irrad., model 8=31148
  Cr, under hydrostatic press., struct. rel. to plasticity, < 18 kbar 8=3556 2
  CsI, rel. to charged dislocation production 8=26669
  Cu, cold-worked, recovery during annealing 8=35709
  Cu, cyclic stressing, shear modulus rel. to resistivity 8=40317
  Cu, ductile mode, exam. by anomalous X-ray transmission 8=26648
  Cu foils, on ultramicrotome-cutting, 8=48850
  Cu, low temp., stored energy rel. to strain and orientation 8=49000
  Cu, rel. to dislocation arrangement at 4.2, 78 and 293°K 8=48854
  Cu, tensile, rel. to dislocation distrib. in surface layer 8=48856
  Cu whiskers, by torsion, rel. to sructural features 8=35254
  Cu whiskers, yield strength, flow stress 8=44566
  Cu-Al, second-phase deformations afer cold-rolling 8=4900
  Cu-Ge alloy foils, on ultramicrotome-cutting, 8=48850
  $Cu_{0.5}Mn_xFe_{2.5-x}O_{4.\gamma}$ spinels, compensated tetragonal, deformation 8=48380
  Cu_2O, exciton band splitting in light and dark blue series by unidirectional pressure 8=35791
  Cu-Sn, second-phase deformations after cold rolling 8=49001
  Cu–38% Zn alloy, polycrystalline, alternating micro deformation 8=35644
  Cu-Zn, second-phase deformations after cold rolling 8=49001
  Fe, high temperature, rel. to vacancy concentration 8=31038
  Fe–Ni–C, austenite alloys, twinning at room temp. 8=4446
  Fe-Ni-C martensites, thermally activated, and solid solution hardening 8=26816
  Ge, brittle mode, exam. by anomalous X-ray transmission 8=26648
  Ge crystals, rel. to dislocation structure from e-microscope exam. 8=31064
  Ge, (111) face, rel. to Jahn-Teller effect, LEED obs. 8=26917
  KCl, acoustic emission, rel. to microscopic model 8=26582
  KCl, rel. to colourability, room temp. 8=31119
  LiF, acoustic emission, rel. to microscopic model 8=26582
  Mg and alloy MA-8, fast deform., slip and twinning contribs. 8=40169
  Mg, of second-order twins 8=44588
  MgO, compressive, rel. to creep curve 8=31221
  Mn-Au alloys, effects on antiferromag. props. 8=31776

Deformation—contd
MnO, deformed, crystal structure 33-157°K and mag. anomaly 8=30906
Mo crystals, in tension, slip line pattern and active systems 8=31091
Mo, under hydrostatic press., struct. rel. to plasticity, < 18 kbar 8=35562
Nb, strain-ageing, oxygen dependence 8=26835
Nb-O, strain-ageing from resitivity meas. 8=26846
Ni, cold-worked, recovery during annealing 8=35709
Ni, high temperature, rel. to vacancy concentration 8=31038
Ni–17%Cr alloy, polycrystalline, alternating microdeformation 7=35644
PbS, investigation by harmonic analysis of form of interference lines 8=31227
Si, due to n-irrad., injection and temp. depend. of transient annealing 8=27122
Si, (111) face, rel. to Jahn-Teller effect, LEED obs. 8=26917
Sn-Sb, second-phase deformations after cold-rolling 8=49001
Ta-O, strain-ageing from resistivity meas. 8=26846
α-U, twinning modes in Bravais lattice, table 8=44090
UN, and oxidation, e microscopy 8=27718
W crystals, in tension, slip line pattern and active systems 8=31091
W, exam. by anomalous X-ray transmission 8=26648
Xe, solid, deform. pots and band struct. 8=44646
ZnO, potentials, and valence band symmetry 8=35782
Zr, corrosion breakaway region, inelastic behaviour of metal and oxide 8=36576
Zr, rel. to corrosion behaviour 8=26852
Zr, tensile, effect of O up to 4.2 at.% 8=44609

de Haas-van Alphen effect
See also Diamagnetism; Magnetic properties/diamagnetic.
f.c.c. transition metals, meas., good agreement with Fermi surface calc. 8=40250
in Fermi surface calcs., inversion scheme 8=40225
Kondo scatt. effect on amplitude 8=31490
metals, mag. breakdown and osc. periods 8=40725
metals, mag. moments in strong fields, charact. props. 8=44962
oscillations, giant, nonlinear effect rel. to time width 8=31489
sample rotation effect on oscillations 8=36067
in tin, white, rel. to Fermi surface 8=31508
Al-based alloys, dilute 8=31494
As, pure and Ge doped 8=49091
Bi, doped, beats rel. to e energy spectrum 8=27376
Bi-Sb-Pb alloys, conc. and temp. dependence, 1.6-4.2°K rel. to e densities over Fermi surface 8=31496
Fe, rel. to Fermi-surface determ. 8=31289
In, meas. 8=49470
In, second band hole surface 8=40226
Ni ferromagnet, rel. to electronic structure 8=31698
Ni, ferromagnetic, rel. to exchange and spin-orbit interactions 8=44649
Ni, rel. to Fermi-surface determ. 8=31289
RuO_2, rutile structure, meas. 8=27382
Sb: Sn(Te), Fermi surface change due to level shift 8=49090
W crystal magnetocaloric oscillations, isothermal, rel. to dHvA effect 8=31514

Delay lines, ultrasonic. See Acoustics; Ultrasonics.
Delbrück scattering. See Photons/scattering.
Demagnetization. See Magnetization process.
Dember effect. See Photoelectromagnetic effects.
Demonstrations. See Teaching/demonstrations.
Dendrites. See Crystallization; Crystals/growth.

Densitometry
blackening, working range extension 8=24360
moon charting and relative heights meas. 8=28143
moon elevation profiles, Ranger 9 photographs 8=28144
photographic plate characts., aperture effects 8=42280

Density
acetone, near crit. pt. 8=34956
benzene, near crit. pt. 8=34956
chloroform, near crit. pt. 8=34956
fluctuations in fluids with internal degree of freedom 8=34789
nuclear matter, rel. to shell model potential 8=25061
Ar plasma, calc. from shock tube obs. 8=34485
gases
fluidized beds, fluctuations 8=48230
low-press., obs. by luminescence induced by electron beam 8=39171
rarefied, determ. by meas. from electron beam scattering 8=47933
rarefied, in boundary layer of plate, corrections 8=34645
wake of hypersonic sphere, fluctuations 8=30264
HCl, at 20, 50, 75°C and 5 and 40 atm. 8=30281
liquids
amyl and isoamyl alcohol, temp. derivatives 8=34803
binary hydrocarbon liq. mixtures 8=48041
n-butyl alcohol, temp. derivatives 8=34803
derivative, isothermal, of optical dielectric consts. empirical reln. 8=39399
monatomic, model for radial density and scatt. 8=34750

Density—contd
liquids—contd
octyl alcohols, evidence for struct. transform. 8=39296
polystyrene solns., depend. on conc. and temp. 8=44065
pressure dependence, to 5000 kg/cm² 8=39401
water, liq. and heavy, max density temp., from significant struct. theory 8=43767
Ar, exptl. determ. 8=28219
CCl_4 with internal degree of freedom, fluctuations 8=34789
CS_2 with internal degree of freedom, fluctuations 8=34789
He II, rotating 8=24049
H_2O in capillaries shift in temp. of maximum 8=34790
$NaClO_3$-$NaNO_3$ molten system 8=48086
HSO_3Cl solns. of simple bases 8=48194
Ne-N mixtures, and supercritical excess vols., 100.78°K and < 8000 lb in $^{-2}$ 8=30592
Pb, over temp. range above liquidus 8=39325
Pb-Sb alloys, rel. to temp. 8=39326
Pb-Sb-Sn alloys, rel. to temp. 8=39326
Pd-Sn alloys 8=48082
Rb near melting point, meas. 8=30421
Su, over temp. range above liquidus 8=39325
$TlMeSO_4$ (Me=alkali metal), 700-1150°C 8=39411
$TlNO_3$, molten 8=39331
Tl_2SO_4, 700-1150°C 8=39411
solids
glass, densification under cutting wheel, using Zeiss interference microscope 8=39724
glasses, effect of mixed γ-n radiation 8=44493
ice, hexagonal 8=49028
polycaprolactam, rel. to cryst. morphology, obs. 8=43907
polyethylene, foled-chain crysts. 8=35248
polyoxymethylene extended chain crysts., X-irrad. effects, < 4.8×10^7 R 8=44509
pyrocarbons compressed at high temps. 8=45941
quartz, rel. to radiation damage 8=26722
AgI, at 3 kbar 8=35316
Ar, exptl. determ. 8=28219
CaF:GdF_3, changes due to pt. defects 8=44559
CuCl film, optical, obs. 8=31982
Fe–Mo alloys, rel. ageing characts. 8=44004
p-H_2, on melting line 8=40575
In–Cd solid solns. 8=43977
KCl, γ-irradiated, by flotation meas. 8=40129
LiF, γ-irradiated, by flotation meas. 8=40129
Mo, effect of S, Se and Te in solution 8=48664
NaCl, γ-irradiated, by flotation meas. 8=40129
NaF, γ-irradiated, by flotation meas. 8=40129
Nb, from X-ray determ. of lattice parameter and hydrostatic meas. 8=48670
PbO-La_2O_3-B_2O_3 optical glasses 8=45214
SiO_2, rel. to radiation damage 8=26722
Tl amalgams 8=48348
UC, irrad. at 77°K, var. during annealing, obs. 8=44605
UO_2, irrad., var. during annealing rel. to fission damage recomb., obs. 8=44605

Density measurement
atmosphere, falling sphere accelerometer 8=41620
critical density determ., effects of sample config. in earth's field 8=30574
gas, rarefied, by e scatt. 8=47933
high-press. capacitance and resist. piezometers 8=39401
metal film, vacuum-evaporated 8=48437
molten metal-salt systems, radiometric method 8=30414
plasma, calc. from r.f. cond. meas. 8=43546
soil, γ back-scatter guage with restricted angle 8=41325
spatial distrib. in closed media, determ. by γ ray absorpt. 8=29083
Ar, liquid, exptl. determ. 8=28219
Ar, solid, exptl. determ. 8=28219
K plasma, absolute density measurement 8=30093

Desorption. See Sorption.

Detonation
See also Explosions; Shock waves.
blasting caps, elec. initiation 8=32905
gas, velocity fluctuation, origin 8=45356
in explosive liq. films, initiation and propag. 8=34748
impact sensitivity testing of explosives, conversion of mech. to thermal energy 8=32907
metal plate shock wave structure, classical validity for condensed explosives 8=44515
nitrocellulose powder, ignition by shock wave 8=23950
nitroglycerin powder, ignition by shock wave 8=23950
physical approach, review 8=46175
propane-O_2-N_2, elec. conductivity of products at cm. wavelengths 8=27731
wave propagation, asymptotic laws 8=46172
wave velocity meas. by piezoelec. coaxial transducer pins 8=41836
waves, interaction with sliding over liq. surface 8=23949
C-H-N-O explosives, detonation velocity prediction 8=41262
C_2N_2/O_2 mixtures limits 8=45357
D_2/O_2 mixture, dual velocity regime 8=45355
H_2/O_2 mixture, dual velocity regime 8=45355

Detonation—contd
of O_2 and H_2 mixtures, mass effects, effects of Ar or He dilution and D replacement of H 8=32115
Deuterium
atom g_J ratio meas. by optical pumping 8=38734
atoms, collisional ionization, e spin polarization obs. 8=29662
atoms, recomb. rate in shock waves 8=25649
atmosphere, isotopic content in H_2, 1958 to 1963 obs. 8=27882
condensation pumping on to liq-He-cooled surface 8=30593
content in Antarctic firn, to depth of 106 m, rel. to climatic variations 8=50088
crystal structure, 4.2 to 0.91°K, neutron diffraction obs. 8=39795
discharge plasma, temp. meas., inverted spectral lines 8=29895
ions, transmission sputtering of Au films 8=44495
liquid, ortho-para solns., neutron scatt. 8=30404
meson-proton coherent prod. and deck effect best with deuterium 8=24911
molecules first excited ${}^1\Sigma^+_g$ state rot. and vibr. levels calc. 8=38823
neutron scatt., 4.6 MeV, apparatus for n polarization meas. 8=47324
optical pumping and D-line ratio in Comet 1962-III 8=37018
origin, in solar system, big bang and solar spallation theory 8=36990
orthodeuterium-inert gas mixtures, rotation 8=30295
ortho/para-D_2 liq. systems, heat of mixing at 20°K 8=30412
paradeuterium, solid far infrared absorpt. spectrum obs. 8=45192
in paramagnetic ion solns., isotope effect on proton spin relax. 8=30536
plasma, ion component from differential n spectrum 8=34512
solid, laser-irradiated target rel. to plasma production 8=39064
solid, rotational excitations 8=44297
spectra, 6 Balmer lines obs. and Rydberg constant calc. 8=47494
in stars and interstellar medium, obs. 8=36927
Θ-pinch, heating with low energy capacitor battery 8=39124
triode ion pump, voltage reduction for thermal stability 8=30325
CD_4 added to D_2, θ pinch at 0.8 m torr filling press. 8=34417
Cs-D_2 collisions, cross-section obs. 8=38957
in CH_4, atmospheric 8=27883
D^+, 5-80 keV, range in Au and Al 8=48912
D^+ formation in H_2 ionization by e-impact, 250-2200 eV 8=29963
D_2, H_2, HD, electronic isotope shifts in Lyman bands 8=34244
D_2^+, collision-induced dissociation 8=25648
D_2^+ in H_2, charge-transfer cross-section obs. 8=47539
D_2^+ photodissoc., theory and calc. 8=47704
DCl, crystal structure and phase transforms. by X-ray and n-diffr. 8=26073
D/H ratio during dehydration of $CuSO_4$, $5H_2O$ 8=30802
D_2/O_2 mixture detonation, dual regime 8=45355
H_2 and D_2, vibr. relax., isotope effect 8=34240
HD, liquid, n. m. r., double 8=34921
K atom collisions, mixing and quenching cross sections 8=29836
Deuterium compounds. See Hydrogen compounds.
Deuterons
See also Cosmic rays/deuterons; Nuclear reactions due to/deuterons.
magnetic moment, cross-section sum rules for Compton scatt. 8=42622
momentum spectra, energetic, from p-nuclei collisions at 1 GeV 8=42667
neutron capture, 3-body scatt. effects 8=43038
n capture, thermal, zero-range approximation theory 8=29219
optical pot., four parameter 8=42826
polarized beam source, in $2S_{1/2}$ metastable state 8=38763
production in nuclear emulsion by high energy p and π beams 8=38099
production in p-p collisions, 1.5 to 3 GeV, differential cross-sections 8=42668
quadrupole moment and neutron electric form factor threshold values depend. 8=47139
width, for transfer reaction or heavy particle stripping process 8=47177
$As^{75}(n, d)Ge^{74}$, transitions angular distrib. rel. to shell model, obs. 8=29468
$Ca^{40}(n, d)K^{39}$, transitions angular distrib. rel. to shell model, obs. 8=29468
$Cl^{35}(n, d)S^{34}$, transitions angular distrib. rel. to shell model, obs. 8=29468
$K^{39}(n, d)Ar^{38}$, transitions angular distrib. rel. to shell model, obs. 8=29468
effects
diamond bombardment, chem. reactions 8=45406
Pt, defect production and recovery, plastic deformation and Au substitution effects 8=39997

Deuterons—contd
effects—contd
disintegration, internal structure influence on diffraction 8=38100
disintegration, pionic, threshold to 300 MeV, covariant theory 8=33843
electrodisintegration, cross-sections and p polarization sensitive to spin-flip radial integrals 8=29095
electrodisintegration problems with d wave function and N core radius 8=33842
$d + He^3 \rightarrow \alpha + p$, single-level resonance formula 8=25007
$D(n, n^2)p$, at 14 MeV, rel. to n-n interact. 8=24951
$D(p, \gamma)He^3$, low energy S wave cross-section 8=42632
d(p, n)2p, Ep = 45.5 MeV, ang. distrib. obs. 8=43017
d(p, n)2p, polarization transfer calc., Ep = 30-150 MeV 8=38101
d(p, 2p)n and p(d, 2p)n rel. to p-n final state interacts. 8=24902
$d + t \rightarrow \alpha + n$, single-level resonance formula 8=25007
K^- d, test of one-meson exchange 8=42586
$K^-d \rightarrow \Lambda n$, $p_{K^-} = 340$ MeV/c and 400 MeV/c 8=33704
$K^-d \rightarrow \overline{Z}p$, $p_{K^-} = 340$ MeV/c and 400 MeV/c 8=33704
$K^+ + d \rightarrow p + p + K^\circ$ rel. to K°-K^+ mass difference 8=29154
$Md \rightarrow \gamma BN$, sensitivity to BN interactions 8=37916
nd, 14-27 GeV/c, total cross-section and Glauber screening correction 8=29196
nd high energy reaction, n cross-section obs. 8=42645
$n + d \rightarrow 2n + p$, 14 MeV, ang. distrib. obs., anomaly rel. to spectator model 8=33768
$n + d \rightarrow p + 2n$, 100 MeV, n-p bound scatt., polarization 8=24961
$\overline{\nu}_p$-d, expt. investigation 8=47078
$pD(1S) \rightarrow H(1S; 2S)D^+$ cross-section calc., 0.02-100 MeV 8=43237
π and photo-disintegration covariant form of Austern model 8=25006
π-D, absorpt., elastic and inelastic, exact iteration calc. 8=33673
π^+d, search for $2\pi^\circ$resonance near 730 MeV 8=42532
$\pi^+d \rightarrow pp$ Miyazawas theory of π absorpt. 8=42531
$t(d, n)He^4$, n energy dispersion obs. rel. to accelerators 8=29220
D_2O, delayed n prod. by U^{235} fission fragment γ-rays, half-lives, obs. 8=33764
$H^2 + \nu \rightarrow e^- + 2p$, cross section obs. 8=47077
$H^3 + d \rightarrow \alpha + \eta$, 3-11 MeV, cross-section obs. 8=24937
He^3, d capture, γ spectra obs. 8=29227
photodisintegration
angular distrib., 140-400 MeV obs. 8=25008
Austern model, covariant form 8=25006
γ-d scattering, dispersion theory, 0-100 MeV 8=38098
$d(\gamma, n)p$, sum rules, employing Yale and Hamada-Johnston potentials 8=38450
symmetry coeffs., rel. to parity-violating N-N potential 8=24876
polarization
Lamb-shift source, enhancement by static field methods 8=37436
in n-d elastic scatt., rel. to phases at low energy 8=29221
Al^{27} parameters obs. in 7-11 MeV d elastic scatt. 8=25265
C^{12} scatt., E_d=12 MeV, obs. 8=29499
D(d, p)T, effects at $\overline{E}_d = 80$ keV, obs. 8=47343
Fe^{56} scatt., E_d=12 MeV, obs. 8=29499
Si, parameters obs. in 7-11 MeV d elastic scatt. 8=25265
Ni^{58} scatt., E_d=12 MeV, obs. 8=29499
Ni^{60} parameters obs. in 7-11 MeV d elastic scatt. 8=25265
scattering
See also Protons and antiprotons/scattering, proton—deuteron.
d-d, 94-595 MeV obs. 8=25007
e-d, quasi-elastic, and n struct. 8=47084
e-d, quasielastic obs., n magnetic form factor deduced 8=24722
electrodisintegration at quasielastic peak 8=33632
by even nuclei, at 28 MeV 8=29498
n-d, Born approximation with tensor interaction 8=24960
n-d, elastic, different phases w. r. t. polarization of n, d 8=20221
n-d, elastic, phase analysis accuracy enhancement 8=29198
nuclei, 52 MeV elastic, ang. distrib. obs. 8=29493
nuclei, various, 52 MeV, levels excited DWBA with collective model 8=42837
optical potential calc. 8=25052
optical pot. model and distorted-wave method 8=29492
p-d bremsstrahlung at 197 MeV obs. 8=29182
p-d real part obs. at 1 GeV 8=24928
$\pi^-d \rightarrow 2n\gamma$ for nn scatt. length obs. 8=42648
π-D, elastic and inelastic, exact iteration calc. 8=33673
π-d, 200 MeV, contrib. of Δ_{33} virtual isobar to amplitude 8=42544
πd, 0.46-2.67 GeV/c obs., π^- cross-section higher than π^+ 8=29139
π^+ d, elastic and differential cross sections obs. 3.65 BeV/c 8=37985
recoil spectra, correction of energy resolving power effects in scintillation counters 8=24513

Deuterons—contd
  scattering—contd
    t-d, 76-660 MeV obs. 8=25007
    Al^{27} 7-11 MeV, polarization parameters obs., optical-model analysis 8=25265
    Ar^{38,40}(d, p) 11.6 MeV L-, J-values obs. 8=38507
    Ar^{38,40}(d, t), L-, J-values, 11.6 MeV 8=38507
    Be^{9}, elastic, differential cross sections for 5 scatt. angles 8=25262
    C^{12}, optical model calc. at 12.4 MeV, in ang. region 60–100° 8=47342
    C^{12}, optical model, spin-orbit and tensor forces 8=43053
    C^{12}(d, d), optical-model analysis includes tensor polarization terms 8=38501
    C^{12}(d, d), tensor polarization of deutron, 5.25, 6.10 and 7.05 MeV obs. 8=38501
    C^{12}, E_d=12 MeV, polarization obs. 8=29499
    C, 13.6MeV, polarization obs. from He^{3}(d, p) He^{4} ang. distrib. 8=38500
    Ca^{40}, optical model parameters 8=29497
    Ca^{40}, optical model, spin-orbit and tensor forces 8=43053
    Dy, 12 MeV, collective vibr. states identified 8=25149
    Fe^{56}, inelastic, energy levels obs. 8=29310
    Fe^{56}, E_d=12 MeV, polarization obs. 8=29499
    Fe^{54}–Sn^{124} isotopes, elastic cross-sections obs. 14.5 MeV 8=43054
    H^{2}(d, d), for He^{4} states search 3-11 MeV 8=38353
    H^{3}-d, 3-11 MeV, anomaly obs. 8=24937
    He^{3}-d elastic scatt. obs., 239-630 MeV 8=25007
    d–He^{4}, elastic, rel. to N exchange, Ed = 0.2–10.3 MeV 8=43052
    K^{-}-d, unitary impulse approx. 8=29142
    $K^{\pm}$ + d, 0.6-2.65 GeV/c obs., Y_0*, Y_1* 8=29159
    K^{39}(d, d′), K^{39}* collective core excitation obs. 8=33908
    Nd isotopes, 12 MeV 8=43056
    Ni^{58}, E_d=12 MeV, polarization obs. 8=29499
    Ni^{58,60}, elastic, optical model analysis, 21.6 MeV 8=29501
    Ni^{60}, polarized d elastic scatt., vector and tensor params. angular distrib., 21.6 MeV 8=29500
    Ni^{60}, 7-11 MeV, polarization parameters obs., optical model analysis 8=25265
    O^{16}(d, d)O^{16}, cross section, 2-3.5 MeV 8=38504
    O^{16}(d, d)O^{16}, for F^{16} energy level determ. 8=47235
    Pb^{208}, polarized d elastic scatt., vector and tensor params. angular distrib., 21.6 MeV 8=29500
    Si, 7-11 MeV, polarization parameters obs., optical model analysis 8=25265
    Si^{28}, elastic, differential cross-sections for 5 scatt. angles 8=25262
    Si^{28}(n, d)Al^{27}, E_n=21.3 MeV, ang. distrib. obs. 8=29467
    Ti^{46}(p, d)Ti^{45}, E_n = 26 MeV, ang. distrib. obs. 8=29307
    U^{233,235}, rel. to ground state rotational bands study 8=47269
    Zr^{90}, polarized d elastic scatt., vector and tensor params. angular distrib., 21.6 MeV 8=29500
Development, photographic. See Photographic process/development.
Diamagnetic resonance. See Cyclotron resonance.
Diamagnetism
    See also Cyclotron resonance; de Haas–van Alphen effect; Magnetic properties/diamagnetic.
  atomic wavefunctions and susceptibilities 8=47466
  cyclic polyene with 4nπ electrons, theory of diamag. anisotropy 8=25434
  ions with $^{1}S_0$ terms 8=38644
  positive column plasma 8=34411
Diamonds
  abrasive grains, frictional coeffs. with metals 8=31184
  atomic vibration spectrum, exptl. evidence, review 8=43922
  band structure rel. to interband optical absorption 8=40233
  damaged layer exam. on bombardment with Li^{7}, B^{11}, P^{31} ions, 20–120 keV 8=35601
  deuteron bombardment, chem. reactions 8=45406
  lattice spikes, reciprocal, on type Ia 8=44209
  luminescence and growth techniques 8=36475
  natural, luminesc. excitation spectra 8=36473
  natural, silicate-mineral inclusions, orientation 8=26179
  natural and synthetic, crystallographic features in stable and metastable regions 8=26192
  neutron irrad., X-ray scattering, random defect distribution 8=40016
  octahedral, (III) face rel. to growth mechanism involving wing trigons 8=26237
  photoconductivity spectrum 8=44914
  proton bombardment, chem. reactions 8=45406
  seed crystal growth by vapour-deposition 8=39669
  semiconductor, isotropic, total single-particle energy calcs. 8=40228
  semiconducting, with Al acceptors, photoconductivity spectrum, photothermal ionization and photo-induced tunneling 8=44913
  spark-erosion shaping method 8=35662
  surface energy of liq. metal interfaces 8=30718
  synthetic, anomalous X-ray refl. obs. 8=30889
  synthetic, crystal habit rel. to nitrogen impurity content 8=48521
  synthetic, reduction of e.s.r. linewidths 8=31847
Diamonds—contd
  synthetic u.v. and X-ray irradiated, thermoluminescence 20-400°C 8=36474
  type II, abundance and u.v. transparency 8=49710
  ultrasonic absorpt. prediction 8=35402
  vibration spectra, freq. along asymmetric dims. 8=30934
Dichroism. See Pleochroism.
Dielectric devices
  capacitor, vibr. with electrostatic drive, for contact pot. meas. 8=28450
  capacitors from high-quality ceramic dielecs. sintered in reducing atmos., 8=49332
  ceramic capacitors, high-quality, production from mat. sintered in reducing atmos. 8=27220
  diodes, SCL, small-signal operation and detection characts 8=49275
  electronic components, conference Washington U.S.A. (1968) 8=31416
  film-covered symmetric contacts, tunnel and thermionic currents 8=40628
  filter, narrowband transmission interference, props. 8=42200
  glass dielectrics for microcircuits, vac. deposition 8=44895
  heterojunction, semiconductor-dielectric, volt-ampere characts. 8=49287
  metal-aluminium oxide contact, rectification at high temps. 8=40630
  metal dielectric boundary, exciton quenching 8=44657
  metal-dielectric-metal, current transmission asymmetry, theory 8=27239
  metal-dielec.-metal structs, temp-depend of tunnel current 8=49146
  metal-dielec.-metal system, effect of dielec. props. on emission: elastic scatt., optical phonons 8=49387
  metal-dielectric-metal system in constant elec. field, non-stationary processes 8=35990
  m.i.m., negative resistance, irreversible break-down 8=40632
  m.i.m. system, conduction processes, transition from electrode-limited to bulk-limited 8=27303
  m.i.m. system, photoelec. emission from Lallemand electron camera exam. 8=27352
  m.i.m. system, symmetric, tunnel current density-energy distrib. 8=40631
  m.i.m. tunnel diode, zero bias anomalies due to paramag. impurities 8=44897-8
  m.i.m., with ferromag metal electrodes or impurities at barrier electrode interface, tunnel current flow 8=44899
  m.n.s. capacitor, memory behaviour 8=40629
  m.o.s. capacitors, radiation effects, determ. from conductance obs. 8=27204
  metal-oxide-metal structures, I-V characts., optical fibres method 8=35950
  multilayer dielectric and mag. film structure, longit. Kerr magneto-optic effect 8=41045
  multiple-Curie-point capacitor dielecs., prep. techniques 8=27286
  narrow-band interference filter with passbands exactly matching specification 8=42202
  photodielectric detector using superconducting cavity 8=40681
  piezoelec. readout, for spark chamber 8=33390
  piezoelectric resonator having N electrodes, eqs. governing elec. behaviour 8=49383
  polar dielectric, capacitor, thermodynamic effects 8=35991
  polymer capacitor, residual charge and dipole moment 8=40633
  pyroelectric ceramic detector for at. beams 8=47544
  quartz-Al capacitor, sputtered, prep. and props. 8=44059
  quartz shorted-guard-ring stress gauge 8=37110
  resonators, appl. as microwave filters 8=31444
  semimetal-insulator-metal junction, tunnelling conductance near saddle pt. 8=44896
  SCL diodes, trapping and transit-time effect in h.f. operation 8=27304
  switch, hardness to transient and steady state ionizing rads. 8=27302
  transducer for heat transfer obs. in hypersonic wind tunnels 8=47953
  waveguide loaded with n-InSb thin plate, field distribution 8=49385
  waveguides, moving, propagation along 8=33135
  m-Al_2O_3-m films, conductivity 8=44894
  Al-Al_2O_3-metal structures, I-V characts. 8=27240
  Al-Al_2C_3-Al, current transmission asymmetry, theory 8=27239
  Al-Al_2O_3-Al doped with Fe impurities at Al_2O_3-Al interface, tunnel current flow 8=44899
  Al-Al_2O_3-Al structures, Schottky current, negative space-charge effect 8=44901
  Al-Al_2O_3-Au structures, reverse conduction and electroluminescence 8=49388
  Al-Al_2O_3-Au tunnel cathode, e emission fluctuation 8=44935
  Al-Al_2O_3-Bi tunnel junctions, characts. 8=40627

Dielectric devices—contd
- AlN film structures, current-voltage characts. 8=44900
- Ca stearate Langmuir films, I-V-temp. characts. and cond. mechanism, obs. 8=44902
- CdS, light demodulator with u. s. amplification 8=27216
- In-CdS-In system in constant elec. field, non-stationary processes 8=35990
- Si–SiO$_2$ solid–solid interface system 8=40504

Dielectric loss. See Dielectric phenomena; Dielectric properties of substances.

Dielectric materials
- ageing, effects of atmosphere 8=40556
- anisotropic, guided wave propagation 8=33134
- antennas, metal reinforced, reflective properties 8=24211
- alumina ceramics, surface resistivity dependence on ambient humidity and cleanness 8=27237
- breakdown in rotating equipment, photomicrography 8=40553
- cellulose nitrate, etchable track formation 8=44492
- ceramic sub-assemblies in klystron, props. and behaviour 8=28602
- ceramics, review 8=49333
- ceramics sintered in reducing atmos. for high-quality capacitor production 8=27220
- ceramics, sintered in reducing atmospheres, prep. constitution and elec. props. 8=49332
- charge prod. determ. method 8=49224
- coating on opaque substrate, reflectance to monodirect. flux 8=31935
- conference, American Ceramic Society 70th annual meeting, Chicago (USA), 1968 8=40085
- diamond and zinc-blende type, band struct. and optical props. 8=44753
- diglycine nitrate, ferro-and paralelectric phases determ. by crystal structure 8=48685
- elastic, controllable states as combination of finite static deform. and static elec. fields 8=44858
- elastic, electro-mech. interactions rel. to polarization gradient, theory 8=44893
- electric field distrib. frequency depend. of stress distrib. 8=49386
- electric insulation and dielectric phenomena, conference 8=31418
- electroceramics of cordierite structure, production 8=30666
- electron deposition at high dose rates 8=27218
- electronic components, conference Washington U.S.A. (1968) 8=31416
- for electro-optic, elasto-optic and u. s. device appls, rel. to low-loss optical transmission 8=27229
- electrostatic pot., 3-dimens., round square array of surface charges 8=41925
- etchable track formation 8=44492
- external X-ray photo-effect, quantum yield obs. 8=36005
- ferromagnetic, acoustic wave velocity changes rel. to magnon-phonon interaction 8=30937
- films, as mirrors, windows and filters for laser work 8=49674
- finite samples, thermal cond. rel. to phonon-phonon interactions 8=35454
- finite size sample, thermal conductivity, theory 8=39939
- insulating ceramics, volume resistivity meas. at high temps. 8=27219
- insulators, analysis using ionoluminescence 8=40555
- Lexan polycarbonate, etchable track formation 8=44492
- liquids, high field electrophoresis of glass and metallic particles 8=30548
- magnetic, light scattering near phase transition of second kind 8=36301
- mechanical deform., theory 8=26752
- metallizing device for e microscopy 8=30853
- mica, etchable track formation 8=44492
- multiple-Curie-point capacitor dielecs., prep. techniques 8=27286
- Nylon 66, doubly oriented, anisotropic cond. rel. to direction and temp. 8=27257
- organic insulators and alkali halides, charge transfer by friction 8=27223
- partial discharge resistance testing 8=24060
- phonon effects, in external elec. field, theory 8=40560
- piezoelectric, sound generation in alternating field rel. to electric. oscills. instability 8=30940
- piezoelectric, transverse wave interacts in elec. and mag. fields 8=27296
- plastic-oil composite, elec. props. 8=40558
- polymer insulators, sheet form, polar and non-polar, losses and consts. 4.2-300°K 8=27253
- polymers, cond. meas. 8=40592
- polymers, conductivity theory 8=40593
- polymethylmethacrylate, thermal radiation during damage by laser light 8=30994
- polystyrene, thermal radiation during damage by laser light 8=30994
- polystyrenesulfonic acid membranes, rel. to adsorbed H$_2$O 8=49357
- porcelain, breakdown when subject to ionizing radiations optimal thickness calc. 8=31417
- pseudoinsulators (conductive at l.f.), dispersion 8=40550
- p-quaterphenyl layers, meas. of space charge limited currents 8=31427

Dielectric materials—contd
- refractory oxide solid solutions, with fluorite, pyrochlore and perovskite structures, anionic conduction 8=27232
- rocksalt films, breakdown strength, anode surface and mats. effects 8=40578
- ruby crystals, conductivity, 20-850°C and Seebeck coeff., 500-850°C 8=27236
- sapphire, crystals, conductivity, 20-850°C 8=27236
- Schottky and Poole-Frenkel effects, distinguishing between 8=27231
- solid, sliding discharge on surface in vacuum 8=27224
- solid, thin, rel. to power losses 8=27228
- surface resistivity meas. 8=28454
- surface topography from e.-mirror micrographs rel. to charge conc. 8=44863
- thiourea, thermal expansion anisotropy in paraelectric phase 8=26597
- track formation by ions, theory 8=40552
- transient radiation effects on electronic components 8=31126
- transparent, charged-particle emission on ruby laser irradiation without physical damage 8=40703
- transparent, constraints developed by luminous wave 8=27524
- transparent, crack orientation, laser destruction, stress effect 8=40191
- transparent, failure under laser rad., stress magnitudes and mechanisms 8=40547
- ultrasonic absorpt., imperfection depend 8=48715
- ultrasonic wave absorpt. in insulators, predominance of Akhiezer effect 8=35402
- CsCl: K$^+$, Rb , Br$^-$, ionic conductivity 8=31419
- KBr doped with KOH and KOD, dielec. relax. 8=27247
- KBr, pure and doped, ionic conductivity temp. dependence 8=27248
- KCl, charge flow during plastic deform., by dislocation movement 8=35961
- KCl, pure, doped and irradiated, ionic, conductivity, temp. dependence 8=27248
- KCl:OH, acoustical paraelec. resonance 8=27246
- KCl:OH, dipole interaction through phonon field 8=40577
- KNb$_3$O$_8$, mica like 8=40568
- MnO$_2$, characts rel. to contact mats. and way of coating 8=31383
- NH$_4$H$_2$PO$_4$, paraelec. phase, crystal structure from e. diffr. exam. 8=39816
- NaCl, ionic cond. and dielec. absorpt. meas. of dispersion of Ca^{2+} ions 8=35965
- NaCl, pure and doped, ionic conductivity temp. dependence 8=27248
- Pb(Zr, Ti)O$_3$ compounds, ferroelectric and antiferroelectric, electrocaloric effects 8=27279
- Sb$_2$Se$_3$, energy spectrum of traps from thermally stimulated depolarization meas. 8=40251
- Si$_3$N$_4$ film on Si, props. rel. to vapour deposition 8=49350
- Si$_3$N$_4$ films, pyrolytic, conduction props. 8=49352
- Si$_3$N$_4$-SiO$_2$ amorphous films on Si, props. rel. to form of m.i.s. devices 8=49319
- SiO$_2$ film on Si, props. rel. to vapour deposition 8=49350
- SiO$_2$ insulating film on Si, polarization effects 8=44854
- SiO$_2$, sputtered, for multilayer interconnects in MOS dev. 8=44855
- Si$_x$O$_y$N$_z$ film on Si, elec. and passivation props. 8=49351
- TiO$_2$-based, Ag diffusion coeffs. 8=31016
- TiO$_2$ single crystals, time-dependent elect. conduction 8=27250
- Xe-solid, deformation pots and band struct. 8=44646

Dielectric measurement
- biological solns., permittivity meas. below 1 MHz 8=28452
- bonded joint adhesives, capacitive stress/strain meas. 8=35639
- breakdown tests on insulating materials, effective factors 8=46322
- bridge for .001-10 000 Hz 8=33023
- capacitance, dynamic, direct meas. method 8=28451
- capacitance, small, use of spiral resonator in oscillation meas. method 8=46319
- capacitance, temp. coeff., new methods 8=24063
- cell for oxide powders, wide temp. range 8=44866
- complex permittivity measurement for high dielectric losses 8=46323
- complex relative permittivity at microwave freqs., in TE$_{10}$ mode rectangular waveguides 8=46346
- crystal photocarrier transport props. 8=35747
- electrode polarization compensated by 4 electrode null technique with high resolution 8=28453
- ferroelectric SHF temp. charact. 8=49365
- foam, complex constant, real component, in GHz 8=48245
- high resistance meas. in insulator range, apparatus 8=24064
- insulator test, allowance for nonsustained breakdown 8=37368
- interference spectrometer for mm. and sub. mm. meas. 8=49323
- in liquids, of complex dielec. constant at u. h. f. using resonant cavity device 8=30506
- m. o. s. capacitance at v. l. f. 8=35945
- optical method with colloidal generator 8=28766
- partial discharge resistance testing 8=24060

Dielectric measurement—contd
- permittivities in m.w. region, errors in spectrometer meas. 8=46343
- permittivity in E-band in low-loss mats. in overmoded waveguide 8=40554
- permittivity, of low loss materials, 2 methods at mm. wavelength 8=46320
- plane specimens, and elec. thickness of radomes, interferometer for 3-5 mm range 8=27222
- polymer capacitor, residual charge and dipole moment 8=40633
- pyreoelectric film, const. meas. in low elec. field, method and app. 8=40599
- solutions, dipole moment heterodyne-beat apparatus 8=34892
- time-to-breakdown curves for insulators under action of partial discharge, statistical determ. 8=44861
- Cu-containing perovskites, rel. to phase transforms. 8=27243
- GaAs, dielec. constant meas. method 8=44775

Dielectric phenomena
- See also Electric strength.
- acoustical paraelec. resonance, theory and appl. to KCl:OH 8=27246
- alkali halides, reorientation time of O_2^- impurities 8=48822
- charge deposition on dielectric rotor surface from semi-insulating fluid rel. to motor action 8=37369
- chemical relax. effects on dielec. dispersion 8=48187
- current injection, regional approximation method 8=40557
- current noise, double injection 8=44748
- dipolar absorpt., molec. rot. freedom model 8=25420
- dipole radiation pattern, effect of dielec. cylinder, calc. 8=28629
- discharges along insulator in vacuum, surface effects on field strengthening at the cathode 8=40562
- dispersion data, anal. into two relax. regions 8=41923
- dissipative instability of light propag. 8=46712
- domain theory of H-bonded fluids in supercrit. region 8=48183
- double charge ejection theory 8=49328
- electron gas, h.f. const. 8=31305
- electron self-trapping in continuous media, math. model 8=28466
- half-space, moving conducting, interaction with plane e.m. waves 8=24213
- hollow reinforced cylinder, effects of polarization under extension, inflation and torsion 8=35947
- ideal crystals, second sound in absence of Umklapp process 8=35957
- insulator wuth blocking electrodes, double injection 8=40551
- insulators, excitons and plasmons, relation 8=35949
- liquid-solid dielectrics, discharge onset, effect of dielec. thickness 8=44859
- liquids, attraction by elec. field 8=43853
- liquids, charge carrier momentum transfer 8=39393
- liquids, interpretation of expt. results 8=43854
- liquids, transient space-charge-limited conduction 8=39392
- many-particle system, optical refraction theory 8=37680
- Maxwell-Wagner effect for study of dielecs. showing dipolar relax. losses and high cond. 8=46345
- 3-methyl 2, 4-heptanediol, dielec. relaxation 8=48189
- mixtures, theory 8=48183
- Onsager reaction field, mol. field theory and spherical model 8=32826
- organic insulators and alkali halides, charge transfer by friction 8=27223
- paraelectric resonance, theory 8=49329
- photo-discharge, theory, accounting for recombination 8=35955
- polarization relax. time after shock wave passage, meas. 8=40563
- polyethylene, behaviour of props. rel. to freq. 8=44875
- polymer capacitor, residual charge and dipole moment 8=40633
- random anisotropic medium, tensor for e. m. wave propag. 8=30074
- relaxation, relation between freq.-temp. representations 8=41924
- relaxation times distribution, numerical evaluation 8=46349
- response to applied d.c. voltages 8=40549
- semiconductors and semimetals, superconducting and insulating mechanisms 8=26886
- semiconductors, charged impurity response model 8=49222
- space-charge conduction in insulators 8=49327
- static dielectric function in zero-gap semiconductors 8=27057
- stress distrib., frequency depend. 8=49386
- surface in water, sliding discharges 8=34397
- thick-walled electrostrictive cylinder, axially symmetric motions 8=46342
- in waveguides, calc. of discontinuities 8=28625
- X-ray reflection on periodic pile of layers 8=49675
- Al_2O_3 layers, constant rel. to temp. 8=44865
- CdS, loss meas. to study lattice defects 8=44867
- CdS, polycrystalline, capacitive changes with optical excitation, temp. effect 8=49414
- NaCl-glycerol soln., relaxation 8=48192

Dielectric phenomena—contd
- $NaNO_2$, relaxation, exptl. study 8=40612
- $NaNO_2$, relaxation mechanism 8=40613
- Te, constant, contribution of free carriers 8=40587
- ZnS: Cu, Cl, thermally stimulated effect, and thermoluminesc. 8=36518

ferroelectric. See Ferroelectric phenomena.

Dielectric properties of substances
- See also Electric strength.
- antennas, basic factors affecting radiation patterns 8=28631
- ceramics, migration polarization from motion of ions along dislocations 8=49322
- composite materials, permittivity 8=26939
- concentrated electrolytes, ion-pair theory 8=41272-3
- constant, meas., of low loss materials, 2 methods at mm. wavelength 8=46320
- constant, theory, recent developments 8=47576
- contact electrification of insulators, appl. to electrets 8=49379
- dicarboxylic acid esters, intramol. mobility and dielec. relax. 8=43340
- electrographic processes, charge transfer meas. 8=24075
- electron gas, Hartree-Fock approximation 8=23900
- emulsions, water-in-oil, effect of temp. 8=30567
- ferroxplane solid solutions 8=49321
- fluorodurene, crystalline, rel. to molecular reorientation movements 8=27256
- hydroxy- and methoxybenzaldehydes in benzene solns., relax. 8=39400
- liquid-solid dielectrics, discharge onset, effect of dielec. thickness 8=44859
- liquids, polar, by ionic thermoconductivity method 8=25944
- metal-dielec. -metal system, effect on emission: elastic scatt., optical phonons 8=49387
- molecules, relaxation time meas. from polarizability plot 8=43267
- muscovite-mica, permittivity press. dependence 8=44874
- nitile, h.f. dielectric consts., h.f. conductivity 8=49331
- permeability and dielectric constant calc. for e.m. waves in polarizable medium 8=24215
- polarizability tensor in cubic and hexagonal II-VI cpds. 8=27545
- polymers, ionic cond., weak-electrolyte theory 8=40590
- pressure dependence, to 5000 kg/cm^2 8=39401
- pyroelectric film, const. meas. in low-elec. field, method and app. 8=40599
- Al alloys corrosion prod. films in NaCl, tan δ rel. to cation impurities, obs. 8=44864
- Ar, Lorentz-Lorenz function, gas, liq. and crit. state 8=47967
- $BaTiO_3$, permittivity in paraelectric state rel. to degree of ionicity 8=35984
- BeO binaries with Al and Fe, elec. cond., activation energy polarization effects 8=27241
- CdTe, semi-insulating, transient currents charact. of deep traps 8=40441
- Cu_2O, constant, and refl. rel. to lattice vibrs., 290°K 8=39873
- KBr: OH , OD , relaxation 8=49344
- NaCl, losses rel. to F-centre thermal destruction 8=44484
- NaCl, pseudopot. calc. of frequency depend. dielec. function 8=41121
- Na-Sr-Cd niobates, and phase transitions 8=35979
- PbO-TiO_2 mixed films, max. permittivity rel. to struct. 8=49347
- $SrTiO_3$, permittivity in paraelectric state rel. to degree of ionicity 8=35984

gases
- polar, relaxation influenced by molecular multipole moments 8=43697
- steam, supercrit. region 8=48183

liquids and solutions
- air, permeability from meas. on N_2, O_2 and Ar at ca. –190°C 8=30512
- alcohols, relaxation, l.f., and viscous flow, mechanism 8=39398
- alcohols, using helix resonator to measure dielectric dispersion 8=39405
- alkylbenzenes, symmetrically substituted 8=34890
- aniline, dielec. relax. 8=43856
- amino acids in aq. soln., dielect. dispersion at 350-4000 MHz 8=30513
- anion radicals, electrolytically prod., phys. props and struct., e.s.r. meas. 8=43860
- anisoles absorption, internal rotation in non-polar solvents 8=43859
- anisole, dielec. relax. 8=43856
- benzenes, mono-substituted, microwave absorpt. 8=34889
- benzodioxane-1, 4 soln., absorpt. spectrum rel. to solvent dielec. constant 8=39376
- benzonitrile-acetonitrile, mixture, dielec. relax. 8=43856
- benzonitrile-propionitrile mixture, dielec. relax. 8=43856
- benzophenone + trichloroacetic acid mixture 8=48190
- binary mixtures of polar liqs., r.f. relaxation spectra 8=48185
- chloroaniline, o.m. and p, in benzene, temp. variation at microwave freqs. 8=48181

Dielectric properties of substances—contd
liquids and solutions—contd
cholesteryl, liq. crysts, dipole moments and transition temps. 8=34893
collagen, in soln., h. f. 8=30510
complex dielec. constant meas. at u. h. f. using resonant cavity device 8=30506
conduction enhancement in presence of insulating particles 8=49945
constant, optical, isothermal density derivative, empirical reln. 8=39399
1, 2-dichloroethane in various solvents potential barrier 8=43855
4, 4′-di-n-alkyloxy azobenzenes, nematic crysts, molec. polarizabilities 8=48068
electric insulation and dielectric phenomena conference 8=31418
electrolytic, aqueous, behaviour 8=39397
electrolyte solns., isothermal equilib. independ. of changes in dielec. const. 8=43761
electron self trapping, math. model 8=28466
ethylenediamine oligomer in soln., —100 to 60°C 8=39404
eugenol, permittivity and relax. time rel. to pressure 8=39395
film, a.c. breakdown voltage 8=48178
haloethanes in p-xylene soln., relax. processes 8=48184
n-hexane, non-linear susceptibility obs. 8=34888
n-hexane, pressure and temp. effects 8=39396
intramolecular barrier in solns., dielec. meas. 8=48186
isoamyl bromide and 2-ethyl 1-hexanol binary solns., complex permittivity 8=48191
isoamyl bromide, low temp. 8=48188
3-methyl 2, 4-heptanediol, dielec. relaxation 8=48189
methylalcohol, dispersion, temp. depend. 8=43857
methyl-heptanols, permittivity rel. to pressure and intermolecular association 8=39394
micromolecules in soln., effect on association 8=30418
mixtures of H-bonded liqs., dielec. const. calc. 8=48183
nitroaniline in benzene, temp. variation at microwave freqs. 8=48181
octanols, permittivity rel. to pressure and inter-molecular association 8=39394
octyl alcohols, isomeric 8=30508-9
octyl alcohols, isomeric, press. depend. 8=48182
oil-solid systems, polarization mechanism 8=34891
partial discharges on points in low-viscosity insulating oil 8=30504
permittivity, complex; calc. for organic liquids from CWCN maser meas. 8=48179
permittivity meas. in low-loss mat. in overmoded waveguide 8=40554
permittivity of biological solns. below 1 MHz 8=28452
permittivity, complex, cell for meas., rel. to temp. 8=30507
photoionization, prod. of charge and mechanism of conduction process 8=43861
polar liquids, temp. variation at microwave freqs. 8=48181
polar viscous soln., relaxation at microwave freqs., expt. and theory 8=43852
pyperine, supercooled, dipole polarization activation, thermodyn. props. 8=39403
radiolysis, effects of dielec. const. 8=32139-40
solutions of substs. having anomalous dipole moments 8=43344
supercooled, dipole polarization activation., thermodyn. props. 8=39403
synthetic insulating materials, properties 8=48180
triethylamine-I_2 complexes in soln. 8=30511
triglycine sulphate, domain and defect structs. in ferroelec. and paraelec. phases, obs. 8=31031
water, dielectric constant calc. from reflectance 8=43752
water, light and heavy, consts. and modification of Onsagers eqn. for polar liq. 8=43767
water-oil system solubilized with Aerosol OT, 5-60°C 8=39406
water, relaxation, l.f., and viscous flow, mechanism 8=39398
water-solid systems, polarization mechanism 8=34891
Ar, permeability meas. at ca. —190°C rel. to liq. air permeability calc. 8=30512
C_6H_4-containing cpds. 8=30505
CCl_4, non-linear susceptibility obs. 8=34888
CCl_4, polarization in refl. shock waves 8=43858
CCl_4, pressure and temp. effects 8=39396
$CoCl_2$ aqueous solns., consts. and loss factors 8=34887
CS_2, non-linear susceptibility obs. 8=34888
CS_2, pressure and temp. effects 8=39396
$CuCl_2$ aqueous solns., consts. and loss factors 8=34487
H_2O, changes during adsorption by solids below O°C. 8=39402
Hg/sulpholane interface, elec. double layer and specific adsorpt. 8=30396
$MnCl_2$ aqueous solns., consts. and loss factors 8=34887
N_2, permeability meas. at ca. —190° C rel. to liq. air permeability calc. 8=30512
NaCl-glycerol soln., relaxation 8=48192
$NiCl_2$ aqueous solns., consts. and loss factors 8=34487
O_2, permeability meas. at ca. —190° C rel. to liq. air permeability calc. 8=30512
solids
actinide cpds, conductivity at low temps. 8=49348

Dielectric properties of substances—contd
solids—contd
alkali halides, dielectric constant, low frequency meas. and review of other meas. 8=40567
alkali halides, electronic polarizability, ionic radius ratio, heat of fusion and melting pt., relationship 8=39474
α-methylstyrene-methyl methacrylate copolymer, stretching effects, 125-150°C 8=49356
alumina, commercial ceramics, loss tangent and permittivity, 20-400°C 8=27238
alumina mats, commercial, loss tangent and permittivity meas. at 9368 MHz and 20-400°C 8=49339
alumina, volume resistivity meas. problems at high temp. 8=49334
anomalies, in phase transitions 8=44860
anthracene, low-mobility, electron and hole generation 8=40595
benzene derivatives, crystalline polysubstituted 8=49629
breakdown tests, effective factors 8=46322
Carnauba wax thermoelectret, heterocharge on ionic addition 8=44879
cellulose, permittivity and dielectric loss, optical meas with colloidal mass emitter 8=28766
ceramics, sintered in reducing atmospheres, prep. constitution and elec. props. 8=49332
coal, constant and loss meas., temp. and freq. dependence 8=40572
complex relative permittivity at microwave freqs., meas. in TE_{10} mode rectangular waveguides 8=46346
conductors with anisotropic conduction band, permittivity 8=26938
corona resistance 8=29914
diamond, imaginary part of constant, interband contrib. 8=40233
dichlorofluoromethane, ice and water clathrates 8=27255
dielectric constant, mm. and sub-mm., and loss tangent value of some common materials 8=27227
dielectric layer in sandwich cathode, electron emission 8=44941
electrets, plastic, surface charge characts. 8=44892
electric insulation and dielectric phenomena conference 8=31418
ferrites, permittivity and loss, effect of freq. and temp. 8=40565
film insulator in integrated monolithic device with metal film, basic technology 8=44852
foams, complex constant, real component meas. in GHz 8=48245
glass, thermal strength rel. to thickness 8=35953
heterogeneous systems, losses 8=44757
hydrate of SF_6 8=49342
hydrates of Ar and N_2 8=49343
ice and water clathrates 8=27255
ice, NH_4F-doped, relax. time actuation energy from dielec. constant and conductivity meas. 8=44869
ice III, transition to antiferroelec. phase 8=31438
ice with HCl impurity 8=31420
insulating films, space-charge conduction theory 8=49327
insulator, excitonic, mag. fields effects 8=40261
insulator transient currents, electrode- and space-charge-limited 8=27221
insulators, electronic transport study, new technique 8=27230
interband, in electric field 8=27226
Maxwell-Wagner effect for study of dielecs. showing dipolar relax. losses and high cond. 8=46345
methanes, tetra-substituted, anomalous dielec. dispersion in low-temp. phases 8=49326
mica, impurity effect on conduction current in d. c. field 8=35948
organic polar cpds. in crystalline phases, dielec. constant transitions rel. to i. r. spectroscopy 8=27617
paper, permittivity and dielectric loss, optical meas. with colloidal mass emitter 8=28766
paraelastic and paraelectric defect systems in solids 8=48798
permittivity meas. in low-loss mat. in overmoded waveguide 8=40554
poly-1, 3-dioxolane dispersion 8=41003
polyethylene, dielec. losses at cryogenic temps. 8=49355
polyethylene, strength, subject to polarity reversals 8=35954
polyethylene terephthalate, losses at cryogenic temps. 8=49355
polyethylene, transparency at mm and sub-mm wavelength 8=44876-7
poly(fluoroalkyl acrylates), permittivity and loss meas. 8=40594
poly(4-methyl pentene-1), losses at cryogenic temps. 8=49355
polymer insulators, polar and non-polar, consts. and losses in temp. range 4. 2-300°K, in sheet form 8=27253
polymethyl methacrylate, permittivity 8=40957
polystyrene, complex dielec. const. 8=27639
polystyrenesulphonate membrane forms, optimum ionic electret 8=44878
polytetrafluoroethylene 8=35952
polytetrahydrofuran, dispersion 8=41003
polyvinyl chloride, losses at cryogenic temps. 8=49355

Dielectric properties of substances—contd
solids—contd
poly-w-undecanolactum, losses at cryogenic temps. 8=49355
powders, highly compressed, crystalline 8=49325
powders, permittivity calc. for dielectric constant detem. 8=49324
quantum structure in dielectric function of metals and anomalous prop. modes. 8=31307
p-quaterphenyl layers, meas. of space charge limited currents 8=31427
rare earth cpds, conductivity at low temps. 8=49348
Rochelle salt, relaxation, –50 to 45. C 8=27289
rubbers, and molec. struct 8=31425
ruby crystals, conductivity temp. dependence 20-850°C 8=49338
sapphire crystals, conductivity temp. dependence, 20-850°C 8=49338
sapphire insulating ceramic, volume resistivity at high temps., 8=49334
sapphire, principle consts., meas. by mech. action method, comments 8=40569
sea ice, constant and loss tangent 8=35956
semiconductor films, surface capacitance rel. to thickness 8=35873
semiconductors, permittivity of free electrons, quantum theory 8=35761
slab between sphere and plane, pot. gradient calc. 8=24074
slabs, permittivity modulated, parametric props. 8=27217
time-to-breakdown curves for insulators under action of partial discharge 8=44861
transition metals, constants and loss calcs. from vacuum u.v. reflectivity data 8=41147
trichlorofluoromethane, ice and water clathrates 8=27255
triglycine sulphate single crystal, differential permeability, effect of impurities 8=27288
uniaxial crystals, effect of dielect. anisotropy on donor ground states 8=31278
wax, u.s. field effects 8=27258
wurtzite, model for electronegativity definition 8=27251
zincblende, model for electronegativity definition 8=27251
Al-Al_2O_3-metal structures, I-V characts. 8=27240
Al_2O_3, chemisorption effects 8=44866
BaF_2, unipolar conduction mechanism from solid-state electrolysis 8=40579
$(Ba_{0.05}Sr_{0.95})TiO_3$, press. depend. of consts., in 20-80°K temp. range 8=27283
$BaTa_2O_6$, hexagonal, polarization relax. in a. c. field, rel. to tunnel struct. 8=35959
$BaTi_{0.75}Sn_{0.25}O_3$ soln., const. and Mössbauer effect –200 – 20°C 8=30639
$BaTiO_3$, repolarization processes, under double freq. excitation 8=31430
$BaTiO_3$, semiconducting, ionic-relax. polarization 8=35974
$BaTiO_3$–$BaFeO_3$ solid solns., transitions, e.p.r. study 8=27488
$BaTiO_3$:MgO(MnO), permittivity changes on ageing in elec. fields 8=27263
$BaTi_3O_7$ and $BaTi_4O_9$ 8=40571
BeO, elec. cond., activation energy, polarization effects 8=27241
BeO, response function exciton line splitting, phonon induction, obs. 8=36331
$BiFeO_3$-$Pb(Fe_{0.5}Nb_{0.5})O_3$ solid soln. system, phase transitions 8=39543
Bi_2O_3 8=49335
$Bi_4Ti_3O_{12}$ crystals, from permittivity temp. dependence meas. 8=27270
BN films, rel. to prep. and uses 8=48445
CaF_2-$Tb_2O_3(Tb(OF)_3)(TbF_3)$ solid solns., permittivity rel. to crystal chemistry 8=39640
CaO, i.r. dielectric response rel. to lattice vibrations 8=41075
CdS, movement of high-field domains, anode-cathode direction 8=40573
CdS, polycrystalline, capacitive changes with optical excitation, temp. effect 8=49414
$CdTiO_3$, perovskite modification, transitions, 20-1000°C 8=27242
Co, permeability tensor freq. dependence from Kerr effect 8=31696
Co-Co oxide-Co, anomalous tunneling rel. to Co ferromag. film use 8=31422
Eu oxides, divalent, permittivity and static conductivity at microwave freqs. and 80-700°K 8=35960
Fe, permeability tensor freq. dependence from Kerr effect 8=31696
Fe-Fe oxide-Al, anomalous tunneling rel. to Fe ferromag. film use 8=31422
GaAs, dielec. constant meas. method 8=44775
GaAs, insulating region, excitonic 8=40514
GaAs lattice microwave permittivity rel. to temp. 8=27090
GeSi alloys, constant, in energy region 1-13 eV 8=36366
H. bonded, dielec. absorption study 8=49330
p-H_2, on melting line 8=40575
α-HgS, nature of photoelectret effect 8=31440
KBr doped with KOH and KOD, dielec. relax. 8=27247
KBr:$SrCl_2$, polarisation effects by thermal depolarisation method 8=27245

Dielectric properties of substances—contd
solids-contd
KCl crystal, polarization by voltage pulses, 100°-350°C 8=40580
KCl, polarisation effects by thermal depolarisation method 8=27245
KCl: LiCl, paraelectric resonance 8=40548
KCl: OH, paraelectric resonance characts. 8=49345
$KD_3(SeO_3)_2$, anomalous, obs. 8=30698
$K_2Mn_2(SO_4)_3$, langbeinite structure, constant meas. rel. to electro-optical props. 8=39678
KNb_3O_8, mica like 8=40568
$K_2Ni_2(SO_4)_3$, langbeinite structure, constant meas. rel. to electro-optical props. 8=39678
$LaNiFe_{11}O_{19}$, persistent polarization after appl. of d.c. field 8=31424
Li ferrites, heat treatment effects 8=35962
LiBr, LiI and LiF films, l.f. polarization effects 8=44870
LiF, ionic cond. rel. to diffusion of anion and cation vacancies 8=35963
LiF: Mg, loss, effects of pre-irrad. isothermal annealing 8=45280
LiF, MgF_2, ionic cond, energy of motion of Li^+ vacancy and assoc. with Mg^{2+} ion 8=31423
$Li(Nb_{0.5}Fe_{0.5})O_2F$, and crystal structure 8=31435
$Li(Nb_{0.5}Fe_{0.5})O_2F$–$Li(Ta_{0.5}Fe_{0.5})O_2F$ system, permeability 8=31435
$Li(Ta_{0.5}Fe_{0.5})O_2F$, and structure 8=31435
$LiTaO_3$ ferroelec., constant temp. dependence, 25-700°C 8=44888
MgO based insulating materials 8=31445
MgO, response function exciton line splitting, phonon induction, obs. 8=36331
Na_3AlF_6 (cryolite) film, l.f. polarization effects 8=44870
NaCl, carrier-mobility temp. dependence, 7. 7-200°K, theory 8=44872
NaCl crystal, polarization by voltage pulses, 100°-350°C 8=40580
NaCl, interfacial polarisation, electrode performance effects 8=40582
NaCl-type ionic crystals, energy loss due to surface optical mode 8=44871
NaCl, unipolar conduction mechanism from solid-state electrolysis 8=40579
NaCl-AgCl, solid soln., conductivity and loss tangent meas. for structural change exam. 8=35060
NaCl:Mn, and pure, ionic cond., and cation vacancy motion 8=35537
$Na(H_xD_{1-x})_3(SeO_3)_2$, permittivity and spontaneous polarisation temp. and field strength dependence 8=40581
$NaH_3(Se_2O_3)_2$, phase transitions and thermal hysteresis 8=44873
$NH_4H_2AsO_4$, (ADA) constants obs. 8=27298
$NH_4H_2PO_4$, antiferroelectric, spontaneous polarization temp. dependence 8=40624
$(NH_4)_2Mn_2(SO_4)_3$, langbeinite structure, constant meas. rel. to electro-optical props. 8=39678
Ni ferrites, losses at microwave freq. 8=49346
Ni, permeability tensor freq. dependence from Kerr effect 8=31696
$NiCl_2.6NH_3$ and $NiCl_2.6ND_3$, dielectric dispersion and proton motional phase transitions 8=40614
Ni-Nioxide-Al, anomalous tunneling rel. to Ni ferromag. film use 8=31422
$PbCd_{0.5}W_{0.5}O_3$, ferrielectric phase transitions between 130-400°C and at 420°C 8=40583
$Pb(Fe_{0.5}Nb_{0.5})O_3$, para- to ferroelec. transition, e.p.r. study 8=27488
$(Pb_xSr_{1-x})TiO_3$ crystals, x ≈ 0. 25 9=44139
$PbTiO_3$–$PbMn_{2/3}W_{1/3}O_3$ system, solid solns., permittivity temp. and comp. dependence 8=40616
$Pb(Ti, Zr)O_3$ ceramics, orientational polarization 8=35980
$PbZn_{1/3}Nb_{2/3}O_3$, and electro-optical props. 8=27280
$PbZrO_3$-$PbTiO_3$ ceramics, effects of hot-pressing 8=39535
$Pb(Zr, Ti)O_3$ compounds, ferroelectric and antiferroelectric, electro-caloric effects 8=27279
PVC, background loss power temp. law for h.f. and μ wave region 8=31426
RbH_2PO_4, Curie–Weiss behaviour in paraelec. phase 8=40617
$RbMnF_3$, constant, loss and conductivity meas. 8=40584
$Rb_2Mn_2(SO_4)_3$, langbeinite structure, constant meas. rel. to electro-optical props. 8=39678
Rh h.f. polarizability, wavelength depend. rel. to cryst. e states, 0. 4-11μm 8=32026
Sb_2S_3 crystals, constant determ. at high freqs. 8=40585
Se, permittivity in phenomenological quant. descript. of optical absorpt. of granular mat. 8=41135
SiC film, breakdown mechanism 8=27249
SiC heater elements, sintered, elec. ageing rel. to oxidation ageing 8=49349
SiC, 6H polytype, low-freq. dielectric constant 8=36407
Si_3N_4 based insulating materials 8=31445
Si_3N_4 films from $SiCl_4$ + NH_3 8=44051
SnO_2, static constant determ. 8=49353
$(Sr_{0.4}Bi_xLa_{0.6-x})MnO_3$, and mag. props. rel. to structure 8=26038
$(Sr_{1-y}Bi_y)MnO_3$, and mag. props. rel. to structure 8=26038

- **Dielectric properties of substances**—contd
  - **solids**—contd
    - SrO, i.r. dielectric response rel. to lattice vibrations 8=41075
    - $SrTiO_3$, press. depend. of consts., in 20-80°K temp. range 8=27283
    - ThF_4 films, dielec. const. meas. 8=35184
    - $Tl_2Mn_2(SO_4)_3$, langbeinite structure constant meas. rel. to electro-optical props. 8=39678
    - ZnO crystals, e. multiplication and surface charge 8=49354
    - ZnO polar crystals, from point-charge model 8=30630
    - ZnO: Li, high-resistivity, electronic drift mobilities and SCL currents 8=40588
    - ZnSe, constant from i.r. lattice vibration meas. 8=49764
    - ZnTe, constant from i.r. lattice vibration meas. 8=49764
    - ZrO_2, effective and intrinsic permittivity 8=40589
  - **solids, ferroelectric.** See Ferroelectric materials.
- **Dielectric relaxation.** See Dielectric phenomena; Dielectric properties of substances.
- **Dielectric strength.** See Electric strength.
- **Differential analysers.** See Calculating apparatus.
- Differential equations
  - as Euler-Lagrange or canonical eqns., first-order linear ordinary eqns. system 8=28230
  - $(\partial^2/\partial x\partial y + ax\partial/\partial x + by\partial/\partial + cxy\partial/\partial t)P = O$, series soln. 8=23799
  - eigenvalue problem, Sturm's fund. theorem appl. 8=28229
  - Hamilton-Jacobi partial eqn., integration using variational princ. and transversality cond. 8=32662
  - Hartree-Fock integro-differential eqns. for atoms 8=29587
  - with hysteretic non-linearity, periodic solns. 8=41632
  - linear partial, asymptotic soln. by ray method 8=41634
  - Lyapunov-type theorem 8=41633
  - molecular transfer, derived from irreversible thermodynamics 8=41792
  - nonlinear system, convolution integral and Volterra kernels 8=37229
  - nonlinear system, high order, soln. by delta method, gen. approach 8=28243
  - perturbed system, motion near neighbourhood of stationary point 8=45981
  - Poisson eqn. for non-neutral plasma 8=34465
  - quadratic, with closed trajectories, obs. 8=45983
  - in quantum mechanics, integral-differential system, numerical soln. 8=46798
  - quantum-mech. pair eqns., numerical soln. 8=47438
  - radiative transfer, numerical soln. 8=37230
  - rear stagnation point in MHD 8=24191
  - Sturm-Liouville boundary value problems, nonlinear perturbations 8=45974
  - system arising from theory of mean atmos. waves, soln. 8=36726
  - two-sided Cauchy problem, solution, for m-dimensional acoustic system 8=46188
  - weakly nonlinear systems, periodic solns. 8=23802
  - SH-waves, by half-plane 8=45998
  - WKB approx: applied to slowly varying propag in waveguide 8=24234
  - WKB soln. of general 2nd order eqn. and propagation problem applic. 8=23803
- Diffraction
  - dielectric wedge, Laplace transform soln. 8=46482
  - of elastic waves, harmonic, by rigid circular disc 8=32894
  - line broadening effects, separation by means of line-width relations 8=45147
  - multisource, slit source, and grating Moiré methods for recording slopes in flexed plates 8=46733
  - nuclear resonant, of γ-rays by perfect crystals, theory 8=48616
  - of plane, dilational pulse by semi-infinite barrier at fluid-solid interface 8=23940
  - radiation from nearby source, h.f. 8=23810
  - scalar, plane wave, by elliptic disc 8=23811
  - by smooth curves, Watson transform. and creeping modes in shadow 8=33281
  - wave reduction problems on non-closed, infinitely thin screens 8=46000
  - wedge diffraction theory 8=23809
  - in wedge-shaped regions, $\psi_{\omega}(Z)$ appl. 8=32684
  - zone plates, Fresnel and sine wave, production 8=37690
  - H atom, e scatt. theory 8=29653
  - SH waves, earth's spheroidal core 8=27844
  - **acoustic waves**
    - at boundary of semi-infinite impedance system 8=32913
    - holography, and appls. 8=24436
    - pulses, by plane interface 8=23963
    - wedge-shaped regions, $\psi_{\phi}(Z)$ appl. 8=32684
  - **acoustic waves, ultrasonic**
    - acoustic transducer, retangular, optical probing of Fresnel and Fraunhofer regions 8=37262
    - holography, and appls. 8=24436
  - **electromagnetic waves**
    - black bodies and absorbing semi-transparent plates 8=42014
    - body scatt. in plasma medium 8=37495

- **Diffraction**—contd
  - **electromagnetic waves**—contd
    - circular aperture, effect of screen geometry 8=33132
    - by conducting cylinder, energy flux, numerical study 8=46484
    - conformal mapping application 8=37488
    - cross-polarized, by knife-edge obstacle 8=37491
    - cylinders, 2 parallel, using equivalent ccts. 8=46478
    - dielectric semiplane, ignoring surface-wave effects 8=42018
    - on disc, ideally conducting, in spherically-symmetric plasma 8=25747
    - dispersive hyperbolic eqn., initial boundary value problems, asymptotic expansions 8=37483
    - focus of converging wave, nonlinear effects 8=37487
    - focusing, multiaperture technique 8=37482
    - in gas, nonstationary diffusion, similarity principle for solns, reduction 8=42019
    - half-plane in transverse plane of uniaxially anisotropic medium 8=37493
    - holograms, microwave, and visible images rel. to antenna array theory, obs. 8=24439
    - holography, microwave, and appls. 8=24436
    - by impedance stripes in anisotropic medium 8=24226
    - inhomogeneous media, transition functions 8=37492
    - knife edge, of radiation from directional antenna, Kirchoff-Fresnel approx. 8=24218
    - partially coherent, spectral density functions 8=42016
    - penetrable half-plane parabolic cylinder 8=37490
    - plane elliptically polarized, in absorbing medium, by plane dioptre 8=28611
    - plane wave incident on non homogeneous sector of impedance plane 8=24219
    - plane wave spectral method 8=37485
    - plasma structures, resonant scatt. 8=37495
    - Poynting vector flux curves for diffr. by reflecting half-plane 8=24223
    - radiation of source moving near comb structure 8=24221
    - r.f. holography 8=46479
    - right-angled dielectric wedge; inverse-transformable soln. calc. 8=46482
    - by screen of finite thickness with evenly distrib. apertures which can be filled with dielectric 8=24220
    - screen, thin black, suitability for meas. 8=46483
    - by slit aperture, plane 8=24224
    - by square grating 8=37484
    - surface wave, obliquely incident on wedge of impedance half plane 8=24222
    - transparent elliptical cylinder 8=37489
    - two-dimensional, theory, advances 8=46464
    - wedge, moving conducting 8=42015
    - Weiner-Hopf equations and applic. 8=46481
    - wide aperture in magnetoionic medium 8=37494
    - zones on rough screen, correl. of amplitude and phase spatial vars 8=24225
  - **electrons.** See Electron diffraction.
  - **light**
    - See also Holography.
    - acoustic imaging by diffracted light, two-dimensional interaction 8=37272
    - coherent, by condensed systems, generalization of 3-D Patterson function to 4-dimens. 8=26356
    - colloidal sphere arrays 8=48237
    - ferromagnetic domains 8=45143
    - Fraunhofer, for extraction of characts. from visual pattern 8=33246
    - Fresnel images, appl. of convolution formulation of diffraction 8=42253
    - Fresnel, in media with variable density, applic. of Huygen's principle 8=37689
    - Fresnel, of nonspherical wave 8=46730
    - Fresnel pattern synthesis by overlapping zone plates 8=28888
    - Fresnel zone plates, optical method for prod. 8=28869
    - gratings, parallel Wood's anomalies 8=28868
    - hologram transmission systems, bandwidth reduction by elimination of vertical parallex 8=28893
    - holograms, bleached 8=42266
    - holographic stereograms, bandwidth reduction for white light illuminated objects 8=37693
    - image of point in focal and out of focus planes 8=42251
    - laser beams by u. s. waves, use in optical correlator 8=28751
    - laser, ruby, coherence function determ. 8=37607
    - latexes 8=48237
    - lensless incoherent correlation, effect of diffraction 8=42255
    - Moiré fringe theory 8=46732
    - opals, gem, crystal structure determ. 8=44254
    - pattern calc. by computer by Fourier transform of aperture elec. field 8=28871
    - patterns of annular aperture with spherical aberration and coma, irradiance distrib. 8=42169
    - patterns, rel. to apparent separation and intensities of two close objects 8=24368
    - phase objects, Fresnel diffr. distrib. 8=33280
    - polarization for diffraction by u. s. waves in isotropic solid 8=36302
    - rabbit psoas muscle, glycerol-extracted, filament lattice studies 8=26458

Diffraction—contd
- **light**—contd
  - scalar integrals of Kirchhoff, appl. to parabolic and plane waves 8=42253
  - sectoral slit, theory 8=24416
  - self imaging, algebraic formulation 8=46731
  - sinusoidal grating, intensity distrib. calcs. and appl. to diffusion meas. 8=41019
  - sinusoidal gratings, theory and appl. to self-diffusion meas. 8=41020
  - spectrometry, Fourier, by transmission grating resons. scanning 8=28787
  - straight edge imaging in partially coherent light with spherical aberration 8=37694
  - ultrasonically, gas, approx. formula 8=34662
  - by ultrasonic pulses 8=24418
  - by ultrasonic waves 8=24417
  - wave aberration function, variance evaluation 8=42254
  - GaAs, calc. by u.s. reflecting lattice 8=36290
  - He-Ne laser radiation field obs. 8=24313
  - Y-Fe garnet, use in study of 1.1 GHz transverse magneto-elastic waves 8=40101
- **neutrons**. See Neutron diffraction.
- **X-rays**. See X-ray diffraction.

Diffraction by acoustic waves. See Acoustic waves/effects; Diffraction/light.

Diffraction gratings
- abnormal behaviour in far u.v. 8=46734
- allowable non-parallelism in incident beams, in high resolution spectrometers 8=42228
- amplitude, f.m., curvature interferometry 8=35616
- concave, aberration calc., approx. formulae 8=24415
- concave, Czerny-Turner arrangement of one and spherical mirror 8=37644
- concave-grating mounting for x.u.v. monochromator 8=28808
- in electron microscope, profile examination 8=37423
- gap effect on Moiré patterns 8=46727
- gear hobbing machine table drives, use in transmission error obs. 8=24373
- laser beam modulation 8=42123
- modulation of laser light 8=42122
- Moiré fringe theory 8=46732
- Moire fringes for system of transparent and reflection gratings 8=28872
- multisource, slit source, and grating Moiré methods for recording slopes in flexed plates 8=46733
- optical, parallel Wood's anomalies 8=28868
- plane, mounting utilizing convergent illumination, theory 8=37692
- radial, moiré pattern form. theory 8=33279
- sinusoidal, intensity distrib. calcs. and appl. to diffusion meas., 8=41019
- sinusoidal, theory and appl. to self-diffusion meas. 8=41020
- with skew incidence illumination, location of poss. anomalous behaviour 8=28870
- spectrography, Girard coding, grating appls. 8=28822
- spectrometer, multiplex grating, 16-channel for near i.r. 8=28798
- stigmatic concave with varying spacing 8=37691
- X-ray, 1Å dispersion 8=28929
- X-ray, ruling engine design and construction 8=33303

Diffrimoscopy. See Diffraction/light; Optical images.

Diffusion
- See also Neutrons and antineutrons/diffusion; for diffusion of matter, see Diffusion in gases; Diffusion in liquids; Diffusion in solids.
- aerosol particles, photodiffusiophoresis 8=30561
- analysis of problems using principle of superposition of singularity solutions 8=46129
- atmospheric eddies, role in W-185 tracer movement 8=50163
- branching process of restricted Brownian particles, averaging process asymptotic behaviour 8=46097
- concentration-dependent, in semi-infinite medium 8=23916
- crystallites, surface-adhered, migration theory 8=44021
- dual variational principles, for error estimation, in approx. solns. 8=28355
- Eaton-Zadeh's method of controlling diffusion processes 8=41796
- electrons in positive column, const. coeff. eqn., validity criteria 8=43447
- Fermi liquid calc. 8=41778
- gas and steam, permeability of synthetic membranes 8=35471
- generalized eqn, complementary variational principles for soln. 8=28353
- group diffusion eqn, 1D, soln. by Laplace transformation 8=47378
- magnetization and interspin-energy diffusion, moment-method calc. 8=27367
- method for solution of problems over regions with time-dependant shape 8=46240
- multicomponent systems containing chem. equiv. pairs 8=30449
- oceanic drogue, large scale 8=45434
- one-dimensional eqn., pseudo-similarity solns. 8=23912

Diffusion—contd
- P_N approximations, for error bounds 8=23915
- plasma, ambipolar → free, transition microwave meas. 8=39078
- plasma, enhanced transverse, rel. to longit. resistivity 8=30028
- plasma, Lorentzian, inhomogeneous, and conductivity tensors, non-linear terms calc. 8=30025
- plasma, thermal nonequilib., and thermodiffusion coeffs. in stationary e.m. field 8=47817
- point-type continuous source, analysis 8=41797
- radiation in anisotropically scatt. plane layer 8=46131
- radiation in spherical envelope surrounding point source 8=41801
- rare earth metals, out of p-irradiated metal foils in vacuum, at 1500-2800°C 8=40081
- region in electrode layer of low temp. plasma 8=39081
- spectral, in e.s.r., and saturation 8=49607
- surface, negative temp. coeffs. in catalysis and chemisorption 8=49898
- turbulent scalar fields, diff. approx. for spectral component transfer 8=47925
- two-media system with moving boundary separation, eqns. 8=46130
- variational principle, virtual limitation 8=23914
- variational theory, time-depend 8=23913
- **acoustic waves**
  - See also Scattering/acoustic waves.
  - decaying sound field, reverberation room obs. 8=23961
- **electromagnetic waves**
  - See also Scattering/electromagnetic waves.
  - No entries
- **light**
  - See also Reflectivity; Scattering/light.
  - liquids, laser resonator instrument for meas. 8=46536
  - non-equilibrium in nonhomogeneous plane-parallel layer 8=28873
  - plant canopy interaction, lab. expt. rel. to theory 8=46735
  - reflected from polished surface 8=24411
  - sodium salicylate on MgO, diffusion indicator in far u.v. 8=49778

Diffusion in gases
- See also Flow/gases.
- atmosphere, exponential, small particles 8=41345
- of atoms, coeff. determ. using graphite cuvette 8=38619
- binary laminar boundary layer eqns., soln. 8=25838
- binary mixtures, diffusion force in transition region of Knudsen number 8=47985
- binary mixture, diffusion phoresis in spherical drops 8=34677
- binary system, mass coeff. meas. based on convective and diffusive flow 8=43706
- diffusion meas., Moiré interference method 8=48119
- electrons, drift rel. and diffusion coeffs. 8=39230
- evaluation of meas., simple method. 8=47984
- flames, laminar, effect on stability 8=28407
- hydrocarbons, vapour-phase fugacities 8=39481
- ionosphere, role in l.f. instabilities 8=45527
- of ions, and mobility, theory and obs. review 8=30318
- ions, and recombination, no. unrecombined particles asymptotic limit 8=34473
- isotope separation, tapered cascade characts. 8=29670
- membrane, time lag depend. on conc. 8=30321
- molecular flow in tubes with particle adsorpt. 8=47983
- nonpolar mixtures, coeffs. at ordinary pressures 8=47981
- oil-gas separator, use of simple diaphragm system 8=30317
- optical orientation by spin-echo 8=39240
- through orifice, cavity filling, rel. to heat-insulating props. of chamber 8=41866
- plasma sheet, m.h.d. flow limit 8=30034
- plasma streaming along uniform mag. field, boundary effects 8=30015
- plasma, turbulent, transfer coeffs. 8=30023
- and pressure diff. at high press. 8=43708
- polyatomic mixtures, velocities, and heat fluxes and viscous stress tensor, eqns. 8=43699
- pumping theory, diffusion and mean-free-patts. aspects using kinetic theory of nonuniform gases 8=47993
- reactant diffusing from point source to infinite surface, steady state reaction 8=36549
- reacting systems 8=41244
- separate components coeff. determ in mixture 8=39342
- turbulent, mass transfer at ordinary rates, rate of concentration of nondiffusing species 8=47978
- Ar, thermal cond. determ. in hot-wire column 8=43683
- Cs vapour, of Cs ions, time-of-flight analysis rel. to conduction studies 8=43705
- CO_2 excited (00°1) state, through pure CO_2 8=38817
- Cs vapour, coeff. meas. from hyperfine relax. 8=47537
- Cs vapour of Cs_2^+, diff. coeff., time-of-flight obs. 8=30314
- H, of electrons, and mobility 8=39228
- He-Ar, mixture, concentration diff. coeff., meas. by two-bulb method 8=34678
- He-Ar mixtures, effect on u.s. attenuation 8=43689
- He^3 and He^4, rel. to low temp. transport props. mutual consistency 8=34671
- He-Kr mixtures, effect on u.s. attenuation 8=43689

Diffusion in gases—contd
- Kr in $N_2O_4 \rightleftharpoons 2NO_2$ system, effect of chem. reaction 8=34681
- N, of electrons, and mobility 8=39238
- Ne-Kr, mixture, concentration diff. coeff., meas. by two-bulb method 8=34678
- NO-N, mixture, Senftleben effect 8=30316
- O atoms through gases 8=49910
- $O^{16}O^{18}$-O_2^{16} mixture, Senftleben effect 8=30316
- RaA, rel. to radiation hazard 8=32257
- **thermal**
  - binary system, meas. using combination of convective and diffusive flow 8=43706
  - Chapman-Enskog kinetic theory 8=30315
  - eqn. from least-dissipation principle of thermodynamics 8=23906
  - hot-wire column for thermal cond. meas. 8=47956
  - isotope separation column, theory and expt. data 8=38766
  - magnetosphere, and multiply charged ion concs. 8=50165
  - measurement in mixtures, trennschaukel 8=39239
  - methane-argon mixtures, influence of atomic mass distrib. 8=43709
  - mixtures, press. depend. 8=47982
  - monatomic-polyatomic gas mixtures 330°-600°K, Chapman-Enskog theory 8=43707
  - separation of gas mixture, thermal diffusion column 8=30319
  - separation of mixtures in chem. equilib. 8=47986
  - spectroscopic investigation 8=30322
  - thermal transpiration in Knudsen gas 8=25837
  - Ar-CO_2 mixtures, composition and temp. depend. 8=47987
  - $Ar/He/NO_2/N_2O_4$, separation 8=47986
  - CO_2, diffusivity in crit. region 8=39241
  - CO_2-inert gas mixtures, comp. depend. 8=34679
  - CO_2-Kr 330°-600°K, Chapman-Enskog theory 8=43707
  - CO_2-Xe 330°-600°K, Chapman-Enskog theory 8=43707
  - Cs vapour, transport coeffs. calc. 8=30306
  - H and He in thermosphere 8=50188
  - H_2-He mixtures, comp. depend. 8=34680
  - H_2-Xe 330°-600°K, Chapman-Enskog theory 8=43707
  - He-Kr mixture, rel. to intermolec. forces 8=34675
  - He-Ne mixture, rel. to intermolec. forces 8=34675
  - He + Ne + CO_2 system 8=30320
  - Ne-Ar and Ne-Xe system 8=39239
  - Ne-Kr mixture, rel. to intermolec. forces 8=34675
  - $2NO_2 \rightleftharpoons 2NO + O_2$, separation 8=47986
  - $ZrCl_4$ and $HfCl_4$ vapours, constant 8=34676

Diffusion in liquids
- See also Flow/liquids.
- alkali halide aq. solns., self-diffusion of H_2O 8=25953
- alkaline earth halide aq. solns., self-diffusion of H_2O 8=25953
- n-alkanes in soln., theoretical calc. 8=30452
- aqueous solution, self-diffusion coeff. by capillary method using radioisotopes 8=25899
- axial, through cylinder connecting two reservoirs, with pulsed flow 8=34811
- binary liq. systems, coeffs. using diaphragm cell 8=43785
- binary systems of neutral components 8=43786
- blood, convective, of O_2, CO_2 and inert gases 8=43793
- carrier and single file, asymm. discrimination 8=25902
- of cavitation bubbles 8=34735
- cell, freezing of u.s. standing waves 8=48135
- cellulose, and sorption of water 8=30785
- convective diffusion in capillaries 8=30447
- diffusivities, modified Eyring eqn. 8=25900
- effect in chem. reactions, statistical anal. 8=34882
- effect on transfer of electronic excitation energy 8=34881-2
- electrolyte solns., diffusion potential decay 8=30448
- electrolytic solns., dil., and thermal diff., 8=49922
- electrolyte solns., rot. and translational diffusion 8=25952
- ethylene, self-diffusion, activation energies 8=30451
- fluorescence quenching kinetics 8=39385
- frequency-dependent friction constant analysis 8=39340
- hexamethylenetetramine aq. solns., differential diffusion coeffs. 8=30446
- high-molecular biopolymers, method and apparatus 8=48116
- hydrocarbons, aromatic and cycloparaffin, in H_2O, 2 to 60°C 8=48118
- isobutyric-acid-water system, diffusion coeff. obs. near critical soln. conc. 8=39341
- limiting rate at surface of rotating electrode in turbulent system 8=30453
- liquid-liquid interface, kinetic of adsorption 8=43792
- at liquid-solid interface, u.s. oscillations effects 8=34814
- liquid spreading about nozzle bed, rel. to irrigation intensity for nozzle dimensions 8=30361
- metal binary systems, coeffs. meas. using conc. cell. 8=43784
- metals, fluctuation model 8=43790
- methane, self-diffusion, activation energies 8=30451
- micellar coeffs., polarographic determ. 8=34941
- Moiré interference method, applic. 8=48119
- multicomponent isothermal, Darken theory 8=43787
- multicomponent systems containing chem. equiv. pairs 8=30449

Diffusion in liquids—contd
- polymer chains, translational, theory 8=48114
- polymer meas. using Zeiss Schlieren equip. 8=48113
- polymer, plane polygonal, translational coeff. 8=34817
- polystyrene in polystyrene, effect of mol. wt. 8=30450
- propane, self-diffusion 8=34812
- pulsation diffusion method, transport increase 8=34816
- relative permeabilities for constant field eqn., expt. determ. 8=48122
- rotational, effects on n.m.r. relax. 8=39426
- salts, molten, self-diff., theory and expt. 8=43789
- sensitivity of meas., increase 8=48117
- separate components coeff. determ in mixture 8=39342
- ternary aq. systems, Darken theory 8=43788
- two-phase flow, axial coefficient meas. 8=48014
- unsteady gas absorption with irreversible first-order reaction, penetration theory 8=48110
- vertical, thermal disturbances due to meas. 8=43791
- Ag of Ni 8=34813
- CO_2, self-diffusion 8=34812
- Fe_2O_3, molten, of Al_2O_3, rate 8=39343
- H burning theory 8=32111
- He^3-He II dilute soln., spin-diffusion coeff. obs. 8=46306
- KCl aq. soln., proton diff. coeff. 8=48115
- Li isotopically pure melts, Li^6 and Li^7 inter-diffusion 8=34807
- Li, self-diffusion, n.m.r. meas. 8=48112
- LiCl aq. soln., proton diff. coeff. 8=48115
- $MgSO_4$ soln., rate constants, three-step ion assoc. model calc. 8=43783
- $Na^{22,24}$ ions, electromigration in molten nitrates 8=43782
- NaCl and $NaClO_4$ aq. soln., proton diff. coeff. 8=48115
- $PbBr_2$ molten, self-diffusion 8=34808
- Pb-Sn alloys, self-diffusion of Ag impurity 8=34806
- $ZnCl_2$ molten, self-diffusion 8=34815
- **thermal**
  - column design, rel. to convective flow rate and plate spacing 8=34810
  - Dufour effect 8=48111
  - electrolytic solns., dil., 8=49922
  - eqn. from least-dissipation principle of thermodynamics 8=23906
  - metals ratio of eddy diffusivities, from turbulent flow temp. profiles 8=34836
  - nonisothermal, variation of coeffs. 8=34809
  - solution heated from below and onset of convection 8=34818
  - spectroscopic investigation 8=30322
  - in supercooling, constitutional, during solidification 8=34974
  - Bi-Sn alloys, coeff. rel. to composition 8=39344
  - In, isotope thermotransport 8=29671

Diffusion in solids
- See also Permeability, mechanical.
- activation energy, temp. dependence 8=39958
- adamantane molecular crystal self-diffusion, n.m.r. and plastic-flow obs. 8=39988
- agar gel, counterdiffusion of Pb^{++} and CrO_4 8=48244
- alkali feldspars, O mobility, by autodiffusion and alkali atom exchanges 8=35477
- alkali halides, migration of gas inclusions 8=39966
- alloys, ordered, of β-brass type, theory rel. to vacancy conc. and migration energy 8=26613
- alloys, ordered f.c.c., rel. to vacancy conc. and migration energy 8=26614
- alloys, self-diffusion mechanism rel. to defect densities 8=26615
- armco Fe in weld joints under transient pressure 8=44373
- atomic translational-diffusion mechanism from NMR spin-relax. time exam. and order parameter calcs. 8=27498
- binary alloys, of vacancies, correlation factors 8=31039
- classical and quantum rate theories 8=35516
- clay, moisture diffusion coeff. and thermograd. coeff. rel. to moisture content 8=30662
- coal, of sat. hydrocarbons 8=48775
- coefficient determ. using X-ray diffr. data 8=35469
- crystals, growing, of impurities rel. to impurity distribution anisotropy 8=26207
- crystals, of isomorphous impurities rel. to compounds of different solubilities 8=26612
- diffused structures, planar, strain effects. 8=48844
- dislocation stress fields, precipitation hardening 8=39537
- electro-graphite, of O_2 8=41266
- Fick's first law, reformulation rel. to atomic jump freq. 8=44376
- fission prods. in coated fuel particles rel. to in-pile release, model 8=38591
- gas-metal permeation, concentration-dependent time-lag measurements 8=48768
- grain boundary, meas. analysis 8=39957
- grain size depend of peak temp. of linear heating curves for rare gas systems 8=26617
- halide crystals, inert gas diffusion following ion bombardment 8=48888
- ice, hydrate of SF_6 8=49342
- ice, surface diffusion at ice-air interface rel. to step propag. across basal plane 8=35145
- ice, water migration in transition layer under influence of elec. and temp. grads. 8=30999

Diffusion in solids—contd
- impurities, coeff. determ., anelastic methods 8=30995
- impurity diffusion coeffs., e microprobe obs. 8=30998
- inert-gas, as probe for lattice defects in ionic crystals 8=39992
- laws, rel. to Boltzmann condition 8=35468
- liquid spreading about nozzle bed, rel. to irrigation intensity for nozzle dimensions 8=30361
- loams, moisture diffusion coeff. and thermograd. coeff. rel. to moisture content 8=30662
- magnetite, of Fe^{2+}, rel. to oxidation to γ-Fe_2O_3 8=27702
- measurement method for activated gas diff. 8=48775
- metal crystals, inert gas diffusion following ion bombardment 8=48888
- metals, grain boundary diff., size effect 8=48349
- metals, of atoms rel. to crystal defects 8=26629
- metals, of Xe, rel. to mech. props. 8=48766
- metals, metastable, annealing time effects on rates 8=35474
- metals, mobility temp. dependence 8=48783
- metals, self-diffusion mechanism rel. to defect densities 8=26615
- meteorite Fayetheville, primordial He, Ne and Ar diffusion 8=37024
- microinhomogeneous, macroscopic coeff., eqn. 8=48741
- molecular solids, self-diffusion, by vacancy mechanism 8=35531
- monatomic crystals, diffusion-jump process theory rel. to phonon system 8=44379
- non-Fickian anomalies, time lags 8=48769
- nuclear materials, inorganic, diffusion rates 8=48772
- nuclear reactor fuels, thermal 8=48776
- oxide crystals, inert gas diffusion following ion bombardment 8=48888
- peat, visco-plastic, internal mass transfer in drying 8=34982
- point defects, appl. of anelasticity 8=31127
- polymer adhesion, metal welding, analogy 8=35515
- polystyrene, atactic, of n-pentane, rel. to second-order transition above glass point 8=44398
- porous materials, moisture diffusion eqn. 8=44374
- porous media, convective salt diffusion, boundary cond. at inlet of system 8=39959
- positronium, annihilation spectra mean lengths and diffusion constants 8=44378
- powder mixture model, diffusion parameters 8=35472
- quartz, irrad., H_2 diffusion 8=48790
- rare gases, and vacancy conc. 8=44415
- reactor fuels, of inert fission-prod. gases rel. to bubbles nucleation 8=31109
- redistribution of diffused layers during epitaxy and other process steps 8=48441
- rotational diff. rates of mols. rel. to molec. struct. and cryst. packing density 8=48767
- scintillation counter plastic, of Kr 8=35499
- second phase, from plane, finite source 8=44375
- semiconductors, instabilities 8=26616
- semiconductors, interactions in sequential processes 8=48770
- semiconductors, of impurities, simultaneous and consecutive, rel. to internal elec. field 8=30997
- semiconductors, piezoelectric, of impurity atoms, coeff. determ. 8=35491
- silica, fused, ion diffusion from molten salts 8=48789
- soda-potash-baria glass, of K and Ba in refractories 8=48780
- solid solution, effect of deviations from Vegard rule under multilateral pressure conditions 8=48765
- spinels, cation migration 8=44377
- steel scale, of reactive gases rel. to simultaneous oxidation and carburisation 8=48777
- surface, activation energy elec. field dependence (10^7–10^8V/cm), theory 8=35512
- surface diffusion in electrochem. cryst. growth 8=48531
- surface meas. using sinusoidal grating diffraction phenomena 8=41019
- surface roughness effects 8=39956
- surface self-diffusivity meas. using sinusoidal grating diffr. phenomena 8=41020
- in temperature gradient, motion of markers and bubbles 8=35470
- tetrafluoroborate salts, ion motion and n.m.r. 8=31905
- thermal, semi-infinite wall rel. to temp. 8=32952
- transient, in composite slab, theory 8=39960
- transition metals, b.c.c., entropy rel. to elastic consts. temp. depend. 8=48984
- Ag^{110}, grain boundary self diffusion coeff. meas. 8=39961
- Ag halides, of Mn^{2+}, 8=39962
- Ag halide particles in glass, thermal bleaching model 8=41094
- Ag–Al films 8=31000
- Ag-Au alloys, data from kinetics of short range order 8=35059
- Ag–Zn solid solns., atomic mobility, vacancy-controlled, Zener relax. studies 8=31040-1
- Al alloys, of dilute impurities, e microprobe obs. 8=31003
- Al crystals, of Cr rel. to impurity ion effect on structure 8=26642
- Al, self-diffusion, activation vol. and press. depend., 0-10kbar, 400-610°C 8=39967

Diffusion in solids—contd
- Al, self-diffusion and quenching studies, analysis 8=35479
- Al, self-diffusion coeff. from annealing kinetics of voids 8=35478
- Al-4% Cu, interfacial, grain boundary precipitates, growth 8=39715
- Al, of Ag^{110} and Sb^{124}, 450–630°C 8=44381
- Al, of Cu, coefficient determ, step annealing procedure 8=48773
- Al, of V, coeffs. 8=35476
- α-Al_2O_3, diffusion of Pu^{239} and Am^{241}, meas. by α-absorpt. method 8=35480
- α-Al_2O_3, of inert gas, high resolution meas. 8=39965
- Al_2O_3 powders, of positronium, annihilation spectra mean lengths and diffusion constants 8=44378
- Al, of Pd, Ag, Cd, In and Sn, due to near surface effect 8=39964
- Au films on Cr underlayers, at grain boundaries 8=26112
- Au, self-diffusion, activation vol. and press. depend., 0. 10kbar, 700-990°C 8=39967
- Au, self-diffusion and quenching studies, analysis 8=35479
- Au-Al bonds, purple plague formation 8=48771
- Be, self-diffusion coeff., 650–1200°C 8=35481
- BeO of Be rel. to radiation damage 8=26722
- BeO, self-diffusion and creep activation energies correl 8=44553
- BeO, thermal, accuracy of pulsed n meas. 8=25308
- BeO, thermal, pulsed n obs. 8=25307
- Bi_2Te_3, of Ag, thermal, and ht. of transport calc. 8=39968
- CaF_2, inert gas diffusion mechanism 8=26619
- CaF_2, Ar, Kr and Xe diffusion U doped CaF_2, Ar, Kr and Xe diffusion 8=26618
- CaF_2:Sm^{2+}, of O 8=44382
- CaF_2:UO_2, UC and U-doped, of inert gases, simultaneous 8=34107
- CaO crysts, neutron irrad., Ar^{37} diff. 8=39969
- CdS, self-, on α- and γ-ray bombardment, radiation-stimulatd coeff. determ. 8=35482
- CdS, of Li 8=44383
- Cs halides, neutron irrad., Xe diffusion 8=39970
- Co, f.c.c., surface coefficient 8=44026
- CoO, volume diffusion of O, meas. by proton activation of O^{18} 8=35483
- Cr coating of hyper-eutectoid carbon steels 8=39973
- Cr_2O_3, of S at 1000°C 8=44384
- Cu alloys, of dilute impurities, e microprobe obs. 8=31003
- Cu crystals and whiskers, of Zn, mechanism 8=35487
- Cu, heated in Zn vapour, activation energies for Zn diff. calc. from weight increase 8=35485
- Cu, self-diffusion, activation vol. and press. depend., 0-10kbar, 700-990°C 8=39967
- Cu-Au films, vol. and surface 8=35486
- Cu_3Au, of Au rel. to vacancies rôle in order-disorder alloys 8=39971
- Cu, of Kr, Xe, elucidation 8=48483
- Cu-Mn interdiffusion kinetics, e microprobe obs., 640-820°C 8=31002
- Cu–Ni, omnidirectional pressure effects 8=35488
- Cu–Ni system, of Cu on Ni side 8=31013
- Cu–Ni–Mn system rel. to thermodynamic activities, obs. 8=31004
- in Cu_2O films struct. defects rel. to Cu(111) oxidation, obs. 8=44042
- α-CuSi, interdiffusion coeffs. by moving interphase boundary method 8=44385
- Cu_3Si phase, activation energy 8=44386
- Cu-Sn system, γ and δ phases, self-diffusion coeffs. and energies 8=35484
- Cu-Zn-Sn solid solutions, ternary 8=39972
- Fe, α and δ, self- and of Co 8=44388
- Fe, annealing time effects on rates 8=35474
- Fe, b.c.c., of O, by interstitial migration 8=48361
- Fe, b.c.c., P stabilized, diffusivity of O 8=44387
- Fe membranes of electrolytic H 8=44389
- Fe, of C, at 350°C, preliminary cold plastic deform. effects 8=35490
- Fe–Cr, of C, at 350°C, preliminary cold plastic deform. effects 8=35490
- Fe-Ni alloys, of Au, lattice parameter change 8=39789
- Fe–Si, of C, at 350°C, preliminary cold plastic deform. effects 8=35490
- Fe_2SiO_4, thermal, at high press. and temp. 8=48762
- n-GaAs, of Cu, rel. to transducer prep. 8=35491
- GaAs, of Mn and Cu, complex formation influence 8=35492
- GaAs, of S through SiO_2 films 8=35493
- GaAs, of Zn 8=39974
- GaAs, of Zn 8=48774
- n-GaAs, of Zn, at 900°C, rel. to high donor conc. 8=31006
- GaAs, of Zn, reproducible, role of phase diagram, diffusion and solubility anals. 8=44390
- GaAs:Zn, of Cu, defect formation from photoluminescence data 8=48819
- nGaSb(Te), of Cd, rel. to p–n junction formation 8=31005
- Ge, of As, rel. to dislocation formation 8=35568
- Ge, of oxygen, distrib. coeff. determ. 8=48779

Diffusion in solids—contd
Ge oxide film on Ge, vel. of H_2O diffusion 8=48778
Ge substrate, of As from epitaxially grown GaAs 8=35494
He, under a.c. conditions 8=38992
Hf, of C, coeff. temp. dependence, 1120–2130°C 8=35495
Hg, preionized flow, intensity relax. of certain lines in flow direction 8=47753
In-Ag alloys, effect of In diffusion on oxidation 8=49874
InAs, of Cu, effect on elec. props. 8=40473
n-InAs, of P, coeff. temp. dependence, 650-900°C 8=35496
K halides, Ar gas, and release, after neutron irrad. 8=35498
KBr, of Br, meas. by isotopic exchange, rel. to dislocations and grain boundaries 8=35497
KCl, diffusion of Bi ions 8=48781
KCl, of Pb and Ca, rel. to impurity ion effect on structure 8=26642
KCl, reciprocal and self-diffusion along dislocations 8=26620
KCl-RbCl mixed cryst., diff. coeffs. 8=39975
KI, reciprocal and self-diffusion along dislocations 8=26620
$K_xNa_{1-x}Fe_7O_{11}$, ion mobility 8=48782
Li borates, glass and cryst., Li^7 n.m.r. 8=31007
Li, electrotransport of lattice defects. 8=35501
Li, isotope inter-diffusion 8=39976
Li, of Ag^{110m}, 67°-160°C 8=31008
Li of Na, obs. btw. 50–176°C 8=31009
LiF, of anion and cation vacancies, rel. to ionic cond. 8=35963
LiF, of Li$^{6\cdot7}$ positive ions from relative difference between ion mobilities meas. 8=35500
LiF, of Ni, rel. to impurity ion effect on structure 8=26642
$LiSO_4$, of Na$^+$, Ag$^+$, K$^+$. Rb$^+$ and Tb$^+$, 590-820°C 8=39977
MgO, of Cr^{3+}, luminesc. determ. 8=31010
MgO powder, of positronium, annihilation spectra mean lengths and diffusion constants 8=44378
Mg_2SiO_4, thermal, at high press. and temp. 8=48762
Mo, of C, mobility determ. from low temp. internal friction peaks 8=35513
Mo, of N 8=39987
Mo, of S, 2220–2470°K 8=35502
Mo, of Si, phase identification 8=48784
Mo, surface, activation energy elec. field dependence (10^7-10^{8}V/cm), 1300-1800°K 8=35512
NaCl, of Pb and Ca, rel. to impurity ion effect on structure 8=26642
NaCl, of Pb^{2+} 8=31011
NaCl, reciprocal and self-diffusion along dislocations and break surfaces 8=26620
NaCl, thermal, at high press. and temp. 8=48762
$NaNO_3$, thermal diffusivity in phase transition 8=48391
Na_2O. 2SiO_2, diffusion processes and interfacial reaction of Fe, kinetics 8=26621
Nb, of V, coeffs. 8=35475
Nb, surface self-, in strong elec. field, field-emission exam. 8=39978
$NbC_{0\cdot64}$, of C, temp. dependence 8=31018
Nb_2O_5 crystals and scales on Nb, of oxygen, rel. to Nb oxidation behaviour 8=48785
Nb–1%Zr, mass transfer in Li, temp. effect determ. in thermal convection loop tests 8=35503
Ni, annealing time effects on rates 8=35474
Ni-base alloys, annealing time effects on rates 8=35474
Ni foil, H diffusion kinetics 8=31014
Ni, of Au, lattice and grain-boundary diffusion, 700–1075°C 8=44391
Ni, Of H_2, isotope effects 8=31012
Ni, of surface self-diffusion and surface energy 8=44028
Ni, of V, coeffs. 8=35476
Ni, pure, ion electron transport temp. dependence, 1000–1400°C 8=39980
Ni, pure, self-diffusion 8=39979
Ni, self-, 980 to 1400°C 8=48786
Ni–Au films, vol. and surface 8=35486
Ni–Au system interdiffusion rel. to comp. 850–925°C 8=31015
PbS + CdO → PbO + CdS, solid state, diff. mech. 8=49840
PbSe, interdiffusion coeffs. rel. to temp. 8=44141
PbSe, of Ni, anomalous 8=39981
$Pb_{1-y}Sn_ySe$, interdiffusion coeffs. rel. to temp. 8=44141
$Pb_{1\ x}Sn_xTe$, interdiffusion coeffs. rel. to temp. 8=44141
δ–Pu–Ga alloys, interdiffusion coeff. obs. 350°–517°C 8=35504
Rb, neutron irrad., of rare gas 8=40079
$RbAg_4I_5$, of Ag rel. to high-conductivity in solid electrolyte 8=48787
Re, interdiffusion with Ta substrate, rel. to emitter performance 8=28502
Sb, grain boundary self-diffusion meas. 8=48788
Sb_2S_3 films, of Al 8=35505
Si epitaxial layers, of P, effects on defect structure 4=48833
Si: Li diode, Li mobility, effects of neutron and electron induced defects 8=39982
Si, localized, rel. to imperfection near oxide film edge, X-ray micrographic obs. 8=35552

Diffusion in solids—contd
Si, of B, controlled by Si-B phase surface layer 8=49264
Si, of B and P, secondary dislocations formation 8=35572
Si, of In and Tl implanted ions, from subst. to interstitial sites 8=40007
Si, of P from oxide film, rel. to model 8=44375
Si, of P, vacuum method using $POCl_3$ as source 8=48792
Si of Sn, effects of P and B codoping 8=48791
Si, of T 8=48346
Si, vacancies at induced dislocations, and dislocation-enhanced in (001) crystals 8=26622
Si_3N_4 films, of Al substrate, coeff. and activation energy temp. dependence 8=31001
Si_3N_4 films, of Na 8=48605
Si–Ni, omnidirectional pressure effects 8=35488
Si: P junctions, intense interjunction strain 8=49046
Si: P planar diffused structure, propag. through strain effects 8=48844
Si, with SiO_x coating, B redistribution 8=48793
n-SiC, of Be, 1700–2250°C, mechanisms and anisotropy 8=35506
SiO_2 films, ion migration, and ordered structure 8=44054
SiO_2-glass, of Na^{22}, α-β quartz transformation effects 8=48794
SiO_2 glass, synthetic, mobility of Na ions 8=48795
SiO_2, of Au 8=39984
SiO_2 powders, of positronium, annihilation spectra mean lengths and diffusion constants 8=44378
TaC, of C, rel. to comp., 2100–2650°C 8=44392
$TaC_{0\cdot66}$, of C, temp. dependence 8=31018
Ta_2C, of C, 2100–2650°C 8=44392
ThO_2, lattice and grain-boundary diffusion of Pa 8=35508
ThO_2, Th^{230} cations self-diffusion, α-spectrometry obs. 8=35510
ThO_2, U lattice and grain-boundary diffusion, obs. 8=35507
ThO_2–UO_2 solid soln., lattice and grain-boundary diffusion of Pa 8=35508
ThO_2–UO_2 solid soln., U lattice and grain-boundary diffusion, obs. 8=35507
Ti, b.c.c. and h.c.p., diffusion of H, 610° to 900°C 8=44393
Ti in weld joints under transient pressure 8=44373
Ti–Ag system, conc.-penetration curves, and phase growth 8=35509
TiC, of C^{14}, coeff. comp-dependence, 1450-2280. C 8=39985
TiO_2-based dielec., Ag diffusion coeffs. 8=31016
Ti-V alloys, self-diffusion comp. -temp. dependence 8=26623
U doped CaF_2, inert gas diffusion mechanism 8=26619
U migration, decay products in minerals 8=48796
UC mobility and trapping of Kr and Xe 8=25318
UO_2, migration of Kr bubbles, before and after annealing 8=26625
UO_2, mobility and trapping of Kr and Xe 8=25318
UO_2, sintered, diffusion and release of Xe, from 400°- 800°C 8=26624
UO_2, surface diffusivity of U ions, 1544°-1915°C obs. 8=35511
UO_2, of O, rel. to oxide films growth on UC, 60-160°C 8=39604
UO_{2+x}, U^{233} cations self-diffusion, α-spectrometry obs. 8=35510
UO_2-CeO_2, thermal 8=48776
V, of V, coeffs. 8=35475
W, of C, mobility determ. from low temp. internal friction peaks 8=35513
W, of N 8=39987
W, of Nb, electrochem. sectioning tech. to determ conc. profiles 8=48797
W, surface, activation energy elec. field dependence (10^7-10^{8}V/cm), 1200-2100°K 8=35512
ZnS crystal, of impurity ions, mechanisms 8=26626
Zr hydride, of H, thermal diffusion eqn. 8=26627
Zr, of O, rel. to oxidation, inhibition by Cr coating, ≤650°C 8=32107
Zr, of oxygen, using O^{16}(d, p)O^{17} reaction 8=31017
Zr, of V, coeffs. 8=35475
$ZrC_{0\cdot56}$, of C, temp. dependence 8=31018
Zr–Cu alloy, of oxygen, using O^{16}(d, p)O^{17} reaction 8=31017
ZrN, of N_2, film-thickness determ. 8=44396
Zr–O solid solns. microprobe and e microscope obs. 8=30658
ZrO_2, self-diffusion coeffs. of O 8=35514

Diffusion columns. See Diffusion in gases/thermal; Isotope separation.
Diffusion pumps. See Vacuum pumps.
Digital computers. See Calculating apparatus/digital computers.
Dilatometers. See Length measurement; Volume measurement.
Dimensions
See also Units.
method, misuse for erroneous relations between units 8=37106
Dimers. See Molecules; Polymers.
Dineutrons. See Neutrons.
Diodes. See Electron tubes; Plasma devices; Rectifiers; Semiconducting devices/diodes and /tunnel diodes.
Dipole moments. See Molecules/moments; Nucleus/electric moment; Nucleus/magnetic moment.

Diquarks. See Elementary particles.
Dirac electron theory. See Electron theory.
Dirac equation. See Quantum theory/wave equations.
Discharge tubes. See Electron tubes; Gas-discharge tubes; Ion sources; Particle accelerators; X-ray tubes.
Discharges, electric
See also Arcs, electric; Breakdown, electric; Corona, electric discharge; Plasma; Sparks, electric.
acetylene-air flame, intensified by discharge, activation energy of origin of excited radicals OH, CH and C_2 8=45359
acoustic vibration spectra. 8=38981
acrylonitrile monomer vapour, formation of polyacrylonitrile films 8=39605
afterglow plasma, anomalous diffusion obs. 8=38984
air afterglow, mechanism 8=32274
air, high press. vortex 8=29894
air, ionic flowmeter appl. 8=34610
air, spark discharge at atmos. press., superradiant laser action obs. 8=24301
along insulator in vacuum, surface effects on field strengthening at the cathode 8=40562
anodic phenomena rel. to d. c. in vacuum 8=29881
arc at atmos. pressure in magnetic field 8=38983
beam-plasma in mag. mirror trap, instability 8=43564
between cold electrodes in supersonic layer of plasma with additives, physical picture 8=43442
capillary, breakdown of cover glasses used in work 8=48983
cold-cathode discharge in magnetron geometry, efficient sputtering 8=25694
continuous reflex, producing quasi rectangular section plasma for interferometric meas. in 8mm band 8=29879
constantin wires, exploding, restrike mechanisms 8=40288
convertor, thermionic, in discharge mode, kinetic eqn. 8=33036
current, modulating He-Ne laser 8=37589
d.c., conductivity in Faraday space 8=47740
electrode pulse heating, elec. contact method 8=29877
electrodeless, high press., mag. field effect on configurations 8=43444
in electron-irradiated sheets of plexiglass and epoxy-resin moulding material 8=29876
flash X-ray discharge continuum with various anode materials 8=25689
flash X-ray, time-resolved spectroscopy 8=34409
gap short-circuit by plasma jet 8=39148
gas, dielectric-bounded, pulsed current calc. 8=34407
gas, electron densities, meas. 8=47743
gas pressure meas., spectral methods 8=38980
gas pumping obs. in Ar. 8=38987
gas, subnanosec. spark generation 8=47771
high-current, plasma properties 8=43440
hollow cathode, emission spectral intensity change rel. to H_2 released from cathode 8=29892
hollow-cathode, gas temp. determ. 8=34402
IG-3 generator, acoustic oscillation spectrum 8=29875
ignition s.c.r. trigger circuit 8=49277
insulated wall pot. stabilization modes 8=34401
insulators, partial discharge testing 8=24060
interelectrode gap microdischarge theory 8=34398
ionic laser, drift velocity rel. to ionization 8=37551
ionizing radiation prod. parameters 8=29930
light source, continuum, in XUV region 8=37671
light sources, review 8=28769
lightning, cloud and ground, comparison of processes 8=27919
liquid-solid dielectrics, discharge onset, effect of dielec. thickness 8=44859
low-pressure, in transverse mag. field, effect of anode orientation 8=34403
low-pressure, in transverse mag. field, instability 8=34404
manometer, "immersion" type with simplified construction 8=47996
m.h.d. instability in longit. mag. field, h.f. stabilization 8=39139
microwave, at. and mol. beam source 8=43241
microwave gas, at 55 GHz, harmonic generation, exptl. studies 8=43438
microwave noise emission from plasma 8=25756
multipactor, e packet motion rel. to photon bursts 8=43439
oscillating electron, charged particles radical distrib. approx. calc. 8=34408
partial, by insulating surfaces 8=24061
partial, formation on points in low-viscosity insulating oil 8=30504
partial, power dissipation calorimetry 8=24059
Penning, anode and cathode power dissipation 8=43445
Penning, primary electron energy spectrum and pot. drop in penetrating plasma 8=34400
Philips ionization gauge, mech. 8=38979
plasma, acoustic pulse reaction 8=34486
plasma conc. profiles, radial density var. obs. 8=43441
plasma, diagnostics 8=30092
plasma non-cylindrical Z pinch, development 8=43553
plasma, pulsed, simulator 8=34399
plasma temp. calc. from quadratic strength distribution of spectral lines 8=47810
plasmas, high-pressure, excited in diatomic gases, energy exchange 8=47742

Discharges, electric—contd
plasmatron, vortex configuration for high current operation 8=30176
positive column, Maxwellian vel. distrib. of electrons 8=34416
positive column plasma with current change, non-stationary processes 8=25695
positive column, radical density distribution in hysterisis region 8=43446
positive column, weakly ionized gas, const. coeff. electron diffusion eqn. criteria validity 8=43447
pre-breakdown (vacuum) current between Cu electrodes in presence of microdischarges 8=43459
pulse, behaviour on cathode surface 8=34435
pulse source of large electron currents of short duration 8=34406
pulsed spark, in air, fast electrons and X-radiation during intial growth 8=39002
radiation, microwave, from positive column 8=28600
reduced pressure, Fe line intensity var. 8=34433
reflex, anisotropy of e velocity distrib. obs. by c.w. laser scatt. 8=30012
ring-electrode systems, transition from low to high em radiation output 8=47741
self-sustained, in supersonic gas flow in transverse mag. field 8=25740
shielded cathode, current density, radial distrib. 8=25691
simultaneous multipolar arc 8=29937
sliding, in water on dielectric surface 8=34397
sliding, on solid dielectric surface in vacuum 8=27224
spark chamber switch controlled by small-amplitude pulse 8=46967
spark light source with plane boundaries 8=28767
spectral and elec. props. excitation freq. depend., obs. 8=29880
spectra of elements, maximum sensitivity 8=29578
striation phenomena in prebreakdown 8=38997
suppressed or arrested discharge in gases, rel. to nanosec impulse technology 8=25693
surface wave, in Hg vapour tube, prod., classical and numerical solns. 8=47750
thermionic diodes, Xe-filled, irradiated in nuclear reactor core, breakdown and maintaining voltages 8=46417
θ-pinch, Scylla IV, mag. field and density integral product from Faraday rot. 8=34530
toroidal, conductivity from Thomson scatt. obs. 8=29878
toroidal, plasma instability causes 8=30169
trap parameters in semiconducting film, determ. by thermally stimulated capacitor discharge 8=27052
on triglycine sulphate crystal surfaces 8=40623
tube heavy current with high temp. capillary 8=38982
vacuum breakdown damage of electrodes, obs. 8=29874
in vacuum gap with commutating impulse current up to 150 kA at 1 MHz, controlled 8=34405
Voigt contours of spectral lines, atom temp. and e concs. obs. 8=29936
voltage drop in spark during pulse discharge in nsec. time range 8=29920
work of electrode in plasma air stream containing K 8=29946
Z-pinch discharge shock wave, dynamics 8=34410
Ar afterglow, ion conversion 8=43452
Ar, high press. vortex 8=29894
Ar, impulse e. densities in disintegrating plasma 8=43458
Ar linear pinch as lens for 3.5 MV electrons in 30 nsec pulses 8=28563
Ar, low press., induction interaction of currents, obs. 8=43451
Ar, plasma-beam, stimulated emission, 4545–5145Å 8=28673
Ar plasma, interferometric meas. in 8mm band 8=38989
Ar, selective enhancement of HD and D_2 spectra 8=25471
Ar-Cs, plasma ionization instability in crossed elec. and mag. fields, obs. 8=34556
Ca atoms in arc discharge, spectral line broadening 8=34437
Cd-Ar(Ne) low pressure, 2288Å and 3261Å radiation intensities 8=38990
CH_4 or CD_4 added to H_2 or D_2, θ pinch at 0.8 m torr filling press. 8=34417
CO, excitation of C h. p. bands, isotope shift obs. 8=34161
Cs, plasma, level populations, recomb. and radiative energy loss 8=34494
Cs vapour, electron-atom collision momentum transfer cross sections from drift velocity meas. 8=29911
Cu atoms in arc discharge, spectral line broadening 8=34437
Cu wires, exploding, restrike mechanisms 8=40288
D plasma, temp. meas., inverted spectral lines 8=29895
He flowing afterglow, atom-e spin exchange 8=43221
He^3, impulse, e. densities in disintegrating plasma 8=43458
He positive column, press. 0.05-0.4 Torr, probe expt. 8=43551
He reflex, electron-density and -temp. meas. by cw Ar^+ laser light scattering 8=38991
He-Ne, low-voltage arc, rel. to cw laser oscillations 8=24315
Hg, low press., induction interaction of currents, obs. 8=43451

Discharges, electric—contd
- Hg vapour, electron energy distribs. and Langmuir paradox 8=34419
- Hg-vapour green-band emission 8=29944
- Hg vapour, oxide cathode, rel. to electrode damage 8=36042
- N_2 evidence for $^3\Delta_u \rightarrow B^3\Pi_g$ transition 8=47608
- N_2, waves of ionization 8=47745
- NH_3-methane mixture, laser emission 8=33190
- N-He mixture, metastable N e.s.r. spectrum 8=25386
- Ne, plasma, interferometric meas. in 8mm band 8=38989
- Ne-Kr mixture, Kr 4p^{5}5s excited levels 8=29882
- N_2 + He$^+$, and O$^+$, reactions in afterglow 8=41253
- O, self-sustaining dipole 8=38995
- O_3 formation, var. across gap 8=25700
- SF_6, electron detachment in swarm conds 8=29978
- Si, avalanche, noise 8=35933
- W wires, exploding in vacuum, undegassed and degassed, discharge currents 8=40294
- Xe lasers, time varying, perturbations of microwave cavity fields 8=24294
- Xe, pulse, spectrum in presence of 2n, 240-300 nm 8=34292
- Zn atoms in arc discharge, spectral line broadening 8=34437
- **glows**
  - afterglow e density decay meas., X-band interferometer using 90°unbalancing 8=25763
  - afterglow plasma, very low e. density meas., microwave diagnostics 8=47848
  - air, hollow cathode in longit. mag. field, cathode surface current distribution 8=29896
  - air, standing striations in pos. column, effect of l.f. acoustic waves 8=47747
  - in atmosphere, vortex-stabilized, threshold conditions 8=32248
  - contracted pinch rotational sensitivity, obs. 8=29891
  - electron beam, high power, prod. from 8=24137
  - formation mechanisms in early afterglow of pulsed discharge 8=47751
  - gas positive column, thermal regime 8=34412
  - hollow cathode, new operation mode 8=29884
  - hollow cathodes, plasma, rot. obs. 8=29885
  - hydrogen, hollow cathode in longit. mag. field, cathode surface current distribution 8=29896
  - Joshi effect under pulsed illumination 8=38985
  - light variations, generation mechanism 8=47749
  - moving striations in plasma, origin 8=47748
  - negative, and Faraday dark space, electron spatial conc. patterns 8=25696
  - negative in cathode region, influence on elementary processes 8=38988
  - positive column, Galerkin's method appl. 8=34413
  - positive column, gas transport due to collisions 8=38986
  - positive column, noise temp. interpretation 8=29886
  - positive column, perturbation density at helical instability onset 8=29888
  - positive column, plasma diamagnetism 8=34411
  - pulsed high current, radiation from plasma 8=29883
  - pulse, light polarization meas. apparatus 8=24425
  - silane + N_2 reaction for prep. of Si_3N_4 film 8=35183
  - sustained by inert gas, appl. in N^{15} spectrochemical estimation 8=27791
  - Al oxide films, sputtering in O or Ar discharges 8=39587
  - Ar linear pinch, acceleration by propag. current 8=34415
  - Ar positive column, e density and collision freq. meas. 8=30052
  - Cd-Xe atom collision cross section calc. 8=34180
  - CO, Asundi bands, quenching 8=38994
  - H_2 large power reflex discharge in magnetic field 8=43450
  - He, afterglow, metastable mol. and at. decay obs. 8=25697
  - He afterglow, obs. of ion diffusion and recombination 8=43448
  - He free-electron gas, negative point-to-plane breakdown 8=39001
  - He, hollow cathode, singlet and triplet excitation mechanism 8=25353
  - He, near-cathode region, space and time dependence on press. 8=47752
  - He, 1.35-2.6 torr, 0.5-2.5 mA, dynamic behaviour at 10 Hz to 50 kHz 8=34420
  - He, negative glow plasma characts., effect of u.h.f. field 8=43453
  - He-Ne afterglow, due to different vels. of 2s and 2p Ne 8=30080
  - Hg, r.f. discharge afterglow spectrum 8=29616
  - Hg-vapour positive column, electron-density profile microwave meas. 8=39113
  - Hg, He and Ne positive column, excitation of helical wave 8=34414
  - Hg-Kr mixture, e energy distrib. rel. to striations 8=34418
  - InI_3, h.p. ionization and dissoc. theory 8=43455
  - InI_3 lamp, temp. distrib. determ. 8=43454
  - Kr, visible afterglow emission 8=47754
  - NO afterglow, chemiluminesc. rate consts. 8=38993
  - NO afterglow, photoionized, e recomb., attachment and ambipolar diffusion obs. 8=47755
  - N_2 afterglow, kinetic and spectroscopic constraints 8=29897

Discharges, electric—contd
- **glows**—contd
  - N_2, first positive system excitation, quenching 8=38994
  - N_2, standing striations in pos. column, effect of l.f. acoustic waves 8=47747
  - N_2, temp. depend. of afterglow in glow discharge shock tube 8=27712
  - N_2, yellow afterglow intensity 8=47756
  - Na vapour lamp, thermal insulation and pressure effects 8=42208
  - Ne, d.c., connection between moving and standing striations 8=47758
  - Ne, ionization waves, effects of cooling 8=47757
  - Ne, normal cathode fall 8=34422
  - Ne, 1.35-2.6 torr, 0.5-2.5 mA, dynamic behaviour at 10 Hz to 50 kHz 8=34420
  - Ne, positive column, Bremsstrahlung emission 8=29898
  - Ne steady state positive column plasma, 2-32 mm Hg 8=29899
  - Ne-He mixture positive column, region of Pupp current limit 8=34421
  - O green line λ 5577, new emission mechanism 8=29625
  - O, prod. of SiO_2 layers in cathode fall area 8=35182
- **high-frequency**
  - air r.f. nonequilibrium. obs. 8=29893
  - argon r.f. nonequilibrium, obs. 8=29893
  - at atm. pressure, characts. and spectrochem. appl. 8=29889
  - axial 8=25688
  - capacitive, conditions for fast electrons at low pressures 8=29907
  - electrodeless lamps for at. fluoresc. spectrometry 8=41301
  - electrodeless, laser pumping appl. 8=33178
  - electrodeless, microwave excitation 8=29873
  - plasma flame prod. when applied to gas jet 8=38977
  - plasma prod. in upper atm., feasibility 8=38978
  - self oscillatory, resonance freq. shift 8=25690
  - sputtering, ion energy distrib. calc. 8=25687
  - Tonks-Dattner resonances damping rel. to microwave field 8=43443
  - unipolar, energetic conditions in plasma 8=47812
  - Ar, energy distrib. of electrons and positive ions in plasma 8=25692
  - Ar induction, stationary, temp. determ. from spectral characts. 8=29900
  - Ar, Tonks-Dattner resonances damping rel. to microwave field 8=43443
  - CaBr molecule u.v. emission spectrum 8=43295
  - H, atom reactions with liquids 8=32101
  - He, energy distrib. of electrons and positive ions in plasma 8=25692
  - He-Ne laser, comparison with arc 8=43456
  - Ne, electron energy distribution 8=43457
  - Ne, energy distrib. of electrons and positive ions in plasma 8=25692
  - Xe induction, stationary, temp. determ. from spectral characts. 8=29900

Disintegration. See Beta-decay theory; Nuclear decay theory; Radioactivity.

Disintegration energies. See Radioactivity.

Dislocations. See Crystal imperfections/dislocations.

Disperse systems
- See also Aerosols; Colloids; Emulsions; Foams; Powders; Sols; Suspensions.
- alcohol, u.s. dispersion of insoluble particles, obs. 8=39442
- atomization of liq. by rotating disc, and 'secondary' break up of droplets 8=30389
- cement-water mixture, rheological behaviour as function of conc. 8=30545
- charged droplets stream, electrostatic lateral instability 8=34944
- conductivity, permittivity and permeability, theory 8=26939
- corundum particle layer, fluidized by gas flow or vib., heat transfer coeffs. 8=39448
- double hydrosilicates of Ca and Na, dispersion structures in aqueous suspensions 8=34937
- electric breakdown, liquid-solid system 8=34891
- filling particles, form factors meas. 8=39533
- fission products deposition in gas conduit from laminar stream, models 8=34060
- fluid containing small particles, viscosity 8=39443
- fluidized beds, radiative heat transfer meas. with immersed body 8=39456
- gas/dust mixtures, channel flow characts. rel. to dimensionless gas rate 8=39179
- gas fluidized beds, density and pressure fluctuations 8=48230
- gas-liq. droplets in condensing medium, sound alternation with mass transfer 8=43688
- granular mats, flow patterns in axisymmetric rotor 8=43884
- graphitic mats. hot worked with dispersed liq. carbide, thermal and elec. conductivities 8=44361
- gravity flow of particles, mechanism 8=48234
- gylceride-water mixture, mesomorphic phase and micelle structure 8=25966
- heat transfer, modified Woodside model 8=44359
- hydrophilic clays, porosity coeff. rel. to sorption and water permeability 8=30661

Disperse systems—contd
  light scattering, verification of single scattering theory app. to narrow beams 8=28874
  particle analysis, e microscope-microprobe for particles, 0.1-10μ 8=34935
  particle-diameter distrib. determ. by small-angle X-ray scattering 8=30553
  particle identification by e microprobe 8=30557
  particle size and residence time distribs, rel. to coupled heat and mass transfer 8=34936
  particle-size meas. by Doppler-shifted laser light, rel. to Stokes-Einstein relation 8=30552
  polydisperse colloidal spheres, number determ. by light scattering 8=34940
  powders, u.s. micromesh sifting 8=35066
  rocket exhaust, drag coeff. small spherical particles 8=30569
  sand-water mixture, rheological behaviour as function of conc. 8=30545
  silica spheres, monodisperse suspensions, controlled growth 8=48235
  solid, heat transfer 8=41860
  solid-plastic, fluidity 8=34938
  soot clouds, plane-parallel, scatt., absorpt. and reflectance 8=39447
  sound attenuation 8=25961-2
  spheres falling in viscous fluid, spatial distrib. 8=30546
  statistical mixtures, thermal conductivity 8=37309
  structure strength rel. to interaction forces between its elements 8=48226
  submicroscopic particle, light scattering obs. 8=39446
  surface area meas., neg. adsorpt. and other methods 8=48228
  suspended particle motion eqns. in rectilinear channel, effects of collisions 8=30544
  turbulent flow, mathematical model for deposition from 8=34586
  two-phase, saturated with different liq. fillers, thermal props. and heat and mass transfer 8=30555
  water-cyclohexane-polyoxyethylene (9.7) nonylphenylether, temp. effect 8=48249
  water, u.s. dispersion of insoluble particles, obs. 8=39442
  Al melts, u.s. dispersion of Al_2O_3, Fe and Ti, 740-800°C 8=39442
  Al slurries in H_2SO_4, heat transfer by forced convection, rel. to Bingham plastics 8=39266
  Al_2O_3 clouds, plane-parallel, scatt., absorpt. and reflectance 8=39447
  Al_2O_3 molten particle cloud, spectral emissivity 8=34939
  BeO molten particle cloud, spectral emissivity 8=34939
  in Co, effect on mag. props. 8=31620
  in Fe, effect on mag. props. 8=31620
  Fe particles in N, Ar or H gas, absorpt. spectra including carrier gas contrib. 8=25968
  Gd_2O_3 in UO_2, behaviour at high temp. 8=35074
  in Ni, effect on mag. props. 8=31620
  SiO_2 clouds, plane-parallel, scatt., absorpt. and reflectance 8=39447

Dispersion, acoustic
  in aerosols, rel. to particulate relax. processes, theory and expt. 8=43889
  in liquids, rel. meas. with u.s. stroboscope 8=28373
  measurements by u.s. stroboscopes 8=46197
  monatomic gas, using relaxation theory 8=30297
  superconducting semiconductors, theory 8=35403
 ultrasonic
  cholesteryl 2-(2 ethoxy ethoxy) ethyl carbonate liquid crystal, from Brillouin scatt., 20-60°C 8=48146
  liquid crystal, from Brillouin scatt., 20-60°C 8=48146

Dispersion, optical
   See also Optical constants; Refractive index/light.
  anomalous, absorpt. line theory in mag. field 8=29570
  anthracene, rel. to exciton-phonon interact. and band struct 8=41161
  anthracene, 5-100μ thickness meas. from refr. index dispersion 8=32043
  crystal, with anomalous dispersion, for backward wave light generator 8=24357
  extinction coeff. meas., accuracy rel. to geometry of expt. 8=24419
  glasses, rel. to composition 8=31996
  in laser emission, rel. to random heterogeneities in refractive index 8=37566
  para-terphenyl, 5-100μ thickness meas. from refr. index dispersion 8=32043
  plasma, Vlasov relativistic 8=30066
  plastic scintillator NE 102A, 5-100μ thickness meas. from refr. index dispersion 8=32043
  proteins, rotary, struct. determ. 8=29862
  quartz, in vac. u.v., from interference in thin parallel plate 8=32034
  rotatory adapter using film polariser and spectrophotometer 8=24370
  rotatory, rel. to circular dichroism, expt. verification 8=41044
  secondary spectrum of two-element lenses in i.r. 8=45144
  self-modulation of nonlinear plane waves 8=28720
  tetracene, 5-100μ thickness meas. from refr. index dispersion 8=32043

Dispersion, optical — contd
  trans-stilbene, 5-100μ thickness meas. from refr. index dispersion 8=32043
  turbid medium illuminated by narrow beam, field 8=24421
  X-rays, 1Å, gratings 8=28929
  CdS, anticrossing of curves due to spatial dispersion 8=36346
  CdS_xSe_{1-x} monocrystal, component conc. calc. by dispersion 8=30803
  CdSe, anticrossing of curves due to spatial dispersion 8=36346
  GaSb near energy gap, from diode laser modes temp. depend., 80°K 8=41088
  n-Ge, and absorption in Q-band 8=27572
  MgO, i.r. and spectral reflectivity 8=41022
  $PbO-La_2O_3-B_2O_3$ glasses, unusual dispersion characts. 8=45214
  ZnO layer 8=36429

Dispersion relations
   See also Field theory, quantum; S-matrix theory.
  angular momentum, of Jost junction, rel. to interpolation formulae 8=28938
  e anomalous magnetic moment, sixth order contrib. 8=29094
  boundary values of analytic functions 8=32661
  centrifugal-barrier effects in N/D calc. 8=42422
  drifting plasma, wave propag. 8=30149
  e-p scatt., inelastic resonances obs. 8=37938
  for form factors 8=37865
  in forward scattering at high energy 8=33576
  forward scatt., new class of sum rules 8=42417
  helicity amplitude applications 8=37961
  hyperon decay, nonleptonic, appl. 8=33829
  for K_{13} decay parameters calc. 8=38003
  KN sum rules agreement between high energy Regge behaviour and low energy parameters 8=37988
  $K^{\pm}p$ forward scatt., calc. 8=24830
  $K^{\pm}p$, $K^{\pm}n$ scatt., real part obtained 8=24831
  Liu-Okobo for πN scatt. 8=29143
  low-energy limits for pion scatt. 8=42418
  low-energy scatt. and high energy limits 8=37894
  meson-meson, meson-baryon scatt. 8=29116
  modified for KNY coupling consts. 8=24828
  optical, for many-particle systems 8=37680
  For partial-wave amplitudes, applied to π photo-prod 8=33840
  partial-wave, semi-phenomenological calc. 8=29066
  π-π phase shift calc. 8=24800
  plasma, for longit. and transverse wave propag. perp. h.f. elect. field 8=43571
  plasma interaction with electron beam, roots transition to Landau-type solns. 8=43510
  plasma, e-ion, e-hole, in constant elect. and mag. fields 8=43576
  plasma, e.m. circularly polarized waves, with parallel elect. and mag. fields 8=43532
  plasma, Vlasov relativistic 8=30066
  N-N forward, for meson-nucleon coupling consts 8=24746
  πN amplitudes, backward 180° applications 8=42548
  πN scatt., sum rules, Cauchy calc. and expt. 8=24797
  πN, subtraction by means of canonical commutation relations 8=24798
  πN sum rules agreement between high energy Regge behaviour and low energy parameters 8=37988
  πN, t channel contrib. rel. to π-π scatt. at low energy 8=33692
  ρ-π superconvergence, approximate saturation 8=38044
  scattering, dispersion sum rules for non-decreasing amplitudes 8=24671
  scattering, meson-baryon, superconvergent sum rule for factorized amplitudes 8=37960
  solid, elastic, kink-capillary oscills. 8=26748
  subtracted, with current algebra for K_{13} decay form factors 8=42578
  subtraction of amplitude for $\pi \rightarrow l\nu\gamma$ 8=33726
  sum rules, in Fubin's current algebra, M-function transformation according to homogeneous Lorentz group 8=37895
  sum rules, new class from equating dispersion relations 8=33585
  superconvergence, analyticity constraints 8=42406
  superconvergence and Regge poles, odd-signature exchanges 8=42423
  superconvergence as a means of coupling particles 8=33680
  superconvergence conditions for 2 particle scatt., t-s channel relationship 8=33579
  superconvergence for particles of arbitrary spin 8=42420
  superconvergence, Drell-Hearn rel. to N Compton scatt. 8=24694
  superconvergence for $\overline{N}N \rightarrow \pi\rho\,(\omega)$, saturation to obtain sum rules and form factors 8=33740
  superconvergence, perturbative approach and current algebra 8=29017
  superconvergence relation for a linear combination of amplitudes 8=37893
  superconvergence rel. to SU_3 symm. breaking in meson decay 8=24769

Dispersion relations—contd
superconvergence, saturation, giving same result as boot strapping 8=33601
superconvergence, single particle representations, no-go theorem in the covariant approach 8=24597
superconvergence sum rules for Compton scatt. 8=24695
superconvergence theory test of quark model in infinite energy cross-sections 8=33649
superconvergent amplitude, diffractionlike possibility 8=37892
superconvergent for πN scatt. and Regge parameters 8=29138
superconvergent, P + P′ Regge model of πp scatt. 8=37994
superconvergent, saturation with $q\bar{q}$ states 8=24669
superconvergent sum rules for KN, Ξ scatt. 8=29157
superconvergent type, used to determ. Regge pole parameters for πN scatt. 8=42431
3-particle scatt., analytic props. in momentum transfer 8=33582
unsubtracted and consistency of pole dominance approx. with current algebra 8=29021
vector and axial-vector, meson decay calc. 8=42597
weak interactions, expt. test of current-current nature 8=24711
Dispersions. See Disperse systems.
Displacement measurement. See Length measurement; Strain gauges.
Dissociation
See also Heat of dissociation; Ionization; Molecules/dissociation.
alkaline-earth oxides, on heating in high vacuum 8=30605
α-cellulose, decomp. with temp., reaction kinetics 8=32094
ethane, dissociative ionization 8=29976
gas mixtures, mols and atoms, relaxed flow calc. 8=36547
gases, diatomic, thermodynamic props. 8=32088
gases, photodissociation waves, as supersonic perturbs 8=39215
grinding, formation of free radicals 8=25656
ionic system, chem. relax. timing by pressure shock technique 8=45360
liquid cpds., calc. of extent including activity coeffs. in formula 8=30415
semiconducting compounds, $A^{III}B^{V}$, by light pulses from laser 8=40437
transition metal carbides, decomp. rel. to interact. with liq. Pt 8=27715
unimolecular, Kossel model modification 8=25646
$CaCO_3$, decomposition and phase transformations, effect of impurities 8=30682
CO, by e beam, O^- prod. cross-section obs. 8=47703
CO_2, dissociative ionization 8=29976
CrO_2, decomp. to Cr_2O_3 at high temp. and press. in 'belt' app. 8=26281
CuO, near equilibrium kinetics 8=41246
β-Cu-Sn alloy, quenched, decomposition products and structure 8=39528
D_2^+, collision induced 8=25648
Fe, commercial, nature of decomposition products and precipitation mech. in age hardening 8=40155
H_2^+, collison induced 8=25648
H_2O, dissociative ionization 8=29976
InI_3 discharge at h.p., theory 8=43455
$MgSO_4$, decomposition kinetics rel. to sample mass and processing press. 8=36565
N_2, dissociative ionization 8=29976
NH_3, to H_2 and N_2, on sorption by Ti 8=32103
NO, by e beam, O^- prod. cross-section obs. 8=47703
O_2, dissociative ionization 8=29976
TiO_2-SnO_2 system, spinodal decomposition 8=39703
electrolytic
See also Ions, electrolytic.
diffuse double layer of weak electrolytes with field dissoc. 8=41277
organic ions in aq. soln., C isotope effect 8=29669
$HClO_4$-$DClO_4$-H_2O-D_2O system, p. m. r. 8=34920
Dissolution. See Solubility; Solutions.
Distillation
See also Isotope separation.
binary batch distillation, time-optimal reflux policy 8=32080
ethyl acetate from acetoacetate, liquid/vapour equilib. data 8=25989
liquid-liquid and vapour-liquid equilibria for binary and ternary systems extractive separation study 8=48270
C, isotope fractionation in CO_2-gas-CO_2 in soln., and HCO_3 HCO_3–CO_2 in soln. system 8=47547
UO_2 from uranyl nitrate-TBP soln., application to fuel reprocessing 8=47413
Domains. See Ferroelectric phenomena; Magnetization state; Superconductivity.
Domains, antiphase. See Alloys; Crystal structure/microstructure; Solids/structure.
Doping. See Semiconducting materials; Semiconductors.
Doppler effect
acoustic, scatt. from moving elastic nonlinearity 8=46192
acoustic shift experiments 8=32909
attenuated waves, relativistic Doppler eqns. and drag effect 8=46470
auditory sequence discrimination thresholds 8=46212
Doppler effect—contd
cosmological applic. and expt verification 8=50261
at electron cyclotron freq., exptl. investigations 8=47823
electrooptic crystals, use in optical frequency shifting of mode-locked laser beam 8=46595
ionosphere electron content determ., comparison with Faraday rot. method 8=32295
ionosphere, v.l.f. Doppler expt. for rocket obs. 8=45537
ionospheric at 2.7 and 4.6 MHz rel. to u.l.f. geomag. fluctuations 8=27976
in laser light meas. of particle size rel. to Stokes-Einstein relation 8=30552
laser scatt., meas. of turbulent velocities 8=39272
laser velocimeter application 8=37553
linewidth narrowing in standing light wave, 8=47970
Mössbauer source, data reduction, graph method 8=38350
in neutron resonant capture, reformulation 8=29455
neutron slowing down, alteration of MUFT programme 8=43132
optical, free surface vel. meas. on impacted projectile 8=41622
plasma spectrum 8=30092
ray theory for time-varying anisotropic medium 8=37527
shift in inhomogeneous anisotropic medium 8=42036
spectral line shift, meas. by optical wedge 8=47471
tropospheric scatter propag., wind produced shifts 8=27921
u. s. velocity monitor for meas. of vocal fold motion 8=32923
Ga, acoustic cyclotron resonance 8=48720
Dosimetry
See also Radiation monitoring; Radioactivity measurement; X-ray measurement.
accelerator stray neutrons, spectrometers and obs., <0.5 and up to 200 MeV 8=33824
α-acetylaminoacrylic acid-N-vinylpyrrolidone copolymer-gelatin emulsion for fast-n dosimetry 8=33800
activation detectors appl. in p-irradiated phantoms 8=24523
air, blurring caused by 4mm diam ionization chamber 8=28975
alumophosphate glows: Li and B, slow-n personnal thermoluminesc. dosimeters 8=33797
depth, effect of ionization chamber size 8=28976
2,4-disulphonic acid benzaldehyde polyvinyl acetate-gelatin emulsion for fast-n dosimetry 8=33800
dose distrib. in water due to 70 MeV π beam 8=37090
electron beam, by fluorescence of polyethylene 8=24729
energy absorpt.-radiation dose conversion operator 8=24495
ethylene, appl. to accelerator radiation meas. 8=24524
fast n monitoring, with Kodak NTA films 8=33812
fluorites, dosimetric parameters, from Bulgarian ore deposits 8=49799
γ and neutron mixed radiation fields, method of rem meas. 8=46923
γ, calorimeter meas., above 5 rad/sec 8=24688
γ, characts. of ORWO3 and 4 films and FD-1 meter 8=47046
γ-fast n, ionization chambers, hexane and CCl filled 8=33811
γ in n background, stilbene scintillation counter 8=33821
γ-n dose-equiv-definition and rem counter 8=33612
γ metaphosphate glass:Ag n activation dosimeters by Cerenkov radiation meas. 8=33798
γ-ray, in air and in depth, spatial freq. characts of ionization chamber 8=46862
γ-rays, reflected by concrete, lead from Co^{60}, Cs^{137}, Ir^{192} point sources; dose rates 8=47393
heavy ion beams 8=50463
hexane ionization chamber, quality factor 8=37787
high-altitude instrumentation system 8=46841
interactions above 10 GeV, classification 8=42720
ionization chamber, hexane 8=37786
ionization chamber, liquid dielec. filled for mixed fields 8=33371
luminescent dosimeter for hard radiation 8=45930
luminescence in vitreous state, appl. 8=36465
manganese arsenic borate glass dosimeter 8=44500
metaphosphate glass:Ag n activation dosimeters by Cerenkov radiation meas. 8=33798
mixed fields with multisphere n detector and tissue-equiv. ionization chamber 8=33793
mixed radiation, dose-equiv., LET-depend. counters meas. 8=33364
n and γ body doses in criticality accident, meas. 8=33767
n-γ, flux and Kerma distance depend., counter and Na activation obs. 8=33771
n and γ radiation element personnel dosimeters 8=33799
n-γ, simultaneous, organic scintillator, $E_n = 0.4-18$ MeV 8=33823
neutron, body-Na activation emergency dosimetry 8=33765
neutron, by emulsion scanning, edge effects and track length meas. 8=33804
neutron dose-equiv. outside sheilding, intermediate, n contribution 8=33766
neutron dosimeters, Al_2O_3, W 8=47162
neutron, fission dosimeters and personnel appls. 8=38080

Dosimetry—contd
- neutron, Geesthacht reactor, p-recoil, rein and BF_3 counters obs. 8=33807
- neutron, fluence-dose conversion rel. to calibration with (α, n) sources 8=33805
- neutron, human phantom, dose distrib. obs. 8=38074
- neutron, in tissue-equiv. human phantom, dose distrib. calc., 100 eV-10 MeV 8=38075
- neutron, personnel monitoring and high-energy meas., review 8=33810
- neutron, stilbene counter with γ discimination 1–10 MeV 8=33822
- neutron survey monitors calibration, thermal-20 MeV 8=33806
- neutron, S activation and tissue-equiv. ionization chamber comparison, 3 and 15 MeV 8=38079
- neutron, thermal and intermediate, with Cd-covered film and track emulsions 8=33803
- n, use of synthetic polymers in nuclear emulsions 8=47152
- neutrons, critical argon dose rel. to dosimeter obs. 8=33796
- neutrons, fast and intermediate, personnel film dosimeter with reson. filters 8=33801
- neutrons, fast, body dose rel. to counter obs., isotropic flux and beam 8=38072
- neutrons, fast, semicond. counters appls. 8=33787
- neutrons in tissue and equivalents, Kerma calc., 0.1–10 MeV 8=33772
- neutrons, in tissue-equiv. human phantom, $\leq$ 5 MeV 8=38073
- neutrons, in tissue, plastic scintillator dosimeter and obs. 8=33809
- neutrons, personnel monitoring, review 8=33808
- neutrons, slow, scintillation counter with spherical polyethylene moderator and Cd shields, 5 eV–17 MeV 8=33791
- organic materials, Megarad techniques for p synchrotron 8=46925
- particle size distribution of radioactive aerosols in selected areas at AERE 8=50159
- personnel n dosimeter for nuclear accident 8=37091
- personnel, of slow neutrons by solid-state nuclear track detector 8=46920
- Perspex dosimeters, photosensitivity 8=37792
- phosphors, radioluminesc. appl. 8=36462
- phosphate glass:Th or U, fission-fragment track registration 8=24538
- in-pile calorimeter for simultaneous meas. of n-induced and γ-induced energies 8=25319
- polytetra fluoroethylene, by quantitative assay of free radicals prod. by ionizing rad. 8=28985
- proton quality factor in water phantom, depth distrib. 8=33758
- radioactive products in the organs of animals and men after inhalation 8=45927
- p-recoil counter, rein sensitivity energy depend., 0.1–6.3 MeV 8=33807
- ruby fluoresc. dosimeter for pulsed ionizing radiation 8=45258
- solid-state radioactivity detector in mammalian tissue, geometrical efficiency 8=32621
- space, proportional counter appl. 8=46858
- stilbene scintillation counter for n flux, 2.5 MeV 8=33817
- thermal n concentric detector 8=38081
- u.v. radiation by use of pyroelectric properties in ZnS 8=46924
- X-rays, powerful pulses, use of photomultiplier 8=46922
- Ag-Br activation in film emulsion, effects 8=33802
- BF_3 short counter with spherical moderator for neutrons in γ background 8=33792
- BF_3 n monitor portable, for pulsed fields, 1–3000 mrem/hr 8=33815
- CaF_2:Mn, read-out, u.v. induced thermoluminesc. rel. to irrad. dose, obs. 8=45261
- $FeSO_4$ Fricke-Miller dosimeter, $G(Fe^{3+})$ yield, 62 keV X-rays 8=42457
- $HgCl_2$ as low level γ-ray dosimeter 8=45409
- Li^6-glass counters for n flux, $<$ 2 MeV 8=33817
- $Li_2B_4O_7$:Mn thermoluminesc. fast-n personnel dosimeter 8=33796
- LiF dosimeters, TLD-100, energy depend. rel. to total dose, obs. 8=42348
- LiF thermoluminesc. fast-n personnel dosimeter 8=33796
- LiF/CaF_2:Mn thermoluminesc. dosimeters in tandem, for X- or γ-ray fields 8=25169
- LiI:Eu n monitor portable, for pulsed and steady fields, 0.5–1000 mrem/hr 8=33815
- Na^{24} in blood activity and $H(n, \gamma)$ autogamma dose calc. from spectrometer obs. 8=38067
- $N_2^{14}O$ and $N_2^{15}O$ for meas. in mixed γ and thermal neutron fields 8=46921
- $P^{31}(n, p)S^{31}$ fast-n activation dosimeters, by Cerenkov radiation meas. 8=33798
- Rh activation foil n personnel dosimeter 8=33795
- $S^{32}(n, p)P^{32}$ fast-n activation dosimeters, by Cerenkov radiation meas. 8=33798
- Si diode dosimeter for fast-neutrons, $<$ 1-15,000 rads. 8=33788
- Si diode dosimeters for p beams 8=38064

Dosimetry—contd
- Si fast-n p–n junction counters 8=33790
- Si n counter, surface-barrier, 2-5 MeV 8=33787
- U-mica foil n fission-fragment dosimeter 8=33794
- U^{235}-depleted U^{238}–Np^{237} fission foil n personnel dosimeter 8=33795

Double refraction

See also Electromagnetic wave propagation; Optical constants; Optical rotation; Polarized light.
- acoustic, in solids, meas. of anisotropy 8=30938
- ammonium oxalate, non-linear props. and double refraction 8=36443
- amphiphiles, lamellar liq. crystalline solns. obs. 8=25919
- in anisotropic crystals, thermally-induced birefringes changes as basis for temp. meas. 8=35420
- birefringence, acoustical, of u.s. waves in deformed isotropic elastic materials 8=46187
- birefringence, gyrotropic, phenomenological theory 8=36303
- birefringence, gyrotropic, theory and appl. to Cr_2O_3 and $MnTiO_3$ 8=45155
- birefringence, sapphire and synthetic quartz, 3000-1500 Å 8=41056
- birefringent filter with high transmission 8=42198
- birefringent networks, single-pass and double-pass 8=33251
- bonded birefringent strip, for obs. of surface deforms of opaque bodies 8=44521
- colloids, induced by laser beam 8=34951
- filters, chain birefringent 8=42260
- gas, due to spin alignment 8=39216
- laser, ruby, birefringent plate control of spectral emission 8=37609
- liquids, mol. optical Kerr consts., calc. 8=34845
- optical, induced by elec. fields, quantum field theory 8=33340
- polarization of light waves in optically active crystals 8=31947
- polarized laser cavity insensitive to birefringence in laser rod 8=46597
- poly(ethylene terephthalate) fibres rel. to amorphous orientation and crystallinity, obs. 8=44175
- CdSe, birefringence, effect of uniaxial stress 8=36342
- $NaNO_2$, birefringence, dispersion and temp. depend. determ. 8=27594
- Nd glass, birefringence dependence on laser pumping pulses 8=41125
- n-Ge, birefringence of microwaves due to hot electrons 8=35903
- H_2, Kerr effect theory 8=34664
- He, optically pumped 8=39216
- MgF_2, birefringence, 3000 to 1500 Å 8=41056
- MgF_2 Soleil compensator, near i.r. 8=37699
- n-Si, birefringence of microwaves due to hot electrons 8=35903
- Si, birefringence rel. to thermally induced stresses 8=49051

electric. See Electro-optical effects.

flow
- cellulose sulphoester solns. 8=34850
- polymer solns., effects of polydispersity 8=39368
- polypropylene, rel. to mol. wt. distrib. obs. 8=43721
- single liquids 8=39369

magnetic. See Magneto-optical effects.

mechanical

See also Photoelasticity.
- photoelastic stress analysis, transmission-microscope polariscope 8=33283
- polymer chains, theory 8=38971

Double resonance. See Nuclear magnetic resonance and relaxation; Paramagnetic resonance and relaxation.

Drops
- approaching plane interface, radius of draining film 8=30381
- disintegration of pairs of drops raised to equal and opposite potentials 8=25852
- electrophoresis, Booth equation 8=34896
- entrainment of small particles by large sphere 8=34736
- evaporation of liq. droplets containing surface impurities 8=48267
- fluid droplets in different fluid, freq. and rate of damping of oscs. 8=43738
- formation in liq.-liq. systems, prediction of vol. 8=39286
- freely falling waterdrops, structure of ventilation coeffs., physical interpretation 8=25854
- freezing and fragmentation of suspended waterdrops influence of environmental parameters 8=25853
- growing droplet profile, use of pressure balance for determ. 8=48048
- interfacial tension meas., eqns for 1/H vs S values in computed calcs. 8=48042
- liquid, approach through viscous liq. to flat plate, rel. to drainage rate 8=30385
- liquid atomization by rotating disc, and 'secondary' break up of droplets 8=30389
- liquid, evaporation rates when coated with insoluble film 8=48272
- liquid, falling through air, drag coeffs. rel. to Reynolds number 8=30384
- liquid, sessile, shape analysis 8=25857
- liquid, spherical, motion at high Reynolds number 8=30386

Drops—contd
liquid spray, evaporation rates 8=48278
mass transfer to drops at high Reynolds no. 8=30387
metal, laser form. and ignition apparatus 8=34740
metal (liquid) falling in viscous dielectric in longit. mag. field 8=30390
nucleation from vapour, free energy of formation 8=43781
nucleation theory, equilib. distrib. of droplets 8=39485
optical back scatter 8=27916
separating due to vol. exceeding crit. value, profile calc. from capillary eqns. 8=48047
spherical, charging and freezing technique 8=48045
spherical, diffusion phoresis in binary gas mixtures 8=34677
spherical liq. droplets, light scatt. using computer-synthesized holograms 8=34848
spherical, with radii under 500A, surface energy and evaporation rate 8=26000
surface tension by drop-weight-volume method, correction factors 8=30441
uniform, prod. by ion drag pump 8=43742
water, charging in ion stream rel. to clouds electrification by selective ion-capture, obs. 8=30517
water, evaporation rate meas. by optical scatter 8=39484
water, falling in air and other gases, supercooling and freezing 8=25984
water, freezing on metal plate, cooling rate and freezing temp. interdependence 8=48263
water, photographed pulsed motion 8=43741
water, photomultiplier investigations 8=48043
water, supercooled, crystallization processes 8=25985
water, time change of radius in evaporation processes, asymptotic soln. 8=30600
H_2 liquid, $15\mu m$ dia., production 8=34741
Zn^{65} extraction, between liq. metals and fused salts 8=27725

Drying
capillary-porous mat., influence of vibration 8=30591
capillary-porous mats., in e. m. field, ht. and mass transfer 8=39487
clay, shrinkage, effect of graphite 8=39709
gas, moisture trap 8=50470
muscovite dehydration, mechanism 8=49876
peat, visco-plastic, internal moisture transfer and evaporation intensity over surface 8=34982
silica-gel spheres, by contact with dry particles, in mixing 8=34978

Ductility. See Plastic flow; Plasticity.

Dusts. See Aerosols; Powders.

Dynamics
See also Ballistics; Kinematics; Rotating bodies; Vibrations.
anharmonic oscillator, perturbations effects, teaching demonstration 8–41803
classical and quantum theory fundamentals 8=46013
conductors, electrical, dynamical theory under e.m. field 8=41642
conservation laws, for system with geodesic trajectories in Riemannian spaces 8=32694
conservation of momentum 8=28255
controlled systems, motion 8=46019
and differential geometry 8=28252
dynamical systems, noisy discrete-time nonlinear, state variables estimation 8=46009
elastic solids, forced motion 8=41674
elastodynamics, transient, direct formulation and numerical solution 8=46054
electrometer needle, parametric resonance obs. 8=37360
eqns. of motion, Lorentz-invariant from Einstein's field eqns. 8=28293
Ergodic theorems for general systems 8=32696
general coords., expression for dynamical quantities 8=28933
inelastic column instability subjected to time-dependent load 8=32706
Keppler motion, general perturbed two body problem 8=46007
Kepler problem, radiationless relativistic, classical soln. in strong coupling limit 8=28250
limiting cycle domain existence of dynamic systems with cylinderical phase space 8=46010
linear air track, Y-T recorder 8=28256
mass on vib. surface, 'frictional viscosity' effect 8=32695
masses, inert and gravitational, exptl. verification of equality 8=46021
motion in relativistic space 8=46011
motion of solid with and without external moments, generalization of Erlenan case 8=46008
nearly periodic Hamiltonian systems, invariant calc. 8=28251
oscillations, active damping of model suspended in stream 8=46143
oscillator, ID, quasirandom 8=46016
particle motion in acoustic field of stagnant waves 8=23819
reaction, chemical heterogeneous, at stagnation point 8=25812

Dynamics—contd
rotary motion of rigid body, precession types 8=23817
rotation of solid with fluid filled cavity 8=46018
satellite, effect of elasticity 8=41640
slippage in systems with collision interactions 8=46014
strings and membranes, travelling forces 8=37241
systems with transient response, method for freq. response calc. 8=41638
triple systems, statistical analysis 8=41639
two-centre Kepler problem, constant of motion 8=46791
ultracentrifuges, rotor deceleration formula 8=30542
wheel, elastic, lateral force property in presence of thrust exptl. study 8=41644

Dynamometers
See also Force measurement.
precision, standardization 8=23795

Dysprosium
electronic structure from positron annihilation studies 8=26906
electronic structure from relativistic augmented-plane-wave calcs. 8=26905
ferromagnetic anisotropy constant temp. dependence 8=31651
ferromagnetic, mag. viscosity 8=45029
generalized susceptibilities and mag. ordering 8=44973
Hall effect, anomalous, 340-4°K 8=44969
isotope shifts and nuclear deform. spectra 8=43188
magnetic-ordering temp., pressure dependence 8=31652
magnetic ordering temps. at high pressures 8=40730
magnetic properties hydrostatic pressure dependence 8=36082
magnetic props. from mag. moment meas. at 4.2°K and high fields 8=31705
magnetization anisotropy and magnetostriction meas. in pulsed fields up to 150 kOe 8=40743
NMR relax. of $Dy^{161,163}$ in metal 8=27504
nuclear spin relaxation, indirect 8=31915
spin-wave spectrum, anomaly in spiral spin structures 8=49572
spin waves and mag. resons: thermal, applied field, and magnetoelastic effects 8=31703
thermal conductivity, temp. dependence, 5-300°K, rel. to mag. transition 8=35458
Dy^{3+}in CeO_2, e.s.r. spectra 8=40918
Dy^{3+} in LaF_3, absorpt. and fluoresc. spectra 8=31985
Dy^{3+}, spin lattice relaxation in CeO_2 8=36222
Dy^{3+}, in ThO_2, e.s.r. spectra 8=40918
SrF_2: Dy^{3+}, e.s.r. in cubic fields 8=36252

Dysprosium compounds
alloys, ferromagnetic, mag. viscosity 8=45029
aluminate, dipolar magnetisation 8=36136
aluminates, antiferromag., thermal props. 8=35435
spectrum, isotopic shift 8=47493
Dy elthyl sulphate, paramag. relax. Mossbauer study 8=27472
DyAl garnet, critical n.-scattering rel. to antiferromag. Ising model 8=31769
DyAl garnet, magnetization and mag. ordering, 0.37°K 8=40866
DyAl garnet, magnetization change below 1.7°K, model 8=45057
DyAl garnet, n.m.r. of Al^{27}, quadrupole splitting and paramag. shifts 8=31893
DyAl garnet, sp. ht. shape dependence 8=35423
Dy_3Al_2, metamagnetic props 8=49544
$DyAlO_3$, absorpt. spectra rel. to mag. props. 8=36356
$DyAlO_3$, nuclear and magnetic structure n diffr. obs. 8—48647
DyC_2, mag. struct. by neutron diffr. 8=40865
$DyEr_x$ $(x = 1, 3)$ alloys with 4f e. conc. = 10, 11; magnetization 8=41654
$DyFeO_3$, absorpt. spectra rel. to mag. props. 8=36356
Dy-Pb system, phase diagram 8=39550
$Dy_{0\cdot2}Y_{1\cdot8}Ti_2O_7$, mag. susceptibility meas., 2-1400°K 8=27429
DyFe garnet, dilute, magnetostriction 8=31724
$DyFe_2$, hyperfine field at Fe from Mössbauer effect 8=36146
$DyFeO_3$, antiferromagnetic props. below 36°K 8=31768
$DyFeO_3$, sp. ht., 1.2–80°K rel. to mag. ordering 8=35429
$Dy_xY_{1-x}Fe_2$, Curie temp. and coercivity comp. dependence 8=31610

E-layer. See Ionosphere/E-region.

ENDOR (electron nuclear double resonance). See Nuclear magnetic resonance and relaxation; Paramagnetic resonance and relaxation.

Ear
See also Hearing.
cat interference between two tones, cochlear response obs. 8=32933
cat, 2-tone inhibition in auditory nerve fibres 8=32932
characteristic curves, subjective sound intensity analyser 8=46196
cochlear pot., nonlinearity model 8=46203
eardrum impedance changes with loudness of sound 8=23976

Ear—contd
middle, acoustic stimulation of muscles 8=28377
monaural bone-conduction threshold, specification 8=37293
pressure generated by audiometric earphone 8=46204
shear waves between longitudinal and tectorial membranes, props. 8=32925
threshold shift rel. to noise 8=46205
Earphones. See Acoustic transducers.
Earth
See also Geodesy; Geophysics.
accretion rate of cosmic dust, use of 'signatures' due to cosmic ray activation 8=28168
Antarctica, late paleozoic glacial geography 8=50087
bow shock plasma wave emission 8=41389
core-mantle boundary struct. rel. to P-waves attenuation 8=27842
core, rigidity and viscosity from wave refl. at mantle-core boundary 8=36664
crust as waveguide for very long radio waves 8=36676
crust, sialic low-vel. channel in S. German Triangle, seismic refr. obs. 8=27836
crust struct., wide angle meas. 8=45428
crustal block, rise, trenches, great faults 8=36670
crustal strength in shallow focus strike slip faulting 8=36668
crustal struct. in Himalayan foothills, from P wave data of shallow earthquakes 8=50068
crustal structure 3D model, middle Atlantic states 8=36674
crustal tectonics and mantle convection inferred from satellite. sea-floor spreading 8=32180
crustal thickness in central USA and Bolivia, from P wave spectrum 8=50071
density, models rel. to seismic equation of state 8=27823
earth-atmos. system, albedo, emitted thermal rad., and rad. balance, global, distrib. maps 8=41316
elastic eqns. consistency rel. to models validity 8=27840
e.m. wave and pulse transmission rel. to shielding props. 8=46471
e.m. wave propagation in jungle medium, conducting-slab model 8=28610
equation of state of periclase and Birch's relationship between velocity and density 8=27851
faults, basin and range, effect of Timber Mountain caldera, mech. analysis 8=32181
finite deformation in interior of earth model 8=50066
γ-ray spectrum obs. by spacecraft 8=45794
geomagnetic activity, dependence on energy density and press 8=45570
gravitational accretion of particles producing rotation 8=50406
gravitational field, effects of convection in mantle, hydrodynamical model for interior 8=50006
gravitational/inertial mass ratio, meas. by lunar laser ranging 8=41748
gravity field, external from artificial satellites motion meas. 8=27819
horizon radiance profiles, 14-16 μ 8=45422
i.r. radiation, angular and spectral distrib., rel. to cloud distrib. 8=36657
latitude of tropics, eccentricity of orbit, perigee and apogee dates obs. 8=45862
mantle inhomogeneities, seismic wave vel. profiles obs. 8=27824
mantle, structure, and obs. of long-period surface waves 8=41322
mantle struct., teleseismic signals obs. 8=27845
mantle, temp. and discontinuities in transition layer 8=36678
mid-oceanic rises, mag. anomalies, crustal spreading and continental drift 8=50089
moon, capture theory and geophys. consequences 8=50401
from moon, return trajectories from surface and satellite orbits 8=32375
natural evaporation from surface, energy balance study on hourly basis 8=36685
orbit, secular perturbations, rel. to climates 8=37009
Pacific, total solar flux obs. 8=27904
radiation in spectral region 8-12μ, surface meas. 8=32175
Ramapo fault in USA, seismic activity 8=50037
river sediments, Th and U concs. and isotope ratios 8=50094
shear component of strain, use of Michelson interferom. as sensor 8=27848
shell, phase transition and critical phenomena 8=50077
stress accumulation at depth, meas. from changes in compressional vel. of seismic waves 8=36673
structural implications of gravitational obs. 8=45429
structure and elastic-gravit. oscill. from gross data, numerical soln. 8=27849
thermal springs in Italy, O isotopic comp. of sulphate ions 8=50093
upper mantle boundaries nature, deep-focus earthquakes hodographs interpretation 8=27833
upper mantle model from seismologic data 8=36672
upper-mantle struct., from travel-time curves of long-period S-waves 8=36661
upper mantle structure in Canada, from seismic obs. using chem. explosions 8=32179
upper mantle to West of Lake Superior, study by P and S wave seismograms 8=50065

Earth—contd
velocity meas. through 3°K background radiation field 8=36653
vibrations, spheroidal, elementary theory 8=50091
v.l.f., wave propag. in earth interior 8=46468
CO_2 horizon profile spatial energy distrib., 15μ 8=27910
Li content, comparison with Sun's composition 8=50292
age
See also Radioactive dating.
exposed lavas in Iceland, oldest, K/Ar ages 8=50083
from Pb isotope abundances in rock, appls of concordia plots for U^{238}/Pb^{204} ratio 8=27856
Zoetlief volcanic system in S. Africa, Pb-isotope dating 8=50082
composition
igneous Icelandic rocks, Pb-isotope studies rel. to formation and age 8=50085
Lake Superior crustal struct., 1963 seismic expt., reinterpretation 8=32178
lithosphere, petrology 8=45427
mantle-core boundary, close continuity of compressibility 8=27847
mantle to core transition region, simulation by thin-layer model 8=50072
mantle, lower shock wave data for minerals, phase implication 8=41321
noble gases, abundance 8=36677
temperature and discontinuities in transition layer in mantle, olivine-spinel transition in Mg_2SiO_4-Fe_2SiO_4 system 8=36678
ultramatic rocks in Alaska, Sb-Rb-K and Sr isotopic relns. 8=50069
upper mantle C-region phase changes 8=50076
vertical discontinuities, true chargeabilities obs., applic. to Pb-Zn ores in Turkey 8=32177
xenolithic rocks, extremely high Ar^{40}/K ratios 8=50084
Ar and He, radiogenic in ultramafic inclusions in Hawaii 8=50073
Hf/Zr ratio of metamorphic rocks from Ontario 8=50067
Mg ilmenites, MgO content rel. to MgO/FeO ratio in host rocks 8=50070
Sr isotope ratios in volcanic rocks of three island arc areas 8=32186
Th, U and K abundances in peridotite inclusions in basalts, rel. to upper mantle 8=50012
electricity
conductivity, calc. from geomag. vars. using e.m. induction 8=36679
conductivity, deep layer, estimation from 30 year mag. cycle 8=41471
currents, rel. to rate of change of Sq geomag. vars. 8=36891
d.c. four point meas., efficiency of geoelec. apparatus 8=50080
e.m. fields from long horizontal line source, two layer conducting earth 8=27853
e.m. induction by s.s.c. mag. vars. with allowance for ocean effect 8=50205
heterogeneities and mag. field anomalies, from mag. field of submerged cable 8=36680
impedances, using magnetotelluric fields 8=32182
lower mantle cond. and geomag. spectrum of internal origin 8=32183
vertical discontinuities, true chargeabilities, determ. and applic. to Pb-Zn ores. 8=41323
weakly bound motion. effect of gas-forming substs. in focus of electric explosion 8=50078
heat
borehole, Camp Century, Greenland, temp. profiles, comp. between meas. and theory 8=32174
continental terrestrial heat flow, glacial effect and significance 8=50019
descending mantle convective flow zones, rel. to high heat flow and volcanism 8=45430
flow pattern 8=32173
geological manifestations of thermal energy 8=50015
i.r. rad. into space, angular and spectral distrib. 8=36657
mantle convection and crustal tectonics inferred from satellite, sea-floor spreading 8=32180
mantle convection, rel. to mid-ocean ridges and geotherm distrib. 8=32172
mantle, effect of selective melting on thermal history 8=50018
sediments, hundreds of meters thick upon crystalline rock, flux meas. 8=50016
thermodynamical study 8=32171
magnetic field
activity diffs. between two hemispheres following sector struct. of interplanetary mag. field 8=41478
anomalies, linear in Bay of Biscay, rel. basalt injections and extrusions 8=50207
anomalies, linear inverse problem soln., and Juan de Fuca ridge appl. 8=28019
anomalous and normal component separation 8=36876
anomaly, S. Atlantic, rel. to F region conjugate enhancement 8=41453
B-L space and field models 8=36874
circular sattelite orbit stability in gravitational and dipole mag. fields 8=50236

Earth—contd
- **magnetic field**—contd
  - components meas. in meridian plane at sea by nuclear precession 8=28005
  - confinement by a beam of ions solar wind 8=36822-3
  - confinement by ion beam 8=32366-7
  - conjugate point location from models of main field 8=41456
  - conjugate points, radio absorption, correlation 8=41402
  - conjugate points rel. to sporadic E at temperature latits 8=41446
  - conjugate places at low latitudes, f_0F2 vars. 8=41455
  - conjugate stations, annual total of simultaneous night hours, contours 8=41457
  - cosmic-ray shower radio emission polarization, exptl. tests 8=38204
  - demagnetization effect of rectangular prism 8=50204
  - dipole, particle motion in, effect of const. elect. field (model) 8=37409
  - dipole, rel. to charged particle motion under action of e. m. pulses 8=36815
  - drift around axis, westward and equatorial components 8=36875
  - dynamo theory test 8=50405
  - equatorial cosmic muon spectra 8=38141
  - free precession expts. in field 8=46518
  - geoelectric variations det. by underground cable 8=33380
  - geomagnetic pulsations of Pi Z type in magneto-conjugated points, investigation 8=50216
  - geomagnetic spectrum of internal origin and lower mantle cond. 8=32183
  - harmonic series, at evaluation for 1100 km height 8=36880
  - high-altitude satellite meas., suggestions 8=28004
  - interaction with solar plasma, importance to theory of generalized Riemann problem 8=45482
  - international geomag. ref. field-1965, proposed model 8=32363
  - and interplanetary, obs. 8=37037
  - intensity, scalar, at 1100 km mid and low latits. 8=36881
  - magnetic anomalies over spheres, standard curves 8=32362
  - magnetometer, two-component gyrostabilized at sea 8=24107
  - magnetosphere, outer, and boundary obs. 8=36878
  - magnetosphere, Pioneer 7 obs. 8=32267
  - magnetospheric boundary, hydromag. stability 8=41385
  - magnetospheric tail, motion of charged particle 8=24127
  - magnetotelluric sounding in Klyuchi settlement of Kamchatka region 8=50079
  - neutron monitor acceptance vectors for 72 stations, for dipole and real fields 8=38273
  - n. m. r. signals in field using "growth effect" 8=30529
  - n.m.r. spectroscopy, high-resolution, in terrestrial field range 8=46516
  - nondipole part, rel. to boundary of magnetosphere 8=45487
  - North Arabian sea aeromag. survey, interpret. 8=50206
  - optimum representation by three dipoles 8=45555
  - paleo-intensities, determ. by Thelliers method 8=45573
  - paleomagnetic field intensity, outline from 2.5×10^{-9} yr to present 8=28017
  - photon mass, geomag. upper limit 8=42446
  - polarity intervals, lengths 8=36879
  - quartz H magnetometer readings, humidity effects 8=41458
  - reversal rate from polarity zones in Icelandic lavas 8=36883
  - satellites, magnetized, passive stabilization 8=32383
  - satellites stabilization, mag. and gravit. fields effects 8=32381
  - second and fourth order sectorial harmonics, determ. from motion of 12 hr satellites 8=28003
  - secondary field, interpretation by analytic continuation 8=45556
  - solar wind effect 8=32584
  - space-time-structure, exploaration problems and methods 8=50203
  - spherical harmonic analysis, S clusters method 8=36877
  - structure 8=50201
- **magnetic field, variations**
  - See also Magnetic storms.
  - activity at high altitudes of northern hemisphere during IQSY 8=45558
  - activity, correlation with spread-F in middle latitude 8=36865
  - activity rel. to heating of upper atmos., relative to solar EUV rad. effect 8=27934
  - activity rel. to satellite scintillation in auroral zone 8=32285
  - of activity, 27-day period, in auroral zones, and inactive intervals during mag. quiet days 8=28008
  - anomalies and their geophysical interpretation 8=41461
  - anomalous, SW Scotland 8=50223
  - bay associated events, simultaneous surface and ATS-1 magnetometer obs. 8=41463
  - conjugate locations, 4 to 0.002 Hz 8=41475
  - core, outer, west drift rel. secular changes 8=50202
  - correlation with cosmic-ray daily var. 8=38289
  - cyclic, 30 years, and deep layer elect. conductivity estimation 8=41471
  - D_n2 rel. to magnetosphere plasma convection 8=41479
  - directional variations of geomag. induction arrows of finite cond. 8=50210

Earth—contd
- **magnetic field, variations**—contd
  - disturbance in Arctic, rel. to solar activity 8=45571
  - diurnal, rel. to drift inhomogeneities in upper ionosphere 8=45525
  - dynamo effect, 2-dimens., numerical simulation 8=28006
  - energy of disturbances, effect of interplanetary field 8=41467
  - events conjugate to Byrd, Antarctica, spatial extent 8=41465
  - F-region, effect on, prod. of intense fluctuations, travelling waves, above Arecibo 8=32331
  - F2-region horizontal drifts, effect on 8=45553
  - geomagnetic activity, dependence on energy density and press. of interplanetary plasma and on mag. field 8=45570
  - geomagnetic activity rel. to red O emission at 6300Å 8=36750
  - geomagnetic micropulsations 8=27971
  - geomagnetotail sudden impulses 8=36887
  - height dependency of Central European mag. field, deriv. from polynomial rep. of geomag. elements 8=36884
  - high latitudes, solar-daily vars., IGY 8=41460
  - horizontal and f_0F2 luni-solar tidal oscills. in quiet period 8=27997
  - ionospheric current system and electrojet from mag. correlation 8=45569
  - ionospheric obs. rel. to stratospheric heating 8=27982
  - Kp disturbance index, review 8=50215
  - late Mississippian red sediments, sample obs. 8=32373
  - long period fluctuations after 1964 Alaskan earthquake 8=28009
  - lunar-period oscillations, obs. 8=28012
  - luni-solar daily, anomalous, at Watheroo, Western Australia, IGY data 8=50209
  - magnetographs thunderstorms and earthquakes effects, on Hyderabad 8=32365
  - magnetosphere, pc 1 micropulsations, longit. spread 8=27945
  - marine anomalies, and reversals 8=36899
  - m. f. radio wave absorption, dependence at mid-latitudes on planetary mag. activity 8=41423
  - microburst, auroral high intensity temporal features 8=36804
  - micropulsation diagnostics of magnetosphere review 8=45486
  - micropulsation sources, polarization 8=28011
  - micropulsations and electron precipitations rel. to magnetospheric substorm 8=41399
  - micropulsations during quiet solar years 8=50213
  - micropulsations, in auroral zone, radiated field from line source of current 8=45568
  - micropulsations, long-period, origin 8=41474
  - micropulsations, long-period, use in determ. of magnetospheric plasma density 8=50167
  - micropulsations, pearl, dot struct. of spectrogram 8=36890
  - micropulsations, pearl, spectral analysis by analogue computer 8=41473
  - micropulsations, PC1, correction at spaced stations 8=36888
  - micropulsations, Pc1, temporal variations 8=32364
  - micropulsations, Pg, at conjugate point (1963 and 1964) 8=41477
  - micropulsations, Pi ⊥, behaviour in magnetically conjugated points 8=50214
  - micropulsations, Pi 1 type, at mag. conjugate points 8=45567
  - micropulsations rel. to auroral substorm electron precipitation 8=41398
  - Norwegian sea, aeromag. obs. 8=50208
  - over underwater mountains 8=45559
  - paleomagnetic, Indian Ocean anomalies and floor spreading 8=36898
  - paleomagnetic, Pacific anomalies and floor spreading 8=36896
  - paleomagnetic, S. Atlantic anomalies and floor spreading 8=36897
  - Pc stable pulsations, dependence of amplitude on phase of moon, statistical study 8=45565
  - PC1 fine struct, phase shift at high-lat. conjugate points 8=36893
  - Pc-1 type oscills, propag. speed 8=41476
  - Pc 1, 2 and 3 hydromag. waves, radial diffusion coeffs. magnetospheric protons 8=41411
  - pc-3 and pc-4, rel to Alfven waves and solar wind-magnetopause interaction 8=50217
  - pc 3 pulsations, transmission through ionoxphere rel. to solar X-ray fluxes 8=41472
  - pearl pulsations, shift of source region rel. to equatorial plane 8=41470
  - Pi 2 type pulsations, behaviour at mag. conjugate points 8=45566
  - polar disturbances, rel. to magnetosheath and interplanetary mag. field 8=41466
  - polar mag. disturbances and currents, laws 8=36886
  - potential fields, smoothing 8=50011
  - pulsations, PP, as Cherenkov radiation 8=41469
  - quartz H variometer, setting rel. to mag. meridian 8=41459
  - rapid, total intensity, auto and cross spectrum analysis 8=36889
  - recent trends, analysis of collected obs. 8=36882

- **Earth**—contd
  - **magnetic field, variations**—contd
    - S_n rel. to solar activity at Yakutsk 8=36892
    - secular, analytical representation, improvement 8=45560
    - secular, in historic time, ancient aurorae study 8=50211
    - secular, Sverdlovsk observatory data rel. to Irkutsk and Kazan obs. 8=36885
    - secular wobble, Reunion Island palesmag. obs. 8=50221
    - solar and luni-solar daily vars. in I.G.Y., Hartland, U.K. 8=28007
    - spread-F and magnetic activity 8=45549
    - Sq in median latits., semi-annual amplitude vars. 8=28010
    - Sq, rate of change rel. to earth currents 8=36891
    - Sq, rel. to ionospheric layer conductivities 8=50178
    - storms, simultaneous surface and ATS-1 magnetometer obs. 8=41464
    - sudden impulse interruption of X rays, persisting periodicity 8=45504
    - u. l. f. rel. to ionospheric Doppler shift at 2.7 and 4.6 MHz 8=27976
    - upper atmosphere heating 8=27931
    - Victoria Magnetic Observatory, observations 1966 8=45557
    - westward drift and displacement of eccentric dipoles 8=45562
    - westward drift, causes 8=45561
  - **rotation**
    - rel. to atmospheric circulation, calc. methods evaluation 8=45827
    - Conference, Stresa, Italy 1967 8=32196
    - by gravitational accretion of particles 8=50406
    - motion, and orbital: nebular momentum coupling 8=50407
    - obliquity of ecliptic secular change and var. with earth's rotation 8=50392
    - radial oscills, decay 8=50412
    - shock-wave effects in atm. 8=36724
- **Earth satellites.** See Satellites, artificial.
- **Earthquakes.** See Seismology.
- **Eberhard effect.** See Photographic materials.
- **Ebullition.** See Boiling.
- **Echelons** See Diffraction gratings.
- Echo
  - See also Architectural acoustics; Reverberation; Sound ranging.
  - backscattering, ionospheric, role of land and sea 8=27977
  - direction perception physiology 8=46207
  - ferrites, amplified ferrimag. obs. 8=31717
  - fluxoid, induced in r. f.-irrad. superconductor 8=27010
  - sound ranging by sea lion 8=37295/6
- **Eclipses.** See Moon; Sun/eclipses.
- **Eddy-currents**
  - braking at high speeds by permanent magnets 8=24115
  - decay, meas. of metal resistivity, analysis 8=46326
  - in ferromagnetic sheets under alternating magnetiz., distrib. and waveform 8=28516
  - flowmeter for liq. metal, analysis 8=48026
  - plate moving in mag. field, theory 8=33027
  - in probe-coil problems, analyt. solns. 8=37402
  - n-Ge, thermoelec. expt. 8=40642
- **Edge emission.** See Luminescence/solids, inorganic; Luminescence/solids, organic.
- **Education.** See Teaching.
- **Effusion.** See Flow/gases.
- **Eightfold way.** See Elementary particles; Field theory, quantum.
- **Einstein–de Haas effect.** See Gyromagnetic effect.
- **Einsteinium**
  - Es^{253} emission spectra, hyperfine structure 8=43189
- **Elastic constants**
  - See also Compressibility; Stress/strain relations.
  - Anderson-Gruneisen parameter for general interatomic potential 8=48939
  - brass rods, Young's and shear moduli, annealing temp. dependence 8=31195
  - butadiene acidic and basic copolymers mixtures rel. to H-bonding, obs. 8=48506
  - butadiene-methacrylic acid copolymers rel. to H-bonding, obs. 8=48506
  - butadiene-2-methyl-5-vinylpyridine copolymers rel. to H-bonding, obs. 8=48506
  - calcite, comparison of values obtained by various methods 8=40132
  - calcite, pressure dependence to 6kbar at 25°C 8=48998
  - calcite, temp. variation, 2-375°C 8=44558
  - calcite, third-order, at 0°C 8=48999
  - chromic steel, change at tempering 8=49003
  - coagulation structures, solid-like, thixotropically hardened, and viscosity 8=40090
  - composite, unidirectional fibre-reinforced, calc. 8=48942
  - crystal, determ., correction for second-order diffuse X-ray scattering 8=40093
  - crystals, mono- and poly-, third-order reln. 8=44511
  - cubic crystals, second- and higher-order, pressure dependence under hydrostatic compression 8=40091
  - cubic crystal, Stoneley wave propag. 8=26746
  - cubic crystal, under moderately high hydrostatic pressure 8=26741
  - glass, rel. to oxide dilution 8=44579
  - glasses, effect of mixed γ-n radiation 8=44493
- **Elastic constants**—contd
  - glycerol, liq., press. depend. 8=34841
  - graphite artefacts, dynamic Young's mod., —196°C to 1000°C 8=26790
  - graphite, isotropic reactor type, meas. before and after n-irrad. 8=26789
  - graphite, isotropic, Young's modulus, shear modulus and Poisson's ratio 8=26793
  - graphite, polycryst., Young's mod. rel. to orientation, by averaging tech. 8=35663
  - graphite, pyrolytic, shear compliance, (C_{44}), effect of neutron irrad. 8=35665
  - Grüneisen solid, h.p. bulk modulus, thermodynamic calc. 8=30972
  - gypsum systems, and hardness and porosity, interrelations 8=40172
  - ice, from u.s. velocity meas., mp to-140°C 8=44581
  - inclusion, spherical effect in anisotropic solid 8=48938
  - intermetallic cpds of β-W structure, shear modulus temp. dependence rel. to lattice instability and supercond., 8=44721
  - invariant, for crystals 8=44512
  - isotropic matrix reinforced with imperfectly oriented fibres 8=40092
  - lamellar composite materials, acoustic wave propag. obs. 8=40100
  - metals, e. -mean free path, and free-e. density, strain coeff. determ. using thin-film technique 8=49081
  - metals, hexagonal, first-, second- and third-order shear, for arbitrary axial ratio 8=35642
  - microelastic solid, linear, inequalities between constants 8=40094
  - molecular crysts., pair potential approx. 8=30925
  - napthalene, tensor temp. dependence, 20-80°C 8=26856
  - plastic resin reinforced with alumina fibres 8=26857
  - Poisson's ratio, anomalies rel. to cryst. anisotropy and internal stresses, $\mu < 0.5$ 8=40095
  - Poisson's ratio, stress depend in plane elasticity 8=41683
  - poly-i-butyl methacrylate, bulk and shear relax. processes 8=40193
  - polyamides, in tension and compression, difference 8=31242
  - polycrystalline media, third-order 8=26740
  - polyethylene, Poisson's ratio in compression 8=31245
  - polyurethane foams, effect of cell membranes 8=48243
  - pyrocarbons compressed at high temps. 8=45941
  - α-quartz, calc. from model 8=44599
  - α-quartz, coeffs. and moduli. polarizing tensor 8=49048
  - quartz plates, third-order consts. for calc. stress depend. of freq. 8=49049
  - quartz, third-order moduli, pulse-echo interferometric obs. 8=49050
  - of quasi-isotropic materials, third-order 8=48940
  - of quasi-isotropic materials, third order, estimation 8=48941
  - of quasi isotropic polycryst. materials, statistical calc. 8=35610
  - reinforced material, compliance tensor 8=28268
  - sapphire whiskers, Young's modulus 8=35661
  - shear modulus meas. in vibr. expts., analysis 8=41810
  - solid, microinhomogeneous, macroscopic coeff., eqn. 8=48741
  - statistical calc. rel. to Kroner soln., for quasi isotropic polycryst. materials 8=35610
  - steel, hardened, Youngs mod., effect of austenite decomp. 8=31208
  - succinonitrile, in plastic phase 8=44611
  - teflon, Poisson's ratio in compression 8=31245
  - transition metal carbides, directional variations 8=49056
  - transition metals, b.c.c., temp. depend. rel. to entropy of self-diffusion 8=48984
  - wire, Young's, longitudinal vibration due to thermal shock 8=40088
  - α-Al_2O_3, Voigt-Reuss-Hill approx. rel. to meas. of moduli 8=40188
  - Al-Zn alloys, Young's mod., temp. depend. rel. to phase diagram 8=48988
  - B fibres, shear modulus, amplitude dependence 8=40131
  - BaF_2, third-order from acoustic meas. 8=26787
  - C artefacts, dynamic Young's mod., —196°C to 1000°C 8=26790
  - C, vitreous, 4-570°K 8=44557
  - CaF_2, temp. dependence, room temp.—420°C 8=35667
  - $CaMoO_4$, and compliances 8=40133
  - CoO, anomalies rel. to mag. phase transition 8=44560
  - CsBr, adiabatic, rel. to press. and temp., expt. and theory 8=44562
  - CsI, adiabatic, rel. to press. and temp., expt. and theory 8=44562
  - Cu, drawn, Young's and shear moduli, annealing temp. dependence 8=31195
  - Cu, n-irradiated, third-order, from u. s. meas. of non-linearity parameters 8=26800
  - Cu, shear modulus rel. to resistivity on cyclic stressing 8=40317
  - Cu, third-order, from third harmonic amplitude obs. of initially u.s. wave 8=26581
  - Fe crystal, stiffness coeffs., room temp. to 500°C 8=44570

Elastic constants—contd

α-Fe, pressure derivs. to 10 kbs at 300°K 8=26823

Fe–Ni–Ti alloys, Young's modulus rel. to texture changes in $\gamma \rightarrow \alpha$ and $\gamma \rightarrow \alpha \rightarrow \gamma$ transforms. 8=35701

$Fe_{0.98}O$, rel. to Neel temp. determ. 8=31772

GaAs, third-order, Keatings theory 8=44578

GaP, from u.s. phase-comparison meas. 8=49021

GaSb, pressure dependence and compression to 80 kbar 8=49022

Ge, modulus temp. and illumination dependence rel. to carrier generation 8=35702

n-Ge:Sb doped, moduli meas., 300–500°K 8=40163

$Hg_5In_2Te_8$ 8=49027

KBr, Young's modulus and relaxation rel. to dislocation pinning by lattice defects 8=26680

KCl, Young's modulus and relaxation rel. to dislocation pinning by lattice defects 8=26680

$KH_2AsO_4(KD_2AsO_4)$, temp. dependence, 20-80°C 8=49368

MgF_2, and thermoelastic behaviour 8=44590

MgF_2, by pulsed u.s. technique 8=44589

MgO, polycrystalline, press. derivs. of moduli, revised data 8=31217

MgO, second-order, pressure derivs., 8=49035

MnF_2, and thermoelastic behaviour 8=44590

NaCl-type alkali halides, and tensile strength 8=49036

NaCl-type alkali halides, Anderson-Gruneisen parameter 8=48939

NaCl, Young's modulus and relaxation rel. to dislocation pinning by lattice defects 8=26680

NaCl, Young's modulus rel. to theoretical strength along body and face diagonals 8=44594

Nb crystals, mono- and poly-, third-order constants 8=40177

NbC-graphite composites, cubes and thin rods, at 23°C 8=49040

NH_4ClSnO_3, determ. by optical method 8=26837

$NH_4H_2AsO_4$(ADA) obs. 8=27298

$PbCl_2$, from vel. meas. of u.s. waves 8=35712

PbTe, and thermal expansion, 4.2-303°K 8=49044

Pu, temp. var. 8=44632

δ-Pu-Ga alloys, temp. depend. below 300°K 8=44598

RbI, Young's modulus and relaxation rel. to dislocation pinning by lattice defects 8=26680

Te crystal, temp. dependence, 270–700°K from ultrasound velocity meas. 8=35719

Ti, temp. dependence, 4.2-36°K rel. to anomaly at 22°K 8=49054

TiNi, temp. dependence, —170 to 800°C 8=26847

TiO_2, Voigt–Reuss–Hill approx. rel. to meas. of moduli 8=40188

U, meas. 2-43°K, rel. to phase transition 8=40185

U oxides, hyperstoichiometric, Young's modulus and internal friction, at room temp. 8=35722

UO_2, temp. dependence rel. to u.s. attenuation 4.2-300°K 8=39898

V_3Si, superconductivity dependence on lattice instability from Young's modulus meas. 8=27037

W, shear modulus freq. and temp. dependence (0.0004–20 cps, 1400–2000°K) 8=35723

$91Y_2O_3 + 9ThO_2$ in solid solution, temp. depend. from 25° to 1100°C 8=35724

ZnO polar crystals, from point-charge model 8=30630

ZnO, Voigt–Reuss–Hill approx. rel. to meas. of moduli 8=40188

measurement

gels, rational geometry 8=32774

glass, strain-optic individual coeffs., u.s. determ. 8=41138

high-temp. short specimen ultrasonic buffer-rod technique 8=40096

third-order, u.s. meas., theory 8=40089

Young's modulus at h.f., apparatus 8=40097

α-SiO_2, changes in electric field 8=44600

Elastic deformation

See also Bending; Stress/strain relations; Torsion.

$A^{III}B^{V}$ crystals, rel. to elec. field gradients at nucleus from n.m.r. obs. 8=31909

adiabatic strain-cycling and temp. rise model, dispersion relations appl. 8=40102

adiabatic, temp. changes in stressed members rel. to meas. 8=44517

b.c.c. metals, mechanisms in 8=26813

bar, flexible, subject to arbitrary discrete loads and boundary conditions 8=46053

bulk material subjected to point load, density and initial stress nonuniform 8=32748

circular cylinder, homogeneous, general soln. 8=41696

circular ring, radially constrained, buckling under distributed loading 8=32731

compression of infinite elastic layer by two rigid punches with different cross sections 8=46028

continuous medium, rate for, exact derivation 8=41668

cosserat surfaces and shells, linear theory 8=41700

crystals, real, elasto-plastic deform. stages, classification 8=26756

dielectric rectangle reinforced with inextensible cords, anal. of flexure 8=23843

discontinuity in finitely deformed medium, thermodynamic relations on surface 8=37142

dynamic, difference method for plane strain 8=23849

Elastic deformation—contd

edge-loaded band, divergence buckling 8=23846

elastic-plastic, relations for high-press. vessel 8=46057

field, interaction with vortex filaments of type II superconductor 8=49186

glass, inorganic, forced frozen deform., in microindentation, obs. 8=35646

glass-reinforced plastics, stress-strain relations 8=31236

glasses, inorganic, delayed, activiation energy spectrum 8=49025

inclusion, circular, in infinite compressible medium, 2nd order effects 8=23841

loading and mass matrix reduction 8=23825

membrane displacements and strains, finite element method 8=41677

metal plate shock waves structure, classical, validity for condensed explosives 8=44515

mirror, parabolic 4 m diam, by dynamic relaxation technique 8=41663

plate, circular, bending singularity for point load 8=32729

plate perforated with ovaloid hole, rigid inclusions under various loadings 8=32742

plate, response to random loading 8=37140

plates, thick, with circular hole, bending and twisting 8=37133

polypropylene fibres, stretching, structural changes 8=49067

rods, small deforms, superposed on large deform. and stability, theory 8=41699

rubber cylinders by compressive end loads, stability 8=44610

satellite, rotating, rel. to stability 8=41487

shell cylindrical, of ideal plastic material 8=46062

shell theory, approx., for unrestricted deformation 8=32726

shells, cylindrical, creep buckling under axial compression 8=32739

shock compression, crystallographic analysis 8=26745

spherical caps buckling under conc. load 8=41697

spherical wedge, analysis 8=41675

thermoelastic, at metal interface 8=41738

tube, compressible reinforced, finite torsion calc. 8=41667

Ag, films, vacuum-condensed, anisotropy rel. to structure 8=44545

AgCl, structural defects in slip-lines 8=48827

Al films, vacuum-condensed, anisotropy rel. to structure 8=44545

Al-$NbAl_3$ dispersion phase alloy, 20-450°C 8=44546

AlSb, rel. to elec. field gradients at nuclei from n.m.r. obs. 8=31909

Au films on amorphous substrate, grain-boundary effects 8=44551

Cu, films, vacuum-condensed, anisotropy rel. to structure 8=44545

Cu, structural defects in slip-lines 8=48827

Fe_3O_4 (magnetite) crystals, remanent and transitory effects 8=31728

GaAs(Sb), rel. to elec. field gradients at nuclei from n.m.r. obs. 8=31909

n-Ge:Sb, effects on longit. and transverse magnetoresistance 8=35899

InAs, rel. to elec. field gradients at nuclei from n.m.r. obs. 8=31909

Nb_3Sn, lattice softening and stiffening at low temps. 8=49039

Ni, films, vacuum-condensed, anisotropy rel. to structure 8=44545

Pb cylindrical bars, elastic-plastic deform. pulse propag., 8=44596

Si-Fe crystals tensile strain effects on domain structure 8=36173

Elastic fatigue

cavitation, high-temp., fractographic obs. 8=26771

crack propagation, gas environment effects 8=31183

crack propagation in metals 8=44586

cracks in railheads, microspectral analysis 8=35633

failure by cavity formation, theory 8=48944

failure rel. to work hardening 8=31171

f.c.c. metals, mechanisms rel. to stress magnitude, ductility and texture 8=26772

high-temp. strain, diametral extensometer 8=35630

metals, fatigues, dislocation distrib., effect of surface-active substs. 8=35556

metals, pure, grain-boundary migration, characts. at elevated temps. 8=39710

metals, theory 8=40116

microfissures appearance, probability 8=35631

nuclear canning material, tension-compression tests at elevated temp. 8=35628

polymers, viscoelastic, due to homogeneous submicrocavitation processes 8=31181

reliability under random loadings 8=35629

steel, appl. of microplastic strain energy criterion 8=35688

steel, ball bearing, crack propag. rel. to crack growth, electron microfractographical studies 8=35696

steel, crack propagation rel. to environment 8=49008

steel, mild and high strength, crack propag. behaviour 8=35697

steel, mild, sharply notched, random and block-loading tests 8=26821

Elastic fatigue—contd
steel, notch effect, specimen design and loading 8=35690
strength, understressing effect, explanation 8=40114
two-parameter theory, corrections 8=40099
Zircaloy-2, crack initiation 8=26854
Al alloys, long-life props, controlling factors 8=48995
Al alloy, 2024-T3, due to broad and narrow-band random loading 8=44547
Al, in reduced partial press. of O_2, H_2O and H_2 gases 8=44540
Al sheets, crack growth rate, local plastic deformation effects 8=35652
Al, surface damage from Au nucleation exam. rel. to fatiguing environments 8=26778
Al-Zn-Mg alloy, hardness changes associated with fatigue-crack propag. 8=26783
Cu, dislocation structure associated with fracture surface 8=40143
Pb alloys with 0.5% Sb, Te, Cu, effect of dopant on alloy lifetime and structure 8=26841
Pb-0.5% Sb, bands developed on reversed bending cycles 8=35714
Si-Fe, collective recrystallization and polygonization during testing 8=48558
Si-Fe, low cycling, dislocation density 8=39963
Si-Mn steel, crack, initiation and propag., previous austenitic grain size effects 8=44575
Elastic limit
See also Slip.
beams for multiple loading, minimum-weight design 8=41682
α-brass, discontinuous yielding rel. to grain size and strain ageing temp., obs. 8=40141
cubic yield condition for incompressihle bodies 8=48961
permalloy, determ. by Barkhausen effect 8=26838
shells, rotationally symmetric, under central boss loadings, limit anal. 8=23840
steel. age-hardened containing γ' precipitates, tensile yield mechanism 8=49014
steel, yield point behaviour 8=44571
Al-Cu alloys, aged, orientation effect on yield strength 8=48991
Fe-C martensite, yield strength and transformation substructure 8=26812
Fe, ferromagnet, determ. by Barkhausen effect 8=26838
KCl, yield point dependence on growth conditions and impurity effects 8=26401
LiF, yield point dependence on growth conditions, impurity effects 8=26401
NaCl, yield point dependence on growth conditions and impurity effects 8=26401
Ni, ferromagnet, determ. by Barkhausen effect 8=26838
Elastic losses. See Internal friction.
Elastic relaxation
See also Creep.
α-brass, stress relax., 78-295°K rel. to dislocation behaviour 8=31193
crystal point defect phenomena 8=31027
b.c.c. transition metals, dislocation in 8=31088
f.c.c. alloys, disordered, Zener, relax. time and jump freq. reln. 8=31188
ice crystals, understanding of relax. phenomena 8=49366
impurity diffusion coeff. determ. 8=30995
metals, thermal activation energy determ. by alternating bending 8=35613
paraelastic and paraelectric defect systems solids 8=48798
poly-α-methylstyrene 8=40198
Snoek effect, orientation dependence 8=26747
viscoelastic, very early-time props. 8=32773
Ag-M solid solns., (M = In, Sn, Sb), activation energies for Zener relax. 8=31190
Ag-Zn solid solns., Zener relax. rel. to vacancy-controlled atomic mobility 8=31040-1
CaF_2:Sm, Nd, relax. flow teeth obs. 8=26794
CdF_2:Sm, Nd, relax. flow teeth obs. 8=26794
Cu-Si-Mn, stress relax. anomalies, 200-400°C 8=35668
Fe, local stress relax., rel. to dislocation structure, strain rate and temp. 8=35676
αFe-C(N), Snoek relax., temp. depend. of mag. losses 8=40880
KBr, rel. to dislocation pinning by lattice defects 8=26680
KCl, rel. to dislocation pinning by lattice defects 8=26680
LiF, of stresses during thermal processing 8=40167
NaCl, rel. to dislocation pinning by lattice defects 8=26680
RbI, rel. to dislocation pinning by lattice defects 8=26680
Elastic waves
See also Acoustic waves; Seismic waves.
attenuation, in nonhomogeneous semispace surface with waveguide 8=41815
axially symmetric, in solid of revolution 8=46146
in bars, anisotropic, of rect. cross-section 8=32891
classical elasticity analogue of linear isotropic plasma waves 8=34538
compressional, refl. at interface, amplitude-distance curves freq. depend 8=23933
crystal, infinite piezoelec. plate, vibr. theory 8=46144
in crystals, anisotropic, surface propag., forbidden directions 8=48946

Elastic waves—contd
cylinder, circular with hexagonal cryst. symmetry, propag. 8=46147
in cylinders, two-layered, of axially symm. waves 8=41817
diffraction in multi-layered spherical geometry rel. to P-waves attenuation 8=27842
eikonal and asymptotic equations 8=32722
in elastic-plastic string, transverse propag. for different plasticity conds. 8=32751
energy flux for two interfering waves 8=41814
epicentre motion of half-space due to buried stationary and moving line sources 8=41818
excitation in piezoelectric slab by plane electromagnetic waves 8=46157
field representation by scalar wave functions 8=23941
in finite bar, with loadings at impact end, numerical soln for 2-dimens propag. 8=23938
in finite elastoplastic bar in contact with elastic bar, with longit impact 8=23934
flexural, reflection from intermediate rod of variable thickness 8=41826
half-space, buried spherical source 8=41820
half-space containing cylindrical cavity 8=23939
half-space with moving boundary load, dynamic reactions along rigid-smooth wall 8=41685
harmonic, diffraction by rigid circular disc 8=32894
in heterogeneous materials, continuum approach to theory 8=37248
interaction of two waves, coupled mode theory 8=32681
in layered solids, linear wave motions of thermoelastodynamics, potential eqns. 8=23829
in layered sphere, prod. by impact, surface wave dispersion, and vels. 8=32887
in layered structs, theoretical surface motion for pulse transmission 8=32888
linear elastodynamics, extremum principles in terms of polarization tensors 8=23847
Love waves propag. along homogeneous and heterogeneous media interface 8=32895
in magnetically polarized conductors, transformation into elastic waves 8=39886
metallic films, magnetoelastic waves, boundary-value-problem 8=40797
in micropolar solids, propag. vels of surfaces of discontinuity of displacements 8=32893
nod, control of dispersion by using one material 8=23932
in nonlinear dissipative materials, existence of steady waves 8=46151
one-dimensional, propagation in homogeneous media 8=46156
oscillations, wave film type, of quantized thickness, propagation 8=46149
piezosemiconductors and dielectrics, instability in alternating field rel. to sound generation 8=30940
plane dilational pulse, transient diffraction at fluid-solid interface 8=23940
in plate, semi-infinite, in contact with harmonically disturbed elastic half-space 8=41822
plates and rods, reflection of mode from free edge, traction-free boundary conds. 8=41824
Plexiglas, dispersion and absorption of transverse waves 8=49069
point and line defect movement in continuum theory 8=48952
propagation equations applied to solid earth 8=50031
propagation in conducting medium in presence of mag. field 8=46154
propagation in cylindrical shell filled with fluid, surrounded by elastic medium 8=41816
propagation in elastic-plastic medium 8=23935
propagation in nonlinear materials, relativistic theory 8=41821
propagation, nonlinear, perturbation theory 8=41819
reflected and refracted at boundary between transversely isotropic media, energy distribution 8=41825
relfection and refraction, transversely isotropic-media 8=46145
Rayleigh wave propag. in elastic half-space inhomogeneous in x and z co-ords 8=23936
Rayleigh wave propag. past step change in elevation, transmission and refl. coeffs. 8=46152
Rayleigh waves in inhomogeneous elastic half-space of waveguide type 8=46148
rod, curved slender, longitudinal-flexural modes 8=41827
in sandwich ring, harmonic wave propag. 8=32892
rel. to seismology, compress. pulse propag. in liquid sphere, wave theory 8=28364
in semilinear viscoelastic mats, velocity (or stress) after impact 8=32886
shear waves in crystals, transucer applics. 8=46195
and shock waves in thin rod 8=46166
solid, kink-capillary, rel. to surface tension 8=26748
in solids, interact. with temp. waves, attenuation and temp. depend. 8=39882
in solids, shock compression, crystallographic analysis 8=26745
spherical elastic-plastic, propagation 8=46153
sphere surface motion due to radial impulsive force and explosive point-source 8=36667

Elastic waves—contd
- standing waves in layered fluid half-space, from compressional waves below 8=32889
- stationary, in spinning disc 8=23937
- Stoneley, propag. in cubic crystal 8=26746
- stress, propagation in half-plane with boundary loading 8=37130
- stress waves in plates, prod. by impulse load on portion of edge 8=23834
- surface, excitation in piezoelectric solid by interdigital transducer 8=46155
- surface, in joined elastic materials, crack propagation along junction 8=46050
- surface in layers with varying thickness, differential equation 8=32890
- surface of elastic isotropic medium, surface impedance effect 8=28365
- surface, production by Hertzian impact 8=32714
- thermoelastic solid in mag. field 8=28278
- travelling, in beams and plates, dynamical finite-element analysis 8=41823
- velocity calc. for case of Birch-Knopoff eqn. 8=26749
- vinyl, dispersion and absorption of transverse waves 8=49069
- viscoelastic medium, disturbances produced by impulsive torsional body forces 8=46150
- in visco-elastic slab due to transient torsional forces 8=32769
- visco-plastic, non-homogeneous bars, propagation 8=28363
- waveform distortion, finite-amplitude, rel. to dissipation and spreading loss 8=37247
- ultrasonic wave scatt. factor effect on calc. of polycrystalline solids 8=30936
- Cu, propagation mode compilation 8=44563
- $LiNbO_3$, 20-2000 Mc/s, excitation and attenuation 8=44584
- in YFe garnet in two-port magnetoelastic delay lines 8=40850
- Y-Fe garnet, magnetoelastic waves, 1.1 GHz, props. from light diffraction obs. 8=40101

Elasticity
- See also Compressibility; Mechanical strength; Stresses, internal; Thermoelasticity; Viscoelasticity.
- adiabatic strain-cycling and temp. rise model, dispersion relations appl. 8=40102
- anelasticity, appl. to radiation damage and point defect diffusion 8=31127
- anelasticity theory due to glide-dislocations motion 8=48943
- asymmetric theory, plane strain 8=46056
- axi-symmetric solid with pit or cavity symmetric inside or on solid 8=41666
- bar, flexible, subject to arbitrary discrete loads and boundary conditions 8=46053
- beam on elastic foundation with moving load, nonlinear effects 8=41652
- beam on Wieghardt-type foundation differential eqn. for deflection curve 8=41679
- beam, under impact loading, closed form solution for transverse vibrations 8=41678
- beams, continuous, 3 dimensional solution 8=37136
- beams, indeterminate, elastoplastic analysis under reverse loadings 8=37135
- beams, min. weight design with inequality constraints on stress and deflection 8=23828
- beams, thick rectangular, higher order effects 8=41705
- bending, intense, of plates, solvability of eqns. 8=37151
- bending of elastic plates, theory, contribution to Reissnerian algorithm 8=41669
- boundary-value problems, dynamic, soln. for circularly symmetric bodies using differential-difference method 8=32743
- cellular shell, multiple anisotropy model 8=32723
- circular plate collapse under two uniform loads 8=41680
- circular plates on elastic foundations, buckling equation roots 8=32725
- classical, analogue of linear isotropic plasma waves 8=34538
- classical, expanding boundary value problems 8=46027
- composite medium, wedge-like waves 8=37159
- contact problems for cylindrical elastic bodies, use of asymptotic solution of class of integral equations 8=45982
- corner singularity due to asymmetric shear loading, couple-stresses effect 8=41692
- couple stress theory, two-dimensional problem of equilib. 8=41686
- couple-stresses, effects on singularities due to discontinuous loading 8=32733
- crack propagation along junction of elastic material 8=46050
- crystal, mech. and shape equilibrium, Gibbs surface model 8=40086
- crystals, theory at low temps. 8=48936
- cracks, elliptical, three-dimensional theory 8=41709
- crystal point defects, anelastic behaviour, thermodynamics 8=31027
- cubic media, fundamental integral 8=46036
- curvilinear cracks in bonded dissimilar mats, elastostatic problems 8=26773

Elasticity—contd
- cylinder, hollow, bonded to thin shell, axial shear vibrations 8=32876
- cylindrical cavity, transient response at boundary 8=41695
- cylinder, hollow, bonded to thin shell, elastic vibrations 8=32875
- cylinders, two in contact, torsion 8=32717
- cylinder, two-layer, in torsional vib., calc. of internal friction 8=28362
- cylindrical bars, press.- step and vel.-impact loaded, strain and stress distribs. 8=23833
- deformation rate for continuous medium, exact derivation 8=41668
- deformed isotropic materials, acoustical birefringence of u.s. waves 8=46187
- dielectrics, controllable states as combination of finite static deform, and static elec. fields 8=44858
- dielectrics, electro-mech. interactions rel. to polarization gradient, theory 8=44893
- discontinuities, one-dimensional, propagation in compressible materials 8=32741
- discontinuity in finitely deformed medium, thermodynamic relations on surface 8=37142
- disc, rigid-workhardening, of initially non-uniform thickness, finite expansion of hole 8=37133
- disks, rotating, elasto-plastic analysis 8=46044
- disks, thin, variable thickness, consistent finite difference equation 8=37145
- displacements in a harmonic type material, energy and uniqueness theorem 8=32747
- dual equations in elasticity theory soln. 8=46039
- dunite and gabbro, brittle-ductile transition 8=48976
- earth, eqns. consistency rel. to models validity 8=27840
- eikonal and asymptotic equations for moving medium 8=32722
- elastic-plastic deformation of high pressure vessel 8=46057
- elastic-plastic problem, analytic method 8=41723
- elastic-plastic problems, plastic stress-strain matrix appl. 8=28258
- elastic-plastic string, transverse vib. for different plasticity conds. 8=32751
- elastic structures, generalised theory of 8=32746
- elasticae, plane extensible; with nonlinear stress-strain laws, general solutions 8=46043
- elastical, deduction of known solns. 8=41681
- elastodynamics, linear, stability of traction boundary, value problem 8=46032
- elastodynamics, transient, direct formulation and numerical solution 8=46054
- elastoplasticity contact problem 8=37152
- elements, curved, isoparametric, "quadrilateral", for finite element analysis 8=41687
- elliptic die press. on elastic half-space 8=32711
- equations, general asymptotic solution for internal stress state of thin layer 8=46029
- equilibrium of plates and shells, hypergeometric functions 8=46038
- equilibrium paths through critical points 8=41672-3
- field in anisotropic solid, effect of spherical
- finite difference method for axially symmetrical and plane problems 8=32730
- glasses, inorganic, delayed 8=49025
- Griffith cracks, two coplanar, in infinite elastic medium 8=46042
- half-space, epicentre motion due to buried stationary and moving line sources 8=41818
- half-space mixed boundary-value problems 8=23845
- half-space of granular material, moving step load on surface 8=41711
- half-space, subject to radial stress distrib., torsional damped vibs. 8=28262
- half-space with moving boundary load, dynamic reactions along rigid-smooth wall 8=41685
- impact of mass on beam 8=37132
- inclusion, circular, in infinite compressible medium, 2nd order effects 8=23841
- inclusion problems, three-dimensional 8=41693
- incompressible, homogeneous materials, quasi-equilibrated motion 8=37124
- inelastic column instability subjected to time-dependent load 8=32706
- integral equations, first kind, reduction to second kind 8=46030
- kinetic stress function determination in elastodynamics 8=46037
- limestone, brittle-ductile transition 8=48976
- linear elastodynamics, extremum principles in terms of polarization tensors 8=23847
- linear problems, soln. using convergence of finite element method 8=32727
- linear problems, solution properties 8=46026
- linear theory, displacement boundary value problem 8=46045
- linear theory, strain-gradient contrib. to potential energy-density 8=41690
- linear theory, variational principles for general boundary conditions 8=41670

Elasticity—contd
micropolar, for stress analysis around circular hole in infinite plate 8=32738
micropolar materials, hereditary, linear theory 8=41708
moment, formulation of statistical problems 8=46040
multiphase media, boundary problem 8=32735
n-degree elliptical ring of non-uniform cross section, analysis 8=46051
non-homogeneous body, stability, general condition 8=32709
noncircular rings under shear load 8=32720
nonlinearly elastic material, self-similar impact-loading problem 8=41671
nonprimitive crystals, rel. between macroscopic and microscopic theory 8=31160
orthotropic circular plate, large deflection under concentrated load 8=32721
oscillations, high-freq., of thin elastic variable-thickness layer 8=41813
permalloy sheet, anisotropy, effect of recrystallization 8=35282
plane, stress depend on Poisson's ratio 8=41683
plane stress theories for stretched plates 8=23848
plate, asymmetrically layered elastic, moderately large deflection 8=37144
plate on elastic half-space, with moving line load, bending moments and stiffness 8=23830
plate, response to random loading 8=37140
plate stability problem solution without preliminary determination of initial stress state 8=46031
plate waves, non-propagating, effects on dynamical stress concentrations 8=41694
plates, dynamic stress concentrations 8=37150
plates, subject to large deflections, equilibrium bifurcation 8=46041
point-force at any point in compressible infinite medium, second-order effects 8=28259
polymers, oriented, macromol. segmental mobility dependence 8=35735
polypropylene melt, behaviour 8=39261
polystyrene melt, behaviour 8=39261
plates, thin, containing internal stress, flexure 8=37137
α-quartz, elastic coeffs. and moduli, polarizing tensor 8=49048
rigid cylinder on elastic layer on rigid base, contact problems, asymptotic solns. 8=37139
and ring force 8=41665
rods, general theory 8=37127
rubber, eqn. of state 8=26858
satellite, dynamics of elastic satellite 8=45578
satellite motion effect of elasticity 8=41640
sheets, overlapping bonded, stress analysis 8=41689
shell, cylindrical, forced axi-symmetric motions 8=32715
shell, elastic of revolution of negative Gaussian curvature, asymptotic solution 8=37148
shell, thin, distortional theory 8=32724
shells and plates, anisotropic, linear theory 8=37149
shells, conical of varying thickness, subjected to lateral loads, solution 8=37146
shells helicoidal, axial extension and tension 8=32734
shells, linear theory, multivaluedness of stress functions 8=32718
shells, long, cylindrical, subject to uniform pressure and ring force 8=41665
shells of revolution, nonlinear boundary layer 8=41707
shells, sandwich, with dissimilar facings, theory for moderately large deflections 8=37128
shells, shallow, multivaluedness of solns. 8=32719
shells, shallow spherical, displacement boundary value problem 8=41701
shells, shallow spherical, membrane and bending stresses 8=37141
shells, thin circular cylindrical behavior, rel. to infinite crack 8=32708
shells, thin, finite element approx. for analysis 8=41688
small-deflection theory, applied to thermal deflection of non-homogeneous rectangular plate 8=41872
snap-through of truss, effect of geom. imperfections 8=46035
solid of revolution with inside cavity subjected to torsion at infinity 8=41666
solid, kink-capillary oscills. rel. to surface tension 8=26748
solids, direct numerical determ. of stresses, as shown by torsion problem 8=41702
solids, forced motion 8=41674
solids of revolution, soln. of 3-dim. theory problems by analytical functions 8=41704
sphere in solid, uniformly stressed at infinity, contact stresses 8=23831
stability, energy concepts 8=32740
stability for incompressible hyperelastic bodies 8=41676
steel frames, in stability in elasto-plastic range 8=40156
step load moving with superseismic velocity on surface of elastic-plastic half-space 8=32749
stress field, strain and density in a bulk with nonuniform initial stress, numerical solution 8=32748
stress, strain and displacement fields analysis in composite material reinforced with discontinuous fibres 8=46049
structures, optimal design for max. stiffness 8=41703

Elasticity—contd
superconductors, type II, effects, theory 8=40357
surface waves produced by Hertzian impact 8=32714
theory, differential operators, reciprocal relations 8=46055
theory of mats. with long range cohesive forces 8=32732
theory in a Riemann space 8=32746
theory, integral equations, approximate solutions 8=45980
theory, solution of equations differing from zero only near surface 8=46149
three-dimensional, problems in the theory 8=32710
time-variant creep, analogy 8=41737
torsion of elastic cylinder welded to elastic half space 8=23827
two solids in isotropic mixture, plane strain, linearized theory 8=32744
vibrations, radial, of cylindrical inhomogeneous annulus of aeolotropic materials 8=32716
viscoelastic fluids, determ. from tangential stress meas. 8=48099
wave velocity, for Birch-Knopoff eqn., calc. 8=26749
wheel, elastic, lateral force property in presence of thrust, exptl. study 8=41644
yield and generalized pyramidal fracture criteria 8=41712
in KMnF$_3$, anomaly at 184°K 8=26827
SiC, properties 8=35717
Zr, corrosion breakaway region, inelastic behaviour of metal and oxide 8=36576

liquids
See also Compressibility/liquids.
elastico-viscous liquids, linear, theory 8=25841
rigid sphere, approach to deformable liquid/liquid

Elastomers. See Rubber.
Elastoplasticity. See Plasticity.
Elastoresistance. See Piezoresistance.
Electrets
See also Electrostatics.
Carnauba wax thermoelectret, heterocharge on ionic addition 8=44879
dipole orientation rel. to thickness and polarizing field. X-ray diffraction obs. 8=44891
naphthalene pure and naphthol-doped, glow peak analysers 8=49378
paraffin, surface charge density meas. and contact electrification 8=49379
plastic, surface charge characts. 8=44892
polystyrene and polyethylene, surface charge density meas. and contact electrification 8=49379
polystyrenesulphonate membrane forms, optimum ionic electret 8=44878
review of phenomenological theories 8=46344
α-HgS, nature of photoelectet effect 8=31440
Electric breakdown. See Breakdown, electric.
Electric charge
See also Space charge.
accelerated, radiation invariance restrictions on momentum change 8=37935
aerosol particles, charging in an electric field, theory 8=25969
alkali halides and organic insulators, transfer by friction 8=27223
aromatic hydrocarbons, injection in liq., soln. and solid forms 8=30518
electret, rel. to thickness, X-ray diffr. obs. 8=44891
electrographic processes, transfer meas. 8=24075
elementary, proposed variation with time laboratory test 8=28212
emission from proton synchrotron targets, beam monitoring 8=33490
extended particle with arbitrary change structure, stability, negative mass. 8=33522
galvanometer, ballistic, appl. to pulsed laser threshold meas. 8=33164
liquids, charge carrier momentum transfer 8=39393
production in semiconductors and insulators, determ. method 8=49224
smoke particles, chain aggregate, obs. 8=30562
H_2O drops in ion stream rel. to clouds electrification by selective ion-capture, obs. 8=30517
Electric discharges. See Discharges, electric.
Electric fields
See also Electromagnetic fields.
in corona discharges in rod/plane gap systems, subjected to impulse voltages 8=29923
cyclotron, central config., mag. analogue 8=46999
cylindrical discharge plasma traversed by current, field strength calc. 8=47820
dielectric slab between sphere and plane, pot. gradient calc. 8=24074
electrostatic, Dirichler's and Thomson's princ. arising in complementary manner 8=28353
equation solution, affected by permanent unipolar ion flux 8=33026
gradient, caused by mag. impurities in metals 8=40962
gravitationally induced in conductors, estimate from statistical electron model 8=26876
gravitationally induced near metals, expt. criticised 8=40297
gravity-induced, near conductor 8=24076

Electric fields—contd
- Heaviside formulae connection with relativity 8=46347
- long horiz. line source above ground 8=24242
- mathematical models and computer soln., book 8=33054
- multidielectric region, numerical solution of Laplace's equation 8=46348
- metals, gravitationally induced elec. field, meas. 8=35814
- plasma, microfield distrib., asymptotic calc. 8=39082
- plasma, weakly ionized, effect of inelastic collisions 8=47821
- plotting experiment, modification 8=37367
- point charge in inhomogeneous medium, elec. pot. 8=33024
- production, by propagation of plane coherent e.m. radiation in stratified medium 8=28613
- quadruprobe for d.c. elec. field meas. in space 8=41381
- quadrupole e.s. lens with concave electrodes, meas. 8=37420
- quadrupole, in circular concave electrodes 8=46350
- α-quartz crystal, refractivity interpret. 8=49756
- space, detect. and meas. 8=27958
- spatially varying, h.f. breakdown of nonuniform gases 8=29908
- static non-uniform, focusing props. 8=28540
- two-dimensional problems, solution by boundary relaxation 8=45994
- Ni ferrite, external field amplification factor determ. from NMR expts. 8=36267

effects
- absorption spectra modulation 8=38881
- a.c. strong, nonlinear excitation of electrons in semiconductors 8=49209
- aerosol particles, charging 8=25969
- p-(anisalamino)-phenyl acetate liq. cryst., on n.m.r. 8=34924
- azulene, broadening of electronic transition 8=45238
- birefringence, optical, quantum field theory 8=33340
- Bloch electron motion in external field, classical and quantum dynamics 8=26875
- on cholesteric liq. crystal struct. 8=34768
- on condensation heat transfer, and thickness of liq. films 8=34990
- conductivity changes, expt. using stationary high-field domain analysis 8=31368
- colour centre alignment to remove macroscopic inversion asymmetry 8=44471
- critical opalascence of dipolar mixtures 8=39312
- critical opalescence, relax. times 8=30473
- crystal electron intraband and donor-band transitions rel. to band structure determ. 8=31281
- crystal electrons, relativistic and spin effects 8=44624
- d.c., on chemisorption of O_2 on ZnO 8=49905
- in dielectrics with high permittivity, theory 8=40560
- impurity centres in crystals, e.p.r. spectra 8=45070
- F-centres, shallow, in ionic cryst., rel. to theory 8=44470
- ferroelectric crystal, Curie temp. var. 8=27259
- ferroelectrics, rel. to soft phonon modes freqs. 8=40604
- field-ionization mass spectra 8=47796
- Franz-Keldysh effect, high-freq. 8=31950
- gases, elec. field induced spectra 8=25582
- ice filaments, growth and destruction 8=35244
- ionic crystals, activated, photoluminesc. spectra 8=36456
- linear, on EPR spectrum of Cu^{2+} ions in tetrahedral cryst. fields 8=49585
- liquids, rel. to gas bubbles formation 8=25855
- on metal epitaxial film growth 8=26109
- metal penetration, prod. of slowly damping oscs. of the pot. 8=40298
- minerals, deformation rates in h.f. e.m. fields 8=35643
- molecules, axially symmetric, spectra 8=29676
- nematic liq. crysts. thermal cond. 8=34833
- non-Kramers doublets, e.p.r. transitions 8=49584
- on paramagnetic resonance, non-linear, theory and appl. to ruby: Cr^{3+} 8=40906
- plasma ion-acoustic waves, electron drift vel. obs. 8=25729
- plasma kinetics, statistical mechanics 8=30019
- plasma l.f. oscillations, radial field effect 8=34539
- plasma spectral line Stark broadening 8=25340
- plasma, weakly ionized, in time-depend. field electron distrib. function 8=43520
- probe, electrostatic, natural vibration freq. 8=47860
- ruby, on mag. resonance of Cr^{3+} pairs 8=40904
- saddle point optical transitions under crossed elec. and mag. fields 8=27543
- scalloping of compressed e beams 8=46405
- semiconductor, impact ionization of impurity atoms in strong fields 8=35864
- semiconductors, diffusion instabilities 8=26616
- semiconductors, diffusion, simultaneous and consecutive, of impurities, rel. to internal elec. field 8=30997
- semiconductors, magneto-optical absorption spectrum in exciton region 8=36305
- semiconductors, rel. to phonon excitation 8=27059
- solids, dielectric props., interband 8=27226
- sorption process 8=39606
- CdTe:Fe, selective abs. changes under influence of high elec. fields 8=36339
- Cu phthalocyanine, rel. to photocarriers 8=36018
- Cu_2O, on exciton quadrupole transitions 8=31984
- H atom, beam foil excitation 8=25376

Electric fields—contd
effects—contd
- H_2 mol., mag. shielding in elec. field 8=47599
- HBr, gas-phase radiolysis 8=49977
- HCl, gaseous, rel. to gamma-radiolysis 8=36622
- KBr: Tl, (In), mono- and di-molecular recombination in luminescence 8=45276
- KI: Tl, (In), mono- and di-molecular recombination in luminescence 8=45276
- Nb surface self-diffusion in strong elec. field, field-emission exam., 8=39978
- ZnO, Brillouin scattering from shear waves in crysts. under high fields 8=44325

Electric strength
See also Breakdown, electric.
- insulator test, allowance for nonsustained breakdown 8=37368
- SiO_2 films, amorphous, temp. dependence. −196 to +50°C 8=40561

Electrical conduction. See Conduction, electrical; Conductivity, electrical.

Electrical current. See Current, electrical.

Electrical measurement
Entries describing measurement methods for specific electrical quantities and effects may also be found listed under the various headings for the subjects concerned.
- ammeter using flux quantization in superconductors 8=4041
- apparatus suspended on flat elastic strings, equilib. and stability of mobile part 8=33009
- capacitance, small, use of spiral resonator in oscillation meas. method 8=46319
- capacitance, temp. coeff., new methods 8=24063
- cascade generator, voltage control using pick-up electrode 8=41917
- coaxial transmission-line r.f. power calorimeter 8=33007
- conductivity of melt up to 1600°C 8=34902
- conductivity tensor of anisotropic crysal 8=26940
- contact pot., vibr. capacitor with electrostatic drive 8=28450
- corona discharge, peak-reading meters and recorders 8=24062
- current, ionization, fluctuation errors 8=42345
- digital phase-sensitive detector 8=28449
- electric fields in space 8=27958
- electrode polarization compensated by 4 electrode null technique with high resolution 8=28453
- feedback Kelvin probe 8=33005
- fluctuation-noise level meter, wideband, transistor 8=46318
- frequency characteristics meas. of photoelectronic devices with tunable laser 8=46317
- frequency response from transient response, practical method 8=41638
- galvanometer ballistic, appl. to pulsed laser threshold meas. 8=33164
- galvanometer, bandpass filter for lock-in amplifiers 8=33011
- high resistance, in insulator range, apparatus 8=24064
- impedance comparator as fast-balancing a.c. bridge 8=24065
- ion beam, intense, collector method 8=46325
- ion counter SI-01 8=47450
- leakage current monitor for semicond. detector 8=37775
- nuclear reactor power, by plasma microwave diagnosis 8=47432
- polymer conductivity, difficulties 8=40592
- proton linear accelerator, beam current and energy calibration 8=33435
- resistance, small rapid change meas. 8=28456
- resistance, variable, automatic meas. of Hg column level 8=28455
- resistivity, eddy-current decay method, analysis 8=46326
- resistivity meas. in megagauss fields, method 8=24066
- rocket probe for ionospheric e density and temp. meas. 8=36847
- scanning e microscope beam current 8=46324
- semiconductor, piezoresistance meas. 8=35876
- semiconductor props., photoelec. method 8=27076
- sheet resistance test apparatus 8=28457
- standards, historical review (1918-1968) 8=28209
- standards of units and transfer of their dimensions to meas. and instruments 8=46315
- superconducting coils, techniques for mag. field determ. 8=37396
- superconducting voltage-detector, high-sensitivity 8=40415
- surface resistivity of dielectrics 8=28454
- transistors, ultra fast, parameters meas. using simulator 8=27197
- two-channel data logger 8=37359
- vector plotting display 8=24057
- v.h.f. square wave generator, type T-402 8=33017
- voltage/current meas. in GHz range using bolometers 8=24058
- voltage, d.c., supercond. parametric amplifier 8=31347
- voltage-freq. converter for integrating digital voltmeter 8=41918
- voltage, high frequency cyclic, on a surface, electron microscope obs. 8=33008

Electrical measurement—contd
voltage, in scanning e microscope 8=41970
voltage, small d.c.. by phase-sensitive detection in double Josephson junction 8=46321
voltmeter, direct reaching attracted-disk, absolute 8=33010
voltmeter, integrating digital, use of timer 8=41920
voltmeter using Josephson junction props. 8=31353
waveguides, characteristic impedances 8=46491
zero-crossing phase meter modifications 8=33006
ZnS electroluminesc. semicond. resistors 8=27145
Electrical properties of substances
See also individual properties, e. g. Conductivity, electrical; Dielectric properties of substances, etc.
air, e temp. in shock waves, microwave meas. 8=39221
aqueous electrolyte solns., surface potentials 8=30516
charge carriers, natural, determ. of mobility 8=43863
clays, potential meas. 8=26947
complexes, charge-transfer, monomeric and polymeric, review 8=26942
conducting mats, theories of mechanical deform. 8=26752
conductors with anisotropic conduction band, permittivity 8=26938
electrolytes, aq. solns., Hall effect meas. 8=48199
electronic parts, reliability in combined temp., vacuum and nuclear rad. environment 8=27192
ethane, mobility of electrons, photoelectrically generated 8=39223
impedance of thin conducting films in longit. mag. field 8=26955
liquid chains, localized electron states, non-exponential range 8=34886
magnetic ceramics, props. rel. to ferrimag. props. review 8=49554
mesitylene-benzonitrile liq., rel. to charge-transfer interacts. 8=30515
metal electrodes in ionized gas flow, voltamp characts. 8=26952
metals, gravitationally induced fields 8=40297
methyl silane, isomeric derivs., elec. dipole moment study 8=43925
plastic-oil composite dielectrics 8=40558
p-n-n$^+$ diode, current-voltage characts., allowing for carrier lifetime variations in base 8=27170
point charge in inhomogeneous medium, elec. pot. 8=33024
polyacetylene, linear, cond. and Seebeck voltage rel. to O content 8=31398
pyridine-benzonitrile liq., rel. to charge-transfer interacts. 8=30515
pyridine-trinitrotoluene liq., rel. to charge-transfer interacts. 8=30515
rubeanato-Cu co-ord. polymer, cryst. compared with amorphous 8=27385
semiconductors, acoustic domains and IV charact. under acoustic instability condns. 8=27053
synthetic insulating materials, properties 8=48180
thin films, contactless meas. 8=49134
transition metal arsenides 8=41079
Xe, conversion to metal-like state on shock compression 8=43851
Al_2O_3, chemisorption effects 8=44866
Ar, e temp. in shock waves, microwave meas. 8=39221
Ar, liquified, ion mobility and liq. motion 8=48193
Ar, solid and liq., charge transport 8=26943
$Ba_2(FeMo)O_6$, and mag. props. 8=36195
Bi, charged carrier diffusion through shock wave front 8=35826
Bi, transverse voltage in longit. mag. field 8=35825
$Ca_2(FeMo)O_6$, and mag. props. 8=36195
$CdGeP_2$, n- and p-type crystals, rel. to conc. 8=49791
Cd-Pb system, electrotransfer inversion, and scatt. of impurity atoms 8=40315
CdS layers, chem. deposited, and photocond. props. 8=44918
CdSe, current saturation and acoustic noise 8=30942
n-CdTe, instability 8=40445
CdTe, pure, and production 8=26239
$Cu_{0.5}Fe_{2.5}O_4$, rel. to constitution 8=48341
Cu-Zn system, conc. dependence, stacking fault energy 8=48869
DNA solns, background noise between 300 Hz and 50 kHz 8=30520
Fe films, and optical props. rel. to absorpt. of bulk Fe 8=41085
Fe layers, thick evaporated, gyroelec. and gyromag. consts, reflected light meas. 8=36141
GaP photodiode, strongly compensated p–i–n junction 8=40509
He gas, energy distrib. functions and drift vels. 8=47975
HgSe-βHgS, mixed crystal 8=31320
HgTe-βHgS mixed crystal 8=31320
HgTe-HgSe mixed crystal 8=31320
KCl-KBr fused mixtures, conductivity and activation energy for ion conduction 8=30519
KCl-LiCl fused mixtures, conductivity and activation energy for ion conduction 8=30519
KCl-NaCl fused mixtures, conductivity and activation energy for ion conduction 8=30519
Kr, solid and liq., charge transport 8=26943

Electrical properties of substances—contd
Mn-Sn alloys, liq., electron config. rel. to conc. curves 8=36214
N_2, e temp. in shock waves, microwave meas. 8=39221
NaCl-NaBr fused mixtures, conductivity and activation energy for ion conduction 8=30519
Nb-45 wt. %Ti and Cu composite conductor for large currents 8=27021
$NiCl_2$, $NiBr_2$ and NiI_2, sublimation 8=39496
NiS, metallic-semiconducting transition 8=31788
PbO, and optical props. 8=26948
Pt-1 at % Co(Fe) alloys, and mag. props., plastic deformation effects. 8=31327
$Sb_xBi_{1-x}SJ$ and $SbS_xSe_{1-x}J$ 8=40670
Si epitaxial films on sapphire 8=40491
SiC compact bodies, compared with sintered lines 8=49142
$Sr_2(FeMo)O_6$, ordered perovskite, and mag. props. 8=36195
Tl-Te alloys, liquid, n-type 8=34897
α-U_3O_8, from meas. of thermoelec. power 8=35999
UO_2 powders, n-irradiated, e.m.f. meas. rel. to electronic props. 8=40290
WS_2 irrad. in nuclear reactor 8=49143
Xe, solid and liq., charge transport 8=26943
Electrical units. See Units.
Electricity
asynchronous induction machine, single-phase, response to variable freq. rectangular wave 8=41930
book, physical aspects 8=28448
conventions and nomenclature 8=24121
d.c. current storage using superconducting flux pumps and transformers 8=41931
illumination and air-conditioning, combined systems 8=41928
illumination improvement by combination with air-conditioning 8=41929
motors, d.c., with electronic commutation, torque-speed curve 8=37373
direct conversion
adsorption integral Cs reservoir converter, Cs contents in components after life test 8=28503
book 8=41932
cells, electrochem. and sealed, internal press. meas. 8=33035
cells, thermal, performance 8=33033
convertor, thermionic, in discharge mode, kinetic eqn. 8=33036
electrochemical devices, possible advances 8=36590
emitter sheath, double, density of trapped positive ions 8=34525
fluidized bed electrode appln. to fuel cells 8=41278
fuel and corrosion cells, cathodic reduction of O_2 8=37374
fuel cell for intermed. temp., with H_3PO_4 paste with dispersed B phosphate 8=33029
fuel cell, intermed. temp., operation on dilute H_2 and O_2, and carbonaceous fuels 8=33030
fuel cell reactions, adsorbed species identification 8=46357
fuel cells, review 8=46358
generator with finite electrodes, conductivity effect on flow 8=28471
heat-pipe converter, with Cs-graphite absorpt. reservoir 8=28490
induction m. h. d. generator expt. 8=28467
inpile thermionic reactor, behaviour of damage flux in critical assemblies 8=28504
m. h. d. generator, analysis using vector diagrams 8=28469
MHD generator channel, operation of cold electrodes 8=28474
m. h. d. generator channel, potential distribution by equivalent circuit method 8=28472
m. h. d. generator, electrodynamic effects of non-uniformity of mag. field and fluid parameters 8=28468
MHD generator, end effects and induced mag. field 8=24198
m. h. d. generators, finite electrodes, end effects on fluid flow 8=28473
m. h. d. generators with sectionalized electrodes, volt/ampere characts. 8=28470
MHD open-cycle generator, applic. of aq. K_2CO_3 for admission of ionizing additive into duct 8=46360
MHD optimum generator with channel of constant cross section 8=46359
MHD pulsed generator with superconducting magnet system 8=37376
MHD subsonic generator, core flow in channel with K seeded Ar 8=41933
new methods 8=24081
power extraction from high speed plasma flow through mag. field 8=24082
power sources in nonaqueous solvents 8=33034
propane-O, K_2CO_3 seeded plasma in m.h.d. duct, pot. distrib. and electrode voltage drop, obs. 8=39084
RD-502 cylindrical diodes, with etched Re emitters, performance comparison 8=28483
Re/Mo cathodes in thermionic converter, post test anal. 8=28501
SIRENE 302, in pile thermionic life test 8=28482
solar cell array performance, computer simulation 8=24084
solar cell flexible deployable array, 500 watt 8=24099

Electricity—contd
- **direct conversion**—contd
  - solar cell irrad. degradation and equiv. 1 MeV e flux, computer calc. 8=24085
  - solar cell Langley plots, anomalies associated with tropopause 8=32231
  - solar cell power systems for satellites, and control 8=24087
  - solar cell power systems for satellites, practical
  - solar cells and arrays for lunar surface operations 8=24098
  - solar conversion and energy storage systems, for satellites 8=24088
  - solar energy dev. with reflectors, calc. of energy distrib. in rad. field 8=46361
  - solar energy thermionic generator assembly, converters and ancillary equipment 8=28488
  - solar energy to electricity, thermionic method, review 8=41934
  - solar power system of Mariner IV, design and performance 8=24097
  - solar/thermionic generator combined with Romashka nuclear reactor 8=28493
  - thermionic, Ac^{227} fuelled, heat source optimization and development 8=28492
  - thermionic, CsF excluded at high temp. 8=24083
  - thermionic, cathode electron cooling, 1400°-1800°C obs. 8=33037
  - thermionic, comparison of Re and Pd as collectors 8=28487
  - thermionic converter, cylindrical, with improved W emitter, characts 8=28478
  - thermionic converter, cylindrical, with UO$_2$ fuelled W emitter, post test exam and anal. 8=28500
  - thermionic converter data, correl. method using 'figure of merit for electrode mats' 8=28498
  - thermionic converter with etched, vapour deposited W emitter, characts 8=28476
  - thermionic converter, ion prod. and contrib. to energy loss rate 8=28496
  - thermionic converter performance characts, theory 8=28505
  - thermionic converter for in-pile tests, fabrication problems and techs 8=28486
  - thermionic converter, plasma transport eqns inc. spacing effects 8=28494
  - thermionic converters, high press., electron cooling of emitter 8=28497
  - thermionic diode, planar emitter surface temp. and efficiency meas. with calorimeter 8=28484
  - thermionic diode, use of Cm$_2$O$_3$ and Tm$_2$O$_3$ as isotopic heat sources 8=35425
  - thermionic diodes, reliability of components 8=37377
  - thermionic diodes with cavity emitters, apparent work function 8=28480
  - thermionic diodes, Xe filled, props. on exposure to nuclear rad. 8=28485
  - thermionic, effect of Xe and Kr and V-I characts of variable spacing converter 8=28481
  - thermionic, electron temp. distrib., density, and gap pot, calc. 8=39010
  - thermionic generator fuelled with Co^{60} utilizing thermal separation between fuel and γ absorber 8=28491
  - thermionic, heat-pipe collector-radiator struct., to reduce collector overheating 8=28487
  - thermionic, interdiffusion of emitter of Re welded on Ta substrate 8=28502
  - thermionic system, based on radiant heat transfer, with demonstrated components 8=28493
  - thermoelectric, review 8=49390
  - thermomagnetic generators with graded mass and gap, performance characts., 8=46388
  - 300 watt flame-heated thermionic power supply 8=28489
  - Al dry cell with Al anode 8=33031
  - Cs converter, possibility of Cs oxide reservoir as source of O$_2$ and Cs 8=28479
  - Cds solar cells for multikilowatt arrays 8=24100
  - CdS solar cells micrometeoroid degradation, simulation obs. 8=24094
  - CdS solar cells, performance after micrometeoroid exposive 8=24093
  - Cs plasma diode, seeding with Cd or Hg, influence on performance 8=28475
  - Cs thermionic converter, anal. of plasma distribs. 8=28495
  - H$_2$-CO cell anodes, electrocatalysts 8=46355
  - H$_3$PO$_4$ paste with dipersed B phosphate, in fuel cell, for intermed. temp. 8=33029
  - Ni-Cd flexible thin-film batteries 8=33032
  - Ni and Mo collectors in thermionic diode, comparison 8=31460
  - Pu and cpds, props. and selection criteria 8=25313
  - p-Si solar cell, electron damage coeffs in orbit, calc. 8=27123
  - n/p-Si solar cells charged particle irrad. degradation, base resist. effects, 1-25 ohm cm 8=24092
  - Si solar cells, e irrad, role of Li in degradation and recovery of diffusion length 8=28508
  - Si solar cells for multikilowatt arrays 8=24100
  - Si solar cells in-flight performance, computer prediction 8=24086

Electricity—contd
- **direct conversion**—contd
  - Si solar cells, Li diffused, radiation damage self-healing 8=24091
  - Si solar cells, n irrad. damage and Li effects, obs. 8=24095
  - Si solar cells, p irrad. damage thermal annealing, 4.6 MeV 8=24101
  - Si solar cells, p-irrad., photovoltaic characts. rel. to thermal annealing 8=24105
  - Si solar cells, surface effects, study with low energy p 8=28506
  - Si: Li solar cells, efficiency and e irrad. damage annealing, obs. 8=24103
  - Si: Li solar cells, experience and future of 8=24104
  - n/p-Si solar cells micrometeoroid degradation, simulation obs. 8=24094
  - Si: Li solar cells, present status 8=24090
  - p$^+$/n-Si: Li solar cells, status 8=24102
  - p/n-Si: Li and n/p-Si solar cells, comparison 8=24089
  - Si:P or B, solar cells, comparison of characts 8=28507
  - Th and cpds. props. and selection criteria 8=25313
  - U and cpds., props. and selection criteria 8=25313
  - W emitter with (110) preferred orientation, thermionic converter test 8=28477
  - W/Mo cathodes in thermionic converter, post test anal. 8=28501
  - Zr phosphate membranes for intermed. temp. fuel cells 8=46354

Electroacoustic transducers. See Acoustic transducers.

Electrocataphoresis. See Electrophoresis.

Electrochemistry
- See also Chemical analysis/electrochemical; Electrolysis; Electrolytic deposition.
- aklali halide solns., microdyn. model 8=25953
- alkaline earth halide solns., microdyn. model 8=25953
- alloys, molten, activities determ. by Touch instant e. m. f. method 8=36592
- anthracene, hole injection by electrochemical mechanisms 8=45376
- coal-I batteries, props. rel. to charge-transfer complexes, obs. 8=45369
- concentration cell, self-discharge 8=49925
- Debye-Hueckel Limiting Law 8=49915
- devices, possible advances 8=36590
- dyes, photosensitive, polarograms and hyper-redox potential rel. to work function 8=40687
- electrochemiluminescent processes 8=27691
- electrolyte adsorption, Debye-Hückel limiting law Gibb's equation 8=36591
- electrolytic hygrometer appl. to evolution of water reaction phenomena 8=45314
- galvanic short-cct. current, monitoring 8=46352
- galvanostatic transient processes, overvoltage and double-layer charge 8=27746
- liquid phase cells: concentrating effect cells, and cells opposing Na + ion to K + ion 8=45390
- metal binary systems, liq., diffusion coeff. meas. using conc. cell. 8=43784
- metal machining theory, Cauchy problem for Laplace eqn. 8=49914
- microsectioning tech. to determ. Nb conc profiles after diffusion in W 8=48797
- oxidation-reduction systems, electronic cond. 8=27749
- polystyrenesulfonic acid membranes, dielec. props. rel. to hydration 8=49357
- power sources in nonaqueous solvents 8=33034
- protium and deuterium, separation factor 8=49919
- sealed electrochem. cells, internal press. meas. 8=33035
- solid state cell based on ion conductive ceramics 8=49927
- steel, mild, corrosion in NaCl, transient charge fluctuations, obs. 8=45368
- steel, stainless, corrosion in H$_2$SO$_4$, inhibition by Na$_3$PMo$_{12}$O$_{40}$ mechanism. 8=45370
- thermal cells, performance 8=33033
- varnish on Fe and Pt anodes, elect. characts. 8=49916
- Ag halides at low temps. 8=45256
- Ag, radioactive, props. 8=36594
- AgNO$_3$, molten, cell pot gravit. component 8=45367
- AgNO$_3$-AgCl, molten. cell pot, gravit. component obs. 8=45367
- Al alloys corrosion in NaCl, transient charge fluctuations, obs. 8=45368
- on Al, anodic oxide films, pore struct. and barrier layer. obs. 8=44038
- Al corrosion in NaCl, transient charge fluctuations, obs. 8=45368
- Al dry cell 8=33031
- AlCl$_3$-NaCl-KCl eutectic, fused, of Zn, Cd and Hg ions 8=49917
- C in austenite, study of thermodynamic properties 8=44327
- E$_{f°}$, determ. from polarographic data 8=41276
- Fe, active, in acid solns with high halide concs, anodic dissolution 8=36598
- Fe in H$_2$SO$_4$ containing ring-substituted anilines, corrosion inhibition 8=45377-8
- n-GaAs single crystals 8=45269
- n-Ge anodic dissolution in aqueous solns., cond. band mechanism, obs. 8=45371

Electrochemistry—contd
  H_2O_2 on Pt microelectrode, polarographic behaviour on periodic renewal of diffusion layer 8=41275
  K and Na ions, active transport through biological membranes 8=50461
  $LiClO_4$, fused, electrolysis reactions and metals anodization obs. 8=45389
  LiF solid, oxide doped, oxide and hydroxide activity determ. 8=36593
  Mg corrosion in NaCl, transient charge fluctuations, obs. 8=45368
  NbO stability, polarization of solid galvanic cell 8=45374
  Ni, as-plated electroless, dissolution in acid rel. to Ni_2O phase existence 8=45383
  Ni–Cd flexible thin-film batteries 8=33032
  $NiCl_2$ in alkali halide melts, cell emf's rel. to thermodynamic props., 8=49946
  NiO in NiO–MgO solid soln., thermodynamic activities, obs. by solid-state galvanic cell 8=43979
  O^{17}–n.m.r. study of aq. electrolyte and nonelectrolyte sons. 8=25956
  $PdCl_2$ in molten eutectic $MgCl_2$-NaCl-KCl, voltammetry 8=32131
  $RbClO_4$ in dioxane-water mixtures, conductance meas. at 25°C 8=41274
  Si, activity in molten Ag-Si alloys by e.m.f. meas. 8=48078
  SnO_2-coated glass analogue system 8=32129
  Ta anodic film activation energies of conduction 8=49924
  V_2O_4 anodic films growth in acetic acid-$Na_2B_4O_7$ solns., obs. 8=45375
  Y, electrotransfer of impurities 8=36596
  Zn corrosion in NaCl, transient charge fluctuations, obs. 8=46368
  Zn, radioactive, props. 8=36594
  $ZnBr_2$ molten, external transport numbers 8=34791
  ZnO crystal, photocurrent sensitization 8=49425
  n-ZnO dissolution, current flow 8=49918
  $(ZrO_2)_{0.85}(CaO)_{0.15}$ thermocell, Seebeck coeff. 8=45392
 electrodes
  adsorbed species in fuel cell reactions 8=46357
  cathode depolarization, electrolyte prep. for capacitors 8=49934
  coherent, development and evaluation, exchange behaviour 8=49935
  diffuse double layer of weak electrolytes with field dissoc. 8=41277
  electroadsorption phenomena 8=45366
  electrodic redox reactions, depend. of rate on substrate 8=32133
  ethylene, electrochem. oxidation, oscillatory kinetics 8=49939
  fluidized bed, appln. to fuel cells 8=41278
  formate, electrochem. oxidation, oscillatory kinetics 8=49939
  noble metals and alloys, Tafel slope rel. to cathodic reduction 8=45380
  polarographic, metallized membrane type for use in Clark cell 8=27775
  porous, current distrib. in and on 8=49933
  silver oxide, charging with 60 cps asymmetric a.c., 8=49937
  transparent electrodes, internal reflect. spectra 8=41280
  Ag(I) in $NaNO_3$-KNO_3 eutectic, linear sweep voltammetry 8=27750
  Al anodic films, high field kinetic processes 8=36603-4
  Al, passivation by chromate solns., 8=45379
  Cd, anodic behaviour in alkali 8=32132
  Cd(II) in $NaNO_3$-KNO_3 eutectic, linear sweep voltammetry 8=27750
  Cr, measured conductance rel. to capacitance and Faradaic current 8=49929
  Cu-Au alloy, surface roughening during dissolution. 8=49938
  Cu in HF (anhydrous), anodization Cu/CuF_2(s) couple and its reversible behaviour 8=49930
  Cu, in 3% NaCl aqueous soln., effect of dissolved O on stability of Cu_2O surface film 8=41279
  Cu(II) in $NaNO_3$-KNO_3 eutectic, linear sweep voltammetry 8=27750
  Cu-Zn disc, selective corrosion in H_2SO_4 8=45381
  Fe, diffusion and permeation of electrolytic H 8=44389
  Fe, oxide films, active, passive and transpassive, e.diffr. exam., 8=49931
  Fe passivation in neutral solns., capacitance studies. 8=49932
  Fe-Cr alloys, anodic passivation, influence of Si and Al additions 8=36602
  Hg drop, double layer capacity determ. 8=27751
  Ge, effect of HF and H_2SO_4 on elect. and chem. surface props. 8=27752
  Ge-electrolyte interface, reln between surface states and radicals 8=36599
  Ge, surface photovoltage, pulse meas. 8=27753
  H_2-CO fuel cell anodes, electrocatalysts 8=46355
  Hg, adsorpt. energy of ions 8=36600
  In(III) in $NaNO_3$-KNO_3 eutectic, linear sweep voltammetry 8=27750

Electrochemistry—contd
 electrodes—contd
  Ni fuel cell, activation with Pt catalyst 8=46356
  $Ni(OH)_2$ in LiH, anodic oxidation and Li migration in n-semiconducting mat. production 8=45382
  Pb, anodic behaviour in alkali 8=32132
  Pb(II) in $NaNO_3$-KNO_3 eutectic, linear sweep voltammetry 8=27750
  Pd-H probe, as microreference electrode 8=36605
  Pt, ellipsometry of O-containing films 8=27754
  Sn, measured conductance rel. to capacitance and Faradaic current 8=49929
  Sn, polycryst., double layer capacitance in aqueous soln. obs. 8=45384
  Ti, measured conductance rel. to capacitance and Faradaic current 8=49929
  U alloy, measured conductance rel. to capacitance and Faradaic current 8=49929
  Zn, adsorpt. of org. materials, pot. vars. 8=36601
  Zn, measured conductance rel. to capacitance and Faradaic current 8=49929
  Zn in KOH solns., anodic behaviour 8=45385
  Zn in KOH solutions, double layer capacitance. 8=49936
Electro-deposition. See Electrolytic deposition.
Electrodes. See Cathodes; Electrochemistry/electrodes.
Electrodynamics
  See also Eddy-currents; Quantum electrodynamics.
  accelerated nonradiating charge distribs., e.m. field 8=28544
  acceleration of particles by dissipative force in rad. flux 8=32515
  cavity formed by corpuscular flux incident on line current, time-depend. motions 8=25728
  charge in superimposed quadrupole and longit. mag. fields 8=33064
  charges in e.m. fields, drift approximation 8=28543
  Cherenkov radiation from point charge moving perpendicularly to a conducting barrier 8=47073
  cyclotron freq. of free electrons in quadrupole cage 8=29096
  diocotron instability, effect of inductive and capacitive walls 8=41950
  Dirac Hamiltonian, non-relativistic approximations 8=37932
  Dirac wave packet, hidden linear momentum rel. to α.E term 8=24716
  eddy current braking at high speeds by permanent magnets 8=24115
  e in stable orbit, eqn. of free oscills. 8=29008
  electron-fluid-dynamical waves, nature 8=28546
  electron motion in plane circularly polarized e.m. wave 8=33637
  electron moving in circularly polarized e.m. wave, intensity and ang. distrib. of radiation 8=33063
  electron and photon two-point functions, perturbation calc. 8=33067
  electron synchrotron radiation in accelerator with megagauss fields 8=46987
  e.m. waves in moving conducting media 8=28599
  extended one-body problem decompostion of Maxwell stress-energy tensor 8=24125
  focusing props. of static nonuniform elect. and mag. fields 8=28540
  free electron in closed metal container 8=28542
  gas, partially ionized, e vel. distrib. inelastic interation effects 8=39024
  harmonics in optical emission of harmonic oscillator 8=42472
  helices interact. with transverse waves in electron beam, optimum dimensions 8=28557
  hodograph method, continuous nonlinearly conducting media 8=46351
  Jupiter's satellite, Io, effects 8=37010
  linear theory of motion in electron storage ring 8=24589
  Lorentz-Fitzgerald contraction explanation 8=33065
  in mag. field reversal zone 8=46398
  in magnetic mirror traps, exptl. investigation 8=47870
  m.h.d. generator, electrodynamic effects of non-uniformity of mag. field and fluid parameters 8=28468
  momentum, velocity, acceleration and spin, relations 8=42313
  motion in field and circularly polarized wave propag. along mag. field and gyroresonance 8=24131
  moving media, rel. to Cherenkov radiation 8=33060
  non-adiabatic motion in inhomogeneous rot. symmetric mag. field, approx. calc. 8=46399
  nonlinear eqns. for $\epsilon(E)$ and $\mu(H)$ reduced to linear 8=28541
  nonlinear, ferromag. media, boundary problem soln. 8=37407
  non-linear, ray vel. diagram 8=46397
  one-dimensional unneutralized flow in bounded system, anal. for several flow models 8=41984
  particle beams, curvilinear, design method 8=24128
  particle in twisted magnetic flux tube 8=24127
  particles in dipole mag. field, effect of const. elect. field on motion 8=37409
  particles in inhomogeneous mag. field, effect of elect. field 8=24130

Electrodynamics—contd
particle-magnet "hidden momentum" reaction 8=41949
photon-mass formulation without potentials 8=28539
plasma, frictional force analysis 8=28545
plasma in a magnetic field, e motion effect on ionization recombination equilibrium 8=29993
radial diffusion in drift-tube expts. 8=41948
radiation, use of reciprocity relation 8=37406
relativistic in large amplitude e.m. fields 8=37405
scalloping of electron beams in varying elect. and mag. fields 8=46405
spin-1 particle in e.m. field, no distinction between classical and quantal descriptions 8=33563
spinor, finite charge renormalization 8=24485
spiralling electrons displacement by elect. field in terms of adiabatic invariants 8=24129
of superconductors with P-pairing, and collective excitations 8=44703
trajectories of scatt. from charge distribs. 8=33066
travelling-wave tube, waveguide excitation theory 8=37515
u.h.f., boundary problem soln., calculated data accuracy 8=37407
world-line of charged particle in const. e.m. field 8=46074
Electroendosmosis. See Electrophoresis.
Electrojet. See Atmosphere/upper; Atmospheric electricity; Ionosphere.
Electrokinetic effects
See also Electrophoresis.
chabazite fryst. plug, hydraulic permeabilitty rel. to ambient salt conc. 8=35473
current-carrying conductor instabilities 8=24079
electro-osmosis in porous capillary systems 8=27744
electro-osmosis, temp. dependence of rate constants for acetone and deionized water 8=32130
fibres, cylindrical, zeta potential 8=41271
phenol sulphonic acid formaldehyde type membranes, electro-osmosis and streaming pots. 8=27745
polyvinyl-alcohol fibres, structural features characterized by electrokinetic potential 8=26154
zeta-potential determ. from viscous damping of elec. driven pendulum 8=27743
zeta potential in cylindrical fibres 8=41271
$Na^{22,24}$ ions, electromigration in molten nitrates 8=43782
Electroluminescence
anthracene, delayed, rel. to charge-transfer exciton and ionic levels 8=27254
capacitor as distributed-parameter system 8=36537
crystals, pure, polarization mechanism 8=41180
9,10-dimethylanthracene in dimethylformamide: spectra of electrochemiluminescence 8=48177
diodes and lasers, thermodynamic limits 8=24382
display system, pulsed power supply 8=46340
films, thin, prep. and props. 8=36454
hydrocarbon, aromatic, in liquid phase below optical excitation threshold 8=30497
isobenzofurans, double-potential step and spectroscopic meas. 8=27691
light source for data recording 8=37668
light sources, review 8=28769
m.o.m. thin sandwiches, correlation with electron emission 8=40700
rubrene, liquid, with luminophor 8=43848
Seignette salt cryst., surface 8=41228
semiconductors, review 8=36464
Al-Al_2O_3-Au structures 8=49388
Al_2O_3 films, brightness waves rel. to electrode mat. effects 8=45260
Au-Si_3N_4-ZnSe diodes, visible 8=41230
CdS, at 77°K, mechanism investigation 8=45264
CdS, MOS diode, at low-voltage, high-current and 77°K 8=27644
CdTe diodes, temp. depend. 8=49790
Cu_2O, rel. to injection-chem. effect 8=45267
GaAs and Si alloyed diodes, and V-I characts 8=32058
GaAs diodes, efficiency rel. to junction depth and doping 8=45268
GaAs laser diodes, luminescence mode, current noise spectra 8=46614
GaAs, unipolar, by tunnel injection of minority carriers 8=36497
$GaAs_{1-x}P_x$ diodes, efficiency rel. to junction depth and doping 8=45268
$GaAs_{1-x}P_x$ injection laser, luminance $> 6 \times 10^9$ cd/m² 8=41192
GaP diodes, depend. of radiative efficiency on heat treatment 8=27179
GaP diodes, prep. from p-on-n liquid phase epitaxial layers 8=41229
GaP p-n junction obs. 8=36509
GaF p-n junctions, 77-420°K 8=45273
GaP p-n junctions grown by liq-phase epitaxy, green electroluminescence 8=41231
GaP p-n junction, synthesis and epitaxial growth by fused salt electrolysis 8=48573
GaP p-n junctions, red-emitting, prep. by soln. growth of p-type thick layers on n-type substrates 8=41232
GaSe, injection, with parallel and perpendicular elect. fields 8=32055
Electroluminescence
Ge p-n junction obs. 8=36509
KH_2PO_4 8=49804
Na_2ZnGeO_4, in constant elec. field 8=45283
Si and GaAs alloyed diodes, and V-I characts. 8=32058
Si p-n junction obs. 8=36509
SiC p-n junction obs. 8=36509
Ta, oxidised films 8=45287
$Zn_xCd_{1-x}S$ graded-band-gap crystals 8=39696
(Zn, Cd) (S, Se): Cu phosphors, red emission and energy levels rel. to comp., obs. 8=45293
ZnO single crysts. 8=32059
ZnO-Cu_2O heterojunctions 8=36516
ZnS crystal, 77°-600°K. obs. 8=45291
ZnS, effect of twist boundaries 8=41214
ZnS films, sublimated, and stimulated cond., 77-294°K 8=32060
ZnS, influence of structure 8=41215
ZnS phosphor powders, enhancement using resin binders 8=41217
ZnS, reabsorpt. of rad. and form. of stimulated state 8=32062
ZnS sublimated layers 8=32061
ZnSe-type phosphors. rel. to temp effects and Mn-band characts. 8=49820
ZnS-type powders, a.c. excitation 8=36521
ZnS-CdSe alloy systems 8=32066
ZnS:Cu, coactivator effect (Cl, Br, I) 8=32069
ZnS: Cu luminophor, two-band emission prep. 8=45307
ZnS: Cu phosphors, freq. dependence 8=41218
ZnS: Cu, spectrum dependence on heating processes 8=36519
ZnS: Mn Cu phosphor sublimate, annealing effect 8=27663
ZnS: Mn, Cu, Cl films, in gap and sandwich cells 8=49818
ZnSe(Cu, I, Cl) sublimated layers, obs. 8=41211
ZnTe, polycrystalline under a.c. and d.c. excitation obs. 8=32064
Electrolysis
See also Conductivity, electrical/liquids, electrolytic; Dissociation/electrolytic; Electrochemistry; Electrolytic deposition; Ion velocity/electrolytic.
analogue computer electrolytic tank for two-port network analysis 8=46005
aqueous, circulation pump 8=32128
cell for corrosive, volatile materials and for subsequent i.r. analysis 8=36606
compressed electrolyte viscosity meas., remote control 8=34793
device operation at low temps, limitations from electrolyte transport behaviour 8=45387
electrolyte relax., laser temp.-jump apparatus 8=36595
Faraday's law breakdown in weakly conducting solutions, expt. evidence 8=45386
fuel cell reactions, adsorbed species identification 8=46357
galvanic cells, primary and secondary, review. 8=49947
liquid phase cells: concentrating effect cells, and cells opposing Na + ion to K + ion 8=45390
mass transfer coeffs., effect of pulsation, ionic mass transfer 8=49940
polymers, weak-electrolyte theory of ionic cond. 8=40590
pulse, kinetics, using e.s.r. 8=49942
pulse, rapid scanning of mag. field 8=33145
sodium alkylbenzene sulfonates, conc. of electrolyte on free energy of adsorption 8=39339
Ag_2O-Zn secondary cells, cycle life performance, surfactant additions to zinc plate, effects 8=49941
Al electro-refining process, study using radioactive tracers 8=36607
BaF_2, solid-state, rel. to unipolar conduction mechanism 8=40579
Cu_2S, anodic dissolution 8=41281
Ga, liq., electrotransfer of Ag, temp. depend. 8=36597
GaP, epitaxially deposited in Si substrate, by fused salt electrolysis 8=48573
H liberation in Cr with various crystal structures, kinetics 8=49943
KCl, impurity anion doped, solid-state electrolytic exam. of conductivity 8=40570
$LiClO_4$, fused, limiting reactions, obs. 8=45389
NaCl, solid-state, rel. to unipolar conduction mechanism 8=40579
NH_4HF_2 in anhydrous HF 8=45391
NH_4HF_2 in HF, and subsequent i.r. analysis, cell requirements and construction 8=36606
Si, activity in molten Ag-Si alloys by e.m.f. meas. 8=48078
WC-Co hard metals, electropolish thinning for transmission e microscopy 8=36608
Electrolytes, theory. See Electrochemistry; Solutions.
Electrolytic conductivity. See Conductivity, electrical/liquids, electrolytic.
Electrolytic deposition
crystal growth and surface diffusion 8=48531
isotope exchange reactions, rate data evaluation 8=45311
kovar, Ni plating for stress-corosion cracking prevention 8=31211
metal surface high-vacuum techniques 8=39572

Electrolytic deposition—contd
  Ag, crystals, structure and orientation during initial stages 8=30822
  Ag on Pt electrode, nuclei form. 8=49948
  Cd, from non-aqueous solns., review and prelim. studies 8=45393
  Co cryst. growth 8=26245
  Cr black coatings, props. 8=45394
  Cr, to form ductile foil, using asymmetrical current 8=36609
  Cu, bright, from $CuSO_4$ solns. containing CN, obs. 8=45395
  Fe, active, in acid solns with high halide concs, anodic dissolution 8=36598
  Fe, rel. to post-natural ageing effects 8=35104
  Fe, to form ductile foil, using asymmetrical current 8=36609
  Fe-Re alloy, to form ductile foil, using asymmetrical current 8=36609
  GaP epitaxial, on Si substrates by fused salt electrolysis 8=48573
  Hg, Ag and Pd, electrocrystallization 8=41283
  KBr, colouration, influence of dislocations 8=44469
  Nb hydride production, pure, by Nb electrode charging with hydrogen 8=27755
  Ni, and charging with H, effect of H on magnetization inversion 8=36170
  Ni, conditions rel. to stacking-fault, microstrain and particle-size production 8=26298
  Ni crystals, structure and orientation during initial stages 8=30822
  Ni, electroless plating on Si p-n junctions 8=45396
  Ni-Fe films rel. to mag. props., obs. 8=31672
  Pd, internal tension of deposits rel. to current density and metal conc. in electrolyte 8=36610
  Pt anodic film, ellipsometric obs. of chemical nature 8=41282
  Pt on Si crystal face, decoration of micro-relief for e.-microscope exam. 8=40496
  Re, internal tension of deposits rel. to current density and metal conc. in electrolyte 8=36610
  Rh, internal tension of deposits rel. to current density and metal conc. in electrolyte 8=36610
Electrolytic tanks. See Calculating apparatus/analogue apparatus.
Electromagnetic fields
  of charge distrib., accelerated, non-radiating 8=28544
  conducting cylinder, excitation by axial dipole 8=28627
  coupled cavity system eqns. 8=37456
  crossed, rel. to shock wave vel. 8=41830
  cylinder, solution for current to produce given 2D field 8=33058
  of dipole over stratified medium, asymptotic soln. 8=28633
  Dirac wave packet, hidden linear momentum rel. to α. E term 8=24716
  director field theory deriv. using Fourier anal. 8=41944
  Einstein-Maxwell axially-symmetric, construction 8=32783
  Einstein-Maxwell fields of embedding class one 8=24126
  electron radiation field, high-energy, statistical characts. 8=28552
  energy and momentum, nonlinearity 8=37403
  equal-time commutators, theory 8=24080
  generated by dipole sources buried in conducting stratified media algorithm for calc. 8=46392
  Green function of electron interacting with electromagnetic field 8=33635
  Lagrange-Sylvester theorem applications 8=33055
  Lehmann-Källen representation, rel. to Schwinger terms 8=24613
  mathematical models and computer soln., book 8=33054
  Minkowski, pulse-energy density tensor 8=41940
  m metal lattices, short range, meas. method 8=35026
  motion of magnetic charges 8=37404
  multi-port junction network analysis 8=37400
  operators, formulae for calc. of correl. functions 8=33062
  origin and numerical solutions, books 8=28538
  of oscillating mag, dipole in streaming plasma 8=30050
  potential field distrib. in plane condenser with additional plates 8=28465
  production in cavity undergoing compression 8=46394
  pulse-energy tensor density 8=28537
  relativistic transform., simplification using test charge at rest 8=32788
  relativity, general, stationary distrib. with dust 8=32803
  in r. f. structures, perturbation meas., theory 8=37453
  shield, large, scaling laws 8=46375
  shock waves of ionized gases 8=47945
  standing-wave cavity field, motion of helical electron beam at cyclotron-freq. harmonics 8=24204
  stationarity, homogeneity and isotropy under translation and rotation in coherence theory 8=37401
  steady dynamics with certain symmetries, impossibility 8=24119
  u. h. f. in plasma, damping model 8=34536
  waveguide, interact with helical electron beam, gain rel. to electron vel. 8=24205
  in Fe, calc. methods 8=26013
Electromagnetic oscillations
    See also Magnetohydrodynamics; Masers; Plasma oscillations.
  cavity-garnet system, coupling parameters 8=24206
  dispersive resonator for retuning laser generation freq. 8=28665
  Fabry-Perot resonator, excitation by small aperture theory 8=46465
  klystron, freq. stabilization in mm range with open resonator 8=46467
  laser resonators, computation of modes by resonance excitation method 8=42074
  oscillator with u.l.f. stability using superconducting cavity 8=46466
  parametric, optical frequency, nonlinear crystal internal to laser cavity 8=46547
  resonator, microwave cavity 8=37455
  resonator-solenoid, superconducting 8=49208
  resonator theory, correspondence with R-matrix theory of nuclear reactions 8=33972
  r. f. system, automatic phase and amplitude control 8=24559
  space charge in cylindrical magnetron 8=42001
  standing-wave cavity field, motion of helical electron beam at cyclotron-freq. harmonics 8=24204
  GaAs laser, junction, continuous microwave oscills. 8=33220
  InSb photoresistors, optical heterodyne effect 8=36372
Electromagnetic radiation. See Electromagnetic waves; Gamma-rays; Light; Radiation; X-rays.
Electromagnetic wave propagation
    See also Absorption; Diffraction, etc.; Plasma/electromagnetic wave propagation.
  anisotropic media 8=46473
  anisotropic media, soln. of Maxwell's eqns. 8=37466
  antenna impedance acoustic wave effect 8=24243
  beam in randomly inhomogeneous medium, correl. function eqns. 8=42004
  boundary waves, surface propag. 8=37469
  Cherenkov radiation from point charge moving perpendicularly to a conducting barrier 8=47073
  coherence functions and wave field densities 8=37474
  coherence functions, correlation props. 8=37475
  coupling in multimode ionized media 8=37464
  delay of microwaves in single crystal YFe garnet 8=49564
  delay time, variable nondispersive, in magnetoelastic two-port devices 8=31745
  dielect. slabs, permittivity modulated, plane wave solns. 8=27217
  dispersive non-linear media, modulation conversion 8=37471
  in earth interior, v.l.f. 8=46468
  in electric field, static, in isotropic medium, refl. and refr. at free space interface 8=28607
  films, thin, after excitation of plasmons by e.m. waves 8=40272
  Gaussian light beam in random medium, fluctuations 8=28717
  ground wave phase velocity over plane earth with constant surface impedance 8=24251-2
  h. f., through dielec. irregularities 8=37462
  h. v. interface crossing at 1 MHz bandwidth 8=33126
  inhomogeneous media, general survey 8=37463
  invested medium, exact solution for steady-state resonant pulse propagation 8=46548
  ionosphere radio scintillation obs. at mid latit. conjugate stations 8=41426
  irregular terrain effects, model analysis 8=46497
  jungle medium, conducting-slab model 8=28610
  laser light scattering in atmosphere 8=32243
  light beam, nonlinear difference method solution 8=33232
  light beam, self-trapped, non-linear Helmholz eqn. analysis 8=46715
  light, dissipative instability in non-linear dielec. 8=46712
  light pulse in nonlinear medium 8=46646
  in magnetically polarized conductors, transformation into elastic waves 8=39886
  medium wave, transistorized field strength meter, portable 8=28634
  microwave filters, appl. of dielec. resonators 8=31444
  microwave gas discharge at 55 GHz, harmonic generation, exptl. studies 8=43438
  microwave horn gain meas. with revised proximity corrections 8=24207
  mixed-path, field of line source near interface 8=37468
  mixed-path, of ground waves, theory and expt. 8=37528
  modulated, 2 Gc band, apparatus for meas. 8=33122
  near smooth caustic, asymptotic soln. 8=37460
  in nonlinear media, beams propag. 8=33125
  over conductor, stratified, nonparallel, directional depend. 8=33127
  in periodic structs., represented as cascade of identical two-ports, theory 8=42009
  phase velocity over open periodic structure 8=37470
  plane coherent radiation in stratified medium, production of electric fields 8=28613
  plane elliptically polarized, in absorbing medium, components of energy-pulse tensor 8=28611
  plane wave transmission by complex metal - dielectric lattices 8=24211

Electromagnetic wave propagation—contd
- plane waves in dissipative media 8=37467
- from plasma wave transform. at plasma-dielec. interface 8=43583
- in polarizable particle system, attenuation, refract. index and permeability calc. 8=24215
- radiation flow, polarized in free electron atmosphere 8=28341
- radiation vertical elec. dipole in inhomogeneous half-space 8=46494
- radio-frequency holography 8=46480
- radio interference, pulse sources, analysis 8=28605
- random and periodic media 8=37461
- random anisotropic medium, dielec. tensor 8=30074
- random discontinuous medium, freq.-space correl. of amplitude and phase 8=42010
- random refractive index media 8=42005
- randomly inhomogeneous medium, mutual coherence function, diffusion analysis 8=42119
- reciprocity relationship for bianisotropic media 8=42007
- refraction at strip, h.f. condition 8=46477
- resonance radiation transfer in infinite medium 8=29635
- r.f. amplitude modulated, demodulation in plasma at resonance 8=30054
- satellite path meas., r.f. refr. and errors calc. 8=28635
- scalar wave in random medium, statistical props. calc. 8=42240
- in semiconductor, rotation of plane of polarization in strong elec. field 8=31364
- spherical boundary-value problem, time-domain treatment 8=37458
- in spherically stratified isotropic media, rel. to refractive index profiles 8=33128
- in Sun's field, between planets general relativistic calc. 8=37163
- surface wave over the earth, launching device use for trapped waves over inductive surface 8=24253
- surface waves, 50-100 km range, higher power if vertical unipole used 8=24254
- theory, conference, Delft, Netherlands Sept. 1966 8=28606
- time-varying media 8=37473
- transients, asymptotic analysis 8=37459
- transients in magneto-ionic media 8=37444
- transmission at moving interfaces, of e. m. power 8=37476
- turbulent media, dielectric 8=46472
- in twisted anisotropic media 8=33124
- v.l.f. ground wave, phase variations in antarctic exploration 8=45431
- WKB soln. in nonhomogeneous media 8=23803
- Cu wire, effect of pulse of high current density 8=42002
- Ge p-n junctions microwave oscillations generation 8=40506
- Si p—n junctions microwave oscillations generation 8=40506
- YFe garnet, excited by mag. field pulses, optimal conditions of re-emission 8=28612
- ZnO, microwave transmission through acousto-electrically excited crystals 8=42011

atmosphere
- absorption affecting solar 10cm obs. 8=37054
- absorption altitude dependence at 4 mm wavelength 8=27909
- absorption near $\lambda = 1.35$ cm, for water content meas. 8=32205
- absorption 35 GHz solar radiation 8=27902
- absorption, vertical at $\lambda = 1.3$ cm, rel. to determ. of water vapour mass in column 8=32204
- atmospheric refractive index distribution, effect of mountain wave 8=27925
- bistatic microwave probing of refractively perturbed clear atmos. 8=32254
- distribution of time intervals between pulses of atmos. noise 8=27924
- ducted whistler-mode propagation in magnetosphere, upper intensity cutoff and associates wave growth phenomena 8=36789
- earth-ionosphere cavity resonance, automatic recorder 8=41427
- earth-ionosphere cavity, resonance mode, frequency tracker 8=36852
- fluctuations on u.h.f. over-water radio path 8=37529
- from geo-stationary satellites, fading rel. to tropospheric gravity waves 8=41434
- ground wave propag. influence of thin inhomogeneous surface layer 8=46498
- laser radiation, 0.63 to 1.15 microns, surface layer transmission 8=27918
- light beam, use of Monte-Carlo method algorithms 8=46714
- line-of-sight propagation through turbulence 8=46499
- lower, radio refractive index, variation with angle of incidence 8=27926
- magnetosphere, e. m. wave guidance along inhomogeneous field aligned plasma stratum 8=32262
- medium wave, at night, S.E. England, pulse meas., change from E to F-modes 8=32309
- microwave line-of-sight paths, analysis of tropospheric waveguides to explain fading 8=37530

Electromagnetic wave propagation—contd

atmosphere—contd
- millimeter wave lens, dielectric sphere 8=27923
- optical signal, heterodyne detect. after one-way propag. on atmos. path 8=27915
- pulsations in freq. range below 1Hz, meas. 8=45469
- pulse u.s.w. signals along earth, distortion analysis 8=41370
- radio climatic charts from India 8=45474
- radio, linear polarization of sky radiation 8=45463
- radio refractive index differences, spectra 8=50153
- radio refractive index in troposphere, var. 8=50154-5
- refractive index, measurements, at 14, 250 feet elevation 8=45475
- transients in freq. band 1 to 100 kHz, digital data collection system 8=32253
- transmission beyond horizon, rel. to struct. of troposphere 8=45476
- troposphere, m to sub-mm, USSR work review 8=36756
- troposphere, psychrometer radiosonde 8=28601
- troposphere, review of Soviet contrib., 1957-67 8=27922
- troposphere, superrefractive with nontrapping surface layer 8=32252
- tropospheric layer, whispering-gallery modes 8=50156
- tropospheric scatter, wind produced Doppler shifts 8=27921
- whistler rate and v.l.f. noise variations, abrupt changes at plasmapause, Alouette 1 and 2 obs. 8=36788
- VHF waves, terrain scattering in Himalayan region 8=24250
- v.l.f. emissions in magnetosphere, polar, "hiss" and "chorus" rel. to auroral substorm 8=41390
- H_2O vapour, attenuation at mm. wavelengths 8=45473

ionosphere
- absorption meas. in freq. range 128-2775 kc/s, diurnal and seasonal varitions 8=32300
- anisotropic and sharply bounded, reflection soln. 8=50183
- antenna admittance calc. for plasma similar to E-region of ionosphere 8=36903
- antenna, dipole, response to electrostatic wave 8=42032
- auroral zone radiowave absorption in Alaska, morphology 8=41403
- back scatter sounding, field strength predictions 8=50190
- backscatter soundings, apparent range variations rel. to irregularities 8=32311
- backscattering, role of land and sea 8=27977
- Brillouin scatt. in plasmas, applic. to ionospheric irregularities 8=41429
- Dopper shift at 2.7 and 4.6 MHz rel. to u. l. f. geomag. fluctuations 8=27976
- Doppler shift in inhomogeneous anisotropic medium 8=42036
- D-region, absorpt. rel. to e bursts in magnetotail 8=41440
- D-region meas. by rockets, rel. to electron height distrib. 8=32327
- D-region, over steep incidence path, effects of solar flares 8=32325
- E-region reflection, continuous, duration variation 8=36859
- earth-ionosphere cavity resonance, automatic recorder 8=41427
- earth-ionosphere waveguide 8=27970
- in earth-ionosphere waveguide 8=50181
- earth-ionosphere waveguide, mode conversion and refraction effects for v. l. f. radio waves 8=41428
- e. l. f. and v. l. f. propag. below curved stratified ionosphere 8=50182
- e.l.f., anisotropic, long distance propag. below 8=45524
- electron density distrib. meas. using stationary phase techs. for angle of incidence calc. 8=32322
- equator, effect of spread-F 8=32335
- F-region apparent reflection coeff. of h.f. waves, influence of focusing 8=32348
- F region radio pulse reflection, 4. 7MHz, near mag . equator (India) 8=45551
- F2 critical freq., post-culmination maximum obs. 8=36873
- fading of ionospheric echoes, periodic, from E, E_s and F-regions 8=41443
- Faraday rot. obs. at 3 stations, rel. to irregularities in electron content 8=36837
- field of v. l. f. Antarctic horizontal dipole 8=37531
- from geo-stationary satellites, fading rel. to refracting irregularities 8=41434
- height distrib. of e density rel. to radio absorpt., soln. of integral eqn. 8=41422
- h.f. radio wave diffraction from irregularities, statistical parameters 8=32304
- h. f. radio waves, ray tracing determ. direction of arrival 8=50184
- influence of auroral zone disturbances on freqs. below 12 kHz and above 16 kHz 8=32307
- intermodulation, effect of electronic and ionic gas coupling 8=27973
- ion effects on v. l. f. whistlers, obs. 8=41425
- layered media, modified reflection coeff. 8=28615
- length of hop and integral absorption of short radio-waves depend. on emergence angle of radio beam 8=45517

Electromagnetic wave propagation—contd
ionosphere—contd
l. f. and v. l. f. reflection coeffs., calc. 8=42035
lightning atmospherics, 27 kHz, multiple reflection 8=27920
lower, reflection loss, l. f. and v. l. f., calc. 8=50185
lower vertically stratified plasma, v. l. f. waves from rad. sources 8=42034
magnetoplasma, pulsed transmission 8=34493
medium wave, at night, S.E.England, pulse meas., change form E to F-modes 8=32309
m. f. radio wave absorption, dependence at mid-latitudes on planetary mag. activity 8=41423
oblique incidence on warm drifting plasma, refractive index calc. 8=30067
oblique soundings near mag. equator, for evening and night-times 8=32312
parameters, investigation using satellite signals 8=50189
phase regressions of v.l.f. waves before and after morning rotation 8=32302
phase variation meas. effect of reference voltage instability 8=36835
plasma, scattering by cylindrical irregularity 8=45520
radar for Faraday rot. meas., error reduction 8=27969
radiated field from line cource of current, in auroral region 8=45568
radio absorption at 2, 2.5 and 3 MHz 8=45541
radio scintillations from satellites, effect of field aligned irregularities 8=45530
radiowave absorption in model ionospheric layers 8=41424
radiowave propag. study in USSR during last 50 years, review 8=27974
ray tracing 8=45522
re-entry transmission using modulated electron beam device, simulation 8=36906
reflection from plane stratified medium 8=28614
reflection of ultralong. radiowaves, correlation of reciprocity principle 8=45519
r.f. waves in inhomogeneous magnetically active ionosphere, geometrical optics calc. 8=28636
rel. to satellite path meas., refr. and errors calc. 8=28635
satellite signals, Faraday rot. rel. to large-scale struct. of F layer at Kiruna 8=32236
scatter intensity, Antarctic, and effect of P(A) 8=36833
scintillation obs. at 136 MHz, diurnal pattern characts. 8=32317
scintillation of satellite signals rel. to irregulatities, correl. with position, sunspot cycle and season 8=32353
scintillation of signals from Discoverer 36, correl. with spread-F 8=32354
scintillation, S. Marco/20.005 MHz satellite signals 8=45518
scintillations, broadband, of Cassiopeia A, correl. with occurrence of spread-F 8=32332
scintillations, radio star and satellite, geophys. aspects 8=32318
spatial fluctuations of v.l.f. wave field in zone close to transmitter 8=32301
spread-F echoes, angular spread of backscatt. signals at 2.4 Mc/s 8=32347
from stars, scintillations and fadeout, rel. to irregularities 8=32516
terrestrial waveguide model, theory and expt. 8=37504
transequatorial characts. at 34, 45, 54 and 77 MHz 8=32310
transmission coeff., v. l. f., calc. 8=27972
U.S.S.R. work since 1900, survey 8=36836
v.h.f. radar reflections, from satellites, scintillations obs. 8=32315
v.h.f. satellite signal scintillation, study of night-time iregularities 8=32356
v. l. f. absorpt. in 3 kc/s range, theory 8=36832
v. l. f. and e. l. f., recent progress 8=27971
v.l.f. characts., influence of meteoric dust 8=32308
v.l.f. field strength and phase meas., rel. to electron profiles 8=32326
v. l. f. in magnetoionic medium 8=42037
v.l.f. mode struture and polarization below anisotropic ionosphere 8=32306
v. l. f. (< 1.5 KHz), effect of ions 8=24255
v. l. f. radiowave scatt. in curved earth-ionosphere waveguide 8=27975
v.l.f. transmission and refl. coeffs. for vertical incidence, determ. of thin film optics tech. 8=32299
v.l.f. wave field near transmitter, FR-1 satellite expt. 8=45523
v.l.f. wave transmitted from ground, structure meas. and refractive index of medium 8=32303
v.l.f. waveguide mode conversion at graded height change 8=50186
waveguide analogue 8=24256
waveguide upper boundary, height and conductivity gradients, SID changes 8=32321
whistler, effect of mag. storms on duct formation 8=50187
whistler mode with longit. static elect. field 8=45521
F-2, fluctuations in critical freq. in Asian zone 8=50198
guided waves
accelerator beam stability in disc-loaded guide 8=37809
in anisotropic dielec. medium with conducting planes, math. analysis 8=33134

Electromagnetic wave propagation—contd
guided waves—contd
boundaries of arbitrary shape, Laplace soln. 8=37509
cable, submerged, vertical grounded, peculiarities of mag. field 8=36680
cavity-garnet system, coupling parameters 8=24206
circular waveguide, asymmetric waves 8=24232
circular waveguide, susceptance of annular iris 8=37512
circular waveguides, coupling by walls of different surface admittance 8=37507
coaxial line with partial plasma filling 8=42028
coaxial transmission-line r.f. power calorimeter 8=33007
common-wall directional coupler for waveguides 8=37519
corrugated elliptical waveguide 8=37511
in cylindrical plasma column 8=39092
earth-ionosphere v.l.f. mode conversion at graded height change 8=50186
earth-ionosphere waveguide 8=50181
earth-ionosphere waveguide, mode conversion and refraction effects for v. l. f. radio waves 8=42428
earth, ionosphere waveguide, planar analogue 8=24256
earth's crust as waveguide for very long radio waves 8=36676
EH_{11} hybrid wave, guide with metal ions, separation of ultrarelativistic particles 8=33073
in electron linear accelerator, perturbation meas., theory 8=37453
excitation of dielect. and plasma slab, harmonic analysis 8=28618
focusing, multiaperture technique 8=37482
glide reflection symmetry props. 8=37505
gyromagnetic media, rel. to theory of exchange spin-wave excitation 8=28619
helices interact. with transverse waves in electron beams, optimum dimensions 8=28557
H_{11} mode, radial scatt. of plasma ions 8=39108
inhomogeneous filling with dielec., metal boundaries 8=37510
ionosphere, anisotropic upper boundary v.l.f. mode structure and polarization 8=32306
iris waveguide, EH_{11} hybrid wave obs. 8=37517
lens, Luneberg microwave, made of foam glass steps 8=37465
lines, active nonlinear, shock 8=46168
liquids, optical beam self-trapping 8=34843
loop-slot radiating element for obtaining circular polarization 8=42029
magnetosphere, along inhomogeneous field aligned plasma stratum 8=32262
microwave waveguide probes, e,m. interference in space between probes 8=24216
mode system for radial wavebeams 8=37457
moving media, first-order theory 8=46492
non-uniform waveguide, computational soln. 8=37508
optical fibres, props. 8=28760
optical, four-layer waveguides, use for phase-matching in second harmonic generation 8=33136
optical glass fibre light guides, manufacture 8=28761
optical resonators and guides with infinite mirrors, modes 8=33121
parallel plates asymmetrically bifurcated by unidirectional conducting half screen 8=28624
parametric coupling in nonlinear media 8=37520
permittivity meas. in E-band, in low-loss mats. in overmoded waveguides 8=40554
plane-parallel waveguide, characts. of resonant ferrite isolator allowing for dielec. and mag. losses 8=28620
plasma waveguide, interact with electron beam, rel to amplification 8=24233
prop constant in dielectric loaded waveguide 8=46489
reactive loads, conformal mapping appl. 8=37518
rectangular hollow conducting cylinder 8=24236
reflection coeff. meas. for plasma parameters 8=30052
resonant helices in mag. res. 8=46500
resonator system with total internal reflection 8=42022
shock in nonlinear active lines, model for detonation wave in gas 8=46169
on shorted helix of spectrometer 8=46488
superconducting meander lines 8=40411
surface wave, launching on unidrectionally conducting screens 8=46490
TEM waves, field pattern, resist. analogue 8=24077
terrestrial waveguide model, theory and expt. 8=37504
terrestrial waveguides 8=37503
theory, conference, Delft, Netherlands, Sept. 1966 8=28606
transmission-line with non-linear parameters, shock front structure 8=42027
transmission lines, nonlinear with active elements 8=37521
travelling-wave tube electrodynamics 8=37515
waveguide, axially magnetized ferrite-filled, mode characts. 8=28622
waveguide, appl. of wave mechanics 8=42025
waveguide, calc. of dielectric discontinuities 8=28625
in waveguide, cylindrical, filled with isotropic plasma with slowly varying electron density 8=39106
waveguide e.m. field interact with helical electron beam 8=24205
waveguide excitation by external currents, theory 8=37514
waveguide filled with moving medium 8=24237

Electromagnetic wave propagation—contd
guided waves—contd
waveguide, hollow plasma, characts. 8=24235
waveguide loaded with n-InSb thin plate, field distribution 8=49385
waveguide moving dielectric 8=33135
waveguide, multimode with corrugated walls, wave transformation 8=37513
waveguide phased array, radiation in anisotropic plasma 8=24239
waveguide, plasma cont., gap coupling, appl. to amplifiers 8=42024
waveguide, rectangular, TE_{10} mode, complex rel. permittivity meas. 8=46346
waveguide, straight and curved multilayer systems, optical ray method for modal struct. 8=28621
waveguide theory, correspondence with R-matrix theory of nuclear reactions 8=33972
waveguide, wave propag. in earth-ionosphere 8=27970
waveguide with losses and large number of discontinuities resulted reflection coeff. 8=24231
waveguide, with sinusoidally varying dielec. const., anal. of e.m. transients 8=42023
waveguides, beam, and optical resonators, scalar theory 8=28669
waveguides, characteristic impedances 8=46491
waveguides, disc-loaded of electron linear accel., non-uniformity effect 8=37516
waveguides, nonuniform 8=33137
waveguides, optical, stability of light beam at bends 8=46642
waveguides, overmoded, admittance of iris 8=42026
waveguides, planar dielectric, physical-optics theory 8=28623
waveguides, slowly varying, using WKB approx. 8=24234
wedge waveguide antenna with plasma sheath, admittance 8=42033
Wiener-Hopf soln., extension of closed-region function-theoretic approach 8=37506

Electromagnetic waves
See also Diffraction; Reflection, etc.; Light/electromagnetic theory.
amplification, electron system with anisotropic impulse distribution 8=42006
amplification by systems with equidistant spectra 8=42008
coupled cavity systems, field eqns. 8=37456
cyclotron waves in degenerate electron Fermi liq. in mag. field 8=37218
delay line, continuously variable, at 720 MHz, obtained by Brillouin effect 8=28609
digital phase-sensitive detector 8=28449
diversity combining of different signals, using lock techniques 8=33120
electrodynamic → MGD wave transformation 8=37441
electron momentum gain, intensity-dependent 8=33634
e.m.-gravitational wave interaction, perturbation theory 8=32778
emission in periodically nonstationary media 8=37472
energy levels of electrons, existence of infinite number of given momentum 8=28598
energy transport velocity, comment and reply 8=28608
energy-transport velocity of induced electromagnetic wave in lossy moving fluids 8=37442
excitation in inhomogeneous media 8=37450
excitation of elastic waves in piezoelectric slab 8=46157
extended thermal source, degree of coherence 8=33238
ferroelectric, magnetically polarized, coupled elasto-spin and excitation of reflected waves 8=27261
gamma source above conducting screen, with long free path in air, elect and mag. field 8=24246
in gravitational fields 8=32806
integration method for inhomogeneous layer 8=46463
interaction of two waves, coupled mode theory 8=32681
interaction with moving conducting dielectric half-space 8=24213
interaction with 3-level system, quantum theory 8=37750
in ion semicond., coupled system with lattice and plasmic waves 8=31304
Maxwell's eqns from Coulomb's law and special relativity 8=41997
microwave cavity resonators, X-band exptl. scaling of optical types 8=41998
microwave cavity, supercond. 8=31350
microwave diagnostics for plasma 8=39117
microwave, discharge prod. of at. and mol. beams 8=43241
microwave dual-mode cavity for gas refractive index meas. 8=47969
microwave mixer of YFe garnet, energy-balance 8=41999
microwave supercond. mixer 8=31351
microwave supercond. oscillator–detector 8=31356
microwave, use in constructing hologram by two-beam interference method 8=46756
microwaves, ferrite applications in USSR 8=24203
millimetre wave image conversion to visual display 8=28775
oscillator, r.f., mismatch refl. power, protection 8=28603
parametric excitation of coupled waves, plasmon-photon interactions 8=43587

Electromagnetic waves—contd
plane, interaction with cylindrical plasma 8=47845
plane, polarization of reflection incident on spherical reflector 8=46474
plasma accel. with travelling waves 8=30013
plasma radiation, photomultiplier radiometer 8=43540
potential equations for anisotropic inhomogeneous media 8=37365
Poynting's vector, additional term, leading to $\vec{\mathcal{E}}.\vec{\mathcal{E}}^*$ or $\vec{H}.\vec{H}^*$ characterizing usual detection processes 8=28597
radio physics interpretation of holography 8=42276
r.f. structures, field strength perturbation meas., theory 8=37453
reflection coeff. of inhomogeneous layer, determ. 8=46015
resonant cavity, Q determ. method 8=37454
self-focusing by density change in medium 8=36310
spherical cavity resonator, concentric shell system 8=37452
superposition of thermal and coherent fields, normal and antinormal correlations 8=46469
theory, conference, Delft, Netherlands, Sept. 1966 8=28606
transformation in piezoelectric crystals 8=35987
radiators
annular slot in compressible plasma, theory 8=30075
Antarctic v.l.f. horizontal dipole, radiation field in ionosphere 8=37531
antenna array, non-uniformly spaced, synthesis, new method. 8=24245
antenna array theory rel. to microwave holograms and visible images, obs. 8=24439
antenna-coil for e.l.f.-atmospherics, highly-sensitive 8=42030
antenna, cylindrical, current distrib. in plasma column expt. and theory 8=24249
antenna, cylindrical, input admittance in magneto-ionic medium 8=28630
antenna, dipole, response to electrostatic wave, in ionosphere 8=42032
antenna gain degradation in beyond-horizon links 8=37526
antenna impedance, acoustic wave effect 8=24243
antenna in compressible plasma, current distrib. 8=28626
antenna in cylindrical plasma, radiation pattern calc. 8=24238
antenna, non-resonant, in weakly ionized plasma 8=42031
antenna, synthetic, data processing by wavefront reconstruction 8=37524
antenna, 20m parabolic, 100 MHz-4.2(10) GHz 8=50460
antennae, in plasma similar to E-region of ionosphere, calc. of admittance 8=36903
antenna, wedge waveguide with plasma sheath, admittance 8=42033
aperture antennas, effects of plasma in near field region 8=24240
array, linear continuous, aperture size rel. to beam width 8=24241
conducting cylinder, excitation by axial dipole 8=28627
cosmic-ray showers, geomag. polarization mechanism exptl. tests 8=38204
dielectric antennas, basic factors affecting radiation patterns 8=28631
dielectric reinforced by metal elements, reflective properties 8=24211
diffraction, knife edge, of waves from directional antenna 8=24218
dipole antenna, radiation in a compressible plasma, numerical solution 8=24248
dipole in Epstein medium, field calc. 8=37522
dipole rad. pattern, calc. of effect of dielec. cylinder 8=28629
dipole short in lossy uniaxial medium 8=46495
dipole over stratified half-space, aymptotic soln. for e.m. fields 8=28633
e.a.s., detection by half-wave dipole system 8=38242
e.a.s. emission at 22 MHz, obs. 8=38200
e.a.s., pulse correl. by arrival directions 8=38201
e.a.s., pulse obs. at 32, 60 MHz 8=38202
ellipsoidal antenna, reactance in magnetoactive plasma 8=28632
Hertzian dipole in centre of sphere, rad. resist. 8=33138
H-polarized rad. from layered medium, effect of metallic array 8=28628
horn, gain meas., comments 8=24247
infinite cylindrical antenna in compressible plasma 8=37525
launching device for trapped surface waves over highly inductive surface 8=24253
leaky-wave beams of multiply layered plasma media 8=30049
loop-slot radiating element for obtaining circular polarization 8=42029
medium wave transmitters, field strength meas. with transistorized meter 8=28634
microwave radiation from magneto-plasma 8=28600
millimeter wave lens, dielectric sphere 8=27923
monopole antenna, cylindrical, in hot plasma, current distribution meas. 8=33139
in moving conducting media, time-depend. Green's function 8=28599
near-zone mag. field of small circular-loop antenna 8=46493

Electromagnetic waves—contd
radiators—contd
oscillating mag, dipole in streaming plasma 8=30050
point source in strongly focussing medium, modal solution 8=23808
power transmission line, electric and magnetic fields 8=24242
pulse emission from e.a.s., theory 8=38203
slot, annular, in magnetoplasma, admittance calc. 8=37523
slot, axial, in dielect. coated metal cylinder, radiation conductors 8=24244
slotted wedge-shaped, in anisotropic plasma, field distrib. 8=30073
spherical, polarization of reflection of incident plane waves 8=46474
surface wave radiation from thick, semi-infinite plane with reactive surface 8=46496
transmitter, pulsed r.f., for n.m.r. spectroscopy 8=33153
u.h.f. investigation of fields in metal lattice 8=35026
vertical elec. dipole in inhomogeneous half-space 8=46494
vertical unipole, for med. freq. and 50-100 km range, higher power than for surface waves 8=24254
waveguide phased array, radiation in anisotropic plasma 8=24239
n-GaAs, UHF emission rel. to acoustoelectric domain 8=27095
Electromagnetism
See also Electrodynamics; Quantum electrodynamics.
Bel-Lapiedra-Montserrat eqns. solved in conformally flat space-time 8=28535
betatron, output doubling by magnet pulsing 8=24586
charged particle radiation in waveguides with gyrotropic filling 8=41939
conventions and nomenclature 8=24121
current loop, force 8=24124
current, magnetic field and temp. distrib. inside cylinder with temp. depend. conductance in elec. field 8=41946
dipole in conducting stratified media, calc. of e.m. field 8=46392
director field theory deriv. using a Fourier anal. 8=41944
displacement currents, contradictory proof 8=41945
dynamic model for material media 8=33056
eddy-current probe-coil problems, analyt. solns. 8=37402
Einstein spaces, new family of solutions 8=24123
e.m. phenomena, statistical thermodynamics 8=32839
e.m. wave diffraction by conducting cylinder, energy flux, numerical study 8=46484
Faraday's law of induction, expt. demonstration 8=24122
ferromagnetic sheets under alternating magnetiz., field eqns. soln. 8=28516
gauge noninvariant theory as extension of Dirac's theory of classical clouds of charge 8=32776
Gauss theorem, generalized form. 8=33059
impulse density vector flux rel. to elec. field amplitude 8=41941
induction, exceptions to flux rule 8=37399
Lorentz cond. for uncoupling scalar and vector potentials 8=24118
magnetic charge, motion in e.m. field 8=37404
magnetic fields, dipole and quadrupole planar, produced by line currents 8=46393
magnetodynamic effect, equivalence of Coulomb's and Ampère's description 8=33057
Maxwell-Einstein eqns., singularity-free soln. 8=33061
Maxwell stress-energy tensor decomposition rel. to extended one-body problem 8=24125
Maxwell's displacement concept 8=33025
medium, magnetized, surface refractive index 8=24214
moving media, eqns. appl. to Cherenkov radiation 8=33060
numerical solution of problems 8=46391
power density in presence of matter 8=28536
Poynting's vector, additional term, leading to $\vec{\mathcal{E}}.\vec{\mathcal{E}}^*$ or $\vec{H}.\vec{H}^*$ characterizing usual detection processes 8=28597
Poynting's vector studies 8=41943
Rayleigh equivalence theorem 8=41942
Stokes theorem, generalized form. 8=33059
symm. tensor formation of general relativity equivalent to Maxwell theory 8=28302
time delay, collision lifetime matrix 8=41947
vector Kirchhoff equations analysis and associated boundary-line charge 8=24120
Electromagnets. See Magnets.
Electromechanical effects. See Electrostriction; Piezoelectricity.
Electrometers. See Electrical measurement.
Electromotive force
induced by Ar supersonic m.h.d. stream, plotting for struct. determ. 8=41992
Penfield-Hans effect, complete theory 8=33057
Ag-Si molten alloys, Si activity by e.m.f. meas. 8=48078
$AlCl_3$-NaCl-KCl eutectic, fused, of Zn, Cd and Hg ions 8=49917
UO_2 powder, n-irradiated, meas. rel. to electronic props. 8=40290
Electron affinity. See Atoms; Ionization; Molecules; Solids.
Electron annihilation. See Electron pairs/annihilation.
Electron avalanches. See Breakdown, electric.
Electron beams
See also Electron optics; Particle accelerators.
accelerated, abnormal energy distribution in guns 8=24140
in anisotropic mats, energy loss meas. in optical constants 8=49672
crossed-field noise, suppression by lateral and transverse mag. fields 8=24139
crossed-field, stability rel. to coherent radiation 8=37415
cylindrical diocotron theory, new results 8=24136
depolarization in target material 8=35592
diffracting, abnormal absorpts. by plasmon 8=44662
dumps, slits and collimators for linear accelerator 8=33424
electron beam scanlaser, theory, design and operating parameters 8=24277
electron-ion beams emitted by cylinder or sphere, steady-state potential distribs. 8=27330
electronic stopping cross-section, Z, depend. 8=48893
energy deposition on traversing matter, formula and combination with δ ray formula 8=40067
energy loss through Al foils 100 to 800 μ thick, for initial energies 0.6 to 1.2 MeV 8=48908
fine structure surrounding undiffracted beam in e diffraction, obs. 8=26288
focusing of relativistic flow 8=46409
Fraunhofer holograms, optical reconstruct. of image 8=46747
gun, demountable 8=46403
gun demountable for laboratories 8=46404
gun for LEED instrument 8=46402
in gun of high area convergence and perveance 8=46410
gun, three-electrode with longit. compression, theory 8=37416
gun using LaB_6 rod cathode, suitable for microscopes and probe app. 8=28555
gun with field-emission source 8=28554
guns, high perveance axi-symmetric, digital simulation 8=46408
guns with pt. cathode in interferometer with mag. lenses 8=41952
helical, interact. with e.m. cavity field at cyclotron-freq. harmonics 8=24204
helical, interact, with e.m. field in waveguide, gain parametered to electron vels. 8=24205
high-power, handling problems 8=33075
high power, pulsed, prod from glow discharge 8=24137
holograms, theory for three-dimens. wavefront-reconstruction imaging 8=24150
injector gun of high-current proton accelerator type, design 8=46401
instability in linear accelerator 8=33416
intense nanosecond, design and diagnosis 8=33078
interact with plasma in waveguide, rel to em. wave amplification 8=24233
interaction with optical grating (Smith-Purcell effect) 8=28559
interaction with plasma in weak mag. field 8=34477
interactions, nonthermal, limitats 8=24133
interaction with plasma e.m. surface waves 8=43539
ionization of alkali metal atoms 8=43477
l.f. beam position monitor 8=33076
linear accelerator, precise control, radiation of required number of pulsed beams 8=42355
of linear accelerator, regulation and meas. of current 8=46993
low-density crossed-field, computer experiments 8=28558
in magnetron, smooth-bore, transport theory 8=24138
microanalysis, e probe current stability 8=28553
in model of axially symmetric, isochronous cyclotron 8=29009
modulation of current by potential or capacitance surface relief 8=33080
monitors for linear accelerator switchyard 8=33077
multiplier pulse-height distribs. 8=37430
nonvacuum, design, behaviour in gases and generation of beam plasma 8=28556
for optical signal production 8=36461
plasma-beam system instabilities control by beam modulation 8=43599
plasma-beam system, wave propag., 8=43537
plasma, charge carrier density rel. to volume and wall recombinations 8=47802
plasma-e. beam system in mag. field, wave propag. and linear amplification 8=39102
plasma, hydrodynamic instability 8=34557
in plasma mag. mirror trap discharge, instability 8=43564
point-cathode gun, anal. of focusing props, aberrations, size limitation etc. 8=24134
positron, production in electron linear accelerator 8=33426
probe, influence of secondary electrons 8=30100
pulsed, from 1 TW accelerators 8=33079
pulsed relativistic, > 10 GW, generation and diagnosis 8=33082
polarization by magnetic systems rel. to e-magnon scattering 8=35754

Electron beams—contd
    radiation field, high-energy, statistical characts. 8=28552
    relativistic, guidance through accelerator 8=33085
    scalloping, in varying elect. and mag. fields 8=46405
    scalloping, with centrifugal electrostatic focusing and h. f. helical electrodes 8=24135
    scanning microscope, current meas. 8=46324
    shift meas., shape of electrodes 8=46395
    spot size in tube screen, effect of space charge on Langmuir limit 8=41959
    stopping power, oscillating behaviour 8=48894
    thin, interact. with helix under broadband amplification and re-rad. of transverse waves 8=28557
    transport system, e.s., with periodic focussing 8=41965
    ultrasonic gas jet excitation for u. v. source 8=38660
    velocity-modulated, nonlinear space charge wave-type klystron theory 8=46420
    Al film, electron energy loss spectra rel. to film thickness 8=48904
    Al, low-energy reflection, charact. energy losses 8=48905
    in Al, stopping distance and absorpt. coeff. at 50 and 1200 keV 8=44494
    C films, evaporated, energy loss spectra rel. to thickness 8=48913
    Cu, low-energy reflection, charact. energy losses 8=48905
    Si, elastic reflection of pulses (20-1000 eV) 8=35605
  absorption. See Electrons/absorption.
  effects
      See also Beta-rays/effects.
    alkali halide crystals, energy losses rel. to band structure and plasmon energy determ. 8=26937
    alloys, disordered, dynamic theory of scattering 8=35596
    annihilation of ortho-positronium form in powder 8=49130
    anthracene, carrier generation and transport 8=49084
    anthracene scintillator excitation, decay obs. 8=49832
    beam plasma generation by nonvacuum beam 8=28556
    desorption by emerging high-energy electrons, kinematics 8=39607
    dielectrics, high-rate deposition, time resolved studies 8=27218
    emulsions, resolution of 7-60 keV images 8=37722
    emulsions, response to 7-60 keV 8=37721
    FET's, effect on carrier mobilities in inversion layers 8=27191
    gas irradiation rel. to production of metastable, thermal energy at. beams 8=29668
    p-n junction active devs, dynamic response anal. 8=44831
    laser pumping, photon loss and gain factor meas. 8=28699
    low-energy impact spectroscopy 8=25384
    MOSFETs, radiation damage thermal annealing characts. 8=27213
    MOS transistors, selective irradiation, transient and steady-state changes 8=27212
    neon-like, ions, X-ray satellite intensities 8=25372
    in plasma, excitation of ion cyclotron harmonic waves 8=34546
    in plasma, generation of h.f. waves 8=47884
    plasma, heating, oscill. of electrostatic field 8=43573
    plasma in inhomogeneous mag. field, instabilities rel. to acceleration 8=43592
    plasma, microwave osc. prod., spatial distrib. of intensity 8=39127
    plasma reson. emission in solids 8=35802
    plasma, uhf emission 8=30048
    plasmons in metal spheres, coulomb-stimulation and radiative decay 8=45145
    polyethylene, Hg lamp excitation of fluorescence 8=24729
    polystyrene, thermal props., low-temp., radiation-induced cross-links effects 8=26606
    positron prod. on W targets 8=33642
    rarefied gas, density obs. by induced luminescence 8=39171
    silicate glasses, surface damage on e-microprobe exam. 8=30865
    on solid, excitation of Alfvén and helicon waves 8=40278
    steel plasticity and mech. strength, 2.5 MeV 8=35694
    surface impurity formation rel. to beam width 8=40010
    thermal lattice vibrs., effect on electron scatt. in crysts. 8=48697
    thin films, heating effects, estimation of transient temp. distrib. 8=30733
    Ag crystal, evaporation and prod. of ion, collection to control flow 8=40712
    Ag, depth dose distribs., energy losses, and ionization 8=31143
    Ag, formation of conducting films 8=39603
    Ag target, $E_e = 1.52, 2.65, 3.66$ MeV, energy loss distrib. obs. 8=31142
    Ag, visible radiation emission 8=36317
    Al, depth dose distribs., energy losses, and ionization 8=31143
    Al, electrical resistivity recovery rel. to lattice defects 8=31147
    Al, hardening effect, rel. to point defect props. 8=31141
    Al, modulus effect after low temp. irrad. 8=48907
    Al, plastically deformed, prestimulation effect on exoelectron emission 8=44942
    Al, radiation from tangential surface plasmons, 50 keV 8=40281

Electron beams—contd
  effects—contd
    Al target, $E_e = 1.52, 2.65, 3.66$ MeV, energy loss distrib. obs. 8=31142
    Al target, thick, bremsstrahlung production on 0.5-2.8 MeV irradiation 8=40071
    Al vapour deposition 8=30744
    Al, visible radiation emission 8=36317
    Au, depth dose distribs., energy losses, and ionization 8=31143
    Au target, $E_e = 1.52, 2.65, 3.66$ MeV, energy loss distrib. obs. 8=31142
    Au, visible radiation emission 8=36317
    $AuAg_3Te_2$, phase transforms during e microprobe analysis, obs. 8=30857
    Be, depth dose distribs., energy losses, and ionization 8=31143
    Be oriented sheets, angular variation of charact. energy losses of 30 kV electrons 8=26936
    CO_2^+ band excitation by 80-1500 eV impact 8=25490
    CaF_2, irrad., product. of colloidal Ca 8=40074
    $CaWO_4$, effect on luminescence props. 8=36481
    CdS, damage, photoelectronic evaluation 8=40654
    CdS thin films, amorphous to crystalline transition 8=43993
    Co at 20°K, point defects, elec. resistivity obs. 8=48914
    Cu, depth dose distribs., energy losses, and ionization 8=31143
    CO, dissoc. attachment cross-section obs. 8=47703
    Cu, lattice defects interactions by elec. resist. recovery 8=31146
    Cu target, $E_e = 1.52, 2.65, 3.66$ MeV, energy loss distrib. obs. 8=31142
    Cu-Al solid solutions, stacking-fault energy, annealing and irrad. effects 8=26702
    Cu_2O, luminescence 8=41189
    Fe target, thick, bremsstrahlung production on 0.5-2.8 MeV irradiation 8=40071
    GaSb, undoped, on temp. depend. of Hall coeff. and mobility 8=27091
    Ge crystals, from sec. electron emission and radiation-induced conductivity meas. 8=44951
    n-Ge, damage production and recovery energy dependence 8=44789
    Ge, defect production and interaction with dislocations 8=40038
    Ge, electron irrad. I-V characts., and negative resistance change at low temps. 8=49244
    Ge etched surfaces, low energy irradiations rel. to charge condition 8=35901
    Ge, irradiated, e.p.r. 8=27476
    p-Ge:Ga, flux dependence of microhardness and carrier-density 8=27101
    n-Ge:Sb, flux dependence of microhardness and carrier-density 8=27101
    He, anisotropic excitation cross-sections 8=38702
    KCl, irradiated, photostimulated electron exo-emission 8=40708
    KI crystal, colour centre form. 8=44475
    LiF, colouring process, absorpt. and luminescence 8=40062
    Mg, irradiation damage recovery at low temps. 8=26734
    MgF_2, plasmon and interband transition excitation 8=26931
    MgO, effect on luminesc. 8=49809
    NO, dissoc. attachment cross-section obs. 8=47703
    N_2 excitation by 1-12 eV electrons 8=29755
    N_2^+ band excitation by 80-1500 eV impact 8=25490
    NaCl crystal, e beam pulse effect 8=44475
    NaCl, irradiated, photostimulated electron exo-emission 8=40708
    NaCl, 33.5-44 keV directional breakdown 8=48925
    NaCl-type ionic crystal, energy loss due to surface optical mode 8=44871
    NaF, colour centres, obs. with oven cryostat 8=48880
    Ni, formation of conducting films 8=39603
    Ni-Fe alloy, e-irradiated, remanence growth during low temp. mag. anneal 8=36156
    O_2^+ band excitation by 80-1500 eV impact 8=25490
    Pb, e.-shower production from 1-GeV incident electrons and charge component 8=44502
    Pt, damage rate meas., by irradiation 8=31155
    RbF, colour centres, obs. with oven cryostat 8=48880
    Se films, amorphous, prep. by vacuum evap., rel. to crystn. 8=39691
    p-Si, damage coeffs. rel. to use in solar cells 8=27123
    n-, p-Si, electrically active defect introduction rates on 1.7MeV irradiation 8=39998
    Si photocells, bombardment rel. to props. 8=27329
    Si, O-rich, Li diffused, annealing of irradiation induced defect 8=26632
    Si p-n junctions, shallow ion-implanted, elec. response rel. to surface structs. 8=27129
    Si, radiation damage rate rel. to depth 8=26736
    on Si solar cells, role of Li in damage and recovery 8=28508
    SiC, luminescence on 20 keV irradiation 8=36510
    β-SiC, on radiation recombination at high energies 8=36508
    Si:Li diode, on diffusion coeffs. of Li 8=39982
    Si:Li, majority carrier removal rates rel. to damage 8=27121

Electron beams—contd
effects—contd
Si: Li solar cells, damage annealing, obs. 8=24103
on SiN insulated gate, field effect transistors 8=27201
Ta, formation of conducting films 8=39603
Te films, resistance increase due to CO_2 desorpt. 8=35829
TiO_2 films, amorphous, prep. by vacuum evap., rel. to crystn. 8=39691
W, desorption of CO 8=48495
W, irradiation and recovery 8=48934
W with adsorbed Cs, Hg and O, low energy electron interactions 8=39623
Zn, formation of conducting films 8=39603
ionization. See Electrons/ionization.
Electron capture. See Ions/recombination; Radioactivity electron capture.
Electron diffraction
absorption, normal and abnormal, theory 8=30845
absorption parameters in theory 8=48628
anomaly due to secondary e. emission 8=48587
biprism interference fringes on illumination from field emission source 8=41953
camera EVR-1, use of scintillation counter 8=42346
diffractometers, design and applics. 8=41972
films, charged, anomalous interference of electrons on edge 8=44030
Friedal's law breakdown and symmetry determ. from zero-layer interactions 8=39759
history, early 8=30885
lattice mechanics of thin films 8=35387
low energy, strong absorption rel. to theory 8=37418
Al(100) face, at low and medium energy rel. to secondary emission 8=27356
H atom, e scatt. theory 8=29653
Electron diffraction crystallography
See also Crystal structure, atomic.
alkali halides, Debye-Waller factors temp. dependence, calcs. 0-900°K 8=39869
n-beam intensities, matrix evaluation 8=48627
diffraction meas. by e microscope 8=44194
diffuse scatt. rel. to electron density, and harmonic osc. of atoms 8=26347
diffuse scattering intensities rel. to short-range ordering 8=39758
domain boundary caused spots, fine structure 8=30846
dynamical theory, using a Green's function constructed of Bloch waves 8=35308
effective field eqns. of model cryst., rel. to self-consistent multiple-scatt. approach to LEED interpret. 8=26350
Friedal's law breakdown and symmetry determ. from zero-layer interactions 8=39759
indexing diagrams and struct. projections for arbitrary crystal orientation 8=35312
LEED complex patterns, laser simulation and interpretation 8=35310
LEED, from crystal surfaces, using multiple scatt. theory 8=26349
line broadening effects, separation by means of line-width relations 8=45147
microdiffr. technique for study of ferroelectrics 8=26430
micro technique for investigating ferroelectrics (magnets) 8=39761
multiphonon scattering of low-energy electrons 8=44193
non-conducting foil mountings to reduce background scattering, errors produced 8=26352
pseudopotential approach to intensity 8=35307
quasi-elastic scatt. contrasts rel. to bonds and polarisation 8=39762
relativistic, abnormal absorpt. coeff. 8=26348
scattering factors, relativistic Hartree-Fock, calc. method 8=39741
scattering of slow electrons by static Gaussian atomic potentials 8=35311
slow electron apparatus 8=26351
two-beam pattern calcs. 8=39760
Bi-O system, new tetragonal phase obs. 8=30888
$GeBi_4Te_7$ obs. 8=30898
GeI_2 obs. 8=30897
Cu, mean inner pot. meas. 8=30628
KBr, mean inner pot. meas. 8=30628
$K_2MoO_2F_4$ obs. 8=30903
$K_{0.23}NiO_{1.8}$ obs. 8=30902
NaCl, mean inner pot. meas. 8=30628
Si, Bragg refl. effect on electron scatt. 8=35354
Electron diffraction examination of materials
alloys, disordered, dynamic theory of scattering 8=35596
chemisorption systems, interpret. of LEED data rel. to interact with adatoms 8=27733
contrast, dynamical theory approximations 8=31020
corundum, heat-treated, surface defects 8=31054
crystals, low energy intensities by propag. matrix methods 8=30848
dickite microcrystals, Au-decorated, growth study 8=26231
diffractometers, design and applics. 8=41972
dispersion surface in rot. cryst., photographs 8=35309
domain boundary caused spots, fine structure 8=30846
electron gun for LEED instrument 8=46402

Electron diffraction examination of materials—contd
epitaxially grown on Ta (100), LEED obs. 8=48469
ferrite, easy magnetization direction, reflection electron diffraction obs. 8=31716
ferroelectrics (magnets), at. structure determ. using microtechnique 8=39761
film, thin, low-energy apparatus 8=35313
gas molecules, EG-100A apparatus 8=38805
inclusions, orientation contrast, theory 8=44156
insulating films, anomalous ring patterns due to secondary e. emission 8=48587
kaolinite microcrystals, Au-decorated growth study 8=26230
layer-type crystals, vapour-deposited, stacking fault obs. 8=26699
magnetic, analysis technique 8=44998
microprobe resolution improvement by deconvolution 8=30847
molybdenite cleavage surface, LEED study 8=48524
multiple scatt. interpret. of complex LEED patterns, comments rel. to superstructures 8=26287
oxide films, active, passive and transpassive, on Fe in electrolyte, e. diffr. exam.. 8=49931
β-poly-γ-methyl-L-glutamate, disordered structural characteristics 8=25677
quartz 8=35355
steel, tempering effects 8=35680
temperature controller for LEED expt. 8=46277
titanocene derivs, $(C_5H_5)_2TiCl_2$ and $C_5H_5TiBr_3$, mol. structure by gas e-diffr. 8=25629
u. h. vacuum camera for energies (10-50 kV), performance rel. to surface struct. 8=26353
Ag, surface structure from electron diffraction examination 8=35153
AlN films, fibre texture 8=30742
Au microcrystals, growth and defect structure 8=39666
Au polycrystalline films, dynamical intensities temp. dependence 8=39769
Au surface, LEED interpret. by coincident site lattices, and phase and spacing modulation 8=26096
B_2Cl_4, internal rotation from gas e-diffr. temp. dependence meas. 8=25446
$BaTiO_3$ (001) face, linear disorder on heating in u.h. vacuum 8=39649
Bi, surface structure, by LEED 8=26106
C films, condensed, structure 8=35162
C_3O_2, gas phase, temp. effects 8=25466
Cd, reflection, 600 to 1200 keV 8=44197
Cr films, vacuum deposited, structure and substructure rel. to deposition temp. 8=35169
Cr–Mo–Co steel R-phase precip., structure analysis 8=44001
Cs_3Sb films on MnO 8=39591
Cu, LEED beams, surface asymmetry origin of fractional order peaks 8=26100
Cu, spherical crysts., LEED spot patterns rel. to surface and reciprocal lattice 8=26098
Cu, surface structs. due to O_2 adsorption 8=26136
Cu-Zn alloys, abraded, surface and subsurface structure 8=26294
α-Fe_2O_3, twinned, bladelike platelet growths on iron, selected area exam. 8=48518
IrF_6. molec. struct. 8=38858
K films, LEED exam 8=48453
LiCl, thermal vibr. and Debye-Waller factor obs. 8=30905
LiF, thermal vibr. and Debye-Waller factor obs. 8=30905
Li-O-W (110) system. structure 8=39593
MgO rot. cryst., dispersion surface photographs 8=35309
Mo(111), faceting from CO adsorpt. 8=48486
Mo–Mn steel R-phase precip., structure analysis 8=44001
NaCl, thermal vibr. and Debye-Waller factor obs. 8=30905
NaCl-type crystals, LEED obs. of (11) beam from (100) surfaces 8=44236
NaCl(Br, I), LEED intensities, electrostatic potential contribution 8=48423
NaF, thermal vibr. and Debye-Waller factor obs. 8=30905
Nb and Ni alloy 79 HM5, reflection 600 to 1200 keV 8=44197
Nb, rolled, orientation distrib. of crystallites 8=35275
Ni, LEED beams, surface asymmetry origin of fractional order peaks 8=26100
Ni-34.5 at. %Cr, alloy ordering from e. diffr. exam. rel. to elec. resistivity 8=35064
NiO (100) face on heating 8=39650
NH_4I, polycrystalline 8=35343
NpF_6, molec. struct. 8=38858
OsF_6, molec. struct. 8=38858
Pb crysts., mean displacement of surface atoms 8=30935
Pb-Bi alloy films at low temp., of structure, new phases obs. 8=35152
$PbBi_2Se_4$, struct. 8=35348
Pb–Sn alloys, reflection, 600 to 1200 keV 8=44197
Pd cryst., mean displacement of surface atoms 8=30935
Pd-Sb system in thin films 8=30909
PuF_6, molec. struct. 8=38858

Electron diffraction examination of materials—contd
- Rb films, LEED exam. 8=48453
- Sb, surface structure, by LEED 8=26106
- SiO_2 films 8=30910
- Ta and Ti, reflection, 600 to 1200 keV 8=44197
- Ti_2O_3 identification as oxide protecting cemented carbide cutting tools 8=48428
- UF_6. molec. struct. 8=38858
- UO_2, LEED from surface steps 8=48429
- UO_2 surfaces, low-energy diffr. 8=48430
- W, LEED beams, surface asymmetry origin of fractional order peaks 8=26100
- W (100) surface, LEED obs. of electron impact effects on adsorbed NH_3 8=26140
- W, (110) surface, LEED 8=48431
- WF_6, molec. struct. 8=38858
- XeF_6, gas-phase, molec. struct. 8=34290-1
- XeF_6, molec. struct. 8=25523

Electron emission
- See also Fluctuations/electrical; Photoelectricity.
- alkali halides, tribo-, and luminescence 8=31462
- alloys, strained, exo-emission and work function irradiation dependence 8=44938
- cathodes with mica layer 8=44941
- cold cathode electron source, brightness obs. 8=47744
- electron-ion beams emitted by cylinder or sphere, steady-state potential distribs. 8=27339
- exo, counter 8=27340
- exoelectron emission photo stimulation in i.r. region 8=49438
- exoelectrons, on solidification of metals in vacuum, nature 8=40692
- ion-electron emission and sputtering coeffs. anisotropy rel. to target lattice thermal vibrations 8=40685
- of metal-dielec.-metal system model with scatt. on phonons and flaws 8=49387
- metals, experimental proof of general theory 8=49434
- molecules, ang. distrib. of photoelectrons 8=25705
- plasma, low temp. from electrode 8=39081
- steel, exoelectronic, during friction 8=44939
- Al, atom, auger electron following K → L de-excitation, chemical effect 8=43227
- Al, exoelectronic, during friction 8=44939
- Al, plastically deformed, effect of u.v. and electron bombardment pre-stimulation 8=44942
- Al, plastically deformed, photostimulated, temp. effect 8=44943
- Al-Al_2O_3-Au tunnel cathode, fluctuation pattern 8=44935
- γ-Al_2O_3, rel. to surface radiational defects 8=44025
- Au films, X-irradiated, emission-event statistics 8=44950
- BaF_2, exoemission, X-ray and thermo-stimulated, obs. 8=36040
- CsI films, X-irradiated, emission-event statistics 8=44950
- Cu, current density coeff. and other characts. 8=40698
- Cu, strained, exo-emission and work function irradiation dependence 8=44938
- Fe, in $\alpha \rightleftharpoons \gamma$ transformation region and positive-ion emission 8=27363
- GaAs, work function, obs. of giant temp. depend. 8=40688
- Ge, exo-, after irradiation and mech. treatment, rel. to surface defects 8=40694
- He liquid, due to vortex ring annihilation 8=37344
- KCl, bombardment with inert gas ions 8=40686
- LaB_6, laser-induced, using ruby and Ar lasers 8=40710
- LaB_6-La system, or with W and Ti added, characts. 8=27348
- LiF, X-irradiated, rel. to dislocations effect on F-centre thermal stability 8=35570
- Mo, from (110) and (111) faces 8=36036
- NaCl, bombardment with inert gas ions 8=40686
- Nb(110), (100), (111) and (116) faces 8=40689
- Ni, cold emission in N_2 with elect. field 8=49439
- S atom, auger electron following K → L de-excitation, chemical effect 8=43227
- Si, atom, auger electron following K → L de-excitation, chemical effect 8=43227
- Si, exo-, after irradiation and mech. treatment, rel. to surface defects 8=40694
- Si, exoemission rel. to surface treatment 8=40693
- SrF_2, exoemission, X-ray and thermo-stimulated, obs. 8=36040
- Ta, laser-induced, using ruby and Ar lasers 8=40710
- W, laser-induced, using ruby and Ar lasers 8=40710
- W, work function with various impurities 8=31461
- **field emission**
  - cathode for coherent illumination of e. biprism 8=41953
  - cathode, thin-film, structure, fabrication, performance and e.-micrography 8=40696
  - dielectric porous thin film, self sustained obs. 8=40695
  - film, thin. semicond., ionization 8=31463
  - source for electron gun 8=28554
  - Gd, polarization in high mag. field 8=27342
  - In_2S_3, hot electron mobility investigation 8=31381
  - Ir, studies rel. to surface migration 8=27343
  - MgO porous thin film, self sustained, obs. 8=40695
  - Re, studies rel. to surface migration 8=27343
  - Rh, studies rel. to surface migration 8=27343
  - Si, characts. rel. to cleaness of surface 8=35148
  - W, coated with Al_2O_3 film, rel. to thickness 8=27341

Electron emission—contd
- **field emission**—contd
  - W, O_2-covered, thermal rearrangement of surface 8=31464
  - W, studies rel. to surface migration 8=27343
  - W, with adsorbed NH_3 8=27734
- **photoelectric**
  - $A^vB_3^{vii}$ iodides, external photoeffect 8=44947
  - alkali metal contacts, into anthracene, obs. 8=31472
  - alkali metals, into anthracene rel. to its band structure determ. 8=31283-4-5
  - alkaline-earth metal contacts, into anthracene, obs. 8=31472
  - anthracene, band gap from threshold energies 8=44640
  - anthracene, study of conduction band structure 8=44639
  - atomic photoeffect, K-shell, relativistic, soln. with Laplace integrals 8=47526
  - from ferromagnetic substs., polarization of electrons 8=40701
  - γ rays, inelastic interaction with K-shell electrons 8=43226
  - light photon counter, photometric characts. 8=31471
  - low light intensities 8=44945
  - m.i.m. system, Lallemand electronic camera exam. 8=27352
  - m.o.m. thin sandwiches, correlation with electroluminescence 8=40700
  - metal work function differences, photoelect. determ. 8=31459
  - organic cpds, donor-acceptor type, for meas. of ionization energy 8=29947
  - photocathodes, light intensity and quantum yield meas. λ=30-100nm 8=27351
  - photoelectron spectroscopic system 8=36050
  - photomultiplier, cathode rel. sensitivity distrib. 8=33094
  - in photomultipliers, grid-controlled, suppression of parasitic photoemission 8=24158
  - semiconductors, calculation methods 8=49441
  - shot noise in detectors, photon bunching effects 8=46418
  - single e recording method, limits of applicability 8=36049
  - spectrometer for photoelectrons, parallel-plate 8=31470
  - spontaneous, existence of correlation between oscillations 8=38712
  - transparent dielectric mats., on ruby laser irradiation without physical damage 8=40703
  - X-ray excited, energy distrib. rel. to secondary emission 8=44946
  - Ag thin films, polycrystalline, obs. 8=27353
  - Ag-O-Cs photo cathode, origin of photoelectrons 8=49440
  - Al crystals, external effect rel. to Fermi surface anisotropy 8=40704
  - Al, exoemission in vacuum external elec. field effects, obs. 8=36041
  - Al, oxide coated, exoemission in plastic deform., obs. 8=36039
  - Ar, double ejection by K_α X-rays 8=38714
  - Au thin films, polycrystalline, obs. 8=27353
  - CdS, wurtzite, electronic structure study 8=31287
  - CdSe, wurtzite, electronic structure study 8=31287
  - Cs_3Sb, i.r. 8=40705
  - Cu thin films, polycrystalline, obs. 8=27353
  - GaAs, broken and cleaved, yield spectra, 82 and 293°K 8=36052
  - GaAs thin films 8=27354
  - Ge, Auger-recombination, indirect band to band 8=35892
  - Ge, field electron-emissive photocell 8=40702
  - Hg, two- and three-photon, in $HClO_4$ solns., obs. 8=40706
  - In, on X-irradiation, energy distrib. 8=40707
  - InSb, on X-irradiation, energy distrib. 8=40707
  - KCl, exoemission in vacuum external elec. field effects, obs. 8=36041
  - Na, two-quantum volume effect 8=44948
  - NaCl, exoemission in vacuum external elec. field effects, obs. 8=36041
  - KCl, exoemission on excitation by electron irradiation 8=40708
  - NaCl, coloured, tribo-photostimulated exoemission, and triboluminesc. 8=40709
  - NaCl, exoemission on excitation by electron irradiation 8=40708
  - NaCl, exoemission, X-ray excited, obs. and model 8=36053
  - NaCl-Ag layers, exoemission, X-ray excited, obs. and model 8=36053
  - NaI(Tl) scintillation counters, primary yield obs. 8=24516
  - Ne, double ejection by K_α X-rays 8=38714
  - Pd, electronic structure by photoemission and optical studies 8=31293
  - Rb films, vacuum-condensed 8=44944
  - Sb, on X-irradiation, energy distrib. 8=40707
  - $SbCs_3$ films, quantum yield, thickness depend. 8=36054
  - Si field electron-emissive photocell 8=40702
  - Si, n-, p-type and caesiated, rel. to surface Fermi level and work function, 80 and 290°K 8=40495
  - $SnSe_2$, energy distrib. 8=36055
- **secondary**
  - accelerator, avalanche effect 8=33394
  - Auger spectroscopy of f.c.c. metal surfaces, e-escape depth determ. and appls. 8=27355

- **Electron emission**—contd
  - **secondary**—contd
    - detector, semiconductor, with flexibility of mech. motion 8=31474
    - detection on scanning electron microscope 8=33091
    - dielectrics, characteristics meas. 8=49442
    - diffusion pump oil DC-705, δ-η anal. 8=48196
    - dynode thin films, mechanical props. 8=31161
    - in electron diffraction ring patterns of insulating films 8=48587
    - emitters, improved, with increased maximum yield 8=49443
    - metal surfaces, effect of contamination 8=49445
    - metals, coeff. rel. to energy of primary electrons 8=36058
    - metals, energy distribution rel. to incidence of primary beam 8=36059
    - reflection-type, noise spectrum obs. 8=31475
    - semiconductors, characteristics meas. 8=49442
    - semiconductors, due to ion beams 8=48892
    - solids due to ion and atom bombard. 8=26861
    - structure of energy spectra 8=31473
    - from X-irradiated target in vacuo 8=49444
    - X-ray excited, energy distrib. rel. to photoemission 8=44946
    - yield curve automatic plotting 8=36056
    - Al crystal-film, angular dependence, fine structure origin 8=40711
    - Al(100) face, obs. rel. to low and medium energy e-diffr. 8=27356
    - Al_2O_3, shot noise fluctuations 8=44949
    - Au, N_2* beam bombarded, 13-200 eV 8=34454
    - Cu crystal-film, angular dependence, fine structure origin 8=40711
    - Cu, energy angular distrib., fine structure meas. 8=40713
    - Ge crystals, rel. to primary electron interactions 8=44951
    - KCl, porous layers, influence of applied fields 8=36057
    - La, coeff. and energy spectrum obs. 8=40716
    - MgO films, porous, field-assisted 8=27359
    - MgO, shot noise fluctuations 8=44949
    - Mo, bombarded by positive ions, Auger, rel. to angle of incidence 8=27357
    - Mo, clean, bombarded by positive, electronically excited ions; Auger emission 8=27358
    - Si crystals, angular dependence for 1000 eV primary beam 8=40714
    - Si crystals angular dependence in primary e. range, 100-2000 eV 8=44952
    - W. shot noise fluctuations 8=44949
    - W variation depend. on absorpt. of primary beam 8=40715
    - W-Mo alloys 8=27360
    - W-Ta alloys 8=27360
    - Y, coeff. and energy spectrum obs. 8=40716
  - **thermionic**
    - See also Cathodes.
    - a. c. and d. c. currents rel. to voltage for N_2 at 900°C 8=36046
    - alkali halide crystals, dependence on excitation methods 8=40697
    - emitters having multiple cavities, apparent work function 8=28480
    - film-covered symmetric contacts, and thermionic currents 8=40628
    - impregnated aluminate cathode on W, Mo or Re base, limiting current 8=27345
    - metallic alloys, props., review 8=36047
    - molecular jet variations, thermo-optical detection 8=43431
    - oxide cathodes, well-activated, temp. range 500 to 1100°K 8=27346
    - plasma from laser vaporized metal 8=449490
    - by semiconductors with rare earth additives, total emissivity and induced rad. emission 8=31465
    - As_2Se_3, dependence on excitation methods 8=40697
    - Ba films on Ni 8=27347
    - CaO, emission props. in BaO stream 8=27349
    - Cs diode, optimum added noble gas pressure 8=41974
    - Ge, dependence on excitation methods 8=40697
    - LaB_6, rod cathode for high-brightness electron gun 8=28555
    - Mo, meas. of O_2 adsorpt. and desorpt. energies 8=31469
    - Mo_2C, in Cs vapour, and ion emission rel. to other refractory metal cpds 8=27350
    - $MoSi_2$, in Cs vapour, and ion emission rel. to other refractory metal cpds 8=27350
    - Os balls, vacuum work function and Richardson consts. 8=31467
    - Re, meas. of O_2 adsorpt. and desorpt. energies 8=31469
    - Re, vapour deposited, effective Richardson work function, and surface characts. 8=31468
    - Si, dependence on excitation methods 8=40697
    - SrO, emission props. in BaO stream 8=27349
    - TaB_2 in Cs vapour, and ion emission rel. to other refractory metal cpds 8=27350
    - $TaSi_2$, in Cs vapour, and ion emission rel. to other refractory metal cpds 8=27350
    - W emitter with (110) preferred orientation, work function characts 8=28477
    - W, in Ba and Cs atom flux 8=36048
    - W, meas. of O_2 adsorpt. and desorpt. energies 8=31469
    - W, with Cs-coverage, spectral rad. distrib. 8=31465

- **Electron emission**—contd
  - **thermionic**—contd
    - WSi_2, in Cs vapour, and ion emission rel. to other refractory metal cpds 8=27350
    - ZrC, in Cs vapour, and ion emission rel. to other refractory metal cpds 8=27350
- **Electron energy states**. See Crystal electron states.
- **Electron gas**
    - See also Metals/theory; Plasma; Solids/theory; Superconductivity.
    - classical, equilib. props., exact lower bounds 8=41783
    - classical, pair distribution function asymptotic behaviour 8=41782
    - collision frequency meas. by open plasma resonators 8=47852
    - degenerate, single particle spectrum 8=26925
    - dielectric const., Hartree-Fock approximation 8=23900
    - degenerate Fermi fluid, spectra of e.m. wave propag. and cyclotron waves 8=37218
    - electric dipoles, permanent and collective excitations 8=37217
    - Fermi-Dirac distrib., magnetoresistance deriv. 8=26870
    - ferromagnetism, interaction with Yukawa potl. 8=40762
    - Hartree-Fock exchange pot. for electron gas adaptation to atoms and solids 8=38617
    - h.f. dielect. const. 8=31305
    - inhomogeneous, variational principle for ground state energy 8=28340
    - loss-cone plasmas, absolute instabilities, effect of electron temp. 8=43602
    - metal, appl. Landau theory of quantum liquids, book 8=30397
    - momentum distrib. discontinuity 8=46121
    - plasma, one dimensional, numerical expt. on nonlinear behaviour 8=43495
    - plasmons and zeroth sound 8=44665
    - radial distrib. function 8=28342
    - radiation flow, polarized, soln for Green's function of matrix transport eqn. 8=28341
    - single crystal, absorpt. due to plasmon excitation 8=35795
    - in solids under arbitrary fields, Boltzmann eqn. stability 8=40275
    - in solids, almost-degenerate, corrections for Grüneison coeff. and sp. ht., 8=39908
    - Vlasov and Poisson oscill. eqns., soln. for linear confining potential 8=34548
    - wave amplitudes associated with particle phase mixing, Landau decrement 8=34550
    - weak periodic field, Peng's perturb. theory 8=34123
    - zero-temp. impurity resistivity, breakdown of conc. expansion 8=31306
- **Electron guns**. See Electron beams.
- **Electron lenses**
    - See also Electron microscopes; Electron optics.
    - aberrations introduced in image of off-axis point source 8=41958
    - asymptctic aberration coeffs. magnification and object position 8=28561
    - cathode-ray, testing 8=41960
    - cathode-ray tube electron focussing-lens systems 8=41957
    - cryo-electron-lenses, review 8=46411-12
    - elements of 2 and 4 fold symmetry 8=41955
    - focussing in mag. optic systems 8=41954
    - microscope objective with higher-than-conventional contrast 8=41961
    - quadrupole, dipole and quadrupole mag. field 8=46393
    - quadrupole lens system, beam stability 8=37414
    - spherical aberration coeffs. of stigmatic doublets of short quadrupole lenses 8=24145
    - spherical aberration, two-section correction, resolving power 8=24144
    - stigmatic doublets of short quadrupole lenses, coeffs. of spherical aberration 8=24145
  - **electrostatic**
    - aberration characts. for rotationally-symmetric fields 8=41963
    - centrifugal focusing and h.f. helical electrodes, for scalloping beams 8=24135
    - electron-impact spectrometer 8=47585
    - potential of axisymmetric electrostatic field in space rel. to given distrib. along axis 8=24143
    - quadrupole field in circular concave electrodes 8=46350
    - quadrupole, two-dimensional, chromatic aberration 8=37421
    - quadrupole, with concave electrodes, field meas. 8=37420
    - tubular or parallel plate, calc. 8=28562
    - three-electrode cathode lens of emission microscope, resolution limit 8=41962
  - **magnetic**
    - chromatic aberration coefficient meas. 8=33087
    - design, applic. of method of least squares 8=41964
    - electron microscope image vel. analyser 8=28565
    - for linear accelerator used as positron source 8=42353
    - magnets for beam transport, focusing props. and params. choice 8=28520
    - microscope advances, book 8=37422
    - as objective, with bifilar superconductors, ultra fine deflection 8=24147
    - photomultiplier defocusing, evaluation 8=41977
    - probe-forming, spherical aberration obs. and calc. 8=33086

Electron lenses—contd
magnetic—contd
quadrupole, mag. centre and axes location 8=28564
superconducting wires as exciting coil 8=24146
variable field distrib., for β spectrometer 8=24731
Ar linear pinch discharge, 3.5 MV electrons in 30 nsec pulses 8=28563

Electron microscope examination of materials
alkali borates, binary, microstructure in subliquidus phases rel. to immiscibility 8=43756
alloy, ticonal-type, oriented modulated structure 8=35056
α-keratin, matrix-microfibril texture 8=39729
amorphous substances, vapor-deposition effect on replicating as error source 8=39707
brass standard, Midwest Probe Users Group report 8=30851
carbonaceous, sample prep. and structural features 8=44164
cathode, thin-film field-emission 8=40696
ceramic coatings of archaelogical specimens 8=43970
dielectric surface topography from e.-mirror micrographs 8=44863
dislocation defects, prismatic, rel. to identification 8=31061
dislocation density meas. 8=35559
epoxide resins, hardened 8=35292
explosion bonded metals, microstructure 8=44157
ferroelectric surface topography from e.-mirror micrographs 8=44863
ferromagnetic films, of individual domains 8=31586
films, thin ferromag., domain obs. by transmission e mic. 8=31590
films transmitted images by scanning microscope 8=30735
graphite, after thermal oxidation 8=44167
graphite, crystal growth rel. to adsorbed impurity effects 8=26236
image profiles of paired and triple dislocations 8=40030
inelastic e scatt. and excitation of surface plasma oscs., for surface exam. 8=26926
insulating, pre-exam. metallizing device 8=30853
light elements using axial illum., lattice fringes resolution 8=39775
metallurgical appls. of scanning microscope 8=50472
molybdenite films, thick, 50 to 1200 kV 8=48602
muscovite heated in vacuum, superstructure phase, study 8=26190
oxide film stripping technique 8=30732
oxides: CdO, CaO, MnO, NiO, struct. 8=48592
phase contrast images of molecular details 8=29710
polymers in soln. and in films, fibrillar structure 8=26153
polypropylene lamellae grown from dil. α-chlornaphthalene solns., twinning obs. 8=35218
precipitates, semi-coherent, interfacial structure 8=26656
single stage C replica of mineral crystals, rapid method of prep. 8=30855
steel, high-carbon, martensite defect structure 8=35272
steel, stainless, thickness limits at high voltages 8=41971
steel, stress-corrosion by transmission 8=45335
tilted foil, with dislocations and stacking faults, computer micrograph 8=40017
Al–In alloys, dilute 8=35265
Al–Mg–Zn alloy, new rupture pattern in replica tech. 8=35658
Al_2O_3, particulate, replication technique 8=44160
Au evaporated particles, structure 8=35317
$AuAg_3Te_2$, phase transforms during e microprobe analysis, obs. 8=30857
$BaTiO_3$, surface domain structure and topography from e.-mirror photomicrographs 8=39576
C films, condensed, structure 8=35162
CdS crystals, surface changes rel. to photoconductivity on ht. treatment, 100–600°C 8=35268
Co electrolytic deposition, cryst. growth 8=26245
Cs layers on refractory metals, field-emission 8=39624
Fe, high-purity, plastically deformed, on heating to 600°C 8=35677
Fe–Al alloys, "K-state" characterization by ordered domains 8=48597
Fe-C standard, Midwest Probe Users Group report 8=30851
Fe-Cr alloy, oxidized surface film interface 8=44074
Fe-Mn alloys, structural changes due to stacking fault conc. rel. to Mn content 8=35576
Fe-Ni standard, Midwest Probe Users Group report 8=30851
Ge crystals, deformed, dislocation structure, method and results 8=31064
K_2O-SiO_2 glasses, comp. vars. in e microanalysis rel. to surface damage, obs. 8=30865
LiF, dislocation multipoles in slip bands 8=44460
NaCl, doped with divalent cations, evaporation structure 8=48603
Na_2O-FeO-SiO_2 glasses, comp. vars. in e microanalysis rel. to surface damage obs. 8=30865
Ni_3Mn alloy thin films, antiphase boundaries obs. 8=35279
Ni_4Mo, long- and short-range order and resulting substructure 8=44009
Si, and incoherent X-ray scattering 8=44155

Electron microscope examination of materials—contd
Si, n-irradiated, defect character from anomalously wide images using stereo e-microscopy 8=31025
Si surface electrically-decorated by Pt, high-resoln. 8=40496
Si, thickness limits at high voltages 8=41971
SiC, microprobe analysis, Philibert's correction for absorpt. 8=27798
SiO_2 films 8=30910
SiP precipitation on high-conc. P diffusion in Si, defect structure 8=39983
Ta_2O_5 thin film, obs. of superstructure 8=26129
Te, transmission microscopy 8=35356
ThO_2 inclusions in W 8=44173
Ti-47%Nb, α-phase formation during heating in microscope 8=35119
US crystals, precip. and groove-etching obs. 8=35286
US, slip behaviour 8=35285
V_3Si, superconducting, martensitic phase transform. 8=26085
W-Mo-Re alloys, structure and surface props. from field emission studies 8=39727
Y Al garnet, planar defects 8=44429
Zn crystal growth forms 8=48562

Electron microscopes
contrast anomalies 8=46416
diaphragm, thin-walled objective aperture 8=24148
diffractometers, design and applics. 8=41972
electron microscopy/microanalyser, and appls. 8=27805
electron microscope-microprobe for small particles analysis 8=34935
EM-9, transmission type, construction and operation 8=41969
emission type, vacuum system and objective 8=28570
field-electron emission shadow 8=24152
field emission, K deposition on W emitters, flicker noise and surface migration 8=44936
field, for whisker formation on W using chloromethane adsorption 8=26272
foot operated electric drive for rotating-tilting stage 8=33089
grating profile, examination method 8=37423
image intensifier 8=33095
interference, mean internal potential determ. 8=46414
lenses, magnetic, use of superconducting wires 8=24146
liquid He stage for accessories 8=28571
as low angle electron diff. camera, arrangements needed, appls. and techs 8=24149
microprobe-microscope combination 8=28574
microprobes, testing and data correction, Scandinavian users assoc. report 8=30852
microprobe-X-ray spectrometer combination 8=28573
multipurpose high-resolution stage 8=46415
objective with higher-than-conventional contrast 8=41961
objective, with intermediate deceleration of electrons 8=41966
oil-free vacuum pump system 8=34684
optics, advances, book 8=37422
photoelectric, displacement comparator 8=46413
resolving power of 1Å, development advances 8=46411-12
scanning, beam current meas. 8=46324
scanning, for films transmitted images exam. 8=30735
scanning, review 8=41968
scanning type, new method of detecting secondary electrons 8=33091
scanning, voltage meas. by e.s. analyser 8=41970
stage for e diffr. crystallographic meas. 8=44194
superconducting wires in magnetic lenses 8=24146
X-ray spectrometer attachment for Phillips EM-200 8=24451
C, tartan film prod. mask 8=35164
He liquid cooled stage 8=46293

Electron microscopy
See also Crystal structure, atomic.
applications for investigation of electrodeposites 8=44154
defocussing dependence of phase contrast in micrograph images 8=24151
fibre purificiation for electronmicroscopic prep. 8=48360
field emission shadow 8=24152
high voltage, e energy losses rel. to multiple inelastic scatt. 8=37417
high-voltage, specimen thickness limits 8=41971
holography, theory for three-dimens, wavefront-reconstruction imaging 8=24150
insulating materials, metallizing device 8=30853
irradiated object size, accurate determ. 8=41956
Lorentz, electron beam coherence and mag. film micrograph interpretation 8=33090
Lorentz, for high resolution exam. of thin films 8=36128
Lorentz, of weak magnetic flux inhomogeneities 8=36132
low-energy 8=41966
low energy scanning probe, anal. of retarding-field systems 8=28568
magnetic lens image vel. analyser 8=28565
micrograph image contrasts images of molecular detail 8=29710
micrometeorites, X-ray spectrometer appl. 8=28156
microprobe analysis, absorpt. correction functions, evaluation 8=27797

Electron microscopy—contd
microprobe analysis absorpt. corrections rel. to target Z 8=27796
microprobe analysis, Philibert's correction for absorpt. 8=27798
microprobe analysis, target absorpt. corrections 8=27799
microprobe analysis, X-ray fluoresc. corrections errors 8=27800
microprobe correction factors, calc. methods evaluation 8=27801
microprobe data statistical analysis 8=30850
microprobe-microanalyser combination, appls. 8=27806
microprobe, specimen heating device 8=28572
microprobe with automatic scanning and data analysis 8=27807
mirror microscopy for meas. of elec. and topological features of biol. mats. 8=41603
mirror voltage resolution 8=28567
orientation effect, improvements 8=35262
perforated foils production 8=45938
phase and amplitude of e wave without spherical aberration 8=30854
phase contrast in micrograph images, defocussing dependence 8=24151
photomicrography, emulsion resolution of 7-60 keV electron images 8=37722
photomicrography, emulsion response to 7-60 keV electrons 8=37721
reflection, microscopic differences in height meas. 8=44023
review of new developments 8=46411-12
scanning techs, limitations rel. to contamination and interpret. 8=30849
scanning type, secondary electron detection 8=33091
single stage C replica of mineral crystals, rapid method of prep. 8=30855
specimen blanks preparation 8=37098
specimen preparation and applications, advances, book 8=37422
stroboscopic scanning 8=33008
thin foils rapid preparation 8=28205
thoria gel, crystallite sizes, equivalence with X-ray diffraction meas. 8=35284
3D object reconstruction from micrographs 8=35260
tilted foil, with dislocations and stacking faults, computed micrograph 8=40017
transmission and scanning, comparison for fracture surfaces 8=48415
transmission-type optimum resolution with small-angle diffraction 8=28569
virus structure determ. 8=32624
Al-Cu alloy, grain boundary precip. 8=26708
Be and alloys, transmission, for temp. dependence of slip and dislocation identification 8=44555
GaAs automatic jet thinning for transmission microscopy 8=33088
Li p-n junction regions in Si, mirror microscope obs. 8=35922
WC-Co hard metals, electropolish thinning for transmission e microscopy 8=36608
Electron multipliers. See Electron tubes; Photomultipliers.
Electron multiplier phototubes. See Photomultipliers.
Electron nuclear double resonance (ENDOR). See Nuclear magnetic resonance and relaxation; Paramagnetic resonance and relaxation.
Electron optics
See also Beta-ray spectrometers; Electron lenses; Ion optics; Particle optics.
asymptotic aberration coeffs. magnification and object position 8=28561
asymptotic quadrupole aberrations, rel. to object position 8=24141/2
betatron oscills. in cyclotron 8=33466
bunching, accelerator injection, space-charge analysis 8=33084
deflection, two-dimensional, study of aberrations 8=46407
diaphragms, axisymmetric e. s. problem 8=33083
distortions in shadow projection mirror images of periodic structs. 8=41967
double-focusing β spectrometer, computation and expt. 8=37940
electrostatic lenses, tubular or parallel plate, calc. 8=28562
electrostatic system aberration functions 8=41963
elements of 2 and 4 fold symmetry 8=41955
extraction field, parameter of path shape 8=29008
field emission cathode for coherent illumination of biprism 8=41953
films, charged, anomalous interference of electrons on edge 8=44030
films, high-resistance, subjected to e-beam scanning, resolving power 8=33096
funs, high perveance axi-symmetric, digital simulation 8=46408
holograms, theory for three dimens. wavefront-reconstruction imaging 8=24150
in infrared image analyzer tube 8=41981
interference on charged C film edge, obs. 8=37419
Electron optics —contd
linear accelerator, waveguide bunching system 8=37815
microscope advances, book 8=37422
mirror voltage resolution 8=28567
non-conducting foil mountings to reduce background scattering, errors produced 8=26352
open channels, axisymmetric e. s. problem 8=33083
potential of axisymmetric electrostatic field in space rel. to given distrib. along axis 8=24143
three-electrode cathode lens of emission microscope, resolution limit 8=41962
trajectory recording with analogue computer 8=46406
transport system, e.s., with periodic focussing 8=41965
Electron pairs
See also Positronium.
colliding beams, pair prod. with spin $^3/_2$ 8=24733
e^-e^+ beam collisions, W-boson prod. 8=24720
annihilation
angular distribs. rel. to single-particle positron wave functions 8=44669
C-parity selection rules 8=37941
$e^+e^- \rightarrow \mu^+\mu^-$ longitudinal circular polarization survival 8=37941
$e^+e^- \rightarrow \pi^\circ\gamma, \eta\gamma$, interference of ρ°, ω states 8=24734
$e^+e^- \rightarrow 2\gamma$ longitudinal circular polarization survival 8=37941
electron-position, two-photon annihilation in strong mag. field 8=42477
3π prod. general method for deriving ang. correls. 8=24687
photons circular polarization at high energies, spin correl. calc. 8=29098
polarization effects for ultrarelativistic electrons 8=37942
positron, line shape meas. using Ge(Li) detector 8=40285
positron, single-quantum, cross sections 8=44670
Al, angular distribs. rel. to single-particle positron wave functions 8=44669
Al, positron, in determ. of Fermi momentum pressure dependence, 0. 100 kbar. 8=44635
Au, positron, single-quantum, cross sections 8=44670
Cu-Al alloys, rel. to Fermi surface 8=31288
Dy, rel. to electronic structure 8=26906
Gd, rel. to electronic structure 8=26906
Ho, rel. to electronic structure 8=26906
Ho-Er alloy, rel. to electronic structure 8=26906
O_2 molecules as paramag. impurity rel. to long lifetime 8=29851
Pb, positron, single-quantum, cross sections 8=44670
Si, angular distribs. rel. to single-particle positron wave functions 8=44669
Sn, positron, single-quantum, cross sections 8=44670
Ta, positron, single-quantum, cross sections 8=44670
Tb, rel. to electronic structure 8=26906
U, positron, single-quantum, cross sections 8=44670
Y, rel. to electronic structure 8=26906
production
in condensed medium, multiple scatt. effect 8=24693
cosmic ray cross-section calc. 8=29387
crystal, thin, high-energy calc. and meas. methods 8=42460
in magnetic field, spontaneous, calc. including electron anomalous magnetic moment effect 8=45590
by μ in nuclear field 8=38257
nuclear multipole transformations 8=25086
in photon-photon collisions, magnetic field effect 8=33643
by photon in const and uniform elec. field, probability 8=37934
photoproduction on C, high energy 8=42990
by π^- in nuclear emulsion, direct prod., 16.2 BeV/c 8=33645
in semiconductor detectors, Fano factor 8=46889
$\Sigma^\circ \rightarrow \Lambda^\circ + e^- + e^+$, Λ° polarization re-estimate 8=29211
vector meson decay, rate, calc. of radiative correction 8=29170
Al, 500 MeV e scatt. 8=29411
Be, 500 MeV e scatt. 8=29411
Pt, 500 MeV e scatt. 8=29411
γ + Al, total cross section, 1.200-4.050 GeV 8=33644
γ + C, total cross section, 1.200-4.050 GeV 8=33644
γ + Cu, total cross section, 1.200-4.050 GeV 8=33644
γ + Pb, total cross section, 1.200-4.050 GeV 8=33644
Electron paramagnetic resonance. See Paramagnetic resonance and relaxation.
Electron—phonon interactions. See Crystal electron states; Crystals/lattice mechanics.
Electron probe analysis. See Chemical analysis/X-ray.
Electron resonance. See Cyclotron resonance; Paramagnetic resonance and relaxation.
Electron spin resonance. See Paramagnetic resonance and relaxation.
Electron states in solids. See Crystal electron states.
Electron structure of solids (crystallography). See Crystal structure, atomic.
Electron structure of solids (energy structure). See Crystal electron states.
Electron theory
See also Quantum electrodynamics.
chain theory for internal structures of elementary particles 8=37866

Electron theory—contd
Dirac electron spin rel. to magnetodynamic effect 8=33629
Dirac equation exact solns. 8=29092
Dirac eqn. for arbitrary spin, e. m. moments 8=33564
Dirac eqn., homogeneous solns. 8=29093
Dirac eqn. in const and uniform elec. field, physical solns. 8=37934
Dirac eqns., solvable potentials for non-relativistic limit 8=33319
Dirac eqn., symmetry algebra calc. 8=46803
Dirac Hamiltonian, non-relativistic approximations 8=37932
Dirac theory reformation in O(4, 2) rel. to antiparticles 8=33627
Dirac wave packet in electric field, hidden linear momentum rel. to α. E term 8=24716
electric charge, proposed variation with time laboratory test 8=28212
Green function of electron interacting with electromagnetic field 8=33635
Hestenes and Dirac theories 8=42467
infinite field mass elimination 8=42466
momentum gain, intensity-dependent, in e.m. waves 8=33634
quantum, with Dirac condition $A^{\mu}A_{\mu} = M_0^2/\epsilon^2$ 8=37933
radiation damping in conformally flat spaces 8=32809
radiation damping, vierbein formalism 8=32808
radiation-induced spin polarization, spiral orbit 8=24715
velocity of field calc., by expressing Dirac spinors as vectors 8=33626
Volkov soln. of Kelin-Gordon eqn., e.m. wave scatt. appl. 8=33633

Electron theory of metals. See Crystal electron states; Metals/theory.

Electron traps. See Crystal electron states.

Electron tubes
See also X-ray tubes.
carcinotron modulation 8=46421
cathode ray, opto-electronic cold cathode 8=44937
cathode-ray tube electron focussing-lens systems 8=41957
c.r.t. mirodensitometer for X-ray crystallography 8=35304
crossed-field, high-vauum devices, wall potential, mag. field dependence 8=37427
cylindrical magnetron, cut-off characts, depend on emission current, reply to comments 8=24154
diode, gas, space-charge-limited, noise suppression 8=28576
diode voltage fluctuations, Fokker-Planck eqn. 8=46353
electron swarm, spatial/time variation of electron energies 8=28575
emitter sheath, double, density of trapped positive ions 8=34525
klystron, ceramic sub-assemblies props. and behaviour 8=28602
klystron, freq. stabilization in mm range with open resonator 8=46467
klystron theory, nonlinear space charge wave-type 8=46420
klystrons, computer design 8=24547
manufacture, vacuum prod. and meas. 8=39257
magnetron, current passage under above-critical conditions, diffusion theory, expt. verification 8=37429
magnetron, cylindrical, comment on cut-off characts. 8=24153
magnetron, cylindrical, electron cloud resolution into concentric multilayers 8=33093
magnetron, cylindrical space charge oscillations 8=42001
magnetron, radial distrib. of end current 8=33092
in magnetron, smooth-bore, electron transport theory 8=24138
magnetron-type microwave amplifiers, ways of increasing gain 8=24202
multiplier, continuous-channel, transformer coupling 8=46423
orotron, electron device with open resonator and reflection grating 8=37428
oscilloscope, multi-trace identification modulation 8=41975
parameter meas., standardization 8=37426
pencil triodes, u. h. f., grid blackout, dynamic behaviour 8=37425
photoelectric detectors, shot noise, photon bunching effects 8=46418
quantitative meas. by shadow projection method 8=33081
RD-502 cylindrical diodes with etched Re emitters, performance comparison 8=28483
surface charges, associated transition processes 8=24155
thermionic diode, cermet seal of Nb-Al_2O_3 powder between Nb slabs 8=28499
thermionic diodes, metallographic evaluation of components 8=37377
thermionic diode with cavity emitters, apparent work function 8=28480
thermionic diode, Xe-filled, V-I characts on exposure to nuclear rad. 8=28485
thermionic diodes, Xe-filled, irradiated in nuclear reactor core, elec. props. 8=46417
travelling-wave tube electrodynamics 8=37515
travelling-wave tubes multiple-large-signal theory 8=41973
trigatron, selection of gas mixture 8=37424
CdSe-Sb_2S_3 vidicon-type targets, props. 8=46419

Electron tubes—contd
Cs thermionic diode, optimum added noble gas pressure 8=41974

Electrons
This heading includes both negative and positive electrons when the differences between them are of no special significance. See also Beta-rays; Cosmic rays/electrons; Crystal electron states: Fluctuations/electrical; Nuclear reactions due to/electrons; Photoelectricity; Plasma; Positronium; Positrons; Space charge.
angular distrib. in cosmic-ray shower, arbitrary boundary conditions 8=38209
angular distrib. rel. to depth in cascade showers 8=38208
anomalous, existence, theoretical and expt. limits 8=33625
auroral microburst and rel. to X-rays, obs. 8=32280-81
aurora, near monoenergetic flux ~4 keV rocket obs. 8=32291
auroral precipitation, average props. determined by satellite obs. 8=27955
bubble in liq. He, vibration freq. estimate 8=37346
capture of fast protons in gases 8=34172
charge, Millikan's expt. modification to eliminate air viscosity valve 8=42468
chemical properties 8=25322
collision freq., effective, in plasma, spatial distrib. determ. by microwave method 8=25764
conduction, effective masses, temp. depend. 8=44637
cyclotron freq. of free electrons in quadrupole cage 8=29096
in dielectric media, self-trapping effect, math. model 8=28466
dipole moment contribution to atom's electric dipole moment 8=38612
dipole moment, upper limit from meas. of elec. dipole moment of Cs 8=29614
Dirac, e. m. and meson fields interacting 8=38015
Dirac equation, perturbation theory 8=24488
Dirac, 2 in bound state = meson 8=24750
discharge, Ne h.f., energy distribution 8=43457
d disintegration at quasielastic peak 8=33632
distribution equilib. function in e. m. cascade 8=38207
drift velocity in gases, new theory 8=39222
e^-e^- beam collisions, W-boson prod. 8=24720
electrodisintegration of d, p polarization sensitive to spin-flip radial integrals 8=29095
(electron charge)^2, possible var. with the age of the universe 8=28028
electroexcitation of baryon resonances, relations between form factors 8=42661
electron-positron g-factor comparison, crossed-field prod. 8=33628
electroprod. of π from protons, radiative correction obs. 8=24775
electroprod. of ρ°, analysis of $e + p \rightarrow e^1 + \rho^\circ + p^1 \rightarrow \pi^* + \pi^-$ 8=24859
e.m. wave scatt., effect of constant uniform mag. field 8=24726
in e.m. waves, energy levels for given momentum, infinite number 8=28598
$e + N \rightarrow e + N + \pi + \pi$, current algebra and PCAC calc. of N axial-vector form factor 8=33738
$e^- p \rightarrow e^- n\pi^+$, pion form factor evaluation 8=37966
$ep \rightarrow eN^*$, quark model, form factors 8=33631
energies in swarm, spatial/time variation 8=28575
excess electron in nonpolar fluid 8=34571
extranuclear, effect on muonic atom energy level 8=34188
g-factor anomaly, recalc. 8=24717
free, liberated in gas by laser beam irradiation 8=29905
heavy, unsuccessful search in e-p 5BeV inelastic scatt. 8=24714
impact excitation of atoms, role of intermediate states 8=43213
in inner rad. zone, model intensity distribs. 8=36816
in ionosphere, altitude distrib. of temp. and conc. 8=27966
ionosphere content, enhancements assoc. with mag. storms 8=45512
in ionosphere D-region, height distrib. rel. to prod. of ionization by solar rads. 8=32327
ionosphere and magnetosphere, temps. obs. 8=32297
in ionosphere, D-region, neutral collision freq. and desnity profiles 8=32326
linear theory of motion in storage ring 8=24589
liquid, degenerate, spin-independ. oscills. 8=34755
low energy, response of anthracene scintillation counter 8=24728
with magnetic moment, anomalous in field of plane e. m. wave 8=33637
magnetic moment anomalous rel. to spontaneous prod. of e pairs in magnetic field 8=45590
magnetic moment, anomalous 6th order term using dispersion relation 8=29094
motion in plane circularly polarized e.m. wave 8=33637
μ-e e.m. differences, by comparison of μ-p and e-p elastic scatt. 8=42480
number in e.a.s., probability distrib. functions 8=38213
in outer radiations belt, intensity time variation rel. to radial diffusion 8=36817

Electrons—contd
ν-e$^{\pm}$ interaction, μ production, exam. using two- and four-component theory 8=29090
positive column, Maxwellian vel. distrib. 8=34416
production in O$^-$ associative detachment reactions 8=39051
quantum electrodynamics with external current and potential 8=28960
quantum electrodynamics mass and charge renormalization 8=28961
quasi-energy spectrum and green function in e. m. wave field 8=47080
reflection by standing light waves 8=47089
relativistic motion in const. mag. field 8=42471
rotational and vibrational excitation of molecular ions 8=38785
radial diffusion coeff. at low L values 8=27961
reflection, specular, from semi-metal films, rel. to Sondheimer effect 8=26957
self-mass guage-independence in g.e.d. 8=28950
solar wind, terrestrial origin upstream beyond bow shock 8=32587
solvated, in polar liqs., oriented dipole model 8=34785
solvated, reactions in radiolysis of alcohols 8=49964
spatial conc. patterns in negative glow and Faraday dark space 8=25696
transport coeffs. and energy distrib. in gas, stochastic model 8=39230
velocity, relativistic, limiting obs. 8=33709
CO adsorbed on W, electron bombard. effect 8=30776
K$^+$ ionization by electron impact 8=39047
Na$^+$ ionizaton by electron impact 8=39047

absorption
See also Beta-rays/absorption.
normal and abnormal, in diffraction, theory 8=30845
silicate glass, irradiated, spectra, and thermoluminesc. and e.p.r. 8=41196
Al, coeff. and stopping distance at 50 and 1200 keV 8=44494
CN, reaction spectroscopy 8=27700
Li$^+$, e capture cross section 8=25392
Na-Ca silicate glasses 8=30792
W, of primary beam, effect on secondary emission 8=40715

ionization
No entries

radiation
See also Bremsstrahlung; Cherenkov radiation; Electrodynamics.
astronomical radio sources, self-absorbed, relaxation 8=50384
bremsstrahlung Mork-Olsen radiative corrections and pair prod. obs. 8=24706
electromagnetic field, high-energy, statistical characts. 8=28552
in e.m. wave, plane circularly polarized 8=33637
harmonics in optical emission of harmonic oscillator 8=42472
invariance restrictions on momentum change of accelerated charge 8=37935
magnetic bremsstrahlung, megagauss Cnare targets for meas. 8=46987
moving in circularly polarized e. m. wave, intensity and ang. distrib. of radiation 8=33063
resonance props. of Cherenkov radiation at longitudinal waves 8=37930
solar flares, r. f. and X-ray emission 8=32601
spark discharge, pulsed in air, fast electrons and X-radiation during initial growth 8=39002
synchrotron, absorption and emission in magnetic field 8=37936
synchrotron, dependence on external radiation props. 8=24721
synchrotron emission of intermediate energy electrons, influence of ionized medium 8=37052
synchrotron, laser action in accelerator, desntiy calc. 8=33636
synchrotron, polarization and emission spectra, relativistic calc. 8=47082

scattering
See also Atoms/electron scattering; Beta-rays/scattering.
alloy, Kondo effect rel. to de Haas-van Alphen oscillations 8=31490
apparatus for meas. at 180° 8=24725
auroral, by atmosphere 8=41394
backscattering, triple 8=49995
Compton effect, multiple, obs. 8=24697
Compton, 1 GeV, near 180, obs. 8=42459
crystal, single, rel. to lattice struct. 8=48889
d electrodisintegration, problems with d wave function and N core radius 8=33842
e-d, quasielastic obs., n magnetic form factor deduced 8=24722
e$^-$e$^+$ → AB processes with polarised beams 8=33646
eigenchannel theory, generalization 8=33981
electron-atom approximation, adiabatic-exchange, orthogonality 8=25381
electron-deuteron, quasi-elastic, and n struct. 8=47084
in electron diffr. crystallography, quasielastic scatt. rel. to bonds and polarization 8=39762

Electrons—contd
scattering—contd
electron-electron at 2 × 160 MeV, bremsstrahlung obs. 8=47085
electron-proton, large momentum transfer, enhancement of 2-photon-exchange effects 8=42470
e.m. wave, momentum gain, intensity-dependent 8=33634
e.m. wave, Volkov soln. of Klein-Gordon eqn. 8=33633
e-ν, rel. to difficulties in weak interaction theory 8=33566
e-p, e$^+$-p ratio obs. equal to unity up to $(5\,\mathrm{GeV/c})^2$ 8=42639
e$^-$ + p → e$^-$ + p + π^0, differential cross-section near N* (1236) reson., obs. 8=33671
e-π, polarization effects for ultrarelativistic electrons 8=37942
ethyl iodide mols., spin polarization calc., 300-400 eV 8=34214-5
by excitons, non-localized of Mott 8=35789
field intensity near focus of laser beam 8=47083
four-magnet system for 180° scatt. 8=24116
gas, e drift vel. rel. to resonance scatt. 8=47979
gas, rarefied, density meas. 8=47933
graphite, low-energy back-scatt., energy distrib. curves rel. to surfaces 8=30730
inelastic at low momentum transfer, model-independent evaluation 8=38457
inelastic, monopole and quadrupole excitations 8=42993
inelastic, Born approximation and DWBA, comparison 8=29408
inelastic, into crystal reflections, dielectric theory 8=26725
in ionosphere F-region, collision freq., 8=50195
in electron microscope, h. v., multiple inelastic scatt. rel. to energy losses 8=37417
Kondo Hamiltonian, off localized moments, equivalence of Nagaoka and Suhl treatments 8=35750
by light wave, Kapitza-Dirac formula modification 8=47090
in magnetic systems, by e-magnon interaction, and beam polarization 8=35754
metal film thickness determ. by fast e.-backscatt. 8=48434
metal surface, line shape theory of radiofrequency size effect 8=44638
metals, specular, rel. to anomalous skin effect 8=49739
by molecules, diatomic, in the approx. of two short-range potentials 8=43425
by molecules, inelastic, theory 8=43279
by molecules, resonance before electron emission or predissociation 8=38949
multiphonon scattering of low-energy electrons 8=44193
negaton-positon, quastipotential approach 8=24719
nuclear matter, response function calc. 8=29407
nuclei, extended, azimuthal asymmetry 8=38459
nuclei, heavy, rel. to models charge and transition densities 8=33861
nucleon, elastic, form factors and vertex amplitudes 8=47086
nucleus, high-energy, geometrical optics analysis 8=47030
$\bar{\nu}$-e, cross-section meas. 8=47079
rel. to nucleus structure, elastic, inelastic and quasi-elastic scatt. 8=33982
π e, polarization and π form factor 8=24767
polarization vector change obs. in nuclear scatt. 8=42994
rel. to nuclear matter, re-arrangement energy calc. 8=29273
overlap integral calc. using single particle orbitals 8=29263
photon-electron, in refracting medium, inducement of additional photon 8=37937
by polar molecules, rel. to dipole moment 8=25441
plasma, multiple scatt., Molière's theory 8=39076
rare-gas liquids, electron-atom scattering length, mobility max. 8=43229
Regge trajectories, conspiracy test 8=42469
relativistic, in plasma, thermodynamic Green's functions 8=34474
relativistic scatt. of laser beam, finite vol. effects, spectral intensity 8=42451
semiconductor impurity states, interaction with optical phonons 8=44629
semiconductors, many-valley, e-phonon inelastic scatt., dissipative effects loss 8=31264
spin-flip scatt. of conduction electrons from impurities 8=40893
stimulated multiple, by strong laser field 8=47087
superconductor, by paramag. impurities 8=40211
thermal lattice vibrs., effect on electron scatt. in crysts. 8=48697
in thin monocryst, with spatial regrouping of particle stream 8=40066
in transition metals, electron-electron scatt. and Baber's model 8=40209
and X-ray prod. in microanalysis specimen, transport eqn. calc. 8=28560
Al, energy loss spectra, quantitative comparison with dielectric theory 8=26727
Al, 500 MeV e trident and pair prod. 8=29411
Ar, energy loss, charact., on transmission 8=34449
Be^9 nuclear mag. transitions obs. 8=25096
Be, 500 MeV e trident and pair prod. 8=29411
Bi-Te-Se semicond., scatt. mechanism 8=40440

Electrons—contd
  scattering—contd
    C^{12}, elastic and quasi-free scatt., short-range correls. 8=38355
    C^{12} giant resonance, inelastic cross section, $E_e = 20-35$ MeV 8=47310
    Ca^{40} rel. to charge distrib., 750 MeV 8=29304
    $Ca^{40,48}$, elastic, 750 MeV 8=29412
    Ca^{40}, elastic, shell model with N-N correls., 750 MeV 8=33911
    Cu, back-scatt., energy loss spectra rel. to plasmon states, 30–350 eV 8=35809
    Cu, low-energy back-scatt., energy distrib. curves rel. to surfaces 8=30730
    Cu-Cr alloys, exhibiting Kondo effect 8=44688
    H_2, rotational excitation, exchange effects 8=34241
    He, back-scatt. in crossed elec. and mag. fields, obs. 8=39232
    He^4, implications of a new approach to Q.E.D. 8=24723
    He^4, 150-400 MeV, 20 MeV O^+ state excited 8=24724
    I_2 mols., spin polarization calc., 300-400 eV 8=34214-5
    n-$InAs_xSb_{1-x}$ alloys, from thermoelec. and Hall coeff. obs. 8=35758
    InSb type semiconductors 8=40217
    K, energy loss spectra, quantitative comparison with dielectric theory 8=26727
    Li^7, Coulomb form factors 8=29289
    Mg^{24}, $E_e = 100-260$ MeV, obs. and α model calc. 8=47311
    Mg^{24}, inelastic 180°, $E_e = 39.56$ MeV, obs. 8=42995
    N excitation spectrum, meson field model 8=29180
    O^{16} giant resonance levels excited 8=42843
    O^{16}, inelastic, energy level obs. to 14 MeV 8=47232
    Pb^{208}, elastic, 175 and 250 MeV 8=29412
    Pt, 500 MeV e trident and pair prod. 8=29411
    Si^{28} giant dipole resonance 8=25115
    Si^{28}, $E_e = 100-260$ MeV, obs. and α model calc. 8=47311
    Si, inelastic, and incoherent X-ray scattering 8=44155
    Si single crysts., effect of Bragg refl. 8=35354
    Sn^{116}, to 2_1^+, 3_1^- states, 2, 4-quasiparticle microscopic theories 8=25143
    $Sn^{116,120,124}$, inelastic, rel. to 2^+ and 3^- states transition probabs. obs. 8=33924
    $Ti^{46,47,50}$, differential cross-sections 8=25210
    W, low-energy back-scatt., energy distrib. curves rel. to surfaces 8=30730
  scattering, electron—proton
    5 BeV, inelastic, search for heavy e 8=24714
    inelastic, obs. of first πN resonance 8=37938
    polarization effects for ultrarelativistic electrons 8=37942
    p polarization obs. at 900 MeV 8=29189
    H atom, diffr. theory 8=29653
Electro-optical effects
    See also Electroluminescence; Optical constants.
    a. m. modulator, 3 stage, obs. 8=33240
    ammonium oxalate, and prep. 8=36442
    amorphous phase of liquid crystals, orientation fluctuations 8=34767
    birefringence meas. of elec. quadrupole moments 8=43271
    colour centre absorption and difference between ground and excited states obs. 8=44471
    controllable-transmitting liquid shutter for Q-modulation of laser 8=42063
    critical opalescence of dipolar mixtures, elec.-field effect 8=39312
    crystals with nonuniform built-in strains 8=36309
    deflection schemes, digital and analogue 8=45161
    dielectric mats for use in dev., rel. to low-loss optical transmission 8=27229
    dipolar mols., quadrupole moments, meas. by electro-optical method 8=29705
    electroreflectivity meas. at low temps., sample package 8=49696
    e.m. waves refl. and refr. at free space-medium interface, static elec. field 8=28607
    ferroelectrics, oxygen octahedra, nonlinear optical tensor coefficients 8=41017
    Franz-Keldysh effect, theory 8=36307
    gases, birefringence, quadrupole moment determ. 8=47584
    image luminance amplification in electro-opt. systems 8=42261
    ionic crystals, activated, photoluminesc. effect of elec. fields 8=36456
    Kerr liquid, laser pulse propagation, steady-state electromagnetic shock solution 8=46549
    laser beams deflection, use of electrooptic prisms 8=42062
    laser beams, phase modulation in small-scale filaments 8=24274
    light modulators, amplitude, synthesis 8=33239
    in light signal processing 8=46637
    liquid crystals, cholesteric electric-field-induced optical rotation 8=43811
    liquid-crystals, Kerr effect in pre-transition region 8=30409
    liquid film flow, hydrodynamic ridge instability 8=34747
    magnetic thin films, obs. 8=36107
    modulators for e.m. distance meas., matrix analysis 8=46648

Electro-optical effects—contd
    nitrobenzene, Kerr effect 8=34898
    nontionite, monodisperse sols., experimental results 8=39459
    optical anisotropy of electrically and magnetically isotropic medium 8=24428
    optical frequency shifting of mode-locked laser beam 8=46595
    piezospectroscopic stress cell 8=49697
    polymer chains, Kerr const. calc. 8=38972
    pulse response of electro-optic modulators and photocond. detectors at 10. 6μ 8=36001
    quartz, Pockels effect meas. at 9GHz 8=41144
    Rochelle salt, props near ferroelec. phase transitions 8=27577
    salt solns., aq., Kerr effect meas. 8=34844
    semiconductor panel, spot illumination 8=49214
    semiconductor plasma in elec. field, nonlinear props. 8=31930
    semiconductors, anisotropy rel. to inversion centres 8=35859
    semiconductors, Green's function calc., general formalism and interband transitions 8=35861
    scanning laser device, selecting one degenerate mode of resonator 8=24277
    triglycine sulphate, induced indicatrix rotation in phase transition region 8=27638
    triglycine sulphate, near phase transitions 8=27637
    triglycine sulphate single crystal, refr. rel. to temp. 8=36439
    wide-band light modulator with travelling v.h.f. wave, high-acc. spatial meas. 8=41617
    Ag_3AsS_3(proustite) 8=45166
    $Ba_2NaNb_5O_{15}$, linear and quadratic coeffs., relationship based on spontaneous polarization obs. 8=27583
    $BaTiO_3$ ionic model for calcs. rel. to nature of bonding in crystal 8=41067
    $BaTiO_3$, near phase transitions 8=27637
    $BaTiO_3$, quadratic, dynamic obs. 8=27268
    CdS, light demodulator with u. s. amplification 8=27216
    CdS, self-scanning optical image sensor using high-field domains 8=27317
    CdS, Stark effect of exciton levels 8=36348
    Cu_2O, electroreflectance spectrum 8=49159
    GaAs, mobile electrical domains 8=44777
    GaP, coeff. meas. between 0. 56 and 3. 39μ 8=41092
    GaP, Franz-Keldysh effect 8=36362
    Ge, electroreflectance at oblique incidence 8=49722
    GeH_4, deuterosubstituted, electro-optical params. and i. r. band intensities, calc. 8=29737
    H_2, Kerr birefringence theory 8=34664
    $K_2Mn_2(SO_4)_3$, langbeinite structure, power meas. 8=39678
    $K_2Ni_2(SO_4)_3$, langbeinite structure, power meas. 8=39678
    KCl, impure crystals 8=32005
    $KH_2AsO_4(KD_2AsO_4)$, deuteration effects 8=49369
    KH_2PO_4, near phase transitions 8=27637
    KH_2PO_4 parametric light generator, electro-optical tuning, obs. 8=41103
    $KTa_fNb_{1-f}O_3$ (KTN) conc. gradient light beam deflector 8=36382
    $LiNbO_3$ crystal Q switch in laser operating at 1.06 μ 8=46604
    $LiNbO_3$, linear and quadratic coeffs., relationship based on spontaneous polarization obs. 8=27583
    $LiNbO_3$, piezoelec., and opt. detection on laser illumination 8=45203
    $LiTaO_3$, linear and quadratic coeffs., relationship based on spontaneous polarization obs. 8=27583
    NaCl, spectra of conductivity, dielectric constant and refractive index 8=45205
    NH_4Cl, linear, electronic contrib. 8=36397
    $NH_4H_2PO_4$, contribution of quadratic effect 8=32015
    $(NH_4)_2Mn_2(SO_4)_3$, langbeinite structure, power meas. 8=396
    $(Na_{0\cdot7}K_{0\cdot3})NbO_3$, spontaneous and induced birefringence 8=27294
    Nd glass laser, modulation at Q-factor 8=24342
    $PbMg_{1/3}Nb_{2/3}O_3$ crystals 8=36400
    $Rb_2Mn_2(SO_4)_3$, langbeinite structure, power meas. 8=39678
    $PbZn_{1/3}Nb_{2/3}O_3$, and dielec. props. 8=27280
    RbH_2PO_4, piezoelec. effect on laser illumination 8=45203
    Se, trigonal at 1. 15μ 8=36402
    $SrTiO_3$ crystals, 23 to −183°C 8=36416
    $SrTiO_3$, electroreflectance near absorpt. edge 8=27609
    $SrTiO_3$, electrorefl. oscills. rel. to h. f. free-carrier mass 8=36415
    $SrTiO_3$, temp. dependence 8=36414
    $Tl_2Mn_2(SO_4)_3$, langbeinite structure, power meas. 8=39678
    ZnS, wurtzite, obs. 8=36431
Electrophoresis
    carbon black suspension in nonpolar media, electrokinetic pot. and stability, H_2O effects, obs. 8=30550
    cell, double-tube flat capilliary 8=24078
    charged droplets stream, electrostatic lateral instability 8=34944
    conduction enhancement in presence of insulting particles, 8=49945
    deposition of luminescent powder 8=45388
    dielectrophoresis, particle separation and deposition, theory 8=45365

Electrophoresis—contd
  drops, liquid, Booth equation 8=34896
  glass particles in low cond. liqs., mobility rel. to surface charge density 8=30548
  ionic laser discharge, drift velocity rel. to ionization 8=37551
  metallic particles in low cond. liqs., mobility rel. to surface charge density 8=30548
  polystyrene latex particles in La, Nd and Th nitrates, mobilities rel. to size and pH 8=49923
  suspensions, mobilities, effect of double layer overlap 8=34942
  $BaSO_4$ suspension in nonpolar media, electrokinetic pot. and stability, H_2O effects, obs. 8=30550
  U_3O_8 layers, h. v. preparation 8=26130
Electrophotography. See Photography.
Electrophotoluminescence. See Electroluminescence.
Electropolishing. See Surface texture.
Electroproduction. See Beta-rays/effects; Electrons; Nuclear reactions/due to electrons.
Electrostatic generators. See High voltage production; Particle accelerators/linear.
Electrostatic lenses. See Electron lenses/electrostatic; Ion optics.
Electrostatics
  See also Electrets; Electric charge; Electric fields.
  accelerator, low-energy, terminal pulsing 8=24556
  charged dust static distrib. in general relativity 8=32815
  electric field with ion flux, soln. of eqns. 8=33026
  electrographic processes, transfer meas. 8=24075
  electron clouds in mag. fields, electrostatic equilibrium 8=33074
  in electron-optical system, propag of field pot. into space rel. to distrib. along axis 8=24143
  generalized diffusion eqn, complementary variational principles 8=28353
  high-voltage generators 8=41926
  imaging methods, computer-animated teaching film 8=37366
  insulators, 3-dimens. pot. round square array of surface charges 8=41925
  ionospheric satellite, electrostat. pot. fields and wake 8=41414
  liquids, attraction by elec. field 8=43853
  magnetostatic boundary-value solns., application 8=33038
  Maxwell's displacement concept 8=33025
  motor, dielectric, liq.-immersed 8=37369
  particle separation at high energies 8=28999
  plane 'infinite' condenser with additional plates, soln. of pot. field distrib. 8=28465
  plasma, Vlasov, test charge effective potential inverse 3rd power law 8=43499
  point charge in inhomogeneous medium, elec. pot. 8=33024
  probe, characts. 8=47859
  vibrating capacitor drive for contact pot. meas. 8=28450
Electrostriction
  See also Piezoelectricity.
  gases, statistical theory 8=39224
  quartz, mixing of light waves to generate acoustic waves 8=45162
  sapphire, mixing of light waves to generate acoustic waves 8=45162
  self-focusing of light in solids, mechanism 8=41046
  thick-walled cylinder, axially symmetric motions 8=46342
  $SrTiO_3$, mixing of light waves to generate acoustic waves 8=45162
  TiO_2, mixing of light waves to generate acoustic waves 8=45162
Elementary particles
  See also Baryons; Field theory, quantum; Hadrons; Leptons; Nucleons and antinucleons; Nucleus; Particle detectors; Particle range; Quantum theory; Quarks; Scattering particles; Strange particles; and individual particles, e.g. Electrons; Mesons.
  Adler-Weisberger sum rules and $D_{13}D_{13*}$ coupling constant 8=33534
  algebra of spin currents, field theoretical model 8=24603
  algebra of current densities, representations 8=37839
  algebra of spin currents, field theoretical model 8=24603
  amplitude of conversion of two particles into three, Feynman graphs asymptotic behaviour 8=37902
  analyticity contraints in πp scatt. 8=33680
  analyticity as fundamental principle 8=29023
  analyticity in momentum transfer in pot. theory 8=37832
  arbitrary spin, interaction invariant amplitudes, exptl. determ. limitations 8=42392
  arbitrary spin-superconvergence relations 8=42420
  autocomposite, introduction of isospin in field theoretic' treatment 8=29019
  axial vector renormalization constant from current algebra 8=33527
  basis 8=32663
  Bethe-Salpeter amplitudes decomposed into standard covariants and invariant amplitudes 8=37848
  Bethe-Salpeter eqn. for bound state of two unequal mass particles, normalization of wave function 8=47022
  Bethe-Salpeter eqn. for Wick-Cutkosky model, method of soln. 8=24675
  Bethe-Salpeter eqn., Regge daughter trajectories 8=37911

Elementary particles—contd
  Bethe-Salpeter eqn., variational solns. 8=37873
  Bethe-Salpeter eqn. with Feynman propagations, cancellation of spurious corrections 8=33561
  bootstrap calc. and saturation of superconvergence relations giving the same result in static model 8=33601
  boot strapping with Regge boundary conditions 8=33600
  boson, 27 plet, mass and decay spectra 8=29033
  branding rules of SU(6) representations, embeddings of simple Lie groups 8=33532
  Bronzan-Lee model, solved by strong coupling theory 8=29026
  Cabibbo angles, relation between vector and axial-vector in broken SU_3 8=24619
  Cabibbo theory, explanation in terms of strange neutrons 8=24708
  Cabbibo theory from vector-meson-lepton-neutrino coupling constant 8=33568
  Casimir operators, eigenvalues 8=24591
  causality for homogeneous spaces of simple Lie groups 8=33540
  centrifugal-barrier effects in N/D calc. 8=42422
  CG coefficients and crossing matrix 8=33542
  character and theory 8=42375
  charge conjugation for integral or half-integral spin 8=37913
  charged, transport, Monte Carlo sampling appls. 8=32855
  Chew-Low model, weak axial vector coupling constant 8=29040
  Chiral $SU(2) \otimes SU(2)$ symmetry and pion mass 8=42378
  chiral symmetry, quantized gauge field theory 8=42445
  chiral transformations, πN system, $\pi\pi$ scatt. η decay 8=24686
  Clebsch-Gordan coefficients, an operator method 8=33307
  Clebsch-Gordon coeffs. for SU(3) calc. method using normalized solid harmonics 8=42366
  Clebsch-Gordon coeffs. of symmetric representations of Su_n 8=37842
  Clebsch-Gordan series for SO_5, SO_4, Sp_4 and G_2, deriv. 8=33362
  cluster model for mesons and square mass relation 8=47104
  complex ang. momentum, continuation of 3-particle discontinuity 8=42390
  composite described as fields in non-relativistic theory, $Z = 0$ conditions 8=42372
  composite, form factors, asymptotic behaviour 8=42385
  composite, introduction of independent particle field in relativistic scalar field theory 8=33521
  composite model of vector mesons, rel. to Lagrangian field theory 8=37869
  composite, relativistic field theory 8=46830
  composite, $V-\theta$ model, bound state operator and physical props. 8=37834
  compositeness conditions, Lagrangian field theory 8=33550
  conference, Liperi Summer School, Finland, 1965 8=24598
  conservation laws mirror relations as nondynamical test 8=24685
  conserved charge operators, additivity 8=37829
  consistency condition for $|\Delta S| = 1$ currents 8=29043
  conspiring trajectories, classification by SU(3) and Lorentz-pole symmetries and exchange degeneracy 8=37885
  convergent, relativistic model theory 8=37871
  coordinates from nonlocal currents 8=42368
  correspondence to composite system, phenomenological approach 8=37826
  Coulomb problem, relativistic symmetric, dynamic symm. in case of cont. spectrum 8=47016
  coupling constants and masses, calc. from saturation of dispersion relations 8=24669
  coupling constant, axial vector, in static Chew-Low model 8=29040
  covariant theory no single-particle function systems which generate acceptable representations 8=24597
  C violation with $\Delta I=3$, semi-strong interaction 8=29032
  CP violation 8=33544
  CPT conservation rel. to π^+ and π^- lifetimes difference 8=42509
  CPT invariances, testing in pp or $p\bar{p}$ collisions 8=24909
  creation in expanding universes 8=42362
  cross-section preasymptotic behaviour, Bethe-Salpeter calc. 8=29028
  current algebra, divergence conditions and current-current equal time commutators 8=29020
  current algebra first-moment operator calc. 8=33553
  currents, (V + A), weak interactions 8=33565
  decay, asymmetry moments of ang. distrib. 8=24631
  decay, correspondence to poles of S-matrix 8=33552
  decay, low-energy photon emission 8=42447
  decay, nonleptonic, $\Delta I = 1/2$ rule in octet dominance 8=37859
  decay, nonleptonic, phenomenological approach 8=37861
  decay, non-leptonic, pole approx., $\Delta I = 1/2$ rule 8=47021
  decay, nonleptonic, possible interrelation to current-current (J^+J) picture 8=37862
  decay, nonleptonic, systematic and steady phenomenological approach 8=37860

Elementary particles—contd
decay, 2-particle of polarized baryons and bosons in terms of coupling constants 8=37863
$\Delta S = \Delta Q$ rule, obs. on upper limit of violation in Σ leptonic decay 8=38090
de Sitter model in nonstatic frame 8=29024
Dirac and anti-Dirac particle, bound state problem 8=42359
Dirac eqn., symmetry algebra calc. 8=46803
Dirac monopole 8=33513
Dolen-Horn-Schmid duality and Deck effect 8=33559
E(2) basis for calc. of form factors involving SL(2, C) group 8=33554
eight-fold way, multilinear couplings 8=33531
electron chain theory, internal structure 8=37866
elementary length, upper limit from πp scattering data and quant. electrodynamics 8=24601
e. m. interaction effects on high energy h. h scatt. 8=37952
e.m. mass difference in Lagrangian field theory, correction anomalies with composite model for mesons 8=37869
e.m. mass shifts and their relation to equal time commutators 8=37761
e.m. moments for arbitrary spin 8=33564
Euclidean group, two-dimens., and partial-wave expansion 8=37851
extended particle with arbitrary change structure, stability, negative mass. 8=33522
F_π relation, Kawarabayashi-Suzuki, queried 8=24595
Fadeev-Lovelace formalism, generalization of Pierls mechanism to ladder diagram for $K\pi\pi$ 8=24848
Fermi-odd interactions, applic. of Wick theorem 8=42393
fermions, conspiring trajectories; reflection symmetry 8=47012
Feynman diagram $O^- + \frac{1}{2} \rightarrow O^- + \frac{1}{2}$ B-exchange reactions rel. to MacDowell symm. 8=29047
Feynman integral and condition of Landau singularity in physical region 8=24652
field-current identities, broken symmetries and gauge invariance 8=42319
Foldy Wouthyusen Hamiltonian, unitary transformation to laboratory system 8=29025
form factor dispersion relations 8=37865
form factors, asymptotic behaviour and renormalization constant ratio 8=42384
form factors, kinematical, relativistic model 8=37864
form factors, Namliu and Barut-Kleinert, derived in E(2) basis 8=33554
form factors, weak, renormalization 8=42386
free particle observables and spectral representations change 8=29022
Fubini-Dashen-Gell-Mann sum rule, current locality problem 8=33514
Fubini-Dashen-Gell-Mann sum rules 8=29038
Fubini operators and partial symmetry 8=37827
G(2) group, Clebsch-Gordan series 8=29264
gauge-field algebra with symmetry breaking 8=37853
gauge fields with noninvariant interactions rel. to Yang-Mills fields 8=32776
Gell-Mann-Okubo mass formula and sum rules derived 8=24625
Goebel's static model, connection between superconvergence and algebra 8=37838
in gravitational field, radiation 8=37831
gravitational pot. determ., lower mass limit predicted 8=29030
gravitons, scatt. low energy form of amplitude 8=29080
Gribov Pomeranchuk poles, third double-spectral function effects 8=24680
Gribov-Pomeranchuk singularity removed by N/D eqns. 8=24679
group theoretical schemes and general conservation laws, test using two-nucleon interact. 8=24866
group theory, review of appl. 8=29014
group theory solution of non-maximally degenerate quantum mechanical systems 8=33306
group transformations of O(2, 1), representations in continuous basis 8=24593
groups, non-compact associated with vertex operator 8=33651
Han-Namliu model, CP violation 8=33524
helicity amplitude correl. and threshold kinematic constraints 8=42404
high-energy exchange models, direct-channel amplitude formulation 8=37897
high energy strong and weak interaction processes, cosmic ray studies 8=24636
high energy, SU(3) symmetry and Regge poles 8=24682
higher-spin wave eqns., consistent when interacts are included 8=33515
Horn–Schmid duality 8=33545
inelastic processes, Reggeon graphs 8=29072
inelastic processes, unitarity for matrix elements 8=37881
interacting radii computed in optical model 8=29044
interaction in 8-dimensional space 8=47025
interactions and props., 800 MeV p beam appl. 8=33512
interactions, causality conditions 8=29046
interactions, high energy analysis of multiplicity and ang. distrib. of secondary particles 8=29238
interactions in eight-dimensional space 8=42395

Elementary particles—contd
interactions, strong, sum rule based on unitarity 8=42399
interactions, SU(3) symm. breaking of current-current form, sum rules 8=29045
interactions two-body, differential cross sections, optical model 8=29041
interactions, weak radiative, vector current conservation 8=37876
internal symmetry and C, P, T operations 8=37870
introduction to advanced field theory 8=33349
isobar masses and coupling consts. rel. to dispersion sum rules 8=29035
isospin or strangeness type, intrinsic degrees of freedom, para-field representation 8=46825
isospin, rel. to field theory of autocomposite particles 8=29019
isovector form factors, ϕ-ω mixing angle and quark models 8=29039
$K = G_o(8) \otimes SU(3)$, new Lie group for scalar SU(3) symm. strong-coupling theory 8=33541
Kawarabayashi-Suzuki-Fayyazuddin-Riazuddin relation, new derivation 8=24600
Lee, as W bosons, consistent with CP nonconservation 8=37837
lepton quantum number multiplicative? 8=33622
Lie algebra, unitary, inhomogeneous, compact number of invariants for two types computed 8=32651
L_3, calc. of Wigner coeffs. 8=28235
Lie group, causality defined for homogeneous spaces 8=33540
local one particle approx. for matrix elements of two four vector currents 8=33530
Lorentz group, representations, geometry and algebra 8=24592
Lorentz group unitary representation in 0(2, 1) basis 8=32663
Lorentz invariance, universality 8=37847
Lorentz pole analysis of $\pi N \rightarrow \omega N^*_{3/2}$ (1236) 8=37974
Lorentz pole structure of vector meson prod. in $\pi\pi$, πN interactions 8=29171
Lorentz poles in equal-mass scatt. from analyticity and factorization 8=42416
magnet, alternating gradient, for secondary beam transport 8=28519
magnetic moments, Coleman-Glashow formulae, correction for symmetry breakup 8=42383
many-particle wave functions, closure property 8=33517
mass formula, dual-mass particle postulate 8=37858
mass formulae from symm. groups 8=33549
mass going through zero, Regge pole model 8=29069
mass, lower limit predicted 8=29030
mass operator, relativistically invariant, a nontrivial Lie algebra 8=37855
mass relations, SU(3) for arbitrary spin 8=42380
mass relationships 8=24622
mass relationships, tamaid-bach theory 8=24630
mass relationships, "tamaid" theory 8=24628
mass relationships, tamaid-bach theory 8=24629
mass renormalization, automorphism of algebra of field operators 8=37856
mass spectrum, degenerate, implied by infinite momentum representation of current algebra 8=33525
mass spectrum in any unitary representation in a Hilbert space of a Lie group 8=37857
mass splitting theorem for general definitions 8=42381
masses, and multitemporal theory of relativity 8=47019
massless, Goldston theorem inconclusive 8=33520
massless, implications of broken symmetry 8=42377
massless, with definite helicity, not weakly localizable 8=47018
model representation rel. to field quantization 8=42370
models from sympletic varieties constructed from Lie groups 8=29016
models, test of validity using equal time commutators of components of e.m. current 8=42365
moment determ. feasibility 8=33563
multiple particle prod., unitary-symmetrical statistical model 8=33546
multiple prod. processes, creation on peripheral trajectories 8=42394
non-compact family of SU(p, 1) groups, unitary representations 8=37841
non-invariance and strong coupling models 8=37843
non-relatistic, study by Galilei invariant wave eqns. 8=33320
O(2, 1), unitary representations in O(1, 1) basis 8=24605
O(4) symmetry, composite model structure of particles 8=47011
O(4, 2) classification of all $I = 1/2, 1$ bosons 8=24788
1^- and 1^+ nonets mass relation based on Weinberg's sum rules 8=37854
O'Raifeartaigh's theorem, proof avoiding questions of domains and denseness 8=37846
pair prod. symm., radiative corrections 8=29075
para-particles, existence of and para-statistics 8=42318
n-particle prod., multi-Regge model exchange of Pomeranchuk trajectories 8=24681
PCAC and current algebra applied to K_{l3} decay 8=29149
PCAC and current algebra, mutual connections 8=47013

Elementary particles—contd
PCAC used to obtain couplings of vector to pseudoscalar mesons 8=33654
PCTC in Σ decay branching ratio calc. 8=24992
phase shifts with cut-off parameter, approximation 8=47027
pion conspiracy, contributions of evasive, conspiring Regge-pion pole for different reactions 8=37909
Poincare group contraction for infinite-momentum kinematics 8=33558
pole dominance approx. combined in a consistent way with current algebra 8=29021
pole of two interacting spinless particle Green function 8=24602
Pomeranchuk intercept, shift due to electromagnetism 8=29071
position operators, quantum mechanical restrictions restrictions 8=42387
production, coherent and incoherent, in nuclei at very high energies, cross section obs. 8=37914
production, general method using vector operators for ang. correls. 8=24687
quark, local current and bootstrapping 8=29073
quasiparticle approx., fluctuation-dissipation theorem 8=24596
radius, upper limit 8=37868
Regge amplitude, ρ for πN charge-exchange scatt. 8=24779
Regge cuts and absorbing hard core 8=42427
Reggeized short range potential and resonance width application to π-π scatt. 8=47036
Reggeon Feynman diagrams 8=28964
Regge parameters for πN scatt. 8=29138
Regge-pole analysis, double for $pp \to \Delta^{++}p\pi^-$ 8=24912
Regge-pole analysis of pot. non-relativistic scatt. 8=28943
Regge-pole model for η photoprod. 8=24839
Regge pole model for K, π photoproduction 8=29124
Regge-pole model for particles whose mass goes to zero 8=29069
Regge-pole model for NN charge-exchange scatt. 8=24888
Regge-pole model for $\pi + N \to \rho + N^*$ 8=24781
Regge-pole model for $\pi + N \to \rho + N^* \to N + 3\pi$ 8=24780
Regge-pole model with π trajectory for πp, Kp, and $\bar{p}$p reactions with Δ(1238) prod. 8=29217
Regge-pole model for ρ°, ω° prod. in p-p collisions 8=24858
Regge singularities in πN charge exchange 8=29130
Regge trajectories for isospin-one mesons 8=24677
Regge trajectories in Wick-Cutkosky model of Bethe-Salpeter eqn. 8=24675
Regge trajectories, Mandelstorm dynamical scheme applied to VP $\to$ PP 8=33658
Regge trajectories, nonlinear and infinitely rising 8=42436
Regge trajectory coupling to integer spin particles, Feynman diagram model 8=29068
Regge trajectory, daughter, predicted by Freedman-Wang, identified, props. 8=29067
relativistic-symmetric Hamiltonian, Foldy-Wouthuysen transform. 8=24634
relativistic two-particle Hamiltonian, bound states 8=47039
and relativity, general, with cosmological const., vacuum props. 8=28292
relativity theory, multitemporal, appl. 8=46076
resonant states, production and decay 8=29037
review of advances in research (since 1911) 8=47009
ρ bootstrap, δ-function and Breit-Wigner exchange compared 8=29074
Riemann space, local forms 8=28284
saturation of sum rules in strong-coupling theory 8=33342
scalar-pseudoscalar weak interactions in Σ decay branching ratio calc. 8=24992
Schrodinger equation for particle with arbitrary spins, relativistic 8=33516
Schwinger's chiral dynamics, review and elaboration 8=24637
second quantization for any spin and internal symmetry 8=42363
single-particle prod., double Regge model and density matrix 8=37901
SL(n, C) unitary representations, new method for analysis 8=46813
SL(6, C) relativistic strong vertex, expansion 8=24632
SL(2, C), e.m. vertex in spin-$\frac{1}{2}$-particle calc. 8=46815
SL(2, C), production vertex of 2 spin $\frac{1}{2}$ particles by a spin 1 particle calc. 8=46814
space-time dilatation, $x_\mu \to \rho x_\mu$, in broken symm., physical interpretation of σ terms 8=33528
spin-$\frac{1}{2}$ particles, depolarization in target 8=35592
spin operator for arbitrary momentum, covariant 8=24635
spin-particle theories, quantal, and eqns. of motion of classical analogue 8=33555
static models in strong coupling limit, rigid rotation model 8=33535
strong-coupling theory, nature of "broken SU(3)" symmetry 8=42397
strong interactions, symmetries 8=24642
structure analysis 8=29031

Elementary particles—contd
structure and dynamical group 8=37845
SU$_n$, build up of tensors, reduction of transformation matrices 8=33539
SU(n) groups, evaluations of Clebsch-Gordan coeffs. 8=37844
SU(n), regular representation, j coeffs. 8=24604
SU$_n$, substitution and mirror refl. symmetry 8=24608
SU$_2$ × SU$_2$, validity of second Weinberg sum-rule in hard π calcs. 8=33536
SU$_3$ and its implications 8=24616
SU$_3$ applic. to 27 plet of bosons 8=29033
SU(3) breaking enhancement, Regge theory 8=42315
SU$_3$, broken, derivation of Gell-Mann-Okubo mass formula 8=24625
SU$_3$, broken, relation between vector and axial-vector Cabibbo angles 8=24619
SU$_3$ Clebsch–Gordan coeffs. 8=37850
SU(3) embedding in SU(8) 8=42379
SU(3) evaluation of Clesbch-Gordan coeffs. 8=37844
SU$_3$ gauge invariant theory rel. to vector-meson scatt. 8=24851
SU(3), Goldberger–Freiman relation, and Cabibbo angle 8=37828
SU(3) invariance in strong interactions in dynamical model for P-violation in hyperon decay 8=33830
SU$_3$ mass splitting interaction and hadron decay 8=24626
SU$_3$ prediction for η decay if η is a pure octet member 8=24837
SU(3) representations 8=33348
SU$_3$ × SU$_3$ = K$_3$, fields with nonlinear transformation laws, construction of effect Lagrangian 8=33341
SU$_3$ symmetry and mass formulae 8=24620
SU$_3$ symm. breaking in η, π decay, use of superconvergence relations and Weinberg sum rule 8=24769
SU$_3$ sym., deviation from in vector meson field theory 8=29168
SU$_3$ symm., tested in $\pi^-p \to \gamma n$, $K^-p \to \gamma\Delta$ 8=37916
SU$_3$ theory fundamental triplet, search for heavy singly-charged particle in cosmic rays 8=42674
SU$_3$ violation in $\eta_Y \to 2\pi/\bar{K}K$ branching ratio 8=29113
SU(3) crossing matrix, simplified form 8=29018
SU(3) symm. strong coupling theory, dynamical group 8=24614
SU$_6$ applic. to 27 plet of bosons 8=29033
SU(6, 6) classification of high-spin resonances, missing SU(3) multiplets 8=37849
SU(9) contraction procedure to give isobar series 8=29034
sum rule, $(K^+p + K^-p) - \frac{1}{2}(K^+n + K^-n) = \frac{1}{2}(\pi^+p + \pi^-p)$ 8=37988
sum rules from charge-charge and charge-density commutators 8=42369
sum rules saturation, role of Schwinger terms 8=24633
sum rules, SU(3) × SU(3) spectral function, derived 8=33551
superconvergence and bootstrap, static models 8=24684
superconvergence and current algebra for spin-$\frac{1}{2}$ target 8=42405
superconvergence and Regge poles, odd-signature exchanges 8=42423
symmetries, field theory and measurement, Pisa Conference 1964 8=24609
symmetry, explained in terms of quarks 8=47015
T-violating effects in weak and e.m. interaction 8=33567
tadpoles members of scalar octet with masses around 1 GeV 8=29113
theory, Hawaii tropical conference, August 1967 8=29027
theory of current, Sugawara extension 8=42391
3-body Amado model, Faddeev perturbation 8=42413
3-body decay and prod., Khuri-Treiman eqns. 8=42382
three-body problem with Lee-type interaction 8=24639
3 π decay, energy distrib. construct 8=24756
3-j symbols recursion relations 8=33547
three-triplet model for baryonic resonances e.m. transitions 8=38095
Toller families, $M = 0, 1$, "mass formula" calc. 8=47020
tunnel effect in double min. pot. 8=24466
2-body compound systems, relativistic and non-relativistic, pot. scatt., and Bethe–Salpeter model 8=37825
two body high energy reactions, SU$_3$ symm. 8=47023
U$_n$, Lie algebra irreducible representations, simple technique for construction 8=33538
U$_{p,n-p}$, Lie algebra irreducible representations, simple technique for construction 8=33538
U(p, p) ladders, physical multiplets assignment consistent with U(6, 6) 8=24618
U(p, q) ladder representations coupling, local and global props. 8=24617
U(p, q) ladder, tensor product of two, existence at most of one ladder 8=24618
U(6) ⊗ U(6) scheme for baryon-meson interactions 8=25001
U$_{6,6}$ symm. rel. to mass-splitting of baryons 8=29179
U(3) harmonics, solid, normalization 8=41627
U$_6$ ⊗ U$_6$ commutation relations rel. to vector-meson dominance in π° decay 8=33662
unequal-mass interactions, conspiracy relations 8=42396
unitary spin and its extension to U(6) 8=33523
unitary symmetry, mass operator 8=24627

Elementary particles—contd
unstable, admissable mass distribs. 8=47017
unstable states, particle transfer reactions as probe 8=29496
V-particle in Lee model, interplating fields 8=37867
wave function normalizable before 2-particle interaction is finite after it 8=33556
weak-interaction cutoff and second-order
weak interaction theory, difficulties 8=33566
weak interactions 8=24646
weak interactions, CP-noninvariance 8=24649
weak interactions, symmetries 8=24645
weak interactions and unitary symmetry 8=24644
Weinberg relation derived using current algebra, pole dominance and meson coupling constants 8=33526
Weinberg sum rule, second, validity in the case of chiral $SU_2 \times SU_2$ 8=33536
Weinberg sum rules and $K^+ - K^0$ mass difference 8=24825
Weinberg sum rules, calc. of hadron decay rates 8=42497
Weinberg sum rules in perturbation theoretic model 8=24623
Weinberg sum rules and π e.m. mass difference, improvements 8=24621
Weinberg sum rules for K_{l3} decay form factor calc. 8=24818
Weinberg sum rules rel. to A_1 width 8=24856
Weinberg's first sum rule applied to axial-vector currents 8=29029
Weinberg's second sum rule derivation assuming isospin structure 8=33543
Weinberg's spin one particles, field theory 8=33355
Wick-Cutkosky model for unequal masses, soln. of Bethe-Salpeter eqns. 8=24675
W, strongly interacting theory 8=24643
Yukawa and Fermi theories, derivation of equivalent coupling constant 8=37833
zero mass particles, group properties of wave eqns. 8=47014

interactions. See Field theory, quantum/interactions; Nuclear reactions. Entries on interactions involving named particles are listed under the particles concerned, e. g. Mesons/interactions; Cosmic rays/effects and interactions.

Elements
in comendite glasses, systematic variation of major ores 8=50075
in glass, ternary silicate, rel. to spectra and struct.. 8=36411
in pantellerite glasses, systematic variation of major ores 8=50075

origin
See also Cosmology; Thermonuclear reactions.
cosmic nucleosynthesis rel. to antimatter-matter annihilation 8=41492
heavy nuclei, synthesis in supernovae explosions 8=41504
nucleosynthesis in big and little bangs 8=36911
teaching aids and literature, review 8=45585
B in solar system, big bang and solar spallation theory 8=36990
Be in solar system, big bang and solar spallation theory 8=36990
H^2 in solar system, big bang and solar spallation theory 8=36990
$Li^{6,7}$ in solar system, big bang and solar spallation theory 8=36990
No, element 102, methods of discovery 8=43154
Th nucleosynthesis in interstellar gas by heavy-ion reactions 8=41505
U, nucleosynthesis in interstellar gas by heavy-ion reactions 8=41505
$Z \leq 5$ in universe, p spallation cross sections, obs. 8=32390

relative abundances
clusters, globular, heavy-element abundances 8=32480
HD33579 Magellanic Cloud 8=36940
metals in τ Bootis, F and G stars 8=45626
moon, surface metals, Surveyor V obs. 8=28140
planets, rel. to condensation theory 8=28147
Saint-Severin meteorite, of $P^{32,33}$ 8=45846
stellar nucleosynthesis by n captive, rel. to mass laws 8=41503
Sun, determ. from spectrum synthesis 8=45872
sun, Pottasch calc. from 33-110Å spectra 8=32575
super-heavy nuclei prod. in thermonuclear explosion, rel. to mass formula 8=38324
B in cosmic rays, galactic, p-fragmentation prod. rel. to dating 8=38176
Be in cosmic rays, galactic, p-fragmentation prod. rel. to dating 8=38176
Be^9 in stars and interstellar medium, obs. 8=36927
C, N_2 and O_2, solar photosphere 8=28171
C_2 in sun rel. to centre-limb spectra vars., calc. 8=45875
CO_2 in Martian atm., 1.05μ spectrometry 8=45828
Fe group elements in Sirius 8=50285
Fe, in solar photosphere 8=28174
Ga in sun, from spot spectra 8=32573
H^2 in stars and interstellar medium, obs. 8=36927
H-He ratio, satellite mass-energy spectrometer 8=32563

Elements—contd
relative abundances—contd
He and metals, overabundance in giant galaxies 8=28106
He, high galactic abundance, evidence 8=45641
He^3 in stars and interstellar medium, obs. 8=36927
Li, in solar, rel. to resonance lines 8=45865
$Li^{6,7}$ in stars and interstellar medium, obs. 8=36927
Li in young (T Tauri) stars, formation process, 8=50297
Mg/O, λ Boo and 6 similar stars 8=50286
Na, Al, P, S and K, in solar photosphere 8=28172
Ne/O, from emission spectra; comparison with cosmic
Si, in solar photosphere 8=28173
$Tc^{97,99}$ in red giant stars rel. to Tc^{97} synthesis 8=45644

Emission spectra. See Luminescence; Spectra; X-ray spectra emission.

Emissivity
ablation chars, visible and near i. r., from 2200 to 3500°K 8=36334
air, shock-tube heated 8=24399
Auer-Welsbach grids in flames, thermal radiation peculiarities 8=26609
cyanine dye soln., stimulated 8=48154
diffuse spherical cavity 8=46222
directional, from semi-infinite slab. of absorb.-scatt. medium 8=23991
Elasser band model, Doppler analog 8=34198
emittance meas., by cyclic incident radiation 8=27566
gases, i. r. radiating, integral eqn. for radiative equilib. 8=34649
glass, cooling rate rel. to coloration 8=44331
glow discharge, light variations, generation mechanism 8=47749
graphite, pyrolytic, correl. with struct. anisotropy 8=36332
graphite, visible and near i. r., from 2200 to 3500°K 8=36334
incandescent, normal spectral emissivity meas. 8=39954
isothermal spherical cavity with gray Lambertain walls 8=46223
light, secondary emission by molecules 8=34195
materials used in multilayer insulation, temp. depend. 8=39955
metals, degree of blackness of normal total radiation, temp. and kinetic dependence 8=35465
metals, plated by plasmic method, compared with uncoated sample 8=35815
molecular crysts., i.r. emission 8=41021
of nongray surface, thermal, determ. 8=26608
radiative heat transfer between two dielectrics, effect of small spacings 8=26607
in radiative transport calcs. 8=41800
rare earth oxides, hemispherical spectral 8=35466
spectral depend., rel. to radiation heat transfer model 8=28390
spectral of materials with low thermal conductivity 8=23988
trapezoidal grooves, emissive power 8=23987
Ag polycrystalline films, photoelec., obs. 8=27353
Al_2O_3, molten particle clouds, optically thick, from extinction and absorpt. meas. 8=34939
Ar, shock-tube heated 8=24399
Au polycrystalline films, photoelec., obs. 8=27353
Be, correl. with struct. anisotropy 8=36332
BeO, molten particle clouds, optically thick, from extinction and absorpt. meas. 8=34939
BN, pyrolytic, correl. with struct. anisotropy 8=36332
C arc, spectral emissivity of anode 8=36333
C, visible and near i. r., from 2200 to 3500°K 8=36334
CO_2, band and total, at press. where rot. hyperfine struct. removed 8=43280
CaF_2 crystal, infrared 8=32006
Cu polycrystalline films, photoelec., obs. 8=27353
Ge, emissive power determ. in range 700-1200°K 8=26610
Ge, emissive power determ. in range 700-1200°K 8=26610
H_2O, band and total, at press. where rot. hyperfine struct. removed 8=43280
H_2O vapour, spectral theoretical expression allowing for line struct. 8=25481
InSb, r. f. emission, elect. and magnetic field effects 8=36371
LaF_3, i. r. dispersion rel. to lattice vibrations 8=45201
LiF crystal, infrared 8=32006
Mo, thermal emittance of small cavities in surface 8=26611
N_2, shock-tube heated 8=24399
Nb-W alloys, normal spectral, temp. and comp. dependence 8=45224
Ne, shock-tube heated 8=24399
Pu, hemispherical emittance, effect of surface cond. and temp. 8=30993
Si, emissive power determ. in range 700-1200°K 8=26610
Si, thermal radiation on laser beam irrad. 8=35467
Ta-W alloys, normal spectral, temp. and comp. dependence 8=45224
U, thermal diffusivity, 20° to 850°C, laser pulse method 8=39952
W, Cs-covered, spectral distrib. during thermionic electron emission 8=31465
W, thermal emittance of small cavities in surface 8=26611
W-Mo alloys, spectral 8=45228

Emulsions
See also Colloids.
butadiene, radiation-induced polymerization, RhCl$_3$ additive effects 8=44081
dielectric props., water-in-oil, effect of temp. 8=30567
emulsifying agents at oil-water interfaces, viscosity 8=48101
rheology 8=39461
van der Waals const. determ. from theological props 8=48241
water-in-oil, dielectric properties, effect of temp. 8=30567
SnO$_2$ in glycerine-alcohol mixture, γ-rays reson. absorpt. 8=24701
Emulsions, nuclear. See Nuclear track emulsions.
Emulsions, photographic. See Nuclear track emulsions; Photographic materials.
Energy bands. See Crystal electron states; Metals/theory; Semiconducting materials; Semiconductors.
Energy gaps. See Crystal electron states; Semiconducting materials; Semiconductors; Superconducting materials and devices; Superconductivity.
Energy levels. See Atoms/structure; Molecules; Nucleus/energy levels; Spectra.
Enthalpy. See Thermodynamic properties.
Enthalpy measurement. See Calorimetry.
Entropy
See also Thermodynamics.
balance eq. for moderately strong coupled classical non-uniform gas 8=30292
Boltzmann equilib. distrib. retention conditions 8=32835
communal, influence on liq. state reappearance 8=25976
cosmological considerations 8=50248
from energy functional using Lagrange multipliers 8=46122
existence in thermodynamics 8=41791
gas mixture outside equilib., relativistic law 8=25821
H-function convexity 8=41761
hard-sphere gas, and H function 8=37220
horizontal wind-vectors, monthly information entropy, Potsdam, 1951 8=50138
invariance in special relativity 8=28288
irreversible processes, theory of changes .8=32854
layer developed around blunt cone 8=30267
lens system transmission 8=46658
quantum counterpart of Gibbs theorem 8=23884
scattering of light, (stimulated temp.), theory 8=24424
solids at high temp., correspondence principle 8=44332
properties of substances
crystalline mats., temp. rise on adiabatic strain-cycling, model and dispersion relations appl. 8=40102
rare earths, h.c.p., associated with mag. transitions 8=49453
steel, austenitic, entropy shock at phase transform. in mag. field 8=39553
volume expansion of gases dissolved in non-polar solvents 8=39288
COF$_2$, from molec. and spectroscopic data 8=30573
Cu-Fe Kondo alloy obs. down to $2 \times 10^{-3} T_K$ 8=44334
He^3, liquid, shielded pot. approximation 8=28338
Hg solute, vaporization and soln. 8=43798
Ne, solid, anharmonic contrib. 8=35431
α-NiSO$_4$.6H$_2$O, 0.4–4.2°K, in mag. field 8=30968
Epitaxy. See Crystals/faces; Crystals/growth; Films/solid.
Equations
See also Differential equations; Integral equations.
De Gennes, for superimposed metal and superconducting films, numerical soln. 8=27011
difference eqns. as infinite order differential eqn., rel. to soln by WKB method 8=23801
difference eqns., second order linear, soln. by 10 KB method 8=23800
dispersive non-linear, model 8=46003
eigenvalue problem $Tu-\lambda Su = O$ with unbounded and nonsymmetric operators T and S 8=32660
eikonal and asymptotic, for moving elastic medium 8=32722
Faddeev, reduction to multichannel 2-particle Lippmann-Schwinger eqns. 8=29054
generalized stochastic, for random system 8=37176
Hartree-Fock, l-averaged exchange term 8=38640
heat conduction, problems with unknown boundaries 8=46241
heat equations, behaviour of solutions 8=23996
heat, over-relaxation parameter determ. 8=41850
heat, solution by iterative process 8=24005
Helmholtz, scalar and vector, relations between solns. 8=37114
Klein-Gordan, integral transformations 8=24453
Korteweg-de Vries, asymptotic relations for soln. 8=28239
Laplace, computing device solving Cauchy problem 8=45984
Laplace, properties of solutions generated by integrals in complex domain 8=45986
Liouville, variational solns 8=37115
Lippmann-Schwinger equivalent of Faddeev eqn. 8=29054
Maxwell-Einstein, singularity-free soln. 8=33061
Maxwell–Minkowksi, integrated, associated Green's function defined 8=28599
multiple wave scattering theory, soln. of eqns. by smooth perturbation method 8=46001
Equations—contd
nonlinear, potential type, solution 8=45988
Reimann's relation on symmetric open Riemann surfaces 8=32658
Schrodinger operator, spectral function, asymptotic behaviour 8=33316
vector Kirchhoff, analysis, and associated boundary-line charge 8=24120
virial, of fourth order 8=23856
wave, reduced, "interior" solns. in platelike region 8=32676
Wiener-Hopf for diffraction of e.m. waves 8=46481
with Zilch type conservation laws 8=28240
Equations of state
See also Thermodynamics.
Benedict-Webb-Rubin, generalization 8=48247
classical fluids, improved eqn. 8=30186
fluids, improvement from modified self-consistent Born-Green eqn. 8=47900
gas near crit. point, density fluctuations rel. to anomalous viscosity and thermal cond. 8=30291
hard-particle systems 8=37219
for monatomic fluid with 6-12 pot., and excess internal energy 8=30191
multicomponent systems, curved operating lines for absorption 8=48248
scaling-law, functional form from Kadanoff generalization 8=23905
second virial coeff. for arbitary potential function 8=34955
Tait and related empirical eqns. 8=30571
Ar, coexistence curve shape near critical state from refractive index meas. 8=30590
Ar, fluid, and direct correlation function 8=34756
Ar, pair and non-pair potential 8=43924
CO$_2$, 273-4000°K for pressures up to 1000×10^5 N/m^2 8=39466
H plasma 8=47806
H plasma, ionized, determ. by Monte Carlo method 8=30000
HCl gas, virial coeff. from density meas. at 20, 50, 75°C and 5 and 40 atm. 8=30281
Hg, and electrical conductivity, at 0-2000°C and 200–5000 atm. pressure 8=25945
UO$_2$, critical constants from low temperature vapour pressure and specific heat date 8=30572
Xe, near critical point, interferometric determ. 8=25977
gases
binary mixtures, component and composite conservation eqns 8=43668
Bogolyubov, binary distrib. function of dense Coulomb gas 8=23881
condensable vapour, determ. without independent meas. of vapour vol. 8=39195
corresponding states, quantum deviations 8=47949
ethane, low-temp. virial coeffs. 8=34643
excited, composed of resonance atoms, effect of dipole-dipole interact 8=39194
formulation according to expt. thermodynamic data 8=30279
methane, low-temp. virial coeffs. 8=34643
mixtures of Lennard-Jones 6-12 mols., 3rd virial coeffs. 8=47950
polar, Kihara core model 8=43677
rarefied, in boundary layer of plate, corrections for density, temp. and vel. 8=34645
steam, virial coeffs, 150°-450°C 8=39195
vibrational energy relaxation with multiple quantum transitions 8=34640
virial coefficient, second, spherically symmetrical molecules 8=47951
Ar 8=39193
Ar, interatomic pot. from second virial coeffs. 8=30282-3
Ar, Percus-Yevick isotherm for exp-6 potential 8=34390
Cs vapours, P, V, T relationship evaluation 8=48296
He^3, near critical point, props. 8=25824
He^4, second virial coeff., 2°-20°K 8=47952
NO, 190°-2000°K 8=43676
N$_2$O$_4$, P-V-T dependence, obs. 8=30280
Ne-Kr system, phase separation 8=43675
Xe 8=39193
liquids
cell theory, Joule-Thomson coeff. 8=48056
density exptl. determ. 8=28219
poly-α-methylstyrene in cyclohexane, temp. rel. to microtacticity, obs. 8=43750
poly(α-methylstyrene) solns., mol. wt. distrib. and 2nd virial coeff. 8=48152
poly-α-methystyrene in toluene, second virial coeff. rel. to microtactivity, obs. 8=43750
6:12 pot. fluids, pair distrib. and direct correl. functions, exact and approx. values 8=25787
CCl$_4$, shocked-compressed, P-T curves from brightness temp. meas. 8=48089
CCl$_4$-C$_6$H$_6$, shocked-compressed, P-T curves from brightness temp. meas. 8=48089
solids
density exptl. determ. 8=28219
ferromagnet in critical region 8=31536
Gruneisen, h.p. props., thermodynamics calc. 8=30972
rubber elasticity, vol. depend. 8=26858
trinitrotoluene, Debye-Einstein construction method 8=48728

Equations of state—contd
  solids—contd
    Al, from determ. of Debye temp. as function of press., 0 to 135 kbars 8=43946
    Cs, and calcs. of Gruneisen constant, volumetric thermal expansion and compressibility 8=30973
    EuS, mag., near Curie point 8=27405
    K, and calcs. of Gruneisen constant, volumetric thermal expansion and compressibility 8=30973
    Na 8=26588
    Na, theory based on lattice free energy concepts in quasi-harmonic approx. 8=35021
    Rb, and calcs. of Gruneisen constant, volumetric thermal expansion and compressibility 8=30973
    ZnO, polar crystals, model for thermal eqn. 8=30630
Erbium
    doping in YFe garnet, effect on mag. domain-wall propag. vel. 8=49565
    electronic structure from positron annihilation studies 8=26906
    electronic structure from relativistic augmented-plane-wave calcs. 8=26905
    glass, oxide, Er^{3+} sensitization of luminesc. by other rare-earth ions 8=36486
    generalized susceptibilities and mag. ordering 8=44973
    L-emission spectrum, dipole transitions 8=34141
    magnetic props. from mag. moment meas. at 4.2°K and high fields 8=31705
    magnetic struct. of three ordered states below Néel temp. 8=44970
    magnetization anisotropy and magnetostriction meas. in pulsed fields up to 150 kOe 8=40743
    Néel temp., effect of hydrostatic press. 8=36212
    thermal conductivity, temp. dependence, 5-300°K rel. to mag. transition 8=35458
    Er 1, Zeeman effect, 3000-5000Å in 26 kOe field, obs. 8=29637
    Er^{3+} in ethylsulphate crysts., Zeeman effect theory 8=36357
    Er^{3+} in ThO_2, spin-lattice relaxation on cubic sites 8=40919
    Er^{3+} in ZnSe, codoped, Zeeman effect 8=30646
Erbium compounds
    chalcogenides: (rare-earth)$^{3+}$, resistivity anomaly 8=35884
    ferrite garnet, mag. anisotropy and Zeeman effect, temp. dependence 4.2-20.4°K 8=36185
    orthoferrites, microwave mag. loss meas. near spin-reorientation temps. 8=36224
    oxides, divalent, dielec. props. at microwave freq. 8=35960
    $ErAl_2$, ferromagnetism and ferromag. relax. study by Mössbauer effect 8=49518
    $ErAl_2$, mag. struct. by neutron diffr. meas. 8=31611
    $ErAl_3$, Er spin relaxation from Mossbauer effect 8=31864
    $ErCrO_3$, ferro-and piezoelectricity, comment 8=27272
    $ErCO_2$, field effects, crystalline, and first order phase transition 8=26014
    Er-D system, thermodynamics 8=44330
    $ErFe_2$, hyperfine field at Fe from Mössbauer effect 8=36146
    ErGa garnet, antiferromag. struct. and metamag. transition, 0.31 and 4.2°K 8=40867
    Er-H system, phase determ. 8=39551
    $ErPO_4$, cryst. struct., neutron diffr. 8=44213
    Er-Th alloys, f.c.c., antiferromag. ordering stabilization by Th 8=36218
    $ErVO_4$, cryst. struct., neutron diffr. 8=44213
    $ErVO_4$, lattice parameters and Miller indices, using computer programmes 8=44252
    $Eu(NO_3)_3 . 6H_2O$ luminesc. aromatic ketones sensitized, energy transfer mechanism, obs. 8=36487
    EuS:Gd, magnetic specific ht. 8=44337
Ergodic theorem. See Statistical mechanics.
Errors. See Measurement/errors; Random processes.
Esaki diodes. See Semiconducting devices/tunnel diodes.
Esaki effect. See Semiconducting devices/p-n junctions.
Etalons. See Interferometers.
Etching. See Crystals/etching.
Ether drift. See Relativity/special; Velocity/light.
Ettingshausen effect. See Magnetothermal effects.
Europium
    activator in industrial fluorescent lamps 8=42212
    antiferromagnetic props. from mag. moment meas. at 4.2°K 8=31706
    atom, core-electron binding energies, chem. effects 8=38620
    from benzophenone, energy transfer, mechanism and sensitized luminesc. obs. 8=36487
    cations, mixed valency, in La phosphors rel. to line and band emission 8=45278
    ground level h.f.s. Stark effect obs. 8=29602
    ions, in YVO_4, Eu^{3+} $(4f)^6$ levels splitting rel. to cryst. field, obs. 8=41152
    iron garnet, sublattice magnetization 8=40839
    spectrochem. and nephelauxetic parameters 8=43927
    Eu and Eu^{++}, hyperfine structures, polarization effect calcs. 8=29615
    Eu II spectrum obs. 8=47495
    Eu^{2+} in KCl, optical absorption 8=36379
Europium—contd
    Eu^{2+} and Eu^{3+}, electron transitions, isotopic shifts and changes in nuclear radii 8=48322
    Eu^{3+}, electronic Raman effect in garnets 8=27612
    Eu^{3+}, fluoresc. in NaLn titanates 8=41191
    Eu^{3+} in $GdVO_4$, spectra and crystal field Hamiltonian 8=31992
    Eu^{3+} ion in $KMnF_3$, luminescence spectra, spin-wave sideline 8=27655
    Eu^{3+} ion, magnetic case history 8=31522
    Eu^{3+}, mag. susceptibilities in YGa garnet 8=49468
    Eu^{3+}, transformation to Eu^{2+} in CdF_2: Eu 8=27473
    Eu^{151}, ^{153}, muonic x-ray spectra rel. to nuclear charge distrib., obs. 8=34194
    in KCl, vacancies and dislocations rel. to dopant conc. 8=40001
Europium compounds
    chalcogenides, refractive index meas. rel. to dispersion theory 8=49716
    chelates, luminesc., D isotope effects 8=30503
    chelates in water-methanol solns., luminesc. spectra 8=30499
    monochalcogenides, high pressure phase transformations 8=26070
    Eu β-diketone chelates, cryst. and in soln., synthesis and fluoresc. props. 8=32071
    Eu-chalcogenide, magnetic and transport phenomena, anomalous 8=31268
    Eu chalcogenides, obs. of ferro- and antiferromag. domains. 8=31613
    Eu^{2+} in alkaline-earth fluorides, absorpt. spectra multiplet structure 8=31986
    EuC_2, vol. variation c.f. other rare earth dicarbides 8=48340
    $EuCl_3$-dipyridyl complexes, fluoresc. spectra 8=41190
    EuF_2, magneto-optical effects rel. to Eu^{2+} absorpt. spectra multiplet structure 8=31986
    $Eu_3Fe_{1.94}Ga_{3.06}O_{12}$, cation distrib. 8=30895
    EuO, Curie-point increases by selective doping 8=31612
    EuO film memory medium in low temp. laser-beam addressable memory 8=36123
    EuO films, ferromagnetic, transverse Kerr magneto-optical effect 8=31987
    EuO, hyperfine fields from Mossbauer spectra 8=36208
    Eu_3O_4, hyperfine fields from Mossbauer spectra 8=36208
    Eu_2O_3 in rare-earth oxide mixtures, u.v. spectrophotometric determ. 8=27786
    Eu_3O_4, low temp. magnetic props. 8=40734
    EuO, magnetoelastic interactions and λ anomaly from magnetostriction meas. 8=45011
    EuO, magnetostriction exchange 8=40870
    EuO, Eu^{115} n.m.r. 8=49641
    EuP, Eu^{3+} spin $\langle S(T) \rangle$ temp. dependence from P^{31} n.m.r. obs. 8=31904
    $Eu(ReO_4)_3$ crystal struct., high-temp. modification, X-ray obs. 8=30914
    EuS, ferromag.-paramag. transitions, critical line existence 8=36137
    EuS, mag., eqn. of state and sp. ht. near Curie point 8=27405
    EuS, mag. sp. ht. in non-zero field 8=27406
    $^{151}Eu_3S_4$, electron hopping obs. by Mossbauer spectroscopy 8=30638
    EuS, Eu^{115} n.m.r. 8=49641
    EuS(Se), photoconductivity 8=27320
    EuSe, magnetocrystalline anisotropy 8=45012
    EuSe, Eu^{115} n.m.r. 8=49641
Evaporation
      See also Vaporization.
    alcohols, of dissolved gases, determ. of heat of evap. 8=39319
    alkaline-earth oxides, on heating in high vacuum 8=30605
    from capillary-porous body, heat and mass transfer for transpiration cooling 8=39488
    capillary-porous materials drying in e.m. field, ht. and mass transfer 8=39487
    from cathodes in (4-8)× 10^3 °K range, cooling effect with autoelectronic emission 8=40698
    clouds and sprays in air 8=48273
    of clouds, in radiation field 8=27898
    and condensation, system with 2 interphase surfaces and arbitrary condensation coeffs. 8=34976
    cooling, effect of depth of surface 8=41861
    cooling, heat and mass transfer equation 8=48290
    corundum, effect on crystal form during high temp. heating at low pressures 8=39643
    crystal, ionic, laser irradiation, obs. 8=39494
    ethylene glycol droplets, effect of n-dibutylphthalate coating film 8=48272
    evaporation, eddy flux instrument for natural evaporation meas. 8=50122
    formamide-dioxane system, evaporation equilib. 8=34825
    ice, diffusion of "steps" across surface 8=35145
    ice, evap/condensation rel. to neck formation between sphere and plane 8=30723
    ice in space 8=48289
    liquid droplets containing surface impurities 8=48267
    liquid in vacuum, rate formulae compared with obs. 8=39480

Evaporation—contd
  liquids from free surface in rarefied atmos., heat and mass transfer 8=30601
  liquids, from porous metals at porous cooling under vacuum 8=30602
  liquids, retardation rel. to monolayers 8=39486
  metal, laser irradiation, obs. 8=39494
  mineral, laser irradiation, obs. 8=39494
  moisture absorbed in porous bodies, thermodynamic functions 8=44070
  natural from land, study on hourly basis, and energy balance 8=33685
  organic material, laser irradiation, obs. 8=39494
  oxides in graphite arc electrodes 8=34436
  particles, spherical, radii less than 500Å, rates 8=26000
  in peat drying, intensity over external surface 8=34982
  semiconductor, laser irradiation, obs. 8=39494
  from sphere, local mass and thermal transport 8=34985
  sprays of pure liquid drops, rates 8=48278
  water droplet, time change of radius, asymptotic soln. 8=30600
  water droplets, effect of n-decanol film coating 8=48272
  water droplets, rate meas. by optical scatter 8=39484
  water, maximum rates 8=43915
  water, wet bulb depression meas. in mass transfer boundary layer 8=25996
  whiskers, Stefan problem soln. 8=39697
  Ag crystal, of ions prod. by e bombard. flow control by ion collection 8=40712
  Ag thin film crystallization 8=30741
  AgMn films prod. by simultaneous condensation, magnetic props. conc. depend. 8=40 802
  Au alloys, containing 1% Sb, evaporation in vacuum 8=34998
  C, tartan film by superimposing two evaporations 8=35164
  CCl_4, maximum rates 8=43915
  Cs_2CO_3, evaporation products, mass-spectrometer obs. 8=48294
  GaAs film, 2-source vacuum arrangements 8=44045
  GaAs, kinetics 8=35003
  Ge film formation on GaAs 8=35174
  He liq. from small Dewars without N_2 cooling, loss calc. 8=28439
  He II, vel. distrib. of evaporating atoms, theory 8=41891
  LiF negative thread crystals, kinetics 8=26256
  Pt, submicron particles in shock tube 8=39493
  Si on sapphire, perfect crystals 8=39595
  Sb from PtSb at 900°C, nature of Sb species from atomic absorpt. meas. 8=30608
  Se, vapour mol. comp. and Se_{1-8} appearance pots., obs. 8=43916
  SiO, from graphite cloth 8=35005
  Ti foils, self-supporting, vacuum deposition method 8=39601
  ZnS on Si, epitaxial growth 8=30740
Evershed effect. See Sunspots.
Examination of materials. See Electron diffraction examination of materials; Electron microscope examination of materials; Neutron diffraction examination of materials; X-ray examination of materials.
Exchanges, chemical
    See also Isotope exchanges.
  cation equilibrium, in uranyl-hydrogen system, fuel reprocessing application 8=47409
  hydration of Al(III) and Ga(III) ions, O^{17} n. m. r. 8=30540
  ion exchange membranes, osmosis 8=25901
  octadecylamine on steel and glass, and desorpt., obs. 8=30768
  quantum mechanics of inelastic collisions 8=37744
  silicate glasses, strengthening by ion exchange 8=26845
  silicate ion exchangers, isotope exchange investigation 8=45313
  stearic acid on steel and glass, and desorpt., obs. 8=30768
  AB-type n. m. r., transient effects 8=37543
  Ba isotope exchange rate, zeolith A and aq. soln., 100-180°C 8=45313
  F, between tetrabutylammonium hexafluorophosphate and BF_3 or PF_5 in CH_2Cl_2 soln., n.m.r. obs. 8=25960
  Gd(III) ion in aqueous soln., water exchange from first co-ord. sphere, n. m. r. study 8=43882
  NH_4-NH_4 proton exchange in liq. NH_3 8=27675
  Na-Ca, in montmorillonite suspensions 8=39450
  Nb oxide, ion exchange separation from columbite 8=36544
  NbF_6^- in F^{19} n. m. r. 8=34914
  Pm 147, pure, exchange preparation 8=49838
  Ta_2O_5, ion exchange separation from columbite 8=36544
Excimers. See Molecules/excitation.
Excitation. See Atoms/excitation; Molecules/excitation; Nuclear excitation; Vibrations/excitation.
Excitons. See Crystal electron states/excitons.
Excitons, molecular. See Molecules; Polymers.
Exoelectron emission. See Electron emission.
Exosphere. See Atmosphere/upper.
exp-6 potential. See Kinetic theory; Molecules/intermolecular mechanics.
Expanding universe. See Cosmology.
Expansion, thermal. See Thermal expansion.
Explosions
    See also Detonation; Shock waves.

Explosions—contd
  in atmosphere, rel. to shock wave propag. upward 8=28371
  bridgewire firing sets, joulemeter 8=32938
  burning and thermal decomposition of explosives 8=32114
  cladding, velocity meas. in collision region 8=28370
  constantin wires, elec. discharges, restrike mechanisms 8=40288
  deep refraction seismic expt., NH_4NO_3-fuel oil explosive as energy source 8=50047
  explosive strength comparison by ballistic mortar 8=41837
  galactic, rel. to dust condensation 8=45728
  impolding shells, e.m. field production 8=46394
  metal plate shock wave structure, classical validity for condensed explosives 8=44515
  metals and alloys, explosive cladding and welding, flow 8=39262
  at ocean surface, due to pressurized spheres 8=27867
  for radial expansion of brass tube obs. 8=31202
  thermal initiation apparatus for 300°-1000°C 8=46288
  thermal, semi-infinite explosive, approximate solns. 8=32116
  thermal, theory, stability of steady-state solutions 8=46173
  underwater, ocean bottom reverberation meas. 8=50099
  unstable cpd, explosion limits, photochem. effects 8=27732
  water, pressure pulse phase shift, interpretation 8=48034
  water, pulse phase shift at caustic 8=48035
  Al foil, fast circuit switching appl. 8=32906
  C, glassy, disruption in K vapour 8=49888
  Cu wires, in elec. discharges, restrike mechanisms 8=40288
  Li wire, extrusion die-electrode combination 8=33028
  Li wire, extrusion technique 8=50473
  W wires, in vacuum, undegassed and degassed, X-ray emission and discharge currents 8=40294
 nuclear
  earth shielding effect rel. to e.m. wave and pulse transmission rel. to shielding props 8=46471
  Greeley, P times 8=50049
  neutron γwx use for radioactive nuclide cross-sections meas., underground explosion 8=38478
  on ocean surface 8=28372
  radio absorption detection following high altitude test 8=45538
  as n source for study of energy depend. n-n scatt. 8=24958
  Starfish, Indian Ocean mag. intensity max. 8=41468
  in stars, $M > 6 \times 10^4 M_\odot$, after compression and stability loss 8=32429
  super-heavy nuclei prod., abundances mass formula 8=38324
  thermonuclear, n capture by heavy isotopes 8=25252
  Fm^{259} abundance in Cyclamen test rel. to predicted half-life 8=38496
  Md^{259} abundance in Cyclamen test rel. to predicted half-life 8=38496
  Pu^{242} target n irrad., heavy-isobar yield rel. to supernovae reactions, obs. 8=38495
  U^{238} target n irrad., heavy-isobar yield rel. to supernovae reactions, obs. 8=38495
Extensive air showers. See Cosmic rays/showers and bursts.
Extensometers. See Strain gauges:, Thermal expansion.
Extra-terrestrial radiation. See Cosmic radiations, radio-frequency; Sun/radiation.
Eye
    See also Vision.
  astigmatism in accommodation 8=37726
  cats, recovery time following high luminance stimulation 8=28916
  cattle rod outer segments, visual pigment fluorescence obs., 575-600 mμ 8=49828
  compound, superposition, form and functioning of diffraction images 8=42253
  corneal contour by slit lamp section photography 8=46772
  human retinal cones, lateral inhibition and subjective light patterns 8=42294
  human, smooth pursuit movements, direct evidence against intermittency or sampling 8=24445
  LGN cells, responses, analysis 8=28926
  light, colour and vision, book 8=42293
  movement, voluntary saccadic, visual suppression prior to onset 8=42296
  primate, photoreceptor orientation, model 8=24444
  protection filters, meas. and characts. of scatt. light 8=28922
  pupil light reflex, optimizing use of criterion response 8=28915
  retina photo coagulation with quasi-continuous ruby laser 8=28912
  retina, struct. model relating obs. trichromatic and opponent-colour responses 8=28924
  retinal image given by correcting glass of progressive power 8=46775
  retinal image motion, effect on critical flicker-fusion obs. 8=37727
  rods, excitation modes 8=37728
  sensitivity curve rel. to multi-beam interometer fringe apparent broadening 8=28866

Eye—contd
SLF photo-slit lamp 8=42203
time course of visual inhibition during voluntary saccades 8=28917
time-varying light signals detection, as meas. by pupillary response 8=28914
triple-function ocular monitor 8=28913
visual suppression during passive movement 8=46773
yellow blur, role in human eye 8=46771

F-centres. See Colour centres.
F-layer. See Ionosphere/F-region.
Faculae. See Sun.
Fallout
See also Atmosphere/radioactivity; Nuclear reactions; Radioactivity.
beta-ray spectroscopy of radioactive fallout 8=46851
condensation nuclei, precipitation form. study 8=41357
fission products, Finland, Dec. 1966 obs. 8=27927
near Milan from 7th Chinese nuclear explosion, γ spectroscopy 8=50162
radon, atmospheric conc. Washington D.C. area 8=27881
stratospheric, transuranium elements, radiochem. anal. and evaluation by α-spectroscopy 8=27928
subcloud level, precipitation of division products 8=27929
trace subst. transport in lower stratosphere and upper troposphere 8=50163
tritium geophysics from 1961/2 nuclear tests 8=32256
C^{14} from 1961-62 tests by U.S.A. and U.S.S.R. time and space distribution 8=27930
$Ce^{141,144}$, concs. in ground-level air after nuclear explosion of 9-5-66 8=36757
H_2, tritium and deuterium content, 1958 to 1963 obs. 8=27882
RaA inhalation hazard rel. to diffusion coefficient, humidity var. 8=32257
U in hot particles, rainwater and soil 8=41373
Faraday effect. See Magneto-optical effects.
Fatigue. See Elastic fatigue.
Fermi gas. See Fermions.
Fermi level. See Crystal electron states/Fermi level.
Fermi surface. See Crystal electron states/Fermi surface.
Fermion systems. See Fermions.
Fermions
See also Elementary particles; Quantum theory/many-particle systems.
conspiring trajectories; reflection symmetry 8=47012
correlation energy of many-fermion system 8=42772
electronic contribution to energy and press. of elements and mixture, high temp. 8=23901
e.m. scatt. polarization expressions 8=24662
Fermi integrals evaluation 8=41779
Fermi-liquid, inequalities, instabilities and renormalization 8=26864
Fermi liquid interactions in alkali metals, magnetoplasma modes prod. 8=40271
Fermi liquid, transport props., calc. 8=41778
Fermi-odd interactions, applic. of Wick theorem 8=42393
field, theory, para-Fermi, nonrelativistic, state vector props. 8=42320
gas, Bloch density matrix calc. of attractive scatt. centre leading to bound states 8=35765
gas rel. to props of high density matter in intense mag. field 8=45601
independent pair model for nuclear matter 8=47211
integral representation of Fermi functions 8=28333
kinematic singularities and Macdowell symm. 8=29047
Landau Fermi liquid theory 8=28434
liquid, entropy in shielded potential approx. 8=28338
liquid, Landau quantum theory, book 8=30397
liquid, nearly ferromagnetic temp. depend. of spin susceptibility 8=28337
liquid, surface wave effects 8=28339
long-range intraction, superconductivity theory 8=26983
odd number, N-representability for density matrices 8=37215
para-fermion relations, second and third order 8=46825
Regge poles and ratios between cross-sections of large angle scatt. 8=42441
Regge trajectories, asymmetric, rel. to πN dynamics 8=24678
Regge trajectories, N_α and N_γ interference to explain dip in π^+p 8=33687
scatt., identical polarized with anomalous magnetic moment, cross-section calc. 8=24660
self-conjugate, field operators and commutation relations 8=37913
as spinors, two-component, helicity of non-zero mass in quantum electrodynamics 8=37767
system collective modes, var. principle for Landau eqn. 8=46118
system, degenerate, method for calc. of transport coeffs. 8=41781
system, dilute, in boson background 8=28334
system, expectation values of observables using cluster expansions 8=32848-9
system Fermi-Bose, mixed, dispersion relation for eigenfrequencies of low-lying states 8=23891

Fermions—contd
system, finite, self-energy part and one-particle Green's function 8=37213
system, finite, theory appl. to deformed nuclei 8=25089
system, gas, low-density, pair collisions 8=32852
system, interacting gas, generalized instability criterion 8=32850
system liquid, transport coeffs., finite temp. corrections 8=46120
system, Luttinger model, random phase approximations 8=23899
system, many-component, theory of transport phenom. 8=32851
system, many-, generalized uncertainty relations 8=28336
system, model yielding lower bound to ground state energy 8=41780
system, phase transitions, quantum field theory 8=46823
system of quarks, nuclear model 8=24743
system, ordering of 2 and n identical particles, dynamical theory of Pauli princ. 8=33519
system, one-dimensional Tomonaga model, ground state momentum distrib. 8=23896
system, 1D, single particle Green's function, with branch cut in complex energy plane 8=28335
system, theory of Sn and Pb first 2^+ levels 8=29325
system, transport coefs. and sp. ht., low-temp. expansion 8=37216
system two-sort, low temps. 8=37214
systems Landau theory 8=23898
2-fermion system, Schrodinger-like eqn. applied to $q\bar{q}$ 8=29104
Fermium
No entries
Fermium compounds
No entries
Ferrimagnetic resonance
See also Ferromagnetic resonance.
linewidth maxima mechanism 8=31828
for magnetostriction constants meas. by ferromag. resonance method 8=31569
nonlinear theory 8=37538
Permalloy films, internal isotropic stresses and demagnetizing factors obs. 8=31223
$CoCr_2O_4$ insulating spiral, freq. and temp. dependence 8=31831
Li ferrite with near-zero defect. concs., linewidth meas. 8=31829
$MnCr_2O_4$ insulating spiral, freq. and temp. dependence 8=31831
$Mn_vFe_{3-x}O_{4+\nu}$, electron-transfer relaxs. 8=31830
$Ni_{1+x}Ge_xFe_{2-2x}O_4$, 4.2-393°K rel. to anisotropy 8=36227
$Y_{3-2x}Ca_{2x}Fe_{5-x-y}V_xIn_yO_{12}$, $(x \leqslant 1.5, y \leqslant 0.5)$, linewidth reduction 8=31833
YFe garnet:Ho, giant-anisotropy linewidth, crystallographic angle and temp. dependence 8=31832
YFe garnet polycrystals, linewidth and off-resonance loss at microwave freq. 8=31834
Y Fe garnet, standing-spin-wave modulation of reflected microwave power 8=40847
Zn_2Y, hexagonal ferrite, two-magnon linewidth 8=36228
Ferrimagnetism
See also Ferromagnetism.
fine-particle assemblies and thin films, interaction effects 8=36130
ferrites, amplified ferrimag. echoies, obs. 8=31717
gases, conditions for occurrence 8=39228
Heisenberg magnet, critical behaviour in susceptibility 8=31714
magnon-phonon interaction rel. to sound-wave attenuation 8=35401
micromagnetism, point singularities 8=31593
spin oscillation instability on parametric acoustic wave excitation 8=40833
spin-reorientation rel. to phase transitions 8=36181
spin waves, freq. shift and damping const. 8=27427
sublattice rotations, mol. field model 8=31725
$RbNi_{1-x}Co_xF_3$, mag. and optical props. 8=49555
Y Fe garnet, spin wave excitation time in first- and second-order nonlinear processes 8=45041
Ferrites
See also Magnetic properties of substances.
amplified ferrimag. echoes, obs. 8=31717
antiferromagnetic and ferrimagnetic props. 8=49460
Bitter patterns rel. to changes in width and domain shape 8=31557
complex permeability and permittivity in mm wave range, meas. tech 8=49551
contrast mats. for X-ray diagnosis 8=37093
cores, magnetoelastic resonance 8=36226
crystal structure and preparation methods, review 8=49547
dielectric permittivity and loss, effect of freq. and temp. 8=40565
easy magnetization direction, reflection electron diffraction obs. 8=31716
effective permeability induced by temperature and stress variations, instability study 8=49552
e.m. transmission properties and appl. non reciprocal networks 8=46473
energy losses on rotating in alternating and direct mag. fields 8=36102

Ferrites—contd
epitaxial growth on metal oxides, prep. methods 8=35175
folded, loaded, for alternating gradient synchrotron 8=24580
garnets, polycrystalline magnetic, use in microwave devices 8=40834
garnets, structure 8=36136
high-permeability, influence of ferric oxide and ferrite powders 8=45035
high-uniaxial-anisotropy, domain-wall mobility 8=27428
hot-pressed, fine-grained, h.f. and microwave props. 8=27435
integral comb model, remagnetisation 8=36182
initial permeability at microwave and natural gyromagnetic resonance 8=31715
manganic, crystal growth techniques 8=26257
magnetic anisotropy, effect of hydrostatic pressure 8=49559
magnetic domains in orthoferrites, props. and device applics. 8=49553
easy magnetization direction, reflection electron diffraction obs. 8=31716
magnetization intensity temp. dependence, 95–300°K 8=40836
magnetoacoustic resonance excitation in non-linear ferromag. resonance 8=49064
magnetoresistance temp. dependence 8=40835
magnetrostriction characts. 8=49452
microwave applications in USSR, bibliography 8=24203
microwave mixer of YFe garnet, energy balance 8=41999
mixed, $M_xM'_{1-x}Fe_2O_4$, (M=Mg, Zn; M'=Mn, Ni) mag. structure from polarized n.-scattering 8=31732
molecular field coeffs. from mag. saturation temp. dependence using Néel-Weiss theory 8=45033
permeability, initial, rel. to freq. 8=45034
Perminvar, meas. of susceptibility in Mc/s range 8=49557
polycrystalline, associated magnetostatic energy 8=49550
rare-earth orthoferrites, antiferromagnets with weak ferromagnetism, anisotropy pressure depend 8=40857
rare-earth orthoferrites, hydrothermal growth 8=35249
rectangular, minimum switching time calc. 8=27430
resonant elastic oscillation excitation in non-linear ferromag. resonance 8=49064
resonators hydrodynamic liquid cooling method 8=33048
rubber ferrite-loaded magnets props. 8=24111
square loop, simulation of domain wall motion and wall behaviour 8=45036
spinel, Faraday effect in far i.r. 8=41133
spinel ferrite lattice, cubic, local Jahn-Teller distortions rel. to phase transitions 8=26408
spinels, split dislocation structure 8=40027
spinels, two-component, vacancy formation and behaviour 8=26638
u.s. transducer with clamped core 8=41840
in waveguides, axially magnetized, mode characts. 8=28622
Ba, mag. props. rel. to magnets for transport appls. 8=24114
$BaCo_2Fe_{16}O_{27}$, rotatory hysteresis losses and anisotropy 8=45037
$BaFe_{12}O_{19}$, as permanent magnet materials 8=36184
$BaFe_{12}O_{19}$ flexible magnets, anisotropic, prep. and props. 8=24110
$BaFe_{12}O_{19}$, rotatory hysteresis losses and anisotropy 8=45037
$Ba\,Sc^{3+}_{1.8}\,Fe^{3+}_{10.2}\,O_{19}$ (M), antiphase spin ordering 8=36183
Ca-Bi-V-ferrites, ferromag. res., effects of defects from U^{235} fission fragments 8=36225
Co-substituted, uniaxial mag. anisotropy rel to Fe, Co ions and vacancies 8=49556
$Co_2BaFe_{16-x}In_xO_7$, mag. props. comp. dependence 8=45038
$Cu_{0.09}Mn_{0.61}Fe_{2.3}O_4$, magnetic anisotropy rel. to temp. 8=31723
DyAl garnet, antiferromag., magnetization and ordering, 0.37°K 8=40866
ErGa garnet, metamag. transition and antiferromag. struct., 0.31 and 4.2°K 8=40867
Fe_5LiO_8, short range order 8=26866
Fe-Ni-Co, induced anisotropy constant angular dependence 8=45039
Fe_2O_3: Co, induced anisotropy, dependence on annealing temp. 8=36186
Fe_2TiO_4, Mössbauer spectra for electronic structure 8=48327
Gd, spontaneous radiation temp. dependence 8=45190
Li, heat treatment effect on resist., dielect. and thermoelect. props. 8=35962
$Li_{0.5}Fe_{2.5}O_4$, n scatt. by spin waves, polarization effects, obs. 8=36187
Mg-Mn, sphere, magnetostatic spectrum, anisotropy dependence 8=40888
Mn, Ba-doped, discontinuous growth 8=39677
Mn-, domain structure from X-ray obs. 8=27434
Mn, Hall effect 8=40841
Mn, Fe-rich, elec. conductivity, low temp. 8=49140
$Mn_{1+x}Fe_{2-x}O_4$, induced anisotropy at low temps. 8=36188
$MnFe_2O_4$ films, single-cryst., pulse switching and static characts., obs. 8=31730
Mn–Zn, mag. props. rel. to sintering conditions effects 8=49561
Mn-Zn, Mössbauer study of hyperfine fields 8=35042

Ferrites—contd
Mn–Zn, with high-permeabilities 8=49560
$Mn_xZn_{1-x}Fe_2O_4$, cation distribs. and lattice parameters from X-ray and n.-exams. 8=44229
$NdFeO_3$, mag. anisotropy 8=31733
Ni, dielectric losses at microwave freq. 8=49346
Ni, epitaxial growth on MgO (111) and (110) surfaces 8=39594
Ni evaporated contact electrode 8=31321
Ni, ultrasonic waves, magnetic hysteresis of velocity, with Co, Mn and Cu impurities 8=31736
Ni, with high saturation magnetization and improved hystersis 8=31734
Ni-Fe, small Co additions, mag. diffusion after-effect 8=36191
$NiFe_2O_4$ films, ferromag. resonance thickness dependence 8=31823
Ni–Zn, hot-pressed, fine-grained, hf and microwave props. 8=49562
Ni-Zn system, ferromag. relax. 8=27491
Pb, with oxide additives, mag. residual induction and energy product 8=40842
$Sm_{1-x}Tm_xFeO_3$, antiferromag. props. 78°-500°K 8=31797
Sr, processes of magnetic reversal 8=31739
$SrFe_{12-x}Ga_xO_{19}$, Mössbauer spectrum of Fe^{57} obs. 8=30624
YFe garnet, e.m. conversion to exchange spin wave energy, coherent i.r. diffraction determ. 8=40848
YFe garnet, magnetoelastic waves, 1.1 GHz, props. from light diffraction obs. 8=40101
YFe garnet, spin wave freq. and amp. in subsidiary absorpt. region 8=49563
YFe garnet, standing-spin-wave modulation of reflected microwave power 8=40847
$Y_3Fe_5O_{12}$, n-scattering by parametrically excited spin-waves 8=36094
Zn_2Y two-magnon ferromag. resonance linewidth hexagonal 8=36228
Ferroacoustic resonance. See Crystals/lattice mechanics; Ferromagnetic resonance.
Ferroelectric devices. See Dielectric devices.
Ferroelectric materials
ammonium oxalate, electro-optical effects 8=36442
bismuth titanate, thermodynamic analysis 8=44887
ceramic, coarse-grained, Rayleigh scatt., polarization-dependence 8=45151
ceramics, energy storage materials 8=35969
displacive, at. displacement rel. to Curie temp. and spontaneous polarization 8=44882
displacive type, coupled mode of sound with soft mode 8=39881
domain struct. config. 8=48577
dynamic polarization and losses 8=40601
glycine sulphate, refractive index n_α, temp. depend. 8=45243
guanidine chromium sulphate hexahydrate, dilution splitting of absorpt. lines of Cr^{3+} 8=41164
ice IX, antiferroelec. phase 8=31438
lattice structure determ. using micro e.-diffr. technique 8=39761
magnetically polarized, coupled elasto-spin e. m. waves and excitation of reflected waves 8=27261
nonlocal connection between polarization and electric field 8=40598
octyl benzoic acid liq. cryst. 8=25882
oxygen octahedra, nonlinear optical tensor coefficients 8=41017
perovskite-type solid solns. and cpds., phase fluctuations in transitions 8=35970
pyroelectric film, const. meas. in low elec. field, method and app. 8=40599
Rochelle salt, deuterated, d.m.r. and dielectric relaxation 8=49651
rochelle salt, deuterated, props. rel. to pressure and temp. 8=40621
Rochelle salt, dielectric relaxation 8=27289
rochelle salt, polarization non-linearities in strong elec. fields, –35 to +35℃ 8=35982
Rochelle salt, props near ferroelec. phase transitions 8=27577
Rochelle salt, relax. sound absorpt. near phase transition 8=39899
rochelle salt, stabilization of domains, effect of γ-irradiation 8=35981
seignette salt, thermal conductivity temp. dependence near Curie salt 8=44358
seignettomagnetics, phase transitions and coupling of ferroelec. and mag. props. 8=27398
shocked, resistivity estimates 8=44880
similarity transformations 8=49360
soft, spectra-struct. correl. 8=27544
space compensating charge rel. to domain structure 8=40605
structure, properties, chemical nature, classification 8=35966
thermocurrent spectra in crystals 8=40634
thiourea and deuterated deriv., crystal structures from n. diffr. above and below transition 8=44251
triglycine fluoberyllate, electrocaloric effect and dielec. constant 8=27291

Ferroelectric materials—contd
- triglycine selenate, electrocaloric effect and dielec. constant 8=27291
- triglycine selenate, optical indicatrix rotation in phase transition region 8=27638
- triglycine selenate, props. at high hydrostatic pressures 8=40622
- triglycine selenate, spontaneous polarization, permittivity and sp. ht. temp. dependence 8=44890
- triglycine-silphate group, temp. -induced changes in the 575 cm^{-1} band at phase transition 8=36438
- triglycine sulphate and isotypes, transition mechanisms from i. r. spectra 8=27290
- triglycine sulphate and isotypic crystals, solid solns., phase transition comp.-dependence 8=27293
- triglycine sulphate, anomalous sp. ht. near Curie pt. 8=39923
- triglycine sulphate as pyroelectric radiation detector 8=28383
- triglycine sulphate crysts., interaction of defect and domain structures 8=40620
- triglycine sulphate crystals; isomorphous with ferroelectrics i.r. spectra 8=49774
- triglycine sulphate, deuterated, conc. depend of props of solid solns. 8=49377
- triglycine sulphate, domains, change in width with time 8=31437
- triglycine sulphate, domain twins in growth 8=27292
- triglycine sulphate, domains and dislocations, interactions 8=27287
- triglycine sulphate, electro-optical props. near phase transitions 8=27637
- triglycine sulphate, elec. resist., effect of atmospheric humidity 8=35985
- triglycine sulphate, fundamental absorpt. edge temp. dependence, room temp. -62°K 8=41172
- triglycine sulphate group crystals and spectral identification 8=49776
- triglycine sulphate, near Curie temp., transition energy and entropy change 8=35430
- triglycine sulphate optical indicatrix rotation in phase transition region 8=27638
- triglycine sulphate, permittivity at 20 kHz obs 8=44889
- triglycine sulphate, polarization in d.c. field and resistivity determ. 8=40618
- triglycine sulphate, polarization process, ultrasound effects under static conditions 8=35986
- triglycine sulphate, pyroelec. effect for rapid temp. change in Curie pt region 8=31443
- triglycine sulphate, second harmonic generation domain structure influence 8=35977
- triglycine sulphate single crystal, differential permeability, effect of impurities 8=27288
- triglycine sulphate single crystal, electro-optical effect 8=36439
- triglycine sulphate, surface sparks 8=40623
- two-dimensional, correlation functions 8=27260
- in two-phase mixture. elec. oscills. damping and dispersion 8=40600
- $A_{V}B_{VI}C_{VII}$-type semiconductors, phase transforms. rel. to elec. and optical props. 8=27077
- $(BaCa)TiO_3$, study of SHF temp. characteristics 8=49365
- $Ba_2NaNb_5O_{15}$, linear and quadratic electro-optic coeffs., spontan eous polarization obs. 8=27583
- Bi perovskites, and antiferroelec. transitions rel. to phase transforms. 8=26063
- $BiFeO_3$, e. -microdiffr. exam 8=26430
- $BiFeO_3$, e.p.r. study 8=27488
- $BiFeO_3$ solid solns., ferro- and antiferroelec. transitions 8=27285
- $BiFeO_3$, spontaneous polarization, elec. field and field gradient calcs. 8=27269
- $BiFeO_3$-$PrFeO_3$ system, phase transitions rel. to mag. props. 8=26064
- $Bi_4Ti_3O_{12}$ crystals, electrical-optical behaviour 8=27271
- $CdTiO_3$, perovskite modification, transitions, 20-1000°C 8=27242
- Cu formate tetrahydrate, antiferroelec., deuteron n. m. r. 8=44269
- $Fa_{0.27}Sr_{0.75}Nb_2O_{5.78}$, cryst. struct. 8=48638
- H-bonded, theory 8=44881
- $K_4Fe(CN)_6.3H_2O$, dielec. constant and birefringence rel. to polytypic transforms, 0 to—100°C 8=31432
- $K_4Fe(CN)_6.3H_2O$, phase transition sequence in —45 to —25°C from permittivity and polarization meas. 8=40610
- KD_2PO_2, automatic thermostatic control 8=31431
- KD_2PO_4, dielec. and electromechanical props. near phase transition 8=27275
- KH_2AsO_4, critical temp. behaviour of As^{75} quadrupole interaction 8=45137
- $KH_2AsO_4(KD_2AsO_4)$, electro-optic and dielec. constants 8=49369
- KH_2AsO_4 (KD_2AsO_4), piezoelec. and elastic constants 8=49368
- KH_2PO_2, automatic thermostatic control 8=31431
- KH_2PO_4, electro-optical props. near phase transitions 8=27637
- KH_2PO_4, ferroelec. mode temp. depend., Raman scatt. obs. 8=36376
- KH_2PO_4, long-range domain interactions, optical obs., 8=49367
- KH_2PO_4-model, modified to include external field 8=27262
- KH_2PO_4, spontaneous polarization, deuteration effect 8=40609
- KH_2PO_4-type crystals, sound attenuation and thermal conduction, critical anomaly 8=48716
- KH_2PO_4-type phase transitions using neutron scattering in hydrogen bonds 8=35017
- KH_2PO_4, vibrational mode disappearance from n. time-of-flight spectra 8=44299
- KH_4PO_4, l. f. oscills. from Raman spectra study 8=36378
- KH_2PO_4 and KD_2PO_4, Curie temp. pressure-dependence 8=27274
- $KNbO_3$, e-microdiffr. exam. 8=26430
- $KNbO_3$, spontaneous polarization, elec. field and field gradient calcs. 8=27269
- KNO_3, dielectric behaviour at high-temp. 8=49370
- KNO_3, phase-III, stable and metastable, props. pressure-dependence 8=27273
- $KSr_2Nb_5O_{15}$–$LaNb_3O_5$ system, props. 8=40611
- $KTa_fNb_{1-f}O_3$ (KTN) conc. gradient light beam deflector 8=36382
- $KTaO_3$, ferroelectric phase transitions, lattice-dynamical theory, elastic and dielectric anomalies 8=27284
- $KTaO_3$, thermal conductivity temp. and field dependence rel. to Cochran modes 8=26605
- Li trihydrogen selenite, optical indicatrix rotation in phase transition region 8=27638
- $LiD_3(SeO_3)_2$, d.m.r. 8=49648
- $LiNbO_3$, Curie temp. as function of melt stoichiometry 8=31433
- $LiNbO_3$, Curie temp. meas. and dielec. anisotropy 8=27285
- $LiNbO_3$, domain wall obs. rel. to dislocation pinning 8=31434
- $LiNbO_3$, electrical conductivity up to 1400°K 8=2 7276
- $LiNbO_3$, linear and quadratic electro-optic coeffs. spontaneous polarization obs. 8=27583
- $LiNbO_3$, phase transitions, 20°–1170°C, X-ray obs. 8=30863
- $LiNbO_3$, Raman and Rayleigh scattering temp. dependence, 90-1100°K 8=27585
- $LiNbO_3$, structural change rel. to ferroelec. transition from x-ray and elec. exam. 8=31435
- $LiNbO_3$-$CdTiO_3$ system, solid solns. of ilmenite structure, Curie temp. comp.-dependence 8=27278
- $LiNbO_3:Cr^{3+}$, polydomain crystal, elec. paramag. resonance of Cr^{3+} 8=27277
- $LiNbO_3:Cr^{3+}$, polydomain crystal, paramag. hypersound absorpt. by Cr^{3+} 8=31873
- $LiNbO_3$–$LiTaO_3$–$Fe(Mg)TiO_3$ system, X-ray exam. 8=27278
- $LiTaO_3$. Curie pt. and lattice consts. 8=49371
- $LiTaO_3$, Curie point rel. to mol. ratio Ta_2O_5/Li_2O 8=49372
- $LiTaO_3$, dielec., thermal and pyroelec. props. 8=44888
- $LiTaO_3$, high-temp., X-ray investigation 8=35978
- $LiTaO_3$, linear and quadratic electro-optic coeffs., spontaneous polarization obs. 8=27583
- $LiTaO_3$, Raman and Rayleigh scattering temp. dependence, 90-1100°K 8=27585
- $LiNbO_3:Mn^{2+}$, e.s.r., spacing of hyperfine sextet 8=45090
- $LiNbO_3$, n.m.r. 8=40987
- $LiTaO_3$, n.m.r. 8=40987
- $LiTaO_3$–$CdTiO_3$ system, solid solns. of ilmenite structure, Curie temp. comp.-dependence 8=27278
- $NaD_3(SeO_3)_2$, d.m.r. 8=49648
- $NaH_3(SeO_3)_2$ and deutero-cpd., props. over transition range and NMR study 8=27511
- $(Na_{0.7}K_{0.3})NbO_3$, antiferroelec., electro-optical effects 8=27294
- $NaNO_2$, charge distrib. of NO_2^- 8=48308
- $NaNO_2$, dielectric relaxation, exptl. study 8=40612
- $NaNO_2$. dielectric relax. mechanism 8=40613
- Na-Sr-Cd niobates, dielectric props. and phase transitions 8=35979
- $NH_4H_2PO_4$, antiferroelec. phase transition, group theory 8=31439
- $NH_4H_2PO_4$, electro-optical props., contribution of quadratic effect 8=32015
- Ni boracites, sector-growth and twinning. exam. by polarized-light microscopy 8=26188
- $PbTiO_3$, at. structure determ. using micro e. -diffr. technique 8=39761
- $PbTiO_3$, e-microdiffr. exam. 8=26430
- $PbTiO_3$–$PbMn_{2/3}W_{1/3}O_3$ system, solid solns., permittivity temp. and comp. dependence 8=40616
- $Pb(Ti, Zr)O_3$ ceramics, orientational polarization 8=35980
- $PbZn_{1/3}Nb_{2/3}O_3$, dielec. props. 8=27281
- $PbZn_{1/3}Nb_{2/3}O_3$, dielec. props. and electro-optical props. 8=27280
- $Pb(Zr, Ti)O_3$ ceramic detector, for differential energy spectrum of pulsed rad. sources 8=28971
- $Pb(Zr, Ti)O_3$ ceramic, 90° domain wall-pt. defect interaction 8=44405
- $Pb(Zr, Ti)O_3$ compounds, electro-caloric effects 8=27279
- RbH_2PO_4, dielec. and electromechanical props. near phase transition 8=27275
- RbH_2PO_4, dielec. props. near phase transiton pt. at u.h.f. 8=40617
- Sb sulpho-iodide, dielectric behaviour with elec. field freq., to microwave range 8=35983
- SbSI, far i.r. spectra 8=41134

Ferroelectric materials—contd
- SbSI, phase transition 8=31436
- SbSI, photodielectric effect 8=40669
- SbSI, photoferroelectric, anomalous props. 8=49373
- SbSI, pressure depend. of props. 8=49374
- Si 8=27442
- $SrTiO_3$, annealed, electric double hysteresis 8=49376
- $SrTiO_3$ crystals, electro-optical effect, 23 to −183°C 8=36416
- $SrTiO_3$, ferroelectric phase transitions, lattice-dynamical theory, elastic and dielectric anomalies 8=27284
- $SrTiO_3$, photocond. and Hall effect 8=40675
- $SrTiO_3$, photoconductivity, anomalous temp. dependence 8=27331
- $SrTiO_3$, vibration mode, 77 to −173°C 8=35984
- $SrTiO_3$, similarity transformations 8=49360
- $SrTiO_3$ solid solution, dielectric relaxation 8=49375
- $SrTiO_3$, thermal conductivity temp. and field dependence rel. to Cochran modes 8=26605
- $YMnO_3$, dielec. constant temp. dependence 8=27285
- **barium titanate**
  - aging in a.c., d.c. and zero fields rel. to oxidation states of impurity ions. 8=49361
  - Curie pt. pressure dependence rel. to electrostrictive constant temp. dependence 8=44886
  - electro-optical effect calcs. using ionic model rel. to nature of bonding in crystal 8=41067
  - electro-optical effect, quadratic, dynamic obs. 8=27268
  - electro-optical props. near phase transitions 8=27637
  - film bending on polarization 8=40608
  - films, domain structure, transmission electron microscope 8=35973
  - films, sputtering prep. 8=35161
  - internal field at Curie point 8=35972
  - natural unipolarity in single crystals grown by Remeika method 8=31429
  - polarization processes, X-ray obs. 8=40607
  - polarization reversal, partial, exam. by square bipolar pulses 8=27267
  - potential distribution in humid atmosphere 8=27266
  - relaxation processes on subjecting to unidirectional mech. pressure pulses 8=35976
  - repolarisation process in weak alternating fields 8=40606
  - repolarization processes, under double freq. excitation 8=31430
  - similarity transformations 8=49360
  - single domain crystal prod. 8=30817
  - solid solutions with $La_{2/3}TiO_3$, $Sm_{2/3}TiO_3$ and $Ba_{1/2}NbO_3$, relax. polarization due to vacancies 8=35975
  - spontaneous polarization, elec. field and field gradient calcs. 8=27269
  - structural changes near transition point 8=35971
  - surface domain nucleation in switching mechanism 3=27265
  - surface properties using semiconductor thin films 8=49364
  - thermal conductivity near transition point 8=48760
  - thermocurrents rel. to phase transition 8=27306
  - transducer, pyroelec. for hypersonic wind-tunnel heat transfer 8=47953
  - vibration mode, 200 to −60°C 8=35984
  - $(Ba, La)TiO_3$ film, production and props. 8=27264
  - $(Ba, La)TiO_3$ films, permittivity and loss tangent substrate temp. dependence, 100-850°C 8=49363
  - $BaTiO_3$, semiconducting, ionic-relax. polarization in ferro- and paraelec. states 8=35974
  - $BaTiO_3$:MgO(MnO), permittivity changes in ageing in elec. fields 8=27263
  - $BaTiO_3$: Sm(La), baked electrophoretic films, semi-conducting and dielec. props. 8=44885
  - $BaTiO_3$, Ti^{3+} electronic transition theory 8=49362
  - Gd doped, non-stoichiometric, barrier capacitance 8=44884

Ferroelectric phenomena
- Curie temp. rel. to elec. field 8=27259
- displacement-type phase transitions, statistics, and dynamics 8=40603
- domains, obs. by X-ray topography 8=35968
- elementary dipole nature, dipole coupling, partition function calc. 8=35967
- lattice problem, combinatorial approach 8=44883
- phase transitions, e.s.r. study 8=49359
- phase transition in KH_2PO_4-type crystals, dynamical theory 8=31428
- phase transitions, lattice-dynamical theory, elastic and dielectric anomalies 8=27284
- phase transitions, study by d.m.r. 8=49358
- phonon modes freqs., soft, elec. field influence 8=40604
- polarization-caused film bending 8=40608
- rare earth orthochromites, studies 8=27282
- rare-earths, props., magnetic structure 8=40619
- temp. characteristics, s.h.f. study method 8=49365
- triglycine sulphate, domain and defect structs. in ferro-elec. and paraelec. phases, obs. 8=31031
- triglycine sulphate, interaction of defect and domain structures in ferro- and paraelectric states 8=40620
- Van der Waals forces between two ferrodielecs. separated by narrow gap 8=40602
- $BaTiO_3$, films, domain structure 8=35973
- $ErCrO_3$, ferroelectricity and piezoelectricity, comment 8=27272
- $HoCrO_3$, ferroelectricity and piezoelectricity, comment 8=27272

Ferroelectric phenomena—contd
- KH_2PO_4-model, modified to include external field 8=27262
- $Pb(Fe_{1/2}Ta_{1/2})O_3$, transition, dielectric constant 8=40615
- Ni-Zn ferrite system 8=27491
- X-ray differential photometric exam. technique 8=26323
- Y manganites, props., magnetic structure 8=40619

Ferromagnetic relaxation
- at Curie temp. and above, model 8=42039
- neutron meas., critical, incident spectrum broadening by inelastic scatt. 8=40795
- ruby, ferromagnetic interactions 8=49580

Ferromagnetic resonance
- See also Ferrimagnetic resonance.
- anharmonicity at l.f. in transversely magnetized film 8=40883
- ferrimagnets, and spin waves 8=49579
- ferrites, resonant elastic oscillation excitation in non-linear ferromag. resonance 8=49064
- ferroglass, modulation of He-Ne laser 8=24359
- films, in microwave cavity, uniform mode growth mechanism 8=36220
- films, permalloy, flash evaporated, use 8=31809
- films, rel. to mag. params., obs. 8=31807
- films, surface waves in spin-wave resonance, theory 8=45068
- foldover effect, double 8=49578
- garnets: Fe^{4+}, linewidth temp. dependence, 4.2°. -300°K at 10 and 25 kMc/sec 8=31827
- Ising spin systems with impurities 8=31836
- laser light modulation, at microwave freq., theoretical anal. 8=42053
- line width, effect of dislocations 8=40884
- magnetic thin films 8=36114
- magnetoelastic instability in uniform precession 8=36221
- metal polycrystals, plastic deformation and annealing effects 8=31811
- nonlinear effects above spin-wave instability threshold 8=31805
- nonlinear, instability 8=13806
- nonlinear, self-modulation anisotropy 8=45069
- parallel resonance, hyperfine, theory and appl. to $K_2CuCl_4.2H_2O$ 8=27454
- permalloy film, "flash-evaporated", Kittel:s model 8=27452
- Permalloy film rel. to internal stresses, obs. 8=31821
- permalloy films, and coupled double layers with Fe–Ni–Mn, at 9.3 GHz 8=31814
- Permalloy films, and off-reson. susceptibility, r.f. 8=31822
- permalloy films, effect of surface conds and Au and Ni layers 8=49581
- permalloy/Gd/Co-permalloy triple layers, spin-wave resonance temp. dependence, 100–400°K 8=31816
- quasi-stationary state-phonon interactions 8=40775
- radiation field interaction rel. to polarization 8=40882
- semiconductors, indirect exchange calcs. 8=40768
- spin cluster, in Ising spin system 8=27450
- theory: natural oscills. of magnetization, spin wave instability in alternating field and nonlinear effects 8=31810
- in thin films, theory or calc. of power absorpt. and polarized r.f. fields 8=31808
- thermal effects of absorbed microwave power 8=49577
- $Ba_2Zn_2Fe_{12}O_{22}$ 8=40885
- Ca-Bi-V-ferrite, effects of rad. defects from U^{235} fission fragments 8=36225
- $CdCr_2Se_4$, spin-wave relax., 4.3°K to near T_c(≈130°K) 8=31812
- Co, hexagonal, film, spin-wave reson. 8=40886
- CoS_2 powder, below T_c 8=49603
- $ErAl_2$, relax. study by Mössbauer effect 8=49518
- EuSe, magnetocrystalline anisotropy from meas. at 1.3°K 8=45012
- Fe, linewidth temp. dependence, 300–1000°K 8=31815
- Fe-Cr films, rel. to exchange constant determ. 8=36147
- Fe-Ni-Co films, s.h.j. reson. absorpt. line width. obs. 8=31629
- Fe-Si, H charged, diffusional relax. effects 8=36223
- $Ga_{2-x}Fe_xO_3$, spectra 1.2–360°K rel. to highly anisotropic ferrimagnetism 8=27453
- Gd/permalloy double layers, spin-wave resonance temp. dependence, 100–400°K 8=31816
- $K_2CuCl_4.2H_2O$, hyperfine parallel resonance 8=27454
- $LiFe_5O_8$, effects of rad. defects from U^{235} fission fragments 8=36225
- LuFe garnets: Fe^{4+}, linewidth temp. dependence, 4.2°–300°K at 10 and 25 kMc/sec 8=31827
- Mg ferrous ferrite, microwave, rel. to magnetic anneal 8=31818
- Mg–Mn ferrite films, thermal, treatment effects 8=31817
- β_1-MnZn films 8=27451
- Ni ferrite films, rel. to structural props. 8=36192
- Ni film rel. to internal stresses and magnetization inhomogeneity, obs. 8=31821
- Ni, linewidth temp. dependence, 300–1000°K 8=31815
- Ni-Fe alloy film, linewidth and relax. processes for main resonance in spin-wave spectra 8=40887
- Ni-Fe alloy films, and domain-wall losses 8=31695
- Ni-Fe films, rel. to magnetoelastic coupling obs. 8=31820

Ferromagnetic resonance—contd
- NiFe$_2$O$_4$ films, rel. to thickness 8=31823
- Ni–Zn ferrite, and non-linear effects 8=31819
- YFe garnet, magnetoelastic instability in uniform precession 8=36221
- YFe garnet, nonlinear, self-modulation anisotropy 8=45069
- YFe garnet, rel. to crystallographic anisotropy 8=31826
- YFe garnets: Fe^{4+}, linewidth temp. dependence, 4.2°–300°K at 10 and 25 kMc/sec. 8=31827
- YFe garnet: Si, temp. dependence, 4.2–400°K at 10 and 30 GHz 8=31825
- YFe garnet: Tb^{3+}, linewidth rel. to energy levels, wave functions and relax. times 8=31824
- Y$_3$Fe$_5$O$_{12}$, effects of rad. defects from U^{235} fission fragments 8=36225

Ferromagnetics. See Magnetic properties of substances/ferromagnetic.

Ferromagnetism

See also Antiferromagnetism; Ferrimagnetism; Ferromagnetic relaxation; Ferromagnetic resonance; Magnetic properties/ferromagnetic; Magnetization process; Magnetization state.
- absence in one and two dimensions in many-band model for interacting electrons in a metal 8=44993
- anisotropic field and position of easy magnetization axis in cylindrical magnet, meas. method 8=40785
- anisotropy and field dependence, induction meas. method 8=31560
- anisotropy temp. dependence 8=31561
- atomic and electron theory 8=49460
- band model, stability 8=31542
- band theory, dipolar corrections to magnon energy 8=31539
- band theory, soluble model 8=27388
- chain of spins $\frac{1}{2}$, susceptibility in oscillating field, calc. 8=44997
- cristobalite lattice, Ising model high-temp props. 8=31570
- critical fluctuations, dynamics 8=37179
- crystals, magnetization curve rel. to uniaxial lattice deform. 8=36104
- domains in films, individually obs. by e-microscope 8=31586
- dynamical critical exponent in isotropic system near transition temp. 8=31553
- electrons, itinerant, with strong correlations 8=49486
- ellipsoidal specimen, internal mag. field recording 8=46372
- energy-band theory 8=31545
- equation of state in critical region 8=31536
- excitations, kinematic and dynamic interactions 8=40759
- Fermi liquid, phase transition 8=35803
- film magnetization, thickness-, anisotropy-and temp.-dependence 8=36116
- films, band structure 8=36117
- films, Néel wall structure model 8=31584
- films, thin, coupling effects through nonmag. interlayer 8=31588
- fine-particle assemblies and thin films, interaction effects 8=36130
- fine-particle theory, fundamental theorem 8=31548
- four-axial, soln of (71°/180°) Bloch wall 8=49503
- in gases, real, conditions 8=34668
- Green function theory first-order 8=49488
- Green's function theory of 2-spin system and teaching appls. 8=40769
- hard-particle systems model 8=49496
- Heisenberg, as an example of quantum field theory 8=36093
- Heisenberg magnet, rotational invariance constraints on Green functions 8=27393
- Heisenberg model, magnon-density fluctuations 8=31551
- Heisenberg model, ultrasonic attenuation near critical point 8=39885
- impurities, non-magnetic, in lattice rel. to local magnetization of neighbouring ions 8=36105
- indirect exchange theory, impurity influence 8=36066
- Ising chain, basic cluster in effective field theory 8=40774
- Ising decorated lattice, 2 phases separated by paramagnetic phase 8=49493
- Ising ferro- and antiferromagnet, spin pair correlation function 8=40779
- Ising ferromagnets, correlation functions, critical behaviour 8=49487
- Ising lattices, impurities and defects effects 8=41758
- Ising lattice with impurities 8=40773
- Ising model, critical behaviour above and below critical temp. 8=36084
- Ising model, finite size effects at critical point 8=27395
- Ising model, inequalities satisfied in mag. field 8=36089
- Ising model, 3-dim., sp. ht. below T_c 8=48731
- Ising system, inelastic n scatt., temp. and freq. depend. 8=31571
- isotope effect in weak itinerant ferromagnets 8=45032
- itinerant electron model for very weak ferromagnets, appl. to ZrZn$_2$ 8=31547
- itinerant electrons, mag. props. 8=40762
- Lorentz microscopy, contrast linked to relief in films 8=45002
- magnetization anisotropy due to screw dislocations 8=40790

Ferromagnetism—contd
- magnetization field near frontal plane rel. to domain formation 8=31554
- magnetization process in polycryst. ferromags., phase model 8=36103
- magnetostatic uniform screening of shells 8=37379
- magnon interaction with longit and transverse phonons (Ho) in [111] direction 8=31567
- magnon-magnon and exciton-magnon interaction effects on antiferromagnetic spectra 8=40843
- magnon-magnon interactions evidence 8=40875
- magnon-phonon interaction rel. to acoustic wave velocity changes 8=30937
- many-spin systems, dynamical spin correlations rel. to sublattice orderings 8=36091
- metals, wave functions symmetry in one-electron band theory 8=44990
- neutrons critical mag. scatt., theory 8=36096
- n.m.r. theory 8=40964
- Permalloy thin films, exchange stiffness const. by pulse switching technique 8=31686
- phenomenological theory near critical points 8=44989
- phonon-paramagnon interactions, effect on u.s. attenuation 8=48714
- polar model, theory 8=40766
- powders, susceptibility calcs. in weak field, model 8=40800
- prolate ellipsoid of revolution in longit. alternating mag. field 8=36092
- sample, free at one end, Procopiu acoustic effect 8=45001
- s-f, dynamic effects of conduction electrons 8=27391
- specific heat, smoothness near critical temp. due to random impurities 8=44987
- spin-$\frac{1}{2}$ Heisenberg ferromagnet, high-temp. susceptibility, Green function theory 8=40770
- superexchange and direct interactions, model calcs. 8=31749
- superexchange in binary mixtures with one mag. component, statistical effects 8=27438
- transitions between uniformly and nonuniformly magnetized states, thermodynamics 8=40788
- uniaxial antiferromagnet, magnetization curve, influence of second uniaxial anisotropy constant 8=36203
- Weiss mol.-field theory, modified rel. to short-range mag. order 8=44991
- Cr chalcogenide spinels, exchange interaction, night-angle nearest-neighbour, systematics 8=31748
- Fe fractionation in solar system 8=28135
- Pt-Mn alloys, and atomic structure 8=26432

spin-wave theory
- Bose operator, applic. to Heisenberg model 8=49495
- complex structures with dislocations, spin wave scattering and thermal conductivity 8=39936
- core polarization in 4d^n and 5d^n configs. from e.s.r. data 8=36087
- critical props., rel. to spin dimensionality 8=27390
- crystals, generating microwave acoustic waves 8=49508
- cubic lattice with dislocations, energy spectrum and local states 8=40761
- dynamics of critical fluctuations 8=44984
- exchange excitation, rel. to guided wave propag. in gyromag media 8=28619
- exchange interactions in magnetic insulators 8=40777
- exchange interactions, orbital effects 8=31544
- Fermi liquid, temp. depend. of susceptibility, contrib. of paramagnons 8=28337
- ferrimagnets, and ferromag. reson. 8=49579
- ferromagnet, quantum wave mechanics 8=40778
- films, Curie temp. thickness depend 8=31576
- films, resonance 8=36114
- films, thin, saturation 8=36113
- films, thin, stationary wave excitation 8=31587
- films, thin, surface anisotropy and pinning 8=31591
- films, with domain structure 8=40798
- Heisenberg chain thermal conductivity, $0 \ll T \ll \infty$ 8=39938
- Heisenberg (classical) model, configurational exam. rel. to critical phenomena 8=31538
- Heisenberg ferromagnet, interactions 8=31543
- Heisenberg ferromagnet, spin-1/2, Green function theory 8=36086
- Heisenberg linear chains finite, time correlations rel. to mag. resonance linewidths 8=31549
- Heisenberg magnet, space-time correlation functions, divergences in one-dimension 8=44988
- Heisenberg magnet, thermodynamic props for arbitrary spin 8=49490
- Heisenberg model, correlation functions, computer calcs. 8=31550
- Heisenberg model, distrib. function and thermodynamics 8=44983
- Heisenberg systems, two-dimensional, expt. verification of spin-wave predictions 8=36088
- Heisenberg, with impurities, sp. ht. calcs. 8=35422
- impurity-induced spin-ordering above Curie temp. 8=49500
- Ising lattices, decorated square and triangle with anisotropic couplings, 3 transition temps. 8=49492
- Ising model, configurational exam. rel. to critical phenomena 8=31538
- Ising model, convergent, bounding, approx. procedures rel. to crit. phenomena 8=31537

Ferromagnetism—contd
  spin-wave theory—contd
    Ising model dynamics near critical point 8=27396
    Ising model, two-dimensional, exact freq. -dependent susceptibility 8=31546
    Ising spins statistical system, ordering rel. to type of magnetism 8=40772
    itinerant electron model, temp. depend. of energy 8=31540
    localized system oscillations, two types, in ferromagnets with plane defects 8=44986
    Mandel'shtam-Brillouin effect 8=36095
    many-spin systems, dynamical spin correlations 8=36091
    metal, model 8=40765
    metals, almost ferromag., impurity effect on spin fluctuations 8=40764
    metals, local-moment-conduction-electron exchange coupling and RKKY spin densities 8=35742
    metals, using perturbation theory 8=49498
    Mössbauer absorpt. spectra rel. to spin relax. 8=43940
    in narrow bands 8=31541
    neutron scattering by parametrically excited spin-waves 8=36094
    nonlinear excitation 8=44985
    ordered magnetic bodies description 8=49499
    parametric processes in medium with space-time periodicity 8=40776
    phase transition of Ising spin systems, effect of lattice vibration 8=36098
    quasi-stationary state-phonon interactions 8=40775
    rare-earth metals, and mag. reson: thermal, applied field and magneto-elastic effects 8=31703
    semiconductors, indirect exchange interactions, intervalley transitions effect 8=40768
    semiconductors, many-valley, indirect exchange inter-actions 8=36085
    single crystals with plane defects, spin excitation 8=31552
    specific heat, spin-fluctuation contributions 8=30960
    spin-correlation function, time-dependent 8=36090
    spin-correlation functions, calc. using Monte Carlo method 8=49494
    in thin films, eigenvalues of energy and amplitudes 8=49512
    spin system, effect of free crystal surface 8=27389
    stability rel. to antiferromag. under s-f interaction 8=40767
    strongly coupled waves, model, connection with coupled oscillators 8=49489
    thin films, standing spin waves 8=49510
    in 3d metals 8=31627
    transient processes with three-magnon non-linear transitions, quantum mechanical treatment 8=49497
    unstable modes, meaning 8=44994
    Co, thermal neutrons, critical scattering 8=31626
    $CoPt_3$, 3 optical and one acoustical branch 8=31649
    Fe, spin diffusion constant, temp. depend. 8=40812
    Fe, thermal neutrons, critical scattering 8=31626
    Fe-(Mn, Er), dilute, neutron scattering, inelastic, by virtual magnon states 8=31625
    Fe-Ni alloys, dispersion relation 8=31624
    He^3, solid, antiferromagnetic, nuclear spin exchange interaction 8=31774
    K 8=31659
    K_2MnF_4, zero-point spin reduction 8=27445
    Na 8=31659
    Ni, and Stoner modes and critical fluctuations 8=36215
    Ni, thermal neutrons, critical scattering 8=31626
    Ni-Fe films, magnetoelastic coupling obs. by spin-wave reson. 8=31820
    Pd-Fe alloys, stiffness constant field dependence 8=45026
Ferromagnets. See Magnetic properties of substances/ ferromagnetic.
Feynman diagrams. See Field theory, quantum/interactions.
Fibre optics. See Optical systems.
Fibres
    alumina, for plastic resin reinforcement 8=26857
    banana, normal and treated, X-ray study 8=48359
    bending strength, three-point tester 8=31172
    broken, in composite materials, load transfer 8=48975
    coir, X-ray diffraction study, spiral orientation and cell walls 8=48358
    cylindrical, zeta potential determ., streaming current relationship 8=41271
    deoxycholic acid, X-ray exam. 8=26491
    fibre-reinforced composite, unidirectional, elastic consts. calc. 8=48942
    fibrous structures with steric constraints 8=30400
    glass, as light guides, technology of manufacture 8=28761
    glass, optical, sintered thermal expansion 8=39925
    glass, optical, viscosity rel. to concentric casings 8=39631
    α-keratin, matrix-microfibril texture, by X-ray diffraction and electron microscopy 8=39729
    orientation distrib. calc. formulae 8=44178
    poly(ethylene terephthalate), birefringence, influence of crystallinity and orientation 8=44175
    polymers in soln. and in films, fibrillar structure 8=26153
    polypropylene, structural changes in stretching process 8=49057
    purification for electronmicroscopic prep. 8=48360
Fibres—contd
    pyrolytic products, mass spectroscopy 8=36632
    rayon, n. m. r. of adsorbed H_2O 8=27508
    sisal, normal and treated, X-ray study 8=48359
    stress, strain and deplacement fields analysis in composite material reinforced with discontinuous fibres 8=46049
    thermal cond., effective, of mats. with irregular struct. 8=35452
    vapor-deposition effect on replication in electron microscopy 8=39707
    wood, small and wide-angle X-ray diffr. patterns 8=26047
    B, internal friction and shear modulus, amplitude dependence 8=40131
    C, recrystallization, Ni stimulated 8=35236
    Fe-50 Ni, reinformemnt rel. to mech. and mag. props. 8=31209
    Fe-1, 35Si, reinforcement rel. to mech. and mag. props. 8=31209
Field emission. See Electron emission/field emission.
Field emission microscopes. See Electron microscopes; Ion microscopes.
Field theory, classical
      See also Electromagnetism; Gravitation; Relativity.
    counterparts of quantum operators 8=32673
    crystal, anharmonic, thermodynamic props. and quantum theory, book 8=30954
    density-fluctuation approach to plasma 8=34462
    electromagnetic director, derivation by Fourier analysis 8=41944
    electromagnetic, mathematical models, book 8=33054
    gauge fields with noninvariant interactions 8=32776
    group of motions of a straight line and field geometrical theory, 8=37117
    electromagnetic, energy and momentum nonlinearity 8=37403
    infinite systems, formalism of creation and annihilation operators 8=28238
    Lehmann-Källen representation, rel. to Schwinger terms 8=24613
    Petrov space type determination 8=32793
    Riemannian space with elliptic slot, Green's function and boundary value problems soln. 8=32711
    scalar field, characteristic values, Cowar limits 8=32683
    semiclassical analysis of weakly coupled reson. systems, validity rel. to zero-point oscills. 8=32674
    slip-line, algebraic geometry, appl. to boundary-value problems 8=23806
    two-dimensional problems, solution by boundary relaxation 8=45994
    vector eqns. obtained using variational principles and tensor analysis 8=32672
    Yang-Mills fields, internal holonomy groups 8=28237
Field theory, quantum
      See also Dispersion relations; Elementary particles: Physics fundamentals; Quantum theory.
    Adler-Weisberger sum rules and $D_{13}D_{13}$ coupling constant 8=33534
    algebra of fields, and divergent part of hadron e.m. mass difference 8=24744
    algebra of spin currents, field theoretical model 8=24603
    algebraic, C* bundles and a possible set of axioms 8=33360
    analyticity in momentum transfer in pot. theory 8=37832
    anharmonic oscillator, field theoretic functional calculus. 8=28942
    axial vector currents, for S and P-wave scatt. 8=42376
    axiomatic, adiabatic hypothesis 8=46836
    axiomatic foundation 8=24490
    axiomatic, Green's functions, (non) renormalized 8=28963
    axiomatic method, dynamic apparatus problem in 8=46837
    axiomatic, observable currents 8=42332
    axiomatic quantum mechanics, lattice of decision effects 8=33359
    axiomatic rel. to Chiral SU(2) ⊗ SU(2) symmetry 8=42378
    axiomatic, validity of current algebra in quasi-local terms 8=37770
    Bethe-Salpeter amplitude singularities 8=42334
    Bethe-Salpeter amplitudes decomposed into standard covariants and invariant amplitudes 8=37848
    Bethe-Salpeter equation, spectra of massless and zero energy-momentum solns. 8=46829
    Bethe-Salpeter eqn., use for asymptotic behaviour of graphs in $\lambda \phi^4$ theory 8=42323
    birefringence, optical, induced by elec. fields 8=33340
    book, introduction to advanced field theory 8=33349
    Born-Infeld classical and quantum S-matrices 8=46826
    boson fields with nonlinear selfinteraction in two dimensions 8=24482
    broken symmetry rel. to massless particles 8=42377
    bubble diagrams, singularity props. 8=24491
    causality conditions applied to elementary particle interactions 8=29046
    chiral-dynamic-Lagrangian calc. of $\chi \rightarrow \eta\pi\pi$ 8=42605
    Clebsch-Gordan coefficients, calc. of product sums 8=46838
    Clebsch-Gordan series for SO_5, SO_4, Sp_4 and G_2, deriv. 8=33362
    complex scalar, Ricci tensor conditions 8=24476
    composite particle field, elimination of coupling constant singularities and ace perturbation theory 8=33521

Field theory, quantum—contd
composite particles described as fields 8=42372
conservation laws mirror relations as nondynamical test 8=24685
conserved charge operators, additivity 8=37829
C violation in η decay 8=24816
CP invariance model within current-current form of weak interactions 8=42325
CP non-conservation and intermediate boson hypothesis 8=37837
CP-nonconserving phase angles, isospin selection rules 8=24484
CP selection rules for e^+e^- annihilation 8=37941
CP violation 8=33544
CP violation in behaviour of weak currents in Han–Namliu model 8=33524
CP violation in current × current weak interaction 8=37877
CP violation in η, K decay 8=24816
CP violation in $K \to 2\pi$, current-current models 8=42575
CP violation in weak interactions and intermediate vector mesons 8=24845
CP violation model from vector meson e.m. interaction 8=29119
CPT invariance in $K \to 2\pi$, π-π phase shift anomaly 8=24815
CPT restriction on $K^\circ \to 2\pi$ 8=42581
CPT test in $K_L^\circ \to \pi^\pm \mu^\mp \nu$ $K_L^\circ \to \pi^\pm e^\mp \nu$ 8=42568
crystal, anharmonic, thermodynamic props, and classical theory, book 8=30954
current algebra, Ward identities and space-space equal-time current commutators 8=42485
current density, quantized, equal-time commutation relations deduced from tensor products of Lie group 8=24599
cutoff, limiting process and auxiliary fields 8=24469
$\Delta S = -\Delta Q$ rel. to $\Delta S = 2$ leptonic decays
differential cross-sections of scattering cross-reactions of particles with arbitrary spin 8=37879
Dirac spinors, covariant currents and Lorentz group 8=33350
and dispersion relations, book 8=28951
Dyson representation in current algebra 8=42336
edge of the wedge theorem, generalized for boundary on an analytic curve 8=32648
e.m. meas. shifts and their relation to equal time commutators 8=37761
elementary length, upper limit 8=24601
elementary particles, and general relativity with cosmological const., vacuum props. 8=28292
Euclidean invariant, correspondence principle between quantum and classical generators 8=28948
Fermi systems phase transitions 8=46823
Feynman diagram analysis of Compton effect, sum rules 8=37918
Feynman diagram, applic. to He-3 reaction with light nuclei 8=38516
Feynman diagram for $\pi \to \mu + \nu$ perturbation theory 8=29121
Feynman diagram for Regge pole coupling 8=29068
Feynman diagram, 2γ, A-meson contrib. rel. to discrepancy in h.f.s. of H 8=33743
Feynman diagrams, behaviour of very-high-order perturbation 8=33363
Feynman diagrams model of relativistic quantum mechanics, Fubini identities rel. to currents 8=24610
Feynman diagrams, Reggeon elementary particles 8=28964
Feynman integral and duality with perturbation term of Wightman function 8=42338
Feynman integrals, homological approach 8=24493
Feynman integrals, homology 8=33338
field-current identities, broken symmetries and gauge invariance 8=42319
Froissart model, nonunique canonical formalism 8=24477
Gell-Mann-Okubo mass formula and sum rules derived 8=24625
generalized free field, possible candidate for broken symm. 8=28957
gravitation, canonical method 8=41750
gravitational field theory 8=32820
Haag-Ruelle of asymptotic fields, processes defined by off-mass-shell part of field operator 8=24471
Heisenberg ferromagnet 8=27394
and Heisenberg ferromagnet 8=36093
higher-spin wave enqs., consistent when interacts are included 8=33515
Josephson junctions, fluctuation phenomena 8=27050
Klein-Gordon eqn., consutruction of solvable potentials 8=33319
Lagrangian, effective, construction rel. to chiral group $K_3 = SU_3 \times SU_3$ 8=33341
Lagrangian theory appl. to compositeness conditions for particles 8=33550
Lagrangian, treatment of vector mesons as composite particles rel. to e.m. mass difference 8=37869
Lagrangian Zachariasen model, anal. of graphs with propagator insertions 8=42324
$\lambda\phi^3$, Regge poles generated by ladder diagrams, mixing with cuts 8=33591

Field theory, quantum—contd
$\lambda\phi^4$, renormalization scheme 8=24472
in lattice space, calc. of Gelfand functionals, and other props. 8=33354
lattice space, strong-coupling perturbation 8=33345
lectures by Dirac 1963-64, book 8=28952
Lee model, interpolating fields for V-particles 8=37867
linear transformations of field operators 8=28950
Lippmann-Schwinger eqns., approximation schemes 8=42335
local field construction for many masses and spins 8=42333
local infinite-component, non-existence demonstrated 8=24597
local one particle approx. for matrix elements of two four vector currents 8=33530
local properties of unrenormalizable theories 8=37760
Lorentz covariant field eqns., sets of solns. for infinite no. of field components 8=33352
Lorentz invariant distribs. and scale transforms., spectral representations, application 8=32792
magnetic moments, Coleman-Glashow formulae, corrections for symmetry breakup 8=42383
many-body theory, applic. of Feynman graphs 8=37771
mass operator, relativistically invariant, geometrical interpret. 8=37855
mass renormalization, automorphism of algebra of field operators 8=37856
massless particles with definite helicity, not weakly localizable 8=47018
measurement anal. in micro-and macrophys., and space extensions 8=28213
methods, review 8=24479
model for daughter Regge trajectory 8=42428
model with spectral functions of fast increase 8=24483
Neumann algebra and translation group unitary representation, Araki theorem, proof 8=33361
with N and Roper resonance symmetrical, compositeness conditions 8=24480
non-relativistic, connection between singularities of matrix elements and physical S-matrix 8=37759
off-mass shell methods for S and P-wave scatt. 8=42376
para-Fermi, nonrelativistic, state vector props. 8=42320
parafield transformation to a system of two fields obeying isotopic symm. 8=46825
partially conserved dilatation current 8=33528
partial-wave unitarity integral evaluation and N/D scatt. method appls. 8=29065
particle-like solns. internal dynamics leading to quantum dynamical predictions 8=28953
particle symmetries and measurement, Pisa Conference, 1964 8=24609
Pauli principle, model of dynamical theory 8=33519
phenomenological Lagrangian method calc. of Compton scatt. of isovector photons with nucleons 8=37920
pole of two interacting spinless particle Green function 8=24602
potential strength analyticity 8=24475
primitive domain, scatt. amp. analyticity rel. to micro-causality and Meyman locality 8=37762
Proca theory, equivalent to Weinberg's spin-one theory 8=33355
quasipotential construction in some models 8=46828
Regge families in zero mass exchange 8=47035
rel. to isobar masses and coupling consts., dispersion sum rules 8=29035
relativistic amplitudes, Poincaré and Lorentz invariant expansions 8=46831
relativistic, composite particles and perturbation expansion 8=46830
relativistic and CP invariances 8=24612
relativistic Lagrangian for composite systems 8=42322
relativistic, symmetry rel. to Coulomb problem double degeneracy 8=37840
saturation of sum rules in strong-coupling theory 8=33342
scattering, non-relativistic, S matrix cluster decomp. in time separated expts. 8=28944
scattering, quasi-potential approach and expansion in relativistic spherical functions 8=33573
scattering, quasi-potential equations, relativistic, particles with spin 8=33574
scattering, Regge pole contrib. to direct-channel amplitudes 8=33597
scattering, time-dependent variational principle 8=33346
Schrodinger equation for particle with arbitrary spins, relativistic 8=33516
Schwinger terms directly from local currents 8=33343
semi-definite metrics 8=28955
Snyders space-time theory generalization 8=28954
statistics, generalized, difference of field and quantum theory formulations 8=42318
stochastically averaged intermediate-time, scalar, condition for satisfying equal-time commutation relations 8=24481
SU(2, 2), irreducible representations, finite and infinite dimens. 8=28232
SU(3) breaking enhancement, Regge theory 8=42315
SU_3, broken sum rules in coupling constants from meson-baryon interactions 8=37958

Field theory, quantum—contd
SU(3) representations 8=33348
$SU_3 \times SU_3 = K_3$, fields with nonlinear transformation laws, construction of effective Lagrangian 8=33341
tensor fields, spectral function sum rules 8=38027
three-body system rel. to nuclear forces 8=33863
3-photon absorpt., coherence effect 8=42316
time reversal in weak N-N interactions 8=24875
T-invariance test through $Mg^{24} + \alpha \rightleftharpoons Al^{27} + p$ 8=43088
T-nonconservation in Mossbauer effect in Ir^{193} 8=25156
Toposanski theorem, generalization 8=33351
tree approx. correspond to semi-classical approx. appl. to S-matrix 8=24492
2-body compound systems, relativistic and nonrelativistic pot. scatt., and Bethe-Salpeter model 8=37825
2-dimensional, Lorentz invariance breakdown 8=42321
unitarity rel. to spin-family soln. 8=24473
unitarity restriction on $K^\circ \to 2\pi$ 8=42581
unitary transformation of Foldy-Wouthyusen Hamiltonian to laboratory system 8=29025
U(p, p) ladders, physical multiplets assignment consistent with U(6, 6) 8=24618
U(p, q) ladder representations coupling, local and global props. 8=24617
U(p, q) ladder, tensor product of two, existence at most of one ladder 8=24618
vacuum quantum fluctuations rel. to theory of gravitation 8=37165
vector field, neutral, from which photon field eqns. may be derived 8=33716
W*-algebra, non-abelian, sequential convergence 8=32654
weak interaction and e.m. currents, identified with boson field 8=29106
weak, interaction theory, difficulties 8=33566
Weinberg's spin one particles, equivalence to Proca theory 8=33355
Wightman functions' holomorphy envelopes, upper bounds 8=28958
Wigner coefficients of SU(1, 1) 8=33347
Yang-Mills bosons, and CP violation in weak interactions 8=24845
Yukawa coupling of fields in two dimens. 8=28949
Zachariasen model, possible condidate for broken symm. 8=28957
zero-charge problem and nonlocalizable theories 8=46824
electromagnetic field. See Quantum electrodynamics.
interactions
See also Elementary particles; Nuclear reactions. Entries on interactions involving named particles are listed under the particles concerned.
approximate formulation using direct mathematic methods 8=46840
axial-vector current partial conservation and Kawarabayashi-Suzuki-Riazuddin-Fayazuddin sum rule 8=33717
Bethe-Salpeter eqn. for π-N, bound-state solns. 8=42534
Bethe-Salpeter eqn., for two scalar particles, appl. of Riemann method 8=33557
Bethe-Salpeter eqn. solns. in ladder approx. with Padé approximants 8=47112
collision matrix, unitary pole resonance form 8=24667
conspiring trajectories, classification by SU(3) and Lorentz-pole symmetries and exchange degeneracy 8=37885
current divergence and equal-time commutation, quark model 8=33529
Dirac, e. m. and meson fields interacting 8=38015
e. m., analytic behaviour, inconsistencies of Fubini-Dashen-Gell-Mann sum rule resolved 8=29015
Fermi-odd interactions, applic. of Wick theorem 8=42393
Feynman diags. for first and second orders for some states of light atoms 8=38657-8
Feynman diagrams of 1st and 2nd orders of light atoms 8=47472
Feynman graphs, asymptotic behaviour of amp. in two-to-three particle conversions 8=37902
fireballs, lifetime possibility 8=29042
internal symmetry and C, P, T operations 8=37870
Jansen perturbation theory of intermol. exchange 8=43428
Lie fields, relativistic, absence of interactions 8=33344
negaton-positon, quasipotential approach 8=24719
operators, general soln. 8=24478
π conspiracy in $t = o$ region, dynamical model 8=33661
scattering amplitude, relativistic, quasipotential type equation 8=37886
scattering, potential, N/D method 8=33586
semi-strong C violation with $\Delta I=3$ 8=29032
three-body problem with Lee-type interaction 8=24639
three-particle prod. amp, compared with two-particle reaction amp. 8=37902
two-body, differential cross sections, optical model 8=29041
interactions, strong
Bethe-Salpeter eqn., variational solns. 8=37873
cross-section preasymptotic behaviour, Bethe-Salpeter calc. 8=29028
fireball prod. in framework of peripheral interact. theory 8=29048
gauge theory, specialized to SU(3), appl. to vector meson system 8=42604

Field theory, quantum—contd
interactions, strong—contd
hadronic currents rel. to self-induced strong interactions 8=29111
Marchenko formalism rel. to N/D eqns. 8=24670
multiple-prod., Dolen-Horn-Schmid duality and Deck effect 8=33559
N/D eqns., crossing-symmetric, solns. 8=24801
Padé approximants, nice features 8=24470
possibility for intermediate boson 8=24643
S-matrix, analytic theory 8=37872
SU(2, 2) with infinite multiplets 8=33562
interactions, weak
ang. mom. requirement for Kronecker δ in current algebra 8=24647
broken symm. leading to massless photons and gravitons 8=33520
Cabibbo theory from vector meson-lepton-neutrino coupling constant 8=33568
CP-noninvariance 8=24649
CP-violating weak currents 8=24814
CPT-invariance test 8=46827
current-current form, model for CP invariance 8=42325
current × current which conserves vector current, universality, CPT but violates CP 8=37877
cut-off rel. to $K_L^\circ - K_S^\circ$ mass difference and $K_L^\circ \to \mu^+\mu^-$ decay 8=33700
$\Delta I = 1/2$ rule in nonleptonic decay 8=37859
$\Delta I = 3/2$ effects in $\Sigma^\pm, K^\pm$ nonleptonic decays 8=29151
Fubini-Dashen-Gell-Mann sum rule inconsistencies solved 8=29015
hadrons with neutral lepton currents 8=29110
intermediate-boson field and e.m. field derivative, symmetries 8=42389
leptonic currents, neutral, normal and strange 8=24708
minimal e.m. extension, use in deriv. of current algebra eqns. 8=42515
nonleptonic, experimental test of current-current nature 8=24711
non-leptonic, parity- and strangeness-changing, unitary struct. 8=37875
non-leptonic rel. to e. m. mass difference of hadrons 8=24744
nuclei, "elementary particle" model 8=33955
peratization of vertex rel. to W-meson 8=46839
radiative, vector current conservation 8=37876
S-matrix formulation, 8-dimensional space 8=47025
S-operator theory of weak interactions 8=37874
two-photon annihilation, charged intermediate vector bosons 8=29161
universal primary interactions 8=24638
rel. to (V + A) currents 8=33565
meson field
See also Mesons; Nuclear forces.
C invariance, obs. of $\eta \to \pi^+\pi^-\gamma$ 8=42590
C invariance test in $\eta \to \pi^+\pi^-\pi^0$ obs. 8=42591
chiral symmetry, Gürsey models 8=42445
e. m. and Dirac field, interactions 8=38015
infinite mass renormalization, some consequences 8=24850
model of N-N interacts. 8=24868
pseudoscalar theory, contraction on SU(9) to give isobar series 8=29034
N, oscills. rel. to e.m. props. and e excitation spectrum 8=29180
vector meson decays, current-density-current-density commutators 8=42337
vector meson, deviation from SU_6 symm. 8=29168
vector meson, employing more general functional derivatives for vector mesons 8=29164
quantization
See also Quantum theory/quantization.
autocomposite particle eqns. 8=29019
elementary particle, model representation 8=42370
generalized procedure 8=28965
gravitational field, modified general relativity theory 8=32819
massless of arbitrary spin, transformation of pot. 8=28956
particles with any spin and internal symmetry, second quantization process 8=42363
Films
Bingham plastic surface flow anal. in canal viscometer 8=30343
fluid, thin, disjoining pressure 8=30195
molecular layers, regular deposition 8=43921
monolayers, role in retardation of evaporation 8=39486
optics, amplitude superposition and boundary condition methods 8=42244
GaP p-on-n liq.-phase epitaxial layers in prep of electroluminescent diodes 8=41229
He II, phase transition 8=24043
Hg monolayer ellipsometer, surface tension and contact pot. obs. 8=48061
Na, intensity of heat transfer in film condensation of pure vapour 8=48132
liquid
See also Adsorbed layers; Contact angle; Helium/liquid; Superfluidity; Surface tension.

Films—contd
liquid—contd
bubble "microtome" for sampling liq. surface 8=30380
condensates on surface normal to body forces, flow rel. to variation in hydrostatic press 8=34989
contact angles rel. to London-van der Waals forces 8=25859
dielectric, a.c. breakdown voltage 8=48178
explosive, shock sensitivity, detonation initiation and propag. 8=34748
falling, mass transfer at low Reynolds numbers 8=34745
flow down inclined plane, ridge instability due to elec. field 8=34747
free, with diffuse elec. double layers, shape fluctuations 8=30394
hydromagnetic stability down an inclined conducting plane 8=28592
laminar rippling, gas absorption rates, method 8=48053
Marangoni, hydrodynamic stability 8=48052
mass transfer through films in wavy motion 8=39327
menisci, advancing, deformation 8=48103
micropolar, flow down inclined plane 8=30391
monolayer, on aqueous substrates at low surface pressures, circulation 8=34746
n-octa decanoic acid on metal oxide, wettability rel. to heat treatment of surface 8=48050
n-octadecyl alcohol on metal oxide, wettability rel. to heat treatment of surface 8=48050
n-octadecylamine on metal oxide, wettability rel. to heat treatment of surface 8=48050
non-Newtonian, flow and heat transfer over rotating surface 8=30392
packed columns, gas absorption, correlation of gravitational force 8=50003
polar, orientation by cell surface elec. fields i.r. absorpt. obs. 8=39302
radius of draining film beneath drop approaching plane interface 8=30381
rupture due to fluctuations in thickness 8=48051
soap, solvation forces 8=27686
solid surfaces, removal from, interfacial mechanism 8=39608
on surface of other liq., suppression of wind-generated waves 8=48037
surfactant, surface tension gradients and Gibbs elasticity 8=30445
thickness meas., mag. reluctance technique 8=39287
ultra-thin free films, light scatt. techs. for meas. of van der Waals-Hamaker pots. 8=30393
visco-elastic, flowing down inclined plane, stability 8=43745
water n-alkane interface, ideal gaseous behaviour of Na alkyl sulphates 8=30395
C_{16}-OH, monomol., surface viscosity rel. to phase transitions, 15-30°C 8=30428
C_{18}-OH, monomol, surface viscosity rel. to phase transitions, 15-30°C 8=30428
C_{20}-OH, monomol, surface viscosity rel. to phase transitions, 15-30°C 8=30428
C_{22}-OH, monomol. surface viscosity rel. to phase transitions, 15-30°C 8=30428
He, discrete flow rates obs. 8=24042
solid
See also Magnetic films; Optical films; Thickness measurement.
alkali-antimonide, photocathode formation, quartz-crystal microbalance technique 8=40683
anodic oxide, on Al, growth mechanism by electron microscope obs. 8=44032
antireflectant, behaviour, theoretical interpretation 8=42243
carotene, absorpt. spectra, effect of gas adsorpt. 8=49773
cellulose acetate, i.r. spectra 8=32048
cellulose, dimens. stability rel. to orientations of phases 8=39634
cellulose, Du-Pont K116-207, fracture toughness, obs. 8=44614
charged, anomalous interference of electrons on edge 8=44030
coating on Cu single crystals, surface damage rel. to strengthening effects 8=40150
coating thickness, beta backscatter meas. 8=48436
collagen, hydrated, d.m.r. 8=49639
complex coatings, effect of decomp. non-uniformity on thermal conds 8=30958
conductors in longit. mag. field, impedance calcs. 8=26955
conductivity, elec., 4-point Hg contact probe 8=41907
copper oxide, epitaxial growth by ion bombardment 8=26116
covered symmetric contacts, tunnel and thermionic currents 8=40628
crystal, epitaxially grown, effect of gaseous etchants 8=30754
crystal violet, photocapacitance and photocurrent "memory" 8=36032
crystalline polymers, optical transmission obs. 8=45245
crystallization from mol. beams, transfer calc. 8=30737
deposition of films thicker than 1μ on optical component surfaces 8=44034
deposition, phase transitions, during and after 8=39544-5

Films—contd
solid—contd
detector films from polyvinyl alcohol 8=24978
dielectric coating on opaque substrate, reflectance to monodirect. flux 8=31935
diffused layer redistribution during epitaxy and other process steps 8=48441
dynodes, mechanical props. 8=31161
electrical negative cond., in transverse mag. field, mechanism 8=40300
electrical parameters meas., contactless method 8=49134
electrodeposited, substrate preparation 8=35177
electroluminescence, d.c. excitation 8=36521
electronic components, conference Washington U.S.A. (1968) 8=31416
electron images, transmitted, scanning microscope exam. 8=30735
epitaxial crystallization from at. beams, mechanism 8=39698
epitaxial layers, thickness meas. with infrared beams 8=26108
epitaxial, on mica and NaCl substrates, stresses causing film curling 8=35157
epitaxial overgrowths, site exchange processes 8=44151
epitaxic, impurity distrib. 8=26208
evaporated, magnetic perpendicular anisotropy 8=36108
evaporated, thickness distrib. reproducibility 8=35151
ferroelectric, bending on polarization 8=40608
ferromag. thin, saturation magnetization 8=36113
ferromag. thin, superparamag. effects 8=36111
field-emission cathode, structure, fabrication, performance and e.-micrography 8=40696
foil target, thickness meas. by Rutherford scatt. 8=46850
granular, optical props. 8=27521
insulating, anomalous e. diffr. patterns due to secondary e. emission 8=48587
insulating, Schottky current, negative space-charge effect 8=44901
insulating, space-charge conduction theory 8=49327
i.r. interf. filters, props. 8=32937
laser material coatings, single layer antireflection, mismatch 8=42060
lattice vibrations, electron diffraction examination 8=35387
magnetic, holograms recording and reconstruction 8=33294
magnetic interaction effects 8=36130
magnetic multilayered, coupling 8=36133
magnetic storage cells using domain propag. 8=24117
magnetic, switching process 8=36115
malachite green, photocapacitance and photocurrent "memory" 8=36032
metal, cubic, thermally induced strains 8=40122
metal deposits, thermal conductivity coeff. 8=35453
metal, e.m. power-transmission coeffs., 8=49698
metal, epitaxial, elec. field effects on growth 8=26109
metal epitaxial, growth by thermal evaporation on ionic crystals in vacuo and air 8=30738
metal, evaporated, intrinsic stress 8=48953
metal foils, time-to-rupture from creep tests under tensile loads of periodically varying orientation 8=35626
metal iodides with layer structures, optical absorpt. spectra 8=45176
metal, mag. props. 8=49461
metal, optical and transport props. 8=26954
metal-oxide-metal structures, I-V characts., optical fibres method 8=35950
metal-supercondutor superimposed films, transition temp., numerical soln. of eqn. 8=27011
metal, temp. meas. during vapour deposition 8=44035
metal, thickness determ. by fast e.-backscatt. 8=48434
metal, vacuum-evaporated, density meas. 8=48437
metal, work function thickness, shape and size factors 8=36037
metallic for thermal insulation in high pressure gas 8=26602
metals, discontinuous resistance changes in oxidation rate-constant determ. at low temps. 8=49883
metals, e. -mean free path and free-e. density, strain coeff. determ. using thin-film technique 8=49081
metals, oxide scale layers growth, effects of size and shape of specimen 8=36552
metals, plasma drifted, elect. and thermal props. 8=35815
microcrystal growth from melt on foreign substrate, thermal conditions mathematically analysed 8=26275
microelectronic device, integrated monolithic, comprising conductor and insulator films, basic technology 8=44852
micrometeoroid penetration, study on Gemini 9 and 12 8=37020
microstructures of thin surface layers, optical ellipsometry 8=48439
molecular beam crystallization, non-isothermic, phenomenological theory 8=30739
molybdenite, thick, electron microscopy at 50 to 1200 kV 8=48602
m.o.m. sandwiches, electroluminescence, correlation with electron emission 8=40700

Films—contd
  solid—contd
    monoatomic, impurities, maximum and optimal concentrations 8=35150
    noble metal, effects on Zr oxidation 8=49882
    nucleatron in evaporated films 8=48440
    optical constants determ. from intensity meas. at normal incidence 8=36289
    optical consts. meas. in vacuo 8=36288
    oxide, active, passive and transpassive, on Fe in electrolyte, e diffr. exam., 8=49931
    oxide layers on Cd and Mg, nature 8=35167
    oxide layers on Ni, formation mechanism 8=45346
    oxide, on Ge, optical consts. 8=49721
    oxide on Si crystals i.r. spectroscopic study 8=39598
    oxide, on Zr-2.7 w/o Nb alloy structure and morphology exam., 300-500°C 8=44064
    oxide, stripping from metals 8=30732
    Permalloy, critical switching curves, obs. 8=31671
    Permalloy, internal isotropic stresses and demagnetizing factors, ferromag. reson. obs. 8=31223
    permalloy, spin-wave resonance 8=27452
    Permalloy, thermal expansion coeff., e diffr. meas., 20-420°C 8=35446
    phases, non-equilib. origin 8=30736
    phospho-silica, on Si substrates, nondestructive determ of P 8=49994
    phosphosilicate glass, on SiO_2, by reaction of gaseous, PSO_5 with SiO_2 8=44048
    plasmons, excitation by e.m. waves 8=42072
    polyacetaldehyde, amorphous, depolymerization in vacuum, 40-80°C 8=45364
    polyacrylonitrile, deposition, semicond. and photoelec. props., obs. 8=39605
    polycarpamide, cryst. unoriented, creep vel. rel. to stress 8=40196
    polychlorotrifluoroethylene copolymer, crystallization 8=39680
    polycrystalline, II-VI compounds, deposition methods and physical props. 8=48444
    polyether coatings, influence of substratum 8=35188
    polyethylene, cryst. unoriented, creep vel. rel. to stress 8=40196
    polyethylene, I-doped, elec. cond. enhancement 8=40596
    polyethylene, stretching processes, X-ray diffr. studies 8=26859
    poly-γ-benzyl-L-glutamate, planar layered structure obs. 8=26131
    polyimide, noncrystal, mech. props. rel. to mol. struct. obs. 8=44619
    polymer-coated bodies, rolling friction and adhesion 8=31186
    polymer coatings, correl. between internal stresses and thermal props. 8=30759
    polymer with ringed spherulites, multiple-order light scatt. 8=45246
    polymeric organosilicon, on glass, strengthening effect 8=49024
    polymers, dielectric breakdown 8=40564
    polymers, fibrillar structures 8=26153
    polymethylsiloxanes, thermal degradation 8=35189
    polypropylene, CCl_4 swollen, n.m.r. rel. to mol. motion, 140-373°K 8=48510
    polystyrene, far u.v. optical props. 8=27639
    polystyrene, film-forming solutions 8=44065
    polystyrene, i.r. transmission rel. to glass transitions, 50-120°C 8=45247
    polystyrene, optical constants in vac. u.v. 8=41174
    polystyrenesulfonic acid membranes, dielec. props. rel. to H_2O adsorpt. 8=49357
    polythene, ionization by giant laser pulses 8=40720
    polyvinyl acetate latex, particle packing 8=48471
    polyvinyl alcohol, Au crystal X-ray sizing 8=30858
    poly (vinyl alcohol), i.r. transmission rel. to glass transitions, 50-120°C 8=45247
    poly (vinyl chloride-co-vinyl acetate), i.r. transmission rel. to glass transitions, 50-120°C 8=45247
    quartz, fused, reflectance in vac. u.v., obs. 8=27558
    radiation hardening during vacuum deposition 8=48965
    refractive index and thickness, simultaneous and independent obs. by ellipsometry 8=31931
    resistance decrease on annealing 8=49135
    resistor material and characts., 8=44675
    rhodamine-B, photocapacitive effect 8=40680
    rhodamine, photocapacitance and photocurrent "memory" 8=36032
    rocksalt, breakdown strength, anode surface and mats. effects 8=40578
    sapphire substrate prep. for Si epitaxial deposition 8=39699
    semiconducting, e.m. power-transmission coeffs., 8=49698
    semiconductor, surface capacitance rel. to thickness 8=35873
    semiconductor thin-platelets, optically pumped, laser emission 8=46613
    semiconductor, thin, single-crystal layers, production and props. 8=40436

Films—contd
  solid—contd
    semiconductors, Hall effect and specific conductivity meas. 8=40424
    semimetal, Sondheimer effect rel. to e-specular reflection 8=26957
    sheet resistance test apparatus 8=28457
    silicide, on Nb chromised, titanised and chromo-titanised, structure and props. 8=35176
    spherulite, radial, Rayleigh-Gans light scatt. 8=36447
    spin waves, energy and amplitudes, theorems and tables 8=49512
    sputtering, duoplasmatron ion source 8=48442/3
    sputtering method for production 8=25694
    sputtering systems, r.f., choice between single-ended and balanced 8=39586
    standard coatings with unchanging radiation props., prep. 8=49673
    steel, growth kinetics in chromate solns., effect of surface prep. 8=44039
    steel, transformer, hot-rolled, oxide film formation at 800-1180°C and structure 8=36561
    stresses, residual, in vacuum deposited films, X-ray diffr. obs. 8=44537
    substrate cooling technology 8=48727
    superconducting and ferromagnetic, proximity effect 8=27008
    superconducting and normal, zero-field proximity effect 8=27006
    superconducting, for radiant-energy detection, microwave-near i.r. 8=37299
    superconducting, modulated flux flow 8=27043
    superconducting props. rel. to degree of crystal lattice distortion 8=35849
    superconducting–superconducting, superconducting-metal, critical magnetic field 8=35846
    supercond. surface nucleation fields, influence of planar defects 8=34834
    superconducting, thin, mixed state condition from crit. field temp. and angular dependences 8=44713
    superconducting, Tomash oscillations in density of states 8=40358
    superconducting transitions obs., with very small mean-free-path 8=26980
    superconducting tunneling junctions, application as negative resistance devices above 4.2°K 8=49207
    surface pressure recording system 8=39573
    temperature coeff. of resistance, effect of expansion mismatch 8=31315
    thermodynamic fluctuations 8=35421
    thickness calc. for transparent film from ellipsometric obs. 8=30734
    thickness determs. effect of numerical aperture of microscope objectives 8=39584
    thickness measurement, interference microscope 8=35149
    thin, electrical conductivity rel. to temp. 8=40296
    thin epitaxial, e diffr. low-energy apparatus 8=35313
    thin, estimation of transient temp. distrib. on electron beam heating 8=30733
    thin, growth monitoring by u.s. interferometry 8=44031
    thin, Kerr magneto-optic apparatus 8=36304
    thin, luminesc., prep. and props. 8=36454
    thin, phase transform. hysteresis, inter-phase potential barrier mechanism 8=43990
    thin, produced in shock. properties 8=48438
    thin, rapid preparation for transmission electron microscopy 8=28205
    thin semiconducting, field ionization 8=31463
    thin superconducting, field effects 8=27007
    thin, thickness of using semjconductor detector 8=44029
    thin-film coil preparation technique 8=44033
    in thin-film resistance thermometer by optical interference method 8=39585
    transducers, insertion loss and coupling factors 8=49380-1
    transition metal sulphide, as lubricant for cpds., at high temp. 8=31219
    on transparent electrodes, internal reflec. spectra 8=41280
    tunnel junction semiconductor, quantum size effect 8=35935
    ultra-thin, fabrication technique 8=35155
    ultrathin, superconductive phenomena 8=40400
    vacuum condensates, growth mechanism and structural defects 8=35156
    vacuum condensates, internal macrostresses form. and classification 8=31164
    vacuum deposition, mask changer 8=30338
    vapor-deposition effect in amorphous mats. on replication in electron microscopy 8=39707
    X-ray emission, surface ionization function rel. to over-voltage and substrate Z, obs. 8=31945
    X-ray interferences fringes exam. 8=48435
    Zircaloy-2 surface oxide film, white spotting rel. to struct. and orientation 8=35187
    Ag, abnormal optical absorpt. in vacuum and Ar atmos. 8=45168
    Ag, absorbent and anisotropic, optical props., theoretical study 8=49707
    Ag, adsorpt. of O_2 and substrate for H_2 and O_2 8=39616

Films—contd
  solid—contd
    Ag, conducting, formation using electron beam 8=39603
    Ag, crystallization rel. to evaporation rate 8=30741
    Ag deposition ions, produced in e bombard. 8=40712
    Ag, electrical resistivity, 4.2 to 295°K 8=26944
    Ag, epitaxial growth on NaCl crystals 8=30745
    Ag, excitation of surface plasma oscillations 8=35804
    Ag, light refl. phase retardation meas. 8=31960
    Ag on mica, growth in ultra-high vacuum 8=44037
    Ag on NaCl and KCl, orientation 8=44085
    Ag, p-bombardment effects on resistance, −13 to −158°C 8=40302
    Ag polycrystalline, photoelec. emissivity obs. 8=27353
    Ag, resistivity, ion-bombardment induced changes 8=49151
    Ag, stacking faults, thermal behaviour 8=40047
    Ag, surface structure from electron diffraction 8=35153
    Ag, thermal expansion coeff., e diffr. meas. 20–420°C 8=35446
    Ag, thin, mean free path of conduction electrons rel. to optical absorption 8=36315
    Ag thin, optical transmission near plasma freq. 8=27547
    Ag, vacuum-condensed, elastic anisotropy rel. to structure 8=44545
    Ag, vacuum deposited, internal friction temp. dependence rel. to prep. 8=35650
    Ag, vacuum-deposited, structural formation rel. to elec. resistance behaviour 8=26110
    Ag, vacuum-deposited, temp. coeff. of resistance 8=35819
    Ag, with C layer, e energy loss spectra obs. 8=35808
    Ag–Al, diffusion 8=31000
    AgBr, AgCl and AgI epitaxial, vacuum deposition 8=44036
    Ag on CaF$_2$ and NaCl, X-ray structure investigations 8=44158
    AgCu alloy, vapour-quenched, structure from X-ray scatt. 8=44159
    AgI, polycrystalline dye-sensitized, thermally stimulated conductivity 8=35994
    AgMn prod. by simultaneous condensation, magnetic props. conc. depend. 8=40802
    β-Ag$_2$S, conductivity and photoconductivity 8=49152
    Al anodic films, high field kinetic processes 8=36603-4
    on Al, anodic oxide, pore struct. and barrier layer, obs. 8=44038
    Al crystal, secondary emission angular dependence, fine structure origin 8=40711
    Al, diffusion of impaired electrons obs. 8=40212
    Al, electron energy loss spectra rel. to film thickness 8=48904
    Al, epitaxial growth on NaCl crystals 8=30745
    Al, evaporated, struct., form of localized growths and whiskers 8=44040
    Al, intrinsic resistivity and e. mean free path 8=49153
    Al, light refl. phase retardation meas. 8=31960
    Al, on BK7 glass, X-ray refl. obs. 8=31961
    Al on NaCl, orientation 8=44085
    Al on Ta(110), interaction of O$_2$ and CO 8=35159
    Al on U, ion-plated, parametric study rel. to max. corrosion protection 8=49844
    Al, oxide film effect on dislocation-surface interacts. 8=26094
    Al oxide films, sputtering in plasma anodization 8=39587
    Al, photocurrent induced by synchrotron radiation 8=27550
    Al, plasma resonance in reflection spectrum 8=30746
    Al, qualification by X-ray fluorescent spectrum line shift 8=41059
    Al, resistance monitoring and nonadhesion effects 8=30743
    Al, size effects in magnetoresist.. 8=44683
    Al size effects in thermal Hall effect (Righi–Leduc effect) 8=40308
    Al, superconducting, granular, prep. and enhanced T$_c$ value 8=27013
    Al, thermal expansion coeff., e diffr. meas., 20–420°C 8=35446
    Al, transmission and reflection of synchrotron radiation near plasma wavelength 8=27549
    Al, transparency, thickness depend. oscills. rel. to e quantization. 4.2°K 8=31957
    Al, unique superconducting energy gap obs. 8=35845
    Al, use of anodisation for measurement 8=35158
    Al, vacuum-condensed, elastic anisotropy rel. to structure 8=44545
    Al, vacuum-deposited, temp. coeff. of resistance 8=35819
    Al, vapour deposition by e beam bombard. 8=30744
    Al-Al$_2$O$_3$-Al struct., e energy loss obs. 8=27316
    Al-CdS-Au diodes, vacuum-deposition prep. and elec. props. 8=27174
    AlN, current-voltage characts. 8=44900
    AlN, prep. by chem. transport 8=30742
    Al$_2$O$_3$, absorption, transmittance and reflectance 8=41057
    Al$_2$O$_3$, elec. conductivity 8=44894
    Al$_2$O$_3$, luminescent brightness waves rel. to electrode mat. effects 8=45260
    As$_2$Se$_3$ and (As$_x$Sb$_{1-x}$)$_2$Se$_3$, energy bandgap, reflectance and refractive index 8=31963
    Au, absorbent and anisotropic, optical props., theoretical study 8=49707

Films—contd
  solid—contd
    Au, current noise power spectrum 8=40310
    Au crystallites on KCl cleavage planes, thermally-deposited, Brownian movement 8=44022
    Au, discontinuous, morphological changes following deposition mechanism 8=39588
    Au, double-positioned, damage on bombardment by He ions 8=40073
    Au epitaxial films in high vacuum 8=30747
    Au. epitaxial on NaCl, electrostatic field effect on initial orientation 8=26111
    Au, evaporated films, water vapour adsorption 8=35194
    Au evaporated particles, multiple-twin struct. and deca- or icosa-hedron shapes 8=35317
    Au, lattice parameter thickness dependence by X-ray diffr. 8=30748
    Au on amorphous substrate, grain boundary effects on elastic deform. and residual resistivity 8=44551
    Au on NaCl and KCl, orientation 8=44085
    Au, polycrystalline, dynamical e.-diffr. intensities temp. dependence 8=39769
    Au polycrystalline, photoelec. emissivity obs. 8=27353
    Au, proton channeling investigation of surface electron states 8=31286
    Au, reflectance in vac. u.v., obs. 8=27558
    Au, resistivity, ion-bombardment induced changes 8=49151
    Au, thin, photoconductivity 8=36009
    Au, (111) epitaxial, vacuum deposition effects on structure 8=35160
    Au, transmission sputtering by low-energy H ions 8=40072
    Au, triode-sputtered, resistivity meas. 8=40309
    Au-Ag bonds, ultrasonically joined, purple-plague formation 8=48771
    Au-Mo laminated metallization in integrated circuits, thickness, e microprobe obs. 8=30749
    B, amorphous, switching and neg. resistance 8=27079
    BN, prep. and props. 8=48445
    Ba, deposited on Ni, nature and thermionic emission 8=27347
    (Ba, La)TiO$_3$, permittivity and loss tangent substrate temp. dependence, 100-850°C 8=49363
    (Ba, La)TiO$_3$, production and dielec. props. 8=27264
    BaTiO$_3$, ferroelectric domain structure 8=35973
    BaTiO$_3$, ferroelec., sputtering prep. 8=35161
    BaTiO$_3$: Sm(La), baked electrophoretic, semiconducting and dielec. props. 8=44885
    Be-Cu foil, thermal and elec. cond. 8=39947
    Bi, cond. in elec. field, quantum size effect oscills., 10^3 v/cm 8=40312
    Bi, quantum effects in resistivity, Hall const. and magneto-resistance, rel. to thickness 8=27082
    Bi, transition to semiconducting state 8=27083
    C, condensed, structure from e.-diffr. and microscope exam. 8=35162
    C, evaporated, electron energy loss spectra 8=48913
    C. evaporated, optical absorpt. edge in near i.r. 8=36335
    C foil, stable 2mg/cm^2, preparation 8=35163
    C, resistance, low-temp. non-linearity 8=31318
    C, tartan film by superimposing two evaporations 8=35164
    Cd, anodic films in alkali 8=32132
    Cd chalcogenides, mono- and multilayer, epitaxially grown, structure and photoelec. props. 8=26115
    Cd$_3$As$_2$, high mobility, prep. by evap. method 8=48447
    CdS, anode blocking contact and carrier injection process rel. to vacancy transport mechanism 8=40442
    CdS, deposition study 8=48446
    CdS diodes, effect of heat treatment 8=27176
    CdS, electromech. coupling coeffs. determ. from admittance meas. 8=40626
    CdS, epitaxial growth and polymorphic transforms. 8=26113
    CdS, epitaxial growth on CdS and ZnS platelets, dislocations and cryst. orientation 8=35165
    CdS, epitaxy and crystal growth 8=26114
    CdS, evaporated by e bombard., props. 8=35166
    CdS, evaporated, conductivity rel. to thickness 8=49233
    CdS, Faraday effect near fundamental absorpt. edge, at 300°K 8=36347
    CdS, forbidden band width film-thickness dependence 8=26904
    CdS in MOS structure, field-effect conductance temp. dependence 8=40544
    CdS layers, chem. deposited, elec. and photocond. props. 8=44918
    CdS, photoeffect, electrically induced, props. 8=27319
    CdS, properties, chemically deposited 8=39589
    CdS, spray deposited, appl. in thin film transistors 8=31414
    CdS, thin, amorphous to crystalline transition 8=43993
    CdS, whisker-formation and structural changes during crystal growth 8=26270
    CdS-CdTe heterojunction diodes 8=49306
    CdS-Cu$_2$S system, photovoltaic effect rel. to thickness and prep. 8=40652
    CdSe, as base for photocells with p-n hetero-transition 8=40647
    CdSe evaporated, photoelectronic props. 8=44922
    CdSe, nonlinear optical absorption 8=36340
    CdSe, photocurrent saturation 8=44923

Films—contd
solid—contd
CdSe, photosensitive, field effect effective mobility freq. and temp. dependence 8=36016
CdSe, surface enhancement by SiO_2 8=49232
CdSe, resistance 8=44772
CdSe transistor, electron Hall mobility in space-charge layer 8=27199
CdSe, transistor instability and stabilization techniques 8=44848
CdSe, vapour deposited, appl. in thin film transistors 8=31414
Cd(SeS) semiconductor thin-platelets, optically pumped, laser emission 8=46613
CdSe-SiO_2 transistors, effects of instability on l.f. characts. 8=27198
$CdSO_4$ single crystal layers 8=44041
CdTe, photovoltaic effect, gas adsorption effects 8=44924
CdTe, preparation by ion bombardment method 8=30750
CO_2 cryodeposits on 77°K surface, refractive index from Bragg interference meas. 8=41068
Co alloys, ferromag., epitaxial growth on LiF and MgO 8=35170
Co, galvanomagnetic effects and domain struct. rel. to thickness, 200-2000Å 8=31598
Co, hexagonal, spin-wave reson. 8=40886
Co, n.m.r. 8=40976
Co, transverse Kerr effect, and application to hysteresis loop plotter 8=49516
Co, single-cryst., epitaxial growth on LiF and MgO 8=35170
Co-CoO, ferro-antiferromagnetic coupling and after effect 8=49517
Co-Ni-Fe, critical thickness and coercivity 8=27400
Cr, prep. by oblique incidence of mol. beam and optical anisotropy 8=31977
Cr, prep., elec. and mag. props. 8=39590
Cr surface species from chemisorpt. of molec. subs., i.r. study 8=45363
Cr, vacuum-deposited, effect of dielectric coating on resist. 8=26964
Cr, vacuum-deposited, structure and substructure from e.-diffr. exam. rel. to deposition temps. 8=35169
Cr/SiO mixture, structural and elec. props. 8=48448
Cs, on refractory metals, work function 8=39624
CsI(Tl) layers fabricated by vac. deposition, scintillation characts. 8=46875
Cs-Sb, photocathode formation, quartz-crystal microbalance technique 8=40683
Cs-Sb photoelectron attenuation length determ. 8=31455
Cs_3Sb, on MnO, e.- and X-ray-diffr. exam. 8=39591
Cu crystal, secondary emission angular dependence, fine structure origin 8=40711
Cu, effect of absorbed Ar on props. 8=49158
Cu, epitaxial growth on NaCl crystals 8=30745
Cu, evaporated films, water vapour adsorption 8=35194
Cu foil, elec. conductivity ht. treatment dependence 8=49161
Cu layer on Pb, proximity effects in supercond. 8=27015
Cu, light refl. phase retardation meas. 8=31960
Cu polycrystalline, photoelec. emissivity obs. 8=27353
Cu single crystal on sapphire, epitaxy 8=30751
Cu sponge, $He^{3,4}$ adsorpt. at 4°K 8=24056
$CuAsSe_2$, semiconducting, phases and crystal structure from e.-diffr. exam. 8=39788
Cu-Au system, surface and vol. diffusion 8=35486
CuO_2 on Cu(111), microstruct. and diffusion in defects rel. to oxidation, obs. 8=44042
Cu_2O, optical and transport props. 8=31983
Cu-S, phase transform kinetics by new e-diffr. procedure 8=26082
Fe alloys, ferromag., epitaxial growth on LiF and MgO 8=35170
Fe, condensed, internal macrostresses form. rel. to substrate temp., obs. 8=31164
Fe ductile foil, electrochem. prep., and study of Fe, Cr, Fe-Re deposits 8=36609
Fe glazes, FeO content rel. to shade 8=49717
Fe, light refl. phase retardation meas. 8=31960
Fe, optical and elec. props. rel. to absorpt. of bulk Fe 8=41085
Fe oxide, growth on Fe in neutral soln. 8=27706
Fe passive layer, presence of H in outer layer 8=35171
Fe, single-cryst., epitaxial growth on LiF and MgO 8=35170
Fe, thin, optical absorption, electrical resistivity, in vacuum 8=36359
Fe-18% Cr alloy, complex scale formation on oxidation 8=45340
Fe-Cr alloy, oxidized surface 8=44074
Fe-Cr-O system, low-temp. oxidation, glancing-angle X-ray diffraction technique 8=27703
Fe-Ni, Faraday effect and optical consts. 8=36358
Fe-Ni-Co, single cryst., mag. anisotropy, domains and saturation magnetization, obs. 8=40809
Fe_3O_4, growth in LiOH solns., two-phase struct., 300°C 8=44043
Fe-Re alloy ductile foil, electrochem. prep., and study of Fe, Cr, Fe-Re deposits 8=36609
GaAs epitaxial, deposited by vacuum evaporation 8=26117
GaAs, epitaxial growth, high electron mobility, rel. to substrate orientation 8=39592

Films—contd
solid—contd
GaAs, epitaxial on Ge, diffusion of As across interface 8=35494
GaAs, epitaxy on rocksalt, 25-430°C 8=35172
GaAs, formation flash evaporation 8=48450
GaAs, high mobility layers, obtained by liq. phase epitaxy 8=30753
GaAs hole deposits, faceted, effect of vapour comp. on growth rates 8=48572
p-GaAs, in tunnel diode prep. by closed-growth using $ZnCl_2$ transport agent 8=44846
GaAs layer growth from Ga and As_2 vapours, kinetic mechanism using mol. beam, technique 8=48449
on GaAs, oxide layer form. in range 400-530°C 8=49870
GaAs, photoemission and prep. 8=27354
GaAs, polycryst., tunnel p-n junctions 8=27188
GaAs, polycrystalline, photoconducting props. 8=27321
GaAs semiconductor thin-platelets, optically pumped, laser emission 8=46613
GaAs, 2-source vacuum evaporation arrangements 8=44045
GaAs, vapour growth on Ge 8=30752
GaAs-InAs solid solns., epitaxial, crystallization kinetics and structure 8=26119
p-Ga(As_xP_{1-x}) in tunnel diode prep. by closed-growth using $ZnCl_2$ transport agent 8=44846
Ga(AsP) semiconductor thin-platelets, optically pumped, laser emission 8=46613
p-GaP, in tunnel diode prep. by closed-growth using $ZnCl_2$ transport agent 8=44846
GaP p-n junctions, red-emitting, prep. by soln. growth of p-type thick layers on n-type substrates 8=41232
GaP_xAs_{1-x}-GaAs n-n heterojunctions, photosensitivity spectra 8=36019
n-GaSb, epitaxial growth from liq. on p-GaSb 8=44044
Ge, amorphous, tunneling 8=31411
n-Ge, dendritic, microwave magnetoresistance 8=27111
Ge epitaxial, defect structure rel. to growth processes 8=26647
Ge, epitaxial, formation on GaAs, thermal evap. in vac. 8=35174
Ge, epitaxial, morphology dependence on gas-flow during growth 8=26118
Ge, epitaxially grown, effect of etching with gaseous HI, HBr and HCl 8=30754
Ge, impurity doped, epitaxial, crystallization kinetics and structure 8=26119
Ge layers, preparation by chem. H plasma transport 8=44781
Ge, photomagnetic effect spectrum 8=27323
Ge, Si monoxide, interf. filters, props. 8=32937
Ge, vacuum-deposited, liquid-like behaviour of crystallites 8=26121
Ge-Al_2O_3-ZnO, I-V characts., conductivity change 8=40488
GeI_2 struct., e diffr. obs. 8=30897
Ge_3N_4, amorphous, prep. and props. 8=44046
Ge_3N_4, prep-on stained Ge surface 8=48451
H adsorbed on solid CO_2, below 100°K, granular and amorphous structure 8=30765
H_2 foils, laser-irradiated rel. to plasma production 8=29995
H_2 liquid containment, windows 8=24035
H_2O, D_2O, and HDO, i.r. intensities of stretching and vibrational bands 8=36369
β-HgS, elec. conductivity and thermal e.m.f. temp. dependence 8=44792
HgS, epitaxial growth on CdS and ZnS platelets, dislocations and cryst. orientation 8=35165
HgSe, structure 8=30755
HgTe, structure 8=30755
In, size effects in magnetoresist. 8=44683
In thin, critical mag. field, influence of structural disorder and defects 8=40382
In, vacuum-deposited, liquid-like behaviour of crystallites 8=26121
In-Al superconducting, Tomash oscillations in density fo states 8=40358
InAs, annealed, elec. props. 8=44794
InAs microminiature Hall probe for liq. He 8=28509
InBi, Mn layers on each side, proximity effect on superconductivity obs. 8=40372
In_2O_3, sputtered, electrical props., intrinsic absorption 8=40469
In_2O_3, sputtered, near i.r. optical props. 8=40470
InP on Ge, epitaxial, prep. 8=44047
In-Pb, superconducting, Tomash oscillations in density of states 8=40358
InSb microminiature Hall probe for liq. He 8=28509
InSb, surface photoconductivity and field effect 8=27326
InSb thin films, production techniques rel. to semiconducting props. 8=26120
InSb:S, electron mobility 8=49255
Ir on Mo, field-ion microscope study of deposition 8=48452
K, LEED exam. 8=48453
K, optical props. for photons 3.96 to 9.69 eV 8=49731
KCl, u.v. reflection and absorpt. spectra 8=32025
KI, u.v. reflection and absorpt. spectra 8=32025
K-Sb, photocathode formation, quartz-crystal microbalance technique 8=40683

Films—contd
solid—contd
LiBr, LiI and LiF, dielectric, l.f. polarization effects 8=44870
Li-O on W(110) face, surface reconstruction, and work function 8=39593
Mg phthalocyanine, barrier effect, photoconductivity 8=40678
MgO, porous, field-assisted secondary electron emission 8=27359
MgO porous, self sustained electron field emission, obs. 8=40695
Mn surface species from chemisorpt. of molec. subs., i. r. study 8=45363
β_1-MnZn, ferromag. resonance 8=27451
Mo, resistance and work function, effect of Ba, BaO and O_2 adsorption 8=40322
Mo, resistors for integrated circuits, fabrication and props. 8=44693
Mo, sticking probabilities of N_2 8=30771
Mo, vapour deposited, orientation rel. to temp. and annealing 8=35154
MoO_3, optical absorpt. and photocond. 8=32013
Na_3AlF_6 (cryolite), dielectric, l.f. polarization effects 8=44870
NaI(Tl) layers fabricated by vac. deposition, scintillation characts. 8=46875
Nb, deposition by d.c. diode and substrate bias sputtering 8=48455
Nb, discontinuous, resistance changes in oxidation rate-constant determ. at low temps. 8=49883
Nb, sputtered cylindrical, flux jumping phenomena 8=49472
Nb_2N, deposited by reactive evaporation 8=48454
Nb_2O_5 insulator, refractive index 8=49763
Nb–Ti–N, reactively sputtered, superconducting props. rel. to comp. 8=40380
Nb–Zr–N, reactively sputtered, superconducting props. rel. to comp. 8=40380
Ni alloys, ferromag., epitaxial growth on LiF and MgO 8=35170
Ni, conducting, formation using electron beam 8=39603
Ni, discontinuous, resistance changes in oxidation rate-constant determ. at low temps. 8=49883
Ni ferrite, epitaxial growth on MgO (111) and (110) surfaces 8=39594
Ni, He-Ne laser TEM_{00q} modes separation, obs. 8=37565
Ni, light refl. phase retardation meas. 8=31960
Ni, magneto elastic resonance props. 8=36164
Ni on NaCl, orientation 8=44085
Ni, single-cryst., epitaxial growth on LiF and MgO 8=35170
Ni, thermal expansion coeff., e diffr. meas., 20–420°C 8=35446
Ni, vacuum-condensed, elastic anisotropy rel. to structure 8=44545
Ni, vacuum-deposited, temp. coeff. of resistance 8=35819
Ni–Au system, surface and vol. diffusion 8=35486
Ni–Cd flexible thin-film batteries 8=33032
NiCoP, chem. deposited, mag. props. stability, up to 100°C and 1600 hr 8=45023
Ni–Cr alloy, vacuum-deposited, temp. coeff. of resistance 8=35819
Ni-Cu alloy, resistivity temp. (20-600°C) and comp. dependence 8=40325
NiFe, coupled, domain wall behaviour 8=49541
Ni-Fe, electrolytically prepared, conditions for formation of hexagonal structure 8=26122
Ni 81%-Fe 19%, ferromag., 180° domain wall energy density rel. to thickness 8=45018
Ni-Fe, magnetoelastic sensitivity, composition gradient effect 8=36111
Ni-Fe, magnon-phonon coupling 8=27421
Ni-Fe polycrystalline alloys, magnetic anisotropy induced during evaporation and annealing 8=36152
76%Ni–Fe, type II stripe domains, obs. 8=40825
$NiFeS_x$ electrodeposited rel. to vacuum deposited 8=35177
Ni_3Mn, alloys, thin, antiphase boundaries obs. 8=35278
Ni–NiO, ferro-antiferromagnetic coupling and after effect 8=49517
Ni-P, Hall effect structure dependence 8=44696
Pb, anodic films in alkali 8=32132
Pb chalcogenides, mono- and multilayer, epitaxially grown, structure 8=26115
Pb, production by diffusion evaporation 8=48456
Pb, supercond. transition, critical fields 8=27028
Pb, thin, critical mag. field, influence of structural disorder and defects 8=40382
Pb-Bi alloys, electron diffraction and resistivity examination of structure 8=35152
PbO vapour deposited, preferred crystal orientation 8=30756
PbO-TiO_2 mixed, struct. and elec. props. 8=49347
PbS, monocrystalline, photosensitivity 8=40667
PbS, polycrystalline, and crystals, photo-e. m. f. force temp. dependence 8=36025
PbS, polycrystalline, polarization currents rel. to oxygen diffusion 8=35909
PbSe epitaxic formation by sublimation in vacuo 8=26123

Films—contd
solid—contd
PbSe, polycrystalline, photoconductive meas. at 77°K rel. to mobility changes and heat treatment 8=27328
Pd on NaCl, orientation 8=44085
Pd-Sb system, electron diff. investig. 8=30909
PbTe, temp. depend. of photoelec. parameters 8=40668
Pt, annealing and substrate temp. effects on props. 8=44698
Pt anodic films, ellipsometry 8=27754
Pt on W, structure, work function and adsorpt. of Cs 8=35178
Pt, sputtered, oriented growth 8=44049
Rb, LEED exam. 8=48453
Rb, vacuum-condensed, photoelec. props. 8=44944
RbI, u.v. reflection and absorpt. spectra 8=32025
Ru foils, prep. by electrolytic deposition 8=36610
Sb, epitaxial growth on disordered substrates 8=26124
$SbCs_3$, quantum yield, thickness depend. 8=36054
Sb_2S_3, diffusion of Al 8=35505
Sb_2S_3, optical consts. meas. for diff. thicknesses 8=49748
Sb_xS_3 and $(As_xSb_{1-x})_2Se_3$, energy bandgap, reflectance and refractive index 8=31963
Se, absorption and reflecting power in fundamental absorpt. region 8=27605
Se, amorphous, prep. by vacuum evap., crystn. by electron irradn. 8=39691
Se electrophotographic layers, current carrier drift mobilities 8=40671
Se, epitaxial on Te, evap. conds effects on struct. 8=48457
Se, linear thermal expansion coeff. meas. and Ag impurity dependence 8=48746
Se, single-crystal, in rectifying Te-Se-Cd structures 8=35930
Se, thin, vacuum-deposition illumination 8=30757
Se, with embedded Hg atoms 8=35179
Se : Ag hexagonal evaporated, struct. and props. 8=48458
Si, analysis by neutron activation 8=40014
Si; chemically grown epitaxial, nucleation study using molecular beam techniques 8=44144
Si, deposited by sputtering through moving mask, low-temp. orientation 8=26127
Si, deposition in u.h.v. on (0001) and IT02) sapphire substrates 8=44056
Si, epitaxial, autodopant transfer from n-type substrate 8=44812
Si, epitaxial deposition conditions at low-temps 8=48461
Si epitaxial deposition on sapphire, substrate prep. 8=39699
Si, epitaxial, doping on deposition of $SiCl_4$ with gaseous impurity, deposition conditions effect 8=44811
Si, epitaxial, growth on Si substrate 8=39597
Si epitaxial, impurity penetration in growing process 8=26128
Si epitaxial layer, impurity conc., non-destructive determ. using metal-silicon Schottky barrier 8=44815
Si epitaxial layers, crystal perfection, effect of substrate surfaces 8=39596
Si epitaxial layers, stacking-fault defect nature 8=40050
Si epitaxial layers, stacking fault disappearance 8=40049
Si, epitaxial on sapphire, carrier transport, 1-2 μ thick 8=40489
Si, epitaxial, on sapphire, vacuum depositionand elec. props. 8=40491
Si, epitaxial on spinel surfaces, carrier mobility 8=35181
Si layers, preparation by chem. H plasma transport 8=44781
Si, masking, stress effects rel. to devices 8=49047
Si, moving mask, growth on amorphous quartz substrates 8=26126
Si on quartz, epitaxial arrangements and multiple orientations 8=48465
Si, on quartz substrate, deposition, struct. and elec. props. 8=35180
Si, on sapphire, crystallog. orientation relations 8=44058
Si, perfect single cryst., on sapphire, by vacuum evaporation 8=39595
Si, vacuum deposition on sapphire 8=44057
Si–B phase formation, removal 8=48463
SiC, dielectric, breakdown mechanism 8=27249
SiC, noncrystalline, prep. and elec. props 8=48467
Si–Cr, resistivity, resistance temp. coeff., stability at 200°C and struct. 8=44818
Si(Ge)-ZnO, I-V characts., conductivity change 8=40488
SiN on Si, from $SiCl_2–NH_3–H_2$ system, anomalous etching rate 8=48464
Si_3N_4, diffusion of Al substrate, coeff. and activation energy temp. dependence 8=31001
Si_3N_4, etching 8=39652
Si_3N_4 insulator, refractive index 8=49763
Si_3N_4 on Si, vapour deposited, elec. props. 8=49350
Si_3N_4, prep. by r. f. discharge reaction of silane and N_2 8=35183
Si_3N_4, prep. from $SiCl_4 + NH_3$ and elec. props 8=44051
Si_3N_4, pyrolytic, conduction props. 8=49352
Si_3N_4, structure and Na migration 8=48605
Si_3N_4, vapour depositon on Si and MNS diodes props., obs. 8=40545
Si_3N_4-SiO_2 mixed amorphous, on Si, struct., opt. and elec. props. 8=49319

Films—contd
solid—contd
SiO amorphous, formation and structure 8=44052
SiO, pulse breakdown voltage obs. 8=40586
SiO_2. amorphous, elec. strength temp. dependence, —196 to + 50°C 8=40561
SiO_2, amorphous, on Si, prod. by oxidation of silane 8=44055
SiO_2, chemically vapour-plated, environmental effects 8=48466
SiO_3 coating for protection of aluminized mirrors operating in u.v. 8=42148
SiO_2 diffusion masks obtained by evaporation, use 8=48459
SiO_2, e diff. and microscope investigation 8=30910
SiO_2, insulating, on Si, polarization effects 8=44854
SiO_2, ordered structure and ion migration 8=44054
SiO_2, oxide layer thickness and nature from i.r. props. 8=26125
SiO_2, pyrolytic deposition under vacuum 8=44050
SiO_2, wetting by water obs. 8=35140
SiO_2 on GaAs, S diffusion through film into GaAs 8=35493
SiO_2 on Si, by oxidation by SiH_4 8=44053
SiO_2 on Si. thickness meas. by i.r. techs 8=48460
SiO_2 on Si. vapour deposited, elec. props. 8=49350
$SiO_{2-x}N_x$, on Si substrate, prep. by chem. vapour deposition and stress-comp. dependence 8=48462
$Si_xO_yN_z$ on Si, elec. and passivation props. 8=49351
Sn chalcogenides, struct. and props. 8=39600
Sn, elec. resistance rel. to impurity conc. 8=35828
Sn, microwave transmission meas. 8=40386
Sn, supercond., clean and dirty, critical mag. field 8=44734
Sn, superconducting, energy gap mag. field and film thickness dependence by e-tunnelling 8=27033
Sn, superconducting, hyperfreq. nonlinearities 8=27030
Sn, supercond. tunneling expts in mag. field 8=44732
Sn–In, superconducting, mag. props. 8=44974
Sn-In, supercond. tunneling expts. in mag. field 8=44732
SnO on glass, transparent and elec. conducting, deposition technique 8=44061
SnO_2, prep. and props. by reactive cathode sputtering 8=44062
SnS, epitaxial, structure and optical props. 8=44060
SnSe, epitaxial, structure and optical props. 8=44060
SnTe, epitaxial, structure and optical props. 8=44060
SnTe(Se)(S), epitaxial deposition on NaCl/KBr substrates at 293-873°K 8=39599
Ta, anodic, activation energies of conduction 8=49924
Ta, conducting, formation using electron beam 8=39603
Ta, oxidised, electroluminescence 8=45287
Ta_2N, deposited by reactive evaporation 8=48454
Ta_2O_5 insulator, refractive index 8=49763
Ta_2O_5, superstruct. obs. with electron microscope 8=26129
Te, e-irradiated, resistance increase due to CO_2 desorpt. 8=35829
Th, epitaxially grown on Ta (100), LEED obs. 8=48469
ThF_4. prod. by vacuum evap., dielec. and optical props. 8=35184
Ti, discontinuous, resistance changes in oxidation rate-constant determ. at low temps. 8=49883
on Ti, in boiling dilute H_2SO_4 and HCl, oxide, differences in struct. 8=39602
Ti, on Nb alloys, non-electrolytic deposition from fused salts at high temps. 8=44063
Ti, resistance and work function, effect of Ba, BaO and O_2 adsorption 8=40322
Ti, resistivity, ion-bombardment induced changes 8=49151
Ti, self-supporting, vacuum deposition method 8=39601
Ti, sticking probabilities of N_2 8=30771
TiO_2, amorphous, prep. by vacuum evap., crystn. by electron irradn. 8=39691
TiO_2 diffusion layer growth on Ti, effect of O_2 pressure 8=36573
TiO_2, vapour deposition from decomp. of tetraisopropyl titanate 8=35185
TlSe, phase transform kinetics by new e-diffr. procedure 8=26082
Tl_2Se, substrate temp. effect on semicond. props. 8=31395
Tl_2Te, substrate temp. effect on semicond. props. 8=31395
UO_2 on UC crysts., growth kinetics rel. to O diffusion through film, 60-160°C 8=39604
U_3O_8, prep. by h. v. electrophoresis 8=26130
V surface species from chemisorpt. of molec. subs., i.r. study 8=45363
VO thin single crystals, epitaxial growth, electrical resistivity rel. to temp. 8=48470
VO_2 on alumina substrates, rel. to device fabrication 8=30758
VO_2, sputtered, transport props. 8=27138
V_2O_4 anodic, growth in acetic acid-$Na_2B_4O_7$ solns., obs. 8=45375
W, evaporated films, superconductivity 8=40393
W, evaporated films, superconductivity 8=40394
W-on-glass, ultrahigh-vacuum-evaporated, elec. conductance 8=40332

Films—contd
solid—contd
W, resistivity, ion-bombardment induced changes 8=49151
W, vapour deposited, orientation rel. to temp. and annealing 8=35154
WC–Co hard metal foils, microstructure 8=35287
Zn chalcogenides, mono- and multilayer, epitaxially grown, structure 8=26115
Zn, cold-rolled, from Hall effect and magnetoresistance anisotropy obs. 8=30810
Zn, conducting, formation using electron beam 8=39603
ZnS: Mn, Cu, Cl, electroluminesc. in gap and sandwich cells 8=49818
Zr, discontinuous, resistance changes in oxidation rate-constant determ. at low temps. 8=49883
ZrN, thickness meas. in determ. of N_2 diffusion coeff. 8=44396
ZnO, polycrystalline dye-sensitized, thermally stimulated conductivity 8=35994
ZnS, epitaxial growth on CdS and ZnS platelets, dislocations and cryst. orientation 8=35165
ZnS, epitaxial growth on Si, vac. evaporation 8=30740
ZnS, stimulated cond. and electroluminesc. 8=32060
ZnSe, on p-Ge, epitaxial layers, growth and elec. characts. 8=44834
ZnSe(Cu, I, Cl) sublimated layers, electroluminesc. obs. 8=41211
Zr, oxidised 300-500°C, structure obs. by e. microscope 8=35186
Zr phosphate membranes for intermed. temp. fuel cells 8=46354
ZrO_2, gamma, neutron and neon damage 8=35607
ZrO_2, permittivity, effective and intrinsic 8=40589

Filters
diffusion coeff. for liq. motion along packing 8=30361
ethylene glycol-methanol (cellulose membrane) syst., ultra-filtration 8=25904
nuclear pulse, tapped delay line appl. 8=33385
particle detector, finite cylindrical, Cd cut-off energies 8=33366
time-dependent, for nuclear spectroscopy, S/N calc. 8=33386
X-ray, automatic balanced filter device, for diffr. expts. 8=44191

Filters, electrical. See Circuits.

Filters, optical
See also Absorption/light; Optical films.
birefringent, chain 8=42260
birefringent, with high transmission 8=42198
Christiansen, shape and bandwidth by multiple scattering calc. 8=37665
Cristiansen-effect, infrared, design and manufacture 8=33252
coloured glasses, luminous transmittance and chromaticity in CIE 1964 colour space 8=37664
computer generated spatial filters for coherent opt. data processing 8=28764
Cristiansen-effect, infrared, design and manufacture 8=33252
dielectric narrow-band interference, with passbands exactly matching specification 8=42202
dielectric narrowband transmission interference, props. 8=42200
eye protection filters, light scatt., meas. and characts 8=28922
fiber polychromator for separating spectra from pulsed plasma 8=37662
glass, for daylight simulation in sensitometric exposure 8=42288
i. r. interf. filters, props. 8=32937
interference all-dielectric, 2500-4000Å 8=28762
interference, bandwidth rel. to refr. index of central layer 8=24376
laser, ruby, birefringent plate control of spectral emission 8=37609
light transmission through aberrated and misaligned lenses, effect 8=46662
liquid, of complementary colours, nomogram 8=24377
magnetic, for Cs vapour hyperfine pumping 8=38693
matched filtering with self-luminous objects 8=37663
multilayer reflection-type interference filter 8=42199
passive optical shutter for reducing fluorescent output of pulsed ruby laser 8=24328
pyrometric, appln. in high temperature meas., theory 8=46266
radiographic images produced by extended sources, degradation compensation 8=28911
Reststrahlen powder, low temp. props. in far i.r. region 8=42197
single-pass and double-pass birefringent networks 8=33251
spatial discrimination increment 8=42201
spatial frequency filter to remove zero frequency 8=46676
for strap light meas. in spectrometers 8=46701
for suppression of part of a spectrum in own transmission band 8=24375
transmission characts., educational expt. 8=37666
ultraviolet, for at. absorpt. spectrophotometry 8=28805
varicon-type for far infrared 8=24378
BCl_3, saturating, for CO_2-N_2-He laser Q-switching 8=46588

- **Filters, optical**—contd
  - NaCl$_3$ for Rb-D$_2$ transmission in student optical in pumping expts. 8=42196
  - PbO layers, characts. rel. to struct. 8=28765
  - ZnS-MgF$_2$ layer Fabry-Perot, max. transmission wavelength, H$_2$O vapour effects 8=28763
- **Finlay—Freundlich red-shift hypothesis.** See Astronomical spectra; Cosmology; Gravitation; Relativity.
- **Fireball model.** See Cosmic rays; Elementary particles; Field theory, quantum/interactions; Nuclear reactions.
- **Fission.** See Nuclear fission.
- **Flames**
  - acetylene, Cu conc., linear absorpt. method 8=27790
  - acetylene-air, intensified by discharge, activation energy of excited radicals OH, CH and C$_2$ 8=45359
  - acetylene-air, low pressure, spectroscopic and thermocouple meas. of temp. 8=41877
  - acetylene-nitrous oxide, atomic emission characts. 8=49985
  - with Auer-Welsbach grids, thermal radiation peculiarities 8=26609
  - diffusion, natural gas, noise meas. 8=28406
  - electric properties, dependant on whether fed by hydrocarbons or pure hydrogen 8=32974
  - fuel rich air-H$_2$, determ of K and Na 8=49990
  - gas and condensed phases temp. meas. by spectral comparison method 8=32977
  - graphite surface burning in stream of dry O$_2$, temp. profile 8=46256
  - halide, C$_2$ Swan emission 8=29727
  - high temp. for atomic absorption spect., review 8=46686
  - ion density and vel. of propag., reln. 8=39022
  - laminar, stability, effect of preferential diffusion 8=28407
  - open turbulent premixed, study of noise prod. 8=32108
  - opposed jet diffusion flame, ignition and extinction problems 8=32971
  - optics in atomic absorpt. spectroscopy 8=42238
  - oxidation of Na, K and Cs 8=49877
  - photometry, design for clinical lab. 8=42134
  - plasma produced when gas jet is subject to electric discharge 8=38977
  - propane diffusion, C particles size and temp. distrib., i.r. spectroscopy 8=46257
  - propane-O$_2$-Al, heat transfer rates to plate, rel. to Al seeding 8=32973
  - quenching of excited Rb(5^2P) atoms 8=34150
  - radiant props, meas. by radiometer without condensing agents 8=28408
  - separated, applic. in analytical flame
  - slot burner for absorpt. spectroscopy 8=36637
  - sooty flames, dispersion of aborpt. coeff. 8=32975
  - spectroscopy, Ca, Mg at. fluoresc. interferences 8=29606
  - temperature, meas. by single-beam photoelec. pyrometer 8=41875
  - temperature meas. by spectral line reversal with objective methods of recording 8=46255
  - 300 watt flame-heated thermionic power supply 8=28489
  - CO, chemiluminesc. 8=27698
  - H$_2$-O$_2$, e.p.r. study of conc. profile of H radicals 8=49892
  - H$_2$S, rarefied, stages in burning 8=36582
  - Mg, temp. meas. by MgO vibr. spectrum obs. 8=24013
  - MgO flame, dispersion of absorpt. coeff. 8=32975
  - MgO, radiometry 8=37312
  - N-I$_2$, i.r. emission 8=49890
- **Flares, solar.** See Sun/flares.
- **Flash photolysis.** See Photochemistry.
- **Flicker noise.** See Electron tubes; Fluctuations/electrical.
- **Floating zone refining.** See Zone melting and refining.
- **Flocculation.** See Sedimentation.
- **Flow**
  - acoustics, geometric energy invariant in moving medium 8=46177
  - aerosol aspiration theory, large Stokes' numbers 8=34945
  - arc, electric, wall-stabilized with transverse mag. field, field flow theory 8=39007
  - axi-symmetric, convection eqns., analogue computer solns. 8=34822
  - axisymmetric, gradient of acoustic line on shock wave 8=30208
  - in axisymmetric rotor, flow of granular mats., appl. of plasticity theory 8=43884
  - axisymmetric, system of boundary layer eqns. 8=34582
  - boundary layer past slender body, axisymmetric free convection 8=41868
  - boundary layer problem, soln. using Prandtl-Mises transformation 8=47910
  - boundary layer, three-dimensional wave packets, development 8=30236
  - boundary-layer unsteady, general theory 8=25795
  - channel, non-homogeneous turbulence theory 8=25799
  - charged droplets, electrostatic lateral instability 8=34944
  - circular, in annular channels between rot. coax. cylinders, turbulence 8=30225
  - clay solution, in pipe with permeable walls, hydraulic resistance 8=48023
  - compressible, turbulent boundary layer development prediction 8=30220
  - conducting incompressible fluid, linearized analysis 8=48017
  - convective, in box, preferred wave-number depend. on Rayleigh number 8=47919
  - convective instability problems, application of Galerkin method 8=47920
  - convective motion between vertical planes, spectrum of perturbations and stability 8=46250
  - Couette flow of anomalous Grad fluid 8=47905
  - Couette, plane parallel, of viscoelastic fluid, linear instability 8=47909
  - Couette rot. stability obs. rel. to numerical results 8=43723
  - Couette, transient thermal response rel. to solid conducting boundary 8=47908
  - convection, interact. with jet at isothermal surface, heat transfer in stagnant zone formed 8=34731
  - convection past vertical porous plate, effect of periodic suction 8=34583
  - convection, stability, of fluid heated from below in a gravitational field 8=46251
  - convection, steady laminar Benard, between conducting plates 8=43641
  - creeping, power-law fluid over Newtonian fluid sphere 8=39163
  - curved, local instability 8=39159
  - cylinder, steady laminar forced convection at low Reynolds numbers 8=30231
  - dipolar fluid, slow flow past sphere and monopolar force experienced 8=25792
  - dynamic laws of fluid free surfaces and interfaces, contribution to generalization 8=30198
  - entropy layers in hypersonic flow 8=30267
  - fluid adherence to wall 8=43638
  - fluid, between rotating and stationary discs 8=30210
  - fluid, conducting, in longitudinal mag. field, and effects 8=24181
  - fluid near intersection of wall and dividing streamline 8=30215
  - fluid, pipe Poiseuille, linear azimuthally periodic disturbances 8=43627
  - fluid, relativistic, generalization of Hugoniot formulae 8=39158
  - fluid, rotating, source-sink flows 8=39156
  - fluid, stratified, past finite flat plate, theory 8=43628
  - fluid, uncompressible, analytic solution of system of eqns. 8=43639
  - fluid, viscous incompressible, boundary on vertical plate 8=34587
  - fluid, with variable physical characts., numerical integration of ht. of propag. eqn., 8=39196
  - fluids, between rotating spherical surfaces 8=43631
  - fluids, linear time-dependent problems 8=47913
  - fluids, micropolar, Couette 8=39162
  - fluids, motion in long pipe, invariant solutions of eqns. 8=39166
  - fluids, stably stratified, selective withdrawal 8=30188
  - fluids, through woven screens, pressure drop correlations, packed bed model 8=47912
  - fluids, turbulence equations 8=47923
  - fluids, viscometric and controllable 8=47914
  - free convection from heated inclined plate, stability of boundary layer 8=30222
  - free, finite disturbance, equilib. state 8=39161
  - free surface dispersion coefficients by particle simulation method 8=39165
  - gas/liquid glandless control valve 8=30203
  - gravity flow of particles, mechanism 8=48234
  - growth of disturbances in both space and time 8=30207
  - halloysite suspensions, behaviour, rheological model 8=39444
  - Hartman boundary layer, stability under parallel mag. field 8=41988
  - high-frequency oscillatory viscous 8=30217
  - homogeneous, isotropic, turbulent flow, probability dist. of velocity difference at two distinct points 8=47924
  - hydro- and thermo-mechanical ratios in cyclindrical vessel rel. to hydrothermal crystallization 8=30354
  - hydromagnetic, due to accelerated plate 8=46454
  - incompressible conducting fluid through channel with rectangular cross section, in mag. field 8=47916
  - incompressible, of uniform stream past semi-infinite plate at zero incidence 8=47918
  - instability, Rayleigh, theory 8=43625
  - interface, thermal unstable 8=30224
  - inviscid, comparison of fine algorithms, rel. to coding, resolution and execution time 8=34632
  - Laminar boundary layer, non isothermal, method for solving eqns. 8=25797
  - laminar boundary layers characts with surface catalysis 8=36587
  - laminar boundary with surface mass transfer and slip 8=34588
  - laminar, entry length reduction 8=34712
  - laminar field of closed streamlines, temp. distrib. at high Péclet number 8=34710
  - laminar forced convection in eccentric annuli 8=46249
  - laminar forced convection in rectangular channels 8=46236
  - laminar, in annular duct, temp. distrib. allowing for energy dissipation 8=39356
  - laminar nonviscous, differential rotation model 8=43640

Flow—contd
laminar, stability 8=43626
laminar through vibrating pipe, cause of friction factor increase 8=30200
laminar-turbulent transitions 8=47922
lee-wave amps and wave drag for thin barrier in stratified flow 8=43659
limiting dynamic and thermal layers, determ. of conditions 8=25798
measurement by thermal methods 8=34591
magnetogasdynamics, effect of finite-magnetic-Reynolds-number 8=46444
m.h.d., boundedness 8=46459
m.h.d., boundedness 8=46460
m. h. d. channel, thermal-entry region heat transfer rel. to axial conduction 8=33110
m.h.d. fluid channel, couple stress effects 8=28590
m.h.d., in pipes in presence of longitudinal elec. current 8=46447
m. h. d., nonstationary satisfying a circulation property 8=24189
MHD, Couette, unsteady with suction, similar solns. 8=46457
MHD, curled, in plane channel, influence of Hall effect on development 8=24187
MHD, electrically driven 8=24173
MHD, in rectangular channel, charact. of boundary layers and their overlapping 8=46443
M.H.D. parallel flows, steady, intrinsic props. 8=46453
MHD, quasi-onedimensional, stability 8=46455
MHD turbulent in channel, velocity profile 8=46461
MHD vortex, confined, for elect. conduct., viscous, incompressible fluid 8=41996
motion of cylinder in viscous elec. cond. medium in mag. field 8=41991
in natural channels, similarity 8=48020
non-Newtonian fluid, impulse theory extended to include rotation 8=25796
non-Newtonian fluids, laminar incompressible boundary layer 8=34585
non-planar parallel, long wavelength disturbances 8=30211
oceanic circulation, wind-driven, overlooked aspect 8=41331
one-dimensional nonstationary and 2-dimensional stationary, problems of geometrical acoustics 8=30205
parallel flows, steady, intrinisc props. 8=46453
parallel, interaction with two-dimensional jet 8=34589
parallel, inviscid ,fluid, stability 8=30212
parallel, unbounded, three-dimensional wave-packets, development 8=39154
plasma, boundary between stream and dipole mag. field 8=43511
plasma, tennous, in magn. field 8=47831
past plate, horiz., with heated side down, rel. to heat transfer by convection 8=39202
past plate with wing element, effect of roughness on heat transfer 8=39208
Poiseuille flow in circular tube, steady conjugated heat transfer including viscous dissipation 8=30253
Poiseuille, micropolar and dipolar fluids in circular channel 8=47907
Poiseuille, thermally stratified plane, stability 8=43629
in porous channel, heat and mass transfer, soln for large suction and injection at walls 8=30214
potential about arbitrary bodies, Laplace eqn. for Neumann conditions, soln. 8=34581
potential, velocity field rel. to vortices distrib. on profile boundary 8=34577
quasi-incompressible fluid, convective instabilities in fully developed flows 8=34580
radial, of viscous non-Newtonian fluids between discs. 8=39160
relativistic turbulence, incompressible fluids, mean flow equations 8=34594
Reynolds crit. numbers for flow with particles 8=47904
rotating Couette, stability, asymmetric waveforms 8=30206
rotating fluid, stirred, mixing of ang. momentum 8=47929
rotating, transformations of boundary-layer eqns. 8=43636
secondary flow between rotating cylinders, meas. with hot thermistor anemometer 8=45449
shear flow with interacting deformable substruct. 8=47901
shear, in stratified fluid, method of prod. 8=39157
shear, inviscid, resonant interaction of neutral disturbances 8=30235
singular points in laminar 2-dim near wake field 8=43633
solid particle motion in rotating potential flow, stabilization 8=30551
spreading of a twisted stream in an infinite space flooded by the same fluid 8=47906
stagnation point forward of circular cylinder, wake induced effects 8=43717
stationary compressible flow as a limit of a non-stationary flow, numerical solution 8=34624
stationary impedance of ordered stacks of spheres, approximations 8=47903
steady hydromagnetic past slender bodies, establishment 8=24186
steady inviscid, vorticity transfer and production 8=34584

Flow—contd
steady, of non-linear viscoelastic fluids, stability against shear waves 8=43635
steady-state, of conducting fluid, at large Hartman numbers 8=41993
Stoke's fluids, linear and non-linear, differences in turbulence props 8=30228
in submerged jets, vels. and vel. fluctuations rel. to initial turbulence 8=30223
suction, past porous sphere, asymptotic theory application 8=34590
supersonic, unsteady, around blunt bodies, theoretical investigation 8=47944
suspended particles, in rectilinear channel, eqns. of motion, effects of collisions 8=30544
in system of disc rotating in cylinder, effects on mass and heat transfer 8=32954
three-layered fluid, development of flow in plane tube in presence of transverse mag. field 8=30204
torsional, of second-order fluids, intertia effects rel. to interpret. of parallel disc viscometer data 8=25842
transient, near rotating disc, after impulsive starting from rest 8=39164
transversal in limiting layer, curvature of polar representation 8=25794
transverse, slow, past obstacles in rapidly rotating fluid 8=30201
turbulent boundary layer on plate, heat transfer and friction forces 8=30245
turbulent heat transfer in drag reducing fluids 8=46233
turbulent in concentric annuli, heat transfer anal. 8=34595
turbulent, in pipes, velocity distribution expression and eddy diffusivity profile 8=47927
turbulent, mathematical model for deposition from 8=34586
turbulent, near smooth wall, conducting sub-layer 8=43642
turbulent, through channels of non-circular cross-section hydraulic resist. coeffs. calc. 8=25800
turbulent through concentric annuli, comments and reply 8=25810-11
turbulent limiting layers with temperature gradient at wall 8=25793
turbulent, over flat plate with heat source, transient heat transfer 8=30250
turbulent Rayleigh shear 8=30219
two-phase, anal dispersion coefficient meas. 8=48014
two-phase, appl. of Reynolds flux concept., deriv. of anal. techniques 8=34983
two-phase flow with phase-change, conservation law 8=25789
two-phase, press. grad. prediction using Reynolds flux concept 8=34984
viscoelastic, dimensional considerations 8=47915
viscous, between eccentric rotating cylinders, stability 8=30216
viscous fluid, boundary problem, small parameter method appl. 8=25846
viscous fluid past heated thin plate, isothermal and non-isothermal motion 8=30358-9
viscous fluids, axisymmetrical motion 8=43630
viscous fluids, near walls and obstacles, boundary limit problems 8=30218
viscous, inertia forces 8=39328
viscous, over corrugated bottom in rot. system, steady state soln. 8=30202
viscous unsteady, past circular cylinder, numerical soln. 8=30199
in visoelastic fluid, secondary, due to rot. oscills of sphere rel. to time-dependent suction or injection 8=39155
visualization, by real-time holographic Moiré patterns 8=37710
wake, axisymmetric, stability 8=30229
water-air horiz. annular, heat transfer and pressure drop 8=43653
water, shallow, wave generation by unsteady flow 8=30374
wedge-type laminar, variable temp. and normal vel. along wall, heat transfer including frictional heat 8=34579

gases
See also Acoustic streaming; Aerodynamics; Anemometers; Supersonic flow.
adiabatic in plane-parallel channel, soln of Prandtl eqns. 8=30242
air—air injection, Mach 10 8=25838
air condensation in hypersonic wind tunnel 8=30599
air, equilib. stagnation point heat transfer calcs. 8=39206
air, in annuli with small cores, max. pts of vel. profiles, heat and momentum transfer 8=34647
air, in inlet region of tube, effect of initial turbulence on heat transfer 8=39203
air in wind tunnel, exchange of momentum, mass and heat with artificial lead 8=34608
air mixture turbulent motion in pipes 8=39176
air velocities in room, distribution due to ceiling fan 8=47941
anemometry with fine hot wires, calculations 8=30258
axisymmetric turbulent wake, slender body, Mach 3 obs. 8=30254
in bed of lump mats, heat transfer for counter flow with heat sources 8=30284

Flow—contd
gases—contd
boundary layer at high temp., optical convertor method for vel. meas. 8=30244
boundary layer, interaction with shock wave 8=47946
boundary layer over semi-infinite plate, temp.-time var. 8=47942
boundary transition, sharp cones at hypersonic speeds, obs. 8=30221
caused by full radial jet distrib. in space restricted by two parallel planes 8=30249
in closed end of axisymmetrical tube, radial and longit. vels, soln via Laplace eqn. 8=30248
combustion, gas flow, electrical control 8=25710
compressible one-dimensional, exact calc. 8=34611
Couette, rarified nonlinear with heat transfer 8=34616
cross flow over right-angled wedge, convective heat transfer 8=28405
through cylinder array, longit. viscous, rel. to press. drop and vel. distrib. charact. 8=39268
cylindrical and spherical, expanding cloud in rarified atmosphere 8=34601
dissociating, nonequilibrium past convex corner 8=43655
in duct, heat transfer and sublimation mass transfer at walls 8=35013
in ducts with accelerated boundaries 8=47939
flowmeter errors, due to expansion coeff. var., automatic compensation 8=25805
flowmeters, calibration equipment 8=25804
flow noise, spoiler generated, obs. 8=32919
forced convection flow over flat plate with heat source, transient heat transfer 8=24003
free convection around isothermal vertical plate 8=34658
free molecule flow, effect of molec, interreflections on concave wedge 8=39174
gas/dust mixtures, parameters in channel flow, rel. to dimensionless gas rate 8=39179
gas-particle mixture, downstream of normal shock in nozzle 8=43688
gas-soid suspension, heat and mass transfer 8=43650
heat exchange, nonstationary, in tube when heat flux and flow rate change 8=47961
heat transfer from circular cylinder at low Reynold's number 8=30259
around heated body, friction coeff. and thermal flux density 8=28389
hypersonic, rarefied, over blunt body 8=25814
hypersonic, rarefied, past flat plate 8=25815
hypersonic 3D, around blunt bodies 8=25816
hypersonic viscous interaction with flat plate, upstream influence 8=43664
ideal, in spherically symmetrical gravitational field allowing for radiant heat conduction and radiant pressure 8=47937
inlet valve, electromagnetic, very quick acting, for plasma expts. 8=47935
interferometric investigation, optimal adjustment 8=39181
inviscid, coupling with compressible boundary layer in entrance region for internal flows 8=25803
inviscid, with surface injection 8=43669
jet, compressible axisymmetric, rotating downstream eqns. 8=43657
laminar boundary-layer eqns., with mass transfer, approx. soln. 8=25813
laminar free convection about inclined isothermal plate 8=28404
laminar free convection near heated plate, boundary layer eqn. with rad. term 8=43685
Laval nozzle, Cauchy's problem soln. 8=34605
at leading edge of plate, mass, impulse and energy fluxes, asymptotic behaviour 8=34609
linear shear flow past flat plate, heat transfer coeffs. 8=34651
luminous region ahead of cylinder, using elec. shock tube 8=47943
across mag. field projecting from plane wall, potential distrib. 8=43634
measurement errors, with differential manometers 8=25806
meas. method and instrums, standardization 8=25791
measurement, condensable gases, by Kr^{85} tracer 8=34621
MGD, axisymmetric mixed flow 8=24195
MGD, steady 2 dimensional general 8=46458
m.h.d. duct, nonconducting wall boundary layer vel. and density profiles calc. 8=28593
m.h.d. shock tube generator, unsteady 8=28594
microporous media, multilayer flow of adsorbed gases 8=48476
momentum and temp.-slip coeffs. with arbitrary accomodation at surface 8=47940
motion in long pipe, invariant solutions of eqns. 8=39166
nonequilibrium, onset of shock waves 8=41833
nongray, in entrance region flow, coupling of radiation with conduction and convection, effects 8=25827
nonisothermal through packed beds, pressure profile 8=43660
in nozzles, effect of convergence angle and uncooled inlet length on heat transfer and boundary layer 8=30252
in nozzle throat, flow-acceleration effects on turbulent heat transfer 8=25808

Flow—contd
gases—contd
in nozzles, particle velocities, analytical and exptl. investigation 8=43652
oil diffusion pump, backstreaming meas. by cooled quartz crystal microbalance 8=39243
optimal suction of fluid from boundary layer on porous plate, effect of initial flow turbulence 8=30256
through orifice, to cavity, effect of heat transfer through walls, rel. to insulation of chamber 8=41866
Oseen eqns. for arbitrary gas, soln. 8=43661
over porous plate, transport processes in reacting boundary layer 8=30308
over surface cavity, heat transfer in turbulent boundary-layer separation 8=30251
over wedge, cone and sphere, soln. for radiating anal. absorbing flow 8=37298
between parallel planes, turbulent 8=34597
parameters of mixing of fine plane turbulent jets 8=30240
past porous surface, transpiration cooled, transient temp. response 8=35450
from pipe, compressed gas two-dimens. nonstationary outflow 8=34603
in porous medium, unsteady, for only slight press. change 8=34620
progress in aeronautical sciences, book 8=34614
pulsed, rel. to thermal convection around cylinders 8=34656
plasma, one dimensional, in m.h.d. energy converter channel 8=30041
radiation boundary layer flow, effect of viscous dissipation and mass addition 8=39180
radiation-heated vapours steady state motion 8=48291
radiating compressible gray gas, near plate set impulsively in motion for finite Mack number 8=43686
rarified in pipe, circular, asymptotic behaviour 8=43658
rarefied, past sphere 8=43663
rarefeld, thermal creeps through cylindrical tube 8=25807
rarified velocity field 8=34615
rarified, viscous, boundary layers, shock structure and ultrasonic propag. 8=34602
rate meas. by pressure drop timing, errors 8=30239
rates, thermal resistance detectors units 8=25802
reactive, one dimens., steady state analysis 8=34617
recording automatic continuous flowmeter 8=43647
relaxed flood mixtures of mols. and atoms generated from dissociation 8=36547
rotating flow with heat transfer, nature of thermal boundary layer 8=43646
satellite in F region, electron-ion collision effect on wake structure 8=34443
shallow-layer thermal convection eqns, based on Boussinesq approx. 8=36727
shear flow in wind tunnels, meas. near axis 8=34613
in shock tube around models, investigation using interferometer with diffraction grating 8=39172
skin friction, incompressible transpired turbulent layers 8=30263
slip, developing, finite difference analysis 8=48016
slow, past circular cylinder, for small stream-cylinder temp. difference 8=43656
solar wind, magnetized, in lunar vicinity 8=37058
sonic-point ht. transfer, effect of press. gradient 8=37303
spherical and cylindrical, expanding cloud in rarified atmosphere 8=34601
stagnation point, axisymmetric, boundary layer containing 4 inert species 8=43654
stagnation point, heterogeneous reaction dynamics 8=25812
steady, over symmetric bodies, soln. for multi-dimens. radiating and absorbing flow 8=37298
subjected to oblique mag. field, rel. to nonuniform shock wave at rest 8=39184
suction, uniform, of rarefied boundary layer, rel. to slipping vel. and temp. jump 8=30246
supersonic, in transverse mag. field, self-sustained electric discharge investigations 8=25740
supersonic rarefied, density disturbance ahead of sphere 8=43672
supersonic with detached shock wave round convex profile 8=34604
supersonic, of viscous gas near wall with corner 8=34606
transonic in Lavalle nozzle 8=39173
transonic, 2D, in presence of normal shock wave 8=47938
in tube, kinetic energy losses 8=43649
turbulent boundary layers, with arbitrary press. gradients 8=25834
turbulent convection from vertical plate, temp. distrib. and vel. in boundary layer 8=32965
turbulent in channel of circular cross-section, obs. 8=34607
turbulent, in concentric annuli 8=39178
turbulent, in entrance region of tube, heat trouble and wall friction for varying props. 8=39201
turbulent over single spheres and packed beds, heat and mass transfer 8=30951
turbulent, past flat disc, heat transfer and temp. boundary layer stability 8=37314

Flow—contd
gases—contd
turbulent Pr number rel. to friction and heat transfer coeffs for immersed plate 8=30255
ultrasonic, excitation and gas temps. 8=30257
velocity fluctuation meas., thermoelec. method 8=39177
viscous, in strong mag. fields 8=34619
viscous, radiation coupled, soln for stagnation region and flat plate 8=39204
vortex tube, Ranque effect at low temp. 8=43648
weakly ionized, rel. to shock struct. with non-equilib. radiation 8=39016
wind meas., shadow effect, scale model launch tower in wind tunnel 8=36732
Ar–air injection, Mach 10 8=25838
Ar–O, dissoc., heat transfer meas. with catalytic flat plate 8=25826
Ar plasma, radiating, relax. 8=25741
CO, vibr. relax. in nozzle flow 8=47586
CO_2–air injection, Mach 10 8=25838
He–air injection, Mach 10 8=25838
He plasma, magnetoacoustic waves 8=25738
N_2 condensation in hypersonic wind tunnel 8=30599
liquids
See also Acoustic streaming; Double refraction/flow; Hydrodynamics; Superfluidity.
alcohols, viscous flow, and l.f. dielectric relax., mech. 8=39398
along permeable plate, heat and hydrodynamic boundary layer solns. 8=39267
batch mixing of viscous liqs. with rotating agitators, model studies 8=30437
Bingham plastic surface flow anal. in canal viscometer 8=30343
boiling crisis, boundary layer analysis 8=43917
boundary layer, non stationary, calc. method 8=43722
capillary flow 8=39283
in channels formed by closely packed rods, turbulence scale 8=34720
compressible, in porous media 8=34716
conducting in mag. fields, unsteady, under influence of const. press. gradient 8=28591
conducting liq. in rectangular ducts situated in transverse mag. field, velocity distribution 8=33114
convective circulation in system and closed vertical circular duct or slots 8=30464
diffusion coeff. for liq. motion along packing 8=30361
dilute polymer solutions, impact tube meas. 8=48015
past disc rotating, heat transfer in laminar flow rel. to large viscosity changes 8=39358
distribution over contact, filtering and other z-shaped apparatus 8=30360
drag reduction by bacterial metabolites 8=34711
drag-reduction in turbulent flow, viscoelastic model and its appln. 8=48093
elastic, dynamic similarity and drag reduction through curved pipes. 8=48018
elasticoviscous, through straight tube with equitateral triangular cross-section 8=34713
elasticovscous, through straight tube with equilateral triangular cross-section 8=34713
emulsions, dilute 8=39461
film condensate, normal to body forces, rel. to hydrostatic press. variation 8=34989
film, falling, mass transfer at low Reynolds numbers 8=34745
film, visco-elastic, down inclined plane, stability 8=43745
films, electrohydrodynamic ridge instability 8=34747
final vel. of capillary motion, particular soln. of moisture transfer eqn. 8=30378
foams, drainage and overflow, test of theory 8=34953
force method of measuring small rates 8=25844
forced, conducting, viscous liquid 8=33118
forced convection flow over flat plate with heat source, transient heat transfer 8=24003
freely falling waterdrops, structure of ventilation coeffs., physical interpretation 8=25854
heated, over flat plate, eqns for one-sided heat transfer 8=28397
horizontal layer on oscillating plane, instability 8=30355
immiscible. in cracked porous medium, capillary pressure effect 8=34714
incompressible, fields of flow rel. to turbulence 8=48031
incompressible, with mass injection, turbulent boundary layer on submerged plate 8=39271
inviscid, struct. of embedded eddies, axially-symmetric 8=48033
in jet viscometer orifices, Poiseuille flow rel. to geometrical shape determ. 8=30362
laminar, excess pres. deep through sudden contraction 8=30356
laminar, in free jet at high Reynolds number 8=30357
metals and alloys in explosive cladding and welding 8=39262
metals, turbulent, effect of internal source on heat transfer characts. 8=48021
MHD, around plane plate 8=41990
MHD boundary layer in uneven mag. field 8=24182

Flow—contd
liquids—contd
micropolar layer, inclined plane 8=30391
non-Newtonian, film flow over rotating surface, and heat transfer 8=30392
non-Newtonian fluids, stability of parallel flows 8=48009
non Newtonian, power law, dimensional problem 8=30353
non-Newtonian pseudoplastic liq., convective mass transfer on circular cylinder, effect of polymer additions 8=30423
around obstacle between straight parallel walls, plane stationary and non-rotational 8=30352
optimal suction of fluid from boundary layer on porous plate, effect of initial flow turbulence 8=30256
in oscillatory conds., mass transport phenom. 8=30351
Oseen, past perpendicular flat plate, numerical study 8=25847
Poiseuille flow in annular channels with radius ratio varying stability 8=43719
polymers, linear, dilute soln, friction factor characts. 8=25845
polymer solns, conc., simple shear flow, molec. theory forstress 8=34699
polymer solns., dilute, turbulent, onset of drag reduction, molec. approach 8=30368
polymer solns., flow-time fluxtuations in capillary viscometer 8=30431
polymer solns., kinetic approach 8=39334
polymer solns., turbulent drag-reduction 8=30364
porous medium, flow of salt water 8=43726
rates, thermal resists. for meas. 8=25802
rot. viscous, forced, with heating from below 8=34718
rotating annulus, rigidly bounded, axisymmetric convective regime 8=39350
rotating between noncircular cylinders, obs. 8=43724
rotating, effect of fixed body of revolution, effect 8=30342
shear flow turbulence, drag reduction 8=30364
sheared suspension, streamlines round cylinders and spheres 8=48227
skin friction and heat transfer in gap btw. rot. coaxial cylinders 8=30463
slip flow developing, finite difference analysis 8=48016
stagnation point flow, approx. integral soln. 8=48019
steady radical, of incompressible, homogeneous ground water towards circular well 8=43725
slug stimulus and laminar dispersion coeff. 8=30379
subterranean effective porosity, definition 8=34715
over surface cavity, heat transfer in turbulent boundary-layer separation 8=30251
suspensions of rigid spheres, through tube, reductions in vol. conc. 8=48229
thermodynamic state and viscosity 8=25848
through porous bodies, anomalies 8=48024
transient heat transfer (single blow) temp. response function, props 8=46234
turbulence, in annular plane channels 8=30365
turbulent boundary layer momentum equation, solutions analysis. 8=48030
turbulent, cond. liq. in channel, convective heat transfer, alt. mag. field effect 8=41994
turbulent, in channel of rectangular section, velocity field calc. 8=48028
turbulent, in concentric annuli, heat transfer and thermal boundary layer at entrance 8=34834
turbulent, mol. transport processes accel. 8=34719
turbulent, transducer for pressure meas. 8=28226
turbulent viscosity reduction by small plastic additives 8=30436
two-dimensional, around immersed bodies, calc. method 8=39269
two-phase dispersed annular, phenomena of liq. transfer 8=34707/8
two-phase laminar, ht. transfer, graphical solns. 8=39352
viscoelastic materials, sudden flow, tensile stresses 8=30376
viscoelastic, multiphase, through porous media 8=39270
viscoelastic, stability in parallel flows, used hereditary stress/strain law 8=43720
visco-plastic medium, rectilinear steady motion 8=34706
viscous flow in annular channel with one heated wall, stability 8=43719
viscous incompressible, in curved channels, streamline motion 8=48022
viscous, study rel. to struct. at aggregates of spheres in space, and non-linear continuum mechanics 8=25894
water, flow, and l.f. dielectric relax., mech. 8=39398
water, in pipe, heat transfer rate, fluctuations induced by turbulence near wall 8=34830
water, laminar over heated and tooled plates, stability rel. to heat transfer 8=34709
water, swirling, in vertical and inclined tubes 8=30366
water, wake of sphere, turbulent vel. and temp. fluctuations 8=34701
water, with DNA additive, vel. profiles and pulsations 8=39265
wave dispersion in rotating, differentially heated cylindrical annulus 8=39277
He film, discrete rates obs. 8=24042
He II, superfluid, velocity 8=43731

Flow—contd
liquids—contd
Hg, caused by travelling mag. field, obs 8=24180
Pu alloys, in oscillating-cup viscometer 8=39330
Flow birefringence. See Double refraction/flow.
Flowmeters
See also Anemometers.
asynchronous, for liq. metals 8=48027
dual-frequency u. s. appl. 8=47911
eddy-current, for liq. metal, analysis 8=48026
electrodynamic passage flow meter 8=43632
e.m. equation, solns. for cylindrical geometries 8=43727
gas, automatic continuous recording 8=43647
gas, calibration equipment 8=25804
gas, direct action 8=25801
gas errors, due to expansion coeff. var., automatic compensation 8=25805
gases and liquids, standardization 8=25791
gases and liquids, thermal resistance detecting units 8=25802
gas, rate meas. by pressure drop timing, errors 8=30239
ionic, for small airflow 8=34610
photoelectric timing system 8=34592
pulmonary ventilation recording 8=37094
recording, for 1 ml/min. 8=30363
thermal, for liquid metals, design 8=48025
vacuum, apparatus and methods of meas. 8=39253
variable gas pressure difference, meas. errors 8=25806
water, low velocity meas. 8=34717
Na, in-core permanent-magnet, calibration and stability 8=48013
Fluctuations
See also Brownian movement; Random processes.
amplitude and phase, in irregular media, probability distrib. calc. 8=46485
beam current, compensation by ratiometer 8=37779
chemically reactive fluid, light scatt. 8=32090
continuous systems, thermodynamic theory 8=37224
cosmic-ray e. a. s., lateral struct. and e transition curve 8=38217
cosmic-ray e. a. s., nuclear-active particle component calc. 8=38219
critical, dynamics 8=37179
at critical point, non-linear effects 8=23904
density, in fluids with internal degree of freedom 8=34789
electric dipoles, permanent and collective excitations 8=37217
e. m. field on u. h. f. over-water radio path 8=37529
fluctuation-dissipation theorem rel. to Brownian motion 8=28313
γ-ray spectrometry peaks, statistics 8=42456
gas detonation velocity, origin 8=45356
gas lasers, statistical analysis 8=37573
of gas mixture in particle spectrometers, minimalization 8=28969
Gaussian beam, laser in random medium 8=46644
light scatt. from liquids, theory 8=30475-6
liquid films, rupture due to spontaneous thickness fluct. 8=48051
many particle systems, relation between response to perturbations and time-depend. correls. 8=23889
muon component in centre of e.a.s. 8=38185
muon component of e. a. s., calc. 8=38218
neutron count in short time interval, third moment 8=38082
noise emission by turbulent flames, rel. to rate of combustion and struct. 8=32108
noise in imagery with coherent light, minimizing 8=37628
plasma, computer model, E field fluctuations 8=34466
in plasmas, weakly turbulent, kinetic-theoretical approach 8=39134
polymer solns., concentration fluctuations 8=30431
pressure, due to shock interactions, obs. and theory 8=32903
pulse amplitude meas. in noise, high resolution 8=37795
random medium, quantum mechanics of waves 8=23880
relaxation phenomena near critical points 8=28317
stability of nonlinear systems, hyapurnov functions 8=41626
stability of nonlinear systems, Lyapunov functions 8=41626
turbulent-boundary-layer pressure, nondimensional form 8=39273
wall-pressure, turbulent, on body of revolution 8=39274
He liquid, theory and λ phase transition 8=32998
electrical
amplifier, coherent 30 Hz-20 kHz 8=28458
amplifier, lock-in, bandpass filter galvanometer 8=33011
arc plasma e beam, propag. 8=39009
crossed-field beam noise, suppression by lateral and transverse mag. fields 8=24139
current noise spectra of GaAs laser diodes in luminescence mode 8=46614
dielectrics, current noise, double injection 8=44748
diode, gas, space-charge-limited, suppression 8=28576
diode voltage, Fokker-Planck eqn. 8=46353
discharge-modulation noise in gas laser, suppression by external modulator 8=24302

Fluctuations—contd
electrical—contd
DNA solns, background noise between 300 Hz and 50 kHz 8=30520
dynamitron, multiloop feedback for voltage stabilization 8=24553
ferromagnetics, sound scatt. of e.m. waves, rel. to magneto-elastic const. 8=40796
flicker noise during K deposition on W emitters in field emission microscope 8=44936
gas laser noise, suppression 8=42082
in Gunn oscillators, X band, freq. modulation noise 8=27143
hot-wire anemometers, analysis 8=30238
insulating films, Schottky current, negative space-charge effect 8=44901
insulators, Schottky and Poole-Frenkel effects, distinguishing between 8=27231
ion beam current, regulator for linac 8=46438
i.r. detector, Ge:Cu, low freq. noise 8=32946
l. f. noise, surface-state related, in p-n junctions and m. o. s. transistors 8=35920
lightning discharge statistical props. of noise from predischarge part 8=45470
magnetic films pulse switching, noise subtraction circuit for gated oscillograph c.r.o. 8=31575
magnetospheric radio noise obs. from satellites 8=45496
microwave noise emission by gas discharge plasma 8=25756
noise from ceramic transducer sensors used in cosmic dust expts. thermal grad. effects 8=41576
noise in star tracker photomultiplier tubes, electron induced 8=28577
noise, l/f, statistics 8=37371
noise props. of systems in local equilib., fluctuation-dissipation theorem 8=37370
noise spectrometer, microwave 8=46501
photoelectric detection, shot noise photon bunching effects 8=46418
photomultiplier output, optimum filter 8=28579
photomultipliers, single-electron component, use in meas. 8=46426
p–n junction, forward-biased, l.f. noise due to charge fluctuations in depletion layer 8=40519
quantum mechanics for noise spectrum and admittance of a system relation 8=28326
radio noise, lightning generated, global survey, Aerial III equipment 8=28026
semiconductor diode junctions, in avalanche, meas. in r.f. and ultra-r.f. region 8=40534
semiconductor laser junction, noise 8=33194
semiconductors, current noise, double injection 8=44748
spurious-count rejection 8=46927
transistor wideband meter 8=46318
Al_2O_3 secondary emission, shot noise 8=44949
Au thin films, current noise obs. 8=40310
CdS, current noise, excited, in non-ohmic region 8=31371
CdS space-charge-limited diode, limiting noise 8=27177
p-Ge, hot current carriers 8=40457
Ge:Au photoresistors, surface charge effects on I-V characts. and excess noise 8=36034
InSb, microwave noise emission stimulated by acoustic wave amplification 8=49249
n-InSb, noise spectrum and photoconductivity kinetics 8=27327
MgO secondary emission, shot noise 8=44949
Nd glass lasers, noise obs. 8=24344
SCL diodes, h. f., source 8=27172
Si avalanche diodes, noise of self-sustaining discharge, microwave meas. 8=40537
Si, avalanche discharge, noise 8=35933
p-Si, due to hot electrons, room temp. and liq. N_2 temp. meas. 8=35759
Si, ^{1}/f noise, due to carrier motion in surface band 8=40213
Si, space charge limited triode, noise parameters 8=31409
Si transistor noise at v. l. f., .05-.0001 Hz, obs. 8=40543
n–Si : Au, noise temp. and light-illumination dependence 8=44824
W secondary emission, shot noise 8=44949
Fluid flow. See Flow
Fluid mechanics. See Hydrodynamics.
Fluidized powders. See Flow; Fluids; Powders.
Fluids
See also Gases; Liquids.
adherence to wall 8=43638
angular momentum mixing by stirring rotating fluid 8=47929
approximate radial distrib. function 8=47897
axisymmetric flow, system of boundary layer eqns. 8=34582
binary mixture, Percus-Yevick-II integral eqns. 8=30193
Born-Green equation, self-consistent, improvement to eqn. of state 8=47900
boundary layer on plane plate in presence of strong longitudinal mag. field 8=33115
boundary layer problem, soln. using Prandtl-Mises transformation 8=47910
classical, new symm. integral eqns. 8=34572
conducting homogeneous in mag. field, with horizontal interface, gravitational instabilities 8=33117

Fluids—contd
- conducting, steady-state flow at large Hartman numbers 8=41993
- convection, classical cellular, with spatial heat source 8=30189
- convection in box, depend. of preferred wave-number of Rayleigh number 8=47919
- convection flow stability, heated from below, in gravitational field 8=46251
- convective instability problems, application of Galerkin method 8=47920
- convective motion between vertical planes, spectrum of perturbations and stability 8=46250
- Couette flow of anomalous Grad fluid 8=47905
- critical region, Ornstein-Zernike theory 8=25975
- deformable directed, simple 8=43615
- dense, non-equilibria, Prigogine theory 8=43618
- density fluctuations, freq. spectrum 8=34789
- dipolar, monopolar force exerted onsphere immersed in slowflow 8=25792
- dissipative systems, symmetry breaking instabilities 8=32836
- drag reducing, turbulent heat transfer 8=46233
- dynamic laws of fluid free surfaces and interfaces, contribution to generalization 8=30198
- dynamical and thermal boundary layers on flat plate for non-Newtonian fluid 8=30213
- elastico-viscous, static stability 8=43616
- electrically conduct., viscous and incompressible, MHD confined vortex flow 8=41996
- electron-fluid-dynamical waves, nature 8=28546
- Enskog eqns., temp. depend. of rigid-sphere dia. 8=30185
- entropy, communal, influence on liq. state reappearance 8=25976
- equation of state of simple fluid 8=30186
- equilibrium configurational properties, appln. of statistical mechanics 8=34573
- equilibrium theory, Born-Green-Yvon and Kirkwood hierarchies 8=47898
- excess electron in nonpolar fluid, localization 8=34571
- films, thin, disjoining pressure 8=30195
- flow across mag. field projecting from plane wall, potential distrib. 8=43634
- flow between rotating and stationary discs 8=30210
- flow growth of disturbances in both space and time 8=30207
- flow, non-planar parallel, long wavelength disturbances 8=30211
- flow, stratified, past finite flat plate, theory 8=43628
- flow through woven screens, pressure drop correlations, packed bed model 8=47912
- flow, transversal in limiting layer, curvature of polar representation 8=25794
- flow viscous, axisymmetrical motion 8=43630
- flow, viscous near walls and obstacles, boundary limit problems 8=30218
- fluidized bed, radiative heat transfer with immersed body 8=39456
- fluidized beds, calc. of impedance of ordered stacks of spheres 8=47903
- friction-constant formalism 8=39150-1
- half-space, layered, standing waves 8=32889
- hard spheres, distrib. function 8=37221
- hard spheres, quantum-mech. pair-correl. function 8=28348
- Hartman boundary layer, stability under parallel mag. field 8=41988
- homogeneous, isotropic, turbulent flow, probability dist. of velocity difference at two distinct points 8=47924
- horizontal layer, subcritical instability and exchange of stability 8=30234
- ideal, Einstein field eqn. sols. 8=37174
- instability, Rayleigh, theory 8=43625
- interface between conducting and nonconducting, stability in varying vertical elect. field. 8=43622
- interface stability with relative motion 8=43620
- inviscid, parallel flow, stability 8=30212
- kinetic theory, small perturbation method 8=30209
- Kirkwood-Salsburg integral eqn. and superposition approx. 8=34570
- laminar boundary layer, non isothermal, method for solving eqns. 8=25797
- laminar flow, stability 8=43626
- laminar forced convection in eccentric annuli 8=46249
- layer, heated from above, stability 8=43619
- layer with finite resistivity, self-gravitational instability 8=43621
- layers, horizontal, thermal convection 8=43614
- magnetofluid dynamics, pressure distrib. meas. around sphere 8=28588
- micropolar and dipolar, Poiseuille flow in circular channel 8=47907
- micropolar, Couette flow 8=39162
- mixtures, effects of molec. sizes on thermodynamic props. 8=47896
- molecular and many-body, optical props. 8=37680
- monatomic, review of theory 8=30190
- monatomic, with 6-12 pot., eqn. of state and excess internal energy 8=30191
- Morse potential, relation with Altenburg's quadratic mean radius 8=47722

Fluids—contd
- motion between rotating spherical surfaces 8=43631
- motion, vertical, of spherical particles 8=47921
- motion in long pipe, invariant solutions of eqns. 8=39166
- multispecies quantum, ground state, var. method 8=37199
- non-Fourier power fluid, thermal boundary layer on variably heated surface 8=39357
- non-Newtonian, flow impulse theory extended to include rotation 8=25796
- non-Newtonian, laminar incompressible boundary layer flow 8=34585
- non-Newtonian viscous, radical flow between discs. 8=39160
- nonspherical mols., transport coeffs. 8=39153
- opalescent, spectrum of doubly scatt. light 8=39152
- oscillations, in cavity in rotating solid body 8=46018
- Poiseuille, flow, thermally stratified plane, stability 8=43629
- pressure at solid boundary, measuring instrument 8=30197
- puffs, inclined buoyant motion 8=39168
- quantum, h.f. elasticity moduli 8=41772
- quasi-incompressible, convective instabilities in fully developed flows 8=34580
- radial distribution function, theory 8=30192
- Rayleigh-Jeffreys problem with boundary slab of finite conductivity 8=30187
- relativistic turbulence, mean flow equations 8=34594
- rotating Couette flow, stability, asymmetric waveforms 8=30206
- rotating cylinder, short, observed motion of sphere 8=30348
- rotating, in container of finite length, rise of body 8=30347
- rotating rapidly, slow transverse flow past obstacles 8=30201
- rotating, source-sink flows 8=39156
- second-order, torsional flow between two parallel discs, inertia effects 8=25842
- spreading of a twisted stream in an infinite space flooded by the same fluid 8=47906
- stratified, shear flow, method of prod. 8=39157
- stratified, spin-up 8=43617
- stratified, stably, selective withdrawal 8=30188
- structured, nonrigid, constitutive eqns. 8=43623
- thermal instability, gravitational effects, effects of surface stresses 8=30290
- thermal stability of completely confined fluids, Hilbert spaces analysis 8=25786
- three-layered, development of flow in plane tube in presence of transverse mag. field 8=30204
- transient flow near rotating disc after impulsive starting from rest 8=39164
- transient upstream temp. changes, anal. by max. slope method 8=34574
- turbulence, distortion by irrotational plane strain 8=39169
- turbulent boundary-layer separation 8=30227
- turbulent boundary layers, external region universal properties 8=34599
- turbulent flow in pipes, velocity distribution expression and eddy diffusivity profile 8=47927
- turbulent flow near smooth wall, conducting sublayer 8=43642
- turbulent motion equations 8=47923
- turbulent separation, motion of, numerical experiment 8=47928
- uncompressible axisymmetrical flow, analytic solution of system of eqns. 8=43639
- velocity meas., tracer-particle laser appl. 8=41623
- viscoelastic, Couette flow, plane parallel, linear instability 8=47909
- viscoelastic flows, dimensional considerations 8=47915
- visco-elastic, non-linear, stability against shear waves of steady flows 8=43635
- viscous flow, boundary problem, small parameter method appl. 8=25846
- viscous, flow past heated thin plate, isothermal and non-isothermal motion 8=30358-9
- viscous, linear wave motions of hydrodynamics, gen. solns from potential eqns. 8=23829
- viscous nonlinear incompressible isotropic, plane deform. fields character 8=47899
- viscous, nonlinear singular boundary value problem, analytical solution 8=47918
- viscous, transient sound propag. theory 8=46183
- visoelastic, secondary flow due to rot. oscills of sphere 8=39155
- volume viscosity, relax. times 8=30194
- Vortex lattices, collective modes. 8=25785
- wave dispersion in rotating, differentially heated cylindrical annulus 8=39277

Fluorescence. See Luminescence.

Fluorescent screens. See Luminescent devices.

Fluorimetry. See Chemical analysis.

Fluorine
- active to passive gravitational mass ratio, comp. with A 8=41743
- active to passive gravitational mass ratio, comp. with B 8=41743
- active to passive gravitational mass ratio, comp. with Br 8=41743
- atom, mag. moment, wave function calc. 8=47531

Fluorine—contd
- atoms, Rydberg orbitals calc. 8=29620
- isoelectronic sequence, spectra of ions from Sc XIII to Cu XXI 8=29628
- molecule F_2, dissoc. energy and band spectrum 8=34376
- reaction with NCN, matrix-isolation 8=47712
- solid, cryst. struct. and intermolec. forces 8=48648
- Zircaloy-2 surface contamination effect on corrosion in water and steam 8=45352
- F^- in aq. soln., determ. by atomic absorpt. spectrometry 8=27788
- F_2, emission spectrum 8=29735
- F^{19} chem-shifts B, P(III), phosphoryl and thiophosphoryl halides 8=43406
- F^{19} in aq. solns., effect of Cu^{2+} on n.m.r. relax. 8=48222
- F^{19} in CaF_2, relaxation, field dependence 8=49634
- F^{19} in CaF_2 : Mn^{2+} nuclear spin-lattice relaxation 8=49633
- F^{19}, n. m. r. in NbF_6^- 8=34914
- KLL Auger spectrum in 3 fluoride salts 8=34166

Fluorine compounds
- five-component fluoride as laser material 8=28706
- fluorite crystals, magneto-optical rotation of Ce impurity centres 8=49718
- hexafluorides, octahedral mols. force fields, calc. 8=38863
- salts, KLL Auger spectrum 8=34166
- FCN, direct l-type doubling transitions 8=34323
- F_2CN, matrix-isolated, i.r. spectrum 8=38946
- FCO radical, potential functions and bonding 8=47713
- FI, vac. u. v. spectrum 8=33264
- $F_2O + H_2$ flash photolysis for HF laser 8=37582
- $F_2SO_3 + SO_3$, reaction kinetics 8=45333
- HF, n.m.r. F^{19} chem. shift in H_2O and D_2O 8=43874
- HOF, i.r. spectrum and vibr. potential 8=43299
- SF_6 + U or U compounds, fission product decontamination 8=43128

Foams
- See also Bubbles.
- dielectric constant, complex, real component meas. in GHz 8=48245
- drainage and overflow, test of theory from fractionation columns and stationary foams 8=34953
- polyurethane, appl. to plate spark chamber 8=24540
- polyurethane, mech props., effect of cell membranes 8=48243

Focused collision sequences. See Sputtering.

Focusons. See Crystals/lattice mechanics; Sputtering.

Fog
- artificial microstructure continuous meas. by small angle method, halo apparatus 8=34946
- backward scattering of laser radiation optical thickness dependence 8=34949
- drops, electrically charged by diffusion 8=36740
- radiation, stationary method 8=32203

Fokker—Planck equation. See Transport processes.

Foldy—Wouthuysen transformation. See Field theory, quantum.

Forbush decreases. See Cosmic rays/variations.

Force. See Dynamics.

Force constants. See Molecules/vibration.

Force measurement.
- gravitational gradient sensors, rotating cruciform-shape, vibrational mode behaviour 8=37168
- in metal cutting at 100-700 m/s 8=35655
- precision trandučers, standardization 8=23795
- quartz shorted-guard-ring stress gauge 8=37110
- in Al cutting at 100-700 m/s 8=35655

Fortran. See Calculating apparatus/digital computer programmes.

Fountain effect. See Helium/liquid; Superfluidity.

4 π counters. See Counters.

Fourier analysis
- See also X-ray crystallography/calculation methods.
- deconvolution of physical data 8=23785
- electromagnetic director field theory appl. 8=41944
- polynomials, orthogonal, general formula for sequence 8=32653
- two-line, influence of cut-off 8=35299

Fourier series. See Series; Transformations, mathematical.

Fourier-transform spectroscopy. See Fourier; analysis; Spectroscopy.

Fractionation. See Distillation.

Fracture
- See also Mechanical strength
- alloys, heat resistant, physical parameters, high temp. and high stresses 8=26760
- biaxial criterion for porous brittle materials 8=48974
- brittle and ductile, material resistance 8=35627
- brittle, energy criterion, crack propagation 8=40115
- brittle in 3-dimens., extension of Griffith's theory for flat elliptical crack 8=26767
- in brittle solids, controlled, rel. to interruption of elec. current 8=35632
- cellulose, Du-Pont K116-207 films, fracture toughness, obs. 8=44614
- ceramics, role of plastic deform. in crack propag., and dislocation mobility 8=31180
- charpy-V specimens, appearance assessment, television microscope 8=40113

Fracture—contd
- cleavage, double-cantilever, discussion on theory 8=26769
- cracked plate, under plane stress 8=46025
- creep rupture parameters 8=44526
- ductile metals, initiation 8=48972
- flaw growth mechanics and applic. 8=48979
- glass, brittle, study by stress wave propag and reflection 8=44531
- glass, mist zone on surface, microstructure 8=30722
- high strength alloys, microstructure dependence of toughness 8=49011
- high-strength mats., toughness dependence on thickness, effect of work hardening exponent 8=26766
- initiation by plasticity relax. and spread from sharp groove, after deform. 8=32766
- invariant criterion, qualitatively correct 8=26770
- metal, test behaviour and working props. 8=40087
- in metallic/brittle aggregates, initiation at reinforcing particles 8=31182
- metals, b.c.c. or h.c.p., effects of alloying elments 8=31189
- metals, under static and repeated loads 8=48971
- mica, obs. of props. 8=49052
- nature, in relation to total potential energy 8=26768
- polycrystalline materials, cleavage, hydrostatic pressure effects 8=48978
- polycrystals, rel. to slip charact. 8=31177
- polymers, linear amorphous, theory inc. viscoelastic and plastic considerations 8=31249
- polymethylmethacrylate, brittle, study by stress wave propag and reflection 8=44531
- polystyrene, brittle, study by stress wave propag and reflection 8=44531
- pyramidal, generalized, and yield interia 8=41712
- quasi-brittle, conditions 8=44530
- quasi-brittle, crack propagation in continuous media 8=44533
- steel, analysis rel. to environment 8=49008
- steel, ball bearing, fatigue crack props. rel. to crack growth, electron microfractographical studies 8=35696
- steel, high-strength, toughness dependence on thickness, effect of work hardening exponent 8=26766
- steel, high tensile, stress-corrosion cracking 8=31212
- steel, rosette, star, tensile 8=35687
- steel, split, layered, cup and cone tensile fracture 8=35685
- steel, stainless, fracture micromechanisms 8=49012
- steels of ultra-high strength, toughness dependence of microstructure 8=49010
- strength, elastic plastic stress distrib. of notched bars 8=46058
- surface fracture study, comparison of transmission and scanning electron microscopy 8=48415
- systems-type anal. including struct., loading, stress, elasticity etc. 8=31179
- tensile, initiation rel. to microstructure 8=31174
- toughness testing, state for WOL specimen 8=48973
- viscoelastic mat., linear, crack initiation rel. to loading history 8=31178
- Al alloys, toughness, effect of specimen type and crack orientation 8=48989
- Al, analysis by acoustic emission 8=48996
- Al, high-strength, toughness dependence on thickness, effect of work hardening exponent 8=26766
- Al-Mg-Zn alloy, new rupture pattern obs. by replica tech. 8=35658
- Al_2O_3 trichites, rupture constraint rel. to structural state 8=26777
- AlSb, surface hydrolysis effects 8=44443
- Al-20%Zn alloy, temp. effects rel. to triple-point cracks 8=48993
- Be, analysis by acoustic emission 8=48996
- CaF_2, fracture surface as function of crystallographic direction and treatment method 8=44593
- Cu, activation energy, temp. effect 8=26797
- Cu, fatigued, dislocation structure associated with surface 8=40143
- Fe, cast, criterion 8=49007
- Fe-21%-Cr-0.05%C alloy, ductile mechanism, 20-600°C 8=26819
- Ir crystals, brittle, scanning e-microscope obs. 8=26825
- KCl, fracture surface as function of crystallographic direction and treatment method 8=44593
- LiF, fracture surface as function of crystallographic direction and treatment method 8=44593
- Mg, of seond-order twins 8=44588
- MgO, cleavage steps interaction with crack front 8=44591
- Mg-Sn alloy, and twinning along $\{10\bar{1}1\}$ planes 8=44592
- NaCl, fracture surface as function of crystallographic direction and treatment method 8=44593
- NaCl work of fracture for crystals containing cavities 8=26834
- Ni alloy high-strength, stage I fatigue, characts. 8=26839
- Pb, activation energy, temp. effect 8=26797
- Ta-Re alloy, cleavage, rel. to conc. and temp. 8=40182
- Ti alloys, fracture toughness parameters 8=49058

Fracture—contd
- Ti alloys, high-strength, toughness dependence on thickness, effect of work hardening exponent 8=26766
- Ti-8Al-1Mo-IV alloy, creep rupture props. 8=49060
- W, sintered, brittle, nucleation at low temp. 8=44608
- in WC-Co alloys, rel. to plastic deformation and microstructure 8=26851

Francium
- No entries

Francium compounds
- No entries

Franck–Condon factors. See Spectra.

Franck–Read sources. See Crystal imperfections/dislocations.

Fraunhofer lines. See Astronomical spectra; Spectra; Sun/spectra.

Free radicals
- aliphatic fragment, proton h. f. s. and spin-spin coupling 8=38943
- alkyl, spin density distrib. calc. 8=43416
- alkyl, spin density distrib. Hartree-Fock calc. hetero-atom model 8=43417
- amino acids, γ-irrad. crysts., e.s.r. 8=40907
- anion type, electrolytically prod., e.s.r. and polarographic studies 8=43860
- apparatus for e. p. r. solid state obs. of radicals formed in gas phase by 5 to 500 eV electrons 8=25652
- aromatic, g-factors, precise meas. and correlation with π-orbital energies 8=47708
- from benzene photochem. oxidation in gas phase 8=41286
- 1, 4-benzoquinone, in soln., e. s. r. spectral linewidth alterations, 20-80°C 8=47681
- benzyl, absorpt. spectrum 8=43420
- benzyl, polarization of vibronic transitions 8=25549
- in cellubiose frozen aq. solns., e. s. r. 8=47707
- chloro-acetyl DL-alanine irrad. crysts., rot. of methyl groups 8=36240
- cometary emission spectra synthetic profile computed, 4050 Å 8=50424
- cyclooctatetraenyl radical anion, electronic spectrum 8=25658
- in crystals, electron resonance and ENDOR spectra 8=40969
- diethylamine radical ($C_4H_{10}N$), ionization at W surface 8=47794
- 2, 5-dimethoxysemiquinone anion, solvation by protic and aprotic solvants 8=45358
- dimethyl (9-fluorenyl) sulphonium bromide, X-irrad. e.s.r. of trapped radicals 8=31883
- 2, 2′-dinitrodiphenyl anion, e.s.r., linewidth effects 8=38945
- di-tert-butyl-nitroxide time dependent interactions, e.s.r. and p relaxation study 8=48207
- di(tetramethyl-2, 2, 66 piperidinyl-4 oxyl-1) terephthalate strong or weak exchange 8=43423
- DPPH, e.s.r. of solns. in weak fields 8=39418
- DPPH in rigid matrix, spin-lattice relax. 8=27471
- dynamic nuclear polarization, relaxation and paramag. shifts of protons 8=38915
- electron spin density attenuation, comp. with molecules and complexes 8=47593
- electrons considered as, chemical properties 8=25322
- ethyl, reactions with SO_2, 28-75°C 8=49848
- fluorinated methyl, MO theory of geometry and hyperfine coupling consts. 8=47564
- fluorocarbons in soln., dynamic polarization of F nuclei 8=48221
- fluoro-organic solns., nuclear-electron interactions and molecular motion 8=39436
- from formamide, hydroxyurea, and malonamide, struct. 8=32138
- formation by autoradiolysis of radioactive labelled organic compounds, e. s. r. study 8=47709
- in gentibiose frozen aq. solns., e. s. r. 8=47707
- glutaric acid, X-irradiated, recombination rel. to polymorphic transform 8=29828
- in glycine γ-irrad., e.s.r. 8=31844
- glycine, irrad. crysts., e.s.r. 8=49610
- hexachloroethane, X-irradiated, recombination rel. to polymorphic transform 8=29828
- from hydrocarbons (isobutane, pentanes, hexanes), irrad., e. s. r. obs. 8=25659
- intermediate stability, e.s.r. 8=48204
- in maltose frozen aq. solns., e. s. r. 8=47707
- mass spectrometry, review 8=29829
- methyl and deuteromethyl radicals adsorbed on Si gel, e. s. r. spectra rel. to tumbling 8=25660
- methyl, e. s. r. on porous glass surface 8=47684
- methyl group, n. m. r. narrowing due to coherent zero-point motion 8=25635
- methyl, isotopically substituted, vibronic effects, MO calc. 8=43421
- methyl, reactions with SO_2, 25-164°C 8=49847
- p-methylbenzyl radical formation from p-xylene 8=36617
- methyleniminyl, electronic absorpt. spectrum 8=34337
- 5-nitro-6-methyluracil, γ-irrad. cryst., e.s.r. 8=49615
- nitroxide bi- and polyradicals 8=25661
- nitroxide from diethylhydroxylamine, dioctylhydroxylamine and N-hydroxypyrrolidine, e. s. r. obs. 8=25655
- nitroxide, proton resonance at 310 MHz 8=43415

Free radicals—contd
- nuclear dynamic polarization, spin-temp. model 8=25653
- nuclear mag. relax. and dynamic nucl. polarization in free radical solns. of toluene 8=39439
- from nucleic-acid bases irrad. in reactor, yields and spectra 8=49891
- organic compounds, formation in solns. from e.s.r. 8=32117
- from organic cpds, γ-irrad., stabilization by nitroso cpds for e.s.r. exam., 8=49980
- organic, in solution, e.s.r. 8=48205
- peroxy, produced by irradiation of tetrafluoroethylene-hexafluoropropylene copolymers, e.s.r. 8=43422
- phenoxy, C^{13} splittings in e.s.r. 8=38947
- phenoxy, n.m.r. 8=43411
- phenoxyl, absorpt. spectrum 8=43420
- p-phenylenediamine cations, u. v. spectra, dimerization of radicals 8=25657
- phosphorus oxyhalide, electronic emission spectra 8=43414
- π-radicals, F hyperfine interactions 8=29816
- planar, conjugated π, σ spin densities calc. 8=34379-80
- polycaprolactam, stressed, behaviour in photodegradation 8=45399
- polyethylene terephthalate, stressed, behaviour in photodegradation 8=45399
- polymer fibres, stressed, behaviour in photodegradation 8=45399
- polymer radicals in aq. soln., e. s. r. 8=34906
- polymers solid, secondary, reactions mech. damage 8=45361
- polyoriented, e. p. r. spectra, interpretation 8=34378
- pyridinyl diradicals, stable, intramolec. assoc. 8=43424
- from pyrimidine nucleosides, irrad. in reactor, yields and spectra 8=49891
- reaction kinetics in capillanes, e.p.r. meas. 8=27690
- recombination kinetics, nonequilib effects 8=27679
- recombination prod. by irradiating various organic compounds with γ rays 8=38939
- semicarbazine hydrochloride, γ-irrad. crysts. 3=49604
- silk, natural stressed, behaviour in photodegradation 8=45399
- solids, formation by grinding 8=25656
- in solution, electron-electron double reson. 8=38940
- solutions, e.s.r. in weak fields 8=39418
- in starch, γ-irradiated, e.s.r. 8=49618
- TEMPAD biradical, paramag. susceptibility, anomalous behaviour 8=40756
- 1, 4-Bis (2, 2, 6, 6-tetramethyl-4-hydroxy-4-piperidyl-1-oxyl) butadiene, stability up to 144°C 8=39417
- tert-butyltropenyl radicals, mono- and tri-, e.s.r. 8=38944
- tetramethyl-2, 2, 6, 6, -piperidinol-4-oxyl-1, in crystal, structure and bonding 8=25654
- tetramethyl tin, e. s. r. detection 8=34382
- thiobenzophenone anion, formed by light excitation in (n, π^*) band 8=29827
- transient, prod. by pulse radiolysis, e.p.r. 8=49970
- trapping matrices, viscosities of organic glasses 8=49065
- trichloromethyl in solid Ar, i. r. spectrum 8=29831
- trifluoromethyl, e. s. r. in inert-gas matrices 8=34381
- in triglycine sulphate, γ-irrad., e.s.r. 8=31844
- sym-trinitrobenzene anion, effect of Li cation on spin density 8=47714
- 2, 4, 6-triphenylpyryl, e. s. r. 8=29832
- yield from γ irrad. of organic compounds, e.s.r, study 8=49967
- C_2 in acetylene-air flame, intensified by discharge, activation energy of origin 8=45359
- C_2 in comets, forbidden intercombination transition 8=28154
- CF_2, matrix-isolated, i. r. spectra 8=29723
- CF_2-$C(CF_3)$-CF_2, photoinduced and thermal conversion to CF_2-$CF(CF_2)$-CF_2 8=49953
- CF_3, matrix-isolated, i. r. spectra 8=29723
- CF_3OOO, e.s.r. 8=38941
- CH, in acetylene-air flame, intensified by discharge, activation energy of origin 8=45359
- CH-radicals, h.f.s. null field reson. 8=43418
- CH^+, $^1\Delta \rightarrow {}^1\Pi$ and $^3\Sigma \rightarrow {}^3\Pi$ band systems 8=38942
- CH_2, ht. of formation 8=29985
- CH_3, high-energy, from photolysis of CH_3Br 8=49961
- CH_3, photoionization 8=29985
- CH_3, reaction with O atoms 8=49880
- C_7H_6D, e. s. r., effect of D substituent 8=47706
- ClCO, potential functions and bonding 8=47713
- ClO_3, in γ-irrad. $NaClO_3$ cryst., e.s.r. 8=49613
- CN, σ-states, electronic configs. and N^{14} quadrupole coupling 8=47710
- D_2O X-irrad., primary radical yields 8=49972
- FCO, potential functions and bonding 8=47713
- F_2CN, matrix-isolated, i.r. spectrum 8=38946
- FNCN, i. r. spectra 8=47712
- H, conc. profile in H_2-O_2 flame, e.p.r. study 8=49892
- H_2O vapour irrad. with 1 MeV He^+ 8=49968
- HCO, potential functions and bonding 8=47713
- NH_3OHCl, X-irradiated, e.s.r. of radical pairs, V_K centres and trapped NO 8=31878
- NO_2, radical pair in cryst. N_2O_4 matrix 8=45096
- OH, in acetylene-air flame, intensified by discharge, activation energy of origin 8=45359

Free radicals—contd
OH, in Li_2SO_4, n-irradiated, thermal decay, e.s.r. study 8=27481
OH, matrix-isolated, i.r. spectrum 8=34276
OH$^+$, $^3\Pi_i$ excited state, fine structure 8=29830
OH*($^2\Sigma^+$) from photodecomp. of H_2O, quenching and relax. 8=47613
OH and OD, spectra in solid Ne, evidence of rotation 8=32020
SO_2^- radical ion, e.p.r. investigation 8=38948
SO_3^-, optical spectrum from photolysis of dithionate ions in soln. 8=49957
$S_2O_6F_2 \rightleftarrows 2SO_3F\cdot$ equilib. in gaeous state. e.s.r. 8=47711
Freezing
See also Melting; Supercooling.
acetone, high press. 8=50477
alkali halides, thin crystals, dislocation arrays microscope examination 8=43902
aqueous solns, dentritic cryst. of ice 8=30835
austenitic stainless weld metal solidification 8=48265
bars, solidifying, temp., distrib., location and shape of solid-liq. interface 8=43908
binary eutectic alloy, with time depend. surface temp., heat transfer anal. 8=34967
clouds, radar refl. obs. 8=32224
enstatite melts, incorporation of rare gases 8=34972
fluids, theory 8=30190
gelatine, vitrification temp. 8=48256
ice, growing cylindrical crystal, morphological stability 8=39673
ice, liq.-like transition layer, survey 8=34975
ice nucleation by AgI, nature of nucleating site 8=32216
ice nucleating props of mineral particles 8=35229
ice nucleation, substrate-ice interface obs. 8=25986
ice on silicate surfaces, existence of liq. like, unfrozen interfacial water layer 8=35142
ice-solution interface, model, rel. to 'freezing potential effect' 8=34970
infinite plate solidification, calc. of thermal stresses 8=39478
ionic solns, very dilute, ionic distrib. and phase boundary pots 8=34971
metals, solidification in vacuum, nature of exoelectrons emitted 8=40692
metals, solification profiles with ultrasonic pulses 8=39477
methylcyclohexane, high press. 8=50477
normal, binary systems with cubic liquidus and solidus lines 8=25983
sea ice, dielectric props., —55°C 8=35956
sea water, cause of haline convection 8=41332
slab solidification, general starting soln. 8=39471
soil, moisture migration and determ. of stratified texture 8=34969
solid-liquid interface stability 8=43910
solidification, grain size dependence 8=35233
supercooling, constitutional, during solidification, thermal diffusion effects 8=34974
supercooled water, nucleation by cavitation 8=25981
suspended waterdrops, and fragmentation, influence of environmental parameters 8=25853
water, contact angle of water on ice for rapidly freezing interface 8=35146
water droplets falling in air and other gases 8=25984
water drops, supercooled, crystallization processes 8=25985
water, supercooled, basal-plane solidification, effects of impurites 8=25982
Ag, bubble formation during solidification 8=30587
Al-Cu alloys, chill zone in ingot solidification 8=43912
Ar, solidification 8=43909
Bi, supercooled liq., effect of u.s. vibs on nucleation 8=48261
H_2O drops on metal plate, cooling rate and freezing temp. interdependence 8=48263
H_2O, in vapour to ice conversion by AgI 8=45458
Hg subcooling 8=30583
NaCl solns., homogeneous nucleation 8=34973
Pb-0.005%Sn alloy, hydrodynamic currents in solidification front region 8=34968
Sb, temp. standard, apparatus 8=30585
Sb, temp. standard, measurements 8=30586
UCl_4-$PbCl_4$ liquidus, obs. 8=30584
Frenkel defects. See Crystal imperfections/interstitials.
Frequency. See Time measurement.
Friction
See also Internal friction.
annular contact tester 8=35637
coal and sandstone, minimum fluidizing vel. 8=26042
Coulomb, damping of chatter vibrations 8=23929
drag-reducing additives, effect on vortex streching 8=34721
drag reduction by bacterial metabolites 8=34711
flow around heated body, coeff. and thermal flux density 8=28389
forces in turbulent boundary layer on plate, rel. to step changed of wall conditions 8=30245
graphite, coeff. changes on condensable vapour
graphite, rate changes on condensable vapour intercalation rel. to lattice expansion 8=44208
Friction—contd
Green, invariant imbedding eqns. from operator theory 8=28228
mass on vib. surface, 'frictional viscosity' effect 8=32695
metal surfaces, rel. to contact area 8=26775
non-stationary contact, analog simulation of heat generation 8=37319
polyformaldehyde, antifriction props. 8=31246
polymers, and wear, effect of C fibre reinforcement 8=40192
rolling, and adhesion process 8=31186
rubbers, effect of load on temp. and velocity depend. 8=31252
skin, fluctuating, in air, meas. with heated thin-film gauges 8=39236
skin, in liquid gap between rot. coaxial cylinders 8=30463
steel, rel. to exoelectronic emission 8=44939
turbulent boundary layer on plate in incompressible liquid with mass injection 8=39271
two-member law, verification rel. to real surface of contact of metals 8=32697
wall/tangential jet, Preston tube and balance meas. 8=30268
wear-stick/slip correlation 8=35638
Al alloys, antifriction props. 8=44544
Al, rel. to exoelectronic emission 8=44939
Cu-Au solid solution alloys, and wear and surface hardness, in abrasion 8=40149
W, chemisorbed gases effects 8=49061
Frictional electricity. See Electric charge; Electrostatics.
Fuel cells. See Electricity/direct conversion.
Fugacity. See Diffusion in gases; Kinetic theory/gases.
Functions
cascade processes, charact. functional 8=25034
extremal norm-determining measures for Hilbert spaces of entire functions 8=46810
generating functionals and eqns. of motion in classical and quantum statistics of nonequilib. systems 8=41770
Green's for 1D Fermi system, props. 8=28335
Green, in spin-1/2 Heisenberg ferromagnet, decoupling scheme 8=36086
Green's, in atomic and molec. calc. 8=34130
Green's, spectral anal. 8=46801
hypergeometric, elastic equilibrium of plates and shells 8=46038
kinetic stress function determination in elastodynamics 8=46037
logarithmic and power, pulse analogue devices, and mult. and division of power fns. 8=45985
Lyapunov generation, topological approach 8=41626
modulating function, ϕ treated as function of standard deviation 8=45947
set, in space-like region, construction 8=45973
spin-weighted, geometric theory 8=23798
H, convexity 8=41761
Fundamental concepts. See Physics fundamentals.
Fundamental constants. See Constants.
Fundamental particles. See Elementary particles.
Furnaces. See Heating
Furry theorem. See Quantum electrodynamics.
Fusion. See Heat of fusion; Melting; Nuclear fusion.

g-factor. See Elementary particles; Gyromagnetic ratio; Nucleus; Spectra.
Gadolinium
Curie temp. variation with hydrostatic press. and anomalous compressibility 8=36149
electronic structure from positron annihilation studies 8=26906
electronic struture from relativistic augmented-plane-wave calcs. 8=26905
electrons, field-emitted, polarization in high mag. fields 8=27342
ferromagnetic, mag. viscosity 8=45029
generalized susceptibilities and mag. ordering 8=44973
Hall effect meas. 4.2°-340°K, in mag. fields to 30 kOe 8=44690
ion sputtering on Al, Ta targets, ang. distrib. obs. 8=48909
Knight shift and pseudopotentials 8=45129
lattice parameters rel. to pressure 8=48669
magnetic fields induced at nuclei 8=49558
magnetic-ordering temp., pressure dependence 8=31652
magnetic ordering temps. at high pressures 8=40730
magnetic props. from mag. moment meas. at 4.2°K and high fields 8=31705
magnetization anisotropy and magnetostriction meas. in pulsed fields up to 150 kOe 8=40743
susceptibility ferromag. impurity dependence near Curie temp. 8=40751
ultrasonic attenuation at Curie pt. 8=35416
Ga^{3+} ions in CaF_2-type crystals, e.p.r. spectral cubic splitting temp. dependence, 77-950°K 8=40909
Ga^{3+} spectrum in $CaWO_4$ cryst., ^8P Stark levels and line polarization 8=31993
Gd/permalloy double layers, spin-wave resonance temp. dependence, 100–400°K 8=31816

Gadolinium—contd
- Gd(III) ion in aqueous soln., n. m. r. and e. p. r. study of water exchange in first co-ord. sphere 8=43882
- Gd^{3+}, electron spin resonance in $BaTiO_3$, orthorhombic and rhombohedral phases 8=31852
- Gd^{3+} in CdF_2, trigonal spectra in e.p.r. 8=49609
- Gd^{3+} in PbF_2, spectrum 8=36250
- in Pd-Ag alloy, resistance anomaly 8=31326

Gadolinium compounds
- aluminates, antiferromag., thermal props. 8=35435
- chelates soln., laser action of organic ligand 8=24349
- ferrite, spontaneous radiation temp. dependence 8=45190
- iron garnet, sublattice magnetization 8=40840
- Gd and Permalloy films, antiparallel exchange coupling 8=40816
- $GdAlO_3$, antiferromag. ordering 8=31773
- GdAs, e.s.r. exchange-narrowed lines, 17-400°K 8=31846
- Gd-Au alloys, resistivity meas., 1.3-20°K 8=40311
- GdBi, e.s.r. exchange-narrowed lines, 17-400°K 8=31846
- $Gd_{2.7}Ca_{0.3}Fe_{4.7}Sn_{0.3}O_{12}$, effective mag. field at Sn^{119} nucleus through compensation point 8=49469
- $GdCl_3$, magnetic specific heat, exchange consts., high freq. meas. 8=40817
- Gd-Er alloys, magnetocrystalline anisotropy rel. to impurity contribution 8=44971
- GdFe garnet, dilute, magnetostriction 8=31724
- $GdFe_2$, magnetic fields induced at Gd nuclei 8=49558
- $Gd_3Fe_5O_{12}$ and fused quartz, chemical interaction 8=41251
- Gd-Ho alloys, magnetocrystalline anisotropy rel. to impurity contribution 8=44971
- Gd_2O_3, dispersion in UO_2, reaction at high temp. 8=35074
- Gd_2O_3, retention of additives 8=39693
- GdP, e.s.r. exchange-narrowed lines, 17-400°K 8=31846
- GdPd, crystal structure and mag. props. 8=44216
- GdSb, e.s.r. exchange-narrowed lines, 17-400°K 8=31846
- Gd $\times_2$ ($\times$ = Rh, Ir, Mn, Pt, Al), g shift rel. to hyperfine fields e.s.r. studies 8=27475
- Gd-Y alloys, spin-disorder resistivity meas., comments 8=49165
- $GdVO_4$:Eu^{3+}, determ. of phenomenological parameters of crystal field Hamiltonian 8=31992

Galaxies
- See also Nebulae.
- Andromeda nebula, novae subsystem 8=45737
- antimatter theory 8=41492
- Arp, excess of radio sources 8=32501
- Arp, excess of radio sources 8=32502
- brightest in rich clusters, luminosity distrib. model 8=45746
- in clusters, near, sculptor-type dwarfs distrib. 8=28109
- clusters, rich, redshifts distribution 8=50386
- by Coma Cluster centre, distribution, 8=50363
- compact blue, in Leo A and B clusters, redshifts rel. to Einstein gravit. effect 8=28113
- compact, n star studded, redshifts rel. to quasars distance 8=28112
- dimensions, rel. to Jeans's criterium 8=50280
- descriptions in morphological catalogue, comparison with classification by Hubble and Vancoulurs 8=32503
- elliptical, diameter-luminosity relation 8=28107
- elliptical, fragmentation form. and unstable clusters props. 8=45752
- elliptical, nuclei classification, obs. 8=45747
- evolution through quasar and radio stages 8=32521
- extragalactic soft X-rays, obs. 8=36923
- five-colour intermediate-band photometry 8=41508
- formation, and microwave background radiation 8=36977
- formation and statistical mechanics of violent relax., 8=50374
- formation in steady state universe 8=50356
- formation, rel. to non-linear eqs. of spherical collapse 8=50258
- formation, thermal instabilities in process, 8=50375
- flattening, distrib. in galactic clusters 8=28114
- 4287 in Hydra, Ursa, Major, Virgo and Evidanus, dimensions, forms and position angles 8=36975
- galactic disc, mag. cut-off of extragalactic protons 8=45739
- galactic explosions, dust condensation 8=45728
- giant, overabundance of He 8=28106
- group in Centaurus containing peculiar galaxy, characts. 8=28104
- HI distrib., mass and distance of small galaxies, 21 cm 8=45748
- H II region temp. calc. 8=28091
- H II, region, morphological study 8=36963
- intergalactic gas density rel. to X-ray and u. v. backgrounds outside atm., obs. 8=32490
- magnetic field, structure 8=36969
- magnitudes determ. integral with electrophotometry and photographs 8=36974
- mass model, Z-vel. dispersions evaluation 8=32507
- MCG 12-7-28, peculiarities 8=45749
- M82, polarization rel. to light scatt. by halo dust, obs. 8=45751
- NGC 224, mass, density, angular momentum and rotational distributions calc. 8=36968
- NGC 1275, flux density at λ 5.2 cm 8=41552
- NGC 1275, 1068, 3077, 3516, 7969, optical variability 8=50360

Galaxies—contd
- NGC 1672, 5236, 7552, 1808, 2997; spectra of peculiar nuclei 8=50358
- NGC 3115, surface photometric symmetry obs. 8=45745
- NGC 3310 nucleus colorimetry condensations rel. to u. v. excess, obs. 8=28110
- NGC3351 nucleus colorimetry condensations rel. to u.v. excess, obs. 8=28110
- NGC3389 distance modulus rel. to M96 Leo group membership 8=28111
- NGC 3955, eccentric explosion, spectral obs. 8=32508
- NGC 4027, barred spiral Magellanic type; photometry, kinematics and dynamics 8=41533
- NGC 4945 southern spiral, nucleus 8=28105
- NGC 4449, structure of irregular galaxy 8=50362
- NGC4245, variable nucleus obs. 8=28115
- NGC 5128, 5253, 6970; radial velocities 8=50357
- NGC 6823 photometric obs. 8=36972
- NGC 7714, emission spectrum obs. 8=45744
- non-circular motions, instabilities 8=50369
- nuclei, of 73 barred spiral galaxies 8=45742
- nucleus as source of energetic particles 8=50368
- Oorts' const. B change, secular change in obliquity of ecliptic 8=50392
- Oort's const. B. revised due to diminishing obliquity of equatorial pole 8=50376
- orientation in clusters, favourable, possible origin and prospects, 8=50372
- origin in oscillating relativistic world model, galaxies origin, 8=50370
- radio, circular polarization, observed limits at radio freq. 8=28133
- radio emission at 11, 21 and 75 cm 8=32504
- radio emission, in Pereus cluster 8=50359
- radio source Sagittarius B2, OH emission, interplanetary scintillation 8=45850
- radio source satellites, single, of spiral galaxies, obs. 8=45773
- radio source VRO 42.22.01, spectrum obs. 8=45771
- radio sources, ang. struct., interferometric obs. 8=32517
- radio sources at 6 cm., spectral indices obs. 8=45779
- radiosources, Australian obs. 8=32610
- radio sources, compact p synchrotron emission 8=45766
- radio sources, discrete, flux density at 11.3 cm obs. 8=45767
- radio sources, ejected, assocs. and parent galaxies struct. obs. 8=45772
- radio sources, Gaussian least-squares fit 8=32514
- radio sources, southern, accurate R. A. meas. 8=32512
- radio sources, variable, 2.8 cm obs. 8=45766
- radiogalaxies, collapse and anticollapse 8=50327
- rapidly rotating, props., mathematical exam., 8=50373
- rotation constant A, determ. from 52 O, B, A stars 8=32509
- rotation curve, using 21cm radiation, excitation temp. obs. 8=50353
- rotation effects on gaseous arm stability 8=50365
- rotational curves for projected mass, angular moment and rotational energy calc. 8=36973
- Seyfert and N-type, rel. to quasars 8=45778
- Seyfert, NGC 1068 and 1275, i. r. radiation surplus,
- Seyfert, optical forms, comparison with N-type 8=45743
- Seyfert, UBV system obs. and luminosity dec. 8=50360
- spectroscopy of emission regions, multi-lens Perot-Fabry assembly 8=32414
- spiral and radio, unified theory 8=50371
- spiral arms, magnetic field configuration 8=50366
- spiral, diameter-luminosity relation 8=28107
- spiral, polarimetric obs. 8=28116
- spiral, r.f. emission rel. to nuclei type and optical activity 8=28108
- spiral structure, importance 8=50367
- spiral, struct. rel. to gas density perturbation 8=32506
- spiral structure stability rel. to stellar orbits 8=50364
- stars absolute proper motions, 14000 obs. 8=45740
- stellar velocity distribs. rel. to system stability 8=50279
- superclusters, collapse and anticollapse 8=50327
- superclusters, statistical characts. 8=45741
- thermal X-ray source, non-thermal radiowave asborpt. model. 8=45770
- III Zw 2, compact, Seyfert-type spectra analysed 5=50361
- 3C 120, compact radio, Seyfert-type spectra analysed 8=50361
- 3C390.3, variable N-galaxy 8=36976
- USSR radioastronomical apparatus and obs. 8=32523
- Vela-X, supernova remnant, radio emission obs. 8=32505
- Virgo cluster, revised identification 8=28117
- H_2 in southern Coalsack, abortive search 8=28093
- Sb, central condensations classification, obs. 8=45750

the Galaxy
- in Casiopeia, starlight polarization rel. to interstellar clouds, obs. 8=50355
- cosmic-ray confinement, rel. to e spectrum >50 BeV 8=32397
- cosmic ray electron energy loss rate in galactic space 8=38165
- cosmic-ray e storage and diffusion 8=32396
- cosmic ray storage, halo and disc components 8=38167
- Cygnus X region, NGC 7000 emission contours, 610.5, 750 and 1414 MHz 8=50354

Galaxies—contd
  the Galaxy—contd
    discontinuity at $l^{II} = 140^\circ$ 8=41532
    fundamental proper motions, precessional consts. 8=32499
    galactic background emission and energy spectrum of electrons in interstellar space 8=32500
    galactic disc near $L^{II} = 140^\circ$, non-thermal emissivity 8=36971
    γ-ray obs. of the centre 8=45795
    halo, star density in SA 57, RGU photometry determ. 8=41531
    halo stars SA51, RGU photometry 8=36967
    magnetic field direction calcs. 8=28103
    magnetic field estimation using cosmic ray electrons 8=41530
    magnetic field, interstellar, meas. using linear polarization of radio emission 8=32495
    mass, density, angular momentum and rotational energy distributions calc. 8=36968
    Milky Way, u.v. radiation, obs. from Venera-4 8=28101
    models for resonant periodic orbits 8=41643
    nebulae, planetary, space orientation rel. to mag. field 8=45736
    novae subsystem struct. 8=45737
    plane orbits in spiral field, deviations 8=45734
    polarized emission at $\lambda = 1.25$ m, synchrotron radiation 8=28102
    radio emission at 85 and 150 MHz 8=32498
    radioemission at 610.5 MHz, longit. 47°-56° obs. 8=32497
    radio sources, catalogue 8=41548
    rotation, rel. to radial vel. of Be stars 8=45735
    stars, near sun, kinematic models 8=36970
    stars vel. relax. rel. to interstellar gas gravit. condensation 8=45733
    structure, by obs. of polarization of 210 Mc/s cosmic radiation, using 3-channel radiometer 8=41543
    third integral of motion 8=32496
    u.v. radiation, high level winter obs. 8=36966
    X-ray background, effect on uniformity of central region 8=45602
    X-ray background, possible source 8=32398
    X-ray survey of central region 8=45738
    H cloudlets, intermediate-velocity 8=45732
    H, neutral, distrib. and possible correl. with Gould's Belt 8=45723
Gallium
    acoustic cyclotron resonance, Doppler-shifted 8=48720
    boundary with non-polar org. liqs., interphase surface tension 8=39338
    crystal growth rel. to supercooling and dislocations, and melting characts. 8=44130
    cyclotron resonance line shape, mass extremum effect 8=26935
    implantation in Si, anomalous penetration 8=48929
    impurities in cooled Ge bolometer, depend. of parameters on conc. 8=41855
    K-absorption edge, comparison with oxide, chloride, nitrate and sulphate 8=31990
    Knight shift 8=27505
    laser emission from optically pumped thin platelets 8=46613
    liquid, cold neutron scatt. cross-section, energy depend. 8=39301
    liquid, electrotransfer of Ag, temp. depend. 8=36597
    liquid, sp. ht. meas. in stable and undercooled states, 611-245°K 8=30459
    liquid, x-ray scatt. 8=34765
    polymorphism, identification of metastable forms 8=35111
    size-dependent oscillatory magnetoresistance effect 8=49164
    sun, abundance from sunspot spectra 8=32573
    superconducting amorphous film, tunnelling obs. 8=40368
    superconducting energy gap of amorphous and β phases 8=40369
    thermal conductivity and Lorentz number meas, 283-673°K 8=39945
    thermal magnetoresist. rel. to heat switch appls., 1-10°K 8=35459
    vapour, absorption spectra in 250-150 nm region, S^2p-Sp^2 transition cross sections obs 8=47486
    x-ray scatt. by liquid 8=34765
    β-Ga, melting curve 8=48260
    Ga(III) coordination no. in aq. solns. determ. by p.m.r. 8=39431
Gallium compounds
    chalcogenides, synthesis and growth in Ga and In melts 8=48563
    $AgNO_3$, fused, elec. cond., effect of inert gas press. and solubility 8=25949
    Ga(III) ions, hydration, O^{17} n.m.r. 8=30540
    $Ga_{1-x}Al_x$) As diodes, epitaxial layers, observation of stimulated emission 8=46619
    in GaAs, activation energies of Cr, Fe and Ni 8=42038
    GaAs bulk oscillators, random one-dimensional doping fluctuations effect, computer study 8=49308
    p-, n-GaAs, conduction band density of states from fluorescence at 300 and 77°K 8=32054
    GaAs crystals grown from supercooling melt, dislocation structure rel. to growth conditions 8=26678
    GaAs epitaxial films, deposited by vacuum evaporation 8=26117

Gallium compounds
    GaAs, epitaxial, n-type from p-type, photo luminescence 8=41193
    p-GaAs, in tunnel diode prep. by closed-growth using $ZnCl_2$ transport agent 8=44846
    GaAs, k. p expansions, double group full-zone 8=44636
    GaAs, quadrupole relax. time and chemical shift rel. to covalence 8=31928
    GaAs, ultrasonically excited, reflection of light 8=36290
    GaAs:Fe, e.p.r. at 77 and 300°K 8=31866
    GaAs–Ge epitaxial combinations, linear defects interpretation as misfit dislocations 8=31078
    GaAs—Ge epitaxial combinations, linear defects interpretation as slip 8=31077
    GaAs: Si grown by liquid-phase epitaxy, luminescence 8=27650
    GaAs: Zn luminescence, near-band-edge 8=45271
    $GaAs_{1-x}P_x$, effect of Te and S donor levels on direct-indirect transition 8=27093
    p-$Ga(As_xP_{1-x})$, in tunnel diode prep. by closed-growth using $ZnCl_2$ transport agent 8=44846
    $GaAs_{1-x}$ P_x injection laser, electroluminescent source, luminance > 6×10^9 cd/m^2 8=41192
    Ga(AsP) laser resonator, pumped by Ga(AsP) junction, photon output energy rel. to band gap 8=33215
    $Ga_{2-x}Fe_xO_3$, highly anisotropic ferrimag., ferromagnetic resonance, 1.2-360°K 8=27453
    $Ga_{0.85}Fe_{1.15}O_3$, mag. ordered, e.s.r. spectrum, external elec. field effects obs. 8=31867
    Ga-In liq. alloys, activities 8=39315
    GaP, band gap from absorpt meas., 0-900°K and diode luminescence, 300-900°K 8=45188
    GaP, crysts. growth from soln., theory 8=35232
    GaP crystalline powders, Raman scatt. cross section temp. dependence, 103-723°K 8=45189
    GaP, cryst. VLS growth and morphology, obs. 8=35208
    GaP, czochralski growth under boric oxide layer 8=44131
    GaP, dislocation creation during spark erosion 8=40037
    GaP, effective electron mass, anisotropy 8=31290
    GaP, elastic constants from u.s. phase-comparison meas., 8=49021
    GaP, electro-optic and piezoelec. coeffs. and refractive index meas., 8=41092
    GaP, electroluminescent p-n, junction obs. 8=36509
    GaP, energy levels of N-N pairs 8=49803
    GaP, exciton absorpt. profile, 77-673°K 8=41087
    GaP, growth of large crysts from stoichiometric melt 8=48543
    p-GaP, in tunnel diode prep. by closed-growth using $ZnCl_2$ transport agent 8=44846
    n-GaP, i.r. absorption impurity photoionization 8=41091
    n-GaP, i.r. absorption, scattering mechanism 8=41090
    GaP, i.r. donor-acceptor pair spectra involving deep oxygen donor 8=36488
    GaP, luminescence band formation, role of vacancies and substitutional impurities 8=45274
    GaP platelet growth, effect of impurities and crystallization conditions 8=26205
    GaP p-n junction, I-V charact., stress effects 8=31403
    GaP p-n junctions, electroluminescence, 77-420°K 8=45273
    GaP p-n junctions, red-emitting, prep. by soln. growth of p-type thick layers on n-type substrates 8=41232
    GaP p-n liq.-phase-epitaxial layers in prep. of electroluminescent diodes 8=41229
    GaP, preparation in bulk ingot form 8=48542
    GaP, quadrupole relax. time and chemical shift rel. to covalence 8=31928
    GaP reverse-biased diode for h.f. light modulation 8=40528
    GaP, strongly compensated p–i–n junction in photodiode, elec. and optical props. 8=40509
    GaP, synthesis and epitaxial growth by fused salt electrolysis 8=48573
    GaP_xAs_{1-x}-based injection lasers, production and props. 8=36360
    GaP_xAs_{1-x}, growth from soln, with temp. distrib. adjustment 8=44147
    GaP_xAs_{1-x}-GaAs n-n heterojunctions, photosensitivity spectra 8=36019
    GaP: Cd-O complexes, optical props. 8=27648
    GaP: Cd(Zn) and O, red pair luminescence 8=27649
    GaP–Cu, photoconducting storage effects 8=49419
    GaP-GaAs solid solns, epitaxially grown, departures from homogeneity 8=30838
    GaP:Te of improved homogeneity, Hall meas. 8=27096
    GaP : Zn(Cd), epitaxial growth by $GaCl_2$ vapour transport 8=48544
    GaP: Zn-O complexes, optical props. 8=27648
    GaP: Zn, O, excitation spectra and quantum efficiency 8=41195
    GaP(Zn, O)/(Cd, O), temp.-dependent radiative recombination mechanisms 8=41194
    GaP:Zn-O, (Te), p-n junctions, red emission time-delay characts. 8=45272
    GaS, band structure, optical props. 8=44774
    n-GaSb, carrier conc. temp. dependence and conduction-band minima 8=49241
    GaSb crystal, dislocation density changes on back-melting 8=44447
    GaSb, elastic moduli and compression to 80kbar 8=49022

Gallium compounds
  n-GaSb, epitaxial growth on p-type substrate 8=44044
  p-GaSb, hole masses, light and heavy, reflectivity meas. 8=35886
  GaSb, i.r. absorption and reflection spectra, band structure 8=41089
  GaSb, optical consts. near energy gap, from laser modes temp. depend., 80°K 8=41088
  n-GaSb, oscillations of longitudinal magnetic resistance in degenerate electron gas 8=40466
  GaSb, optical transmittance curves, room temp., from 0.2 to 3.0μ 8=45187
  GaSb, quadrupole relax, time and chemical shift rel. to covalence 8=31928
  GaSb, undoped, electron irrad. effects on Hall coeff. and mobility 8=27091
  GaSb-InSb heterojunction, lattice mismatch accommodation. 8=48857
  n-GaSb:S, (Se), (Te), conduction-band structure, from resistivity-pressure dependence to 50kbar 8=49236
  n-GaSb(Te), diffusion of Cd rel. to p-n junction formation 8=31005
  GaSe, band structure, optical props. 8=44774
  GaSe, electroluminescence, injection obs. 8=32055
  GaSe(S), one- and two-phonon absorpt. 8=27571
  $Ga_2(SO_4)_3$ hydrated crysts., n.m.r. evidence of H_3O^+ ions 8=49643
  Ga_2Te_3:Cu, lattice parameters 8=30896
 gallium arsenide
  absorption coeff. at microwave and mm. freqs. 8=27568
  automatic jet thinning for transmission electron microscopy 8=33088
  diffusion of As across epitaxial interface to Ge substrate 8=35494
  diffusion of Mn and Cu, complex formation influence 8=35492
  diffusion of S through SiO_2 films 8=35493
  diffusion of Zn 8=39974
  diffusion of Zn 8=48774
  electroreflectance rel. to interband transitions 8=49728
  elastic constants, third-order, Keatings theory 8=44578
  elastically deformed, elec. field gradient at nuclei from n.m.r. obs. 8=31909
  electronic charge transfer 8=31266
  epitaxial layers on Ge, vapour growth 8=30752
  epitaxially grown on Ge, twin structure obs. 8=26276
  evaporation kinetics 8=35003
  films epitaxy on rocksalt, 25-430°C 8=35172
  films, polycrystalline, photoconducting props. 8=27321
  growth from soln., theory 8=35232
  growth on insulating substrates 8=30826
  hole deposits, faceted, effect of vapour comp. on growth rates 8=48572
  injection-laser, far-field patterns with Gaussian profiles in junction plane 8=37597
  interband Faraday rotation 8=41086
  intracavity acousto-optic loss modulator, use in mode locking CO_2 laser 8=24305
  junction laser, internal Q switching 8=37612
  junction lasers, obtaining Gaussian beams 8=33203
  laser action, field-ionized 8=24340
  laser, bulk field-ionized, stimulated emission 8=33207
  laser, c. w. operation noncatastrophic degradation 8=33205
  laser diode soln. grown, gain and loss rel. to orientation 8=33214
  laser, far field patterns 8=33202
  laser, injection, self damage 8=33208
  laser junction, internal Q switching 8=33212
  laser junction, output light spikes at room temp. 8=33204
  laser junction, transverse modes 8=33206
  laser, semiconductor injection, mode self-synchronization 8=46565
  laser transmitter for optical communications 8=37611
  layer growth from Ga and As_2 vapours, kinetic mechanism using mol. beam technique 8=48449
  light scatt. by screened single—particle e excitations, obs. 8=36363
  liquid, x-ray scatt. 8=34765
  luminescence due to Ge acceptors 8=49801
  optical transmittance curves, room temp., 0.2 to 3.0μ 8=45187
  oxide layer form. in range 400-530°C. struct. 8=49870
  photoelectric yield spectra of broken and cleaved surfaces, 82 and 293° K 8=36052
  radiative lifetime, quantum efficiency 8=49802
  thin films, photoemission 8=27354
  work function of cesiated n-type, temp. depend. due to band bending 8=40688
  x-ray scatt. by liquid 8=34765
  n-GaAs, electroluminescence 8=45269
  GaAs:Cu, recombination centres, parameters determ. from photoconductivity 8=36020
  GaAs:Te, large imperfections, obs. 8=40013
  $GaAs_{1-x}P_x$ injection laser, delay and memory effects 8=33209
  $GaAs_{1-x}P_x$, laser, optical filling of delay inducing traps 8=46618
  GaAs:Te, microprecipitates 8=40012
  GaAs:Te, 1.6×10^{18} carriers 1 cm^3, helical dislocations, obs. 8=40036

Gallium compounds—contd
 gallium arsenide—contd
  n-GaAs:Te, schlieren pattern, recombination radiations 8=45270
  GaAs:Zn, defect formation during Cu diffusion from photoluminescence data. 8=48820
  GaAs:Zn, 1.370eV photoluminescence emission band, heat treatment effects 8=49800
  p-GaAs:Zn, schlieren pattern, recombination radiation 8=45270
  (Ga, In)As, electroreflectance rel to interband transitions 8=49728
  Ge film formation, thermal evap. in vac. 8=35174
  Ge–GaAs system, heteroepitaxy from liq. phase on contact fusion 8=48546
Galvanomagnetic effects. See Magnetoelectric effects.
Galvanothermomagnetic effects. See Magnetoelectric effects; Magnetothermal effects.
Gamma-ray sources. See Gamma-rays.
Gamma-ray spectra
   See also Nuclear decay theory.
  (α, xn) reactions on heavy deformed nuclei rel. to intermediate stages 8=25201
  analysis for low radioactivity samples 8=47043
  asymmetric doublet rel. to magnetic hyperfine splitting for levels of even-even nuclei in muonic atoms 8=42809
  biological material assay 8=47065
  biomedical, data collection by computer 8=50462
  n capture γ-rays, calc. 8=33886
  energy and intensity in $As^{75}(n, \alpha)As^{76}$ obs. 8=34010
  γ-γ directional correl., computer analysis 8=24703
  high-energy interactions, obs. at 2900m 8=25038
  high resolution with Ge(Li) detector, analysers using Gaspan computer code 8=30390
  high resolution with Ge(Li) detector, analysis using Gaspan computer code 8=46846
  intensities of transitions to ground and first excited state in 23 resonances of $Gd^{155}(n, \gamma)Gd^{156}$ 8=38389
  light nuclei multipolarities and short-lived activities meas. 8=24705
  n capture, (n, n′γ) and (d, pγ) rel. to mechanisms, 15 keV-15 MeV 8=25235
  neutron-induced prod., formalism 8=29453
  nuclear excit. and vibr. levels analysis multipole sum rules appls. 8=25078
  nuclear reactions rel. to intermediate stages 8=25201
  nuclear structure determ using resonant absorpt. and fluorescence exam. 8=47222
  odd mass deformed nuclei, E1 and E2 transitions 8=29285
  pulse-height analyser for space expts. 8=47064
  radioactive products of linear accelerator 8=33953
  (p, γ) resonances rel. to analogue states in s-d shell, obs. 8=25079
  in resonance capture, internal and channel, radiative transitions 8=25233
  spectral analysis, noise errors 8=46847
  from 10 MeV protons on natural targets 8=47214
  true spectrum with digital filtering 8=47063
  wavelength standard selection and line shifts, 10-100 keV 8=29084
  $Ac^{224} \xrightarrow{\alpha} Fr^{220}$ 8=47299
  $Ag^{108}(T_{1/2} \geqslant 5$ years) transition 8=42953
  $Ag^{110m} \rightarrow Cd^{110}$ decay, intensities 8=47288
  Al^{27} following neutron inelastic scatt. 8=38481
  $Al^{27}(n, \gamma)Al^{28}$, E_n=14 MeV, radiative capture cross section 8=29466
  Al^{28} n capture γ-rays, calc. 8=33886
  As^{74} decay, additional γ obs. 8=42947
  As^{75}, 280 keV level decay 8=29317
  Au^{200} decay, γ obs. attributable to Hg^{200} 8=42969
  B^{10}, from $B^{11}(He^3, \alpha)$, γ decay obs. 8=42834
  $Ba^{128} \rightarrow Cs^{128} \rightarrow Xe^{128}$ decay 8=42956
  $C^{12}(d, p)C^{13}$, emission, 170 keV, plane polarisation 8=43058
  $C^{12}(p, \gamma)N^{13}$, from lowest T=$^3/_2$ N^{13} state 8=29440
  from Ca^{43} levels transitions 8=43027
  $Ca^{48}(p, p')Ca^{48}$ at 4.51 MeV 8=47242
  Cd^{109}, energy meas., 88.2 KeV 8=42888
  Cd^{115} γ decay, directional correl. obs. 8=38377
  $Cd^{115m} \rightarrow In^{115}$, rel. to decay obs. 8=25184
  Ce^{138} levels, from Pr^{138} decay 8=29368
  $Ce^{145,146}$ rel. to decay schemes, obs. 8=38430
  Ce^{146}, β decay and transitions obs. 8=42959
  Cf^{252} spontaneous fission fragments 8=25278
  Cl^{38}, β, γ-transitions obs. 8=29359
  Co^{56}, γ-γ coincidence obs. 8=29364
  $Co^{57,59}$, lifetimes and g-factors of first excited states, obs. 8=29314
  Co^{58} 8=29313
  Cr^{50} low levels 8=29309
  Cs^{133}, relative intensities of weak rays 8=29086
  $Cu^{63,65}$ following neutron inelastic scatt. 8=38481
  $Cu^{63,65}$ n capture, 10-60 keV, obs. 8=25247
  from $Cu^{63,65}(n, \gamma)$, in 100-1500 KeV and 5000-8000 KeV ranges obs. 8=42881
  Cu^{64} n-capture γ-rays, obs. 8=29470
  Cu^{65}, 1115 keV level 8=29365
  Cu^{66} n-capture γ-rays, obs. 8=29470
  Er^{166}, energy shift in presence of μ in 1s state 8=42902

Gamma-ray spectra—contd
  from Er^{171} decay, Tm^{171} level schemes obs. 8=47259
  Eu^{144}, rel. to Sm^{144} 1659 and 2481 keV levels population in (p, p'), obs. 8=38435
  Eu^{154} decay to Sm^{154}, Gd^{154}, obs. 8=42962
  F^{19}, inelastic n scatt. excitation, ⩽200 keV 8=29088
  Fe^{56} following neutron inelastic scatt. 8=38481
  Fe^{57}, decay scheme from thermal n capture 8=47246
  Ga^{65} decay to Zn^{65}, obs. 8=25178
  Ga^{70,72}, slow n capture γ-rays rel. to low-lying levels, obs. 8=29316
  Gd, fluorescent yield 8=42905
  Gd^{154}, energy shift in presence of μ in 1s state 8=42902
  Gd^{159} → Tb^{159} decay 8=29372
  Gd^{159}, 68 keV 26 nsec isomeric state decay 8=29335
  Ge^{69}, from Ga^{69}(d, 2n) obs. 8=25132
  Ge^{77} → As^{77} decay obs. 8=29366
  He^{3}(d, γ)Li^{5} obs. 8=29227
  Hf^{180m}, decay studies 8=29341
  Hg$^{192, 194, 196, 198}$, and decay schemes, obs. 8=38394
  I^{121,123} decay rel. to Te^{121,123} low-lying levels, obs. 8=29327
  I^{127}, inelastic n scatt. excitation, ⩽200 keV 8=29088
  I^{127}(n, γ)I^{128}, E_n=14 MeV, radiative capture cross section 8=29466
  I isotopes (γ, xn) prod., E_γ < 900 MeV 8=38456
  In^{115} de-excitation, rel. to vibr. states, 900-1600 keV 8=29323
  In isotopes, decay 8=47251
  In Se^{75}, gamma gamma angular correlation 8=33916
  Ir fraction of p irrad. Au, 660 MeV 8=29342
  Kr^{90,91,92,93} from U^{238}O$_2$-stearate fission source, obs. 8=38549
  La^{134,136} decay obs. 8=42958
  Lu^{168m} rel. to Yb^{168} levels, obs. 8=29339
  Mg^{24} dipole transitions 8=29300
  Mg^{25} levels 8=29301
  Mg^{25} n capture γ-rays, calc. 8=33886
  Mn^{56}, γ–γ coincidence obs. 8=29364
  N^{15} from N^{14}(n, γ), 9.15 MeV doublet energies and decay modes 8=42839
  N^{15} levels 8=29294
  NaI(Tl) single-crystal with anticoincidence scintillator 8=47066
  Nd^{141g,m} decay, obs. 8=42960
  Nd^{150}, energy shift in presence of μ in 1s state 8=42902
  Ne^{20,22}(n, γ)Ne^{21,23}, gamma rays obs. 8=47329
  Ne^{22}, up to 6.68 MeV level 8=29298
  O^{15} levels 8=29294
  O^{16} radiative π capture, giant resonance obs. 8=47334
  O^{16}(α, γ)Ne^{22}, e.m. deexcitation of Ne^{22} at 11.89 and 12.28 MeV 8=47240
  Pa^{234}(UZ, $T_{1/2}$ = 6.7h) → U^{234}, rel. to U^{234} energy levels 8=47270
  Pb daughters of Po$^{197-203}$, obs. 8=38440
  Pb scatt. of Co^{60} γ, Ge : Li remeas. 8=33978
  from Pb^{211} β decay 8=47267
  (p, γ) and (α, γ) on low and medium Z nuclei, E_p = 16-160 MeV, E_α = 59 MeV 8=38462
  Po–B source, and n spectrum, fast-slow n-γ coincidence obs. 8=33783
  Po–Be source, and n spectrum, fast-slow n-γ coincidence obs. 8=33783
  Pr^{139} decay 8=47251
  from Pr^{142} → Ce^{142} and Nd^{142} decay obs. 8=38432
  Pt, following thermal neutron capture 8=38492
  Pt, reson. n capture partial γ width distrib. rel. to levels, obs. 8=29343
  Pt^{192}, e–γ directional correlation meas. 8=33935
  Ra^{223} and derivs. 8=42972
  Rb^{90} rel. to isomer, obs. 8=29367
  Rb^{91} obs. 8=25181
  Re^{186} 8=29377
  Re^{188} decay to Os^{188}, scheme 8=25192
  Ru^{95}, and β-spectra and decay scheme, obs. 8=42952
  Ru^{100}, excited states study by decay of Rh^{100} 8=29321
  Ru^{219} rel. to energy levels, obs. 8=29346
  Sb and Te decay, Sb even isotopes spectroscopic study 8=47252
  Sb^{125}, oriented, anisotropies and spins obs. 8=42892
  Se^{83m}(69 sec), and β-spectrum, rel. to to decay scheme, obs. 8=38420
  Si^{28} dipole transitions 8=29300
  Si^{28}, nucl. reson. fluoresc. anisotropy meas. 8=30631
  Si^{30}(p, γ)P^{31}, 26 resonances 8=29444
  Sm^{143} decay 8=47251
  Sm^{155} → Eu^{155} and level scheme, obs. 8=29334
  μ-Sm^{152}, 1st rot. transition, energy rel. to isomer shift, obs. 8=29332
  Sn isotopes, decay 8=47251
  Sn, reson. n capture partial γ width distrib. rel. to levels, obs. 8=29343
  Sn^{119m}, in Pb, In, Cd, Cu, ag, isomer shifts 8=26015
  Ta^{177} rel. to energy levels, W^{177} decay time-to-amplitude coincidence obs. 8=29376
  Te$^{118-126}$ rel. to energy levels, 0-3 MeV 8=29326
  Te^{133g,m} decay obs. 8=42897
  Th^{233} β, Pa^{233}, obs. 8=29380
  Ti^{48}(n, γ)Ti^{49}, angular correl. and γ-γ coincidence, obs. 8=29470
  Ti^{48}(p, γ)V^{49} 8=29445

Gamma-ray spectra—contd
  Tl daughters of Po$^{197-203}$, obs. 8=38440
  Tl$^{192, 194, 196, 198}$, and decay schemes, obs. 8=38394
  U, in ore, new log for direct determ. 8=32184
  U^{235} fission prods., 30-300 keV 8=38547
  U^{235} fission, obs. 8=47365
  U^{235,238} isotopic ratio determ. by activation analysis 8=47546
  U^{238} fission fragments, Ne^{22} ion induced, mass distrib. analysis 8=29539
  V^{51}(n, γ)V^{52}, angular correl. and γ-γ coincidence, obs. 8=29470
  W^{182,184,186} energy shift in presence of μ is 1s state 8=42902
  W, reson. n capture partial γ width distrib. rel. to levels, obs. 8=29343
  Xe^{127m} rel. to transitions assignments, 125 and 175 keV 8=38427
  Yb^{168}(n, γ)Yb^{169} obs. 8=42909

Gamma-ray spectrometers
    See also Beta-ray spectrometers; X-ray spectrometers.
  for activation resonance integral and resonance spectrum meas. 8=47067
  bent-crystal, for Ge detector 8=33619
  Cauchois, precision angle meas. device 8=25236
  characteristics, influence of conical light guides 8=47061
  for fission prods. meas. bent crystal spectrometer, 30-300 keV 8=38547
  e-γ coincidence spectrometer 8=29333
  high resolution, hypercryogenic detector–f.e.t. unit-care 8=47056
  low-level β-γ coincidence spectroscopy 8=24704
  magnetic pair, light nuclei multipolarities meas. 8=24705
  Mössbauer, electromech. servomechanism 8=37783
  Mössbauer, velocity calibration, interferometric method 8=37927
  Mössbauer, with constant velocities ⩽ 30 cm/sec 8=47062
  Mössbauer, with constant velocity or constant acceleration 8=47052
  peaks, statistical fluctuations 8=42456
  pulse-height analyser, large-memory 8=33383
  scintillation, for spectra of radioative capture of neutrons with Pd^{108} and Pt^{198} resonances 8=47068
  scintillation, statistical accuracy of measured resolution 8=47060
  single-channel, keyed stabilizing system 8=29085
  slow down time lead for obs. of n resonance parameters 8=24972
  stilbene scintillation for use in n background 8=33821
  sum coincidence, for relative intensity determ. of weak rays from complex nuclei 8=29086
  CdTe p-n counters 8=33618
  CdTe surface barrier detectors for γ-ray spectroscopy 8=47069
  Ge counter for inelastic n scatt. excitation, ⩽ 200 keV 8=29088
  Ge, review 8=47070
  Ge(Li), anticoincidence-shielded, for high sensitivity counting 8=47058
  Ge(Li), degradation of performance below 20°K 8=46901
  Ge(Li) detector, anti-Compton 8=47057
  Ge(Li) detectors coincidence experiments with coaxial detector in low energy range 8=47059
  Ge(Li) diode detector, energy resolution rel. to appl. in space expts. 8=29087
  Ge(Li), for Compton suppression 8=47054
  NaI(Tl), for neutron-capture γ-ray activation anal. 8=32168
  NaI(Tl), GeV range 8=47055

Gamma-rays
    See also Cosmic rays/photons.
  branching ratios from N^{15} 9.16 MeV level decay obs. 8=33898
  dislocation pinning by pt. defects during continuous irrad., appl. to stage III in Cu 8=39995
  n-γ, flux and Kerma distance depend., counter and Na activation obs. 8=33771
  hard radiation in atmos. 8=45477
  neutron-induced prod. cross sections and spectra, formalism 8=29453
  nuclear resonant diffraction by perfect crystals, theory 8=48616
  particle nature, teaching demonstration 8=29082
  (p, γ) and (α, γ) on low and medium Z nuclei, cross sections and spectra, Ep = 16-160 MeV, E_α = 59 MeV 8=38462
  point source above conducting screen, with long free path in air, elect. and mag. field 8=24246
  production by Compton effect with relativistic electrons colliding with laser beam photons 8=47045
  pulsed source using remodelled electron linear accelerator 8=46986
  transfer and scattering, solutions for coupled equations 8=33609
  two-layer barrier transmission, radiation field calc. using perturbation method 8=44489
  in upper atmos., above 50 MeV, obs. rel. to discrete sources 8=42686
  vertical intensity of hard γ-radiation at sea level 8=45478
  Ar, thermal neutron capture, γ-ray obs. 8=25242

Gamma-rays—contd
- from $C^{12}(He^3, p\gamma)N^{14}$ reaction, study 8=47354
- Fe^{57} monochromatic polarized source 8=37924
- Pb shield, leakage through slit. 8=38595
- Pu-α-Be calibrated 4.43 MeV source 8=37925
- Sn^{119m}, Mössbauer beam correl. props., 23.8 keV 8=37923
- Ti^{46}, γ-γ correlations 8=47244
- **absorption**
  - See also Mössbauer effect.
  - for density spatial distrib. determ. in closed media 8=29083
  - Mössbauer emission from atoms in relaxing localized modes 8=48319
  - oxybromine cpd. radiolysis, $BrO_{1,2}$ spectra 8=27768
  - shielding penetration, Monte Carlo calc., self-optimized exponential biasing 8=34075
  - slab penetration, invariant imbedding calc. 8=31131
  - 3-photon, coherence effect, quantum field theory 8=42316
  - two-layer slabs penetration and composite slabs buildup, factor, invariant imbedding calc. 8=37921
  - Cd-$CdCl_2$ liq. system, vol. change on mixing 8=30414
  - from Co^{60}, barrier and geometry attenuation by vertical steel slab 8=37922
  - H, C, H_2O, Al, Ar, Fe, Mo, Pb, and U, absorpt. coeffs. calc. 8=47411
  - SnO_2 colloidal soln. in glycerine-alcohol mixture, reson. absorpt. 8=24701
- **angular distribution**
  - α-γ correl. meas., gridding ionization chamber 8=33952
  - from (α, n) and (p, n) reactions 8=34037
  - annihilative, obtained by positron annihilation in In and Sb 8=49128
  - complex radiation shielding calc. 8=24700
  - cyclotran meas., accidental coincidence background reduction 8=29005
  - in ferromagnetic host, follow ion Coulomb excitation and implantation 8=26011
  - inelastic n scatt. near threshold 8=34006
  - isotropic, interpretation for final state of spin 3/2 8=33887
  - Mössbauer resonance scatt., crystal lattice interference effects 8=48320
  - perturbed, for parity test 8=33890
  - $Ca^{40}(d, p\gamma)Ca^{41}$, angular correl. 8=29303
  - in $Ca^{48}(p, n)$, n-γ angular correl. rel. to Sc^{48} excited states, obs. 8=33997
  - Ce^{140}, $3^+ \rightarrow 4^+ \rightarrow 2^+$ cascade correl., extranuclear field effects, obs. 8=29329
  - $Li^7(p, \gamma)Be^8$ 1.4–2.5 MeV and levels of Be^8 8=47320
  - $Ne^{20}(\alpha, \alpha'\gamma_{1.63})Ne^{20}$, $E_\alpha = 3.96$-6.08 MeV, obs. 8=38517
  - $Ne^{20}(\alpha, p\gamma_{0.44})Na^{23}$, $E_\alpha = 3.96$-6.08 MeV, obs. 8=38517
  - Ra^{223} decay, α-γ angular correl. rel. to Rn^{219} levels, 270 keV 8=33942
  - rel. to Rn^{219} levels, α-γ angular correl. obs. 8=29346
  - $Ti^{48}(n, \gamma)Ti^{49}$, correl. and γ-γ coincidence obs. 8=29470
  - $V^{51}(n, \gamma)V^{52}$, correl. and γ-γ coincidence obs. 8=29470
- **detection, measurement**
  - See also Dosimetry; Gamma-ray spectrometers; Particle detectors; Radioactivity measurement.
  - angular distribs. and correls. and short-lived activities meas. 8=24705
  - background, by NaI(Tl) scintillation counter, absolute method 8=50157
  - in coincidence with e, Ge pin diode 8=46894
  - collimators, focused, for scanning extended sources, dig. recording of line-source response 8=24702
  - collimators, multihole focusing, longit. and lateral response 8=42342
  - collimators, scanning, single- and double-head, sensitivity depth depend. 8=42343
  - dosimeter, FD-1, ORWO3 and 4 films 8=47046
  - dosimeters radiation element, personnel 8=33799
  - dosimetry, blurring caused by ionization chamber, energy depend. 8=46862
  - dosimetry, calorimeter, above 5 rad/sec. 8=24688
  - external, internal and intramuscular radiation, dosimeter meas. 8=45930
  - fast n-γ detector for space research 8=47158
  - 4-detector apparatus for angular correlations 8=37926
  - γ-γ and particle-γ coincidence, 2-dimens. pulse height analysis 8=24532
  - γ-γ coincidence meas., digital windows for 8=37799
  - image intensifier detectors, gas filled 8=46855
  - manganese arsenic borate glass dosimeter 8=44500
  - n and γ body doses in criticality accident meas. 8=33767
  - n spectrometer γ background discriminator, $E_n \geqslant 0.2$ MeV 8=33384
  - organ scintiscanning, 2-isotope for overlapping tissues localization, theory 8=42454
  - Penning gauge with quenching circuit 8=37784
  - polarization meas., γ-γ linear 8=24699
  - pulse height spectra, time-dependent, vector analysis 8=46945
  - rem meas. method for mixed γ-neutron radiation fields 8=46923
  - scintillation detector, multilayer 8=47051
  - scintillation spectrometer for spectra of resonance neutron capture 8=47068

Gamma-rays—contd
- **detection, measurement**—contd
  - spectrometry, peaks statistical fluctuations rel. to background, obs. 8=42456
  - thermometer, fast-response for in-core flux monitoring 8=47050
  - wavelength standard selection and line shifts, 10-100 keV 8=29084
  - X-rays, soft, detectors employing channel electron multipliers 8=47041
  - CdS, growth of crystals and determ. of characts. rel. to detection 8=26241
  - CdTe surface barrier detectors, high energy resolution 8=46900
  - Cs^{137} determ. by β-γ coincidence counting while meas. γ ray spectrum with NaI(Tl) analyzer 8=47360
  - Cu foils for use in meas. nuclear deexcitation, texture 8=49663
  - Ge(Li) cylindrical double-open-end coaxial γ-ray detectors, charge collection 8=46908
  - Ge(Li) detector, average energy per e-hole pair, temp. dependence 8=47007
  - Ge(Li) detector degradation by fast n bombard 8=42453
  - Ge(Li) detector pulse timing system 8=47049
  - Ge(Li) detectors coincidence experiments with coaxial electric in low energy range 8=47059
  - Ge(Li) detectors, efficiencies and operating characteristics 8=46902
  - Ge(Li) detectors, time resolution in γ-γ coincidence 8=47048
  - Ge(Li) planar detector, slow rising pulse obs. 8=37791
  - NaI well type, photopeak efficiency determ. 8=28980
  - NaI(Tl) low-level counter 8=33614
  - from Nd^{144} following Pr^{144} β decay 8=38434
  - PbF_2 Cherenkov counter 8=46885
  - PbF_2 crystal Cherenkov shower detector 8=33613
- **effects**
  - See also Nuclear reactions due to/photons.
  - acetonitrile-d_3, irradiated, trapped electron and its reversible reaction, e.s.r. evidence 8=49955
  - alloys, strained, on work function 8=44938
  - amino acid crysts., free radicals 8=40907
  - amino acids, γ-irradiated, e.s.r. and optical spectral investigation of defects 8=26634
  - aqueous solns., γ-radiolysis at high press., reaction of hydrated electron 8=32143
  - Compton virtual proton effect on wide angle bremsstrahlung and polarization phenomena 8=42458
  - concrete, attenuation 8=48891
  - elastic quasi-mosaic effect after diffraction from elastically deformed crystals 8=39706
  - electron transfer between acceptor and donor atoms in rare gas matrix 8=40202
  - electronic components, transient effects 8=31126
  - ethylene-silica gel system, ionization-polymerization, e.p.r. obs. 8=32127
  - films, excitation of plasmons in thin films 8=40272
  - free radical recombination induced in various organic compounds 8=38939
  - $\gamma + p \rightarrow \pi^+ + n$, $E_\gamma = 165$-230 MeV, differential cross-section obs. 8=29126
  - glasses, physicochem. props., effect of mixed γ-n radiation 8=44493
  - hexafluoropropylene copolymer, γ-irradiated, photoinduced and thermal radical conversions 8=49953
  - hexane ionization chamber rel. to dosimetry 8=37787
  - hydrocarbon glasses, electron trapping sites, saturation and removal 8=40082
  - ice, alkaline, trapped dielectrons, optical absorpt. spectrum 8=45194
  - ionization chamber n detector, transient-field behaviour 8=47160
  - isobutene-silica gel system, ionization-polymerization, e.p.r. obs. 8=32127
  - leucosapphire, on optical props. 8=41054
  - methanol-d_1, isotopic comp. of H prod. 8=32136
  - methyl oleate, γ-induced oxidation 8=41293-4
  - 3-methylpentane glass, trapped electrons 8=27483
  - π^+ photoprod., linear polarized γ, apparatus and method 8=29125
  - piezoelectric annular disc, heating rel. to radial deform. 8=31441
  - polyethylene, elec. cond. obs. 8=40084
  - quartz, defects study by thermoluminesc. 8=49812
  - recoil-free fractions of Fe^{57} in cubic lattices, appl. of Gruneisen's formula 8=44498
  - ruby, on optical props. 8=41054
  - semiconductors based on GeTe: (Bi, Cu), electrical conductivity, thermoelectricity compressive strength 8=40637
  - starch, γ-irradiated, e.s.r. of free radicals 8=49618
  - T three-body photodisintegration 8=29223
  - tetrafluoroethylene copolymer, γ-irradiated, photoinduced and thermal radical conversions 8=49953
  - Al, analysis of total cross sections 8=26728
  - Bi-Te-Se(Sb) system, on elec. and thermal conductivities and thermoelec. force 8=44763
  - CaF_2, irrad. at 77°K, thermoluminesce. activation energies and emission spectra 8=36477
  - CaF_2, synthetic, irradiated, thermoluminescent spectra and transition kinetics 8=45262

Gamma-rays—contd
effects—contd
CdS, self-diffusion, radiation-stimulated coeff. determ. 8=35482
CrO_4K_2, γ-irradiated, e.s.r. 8=49605
$CrO_4(NH_4)_2$, γ-irradiated, e.s.r. 8=49605
Cu, analysis of total cross sections 8=26728
Cu, strained, on work function 8=44938
D_2O, delayed n prod. by U^{238} fission fragment γ-rays, half-lives, obs. 8=33764
n-Ge, radiation defects, reduction of rate of formation by heat treatment 8=31152
Ge single crystal, Co^{60} γ irrad. induced surface layer 8=36365
$HClO_4$, release of H atoms, e.s.r. obs. 8=49963
He^3 three-body photodisintegration 8=29223
H_2SeO_3, e.p.r. of γ-irrad. cryst. 8=31884
on I vapour reaction rate with 8 metals at room temp. 8=36555
K halides, Bremstrahling energy losses rel. to beam collimation and crystal thickness 8=31310
KCl, density changes 8=40129
KCl, hardening from critical shear stress analysis 8=49037
LiF, density changes 8=40129
LiH buildup factors and fission neutron attenuation by Monte Carlo method 8=47401
NaCl, Co^{60} γ-irradiated, F-centres, chemical determ. 8=48884
NaCl, density changes 8=40129
NaCl, hardening from critical shear stress analysis 8=49037
NaCl, surface F-centre formation rel. to Au nucleation 8=44152
$NaClO_3$, e.s.r. of γ-irrad. cryst. 8=49613
NaF, density changes 8=40129
NaOBr, γ-radiolysis, radical yields 8=27767
NaOH ice, γ-irrad. electron traps 8=31153
Nb glasses, e.s.r. of Nb centres 8=40937
Pb, analysis of total cross sections 8=26728
Pb halides, colour centre prod. by vacancy trapping of electrons or holes 8=36249
$Pb(NO_3)_2$, annealing of damage, kinetics 8=44414
Si, Co^{60} γ irrad., effects on surface and bulk recomb. rates 8=27120
Si, recombination-active defect lifetimes 8=49424
V_2O_5-P_4O_{10} semicond. glasses, effect on elec. cond. 8=27137
ZrO_2 films, damage and effect on props. 8=35607
internal conversion
See also Beta-ray spectra/conversion electrons.
in α-recoil atoms, e spectra deform. in elec. field 8=29287
coefficient meas. with Si(Li) and Ge(Li) detectors for obs of electrons and γ-rays 8=42970
coefficients, theoretical, Rose's, Sliv and Band's tables compared 8=47223
coincidence circuit, $4\pi\beta$-γ, correction 8=24727
Orgel-type cluster, D_2O lattice obs. 8=25305
Ag^{110}, electrons, and transition multipolarities 8=33920
in Au^{197} α-bombard. rel. to $Au^{197}(\alpha, pn)Hg^{199}$, 25 MeV 8=29361
Co^{58M}, for 25 KeV isomeric transition 8=33966
Dy^{165}, β-decay, new γ transitions 8=47296
Eu^{155}, low energy, rel. to nuclear levels, obs. 8=29371
Fe^{57} 14.4 KeV transition coeffs. calc. 8=42876
Gd^{155}, 86.5 KeV transition coeff. determ. from $Eu^{155} \rightarrow Gd^{155}$ decay 8=42905
Hf^{179}, K-coeff. determ. of 161 KeV transition 8=47261
Hf^{180m}, decay studies 8=29341
Ir^{192m}, coeffs. for an isomeric transition 8=33966
Lu^{175}, dynamic penetration effects 8=33932
$Os^{180, 181}$ decay, conversion coeffs. obs., transition multipolarities calc. 8=38438
Pa^{231}, 58.5 KeV transition, obs. of L subshell fluorescence 8=43200
Pt^{195}, directional correl. meas. with conversion electrons 8=38392
Po^{210}, K-conversion coeffs. 8=25195
Re^{178} decay, conversion coeffs. obs., transition multipolarities calc. 8=38438
Sb^{124}, disintegration scheme 8=47289
Se^{81m}, K conversion coeff. obs. for 102.7 keV transition 8=29370
Sm^{150} excited levels, e-γ coincidence obs. 8=29333
Tm^{168} decay 8=25191
Tm^{169}, L and M internal conversions of E_2 transitions 8=33931
Tm^{169}, rel. to chem. environment and Mössbauer isomer shift 8=29336
U^{235m}, low lying level, environmental effects on lifetime meas. 8=25164
scattering
See also Compton effect.
back-scatter guage, meas. with restricted angle 8=41325
Bijoveet type generalized eqns. 8=35297
Compton, freq. and direction, centre-of-mass calc. 8=42452

Gamma-rays—contd
scattering—contd
complex radiation shielding calc. 8=24700
flux near ground-air interface, image source calc. 8=33610
γN, forward matrix amplitude reconstruction 8=24672
γP Compton scatt., < 150 MeV, expt. and calc. 8=24696
Mössbauer resonance, by crystals, interference effects 8=48320
nuclear resonance scatt., ang. distribs., effect of local environment 8=39511
on plane surface semi-infinite, emanating from point sources 8=47393
polyethylene slabs, backscatt. spectra rel. to thickness, and energy albedo 8=25207
Al, photoelec. cross-section determ. 50-208 keV 8=36004
Al slabs, back scatt. spectra rel. to thickness, and energy albedo 8=25207
Au, photoelec. cross-section determ. 50-208 keV 8=36004
C, total cross section, E_{γ} = 84-662 KeV, calc. 8=38449
Cu, photoelec. cross-section determ. 50-208 keV 8=36004
Fe, n capture, resonant γ scatt. obs. 8=25245
Pb, of Co^{60} γ, Ge : Li remeas. 8=33978
Pb, natural, inelastic and elastic cross sections, ⩽ 21 MeV 8=29399
Pb, photoelec. cross-section determ. 50-208 keV 8=36004
Pb slabs, back scatt. spectra rel. to thickness, and energy albedo 8=25207
Pt, total cross section, E_{γ} = 84-662 KeV, calc. 8=38449
Sn, photoelec. cross-section determ. 50-208 keV 8=36004
Sn slabs, rel. to thickness 8=41035
Sn, total cross section, E_{γ} = 84-662 KeV, calc. 8=38449
W, photoelec. cross-section determ. 50-208 keV 8=36004
W, total cross section, E_{γ} = 84-662 KeV, calc. 8=38449
Gamow—Teller transitions. See Beta-decay theory; Nucleus/energy levels.
Garnets
See also Ferrites.
cavity-garnet system, coupling parameters 8=24206
ferrite-garnet crystals, dislocations and hydrothermal synthesis conditions on their formation 8=26660
garnets: Fe^{4+}, linewidth temp. dependence, 4.2°-300°K at 10 and 25 kMc/sec 8=31827
magnetic, polycrystalline, use in microwave devices 8=40834
magnetic structure 8=36136
rare earth iron, mag. moments at 0°K substitution dependence, mol.-field model 8=45027
zoned, from Galway granite, governed by Rayleigh fractionation princ. 8=27852
$Bi_{3-2x}Ca_{2x}Fe_{5-x}V_xO_{12}$, two-sublattice cpd., first magneto-crystalline anisotropy constant temp. dependence 8=45042
$Ca_3Al_2(O_4D_4)_3$, garnetoid, cryst. struct. 8=39777
DyAl garnet, magnetization change below 1.7°K, model 8=45057
DyFe, crystal growth form and solubility obs. 8=30807
$Eu_3Fe_{1.94}Ga_{3.06}O_{12}$, cation distrib. 8=30895
$Gd_{2.7}$ $Ca_{0.3}$ $Fe_{4.7}$ $Sn_{0.3}$ O_{12}, effective mag. field at Sn^{119} 8=49469
GdFe, crystal growth form and solubility obs. 8=30807
Y, dispersion of magnetoelastic waves 8=40186
Y garnets, synthetic, high-pressure decomp. 8=26087
YAG, morphology rel. to growth on seed by flux technique 8=26198
YAl garnet, planar defects from e. microscope exam. 8=44429
$Y_{3-2}Ca_{2x}Fe_{5-x-y}V_xIn_yO_{12}$, ($x \leqslant 1.5$, $y \leqslant 0.5$), linewidth reduction 8=31833
YFe, crystal growth form and solubility obs. 8=30807
YFe, ferromag. resonance field rel. to crystallographic anisotropy 8=31826
YFe garnet, mag. domain-wall propag. vel., effect of Er doping 8=49565
YFe garnet, para process in h.f. mag. field near Curie point 8=49566
YFe garnet, single crystal, delay of microwave signals 8=49564
Y Fe garnet, spin wave excitation time in first- and second-order nonlinear processes 8=45041
Y Fe, magnetoelastic pulse excitation and propag. in non-uniform field, loss meas. 8=45043
YFe, nonlinear ferromag. resonance, self-modulation anisotropy 8=45069
YFe rods, axially magnetized, abs. spectra 8=36426
$Y_3Fe_{5-x}In_xO_{12}$, two-sublattice cpd., first magneto-crystalline anisotropy constant temp. dependence 8=45042
YGa garnet: Eu, electronic Raman transitions 8=27612
YGa garnet : Eu^{3+}, mag. susceptibilities 8=49468
YGa garnet: Nd, crysts. growth and laser oscills., obs. 8=39694
YGa garnet: Nd, electronic Raman transitions 8=27612
YGdAl: Nd^{3+} growth and laser characts. 8=39692
Gas analysis. See Chemical analysis.
Gas-discharge tubes
See also Counters; Ion sources.
anodic-bore ion laser tube 8=37571
cold cathode e emission, brightness obs. 8=47744

Gas-discharge tubes—contd
- corona, high-voltage stabilizing circuit application 8=41921
- electrodeless, microwave excited, applics in atomic spectroscopy 8=46707
- electron swarm, spatial/time variation of electron energies 8=28575
- Faraday dark space, electron conc. patterns 8=25696
- fluorescent tube operation, temp. and freq. influence 8=46681
- hollow-cathode, as extreme u.v. source 8=24381
- hollow-cathode demountable design 8=29887
- hollow-cathode, gas fed, rot. and plasma waves 8=29926
- laser design with small tube 8=37570
- laser, perpendicularly disposed windows 8=24298
- light source, pulsed, high intensity 8=42204
- mercury, low pressure, current limitation and gas rarefaction 8=47767
- moving striations in positive columns, origin 8=47748
- negative glow, electron conc. patterns 8=25696
- Penning, anode and cathode power dissipation 8=43445
- plasma properties, high-current discharges 8=43440
- positive column, collision-induced transport processes 8=38986
- positive column plasma with current change, non-stationary processes 8=25695
- radial var. of pot., vel. spread of ions, effect, appearance sheath 8=29890
- ring-electrode systems, transition from low to high em radiation output 8=47741
- thyratron as switch for 70 MW, 250 kV compact modulator 8=28994
- trigatron, selection of gas mixture 8=37424
- work of electrode in plasma air stream containing K 8=29946
- Cs, low voltage arc with non-isothermal cathode 8=25703
- H-filled SC1 corona tubes, sheath radius obs. 8=47769
- He, rotating mag. field pinch 8=25770
- Ne, noiseless tube 8=47746
- Hg, surface wave prod. device and soln. 8=47750

Gas flow. See Flow/gases.

Gases
- See also Kinetic theory/gases.
- absorption in liquids in wetted-walls columns, acceleration by corona discharge 8=32119
- absorption in packed columns, correlation of gravitational force 8=50003
- absorption rates into laminar rippling liquid films, method 8=48053
- active medium, dip parameters in transition line 8=46576
- air, composition and props. in system with temp. gradient 8=47947
- analysis, differential thermal cond. analyser, theory and design 8=27774
- analytical determ. of nitrogen and oxygen conc. in mixtures by interferometry 8=49988
- autoionization in u. v., Ladenburg-Reich integral, generalized, anal. 8=34438
- binary mixture, structure of normal shock waves 8=30261
- binary mixtures, shock wave struct 8=43668
- Boltzmann, dense, divergence free kinetic equation 8=23910
- Boltzmann equation, linear and stationary, solution 8=28352
- Brillouin scattering in resonator, threshold scatt. for large and small angle 8=34661
- classical ideal, correlation of density fluctuations 8=23883
- convection-radiation interacts, role of optically thick approx. 8=25825
- critical, anomalous transport 8=47963
- critical region, transport coeffs. 8=39229
- dense real, transport processes, failure of weak-coupling model 8=39234
- double refraction due to spin alignment 8=39216
- electron capture of fast protons 8=34172
- electron drift velocity, new theory 8=39222
- electron drift vel. rel. to resonance scatt. 8=47979
- electron transport coeffs. and energy distrib., stochastic model 8=39230
- electrostriction, statistical theory 8=39224
- ferromagnetism, conditions for occurrence 8=39228
- ferromagnetism in real gases 8=34668
- flow, standardization of meas. method and instrums. 8=25791
- free electrons liberation by laser irradiation 8=29905
- gravitating, with homogeneous deform. and transverse vel. compts., exact solns. of eqn of motion 8=34628
- grey, similarity to effect of bundle of black screens with radiation 8=37297
- gun performance rel. to valve opening time 8=47934
- hard core quantum gas at high temps. 8=41785
- homogeneous, isotropic, energy transition probabilities in molecular collisions 8=34642
- humidity meas. microsensor 8=43644
- humidity, Soviet coulometric and diffusion hygrometers 8=27878
- humidity transducers, test apparatus 8=26001
- ion motion, homogeneous elec. field effect, analysis rel to numerical soln. 8=25711

Gases—contd
- ionized, radiation smoothing of small shocks to prod-continuous temp. profile 8= 39200
- ionized, shock waves in e. m. field 8=47945
- i. r. radiating, radiative equilib., integral eqn. 8=34649
- i.r. radiation, calc. of mean absorpt. coeffs. 8=25822
- at leading edge of plate, mass, impulse and energy fluxes, asymptotic behaviour 8=34609
- light diffraction by ultrasonics, approx. formula 8=34662
- light scattering, molecular collision-induced 8=30474
- liquified, solutions, apparatus for study of abs. spectra 8=30486
- masses, adiabatic pulsation and convective 8=50321
- mixing, laminar free, method of integral relations 8=25819
- mixing, mag. roller device 8=30237
- mixtures, light scatt. rel. to mol. correls. 8=34663
- molecules, gaseous radiationless e relax 8=25546
- monatomic, unsteady cylindrically symmetric expansion into vacuum, Boltzmann eqn. soln. 8=30276
- motion in long pipe, invariant solutions of eqns. 8=39166
- near critical point, density fluctuations rel. to anomalous viscosity and thermal cond. 8=30291
- non-isothermal radiation in superposed vibr. rot. bands 8=43680
- nonpolar, scatt. of polar mols, comment on $1/r^6$ potential 8=29853
- n.m.r., apparatus for study 8=39225
- oscillations in resonant tube 8=30266
- partially ionized, ion velocity distribution 8=29955
- photodissociation waves, vel., supersonic perturb 8=39215
- photon echo rel. to optical pulse separation 8=39213
- polyatomic, Boltzmann eqn. 8=30309
- polyatomic mixtures, transfer and relax. phenomena 8=43699
- pressure meas. with Mcleod gauge 8=39248
- radiation nonstationary diffusion, similarity principle for solns. reduction 8=42019
- radiative props. and Planck mean absorpt. coeff., for appls. in fluid mech. 8=39198
- rarefied, in boundary layer of half-plane corrections for density, temp. and vel. 8=34645
- real, width of jet boundary layer, and dimensionless profile of vel. head 8=39187
- residual, in multi-layer insulation, heat transfer studies 8=25823
- separation of mixture, thermal diffusion column 8=30319
- shock wave propag., fading in transverse mag. field 8=33106
- spectral radiant heat flux. distrib. in cylinder, for temp-depend absorpt. coeff. 8=39197
- spheres, finite isothermal, Jean's type gravitational instability 8=45618
- spherical bulb, unmovable, growth in spherical liq. volume, Rayleigh eqn. 8=30382
- temperature distrib. at high temp., by two-seeding method 8=34650
- ternary mixtures, constancy of dynamic viscosities 8=25836
- thermal radiating, wall temp. sudden change, effect 8=30288
- thermal regenerator, simulation 8=43687
- thermomagnetic effect, obs. with modulating magnetic field 8=39227
- transport prop. tables, dilute, validity range for real gases 8=34672
- u.s. relax. time, origin of temp. depend 8=39209
- van der Waals gas in critical region, anomalous transport props. 8=30305
- X-ray emission, carbon spectra 8=47652
- Ar, correlation function, direct, and equation of state 8=34756
- Ar, dense, three body forces contribution to thermodynamic properties 8=37198
- Ar, intermolecular pot., X-ray scatt. obs. 8=30274
- Ar, pair and non-pair potential 8=43924
- CO, Cl, NO_2, reactions at 381-473°C, kinetic eqn. setup 8=49857
- CO_2-H_2O vapour, optical-acoustic radiation and absorpt., press., temp. effects 8=30298
- Rb resonance radiation quenching by N_2 and inert gases 8=29626

Gegenschein. See Zodiacal light.

Geiger counters. See Counters/Geiger.

Gelatin
- drying, decomposition of introduced calcium acetate with acetic acid loss, mechanism 8=25973
- melting mechanism, from elec. cond. 8=34962
- rigidity and bond energy 8=25972

Gels
- agar, counterdiffusion of Pb^{++} and $CrO_4^{=}$ 8=48244
- alkali silicate, melt structure transition by high temp. flow 8=34757
- elastic parameter meas., rational geometry 8=32774
- gelatin, drying, decomposition of introduced calcium acetate with acetic acid loss, mechanism 8=25973
- gelatin, rigidity and bond energy 8=25972
- silica "adsorbed, adsorbent" interactions 8=34954
- silica, AgI single crystal growth 8=26227
- silica, complete pore struct. anal., surface areas of micropores 8=48351

Gels—contd
silica, entire pore surface accessible to N_2 8=48350
silica, O_3 adsorpt. rel. to annealing temp., −80°C 8=30786
thoria, crystallite sizes, equivalence of X-ray and electron microscopy 8=35284
$Al(OH)_3$, structure 8=25971
Ca tartrate crystal growth in gel media 8=35246
SiO_2 gel, adsorpt. of mols., n.m.r. signal shifts 8=39462
SiO_2 spheres, wet, drying through constant with dry SiO_2-gel particles in mixing 8=34978
Geochemistry. See Earth/composition.
Geochronology. See Earth/age; Radioactive dating.
Geodesy
See also Gravity.
gravity harmonics, low order resonant from satellite drift 8=50009
polar flattening and gravity formula in Geodetic Reference System (1967) 8=50007
Stokes-Poincaré theorem, meaningful choice of Stokes elements 8=32170
Geoelectricity. See Earth/electricity.
Geomagnetism. See Earth/magnetic field.
Geometrical optics. See Optics/geometrical.
Geometry
differential, dynamical content 8=28252
differential, techniques in canonical quantization 8=37746
internal force distrib. theorem expressed as a principle of maximum uniformity 8=37121
pregeometric functions, applic. to relativistic plasma 8=28327
rational, for gel elasticity meas. 8=32774
wave, geometrization of physical laws 8=32682
Geons. See Gravitation.
Geophysical prospecting
borehole direction surveying, photographic equipment 8=28906
mineral, radioactive, pulse-height spectrum analysis 8=46939
telluric "relative ellipse area", meas. by "vectograms" 8=50044
two-layer freq. prospecting curves, interpretation 8=50029
water table and alluvium depth, refraction determ. 8=50057
U in ore, natural selective γ-logging 8=32184
U, presence in rocks and minerals from fission fragment tracks made visible by chemical etching 8=32185
Geophysics
See also Atmosphere; Earth; Oceanography; Seismology.
andesite suites from circum Pacific arcs, systematic potash content vars. 8=36675
antarctic exploration with phase variations in v.l.f. ground wave propagation 8=45431
aspects in ionosphere scintillations for satellites and radio stars 8=32318
basalt and granite fracture mechanisms 8=48985
Colorado, NE Front Range, precambrian history 8=36686
common data point, effect of vel. layering and steep dip 8=50052
concretion formation, stages, and thermoluminescence 8=50004
continental drift, secular motion of pole and earth rotation, Conference, Stresa, Italy 1967 8=32196
convective phenomena, contrib. to theory 8=50017
core, outer, west drift rel. to secular mag. changes 8=50202
crustal structure 3D model, middle Atlantic states, by time term technique 8=36674
descending mantle convective flow zones, rel. to high heat flow and volcanism 8=45430
earth's strain, use of Michelson interferom. as sensor 8=27848
e.m. field generated by dipole sources buried in conducting stratified media, algorithm for calc. 8=46392
faults, basin and range, effect of Timber Mountain caldera, mech. analysis 8=32181
geoelectrical apparatus for d.c. four point meas. 8=50080
implications of gravitational field satellite obs. 8=45429
India, middle-dorsal region between 20 and 40°S, data 8=27850
infrasonic waves in atmosphere and earth's crust due to marine storms, limitations on determ. of wave vector 8=36666
magnetic anomalies and their geophysical interpretation 8=41461
mantle-core boundary, close continuity of compressibility 8=27847
mantle, selective melting effect on thermal history 8=50018
metamorphic garnets, zoning due to Rayleigh fractionation princ. 8=27852
micropaleontology of deep sea cores, and paleomag. stratigraphy 8=50102
oldest exposed lavas in Iceland, K/Ar ages, rel. to ocean floor spreading and crustal drift 8=50083
petrology of lithosphere rel. to geophys. discontinuities 8=45427
river sediments, Th and U concs. and isotope ratios 8=50094

Geophysics—contd
rock, brittle, creep mechanism 8=40111
rocks, determ. of Si content by n activation analysis 8=50062
sand movements, labelling with Cr^{51} 8=50092
sediments, hundreds of meters thick upon crystalline rock, heat flux meas. 8=50016
soil permeability, field determinations by nuclear methods 8=27858
subterranean effective porosity 8=34715
tectonic deformation and atmospheric press. waves, 28 March 1964 Alaskan earthquake 8=41317
time series, filtering 8=41637
transform fault concept, spherical surface, and verification with Africa-S. America data 8=36670
20th Annual Southwestern IEEE, conference 8=28645
underwater rad. distrib. meas., directional photometer 8=42136
upper mantle C-region phase changes 8=50076
v.l.f., wave propag. in earth interior 8=46468
water from lakes and rivers, O isotope meas. SO_4 ions 8=50095
Sr and Pb, isotopes evolution model with crustal material recycling through mantle 8=36682
Germanium
See also Semiconducting devices; Semiconducting materials/germanium.
adsorption-desorption mechanism rel. to electrophysical parameters of surface 8=48484
amorphous, structure obtained by Ar ion bombardment of crystalline form. 8=39723
annealed and cleaved surfaces, structure transformations 8=48419
annealing effect on i.r. absorption of γ induced surface layer 8=36365
Brillouin scattering, stimulated, and intensity limiting 8=45191
crystal breaking strength, effect of smooth surface defects at 300°K and 4.2°K 8=40161
crystal, ion-bombarded, structural defects from e.-diffr. exam. 8=39793
crystal temp. field on growing by Czochralski method 8=30827/8
crystals, deformed, dislocation structure from e-microscope exam. 8=31064
deformation mode, brittle, anomalous X-ray transmission exam. 8=26648
dendrite growth mechanism 8=48567
dendritic ribbons crystals, lateral growth 8=26271
diffusion from GaAs of As into Ge substrate 8=35494
diode, p–i–p, multiple negative resist. rel. to filamentary current paths 8=40529
diode, p–i–p, negative resist. mag. field depend., 77°K 8=40530
dislocation density meas. by radioactive tracer decoration 8=40039
dislocation formation during As diffusion 8=35568
dislocation line resonant vibrations 8=35563
dislocation lines, space orientation determ. from topograms obtained by Borman's method 8=40040
dislocation loops, prismatic, in As-doped mat., e-microsc. obs. on annealing 8=35567
dislocation structure at stages of work hardening curve 8=35566
electrodes, effect of HF and H_2SO_4 on elect. and chem. surface props. 8=27752
electron beam interactions from sec. e.-emission and radiation-induced conductivity meas. 8=44951
emission of energy deficient photons subjected to uniaxial compression 8=45275
epitaxial films, defect structure rel. to growth processes 8=26647
epitaxial films, morphology dependence on gas-flow during growth 8=26118
epitaxial layer growth by close-spaced system 8=48574
exoelectron emission after irradiation and mech. treatment rel. to surface defects 8=40694
far infrared spectroscopic bolometer appl. 8=32939
field electron-emissive photocell 8=40702
films, epitaxially grown, effect of etching with gaseous HI, HBr and HCl 8=30754
films, formation on GaAs, thermal evap. in vac. 8=35174
films, vacuum-deposited, liquid-like behaviour of crystallites 8=26121
γ-ray counter for inelastic n scatt. excitation, ⩽ 200 keV 8=29088
γ-ray spectrometers, review 8=47070
grown by Czochralski method, shielding conditions invest. 8=26253
internal friction 100 to 300°K, pure and In doped, peak rel. to dislocations 8=35703
ion implantation analysis by 1 MeV He^+ scatt. 8=48927
ions, multiply-charged, production and acceleration in cyclotron 8=46433
irradiated, e.p.r. 8=27476
i.r. interf. filters, props. 8=32937
k.p expansions, double group full-zone 8=44636
lattice constants determ. from pseudo-Kossel lines 8=48653

Germanium—contd
- lenses, corrosion resistance 8=40162
- luminescence and growth techniques 8=36475
- melt temp. field in growing crystals by the Czochralski method 8=30829
- modulation, far i.r., crossed field, free carrier 8=41093
- monocrystals, growth from Sn-Pb mixtures 8=26252
- n-type, anodic dissolution in aqueous solns., cond. band mechanism, obs. 8=45371
- n-type, diffusivity by temp. waves meas., 20°C 8=39953
- n-type, Sb-doped, elastic moduli, 300–550°K 8=40163
- n-type, photomagnetoelec. effect in pulsed mag. fields 8=36021
- neutron-irradiated, defect detection using anomalous X-ray transmission 8=48834
- optical difference mixing 8=31995
- oxygen distrib. coeff. determ. 8=48779
- particle spectrometer, calibration by Ra and decay products 8=37781
- photoconductivity assoc. with ionization of H-like acceptors 8=44954
- photomechanical effect, wavelength dependence 8=36368
- radiation defects and dislocations interactions 8=40038
- scattering of lattice waves by dislocations 8=30933
- Schottky defect formation energy 8=44411
- surface preparation, stabilization and chemical treatment 8=48420
- thermal expansion from X-ray powder diffr. exam. 8=44347
- thermal diffusivity of n-type by temp. waves meas., 20°C 8=39953
- thermal expansion coeff. temp. depend., theory and obs. 8=26594
- transistor emitter injection efficiency meas. 8=44850
- vapour crystallization droplet mechanism and overgrowth defect formation 8=26277
- vapour crystallization processes 8=26278
- vibration spectra, freq. along asymmetric dims. 8=30934
- X-ray emission spectrum, L-series 8=49719
- X-ray thermal scattering accompanying Bragg reflection, direction dependence of intensity 8=44217
- Ge:Cu i.r. detectors 8=46226
- Ge–GaAs epitaxial combinations, linear defects interpretation as misfit dislocations 8=31078
- Ge–GaAs epitaxial combinations, linear defects interpretation as slip 8=31077
- Ge–GaAs system, heteroepitaxy from liq. phase on contact fusion 8=48546
- Ge^{73}, Mossbauer expts. after Coulomb recoil implantation 8=39525
- ZnTe, hole-traps, Ge-associated 8=26884

Germanium compounds
- digermane Ge_2H_6, Ge_2D_6 frequencies and Coriolis constants calc. for digermane force field 8=48711
- germane, thermal decomp., accel. by Pt–Ge contacts 8=32123
- germania, vitreous, vibrational spectra 8=35392
- oxide film on Ge, vel. of H_2O diffusion 8=48778
- oxide films, optical consts. 8=49721
- Al–Ge solid solns., stacking faults in precip. particles and elastic stresses 8=31096
- Ge periodate, i.r. absorpt. spectrum 8=43300
- Ge-Al_2O_3-ZnO films, I-V characts., conductivity change 8=40488
- Ge-As-Cu system, complex formation 8=49871
- $GeBi_4Te_7$ struct., e diffr. obs. 8=30898
- Ge–C system at high press., absence of carbide formation 8=48382
- $Ge(C\equiv H)_4$, i. r. and Raman spectra 8=25625
- $GeCl_4$, Coriolis coupling consts. and force fields 8=38822
- $GeCl_4$, vibr. relax. and u.s. attenuation 8=39360
- $GeFe_2O_4$, electronic and mag. props. from Mossbauer spectra 8=31726
- $Ge[Fe_2]O_4$, Mössbauer quadrupole splitting of Fe^{2+}, theory 8=43942
- Ge–Ga–Zn, application to low temp. thermometry 8=41874
- GeH_4, deuterosubstituted, electro-optical params. and i. r. band intensities, calc. 8=29737
- GeI_2 struct., e diffr. obs. 8=30897
- GeI_4, Mossbauer effect 8=39520
- $Ge_{1-x}Mn_xTe$, $0.01 < x < 0.1$, Hall const. and s-d scatt. resist., 4.2-400°K 8=40456
- Ge_3N_4 amorphous films prep. and props. 8=44046
- Ge_3N_4, growth on clean and stained Ge surfaces 8=48451
- GeO, ground state reduced potential curves 8=29717
- GeO, molecular u.v. absorpt. spectrum 8=43301
- GeO_2, heat capacity, enthalpy and entropy 8=44339
- GeO_2 in glass polishing slurry, hexagonal to tetragonal transition 8=39558
- GeO_2, tetragonal, prep. for passivation of Ge devices 8=40502
- GeO_2-SiO_2 glasses, binary, non-ideal mixing 8=44080
- $Ge_2Sb_2Te_5$, crystal structure from e. -diffr. exam. 8=39794
- $GeSb_4Te_7$, crystal structure from e.-diffr. exam. 8=39794
- GeSe, optical and photoelectric props. in energy range 0.5-1.5eV 8=49727
- $GeSe_{0.75}Te_{0.25}$, optical absorption 8=31994
- Ge-Si alloys, elec. resistivity and Hall coeff. meas. 8=35893

Germanium compounds—contd
- GeSi alloys, optical props. in energy region 1-13 eV 8=36366
- GeTe, optical and elec. meas. rel. to band structure determ. 8=49726
- $HGeCl_3$ mol. crystals, n.q.r. multiplicity and spin lattice relax times rel. to phase transforms 8=41010

Getters. See Adsorption; Electron tubes; Vacuum technique.
Giant pulsations. See Earth/magnetic field; Magnetic storms.
Gibbs functions. See Thermodynamic properties.
Ginzburg—Landau theory. See Superconductivity.

Glaciers
- Antarctic firn, D content to depth of 106 m, rel. to climatic variations 8=50088
- in Antarctica, late paleozoic geography reconstruction 8=50087
- Arctic basin, ice-field drifts and currents 8=36684
- borehole, Camp Century, Greenland, temp. profiles, comp. between meas. and theory 8=32174
- Filchner ice shelf, thickness and dielect. const. from ionosonde obs. 8=45533
- melting pt. behaviour 8=50086
- radio wave reflection and scattering, MF-HF band, by melted surface 8=24209

Glass
- See also Optical materials; Vitreous state.
- aliphatic alcohol, γ irrad. at 77 °K 8=49966
- alkali-arsenate, γ-irrad., e.s.v. spectra 8=45074
- alkali borates, binary, phase boundaries and microstructures rel. to subliquids immiscbility 8=43756
- alkali-germanate, γ-irrad., e.s.v. spectra 8=45074
- alkali-phosphate, γ-irrad., e.s.v. spectra 8=45074
- alkali silicate, ionic conduction 8=44676
- alkaline-silicate, irradiated, nature of hole centres 8=40218
- aluminoalkalisilicate, Al^{27} n.m.r. 8=40971
- alumophosphate: Li and B, slow-n dosimeters, personnel 8=33797
- angle meas, comparative reflection method 8=32637
- binary, metastable struct. bonds 8=30620
- BK7 substrate for Al film, X-ray refl. obs. 8=31961
- borate, X-ray exam. of dissociated regions 8=39630
- borated, lattice defects, e.p.r. study 8=26628
- breakdown of cover glasses used in work with powerful elec. capillary discharge 8=48983
- breakdown when subject to ionizing radiations, optimal thickness calc. 8=31417
- brittle fracture, study by stress wave propag. and reflection 8=44531
- capillary sealing under pressure 8=50469
- chemical analysis, acceleration by SiO_2, precip. into $H_2Si_2O_5$ 8=45413
- coloured filter, luminous transmittance and chromaticity 8=37664
- compression under 10-65 kbar pressure, rel. to optical and mechanical props. 8=40164
- computer appls. in container prod. system 8=50471
- Corning 7560, specific heat between 4. 5° and 20° K 8=26589
- Corning Works, materials and appl., review 8=37660
- covalency estimate from effective mag. field at Mn^{2+} nuclei 8=48304
- densification under cutting wheel, using Zeiss interference microscope 8=39724
- dielectrics for microcircuits, vac. deposition 8=44895
- elastic deformation, delayed, activation energy spectrum 8=49025
- emerald green, u.v. absorbing, colour characts. 8=49720
- emissivity and cooling rate rel. to colour 8=44331
- ferroglass, ferromag. resonance modulation of light 8=24359
- fibres as light guides, technology 8=28761
- fibres, thermal-elastic relax., obs. in transverse vibs. 8=44513
- fluoroberyllate, e.s.r. of Fe transition group ions 8=40922
- foam, compressive deform., obs. 8=35647
- formation prediction, cooling rate rel. to melting temp. and diffusion coeff. 8=48501
- fracture surfaces, microstructure of mist zone 8=30722
- germania, vitreous, vibrational spectra 8=35392
- hot, transfer of ht. by rad. 8=44371
- impression by high intensity laser beam 8=33248
- industrial, thermoluminesc. rel. to heat treatment 8=36460
- for i. r. optics 8=31954
- inorganic, forced frozen elastic deform. in microindentation, obs. 8=35646
- inorganic, fracture strength, rel. to surface conds., loading and chem. comp. 8=31176
- iron phosphate diffusion, electronic carriers, thermally activated 8=49079
- laser rod, birefringence, insensitivity of polarized laser cavity 8=46597
- light-pulse, picosecond, self-trapping 8=43810
- luminescence following proton bombard., rel. to lunar phenomena 8=28145
- manganese arsenic borate glass dosimeter 8=44500
- metaphosphate: Ag, fast-n dosimetry by Cerenkov radiation meas. 8=33798
- mixed alkali silicate type, elec. conductivities and densities 8=27235

Glass—contd
modified fused silica with ultralow thermal expansion coeff., physical props. 8=39930
molten, high-temp. shear u.s. interferometry 8=39280
octadecylamine desorpt. and exchange, obs. 8=30768
optical absorption, special effect of As_2O_3 8=41097
optical, annealing for low residual stress and refractive index homogeneity 8=41141
optical, corrision resistance 8=41241
optical indices of internal strains, glasses in optical glass catalogue 8=41096
optical, mean reference index for F and C achromatism, simplified expression 8=42161
optical props, production techniques 8=31996
optical, refractive index determ. 8=37636
organic, used as trapping matrices, viscosities 8=49065
oxide, absorpt. and luminesc. of Sm^{3+} 8=36412
oxide, rel. to "ideal glass" concept 8=30788-9
oxide, Er^{3+} luminesc., senisitzation by other rare-earth ions 8=36486
particles in low cond. liqs., high field electrophoresis 8=30548
phosphate, Mo^{3+} doped, e.s.r. and optical absorpt. 8=31879
photochromic glasses 8=41095
photochromic, kinetics of bleaching 8=41094
photochromic, production by Ag^+ exchange 8=41140
phsopholsilicate film on SiO_2, form. and composition 8=44048
physicochemical props., effect of mixed γ-n radiation 8=44493
plexiglass, creep 8=31250
plexiglass, polarization relax. time in shock wave, meas. 8=40563
Poisson's ratio rel. to oxide dilution 8=44579
porous, adsorpt. of HCN, i.r. spectrum, surface reaction and polymerization 8=48491
porous Vycor, e. s. r. of methyl radicals on surface 8=47684
porous with impregnated Ins, superconducting props. 8=40370
pyrex, adsorpt. of Xe+Kr 8=30774
pyrex, vacuum coated, refraction of polarized light obs. 8=36319
quartz-glass-coesite, phase transforms. under high-temp. and pressure 8=48400
quartz, X-ray exam. of structure 8=39629
refractive index, reference proposal 8=36410
refractive index variation in strong field of ruby laser 8=41098
second-harmonic generation of light obs. 8=27555
semiconducting, and props. in comparison with ordered lattice 8=44806
semiconducting oxide type, role of network former in elec. props. 8=27085
semiconducting, radiation effects on conduction 8=27137
sheet strength, ambient humidity dependence 8=41065
silica, densified at very high press., quasi-crystalline atomic arrangements 8=48504
silica, fused, ion diffusion from molten salts 8=48789
silica, vitreous, vibrational spectra 8=35392
silicate-alumina at 600°C, i. r. emission spectra 8=38842
silicate, containing As, Sb oxides, vibr. spectra and struct. 8=31964
silicate glasses, phase separation and submicroscopic structure 8=30787
silicate, irradiated, thermoluminesc, e.p.r. and electron absorpt. spectra 8=41196
silicate K-8, stimulated Mandel'shtam–Brillouin scatt. threshold, 0.35, 0.69 and 1.06μ 8=32032
silicate: Nd, Yb stimulated emission 8=36512
silicate, strengthening by ion exchange 8=26845
silicate, substructures 8=30794
sintered optical fibres, thermal expansion 8=39925
soda-potash-baria, diffusion of K and Ba in refractories 8=48780
soft, far i.r. absorpt. rel. to inherent disorder 8=49681
solid and melt, structural similarities 8=30790
stearic acid desorpt. and exchange, obs. 8=30768
strain-optic individual coeffs., u.s. determ. 8=41138
strengthening effect of polymeric organosilicon film 8=49024
surface composition using spark source mass spectrometer 8=41300
surface porosity, rel. to aq. attack 8=26149
surface structure after etching, i.r. spectroscopy 8=39578
sytalls, degree of ordering dependence on thermal treatment and radiations 8=26147
ternary silicate, spectra and struct. rel. to chem. elements 8=36411
thermal cond. rel. to oxide dilution 8=44579
thermal dielectric strength rel. to sample thickness 8=35953
thermal expansion rel. to oxide dilution 8=44579
thermal props. at low temp., rel. to vib. density of states, review 8=35455
thermal stress problems 8=26824
thermophosphate, F^{19} n. m. r. studies 8=45121
tubing, technique for production of extremely thin walls and small holes 8=32629

Glass—contd
uranyl glass, photo-induced absorpt. 8=27610
vanadate, structural characterization and phase separation 8=26152
viscosity of fibres with and without concentric glass casings 8=39631
vycor glass, adsorpt. of binary, org., liq. mixtures 8=48477
Vycor, porous, surface conduction current variation by water vapour adsorption 8=27252
weakening defects 8=44580
Young's modulus rel. to oxide dilution 8=44579
with Ag elongated particles, selective light polarization by absorption 8=41051
Ag atom impurity stabilization and atomic centre production by X-rays and e. p. r. 8=31114
BaO, heat capacity as function of composition and temp. 8=44333
BaO-TiO_2-SiO_2 system, structural states of TiO_2 8=44078
Be phosphate, struct., i. r. spectroscopy of $NaBeF_3$-$NaPO_3$ system 8=30791
BeF_2, vitreous, vibrational spectra 8=35392
B_2O_3–PbO–Al_2O_3 system, spinodal decomposition from X-ray diffr. studies 8=26061
BaO-B_2O_3 system, n. m. r. studies 8=27499
CdS particles in, light absorption with a.c. elect. field modulation, obs. 8=40267
Cr, effect of press. and comp. on nature of Cr^{3+} sites 8=39632
GeO_2-SiO_2, binary, non-ideal mixing 8=44080
K_2O-B_2O_3-Al_2O_3 system, structural units 8=35201
K_2O-RO-B_2O_3 system, R=(Ca, Sr, Ba), u. v. absorpt. of Cr(VI), and basicity 8=36325
K_2O-SiO_2 glasses, comp. vars. in e microanalysis rel. to surface damage, obs. 8=30865
Li borate, γ-irrad., e.s.r. 8=49612
Li borates, n.m.r., diffusion of Li^7 8=31007
Li^6-glass scintillation n counter, < 2.5 MeV 8=33817
$Li_2Al_2O_4$-SiO_2 system, titania and zirconia nucleated for casting mirror blanks 8=41137
LiC-SiC_2, crystallization kinetics, comp. and ht. treatment effects 8=44133
Li_2O. 2. 5 SiO_2 fibres, ion-exchanged, internal friction 8=40168
Na aluminosilicate, ion-exchange hardening, i. r. spectroscopy 8=30864
Na silicate, high-temp. internal friction and transport mechanisms 8=40176
Na-Ca silicate, thermoluminesc., e. s. r. and e absorpt. spectra 8=30792
Na_2O-FeO-SiO_2 glasses, comp. vars. in e microanalysis rel. to surface damage, obs. 8=30865
Nb_2O_5-Na_2O-SiO_2, γ-irrad., e.s.r. of Nb centres 8=40937
Nd, birefringence dependence on laser pumping pulses 8=41125
Nd glass stimulated emission spectrum and quasi-continuous generation, 4.2°K 8=36503
Nd laser, energy characts. of radiation with Q switching 8=24348
Nd, laser, single-mode, waveguide type 8=24346
Nd, self-focusing in disperse medium 8=36310
Pb crystal, determ. of Pb by atomic absorpt. spectrometry 8=27789
PbO-La_2O_3-B_2O_3, exhibiting unusual dispersion characts. 8=45214
RO-B_2O_3 system, R=(Ca, Sr, Ba), u. v. absorpt. of Cr(VI), and basicity 8=36325
R_2O-B_2O_3 system (R=K, Na, Li), optical absorpt. of Co(II) and basicity of glass 8=36324
R_2^1O-$R_2^{11}O$-B_2O_3 system, R^1, R^{11}=(K, Li or Na), u. v. absorpt. of Cr(VI) and basicity 8=36325
RO-TiO_2-SiO_2 systems (R = Ca, Sr, Ba, Zn, Cd), glass formation 8=44079
Se–Cd, nonlinear optics 8=32029
SiO_2, synthetic, mobility of Na ions 8=48795
Si_2O_3, struct determ. by X-ray diffr. 8=48503
SnO_2-coated, analogue for electrochem. system 8=32129
Tl silicate, ionic conduction 8=44676
TiO_2-containing, small polaron as charge carrier 8=40499
UO_2^{+2}:Nd^{+3} laser glass, Ce-stabilized 8=28710
V-containing, e.p.r. spectra of varadyl ion, hyperfine structure 8=40923
V_2O_5-containing, small polaron as charge carrier 8=40499
V_2O_5-P_2O_5-(La_2O_3, Nd_2O_3 or CeO_2) systems, i. r. transmission 8=36425
in V_2O_5–P_2O_5–WO_3 system, elec. conduction mechanism from e.s.r. 8=40291

Glass—metal seals
ceramic-to-metal seals, graded, fabrication by isostatic gas, bonding 8=34692
cryostat leakage current, improvement 8=41885

Glow discharges. See Discharges, electric/glows.

Goks. See Hypernuclei.

Gold
absorption in 50-340Å range, calc. of partial oscillator sums 8=31981
adsorption on Si, influence of elec. props. 8=27134
α-ray absorpt. at 54.4 MeV, obs. 8=48919

Gold—contd
  anomalous surface structs., as props. of clean metal surfaces 8=26097
  atom, inelastic e scatt., E_e=200, 400 keV, cross-section 8=38719
  cold drawn, relaxation peaks 8=48997
  cold-worked, stored energy, electrical resistivity, tensile props. 8=40130
  corrosion in autoclave liners during hydrothermal crystal growth reactions 8=49855
  crystals in polyvinyl alcohol films, X-ray sizing 8=30858
  Debye-Waller factor of Fe, mössbauer meas., 8=39873
  decorant for graphite surface microtopography, and epitaxial growth 8=44099
  defect tetrahedra, stability and growth, effect of multiple quenching 8=44464
  depth dose distrib. prop. by electron irrad., energy losses and ionization 8=31143
  diffusion in Al, purple plague formation 8=48771
  diffusion in Fe-Ni alloys, lattice parameter change 8=39789
  diffusion in Ni, lattice and grain-boundary type, 700–1075°C 8=44391
  diffusion through SiO_2 films 8=39984
  disk cutting from sheet by HCl jet 8=32632
  doping in Si diodes, computer simulation of effects on electronic states 8=27182
  electron beam energy loss distrib. obs. 8=31142
  energy band structure 8=44642
  energy loss of 400keV p and 800 keV He^+ 8=49133
  epitaxial growth on NaCl, electrostatic field effect on initial orientation 8=26111
  evaporated film, water vapour adsorption 8=35194
  evaporated particles, multiple-turn struct. and deca- or icosa-hedron shapes 8=35317
  Fermi surface, effect of lattice parameters change 8=40237
  film, absorbent and anisotropic, optical props., theoretical study 8=49707
  film, double-positioned, damage on bombardment by He ions 8=40073
  film, holographic grating prep. 8=33290
  film, (111) epitaxial, structure rel. to vacuum deposition conditions 8=35160
  film, polycrystalline thin, photoelec. emissivity obs. 8=27353
  film, single-crystal, surface electron states investigated by proton channeling 8=31286
  films, discontinuous, morphological changes following deposition mechanism 8=39588
  films, epitaxial growth in high vacuum 8=30747
  films, lattice parameter thickness dependence by X-ray diffr. 8=30748
  films on amorphous substrate, grain-boundary effects on elastic deform. and residual resistivity 8=44551
  films, orientation after deposition on NaCl and KCl 8=44085
  films, polycrystalline, dynamical e.-diffr. intensities temp. dependence 8=39769
  films, thin, photoconductivity 8=36009
  films, transmission sputtering by H and D ions 8=44495
  films, transmission sputtering by low-energy H ions 8=40072
  films, triode-sputtered, resistivity meas. 8=40309
  films, X-irradiated, e.-emission-event statistics 8=44950
  foil, Ar ion bombard., lattice defect penetration 8=48815
  interstitial atom cluster form. by Au ion bombard. 8=44418
  ion penetration, chem. film technique 8=48920
  ions, 40 kV, dechannelling at planar defects in Ag and Au 8=35599
  microcrystals, growth and defect structure 8=39666
  multiply-charged impurity in Si p-n junctions, effects on breakdown voltage 8=27161
  nucleation on NaCl crystals rel. to surface F-centre formation in γ-irrad. 8=44152
  photoelectric effect rel. to temp. 8=36008
  photoelectric γ cross-section determ. 50-208 keV 8=36004
  plasma, laser-induced, ion energy and abundances 8=36051
  positron annihilation, single-quantum, cross sections 8=44670
  quartz, fused, reflectance in vac. u. v., obs. 8=27558
  quenched, activation energy spectrum, effect of impurity atoms 8=31052
  quenched and deformed, annealing kinetics of vacancies to dislocations 8=26637
  quenched, annealing kinetics of vacancy defects at elevated temps. 8=31044
  quenched, black spot defects, nature 8=44465
  quenched, plastic deformation rel. to vacancy clustering 8=31045
  self-diffusion, activation vol. and press. depend., 0-10kbar, 700-990°C 8=39967
  self-diffusion and quenching studies, analysis 8=35479
  single crystal, sputtering by fast neutrons 8=48911
  specific heat in pure samples below 3°K 8=39912
  specific ht. and ht. of melting 8=35424
  sputtered atoms, energy distrib. analysis by mechanical spectrometer 8=48915

Gold—contd
  sputtering, by 1 to 5 keV Ar^+ 8=40069
  sputtering, energy spectrum of ejected atoms 8=48916
  stacking fault energies 8=31097
  stacking fault tetrahedra nucleation and growth, in quenched Au, obs. 8=48866
  structure in liquid state 8=39307
  surface energy and impurity adsorpt. on heating in air 8=26095
  surface structures, LEED pattern interpret. via coincident site lattices, and phase and spacing modulation 8=26096
  thin film, current-noise power spectrum obs. 8=40310
  thin film, resistivity, ion-bombardment induced changes 8=49151
  u.s. attenuation, low temp, rel. to dislocation motion effects 8=39894
  vacancy activation energies, temp. depend. 8=44408
  vacancy resistivity rel. to temp. 8=44409
  visible radiation produced by electron bombardment 8=36317
  wetting by H_2O 8=48418
  and Ag, dechannelling of 40 kV Au ions at planar defects 8=35599
  Au(I) in cyanide solns., at. absorpt. spectrometry 8=32162
  Au I resonance doublets, absolute line strengths, quantum-mechanical calcs. 8=43216
  Au(100) surface, purity and structure from Auger spectroscopy and LEED 8=27355
  Au^{197} impurity in metallic matrices, Mössbauer absorpt. spectra, interpret. of isomer (chem.) shift 8=48318
  Au^{197} in Fe, Mössbauer effect rel. to hyperfine structure determ. 8=43948
  Au–n-Si, contact, potential barrier 8=35924
  D^+, 5-80 keV, range obs. 8=48912
  in Fe meteorites and inclusions, n activation determ. 8=28159
  Kr bombard., thermal desorption obs. 8=48483
  N_2^* beam bombarded, secondary e and negative ion emission, 13-200 eV 8=34454
  Pt, substitution effects on defect production and recovery 8=39997
  on Si, ohmic contacts 8=49286
  in Sn/Pb solder, X-ray spectrometric analysis 8=27816
  Xe bombard., thermal desorption obs. 8=48483
  Xe^{133} ions, 40 keV, depth distrib. 8=48935
Gold compounds
  alloys containing 1% Sb, evaporation in vacuum 8=34998
  magnetic alloys, dil., solute Knight shifts rel. to rigid band theory 8=45117
  rare-earth alloys, (Gd, Tb, Ho), resistivity meas., 1.3–20°K 8=40311
  transition metal alloys, very dilute, specific heat below 3°K 8=39912
  Au(III)-dimethyl hydroxide, cryst. and molec. struct. 8=39770
  Au-rare-earth alloys, resistivity temp. dependence, 1.3-20°K 8=31317
  Au–Ag alloy, vacancy conc. 8=31046
  $AuAg_3Te_2$, phase transforms during e microprobe analysis, obs. 8=30857
  Au-Cd alloys, hexagonal, stacking faults 8=26701
  Au–Cd alloys, hexagonal, structural, imperfections, from X-ray diffraction 8=44426
  β-Au-Cd alloys, structure of martensites 8=26035
  Au–Cd system, phase transformation diffusion energetics 8=48373
  Au-Co, ferromagnetism in liq. state, and elec. resist. 8=43871
  Au-Cr alloys, electrical resistivity rel. to temp., 8=44685
  Au-Cu alloys e probe microanalysis, absorpt., fluoresc. and 2 corrections 8=27802
  AuCu-type ordered alloys, dislocation damping mechanism 8 =40031
  $AuCu_3$, antiphase-domain growth rel. to antiphase-boundry reactions 8=26060
  Au_3Cu ordering after quenching, rel. to energy and resistivity changes 8=26059
  Au–Cu–Zn alloy, martensitic θ-struct. 8=48633
  Au-Fe alloy, dil, low temp. susceptibility rel. to spin compensation 8=31604
  Au-Fe alloy thermocouple wire, props. 8=35995
  Au-Fe, hyperfine coupling constants from nuclear sp. hts. down to 0.02°K 8=31495
  Au-Ge alloy, eutectic, as ohmic contacts for Gunn elements 8=49282
  Au-Ge-Si alloys, glass-liq. transition 8=39470
  Au_2Mn, antiferromagnet, exchange striction and exchange coupling consts. 8=31755
  Au_2Mn, antiferromagnet, magnetostriction at high mag. field 8=31754
  Au_2Mn, magnetostriction at high mag. fields 8=40858
  Au_4Mn, saturation magnetization, press. effect 8=36069
  Au_5Mn_2, ordered, antiferromag. 8=31756
  Au-Mo laminated metallization in integrated circuits, thickness, e microprobe obs. 8=30749
  Au-Ni, ferromagnetism in liq. state, and elec. resist 8=43871
  Au-Ni thin film thermocouples for temp. variation across thin semiconductors, obs. 8=40638

- **Gold compounds**—contd
  - Au-Pt alloy, dil, vacancy-impurity interaction from quenching resistance 8=48805
  - Au-Pt alloys, annealed and quenched, thermal conductivity 8=48759
  - n–Au–Si surface barrier photodiode, h.f., technology and props. 8=49432
  - Au-Si surface barrier, rectification characteristics 8=49294
  - Au-Sn system, liquidus in phase, diag. 8=48072
  - Au-V dilute solid solns., V^{51} n. m. r. 8=27514
  - Au–V solid solns., lattice parameter comp. dependence, 0–10 at.% V 8=44205
  - Au_4V, ferromagnetic, mag. disorder induced by plastic deform. 8=27399
  - Au_4V, Mossbauer effect determ. of V moment 8=26016
  - Au_4V, ordered, mag. moment 8=49463
  - Au-W thick-target bremsstrahlung spectra 8=33621
  - Ni–Au system interdiffusion rel. to comp., 850–925°C 8=31015
- **Grain boundaries.** See Crystal imperfections; Crystal structure/microstructure.
- **Gramophones.** See Sound reproduction.
- **Granato–Lücke theory.** See Crystal imperfections/dislocations.
- **Granular structure**
  - α-brass, discontinuous yielding and stretcher strains rel. to grain size obs. 8=40141
  - α-brass, influence of Fe and P additions on grain size 8=48594
  - aggregate, ultrasonic wave scatt. factor, elastic wave vel. effect 8=30936
  - coal and sandstone, interparticle friction 8=26042
  - disperse, flow patterns in axisymmetric rotor 8=43884
  - elastic-plastic material, moving step load on surface of half-space 8=41711
  - films, thin, optical props. 8=27521
  - grain size and distrib. meas. 8=44153
  - grain size determ. by X-ray method 8=30841
  - grain size distrib. reln. with dimension distrib. of planar and linear intercepts. 8=43986
  - insulations, thermal conductivity CO_2 gas pressure dependence 8=26600
  - metals, grain size reln. with diffusion 8=48349
  - metals, non-ferrous annealed, grain refining rel. to heating speed and dispersion 8=39714
  - observation by X-ray diffraction camera 8=26331
  - particle size distrib. meas. by small-angle X-ray scatt. 8=26041
  - plastically torsioned hollow cylinders rel. to length change 8=44523
  - steel, 18/8 stainless, corrosion and powder formations 8=43983
  - steel, quench-hardened, austenitic grain struct. formation 8=35110
  - tensile strength, theory and expt. in whole moisture range 8=31173
  - Al, annealing, grain refining rel. to heating speed and dispersion 8=39714
  - Al macrocrysts. plastic deform., grain boundary props., EPMA-Kossel obs. 8=30856
  - Al sheet, grain size in forming rel. to ribbing 8=39713
  - Al-Al_2O_3, influence of grain size on high-temp. ductility 8=26779
  - AlMn, annealing, grain refining rel. to heating speed and dispersion 8=39714
  - Au evaporated particles, multiple-twin struct. and deca- or icosa-hedron shapes 8=35317
  - Cd, grain size rel. to vibr. during crystallization, obs. 8=35269
  - Cu55%- Zn45% α and β phases location and comp., obs. 8=30688
  - of H adsorbed on CO_2 80-100°K 8=30765
  - KCl, grain boundary mobility, meas. technique 8=40052
  - NaCl, grain boundary energies, rigid lattice approx. 8=40053
  - Ni–Fe films, columnar structure obs., anisotropy existence and origin 8=44169
  - U alloys, α-phase grain refinement by B addition, obs. 8=44171
  - UC, grain boundary grooving rel. to surface energy 8=30871
  - UO_2, columnar grain growth under steep thermal grads 8=26301
  - UO_2 with dispersed Gd_2O_3, after high temp firing 8=35074
  - Zn macrocrysts. plastic deform., grain boundary props., EPMA-Kossel obs. 8=30856
- **Graphite**
  - adsorption of CCl_4 8=48473
  - artefacts, dynamic Young's mod., from −196°C to 1000°C 8=26790
  - Auger spectra for surface structure 8=44656
  - carbide mats., hot worked with dispersed liq. carbide, thermal and elec. conductivities 8=44361
  - in clay, effect on microstructure and drying shrinkage 8=39709
  - creep behaviour, high-temp., influence of cryst. orientation 8=35664
  - creep rate tensile stress dependence 8=26792
- **Graphite**—contd
  - crystal growth and characterization 8=44123
  - crystal growth mechanism in Fe-C-Si 8=39670
  - crystal growth rel. to adsorbed impurity effect, scanning-e-microscope obs. 8=26236
  - crystal structure and defects at >2000°C from X-ray diffr. exam. 8=39792
  - cuvette for atomic spectroscopy 8=38619
  - dimensional changes due to neutron irrad., influence of crystallite size 8=35600
  - electron microscope exam., lattice fringes resolution, 100 kV 8=39775
  - electron plasma, energy loss spectrum at different angles of incidence with crystal axis 8=26929
  - electronic structure, optical study 8=31279
  - emittance and reflectance, visible and near i. r., 2200 to 3500°K 8=36334
  - empty-channel lattice, pulsed-source obs. 8=30890
  - energy calcs., anisotropy 8=48299
  - field-ion microscopy 8=26292
  - grade A reactor, n-irrad. at 80°K and annealed at temps. up to 300°K, e.s.r. 8=45081
  - grain condensation in cool stars 8=45645
  - graphite/H_2O and /D_2O interfaces, n diffusion waves refl. and refr. at, theory 8=38071
  - graphitoplastics, mech. props. 8=31247
  - insertion compounds, possible structs. rel. to superposed 2-dimens. lattices 8=35320
  - intercalatron isotherm of $FeCl_3$ vapour from 300 to 350 C 8=27697
  - internal friction rel. to preparation, damping coeff. expt. and theory 8=26791
  - interstitial formation on n-irradiation below 200°C, cluster size and temp. dependence 8=44419
  - isotropic, elastic properties 8=26793
  - isotropic, kinetics of O-atom and O_2 attack to 2100°K 8=36556
  - lattice defect energies, extended Huckel theory calc. 8=31021
  - lattice expansion on condensable vapour intercalation rel. to friction and wear 8=44208
  - lattice vibration 8=35383
  - membranes, sorption time-lag and blind pore behaviour 8=26134
  - microscopy, opt. and electron 8=44164
  - microstructure, changes on creep strain at 2500°C 8=44163
  - neutron-irradiation damage, annealing studies by ESR 8=26729
  - neutron irrad. obs. 8=43143
  - neutron thermal wave propagation and effect of Bragg continuum 8=47374
  - neutron wave propagagion expt., group coupling through Bragg cut-off energy 8=47375
  - nitrates, first and sec. sequences, elec. props. and phase transforms. 8=35827
  - optical constants from e.-energy loss meas. 8=49672
  - oxidation anisotropy 8=41239
  - oxidation, inhibiting effects of Cl and CCl_4 8=27696
  - oxidation, thermal, structure after 8=44167
  - polycrystalline, Young's mod. and thermal expansion coeffs. rel. to orientations averaging tech. 8=35663
  - powder in Ar compressor, effect on absorpt. and emission of purity lines 8=34138
  - proton reactions, 24 GeV/c, energy of n prod. 8=29439
  - pyrolytic, carrier density rel. to pressure 8=35756
  - pyrolytic, electron and hole location from laser magnetoreflection data 8=35757
  - pyrolytic, Esaki effect at liquid N_2 temp. 8=44764
  - pyrolytic, kinetics of O-atom and O_2 attack to 2100°K 8=36556
  - pyrolytic, preferred orientation 8=39646
  - pyrolytic, structural anisotropy correl. with normal spectral emissivity 8=36332
  - reactor damaged, change of e.s.r. with annealing 8=36237
  - reactor type, elastic consts, stress/strain relns, strength and hardness meas. 8=26789
  - resistance furnace for fuel element heating simulation 8=34112
  - under restraint, struct. changes on n-irrad. 8=31149
  - rhombohedral, mag. props and transform. into hexagonal struct 8=31497
  - shear compliance (C_{44}), effect of neutron irrad., rel. to 'pinning' defects 8=35665
  - surface burning in stream of dry oxygen, temp., profile by spectrum-line reversal temperature 8=46256
  - surface energy of liq. metal interfaces 8=30718
  - surfaces, energy anal. of back-scattered electrons rel. to structs. 8=30730
  - surfaces, gold decoration and epitaxial growth 8=44099
  - synthetic, porosity, access of gases at high temps. 8=48353
  - thermal conds. rel. to high orientation, theory of effect of crystallite boundaries 8=35457
  - trigonal warping of bands and Hall effect 8=35767
  - Vickers hardness before and after neutron irrad. 8=35666
  - X-ray diagrams, line intensity 8=35319
  - Cs-graphite absorpt. reservoir system for heat-pipe converter 8=28490

Graphite—contd
Cs-graphite lamellar cpds rel. to Cs vapour press. and temp. 8=35011
H reactions at high temp. and press. 8=47422
K graphites, formation and structure 8=30904
K, order-disorder transformation obs. 8=26074
in NbC composites, elastic props., 8=49040
SiO evaporation from cloth 8=35005
Graphs
See also Nomograms.
for analysis of transverse vib. of elastic-plastic string 8=32751
cubic lattice characterization 8=46002
curve fitting for n cross section computation 8=33789
delta method for soln. of higher order nonlinear systems, gen. approach 8=28243
in $\lambda\ \phi^4$ theory, asymptotic behaviour soln. using Bethe-Salpeter eqn. 8=42323
logarithmic Gaussian beam chart, for laser propag. and matching 8=28646
Mössbauer source with Doppler effect, data reduction 8=38350
perturbation theory diagrams with composite particles, analytical props. 8=42324
Reggeon, for inelastic processes 8=29072
secondary emission yield, automatic plotting 8=36056
smoothing, appl. of statistical props. of noise 8=32688
x-y charts reading into computer for processing 8=23813
Gratings. See Diffraction gratings; X-ray diffraction.
Gravimeters. See Gravity.
Gravitation
See also Relativity.
active and passive mass for extended body, equivalence 8=41743
Bondi's active and passive mass, expt. investigation 8=32816
Brans-Dicke coupling constant, necessarily positive 8=45589
circular motion in relativistic Kepler problem, stability 8=37123
classical, renormalized mass definition 8=28282
collapse, appl. of event horizons in static electrovac space-times 8=32807
collapse, freq. shift in expanding universe 8=36915
collapse in presence of mag.-field 8=50264
collapse of gaseous ellipsoid 8=32393
collapse of isothermal sphere, protostar form. 8=32432
collapse of protostar, evolution 8=45640
collapse or expansion in general relativity 8=50250
collapse problems, numerical methods 8=50265
collapse, props. of high density matter in intense 8=45601
collapse rel. to Schwarzschild singularity 8=32812
collapse, protostellar cluster, runaway star evolution 8=36960
collapsing and radiating body, Bondi model 8=45600
collapsing clouds, fragmentation, rotation and pressure gradients effects, 8=50256
constant, rel. to cosmic microwave radiation 8=32795-6
constant, universal, pendulum meas. 8=32780
Curzon metric, structure 8=37172
deflection of light, effect on lunar star occultation time 8=32801
Dirac particle, anomalous interaction due to breakdown of Bianchi identities 8=46081
earth satellites stabilization, gravit. and mag. fields effects 8=32381
effects on thermal instability of heated fluids 8=39290
Einstein eqns., free, soln. in Gaussian co-ords. with only one singularity 8=37167
Einstein field eqns. used to derive Lorentz-invariant eqns. of motion 8=28293
Einstein's field eqns., new general relativistic dust metrics 8=28289
Einstein-Maxwell field eqns. reformulated for axially symm. problem 8=28303
Einstein's theory, gauge noninvariant interactions 8=32776
electric field induced near metals, criticism of an expt. 8=40297
elec. field induction in conductors, from statistical electron model 8=26876
elementary particle gravitational coupling constant 8=29030
e. m. field effect on motion of changed hypersurface in general relativity 8=28291
e. m.-gravitational wave interaction, perturbation theory 8=32778
e.m. wave propag. in Sun's field, general relativity calc. 8=37163
e. m. waves in gravitational fields 8=32806
field, cylindrical non stationary solution 8=28301
field energy, chronometrically invariant definition 8=32799
field energy-momentum, timelike character 8=32802
field equations for fluid spheres, solns. for $e^{-\lambda}$ 8=41740
field-induced contact pot. difference, rel. to surface-stress concept 8=44679
field of constant-mass-density sphere 8=32800
field nature and metric principle validity 8=28290
field quantization, canonical 8=41750
Gravitation—contd
field quantization, modified general relativity theory 8=32819
field, zero rest-mass, asymptotically flat, conservation laws 8=28281
flow of ideal gas in spherically symmetrical field with allowance for radiant heat conduction and radiant press. 8=47937
fluid heated from below in gravitational field, stability onset analysis 8=46251
gradient sensors, rotating cruciform-shape, vibrational mode behaviour 8=37168
gravitation/inertial mass ratio, meas, by lunar laser ranging 8=41748
gravitational waves, detection by electromag. radiation 8=23864
graviton mass and light deflection 8=46079
graviton non-zero mass and metric theory incompatibility 8=28298
gravitons, from broken symmetry in weak interactions 8=33520
gravitons, scatt., low energy form of amplitude 8=29080
instability in isothermal nebula 8=50341
instability of interface separating two streams of homogeneous medium 8=28100
instability rel. to interstellar matter and stellar formation 8=50348
Kerr metric, formula for constructing interior solns. 8=23867
Kerr metric, spinning mass shell source 8=41749
Lorentz invariant theory, cosmological solns. 8=28032
mass-energy relation 8=23862
mass, gravitational and inertial, equiv. tested in solar system 8=32817
mass, inertial and gravitational, equiv. principle in Einstein and Brans-Dicke theories 8=32818
masses, inert and gravitational, exptl. verification of equality 8=46021
metals, induced external elec. field, meas. 8=35814
Minkowski formulation of Einstein's theory by Rosen method 8=46083
neutron star, mass infall as source of cosmic and X-rays 8=45676
Newtonian orbit in pulsating Universe 8=46082
particle in field of particles, 5D relativistic theory 8=28300
plasma, gravit. instability 8=32492
plasma instability study with Chew-Goldberger-Low eqn. 8=41528
potential of arbitrary body, study of coeffs. by tesseral harmonics 8=36912
pulsating object, spectral shift of emitted light 8=28033
quantum theory, via correspondence principle applied to Hamilton-Jacobi theory 8=32777
radiation from pulsars, gravitational, possible obs. on earth 8=45782
radiation from uniformly accelerated particles in general relativity 8=23868
radiation interact. with coupled and uncoupled test particles 8=41742
radiation metric logarithmic terms from radiative corrections 8=28299
radiation, outgoing/incoming mixture, mass transfer from source 8=32804
scalar particle in its own field, stable states 8=28296
scalar-tensor theory rel. to cosmic fireball 8=23858
scalar theories with variable velocity of light 8=46086
Schwarzschild singularity, scatt. of massless scalar waves 8=36929
self-gravitating gas, one dimensional, Vlasov equation 8=50251
self-gravitating stellar system with uniform rotation, stability of density waves 8=28037
shells, charged, gravitational collapse 8=46088
static axial symmetry, exact soln. for metric 8=37166
static electrovac spacetimes, event horizons 8=32807
Stokes-Poincaré theorem, meaningful choice of Stokes elements 8=32170
sun's internal field rel. to light waves bending, metric theory 8=32569
superdense matter, scaler interaction energy density 8=45599
unified quantum field theory 8=32820
vacuum quantum fluctuations rel. to Einstein's theory 8=37165
virial eqns. of fourth order 8=23856
wave-detector-events 8=36654
waves and radiation 8=46085
waves, detectability in scintill. of starlight 8=37164
waves emitted by pulsating star, damping of pulsations 8=41516
waves, generation, due to emission and absorpt. of em. waves, criticism of Weber's results 8=41744
waves, intrinsic freq. and energy conservation 8=23807
waves, plane, without polarization, Klein-Gordon eq. sol. 8=32813
$AgNO_3$, molten electrolyte, cell pot. gravit. 8=45367
$AgNO_3$-AgCl, molten electrolyte, cell pot. gravit. comparent, obs. 8=45367
He^4, field effect on superfluid transition 8=41899

Gravitational collapse. See Gravitation.
Gravitational red shift. See Relativity/general.
Gravitons. See Gravitation.
Gravity
See also Geophysical prospecting.
anomalies interpretation, computer soln. 8=27821
atmospheric waves, transient, calc. 8=27886
circular sattelite orbit stability in dipole mag. and gravitational fields 8=50236
closure problem in system of random waves 8=36656
critical density determ., effects of sample config. in earth's field 8=30574
earth's external field from artificial satellites motion meas. 8=27819
earth's field, effects of convection in mantle, hydrodynamical model for interior 8=50006
earth's topography gravit. attraction, computer calc. 8=27820
effect on boiling heat fluxes, peak and min., interact with geometry effects 8=34997
Eotvos corrections for airborne gravimetry 8=50010
field in Hudson Bay and vicinity, structural implications 8=32169
formula and polar flattening in Geodetic Reference System (1967) 8=50007
free fall in a rarified atmosphere 8=28257
global variations with time 8=50014
gravity meter meas., comparison with satellite obs. results 8=50008
harmonics, low order resonant from satellite drift 8=50009
liquid jet leaving Poisseuille tube, effect 8=48039
liquid sessile drops, rel. to shape analysis 8=25857
potential fields, smoothing 8=50011
satellite obs. geophysical implications 8=45429
shipboard meters, La Coste-Romberg performance (1963 and 1964) 8=36655
superconducting gravimeter 8=31352
superconducting gravimeter 8=50013
unknown parts of earth's field, obs. from successive satellite passages 8=41315
vertical gradient in motion, determ. with group of accelerometers 8=50005
wave-detector-events 8=36654
G, possible var. evidence from solar structure 8=45861
Grey atmosphere. See Radiative transfer; Stars/radiation.
Group theory
algebra and superconvergence in Goebel's static model 8=37838
Baer*-semigroups and ortholattices, quantum logic 8=32823
Casimir operators, eigenvalues 8=24591
causality groups of S-matrix 8=33584
Clebsch-Gordan series for SO_5, SO_4, Sp_4 and G_2, deriv. 8=33362
conformal, violation of causality 8=32779
conspiracy problem solutions 8=47037
Coulomb problem, relativistic symmetric, dynamic symm. in case of cont. spectrum 8=47016
de Sitter group in molec. quantum mech. 8=25430
eight-fold way, multilinear couplings 8=33531
four-spinors 8=24594
groups, non-compact associated with vertex operator 8=33651
G(2), Clebsch-Gordan series 8=29264
Hilbert space, critical point theory 8=45989
homotopy groups, unstable, of classical groups, odd primary components 8=32665
$K = G_0(8) \otimes SU(3)$, new Lie group for scalar SU(3) symm. strong-coupling theory 8=33541
Kronecker squares of representations, decomposition 8=28236
L_3, calc. of Wigner coeffs. 8=28235
lattice vibrs. in molec. crysts. 8=39861
Lie algebra representations, multiplicities 8=45993
Lie algebras, Poisson bracket realization by analytic functions of generators 8=28231
Lie groups and Lie algebras, representation theory methods and results 8=45992
Lie, in construction of models for elementary particles 8=29016
Lie, tensor products of representations over a continuous variable 8=24599
Lagrangian, effective, construction rel. to chiral group $K_3=SU_3 \times SU_3$ 8=33341
Lorentz, irreducible representations, reduction of relativistic wave functions 8=33314
Lorentz, representations, geometry and algebra 8=24592
Lorentz, unitary representation functions 8=24456
Lorentz, unitary representation in O(2, 1) basis 8=32663
Lorentz, Zeeman causality theorem, algebraic analogue 8=23857
magnetic groups and corepresentations 8=26159
matrix groups, exponential representations and canonical forms 8=45990
Minkowski space, Wightman set theory, generalization 8=32781
molecular vibration application 8=34201
Group theory—contd
non-compact, construction of physically acceptable representations 8=37846
non-compact groups, matrix elements of representations in continuous basis 8=24593
non-compact in particle physics and their relaxations 8=37845
O(2, 1), unitary representations in O(1, 1) basis 8=24605
$O_{3,1}$ symmetry and Lorentz states of exchanged trajectories for $0 + \frac{1}{2} \to 1 + \frac{3}{2}$ spin processes 8=37900
$O_{3.1}$ symmetry and $N\bar{N} \to Y\bar{Y}$ high energy reactions 8=3805
$O_{4.1}$ of H atom additional generators 8=38650
O(4) symmetry, composite model structure of particles 8=47011
O(4, 2) dynamics, relativistic current of H atom 8=29594
O_8 broken symmetry and mass relations 8=38317
S-operator theory of weak interactions 8=37874
orthogonal and pseudo-orthog., unified representation theory 8=33537
permutations, timelike, definition and properties 8=37116
Poincaré, for infinite momentum kinematics of interacting particles 8=33558
Poincaré modification rel. to combination of relativity and internal symm. 8=37847
Poincaré subgroups, quantum numbers 8=24457
relative ideals in semigroups 8=23805
quarks and non-relativistic particle dynamics 8=37847
representations and orbital ang. momentum 8=33309
review of appl. in particle physics 8=29014
rotation, canonical realizations 8=24607
rotation group with complex spin, infinite-dimens. representations with entire functions 8=32664
semigroups, complete ideals 8=32666
semigroups, direct product, nilpotent elements and radicals 8=32668
semigroups, Ševrin radical 8=32667
$SL_{2,c}$ broken, mass formula and applications to nucleon and delta Regge trajectories 8=37904
SL(2, C), form factors calc. in E(2) basis 8=33554
SL(6, C), relativistic strong vertex, expansion 8=24632
SO(n)-symmetric field equations 8=33518
SL(n, C) unitary representations, new method for analysis 8=46813
SL(2, C), e. m. vertex in spin-$\frac{1}{2}$-particle calc. 8=46815
SL(2, C), production vertex of 2 spin $\frac{1}{2}$ particles by a spin 1 particle calc. 8=46814
SL(6, C), baryon-meson vertex 8=47098
$SO_0(N, 1)$, $N \geq 3$, unitary irreducible representations, classification 8=32670
$SO(3) \otimes SO(2, 1)$ non-invariant group and broken symmetry 8=33306
SO_4, algebra and point rotor, rel. to H atomic symmetry 8=34128
SO(4) symmetry in πN scatt., applications 8=42550
space-momentum commutation, general relation 8=28234
spin-S spherical harmonics and ∂ 8=23804
strong coupling groups, representations 8=33535
strong interactions, symmetries 8=24642
SU_n, build up of tensors, reduction of transformation matrices 8=33539
SU(n), regular representation, j coeffs. 8=24604
SU_n, substitution and mirror refl. symmetry 8=24608
SU_n symm., non-isotropic harmonic oscillators 8=24467
SU_n, symmetric representations, Clebsch-Gordon coeffs. 8=37842
SU(p, 1), representations constructed from irreducible representations of U(p) 8=37841
SU(1, 1), Wigner coefficients, general study 8=33347
SU(2) realization by boson operators rel. to 3-j symbols 8=33547
SU(2, 2), irreducible representations, finite and infinite dimens. 8=28232
SU(2, 2) with infinite multiplets 8=33562
$SU(2) \otimes SU(2)$ Lagrangian rel. to ρ couplings and mass depend. of $\gamma_{\rho\pi\pi}$ 8=38041
SU_3 and its implications 8=24616
SU_3 assignments 8=25004
SU(3), broken and P_{11} π-N scatt. 8=42546
SU(3) broken symmetry in strong-coupling theory 8=42397
SU_3 Clebsch-Gordan coeffs. 8=37850
SU(3) crossing matrices 8=33542
SU(3) embedding in SU(8) 8=42379
SU(3) evaluation of Clebsch-Gordan coeffs. 8=37844
SU(3), Goldberger-Freiman relation, and Cabibbo angle 8=37828
SU(3) leading to mass formulae 8=33549
SU_3 reducible representation, classification of baryon resonances 8=42663
SU(3) representations 8=33348
SU_3, substitution group and mirror reflection symmetry 8=45991
SU_3 symmetry and mass formulae 8=24620
SU(3) symm. breaking and K decay parameters 8=38002
SU_3 symm. in two-body high energy reactions 8=47023
SU(3) symm. strong coupling theory, dynamical group 8=24614
SU(3) symmetry broken, baryon spectrum 8=47125
SU(3) validity in high energy two-body and quasi-two-body, scatt. 8=37852

Group theory—contd
    $SU(3)^{11}$ excitation of baryon resonances 8=25002
    $SU(3) \otimes SU(3)$ chiral algebra, sum rules for baryon mixing angles, infinite momentum 8=38047
    $SU(3) \times SU(3)$, baryon-meson interaction Lagrangian 8=47127
    $SU(3) \times SU(3)$ spectral function derivation, sum rules 8=33551
    $[SU(3) \otimes SU(3)]_{c.m.}$ symmetry and vector meson prod. 8=42603
    SU(4), axial vector renormalization constant derivation 8=24615
    SU(6), branching rules, and embeddings of simple Lie groups 8=33532
    $SU_W(6)$, broken symmetry and the ninth pseudoscalar meson 8=33655
    SU(6), classification of 2^+ meson 8=33549
    SU(6) 405-plet classification of meson resonances 8=38020
    SU(6) leading to mass formulae 8=33549
    SU(6, 6) selection rules, missing SU(3) multiplets 8=37849
    SU(n), evaluation of Clebsch-Gordan coeffs. 8=37844
    symmetry broken for e.m. weak hadron current gauge field models 8=37853
    unitarity corrections in spectral-function sum rules, meson propagators 8=37954
    unitary, compact, inhomogeneous, invariants and scalars 8=32650
    unitary, inhomogeneous, compact number of invariants for two types computed 8=32651
    unitary irreducible representation, basis from bound states of Hamiltonian 8=37843
    unitary, tensor operators, pattern calculus 8=32669
    U(p, p) ladders, physical multiplets assignment consistent with U(6, 6) 8=24618
    U(p, q) ladder representations coupling, local and global props. 8=24617
    U(p, q) ladder, tensor product of two, existence at most of one ladder 8=24618
    U(3) harmonics, solid, normalization 8=41627
    U(3, 1) broken symmetry, soln. 8=42307
    U_6 composite quark model for baryons and resonances 8=47100
    U(6), extension of unitary spin 8=33523
    $U(6) \otimes U(6)$, internal quark dynamics of hadrons 8=33648
    $U(6) \otimes U(6)$ Reggeization 8=42439
    H atom, relativistic, partial treatment 8=29593
Grüneisen coefficient. See Specific heat; Thermal expansion.
Gudden–Pohl effect. See Electroluminescence.
Guinier–Preston zones. See Crystal structure/microstructure.
Gunn effect. See Crystal electron states/plasma; Semiconducting materials; Semiconductors.
Gyromagnetic effect
    No entries
Gyromagnetic ratio
    deformed nuclei, effective spin, calc. 8=25089
    electron, g-factor anomaly recalc. 8=24717
    ferrihaemoglobin, g factor anisotropy rel. to dynamical Jahn-Teller effect 8=36234
    for ground state rot. band in deformed nuclei, using cranking-model 8=25088
    nuclei embedded in magnetized ferromag. foil, meas. 8=38401
    in pairing-plus-quadrupole model 8=25055
    g-tensor, perturbation corrections 8=43160
    Ba, of lowest $^1P_1$, $^3P_1$ states 8=38691
    CaF_2: Ho^{2+}, g-factor stress dependence 8=31510
    D, g_J ratio meas. by optical pumping 8=38734
    Dy^{161}, 74.5 MeV level rel. to ground level using Mossbauer effect 8=25150
    Fe layers, thick evaporated, and gyroelectric consts., reflected light meas. 8=36141
    H, g_J ratio meas. by optical pumping 8=38734
    I isotopes, meas. by Xe nuclei magnetized ferromag. foil 8=38401
    Ni-Pd alloy, g factor and saturation magnetization meas. 8=31666
    $Rb^{85,87}$, g_J ratio meas. by optical pumping 8=38734
    ThO_2: Yb^{3+}, g-factor stress dependence 8=31510
Gyroscopes
    laser gyro, fundamentals and advantages 8=46012
    motion in universal suspension on uniformly rotating base 8=41645
    superconducting, drift data and mathematical model 8=23820
    superconducting, for relativity verification 8=29000

Hadrons
    absorption model consistent with elastic unitarity for high energy collisions 8=42488
    baryon-meson supermultiplet symmetry from spinor currents 8=42483
    baryon-meson vertex in SL(6, C) 8=47098
    bootstrap model, asymptotic vertex function 8=42484
    bootstrap of vector and tensor trajectories from superconvergence 8=33602
    cluster model, mesons decay and mass spectrum 8=42486
Hadrons—contd
    component of e.a.s., multiple core struct. 8=38231
    current algebra, Ward identities and space-space equal-time current commutators 8=42485
    current in reaction $\nu + N \to N^* + \mu$ 8=25004
    currents, crucial test of theory 8=42371
    baryon-antibaryon-meson vertices, phenomenological symms. rel. to channel dependence 8=33651
    composite model and Regge pole 8=37953
    Compton scatt., kinematic singularity of helicity amplitudes 8=29079
    decay in symm. schemes, incomplete without SU_3 mass splitting interaction 8=24626
    decay, leptonic, radiative corrections finiteness conditions 8=37948
    decay, nonleptonic, possible interrelation to current-current (J^+J) picture 8=37862
    decay, nonleptonic, systematic and steady phenomenological approach 8=37860
    decay of resonances, quark model 8=42493
    decay rate calc. using quark model 8=42497
    decay widths 8=37949
    diffraction theories of collisions, appls. 8=29109
    e.m. corrections to mass shifts and decays of weak interaction currents identified with boson field 8=29106
    e.m. mass difference, using algebra of fields and non-leptonic weak interactions 8=24744
    e.m. mass shifts, current-algebra anomalies rel. to equal-time commutator and N form factor 8=33652
    form-factors of half-integer spin particles, asymptotic behaviour 8=47097
    form factors asymptotic behaviour rel. to compositeness 8=33650
    $\gamma + \gamma \to \rho^\circ + \rho^\circ$, high energies 8=47040
    gauge-field algebra with symmetry breaking 8=27853
    hadrons-nucleus collisions, semiclassical theory 8=42491
    h-h elastic scatt., quark model, cross-section relations 8=29112
    Horn–Schmid duality 8=33545
    interacting radius, excited state smaller than ground, energy depend. 8=29044
    interaction with neutral lepton currents 8=29110
    mass relations, empirical 8=42498
    mass splitting, dynamical mechanism 8=29107
    model which gives rise only to irreducible representations of zero triality 8=42496
    S-operator theory of weak interactions 8=37874
    photoproduction, rel. to vector meson prod. by meson-nucleon collisions, photon-vector-meson analogy 8=42503
    production, multiple, in theory of complex ang. momenta, statistical charact. 8=37950
    production with identical L and S but different in quark model 8=37951
    pseudoscalar meson-hadron scatt., decuplet sum rules 8=42499
    quark dynamics in $U(6) \otimes U(6)$, mass formulae 8=33648
    quark factorization model, large momentum transfer scattering 8=37945
    quark model for high energy elastic scatt. 8=37947
    quark models for struct. and interactions 8=29103
    quark model, search for $^2/_3e$ charged particle in cosmic rays 8=42489
    resonance decay in the quark model, relationships 8=42494
    resonance, direct channel, scatt. amplitudes at high energies 8=47102
    sakaton rearrangement interactions and high energy hadron-hadron scatt. 8=47103
    scatt. current algebra restrictions deducible from conspiracy theory 8=29136
    scattering, additional meson production, quark model 8=47101
    scattering, high-energy currents model 8=29105
    scattering, high energy e. m., cross-section behaviour 8=37952
    scattering, high energy, quadratic and cubic sum rule using quark model 8=33653
    scattering, interference model and finite energy sum rules 8=24745
    scattering, 2-hadron elastic high-energy model 8=42407
    spectroscopy, Hawaii tropical conference August 1967 8=29027
    spectrum generating algebras 8=33523
    state classification according to representations of local algebra 8=37839
    strange spin formalism 8=42487
    strong interaction, self-induced, matrix elements of currents deduced 8=29111
    theory, complete from Chew's nuclear democracy 8=37872
    triplets of integral charge, dynamical symmetry 8=24740
    Weinberg's second sum rule derivation assuming isospin structure 8=33543
Haemoglobins. See Proteins.
Hafnium
    analysis of O content by He^3 irrad. 8=27818
    diffusion of C, coeff. temp. dependence, 1120–2130°C 8=35495
    polycrystalline, optical consts. from reflectance ratios 8=45164

Hafnium—contd
stacking fault probab. of cold-worked, X-ray obs. 8=26704
Hf/Zr ratio, metamorphic rocks from Ontario 8=50067
Hafnium compounds
diborides, conduction e-parameters calc. based on single zone method 8=35830
HfC, oxidation 1790-2000°K 8=45351
$HfCl_4$ and $ZrCl_4$ vapours, thermal diffusion constant 8=34676
HfN, f.c.c. superconducting props., anomalous 8=27022
HfO_2, rare-earth impurity ion doping in melt-grown crystals 8=26645
$HfSb_2$, at. structure rel. to quasi-homologs 8=35360
Hf-X, (X = Os, Ir, Pt), crystal structure rel. to phase transforms 8=30899
(Hf, Zr)N, f. c. c. superconducting props., anomalous 8=27022
Half-lives. See Radioactivity/decay periods.
Hall effect
See also Semiconducting materials; Semiconductors.
curled MHD flow in plane channel, influence of Hall effect on development 8=24187
electrolyte aq. solns., meas. 8=48199
e.m.f. rel. to sample thickness 8=35812
ferromagnetic films, optimization 8=44681
graphite, and trigonal warping of bands 8=35767
gravitation induced, in type I superconductor 8=31333
ice, and proton mobilities 8=35958
ionized gases, comparison with solids 8=43695
magnetic field probe system 8=28510
measurement by pulse method 8=49149
in MHD channel flow 8=37445
microminiature probe for use in liq. He 8=28509
multiplier for pressure-squaring acoustic power meter 8=32915
poly(N-vinyl carbazole)I complex, mobility for charge-transfer state 8=27462
probes for magnetic field meas. at cryogenic temp. 8=24031
pyrocarbons, B-doped, rel. to electron states 8=27084
pyrocarbons compressed at high temps. 8=45941
quantum oscillations of Hall constant 8=31265
semiconductor plaquettes 8=44752
semiconductor thin films, meas. 8=40424
semiconductors, high resistivity, single electrometer method of meas. 8=27060
semiconductors, remote meas. apparatus 8=49220
single crystals at 70kb, meas. 8=44680
sondes of magnetic fields 8=33041
in 3d ferromagnets, giant spontaneous 8=31562
Al, coeff. determ. using helicon wave resonaces rel. to surface-mode loss 8=44682
Al films, size effects and Righi-Leduc coeff. 8=40308
Ar plasma, radial mag. field in shock tube, obs. 8=34485
B, coarse-grained, coeff., 150-850°C 8=35824
B, temp. dependence, 300-1200°K 8=35823
Bi films, thickness depend. and quantum effects 8=27082
n and p-Bi_2Te_3, conductivity, carrier lifetime 8=40439
Cd_3As_2, evaporated Hall elements, props. 8=27088
$Cd_xCa_{1-x}O$, and elec. conductivity and optical props. 8=49137
n-CdS, Hall mobility, 1.9 to 294°K 8=31369
CdS, p type high conductivity 8=40444
CdSb, Ag doped, at low temp. 8=44773
CdSb: In(Cu), rel. to temp. 8=44768
n-CdSe, prepared under 100 atm. of N, Hall constant meas. 8=49230
$Cd_xSr_{1-x}O$, and elec. conductivity and optical props. 8=49137
CdTe, low temp. 8=44771
n-CdTe, thermal n irrad., rel. to Cd vacancies, obs. 8=35533
Co film, ferromag., planar effect, thickness (100-1500Å) and temp. (77-293°K) dependence 3=31687
Co films, polycryst., thickness depend., 200-2000Å 8=31598
Cr, coeff. temp. dependence, 77-330°K rel. to "mag. cooling" effects 8=45054
$CrTe_{1-x}Sb_x$ alloys, comp. and temp. dependence 8=35883
Cu alloys, constant changes on plastic deform. rel. to order and stacking fault energy 8=44689
Cu, coeff. and magnetoresistance, mag. field, temp. and orientation dependence 8=49157
$Cu_{2-x}S(0 \leqslant x \leqslant 0.2)$ 8=49156
Dy, anomalous, 340-4°K 8=44969
Fe, coeff., ordinary, theory at low temps. 8=49162
Fe film, ferromag., planar effect, thickness (100-1500Å) and temp. (77-293°K) dependence 8=31687
Fe-Ni alloy, plane effect, temp. depend. and role of scatt. mechanisms 8=40324
β-$FeSi_2$:Co, Al, coefficient, conduction mechanism 8=35885
GaAs, conductivity 8=44779
GaAs, microwave mobility of hot electrons 8=49239
GaP:Te of improved homgeneity, meas. 8=27096
p: GaSb, rel. to impurity conc. 8=44780
GaSb, undoped, electron irrad. effects on mobility and coeff. 8=27091
Gd, rel. to Fermi surface, 4.2-340°K, mag. fields to 30 kOe 8=44690
Hall effect—contd
Ge, complex factor from microwave magneto-Kerr effect 8=27127
n-Ge, deformed mobility 8=44784
n-Ge, rel. to dislocation, acceptor level position 8=35891
p-Ge, field and temp. dependence 8=44790
$Ge_{1-x}Mn_xTe$, $0.01 < x < 0.1$, Hall const. and s-d scatt. resist., 4.2-400°K 8=40456
Ge-Si alloys, hot-pressed, 300-850°K 8=35893
Ge-Si alloys: Au, coeff., electrical conductivity, donor level 8=40460
p-Ge-Si alloys, rel. to alloy scattering 8=31377
Hf diborides, rel. to conduction e-parameter calcs. based on single zone model 8=35830
Hg amalgams, liq. 8=43869,
In, coeff. determ. using helicon wave resonances rel. to surface-mode loss 8=44682
p-InAs, coefficient, and electrical cond. and magneto-resist. 8=27114
n-$InAs_xSb_{1-x}$ alloys, high-temp. obs. 8=40475
n-$InAs_xSb_{1-x}$ alloys, obs. and e scatt. calc. 8=35758
n-InSb, Hall angle at 77°K, rel. to angle between current and mag. field 8=27109
n-InSb, inhomogeneous, at 77°K 8=27117
n-InSb single crystals with high density dislocations 8=49248
n-InSb, 2-5°K, in 15kG mag. field 8=49250
InSb, voltage caused by instability, transverse breakdown 8=40468
InSb-InAs alloys, coeff. and conductivity meas., 300-700°K 8=40472
InSb: Mn, rel. to temp., Mn behaviour 8=44799
K, coeff. determ. using helicon wave resonances rel. to surface-mode loss 8=44682
K, field-dependent coeff. rel. to Fermi surface 8=26969
LaSb, coeff. temp. dependence rel. to semi-metal charact., 8=39948
Lu, anisotropy rel. to Fermi surface 8=44690
Mn ferrites 8=40841
MnO, electron and hole mobilities at 943°C 8=27118
MnO: Li, rel. to conduction 8=44801
Na, coeff. determ. using helicon wave resonances rel. to surface-mode loss 8=44682
Nb, superconducting, obs., 8=44724
Nd-H system 8=49141
Ni film, ferromag., planar effect, thickness (100-1500Å) an temp. (77-293°K) dependence 8=31687
Ni, plane effect, temp. depend. and role of scatt. mechanisms 8=40324
$Ni_{1-3x}Cu_{2x}Fe_x$, reconciliation of low temp. sp. heat with Hall effect data 8=39919
Ni-Fe film, ferromag., planar effect, thickness (100-1500Å and temp(77-293°K) dependence 8=31687
Ni-P films, obs. 8=26970
Ni-P films, structure dependence 8=44696
Ni-Sn ferromag. alloys 8=27425
PbO, coefficients obs. 8=26948
n-PbS, rel. to conduction band structure, 77-300°K 8=2711
PbSe:Gd, doping effects 8=44805
PbTe, 77-450°K, valence band, effective mass 8=44804
PbTe:Sb, and elec. cond. 8=40478
PbTe-SnTe-PbS system, meas. rel. to current carrier scattering mechanism 8=31385
Sb_2T_3, coeff. temp dependence rel. to complex valence band structure 8=44808
Si, complex factor from microwave magneto-Kerr effect 8=27127
Si, ion-implanted layers 8=44822
p-Si, n-irradiated, rel. to dimensions and conductivity of disordered regions temp. dependence 8=35913
p-Si:Cu, and resist. 8=49262
Si:P, Li, B obs. 8=49268
$SrTiO_3$, a.c. obs., 190 to 500°K, depend of Hall mobility on charge-carrier density 8=31392
$SrTiO_3$, and photoconductivity 8=40675
TaC_x, coeff. comp. and temp. dependence 8=26972
Te crystals, pulse-heated, anomalous reversal at 515°K rel. to vacancy behaviour 8=31329
Te, meas. in mag. fields up to 150kg 8=49171
Te, molten 8=34965
Te, rel. to galvanomagnetic effects, anisotropy, statistical interpret. 8=31394
Ti diborides, rel. to conduction e-parameter calcs. based on single zone model 8=35830
in Ti-16 at.%Mo alloys, type II superconductor, mixed-state 8=27035
V, type II superconductor 8=40392
VO_2 sputtered films, coeff. rel. to transport props. 8=271
Y, anisotropy rel. to Fermi surface 8=44690
Y single crystals, temp. depend. 8=26975
Zn films, anisotropy meas. rel. to preferred crystal orientation studies 8=30810
ZnSb, anisotropy 80°-420°K 8=44910
$ZnSnP_2$ platelets, coeff. and mobility meas., 190-400°K 8=26267
Zr diborides, rel. to conduction e-parameter calcs. based on single zone model 8=35830
Hall generators. See Electricity/direct conversion; Semiconducting devices.

Hall mobility. See Semiconducting materials; Semiconductors.

Halogens
  adatoms on metal surface, work function and desorpt. energy 8=35193
  atoms, electronically excited, spin orbit relax. 8=25373
  cpds., relation between nucl. quadrupole reson. and polarizability 8=29811
  molecules, photoelectron spectra 8=25486
  phosphorous oxyhalide radicals, electronic 8=43414
  tetrahalogens, mean amplitude quantities and bond covalency correl. 8=34228
  H halides, correl. between mean amplitude quantities and bond covalency 8=34228

Hamidashi effect. See Ferroelectric materials; Ferroelectric phenomena.

Hard-sphere gases. See Quantum theory/many-particle systems; Statistical mechanics.

Hardness
  See also Abrasion; Work hardening.
  α-brass, surface hardening, preferential, in early stage II 8=40145
  austenitic alloys, increase on ageing with plastic deformation at 600°C 8=35699
  austenitic stainless steel, irrad. hardening, substructure 8=49015
  crystals for u.v. and i.r. optics 8=42116
  explosive claddings, microhardness rel. to primary and secondary shock waves 8=48945
  films, radiation hardening during vacuum deposition 8=48965
  graphite, Vickers hardness before and after neutron irrad. 8=35666
  gypsum systems, and modulus of elasticity and porosity, interrelation 8=40172
  knoop, anisotropy, stereographic representation 8=40118
  metallic materials, determ. of C content 8=40119
  microhardness of thermionic diode components rel. to reliability 8=37377
  n- and γ-irradiation hardening from critical shear stress analysis 8=49037
  polymers, amorphous, temp.-time charact. 8=31234
  precipitation hardening by coherent particles, review 8=48980
  quartz brittle crystals, microhardness rel. to dislocation mobility 8=26796
  silicide films on Nb chromised, titanised and chromotitanised 8=35176
  solid-solution hardening in conc. solns., 8=48964
  solid solutions, ternary f.c.c. substitution, hardening action of short range order 8=26806
  steel, low C castings, effect of rare-earth metal additions 8=49009
  steel, low C, strain age-hardening, time law 8=40158
  steel Templugs, heat prod. softening as temp. meas., 70-850°C 8=24024
  tin sheet, bound by Araldite or Cemendine 3000 8=40121
  Vickers indentation, crack length 8=49053
  Ag, increased by internal oxidation of dispersed Al 8=35649
  Al, electron irradiation hardening, rel. to point defect props. 8=31141
  Al, zone-refined, changes during recrystallisation after low-temp. deformation 8=35660
  AlSb, microhardness temp. dependence rel. to dislocation distribs. 8=44443
  Al-Zn-Mg alloy, changes associated with fatigue-crack propag. 8=26783
  Be-Cu alloy, anisotropy rel. to slip resist., Cu conc. effect obs. 8=44552
  CaF_2, microhardness rel. to Rebinder effects occurrence and mechanism 8=40136
  CdS brittle crystals, microhardness rel. to dislocation mobility 8=26796
  CdS, microhardness i.r. illumination dependence rel. to photoconductivity 8=40137
  Cu alloys, improvement by increasing Pb content 8=40144
  Cu, cold-worked, recovery during annealing 8=35709
  Cu, increased by internal oxidation of dispersed Be or Al 8=35649
  Cu, surface hardening, preferential, in early stage II 8=40145
  Cu ternary chalcogenides, microhardness and thermoelec. props. 8=31448
  Cu-Al alloys, rel. to solute atom segregation on stacking faults 8=26643
  Cu-Al-Ni and Cu-Al-Fe, hardening action of short range order 8=26806
  Cu-Au solid solution alloys, surface, and wear and friction, in abrasion 8=40149
  Cu_3Si, gaseous impurity segregation from microhardness meas. 8=35673
  Fe, commercial, age hardening, precipitation mechanism and nature of decomposition products 8=40155
  Fe, high-purity, plastically deformed, softening on heating to 600°C 8=35677
  Fe-Mo alloys, rate of hardening rel. to treatment temp. 8=44004
  Fe-Ni-C martensites, solid solution hardening and thermally activated deformation 8=16816

Hardness—contd
  Fe-Ni-Ti alloys, increase on ageing with plastic deformation at 600°C 8=35699
  Ge, effect of γ-irrad. 8=40637
  p-Ge:Ga, e-irradiated, microhardness and carrier-density, e-flux dependence 8=27101
  n-Ge:Sb, e-irradiated, microhardness and carrier-density, e-flux dependence 8=27101
  KCl, dependence on growth conditions and impurity effects 8=26401
  KCl, hardening by F_A centres 8=44583
  KCl, microhardness F-centre density dependence 8=26690
  LiF, dependence on growth conditions and impurity effects 8=26401
  MgO, critical resolved shear stress rel. to low dose n irrad. 8=26829
  Mg-Zn alloys, age hardening characts., effects of 1%Au addition 8=26832
  Mo, hydrostatically-extruded 8=35706
  Na aluminosilicate glass, ion-exchange hardening, i.r. spectroscopy 8=30864
  NaCl, dependence on impurity effects 8=26401
  NaCl, microhardness F-centre density dependence 8=26690
  NaCl, n- and γ-irradiation hardening from critical shear stress analysis 8=49037
  Nb-O-N supersaturated solid solns., age hardening obs. 8=30831
  Ni, cold-worked, recovery during annealing 8=35709
  Ni_3Ge, gaseous impurity segregation from microhardness meas. 8=35673
  Ni_3Sn_2, gaseous impurity segregation from microhardness meas. 8=35673
  Pb rich alloy of Pb-Sn-Sb ternary system, aging 8=26764
  Pb, zone-refined, solute-induced hardening near grain boundaries 8=26842
  PbTe, effect of γ-irrad. 8=40637
  Pt, n-irradiated, hardening 8=35716
  Sn, zone-refined, solute-induced hardening near grain boundaries 8=26842
  U/10% Pu/10% Fz, changes on annealing 8=30711
  W, anisotropy rel. to plane of testing 8=44607
  W-C-Co system alloys, cracks around Vickers indentation 8=49063
  Zn, zone-refined-solute-induced hardening near grain boundaries 8=26842
  ZnS brittle crystals, microhardness rel. to dislocation mobility 8=26796
  Zr-O solid solns., interdiffusion zone obs. 8=30658

Hardness, magnetic. See Magnetic properties of substances/ferromagnetic.

Harmonic analysis. See Acoustic analysis; Calculating apparatus; Fourier analysis.

Harmonic generation, optical. See Lasers; Optics.

Harmonic oscillators. See Quantum theory.

Hartree–Fock method. See Atoms/structure; Solids/structure.

Hearing
  See also Ear; Speech.
  acoustic meas. errors 8=28375
  aid, temporary threshold shift and recovery 8=37291
  airliner noise, subjective, air speed and duration effect 8=41847
  auditory distance determ., dual rôle of freq. spectrum 8=46214
  auditory feedback delay effects on speech 8=23975
  Békésy threshold, variation of attenuation rate, and starting intensity, effect 8=23979
  BUDTIF adaptice threshold procedure 8=46206
  bullfrog, complex units in 8th nerve, best inhibitory freqs. 8=46220
  cat interference between two tones, cochlear response obs. 8=32933
  cat, 2-tone inhibition in auditory nerve fibres 8=32932
  central masking, freq. distrib. 8=37287
  characteristic curves, subjective sound intensity analyser 8=46196
  condenser-earphone, distortion compensating for physiological studies 8=32926
  cutaneous localization, phase-difference cues 8=37294
  detection and localization, prob. of correct answer 8=23977
  discriminating between simple tones 8=23982
  echo direction perception physiology 8=46207
  echolocation by sea lion 8=37295/6
  frequency analyzing power 8=23980
  frequency discrimination uncorrel. with critical ratio 8=23983
  Haas effect, historical background 8=37292
  interaction with visual stimulation 8=46209
  interval in filtered auditory pulse trains, discrimination 8=32930
  lateralization of tones and clicks 8=46208
  localization in vertical plane, influences 8=37288
  localization of tonal stimuli in vertical plane 8=37289
  loudness calc., exponent in power law 8=46216
  loudness, reflex changes in eardrum impedance 8=23976
  masking by competing signals, interaural time delay effects 8=37286

Hearing—contd
- masking difference harmonics produced in response to single tone 8=23981
- monaural bone-conduction threshold, specification 8=37293
- monaural detection, internal correlation of masking noise, effect 8=23984
- monaural loudness functions rel. to masking 8=46219
- periodicity discrimination in pulse trains 8=32931
- pitch, practice effects in absolute judgement 8=32928
- polyacusis, binaural anomalous pitch perception 8=37290
- porpoise, relation between threshold and pulse duration similar to human 8=23985
- precedence, historical background 8=37292
- pulsed Doppler sequence, discrimination thresholds 8=46212
- pure-tone intensity discrimination 8=46210
- shift from center detection 8=23978
- sonic boom, comments and reply on Farfeld spectrum 8=25817-18
- sound range perception expt. 8=46217
- supernormal individuals, threshold assessment 8=46215
- temporary threshold shift and recovery after use of aids 8=37291
- temporary threshold shift, exposure and recovery models 8=28378
- threshold shift rel. to noise in ear 8=46205
- tonal complexes, meaningless, identification 8=46213
- tone burst duration and rise time effect on cortical pot 8=46211
- tone sensitivity theory 8=46218
- tones masked by noise, unmasking obs. 8=32929

Heat
- See also Radiation/heat; Thermodynamics.
- diffusion equation, solution using continuous method of approximation 8=32934
- equation, over-relaxation parameter determ. 8=41850
- equation, solution by iterative process 8=24005
- generalizing the meaning, by changing structure of thermodynamics 8=23986
- numerical methods applied to heat problems 8=46221

Heat capacity. See Specific heat.

Heat conduction
- See also Conductivity, thermal.
- α-quartz, pulse-shape, phonon dispersion effects 8=48753
- bar, and loss, demonstration 8=32956
- in bodies of arbitrary shape, transient and steady, for arbitrary boundary and initial conds. 8=32961
- bodies of complex config., method for estimating heat resistance 8=28398
- carbon black, use as load-bearing high-temp. insulator 8=35456
- casings of different shapes, calc. of thermal resistance 8=37308
- cavity, gas-filled, effect on acoustic impedance 8=46186
- composite materials, transport coeffs. 8=26939
- of composite rectangle, with mixed boundary conds., steady state soln. 8=37307
- cooling of substrates containing multiple heat sources 8=48727
- dielectric crystals, one-particle densities, thermal propagation and second sound 8=26587
- electrical analogue of periodic heat flow through brick wall 8=46248
- equation, asymptotic soln. by ray method 8=41634
- equation, deviation, finite heat propagation velocity for half-space coupled thermoelasticity problem 8=46068
- eqn. from least-dissipation principle of thermodynamics 8=23906
- equation, problems with unknown boundaries 8=46241
- extremum principles for rigid conductors 8=32962
- in fins, with surface heat transfer of convection and rad. 8=28392
- flow in right circular cylinder with internal heat generation, applic. to thermal cond. determ. 8=46246
- in frost and snow, model 8=32219
- fuel element, current heated with temp. dependent elect. cond., nonlinear therm. cond. calc. 8=30976
- in gas layer, bounded, static, horiz., appl, of wide-band nongray gas model 8=34659
- gas, polyatomic between concentric cylinders at different temps. 8=34638
- glass, hot, radiative transfer 8=44371
- heat transfer with conduction and radiation, soln. of matrix. eqn. 8=32953
- insulating props. of chamber envelope, from gas flow through orifice 8=41866
- liquids, local equilib. model 8=25908
- metallic foil insulation in high pressure gas 8=26602
- metals and alloys, phonon conductivity calc. 8=30928
- method for solution of problems over regions with time-dependant shape 8=46240
- near metal surface exposed to blackbody radiation, modified kinetic theory 8=44353
- nongray gas model appl. to cond.-rad. interact. in bounded static horiz. gas layer 8=34659
- nonlinear problems involving plate heating and cooling, soln by Kantorovichs method 8=24004
- non-metallic crystals 8=44356

Heat conduction—contd
- in plate of regular polygonal shape, unsteady problem using conformal mapping 8=28401
- in plate, transient, subjected to combined convection and radiation 8=28402
- prismatic elements, bar heated at one end 8=35441
- pulse-shape, phonon dispersion effects 8=48753
- radiant, calc. of coeff., in presence of molecular spectrum 8=46242
- reference materials for high-temperature measurements 8=46224
- solid, semi-infinite, heating allowing for mass loss and physico chemical conversions 8=32960
- in solids, with boundary conds. as functions of time, soln. techs. 8=37310
- in solids with temp. depend. conductivity, variational princ. soln. 8=30982
- steady-state, in layer with heat transfer conditions at boundary 8=46239
- temperature field under conditions of monotonic heating 8=37316
- temperature fields in rigid bodies 8=46245
- thermal effectiveness determ. 8=46254
- through fin, tapered, downward projecting in fluid, and laminar free convection 8=32964
- transient eqn. soln., successive block over relax. convergence accel. 8=32963
- transient, use of transcendental profile function approx. 8=28403
- waves through brick wall, Beuken's method 8=46243
- waves through wall, transient conditions, Liebmann method 8=46244
- Fe_2SiO_4, thermal diffusivity at high press. and temp. 8=48762
- He II, Kapitza conductance from metals 8=28444
- MgO:Fe, detection of microsec. heat pulses in large mag. field 8=44366
- Mg_2SiO_4, thermal diffusivity at high press. and temp. 8=48762
- NaCl, thermal diffusivity at high press. and temp. 8=48762
- Pu, hemispherical emittance, effect of surface cond. and temp. 8=30993

Heat exchange. See Heat transfer.

Heat flow. See Convection; Heat conduction; Heat transfer.

Heat losses. See Heat transfer.

Heat measurement. See Calorimeters; Calorimetry.

Heat of adsorption
- chemisorption, calc. using H-MO approx. to localized molec. orbitals 8=36585
- porous mats, N_2 isotherms, pore struct. anal. on capillary condensation regions 8=30659
- Cu, of Sr, Ba and alkaline atoms, quantum calc. 8=35199
- H on Pd-Au alloys 8=26139
- ThO_2, adsorpt. of H_2O rel. to specific surface area 8=48493
- W, of Sr, Ba and alkaline atoms, quantum calc. 8=35199

Heat of combustion
- copolymers of methylmethacrylate with methacrylic acid 8=39917

Heat of crystallization. See Crystallization.

Heat of dissociation
- variable model appl. to equilib. air stagnation point, transfer calcs. 8=39206
- Xe_2, from photo-attenuation, 1050-1550Å 8=43206

Heat of formation
- hydrogen bonded complexes, and equilib. const., calorimetric determ. 8=36543
- methane, SCF-MO-LC(LCGO) calc. 8=47628
- prediction, semiempirical quantum-mech. eqns. 8=49851
- solid, semi-infinite, heating allowing for physicochemical conversions 8=32960
- B_4C 8=49856
- CH_2 8=29985
- CHO^+ 8=36557
- Cs_2O gas, −34 ± 3 kcal mole^{-1} 8=32096
- Cs_2O_2 gas, −55 ± 5 kcal mole^{-1} 8=32096
- KAg_4I_5 8=48396
- Li_3AlF_6, meas. from $LiF + AlF_3$ reaction 8=36564
- MnSe(s) 8=39498
- $NH_4Ag_4I_5$ 8=48396
- OCN^- 8=29980
- OF_2 8=49864
- P_3N_5 8=43413
- $RbAg_4I_5$ 8=48396
- SCN^- 8=29980
- SnTe-PbTe solid soln., exothermic rel. to binary cpds 8=43981
- TaF_5 and $TaOF_3$ 8=38938

Heat of fusion
- alkali halides, and melting pt., electronic polarizability and ionic radius ratio, relationship 8=39474
- alloys by contactless thermal analysis, 20-2800°C 8=28411
- flux eqns., free boundary problem 8=25980
- metals by contactless thermal analysis, 20-2800°C 8=28411
- polycaprolactam, rel. to cryst. morphology, obs. 8=43907
- polyethylene, crystallized from diluent mixtures, enthalpy 8=34966
- polyethylene, enthalpy of fusion and crystallinity 8=30578

Heat of fusion—contd
polyethylene, folded-chain crysts. 8=35248
Ar, pressure depend, from volume change obs. 8=28219
COF_2 8=30573
$NaClO_3$-$NaNO_3$ system 8=48087
$PbO.2B_2O_3$ 8=43905
Pu, reactor fuel 8=47407
Se, and heats of vaporization of Se_{2-8}, obs. 8=43916
UO_2, high temp. 8=39902
Heat of mixing. See Heat of solution.
Heat of reaction
biochemical reaction studies, differential microcalorimeter 8=27687
by calorimetry, compensated power differential 8=24029
chemisorption, calc. using H-MO approx. to localized molec. orbitals 8=36585
complex mixtures, comp. equilib., calc. by generalized free energy method 8=36542
enthalpies of reactions, from matrix formulation of Hess's law 8=36546
explosions, thermal, semi-infinite explosive 8=32116
isothermal titration calorimeter 8=46282
second- and third-laws, obtained from equilib. press. meas., comparison 8=32091
vandyl acetylacetonate in nitrobenzene soln, enthalpy changes 8=43872
water-organic basic mixtures in acid, thermometric analysis 8=27771
α-Al_2O_3, immersion in aqueous Na dodecyl sulfonate, rel. to adsorpt. of detergent ions 8=49854
Au_3Cu, energy changes on ordering after quenching 8=26059
$BaO-Li_2O-SiO_2$ system, calc. of silica activities, and metastable immiscibility 8=30413
$BeO(s) + BeF_2(g)$ 8=35012
$VO_{2\cdot5}$, molten, thermal dissoc., obs. 8=27724
Heat of solution
alkali metal alloys, calcs., 8=43796
aniline, mixing, in polar solvents 8=34821
benzene, enthalpy of mixing with CCl 8=39348
calorimeter, differential, for mixtures 8=32989
decylhexaoxyethylene glycol monoether + water systems, heat of mixing obs. 25°C 8=48126
n-hexane, enthalpy of mixing with cyclohexane 8=39348
high-dilution differential calorimeter 8=41879
isothermal titration calorimeter 8=46282
mixing of liquids, calorimeter 8=39348
molten salts, theory 8=34784
nitrates, fused, ethalpies of mixing in ternary systems 8=48080
octylhexaoxyethylene glycol monoether + water systems heat of mixing obs. 25°C 8=48126
ortho/para-D_2 liq. systems, mixing at 20°K 8=30412
ortho/para-H_2 liq. systems, mixing at 20°K 8=30412
n-pentane in polystyrene rel. to second-order transition above glass point 8=44398
Hg, in dimethylcyclohexanes and alcohols 8=48071
Hg, in various liqs. 8=30416
Pb in liquid Na 8=43762
Pd in liq. Sn, as function of temp. and conc. 8=48082
Heat of sublimation
AlF_3 8=30607
As 8=39497
Ba_2O_2 8=30606
Ca_3N_2 8=48295
Cs_2CO_3 8=48294
$NiCl_2$, $NiBr_2$ and NiI_2 8=39496
Heat of transformation
aromatic liq. cryst-forming mats, and temps. 8=34772
solid-solid non-polar phase transformations, physical significance 8=35075
solid state transition energies by differential calorimetry, obs. 8=30674
Heat of vaporization
solutes, in rel. to diffusivity 8=25900
$AlBr_3$, enthalpy 8=43895
COF_2 8=30573
Hg, from various solvents 8=30417
Hg solute, heats and entropies calc. 8=43798
$Se_{2,5,6,7,8}$, and appearance pots., 625°K 8=43916
Heat of Wetting. See Wetting.
Heat pumps. See Heat transfer.
Heat radiation. See Radiation/heat.
Heat transfer
See also Convection; Heat conduction; Radiation/heat; Radiative transfer.
across brass/copper pressed contacts, at reduced press. and low temp. 8=23997
in air, at equilib. stagnation point boundary layers 8=39206
in air flow in inlet region of tube, effect of initial turbulence level 8=39203
in air flow through annuli with small cores, turbulent, and momentum transfer 8=34647
in air operated nozzles, effects of uncooled inlet length and nozzle convergence angle 8=30252
in air, turbulent pipe flow, effect of Prandtl number on temp. profile 8=30367
anemometry with fine hot wires, calcs. 8=30258

Heat transfer—contd
in bed in burning zone with moving fluxes, rel. to temp. difference of gas and mat. 8=37313
in bed of lump mats, in counter flow with heat sources 8=30284
between aggregate of particles and gas during surface reaction, rel. to ignition 8=32970
between concentric spheres, by natural convection at low Rayleigh numbers 8=32966
between leaf, artificial, and air flow in wind tunnel 8=34608
between liquid metal and crystallized crust on Cu wall, water cooled 8=30974
between spherical solid and turbulent gas flow 8=30951
bibliography, mainly (1966) 8=32950
bibliography of Japanese works, (1966-67) 8=28387
bibliography of Russian works, (1964-66) 8=37304
in binary eutectic alloy system freezing with time depend. surface temp. 8=34967
to Bingham plastic in tube flow with int. heat generation, by forced convection 8=39266
boiler, coal-fired, radial disk meter 8=32955
boiling, nucleate, transition and film, transfer functions, evaluation and development 8=48282
in boiling org. liqs. rel. to state of heating surface 8=35001
boundary layer following shock wave over semi-infinite plate in tube 8=28386
boundary layer problem of non-Newtonian fluid over flat plate 8=30213
boundary problems, analogue computer soln. 8=41863
in bubble boiling, rel. to evaporation and liq. mixing 8=39489
capillary-porous mats., on drying in e. m. field 8=39487
from circular cylinder at low Reynold's number 8=30259
in closed streamlines of laminar flow at high Péclet number 8=34710
coefficients for sphere in randomly packed bed, meas. 8=46231
composite coatings, effect of lining decomposition non-uniformity on heat regime 8=30958
concentric spheres and cylinders, effect of incomplete accommodation 8=46235
with condensation, effect of molecular-kinetic resistance 8=25990
condensation rate, rel. to presence of non-condensable gases 8=25993
contact between solid and liq, local study of temp. field 8=26601
contact thermal resistances, short signal method of meas. 8=24006
convection and conduction cooling of substrates containing multiple heat sources 8=48727
convection and rad. combined, rel. to transient heating or cooling of plate 8=28402
by convection, from horiz. surfaces with heated side down, for two flow regions 8=39202
in convective gas flow-near heated plate, rel. to absorpt. and emission props. 8=43685
cooling loop, space vehicle, heat carrier choice 8=32389
in corundum bed, fluidized by gas flow or vibs., comparison of coeffs. 8=39448
counter-flow exchanger with cross-flow headers, numerical solns. 8=32949
crystallization on constant temp. surface, effect 8=48529
to cylinder in liquid, temp. depend. rel. to induced thermal stresses 8=37321
in cylindrical tube, convective, calc. of temp. and heat fluxes by Bubnov–Galerkin tech. 8=37311
in diphenyl, terphenyl and mixtures, rel. to use as coolant in reactors 8=30422
to disc, cooled, rotating in its environment, and temp. profiles 8=32967
from disc, rotating, to fluid, for large changes in viscosity and laminar flow 8=39358
in dispersions, coupled with mass transfer, rel. to residence time and particle size distribs. 8=34936
earth's mantle, and effect of selective melting 8=50018
in electric arc in cross flow, turbulent transfer 8=29939
energy converter staging, thermoelectric-thermomagnetic 8=46238
ethyl alcohol, press. oscills. accompanying transfer in tubes 8=34832
in ethylene glycol aqueous soln., turbulent pipe flow, effect of Prandtl number on temp. profile 8=30367
evaporation cooling, Merkel Main Equation for heat and mass transfer 8=48290
in film flow of non-Newtonian liq. over rotating surface 8=30392
to finite cylinders with variable temps. at uninsulated plane surface, anal. 8=28394
fin immersed in fluid, conduction through, and free convection from 8=32964
fins, with convective and rad. surface heat transfer, one-dimens. conduction 8=28392
in flash boiling system, effect of u. s. field 8=25994
to flat disc in transverse low-turbulence flow, temp. boundary layer 8=37314
to flat plate immersed in laminar flow of heated liq. 8=28397

Heat transfer—contd
to flat plate in linear shearing flow, rel. to temp. distribs. 8=34651
flow around heated body, friction coeff. and thermal flux density 8=28389
in flow in annular duct, allowing for mech. energy dissipation 8=39356
flow in right circular cylinder with internal heat generation, applic. to thermal cond. determ. 8=46246
in flow systems, interphase heat and mass transfer, and Onsager relns. 8=34828
fluid between horiz. plates heated from below, effect of side walls on natural convection 8=25909
in fluid flow with variable physical characts., numerical integration of ht. of propagation eqn., 8=39196
fluid Laminar boundary layer, non isothermal, method for solving eqns. 8=25797
fluid, numerically calc. flux rel. to supercritical transition 8=32951
fluidized bed, dilute-phase 8=41865
flux along elec. leads to liq. He cryostat, rel. to supercond. dev. 8=31361
forced laminar convective transfer in heated horiz. tubes theory 8=24007
in Freon-22-dibutylphthalate soln. boiling on horiz. tube 8=34999
in frost and snow, model 8=32219
fuel element, current heated with temp. dependent elect. cond., nonlinear therm. cond. calc. 8=30976
gas, absorbing-emitting, effects of mass addition on boundary layer flow 8=39180
gas agitation of liquids 8=48029
in gas cross-flow over right-angled wedge, convective transfer 8=28405
in gas flow in entrance region of tube, effect of varying fluid props. 8=39201
from gas flow in duct, rel. to sublimation mass transfer at walls 8=35013
gas, in Couette nonlinear flow 8=34616
in gas layer, bounded, cond.-rad. interact., appl. of nongray gas model 8=34659
gas-solid suspension flow 8=43650
in gas/solid suspension, turbulent flow, hydrodynamic theory 8=39457
gas thermal regenerator, simulation 8=43687
in gases, convection-radiation interacts, role of optically thick approx. 8=25825
hailstones, artificial, rough, rate of melting 8=34963
heat equations, behaviour of solutions 8=23996
heat exchanger, high temp., with cross blast of intermediate heat carrier 8=46287
heat exchanger, surface temp., accurate meas. 8=46237
from heated plates, vert. and horiz., at small Grashof numbers, conduction and convection 8=32968
high flux density apparatus 8=28393
high-temperature solar devices, calorimetric investig. 8=41864
in hollow circular cylinder, two solns., rapidly convergent for numerical computation 8=32959
hypersonic wind-tunnel, $BaTiO_3$ pyroelec. transducer meas. 8=47953
insulation, thermal rel. to cryogenics 8=46298
intensification in magnetic field 8=41857
interferometry, refr. error evaluation 8=28395
internal heat and mass, irreversible thermodynamics 8=46128
interphase mass transfer in flow systems, effect of surface chem. reactions 8=34829
Joule's dissipation of m.h.d. flow in const. transverse mag. flux 8=33113
laminar forced convection in eccentric annuli 8=46249
laminar forced convection in rectangular channels 8=46236
in laminar free convection flow about inclined isothermal plate 8=28404
in laminar radial slot gas jets propag. along plane wall 8=30247
limiting heat removal rates from horiz. wires heated in liq. He II 8=28442
liquid alkali earth metals in short vertical tubes with natural convection 8=30460
in liquid evaporation from free surface in rarefied gas atmos. 8=30601
liquid film breaking on vert. surface, ht. transfer condns., contact angles meas. 8=25895
in liquid film condensation, effects of strong elec. fields 8=34990
in liquid flow along permeable plate, rel. to boundary layer soln. 8=39267
in liquid gap between rotating coaxial cylinders 8=30463
in liquid-metal reactor coolants, effect of variable wall heat flux 8=25309
in liquid metal, review 8=39353
liquid metals, effect of internal source. 8=48021
in liquid/solid suspension, turbulent flow, hydrodynamic theory 8=39457
from loose layer to wall, for wide temp. range 8=28396
in low-boiling liquids 8=46289
mass and heat, irreversible thermodynamics 8=46127

Heat transfer—contd
mass-flow meas. appl. 8=34591
mechanism in spray column heat exchanger 8=46232
metallic surfaces, planar, during contact 8=37305/6
in m.h.d. aligned flow past flat plate 8=28589
m. h. d. channel, thermal-entry region heat transfer rel. to axial conduction 8=33110
in m. h. d. field-aligned flow past plate, local coeffs. 8=33111
m. h. d. gas duct, nonconducting wall boundary layer 8=28593
moist mats., simultaneous determ. of thermophys. characts. for any values of Fourier no. 8=37315
nonstationary exchange in tube when heat flux and gas flow rate change 8=47961
nuclear thin rotating target, calc. 8=37780
outer walls, thermal characts. determ. using Pontryagin optimization princ. 8=41862
to plate, cooled, temp. slip coeff. dependence on model 8=43684
at plate immersed in gas stream, influence of turbulent Pr number 8=30255
from plate to rarefied gas boundary layer 8=34645
plate with wing element, calc. of wing profile flow rel. to roughness 8=39208
in Poiseuille flow in circular tube, steady conjugated problem including viscous dissipation 8=30253
polar organic vapours, thermal cond. obs. 38°-200°C 8=34657
pool boiling, to cryogenic liquids 8=48127-9
porous and disperse media, modified Woodside model 8=44359
in porous channel, 2-dimens., soln for large suction and large injection at walls 8=30214
porous medium, three-phase 8=37301
to porous surface, transpiration cooled, transient temp. response in forced convection surroundings 8=35450
from propane-O_2-Al flame to cooled plate, rel. to Al seeding 8=32973
radiant, from isothermal dispersions with isotropic scatt. for plane-parallel geometry 8=23990
in radiating and absorbing steady gas flow over symmetric bodies 8=37298
radiative in nongrey gas near equilibrium, differential approximation 8=30289
random temp. field in plate under conditions of turbulent transfer, statist. characts. 8=46230
reactor fuel elements, He cooled, surface roughening effects in-pile obs. 8=34104
in reactor transient boiling 8=47373
to rectangular fin with vapour condensation 8=34991
reduction by bundles of shields of black screens, similarity to grey gas 8=37297
in regenerator, design for fluids with variable thermophys. props. 8=30293
relative conformity and appl. to problems 8=23998
by residual gases in multi-layer insulation, at low temp. 8=25823
review and bibliography for (1965, 66) 8=28388
rotating annulus, rigidly bounded, axisymmetric convective regime 8=39350
rotating disk in stationary cylinder, effects of flow 8=32954
in rotating gas flow, nature of thermal boundary layer 8=43646
sensors, with varying medium temp. and transfer coeff. 8=28385
shock-tube end-wall, secular change obs. 8=34653
solid dispense systems 8=41860
to solid-liquid suspensions in agitated vessel 8=48232
sonic-point transfer, effect of press. gradient 8=37303
sphere in stream of small Reynolds number 8=30457
sphere in turbulent air jet, rel. to flow regime and distance from nozzle 8=39205
from spheres, local, rel. to Reynolds number, turbulence and polar angle 8=34985
in stagnant zone due to jet interact. with convection flow at isothermal surface 8=34731
stagnation point forward of circular cylinder, wake induced effects 8=43717
steady-state heat conduction in layer with heat transfer conditions at boundary 8=46239
steady-state with conduction and radiation, soln. of matrix eqn. 8=32953
in steam condensation on Cu at low steam press. 8=34993
superconductor-substrate systems rel. to stabilization, obs. 8=27002
in superfluid He filled capillaries connecting points at different temps. 8=28443
in system of plane turbulent layers in presence of diffusion combustion 8=43666
thermal stress induced plastic zone in infinite solid containing penny-shaped crack 8=37156
thermal transport coefficients in magnetic field 8=37302
rel. to transient arbitrary upstream temp. changes, anal. by max. slope method 8=34574
transient, for forced connection flow over flat plate containing heat source 8=24003
transient, for turbulent flow over flat plate cont. heat source 8=30250

Heat transfer—contd
- transient heat transfer (single blow) temp. response function, props. 8=46234
- transient, in composite slab, theory 8=39960
- in transition pool boiling, stability anal. and methods of meas. 8=35002
- transition regime, approx. method 8=23999
- in transpiration cooling by liq. evap. from capillary porous mat. 8=39488
- in turbulent boundary layer on plate, rel. to step changed wall conditions 8=30245
- in turbulent flow in concentric annuli 8=34595
- in turbulent flow in entrance regions of concentric annuli 8=34834
- turbulent free convection from vertical plate 8=41869
- turbulent, in drag reducing fluids 8=46233
- turbulent, in nozzles, effects of gas flow-acceleration 8=25808
- turbulent, in rotating pipe with forced convection 8=41858
- in turbulent separated flow boundary-layer over surface cavity 8=30251
- in two-phase disperse system saturated with different liq. fillers 8=30555
- in two-phase laminar flow, graphical soln. . 8=39352
- in vertical cylinder with vol. heat sources, combined forced and free turbulent convection 8=24010
- from vibrating surface to air, by free convection, appl. to Danckwerts-Mickley model 8=34646
- on viscous fluid flow past heated thin plate, rel. to isothermal and non-isothermal motion 8=30358-9
- wall temp prediction in post burnout region 8=46229
- water-air horiz. annular flow, coeffs. and pressure drop 8=43653
- in water at 4°C, rel. to free convection about a flat plate 8=34838
- in water flow over heated and cooled plates, effects on stability 8=34709
- in water, min. effect for free convection at temps below 277°K 8=34837
- by water pipe flow, turbulence induced fluctuations near wall 8=34830
- in wedge-type laminar flow with variable temp. and normal vel. along wall, including frictional heat 8=34579
- to CO_2, in crit. region, by free convection from horiz. Pt wire 8=34823
- H forced convection boiling, cryogenic fluids 8=32957
- He^4 gas-solid, Kapitza resist. rel. to adsorpt., 1.5-4°K 8=34652
- He liquid-metal heat transport, kinetic theory model 8=37338
- in Hg-Hg turbulent co-current flow exchanges, expt. rel. to theory 8=34835
- Na, in film condensation of pure vapour, intensity 8=48132
- in Na liq., forced-convection transfer from moving spheres 8=34839
- Nb and V, superconducting, in mixed state, dissipation and nonlinear resistivity 8=27027
- O, dissoc., catalytic flat plate meas. 8=25826

Heat treatment
- alloys, liquid, quenching by torsion-catapult method 8=43746
- alumina (96%) rods, thermally conditioned, residual stress and flexural strength 8=35659
- annealing crystals in specimen-holder of diffractometer, thermoelec. element 8=39755
- annealing kinetics of vacancies to dislocations 8=26637
- basalt and granite, strength rel. to temp. 8=48985
- carbons, graphitized, effect on interstitials and layer distortions 8=35553
- clays, electrical potential meas. rel. to physical and chem. changes during heating 8=26947
- coronene in cryst. matrices, effect on spectra 8=45242
- corundum, rel. to surface defects and suitability as substrate for epitaxial growth 8=31054
- film resistance decrease on annealing 8=49135
- glass, optical, annealing for low residual stress and refractive index homogeneity 8=41141
- glass, residual stresses 8=26824
- glasses, industrial, effect on thermoluminesc. 8=36460
- graphite, grade A reactor, n-irradiated at 80°K, and annealed at temps. up to 300°K, e.s.r. 8=45081
- graphite, radiation damage annealing studies by ESR 8=26729
- graphite, reactor damaged, annealing and e.s.r. behaviour 8=36237
- hot-pressing, deformation theory giving density eqn. 8=26755
- magnetic films, uniaxial-anisotropy relax. process excitation by rotating mag. anneal 8=31581
- metal polycrystals, annealing effect on ferromag. resonance 8=31811
- metals, f. c. c., annealing rel. to internal friction 8=26742
- metals, metastable, annealing time effects on diffusion rates 8=35474
- metals, non-ferrous, grain refining rel. to heating speed and dispersion 8=39714
- metals, quenched, annealing and excess vacancy coalescence, theory 8=35527

Heat treatment—contd
- MOSFETs, radiation damage thermal annealing characts. 8=27213
- muscovite mica, U^{235} fission fragment track annealing anisotropy 8=44505
- perovskites, high-temp. phase transformations 8=39538
- polytetrafluoroethylene, post irrad., effect of temp. on n.m.r. spectra 8=49640
- poly-2, 2′-octamethylene-5, 5′-dibenzimidozole amorphisation in annealing, obs. 8=26158
- polyvinylidene fluoride, $\alpha \rightleftharpoons \beta$ transform. on stretching in temps., 20-150° and annealing 8=26155
- recrystallization of metals and alloys, high-temp., microscope for study 8=42183
- semiconductors, during prep. rel. to dislocation distrib. 8=26679
- solid solns., rel. to short-range ordering 8=26033
- stainless austenitic steel, annealing twin freq., compositional effects 8=40157
- steel, stainless, explosive shock-loaded thermal recovery 8=49004
- step annealing process for diffusion coeff. determ. 8=48773
- sulphide ores, grain boundary movement 8=26843
- sytalls, rel. to degree of ordering 8=26147
- talc, structural changes, thermal and X-ray analysis 8=48601
- trans-$[Co\ en_2(NO_2)_2]NO_3$ annealing of interstitials formed by Szilard-Chalmers recoil, crystal size effect 8=31049
- Ag, annealing in air effect on creep rate at low pressures 8=26803
- AgMn films, annealing, effect on magnetic props. 8=40802
- Al, annealing twin boundaries 8=44161
- Al, grain refining rel. to heating speed and dispersion 8=39714
- Al, self-diffusion coeff. from annealing kinetics of voids 8=35478
- Al, strained, substructure changes 8=44162
- Al, thermomechanical effects on critical deformation and structure 8=35672
- Al: (Fe, Si) sheet, final anneal, precipitation effect on texture formation 8=35267
- AlMn, grain refining rel. to heating speed and dispersion 8=39714
- Al-0.04 wt % Fe, recryst. and recovery, rel. to Fe precip., obs. 8=39664
- α-Al_2O_3, annealing effect on n-induced defects 8=26666
- Al_2O_3:Fe^{57}, effect on Mössbauer spectra rel. to iron clustering and cation valence states 8=43943
- Ag pastes hardened at 20-150°C, conductivity 8=35820
- Ag-Sn solid solutions, annealing rel. to extended dislocation nodes 8=35561
- Au, quenched, annealing kinetics of vacancy defects at elevated temps. 8=31044
- Au, quenched, black spot defects, nature 8=44465
- Al, self-diffusion and quenching studies, analysis 8=35479
- Au, defect tetrahedra, effect of multiple quenching on stability and growth 8=44464
- C, glassy, effects on mag. susceptibility 8=44966
- CdS diodes, thin-film, in various ambients 8=27176
- CdS, effect on parameters of slow recombination centres 8=50655
- CdS, 100-600°C, rel. to surface topography and photoconductivity 8=35268
- CdS : Au, annealing rel. to precipitation and dislocations 8=48375
- CdS : Cu, annealing rel. to precipitation and dislocations 8=48375
- $[Co(NH_3)_6](NO_3)_3$ annealing of interstitials formed by Szilard-Chalmers recoil, crystal size effect 8=31049
- Cr_2O_3/C compacts, shrinkage and cavitation in reduction sintering 8=35072
- Cu, annealing in air effect on creep rate at low pressures 8=26803
- Cu, annealing stage I after α-irrad., influence of defect conc. 8=48926
- Cu, continuous casting, heat dissipation problems 8=28207
- Cu crystal, n-irradiated, radiation hardened, critical shear stress temp. and strain rate dependence 8=31196-7
- Cu, drawn, Young's and shear moduli, annealing temp. dependence 8=31195
- Cu foil, effect on conductivity 8=49161
- Cu, grain boundary cavity stability during annealing 8=26802
- Cu, rel. to pore formation during creep 8=35524
- Cu wire, heavily drawn, annealing spectrum 8=26808
- Cu, wold-worked, recovery during annealing 8=35709
- Cu-Al solid solutions, stacking-fault energy, annealing and irrad. effects 8=26702
- Cu_2O, annealing, stoichiometric defects prod. rel. to absorpt-spectrum, obs. 8=41083
- Cu_5Si, rel. to gaseous impurity segregation 8=35673
- β-Cu-Sn alloy, quenched, structure and decomposition products 8=39528
- Fe, annealing after wet H treatment, effect on tensile yield and flow stresses 8=49018

Heat treatment—contd
Fe, annealing time effects on diffusion rates 8=35474
Fe, high-purity, plastically deformed, softening on heating to 600°C 8=35677
Fe-27% Cr, annealing, Guinier-Preston zones form., 475°C 8=35273
Fe-3% Si secondary recryst., cube textured, rel. to impurities and processing 8=26265
GaAs, effect on current carrier lifetime 8=40449
GaAs : Zn, effects on 1.370eV photoluminescence emission band 8=49800
GaP diodes, depend. of radiative efficiency 8=27179
Ge, annealing effect on i.r. absorption of γ induced surface layer 8=36365
Ge, epitaxial, annealing, effect on packing defects 8=31099
n-Ge, radiation defects, rel. to reduction of rate of formation 8=31152
Ge, thermal quenching of interimpurity radiative recombination 8=36364
InAs, films, annealed, elec. props. 8=44794
InSb, extraction of Cu 8=44582
KCl, X-irrad., thermal annealing Frenkel defect recombination 8=40166
Li ferrites, effect on resist., dielect. and thermoelect. props. 8=35962
LiF crystals, plastic deformation and annealing rel. to thermal conductivity 8=30989
LiF, F band, annealing and re-irradiation behaviour between 80°K and 300°K 8=49738
LiF, quenching effect on plastic deformation mechanism 8=26828
LiF, stress relax. during process 8=40167
LiF :Mg, pre-irrad. annealing effect on thermoluminesc. 8=45280
Li_2SO_4, n-irradiated, OH radical thermal decay, e.s.r. study 8=27481
Mg, e-irradiated, low temp. annealing spectrum 8=26734
$MgAl_2O_4$, vacuum hot-pressing, densification kinetics 8=40174
Mo, hydrostatically extruded, annealing effects on ductility 8=35705
Mo wire and foil Hg quenching 8=31218
NaCl:$Pb(NO_3)_2$, at 300°C rel. to structural changes 8=26689
NaF crystals, R_N and N centre annealing after p.-irrad. at liq. N_2 temp. 8=48883
Nb_3Al-20 %Nb_3Ge, sintered, annealing rel. to critical temp. increase, obs. 8=27019
Nb-O-N supersaturated solid solns. annealing, oxide and nitride precip. obs. 8=30831
$(NH_4)_2CrO_4$ annealing of interstitials formed by Szilard-Chalmers recoil, crystal size effect 8=31049
Ni, annealing time effects on diffusion rates 8=35474
Ni, cold-worked, recovery during annealing 8=35709
Ni, strongly deformed, annealed in mag. field, onset of uniaxial anisotropy 8=36216
Ni, vacancy clustering during quenching 8=44413
18 Ni-9 Co-5 Mo maraging steel, investigation in 520-700°C temp. range 8=44572
Ni_3Ge, rel. to gaseous impurity segregation 8=35673
Ni_3Sn_2, rel. to gaseous impurity segregation 8=35673
Pd surface annealing changes, effect on CO adsorption 8=48424
$Pb(NO_3)_2$, annealing of γ-irrad. damage, kinetics 8=44414
PbSe films, polycrystalline, rel. to photoconductivity and mobility changes 8=27328
$PbZrO_3$-$PbTiO_3$ ceramics, sintering by hot-pressing, and elec. props 8=39535
Pt, defect recovery, plastic deform. and Au substitution effects 8=39997
Pt films, effect on props., 8=44698
α-Pu, at press. over 30 kbar, study of microstructs. prod. 8=35281
Pu rods, for microcracks elimination 8=31228
Se, effect on crystallization 8=30834
Si annealed surfaces, nature 8=30727
Si crystals with oxygen and carbon impurities, precip. of SiO_2 and SiC 8=39702
Si, influence on electronic structure of surface 8=40487
Si, n-irrad., injection level and temp. depend. of transient annealing 8=27122
Si solar cells, annealing of p irrad. damage, 4.6 MeV 8=24101
Si solar cells, p-irrad., thermal annealing rel. to photovoltaic characts. 8=24105
Si, surface imperfections 8=30728
Si surfaces, vacuum-crushed, air-crushed or mechanically polished, effect on e.p.r. 8=39580
SiC films, noncrystalline, annealing effect on conductivity 8=48467
SiO_2 powder from pyrolytic decomp. of silicon, crystallization by annealing 8=35251
SiO_2 slip refractory for melting optical glasses 8=45936
$SmFeO_3$, in hydrogen, effect on mag. reorientation temp. 8=40876
Te crystals, pulse-heated, anomalous Hall reversal at 515°K rel. to vacancy behaviour 8=31329
Ti-6 % Mo alloy, quenched, structure study by electron microscopy 8=30869
U, quenching, and anomalous thermal arrest in β phase, origin rel. to cryst. struct. 8=35129

Heat treatment—contd
UO_2, with dispersed Gd_2O_3, reaction and diffusion at high temp. 8=35074
W, n-irradiated, stage III recovery 8=31157
W, O_2-covered field emitters, surface rearrangement 8=31464
ZnS: Cu, effect on electroluminescence spectrum 8=36519
$ZrOCl_2.8H_2O$, ZrO_2 grain growth and phase transition 8=48357
$Zr(OH)_4$, ZrO_2 grain growth and phase transition 8=48357
alloys
7-3 brass, heavily rolled, annealing texture 8=40151
brass rods, Young's and shear moduli, annealing temp. dependence 8=31195
permalloy films, annealing kinetics and increasing S conc. 8=31222
steel, effect on mag. props. 8=45014
steel, 18/8 stainless integranular corrosion and power formation 8=43983
steel E 1702 holding time effects at different quenching temps. on γ^1-phase precip. 8=35108
steel, EI 702, rel. to γ' and η' phase precip. or dissoln. 8=43998
steel, quench-hardened, tempering rel. to martensite decomp. C conc. effects 8=35099
steel, quench-hardening, and austenitic grain struct. formation 8=35110
steel, tempering effects on structure, e-diffr. exam. 8=35680
steel, transformer, annealing effects at high-temp and vacuum 8=35107
steel, transformer, in cubic texture perfection rel. to mag. props. 8=36140
steel U8, quenched, tempering under high hydrostatic pressures 8=35679
steels, cast austenitic, thermal cycling to increase strength through phase transforms. 8=35698
steels with f.c.c. lattice of solid soln., rel. to internal friction peak 8=35678
ticonal, structure formation after thermomagnetic treatment 8=35055
vicalloy, annealed, domain structure on straining in tension 8=40804
vicalloy strip, thermomechanical treatment effects in mag. props. 8=36135
Ag_3Mg, long range order, quenching temp. dependence 8=44200
Ag-Zn solid solns., vacancy quenching rel. to atomic mobility control, Zener relax. studies 8=31041
Al alloys, annealing characts rel. to precipitate interact. with dislocations 8=48849
Al, hardening curves similarities from elec. resistivity meas. on ageing up to 100°C 8=35654
Al-5 wt. %Mg, thin foils from quenched specimens, vacancy lifetimes 8=31042
Al-25 wt. % Zn, effect of quenching conditions on precip. 8=26058
Al-V, plasma-jet spray-quenching in dispersion hardening 8=26780
Au_3Cu ordering after quenching, rel. to energy and resistivity changes 8=26059
Au-Pt alloy, dil, quenching resistance in vacancy-impurity interaction determ. 8=48805
Au-Pt alloys, annealed and quenched, thermal conductivity 8=48759
C-Mn steel, creep under cyclic stress and temp. conds. 8=26822
Co-C, splat-quenching effect on metastable extension of C solubility 8=30656
Co-Fe-Au, low-magnetostrictive, effect on coercive force 8=31599
Cu-Al alloys, continuous cooling, transform. of β-phase 8=26069
Cu-10.5 at. % Ge, resistance recovery folliwing quenching 8=49160
Fe, deformed, annealing effects on X-ray diffr. line intensities 8=35332
Fe-Cr, post-deformation annealing, effect on hydrogen permeability temp. dependence 8=35489
Fe-Ni binary, effect of cyclic process on martensitic transformation 8=26071
Fe-0.025% N, enhanced aging due to γ-α transform 8=445
Fe-Pd, structural transforms and mag. props 8=35102
KCl-KI solid solns, decomposition rel. to effect on spectral characts. 8=36395
Mg-Mn ferrite films, FMR, thermal treatment effects 8=31817
Mg-Zn-Mn alloy, wrought, effects on tensile props. 8=35704
Mn-Au, ageing effects on antiferromag. props. 8=31776
Mo-Fe(8wt. %), annealing rel. to precipitation behaviour 8=35115
NaCl-KCl solid solns, decomposition rel. to effect on spectral characts. 8=36395
Nb_3Sn, hot pressing rel. to supercond. transition temp. 8=49190
Ni-10 at. %W, rel. to local at. arrangements 8=44244
Ni-base, annealing time effects on diffusion rates 8=35474
Ni-Au, fibre-reinforced, prep. 8=28208

Heat treatment—contd
- **alloys**—contd
  - Ni-C, splat-quenching effect on metastable extension of C solubility 8=30656
  - Ni-2%Cu solid soln., quenching 8=44410
  - Ni-Fe-Ni strip, rel. to gas emission in vacuum apparatus 8=39254
  - Ni-Te alloys, permanent magnet, extrusion effects on texture and props. 8=33046
  - Pb-Sb (to 2 wt.%), quenching, and subsequent ageing 8=35121
  - PbSe, annealing rel. to carrier conc. and mobility 8=44141
  - $Pb_{1-y}Sn_ySe$, annealing rel. to carrier conc. and mobility 8=44141
  - $Pb_{1-x}Sn_xTe$, annealing rel. to carrier conc. and mobility 8=44141
  - Pt-50% Co alloy, uniaxial mag. anisotropy induced by tempering under stress 8=31702
  - SAP, (sintered Al/Al_{203} alloy), lattice defects, behaviour on quenching, resistometric exam.. 8=48816
  - Si-O solid soln, rel. to periodicity changes on decomp. and anomalous X-ray transmission 8=36409
  - Ti-6Al-4V, addition of Co, properties 8=49055
  - Ti-22at.%Nb/Cu composite conductors ω precip. 8=40419
  - Ti–V, rel. to superconducting critical current densities 8=40391
  - U-1. 5% Mo, rapid cooling from γ-phase, transform. mechanism 8=35130
  - U/10% Pu/10% Fz, annealing rel. to changes in structure, hardness and elastic modulus 8=30711
  - Zr–Nb, anti-hydrogenation, with molten $NaNO_3$ 8=32105

Heating
- of blunt body during superorbital re-entry, effected non-grey self-absorpt. and energy loss 8=41488
- boiling of liq. with free convection, heater size effects on critical heat loads 8=48280
- electrical circuits for calorimetry, resistance stabilization 8=28423
- energy converter staging, thermoelectric-thermo magnetic 8=46238
- fluid layer, from above, stability 8=43619
- fluids, effects of gravitational field changes on thermal stability 8=30290
- by frictional contact, non-stationary, analog simulation 8=37319
- furnace, graphite, fuel element thermal stress simulation 8=34112
- furnace, imaging, for X-ray diffractometry 8=33304
- inner face of hollow circular cylinder of reactive solid, rel. to thermal ignition 8=32976
- laser, by pumping, change in active element 8=24325
- particle of dispersed mat, transient heating without temp. grad. for small Fo nos. 8=30957
- plasma heating by e.m. waves 8=47814
- plasma, turbulent, by mag. field annihilation 8=34467
- of plate, transient, by combined convection and radiation 8=28402
- plate, with thermal characts depend on temp., soln by Kantorovich's method 8=24004
- of porous surface, transpiration cooled, by forced convection, transient temp. response 8=35450
- radiant, of absorbing and scatt. slab 8=46228
- r.f. induction, temp. control by photoconductive cell 8=46276
- simple arrangement for use in neutron scattering experiments 8=34762
- spheres, transient, via thermal rad. at bounding surface 8=41859
- strip-heated flat plate, temp-variations of surface 8=24018
- volume sources in vert. cylinder, combined forced and free turbulent convection 8=24010
- wall, semi-infinite, 2nd order approximate soln. 8=32952
- He II by small wires scintillation obs. 8=24044

Heaviside layer. See Ionosphere.
Heavy water. See Water.
Height measurement. See Length measurement.
Heisenberg model. See Ferromagnetism; Statistical mechanics.
Helicity. See Elementary particles; Field theory, quantum.
Helicons. See Crystal electron states.
Helions. See Alpha particles and helium nuclei; Alpha rays.
Heliotron. See Plasma/devices.

Helium
- abundance in Population II stars 8=45641
- afterglow in near-cathode region 8=47752
- afterglow, mass spectrometric obs. of diffusion and recombination 8=43448
- afterglow plasma, Langmuir probe obs. of ion conversion and diffusion 8=43449
- annihilation of slow positrons, theory 8=38740
- arc, unipolar, Sn-Bi alloy substance entering 8=47777
- atom, differential excitation function for n=2 states 8=38729
- atom-e collision, excitation cross section calcs. 8=38703
- atom, e scatt., transport cross section calc. 8=25383
- atom, excitation by electron impact, effect of electron exchange 8=38701
- atom, excitation by fast electrons 8=38700
- atom, excitation by fast electrons to 2^1P state 8=38699

Helium—contd
- atom, excitation by fast protons 8=38698
- atom, extended Hartree-Fock calc. for ground state 8=47483
- atom, ground state calc. using 3-body problem solution 8=33315
- atom, Hartree-Fock calc. refr. index, dynamic polarizability and Verdet coeffs. 8=47485
- atom, incoherent-scatt. function and pair prod. length 8=43174
- atom in 2^1P state, lifetime obs. oscillator strength for 2^1P-2^1S transition 8=38654
- atom, low-energy e scatt., data analysis 8=25385
- atom, metastable, lifetime rel. to population inversion in He-Ne lasers 8=24312
- atom, neutral, number density in upper atmos. rel. to altitude and latitude 8=36777
- atom, numerical soln. of S-limit Schrodinger eqn. 8=29596
- atom, pair function calc. 8=47438
- atom, S-type wavefunctions, natural occupation amplitudes 8=38655
- atom, slow e scatt., short-lived compound excited states 8=47528
- atom, 6-8 Torr, spectrum from 20-40 keV electron beam scatt. 8=29651
- atomic beam, fast metastable atoms in electron-loss collisions 8=38764
- atoms, anisotropic excitation by electrons and protons 8=38702
- atoms, doubly excited states, R_4 invariants 8=25352
- atoms, excited, apparent lifetimes of levels and excitation transfer 8=43219
- atoms, forbidden transitions by low-energy electron impact 8=25384
- atoms, He-like, saddle point character of h. f. energies 8=38652
- atoms, high velocity scatt. by H_2 and D_2 8=25667
- atoms, singlet and triplet excitation mechanism in hollow cathode discharge 8=25353
- BD + 10°2179 star, C content 8=28066
- birefringence due to spin alignment 8=39216
- cooling effect in high-vel. streams, on injection into reacting or non-reacting boundary layer 8=32958
- cosmic fireball conversion, test for gravitation theories 8=23858
- cosmological prod., rel. to n half-life 8=24945
- cyrostat for use in neutron diffraction studies, 3°-300°K 8=39763
- discharge, negative glow plasma characts., effect of u.h.f. field 8=43453
- discharge positive column, press. 0. 05-0. 4 Torr, probe expt. 8=43551
- discharge tube, rotating mag. field pinch 8=25770
- discharges, microwave and h. f., energy distrib. of electrons and positive ions in plasma 8=25692
- elastic scattering of electrons from atoms 8=38730
- electron impact, 2^1S, 3^1S states excited by, Born cross sections 8=38695
- electron scatt., correlation importance in Born cross sections evaluation 8=38728
- electron scatt. resonances, exchange and product wave function 8=38726-7
- emission at 10 830Å in twilight aurora, 2^3P-2^3S transition 8=32287
- emissions in auroral zone, search 8=36796
- free-electron gas, negative point-to-plane breakdown 8=39001
- gas, shock wave of Z-pinch discharge, dynamics 8=34410
- glow discharge, 1. 35-2. 6 torr, 0. 5-2. 5 mA, dynamics 8=34420
- incorporation in solidifying enstatite melts 8=34972
- ion refl. from Cu single crystal 8=48918
- ion, 2^3S, e affinity meas. by laser photodetachment 8=29970
- ions, damage to double-positioned Au films on bombardment 8=40073
- ions He^+, charge exchange with Ar, Kr, N_2, O_2 and CO_2, 2-250 eV 8=38758
- ionization, double, by electron impact, importance of exchange scatt. 8=39032
- lamp, with double helix, as Raman light source 8=46711
- lines in γ-Pegasi spectrum, equiv. width rel. to electron density in atmos. 8=32422
- liquid, bubbles due to zero-point motion of positronium atoms 8=30388
- Maxwellian beam scattered by room temp. H_2 and He, total collision cross-sections 8=47729
- metallic screen insulation in helium 8=48755
- mobilities α particles from 10-300°K obs. 8=38836
- molecules triplet state lifetimes, low energy e impact spectrometry excit. meas 8=25528
- neutron scintillation counter with sodium salicylate wavelength converter, 14 MeV 8=33825
- nightglow, 304- and 584-Å, upper limits 8=27941
- number density, with Ar, in thermosphere, rel. to altitude of turbopause 8=36775
- overabundance in giant galaxies 8=28106
- photoionization by diagonalization method for calc. atomic system reson. 8=43220

Helium—contd
pinch shock tube current sheet 8=34448
in planetary nebulae, triplet state emissions 8=45710
plasma, containing trace of Cs, phys. props. 8=47818
plasma, electron temp. from spectral line intensities, effects of cascading and metastable atoms 8=34468
plasma, flowing, magnetoacoustic waves 8=25738
plasma, highly ionized, decay mechanisms 8=43516
plasma, in T-tube, flow deceleration in transverse mag. field, obs. 8=47832
plasma, non-equilibrium, optimum seeding with Cs 8=29997
plasma, press. build-up 8=29990
plasma, rad. below 800Å rel. to photo-ionization of H_2 8=34529
position and width of $2p^2\ {}^1D$ resonance by configuration interaction method 8=38756
primordial, diffusion in Fayetheville meteorite 8=37024
protons mobilities from 1-600°K obs. 8=38836
radiogenic in ultramafic inclusions, Hawaii 8=50073
red giants, N^{14} burning before He flash 8=28055
reflex discharge, e-density and -temp. meas. by cw Ar^+ laser light scattering 8=38991
Rutherford scatt. of H and H^+ 8=38754
spark channel, high press. μ sec., turbulent eddies 8=29924
spectra line intensities, rel. to electron temp. meas. and effect of plasma conc. 8=30084
Stark broadening of 3889, 5016 Å lines, obs. 8=47841
Stars, H shells thermal instability 8=45624
thermosphere, thermal diffusion 8=50188
3^3D fine structure 8=29598
in upper atmos., winter diurnal bulge, characts. 8=36776
X-rays, soft, absorpt. cross sections, calc. 8=45727
and Ar gas mixture, structure of normal shock waves 8=30261
Br^- ions collision with atoms, detached electrons energy obs. 8=29972
Cl^- ions collision with atoms, detached electrons energy obs. 8=29972
Ge implantation, scatt. analysis 8=48927
H_2^+ collision, Born cross-section calc. from e scatt. data 8=38951
HeI, combined Zeeman and Stark effects on hydrogenic lines 8=38653
He I, 5876 Å, nightglow, S. America photometric obs. 8=45498
He I λ 584 line, oscillator strength 8=43173
He I, probability of 2γ decay from 2^3S_1 metastable level 8=43175
$pHe(1S^2) \rightarrow H(1S)He^+(1S)$ cross-section calc., 0.1-100 MeV 8=43237
He II emission lines 4686 and 5411 in eclipsing binary star, spectrophotometric obs. 8=45654
He II, enhancement of λ4686 by mag. field 8=34132
He II, 3203Å stark broadening 8=43225
He II λ 4686 line in quiescent prominences, excitation 8=28179
He II, injection of electrons from immersed tungsten filament up to 2500°K 8=37351
He field-ion microscopy of Re and Ru h. c. p. metals, rel. to surface structs. 8=26105
He line λ10830Å in late-type stellar spectra 8=28071
$He(1^1S \rightarrow 2^3S)$ transition, inapplicability of Born approx. 8=34173
$He3^1P_1$ state lifetime determ. 8=29597
He^-, autoionization of $1s2s2p^4P_{5/2}$ state 8=39041
He^- free-free absorpt. coefficient 8=47484
He^+, distribution in plasmasphere 8=27947
He^+ in He, mobility and total, charge-transfer, diffusion and viscosity cross sections obs. 8=38835
He^+, Lamb shift of $n = 4$ level, meas. by r.f. spectroscopy 8=43172
He^+, reaction with vibr. excited N_2 8=41253
He^+, reactions with O_2, N_2 in upper atm. 8=27937
He^{++} in magnetosphere, concs. 8=50165
He_2 and He_2^+, potential energy, scaled atoms-in-mols. calc. 8=29750
$He_2(a^3\Sigma_u(\sigma = O))$ at 77°K, metastability 8=34227
He_2, LCGTO SCF MO wavefunctions 8=47603
He_2 molecules, formation mechanisms in early afterglow of pulsed discharge 8=47751
He_2, triplet states 8=34250
He_2^+ -e recomb. coeff. 8=39038
He^{2+} ion accel. in U-120 cyclotron 8=47006
He^{2+}, LCGTO SCF MO wavefunctions 8=47603
He_2^+, orbital exponent in ground state calc. 8=25487
He^3, disintegrating plasma in impulse discharge, e-densities 8=43458
He^3 in meteorites, cosmic ray produced 8=50428
He^3 positive polarized ion beam prod. 8=24168
He^3, radiooptical resonance 8=47517
He^3, thermomolecular press. ratio down to 0.3°K expt. 8=28438
He_3^+, evidence for 8=39037
He_3^+, geometry and binding energy 8=34249
He^3 in stars and interstellar medium, obs. 8=36927
He^4 atom, 2^3P_1-2^3P_2 fine structure obs. 8=38651
^4He films, bose systems, two dimensional, rel. to superfluid transition 8=23892

Helium—contd
He^4 lattice thermal cond. calc. 8=39940
He-Ar mixture, concentration diffusion coeff., meas. by two-bulb method 8=34678
He-CO_2 mixture, 43.7 MeV p-irradiated, energy deposited freq. distrib. 8=29663
He-CO_2 mixtures, thermal diffusion 8=34679
He-Cs plasma, shock wave structure 8=30046
He-H mixtures, thermal cond. 8=47957
He-H system, normal and equilib., press.-temp-co-ords of three-phase locus 8=43893
He-H vapour-liq. phase equilib., to 100 atmos. 8=43913
He^+-H, H_2 collisions, Lyman-α emission cross sections and polarization obs. 8=38755
He^{2+} + H(1s), impulse-approx. calc. 8=38743
He-He interaction potential 8=34181
He-Kr mixture, thermal diffusion and intermolec. forces 8=34675
He-N mixture, mass and thermal diffusion coeff. meas. 8=43706
He-Ne gas, effect of one laser beam on the transmission of another 8=46576
He-Ne laser, absorpt. saturation effects, and freq. reproducibility 8=37591
He-Ne laser, coherence length extension 8=37586
He-Ne laser, eigenstates of polarization with partial polarizers 8=46559
He-Ne laser, intensification line shape, change due to saturation 8=37590
He-Ne laser, multimode, initial transients 8=37585
He-Ne laser, Ne as nonlinear absorber for mode locking 8=37588
He-Ne laser operating at 633 nm, reproducibility of wavelengths 8=28685
He-Ne laser, output power rel. to gas temp. 8=33186
He-Ne laser, saturation behaviour in various polarization states 8=46591
He-Ne laser, single-mode, amplitude stabilization 8=33187
He-Ne laser TEM_{009} modes separation with Ni film, obs. 8=37565
He-Ne mixture, thermal diffusion and intermolec. forces 8=34675
He-Ne, multimode, initial transients 8=37585
He-Ne plasma afterglow kinetics 8=30080
He + Ne + CO_2 system, thermal diffusion 8=30320
I^- ions collision with atoms, detached electrons energy obs. 8=29972
Si implantation, scatt. analysis 8=48927
Zn 3075.9 Å, perturbation of resonance line 8=47512
gas
atom collision excitation transfer cross-section calc. 8=47540
atom, 2^3S excitation by e impact, ang. depend. approximation 8=38696
2, 3-atom nonretarded van der Waals coeffs., Padé approximants 8=38757
breakdown by laser beam, threshold parameter meas. 8=47761
breakdown rel. to laser appl. 8=29910
charge transfer from p and H atom, cross-sections 8=38737
collision with N_2 mol., rotational excitation 8=25666
discharge, afterglow, metastable mol. and at. decay obs. 8=25697
discharges under a.c. condns. 8=38992
elastic e scatt. cross-sections, Born approximation tests 8=38731
electron back-scatt. in crossed elec. and mag. fields, obs. 8=39232
electron transport coeffs. 8=39230
energy distrib. functions and e drift vels. 8=47975
excited by H^+ and H_2^+ impact, polarization of 4^1D-2^1P transition 8=38697
flowing afterglow, atom-e spin exchange 8=43221
heat transfer to solid, Kapitza resist. rel. to adsorpt., 1.5-4°K 8=34652
high heat flux convection correls 8=24008
ionized, partially, transport coeffs. at several press. and temps. to 35000°K 8=29968
light, from e impact, polarization obs. 8=29641
microwave breakdown at 9 GHz 8=47768
Rayleigh scatt. and atomic e. m. susceptibility 8=25375
refrigerator, closed-cycle, for Mössbauer expt. 8=46301
scintillation induced by α-particles, recombination luminesc. 8=29642
shock front propag., e. m. excited, for press. 0.1 to 20 mm Hg 8=34635
water droplets falling in, supercooling and freezing 8=2598
weakly ionized, collision and radiative mechanisms 8=29969
H^+ ion cooling by elastic collisions 8=43681
He^{++} pulsed beam from van de Graaff accelerators 8=33098
He^3 activation analysis cyclotron 8=33470
He^{3+}, 15-25 transition obs. 8=29971
He^3, near critical point, props. 8=25824
He^3 nuclear spin, optical polarization rel. to temp. and press. 8=47689
He^3, purification from He^4 using He^3 refrigerator as rectifying column 8=30271

Helium—contd
gas—contd
He^3 and He^4, low temp. transport props. mutual consistency rel. to quantum effects 8=34671
He^4 pair distrib. function, 3-particle density matrix 8=41759
He^4, pressure-density-temp. surface near critical point 8=37342
He^4, second virial coeff., 2°-20°K 8=47952
He-air, thermodynamic and transport props., 50° to 3500°K 8=25838
He-Ar mixtures, u.s. absorpt., effect of diffusion 8=43689
He-Kr mixtures, u.s. absorpt., effect of diffusion 8=43689
He-Ne arc discharge, low-voltage, rel. to cw laser oscillations 8=24315
He-Ne gas laser, side light investigations 8=24320
He-Ne laser amplification and loss meas. 8=37587
He-Ne laser at 0.62μ, freq. fluctuation and natural width determ. 8=24318
He-Ne laser, Faraday rotation temp. meas. anomaly 8=42094
He-Ne laser, forced and spontaneous phase locking of transverse modes 8=42093
He-Ne laser, hysteresis and "hard" excitation, 0.63μ 8=37584
He-Ne laser, intensity fluctuations at 0.63 and 3.39μ 8=24316
He-Ne laser, optical freq. doubling and mixing 8=42095
He-Ne laser, output power at 6328Å, optimum diameter for various tube lengths 8=24314
He-Ne laser photons correlation, obs. 8=28686
He-Ne laser radiation field obs., diffr. struct. 8=24313
He-Ne laser, saturation peaks by tuned laser differential spectrometry obs. 8=42091
He-Ne laser, small optical loss meas. 8=28689
He-Ne laser, spontaneous modulation on beam switching 8=42090
He-Ne laser tube, sputtered cathode particles 8=24317
He-Ne laser type LG-75 8=24311
He-Ne laser, with folded optical path 8=42096
He-Ne 6328Å laser, competition and stimulated switching of transverse modes 8=42092
He-O$_2$ diving atmosphere, non-combustion region 8=49884
liquid
See also Quantum theory/many-particle systems; Superfluidity.
Bose-Einstein gas, comparison 8=28344
bose liquids, survey of elementary excitations 8=28331
breakdown by laser beam, threshold parameter meas. 8=47761
breakdown, elect., destruction of electrodes 8=46303
breakdown voltage dispersion, external ionization source effects 8=41890
cerium magnesium nitrate thermometry, corrections 8=37332
charged vortex ring formation below 0.8°K 8=28435
coolant for e microscope stage 8=46293
dewar, modified 8=28427
Dewar, narrow-tail glass 8=32994
electron bubble vibration, freq. estimate 8=37346
elementary excitations, dispersion curve rel. to interact. of atoms 8=41886
evaporation loss from small Dewars without N_2 cooling, calc. and nomograms 8=28439
excess electron, localization 8=34571
with excess electron, optical props., theory 8=34854
film, discrete flow rates obs. 8=24042
fluctuations and λ phase transition 8=32998
free surface, superfluid eddy emergence 8=37352
λ point shift in rotating angular gap, obs. 8=37348
ion-vortex-ring transition, velocity rel. to elec. field 8=24047
isotope solns, enthalpy and osmotic pressure 8=28436
isotropic solns., irreversible osmotic relax 8=24037
Kapitza resistance theory 8=37338
Landau Fermi phenomenological theory 8=28434
laser light transmission, spectrum and fluctuations 8=32993
microminiature Hall probe 8=28509
monolayers, mobility 8=37336
phenomenological theory near critical points 8=44989
phenomenological theory near λ-transition 8=46304
photoeffect on negative charges, current wavelength depend. 8=28437
polarimeter for fast n, analysing power calc. 8=33810
polarimeter for fast neutrons, description 8=33819
pressure transducer for velocity meas. 8=32995
protons mobilities from 1-600°K obs. 8=38836
referigerator as liquefier 8=32990
rotating, motion of negative ions trapped in vortex lines 8=37334
stage for e microscope accessories 8=28571
superfluid He^4, vortex ring prod. effect of He^3 impurities 8=37339
superfluid, heat torques and circulation 8=37345
superfluid, ion mobility discontinuities, inadequacy of Huang-Olinto theory 8=41897
superfluid, neutral excitation with Po^{210} α source 8=24045
superfluid, persistent flow and pot. motion 8=33002
superfluid, rotating, hydrodynamic theory of relaxation 8=37347

Helium—contd
liquid—contd
superfluid, vortex ring annihilation at surface with electron ejection 8=37344
superfluid, vorticity in flow 8=43731
thermalized ions movement, in external fields 8=37335
vortex resonance theory 8=24046
vortex-ring interaction cross section, superfluid 8=41895
He, dynamics of lattices of rectilinear vortices 8=25785
He II, bubble states, photoejection of trapped electrons 8=41901
He II, capillary wave modes 8=37350
He II films, phase transition 8=24043
He II, heat conduction in capillaries connecting points at different temps. 8=28443
He II, heating of small wires 8=24044
He II, Kapitza conductance from metals 8=28444
He II, max, low temp. dissipation rates from single horiz. wires 8=28442
He II, osc. of cylinder pairs rel. to fluid and superfluid viscosity 8=41902
He II, phenomenological theory of superfluidity 8=46311
He II, quantized circulation round vib. wire 8=41903
He II, rotating, effect on density 8=24049
He II, rotating, λ-point anomaly 8=28440
He II rotating, props. of deeply penetrating S-wave 8=24048
He II, rotating, vortex density from computer calcs. 8=24051
He II, superfluid, particle motion and heat exchange 8=37349
He II, superfluid, vortex wheels 8=41900
He II, thermal props., Landau phase transition theory 8=33001
He II, thermodynamic potential function near T_λ 8=24052
He II, vel. distrib. of evaporating atoms, theory 8=41891
He II, vortex ring production by neg. ions, 16 atm. pressure, ≤ 0.3°K 8=41896
He II, vortices distrib. in rotating cylinder 8=24050
He^3 and mixtures, spin echo effect 8=24038
He^3, binding energy calc. from 2-body correls. 8=37341
He^3, charge mobility of crit. point 8=41888
He^3 direct-access cryostat 8=46297
He^3, entropy, shielded pot. approximation 8=28338
He^3, ground-state and low-excited props., two-body potential calc. 8=32996
He^3, h.f. sound vel. and X-ray zero-point scatt., obs. 8=32999
He^3 in liquid He^4, dilute mixture, transport coeffs. for degenerate Fermi system 8=41781
He^3, ion mobility obs. below 1°K 8=24039
He^3, Landau theory of quantum liquids, book 8=30397
He^3, liquid/solid comparative theory 8=37357
He^3 nuclear polarization by optical pumping 7=37337
He^3 repulsive forces, appl. of Fermi gas pair collision theory 8=32852
He^3 soln. in He^4, Fermi-liq. transport coeffs. 8=37340
He^3 soln. in superfluid He^4, phonon Boltzmann eqn. and first viscosity calc. 8=41898
He^3, surface phenomena 8=28339
He^3, 3-body contrib. to binding energy 8=41887
He^3 vapour press. increase in mag. field, 3°K, 40-80 kOe 8=28433
He^3, X-ray scattering at 0.65, 1.25 and 2.29°K 8=24036
He^{3,4} mixture, transition temp. Tλ rel. to pressure and He^3 conc. 8=24041
He^4, and solid He^4, phase diag. below 1.2°K 8=37333
^{4}He, anomalous Green's function 8=46307
He^4, critical exponent δ and Griffiths inequality 8=24040
He^4 film, rel. to condensation of a Bose gas 8=32845
He^4 in rotating annulus, λ-point 8=46309
He^4 near λ transition, Green's functions 8=32997
He^4, pressure-density-temp. surface near critical point 8=37342
He^4, superfluid transition, gravit. field effect 8=41899
He^3-He II dilute soln., diffusion coeffs. and nuclear mag. susceptibility 8=46306
He^3-He^4 mixture, isotope refrigerator for temps. below 0.1°K 8=46292
He^3-He^4 solutions, mobility of positive ions, 1.4 to 2.15°K 8=46312
Nb_3Sn, sintered, supercond. stabilization by liquid He flow through pores, obs. 8=27020
liquid, sound propagation
dielectric ideal crystals, second sound in absence of Umklapp process 8=35957
first-sound dispersion prod. by normal component deceleration, obs. 8=28441
first sound, velocity and attenuation near λ-point 8=37343
pressure amplitude in second sound wave, obs. 8=28445
second sound, anomalous dispersion examination of Ferrell-Menyhard-Schmidt-Schwabl-Szepfalusy theory 8=46313
third, in unsaturated superfluid films, generation and detection 8=24054
vel. of second sound obs. near λ point 8=37353
wave modes in capillaries 8=24053
He I, first sound damping, dynamical scaling 8=41892
He II, critical velocities 8=33000
He II, dispersion, first and second, in cylindrical capillary 8=41904

liquid, sound propagation
HeII, second sound, exptl. demonstration 8=33003
HeII, study of Moris theory 8=46305
He^3, acoustic impedance 8=46310
He^3, zero sound, transverse, excitation 8=46308
He^3–He^4, velocity rel. to He^3 conc. for three freq., nonlinearity obs. 8=41893
solid
crystal, correlation theory 8=28446
lattice dynamics, dispersive anharmonic effects 8=44292
phonon scatt., effect of isotopes 8=37355
He^3, b. c. c., sp. ht. and thermodynamic props. 8=37356
He^3, compressibility and thermal expansion obs. 8=37358
He^3, exchange operator matrix elements calc. 8=28447
He^3, liquid/solid comparative theory 8=37357
He^3, magnetized, nuclear spin interaction rel. to thermodynamic props. 8=41905
He^3 melting curve, pressure to 17 m deg K and molar volume change on melting to 300 m deg K 8=41889
He^3, nuclear-spin exchange interaction 8=31774
He^3, spin-lattice relax. from negative temps. 8=33004
He^3, spin-lattice relax. time, temp. depend. 8=24055
$He^{3,4}$ adsorpt. on Cu sponge at 4°K 8=24056
He^4, and liquid He^4, phase diag. below 1.2°K 8=37333
He^4, $(\partial P/\partial T)_v$ meas. 8=37354
He^3-He^4 mixtures, props computed from model 8=46314
Helium compounds
HeAr, interatomic potential 8=29749
HeH and HeH^+; potential energy, scaled atoms-in-mols. calc. 8=29750
HeNe, interatomic potential 8=29749
Hellmann–Feynman theorem. See Quantum theory.
High-pressure phenomena and effects
acetone, freezing press. 8=50477
alkali-metal nitrates, fused, elec. cond 8=39410
alkali metals, hydrostatic compression effects on phonon spectra 8=35380
alkali metals, melting curves up to 80 kb 8=34961
anthracene crysts., excimer emission 8=49823
anthracene, fluoresc. in host crysts. 8=49822
anthracene, fluoresc. of doped crysts. 8=49824
aqueous solns., γ-radiolysis 8=32143
aromatic hydrocarbons, phosphoresc. 8=49825
autoclave liners (noble metal), corrosion during hydrothermal crystal growth reactions 8=49855
benzene, liq. -solid transform 8=26327
benzene, proton spin-lattice relax. T_1 8=39432
chamber for working at liq. He temp. at press. to 18 kbar 8=24034
chemical and polymorphic equilibria under hydrostatic press., X-ray obs. 8=43901
chemical reaction thermobalance 8=45316
cubic crystal, elastic constants 8=26741
cylindrical shell, dynamic pulse buckling under lateral transient press. 8=32712
deformation, elastic-plastic, relations for high-press. vessel 8=46057
electrolyte cond. rel. to viscosity, remote meas. 8=34793
gas circuits, sound propag. corrections 8=23960
gas, pressure diffusion 8=43708
gas viscometer, absolute, low-temp. design 8=34674
general solids, low temp. melting, rel. to cores of planets 8=32535
glass powders under 10-65 kbar pressure, optical and mechanical props. 8=40164
Grüneisen solid, thermal expansion and bulk modulus, thermodynamic calc. 8=30972
Hall effect in single crystals at 70kb 8=44680
hematite, mag. moment direction, 41 kbar obs. 8=45059
high pressure engineering, conference, London, England, 1967 8=32634
hot-pressing, deformation theory giving density eqn. 8=26755
hydrocarbons in solvents, vapour-liq. equilib. 8=39481
hydrocarbon-TCNE complexes, effects of press. on charge transfer absorpt. 8=36433
ice, H_2O and D_2O, phase diagrams 8=48383
ice VII, H_2O and D_2O, vol. change 8=49026
inert gas solubility in fused $AgNO_3$, elec. cond. 8=25949
inorganic crystals, phase transforms under impact pressure 8=26057
liquid-liquid-gas equilib., expt. determ 8=34773
liquid u. s. absorpt., meas. method and error analysis 8=48137
liquids, dielec. const. and density 8=39401
magnetization meas. 8=27371
methylcyclohexane, freezing press. 8=50477
muscovite-mica, on dielec. permittivity 8=44874
naphthalene crysts., excimer emission 8=49823
naphthalene, fluoresc. of doped crysts. 8=49824
octyl alcohols, density and struct. transform 8=39296
octyl alcohols, isomeric, dielec. props. 8=48182
perdeuteronaphthalene, triplet-triplet absorpt. 4500-3800Å, obs. 8=30491
perylene, cryst. spectra 8=41168
phase transformations and crystal radii 8=26054
phase transformations, solid-state, high-press technique for n.m.r. study 8=48362
phenanthrene crysts., excimer emission 8=49823
High-pressure phenomena and effects—contd
phenanthrene, fluoresc. of doped crysts. 8=49824
piezometers, capacitance and resist. 8=39401
polyethylene, mech. props. 8=44620
polytetrafluoroethylene, mech. props. 8=44620
pressure calib. to 20 kbar by spectral shift 8=50477
pressure indicator, differential, calibration technique 8=32645
pyrocarbons compressed at high temps., optimum conditions 8=45941
radial nozzles in spherical pressure vessels, shakedown loads 8=32750
Raman spectra, laser-excited, expt. 8=41031
rubrene, cryst. spectra 8=49779
samples and leads, vapour deposition technique 8=45942
shock-compressed liq., elec. cond. meas. 8=34903
shock technique for chem. relax. timing 8=45360
steel U8, quenched, during tempering, on phase transformations 8=35679
stress difference in tetrahedral lattice 8=45943
tetracene, cryst. spectra 8=49779
tetracene, fluoresc. in host crysts. 8=49822
trinitrobenzene cryst. complexes, absorpt. and fluoresc. 8=27635
trinitrofluorenone cryst. complexes, absorpt. and fluoresc. 8=27635
water, liq. -solid transform 8=26327
windows for infrared meas. 8=33249
AgI, cryst. struct. at 3 kbar 8=35316
AgI, elec. cond. to 100 kbar 8=31311
Al, on Debye temp., 0 to 135 kbars, rel. to eqn. of state 8=43946
Al powder, on nuclear spin-lattice relax. times 8=45110
$AlBr_3$, critical press. 8=43895
Ar, liq., u. s. velocity 8=48138
Ar, solid, compression up to 20 kbar at 38 and 77°K 8=26836
$(Ba_{0\cdot05}Sr_{0\cdot95})TiO_3$, press. depend., to 1600 atmos., of dielec. const. at low temp. 8=27283
Bi, phase changes 8=35093
Bi trihalides, phase diagrams 8=39468
BN, hexagonal, irreversible transformation by shock compression 8=26062
BN, rel. to production of dense modifications 8=48374
$Cd_{0\cdot11}Hg_{0\cdot89}Te$, semi-metal → semiconductor transition induced by hydrostatic press. 8=27086
Cr glasses, absorpt. spectra 8=39632
Cr, mag. props., n-diffr. exam. 8=31766
CrO_2, stability at high press. and temp. rel. to decomp. to Cr_2O_3 8=26281
Cs, on melting curve and elec. resistance of melt 8=39473
Cs, melting-curve maxima 8=34965
Cu–Ni, on diffusion phenomena 8=35488
Dy, magnetic ordering temps. 8=40730
Eu monochalcogenides, phase transformations 8=26070
Fe, on Fe^{57} Mössbauer spectrum, rel. to $\alpha \rightarrow$ h. c. p. transition 8=43946
Fe^{57} Mossbauer spectra, 0-85 kbar, obs. 8=43949
β–Ga, melting curve 8=48260
Gd, magnetic ordering temps. 8=40730
n-Ge, current oscillations, effect of hydrostatic press. 8=35902
Ge–C system, absence of carbide formation 8=48382
p-H_2, dielec. consts., density, melting 8=40575
HBr aq. solns., elec. cond. 8=43864
HDO in H_2O, effect on i. r. absorpt. spectra, with high temp. 8=25930
KD_2PO_4, on Curie temp. shift 8=40818
KCl in H_2O-alcohol solns., elec. cond. 8=39407
KCN, melting and polymorphism 8=48385
KH_2PO_4, on Curie temp. shift 8=40818
Kr, solid, compression up to 20 kbar at 81 and 115°K 8=26836
KSCN, melting and polymorphism 8=48385
Mg borides prepared under superhigh-pressure condns. 8=35245
MnSb, effect on lattice parameters 8=26407
NH_4F, phase diagram to 20 kbar 8=34960
NaBr aq. solns., elec. cond., 0°-800°C 8=48195
NaCl, X-ray study 8=35303
NaCN, polymorphism and melting 8=30701
NaSCN, polymorphism and melting 8=30701
Ne, solid, compression up to 20 kbar at 18°K 8=26836
Ni dimethylglyoxime spectral shift for calib. 8=50477
Ni, on Fe^{57} Mössbauer spectrum 8=43946
P black, plate crystal growth from vapour phase 8=30832
P, yellow–black transition, thermal analysis 8=30703
Pd, elec. resist., room temp. 8=44697
PtO_2, synthesis and properties 8=35205
$RbNiF_3$, phase transform. and mag susceptibility charges 8=48661
RhO_2, synthesis and properties 8=35205
Sb, crystalline structure changes, investigation 8=44010
Si–Ni, on diffusion phenomena 8=35488
Sm monochalcogenides, phase transformations 8=26070
β-Sn, Mössbauer line shift during phase transform. under pressure 8=43941
$SrTiO_3$, press. depend., to1600 atmos., of dielec. consts. at low temp. 8=27283

High-pressure phenomena and effects—contd
Tb, magnetic ordering temps. 8=40730
Te, melting-curve maxima 8=34965
TeO$_2$, phase transform. at high pressures (p = 60 kbar) 8=26081
Xe, shock compression rel. to conversion to metal-like state 8=43851
Y garnets, synthetic, on decomposition 8=26087
Yb monochalcogenides, phase transformations 8=26070

High-speed photography. See Cinematography; Photography/high-speed.

High-temperature production and effects
air plasma, radiated power 8=34509
arc furnace for growing MgO crystals 8=48549
brittle solids, rapid bend testing 8=44532
calibrated multichamber source 8=24030
carbon black, suitability as load-bearing high temp. insulating mat. 8=35456
concrete, heat-resistant high-alumina-cement thermal cond., 200-1500°C 8=48756
cristobalite lattice, Ising model props. 8=31570
cuvette for i. r. absorpt. spectroscopy 8=37679
elastic moduli, ultrasonic buffer-rod meas. 8=40096
explosives, 300°-1000°C thermal initiation apparatus 8=46288
furnace cell with "rectangular" temp. field 8=46708
heat exchanger with cross blast of intermediate heat carrier 8=46287
parallel susceptors, temp. difference maintained by r. f. furnace 8=28425
sample furnace for 50°-1000°C, spectrometer 8=33266
strain fatigue, diametral extensometer 8=35630
tensile strength meas. apparatus 8=31175
Ac^{227} heat source for thermionic generation 8=28492
Ar, in explosive-driven shock tube 8=25830
Cs$_2$CO$_3$, evaporation products, mass-spectrometer obs. 8=48294
K vapour, thermal cond. 841 to 1241°K 8=47964
N, thermal cond. and total emission coeffs., 10 000 to 15 000°K 8=47955
Na, vapour, thermal cond., 886 to 1264°K 8=47964
Pt, evaporation of submicron particles in shock tube 8=39493
PuC$_2$, structure by X-ray diffraction 8=44196
S^{35} amino acid attempted synthesis 8=41261

High voltage production
cascade generator, voltage control using pick-up electrode 8=41917
electrostatic generators 8=41926
laser-triggered spark gap 8=34431
power supply for Nimrod failure of alternators 8=33411
pulsed, phased power supply, low ripple without use of a filter 8=33412
supply circuit for solid-state particle detectors 8=37364

History
electron diffr. 8=30885
Haas and/or precedence effect in hearing 8=37292
journals on astronomy and Astrophysics (1823-1968) 8=36907
measurement standards, length, time, freq. (1918-1968) 8=28209
nuclear instruments (1918-1968) 8=28967
spectrograph design (1918-68) 8=33268
thermodynamics, Thomson's dilemma 8=41789
O$_3$, atmospheric, 40 years research at Oxford 8=36723

Hodoscopes. See Cosmic rays/apparatus; Particle detectors.

Hole theory of liquids. See Liquids/theory.

Holes. See Crystal electron states; Semiconducting materials; Semiconductors.

Holmium
electronic structure from positron annihilation studies 8=26906
magnetic props. from mag. moment meas. at 4.2°K and high fields 8=31705
Néel temp., effect of hydrostatic press. 8=36212
neutron paramagnetic scattering 8=31523
X-ray L emission spectrum 8=45193
Ho, $L_I N_{IV\ V}$ and $L_I O_I$ transitions, obs. 8=31999
Ho, s, t doublet in L-spectrum 8=47499
μ-Ho^{165} atoms, dynamic quadrupole interaction, K and L x-rays obs. 8=34191
Ho^{2+} in CaF$_2$, g-factor stress dependence 8=31510
Ho^{3+}, absorpt. spectrum in Ho ethylsulphate 8=49777

Holmium compounds
orthoferrites, microwave mag. loss meas. near spin-reorientation temps. 8=36224
Ho ethylsulphate, absorpt. and Zeeman effect of $^5I_8 \rightarrow {}^3K_8$ and $^5G_4$ transitions 8=49777
HoAl, magnetic props. and structure 8=31650
Ho-Au alloys, resitivity meas., 1.3-20°K 8=40311
HoCo$_5$, magnetic structure and magnetocrystalline anisotropy 8=40737
HoCrO$_3$, ferro- and piezoelectricity, comment 8=27272
Ho-Er alloy, electronic structure from positron annihilation studies 8=26906
Ho$_x$Er$_y$ alloys with 4f e. conc = 10, 11; magnetization 8=31654
HoFe$_2$, hyperfine field at Fe from Mössbauer effect 8=36146
HoFeO$_3$, absorpt. spectra rel. to mag. props. 8=36356

Holmium compounds—contd
Ho-Th alloys, f.c.c., antiferromag. ordering stabilization by Th 8=36218

Holography
acoustic, electronic simulation of variable inclination reference via u.s. camera 8=37275
acoustic imaging 8=37273
acoustic, 3-D information storage 8=46752
acoustical holograms, ultrasound camera system for viewing 8=37276
aerodynamics applications 8=46745
applications to problems in coherent optics 8=46742
atmospheric wavefront distortion compensation, holographic simulation 8=37708
biasing for single and multiple exposure 8=42271
bibliography, (655 refs) 8=37709
blazed hologram production 8=33287
bleached grams, diffraction theory 8=42266
carrier freq. gram formation with on-axis reference beam 8=42268
character recognition application 8=24440
coarsely sampled holograms, aliasing effect 8=24438
colour, recording and reconstruction 8=24437
conference, 1967 8=24279
copying reflection holograms 8=33292
correlation meas., improved by use of additional spatial filter 8=37719
data reduction 8=42267
with double-focus lens, simple lecture demonstration 8=46758
effect of light source coherence 8=46743
electron-beam type, 3-dimens. wavefront-reconstruction imaging, theory 8=24150
electron, laser light reconstruction 8=46757
electronic shutter for holographic applics. 8=46753
extended source hologram, compensation using a positive of a second hologram 8=28884
film-grain noise effect 8=28899
finite sampling effect 8=28886
Fourier-transform division, photographic realization of image-deconvolution filter 8=42262
Fourier-transform holograms with partially coherent light, spatial coherence obs. 8=28890
Fraunhofer electron type, optical reconstruct. of image 8=46747
Fraunhofer, 'in-line', use of time-varying diffused illumination 8=46750
Fraunhofer type, appl. to, in determ. of particle-size distribs, and dynamic situations 8=24429
Fraunhoffer, two-beam, diffuse illumination, spatial
Fresnel diffraction pattern synthesis by overlapping zone plates 8=28888
fringe visibility rel. to speckling 8=33277
fundamental princ., and technical problems arising by imaging process 8=33291
grating on thin metal film 8=33290
hologram construction using ruby laser 8=24431
hologram copying method 8=28885
hologram filters for target recognition, simplified method for production 8=28898
hologram, Fresnel, binary computer generated, 3 dim. images showing grey scale 8=46749
hologram information reduction by spatial freq. sampling 8=37712
holograms, local reference beam, rel. to information retrieval 8=46751
holograms, very small and very large, techniques for production and use 8=42269
human subject, front-lighted hologram of nonstationary scenes, use of ruby laser 8=46759
image grid formation using spatially incoherent illumination 8=42263
image restoration, sharp-focus, from blurred photographs taken in white light 8=24433
image transmission by television 8=33293
imaging, equivalent-lens theory 8=46748
imaging through randomly inhomogeneous medium by wavefront reconstruction 8=28889
imaging through random medium 8=24434
imaging through scatterers 8=24435
incoherent light, one dimensional 8=28892
information decoding method 8=37718
information reduction for visual display 8=28900
interference microscopy, applic. of holography 8=37656
interferometric control of apparatus 8=33289
interferometry, anal. and appl. for determ. of real-time deform. 8=42263
interferometry, applic. to comp. of highly polished reflecting surfaces 8=31936
interferometry with u. v. light 8=33286
interferrogram cinematographic recording for time-dependent object changes 8=46760
isolines of principal stress, aid to determ. 8=24432
light absorption, meas. 8=24410
light flux in image, effects of photographic characts. 8=42272
light scatt. by spherical liq. droplets using computer-synthesized holograms 8=34848

Holography—contd
luminance of hologram reconstructions, effect of photographic gamma 8=24430
magnetic films appls., recording and reconstruction 8=33294
with Hg lamp 8=46754
microscopes, theory 8=33247
microscopy in X-ray and u.v. regions, possibility in terms of Fresnel transforms. 8=42253
microwave, and visible images rel. to antenna array theory, obs. 8=24439
microwave, two-beam interference method, optical reconstruction 8=46756
Moiré-hologram interferometry, transparent objects 8=37706
Moiré patterns, real-time, for flow visualization 8=37710
motion picture film with constant velocity transport 8=33285
of moving scenes 8=28894
nonoptical 8=46480
object and detector, simultaneous illumination scanning 8=42275
optical activity meas. technique 8=28887
optical filtering and best conditions for achieving holograms 8=46744
optical transfer functions meas. 8=37704
phase object measurement for phase hologram 8=37715
photograph image-deblurring restoration appl., using "extended source" lensless Fourier-transform compensation 8=46763
photographic image integration 8=46755
photographic, emulsion, comparative noise performance in holographic and conventional imagery 8=28901
photographic plate sensitivity increase in partial vacuum, appl. 8=42281
photographic relief images 8=28883
polarization effects recording 8=28878-9
pulsed laser holography 8=42270
radar system, sidelooking, with coherent optical processor, holographic analysis 8=37524
radio physics interpretation 8=42276
record, effect of nonlinear rel. between amplitude transmission and exposure 8=37707
recording props., comp. with photographic method 8=46746
with reference beam differing from scatt. radiation wavelength 8=33288
without reference beam 8=37714
restitution of coherent wave deformed by traversing inhomogeneous medium 8=42265
r.f. 8=46479
semiconducting devices, motion due to self-heating, holographic detection 8=49279
shape definition, use of coherent optics 8=46669
shearing interferometry by wavefront reconstruction 8=42274
single-sideband for twin image suppresion 8=28891
spatial freqs. in holograms, reduction without decreasing field of view 8=28895
stereogram prod., lenticular, direct method 8=28904
stereograms, transmission bandwidth reduction for white light illuminated objects 8=37693
stroboscopic, for vibration analysis 8=23919
stroboscopic hologram interferometry, rel. to surface vibr. modes 8=32883
for student laboratories 8=28897
surface contouring by limited depth focusing 8=37705
surface displacement interferometry 8=37713
synthetic hologram, expt. production 8=37711
10μ i.r. 8=37717
time-varying diffuse illumination effects 8=37720
total internal reflection holograms, improved resolution and S/N ratio 8=37716
transmission systems, bandwidth reduction by elimination of vertical parallex 8=28893
ultrasonic image convertor for image visualisation in opaque media 8=28374
wavefront reconstruction, developments 8=37702
white-light reflection, spectroscopy and interferometry appls 8=28896
in X-ray, microwave and acoustic fields, and appls. 8=24436
zone plates, partially achromatic, production and evaluation 8=42273
Hot-atom chemistry. See Chemical analysis/radioactive; Nuclear reactions/chemical effects; Radiochemistry.
Hubble model. See Cosmology.
Hugoniot diagrams. See Equations of state.
Humidity
See also atmosphere/humidity; Hygrometers; Moisture.
gas, moisture trap 8=50470
gas stream, microsensor 8=43644
gases, Soviet coulometric and diffusion hygrometers 8=27878
transducers, for air-vapour mixtures and gases, test apparatus 8=26001
Hydrodynamics
See also Flow/liquids; Jets; Liquid oscillations; Liquid waves; Magnetohydrodynamics; Viscosity/liquids.
Cauchy-Poission problem, long-time behaviour of soln. 8=34703
in curvilinear co-ord. systems, conservation form of eqns. 8=34578
Hydrodynamics—contd
dilute polymer solutions, impact tube meas. 8=48015
elastico-viscous fluid, drag on oscill. cylinder 8=47930
electro-, free surface gravity waves 8=30344
entrance region of parallel plate channel and plain tube, developing slip flow 8=48016
epihydrodynamics, optimization techniques 8=34704
evolution of protostars, calc. method 8=45646
field around an ellipsoid of resolution 8=34576
flow along permeable plate, soln of boundary layers 8=39267
flow, suction, past porous sphere, asymptotic theory application 8=34590
flow, viscous unsteady, past circular cylinder, numerical soln. 8=30199
fluid containing nonrigid structures, constitutive eqns 8=43623
fluid interface between conducting and non conducting stability in varying vertical elect. field. 8=43622
fluid moving with temp. gradient, Brownian movement 8=46096
fluids with relative motion, interface stability 8=43620
Green's functions for thermodynamic correl. functions 8=46101
Hamiltonian principle appl. to free surfaces 8=34702
hydrofoils, swimming flexible, of finite thickness, propulsion efficiency 8=30350
hydromechanical ratios in cyclindrical vessel rel. to hydrothermal crystallization 8=30354
integral equations, first kind, reduction to second kind 8=46030
inviscid fluid, struct. of embedded axially-symmetric eddies 8=48033
in liquid film flow, ridge instability due to elec. field appl. 8=34747
liquid rotating, fixed body of revolution on axis, effect 8=30342
liquid, viscous, pressure drop created by sphere settling, Reynolds no. 0. 2 to 21, 000 8=39263
material burnup rate selection for radiation-heated solid vaporization 8=48291
menisci, advancing, deformation 8=48103
metals, mechanism of elec. cond. in mag. field 8=49150
motion, free, of floating body, decay: force coeffs. at large complex freqs. 8=30345
Navier-Stokes eqn. from least-dissipation principle of thermodynamics 8=23906
nonequilibrium, characteristic manifolds 8=47902
pipe flow, transition regime, effect of vibrations 8=25843
Poiseuille flow in circular tube, steady conjugated heat transfer including viscous dissipation 8=30253
potential flow about arbitrary bodies 8=34581
quantum liquids, rotation, statistical mechanics 8=23879
Rayleigh instability, theory 8=43625
relativistic, class of solution for equations 8=30196
relaxation in superfluid rotating He 8=37347
rigid sphere in ideal compressed fluid, motion under influence of acoustic pressure wave, 8=39264
rotating, in container of finite length, rise of body 8=30347
rotating cylinder of fluid, short, observed motion of sphere 8=30348
rotating fluid, ang. momentum mixing by stirring 8=47929
rotating fluid in container of finite length, rise of body 8=30347
rotating surface of two-layer liq., equation 8=46659
shear flow with interacting deformable substruct. 8=47901
shock-wave, tiple, configuration and propag. in liquid explosives 8=30341
shock-wave, triple, configuration and propag. in liquid explosives 8=30341
smooth flow, primitive equations, second order numerical approx. 8=34575
sphere moving in viscous liq., force experienced for small gap widths, inc. inertial effects 8=43718
stability, Liapunov method 8=34705
stagnation-point flow near front of blunt body, general and accurate anal. 8=43624
stationary flow impedance of ordered stacks of spheres, approximations 8=47903
statistical hydromechanics with random force action 8=46100
Stoke's fluids, linear and non-linear, differences in turbulence props 8=30228
Stoke's oscillating plate transient, tabulated functions as solution 8=30346
sun, lower photosphere, obs. 8=32593
thermal instability, gravitational effects 8=30290
tides in cruciform oceanic basins 8=36699
transducer for pressure meas. in turbulent flow 8=28226
velocity field in profiles, singularity method 8=34577
vibration damping in fluid coupling, quantitative analysis 8=25788
viscoelastic liq., magnetostrictive meas. 20-100 kHz 8=30429
viscous fluids, linear wave eqns, governing potential eqns. 8=23829
viscous stratified fluid, slow motion of flat plate 8=30349

Hydrodynamics—contd
wake of sphere in water, turbulent vel. and temp. fluctuations 8=34701
wave-packets, three-dimensional, in unbounded parallel flows, development 8=39154
wavetrains, intrinsic freq. and wave energy conservation 8=23807
He liquid, rotating, motion of negative ions trapped in vortex lines 8=37334
He, liquid, vortex ring annihilation with electron ejection 8=37344
He liquid, vortex ring prod. by negative ions, effect of He^3 impurities 8=37339

Hydrogen
See also Deuterium; Protons and antiprotons; Tritium.
adsorption on Pd-Au alloys, electron-donation model 8=26139
adsorption on solid CO_2 below 100°K 8=30765
arc in axial parallel mag. field 8=43467-8
atmospheric molecular, tritium and deuterium isotopic content, 1958 to 1963 obs. 8=27882
beam, reflection at Pt surface at different temps. 8=25668
behaviour in porous cast steel, rel. to defects 8=30663
bond, induced dipole moment calc. 8=34219
bonded systems, infrared spectra, review 8=38887
bonding in water, mol. orbital treatment 8=43313
bonding, n.m.r. study, review 8=48219
bonds, H, bent O-H---O in crysts. 8=48300
bonds, strong, n.m.r. and i.r. study 8=48301
breakdown electric, formative time in strong crossed fields 8=29903
breakdown voltage of cylindrical positive corona discharges 8=47765
in chemiluminescent reactions involving atomic N, and CH_4, N_2 and Ar 8=41245
chemisorbed on Rh, i.r. spectra 8=25470
chemisorption on Ni film, kinetics at adsorbate–adsorbent interface 8=27737
condensation pumping on to liq-He-cooled surface 8=30593
cooling effect in high-vel. streams, on injection into reacting or nonreacting boundary layer 8=32958
deposition and chemisorption on W 8=49904
D/H ratio during dehydration of $CuSO_4, 5H_2O$ 8=30802
diffusion and permeation of Fe membranes 8=44389
diffusion in h.c.p. and b.c.c. Ti, 610° to 900°C 8=44393
diffusion in irrad. quartz 8=48790
diffusion in Ni, isotope effects 8=31012
diffusion in Ni, kinetics 8=31014
dilute, use in operation of intermed. temp. fuel cell 8=33030
discharge, hollow cathode in longit. mag. field, cathode surface current distribution 8=29896
discharge tubes, H-filled SC1 corona, sheath radius obs. 8=47769
electric dipole moment contribution of electron electric dipole moment 8=38612
electrolytic charging of Nb to produce pure hydride 8=27755
electron diffusion coeff. rel. to mobility 8=39238
foils, laser-irradiated rel. to plasma production 8=29995
forced convection boiling heat transfer 8=32957
formation in radiolysis of gaseous HCl 8=27764
in galaxies, small, HI distrib., 21 cm obs. 8=45748
gas electron transport coeffs. 8=39230
gas, Fe particles dispersed, absorpt. spectra including carrier gas contrib. 8=25968
gas, stimulated scattering of light at low press. 8=47971
gaseous, in Pd, elec. resist at high pressures, room temp. 8=44697
glow discharge, prod. of focused, pulsed electron beams 8=24137
graphite, reactions at high temp. and press. 8=47422
heliosphere radius, and interplanetary neutral H 8=41573
internal friction of Ni modification 8=49041
liberation, electrolytic in Cr with various crystal structures 8=49943
lines in γ-Pegasi spectrum, equiv. width rel. to electron density in atmos. 8=32422
liquid, and solns., absorpt. spectra, translation-vibrational branches, theory 8=34860
liquid, bubbles, due to zero-point motion of positronium atoms 8=30388
liquid, containment, thin-film windows 8=24035
liquid, diffusion theory of burning 8=32111
liquid droplet, 15 μm dia., production 8=34741
liquid nuclear target, mech. refrigeration 8=46849
liquid, Scotchlite sheeting reflectivity obs. 8=36312
rel. to magnetization inversion in Ni films charged with H 8=36170
maser, automatic tuning 8=46530
maser, synchronised, oscillation amplitude freq. dependence 8=42050
Maxwellian beam scattered by room temp. H_2 and He, total collision cross-sections 8=47729
microdetermination in B, Si polymeric cpds. 8=36628
naphthalene crystal, rel. to band structure 8=31291

Hydrogen—contd
neutral atoms H_n-system, nuclear motion 8=29739
neutral, Galactic distrib. and possible correl. with Gould's Belt 8=45723
normal, cryst. struct. and phase transition, 4.2 to 0.91°K 8=39795
normal solns. in Ne, surface tension, 24.59 to 29°K 8=43780
ortho-hydrogen, solid below T_λ n.m.r. spin lattice relax. 8=45124
ortho/para-H_2 liq. systems, heat of mixing at 20°K 8=30412
para-H, cryst. struct. in range 4.2 to 0.91°K 8=39795
parahydrogen-inert gas mixtures, rotation 8=30294
para and ortho, rotational excitation on collision with He 8=47720
parahydrogen, solid, rot. and vibr. excitation and spectra freq. analysis 8=43967
permeation through W and Mo 8=39986
π meson capture, in hydrogeneous substs. 8=47739
pinch shock tube current sheet 8=34448
plasma, conductivities elect. and thermal, and effective current density meas. 8=43518
plasma, heating by fast large amplitude magnetoacoustic wave, investigation 8=47839
plasma, line broadening of excited atoms, for $n \rightarrow n^1$ transition 8=34505
plasma mag. well in coil, obs. 8=30126
plasma, non-thermal population densities meas. 8=29996
plasma radiation from flat isothermal layers, 1-100 atm, 0.6-20 eV, 0.1-100 cm 8=47837
presence in outer layer of passive film on Fe 8=35171
protium and deuterium, electrolytic separation factor 8=49919
proton scatt. variable effective charge, cross sections calc. 25 keV 8=38752
radicals, conc. profile in $H_2 \cdot O_2$ flame, e.p.r. study 8=49892
Raman laser emission, combination freq. generation 8=25598
Raman stimulated spectra, Q|1| vibr. line shift depend. on press. temp. 8=43306
Rayleigh scattering, depolarized, as new probe of intermolecular forces 8=39212
reaction with O_2 in combustion peninsular region 8=45354
recombination in hot model of universe 8=45592
relaxed flow calc. with mols and atoms generated from dissoc. 8=36547
released in hollow cathode discharge, rel. to anomalous charge in spectral intensity 8=29892
in solar chromosphere, lower, density 8=45914
solar emission spectrum, computation 8=45876
solid, f.c.c., oriental phase transition, nonexistence 8=35112
solid orthohydrogen far infrared absorpt. spectrum obs. 8=45192
solid, ortho-, theory of ang. mom. waves 8=35743
solid, production of temps. of 14-6°K by pumping of vapour over its surface 8=46290
Stark effect intensity distrib. 8=47480
stars, Hγ profiles 8=28056
in stellar spectra, Hβ-Hζ equivalent widths, obs. 8=28057
thermal diffusion in Zr hydride 8=26627
thermosphere, thermal diffusion 8=50188
transitions, high-level, oscillator strengths 8=41546
Venus upper atmosphere, molecular and atomic, in Mariner 5 obs. 8=32550
X-rays, soft, absorpt. cross sections, calc. 8=45727
Zeeman effects for large quantum no.s and freqs. 5-20 MHz 8=47501
CH_4 added to H_2, θ pinch at 0.8 m torr filling press. 8=34417
CO_2 laser-system, sealed-off, effect on gas composition 8=46584
in Fe, effect on internal friction 8=31207
H-bonded, ferroelectrics, theory 8=44881
H-bonds, two-dimens. double-minimum model 8=47602
o-H, f.c.c., elementary excitations, spin-wave treatment 8=26908
H_2, solid, e.p.r. at 4.2°K after radiation damage 8=40924
p-H_2, solid on melting line, dielec. const., density 8=40575
from H_2-Ar solns., adsorption, 87-120°K 8=25898
He-H vapour-liq. phase equilib. to 100 atmos. 8=43913
Li ion beam, charge equilib. 8=28584

ions
beam, polarized, apparatus for altering spin orientation 8=46437
charge transfer to various gases, cross-section obs. 8=38737
clusters, energy analyzed, mass spectra 8=47787
hydride ion reaction with HF and H_2, MO theory 8=27676
hydride ion reaction with H_2O, MO theory 8=27677
hydride ion reaction with NH_3 and CH_4 8=27678
initial plasma of θ-pinch, photo-ionized by Li filled z-pinch light source 8=34528
Penning discharge getter-ion pumps, improvement 8=34683
photoionization, ion-mol. and chemi-ionization reactions 8=36611
plasma at 10^5°K, optical emission from α particle and Fe ion slowing down 8=43542

Hydrogen—contd
ions—contd
plasma, dense, spectral and total rad. calc. 8=34508
plasma formed by neutral injection, Fokker-Planck eqns., for vel. distrib. soln. 8=34470
Plasma + 10% He, at 5 × 10^4°K, optical emission from α particle and Fe ion slowing down 8=43542
plasma, highly ionized decaying, neutral atom density determ by photoabsorption 8=43545
in plasma, ionization and recomb., and reabsorpt. of rad. 8=34495
plasma, ionized, equation of state determ. by Monte Carlo method 8=30000
plasma, partially ionised, non-Maxwellian deviation of fast electrons, effects on ionisation equilib. 8=47804
plasma, rad. below 800Å rel. to photo-ionization of H_2 8=34529
plasma, radiative decay spectra, T-tube obs. 8=30057
plasma, spectral-line broadening of highly excited atoms 8=34505
plasma, variable ionization equilib. 8=30004
recombination in primeval fireball plasma, theory 8=45596
scattered on metallic surface, luminesc. 8=49787
transmission sputtering of Au films at low energies 8=40072
transmission sputtering of Au films 8=44495
Fe-Si, H charged, diffusional relax. effects 8=36223
H^-, effect of forbidden continuum in solar atmosphere 8=50440
H^-, electron correlation 8=34238
H^- e detachment by e impact, cross-section obs. 8=39036
H^- + F collisions, electron detachment 8=34451
H^-, laser photodetachment, ang. depend 8=25713
H^-, 1.5MeV accelerator source and energy stabilization system 8=46434
H^-, polarized, K vapour charge-exchange source 8=33099
H^-, prod. and extraction from h.f. source 8=46431
H^-, stability, wave function calc. 8=47482
H^+ cooling by elastic collisions in He gas 8=43681
H^+, diff. in aq. salt solns. 8=48115
H^+, distribution in plasmasphere 8=27947
H^+, H° and H^- interaction with Xe atom, charge state changes, investigation by coincidence method 8=43238
$H^+ + H(1s)$, impulse-approx. calc. 8=38743
$H^+ + (H(1s) \rightarrow H(2s)) + H^+$ collision, cross-section, for metastable 2s state 8=38753
H^+ implantation in metals, rel. to sputtering 8=30764
$H^+ + Li^+ \rightarrow H(n) + Li^{++}$, cross-section calc. 8=25392
H^+, mass-identified, in H_2, drift mobility obs. 8=39033
H^+, Rutherford scatt. by He, Ne and Ar 8=38754
H^+ velocity distributions in ionosphere 8=41412
H II region electron temp. for NGC 2024, Orion nebulae, radio obs. 8=50338
H_2 photoionization calc. not giving obs. cross-section undulations 8=43482
H_2 pot. energy, complex restrictions from analyticity and unitarity 8=43308
H_2-He plasmas, isothermal, equilib. spectra, calc. 8=43544
H_2^-, attempt to produce 8=43481
H_2^-, resonant and autoionizing states, energy calc. 8=43307
H_2^-, potential energy, scaled atoms-in-mols. calc. 8=29750
H_2^+ beam bunching solid-state for tandem accelerator 8=46436
H_2^+, collision-induced dissociation 8=25648
H_2^+ collision with He, Born cross-section from e scatt. data 8=38951
H_2^+, const. of motion for two-centre Kepler problem 8=46791
H_2^+ decomp. in analyser tube 8=47454
H_2^+, electronic terms and wave functions for large internuclear separation 8=43310
H_2^+, electronic terms, eigenparameters for large distances 8=34243
H_2^+, hyperfine transitions, nuclear and e polarization 8=29743
H_2^+ photodissoc., theory and calc. 8=47704
H_2^+ radio-frequency spectrum, interstellar abundance obs. 8=45722
H_2^+ and D_2^+, vibr. struct. 8=39034
H_2^+ in H_2, D_2, Ar, charge-transfer cross-section obs. 8=47539
H^3He^+, reactions with gaseous methane and ethane 8=45341
H_3^-, configuration-interaction calc. 8=38831
H_3^- system, interaction energy 8=29738
H_3^+, excited singlet states, diatomics-in-mols. calc. 8=34245
H_3^+, excited triplet states, diatomic-in-mols. calc. 8=47598
H_3^+, mass-identified, in H_2, drift mobility obs. 8=39033
H_3^+, nature of chem. bond 8=29742
H_3^+, reactions with propane or butane 8=39057
H_4^+, linear, LCGTO SCF MO wavefunctions 8=47603
neutral atoms
beam foil excitation, elec. field and multi-foil effects 8=25376
charge transfer to gases, cross-sections obs. 8=38737

Hydrogen—contd
neutral atoms—contd
chemisorbed, long-range forces 8=47533
cloudlets in Galaxy 8=45732
collision with inert gases, Lyman-α excitation cross-sections 8=38760
collision with inert gases, Lyman-α polarization 8=38759
conc. determ. in mixture with mols, by Faraday effect 8=29639
diffraction theory of e scatt. 8=29653
elastic e scatt. phase shift calc. 8=38723
electron scatt., integral eqn. approach 8=38724
electron scatt., optical-potential calc. 8=38725
from electric discharge, reactions with liquids 8=32101
excitation of n = 2 states by electron impact 8=29640
excited states, charge exchange into from $H^+ + Li^+ \rightarrow H(n) + Li^{++}$ 8=25392
galactic structure in Cygnus region 8=50347
Green's function calculations 8=34130
Green's function, spectral analysis 8=46801
interaction energy, third-order 8=29656
interstellar abundance rel. to dust 8=45731
interstellar, maser action at 21 cm 8=28090
ionization, electron impact, extension of Gryzinskis theory to degenerate levels 8=43483
ionization, multiphoton H, atom, cross section calc. 8=25715
ionization, multiphoton in ground state, theory 8=47788
Lamb shift, exptl. correction 8=25351
latent symmetry 8=47481
magnetic moment, g_J ratio meas. by optical pumping 8=38734
maser freq. shifts, due to coherently excited $\Delta m_F = \pm 1$ transitions between F = 1 levels of ground state 8=25350
metals, H, O, N joint determ., isotope method 8=27784
neutral, number density in upper atmos. rel. to altitude 8=36777
non-closed-shell linear chain system low-lying energy levels 8=44644
non-invariance group for dynamical systems 8=37843
nonrelativistic, Runge-Lenz vector, physical interpret. 8=38649
1s-2s excitation by slow electrons, theoretical and numerical study 8=38694
2s state two-photon decay, analytic soln. 8=38647
O(4, 2) description, relativistic current operator 8=29594
$O_{4.1}$ group additional generators 8=38650
O_4 symmetry, from factorization of Schrödinger eqn. with α/r central pot. 8=34129
photoionization cross section meas. 8=29949
plasma emission 2 keV-1 MeV spectrum, meas. and display 8=38646
positron scatt., resonance mechanism 8=38722
proton collision, Sturmian coupled-state calc. 8=38736
$pH(1S) \rightarrow pH(2s)$ 1-500 keV, invalidity of peaking approx. method 8=43218
p-H scatt., impact parameter representation 8=46821
in radiation belts, interaction with charged particles, consequent Ly-α emission 8=36818-19
recombination rate 8=36563
recombination rate at room temp., e. p. r. spectroscopy 8=34377
relativistic, partial group-theory treatment 8=29593
release from $HClO_4$, by γ-irradiation, spatial distrib. e.s.r. obs. 8=49963
SO(4, 1) group generators, construction 8=43171
Rutherford scatt. by He, Ne and Ar 8=38754
in solar photosphere, collisional damping of Fraunhofer lines 8=37049
solar, profiles photometric obs. 8=37042
Sommerfeld fine-structure constant measurement 8=38648
statistical analysis of structure 8=29595
stripping analyzer, sensitivity in 50 to 300 eV range 8=43236
sym. generalization applic. in quantum mechanical treatment 8=33523
symmetry group, use of SO_3, algebra, point rotor and stereographic mapping 8=34128
transfer reactions, activation energies 8=27708
$2l_0$-$3l$ transitions, meas. of electron collision cross sections 8=38721
transport mechanism in chem. reactions 8=41252
two-dimens. analogue, Schrodinger equations 8=34131
in CaF_2 as interstitials, localized vibrations 8=41072
Hα-line spectra of sunspots, rel. to velocity fields at chromospheric heights 8=28184
H_α profile, strong-collision effects 8=38645
Hβ 4861 Å, nightglow S. America photometric obs. 8=45498
H_β profile in spectrum, meas. absorpt. and emission lines in Zodiac light 8=41353
H_β radiation in night sky spectrum 8=41354
H(2S) in weak electric fields, Lyman-α radiation polarization 8=25349
H isotope-inert gas mixtures, rot., theory and obs. 8=30296
H+D and D+D, hyperfine splitting of interaction energy 8=38751
H + D_2, energetic atom reaction 8=41242

Hydrogen—contd
  neutral atoms—contd
    $H + F^-$ collisions, electron detachment 8=34451
    $H + H^- \rightarrow H_2^* + e$, associative detachment 8=25391
    $H + H^+$, high-energy electron capture cross-sections 8=38744
    $H + H_2 = H_2 + H$ isotopic reactions, permeabilities 8=45312
    H-He mixtures, thermal cond. 8=47957
    H-He system, normal and equilib., press.-temp-co-ords of three-phase locus 8=43893
    $H + NO_2$, free electron generation 8=49872
    $H + O_3$, i.r. chemiluminesc. 8=32099
    He^+ collisions, Lyman-α emission cross sections and polarization obs. 8=38755
    O and α-Ti mixed crystals, lattice struct. rel. to hydrogenation, n diffr. obs. 8=35357
  neutral molecules
    absorption into turbulent jets of water 8=30425
    bare-nucleus perturbation theory 8=38829
    bond formation process 8=34221
    charge transfer from p and H atom, cross-sections 8=38737
    chemisorption on MgO, i.r. spectros. 8=49894
    electronic energy, variation-perturbation calc. 8=38832
    formation in dehydration of single crystals 8=36554
    gaseous jet in vacuum, forming and trapping 8=43645
    h.f.s. discrepancy, A meson contrib. to Feynman diagram, quark model of proton 8=33743
    high energy, nonadiabatic trapping in mag. mirror machine 8=30120
    high-velocity scatt. by He atoms 8=25667
    impact with Hg, 2537 Å line broadening and shift 8=43194
    impurity in O_2, effect on acoustic absorpt. 8=39211
    interaction with Ti, and form. by Ti sorption and diss. of NH_3 8=32103
    interstellar, in southern Coalsack, abortive search 8=28093
    ionization, double, Franck-Condon calc. 8=29967
    ionization by e-impact, 250-2200 eV, and D^+ ion formation 8=29963
    ionization of gas at 10^{-3} torr, by laser-irradiation rel. to multiphonon theory 8=29964
    ionization, test of Franck-Condon principle 8=29966
    i. r. absorpt. spectrum in cryst. Ar 8=27573
    Kerr elec. birefringence theory 8=34664
    Lyman bands, isotope effects on Franck-Condon factors 8=34271
    Lyman bands, oscillator strengths 8=43309
    magnetic shielding in elec. field 8=47599
    photoionization, ion-mol. and chemi-ionization reactions 8=36611
    polarizability 8=47600
    plasma source, action of 3cm microwaves 8=34565
    reaction with hydride ion, MO theory 8=27676
    recombination rate at room temp., e. p. r. spectroscopy 8=34377
    relfex discharge in magnetic field of 10-1500 Gauss 8=43450
    rotational excitation and de-excitation by slow electrons, absolute total cross section, energy and angular var. 8=43311
    shape and dimensions 8=34248
    $^1\Sigma^+_g$ first excited state, rot. and vibr. levels, calc. 8=38823
    spectroscopy 850 to 792 Å 8=43303
    spin-lattice relax., h. p., timing by data acquisition system 8=29805
    u.v., spectra, absolute transition probabilities 8=34230
    vacuum u. v. emission from p and H-atom impact 8=38834
    vibrational and rot. energies for $B^1\Sigma_u^+$ and $a^3\Sigma_g^+$ states 8=38827
    vibrational solvent shifts in induced i.r. spectra 8=43837
    viscosity with const. density, 16. 6-300°K 8=43703
    on Ag films, reaction with O_2 8=39616
    Cs-H collisions, cross-section obs. 8=38957
    D_2, spectra, selective enhancement in Ar discharge 8=25471
    HCl mol., first rotational linewidths determ. 8=38825
    HD, liquid, n. m. r., double 8=34921
    HD, solid and liquid, proton spin-lattice relax. 8=31908
    HD, spectra, selective enhancement in Ar discharge 8=25471
    H_2 dissolved in solid Ar, induced i. r. fund. band obs. 8=36326
    H_2, HD, D_2 electronic isotope shifts in Lyman bands 8=34244
    H_2 gas, ionization by 0. 2-1. 8 MeV He^+ ions, effective cross sections 8=39035
    H_2 gas, simultaneous fundamental and second harmonic laser radiation 8=46592
    H_2 ground state rot. and vibr. consts., calc. 8=38792
    H_2, large vibr.-rot. interaction effects in Franck-Condon factors 8=43304
    H_2, numerical single-centre SCF function 8=47601
    H_2, photoionization near threshold 8=47786
    $H_2 + Cl \rightleftarrows HCl + H$, reaction kinetics, e. s. r. study 8=49861
    H_2 and D_2, photoionization, threshold electrons 8=39034
    H_2 in H_2-Ne mixture, pressure-induced i. r. absorpt. of fund. band 8=38833

Hydrogen—contd
  neutral molecules—contd
    H_2, HD and D_2, vibr. consts. of singlet states 8=43305
    H_2-He gaseous mixtures, thermal diffusion 8=34680
    H_2-O_2 flame, e.p.r. study of conc. profile of H radicals 8=49892
    H_2/O_2 mixture detonation, dual regime 8=45355
    $O_2 + H_2$ mixtures, detonation limits, influence of molec. mass 8=32115
    H_2-O_2 mixtures, combustion in shock waves 8=32109
    $H_2 + O_2$ reaction in shock tube, OH chemiluminesc. 8=49889
    H_2-Xe thermal diffusion 330°-600°K, Chapman-Enskog theory 8=43707
    H_3, config.-interaction calc. 8=29744
    H_3, linear, LCGTO SCF MO wavefunctions 8=47603
    H_3, potential-energy surface 8=34246
    H_4, linear, LCGTO SCF MO wavefunctions 8=47603
    H_2 and D_2, vibr. relax., isotope effect 8=34240
    $H_2 + D_2 \rightleftarrows 2HD$, catalyzed by Mo 8=49907
    H_2-H_2 interaction, quantum mech. calc. 8=34387
    H_2-H_2 interaction, valence-bond calc. 8=29844
    H_2, in H_2-Kr mixture, pressure-induced i. r. absorpt. of fund. band 8=38833
    H_2S, mm. spectrum h.f.s., elec. resonance spectroscopy 8=38826
    He^+ collisions, Lyman-α emission cross sections and polarization obs. 8=38755
    OH surface groups, effect of adsorbed benzene on n. m. r. 8=38923
    K atom collisions, mixing and quenching cross sections 8=29836
    Ni, desorpt. obs. 78°-300°K 8=30772
    Ti, desorpt. obs. 78°-300°K 8=30772
Hydrogen compounds
    See also Ice; Steam; Water.
    halides, dissociative electron attachment 8=29965
    hydrate binary systems, thermal analysis under pressure, ⩽ 500°C 8=28413
    hydrates, crystalline, H atom position determ. by NMR 8=44219
    hydrides, AH, second row, Hartree-Fock wave functions and energy quantities 8=34257
    hydrides, first-row, floating spherical Gaussian orbital model 8=38811
    hydrides, first-row, Hartree-Fock wavefunctions and energy quantities 8=34256
    μ^- depolarization obs. 8=29673
    Uranyl-hydrogen system, cation exchange equilibria 8=47409
    DBr, solid, crystal struct. rel. to phase transition 8=26396
    DCN, assignment of laser lines 8=28682
    DCN laser, new c.w. sub-mm lines, absolute freq. obs. 8=28683
    DCl, calc. D quadrupole coupling consts. 8=38921
    DCl, cubic, crystal structure 8=35330
    DCl spectra by double-beam, two-beam interferometry far i.r. 8=28818
    DF, calc. D quadrupole coupling consts. 8=38921
    D_2O, at 4°C, X-ray study of struct. and distrib. functions 8=25872
    D_2O, hyperfine structure by beam maser microscopy 8=25923
    D_2S, ν_2 fundamental vibr. 8=25484
    D_2S solns., in ethers, ionic reactions in γ-radiolysis 8=45402
    H halide mols., photoelectron spectra 8=25486
    H Halides, mean amplitude quantities and bond covalency correl. 8=34228
    H_xA gases, adsorpt. on CdS powders, comp. with O_2 8=26135
    H_2Ar, bound states, i. r. absorpt. 8=25472
    H_2-Ar solns. surface tension, temp. and conc. depend., 87-120° K 8=25898
    HBr aq. solns., elec. cond., 0°-800°C, to 4000 bar 8=43864
    HBr, gas-phase radiolysis 8=49977
    HBr, line broadening rel. to Debye forces of dispersion and induction 8=25407
    HBr, n.m.r. of solid phases 8=49645
    HBr, photoelectron spectra and ionized states 8=34229
    HBr, radiolysis mechanism 8=32142
    HBr, trapped in matrices, far i. r. dimer bands 8=27575
    HBr in DBr, solid solutions n.m.r. 8=36269
    HCN, adsorbed on porous glass, i.r. spectrum. polymerization 8=48491
    HCN, assignment of laser lines 8=28682
    HCN laser, multiple pulse emission 8=24309
    HCN, matrix- isolated dimer 8=29740
    HCN, molec. bending calc. 8=25474
    HCN, photoionization 8=47789
    HCN pulsed laser, acoustic perturbations 8=46593
    HCO radical, potential functions and bonding 8=47713
    HCN, SCF minimal basis set calc. 8=29719
    H_2CO, and halogen analogs, spin-orbit coupling 8=25473
    $(HCO_3)_2^{2-}$ in $KHCO_3$, structure from NMR study 8=26032
    HCP, molec. bending calc. 8=25474
    HCl, crystal structure and phase transforms. by X-ray and n-diffr. 8=26073
    HCl, dissoc. behind shock waves 8=38931

Hydrogen compounds—contd
HCl, gas, density at 20, 50, 75°C and 5 and 40 atm. 8=30281
HCl, gaseous, gamma-radiolysis, effect of applied elec. field 8=36622
HCl, gaseous, radiolysis, mechanism of H formation 8=27764
HCl, line broadening rel. to Debye forces of dispersion and induction 8=25407
HCl, i. r. spectra in solvents, rotation-like motion 8=25928
HCl mass transfer in water, in cylinder with pulsed flow 8=34811
HCl, n.m.r. of solid phases 8=49645
HCl, photoelectron spectra and ionized states 8=34229
HCl, second harmonic vibration-rotation band in liq., cubic, orthorhombic phases 8=25929
HCl, solid, low-temp. phase, phonon freq. distrib. 8=35384
HCl, solid, n.m.r. 8=40965
HCl, trapped in matrices, far i. r. dimer bands 8=27575
HCl and DCl, solid, n.q.r. and n.m.r. study of molecular motion 8=31903
HCl in DCl, solid solutions, relax 8=36270
$HClO_4$, e.s.r. study spatial distrib. of H atoms after γ irrad. 8=49963
HD, Cs-HD collisions, cross-section obs. 8=38957
HD, elec. dipole moment obs. 8=34242
HD, solid, radiation damaged e.p.r. of H atoms 8=40924
HDO in H_2O, i.r. absorpt. at high press. and temp. 8=25930
HDO, hyperfine structure by beam maser microscopy 8=25923
HF, chem. laser 8=37582
HF, chem. laser 8=46590
HF, dissociation in shock waves 8=25650
HF effect on Ge electrode surface 8=27752
HF fractionation column 8=41608
HF, gaseous, n. m. r. 8=29817
HF(g), i. r. spectrum of trimer and dimer 8=29747
HF and DF, ionization energies 8=29962
HF, line broadening rel. to Debye forces of dispersion and induction 8=25407
HF, nuclear shielding and spin-rot. consts., vibr. corrections 8=38924
HF, 1-0 and 2-0 bands 8=25476
HF, photoelectron spectra and ionized states 8=34229
HF, pure rotation spectrum 8=29734
HF, reaction with hydride ion, MO theory 8=27676
HF solution of NH_4HF_2, electrolysis and subsequent i. r. analysis, cell requirements and construction 8=36606
HI, line broadening rel. to Debye forces of dispersion and induction 8=25407
HI, n.m.r. of solid phases 8=49645
HI, photoelectron spectra and ionized states 8=34229
H_2Kr, bound states, i. r. absorpt. 8=25472
$HNCLO_3^-$ ion, structure from i.r. absorpt. obs. 8=34247
HNO_3, absorption in lower stratosphere 8=27877
HNO_3 etching of UO_2 rel. to cryst. orientation 1-37 molar 8=30818
H_2O^{16} and H_2O^{18}, high-resolution i. r. spectrum 8=25478
H_2O dimer, MO calc. for H-bond 8=38828
H_2O, isotopic, force const. displays 8=43302
H_2O, matrix-isolated, i. r. obs. of nuclear-spin-species conversion 8=38830
H_2O, molec. bending calc. 8=25474
H_2O molecule, Rydberg terms calc. 8=25479
H_2O, Rydberg states calc. 8=29746
H_2O, vac. u. v. photodecomp. 8=47613
H_2O vapour, band and total emissivities 8=43280
H_3O mol., evidence 8=47610-11
H_3O^+ ion, in hydrated $Ga_2(SO_4)_3$ crysts., n.m.r. evidence 8=49643
$H_3O.NO_3$ crysts. n scatt. rel. to mol. and lattice vibr., obs. 8=35385
H_2O-CO_2 mixture, 80-230°K obs. rel. to composition of Martian icecaps 8=32547
HOCl, i. r. spectrum 8=25475
H_2O_2 frozen solns., irrad., e.s.r. 8=40925
H_2O_2 on Pt microelectrode, polarographic behaviour on periodic renewal of diffusion layer 8=41275
$H_2PO_4^-$ crystals, growth rel. to morphology, impurity effects and crystallization conditions 8=26254
H_3PO_4, for crystallization of $CaSO_4$, conc. and suspension density effects 8=35239
H_3PO_4 paste electrolyte in fuel cell, for intermed. temp., operating on H_2 and O_2 8=33029
H_2S, accidental Coriolis resonance 8=25482
H_2S flame, rarefied, stages in burning 8=36582
H_2S, isotopic. force const. displays 8=43302
H_2S, mm elec. reson. spectra 8=25483
H_2S, nonempirical SCF calc. 8=47596
H_2S, proton affinity 8=32100
H_2S, three solid phases, pulse and steady state n.m.r. 8=40982
H_2S_2, mm-wave spectrum and molec. consts. 8=25485
H_2Se, isotopic, force const. displays 8=43302
H_2SO, nonempirical SCF calc. 8=47596
H_2SO_4 mixed with HF, effect on Ge electrode surface 8=27752
$H_2SO_4.H_2O$, H bonding rel. to crystal structure 8=26400
H_xWO_3, X-ray and neutron diffraction studies 8=35336

Hydrogen compounds—contd
H_2Xe, bound states, i. r. absorpt. 8=25472
$OH^*({}^2\Sigma^+)$, in photodecomp. of H_2O 8=47613
Hydrogen ion concentration. See Electrochemistry.
Hydromagnetics. See Magnetohydrodynamics.
Hydrometry. See Flowmeters.
Hydrophones. See Acoustic transducers: Oceanography.
Hydrostatics
No entries
Hygiene. See Medical science.
Hygrometers
coulometric and diffusion, Soviet types 8=27878
electrolytic, appl. to evolution of water reaction phenomena 8=45314
thermistor, soil moisture free energy meas. 8=50090
Hyperfine structure See Paramagnetic resonance and relaxation; Spectra.
Hyperfragments. See Hypernuclei.
Hypernuclei
heavy spallation, by K^-, 800 MeV/c prod. 8=25166
hyperfragment prod. from K^- and emulsion nuclei, 10.1 GeV/c obs. 8=29487
hypertriton n-p tensor interactions from Λ-p scatt. 8=25012
Λ-N and Λ-Λ interactions and p-shell nuclei props. rel. to spectroscopy 8=33947
π^+ decays, binding energy, Λ-Λ interactions and nuclear struct. appls. review 8=29349
p-shell, ΛNN 3-body repulsion rel. to binding energies 8=29350
Ξ, decay by $\Xi N \rightarrow \Lambda\Lambda$ conversion rel. to double hyperfragment prod. in K^- interactions 8=33832
${}_{\Lambda\Lambda}C^{14}$, analysis 8=42932
$C^{14}{}_{\Lambda\Lambda}$, binding energy of Λ-Λ interaction 8=33948
${}_{\Lambda}H^3$ binding energy, effect of Λ-Σ conversion 8=42657
${}_{\Lambda}H^3$ lifetime obs. 8=25011
${}_{\Lambda}H^3 \rightarrow e^- + \bar{\nu} + He^3$, all e^- β-decay rate calc. 8=29351
${}_{\Lambda}H^3$, lifetime determ. 8=38400
${}_{\Lambda}H^4 \rightarrow e^- + \nu^- + He^4$, all e^- β decay rate calc. 8=29351
${}_{\Lambda}H^4 \rightarrow \pi^- + He^4$ using s-wave π-He^4 scatt. data at 139 MeV/c calc. of final state interaction effects 8=25168
${}_{\Lambda}He^4 \rightarrow$ all e^-, β-decay rate calc. 8=29351
$He^4 \rightarrow He^3 + p + \pi^-$ decay, final state interactions and excited states, obs. 8=33949
$He^5 \rightarrow He^4 + p + \pi^-$ decay, final state interactions and excited states, obs. 8=33949
${}_{\Lambda}He^6$ binding energy calc. rel. to Λ-N interaction 8=38399
${}^6He_{\Lambda\Lambda}$ with nonlocal separable interactions with hard shell Λ-Λ replusion 8=42931
He^7 excited levels rel. to γ transitions 8=33947
${}_{\Lambda}Li^6$, existence 8=38399
${}_{\Lambda}Li^6$, existence questioned 8=25167
Li^7 excited levels rel. to γ transitions 8=33947
Li^8 fragment prod. from K^- and emulsion nuclei, 10.1 GeV/c obs. 8=29487
$O^{18}{}_{\Lambda\Lambda}$, binding energy of Λ-Λ interaction 8=33948
Hyperons
lifetimes and branching ratios 8=24827
Λ polarization in $\gamma p \rightarrow K^+\Lambda$ reaction 8=42658
Λ° polarization in $\Sigma^\circ \rightarrow \Lambda^\circ + e^+ + e^-$ 8=29211
Σ^- polarization in $\pi^- + p \rightarrow \Sigma^- + K^+$, 1145 MeV/c 8=24996
absorption
No entries
capture
No entries
decay
Λ β-decay coupling constant meas. 8=29351
Λ-Σ conversion effect on ${}_{\Lambda}H^3$ binding energy 8=42657
Λ° lifetime, from $\Sigma^- p \rightarrow \Lambda^\circ n$ reaction obs. 8=38092
$\Lambda^\circ \rightarrow N\pi$, radiative corrections 8=33833
nonleptonic, and equal time commutation relations 8=4265
nonleptonic, based on composite scheme, P-wave decay props. 8=38085
nonleptonic, chiral dynamics 8=42619
nonleptonic, current-algebra and hard-pion calc. 8=42654
nonleptonic, parity-conserving in SU(3) 8=42655
nonleptonic, rel. to current algebra, asymptotic SU(3) symmetry, Regge poles and dispersion relations 8=33829
non-leptonic s-wave, rel. to baryon models 8=24987
nonleptonic, tadpole model, partity violation explained with baryon octet and decuplet poles 8=33830
nonleptonic, U-spin pole model 8=24986
nonleptonic, vector meson dominance 8=38086
Ω^-, nonleptonic, using pole approx. calc. 8=37861
P-violation explained with baryon octet and decuplet poles 8=33830
rel. to a test of current-current nature of weak interactions 8=24711
semileptonic in sum-rules for SU(3) breaking interactions 8=29045
s-, p-wave amplitudes from extrapolation of $K_1 + Y \rightarrow \pi + N, \kappa_1 + Y \rightarrow \pi + N$ 8=24988
S P-wave with matrix element structure of Hamiltonian and current-algebra 8=29210
$\Sigma \rightarrow ne^-\bar{\nu}, n\pi^-$ branching ratio obs. 8=38090
$\Sigma^- \rightarrow n + e + \bar{\nu}$, Cabibbo theory status 8=38009
$\Sigma^- \rightarrow nl\nu$, measurement of asymmetry parameter 8=38089
$\Sigma^\circ \rightarrow \Lambda^\circ + e^- + e^+, \Lambda^\circ$ polarization re-estimate 8=29211

Hyperons—contd
decay—contd
$\Sigma^\circ \to \Lambda^\circ$ in K^- interaction with complex nuclei in bubble chamber 8=25254
Σ°-Λ transition magnetic moment possibility of meas. in $\pi^- p \to \Lambda K^\circ \gamma$ 8=33835
$\Sigma^+ \to n\pi^+$ and $K^\pm \to \pi^\pm \pi^\circ$ related by $\Delta I = 3/2$ effects 8=29151
$\Sigma^+ \to p + \gamma$, branching ratio calc. 8=24992
$\overline{\Sigma}^\pm \to n + \pi^\pm$, p- and s-waves decays, $|\Delta I| = 1/2$ and triangle relation validity 8=38088
SU(3) model with CP invariance reproducing parity violation 8=33831
3-body weak photonic, calc. from SU(3) $\otimes$ SU(3) 8=42653
Ξ^- parameters from K^-p, 1.7-2.7 BeV/c interactions 8=24997
$\Xi^- \to \Lambda^\circ e^- \bar{\nu}$, branching ratio 8=24998
$\Xi^- \to \Sigma^\circ e\bar{\nu}$, e.m. T-odd correl. calc. 8=47176
$\Xi^0 \to \Sigma^+ + e^- + \bar{\nu}$, calc. of renormalization of weak axial-vector coupling constant 8=24619
$\Xi^*_{1817} \to \Lambda + \bar{K}$ analysis, from $K^- p$, 1.7-2.7 BeV/c 8=24997
$\Xi^*_{(1817)} \to \Xi^*_{(1530)} + \pi$ analysis from K^-p, 1.7-2.7 BeV/c 8=24997
PCTC, scalar-pseudoscalar assumptions 8=24992
decay observations
Ω^-, β-decay 8=42659
Σ^-, mean lifetime obs. 8=24993
detection, measurement
I = 2, search from K^- n interactions; 2-11, 2.65 GeV/c 8=42656
effects
Σ^- conversion in light nuclei, impulse-model calc. 8=38094
interaction
See also Hypernuclei.
Λ-Λ rel. to hypernuclear spectroscopy 8=33947
Λ-N from ${}_\Lambda H^3$ lifetime 8=25011
Λ-N nuclear rel. to hyernuclear spectroscopy 8=33947
Λ-N rel. to hypernuclear spectroscopy 8=33947
ΛNN in p-shell hypernuclei, 3-body repulsion rel. to binding energies 8=29350
Λ-p, low energy obs. 8=33838
extrapolation to s, p-wave amplitudes in Y decay 8=24988
$\Sigma^- + He^4 \to \Lambda^\circ + n + t$, impulse-model calc. 8=38094
Σ^--p $\to \Sigma^\circ n$ and $\to \Lambda^\circ n$, capture ratio Λ° lifetime and Σ^--Λ° mass difference 8=38092
Σ^--p, low energy obs. 8=33838
$\Sigma^+ n \to \Lambda p$ obs. in $K^- d \to \pi^-(\Sigma^+ n) \to \pi^-(\Lambda p)$ 8=38093
Σ^+-p, low energy obs. 8=33838
$\kappa_1 + Y \to \pi + N$, extrapolation to s, p-wave amplitude in Y decay 8=24988
$C^{14}{}_{\Lambda\Lambda}$ hypernucleus, binding energy calc. 8=33948
$O^{18}{}_{\Lambda\Lambda}$ hypernucleus, binding energy calc. 8=33948
Y-N, final state, low energy obs. 8=33838
magnetic moment
Σ°-Λ transition, possibility of meas. in $\pi^- p \to \Lambda K^\circ \gamma$ 8=33835
Σ^+ 8=38091
Σ^+, broken, vector-current sum rule 8=29212
mass
Σ^--Λ° difference, rel. to p capture ratio 8=38092
production
Λ in $K^- p$ interactions, 10 GeV/c cross-section decrease depend. one strange meson exchange 8=33834
$\overline{\Lambda}$ in $K^+ p$ reaction at 9 BeV/c, mass enhancement 8=24991
Λ and Σ°, in K°_L + Pb, cross section at E = 150 MeV 8=24989
Λ in $\Sigma^+ n \to \Lambda p$ obs. in $K^- d \to \pi^-(\Sigma^+ n) \to \pi^-(\Lambda p)$ 8=38093
Λ° in $K^- p$ interactions, 6 GeV/c 8=38087
Ω^- in $K^- p$, 5.5 GeV/c, 3 events obs. 8=29213
p-p interactions, 2.4, 2.85 BeV 8=29188
from π^- interaction in heavy emulsion nuclei, strange particle prod. p_π = 17 GeV/c 8=33837
$\Sigma\pi$ pair prod. by K^- on emulsion nuclei 8=33836
Σ° in K^- interactions with complex nuclei in bubble chamber 8=25254
$\overline{\Sigma}^0$ in $K^+ p$ reaction at 9 BeV/c 8=24991
$\Sigma^+ K^+$ and $\Sigma^+ K^{*+}$, diff. cross sections and Regge pole model 8=24994
Σ^+ in $pp \to \Sigma^+ K^\circ p$, 5 GeV/c 8=24913
Ξ, from π^-N interactions at 4.0 GeV/c 8=24999
In K^- interaction with heavy nuclei, double hyperfragment emission, 1.5-5 MeV 8=33832
Y_1^* in p-p collisions, 6.92 BeV/c final states 8=24916
resonances
strangeness = −1 and −2 8=29214
$Y_0^*(1520)\pi$ prod. in $K^- p \to \bar{K} N \pi$, 1.33 GeV/c 8=33706
scattering
$K\Xi$, superconvergent sum rules 8=29157
$K^- \Xi^\circ$, consistency condition for $|\Delta S| = 1$ currents 8=29043
Λ-N potential calc. 8=24990
Λ-p rel. to n-p tensor interaction in ${}_\Lambda H^3$ 8=25012
spin and parity
Σ parity in $\pi^+ p \to K^+ \Sigma^+$ 8=24995
Ξ^- decays, from $K^- p$, 1.7-2.7 BeV/c 8=24997
Ξ^* decays, from $K^- p$, 1.7-2.7 BeV/c 8=24997
Hypersonics. See Ultrasonics.
Hypertritons. See Hypernuclei: Tritons.
Hypervirial theorem. See Quantum theory.
Hypochromism. See Absorption/light: Polymers.
Hysteresis
See also Dielectric phenomena; Dielectric properties of substances; Ferroelectric phenomena; Magnetization process.
dynamical loop representation 8=44961
ferromagnetic films, loops, from transverse Kerr effect, azimuthal variation effect 8=40786
ferromagnetic films, teaching demonstration 8=27397
internal friction, rel. to thermomechanical unpinning of dislocations. 8=48839
loop plotter, rel. to transverse Kerr effect in Co films 8=45007
magnetic and surface superconductivity, Ginzburg-Landau theory 8=44718
mechanical, in microstrain regions, rel. to dislocation substructure and friction stress 8=26744
oscillating, losses in multiple mag. thin films 8=31585
phase transform., bulk and thin-film, inter-phase potential barrier mechanism 8=43990
thixotropic props. determ. 8=25965
$BaCo_2Fe_{16}O_{27}$, mag. rotatory losses and anisotropy 8=45037
$BaFe_{12}O_{19}$, mag. rotatory losses and anisotropy 8=45037
Co films, polycryst., field and coercive force, thickness depend., 200-2000Å 8=31598
Fe-3% Si, magnetostriction and mag. loss in rotating fields up to 2000 Oe 8=31680
$NaH_3(SeO_3)_2$, thermal, in both phase transitions 8=44873
Nb-Sb superconducting alloys, mag., at 4.2°K 8=27024
Nb-Sn superconducting alloy, mag., causes 8=44972
Ni ferrites, velocity of ultrasonic waves., with Co, Ma and Cu impurities 8=31736
Ni film, oscillating 8=45021
Ni, magnetostriction and mag. loss in rotating fields up to 2000 Oe 8=31680
$SrTiO_3$, annealed, electric double hysteresis 8=49376

INDOR (internuclear double resonance). See Nuclear magnetic resonance and relaxation.
Ice
See also Glaciers: Snow.
absorption spectra, vacuum u.v. 8=31998
adhesion bond strengths with plastics, correl. with phys. and chem. props. 8=31215
alkaline, optical absorption spectrum of trapped dielectrons 8=45194
Antarctic firn, deuterium content in layers to 106 m. rel. to climate 8=50088
clathrates, dielec. props. 8=27255
cloud radar refl. obs. 8=32224
conversion from H_2O vapour by AgI 8=45458
crystal dielec. and mech. relaxation 8=30995
crystals growing in supercooled water, morphology 8=26176
dendritic crystallization from aq. soln. 8=30835
dielect consts, compared with light and heavy water 8=43767
dielectric props. with HCl impurity 8=31420
elastic moduli from u.s. velocity meas., mp to -140°C 8=44581
far i.r. absorpt., disorder induced rel. to Bjerrum type defects 8=49681
far i.r. spectrum and long-range forces 8=31997
filaments, growth and destruction in elec. field 8=35244
firn samples from Antarctica, dating by meas. of natural and artificial radioactivity 8=27855
forming in supercooled aerosol flow, density and struct. 8=27899
free growth rate in supercooled aqueous solns., rel. to ice-soln. interface 8=35242
freezing nuclei conc. in atmos., meas. 8=36737
growing cylindrical crystal, morphological stability 8=39673
grown from dilute ionic solns., ionic distrib. and freezing pots 8=34971
habit and charge of crystals, modification by vapour contamination 8=32220
hailstones, artificial, lobe-like growth and surface config., drag. coeffs. 8=35228
hailstones, artificial, rough, rate of melting and heat transfer 8=34963
Hall effect and proton mobilities 8=35958
hexagonal, density 8=49028
hexagonal, freq. spectrum from neutron scatt. 8=39875
hexagonal, proton spin-lattice relax. 8=49644
void formation during non-basal glide under tension 8=44402
ice on silicate surfaces, existence of liq. like, unfrozen interfacial water layer 8=35142
ice I and III, equilib. line 8=30696
ice VII, H_2O and D_2O, effect of press. on vol. 8=49026
ice IX, antiferroelec. phase 8=31438
ice-solution interface, model, rel. to 'freezing potential effect' 8=34970
irradiated, l.f. e.s.r. 8=40925
liquid-like transition layer, survey 8=34975
lunar, rel. to maria and craters 8=45815
mass transfer along surface, neck growth and particle migration 8=30723

Ice—contd
melting. submicroscopic gaseous inclusions, nuclei for Tyndall figures 8=30579
multiplication in atmos. possibilities 8=45454
nucleation by AgI, nature of nucleating site 8=32216
nucleation props of mineral particles 8=35229
nucleation, substrate-ice interface obs. 8=25986
oceans as source of nuclei 8=41337
1h and 1c, orientationally-disordered crysts, far i. r. spectra 8=27574
phase transform. of water, by shock compression 8=48262
phonon frequency distrib. from inelastic neutron scatt. 8=26574
proton dynamics from slow n. inelastic scatt., at. 268. 7°K 8=39303
powder, adsorpt. isotherms for N_2, rel. to surface struct. 8=30769
powdered spheres, sintering and rate of decrease of surface area, due to plastic flow 8=35073
relaxation phenomena in ice crystals 8=49366
sea, dielectric props. 8=35956
seawater microwave emission, effect of thin layer 8=50113
on solid surface, water mols. mobility in transition layer 8=30999
in space, evaporation 8=48289
sp. heat near ferroelectric transition temp. 8=48737
step propag. across basal plane, rel. to surface diffusion at ice-air interface 8=35145
spheres, i. r. optical properties; application to radiative transfer in planetary cloud layers 8=50140
sun's image on airborne ice crystals 8=36745
surface features obs. during thermal etching 8=35147
vapour pressure, isotope effects 8=39491
water drops, supercooled, crystallization processes 8=25985
water-ice contact angle for rapidly freezing interface 8=35146
H disorder effect on dislocation and plastic deform. 8=35569
H_2O and D_2O, phase diagrams at high press. 8=48383
H_2O, D_2O, and HDO, i. r. intensities in solid films 8=36369
NH_4F-doped, dielec. relax. time actuation energy 8=44869
SnIV isomer shifts, conc. depend. 8=43957

Illumination
See also Brightness.
convergent, for plane grating mounting, theory 8=37692
electrical, combination with air-conditioning systems 8=41928
electrical, improvement by combination with air-conditioning 8=41929
focon reflecting system 8=42124
pulsed, rel. to Joshi effect 8=38985
scanning of object and detector simultaneously in holography 8=42275
time-varying diffuse, effect on holography 8=37720
GaP p-n junction, effect on I-V characts., and mech. stress effects 8=49288

Image convertors and amplifiers
for cosmic ray shower photography 8=33847
cascade intensifier, use in Coudé spectroscopy 8=28773
electro-optical converter, M-9, in visual u.v. microscope 8=42214
electron-optical, resolving power 8=41978
electrostatic "memory" for image storage 8=46682
films, high-resistance, subjected to e-beam scanning, resolving power 8=33096
holography, ultrasonic, for image visualisation in opaque media 8=28374

Image orthicons. See Electron tubes.

Impact
See also Ballistics.
image-tube framing camera, time dispersion effects 8=37433
infrared tube, electron optics by pot. distrib. 8=41981
infrared tube, epitaxial growth of mosaic of p-n junctions 8=44844
infrared tube with Ge mosaic 8=41980
intensifier for e microscope 8=33095
intensifier for thermal n TV radiography 8=37725
intensifiers, gas-filled detectors for X and gamma-rays 8=46855
i.r. viewer 8=32948
low-light level performance of image intensifer systs. 8=33255
luminance amplification in electro-optical systems 8=42261
millimetre-wave, to visual display 8=28775
objective design 8=42178
photodiode mosaic technology 8=41982
target, junction mosaic, contrast sensitivity variations 8=41979
thermal, i.r. scanning system 8=42213
X-ray image intensifier, electron-optical, development 8=46781
drop-weight impact sensitivity testing explosives 8=32907
on finite elastoplastic bar, compression wave propag. 8=23934

Impact
See also Ballistics.
of flat body on free surface, effect of air compressibility 8=41648
metallic materials, determ. of C content 8=40119
microparticles, hypervelocity, appl. to data anal. from cosmic dust microphone sensors 8=41577
Newtonian theory, aerodynamic relns rel. to drag and config. 8=32704
one-dimensional collisions, energy transfer 8=28254
of micrometeoroids, simulation, study of craters, penetration and emission of charges 8=37028
rigid sphere on linear visco-elastic half-space, numerical soln. and comparison with expt. 8=41736
of rigid sphere on thin viscoelastic plate, resulting eqns. of motion 8=23853
on viscoplastic rods, nonlinear soln. 8=41724
on viscoelastic, semilinear, bar, rel. to wave propag. 8=32886
Cu–Ni alloy, obliquely with steel plate, temp. developed 8=32981
Fe and Fe–C alloys, effect of Mn and Ni on impact properties 8=35693

Impedance, acoustic. See Acoustic impedance.

Imperfections in solids. See Alloys; Crystal imperfections; Solids/structure.

Impurities. See Crystal imperfections; Crystal/growth; Semiconducting materials.

Independent particle model. See Nucleus/models.

Indeterminacy
extension of measurement 8=28215
measurement effects on relativistic quantum mechanical systems 8=46790
meas. in quantum mechanics, idealized trajectory determ. 8=24458
measurement theory with degeneracy 8=24459
measuring process, quantum-statistical model 8=34097
particle moment determ. by Stern-Gerlack-like expts. 8=33563
of photon phase, degree of indefiniteness for any coeffs. representing state 8=33604
photon det., quantum theory 8=29081

Indium
alkali halide molecules, surface ionization on Ir 8=27365
atomic, photoionization cross section meas. 8=29949
cold rolled, effect of alloying additions on twinning activation energies 8=35217
cubic phase, n.m.r. 8=36271
de Haas-van Alphen meas. 8=49470
diffusion in Al, due to near surface effect 8=39964
film, size effects in magnetoresist., interpret. using two-band model 8=44683
film, superconducting, props. rel. to degree of crystal lattice distortion 8=35849
films, vacuum-deposited, liquid-like behaviour of crystallites 8=26121
γ-quanta, annihilative, obtained by positron annihilation, ang. distrib. 8=49128
helicon-wave resonances in Hall coeff. determ. rel. to surface-mode loss 8=44682
hole surface, second band, de Haas–van Alphen study 8=40226
implantation in Si, anomalous penetration 8=48929
intermediate state, quadratic response to transverse alt. mag. field 8=35835
ion-implanted in Si, diffusion from subst. to interstitial sites 8=40007
liquid, adhesion to Al 8=39336
liquid, structure temp. dependence by X-ray diffr. exam. 8=25873
non-Londonean resistance jump 8=40371
oxidation, formation of surface "molecular clusters" 8=45343
phonons, transverse microwave, e.m. generation freq. depend. 8=49087
photoelectron emission on X-ray excitation, energy distrib. 8=40707
photoeffect, I-V characts. on X-irradiation and at 6000 V 8=27325
resonance radiation, electrodeless h. f. source 8=24380
stopping power for 3. 75–5. 5 MeV proton, using (p. n) obs. 8=43030
surface impedance in mag. field perp. to surface of metal 8=49125
surface migration, from field-emission studies 8=27343
thermal expansion from X-ray powder diffr. exam. 8=443
thin films, critical field, influence of structure disorder and defects 8=40382
vapour, absorption spectra in 250-150 nm region, S^2p-Sp^2 transition cross sections obs. 8=47486
CdS-In contact region, dark current relax. obs. 8=44916
In(III) coordination no. in aq. solns. determ. by p.m.r. 8=39431
In(III) electrode in $NaNO_3$-KNO_3 eutectic, linear sweep voltammetry 8=27750
In-CdS-In system in constant elec. field, non-stationary processes 8=35990
Sn^{119m} isomer shift 8=26015

Indium compounds
alloys, cold rolled, effect of alloying additions on twinning activation energies 8=35217
In-Ag alloys, internal and external oxidation 8=49874
InAs, alloyed diodes, capacitance depend. on reverse voltage 8=27181
InAs, elastically deformed, elec. field gradient at nuclei from n.m.r. obs 8=31909
InAs electroreflectance rel to interband transitions 8=49728
InAs, energy band parameters at 20, 80 and 298°K 8=40240
InAs film microminiature Hall probe 8=28509
InAs, films, annealed, elec. props. 8=44794
n-InAs, magnetophonon oscillations in longitudinal thermoelec. power 8=27308
InAs, magnetoresistance, anomalous, in two dim. transport below 4.2°K 8=35905
InAs p-n junction, radiative recombination mechanism 8=36489
InAs, quadrupole relax. time and chemical shift rel. to covalence 8=31928
InAs solid solns. with $A^{I}B^{VI}$ type cpds., reflection spectra 8=41099
InAs:Cu, elec. props. rel. to effect of Cu and decomp. of solid soln. 8=40473
InAs-GaAs alloys photocond. and impurity levels, obs. 8=27324
n-$InAs_xSb_{1-x}$ alloys, e scatt. from thermoelec. and Hall coeff. obs. 8=35758
n-$InAs_xSb_{1-x}$ alloys, free-carrier Faraday rot. obs. 6-25μ 8=36370
n-$InAs_xSb_{1-x}$ alloys, Hall coeff., elec. cond. and thermoelec. power obs. 8=40475
In-Bi complex eutectic liq. alloys, atomic distrib. character 8=25871
InBi film, Mn layers on each side, proximity effect obs. via thermal conductivity 8=40372
In-Cd solid solns., densities 8=43977
In-Ce solid solns., superconductivity, resistivity and thermoelec. power rel. to localized moments 8=31339
InGa alloyed junctions, tunnelling electrons scatt. by impurity vibrs., 1-10°K 8=35938
InGaAs:Cr photocond. rel. to InAs trap level, obs. 8=27324
InGaAs:(Cr, Zn) photocond. rel. to trap and acceptor levels, obs. 8=27324
$In_{1-x}Ga_xSb$, solid solutions, thermal conductivity temp. dependence 8=44363
InI_3 discharge lamp, temp. distrib. determ. 8=43454
InI_3 h.p. discharge, ionization and dissoc., theory 8=43455
$In_2(MoO_4)_3$, mol. struct., X-ray obs. 8=30900
In_2O_3 grown from PbO-B_2O_3, etch pits and tubes rel. to crystal growth 8=44103
In_2O_3 sputtered films, electrical props., intrinsic desorption 8=40469
In_2O_3 sputtered films, near i.r. optical props. 8=49470
InP, by screened single-particle e excitations, obs. 8=36363
InP diffused p-n junctions, I-V characts., 77-590°K 8=35921
InP, p-n junction radiative recomb. mechanism 8=27159
InP, p-n junctions, radiative recombination mechanisms 8=41197
InP, quadrupole relax. time and chemical shift rel. to covalence 8=31928
In-Pb alloy, upper crit. field, temp. and mean free path depend. 8=31340
In-Pb alloys, dil., NMR 8=45125
In-7.05 wt.% Pb alloy, type II superconducting, sp. ht. rel. to irreversibility effects on Maki's parameters 8=44342
In-Pb alloys, type II superconductors, comparison with Caroli-Cyrot theory 8=39946
InS, synthesis in Ga and In melts 8=48563
β-In_2S_3, domain struct. due to ordering of In vacancies 8=48599
InSb, extraction of Cu 8=44582
p-InSb, impurity photoconductivity spectra 8=44926
InSb, magneto-optics, polaron effect 8=49729
InSb, microwave instabilities in plasma, theory 8=26930
InSb, quadrupole relax. time and chemical shift rel. to covalence 8=31928
p-InSb, surface photoconduction 8=44927
InSb(As, P), transformation produced by Ga 8=48384
n-InSe, absorpt. and reflection spectra, optical transitions 8=45196
n-InSe, fundamental absorpt. spectra and optical transitions 8=41100
InSe, thermal cond., 100 to 600°K 8=44364
α-In_2Se_3, h.f. conductivity 8=27244
In-Sn alloys, dil., NMR 8=45125
In_3Te_4 thin layers, crystallographic, optical and photoconducting props. 8=39796
indium antimonide
See also Semiconducting materials/indium antimonide.
bolometer, Rollin free-carrier, heterodyne detection at mm wavelengths 8=23995
crystal growth characts. and impurity incorporation during facet growth 8=48820
crystal orientation determ. by light reflection 8=39645
far infrared spectroscopic detector appl. 8=32939

Indium compounds—contd
indium antimonide—contd
Faraday rotation, use for making circulators and isolators 8=49693
lattice vib. curves and phonon spectra 8=26576
magneto-optical interband transition linear-$\vec{k}$ valence-band splitting, obs. 8=36373
photoelectron emission on X-ray excitation, energy distrib. 8=40707
photomagnetic effect oscills. in n-type rel. to e heating 8=31456
photon absorpt, with phonon creation and excitation of electronic impurity state 8=40665
photoresistors, optical heterodyne effect 8=36372
plasma coherent emission prod. mag. field, obs. 8=32001
n-type, high mobility, resonant and round trip acoustoelect. gain 8=44797
r.f. emission, 10MHz to 10GHz, under influence of mag and elec. fields 8=36371
u.s. wave amplification under d.c. operating conditions and transverse mag. field 8=39893
InSb, resonant-polaron-coupling from cyclotron resonance and magneto-optical exam. 8=40270
InSb-GaSb alloys photocond. and impurity levels, obs. 8=27324
InSb-GaSb heterojunction, lattice mismatch accommodation, 8=48857
InSb:Te, impurity heterogeneities from multiple-beam interferometry, 8=48821
Inductance
superconducting structure, self and mutual 8=27009
superconductor, modulation by mag. field, appl. 8=31348
Inert gases
See also the individual gases.
absorption spectra in vac. u.v. region 8=43196
adsorption on Ar and Xe crystals at (100) face, Van der Waals interactions 8=39617
adsorption on Ar and Xe crystals at (111) face, Van der Waals interactions 8=39618
alkali metal collisions, interactomic pot. 8=47541
alkali-metal-seeded, breakdown voltage 8=47759
analytical potential models and props. 8=30272
arcs, low-voltage, pressure and impurity effects 8=47773
atomic beam, e scatt. 40-150 eV spin polarization obs. 8=34175
convective diffusion in blood, rel. to membrane-type artificial lungs 8=43793
couples, translation band, transition probability at l.f. 8=29711
crystal lattice props., theory and expt. 8=35390
depth distrib. in solids, sputtering obs. 8=48923
diffusion in α-Al_2O_3, high resolution meas. 8=39965
diffusion in CaF_2 and U doped CaF_2, mechanism 8=26619
diffusion in ionic crystals as probe for lattice defects 8=39992
diffusion in neutron irrad. Rb halides 8=40079
dynamic viscosity meas. and statistical-mech. correls. 8=43704
energy transfer in collisions with Na atoms, rel. to fluoresc. 8=34182
fission gases, release from UO_2 fuel rods 8=34108
fission products, isotope separation and decay schemes, obs. 8=38545
in flash lamps with quartz enveloped, for research in solar engineering 8=46680
ion-atom and mol. collisions, 1-100 eV charge transfer obs. 8=38735
ionization at 10^{-3} torr, by laser-irradiation rel. to multiphonon theory 8=29964
ionization by 0.2-1.8 MeV He^+ ions, effective cross sections 8=39035
ionized magnetically, to plasma with electron temp. > gas stagnation temp. 8=37448
ions, secondary electron emission from metals, struct. of energy spectra 8=31473
ions, sputtering of metals, rel. to trapped gas 8=26726
liquid, far u.v. reflectivity cell 8=34846
matrices for e.s.r. meas. on Cd^+, Cr^+, Mn^+ 8=40202
mixture, collision-induced translational absorpt. theory 8=34384
metastable excitation by e impact, total cross sections 8=25377
optical third-harmonic coeff. calc. 8=39214
photoionization cross section meas. 8=29949
Rayleigh light depolarisation, press-induced 8=39217
rare gas diffusion in solids, appl. of linear heating tech., depend-on grain size 8=26617
in reactor fuels, fission-prod. bubbles nucleation 8=31109
scattering from Ag surface 8=39575
solid, vibrational energy, zero-point 8=48692
solids, vacancy conc. and diffusion 8=44415
solubility at high press. in fused $AgNO_3$ 8=25949
solubility in alcohols, heats of evaporation and free enthalpy 8=39319
solutions in H_2O 8=48077
terrestrial abundance 8=36677
van der Waal's const. with alkali atoms 8=25388
Cd 6^3S_1 level depolarisation in collisions, cross section, obs. 8=38692

Inert gases—contd
Cs collision excitation transfer cross-section calc. 8=47543
Cs thermionic diode, optimum pressure 8=41974
H collisions, Lyman-α excitation cross-sections 8=38760
H collisions, Lyman-α polarization 8=38759
Hg^{198} atom collisions, relax. cross sections, temp. effect 20°-600°C 8=29664
N^{15} spectrochemical estimation, enhancement 8=27791
Ne-Kr system, phase separation 8=43675
Rb collision excitation transfer cross-section calc. 8=47543
W bombard., thermal desorption obs. 8=48497
Inflammability. See Combustion.
Information theory
See also Entropy; Random processes; Statistical analysis/applications.
Calen and Welton formula, discrepancy 8=32671
computer retrieval of papers in acoustics 8=37254
correlated and single events, simultaneous analysis by sampling 8=46854
holographic television system loss 8=33293
image quality, theoretical prediction 8=28741
kinetic eqns. derivations 8=37189/90/91
local equilib. distrib. appl. 8=23876
nuclear reactions, communication theory 8=33969-70
optical systems, information-processing, optimization by transcorrelation-function maximization 8=28740
optimal algorithm, principles, consequences and applications 8=23783
photon beam, superposition of 2 thermal beams 8=41852
pulsed nuclear rad. meas., appl. to prod. new circuit 8=46935
radiographic images, calc. of max. entropy or information capacity 8=46770
transfer function applic. in image optics 8=28736
Infrared detectors. See Bolometers; Radiation detectors.
Infrared sources. See Light sources; Radiation/heat.
Infrared spectra. See Spectra.
Instruments
See also Laboratory apparatus and technique; Measurement; Recording; and under specific subjects, e.g. Astronomical instruments. Some specific instruments are listed separately, e.g. Spectrometers; Thermometers. Where no separate headings exist, entries describing instruments may be found included under the headings of the appropriate quantities or subjects.
cross-correlation, effect of instrumental time-lag or filtering 8=45948
electronic graph-signal convertor 8=46316
joulemeter for exploding bridgewire firing sets 8=32938
Insulating materials, acoustic. See Noise abatement.
Insulating materials, electrical. See Dielectric properties of substances.
Insulating materials, thermal. See Conductivity, thermal.
Integral equations
approximate solutions, in theory of elasticity and mathematical physics 8=45980
adhesive contact with incremental loading, Wiener-Hopf eqn. 8=28270-1
excluded-volume effect in polymers 8=29869
first kind, reduction to secondkind 8=46030
Fredholm, reducible to initial value problems 8=45987
Fredholm simultaneous, soln. rel. to distributed-parameter reactor control 8=34098
Fredholm system, soln. in power series 8=46028
Hartree-Fock integro-differential eqns. for atoms 8=29587
ionosphere e density, height distrib., rel. to radio absorpt. 8=41422
Kirkwood-Salsburg, superposition approx. 8=34570
nonsingular, for partial-wave amplitudes 8=42419
Percus-Yevick-II, for binary fluid mixture 8=30193
in quantum mechanics, integral-differential system, numerical soln. 8=46798
radial distribution function 8=30192
series-expansions for functions satisfying the equations 8=32659
special class of first kind, applic. to contact problems for cylindrical elastic bodies 8=45982
Integrals
See also Calculus.
atomic, containing $r_{23}^{\lambda} r_{31}^{\mu} r_{12}^{\nu}$ 8=29583
collision integrals for high-temp. gases 8=34670
complex domain, Laplace equation solution generation 8=45986
Dirichlet problem, soln. by block iteration 8=41628
electronic transition moment integrals 8=25460
Fermi, evaluation 8=41779
Feynman, and homology, book 8=33338
Fourier, involving $\tan^{-1}t$, expression in closed form 8=32657
Fourier, numerical evaluation 8=37112
Fourier, series representations 8=45975
functional, theory of Brownian movement 8=37182
Ladenburg-Reiche, generalization anal. 8=34438
of motion in Poincaré subgroups 8=24457
multicentre, of r_{12}^{-1} in Slater-type orbitals 8=38600-2
relations method, in laminar free mixing problem 8=25819

Integrals—contd
sine and cosine 8=45976
thermal neutron scatt., convergent approximation 8=26354
Pu atom, configuration-interaction calc. 8=38679
Intensity measurement
two close objects, and apparent separation 8=24368
wedge crystals, multi-beam intensity profiles, absorpt. effect 8=45150
acoustics
sound distribution at low freq. in rectangular enclosure 8=23951
surface-integral directive power meter 8=32915
Interatomic forces, between bound atoms. See Bonds; Molecules/internal mechanics; Solids.
Interatomic forces, between free atoms. See Collision processes.
Interface tension. See Surface tension.
Interference
electrons, on charged C film edge, obs. 8=37419
e microscopes, mean internal potential determ. 8=46414
i.r. interf. filters, props. 8=32937
waves, sub.-mm., over 450m. path diff. 8=33278
X-ray, in thin films 8=48435
acoustic waves
No entries
electromagnetic waves
bar, oscillating, microwave meas. of deflection 8=37238
Cherenkov, proximity of conductor 8=24707
plane waves in anisotropic medium, nonlinear interaction 8=37486
Michelson, multiple-refl. correction in velocity meas. 8=42017
in space between probes in microwave radiographic devices 8=24216
wavefront reconstruction for synthetic antenna data processing 8=37524
light
beams from same and difference sources, intensities derived 8=28718
coherent averaging of interferograms, and digital minimizing of errors 8=28862
diffusion constants of dil. polymer solns. by Moiré fringe patterns, increase in sensitivity of meas. 8=48117
diffusion meas., Moiré interference method 8=48119
filters, all-dielectric, 2500-4000Å 8=28762
filters, bandwidth rel. to ref. index of central layer 8=24376
fringes of equal thickness, use in photoelectricity 8=46741
fringes produced by photographic scatterers 8=46721
Huyghen's principle in media of variable density 8=37689
independent beams and resulting phenomena 8=46725
laser material coating, single layer antireflection, mismatch 8=42060
microscope, out-of-focus transfer function 8=28755
Moiré effect used in determ. of slip component parallel to a marker line 8=40046
Moiré fringes, applic. to accurate meas. of minute displacements 8=46729
Moiré fringes, effect of gap between gratings 8=46727
Moire fringes for system of transparent and reflection gratings 8=28872
Moiré obs. mismatch by diffraction effect 8=33273
Moiré patterns formed by inclined gratings 8=42247
Moiré patterns, real-time holographic, for flow visualization 8=37710
photographic emulsions, thick, verification of Wiener's expts. 8=46766
photon beams, independent at low intensity, laser expt. 8=42248
photons, statistically independent monochromatic, theory 8=46726
projection screen scintillation 8=46723
quartz, laser-illuminated, interferometric analysis and separation of three Brillouin scattering components 8=36408
refractive index small changes meas. 8=46722
scanning confocal, high resolution 8=42245
spectrum meas., photographic appl. 8=28792
teaching demonstration, lower-order multiray fringes 8=28854
two-beam, path-difference in dispersive medium rel. to temperal coherence 8=28852
two independent laser beams of small intensity 8=42249
visibility of fringes, effect of slit width and nonmonochromaticity 8=28867
Kr^{86}, wavelength standard, reproducibility for abs. meas., discussion 8=23789
ZnS-MgF_2 layer Fabry-Perot filters, max. transmission wavelength, H_2O vapour effects 8=28763
Interference spectroscopy. See Spectroscopy.
Interferometers
automatic, with digitalor analog readout, for refractometric anal. 8=28750
dielectric meas., mm. and sub-mm., with interference spectrometer 8=49323
electron, point cathode source 8=41952
Fabry-Perot, defocused, for pulsed laser sources 8=42250
Mack-Zehnder with colour film for electron density meas. in plasma 8=30094
Michelson, with cats eye reflectors, for wide range Fourier spectroscopy 8=28813

Interferometers—contd
    multi-ray, for use in gas dynamic investigations, optimum adjustment 8=39181
    refractive index meas. in i.r. region 8=42246
    X-ray, Z-crystal, construction and operation 8=37733
  acoustic waves
    No entries
  electromagnetic waves
    dispersion types, differential and absolute, gen. props and 2-freq. and 3-freq. cases 8=24217
    microwave, multiple-refl. correction in velocity meas. 8=42017
    in 3-5 mm range, for meas. dielec. const of plane specimens, and elec. thickness of radomes 8=27222
    X-band using 90° unbalancing, for plasma e density decay 8=25763
  light
    for astronomical spectroscopy, Mock interferometer, telescope mounted, visible and near i.r. 8=32412
    beamsplitters, thin-film far i.r., polarization props. 8=28851
    cube corners, and assoc. electronics 8=28780
    with diffraction grating, for investigating flow round models in shock tube 8=39172
    displacement meas. optical system 8=41619
    Fabry-Perot, astronomical, for rocket appls., 1700-5500Å 8=32411
    Fabry-Perot, astronomical, improvements 8=32415
    Fabry-Perot, astronomical, use with telescope, non-uniform illum. effects 8=32410
    Fabry-Perot confocal resonator, curvature deviation 8=42215
    Fabry-Perot confocal spherical mirror, theory and use 8=37685
    Fabry-Perot etalon analysed 8=28718
    Fabry-Perot, method for increasing the transmitted light 8=46728
    Fabry-Perot plates charting, Michelson interferometer meas. 8=28849
    Fabry-Perot, plate spacing automatic control 8=28819
    Fabry-Perot, wedge-shaped, appl. to study of rarefied, supersonic air flow 8=30243
    Fabry-Perot, with electromechanical scanning system 8=46696
    Fabry-Perot, with remote control 8=46724
    Fizeau, for flatness testing of optical surfaces to 240mm. dram. 8=28859
    lamellar with saw-tooth drive as Fourier spectrometer for far i.r. 8=28812
    Mach-Zehnder, astigmatism 8=28863-5
    Michelson, balloon-borne for solar Fourier spectroscopy, 10-100μ 8=32571
    Michelson, double-passed, photometric-setting accuracy effect of surface errors and misalignment of end mirrors 8=28858
    Michelson, effect of sinusoidal polish errors 8=24414
    Michelson, for absorption, spectroscopy and refractometry 8=33272
    Michelson's spatial coherence calc. 8=28718
    Michelson stellar, variant, converged beams coincident 8=33276
    Michelson, thin film beamsplitters efficiency, far i.r. 8=28850
    Michelson, use as earth strain sensor 8=27848
    Mobius band, tilt compensated, use of Fourier spectroscopy 8=28814
    multi-beam, fringe apparent broadening rel. to eye response curve 8=28866
    multibeam, multiple wavelength systems 8=37688
    1 km laser, for earth strains 8=50061
    1-metre line-standard interferometer 8=45951
    for plasma meas., multichannel Fabry-Perot with Fresnel lenses 8=30089
    plasma transient Stark and Zeeman shifts, Fizeau interferometer meas. 8=30088
    for plasma u. v. emission lines Doppler breadth, multi-channel fast scan Michelson interferometer 8=30090
    precision with 3 slits, and Frucoutt gratings 8=28860
    Rayleigh's spatial coherence calc. 8=28718
    refractive index distrib. direct recording 8=28861
    reference equipment for reproducing unit of length 8=45949
    for solar and dayglow meas., photoelec. Fabry-Perot, magnetostriction scanned 8=32272
    for solar monochromatic images, Fabry-Perot etalon appls. 8=45857
    spectrometer, double Fabry-Perot, scanning synchronization and plates parallel spacing, servocontrols 8=28821
    spectrometer, double Fabry-Perot, press. scanned and digital recording 8=28796
    spectrometer, PEPSIOS scanning three Fabry-Perot, high resolution 8=37674
    spectrometer, photoelec. Fabry-Perot, press. scanned for low intensities 8=28820
    spectrometer, photoelectric multi-channel, Fabry-Perot etalon and axicon mapping 8=28804
    spectroscopy, Fourier interferometers and computer system for far i. r. 8=28799
    stellar, at Narrabi Observatory 8=41510

Interferometers—contd
  light—contd
    stellar, precision meas. 8=28752
    triangle path 8=37687
    for twilight and zodiacal light, press. scanned Fabry-Perot 8=32568
    two-beam, use as i.r. Fourier transform spectrometer 8=28815
    upper atm. spectroscopy, Fabry-Perot appls. 8=32271
    visibility phase meas. in presence of atmos, seeing, technique 8=28857
    Young's, spatial coherence calc. 8=28718
    Zeiss interference microscope, densification of glass under cutting wheel 8=39724
Interferometry
    alignment of 2 mile accelerator using large rectangular Fresnel lenses 8=42173
    Gaussian light beam width obs. 8=33166
    hologram, anal. and appl. to determ. of deforms 8=42263
    laser, for plasma jet e density meas. 8=30085
    Mach-Zender, free convection field obs. 8=23009
    Michelson, velocity calibration of Mössbauer spectrometer 8=37927
    piezoelectric plate mode determ. 8=41828
    quartz, third-order elastic moduli, pulse-echo obs. 8=49050
    radar, plasma width determ. for turbulent column 8=47857
    shearing, by wavefront reconstruction 8=42274
    stroboscopic hologram, rel. to surface vibr. modes 8=32883
    zone plates, partially achromatic, holographic production and evaluation 8=42273
    Be plasma, laser produced, e density profile 8=25760
    CS, Zeeman effect from millimeter interferometry 8=38814
  acoustic waves
    ethane-Ar mixtures, u.s. vel. dispersion meas. 8=47966
    ultrasonic, high-temp. shear in molten glass 8=39280
    ultrasonic, monitoring of thin film growth 8=44031
  electromagnetic waves
    long-baseline, effect of earth tides 8=45423
    microwave spectrum, coherence function meas. 8=37451
  light
    angle meas. using lasers 8=45950
    aurora, 5577 Å emission temp. meas. 8=41400
    curvature definition by f.m. amplitude gratings 8=35616
    Fabry-Perot automatic scanning etalon 8=28848
    Fabry-Perot with confocal spherical mirrors, use 8=37685
    Fizeau fringe separation, moiré meas. 8=33275
    fringe projection for non-optical surface topography 8=26093
    glasses, refractive index meas. 8=37636
    heat transfer, refr. error evaluation 8=28395
    hologram-Moiré, transparent objects 8=37706
    holographic apparatus, control of vibr. and limited coherence effects 8=33289
    holographic applic. to comp. of highly polished reflecting surfaces 8=31936
    holographic interferrogram cinematographic recording for time-dependent object changes 8=46760
    holographic surface contouring by limited depth focusing 8=37705
    holographic, with u. v. light 8=33286
    holography, white-light reflection, appls. 8=28896
    interferogram phases rel. to spectra analysis 8=28782
    interferograms zero-order correction and extrapolation 8=28783
    laser, fringe visibility rel. to speckling 8=33277
    laser surfaces, parallelism determ. using coherent light 8=37550
    microscopy, applic. of holography 8=37656
    moiré fringe obs., anti-parallax grating system 8=33274
    moiré pattern form. by radial gratings, theory 8=33279
    multibeam, multiple wavelength systems 8=37688
    multiple-beam, of impurity heterogeneities, 8=48821
    nitrogen conc. determ. in gaseous mixtures 8=49988
    1-metre line-standard interferometer 8=45951
    optical flats, contour determ. 8=37686
    optical materials, small samples, thermal expansion meas. 8=35439
    optical wave-front mapping by dual interferometry 8=28853
    oxygen conc. determ. in gaseous mixtures 8=49988
    phase object measurement for phase hologram 8=37715
    polarization using props. of plane waves on isotropic and anisotropic media 8=28856
    reflection multi-beam, transmission fringes 8=24413
    review of pre-laser advances, precision techniques 8=28855
    spectrometry, Fourier, by transmission grating resons. scanning 8=28787
    spectroscopy, Fourier, intensity error from finite series approx. 8=28781
    spectroscopy, Fourier, interferograms modulation by source noise 8=28780
    surface displacement holographic meas. 8=37713
    transmittance, from far i. r. asymmetric Michelson interferograms, pseudo-coherence effect 8=28844
    two wave fringe, evaluation of accuracy of localization 8=46720

Interferometry—contd
- **light**—contd
  - vacuum differential manometer appl. 8=39249
  - vibration displacement meas. rel. to wavelength 8=28357
  - visibility phase meas. in presence of atmos. seeing, technique 8=28857
  - InSb: Te, multiple-beam, of impurity heterogeneities. 8=48821
  - Xe, near-critical isotherms 8=25977

Intergalactic matter. See Galaxies.

Intermetallic compounds. See Alloys; Semiconducting materials and under the compounds and alloys of the individual metals.

Intermolecular forces. See Molecules/intermolecular mechanics.

Internal conversion. See Beta-ray spectra/conversion electrons; Gamma-rays/internal conversion.

Internal friction
- alkali halides crystals., rel. to dislocation mobility dependence on electrostatic field 8=26667
- alumina, spectrum rel. to l.f. grain-boundary relax. 8=44549
- b.c.c. metals, mechanisms 8=26813
- Bordoni peak meas. in f.c.c. metals 8=26742
- calculations from statistical theory of dislocations 8=26654
- crystal point defects, thermodynamics 8=31027
- f.c.c. alloys, rel. to dislocation viscous movement 8=35615
- glass fibres, as function freq. for transverse vibs. obs. of thermal elastic relax 8=44513
- graphites, rel. to prep. process, damping coeff., expt. and theory 8=26791
- h.f., measuring apparatus 8=40097
- high-temperature, theory rel. to dislocation behaviour 8=44435
- hysteresis in microstrain regions, rel. to dislocation substructure and friction stress 8=26744
- hysteretic contrib. rel. to thermomechanical unpinning of dislocations 8=48839
- kinks in dislocation lines, effects 8=26743
- metals in alternating bending, thermal activation energy determ. 8=35613
- polycrystalline specimens, amplitude depend. 8=40098
- spodumene, twinned, meas. and mechanism 8=49033
- steel, austenitic stainless, meas. rel. to stress corrosion cracking study 8=40159
- steel, Snoek effect 8=26747
- steels, with f.c.c. lattice of solid soln., diffusion peak comp., ht. treatment, n-bombardment, grain size and texture dependence 8=35678
- for torsional oscs. of two-layer cylindrical rod 8=28362
- Ag, after cold drawing and irradiation 8=48986
- Ag films, vacuum-deposited, temp. dependence rel. to prep. 8=35650
- Al, amplitude dependent, at high deformation amplitudes 8=26776
- Au, cold drawn, relaxation peaks 8=48997
- B fibres, amplitude dependence 8=40131
- of C in α-Fe solid soln., effect of osc. modes on quantitative anal. 8=35695
- C, vitreous, 4-570°K 8=44557
- CoO, anomalies rel. to mag. phase transition 8=44560
- Cu-Zn alloys, abraded, rel. to surface and subsurface structure 8=26294
- Fe, changes during $\alpha \rightleftharpoons \gamma$ transform. 8=40152
- Fe, effect of H 8=31207
- Fe, high-purity, multiple $\alpha \rightleftharpoons \gamma$ transforms. effect 8=35700
- Fe, peak due to dislocation dragging by interstitial impurities 8=26814
- Ge, pure and In doped, peak rel. to dislocations in 100 to 300°K range 8=35703
- K, O contaminated, relax. peak at 160°K, rel. to precipitates 8=49029
- LiF, rel. to crystal orientation under application of static compressive load 8=44585
- LiF, rel. to dislocation interaction with point defects 8=26683
- Li_2O. 2.5 SiO_2 ion-exchanged glass fibres 8=40168
- Mo–C, rel. to C diffusion mobility determ. 8=35513
- Na, nomially pure 8=49029
- Na silicate glasses, at high-temps. rel. to vacancy model for ionic transport 8=40176
- NbC-graphite composites, thin rods 8=49040
- Ni, effect of H 8=49041
- Ni, from grain boundary relax. and damping peaks 8=48872
- Pb(Zr, Ti)O_3 ferroelec. ceramic, temp. dependence rel. to 90° domain wall-pt. defect interaction 8=44405
- Ta wire, loaded with N rel. to Snoek damping 8=48468
- Tb, variation with strain amplitude 8=49475
- TiNi, temp. dependence, –170 to 800°C 8=26847
- U oxides, hyperstoichiometric, and Young's modulus, at room temp. 8=35722
- UO_2, relax. peaks rel. to reorientation of interstitial O atoms 8=35545
- W–C, rel. to C diffusion mobility determ. 8=35513
- Zn twinned crystals, peak at 265°K due to stress relax. at twin boundaries 8=35727
- Zr, corrosion in breakaway region, rel. to inelastic behaviour of metal and oxide 8=36576

- **liquids**. See Liquids: Viscosity/liquids.

Internal stresses. See Stresses, internal.

Internuclear double resonance (INDOR). See Nuclear magnetic resonance and relaxation.

Interplanetary magnetic fields
- axisymmetric dynamo, steady 8=41524
- cosmic ray accel. at solar wind boundary 8=47182
- cosmic ray periodic variations associated with field's sector structure 8=42750
- cosmic ray variation w.r.t. fields' sector structure 8=42748
- cosmic rays propag., regular and random 8=42703
- direction distribs. rel. to polar mag. disturbances 8=41466
- effect on energy of geomag. disturbances 8=41467
- galactic, structure 8=36969
- influence on geomag. activity 8=45570
- interaction with solar wind 8=50438
- interstellar field 8=45852
- macro- and micro-structure 8=41575
- micro-scale ($\lesssim$0.01AU) structures in combined mag. field and plasma data 8=37030
- Moon's wake of solar wind 8=50395
- orientation, deduced from second spherical harmonic of diurnal variation 8=42752
- perturbations by linear wake 8=37031
- power spectrum rel. to low rigidity cosmic ray modulation, 1962-5 8=42677
- protons associated with solar activity centres, propag. in field corot. sun 8=41587
- quiet, sector struct., distrib. of energy density and press. 8=45849
- re-connection at tangential discontinuities in solar wind 8=45854
- regular, magnitude estimate from anisotropic stage of cosmic ray bursts 8=37038
- sector struct. rel. to mag. activity diffs. between two hemispheres 8=41478
- slope from cosmic ray diurnal variation 8=42744
- small-scale inhomogeneities of mag. field of solar corona and of interplanetary plasma 8=45848
- solar cosmic ray particles, effect of interplanetary magnetic field on propagation 8=38152
- solar magnetic pattern extending over equatorial latitudes 8=41580
- solar origin and terrestrial effects 8=32566
- structure in plane perpendicular to ecliptic 8=37037
- variation and cosmic ray intensity, short period fluctuations 8=47192

Interplanetary matter
- blast waves, singular var. near contact discontinuity 8=45853
- cosmic dust, activation by cosmic rays, as 'signature' for accretion by Earth 8=28168
- cosmic dust collection on Luster I and II, and of exposed surfaces, and of particles 8=41372
- cosmic dust, detect. by impact ionization 8=50437
- cosmic dust sensors, microphone type, appl. of microparticl hypervel. impact studies 8=41577
- cosmic rays transport 8=42673
- density in moon vicinity, rel. to halo or passage thro' dust aggregate 8=37033
- dist., distrib. model rel. to obs. of brightness of zodiacal light 8=45856
- distribution, from photometry of zodiacal regions in quadrature to Sun 8=45855
- dust, anal. of data from various sources to obtain inter comparisons 8=37035
- dust, 'effective collection time' in rocket expts., standard basis for comparison of results 8=37029
- dust, noise from ceramic transducer sensors, effects of thermal grad. and temp. 8=41576
- dust particle data during meteor showers, flux of microparticles 8=41346
- environment, effect on thermal-control coatings 8=32562
- German radioastronomical obs. 8=32612
- inhomogeneities rel. to solar spicules 8=37079
- ion flux, positive, energy distrib. and flow characts., to 75 earth radii 8=37036
- meteoritic-dust, space density of particles from craters and contamination of thin films 8=37027
- micrometeorite expts, by Gemini spacecraft, equipment, techs. and exposure conds. 8=41578
- micrometeorite impact data on mats, and influx model 8=41579
- micrometeoroid collection by Gemini 9 and 12, flux anal. from study of exposed surfaces 8=37026
- micrometeoroid impact simulation, study of craters and penetration 8=37028
- micro-scale ($\lesssim$0.01AU) structures in combined mag. field and plasma data 8=37030
- plasma, collisionless anisotropic, hydromag. wave propag. 8=34484
- plasma, energy density and press., rel. to geomag. activity 8=45570
- plasma, small scale inhomogeneities of mag. field 8=45848
- plasma, struct. heterogeneities rel. to temp. anisotropy 8=45851
- protons associated with solar activity centres, propag. in mag. field corot. sun 8=41587
- scintillation of OH emission from Sagittarius B2 8=45850

Interplanetary matter—contd
scintillation obs. and effect of finite receiver bandwidth 8=41574
solar particle energetic propagation and space structure 8=41589
solar wind, Parker's, plasma flow with 3D heat source 8=37061
USSR apparatus and obs. 8=32523
zodiacal dust meas., and in cis-lunar space, from OGO III and Mariner IV expts. 8=37034
H, neutral, and helosphere radius 8=41573

Interstellar matter
absorption bands, diffuse, origin 8=28062
absorption, continuous, effect on spectral line formation 8=50337
absorption, galactic nebulae photography 8=28098
atomic and molecular abundances of specific medium, from interstellar line spectrum of ζ Oph 8=32442
axisymmetric dynamo, steady 8=41524
colour centres in grains, 8=50349
contracting gas cloud, effect of ohmic diffusion on mag. field distrib. 8=36965
cosmic dust, activation by cosmic rays, as 'signatures' for Accretion by Earth 8=28168
cosmic ray nuclei confinement 8=41494
Cygnus region, structure of galactic neutral hydrogen 8=50347
diffuse absorpt. bands, origin 8=28099
diffuse galactic radiation scatt. 8=28092
dust condensation in galactic explosions 8=45728
dust, refl. nebulae brightness, colour and optical polarization 8=28097
dust scattering props. from diffuse galactic light 8=45730
extinction law, non-uniformity 8=50351
galactic plasma, confinement by mag. fields 8=41527
galactic plasma, dynamics 8=50346
in Galaxy, gas gravit. condensation rel. to stars vel. relax. 8=45733
garden-hose instability, growth rate due to cosmic rays 8=45729
gas and dust clouds, collision 8=45725
gas cloud, collapsing, stability against fragmentation 8=50301
gas cloud, homogeneous rotating, ang. momentum and energy rel. to evolution of young stars 8=32431
gas clouds model, numerical methods 8=50265
gas, condensation, struct. changes in contracting HI cloud 8=50293
gas, cooling after collisional heating 8=50350
gas density rel. to u. v. and X-ray backgrounds outside atm., obs. 8=32490
gas, properties and problems 8=50352
gaseous arm stability, galactic rotation effects, 8=50365
gaseous sphere, rotating, equilib. state and meridian circulation 8=32491
grains temperature 8=36964
gravitational instability of interface separative two streams of homogeneous medium 8=28100
gravitational matter contribution rel. to stellar formation 8=50348
horizintal-branch stars at high altitude 8=32479
interaction with supernovae remnants 8=50326
intergalactic gas, possible thermal history 8=50345
magnetic field, meas. from radio waves of CPO950 8=45724
magnetic field, meas. using linear polarization of radio emission 8=32495
magnetic field, random walk of lines and cosmic particle trajectories 8=41526
optical absorption features 8=41525
Orion, 8 GHz continuum and H II recomb. line obs. 8=32489
plasma, gravit. instability 8=32492
plasma, magnetized, collisionless, self-gravitating, cylindrical wave propag. and instability 8=30143
plasma, gravitational instability, Jeans criterion determ. 8=41528
quartz grains, extinction curves 8=28096
stellar plasma, self-trapping and redshift of incoherent light 8=45726
X-rays, soft, absorpt. cross sections, calc. 8=45727
Be^9 abundance, obs. 8=36927
H atoms and dust, relative abundance and grain density 8=45731
H, neutral, in Galaxy, distrib. and possible correl. with Gould's Belt 8=45723
H, neutral, maser action at 21 cm 8=28090
HI clouds interactions with cosmic rays 8=42712
HI regions, heating by energetic particles 8=50344
H II region temp. calc. 8=28091
H II regions, excited H lines 126, 127α obs. 8=32488
H^2 abundance, obs. 8=36927
H_2 in southern Coalsack, absortive search 8=28093
H_2^+ radio-frequency spectrum, abundance obs. 8=45722
He^3 abundance obs. 8=36927
$Li^{6,7}$ abundance, obs. 8=36927
OH prod. in shock waves 8=28095
OH, stimulation by phonons 8=28094
Th nucleosynthesis by heavy-ion reactions 8=41505

Interstellar matter—contd
U nucleosynthesis by heavy-ion reactions 8=41505

Interstitials. See Crystal imperfections/interstitials.

Iodine
adsorption on oxides, refl. spectra 8=48479
atom, absorpt. series and ionization potential 8=38663
atom, core-electron binding energies, chem. effects 8=38620
atom, e scatt., E_e=20 eV-150 keV, relativistic effects 8=38720
bonds, 5p electron population 8=35040
deep sea sediments, abundance 8=36688
diffusion in UO_2, UC and U doped CaF_2 8=34107
electrical conductivity, anisotropy in single crysts, a. c. and d. c. meas. 8=27107
electrical resistivity effect of dissociating and thermally stable gaseous impurities at 350°C 8=48203
ions, electron capture between 19 and 55 MeV 8=39040
ions I^- collisions with He, Ne, Ar and Kr atoms, detached electrons energy obs. 8=29972
molecule, vibrational deactivation depend. on ratio of collision time to period of vibr. 8=34252
molecules spin polarization calc., 300-400 eV 8=34214-5
n.q.r. spin echo, indirect spin-spin interactions, beats 77°K 8=41011
photoionization, 2 photon, discrepancy 8=34453
polyethylene doping, elec. cond. enhancement 8=40596
reaction with active N rel. to u. v. chemiluminescence 8=49887
reactions activated by radiative neutron capture in liq. hydrocarbons 8=41296
u.v. absorption of ions in aqueous solution 8=34820
u.v. photon counter props. 8=46672
vapour reaction with metals at room temp., effects of Co^{60} γ-irrad. 8=36555
I^{127} in Te crystals, quadrupole coupling 8=36284
I^{127} ion beams in mylar, stopping powers 8=44508
I^- centre in AgCl, excited-state structure 8=45257
I_2, dissoc. e attachment at 295°K, obs. 8=47790
I_2, freq. shift of stretching vibr. in liq. mixtures 8=34875
I_2^- centres in PH_4I, e. p. r. 8=31124
I_3^- in $N(CH_3)_4I_3$, structure studies 8=30649
$I_2(B^3\Pi_{ou^+})$, time resolved emission 8=34251
N-I, flames, i.r. emission 8=49890

Iodine compounds
α-HIO_3 crystal, soln. grown, nonlinear, optical obs. and appl. 8=32000
$I^{129}CN$, Mossbauer effect 8=30643
IBr, ICl and ICN, reactions with active N rel. to u.v. chemiluminescence 8=49887
IBr, Mössbauer effect in I^{129}, chem. bonding 8=35040
IBr, Mössbauer effect in I^{129}, lattice dynamics 8=35041
$IBrCl^-$ in NH_4BrICl, structure studies 8=30649
ICl, Mossbauer effect in I^{129}, chem. bonding 8=35040
ICl, Mössbauer effect in I^{129}, lattice dynamics 8=35041
ICl, Stark effects in $A^3\Pi_1$-$X^1\Sigma^+$ transition 8=25488
ICN, laser emission at 538μm, mechanism and time behaviour 8=37615
I_2Br^- in CsI_2Br, structure studies 8=30649
I_2Cl_6, Mössbauer effect in I^{129}, chem. bonding 8=35040
I_2Cl_6, Mössbauer effect in I^{129}, lattice dynamics 8)35041
I_2Cl_6, Raman spectrum 8=45195
KIO_4, metaperiodate, thermal expansion 8=35444

Ion beams
See also Ion optics; Mass spectrometers; Particle accelerators: Particle range: Sputtering.
aberration and lateral displacement by 2-D fringing fields 8=41985
bunched, defocusing by space charge 8=33103
chopper for mass spectrographic analysis 8=27779
cross sectional distrib. monitor 8=46439
current regulator for linac 8=46438
duoplasmatron, ion sources 8=46435
duoplasmatron source for thin film sputtering 8=48442/3
electronic stopping cross-section, Z, depend. 8=48893
electron-ion beams emitted by cylinder or sphere, steady-state potential distribs. 8=27339
elliptical, calc. of space charge pot. 8=33072
extraction from plasma 8=37434
focussed, uses with high current density 8=24167
focusing by mag. field with circular boundaries, fringe effect, dispersion and aberrations 8=33102
guides with few repetitions, acceptance 8=46442
heavy ion irrad. of mammalian cells in vitro 8=50463
high-current, scanning system 8=33100
implantation sources for semiconds, description rel. to types of metals used 8=27068
injection and acceleration in tandem accelerators 8=24569
instability in orbital accelerators 8=33467
intense, current meas., collector method 8=46325
magnets, superconducting for beam handling 8=28995
modulated, interaction with plasma in mag. field 8=34542
negative heavy ion intense beams, ion source 8=24163
neutralization with electrons, steady state flow soln. 8=41984
in plasma hydrodynamic instability, nonlinear theory 8=43515
polarization, enhancement from Lamb-shift source, static field methods 8=37436

Ion beams—contd
- polarized, direct conversion of atomic beam 8=42352
- polarized hydrogen, spin orientation change 8=46437
- profile meas. 8=24169
- profile measurement 8=28581
- proton accelerating tube, Alvarez-type 8=24551
- r.f. separator superconducting, for accelerators 8=24550
- ribbon in short rectangular tube, pot. distrib. 8=24165
- rotating neutron target system 8=33396
- secondary beam targetry for accelerators 8=33367
- separator, superconducting, r.f., for accelerator 8=24543
- shift meas., shape of electrodes 8=46395
- in solids, charge determ. of fast beams electronic structure effects 8=44671
- in solids, penetration depth and distrib. 8=31138
- space charge neutralisation by injection of thermionic electrons 8=46441
- superconducting quadrupole magnets rel. to accelerators 8=33404
- tracks in photographic emulsions, width meas. 8=44488
- transport system for cyclotron 8=33474
- transverse current density calc., 8=24166
- trapping technique for pulsed-source mass spectrometry 8=29577
- ungridded 90° electrostatic mirror 8=37437
- water-cooled targets 8=33397
- windowless gas target as 14.2MeV n source 8=33395
- B in SiO_2, distribution and range 8=35604
- H^-, up to 1.5MeV and 1mA, production 8=46434
- H_2^+ bunching solid-state system for tandem accelerator 8=46436
- He^{2+}, acceleration in U-120 cyclotron 8=47006
- He^3, positive, polarized, prod. 8=24168
- K^+, ionization to K^+ by electron impact 8=39047
- K^+ profile obs. 8=24169
- Li^+ ions in H_2 and air, charge equilib. 8=28584
- Li^+ source for low energy expts. 8=41983
- N^+, contamination by N_2^{2+} 8=29974
- N^+, N_2^{2+} conc. in mass-14 beam 8=28583
- N_2^{2+}, charge exchange in N_2, CO_2 and Ar 8=29974
- $N^+ + O^-$ neutralization, cross section, superimposed beam obs. 8=34455
- Na^+, ionization to Na^{2+} by electron impact 8=39047
- Ne^+, bombardment damage in Si 8=44503
- O^+, abundance of excited ions in beam 8=28582
- O_2^+, abundance of excited ions in beam 8=28582
- P in SiO_2, distribution and range 8=35604
- **effects**
  - bevatron secondary beam extraction targetry 8=33486
  - bombardment-enhanced solubility, removal of thin layers from insulator and semiconductor surfaces 8=40068
  - crystal defect obs. by channelling 8=49132
  - δ-ray component calc. 8=37801
  - diamond, damaged layer exam. on bombardment with Li^7, B^{11}, P^{31} ions, 20-120 keV 8=35601
  - electric field with ion flux, soln. of eqns. 8=33026
  - elect. fields, variable, produced in beam interacting with rarified gas 8=28580
  - in ferromagnetic host, implantation hyperfine transient fields and X-ray ang. correl. 8=26011
  - films of semiconducting cpds., preparation by bombardment method 8=30750
  - magnetic field confinement 8=36822/3
  - metal polycrystals, sputtering ratio rel. to incidence 8=48899
  - metallic surface, particle luminesc. on scattering of H ions 8=49787
  - metals, low-energy inert gas bombarded, sputtering, rel. to trapped gas 8=26726
  - molecular crystals, chemical effects 8=45404
  - molecular states, accelerated beam rel. to lifetime meas. 8=43251
  - mylar, S^{32}, Cl^{35}, Br^{79} and I^{127} stopping powers 8=44508
  - noble gas ions, secondary electron emission from metals, struct. of energy spectra 8=31473
  - oxygen, rel. to copper oxide epitaxial growth 8=26116
  - penetration in channelling diodes of p-i junctions 8=44490
  - photographic plates, background blackening 8=28903
  - plasma-beam bounded system with sharp interface between 2 media, small amplitude oscills. 8=43590
  - plasma-stream system, heated, steady state oscills. 8=43580
  - permalloy films of Ar^+ on induced uniaxial anisotropy 8=31694
  - porous metals, sputtering 8=35594
  - semiconductor interactions, regularities 8=48892
  - shallow Si p-n junctions 8=40505
  - solids bombardment 8=48886
  - Ag, Kr, Xe bombard., thermal desorption obs. 8=48483
  - Al crystal, 50 keV Al^+, Cu^+ bombard., damage obs. 8=48910
  - Al crystal, K-shell fluoresc. 100-200keV 8=49788
  - Ar, on crystalline Ge, conversion to amorphous state 8=39723
  - Ar^+, X-ray production from metal surfaces 8=31130
  - As^+, type conversion and p-n junction production in n-CdTe by ion implantation 8=35882
  - Au, double-positioned, damage on bombardment by He ions 8=40073
  - Au film, transmission sputtering by H and D ions 8=44495

Ion beams—contd
- **effects**—contd
  - Au, 40 kV, dechannelling at planar defects in Ag and Au 8=35599
  - Au foil, Ar ion bombard., lattice defect penetration 8=48815
  - Au, interstitial atom clusters form. by low energy Au ion bombard 8=44418
  - Au, Kr, Xe bombard., thermal desorption obs. 8=48483
  - CdS luminescence low-temp, spectrum rel. to vacancies creation 8=36483
  - CdSe crystals. photocurrent instabilities obs. 8=49415
  - CdTe films, preparation by bombardment method 8=30750
  - Cu crystal, Xe^+ thermal desorption obs. 8=48482
  - Cu foil, Ar ion bombard., lattice defect penetration 8=48815
  - Cu, sputtering intensity in directions of dense packing rel. to incidence angle of ions angle 8=26731
  - Cu, Kr, Xe bombard., thermal desorption obs. 8=48483
  - Ge crystal, Ar^+-bombarded, structural defects, e.-diffr. exam. 8=39793
  - Ge crystal, IIIA-VA ion bombard., damage and chem. impurity obs. 8=48922
  - Ge, implantation analysis by 1 MeV He^+ scatt. 8=48927
  - H^+ and H_2^+-impact on He, rel. to polarization of 4^1D-2^1P transition 8=38697
  - H_2O drops charging rel. to clouds electrification by selective ion-capture, obs. 8=30517
  - He^+, 1 MeV, on H_2O vapour 8=49968
  - KCl, electron emission 8=40686
  - KCl lattice, channeling of K^+, Na^+ and Cl^-, computer analysis 8=40075
  - Mo, bombarded by positive ions, Auger electron emission, rel. to incident angle 8=27357
  - Mo, clean, bombarded by positive electronically excited ions, Auger electron emission 8=27358
  - N^{14}, 115 MeV, radiation chemical studies 8=41289
  - N_2, on p-Si, donor properties 8=27128
  - NaCl, electron emission 8=40686
  - NaCl lattice, channeling of K^+, Na^+ and Cl^-, computer analysis 8=40075
  - NaI(Tl) response to ions, $Z > 5$, 1-10 MeV/amu 8=44501
  - Ne, pumped on glass, desorption temp dependence 8=48485
  - Ne^{20}, 21 MeV, radiation chemical studies 8=41289
  - Ni sputtering by Ar^+, ⌊110⌋ and ⌊100⌋ close-packed directions yields, 25-600 eV 8=40078
  - Si detector, pulse height defects due to nuclear collisions 8=46896
  - Si, doping by Al ion implantation 8=40485
  - Si, Ga implanted, anomalous penetration 8=48929
  - Si, implantation analysis by 1 MeV He^+ scatt. 8=48927
  - Si, In, implanted, anomalous penetration 8=48929
  - Si, injected ion profiles and channelling dose depend., obs. 8=44813
  - Si, irrad. with pions, carrier density rel. to conductivity 8=44814
  - Si, junction formation by implantation 8=49263
  - Si, P^+ bombard., struct. defect conc. rel. to temp. 8=48831
  - SiC, luminescence on irradiation with H and D ions of 20 keV 8=36510
  - W, inert gas bombard., thermal desorption obs. 8=48497
  - W(110) surface, damage due to Ne^+, Ar^+, Kr^+ or Xe^+ ions 8=26104
  - ZrO_2, films, Ne bombard, damage and effect on props. 8=35067

Ion counters. See Counters.

Ion emission
- electron-ion beams emitted by cylinder or sphere, steady-state potential distribs. 8=27339
- field evaporation, low temp., mass spectrometric analysis 8=27362
- field evaporation, relative abund. of species rel. to emitter temp., theory 8=36060
- field, production using heated filaments 8=47448
- ion-electron emission and sputtering coeffs. anisotropy rel. to target lattice thermal vibrations 8=40685
- mass spectrometry, field ionization, comparison 8=29573
- metal tip in FEM, rel. to gas interact. with surface 8=35143
- metals, on giant-pulse laser irrad., energy rel. to surface temp. 8=27361
- plasma, low temp. from electrode 8=39081
- solid source, energy spread obs. 8=24162
- transparent dielectric mats., on ruby laser irradiation without physical damage 8=40703
- Al, laser induced, mobility obs. 8=36051
- Au, laser induced, mobility obs. 8=36051
- Cs^+ field desorption, theory 8=44953
- Cs^+, from 50-75μ diam. hole in W(110) face 8=49446
- Cu, laser induced, mobility obs. 8=36051
- Fe, in $\alpha \rightleftharpoons \gamma$ transformation region, and electron emission 8=27363
- Pt films on W, field-emission image of clean W surface 8=35178
- Pt, ion microscope tips smoothing by field evaporation, 10 and 78°K 8=39708
- W, field-ion microscope exam. of screw dislocations 8=31089

Ion emission—contd
secondary
energy and angular distribution 8=49447
impurities on Pt, W surfaces investigated by this method 8=35549
metals, inert gas bombard., Auger de-excitation of ions, obs. 8=40718
transition metals, first series, rel. to ionization process 8=40717
Al polycrystal, Ar$^+$ 40 keV bombard., mass
Au, N_2* beam bombarded, negative ion emission, 13-200 eV 8=34454
Co polycrystal, Ar$^+$ 40keV bombard., mass spectrum 8=49448
Mn polycrystal, Ar$^+$ 40keV bombard., mass spectrum 8=49448
Mo, due to K$^+$ scatt., ang. depend. of energy spectra of secondary ions 8=40719
Ta polycrystal, Ar$^+$ 40keV bombard., mass spectrum 8=49448
thermionic
Fe, positive ion emission peak rel. to $\alpha \rightleftarrows \gamma$ struct. transform 8=44955
Ir, wires, props. 8=36061
Mo_2C in Cs vapour, and e-emission rel. to other refractory metal cpds 8=27350
$MoSi_2$ in Cs vapour, and e-emission rel. to other refractory metal cpds 8=27350
Pt, wires, props. 8=36061
Pt, of Na$^+$, K$^+$, oxide reaction effects 8=35549
TaB_2 in Cs vapour, and e-emission rel. to other refractory metal cpds. 8=27350
$TaSi_2$ in Cs vapour, and e-emission rel. to other refractory metal cpds 8=27350
Ti ions from W surface in strong electric field 8=35197
WSi_2 in Cs vapour, and e-emission rel. to other refractory metal cpds 8=27350
ZrC in Cs vapour, and e-emission rel. to other refractory metal cpds 8=27350
Ion exchange. See Exchanges, chemical; Ions, electrolytic.
Ion microscopes
field-ion, photographic recording time reduction 8=28585
field type, interact. of gases with metal tip 8=35143
radiation damage investigations by liq. He field-ion microscope 8=31128
stacking faults and partial dislocations, rel. to contrast in field-ion microscope 8=31092
He field-ion microscopy of Re and Ru h. c. p. metals, rel. to surface structs. 8=26105
Pt tips initial smoothing by field evaporation, 10 and 78°K 8=39708
PtCo alloys, surface charge distrib. rel. to field ion image formation 8=27366
Ion mobility. See Ion velocity.
Ion optics
See also Alpha-ray spectrometers; Ion microscopes; Mass spectrometers; Particle optics.
aberrations in focusing by mag. field with circular boundaries 8=33102
beam guides with few repetitions, acceptance 8=46442
cyclotron beam handling, solid-state control and logic system 8=33441
cylindrical electrostatic analyser, 127°, used as monochromator for slow ions, resolving power 8=37438
defocusing of bunched ion beams 8=33103
in gas in homogeneous elect. field, analytical rel. to numerical soln. 8=25711
isotope separators, retardation, electrostatic lenses 8=34186
magnetic spectrograph, constant-deviation, optimum parameters 8=46853
metal microanalysis appl. 8=27777
mirror, electrostatic, cylindrical-field focusing 8=37411
negative heavy ion intense beams, ion source 8=24163
plasma lens parameters calc. 8=41986
prisms, magnetic, aberrations and lateral displacement by fringing fields 8=41985
quadrupole e. s. lens with concave electrodes, field meas. 8=37420
quadrupole two-dimensional e. s. lens, chromatic aberration 8=37421
r. f. mass spectrometer, 7-5 and 9-7 cycle, energy gain 8=34119
in tandem accelerators 8=24569
Cu single crystal, Ar$^+$, Ne$^+$, He$^+$ refl. obs. 8=48918
Ion pumps. See Vacuum pumps.
Ion sources
See also Ion emission/thermionic.
a.c. generator excitation cct. 8=46327
charge particles radial distrib. in oscillating electron discharge, approx. calc. 8=34408
duoplasmatron, extraction and emission theory 8=24164
duoplasmatron, properties 8=46435
for electrostatic accelerators 8=24573
ETH, Stark field ionizer 8=46430
filament current regulator for solid source mass spectrometers 8=34120
Ion sources—contd
high-yield generator for thermal n TV radiography 8=37725
Lamb-shift, polarization enhancement, static field methods 8=37436
mass spectrometer, modification for field-ionization 8=34447
mass spectrometry, field ionization, comparison 8=29573
for negative heavy ion intense beams 8=24163
Penning type neutron generating tube 8=24949
plasma chamber, dense beam extraction 8=37434
plasma, vacuum system 8=30180
plasma Ti source, nonlinear effects in operation 8=34569
polarized, direct conversion of atomic beam 8=42352
polarized, -ve ions and protons 8=24161
polarized, nuclear spin filter 8=34124
preinjector for Bevatron, Cu-tape-wound edge cooled solenoid 8=33052
for semiconductor implantation, description rel. to types of metals used 8=27068
solid, energy spread obs. 8=24162
for tandem accelerators 8=24569
tritium, method of economizing working gas 8=46432
Van de Graaf accelerator, X-radiation reduction 8=24545
C$^-$, prod and extraction from h.f. source 8=46431
Cs$^{+,2+,3+}$ polarized ions, by e bombardment of Li° 8=24160
Ge, multiply-charged 8=46433
H$^-$, for 1.5MeV accelerator 8=46434
H$^-$, polarized, K vapour charge exchange 8=33099
H$^-$ polarized, Lamb-shift improvement 8=37435
H$^-$, prod. and extraction from h.f. source 8=46431
He^{++}, van de Graaff accelerator 8=33098
Li, $^-$, for van de Graaff accelerators 8=24159
Li$^-$, prod and extraction from h.f. source 8=46431
Li$^+$ emitter for low energy beam expts. 8=41983
Li$^{+,2+}$ polarized ions, by e bombardment of Li° 8=24160
O$^-$, prod. and extraction from h.f. source 8=46431
Ion velocity
acceleration in Crab nebula, with hydromagnetic waves 8=41522
air, dry, positive-ion mobility obs. 8=39027
atmosphere ions, mobility spectra, law and medium A 8=39043
Blanc's law of mobilities, kinetic-theory deviations 8=39021
distribution in partially ionized plasma 8=29955
Doppler shift of spectral line, with optical wedge 8=47471
of flame in electric field 8=25710
flame, propag. and in ion density, reln. 8=39022
ionosphere, lower, use of ionic mobilities for meas. 8=36846
oxygen/water vapour mixture, ion mobility of different species 8=39023
positive, small ions, meas. by time-of-flight method 8=43474
sputtering, r. f., energy distrib. calc. 8=25687
Al, in plasma induced near crystal surface by laser 8=36051
Ar afterglow plasma, and conversion rates 8=43480
Ar, liquified, ion mobilities 8=48193
Au, in plasma induced near crystal surface by laser 8=36051
Cs vapour, Cs_2^+ diffusion, time-of-flight analysis rel. to conduction 8=43705
Cu, in plasma induced near crystal surface by laser 8=36051
in He afterglow, obs. 8=43448
He in afterglow plasma, obs. with Langmuir probe 8=43449
He liquid, rotating, trapped in vortex lines 8=37334
in He, of He$^+$ 8=38835
in He, p and α 8=38836
He, superfluid, mobility discontinuities, inadequacy of Huang-Olinto theory 8=41897
H$^+$, mass-identified, in H_2, drift mobility obs. 8=39033
H_3^+, mass-identified, in H_2, drift mobility obs. 8=39033
He^3, charge mobility at crit. point 8=41888
He^3 liquid, mobility obs. below 1°K 8=24039
$K_xNa_{1-x}Fe_7O_{11}$, ion mobility 8=48782
Li^{6,7} positive ions in LiF, relative difference between mobilities rel. to isotope self-diffusion effect 8=35500
Ne afterglow plasma, and conversion rates 8=43480
Ne$^+$ and Ne_2^+, mobility and reaction rate obs. 300°K 8=39049
electrolytic
See also Conductivity, electrical/liquids, electrolytic; Electrophoresis.
adsorption energy at Hg electrode 8=36600
cyclooctatetraenyl radical anion, electronic spectrum 8=25658
Raman spectra of aq. soln. 8=34863
p-phenylenediamine cations, dimerization 8=25657
$HNClO_3^-$, structure from i.r. absorpt. obs. 8=34247
NH_4-NH_4 proton exchange in liq. NH_3 8=27675
Ionization
See also Dissociation; Electrons/ionization.
acetaldehyde, by electron impact, dissoc. 8=39056
acetic acid, by electron impact, dissoc. 8=39056

Ionization—contd

- acetone, by electron inpact, dissoc. 8=39056
- acetonitrile, photoionization 8=47789
- alcohols, lower aliphatic, photoionization 8=47793
- alkali metal atoms by slow electrons 8=43477
- atom, by colliding with excited atom, formula without rotating-atom approx. 8=25706
- atom, by e impact, quantum theory 8=43470
- atoms during plasma heating for short-wave radiation amplification 8=47780
- atoms, Z=41-98, by electron impact, calc. 8=39013
- current measurement, fluctuation errors 8=42345
- diethylamine radical ($C_4H_{10}N$), at W surface 8=47794
- electron-impact dissoc., translational energies of products 8=38929
- elimination of CO_2 from ions in mass spectrometer 8=38607
- energies, semiempirical calc., isoelectronic atoms 8=47478
- field-ionization mass spectra 8=47796
- gauges and vacuum technique 8=30323
- hologen negative ions, electron energies from inert gas collisions 8=29972
- hydrocarbons, ion impact, charge and proton transfer 8=29984
- ionometer for continuous meas. on a fluid in the dispersed state 8=25709
- ion-polar mol. reactions, preferred dipole orientation 8=34444
- mechanisms, rel. to Alfven's critical vel. hypothesis 8=36989
- methanol-acetaldehyde mixtures, H atom and proton transfer 8=34444
- methyl phenanthrene, by electron impact 8=47797
- molecular plasma 8=43493
- molecules, photoionization and electron structure 8=47582
- multiple, Auger effect theory 8=39019
- organic compounds, metastable ion detector for mass spectra 8=43152
- organic molecules, energies in vapour state and in molec. cryst. 8=29947
- phenanthrene, by electron impact 8=47797
- photo and auto, parametrization for attenuation cross-sections in atoms 8=38684
- photoelectrons, ang. distrib. 8=25705
- plasma, magnetoactive, equilibrium with recombination 8=29993
- propylene, ion-mol. reactions 8=43492
- radiation prod. in arc discharge, optimum parameters 8=29930
- solar corona, revaluation of temp. 8=45923
- tetramethyl-p-phenylene diamine in soln, biphotonic ionization 8=43861
- total energy of atom 8=34439
- ArII multiplets, Stark broadening, temp. depend. 8=39028
- Be atom, photo-ionization cross-section near threshold, calc. 8=39029
- C^-, laser photodetachment, ang. depend 8=25713
- Ca, autoionization resonance structure of spectrum fitted to Shore parameter 8=43185
- Cd atoms by e impact, direct and stepwise cross-sections 8=29961
- Cd, autoionization up to 19 eV 8=39031
- $pD(1S) \rightarrow H(1S, 2S)D^+$ electron capture cross-section calc, 0.02-100MeV 8=43237
- H, electron impact, extension of Gryzinskis theory to degenerate levels 8=43483
- H^-, laser photodetachment, ang. depend 8=25713
- $H^- + F$ and $H + F^-$ collisions electron detachment 8=34451
- H_2, photo calc. not giving obs. cross-section undulations 8=43482
- HCN, photoionization 8=47789
- He, autoionizing $2p^2\ ^1D$ state, calc. of position and width 8=38756
- He, liq., external source effects on breakdown voltage dispersion 8=41890
- $pHe(1S^2) \rightarrow H(1S)He^+\ 1S$, electron capture cross-section calc. 8=43237
- He, photoionization, by diagonalization method for calc. atomic system reson. 8=43220
- He^-, autoionization $1s2s2p^4P_{5/2}$ state 8=39041
- Hg autoionization, up to 17.7 eV 8=39031
- K, autoionizing states, new magnetic resonance method 8=43244
- K^+ to K^{2+}, by electron impact 8=39047
- Kr^+–Kr, sudden change in number of electrons at 25 keV 8=39018
- I ions, electron capture between 19 and 55 MeV 8=39040
- Li, autoionization $1s2s2p^4P_{5/2}$ state 8=39041
- $Li^{6,7}$, atom, autoionizing $(1s2s2p)^4P_J$ states, energies and lifetimes 8=43243
- Li^+ in $H^+ + Li^+ \rightarrow H(n) + Li^{++}$ cross-section calc. 8=25392
- $Mg^+e \rightarrow M^{++}2e$, threshold to 2000 eV, cross section meas. 8=43486
- N, photoionization cross-sections 8=39044
- N_2 discharge, excited waves 8=47745
- $N_2^+ + H_2$ and $N_2^+ + D_2$, low energy ion-mol. reactions 8=27711
- $N_2^* + Ar$ collisions, cross section enhancement by excited mols., obs. 8=34454

Ionization—contd

- Na^+ to Na^{2+}, by electron impact 8=39047
- Ne–Ne, Ne^+–Ne, Ne^{++}–Ne, ratio of prod. of fast electrons 8=39018
- O atom, auto-ionizing e energy spectra 8=39050
- O^-, laser photodetachment, ang. depend 8=25713
- O^+, photoionization cross-sections 8=39044
- gases
  - See also Plasma.
  - in accelerating space of gas-filled neutron tube 8=47141
  - acetylene, Frank-Condon factors 8=29982
  - acetylene, reactions with 0.5-1200 keV positive ions 8=43491
  - air, by shock wave, e temp. meas. 8=39221
  - air, dry, positive-ion mobility obs. 8=39027
  - alkali-like ions in plasma, variable ionization equilib. 8=30004
  - alkali metal atoms, oscillator strengths of photoionization continua 8=29603
  - aromatics, polycyclic, cross sections and ionization pot., 1120-1770Å 8=38860
  - atomic, by multi-photon tech., effect of contours interact. 8=39017
  - atomic, photoionization cross section meas. 8=29949
  - atoms, highly excited, near metallic surface, calc. 8=25707
  - autoionization in u.v., anal. of generalized Ladenburg-Reiche integral 8=34438
  - in cathode-fall region of moving arcs 8=29938
  - charge transfer, thermal and low-eV region, energy depend. 8=39025
  - classical expression based on Thomson theory for atom-atom collisions 8=29951
  - compound state e spectra, obs. 8=34224
  - conductivity components in magnetic field 8=47783
  - controlled ion conc. apparatus 8=43469
  - cyanocarbons, electron capture 8=34457
  - dissociative electron attachment to mols., theory 8=29953
  - electric field, effect of inelastic collisions 8=47821
  - electrons in weakly ionized gas, appl. expanded Boltzmann eqn. 8=34442
  - equilibrium of low density plasma, collision effect 8=25722
  - ethane, dissociative ionization 8=29976
  - ethane 10^{-4}, due to electron collision, calc. of mean free path 8=34458
  - flame, ion density and vel. of propag., reln. 8=39022
  - Hall effect, comparison with solids 8=43695
  - halogen acids, to $^2\pi$ and $^2\Sigma^+$ states, study by photoelectron spectra 8=34229
  - inert gases, by 0.2-1.8 MeV He^+ ions, effective cross sections 8=39035
  - inert gases, in m.h.d. generator, to plasma with electron temp.> gas stagnation temp. 8=37448
  - ion motion, steady state in elect. field, controlled by charge exchange alone 8=25712
  - ion waves dispersion near and above plasma freq. 8=30152
  - by laser pulse, mechanism theory rel. to inverse bremsstrahlung process 8=29952
  - laser, rel. to drift velocity of ions 8=37551
  - mass spectra, field-ionization 8=34447
  - m.h.d. channel, enhancement using peroxides 8=30043
  - methane, photoionization, mass spectra 8=29986
  - methanol ion-mol. reactions, ion cyclotron reson. 8=27709
  - methyl halides, prebreakdown current growth 8=25708
  - microwave absorpt. near electron cyclotron frequencies in magnetic field 8=39020
  - mixture of charged and neutral particles, statistical equilibrium 8=28330
  - monatomic, precursor ionization, effect of line rad. 8=39015
  - partial, e vel. distrib., inelastic interaction effects 8=39024
  - I,2 photon photo-process, discrepancy 8=34453
  - photo-ion kinetic energy analysis with photoelectron spectrometer 8=47784
  - photoionization, multichannel u.v. chamber 8=29948
  - photon scatt. by electrons, and Fokker-Planck operator 8=43475
  - pinch shock tube, current sheet dynamics 8=34448
  - plasma, charge exchange meas. of emitted fast atoms flux distribution 8=43501
  - plasma diode, density distribution rel. electron temp. for equilibrium 8=43606
  - propane, 10^{-4}, due to electron collision, calc. of mean free path 8=34458
  - pure and binary, by Pb^{206} 103 keV recoil particles 8=29950
  - radiation smoothing to prod. continuous temp. profile 8=39200
  - rare at 10^{-3} torr, by laser-irradiation rel. to multiphonon theory 8=29964
  - rate meas. in shock heated gases, microwave method 8=39014
  - shock wave in e.m. tube, separation of electron density transition from sheet 8=43472
  - shock wave, transverse elect. field ahead (Alfven Mach > 2) 8=34440
  - shock waves, ionizing, simple model 8=47781

Ionization—contd
gases—contd
source of molecular ions, multimomentum 650 mA for producing trapped plasma 8=43609
spectro-ionometer, electronic for meas. in air, aerosols. 8=25709
Stark field ionizer for ETH ion source 8=46430
tetra alkyl metal compounds, total cross section 8=25719
in thermal equilibrium, review 8=47782
transient radiation, effects on electronic components 8=31126
transport props using modified Chapman-Enskog tech for collision terms 8=43473
two-atom, thermodynamic functions, approx. calcs. 8=47954
vacuum gauges standardization 8=39250
Vlasov eqn; linearized, soln. for space-time dependent distribution function 8=29954
wave coupling across shock front, theory 8=46165
Ar afterglow plasma, conversion rates and ion velocity 8=43480
Ar and Ar-C_2H_6 mixture, ionization coeffs. and sparking voltages 8=25701
Ar arc plasma rel. to equilib. disturbance 8=29942
Ar, at high-temps, e. attachment on SF_6 injection 8=43478
Ar, electron energy loss, charact., on transmission 8=34449
Ar flash as light source for high-speed photography 8=28768
Ar: freon-12, multiphoton, evidence for cascade breakdown 8=39000
Ar plasma, waves, characteristic pots. rel. to press. and current for three types 8=25742
Ar radiation frequencies absorption, resonance rel. to transfer shock precursor radiation 8=34441
Ar, by shock waves, e temp. meas. 8=39221
Ar, shocked in mag. field, microwave signal attenuation 8=29960
Ar, supersonic m.h.d. stream, struct. obs. by induced e.m.f. 8=41992
Ar-C_3H_8, ionization coefficient and sparking voltage 8=43479
Ar-CH_4, ionization coefficient and sparking voltage 8=43479
Ar-Co discharge plasma, instability in crossed elec. and mag. fields, obs. 8=34556
CF_4, current growth 8=29983
C_2F_6, current growth 8=29983
C_3F_8, rate of electron attachment, two body process 8=43471
C_7F_{14}, rate of electron attachment, two body process 8=43471
CHO^+ ion-mol. proton transfer reactions 8=49869
CH_3, photoionization 8=29985
C_2H_5I and CH_3CD_2I, fragment ions from X-irrad. 8=47795
CO, e beam dissoc., O^- prod. cross-section obs. 8=47703
CO, electronic transition moment integrals 8=25460
CO_2, dissociative ionization 8=29976
CO_2, 10^{-4}, due to electron collision, calc. of mean free path 8=34458
CO_2, photoionization and Franck-Condon principle 8=39030
Cs discharge, rel. to plasma params. and wall ion current, 0.03-0.3 torr 8=25714
Cs, partial, effect on viscosity in temp. range 1000° to 2400°K 8=30310
Cs, vapour arc, low voltage short gap 8=43465
Cs vapour, Cs_2^+ diffusion, time-of-flight analysis rel. to conduction 8=43705
H atom, multiphoton, cross section calc. 8=25715
H, atomic, multiphoton absorpt., theory 8=47788
H, equilib. effects on non-Maxwellian deviation of fast electrons 8=47804
H halides, dissociative electron attachment 8=29965
H-like ions in plasma, variable ionization equilib. 8=30004
H plasma, and recomb., rel. to reabsorpt. of rad. 8=34495
H^- e detachment by e impact, cross-section obs. 8=39036
H^- source, K vapour charge exchange 8=33099
H_2 and D_2, photionization, threshold electrons 8=39034
H_2, as initial plasma of θ-pinch, by intense light source 8=34528
H_2, at 10^{-3} torr, by laser-irradiation rel. to multiphonon theory 8=29964
H_2, by e-impact, 250-2200 eV, and D^+ ion formation 8=29963
H_2, photoionization near threshold 8=47786
H_2, by 0.2-1.8 MeV He^+ ions, effective cross sections 8=39035
H_2, by rad. from dense He and H plasmas below 800Å 8=34529
H_2, double ionization, Franck-Condon calc. 8=29967
H_2, double ionization, test of Franck-Condon priniciple 8=29966
H_2, drift mobility of mass-identified H_3^+ and H^+ 8=39033
H_2, photoionization, ion-mol. and chemi-ionization
H_2^+, hyperfine transitions, nuclear and e polarization 8=29743
He(2^3S) e affinity meas. by laser photodetachment 8=29970
He, by p bomb, e cross-sections 8=34452

Ionization—contd
gases—contd
He, double ionization by electron impact, importance of exchange scatt. 8=39032
He, transport coefficients 8=29968
He^+, reaction with vibr. excited N_2 in afterglow 8=41253
He_3^+, evidence for 8=39037
He^{3+}, 15-25 transition obs. 8=29971
Hg vapour, associative ionization cross section 8=25716
H_2O, dissociative ionization 8=29976
I_2, dissoc. e attachment at 295°K, obs. 8=47790
InI_3 discharge at h.p. theory 8=43455
K, vapour, photoionization absorpt. continua 8=29973
Kr, by impact of monoenergetic electrons 8=43485
N, coeffs. 8=39042
N, states of some unidentified lines 8=43223
N_2^{2+}, charge exchange in N_2, CO_2 and Ar 8=29974
N_2, by collisions with atomic ions, transfer of rot. and vib. energies 8=39046
N_2, by 0.2-1.8 MeV He^+ ions, effective cross sections 8=39035
N_2, by shock wave, e temp. meas. 8=39221
N_2, dissociative ionization 8=29976
N_2 thermodynamic functions, approx. calcs. 8=47954
N_2, vac. u.v. photon impact 8=47609
N_2, with simultaneous excitation by e impact 8=25717
NH_2^- ion reactions with triatomic mols. 8=29980
NH_3 ionization energy from NH_4I and $NH_4I(Tl)$ spectra 8=32014
NH_3, photoionization, ion-mol. reactions 8=36612
N I, limits 8=43488
NO, e beam dissoc., O prod. cross-section obs. 8=47703
NO, rate consts. for charge exchange with quasithermal ions 8=29975
NO_2, first ionization potl. and vibr. struct. obs. 8=43487
NO_2 + H, free electron generation 8=49872
Ne afterglow plasma, conversion rates and ion velocity 8=43480
Ne, auto-ionizing levels, excitation by ion impact 8=39048
Ne, growth time analysis 8=29912
Ne, ion mobility and reaction rate obs. 300°K 8=39049
Ne, low-voltage arc mode in plasma diode, predominant mechanism 8=47779
O, oscillator strengths, exptl. determ. 8=34456
O^-, associative detachment reactions, electron prod. 8=39051
O^- e detachment by e impact, cross-section obs. 8=39036
O^+, reaction with vibr. excited N_2 in afterglow 8=41253
OCN^- formation in ion-mol. reactions 8=41259
O_2, dissociative ionization 8=29976
O^-_4, stability 8=25718
$Pb(CH_3)_4$, fragment ions from X-irrad. 8=47795
Rb, vapour, photoionization absorpt. continua 8=29973
S_n, high-temp. vapours, photoionization 8=47791
S^- ion reactions with triatomic mols. 8=29979
SF_6, rate of electron attachment, two body process 8=43471
SiF_4, rate of electron attachment, three body process 8=43471
on Ti Br_4-Br mixture, Ti I, II absolute gf-values determ. 8=43489
Tl halides, and recomb. rate rel. to Ar and Xe press 8=43490
Xe, ionic ground state alignment by e impact 8=39052
Xe-methane mixtures, charge exchange 8=47792
Xe, photoionization cross sections of M shell 8=29981
liquids
aromatic hydrocarbons in soln., free carriers from triplet-triplet collisions 8=48201
benzenes, F-substituted, ionization ptl. calc. 8=43868
insulators, transient radiation effects on electronic components 8=31126
radiolysis, geminate recomb. 8=45403
scavenging of ions in irrad. liqs. 8=39413
He, superfluid, mobility discontinuities, inadequacy of Huang-Olinto theory 8=41897

solids
anthracene, crystalline, photo-ionization 8=31267
dielectric, track formation theory 8=40552
film, thin semicond. field ionization 8=31463
hydrocarbon glasses. radiation-induced trapped electrons 8=45401
insulators, transient radiation effects on electronic components 8=31126
metals, transient radiation effects on electronic components 8=31126
polythene films, by giant laser pulses 8=40720
rare gas matrix of trapped atoms, photo-prod. 8=40202
semiconductor diode junctions, charact. magnitudes determ by avalanche noise meas. 8=40534
semiconductor impurity atoms, in strong elec. fields 8=35864
semiconductors, transient radiation effects on electronic components 8=31126
$Cd_{0.23}Hg_{0.77}Te$ alloy, thresholds determ. by quantum yield of internal photoelectric effect 8=35879
n-GaP, impurity photoionization 8=41091
Ge, photothermal, of H-like acceptors, and assoc. photoconductivity 8=44954

Ionization—contd
- solids—contd
  - Ge, Li drifted, energy determ. 8=24522
  - InSb, impact ionization rates and instabilities, effect of mag. fields 8=31303
  - InSb, impact, rel. to avalanche plasma prod. 8=35794
  - La, K-ionized, L-K X-ray ang. correl. obs. 8=41111
  - Si, Li drifted, energy determ. 8=24522
  - SiO_2, collision ionization during anodic growth mechanism 8=39687
  - UO_2, surface diffusivity of U ions, 1544°-1915°C obs. 8=35511

Ionization, atmosphere
- See also Atmosphere/radioactivity; Ionosphere.
- aurora, e flux and luminosity, simultaneous obs. 8=32286
- controlled ion conc. apparatus 8=43469
- corpuscular and wave radiation effects on ionosphere 8=45508
- E region, equatorial evening twilight Langmuir probe obs. 8=45545
- in equatorial F-layer, seasonal depend. of osc. movement and turbulence 8=32342
- field-aligned structure at boundaries of spread-F in middle latitudes 8=32346
- ionometer for continuous meas. on a fluid in the dispersed state 8=25709
- ionosphere, electron content, annual and seasonal anomalies 8=45511
- ionospheric, electrons and ions, temp. and composition 8=45513
- plasmasphere, thermal ion struct. 8=45492
- positive-ion distrib. in F-region, 140-300km., calc. and obs. 8=45552
- var. horizontal and vertical, 15° to 30° South latitude 8=27984
- F2 layer ionization rate variations at high altitudes during solar activity max. 8=45550
- F2 layer, rate meas. 8=36871

Ionization, surface
- See also Electron emission thermionic; Ion emission/thermionic; Work function.
- alkali halide molecules on metals of Pt group, e.g. Ir 8=27365
- alkali halide molecules on Pt 8=36062
- alkali on porous substrate, analysis 8=49449
- charges due to electron beam incident on metallic surface, temp. effect 8=27364
- diethylamine radical ($C_4H_{10}N$) 8=47794
- lanthanides, 8=31477
- Al, laser-induced plasma, ion energy and abundances 8=36051
- Au, laser-induced plasma, ion energy and abundances 8=36051
- Cu, laser-induced plasma, ion energy and abundances 8=36051
- Ir, wires, use in ion sources 8=36061
- Pt, of Na atoms, coeff. absolute meas. 8=31476
- PtCo alloys, charge distrib. rel. to field ion image formation 8=27366
- W, of Na atoms, coeff. absolute meas. 8=31476
- ZnO crystals, e. multiplication and surface charge 8=49354

Ionization chambers
- α-γ, gridded, ang. correl. meas. 8=33952
- blurring caused by 4mm diam. chamber in air dosimetry 8=28975
- calorimeter, principles and applic. 8=37782
- cosmic ray recording of "stars" 8=29233
- in depth dosimetry, effect of chamber size 8=28976
- for n dosimetry, and S activation, comparison, 3 and 15 MeV 8=38079
- fluctuation errors, validity of conclusions drawn from ratemeter 8=42345
- double pulsed for nuclear reactions 8=24512
- flowmeter for small airflow 8=34610
- γ-compensated, for reactor n flux meas. 8=47156
- for γ-fast n dosimetry, ionization chambers, hexane and CCl filled 8=33811
- hexane filled, for dosimetry 8=37786
- hexane, quality factor in mixed γ-n fields 8=37787
- liquid dielec. filled for mixed field dosimetry 8=33371
- neutron detector, transient γ field behaviour 8=47160
- Penning gauge for particle and γ detection 8=37784
- spatial freq. characts in γ-ray dosimetry, in air and depth 8=46862

Ionization gauges. See Vacuum gauges.

Ionization potential
- aromatic compounds 8=34297
- aromatics, polycyclic, and photoionization cross sections, 1120-1770Å 8=38860
- B atom, e affinity calc. 8=38661
- benzene, SCF-MO-LC(LCGO) calc. 8=47624
- benzenes, F-substituted, vertical potl. calc. 8=43868
- cyclopropane, SCF-MO-LC(LCGO) calc. 8=47625
- electron subshell binding energies, H to Zn 8=43156
- ethane, from electron spectra 8=34459
- ethylene, SCF-MO-LC(LCGO) calc. 8=47626
- free radicals, appearance pot. meas. 8=29829

Ionization potential—contd
- Koopman's theorem, analysis 8=34116
- lanthanides, from surface ionization 8=31477
- methane, from electron spectra 8=34459
- methane, SCF-MO-LC(LCGO) calc. 8=47628
- nitrogen heterocyclics 8=39060
- oxygen/water vapour mixture, ion cross-sections of different species 8=39023
- Ar-CH_4 mixture 8=43479
- Ar-C_3H_8 mixture 8=43479
- BF_3, BCl_3 and BBr_3 8=34450
- C_7H_{12}, mono- and bicyclic isomers 8=39059
- CHO^+, appearance potential 8=36557
- $C_5H_5^-$, SCF-MO-LC(LCGO) calc. 8=47623
- CNDO/2 method calc. 8=47785
- Cl, atomic 8=38663
- HF and DF, ionization energies 8=29962
- H_3O 8=47610-11
- I, atomic 8=38663
- N, states of some unidentified lines 8=43223
- NH_4 8=47610-11
- NO_2, first potl. and vibr. struct. obs. 8=43487
- O_2^+, energies of $b^4\Sigma^-_g$ and $B^2\Sigma^-_g$ states 8=47615
- S_n, high-temp. vapours, photoionization 8=47791

Ionized gases. See Ionization/gases; Plasma.

Ionosondes. See Ionosphere measuring apparatus.

Ionosphere
- See also Electromagnetic wave propagation/ionosphere.
- absorption in freq. range 128-2775 kc/s, diurnal and seasonal variations 8=32300
- acoustic waves up to 120 km at 0.01 and 10 Hz, model 8=45534
- Alfven waves rel. to pc-3 and pc-4 pulsations 8=50217
- auroral X-rays during slowly varying absorption events, simultaneous balloon obs. 8=27956
- auroral zone disturbances rel. to propag. characts. of freqs. below 12 kHz and above 16 kHz 8=32307
- auroral zone, 129 to 212 km daytime, temp. profile from N_2^+ rocket spectra 8=45483
- auroral zone satellite scintillation at Kiruna, rel. to time and mag. activity 8=32285
- back scatter sounding, field strength predictions 8=50190
- bithermal, double scatt. of plasma streams 8=45531
- characteristics, CCIR atlas 8=27980
- charged particle motion in geomag. dipole field, under action of e.m. pulses 8=36815
- composition and mean molecular weight, diurnal and latit. effects 8=36770
- conductivity components in mag. field, model 8=47783
- conductivities, layer, rel. to Sq vars. 8=50178
- corpuscular and wave radiation effects 8=45508
- cosmic rays in radiation belts 8=25023
- current system, general, rel. to equatorial electrojet 8=45569
- current systems, daily automatic calc. 8=50180
- current systems due to Sun and Moon 8=50179
- curved stratified, e.l.f. and v.l.f. propag. below 8=50182
- disturbances, quasi-sinusoidal 8=41432
- drift obs., analysis method 8=45535
- earth-ionosphere cavity, resonance mode, frequency tracker 8=36852
- effects associated with appearance of energetic electrons in magnetospheric tail 8=45510
- electric currents calc. by equiv. circuit method 8=41439
- electric field, meas. by ejected probe 8=36849
- electrojet over Thumba, India, quiet day obs. 8=41406
- electron and ion temp. and composition 8=45513
- electron and ion temp. profiles at temperate latits., review 8=27985
- electron conent, and [01] 6300Å nightglow 8=36827
- electron content, annual and seasonal anomalies 8=45511
- electron content, enhancements assoc. with mag. storms 8=45512
- electron content, Faraday rot. and Doppler determ. methods, comparison 8=32295
- elecron content, incoherent radar back scatter obs. 8=32296
- electron content near mag. equator, Faraday rot. obs. 8=32294
- electron content, nighttime changes 8=36825
- electron content, total, at mid-latits. during sunspot min. 8=27967
- electron cooking due to induced transitions amongst fine struct. levels of O 8=32298
- electron density, by ground-based obs. of radio signals from cosmic vehicles, review 8=41415
- electron density meas. in transition region with magnetosphere 8=36829
- electron density profiles, 55-105km, 1QSY seasonal var. Wallops Island 8=45528
- electron density profiles above Antarctica, during solar event of Jan. 28, (1967) 8=36768
- electron density profile, microstruct. meas. by gyro-plasma probe 8=36828
- electron conc. meas. apparatus 8=36845
- electron, ion and neutral particle temps., rocket and satellite obs. review 8=32297
- electron production rate in ionosphere of bolar cap due to solar cosmic rays 8=50177

Ionosphere—contd
electron temp. and conc., altitude distrib. meas. by geophys. rockets 8=27966
electron temp. and density, v. l. f. rads and noise 8=41438
electrostatic waves and ionization irregularities 8=32314
energy deposition, nonlocal for thermal disequilibrium and allowing for photoelectron escape 8=45526
equatorial, oblique sounding and spread echoes 8=32312
F-region drift speed, rel. to sunspot activity 8=28175
fine structure by aperture synthesis 8=45529
geomag. obs. rel. to stratospheric heating 8=27982
heating, presunrise at Arecibo, due to conjugate point. photoelectrons 8=41421
hydromagnetic wave propag. and Schumann resonance 8=45532
ice shelf, Filchner, directional characts. ionosonde interference patterns 8=45533
inhomogeneities, dimensions from satellite signal fading at 20 and 40 MHz 8=36841
inhomogeneites from electron density profiles once Wallops Island 8=32319
inhomogeneities, moving, lifetime and spreading, model 8=36840
initial height determ., absorpt. meas. method 8=36824
ion and electron densities and temps., effective recomb. coeff. 8=41378
ion and electron densities and temps, rocket meas. in Indonesia 8=36830
ion density meas. with blunt probes 8=36853
ionization var. vertical and horizontal obs. 15°to 30° South latitude 8=27984
ionogram analysis, correlation with lab. obs. 8=45509
ionosphere and magnetosphere, temps. obs. 8=32297
irregularities, field aligned, effect on radio scintillations from BEB and BEC satellites 8=45530
irregularities in electron content, from Faraday rot. obs. at 3 places 8=36837
irregularities, refracting, determ. from fading of signals from stationary satellites 8=41434
irregularities, small scale formation, linear analysis 8=41433
irregularities, statistical and of h.f. radio wave diffraction 8=32304
Langmuir probe, spherical, charact. of ion collection in drifting Maxwellian distribution 8=25765
low, cosmic ray electron production obs. 8=50176
lower, electron density, wave propag. and r.f. capacitance probe obs. 8=45515
lower, region of development of disturbance systems, non-isolated, rel. to meteorology 8=32316
lower, use of ionic mobilities for meas. 8=36846
magnetically conjugate photoelectron flux heating, low latitude effects 8=41410
m.f. radio wave absorption, dependence at mid-latitudes on planetary mag. activity 8=41423
middle, effects of superposition of two anomalous X-ray emissions 8=45516
movements, detection by freq. swept backscatt. soundings 8=32311
night-time electron density, meas. by v.l.f. Doppler shift method 8=36848
North and South hemisphere, current rels. 8=45569
observations at mag. conjugate points Kerguelem-Sogra 8=45507
observations (Nov. 1967) 8=50173
observations, October 1967 8=27963
observations, September 1967 8=27962
observations, May 1968, Belgium 8=50174
over Europe, total e content (Jan. 1965) 8=41418
Pc-3 pulsation transmission, effects of solar X-ray fluxes 8=41472
photoelectron escape 8=41417
plasma l.f. instability, theoretical discussion 8=45527
polar cap absorption event, recent, nonconjugate aspects 8=36834
of polar caps, electric current, mean intensity rel. to planetary mag. activity 8=27964
polar, electron density, temp. and flux in altitude range 2000 to 3000 km 8=36826
radio absorption detection, late time following high altitude nuclear explosion 8=45538
radio absorption, solar eclipse 12 Nov. 1966 8=27978
radio star scintillations and fadeout 8=32516
radio-star visibility fades in Alaska near solar minimum 8=41437
radio-star visibility fades, phase variance and autocorrelation obs. 8=41436
radiowave absorption in model ionospheric layers 8=41424
real-height problem, generalization of Abel's soln. for both magnetoionic components 8=27965
refractive index for v.l.f. wave transmitted from ground 8=32303
resonances at 2nd, 4th and 5th harmonic of electron gyro-freq., Explorer 20 obs. 8=27968
satellite signal utilization for investigation 8=50189
scintillation, Canadian obs. 8=32609
scintillation obs. at 136 MHz, diurnal pattern characts. 8=32317
scintillations in satellite signals, latitudinal var. 8=41431
scintillations obs. by v.h.f. radar reflections from satellites 8=32315
scintillations, radio star and satellite, geophys. aspects 8=32318
slab thickness, equivalent, incoherent radar backscatter obs. 8=32296
solar flare effects, theory 8=41413
solar proton flare disturbances 8=36838
space research, conference, London (1967) 8=28020
spherical satellite, electrostatic pot. fields and wake 8=41414
Sq midlatitude current system, vector obs. 8=41416
sub protonospheric whistlers, existence of electron density 8=36844
thermosphere, diurnal variation of electron temp. 8=50175
thermosphere, lower, air densities from jet radii 8=36759
topside, ionization var. during mag. storm, obs. 8=41435
topside, night-time plasma transport, using back-scatter N profiles 8=41419
total electron content, anomalous variations at sub-auroral latitudes 8=41420
transmission and refl. coeffs. as vertical incidence for v.l.f. waves 8=32299
travelling disturbances caused by nuclear explosions, rel. to acoustic and gravity-wave modes 8=27979
travelling disturbances, review 8=27981
turbulent process stratification below turbopause 8=36839
upper, charged particle density, relation with sunspot number 8=32293
upper, drift inhomogeneities, rel. to diurnal variations of geomag. field 8=45525
v.l.f. emissions, stations close to auroral zone and at lower latits 8=45505
v.l.f. hiss decrease rel. to sudden commencement 3 Sept., 1966 8=32305
whistlers and hiss, characts and variations, review 8=32263
wind oscillations, short period, exptl. demonstration 8=27983
winds, over Yuma, Arozona, obs. by gun-launched projectiles 8=36843
wind profiles, 85 to 160 km altitude, circulation patterns seasonal and time difference 8=36842
Ar and He concentrations rel. to turbopause altitude 8=36775
H and He, thermal diffusion 8=50188
H^+ velocity distributions from Boltzmann eqn., collision model and Maxwellian distributions 8=41412
He^+ conc. calc. and escape rates 8=27937
N(h) profile calc., assigning reference elements for computer memory 8=36831
N_2 density and temp., diurnal 8=36774

D-region
annual behaviour, similarities with stratosphere 8=50117
conduction, low field, in presence of high field signal 8=45540
conductivity gradients, SID changes 8=32321
electron collision, energy loss factor 8=27990
electron conc. profiles, day and night, method of calc. 8=36855
electron concentration profile sunrise development, Virginia rocket obs. 8=27988
electron concentrations and negative ions, pre-sunrise rocket and ground v. l. f. obs. 8=27989
electron density distrib., meas. from v.l.f. radio wave propag. 8=32322
electron density distribution during winter anomalous radio absorption 8=45542
electron density, height distrib. rel. to ionization prod. by solar rads., rocket meas. 8=32327
electron-neutral collision freq. and density profiles, v.l.f. meas. 8=32326
focused atenna, transient electron growth due to intense e.m. wave 8=43504
gyro-wave interaction obs. 8=45539
mag. storm long lasting effects on amplitude of 245 kHz signals 8=27987
middle-latitude, ionization changes associated with geomag. storms 8=41441
negative ion. concentration estimation 8=50192
radio absorpt. rel. to e bursts in magnetotail 8=41440
radio absorption at 2MHz and rel. to solar zenith angle 8=45541
reflection loss, l. f. and v. l. f. calc. 8=50185
NO in non-polar region, height distribution and recombination coeff. 8=50191
NO production and $O_2(^1\Delta)$ metastable ionization by 1027–1118Å 8=32323
NO production around 100 km 8=41442
O and O_3, associative detachment and dissociative attachement, l.f. obs. 8=32324
$O_2(^1\Delta)$ metastable, ionization by 1027–1118Å and NO production 8=32323

E-region
anisotropy parameters of irregularities 8=45546
annual behaviour, similarities with stratosphere 8=50117

- **Ionosphere**—contd
  - **E-region** contd
    - auroral elect. field estimates 8=27991
    - critical freq. depend. on sun and latitude 8=36863
    - electron concentration distribution new mag. equator, rocket obs. 8=41450
    - electron density distribution during winter anomalous radio absorption 8=45542
    - electron temp., rocket obs. 8=41444
    - equatorial electrojet, contour maps 8=41445
    - equatorial, evening twilight, Langmuir probe obs. 8=45545
    - E-2, appearance, dependence upon solar activity 8=50193
    - E_s formations, connecting with preceding F_2 iregularities 8=32359
    - Es, correlation of zenith radiation depolarization 8=32273
    - Es in subauroral zone based on obs. in Yakutsk 8=45543
    - E_S lifetime rel. to f_0E_S max. 8=41449
    - Es, patterns of occurrence and spatial characts. 8=45544
    - Es, rel. to computation of nighttime F-region ionization 8=45547
    - Es, rel. to electron conc. in surrounding medium 8=45514
    - E_S rel. to sporadic meteors 8=41448
    - fading of ionospheric echoes, periodic, from E and E_S regions 8=41443
    - f_0F2; 20 May 1966 solar eclipse 8=50200
    - irregular type sporadic-E, obs. by rocket borne gyro-plasma probe at temperate latitude 8=32328
    - metal-ions layering process, and effects of NO^+ and O_2^+ ions 8=36858
    - motion, non-uniform, u.h.f. scatt. obs. 8=36856
    - radio absorption at 2MHz 8=45541
    - reflections, continuous, duration variation 8=36859
    - seasonal changes in appearance 8=36862
    - sporadic, blanketing, solar cycle var. 8=41447
    - sporadic classification from rocket obs. 8=27992
    - sporadic E and f_0F2 at mid-latit. in summer during sunspot min. 8=27993
    - sporadic E, connection with nightglow and spread-F 8=32278
    - sporadic E in polar cap, occurrence 8=36860
    - sporadic-E, space distrib. 8=32330
    - sporadic, intense, temperate latit., conjugate point dependence 8=41446
    - sporadic layers in middle latitutdes 8=32329
    - sunrise behaviour at midlatitudes 8=36864
    - at sunrise, role of NO in molec. ionization 8=36857
    - winter anomaly 8=50194
    - NO production around 100 km 8=41442
  - **F-region**
    - apparent rotation 8=41379
    - beacon obs. compared with theory for electron content variations 8=32333
    - conjugate enhancement rel. to S. Atlantic mag. anomaly 8=41453
    - electron collision freq. in region, 8=50195
    - electron content variations, beacon obs. compared with theory 8=32333
    - electron heating effects, optical heating discrepancy 8=27995
    - electron temps. over Ahmedabad from cosmic noise absorption 8=27996
    - electrons, ions, temp. and concentration for mag. quiet and disturbed conditions 8=41451
    - equatorial ionization, seasonal depend. of osc. movement and turbulence 8=32342
    - fading of ionospheric echoes, periodic 8=41443
    - F2, effect of diurnal temp. changes, temp. depend. loss rate 8=41454
    - F2, $\Sigma\sqrt{f_0F2}$ at conjugate mag. latits., seasonal and secular characts. 8=27998
    - F2 critical freq. at low latits., semi-diurnal lunar perturbation 8=28001
    - F2 critical, horizontal gradients rel. to solar time 8=36868
    - F2, ion drag with electrodynamic drift 8=50197
    - F-2, fluctuations in critical freq. in Asian zone 8=50198
    - F_2, field-aligned irregularities, as effect of increased electron temp. 8=32361
    - F_2, max., irregularities obs. and meas. of travelling vels. 8=32360
    - F2 horizontal drifts, effect of geomag. activity, obs. 8=45553
    - F2, horizontal drift meas. at Waltair 8=45554
    - F2 ionization rate, meas. 8=36871
    - F2, ionization rate variations at high altitudes during solar activity max. 8=45550
    - F_2 irregularities, focusing props. and connection with E_S formations, backscatt. study 8=32359
    - F2 layer, ionization depression, formation, and thermal effect of photoelectrons at mag. equator 8=27999
    - F2 layer, time depend. effects of general electrodynamic drifts, tech. for eval. 8=32357
    - F-2, max. electron density, v.l.f. Doppler expt. 8=45537
    - F2, reflection coeff. rel. to fine structure parameters 8=36872
    - F2 undisturbed, critical freq. at solar maximum 8=36870
    - f_0F2 and horizontal mag. intensity, luni-solar tidal oscills. in quiet period 8=27997
    - f_0F2 equatorial anomaly 8=36869
    - f_0F2 and M(3000)F2, statistical model for monthly distributions 8=28000

- **Ionosphere**—contd
  - **F-region**—contd
    - f_nF_2, indices for prediction 8=50199
    - f_0F2 and sporadic E at mid-latit. in summer during sunspot min. 8=27993
    - f_0F2 vars. at conjugate places in low latitudes 8=41455
    - f_0F2 var. in mag. storm, N-S asymmetry 8=28002
    - f_0F2 solar cycle variation 8=36867
    - height of peak rel. to electron content, backscatter obs. 8=32296
    - heights of nighttime F region during intense mag.-ionospheric storms in IGY and IQSY 8=45548
    - horizontal drifts over Ahmedabad 8=50196
    - ionization, and solar wind 8=41452
    - irregularities after detonation of July 9, (1962), spread-F and crit. freqs. change 8=32340
    - irregularities, elongation over mag. equator (India) 8=45551
    - irregularities, satellite radio signal scintillation study 8=32353
    - irregularities, size, movements, effects of mag. disturbance 8=32337
    - large-scale behaviour, review 8=32334
    - large-scale strut. at Kiruna, by Faraday rotation of satellite signals 8=32336
    - nighttime ionization in presence of Es, computation 8=45547
    - night-time irregularities, equatorial, study by scintillation of v.h.f satellite signals 8=32356
    - photoelectron escape and heating of protonosphere, model 8=36866
    - plasma lines, characts. by Thomson scattering probe 8=27994
    - positive-ion distrib. 140-300km., calc. and obs. 8=45552
    - reflection coeff., apparent, of h.f. waves, focusing influence 8=32348
    - satellite, electron-ion collision effect on wake structure 8=34443
    - scintillation of signals from Discoverer 36, correl. with spread-F 8=32354
    - spread-F and magnetic activity 8=45549
    - spread-F in Antartica, freq. of occurrence in IGY period 8=32352
    - spread-F, connection with nightglow 8=32278
    - spread-F, correl. with geomag. activity in middle latitude 8=36865
    - spread-F at Djibouti and Dakar, hourly and seasonal variations 8=32341
    - spread-F echoes, angular spread 8=32347
    - spread-F, effect on radio propag. near equator 8=32335
    - spread-F in Greenland, variations, diurnal, annual, latitudinal and through sunspot cycle 8=32350
    - spread-F, high latitude, anal. of data from oblique incidence soundings 8=32349
    - spread-F, irregularities, equatorial type, survey of obs., variations and props. 8=32343
    - spread-F irregularities, field-aligned, spiralline charged particle prod. 8=32339
    - spread-F irregularities, main props. and theories of production 8=32338
    - spread-F, in middle lattitudes, field-aligned struct. of ionization at boundaries 8=32346
    - spread-F, in mid-Pacific, (Oct. 27, 1962), onset and developmetn from ionograms 8=32344
    - spread-F occurrence, correl. with broadband scintillations of Cassiopeia A 8=32332
    - spread-F occurrence probability, partial correl. coeffs. with solar, ionospheric and geomag. parameters 8=32351
    - spread-F and radio-star scintillations in auroral zone, review 8=32355
    - spread-F, topside, in mid and high latitudes, meas. from Alouette satellite 8=32345
    - spread, topside, midlatitudes and global solar influence 8=32358
    - travelling waves over Arecibo, assoc. with mag. disturbance 8=32331
    - wind vel. 400 m/s obs. 8=27949
- **Ionosphere measuring apparatus**
  - in Ariel III, for electron temp. and density 8=41438
  - blunt probes, ion density meas., theory and expt. results 8=36853
  - ejected probe meas. of elec. field 8=36849
  - gyro-plasma probe for electron density magnetosphere transition region 8=36829
  - ionospheric diagnostics using resonances of electric dipole impedance 8=27986
  - irregular type sporadic-E, obs. by rocket borne gyro-plasma probe at temperate latitude 8=32328
  - Langmuir probes, cylindrical, and effect at satellite speeds 8=32320
  - probe, electrostatic, for e density and temp., principles 8=36847
  - probe techniques for electron conc. meas., comparison 8=36845
  - quadruprobe for d.c. field meas. 8=41381
  - radio absorption at 5 fixed freq., installation 8=36850
  - r.f. impedance probes, theory, appl. to different configs. and plasma conds. 8=36854
  - in situ probe system with thermal equalization, pulse and Langmuir probes 8=45536

Ionosphere measuring apparatus—contd
- stations, small and fixed freq., realization 8=36851
- v.l.f. Doppler expt. for rocket obs. of ionosphere 8=45537

Ions
- See also Atoms; Ion emission/thermionic; Molecules; Plasma.
- acetone condensation products, mass spectra 8=29840
- alkyl, prod. by H_3^+ reactions with propane or butane 8=39057
- atmospheric, structure 8=50133
- atom collisions, boundary condition for theoretical treatment 8=29655
- atomic, dipole hyperpolarizabilities 8=25334
- carbonium, electronic struct. 8=38876
- cations in aq. soln., coordination numbers 8=34779
- cometary, and radicals, photochemical effects in production 8=50425
- counter, SI-01 8=47450
- in crystal fields, mag.-field-induced quadrupole splitting 8=43939
- cyclic aromatic hydrocarbon ions, electronic ang. momentum 8=25538
- d^3 in α-Al_2O_3, trigonal splittings, stress dependence 8=43929
- $d\epsilon^1$ and $d\epsilon^5$, dynamical Jahn-Teller effect rel. to mag. anisotropy 8=36234
- diamagnetic susceptibility of ions with $^1S_0$ terms 8=38644
- diffusion in gases and mobility, theory and obs. review 8=30318
- double molecular, metastable, formation 8=29834
- effect on v.l.f. e.m. wave propag. through ionosphere 8=24255
- electric dipole moment, calc. for open electron shells 8=34127
- electron capture, rel. to chemical properties of electrons 8=25322
- electron-impact linewidths, formulae 8=38718
- in gas, motion in homogeneous elect. field, analytical rel. to numerical soln. 8=25711
- implanted in semiconds., impurity profile calc. from statistical model 8=27132
- inert-gas, collision with atoms and mols., 1-100 eV charge transfer obs. 8=38735
- ion-molecule reaction kinetics 8=27679
- of iron group elements, spectra, theory 8=43202
- level population in stationary nonthermal plasma 8=39069
- mesosphere, chemistry rel. to electron concs. 8=27880
- metastable, in cycloidal mass spectrometer 8=39026
- metastable organic, detector for mass spectra 8=43152
- motion along dislocations rel. to migration polarization 8=49332
- motion in tetrafluoroborate salts, n.m.r. 8=31905
- motion, steady state, in elect. field, controlled by charge exchange alone 8=25712
- multiply charged, metastable states 8=43217
- neon-like, X-ray satellite intensities 8=25372
- nitrosylruthenium, sorption on $Fe(OH)_2$, obs. 8=44073
- paramagnetic, in solids, axial-field-splitting, covalency effects 8=35046
- plasma current layer, moving interaction 8=29989
- populations of excited states analysis, and applic. to electron temp. and density obs. 8=30027
- r.f. transitions, spectroscopic methods 8=38596
- species from field emission, rel. to emitter temp., theory 8=36060
- $3d^n$, energy levels in crystal field of symmetry C_{4v} 8=47516
- visualization in supercooled fluids, by cryst. form. on ions as nuclei 8=39656
- wave propagation in plasma, harmonics 8=47874
- Ag^- orbitals, reduced basis set expansions 8=43176
- Ar laser, c.w., excitation processes 8=28675
- $Ar^+ + C_3H_6$, charge transfer reaction, obs. by He resonance line 8=34445
- $Ar^+ + D_2$ and $Ar^+ + H_2$, reaction kinetics 8=45323
- B^{++}, new type of wave function 8=38672
- Be^+, new type of wave function 8=38672
- BF_4^-, motion in $NaBF_4$ 8=31912
- Br^- collisions with He, Nr, Ar and Kr atoms, detached electrons energy obs. 8=29972
- $BrICl^-$ in NH_4BrICl, structure studies 8=30649
- CHO^+, ht. of formation 8=36557
- $CH_4^+ + C_3H_6$, charge transfer reaction, obs. by He resonance line 8=34445
- CO_3^{3-}, Y^{3-}-stabilized mol.-ion in calcite 8=49620
- $C_5H_5^-$, SCF-MO-LC(LCGO) calc. 8=47623
- Ca XV and XVI spectra, laser prod. plasma, 120-240 Å 8=29608
- Cd I series, intercombinational transition probabilities 8=38711
- Cl^- collisions with He, Ne, Ar and Kr atoms, detached electrons energy obs. 8=29972
- Co^{2+} in ZnS, CdS, ZnSe and ZnS-CdS, absorpt. and emission rel. to impurity levels, 3500 cm^{-1} 8=27613
- Cr, positive, spin-orbit coupling 8=38665
- Cr^{2+} in MgO, dynamic lattice couplings, from microwave u.s. and thermal-conductivity studies 8=35053

Ions—contd
- Cr^{3+} in $LiNbO_3$, acoustic paramag. reson., 4.2°K 8=44318
- in Cs seeded Ar plasma, species present, relative abundance and ion signals 8=29987
- Cs vapour of Cs_2^+, diff. coeff., time-of-flight obs. 8=30314
- $Cs^{+,2+,3+}$ polarized ions, production by e bombardment on Cs° 8=24160
- Cu^{2+}, bonding in Rochelle salt and triglycine sulphate e.p.r. obs. 8=36243
- D_2^+, collision-induced dissociation 8=25648
- D_2^+ photodissoc., theory and calc. 8=47704
- Eu^{3+} in YVO_4, absorpt. and fluorcoc., $(4f)^6$ level splittings rel. to cryst. field, obs. 8=41152
- Fe, positive, spin-orbit coupling 8=38665
- Fe^{3-} in $CdWO_4$, e.p.r. lines splitting by elec. field, 320 kv/cm 8=40929
- $FeCl_4^-$ anion, intensities of d-d transitions 8=29736
- H cluster ions, condensed, mass spectra 8=47787
- H^-, electron correlation 8=34238
- H^-, stability, wave function calc. 8=47482
- H_2^-, attempt to produce 8=43481
- H_2^+, collision-induced dissociation 8=25648
- H_2^+ photodissoc., theory and calc. 8=47704
- $(HCO_3)_2^{2-}$ in $KHCO_3$, structure from n.m.r. study 8=26032
- H_3O^-, in hydrated $Ga_2(SO_4)_3$ crysts., n.m.r. 8=49643
- H^3He^+ reactions with gaseous methane and ethane 8=45341
- He_3^+, evidence for 8=39037
- $He^+ \rightarrow He_2^+$ in afterglow plasma, obs. of rate 8=43449
- He^3-He^4 solutions, mobility of positive ions, 1.4 to 2.15°K 8=46312
- Hg, in supersonic jet, charge exchange of polarized ions 8=39039
- Hg I series, intercombinational transition probabilities 8=38711
- I^- collisions with He, Ne, Ar and Kr atoms, detached electrons energy obs. 8=29972
- I_3^- in $N(CH_3{}_4)I_3$, structure studies 8=30649
- I_2Br^- in CsI_2Br, structure studies 8=30649
- Ir^{4+}, exchange coupling in $(NH_4)_2Ir$; $PtCl_6$ 8=32002
- $Kr^+ + C_3H_6$, charge transfer reaction, obs. by He resonance line 8=34445
- Li^-, stability, wave function calc. 8=47482
- $Li^{+,2+}$ polarized ions, production by e bombardment on Li° 8=24160
- Li^{7+}, ^1D, ^3D, ^1F and ^3F states, mag. h.f.s. calc. 8=38673
- Mn, positive, spin-orbit coupling 8=38665
- Mn^{2-} in $CdWO_4$, e.p.r. lines splitting by elec. field, 320 kv/cm 8=40929
- N_2, excited states rot. and vibr. consts. calc. 8=38792
- NO^+, electronic states 8=47606
- NO_2^-, charge distrib. in ferroelec. $NaNO_2$ 8=48308
- Nd^{3+}, approx. analytical wavefunctions 8=38674
- Nd^{3+} in $NdCl_3$, annihilation between excited states 8=41205
- O^+, reaction with O_2 and N_2, temp. depend. of rate coeffs. 8=29977
- O^-_4, stability 8=25718
- Pb III series, intercombinational transition probabilities 8=38711
- Ru, sorption on $Fe(OH)_2$, obs. 8=44073
- in SF_6, in swarm conds., electron detachment, rel. to corona studies 8=29978
- in Si, implanted impurity distribs. of B, N, P and As 8=27131
- SiII, IV, spectra, doublets oscillator strength ratios, Fermi calc. and obs. 8=34152
- Ti^{3+} in $BaTiO_3$, electronic transition theory 8=49362
- UO_2^{2+} excitation in β-diketone + N-containing organic bases triple complexes by intramol. energy transfer. obs. 8=34288
- X_2O_7, type, vibration spectra and chemical structure 8=47475
- XY_4 type, force consts. vibr. amplitudes and Coriolis coupling consts. 8=34206
- Zn I series, intercombinational transition probabilities 8=38711
- recombination
  - rate consts., gaseous ions 8=34446
  - capture radius 8=29956
  - and diffusion, no. unrecombined particles, asymptotic limit 8=34473
  - gases, dense neutral, in e-atom collisions, calc. from Thomson's theory 8=29951
  - isolated ion pair, theory of neutralization 8=29957
  - in plasma diffusion decay 8=30011
  - plasma, magnetoactive, equilibrium with ionization 8=29993
  - plasma, volume coeffs. from atomic flux emergence meas. 8=47849
  - primeval fireball plasma, theory 8=45596
  - satellite in F region, electron-ion collision effect on wake structure 8=34443
  - solar corona, revaluation of temp. 8=45923
  - Ar ionized flows at high temps, e. attachment on SF_6 injection 8=43478
  - in Cs discharge plasma, rel. to level populations and rad. loss 8=34494
  - in He afterglow, obs. 8=43448
  - He_2^+-e recomb. coeff. in afterglow plasma 8=39038
  - NO afterglow discharge, photoionized, obs. 8=47755
  - NO afterglow, chemiluminesc. rate consts. 8=38993

Ions—contd
- **recombination**—contd
  - NO$^+$ + e dissociative-recombination-rate coeff. temp. dependence 8=29958
  - N_2O, electron attachment, structural resolution 8=39045
  - in $PbBr_2$ weakly ionized gas, press. depend. 8=43476
  - in PbI_2 weakly ionized gas, press. depend. 8=43476
  - after Tl halide photo-ionization, rel. to press. and inert gas presence 8=43490
  - in TlI, weakly ionized, press. and temp. depend of coeff. 8=43476
- **scattering**
  - angular distributions and excitation functions obs. 8=38523
  - deformed nuclei, backscatt., test for pulse approximation in multiple Coulomb excitation 8=29280
  - string effect, energy and temp. depend. 8=48897
  - Ar, 10-20keV, effect of lattice thermal oscillations 8=46440
  - Cu single crystal, Ar$^+$, Ne$^+$, He$^+$ refl. obs. 8=48918
  - Gd, on Al, Ta targets, ang. distrib. obs. 8=48909
  - K$^+$ on (100) and (110) Mo surfaces, ang. depend. of energy spectra of secondary ions 8=40719
  - Kr, on Al, Mo, Ta targets, ang. distrib. obs. 8=48909
  - Mg, on Al, Mo, Ta targets, ang. distrib. obs. 8=48909

Ions, electrolytic
- See also Conductivity, electrical/liquids: electrolytic; Dissociation/electrolytic.
- alkali ion motion in soln., i.r. bands 8=25931
- amide ion and ion aggregates, in solns. of KNH_2 in liq. NH_3, absorption spectra 8=39380
- cation coordination no. in aq. solns. determ. by p.m.r. 8=39431
- chlorinated diphenyls, ion purification 8=45310
- 2, 2′-dinitrodiphenyl anion, e.s.r., linewidth effects 8=38945
- electroadsorption phenomena 8=45366
- hydration in aq. solns., i.r. spectra 8=39373
- ion-pair theory of conc. electolytes 8=41272-3
- ion-solvent interaction, preferential solvation in mixed solvents 8=39314
- liquid phase cells, dissymmetry due to difference in ion nature 8=45390
- multi-ionic reaction rates, strength independ. 8=49845
- naphthalene anion in soln., e.p.r., ion paring effects 8=39416
- 1-nitro-4-trifluoromethoxybenzene anion radicals ion pairing 8=39415
- polar double membranes, current-voltage and time meas. 8=27748
- polar double membranes, static effects 8=27747
- sym-trinitrobenzene anion, effect of Li cation on spin density 8=47714
- $Al(NO_3)_3$, hydration no. determ. by n.m.r. 8=48215
- $AlCl_3$ in aq. solvent mixtures, proton magnetic resonance coordination number study 8=25954
- Cd, in fused $AlCl_3$-NaCl-KCl, electrochem. 8=49917
- F$^-$ in aq. soln., determ. by atomic absorpt. spectrometry 8=27788
- Hg, in fused $AlCl_3$-NaCl-KCl, electrochem. 8=49917
- K and Na, active transport through biological membranes 8=50461
- $N_2H_4{}^+$, e.s.r., temp. depend. 8=47685
- Ni(II) in aq. soln., primary solvation no. determ. by p.m.r. 8=39423
- Sn(IV), isomer shifts in ice, conc. depend. 8=43957
- SO_3Cl^-, mobility 8=48194
- Zn, in fused $AlCl_3$-NaCl-KCl, electrochem. 8=49917

Irasers. See Lasers.

Iridium
- crystal, brittle fracture, scanning e-microscope obs. 8=26825
- Fermi surface, effective mass 8=40250
- susceptibility in Pt-Ir alloys, n.m.r. meas., Knight shift, 8=40998
- thin films on Mo, field-ion microscope study 8=48452
- wires, thermionic props. 8=36061
- with Fe dissolved, solute resistivity temp. dependence 8=40318
- Ir^{4+}, exchange coupling in $(NH_4)_2Ir; PtCl_6$ 8=32002
- Xe^{133} ions, 40 keV, depth distrib. 8=48935

Iridium compounds
- complexes, anisotropic, electrical conductivity, temp. dependence 8=40320
- $IrBr_6{}^{2-}$ complexes, mag. circular dichroism 8=49730
- $(IrCl_6)^{2-}$ complex in $(NH_4)_2PtCl_6$ and K_2PtCl_6. spin-lattice relax. 8=49622
- $(IrCl_6)^{2-}$ complexes in $(NH_4)_2PtCl_6$, nearest-neighbour exchange coupled pairs. spin-lattice relax. 8=49623
- $IrCl_6{}^{2-}$ complexes. mag. circular dichroism 8=49730
- IrF_6, electron diffr. and molec. struct. 8=38858
- Ir–Pt alloy with dissolved Fe, solute resistivity temp. dependence 8=40318
- $(IrX_6)^{2-}$ complexes (X = F, Cl, Br), mag. props. 8=49471

Iron
- abundances in solar photosphere 8=28174
- active, anodic dissolution in acid solns with high halide concs 8=36598
- aerosols, spectral absorpt. of excited molecules 8=34950
- α and δ, self-diffusion and diffusion of Co 8=44388

Iron—contd
- α to h. c. p. transition, followed by Mössbauer spectrum 8=43946
- α-iron, elastic constants pressure derivs. to 10 kbs at 300°K 8=26823
- anode, varnish deposit, elect. characts. 8=49916
- armco, n.-bombardment effects on ferromag. props. 8=36169
- armco diffusion processes in weld joints under transient pressure 8=44373
- atom, electronic struct. effect on Mossbauer spectra 8=39514
- atomic energy levels, X-ray, effect of pressure 8=47497
- b.c.c., discrete-atom model for interstitial aggregates 8=35544
- b. c. c., edge disloc-impurity interaction, force-distance curve calc. rel. to hardening model 8=26674
- b.c.c. lattices, energy of interstition of impurity atoms into octahedral and tetragonal positions 8=35542
- b.c.c., solubility and interstitial migration of O 8=48361
- Bloch law deviations, temp. depend. 8=27411
- bremsstrahlung production in thick targets on 0. 5-2. 8 MeV e.-irradiation 8=40071
- carbonyl complex, $C_{13}H_{12}Fe_2(CO)_8$ 8=26446
- cascade e ang. distrib. in shower maximum, calc. 8=38181
- case, with spherical graphite, notch impact and impact bend strength, testing 8=49017
- cast, fracture criterion 8=49007
- cations in AgCl, valency state determ. of Fe impurities 8=35550
- cementation of Cu, kinetics, and activation enthalpy 8=43898
- charged states in Co cpds Mössbauer spectral determ. 8=35034
- colour centres in amethyst 8=31116
- commercial, precipitation mechanism and nature of decomposition products in age hardening 8=40155
- compressibility, comparative to Pb, under impact press. 31 to 34 m bars 8=40108
- Compton profile 8=31989
- corrosion in H_2SO_4, inhibition by dissolved ring-substituted anilines 8=45377-8
- cosmic-ray μ high-energy e. m. interactions 8=38250
- crystal, elastic stiffness coeffs., room temp. to 500°C 8=44570
- crystal growth by strain-anneal, and dislocation density and distrib. 8=26250
- deformed, X-ray diffraction line intensity changes on annealing 8=35332
- diffused into Na disilicate glass, mag. susceptibility rel. to Fe content 8=27381
- diffusion and surface reaction in Fe:Na_2O. $2SiO_2$ system 8=26621
- diffusion of C at 350°C, preliminary cold plastic deformation effects 8=35490
- diffusion rates, annealing time effects 8=35474
- dispersion-strengthened, mag. props. dispersoid effects 8=31620
- domain-wall dynamics from pulsed n.m.r. expts. 8=31621
- ductile foil, electrochem. prep., study of Fe, Cr and Fe-Re deposits 8=36609
- electrochem. behaviour in neutral solns 8=49932
- electrodeposited, natural ageing effects rel. to deposition conditions 8=35104
- electromagnet core, field accuracy rel. to excitation rate and induction history 8=28523
- electropolishing, "Universal" technique applications 8=44027
- electron spectrum computation using Slater–Koster interpolation method 8=35770
- Fermi-surface from galvanomag. coeffs. and de Haas-van Alphen effect 8=31289
- ferromagnet, elastic limit determ. by Barkhausen effect 8=26838
- ferromagnetic films, planar Hall effect, thickness (100-1500Å) and temp. (77-293°K) dependence 8=31687
- ferromagnetic properties rel. to band structure 8=31632
- ferromagnetic resonance linewidth temp. dependence, 300-1000°K 8=31815
- ferromagnetic, thermal neutrons, critical scattering 8=31626
- film, coercivity meas. as function of temp., 0 to -175°C 8=31583
- film on glass, light refl. phase retardation meas. 8=31960
- films, condensed, internal macrostresses form. rel. to substrate temp., obs. 8=31164
- films, domains and coercive force in supercritical transition, obs. 8=31629
- films, domains and mag. fine structures form., e microscope obs. 8=31640
- films, epitaxial, anisotropy constant 8=31631
- films, Richter-type aftereffect 8=31633
- filoform microcrystals, effect of dislocation on magnetization process 8=26677
- Fisher's correlation function, evidence from critical neutron scattering 8=27412
- group, 2nd spectra, interactions between d electrons 8=43190

Iron—contd
Hall coeff., ordinary, theory at low temps. 8=49162
in hemoproteins, fine structure of ions 8=35044
high-purity, internal friction, multiple $\alpha \rightleftharpoons \gamma$ transforms. effect 8=35700
hyperfine field at Mn, temp. dependence 8=40814
impurity ions in AgCl and NaCl, Mossbauer effect study 8=39510
interaction energy with the magnetization of interstitial atoms and solute atom pairs 8=31614
internal friction and fatigue mechanisms 8=26813
internal friction changes during $\alpha \rightleftharpoons \gamma$ transform. 8=40152
internal friction, effect of H 8=31207
internal friction peak due to dislocation dragging by interstitial impurities 8=26814
ion slowing down in H plasma, optical emission 8=43542
ions, Fe^{3+} in $CdWO_4$, e.p.r. lines splitting by elec. field, 320 kv/cm 8=40929
irradiated and quenched, interstitial C and N solute trapping 8=44420
isomer shift temp. dependence and hyperfine field near Curie point 8=31636
Kerr effect in dielec. permeability tensor freq. dependence determ. 8=31696
layers, thick evaporated, gyroelectric and gyromag. consts. reflected light meas. 8=36141
line intensity rel. to discharge gas pressure 8=34433
liquid, atomic structure from X-ray diffr. exam. 8=25874
liquid, initial O content as formation factor for alumina inclusions group 8=35651
magnetic films, anisotropy from Mossbauer meas. 8=31641
mag. moment disturbance distrib. from dissolved impurity atom, n. scattering obs. 8=31637
magnetic props. deduced from tight-binding calcs. 8=36145
magnetization field near frontal plane rel. to domain formation 8=31554
Magnetocrystalline anisotropy constant, first-order, pressure dependence 8=27407
magnetostriction, rel. to temp., mag. field and mag. field orientation 8=31619
membranes, diffusion and permeability of electrolytic H 8=44389
metal and alloys, high field susceptibility 8=45013
meteorites, anal. of Ar^{40}-K^{40} ages of silicate inclusions 8=28157
meteorites, determ. of Au conc. 8=28159
meteorites, K spatial distrib. rel. to determ of K-Ar ages 8=45844
molten, viscosity by oscillating crucible method 8=34798
Mossbauer effect pressure dependence, 0-85 kbar 8=43949
Mössbauer six-line spectra position analysis for Fe^{57} 8=48330
Mössbauer spectra in cytochrome c 8=48331
muon spectrograph, interpretation of bursts 8=38221
neutrons, fast, shielding and collimation props. 8=33793
optical absorpt. in bulk, determ. from Fe thin film exam. 8=41085
particles dispersed in N, Ar or H gas, absorpt. spectra including carrier gas contrib. 8=25968
passive layer, presence of H in outer layer 8=35171
permeability changes on rotation in continuous mag. field 8=40811
points defects created by strong rolling in liq. N_2 elimination 8=31024
polycrystals, magnetic after effect rel. to plastic deform. 8=36143
positive-ion and electron emission, from $\alpha \rightleftharpoons \gamma$ transformation region 8=27363
positive ion emission, rel. to $\alpha \rightleftarrows \gamma$ struct transform 8=44955
positive ions, spin-orbit coupling 8=38665
positrons, polarized, annihilation 8=49129
pressurized, yielding phenomena 8=31206
proton accelerator target, residual radiation dose rate 8=33402
pure, surface struct. and corrosion, effect of reactor irrad. 8=30720
purification of α-Febar by γ-phase zone displacement 8=30825
recrystallization diag. obtained by vacuum melting low-C 8=35240
residual strain distrib. 8=31214
rolling textures rel. to deformation mechanism and sample orientation 8=26820
saturation magnetization determs. 8=31618
secondary recrystallization 8=39672
softening on heating to 600°C in high-purity, plastically deformed mats. 8=35677
solar, abundance rel. to Si 8=37084
in solar chromosphere, lower, Fe^+ emission regions 8=45914
solar emission spectrum obs. 8=28165
solid, e. m. internal field, calc. methods 8=26013
spin-wave renormalization effects, obs. 8=49520
spin waves 8=31627
stacking fault energies on {111} planes in b.c.c. lattice 8=48870
strain-rate sensitivity and temp. dependence of flow stress over wide range 8=44573

Iron—contd
stress relax. local, rel. to dislocation structure, strain rate and temp. 8=35676
susceptibility above Curie temp., temp. depend. of 8=40812
temperature cond. at 0° to 1000°C 8=39944
tensile yield and flowstresses, rel. to annealing after wet H treatment 8=49018
thermal conductivity, and elec. resistivity 8=48761
thin films, optical absorption, electrical resistivity, in vacuum 8=36359
twin interlayers, volumetric form 8=44467
unmagnetized, mag. small angle scatt. of thermal neutrons 8=31642
vacancy concentration during high temp. deformation 8=31038
whiskers, plastic flow, 4-300°K 8=49032
white cast, Bi, Al, B determ. by hollow-cathode discharge spectrum 8=36642
X-ray diffraction line intensity changes on plastic deform. 8=44166
x-ray line intensity and lattice consts. rel. to temp. 8=48649
in Al melts, u. s. dispersion, 740-800°C 8=39442
Au^{197} Mössbauer effect rel. to hyperfine structure determ. 8=43948
in CoO, multiple charge states 8=39521
in Cu, singlet ground state n.m.r. 8=31900
in Cu, spin compensated state rel. to Mössbauer effect 8=35036
in ε Cu-Zn, local moment formation from susceptibility meas. 8=31617
Fe^{55} X-ray source for Debye-Scherrer diffractometry 8=28930
Fe^{57}, acoustic sidebands in Mössbauer spectrum due to r.f. magnetic field 8=39513
Fe^{57} isomer shift pressure dependence in b.c.c. phase 8=43950
Fe^{57} Mössbauer scattered radiation time dependence 8=43947
Fe^{57}, spectrum (I) following Co^{57} decay in AgCl 8=39519
α-Fe, cold-deformed, solid solubility of C and N, normal and in stacking faults 8=35543
α-Fe, damping peak, cold-working 8=31204-5
α-Fe, neutron-irradiation effects saturation 8=31151
α-Fe solid solution, internal friction of C, effect of osc. modes on quantitative anal. 8=35695
α-Fe, solubility and permeability of S 8=43974
FeI, lifetimes of energy levels calc. from transition probabilities of spectra 8=47496
Fe I u.v. lines, gf shock tube meas. 8=29638
Fe(111) type film, energy and spin wave amps. eigenvalues 8=49512
FeIX to XIV, oscillator strengths 8=38668
Fe XV in solar corona, lines relative intensities 8=37082
Fe^{2+}, high-spin, electronic factors in paramag. relax. 8=40921
Fe^{2+} in $KMgF_3$, magnetoelastic coeffs. from acoustic paramag. resonance 8=31817
Fe^{2+} in MgO, low-lying energy level from spin-relaxation time meas., 4.2–13°K 8=45086
Fe^{3+} in $Al_2SiO_4F_2$, isotropic and dipolar contribs. to s.h.f.s. tensor 8=36244
Fe^{3+}, in CaO, uniaxial stress meas. at impurities, strain coeffs. 8=40134
Fe^{3+} in LiF, e.s.r. and n.m.r. 8=40920
Fe^{3+} in ZnSe, e.p.r. rel. to Fe^{3+} in cubic and axial fields 8=40949
Fe^{3+}/Fe^{2+} ratios in phosphate and oxide mixtures, Mössbauer quantitative anal. 8=27778
Fe^{+m}, $(8 \leq m \leq 15)$, ionization cross sections rel. to solar corona temp. 8=37085
Fe:Co^{60}, spin lattice relax., low temp. deviations from Korringa law 8=45106
Fe^{2+}:MgO, spin-lattice relaxation by phonon avalanche 8=40941
Fe : Pd, magnetic hyperfine field, temp. depend. 8=45016
Fe:Sb^{125}, mag. hyperfine fields and spin-lattice relax., from n.m.r. 8=31891
in GaAs, activation energies 8=40238
in Ir, Os-Ir and Ir-Pt alloys, resistivity temp. dependence 8=40318
on LiF, films, single-cryst., epitaxial growth 8=35170
on MgO, films, single-cryst., epitaxial growth 8=35170
Mn effects on impact properties 8=35693
$2MnO.SiO_2$ inclusions, e microprobe obs. 8=27802
from NH_3 synthesis, and N chemisorption 8=41265
Ni effects on impact properties 8=35693
in Ni_3Ga, giant mag. moment inducement 8=27423
P stabilized, b.c.c., diffusivity of O 8=44387
Tm^{169} implanted, time-dependent hyperfine interaction 8=39524

Iron alloys
See also Iron compounds; Steel.
Alni alloy, chem. comp. and magnetization ageing dependence, Mössbauer exam. 8=49514
austenitic Fe base alloys, statistical thermodynamics of C 8=39903
austenitic, plastic deform. effects on phys. props. during ageing 8=35699

Iron alloys—contd
  electron probe microanalysis, absorpt., fluoresc. and 2 corrections 8=27802
  electropolishing, "Universal" technique applications 8=44027
  f.c.c., containing Pt group elements, magnetization saturation 8=40736
  ferrite, diffuse x-ray scattering from doublet defects 8=39996
  Invar alloys, magnetostriction, anomalous volume 8=36138
  Invar, magnetization, pressure depend. from 30-450 kbar 8=31622
  kovar, stress-corrosion cracking prevention by Ni plating 8=31211
  liquid, containing S, phase equilibrium 8=41249
  martensite, diffuse x-ray scattering from doublet defects 8=39996
  martensite nucleation in Ni-Fe alloys showing disrupture transform. kinetics 8=39555
  n.m.r., rel. to dilute impurities of 4d and 5d elements of group VIII 8=49642
  permalloy sheet obs. of texture during recrystallization 8=35282
  Silectron, magnetization, pressure depend. from 30-450 kbar 8=31622
  silicon bronze, with low stacking fault energy, shock loading effects on lattice 8=31098
  Al-0.04 wt % Fe, recryst. and recovery rel. to Fe precip., obs. 8=39664
  Cr-Fe, catastrophic grain boundary corrosion 8=45329
  Fe base, thermodynamic props. of interstitial solutions 8=44328
  Fe-based sintered metals, self-lubricating, sliding wear characts. 8=31187
  Fe-rich solid solution alloys with non-transition elements, saturation magnetization 8=49519
  Fe-Ag associated in II-VI cpds., paramag. reson. 8=27474
  Fe-Al alloys, magnetization and spin-wave stiffness in Heisenberg model 8=31645
  Fe–Al, detailed spin-echo spectra rel. to hyperfine interactions 8=31906
  Fe-Al, ferro-, antiferro- and superparamag. props. 8=31615
  Fe-Al interaction energy with the magnetization of Al solute pairs 8=31614
  Fe-Al, order-disorder transformations 8=39557
  Fe-Al, structure and mechanical props. 8=39720
  Fe-Al, K-state effect on mag. props and residual elec. resistance 8=49525
  Fe-Al, "K-state" transmission electron microscopic study 8=48597
  Fe-Be, 3-D modulation of struct 8=30650
  Fe-Be, Mossbauer effect and mag. props. 8=26024
  Fe-C martensite, Mössbauer effect during tempering 8=48323
  Fe-C martensite, Mössbauer studies 8=26020
  Fe–C martensite, yield strength and transformation substructure 8=26812
  Fe-C, X-ray microanalysis of standard, Midwest Probe Users Group report 8=30851
  αFe-C(N), mag. losses in case of Snoek relax., temp. depend. 8=40880
  Fe-Co alloys, deviations from Bloch law, temp. depend. 8=27411
  Fe–Co, high field susceptibility 8=45013
  Fe-Co, hyperfine field distrib. from Fe^{57} and Co^{57} NMR 8=45120
  Fe-Co in fine particles, order-disorder transform. 8=39556
  Fe-Co powders, mag. permeability meas. at 400-40 000 Mc 8=40810
  FeCo, 3d-electron redistrib. from X-ray spectra 8=35780
  Fe-Co-Ni-Al-Cu system alloys with added Nb and Ti, high-coercive phases rel. to anisotropy 8=27415
  Fe-Co-Ni-Al-Ti, ticonal-type, oriented modulated structure 8=35056
  $Fe_{2-\delta}Co_{\delta}W$ solid soln., magnetostriction of polycryst. samples 8=40815
  Fe-Cr, activation anal. of Cr contents in inclusions 8=36652
  Fe-Cr, alloy-oxide interface texture obs. 8=26103
  Fe-Cr alloys, oxidation study by glancing angle X-ray diffr. technique 8=49868
  Fe-Cr, anodic passivation, influence of Si and Al additions 8=36602
  Fe-Cr binary, oxidation 8=36559
  Fe-18% Cr. complex scale formation on oxidation 8=45340
  Fe–Cr, diffusion of C at 350°C, preliminary cold plastic deformation effects 8=35490
  Fe-Cr films, exchange constants from spin-wave resonance spectra 8=36147
  Fe–Cr, high field susceptibility 8=45013
  Fe-Cr, hydrogen permeability temp. dependence rel. to deformation and annealing effects 8=35489
  Fe-Cr, oxidized surface film interface 8=44074
  Fe-16 Cr, pitting corrosion in solns. of Cl^- 8=44102
  Fe–Cr system, athermal martensitic transforms. 8=44000
  Fe-Cr, X-ray microanalysis of standard, New York Metropolitan Probe Users Group report 8=27813

Iron alloys—contd
  Fe-Cr-C, bainite transform., transmission e-microscope exam. 8=30694
  Fe-8%Cr-1.1%C alloy bainite transformation crystallography 8=30693
  Fe–21%–Cr–0.05%C, ductile fracture mechanism, 20-600°C 8=26819
  Fe-Cr-Ni, antiferromag. investigation 8=36209
  Fe-Cr-O, system, low-temp. oxidation, glancing angle X-ray diffraction technique 8=27703
  Fe-Cu associates in II-VI cpds, paramag. reson. 8=27474
  Fe–Ir, equilib. with Fe oxide and CO_2–Co atmos. 8=43999
  Fe-Li associates in II-VI cpds., paramag. reson. 8=27474
  γ-FeMn, antiferromagnetism 8=31770
  Fe-Mn internal oxidation rate rel. to temp. 8=45336
  Fe–Mn, structural changes due to stacking fault conc. rel. to Mn content 8=35576
  Fe-Mn-N, high temp. strengthening. Mössbauer study 8=49019
  Fe–Mo, ageing charact., precipitate growth 8=44004
  Fe–Mo system, phase identification using diffusion couples 8=48381
  Fe-0.025% N, enhanced aging due to γ-α transform 8=44577
  Fe-N martensite, structure electron transmission 8=39721
  Fe-N, resistivity mag. field dependence at 4.2°K 8=31319
  Fe-Ni binary martensitic transformation, effect of cyclic heat treatment 8=26071
  Fe-Ni, deformed, return of saturation magnetization and resistance 8=31639
  Fe-Ni, diffusion of Au, lattice parameter change 8=39789
  FeNi electrodeposited films, magnetization reversal obs. 8=31644
  Fe-Ni, f.c.c., Curie temp. and C effect 8=31646
  Fe–50Ni, fibre-reinforced, mech. and mag. props. 8=31209
  Fe-Ni, films, domains and mag. fine structures form., e microscope obs. 8=31640
  Fe-Ni films, Faraday effect and optical consts. 8=36358
  Fe-Ni films, switching along easy axis above nonuniform rot. threshold field 8=31630
  Fe-Ni(50-50) crystals, n-irradiated in mag. field, magnetization curves 8=36144
  Fe–Ni, high field susceptibility 8=45013
  Fe-Ni, isothermal compression up to 300kb, crystallographic obs. 8=49006
  Fe–Ni magnetic thin films, exchange stiffness const. 8=49522
  Fe Ni, Mössbauer eff., temp. depend., and exchange anisotropy 8=48328
  γ Fe–Ni, Mössbauer study 8=48333
  Fe-Ni, plane Hall effect, temp. depend. and role of scatt. mechanisms 8=40324
  Fe-Ni single crystal, Mössbauer effect 8=35037
  Fe-Ni, spin-wave dispersion, relation 8=31624
  Fe-Ni, X-ray microanalysis of standard, Midwest Probe Users Group report 8=30851
  Fe-Ni, X-ray microanalysis of standard, New York Metropolitan Probe Users Group report 8=27813
  Fe-Ni-Al-Ti, Laves phase of comp. $(Fe, Ni)_{2-3.5}(Ti, Al)$ 8=35106
  Fe–Ni–C, austenite, deform. twinning at room temp. 8=44468
  Fe–Ni–C martensites, solid solution hardening and thermally activated deformation 8=26816
  Fe-Ni-Co ferrites, induced anisotropy constant angular dependence 8=45039
  Fe-Ni-Co ferromag. films, anisotropy, review 8=36148
  Fe-Ni-Co films, anisotropy, coercive force and s.h.f. reson. absorpt., obs. 8=31629
  Fe-Ni-Co films, mag. anisotropy, domains and saturation magnetization, obs. 8=40809
  Fe-Ni-Cr-Nb, strengthening identification 8=44574
  Fe–Ni–Ti, plastic deform. effects on phys. props. during ageing 8=35699
  Fe–Ni–Ti, Young's modulus rel. to texture changes in $\gamma \rightarrow \alpha$ and $\gamma \rightarrow \alpha \rightarrow \gamma$ transforms. 8=35701
  FeNi-FeNiMn multilayer films, mag. coupling 8=36133
  $Fe_{0.98}O$, Neel temp. determ. by elastic modulus method 8=31772
  $Fe_{80}P_{12.5}C_{7.5}$, amorphous ferromagnet, magnetization and hyperfine field temp. dependence 8=40813
  Fe-Pd, dil., hyperfine field at Fe, mag. field dependence 8=36081
  FePd, resistive anomaly near Curie point 8=49163
  Fe-Pd, structural transforms. and mag. props. 8=35102
  $FePd_x$, $(x = 3.1)$, Fe^{57} hfs temp. dependence near Curie temp. 8=45015
  $Fe(Pd_xPt_{1-x})_3$, antiferro-ferromag. transition mechanism obs. 8=40808
  Fe-Re, ductile foil, electrochem. prep., study of Fe, Cr and Fe-Re deposits 8=36609
  Fe–Rh, equilib. with Fe oxide and CQ–CO atmos. 8=43999
  Fe-Rh, mag. transitions pressure dependence 8=40735
  Fe–Ru, magnetic properties, electrical resistivity 8=49481
  Fe–Si, creep mechanisms 8=40154
  Fe-3% Si, cube texture secondary recryst. and mag. props., obs. 8=26265

Iron alloys—contd
- Fe–Si, diffusion of C at 350°C, preliminary cold plastic deformation effects 8=35490
- Fe–1.35Si, fibre reinforced, mech. and mag. props. 8=31209
- Fe-Si, H charged, diffusional relax. effects 8=36223
- Fe-3%Si, critical shear stress and plastic flow 8=44568
- Fe-Si crystals X-ray diffr. contrast at ferromagnetic domain walls 8=27409
- Fe-3% Si, hysteresis loss and magnetostriction hysteresis in rotating fields up to 2000 Oe 8=31680
- Fe-3%Si, magnetization by Barkhausen jumps, hysteresis freq. depend., obs. 8=40789
- Fe-Si, magnetization curve and energy losses in alt. mag. fields, effect of dislocations 8=36142
- Fe-3%Si (100) and (110) surfaces, surface energy by surface relax. meas. 8=26101
- Fe-Si shade etchings, orientation dependency 8=35222
- Fe-3.14%Si, single and polycrystalline, dislocation velocity 8=26675
- Fe-Si, slip bands after two bendings in opposite directions 8=48863
- Fe-3% Si, surface and grain boundary energies in presence of O_2 8=26102
- Fe–3%Si, twinned, creep at 600°C 8=35681
- Fe–V, high field susceptibility 8=45013
- Fe–W system, equilib. diagram and lattice parameters 8=30692
- on LiF, ferromag. films epitaxial growth 8=35170
- Mg alloyed cast iron, laser spectrochemical analysis 8=32157
- on MgO, ferromag. films epitaxial growth 8=35170
- NiFe, film, electrodeposited, mag. switching behaviour 8=27419
- Ni-Fe, magnetoelastic sensitivity, composition gradient effect 8=36111
- Ni-Fe polycrystalline, mag. anisotropy induced during evaporation and annealing 8=36152
- Si–Fe, collective recrystallization and polygonization in fatigue testing 8=48558

Iron compounds
- See also Ferrites; Iron alloys; Steel.
- botryogen, crystal structure 8=39790
- calcined ferric oxides, dissolution behaviour rel. to calcining temp. 8=45337
- carbides, phase transformations thermally induced 8=44003
- carbonyl complex, $Fe(en)_3Fe_2(CO)_8$, crystal structure 8=26380
- chalcopyrite, $CuFeS_2$, Mossbauer spectra, 300–448°K 8=26019
- chromites, phase transformation, X-ray and Mössbauer effect study 8=35101
- disc, energy losses on rotating in alternating and direct mag. fields 8=36102
- ferric complexes in acid solns., p.m.r. 8=43879
- ferric complexes with desoxyribonucleotides, p.m.r. 8=43880
- ferrites with spinel struct, Kβ-group of X-ray lines 8=31988
- haematite crystal growth by vapour-solvent method 8=26251
- hematite, mag. moment direction pressure dependence to 41 kbar, n. diffr. exam. 8=45059
- hematite, magnetic domains and evidence for new wall structure 8=27408
- hematite, specular, temp. variation of mganetisation and susceptibility 100°K–1000°K 8=40791
- limonite, Mössbauer effect study 8=35031
- magnetite oxidation to γ-Fe_2O_3, mechanism rel. to Fe^{2+} diffusion 8=27702
- magnetite, single domain, in pyroxene grains, rel. to total thermoremanence of rock 8=50230
- oxides, Fe Kβ X-ray spectra rel. to valency energy bands 8=41084
- oxide film growth in neutral soln. 8=27706
- oxides, thermodynamic props. by e.m.f. meas. 8=48729
- oxides with spinel struct, Kβ-group of X-ray lines 8=31988
- phosphate glasses electronic carriers, thermally activated diffusion 8=49079
- prophyrins, Mossbauer spectroscopy 8=26021
- Prussian blue, Mossbauer effect 8=39518
- -rare-earth intermetallics, hyperfine field at Fe from Mössbauer effect 8=36146
- semi-borides, thermoelectric power 8=40640
- Turnbull's blue, Mossbauer effect 8=39518
- wustite($Fe_{1-y}O$), composition-oxygen partial pressure diag., thermogravimetric determ. 8=36540
- Fe carbonyl, cyclopentadienylcarbonyliron mercury tetracarbonyl cobalt, crystal structure 8=26398
- Fe carbonyl, $[(C_6H_5)CSFe(CO)_3]_2$, crystal structure 8=26398
- Fe complex, bis(1,2-cyclohexanedionedioxime) FeII XY, Mossbauer spectral 8=30640
- Fe complex, cyclopentadienyl iron sulphide, crystal and mol. structure 8=26537
- Fe complex, phthalocyanine $Fe(II)[Z_2$, Mossbauer spectra 8=30640
- σ-Fe diarylene, Mössbauer investigation 8=35039
- Fe glazes, FeO content rel. to shade 8=49717
- Fe(II) octahedral complexes, Mössbauer effect, $^5T_2$-'A, crossover 8=35038

Iron compounds—contd
- Fe(III) complex, tetra-(n-butyl)-ammonium bis-(maleonitriledithiolate)Fe(III) structure 8=25469
- Fe(III) coordination no. in organic complexes, Mossbauer determ. 8=39516
- Fe(III) porphyrin cpds., zero-field splitting 8=30623
  - Fe_3Al, internal mag. field temp. dependence for two sublattices 8=27410
- $FeAl_2O_4$, cation distrib., Mossbauer and X-ray diffraction study 8=35331
- Fe_xB, (x = 1, 2), electron sp. ht. 8=30965
- FeC_x in carbon steel, particle coarsening 720°and 675°C 8=30691
- $Fe(C_{12}H_8N_2)_3Sb_2(C_4H_2O_6)_2.8H_2O$ crystal and mol. structure 8=26397
- Fe(III)Cl-methanol solns, Fe(III)-chloride distance 8=43764
- $FeCl_2$, Mössbauer fraction temp.-dependence, 10-300°K, anomalous, low-temp anharmonicity interpretation 8=48326
- $FeCl_3$. Mossbauer effect, 3°-310°K. obs. 8=30641
- $FeCl_3$ vapour, intercalatron isotherm on graphite 8=27697
- $FeCl_4^-$ anion, intensities of d-d transitions 8=29736
- $FeCl_2.H_2O$, Mossbauer effect, 3°-310°K. obs. 8=30641
- $FeCl_2.2H_2O$, antiferromagnet, nuclear spin-lattice relax., 1.3° to 12°K 8=31898
- $FeCl_2.4H_2O$, Mossbauer study, 4.2-0.025°K rel. to mag. props. 8=36211
- $4(FeCl_2.H_2O)$ stilbene, Mossbauer effect, 3°-310°K. obs. 8=30641
- $Fe(CN)_6^{3-}$, n.m.r. of aq. soln. 8=48225
- $Fe(CN)_6^{4-}$. n.m.r. of aq. soln. 8=48225
- $Fe(CN)_5NO^{3-}$, e.p.r., hyperfine anal. 8=47683
- $Fe(CO)_5$. semiempirical MO model 8=47594
- $Fe_xCo_{1-x}S_2$ pyrite solid solutions. prep. and lattice parameters 8=48342
- $FeCr_2O_4$, electronic and mag. props. from Mossbauer spectra 8=31726
- $FeCr_2S_4$, magnetically induced quadrupole interactions 8=45060
- $FeCr_2S_4$. NiAs-type structure. magnetization. 1.5°K to room temp. 8=45064
- $FeCr_2S_4$-$CuCr_2S_4$ spinels, elec. transport props. 8=31373
- $Fe_{1-x}Cu_xCr_2S_4$. Mössbauer effect, indication of ion existence 8=39515
- FeF_2, antiferromagnetic, zero-magnon lines in 3800Å and near i.r. region 8=45061
- FeF_2, effects of exciton-magnon interactions on spin-allowed optical transitions 8=45062
- FeF_2, mag. susceptibility rel. to i.r. spectra 8=36210
- FeF_2 rutile antiferromagnet, spin-wave light scattering 8=36387
- FeF_2, spin-wave dispersion relations from n.-scattering 8=31771
- FeF_2, uniaxial antiferromagnet. props. exam. by cluster-variation method 8=45058
- FeF_3 crysts. cubic–rhombohedral transition. 410°C 8=44005
- FeF_3, sublattice magnetization near critical point 8=27416
- FeF_3 twinned crystals, antiferromag. resonance 4.2–400°K 8=31838
- FeF_3-FeF_2-MF(M = Li, Na, K, Rb, Tl) system, crystallog. classification of phases appl. to mag. props. 8=48651
- $Fe_xGa_{2-x}O_3$, ferrimagnetic props. from polarized n.-scattering 8=31727
- $Fe_xGa_{2-x}O_3$, magnetic structure 8=36139
- $FeHo_4S_7$ and certain isotypic cpds., crystal structure 8=44214
- $FeLiO_2$(β phase) Mossbauer effect, study 8=26022
- Fe_5LiO_8, short range order 8=26866
- $Fe(MSO_4)_2$, M = NH_4^+, K^+, Rb^+, Cs^+, crystal field splitting. Mossbauer studies 8=26023
- Fe(III) N, N-dialkyldithiocarbamates. Mössbauer effect 8=48329
- Fe-N single crystals, solid solution strengthening 8=49013
- Fe_2N composition, Mössbauer effect study of ε and ζ phases 8=30695
- Fe $Nb_{0.2}Ta_{1.8}O_6$ (tapiolite), neutron and X-ray diffraction studies 8=48614
- $Fe(NH_4SO_4)_2.6H_2O$ crystals, nuclear electric-field-gradient determ. 8=30626
- $Fe(NH_4SO_4)_2.6H_2O$, quadrupolar hyperfine anisotropy and mag. susceptibility 8=43951
- $FeNH_4(SO_4)_2.12H_2O$, Mossbauer spectrum, rel. to atomic spin time fluctuations 8=30642
- $Fe_{1-x}Ni_xCr_2O_4$. cooperative Jahn-Teller distortions 8=35052
- FeO content in Fe glazes, rel. to shade 8=49717
- $Fe_{0.98}O$, Neel temp. determ. by elastic modulus method 8=31772
- Fe_xO, sp. ht. comp-dependence 8=39916
- Fe_2O_3 compacts, shrinkage in range 800-1000°C, effect of additives 8=35067
- Fe_2O_3, Fe K_α line shift rel. to e microprobe analysis, obs. 8=27804
- Fe_2O_3, longit, magnetostriction, and antiferro-weak ferromag. transition 8=40868
- Fe_2O_3, molten, diffusion of Al_2O_3, rate 8=39343

Iron compounds—contd
- Fe_2O_3, spin-wave excitation-energy changes from n. scattering meas. 8=31638
- α-Fe_2O_3, chemical reduction to Fe_3O_4 and substrate-product topotaxy 8=26072
- α-Fe_2O_3, crystal growth by temp.-alternating method 8=44107
- α-Fe_2O_3, ferromag. domain structure of natural and synthetic crysts. 8=31648
- α-Fe_2O_3 fine particles, spin flip temp. shift particle size dependence rel. to lattice dilation 8=27414
- α-Fe_2O_3, mag. memory rel. to neg. pressure effects on Morin transition pt. 8=31616
- α-Fe_2O_3, n scatt scatt. by antiferromag. spin waves, polarization effects, obs. 8=36187
- α-Fe_2O_3, superparamagnetism obs. by Mössbauer effect 8=49521
- α-Fe_2O_3, synthetic and natural, variation of remanent magnetization with temp. 8=31647
- α-Fe_2O_3, twinned, bladelike platelet growths on iron, selected area e.diffr. exam. 8=48518
- α-Fe_2O_3, whiskers and twinned platelets, defect diffusion during growth rel. to gaseous oxidation 8=44150
- α-Fe_2O_3 whiskers, growth and props. 8=35255
- δ-Fe_2O_3 (hydrate), cryst. structure 8=44215
- γ-Fe_2O_3 particles, acicular, mag. props. crystallite size dependence 8=31635
- Fe_3O_4, films growth in LiOH solns., two-phase struct., 300°C 8=44043
- Fe_3O_4, (magnetite) crystals, elastic deformation, remanent and transitory effects 8=31728
- Fe_3O_4 powder, influence on ferrite synthesis 8=45035
- Fe_2O_3: Co, induced anisotropy, dependence on annealing temp. 8=36186
- Fe_2O_3-$3La_2O3$-SnO_2, crystal structure and formation kinetics 8=48650
- α-Fe_2O_3: Ti, mag. resonance rel. to doping and canted antiferromagnetic structure 8=36231
- $Fe(OH)_2$. Fe^{57} Mossbauer effect 8=39517
- $Fe(OH)_2$, sorption of Ru and nitrosylrothenium, ionic and colloidal, obs. 8=44073
- $Fe(OH)_3$, absorpt. and coprecipitation of Ag 8=48478
- α-FeOOH, crystal and mag. structures, n-diffr. exam., —190 to 120°C 8=30894
- β-FeOOH rod crysts. sizing by light scatt. from streaming suspension, obs. 8=30549
- FeP, magnetic and thermodynamic props. 8=27378
- $Fe_3(PO_4)_2 . 4H_2O$, ludlamite, single crystal susceptibility obs. 8=27379
- $Fe_3(PO_4)_2 . 4H_2O$, ludlamite, static magnetization obs. below 15. 3°K 8=27413
- Fe–Se systems, phase diagram 8=48254
- FeS, magnetic structure 8=36139
- FeS_2 pyrites, mag. props. 8=36078
- FeS_2, pyrites struct., growth by Cl_2 transport 8=26249
- Fe_2S, thermal decomposition in fluidized bed 8=41250
- Fe_3S_4, magnetic synthesis 8=41248
- Fe_7S_8, mag. anisotropy energy origin 8=31634
- Fe_7S_8, pyrrhotite, ferrimagnet, sublattice rotations, mol. field model 8=31725
- $FeSO_4$ Fricke-Miller dosimeter, G(Fe^{3+}) yield, 62 keV X-rays 8=42457
- $FeSO_4 . 7H_2O$ crystals, nuclear electric-field-gradient determ. 8=30626
- Fe_7Se_8 mag. anisotropy energy origin 8=31634
- FeSi band structure from elec. meas , 100–450°K 8=35769
- FeSi, ferromag. domains by magnetization in alternating fields up to 20 kcpsec. 8=49524
- $FeSi_2$, β-phase, struct. 8=30862
- β–$FeSi_2$, space group symmetry, Mössbauer determ. 8=48325
- Fe_3Si, internal mag. field temp. dependence for two sublattices 8=27410
- Fe_5Si_3, C-stabilized, mag. moments and hyperfine interactions 8=31623
- β-$FeSi_2$:Co, Al, electrical conduction mechanism 8=35885
- Fe_2SiO_4, thermal diffusivity at high press. and temp. 8=48762
- Fe_2SiO_4-Mg_2SiO_4 system, olivine-spinel transition, geophys. applic. 8=36678
- $FeTa_2O_6$, neutron and X-ray diffraction studies 8=48614
- $FeTbO_3$, magneto-electric effect 8=36217
- Fe_2TeO_6, Mössbauer effect, magnetic structure 8=49457
- Fe_2TiO_4, Mössbauer spectra for electronic structure 8=48327
- FeV_2O_4, electronic and mag. props. from Mossbauer spectra 8=31726
- $H_4Fe(CN)_6$, twinning rel. to H bonding 8=26186
- $NiFeS_x$ films, electrodeposited rel. to vacuum deposited 8=35177
- YFe garnet, excited by mag. field pulses, optimal conditions of re-emission 8=28612

Irradiation effects. See Biological effects of radiations; Chemical effects of radiations; Physical effects of radiations.

Ising lattice. See Statistical mechanics.

Ising model. See Alloys; Ferromagnetism.

Isomerism
- See also Nuclear isomerism.
- acryloyl fluoride, rotational isomers 8=38864

Isomerism—contd
- $\alpha\beta$-unsaturated ketones 8=29788
- alkyl derivatives of benzene, photoisomerization 8=49949
- allyl cyanide, microwave dipole moment obs. 8=34304
- difluoroacetone, symmetrical, rotational isomerism 8=29783
- ethyl formate, rotational isomers 8=25572
- methallyl iodide, rotational 8=43370
- methyl vinyl ether, rotational 8=29790
- phthalic acid distribs., infrared spectroscopic determ. of isomers 8=34346
- rotational, obs. by partial saturation in double n. m. r. 8=29812
- 3-butenenitrile, vibr. spectra and rot. isomerism 8=25551
- 2-butenes, cis-trans isomerization, benzene photosensitization 8=49959
- 2-butenes, n. m. r. and steric effects 8=47698
- octyl alcohols, liq., intermolec. assoc. 8=30508-9
- octyl alcohols, intermolec assoc. and dielec. props. 8=48182
- C_7H_{12}, mono- and bicyclic isomers, mass spectra 8=39059
- $[(C_6H_5)_3FC_4]_2$, isomerization 8=39642
- N_2F_4 8=38839
- N_2H_2, extended Huckel calc. 8=25509

Isomerization. See Isomerism.

Isotope effects
- alkali halides, U centre, in absorpt. bands rel. to e-phonon interaction 8=27557
- alkaline-earth carbonates, C-isotope effects on i. r. spectra 8=31966
- aromatics, triplet-state lifetimes, effect of partial deuteration 8=34306
- benzene isotopic mixed crysts., phosphorescence, fluorescence and absorpt. spectra 8=49771
- benzene, isotopic mixed crystals., trap-trap triplet energy transfer 8=36527
- benzene, isotopic mixed crysts., triplet-triplet annihilation and delayed fluoresc. 8=41225
- benzene, phosphoresc. decay, deuteration effects 8=49826
- chlorobenzenes, effect of D substitution on Cl n. q. r. 8=27517
- in crystal-field splitting 8=26012
- energy transfer in isotopically mixed crysts. 8=27668
- Franck-Condon factors 8=34271
- hydroxyl radical kinetics, deuterium isotope effects 8=27707
- ice VII, H_2O and D_2O, effect of press. on vol. 8=49026
- isotope labelling of cpds., for probing chemistry underlying mass spectra 8=25393
- laser i.r. line shifts, variable length cavity meas. 8=28652
- lattice vibration, rel. to isotopic mass 8=35375
- magnetic ions in host lattices, shift temp. dependence 8=49451
- methanol-d_1, irrad., isotopic comp. of H prod. 8=32136
- molecules, reduced partition function 8=29702
- nuclear potential radius shift calc. 8=25044
- quantum correction to effects on transport props. 8=37187
- shift in crystal-field splitting 8=39506
- temperature dependences 8=41235
- on vapour pressure differences in liqs, appl. of significant struct. theory 8=43755
- water and ice, vapour press. 8=39491
- Ar:H(D), solid, in absorpt. bands rel. to e-phonon interaction 8=27557
- C isotope effects on electrolytic dissoc. of org. ions 8=29669
- Ca region, calc. with density depend. N-N interaction 8=42802
- CH_4 and CD_4, liq. and gaseous, phys. props. 8=30588-9
- C_7H_6D radical, vibronic near degeneracy 8=47706
- D in proton spin relax. in paramag. ion solns. 8=30536
- D/H ratio during dehydration of $CuSO_4 . 5H_2O$ 8=30802
- D_2O–D_2H_2OD vapour press. 8=48283
- Dy spectrum, shift 8=47493
- Eu chelates, D isotope effects on luminesc. 8=30503
- Eu^{2+} and Eu^{3+}, shifts in electron transitions and changes in nuclear radii 8=48322
- GeO, molecular u.v. absorpt. spectrum 8=43301
- H and D halides, dissociative electron attachment 8=29965
- H_2 and D_2, chemisorbed on Rh, i. r. spectra 8=25470
- H_2 and D_2, vibr. relax 8=34240
- H_2, diffusion in Ni 8=31012
- H_2O, HDO and D_2O in non-aq. solvents, i.r. intensities 8=39377
- H_2O^{16} and H_2O^{18}, high-resolution i. r. spectrum 8=25478
- H_2O-C_2H_5OH vapour press. 8=48283
- He, solid, differential phonon scatt. 8=37355
- I_2 reactions activated by radiative neutron capture in liq. hydrocarbons 8=41296
- In. liq., isotope thermotransport 8=29671
- K oxalate hydrate, partly deuterated, d. m. r. 8=45122
- KBr:Li^+, on lattice resonant mode, from far i. r. spectra 8=36393
- KI:Ag^+, on lattice resonant mode, from far i. r. spectra 8=36393
- $Li^{6,7}$ positive ions self-diffusion effect in LiF from relative difference between ion mobilities meas. 8=3550

Isotope effects—contd
Li^{6,7}F, induced acoustic band far i. r. absorpt., 7°K 8=36396
Na^{22,24} ions, electromigration in molten nitrates 8=43782
NaCl^{35,37}, induced acoustic band far i. r. absorpt., 7°K 8=36396
NaCl:Cu^{+}, on lattice resonant mode, from far i. r. spectra 8=36393
Pb^{208} calc. with density depend. N-N interaction 8=42802
Si spectrum rel. to Si$_2$O vibr. states, 9μ 8=27607
Tb chelates, D isotope effects on luminesc. 8=30503
Xe, isotopic shifts of 13 i. r. laser lines, meas. 8=25367
Xe laser i.r. line shifts, obs. 8=28652
Isotope exchanges
rate data evaluation of electrodeposition method 8=45311
temperature effects 8=41235
Ba isotope exchange rate, zeolith A and Ag. soln. 100-180°C 8=45313
H between alcohol and mercaptan, i. r. spectroscopy 8=36545
$H_2 + D_2 \rightleftarrows 2HD$, catalyzed by Mo 8=49907
$H + H_2 = H_2 + H$ and isotopes, permeabilities 8=45312
in KBr, use in meas. Br diffusion 8=35497
$N_2^{28} + N_2^{30} \rightleftarrows 2N_2^{29}$ catalyzed by Mo 8=49908
NO and NO_2^-, exchange and fractionation of N 8=27674
NO_2^- and $NO^-{}_3$, exchange and fractionation of N 8=27673
O_2 on Pt powder 8=41236
Te isotope fractionation 8=41234
Isotope separation
See also Radiochemistry.
alkaline earth metal stearate targets and container CERN ISOLDE 8=38768
by carrier diffusion, for low-abundance isotopes 8=47550
chemical reactions contribution, theoretical remarks; ion exchange and solvent extraction 8=47549
Clusius-Dickels new type separation column 8=25395
concentration distrib. in separation columns 8=29672
e.m., retardation devices, comparison 8=34186
fast-acting e.m. separators, review 8=38765
fission fragments, primary, for yield and decay meas. 8=38543
fission prods., focusing parabola mass spectrometer 8=43129
fission product gases, short-lived, on-line system 8=38771
fission product inert gases and decay schemes, obs. 8=38545
fission products, mass-spectroscopic principles and gas-filled separator 8=38544
fission prods., short-lived, mass spectrometer 8=43130
gaseous diffusion, tapered cascade characts. 8=29670
liquid target, circulating, for on-line isotope separator 8=38605
on-line systems, review 8=38770
polyatomic gases by thermal-diffusion, theory and expt. data 8=38766
radiochemical of gases, solids and solns., rapid methods review 8=38767
in reactor, fuel, irradiated, mass spectroscopic determ. 8=29567
Sareq e. m. on-line separator with fission source 8=38769
stable isotopes, review of methods 8=34187
Ar^{36}, by thermal diffusion 8=47548
B^{10,11} by BF_3 distillation, pressure effect 8=25394
Ce^{145,146,147} by column partition chromatography, obs. 8=38430
He^{8} iron p-irrad. cotton fibres, obs. 8=38414
Hg from Pb p-spallation target 8=38394
In, liq., isotope thermotransport 8=29671
Kr and Xe from U^{238}O$_2$-stearate fission source, obs. 8=38549
N, between NO and NO_2^- 8=27674
N, between NO_2^- and NO_3^- 8=27673
Tl from Pb p-spallation target 8=38394
U^{235} and U^{238}, on commercial basis 8=47399
Isotope shifts. See Isotope effects; Spectra.
Isotopes
applications review for humidity meas., moderators, shielding, reactor materials, neutron detectors, optical standards 8=43245
in atmosphere, prod. by cosmic ray nucleons 8=29254
element 102, synthesis and study, review 8=29381
particle beam prod. in thick targets, conc. 8=37025
meteorites and moon surface, nuclide prod. by cosmic rays 8=37025
oxygen, bibliography of uses, 1963-66 8=34185
radioisotope production in JRR-3, n irradiation conditions 8=24947
C, fractionation in CO_2-gas-CO_2 in soln., and HCO_3-CO_2 in soln. systems 8=47547
Cd^{111,114} polarization of light emitted by optical resonance of 2288Å radiation 8=34158
Cd, optical resonance, polarization of radiation (2288Å) emitted 8=25359
Li^{6} and Li^{7} interdiffusion unisotopically pure Li melt 8=34807
Li metal, isotope inter-diffusion 8=39976

Isotopes—contd
Sb odd mass, low level props. calc. from core-particle-coupling model 8=42894
Sn^{117} and Sn^{119}, level crossing investigation of hyperfine struct. 8=29629
detection
See also Mass spectra; Radioactivity.
mass spectrometer for isotopic ratio of trace amounts of noble gases 8=47452
N^{15}, spectrochemical estimation, enhancement by inert gas 8=27791
relative abundances
See also Elements/relative abundances.
recording servoamplifier for mass spectrometer ion current ratios 8=38610
Be^{7,9} in solar cosmic rays, calc. 8=37057
C$^{16-18}$ and O$^{12-13}$ in Venus 8=28153
C and O composition variation in calcereous cave concretions 8=50096
Ca^{43,48}, determ. by neutron time-of-flight 8=36648
Co^{56,59} in solar cosmic rays, calc. 8=37057
Cs, $128 \leqslant A \leqslant 144$, U p-fission yield, 150 MeV 8=38542
Cs, fragments from p-reactions on U, Th, Ta 8=34001
N, determ. by recording spectrometer 8=28817
Na, $20 \leqslant A \leqslant 25$, Si p-spallation yield, 150 MeV 8=38542
Na, fragments from p reacts on Mo^{100}, Ta, Ir, U 8=34000
Os^{187} conc., spectrographic determ. 8=36635
Rb, $83 \leqslant A \leqslant 98$, U p-fission yield, 150 MeV 8=38542
Rb, fragments from p-reactions on U, Th, Ta 8=34001
Sr, ratios in volcanic rocks of three island arc areas 8=32186
Th and U concentrations and ratios in river sediments 8=50094
U^{235,238}, activation analysis by γ spectrometry 8=47546
U^{235,238} in natural U, Fabry-Perot spectrometer, meas. 8=28803
Zr in star HR1105 8=28069

Jahn–Teller effect. See Molecules.
Jet stream. See Atmosphere/movements.
Jets
See also Sprays.
air, free circular, velocity and temp. fields, osc. intensity 8=39190
air, turbulent, heat transfer and flow parameters to sphere 8=39205
axisymmetrical, averaged vels and vel. fluctuations rel. to initial flow turbulence 8=30223
bubble "microtime" for sampling liq. surface 8=30380
capillary action, impinging on liquid surfaces 8=34730
compressible, two-dimens.; hydromagnetic stability 8=46462
drop formation in liq.-liq. systems 8=39286
fluid, condensation of moving vapour stream 8=30598
fluid, ideal, one-dims., incompressible constitutive eqns. 8=48040
gas agitation of liquids 8=48029
gas flow caused by full radial jet distrib. in space restricted by two parallel planes 8=30249
gas, real, width of boundary layer and dimensionless profile of vel. head 8=39187
gas, subject to elect. discharge, prod. of plasma flame 8=38977
gas, transfer processes in mixing of two plane non-uniform jets 8=30241
impinging on wall of combustible mat., ignition problems 8=32971
Lavalle nozzle, transonic gas flow 8=39173
liquid, free, laminar flow at high Reynolds number 8=30357
liquid leaving Poisseuille tube, effects of gravity and surface tension 8=48039
liquid, non-linear capillary instability 8=43740
molecular, jet variations, thermo-optical detection 8=43431
mixing of five plane turbulent jets, expt. study of flow parameters 8=30240
radial-slot gas jets along plane wall, flow and heat transfer problems 8=30247
radiation-heated solid vapour jet 8=48291
recompression zone when deflected by a front wall 8=34612
rectangular, collection of particles by impaction, efficiency 8=48240
rotating free, compressible axisymmetric, down-stream flow eqns. 8=43657
spreading wall jets in mag. field, change of conductivity across jet 8=25790
stagnant region due to interact. with natural convection flow, heat transfer 8=34731
submerged in power fluids, numerical soln of movements 8=39281
supersonic, noise visualization 8=46194
tangential/wall friction meas. using Preston tube and balance 8=30268
turbulent, axis shape in unbounded horizontal cross flow 8=39167
2 dimensional, interaction with parallel flow 8=34589
viscoelastic materials, sudden flow, tensile stresses 8=30376

Jets—contd
  wall-jet, two-dimensional, impervious wall effectiveness rel. to upper lip boundary layer thickness 8=25851
  water, turbulent, CO_2 and H_2 absorpt. 8=30425
  water, vertical to free surface, vel. distribs. and expt. study 8=34732
  H_2, gaseous, forming and trapping in vacuum 8=43645
  HCl cutting of Au disk from sheet 8=32632
  Hg vapour supersonic, use for charge exchange of polarized ions 8=39039
  Rb, atomic clock, optical pumping 8=47525
Jets, cosmic-ray. See Cosmic rays/showers and bursts.
Jogs. See Crystal imperfections/dislocations.
Johnsen–Rahbek effect. See Adhesion; Electrostatics.
Johnson noise. See Fluctuations/electrical.
Jordan–Thiry field. See Cosmology; Relativity/general.
Josephson tunnelling effect. See Superconductivity.
Joshi effect. See Discharges, electric/glows.
Joule–Thomson effect
  i.r. detectors, coolers design 8=32944
  i.r. detectors, cooling techniques 8=32947
Jupiter. See Planets.

K-capture. See Radioactivity/electron capture.
KDP. See Potassium compounds.
Kaons. See Mesons.
Keratin. See Proteins.
Kerr effect. See Electro-optical effects; Magneto-optical effects.
Kicksorters. See Counting circuits.
Kikuchi lines. See Electrons/scattering.
Kinematics
  2-body relativistic collisions, kinematic broadening 8=47028
  n-body relativistic, covariant treatment 8=32699
  conservation of momentum, pitfalls in demonstration 8=28255
  controlled systems, motion 8=46019
  device for creating constant angular acceleration 8=46017
  infinite-momentum, of interacting particles 8=33558
  linear air track, strobe photography, demonstration 8=28253
  motion of solid with and without external moments, generalization of Eulenian case 8=46088
  motion problems, vector approach, quantum theory 8=46787
  oscillator, ID, quasirandom 8=46016
  plane elliptical restraint problem, regularization 8=32705
  rigid body finite displacements 8=32702
  rotation of solid with fluid filled cavity 8=46018
Kinetic theory
  from BBGKY expansions, and compatibility requirements 8=28320
  Boltzmann kinetic equation dependent on particle velocity 8=46125
  Boltzmann's H function, proof that successive derivatives alternate in sign 8=30278
  catalysis in cylinder 8=48109
  equations, derivations 8=37189/90/91
  many-particle system, operator relations 8=46115
  mass transfer in cylinder 8=48109
  non conservative interactions, statistical mechanics 8=46108
  nonspherical mols., transport coeffs. 8=39153
  operator props. 8=46109
  3-particle correlation function in a many particle system 8=28329
  plasma, energy exchange between components 8=30021
  plasma, inhomogeneous, in mag. field 8=43502
  plasma, ion-cyclotron waves 8=30148
  plasma-wave motion in presence of collisions 8=30155
  plasmas, weakly turbulent, approach to fluctuations 8=39134
  plasma, weakly turbulent, electron viscosity coefficient in strong mag. field 8=43514
  plasma, weakly turbulent, fundamental eqs. 8=43503
  small perturbation method 8=30209
  He liquid–metal heat transport, kinetic theory model 8=37338
 gases
   See also Association/gases; Brownian movement; Collision processes; Diffusion in gases; Equations of state/gases; Joule–Thomson effect; Molecules/intermolecular mechanics.
  air at high temp. 8=30273
  atmospheres, thermal escape, transition domain in spherical geometry 8=37008
  Boltzmann, dense, divergence free equation 8=23910
  collision integrals for high-temp. gases 8=34670
  dense gases, nuclear spin relax. and collision freq. 8=34669
  dense, space-time correl. functions for Enskog theory 8=43674
  density fluctuations, spectrum from soln. linearized Boltzmann eqn. 8=30285
  diatomic gas, transport coeffs. calc. 8=30307
  diffusion, thermal, Chapman-Enskog eqns. 8=30315
  energy transition probabilities in molecular collisions 8=34642
  globular mols., transport collision integrals 8=29848
Kinetic theory—contd
 gases—contd
  high temp. props. 8=30273
  ideal quantum, pressure calc. 8=37185
  ion mobilities, deviations from Blanc's law 8=39021
  Lennard-Jones pot., parameters from scatt. data 8=39192
  mass transfer between concentric spheres at low press 8=39235
  masses, adiabatic pulsations and convective instability 8=50321
  Maxwell molecules, 2 temp. uniform, mixture equilibration 8=34639
  model replacing statistical hypothesis 8=30277
  molecular streams from gas layers escaping into vac. 8=43673
  momentum and temp.-slip coeffs. with arbitrary accomodation at surface 8=47940
  monatomic, appl. to light scatt. 8=25829
  nonconservative forces, under action of 8=34641
  plasma, stable and weakly unstable 8=25723
  plasma, sub-relativistic 8=30002/3
  plasma, weakly turbulent, with collisions 8=43497
  polyatomic, between concentric cylinders at different temps., heat conduction 8=34638
  rarified, boundary layers in viscous flow 8=34602
  rarefied gases, approx. kinetic eqs. in theory 8=30275
  relativistic entropy law for mixture outside equilib. 8=25821
  relaxation, in monatomic gases for representation of viscosity 8=30297
  relaxation towards Maxwellian distribution of gas described by Boltzmann equation 8=47948
  slip velocity, thermal, near solid surface, gas-kinetic analysis 8=39175
  transport coeffs., rigid sphere perturbation calc. 8=30303
  variational principles for eqns. 8=34637
  virial coeff., second and intermolecular pot for spherically symm. mols. 8=47951
  Ar plasma, dense, weakly ionized, kinetic energy exchange 8=47805
  Ar_2 rarefied, stationary between concentric cylinders, wire probe equilibrium temp. 8=34655
 liquids. See Liquids/theory.
Kink pairs. See Crystal imperfections/dislocations; Plastic deformation.
Kirkendall effect. See Diffusion in solids; Precipitation.
Klystrons. See Electron tubes.
Knight shift. See Nuclear magnetic resonance and relaxation.
Knudsen number. See Flow; Hydrodynamics.
Kohn effect. See Crystal electron states; Crystals/lattice mechanics.
Kramers–Kronig relations. See Dielectric phenomena; Optical properties of substances.
Krypton
  in achondrites, U and Ca rich, anal. 8=28160
  adsorption on pyrex 8=30774
  adsorption on Zn, effect of chemisorbed O_2 8=48500
  afterglow, visible emission 8=47754
  atom, charge exchange with He^+ and Ne^+, 2-250 eV 8=38758
  atom, e scatt., E_e=20 eV-150 keV, relativistic effects 8=38720
  atom, $4p^55s$ levels excited by elec. discharge of Ne-Kr mixture 8=29882
  atom scatt. on Kr, total scattering cross sections 8=34178
  atomic collision Kr^+–Kr, sudden change in number of lost electrons at 25 keV 8=39018
  bubbles in UO_2, migration before and after annealing 8=26625
  charge transfer from p and H atom, cross-sections 8=38737
  crystal intrinsic luminesc., 20°-110°K obs. 8=27656
  diffusion in CaF_2 and U doped CaF_2 8=26618
  diffusion in $N_2O_4 \rightleftharpoons 2NO_2$ system, effect of chem. reaction 8=34681
  diffusion in scintillation counter plastic 8=35499
  diffusion in UO_2, UC and U doped CaF_2 8=34107
  electron-atom scattering, mobility max. 8=43229
  gas, shock wave of Z-pinch discharge, dynamics 8=34410
  ion sputtering on Al, Mo, Ta targets, ang. distrib. obs. 8=48909
  ionization by impact of monoenergetic electrons 8=43485
  solid and liquid, charge transport 8=26943
  solid, compression up to 20 kbar at 81 and 115°K 8=26836
  solid, equilibrium vacancy conc. meas 8=48809
  solid, model potentials and phonon dispersion curves 8=35389
  solid, pair pot. calc. 8=30615
  solid, thermodynamic props. from thermal expansion, sp. ht., compressibility and vacancy equil. conc. meas. 8=48745
  thermal cond., Langmuir calc. for incandescent lamps 8=42210
  in thermionic converter, effect on V-I characts 8=28481
  viscosity, low-temp. 8=39237
  Ag thermal desorption obs. 8=48483
  Au thermal desorption obs. 8=48483
  Br^- ions collision with atoms, detached electrons energy obs. 8=29972

Krypton—contd
- Cl^- ions collision with atoms, detached electrons energy obs. 8=29972
- Cu thermal desorption obs. 8=48483
- Hg-Kr glow discharge, e energy distrib. rel. to striations 8=34418
- I^- ions collision with atoms, detached electrons energy obs. 8=29972
- Kr^{83}, Mossbauer effect with Se^{83} sources 8=43952
- Kr^{83} n.m.r., local mag. field shift, obs. and theory 8=39226
- Kr^{85} leak test for evacuated tubes 8=47990
- Kr^{86} spectral line profiles from complex visibility Fourier transform, obs. 8=29619
- Kr^{86}, wavelength standard, reproducibility, discussion 8=23789
- Kr-propylene system, liq.-vapour phase equilib., and solubility 8=39479
- Kr^+ charge transfer dissociative reaction with propylene 8=34445
- Zn 3075.9 Å, perturbation of resonance line 8=47512

Krypton compounds
- H_2Kr, bound states, i.r. absorpt. 8=25472

Kuhn–Thomas sum rule. See Molecules/electronic structure.
Kurie plots. See Beta-decay theory; Beta-ray spectra.
Kyropoulos method. See Crystals/growth.

LCAO calculations. See Molecules/electronic structure; Orbital calculation methods.
LS coupling. See Atoms; Spectra/atoms.
Laboratories
- See also Acoustical laboratories.
- for cosmic rays, underground, near Turin (the Monte Cappucini lab.) 8=38133

Laboratory apparatus and technique
- adsorptive pumps for low temp. serial mass spectrometer evacuation 8=38608
- apparatus to achieve temps from 4.2 to 300°K, with temp. stabilization 8=28432
- autoclave liners (noble metal), corrosion during hydrothermal crystal growth reactions 8=49855
- bonding of thermoelements in thermoelec. dev. 8=49398
- ceramic-to-metal seals, graded, fabrication by isostatic gas, bonding 8=34692
- comparator for photoelectric microscope 8=46413
- control wiring, recording by computer 8=37808
- crystallographic specimen-holder, thermoelec. annealing 8=39755
- Dewar for cathodoluminescence meas. 8=41878
- Dewar, narrow-tail glass for liquid He 8=32994
- diaphragm cutter, fast acting 8=32630
- diffusion meas. apparatus for polymer solns. 8=48113
- electro measuring app. with strings, stability of mobile part 8=33009
- electron gun demountable 8=46404
- for electron paramagnetic resonance solid state obs. of radicals formed in gas phase by 5 to 500 eV electrons 8=25652
- electroreflectivity meas. at low temps., sample package 8=49696
- extraction efficiency flow distrib. and droplet boundary-layer behaviour dependences 8=48123
- film gauge for low density shock tubes, highly sensitive 8=32899
- flatness control in optical polishing 8=37652
- flow distrib. over contact, filtering and other Z-shaped app. 8=30360
- gas-cap radiation from simulated Martian atmos. probes 8=41569
- gas drying, moisture trap 8=50470
- gas fluidized beds, density and pressure fluctuations 8=48230
- gas humidity transducers, test rack 8=26001
- gas inlet valve, electromagnetic, very quick acting, for plasma expts. 8=47935
- gas mixtures, explosive, continuous flow mixing 8=34618
- gear hobbing machine table drives, diffraction gratings for error obs. 8=24373
- general relativity verification expt., synthesis 8=41745
- glass capillary sealing under pressure 8=50469
- glass tubing, production of extremely thin walls and small holes 8=32629
- goniometer head for low-temp crystal rotation 8=30815
- graphite cuvette for atomic spectroscopy 8=38619
- HF fractionation column 8=41608
- high heat flux density prod. 8=28393
- hydrothermal crystal growth, large noble metal can technique 8=44112
- internal friction and Young's modulus at h.f., meas. 8=40097
- isotope labelling of cpds., for probing chemistry underlying mass spectra 8=25393
- KCl, grain boundary mobility, meas. 8=40052
- labelling sand with Cr^{51} 8=50092
- laser beam splitting devices 8=37554
- liquid metal level meas. by induction probe. 8=38594
- low angle electron diff. camera, appl. to physics and biology 8=24149

Laboratory apparatus and technique—contd
- low-background radiation meas., alternating method, liquid scintillation counter 8=37772
- micro AgCl tech. for i.r. spectrophotometry 8=24403
- micrometeoroid impact simulation, study of craters and penetration 8=37028
- Mössbauer effect demonstrator 8=38350
- neutron generator for undergraduate lab. 8=38076
- optical instrument parts, machining with diamond-tipped tools on metal-cutting lathes 8=45939
- optical method for prod. Fresnel zone plates 8=28869
- organic coatings, book 8=32628
- packed bubble columns, filled with Raschig rings, performance 8=25858
- packed liquid extraction column, dynamic behaviour 8=49833
- particle accelerators and thermonuclear plasma, common problems 8=34064
- pipetter, remotely operated, for highly radioactive liquid samples 8=41295
- polishing, disproving previous hypotheses 8=50468
- pressure vessels, triaxial elec. lead-in 8=50474
- Pyrex toroidal section prod 8=41607
- quartz toroidal section prod. 8=41607
- regenerators, heat transfer surface, and design for fluids with variable thermophys. props. 8=30293
- rotating agitators for batch mixing of viscous liqs, model study of seven mixer types 8=30437
- rotor-position indicator, anal. of mag. irons for shape and size 8=33051
- sample holder for simultaneous gas sorpt. and X-ray obs. 8=33301
- sample holders for solution calorimetry 8=34831
- sample orientation in solenoid 8=45934
- seal faces, mean surface profile meas. 8=35138
- semiconductor detector for thin film thickness meas. 8=44029
- separation of particles by controlled cycling, apparatus and theory 8=35065
- silicides of transition metals, auxiliary metal bath procedure for synthesis 8=49835
- solar simulator for 3m space environment chamber, geometric optics princ. 8=28734
- spark timer, transistorized 8=28221
- specimen blanks for electron microscope, preparation 8=37098
- spring strip mounts control with piezoelectric 8=37249
- step annealing process for diffusion coeff. determ. 8=48773
- stress corrosion cell for uniaxial tensile tests 8=48970
- structure models, ball-drilling methods 8=32631
- surface-roughness measurement techniques, development in U.S.S.R. 8=48416
- surface texture profilometry, relocation 8=44019
- synthesis of oxidation resistant metal dibonde composites 8=45317
- for thermoluminescence with spectral dispersion 8=45252
- thin film coercivity rel.-to-temp.-, app.-for automatic meas. 8=31583
- torsion pendulum technique for internal friction meas. of glass fibres 8=40168
- for transferring crystal from one goniometer head to another 8=26345
- transmission electron microscope rapid thin foil preparation 8=28205
- u.h.f. investigation of e,m. fields in metal lattice 8=35026
- ultramicrotome cutting of f.c.c. metals, deformation produced, 8=48850
- vacuum apparatus for student practical work 8=30324
- wakes and shock caps of re-entry models, time-resolved spectra 8=41485
- water cooling system, leak detection by aspirin tablet 8=37097
- welding, explosive 8=28202
- Al extrusion temp. meas. using BACO radiation pyrometer 8=32982
- Al powder briquets, prep. for spectrochem. anal. 8=32158
- Al_2O_3, particulate, replication for e. microscope exam. 8=44160
- Au disk cutting from sheet by HCl jet 8=32632
- C articles, monolithic, semi-isostatic forming 8=45933
- GaP bulk ingot prep. 8=48542
- Li wire extrusion for exploding-wire system 8=50473
- $NaCl_3$ Rb–D_2 filter for student optical pumping expts. 8=42196
- p-Si crystal, ohmic contact with Al wire 8=40483
- Si soldered contact prep., metal hydride flux 8=45931
- Sn^{113} source, radioactive, fractional distillation from In^{113} 8=42954
- ZnS luminophors, preparation, effect of halide addition 8=49819

Lamb shift. See Spectra/atoms.
Lambda (λ) point. See Helium/liquid; Phase transformations.
Lamps. See Light sources.
Landé splitting factor. See Spectra; Zeeman effect.
Langmuir probes. See Discharges, electric; Plasma/measurement technique; Space vehicles/instrumentation.
Lanthanides. See Rare earth metals.

Lanthanons. See Rare earth metals.
Lanthanum
  $\beta \to \alpha$ phase transform., model and nucleation 8=44006
  K-ionized, L-K X-ray ang. correl. obs. and partial fluoresc. yield 8=41111
  secondary e emission coeff. and energy spectrum obs. 8=40716
  superconducting, structure in tunneling characteristics of thin film diodes 8=35850
  thermal expansion and magnetostriction, 1.5-40°K, rel. to superconducting transition temp. pressure dependence 8=35438
  La III spectra, principle series, transition probabilities in doublets 8=47506
Lanthanum compounds
  electron emission, laser-induced using ruby and Ar lasers 8=40710
  ethylsulphate:Er^{3+}, spin-lattice relax. times 8=45089
  La complex, ethylene diaminetetra-acetic, La(III), cryst. struct. 8=44223
  La nitrate soln, electrophoretic behaviour of monodisperse polystyrene latex particles 8=49923
  La tetrahydrate perrhenate, i.r. absorpt. obs. 8=36384
  LaB_6, rod cathode in high-brightness electron gun 8=28555
  LaB_6-La system cathodes, emission characts. 8=27348
  $La_{1-x}Ba_xEu_xLi_xPO_4$, luminescence rel. to mixed valency Eu centres 8=45278
  $La_2Be_2O_5$, crystal structure 8=39799
  LaC_2, crystal structure changes on phase transform at 1060°C 8=26405
  La–Ce alloys, susceptibility above magnetic ordering temp. evidence for spin compensation 8=40750
  $LaCl_3$, first-order Raman scattering depolarization 8=27578
  $LaCl_3$:Ce^{3+}, i.r. Zeeman effect at 77 and 27°K 8=36383
  $LaCl_3$: Gd^+ e.p.r. determ. of Gd^{3+} pair-interaction constants determ. 8=31775
  La-Cu double nitrate, heat capacity below 1°K 8=44336
  $La_{3\cdot33}Cu_2S_6$, double sulphide, crystallographic and structural data 8=30800
  in LaF_3, energy transfer between rare earth ions, temp. depend. 8=45138
  LaF_3, i.r. dispersion rel. to lattice vibrations 8=45201
  LaF_3, lattice defects and F motion 8=31048
  LaF_3, tysonite-type crystals, NMR and electronic structure 8=27506
  LaF_3, vapour press., enthalpies and entropies in range 1050°-1200°C 8=35015
  LaF_3:Dy^{3+}, absorpt. and fluoresc. spectra 8=31985
  LaF_3: Pr^{3+}, spontaneous emission probabilities and quantum efficiences 8=49805
  LaF_3:Nd^{3+} laser, continuous stimulated rad. at 300°K 8=37616
  LaF_3:Pr^{3+}(Nd^{3+}), NMR of F^{19}, relax. times, 150-800°K 8=45127
  LaF_3-SrF_2:Nd^{3+} laser operating at 300°K 8=27579
  $LaFeO_3$, e.p.r. rel. to weak ferromagnetism 8=27488
  $La_{1-x}Gd_xAl_2$, superconducting, transition temp. dependence on Gd spin conc. 8=27016
  $La_{2-x}Gd_xCoMnO_6$, mag. interactions and structure 8=27417
  $(La, Gd)_2CoMnO_6$ system, mag. interactions and crystal structure 8=49527
  $La_2M_3''(NO_3)_{12}.24H_2O$: Gd, ($M''$ = Zn or Mg), e.p.r. angular spectra, anomalous 8=45080
  $La_2Mg_3(NO_3)_{12}.24H_2O$: Cu^{2+}, spin-lattice relax 8=40950
  $La_2Mg_3(NO_2)_{12}.24H_2O$:$Mn^{2+}$, e.p.r. 8=40928
  $La_2Mg_3(NO_3)_{12}.24H_2O$:$Mn^{2+}$ zero-field splitting 8=30627
  $La_2Mg_3(NO_3)_{12}.24H_2O$: Nd, electron spin lattice relax. of Nd 8=31872
  $La_{3\cdot33}MnS_6$, double sulphide, crystallographic and structural data 8=30800
  $LaNbO_4$: Nd^{3+} luminescence obs. 8=36515
  $LaNiFe_{11}O_{19}$, persistent polarization after appl. of d.c. field 8=31424
  LaO spectral high resolution using hollow cathode lamp and Fabry-Perot spectrometer 8=29675
  La_2O_3, retention of additives 8=39693
  $La_2O_3.3B_2O_3$, crystal structure and isotypism 8=48657
  La_2O_3 (Bi) phosphor, excitation and emission spectra 8=45279
  LaOOH, synthetic, crystal structure 8=48658
  $La_4Re_6O_{19}$, metal-metal bonding 8=48305
  $LaRu_2$: Gd^{+++}, magnetic susceptibility and e.p.r. study 8=31502
  LaS, vaporization and dissoc. energy 8=48287
  LaSb, thermal and elec. props. rel. to semi-metal charact., 8=39948
  LaSb, thermoelec. power temp. dependence, 80-500°K 8=27309
  La_3Se_4, superconductivity rel. to lattice and electronic props. 8=27017
  $(La, Sr)CoO_3$, localized- to collective-electron transition 8=35773
  $LaTaO_4$: Nd^{3+} luminescence obs. 8=36515
  La-Tb alloys, antiferromagnetism rel. to h.c.p. and d.h.c.p. structures 8=31792
  $LaTO_3$, (T = Ho, Y, Er, Tm, Yb, Lu), crystallography and mag. props. 8=48656
Lasers
  See also Light/coherence.
Lasers—contd
  active isotropic medium, temp. pot. 8=24273
  air spark induction, shock wave theory 8=28369
  for angular meas. 8=45950
  anisotropic, polarization characts., Poincaré sphere calc. 8=33170
  with aspherical lens, for increased brightness 8=28728
  atmosphere irradiation, water vapour luminescence 8=3882
  atomic models for nonlinear interactions of e. m. waves in population-inverted medium 8=33159
  autoresonance energy transfer in active media, investigation methods 8=46543
  axial mode, influence of length limitation 8=37560
  beam-addressable memory device, low temp. with EuO film 8=36123
  beam damage on metal crystals 8=30716
  beam deflection, use of electrooptic prisms 8=42062
  beam expander for divergence correction 8=28743
  beam focusing by CdS active oscillator 8=28882
  beam focusing by spherical lens 8=36377
  beam modulation using grating diffraction effects 8=42123
  beam narrowing in colloids 8=34951
  beam phase fluctuations, effect of lab. generated turbulence 8=42058
  beam scan enhancement through periodic aperture transfer 8=28659
  beam scattering by bound electrons into their natural frequency 8=42259
  beam splitting devices for laboratories 8=37554
  bibliography, 4357 original refs. 8=33171-2
  bibliography, July to December (1967) 8=33161
  breakdown of He, (liq. and gas), threshold parameter meas. 8=47761
  breakdown of Hg vapour, threshold values 8=47766
  Brillouin scatt., thermal, stimulated 8=28649
  chemical, analysis by rapid-scan monochromator 8=28816
  with combined active medium 8=46545
  communications, search for nonlinear optical materials 8=27520
  conference, 1967 8=24279
  coupled mode oscillation. with axial
  cryptocyanine, alcohol soln., optical width var. during giant pulse generation 8=25921
  crystal irradiation, evaporation obs. 8=39494
  cyanine dye solutions as working subst., stimulated emission 8=48154
  diagnostics of theta pinch plasma 8=43552
  diameter meas. on moving sphere 8=23788
  diameter meas. on moving sphere 8=32638
  3, 3′-diethyloxatricarbocyanine iodide in methanol, frequency shift in emission band 8=37622
  discharge applic. for absorpt. spectra 8=34122
  dispersion of emission, rel. to random heterogeneities in refractive index 8=37566
  dispersive resonator for retuning generation freq. 8=28665
  Doppler-velocimeter application 8=37553
  dye pulses, ultrashort, generation by mode-locking 8=4211
  dye, with saturable absorbers, self-mode-locking 8=28711
  electron beam scanlaser, theory, design and operating parameters 8=24277
  emissive power meas. with ultrasonic device 8=46534
  evaporation of metal 8=26003
  excited rotation-vibration Raman scatt. in ultra-small gas samples 8=29683
  f. m. and a. m., amplification obs. 8=33160
  far i. r., rel. to observation of Stark effect on NH_3 rotational lines 8=38845
  ferromagnetic resonance modulation at microwave freq., theoretical anal. 8=42053
  flatness control in optical polishing 8=37652
  focussing, effects on optical second harmonic generation 8=45139
  Fokker-Planck equation for multimode action, exact stationary soln. 8=46561
  freq. conversion systems with 2 photon pumping 8=33241
  freq. modulation of single mode by multicavity resonator adjustment 8=24295
  γ quanta production by Compton effect with relativistic electrons colliding with laser beam photons 8=47045
  gas ionization and breakdown theory, rel. to inverse bremsstrahlung process 8=29952
  gates, with saturable absorbers, certain characts 8=24272
  Gaussian beam fluctuation in random medium, autocorrelation 8=46644
  Gaussian beams, focused, parametric interaction 8=49671
  Gaussian beams, logarithmic chart for propag. and matching problems 8=28646
  Gaussian light beam width obs. 8=33166
  giant-pulse irrad. of metal surface, rel. to ion emission and surface temp. 8=27361
  giant pulse, spectroscopy, ruby time-dependent freq. shifts 8=42054
  Green's function, two-time, theory 8=33169
  gyro, fundamentals and advantages 8=46012
  high intensity beam, impression of glass surfaces 8=33248
  IEEE Region 3 convention, USA (1968) 8=29991
  IEEE, 20th Annual Southwestern conference 8=28645

Lasers—contd
inelastic scatt. in binary mixtures by fluctuations of conc. 8=25918
interferometry of transient Ar arc for determ. of electron mobility and elec. cond. 8=39231
intensity near beam focus by electron scattering 8=47083
injection, optical operation determ. 8=28663
interaction of self-trapped laser beams 8=28877
interference between two beams of small intensity 8=42249
1 km interferometer for earth strains 8=50061
interferometer for plasma jet e density meas. 8=30085
interferometry, fringe visibility rel. to speckling 8=33277
ionic, drift velocity rel. to ionization in discharge 8=37551
i.r. and far i.r. freq. mixing using metal-metal point contact diodes 8=46634
irradiated gas, liberation of free electrons below breakdown threshold 8=29905
irradiation of Ar gas and Cs vapour and resulting light emission 8=29906
isotope shifts, i.r., variable length cavity meas. 8=28652
with large pulsed power, energy parameters meas. 8=46540
laser acoustic techniques for variable time compression, expansion and reversal of r.f. signals 8=28721
laser-Raman spectroscopy, current progress 8=25307
light modulation 8=46542
light pulse, short, two-quantum amplification of short light pulse 8=46546
light scattering in atmosphere 8=32243
light source for high-resolution Brillouin spectroscopy in solids 8=49686
light sources, review 8=28769
line-narrowing effects, freq. spectrum, theory 8=29589
liquid, Nd(III), room-temp. 8=46632
liquid, organic anthracene derivative (9,10-diphenylanthracene) laser-pumped 8=46630
lunar ranging for earth gravitational inertial mass ratio meas. 8=41748
metal irradiation, evaporation obs. 8=39494
mineral irradiation, evaporation obs. 8=39494
miniature linac with grating, proposal 8=37810
mirrors, dielectric, high efficiency, for laser techniques, technology 8=42079
mirrors, laser windows and optical filters for laser work 8=49674
mode coupling by cavity-length modulation, theory 8=28658
mode locked, output characteristics 8=28666
mode locking and ultrashort pulses with anisotropic molecular liquid in resonator 8=42071
modes of optical resonator, computation by resonance excitation method 8=42074
modes, TEM_{009}, separation with absorbing film 8=37565
modulation and demodulation of light 8=46647
modulation using grating diffraction effect 8=42122
nanosecond fluorescence decay times meas. 8=34884
nonlinear optical phenomena, anharmonic oscillator model 8=28657
operation and amplification 8=28653
optical cooling of solids, by transfer of energy into atomic vibration 8=39900
optical pulse generator, extended path and digitally scanned 8=46679
optical pumping efficiency calc. by graphical method 8=42067
optical spectrometers, laser calibration for colour blind spectroscopists 8=37675
opto-mechanical shutter for Q-modulation of resonator 8=42077
organic dye, flashlamp pumped 8=46629
organic dye solutions, cryptocyonine in glycerol and CAP in ethanol, time-resolved spectra 8=33230
organic dye, time-resolved stimulated emission spectra 8=28712
organic luminophore solns. in systems under optical pumping, as light transformers 8=28650
organic matter irradiation, evaporation obs. 8=39494
oscillator for meas. relaxation rates for atomic moments 8=29588
oscillator, obs. of quantum phase noise 8=28667
output energy meas., review 8=42059
output mirror, determination of optimum transmission coefficient 8=46566
parallelism of surfaces, interferometric determ. using coherent light 8=37550
parameters measurement, equipment 8=46555
parametric noise emission, noncollinear phase matching 8=24281
parametric oscillations, nonlinear crystal internal to cavity, theory 8=46547
parametric oscilln. using doubly and singly resonant cavities 8=42072
parametric resonance, theory 8=33167
passively switched, mode locked pulse generation 8=28651
passively switched, short-pulse emission origin 8=37558
phase-modulated, internally, quantum theory 8=28660
phase modulation in small-scale filaments 8=24274
photodetachment meas. of the e affinity of He 8=29970
photometric meas. by photoelec. devices 8=42138

Lasers—contd
photon distribution function equation of motion derivation 8=42051
photon statistics 8=28647
plasma production from interaction with solid D targets 8=39064
plasma production, high temp. and press. 8=29994
plasma production in air and air/D_2, and high-temp. meas. 8=47799
plotting of component parameters to build or modify nomal-mode pulsed systems 8=46554
polarizers, prism for use with lasers 8=33158
polymethine dyes, nineteen, stimulated emission over continuous range 710-1060 mμ 8=28713
polymethyl methacrylate rods containing rhodamine dyes, stimulated emission when flashlamp excited 8=28714
principles, operating characts. and appl. 8=33165
prism, regular, triangular, thermal state calc. 8=24276
propagation of pulse in Kerr liquid, steady-state electromagnetic shock solution 8=46549
propionitrile, competition between modes, polarization, magnification of some lines 8=33231
pulse formation from exact soln. of nonlinear eqns. in transient and steady state region 8=46560
pulse production of quasi-stationary phenomena in Fabry-Perot cavity 8=42070
pulse width meas. with two-photon excitation of fluoresc. 8=46533
pulsed light source, spectroscopy by defocused Fabry-Pérot interferometer 8=42250
pulsed mode-locking, dynamics of generation 8=37562
pulsed, synchronization of light pulse output 8=37564
pulsed, threshold meas. by ballistic galvanometer 8=33164
pulses, giant, rel. to ionization of thin polythene films 8=40720
pulses, rel. to dissociation of $A^{III}B^{V}$ semiconducting compounds 8=40437
pumping by electrodeless h.f. discharge 8=33178
pumping pulse effect on birefringence in Nd glass 8=41125
pumping source, power supply, optimum capacitance 8=42052
Q-modulation by controllable-transmitting liquid shutter 8=42063
Q-modulated, memory tube recording of pulse 8=46535
Q-switch using $LiNbO_3$ as electrooptic material, 1.06 μ operation 8=46604
Q-switched, emission of pulse trains, application of Maxwell and density matrix eqns. 8=37549
quantum electronics, effect on technology 8=28655
quantum fluctuations 8=24282-3
quantum noise, multitime correspondence between quantum and classical stochastic processes 8=42055
quantum noise, six-classical variable description 8=42056
quantum optics fundamentals, book 8=24352
quartz-stimulation of Brillouin effect hypersound parametric amplification 8=26583
radiation characts. rel. to resonator switching rates 8=24286
radiation, transformation in stimulated induced combinational scattering 8=46564
Raman, pulse generation by focusing ruby output on H_2 cell 8=28684
Raman scattering, stimulated in H_2 gas by simultaneous fundamental and 2nd harmonic ruby laser radiation 8=46592
Raman scattering, stimulated, mixtures of acetone and CS_2, distribution of anti-Stokes emission 8=46631
Raman spectroscopy of crystal powders 8=49685
rate eqns., Lyapunov's second method 8=28656
rate equations, singular periodic soln., with saturable absorber 8=24284
rays, scattering on plasma 8=39110
reconstruction of images, microwave hologram. 8=46746
reflectivity of metal, changes during pulse 8=45169
resonator appl. meas. freq. spectra laser and passive resonators 8=24292
resonator, confocal, mode obs. 8=24293
resonator mirror, angular oscillatory modes 8=28664
resonator modes, equations for amplitudes 8=46563
resonator, molecular, stability and selectivity 8=46557
resonator, open two-mirror astigmatic 8=33174
resonator with partial polarizers, eigenstates of polarization 8=46559
resonator with radial gain profile, Gaussian mode 8=37563
resonator, X-band microwave exptl. scaling 8=41997
resonators and beam waveguides, scalar theory 8=28669
resonators and waveguides with infinite mirrors, modes 8=33121
resonators, scalar theory 8=28668
rhodamine dyes in polymethyl methacrylate rods, stimulated emission when flashlamp excited 8=28714
ring applications 8=46541
ring device 8=46572
ring, field spatial distribution 8=42073
ring, locking zone phase relations and optical phasemeter 8=28662
rod between parallel plates which act as mirrors, frequency of axial modes 8=24291

Lasers—contd
ruby, R-line quantum efficiency and spatial distrib. of fluorescence 8=42101
satellite, use for atmospheric surface press. meas. 8=45439
scattering by relativistic electrons, spectral intensity and finite vol. 8=42451
scattering Doppler shift, meas. of turbulent velocities 8=39272
scattering for meas. of ion temp. in plasma 8=39114
scattering for plasma e density profile 8=30082
scattering, multiple stimulated, of electrons by strong laser field 8=47087
second-harmonic generation, coherence functions 8=24358
second harmonic generation in crysts. due to field depend. of dipole moment operator 8=36287
second harmonic generation, nonlinear crystal inserted into cavity, optimum coupling 8=46551
selective-loss, single-freq. regime generation 8=33163
with self-resonant feedback, theory 8=24270
semiconducting and recombination radiation 8=31953
semiconductor irradiation, evaporation obs. 8=39494
semiconductor, variable wavelength as spectroscopy light sources 1-20μ 8=28838
shock-wave generation in rarefied gases by impact in Be targets 8=47833
simulation and interpret. of complex LEED patterns 8=35310
spark gap trigger mechanism 8=34431
spark light source for wide band-gap drift mobility meas. 8=42205
spark production, expansion mechanism 8=34432
spark, travelling, ignition below breakdown threshold intensity 8=42061
spectra, single-pulse operation 8=24268
in spectrochemical analysis 8=32157
spectrochemical analysis, substance utilization improvement 8=36645
spectrophone for meas. light absorpt. in gases 8=39218
statistics of fluctuations 8=46538
statistics, photocount versus photon distributions 8=46532
stimulated Brillouin scattering, large and small angle, threshold condition 8=34661
stimulated emission by emission wave-second order wave beats 8=33173
stimulated emission cross section meas. using laser 8=24280
stimulated Raman scatt., relativistic theory 8=24278
stimulated recomb. luminesc. in rigid organic soln. 8=41222
stress prod. in transparent dielecs., and failure 8=40547
temp. determ. of working substance by dilatometric method 8=28661
Theory, averaging of products of Lorentzian line shapes over thermal velocities 8=43214
theory, exact solution for steady-state resonant pulse propagation on inverted medium 8=46548
theory, mode locking by loss modulation 8=42065
theory of phase locking the transverse modes, application
thermal blooming of beams, time dependence 8=37556
thermodynamic limits 8=24382
threshold excitation conditions and interacting fields phase relations 8=28648
tracer-particle fluid velocity meas. 8=41623
two-coupled. theory 8=42064
two-dimensional resonator 8=24290
two mode field, quantum and classical descriptions 8=42066
two-photon enhanced emission, strong radiation 8=37555
ultrashort light pulse formation, nonlinear, nonstationary optical eff. 8=46544
ultrashort pulse, development and uses 8=24275
ultrashort pulses form. dynamics 8=37552
unidirectional optical heterodyne system over 2.6 km atmos. path, design and output 8=27915
up-conversion of 10.6μ beam to visible in HgS crystal, second harmonic generation 8=46552
u.s. diffraction, appl. in optical correlation, anal. and performance 8=28751
u.v., rel. to luminescence of AgCl 8=36469
vaporization of subst. by laser radiation action 8=48288
vessel for resonator for liquid light diffusion studies 8=46536
waves and harmonics appl. to molecular optical anisotropy dispersion studies 8=38774
welding and connected techniques 8=42057
Al plasma form. by surface irrad., ion energy and abundances 8=36051
Ar, ionized gas, construction and theory 8=42085
Ar plasma-beam discharge stimulated emission 4545–5145Å 8=28673
Au plasma form. by surface irrad., ion energy and abundances 8=36051
CO_2-N_2-He, increased efficiency through addition of Xe 8=46583
Cu plasma form. by surface irrad., ion energy and abundances 8=36051
$GaAs_{1-x}P_x$ injection, electroluminescent source, luminance $> 6 \times 10^9$ cd/m² 8=41192

Lasers—contd
Gd chelates soln., stimulated emission from organic ligand 8=24349
Ge film thickness meas. by i.r. absorpt. 8=35173
He-Ne, echoes from atmos. constituents, freq. spectrum, aerosol content of air obs. 8=45442
He-Ne, TEM_{009} modes separation with Ni film, obs. 8=37565
Nd glass stimulated emission spectrum and quasi-continuous generation, 4.2°K 8=36503
Nd(III), room-temp. liq. 8=46632
$Nd^{3+}SeOCl_2$ liquid, self-Q-switching 8=46633
Nd^{3+}-$SeOCl_2$ liquid, stimulated emission in $^4F_{3/2} \rightarrow {}^4I_{13/2}$ transitions 8=46628
RbH_2PO_4 freq. doubling crystal 8=37557
$SeOCl_2$:Nd^{3+}, liq., improvements 8=37624
$SeOCl_2$-Nd^{3+}, liquid Q-switched, 20°C 8=37623
YAG:Nd^{3+}, pumping efficiency of Kr and Xe flash tubes 8=46550
gaseous
active medium, dip parameters in transition line 8=46576
air superradiant laser action in spark discharges at atmos. press. 8=24301
amplification of modulated light signal 8=24269
anodic-bore ion laser tube 8=37571
axial oscillation mode, radiation field 8=24288
design with small discharge tube 8=37570
discharge-modulation noise, suppression using external KDP cell 8=24302
discharge tube, perpendicularly disposed windows 8=24298
coherent axial mode mixing in InSb photo-resistors 8=36372
field theory, nonperturbative, use to explain inhomogeneous effects 8=33175
fluctuations, statistical analysis 8=37573
for frequency characteristic meas. of photoelectronic devices 8=46317
frequency shifting and modulation 8=46568
gain distribution, population densities and rotational temperature for rotation-vibration transition 8=33183
high power, parameters affecting power output 8=37572
in homodyne arrangement for plasma electron density meas. 8=25761
influence on fluoresc. emitted by gas in magnetic field 8=47515
infrared transitions, pulsed excitation of calcium and strontium vapours 8=42088
intra-cavity reflector for Q control 8=28670
K vapour, four wave parametric interaction 8=33177
mirror refl. coeff. meas. 8=24297
mode locking theory, stability conditions 8=28672
molecular gas breakdown obs. 8=29904
moving striatron modes, obs. rel. to modulation of beam 8=24296
nonlinear absorption, theory 8=46575
oscillation build-up, resonator tuning dependence 8=46570
output coupling, optimum, from inhomogeneously broadene lines 8=37567
output power calculation 8=37574
output power calc., multiple vibr. modes 8=33176
plasma instability, influence in working of laser 8=46574
power system, use of cable pulse transformer 8=46577
pressure broadening effects in output 8=24300
in Raman spectroscopy of natural products 8=27793
resonator, single-freq. parameter optimization 8=33188
review, investigations and applications 8=42080
ring, single-frequency operation, frequency stabilization method 8=46578
single mode, polarization in transverse mag. field 8=3756
theoretical applications 8=46571
travelling wave, unidirectional oscillation 8=37569
trifluoromethyl iodide laser, Q switching and mode locking 8=37576
water vapour, meas. of three lines in 7 micron region 8=33189
water vapour, pulsed, gain characts. 8=24310
Zeeman, g value meas. for atomic levels of Ne 8=43198
Ar, breakdown characts. 8=29910
Ar, continuous, saturation, obs. 8=28677
Ar, excitation of CdS rel. to hole and electron behaviour 8=36012
Ar, excitation of $LiNbO_3$ and parametric luminesc 8=4120
Ar ion, anomalous competition between transitions 8=3757
Ar ion, c.w., excitation processes 8=28675
Ar ion, extension of range of laser oscillation 8=46573
Ar ion, 4880, 4765, 5145 Å intensification, saturation 8=243
Ar ion, high current continuous-action cathode 8=46579
Ar^+, light scattering by He reflex discharge rel. to e-density and -temp. meas. 8=38991
Ar, low voltage, pulsed, possible methods of populating working level 8=28671
Ar, pulsed ion, saturation of power output in very high current regions 8=28676
Ar, pulsed ion, with axial mag. field, improved performance 8=24304
Ar, pulsed, output power characteristics 8=42083
Ar, rel. to induced electron emission from W, Ta and LaB_6 8=40710

Lasers—contd
- **gaseous**—contd
  - Ar II, pulse type, effects of mag. field on output 8=28674
  - Ar II, transition probabilities in lower states 8=46580
  - Ar^+, c.w. scatt. obs. of e vel. distrib. in reflex discharge 8=30012
  - Ar^+, pulsed ion, resonance radiation trapping 8=42084
  - CN, far i.r., pulsed output, mode pattern and polarization characts. 8=46582
  - CN, 337 μm, use in meas. electron densities of plasma 8=47856
  - CO_2, c.w., high power generation and appl. as heat source in welding 8=28678
  - CO_2, 4.3μ transient oscill. 8=28680
  - CO_2, heterodyne detection of beat freq. with $Pb_{0.88}Sn_{0.12}Te$ diode laser 8=42098
  - CO_2 high-power, sealed-off, theory and design 8=42087
  - CO_2, induced fast photocond. in Te 8=40676
  - CO_2, intensity of generated pulses, effect of moment of Q-switching 8=37580
  - CO_2, mode locking using GaAs intracavity acousto-optic loss modulator 8=24305
  - CO_2, output timing by selective intracavity absorpt. 8=46586
  - CO_2, passive Q switching by vinyl chloride 8=28679
  - CO_2, population inversion, thermal production 8=37578
  - CO_2, power-dependent distortion of i.r. beam from laser during propag. in liquids 8=25916
  - CO_2, production of multijoule pulses 8=33180
  - CO_2, quartz welding 8=33179
  - CO_2, repetitive pulsing by means of CO_2 gas and other absorbers 8=24306
  - CO_2 sealed-off system, effect of H and O on gas composition 8=46584
  - CO_2-, sealed-off, gas comp. rel. to water vapour and hydrogen effects 8=24307
  - CO_2, sealed-off, influence of Xe as gas additive 8=33184
  - CO_2, stabilization using 3-mirror system 8=46587
  - CO_2, use of pyroelectric detector to meas. Q-switched pulses 8=46581
  - CO_2, vibr. levels population, 9-11μ 8=24374
  - CO_2, vibration-rotation transitions, sequential Q-switching 8=24308
  - CO_2 with near confocal optical resonator, obs. 8=42076
  - CO-N_2, line selection, amplification and vibrational population 8=28681
  - CO_2-He-N_2, composition and power output, gas flow dependence 8=46585
  - CO_2-N_2-He, dependence of discharge current on laser action 8=33182
  - CO_2-N_2-He mixture, increasing output 8=37577
  - CO_2-N_2-He, output power rel. to pump current and length 8=42086
  - CO_2-N_2-He, passive mode locking 8=37579
  - CO_2-N_2-He, use in determ. of CO_2 line parameters 8=29720
  - CO_2-N_2-He, Q-switching with BCl_3 saturating filter 8=46588
  - CO_2, Q-switching and pulse sharpening, analysis 8=33162
  - CO_2, Q-switching, technique to provide h.f. output pulse repetition rate 8=33185
  - CS_2-O_2 chemical, analysis showing new lines and selective excitation 8=46569
  - DCN, assignment of lines 8=28682
  - DCN, new c.w. sub-mm lines, absolute freq. obs. 8=28683
  - HCN, assignment of lines 8=28682
  - HCN, multiple pulse emission 8=24309
  - HCN pulsed, acoustic perturbations 8=46593
  - HF, chemical 8=46590
  - HF, prod. by flash photolysis 8=37582
  - H_2O, far i.f. spectrum calc. 8=42089
  - H_2O lines identification 8=29745
  - H_2O, molecular level parameters rel. to identification 8=29748
  - H_2O spectrum, transitions in $2\nu_2$, ν_3 and ν_1 states 8=29741
  - H_2O vapour, identification of lines 8=42097
  - H_2O + H_2, sub-mm. sealed-off 8=37581
  - He, breakdown characts. 8=29910
  - He-Ne, absorpt. saturation effects, and freq. reproducibility 8=37591
  - He-Ne, aerosol surface meas. appl. 8=34948
  - He-Ne, amplification and loss meas. 8=37587
  - He-Ne, appl. to breakdown plasma afterglow obs. 8=34504
  - He-Ne, arc and h.f. discharges, comparison 8=43456
  - He-Ne at 0.62μ, freq. fluctuation and natural width determ. 8=24318
  - He-Ne, coherence length extension 8=37586
  - He-Ne, cw oscillations from low-voltage arc discharge 8=24315
  - He-Ne, decay of metastable He atoms rel. to condition for population inversion 8=24312
  - He-Ne, Faraday rotation obs. temp. meas. anomaly 8=42094
  - He-Ne, focussing, effects on optical second harmonic generation in $NH_4H_2PO_4$ 8=45139
  - He-Ne, generation of high repetition rate optical pulses 8=28690
  - He-Ne, hysteresis and "hard" excitation, 0.63μ 8=37584
  - He-Ne, intensification line shape, change due to saturation 8=37590
  - He-Ne, intensity fluctuations at 0.63 and 3.39μ 8=24316
  - He-Ne laser beam Faraday rotation on passage through θ-pinch plasma 8=37583
  - He-Ne laser, forced and spontaneous phase locking of transverse modes 8=42093
  - He-Ne laser freq. rel. to at. freq. 8=28688
  - He-Ne laser operating at 6328 Å π transition for Ne double resonance studies 8=47502
  - He-Ne, lifetime of $3P_4$ level in Ne 8=34184
  - He-Ne, light source for Raman spectrometer, resolution improvement 8=24398
  - He-Ne, meas. plasma θ-pinch end loss 8=30115
  - He-Ne, meas. small thermal expansion coeff. 8=35440
  - He-Ne, mode-locked frequency shifting by use of electrooptic effect 8=46595
  - He-Ne, modulated by discharge current, transient behaviour 8=37589
  - He-Ne, modulation by ferromag. resonance of ferroglass 8=24359
  - He-Ne, Ne as nonlinear absorber for mode locking 8=37588
  - He-Ne, observation of saturation peaks by tuned laser differential spectrometry 8=42091
  - He-Ne, optical freq. doubling and mixing 8=42095
  - He-Ne, oscillation noise, suppression 8=42082
  - He-Ne, output at 6328Å, optimum diameter for various tube lengths 8=24314
  - He-Ne, photons correlation, obs. 8=28686
  - He-Ne, photon statistics for threshold light with finite counting time 8=24319
  - He-Ne, power broadening, observation by tuned laser differential spectrometry 8=46594
  - He-Ne, radiation backward scattering from smokes and fogs, optical thickness dependence 8=34949
  - He-Ne, radiation field diffr. struct. 8=24313
  - He-Ne, saturation behaviour in various polarization states 8=46591
  - He-Ne, single-mode, amplitude stabilization 8=33187
  - He-Ne 6328Å, competition and stimulated switching of transverse modes 8=42092
  - He-Ne, 6328Å, side light investigations 8=24320
  - He-Ne 6328Å, unsaturated gain and output power 8=28687
  - He-Ne, small optical loss meas. 8=28689
  - He-Ne, spectroscopic meas. 8=42081
  - He-Ne, spontaneous emission of $Ne(2p_4 \rightarrow 1s_4)$ along axis 8=25363
  - He-Ne spontaneous modulation on beam switching 8=42090
  - He-Ne, sputtered cathode particles 8=24317
  - He-Ne, stabilized at 633 nm, reproducibility of wavelengths 8=28685
  - He-Ne, temp. effect on output power 8=33186
  - He-Ne, type LG-75 8=24311
  - He-Ne, with folded optical path 8=42096
  - He-Xe, spectroscopic meas. 8=42081
  - Ne, spectroscopic meas. 8=42081
  - Ne, superradiant 5401Å pulsed, coherence props. 8=28691
  - Ne-O, O 3^3p level population inversion mechanism, obs. 8=28692
  - NH_3-methane, deuterated, discharge emission spectral obs. 8=33190
  - Te vapor-Ne, pulsed discharge, assignment of transitions to Te II spectrum 8=46596
  - Xe, discharges, time varying, perturbations of microwave cavity fields 8=24294
  - Xe, isotope shifts on i.r. lines, obs. 8=28652
  - Xe-He, c.w. with diffuse mirror non-reson. feedback, freq. characts., 3.50μ 8=37592
- **solid**
  - absorber saturated by strong light pulse, amplification of simultaneous weak pulse 8=37593
  - active material, thermal conditions 8=46599
  - amplification irregularity distrib. obs. 8=33192
  - amplifier chain, high-gain, optical isolation technique 8=46600
  - coatings, single layer antireflection, mismatch 8=42060
  - current pulse generator, short rise time, high current 8=46333
  - diodes, effect of band-tailing on linewidth of spontaneous emission 8=46602
  - electron-beam-pumped, effect of inhomogeneous minority carrier distributions 8=28696
  - electron pumped, photon loss and gain factor meas. 8=28699
  - electron pumped, power and quantum efficiencies 8=33201
  - epitaxial diodes, temp. dependence of linewidth of spontaneous emission 8=42099
  - with external mirrors for low-temp. expts. 8=46537
  - five-component fluoride as laser material 8=28706
  - frequency stabilization by tuned mirrors 8=24321
  - glass:Nd, induced "blow-off" plasma 8=40065
  - with half-wave Q-factor modulator based on ADP crystal 8=24323
  - heating by pumping, change in active element 8=24325
  - injection, elect. modelling 8=33168
  - insulating materials, luminesc. 8=36468
  - junction, carrier lifetime meas. by direct modulation 8=33191
  - Kerr cell shutter, use of reft. prisms 8=24285

- **Lasers—contd**
  - **solid—contd**
    - loss due to non-uniform pumping 8=37600
    - luminescence in vitreous, state, appl. 8=36465
    - mode-locked, pulse trains 8=28697
    - non-linear mode interaction rel. to line breadth 8=33193
    - organic mols., laser flash spectroscopy 8=43341
    - oscillation threshold, c.w. operation of lasers pumped by pulsed argon ion laser 8=37594
    - oscillator, tandem giant pulse using Nd doped glass rods 8=42075
    - p-n junction, internal parameters, determ. 8=28701
    - polarized laser cavity insensitive to birefringence in laser rod 8=46597
    - pumping rel. to rod side surface matting 8=37598
    - radiation effects, mechanisms, rel. to use in the space environment 8=28694
    - Raman laser emission, combination freq. generation 8=25598
    - rectangular bar element, temp. field 8=24322
    - resonator modes rel. to deform. by pumping pulse 8=42068-9
    - ring, close-lying mode suppression 8=46558
    - rods, pumping distrib., photographic meas. 8=24324
    - ruby, and Nd, beam superposition in freq. mixing 8=24333
    - ruby and Nd with external tilted mirrors, field genesis and structure 8=37608
    - ruby, axial mode discrimination calc. 8=33197
    - ruby, axial mode separation, generation kinetics and emission spectrum 8=24334
    - ruby, birefringent plate control of spectral emission 8=37609
    - ruby, characts at 78˚K, generation threshold and axial mode distrib. 8=37601
    - ruby, coherence function determ. from diffraction 8=37607
    - ruby, construction of hologram 8=24431
    - ruby, crystal thermal deform. 8=24335
    - ruby, damage associated with liq. Raman freq. changer 8=42108
    - ruby, energy of giant pulse, dependence on crystal temp. 8=24329
    - ruby, giant pulse field development with saturating filter in resonator 8=42100
    - ruby, giant pulsing, new method 8=37606
    - ruby, giant pulse production 8=42102
    - ruby, giant-pulse, saturable absorber, system parameter calc. 8=42113
    - ruby, ground-based, backscatter correlation with turbulent regions of atmosphere 8=27917
    - ruby, in constant resonator Q mode, generation energy and threshold, engineering evaluation 8=42107
    - ruby, inducing breakdown in ionic crysts. and polymer 8=40566
    - ruby, influence of defects on radiation characts. 8=42105
    - ruby, irrad. effect on discoloured NaCl crysts. 8=44485
    - ruby, irradiation of transparent dielec. mats. inducing charged-particle emission without causing physical breakdown 8=40703
    - ruby, internal scanning rel. to time charact.. improvement 8=46611
    - ruby, limitation by adiabatic crystal heating 8=37602
    - ruby, large angle scattering in liquids 8=48158
    - ruby laser loss meas. 8=28703
    - ruby, μsec pulse production 8=42114
    - ruby, nanosec. pulse production 8=42106
    - ruby, oscillation characts. by interaction between two lasers 8=42103
    - ruby, passive Q-switched, rooftop prism cavity, single mode beam 8=46606
    - ruby, passively Q-switched, transient interference pattern 8=37596
    - ruby, photocoagulation of retina 8=28912
    - ruby, pulse excitation of organic crystal solns. 8=30479
    - ruby, pulsed, as holographic source 8=42270
    - ruby, pulsed, passive optical shutter for reducing fluorescent output 8=24328
    - ruby, pumped by Ar ion laser 8=28704
    - ruby, Q-modulated, actuated by external signal, time characts. investigation 8=46609
    - ruby, Q-modulated, excitation of org. mols. 8=34295
    - ruby, Q-switch, dye fluoresc. and bleaching 8=28693
    - ruby, Q-switched, periodic pulse generation and diffraction limited osc. 8=28702
    - ruby, Q-switching by natural chlorophyll and effect of solvents 8=33199
    - ruby, Q-switching speeded by rotary prism 8=24332
    - ruby, Q-switching by pheophytin and its derivatives 8=46605
    - ruby, radial temp. distribution during pumping 8=39909
    - ruby, rel. to CuCl luminescence 8=32053
    - ruby, rel. to flash method of thermal diffusivity meas. 8=39950
    - ruby, rel. to induced electron emission from W, Ta and LaB_6 8=40710
    - ruby, relation between total energy and Q-switching time 8=24338
    - ruby, resonator filter, loss calc. 8=37603
    - ruby, ring, for ultrashort pulses 8=33200
    - ruby, second-harmonic generation in Ag 8=27548
    - ruby, self-Q-switching 8=37604
    - ruby, single mode generation 8=33196
    - ruby, single-mode giant-pulse 8=46607
    - ruby, single pulse spectrum 8=42104
    - ruby, strong field, refractive index variation of glass and liquids 8=41098
    - ruby, time depend. of spectrum of modes 8=46610
    - ruby, TiO_2 doping, reduction of laser prod. damage 8=33198
    - ruby, undamped regular spiking, in misaligned cavity 8=37605
    - ruby, with spatially homogeneous inverse population, generation kinetics, radiation spectrum and direction 8=46608
    - sapphire, TiO_2 doping, reduction of laser prod. damage 8=33198
    - semiconductor, band tail spreading energy rel. to temp. 8=28698
    - semiconductor diode, minority carrier lifetime rel. to impedance 8=33195
    - semiconductor electron pumped, far field patterns 8=33202
    - semiconductor, increase of generation efficiency using a resonator 8=28695
    - semiconductor, intrinsic, emission by direct band-band transitions 8=36291
    - semiconductor, laser structure and applications 8=44778
    - semiconductor, many-body wavelength shift 8=28700
    - semiconductor, noise, quantum mechanical Fermi and Bose analysis 8=33194
    - semiconductor, rate of recomb. at threshold, effect of doping 8=46601
    - semiconductor thin-platelets optically pumped 8=46613
    - semiconductors, thermal operating conditions, continuous generation region 8=37599
    - spherical pumping reflector 8=46598
    - spiking behaviour, filamentary mechanism 8=24326
    - stimulated Raman scatt., two-photon absorpt. as quenching mech. 8=24337
    - synchronisation of 2 Q switched lasers 8=24327
    - temperature-jump apparatus for electrolyte relax. 8=36595
    - theory of optical pulse generator using saturable absorber 8=46553
    - $Ba_2NaNb_5O_{15}$ low threshold optical parametric oscillator 8=46612
    - CO_2 plasmas, influence of Xe 8=33181
    - CaF_2:Dy^{2+}, emission mechanism 8=37610
    - CaF_2: Sm^{2+}crystal generation, spectrum-time studies for ruby laser excitation 8=41071
    - $CaWO_4$:Nd, air cooling system 8=28705
    - CdS, e-beam excited, photocurrent, luminescence and absorption saturation 8=31973
    - CdS, electron pumped, power and quantum efficiencies 8=33201
    - CdS far field patterns 8=33202
    - CdSe, coherent radiation of free excitons 8=36343
    - CdSe, e-beam pumped, coherent emission of free excitons 8=31972
    - CdSe semiconductor, two-photon absorpt. anisotropy in the optical excitation 8=36341
    - CdSe thin platelet resonator, pumped by Ga(AsP) junction photon output energy rel. to bandgap 8=33215
    - Cd(SeS) semiconductor thin-platelets optically pumped 8=46613
    - CdTe, electron pumped, power and quantum efficiencies 8=33201
    - $Ga_{1-x}Al_x$) As diodes, epitaxial layers, observation of stimulated emission 8=46619
    - GaAs amplifiers 8=33219
    - GaAs, bistable operation 8=37614
    - GaAs, bulk field-ionized, stimulated emission 8=33207
    - GaAs, c. w. operation noncatastrophic degradation 8=33205
    - GaAs, critical temp. for excited carriers in exponential of band tail 8=35749
    - GaAs diode, near-field pattern, effect of material inhomogeneities 8=42109
    - GaAs diode, oblique angles betw. resonator mirrors and p-n junction 8=46603
    - GaAs diode, short-wavelength radiation emission spectrum 8=37613
    - GaAs diode spectrograph, temp. tunable 8=46589
    - GaAs diode, 300˚K, transient temp. distribution and o/p pulse duration 8=33217
    - GaAs diodes, luminescence mode, current noise spectra 8=46614
    - GaAs diodes, optical losses and efficiency 8=33213
    - GaAs diodes, temp. depend. of delay time between current pulse and laser emission 8=24339
    - GaAs, effect of multiple Zn diffusions on threshold and c.w. output power 8=46615
    - GaAs, electron-beam pumped, nonradiative surface recombination 8=49226
    - GaAs, electron pumped, power and quantum efficiencies 8=33201
    - GaAs, emission delays rel. to temp., trapping model 8=3322
    - GaAs, epitaxial compensated, recombination rel. to temp., and band tailing 8=33225
    - GaAs far field patterns 8=33202
    - GaAs injection diode, internal mode excitation 8=24341

Lasers—contd
solid—contd
GaAs injection, multilayer 8=33210
GaAs injection, optimum stimulation 8=33218
GaAs injection, phase locking and external cavity coupling 8=33211
GaAs, injection, self damage 8=33208
GaAs injection-type, far-field patterns with Gaussian profiles in junction plane 8=37597
GaAs injection, with two junctions, mutually pumped 8=33226
GaAs, ionized by passage of Gunn domains, laser action 8=24340
GaAs junction, compensation effects of Zn and Te impurities 8=46616
GaAs junction, continuous microwave oscills. 8=33220
GaAs junction, internal Q switching 8=33212
GaAs junction, internal Q switching 8=37612
GaAs junction, obtaining Gaussian beams 8=33203
GaAs junction, output light spikes at room temp. 8=33204
GaAs junction, transverse modes 8=33206
GaAs near room temp., delay characts. 8=33222
GaAs, n-type at 77°K, threshold current, power output and quantum efficiency 8=33216
GaAs p-n junction, applic. to phase-modulated optical ranging systems 8=42110
GaAs semiconductor injection, mode self-synchronization 8=46565
GaAs semiconductor, liquid N_2 temp., spectral characts. 8=24336
GaAs semiconductor thin-platelets optically pumped 8=46613
GaAs soln. grown, gain and loss rel. to orientation 8=33214
GaAs structures, thermal impedance meas. 8=33223
GaAs transmitter for optical communications 8=37611
Ga(AsP) semiconductor thin platelets optically pumped 8=46613
Ga(AsP) thin platelet resonator, pumped by Ga(AsP) junction, photon output energy rel. to bandgap 8=33215
$GaAs_{1-x}P_x$ injection, delay and memory effects 8=33209
$GaAs_{1-x}P_x$ injection laser diode, pulsed, temporal-line shift 8=49307
$GaAs_{1-x}P_x$ injection lasers 8=46617
$GaAs_{1-x}P_x$, optical filling of delay inducing traps 8=46618
$GaAs_{1-x}P_x$, threshold and emission efficiency temp. dependence 8=33224
$GaAs_xP_{1-x}$ p-n junction, applic. to phase-modulated optical ranging systems 8=42110
GaP_xAs_{1-x}-based injection-type, production and props. 8=36360
GaSb, modes temp. depend. rel. to optical consts near energy gap, 80°K 8=41088
H_2 foil irradiation, plasma production 8=29995
ICN. 538μm emission, mechanism and time behaviour 8=37615
LaF_3:Nd^{3+}, continuous stimulated emission at 300°K 8=37616
LaF_3-SrF_2:Nd^{3+}, operating at 300°K 8=27579
LiF/U^{6+}, suitability of fluorescence props. for laser 8=46620
$LiNbO_3$, pulsed parametric oscilln. and power limiting 8=42078
Nd, and ruby, beam superposition in freq. mixing 8=24333
Nd glass, band narrowing with passive shutter 8=24345
Nd glass, coupled, three-mirror system 8=37619
Nd glass, electro-optical modulation of Q-factor 8=24342
Nd glass, energy characts. of radiation with Q switching 8=24348
Nd glass, form. and ignition of metal droplets 8=34740
Nd glass in Fabry-Perot resonator, polarized emission 8=42111
Nd glass, noise obs. 8=24344
Nd glass, nonlinear resonator 8=33227
Nd glass, parameters determ. 8=24343
Nd glass rod pumping with compressed Xe_2 light source 8=28709
Nd glass, self-focusing by density change 8=36310
Nd glass, single-mode, waveguide type 8=24346
Nd glass, with unstable resonator, props 8=46625
Nd, plane mirror resonator, spectral effects 8=24287
Nd, polarization of radiation 8=37617
Nd, self-focusing of 1.06μ radiation 8=24347
Nd, spectral effects of resonator elements 8=24289
Nd, use of Q-switch dyes 8=42112
Nd, with plane mirrors, internal modulation 8=33228
Nd^{3+} activated, stimulated emission studies rel. to laser generation 8=37595
Nd^{3+} doped calcium fluorophosphate, optical pumping and oscillations 8=37620
Nd^{3+}, spectroscopic investigations of stimulated radiation 8=46621
Nd:YAG oscillator, intracavity tuning, polarization and Q switching 8=28707
Nd:YAG, picosec. pulses, obs. 8=37618
Nd:YAG, repetitively pump-pulsed, dynamics 8=46623
Nd:YAG, thermal effects and transverse mode control 8=28708
Nd:YAl garnet, mode-locked, characts., 8=46622
$Pb_{0.88}Sn_{0.12}Te$ diode, tunable, heterodyne detection of beat freq. with CO_2 laser 8=42098

Lasers—contd
solid—contd
$Pb_{1-x}Sn_xTe$ diode, i.r. up to 28μ, props. at 12° and 77°K 8=37621
$SeOCl_2$:Nd^{+3}, absorption cross section of Nd^{+3} transition 8=46624
UO_2^{+2}:Nd^{+3} laser glass, Ce-stabilized 8=28710
YAG-Nd, single-mode, static and dynamic behaviour 8=46626
YAG:Nd, CW laser transitions at room temperature 8=46627
YAl garnet: Nd^{3+} ring, close-lying mode suppression 8=46558
YAlG:Nd, continuous 0.532μ solid-state source using $Ba_2NaNb_5O_{15}$ in cavity 8=33253
YGa garnet: Nd single crysts. and growth, obs. 8=39694
YGdAl:Nd^{3+} growth and characts. 8=39692
YVO_4 tetragonal crystals containing Nd^{3+}, induced emission at 300°K 8=33229
ZnO crystals, electron-beam pumped 8=49765
ZnO far field patterns 8=33202
Latent heat
See also Heat of adsorption, etc.; Thermodynamic properties.
fusion, by differential thermal analysis 8=30575
Latent image. See Photographic process.
Lattice constants. See Crystal structure, atomic.
Lattice dynamics. See Crystals/lattice mechanics.
Lattice energy. See Bonds; Crystals; Solids.
Lattice gas. See Statistical mechanics.
Laves phases. See Alloys; Phase transformations/solid-state.
Lawrencium
translawrencium elements, SCF calcs. 8=47513
Lawrencium compounds
No entries
Lead
absorption, infra-red, at 4.2°K 8=27551
anodic behaviour in alkali 8=32132
arc spectrum 8=38678
cascade e ang. distrib. in shower maximum, calc. 8=38181
compressibility, comparative to Fe, under impact press. 31 to 34 m bars 8=40108
creep, at high temp., activation energy and stress depend of secondary stages 8=49043
cylinders, compressive engineering strain-time, strain-rate and force-time characts. 8=35711
deformation pulses, elastic-plastic, propagation in cylindrical bars 8=44596
effective masses of holes on Fermi surface, and anisotropy on (001) and (011) surfaces 8=40328
electron-irradiated, e.-shower production and its charge component 8=44502
films and foils, parallel and perpendicular mag. transitions, 1-4.2°K 8=40741
films, epitaxially grown on PbTe, domain structure from Lorentz microscopy 8=36171
films, thin, supercond. transition, critical fields 8=27028
flow under simple shear, rel. to grain size and boundaries, from 27° to 80°C, and 150°C 8=35713
fracture, activation energy, temp. effect 8=26797
gamma-ray cross sections, analysis 8=26728
ions Pb^{++}, polarographic investigation in $LiNO_3$-$NaNO_3$-KNO_3 melt 8=45414
ions, Pb^{2+} for activation of $Zn(SCN)_2$, luminesc. 8=36520
isotopes evolution model with crustal material recycling through mantle 8=36682
in lead crystal, determ. by atomic absorpt. spectrometry 8=27789
lifetime and oscillator strength of $^3P_1^0$ state 8=38707
liquid and solid, Brillouin scatt. of neutrons rel. to collective particle motion 8=25869
liquid, cooperative modes of motion 8=34725
liquid, cooperative modes of motion, temp. depend. 8=34726
liquid, density 8=39325
liquid, mass-current fluctuations 8=25890
liquid, nucleated by solid Cu, Fe and Sb, undercooling 8=43911
liquid, structure factor 8=48062
neutrons, fast, shielding and collimation props. 8=33793
optical properties in the far u.v. 8=31978
phonon states, tunnelling and neutron-derived densities, origin of discrepancy 8=26883
photoelectric γ cross-section determ. 50-208 keV 8=36004
positron annihilation, single-quantum, cross sections 8=44670
rock isotope abundances, concordia plots rel. to age of earth 8=27856
shield, γ-ray leakage through slit 8=38595
slip bands, orientation distrib. under pure shear 8=48864
solubility in liq. Na 8=43762
superconducting, complex elec. cond., strong-coupling calc. 8=35854
supercooling nucleation behaviour 8=48257
surface atoms, mean displacement 8=30935
superconducting shell, zero mag. field attainment 8=27044
superconducting, surface resistance meas. at 2.868 GHz 8=40383
superconductivity predictions from phonon spectrum and e.-phonon interactions 8=44719
thin films, critical field, influence of structure disorder and defects 8=40382

Lead—contd
thin films, production by diffusion evaporation 8=48456
tunnel effect under pressures up to 15kbar at 1.3°K 8=44737
u.s. attenuation, longit., low-temp. amplitude-independent 8=44321
u.s. attenuation, longit., low-temp. amplitude-independent 8=44322
X-ray Lα, emission, depth distrib. and absorpt. in anticathode, 17-29 kV 8=36420
Cu film on Pb, proximity effects in supercond. 8=27015
Pb$^{206-8}$, muonic, hyperfine interactions obs. 8=38772
Pb(II) electrode in NaNO$_3$-KNO$_3$ eutectic, linear sweep voltammetry 8=27750
Pb III series, intercombinational transition probabilities 8=38711
Pb^{2+}, diffusion in NaCl crysts. 8=31011
Sn^{119m} isomer shift 8=26015
ZnTe, hole-traps, Pb-associated 8=26884
in ZrSiO$_4$, e microprobe meas. 8=27811

Lead compounds
alloys, grain growth dependence on low solubility additions during recrystallization 8=35280
alloys, superconducting transition temps. 8=44729
chalcogenide films, mono- and multilayer, epitaxially grown structure 8=26115
ferrites with oxide additives, mag. residual induction and energy product 8=40842
halides, planar, γ-irrad., colour centre prod., e.s.r. and optical meas. 8=36249
lead(II) hydroxide, structure 8=44255
magnetoplumbite, Bitter patterns rel. to changes in width and domain shape 8=31557
oxides, thermodynamic props. by e.m.f. meas. 8=48729
perovskites, phase transforms. 8=26063
thioborate, crystal structure, new type 8=35349
BiFeO$_3$-Pb(Fe$_{0.5}$Nb$_{0.5}$)O$_3$ solid soln. system, phase transitions 8=39543
Pb rich alloy of Pb-Sn-Sb ternary system, aging 8=26764
Pb-Ag eutectic alloy, structure during solidification 8=26037
Pb-Bi alloys, films at low temp., electron diffraction examination of structure 8=35152
Pb–Bi alloys, superconducting, mag. field spatial distrib. and crit. current density 8=40381
Pb-Bi alloys, superconducting, pinning of flux vortices 8=49200
Pb-Bi solid soln., indirect nuclear spin-spin interactions in Pb by spin echo 8=40996
Pb-Bi system, metastable phases 8=30704
Pb–Bi system, superconducting transition temp. in amorphous phase 8=35844
Pb-BiCl$_3$ molten mixtures, absorpt. spectra 440-1000 mμ to interact. 8=34878
PbBi$_2$Se$_4$, struct. electron diff. exam. 8=35348
PbBr$_2$, anion vacancies in single crystals 8=48812
PbBr$_2$, ionic recomb. rates for weak ionization 8=43476
PbBr$_2$ molten, self-diffusion 8=34808
PbCa$_2$Si$_3$O$_9$, margarosanite, struct. and cryst. chem. 8=44248
PbCd$_{0.5}$W$_{0.5}$O$_3$, ferrielectric phase transitions between 130-400°C and at 420°C 8=40583
PbCl$_2$, crystal growth, effect of bivalent cation addition to soln. before crystallization 8=44120
PbCl$_2$, elastic consts. from vel. meas. of u.s. waves 8=35712
PbCrO$_4$, counterdiffusion of Pb^{++} and CrO$_4$ in agar gel 8=48244
Pb-0.5% Cu alloy, effect of dopant on alloy structure and fatigue life 8=26841
PbF, dissoc. energy 8=38933
PbF$_2$ Cherenkov counter for gamma rays and e$^{\pm}$ 8=46885
PbF$_2$ crystal Cherenkov shower detector 8=33613
PbF$_2$, e.p.r. and spin lattice relaxation of Yb^{3+} 8=36253
PbF$_2$, mass spectra of vapour 8=38933
PbF$_2$: Gd^{3+}, spectrum rel. to excited levels of Gd^{3+} at 77°K 8=36250
Pb(Fe$_{0.5}$Nb$_{0.5}$)O$_3$, e.p.r. rel. to para- to ferroelec. transition 8=27488
Pb(Fe$_{1/2}$Ta$_{1/2}$)O$_3$, dielectric and magnetic props. 8=40615
Pb-Ga, liq., critical opalescence, temp. depend. 8=48149
Pb-Hg solid soln., indirect nuclear spin-spin interactions in Pb by spin echo 8=40996
PbI, Zeeman effect and intensity anomalies 8=34148
PbI$_2$, defect energy level structure from photo-excitation studies 8=44650
PbI$_2$, ionic recomb. rates for weak ionization 8=43476
PbI$_2$, polytypism as high-order transformation 8=44012
Pb-In alloy, intermediate state structures, transition from flux lattice 8=44731
Pb–In alloys, stacking fault formation during deformation rel. to alloy comp. 8=35578
Pb-6.3 at.% In foils, type II superconductor, flux line arrangement 8=40384
Pb-In solid soln., indirect nuclear spin-spin interactions in Pb by spin echo 8=40996
Pb$_{85}$In$_{15}$ superconductor, resistive and mag. props., demonstration 8=35855
Pb-Mg solid solns., decay 8=35062
PbMg$_{1/3}$Nb$_{2/3}$O$_3$ crystals, electro optical effects 8=36400
Pb(Mg$_{1/3}$Nb$_{2/3}$)O$_3$-PbTiO$_3$-PbZrO$_3$ ceramics with Ba or Sr substitutions, piezoelectric props. and phase relations 8=31442

Lead compounds—contd
PbMoO$_4$, i.r. spectra 8=45179
PbMoO$_4$, laser-induced Raman spectra 8=31969
PbMoO$_4$: Ce^{3+}, Yb^{3+}, spin-lattice relax., contrib. processes 8=40911
α-PbN$_6$, cryst. struct., neutron diffr. 8=30908
Pb$_2$(NiW)O$_6$ synthesized under high pressures, phase transitions 8=35122
Pb(NO$_3$)$_2$, annealing of γ-irrad. damage, kinetics 8=44414
Pb(NO$_3$)$_2$, crystal growth, effect of methylene blue impurity 8=39679
PbO, electrical and optical props. 8=26948
PbO layers, microstruct. rel. to optical filter characts. 8=28765
PbO polycrystalline, SCL currents and trap distrib. from photoconductivity 8=36024
PbO vapour deposited layers, preferred crystal orientation 8=30756
PbO, yellow, forbidden band width, determ. 8=32022
PbO. 2B$_2$O$_3$, enthalpy of fusion 8=43905
PbO-B$_2$O$_3$-PbF$_2$ melts, solubility of trivalent oxides, temp. dependence, 1000-1500°C 8=39320
PbO-B$_2$O$_3$-SiO$_2$, phase equilibria and liq. immiscibility 8=34749
PbO-La$_2$O$_3$-B$_2$O$_3$ optical glasses exhibiting unusual dispersion characts. 8=45214
PbO–SiO$_2$ silicates, crystalline and vitreous, spectra 8=32021
PbO-TiO$_2$ mixed films, elec. props and permittivity rel. to struct. 8=49347
PbS, artificial, morphology rel. to hydrodynamic flow theory 8=26197
PbS, chemically deposited, influence of impurities on photosensitivity 8=44931
n-PbS, conduction band nonparabolicity 8=35776
n-PbS, conduction band structure, 77-300°K 8=27119
PbS crystals, steady-state creep, stoichiometric defects and foreign atom addition effects 8=40179
PbS, deformation state, investigation by harmonic analysis of form of interference lines 8=31227
PbS, effect of temp. on photoconductivity 8=44930
PbS film, monocrystalline, photosensitivity 8=40667
PbS films, polycrystalline, and crystals, photo-e.m.f. force temp. dependence 8=36025
PbS films, polycrystalline, polarization currents rel. to oxygen diffusion 8=35909
PbS, growth in silica gels, thioacetamide ion donor 8=48555
PbS on Si, mica and PbS single-crystal substrate, growth process rel. to substrate defect structure 8=26280
PbS, thermal conductivity lattice and electronic components, separate meas., 3-100°K 8=39951
PbS + CdO → PbO + CdS, solid state, reaction kinetics and diff. mech. 8=49839-40
PbS(Te) lattice parameters rel. to pressure 8=48669
Pb-0.5% Sb alloy, effect of dopant on alloy structure and fatigue life 8=26841
Pb-Sb alloys, liquid, density rel. to temps. 8=39326
Pb–Sb alloys, (to 2 wt.% Sb) ageing after quenching 8=35121
Pb–0.5% Sb, fatigue bands developed on reversed bending cycles 8=35714
Pb-Sb system, metastable phases 8=30704
Pb-Sb-Sn alloys, liquid, density rel. to temp. 8=39326
PbSe, anomalous diffusion of Ni 8=39981
n-PbSe, conduction band nonparabolicity 8=35776
PbSe epitaxic film formation by sublimation in vacuo 8=26123
PbSe films, polycrystalline, photoconductive meas. at 77°K rel. to mobility changes and heat treatment 8=27328
PbSe, growth, annealing and diffusion coeffs. 8=44141
PbSe, thermal conductivity lattice and electronic components, separate meas., 3-100°K 8=39951
PbSe:Gd, doping rel. to elec. props. 8=44805
Pb-Sn alloys, cell boundary diffusivity, calcs. from Cahn and Turnbull theories 8=30670
Pb–Sn alloys, electron reflection, 600 to 1200 keV 8=44197
Pb-0.005% Sn alloy, hydrodynamic currents in solidification front region 8=34968
Pb-Sn alloys, liq. self-diffusion of Ag impurity 8=34806
Pb-Sn solid solns, decay 8=35062
Pb–Sn system, cell growth, calc. of limiting boundary diffusivities 8=48533
PbSnO$_3$, perovskite, high press. synthesis and lattice consts. 8=48554
Pb$_{1-x}$Sn$_x$ Se alloys, phase diag. 8=48594
Pb$_{1-x}$Sn$_x$Se, solid solubility, optical props. and band struct. 8=43980
Pb$_{0.88}$Sn$_{0.12}$Te laser diode, tunable, detection of beat freq. with CO$_2$ laser 8=42098
Pb$_{1-x}$Sn$_x$Te alloys, T — x phase diagrams and lattice parameter values 8=26077
Pb$_{1-x}$Sn$_x$Te, growth, annealing and diffusion coeffs. 8=44141
Pb$_{1-x}$Sn$_x$Te laser, i.r. up to 28μ, props. at 12° and 77°K 8=37621
Pb$_{1-x}$Sn$_x$Te, solid solubility, optical props. and band struct. 8=43980
Pb$_{1-x}$ Sn$_x$Te, two valence band evidence and thermal energy gap 8=44651

Lead compounds—contd
- $(Pb_xSr_{1-x})TiO_3$, crystal growth by traveling heater method 8=44139
- $Pb(SSCOC_4H_9)_2$, crystal struct. 8=39855
- Pb-0.5% Te alloy, effect of dopant on alloy structure and fatigue life 8=26841
- PbTe, elastic constants, thermal expansion and Debye temp., 8=49044
- PbTe films, temp. depend. of photoelec. parameters 8=40668
- PbTe, high pressure transformations 8=35082
- PbTe, Knight shift calcs. using augmented-plane-wave method 8=40995
- PbTe, localized energy levels in forbidden gap, $PbTe-Al_2O_3$ junction tunnelling obs. 8=35910
- PbTe, thermal conductivity lattice and electronic components, separate meas. 3-100°K 8=39951
- PbTe, valence band using transport phenomena 8=44804
- p-PbTe-CdTe alloy, magnetoresistance at 77°K 8=49257
- PbTe-SnTe, cryst. growth, phase diagram and props. 8=44140
- PbTe-SnTe-PbS system, current carrier scattering mechanism 8=31385
- PbTe:In p-n junctions, tunnelling electrons scatt. by impurity vibrs., 1-10°K 8=35938
- PbTe: Na, drift mobility of light-mass holes 8=49258
- PbTe:Sb, electrical cond. and Hall effect 8=40478
- $PbTe_{0.5}Se_{0.5}$, I^+ doping effects on thermal conducitivity, 100-400°K 8=35461
- $PbTe_xSe_{1-x}$ solid solns., forbidden band width temp. dependence 8=40247
- $PbTiO_3$ ceramics, piezoelec. coupling factors and ageing rates 8=49384
- $PbTiO_3$, e-microdiffr. exam. 8=26430
- $PbTiO_3$ ferroelec., at. structure determ. using micro e.-diffr. technique 8=39761
- $PbTiO_3$, formation mechanism 8=36569
- $PbTiO_3-PbMn_{2/3}W_{1/3}O_3$ system, solid solns., structures and permittivities 8=40616
- Pb-Tl alloys, superconducting critical currents 8=40385
- Pb-Tl alloys, superconducting transition temp. comp. dependence 8=44730
- $PbWO_4$, i.r. spectra 8=45179
- $PbWO_4$, laser-induced Raman spectra 8=31969
- Pb-Zn ores, applic. of method of determ. true chargeabilities of vertical discontinuities 8=41323
- Pb-Zn ores in Turkey, true chargeability obs. 8=32177
- $PbZn_{1/3}Nb_{2/3}O_3$, and dielec. props. 8=27280
- $PbZn_{1/3}Nb_{2/3}O_3$, dielec. props. 8=27281
- $PbZrO_3$, phase boundaries below 500°C 8=48366
- $PbZrO_3-PbTiO_3$ ceramics, sintering process by hot-pressing, and elec. props. 8=39535
- $PbZrO_3-TiO_3$ ceramics, PbO deficiency on vaporization rel. to piezoelectric props. 8=35010
- $Pb(Zr_{0.65}(Ti_{0.35})_3$, cold-pressed, vaporization in vacuo, 690-1130°C 8=35009
- $Pb(ZrTi)O_3$ ceramics, mechanical quality and microstruct. 8=44597
- $Pb(Zr, Ti)O_3$, ferroelectric and antiferroelectric, electrocaloric effects 8=27279
- $Pb(Zr, Ti)O_3$ ferroelec. ceramic, 90° domain wall-pt. defect interaction 8=44405
- $Pb(Zr_{0.52}-Ti_{0.48})O_3$, thermal diffusivity meas. by laser flash method 8=39950
- $Pb(Zr_{0.65}Ti_{0.35})O_3$, vaporization of hot pressed pellets of near theoretical density 8=43919

Leak detection
- analysis cells, French development 8=39259
- apparatus, highly sensitive 8=47995
- combined leak detector and high sensitivity vac. gauge 8=30337
- instruments and methods review 8=30323
- ionic sorption pump appl. 8=39260
- mass-spectrometer type and NH_3 apparatus 8=39258
- water cooling system, flood protection by aspirin tablet 8=37097
- Kr^{85} leak test. 8=47990

Leather. See Materials.

Lee model. See Field theory, quantum.

Length measurement
- See also Micrometry; Strain gauges; Thickness measurement.
- displacements, very small, using open circuit voltage of symmetric photodiode 8=41618
- e.m. distance meas. by electro-optical light modulators matrix analysis 8=46648
- expansion, longitudinal, of cylinder under uniaxial constraint, precise method 8=28217
- high-accuracy spatial meas. using v.h.f.-modulated light 8=41617
- magnified interferometric, of small displacements 8=41619
- 1-metre line-standard interferometer 8=45951
- Moiré fringes, applic. to accurate meas. of minute displacements 8=46729
- moving sphere, diameter meas. by laser beam 8=23788
- optical ranging systems, phase-modulated, applic. of p-n junction lasers 8=42110
- parallelism of surfaces meas. with laser 8=37550
- pneumatic contactless systems 8=23786

Length measurement—contd
- precise and reproductible standard definition 8=45946
- radius of curvature by contact spherometer 8=42184
- recording dilatometer for −150° to +1500°C 8=28216
- reference interference equipment for reproducing unit of length 8=45949
- standards, historical review (1918-1968) 8=28209
- Kr^{86}, wavelength standard, reproducibility, discussion 8=23789

Length standards. See Standards.

Lennard-Jones and Devonshire theory. See Liquids/theory.

Lennard-Jones potential. See Kinetic theory; Molecules/intermolecular mechanics.

Lenses
- See also Electron lenses.
- apochromatic flat-field objectives for biological microscopes 8=42189
- arbitrary system, coherent transfer characts. 8=37648
- astigmation correction in Czerny-Turner spectrograph 8=46664
- automatic lens design, use of merit functions based on wavefront aberrations 8=28726
- catadioptric system 8=46667
- coherent optical noise suppression 8=37641
- condenser, design 8=28753
- correcting, of progressive power, retinal image 8=46775
- curvature correction in images produced by concentric systems by means of fibre 8=42194
- dome-shaped, for signal lights, graphical analytic design 8=42156
- eye, astigmatism in accommodation 8=37726
- fluid, luneberg, acoustic wave theory 8=30466
- gas, tubular, in guide, beam deformation obs. 8=37639
- gas, using Peltier effect 8=42155
- Gaussian type (F/1.8), in direct and reversed system, comparison of aberrations 8=33245
- gradual correction, for focus shift on stigmatic eye 8=46661
- image formation, matrix approach 8=28725
- magnetic, quadrupole, design for accelerator 8=33104
- magnetic, with periodic longit. field, equivalence with hexapolar magnet 8=37439
- meniscus mirrors, in optical systems 8=42149
- microwave Luneberg made of foam glass steps 8=37465
- mirror-lens variable magnification systems 8=42150
- objectives, cemented 2-lens, computerized design in region of third-order aberrations 8=42163
- objectives for image converters and intensifiers, design 8=42178
- objectives, variable focal length and zoom 8=42157
- perfect defocused, modulation transfer function tables 8=37637
- plasma, parameters calc. 8=41986
- replacement of single-lens components by two-lens components 8=42158
- spherical, laser beam focusing 8=36377
- Strehl ratio, depend. on magnitude of variance of wave aberration 8=28731
- system, entropy transmission 8=46658
- transfer coefficients in lens system 8=42176
- two-element, secondary spectrum in i.r. 8=45144
- variable focal length objectives with mechanical compensation 8=42152
- CdS plate with internal elect. field causing u.s. oscills., effect on laser beam 8=28882
- Ge, corrosion resistance 8=40162
- **aspherical**
  - crystalline (rabbit), refractive index distribution model 8=46779
  - with laser, for increased brightness 8=28728
  - surface calc. method 8=24363
  - surfaces, correction of aberrations by insertion in optical systems 8=46663
- **photographic**
  - amber coating and colour of objectives 8=42289
  - asymmetrical wide angle, struct. and image forming props. 8=28910
  - objective corrected to u.v. using quartz glass and fluorite 8=37724
  - objective, image plane light distribution, wave optics calc. 8=46764
  - telecentric, for bubble chamber photography 8=46956
  - transfer and line spread functions, automatic testing intrument 8=28909
  - variable focal length objectives with mechanical compensation 8=42152

Leptons
- See also Electrons; Mesons; Neutrinos and antineutrinos.
- in baryon decay, rate calc. 8=33734
- currents, neutral, weak interaction with hadrons 8=29110
- Dirac current tests 8=46833
- e.m. corrections to mass shifts and decays of weak interaction currents identified with boson field 8=29106
- lepton-baryon interactions with neutrino production 8=47075
- multiplicative quantum numbers 8=33622
- nucleon e.m. scatt., polarization dependence calc. 8=42462
- pair annihilation into two photons, matrix element calc. with anomalous magnetic moment and polarization 8=29089

Leptons—contd
- pair, symm. photoprod., Bethe-Heitler and Compton amplitudes 8=33623
- pair photoprod. cross section, Compton graph contrib. 8=24709
- pairs, boson coupling and the anomalous magnetic moment of μ 8=29102
- l^+l^- prod. in vector meson decay, calc. of radiative correction 8=29170
- strange, experimental evidence against their existence 8=42461
- strange, neutral leptonic currents 8=24708
- weak interactions, symmetry scheme 8=47074

Lie groups. See Group theory. For applications see Elementary particles; Field theory, quantum.

Ligands. See Bonds; Molecules.

Light
- See also Diffraction; Interference, etc.; Doppler effect; Radiation.
- above atmosphere, u. v. and X-ray backgrounds, rel. to intergalactic gas density, obs. 8=32490
- amplification, non-linear propag. conditions 8=46646
- amplification of modulated signal by gas laser 8=24269
- beam modulation in GHz range, examination with photomultiplier 8=46643
- beam, monochromatic, e.m. field strength, energy, impulse and stationary mass 8=42241
- beam nonlinear difference method solution 8=33232
- beam, self-trapped, non-linear Helmholz eqn. analysis 8=46715
- emission by e in harmonic oscillator, harmonic generation 8=42472
- Gaussian beam fluctuation in random medium, autocorrel. 8=46644
- Gaussian beam, modulation by u. s. wave, Fourier intensity 8=37630
- Gaussian beam propagation in random medium 8=46636
- Gaussian, beam, width obs. 8=33166
- gravitational bending rel. to Sun's internal field nature 8=32569
- gravitational deflection, effect on lunar star occultation time 8=32801
- interaction with plant canopy 8=46735
- laser, ferromag. reson. modulation at microwave freq., theoretical anal. 8=42053
- laser modulation 8=46542
- laser, modulation and demodulation 8=46647
- modulation, amplitude, electro-optic device 8=33239
- modulation by double-quantum resonant optically-pumped Rb^{85} vapour 8=37629
- modulation, by ferromag. resonance of ferroglass 8=24359
- modulation, h.f., by reverse-biased GaP diodes 8=40528
- modulation of laser beams using grating diffraction effects 8=42122
- modulation transfer function for perfect defocused lens 8=37637
- modulation, v. h. f. broadband 8=42121
- modulator, photoelectroplating 8=37631
- primary standard, thermodynamic consideration 8=46654
- propag. in anisotropic medium 8=33270
- Q-modulation of laser by controllable-transmitting liq. shutter 8=42063
- Q-modulation of laser resonator, use of opto-mechanical shutter 8=42077
- screen scintillation due to interference 8=46723
- second harmonic generation in KH_2PO_4 crystal 8=41102
- self-modulation in dispensive media of nonlinear plane waves 8=28720
- stray in optical instruments 8=46670
- transformer using org. luminophore solns. in laser system under optical pumping 8=28650
- wave, dissipative instability in non-linear dielec. 8=46712
- wave packet, kinetic behaviour 8=37625
- KH_2PO_4, second harmonic generation using a laser 8=41102
- **coherence**
  - See also Lasers.
  - beam, monochromatic, e.m. field strength, energy, impulse and stationary mass. 8=42241
  - coherent optical processors 8=46637
  - double quantum light scatt. by mols. 8=25400
  - e. m. field theory, introducing stationarity, homogeneity and isotropy under translation and rotation 8=37401
  - effect in holography 8=46743
  - extended thermal source, degree 8=33238
  - Fourier-transform holograms with partially coherent light, spatial coherence obs. 8=28890
  - Fourier transform spectroscopy, pseudo-coherence effect 8=24390
  - fourth order correl. function, theory of exptl. determ. 8=42118
  - frequency conversion in USSR, bibliography 8=28719
  - frequency mixing by lasers beam superposition 8=24333
  - functions of order, N, M with N ‡ M 8=46641
  - Gaussian beam in random medium, fluctuations 8=28717
  - Gaussian beam propagating through random medium, fluctuation distribution 8=33235
  - Green's function, applic. in theory 8=33237

Light—contd
- **coherence—contd**
  - heterodyne photon signal intensity, spacial coherence effects 8=42120
  - higher-order coherence functions of optical fields and phase fluctuations 8=33236
  - imagery, minimizing noise 8=37628
  - interference of independent laser photon beams at low intensity 8=42248
  - interferences, two-beam, temporal coherence rel. to path-difference in dispersive medium 8=28852
  - laser beam phase fluctuations, effect of laboratory generated turbulence 8=42058
  - laser, coherence function determ. from diffraction 8=37607
  - laser Doppler velocimeter system 8=37553
  - mutual, propagation in randomly inhomogeneous medium, diffusion analysis 8=42119
  - nonlinear optic effects rel. to spectrum expansion 8=33241
  - optical image form. and filtering 8=37649
  - optical noise suppression 8=37641
  - optical parametric amplifier, second-harmonic generation 8=24358
  - photon beats rel. to spectral composition 8=33259
  - photon-phonon interactions, theory 8=46638
  - picosecond pulse of laser light, meas. by photographic method 8=32290
  - pinhole camera, general transfer function, by partial coherence theory 8=28908
  - propagation of coherence function through random media 8=28715
  - quantum optics fundamentals, book 8=24352
  - quantum theory, normal and antinormal ordering of field operators 8=46639
  - radiation field interaction with two-level atoms, quantitative classical analogy 8=25371
  - Raman scatt., spontaneous, partial coherence possibility 8=38778
  - scattering by latex hydrosols, coherent and incoherent light 8=34932
  - second harmonic generation by discrete spectra 8=24354
  - shape definition, applic. of coherent optics 8=46669
  - spatial freqs. in holograms, reduction without decreasing field of view 8=28895
  - statistical props. of coherent radiation 8=46640
  - superposition of thermal and coherent fields, normal and antinormal correlations 8=46469
  - theory partial and spatial and applic., review 8=28718
  - ultrashort pulses form. dynamics 8=37552
  - CdSe radiation of free excitons 8=36343
  - He-Ne laser, coherence length extension 8=37586
  - Hg, scattering, 6^1P_1 level lifetime 8=47498
- **electromagnetic theory**
  - amplitude superposition rel. to boundary condition methods in film optics 8=42244
  - beam propagation theory, use of Monte-Carlo method algorithms 8=46714
  - dissipation functions of anisotropically scatt. invariant imbedding eqns. 8=28843
  - propag. in isotropic and anisotropic media, applic. to interferometry. 8=28856
  - quantum, of fluctuating laser-active medium 8=37626
  - self-focusing pulses freq. spectrum broadening 8=28842
- **quantum theory**. See Photons; Quantum electrodynamics; Quantum theory.
- **velocity**. See Velocity/light.

Light guides. See Optical instruments.

Light modulation. See Light; Optics.

Light sources
- See also Lasers; Monochromators; Photometry/light sources; Spectroscopy/light sources.
- ablative, elect. and optical props. 8=37669
- c.r.t. microdensitometer for X-ray crystallography 8=35304
- colloidal mass emitter for optical meas. of permittivity and dielectric loss 8=28766
- continuum, in XUV region, type of discharge tube 8=37671
- electroluminescent diodes, thermodynamic limits 8=24382
- electroluminescent fiducial display system, pulsed power supply 8=46340
- electroluminescent, for data recording 8=37668
- flash lamp for laser pumping 8=46539
- flash photolysis lamp 8=42206
- flash X-ray discharge continuum with various anode materials 8=25689
- flashlamp for organic-dye lasers 8=46629
- fluorescent lights viewing of Melde expt. 8=28724
- gas-filled, Langmuir theory 8=42210
- generator, backward wave, steady-state oscills. 8=24357
- high intensity, pulsed type 8=42204
- high temp. solids, gases, gas discharges, electro luminescent materials and lasers 8=28769
- hollow-cathode demountable discharge tube 8=29887
- hollow-cathode discharge, for extreme u.v. 8=24381
- for holography, effect of coherence 8=46743
- incandescent, photometric, calibration and standardization 8=42211
- inert gas filled flash lamps, for research in solar engineering 8=46680

Light sources—contd
  i. r. pulse generator 8=28770
  lamp, hollow-cathode for atomic absorpt. spectroscopy 8=36638
  laser, pulsed, spectroscopy by defocused Fabry–Pérot interferometer 8=42250
  lasers for new image recording techniques 8=46669
  lasers, thermodynamic limits 8=24382
  monochromatic generation by amplitude modulation 8=24355
  optical pulse generator, extended path and digitally scanned 8=46679
  z-pinch, dynamically Li vapour filled, for photo-ionization of H$_2$ 8=34528
  polar mols., charact. of absorpt. in far i. r. 8=34859
  projector, enlargement 8=37667
  pulsed, for spark chamber calibration 8=46962
  pulses of 0.2 μsec from z-pinch, for flash photolysis 8=28771
  Schottky barrier meas., source control 8=35875
  short light pulse generation, convenient method 8=24379
  spark discharge between glass plates 8=28767
  spark, for shock tube densitometry 8=33254
  spark, laser-induced, for wide band-gap drift mobility meas. 8=42205
  standard, for simulation of air-glow 8=46678
  standard of low luminance 8=28772
  tungsten-hologen incandescent lamps 8=37670
  u. v. ultrasonic gas jet with e beam excitation 8=38660
  Ar, explosive-driven shock tube 8=25830
  Ar flash for high-speed photography 8=28768
  Ba$_2$NaNb$_5$O$_{15}$ in continuous 0.532μ solid-state source 8=33253
  Cd vapour lamp, possible practical use 8=38990
  Eu activator in industrial fluorescent lamps 8=42212
  GaAs$_{1-x}$ P$_x$ injection laser, electroluminescent source, luminance $> 6 \times 10^9$ cd/m^2 8=41192
  He-Ne laser for Raman spectrometer, resolution improvement 8=24398
  Hg h.p. lamp with iodide additive 8=42207
  Hg lamp for holography 8=46754
  In, resonance radiation, electrodeless h. f. source 8=24380
  InI$_3$ discharge lamp, temp. distrib. determ. 8=43454
  KH$_2$PO$_4$ parametric generator, electro-optical tuning obs. 8=41103
  Kr flash tube pumping efficiency of YAG: Nd^{3+} laser 8=46550
  Na vapour, thermal insulation and pressure effects 8=42208
  Nd glass, generation and amplification of light pulses 8=41126
  Seyfert and N-type galaxies and quasars, common source 8=45778
  SLF photo-slip lamp 8=42203
  Tb activator in industrial fluorescent lamps 8=42212
  Ti, resonance radiation, electrodeless h. f. source 8=24380
  Xe arc lamp, simple power supply system for stable operation 8=24073
  Xe flash tube with delay line 8=42209
Lighting. See Illumination.
Lightning
  ball within metal aircraft 8=45472
  channel paths, tortuosity analysis 8=36754
  cloud and ground, comparison of discharge processes 8=27919
  current moments at e. l. f. of discharges associated with mature tropical hurricane 8=32251
  discharge, statistical props. of noise from predishcarge part 8=45470
  electrical discharges, vortex-stabilized, in atmosphere, threshold conditions 8=32248
  flash counter calibration using elect. field changes 8=36755
  pressure pulse from triggered lab. stroke 8=36752
  radio noise survey, Aerial III equipment 8=28026
  return stroke diameter, elect. circuit model calc. 8=36753
  shock wave from discharge 8=41369
  single-stroke flash, peak power and energy dissipation 8=36751
Linear accelerators. See Particle accelerators/linear.
Linewidths. See Spectral line breadth.
Liouville equation. See Statistical mechanics.
Liquefaction, gases
    See also Low-temperature production.
  C$_v$ discontinuity across liquid-vapour coexistence curve near critical point 8=25988
  Ne, separation from He-Ne mixture 8=46302
Liquid crystals
  4, 4′-di-n-alkyloxy azobenzenes, nematic, molec. polarizabilities 8=48068
  4, 4′-di-n-alkyloxy azoxybenzenes, nematic, molec. polarizabilities 8=48068
  from n-iso-alkoxybenzal-1-aminonaphthalene-4-azobenzene derivs. mixture comp. -and structure 8=39308
  amorphous phase, orientation fluctuations, electrooptic props. 8=34767
  amphilphile aqueous solns., fibrous structs. for M$_1$ and M$_2$ phases 8=30408
  amphiphiles, lamellar solns., birefringence sign reversal 8=25919

Liquid crystals—contd
  p-(anisalamino)-phenyl acetate, elec. field effect on n. m. r. 8=34924
  aromatic pure cpds, heats and temps. of transition 8=34772
  p-azoxyanisole optical rot. obs. of two forms 8=43826
  p-azoxyanisole, struct. in constant elect. fields 8=34771
  p-azoxyanisol, structure in permanent and variable elec. fields, X-ray study 8=25881
  p-azoxyanisole, X-ray structural exam. in strong mag. field 8=39309
  azoxybenzones, sound velocity and absorpt. meas. and phase transforms. 8=25882
  p-benzoquinone, n. m. r. in nematic phase 8=34913
  carbonized coal-tar pitch, microstruct. of coalesced mesophase 8=30576
  chemical shift anisotropies, n.m.r. obs. 8=30411
  cholesteric, electric-field-induced optical station 8=43811
  cholesteric, elec. field induced phase change, 10^5 V/cm 8=34766
  cholesteric, for electrophotographic imaging 8=42279
  cholesteric, optical rotary power, theory 8=43812
  cholesteric, structure distortion by mag. field 8=30407
  cholesteric, struct., effects of elec. and mag. fields 8=34768
  cholesterol derivatives, struct. 8=48069
  cholesterol-type, light scattering meas. 8=25882
  cholesteryl, dielec. props., dipole moments and transition temps. 8=34893
  cholesteryl 2-(2 ethoxyethoxy) ethyl carbonate, Brillouin scatt., 20-60°C 8=48146
  cholesteryl 2-(2-ethoxyethoxy)ethyl carbonate, refractive index obs. 8=30482
  p-n-heptylhydroxybenzoic acid, nematic and smectic phases, domain formation 8=34769
  mesophase transitions, theory 8=39311
  p-methoxybenzylidene-p′-cyanoaniline, nematic, X-ray struct. study 8=48067
  mixtures, structural and stability characts., x-ray exam. 8=39310
  nematic, thermal cond., interfacial and elec. field effects 8=34833
  nematic, weak wave propag. 8=48133
  n. m. r., effect of sample spinning 8=30530
  n. m. r. of 3, 3, 3-trifluoropropyne in nematic cryst. solns. 8=34930
  n.m.r. shielding anisotropics of solutes in liq. cryst. solvents 8=43875
  octylbenzoic acid, ferroelec. behaviour 8=25882
  optically active, n.m.r. of dissolved enantiomers 8=39422
  ordered glass matrix, polarized absorpt. 8=49767
  polymesomorphic type, phase transitions 8=34770
  pre-transition phenomena and electro-optical props. 8=30409
  pyrazine, n. m. r. in nematic phase 8=34913
  t-RNA, formation and study by X-ray diffr. 8=25875
  water in mesomorphic phases, d.m.r. 8=48220
  X-ray examination in mag. fields, apparatus 8=30410
  K$_2$HPO$_3$, lattice energy from ultrasonic velocity 8=25880
Liquid-drop model. See Nucleus/models.
Liquid flow. See Flow/liquids.
Liquid helium. See Helium/liquid.
Liquid oscillations
  Benard cell with molten Ga, unrotated, convective temp. 8=30377
  of droplet immersed in different fluid, freq. and rate of damping 8=43738
  electron liquid, degenerate, spin-independ. oscills. 8=34755
  free, in motionless container, calc. 8=30375
  Marangoni films, hydrodynamic stability 8=48052
  Pb, cooperative modes of motion 8=34725
  Pb, cooperative modes of motion, temp. depend. 8=34726
Liquid waves
    See also Acoustic waves.
  beach, uneven bottom 8=50109
  complex laboratory wave by beating paddle, verification of theory 8=43737
  crystal, nematic, weak wave propag. 8=48133
  dispersion, in rotating, differentially heated cylindrical annulus of liquid 8=39277
  gravity waves in shallow water, damping 8=39276
  shear, in molten glass, high-temp. u.s. interferometry 8=39280
  standing internal gravity waves, profiles, theory and expt 8=48038
  surfactant, solns., capillary nipple damping 8=30445
  water, one-dimensional Lagrangian meas. 8=34729
  water, shock, isothermal at max. density 8=34728
  He II, capillary modes 8=37350
 surface
    See also Oceanography.
  breaking characts., note on integro-differential eqn. model 8=30373
  free gravity waves, electrohydrodynamics 8=30344
  gravity, in uniform channel of arbitrary cross-section 8=30372

Liquid waves—contd
  surface—contd
    gravity, nonlinear and linear motion 8=39279
    after interaction with sliding detonation and shock waves 8=23949
    interfacial ripples, propagation theory 8=39284
    laminar rippling flow, gas absorption rates, method 8=48053
    m.h.d., conducting surrounded by flowing gas 8=48036
    propagation laws and capillary wave attenuation 8=43736
    resonant oscillatins in tank, obs. 8=34724
    resonant oscillations in tank, theory 8=34723
    ripple amplitude meas., off-crest optical method 8=34727
    solid interface 8=43734
    surge and bore, undular, run-up rel. to slope and bottom roughness 8=50116
    water, on vertically uniform current, intrinsic freq. and energy conservation 8=23807
    transmission dynamic action on vertical wall 8=43739
    water phase jumps 8=39278
    water, shallow, wave generation by unsteady flow 8=30374
    wind generated, suppression by surface film 8=48037
Liquids
    See also Association/liquids; Diffusion in liquids; Solutions.
  absorption of gases in wetted-wall columns, acceleration by corona discharge 8=32119
  adsorption on carbon, H^1 and F^{19} n. m. r. lineshift study 8=30766
  acetic acid, microscopic transport props., use of atomic substitution in n scatt. studies 8=30403
  alloys of alkalis in alkalis, thermoelectric powers 8=27305
  amyl and isoamyl alcohol, refractive index, density and viscosity temp. derivatives 8=34803
  aqueous systems, enhanced mass transfer due to detached turbulence promoters 8=34792
  binary, critical phenomena 8=34980
  binary mixtures, near crit. point, inelastic photon scatt. by fluctuations of conc. 8=25918
  binary systems, diffusion coeffs. using diaphragm cell 8=43785
  Brillouin scatt. of neutrons, rel. to collective particle motions 8=25869
  n-butyl alcohol, refractive index, density and viscosity temp. derivatives 8=34803
  charge carriers, natural, determ. of mobility 8=43863
  condensates, effects of strong elec. fields 8=34990
  convective circulation in system and closed vertical circular duct or slots 8=30464
  critical state study using gravitational waves 8=48055
  dielectric dispersion, interpretation of expt. results 8=43854
  dissociation, calc. of extent from freezing pt. curves, inc. of activity coeffs. in formula 8=30415
  double quantum light scatt. by mols. 8=25400
  elastic, flow through curved pipes, dynamic similarity and drag reduction 8=48018
  elastico-viscous, linear, non-Newtonian viscosity and elastic props., theory 8=25841
  e.m. wave self-trapping 8=34843
  flow, standardization of meas. method and instrums. 8=25791
  Freon-113, condensed inside tube, effect of strong elec. fields 8=34990
  interfaces, agitated by large bubbles, mass transfer expts. 8=43743
  light scatt., elastic second harmonic 8=25917
  light scatt., fluctuation theory 8=30475-6
  light scattering, combination meas. using standard, line intensity determ. 8=43808
  light scattering, molecular collision-induced 8=30474
  metal, collective excitation. 8=48054
  metals, automatic manometer for pressure meas. 8=48011
  metals, solid state and liq. state physics, links and review 8=30398
  methanol, microscopic transport props., use of atomic substitution in n scatt. studies 8=30403
  molecular motion, effects on n.m.r. relax. 8=39426
  molecular motion study by nuclear relax. 8=30399
  optical Kerr mol. consts., calc. 8=34845
  organic, bubble growth rel. to Jakob. number 8=34996
  organic mixtures, concs., by internal filling counters 8=27817
  polar dielecs., props. by "ionic thermoconductivity" method 8=25944
  refractive index variation in strong field of ruby laser 8=41098
  radiation nucleation, model of thermal spike effect 8=41292
  rotationlike motion of mols. 8=48157
  salinity gradient, stable, heated from below, behaviour 8=43716
  sliding of detonation and shock waves over surfaces 8=23949
  solid matter solubility in liquid phases, equation 8=48070
  spin-lattice relax. time rel. to molec. rotation and re-orientation 8=30531
  supercooled, viscoelastic relaxation 8=30430
  viscous, pressure drop created by sphere settling, Reynolds no. 0. 2 to 21, 000 8=39263
Liquids—contd
  wake of three cylinders, low Reynolds number, smoke obs. 8=30371
  water in capillaries, shift in temp. of max. density 8=34790
  water, proton dynamics from slow n. inelastic scattering 8=39303
  weightless, outside earth's gravitational field 8=48104
  Ar, liquified, motion, and ion mobilities 8=48193
  CO_2, in crit. region, heat transfer by free convection from Pt wire 8=34823
  Ge melt temp. field in growing crystals by the Czochralski method 8=30829
  $PbO-B_2O_4-SiO_2$, immiscibility and phase equilibria 8=34749
  structure
    in above-critical region, theory 8=25995
    acetonitrile, spin-lattice relax. and molec. reorientation in liq. 8=30539
    alcohols, hydrogen bonding 8=48059
    alkali metal nitrate melts 8=39378
    ammonia, liquid, rel. to absorpt. spectra of $Li\cdot NH_2$ solns. 8=39380
    amphiphile aqueous cryst. solns., phase structs. 8=30408
    p-azoxyanisol liquid crystals, in permanent and variable elec. fields, X-ray study 8=25881
    benzene, x-ray diffrn. 8=34764
    carbon tetrachloride, neutron diffraction 8=34761
    cholesteric crystal, distortion by mag. field 8=30407
    cholesteric liq. crystals, effects of elec. and mag. fields 8=34768
    cholesterol derivatives, liq. crysts. 8=48069
    density expansions of radial distrib., correl. and scatt. intensity functions 8=25876
    deuterium, ortho-para solns., neutron scat. 8=30404
    diborane, significant struct. rel. to phys. props. 8=43755
    ethyl alcohol, i.r. spectroscopic study of non-H-bonded OH groups 8=30401
    feldspar and silica mixtures 8=39297
    flow birefringence of simple liqs. 8=39369
    formamide, and K1 solns., X-ray diffr. 8=39306
    free volume 8=34760
    glass, melt and solid, similarities 8=30790
    hydrated electron, model 8=34752
    hydrazine, significant struct. rel. to phys. props. 8=43755
    hydrogeneous, neutron scatt. cross-section meas. 8=48065
    inert gases in H_2O 8=48077
    metal melts ordering states 8=34759
    metal melts, paracrystalline lattice with vacancies model 8=25979
    metal, theory and exptl. technique 8=34758
    metals, book 8=34753
    methyl alcohol, i.r. spectroscopic study of non-H-bonded OH groups 8=30401
    mixtures, X-ray or neutron scatt. data anal. 8=39628
    molecular groups, correl. between positions and orientations, distrib. functions 8=25868
    molecular motion study by nuclear relax. 8=30399
    molecular rot. influence on viscosity and shear relax. times 8=30426
    molecular, thermal agitation coeff. determ. for diffr. studies 8=25878
    neutron scatt. heating arrangement up to 900° C 8=34762
    nematic from obs. of optical rotation 8=43826
    octyl alcohols, transform., evidence from PVT meas. 8=39296
    organic liqs., correl. with positronium annihilation 8=30406
    polar films orientation by cell surface elec. fields, i.r. absorpt. obs. 8=39302
    polyethylene, oligomeric, conformational struct. in aromatic nonaromatic solvent mixtures, n.m.r. obs. 8=43765
    scattering studies with X-rays and neutrons, comparison 8=30402
    solutions, x-ray and n diffr. methods 8=34763
    spin-lattice relax., theory 8=39427
    thermal motion 8=48063
    water, and distrib. functions, by X-ray scatt. from free surface in equilib. with vapour 8=25872
    water, effect of solutes and temp. 8=39295
    water, exciton and interband transition, band gap 8=43752
    water, i.r. spectroscopic study of non-H-bonded OH groups 8=30401
    water, light, molec. motion models, comp. with results from neutron scatt. 8=39304
    water, modification of Nemethy-Scheraga theory 8=43754
    water, study by i.r. absorpt. of HEO mols. in H_2O at high press. and temp. 8=25930
    water, theory of solvent power for hydrocarbons 8=48085
    water, urea as struct. breaker 8=48085
    water-alcohol solns. of KCl 8=39407
    Al, coordination number transforms, viscosity obs. 8=2586
    Al, radial distrib. function from Percus-Yevick and convolution hypernetted-chain eqns. at high densities 8=48058
    Al-Cu, coordination number transforms., viscosity obs. 8=25866
    Al-Ge alloys, eutectic, atom distribution 8=39298
    Al-Mg, coordination number transforms., viscosity obs. 8=25866

- **Liquids**—contd
  - **structure**—contd
    - Al-Si, coordination number transforms., viscosity obs. 8=25866
    - Ar, correlation function, direct, and equation of state 8=34756
    - Ar, intermolec. pot. and correl. functions, determ. from X-ray diffraction 8=25877
    - Ar, radial distrib. and distrib. functions, X-ray study and theory 8=43759
    - Au, x-ray intensity, Fourier analysis 8=39307
    - Bi, near melting point, and correlation function 8=48062
    - CS$_2$, light scatt. by fluctuations of anisotropy 8=25920
    - Co, atomic structure from X-ray diffr. exam. 8=25874
    - Cu, atomic structure from X-ray diffr. exam. 8=25874
    - Fe, atomic structure from X-ray diffr. exam. 8=25874
    - Ga, x-ray scatt. 8=34765
    - GaAs, x-ray scatt. 8=34765
    - He^3, from X-ray scattering at 0.65, 1.25 and 2.29°K 8=24036
    - Hg-CN-SCN complex, aqueous soln, mixed ligand study 8=43842
    - In, temp. dependence, from X-ray diffr. exam. 8=25873
    - In-Bi complex eutectic alloys, atomic distrib. character 8=25871
    - K, X-ray intensity, Fourier analysis 8=39307
    - Mg-Sn allov melts. atomic distrib. curves 8=39300
    - Na, dynamic three-dimensional structure 8=25867
    - Na$_2$(H$_2$SiO$_4$).4H$_2$O, in soln. 8=48081
    - Ni, atomic structure from X-ray diffr. exam. 8=25874
    - Pb, as function of temp. 8=48062
    - PCl$_3$, POCl$_3$ and POF$_3$, molec. motions 8=34912
    - Pd-Sn alloys 8=48082
    - Sb, x-ray scatt. 8=34765
    - Sn, near melting point, and correlation function 8=48062
    - Sn, 226-1140°C, distrib. curve 8=39299
    - Te, molten 8=34965
    - Tl, near melting point, and correlation function 8=48062
    - Tl, temp. dependence, from X-ray diffr. exam. 8=25873
    - Xe, radial distrib. and distrib. functions, X-ray study and theory 8=43759
    - Zn, near melting point, and correlation function 8=48062
    - Zn-CN-NH$_3$ complex, aqueous soln, mixed ligand study 8=43842
  - **theory**
    - See also Dielectric phenomena; Equations of state/liquids.
    - Benard cell with molten Ga, unrotated, convective temp. oscillations 8=30377
    - binary mixtures, proton mag. relaxation 8=39425
    - boiling, nucleation rate in rel. to superheat 8=25999
    - cell theory, equilibrium and thermodynamical functions 8=48057
    - cell theory, Joule-Thomson coeff. 8=48056
    - close-packed random-model, effect of introducing holes, and resulting distrib functions 8=25862
    - compressibility, isothermal, temp. dependence, calcs. 8=43766
    - distribution functions for correl. between positions and orientations of molec. groups 8=25868
    - electrolyte adsorpt., Debye-Hückel limiting law appl. to Gibb's eqn. 8=36591
    - electron, degenerate, spin-independ, oscills. 8=34755
    - electronic states in mixed disordered systems, optical model 8=39293
    - emulsions, van der Waals const determ. from theological props 8=48241
    - entropy, communal, influence on liq. state reappearance 8=25976
    - excess electron in nonpolar dense liqs. 8=34571
    - excitons, scatt. of polarization waves 8=34754
    - Fermi, charged impurity mobility calc. 8=23897
    - frequency-dependent direct correl. function, rel. to fluctuations in equilib. fluid 8=25864
    - internal press. calc. 8=43748
    - kinetic eqns. in vortex field 8=39275
    - metals, book 8=34753
    - mixtures, light scatt. rel. to mol. correls. 8=34663
    - molecular reorientation 8=39433
    - molecular reorientational motion in "classical" liquids 8=39292
    - monatomic, model for radial density and scatt. 8=34750
    - monatomic, quasicrystalline vacancies affecting at. motion 8=34751
    - monatomic, review 8=30190
    - momentum auto-correl. function 8=30424
    - momentum density correl. functions, fourth freq. moments 8=39294
    - optical absorpt. and emission rel. to molecular Einstein coeffs. 8=39367
    - 1D system, energy spectrum gaps 8=32844
    - order defects and intermolecular pots in modified cell model 8=25865
    - positron lifetime, paramagnetic impurity effect 8=29851
    - 6:12 pot. fluids, pair distrib. and direct correl. functions, exact and approx. values 8=25787
    - semiempirical model 8=43747
    - surface props. of simple liqs. and mixtures, statistical-mech. calc. 8=48107-8
    - radial distrib. functions, from small packings of spheres 8=25860

- **Liquids**—contd
  - **theory**—contd
    - Tait's eqn., soln., 8=43749
    - ternary systems, decorated lattice model 8=34781
    - three-body forces contribution 8=25861
    - Voronoi polyhedron anal. of random packing, rel. to density of close-packing 8=25863
    - Al, radial distrib. function from Percus-Yevick and convolution hypernetted-chain eqns. at high densities 8=48058
    - Ar, semiempirical model 8=43747
    - Si, activity in molten Ag-Si alloys by e.m.f. meas. 8=48078
- **Lithium**
  - adsorption on O covered W, and struct. resultant film 8=39593
  - atom, autoionization of $1s2s2p\,^4P_{5/2}$ state 8=39041
  - atom, $H^+ + Li^+ \rightarrow H(n) + Li^{++}$, cross-section calc. 8=25392
  - atom, new type of wave function 8=38672
  - atom, ^2S ground state, Hylleraas wave function calc. 8=38671
  - atom, Schrödinger wave eqn., numerical soln. 8=29579
  - atoms, glory scatt. by diatomic mols. 8=38959
  - atoms, quadrupolar birefringence in excited states 8=43271
  - atoms, Rydberg orbitals calc. 8=29620
  - band struct., Fermi surface and density of states 8=49103
  - conduction-ESR g value meas. 8=27482
  - in cosmic rays and T Tauri stars, calc. 8=36926
  - crystal electron transition probability from bound to excited states under e-bombardment 8=40243
  - diffusion in CdS single crystals 8=44383
  - diffusion in O-rich Si, annealing of e irradiation induced defect 8=26632
  - diffusion of Ag^{110m}, 67°-160°C 8=31008
  - diffusion of Na, obs. btw. 50-176°C 8=31009
  - dipole spectrum 8=34143
  - electrical resistivity effect of dissociating and thermally stable gaseous impurities at 300°C 8=48203
  - electron momenta from X-ray meas. 8=44647
  - electron scattering, slow, elastic 8=43231
  - energy band struct., calc. by tight-binding method 8=44692
  - exploding wire, extrusion die-electrode combination 8=33028
  - exploding wire, extrusion technique 8=50473
  - ion emitter for low energy beam expts. 8=41983
  - ions Li$^+$ beams in H$_2$ and air, charge equilib. 8=28584
  - isotopic comp. and distrib. in the Holbrook meteorites 8=28161
  - liquid, isotope thermotransport 8=29671
  - liquid, self-diffusion, n.m.r. meas. 8=48112
  - liquid, use in thermal convection loop tests of Nb-Zr alloys 8=35503
  - Knight shift and pseudopotentials 8=45129
  - metal, isotope inter-diffusion 8=39976
  - melting curve up to 80 kb 8=34961
  - pair interaction, phase change 8=35027
  - plasma in arc discharge, exam. from emission spectrum 8=47778
  - precipitation in Si, nucleation and growth 8=44105
  - red giant stars, composition of core and photosphere 8=50292
  - resonance lines rel. to solar abundance 8=45865
  - solid, electrotransport of lattice defects 8=35501
  - in stars, T Tauri, formation 8=50297
  - sunspot high dispersion spectra, abundance calc. 8=50452
  - Li^{6,7}, atom, autoinizing $(1s2s2p)^4P$ states, energies and lifetimes 8=43243
  - Li^{6,7} in stars and interstellar medium, obs. 8=36927
  - Li^6 and Li^7 interdiffusion unisotopically pure Li melt 8=34807
  - Li^{6,7} origin in solar system, big bang and solar spallation theory 8=36990
  - Li^{6,7} positive ions self-diffusion effect in LiF from relative difference between ion mobilities meas. 8=35500
  - Li^7 n.m.r. line in soln., effect of paramag. ions 8=34915
  - Li^{7+}, ^1D, ^3D, ^1F and ^3F states, mag. h.f.s. calc. 8=38673
  - Li$^-$, prod and extraction from h.f. source 8=46431
  - Li$^-$, stability, wave function calc. 8=47482
  - Li$^+$, numerical soln. of S-limit Schrodinger eqn. 8=29596
  - Li-Li$^+$ charge transfer collisions $<$ 10 keV, oscills. in total cross-section 8=38762
  - Li$_2$, bond formation process 8=34221
  - Li$_2$, pseudopotential theory calc. 8=38838
  - Li$_2$, wave functions and binding energies calc. using quantum defect method 8=25489
  - NH$_3$ soln., u.s. vel. obs. and compressibility calc. 8=30468
  - in Si diode, diffusion coeffs. rel. to electron and neutron irrad. 8=39982
  - Si dopant, Hall effect and elec. cond. obs. 8=49268
- **Lithium compounds**
  - borates, glass and cryst., n.m.r., diffusion of Li^7 8=31007
  - ferrite with near-zero defect conc., linewidth meas 8=31829
  - in graphite, buffers in DC-arc spectrographic anal. 8=27792
  - trihydrogen selenite, optical indicatrix rotation in phase transition region 8=27638

Lithium compounds—contd
- ions in NiO-MgO solid soln., struct. and mag. props., 98°-298°K 8=35061
- niobate, melt-grown, refractive index and second-harmonic generation rel. to comp. 8=41114
- salts, 1MHz u.s. velocity in aq. solns., obs. 8=43806
- soaps in alcohols, physical props. 8=39316
- spodumene, twinned, internal friction 8=49033
- Fe_6LiO_8, short range order 8=26866
- Li borate glasses and cpds., γ-irrad., e.s.r. 8=49612
- Li ferrite, heat treatment effect on resist., dielect. and thermoelect. props. 8=35962
- Li^6-glass scintillation n counter, <2.5 MeV 8=33817
- Li metagallate, Czochralski growth in Ar or CO_2 8=48548
- Li(Ag, Au). Li(In, Tl, Pb, Sb, Bi) system, Zinth phases, width, valence electron conc. 8=49102
- Li_9Al_4, crystal structure 8=39801
- Li_3AlF_6, heat of formation and transition temps. 8=36564
- $LiAl_{5-x}Fe_xO_8$, Mossbauer spectra 8=43953
- $LiAlSiO_4$, X-irradiated, e.p.r. and luminescence 8=40936
- $Li_2B_4O_7$:Mn, fast-n personnel dosimeter 8=33796
- LiBr films, dielectric, l.f. polarization effects 8=44870
- Li Br solns., elec. cond., association const. calc. 8=48198
- LiCl aq. soln., diff. of protons 8=48115
- LiCl, Debye-Waller factors from X-ray diffr. meas., 298 and 78°K 8=44224
- LiCl in n-alcohols, effect on relax. time and rotary diffusion 8=34778
- LiCl solns., proton relax. 8=30533
- LiCl, thermal vibr. and Debye-Waller factor obs. 8=30905
- $LiClO_4$, fused, electrolysis reactions and metals anodization obs. 8=45389
- $LiClO_4 . 3H_2O$, struct. by n diff. exam. 8=35339
- $LiD_3(SeO_3)_2$, d.m.r. 8=49648
- $LiD_3(SeO_3)_2$, d.m.r. and molec. struct. 8=49638
- LiF_5O_8, ferromag. res., effects of defects from U^{235} fission fragments 8=36225
- $Li_{0\cdot5}Fe_{2\cdot5}O_4$, n scatt. by ferrimag. spin-waves polarization effects, obs. 8=36187
- Li_5GaO_4 and Li_5 AlO_4 crystal chemistry 8=48513
- LiH, fission neutron attenuation and γ-ray buildup factors by Monte Carlo method 8=47401
- LiH, ground state, pair correl. calc. 8=29604
- LiH, lattice dynamics 8=35386
- LiH, pseudopotential theory calc. 8=38838
- Li H, reduced density matrices, and natural orbital and geminal expansions 8=43182
- LiH, valence-only correl. calc. 8=34254
- LiH-LiD mixed crystals, i.r. absorpt. freq. rel. to lattice dynamics 8=45202
- LiH_2, stable mol., prediction from atoms-in-mols. theory 8=29751
- Li_2H, stable mol., prediction from atoms-in-mols. theory 8=29751
- $LiH_3(SeO_3)_2$. p.m.r. 8=31910
- LiI, films, dielectric. l.f. polarization effects 8=44870
- LiI:Eu n monitor, portable, 0.5-1000 mrem/hr 8=33815
- Li_2MgX, f.c.c. lattices with body-centred substructs., obs. 8=39800
- $LiNO_3$, molten, γ-radiolysis 8=49973
- $LiNO_3$ molten, optical determ of thermal cond. 8=39355
- $LiNO_3$, neutron radiolysis 8=49974
- $LiNO_3$-$NaNO_3$-KNO_3 melt, polarographic investigation of Tl^+, Cd^{++}, Pb^{++}, Zn^{++}, Ni^{++} 8=45414
- $Li(Nb_{0\cdot5}FeO_{0\cdot5})O_2F$, structure and dielec. props. 8=31435
- $Li(Nb_{0\cdot5}Fe_{0\cdot5})O_2F$-$Li(Ta_{0\cdot5}Fe_{0\cdot5})O_2F$ system, phase diag. and dielec. props. 8=32435
- $LiNbO_2$, ferroelectric, n. m. r. of Nb^{93} 8=45128
- $LiNbO_3$, Curie temp., birefringence and phase-matching temp. as function of melt stoichiometry 8=31433
- $LiNbO_3$ crystal in optical cavity pumped by laser, parametric oscilln. 8=42072
- $LiNbO_3$, elastic waves, 20-2000 Mc/s, excitation and attenuation 8=44584
- $LiNbO_3$, electrical conductivity 8=27276
- $LiNbO_3$, ferroelec. Curie temp. meas. and anisotropy 8=27285
- $LiNbO_3$, ferroelec. domain wall obs. rel. to dislocation pinning 8=31434
- $LiNbO_3$, ferroelec., n.m.r. 8=40987
- $LiNbO_3$ laser, pulsed parametric oscilln. and power limiting 8=42078
- $LiNbO_3$, linear and quadratic electro-optic coeffs., relationship based on spontaneous polarization obs. 8=27583
- $LiNbO_3$, n.m.r. 8=36274
- $LiNbO_3$, n.m.r. of Li^7 8=40988
- $LiNbO_3$, parametric luminesc., excited by Ar laser 8=41201
- $LiNbO_3$, phase transitions, 20°-1170℃, X-ray obs. 8=30863
- $LiNbO_3$, piezoelec. effect on laser illumination 8=45203
- $LiNbO_3$, piezo- and thermo-optic behaviour 8=27582
- $LiNbO_3$, Raman and Rayleigh scattering temp. dependence, 90-1100°K 8=27585
- $LiNbO_3$, Raman scattering, near forward, dispersion characts. 8=27584
- $LiNbO_3$, spontaneous parametric emission power and bandwidth 8=27586
- $LiNbO_3$ spontaneous scatt. of intense light, quantum theory 8=27538

Lithium compounds—contd
- $LiNbO_3$, structural change rel. to ferroelec. transition from x-ray and elec. exam. 8=31435
- $LiNbO_3$, thermal props. 8=44341
- $LiNbO_3$-$CdTiO_3$ system, solid solns. of ilmenite structure rel. to ferroelectricity 8=27278
- $LiNbO_3$:Cr^{3+}, acoustic paramag. reson., 4.2°K 8=44318
- $LiNbO_3$:Cr^{3+}, polydomain crystal, elec. paramag. resonance of Cr^{3+} 8=27277
- $LiNbO_3$: Cr^{3+}, polydomain crystal, paramagn, hypersound absorpt. by Cr^{3+} 8=31873
- $LiNbO_3$-$LiTaO_3$-$Fe(Mg)TiO_3$ system, X-ray exam. 8=27278
- $LiNbO_3$:Mn^{2+}, e.s.r., spacing of hyperfine sextet 8=45090
- $LiNiF_4$, stable clusters in LiF:Ni, with inverted spinel struct. 8=35219
- Li_2O-SiO_2 glasses, crystallization kinetics 8=44133
- $Li_2O. SiO_2$-$Li_2O. Al_2O_3. 4SiO_2$-SiO_2 system, liquation isostructure and correl. 8=48255
- $Li_2O. SiO_2$-$Li_2O. Al_2O_3. 4SiO_2$-SiO_2 system, metastable mixture 8=48386
- Li_2SO_4, diff. of Na^+, Ag^+, K^+, $Rb^+$and Tb^+, 590-820°C 8=39977
- Li_2SO_4, n-irradiated, OH radical thermal decay, e.s.r. study 8=27481
- Li_2SO_4-H_2O, phase boundaries below 500°C 8=48366
- Li_2SO_4-Na_2SO_4 phase diagram. 8=39559
- $Li(Ta_{0\cdot5}Fe_{0\cdot5})O_2F$, structure and dielec props 8=31435
- $LiTaO_3$, Curie pt. and lattice consts. 8=49371
- $LiTaO_3$, ferroelec. Curie pt. rel. to mole ratio Ta_2O_5/Li_2O 8=49372
- $LiTaO_3$ ferroelec., dielec., thermal and pyroelec. props. 8=44888
- $LiTaO_3$, ferroelectric, n.m.r. 8=40987
- $LiTaO_3$, high-temp., X-ray investigation 8=35978
- $LiTaO_3$, linear and quadratic electro-optic coeffs., relationship based on spontaneous polarization obs. 8=27583
- $LiTaO_3$, optical transmission variations 8=36385
- $LiTaO_3$, Raman and Rayleigh scattering temp. dependence, 90-1100°K 8=27585
- $LiTaO_3$-$CdTiO_3$ system, solid solns. of ilmenite structure rel. to ferroelectricity 8=27278

lithium fluoride
- acoustic emission rel. to dislocation movement 8=44317
- acoustic emission, rel. to microscopic deform. model 8=26582
- aggregate defect centres, Mollwo-Ivey relations 8=31032
- colouring process on e-irradiation from absorpt. and luminescence 8=40062
- crystal infrared emissivity 8=32006
- crystal, luminescence of O^{2-} impurity 8=36499
- crystal structure and mech. and optical props. growth conditions and impurity effects 8=26401
- crystal, X-ray diffr., Debye-Scherrer obs. with Fe^{55} source 8=28930
- crystals in organic liquids, interfacial energy calcs. rel. to abrasive wear and adhesion 8=30724
- crystals, plastically deformed and annealed, thermal conductivity 8=30989
- density changes on γ-irradiation 8=40129
- dislocation distrib. rel. to loading 8=31082
- dislocation interaction with point defects from internal friction meas. 8=26683
- dislocation mobility in programme-hardened material 8=44450
- dislocation mobility pressure dependence 8=44451
- dislocation multipoles in slip bands, electron microscopy obs. 8=44460
- dislocation structure formation by plastic deformation 8=31080
- dosimeter for fast-neutrons, personnel 8=33796
- dosimeters, TLD-100, energy depend. rel. to total dose, obs. 8=42348
- edge disloc.-impurity interaction force-distance curve calc. rel. to hardening model 8=26674
- electron microscope exam., lattice fringes resolution, 100 kV 8=39775
- electron momenta from X-ray meas. 8=44647
- F band, annealing and re-irradiation behaviour between 80°K and 300°K 8=49738
- F-centres, hyperfine interaction constants, temp. dependence 8=35587
- F_3^+ centre, linear Stark effect 8=31120
- F_3^+-centres conversion and R-centres destruction on R light bleach 8=44482
- fatique propagation in metals 8=44586
- ferromagnetic films epitaxial growth substrate 8=35170
- films, dielectric, l.f. polarization effects 8=44870
- fracture surface as function of crystallographic direction and treatment method 8=44593
- infrared reflectance data, improved Kramers-Kronig dispersion analysis 8=27580
- internal friction under static compressive load rel. to crystal orientation 8=44585
- ionic cond. and diffusivity of cation and anion vacancies 8=35963
- lattice dynamics at 298°K 8=35388
- lattice vibrations in thin film, electron diffraction obs. 8=35387

Lithium compounds—contd
- **lithium fluoride**—contd
  - luminescence after shock compression 8=49806
  - negative thread crystals, growth and evaporation kinetics 8=26256
  - oxide doped, oxide and hydroxide activity determ. 8=36593
  - photomechanical effect, wavelength dependence 8=36368
  - point defect formation on plastic deform. 8=44403
  - polishing of crystals for investigations in far u.v. 8=41112
  - powders, ground, microstrain and crystallite size determ. from X-ray diffr. line-broadening profile analysis 8=48600
  - pressure sintering, densification data rel. to plastic deform. 8=35070
  - quenching effect on plastic deformation mechanism 8=26828
  - radiation-induced macrodefects 8=26711
  - R′ centre, Jahn-Teller vibronic structure 8=44481
  - R'centre, magnetic circular dichroism 8=48878
  - r.f. spectra by elec-resonance method, rel. to struct of mol. 8=43316
  - second harmonic generation obs. in transmission through thin platelets 8=27555
  - single-crystal scatt. centres, Raman spectra 8=49737
  - Stark effect, linear, on colour centres zero-phonon absorpt. lines, obs. 8=27581
  - stress relax. during thermal processing 8=41067
  - thermal vibr. and Debye-Waller factor obs. 8=30905
  - thermoluminescence, spectral emission of intense peaks rel. to heating and irrad. 8=36498
  - thermoluminescence stimulation by excitation of a centre 8=41200
  - transparency, investigation of influencing factors 8=32007
  - ultrasonically irradiated, dislocation behaviour 8=26688
  - X-irradiation effects on F-centres, electrical conductivity, lattice constant 8=35603
  - X-irradiated, dislocations effect on F-centre thermal stability, e-emission exam. 8=35570
  - X-irradiated, [111] defect, e.s.r. exam. 8=40006
  - X-ray scatt. rel. to dislocation density and distrib. 8=45198
  - Fe^{3+} in single crystals, e.s.r. and n.m.r. 8=40920
  - $Li^{6,7}$ positive ions, isotope self-diffusion from relative difference between ion mobilities meas. 8=35500
  - Li^6F and ZnS(Ag) registration of slow neutrons for luminphor 8=47153
  - $Li^{6,7}F$, isotope-induced acoustic band far i.r. absorpt., 7°K 8=36396
  - Li^6F^{19}, mm elec. reson. spectra 8=25483
  - LiF : Cu, Ag, thermoluminescence rel. to doping and dosimetric props. 8=49807
  - LiF:Fe^{3+}, e.s.r. and n.m.r. crystal field distortions 8=48810
  - LiF: Mg thermoluminesc. and optical absorpt. effect of pre-irrad. annealing 8=45280
  - LiF:Ni, impurity ion effect on crystal structure 8=26642
  - LiF:Ni^{2+}, impurity ion clustering from small-angle X-ray scattering exam. 8=44422
  - LiF:Ni^{2+}, struct. of monocryst. clusters of same orientation as matrix 8=35219
  - LiF/U^{6+}, suitability of fluorescence props. for laser 8=46620
  - MgF_2 doped, ionic cond., energy of motion of Li^+ vacancy and assoc. with Mg^{2+} ion 8=31423

Lithosphere. See Earth.
Loges (molecular bonds). See Bonds; Molecules/electronic structure.
Lorentz–Lorenz relation. See Dielectric phenomena.
Lorentz transformation. See Relativity/special.
Lorenz number. See Conductivity, electrical/solids; Conductivity thermal/solids.
Loschmidt number (= Avogadro number). See Constants.
Loudness. See Hearing; Intensity measurement, acoustics.
Loudspeakers. See Acoustic radiators.
Love waves. See Elastic waves; Seismic waves.

Low-temperature phenomena
See also Helium/liquid; Helium/solid; Joule–Thomson effect; Superconducting materials and devices; Superconductivity; Superfluidity.
- amorphous solids, thermal cond. at low-temp. 8=30975
- Fermi liquid, transport coeff. and sp. ht. expansion 8=37216
- heat flux determ. along elec. leads to cryostat with liq. He, rel. to supercond. dev. 8=31361
- heat transfer in low-boiling liqs. 8=46289
- inert gases, liq., far u.v. reflectivity 8=34846
- integral emissivities below 300°K, temp. depend., and 8=39955
- metals, elec. cond., dimensional effects 8=26951
- micromachine for deform of metallic specimens at temps. down to 1.3°K 8=44522
- ortho-H, solid, theory of ang. mom. waves 8=35743
- ortho/para-D_2 liq. systems, heat of mixing at 20°K 8=30412
- ortho/para-H_2 liq. systems, heat of mixing at 20°K 8=30412
- polyethylene, dielec. losses at cryogenic temps. 8=49355
- polyethylene terephthalate, dielec. losses at cryogenic temps. 8=49355
- polymerization by radiation, obs. and theory 8=27742
- poly (4-methyl pentene-1), dielec. losses at cryogenic temps. 8=49355

Low-temperature phenomena—contd
- poly-ω-undecanolactum, dielec. losses at cryogenic temps. 8=49355
- polyvinyl chloride, dielec. losses at cryogenic temps. 8=49355
- residual gas heat transfer in multi-layer insulation 8=25823
- Al films transparency, thickness depend. oscills. rel. to e quantization, 4.2°K 8=31957
- Ar, solid phase transition obs. 8=39567
- $(Ba_{0.05}Sr_{0.95})TiO_3$, dielec. const., press. depend., to 1600 atmos. 8=27283
- C films, non-linear resistance 8=31318
- Cu, nuclear spin-lattice relax. time at temps. below 2×10^{-2}°K 8=31902
- Cu_3Au, sp. ht. below 3°K, effect of ordering 8=35427
- $CuSO_4.5H_2O$, ht. capacity at 0.4°-4.2°K in mag. fields 8=39915
- $CuSO_4.5H_2O$, thermodynamic props. in mag. fields 8=39914
- Ge f.e.t. characts. obs. to 1°K 8=35942
- Ge–Ga–Zn, application to thermometry 8=41874
- GaAs semiconductor laser spectral characts. 8=24336
- InSb p-n junctions at liq. He temp., V-I characts. 8=27160
- MgO: Cu^{2+}, e.p.r. at 1.2°K, Jahn-Teller effect 8=27470
- Nb_3Sn hard supercond. tubes, mag. flux jumps, 4.2°K 8=31341
- Nb-Zr hard supercond. tubes, mag. flux jumps, 4.2°K 8=31341
- Ni-Fe alloys, sp. ht. 1.2-4.2° K obs. 8=26592
- α-$NiSO_4.6H_2O$, ht. capacity, mag. moment 8=30968
- $SrTiO_3$, dielec. const., press. depend., to 1600 atmos. 8=27283
- U^{233} aligned nuclei, α ang. distrib., obs. 8=30634
- α-U, phase transition obs. at 4.2°K 8=39567
- V_3Si, phase transition obs. 8=39567
- ZnO crystal, recomb. radiation of bound excitons, 4.2°-90°K 8=31301
- Zr polycrystals, e-irradiated, resistivity recovery 8=31158

Low-temperature production
See also Joule–Thomson effect; Liquefaction/gases; Magnetic cooling.
- automatic system for single-crystal diffractometry 8=30884
- continuous cooling between 1° and 293°K 8=37328
- Dewar, variable-temp. for cathodoluminescence 8=41878
- refrigeration process for very low temp. 8=20252
- refrigeration process for very low temp. 8=37329
- refrigerator as helium liquefier 8=32990
- 0.55°K, by pumping He^3 8=46294-5
- H, solid, 14-6°K by pumping of vapour over its surface 8=46290
- He isotope refrigerator using He^3-He^4 mixtures 8=46292
- He liquid cooled e microscope stage 8=46293
- He refrigerator, closed-cycle, for Mössbauer expt. 8=46301

Low-temperature technique
- adsorptive pumps for serial mass spectrometer evacuation 8=38608
- apparatus to achieve temps from 4.2 to 300°K, with temp. stabilization 8=28432
- astatic follower system for stabilizing block temp in range 10-150°K 8=24027
- cerium magnesium nitrate scale, evidence from critical magnetic field curve of superconducting W 8=37331
- cerium magnesium nitrate thermometer, props. 8=30962
- cerium magnesium nitrate thermometry, use in liquid He 8=37332
- Cerous magnesium nitrate, high field magnetization anomaly obs. 8=44968
- chamber for working at liq. He temp. at press. to 18 kbar 8=24034
- creep meas. apparatus fr 10^{-7} min^{-1} at 77°K 8=44525
- cryogenic fluids, study of forced convection boiling heat transfer 8=32957
- cryogenic rad. receiver for use with astrophotometer, 8–14μ 8=36920
- cryogenic vacuum chamber, parameters calc. by Monte Carlo method 8=30340
- cryopump system, fast, for ultra-high vac. 8=47992
- cryopumping, theory 8=39247
- electrical feed-through, epoxy, appl. 8=28431
- Epibond moulding for cryogenic apparatus 8=41883
- gas stream temp. control device for range −195° to 250°C 8=28421
- gas viscometer, absolute, h.p. design 8=34674
- goniometer head for crystal in supercond. solenoid 8=30815
- Hall effect probes with diameters ≤ 1 mm, for axial mag. fields at cryogenic temps. 8=24031
- hypersonic wide-band meas., sample holder and tuning technique 8=28376
- insulation, thermal and container design 8=46298
- laser with external mirrors 8=46537
- magnetic anisotropy meas., torque balance 8=31723
- for magnetic properties of solids 8=31485
- magnetothermodynamic props., high-field apparatus with supercond. magnet 8=41882
- mechanical loss meas. 8=35614
- Mössbauer expt., He^3/He^4 dilution refrigerator 8=41880
- paramagnetic absorpt. meas. with RE-1301 radiospectrometer at 4.2°K 8=24261
- phase transformations, X-ray apparatus 8=35078

Low-temperature technique—contd
pool boiling heat transfer to cryogenic liquids 8=48127-9
thermal conductivity meas., a. c. bridge, 0.25% accuracy, 1-4°K 8=28426
tunnel junction, supercond., for 1m° meas. 8=31358
volume expansion for very low mag. field 8=28513
C self-supporting resistance thermometers 8=32983
H_2 liquid containment, thin-film windows 8=24035
He dewar, modified 8=28427
He^3 purification using unmodified He^3 refrigerator as rectifying column 8=30271
N_2 liquid pipe, vacuum insulated 8=46300
Ne liquefaction, separation from He-Ne mixture 8=46302
Pt resistance thermometry below 10°K 8=28428
Lubrication
See also Friction.
annular contact tester 8=35637
mineral oils, and component fractions, viscoelastic relax. spectra 8=34698
surface-active, effect on internal stresses in reversing sliding 8=35617
Fe-based sintered metals, self-lubricating, sliding wear characts. 8=31187
Ludwig–Soret effect. See Diffusion in solids.
Luminescence
See also Electroluminescence; Luminescent devices; Thermoluminescence.
of activated levels of a trap, population calc. 8=36451
activated levels of trap during vacation, perturbation of Boltzmann distrib. 8=36450
anthracene $S_0 \rightleftharpoons T_1$ radiative transitions, mag. dipole contribs. calc. 8=25545
aromatic mols., paramag. reson. effects rel. to singlet-triplet admixing 8=27461
aromatics $S_0 \rightleftharpoons T_2$ radiative transitions, mag. dipole contribs. calc. 8=25545
aromatics triplet state lifetimes, delayed fluoresc. obs. 8=25610
atomic fluoresc. excited by molec. dissoc. 8=38687
Beckman photometer type DK, combined luminesc. and absorpt. meas. 8=33243
benzene $S_0 \rightleftharpoons T_1$ radiative transitions, mag. dipole contribs. calc. 8=25545
cathodoluminescence meas., e microprobe monochromator-photomultiplier attachment 8=36463
cathodoluminescence, variable-temp. Dewar 8=41878
chemiluminescence, vacuum u.v., from reactions of active N with I_2, IBr, ICl and ICN 8=49887
complex mols, fluoresc. duration, spectral depend. 8=29677
cubic crystals with impurity ions in Jahn-Teller states polarization and exciting light freq. dependence 8=41176
delayed luminesc., growth and decay 8=32073
electron microprobe analysis, X-ray fluoresc. corrections errors 8=27800
electron microprobe meas. 8=36461
empirical criterion for occurrence 8=41207
excimer, semiempirical theory 8=38801
extinction by exchange interactions, study by e.p.r. 8=36448
fluorescence and reson., stimulated emission role 8=38638
fluorescence by two-photon excitation, rel. to laser pulse width meas. 8=46533
fluorescence decay meas. instrum. response time corrections 8=32051
fluorescence, glass standard 8=45945
fluorescence maser spectroscopy of molecules 8=38782
fluorescent spectroscopy of regularly deposited thin layers of mols. 8=43921
impurity centres, two-e correlation, in model pot. approx. 8=32049
insulating mats., ionoluminescence in analysis 8=40555
ionic crystals, activated, photoluminesc. effect of elec. fields 8=36456
ionic crystals, review of Russian research 8=36455
molecular crystals, review 1930-67 8=36452
molecular crysts. β- and photo-excitation, recombination problems 8=49399
molecules, photoselection effects on intensity and polarization 8=47579
molecules reson. energy transfer, statistics 8=25404
organic media, radioluminescence, kinetic study 8=47630
organic mol. complexes rel. to charge transfer triplet states, obs. 8=25526
organic molecules, after multiphoton excitation by Q-modulated ruby laser 8=34295
organic scintillators conference, 1966 8=45250
particle, on scattering of H ions on metallic surface 8=49787
phenanthrolines, deactivation of excited states 8=43383
phosphor screen after cathode-ray excitation determ. of persistence characts. 8=49786
phosphorescent T-S band decay rate meas., effect of absorpt. $T^* \leftarrow T$ bands 8=38777
phosphors for detection of vac. u.v. radiation 8=41179
photoluminophors, conversion efficiency investigation 8=36466
photoselection effects on polarization of mols. 8=47579
polarization quenching by excitation transfer 8=43845

Luminescence—contd
powder, deposition by electrophoresis 8=45388
quinoxaline triplet state, and excit. paths rel. to mag. interactions 8=25624
rigid polymer solutions, molecular orientation of luminophors 8=32078
rise-time in phosphoresc. and delayed fluoresc. 8=27640
semiconductors, vitreous 8=36453
solid solutions, photoluminesc. quenching, energy transfer model 8=36459
solid-state, theory and models 8=36458
solids, absorption and excitation spectra 8=36449
solids, ion bombard. excited 8=26861
solids rel. to molecular Einstein coeffs. 8=39367
spectrofluorimeter, fully compensated 8=33263
spontaneous, change of intensity under laser radiation, stimulated emission cross section meas. 8=24280
transition metal cpds., at high temp., by H_2S gas forming metal sulphide surface film 8=31219
uranyl cpds., fluorescence and oscillator model 8=34286
rel. to X-ray emission, secondary fluorescence effects calc. 8=32050
Ca, at. fluoresc. interferences 8=29606
Cu^{65} nuclear resonance fluoresc. obs. 8=42883
K atoms in N_2 and H_2 mixtures, quenching cross sections 8=29836
Mg, at. fluoresc. interferences 8=29606
N_2 active, chemiluminesc. reaction with anhydrous $Na_2 50_4$ 8=41255
OH chemiluminesc. in $H_2 + O_2$ reaction in shock tube 8=49889

gases
anthracene delayed fluoresc. rel. to excit. states decay and intersystem crossing. obs. 8=25537
basalt vapour, emission spectrum time scanning 8=34231
benzene-biacetyl mixts. phosphoresc., inter-cpd. energy transfer and triplet benzene lifetime obs. 8=25544
benzene, press. depend. 8=47640
benzene, yields below 0.1 torr 8=47641
biacetyl, spectrum at 100°C, vibrational analysis 8=43347
carbonyl-containing compounds, vapour $n \leftarrow \pi^*$ 8=34199
density of rarefied gases, obs. by electron beam induced luminescence 8=39171
metals in vapour phase, quenching cross-sections 8=38748
methane, laser-excited vibr. fluoresc. 8=25605
molecules in gaseous phase, review of Russian work to 1967 8=38776
phenanthrene delayed fluoresc. rel. to excit. states decay and intersystem crossing. obs. 8=25537
ruby vapour, emission spectrum time scanning 8=34231
steel, vapour, emission spectrum time scanning 8=34231
in u.v. photolysis of simple gases 8=34266
water vapour in atm., laser irradiation 8=38824
Ar, α-particle induced, obs. 8=47521
CCl_4-Na, K flames chemiluminesc., C_2 high-press bands excitation mechanism, obs. 8=38816
CO, chemiluminesc. from flames 8=27698
CO, Xe-sensitized, excited by 1470 Å radiation 8=25457
Cd atomic vapour, double resonance excited by modulated light 8=38685
Cs, fluoresc. quenching cross-sections, determ. by flame tech. 8=29617
$H + O_3$, i.r. chemiluminesc. 8=32099
H_2O, vac. u. v. photodecomp. 8=47613
He, high-pressure, scintillation induced by α-particles, recombination 8=29642
Hg-vapour green-band emission 8=29944
K, fluoresc. quenching cross-sections, determ. by flame tech. 8=29617
NO afterglow, temp. depend. 8=38993
N_2 afterglow, temp. depend. of chemiluminesc. 8=27712
N_2^+, from vac. u. v. photon impact 8=47609
Na, fluoresc. and energy transfer in collisions with inert gases 8=34182
Ne, $^2P_4$ fluoresc. under laser reson. illum., 6328A 8=38675
Ne, $^3P^0$ and $^1P^0$ populations time dependence during post-luminescence under c. m. wave pulses 8=38686
Rb, fluoresc. quenching cross-sections, determ. by flame tech. 8=29617
SiC, vapour, emission spectrum time scanning 8=34231
Tl, fluoresc. quenching cross-sections, determ. by flame tech. 8=29618
liquids and solutions
acridine-biacetyl-benzene, triplet acridine form. by triplet biacetyl energy transfer, obs. 8=25925
acridine, quenching in ethanol soln. 8=41284
aminobenzoic acids, fluorescence quenching by dinitrobenzenes. 8=43846
aminopyridines in soln. 8=48169
anthracene in n-paraffin rel. to phase transitions of solvent 8=25938
anthracene-perylene fluorescence in benzene solns. energy transfer 8=39387
aromatic hydrocarbons, effect of alcoholic solvents on fluoresc. yield 8=48171
aromatic hydro carbons, fluoresc. yield and triplet state form efficiencies 8=43832

Luminescence—contd
liquids and solutions—contd
aromatic hydrocarbons, oxygen quenching of singlet states 8=48170
aromatics solns., delayed luminesc. and triplet quantum yields, obs. 8=25941
aromatic hydrocarbon solns, p-type delayed fluoresc. 8=30498
benzene and derivatives, excitation by electron impact 8=48172
benzene excimers, semiempirical MO calc. 8=34313
benzodioxane-1, 4, O-substituted 8=48173
chemiluminescence, preannihilative, mechanism 8=27692/3
coronene in n-paraffin rel. to phase transitions of solvent 8=25938
cryptocyanine solns., laser flash 8=48162
crystal with impurity centre, density matrix method considerations 8=45249
diacetyl, sensitized, benzene and toluene triplet-triplet energy transfer 8=34316
DNA, in nucleosides and nucleotides in soln., rel. to energy transfer and excited states in DNA 8=25939
9, 10-diphenylanthracene as fluoresc. standard 8=39391
2, 5-diphenyloxazole in benzene, toluene, p-xylene and mesitylene, excimer, fluoresc. solvent-solute energy transfer 8=25940
fluoranthene and derivatives, anomalous fluoresc. 8=30500
fluorenon, absorpt. bands 8=34328
Hafner's hydrocarbons, substituted, anomalous emission 8=48175
hexafluoroacetone-hexafluorobiacetyl mixtures, energy transfer 8=48168
laser dyes, nanosecond fluorescence decay times meas. 8=34884
liquid scintillators, organic, temperature dependence of energy degradation 8=46869
liquid scintillators with high-speed and efficiency, excited by gamma rays 8=46866
luminophors, org. and inorg., for u.v. radiation meas. with photoresistors 8=48166
rel. to molecular Einstein coeffs. 8=39367
napthacene in n-paraffin rel. to phase transitions of solvent 8=25938
naphthalene + 1, 4-dicyanobenzene, triple complex formation 8=48176
naphthalene in soln., monomer and excimer phosphoresc. 8=30501
N-(α-naphthyl)-carbazole in soln., phosphoresc. 8=43849
nonradiative energy transfer in systems with frozen rot. Brownian motion 8=34883
nucleosides, nucleotides and DNA in soln., rel. to energy transfer and excited states in DNA 8=25939
organic dyes for Q-switch laser, fluoresc. and bleaching 8=28693
organic, phosphoresc. and delayed fluoresc., kinetics and chem. appls. 8=25936
organic, radioluminesc. rel. to mol. excitation kinetics, obs. 8=39384
oxazole, and derivatives, excimer formation 8=29796
perylene-N in N-dimethylaniline, fluoresc. quenching via charge transfer 8=34885
phenanthrene in soln., monomer and excimer phosphoresc. 8=30501
phenanthrolines, fluoresc. and phosphoresc. spectra 8=43382
phenolic binary complexes, hydrophobin bond formation 8=43850
photoluminescence, polarization spectra 8=39386
phthalamides, polarisation in fluorescence spectrum, temp. dependence 8=30502
pyrene in cyclohexane and ethanol, delayed luminesc. and triplet quantum fields, obs. 8=25941
pyrene in n-paraffin rel. to phase transitions of solvent 8=25938
pyrene, in solns. 8=25942
quenching, effect of diffusion 8=34882
quenching, transient and solvent effects, kinetics 8=39385
quinine bisulphate as fluoresc. standard 8=39391
rare earths in H_2SO_4, chemiluminesc. in visible and u. v. range 8=30495
radiation-induced scintillator luminesc. in cyclohexane, mechanism 8=43847
relaxation of local temp. of centres 8=39388
rhodamine B in ethylene glycol, fluoresc. meas. of photon flux 8=46653
rhodopsin extracts in 29° digitonin, 575-600 mμ 8=49828
scintillation mixes for aq. T counting, efficiencies and costs 8=28979
scintillator solns., u. v. excited, decay times 8=30496
scintillators, time dependence of scintillations and the effect on pulse-shape discrimination 8=46868
sonoluminescence produced in liqs. under cavitation. thermal and elec. hypotheses 8=48167
spectrophotofluorometer for absorpt. and transmission 8=46694
tetraphenylbutadienes in soln., effect of intramolec. twisting 8=39390

Luminescence—contd
liquids and solutions—contd
toluene scintillators, max. H_2O conc., dioxane and naphthalene effects 8=43844
transfer of electronic excitation energy, effect of diffusion 8=34881-2
trypaflavine, photoluminesc. quenching by rhodamine in glycerine solns 8=48174
Ce^{3+} organic complexes 8=34873
Eu β-diketone chelates, in soln., fluoresc. characts. 8=32071
Eu chelate cpds., in water-methanol 8=30499
Eu chelates, D isotope effects 8=30503
H_2O, sonoluminescence, temp. depend. 8=39389
KI soln., effect of ultrasonic irradiation cavitation 8=37278
Tb chelates, D isotope effects 8=30503
UO_2^{2+} in β-diketone + N-containing organic bases triple complexes, intramol. energy transfer, obs. 8=34288
$UO_2(NO_3)_2$ water solns. in presence of $Na_4P_4O_{12}$ photoluminescence 8=25943
Xe, liquid, in electric field, induced by α-particle 8=25937
solids, inorganic
alkali halide crystal phosphors, F centers interaction with microdefects in crystal lattice 8=31123
alkali halide crystals, relaxation processes, effect of cryst. lattice microdefects 8=36472
alkali halides, and tribo-electron emission 8=31462
alkali metal halides: Tl^+, rel. to lattice structure 8=36470
alkaline earth aluminates: Eu^{2+}, u. v. excitation and emission mechanisms 8=45253
alkaline earth cpds.: Eu^{2+}, 390-520 nm emission 8=45254
anthracene, crystalline, phosphorescence, triplet exciton 8=27665
anthracene, X-ray excited, prompt and delayed fluoresc. 8=27666
antimonates, Nb^{5+}-activated 8=41207
cathodo-and radioluminesc., theory 8=36462
crystals, co-operative, donor-acceptor mechanisms 8=31942
diamond, and similar lattices 8=36475
diamond, natural, excitation spectra 8=36473
diamond, rel. to at. vibration spectrum, review 8=43922
films, thin, prep. and props. 8=36454
glass, oxide: Er^{3+}, sensitization by other rare-earth ions 8=36486
insulators, for lasers 8=36468
leucosapphire, grown from tungstate melts 8=39648
magnetic props. of centres, rel. to luminesc., 8=41178
measurements rel. to e.s.r. 8=31840
meteorites, rocks and glasses under proton bombard. rel. to transient lunar events 8=28145
niobates, oxidic, cryst. struct. effect on luminesc. 8=45284
nitrite salts 8=49810
phosphors, Eu^{3+}-activated, quantum efficiency meas. using excitation to selected Cu^{3+} levels 8=49798
phosphor: Mn^{2+}, characteristics rel. to crystal lattice obs. 8=27641
plastic, transient nonlinear response to electron irradiation 8=46865
polyethylene, e-irradiated, Hg lamp excitation 8=24729
radical-recombination, on H excitation, temp. effects, 270-470°C 8=36457
rare-earth-activated phosphors, mechanism 8=32052
rare earth crystalline complexes, tests on structural forms 8=36467
rare earth phosphate based phosphors with fast decay rates 8=45285
rare earth phosphate-based phosphors, spectral props. 8=49747
rare earth phosphors and scintillators, survey of electron- and X-ray-stimulated luminescence 8=46874
rare earths, cathodoluminesc. analysis 8=36643
ruby, fluoresc. dosimeter for pulsed ionizing radiation 8=45258
ruby, grown from tungstate melts 8=39648
ruby, spatial distrib. of fluorescence and R-line quantum efficiency 8=42101
ruby, two-photon excitation 8=45259
semiconductors, cathodoluminesc., obs. 8=41187
semiconductor donor-acceptor pairs as radiative recombination centres, review 8=27055
silicate glass: Nd, Yb, stimulated emission 8=36512
tantalates, oxidic, cryst. struct. effect on luminesc. 8=45284
titanates, oxidic, cryst. struct. effect on luminesc. 8=45284
tungstates, oxidic, cryst. struct. effect on luminesc. 8=45284
III-V compound semiconds., electron-hole radiative recomb. mechs. 8=45248
II-VI cpds., V-doped 8=45251
uranyl cpds., fluorescence spectra, interpret. 8=49758
uranyl salts, fluoresc. decay rel. to temp., obs. 8=45288
uranyl nitrates, complexed, fine struct. rel. to anion and cation vibrs., 77°K 8=36514
vitreous, rel. to struct. and phys. props. 8=36465
Ag halides, temp. extinction range, behaviour 8=41181
Ag halides: Tl^+, rel. to lattice structure 8=36470

Luminescence—contd

- **solids, inorganic**—contd
  - AgBr containing iodide, and mirror-like absorpt. 8=41050
  - AgBr, induced by Q-switched ruby laser 8=45255
  - AgCl, excited by u.v. laser 8=36469
  - AgCl, induced by Q-switched ruby laser 8=45255
  - AgCl, radiative lifetime of I^-, rel. to excited state structure 8=45257
  - AgI, powdered, phosphorescent excitation spectra recording 8=36484
  - Al crystal, K-shell fluoresc. under ion bombard. 100-200keV 8=49788
  - $Al_xGa_{1-x}P$, photoluminescence, and preparation 8=26233
  - AlP, fluoresc. rel. to temp. of synthesis 8=44115
  - AlSb, Se-doped, sharp-line donor-acceptor pair spectra 8=36471
  - BaI_2, for X-ray and photo-excitation 8=41182
  - $(Ba_xSr_yCa_z)MgSi_2O_8$: Eu, rel. to equilibria in subsolidus phases 8=49789
  - C_2N_2 (cyanogen) condensed in solid N_2 and Ar 8=25455
  - Ca halophosphate (As, Mn), decay obs. 8=27642
  - CaF_2:Ce^{3+}, constant-temp., rel. to 4f ↔ 5d transitions 8=45263
  - CaF_2: Ce^{3+}, f-d transitions, relative intensities calc. 8=36476
  - CaF_2-ErF_3: Tm^{3+}, $Er^{3+} \rightarrow Tm^{3+}$ energy transfer, conc. and temp. depend. 8=41185
  - CaF_2-ErF_3: Ho^{3+}, $Er^{3+} \rightarrow Ho^{3+}$ energy transfer, conc. and temp. depend. 8=41185
  - CaF_2:Eu^{2+}, rel. to Zeeman effect 8=45177
  - CaF_2:Ho^{3+}, on laser illumination rel. to two-photon absorpt. 8=45180
  - CaF_2:$Pu^{3+,4+}$ 8=31968
  - CaF_2:Y, X-irradiated, polarized, and structure of centres 8=36478
  - CaF_2: Yb + Nd, multiple sensitization effects 8=41183
  - CaO, phosphoresc., u.v. and γ excited, decay rel. to trap depths distrib. 8=41186
  - CaO, radical-recombination mechanism on excitation with H 8=41177
  - $Ca_3(PO_4)_2$ activated by Hg-like ions 8=36479
  - CaS: Zr phosphors, mag. susceptibility obs. 8=44967
  - $CaWO_4$, effect of electron irradiation 8=36481
  - $CaWO_4$ luminophor, pulse-excited, decay rel. to temp. 8=45290
  - $CdGeP_2$, recombination radiation 8=49791
  - CdO, powdered, phosphorescent excitation spectra recording 8=36484
  - CdS, cathodoluminesc., high density bombard. obs. 8=41187
  - CdS, e-beam excited, rel. saturation 8=31973
  - CdS, emission bands in 2.0eV region 8=49792
  - CdS, green edge emission, a.c. modulated 8=49794
  - CdS low-temp. spectrum, ion bombard. effects rel. to vacancies creation 8=36483
  - CdS luminophor, emission spectra 8=45295
  - CdS, pure and doped, donor-acceptor pairs, 77° and 4.2°K 8=27643
  - CdS, recombination kinetics 8=27645
  - CdS, trapping level disposition 8=49793
  - CdS: rare earth heterojunctions, injection luminesc. 8=45265
  - CdSe crystal, 0.93μ, rel. to photoconductivity 8=36482
  - CdSe, effect of uniaxial stress 8=36342
  - CdSe, i.r., ($\lambda_m = 1.2\mu$), mechanism rel. to photoconductivity 8=45266
  - CdTe, emission at 77°K 8=49795
  - $[Cr\ urea_6][Cr(CN)_6]$. $3H_2O$, energy transfer Cr-Cr 8=41188
  - Cr(III) compounds, spectra 8=49796
  - CsBr, after shock compression 8=49806
  - CsI(Tl) in plastic double layered scintillator for separating and detecting low energy protons and electrons 8=46877
  - CsI(Tl), long-lived phosphoresc components 8=27657
  - CsI(Tl) scintillation characteristics, vacuum deposited 8=46875
  - Cs_2PtCl_6 8=36505
  - Cu halide crystals, grown from melt 8=36485
  - Cu halides: Tl^+, rel. to lattice structure 8=36470
  - CuCl, laser excited 8=32053
  - Cu_2O, due to electron bombardment 8=41189
  - Cu_2O, exciton, at 77 and 4.2°K 8=49797
  - $EuCl_3$-dipyridyl complexes 8=41190
  - $Eu(NO_3)_3$. $6H_2O$, aromatic ketones sensitized, energy transfer mechanism, obs. 8=36487
  - p-, n-GaAs, e-irradiated, fluorescence at 300 and 77°K rel. to conduction band density of states 8=32054
  - GaAs, epitaxial, n-type from p-type, photo luminescence 8=41193
  - GaAs p-n junction obs. 8=36509
  - GaAs, radiative lifetime, quantum efficiency 8=49802
  - n-GaAs, self-activated, rel. to Ga vacancy-donor centres 8=36495
  - GaAs, with Cu as substitutional impurity, charact. recomb. times 8=27089
  - GaAs: Ge, due to Ge acceptors 8=49801
  - GaAs: Si grown by liquid-phase epitaxy 8=27650
  - n-GaAs: Te, schlieren pattern 8=45270
  - GaAs: Zn, near-band-edge 8=45271
  - GaAs: Zn, 1.370eV photoluminescence emission band, heat treatment effects 8=49800

Luminescence—contd

- **solids, inorganic**—contd
  - GaAs: Zn, rel. to defect formation during Cu diffusion 8=48820
  - p-GaAs: Zn, schlieren pattern 8=45270
  - GaP, band formation, role of vacancies and substitutional impurities 8=45274
  - GaP diodes, 300-900°K, rel. to band gap determ. from absorpt. meas., 0-900°K 8=45188
  - GaP, energy levels of N-N pairs 8=49803
  - GaP, i.r. donor-acceptor pair spectra involving deep oxygen donor 8=36488
  - GaP, photoluminescence excitation spectra above intrinsic interband absorpt. threshold 8=27647
  - n-GaP, photoluminescence, influence of Si 8=36496
  - GaP p-n junctions, electroluminescent synthesis and epitaxial growth by fused salt electrolysis 8=48573
  - GaP p-n junctions, forward-biased, edge-spectra 8=36490
  - GaP: Cd(Zn) and O, red pair 8=27649
  - GaP: Zn, O, excitation spectra and quantum efficiency 8=41195
  - GaP(Zn, O)/(Cd, O), temp.-dependent radiative recombination mechanisms 8=41194
  - GaP: Zn-O, (Te), p-n junctions, red emission time-delay characts. 8=45272
  - Ge, and other diamond-type lattices 8=36475
  - Ge, energy-deficient photons subjected to uniaxial compression 8=45275
  - Ge, interimpurity radiative recombination, thermal quenching 8=36364
  - $GdVO_4$, fluorescence of Eu^{3+}, determ. of phenomenological parameters of crystal field Hamiltonian 8=31992
  - InAs, p-n junctions, mechanism 8=36489
  - InP, p-n junctions radiative recombination mechanisms 8=41197
  - KBr-KCl solid solutions, intrinsic, induced by X-ray 8=41198
  - KBr, M-centre 8=41199
  - KBr: Tl, F scintillations, and recomb. luminesc. 8=36493
  - KBr: Tl, (In), mono- and di-molecular recombination, elec. field effects 8=45276
  - KCl, M-centre 8=41199
  - KCl, X-irradiated, under mechanical impact 8=36491
  - KCl: Ag^+, transitions, electronic, of impurities, symm. assignment by two-photon-induced emission 8=36494
  - KCl–KBr with Pb admixture, absorption spectra and fluorescence 8=49735
  - KCl: I, from ICl^- V_K-centre-electron recombination and localized exciton decay 8=27651
  - KCl: In, kinetics of F-scintillations 8=36492
  - KCl: Pb, kinetics of F-scintillations 8=36492
  - KCl: Tl, two-e correlation in impurity centres in model pot. approx. 8=32049
  - KCl: Tl, F scintillations, and recomb. luminesc. 8=36493
  - KI: Cu phosphor, complex activation centres 8=45277
  - KI: Tl, host sensitized 8=27653
  - KI: Tl, F scintillations, and recomb. luminesc. 8=36493
  - $KMnF_3$: Eu^{3+}, spin-wave wideline in spectra 8=27655
  - K_2PtBr_6 8=36505
  - K_2PtCl_6 8=36505
  - Kr crystal, intrinsic, 20°-110°K obs. 8=27656
  - K_2SnCl_6: Pt 8=36505
  - La, K-ionized, partial fluoresc. yield 8=41111
  - $La_{1-2x}Ba_xEu_xLi_xPO_4$, rel. to mixed valency Eu centres 8=45278
  - LaF_3: Dy^{3+} 8=31985
  - LaF_3:Nd^{3+}, continuous stimulated emission at 300°K 8=37616
  - LaF_3 : Pr^{3+}, spontaneous emission probabilities and quantum efficiencies 8=49805
  - $LaNbO_4$: Nd^{3+} 8=36515
  - La_2O_3 (Bi) phosphor, excitation and emission spectra 8=45279
  - La_2O_3:Bi^{3+}, configuration curves calc. rel. to band widths and phonon emission 8=40058
  - $LaTaO_4$: Nd^{3+} 8=36515
  - $LiAlSiO_4$, X-irradiated, and e.p.r. 8=40936
  - LiF, after shock compression 8=49806
  - LiF, e-irradiated, rel. to colouring process 8=40062
  - LiF: O^{2-}, impurity effect 8=36499
  - LiF/U^{6+}, suitability of fluorescence props. for laser 8=46620
  - $LiNbO_3$, parametric, excited by Ar laser 8=41201
  - $MgAl_2O_4$:Cr^{3+}, fluorescence spectra 8=49715
  - MgO cryst., phosphorescence and X-ray stimulated luminescence 8=49809
  - MgO:Cr^{3+}, diffusion determ. 8=31010
  - MgS: Sb, K luminophor, pulse-excited, decay rel. to temp. 8=45290
  - $MgTiO_3$: Mn^{4+}, fluorescence, transitions 8=36500
  - Mn^{2+} in spinel, spin temp. equalization between excited and fundamental states 8=45282
  - Mn^{4+} activated oxygenated cpds, excitation spectra 8=41202
  - MnF_2 :$Mg^{2+}(Zn^{2+})(Ca^{2+})$, impurity-induced fluorescence 8=45281
  - Na_3AlF_6: Eu^{3+}, obs. 8=36502
  - $NaAlSi_3O_8$, X-irradiated, and e.p.r. 8=40936
  - NaCl, after shock compression 8=49806
  - NaCl, coloured, triboluminesc., and tribo-photostimulated electron exoemission 8=40709

Luminescence—contd
solids, inorganic—contd
NaCl: Ag excited with extreme u.v. radiation 8=36501
NaCl-Tl, -Ag, phosphors, recombination efficiency after photo thermal destruction of F centres 8=48881
NaF, delayed, of M centre in F-to-M conversion 8=41203
NaI(Tl), emission bands, excited by X-irradiation, 5-80°K 8=46856
NaI(Tl), long -lived phosphoresc components 8=27657
NaI(Tl), pulse shape rel. to Tl conc. and temp. 8=46876
NaI(Tl) scintillation characteristics, vacuum deposited 8=46875
NaI: Tl, temp. (15-300°K) and conc. dependence rel. to Tl$^+$ dimer centre characts. 8=27658
NaI: Tl$^+$, temp. and conc. dependence rel. to energy transfer 8=27659
NaLn$_{1-x}$ Eu$_x$ TiO$_4$, Eu^{3+} fluoresc. 8=41191
Na$_2$ZrSiO$_5$ phosphor, zone scheme 8=41219
Nd glass stimulated emission spectrum and quasi-continuous generation, 4.2°K 8=36503
Nd^{3+} activated, high temp. spectroscopy of stimulated emission 8=37595
Nd^{3+} fluorescence in glass, concentration quenching 8=41206
NdCl$_3$, fluorescence obs. rel. to annililation between excited states of Nd^{3+} ions 8=41205
NH$_4$I and NH$_4$I(Tl), spectra 8=32014
NiCl$_2$, matrix-isolated mols., fluoresc. spectrum 8=29757
O-dominated lattices 8=36504
OH and OD in solid Ne, evidence of rotation 8=32020
PbI$_2$, spectra rel. to defect energy-level structure determ. 8=44650
Pt^{4+} in octahedral complexes 8=36505
RbI: Tl, exciton scintillations, form, decay time and relative efficiency 8=36506
RbMnF$_3$, broad-band fluorescence rel. to temp. 8=49811
RbMnF$_3$:Nd^{3+}, antiferromag., intensity and decay time temp. depend., 20-100°K 8=32057
Rb$_2$PtCl$_6$ 8=36505
Ru(II) complexes, mechanism 8=32027
in Sc$_2$O$_3$, Nd^{3+} rel. to Stark splitting scheme and $^4F_{3/2}$ lifetime, 4.2-293°K 8=32017
Si, and other diamond-type lattices 8=36475
Si, recombination radiation at high excitation levels 8=41209
SiC, and other diamond-type lattices 8=36475
SiC, energy levels and capture centres 8=41210
β-SiC, fast electron bombardment effects 8=36508
SiC, irradiated with electrons, H and D ions of 20 keV 8=36510
α-SiC (6H), high-resistivity, doped accidentally, rel. to band scheme 8=35779
α-SiC (6H), photoluminesc. of single crystals 8=36511
α-SiC: Ni and Al complexes, luminescence 8=36507
Sm, trivalent, in oxide glasses 8=36412
Sr$_3$(PO$_4$)$_2$: Tb, bluish-white emitting cathode-ray phosphor with long decay time 8=49813
Tb(NO$_3$)$_3$.6H$_2$O, aromatic ketones sensitized, energy transfer mechanism, obs. 8=36487
TiO$_2$ (rutile), thermally stimulated currents and luminescence 8=36513
U-activated cpds with rocksalt lattice, fluorescence and co-dopant quenching 8=49808
YGdAl:Nd^{3+} laser characts. 8=39692
YNbO$_4$: Nd^{3+} 8=36515
Y$_2$O$_3$: Ln^{3+}, (Ln=Pr, Nd, Eu, Er, Tm), radiative and multiphonon relax of Ln^{3+} 8=45289
In Y$_2$O$_3$, Nd^{3+} rel. to Stark splitting scheme and $^4F_{3/2}$ lifetime, 4.2-293°K 8=32017
Y$_2$O$_3$: R^{3+}, (R = rare earths), cathodoluminescence 8=49814
YTaO$_4$: Nd^{3+} 8=36515
YVO$_4$: Eu^{3+}, spectrum (4f)^6 level splittings rel. to internal field, obs. 8=41152
Zn, K-fluoresc. yield from Zn^{69m} β decay obs. 8=38418
ZnAl$_2$O$_4$:Cr^{3+}, fluorescence spectra 8=49715
(Zn, Cd)O phosphors 8=45292
Zn$_x$Cd$_{1-x}$S graded-band-gap crystals, and elec. props. 8=39696
(Zn, Cd)(S, Se) :Cu phosphors, photo- and electro-luminesc., obs. 8=45293
ZnO crystal, recomb. radiation of bound excitons, 4.2°-90°K 8=31301
ZnO, edge, exciton contribution 8=27660
ZnS luminophor, emission spectra 8=45295
ZnO luminophor, pulse-excited, decay rel. to temp. 8=45290
ZnO phosphors 8=45292
ZnO, u.v. spectrum, 4.2°-77°K 8=41216
ZnO, Ga scintillation due to α, obs. 8=37789
ZnS activated with Group IVB elements, e.p.r. investigation 8=49815
ZnS and similar lattices, props. 8=36522
ZnS, coherent fluorescence for excitation by 2 photon absorption 8=32063
ZnS crystal, photolum. 77°-600°K, obs. 8=45291
ZnS, excitation at low temp. 8=27661
ZnS luminophors, preparation, effect of halide addition 8=49819
ZnS phosphors, temp. shift of green-Cu band 8=32068
ZnS(Ag) based, scintillation output rel. to α-radiation of surface 8=27662

Luminescence—contd
solids, inorganic—contd
ZnSAg monocrystal, rel. to e.s.r. 8=36523
ZnS:Al(Ga), self-activated polarization 8=32067
ZnS$_x$ -CdS$_{1-x}$, exciton type, edge emission and long-wave rad. 8=41212
ZnS: Cl luminophor, pulse-excited, decay rel. to temp. 8=45290
ZnS: Cu, Al(Ag, Al), rel. to i.r. absorpt. due to donor states 8=41156
Zn(SCN)$_2$, Pb^{2+} or Sn^{2+} activated 8=36520
ZnSe, photoelectronic props. in p-type-Cu-activated and n-type-self-activated 8=45296
ZnSe, photoluminescent props. of activated emissions 8=49816
Zn(S: Se) phosphors, activator free 8=36517
p-ZnSe: Cu, radiative pair transitions 8=45294
ZnSe: Tm^{3+}(Er^{3+})(Ho^{3+}), with Li or Cu codopants, 8=27664
Zr silicates activated by Mn, Cr, Hf and rare-earth's props. 8=41219
ZuSnP$_2$, radiative recombination, photoluminesce. spectra 8=41213
solids, organic
acetophenone in soln. at 77°K, time-resolved phosphorescence, medium effects 8=45297
alkyl aromatics, radiationless decay 8=32072
anthracene, blue fluorescence from triplet exciton interaction, magnetic field effects 8=41223
anthracene, dimezo substituted, 1, 2 benzanthracene composite excimers 8=49821
anthracene, doped crysts., at high press. 8=49824
anthracene, excimer emission at v. high press. 8=49823
anthracene, in host crysts. at high press. 8=49822
anthracene, polarization diagrams for impurity mol. orientation 8=36531
anthracene, scintillation pulses excited by α bombard., temp. pressure depend. 8=36526
anthracene, scintillation response to heavy charged particles, directional anisotropy 8=46870
aromatic hydrocarbons, triplet decay, high press. effects 8=49825
aromatics, triplet-state lifetimes, effect of partial deuteration 8=34306
benzene-cyclohexane, solid solns. at 77°C 8=27624
benzene, energy transfer in isotopically mixed crysts. 8=27668
benzene isotopic mixed crysts., fluorescence and phosphorescence, static cryst. effects 8=49771
benzene, isotopic mixed crysts., trap-trap triplet energy transfer 8=36527
benzene, isotopic mixed crysts., triplet-triplet annihilation and delayed fluoresc. 8=41225
benzene, nonradiative decay, deuteration effects 8=49826
1, 12-benzoperylene quasiline fluoresc. line-widths temp. depend., 4-175°K 8=36528
benzophenone, at 77°K 8=41224
biphenyl, solid soln. in cyclohexane, delayed fluoresc. 8=36529
cattle rod outer segments 575-600 mμ 8=49828
chlorobenzenes in rigid solns., polarization 8=27669
chromophores, intramolec. energy transfer between triplet states 8=41157/8
chrysene, delayed luminesc., growth and decay 8=32073
coronene, in cryst. matrices, effect of thermal treatment 8=45242
4-dimethylamino-4′-nitrodiphenyl in binary soln., phosphor-impurity group centres props., 77°K 8=36532
dinucleotides, at 77°K 8=41227
1, 6-diphenyl-hexatriene-1, 3, 5, polarization diagrams for impurity mol. orientation 8=36531
$\alpha\alpha'$ and $\gamma\gamma'$ dipyridol in n-paraffins, structural spectra of phosphorescence 8=36530
energy transfer in isotopically mixed crysts. 8=27668
ferrocene, matrix-isolated 8=49775
fluoro-aromatics, h.f.s. in $\Delta m=2$ transitions 8=31851
formaldehyde derivatives, phosphoresc. lifetimes 8=25473
halogenated benzenes, singlet-triplet emission 8=27625
hydrocarbons aromatic, quasilinear phosphoresc. spectra 8=36524
p-methylbenzyl radical in Ar matrix 8=36617
mixed crysts., intermolec. triplet decay processes 8=32070
naphthacene, fluorescence in mag. fields 8=41226
naphthalene d$_8$-naphthalene mixed crysts., phosphoresc. spectra 8=32074
napthalene, delayed luminesc., growth and decay 8=32073
naphthalene, doped crysts., at high press. 8=49824
napthalene, e.s.r. emission in triplet state 8=45298
naphthalene, excimer emission at v. high press. 8=49823
naphthalene, fluorescence and absorpt. conc. depend. in n-heptane, cyclohexane 77°K 8=49830
naphthalene mixed crysts., phosphoresc. and delayed fluoresc. 8=32075
naphthalene, polarization diagrams for impurity mol. orientation 8=36531
naphthalene, quenching of triplet state 8=34341
nucleic acid derivative aggretates, energy transfer in frozen solns. 8=45304
organophosphors, photoluminesc. reabsorpt. 8=36525

Luminescence—contd
  solids, organic—contd
    orthodiazines, electronic states and radiationless processes 8=27667
    perylene, α-and β-type crysts., high press. 8=41168
    phenanthrene, delayed luminesc., growth and decay 8=32073
    phenanthrene, doped crysts., at high press. 8=49824
    phenanthrene, excimer emission at v. high press. 8=49823
    m-phenylene-bis-phenylmethylene, quintet mol. 8=47669
    phosphorescence and delayed fluoresc. in solid solns., kinetics and chem. appls. 8=25936
    phosphors 8=41221
    plastic scintillators, mixed preparation and efficiency 8=49829
    polymers of acetylene series 8=32079
    pyrazine, decay at low temp. 8=36535
    pyrazine, phosphorescence, at 4.2°K 8=36534
    pyrene in biphenyl, delayed excimer fluoresc. 8=32076
    pyrene, in mixed cryxts. 8=25942
    pyrene monomer in solid soln. 8=45300
    pyrene, spectrum rel. to carrier photogeneration 8=40679
    radioluminescence of single crysts. rel. to mol. excitation kinetics, obs. 8=39384
    rigid soln., laser-stimulated recomb. 8=41222
    rubrene, crysts. under press. 8=49779
    salicylic acid and salts, polarization diagrams 8=32077
    salicylidene aniline, photochromism 8=45302
    sodium salicylate, fluorescent emission band shape interpretation 8=45303
    sodium salicylate, temp. effects 8=45301
    tetracene, cryst. under press. 8=49779
    tetracene, in host crysts. at high press. 8=49822
    tetracene, temp. depend. 8=36536
    tetraphenylbutadienes, effect of intramolec. twisting 8=39390
    trinitrobenzene cryst. complexes, high press. 8=27635
    trinitrofluorenone cryst. complexes, high press. 8=27635
    triphenylene, delayed luminesc., growth and decay 8=32073
    triphenylene-d$_{12}$-Rhodamine B solns., triplet-singlet energy transfer kinetics, obs. 8=36533
    tris-oxalato Cr(III), low temp. 8=27670
    vanadyl prophyrin complexes 8=45299
    Eu β-diketone chelates, fluoresc. props. 8=32071
    KI, from α-centre, polarization 8=27654
    LuVO$_4$: Eu^{3+}, rel. to Hamiltonians at Eu^{3+} site 8=41208
    NaCl: Cu, fluoresc. spectral comp. after period of storage 8=49741
    ScVO$_4$: Eu^{3+}, rel. to Hamiltonians at Eu^{3+} site, 8=41208
Luminescence chambers
    He gas, high-pressure, scintillation induced by α-particles, recombination 8=29642
Luminescent devices
    See also Counters/scintillation.
    anthracene scintillator, α, e-excited, decay obs. 8=49832
    capacitor, electroluminesc., as distributed-parameter system 8=36537
    cells, electroluminesc., phys. props. 8=36521
    phosphor, photometric standards for chem. testing 8=45418
    phosphor powder, radioactive isotope analysis 8=43987
    phosphors, radioluminesc. dosimetry 8=36462
    scintillator, decay time meas. by simulated photomultiplier pulses 8=46883
    thermoluminescent, for low and high temperatures 8=49831
    Au-Si$_3$N$_4$-ZnSe diode, visible electroluminesc. 8=41230
    CaS: Ce phosphor, decay and thermoluminesc. obs. 8=45305
    CaS: Zr phosphors, mag. susceptibility obs. 8=44967
    Cd-In alloyed diode, spectra at 78 and 300°K, I-V characts. at 300°C 8=36538
    GaP diodes, solution-grown, photoluminesc. at 77°K, effect of donor conc. on optical efficiency 8=44843
    GaP electroluminescence diodes, prep. from p-on-n liquid-phase epitaxial layers 8=41229
    GaP electroluminescent p-n junction, prep. by fused salt electrolysis 8=48573
    GaP p-n junctions grown by liq-phase epitaxy, green electroluminescence 8=41231
    GaP p-n junctions, red-emitting, prep. by soln. growth of p-type thick layers on n-type substrates 8=41232
    CaS: Zr phosphor, thermoluminesc. peak shift obs. 8=45306
    Si-intermetallic cpds.-SiC light diodes, V-I depend. of recomb. rad. intensity 8=27184
    ZnS electroluminesc. resistor props. 8=27145
    ZnS phosphor, trace metal determ. by n. activation 8=50001
    ZnS-type phosphors 8=36522
    ZnS: Cu luminophor, two-band electrolum. emission 8=45307
    Zn$_2$SiO$_4$ phosphors on glass base in u.v. radiation detectors 8=24372
Lumino(pho)rs. See Luminescence/solids, inorganic; Luminescence/solids, organic; Luminescent devices.
Lutetium
    electronic structure from relativistic augmented-plane-wave calcs. 8=26905
    generalized susceptibilities and mag. ordering 8=44973
    Hall effect meas. 8°-320°K, mag. fields to 7.8 kOe 8=44690
    thermal conductivity, temp. dependence, 5-300°K 8=35458
Lutetium compounds
    iron garnet, sublattice magnetization 8=40840
    LuFe garnets: Fe^{4+}, linewidth temp. dependence, 4.2°-300°K at 10 and 26 kMc/sec 8=31827
    LuFeO$_3$, paramagnetic susceptibility, semi-empirical expression by Padé approximant 8=27386
    Lu(ReO$_4$)$_3$ crystal struct., high-temp. modification, X-ray obs. 8=30914
    LuVO$_4$: Eu^{3+}, luminescence rel. to Hamiltonians at Eu^{3+} site 8=41208
Luxemburg effect. See Electromagnetic wave propagation/ionosphere.

M-centres. See Colour centres.
M-regions. See Sun.
Mach number. See Aerodynamics; Shock waves; Supersonic flow.
Mach's principle. See Relativity.
Macromolecules. See also Molecules/configuration and dimensions, macrmolecules; Polymers; Proteins.
    adsorption, theory 8=39614
    amylose structure, i.r. spectra and molec. interactions 8=30485
    cellulose triacetate, existence in different conformations in different solvents 8=43820
    chemistry, conference, Prague, Aug.-Sept. 1965 8=34392
    cholesteryl, liq. crysts, dielec. props. dipole moments and transition temps. 8=34893
    collagen, hydrated, d.m.r. 8=49639
    crystals, chem. bonding 8=43923
    cyclotetratriacontane, and mol. structure 8=39831
    desoxyribonucleotide complexes with Fe, p.m.r. 8=43880
    dinuclecleotides, luminescence at 77°K 8=41227
    DNA, double-stranded, pairon condensation 8=32620
    DNA, irradiated, e.s.r. obs. 8=34366
    DNA model, helix-coil transition 8=47733
    fibrous structures with steric constraints 8=30400
    glass, alkali silicate, melt, structure transition by high temp. flow 8=34757
    helical parameters 8=38965
    helix → coil transition, transitory regimes 8=43432
    heterogeneous chains, helix-coil transition, protein model 8=47733
    high-molecular biopolymers, diffusion meas., method and apparatus 8=48116
    hyperchromism, two-band model 8=39365
    infrared spectrum analysis, review 8=34393
    long-chain, Markov model, end effects 8=25672
    monodisperse rigid rods, spectral distrib. 8=39362
    monomolecular chain Raman linewidth calcs., and appl. to molecular crystal 8=36300
    nucleic-acid bases irrad. in reactor, free radical yield 8=49891
    nucleic acid derivative aggregates, energy transfer in frozen solns. 8=45304
    nucleic acids, molec. interactions and helical struct. 8=29859
    nucleoside derivs, struct. and chem. substitution effects, rotatory and dichroism studies 8=43434
    organic, possible superconductivity near room temp. 8=27038
    in polymers, oriented, segmental mobility rel. to bulk elasticity 8=35735
    polypeptides, helix-coil transition, comparison of theories 8=43433
    pyrimidine nucleosides irrad. in reactor, free radical yield 8=49891
    Rayleigh scatt. from real chain mols. 8=47732
    rayon fibres, n.m.r. of adsorbed H$_2$O 8=27508
    in solution, effect of dielec. const. of solvent 8=30418
    solns., normal stress difference meas. 8=25893
    in solution, theory of diffuse small-angle X-ray scattering 8=25870
    spectra, i.r., vibr. band intensities and terminal group effects in periodic mols., calc. 8=29857
    starch, γ-irradiated, e.s.r. of free radicals 8=49618
    symmetry of helical structures 8=29858
    wormlike chains, intrinsic viscosity with excluded vol. effects 8=30434
Madelung constant. See Solids/structure.
Maggi-Righi-Leduc effect. See Magnetothermal effects.
Magnesium
    atom, lifetime of 4 ^{1}D term, determ. 8=34164
    atomic, photoionization cross section meas. 8=29949
    chemisorption of diphite molecules 8=49899
    corrosion in NaCl, transient charge fluctuations, obs. 8=45368
    deformation, fast, slip and twinning contribs. to mechanism 8=40169
    electron-irradiated, low temp. annealing spectrum 8=26734
    electron momenta from X-ray meas. 8=44647
    emission spectra, L$_{23}$, rel. to Al X-ray band spectra interpret 8=45172
    flame temp. meas. by MgO vibr. spectroscopy 8=24013
    ionization of Mg$^+$ to Mg^{++} by electron impact from threshold to 2000 eV, cross section meas. 8=43486
    ion sputtering on Al, Mo, Ta targets, ang. distrib. obs. 8=48909

Magnesium—contd
- K-type stars, abundance by photometric meas. 8=45633
- λ Boo, abundance ratio Mg/O calc. from i.r. spectra 8=50286
- lattice mechanics, elec. and electronic props., 8=48707
- π 'Ori', abundance ratio Mg/O calc. from i.r. spectra 8=50286
- single crystal, nature of oxide layers on surface 8=35167
- single crystal, optical consts. from reflectance ratios 8=45164
- Sirius, abundance calc. from Mg II lines 8=50285
- spectrochemical anal. in blood plasma, using improved plasma jet equipped with inexpensive analyzer 8=47894
- spectrochemical detect. in Ta 8=45416
- sputtering by 1- to 5 keV Ar^+, rel. to orientation dependence 8=40076
- strained elastically, inner-displacement tensor 8=26406
- talc, structural changes during heating 8=48601
- θ Hya, abundance ratio Mg/O calc. from i.r. spectra 8=50286
- twins, second-order, internal deformation and fracture 8=44588
- weak line transition probability calc. 8=29621
- Mg1, f-values calc. 8=34135
- Mg(II) coordination no. in aq. solns. determ. by p.m.r. 8=39431
- Mg II, e impact line broadening calc. 8=47507
- Mg^{25} in aq. soln., NMR line, chemical shift 8=39440
- Mg^+, electron scatt., autoionization states, excitation of 3s → 3p, 3s → 3d transitions 8=43232

Magnesium compounds
- alloy, h.c.p., fast deformation, slip and twinning contribs. to mechanism 8=40169
- basic sulphate, composition determ. by thermogravimetry, differential thermal anal. and i.r. absorpt spectrophotometry 8=27671
- brucite-like layer ions in double-layer structures formation 8=48514
- brucite, structure from n. -diffr. exam. 8=39804
- chrysotile asbestos suspensions, stability rel. to surface charge on fibres 8=48242
- chrysotile, X-ray diffr. profiles of faulted cylindrical lattice 8=39805-6
- ferrous ferrite, mirowave resonance rel. to magnetic anneal 8=31818
- gypsum systems, hardness, modulus of elasticity, and porosity, interrelation 8=40172
- magnesia spinel, reactive, prep. and props. 8=43989
- magnesioferrite, precip. and coarsening in MgO–Fe solid soln. 8=44007
- olivine, in carbonaceous meteorite 8=28158
- pyroavrite, crystal structure 8=39803
- sepiolite, sorption of vapours 8=26137
- talc, structural changes on heating 8=30699
- Mg alloyed cast iron, laser spectrochemical analysis 8=32157
- Mg ammonium metaphosphates, rhombohedral 8=44245
- Mg borides prepared under superhigh-pressure condns. 8=35245
- Mg phthalocyanine, films, barrier effect, photoconductivity 8=40678
- Mg(II) oxalate complex, conc. soln, raman spectra rel. to co-ord. and coupling 8=43843
- Mg-Al alloys, valence electron distrib. investigation 8=44648
- Mg-Al spinel, Czochralski growth 8=39675
- Mg-Al spinel, epitaxial deposition on Si layers, defect formation 8=48832
- ϵ-$Mg_{23}Al_{30}$, crystal structure 8=44227
- $MgAl_2O_4$, microwave phonon attenuation 8=39895
- $MgAl_2O_4$, single crystal growth by travelling isotherm technique 8=44135
- $MgAl_2O_4$ spinel, plastic deform., slip planes and stoichiometry 8=31216
- $MgAl_2O_4$ spinel, etching investigations for visibility of dislocations and slip planes 8=48526
- $MgAl_2O_4$, vacuum hot-pressing, densification kinetics 8=40174
- $MgAl_2O_4$:Cr, emission and absorpt. spectra, visible and u.v. 8=45210
- $MgAl_2O_4$:Cr^{3+}, optical spectra 8=49715
- $MgBr_2$-diethylether coordination compound, i. r. spectrum 8=25569
- Mg-Cd alloys, ordering effect on residual resistivity and mag. susceptibility 8=40321
- Mg-Cd alloys, ordering transforms., 50-220℃ 8=35113
- $Mg(Cr,Al)O_4$, disorder, X-ray diffraction study 8=44226
- $MgCr_2O_4$, mag. structure from n. diffr. exam., 8=45063
- Mg-Cu-F, high-temp. gaseous equilibria 8=34375
- MgF_2, birefringence, 1500 to 3000 Å 8=41056
- MgF_2, elastic and thermoelastic behaviour 8=44590
- MgF_2, elastic consts. 8=44589
- MgF_2, plasmon and interband transition excitation on e-bombardment 8=26931
- MgF_2, rutile type crystals, NMR and electronic structure 8=27506
- MgF_2 Soleil compensator, near i.r. 8=37699

Magnesium compounds—contd
- MgF_2, vibr. freq. determ. by n. scatt. rel. to Raman scatt. 8=44302
- $MgFe_2O_4$, disorder, X-ray diffraction study 8=44226
- $MgFe_2O_4$, Mossbauer Faraday effect 8=45158
- $MgFe_2O_4$ superparamag. precip. in MgO, Mossbauer spectroscopy 8=31729
- Mg–Mn ferrite films, FMR, thermal treatment effects 8=31817
- Mg–Nd–Mn–Ni system, phase equilib. 8=48387
- MgO, ads. of Br_2 and I_2, refl. spectra 8=48479
- MgO, adsorption of CO_2 and H_2O, i.r. study 8=47974
- MgO based insulating materials, phase composition and electrophysical props. 8=31445
- MgO, chemisorption of H_2 and surface OH, i.r. spectros. 8=49894
- MgO, colour centre bands, Faraday rot. anal. 8=35588
- MgO, colour centres after neutron irrad., study by optical absorpt. bands 8=35589
- MgO, compression creep curve, shape 8=31221
- MgO content in ilmenites, rel. to MgO/FeO ratio in host rocks 8=50070
- MgO, crack front interaction with cleavage steps 8=44591
- MgO, effective atomic charges by X-ray exam. 8=26169
- MgO, e microscope exam., lattice fringes resolution, 100 kV 8=39775
- MgO, exciton line splitting, phonon induction, obs. 8=36331
- MgO, F band, temp. depend. 8=45209
- MgO, F-centre absorpt. spectrum, expt. compared with theory 8=44472
- MgO, ferromagnetic films epitaxial growth substrate 8=35170
- MgO films, porous, field-assisted secondary electron emission 8=27359
- MgO flame, dispersion of absorpt. coeff. 8=32975
- MgO flame, radiometry 8=37321
- MgO, irradiated, defect clusters, very small, study by neutron scattering meas. 8=35525
- MgO, irradiated, phonon-assisted optical absorpt. 8=41049
- MgO, i.r. spectral reflectivity and dispersion 8=41022
- MgO, isostatically hot-pressed, fabrication and characterization 8=26045
- MgO, lattice vibrations in thin film, electron diffraction obs. 8=35387
- MgO(magnesia), high temp., creep, effect of additives 8=40171
- MgO(magnesia), high temp. creep, effect of simultaneous grain growth 8=40170
- MgO, microwave phonon attenuation 8=30948
- MgO, n/e-irradiated, aggregate defect centres, Mollwo-Ivey relations 8=31032
- MgO, neutron irrad., negative-ion vacancies 8=44412
- MgO, neutron irradiated, $(OF)^{2-}$ molecular ion as paramag. defect. 8=44404
- MgO, n-induced damage and macroscopic props. changes, review 8=44496
- MgO, n-irradiated at 80°K, colour centres, zero-phonon lines and phonon-coupling 8=27588
- MgO, n irrad. ($< 10^{18}$ nvt), rel. to hardening, lattice damage, colour centre conc. 8=26829
- MgO, Ni ferrite epitaxial growth on (111) and (110) surfaces 8=39594
- MgO, optical constants from electronic band structure by pseudo-potential calc., 7-28eV 8=27587
- MgO, phosphorescence and X-ray stimulated luminescence 8=49809
- MgO, polycrystalline, press. derivs. of elastic moduli, revised data 8=31217
- MgO porous thin film, self sustained electron field emission, obs. 8=40695
- MgO powder, ortho-positronium form. and annihilation 8=49130
- MgO powder, positronium diffusion constant and annihilation spectra mean length 8=44378
- MgO, pressure sintering, densification data rel. to plastic deform. 8=35070
- MgO, Rebinder effects, obs. 8=31083
- MgO, resistance at high temp., impurity effects 8=26950
- MgO rot. cryst., dispersion surface, electron diffr. pattern 8=35309
- MgO, scattering of lattice waves by dislocations 8=30933
- MgO, second-order, elastic constants pressure derivs., 8=49035
- MgO, secondary emission, shot noise fluctuations 8=44949
- MgO, second order Raman scattering spectrum 8=36386
- MgO single crystal whiskers, spontaneous growth 8=35257
- MgO, spin-lattice relax. anisotropies, theory 8=31874
- MgO, toughness, effect of water 8=40173
- MgO, V^1 centre thermal decay temp. dependence, 18°-50℃ 8=31121
- MgO:Cr^{2+}, acoustic paramag. reson. 8=45092
- MgO: Cr^{2+} dynamic lattice couplings from microwave u.s. and thermal conductivity exam. 8=35053
- MgO:Cr^{3+}, diffusion determ. from luminesc. 8=31010
- MgO: Cr^{3+}, ENDOR 8=40977
- MgO:Cr^{3+}, V^{2+}, e.p.r. of excited ^2E levels 8=45091
- MgO:Cr^{3+}, (V^{2+}), e.s.r. of excited $^2E(3d^3)$ level 8=27484

Magnesium compounds—contd
- $MgO-Cr_2O_3-Fe_2O_3$ at 1300°C in air, phase relations 8=39529
- MgO: Cu^{2+}, e.p.r. at 1.2°K, Jahn-Teller effect 8=27470
- MgO:Fe, detection of microsec. heat pulses in large mag. field 8=44366
- MgO:Fe^{2+}, far i.r. spectra at low temps. 8=27589
- MgO:Fe^{2+}, spin-relaxation time temp. dependence, 4.2–13°K rel. to Fe^{2+} low-lying energy level 8=45086
- MgO: Mn_2^+, charge transfer at surface, e.s.r. study 8=48422
- MgO:Mn^{2+}, e.s.r. at 1.3HGz 8=40930
- MgO–MnO solid solns., and with LiO_2, struct. and mag. props. 8=48662
- MgO-NiO solid solns., formation on thermal decomp. of mixed hydroxides 8=39532
- MgS: Sb, K luminophor, pulse-excited, decay rel. to temp. 8=45290
- Mg_2SiO_4, thermal diffusivity at high press. and temp. 8=48762
- $Mg_2SiO_4-Fe_2SiO_4$ system, olivine-spinel transition, geophys. applic. 8=36678
- Mg-Sn alloy melts, atomic distrib. curves 8=39300
- Mg-Sn alloy, twinning and fracture 8=44592
- n-Mg_2Sn, piezoresistance tensor components, 50-300°K rel. to many-valley processes 8=44800
- n-Mg_2Sn, thermal conductivity from 4.2 to 300°K 8=26603
- n-Mg_2Sn, thermal conductivity, 4.2 to 300°K 8=44365
- $Mg_2SnO_4-MgFe_2O_4$, solid solutions 8=40738
- $MgSO_4.7H_2O$ and $MgSO_4.7D_2O$, vibr. spectra 8=35382
- $MgSO_4.7H_2O$, crystal growth rate dependence on supersaturation of soln. 8=39676
- $MgSO_4$ soln., diffusion rate constants calc. 8=43783
- $MgSO_4$, decomposition kinetics rel. to sample mass and processing press. 8=36565
- $MgSO_4.7H_2O$, left form predominance, crystallization conditions effect 8=26177
- $MgTiO_3$: Mn^{4+}, fluorescence, transitions 8=36500
- Mg–Zn alloys, age hardening characts., effects of 1% Au addition 8=26832
- Mg–Zn–Mn alloy, wrought, tensile and mech. props. rel. to heat treatment 8=35704
- Mg-6 wt.% Zn-0.5 wt.% Zr alloy, diffusional creep with low strain rate sensitivity 8=26830
- Mg–Zr alloy, diffusion-creep and form. of denuded zones 8=26831
- Mg–Zr alloys, fine grain effect through Zr 8=48343

Magnetic amplifiers. See Amplifiers; Magnetic devices.

Magnetic anisotropy. See Magnetic properties of substances; Magnetization state.

Magnetic bays. See Earth/magnetic field, variations; Magnetic storms.

Magnetic bottles. See Magnetic fields; Plasma/confinement.

Magnetic cooling
- CMN crystal container for adiabatic demagnetization 8=32991
- thermodynamic and statistical aspects 8=31518

Magnetic devices
- balances of Sucksmiths type, thermostat for temps to 1100°C 8=46278
- data recording system, effective gap length estimation 8=28534
- digital data collection system for v.l.f. transient waveforms, appl. to atmospherics 8=32253
- eddy current braking at high speeds by permanent magnets 8=24115
- ferromagnetic films, strain-sensitive for sonic film memory 8=36125
- ferrimagnets, based on magnetoelastic effects 8=31713
- ferrite cores, magnetoelastic resonance 8=36226
- ferrite resonators, hydrodynamic liquid cooling method 8=33048
- film storage cells using domain propag. 8=24117
- film storage-elements, controlled easy-axis distrib. 8=49511
- films, coupled, for associative memories 8=36121
- films for magneto-optic readout using media modulation 8=40799
- four-magnet system for 180°e scatt. 8=24116
- hyperfine, caused by mag. impurities in metals 8=40962
- hysteresis, dynamical loop representation 8=44961
- information storage system, energetic model 8=46390
- lens, design, applic. of method of least squares 8=41964
- magnetoelastic two-port: nondispersive variable delay line 8=31745
- magnetoresistor for supercond. magnet field meas. 8=41938
- memory, using incremental permeability round different quiesient flux points 8=28533
- microwave ferrite 8=49547
- multilayer film-, magnetization reversal 8=36120
- orthoferrites, device applics. of mag. domains 8=49553
- permalloy film memories, keepered and nonkeepered, internal field distrib. 8=40820
- Perminvar toroidal magnetic cores, charact. determ. 8=49557
- pulsed magnetic field apparatus for up to 1.2 MOe 8=46383
- racetrack system, influence of form and stretch of azimuthel-edge fields 8=33472

Magnetic devices—contd
- readout, magneto-optic, amplitude, modulated 8=36122
- recording, theory and expt., review 8=33053
- roller for gas mixing 8=30237
- rotor-position indicator, comparative anal. of iron shapes and sizes 8=33051
- sharp film NDRO bit organized memory 8=36124
- shield against e.m. fields, scaling laws 8=46375
- shields for space vehicles, analog simulation and meas. of forbidden volume 8=41481
- solenoid, Cu-tape-wound, edge-cooled for Bevatron preinjector 8=33052
- spiral tape core, flux pattern 8=37398
- strip mag. balance with controllable sensitivity modification 8=46364
- superconducting system in pulsed MHD generator 8=37376
- superconductor-normal metal sandwich (Cooper pair), reduction in spin flip breaking 8=49502
- synchronous drum for n time-of-flight data 8=47155
- tape recording of photographically recorded data 8=42351
- thermomagnetic generators with graded mass and gap, performance characts., 8=46388
- vibrators, magnetostricture, mechanical power limitations 8=49452
- Z-pinch, megagauss pulsed fields prod. 8=28532
- EuO memory medium in low temp. laser-beam addressable memory 8=36123
- MnBi films, memory appls. rel. to props. 8=49531
- Mo permalloy tapes, rolled 4-79, magnetostriction and coercivity process variables dependence 8=31658
- Na flowmeter for reactor core, calibration and stability 8=48013

Magnetic domains. See Magnetization state/domains.

Magnetic field measurement
- automatic magnetometer for e.s.r. 8=46370
- beam bending 90° magnets field uniformity 8=28997
- components meas. in meridian plane at sea by nuclear precession 8=28005
- earth's, maritime two component gyrostabilized magnetometer 8=24107
- earth's, quartz H variometer, setting rel. to mag. meridian 8=41459
- ellipsoidal specimen, internal field recording method 8=46372
- gradient meter, advantages 8=41936
- Hall effect high stability probe system 8=28510
- Hall effect probes with diameters ≤ 1 mm, for axial mag. fields at cryogenic temps. 8=24031
- Hall-effect sondes, construction of suitable electromagnet 8=33041
- Hall probe, microminiature for use in liq. He 8=28509
- Lorentz microscopy, contrast linked to relief in ferromagnetic films 8=45002
- Lorentz microscopy of weak flux inhomogeneities 8=36132
- magnetometer, employing turbine 8=33043
- magnetometer, nuclear, with remote control 8=46369
- magnetometers in satellites, magnetodynamically induced ambiguities 8=36904/5
- proton-resonance automatic calibrator 8=37382
- pulsed distrib. determ. by low voltage capacitor bank 8=33044
- quartz H magnetometer readings, humidity effects 8=41458
- r.f., amplitude meas. by e.p.r. in effective field 8=46366
- size-dependent oscillatory magnetoresistance appl. 8=28517
- spinner magnetometer static charge elimination 8=50231
- static fields, inhomogeneous, several meas. devices 8=33045
- sunspots and pores, spectrography 8=32598
- superconducting loop magnetometer 8=28511
- superconducting magnet. by magnetoresistor 8=41938
- superconducting persistent current magnetometer 8=31355
- superconducting quantum interference device, shielding 8=31349
- n-InSb magnetoresistance probe at liquid He temp. 8=46371
- InSb magnetoresistive sensor for He temps. 8=46367

Magnetic fields
- See also Earth/magnetic field; Electromagnetic fields; Interplanetary magnetic fields; Sun/magnetism.
- absorption line form., anomalous dispersion 8=29570
- analogue of cyclotron central elec. field config. 8=46999
- axially symmetric, conducting ring interaction, induced voltage 8=47829
- of cable, submerged peculiarities rel. to geoelec. variations 8=36680
- confined, boundary layer with warm, streaming plasma 8=34520-1
- confinement by beam of ions 8=36822/3
- constant uniform, effect on e.m. wave scatt. by free electron 8=24726
- of coil, calculation by Kantorovich method 8=28518
- computer calc. of 3-dimens. fields of arbitrary current geometry 8=28515
- cylinders and annular shims, second-order approximation 8=33040
- dipole and quadrupole planar, produced by line currents 8=46393
- distribution in knot of 3-ph. core of cold rolled steel sheet 8=46377
- distribution in layers of sheets with mutually perpendicular rolling direction in knot of 3-ph core, at 90° 8=46378

Magnetic fields—contd
distribution inside cylinder with temp. depend. conductance in const. longit. elec. field 8=41946
electron clouds in mag. fields, electrostatic equilibrium 8=33074
in ferromagnetic sheet under alternating magnetiz., flux distrib. and waveform 8=28516
ferromagnetic susbts., nuclei of impurity atoms 8=40760
film, distrib. determ. technique, comments 8=46389
forces on conductors and field energy in 2-dimens. fields 8=28514
Heaviside formulae connection with relativity 8=46347
homogeneity meas. and control 8=46374
homogeneous, spectral line form. theory 8=43250
implosive megagauss field prod., travelling wave nature 8=24109
inhomogeneous, pole face profile calc. 8=33042
interaction with micro-elastic wave motion, in conducting medium 8=46154
kinetic eqn. for inhomogeneous plasma 8=43502
leakage into semi-infinite pipe, calc. 8=37383
long horiz. line source above ground 8=24242
mathematical models and computer soln., book 8=33054
megagauss, Faraday rot, meas. 8=46683
m. h. d. generator, electrodynamic effects of non-uniformity of mag. field and fluid parameters 8=28468
min. $\bar{B}$ field, equivalent potential and other props 8=46473
near-zone mag. field of small circular-loop antenna 8=46493
planetary, as test of dynamo theory 8=50405
plasma, annihilation and turbulent heating 8=34467
poloidal, in rotating stars 8=41500
prod. by plasma compression 8=30125
production in cavity undergoing compression 8=46394
pulse production for up to 80 kG intensity and appl. 8=36021
pulsed, Z-pinch flux compression to 3 MG 8=28532
pulsing, radar modulator techniques 8=46368
reduction by superconducting volume expansion 8=28513
resistivity meas. in megagauss fields, method 8=24066
scaling laws for large shields in quasi-stationary fields 8=46375
small uniform, prod. by current loops 8=28512
solenoid, maximum attainable field, calc. 8=37384
spherical multipole as plasma mag. trap 8=47868
static non-uniform, focusing props. 8=28540
sunspot group, Evershed effect 8=32596
superconducting coils, meas. techniques 8=37396
toroidal, negative V^{11} system and its equilibrium 8=47869
travelling, interact. with rigid conducting spheres or cylinders 8=24108
two dimensional problems, solution by boundary relaxation 8=45994
two-dimensional, with rectangular boundaries, solution 8=46376
ultra-quantum, kinetic coeffs. theory 8=35737
uniform, quantum mechanics of charged particle 8=42328
uniform transverse, winding optimization 8=28524
vertical dipole above a two-layered medium 8=50120
Mn^{2+} nuclei, effective, covalency effect 8=40739
Mn^{2+} nuclei in glasses, hyperfine splitting rel. to covalency estimate 8=48304
Pb-Bi alloys, superconducting, spatial distrib. 8=40381
effects
air, laser-induced breakdown and spark emission, 210 kG 8=29925
alternating field on convective heat transfer during turbulent flow of cond. liq. in channel 8=41994
anthracene, blue fluorescence from triplet-exciton interaction 8=41223
anthracene, photoconductivity 8=27336
antiferromagnets, in external field, non-linear spin waves 8=40856
on aqueous solns., metastable formations as crystallization centres 8=34776
arc at atmos. pressure 8=38983
arc, electric, wall-stabilized, with transverse field, field flow theory 8=39007
arc, electric, wall-stabilized, with transverse field, adjustable characts. 8=39008
p-azoxyanisol, liq.-crystal, on X-ray structural exam. 8=39309
Bloch electron motion in external field, classical and quantum dynamics 8=26875
on breakdown localization in p-n junctions, longit. and transverse fields 8=27153
on cholesteric liq. crystal struct. 8=34768
cholesteric liquid crystals, structure distortion 8=30407
crystal electrons, relativistic and spin effects 8=44624
drifting plasma, wave propag. 8=30149
electron diffusion, theory 8=24138
on excitonic insulator 8=40261
F-centres, shallow, in ionic cryst., rel. to theory 8=44470
ferromagnetic alloy, on martensitic transform. 8=35109
ferromagnetic discs, rotating in alternating and direct fields, energy losses 8=36102
ferromagnetic shells, uniform screening to obtain uniform field 8=37379

Magnetic fields—contd
effects—contd
films uniaxial-anisotropy relax. process excitation by rotating mag. anneal 8=31581
gas-discharged plasma, resonance in mag. field 8=39128
gas, thermomagnetic effect, obs. 8=39227
growing surface waves in semicond. in presence of transverse mag. field 8=35868
heat transfer intensification 8=41857
ions in cryst. fields, induced quadrupole splitting 8=43939
lateral and transverse, for suppression and crossed-field beam noise 8=24139
magnetism, in high fields 8=31478
on magnetodynamic shock waves, device for obs. 8=23942
magnetoelasticity and magneto-thermoelasticity 8=28278
magnetoplasma propag. 11 to field, Fermi liquid interactions 8=40271
Mössbauer spectrum, prod. of r. f. acoustic sidebands 8=39513
motion of anisotropic crystal in rotating field 8=30435
naphthacene, fluorescence 8=41226
paraffin, liquid, n.m.r. in rotating field 8=25958
parallel, rel. to stability of Hartmann boundary layer 8=41988
piezo-electric, semi-infinite rod in magnetic field longitudinal disturbances 8=40625
plasma, avalanche semiconductor, rel. to hole wave instabilities 8=35797
plasma column, hollow, rel. to helical instability 8=30175
plasma, cylindrical electron-hole, behaviour 8=35799
plasma instabilities due to two-lumped electron vel. distrib., computer expt. 8=30173
plasma jet, current sheet meas. on field interaction 8=39145
in plasma, linear waves, quasi electrostatic, low freq. 8=30156
plasma, spectral line Stark broadening 8=25340
plasma, streaming, transverse field strength rel. to e penetration 8=30022
plasma, weakly ionized, in time-depend. field, electron distrib. function 8=43520
polaron, energy spectrum changes 8=40268
saddle point optical transitions under crossed elec. and mag. fields 8=27543
scalloping of compressed e beams 8=46405
semiconductors, quantizing fields, negative conductivity 8=49403
semiconductors, thermogalvanomagnetic phenomena 8=44751
spin echo signal formation by simultaneous action of local elec. and mag. fields 8=40881
stars, single and multiple, effect on formation 8=50294
steel, martensitic transformation 8=39554
steel, stainless, austenitic, on phse transforms. 8=39553
superconducting alloys, dil. mag., behaviour 8=27004
superconducting ring, current attenuation in alternating field, obs. 8=44704
superconductors, type I, elect. field obs. in presence of quasistatic magnetic field 8=26991
ticonal, structure formation after themomagnetic treatment 8=35055
toroidal, l.f. instabilities in multiple plasma machine 8=39140
transistor, alloy junction, diffusion of minority carriers in base region 8=27196
transverse alternating, rel. to quadratic response of intermediate state 8=35835
triplet excitons, mutual annihilation 8=40260
viscous flow of gases in strong fields 8=34619
Al, Righi-Leduc effect in high fields 8=40727
on ArII pulse laser, output enhancement and quenching 8=28674
Au_2Mn, antiferromagnet, magneto-striction at high field 8=31754
Bi, longit., rel. to transverse voltage 8=35825
Bi, reluctance anisotropy at 77°K 8=40729
Bi-Sb alloys, large changes in seebeck coeff. 8=44905
C arc, magnetized, l.f. oscills 8=25779
C, glassy, on susceptibility 8=44966
$Cd^{111,114}$, 2288Å emission polarization 8=34158
Co^{57} Mössbauer effect sources mag., r.f. field destruction of hyperfine Mössbauer spectrum 8=43945
Cr, mag. props., n. -diffr. exam. 8=31766
Cu_2O, on exciton quadrupole transitions 8=31984
$CuSO_4 . 5H_2O$, ht. capacity and mag. moment, 0.4°-4.2°K 8=39915
$CuSO_4 . 5H_2O$, thermodynamic props., 4°K 8=39914
Fe-N solid solns, on elec. resistivity at 4.2 °K 8=31319
Fe-Si, magnetization curve and energy losses in alt., effect of dislocations 8=36142
Gd, electrons, field-emitted, polarization 8=27342
n-Ge in pulsed fields, photomagnetoelec. effect 8=36021
Ge p-i-p diode negative resist., 77°K 8=40530
Ge tunnel diodes, rel. to reverse current, oscillatory behaviour 8=27189
H arc in axial parallel mag. field 8=43467-8
H_2, breakdown electric, formative time in strong crossed fields 8=29903
He II, enhancement of λ4686 line 8=34132

Magnetic fields—contd
effects—contd
He-3, vapour pressure increase at 3°K 8=28433
Hg flow, travelling field induced, obs 8=24180
n-InAs, magnetophonon oscillations in longitudinal thermoelec. power 8=27308
InSb, on impact ionization rates and instabilities 8=31303
n-InSb, rel. to impurity states 8=49250
NO-N_2 mixture, diffusion 8=30316
Ni steel phase transforms 8=30702
Ni, strongly deformed, onset of uniaxial anisotropy after mag. annealing 8=36216
Ni-Cu and Ni, var. of thermal cond. in mag. field 8=45022
Ni-Fe, electrolytically prepared, conditions for formation of hexagonal structure 8=26122
α $NiSO_4.6H_2O$, magnetothermodynamics, theory 8=39920
$O^{16}O^{18}$-O_2^{16} mixture, diffusion 8=30316
O, sound absorption 8=39210
O_2 thermal cond., field gradient depend., obs. 8=39199
on Si avalanche diode, effects on oscillation 8=27185
YFe garnet, h.f., rel. to para process near Curie point 8=49566
Magnetic films
betatron, inhomogeneities calc. and correction 8=37823
characteristics, local static and pulse, Kerr effect apparatus 8=49513
coercivity as function of temp., app. for automatic and continuous recording 8=31583
coupled, device for associative memories 8=36121
coupled, transverse initial susceptibilities 8=45003
domain struct., hysteresis and magnetooptical effects, teaching demonstration 8=27397
domain structure and reversal mechanisms, electro- and magneto-optical obs. 8=36107
epitaxial growth of ferrites on metal oxides 8=35175
evaporated, perpendicular, anisotropy 8=36108
ferromagnetic and superconducting, proximity effect 8=27008
ferromagnetic, anisotropy of localized sections rel. to pulse switching, obs. 8=31580
ferromagnetic, band structure 8=36117
ferromagnetic, contrast linked to relief in Lorentz microscopy 8=45002
ferromagnetic, Curie temp. thickness depend., spin-wave theory 8=31576
ferromagnetic, density of states formulae in band theory generalization 8=31592
ferromagnetic, domain-propagation technique 8=36126
ferromagnetic, in microwave cavity, uniform mode growth mechanism 8=36220
ferromagnetic, mag. domains individually obs. by e-microscope 8=31586
ferromagnetic, magnetization, thickness-, anisotropy- and temp.-dependence 8=36116
ferromag. magnetization, walls, Bloch, Neel and intermediate 8=36106
ferromagnetic Néel wall energy 8=31574
ferromagnetic, Néel wall structure model 8=31584
ferromagnetic, 180° domain wall energy densities 8=45018
ferromagnetic, partial switching in rot. field 8=31572
ferromagnetic, plane Hall effect optimization 8=44681
ferromagnetic, pulse switching, noise subtraction circuit for gated oscillograph c.r.o 8=31575
ferromag. reson. rel. to mag. params., obs 8=31807
ferromag., surface waves in spin-wave resonance, theory 8=45068
ferromagnetic resonance, l.f., anharmonicity for transversely magnetized film 8=40883
ferromagnetic, single-crystal, transverse susceptibility 8=36127
ferromagnetic, standing spin waves 8=49510
ferromagnetic strips-conductor sandwich, switching processes, obs. 8=31579
ferromagnetic, theory of spin wave resonance 8=31808
ferromagnetic uniaxially anisotropic, magnetization axis rotation under external stress 8=36131
ferromagnetic, with domain structure, spin waves 8=40798
holograms appls., recording and reconstruction 8=33294
hysteresis loops obtained from transverse Kerr effect, azimuth variation effect 8=40786
interaction effects 8=36130
Lorentz microscopy, electron beam coherence and micrograph interpretation 8=33090
Lorentz microscopy, high-resolution 8=36128
Lorentz microscopy of weak flux inhomogeneities 8=36132
magnetization increments near saturation rel. to anisotrpy dispersion, obs. 8=31578
magnetization ripple, linear and nonlinear theories 8=36109
magnetoelastic oscillations, coupled, mag. and acoustic excitation 8=31582
magneto-optic effect, longitudinal Kerr, in multilayer structs. 8=41045
magneto-optic readout, amplitude-modulated 8=36122
for magneto-optic readout using media modulation 8=40799
metallic, magnetoelastic waves, boundary-value-problem 8=40797
Magnetic films—contd
moment subharmonic oscills. in rot. field 8=31573
multilayer, coupled wall configurations 8=36129
multilayer devices, magnetization reversal 8=36120
Permalloy, abnormal Bloch wall motion under hard axis nanosec. pulse drive 8=31668
Permalloy anisotropy and blocking fields rel. to r.f. losses, obs. 8=31678
permalloy, annealing kinetics and increasing S conc. 8=31222
Permalloy, coercive force and blocking field rel. to substrate temp., obs. 8=31676
permalloy, and coupled double layers with Fe-Ni-Mn, spin-wave resonance 8=31814
Permalloy, critical switching curves, obs. 8=31671
permalloy, cylindrical, annealed, bimodal state of magnetization 8=49540
permalloy, domain boundary dynamic props. 8=36167
permalloy, domain wall movement, thermally activated 8=45020
Permalloy, domain walls and mag. fine struct. in switching, stroboscopic transmission e microscope obs. 8=31674
Permalloy domains and coercive force in supercritical transition, obs. 8=31629
Permalloy, exchange stiffness constant by pulse switching technique 8=31686
Permalloy, ferromag. reson. and off-reson. suseptibility, obs. 8=31822
Permalloy, ferromag. reson. rel. to internal stresses, obs. 8=31821
permalloy, flash evaporated, for investigation of spin-wave resonance 8=31809
permalloy/Gd/Co-permalloy triple layers, spin-wave resonance temp. dependence, 100-400°K 8=31816
permalloy, induced uniaxial anisotropy on n.- and Ar^+ bombardment 8=31694
Permalloy, internal isotropic stresses and demagnetizing factors, ferromag. reson. obs. 8=31223
permalloy, in contact with FeNiMn or Gd, spin-wave resonance obs. 8=31681
permalloy, domain boundary energy meas. rel. to thickness 8=40826
permalloy, mag-moment motion in h.f. rotating field 8=36157
Permalloy, mag. struct. stability in pulsed orthogonal fields, obs. 8=31691
permalloy, memories, keepered and nonkeepered, internal field distrib. 8=40820
Permalloy, narrow strips for meas. of domain wall energy 8=27420
permalloy, 1000Å, Néel wall structure and energy 8=31663
Permalloy, pulse switching, induction and magneto-optical meas. comparison 8=31688
Permalloy, pulse switching rate, −180-250°C 8=31675
Permalloy 78, demag. rel. to alternating field freq., obs. 8=31692
Permalloy spots nucleation, struct. and field rel. to dimensions, obs. 8=31673
permalloy stripe-films, domain structure 8=31693
permalloy, supercritical, domain structure, theory 8=31684
permalloy, susceptibility at 5000 Hz, easy and hard directions 8=36110
permalloy, 360° walls and strong stripe domains 8=45024
Permalloy, uniaxial anisotropy, mag. annealing effects, 20-400°C 8=31677
permalloy, wall streaming obs. 8=31558
polycrystalline, susceptibility and ripple 8=36118
ripple relax. times, models 8=36119
rotational initial susceptibility mechanisms 8=31577
saturation magnetization, ferro-, thin 8=36113
sharp film NDRO bit organized memory 8=36124
spin wave resonance 8=36114
spin waves, theorems and tables 8=49512
storage-elements, controlled easy-axis distrib. 8=49511
strain-sensitive ferromag., for sonic film memory 8=36125
superparamagnetic effects ferromag., thin 8=36112
switching process 8=36115
thin ferromag., Bloch wall transitions 8=31589
thin ferromag. coupling effects through nonmag. interlayer 8=31588
thin ferromag., domain obs. by transmission e mic. 8=31590
thin ferromag., spin-wave theory and expt. 8=31591
thin ferromag., stationary spin-wave excitation 8=31587
thin, magnetization and field distrib. determ. technique, comments 8=46389
thin multiple, oscillating hysteresis losses 8=31585
transition layers between domains 8=31555
two-layer, Néel bonding energy interlayer thickness dependence 8=45004
uniaxial-anisotropy relax. process excitation by rotating mag. anneal. 8=31581
Co alloys, ferromag, epitaxial growth on LiF and MgO 8=35170
Co, domains and coercive force in supercritical transition, obs. 8=31629
Co, domains and fine structure form., e microscope obs. 8=31640

Magnetic films—contd
  Co, epitaxial, anisotropy constant 8=31631
  Co ferromag., in Co-Co oxide-Al device, rel. to anomalous tunneling 8=31422
  Co, ferromag., planar Hall effect, thickness (100-1500Å) and temp. (77-293°K) dependence 8=31687
  Co, galvanomagnetic effects and domain struct. rel. to thickness, 200-2000Å 8=31598
  Co, high-coercivity, magneto-optic domain obs. 8=36134
  Co, Kerr effect and application to hysteresis loop plotter 8=45007
  Co, magneto-optic and mag. props. 8=32018
  Co, single-cryst., epitaxial growth on LiF and MgO 8=35170
  Co-CoO, separated by Pd film, magnetization coupling 8=36133
  Co-Ni domains and fine structure form., e microscope obs. 8=31640
  Cu-Ni film thermocouple for substrate temp. meas. 8=31676
  Co-Ni-Fe, critical thickness and coercivity 8=27400
  Co-Ni-Fe, stress, production parameter dependence 8=31192
  Co-P, coercivity rel. to substructure 8=27402
  Cr, antiferro-paramag. transition rel. to resistivitv 8=39590
  EuO, ferromagnetic, transverse Kerr magneto-optical effect 8=31987
  EuO memory medium in low temp. laser-beam addressable memory 8=36123
  Fe alloys, ferromag., epitaxial growth on LiF and MgO 8=35170
  Fe, anisotropy from Mossbauer meas. 8=31641
  Fe, domains and coercive force in supercritical transition obs. 8=31629
  Fe, domains and fine structure form., e microscope obs. 8=31640
  Fe, epitaxial, anisotropy constant 8=31631
  Fe, ferromag., planar Hall effect, thickness (100-1500Å) and temp. (77-293°K) dependence 8=31687
  Fe ferromag., in Fe-Fe oxide-Al device, rel. to anomalous tunneling 8=31422
  Fe, single-cryst., epitaxial growth on LiF and MgO 8=35170
  Fe, Richter-type aftereffect 8=31633
  Fe-Cr, exchange constants from spin-wave resonance spectra 8=36147
  Fe-Ni domains and fine structure form., e microscope obs. 8=31640
  Fe-Ni, exchange stiffness const. 8=49522
  Fe-Ni, switching along easy axis above nonuniform, rot. threshold field 8=31630
  Fe-Ni-Co, anisotropy. coercive force and s.h.j. reson. absorpt. obs. 8=31629
  Fe-Ni-Co, anisotropy, review 8=36148
  Fe-Ni-Co, single cryst. anisotropy, domains and saturation magnetization, obs. 8=40809
  FeNi, electrodeposited, mag. switching behaviour 8=27419
  FeNi electrodeposited, magnetization reversal obs. 8=31644
  FeNi-FeNiMn, separated by Pd film, magnetization coupling 8=36133
  Gd-Permalloy, antiparallel exchange coupling 8=40816
  Gd/permalloy double layers, spin-wave resonance temp. dependence, 100 400°K 8=31816
  Mg-Mn ferrite, FMR, thermal treatment effects 8=31817
  Mn ferrites epitaxially grown on MgO, prep. methods 8=35175
  MnBi, props. rel. to memory appls. 8=49531
  $MnFe_2O_4$, single-cryst., pulse switching and static characts., obs. 8=31730
  Nb_3Sn superconducting ribbons, vapor-deposition rel. to e.m. performance 8=40418
  Nb_3Sn strip superconductor, plasma-plated, critical current angular dependence 8=40420
  $NdCo_5$ and Nd_2Co_{17}, magneto-optic and mag. props. 8=32018
  Ni alloys, ferromag.. epitaxial growth on LiF and MgO 8=35170
  Ni, domains and fine structure form., e microscope obs. 8=31640
  Ni, electrodeposited, and charged with H, effect of H on magnetization inversion 8=36170
  Ni, epitaxial, anisotropy constant 8=31631
  Ni ferrite, structural properties and ferromag. resonance 8=36192
  Ni ferromag., in Ni-Ni oxide-Al device, rel. to anomalous tunneling 8=31422
  Ni, ferromag., planar Hall effect, thickness (100-1500Å) and temp. (77-293°K) dependence 8=31687
  Ni, ferromag. reson. rel. to internal stresses and magnetization inhomogeneity, obs. 8=31821
  Ni films, oscillating hysteresis 8=45021
  Ni-magneto-optical parameter temp. dependence, 20-400°C 8=36398
  Ni, p-bombardment effects on mag. props. at 850 keV 8=36168
  Ni, single-cryst., epitaxial growth on LiF and MgO 8=35170
  Ni, ultrasound from stripe domain resonance 8=31682
  Ni, u. v. reflection, near Curie point 8=36399
  Ni-Fe alloy, domain-wall motion and ferromagnetic resonance losses 8=31695
  Ni-Fe alloy, spin-wave spectra, linewidth and relax. processes for main resonance 8=40887
  Ni-Fe, anisotropy dispersion, temp. depend. 8=40821
  Ni-Fe, electrochem. deposited, coercive force, obs. 8=31672
  Ni-Fe, ferromag., planar Hall effect, thickness (100-1500Å) and temp. (77-293°K) dependence 8=31687
  Ni-Fe, ferromagnetic, thick, domain-wall width determ. by Lorentz microscopy 8=27422
  Ni-Fe films, single and double, reversible rotation regions, obs. 8=31690
  Ni-Fe, magnetization, static reversal, effect of anisotropy dispersion 8=36155
  Ni-Fe, magnetoelastic sensitivity, composition gradient effect 8=36111
  Ni-Fe, magnetoresist. and resist. studies 8=44695
  Ni-Fe, polycrystalline alloy, anisotropy induced during evaporation and annealing 8=36152
  Ni-Fe, polycrystalline, susceptibility strain-dependence 8=40824
  Ni-Fe, ripple-comp.- meas. temp.- and substrate temp.-dependence 8=36159
  Ni-Fe, s. h. f. susceptibility, < 30 Oe 8=31689
  Ni-Fe, stress, production parameter dependence 8=31192
  76%Ni-Fe, type II stripe domains, obs. 8=40825
  Ni-Fe-Al films, single and double, reversible rotation regions, obs. 8=31690
  Ni-Fe-Co films, single and double, reversible rotation regions, obs. 8=31690
  Ni-Fe-Co, s. h. f. susceptibility, < 30 Oe 8=31689
  NiFe, coupled, domain wall behaviour 8=49541
  48 Ni/52Fe (111), epitaxial, ferromag; flat, of few atomic layers 8=36166
  NiFe, sputtered, reduced sensitivity to impurities by neg. bias appl. during deposition 8=31679
  NiFe, 2-200Å, magnetization anomalies rel. to surface anisotropy 8=36158
  NiFeCo, props., effect of Cu layer 8=40822
  $NiFe_2O_4$, ferromag. resonance thickness dependence 8=31823
  $NiFeS_x$ electrodeposited rel. to vacuum deposited 8=35177
  Ni-NiO, separated by Pd film, magnetization coupling 8=36133
  Ni-P, Hall effect obs. 8=26970
  Pb, epitaxially grown on PbTe, domain structure from Lorentz microscopy 8=36171
  Pb, parallel and perpendicular transitions, temp. (1-4.2°K) and thickness dependence 8=40741
  Sn, parallel and perpendicular transitions, temp. (1°K-T_c) and thickness dependence 8=40741
Magnetic flux. See Magnetic field measurement; Magnetic fields.
Magnetic hysteresis. See Magnetization process.
Magnetic lenses. See Electron lenses/magnetic; Ion optics.
Magnetic materials
  alloy, dilute, Green's function theory of Kondo effect 8=31263
  alloys, dilute, singlet-triplet formulation, s-d exchange and Anderson models 8=27369-70
  alnico, high-coercivity, powder pattern exam. 8=35346
  antiferromagnetic dielectrics, near phase transition of second kind 8=36301
  birefringence, gyrotropic, phenomenological theory 8=36303
  ceramics, structure rel. to ferrimagnetism, review 8=49554
  commercial, prep and permanent magnet props. 8=46380
  congress, international, USA (1967) 8=27368
  crystals, Faraday rotation, origin and uses 8=36306
  exchange enhanced susceptibility, effect of spin-flip scattering 8=40747
  ferromagnet in two-phase mixture, mag. oscills. damping and dispersion 8=40600
  ferromagnetic alloy, martensitic transform. mag. field effects 8=35109
  ferromagnetic binary alloys, vapour pressure temp. dependence rel. to mag. and structural transitions 8=35014
  ferromagnetic dielectrics, near phase transition of second kind 8=36301
  ferromagnetic, magnetization direction distributions around spherical cavity 8=40757-8
  ferromagnetic, polarization of emitted photo-electrons 8=40701
  ferromagnets, lattice structure determ. using micro. e.-diffr. technique 8=39761
  Hyhro Radio metal, development, props. and appls. 8=27387
  light absorpt. and scattering in crystals 8=36297
  magnetism, in high magnetic fields 8=31478
  magnetostricture, dynamic properties and applns. 8=49452
  Mumetal, permeability temp. vars. stabilization and appls. 8=27387
  paramagnetic crystals, proton spinlattice relax. in high fields and low temps. 8=31889

Magnetic materials—contd

- properties. book 8=49459
- Satmumetal, development, props. and appls. 8=27387
- superconducting, shielding for He^3 nucleus elec. moment meas. 8=29000
- theoretical applications. properties 8=49460
- thermodynamic props., shape dependence 8=44326
- 3d ferromagnets, giant spontaneous Hall effect 8=31562
- $BaFe_{12}O_{19}$, as permanent magnet materials 8=36184
- Fe-Ni alloy, ferromag., plane Hall effect 8=40324
- Fe–50Ni alloys, fibre-reinforced, mag. and mech. props. 8=31209
- Fe–1.35Si alloys, fibre-reinforced, mag. and mech. props. 8=31209
- Ni, creep near Curie pt., rel. to stacking fault energy 8=35710
- Ni, ferromag., plane Hall effect 8=40324
- Ni-Fe alloys, high-permeability, classification by props. 8=31662

Magnetic measurement

See also Magnetic field measurement. Entries describing measurement methods for specific magnetic quantities and effects may also by found listed under the various headings for the subjects concerned.

- anisotropy and field dependence, induction meas. method 8=31560
- anisotropy, low-temp. torque balance 8=31723
- balance electrodynamic, for meas. magnetic anisotropies of single crystals 8=40721
- core loss at high mag. flux density 8=46365
- crystallographic texture analysis. instruments 8=48579
- ferromagnets. cylindrical, anisotropic field and position of easy magnetization axis, meas. methods 8=40785
- gradient meter, advantages 8=41936
- induction of hard mag. materials 8=46379
- magnetometer, torque, elec. microbalance 8=37381
- magnetostriction, ferro- and ferrimagnetics, low-temp. supercond. solenoid appl. 8=45000
- pulsed field magnetization, apparatus 8=46362
- relaxation time of paramagnetic materials using optical Faraday rotation technique 8=49479
- reluctance technique for liq. film thickness 8=39287
- static-characteristics of ferrous materials, equipment 8=46363
- static susceptibility, by e.p.r. line broadening 8=46508
- susceptibility, direct-reading bridge for soil samples 8=37380

Magnetic memories. See Calculating apparatus; Magnetic devices

Magnetic mirrors. See Magnetic fields; Plasma/confinement.

Magnetic properties of substances

See also Magnetic films.

- actinide cpds, susceptibility and elec. meas. rel. to ordering 8=27234
- actinide cpds, susceptibility at low temps. 8=49348
- alloy. dil., neg. magnetoresistivity calcs. from s-d exchange 8=40723
- alloys, dilute, electronic correlation effect variational treatment 8=26892
- alloys, dilute, Kondo effect, Takano-Ogawa theory exam. and mag. susceptibility calc. 8=44956
- alloys, dilute, low temp. exchange interactions uniquely defined by logarithmic accuracy 8=31492
- alloys, dilute, rel. to electronic structure 8=31270
- alloys, dilute, superconductivity below Kondo temp., Nagaoka's model 8=26988
- alloys, dilute with impurities scattering problem 8=31271
- alloys, nuclear indirect exchange and pseudodipolar interactions by spin-echoes 8=36068
- anisotropy defects, impurities and ripples 8=49454
- anisotropy rel. to dynamical Jahn-Teller effect 8=36234
- anisotropy, states of theories 8=31479
- band structure, model calculations 8=26894
- coal, 7 types; susceptibilities obs. in magnetic fields parallel, perpendicular to bedding planes 8=49478
- composite materials, permeability 8=26939
- congress, international, USA (1967) 8=27368
- critical points, ultrasonic attenuation and e.s.r. linewidth near 8=30939
- crystalline internal mag. fields, Shubnikov group representation 8=27375
- crystals, single, mag. anisotropies meas. by balance 8=40721
- cut-off of extragalactic protons in galactic disc 8=45739
- diluted systems, hyperfine field distrib. calcs. 8=31486
- films, metallic 8=49461
- formaldehyde, molec. susceptibility tensor 8=29784
- gas, spin diff., mag. field effect 8=43698
- gas thermomagnetic effect of applying modulating field 8=39227
- h.c.p. crystals, susceptibility component meas. rel. to arbitrary orientation 8=49450
- impurities in superconductors, appearance of local bound states 8=44710
- impurities, rel. to resistivity anomaly, effect of ordinary scatt. 8=44673
- intermediate state, quadratic response (or susceptibility) to transverse alt. mag. field 8=35835
- isotope shifts temp. dependence and phonon-induced zero-field splitting 8=49451

Magnetic properties of substances—contd

- kinetic coeffs. in ultra-quantum field, theory 8=35737
- liquid, volume susceptibility meas. 8=34904
- linear magnetic chain, diffuse collective mode 8=44995
- luminescence centres, inorganic, susceptibility and resons., meas. 8=41178
- magnetoplumbite, Bitter patterns rel. to changes in width and domain shape 8=31557
- magnetostatic wave propag. at singular turning points, effect of finite linewidth 8=27372
- Malcalloy (Co-Al) alloy, effect of Mn additions 8=36071
- Malcalloy (Co-Al alloy), effect of W additions 8=36070
- Malcalloy, magnetic alloy, (in Co–Al system), Cr additions rel. to props. 8=31602
- materials, book 8=49459
- metal: dilute-magnetic-ion system, localized magnetic moments study 8=27459
- metal, impurities rel. to methods of approaching Kondo's problem 8=35816
- metals, breakdown, de Haas-Van Alphen effect and osc. periods 8=40725
- metals. conditions of existence for localized moment 8=44957
- metals. effective mag. field seen by one electron 8=40722
- metals, local moments 8=44963
- metals, mag. moments in strong fields, charact. props. 8=44962
- metals, IB. IIB groups, susceptibility 8=49466
- metals with impurities, rel. to electronic structure 8=31270
- metals with impurities, scattering problem 8=31271
- metals with mag. impurity, ordinary scattering rel. to exchange scattering 8=26863
- metals with paramag. impurity, form. of localized mag. moment 8=31519
- mineral, anomalously magnetic, thermal changes 8=31595
- Mössbauer absorption spectra of magnetically ordered systems rel. to spin relax. 8=43940
- noble metal-rare earth, susceptibility meas. rel. to local moments 8=31882
- Onsager reaction field, mol. field theory and spherical model 8=32826
- pyridine Cu(II) chlorobenzoates 8=36072
- pyrite dichalocogenide cpds. 8=31493
- quartz, non-linearities and isochronism defect 8=27301
- rare-earth-cobalt cpds, R_xCo_y, comp. dependence 8=31506
- rare earth cpds, low-lying crystal-field spectra 8=36296
- rare earth cpds, susceptibility and elec. meas. rel. to ordering 8=27234
- rare earth cpds, susceptibility at low temps. 8=49348
- rare-earth cpds with singlet crystal-field ground state, collective excitations and mag. ordering 8=44964
- rare-earth hydroxides 8=31507
- rare-earth metal impurities in noble metals rel. to electron transport of dil. alloy 8=31316
- rare-earth metals, mag. anisotropies 8=31505
- rare-earth-nickel cpds, R_xNi_y, comp. dependence 8=31506
- rare-earth orthoferrites, in anisotropy change region 8=31793
- rare-earth perovskites, ordering between 1.2° and 5°K 8=39921
- rare-earth-Th alloys, f.c.c., Th effect in ordering 8=36218
- rare-earth-transition-metal cpds., electron moment, itinerant, in cubic Laves phase 8=49473
- rare earths, heavy, generalized susceptibilities and mag. ordering 8=44973
- rare-earths, structure, ferroelectric props. 8=40619
- rubeanato-Cu co-ord. polymer, cryst. compared with amorphous 8=27385
- selenospinels, binary, rel. to misibility studies 8=30653
- semiconductors, wurtzite type. mag. levels in valence band 8=49094
- space groups and their irreducible representation 8=31488
- spectra, sharp, of magnetic ions, magnon effects 8=27373
- spectroscopy, far-i.r., techniques, mag. ion spectra and magnon absorpt. in antiferromagnets 8=36294
- steel, transformer, annealing effects at high-temp and vacuum 8=35107
- sulphospinels, binary, rel. to misibility studies 8=30653
- susceptibility, complex, effect of mag. diffusion after-effect and logarithmic distrib. of time consts. 8=49549
- susceptibility, nonlinear, diagrammatic approach 8=48297
- systems with dipole interactions, thermodynamic props. shape-dependence 8=44329
- transition metal alloys, dynamic susceptibilities 8=31491
- transition metal alloys, local moments, statements from macroscopic meas. 8=31509
- transition metal arsenides 8=41079
- transition metal carbides, nitrides and oxides, M-M interaction effects 8=26441
- transition metals. nearly ferromag., spin fluctuations effect on susceptibility 8=44992
- AgMn films, evaporation prod., conc. depend. 8=40802
- $Al_2O_3 : V^{3+}$, anisotropy meas. 1.5-5.0°K rel. to g factor and zero-field splitting 8=44965
- Au-Fe alloys, hyperfine coupling constants from nuclear sp. hts. down to 0.02°K 8=31495
- BF molecule, Hartree-Fock calc. 8=25447
- BH molecule, Hartree-Fock calc. 8=25447

Magnetic properties of substances—contd
Bi, reluctance anisotropy mag. field dependence at 77°K 8=40729
Ca manganates, rel. to comp. and lattice geometries 8=31757
CdSb: (Mn, Fe, Ni and La), susceptibility, temp. depend. 8=49464
α, β, Ce, susceptibility above magnetic ordering temp., temp. depend. 8=40750
CeSb, magnetic state phase diagram 8=49465
Co films, and magneto-optic props. 8=32018
Co solid solution with P, moment rel. to P content 8=45006
Co^{2+} in fluoride salts, ordering effects on optical-absorpt. transitions 8=36350
Co_5(rare-earth) high-coercive force mat., domain-boundary model 8=31500
$Co_2BaFe_{16}O_{27}$ crystals, energy anisotropy constants and temp. dependence, 20-500°C 8=40732
Co-Rh alloys, enhanced susceptibilities and n.m.r. relax. rates 8=31499
Cr binuclear complex cpds., biquadratic exchange interaction 8=49467
Cr-Mo(W) alloys, T_N comp. -dependence, from resistivity meas. 4-325°K 8=31763
Cs_3CoCl_5, and optical and e.p.r. props. 8=31501
Cs_3ZnCl_5: Co^{2+}, and optical and e.p.r. props. 8=31501
Cu acetate monohydrate, rel. to optical behaviour 8=36434
Cu alloys, dil., mag. impurity problem, ground state, rel. to NMR meas. 8=45116
Cu-Al, susceptibility of dilute solutions of Fe 8=27403
$CuCr_{1+x}Rh_{1-x}Se_4$, $-1 < x \leq 1$, and electrical conduction 8=31609
$CuCr_2Se_xS_{4-x}$ solid solution 8=40733
$CuCr_{1+x}Ti_{1-x}S_4$, $0 < x \leq 1$, and electrical conduction 8=31609
$CuCr_{1+x}Ti_{1-x}S_4$, $0 \leq x \leq 1$, and electrical conduction 8=31609
$CuSO_4.5H_2O$, mag. moment in mag. field at 0.4°-4.2°K 8=39915
$CuSO_4.5H_2O$, 4°K 8=39914
Dy, generalized susceptibilities and mag. ordering 8=44973
$DyFe_2$, hyperfine field at Fe from Mössbauer effect 8=36146
Er, generalized susceptibilities and mag. ordering 8=44973
$ErFe_2$, hyperfine field at Fe from Mössbauer effect 8=36146
ErO_2S, and structures from n. diffr. meas. 8=40869
Eu-chalcogenide, anomalous props. 8=31268
Fe-Be, and Mossbauer effect 8=26024
FeF_3-FeF_2-MF, (M = Li, Na, K, Rb, Tl) system, of phases rel. to crystallog. classif. 8=48651
$Fe(NH_4SO_4)_2.6H_2O$, susceptibility and quadrupolar hyperfine anisotropy 8=43951
FeP, and thermodynamic props. 8=27378
Gd, generalized susceptibilities and mag. ordering 8=44973
Gd-Er alloys, magnetocrystalline anisotropy rel. to impurity contribution 8=44971
Gd-Ho alloys, magnetocrystalline anisotropy rel. to impurity contribution 8=44971
He^3-He II dilute soln., nuclear mag. susceptibility obs. 8=46306
HgTe, oscillations of longitudinal magnetic resistance in degenerate electron gas 8=40466
$HoCo_5$, structure and magnetocrystalline anisotropy 8=40737
$HoFe_2$, hyperfine field at Fe from Mössbauer effect 8=36146
In-Ce solid solns., localized moments from elec. meas. 8=31339
$(IrX_6)^{2-}$ complexes (X = F, Cl, Br) 8=49471
$KNiF_3$ and K_2NiF_4, ordered crystals, effect of electron-magnon interaction on Ni^{2+} absorption band 8=41127
La-Ce alloys, susceptibility above magnetic ordering temp., evidence for spin compensation 8=40750
$LaRu_2$: Gd^{+++}, susceptibility and e.p.r. study 8=31502
$LaTO_3$, (T = Ho, Y, Er, Tm, Yb, Lu) 8=48656
Lu, generalized susceptibilities and mag. ordering 8=44973
Mg-Cd alloys, susceptibility, effect of ordering 8=40321
MgO-MnO solid solns., and with LiO_2, susceptibilities 8=48662
Mg_2SnO_4-$MgFe_2O_4$, solid solutions, existence of magnetic fields 8=40738
$MnAs_{0\cdot 92}P_{0\cdot 08}$, polycrystalline, and crystallographic props. 8=31503
$Mn_{1-x}Fe_xP$ solid solutions, rel. to props. of FeP 8=27378
Mn-Sn alloys in liq. state, links in Curie-Weiss curves 8=36214
Na disilicate glass, with diffused Fe, susceptibility rel. to Fe content 8=27381
Nb films, sputtered cylindrical, flux jumping phenomena 8=49472
Nb, superconducting, anomalous behaviour 8=27383
Nb-Sb superconducting alloys, mag. hysteresis, at 4.2°K 8=27024

Magnetic properties of substances—contd
Nb_3Sn, hard supercond. tubes, flux jumps, 4.2°K 8=31341
Nb-Ti-Zr alloys, supercond., critical fields 8=35851
Nb-Zr, hard supercond. tubes, flux jumps, 4.2°K 8=31341
Nd^{3+} in ethyl sulphate lattice, anisotropy 8=43932
$NdCo_5$ and Nd_2Co_{17} films, and magneto-optic props. 8=32018
Ni, reversible magnetic susceptibility, dependence on temp. and stress 8=36154
NiO-MgO solid soln. 8=35061
α-$NiSO_4.6H_2O$, mag. moment, 0.4-4.2°K 8=30968
α $NiSO_4.6H_2O$, magnetothermodynamics, theory 8=39920
OCS, magnetic susceptibility anisotropy 8=25511
Pb films, epitaxially grown on PbTe, domain structure from Lorentz microscopy 8=36171
Pb-Bi alloys, superconducting, field spatial distrib. 8=40381
$Pb_{85}In_{15}$, exptl. demonstration, superconductivity 8=35855
Pd_3Fe alloy, hyperfine interaction constants from nuclear sp. hts, 0.15-1°K 8=31504
Pd-Fe alloys, hyperfine coupling constants from nuclear sp. hts. down to 0.02°K 8=31495
Pd-NO sorption systems 8=44075
Pd-Ni alloys, dynamic susceptibilities 8=31491
Pt_3Fe alloy, hyperfine interaction constants from nuclear sp. hts, 0.15-1°K 8=31504
$Pu(C_2O_4)_2.3H_2O$-$Th(C_2O_4)_2.2H_2O$, susceptibility 8=36073
$RbNiF_3$, exchange interactions exam. by n.m.r. 8=41001
$RbNiF_3$, ordered crystals, effect of electron-magnon interaction on Ni^{2+} absorption band 8=41127
$SmFe_2$, hyperfine field at Fe from Mössbauer effect 8=36146
Sn magnetic breakdown rel. to quantum oscills. in thermo-electric e.m.f. 8=40643
Sn-Ce solid solns., localized moments from elec. meas. 8=31339
Sn-In films, superconducting 8=44974
$(Sr_{0\cdot 4}Bi_xLa_{0\cdot 6-x})MnO_3$, and dielec. props. rel. to structure 8=26038
$Sr_{1-y}Bi_y)MnO_3$, and dielec. props. rel. to structure 8=26038
Tb, damping 8=49475
$TbFe_2$, hyperfine field at Fe from Mössbauer effect 8=36146
Tb-Y alloys, helicoidal struct., effect of replacing Tb by Y 8=40742
ThO_2: Yb^{3+}, g-factor stress dependence 8=31510
$TiCr_2S_4$, mag. struct., comparison with $TiCr_2Se_4$ 8=35358
$TiCr_2Se_4$, mag. struct., comparison with $TiCr_2S_4$ 8=35358
Ti-H systems, susceptibility maximum 8=49658
Ti_2O_3, order, and resistivity 8=31313
Ti_5O_9, susceptibility, anomalous, 77° -160°K 8=31511
$TmAl_3$, cryst. stark splitting 8=48309
TmSb, magnetization anisotropy 8=31512
TmFe garnet, sublattice magnetization 8=40840
V, superconducting, anomalous behaviour 8=27383
VAu_4, effect of at. environment, correction to paper 8=31513
VO_2, and elec. props. 8=40293
Y-Ce alloys, bound state, magnetoresistance at low temp. 8=49476
Y-Ce dilute alloys, susceptibility and thermopower due to s-f anomaly 8=27384
YFe garnet, e.m. conversion to exchange spin wave energy, coherent i.r. diffraction determ. 8=40848
$ZnNi_xMn_{2-x}O_4$, susceptibility temp. dependence 8=40745
antiferromagnetic
See also Antiferromagnetism.
alloy, dil., with mag. impurity distrib. symmetrical rel. to sublattices 8=40851
critical relaxation below Neél point 8=49567
tris(dihydroxobis(diethylamine)chromium)chromium (III) sulphate decahydrate, suscept. 8=40860
geothite, natural, rel. to thermoremanence 8=49523
Heisenberg antiferromagnet with uniaxial anisotropy, anomalous behaviour of sound near crit. pt. 8=39883
Heisenberg, ground-state sublattice magnetization 8=36200
Heisenberg, with spinless impurities, zero-point spin deviation 8=27437
hematite, moment direction pressure dependence to 41 kbar, n. diffr. exam. 8=45059
Kondo instability, anal. using Schrieffer-Wolf model 8=49501
magnon absorpt. from far i. r. spectroscopy 8=36294
manganites of perovskite structure, behaviour rel. to lattice distortions 8=49534
moments in crystals, local distrib. by neutron diffraction 8=31643
perovskites, $ATbO_3$, (A=Fe, Cr, Al, Co), ordering of Tb 8=31799
rare-earth-Al alloys 8=36176
rare-earth antimonides, mag. anisotropies 8=31791
rare earth chromites, magnetostatic props. 8=31790
rare earth crystals, mag. -ordering temp., pressure dependence 8=31652
rare earth manganites, magnetostatic props. 8=31790
rare-earth monochalcogenides, susceptibility temp. dependence, 4-1300°K 8=31761
rare-earth ortho-aluminates, thermal props. in Neel point neighbourhood 8=35435

Magnetic properties of substances—contd
antiferromagnetic—contd
rare-earth orthoferrites with weak ferromagnetism, anisotropy pressure depndence 8=40857
seignettomagnetics, phase transitions and coupling of ferroelec. and mag. props. 8=27398
seignettomagnetics, phase transitions from Mossbauer studies 8=27442
semiconductor, coupled spin, plasmic and e. m. waves in const. fields 8=40771
semiconductor, new type of auto-localized conductivity 8=40429
semiconductors, spin-disorder scattering of carriers 8=27058
slow neutron scatt. near mag.-acoustic res., rel. to mag.-elastic coupling 8=40855
spin relaxation, anomalous, near mag. transition 8=49582
spin-wave spectrum, anomaly in spiral spin structures 8=49572
spin waves, instability 8=36202
2, 2, 6, 6 tetramethyl 4-piperidinol 1-oxyl, exchange interaction 8=30969
transition metal salts, transferred hyperfine interactions and spin deviations 8=31919
transition metal boracites, temp. between 1, 8°and 300°K 8=45065
transition metals, atomic mag. moment rel. to localized d electrons 8=35047
two-magnon scattering of neutrons involving orbital transitions 8=45047
uniaxial, sound attenuation, anomalous, near spin-flop transition point 8=26580
AgCrS(Se)$_2$, and crystal structure 8=39810
AlTbO$_3$, magneto-electric effect 8=36217
Au-Cr disordered alloys, susceptibility meas. 8=44685
Au$_2$Mn, exchange striction and exchange coupling consts. 8=31755
Au$_5$Mn$_2$, ordered 8=31756
Ba$_{0.15}$Ca$_{0.85}$MnO$_3$, at. mag. structure from n-diffr. exam. 8=40859
BaCo$_2$Fe$_{16}$O$_{27}$, rotatory hysteresis losses and anisotropy 8=45037
BiFeO$_3$ 8=27285
BiFeO$_3$, e.p.r. study 8=27488
BiFeO$_3$-PrFeO$_3$ system, phase transitions and ferroelec. props. 8=26064
(1-x)BiFeO$_3$-xSr(Sn$_{1/2}$Mn$_{2/3}$)O$_3$, solid solns., transitions from Mossbauer studies 8=27442
CaCrO$_3$ perovskite, band antiferro., and parasitic ferromag. below T_N 8=49570
CaF$_2$: Ho^{2+}, g-factor stress dependence 8=31510
Ca$_2$FeAlO$_5$, and spin orientation 8=31758
Ca$_2$Fe$_2$O$_5$, magnetic structure 8=31759
CaRuO$_3$, rel. to band structure 8=36177
CdAlO$_3$, ordering from sp. ht, susceptibility and optical meas. 8=31773
Cd-Mn alloys, dil., ordering from elec. resistivity and susceptibility meas. 8=31760
Ce, monochalcogenides, susceptibility temp. dependence, 4-1300°K 8=31761
CeAs, from neutron scattering data 8=45052
CeCl$_3$, interaction constants determ. 8=36239
CeSb, from neutron scattering data 8=45052
CoBr$_2$·6H$_2$O, spin-flopping 8=45053
CoBr$_2$. 6H$_2$O, susceptibility and reson. expts. 8=36204
Co-CoO films, ferro-antiferromagnetic coupling and after effect 8=49517
CoCr$_2$S$_4$, NiAs-type structure, magnetization, 1. 5°K to room temp. 8=45064
CoF$_2$, behaviour in high mag. field normal to c axis 8=36230
CoF$_2$, excitations near Neel pt. from n. scattering meas. 8=31762
CoO(I) and (II), hyperfine Mossbauer spectra of Fe^{57} below Neel temp. 8=26018
CoO(I) and (II), Neel temp. shifts rel. to Mossbauer studies 8=26017
CoSe$_2$ pyrite, 8=31493
Co-Ti system, Laves phase, susceptibility rel. to temp. 8=49571
Cr and alloys, spin density waves 8=36205
Cr alloys, spin-density-wave periodicity conc. dependence 8=36207
Cr alloys, spin density wave to antiferromagnetic transition, pressure effect 8=31767
Cr, critical n. scattering rel. to itinerant e.-model 8=31764
Cr, electrical resist. 8=40316
Cr, field-cooled, domain state, fermi surface change 8=39891
Cr, Hall coeff. temp. dependence, 77-330°K rel. to "mag. cooling" effects 8=45054
Cr, high-pressure changes by neutron-diffractometry 8=26361
Cr, Néel temp., effect of plastic deform. 8=45055
Cr, pressure and mag. field effects, n.-diffr. exam. 8=31766
Cr, rel. to band structure 8=36201
Cr, rel. to sinusoidal spin-density waves, band model 8=36206

Magnetic properties of substances—contd
antiferromagnetic—contd
Cr, spin-density-wave distribs. 8=31765
CrH$_x$, ($x < 1$), contrib. to anomalous paramag., rel. to H-orbital expansion effects 8=49480
Cr-Mn alloys, structure stabilisation 8=48735
Cr-Mo alloys, absolute thermoelectric power between 100 and 600°K 8=49393
Cr-Mo(W) alloys, from resistivity meas. 4-325°K 8=31763
Cr$_2$O$_3$, Neel temp. pressure dependence up to 13. 3 kbar 8=27443
Cr$_2$O$_3$ powder, Néel temp. depend. on particle size 8=40861
Cr$_2$O$_3$, sublattice magnetization, susceptibility 8=40862
Cr$_2$O$_3$-Fe$_2$O$_3$ system, structure 8=27444
Cr$_2$TeO$_6$, structure by neutron diffraction 8=40863
Cr$_2$WO$_6$, structure by neutron diffraction 8=40863
CsMnCl$_3$. 2H$_2$O, and n. m. r. 8=36275
Cs$_2$MnCl$_4$. 2H$_2$O, and n. m. r. 8=36275
CuCl$_2$. 2H$_2$O-d$_x$, deuteration effects, from PMR 8=36264
CuCl$_2$. 2H$_2$O, proton relaxation 8=49635
CuCrS(Se)$_2$, and crystal structure 8=39810
CuFe$_2$S$_3$, ordering from Mössbauer spectroscopy 8=40864
Cu-Mn-Sb system, phase equilibrium 8=45056
Cu(NH$_3$)$_4$SO$_4$. H$_2$O, order from PMR 8=36263
Cu(NO$_3$)$_2$. 2. 5H$_2$O, rel. to ht. capacity, 0. 5-4. 2°K 8=35428
Cu(NO$_3$)$_2$. 3H$_2$O, ordering from PMR 8=36263
CuSO$_4$. 5H$_2$O, proton magnetic resonance down to 0. 3°K 8=49637
CuSeO$_4$. 5H$_2$O, proton magnetic resonance down to 0. 3°K 8=49637
Dy, anisotropy constant temp. dependence 8=31651
Dy, mag. -ordering temp., pressure dependence 8=31652
Dy, spin-wave spectrum, anomaly in spiral spin structures 8=49572
DyAl garnet, critical n. -scattering rel. to Ising model 8=31769
DyAl garnet, magnetization and mag. ordering. 0. 37°K 8=40866
Dy$_3$Al$_2$, metamagnetic 8=49544
DyAlO$_3$, neutron diffraction study 8=48647
DyAlO$_3$, rel. to absorpt. spectra 8=36356
DyC$_2$ 8=40865
DyFeO$_3$, below 36°K 8=31768
DyFeO$_3$, ordering rel. to sp. ht., 1. 2-80°K 8=35429
DyO$_2$S, and structures from n. diffr. meas. 8=40869
Er, Néel temp., effect of hydrostatic press. 8=36212
Er, structure of three ordered states below Néel temp. 8=44970
ErAl$_2$, neutron diffr. meas. 8=31611
ErGa garnet, antiferromag. struct. and metamag. transition, 0. 31 and 4. 2°K 8=40867
Er-Th alloys, f.c.c., ordering stabilization by Th 8=36218
Eu, from mag. moment meas. at 4. 2°K 8=31706
Eu$_3$O$_4$, hyperfine fields from Mossbauer spectra 8=36208
Eu$_3$O$_4$, interaction between linear arrays 8=40734
Fe-Al alloys, below 40°K, 8=31615
FeCl$_2$. 4H$_2$O, Mossbauer study, 4. 2-0. 025°K 8=36211
Fe-Cr-Ni alloys, mag. investigation 8=36209
FeCr$_2$S$_4$, effective-field parameters at Fe^{57} temp. dependence, 60-298°K rel. to magnetically induced quadrupole interaction model 8=45060
FeCr$_2$S$_4$, NiAs-type structure magnetization, 1. 5°K to room temp., 8=45064
FeF$_2$, effects of exciton-magnon interactions in spin-allowed optical transitions 8=45062
FeF$_2$ rutile, spin-wave light scattering 8=36387
FeF$_2$, spin-wave dispersion relations from n.-scattering 8=31771
FeF$_2$, susceptibility rel. to i.r. spectra 8=36210
FeF$_2$, uniaxial, exam. by cluster-variation method 8=45058
FeF$_2$, zero-magnon lines in 3800Å and near i.r. region 8=45061
γ-FeMn alloys, rel. to mag. moment and hyperfine field temp. and comp. dependence 8=31770
Fe$_{0.98}$O, Neel temp. determ. by elastic modulus method 8=31772
α-Fe$_2$O$_3$, n scatt. by spin-waves, polarization effects, obs. 8=36187
α-Fe$_2$O$_3$: Ti, canted structure and doping rel. to mag. resonance 8=36231
Fe(OH)$_2$, hyperfine fields from Fe^{57} Mossbauer meas. 8=39517
α-FeOOH, structure from n-diffr. meas. at < 80°C 8=30894
Gd, anisotropy constant temp. dependence 8=31651
Gd$_2$O$_3$, and structures from n. diffr. meas. 8=40869
He^3, solid, nuclear spin exchange interaction 8=31774
Ho, Néel temp., effect of hydrostatic press. 8=36212
Ho-Th alloys f.c.c., ordering stabilization by Th 8=36218
HoO$_2$S, and structures from n. diffr. meas. 8=40869
K$_2$IrCl$_6$, ordering from n. diffr. exam. 8=40870
KMnCl$_3$. 2H$_2$O, and n. m. r. 8=36275
KMnF$_3$, zero-point spin reduction rel. to low temp. heat capacity 8=44340
K$_2$MnF, zero-point spin reduction rel. to low temp. heat capacity 8=44340

Magnetic properties of substances—contd
- **antiferromagnetic**—contd
  - $KNiF_3$, ordering effect on lattice vibration 8=48706
  - K_2ReBr_6, ordering from n. diffr. exam. 8=40870
  - K_2ReCl_6, ordering from n. diffr. exam. 8=40870
  - La-Tb alloys, rel. to h.c.p. and d.k.c. p structures 8=31792
  - $MgCr_2O_4$, structure from n. diffr. exam., 8=45063
  - γ-Mn, rel. to band structure 8=36201
  - Mn-Au alloys, rel. to phase transforms. on deform. and ageing 8=31776
  - Mn_3B_4, Mo- or W- substituted 8=27418
  - $MnCl_2.4H_2O$, ordering rel. to thermal expansion anomaly near Neel pt. 8=35445
  - $MnCr_2S_4$, NiAs-type structure, magnetization, 1.5°K to room temp., 8=45064
  - MnF_2, n. scattering near critical pt., temp. dependence 8=31784
  - MnF_2 rutile, spin-wave light scattering 8=36387
  - MnF_2, spin-wave sidebands 8=36388
  - MnF_2, stressed, magnon sideband shapes rel. to exciton dispersion and exciton-magnon interactions 8=36389
  - MnF_2, susceptibility meas. rel. to spin-wave theory 8=31783
  - MnF_2, uniaxial, first- and second-neighbour exchanges, statistical mech, 8=31782
  - MnF_2, u. s. attenuation near and above spin-flop transition, field dependence 8=44319
  - MnF_2:Co, localized magnon obs. by neutron scattering 8=27380
  - MnF_2: Co, localized magnon obs. from n. -scattering at 4.2°K 8=31785
  - Mn_3GaN, ordering of Mn spins 8=40871
  - $MnIn_xCr_{2-x}S_4$, $(0.4 \leqslant x \leqslant 1.0)$, and crystallographic props. 8=36190
  - Mn_2N, mag. and crystal struct. 8=49573
  - Mn-Ni, (CuAu-I type alloy), structure and phase transform 8=31780
  - MnO, covalency parameters 8=30617
  - MnO, deformed, rel. to crystal structure, 33-157°K 8=30906
  - MnP, by torque meas. 8=49529
  - MnP, hydrostatic pressure rel. to props. 8=31657
  - MnP–MnAs solid solutions, domains 8=48388
  - Mn-Pd, (CuAu-I type alloy), structure and phase transform 8=31780
  - Mn-Pt, (CuAu-I type alloy), structure and phase transform 8=31780
  - Mn–Pt system, structures and transforms. rel. to exchange interactions 8=45017
  - Mn_3Pt, structure, effect of Fe substitution 8=27446
  - α-MnS, covalency parameters 8=30617
  - $MnSeO_4$, Neél temp., obs. using continuous flow cryostat 8=49548
  - $MnSeO_4$, structure from n. diff. data 8=31778
  - $MnSn_2$ 8=36214
  - $MnSn_2$, weakly coupled moments 8=31781
  - Mn_3Sn 8=36214
  - $MnSo_4$ powders, anhydrous and monohydrate 8=31786
  - $MnSO_4$, spin configuration 8=36213
  - $Mn(TiMn)O_4$, structure, ordering 8=40872
  - $(NH_4)_2Ir$; $PtCl_6$, exchange coupling between Ir^{4+} ions 8=32002
  - $NaCrS(Se)_2$, and crystal structure 8=39810
  - Nd monochalcogenides, susceptibility temp. dependence 4-1300°K 8=31761
  - $NiCl_2$, specific heat rel. to mag. energy spectrum, 1.8-16°K 8=39918
  - $NiCr_2S_4$, NiAs-type structure, magnetization, 1.5°K to room temp. 8=45064
  - NiF_2, ordered crystals, effect of electron-magnon interaction on Ni^{2+} absorption band 8=41127
  - NiMn, rel. to band structure 8=36201
  - Ni–NiO films, ferro-antiferromagnetic coupling and after effect 8=49517
  - NiO, covalency parameters 8=30617
  - NiO, magnon dispersion and density of states 8=40874
  - NiS, moments and susceptibility temp. dependence 8=31788
  - NiS_2 pyrite, 8=31493
  - $Pb(Fe_{1/2}Ta_{1/2})O_3$, onset of ordering 8=40615
  - Pd_2MnAl, rel. to order in Pd_2MnIn, Pd_2MnSn, Pd_2MnSb (Heusler alloys) 8=31700
  - Pd_2MnIn, (Heusler alloy), ordered, rel. to mag. and chem. order in Pd_2MnAl 8=31700
  - Pr monochalcogenides, susceptibility temp. dependence, 4-1300°K 8=31761
  - $PrCl_3$, rel. to Cl^{35} NQR line splitting below 0.4°K 8=36283
  - $RbFeF_3$, Fe^{57} hyperfine structure from Mossbauer effect 8=31795
  - $RbFeF_3$: Fe^{3+} octahedral, magnetically induced elec.-field gradients 8=31794
  - $RbMnF_3$, inelastic n. scattering near Neel pt. rel. to spin fluctuatuons 8=31796
  - $RbMnF_3$, magnon-magnon interactions evidence 8=40875
  - $RbMnF_3$ spectra, magnon-magnon and exciton-magnon interaction effects 8=40843
  - $RbMnF_3$, spin correlations in paramag. state 8=49484
  - $RbMnF_3$:Nd^{3+}, luminesc. intensity and decay around mag. ordering temp. 8=32057
  - Sm, from mag. moment meas. at 4.2°K 8=31706

Magnetic properties of substances—contd
- **antiferromagnetic**—contd
  - $SmFeO_3$, reorientation temp., hydrogen ht. treatment effects 8=40876
  - $Sm_{1-x}Tm_xFeO_3$, obs. 78°-500°K 8=31797
  - $Sr_2(FeMo)O_6$, ordering from n-diffr. studies 8=27436
  - Tb, anisotropy constant temp. dependence 8=31651
  - Tb in perovskites, ordering 8=31799
  - Tb, mag. -ordering temp., pressure dependence 8=31652
  - $TbAg_2$ 8=40877
  - TbAl, structure, neutron diffraction study 8=27447
  - Tb_3Al_2, metamagnetic 8=49544
  - $TbAlO_3$, interactions from optical spectroscopy 8=45066
  - $TbAlO_3$, metamagnetic transitions at 1.5°K 8=31798
  - TbO_2S, and structures from n. diffr. meas. 8=40869
  - Tb-Th alloys, f.c.c., ordering stabilization by Th 8=36218
  - TiH_x, $(x < 2)$, contrib. to anomalous paramag., rel. to H-orbital expansion effects 8=49480
  - Tm, Mossbauer hyperfine structure below, Neel temp., analysis 8=30644
  - UAs, magnetic ordering from n. diffr. study 8=40878
  - UO_2, canted structure and domains rel. to weak ferromagnetism 8=49574
  - UO_2, exchange interactions, orbital effects 8=31544
  - UO_2, excitations temp. dependence 8=31802
  - UO_2, rel. to u. s. attenuation and elastic constants 8=39898
  - U_3O_8, neutron diffraction study 8=31801
  - UP-ThP and UP_2-ThP_2 solid solns. 8=45067
  - $(U_{1-x}Th_x)O_2$, susceptibility temp. dependence 8=31803
  - UX, (X=N, P, As, Sb), explanatory model 8=36179
  - $YMnO_3$ 8=27285
  - $ZnCr_2Se_4$ distant-neighbour interaction analysis 8=31596
- **diamagnetic**
  - See also de Haas-van Alphen effects; Diamagnetism.
  - cyclopropane ring systems, susceptibility anisotropy, interatomic contrib. 8=25619
  - epoxide ring systems, susceptibility anisotropy, interatomic contrib. 8=25619
  - hexachlorocyclohexane, cryst. 8=31515
  - hyperfine interactions at ions in ferrimagnetic insulators 8=40832
  - with paramagnetic impurity, e. spin correlation function 8=40726
  - pyrocarbons, B-doped, anisotropy between 77 and 1400°K 8=27084
  - C, glassy, susceptibility field strength, ht. treatment and deform. dependence 8=44966
  - CaS: Zr phosphors, susceptibility obs. 8=44967
  - Tl amalgams 8=48348
- **ferrimagnetic**
  - See also Ferrimagnetism
  - BVC garnets, two-magnon-one-phonon confluence process 8=40837
  - copper chromium halochalcogenides, spinel structure 8=40806
  - ferric oxide and ferrite powders, influence on ferrite synthesis 8=45035
  - ferrites, anisotropy, effect of hydrostatic pressure 8=49559
  - ferrites, Co-substituted, uniaxial mag. anisotropy rel to Fe, Co ions and vacancies 8=49556
  - magnetostriction, meas. at low temps. using superconducting solenoid 8=45000
  - oxidic spinels, aftereffect spectra, mechanisms 8=31718
  - rare-earth ion interactions in insulators 8=31775
  - rare-earth iron garnets: Eu^{153} Mossbauer determ. of exchange interactions 8=36194
  - rare-earth iron garnets, mag. moment at 0°K substitution dependence, mol.-field model 8=45027
  - rubber ferrite-loaded magnets 8=24111
  - saturation temp. dependence in mol. field coeff. determ. using Néel-Weiss theory 8=45033
  - spinels, insulators, hyperfine interactions at diamagnetic ions 8=40832
  - thermoplastic ferrite-loaded magnets 8=24111
  - two-sublattice cpds., first magneto-crystalline anisotropy constant temp. dependence 8=45042
  - Ba ferrites rel. to magnets for transport appls. 8=24114
  - $Ba_2(FeMo)O_6$, and elec. props 8=36195
  - $BaFe_{12}O_{19}$ flexible magnets, anisotropic, and prep. 8=24110
  - $BaFe_{12}O_{19}$, rotatory hysteresis losses and anisotropy 8=45037
  - $Ba_4Zn_2Fe_{36}O_{60}$, 8=31719
  - $Bi_{3-2x}Ca_{2x}Fe_{5-x}V_xO_{12}$, two-sublattice cpd., first magneto-crystalline anisotropy constant temp. dependence 8=45042
  - $Ca_2(FeMo)O_6$, and elec. props. 8=36195
  - $CdCr_2Se_4$, distant-neighbour interaction analysis 8=31596
  - $Co_2BaFe_{16-x}In_xO_{27}$, Curie pt. comp. dependence 8=45038
  - $CoCr_2O_4$, structure from n. -diffr. 8=31721
  - $CoFe_2O_4$, spinel, cation distrib. in octahedral and tetrahedral sites, Mössbauer determ. 8=35035
  - DyAl garnet, sp. ht. shape dependence 8=35423
  - $Dy_{0.2}Y_{1.8}Ti_2O_7$, susceptibility meas. 2-1400°K 8=27429
  - Er ferrite garnet, anisotropy temp. dependence, 4.2-20.4 °K 8=36185
  - Er, orthoferrites, microwave mag. loss meas. near spin-reorientation temps. 8=36224

Magnetic properties of substances—contd
  ferrimagnetic—contd
    EuFe garnet, sublattice magnetization 8=40839
    $FeCr_2O_4$, and electronic props. of Fe^{2+} from Mossbauer spectra 8=31726
    Fe-Ni-Co ferrites, induced anisotropy constant angular dependence 8=45039
    Fe_3O_4(magnetite) crystals, remanent and transitory effects if elastic deformation 8=31728
    Fe_7S_8, pyrrhotite, sublattice rotations, mol. field model 8=31725
    FeV_2O_4, and electronic props. of Fe^{2+} from Mossbauer spectra 8=31726
    $Ga_{2-x}Fe_xO_3$, anisotropy rel. to ferromagnetic resonance, 1.2–360°K 8=27453
    GdFe garnet, sublattice magnetization 8=40840
    $GdFe_2$, induced fields at Gd nuclei 8=49558
    $GeFe_2O_4$, and electronic props. of Fe^{2+} from Mossbauer spectra 8=31726
    Ho, orthoferrites, microwave mag. loss meas. near spin-reorientation temps. 8=36224
    $Li_{0.5}Fe_{2.5}O_4$, n scatt. by spin-waves, polarization effects, obs. 8=36187
    Li-Zn ferrites, hot-pressed fine-grained, h.f. and microwave props. rel. to microstructure 8=27435
    LuFe garnet, sublattice magnetization 8=40840
    $MgFe_2O_4$ superparamag. precip. in MgO, Mossbauer spectroscopy 8=31729
    Mg–Mn films, FMR, thermal treatment effects 8=31817
    $(Mn, Co)_4C$, structure from polarized n. scattering 8=31732
    $MnCr_2O_4$, ferrimagnetic spiral, n.m.r. of Mn^{55} 8=45130
    $MnCr_2O_4$ spiral, far i.r. absorption 8=45204
    $MnCr_2O_4$, structure from n. -diffr. 8=31721
    $Mn_{2-x}Cr_x$ Sb (x=o, 0.03), spin-reorientation rel. to phase transform, 180-280°K 8=36189
    $MnFe_2O_4$ films, single-cryst., pulse switching and static characts., obs. 8=31730
    $Mn_{1+x}Fe_{2-x}O_4$, induced anisotropy at low temps. 8=36188
    $MnIn_xCr_{2-x}S_4$, $(0 \leqslant x < 0.4)$, and crystallographic props. 8=36190
    $Mn_2Sb_{1-y}As_y$, four different ordered states from X-ray diffr. and magnetization meas. 8=27433
    Mn_2Sn 8=36214
    $Mn(TiMn)O_4$, structure, ordering 8=40872
    Mn–Zn ferrite, effect of sintering conditions 8=49561
    Mn-Zn ferrite, sintering conditions effect 8=27432
    Mn–Zn ferrites with high-permeabilities 8=49560
    Mn–Zn ferrites, permeabilities rel. to micro- and chemical structures 8=27431
    $Mn_{0.825}$-ZnY ferrites, from Mossbauer spectroscopy 8=36198
    $NdFeO_3$, mag. anisotropy 8=31733
    Ni films, structural properties and ferromag. resonance 8=36192
    $Ni_{1+x}Ge_xFe_{2-2x}O_4$, anisotropy rel. to resonance props, 4.2-393°K 8=36227
    $Ni_{1+x}Ge_xFe_{2-2x}O_4$, internal fields at two sites, Mossbauer determ. 8=36193
    Ni–Zn ferrite, hot-pressed, fine-grained, hf and micro-wave props. 8=49562
    NiFe ferrite, magnetization by Barkhausen jumps, hysteresis freq. depend., obs. 8=40789
    Ni-Fe ferrites with small additions of Co, diffusion after-effect 8=36191
    Ni-Zn ferrites, hot-pressed fine-grained, h.f. and microwave props. rel. to microstructure 8=27435
    $Ni_{1-x}Zn_xFe_2O_4$, effective anisotropy, contributing factors 8=31735
    Pb ferrites with oxide additives, residual induction and energy product 8=40842
    $RbNi_{1-x}Co_x$ F3, magnetization axis rot. at 77°K 8=49555
    $RbNiF_3$, meas. in strong pulsed fields at 4.2 and 77°K 8=40844
    $RbNiF_3$, spin-ordering on Ni ion substitution 8=31738
    $RbNiF_3$, structure 8=31737
    SmFe garnet, Sn^{3+} mag. moment and hyperfine field temp. dependence from Mossbauer effect 8=31740
    SmFe garnets, from Mossbauer effect, 85-600°K 8=36196
    Sr, processes of magnetic reversal 8=31739
    $SrFe_{12-x}Ga_xO_{19}$, hyperfine field at Fe^{57} nuclei 8=30624
    $Sr_2(FeMo)O_6$, ordering from n-diffr. studies 8=27436
    $Sr_2(FeMo)O_6$, ordered perovskite, and elec. props. 8=36195
    $SrO.4Fe_2O_3.2Al_2O_3$ single crystal, magnetization process and reversal 8=31741
    Tm, orthoferrites, microwave mag. loss meas. near spin-reorientation temps. 8=36224
    TmGa garnet, susceptibility rel. to low-lying energy levels 8=31742
    Y garnets, Si-substituted, permeability and coercive force, spectral dependance 8=40845
    YFe garnet, delay of microwave signals 8=49564
    Y-Fe garnet, magnetoelastic waves, 1.1 GHz, props. from light diffraction obs. 8=40101
    YFe garnet, para process in h.f. mag. field near Curie point 8=49566
    YFe garnet rods, axially magnetized, containing turning pt., magnetostatic mode propagation 8=40846
    Y Fe garnet, spin wave excitation time in first- and second-order nonlinear processes 8=45041

Magnetic properties of substances—contd
  ferrimagnetic—contd
    YFe garnet, spin wave freq. and amp. in subsidiary absorpt. region 8=49563
    YFe garnet, Fe^{3+} anisotropy 8=31743
    $Y_3Fe_{5-x}In_xO_{12}$, two-sublattice cpd., first magnetocrystalline anisotropy constant temp. dependence 8=45042
    YGa garnet: Eu^{3+} 8=49468
    Y_6Mn_{23}, mag. struct., polarized n obs. 8=40849
    $ZnY(Ba_2Zn_2Fe_{12}O_{22})$, from Mossbauer spectroscopy 8=36198
  ferromagnetic
      See also Ferromagnetic relaxation; Ferromagnetic resonance; Ferromagnetism; Magnetization process; Magnetization state.
    alloys dilute, e.s.r. line widths, theory 8=27460
    alloys, rel. to diffuse elastic neutron scattering, second-order effect 8=49491
    Alni alloy, coercive force and structural changes in ageing 8=35090
    Alni alloy, magnetization ageing dependence from Mössbauer exam. 8=49514
    anisotropy energy, magnetocrystalline, temp. dependence 8=44996
    armo iron, n-bombardment effects 8=36169
    austenitic alloys, absence of changes on hardening by ageing with plastic deform. at 600°C 8=35699
    Barkhausen jumps, existence of 2 independent mechanisms 8=49504
    Barkhausen noise, obs. of temp. depend. 8=40792
    ceramics, rel. to structure and elec. props. review 8=49554
    coercive force, continuous recording apparatus 8=49505
    copper chromium halochalcogenides, spinel structure 8=40806
    crystals, tri- and quadri-axial, coercivity anisotropy 8=44999
    domain boundary interact. with dislocations, thermal effect meas. of energy 8=40784
    domain struct. config. 8=48577
    domain wall dynamics 8=36100
    effective permeability induced by temperature and stress variations, instability study 8=49552
    excitations, kinematic and dynamic interactions 8=40759
    Fermi liquid, phase transition 8=35803
    ferrihaemoglobin, g factor anisotropy rel. to dynamical Jahn-Teller effect 8=36234
    ferrites, initial permeability rel. to freq. 8=45034
    ferrites, mixed, $M_xM'_{1-x}Fe_2O_4$, (M=Mg, Zn: M'=Mn, Ni), structure from polarized n. scattering 8=31732
    fields on nuclei of impurity atoms 8=40760
    film, mag. moment subharmonic oscills. in rot. field 8=31573
    film, partial switching in rot. field 8=31572
    film strips-conductor sandwich, switching processes, obs. 8=31579
    films, density of states formulae in band theory generalization 8=31592
    films, domain struct., hysteresis and magnetooptical effects, teaching demonstration 8=27397
    films, ferromag. reson. rel. to mag. params., obs. 8=31807
    films, pulse switching, noise subtraction circuit for gated oscillograph c.r.o. 8=31575
    films, uniaxially anisotropic, magnetization axis rotation under external stress 8=36131
    gases, real, conditions for ferromagnetism 8=34668
    geothite, natural, parasitic ferromagnetism 8=49523
    Heisenberg ferromagnet with uniaxial anisotropy, anomalous behaviour of sound near int. pt. 8=39883
    Heisenberg, high temp. susceptibility and specific ht., for general spin 8=40780
    Heisenberg, quantum field theory approach 8=27394
    hematite, domains and evidence for new wall structure 8=27408
    hematite, specular, temp. variation of magnetisation and susceptibility 100°K–1000°K 8=40791
    hyperfine transient fields for ion implantation 8=26011
    Invar alloys, rel. to anomalous thermal expansion 8=36162
    Ising ferromagnet, magnetization, Green's function method 8=36097
    Kondo instability, anal. using Schrieffer-Wolf model 8=49501
    magnetization, continuous recording apparatus 8=49505
    magnetization direction distributions around spherical cavity 8=40757/8
    magnetoelastic instability in uniform precession 8=36221
    magnetomechanical damping rel. to internal stress distrib. effects 8=31568
    magnetoresistance, anisotropic, theoretical exam. 8=31563
    magnetostriction, meas. at low temps. using superconducting solenoid 8=45000
    Malcolloy (Co–Al), magnetic alloy, effect of Ti additions on props. 8=40803
    manganites of perovskite structure, behaviour rel. to lattice distortions 8=49534
    mu Metal permeability, n irrad. effects 6×10^{19} n/cm², > 1 MeV 8=29553
    metals, energy spectrum of Fermi excitations 8=49093

Magnetic properties of substances—contd
ferromagnetic—contd
metals, wave functions symmetry in one-electron band theory 8=44990
micromagnetism, local field theory 8=31566
mischmetal-Co alloy powders, coercivity milling dependence 8=31597
moments in crystals, local distrib. by neutron diffraction 8=31643
M1040 Vacodur 16 permeability, n irrad. effects, 6×10^{19} n/cm^2, > 1 MeV 8=29553
Nimalloy (in Ni-Mn system), high mag. permeability, V additions rel. to props. 8=31685
particles in airborne dust, e.s.r. 8=36233
permalloy, anisotropy rel to vacancies and interstitials formed on H charging 8=49538
permalloy annealed cylindrical films, bimodal magnetization 8=49540
permalloy cores, testing at low temperatures 8=49542
permalloy, elastic limit determ. by Barkhausen effect 8=26838
permalloy film, in contact with FeNiMn or Gd, spin-wave resonance obs. 8=31681
permalloy film memories, keepered and nonkeepered, internal field distrib. 8=40820
permalloy films, anisotropy change kinetics on stabilization in hard-axis film 8=31222
Permalloy films, coercive force and blocking field rel. to substrate temp., obs. 8=31676
Permalloy films, critical switching curves, obs. 8=31671
permalloy films, induced uniaxial anisotropy of n.- and Ar$^+$ bombardment 8=31694
permalloy films, mag-moment motion in h. f. rotating field 8=36157
Permalloy films, pulse switching, induction and magneto-optical meas. comparison 8=31688
Permalloy films, pulse switching rate, −180-250°C 8=31675
permalloy films, supercritical, domain structure, theory 8=31684
permalloy films, wall streaming obs. 8=31558
permalloy, magnetization axis 8=49543
Permalloy, single-crystal platelets, domains 8=31664
permalloy stripe-films, domain structure 8=31693
permalloy, susceptibility at 5000 Hz, easy and hard directions 8=36110
for permanent magnets, interpretation of props. using fine particle theory 8=46380
permanent magnet materials containing rare-earths 8=40801
permeability and magnetization curve calc. 8=37408
rare-earth-Al alloys, 8=36176
rare earth alloys with 4f e. conc = 10, 11; magnetization 8=31654
rare earth compounds, mag. viscosity 8=45029
rare earth crystals, mag. -ordering temp., pressure dependence 8=31652
rare earths, mag. viscosity 8=45029
rare-earth metals and alloys, hyperfine interactions from n. m. r. 8=36280
rare-earth metals, enhanced effective exchange interaction due to localized spins 8=31594
rare earth metals, heavy, indirect nuclear spin relax. 8=45132
rare-earth metals, heavy, rel. to lattice parameters 8=35350
ruby, ferromagnetic interactions 8=49580
seignettomagnetics, phase transitions and coupling of ferroelec. and mag. props. 8=27398
semiconductor, coupled spin, plasmic and e. m. waves in const. fields 8=40771
semiconductors, spin-disorder scattering of carriers and magnetoresistance 8=27058
semiconductors, temperature range 8=49509
slow neutron scatt. near mag.-acoustic res., rel. to mag.-elastic coupling 8=40855
spin-phonon interaction, Curie temp. shift 8=40763
spin relaxation, anomalous, near mag. transition 8=49582
spin system spectrum and h.f. props. of crystals with plane defects 8=44986
static characteristics of ferrous materials, measuring equipment 8=46363
steel, ht. treatment dependence 8=45014
steel, transformer, cubic texture perfection dependence 8=36140
steel, transformer, hot-rolled, changes on internal oxidation zone formation 8=36562
susceptibility, complex, effect of mag. diffusion after-effect and logarithmic distrib. of time consts. 8=49549
susceptibility, rel. to sp. ht. and expansion coeff. at Curie pt. 8=30959
thermally activated mag. viscosity in multidomain particle of ferromag. subst., theory 8=50226
transition metal alloys, dilute, moments 8=45031
transition metal alloys, dilute, rel. to impurity states 8=45005
3d transition metal alloys, localized moments and Pauling valence 8=49528
transition metal baracites, temp. between 1, 8°and 300°K 8=45065

Magnetic properties of substances—contd
ferromagnetic—contd
transition metal compounds, spin-orbit coupling effects 8=45028
transition metals, atomic mag. moment rel. to localized d electrons 8=35047
transition metals, e. -magnon interaction 8=36178
transition metals, rel. to band structure 8=31632
Ultraperm 10 permeability, n irrad. effects, 6×10^{19} n/cm^2, > 1 MeV 8=29553
uniaxial, Bloch wall energies in ext. mag. field pep. to hexagonal axis 8=40783
vicalloy strip, thermomechanical treatment effects 8=36135
16 AlFe Vacodur 16 permeability, n irrad. effects, 6×10^{19} n/cm^2, > 1 MeV 8=29553
Au-Co, in liquid state, and elec. resist 8=43871
Au-Fe, dil. alloy, low-temp. susceptibility rel. to spin. compensation 8=31604
Au-Ni, in liquid state, and elec. resist. 8=43871
Au_4V, disorder, deformation induced 8=27399
$CdCr_2Se_4$, mangetization and m.n.r. 8=31895
$CeSn_3$, phase at 4.2°K, Mössbauer study 8=43944
Co, after-effect 8=45008
Co, after-effect 8=49515
Co, dispersion-strengthened, rel. to dispersoid effect 8=31620
Co film, planar Hall effect, thickness (100-1500Å) and temp. (77-293°K) dependence 8=31687
Co films, anisotropy field and coercive force, thickness depend., 200-2000Å 8=31598
Co films, epitaxial, anisotropy constant 8=31631
Co, form factor anisotropy rel. to band structure 8=31600
β-Co, superparamagnetism obs. by Mössbauer effect 8=49521
Co–CoO films, ferro-antiferromagnetic coupling and after effect 8=49517
$CoCr_2O_4$, spin-structure determ. from magnetization and resonance 8=31731
Co-Fe-Au alloys, low-magnetostrictive, coercive force rel. to cold working and ageing 8=31599
$CoMn_2O_4$, structure from low-temp. n. -diffr. 8=31722
Co-Ni-Fe films, critical thickness and coercivity 8=27400
CoS_2 pyrite, 8=31493
CoS_2 pyrites, rel. to valence and spin states 8=36078
$Co(S_xSe_{1-x})_2$ pyrite with 12% Se at 0°K 8=31493
Co-W high-temp. structural alloy, development 8=31601
$CrBe_{12}$, at low temps. 8=45009
$(CrFe)_{23}C_6$, austenitization influence on contents and Curie point 8=30684
$Cr_{1-x}Mn_xO_2$ $(0 \leqslant x \leqslant 0.7)$, mixed mag. oxides crystallizing in rutile structure 8=31603
CrTe, spin relaxation of Fe^{57} below Curie point 8=49532
$Cs_3ZnBr_5:Co^{2+}$, exchange interactions in pairs of coupled Co^{2+} ions 8=49606
$Cs_3ZnCl_5:Co^{2+}$, exchange interactions in pairs of coupled Co^{2+} ions 8=49606
Cu-Au alloys with Fe, mag. ordering rel. to spin compensation of Fe from Kondo temp. meas. 8=27404
$CuCr_2Se_3Br$, from n. diffr. exam. 8=31606
$CuCr_2Te_4$, Te^{125} hyperfine field determ. by NMR at 1.4°K 8=27503
$CuCr_2X_3Y$, $(X = Se^{2-}, Te^{2-}; Y = Cl^-, Br^-, I^-$, 8=31605/6
Cu-Fe alloys, s-d exchange model analysis 8=31608
Cu-Fe, dil. alloy, low-temp. susceptibility rel. to spin compensation 8=31604
$CuK_2Cl_4.2H_2O$, spin-wave theory analysis 8=31607
Cu-Mn alloys, s-d exchange model analysis 8=31608
Cu-Mn, dil. alloy, low-temp. susceptibility rel. to spin compensation 8=31604
Cu_2MnAl, ordering temp. 8=45010
Cu–Mn–Sb system, phase equilibrium 8=45056
Cu-Ni system, ferromag. ordering rel. to Debye temp. conc. depend., obs. 8=39913
Dy, anisotropic high field props. from mag. moment meas. at 4.2°K 8=31705
Dy_3Al_2, metamagnetic 8=49544
$DyEr_x$ $(x = 1, 3)$ alloys, with 4f e conc = 10, 11; magnetization 8=31654
$DyFeO_3$, ordering rel. to sp. ht., 1.2–80°K 8=35429
$DyFeO_3$, rel. to absorpt. spectra 8=36356
$Dy_xY_{1-x}Fe_2$, Curie temp. and coercivity comp. dependence 8=31610
Er, anisotropic high field props. from mag. moment meas. at 4.2°K 8=31705
$ErAl_2$, and relax. study by Mössbauer effect 8=49518
$ErAl_2$, neutron diffr. meas. 8=31611
Eu chalcogenides: (rare-earth)$^{3+}$, magnetoresistance rel. to resistivity anomaly 8=35884
EuO, λ anomaly and magnetoelastic interactions from magnetostriction meas. 8=45011
EuO, hyperfine fields from Mossbauer spectra 8=36208
EuO, magnetically ordered, Eu^{115} n.m.r. 8=49641
Eu_3O_4, magnetic structure, coupled spins by interactions 8=40734
EuS, Eqn. of state and sp. ht. near Curie point 8=27405
EuS, magnetically ordered, Eu^{115} n.m.r. 8=49641
EuS, sp. ht. in non-zero field 8=27406
EuSe, magnetically ordered, Eu^{115} n.m.r. 8=49641

Magnetic properties of substances—contd
ferromagnetic—contd
EuSe, magnetocrystalline anisotropy from ferromag. resonance at 1.3°K 8=45012
Fe, anisotropy constant, first-order, pressure dependence 8=27407
Fe, deduced from tight-binding calcs. 8=36145
Fe, deviations from Bloch law, temp. depend. 8=27411
Fe, dispersion-strengthened, rel. to dispersoid effect 8=31620
Fe, elastic limit determ. by Barkhausen effect 8=26838
Fe film, planar Hall effect, thickness (100-1500Å) and temp. (77-293°K) dependence 8=31687
Fe films, anisotropy from Mossbauer meas. 8=31641
Fe films, epitixial, anisotropy constant 8=31631
Fe films, Richter-type aftereffect 8=31633
Fe filoform microcrystals, effect of dislocations on magnetization process 8=26677
Fe, Fisher's spin pair correlation function, evidence from critical neutron scattering 8=27412
Fe, high field susceptibility 8=45013
Fe in Cu, spin compensated state rel. to Mòssbauer effect 8=35036
Fe in ϵ Cu-Zn, local moment formation from susceptibility meas. 8=31617
Fe, interaction energy with the magnetization of interstitial atoms and solute atom pairs 8=31614
Fe, isomer shift temp. dependence and hyperfine field near Curie point 8=31636
Fe, magnetization field near frontal plane rel. to domain formation 8=31554
Fe, mag. moment disturbance distrib. from dissolved impurity atom, n. scattering obs. 8=31637
Fe(II) octahdral complexes 8=35038
Fe. permeability changes on rotation in continuous mag. field 8=40811
Fe polycrystals, after effect rel. to plastic deform. 8=36143
Fe, rel. to band structure 8=31632
Fe, saturation magnetization determs. 8=31618
Fe, spin-wave renormalization effects, obs. 8=49520
Fe, susceptibility above Curie temp., depend. 8=40812
Fe-Al alloy, interaction energy with the magnetization of Al solute pairs 8=31614
Fe-Al alloys, below 40°K, and superparamagnetic behaviour, > 40°4 8=31615
Fe-Al alloys, K-state effects 8=49525
Fe-Al alloys, magnetization and spin-wave stiffness in Heisenberg model 8=31645
Fe_3Al, internal-field temp. dependence for two sublattices 8=27410
Fe-Co alloy, high field susceptibility 8=45013
Fe-Co alloy powders, permeability meas. at 400-40 000 Mc 8=40810
Fe-Co alloys, deviations from Bloch law, temp. depend. 8=27411
Fe-Co-Ni-Al-Cu system alloys with added Nb and Ti, high-coercive phases rel. to anisotropy 8=27415
Fe-Cr alloy, high field susceptibility 8=45013
Fe-Cr films, exchange constants from spin-wave resonance spectra 8=36147
FeF_3, sublattice magnetization near critical point 8=27416
$Fe_xGa_{2-x}O_3$, from polarized n.-scattering 8=31727
$Fe_xGa_{2-x}O_3$, structure 8=36139
Fe:Mn, hyperfine field at Mn, temp. dependence 8=40814
FeNi electrodeposited films, switching behaviour 8=27419
Fe-Ni alloy, high field susceptibility 8=45013
Fe-Ni alloys, f.c.c., Curie temp. and C effect 8=31646
Fe-50Ni, alloys, fibre-reinforced, rel. to mech. strength 8=31209
Fe-Ni alloys, Mössbauer effect and exchange anisotropy 8=48328
Fe-Ni(50-50) crystals, n-irradiated in mag. fields, magnetization curves 8=36144
Fe-Ni films, exchange stiffness const. 8=49522
Fe-Ni films, switching along easy axis above nonuniform rot. threshold field 8=31630
Fe-Ni-Co films, anisotropy. coercive force and s,h. f. reson. absorpt. obs. 8=31629
Fe-Ni-Co films, anisotropy, domains and saturation magnetization, obs. 8=40809
Fe-Ni-Co films, anisotropy, review 8=36148
Fe-Ni-Ti alloys, absence of changes on hardening by ageing with plastic deform. at 600°C 8=35699
α-Fe_2O_3, domain struct. close to low temp. transition 8=31648
α-Fe_2O_3 fine particles, spin flip temp. shift particle size dependence rel. to lattice dilation 8=27414
α-Fe_2O_3, memory effect rel. to neg. pressure effects on Morin transition pt. 8=31616
γ-Fe_2O_3 particles, acicular, crystallite size dependence 8=31635
Fe_2O_3, spin-wave excitation-energy changes from n. scattering meas. 8=31638
α-Fe_2O_3, superparamagnetism obs. by Mössbauer effect 8=49521
Fe_2O_3: Co, induced anisotropy, dependence on annealing temp. 8=36186

Magnetic properties of substances—contd
ferromagnetic—contd
$Fe_{90}P_{12.5}C_{7.5}$, amorphous, magnetization and hyperfine field temp. dependence 8=40813
Fe-Pd alloys, changes on annealing and plastic deformation rel. to structural transforms 8=35102
Fe-Pd alloys, dil., hyperfine field at Fe, mag. field dependence at 1.2°K (T_c ≈ 5°K) 8=36081
Fe : Pd, hyperfine field, temp. depend. 8=45016
$FePd_x$, (x = 3.1), Fe^{57} hfs temp. dependence near Curie temp. 8=45015
$Fe_3(PO_4)_2.4H_2O$, ludlamite, static magnetization obs. below 15.3°K 8=27413
FeS, structure 8=36139
Fe_3S_4, synthesis 8=41248
Fe_7S_8, anisotropy energy origin 8=31634
Fe_7Se_8, anisotropy energy origin 8=31634
Fe-1.35Si alloys, fibre-reinforced, rel. to mech. strength 8=31209
Fe-Si crystals, X-ray diffr. contrast at domain wall 8=27409
Fe-3% Si, cube textured rel. to Goss oriented, obs. 8=26265
Fe-3% Si, hysteresis loss and magnetostriction hysteresis in rotating fields up to 2000 Oe 8=31680
Fe-3% Si, magnetization by Barkhausen jumps, hysteresis freq. depend., obs. 8 =40789
Fe-Si, magnetization curve and energy losses in alt. mag. fields, effect of dislocations 8 =36142
Fe_3Si, internal-field temp. dependence for two sublattices 8=27410
Fe_5Si_3, C-stabilized, mag. moments and hyperfine interactions 8=31623
Fe_2TeO_6, structure, transition temp. by Mössbauer effect 8=49457
Fe-V alloy, high field susceptibility 8=45013
Gd, anisotropic high field props. from mag. moment meas. at 4.2°K 8=31705
Gd, Curie temp. variation with hydrostatic press. and anomalous compressibility 8=36149
Gd, induced fields at nuclei 8=49558
Gd, mag.-ordering temp., pressure dependence 8=31652
Gd-Permalloy films, antiparallel exchange coupling 8=40816
Gd, susceptibility ferromag. impurity dependence near Curie temp. 8=40751
Gd^{3+} pair-interaction constants in $LaCl_3$ from e.p.r. determ. 8=31775
$GdCl_3$, specific heat, exchange consts., high freq. meas. 8=40817
GdPd, and structure 8=44216
$HgCr_2S_4$, structure and metamagnetism 8=31653
Ho, anisotropic high field props. from mag. moment meas. at 4.2°K 8=31705
HoAl, and structure 8=31650
Ho_xEr_y, alloys with 4f e conc = 10, 11; magnetization 8=31654
$HoFeO_3$, rel. to absorpt. spectra 8=36356
$LaFeO_3$, e.p.r. study 8=27488
$(La, Gd)_2CoMnO_6$ system, exchange interactions rel. to ordering 8=49527
$La_{2-x}Gd_xCoMnO_6$, exchange interactions and structure 8=27417
$(La, Sr)CoO_3$, rel. to localized- to collective-electron transition 8=35773
Mn, localized moments and Pauling valence 8=49528
Mn_3B_4, Mo- or W- substituted 8=27418
$MnCO_3$, magnon sidebands in absorpt. spectra at 4.2°K 8=32010
$MnCr_2O_4$, spin-structure determ. from magnetization and resonance 8=31731
Mn_5Ge_3, uniaxial anisotropy consts., temp. depend. of energy 8=36150
MnO. OH, structure 8=49533
MnP. by torque meas. 8=49529
MnP, helical spin structure, stability 8=36151
MnP, hydrostatic pressure rel. to props. 8=31657
MnP, metamagnetic interactions pressure dependence 8=31656
MnP-MnAs solid solutions, domains 8=48388
Mn-Pt system, structures and transforms. rel. to exchange interactions 8=45017
MnSb, spin relaxation of Fe^{57} below Curie point 8=49532
MnSb-Sb aligned eutectic, anisotropy 8=49535
MnSi, mag. moment spacial distrib. from n. scattering 8=31655
Mn-Zn alloys with CsCl-type structure, magnetization and structure 8=40819
Mn-Zn-Ga alloys with CsCl-type structure, magnetization and structure 8=40819
Mo permalloy tapes, rolled 4-79, magnetostriction and coercivity, process variables dependence 8=31658
$NaNiF_3$, orthorhombic, canting from AFMR 8=31839
Ni alloys, saturation magnetization rel. to conc. fluctuation 8=49537
Ni, anisotropy constant, first-order, pressure dependence 8=27407
Ni, anisotropy of energy and magnetization, torque meas. 8=31667

Magnetic properties of substances—contd
ferromagnetic—contd
Ni, anisotropy temp. dependence from magnetostriction and elastic constants 8=31561
Ni crystals, coercivity rel. to dislocation distrib. effects 8=31699
Ni, dispersion-strengthened, rel. to dispersoid effect 8=31620
Ni, elastic limit determ. by Barkhausen effect 8=26838
Ni, electroplated, anisotropy rel to vacancies and interstitials formed on H charging 8=49538
Ni, exchange and spin-orbit interactions rel. to mag. breakdown and de Haas-van Alphen effect 8=44649
Ni film, planar Hall effect, thickness (100-1500Å) and temp. (77-293°K) dependence 8=31687
Ni films, epitaxial, anisotropy constant 8=31631
Ni films, p-bombardment effects at 850 keV 8=36168
Ni films, u. v. reflection, near Curie point 8=36399
Ni, form factor anisotropy rel. to band structure 8=31600
Ni, hysteresis loss and magnetostriction hysteresis in rotating fields up to 2000 Oe 8=31680
Ni, lattice dynamics 8=35391
Ni, mag. moment disturbance distrib. from dissolved impurity atom, n. scattering obs. 8=31637
Ni, magnetization near Curie pt. 8=31697
Ni, magneto elastic resonance props. 8=36164
Ni, magnetostrictive crystalline energy of dislocations from anisotropy of approach to saturation 8=35571
Ni, n-bombardment effects 8=36169
Ni, rel. to band structure 8=31632
Ni, saturation curve anisotropy, edge-dislocation contribution 8=49536
Ni, saturation magnetization determs. 8=31618
Ni, spin-wave renormalization effects, obs. 8=49520
Ni, strongly deformed, onset of uniaxial anisotropy after mag. annealing 8=36216
Ni superparamag. particles, Mossbauer spectra of Fe^{57}, temp and mag. field effects 8=36161
Ni, susceptibility, generalized, temp. depend. 8=31665
Ni, 3d-band, density of states curve 8=40246
Ni, transition temp. pressure-dependence, itinerant-electron theory 8=27424
Ni$_3$B$_7$O$_{13}$I 8=49539
Ni$_3$B$_7$O$_{13}$I, ferromagnetoelectric, props. 8=31670
Ni: Cd^{111}; (Ru^{99}), hyperfine fields at solutes from perturbed-angular-correlation exam. above and below T_c 8=40992
NiCo-C alloys, C anisotropy 8=49526
NiCoP films, chem. deposited, stability, up to 100°C and 1600 hr 8=45023
NiCr$_2$O$_4$, spin-structure determ. from magnetization and resonance 8=31731
Ni-Cu alloys, transition temp. pressure-dependence, itinerant-electron theory 8=27424
Ni-Cu and Ni, var. of thermal cond. in mag. field 8=45022
Ni-Fe alloy, e-irradiated, remanence growth during low temp. mag. anneal. 8=36156
Ni-Fe alloys, high-permeability, classification by props. 8=31662
Ni-Fe film, magnon-phonon coupling 8=27421
Ni-Fe film, planar Hall effect, thickness (100-1500Å) and temp. (77-293°K) dependence 8=31687
Ni-Fe films, electrochem. deposited, coercive force, obs. 8=31672
Ni-Fe films, polycrystalline, susceptibility strain-dependence 8=40824
NiFe films, rel. to neg. bias appl. during sputtering deposition 8=31679
Ni-Fe films, ripple, comp.- meas. temp.- and substrate tem.-dependence 8=36159
Ni-Fe films, s. h. f. susceptibility, < 30 Oe 8=31689
NiFe films, 2-200Å, magnetization anomalies rel. to surface anisotropy 8=36158
Ni-Fe thick films, domain-wall width determ. by Lorentz microscopy 8=8=27422
NiFe-C alloys, C anisotropy 8=49526
NiFeCo film, effect of Cu layer 8=40822
Ni-Fe-Co, films, s. h. f. susceptibility, < 30 Oe 8=31689
NiFe$_2$O$_4$, effect of tetrahedral site Ni^{2+} ions 8=27455
NiFe$_2$O$_4$ superparamag. particles, hyperfine splitting in mag. field from Mössbauer spectra of Fe^{57} 8=36160
Ni$_3$Ga with dissolved Fe, giant moments induced by Fe 8=27423
Ni-18 at. % Mn-8 at. % Fe alloy, longit. galvanomagnetic effect magnetization dependence rel. to anisotropy 8=40827
Ni-NiO films, ferro-antiferromagnetic coupling and after effect 8=49517
Ni-Rh alloy, nearly ferromag., susceptibility and sp. ht. 8=31660
Ni-SOCo alloy, induced anisotropy on cold-rolling 8=31661
Ni-Sn, alloys, Hall effect 8=27425
Ni-V, (Rh), (Pt), and paramag. props., 14-1000°K 8=31683
Pd, exchange interactions, strain depend. 8=45025
PdFe alloys, dilute, exchange interactions, strain depend. 8=45025
Pd-Fe alloys, dil, Fe hyperfine fields, 1.3-4.2°K 8=31701
Pd-Fe alloys, high-field susceptibility conc. dependence 8=36080
Pd-Fe alloys, very dil., low temp. magnetization 8=36079

Magnetic properties of substances—contd
ferromagnetic—contd
PdFe, polarization, distrib. 8=36099
PdFe, spontaneous magnetization 8=36172
Pd$_2$MnSn and Pd$_2$MnSb(Heusler alloys), rel. to mag. and chem. order in Pd$_2$MnAl 8=31700
Pt-50% Co alloy, uniaxial anisotropy induced by tempering under stress 8=31702
Pt-Co ordered crystals, rel. to crystallite distrib. (texture) 8=36175
RbNiF$_3$, susceptibility and press. depend. of Curie temp. 8=48661
Rh-Fe, magnetic impurity, ordinary scattering rel. to exchange scattering 8=26863
Si steel, coercive forces temp. dependence in deformed crystals 8=36174
Si-Fe crystals, coercivity rel. to domain structure 8=31704
Si -Fe single crystals, effect of dislocations on magnetization process 8=26677
Sn-Co, in liquid state, and elec. resist. 8=43871
Sn-Ni, in liquid state, and elec. resist. 8=43871
SrRuO$_3$, rel. to band structure 8=36177
Tb, anisotropic high field props. from mag. moment meas. at 4.2°K 8=31705
Tb, exchange interactions, from inelastic n. -scattering 8=31709
Tb, magnon energies and exchange interactions 8=45030
Tb, spin-wave spectrum and exchange interactions 8=31707
Tb-10% Ho, exchange interactions, from inelastic n. -scattering 8=31709
Tb$_3$Al$_2$, metamagnetic 8=49544
TbAu$_2$, mag. structs. 8=27426
Tb-Y alloy, mol. field soln. 8=31708
Te^{125} hyperfine struture in Fe-rich (ferromag.) mats. from Mossbauer spectra 8=26027
TiCo alloys, susceptibility comp. dependence at 295°K and 77°K 8=31920
TiFe$_x$Co$_{1-x}$ alloys, localized magnetization from n-scattering 8=30912
Tm, from mag. moment meas. at 4.2°K 8=31706
U$_6$M, (M=Mn, Fe, Co, Ni) and alloys, rel. to superconductivity 8=27036
UO$_2$, antiferromag., weak ferromagnetism rel. to canted structure and domains 8=49574
US-ThS system 8=49545
UX, (X=S, Se, Te), explanatory model 8=36179
Y$_{2.1}$Ca$_{0.9}$Fe$_{4.1}$Sn$_{0.9}$O$_{12}$, effective mag. fields at Fe^{57} and Sn^{119} nuclei, rel. to non mag. Sn^{4+} conc. 8=36197
Y$_y$(Mn$_x$Fe$_{1-x}$)$_z$, ($y = 1, 6$; $z = 2, 23$) magnetisation and susceptibility, 80-1500°K 8=31710
YFe garnets, from Mossbauer effect, 85-600°K 8=36196
YFe garnet, magnetoelastic instability in uniform precession 8=36221
YFe garnet: Yb, ion-ion interaction via magnon field 8=40830
ZnCr$_2$O$_4$, spin-structure determ. from magnetization and resonance 8=31731
ZnCr$_2$Se$_4$, spin magnetism 8=36136
(ZrCo$_2$)$_x$(ZrFe$_2$)$_{1-x}$ alloys, hyperfine field distribs. from Mossbauer spectra 8=31712
Zr$_{1-x}$Gd$_x$Zn$_2$, and NMR rel. to localized mag. moments effect in ZrZn$_2$ 8=36180
in (Zr$_{1-x}$Hf$_x$)Zn$_2$ system 8=40831
Zr$_{1-x}$M$_x$Zn$_2$ where M = Ti, Y, Nb or Hf, magnetization, Curie temp 8=49546
ZrZn$_2$, rel. to itinerant electron model 8=31547
paramagnetic
See also Paramagnetic resonance and relaxation; Paramagnetism.
alloy, dil., ground state analysis 8=40200
alloys, dilute, enhanced effective exchange interaction due to localized spins 8=31594
alloys, dilute, superconducting, order parameter spacial variations 8=31332
alloys, dil., with spin-½ impurities, s-d scatt. theory 8=44980
alloys, susceptibility of quasi-bound state 8=44979
dilute, Curie temp. variation rel. to ion conc. 8=36076
di(tetramethylammonium)bis(maleonitriledithialato)CuII, X-ray and e.s.r. studies 8=35364
exchange enhanced Curie Weiss θ's, effect of spin-flip scattering 8=40747
impurities, electron scattering, analytic structure solution 8=40748
impurities in oxide layer of tunnel diode anomalous tunneling theory 8=31410
ketene molecule 8=25589
magnesioferrite, superparamagnetism rel. to precipl. and coarsening in MgO-Fe solid solns. 8=44007
magnetic cooling, thermodynamic and statistical aspects 8=31518
metals, rel. to virtual spin-wave effects 8=31517
methylene fluoride, molec. susceptibility 8=34339
moment fluctuations, temporal, by neutron diffraction 8=31516
p-phynylenediamine-chloranil charge-transfer complex, mag. excitations 8=31880

Magnetic properties of substances—contd
paramagnetic—contd
pyrocarbons, B-doped, susceptibility at room temp. 8=27084
rare earth h.c.p. crystals, field effects on inelastic n scatt. 8=40749
rare-earth sodium molybdates, axial anisotropy from susceptibility meas., 2-300°K 8=31528
salt soln., mag. resonance in eddy solenoidal field 8=34905
spin lattice vibrations 8=36075
spin relaxation, anomalous, near mag. transition 8=49582
superconductors with impurities, conc. non-uniformity, effect on props. 8=44705
TEMPAD biradical, susceptibility, anomalous behaviour 8=40756
transition metal alloys, dilute, moments 8=45031
transition metal alloys, spin susceptibility, exchange enhancement rel. to. rigid-band model breakdown 8=31532
transition metals, orbital susceptibility calc. from band structure 8=31529
transition metals, 3d, stability of non-magnetic state 8=40746
vinylidene fluoride, MO theory 8=29803
B-C cpds, paramag. centre comp. dependence 8=45077
B.C. cpds, susceptibility conc. dependence 8=31520
$CaF_2:Eu^{2+}$ relaxation time meas. using optical Faraday rotation technique 8=49479
CaS : Zr phosphors, susceptibility obs. 8=44967
CoO, rel. to anomalous elastic props. and internal friction from u.s. meas. 8=44560
Cr-Cs alum, susceptibility rel. to cross relax 8=27486
CrH_x, (x < 1), anomalous behaviour rel. to H-orbital expansion effect on d-electron exchange 8=49480
Cr_2O_3 powder, Néel temp. depend. on particle size 8=40861
CrX_3 (X=Br, F), n. scattering energy distrib. 8=31521
Cu diethyldithiocarbamate 8=49485
Dy, effect of hydrostatic pressure 8=36082
Er, neutron scattering, rel. to interactions 8=31523
Eu^{3+} ion, magnetic case history 8=31522
Eu_3O_4, Curie temp., from inverse susceptibility 8=40734
EuO_2S, and structures from n. diffr. meas. 8=40869
EuP, Eu^{3+} spin $\langle S(T)\rangle$ temp. dependence from P^{31} n.m.r. obs. 8=31904
$Fe(OH)_2$, hyperfine fields from Fe^{57} Mossbauer meas. 8=39517
Fe-Pd alloys, dil., hyperfine field at Fe, mag. field dependence at 1.2°K (T_c < 1.2°K) 8=36081
$Fe_3(PO_4)_2 \cdot 4H_2O$, ludlamite, single crystal susceptibility obs. 8=27379
Fe–Ru alloys, susceptibility, Mössbauer eff. 8=49481
FeS_2 pyrites, rel. to valence and spin states 8=36078
Gd, susceptibility forromag. impurity dependence near Curie temp. 8=40751
n-Hg Te, susceptibility singularity 8=44981
Ho, neutron scattering, rel. to interactions 8=31523
K-chloranil, susceptibility transition in 210-260°K region 8=31535
$KMnF_3$, susceptibility, semi-empirical expression by Padé approximant 8=27386
$LuFeO_3$, susceptibility, semi-empirical expression by Padé approximant 8=27386
$MnAs_x\ Sb_{1-x}$ solid solns, susceptibility and structure 8=49482
Ni films, u.v. reflection, near Curie point 8=36399
Ni, lattice dynamics 8=35391
Ni, Stoner modes, spin waves and crtical fluctuations 8=36215
Ni, susceptibility calc. 8=49483
Ni, susceptibility calc. contrib. of intra-atomic exchange enhancement 8=31524
Ni: Cd^{111}, (Ru^{99}), hyperfine fields at solutes from perturbed-angular-correlation exam. above and below T_c 8=40992
Ni-I boracite, susceptibility temp. dependence 8=31525
$NiSe_2$ pyrite 8=31493
$NiSiF_6$, susceptibility rel. to cross relax 8=27486
Ni-V, (Rh), (Pt), and ferro-props., 14-1000°K 8=31683
Pd alloys, susceptibility rel. to band structure and exchange-enhancement effects 8=31294
Pd, susceptibility calc. 8=49483
Pd, susceptibility meas. vs field and temp., rel. to exchange enhancement 8=31526
Pd–Fe alloys, high-field susceptibility 8=40752
Pd-Fe alloys, high-field susceptibility conc. dependence 8=36080
Pd-Fe alloys, very dil., low temp, magnetization 8=36079
Pd-x at. % Ni alloys (x ⩾ O), s-electron-paramagnon scattering rel. to low temp. elec. resistivity 8=31323-4
Pt alloys, susceptibility rel. to band structure and exchange-enhancement effects 8=31294
Pt, susceptibility calc. 8=49483
Pt, susceptibility meas. vs field and temp., rel. . to exchange enhancement 8=31526
Pt-1 at % Co(Fe) alloys, and elec. props., plastic deformation effects 8=31327
Pt-Co(Fe) alloys, local-moment saturation from NMR obs. 8=31527
PuO_2, susceptibility, Van Vleck paramagnetism 8=40753
$RbMnF_3$, spin correlations in paramag. state 8=49484

Magnetic properties of substances—contd
paramagnetic—contd
Tb, critical n.-scattering inelasticity above Néel temp. 8=31530
Tb, effect of hydrostatic pressure 8=36082
Th carbides, carbonitrides and nitrides 8=31531
TiH_x, ($x < _2$), anomalous behaviour rel. to H-orbital expansion effect on d-electron exchange 8=49480
UO_2, rel. to u.s. attenuation and elastic constants 8=39898
US–ThS system 8=49545
V_2O_3, susceptibility, 300°-700°K 8=31534
V_2O_5, susceptibility meas. and calcs. 8=36083
V_3Si, absence of neutron scattering rel. to d electrons in conduction band 8=40754
$Y_3Al_5O_{12}$ system, wavelength dependence of Faraday rotation 8=44982
Yb, susceptibility from mag. moment meas. at 4.2 ~300°K 8=31706
Zr, susceptibility anisotropy temp. dependence 8=40755
transitions
antiferromagnets, orbital, in two-magnon scattering of neutrons 8=45047
binary alloys, effect on vapour pressure temp. dependence 8=35014
crystals with domain structures, local temps. 8=40781
Heisenberg systems, two-dimensional, expt. verification of spin-wave predictions 8=36088
magnetic system distortion 8=36064
neutron diffraction investigation 8=36136
paramagnet, diluted by diamag. ions, Curie temp. variation rel. to mag. ion conc. 8=36076
rare earth crystals, mag.-ordering temp., pressure dependence 8=31652
rare earth ferrite garnets, para-process near Curie temp. 8=45040
rare earths, h.c.p., associated entropy 8=49453
seignettomagnetics, from Mossbauer studies 8=27442
spin relaxation, anomalous, near mag. transition 8=49582
transition metals and alloys, electronic sp. ht. enhancement near paramag. to antiferromag. instability 8=31922
$BaTiO_3$–$BiFeO_3$ solid solns., e.p.r. study 8=27488
$Bi_{1-x}Ca_xMnO_3$, solid solns., temp.-comp. dependence rel. to structural transitions 8=27377
$BiFeO_3$ solid solns. 8=27285
$BiFeO_3$-$Pb(Fe_{0.5}Nb_{0.5})O_3$ solid soln. system 8=39543
$(1-x)BiFeO_3$–$xSr(Sn_{1/2}Mn_{2/3})O_3$, solid solns., from Mossbauer studies 8=27442
$Co_2BaFe_{16-x}In_xO_{27}$, Curie pt. comp. dependence 8=45038
CoO, rel. to anomalous elastic props. and internal friction from u.s. meas. 8=44560
Cr films, antiferro-paramag., rel. to resistivity anomaly 8=39590
Cr, Neel pt. and spin-slip, pressure and temp. dependence 8=31766
Cr_2O_3 powder, Neel temp. depend. on particle size 8=40861
Dy, effect of hydrostatic pressure 8=36082
Dy, effect on thermal conductivity anisotropy, 5-300°K 8=35458
Dy, mag.-ordering temp., pressure dependence 8=31652
Dy, ordering temps. at high pressures 8=40730
Dy_3Al_2, metamagnetic 8=49544
$DyFeO_3$, rel. to sp. ht. meas., 1.2–80°K 8=35429
$Dy_xY_{1-x}Fe_2$, Curier temp. and coercivity comp. dependence 8=31610
Er, effect on thermal conductivity anisotropy, 5-300°K 8=35458
ErGa garnet, metamag. transition and antiferromag. struct., 0.31 and 4.2°K 8=40867
EuO, Curie-point increases by selective damping 8=31612
EuO, λ anomaly and magnetoelastic interactions from magnetostriction meas. 8=45011
Eu_3O_4, antiferromagnetic temp., rel. to susceptibility peak 8=40734
EuS, ferromag.-paramag., critical line existence 8=36137
Fe:Mn, transition impurities, hyperfine field at Mn 8=40814
Fe-Ni alloys, f.c.c., Curie temp. and C effect 8=31646
Fe_2O_3, antiferro- to weak ferromag. from magnetostriction study 8=40868
$Fe(Pd_xPt_{1-x})_3$, antiferro-ferromag., mechanism, obs. 8=40808
Fe-Rh alloys, pressure dependence 8=40735
Fe_2TeO_6, temp. determ. by Mössbauer effect 8=49457
Gd, mag.-ordering temp., pressure dependence 8=31652
Gd, ordering temps. at high pressures 8=40730
Gd, u.s. attenuation at Curie pt. 8=35416
K-chloranil, in paramag-susceptibility in 210-260°K region 8=31535
KD_2PO_4, Curie temp. shift on hydrostatic pressure, theoretical explanation 8=40818
KH_2PO_4, Curie temp. shift on hydrostatic pressure, theoretical explanation 8=40818
Mn, lattice params. and thermal expansion rel. to para-antiferromag. transition, –180-1500°C 8=44253
Mn, paramag. to ferromag., rel. to cryst. structure 8=48663
MnF_2, u.s. attenuation meas. near Néel point 8=48720
MnP, Curie screw-ferromag. pts, pressure dependence 8=31656

- **Magnetic properties of substances**—contd
  - **transitions**—contd
    - Mn- Pt system, structures and transforms. rel. to exchange interactions 8=45017
    - Mn_3Pt, transformation, first-order, x-ray and susceptibility study 8=31777
    - MnSb, high-press. 8=26407
    - $MnSn_2$, antiferromagnetic, neutron-diffraction study 8=31779
    - NdB_6, antiferromagnetic to paramagnetic 8=40873
    - Ni alloys, Curie point, change after plastic deform 8=40823
    - Ni, ferromag., temp. pressure-dependence, itinerant-electron-theory 8=27424
    - Ni near Curie point, magnetic eqn. of state 8=40828
    - Ni-Cu alloys, ferromag., temp pressure-dependence, itinerant-electron theory 8=27424
    - NiS, first-order-paramag-antiferromagnetic 8=31788
    - Pb films and foils, parallel and perpendicular, temp. (1-4.2°K) and thickness dependence 8=40741
    - $(Pb_xSr_{1-x})TiO_3$ crystals, $x \approx 0.25$, Curie temp. 8=44139
    - Pd:Ni dilute alloys, conc. depend., localized exchange enhancement model 8=35432
    - Pt_3Fe, ordered, mixed antiferromag. -ferromag. state 8=31789
    - Sc, lattice params. and thermal expansion rel. to para-antiferromag. transition, 20-660°C 8=44253
    - Sn films and foils, parallel and perpendicular, temp. (1°K-T_c) and thickness dependence 8=40741
    - Tb, effect of hydrostatic pressure 8=36082
    - Tb, mag. -ordering temp., pressure dependence 8=31652
    - Tb, ordering temps. at high pressures 8=40730
    - $TbAg_2$, antiferromag. 8=40877
    - Tb_3Al_2, metamagnetic 8=49544
    - $TbAlO_3$, metamagnetic, at 1.5°K 8=31798
    - $TbAu_2$ 8=27426
    - Ti, lattice params. and thermal expansion rel. to para-antiferromag. transition, —180-1500°C 8=44253
    - Ti_2O_3, neutron-diffraction data 8=31800
    - $(U_{1-x}Th_x)O_2$, first -order paramag.-antiferromag. 8=31803
    - V, lattice params. and thermal expansion rel. to para-antiferromag. transition, —180-1500°C 8=44253
    - V_2O_3, neutron-diffraction data 8=31800
    - V_2O_3, susceptibility, 300°-700°K 8=31534
    - Zr compounds with Laves structure, ferromag. to paramag., rel. to crystal structure 8=31711
- **Magnetic resonance and relaxation**
  - See also Antiferromagnetic resonance; Ferrimagnetic resonance; Ferromagnetic relaxation; Ferromagnetic resonance; Nuclear magnetic resonance and relaxation; Paramagnetic resonance and relaxation.
  - adiabatic rapid-passage expts. in solids for spin-lattice relax. determ. 8=31804
  - alkali atom, elec. dipole moment upper limit determ. 8=43177
  - alloys, dil., elec. field gradients around impurities, direct meas. 8=48313
  - asymmetry in mag. second-rank tensor quantities 8=49575
  - Bloch equations, remarks 8=47675
  - Bloch's magnetodynamic eq., two modifications and generalizations 8=47678
  - in complex semiconductors 8=40889
  - dialkyl ketones, protonated, (dialkylhydroxycarbonium ions), protons spectra 8=38907
  - dipolar temp. concept in solid state spin systems, physical consequences 8=49576
  - in effective field 8=38908
  - exchange narrowing, quantum statistical theory 8=40967
  - ferrite cores, magnetoelastic resonance 8=36326
  - ferrites initial permeability at microwave and natural gyromagnetic resonance 8=31715
  - ferrites, magnetoacoustic resonance excitation in non-linear ferromag. resonance 8=49064
  - Gaussian absorption lines, unsaturated, modulation broadening of shape 8=25633
  - Heisenberg linear chains finite, linewidths rel. to time correlations 8=31549
  - macroscopic spin quantities, equations of motion 8=37532
  - in magnetically ordered systems with two sublattices, phenomenological theory 8=40879
  - magnetostatic mode freq. and pattern, determ. method 8=37533
  - metallic powders, echo phenomenon 8=27448
  - microwave resonance, saturation phenomena, diagrammatic approach to nonlinear susceptibility 8=48297
  - modulation broadening of unsaturated mag. resonance line shapes 8=47674
  - new technique for studying metastable autoionizing states of atoms 8=43244
  - non-Kramers paramag. ions, spin-lattice relax. rate $\propto T^5$, theory 8=40952
  - organic triplet states spectra, rel. to mol. and cryst. struct. 8=27449
  - organophosphorus cpds., C^{13} and P^{31} double resonance obs. 8=43401
  - pulse spectrometer, 8-mm 8=46502
  - rare earth ions in soln., p relax time and cluster asymmetry obs. 8=43870
  - rare-earth metals, and spin waves: thermal, applied field and magneto-elastic effects 8=31703
  - resonant helices in mag. res. 8=46500
  - ruby, spin-lattice relaxation and effect of Cr distribution on interaction 8=49621
  - salt soln., paramag., in eddy solenoidal field 8=34905
  - separation of unresolved lines by action of light radiation 8=47530
  - spectrometer, bidirectional square-wave generator 8=33141
  - spin echo signal formation by simultaneous action of local and mag. fields 8=40881
  - spin-lattice relax. time of impurity centres, role of exchange interact. 8=40953
  - spin-spin relaxation, problems and techniques 8=47676
  - spin systems, stochastic processes 8=29804
  - stochastic model for low field resonance and relaxation 8=47673
  - strain broadened spin resonance line shapes, broadening by point defects 8=49589
  - superconducting solenoids with high homogeneity mag. fields 8=28528
  - Ag-Mn alloy, transmission spin resonance of conduction electron-local-moment obs. 8=31860
  - CeO_2, spin lattice relaxation of Dy^{3+} and Yb^{3+} 8=36222
  - $CoCl_2$, far i.r. absorption in ferro-, ferri- and antiferromag phases 8=31813
  - CoF_2, antiferromagnet, in high mag. field normal to c axis 8=36230
  - Cu tutton salts, spin lattice relaxation, field dependence 8=40954
  - Cu-Mn alloy, transmission spin resonance of conduction electron-local-moment obs. 8=31860
  - D atom g_J ratio meas. 8=38734
  - Er orthoferrites, microwave mag. loss meas. near spin-reorientation temps. 8=36224
  - αFe-C(N), losses in case of Snoek relax., temp. depend. 8=40880
  - Fe:Co^{60}, spin lattice relax., low temp. deviations from Korringa law 8=45106
  - α-Fe_2O_3: Ti, rel. to doping and canted antiferromagnetic structure 8=36231
  - Gd hexa-antipyrene iodide, spin-lattice suppression as Raman relaxation 8=40951
  - H atom g_J ratio meas. 8=38734
  - H_2, compressed, spin-lattice relax. timing, data acquisition system 8=29805
  - H_2 mol., mag. shielding in elec. field 8=47599
  - He^3, spin-lattice relax. from negative temps. 8=33004
  - Hg, double-resonance broadening, 6^3P_1 state 8=38732
  - Ho orthoferrites, microwave mag. loss meas. near spin-reorientation temps. 8=36224
  - $(IrCl_6)^{2-}$ complex in $(NH_4)_2PtCl_6$ and K_2PtCl_6, spin-lattice relax. 8=49622
  - $(IrCl_6)^{2-}$ complexes in $(NH_4)_2PtCl_6$, nearest-neighbour exchange coupled pairs, spin-lattice relax. 8=49623
  - $La_2Mg_3(NO_3)_{12}.24H_2O:Cu^{2+}$, spin-lattice relax 8=40950
  - Mg-Mn ferrite sphere, magnetostatic spectrum, anisotropy dependence 8=40888
  - $Mn_xFe_{3-x}O_{4+\gamma}$, Richter type relax., details 8=36219
  - NH_4I, cubic and tetragonal magnetizations, coexistence 8=40740
  - NaCl type crysts., anistropy of spin-lattice relax. time in strong mag. field 8=27492
  - Nb-Zr alloys, type II superconductors, spin lattice relaxation 8=44744
  - O-H_2 and HD solid mixtures, spin-lattice relax. time 8=27493
  - PbF_2: Yb^{3+}, spin-lattice relaxation 8=36253
  - $Rb^{85,87}$ atom g_J ratio meas. 8=38734
  - n-Si, spin-lattice relax., concentration depend. 8=45107
  - Sm^{155} nuclear spin obs. method 8=29331
  - Tm orthoferrites, microwave mag. loss meas. near spin-reorientation temps. 8=36224
  - V-Ti alloys, type II superconductors, spin lattice relaxation 8=44744
  - YFe garnet, subsidiary absorpt. region, freq. of spin waves 8=49563
- **Magnetic storms**
  - cosmic-ray intensity increase, storm-time increase 8=42747
  - DS field, low-latitude rotation, and westward drift of ring current 8=50212
  - effect on duct formation for whistler propagation 8=50187
  - electrons, energetic, effects at 6.6 Re equator and auroral subzone, correl. 8=41405
  - f_0F2, N-S asymmetry in storm time var. 8=28002
  - geomagnetic, and solar activity, 1966 8=28176
  - heights of nighttime F region during intense mag.-ionospheric storms in IGY and IQSY 8=45548
  - ionization changes in middle latitude D-region 8=41441
  - ionosphere D region, long lasting effects on amplitude of 245 kHz signals 8=27987
  - inosphere e content enhancements assoc. 8=45512
  - ionosphere, topside, variation of, obs. 8=41435
  - micropulsation sources, polarization 8=28011
  - polar, correl. with DR-variation 8=45563

Magnetic storms
- polar disturbances and currents, laws 8=36886
- polar substorms in conjugate areas, rel. to solar wave radiations and electrojet 8=41462
- polar substorms, rel. to v.l.f. emissions in magnetosphere 8=41390
- radiation belts, storm-time, growth during magnetospheric substorm 8=50172
- radiation zones, temporary, caused by storm 8=45564
- ring current effects on cosmic rays 8=38288
- s.s.c., e.m. induction in earth model allowing for ocean effect 8=50205
- Starfish effect, Indian Ocean intensity max. 8=41468

Magnetic traps. See Plasma/confinement.

Magnetic wells. See Plasma/confinement.

Magnetism

See also Antiferromagnetism; Diamagnetism; Earth/magnetic field; Ferrimagnetism; Ferromagnetism; Gyromagnetic effect; Magnetohydrodynamics; Paramagnetism; Rock magnetism; Stars/magnetism; Sun/magnetism.
- book, physical aspects 8=28448
- conference in Boston, Sept. 1967, review 8=49454
- congress, international, USA (1967) 8=27368
- conventions and nomenclature 8=24121
- critical phenomena in magnetic systems, expt. obs. 8=34980
- crystals, magnetic-ion multiplicity effects in exchange interactions 8=31254
- demagnetization effect of rectangular prism 8=50204
- electron-magnon scattering and polarization of scattered beam 8=35754
- magnetic impurities, in a metal, methods of approaching Kondo's problem 8=35816
- magnetostatic boundary-value problems and soln. 8=33038
- magnetostatic waves at singular turning points, effect of finite linewidth 8=27372
- piezomagnetism and magnetostriction, temp. depend., rel. to single-ion model 8=31483
- quantum theory, kinematic interactions 8=49456
- shape anisotropy in polygonal prisms 8=31484
- in solids, in high magnetic fields 8=31478
- specific ht. shape dependence in systems with long-range interactions, shape dependence 8=35423
- surface levels in prescence of superconductivity 8=44958
- theory, quantum statistical methods 8=24106
- $ZnCr_2Se_4$, spin 8=36136
- Zr compounds, with Laves structure, and crystal structure 8=31711

Magnetization process

See also Ferromagnetic relaxation.
- anhysteretic, curves for processes of reversible 180°domain wall motion 8=31565
- Barkhausen discontinuities, size distrib. calc. from simple model 8=31669
- Barkhausen effect, statistical models 8=40787
- by Barkhausen jumps, hysteresis freq. depend., model 8=40789
- Barkhausen jumps model 8=40782
- Barkhausen jumps in Ni, ultrasound influence 8=36163
- Barkhausen noise, temp. depend. anomalous effect obs. 8=40792
- bimodal state in permalloy annealed cylindrical films 8=49540
- chain of spins ½, susceptibility in oscillating field, calc. 8=44997
- curve measurement in superconductors by electronic integration 8=49458
- demagnetization effect of rectangular prism 8=50204
- demagnetization tensors in composite bodies, diagonal sum rule 8=40724
- ferrites, hard, magnetic reversal 8=31739
- ferromag. thin films, saturation, extension of Heisenberg trace and spin wave methods 8=36113
- ferromagnet, direction distributions around spherical cavity 8=40757-8
- ferromagnet, polycryst., phase model 8=36103
- ferromagnets, Barkhausen jumps, existence of 2 independent mechanisms 8=49504
- ferromagnetic crysts., curve rel. to uniaxial lattice deform. 8=36104
- ferromagnetic discs, rotating in mag. fields, energy losses 8=36102
- ferromagnetic film, walls, Bloch, Neel and intermediate 8=36106
- ferromagnetic films, thickness-, anisotropy- and temp.-dependence 8=36116
- ferromagnetic powders, susceptibility calcs. in weak fields, model 8=40800
- film coercivity meas. rel. to temp., automatic recording 8=31583
- film storage-elements, controlled easy-axis distrib. 8=49511
- films, ripple, linear and nonlinear theories 8=36109
- films, spin wave resonance 8=36114
- films, thin, electro- and magneto-optical obs. 8=36107
- hysteresis, dynamical loop representation 8=44961
- incremental permeability round different quiesient flux points, use in memory 8=28533

Magnetization process—contd
- interaction energy of interstitial atoms and solute atoms pairs with the magnetization 8=31614
- micromagnetism, local field theory 8=31566
- permalloy, ferromagnet, Barkhausen effect in determ. elastic limit 8=26838
- Permalloy film spots nucleation, struct. and field rel. to dimensions, obs. 8=31673
- Permalloy films, coercive force in supercritical transition, obs. 8=31629
- Permalloy films demagnetization factors, ferromag. reson. obs. 8=31223
- Permalloy 78 films, demag. rel. to alternating field freq., obs. 8=31692
- plate, boundless homogeneous, micromagnetic analysis of reversal 8=36101
- rare-earth alloys with 4f e conc = 10, 11 8=31654
- Rayleigh region, Neel theory and experimental results contradiction 8=31564
- time constant and impedance calc., empirical formula 8=33049
- $BaCo_2Fe_{16}O_{27}$, rotatory hysteresis losses and anisotropy 8=45037
- $BaFe_{12}O_{19}$, rotatory hysteresis losses and anisotropy 8=45037
- Co borides, density of states curve 8=35426
- Cu-Pb superconducting alloys, rel. to microstructure 8=44723
- Dy aluminate, dipolar 8=36136
- $DyEr_x$ ($x = 1, 3$) alloys with 4f e. conc = 10, 11 8=31654
- Fe ferromagnet, Barkhausen effect in determ. elastic limit 8=26838
- Fe films, coercive force in supercritical transition, obs. 8=31628
- Fe films, Richter-type aftereffect 8=31633
- Fe filoform microcrystals, effect of dislocations 8=26677
- Fe–Al alloys, effect of K-state 8=49525
- Fe-Ni(50-50) crystals, n-irradiated in mag. field, curves 8=36144
- Fe–3%Si by Barkhausen jumps, hysteresis freq. depend., obs. 8=40789
- Fe-Si single crystals, effect of dislocations 8=26677
- FeSi, in alternating fields up to 20 kcpsec. rel. to ferromag. domain behaviour 8=49524
- Ho_xEr_y alloys with 4f e. conc = 10, 11 8=31654
- MnSb, crystal anisotropy 8=49530
- NH_4I, cubic and tetragonal, coexistence, proton spin-lattice relaxation determ. 8=40740
- Nb, supercond., n-irrad. induced hysteresis, obs. 8=40373
- Nb_3Sn, hard supercond. tubes, flux jumps, 4.2°K 8=31341
- Nb-Zr, hard supercond. tubes, flux jumps, 4.2°K 8=31341
- Ni, Barkhausen discontinuities, size distrib. calc. from simple model 8=31669
- Ni, Barkhausen jumps, ultrasound influence 8=36163
- Ni ferromagnet, Barkhausen effect in determ. elastic limit 8=26838
- Ni, near Curie point, spontaneous, by neutron depolarization meas. 8=45019
- Ni-Fe films, static reversal, effect of anisotropy dispersion 8=36155
- NiFe ferrite by Barkhausen jumps, hysteresis freq. depend., obs. 8=40789
- Pd–Fe alloys, spin-wave stiffness constant field dependence 8=45026
- PdFe alloys, spontaneous magnetization 8=36172
- $SrO.4Fe_2O_3.2Al_2O_3$, with high anisotropy field 8=31741

Magnetization state
- analysis by e diffraction technique 8=44998
- anisotropy, and of energy, torque meas. 8=31667
- anisotropy due to screw dislocations, calc. 8=40790
- antiferromagnet ground state in mag. field of arbitrary direction 8=45045
- antiferromagnet, ground-state sublattice 8=36200
- cerous magnesium nitrate, high field magnetization anomaly obs. 8=44968
- ferrite, polycrystalline, associated magnetostatic energy 8=49550
- ferromagnet, continuous recording apparatus 8=49505
- ferromagnet with non-magnetic impurities, local magnetization of neighbouring ions 8=36105
- ferromagnetic materials, calc. of curve 8=37408
- ferromagnets, cylindrical, anisotropic field and position of easy magnetization axis, meas. methods 8=40785
- ferromagnets, transitions between uniformly and nonuniformly magnetized states, thermodynamic 8=40788
- film, determ. technique, comments 8=46389
- films, anisotropy dispersion rel. to magnetization increments near saturation, obs. 8=31578
- films, ferromag., anisotropy of localized sections rel. to pulse switching, obs. 8=31580
- films, multilayer, coupling 8=36133
- fluctuations, critical, neutron-scattering studies 8=31481
- impurity states rel. to electronic props. 8=35741
- Invar, pressure depend. from 30-450 kbar 8=31622
- Keweenewan rocks, partial self-reversal, magnetization of Portage Lake lavas 8=32369
- Keweenawan rocks, partial self-reversal, magnetization of upper lavas and sediments and lower dikes 8=32370

Magnetization state
- measurement to high pressures 8=27371
- metal surface levels, obs. in surface impedance meas. geom. modifications effects 8=44655
- moment-method calculation, and interspin-energy diffusion 8=27367
- Permalloy films, anisotropy and blocking fields rel. to r.f. losses, obs. 8=31678
- Permalloy films, struct. stability in pulsed orthogonal fields, obs. 8=31691
- Permalloy films uniaxial anisotropy, mag. annealing effects, 20-400°C 8=31677
- prolate spheroids of saturated, ferro-mag. polycryst. materials, form effect 8=40793
- prolate spheroids of saturated polycryst. materials, form effect 8=40794
- pulsed field, meas. apparatus for 500kOe 8=46362
- Silectron, pressure depend. from 30-450 kbar 8=31622
- single crystals for n.q.r. obs., orientation determ. of mag. axes 8=44959
- space groups and their irreducible representation 8=31488
- structure analysis, mag. symmetry invariance and classical representation theory 8=31482
- superconductors, two band, localized mag. states 8=49455
- uniaxial antiferromagnet, weak ferromagnetism, magnetization curve, influence of second anisotropy constant 8=36203
- Au$_4$Mn, pressure effect 8=36069
- Au$_4$V, ordered, V moment 8=49463
- Dy, anisotropy meas. in pulsed fields up to 150 kOe 8=40743
- DyAl garnet, and mag. ordering, 0.37°K 8=40866
- DyAl garnet, change below 1.7°K, model 8=45057
- Er, anisotropy meas. in pulsed fields up to 150kOe 8=40743
- ErGa garnet, antiferromag. struct. and metamag. transition, 0.31 and 4.2°K 8=40867
- EuFe garnet, of sublattices 8=40839
- Fe alloys, f.c.c., containing Pt group elements, saturation 8=40736
- Fe, deviations from Bloch law 8=27411
- Fe-rich solid solution alloys with non-transition elements 8=49519
- Fe-Co alloys, deviations from Bloch law temp. depend 8=27411
- FeF$_3$, sublattice magnetization near critical point 8=27416
- Fe-Ni alloys, deformed, return of saturation state and resistance 8=31639
- FeNi electrodeposited films, reversal obs. 8=31644
- Fe-Ni-Co films, anisotropy, obs. 8=31629
- α-Fe$_2$O$_3$, remanent magnetization, variation with temp. of natural and synethic crysts. 8=31647
- Fe(Pd$_x$Pt$_{1-x}$)$_3$ rel. to antiferro-ferromag. transition, obs. 8=40808
- Gd, anisotropy meas. in pulsed fields up to 150kOe 8=40743
- GdFe garnet, of sublattices 8=40840
- He^3, solid, nuclear spin interaction rel. to thermodynamic props. 8=41905
- LuFe garnet, of sublattices 8=40840
- Mn$_{1+x}$Fe$_{2-x}$O$_4$, induced anisotropy at low temps. 8=36188
- Mn-Zn alloys of CsCl type structure, and mag. structure 8=40819
- Mn-Zn-Ga alloys of CsCl type structure, and mag. structure 8=40819
- Ni alloys, effect of plastic deform. 8=40823
- Ni, anisotropy due to screw dislocations, calc. 8=40790
- Ni, disturbances rel. to substitutional impurities 8=36153
- Ni film, ferromag. reson. rel. to inhomogeneity, obs. 8=31821
- Ni, films electrodeposited and charged with H, effect of H on magnetization inversion 8=36170
- Ni-Fe films, single and double, reversible rotation regions, obs. 8=31690
- Ni-Fe-Al films, single and double, reversible rotation regions, obs. 8=31690
- Ni-Fe-Co films, single and double, reversible rotation regions, obs. 8=31690
- Ni$_3$Fe, anisotropy due to screw dislocations, calc. 8=40790
- Ni-Pd alloy, saturation, and g factor meas. 8=31666
- Tb, anisotropy meas. in pulsed fields up to 150 kOe 8=40743
- TmFe garnet, of sublattices 8=40840
- YFe garnet, demagnetization, shock-induced 8=31744
- Y$_6$Mn$_{23}$, ferrimag. coupling, polarized n obs. 8=40849

domains
- alnico, high-coercivity, powder pattern exam. 8=35346
- alnico, meas. using magneto-optical Kerr effect 8=36165
- basalt, white pattern zones of titanomagnetite grains, obs. 8=48588
- Bloch wall fast irreversible displacements model 8=40782
- Bloch wall friction, possible mechanisms 8=31564
- ferrites, high-uniaxial-anisotropy, domain-wall mobility 8=27428
- ferrites, rel. to initial permeability at microwave and natural gyromagnetic resonance 8=31715
- ferrites, square loop, simulation of wall motion and wall behaviour 8=45036
- ferromagnet, magnetization field near frontal plane rel. to domain formation 8=31554

Magnetization state—contd

domains—contd
- ferromagnet, uniaxial, Bloch wall energies in ext. mag. field perp. to hexagonal axis 8=40783
- ferromagnetic films, individually obs. by e-microscope 8=31586
- ferromagnetic films, teaching demonstration 8=27397
- ferromagnetic films with domain structure, spin waves 8=40798
- ferromagnetics, boundaries, interact. with dislocations 8=40784
- ferromagnetic, from light diffr. 8=45143
- ferromagnetic wall dynamics 8=36100
- ferromagnets and antiferromagnets, local transition temps. 8=40781
- film storage-elements, two-domain state and separating wall rel. to easy-axis distrib. 8=49511
- films electron microscope investigation of domain walls 8=33090
- films, thin, Bloch wall transitions 8=31589
- films, thin, transmission e microscope obs. 8=31590
- films, transition layers between domains 8=31555
- four-axial ferromagnets, (71°/180°) Bloch wall soln 8=49503
- hematite, and evidence for new wall structure 8=27408
- in imperfect crystals 8=35573
- Kittel open structure, modification 8=31557
- in martensite crystals of high-C Cr steel, e-microscope exam. 8=40805
- Néel wall energy in ferromag. films 8=31574
- orthoferrites, props. and device applics. of domains 8=49553
- oscillating walls, direct study 8=44960
- Permalloy films, abnormal Bloch wall motion under hard axis pulse drive 8=31668
- permalloy films, boundary dynamic props. 8=36167
- permalloy films, boundary energy meas. rel. to thickness 8=40826
- permalloy film, 1000Å, Néel wall structure and energy 8=31663
- Permalloy films, rel. to supercritical transition, thickness depend obs. 8=31628
- permalloy films, strong stripe, and 360° walls 8=45024
- permalloy film, wall movement, thermally activated 8=45020
- Permalloy films, walls and mag. fine struct. in switching, stroboscopic transmission e microscope obs. 8=31674
- Permalloy, single-crystal platelets, ferromagnetic 8=31664
- permalloy stripe-films 8=31693
- Permalloy thin film strips, meas. of wall energy 8=27420
- reversible 180° domain wall motion controlled by magnetostatic effects, magnetization curves derivation 8=31565
- vicalloy, in various structural states strained in tension 8=40804
- wall models, 180°, self-consistency meas. 8=31556
- wall streaming and obs. in permalloy films 8=31558
- wall structure in ferromagnet, perturbation theory 8=31559
- Co, crystals, tensile elastic strain effects 8=36173
- Co film, high-coercivity, magneto-optic obs. 8=36134
- Co films, fine structure form., e microscope obs. 8=31640
- Co films, polycryst., in switching, obs. 8=31598
- Co films, rel. to supercritical transition, thickness depend obs. 8=31628
- Co, 20° to 400°C 8=31498
- Co^{57} Mössbauer effect sources, mag., in mechanism of r.f. mag. field destruction of hyperfine Mössbauer spectrum 8=43945
- Co-Ni films, fine structure form., e microscope obs. 8=31640
- Co$_5$(rare-earth) high-coercive force mat., domain-boundary model 8=31500
- Eu chalcogenides, ferro- and antiferromag. 8=31613
- Fe films, fine structure form., e microscope obs. 8=31640
- Fe films, rel. to supercritical transition, thickness depend. obs. 8=31628
- Fe, unmagnetized, scatt. of thermal neutrons at boundaries 8=31642
- Fe, wall dynamics from pulsed n.m.r. expts. 8=31621
- Fe-Ni films, fine structure form., e microscope obs. 8=31640
- Fe-Ni-Co films, single cryst., and anisotropy, obs. 8=40809
- α-Fe$_2$O$_3$, ferromag, struct. close to low temp. transition 8=31648
- Fe-Si crystals, X-ray diffr. contrast at ferromagnetic domain walls 8=27409
- FeSi, ferromag., by magnetization in alternating fields up to 20 kcpsec, stroboscopical obs. 8=49524
- Mn-ferrite, structure from X-ray obs. 8=27434
- Ni films, fine structure form., e microscope obs. 8=31640
- Ni film, ultrasound from stripe domain resonance 8=31682
- Ni-Fe alloy films, -wall motion and ferromagnetic resonance losses 8=31695
- Ni-Fe films, rel. to anisotropy dispersion, temp. depend. 8=40821

Magnetization state—contd
domains—contd
Ni 81%-Fe 19% film, 180° domain wall energy density, rel. to thickness 8=45018
76%Ni-Fe films, type II stripe domains, obs. 8=40825
NiFe, thin coupled films, wall behaviour 8=49541
Pb films, epitaxially grown on PbTe, from Lorentz microscopy 8=36171
Si-Fe crystals, structure rel. to coercivity 8=31704
Si–Fe crystals, temp. dependence up to 650°C 8=40829
Si-Fe crystals, tensile elastic strain effects 8=36173
YFe garnet, -wall propag. vel., effect of Er doping 8=49565
Y Fe garnet, X-ray topographic and optical obs. 8=45044
YFe garnet: Si, wall mobility 8=31746
Magnetoacoustic effects
current loops, levitation 8=28522
echo phenomena in superconductors and normal metals 8=40364
ferrites, resonant elastic oscillation excitation at non-linear ferromag. resonance 8=49064
in ferromagnetics, near resonance, scatt. of l.f. e.m. waves by sound 8=40796
microwave acoustic waves, possibility of generation in ferromag. crystals 8=49508
piezoelectric mats., acoustic wave ineract. with cyclotron and helicon waves 8=27296
Procopiu, in ferromag. sample free at one end 8=45001
streaming in elec. conducting fluid, due to small disturbance waves 8=41845
wave, fast large amplitude, rel. to heating of H plasma 8=47839
Fe^{57} Mössbauer effect sidebands due to r.f. magnetic field 8=30513
Ga, cyclotron resonance, Doppler-shifted 8=48720
He plasma, flowing, waves 8=25738
$LiNbO_3$:Cr^{3+}, acoustic paramag. reson., 4.2°K 8=44318
Ni film, ultrasound from stripe domain resonance 8=31682
Sb, galvanomagnetic effects, 50-300°K rel. to band model 8=40330
Y garnet, resonance in 3-cm wavelength range, obs. using transverse pumping 8=35419
YGd garnet, resonance in 3-cm wavelength range, obs. using transverse pumping 8=35419
Magnetocaloric effects. See Magnetothermal effects.
Magnetocrystalline anisotropy. See Magnetic properties of substances; Magnetization state.
Magnetoelastic effects. See Magnetomechanical effects.
Magnetoelectric effects
See also Hall effect; Magnetoresistance.
eddy currents, plate moving in mag. field 8=33027
excitonic insulator in mag. fields 8=40261
films, negative cond. in transverse mag. field, mechanism 8=40300
galvanomagnetic effects, high-elect.-field, in piezoelectric semiconductors 8=31366
galvanomagnetic effects in strong mag. field, semiclassical transport theory 8=35755
higher-orders in Gibbs function 8=27374
magneto-conductivity in a.c. elec. field, nonlinear Boltzmann eqn. soln. 8=35748
magnetostatic waves at singular turning points, effect of finite linewidth 8=27372
metals, galvanomagnetic studies by heliconlike waves 8=26961
rigid cond. sphere or cylinder, travelling relative to sinusoidal mag. field, electromech. characts of interact 8=24108
saddle point optical transitions under crossed elec. and mag. fields 8=27543
semiconductors, many-valley rel. to dissipative effects disappearance 8=40427
semiconductors, thermogalvanomagnetic phenomena at high mag. fields 8=44751
susceptibility upper bound 8=26941
$AlTbO_3$, magneto-electric effect 8=36217
As, and galvanomagnetic effects and Fermi surface, correlation 8=40232
As, energy bands, galvanomagnetic investigation 8=26902
Bi, charge-carrier density from galvanomag. data at 4.2°K 8=26963
Bi-Sn-Te alloys, magnetothermoelec. and thermoelec. props. 8=35996
Bi–Te, in arbitrary mag. fields 8=31312
Fe, galvanomagnetic coeff. rel. to Fermi-surface determ. 8=31289
$FeTbO_3$ magneto-electric effect 8=36217
Ge, galvanomagnetic recombination effect 8=40461
Ge, galvanomagnetic recombination effect, with unequal Lorentz forces 8=40462
n-Ge with dislocations, magnetocond. and low-field magnetoresist. 8=35890
n-InSb, galvanomag. props. at 77°K 8=27117
in InSb, magnetoconductance of nonequilib. plasmas 8=44667
Ni, galvanomagnetic coeff. rel. to Fermi-surface determ. 8=31289
$Ni_3B_7O_{13}I$, ferromagnetoelectric, props. 8=31670
Ni-18 at.% Mn-8 at.% Fe alloy, longit. galvanomagnetic effect magnetization dependence rel. to anisotropy 8=40827
Magnetoelectric effects—contd
Os, galvanomag. props. and Fermi surface anal. 8=40327
Sb, galvanomag. props. in transverse fields up to 100kOe at 4.2, 20.4 and 77°K 8=49170
SiP_2 and $SiAs_2$, meas. 8=40484
Te, down to 0.05°K 8=35916
Te, galvanomagnetic effects, anisotropy, statistical interpret. 8=31394
Magnetogasdynamics. See Magnetohydrodynamics.
Magnetohydrodynamic generators. See Electricity/direct conversion; Magnetohydrodynamics.
Magnetohydrodynamic waves. See Magnetohydrodynamics; Plasma/magnetohydrodynamics; Plasma/oscillations.
Magnetohydrodynamics
See also Plasma/magnetohydrodynamics.
Alfvèn waves, intrinsic freq. and energy conservation 8=23807
Alfven waves in viscous fluid due to introduction of magnetic dipole 8=24171
aligned flow past flat plate, steady-state heat transfer phenom. 8=28589
axisymmetric rot. in viscous fluid of finite conductivity 8=46451
axi-symm. steady flow, effect of mag. field 8=46452
boundary layer on plane plate in presence of strong longitudinal mag. field 8=33115
boundary stability increase by crossing elect. and mag. fields 8=24196
boundedless at flows 8=46459
boundedness at flows 8=46460
channel flow, book 8=34614
channel flow, incompressible, viscous, steady and laminar 8=37445
conducting fluid flow in longitudinal mag. field, end effect 8=24181
conducting fluid motion due to flow rot. of disc in cylinder subject to axial mag. field 8=24184
conducting liquid boundary layer in uneven mag. field 8=24182
conducting liq. in rectangular ducts situated in transverse mag. field, velocity distribution 8=33114
conducting liquid, rot. under stationary disc in mag. field 8=24188
convective heat transfer during turbulent flow of cond. liq. in channel, alt. mag. field effect 8=41994
core flow in subsonic m.f.d. generator channels 8=41933
Couette, flow, unsteady with suction, similar solns. 8=46457
couple on slowly rotating solid 8=24190
curled flow in plane channel, influence of Hall effect on development 8=24187
current, azimuthal, excited in rot. cond fluid 8=24170
diocotron instability model 8=41950
duct with sectionized electrodes, space effects 8=24201
electrodynamic → MGD wave transformation 8=37441
electrolyte in crossed elect. and mag. fields, transport process simulation 8=41989
e.m. pump based pn pinch effect with constant metal flow 8=24178
energy-transport velocity of induced electromagnetic wave in lossy moving fluids 8=37442
epihydrodynamics, optimization techniques 8=34704
field-aligned flow past plate, porous or sublimable, skin friction, heat and mass transfer 8=33111
finite-magnetic-Reynolds-number effects in flows 8=46444
flow around plane plage 8=41990
flow due to accelerated plate 8=46454
flows, electrically driven, theory 8=24173
flow in infinite cylindrical configurations, boundary conditions and EMF calculations 8=37443
flows in pipes in presence of longitudinal elec. current 8=46447
flow in rectangular channel, charact. of boundary layers and their overlapping 8=46443
flow limited by insulating wall, study 8=46448
flow, non stationary satisfying on circulation property 8=24189
flow past a sphere, pressure distrib. 8=24192
flow past insulator 8=46449
flow-past profiles, relativistic 8=24183
flow, quasi-onedimensional, stability 8=46455
flow stability in infinitely long cylindrical pips, radial magnetic field 8=46456
flow through rectangular duct due to periodic pressure gradient 8=46450
flow, turbulent in channel, velocity profiles 8=46461
flow, unsteady, under influence of const. press. gradient 8=28591
fluid channel flows, couple stress effects 8=28590
fluid layer with finite resistivity, self-gravitational instability 8=43621
fluids, conducting homogeneous with horizontal interface, gravitational instabilities 8=33117
forced oscillatory motion of conducting, viscous liquid 8=33118
gas duct, nonconducting wall boundary layer 8=28593
gas subjected to oblique mag. field, rel. to nonuniform shock wave in gas at. rest 8=39184

Magnetohydrodynamics—contd
  generator channel, operation of cold electrodes 8=28474
  generator channel, potential distribution by equivalent circuit method 8=28472
  generator, electrodynamic effects of non-uniformity of mag. field and fluid parameters 8=28468
  generator, end effects and induced mag. field 8=24198
  generator, homopolar, d.c. pump 8=24199
  generator, open-cycle, applic. of aq. K_2CO_3 for admission of ionizing additive into duct 8=46360
  generator, optimum, with channel of constant cross section 8=46359
  generator, vector analysis 8=28469
  generator with finite electrodes, elect. conductivity effect on flow 8=28471
  generators, finite electrodes, end effects on fluid flow 8=28473
  generators with sectionalized electrodes, volt/ampere characts. 8=28470
  Hartmann boundary layer, stability 8=41988
  heat transfer in channel flow, thermal-entry region props. rel. to axial conduction 8=33110
  heat wave, cylindrical with uniform axial mag. field, obs. 8=28595
  hydromagnetic waves excited by slowly streaming cosmic rays 8=47191
  hydromag. waves propag. under action of Coriolis force 8=28596
  induction generator experiment 8=28467
  inviscid boundary layer problems 8=28586
  ion accel. mechanism, with hydromagnetic waves, in Crab nebula 8=41522
  jets, compressible, two-dimens.; hydromagnetic stability 8=46462
  Joule's dissipation of flow in const. transverse mag. flux 8=33113
  linear solution determination 8=33107
  linearized, flow past semi-infinite flat plate in transverse magnetic field 8=46446
  liquid film down inclined conducting plane, hydromagnetic stability 8=28592
  liquid metal automatic metering device for die casting machine 8=24174
  liquid metal drops falling in viscous dielectric in longit. mag. field 8=30390
  magnetofluid dynamics, pressure distrib. meas. around sphere 8=28588
  magnetoionic wave eqns. in cylindrical geometry 8=37440
  MGD, axisymmetric mixed flow 8=24195
  MGD flow, steady 2 dimensional general 8= 46458
  MGD, non-ideal, discontinuities 8=24175
  MGD shock wave, unsteady, curvature and torsion of mag. lines behind wave 8=46167
  molten metal in d.c. pump duct, static equilibrium 8=24179
  motion of cylinder in viscous elec. cond. medium in mag. field 8=41991
  noble gases in generator, mag. induced ionization 8=37448
  past thin bodies, with inwardly diffusing mag. field, flow modification 8=41995
  phenomena similarity, non-dimensional groups definition 8=24172
  plane flow, laminar mass transfer in oriented mag. field 8=33112
  plane shock wave in gas, fading in transverse mag. field 8=33106
  plane waves, influence of imperfect boundaries 8=23923
  plastic —viscous medium, vel. profile through slot in transverse mag. field 8=37446
  propane-O, K_2CO_3 seeded plasma in duct, pot. distrib. and electrode voltage drop, obs. 8=39084
  pulsed generator with superconducting magnet system 8=37376
  Rayleigh-Taylor instabilities, experiment and theory 8=24197
  rear stagnation point, differential eqn. 8=24191
  relativistic, shock waves and compressibility hypotheses 8=28587
  relativistic, simple waves 8=41987
  relativistic, solution to propagation problem 8=24176
  shock tube generator, unsteady flow 8=28594
  shock wave, magnetogasdynamic, with conductivity jump 8=33119
  shock waves decay 8=33108
  sliding mag. field generation in linear machine with finite dimensions 8=37375
  solar processes, laboratory simulation 8=33109
  stagnation-point flow near front of blunt body, general and accurate anal. 8=43624
  stators, max. pondermotive force at in-phase connection 8=24200
  steady flow past slender bodies, establishment 8=24186
  steady-state flow of conducting fluid at large Hartman numbers 8=41993
  theory applied to plasma 8=39086
  thermal instability of magneto fluid in vertical rectangular channel 8=24185

Magnetohydrodynamics—contd
  three-layered fluid, development of flow in plane tube in presence of transverse mag. field 8=30204
  transients in magneto-ionic media 8=37444
  turbulence damping in pipes by longit and transverse mag. fields 8=24194
  turbulence, numerical expt. with incompressible eqns. 8=33116
  turbulent boundary with longitudinal press. gradient 8=24193
  viscous, incompressible and elect. conducting fluid, confined vortex flows 8=41996
  waves, conducting liquid surrounded by flowing gas 8=48036
  waves in second-order fluids 8=37447
  Ar, ionized, struct. of supersonic stream moving in alt. mag. field by plotting induced e.m.f. 8=41992
  Hg flow caused by travelling mag. field obs. 8=24180
  Hg, transient mag. field induced motion in shallow layer, obs. 8=24177
  Na, liquid, Alfven waves, Faraday rotation 8=46445
Magnetomechanical effects
  See also Gyromagnetic effect; Magnetostriction.
  elastic wave transformation into e.m. waves 8=39886
  ferrimagnets, magnetoelastic effects and app. to devices 8=31713
  ferrite cores, magnetoelastic resonance 8=36226
  ferromagnet, magnetoelastic instability in uniform precession 8=36221
  ferromagnets, damping rel. to internal stress distrib. effects 8=31568
  magnetic film, thin, magneto-elastic oscillations, coupled mag. and acoustic excitation 8=31582
  magnetodynamic effect, rel. to effects of Dirac electron spin 8=33629
  magnetoelastic two-port device nondispersive variable delay line 8=31745
  magneto elastic waves, parallel pump instability thresholds, method for calculation 8=49506
  magnetoeleastic waves in non-uniform field, propag. time and excitation mechanisms 8=31487
  magnetoelasticity and magneto-thermoelasticity 8=28278
  magnon interaction with longit. and transverse phonons (Ho in [111] direction) 8=31567
  metallic films, magnetoelastic waves, boundary-value-problem 8=40797
  micro-elastic wave motion and mag. field, interaction, in conducting medium 8=46154
  rare earth ions, magnetoelastic coupling constants, from optical-spectroscopic data 8=31229
  Ca-Bi-V-Fe garnet, excitation of magnetoelastic waves 8=40838
  Co^{2+} in $KMgF_3$, magnetoelastic coeff. from acoustic paramag. resonance 8=31871
  Fe^{2+} in $KMgF_3$, magnetoelastic coeff. from acoustic paramag. resonance 8=31871
  Ni rods, magnetoelastic parametric interaction due to ΔE effect 8=26840
  Ni^{2+} in $KMgF_3$, magnetoelastic coeff. from acoustic paramag. resonance 8=31871
  Ni-Fe film, magnon-phonon coupling 8=27421
  Ni-Fe films, magnetoelastic coupling obs. by spin-wave reson. 8=31820
  Ni-Fe, magnetoelastic sensitivity, composition gradient effect 8=36111
  Y garnet, dispersion of magnetoelastic waves 8=40186
  YFe garnet in two-port magnetoelastic delay lines 8=40850
  Y Fe garnet, magnetoelastic pulse excitation and propag. in non-uniform field, loss meas. 8=45043
  Y-Fe garnet, magnetoelastic waves, 1.1 GHz, study using light diffraction 8=40101
  YFe garnet, magnetoelastic instability in uniform precession 8=36221
Magnetometers. See Magnetic field measurement.
Magneto-optical effects
  See also Optical constants; Zeeman effect.
  absorption by hyperbolic excitons 8=49694
  alnico, domain structure tracking by Kerr effect 8=36165
  circulators for i.r. 8=49693
  cryostats, for study 8=41881
  crystals, cubic, with anisotropic impurity centres, rotation of plane of polarization 8=45159
  diffusion in matrix density formalism 8=41935
  Faraday effect, determination of atomic transition probabilities 8=38676
  Faraday effect, molec. aromaticity determ. 8=47644
  Faraday effect rel. to Mossbauer resonant absorpt. 8=45158
  Faraday rotation in mag. crystals, origin and uses 8=36306
  Faraday rot. meas. in MG fields 8=46683
  Faraday rotation rel. to resonant absorpt. 8=45157
  Faraday rotation technique for relax. time meas. in paramagnetic mats. 8=49479
  ferromagnetic films, teaching demonstration 8=27397
  ferromagnetic films, transverse Kerr effect rel. to hysteresis loops, azimuthal variation effect 8=40786
  films, coupled, transverse initial susceptibilities 8=45003
  film, thin, Kerr apparatus and meas. 8=36304
  fluorite crystals, rotation of Ce impurity centres 8=49718

Magneto-optical effects—contd
- graphite, magnetoreflection of laser light rel. to location of electron and hole carriers 8=35757
- ionic soln., rot. meas. by sample exchange 8=34847
- ionospheric electron content determ., Faraday rot. rel. to Doppler method 8=32295
- laser beam Faraday rotation on passage through θ-pinch plasma rel. to mag. field determ. 8=37583
- longitudinal Kerr, in multilayer structs. of dielec. and mag. films 8=41045
- magnetic circular dichroism, meas. apparatus 8=27615
- magnetic circular dichroism, theory 8=27542
- magnetic thin films, obs. 8=36107
- metal complexes, mag. circular dichroism 8=27616
- metal complexes, mag. circular dichroism, interpretation 8=27614
- metal halide complexes, mag. circular dichroism 8=27615
- metals, ferromagnetic, anomalous effects, electron-phonon scattering contrib. 8=31949
- magnon-sidebands in antiferromagnetic insulators 8=36298
- nucleoside derivs. cotton effect, rel. to chem. substitution 8=43434
- optical anisotropy of electrically and magnetically isotropic medium 8=24428
- organic mols, Faraday effect rel. to nature of charge-transfer complexes 8=43820
- polymer chains, Kerr const. calc. 8=38972
- radar for Faraday rot. meas., error reduction 8=27969
- rare earth cpds, ordered, experiments status 8=36401
- rare-earth iron garnets, Faraday effect in far i.r. 8=41133
- rotatory dispersion and circular dichroism meas., applications 8=33257
- rotatory dispersion, auto-recording type spectrometer for meas. 8=37673
- second harmonic, mag. field induced, search using ADP and quartz 8=45140
- semiconductor absorpt. spectrum in exciton region, elec. field effects 8=36305
- semiconductors absorpt. in strong e.m. wave rel. to interband transition 8=31261
- semiconductors, interband absorpt., effect of spatial dispersion of optical phonons 8=45160
- semiconductors interband absorpt. line splitting rel. to spin-e-phonon coupling const. meas. 8=27074
- semiconductors, mag., edge shifts rel. to strain 8=36299
- semiconductors, multiphonon magnetoabsorpt., theory 8=45156
- signal modulation and detection, new method 8=33284
- spinel ferrites, Faraday effect in far i.r. 8=41133
- superconductor, mag. struct., high-res. magneto-optical obs. 8=31336
- survey and applications 8=49695
- As, magnetoreflectivity, infrared rel. to interband transitions 8=26900
- $BaF_2:U^{3+}$, complex rotatory power, and struct. of U^{3+} centre 8=36336
- Be atom Verdet coeffs., Hartree-Fock calc. 8=47485
- $CaF_2:U^{3+}$, complex rotatory power, and struct. of U^{3+} centre 8=36336
- CaO, Faraday rot. anal. of colour-centre bands 8=35588
- CaO, Faraday rotation of F band and 3557 Å zero-phonon peak 8=45178
- $CdCr_2Se_4$, ferromagnetic, Faraday rotation 8=41078
- CdS films, Faraday effect near fundamental absorpt. edge, at 300°K 8=36347
- Co film, high-coercivity, domain obs. 8=36134
- Co films, and mag. props. 8=32018
- Co films, Kerr effect and application to hysteresis loop plotter 8=45007
- Co films, transverse Kerr effect, and application to hysteresis loop plotter 8=49516
- Co, Kerr effect in dielec. permeability tensor freq. dependence determ. 8=31696
- EuF_2, rel. to Eu^{2+} absorpt. spectra multiplet structure 8=31986
- EuO films, ferromagnetic transverse Kerr effect 8=31987
- Fe, Kerr effect in dielec. permeability tensor freq. dependence determ. 8=31696
- Fe-Ni films, Faraday effect and optical consts. 8=36358
- n-GaAs, Faraday effect in determ. of e-concs. and conc-profiles 8=40239
- GaAs, interband Faraday rotation 8=41086
- Ge, microwave Kerr effect rel. to complex Hall factor determ. 8=27127
- Ge, microwave Kerr effect rel. to relax time and effective mass determ. 8=49261
- H, Faraday determ. of at. conc. 8=29639
- He atom Verdet coeffs., Hartree-Fock calc. 8=47485
- n-$InAs_xSb_{1-x}$ alloys, free-carrier Faraday rot. obs. 6-25μ 8=36370
- InSb, interband transition linear-$\vec{K}$ valence-band splitting, obs. 8=36373
- InSb, polaron effect 8=49729
- InSb, rel. to resonant-polaron-coupling 8=40270
- $IrBr_6^{2-}$ complexes, mag. circular dichroism 8=49730
- $IrCl_6^{2-}$ complexes, mag. circular dichroism 8=49730
- $MgFe_2O_4$, Mossbauer Faraday effect 8=45158
- MgO, Faraday rot. anal. of colour-centre bands 8=35588
- MnF_2 antiferromagnet, Faraday effect, h.f. optical transitions contrib. 8=41116
- Na, liquid, Faraday station of Alfvén waves 8=46445
- $NdCo_5$ and Nd_2Co_{17} films, and mag. props. 8=32018
- Ne atom Verdet coeffs., Hartree-Fock calc. 8=47485
- Ni films, parameter temp. dependence, 20-400°C 8=36398
- Ni, Kerr effect in dielec. permeability tensor freq. dependence determ. 8=31696
- $RbNiF_3$, and n.m.r. studies 8=32023
- $RuBr_6^{3-}$ complexes, mag. circular dichroism 8=49730
- Si, interband Faraday rotation and ellipticity at absorpt. edge 8=36404
- Si, microwave Kerr effect rel. to complex Hall factor determ. 8=27127
- Si, microwave Kerr effect rel. to relax. time and effective mass determ 8=49261
- TbFe garnet, Faraday effect in i.r. 8=32037
- TbFe garnet, Faraday rotation, 100°-450°K 8=32039
- Y garnets, Si-substituted, permeability and coercive force, spectral dependence 8=40845
- YFe garnet, Faraday rotation, 100°-450°K 8=32039
- $Y_3Al_5O_{12}$, Faraday rotation for Eu^{3+}, wavelength dependence 8=44982

Magnetoresistance
- See also Magnetoelectric effects.
- alloy, dil., neg. magnetoresistivity calcs. from s-d exchange 8=40723
- carbon thermometers, Allen-Bradley type, ¼ W, 100 Ω 8=24020
- for Fermi-Dirac distribs. extension of Kittels deriv. for Maxwellian distrib. 8=26870
- ferrites, temp. dependence 8=40835
- ferromagnetic semiconductors 8=27058
- in ferromagnets, anisotropic, theoretical exam. 8=31563
- field meas. in supercond. magnet 8=41938
- films, thin, review of results 8=26954
- magnetic alloys, dilute, calc. by S-matrix theory using s-d model 8=26965
- metal, short-range spin fluctuation effect, temp. depend. 8=26958
- network of coupled orbits, phase-coherent 8=44975
- noble-metal-rare-earth, alloys, dil., rel. to impurity mag. effects 8=31316
- oscillatory, size-dependent, appl. to mag. field meas. 8=28517
- pyrocarbons, B-doped, rel. to electron states 8=27084
- pyrocarbons compressed at high temps. 8=45941
- semiconductors, doped, rel. to impurity, at low temp. 8=27069
- semiconductors with spherical energy band, transverse in strong mag. field 8=49217
- Al films, size effects, interpret. using two-band model 8=44683
- Al, magnetic breakdown 8=49462
- B, at 300°K 8=35823
- Be, oscills. rel. to mag. breakdown, 45-80 kOe 8=26962
- Bi, anomalous longit., rel. to purity of sample 8=40728
- Bi, boundary surface influence 77 and 4.2°K 8=49155
- Bi films, thickness depend. and quantum effects 8=27082
- p-CdSb, negative, rel. to impurity band conduction 8=35880
- CdTe, low temp. 8=44771
- CdTe, magnetophonon resist. oscillations, polaron effect enhancement 8=44661
- Co films, polycryst., thickness depend., 200-2000Å 8=31598
- Cu, and Hall coeff., mag. field, temp. and orientation dependence 8=49157
- Cu-Mn(Cr), calc. by S-matrix theory using s-d model 8=26965
- Eu chalcogenides: (rare-earth)$^{3+}$, temp. dependence meas. rel. to resistivity anomaly 8=35884
- Fe-N solid solns, at 4.2°K 8=31319
- Fe-Ni alloys, deformed, return with saturation magnetization 8=31639
- Ga, size-dependent oscillatory effect 8=49164
- Ga, thermal resist., 1-10°K and < 13 kG 8=35459
- n-GaAs, epitaxial, magnetophonon oscillations 8=40448
- p-GaSb, rel. to impurity conc. 8=44780
- Ge, bulk, galvanomagnetic effect and negative resistance of hot electrons 8=31379
- n-Ge, deformed transverse 8=44784
- n-Ge with dislocations, low-field, and magneto cond. 8=35890
- n-Ge films, dendritic, in microwave region 8=27111
- p-Ge, transverse, field and temp. dependence 8=44790
- n-Ge:Sb, longit. and transverse, elastic deformation effects 8=35899
- Hg, crystalline, and Fermi surface topology 8=26968
- HgTe, oscillations 8=35811
- n-HgTe, Shubnikov-de Haas effect 8=27106
- In films, size effects, interpret. using two-band model 8=44683
- InAs, anomalous, in two dim. transport, below 4.2°K, new type 8=35905
- p-InAs, and Hall coeff. and elec. cond. 8=27114

- **Magnetoresistance**—contd
  - InSb, field sensor for He temps. 8=46367
  - n-InSb, inhomogeneous, at 77°K 8=27117
  - p-InSb, longit., magnetophonon oscills. 8=35904
  - n-InSb probe for mag. fields at liquid He temp. 8=46371
  - InSb, rel. to method of preparation of crystals 8=44798
  - n-InSb single crystals with high density dislocations 8=49248
  - K, rel. to band structure 8=44691
  - K, strain-dependent 8=49166
  - Ni polycrystalline foils, residual resistivity and Kohler's rule 8=26971
  - Ni-Fe thin films, and resist. 8=44695
  - p-PbTe-CdTe alloy, at 77°K 8=49257
  - Si crystal (100) face, inversion layer, 77°K obs. 8=27130
  - Sn, at 1.3°K, structure due to magnetic breakdown 8=40643
  - Sn, over large range of mag. fields and at liq. He temps. 8=27031
  - Sn, quantum oscillations, obs. 8=44975
  - Sn, white, anomalous 8=49474
  - SrTiO$_3$, photomagnetoresistance by dc method at 10°K 8=44976
  - Te, rel. to galvanomagnetic effects, anisotropy, statistical interpret. 8=31394
  - Te, monocrysts, Shubnikov-de Haas effect, struct. of isoenergetic surface 8=40331
  - Yb, Fermi surface 8=40744
  - Zn films, anisotropy meas. rel. to preferred crystal orientation studies 8=30810
- **Magnetosphere**. See Atmosphere/upper; Earth/magnetic field.
- **Magnetostriction**
  - composite rotating cylinder, stress analysis 8=28261
  - constants, meas. by ferromag. resonance method 8=31569
  - ferrimagnetic materials, measurement at low temp. with superconducting solenoid 8=49507
  - ferrite cores, magnetoelastic resonance 8=36226
  - ferro- and ferrimagnetics, meas. at low temps. using superconducting solenoid 8=45000
  - ferromagnetic materials, measurement at low temp. with superconducting solenoid 8=49507
  - interferometer, Fabry-Perot, magnetostriction scanned 8=32272
  - Invar alloys, anomalous volume 8=36138
  - liquid viscoelasticity meas. appl., 20-100 kHz 8=30429
  - load cell for tensile testing under high hydrostatic pressures 8=40103
  - materials, dynamic properties and applns. 8=49452
  - readout of spark chambers in mag. field 8=37803
  - review, work since 1961 8=31480
  - temperature dependence, and piezomagnetism, rel. to single-ion models 8=31483
  - torsion of circular bar, permeated by longit. mag. field, problem 8=33039
  - transition metal alloys, paramagnetic 8=31533
  - transition metals, paramagnetic 8=31533
  - Au$_2$Mn, antiferromagnet, exchange striction and exchange coupling consts. 8=31755
  - Au$_2$Mn, antiferromagnet, at high mag. field 8=31754
  - Au$_2$Mn, at high mag. fields 8=40858
  - Co ferrite, exam. by X-ray differential photometry 8=26323
  - Co^{57} Mössbauer effect sources, mag., in mechanism of r.f. mag. field destruction of hyperfine Mössbauer spectrum 8=43945
  - Co-Fe-Au alloys, low values and coercive force rel. to mechanical treatment 8=31599
  - Dy, meas. in pulsed fields up to 150 kOe 8=40743
  - DyFe garnet, dilute 8=31724
  - Er, meas. in pulsed fields up to 150 kOe 8=40743
  - EuO, exchange 8=40807
  - EuO, in magnetoelastic interaction characterization and λ anomaly studies 8=45011
  - Fe, rel. to temp., mag. field and mag. field orientation 8=31619
  - Fe^{57} Mössbauer spectra, sidebands due to r.f. magnetic field 8=39513
  - Fe$_{2-o}$Co$_o$W solid soln., polycryst., and initial permeability 8=40815
  - Fe$_2$O$_3$, longit. in pulsed fields to 150 kOe, rel. to change in antiferro. vector 8=40868
  - Fe-3% Si, hysteresis and mag. hysteresis loss in rotating fields up to 2000 Oe 8=31680
  - Gd, meas. in pulsed fields up to 150 kOe 8=40743
  - GdFe garnet, dilute 8=31724
  - La, 1.5-40°K, rel. to superconducting transition temp. pressure dependence 8=35438
  - Ni, hysteresis and mag. hysteresis loss in rotating fields up to 2000 Oe 8=31680
  - Tb, anisotropic single-ion props. 8=44977
  - Tb, exchange props. 8=44978
  - Tb, forced, and thermal expansion and forced magnetostriction 8=35447
  - Tb, meas. in pulsed fields up to 150 kOe 8=40743
- **Magnetothermal effects**
  - energy converter staging, thermoelectric-thermomagnetic 8=46238
  - magnetic specific heat, behaviour compared to magnetoresistance of metals 8=26958
  - phonon drag, thermomagnetic coefficients, quantum oscillations 8=36065
- **Magnetothermal effects**—contd
  - semiconductors, thermogalvanomagnetic phenomena at high mag. fields 8=44751
  - temperature-oscillation method for low-temp. studies 8=31485
  - thermomagnetic generators with graded mass and gap, performance characts., 8=46388
  - ticonal, structure formation after thermomagnetic treatment 8=35055
  - Ag, oscillations from modulated mag. field, rel. to Fermi surface 8=44686
  - Al films, Righi-Leduc effect, size effects 8=40308
  - Al, Righi-Leduc effect in high mag. fields 8=40727
  - Be, oscillations from modulated mag. field, showing mag. interact. 8=44686
  - Bi, oscillations from modulated mag. field, rel. to Fermi surface 8=44686
  - Bi-Sn-Te alloys, magnetothermoelec. and thermoelec. props. 8=35996
  - Bi-Te, in arbitrary mag. fields 8=31312
  - Cd arsenide, 65-300°K 8=40731
  - CuSO$_4$.5H$_2$O, ht. capacity, below A°K 8=39914
  - CuSO$_4$. 5H$_2$O, ht. capacity at 0.4°-4.2°K in mag. fields 8=39915
  - Ga, thermal magnetoresist. rel. to heat switch appls., 1-10°K 8=35459
  - Hf diborides, Ettingshausen-Nernst coeff. rel. to conduction e-parameter calcs. from single zone model 8=35830
  - n-InSb, Nernst-Ettingshausen effect, magnetophonon oscs. 8=27113
  - N gas, dilute, thermomagnetic torques, exptl. investigation 8=30287
  - α-NiSO$_4$. 6H$_2$O, ht. capacity, entropy 8=30968
  - n-PbS, Nernst coeff. rel. to conduction band structure, 77-300°K 8=27119
  - Sb, Nernst-Ettingshausen effect, 5-300°K rel. to phonon drag effects 8=40219
  - Sb, oscillations from modulated mag. field, rel. to Fermi surface 8=44686
  - p-Si, 100-400°K rel. to phonon drag 8=35912
  - Ti diborides, Ettingshausen-Nernst coeff. rel. to conduction e-parameter calcs. from single zone model 8=35830
  - W crystal, isothermal magnetocaloric oscills. 8=31514
  - Zn, oscillations 8=49477
  - Zr diborides, Ettingshausen-Nernst coeff. rel. to conduction e-parameter calcs. from single zone model 8=35830
- **Magnetrons**. See Electron tubes.
- **Magnets**
  - alloy, new, for permanent magnets 8=31599
  - for alternating gradient for secondary beam transport 8=28519
  - applied superconductivity, conference 8=31338
  - beam bending 90° magnets, field uniformity meas. 8=28997
  - for beam transport, focusing props. and params. choice 8=28520
  - betatron electromagnet, pulse operation 8=24586
  - coils, hydrodynamic liquid cooling method 8=33048
  - conductors, stabilized for superconducting bending magnet 8=27001
  - for cyclotron, isochronous, poles design and permeability errors effects 8=29003
  - for cyclotron, separated-orbit 8=33475
  - for cyclotron, 10-50 MeV, separated orbit 8=33476
  - electromagnet coil pairs, optimum spacing 8=46382
  - electromagnet suitable for Hall-effect sondes of magnetic fields 8=33041
  - electromagnet winding optimization 8=28524
  - electro-, sector-wise gap field calc. 8=24112
  - epoxy resins for coil insulation, radiation damage, obs. 8=31159
  - fast, kicker, for 200 GeV accelerator 8=33478
  - gradient, for omnitron, prototype 8=33471
  - "hidden momentum" reaction from charged particle 8=41949
  - for high-energy physics, design 8=28996
  - laminated for fast cycling AGS 8=33437
  - laminations, ferromagnetic, under alternating matnetiz., eddy current distrib. 8=28516
  - lattice, magnetic separated funtion for accelerator 8=33473
  - microtron minimum-volume electromagnet 8=33047
  - multipole, quality, computer meas. 8=28521
  - permanent, for future transport applications 8=24114
  - permanent, for n.m.r. spectrometer 8=33152
  - permanent, new materials 8=40801
  - permanent, preparation and properties of commercial materials 8=46380
  - permanent, review 8=46381
  - permanent, stability 8=46379
  - power supply, current regulated, simple electronic sweep circuit 8=24069
  - power supply, s.c.r. preregulator 8=24068
  - proton synchrotron, supercond, energy storage system 8=29011
  - pulse, 60 kOe, for bubble chamber 8=46958
  - quadrupole for drift tubes in 200 MeV proton linac. 8=33105
  - quadrupole lenses for accelerator 8=33104
  - rare-earth pole-pieces for supercond. magnets field enhancement 8=28530

Magnets—contd
- rubber, ferrite-loaded, mag. props. 8=24111
- solenoid, bonded plain helical, mechanical stresses 8=31166
- solenoid, maximum attainable field, calc. 8=37384
- spectrometer permanent magnet with columnar crystal material 8=33152
- superconducting, absolute calibration rel. to helicon propag. 8=44663
- superconducting, advantages of coils, future development 8=33050
- superconducting, apparatus for high-field low-temp. magnetothermodynamic props. 8=41882
- superconducting coil, high-homogeneity tape-wound 8=37397
- superconducting coil optimum shape 8=28531
- superconducting coils, meas. techniques 8=37396
- superconducting, construction, state-of-the-art 8=46387
- superconducting, degradation and stabilization 8=28527
- superconducting, ferromag. pole piece solenoids and magnets optimum design 8=28525
- superconducting, field meas. by magnetoresistor 8=41938
- superconducting, for ANL 12-ft. hydrogen bubble chamber 8=37802
- superconducting for beam handling and accelerators 8=28995
- superconducting, for beam handling in accelerator 8=33404
- superconducting, for high-energy physics 8=24113
- superconducting for polarized π-p scatt. expts., 400 kJ 8=28529
- superconducting for 200 BeV accelerator 8=33403
- superconducting, high-current-density, high-field, stabilization 8=37389
- superconducting, high-field for use in Mössbauer spectroscopy 8=37387
- superconducting, high-field (up to 20 kg) 8=37393
- superconducting, methods for reducing degradation effects and applications 8=46386
- superconducting NbZr coil, effects of n irradiation 8=33405
- superconducting, pulsed, for p synchrotrons 8=29010
- superconducting rel. to type II superconductors 8=28526
- superconducting rings, stabilized, levitated 8=37395
- superconducting solenoid, composite, partially stable 90 kG 8=37394
- superconducting solenoid, 88-kG, 51-cm-bore diam. 8=37390
- superconducting solenoids, flux linkage and self-inductance, rel. to self-excitation 8=31354
- superconducting solenoids with high homogeneity fields 8=28528
- superconducting system, 88-kG, 20-in-bore 8=37391
- superconducting systems, nonaxisymmetrical 8=37388
- superconducting, using NbZr alloy wire, 85KG 8=46385
- synchrotron beam-line magnets, thyristor controlled rectifier for power supply 8=47003
- for synchrotron, flat topping 8=33469
- for synchrotran, separated function lattice 8=29007
- thermoplastic, ferrite-loaded, mag. props. 8=24111
- Al electromagnet for plasma diagnostics 8=46384
- $BaFe_{12}O_{19}$ flexible, anisotropic, prep. and props. 8=24110
- Fe core electromagnet, field accuracy rel. to excitation rate and induction history 8=28523
- Nb_3Sn composite ribbon transient stabilization 8=37392
- Nb–25% Zr superconducting solenoid, persistent current decay rate, field dependence 8=27039
- Nb + 75% Zr superconducting, for 85 kG 8=41937
- Ni-containing, extruded, permanent, texture and mag. props. 8=33046

Magnons. See Ferromagnetism.

Magnus effect. See Aerodynamics.

Majorana effect. See Magneto-optical effects.

Majorana forces. See Nuclear forces.

Malter effect. See Electron emission/secondary; Photomultipliers.

Mandelstam representation. See Scattering, particles.

Manganese
- α, phase transition, second order, Landau-Lifshitz theory, quant. vertification 8=30700
- corrosion effect in steel 8=49866
- crystal structure at 77-300°K 8=48663
- diffusion in GaAs, complex formation influence 8=35492
- doping in InSb, Hall effect, electrical conductivity and mobility rel. to temp. 8=44799
- lattice params. and thermal expansion rel. to para-antiferromag. transition, −180-1500°C 8=44253
- layers on each side of superconducting InBi film, proximity effect obs. 8=40372
- magnetic moments, localized, and Pauling valence 8=49528
- in organic liquids at liq. N temp. atoms stabilized by condensation method e. p. r. spectra 8=30526
- phosphor: Mn^{2+} spectra characteristics rel. to crystal lattice obs. 8=27641
- polycrystal, secondary ionization by 40keV Ar^+, mass spectrum 8=49448
- positive ions, spin-orbit coupling 8=38665
- spectra, rel. to band structure 8=41115
- vacancy pairs in NaCl, temp. depend. 8=48811

Manganese—contd
- Ag, spin relax. of localized mag. moments and conduction electrons 8=31875
- CdS/ZnS mixture, e. p. r. of Mn^{2+} exchange-coupled pairs 8=45105
- Cu–Mn interdiffusion kinetics, e microprobe obs., 640–820°C 8=31002
- Fe and Fe–C alloys, effects on impact properties 8=35693
- Mn^+, e.s.r. in rare gas matrix 8=40202
- Mn^+ in $2(H_2Ca_2Mg_5(SiO_3)_8)$, e.s.r. lines intensity 8=36245
- Mn^{2+}, diffusion in Ag halides 8=39962
- Mn^{2+} e.p.r. in $Cd_2V_2O_7$ obs. 8=31856
- Mn^{2+} e.p.r. in halide host cpds. 8=36246
- Mn^{2+} in calcite, e.s.r. 8=40932
- Mn^{2+} in CaF_2, hyperfine coupling temp. depend 8=31876
- Mn^{2+} in CaF_2, F^{19} nuclear spin-lattice relaxation 8=49633
- Mn^{2+}in (Ca, Mg, Fe)CO_3, e.s.r. allowed and forbidden transitions 8=40933
- Mn^{2+}, in CaO, uniaxial stress meas. at impurities, strain coeffs. 8=40134
- Mn^{2+} in Cd_xHg_{1-x} Te, e.p.r. 8=40934
- Mn^{2+} in $CdWO_4$, e.p.r. lines splitting by elec. field, 320 kv/cm 8=40929
- Mn^{2+}in $La_2Mg_3(NO_3)_{12}.24H_2O$, e.p.r. 8=40928
- Mn^{2+} in $La_2Mg_3(NO_3)_{12}.24H_2O$, zero-field splitting 8=30627
- Mn^{2+} in MgO, charge transfer at surface, e.s.r. study 8=48422
- Mn^{2+} in MgO, e.s.r. at 1.3 GHz 8=40930
- Mn^{2+} in pyrosilicate and pyrogermanate isomorphs of barvsilite, e.p.r. 8=40931
- Mn^{2+} in spinel, spin temp. equalization between excited and fundamental states 8=45282
- Mn^{2+} nuclei, effective magnetic field, effect of covalency 8=40739
- Mn^{2+} nuclei in glasses, hyperfine splitting rel. to covalency estimate 8=48304
- Mn^{3+} in α-Mn_2O_3-type structures, bonding 8=39501
- Mn^{4+} in α-Al_2O_3, trigonal splittings stress dependence 8=43929
- Mn^{4+} activated oxygenated cpds, excitation spectra 8=41202
- Mn^{4+} in TiO_2, ENDOR 8=41007
- Mn^{55} in $Mn_2(CO)_{10}$, n.m.r. spectrum, quadrupole coupling effects 8=49653

Manganese compounds
- ardennite, crystal structure rel. to Si_3O_{10} group positioning 8=39808
- chlorides, complex, hydrated, NMR and antiferromag. props. 8=36275
- ferrite: Ba, discontinuous growth 8=39677
- ferrite, domain structure from X-ray obs. 8=27434
- ferrites, epitaxial growth on metal oxides, prep. methods 8=35175
- ferrites, Fe-rich, electrical cond. at low temps. 8=49140
- ferrites, Hall effect 8=40841
- ferrites, manganic, crystal growth techniques 8=26257
- Mag–Mn ferrite films, FMR, thermal treatment effects 8=31817
- manganese arsenic borate glass dosimeter 8=44500
- manganic acetylacetonate and related chelates, vinyl polymerization initiation 8=32124
- manganites of perovskite structure, magnetic behaviour rel. to lattice distortions 8=49534
- oxides, thermodynamic props. by e.m.f. meas. 8=48729
- oxides with spinel struct, Kβ-group of X-ray lines 8=31988
- spinel ferrite lattice, cubic, local Jahn-Teller distortions rel. to phase transitions 8=26408
- steels, $\gamma \rightleftharpoons \epsilon^1$ and $\gamma \rightleftharpoons \epsilon$ transforms. dilatometric and X-ray diffr. exam. 8=35114
- Cu–Ni–Mn system, diffusion rel. to thermodynamic activities, obs. 8=31004
- Mn complex, diaquobisacetylacetonatomanganese (II), crystal structure 8=44228
- Mn complex, phthalocyanatopyridinemanganese(III)-μ-oxo-phthalocyanatopyridine-manganese(III) dipyridinate 8=26409
- MnAs, n.m.r. hydrostatic pressure and temp. dependence 8=31911
- $MnAs_{0\cdot9}P_{0\cdot1}$, crystal structure at 119°K and 298°K, X-ray powder pattern determ. 8=35341
- $MnAs_{0\cdot92}P_{0\cdot08}$, polycrystalline, mag. and crystallographic props. 8=31503
- Mn As_xSb_{1-x} solid solns., magnetic props. and structure 8=49482
- Mn-Au alloys, antiferromag. props. on thermal and mech. treatment 8=31776
- Mn_3B_4, Mo-or W- substituted, mag. props 8=27418
- MnBi film, mag. props. rel. to memory appls. 8=49531
- $MnCl_2$, aqueous soln, dielec. consts. and loss factors 8=34887
- $MnCl_2$, new absorpt. band 8=32012
- $MnCl_2.4H_2O$, thermal expansion anomaly near Neel pt. due to antiferromag. ordering 8=35445
- $MnCl_4^{2-}$-$ZnCl_4^{2-}$ mixed crysts., spectra at 4°K 8=27590
- $Mn_3Cl_2(NO_3)_{12}.24H_2O$, Zeeman splitting of blue lines, theory and obs. 8=41117
- $MnCO_3$, absorpt. spectrum at 4.2°K rel. to magnon side bands 8=32010
- $MnCO_3$, vis. and u.v. absorpt. spectra 8=32008
- $Mn_2(CO)_{10}$, Mn^{55} n.m.r. spectrum, nuclear quadrupole coupling effects 8=49653

Manganese compounds—contd
$(Mn, Co)_4C$, mag. structure from polarized n. -scattering 8=31732
$MnCr_2O_4$, ferrimagnetic spiral, far i. r. absorption 8=45204
$MnCr_2O_4$, ferrimagnetic spiral, n. m. r. of Mn^{55} 8=45130
$MnCr_2O_4$ insulating spiral, ferrimag. resonance freq. and temp. dependence 8=31831
$MnCr_2O_4$, spin-structure determ. from magnetization and resonance 8=31731
$MnCr_2O_4$, mag. structure determ. from n. -diffr. 8=31721
$MnCr_2S_4$, NiAs-type structure, magnetization, 1. 5°K to room temp. 8=45064
$Mn_{2-x}Cr_xSb$ (x=o, 0. 03), spin reorientation rel. to phase transform, 180-280°K 8=36189
Mn–Cu null-matrix alloy for n diffr. exam. 8=44195
MnF_2, antiferromagnet, uniaxial, first-and second-neighbour exchanges, statistical mech. 8=31782
MnF_2, elastic and thermoelastic behviour 8=44590
MnF_2, n. m. r., extremely narrowed, applications 8=27509
MnF_2, u. s. attenuation near and above spin-flop transition 8=44319
MnF_2, Fe^{2+} impurity, critical-point magnetization 8=31787
MnF_2, n. scattering near critical pt., temp. dependence 8=31784
MnF_2, octahedral symmetry, i.r. absorpt. spectra of Co^{2+} ions 8=32011
MnF_2 rutile antiferromagnet, spin-wave light scattering 8=36387
MnF_2, spin-wave sidebands 8=36388
MnF_2, stressed, magnon sideband shapes rel. to exciton dispersion and exciton-magnon interactions 8=36389
MnF_2, susceptibility meas. rel. to spin-wave theory 8=31783
MnF_2, u.s. attenuation meas. near Néel point 8=48720
MnF_2:Co, localized magnon obs. by neutron scattering 8=27380
$MnF_2:Mg^{2+}(Zn^{2+})(Ca^{2+})$, impurity-induced fluorescence 8=45281
MnFE antiferromagnet Faraday effect, h.f. optical transitions contrib. 8=41116
$MnFe_2O_4$ films, single-cryst., pulse switching and static characts., obs. 8=31730
$MnFe_2O_4$, Mossbauer effect 8=43954
$Mn_{1+x}Fe_{2-x}O_4$, induced anisotropy at low temps. 8=36188
$Mn_xFe_{3-x}O_{4+\gamma}$, Richter type relax, details 8=36219
$Mn_xFe_{3-x}O_{4+\nu}$, electron-transfer relaxs. 8=31830
$Mn_{1-x}Fe_xP$ solid solutions, magnetic props. rel. to props of FeP 8=27378
Mn_3GaN, antiferromagnetic ordering of Mn spins 8=40871
Mn_5Ge_3, ferromag., uniaxial anisotropy consts., temp. depend. of energy 8=36150
Mn_2GeO_4, high-pressure form, crystal structure 8=39807
MnI_2 insulating spiral, antiferromag. resonance freq. and temp. dependence 8=31831
$MnIn_xCr_{2-x}S_4$, $(0 \leq x \leq 1.0)$, mag. and crystallographic props. 8=36190
$Mn(Mn_xV^{4+}_xV^{3+}_{2-2x})O_4$, $x < 0.68$ elec. props. and structures 8=35340
Mn_2N, antiferromagnetic and crystal struct. 8=49573
Mn-Ni, Mn-Pd and Mn-Pt (CuAu-I type alloys), mag. structures and phase transformations 8=31780
MnO, covalency parameters 8=30617
MnO, deformed, crystal structure 33-157°K and mag. anomaly 8=30906
MnO, Hall mobility of electrons and holes at 943°C 8=27118
MnO inclusion in steel, thermal expansion and reln. to tessellated stresses 8=44350
MnO, struct. exam. 8=48592
MnO substrate for Cs_3Sb films 8=39591
MnO, thermoelectric force, electrical resistivity 8=40477
MnO_2 effect on corundum recrystallization 8=48536
MnO_2, semicond. and dielec. props rel. to contact mats and way of coating 8=31383
$MnO.Al_2O_3$ inclusion in steel, thermal expansion and reln. to tessellated streses 8=44350
MnO : Li, electrical conduction 8=44801
MnO. OH, mag. structure and H location 8=49533
$2MnO.SiO_2$ inclusions in Fe, e microprobe obs. 8=27802
Mn_2O_3-NiO-Cu_2O system, thermistor with negative temp. coeffs. 8=49280
MnP, helical spin ordering, development of theory 8=31309
MnP, helical spin structure, stability 8=36151
MnP, magnetic properties by torque meas. 8=49529
MnP, magnetic props, hydrostatic pressure effects 8=31657
MnP, metamagnetic interactions pressure dependence 8=31656
MnP–MnAs solid solutions, magnetic and structural study 8=48388
Mn–Pt system, mag. structures and transforms. rel. to exchange interactions 8=45017
Mn_3Pt, magnetic structure, effect of Fe substitution 8=27446
Mn_3Pt, magnetic transformation, first-order, x-ray and susceptibility study 8=31777
α-MnS, covalency parameters 8=30617
α-MnS., lattice parameters rel. to pressure 8=48669

Manganese compounds—contd
α-MnS, paramagnetic, S^{33} NMR temp. dependence, 175-300°K 8=45131
α-MnS, parameters rel. to pressure 8=48669
MnS inclusion in steel, thermal expansion and reln. to tessellated stresses 8=44350
$MnSO_4$, antiferromagnetic spin configuration 8=36213
$MnSO_4$ powders, anhydrous and monohydrate mag. props. 8=31786
MnSb, dilute solutions in superconducting PdSb 8=27029
MnSb, magnetization and crystal anisotropy 8=49530
MnSb, n.m.r. hydrostatic pressure and temp. dependence 8=31911
MnSb, spin relaxation of Fe^{57} below curie point 8=49532
MnSb–Sb aligned eutectic, mag. anisotropy 8=49535
MnSe, sublimation 8=39498
$MnSeO_4$, antiferromag. structure from n. diffr. data 8=31778
$MnSeO_4$, Neél temp., obs. using continuous flow cryostat 8=49548
MnSi, mag. moment spacial distrib. from n. scattering 8=31655
Mn-Sn system, mag. props of phases and liq. state 8=36214
$MnSn_2$, antiferromagnet, strong weakly coupled moments 8=31781
$MnSn_2$, antiferromagnetic, neutron-diffraction study rel. to structure transitions 8=31779
Mn_3Sn, helical spin ordering, development of theory 8=31309
MnTe, antiferromagnetic semiconductor magnon drag at optical freq. and i.r. spectrum 8=32009
p-MnTe : Ag, thermoelec. props. 300°-1000°K 8=44908
$Mn(TiMn)O_4$, magnetic and crystalline structure 8=40872
$MnTiO_3$, gyrotropic birefringence 8=45155
Mn-V alloys, X-ray investigation of σ-phase 8=49713
Mn– Zn alloys of CsCl type structure, magnetization and mag. structure 8=40819
Mn–Zn ferrite, mag. props. rel. to sintering conditions effects 8=49561
Mn-Zn ferrite, sintering conditions effect on mag. props. 8=27432
Mn-Zn ferrites, Mössbauer study of hyperfine fields 8=35042
Mn-Zn ferrites, permeabilities rel. to micro-and chemical structures 8=27431
Mn–Zn ferrites with high-permeabilities 8=49560
β_1-MnZn films ferromag. resonance 8=27451
$Mn_xZn_{1-x}Fe_2O_4$, cation distribs. and lattice parameters from X-ray and n.-exams. 8=44229
Mn– Zn–Ga alloys of CsCl type structure, mangetization and mag. structure 8=40819
$Mn_{0.625}$-ZnY ferrites, Mossbauer spectroscopy 8=36198
Manometers
See also Vacuum gauges.
all-glass recording membrane 10-760 torr instrument 8=41625
automatic, for press. of liq. metals meas. 8=48011
Bayard-Alpert, X-radiation residual current 8=34685
butyl phthalate oil, correction for variations in room temp. 8=32646
differential, in gas flowmeters, meas. errors 8=25806
dual-range for mercury or oil 8=28224
electric discharge "immersion" with simplified construction 8=47996
high-vacuum measurements, achievements 8=48000
oil, with continuous elec. readout 8=32644
for plasma neutral gas in mag. field var. direction and magnitude 8=43548
thermocouple manometric transducers, thermal rating 8=45961
vacuum, apparatus and methods of meas. 8=39253
vacuum, interferrometric differential apparatus 8=39249
Hg, collinear-arm instrument 8=32643
Many-particle systems. See Quantum theory/many-particle systems.
Markov processes. See Statistical analysis.
Mars. See Planets.
Masers
active medium, nonlinear, excitation by beam of oscillators 8=33155
c. w. 337μ, rel. to interference of sub.-mm waves over 450m path diff. 8=33278
on earth satellite, freq. stability obs. 8=28643
material Q rel. to pump intensity and freq. 8=37548
molecular-beam, oscillation quenching 8=46531
molecular spectroscopy application 8=38782
quantum electronics, effect on technology 8=28655
rate eqns., Lyapunov's second method 8=28656
resonators, optimization 8=33156
ruby, preamplifier for e. p. r. spectrometer 8=33146
theoretical and exptl. work in USSR, review and bibliography 8=28644
three level, intermittent pumping rel. to enhanced action 8=28642
travelling wave, amplification at 36GHz 8=28641
USSR, review 8=33157
H, automatic tuning 8=46530
H, freq. shifts, due to coherently excited $\Delta m_F = \pm 1$ transitions between $F = 1$ levels of ground state 8=25350

Masers—contd
- H, $\Delta m = O$, triplet decomp. 8=42049
- H, synchronised, oscillation amplitude freq. dependence 8=42050
- NH_3 molecular beam oscillator with two cavities in series, characts. 8=37547
- NH_3, two cavity, meas. of 3-2 inversion freq. and freq. stability 8=24267
- Rb^{87}, theory rel. to relax. times 8=24266

optical. See Lasers; Optical pumping.

Mass spectra

See also Chemical analysis/by mass spectrometry.
- acetone condensation products 8=29840
- acetylene, decomp. by 0. 5-1200 keV positive ions 8=43491
- alcohols, lower aliphatic, photoionization 8=47793
- alkyl ions, prod. by H_3^+ reactions with propane or butane 8=39057
- biphenylene 8=39058
- cyclic alkanes, fragmentation of skeletal bonds 8=29824
- deciphering, for high temp. thermodynamic reactions 8=38609
- digital recording systems, design theory 8=38604
- doublet mass difference discrepancies, 1954-1958, analysis 8=29667
- ethanes, deuterated (d_0-d_6) 8=47446-7
- field-ionization, production using heated filaments 8=47448
- for fission products separation 8=38544
- free radicals, techniques and results 8=29829
- group IIA fluorides, bond energies 8=38934
- hydrocarbons and mono-chloro derivatives, field-ionization 8=47796
- hydrocarbons, ion impact, charge and proton transfer 8=29984
- of labelled compounds, for probing underlying chemistry 8=25393
- α- and β-mercaptoesters, skeletal rearrangement on electron impact 8=47456
- 1^+ mesons, O(4, 2) theory 8=42594
- metastable ions in cycloidal spectrometer 8=39026
- methane, photoionization 8=29986
- methyl phenanthrene rel. to ionization and dissoc. by e. impact 8=47797
- molecular dissociation processes 8=38930
- molecular orbital theory 8=29824
- neutral constituents, N_2, O_2, O and Ar in lower thermosphere above Sardinia, determ. 8=27939
- nontrivial, current algebra model 8=24611
- organic, metastable ion detector 8=43152
- organometallic cpds. of transition metals 8=39053-5
- phenanthrene, rel. to ionization and dissoc. by e. impact 8=47797
- propylene, ion-mol. reactions 8=43492
- pyrolytic fibre products, gaseous and volatile 8=36632
- 2-pyrone, C_4H_4O radical cation 8=39061
- reactor irradiated fuel, using isotope separator 8=29567
- Al polycrystal, secondary ions from Ar^+ at 40 keV 8=49448
- BaO, 1365°-1917°K 8=30606
- BeO-BeF_2 system at high temp. 8=35012
- C_7H_{12}, mono- and bicylic isomers 8=39059
- Co polycrystal, secondary ions from Ar^+ at 40 keV 8=49448
- Cs, from U, Ta(p, $Cs^{119-132}$), isotope distrib. obs. 8=34001
- Cs, $128 \leqslant A \leqslant 144$, U p-fission yield, 150 MeV 8=38542
- H cluster ions, energy-analyzed 8=47787
- H_3O 8=47610-11
- Mg-Cu-F, high-temp. gaseous equilibria 8=34375
- Mn polycrystal, secondary ions from Ar^+ at 40 keV 8=49448
- NH_4 8=47610-11
- Na, from Mo^{100}, Ta, Ir, U(p, Na^{21-29}), isotope distrib. obs. 8=34000
- Na, $20 \leqslant A \leqslant 25$, Si p-spallation yield, 150 MeV 8=38542
- PbF_2, high-temp. vapour 8=38933
- Rb, $83 \leqslant A \leqslant 98$, U p-fission yield, 150 MeV 8=38542
- Rb, from U, Th, Ta(p, Rb^{78-96}), isotope distrib. obs. 8=34001
- SnF_2, high-temp. vapour 8=38933
- Ta polycrystal, secondary ions from Ar^+ at 40 keV 8=49448
- TaF_5 and $TaOF_3$, high-temp. 8=38938

Mass spectrometers

See also Ion sources.
- cycloidal, metastable ion formation 8=39026
- electrical r.f. field replaces mag. field, improvement 8=47457
- field ionization, emitters, comparison 8=29573
- field-ionization, modified ion source 8=34447
- filament current regulator to study temp. depend. of alkali ion emission 8=34120
- for fission prod. separation, focusing parabola mass spectrometer 8=43129
- for fission prods., gas-filled separator 8=38544
- for fission prods., short-lived, separation 8=43130
- ironless time-of-flight, review 8=34121
- with magnetic prism, 2D, and quadrupole lenses 8=29574
- magnetic spectrograph, ang. resolution improvement 8=38606

Mass spectrometers—contd
- magnetic, varying field, characts. 8=28970
- MI 13-05, modified, for measuring isotopic ratio of trace amounts of noble gases 8=47452
- omegatron, performance rel. to dimensions 8=29576
- pulsed-source, ion trapping technique 8=29577
- quadrupole, bakeable ceramic 8=29575
- r.f., 7-5 and 9-7 cycle, ion energy gain 8=34119
- sample introduction in form of molecular beams 8=43153
- satellite plasma ion instrument 8=32563
- 60° single focus, performance testing 8=47453
- table, specifications of instruments and applics. 8=47455
- H_2^+ decomp. in analyser tube 8=47454

accessories

See also Ion sources.
- adsorptive pump for low temp. evacuation 8=38608
- alkaline earth metal stearate targets for CERN isotope separator ISOLDE 8=38768
- detector for metastable organic ions 8=43152
- digital recording systems, design theory 8=38604
- ion counter SI-01 8=47450
- liquid target, circulating, for on-line isotope separator 8=38605
- quadrupole, electron multiplier for improved characteristics 8=47449
- sample vaporization system with temperature regulation 8=47451
- servoamplifier for ion current ratio recording 8=38610
- source mounting for thermal-source type 8=25328

applications

See also Chemical analysis/by mass spectrometry.
- auroral α's and protons, rocketborne mag. spectrometer meas. 8=32283
- elimination of CO_2 from ions in spectrometer 8=38607
- field ionization and evaporation, low temp., analysis 8=27362
- glass, surface composition, spark source mass spectrometer 8=41300
- ion-molecule reactions, elevated press, investigation by modified time-of-flight spectrometer 8=29843
- omegatron, residual gas analysis in ultra-high vacuum system 8=36630
- review of instruments and their applics. 8=47455
- surface scanning with electron probe and ion desorption exam. 8=30760
- Cs_2CO_3, evaporation products obs. 8=48294

Mass standards. See Standards.

Mass transfer. See Transport processes.

Master equation. See Transport processes.

Materials

See also individual materials (if separately named) e.g. Ruby.
- bed of lumps, heat transfer for gas counter flow with heat sources 8=30284
- bone, transmission and attenuated total refl. i.r. spectra rel. to protein bands 8=32041
- carbon black, suitability as load-bearing high-temp. insulation 8=35456
- coir, X-ray diffraction study 8=48358
- defects, ultrasonic spectroscopy 8=23964
- Epibond moulding for cryogenic apparatus 8=41883
- fatigue, two-parameter theory, corrections 8=40099
- fibre-glass spacers, influence on radiant heat transfer below 300°K 8=39955
- hot gunning for basic O_2 furnace maintenance 8=50475
- lamellar composite, acoustic wave propag. 8=40100
- metallic/brittle aggregates, fracture initiation and modes of failure 8=31182
- peat, visco-plastic, internal mass transfer in drying 8=34982
- polypropylene, stretching technique for X-ray detector windows 8=50476
- Pyrex toroidal sectioning machine 8=41607
- refractory facing with decomposing lining, heat regime 8=30958
- rubber gasket sizing and shaping 8=45932
- silicates, with ice on surface, existence of unfrozen interfacial layer of water 8=35142
- silicides of transition metals, auxiliary metal bath procedure for synthesis 8=49835
- solders, silver pastes hardened at 20-150 °C, conductivity 8=35820
- Teflon, high finish polishing 8=37096
- testing, high-speed photography 8=42291
- vacuum behaviour with radiation and heat, rel. to synchrotron application 8=37822
- wool, equilib. adsorpt. isotherms of Na hexadecyl sulphate 8=30781
- wool, equilib. adsorpt. of Na dodecyl sulphate, at 40° and 60°C 8=30780
- polishing compounds, i.r. spectra 8=31933
- ZnS luminophors, preparation, effect of halide addition 8=49819

Materials testing. See Mechanical strength.

Mathematical methods. See Calculation; Statistical analysis.

Mathematics
- analytic function from extension of cont. function and Schwartz distrib., boundary values 8=32661

- **Mathematics**—contd
  - analyticity as fundamental principle in physics 8=29023
  - Banach space techniques in perturbation theory of self-adjoint operators with continuous spectra 8=46812
  - calculus for space-coherent e. m. radiation 8=37449
  - cluster expansions in many-fermion system 8=32848-9
  - convolution transforms whose inversions have the same kernel 8=45978
  - eigenvalue problem $Tu-\lambda Su = O$ with unbounded and nonsymmetric operators T and S 8=32660
  - elliptic boundary value problems, asymptotic distribution of eigen values and eigen functions 8=46110
  - Fredholm integral equations reducible to initial value problems 8=45987
  - Froissart model and massless second-order pole, modification of solns. 8=37111
  - Gauss theorem, generalized form. 8=33059
  - Green's functions concepts and appl. 8=24452
  - group transformations of O(2, 1), representations in continuous basis 8=24593
  - Hilbert space, construction of fixed points of nonlinear mappings 8=45967
  - homology and Feynman integrals, book 8=33338
  - integral eqs., approx. solns. 8=45980
  - Kronecker delta in current algebra for weak interaction 8=24647
  - Laplace's equation, numerical solution in multidielectric region 8=46348
  - limits, approximation of double by single, and Kaplun extension theorem 8=41629
  - linearization of expt. curves 8=27680
  - Liouville eqns. variational solns 8=37115
  - Minkowski space, Wightman set theory, generalization 8=32781
  - nonlinear boundary-value problems, expansion method 8=23812
  - operator functionals, derivation and commutation 8=28227
  - operator theory, invariant imbedding eqns. for Green's function 8=28228
  - Pade approximants, convergence 8=32656
  - Padé approximants, rel. to series of Stieltjes 8=32652
  - parabolic system, transform. 8=32647
  - perturbation problems, singular 8=45996
  - perturbation problems, singular 8=45997
  - for physics, book 8=32686
  - for physicists, book for students 8=41631
  - polynomials, orthogonal, sequence from Fourier expansions 8=32653
  - Reimann's relation on symmetric open Riemann surfaces 8=32658
  - Riemannean spaces, generalized motions 8=45968
  - relationship with physics 8=32635
  - similarity principle for soln. of magnetic current source in plasma 8=34498
  - solid angle subtended by one circular disc at another, FORTRAN prog. for calc. 8=32639
  - stationary processes, linear predictors and filters 8=37113
  - Stokes theorem, generalized form. 8=33059
  - Sturm-Liouville boundary value problems, nonlinear perturbations 8=45974
  - Svensson representation with local commutativity 8=45970
  - uniqueness theorem for fields of elliptic modular functions 8=23797
  - variatinal principles, complementary, and n transport appls. 8=33328
  - variational principles, continuum mechanics 8=23815
- **Matrices**
  - correction matrices for d^5 config. in cubic symmetry 8=48306
  - Coulamb-Divac multipole radial elements, analytic props. 8=28941
  - density, for odd number of fermions, N-representability 8=37215
  - off-diagonal square of modulus, variational calc. 8=32685
  - Dirac Hamiltonian as member of hierarchy of matrices 8=46807
  - groups, exponential representations and canonical forms 8=45990
  - helicity and energy as members of hierachy of eigenvalues 8=46808
  - K-matrix, three-particle scatt. 8=29059
  - loading and mass, reduction of 8=23825
  - low-energy collision, unitary model 8=29388
  - 9 × 9 treatment of e. m. wave propag. in anisotropic plasma 8=30058
  - nuclear collision, unitary resonance form for elastic scatt. 8=42985
  - plastic stress-strain for elastic-plastic problems 8=28258
  - quantum-statistical model, for measuring process 8=34097
  - quasi-three-body reaction, non-local model t-matrix 8=29426
  - R-matrix theory of nuclear, correspond. with waveguide and resonator theory 8=33972
  - random, asymptotic distribution of eigenvalues 8=45971
  - random, in physics 8=46090
  - reduced density, n-representability 8=28940
  - spin-spin interaction for f^3 e config. 8=38637
- **Matrix-isolation methods.** See Free radicals; Molecules.
- **Matteucci effect.** See Magnetoelectric effects; Magnetomechanical effects.
- **Maxwell-Boltzmann distribution.** See Kinetic theory; Statistical mechanics.
- **Maxwell effect.** See Double refraction/flow.
- **Maxwell equations.** See Electromagnetism.
- **Measurement**
  - See also Instruments; Recording; Standards; Units; Acoustical measurement; Dielectric measurement; Electrical measurement; Magnetic measurement; Mechanical measurement; Radioactivity measurement; Thermal measurement; X-ray measurement. Some specific quantities are listed separately, e.g. Calorimetry; Density measurement. Where no separate heading exists, measurement methods and instruments are included among the other entries under the heading of the appropriate quantity or subject.
  - cross-correlation, effect of instrumental time-lag or filtering 8=45948
  - deconvolution of physical data 8=23785
  - displacements, very small, using open circuit voltage of symmetric photodiode 8=41618
  - extension 8=28215
  - ion, Doppler shift of spectral line, meas. with optical wedge 8=47471
  - in macro- and microphysics, anal. and space extensions 8=28213
  - moment of inertia, inclined-plane and slip methods 8=37109
  - precision electromagnetic, conf. Boulder (1968) 8=41906
  - techniques, use of new physical effects 8=41614
  - vacuum metrology, apparatus and methods 8=39253
  - **errors**
    - See also Statistical analysis.
    - e.a.s. particle density meas., instrumental effects 8=38240
    - ionization current, fluctuation errors 8=42345
    - i.r. intensities, statistical errors in normal coords. 8=25435
    - liquid u.s. absorpt. at h.p., analysis 8=48137
    - luminescent, due to "thick" specimens, elimination 8=37657
    - modified normal distribs., generalized theory 8=45947
    - optimal algorithm, principles, consequences and applications 8=23783
    - selective rejection of data, statistical analysis 8=28214
    - of single quantity by several instruments, precision 8=23784
    - spectrometer continuously scanning, recording error 8=42233
    - spin conc. determ. using e.s.r. 8=49590
    - strip-chart astrophotometry, inefficiency of visual reading 8=42139
    - X-ray wavelengths, statistical counting errors 8=46784
- **Mechanical measurement**
  - Individual quantities and instruments are listed separately e.g., Length measurement.
  - coaxiality and linearity of axes of holes 8=23787
  - frequency response from transient response, practical method 8=41638
  - pneumatic contactless systems 8=23786
  - vibrations, piezoelectric probe 8=32868
  - Ni, torque meas. of anisotropy of energy and magnetization 8=31667
- **Mechanical properties of substances**
  - See also Individual properties, e.g. Abrasion; Elastic deformation; Mechanical strength; Plastic deformation; Slip; Wear; etc.
  - alumina inclusions group, initial O content in liq. Fe as formation factor 8=35651
  - aviation and aerodynamics, conference 8=30265
  - butadiene acidic and basic copolymers mixtures, H-bonds mech. lability, obs. 8=48507
  - butadiene copolymer mixtures rel. to butadiene-methyl (2-methyl-5-vinyl)-pyridinium iodide copolymers rel. to ionic bonds, obs. 8=48508
  - butadiene copolymer mixtures rel. to ionic bonds, obs. 8=48508
  - butadiene copolymers rel. to ionic bonds lability, obs. 8=48509
  - butadiene-lithium methylacrylate copolymers, rel. to ionic bonds, obs. 8=48508
  - butadiene-methyl (2-methyl-5-vinyl)-pyridinium iodide copolymers rel. to ionic bonds, obs. 8=48508
  - cermets, rel. to geometry and phase distrib. 8=35263
  - ceramics, brittle-to-ductile transition, effect of temp. on slip band struct. 8=31180
  - ceramics, forsterite lapping characts. using diamond abrasives 8=48949
  - ceramics, lapping characts. with ordinary abrasives 8=48948
  - circular cylindrical shells, parametric instability due to in-plane longit. inertia loading 8=23821
  - circular ring, radially constrained, instability due to thermal stress rel. to initial imperfections 8=23823
  - diamond, abrasive grains, frictional coeffs. with metals 8=31184
  - dynode thin films 8=31161
  - explosive claddings, max. shear strength and microhardness 8=48945
  - for extrusion, geometric props. of slip-line fields 8=40112

Mechanical properties of substances—contd
foam plastics for one shot shock absorption, vibration characts. 8=44514
glass breakdown in covers used in elec. discharges 8=48983
graphite, reactor type, meas. before and after n-irrad., rel. to crack propag. etc. 8=26789
graphitoplastics 8=31247
gravitational stresses, determ. using immersion analogy, generalization 8=23832
hollow dielectric, effects of polarization under extension, inflation and torsion 8=35947
loss meas. for low loss materials 8=35614
materials at low temp., review rel. to strength plasticity deform. etc. 8=26738
metal cutting at 100–700 m/s, force meas. method 8=35655
metal thin sheet, simple and constrained acoustic damping layers, loss factor obs. 8=35612
metal, working props. and test behaviour 8=40087
metals, stress corrosion susceptibility rel to ambient press. 8=49034
mischmetal-Co alloy powder, milling effects on coercivity 8=31597
momentum transfer rel. to Schrodinger eqn. in crystals 8=35609
muscovites, shearing force anisotropy rel. to surface condition 8=44602
plastic structures, free vibrations 8=28263
plastics, aging problems 8=44612
plasticity, stress-strain relations, statistical theory 8=40104
plate on elastic half-space, with moving line load, bending moments and stiffness 8=23830
polyimide films, noncryst., rel. to mol. struct., obs. 8=44619
polyurethane foams, effect of cell membrane 8=48243
polyvinyl alcohol, rel. to structural features 8=26154
porous rubber, axial compression of cylinders in torsion 8=31253
quartz, shock-loaded x-cut, 573°K 8=26844
radiation effects, conference Ashevill, North Carolina, USA, Sept. 1965 8=35593
shells, rotationally symmetric, under central boss loadings, limit anal. 8=23840
Steel, 40KhN5S, effect of programmed loading 8=49005
steel, low-carbon, deformation and recrystallization textures, rolling temp. dependence 8=26818
steel, 17% Cr stainless, ridging formation mechanism 8=26810
stress corrosion cracking by wedge force loading 8=48977
torsion of elastic cylinder welded to elastic half space 8=23827
welding, explosive, wave-like profile of interface 8=28203
Al cutting at 100–700 m/s, force meas. 8=35655
Al recovery, models and stage III mobile defects nature 8=39991
Al-Al_2O_3 alloys, ball-milled and blended 8=26782
Al-Mg alloys, dynamic recovery 8=48992
Al-Mg-Zn alloys, rel. to precip.-free zone effects 8=26785
Al_2O_3, abrasive grains, frictional coeffs. with metals 8=31184
Al_2O_3 trichites, rupture constraint rel. to structural state 8=26777
AlSb, rel. to dislocation structure 8=44443
Ar-air mixtures, equilib. props. behind shock waves 8=34625
Au, cold-worked, tensile props. 8=40130
BeO, rupture mod., effect of strain rate, environment and surface cond. 8=26788
C articles, monolithic, semi-isostatic forming 8=45933
$Ca_2V_2O_7$ 8=30798
CaV_2O_6. 8=30798
$Ca_3V_2O_8$ 8=30798
Co-W ferromag. high-temp. structural alloy development 8=31601
Cu, commercially pure, tension and torsion creep recovery 8=26805
Cu, fatigue softening after cyclic loading 8=44565
Cu, grain boundary cavity stability during annealing 8=26802
Cu, polycrystalline, explosively shocked, dislocation damping 8=26672
Cu-Al alloys, fatigue softening after cyclic loading 8=44565
Cu–Al–Ni and Cu–Al–Fe solid solutions, hardening action of short range order 8=26806
Cu-Nb_3Sn-stainless steel composite superconductors, obs. 8=27014
Cu-Zn system, conc. dependence, stacking fault energy 8=48869
Fe-Al alloys, yield stress max. 8=39720
Fe_2O_3, compacts, shrinkage in range 800-1000°C 8=35067
Mg–Zn–Mn alloy, wrought, heat treatment effects 8=35704
Mo, hydrostatically-extruded 8=35706
Nb_3Sn–Cu–steel composite conductors, and e.m. performance 8=40401
Pb(ZrTi)O_3 ceramics, rel. to microstruct 8=44597
Si bronze, with low stacking fault energy, shock loading effects on lattice 8=31098

Mechanical properties of substances—contd
SiC, abrasive grains, frictional coeffs. with metals 8=31184
Ti-6Al-4V alloy, addition of Co 8=49055
TiNb33:N and O, workability, and supercond. and micro-struct., obs. 8=44742
TiNb40: N and O, workability, and supercond. and micro-struct., obs. 8=44742
$(Zn_{0.65}Mg_{0.35})_2SiO_4$, high-temp. 8=35725

Mechanical strength
See also Elasticity; Hardness.
adhesive joints, time depend., effect of relaxation processes 8=48967
alumina (96%) rods, thermally conditioned, flexural, and residual stress 8=35659
basalt and granite, stress rate and temp. effects 8=48985
basalt in ultra high vacuum 8=41320
brass, diaphragm, square, plastic deform. and failure 8=37155
cast iron with spherical graphite, notch impact and impact bend strength, testing 8=49017
cellulose, Du-Pont K116-207 films, fracture toughness, obs. 8=44614
ceramics 8=48968
cleavage, double-cantilever, discussion on theory 8=26769
fatigue, understressing effect, explanation 8=40114
diaphragms, rectangular, bursting strength under hydrostatic press. 8=37154
fracture in notched bars, and elastic-plastic stress distrib. 8=46058
fracture toughness of high strength alloys, effect of microstructure 8=49011
fracture toughness testing, state for WOL specimen 8=48973
glass, effect of polymeric organosilicon film 8=49024
glass, inorg., fracture strength, rel. to surface conds., loading and chem. comp. 8=31176
glass-reinforced plastics in oil, long-time strength 8=31239
glass sheet, ambient humidity dependence 8=40165
glass, weakening defects 8=44580
graphite, reactor type, meas. before and after n-irrad. 8=26789
metallic/brittle aggregates, fracture initiation and modes of failure 8=31182
microsamples, test apparatus for 1.3-1200°K 8=48950
optical contacts 8=44528
oriented media, time-dependence, theory 8=44529
plane stress problems, finite element representations 8=23824
plastics, scale and temp. effects 8=31238
polymers, amorphous, tearing 8=31237
polymers, amorphous, temp.-time charact. 8=31234
polymers, tear strength increase 8=49066
porous solid, effect of surface energy 8=48969
radial nozzles in spherical pressure vessels, shakedown loads 8=32750
shock waves, spherical and plane, propag. and attenuation, rel. to solid strength 8=26751
silicate glasses, strengthening by ion exchange 8=26845
steel, diaphragm, square, plastic deform. and failure 8=37155
steel, e bombard. effects, 2.5 MeV 8=35694
steel, low C castings, effect of rare-earth metal additions 8=49009
steels, Fe–C and Fe–Ni–C, martensite strength, contribution factors 8=26815
steels of ultra-high strength, fracture toughness, effects of microstructure 8=49010
Al alloys, fracture toughness, orientation dependence 8=48989
Al alloys, serrated yielding, dislocation model of temp. and strain rate depend. 8=44548
Al, increase on low temp. deformation due to mosaic block misalignment 8=35653
Al–MeO, dispersion strengthened, elevated temps. 8=40124
BeO, rupture mod., effect of strain rate, environment and surface cond. 8=26788
Co-W ferromag. high-temp. structural alloy development 8=31601
Cr black coatings, electrolytically deposited 8=45394
Cu diaphragm, square, plastic deform. and failure 8=37155
Cu, n-irradiated, strengthening mechanism after mild annealing 8=31198
Cu, reduction by presence of thin epitaxial Ni overgrowth 8=40146
Cu single crystals, film coating on, increase rel. to surface damage 8=40150
Cu, yield surfaces, effects of plastic deform and neutron irrad. 8=44564
4% Cu–Al alloys, rel. to time and temp. 8=31201
Cu-Cr alloys, stress limitation rel. to cavity formation, 8=48871
Fe–C martensite, yield strength and transformation substructure 8=26812
Fe-Mn-N, alloys, high. temp. strengthening, Mossbauer study 8=49019
Fe-N single crystals, solid solution strenthening 8=49013
Fe-Ni-Cr-Nb alloys, strengthening phase identification 8=44574

Mechanical strength—contd
- Ge crystals, smooth surface defects, effect at 300°K and 4.2°K 8=40161
- MgO, toughness, effect of water 8=40173
- NaCl, along body and face diagonals theoretical 8=44594
- NaCl:Mn, yield strength 8=40175
- Ta–Mo alloys, effect of Mo conc. on yield stress 8=35718
- Ta–Nb alloys, effect of Mo conc. on yield stress 8=35718
- Th, effect of C content, 0.008 to 2.83 at % 8=44603
- Th, effect of C solid solution 8=40183
- Ti alloys, fracture toughness parameters 8=49058
- WC-Co alloys, transverse-rupture strength increase on porosity decrease 8=49062
- **compressive**
  - of columns with cracks, load carrying capacity 8=44520
  - cylindrical shells eccentrically stiffened, stability 8=41651
  - rings, diametral compression by "point" loads 8=31168
  - rubber cylinders under end loads, stability 8=44610
  - semiconductors based on GeTe: (Bi, Cu), effect of n and γ irrad. 8=40637
  - Mo, hydrostatically-extruded 8=35706
- **shear**
  - glass, molten, high-temp. u.s. interferometry 8=39280
  - longitudinal shear crack with infinitely narrow plastic zone 8=46061
  - powder, split-ring annular cell meas. 8=35611
  - W, modulus freq. and temp. dependence (0.0004–20 cps, 1400–2000°K) 8=35723
- **tensile**
  - alkali halides, NaCl-type, and elastic consts. 8=49036
  - apparatus for micro-specimens in 1.3 to 1200°K range 8=48947
  - brittle fracture initiation, rel. to microstruct. 8=31174
  - ethylene-propylene copolymer single crysts. mats. obs. 8=44616
  - fibres, three-point bend tester 8=31172
  - flat plate with circular hole under uniaxial tension 8=41723
  - granular materials, theory and expt. in whole moisture range 8=31173
  - high-temperature meas. apparatus 8=31175
  - magnetostrictive load cell for tensile testing under high hydrostatic pressures 8=40103
  - martensitic steel, C content, effect on notch toughness 8=35684
  - metal foils, time-to-rupture from creep tests under tensile loads of periodically varying orientation 8=35626
  - metal samples at 1.3°K, micromachine 8=48959
  - metals, sheet, tensile straining, high temp. effect 8=48982
  - plastic resin reinforced with alumina fibres 8=26857
  - polyethylene, rel. to mol. chain mobility, ≤ 40 000 psi 8=44620
  - polytetrafluoroethylene, rel. to mol. chain mobility, ≤ 60 000 psi 8=44620
  - steel, austenitic stainless, He embrittlement, 540–760°C 8=31213
  - steels, cast austenitic, increase by phase transformations on thermal cycling 8=35698
  - tension tests, stability conditions 8=26739
  - testing apparatus in range -76°C to + 100°C, simple 8=48966
  - testing, remedy for scatter 8=26765
  - uniaxial tests using stress corrosion cell 8=48970
  - Al, zone-refined, changes during recrystallisation after low-temp. deformation 8=35660
  - CsI crystals 8=40139
  - Cu alloys, improvement by increasing Pb content 8=40144
  - Cu, Hg addition effects 8=31203
  - Fe, yield, effect of annealing after wet H treatment 8=49018
  - Fe–50Ni alloys fibre-reinforced, rel. to mag. props. 8=31209
  - Fe–1.35Si alloys, fibre-reinforced, rel. to mag. props. 8=31209
  - KCl, dependence on growth conditions and impurity effects 8=26401
  - LiF, dependence on growth conditions and impurity effects 8=26401
  - Mg–Zn–Mn alloy, wrought, effects of heat treatment 8=35704
  - Mo, hydrostatically-extruded 8=35706
  - NaCl dependence on impurity effects 8=26401
  - NiCoMo steels, constant properties in wide temperature range 8=49016
  - Ni_3Fe, ordered and disordered, behaviour 8=44595
  - Zr, effect of up to 4.2 at.% O on deform 8=44609

Mechanics
- See also Dynamics.
- book 8=37102
- cantilevered bars, instability modes, induced by fluid flow through attached pipe 8=37239
- central force motion, without calculus 8=32703
- chain, composed of two homogeneous parts, small oscills 8=41647
- circular motion in relativistic Kepler problem, stability 8=37123
- classical and quantum theory, fundamentals 8=46013
- classical, canonical transformation governing temperal development 8=28248

Mechanics—contd
- classical, Hamiltonian, relativistically invariant 8=28249
- classical motion problem, quantum vector approach 8=46787
- continuous media in pseudo-Riemann space, models construction, theory 8=32692
- continuum, variational principles 8=23815
- controlled systems, motion 8=46019
- coupled systems subjected to determinate and random input 8=37240
- extremum stiffness of structure 8=23816
- energy transfer in one-dimensional collisions of many objects 8=28254
- flow graphs, boundary value problems 8=32691
- free fall structure design 8=23818
- free fall in a rarified atmosphere 8=28257
- Hencky-Prandtl nets 8=32693
- heterogeneous media with indep. coupling motions 8=32701
- internal force distrib. theorem expressed as a principle of maximum uniformity 8=37121
- Lagrange multipliers for system with constraints, geometrical view 8=23887
- Lie algebras, Poisson bracket realization by analytic functions of generators 8=28231
- product of two rotations 8=28247
- resonant periodic orbits 8=41643
- rotating sphere, deformation soln. 8=32698
- shell, toroidal segments, post buckling behavior 8=37147
- thought-provoking problems for students 8=37103
- three-body problem 8=45605
- three-body problem, periodic orbits distrib. 8=32406

Mechanics of gases. See Aerodynamics.

Mechanics of liquids. See Hydrodynamics.

Medical science
- See also Physiology; Radiation protection.
- acetylcholine ionic environment in the chemical transmission of nerve impulses 8=28201
- antitubercular cpds., structure of ethionamide hydrochloride 8=26502
- antitubercular cpds., structure of ethionamide hydrobromide 8=26503
- aspirator, dry, clock-driven 8=37095
- γ spectroscopy, data collection by computer 8=50462
- instrumentation, 1918-68, bibliography 8=41604
- mammalian tissue, geometrical efficiency of solid state radio-activity detector 8=32621
- membrane-type artificial lungs, convective diffusion of gases in blood 8=43793
- organ scintiscanning, 2-isotope for overlapping tissues localization, theory 8=42454
- pulmonary ventilation recording 8=37094
- retina photocoagulation with ruby laser 8=28912
- tracer kinetics, nomenclature 8=32617
- X-ray diagnosis, ferrites as contrast mats. 8=37093
- Cs^{137} in human infants, 4π plastic scintillation counter 8=42934
- I^{123} for diagnostic use, prod. 8=45408
- K^{40} in human infants, 4π plastic scintillation counter 8=42934

Meissner effect. See Superconductivity.

Melting
- See also Zone melting and refining.
- alkali halides, thin crystals, dislocation arrays microscope examination 8=43902
- alloy, binary, stability of planar interface 8=30582
- cause, rel. to spontaneous generation of dislocations 8=31058
- earth's mantle, selective, effect on thermal history 8=50018
- gelatine gels, mechanism, from elec. cond. 8=34962
- hailstones, artificial, rough, rate of melting in airstream, and heat transfer 8=34963
- heat eqn., free boundary problem 8=25980
- ice, submicroscopic gaseous inclusions, nuclei for Tyndall figures 8=30579
- metals, cubic, theory of criterion 8=34964
- metals, disorder model 8=25979
- metals, refractory, by induction in self formed lining 8=30580
- Moon, Mars and Venus, effect of selective fusion on thermal history 8=50403
- observation by n.m.r. 8=48259
- polyethylene, linear fractions, mol. dispersed eutectic systems 8=44095
- polyethylene, temp. range from vol. expansion coeff. 8=39472
- polymer chains, effect of mol. wt. 8=44108
- poly(tetramethylene oxide), high-mol. wt., dilatometry 8=44134
- slabs, general starting soln. 8=39471
- solid-liquid interface, morphology during melting 8=43897
- solids, general, under very high press., low temp., rel. to cores of planets 8=32535
- Ag 8=35424
- Ag, small crystals, fusion and thermal expansion 8=39928
- Ar, meas. of molar volume along melting curve 8=43904
- Au 8=35424
- Am, melting curve, rel. to pressure 8=39541
- Cs, curve shape rel. to press., to 30 × 10^3 kg/cm^2 8=39473

Melting—contd
  Cs, high press., melting-curve maxima 8=34965
  Cu 8=35424
  Ga, at cryst. interfaces, rel. to superheating 8=44130
  He^3 curve, pressure to 17 m deg K and molar volume change on melting to 300 m deg K 8=41889
  K, curve to 80 kb 8=34961
  KCN, high press. 8=48385
  KSCN, high press. 8=48385
  Li, curve up to 80 kb 8=34961
  Li_2O, $SiO_2-Li_2O.Al_2O_3.4SiO_2-SiO_2$, system liquation isostructure and correl. 8=48255
  Na, curve to 80 kb 8=34961
  $NaClO_3$-$NaNO_3$ molten system, change of vol. 8=48086
  Pu, reactor fuel 8=47407
  Rb, curve to 80 kb 8=34961
  Rb liquid density near fusion, meas. 8=30421
  SiO_2, structural changes 8=48264
  Te, high press., melting-curve maxima 8=34965
  TiO_2-WO_2 system, relation 8=39476
  (U, Pu)O_2 solid soln. production and Pu distribution 8=29562
Melting point
  alkali halides, and ht. of fusion, electronic polarizability and ionic radius ratio, relationship 8=39474
  crystals for u.v. and i.r. optics 8=42116
  DNA, X-irrad., effects of binding agents 8=48903
  of glacier ice, behaviour 8=50086
  polybutene-1, isotactic, rel. to crystallization nucleation, obs. 8=44122
  polycaprolactam, rel. to cryst. morphology, obs. 8=43907
  polyethylene, branched, for lamellar struct. determ. 8=44096
  polyoxymethylene extended chain crysts., X-irrad. effects, $< 4.8 \times 10^7$ R 8=44509
  trifluoromethylphosphonylchloride 8=34330
  waxes, technique for determ. 8=43906
  Bi trihalides, high-press. 8=39468
  Cm_2O_3, rel. to use as heat source in thermionic diode 8=35425
  Fe–Se system 8=48254
  β–Ga, curve to 14.5 kbar 8=48260
  p-H_2, high press. 8=40575
  NaCN, to 40 kbar 8=30701
  NaSCN, to 40 kbar 8=30701
  Ta-Mo-C alloys, phase diagram through melting range 8=39475
  Tm_2O_3, rel. to use as heat source in thermionic diode 8=35425
  in U-H system, from press.-comp.-temp. diagrams 8=30713
  in U/UO_2 system, meas. of solidus and liquidus temp. 8=30581
  XeF_2 and XeF_4 8=39492
Membranes
  chlorinated diphenyls, ion purification 8=45310
  circular, composite, transverse vibrs. 8=32881
  circular, variable density, transverse vibration 8=28358
  diffusion, carrier and single file, asymm. discrimination 8=25902
  displacements and strains, finite element method 8=41677
  gas diffusion, time lag depend. on conc. 8=30321
  interfacial mass transfer in membrane transport in batch dialyzer 8=48120
  intramembrane transport 8=39346
  ion-exchange, osmosis 8=25901
  ion transport, Nernst-Planck eqns. and electroneutrality 8=39345
  permeability, elongation dependence 8=44397
  phenol sulphonic acid formaldehyde type, electro-osmosis and streaming pots. 8=27745
  polar double membranes, current-voltage and time meas. 8=27748
  polar double membranes, static effects 8=27747
  polymer, gas diffusion, time lag depend. on conc. 8=30321
  polymer, transport processes 8=26049
  relative permeabilities for constant field eq., expt. determ. 8=48122
  review of history and problems 8=26048
  synthetic, permeability to gas and steam 8=35471
  transport processes in ternary systs. 8=25903
  transport properties and performance in tubular and flat plate equipment 8=48124
  travelling forces on 8=37241
  spinning disc, stationary waves 8=23937
  $Cu_2[Fe(CN)_6]$, H_2O transport kinetics 8=48121
  Fe, diffusion and permeation of electrolytic H 8=44389
  Zr phosphate, for intermed. temp. fuel cells 8=46354
Memory devices. See Calculating apparatus; Magnetic devices; Superconducting materials and devices.
Mendelevium
  No entries
Mendelevium compounds
  No entries
Mercury (planet). See Planets.
Mercury
  addition to Cu, effect on tensile props. 8=31203
  arc plasma, i. r. bremsstrahlung calc. 8=30069
  atom, double-resonance broadening, 6^3P_1 state 8=38732
Mercury—contd
  atom, elastic electron scatt., cross section and Mott asymm. function calc. 8=34174
  Atom, electron scatt., Mott theory, influence of screening 8=34171
  atom, internal conversion coeff. for e. m. transition between shells 8=38670
  atom, $\lambda = 1850$ Å line, isotope shift and hyperfine structure 8=43192
  atom, metastable 6^3P_2 state, Zeeman sublevel decay constant is relaxation time of longitudinal component of quadrupole moment 8=34142
  atom, 6s6p$^3P_2$ metastable state, elec. dipole polarizabilities meas. 8=38704
  atom, 7^3S_1 state, lifetime and depopulation rate 8=38706
  atom, 2537 Å line broadening and shift by H_2 impact 8=43194
  atomic levels by optical methods 8=43191
  atoms collisions in Na-Hg system, meas. 8=29665
  atoms, excited ^3P, state, inelastic collisions of second kind with electrons 8=43230
  atoms in Se film, distrib. study by e. p. r. 8=35179
  column level meas., by variable resistance, automatic method 8=28455
  conductivity, electrical, and eqn. of state at 0-2000°C and 200-5000 atm. pressure 8=25945
  crystal Knight shift at 1.2°K 8=49646
  crystalline, glide and deformation twinning, –39°C to –196°C 8=26706
  crystalline, magnetoresistance and Fermi surface topology 8=26968
  crystals, deformation twinning modes 8=26187
  desorption from W on interaction with low energy electrons 8=39623
  detection on surfaces in vac. systems using ellipsometer 8=39255
  discharge excitation of Raman spectra in α-quartz 8=49753
  discharge h.p. lamp with iodide additive 8=42207
  discharge, low press., induction interaction of currents, obs. 8=43451
  discharge, r.f., afterglow spectrum 8=29616
  discharge, vapour, surface wave prod. device and soln. 8=47750
  discharges, Tonks, Dattner resonances damping rel. to microwave field 8=43443
  electrocrystallization 8=41283
  electrode, adsorpt. energy of ions 8=36600
  excitation by $N_2(A^3\Sigma_u^+)$ 8=34163
  flow caused by travelling mag. field, obs 8=24180
  fluorescent tube operation, vapour pressure influence when frequency rises to 28 KHz 8=46681
  4-point contact probe for thin film elec. cond. meas. 8=41907
  halide complex with azines, prep. and infra-red study 8=36432
  ions, electrochem. in fused $AlCl_3$-NaCl-KCl 8=49917
  jet supersonic vapour, use for charge exchange of polarized ions 8=39039
  lamp for holography 8=46754
  lifetime of 6^1P_1 level, coherence scattering of light 8=47498
  liquid evaporation rate in vacuum 8=39480
  liquid in reactor boilers, corrosion, inhibited by Ti or Zr 8=47426
  liquid, Knight shift 8=39438
  liquid, temp. profiles in turbulent flow, effect of superimposed free convection 8=34836
  liquid, thermal conductivity, 350°K-500°K 8=48130
  low pressure gas discharge, current limitation and gas clean-up 8=47767
  mag. field induced motion in shallow layer, obs. 8=24177
  manometer with collinear arms 8=32643
  monolayer ellipsometer, surface tension and contact pot. obs 8=48061
  photoemission, two- and three-photon, in $HClO_4$ solns., obs. 8=40706
  porosimeter, low pressure for macropores meas. 8=30660
  preionized vapour flow, intensity relax. of certain lines in flow dirn. 8=47753
  reservoir, control by greaseless valve 8=34691
  resonance radiation, rel. to monochromatic flash spectroscopy 8=24389
  seeding in Cs plasma diode, rel. to performance 8=28475
  6^1P_1, $6^3P_{0,1,2}$ states excited by electron impact 8=38705
  solubility in dimethylcyclohexanes and alcohols 8=48071
  solubility in various liqs. 8=30416
  solubility in various liqs., free-vol. theory 8=30417
  solubility, temp. depend, entropies and solute solvent interacts 8=43798
  spectral line broadening, 2537 Å, in presence of Cd, Zn and Mg vapour 8=43193
  spectroscopy, Fourier, 15.295 Å line h. f. s. 8=28830
  subcooling 8=30583
  vapour, associative ionization cross section 8=25716
  vapour, breakdown by laser beam, threshold values 8=47766
  vapour discharge, electron energy distribs. and Langmuir paradox 8=34419

Mercury—contd
  vapour-discharge, positive column, electron-density profile microwave meas. 8=39113
  vapour, electrical breakdown, mechanisms 8=43484
  vapour, green-band emission 8=29944
  vapour, photoionization curves up to 17.7 eV 8=39031
  viscosity under press. between 40 and 440 kbars 8=48094
  Hg^{119}, hyperfine structure constants in $6\,{}^1P_1$ level, and hyperfine structure of line $6\,{}^1P_1$-$8\,{}^1S_0$ 8=43195
  Hg^{198} atom collisions with inert gases, relax., temp. effect 20°-600°C 8=29664
  Hg^{201}, dispersion and optical props. in vapour on optical pumping and in pulsating e.m. field 8=43222
  γ-Hg, structure 8=44220
  Hg^+ sputtering, yield and ang. distrib. rel. to random and preferential ejection correlation 8=44499
  HgI series, intercombinational transition probabilities 8=38711
  Hg/sulpholane interface, specific adsprt. rel. to elec. double layer 8=30396
  Hg + Cl atom combination 8=49960
  Hg-Hg turbulent co-current flow heat exchanges, expt. rel. to theory 8=34835
  Hg-Kr glow discharge, e energy distrib. rel. to striations 8=34418
  Mo wire and foil quenching 8=31218
Mercury compounds
  alloys, liquid, Knight shift 8=39438
  amalgams, liq., hall effect 8=43869
  β-HgS films, elec. conductivity and thermal e.m.f. temp. dependence 8=44792
  liquid alloys, elec. cond., invalidity of Mott model 8=25948
  mercury di-n-hexyl, liquid: radiolysis to identify composition 8=49976
  HgCl, dimerization 8=49960
  $HgCl_2$ as γ-ray dosimeter, radiolytic and photolytic consts. 8=45409
  Hg-CN-SCN complex in aqueous soln, Raman spectra rel. to mixed ligands 8=43842
  $Hg(CNO)_2$, bonding and stability 8=26006
  $HgCr_2S_4$, mag. structre and metamagnetism 8=31653
  $HgCr_2Se_4$, n.m.r. of Cr^{53} and Se^{77} at 4.2°K 8=31896
  HgD, hyperfine struct. in spectra 8=43314
  $Hg_5In_2Te_8$, elastic consts. 8=49027
  $Hg(OHg)_4Br_2$, least-squares refinement 8=48654
  $[HgOSi(CH_3)_4]_2$, crystal structure 8=48683
  HgS crystal, up-conversion of 10.6μ beam to visible 8=46552
  HgS, films epitaxial growth on CdS and ZnS platelets, dislocations and cryst. orientation 8=35165
  α-HgS, nature of photoelectret effect 8=31440
  HgS_xSe_{1-x}, $O \leqslant x \leqslant 0.4$, cond., Hall effect and i.r. absorpt., 25-300°K 8=40319
  HgS_xTe_{1-x}, $O \leqslant x \leqslant 0.4$, elec. cond. and Hall effect, 25-300°K 8=40319
  HgSe thin films, structure 8=30755
  HgSe-βHgS mixed crystal, elect. props. and band struct 8=31320
  HgT, hyperfine struct. in spectra 8=43314
  Hg-Tb(Yb) systems, phase diags. 8=30706
  HgTe, density of states, effective mass of holes 8=40242
  HgTe, lattice dilatation, constant and thermal expansion coefficient rel. to temp. 8=48744
  Hg Te, magnetoplasma reflection rel. to temp. 8=49247
  HgTe, magnetoresistance oscillations 8=35811
  HgTe, oscillations of longitudinal magnetic resistance in degenerate electron gas 8=40466
  HgTe, phonon viscosity attenuation of u.s. waves 8=30946
  n-HgTe, Shubnikov-de Haas effect 8=27106
  HgTe thin films, structure 8=30755
  HgTe-βHgS mixed crystal, elect. props. and band struct. 8=31320
  HgTe-HgSe mixed crystal, elect. props. and band struct. 8=31320
  Hg_3Te_3-Im_2Te_3 alloy system, phase diagram 8=30697
  Hg_3Te_3-In_2Te_3 alloys, elec. props. 8=40464
  Hg-Tl eutectic, interfacial reactions with metals, dielectrics and polymers 8=49873
  Hg–3% Zn liquid, rel. to ductile-brittle transition temp. of Al, strain-rate depend. 8=35657
  Hg–3% Zn liquid, rel. to ductile-brittle transition in Al 8=35656
Mesic atoms. See Atoms, mesic.
Mesic molecules. See Molecules, mesic.
Mesomorphic state. See Liquid crystals.
Meson field theory. See Field theory, quantum/meson field.
Mesons
    See also Atoms, mesic; Cosmic rays/mesons; Hyperons; Molecules, mesic; Pions.
  baryon-meson coupling constants, sum rules derived 8=24625
  baryon-meson supermultiplet symmetry from spinor currents 8=42483
  baryon-meson vertex in SL(6, C) 8=47098
  bootstrap general scheme 8=33602
  composite of 2 Dirac particles 8=24750
  coupling consts., vector and scalar with nucleon, from low-energy p-p scatt. 8=24748
  classification in boson 27-plet 8=33533
Mesons—contd
  cluster model and square mass relation 8=47104
  coupling constants, quark model calc. 8=42497
  η as bound state of 3π 8=29177
  η_{00} phase meas. in $K^\circ \rightarrow 2\eta$ 8=42581
  exchange adiabatic local potential model for N-N interacts. 8=24868
  exchange and coupling consts. in n-n, pn and pp scatt. 8=24931
  exchange effects rel. to β decay 8=25174
  exchange in relative s state rel. to N-N interacts. 8=24874
  field, vector using more general functional derivatives for vector mesons 8=29164
  $F_K/F_\pi = 1$ from spectral function sum rules 8=29119
  $F_K/F_\pi = 1$ from splitting of Weinberg's first sum rule 8=29029
  $g_{\rho\omega\pi} = 21\ (GeV)^{-1}$, $g_{\phi N}/g_{\omega N} \simeq 0.06$ from saturating superconvergence relations in $\overline{N}N = \pi\rho\,(\omega)$ 8=33740
  $g^2{}_{FK\bar{K}}/4\pi = 0.65$ sum rule from convergence relation for a linear combination of amplitudes 8=37893
  interactions baryon-meson interaction lagrangian, $SU(3) \times SU(3)$ 8=47127
  intermediate states in $\pi^+d \rightarrow \pi^+\pi^-\pi^\circ pp$ reaction at 3.65 BeV/c 8=42529
  K°, mirror, possible experimental search 8=38013
  K_0-$\overline{K}_0$ transition in Dirac and e.m. fields 8=38015
  K^*, search for production below $K\pi$ threshold K^+, H scatt. 1 BeV/c 8=38014
  lifetimes and branching ratios 8=24827
  mass spectrum formula 8=29114
  meson-baryon composity structure of high-spin baryons 8=29178
  meson-nucleon coupling consts. from N-N forward dispersion relations 8=24746
  negatively charge near 960 MeV, search 8=33657
  non-linear Lagrangian models invariant under generalized chiral groups SL(4, C) and SL(12, C) 8=24752
  non-strange, Regge trajectory contrib. to scatt. cross-section 8=42432
  non-strange, theory 8=42500
  one-boson-exchange model, coupling consts. 8=24747
  ϕ_{00} phase meas. in $K^\circ \rightarrow 2\pi$ 8=42581
  polarization correl. with B prod. in ν-N interactions 8=29091
  propagators, unitarity corrections in spectral-function sum rules 8=37954
  pseudoscalar, ninth, and broken $SU_W(6)$ 8=33655
  quark model, semirelativistic 8=42360
  scale factor in algebra of factorized Regge residues 8=42440
  theory, rel. to smooth NN interactions 8=33741
  2^+, props. similar to 1^- octet, possible assignments into SU(6) 8=33549
  vector meson interact. with Coulomb pot., singularities in wave function 8=42596
  vector meson system, Born exchange terms, appl. of gauge theory 8=42604
  vector-pseudoscalar couplings from PCAC in broken SU(3) 8=33654
 absorption
  No entries
 capture
  K^- absorpt. by light nuclei, pair-absorpt. model 8=34019
  by nucleus in mesic atom, approx. calc. 8=47333
  O^{16} radiative π capture, shell model calc. 8=47334
  π^-, by H in hydrogeneous substs. 8=47739
 decay
  $A_1 \rightarrow \rho\pi$ and $\pi^\pm - \pi^\circ$ mass difference, Schwinger theory 8=24854
  $A_1 \rightarrow \rho\pi$ in quark model 8=29175
  $A1 \rightarrow \rho\pi$ using current algebra, pole dominance and meson coupling constants 8=33526
  A_1 width calc. using Lagrangian model of $\pi - A_1$ mixing 8=24855
  $A_2 \rightarrow \pi\gamma$, width calc. from saturating sum rule from $\pi \rightarrow \pi^\circ l\nu\gamma$ 8=33726
  $B \rightarrow \omega\pi$, rel. to spin and parity determ. of B 8=38040
  boson resonances decaying determ. of spin, parity 8=33715
  Cabibbo theory status 8=38009
  χ°, using current algebra rel. to $\eta \rightarrow \gamma\gamma$ 8=24837
  $\chi \rightarrow \eta\pi\pi$, chiral-dynamic-Lagrangian calc. 8=42605
  e.m. rel. to quark charge-commutation relations 8=29108
  κ, lifetime and $K\pi$ coupling calc. 8=29153
  η, CP violation, assuming $\Delta I = 2$ selection rule 8=24816
  $\eta \rightarrow l^+l^-\gamma$ or $\rightarrow l^+l^-$, $l = 3$ or μ, branching ratios calc. 8=42589
  η, rate calc. from Schwinger's chiral dynamics 8=24637
  η, rel. to C nonconservation, obs. review 8=33711
  $\eta \rightarrow 2\gamma$, assuming the interaction for 3π decay transforms. like the third member of an octet 8=24836
  $\eta \rightarrow 2\gamma/\pi^\circ \rightarrow 2\gamma$ ratio rel. to SU_3 symm breaking 8=24769
  $\eta \rightarrow \gamma\gamma$, using current algebra 8=24837
  $\eta \rightarrow 2\gamma/\pi^\circ \rightarrow 2\gamma$ widths ratio by soft-photon emission calc. with SU(3) symmetry breaking 8=38019
  $\eta \rightarrow 2\gamma$, $X^\circ - \eta$ mixing in quark model 8=24835
  η, modes, current algebra and PCAC discussion 8=38025
  $\eta \rightarrow \pi^\circ e^+e^-$, C violation 8=24816

Mesons—contd
  decay—contd
    $\eta \rightarrow \pi\pi\gamma$, C violation 8=24816
    $\eta_V \rightarrow 2\pi$, $\overline{K}K$ branching ratio and SU_3 violation 8=29113
    $\eta \rightarrow \pi^+\pi^-\pi^\circ$, Dalitz plot analysis, possible $\Delta I = 0$, $\Delta I = 2$ C-violating amplitude 8=33712
    $\eta \rightarrow \pi^+\pi^-\pi^0$, $K \rightarrow 0$ replaces $K_u \rightarrow 0$ 8=38005
    $\eta \rightarrow \pi^+\pi^-\pi^0$, obs. test of invariance 8=42591
    $\eta \rightarrow \pi^+\pi^-\gamma$, test of C invariance, obs. 8=42590
    η_{+-} phase, $Re\epsilon$ and superweak model 8=38008
    $\eta^\circ \rightarrow 2\gamma$ derived from N Compton scatt. 8=33663
    $\eta^* \rightarrow \eta + 2\pi$, meson chiral transformation 8=24686
    $f^\circ \rightarrow 2\gamma$ width, $\gamma + \gamma \rightarrow \pi^\circ + \pi^\circ$ dispersion sum rule calc. 8=29173
    h, properties and implications 8=24759
    isospin-one on Regge trajectories, classification, decay modes 8=24677
    K amplitude/π amplitude = 1 to all orders of SU(3) breaking interaction calc. 8=38011
    K decay constant, Goldberger-Freiman relation validity 8=37828
    $K \rightarrow \gamma + e + \nu$, weak vector current conservation 8=37876
    $K \rightarrow l\nu\ \pi l\nu\ \pi\pi l\nu$ current algebra approach 8=37830
    K obs., consistency with soft-pion prediction of current algebra 8=42569
    $K \rightarrow 1 + \nu_1 + \gamma$ applic. of Cabibbo theory 8=24753
    $K \rightarrow \pi e^+e^-$, using vector meson dominant model calc. 8=38004
    $K \rightarrow 2\pi$, CP violation, current-current models 8=42575
    $K \rightarrow 2\pi$, formalism, singularities, and dumps with one π only off mass shell 8=33697
    $K \rightarrow 2\pi$ rel. to CPT invariance and π-π phase shift anomaly 8=24815
    $K \rightarrow 2\pi$, violation of $\Delta T = 1/2$ rule 8=29148
    $K \rightarrow 3\pi$, current algebra constraints, comparison with expt. in τ decay 8=33697
    $K \rightarrow 3\pi$, like-π spectra and non-linear effects 8=24819
    $K \rightarrow 3\pi$, nonleptonic, $\Delta T = 1/2$ violation 8=24823
    $K \rightarrow 3\pi$, odd-π spectral shape rel. to low-energy π-π scatt. 8=33692
    $K \rightarrow 3\pi$ rates, e.m. corrections calc. 8=47116
    $K \rightarrow 3\pi$, simple model for amplitude 8=29152
    $K \rightarrow 3\pi$, vector meson dominance model 8=42577
    $K \rightarrow \pi\pi\pi l\nu_e$, form factors from current algebra and PCAC 8=29149
    K, radiative form factors 8=42566
    K resonance quark model 8=33731
    K, semi-leptonic, phenomenological model 8=24771
    K, with matrix element structure of Hamiltonian and current algebra 8=29210
    K_A strong, calc. using Weinberg-Schnitzer model 8=33730
    $K_A \rightarrow K + \omega$ current algebra calc. using Schnitzer-Weinberg technique 8=33723
    $K_A \rightarrow K + p$ current algebra calc. using Schnitzer-Weinberg technique 8=33723
    K_{13}, calc. of $f_-(0)/f_+(0)$ from algebra of currents and spectral function sum rules 8=42572
    K_{13} current algebra calc. of form factors with SU(3) symm. breaking 8=38002
    K_{13}, discrepancies in ξ determ. 8=29150
    K_{13} form factor calc. using current algebra and dispersion relations 8=38003
    K_{13} form factors, current algebra and subtracted dispersion relations 8=42578
    K_{13} form factors, from chiral dynamics and field-current identity 8=24820
    K_{13} form factors from current algebra and Weinberg spectral function sum rules 8=24818
    K_{13} form factors studied using current algebra 8=33699
    K_{13} mode, matrix element of divergence or vector current 8=42580
    K_{13}, K_{14} from factors, using soft pion techniques and current algebras calc. 8=33694
    K_{14}, extraction of form factors 8=42576
    K_{14}, form factors for calc. of π-π phase shifts 8=29137
    K_{e3} amplitude rel. to renormalization corrections 8=42386
    K_{e3}, Cabibbo theory status 8=38009
    K_{e4} characteristics rel. to low-energy π-π scatt. 8=33692
    K_{e5}, vector form factors, current algebra calc. 8=42579
    $K_{\mu 4}$ spectrum calc. from current algebra 8=24822
    K°, CP violation estimated with a Cabibbo transformation 8=24816
    K°, CP violation phenomena, possible explanation of anomalies 8=33693
    K°, $\Delta S = -\Delta Q$ selection rule 8=33696
    K°, $\Delta S = \Delta Q$ test in leptonic decay 8=42570
    K°, effects of $\Delta S = \Delta Q$ on CP-nonconservation in decay 8=38001
    $K^\circ \rightarrow e^\pm + \nu + \pi$, $\Delta S = \Delta Q$ conserved 8=38007
    K°, pion decay 8=47115
    K°, time-dependent K_S, K_L interference in $\pi^+\pi^-$ decay channel obs. 8=42564
    $K^\circ \rightarrow 2\pi$ rel. to CP 8=24612
    $K^\circ \rightarrow 2\pi$, restrictions imposed by TCP and unitarity 8=42581
    $\overline{K}^\circ \rightarrow K^- + e^+ + \nu_e$, probability predicted in phenomenological model 8=24771

Mesons—contd
  decay—contd
    K°_{13}, μ_3, charge asymmetry rel. to K°-$\overline{K}^\circ$ system params. 8=42584
    K_{e3}°, radiative corrections 8=42573
    $K^\circ_{\mu 3}$ and $\overline{K}^\circ_{\mu 3}$ differential probabs. 8=29147
    $K^\circ_{\mu 3}$, $Re\xi$ meas. from μ polarization 8=42567
    K^0_L, leptonic, T-violating effects 8=33567
    $K^\circ_L \rightarrow \mu^+\mu^-$ and weak-interaction cut-off 8=33700
    $K_L \rightarrow \pi e\nu$, decay mode study 8=29146
    $K_L^\circ \rightarrow \pi^\pm e^\mp$, charge asymm. implying CPT test 8=42568
    $K_L^\circ \rightarrow \pi^\pm\mu^\mp\nu$ charge asymm. implying CPT test 8=42568
    $K^\circ_L \rightarrow 2\pi^\circ$, CP violation 8=24814
    $K_L \rightarrow 2\pi$ CP violation rel. to model $W \equiv a$ 8=38012
    K_2° lifetime meas. 8=33709
    K°_s, mean life $= 0.856 \times 10^{-10}$ sec obs. 8=33695
    $K_s \rightarrow 2\pi$, radiative corrections 8=33833
    $K^0_1 \rightarrow \pi^+\pi^-$ mass-amplitude relation 8=38010
    $K_2^\circ \rightarrow 2\pi^\circ$, $K_1^\circ \rightarrow 2\pi^\circ$, ratio $[\eta_{00}|^2 = (-2 \pm 7) \times 10^{-6}]$ 8=42571
    $K^0_2 \rightarrow \pi\pi\pi$, $K^2 \rightarrow 0$ replaces $K_u \rightarrow 0$ 8=38005
    $K_2^\circ \rightarrow \pi^+\pi^-\pi^\circ$ incorrect assumption that integral over phase space of first-order term is zero 8=33701
    $K^\circ_2 \rightarrow \pi^+\pi^-\pi^\circ$ spectrum rel. to π scatt. lengths, obs. 8=29135
    K^+ $\Delta S = \Delta Q$ selection rule 8=33696
    $K^+ \rightarrow \pi^+ + \pi^- + e^+ + \nu$, π-π phase shift review 8=24805
    $K^+ \rightarrow \pi^+\pi^\circ$ mass-amplitude relation 8=38010
    $K^+ \rightarrow \pi^\circ + \mu^+ + \nu$, parameter $E(q^2)$ determ. 8=24817
    $K^+ \rightarrow \pi^\circ\pi^\circ\pi^+$ spectrum rel. to π scatt. lengths, obs. 8=29135
    K^+_{e2} branching ratio, meas. in spark chamber and counter expt. 8=42565
    $K^+_{e3} \rightarrow \pi^\circ + e^+ + \nu$, π° momentum meas. from its e-pair decay 8=33698
    $K^+_{\mu 3} \rightarrow \pi^\circ + \mu^+ + \nu$, π° momentum meas. from its e-pari decay 8=33698
    $K^\pm \rightarrow \pi^\circ + \mu^\pm + \nu$, radiative corrections with finite ν mass 8=24821
    $K^\pm \rightarrow \pi^\pm\pi^\circ$, and $\Sigma^+ \rightarrow n\pi^+$ related by $\Delta I = 3/2$ effects 8=29151
    $K^\pm\pi^\circ\pi^\circ\pi^\pm$ incorrect assumption that integral over phase space of first order term is zero 8=33701
    K^*(890)(1420) in K^-p, 10 GeV/c comparison with Regge pole model 8=33732
    $K^* \rightarrow K\pi$, $K\pi\pi$ rel. to baryon model for bosons 8=33548
    K^* strong, calc. using Weinberg-Schnitzer model 8=33730
    K^* widths from vertex functions 8=42598
    mass spectrum, using cluster model of hadrons 8=42486
    non-leptonic, amplitudes rel. to current divergence 8=33529
    $\omega \rightarrow e^+e^-$ new data 8=33721
    $\omega \rightarrow l^+l^-$, non-existent consequence, protoprod. 8=33728
    $\omega \rightarrow l^+l^-$, radiative correction calc. 8=29170
    $\omega \rightarrow$ neutrals/$\omega \rightarrow$ total, branching ratio meas. 8=38032
    ω, ϕ, $\rho \rightarrow 2\pi\gamma$, soft-photon emission approach 8=29174
    $\varphi \rightarrow e^+e^-$ obs. 8=33721
    $\phi \rightarrow e^+e^-$, partial width obs. 8=33722
    $\phi \rightarrow l^+l^-$, radiative correction calc. 8=29170
    ϕ, isospin violations assuming asymptotic symmetry 8=42606
    $\phi \rightarrow K + K$, current algebra calc. using Schnitzer-Weinberg technique 8=33723
    $\phi \rightarrow K\overline{K}$, width calc. 8=33654
    ϕ strong, calc. using Weinberg-Schnitzer model 8=33730
    ϕ widths from vertex functions 8=42598
    pseudoscalar, applic. of Cabibbo theory 8=24753
    pseudoscalar, two-body radiative using current algebra, PCAC 8=37955
    Q widths from vertex functions 8=42598
    quark model calc. 8=42497
    radiative, connection with current algebra 8=38025
    radiative, correction with current algebra 8=38025
    resonance, 3-particle, spin and parity determ. 8=38021
    $\rho \rightarrow e^+e^-$ new data 8=33721
    $\rho \rightarrow e^+e^-$, vector-meson-dominance prediction, finite-width corrections 8=42607
    ρ, $f_{\rho\pi\pi}(-m^2_\rho, o, o)$ calc. 8=33727
    $\rho \rightarrow l^+l^-$, protoprod. 8=33728
    $\rho^\circ \rightarrow l^+l^-$, radiative correction calc. 8=29170
    $\rho \rightarrow 2\pi$ and $\pi^\pm - \pi^\circ$ mass difference, Schwinger theory 8=24854
    ρ width calc. using Lagrangian model of $\pi - A_1$ mixing 8=24855
    soft-pion emission, quark model 8=24755
    $V \rightarrow l^+l^-$, radiation correction to decay rate, calc. 8=29170
    vector and axial-vector, current-algebra calc. 8=42597
    vector, current-density-current-density commutators 8=42337
    vector two-body radiative using current algebra, PCAC 8=37955
    vector $\rightarrow$ 2 pseudoscalars, deviation from SU_3 symm. in vector meson field theory 8=29168
    widths, scalar 8=37956
    $W^\pm$, leptonic, T-violating effects 8=33567
    Ξ° $\Delta S = \Delta Q$ selection rule 8=33696

Mesons—contd
decay observations
$K^+ \rightarrow e^+ + \nu_e$, branching ratio 8=42574
$K_L^\circ \rightarrow \pi^+\pi^-\pi^\circ$, streamer chamber for n beam 8=46978
$K_S \rightarrow \pi^+ + \pi^-$, lifetime meas. 8=42582
$\eta \rightarrow \pi^+\pi^-\pi$ and $\eta \rightarrow 3\pi^\circ$, branching ratio 8=47117
$\eta \rightarrow 3\pi^\circ$ and $\eta \rightarrow \pi^+\pi^-\pi$, branching ratio 8=47117
detection measurement
energy estimation from ionization meas. in nuclear emulsions 8=47114
streamer chamber, proportional counter controlled, for slow-meson stops 8=47105
effects
No entries
interactions
See also Nuclear reactions due to/mesons.
annihilation into vacuum rel. to quark model of hadron decay 8=42497
axial-vector current partial conservation and Kawarabayashi-Suzuki-Riazuddin-Fayazuddin sum rule 8=33717
baryon-meson, $U(6) \otimes U(6)$ scheme SU(6) mixing 8=25001
baryon-pseudoscalar meson coupling consts., dispersion sum rules 8=37959
electromagnetic and Dirac fields, K_0-$\overline{K}_0$ transitions 8=38015
η_{+-} phase, Reϵ and superweak model 8=38008
$K + p \rightarrow K + N^*$, Regge pole model, N^* matrix elements 8=33839
KN, low energy between threshold and $Y_0^*(1520)$ resonance, anal. 8=42585
KN, resonance prod., differential cross section 8=24843
KN, superconvergence relations 8=29115
$\overline{K}N$, superconvergence relations 8=29115
KNY coupling consts., modified dispersion relations 8=24828
Kp with $\Delta(1238)$ prod., π trajectory Regge-pole analysis 8=29217
$K\pi$, existence of κ resonance 8=24861
$K\pi$, s-wave in K_{13} decay mode 8=42580
K^--emulsion nuclei, short range hyperfragments, $p_K = 1.5$ GeV/c 8=33702
K^--emulsion nuclei, $\Sigma\pi$ pair prod. obs. 8=33836
$K^- + p \rightarrow K^\circ + n$, K° leptonic decay test of $\Delta S = \Delta Q$ 8=42570
K^- with heavy nuclei, double hyperfragment emission, 1.5–5 MeV 8=33832
K^- with propane freon in bubble chamber $\Sigma^\circ\pi^\circ$ prod. which decay to Λ°, γ 8=25254
$K^- + He^4 \rightarrow (\Sigma + \text{nucleus}) + \pi^- \rightarrow \Lambda^\circ + p + d + \pi^-$, impulse model calc. 8=38094
$K + N \rightarrow Y + M$, amplitude determ. in quark model 8=33703
K^-d, at 2.24 BeV/c, prod. of $Y_1^*(1385)$ state 8=42666
K^-d, resonances rel. to $I = 2$ hyperons search; 2.11, -2.65 GeV/c 8=42656
K^-d, test of one-meson exchange 8=42586
$K^-d \rightarrow \Lambda n$, $p_{K^-} = 340$ MeV/c and 400 MeV/c 8=33704
$K^-d \rightarrow \overline{Z}^-p$, $p_{K^-} = 340$ MeV/c and 400 MeV/c 8=33704
$K^-n \rightarrow \Sigma^-\pi^+\pi^-$, 1660 to 1900 MeV, study of baryon resonances 8=42665
$KN \rightarrow \Lambda\pi$, 1900-2,215 MeV $Y_1^*(1910)$, $J^P = 5/2^+$ 8=33841
K^-p and $Y_1^*(1660)$ and $Y_1^*(1695)$ prod. 8=25005
K^-p at 1.33 GeV/c, 2-body final states 8=42588
K^-p, 1.7-2.7 BeV/c, Ξ^-, Ξ^* prod., spin and decay parameters 8=24997
K^-p at 4.6 and 5.0 GeV/c, 3π effect near 960 MeV obs. 8=38043
K^-p, 5.5 GeV/c, Ω^- prod. obs. 8=29213
K^-p, 6 GeV/c, cross-sections obs., density-matrix elements estimate 8=33705
$K^-p \rightarrow \gamma\Lambda$, rel. to isospin props. of e.m. interactions, predictions of quark model 8=37916
K^-p, Λ prod. cross-section, 10 GeV/c 8=38834
$K^-p \rightarrow \Lambda\eta$ in modified exchange model 8=33707
K^-p, Λ° production, 6 GeV/c 8=38087
$K^-p \rightarrow \overline{K}N\pi$, 1.33 GeV/c, $\overline{K}^*(890)N$, $N^*(1236)\overline{K}$ and $Y_0^*(1520)\pi$ prod. 8=33706
$K^-p \rightarrow \overline{K}^\circ n$, SU(3) symmetry validity 8=37852
$K^-p \rightarrow K^\circ p$, SU(3) symmetry validity 8=37852
K^-p, $K^*(890)(1420)$, prod. obs. comparison with Regge pole model 8=33732
K p, mass dependence of small angle differential cross section, 10 GeV/c 8=42542
$K_2^\circ + p \rightarrow K_1^\circ + p$, domination by ω exchange 8=42587
$K^+ + d \rightarrow p + p + K^\circ$ rel. to K°-K^+ mass difference 8=29154
K^+p, 5.5 GeV/c, K(1300) prod. 8=38024
K^+p at 9 BeV/c, hyperon prod. 8=24991
$K^+p \rightarrow K^+\pi^+n$, double peripheral model 8=29156
K^+p, $S = 2$ boson resonance in mass region 1.0-3.1 GeV search 8=38045
K_S and L_S regeneration phase in Cu at 2.5 GeV/c 8=38006
$K_1 + Y \rightarrow \pi + N$, extrapolation to s, p-wave amplitude in Y decay 8=24988
$Md \rightarrow \gamma BN$, sensitivity to BN interactions 8=37916
meson-baryon coupling consts. in broken SU(6) static model 8=24749

Mesons—contd
interactions—contd
meson-baryon in derivative coupling model, sum rules in coupling constants 8=37958
meson-baryon, prod. of neutral vector and pseudoscalar mesons, quark model 8=37957
meson-baryon, strangeness-exchange, quark model 8=33659
meson-meson, using current algebra and PCAC 8=38025
meson $+ N \rightarrow \gamma B$ for determ. of e.m. couplings of MN resonances 8=37916
meson-nucleon, vector meson prod. rel. to hadron photoprod., photon-vector-meson analogy 8=42503
meson-nucleon, very-high-energy polarization theory 8=37963
meson-proton coherent prod. and deck effect best with deuterium 8=24911
one-boson-exchange, PVS theory, rel. to N-N interacts. 8=24751
two-body, polarization and reson. decay rel. to transversity amplitudes 8=33737
$VP \rightarrow PP$, bootstrapping of Regge trajectories 8=33658
$w, \pi + w \rightarrow \pi + \pi$, thin d double spectral function effects 8=24680
W, weak, peratization of vertex 8=46839
magnetic moment
No entries
mass
A_1, derivation of $J_{A\pi} = {}_A$ 8=42608
f_0, from Padé approximants in Lagrangian field theory 8=24470
formula, empirical, and classification 8=33656
formula, $3\mu_{V2} = \mu_{T2} + 3\mu_{P2}$ (P, V, T) one pseudoscalar, vector and tensor mesons 8=33658
Gell-Mann-Okubo relation for pseudoscalar improved 8=29113
κ, rel. to K_{13} decay from factors 8=33699
K, e.m. mass difference, new sum rule 8=29155
K using current algebra and SU(3) symm. breaking 8=38002
K°-K^+ difference using $K^+ + d \rightarrow p + p + K^\circ$ 8=29154
$K^\circ\overline{K}^\circ$ system, mass resonance ~1300 MeV 8=24847
$K_L^\circ - K_S^\circ$ difference and weak-interaction cut-off 8=33700
K_S° and K_L°, mass difference, calc, 8=42583
$K_1^\circ \sim K_2^\circ$ difference obs. 8=24826
$K_1^\circ \sim K_2^\circ$ difference, intermediate-boson calc. 8=24824
K_1°-K_2° mass difference 8=33697
$K_1^\circ - K_2^\circ$, rel. to low energy π-π scatt. 8=33692
$K^+ - K^\circ$ mass difference calc. using Weinberg sum rules 8=24825
$m_\omega = m_\rho$ from saturating superconvergence relations in $\overline{N}N = \pi\rho(\omega)$ 8=33740
mass formula for vector mesons using current commutators in broken SU_3 8=33720
1^+ mass spectrum and strong decays, O(4, 2) theory 8=42594
$\pi^-\pi^-\pi^+$ mass spectrum, prod. in π^-p interactions, 5 BeV/c 8=37977
$\pi^+\pi^-$, $\pi^-\pi^\circ$, $\pi^-\pi^-\pi^+\pi^\circ$ spectra, g meson obs. 8=38028
pseudoscalar mass splitting, spectral-function sum rules 8=42501
ρ e.m. mass and form factor calc. 8=42510
ρ, from Padé approximants in Lagrangian field theory 8=24470
ρ, virtual mass depend. of $\gamma_{\rho\pi\pi}$ 8=38041
2^+, spectral function sum rules and stress-energy tensor 8=24757
vector and axial vector with the same unitary spin, relation 8=47122
vector mass splitting, spectral-function sum rules 8=42501
W, corrections rel. to vertex peratization in weak interacts. 8=46839
production
A_1 by pions on heavy nuclei by diffraction dissociation 8=42608
$A_2^+\pi^+$ in four-prong annihilation of 1.2 GeV/c $\bar{p}$ in hydrogen 8=38066
additional, at hadron scattering, quark model 8=47101
D(1280) prod. in $\bar{p}p \rightarrow K\overline{K}\,3(4)\pi$, 1.2 GeV/c 8=33759
δ^- in $K^-n \rightarrow \Lambda\delta^-$, cross section upper limits 8=24842
η, from $\gamma + p$, 775-850 MeV, ang. distrib. 8=24840
η in $\pi^-p \rightarrow \eta^\circ n$, 10 GeV/c obs. 8=29160
η, in $\bar{p}p$ scatt. at 1.2 GeV/c 8=33759
η in p-p at 6 GeV/c obs. 8=29187
η, photoprod. on nucleons, expt. and theory 8=33667
η photoprod., theoretical cross section 8=24838
η, photo-, Regge-pole model, forward peaking 8=24839
η°-, photoformation, dispersion rules of sum 8=47118
η° prod. in $\gamma p \rightarrow$ multipion, 4.8–6.0 BeV 8=33669
f° in four-prong annihilation of 1.2 GeV/c $\bar{p}$ in hydrogen 8=38066
κ in $K\pi$ scatt, $SU(3) \otimes SU(3)$ current algebra 8=29158
K by p annihilation in emulsion, interaction vol., 3 GeV/c 8=42528
K, from π^- interaction in heavy emulsion nuclei, $p_\pi = 17$ GeV/c 8=33837
K, photo-, Regge-pole model 8=29124
K photoprod., conspiracy and evasion 8=42526
K, π in π^-N, 17.2 GeV/c 8=42535

Mesons—contd
- **production**—contd
  - K, pseudoscalar, photoprod. on nucleons, Regge pole model 8=29127
  - K(1300) system prod. in K^+p, 5.5 GeV/c 8=38024
  - K^-, from Cu and U by 8 GeV/c protons 8=25231
  - K^- photoprod. on H, momentum distrib. rel. to ϕ and ρ° prod., 15 GeV 8=33724
  - $K_1^\circ K_1^\circ$ in $\pi^- p \to K_1^\circ K_1^\circ n$, 4, 5GeV/c, fitted by complex scatt. length or resonance form 8=42537
  - K^+ from $\gamma p \to K^+\Lambda^\circ\Sigma^\circ$, k via "u channel, high-energy 8=42525
  - K^+ in 2.4, 2.85 BeV interactions 8=29188
  - $K^+\Sigma^+$ and $K^{*+}\Sigma^+$, diff. cross sections and Regge pole model 8=24994
  - K^* (890), in $\bar{p}p$ scatt. at 1.2 GeV/c 8=33759
  - K^*(890)(1420) in K^-p, 10 GeV/c 8=33732
  - L, Q, from $K^-d \to K^-\pi^+\pi^-d$, 12.6 GeV/c 8=29163
  - ω, from γp reactions, up to 5.8 GeV 8=33719
  - ω, in $\bar{p}p$ scatt. at 1.2 GeV/c 8=33759
  - ω in $p\bar{p} \to 3\pi^+3\pi^-\pi^\circ$, 5.7 GeV/c, cross-section 8=24940
  - ω° in p-p collisions, double Regge-pole model 8=24858
  - ω, photoproduction from nucleons 8=33725
  - ω, photoprod. on nucleons, expt. and theory 8=33667
  - ω, ω-ρ° interference in $e^+e^- \to \pi^\circ\gamma, \eta\gamma$ 8=24734
  - p-p collisions, bremsstrahlungs model taking phase space into account 8=24758
  - ϕ, from γp reactions, up to 5.8 GeV 8=33719
  - ϕ in cosmic ray nuclear interactions above 10^{12} eV 8=42734
  - ϕ on C, photoprod. cross section, 1800 MeV 8=38033
  - ϕ photoprod. on H, cross section, 15 GeV 8=33724
  - ϕ, photoproduction from H_2 differential cross-section obs. 6.5-17.8 GeV 8=42602
  - photoproduction from mesons, possibility 8=47120
  - $\pi^+\pi^-\pi^\circ$ from $\bar{p}p$ annihilations at rest 8=38042
  - π°, photoproduction from neutrons around $N_{1/2}^*$(1525) resonance 8=47108
  - h, properties and implications 8=24759
  - pseudoscalar in coulomb field of nucleus 8=47120
  - pseudoscalar, neutral in meson-baryon processes, quark model 8=37957
  - pseudoscalar, photoprod. on nucleons, Regge pole model 8=29127
  - resonance, radiative correction 8=38038
  - ρ, and chiral symmetry prediction 8=38041
  - ρ from meson which explains double-pole character of A_2^- (1300) 8=24857
  - ρ, from $\pi p \to \rho N^*, \pi p \to \rho n^*$, energy- and momentum-transfer dependence of cross-sections 8=37981
  - ρ, general method for deriving ang. correls. 8=24687
  - ρ, in $\bar{p}p$ scatt. at 1.2 GeV/c 8=33759
  - ρ in $p\bar{p} \to 3\pi^+3\pi^-\pi^\circ$, 5.7 GeV/c, cross-section 8=24940
  - ρ, photoproduction from nucleons 8=33725
  - ρ, photoprod. on nucleons, expt. and theory 8=33667
  - ρ°, electroprod., analysis of $e + p \to e^1 + \rho^\circ + p^1 \to \pi^* + \pi^-$ 8=24859
  - ρ°, from γp reactions, up to 5.8 GeV 8=33719
  - ρ° in four-prong annihilation of 1.2 GeV/c $\bar{p}$ in hydrogen 8=38066
  - ρ^0 photoprod. ang. distrib. 8=37914
  - ρ°, photoproduction from H_2 differential cross-section obs. 6.5-17.8 GeV 8=42602
  - ρ° photoprod. on H, cross section, 15 GeV 8=33724
  - ρ° in $\pi^- p \to \rho^\circ n$, 4 and 8 GeV/c comparison with $\gamma p \to \pi^+ n$. Vector dominance model 8=37972
  - ρ° in p-p collisions, double Regge-pole model 8=24858
  - ρ°, ω-ρ° interference in e^+e^- $\pi^\circ\gamma, \eta\nu$ 8=24734
  - V° photoprod. on nucleon 8=24852
  - vector in $\pi N, \pi\pi$ interactions, Loretnz pole structure 8=29171
  - vector, Regge trajectory conspiracy relations in $\gamma N \to VN$ 8=38026
  - vector, in π-N reactions, conspiracy relations 8=24846
  - vector meson photoprod., polarized-photon parity filter 8=42599
  - vector meson photoprod., Regge-pole model 8=42600
  - W in $\pi N \to WN, NN \to NNW$, one pion model, N form factor included 8=38022
  - W prod. in nuclear Coulomb field, electroproduction 8=42595
- **resonances**
  - A, Deck model and Dolen-Horn-Schmid duality 8=33559
  - A(1200) and A(1300) spin parity analysis 8=37979
  - $A\rho\pi$ system sum rules from current algebra and pole dominance approx. 8=29021
  - A_2, e.m. coupling determ. 8=42610
  - A_1 enhancement and recoupling mechanism 8=38039
  - A_1-π mixing and prod. of A_1 by diffraction dissociation 8=42608
  - $A_1 \to \rho\pi, \rho \to 2\pi$ and $\pi^\pm - \pi^\circ$ mass difference, Schwinger theory 8=24854
  - A_1-ρ-π system and $\pi \to l\nu\gamma$ decay 8=42609
  - A_1 and ρ dominance in $\pi \to e\nu\gamma$ 8=29176
  - $A_1 \to \rho\pi$ in quark model 8=29175
  - A_1 width from Weinberg sum rules 8=24856
  - $A_{1\,2}$ obs. in $p\bar{p} \to 3\pi^+3\pi^-\pi^\circ$, 5.7 GeV/c 8=24940
  - A_2 from $\bar{p}p$ annihilation at rest 8=38042
  - A_2(1300) region structure in $\pi^- p$ interactions at 6 GeV/c 8=38035
  - $A_2 \to \pi\gamma$, decay width calc. from saturating a sum rule from $\pi \to \pi^\circ l\nu\gamma$ 8=33726

Mesons—contd
- **resonances**—contd
  - A_2 trajectory in π photoprod., generalized dispersion sum rules 8=42519
  - A_2 trajectory no-compensation mechanism rel. to KN scatt. finite-energy sum rules 8=42612
  - A_2 trajectory and residue functions obtained 8=24853
  - A_2^-, in $\pi^- p \to {}^-\pi p\eta^\circ$ at 5 BeV/c 8=38036
  - A_2^- (1300) double-pole characteristics explained by nondegenerate mass matrix for 2 mesons 8=24857
  - $A_2^\pm\pi^+$ in four-prong annihilation of 1.2 GeV/c $\bar{p}$ in hydrogen 8=38066
  - analysis of $e + p \to e^1 + \rho^\circ + p^1 \to \pi^* + \pi^-$ 8=24859
  - axial mesons, axial current sources 8=33713
  - axial-vector current partial conservation and Kawarabayashi–Suzuki–Riazuddin–Fayazuddin sum rule 8=33717
  - B° in pion, η photoprod. on p, 6-17.8 GeV 8=42523
  - boson, use of nuclear targets obs. 8=24841
  - $\chi \to \eta + 2\pi\pi$ decay, chiral-dynamic-Lagrangian calc. 8=42605
  - coupling consts., vector and scalar, with nucleon, from low-energy p-p scatt. 8=24748
  - current-algebra calc., vector and axial-vector 8=42597
  - D, mass eigenvalues 8=47122
  - D(1280) prod. in $\bar{p}p \to K\bar{K}\ 3(4)\pi$, 1.2 GeV/c 8=33759
  - δ and η', possibility of being same particle 8=24842
  - $\eta\pi\pi$ enhancement near 960 MeV 8=33657
  - η, photoprod. on nucleons, expt. and theory 8=33667
  - f° in $I = 0, J = 2$ channel of π-π scatt. 8=33692
  - f° in four-prong annihilation of 1.2 GeV/c $\bar{p}$ in hydrogen 8=38066
  - f_0, Regge trajectory and mass calc. 8=24470
  - $f^\circ \to 2\gamma$ decay width, $\gamma + \gamma \to \pi^\circ + \pi^\circ$ dispersion sum rule calc. 8=29173
  - g in multipion mass spectra 8=38028
  - g, rel. to new resonance prod. in $\pi^- p \to p\rho^-\rho^\circ$ 8=38023
  - g_A evaluation rel. to chiral algebra 8=24849
  - infinite mass renormalization, some consequences 8=24850
  - isospin-one on Regge trajectories, classification 8=24677
  - κ, possible existence in $K\pi$ system 8=24861
  - $K_T \to K\pi, K^*\pi$ quark model 8=33731
  - $K_A \to K^*\pi$, quark model 8=33731
  - K_A strong decay calc. using Weinberg-Schnitzer model 8=33730
  - K(1300) system prod. in K^+p, 5.5 GeV/c 8=38024
  - $KKn\pi\ (\pi \geq 1)$ final state S = 2 boson search with mass 1.0-3.1 GeV 8=38045
  - KN collisions, Regge-pole model 8=24843
  - $K\pi\pi$, appearance in eigenchannels with definite quantum numbers 8=24848
  - $K\pi\pi$ system, interference 8=42613
  - $K^\circ\bar{K}^\circ$ system, mass resonance ~1300 MeV 8=24847
  - $K^\circ K^+$ final state S = 2 boson search with mass 1.0-3.1 GeV 8=38045
  - K^+K^+ final state S = 2 boson search with mass 1.0-3.1 GeV 8=38045
  - K^* -κ mutual supporting mechanism rel. to $K\pi$ system 8=24861
  - K^*, $K\pi$ and $K\pi\pi$, decay, rel. to baryon model for bosons 8=33548
  - $K^* \to K\pi$, quark model 8=33731
  - $\bar{K}^*N$ prod. in $K^-p \to \bar{K}N\pi$, 1.33 GeV/c 8=33706
  - $K^{*+}\Sigma^+$ production, diff. cross sections and Regge pole model 8=24994
  - K^* strong decay calc. using Weinberg-Schnitzer model 8=33730
  - K^*(890), (1420) obs. in K^-p, 10 GeV/c, decay ang. distrib., comparison with Regge Pole and absorption models 8=33732
  - modified amplitude 8=24851
  - neutral vector in meson-baryon processes, quark model 8=37957
  - neutral vector mesons, leptonic decays, ρ-ω interference 8=38029
  - new, in $\pi^- p \to p\rho^-\rho^\circ$ decay mode and relation to g 8=38023
  - octet, rel. to current algebra and PCAC 8=24624
  - $\omega \to e^+e^-$ new data 8=33721
  - ω exchange in K^{*-}(890) prod. in K^-p at 10 GeV/c 8=33732
  - ω, from $\gamma p \to p\omega$ and $\gamma p \to p\omega\pi^+\pi^-$, up to 5.8 GeV 8=33719
  - ω in p-p at 6 GeV/c obs. 8=29187
  - ω in $p\bar{p} \to 3\pi^+3\pi^-\pi^\circ$, 5.7 GeV/c, cross-section 8=24940
  - $\omega \to l^+l^-$, non-existent consequence, photoprod. 8=33728
  - ω, photoproduction from nucleons 8=33725
  - $\omega, \phi, \rho \to 2\pi\gamma$, decay, soft-photon emission approach 8=29174
  - ω, photoprod. on nucleons, expt. and theory 8=33667
  - $\omega\rho^\circ$ interference in $e^+e^- \to \pi^\circ\gamma, \eta\gamma$ 8=24734
  - ω° prod. in $\gamma p \to$ multipion, 4.8-6.9 BeV 8=33669
  - ω° prod. in p-p collisions, double Regge-pole model 8=24858
  - 1^- and 2^+ nonets self-consistent couplings 8=33718
  - 1^+ mass spectrum and strong decays, O(4, 2) theory 8=42594
  - ϕ decay isospin violations assuming asymptotic symmetry 8=42606
  - ϕ decay width from vertex functions 8=42598
  - ϕ, from $\gamma p \to p\phi$ and $\gamma p \to p\phi\pi^+\pi^-$, up to 5.8 GeV 8=33719

Mesons—contd
- **resonances**—contd
  - Φ, mass eigenvalues 8=47122
  - ϕ, photoprod. on C, cross section, 1800 MeV 8=38033
  - ϕ photoprod. on H, cross section, 15 GeV 8=33724
  - ϕ strong decay calc. using Weinberg-Schnitzer model 8=33730
  - ϕ-ω mixing in model for isovector form factors 8=29039
  - ϕ°, photoproduction from H_2 differential cross-section obs. 6.5-17.8 GeV 8=42602
  - photoproduction and application of optical theorem for quasi-elastic scatt. 8=42601
  - photoproduction, Regge-pole model 8=42600
  - photoproduction rel. to cross sections and photon energy dependence 8=47123
  - photoproduction using polarized-photon parity filter 8=42599
  - πN collisions, Regge-pole model 8=24843
  - $\pi N \rightarrow VN$ and π photoprod., γ–V analogy model 8=33666
  - $\pi\pi$ and $\gamma\pi$, from $\gamma\pi$, of any spin 8=47119 ,
  - $\pi\pi$, I = 0, J = 4 near 2 GeV in π-π scatt. 8=37998
  - $\pi\pi$ interaction, vector meson exchange 8=29166
  - π^+ multipion in π^+p collisions, 1630 MeV 8=33729
  - $\pi^+\pi^-\pi^\circ$ from $\bar{p}p$ annihilations at rest 8=38042
  - 3π near 960 MeV in K^-p interaction at 4.6 and 5.0 GeV/c 8=38043
  - in π photoprod. and N Compton scatt. 8=29162
  - p in πp scatt., analyticity constraints, soln. by means of resonance and Regge trajectories 8=33680
  - in $\bar{p}p \rightarrow K\bar{K}\ 3(4)\pi$, 1.2 GeV/c 8=33759
  - $\varphi \rightarrow e^+e^-$ obs. 8=33721
  - quantum number determ. and phenomenological description of states 8=24844
  - radiative correction to prod. 8=38038
  - ρ and A_1, dominance in $\pi \rightarrow e\nu\gamma$ 8=29176
  - ρ and e.m. coupling determ. 8=42610
  - ρ bootstrap, δ-function and Breit-Wigner exchange compared 8=29074
  - ρ contrib. to π form factor at high momentum transfer 8=24768
  - ρ, coupling consistency with $SU(2) \otimes SU(2)$ theories 8=38041
  - ρ coupling constant in terms of πN coupling constant 8=37992
  - ρ dominance and current algebra 8=38034
  - $\rho \rightarrow e^+e^-$ new data 8=33721
  - $\rho \rightarrow e^+e^-$, vector-meson-dominance prediction, finite-width corrections 8=42607
  - ρ, f bootstrap model, in π-π scatt., high-and low-energy amplitudes simultaneously calc. 8=37912
  - ρ, $f_{\rho\pi\pi}(-m^2, o, o)$ calc. 8=33727
  - ρ in I = 1, J = 1 channel of π-π scatt. 8=33692
  - ρ in $\pi + N \rightarrow \rho + N^* \rightarrow N + 3\pi$, Regge-pole model 8=24780
  - ρ in $p\bar{p} \rightarrow 3\pi^+3\pi^-\pi^\circ$, 5.7 GeV/c, cross-section 8=24940
  - $\rho \rightarrow l^+l^-$, photoproduced 8=33728
  - ρ, photoproduction from nucleons 8=33725
  - ρ, photoprod. on nucleons, expt. and theory 8=33667
  - ρ position in proton form factor in time like region 8=29184
  - ρ prod. and decay ang. distribs. in π^-p interact. 8=42614
  - ρ prod in $\pi + N \rightarrow \rho + N^*$, ang. decay correls. at 8 GeV 8=24781
  - ρ Regge amplitude for πN charge-exchange scatt. 8=24779
  - ρ Regge pole in t-channel generated by $\pi\pi$ channel 8=24860
  - ρ, Regge trajectory and mass calc. 8=24470
  - ρ width and Reggeized short range potential 8=47036
  - ρ, width calc. in π-π scattering 8=29145
  - $\rho\gamma$ enhancement near 960 MeV 8=33657
  - $\rho\pi$, I=2, in 27 plet of bosons 8=29033
  - $\rho\pi$ spectrum from π^-p interaction at 6.7 GeV/c 8=37979
  - ρ-π superconvergence relation, approx. saturation 8=38044
  - $\rho + \rho'$ dominance, s-wave π-N scatt. length and current algebra 8=24799
  - ρ-ω interference and neutral vector meson leptonic decays 8=38029
  - ρ^- prod. in multipion photoprod. on protons, 4.8-6.0 BeV 8=33669
  - ρ°, from $\gamma p \rightarrow p\rho^\circ$ and $\gamma p \rightarrow p\rho^\circ\pi^+\pi^-$, up to 5.8 GeV 8=33719
  - ρ° in four-prong annihilation of 1.2 GeV/c $\bar{p}$ in hydrogen 8=38066
  - ρ^0 photoprod. ang. distrib. 8=37914
  - ρ° photoprod. on H, cross section, 15 GeV 8=33724
  - ρ°, photoproduction from H_2 differential cross-section obs. 6.5-17.8 GeV 8=42602
  - ρ° photoprod., rel. to lepton-pair cross section 8=24709
  - ρ° prod. in $\pi^-p \rightarrow \rho^\circ n$, 4 and 8 GeV/c comparison with $\gamma p \rightarrow \pi^+ n$, Vector dominance model 8=37972
  - ρ° prod. in p-p collisions, double Regge-pole model 8=24858
  - ρ°, ω interference in $e^+e^- \rightarrow \pi^\circ\gamma, \eta\gamma$ 8=24734
  - ρ^+ multipion in π^+p collisions, 1720 MeV 8=33729
  - R, S, T, U mesons classification, adopting spin-orbit and spin-spin forces 8=42593
  - shape, $\pi p \rightarrow \rho N \rightarrow \pi\pi N$ 8=38037
  - σ as bound state of 4π 8=29177
  - spin and parity from 3-particle decay 8=38021
  - spin density matrix for prod. mechanisms 8=42592
  - SU(6), 405-plet classification 8=38020

Mesons—contd
- **resonances**—contd
  - tensor fields, spectral function sum rules 8=38027
  - 2^+, of mass 1085 MeV, and existence of three Regge trajectories 8=33714
  - $V \rightarrow l^+l^-$, radiative correction to decay modes calc. 8=29170
  - $VP \rightarrow PP$, bootstrapping of Regge trajectories 8=33658
  - V° photoprod. on nucleon 8=24852
  - vector boson, Pauli approx. 8=24640
  - vector boson, rel. to N e.m. form factors 8=29165
  - vector bosons, charged intermediate, consequences for stellar evolution 8=29161
  - vector dominance and polarization 8=38031
  - vector dominance in photoproduction 8=38030
  - vector, treated as composite particles rel. to Lagrangian field theory 8=37869
  - vector field approach to N-N interacts. with auxiliary conditions 8=29167
  - vector field treatment of N-N interacts, rel. to relativistic terms and Born phase shifts 8=24872
  - vector field, unified treatment to include photon field 8=33716
  - vector, in uniform e.m. fields 8=29172
  - vector, mass formula, using current commutators in broken SO_3 8=33720
  - vector meson dominance in hyperon nonleptonic decay 8=38086
  - vector meson e.m. interaction, CP violation model 8=29169
  - vector meson eqn. for photon description 8=47121
  - vector meson prod. by meson-nucleon collisions, rel. to hadron photoprod., photon-vector-meson analogy 8=42503
  - vector production and $[SU(3) \otimes SU(3)]_{coll}$ symmetry 8=42603
  - vector prod. in πN, $\pi\pi$ interactions, Lorentz pole structure 8=29171
  - vector prod. in π-N reactions, conspiracy relations 8=24846
  - vector prod., Regge trajectory conspiracy relations in $\gamma N \rightarrow VN$ 8=38026
  - vector state in photoprod., simulating photon absorpt. 8=24690
  - vector $\rightarrow$ 2 pseudoscalar decay, deviation from SU_3 system field theory 8=29168
  - vector, Yang-Mills and CP violation in weak interactions 8=24845
  - p-wave, self-consistent bootstrap calc. in $\pi\pi$ and $\pi\omega$ scatt. 8=42615
  - W prod. in nuclear Coulomb field, electroproduction 8=42595
  - W prod. in $\pi N \rightarrow NW$, $NN \rightarrow NNW$, one pion model 8=38022
  - $X^\circ - \eta$ mixing in quark model for $\eta \rightarrow 2\gamma$ 8=24835
- **scattering**
  - analyticity constraints, soln. by means of resonances and Regge trajectories 8=33680
  - baryons, effective range formulae, extrapolated below threshold 8=37962
  - bootstrap with finite-energy sum rules 8=24860
  - boson resonances decaying determ. of spin, parity 8=33715
  - C, 0.66-2.6 GeV/c, cross-section obs. 8=29159
  - KN dispersion sum-rules, agreement between Regge behaviour and low energy parameters 8=37988
  - K–N, finite energy sum rules and crossover problem 8=24832
  - KN, finite-energy sum rules, Regge-exchange amplitudes rel. to polarization and K^+n charge exchange 8=33710
  - KN finite-energy sum rules rel. to A_2 trajectory no-compensation mechanism 8=42612
  - $\overline{K}N$ low energy with complex singular pot. 8=24829
  - KN, new dispersion sum rules for testing low-energy phase-shift analysis 8=42417
  - KN, Regge trajectories, P and P^1, props. 8=42442
  - $\overline{K}$-N scatt. lengths 8=37984
  - KN, superconvergent sum rules 8=29157
  - KN, s-wave length determ. from obs. of K_2°–p, 168-343 MeV/c 8=33709
  - $K\pi$ rel. to K_{l5} decay 8=29149
  - $K\pi$, using $SU(3) \otimes SU(3)$ algebra of currents, π, K pole dominance, κ meson predicted 8=29158
  - $K + p \rightarrow K + \pi + p'$, cuts in complex l-plane 8=24834
  - $K\Xi$, superconvergent sum rules 8=29157
  - $K^-\Xi^\circ$, consistency condition for $|\Delta S| = 1$ currents 8=29043
  - K^--d, unitary impulse approx. 8=29142
  - K^-p (polarized), elastic, between 1.4-2.4 GeV/c 8=38017
  - K^--p, 6 GeV/c obs. 8=42553
  - K^+-H, search for K^* production below $K\pi$ threshold, 1 BeV/c 8=38014
  - $K^+ + n \rightarrow K^\circ + p$, differential cross section at high energy 8=24682
  - K^+-p differential cross sections rel. to residues of π and $\Lambda + \Sigma$ 8=38016
  - K^+p, forward scatt. amplitude, prediction of ΛKN and ΣKN coupling constants 8=24833
  - K^+-p potential, 2π exchange contrib. 8=33708
  - K^+-p, rel. to diffraction amplitude, ρ and hyperon exchanges, elastic at 3.5 and 5 GeV/c 8=38018
  - $K^\pm$ + d, 0.6-2.65 GeV/c obs., Y_0^*, Y_1^* 8=29159
  - $K^\pm n$ real part predicted by dispersion relation 8=24831
  - $K^\pm p$, forward, dispersion relations calc. 8=24830

Mesons—contd
  scattering—contd
    $K^{\pm}p$ real part predicted by dispersion relation 8=24831
    $K^{\pm} + p$, 0.6-2.65 GeV/c obs., Y_1^*, Y_0^* resonances obs. 8=29159
    K_2°–p, 168-343 MeV/c meas. for determ. of $\bar{K}N$ s-wave scatt. length 8=33709
    meson-baryon and baryon mass-splitting in broken $U_{6,6}$ symm. 8=29179
    meson-baryon, dispersion relations and backward amplitudes 8=29116
    meson-baryon, off mass shell method 8=42376
    meson, baryon, peripheral collisions, multichannel approach 8=42504
    meson-baryon, quark model calcs. 8=24765
    meson-baryon, superconvergent sum rule for factorized amplitudes 8=37960
    meson-baryon s-wave, incorporation of SU(6) invariance 8=33660
    meson-baryon, threshold and pseudothreshold relations 8=42505
    meson-baryon, vector dominance sum-rules 8=24761
    meson-hadron, pseudoscalar, decuplet sum rules 8=42499
    meson-meson, dispersion relations and backward amplitudes 8=29116
    meson-nucleon, forward matrix amplitude reconstruction 8=24672
    meson-nucleon, spin flip effect meas. 8=24764
    neutral scalar, by spinless nucleon, static limit theory 8=24766
    nuclear, K_2° off 7 nuclei, total cross sections obs. 8=33709
    nucleus, K, review 8=29483
    ω, Regge trajectory from $K_2^{\circ} + p \rightarrow K_1^{\circ} + p$ exchange 8=42587
    one-particle-exchange model for low energies 8=24762
    pseudoscalar, 2 in nonet states, zeros 8=42506
    vector, amplitude calc. with one vector-meson exchange 8=24851
  spin and parity
    B, $J^P = 1^+$ or $2^+, 3^-, 4^+$ from $B \rightarrow \omega\pi$ 8=38040
    η triple orbitals in baryon-antibaryon model for bosons 8=33548
    g, $J^P = 3^-$ indicated 8=38028
    isospin-one on Regge trajectories, classification 8=24677
    K in $\pi^+ p \rightarrow K^- \Sigma^+$ 8=24995
    K, triple orbitals in baryon-antibaryon model for bosons 8=33548
    resonance, from 3-particle decay 8=38021
    symmetries for both parities, induction 8=42502
Mesosphere. See Atmosphere
Metallo-organic compounds. See under appropriate metal compound headings.
Metallurgy
      See also Zone melting and refining.
    alumina inclusions group, initial o content in liquid Fe as formation factor 8=35651
    basic O_2 furnace maintenance, hot gunning materials 8=50475
    electron microscope, scanning, appls. 8=50472
    flow of gases through packed beds 8=43660
    high-strength mats., fracture toughness dependence on thickness, work-hardening exponent effect 8=26766
    hot galvanized coatings with variable quantities of Al, structure of 8=39704
    hot-pressing, deformation theory giving density eqn. 8=26755
    melts, u.s. dispersion of heterogeneous phases, obs. 8=39442
    microphotoplasticity techniques using laser systems in metal working problem analysis 8=48954
    plane strain extrusion, upper bound solns. 8=35618
    specimen blanks for electron microscope, preparation 8=37098
    steel, B content determ. from neutron flux depression 8=37100
    steel, 0.2% carbon, ingot, non-metallic inclusion behaviour during hot rolling 8=49020
    steel, cladding with refractory metals, shock wave technique 8=28206
    steel, reversible temper brittleness development rel. to C content changes in grain-boundary regions 8=35683
    steel, transformer, annealing effects at high-temp and vacuum 8=35107
    steel, U8, quenched, tempering under high hydrostatic pressures 8=35679
    steels, austentic stainless, growth in oxidising gases 8=45338
    steels, cast austenitic, thermal cycling to increase strength through phase transforms. 8=35698
    superconductors, effect of factors on flux distrib. 8=40365
    thermionic diode components of refractory metals, microhardness and reliability 8=37377
    welding, cold, deformation on symm. axis and area of joint 8=37099
    welding, cutting and drilling, appl. of CO_2 gas laser as heat source 8=28678
    welding, explosive, wave-like profile of interface 8=28203
    working props. and test behaviour 8=40087
Metallurgy —contd
    Al alloy, crude, production by reduction of bauxites, thermal props. of bauxites 8=30956
    Al alloy, crude, production from and thermal props. of Japanese colloidal earth 8=30955
    Al, casting effects on grain size and orientation 8=48589
    Al melts, u.s. dispersion of Al_2O_3, Fe and Ti, 740-800°C 8=39442
    Al, surface structure appearance during brightening and anodizing 8=48417
    Al–Si alloys, modification 8=43975
    Al-V, plasma-jet spray-quenching in dispersion hardening 8=26780
    β-Au-Cd alloys, structure of martensites 8=26035
    Cr molybdenum steels, CO_2 oxidation resistance effects of chem. comp., mech. treatment and remelting 8=45339
    Cu–2 wt.% Be alloy, ageing characts. with or without additional elements 8=35674
    Cu, continuous casting, heat dissipation problems 8=28207
    Fe and Fe alloys, electropolishing, "Universal" technique applications 8=44027
    FeC_x in carbon steel particle coarsening at 720°C 8=30691
    Mo wire and foil, Hg quenching 8=31218
    Nb, strain-ageing, oxygen dependence 8=26835
    Nb-O, strain-ageing from resistivity meas. 8=26846
    TaO, strain-ageing from resistivity meas. 8=26846
    WC–Co hard metal foils, microstructure 8=35287
    WC-TiC-TaC-10%Co, properties rel. to C content 8=30657
Metals
      See also Alloys; Semiconductors.
    with adsorbed Cs layer, work function and Langmill S-curves 8=31466
    alloys, particle size distrib. in dispersed phases 8=26295
    anharmonicity of thermal vibrations 8=35367
    b.c.c. or h.c.p., effects of solutes on fracture behaviour 8=31189
    b.c.c., sessile splitting of screw dislocations 8=48847
    bonded ceramic-metal components, fast neutron damage study in isothermal irrad. assembly 8=35597
    bonding with high polymer adhesive, strength rel. to appl. of elec. field 8=31185
    catalysts, combined action with semiconductors 8=49906
    cermets, structure rel. to geometry and phase distrib., effects on props. 8=35263
    coated with electroneg. adsorbates O and halogens, work function and desorption energy 8=35193
    conduction electrons, appl. Landau theory of Fermi quantum liquids, book 8=30397
    conductivity, elec., in mag. field, hydrodynamic mechanism 8=49150
    creep, equation describing 8=35648
    creep, high-temp., in high stacking-fault energy metals, mechanism 8=35622
    crystal defects, diffusivity of atoms and plastic deform. mechanism 8=26629
    crystal mosaic block size and disorientation changes on crystallization 8=40051
    crystals, localized damage by laser irradiation 8=30716
    crystals on glass, vacuum-condensed, growth and orientation, rel. to deposition conditions 8=26226
    cubic, thermal expansion, Grüneisen parameters rel. to temp. 8=48743
    cutting at 100–700 m/s, force meas. method 8=35655
    cyclotron resonance in inclined mag. field, characts. 8=40284
    deformation state, and shears, after cold-welding by pear-shaped method 8=37099
    deposited layers, thermal conductivity coeff. 8=35453
    diffusion in liq. metals, fluctuation model 8=43790
    diffusion mobility temp. dependence 8=48783
    dislocations as sources and sinks for point defects 8=31071
    ductile, crack initiation of fracture 8=48972
    ductility, workability 8=26758
    e. m. wave transformation into elastic waves 8=39886
    electric field penetration leading to slowly damping of the pot. 8=40298
    elect. fields, gravitationally induced, criticism of an expt. 8=40297
    electrical cond., low-temp. dimensional effects 8=26951
    electrical conductivity transverse 8=49148
    electrochemical machining theory, Cauchy problem for Laplace eqn. 8=49914
    electrodeposited, aplication of electron microscopy of investigation 8=44154
    electrodeposited, internal stress due to hydrogen 8=31167
    electron emission, experimental proof of general theory 8=49434
    electron gas, new formulation of ground state energy 8=28340
    epitaxial films, growth by thermal evaporation on ionic crystals in vacuo and air 8=30738
    epitaxial films, elec. field effects on growth 8=26109
    epitaxial films on mica and NaCl substrates, stresses causing film curling 8=35157
    evaporation by laser irradiation, obs. 8=39494
    exoelectrons, on solidification of metals in vacuum, nature 8=40692

Metals—contd
external X-ray photo-effect, quantum yield obs. 8=36005
face-centred, work hardening theories rel. to flow stress and dislocation density 8=35558
f.c.c., Bordoni peak meas. 8=26742
f. c. c., plasticity by meas. viscosity of wire samples 8=31169
f.c.c., point defects, energies and atomic configurations 8=31026
f.c.c. quenched, small vacancy clusters 8=31036
f. c. c., stacking fault energy determ. from anisotropic elasticity theory 8=26700
fast cracking during fatigue propagation 8=44586
fatigued, dislocation distrib., effect of surface-active substs. 8=35556
fatigue, theory 8=40116
ferromagnetic, energy spectrum of Fermi excitations 8=49093
ferromagnetic, magneto-optical effects, anomalous, electron-phonon scattering contrib. 8=31949
film conductor in integrated monolithic device with insulator film, basic technology 8=44852
film, mag. props. 8=49461
film thickness determ. by fast e.-backscatt. 8=48434
films, cubic, thermally induced strains 8=40122
films, e.m. power-transmission coeffs., 8=49698
films, temp. meas. during vapour deposition 8=44035
films, vacuum-evaporated, density meas. 8=48437
films, work function thickness, shape and size factors 8=36037
Flow in explosive cladding and welding 8=39262
foil thermal insulation in high pressure gas 8=26602
foils, time-to-rupture from creep tests under tensile loads of periodically varying orientation 8=35626
fracture under static and repeated loads 8=48971
friction, two-member law, verification rel. to real surface of contact 8=32697
galvanomagnetic studies by heliconlike waves 8=26961
gravitationally induced external elec. field, meas. 8=35814
h. c. p., elastically strained, inner-displacement tensor 8=26406
heat conduction near surface exposed to blackbody radiation, modified kinetic theory 8=44353
heat conduction to liq. He II, Kapitza theory 8=28444
heat transfer at interface, thermoelasticity 8=41738
helicon wave propag., standing wave resonances mode struct. 8=44663
hexagonal, first-, second- and third-order shear constants, for arbitrary axial ratio 8=35642
hydrides, positron annihilation, two exponential decays 8=40286
impurity diffusion rel. to elec. resistivity due to impurities 8=30996
with incomplete inner shells, superconductivity 8=35837
i. r. spectral reflectances at low temp. 8=27526
iodide crystals, exciton peak, position rel. to lattice parameter 8=49113
iodination, by I vapour at room temp., effects of Co^{60} γ-irrad. 8=36555
ion emission on giant-pulse laser irrad., and surface temp. 8=27361
ions in ionosphere, E-region, layering processes, effects on NO^+ and O_2^+ 8=36858
ions, secondary, Auger de-excitation, obs. 8=40718
irradiated, porosity formation mechanism 8=35518
Knight shift, review 8=27494
lattice, short range e.m. fields meas. method 8=35026
layer, resistances, stability condns. 8=35818
liquid, asynchronous flowmeter dos. 8=48027
liquid, book 8=34753
liquid, collective excitation 8=48054
liquid, eddy-current flowmeter, analysis 8=48026
liquid, heat transfer characts. of turbulent flow, effect of internal source. 8=48021
liquid, heat transfer, review 8=39353
liquid, laser droplet form. and ignition 8=34740
liquid, links between liq. state physics and metal physics, review 8=30398
liquid, ordering states 8=34759
liquid, sound vel. calc. 8=43803
liquid, structure factor by neutron diffractions techniques 8=43757
liquid, struct. theory and exptl. technique 8=34758
liquid, supercooled, effect of u.s. vibs on nucleation 8=48261
liquid, surface energies of interfaces with graphite and diamond 8=30718
liquid, thermal flowmeter, design 8=48025
liquid, velocity of sound 8=25911
localized states, survey 8=35741
magnetic breakdown, osc. periods and de Haas-Van Alphen effect 8=40725
with magnetic impurities, electronic scattering problem 8=31271
with magnetic impurities, electronic structure 8=31270
with magnetic impurities, Kondo effect 8=31272
magnetic impurities, methods of approaching Kondo's problem 8=35816

Metals—contd
mechanical props at low temp., review 8=26738
melting and melts, disorder model 8=25979
metal-dielec.-metal structs, temp-depend of tunnel current 8=49146
metastable, diffusion rates, annealing time effects 8=35474
microscope for high-temp. study of microstruct. deformation and recryst. 8=42183
microwave surface impedance, reason for oscillations 8=36311
monovalent, interionic potentials 8=35813
on moon surface, Surveyor V obs. 8=28140
noble, energy band structures 8=44642
noble, optical spectra rel. to band structure 8=32036
noble Tafel slope rel. to cathodic reduction kinetics 8=45380
non-ferrous, annealing, grain refining rel. to heating speed and dispersion 8=39714
with nonmag. impurities, temp. depend. of EPR line width 8=49583
non-transitional, stacking fault energy correlations 8=44462
nuclear quadrupole-quadrupole interactions through conduction electrons 8=41007
IB, IIB groups, mag. susceptibility 8=49466
oxidation at high temp., influence of specific area and core dimension changes 8=36551
oxidation, oxide scale layers, effects of size and shape of specimen 8=36552
oxidation rate-constant determ., low-temp., from discontinuous film resistance changes 8=49883
oxide film stripping technique 8=30732
oxides, e probe microanalysis standards 8=41307
with paramagnetic impurity, cond. for form. of localized mag. moment 8=31519
paramagnetic, props. rel. to virtual spin-wave effects 8=31517
paramagnetic resonance and relaxation of impurities calc. by perturbation method 8=49591
particles in low cond. liqs., high field electrophoresis 8=30548
phonon conductivity calc. 8=30928
plasma zero-point energy, exchange and correl. contrib. 8=26922
plasticity by meas. viscosity of wire samples 8=31169
plated by plasmic method, thermal and elec. cond., emissivity and expansion 8=35815
point defect migration. 8=48801
polaritons 8=44660
polycrystalline, ferromag. resonance, plastic deformation and annealing effects 8=31811
porous, cooling under vacuum, rate of water evaporation 8=30602
powder compacts, pressure distrib. meas. 8=48950
powders, echo phenomonon 8=27448
quenched, excess vacancy coalescence during annealing, theory 8=35527
proton-irradiated, diffusion-out of rare earth impurities on heating in vacuum, 1500-2800°C 8=40081
pure, under fatigue, grain-boundary migration, characts. at elevated temps. 8=39710
radiation of heat, black-body laws, correction for a real body 8=32935
refractory, absolute elec. conductivity above 1000°C meas. and obs. 8=31314
refractory, b. c. c., creep analysis 8=26759
refractory, Cs layer adsorpt., field e microscopy 8=39624
refractory, induction melting in self formed lining 8=30580
reflectivity changes during laser pulse 8=45169
resistance at magnetic critical points, spin-fluctuation effects 8=26958
resistivity, eddy-current decay meas., analysis 8=46326
resistor, thin film, material and characts., 8=44675
rough surface, i.r. reflection spectra 8=31932
rupture characts. on basis of short-term creep data 8=44526
second electron energy distribution rel. to incidence of primary beam 8=36059
secondary electron emission coeff. rel. to energy of primary electrons 8=36058
secondary electron energy spectra, structure 8=31473
self-diffusion mechanism rel. to defect densities 8=26615
semimetals in crossed elec. and mag. fields, u.s. amplification 8=35408
semimetals, carrier density pressure dependence 8=40313
semimetals, electric field penetration leading to slowly damping of the pot. 8=40298
semi-metals, superconducting and insulating mechanisms 8=26886
sheet, tensile straining, high temp. effect 8=48982
sheet texture determ., neutron diffraction method 8=35261
shock resistance of metals, effect of deformation speed 8=41714
single crystals, pulsed n.m.r. 8=40959
singlet ground state of localized spin, Schrödinger equation solved 8=40223
solidification profiles with ultrasonic pulses 8=39477
specific heat, modified modulation method 8=48732
spin-paramagnetism, effect of electron-lattice interactions 8=36077

Metals—contd
- sputtering, with low-energy inert gas ions, rel. to trapped gas 8=26726
- stacking fault energy rel. to density of electron states 8=26698
- strain ratio meas. method 8=35641
- stress corrosion susceptibility rel. to ambient press 8=49034
- surface cleanness, industrial vacuum technology aspects 8=39572
- surface, molec. orbital model, and gas interact. in field ion microscope 8=35143
- surface radio frequency size effect for drift motion of electron 8=44638
- structure, protonographic exam. 8=26363
- temperature-gradient instability in low-symmetry, highly conducting crystals 8=35022
- thermal activation energy determ. by alternating bending 8=35613
- thermal analysis, contactless, 20-2800°C 8=28411
- thermal and elec. cond. when coated by plasmic method 8=35815
- thermal emissivity, temp. and kinetic dependence 8=35465
- three dimensional, periodic distortion 8=49095
- transient radiation effects on electronic components 8=31126
- transition, 3d, stability of non-magnetic state 8=40746
- vacancy-impurity pairs, binding entropy, and validity of nearest-neighbour interaction model 8=31037
- vapour condensation coeff. meas., improvement on Knudsen's method 8=34988
- wire thermally shocked into longitudinal vibration by current pulse 8=40088
- working, microphotoplasticity techniques using laser systems 8=48954
- X-ray emission, soft, quantum-mechanical many-body treatment 8=27541
- zone-refined, solute-induced hardening near grain boundaries 8=26842
- Bi-type, elec. conductivity temp. dependence, 80-300°K 8=40301
- Cd, Mg and Sn single crystals, opt. consts. from reflectance ratios 8=45164
- Cr, He, Ni and Zr, polycrystalline, opt. consts. from reflectance ratios 8=45164
- He liquid-metal heat transport, kinetic theory model 8=37338
- O determ. through $O^{16}(n,\gamma)N^{16}$ 8=32167
- TiNb33, metallic additions rel. to supercond., microstruct. and workability, obs. 8=44742
- TiNb40, metallic additions rel. to supercond., microstruct. and workability, obs. 8=44742
- VO_2 crystal, semiconductor-metal transition rel. to reflection spectra 8=41150
- VO_2, optical props. between 0.25 and 5eV rel. to band structure 8=49760
- Xe^{133} diff. and mech. props. 8=48766
- **theory**
  - See also Crystals; Electron gas; Plasma.
  - alkali, local pseudopotential form factors, calcs. errors on omitting conduction-electron exchange potential 8=44630
  - atomic capture coeff. and desorpt. rate in one-dimensional model at very low temps. 8=30762
  - b.c.c., zero-point energy and Θ_c^{∞} 8=30932
  - diffusion thermoelec. power, appl. of integral over Fermi surface 8=40220
  - dislocations, dissociation and sliding on prismatic planes 8=44440
  - divalent simple, structures 8=26364
  - effective mag. field seen by one electron 8=40722
  - electron mean free path and free-electron density, elastic strain coeff. determ. using thin-film technique 8=49081
  - f.c.c., binding and vibrational characts. rel. to structure 8=39500
  - Fermi-liquid, inequalities, instabilities and renormalization 8=26864
  - ferromagnetic, wave functions symmetry in one-electron band theory 8=44990
  - ferromagnets, spin-waves, model 8=40765
  - hyperfine mag. fields and elect. field gradients caused by mag. impurities 8=40962
  - with impurities, energy spectrum and props., 8=35760
  - h.f. wave propag., Fermi-liquid effects 8=49120
  - indirect exchange interaction 8=31256
  - localized mag. impurities 8=26865
  - localized magnetic moment, conditions for existence 8=44957
  - local-moment-conduction-electron exchange coupling and RKKY spin densities 8=35742
  - magnetic moments in strong mag. fields, charact. props. 8=44962
  - magnetic moments, local 8=44963
  - magnetic surface levels, obs. in surface impedance meas. geom. modifications effects 8=44655
  - many-band model for interacting electrons, absence of mag. ordering in one and two dimensions 8=44993
  - melting criterion for cubic metals 8=34964

Metals—contd
- **theory**—contd
  - minute particles, discrete electron energy levels, evidence from mag. resonance 8=40894
  - model for lattice dynamics 8=30927
  - monovalent, e-phonon interaction, screening and e,-correlation effects 8=49074
  - noble, localized impurity d state splitting 8=26868
  - nuclear spin interaction, indirect, divergences 8=26877
  - optical effects, thermodynamic approach 8=27518
  - phonons, transverse microwave, freq. depend. of e.m. generation 8=49087
  - plasmons in metal spheres, e. bombardment stimulation and radiative decay 8=45145
  - pseudopotential form factors, local, in alkali metals errors on omitting conduction-electron exchange potential 8=44630
  - quantum structure in dielectric function of metals and anomalous prop. modes. 8=31307
  - screened interionic potential 8=40204
  - semimetals, piezogalvanomagnetic effects., meas. using stress modulated Alfven waves 8=49147
  - semimetals, superfluidity possibility at dielec. transition 8=44627
  - skin effect, anomalous, for specular e.-scatt. and opt. expts at non-normal angles of incidence 8=49739
  - spin fluctuations in almost ferromagnets, impurity effects 8=40764
  - strong-coupling, quasiparticle approximation breakdown 8=26862
  - thermodynamic props. rel. to band structure 8=39904
  - thermoelectricity, thermodynamic and free electron gas theories 8=40636
  - transport props. in e.m. field 8=35451
  - tunnel current between normal metals due to electron-phonon interaction 8=26956
  - ultrasonic wave propag., quantum theory 8=35407
  - vacancy migration, thermodynamics 8=35528
  - X-ray spectrometry, soft-, rel. to e. theory 8=49687
  - zero-temp. impurity resistivity, breakdown of conc. expansion 8=31306
  - Cs, indirect nuclear interactions 8=43937
  - Ga, size-dependent oscillarotry effect magneto-resistance effect 8=49164
  - Rb, indirect nuclear interactions 8=43937

Metamagnetism. See Antiferromagnetism; Ferromagnetism.

Meteorites
- See also Meteors.
- alloys, sulphide inclusion structures and e.-microbe analyses 8=39722
- anal. of $Ar^{40}-K^{40}$ ages of silicate inclusions 8=28157
- asteroid belt, scatt. of bodies 8=45835
- carbonaceous, occurrence of olivine 8=28158
- chondrites, bronzite, ferromagnesian silicate abundance using Mossbauer effect obs. 8=45847
- chondrites, type I carbonaceous, significance of olivine microchondrule content 8=50431
- chondritic, origin and investigation of observed afternoon excess 8=50433
- cosmic dust, e microscope-microprobe analysis 8=34935
- by cosmic rays, nuclide prod. in Fe and stone meteorites 8=37025
- early heat generation rel. to solar p-irrad. of gases before solidification 8=50435
- extraterrestrial material influx estimation during Silurian 8=45843
- Fayetheville, diffusion of primordial He, Ne and Ar 8=37024
- flux, Asteroid collisions and evolution of mass distribution 8=50411
- in Holbrook, isotropic comp. and distrib. of Li 8=28161
- hypersthene achondrites, K-Ar and radiation ages 8=37023
- impact density on moon 8=45814
- Leighton, Kr and Xe isotopic abundances in dark phase 8=37022
- luminescence following proton bombard., rel. to lunar phenomena 8=28145
- magnetic props. and determ. mag. fields planets 8=37021
- micrometeroid exposive, simulated, on CdS solar cells 8=24093
- micrometeoroids, simulation and detect. techs by impact ionization 8=50437
- micrometeoroids, thin-film penetration, study on Gemini 9 and 12 8=37020
- micrometeorite expts, by Gemini spacecraft, equipment, techs. and exposure conds. 8=41578
- micrometeorite impact data on mats exposed by Gemini craft 8=41579
- micrometeorites, X-ray spectrometer appl. 8=28156
- moon origin 8=50432
- olivine from G pallisites, K-Ar and radiation ages 8=37023
- Saint-Severin, $P^{32,33}$ abundance 8=45846
- tektites, origin 8=50430
- CdS solar cells micrometeoroid degradation simulation obs. 8=24094
- Fe, conc. and isotopic comp. of Xe in inclusions 8=50436

- **Meteorites**—contd
  - Fe, determ. of K–Ar ages, rel. to K spatial distrib. 8=45844
  - Fe, K/Ar age determs, improved neutron activation
  - Fe, n activation determ. of Au, in nodules and inclusions 8=28159
  - H^3 and He^3, cosmic ray produced 8=50428
  - Ni^{59} produced in meteorites and micrometeorites 8=43003
  - Pu^{244}/xenon and I^{129}/xenon decay intervals for achondrites rel. to early solar system synthesis 8=45845
  - n/p-Si solar cells micrometeoroid degradation,
  - U-rich achondrites, Ar, Kr and Xe anal., and case for two types of fission Xe 8=28160
- **Meteoroids.** See Meteorites.
- **Meteorological instruments**
  - See also Anemometers; Hygrometers; Ionosphere measuring apparatus.
  - balloon flights, EOLE, from New Caledonia, at 400, 300 and 200 mb levels 8=36706
  - balloon flights, GHOST, from New Zealand, results at all altitudes 8=36707
  - evaporation, eddy flux instrument for natural evaporation meas. 8=50122
  - Nimbus II satellite, for obs., of cloud systems in 7 spectral bands and four size scales 8=41338
  - satellites, data analysis and transmission 8=45438
  - soundings, in upper atmosphere 8=36705
  - surface instrumentation 8=36702
  - upper air obs. 8=36703
- **Meteorology**
  - air mass motion quasilinear eqns., group invariance soln. 8=27890
  - atmosphere model based on isentropic surfaces 8=27873
  - balloon flights, EOLE, from New Caledonia, at 400, 300 and 200 mb levels 8=36706
  - balloon flight, superpress., at all altitudes, tech. of location and data telemetry 8=36707
  - boundary layer influence on dynamics of large scale processes 8=32197
  - chart records, A/D convertor 8=28244
  - climates rel. to secular orbital perturbations 8=37009
  - climatic and auroral cycles, from 2260 B.C. 8=50228
  - cloud and frontal systems obs. from Nimbus II satellite 8=41338
  - collection and processing of field data, symposium Canberra, Australia (1966) 8=45437
  - developments and world weather watch 8=50125
  - dynamic events development in lower ionosphere, review 8=32316
  - frontal waves, instability 8=32198
  - gas laser, applic. 8=42080
  - higher atmosphere soundings 8=36705
  - mass flow of air and H_2O vapour to stratosphere, using tritium tracer 8=36725
  - observing techniques in satellite 7=36704
  - planetary atmospheric waves, structure and motion 8=50134
  - probabilities of movingtime averages of variate 8=50123
  - of S.W. monsoon in India, rel. to vorticity considerations and N. hemisphere circulation 8=36708
  - satellite study of cloud and earth-atmosphere radiative energy balance review 8=45438
  - stratosphere over Minicoy Island turbulence obs. 8=45445
  - tensor theory of differential operators 8=50124
  - vertical thermal struct. from inverse radiative transfer problem 8=41363
- **Meteors**
  - See also Meteorites.
  - Canadian radioastronomical obs. 8=32609
  - Czechoslovak radioastronomical obs. 8=32611
  - destruction in atmosphere 8=32561
  - drifts in 80-100 km region, rel. to wind shear determ. 8=36779
  - flux data, photographic and radio, appl. of revised luminous efficiency and ionization probability 8=37019
  - fragmentation from instantaneous photographs 8=50427
  - high activity, rel. to H emissions in upper atmos., and noctilucent clouds 8=36794
  - indochinites chemical homogeneity, and teletites origin 8=50429
  - ion spectra 8=41571
  - luminosity rel. to separation of particles in earth's atm. 8=45842
  - meteoric dust in ionosphere, influence on v.l.f. wave propag. 8=32308
  - micron size stratosphere, cosmic dust 8=41359
  - radio echoes, influence of ambipolar diffusion 8=41572
  - showers, meas. of microparticle dust influx into atmos. 8=41346
  - sporadic radiants distribution and efficiency determ. 8=28155
  - sporadic, rel. to E_s 8=41448
  - teketites origin and indochinites chemical homogeneity 8=50429
  - USSR radar obs. 8=32523
- **Metrology.** See Measurement; Mechanical measurement.
- **Mica**
  - ancient cosmic ray tracks? 8=25036
  - characterisation by p.m.r. 8=40985
- **Mica** —contd
  - cleavage surfaces, fission-fragment tracks and dislocation-type defects 8=26693
  - dielectric layer in sandwich cathode, electron emission 8=44941
  - etchable track formation 8=44492
  - fracture props. obs. 8=49052
  - gumbelite fibre crystallites, microstructure exam. 8=26174
  - impurity effect on conduction current in d.c. field 8=35948
  - insulating films, space-charge conduction theory 8=49327
  - knick-band indexing using the X-ray universal stage 8=26714
  - muscovite dehydration, mechanism 8=49876
  - muscovite, dielec. permittivity pressure dependence 8=44874
  - muscovite, U^{235} fission fragment track annealing anisotropy 8=44505
  - muscovites, shearing force anisotropy rel. to surface condition 8=44602
  - natural and synthetic, spherically bent cryst., soft X-ray spectroscopy 3 to 30Å 8=32033
  - U-mica foil neutron dosimeter 8=33794
  - pre-heated, acid treated, rel. to interstratified structure formation 8=36572
  - removal of thin layers from surfaces, ion bombardment-enhanced solubility 8=40068
  - sheets, thin, kinetics of healing of fission-fragment tracks 8=40055
  - zinnwaldite, Mossbauer effect spectroscopy investigations 8=43960
- **Micelle systems.** See Colloids.
- **Microanalysis.** See Chemical analysis.
- **Microhardness.** See Hardness.
- **Micrometeorites.** See Meteorites.
- **Micrometry**
  - See also Interferometry; Strain gauges; Thickness measurement.
  - binary stars, 1164 examples 8=32475
- **Microphones**
  - See also Acoustic transducers.
  - cardioid, meas. of acoustic intensity and refl. coeff. 8=46190
  - pressure-gradient, second-order, random efficiency and back-to-front random ratio 8=37263
  - for spark chambers, in multiple particle detection 8=46963
  - transducer longit. freq. response functions generation, computer programme 8=23952
  - transducers, electrostatic 8=23954
- **Microphotometers.** See Densitometry.
- **Microprobe analysis.** See Chemical analysis/X-ray.
- **Micropulsations.** See Earth/magnetic field, variations; Magnetic storms.
- **Microscopes**
  - See also Electron microscopes; Ion microscopes.
  - attachment for metallography, −196 to +250°C 8=28745
  - design, principles 8=28753
  - biological, apochromatic flat-field objectives 8=42189
  - flow ultramicroscope for latex particle size anal. 8=30543
  - for high-temp. (2000-3000°C) study of materials 8=42183
  - holographic, theory 8=33247
  - interference, out-of-focus transfer function 8=28755
  - interference, transfer functions 8=37654
  - inverted, TELAVAL, specifications 8=42191
  - i.r. using InSb RPY51 detector, for temp. distribution over small areas 8=28380
  - MICROVAL-series, new types, specifications 8=42193
  - particle tracks in nuclear emulsions, semiautomatic microscope for ionization parameters 8=46983
  - polarizing, AMPLIVAL POL-D and AMPLIVAL POL-U, new types 8=42192
  - quantitative television microscope, fracture of charpy-V specimens, appearance assessment 8=40113
  - synthetic immersion oil for objectives 8=39363
  - tandem-scanning reflected-light 8=28757
  - transmission, polariscope for photoelasticity 8=33283
  - travelling, with digital output 8=28754
  - visual u.v., employing M-9 electro-optical converter 8=42214
- **Microscopy**
  - See also Electron microscopy.
  - bubble chamber, digitized data, computer processing 8=46957
  - carbonaceous mats., opt. and electron 8=44164
  - in film thickness determ., effect of numercial aperture of objective 8=39584
  - graphite, field-ion, rel. to crystal structure 8=26292
  - interference, applic. of holography 8=37656
  - microellipsometry in microstructure exam. of thin surface layers 8=48439
  - polymers, supramolec. struct. 8=30795
  - refractory metal carbides, field ion 8=26289
  - steel, alloy, field ion study 8=48596
  - tandem-scanning reflected-light microscope 8=28757
  - X-ray point-projection, technique and limitations 8=48582
  - X-ray, for selected-area diff. patterns and magnified Lane-diffr. images 8=48586
  - Ir films on Mo, field-ion 8=48452
  - W-Mo-Re alloys, structure and surface props. from ion microscope exam. 8=39727

Microscopy—contd
Zn crystal growth forms 8=48562
Microstructure of crystals. See Crystal structure/microstructure; X-ray examination of materials/microstructure.
Microtomes. See Biological technique and instruments; Laboratory apparatus and technique; Microscopy.
Microtrons. See Particle accelerators/orbital.
Microwave spectra. See Spectra.
Microwave spectrometers. See Spectrometers, radiofrequency.
Mie theory. See Scattering.
Milky Way. See Galaxies/the Galaxy.
Mineralogy. See Minerals.
Minerals
See also Mica; Quartz; Ruby.
absorbing anisotropic, refractive index and absorpt. coeff. 8=41061
adularia, O mobility study 8=35477
albite, O mobility study 8=35477
andesite, crystallization under high press. hydrous conds. 8=35227
andesite from circum Pacific arcs, systematic potash content vars. 8=36675
anomalously magnetic, thermal changes in mag. props. 8=31595
apatite structure, paramag. centres 8=31848
apatites, i.v. spectra 8=41047
ardennite, crystal structure, rel. to Si_3O_{10} group positioning 8=39808
barysilite, pyrosilicate and pyrogermanate isomorphs, e.p.r. of Mn^{2+} 8=40931
basalt and granite, strength rel. to stress rate and
basalt in ultra high vacuum, strength characts. 8=41320
basalt, paleomag. meas. 8=50232
basalt, synthetic, crystallization under high press. hydrous conds. 8=35227
basalt vapour scintillation, emission spectrum time scanning 8=34231
basalt, white pattern zones of titanomagnetite grains, obs. 8=48588
basalts, Pliocene, from S.W. U.S.A. paleomagnetism 8=32371
bayerite, structure from n.-diffr. exam., 8=39804
bernankite, struct., X-ray exam. 8=35345
borate, systematology 8=48511
botryogen, crystal structure 8=39790
brucite, structure from n.-diffr. exam. 8=39804
Bulgarian andesites, palaeomag. stability and petrology 8=28013
calcereous cave concretions, C and O isotopic composition var. 8=50096
calcic amphiboles, unit-cell volume and packing density, isotypic replacement effects 8=26372
calcite as neutron monochromator, structure factors 8=42651
calcite, growth shapes rel. to twinning 8=26238
calcite, synthetic, morphology and optical props. 8=26194
chabazite cryst. plug, hydraulic permeability rel. to ambient salt conc. 8=35473
comendite glasses, systematic variation of major elements 8=50075
cristobalite, polymorphic transform., impurity effects 8=26079
cristobalite, stacking fault conc. calc. from X-ray diffr. line profiles 8=26703
crystal-chemical classification based on i.r. spectroscopy 8=39637
deformation rates in h.f. e.m. fields 8=35643
dickite microcrystals, Au-decorated, growth study by e-diffr. exam. 8=26231
dolerites from Spitsbergen, late Mesozoic, anomalous paleomag. poles 8=50224
dunite and gabbro, brittle-ductile transitions 8=48976
ettringite, crystal structure 8=44210
evaporation by laser irradiation, obs. 8=39494
felspars, X-irradiated, structure defect exam. by e.p.r. and thermoluminescence 8=26710
fluorites, dosimetric parameters, from Bulgarian ore deposits 8=49799
Galway granite, zoning of garnets due to Rayleigh fractionation princ. 8=27852
geothite, natural, thermoremanence rel. to parasitic ferromag. and antiferromag. 8=49523
granite, Rb and Sr isotopes post-crystalline movement rel. to feldspar alteration 8=50081
granite, Westerly, permeability rel. to press. up to 4 kB 8=36687
haidingerites, $CaHAsO_4.H_2O$ and $SrHAsO_4.H_2O$, cry. struct. 8=48641
halloysite, water mol. arrangement 8=26143
Iceland spar, prism cutting 8=42160
Iceland spar, rational utilization of geometry in cutting polarizing prisms 8=42159
isotopic abundances of Pb, rel. to age of earth from concordia plots 8=27856
kaolinite microcrystals, Au-decorated, growth study by e-diffr. exam. 8=26231
kröhnkite, cryst. struct. and n.m.r. 8=48660
limestone, brittle-ductile transition 8=48976
magnetite at margins of crystallites, domain struct. behaviour 8=50225

Minerals—contd
magnetite crystals, elastic deformation, remanent and transitory effects 8=31728
metamorphic rocks from Ontario, Hf/Zr ratio 8=50067
metavauxite, crystal structure 8=48631
meteorites, hypersthene achondrites radiation ages 8=37023
meteorites, olivine from 6 pallasites, radiation ages 8=37023
mica, ancient cosmic rays tracks? 8=25036
mica, u.s. transmission coeff. rel. to freq. 8=30947
molecular sieve, type A Linde, containing Ni^{2+} ions, spectra 8=41143
montmorillonite with adsorbed cations, particle size by optical absorption 8=34943
muscovite samples, etchable length of fission tracks rel. to age 8=27854
olivine microchondrules in type I carbonaceous chondrites 8=50431
ores, state of flux in grain boundary movement 8=26843
orthopyroxenes, cation distribution, Mössbauer determ. 8=48324
pantellerite glasses, systematic variation of major elements 8=50075
parawollastonite, cryst. structure 8=48643
particles, ice nucleating props 8=35229
peridotite inclusions and host basalts, Th, U, and K abundances 8=50012
phosphate and oxide mixture, Mössbauer quantitative anal. of Fe^{3+}/Fe^{2+} ratios 8=27778
plagioclases from basic rocks, Sr and Ca fractionation trends, reinterpret. 8=50074
potassium feldspar and plagioclase, simultaneously crystallized at 600 °C, distrib. of trace elements 8=36627
proustite for optical conversion det. of $10 \mu m$ radiation 8=33123
pyrite, elastic field, effect of spherical inclusions 8=48938
pyroavrite, crystal structure 8=39803
pyrrhotite samples, mag. phases 8=50222
quartz, hydrothermal crystallization kinetics 8=26230
quartz-glass-coesite, phase transforms. under high-temp. and pressure 8=48400
radioactive, determ. using low energy (20-610 KeV) γ spectrometry 8=36651
radioactive, pulse-height spectrum analysis 8=46939
recent rhyolites of Mono and Inyo craters, appl. of K-Ar age anal. 8=27857
sapphire, crystals, conductivity, 20-850 °C 8=27236
sapphirine, crystal structure 8=35352
sepiolite, sorption of vapours 8=26137
serendibite, space group, cell dimens. 8=48644
silicate-mineral inclusions, orientation in natural diamond 8=26179
silicates, quantitative microprobe analysis, obs. 8=27809
silicates, surface and bond-forming props. 8=48427
silicates, surface area by Xe adsorb. 8=48426
single stage C replica for electron microscopy, rapid method of prep. 8=30855
sintering kinetics, thermal analysis, meas. 8=30665
spodumene, twinned, internal friction 8=49033
talc, structural changes during heating 8=48601
talc, structural changes on heating 8=30699
tectosilicates, elec. cond., method and exptl. results 8=40289
thaumasite, $Ca_3H_2(CO_3/SO_4)SiO_4.13H_2O$, thermal decomposition, i.r. study 8=26065
titanomagnetite transform. to titanomaghemite on cryst. margin 8=35125
triploidite, crystal structure 8=48652
ultramatic rocks in Alaska, Sb-Rb-K and Sr isotopic relns. 8=50069
Vanda porphyry dikes in Wright Valley, Antarctica, age 8=27859
villamaninite, chem. and structural analyses 8=48646
volcanic from Mono and Inyo Craters, Th^{230} dating 8=27860
whitlockites, crystal chemistry 8=39639
X-ray powder crystallography, peak intensity errors 8=26285
zeolite, H_2O adsorption, translational diffusion, model 8=39619
Zeolite Linde 13x, temp. depend. of mag. proton and cation reson. 8=49656
zeolite, synthetic, surface state evolution from r.f. spectrometry during dehydration 8=39581
zeolites, i.r. spectra of adsorbed NO, N_2O and NO_2 8=27553
zeolites, i.r. spectra rel. to chem. struct. 8=27552
zeolites, surface area determ. 8=48432
zeolites, synthesis 8=36541
zeolites, synthetic, containing transition metal ions, spectra, theory 8=41142
zeolites, synthetic, containing transition metal ions, spectra 8=41143
AlOOH crystals, preferential orientation 8=26183
B polycrystals etched by H_2SO_4, photomicrographs 8=39651
$CaAl_2Si_2O_8$, anorthite, n.m.r. of Al^{27}, obs. 8=40972
(Ca, Mg, Fe) CO_3: Mn^{2+}, e.s.r., allowed and forbidden transitions 8=40933
Mg ilmenites, MgO content rel. MgO/FeO ratio in host rocks 8=50070

Minerals—contd
- Mn_2GeO_4(olivine type) high-pressure form, crystal structure 8=39807
- MoS_2, molybdenite, surface point defects and non-basal dislocations 8=35526
- Pb-Zn ores, applic. of method of determ. true chargeabilities of vertical discontinuities 8=41323
- Pb-Zn ores in Turkey, true chargeability obs. 8=32177
- Sr and Pb, isotopes evolution model with crustal material recycling through mantle 8=36682
- U, presence in rocks and minerals from fission fragment tracks made visible by chemical etching 8=32185
- YFe garnet, e.m. conversion to exchange spin wave energy, coherent i.r. diffraction determ. 8=40848
- ZrO_2:Ce, baddeleyite, impurity positions 8=30917

Minor planets. See Planets.

Mirages. See Atmospheric optics.

Mirrors
- See also Telescopes/astronomical.
- aluminized, protection by SiO_2 coating 8=42148
- aplanatic systems, grazing-incidence results 8=46660
- astigmatic open optical resonator 8=33174
- blanks, glass-ceramics casting 8=41137
- coelostat for Catania observatory 8=28163
- concave, testing with spheres 8=28744
- coplanar mirror prisms, wedge error and zero error, approx. formulae 8=42151
- dielectric, high efficiency, for laser techniques, technology 8=42079
- dielectric thin films for laser work 8=49674
- electron, shadow-projection image distortions of periodic structs. 8=41967
- electrostatic, cylindrical, ion beam focusing 8=37411
- electrostatic, ungridded, for ion beam 8=37437
- gas laser, refl. coeff. meas. 8=24297
- glass, fused silica modified, with thermal expansion coeff. $\sim 10^{-7}/°C$ 8=39930
- laser output, transmission coeff., optimum, determ. 8=46566
- laser resonator, angular oscillatory modes 8=28664
- meniscus lens, in optical systems 8=42149
- misalignment of end mirrors in double-passed Michelson interferometer, effect on photometric-setting accuracy 8=28858
- mosaic, use in solar simulator for 1.5m diam. test objects 8=28734
- objectives for image converters and intensifiers, design 8=42178
- parabolic, 4 m diam, elastic deformations by dynamic relaxation technique 8=41663
- paraboloidal, made by rotation method, surface shape investig. 8=46659
- paraffin, for X-rays $\lambda > 20Å$ 8=24449
- spherical, Czerny-Turner arrangement of 2, and of 1 and concave grating 8=37644
- supports for minimum deflection 8=42182
- systems, design in matrix terms 8=28753
- telescope, large aperture Al alloys 8=46677
- two-component mirror and mirror-lens variable magnification systems 8=42150
- Nd glass coupled lasers, three-mirror system 8=37619
- Nd laser resonator, spectral effects 8=24287

Mixing. See Heat of solution; Solubility; Solutions.

Moderation. See Neutrons and antineutrons/moderation.

Moderators. See Nuclear reactors, fission/materials.

Modulation of light. See Light; Optical properties of substances; Optics.

Moiré fringes. See Interference/light.

Moisture
- See also Atmosphere/humidity; Humidity; Permeability, mechanical

See also Atmosphere/humidity; Humidity; Permeability, mechanical.

- absorbed by porous bodies, thermodynamic functions 8=44070
- diffusion in porous materials 8=44374
- extraction from porous materials 8=45935
- gas coolant in nuclear reactors, dewpoint optical detector 8=47932
- gas, drying trap 8=50470
- soil, free energy meas. using thermistor hygrometer 8=50090

Molar volume. See Density.

Molecular beams
- See also Particle velocity, analysis.
- alkali halides, dipole moments by elec. reson. 8=34232
- alkali halides, elec. reson. spectra 8=25670
- charge transfer, thermal and low-eV region, energy depend. 8=39025
- chemical reaction studies applic. 8=27683
- collision with hot filament, rel. to pyrolytic reactions 8=36577
- crystallization of epitaxial films, transfer calc. 8=30737
- crystallization from, phenomenological theory of non-isothermic process 8=30739
- d, polarized in metastable $2S_{1/2}$ state 8=38763
- deflection at high temps. 8=25671
- density fluctuations, optoelectron study system 8=47730
- electric reson. spectroscopy, at Berkeley 8=25405
- free molecule flow, effect of molec. interreflections on concave wedge 8=39174

Molecular beams—contd
- free radicals, mass spectrometry appl. 8=29829
- gas layer escape into vacuum, kinetic theory 8=43673
- high intensity and energy, techniques 8=29855
- hypersonic flow upstream of shock wave, conversion to continuum flow downstream 8=43667
- jet variations, thermo-optical detection 8=43431
- long-lived complexes in crossed beams 8=25669
- metastable states 8=25459
- microwave discharge source 8=43241
- polar diatomics, state selection and focusing 8=38964
- polar, scatt. by nonpolar gases, $1/r^6$ pot, comment 8=29853
- reflection indicatrix on surface, theoretical study 8=29856
- shaper, multichannel 8=47731
- sinusoidal chopper generating phase ref. signal 8=47727
- thermal energies, intermol. pot. 8=29846
- Ar, reflection at Pt surface at different temps. 8=25668
- B_2O_3, molec. struct. determ. 8=38809
- $CD_3^+ + CD_4 \rightarrow C_2D_5^+ + D_2$, collision mechanism 8=38963
- $CD_4^+ + CD_4 \rightarrow CD_5^+ + CD_3$, stripping-complex mechanism 8=38962
- CH_3I reactive scatt. with Rb atoms, asymmetry 8=47728
- CO, metastable state 8=25459
- CO_2, scatt. of K at. beam, time-of-flight anal. 8=38952
- Cl_2, reactions with K, Rb and Cs in crossed-beams 8=49875
- CsF, state selection and focusing 8=38964
- H_2 Maxwellian, scattered by room temp. H_2 and He, total collision cross-sections 8=47729
- H_2, reflection at Pt surface at different temps. 8=25668
- He Maxwellian, scattered by room temp. H_2 and He, total collision cross-sections 8=47729
- N clusters, interaction with stainless steel surface 8=29854
- $N_2^+ + H_2$ and $N_2^+ + D_2$, low energy ion-mol. reactions 8=27711
- O_2, reflection at Pt surface at different temps. 8=25668
- OCS, elec. dipole moment determ. 8=47587
- RbCl, state selection and focusing 8=38964
- $Rb^{85}F^{19}$, h.f.s., Stark and Zeeman effects 8=25514

Molecular orbitals. See Molecules/electronic structure; Orbital calculation methods.

Molecular relaxation. See Molecules/relaxation.

Molecular spectra. See Spectra/inorganic molecules; Spectra/organic molecules and substances

Molecular structure. See Molecules/configuration and dimensions.

Molecular weight
- carbon black, by light scatt. 8=43885
- macromolecules, effect on adsorpt. 8=39614
- poly-γ-benzyl-L-glutamate, rel. to proton resonance spectra linewidth 8=43873
- poly(α-methylstyrene), light-scatt. and mol. wt. distrib. 8=48152
- polymer chains, effect on crystallization and melting 8=44108
- Se vapour, and heats of vaporization of Se_{2-8}, obs. 8=43916

Molecular weight determination
- polymers, by equilib. ultracentrifugation 8=38967-8

Molecules
- See also Kinetic theory; Spectra.
- n-alcohols, with LiCl solute, relax. time of reorientation 8=34778
- Altmann's Schrödinger supergroup symmetry criticism 8=34212
- aromatic free radicals, g-factors, precise meas. and correlation with π-orbital energies 8=47708
- axially symmetric, elec. field spectra 8=29676
- with broadening, non-uniform, of operating transition line, effect on dynamics of processes 8=43247
- charge-transfer transitions in solns., band shape and polarization, calc. 8=34200
- complex formation in excited state with short-wave absorbent aromatics 8=47629
- complex, water glycerol confirmed from ultrasonic absorpt. 8=34840
- conjugated, charge distrib. 8=43270
- cyclotron double resonance for spectroscopic study of ion-molecule reaction mechanisms 8=47554
- deposition in successive thin layers, arranged in organized way 8=43921
- diamagnetic, quantum theory of magnetic birefringence 8=47567
- diatomic band systems, matrix multiplication property 8=43255
- diatomic, electron scattering in the approx. of two short-range potentials 8=43425
- dielectric constant theory, recent developments 8=47576
- dimers on a quadratic lattice, statistical mechanics 8=28315
- electron capture, rel. to chemical properties of electrons 8=25322
- electron photoejection, ang. distrib. 8=25706
- ethyl iodide, e scatt., spin polarization calc., 300-400 eV 8=34214-5
- excitonic, binding energy 8=40262
- FEMO model, three dimensional, homonuclear diatomic 8=47577
- ferrihaemoglobin, dynamical Jahn-Teller effect in g factor anisotropy 8=36234

Molecules—contd
- gyration radius of linear mol., boson representation 8=38974
- halogen cpds., polarizability, correl. with nucl. quadrupole reson. 8=29811
- halogens, photoelectron spectra 8=25486
- interacting mixtures, optical anisotropy theory 8=46635
- interchange symmetry for mols. and crysts. 8=25410
- ion-lattice interaction as dynamic Jahn-Teller effect 8=48339
- Jahn-Teller effect, dynamical, rel. to mag. anisotropy 8=36234
- Jahn-Teller effect in octahedral systems, calcs. 8=29687
- Jahn-Teller effect, induction of phase transformations in spinels 8=35076
- Jahn-Teller effects in mag. resonance 8=38910
- Jahn-Teller-splitting of e.s.r. lines of ions in cubic lattice sites 8=31841
- Jahn-Teller states of impurity ions in cubic crystals, luminescence 8=41176
- laser light scattering in dense isotropic media 8=34223
- light scatt., double quantum 8=25400
- long, spiral-tangle transitions, theory 8=43246
- luminescence in gaseous phase, review of Russian work to 1967 8=38776
- metastable double mol. and double mol. ions, formation 8=29834
- metastable quasi-mols, form in excited gas of resonance atoms 8=39194
- microwave spectroscopy, review of developments at Duke 8=37534
- molecular physics, book 8=37102
- motion in simple heat engine obs. 8=34196
- n. m. r.-line-shape of adsorbed, with p-p-interaction 8=34370
- n.m.r. parameters, for high-resolution, semi-empirical calc. 8=43405
- n.m.r. signal shifts, mols. adsorpt. on SiO_2 gel 8=39462
- nonspherical, free energy of assembly with hard core 8=41771
- N-particle system in radiation field, dipole coupling 8=39191
- organic, triplet state props. and spin-orbit and spin-spin interactions 8=25409
- perturbation theory, appl. of separable pots. 8=47477
- p-phenylenediamine cations, dimerization 8=25657
- polar, in liq. state, charact. of absorpt. in far i. r. 8=34859
- polar, scatt. by nonpolar gases, comment on $1/r^6$ potential 8=29853
- polarizability, analytical calc. 8=34220
- polarizability, empirical correl. with elect. field gradients 8=29811
- radiation in absorbing medium, effects of conversion to non-wave zone heat 8=38629
- Rayleigh scatt., finite-size effects 8=39219
- reactivity rel. to electronic absorpt. spectra 8=34225
- resonance energy transfer, statistics 8=25404
- semiconductors, chemisorbed, reactivity 8=41267
- spectroscopy and quantum chemistry 8=47553
- spectroscopy, role of wave mechanics 8=38775
- spin systems, stochastic processes 8=29804
- spinel ferrite lattice, cubic, local Jahn-Teller distortions rel. to phase transitions 8=26408
- tropylium salts, molec. motion in solid 8=49659
- turbulent, mol. transport processes accel. 8=34719
- Al_2O_3:V^{3+}, Jahn-Teller effect in $^3T_{2g}$ state, Zeeman study 8=43965
- CN violet emission, shock heated CO_2-N_2 mixture, chemical model 8=29722
- Cr^{2+} in MgO, Jahn-Teller lattice couplings 8=35053
- CS_2, motion in solid 8=39776
- $Cu_{1-x}Ni_xCr_2O_4$, cooperative Jahn-Teller distortions 8=35052
- $Fe_{1-x}Ni_xCr_2O_4$, cooperative Jahn-Teller distortions 8=35052
- Ge, (111) face, Jahn-Teller effect rel. to deformation, LEED obs. 8=26917
- H halides, photoelectron spectra 8=25486
- HBr, trapped in matrices, far i. r. dimer bands 8=27575
- HCN dimer, matrix-isolated 8=29740
- HCl, trapped in matrices, far i. r. dimer bands 8=27575
- He_2 formation mechanisms in early afterglow of pulsed discharge 8=47751
- I_2, e scatt., spin polarization calc., 300-400 eV 8=34214-5
- LiH_2, prediction from atoms-in-mols. theory 8=29751
- Li_2H, prediction from atoms-in-mols. theory 8=29751
- N-methylpyrol, quadrupole coupling consts. 8=29798
- Si, (111) face, Jahn-Teller effect rel. to deformation, LEED obs. 8=26917
- VCl_4, e.s.r., Jahn-Teller distortion 8=49619
- XY_4 type, Coriolis coupling consts. 8=34206

configuration and dimensions
- See also Chemical structure; Crystal structure, atomic.
- antiferromagnetic ordering, impossibility in one-dimensional and two-dimensional 8=34226
- conformational energy barriers in small mols. 8=25421
- contrifugal distortion consts. D_J and D_{JK} 8=47560
- in crystals, rel. to rotational diffusion rates 8=48767

Molecules—contd

configuration and dimensions—contd
- d, polarized in $2S_{1/2}$ metastable state 8=38763
- gas-phase electron diffractometry, EG-100A apparatus 8=38805
- high-pressure effects, Raman spectral data 8=41031
- intramolecular distances, semi-empirical calc. 8=29708-9
- by molecules, resonance before electron emission or predissociation 8=38949
- polytetrafluoroethylene oxide 8=35366
- potential curves, free parameters for linear eqns. 8=38958
- shape factors in vapour-liquid equilibrium calcs. 8=48269
- in solutions, reversible oritentation, mech. 8=39322
- structure models, ball-drilling methods 8=32631
- H_2, and shape 8=34248

configuration and dimensions, inorganic
- uranine, plus solvation shell, vol. in glycerol-ethyl alcohol and glycerol-H_2O solns., obs. 8=34285
- uranyl cpds., U-O bond distance calc. from i.r. spectra 8=34287
- hydrides, first-row, floating spherical Gaussian orbital model 8=38811
- Ag complex, bis(8-hydroxyquinoline)Ag(I) pyridine solvate 8=39765
- Au(III)-dimethyl hydroxide 8=39770
- B compounds, i.r. evidence for single H bridges 8=38808
- BF_3 8=29715
- B_2O_3 8=38809
- $BrICl^-$ in NH_4BrICl 8=30649
- Ca complex, $CaBr_2 . 10H_2O . 2(CH_2)_6N_4$ and crystal structure 8=26370
- Cd complex, diethyldithiocarbamate, and crystal structure 8=26375
- Cd complex, diethyldithiocarbamate and crystal structure 8=26376
- Cd complex, L-α-glycerophosphorylcholine cadmium chloride trihydrate 8=35325
- CF_2 8=25453
- CO_3 8=25464
- C_3O_2, gas electron diffr. 8=25466
- Co complex, nitropentamminocobalt(III) bromide and cryst. structure 8=26386
- Fe(111) complex, tetra-(n-butyl)-ammonium bis-(maleonitriledithiolate)Fe(III) 8=25469
- $Fe(C_{12}H_8N_2)_3Sb_2(C_4H_2O_6)_2 . 8H_2O$ and crystal structure 8=26397
- Ge periodate, i.r. absorpt. spectrum 8=43300
- H_2S_2 8=25485
- HCO radical 8=47713
- $(HCO_3)_2^{2-}$ in $KHCO_3$, structure from NMR study 8=26032
- $HNCLO_3^-$ ion, i.r. absorpt. obs. and structure 8=34247
- H_2O dimer, MO calc. for H-bond 8=38828
- HOCl 8=25475
- HPF_4 8=34279
- He_3^+ 8=34249
- I_3^- in $N(CH_3)_4I_3$ 8=30649
- I_2Br^- in CsI_2Br 8=30649
- IrF_6, electron diffr. 8=38858
- $K_4Mo(CN)_8 . 2H_2O$, mol. struct. 8=43317
- $K_4W(CN)_8 . 2H_2O$, mol. struct. 8=43317
- Mn complex, phthalocyanatopyridinemanganese(III)-μ-oxo-phthalocyanatopyridine-manganese(III) dipyridinate 8=26409
- $Mo(CN)_8^{4-}$ 8=41118
- N_2F_4 8=38839
- N_2H_2, extended Huckel calc. 8=25509
- NH_3 and ND_3, average struct. 8=29753
- NH_3, use of wavefunctions of double minimum potentials 8=25507
- NO_3 in $Ba(NO_3)_2$ crystals, from n-diffr. 8=39773
- $NOIrF_6$ and isotypes, by n-diffr. 8=25469
- $NOPtF_6$ and isotypes, by n-diffr. 8=25469
- Ni complex, bis(N, N-di-n-propyl-dithiocarbamate)Ni(II), and crystal structure 8=26419
- Ni complex, Ni glyoxime, mol. structure 8=26417
- NpF_6, electron diffr. 8=38858
- O_2AsF_6 and isotypes, by n-diffr. 8=25469
- O_2SbF_2 and isotypes, by n-diffr. 8=25469
- OsF_6, electron diffr. 8=38858
- PHF_2 and PDF_2 8=38849
- $Pd(SO_3)(NH_3)_3$ and crystal structure 8=26431
- PuF_6, electron diffr. 8=38858
- Ru complex, diethyldithiocarbamate, and nitrosyl salt and crystal structure 8=26375
- Ru complex, tetraphenyl arsonium tetrachloro cis-diaquo ruthanate monohydrate 8=35351
- $[RuBr_2(CO)_3]_2$ and crystal structure 8=26438
- $SbF_5 . SO_2$ 8=39820
- TaF_8^{3-} 8=41118
- $TmCl_3$, from Mossbauer effect 8=43959
- TmF_3, from Mossbauer effect 8=43959
- V_2O_5, from mag. susceptibility meas. and calcs. 8=36083
- UF_6, electron diffr. 8=38858
- $W(CN)_8^{4-}$ 8=41118
- WF_6, electron diffr. 8=38858
- XeF_6, electron diffraction 8=25523
- XeF_6, from gas-phase electron diffr. 8=34290-1
- $XeOF_4$ 8=43339

Molecules—contd
- **configuration and dimensions, inorganic**—contd
  - Zn complex, bis(acetylacetonato)zinc(II), and crystal structure 8=39824
  - Zn complex, tris(thiourea) zinc (II) sulphate, and crystal structure 8=39825
- **configuration and dimensions, organic**
  - para-acetotoluidide crystals, monoclinic modification X-ray study 8=44262
  - 3β-acetoxy-17α-hydroxy-16β-bromo-5α-pregnan-11, 20-dione, and crystal structure 8=26459
  - adenosine-3′-phosphate dihydrate, and crystal struture 8=35361
  - o-aminobenzoic acid, phase determ. and X-ray obs. 8=43359
  - 1, 2-0-aminoisopropylidene-α-D-glucopyranose, from crystal structure 8=25623
  - azaridines and N-deutero derivs., from i. r. spectra 8=34309
  - p-benzoquinone 8=34913
  - bigeranyl tetrahydrochloride and crystal structure of triclinic form 8=39827
  - biphenyl, config. 8=34348
  - α, α'-bipyridil in cryst. and liquid states, Raman obs. 8=34355
  - γ, γ'-bipyridil in cryst. and liquid states, Raman obs. 8=34355
  - bonds, two photon sensitized breaking, at 77°K, mech. 8=29704
  - 12α-bromo-11β-hydroxyprogesterone, and crystal structure 8=39828
  - 1-bromotriptycene $BrC_{20}H_{13}$, and crystal structure 8=44266
  - 5-bromouridine and dimethylsulphoxide 1:1 complex, bond lengths and angles 8=26471
  - 1, 3-butadienes 8=38918-20
  - calcium hexa-antipyrine perchlorate, and crystal structure rel. to other metal hexa-antipyrine perchlorates 8=44268
  - carborane and derivs, gas e-diff. study 8=25552
  - cellulose triacetate, different conformations in different solvents 8=43820
  - 1-chloroaziridine 8=25556
  - chloroformates (alkyl and phenyl), comparison with butyl formate, dipole moments obs. 8=25555
  - 2, 3-bis-(cis-chloro-1-methylcyclohexyl)-trans-2-butene, and crystal structure 8=39830
  - 2-chloropropene-1, 3-d_1, conformation of methyl group 8=25558
  - 2-chlorotropene, crystal structure 8=26476
  - cumene, by gas e-diffr. rel. to nature of conjugating system 8=25587
  - cyclobutyl monohalides, conformational behaviour 8=25563
  - cis, cis, cis, -1, 4, 7-cyclononatriene $AgNO_3$ adduct and crystal structure 8=26485
  - cyclooctane analogues, conformation rel. to crystal structure 8=26483
  - cyclooctanone, in crystalline phases above and below −87℃ 8=26091
  - cyclopentadienyl iron sulphide, and crystal structure 8=26537
  - cyclopropanone 8=29774
  - L-cysteine, and crystal structure 8=44271
  - demissidine hydroiodide, $C_{27}H_{46}INO$, crystal structure rel. to config. 8=26489
  - 1, 2, dibromoethane, rot. isomerism, n. m. r. study 8=47646
  - 1, 1-dibromo-3-fluorobutadiene-1, 3, energies of conformations, n. m. r. study 8=47631
  - dicarboxylic acids, $COOH[CH_2]_{2n+1}COOH$, and crystal structure 8=26478
  - 3, 6-dichloro-2, 5-diaminobenzoquinone-(1, 4), and crystal structure 8=26493
  - 1, 2, dichloroethane, rot. isomerism, n. m. r. study 8=47646
  - 1, 1-dichloro-3-fluorobutadiene-1, 3, energies of conformations, n. m. r. study 8=47631
  - diferrocenyl and derivs., and crystal structure 8=26497
  - difluorostilbene derivs., and crystal structure 8=26559
  - dihydrothymine 8=30918
  - $3\beta, 17\alpha$-dihydroxy-21-bromo-5α-pregnan-11, 20-dione, and crystal structure 8=39834
  - dimethylamine 8=47660
  - 2, 3-dimethylbutadiene 8=43375
  - dimethyline sulphonyl chloride, $(CH_3)_2NSO_2Cl$ 8=25607
  - 1, 3-dimethyl-2-thioxo-4-oxo-1, 2, 3, 4, 6, 7, 8 heptahydro-pyrimido [1, 2-a] [1, 3, 5] triazine 8=48686
  - eperuic acids, config. at C(13) from p-bromophenacylester of labdanolic acid structural analysis 8=39840
  - fluorinated methyl radicals, MO theory of geometry 8=47564
  - galactose, rel. to sp. ht. and enthalpy, 15-45℃ 8=30966
  - glucose, rel. to sp. ht. and enthalpy, 15-45℃ 8=30966
  - gramicidine S in soln., n. m. r. obs. 8=34332
  - hexamethylethane, steric deformations from gas-e-diffr. study 8=25606
  - hydrocarbons, floating spherical Gaussian orbital model 8=38886
  - 2-hydroxy-1-phenazine carboxylic acid from pseudomonas aureofaciens and crystal structure 8=26541
  - iso-eremolactone, and crystal structure 8=44273
  - isoprene, by gas e-diffr. rel. to nature of conjugating system 8=25587

Molecules—contd
- **configuration and dimensions, organic**—contd
  - ketones, $\alpha\beta$-unsaturated 8=29788
  - labdanolic acid, config. at C(13) from its p-bromophenacylester structural analysis 8=39840
  - leurocristine methiodide dihydrate, by anomalous scatt. methods 8=25590
  - mannose, rel. to sp. ht. and enthalpy, 15-45℃ 8=30966
  - α- and β-mercaptoesters, skeletal rearrangement on electron impact, mass spectra 8=47456
  - metal-metal carbonyl derivatives, X-ray study 8=26474
  - methyl chloroform, microwave spectra 8=29773
  - methyl group, electronic rel. to steric effects 8=25593
  - methyl halides 8=25596
  - 1-methylpentaborane 8=25600
  - 1-methylpentaborane(9) 8=29791
  - methyl vinyl ether 8=29790
  - micrococcinic acid bis-4′-bromoanilide and crystal structure 8=26531
  - molecular-crystals, structure determ. from potential energy-rotation angle minima 8=26455
  - monobromoduclauxin, and crystal structure rel. to duclauxin structure 8=44272
  - monoselenoparaldehyde, from crystal structure analysis 8=35365
  - natural products, from crystal structures 8=26457
  - nitrogen derivatives, stereochemistry from gas e-diffr. study 8=25608
  - nitroxide radicals from diethylhydroxylamine, dioctylhydroxylamine and N-hydroxypyrrolidine, e. s. r. obs. 8=25655
  - norbormide, stereochemistry from X-ray investigations 8=26165
  - octahydroxycyclobutane 8=44267
  - perhydrotriphenylene (PHTP) + n-hydrocarbons; + chloroform; + cyclohexane, inclusion cpds. 8=30920
  - phenol, in ground and first excited state 8=25614
  - phenylcyclopropane, by gas e-diffr. rel. to nature of conjugating system 8=25587
  - phenyldichlorophosphine oxide, by gas e-diffr. rel. to nature of conjugating system 8=25587
  - phthalazine, n-π* transitions 8=41170
  - poly-L-proline II, rel. to crystal structure 8=26547
  - porphyrin diacids 8=44282
  - propargyl alcohol and amine, isomers from microwave spectra 8=25532
  - pyrazine 8=34913
  - 2-pyrone electron-impact fragments 8=39061
  - selenophene 8=43395
  - silacyclobutane, puckered-ring angle 8=29800
  - steroids 8=25626
  - testosterone: mercuric chloride 2:1 complex, absolute config. and crystal structure 8=44283
  - tetrabenzonaphthalene, M-O-calcs. 8=34312
  - 1, 2, 3, 4-tetrabromo-1, 2, 3, 4-diphthaloyl-cyclobutane 8=48688
  - tetracyanoethylene-Pt complex 8=34322
  - tetramethylethane, steric deformations from gas-e-diffr. study 8=25606
  - tetramethylbiphosphine-bis(monoborane), and crystal structure 8=39851
  - N, N, N′, N′-tetramethyl-p-diaminobenzene iodide, and crystal structure 8=26524
  - tetramethyl-2, 2, 6, 6, -piperidinol-4-oxyl-1, free radical in crystal 8=25654
  - s-tetrazine, bond lengths in ${}^1A_g$ and $\tilde{A}\,{}^1B_{3u}$ states 8=25627
  - thulium acetylacetonate trihydrate, from Mossbauer effect 8=43959
  - thulium benzoate, from Mossbauer effect 8=43959
  - thulium oxinate, from Mossbauer effect 8=43959
  - titanium tetramethoxide, and crystal structure 8=44284
  - titanocene derivs, $(C_5H_5)_2TiCl_2$ and $C_5H_5TiBr_3$, by gas e-diffr. 8=25629
  - trifluoromethylphosphine 8=25574
  - trimethylamino borontrichloride and crystal structure 8=44264
  - from triplet states mag. reson. spectra 8=27449
  - triselenoparaldehyde, from crystal structure analysis 8=35365
  - Tschitschibabin carbohydrates in benzolic solution 8=48064
  - Wurster's blue iodide, and crystal structure 8=26524
  - CF_2, unstable mol. 8=25468
  - CF_3, orbital calc. 8=47664
  - $(CF_3)_4As_2$ 8=25604
  - $(CF_3)_2PF_3$ 8=25576
  - CF_3PF_4 8=25576
  - CH_3 in methyl aromatic hydrocarbons 8=29789
  - CH_3, orbital calc. 8=47664
  - $C^{13}H_3NC$, n. m. r. determ. 8=34336
  - $(C_5H_5)_2TiAl(C_2H_5)_2$, crystal and mol. structure 8=26504
  - σ-Fe diarylene, Mössbauer investigation 8=35039
  - H_2CO, use of wavefunctions of double minimum potentials 8=25507
  - $2SbCl_3$. dibenzyl, mol. complex, and crystal structure 8=35353
  - $4SbCl_3$. dibenzyl, mol. complex, and crystal structure 8=35353

Molecules—contd
  configuration and dimensions, organic—contd
    4:1$SbCl_3$. stilbene, mol. complex and crystal structure 8=35353
    $Sn_3(CH_3)_4Fe(CO)_{16}$, and crystal structure 8=26537
    Ti methoxide, and crystal structure 8=26523
  configuration and dimensions, macromolecules
    actin structure by X-ray scattering and diffr. 8=25674
    carboxypeptidase A, by low resolution technique 8=25675
    cellulose propylene phosphite, transformation, by spectroscopy 8=38966
    cyclotetratriacontane, and crystal structure 8=39831
    DNA, conformation in soln. 8=29860
    DNA of phage T2, and lattice structures rel. to glucoside residue effect 8=26490
    DNA, rel. to RNA and DNA-RNA hybrids and synthetic analogs 8=26556
    NaDNA, segment length and helix dia. 8=30434
    ferritin, and crystal structure 8=26506
    gyration radius of linear mol., boson representation 8=38974
    helical macromols. in soln., size and shape determ. 8=30420
    helical parameters 8=38965
    intramolecular energy functions for conformation anal. 8=29861
    β-lactoglobulin, Fourier maps from 2 different crystals 8=26516
    maleic anhydride-styrene copolymer, chain length and steric param., obs. 8=43776
    Markov chain model, end effects 8=25672
    1-methyl-5-bromouracil: 9-methyladenine, and crystal structure 8=26566
    polyacrylonitrile, neutron scatt. 8=25686
    poly-γ-benzyl-L-glutamate in soln., conformations 8=48096
    polybutadiene, chlorinated, n.m.r. obs. 8=38914
    polymer chain, eqn. of repeat angle 8=25685
    polymer chains, geometry 8=25684
    polymethacrylic acid, aqueous and methanol solns., rel. to small-angle X-ray scattering 8=25888
    β-poly-γ-methyl-L-glutamate, disordered structural characteristics 8=25677
    polypeptide chains, conformational analysis 8=25673
    polystyrene, chain dimens. temp. depend. below O point, obs. 8=43774
    PVC, chlorinated, n.m.r. obs. 8=38914
    protein, secondary structure small deformation model 8=25678
    protein structure refinement 8=25679
    proteins, determ. from rotary dispersion 8=29862
    rel. to protein coating of viruses 8=32624
    PVC conformational struct. from vib. anal. 8=43436
    RNA, and crystal structure of double helix 8=26555
    RNA rel. to DNA and DNA-RNA hybrids and synthetic analogs 8=26556
    s-RNA, from X-scattering study of mols. in water 8=25885
    t-RNA, from X-ray diffr. exam. at different concs. and ionic strengths 8=25875
    trypsin and DIP deriv., from X-ray scattering of mols. in soln. 8=25681
    vinyl polymers, mean dimens., effect of side-group interactions 8=29863
  dissociation
      See also Heat of dissociation.
    ABCD → AB + C + D vibr.-rot. populations of diatomic product 8=29682
    acetaldehyde, in ionization by electron impact 8=39056
    acetic acid, in ionization by electron impact 8=39056
    acetone, in ionization by electron impact 8=39056
    acrolein, photodissoc. 8=32135
    biphenylene, thermal fragmentation 8=39058
    1, 3-butadiene, photodissoc. 8=32135
    1-butene, photodissoc. 8=32135
    direct and indirect, recombination theory and dependence on temp. 8=38928
    dissociative electron attachment, theory 8=29953
    electron-impact, translational energies of products 8=38929
    excitation of atomic fluoresc. 8=38687
    guanidine 8=25583
    hexanitromethane, thermal decomposition in gaseous phase 8=49879
    hydrazine, photodissoc. 8=32135
    kinetics, influence of restricted intramolec. energy, flow 8=34374
    methyl phenanthrene, by electron impact 8=47797
    nonequilibrium flow past convex corner 8=43655
    phenanthrene, by electron impact 8=47797
    processes in mass spectrometry 8=38930
    tetranitromethane, thermal decomposition in gaseous phase 8=49879
    two-atom, thermodynamic functions, approx. calcs. 8=47954
    unimolecular reaction rates, Monte Carlo calc. 8=25645
    unimolecular reacts. in thermal systems 8=25647
    water, vac. u.v. photodecomp. 8=47613
    p-xylene, intramolec. formation of p-methylbenzyl 8=36617
    CO_3, photodecomp. 8=25464
    C_2, dissoc. through rot. 8=29826

Molecules—contd
  dissociation—contd
    D_2, recomb. rate 8=25649
    D_2^+ photodissoc., theory and calc. 8=47704
    H halides, dissociative electron attachment 8=29965
    H recomb. rate at room temp., spectroscopic obs. 8=34377
    H_2 by e attachment, restrictions on complex pot. energy 8=43308
    H_2^+ in mass spectrometer 8=47454
    H_2^+ photodissoc., theory and calc. 8=47704
    HCl, behind shock waves 8=38931
    HF, in shock waves 8=25650
    $I_2(B^3\pi_{0u^+})$, time-resolved emission 8=34251
    N_2, in shock tube, using vac. u. v. absorpt. 8=25651
    N_2, thermodynamic functions, approx. calcs. 8=47954
    $N_2O_4 \rightleftharpoons 2NO_2$ system, diffusion of Kr 8=34681
    Na vapour, association rel. to electrical conductivity 8=39220
    O_2, in the atmosphere from twilight and night spectral obs. 8=27949
    O_2, radiative combination of atoms by inverse predissoc. 8=38932
    S_8, dissociative ionization 8=47791
    $S_2O_6F_2 \rightleftarrows 2SO_3F\cdot$ free radicals in gaseous state 8=47711
    T_2 adjacent to solid propane or propene, by electron beam 8=27770
    TaF_5 and $TaOF_3$, stabilities 8=38938
  dissociation energies
    determination, effusion method 8=38935
    diatomic, calc. from spectroscopic consts. 8=25595
    fluorine organic compounds 8=47702
    group IIA fluorides, from mass spectra 8=38934
    methane, photoionization 8=29986
    methanes, substituted, calc. from spectroscopic consts. 8=25595
    prediction, semiempirical quantum-mech. eqns. 8=49851
    BO, mass spectrometric determ., value obtained 191.2 ± 2.3 kcal/mole 8=29825
    BeH^+, valence-only correl. calc. 8=34254
    CuF 8=34375
    F_2, determ. 8=34376
    H_2, HD and D_2 8=43305
    He_3^+ 8=34249
    He_3^+ 8=39037
    LaS 8=48287
    LiH, valence-only correl. calc. 8=34254
    NaF, MO calc. 8=34269
    NdC_4 8=47705
    $NiCl_2$ and $NiBr_2$ 8=39496
    PbF 8=38933
    PN 8=43413
    S_2 8=38935
    Se_2 8=38936
    SnF 8=38933
    Te_2 8=38937
  electronic structure
      See also Bonds.
    absorption spectra rel. to reactivity 8=34225
    aromaticity determ. by Faraday effect 8=47644
    atomic-orbital bases, choice and definition 8=43265
    band intensity, solvent depend. 8=47583
    binding energies measured by photoionization 8=47582
    bond formation in terms of charge distrib. 8=34221
    bounds on polarizaibilities, Rebane, and Kohn 8=25324
    closed-shell, paramagnetism 8=25439
    conformational energy barriers, MO calc. 8=25421
    conjugated, molecular orbital theory of spin 8=29707
    coordinate wavefunctions in computing basis functions 8=38798
    coordination cpds., paramag., e. spin density attenuation in ligands, n. m. r. 8=47593
    correlated wavefunctions, using limited Gaussian basis sets 8=29571
    corresponding orbitals and cofactors 8=47574-5
    d^2 and d^8 configs. in axial model field 8=30647
    de Sitter group in quantum calcs. 8=25430
    density functional representation of quantum chem. 8=47569
    distinguishable electron method for struct. calc. 8=34118
    distortion rel. to light pulse trapping in viscous liquids and glass 8=43810
    electron affinity, theory and exptl. determ. 8=25338
    electron phase contrast images 8=29710
    electronic terms and wave functions for large internuclear separation 8=43310
    electronic wave functions, correl. coeffs. 8=47462
    forbidden transitions, variational principle for intensity 8=47443
    harmonic oscillator methods 8=38597
    Hartree-Fock method, unrestricted, density matrix 8=38797
    Hartree product wavefunctions, projected 8=29572
    heterocycles, five-membered, N^{14} nuclear quadrupole reson. obs. 8=25638
    Hückel theory, self-consistent methods 8=38796
    intramolecular distances, semi-empirical calc. 8=29708-9
    iterative extended Hückel theory 8=25432
    large mols., MOs from SCF matrices of related small mols. 8=47570
    localized MO's, method of steepest ascents 8=29700

Molecules—contd
- **electronic structure**—contd
  - many-electron systems, GF wavefunctions 8=47439
  - optical activity, electron correl. models 8=29706
  - orbital calc., INDO method 8=34211
  - orbital degeneracy, effect on interactions and spin-orbit coupling 8=49568
  - orbitals and classical motion 8=25346
  - π-electron computation, general parameters 8=25440
  - π-electron Hamiltonian, inclusion of self-consistent screening 8=38804
  - π planar radicals, σ spin densities calc. 8=34379-80
  - polyatomic mols., MO calc., improving precision 8=25431
  - polyatomic, uniformly localized MO calc. 8=25428
  - quantum mechanics, Fermionic-Bosonic approx. 8=43264
  - radiationless transitions and molec. quantum beats 8=34209
  - radiationless transitions, theory 8=25406
  - radiative transition, relativistic effect and spin-orbital forces 8=38800
  - resonance integrals, approximations in semi-empirical calcs. 8=34210
  - separated group theory, possibilities in calc. 8=25438
  - separated groups, special config. interaction 8=25437
  - spectroscopy, role of wave mechanics 8=38775
  - spin density in quantum chem. 8=27672
  - spin-forbidden transition probabilities, correct operator 8=25327
  - spin functions in molecular system, irreducible representations 8=47581
  - substitution reactions in octahedral complexes, ligand field theory 8=45318
  - superconductivity appl. 8=34113
  - tetrahedrally localized orbitals, correl. 8=34117
  - Thomas-Fermi energy, upper and lower bounds 8=38636
  - triplet enhancement, presence when singlet effect is small 8=38779
  - triplet yield determ. by e.s.r. 8=29806
  - wavefunctions calc., check by n.q.r. 8=29701
  - PO radical β-systems obs. 8=34280
- **electronic structure, inorganic**
  - halogens, energy levels, from photoelectron spectra 8=25486
  - hydrides, first-row, floating spherical Gaussian orbital model 8=38811
  - Prussian blue 8=39518
  - radiative lifetimes of u.v. transitions 8=25442
  - second-row mols., CNDO calcs. 8=47573
  - tris(α-diimine)Fe(II) complexes, calc. 8=43365
  - Turnbull's blue 8=39518
  - water dimer, MO calc. for H-bond 8=38828
  - water, Rydberg states calc. 8=29746
  - water, Rydberg terms calc. 8=25479
  - AH, first row hydrides, ground states, Hartree-Fock wave functions 8=34256
  - AH, second-row hydrides, from spectra and energy quantities 8=34257
  - AlO, uniqueness of vibronic transition moment expression 8=43283
  - BBr, radiative lifetimes 8=38807
  - BF, mag. props., Hartree-Fock calc. 8=25447
  - BH, mag. props., Hartree-Fock calc. 8=25447
  - B_2H_6, electronic density distrib. 8=43285
  - BeH^+, valence-only correl. calc. 8=34254
  - BeH_2, diatomics-in-mols. calc. 8=25450
  - C_2, population inversion in $A^3\Pi g$ state by chem. reaction 8=29727
  - CF_2 8=25453
  - CN, σ-states, electronic configs. 8=47710
  - CN, transition probabilities 8=47591
  - CN^-, polarization, perturbation point charge calc. 8=25454
  - CN^-, SCF minimal basis set calc. 8=29719
  - CO, distortion in intense elec. fields 8=43291
  - CO, electronic transition moment integrals for ionization 8=25460
  - CO, ground and ionized states, LCAO calc. 8=25492
  - CO, transition probabilities 8=47591
  - CO^+, electronic transition moment integrals 8=25460
  - $Cr(CO)_6$, rel. to Cr-C bond length 8=38821
  - $Cr(CO)_6$, semiempirical MO model 8=47594
  - CrH, CrD, ${}^6\Sigma^+-{}^6\Sigma^+$ infrared obs. 8=47595
  - D_2, first excited ${}^1\Sigma^+_g$ state rot. and vibr. levels calc. 8=38823
  - DCN, assignment of laser lines 8=28682
  - DCN laser, new c.w. sub-mm lines, absolute freq. obs. 8=28683
  - $Fe(CO)_5$, semiempirical MO model 8=47594
  - $FeCl_4^-$ anion, intensities of d-d transitions 8=29736
  - H^-, electron correlation 8=34238
  - H_2, excited states, bare-nucleus perturbation theory 8=38829
  - H_2, first excited ${}^1\Sigma^+_g$ state rot. and vibr. levels calc. 8=38823
  - H_2, mag. shielding in elec. field 8=47599
  - H_2, numerical single-centre SCF function 8=47601
  - H_2, variation-perturbation calc. 8=38832
  - H_2^+, eigenparameters for large distance terms 8=34243
  - H_3, config.-interaction calc. 8=29744
  - H_3, linear, LCGTO SCF MO wavefunctions 8=47603

Molecules—contd
- **electronic structure, inorganic**—contd
  - H_3, potential-energy surface 8=34246
  - H_3^-, configuration-interaction calc. 8=38831
  - H_3^+, excited singlet states, diatomics-in-mols. calc. 8=34245
  - H_3^+, excited triplet states, diatomic-in-mols. calc. 8=47598
  - H_4, H_4^+, linear, LCGTO SCF MO wavefunctions 8=47603
  - H_2CO, and halogen analogs, spin-orbit coupling 8=25473
  - HCN, assignment of laser lines 8=28682
  - HCN, SCF minimal basis set calc. 8=29719
  - H_2-H_2 interaction, valence-bond calc. 8=29844
  - HNCO, SCF minimal basis set calc. 8=29719
  - HN_3, SCF minimal basis set calc. 8=29719
  - H_3O, theoretical evidence 8=47610-11
  - H_2S, nonempirical SCF calc. 8=47596
  - H_2SO, nonempirical SCF calc. 8=47596
  - He_2, triplet states 8=34250
  - He_2, He_2^+, LCGTO SCF MO wavefunctions 8=47603
  - He_2^+, orbital exponent in ground state calc. 8=25487
  - K_2, pseudopotential theory calc. 8=38838
  - KH, pseudopotential theory, calc. 8=38838
  - Li-acetylene 8=34255
  - Li_2, pseudopotential theory calc. 8=38838
  - Li_2, wave functions and binding energies calc. using quantum defect method 8=25489
  - LiH, ground state, pair correl. calc. 8=29604
  - LiH, pseudopotential theory calc. 8=38838
  - LiH, valence-only correl. calc. 8=34254
  - N cpds., charge distribution, molecular spectroscopy 8=47604
  - N_2, ground and ionized states, LCAO calc. 8=25492
  - N_2, potential energy curves of ground and ionized states, LCAO calc. 8=43320
  - N_3^-, SCF minimal basis set calc. 8=29719
  - NCN, singlet and triplet states 8=25495
  - NCO^-, SCF minimal basis set calc. 8=29719
  - NF, $b^1\Sigma^+-X^3\Sigma^-$ band system 8=25497
  - $N^{15}H_3$, h.f.s. inversion transition obs. 8=47607
  - NH_3, wavefunctions of double minimum potentials in struct. determ. 8=25507
  - NH_4, theoretical evidence 8=47610-11
  - N_2H_2, extended Huckel treatment 8=25509
  - NO, Λ doublets in mag. field 8=29758
  - NO^+ 8=47606
  - NO_2 8=45094-6
  - NO_2, 2491 Å transition 8=25503
  - NO_2^-, double-ζ LCAO SCF MO calc. 8=29756
  - $N^{14}O^{16}O^{17}$ 8=25504
  - Na_2, pseudopotential theory calc. 8=38838
  - NaF, SCF-LCAO-MO calc. 8=34269
  - NaH, pseudopotential theory calc. 8=38838
  - $(Nb_6Cl_{12})^{n+}$ (n=2, 3, 4) 8=27595
  - $Ni(CO)_4$, semiempirical MO model 8=47594
  - $NiCl_2$, energy levels, from fluoresc. of matrix-isolated mols. 8=29757
  - NiF_6^{-4}, electron delocalization 8=25510
  - O_2, ab initio calc. on 62 low-lying states 8=47614
  - O_2, Tanaka-Takamine Rydberg series 8=25512
  - O_2^- centers in alkali halides 8=49703
  - O_2^-, free parameters and effect of substitution in alkali halide 8=49704
  - OF_2, double-ζ LCAO SCF MO calc. 8=29756
  - PO_2^-, SCF matrix elements 8=47616
  - $RbMnF_3$, fine structure in ${}^6A_1 \rightarrow {}^4T_1$ (${}^4G$) obs. transition 8=32024
  - SO_2, lifetime of lowest triplet state 8=38853
  - T_2, first excited ${}^1\Sigma^+_g$ state rot. and vibr. levels calc. 8=38823
  - XeF_4, semiempirical MO energy levels 8=25524
- **electronic structure, organic**
  - acetylene, triplet states, by electron impact 8=34302
  - acetylene, two-centre calcs. 8=47632
  - 2-acyl-1, 3-diketones, anal. by MO-LCAO method 8=25588
  - alkyl radicals, spin density distrib. calc. 8=43416
  - alternant hydrocarbons, pairing theorem 8=47650
  - alternant hydrocarbons, rules 8=25584
  - aliphatic fragment, spin-spin coupling 8=38943
  - aminobenzenes, ground state 8=25534
  - aminopyridines, excited states and fluoresc. 8=48169
  - aniline, excited singlet states 8=25534
  - anthracene, low-lying triplet excit. states, 0.4-1.0μ 8=25616
  - aromatic carbonyl cpds., perturbation of singlet-triplet transitions 8=34296
  - aromatic hydrocarbons, localized benzene-like regions 8=47635
  - aromatic hydrocarbons, triplet factor group states 8=27622
  - aromatic, superconducting-type pair correlations 8=47636
  - aromatics, triplet-state lifetimes, effect of partial deuteration 8=34306
  - aryldiazonium cations 8=34363
  - azanologues of benzenoid hydrocarbons, polarization of electronic transitions 8=25548
  - benzene, condensed-pair and separated-pair models calc. 8=38870

- Molecules—contd
  - electronic structure, organic—contd
    - benzene dimers, semiempirical MO calc. 8=34313
    - benzene, excited states, AMO calc. 8=34314
    - benzene, in inert-gas matrix, higher excited states 8=49770
    - benzene, oscillator strengths from transition gradients 8=29780
    - benzene ring substituents, mesomeric effect 8=34311
    - benzene, SCF-MO-LC(LCGO) calc. 8=47624
    - benzenes, methyl-substituted, SCF-MO calc. 8=38897
    - benzenes, monosubstituted, CNDO SCF calcs. 8=25547
    - benzene-halogen complexes, electrostatic contribs. to ground-state props. 8=29768
    - benzothiophenes, mol. orbital calcs. 8=43355
    - benzyl radical, assignment of excited states by three-step photoselection 8=25542
    - boroxine and trialkyl derivatives, aromaticity 8=47644
    - carbonium ions, SCF MO calc. 8=38876
    - carbonyl group, assignment of lowest triplet state 8=25560
    - chromophore groups, LCAO calc. 8=43266
    - chromophores, intramolec. energy transfer between triplet states 8=41157/8
    - chrysene, low-lying triplet excit. states, 0.4-1.0μ 8=25616
    - complexes and components rel. to long-lived emission, obs. 8=25526
    - conjugated systems, intermolec. orbital theory 8=27684
    - Corrin analogue, synthetic 8=25561
    - cyanocobalamin monoacid deriv., by n diffraction 8=25676
    - cyclic aromatic hydrocarbon radicals and ions, electronic ang. momentum 8=25538
    - cyclopropane, SCF-MO-LC(LCGO) calc. 8=47625
    - 1,4-dibromonaphthalene, electronic Zeeman meas. 8=27629
    - p-di-tert-butylbenzene, π e chord symmetry in crysts., 20°K 8=30648
    - p-diiso-propylbenzene, π e chord symmetry in crysts., 20°K 8=30648
    - β-diketones structure and spectra 8=47651
    - ethane, ab initio bond-orbital calc. 8=38891
    - ethylene, oscillator strengths from transition gradients 8=29780
    - ethylene, SCF-MO-LC(LCGO) calc. 8=47626
    - ethylene, u.v. spectra assignments 8=47667
    - ethylenes, methyl-substituted, electronic transitions 8=47647
    - ferrocene 8=29782
    - fluoranthene, moment directions of electronic transitions 8=34329
    - five-membered ring, CNDO calc. 8=38862
    - formaldehyde, all-electron calc. 8=25578
    - formaldehyde, excited states, nonempirical calcs. 8=47648
    - formaldehyde, molec. g value and mag. susceptibility 8=29784
    - furan, anomalies in Parisen-Parr-Pople calcs. 8=38882-3
    - furan, applic. of self-consistent field calc. in differential overlap approx. 8=34357
    - helical polymers, spectral effects of interactions 8=29868
    - heterocyclic anions, N^{14} hyperfine coupling factors 8=34340
    - heterocyclic aromatic cpds., molec. fragments, atomic-orbital calc. 8=29785
    - hydrocarbon, lowest triplet state similar to dinegative ion 8=38884
    - hydrocarbon radicals, spin-extended PPP SCF spin densities 8=47649
    - hydrocarbons, CNDO calc. of nuclear spin-spin coupling 8=47663
    - hydrocarbons, conjugated radicals, ground states, MO calc. 8=38885
    - hydrocarbons, floating spherical Gaussian orbital model 8=38886
    - hydrocarbons, full config. interaction calc. 8=25585
    - hydrocarbons, valence-bond theory 8=29786
    - INDO spin unrestricted wavefunctions, spin contamination 8=47508
    - inner electrons of C atoms, bond participation 8=47627
    - p-isopropyltoluene, π e chord symmetry in crysts., 20°K 8=30648
    - ketene, g values and paramag. susceptibility 8=25589
    - α- and β-mercaptoesters, skeletal rearrangement on electron impact, mass spectra 8=47456
    - methane, ab initio bond-orbital calc. 8=38891
    - methane I^{129} derivatives, Mössbauer effect 8=48332
    - methane, intrapair correl. energy 8=38893
    - methane, SCF-MO-LC(LCGO) calc. 8=47628
    - methylborazines, SCF-MO calc. 8=38897
    - methyl group, rel. to steric effects 8=25593
    - p-methyl-2′-methoxybutylbenzene, π e chord symmetry in crysts., 20°K 8=30648
    - methyl radicals, isotopically substituted, vibronic effects, MO calc. 8=43421
    - methylene fluoride, molec. g-values and mag. susceptibility 8=34339
    - MO LCAO calcs. for compounds with 2 phenyl rings linked via O atom 8=25429
    - naphthalene, deuterated, optical anisotropy of excited state 8=25611
    - naphthothiophenes, mol. orbital calcs. 8=43355

- **Molecules—contd**
  - **electronic structure, organic—contd**
    - nitriles, saturated, N^{14} nuclear quadrupole coupling consts. 8=25642
    - nitrovinylbenzoate, structural group interactions, MO calcs. 8=34347
    - nonbenzoid, monocyclic conjugated systems with 4n and (4n + 2)π electrons 8=25436
    - nucleic purines first excit. triplet states, orbital calcs. 8=25621
    - nucleic pyrimidines first excit. triplet states, orbital calcs. 8=25621
    - olefins, u.v. spectra assignments 8=47667
    - orbital energies in coord. cpds. with strong ligand-ligand interactions 8=29703
    - oxalyl halides 8=25612
    - periodic systems, LCAO-SCF-CO calc. 8=47572
    - periodic systems, LCAO-HCO calc. 8=47571
    - phenanthrene, low-lying triplet excit. states, 0.4-1.0μ 8=25616
    - phenoxy radicals, π-electron spin densities 8=38947
    - m-phenylene-bis-phenylmethylene, quintet mol. 8=47669
    - π-radicals, F hyperfine interactions 8=29816
    - picene, low-lying triplet excit. states, 0.4-1.0μ 8=25616
    - polarization of mols. assigned anomalous dipole moments 8=43344
    - polyenes, oscillator strengths from transition gradients 8=43386
    - polymers, theory of optical props. 8=29867
    - polypeptides, helical, generalized susceptibility theory 8=25680
    - propane, ab initio bond-orbital calc. 8=38891
    - propylene, ab initio bond-orbital calc. 8=38891
    - pyrazine, SCF calc. 8=25622
    - pyrazine, SCF wavefunction, all-electron 8=34360
    - pyrene, low-lying triplet excit. states, 0.4-1.0μ 8=25616
    - pyridazine, by N^{14} quadrupole coupling consts. meas. 8=25643
    - pyridine, applic. of self-consistent field calc. in differential overlap approx. 8=34357
    - pyridine, SCF calc. 8=25622
    - pyridine, SCF wavefunction, all-electron 8=34359
    - pyridines, substituted, by N^{14} quadrupole coupling consts. meas. 8=25643
    - pyrimidine, by N^{14} quadrupole coupling consts. meas 8=25643
    - pyrrole, applic. of self-consistent field calc. in differential overlap approx. 8=34357
    - pyrrole, wavefunction, ground-state 8=34358
    - quinonediazide cations 8=34363
    - thiobenzophenone, excitation in (n, π*) band rel. to anion radical form 8=29827
    - sym-trinitrobenzene anion, effect of Li cation on spin density 8=47714
    - from triplet states mag. reson. spectra 8=27449
    - trypsin and DIP deriv., density from X-ray scattering of mols. in soln. 8=25681
    - vinylidene fluoride, molec. g values and paramag. susceptibility 8=29803
    - CF_3, orbital calc. 8=47664
    - CH_3, orbital calc. 8=47664
    - CH_2X, hybrid orbital force field calcs. 8=29781
    - $C_5H_5^-$, SCF-MO-LC(LCGO) calc. 8=47623
    - CO group, assignment of second singlet 8=32045
    - Cu^{2+} blue proteins, noncovalent model 8=49782
    - H_2CO, wavefunctions of double minimum potentials in struct. determ. 8=25507
  - **excitation**
    - acetophenone energy transfer to Eu and Tb, obs. 8=36487
    - alkyl diradicals, rotation about carbon-carbon bonds 8=27759
    - anthracene, excit. states decay and intersystem crossing obs. 8=25537
    - anthracene $S_0 \rightleftharpoons T_1$ radiative transitions, mag. dipole contribs. calc. 8=25545
    - anthraquinone, optically induced Overhauser effect 8=48210
    - aromatic hydrocarbons in soln., free carriers from triplet-triplet collisions 8=48201
    - aromatic hydrocarbons, oxygen quenching of singlet states 8=48170
    - aromatic hydrocarbons radiationless triplet decay and intersystem crossing Franck-Condon factors 8=25527
    - aromatics triplet state lifetimes, delayed fluoresc. obs. 8=25610
    - aromatics $S_0 \rightleftharpoons T_1$ radiative transitions, mag. dipole contribs. calc. 8=25545
    - benzene excimers, semiempirical MO calc. 8=34313
    - benzene, excited states in pulse radiolysis 8=49979
    - benzene, higher excimer states 8=34872
    - benzene, singlet and triplet π electron states 8=25543
    - benzene $S_0 \rightleftharpoons T_1$ radiative transitions, mag. dipole contribs. calc. 8=25545
    - benzene to diacetyl triplet-triplet energy transfer in solns., obs. 8=34316
    - benzophenone energy transfer to Eu and Tb, obs. 8=36487
    - benzyl radical, assignment of excited states by three-step photoselection 8=25542

Molecules—contd
excitation—contd
beta-diketone negative ions, triplet state e.s.r. 8=47682
carbonyl-containing compounds n ←π* luminescence in vapour 8=34199
close-coupled rot. excitation, computation 8=47719
complex formation in excited state with short-wave absorbent aromatics 8=47629
degenerate electronic states, asymmetric vibronic effects 8=43252
diatomic, energy of core excited and single-particle resonances 8=43307
diatomic mols., rot. excitation in scatt. by atoms 8=47719
1, 2-dichloroethane, vibr. excited, from Hg-photo-sensitized dichloromethane 8=27761
2, 5-dipheyloxazole in benzene, toluene, p-xylene and mesitylene, excimer, fluoresc. solvent-solute energy transfer 8=25940
electronic energy transfer, effect of diffusion 8=34881-2
electron impact, threshold excitation 8=25402
energy bands, pseudopotential method for calc. ultra-localized functions 8=40231
excimer formation with polar mols. 8=29796
excimer, semiempirical theory 8=38801
exciton model for dimers and trimers 8=38779
o-fluorotoluene, photoexcit. triplet state yield rel. to vibr., gas-phase obs. 8=25630
hexafluorobenzene, photoexcit. triplet state yield rel. to vibr., gas-phase obs. 8=25630
hydrocarbons, double photon excitations 8=25585
lifetime meas. of states with accelerated ion beam 8=43251
metastable, review of unusual props. 8=29591
monofluorobenzene, photoexcit. triplet state yield rel. to vibr., gas-phase obs. 8=25630
naphthalene, quenching of triplet state 8=34341
naphthalene, singlet and triplet π electron states 8=25543
naphthalene, triplet state, excitation exchange and optical spin polarization, e.s.r. study 8=47686
β-naphthol, triplet state, acidity determ. by e.p.r. 8=34342
2-napthyl methylketane energy transfer to Eu and Tb, obs. 8=36487
nonradiative energy transfer in systems with frozen rot. Brownian motion 8=34883
optical anisotropy dispersion, by appl. of laser waves and certain harmonics 8=38774
organic, dye (Eastman 9860)electronic transition, picosec. lifetime direct obs. using Nd glass laser 8=43346
organic, multiphoton, by Q-modulated ruby laser 8=34295
organic, radioluminescence, kinetic study 8=47630
organic triplet energy transfer in cysts. from mag. reson. spectra 8=27449
organic triplet states and low-energy e impact spectrometry 8=25528
organic triplet states de-excit. in condensed media rel. to mol.-host interactions 8=26029
oxazole, and derivatives, excimer formation 8=29796
parahydrogen, solid, rot. and vibr. theory 8=43967
phenanthrolines, fluoresc. and phosphoresc. spectra 8=43382
phenanthrene, excit-states decay and intersystem crossing, obs. 8=25537
phenanthrolines, deactivation of excited states 8=43383
phosphorescent T-S band decay rate meas., effect of absorpt. T*←T bands 8=38777
photoselection effects on polarization of luminesc. mols. 8=47579
photoselection, tandem two-photon processes 8=49692
polarization in static elec. field rel. to even harmonic radiation 8=43249
pyrene, flash excited absorpt. spectrum 8=43840
pyridine, photoexcit. triplet state yield rel. to vibr., gas-phase obs. 8=25630
quantum beats 8=34209
quinoxaline triplet state, and radiative decay, paths rel. to mag. interactions 8=25624
radiative lifetimes of excited states 8=34230
rotational and vibr., by low-energy electrons 8=25418
rotational and vibrational excitation of molecular ions by electrons 8=38785
in solids and liquids, excited state lifetime 8=39367
tandem two-photon processes, polarization correl. 8=49692
toluene, excited states in pulse radiolysis 8=49979
toluene, higher excimer states 8=34872
toluene, photoexcit. triplet state yield rel. to vibr., gas-phase obs. 8=25630
toluene to diacetyl triplet-triplet energy transfer in solns., obs. 8=34316
triplet absorpt., extinction coeff. meas. 8=25401
triplet form., quantum yields meas. 8=25401
triplet yield determ. by e.s.r. 8=29806
C_2 high-press. bands in CCl_4-Na, K flames, mechanism, obs. 8=38816
CN, in active N_2, reaction kinetics 8=27699
CO, Asundi bands, in gas discharge 8=38994
CO, energy relax. for thermal e 8=38818
CO, in pulse radiolysis 8=45405
CO, selective, in CS_2O_2 chem. laser analysis 8=46569

Molecules—contd
excitation—contd
CO, Xe-sensitized fluoresc. 8=25457
CO^+ and CO, lifetimes and decay cross-sections 8=34261
CO_2, wall de-excitation of 00°1 state 8=38817
CO_2^+ band, by e-impact (80-1500 eV) 8=25490
CaBr, h.f. discharge, u.v. emission spectrum 8=43295
H_2, para and ortho, rotational excitation on collision with He 8=47720
H_2, rotational excitation and de-excitation by slow electrons, absolute total cross section, energy and angular var. 8=43311
H_2, rotational, by slow e, exchange effects 8=34241
H_2^-, resonant states, and auto-ionizing energy calc. 8=43307
HF, chem. laser 8=37582
He triplet state lifetimes, low-energy e excit. meas. 8=25528
Hg-vapour, rel. to green-band emission 8=29944
Kr, visible afterglow emission 8=47754
$N_2(A^3\Sigma_u^+)$, excitation of NO 8=25494
$N_2(A^3\Sigma_u^+)$ in active N 8=38340
$N_2(A^3\Sigma_u^+)$, reaction with N atoms 8=25493
N_2, band systems, $b'\,^1\Sigma_u^+ \rightarrow X^1\Sigma_g^+$ and $g^1\Sigma_u^+ \rightarrow X^1\Sigma_g^+$, selective enhancement in vacuum u.v. 8=38841
N_2, by electronic energy transfer from metastable Xe atom 8=29847
N_2, by 1-12 eV electrons 8=29755
N_2, by 2-3eV electron scatt., explanation of oscillatory energy depend. 8=43321
N_2, first positive system, in gas discharge 8=38994
N_2, rotational, in He collisions 8=25666
N_2, vac. u.v. photon impact 8=47609
N_2, with simultaneous ionization by e impact 8=25717
N_2^+ band, by e-impact (80-1500 eV) 8=25490
NO, rotating resonance on transitions between Zeeman levels in mag. field rel. to hyperfreq. elec. field meas. 8=38846
N_2O^+ and NO, lifetimes and decay cross-sections 8=34261
O_2, by 0.15-1.0 MeV protons 8=38847
O_2^+ band, by e-impact (80-1500 eV) 8=25490
O_2^+ lifetimes and decay cross-sections 8=34261
O_3, vibr., in radiolysis and photolysis of O_2 8=36620
OH^+, $^3\Pi_i$ excited state, fine structure 8=29830
$OH^*(^2\Sigma^+)$, in photodecomp. of H_2O 8=47613
SF_6, coherent by CO_2 lasers, photon echoes, obs. 8=34282
UO_2^{2+} 8=39382
UO_2^{2+} in β-diketone + N-containing organic bases triple complexes by intramol. energy transfer, obs. 8=34288
intermolecular mechanics
See also Association; Collision processes; Kinetic theory/gases; Liquids/structure; Liquids/theory; Solids/theory.
acetone condensation products, mass spectra 8=29840
adamantane, van der Waals interactions and mol. crystal packing 8=35050
adiabatic phase shifts, lower bounds 8=29842
asymmetric diatomic, vibr. transitions, most favourable orientation 8=43254
BCK potential for nonpolar mols. 8=47718
benzene crystal, rel. to lattice energy 8=35395-6
in binary inert gas mixtures, from thermal diffusion coeffs. 8=34675
chlorophyll-ligand interactions, from n.m.r. 8=29850
collision broadening of rot. and vibr.-rot. line shifts and widths 8=47556
collision cross-sections, diagrammatic methods 8=29838
collision integrals for high-temp. gases 8=34670
collisions, nuclear spin and statistics effects 8=47723
collisional transfer of rotational energy 8=25662
conference, Vatican City, April 1966 8=38960
conjugated systems, intermolec. orbital theory 8=27684
correspondence principle, anomalous potentials 8=25663
crystals, molecular, symmetry of pot. functions 8=34391
diatomic mols., rot. excitation in scatt. by atoms 8=47719
dipolar mol., interaction with spherical atom 8=38954
distorted-wave Magnus approximation 8=43426
double bonds, one and two centre electron repulsion integrals, semi-empirical 8=34218
dye solns., conc., spectroscopy 8=29841
effect on line shapes and depolarization factors of highly polarized Raman lines 8=34858
exchange interactions, Jansen perturbation theory 8=43428
exchange interactions, perturbation theory 8=38738
gases, light scattering, molecular collision-induced 8=30474
gas mixture, thermal diffusion method 8=30315
globular mols., intermolec. forces and octopole moments 8=29849
globular mols., transport collision integrals 8=29848
hydrocarbons, dimers in vapour phase 8=34388
inelastic scatt., semiclassical theory 8=46822
inert gas adsorpt. on solid Ar and Xe, van der Waals interactions at (100) face 8=39617
inert gas adsorpt. on solid Ar and Xe, Van der Waals interactions at (111) face 8=39618
inert gases, analytical potential models 8=30272
inert gases rel. to Rayleigh light press-induced depolarisation 8=39217

Molecules—contd
  intermolecular mechanics—contd
    ion-mol. reaction rates, anomalous, in drift tube 8=29835
    ion pairs and third bodies collision energy change rate coeff. calc. 8=38950
    Lennard-Jones pot., parameters from scatt. data 8=39192
    rel. to light scatt. second harmonic, in dense isotropic media 8=34222
    liquid and gas mixtures, correls. rel. to light scatt. 8=34663
    liquids, hydrodynamic interaction rel. to mag. relax. time 8=34923
    liquids, light scattering, molecular collision-induced 8=30474
    liquid, organic, effect on i.r. absorpt. spectra 8=34861
    London-van der Waals forces, liq. film contact angles obs. 8=25859
    metastably bound double polar mols, lifetime 8=34217
    methane, compressed, mean-squared torque calc. 8=38894
    methane, gaseous, rel. to scattering of slow neutrons 8=38898
    molecular-kinetic resistance, rel. to heat transfer with condensation 8=25990
    Morse potential, relation with Altenburg's quadratic mean radius 8=47722
    organic mixed crysts., intermolec. triplet decay of luminesc. 8=32070
    pair interaction potential between adsorbed mols. 8=48472
    Percus-Yevick isotherm for exp-6 potential 8=34390
    perturbation theories for exchange forces, appl. to simple model 8=25664
    perturbation theories of intermolec. forces 8=25665
    pigment solvents, spectroscopic explanation 8=34383
    polar mols., energy transfer, temp. depend. 8=47716
    potential curves, free parameters for linear eqns. 8=38958
    potential of spherically symmetrical mols. 8=47951
    potentials, degenerate perturbation theory, exchange effects 8=38955
    potentials, derived from cryst. props, effects of anharmonicity 8=35049
    potentials, mol. beams at thermal energies 8=29846
    pressure broadening of rot. and vibr.-rot. transitions, scatt. theory 8=47558
    quadrupolar and octopolar, interacting, double photon scattering 8=47717
    quadrupole-quadrupole interactions 8=25835
    rel. to organic triplet states de-excit. in condensed media 8=26029
    retarded van der Waals potential 8=38961
    scattering, large-angle, perturbation calc. 8=29569
    scattering, multiple turning-point, semiclassical calc. 8=28945
    scattering, reactive and elastic, appl. of R-matrix theory 8=43427
    time-correlation functions of random motions 8=34386
    transitions, rot. and. vibr., prod. 8=29845
    van der Waals forces between macroscopic bodies 8=30610
    van der Waals interactions, calc. 8=29852
    vibrational energy transfer to oscillator by collision with particle 8=47721
    vibrational relax. of anharmonic oscillators in collisions 8=29839
    vibrational transition probabilities, WKB calc. 8=38953
    Ar gas, X-ray scatt. obs. 8=30274
    Ar, pair and non-pair potential 8=43924
    Br_2, vibr-relax. in Ar 8=47726
    CN, dipole-dipole interaction rel. to infrared absorpt. in CCl_4 8=34319
    CO_2, collisional relax. in $10^{0}0$ state 8=47715
    CO_2, Rayleigh scattering, depolarized, as new probe of forces 8=39212
    CO_2 + N_2O, near-resonant energy transfer between i.r.-active vibrs. 8=47725
    Cl_2, intermolec. forces in cryst. 8=48648
    Co complex, bispyridinocobalt(II)dichloride, structural isomers, interaction by Mössbauer spectroscopic study 8=29837
    F_2, intermolec. forces in cryst. 8=48648
    H_2 and D_2, vibr. relax., isotope effect 8=34240
    H_2, para and ortho, rotational excitation on collision with He 8=47720
    H_2, Rayleigh scattering, depolarized, as new probe of forces 8=39212
    H_2-H_2 interaction, quantum mech. calc. 8=34387
    H_2-H_2 interaction, valence-bond calc. 8=29844
    H_3^- system, interaction energy 8=29738
    H_2O-H_2O collisions, vibr. transition probabilities 8=34389
    He-H_2(D_2), high-velocity scatt. 8=25667
    N_2 afterglow, kinetic constraints 8=29897
    $N_2(A^3\Sigma_u^+)$, excitation of Hg 8=34163
    N_2, electronic energy transfer from metastable Xe atom 8=29847
    N_2, Rayleigh scattering, depolarized, as new probe of forces 8=39212
    N_2, rotational excitation in He collisions 8=25666

Molecules—contd
  intermolecular mechanics—contd
    NH_3, collision-induced transitions between rot. levels 8=47612
    O_2, interaction with excited organic mols. 8=38956
    O_2, quenching effect on muonium in Ar, and effect on polarization 8=42482
  internal mechanics
    alkali halide, interatomic potl. calc. 8=43281
    alkali halides, parameter calc., improved potential function 8=43323
    alkali halides, parameter calc. from Wasastjerna potential function 8=43324
    alkali hydride, interatomic potl. calc. 8=43281
    bond properties, review 8=38803
    bracketing theorems for lower bounds 8=38795
    Coriolis interaction between vibrational levels 8=38791
    cyclopropanes, symmetry species correl. and group freqs. 8=25564
    1, 1-dibromo-3-fluorobutadiene-1, 3, energies of conformations, n.m.r. study 8=47631
    1, 1-dichloro-3-fluorobutadiene-1, 3, energies of conformations, n.m.r. study 8=47631
    dielectric meas. of intramolecular barrier in solns. 8=48186
    hindered rotation between orientation sites, explanation of anomalous dielec. dispersion in tetra-subst. methanes 8=49326
    integral virial theorem and generalized differential Hellmann-Feynman formula 8=25323
    intramolecular regroupings, quantum theory 8=45320
    Jahn-Teller principle, formulation 8=38793
    ketones, optical activity, theory 8=38888
    local energies, integral Hellmann-Feynman method 8=25325
    macromolecules in soln., rel. to theory of diffuse small-angle X-ray scattering 8=25870
    macromolecules, intramolec. energy functions for conformation and vibr. anal. 8=29861
    metastable states, molec. beams 8=25459
    nearly-free rotation, vibrational problem 8=34201
    nucleic acids, molec. interactions and helical struct. 8=29859
    organic, bonds, two photon sensitized breaking, at 77°K, mech. 8=29704
    polymethylbenzenes, CH_3 group reorientation at low temp., n.m.r. study 8=49654
    positronium, binding energy calc. 8=43430
    potential-energy function for diatomic mols. 8=29697
    quantitative data from microwave spectrum, improved determ. 8=24258
    resonance valence state, alternative definition 8=25433
    BeH_2, total energy calc. 8=25451
    C-H valence oscills. in vinyl ether 8=30493
    $\lfloor(C_6H_5)_3P^+ - CH_2\rfloor$ radical in crystalline matrix, hindered rotation of CH_2, e.s.r. study 8=49616
    CO, ground and ionized states, potential energy curves 8=25492
    C=O valence oscills. in vinyl ether 8=30493
    $GeCl_4$, Coriolis coupling consts. and force fields 8=38822
    H_2^-, potential energy, scaled atoms-in-mols. calc. 8=29750
    H_2^+, const. of motion for two-centre Kepler problem 8=46791
    H_3-system, nuclear motion 8=29739
    HeAr, interatomic potential 8=29749
    He_2 and He_2^+, potential energy, scaled atoms-in-mols. calc. 8=29750
    HeH and HeH^+, potential energy, scaled atoms-in-mols. calc. 8=29750
    HeNe, interatomic potential 8=29749
    N_2, ground and ionized states, potential energy curves 8=25492
    NH oscills. formed in the spectra of 2, 3, 4-trimethyl-5-carbetoxypyrrol, pyrrol-2-aldehyde, and CCl_4 8=34353
    NO, quenching effect on muonium in Ar, and effect on polarization 8=42482
    NeAr, interatomic potential 8=29749
    $S(CN)_2$, force field and Coriolis coupling coeffs. calc. 8=43333
    $SnCl_4$, Coriolis coupling consts. and force fields 8=38822
    XF_6, octahedral, orbital valency force field calc. 8=38863
  moments
    acryloyl fluoride, rotational isomers 8=38864
    adiabatic inversion with light pulses 8=47437
    alkali halides, dipole, by molec. beam elec. reson. 8=34232
    alkylbenzenes, symmetrically substituted, dipole 8=34890
    bounds on polarizabilities, Rebane, and Kohn 8=25324
    butyl formate, dipole, in dil. benzene, comparison with chloroformates, rel. to configs. 8=25555
    carbon tetrafluoride, octopole 8=29849
    chloroformates (alkyl and phenyl), dipole, in dil. benzene, rel. to configs., and comparison with butyl formate 8=25555
    conjugated, dipole moments, observed and calculated 8=43270
    conjugated systems, quadrupole, polarizabilities, π-electron theory 8=43268
    cyclic polyene with $4n\pi$ electrons, theory of diamag. anisotropy 8=25434

Molecules—contd
- **moments**—contd
  - cyclopropane ring systems, diamag. susceptibility anisotropy interatomic contrib. 8=25619
  - cyclopropanone, dipole 8=29774
  - diatomic ionic mols., dipole moment and effective charge 8=43273
  - dicarboxylic acid esters, intramol. mobility and dielec. relax 8=43340
  - 2,2-difluoro-1-methylcyclopropane, dipole 8=29792
  - difluorodiazirine, dipole, of π^* state 8=25579
  - dimethylamine, dipole 8=47660
  - dipolar mols., quadrupole moments 8=29705
  - dipole derivatives, perturbed Hartree-Fock calc. 8=25425
  - dipole, interaction, elastic in solids 8=48335
  - dipole, molecular field theory, Onsager reaction field and spherical model 8=43269
  - dipole-moment derivatives, statistical errors 8=25435
  - dipole moment determ. of mols. in aq. soln. 8=34213
  - dipole, polar mols. in non-polar solvents, formulae 8=34216
  - dyes, quadrupole, π-electron theory 8=43268
  - dynamic polarizability, variational bounds 8=47580
  - electric dipole, atomic orbital calc. 8=43265
  - electric dipoles, permanent and collective excitations 8=37217
  - electric quadrupole in excited states, meas. method 8=43271
  - epoxide ring systems, diamag. susceptibility anisotropy interatomic contrib. 8=25619
  - formaldehyde, dipole 8=38881
  - formaldehyde, dipole moment of triplet state 8=25580
  - formaldehyde, sign of elec. dipole 8=29784
  - formyl fluoride, dipole, of π^* state 8=25579
  - glycerol, dipole 8=34331
  - haloethanes in solns. 8=48184
  - hydrocarbons, quadrupole, π-electron theory 8=43268
  - inert-gas couples, translation band, transition probability at l.f. 8=29711
  - isobutyl alcohol, dipole 8=34331
  - isopropyl alcohol, dipole 8=34331
  - ketene, g values and paramag. susceptibility 8=25589
  - rel. to light scatt. second harmonic, in dense isotropic media 8=34222
  - methane, octopole 8=29849
  - methyl chloroform, dipole moment 8=29773
  - methylcyclopropane, dipole 8=47665
  - 1-methylpentaborane, dipole 8=25600
  - 1-methylpentaborane(9), dipole 8=29791
  - methyl vinyl ether, dipole 8=29790
  - myristic acid, dipole, in gaseous monolayer at air/water interface, obs. 8=30438
  - organic mols. in dilute benzene solns., dipole 8=34333
  - ortho-alkoxyphenylhydrazones of trimethylene sulphone, dipole obs. 8=38868
  - palmitic acid, dipole in gaseous monolayer at air/water interface, obs. 8=30438
  - pivaldehyde, dipole 8=25618
  - polar, rel. to slow electron scattering 8=25441
  - polarizability, from refractive index of gases having non-resonant absorpt. in microwave region 8=47972
  - polarization in static elec. field rel. to even harmonic radiation 8=43249
  - polarization of mols. assigned anomalous dipole moments 8=43344
  - polymethylmethacrylate, dipole calc. 8=38969
  - polypropylene, second moments transition, CCl_4 effects, 140-373°K 8=48510
  - propionic acid, dipole 8=25620
  - quadrupole, meas. by Zeeman effect 8=47555
  - quadrupole, of simple mols. 8=47584
  - solutions, dipole moment heterodyne-beat apparatus 8=34892
  - tetrahedral mols., octopole, from virial coeffs. 8=29849
  - triethylamine-I_2 complexes, dipole 8=30511
  - trifluoromethylphosphine, dipole 8=25574
  - III-V cpds, bond dipole, rel. to second-order optical susceptibility 8=36314
  - AlO, electronic transition moment variation 8=43283
  - CH_3D, elec. dipole 8=38896
  - CHF_3, quadrupole, from microwave spectral broadening 8=29729
  - CO, dipole, function 8=47589
  - Fe(II) octahedral complexes, mag. moment 8=35038
  - H bond, induced dipole moment calc. 8=34219
  - H_2, polarizability 8=47600
  - HD, elec. dipole moment obs. 8=34242
  - H_2O, dipole, from i.r. absolute intensity meas. 8=38837
  - HPF_4, dipole 8=34279
  - ICl, elec. dipole, of $^3\Pi_1$ state 8=25488
  - N-methylpyrol, dipole moment 8=29798
  - $N_2(1+)$ band system, e transition moment obs. 8=34262
  - N_2O, quadrupole, from microwave spectral broadening 8=29729
  - NaF, MO calc. 8=34269
  - O_2^-, elastic coupling in KCl 8=48337
  - OCS, elec. dipole 8=47587
  - OCS, mag. susceptibility and quadrupole moment 8=25511

Molecules—contd
- **moments**—contd
  - OCS, quadrupole, from microwave spectral broadening 8=29729
  - PHF_2 and PDF_2, dipole 8=38849
  - S_2^-, paraelastic behaviour in KI 8=48336
  - $XeOF_4$, dipole 8=43339
- **nuclear coupling**
  - aliphatic fragment, spin-spin coupling 8=38943
  - allyl bromide, C-C-H and C-H coupling consts. 8=29813
  - p-benzoquinone, n.m.r. spin coupling constants, calc. using σ M.Q. theory 8=47690
  - cis-1-chloro-2-fluoropropene, Cl quadrupole coupling consts. 8=34320
  - 1-chloroaziridine, quadrupole coupling 8=25556
  - m-chlorobenzene, ^1H-^1H coupling constants 8=25641
  - contact spin-spin coupling, valence-bond theory 8=47565-6
  - difluoro-1-1-chloro-1-ethane, quadrupole coupling consts. 8=25575
  - dimethylamine, N^{14} quadrupole coupling consts. 8=47660
  - electron-nucleus interactions 8=47693
  - ethylene, n.m.r. spin-spin consts. calc. 8=25640
  - fluorinated methyl radicals, MO theory of hyperfine coupling consts. 8=47564
  - fluoroberyllate complexes, spin-spin coupling 8=48209
  - fluoro-organic solns. of free radicals, nuclear-electron interactions and molecular motion 8=39436
  - group VI cpds., indirect spin coupling 8=29822
  - heterocyclic anions, N^{14} hyperfine coupling factors 8=34340
  - hydrocarbon, saturated, p-p geminal coupling constant, calc. 8=47692
  - hydrocarbons, F-substituted, n.m.r. spin coupling constants, calc. using σ M.O. theory 8=47690
  - hydrocarbons, planar, long-range trans and cis coupling constants, analysis 8=47691
  - hydrocarbons, spin-spin coupling, CNDO calc. 8=47663
  - methane in solid Ar, nuclear-spin conversion 8=27634
  - methylated, dimeric trihalide of aluminium, Coriolis coupling coeffs. 8=43348
  - molecular rot. transitions, n.g. h.f.s. multiplets 8=34205
  - m-nitrobenzene, ^1H-^1H coupling constants 8=25641
  - n.m.r. spectra, methods of analysis 8=37541
  - n.m.r. spin coupling constants, calc. using σ M.O. theory 8=47690
  - organometallic cpds., C^{13} coupling consts. 8=38925
  - quadrupole coupling consts. calc. for polyatomic mols. 8=29809
  - relaxation mechanism in e.s.r. of liquids 8=34907
  - saturated hydrocarbons substituent effects on C^{13}-H^1 coupling 8=43343
  - solvent depend. of spin-spin couplings 8=43881
  - trans 1-bromopropylene, quadrupole coupling consts. 8=25550
  - trimethyl aluminium dimer, Coriolis coupling coeffs. 8=43348
  - Al_2Cl_6, Coriolis coupling coeffs. 8=43348
  - CH_3SeH, indirect spin coupling 8=29822
  - CN, σ-states, N^{14} quadrupole coupling 8=47710
  - $Cd(CH_3)_2$, indirect nucl. spin coupling consts. 8=43408
  - DF and DCl, calc. D quadrupole coupling consts. 8=38921
  - F hyperfine interactions in π-radicals 8=29816
  - $H-C{=}N^{15}$, relative signs of geminal coupling consts. 8=43409
  - $Mn_2(CO)_{10}$, quadrupole coupling effects in Mn^{55} n.m.r. spectrum 8=49653
  - N_2O, N^{14} quadrupole coupling const. 8=25505
  - NH_2CN, N^{14}-quadrupole coupling 8=43297
  - NH_4^+, relative signs of n.m.r. coupling consts. 8=29820
  - $NaSO_4$, Na^{23} quadrupole coupling 8=49667
  - $Se(CH_3)_2$, indirect spin coupling 8=29822
  - SeH_2, indirect spin coupling 8=29822
  - $Si^{29}H$ in $P(SiH_3)_3$ 8=34918
  - $Te(CH_3)_2$, indirect spin coupling 8=29822
  - VO ground state hyperfine interactions 8=25522
  - XY_6 type, Coriolis-coupling constants, mass effects 8=47688
  - XY_3ZW type, Coriolis coupling and shrinkage effects 8=25413
- **relaxation**
  - See also Acoustic wave propagation; Dielectric phenomena; Liquids/theory; Nuclear magnetic resonance and relaxation; Paramagnetic resonance and relaxation.
  - benzene, gaseous, radiationless transitions 8=25546
  - benzene, long transversal relax. time, obs. using spin-echo technique 8=48218
  - Bloch's magnetodynamic eq., two modifications and generalizations 8=47678
  - DNA, irradiated, e.s.r. obs. 8=34366
  - gases, radiationless transitions 8=25546
  - haloethanes, dielec. relax. in soln. 8=48184
  - intramolecular radiationless transitions 8=25406
  - liquid using neutron scattering 8=39305
  - long transversal relax. time, obs. using spin-echo technique 8=48218
  - methane, vibr.-vibr. relax. 8=25605
  - methyl and deuteromethyl radicals adsorbed on Si gel, e.s.r. spectra rel. to tumbling 8=25660

Molecules—contd
relaxation—contd
multiple processes, anal. 8=38906
multispin molecules with dissimilar nuclei 8=47694
nonlinear, n. m. relax. by spin-rot. interaction 8=29808
nuclear mag. relax. and dynamic nucl. polarization in free radical solns. of toluene 8=39439
spin-spin, problems and techniques 8=47676
stochastic model for low field resonance and relaxation 8=47673
time meas. from polarizability plot 8=43267
vibrational, anharmonic oscillators in collisions 8=29839
Ar plasma flow, non-equilibrium, shock heated 8=25741
Br_2, vibr.-relax. in Ar 8=47726
C_6H_6 on silica gel, proton spin relax. 8=29814
CO, vibr. relax. in nozzle flow 8=47586
CO_2, collisional relax. in 10^00 state 8=47715
H_2 and D_2, vibr. relax. isotope effect 8=34240
H_2O in electrolyte solns., intermolec. proton relax. rate 8=25957
Kr, collision-induced vibr. relax. 8=47754
N_2, effect of O atoms on vibr. relax. 8=47724
$OH^*(^2\Sigma^+)$ from photodecomp. of H_2O, rot. relax. 8=47613
rotation
acetonitrile, Brownian rotary motion, rel. to dipole-dipole intermol. forces in vibr. 8=43827
acetylene-t_2 8=25529
acryloyl fluoride, rotational isomers 8=38864
adiabatic rotations in unimolec. rate theory 8=41243
alkali halides, α_e calc. from Wasatjerna potential function 8=43324
alkali halides, parameter calc., improved potential function 8=43323
allene, barrier, SCF MO calc. 8=29764
allyl cyanide, microwave dipole moment obs. 8=34304
allene-h_4(-d_4), vib.-rot. transitions by i. r. spectroscopy 8=47633
asymmetric internal rotors, torsional effects 8=38788
asymmetric rotors, centrifugal distortion corrections, semi-classical theory 8=25419
asymmetric rotors, quadratic Zeeman effect 8=47555
asymmetric rotors, vibr. rot. calc. 8=25417
asymmetric tops, centrifugal distortion, sextic coeffs. 8=47563
benzene, intermolec. rots. and barrier heights, in solid and liq. form 8=43963
benzonitrile, Brownian rotary motion, rel. to dipole-dipole intermol. forces in vibr. 8=43827
bis(trifluoromethyl)-peroxide internal barrier 8=43366
trans 1-bromipropylene, barrier height 8=25550
3-butenenitrile, vibr. spectra and rot. isomerism 8=25551
2-butenes, barrier, steric effects 8=47698
centrifugal distortion consts., calc. method 8=34208
2-chloropropene-1, 3-d_1 8=25558
cis-1-chloro-2-fluoropropene, rot. consts. and internal barrier 8=34320
collision broadening of rot. and vibr.-rot. line shifts and widths 8=47556
collisional transfer of rotational energy 8=25662
conformational energy barriers in small mols. 8=25421
Coriolis reson. effect on symmetric-top transitions 8=34203
in crystal, rel. to packing density and diffusion rates 8=48767
cyclopentene, rot.-vibr. interaction and barrier to ring inversion 8=38878
diatomic, constants from spectra, computer programmes 8=38790
diatomic, most favourable orientation for vibr. transitions 8=43254
diatomic, prod. in breakup of 4-atom complex., vibr.-rot. populations calc. 8=29682
diatomic, rotational constants of normal electronic states, approx. determ. 8=43258
diatomic, spectrum computer analysis, line rot. quantum numbers 8=29684
1, 2-dichloroethane in various solvents potential barrier 8=43855
difluoro-1-1-chloro-1-ethane, microwave 8=25575
2, 2-difluoro-1-methylcyclopropane, internal barrier 8=29792
dimethylamine 8=25599
ethane-1, 1, 1-d_3 8=25570
ethylene, barrier, SCF MO calc. 8=29764
excitation and de-excitation by slow electron, absolute total cross section, energy and angular var. 8=43311
excitation by low-energy electrons 8=25418
formaldehyde, 3500Å $^1A_2 \leftarrow {}^1A_1$ transition 8=25581
of free radicals on recombination, n. m. r. obs. 8=38939
hindered internal rot., mols. with heavy groups 8=38789
inertial effects in discrete sites model of rot. freedom 8=25420
internal rotation, computer program 8=25423
isoxazole 8=25613
liquids, effects on n.m.r. relax. 8=39426
in liquids, influence on viscosity and shear relax. times 8=30426
liquids, rotationlike motion 8=48157

Molecules—contd
rotation—contd
matrix-isolated mols., rotation-translation coupling 8=27536
methane, compressed, correl. functions and intermolecular torque calc. 8=38894
methane in solid Ar 8=27634
methaneselenol, internal barrier 8=25602
methanol, torsion-vibr.-rot. interactions 8=47654
methyl BF_2, complex rel. to fine struct. in i. r. spectra 8=29793
methylamines, internal rot. effects in i. r. spectra 8=47655
methyl bromide, vibration-rotation spectra, near $600\ cm^{-1}$ 8=47659
methyl chloroform, microwave spectra and internal rot. 8=29773
methylcyclopropane, internal barrier 8=47665
1-methylpentaborane 8=29791
1-methylpentaborane, internal barrier 8=25600
methyl groups in radicals in irrad. chloro-acetyl DL-alanine irrad. crysts. 8=36240
methyl vinyl ether, internal barrier 8=29790
microwave transitions, radiation power and field change 8=25422
molecular-crystals, structure determ. from potential energy-rotation angle minima 8=26455
nearly-free, vibrational problem 8=34201
near-symmetric rotor in triplet state, rot. energy levels 8=25424
neopentane, methyl group librations, n scatt. obs 8=34345
neutron scatt. cross section, rot. correl. functions 8=43277
nitromethane, complex rel. to fine struct. in i. r. spectra 8=29793
nuclear quadrupole h.f.s. multiplets of mol. rot. transitions 8=34205
nuclear spin effects in molec. collisions 8=47723
nuclear-spin-species conversion, matrix isolation 8=38830
o-, m-, p-xylene solid, hindered rot. 8=31924
paracyclophanes, substituted, hindered rot. 8=34326
parahydrogen, solid, excitation theory 8=43967
phenol, coeffs., contrib. of internal rot. 8=47668
piperidine, non-rigid rotor transitions 8=25617
pivaldehyde, internal barrier 8=25618
p motions in hydrogeneous liquids by n scatt. 8=48065
polyatomic mols., anomalies in intensity distrib. of rot. -vibr. lines 8=43257
polymethylmethacrylate, internal rot. in side groups 8=38969
pressure broadening of rot. and vibr.-rot. transitions, scatt. theory 8=47558
propargyl alcohol, from microwave spectrum 8=43389
propionic acid 8=25620
propylene, deuterated 8=43390
restricted, factors and effects 8=43259
rotating resonance relns., 8=43261
rotational constants determ. 8=38794
rotational excitation of molecular ions by electrons 8=38785
rotator strengths, f-sum rule 8=29688
screw rotation coeffs. from lattice dynamical coeffs. 8=26569
selenophene 8=43395
$'\Sigma$-state diatomic mols., expectation values as functions of internuclear separation 8=29689
simple freq. standards for mm. waves 8=45959
small mols. in solvents, rotation-like motion, spectral evidence 8=25928
spectrum, collision-induced, theory 8=47658
s-tetrazine 8=25628
s-tetrazine, J-structure determ. of bond lengths 8=25627
stimulated Raman transitions, competition 8=25399
symmetric top mols., vibr. -rot. transition moment 8=29692
ternary symmetry, hyperfine structure of rotation levels, vibr. effects 8=29698
trifluoromethylphosphine, internal barrier 8=25574
vibration-rotation energy-level density calc. 8=29685
B_2Cl_4, from gas e-diffr. temp. dependence meas. 8=25446
BF_3 8=29715
BS 8=25448
BiF rotational structure of 2650-2850 A system 8=38813
C_2, dissoc. through rot. 8=29826
C_2 in acetylene-air flames, temp. by spectroscopic and thermocouple meas. 8=41877
C_2 mol., new $c'\,^1\Pi_g$-$b\,^1\Pi_u$ band syst. 8=29725
CF_2 8=25453
CF_3COOH-HCOOH, microwave spectra, K splitting 8=25577
CH in acetylene-air flames, temp. by spectroscopic and thermocouple meas. 8=41877
$(CH_3)_2CHX$, (X=halogen), internal barrier 8=25601
$(CH_3)_2CX_2$, (X=halogen), internal barrier 8=25601
CN^- in KCN, hindered, above 168°K 8=26030
CO, rel. to CS_2-O_2 chem. laser analysis 8=46569
CO, theory of order-disorder transition in solid 8=39546
CO, vib.-rot. constants 8=47589
CO_2, bands at 4.3μ 8=29730
$C^{13}H_3Cl$ 8=29794
$C^{12,13}O_2^{16}$, D_{eff} numerical values determ. 8=47592
Ca_2, rel. to orange bands 8=43296

Molecules—contd
rotation—contd
CaH and CaD 8=38820
CaO 8=34237
Co(III) complex, aquopentammine Co perchlorate of complex ion 8=26384
CrH, CrD structure obs. 8=47595
Cs_2, 6250Å band system 8=29733
$Cs^{133}F^{19}$, J=1 state, hyperfine struct. 8=43298
D_2, first excited $^1\Sigma^+_g$ state rot. and vibr. levels calc. 8=38823
F_2 8=29735
H_2, $B^1\Sigma_u^+$, $a^3\Sigma_g^+$ states, rot. energies 8=38827
H_2, first excited $^1\Sigma^+_g$ state rot. and vibr. levels calc. 8=38823
H_2, para and ortho, rotational excitation on collision with He 8=47720
HCl, first linewidths determ. 8=38825
HCl, second harmonic vibration-rotation band in liq., cubic, orthorhombic phases 8=25929
HD, elec. dipole moment obs. 8=34242
HF 8=29734
H_2O^{16} and H_2O^{18} 8=25478
H_2O vapour laser spectrum, transition 8=29741
HOCl 8=25475
HPF_4 8=34279
H_2S, elec. reson. 8=25483
H_2S_2 8=25485
Li^6F^{19}, elec. reson. 8=25483
N-methylpyrol, hindrance pot. of internal rot. from microwave spectra 8=29798
N, N-di-sec-alkyl amides, slow rot. around alkyl-N bond 8=38927
N_2, relax. in freejet expansion from sonic orifice, rel. to temp. 8=34629
N_2 in solid from meas. thermal capacity, 2.6–15°K 8=30967
NCN 8=25495
NCN_3 8=25496
ND, $(A^3\pi_i - X^3\Sigma^-)$ system, analysis of (2, 2) band 8=38843
NF, $b^1\Sigma^+ - X^3\Sigma^-$ band system 8=25497
NH_3, collision-induced transitions between rot. levels 8=47612
NH_3, lines, Stark effect observed by far i. r. laser 8=38845
NH_4 ions in NH_4 salts, barriers 8=48393
NO, resonance rel. to hyperfine elec. field meas. 8=38846
NO, rot. consts. 8=25500
NO_2 in cryst. N_2O_4 matrix, effect on e.s.r. 8=45095
$N^{15}O^{18}$, vibr. rot. bands 8=25502
OD^- in KCl, ang. correlation function of rotator 8=43968
OH^- in KCl, ang. correlation function of rotator 8=43968
OH and OD in solid Ne 8=32020
PO radical β-system obs. 8=34280
PO, rotational analysis of u.v. systems 8=34281
PHE_2 and PDF_2 8=38849
PtC 8=25513
RhC 8=25513
S_2, g-a system 8=38851
SF_5Cl, spectrum at 8 mm. 8=25515
SO, constants for $^1\Sigma^+$ state, obs. 8=38852
$SOCl_2$, rel. to spectrum, 8000-18000 MHz 8=43335
ScO, red system 8=25518
SiF, ν bands anal. 8=38855
SrO 8=34237
T_2, first excited $^1\Sigma^+_g$ state rot. and vibr. levels calc. 8=38823
vibration
acenphthenequinone, vibrational spectrum 8=43282
acetic acid, monomer and dimer, normal coords. 8=25531
acetonitrile, dipole-dipole intermol. forces and Brownian rotary motion 8=43827
acetylene monoderivatives, $C \equiv C$ group oscillation and absorpt. band calc. 8=34300
acetylene-t_2 8=25529
acrylonitrile-metal complexes, twist and wag 8=38865
actinide complexes, octahedral, free and in crystals, vibronic level Zeeman splitting 8=43964
aliphatic amines, normal coordinates calc. 8=38866
aliphatic mononitriles 8=38867
alkali halides, calc. from improved potential function 8=43323
alkali halides, ω_eX_e calc. from Wasastjerna potential function 8=43324
alkyl-Hg(II) cpds 8=43350
allene-h_4(-d_4), vib.-rot. transitions by i. r. spectroscopy 8=47633
αβ-unsaturated ketones, C=O and C=C, fundamentals and overtones 8=29788
aminopyridines and deuterated analogues, i.r. spectra 8=43391
anharmonic oscillator, vibr. relaxation, difference from harmonic oscill. 8=43263
anthracene-d_2(9, 10), i. r. vibr. spectrum, 400-3100cm^{-1} 8=38869
aryl-Hg(II) cpds 8=43350
bending, "nearly linear" formalism 8=25474
benzene and deuterobenzenes, new force consts. 8=38871
benzene, disubstituted, intramol., l.f.s. calc. from model 8=34317

Molecules—contd
vibration—contd
benzene, force consts. and normal coords. 8=29766
benzene, in inert-gas matrix, higher excited states 8=49770
benzene mixed isotropes, vibronic struct., static cryst. effects 8=49771
benzene-2, 1, 3-thio(seleno)diazoles, from i.r. and combination scatt. spectra 8=43356
benzenes, chlorinated, nonplanar group vibrs. 8=38872
benzenes, substituent effects on l. f. vibrs. 8=47642
benzonitrile, dipole-dipole intermol. forces and Brownian rotary motion 8=43827
benzyl, free radical 8=43420
benzyl radical, polarization of vibronic transitions 8=25549
benzyl and substituted benzyltin cpds. 8=29765
biacetyl, rel. to fluorescence spectrum at 100°C 8=43347
biphenylene 8=29770
biphenyl, fundamental freqs., normal coords. 8=34349
biphenyl, symmetry coords 8=43376
biphenyl, vibr. spectrum, re-anal. 8=34348
bismuthyl halides, rel. to i.r. absorpt. and Raman spectra 8=38812
bis(trifluoromethyl)-peroxide 8=43366
bond length and freq., empirical relation 8=38783
bromocyclobutane, and 3 isotopic species, freq. from i. r. spectra 8=29771
3-butenenitrile, vibr. spectra and rot. isomerism 8=25551
2-butenes, cis and trans 8=25552
carbonyl group of semicarbazides, semicarbazones and pyrazolecarboxamides, i. r. abs. 8=47645
2-chloropropene-1, 3-d_1 8=25558
collision broadening of rot. and vibr.-rot. line shifts and widths 8=47556
complex octahedral anions in crystals, cation effects from i.r. and Raman spectra 8=49683
Coriolis coupling consts., effect of orientation of degenerate coords. 8=34202
Coriolis interaction effects 8=38791
Coriolis reson. effect on symmetric-top transitions 8=34203
coronene in cryst. matrices, effect of thermal treatment 8=45242
in crystals, NQR investigations 8=27516
in crystal, thermal, rel. to periodic bond chain theory 8=26005
cubic XY_8, mean amplitudes 8=43262
cyanoacetylene, direct *l*-type doubling 8=34323
cyclic vicinal dihalogenides 8=34324
cyclooctanone, in crystalline phases above and below −87°C 8=26091
cyclopentene, ring puckering 8=34325
cyclopentene, rot.-vibr. interaction and barrier to ring inversion 8=38878
cyclopropane-H_6, vibr.-rot. bands 8=43363
deformation vibrations characterization by vectors nonperpendicular to bonds 8=29679
dialkyl disulphides 8=43349
dialkyl-Tl(III) cpds 8=43351
dialkylamido-transition metal cpds., metal-N_2 i. r. stretching frequencies 8=29712
diaryl disulphides 8=43349
diatomic, avoided crossings in potential energy curves 8=47557
diatomic, force consts. and zero-point energies calc. 8=25595
diatomic, most favourable orientation for transitions 8=43254
diatomic, potential energy and force consts. calc. 8=25426
diatomic, prod. in breakup of 4-atom complex., vibr.-rot. populations calc. 8=29682
diatomic, spectrum computer analysis, line rot. quantum numbers 8=29684
dichlorocarbene 8=29775
1, 2-dichloroethane, vibr. excited, from Hg-photosensitized dichloromethane 8=27761
dicyanodiacetylene Σ_g^+ modes, mean amplitudes 8=26031
diethylether, coordination compounds with Lewis acids, vibrs. sensitive to complex formation, i. r. spectra obs. 8=25569
difference band systems, temp. depend. of total intensity 8=25463
2, 2-difluoro-1-methylcyclopropane, torsional 8=29792
dimethylamine, inversion barrier 8=47660
dimethylphenylarsine 8=43381
di-n-butyl diselenide 8=43349
diphenyl-Tl(III) cpds 8=43351
ethylene and perdeuteroethylene 8=25573
excitation by low-energy electrons 8=25418
o-fluorobenzene, photoexcit., rel. to triplet state yield, gas-phase obs. 8=25630
force consts. calc. for mols. with free internal rotation 8=25427
force const. displays 8=43302
force constants of Si-O bonds, rel. to nature of substituents at Si and O 8=38784
force consts., multiplicity 8=29691

Molecules—contd
vibration—contd
force consts., perturbed Hartree-Fock calc. 8=25425
force field calc., improving convergence 8=29686
formaldehyde, normal-coordinate anal. of singlet excited state 8=43367
formaldehyde, 3500A $^1A_2 \leftarrow {}^1A_1$ transition 8=25581
Franck-Condon principle for polyatomic mols. 8=39030
furan, methyl-substituted, spectra interpret 8=43368
halides, Sc subgroup, freq. calc. 8=29761
hexafluorobenzene, photoexcit., rel. to triplet state yield, gas-phase obs. 8=25630
imidazole 8=29787
imidazole, H-bond freqs. 8=41165
inert-gas couples, translation band, transition probability at l. f. 8=29711
infra-red and Raman spectroscopy 8=24405
i.r. intensities correl. with chem. reactivity 8=43253
i. r. intensities, statistical errors in normal coords. 8=25435
isotopic mols., reduced partition function 8=29702
lanthanide complexes, octahedral, free and in crystals, vibronic level Zeeman splitting 8=43964
levels for pair of potential curves having small avoided crossing 8=25415
macromolecules, intramolec. energy functions for vibr. anal. 8=29861
mean amplitudes, comparison 8=29690
metal thiocyanate molten solns., force consts. 8=25934
methane in solid Ar 8=27634
methane, SCF-MO-LC(LCGO) calc. 8=47628
methane, vibr.-vibr. relax. 8=25605
methanes, substituted, force consts. and zero-point energies calc. 8=25595
methaneselenol 8=25602
methyl bromide, vibration-rotation spectra, near 6000 cm^{-1} 8=47659
methyl chloride, $2\nu_5$ band near 2880 cm^{-1}, parallel component 8=43374
methyl chloride, perturbations in ν_4 band 8=34334
methyl cyanide, direct l-type doubling 8=34323
methyl fluoride 8=43371
methyl halides, anharmonicity 8=38895
methyl halides, C-H bond, i.r. absorpt. intensities rel. to electron cloud distrib. 8=43373
methyl iodide, resonances perturbing ν_5 band 8=25594
methyl vinyl ether 8=29790
methyldiphenylarsine 8=43381
1-methylpentaborane(9), vibr.-rot. interaction 8=29791
methylstannane 8=43369
methylvinylsulphide 8=38899
mode interactions, anharmonic 8=25411
mono-deuterobenzene p-derivs., ν(CH) and ν(CD) 8=34315
monofluorobenzene, photoexcit., rel. to triplet state yield, gas-phase obs. 8=25630
naphthalene, symmetry coords. 8=43376
naphthalenes, isotopic, mean amplitudes calc. 8=43377
organotrichlorosilanes, l. f. vibs. 8=47620
oxalyl halides 8=24612
parahydrogen, solid, excitation theory 8=43967
perbromocyclopropane 8=25565
perchlorocyclopropane 8=25565
perfluorocyclopropane 8=25565
phenol, in ground and first excited state 8=25614
phenol, out-of-plane freqs. 8=43378
phenyl group IV-A cpds. 8=38901
o-phenylenebis(dimethylarsine) 8=43381
polyatomic, first approx. method for force field 8=47562
polyatomic, models, symmetry coordinates 8=25414
polyatomic mols., anomalies in intensity distrib. of rot. -vibr. lines 8=43257
polyatomic, use of dependent coords. 8=47561
polymer chain, dispersion curves and freq. distrib. 8=38975
polymers frequency distributions 8=47736
polymers, random, freq. distrib. 8=38970
polyvinylchloride, normal vib. anal. rel. to conformational struct. 8=43436
potential energy calc. 8=38799
pressure broadening of rot. and vibr.-rot. transitions, scatt. theory 8=47558
pyridazine, and deuterium analogues 8=25933
pyridine derivs., ν(CH) bands near 3000 cm^{-1}, i. r. absorpt. study 8=29799
pyridine, photoexcit., rel. to triplet state yield, gas-phase obs. 8=25630
pyrimidines, polysubstituted, i. r. spectra in 700-200 cm^{-1} range 8=47670
quinoline and isoquinoline, at liq. N_2 temp., interpret. and i. r. spectra 8=34362
rare-earth halide-terpyridyl complexes 8=41131
redundant coords. in harmonic approx. 8=47559
relaxation of anharmonic oscillators in collisions 8=29839
rigid-body motion analysis in crystals 8=26028
$^1\Sigma$-state diatomic mols., expectation values as functions of internuclear separation 8=29689
silacyclobutane, ring puckering 8=29800
silicate glasses, containing As, Sb oxides, vibr. and struct. 8=31964
stimulated Raman transitions, competition 8=25399

Molecules—contd
vibration—contd
symmetric top mols., vibr. -rot. transition moment 8=29692
symmetric tops, computer anal. of bands 8=25412
symmetric tops, Coriolis reson., computer anal. 8=25416
ternary symmetry, hyperfine structure of rotation levels, effects 8=29698
tert-butylropenyl radicals, vibronic near degeneracy 8=38944
tetracyanoethylene, assignment on basis of i. r. polarized spectra of charge transfer complexes 8=38879
tetrahalogens correl. between mean amplitude quantities and bond covalency 8=34228
tetrahydrofuran and deutero-substitutes, spectra interpretation 8=43397
tetraiodoethylene, vibrational spectra and force consts. 8=43396
tetraphenylbutadienes, effect of intramolec. twisting on fluoresc. 8=39390
s-tetrazine 8=25628
theory, second-order secular eqn. 8=34204
thiophene, monoalkyl substitutes, oscillation spectra 8=34364
toluene, photoexcit., rel. to triplet state yield, gas-phase obs. 8=25630
transition probabilities in molec. collisions, WKB calc. 8=38953
1, 3, 5-trichlorobenzene, NQR investigation 8=27516
trichloromethyl radical in solid Ar 8=29831
trifluoromethylphosphonylchloride 8=34330
trimethylene selenide, ring-puckering 8=29802
triphenylarsine 8=43381
triphenylarsine, mol. addition compounds with SnX_4 (X=halogen), i. r. spectra obs. 8=25631
triphenylphosphine, and complexes 8=43380
triphenylphosphine, mol. addition compounds with SnX_4 (X=halogen), i. r. spectra obs. 8=25631
triphenylphosphine oxide, and complexes 8=43380
uranyl cpds., bending freq. and U-O bond distance calc. 8=34287
urea and deuterated urea, spectra, force constants and mean amplitudes of vibrs. 8=38904
vibration-rotation energy-level density calc. 8=29685
vibrational excitation of molecular ions by electrons 8=38785
vinyl fluoride and deuterovinyl fluorides, normal coords. 8=25632
zig-zag chains, randomly folded, vibr. freq. 8=47735
AsH_3, K-type doubling in ν_3 band 8=25445
AsI_3, far i. r. cryst. spectra 8=45223
BF_3-dimethyl selenide and sulphide complexes 8=38806
BO_4 group complexes, asymmetric stretching, rel. to i. r. spectra 8=29714
B_2O_3 in crystallite from radial distrib. functions, rel. to lattice dynamics contrib. 8=44206
Ba tetraoxometalates 8=31965
Be halides 8=25449
BeF, ground state reduced potential curves 8=29717
BeH_2, diatomics-in-mols. calc. 8=25450
$BiCl_3$, far i. r. cryst. spectra 8=45223
Br_2, vibr. relax. in Ar 8=47726
C_2 in acetylene-air flames, low press., spectroscopic and thermo-couple meas. of temp. 8=41877
C_2 mol., new $c'\,{}^1\Pi_g$-$b^1\Pi_u$ band syst. 8=29725
CCl_4, Raman intensity in various solvents 8=30488
$C_6D_5GeCl_3$ 8=25615
$C_6D_5GeCl_3$ 8=34351
CF_2 radical 8=29723
CF_3 radical 8=29723
$(CF_3)_4As_2$ 8=25604
CF_3SF_5 8=25516
CH force consts. 8=29789
CH in acetylene-air flames, temp. by spectroscopic and thermocouple meas. 8=41877
CH_3 in methyl aromatic hydrocarbons 8=29789
CH_3 one and two top mols., torsional vibr. 8=25601
C_2H_6, CH_3CD_3, and C_2D_6, torsional vibr. 8=29778-9
$C^{13}H_3Cl$ 8=29794
$(CH_3)_3CNCO$ 8=29732
C_7H_6D radical, vibronic near degeneracy 8=47706
in CH_2I_2, crysts., and lattice vibr., n inelastic scatt. obs. 8=35385
in CH_3I, crysts., and lattice vibr., n inelastic scatt. obs. 8=35385
CH_3NF_2 and CD_3NF_2, rotational coupling 8=25597
$(CH_3)_2NPX_2$. (X=F, Cl, Br), from i.r. spectra, fundamentals assignment 8=43372
CH_3OPCl_2 8=38892
CH_3SiHD_2 8=34338
CH_2X, hybrid orbital force field calcs. 8=29781
ClCO radical, potential functions calc. 8=47713
$ClSi(NCO)_3$ 8=29732
Cl_3SiNCO 8=29732
Cl_3SiNCS 8=29732
CN, 10th level of $A^2\pi_{3/2}$ state, transitions between hyperfine levels of $J=7/2$ γ doublet 8=38819
CO, adsorbed on Si-supported Pt 8=30773
CO, rel. to CS_2-O_2 chem. laser analysis 8=46569

- **Molecules**—contd
  - **vibration**—contd
    - CO, vib.-rot. constants 8=47589
    - CO, vibr. relax. in nozzle flow 8=47586
    - CO_2, anharmonic force consts. 8=43292
    - CO_2, bands at 4.3μ 8=29730
    - CO_2, collisional relax. in $10^{0}0$ state 8=47715
    - CO_4 group complexes, asymmetric stretching, rel. to i.r. spectra 8=29714
    - C_3O_2, amplitudes and shrinkage effects, temp. effect 8=25466
    - C_3O_2, mean amplitudes and shrinking effects 8=25465
    - $^{12}C^{16}O_2$, analysis 8=47590
    - COF_2, $COCl_2$ and $COBr_2$, integrated intensities 8=38875
    - CO_2 + N_2O, near-resonant energy transfer between i.r.-active vibrs. 8=47725
    - CS, ground state reduced potential curves 8=29717
    - C_3S_2, mean amplitude rel. to temp., from spectrum obs. 8=43290
    - CaO 8=34237
    - $Ca(OH)_2$ 8=27563
    - $CaSO_4.2H_2O$, i.r. combination vibr. spectrum, 10,000-12,000 cm^{1} 8=41074
    - $Co(CO)_3NO$, symmetry force consts. 8=48161
    - Cs_2, 6250Å band system 8=29733
    - D_2, first excited $^1\Sigma^+_g$ state rot. and vibr. levels calc. 8=38823
    - D_2O deform. vibrs. characterization by vectors nonperpendicular to bonds 8=29679
    - D_2S_2, force field from i.r. spectra 8=43331
    - D_2S, ν_2 fundamental 8=25484
    - FCN, direct l-type doubling 8=34323
    - F_2CN, matrix-isolated 8=38946
    - FCO radical, potential functions calc. 8=47713
    - GF method generalisation, inter- and intramolecular coupling 8=43961
    - GeO, ground state reduced potential curves 8=29717
    - H-bonded systems, theory of i.r. spectra 8=38787
    - H halides, correl. between mean amplitude quantities and bond covalency 8=34228
    - H_2, $B^1\Sigma_u^+$, $a^3\Sigma_g^+$ states, vibr. energies 8=38827
    - H_2, first excited $^1\Sigma^+_g$ state rot. and vibr. levels calc. 8=38823
    - H_2, large vibr.-rot. interaction effects in Franck-Condon factors 8=43304
    - H_2 and D_2, chemisorbed on Rh 8=25470
    - H_2 and D_2, vibr. relax., isotope effect 8=34240
    - H_2^+ and D_2^+, vibr. struct. 8=39034
    - HCCH, isotopic, force const. displays 8=43302
    - HCN, bending, "nearly linear" formalism 8=25474
    - HCO radical, potential functions calc. 8=47713
    - HCP, bending, "nearly linear" formalism 8=25474
    - HD, and D_2 8=25471
    - HDO deform. vibrs. characterization by vectors nonperpendicular to bonds 8=29679
    - HF, nuclear shielding and spin-rot. consts., vibr. corrections 8=38924
    - H_2, HD and D_2, vibr. consts. of singlet states 8=43305
    - HCl, second harmonic vibration-rotation band in liq., cubic, orthorhombic phases 8=25929
    - H_2O, bending, "nearly linear" formalism 8=25474
    - H_2O deform. vibrs. characterization by vectors nonperpendicular to bonds 8=29679
    - H_2O, isotopic, force const. displays 8=43302
    - HOF, potential function 8=43299
    - H_2O, D_2O, and HDO. i.r. intensities in solid films 8=36369
    - H_2O, HDO and D_2O in non-aq. solvents, i.r. intensities 8=39377
    - H_2O-H_2O collisions, vibr. transition probabilities 8=34389
    - in $H_3O.NO_3$ crysts., and lattice vibr., n inelastic scatt. obs. 8=35385
    - H_2S, accidental Coriolis resonance 8=25482
    - H_2S_2, force, field from i.r. spectra 8=43331
    - H_2S, isotopic, force const. displays 8=43302
    - H_2Se, isotopic, force const. displays 8=43302
    - I, deactivation depend. on ratio of collision time to period of vibr. 8=34252
    - I_2, freq. shift of stretching vibr. in liq. mixtures 8=34875
    - I_2Cl_6 8=45195
    - ICN charge-transfer complexes 8=48163
    - N_2, effect of O atoms on vibr. relax. 8=47724
    - N_2, vibr. excited, reactions with He^+ and O^+ 8=41253
    - NF, $b^1\Sigma^+$-$X^3\Sigma^-$ band system 8=25497
    - NF_3, force field 8=43319
    - NH_3 adsorbed on Si, rel. to bonding strength 8=25508
    - NH_3, anharmonic effects on thermodynamic props. 8=47960
    - NH_3 and ND_3, anharmonic consts. 8=29753
    - NH_3^- groups in sulphonic acids 8=29801
    - NH_4 quaternary halides, ν_{C-N} and δ_{C-N} 8=38844
    - N_2 discharge, evidence for $^3\Delta_u \rightarrow B^3\Pi_g$ transition 8=47608
    - $N_2H_4^+$, torsional 8=47685
    - NO_3 in $NaNO_3$, KNO_3 and $CsNO_3$ near 600°C, i.r. spectroscopic emission obs. 8=38842
    - $N^{15}O^{18}$, vibr. rot. bands 8=25502
    - $NaClO_3$, i.r. reflectance bands, dispersion anal. 8=27593
    - $Ni(CO)_4$, force consts. from vibr. spectra of isotopic species 8=34270
    - O_2^+ state, vibrational constants 8=25512

- **Molecules**—contd
  - **vibration**—contd
    - O_3 8=34278
    - P_2, ground state reduced potential curves 8=29717
    - PO radical β-systems obs. 8=34280
    - PX_5, force fields 8=38850
    - Pt-ammine complexes 8=43330
    - S_6, force and torsional consts. comparison with S_8 values 8=43332
    - $S(CN)_2$, force field and Coriolis coupling coeffs. calc. 8=43333
    - SF_5Cl 8=25516
    - SO, constants for $^1\Sigma^+$ state, obs. 8=38852
    - SO_3^- groups in sulphonic acids 8=29801
    - $SPCl_2F$ 8=25517
    - $SPCl_3$ 8=25517
    - $SPClF_2$ 8=25517
    - SbF_3 normal oscillation freq. calc. 8=34283
    - Sc subgroup halides, freq. calc. 8=29761
    - SeF_6, force fields 8=25519
    - SeO, force constants. correl. with SO 8=38854
    - SiF_2 8=25520
    - SiN, ground state reduced potential curves 8=29717
    - SiS, ground state reduced potential curves 8=29717
    - SnBr, $B^2\Sigma$-$X^2\pi$ system, from u.v. absorpt. spectra 8=34284
    - SnH_3CH_3 and $SnCl_3CH_3$, force consts. 8=38890
    - SnI_4, far i.r. cryst. spectra 8=45223
    - SnI, $B^2\Sigma$-$X^2\pi$ system, from u.v. absorpt. spectra 8=34284
    - SrO 8=34237
    - T_2, first excited $^1\Sigma^+_g$ state rot. and vibr. levels calc. 8=38823
    - Te cpds., isotope effects 8=41234
    - $TeBr_4$, far i.r. cryst. spectra 8=45223
    - $TeCl_4$, far i.r. cryst. spectra 8=45223
    - $ThCl_6^{2-}$ 8=47619
    - UCl_6^{2-} 8=47619
    - WCl_6, fundamental modes assignment. obs. 8=38859
    - WF_6, force fields 8=25519
    - X_2O_7-type, vibration spectra and chemical structure 8=47475
    - XY_4 type force consts. and vibr. amplitudes 8=34206
    - XY_4-type of T_d symmetry, vibr. amplitudes and Coriolis coupling 8=43256
    - XY_n-type, mass influence on Coriolis coupling 8=43260
    - XY_3Z type Si cpds., and Coriolis coupling consts., mean amplitudes 8=38786
    - XY_3ZW type, mean square amplitudes and shrinkage effects 8=25413
    - XeF_6, from gas-phase electron diffr. 8=34290-1
    - XeF_6, inversion 8=25523
    - XeO_4, root-mean-square amplitudes 8=34289
    - $XeOF_4$, vibr. satellites 8=43339
- **Molecules, mesic and muonic**
    - S states involving H isotopes, p.μd ground state rel. to N-D capture and pμd fusion 8=42632
    - water, with K^+, π^+ or Σ 8=29872
    - π^- by H in hydrogenous substs 8=47739
- **Mollier diagrams**. See Thermodynamic properties.
- **Molybdenum**
    - absorpt. of K ions, 960-1200°K 8=30770
    - adsorption of O_2 on (100) face 8=35195
    - adsorption of O_2, CO_2, N_2 and N, on (001) and (110) faces 8=41269
    - analysis of O content by He^3 irrad. 8=27818
    - breakdown and pre-breakdown voltages of electrodes in vacuum, effect of conditioning processes 8=34426
    - catalysis of H_2 + D_2 $\rightleftarrows$ 2HD reaction 8=49907
    - catalysis of NH_3 synthesis 8=49909
    - catalysis of N_2^{28} + N_2^{30} $\rightleftarrows$ N_2^{29} reaction 8=49908
    - cladding of steel, shock wave technique 8=28206
    - collector in thermionic diode, effective work function, comp. with Ni 8=31460
    - corrosion resistance of austenitic stainless steel, influence 8=49867
    - creep properties at 650-750°C 8=35707
    - crystal, X-ray topographic investigation 8=35274
    - crystals, deformed in tension, slip line pattern and active systems 8=31091
    - deformation under hydrostatic press., struct. rel. to plasticity, $<$18 kbar 8=35562
    - dendrites, structure and morphology 8=48568
    - diffusion of C, mobility determ. from low-temp. internal friction peaks 8=35513
    - diffusion of S, 2220-2470°K 8=35502
    - diffusion of Si, phase identification 8=48784
    - dislocation velocity stress dependence at 77 and 300°K 8=26684
    - electron emission, Auger, on bombardment by positive, electronically excited ions 8=27358
    - electron emission, Auger, on bombardment with positive ions, rel. to incident angle 8=27357
    - electron emission from (110) and (111) faces 8=36036
    - extruded, hydrostatically, annealing effects on ductility 8=35705
    - extruded hydrostatically, mech. props. 8=35706
    - Fermi surface 8=49104
    - Fermi surface and correlation effects in optical props. 8=36392
    - films, resistance and work function rel. to adsorpt. of Ba, O_2 and BaO 8=40322

Molybdenum—contd
- films, sticking probabilities of N_2 8=30771
- foil, Hg quenching 8=31218
- isochromat obs. 8 kV 8=45227
- lattice consts, densities and thermal expansions, effect of solution of S, Se and Te 8=48664
- lattice parameters rel. to temp. 8=44233
- in liquid steel, conc. rel. to C activity 8=30458
- lubrication at high temp., by exposure to H_2S and film form. 8=31219
- neutron irradiation creep obs. at 100℃ 8=26833
- (001) and (110) surfaces, damage due to Ne^+, Ar^+, Kr^+ or Xe^+ bombard., study by LEED 8=26104
- optical consts., reflectance meas. 537-5770Å 8=27591
- orientation when deposited from MoF_6, rel. to temp. and annealing 8=35154
- permeation, diffusion and soln. of N 8=39987
- permeation of H 8=39986
- radiation defects, thermal stability 8=40077
- scattering of K^+ ions, ang. depend. of energy spectra of secondary ions 8=40719
- silicides, electron microprobe identification 8=48389
- solubility of IV A-group metal carbides 8=48344
- sorption of N_2 8=49908
- spectrum, successive onsets rel. to excitation pot. 8=29643
- sputtering by Ar^+ ions, mechanism 8=35606
- substrate for Ir thin films, field-ion microscope study 8=48452
- surface diffusion, activation energy elec. field dependence, (10^7–10^8V/cm), 1300–1800°K 8=35512
- thermal emittance of small cavities in surface, rel. to temp. 8=26611
- thermal expansion coefficient 8=44233
- thin film resistors, for integrated circuits, fabrication and props. 8=44693
- vacuum-gap cathode erosion by discharge 8=34424
- wetting by Cs and Na, rel. to bare work function 8=35168
- wire, Hg quenching 8=31218
- work function and desorpt. energies of O_2, thermionic meas. 8=31469
- work-functions for clean and gas-covered Mo 8=34422
- Cs adsorpt. and work function, theory comp. with expt. 8=31466
- Kr ion sputtering, ang. distrib. obs. 8=48909
- Mg ion sputtering, ang. distrib. obs. 8=48909
- Mo-gate m.o.s.f.e.t., self-registered 8=49316
- Mo(111), faceting from CO adsorpt. 8=48486
- Mo^{5+}, paramag. relax. in TiO_2 8=36247

Molybdenum compounds
- arsenate complexes, e.s.r. spectrum, superfine structure 8=45099
- molybdenite cleavage surfaces, LEED exam. 8=26199
- molybdenite cleavage surface. LEED study 8=48524
- molybdenite films, thick, electron microscopy at 50-1200 kV 8=48602
- pentavalent, containing dimeric and monomeric oxygen, e.s.r. 8=47677
- permalloy tapes, rolled 4-79, magnetostriction and coercivity, process variables dependence 8=31658
- $K_4Mo(CN)_8 . 2H_2O$, mol. struct. 8=43317
- Mo bronzes, electronic struct. 8=40245
- Mo complex halides, electron spectra 8=38857
- Mo complex, π-cyclopentadienyl molybdenum tricarbonyl chloride, crystal structure 8=26488
- Mo complex, thiocyanate, $K_3Mo(NCS)_6H_2O . CH_3COOH$, crystal structure 8=26410
- MoC, supercond., upper critical fields at 4.2°K 8=27018
- Mo_2C, supercond., upper critical fields at 4.2°K 8=27018
- Mo_2C in Cs vapour, e- and ion-emission rel. to other refractory metal cpds 8=27350
- Mo_6Cl_{12}-2, 5-dithiahexane complex, i.r. spectrum 8=43318
- $Mo(CN)_8^{4-}$, spectra and struct. 8=41118
- MoCoB and related $PbCl_2$-type crystals, crystal structure 8=39809
- Mo_3CoSi, crystal structure 8=35342
- Mo-Fe solid soln, precipitation behaviour and lamellae form 8=35115
- $Mo_{13}Ge_{23}$, crystal structure 8=39782
- $MoNb_{15}O_{40}F$, crystal structure 8=44232
- MoO_2, distorted rutile, metal-metal bonding 8=48305
- MoO_3, optical absorpt. and photocond. for films and crysts. 8=32013
- $Mo_3O_4(C_5H_7O_2)(C_2H_5O)_3$, crystal structure 8=26461
- $MoOF_5^{2-}$ ions, X- and Q-band e.s.r. spectra, comparison 8=38911
- MoS_2, lattice parameter meas. 8=44231
- MoS_2, molybdenite, surface point defects and non-basal dislocations 8=35526
- MoS_2, spherically bent cryst., soft X-ray spectroscopy 3 to 30Å 8=32033
- $MoSi_2$ in Cs vapour, e- and ion-emission rel. to other refractory metal cpds 8=27350
- $MoZn_{\sim 22}$, crystal structure 8=44230

Monitoring. See Radiation monitoring.

Monochromators
- See also Filters, optical; Light sources; X-ray monochromators.
- for cathodoluminescence meas., e microprobe monochromator-photomultiplier attachment 8=36463

Monochromators—contd
- constant output, 100 ± 2μW 8=28810
- monochromatic generation by amplitude modulation 8=24355
- neutron, curved-slit chopper 8=24985
- neutron, double reflection appratus 8=24977
- rapid-scan, for analyzing chemical lasers 8=28816
- Seya-Namioka, for vac. u. v. 8=33264
- single, instrument function for partially-coherent illum. of entrance slit 8=24400
- two-beam, with compensating recorder 8=24393
- u. v., spurious obs. of scatt. light 8=28807
- x. u. v., concave-grating mounting 8=28808

Monolayers. See Adsorbed layers.

Monomers. See Molecules.

Monomolecular layers. See Adsorbed layers.

Monte Carlo method. See Statistical analysis.

Moon
- absolute coordinates for 917 lunar features 8=45813
- attitudes, relative, meas. and reduction 8=28142
- basalt in ultra high vacuum, strength characts. 8=41320
- Birt crater, anomaly in length of internal shadow 8=50399
- bow and wake shock waves, hypothesis for absence 8=36997
- capture by earth, theory and geophys. consequences 8=50401
- capture hypothesis 8=36993
- cis-lunar space, zodiacal dust meas. by OGO III and Mariner IV, (1966) 8=37034
- by cosmic rays, nuclide prod. on surface 8=37025
- Copernicus crater, cometary impact origin 8=32526
- crater array analysis 8=28146
- craters, computer simulation 8=45816
- craters, dark-haloed, origin 8=36991
- craters diameter-frequency relation, photographed by Rangers VII, VIII and IX 8=45810
- craters, large, surface density 8=45808
- dimensions and geometric shape, anomalies obs. 8=45802
- diurnal atmospheric tide 8=36992
- earth-moon system, early history from waves in marine sandstones and calcarenites 8=50115
- to earth, return trajectoreis from surface and satellite orbits 8=32375
- eclipse of 1964 Dec. 19, occultation obs. 8=45807
- electrical conductivity 8=37002
- elevation profiles by isodensitometry, Ranger 9 photographs 8=28144
- emission, mm and sub-mm range 8=45804
- Encke C region, crater alignments 8=41554
- γ-ray intensities due to Al^{26}, Na^{22}, Mn^{54} 8=32531
- γ-ray obs. 8=45795
- glows, transient, due to bombard. of surface by solar protons 8=28145
- ground, struct. and mech. props., density of surface layer, meas. from 'Luna 13' 8=36995
- Hamsteed region, crater alignments 8=41554
- Herodotus and Schroter's valley, obs. 8=32528
- hot spots during eclipse, temp. enhancement proportional to crater depth/diam. ratio 8=36998
- interplanetary mag. field, perturbations by lunar wake 8=37031
- interplanetary matter in vicinity, density rel. to halo or passage thro' dust cloud 8=37033
- isodensitometry charting and relative heights meas. 8=28143
- isostatic equilibrium, model 8=32527
- Laser ranging for earth gravitational/inertial mass ratio meas. 8=41748
- libration in longitude, approx. soln. 8=28138
- lunar radial bands, dark, formation 8=45805
- magnetic field in solar wind wake 8=50395
- magnetic field structure in plasma void leeward of solar wind, model 8=41559
- magnetic tail and wake 8=32529
- magnetospheric interaction with solar wind, models 8=41558
- maria and craters rel. to collision with ice 8=45815
- meteorite impact density 8=45814
- meteorite origin 8=50432
- observation when highly illuminated 8=32525
- occultations, tables for 1966 at Sydney Observatory 8=50398
- orbital history and new integrals of motion 8=41556
- outgassing, frequency limit of bursts 8=41553
- phase, effect on amplitude of type Pc stable pulsations, statistical study 8=45565
- photoelectron atmos., density rel. to height, models 8=45809
- photography, earth-based high-resolution 8=28137
- photography, light rays struct. anomalies rel. to craters struct. 8=45801
- photography, techniques and results 8=36994
- Plato J, nature of crater 8=50397
- profile deviations from circle, annular solar eclipse January (1963) 8=28319
- proton and electron intensities in vicinity, meas. from Luna II 8=37060
- radar aperture synthesis, appl 8=32616
- radar astronomy, two-dimens. aperture synthesis and brightness distrib. 8=32524
- radio scattering cross section, models in optical range 8=45803

Moon—contd
- reflection coeff. of upper layer 8=28136
- rille pattern in crater Humboldt 8=37001
- ring structures and nature of maria 8=41555
- sedimentary rocks, obs. evidence 8=32532
- shadow, accuracy estimates 8=45818
- shadowing of energetic particles obs. 8=37003
- soil, particle size distrib. 8=32530
- solar wind, magnetized, free molecule flow 8=37058
- spectra, Fourier i. r. obs. 8=28780
- specular reflection, lunar satellite tracking possibility 8=50394
- star occultation time, effect of gravit. deflection of light 8=32801
- surface 8=45806
- surface characteristics inferred from optical properties 8=50400
- surface, colour opposition effect obs. 8=45812
- surface material size distribution, Surveyor I data interpretation 8=36995
- surface metals distrib., Surveyor V obs. 8=28140
- surface, nocturnal heat sources 8=41557
- surface, photometric props., in situ meas. 8=36999
- surface samples, contamination by lunar module exhaust 8=37000
- surface, thermal behaviour of rock on equator 8=45811
- thermal history, effects of selective melting 8=50403
- three-channel photoelec. spectropolarimeter obs. 8=36921
- topography, grand-based photography under oblique illum. 8=28141
- transient phenomena obs. 8=50396
- transient phenomena, possibility of explanation by gaseous volumes 8=45817
- solar cells and arrays for lunar surface operations 8=24098
- USSR radioastronomical apparatus and obs. 8=32523
- rel. to vertical deviations of astronomical obs. 8=36924

Morse potential. See Kinetic theory; Molecules/intermolecular mechanics.

Mosaic structure. See Crystal structure/microstructure.

Mössbauer effect
- See also Gamma-rays/absorption; nuclear excitation.
- alkali halides, quadrupole splitting, and elec. field gradient at (100) surface 8=30717
- Alni alloys, chem. comp. and magnetization ageing dependence 8=49514
- benzene, supercooled glassy and polycrystalline states, obs. of mol. motion 8=43751
- chalcopyrite, $CuFeS_2$, spectra, 300-448°K 8=26019
- cryostat, demagnetization, ≥ 0.025°K 8=37330
- crystal lattice interference effects 8=48320
- using cryostat, He^3/He^4 dilution refrigerator, for expt. at 0.03°K 8=41880
- cytochrome c, Fe spectra 8=48331
- Debye-Waller factor in single crystal absorbers, obs. 8=39745
- emission from atoms in relaxing localized modes 8=48319
- Faraday effect 8= 45158
- with Faraday rotation 8=45157
- ferrites, Ga substituted, obs. on Fe^{57} 8=30624
- for ferromagnesian silicate abundance in bronzite chondrites obs. 8=45847
- ferro-spinels, quadrupole splitting of spectra 8=43942
- gadolinum garnet: Sn^{119}, effective mag. field change at compensation point 8=49469
- glycerol, supercooled, glassy and polycrystalline states, obs. of mol. motion 8=43751
- ice: Sn(IV), conc. depend. of isomer shifts 8=43957
- iron-stilbene, 3°-310°K. obs. 8=30641
- limonite, study 8=35031
- local environment effect on ang. distrib. of resonantly scatt. γ-quanta 8=39511
- low-temp., closed-cycle He refrigerator 8=46301
- magnetic-field-induced quadrupole splitting 8=43939
- magnetically ordered systems, absorpt. spectra rel. to spin relax. 8=43940
- metallic matrices, of Sn^{119} and Au^{197} impurity, interpret. of isomer (chem) shift 8=48318
- methane I^{129} derivatives 8=48332
- natural line widths of Mossbauer absorbers at variable low temps. 8=30635
- nucleus, refined constitution analysis methods 8=49624
- optics, gamma-ray and x-ray, quantum theory 8=30636
- orthopyroxenes cation distribution determ. 8=48324
- oscillations of separate atoms in system, and effective Debye freq. 8=39509
- paramagnetic and magnetically ordered substs., spectrum rel. to atomic spin time fluctuations 8=30642
- peroxidase and derivs. rel. to spin states 8=29823
- Prussian blue and Turnbull's blue 8=39518
- radiation, rel. to quantized space-time 8=24689
- rare-earth iron garnets: Eu^{153}, rel. to exchange interaction determ. 8=36194
- rare earths, electronic shielding 8=39508
- review of study of nuclear hyperfine interactions in solids 8=48317
- solid solns. order-disorder transforms. effects 8=35032
- solid state applications, review 8=43938
- source Doppler shift, data reduction, graph method 8=38350

Mössbauer effect—contd
- spectra in presence of e.s.r. 8=35030
- spectral parameters and standard errors using least-squares method 8=47044
- spectrometer, velocity calibration, interferometric method 8=37927
- spectrometer, with constant velocities ≤ 30 cm/sec 8=47062
- spectrometer, with constant velocity or constant acceleration 8=47052
- spectrometry, electromech. servomechanism 8=37783
- spectroscopy using high-field superconducting magnets 8=37387
- surface chemistry, review, 8=49902
- time correlation function formalism 8=29386
- zinnwaldite mica, absorpt. spectra 8=43960
- AgCl, Fe impurity ions 8=39510
- Al-Fe alloy, Fe precip. exam. 8=30678
- Al_2O_3:Fe^{57}, heat treatment effects rel. to iron clustering and cation valence states 8=43943
- Au_4V, of Au^{197} rel. to V moment determ. 8=26016
- $BaTi_{0.75}Sn_{0.25}O_3$ solid soln., temp. depend. rel. to dielec. props., —200 - 20°C 8=30639
- $CeSn_3$, of Sn^{119}, phases at 4.2°K 8=43944
- Co^{57} sources, mag., r.f. mag. fields effects 8=43945
- Co complex, bispyridinooobalt(II)dichloride, structural isomers, rel. to intermolecular interaction 8=29837
- β-Co, superparamagnetism obs. 8=49521
- $CoFe_2O_4$, ferrimag. spinel, cation distribs. in octahedral and tetrahedral sites, determ. 8=35035
- Co_2MnSn, Heuser alloy 8=35033
- CoO, containing Fe, multiple charge states 8=39521
- CoO(I) and (II), hyperfine spectra of Fe^{57} below Neel temp. 8=26018
- CoO(I) and (II), rel. to valency states 8=26017
- Cr_2O_3-Fe_2O_3 system, magnetic structure 8=27444
- Cu-Fe alloys, "doublet" line structure 8=39512
- Cu : Fe^{57}, f number and isomer shift pressure dependence 8=48321
- Cu: Fe, rel. to spin compensated state 8=35036
- $CuFe_2S_3$, rel. to antiferromag. ordering 8=40864
- $Cu_{1-x}M_xFe_2O_4$, (M = Cu, Zn, Cd), Fe^{57} resonance, 4.2-1000°K 8=31907
- Cu-Ni-Fe alloys, "doublet" line structure 8=30512
- Dy^{161}, 74.5 keV level, g factor, elec., mag. moment obs. 8=25150
- Dy ethyl sulphate, paramag. relax. 8=27472
- $DyFe_2$, rel. to hyperfine fields at Fe 8=36146
- $ErAl_2$, ferromagnetism and ferromag. relax. study 8=49518
- $ErAl_3$, rel. to Er spin relax 8=31864
- $ErFe_2$, rel. to hyperfine fields at Fe 8=36146
- Eu^{2+} and Eu^{3+}, electron transitions, isotopic shifts and changes in nuclear radii 8=48322
- EuFe garnet, rel. to exchange interactions in sublattice and its magnetization 8=40839
- EuO, hyperfine field study 8=36208
- Eu_3O_4, hyperfine field study 8=36208
- $^{151}Eu_3S_4$, electron hopping obs. by Mossbauer spectroscopy 8=30638
- F^{19}, Coulomb excitation of decelerated ions, probab., calc. 8=42878
- Fe^{57} acoustic sidebands due to r.f. magnetic field 8=39513
- Fe^{57}, Coulomb excitation of decelerated ions, probab., calc. 8=42878
- Fe^{57} γ-rays scattering time distribs. 8=43947
- Fe^{57}, spectrum (I) following Co^{57} decay in AgCl 8=39519
- Fe, b.c.c., of Fe^{57} rel. to isomer shift pressure dependence up to 130 kbar 8=43950
- Fe, charged states in Co cpds., spectra 8=35034
- Fe chromites, phase transformation study 8=35101
- Fe complex, bis(1,2-cyclohexanedionedioxime)Fe(II)XY, XY ligands ataxial posns. 8=30640
- Fe compounds, effect of electronic struct. of Fe atom 8=39514
- σ-Fe diarylene: Fe^{57}, spectra 8=35039
- Fe film magnetic anisotropy meas. 8=31641
- Fe in CoO, Fe multiple charge states 8=39521
- Fe in Cu and Au, Debye-Waller factor obs. 8=39874
- Fe, isomer shift temp. dependence and hyperfine field near Curie point 8=31636
- Fe, of Fe^{57}, effect of high press. to 140 kbars, rel. to $\alpha \rightarrow$ h.c.p. transition 8=43946
- Fe, of Fe^{57}, six-line spectra position analysis 8=48330
- Fe porphyrins, spectroscopy 8=26021
- Fe, pressure dependence, 0-85 kbar 8=43949
- Fe(II) octahedral complexes, $^5T_2$-$'A$, crossover 8=35038
- Fe(III) coordination no. determ. in organic complexes 8=39516
- Fe(III) N, N-dialkyldithiocarbamates 8=48329
- Fe^{2+}, line broadening due to orbit-lattice interaction 8=40921
- Fe^{3+}/Fe^{2+} ratios in phosphate and oxide mixtures, quantitative anal. 8=27778
- Fe_3Al, internal mag. field temp. dependence meas. for two sublattices 8=27410
- $FeAl_2O_4$, rel. to cation distrib. 8=35331
- Fe:Au^{197}, hyperfine structure determ. 8=43948
- Fe-Be system, and mag. props. 8=26024
- Fe-C martensite, during tempering 8=48323

Mössbauer effect—contd
Fe–C martensite, rel. to internal mag. field, Q.S. and isomer shift 8=26020
$FeCl_2$, anomalous temp.-dependence, 10-300°K, low-temp. anharmonicity interpretation 8=48326
$FeCl_2.H_2O$, 3°-310°K. obs. 8=30641
$FeCl_2.4H_2O$, 4.2-0.025°K rel. to mag. props. 8=36211
$FeCl_3$. 3°-310°K. obs. 8=30641
$FeCr_2O_4$, rel. to electronic and mag. props. of Fe^{2+} 8=31726
$FeCr_2S_4$, of Fe^{57}, 60-298°K, effective-field parameters rel. to magnetically induced quadrupole interactions 8=45060
$Fe_{1-x}Cu_xCr_2S_4$, indication of ion existence 8=39515
$FeLiO_2$ (β phase), study 8=26022
Fe-Mn-N alloys, study of high temp. strengthening 8=49019
$Fe(MSO_4)_2$, $M = NH_4^+, K^+, Rb^+, Cs^+$, rel. to crystal field splitting studies 8=26023
Fe_2N composition, study of ϵ and ζ phases 8=30695
$Fe(NH_4SO_4)_2.6H_2O$, of Fe^{57}, quadrupole hyperfine anisotropy determ. 8=43951
$FeNH_4(SO_4)_2.12H_2O$, spectrum, rel. to atomic spin time fluctuations 8=30642
Fe Ni alloys, exchange anisotropy 8=48328
γ Fe–Ni alloys, low Ni conc. 8=48333
Fe-Ni single crystal 8=35037
α-Fe_2O_3, superparamagnetism obs. 8=49521
$Fe(OH)_2$, Fe^{57} rel. to mag. fields at 4.2°K 8=39517
$FePd_x$, (x = 3.1), Fe^{57} hfs temp. dependence near Curie temp. 8=45015
Fe-Pd alloys, dil. hyperfine field at Fe, mag. field dependence 8=36081
Fe–Ru alloys, mag. susceptibility 8=49481
β–$FeSi_2$, space group symmetry determ. 8=48325
Fe_5Si_3, C-stabilized, mag. moments and hyperfine interactions 8=31621
Fe_2TeO_6, transition temp. determ. 8=49457
Fe_2TiO_4, spectra for electronic structure, 4.2-800°K 8=48327
FeV_2O_4, rel. to electronic and mag. props. of Fe^{2+} 8=31726
$Gd^{155,157}$ rel. to ratio of quadrupole moments and isomer shifts 8=33930
Ge^{73}, coulomb excited after recoil implantation 8=39525
$GeFe_2O_4$, rel. to electronic and mag. props. of Fe^{2+} 8=31726
GeI_4, I^{129} transition 8=39520
$HoFe_2$, rel. to hyperfine fields at Fe 8=36146
$I^{129}CN$ 8=30643
IBr, ICl, I_2Cl_6, using I^{129}, chem. bonding 8=35040
IBr, ICl, I_2Cl_6, using I^{129}, lattice dynamics 8=35041
Ir^{193}, no evidence for T-violation 8=25156
K^{40}, nuclear props. and target Debye temp. calcs. 8=42859
$K_3Fe(CN)_6$, h.f.s. and internal mag. field, 0.025-0.04°K 8=37330
$K_4Fe(CN)_6$, radiation scattering by nucl. resonance, diffr. and interference effects 8=26025
Kr^{83} with Se^{83} sources 8=43952
$LiAl_{5-x}Fe_xO_8$, spectra 8=43953
$MgFe_2O_4$, rel. to Faraday effect 8=45158
$MgFe_2O_4$ super paramag. precips in MgO, spectroscopy 8=31729
Mg_2SnO_4-$MgFe_2O_4$, hyperfine structure of absorption spectra 8=40738
$MnFe_2O_4$ 8=43954
Mn-Zn ferrites, hyperfine fields 8=35042
$Mn_{0.625}$-ZnY ferrites, rel. to hyperfine mag. fields and elec. quadrupole interactions 8=36198
NaCl, Fe impurity ions 8=39510
Ni superparamag. particles: Fe^{57}, spectral dependence on temp. and mag. field 8=36161
Ni, of Fe^{57}, effect of high press. 8=43946
$NiFe_2O_4$ superparamag. particles of Fe^{57}, rel. to hyperfine splitting in mag. field 8=36160
$Ni_{1+x}Ga_xFe_{2-2x}O_4$, internal fields at two sites, determ. 8=36193
Np^{237}, isomer shift and hyperfine splittings of 59.6 keV resonance 8=43955
Np^{237} spectrum after α-decay of Am^{241} in Th lattice 8=42929
Pt-1 at% Co(Fe) alloys, plastic deformation effects 8=31327
$RbFeF_3$:Fe^{2+} octahedral, magnetically induced elec.-field gradients Mossbauer determ. 8=31794
$RbFeF_3$, Fe^{57} hyperfine field determ. 8=31795
Sb halides, trivalent, isomer shifts of γ line 8=43956
SiI_4. I^{129} transition 8=39520
SmFe garnets, 85-600°K, rel. to mag. props. 8=36196
SmFe garnet, Sm^{3+} mag. moment and hyperfine field temp. dependence 8=31740
SmFe garnet, Sm^{3+} mag. moment and hyperfine field temp. dependence from Mossbauer effect 8=31740
$SmFe_2$, rel. to hyperfine fields at Fe 8=36146
Sn cpds., isomer shifts and nuclear radius change 8=26026
β-Sn, line shift during phase transform. under pressure 8=43941
Sn^{119}, resonant radiation, diffraction on electrons and nuclei, obs. 8=48334
SnTe, of Sn^{119} and Te^{125}, rel. to Debye temp. determ. 8=44344
SnX_4, (X = Cl, Br, I, H, Li, Na), Sn^{119} isomeric shift dependence on at. radius of X 8=30637
$SrTiO_3$:Fe^{57}, rel. to iron sites in lattice and oxygen vacancies 8=43958
$TbFe_2$, rel. to hyperfine fields at Fe 8=36146
Te^{125} hyperfine structure in Fe-rich (ferromag.) mats. 8=26027
Ti : Fe^{57}, f number and isomer shift pressure dependence 8=48321
$TiFe_{1-x}Co_x$:Fe^{57}, line profile comp., temp. and stoichiometry dependence 8=31921
Tm cpds, rel. to structure determs. 8=43959
Tm metal, hyperfine structure analysis below Neel temp. 8=30644
Tm^{169}, shift rel. to internal conversion 8=39226
V : Fe^{57}, f number and isomer shift pressure dependence 8=48321
W^{183}, following Coulomb excitation with protons 8=47262
Xe chlorides: Xe^{129} 8=30645
$Y_{2.1}Ca_{0.9}Fe_{4.1}Sn_{0.9}O_{12}$, effective mag. fields at Fe^{57} and Sn^{119} nuclei, rel. to nonmag. Sn^{4+} conc. 8=36197
YFe garnets, 85-600°K, rel. to mag. props. 8=36196
Y-Sn alloys. at room and liq. N_2 temp. 8=35043
$ZnY(Ba_2Zn_2Fe_{12}O_{22})$, rel. to hyperfine mag. fields and elec. quadrupole interactions 8=36198
$(ZrCo_2)_x(ZrFe_2)_{1-x}$ alloys, hyperfine field distrib. determ. 8=31712
Multiple stars. See Stars.
Muonium
coupling of muonium to antimuonium, probability and weak interact. calc. 8=42481
e. s. r. rates close to splitting freqs., rel. to residual polarization 8=38773
quenching of hyperfine resonance and polarization of bound muon rel. to O_2 and NO conc. 8=42482
Muons
arrival time distrib. in e.a.s. 8=38189
charge ratio in e.a.s. 8=38184
component in centre of e.a.s., fluctuations 8=38185
component in centre of e.a.s., lateral distrib. 8=38187
component of e.a.s., fluctuations calc. 8=38218
component of large e.a.s., high momentum excess obs. 8=38183
direct prod. in cosmic rays, review of evidence 8=25039
electron pair prod. in nuclear field 8=38257
flux meas. in cosmic ray burst 8=38134
high-energy in e.a.s., obs. 8=38186
lateral distrib. in e.a.s., obs. 8=38194
low-energy, in e.a.s. obs. 8=38182
magnetic moment, anomalous, suggested boson-lepton pair couplings 8=29102
magnetic moment, anomalous as test for q.e.d. 8=29099
magnetic moment, anomalous rel. to existence of neutral vector boson 8=42361
magnetic moment, using pion form factor data 8=24737
mass, evidence 8=29099
mass relationships, tamaid-bach theory 8=24629
moment, anomalous magnetic, and Lamb shift in H atom, hadronic contrib. 8=37944
μ^+-mesons depolarization in media, muon mechanism 8=38773
μ^+, polarization in various media, and relax. of spin 8=37943
number in e.a.s., probability distrib. functions 8=38213
polarization from $K^{\circ}_{\mu 3}$, Reξ meas. 8=42567
polarization meas. in $K^+ \rightarrow \pi^{\circ} + \mu^+ + \nu$ 8=24817
spin, evidence 8=29099
theoretical survey, decay and capture processes 8=24735
Mu–Ni alloys, electronic structure of Ni atoms 8=49744
capture
μ^-, by He^4, total capture rate 8=29229
radiative, angular correl. calc. 8=25214
Ca, n ang. distrib. asymmetry obs. 8=29416
Ca, n spectrum 7.7-52.5 MeV obs. 8=29415
He^4, μ^- capture rate obs. 8=38460
S, n ang. distrib. asymmetry obs. 8=29416
S, n spectrum 7.7-52.5 MeV obs. 8=29415
Si, n ang. distrib. asymmetry obs. 8=29416
Si, n spectrum 7.7-52.5 MeV obs. 8=29415
decay
electron spectrum, low energy, exact 8=29100
energy losses due to pair prod. 8=24738
μ^+ spectrum, low-energy end, obs. 8=24736
$\mu^{\pm}$ and μ^- in Cu, comparison of spectra 8=42478
$\mu^{\pm}$ in Cu, spectra comparison 8=29101
$\mu^{\pm}$, leptonic, T-violating effects 8=33567
underground decay, identification 8=38150
detection, measurement
spectrograph, cosmic ray bursts in iron, interpretation 8=38221
interactions
cosmic-ray, high-energy nuclear and e.m., obs. 8=38255
and e.m. stucture 8=24739
inelastic, 5 GeV/c, in emulsion 8=25213

Muons—contd
- **production**
  - cosmic ray N induced showers, 10^{12}-10^{14} eV 8=29250
  - cosmic ray, prop. rel. to shower size 8=29244
  - cosmic rays, spectrum obs. direct prod. not confirmed 8=25037
  - $\mu^+\mu^-$ asymmetric pairs, photoprod. on H rel. to quantum electrodynamics breakdown, 850 MeV 8=33647
  - $\mu\bar{\mu}$ pair, from W decay and πN, NN reactions 8=38022
- **scattering**
  - in emulsion, single, 5 GeV/c, distrib. obs. 8=25212
  - large-angle, by e. m. and photonuclear interactions 8=38254
  - $\mu^{\pm}$e, counter expt. 8=42479
  - μ-p, elastic, high momentum transfers, rel. to μ-e e.m. differences 8=42480
  - by nucleus 8=29099

Music. See Acoustics/musical.

Musical instruments
- clarinet, resonance freq. plotting 8=37269

Navier–Stokes equations. See Flow; Hydrodynamics.

Nebulae
- See also Galaxies.
- absorption in M17 direction 8=32482
- Andromeda, ellipsoidal subsystem of globular clusters 8=32477
- collisionally excited, effect of diffuse ionizing radiation 8=50340
- Cometary, S130, condensations i. r. emission and gas density, 1.6–21 μ 8=45783
- Crab, γ-spectrum obs. 8=45796
- Crab, linear polarization at 4170 and 6390 MHz 8=36961
- Crab, mechanism of ion accel. 8=41522
- Crab, neutron star mass infall as source of cosmic rays 8=45676
- Crab, obs. of γ-rays 8=45799
- Crab, radiobrightness distrib. at f=535 MHz, and centre of gravity 8=32483
- Crab, X-ray obs. 8=45720
- Crab, X-ray obs. 8=45776
- Cygnus X region II, obs. at 610.5 MHz 8=41544
- diffuse, review of obs. and theory 8=28089
- diffuse, stretched dark canals form. rel. to magnetogravit. instability 8=45714
- galactic, interstellar absorpt. obs. 8=28098
- gaseous, e temp. from Balmer decrement obs. 8=45718
- gaseous, e temp. from continuum-to-line ratio obs. 8=45719
- gaseous, radio emission rel. to distance and exciting star characts. 8=32484
- H II region temp. calc. 8=28091
- H II regions, 4170 MHz radio obs. 8=32493
- H II regions, optical obs. of H_α emission 8=32494
- H II regions, spherically symmetric expansion theory 8=45721
- IC 446, polarization of light 8=45715
- IC 2165, emission-line intensities and excitation 8=45708
- interstellar refl. brightness, colour and optical polarization 8=28097
- ionized, thermal instability and condensations 8=45716
- isothermal, gravitational instability 8=50341
- Magellanic Cloud, Small, star finding list 8=32485
- N Her 1963, stellar temp., electron density, and electron-density of shell 8=36935
- NGC 2024, electron temps. of H II regions calc. radio. obs. 8=50338
- NGC 2024, electron temp. radio recombination lines obs. 8=50339
- NGC 7027, oxygen abundance obs. 8=45713
- Orion, condensations 8=50342
- Orion, 8 GHz continuum and H II recom. line obs. 8=32489
- Orion, electron temp. radio recombination lines obs. 8=50339
- Orion, electron temps. of H II regions calc. radio. obs. 8=50338
- Orion OII lines, intensity errors in Fabry–Perot use with telescope 8=32410
- planetary, absolute proper motions and space vels. 8=50343
- planetary, dynamical models 8=32481
- planetary, effects of variation in surface gravity on emergent flux of central stars 8=41513
- planetary, evolution from FG Sagittae, obs. 8=45692
- planetary, Hβ interstellar absorpt., obs. 8=45712
- planetary, mass, radius and distance from OII, III and radio obs. 8=45709
- planetary model, ionization stratification and thermal stability 8=50336
- planetary, space orientation rel. to Galactic mag. field 8=45736
- planetary, spectrum lines excitation by absorption of stellar radiation rel. to ion abundances 8=45713
- planetary, spatial and kinematic models 8=45707
- planetary, symposium, Czechoslovakia (1967) 8=45711
- planetary, triplet state emissions of neutral He 8=45710
- planetary, two new, on maps of Palomar Atlas 8=45706

Nebulae—contd
- R Monocerotis, struct. and spectrum obs. 8=32487
- radiation diffusion 8=41801
- reflection, star photometry and spectroscopy 8=32472
- Rosette, Fabry-Perot obs. of radial velocity 8=32486
- Sharpless 261, continuum radio emission obs. 8=45717
- spherical, modeling of light scatt. using digital computer 8=36963
- 30 Doradus nebula at 408 NHz high resolution obs. 8=41523

Néel temperature. See Magnetic properties of substances.

Negatons. See Electrons.

Nematic phase. See Liquid crystals.

Neodymium
- in complexes, fund. level splitting obs. 8=29623
- glass laser, band narrowing with passive shutter 8=24345
- glass laser, electro-optical modulation of Q-factor 8=24342
- glass laser in Fabry-Perot resonator, polarized emission 8=42111
- glass laser, single-mode, waveguide type 8=24346
- glass laser, with unstable resonator, props 8=46625
- ion in silicate glass, stimulated emission 8=36512
- laser, and ruby, beam superposition in freq. mixing 8=24333
- laser, glass, coupled, three-mirror system 8=37619
- laser, glass, energy characts. of radiation with Q switching 8=24348
- laser, plane mirror resonator, spectral effects 8=24287
- laser, resonator nonlinearity rel. to radiation flux 8=33227
- laser, selective resonator, spectral effects 8=24289
- laser, self-focusing of 1.06μ radiation 8=24347
- laser with external tilted mirrors, field genesis and structure 8=37608
- laser, with plane mirrors, internal modulation 8=33228
- self-focusing produced in laser 8=36310
- Nd-doped YAG laser, single-mode, static and dynamic behaviour 8=46626
- Nd glass laser, parameters determ. 8=24343
- Nd(III) liq. room-temp. laser 8=46632
- Nd^3 in glass, fluorescence, concentration quenching 8=41206
- Nd^{3+} activated subs, stimulated emission studies rel. to laser generation 8=37595
- Nd^{3+}, approx. analytical wavefunctions 8=38674
- Nd^{3+} doped calcium fluorophosphate, laser characts. 8=37620
- Nd^{3+}, electronic Raman effect in garnets 8=27612
- Nd^{3+} in CaF_2, ions in sites of tetragonal symmetry, direct one-phonon spin-lattice relaxation times 8=40938
- Nd^{3+} in CaF_2, spin-lattice interactions in uniaxially stressed crystal, e.s.r. obs. 8=40939
- Nd^{3+} in ethyl sulphate lattice, mag. anisotropy and field parametrization 8=43932
- Nd^{3+} in LaF_3-SrF_2, induced emission at 300° K 8=27579
- Nd^{3+} in tetragonal YVO_4 crysts., induced emission at 300° K 8=33229
- Nd^{3+} laser, spectroscopic investigations of stimulated radiation 8=46621
- Nd^{3+} spectra in Y_2O_3 and Sc_2O_3, Stark splitting scheme and $^4F_{3/2}$ lifetime, 4.2–293°K 8=32017
- $Nd^{3+}SeOCl_2$ liquid laser, self-Q-switching 8=46633
- Nd^{3+}-$SeOCl_2$ liquid laser stimulated emission in $^4F_{3/2} \rightarrow {}^4I_{13/2}$ transitions 8=46628
- Nd:YAG laser, picosec. pulses, obs. 8=37618
- Nd:YAG laser repetitively pump-pulsed, dynamics 8=46623
- Nd:YAG laser, thermal effects and transverse mode control 8=28708
- Nd:YAl garnet, mode-locked laser 8=46622
- in Pd-Ag alloy, resistance anomaly 8=31326
- $SeOCl_2$:Nd^{+3}, absorption cross section for laser transition 8=46624
- $SeOCl_2$-Nd^{3+} liquid laser, Q-switched, 20°C 8=37623
- YAG:Nd, CW laser transitions at room temperature 8=46627

Neodymium compounds
- glass, birefringence dependence on laser pumping pulses 8=41125
- glass laser, use of spherical pumping reflector 8=46598
- monochalcogenides, antiferromag. props., 4-1300°K 8=31761
- Nb-Ta alloys, oxidation kinetics, 550-1050°C 8=36566
- Nd-alkali metal tungstates, hydrothermal synthesis and morphology 8=26259
- Nd glass, generation and amplification of light pulses 8=41126
- Nd glass stimulated emission spectrum and quasi-continuous generation, 4.2°K 8=36503
- Nd nitrate soln, electrophoretic behaviour of monodisperse polystyrene latex particles 8=49923
- Nd(III) complex of nitrilotriacetic acid, crystal structure 8=26415
- NdB_6, magnetic susceptibility, transitions 8=40873
- NdC_4, atomization energy 8=47705
- $NdCl_3$, fluorescence obs. rel. to annihilation between excited states of Nd^{3+} ions 8=41205
- $NdCl_3$ Rb–D_2 filter for student optical pumping expts. 8=42196
- $NdCo_5$ and Nd_2Co_{17} films, magneto-optic and mag. props. 8=32018
- $NdFeO_3$, mag. anisotropy 8=31733
- Nd-H system, Hall effect and cond. 8=49141
- $Nd_2W_2O_9$, structure and hydrothermal synthesis, obs. 8=39636

Neodymium compounds—contd
- NdWO$_4$Cl, synthesis, struct. and thermal decomp., obs. 8=39815

Neon
- afterglow plasma, conversion rates and ion velocity 8=43480
- arc, low-voltage mode in plasma diode, predominant ionization and loss mechanism 8=47779
- atomic collisions, Ne-Ne, Ne$^+$-Ne, Ne^{++}-Ne, prod. of fast electrons obs. 8=39018
- atom, double resonance in He-Ne laser operating at 6328 Å π transitions 8=47502
- atom, Hartree-Fock calc. refr. index, dynamic polarizability and Verdet coeffs. 8=47485
- atom, low-energy e scatt., data analysis 8=25385
- atom, Ne, 2p^6, 2p^{5}3s, 2p^{5}3p, 2p^{5}4s states, wave functions 8=29624
- atomic levels in Zeeman laser, g value meas. 8=43198
- atomic transition probabilities determ. by Faraday effect 8=38676
- atoms, excited, collisional disalignment 8=34183
- atoms, $2p_4 \rightarrow 1s_4$ spontaneous emission along axis of He-Ne laser 8=25363
- atoms, $^3P^0$ and $^1P^0$ populations time dependence during post-luminescence under c. m. wave pulses 8=38686
- atoms, radiative transition probabilities 8=34146
- discharge, d.c. glow, connection between moving and standing striations 8=47758
- discharge, h.f., electron energy distribution 8=43457
- discharge, positive column, Bremsstrahlung emission 8=29898
- discharge tube, noiseless 8=47746
- discharge, 2-32 mm Hg, steady state positive column plasma 8=29899
- discharges, microwave and h. f., energy distrib. of electrons and positive ions in plasma 8=25692
- with dissolved H normal solns., surface tension, 24. 59 to 29°K 8=43780
- energy widths of X-ray levels 8=29649
- fluorescence, $^2P_4$ emission under laser reson. illum., 6328Å 8=38675
- gas, Fe particles dispersed, absorpt. spectra including carrier gas contrib. 8=25968
- glow discharge, ionization waves, effects of cooling 8=47757
- glow discharge, 1. 35-2. 6 torr, 0. 5-2. 5 mA, dynamics 8=34420
- glow discharge, normal cathode fall 8=34422
- incorporation in solidifying enstatite melts 8=34972
- ion mobility and reaction rate obs. 300°K 8=39049
- ion refl. from Cu single crystal 8=48918
- ionically pumped on glass, desorption temp. dependence 8=48485
- ionization growth times analysis 8=29912
- ions Ne$^+$, charge exchange with Ar, Kr, N$_2$, O$_2$ and CO$_2$, 2-250 eV 8=38758
- laser, He-Ne, population inversion condition 8=24312
- laser, superradiant 5401Å pulsed, coherence props. 8=28691
- lattice thermal cond. calc. 8=39940
- liquid, 24. 6 to 27°K, sound velocity meas., Debye-Sears method 8=25913
- microwave breakdown at 9 GHz 8=47768
- nonlinear absorber, for mode locking of He-Ne laser 8=37588
- optically pumped, 3S$_2$ level relax. rel. to theory of multiple coherent scattering 8=43224
- photoabsorption of K$_\alpha$ X-rays, double e ejection 8=38714
- plasma, interferometric meas. in 8mm band 8=38989
- plasma, negative conductivity 8=25733
- primordial, diffusion in Fayetheville meteorite 8=37024
- Rayleigh scatt. and atomic e. m. susceptibility 8=25375
- Rutherford scatt. of H and H$^+$ 8=38754
- solar emission spectrum obs. 8=28165
- solid, anharmonic contrib. to entropy 8=35431
- solid, compression up to 20 kbar at 18°K 8=26836
- solid, ground-state energy 8=48709
- solid, model potentials 8=35389
- solid, pair pot. calc. 8=30615
- spark, laser-prod., expansion mechanism, obs. 8=34432
- spectral radiation intensity, shock-tube heated 8=24399
- thermal cond. 8=47956
- 3P$_4$ level lifetime in He-Ne laser 8=34184
- Zeeman effects for large quantum no.s and freqs. 5-20 MHz 8=47501
- Ar II transition probabilities and continuous spectra meas. 8=43179
- Br$^-$ ions collision with atoms, detached electrons energy obs. 8=29972
- Cl$^-$ ions collision with atoms, detached electrons energy obs. 8=29972
- He-Ne plasma afterglow kinetics 8=30080
- I$^-$ ions collision with atoms, detached electrons energy obs. 8=29972
- Ne^{20} ions, 21 MeV, radiation chemical studies 8=41289
- Ne I solar isoelectronic sequence, spectral resonance line strength 8=45871
- Ne I, 3p level, lifetime meas. using ion beam 8=29645
- Ne IV-VIII solar emission lines obs. and abundance determ. 8=50443

Neon—contd
- Ne IX plasma, 2-proton continuum emission 8=29599
- Ne-Ar mixture, concentration diffusion coeff., meas. by two-bulb method 8=34678
- Ne-Ar mixtures, thermal diffusion 8=39239
- Ne-CO$_2$ mixtures, thermal diffusion 8=34679
- Ne-Kr mixture, thermal diffusion and intermolec. forces 8=34675
- Ne-Li plasma, shock wave structure 8=30046
- Ne-O laser, O 3^{3}p level population inversion mechanism, obs. 8=28692
- Ne-O$_2$, phase equilib., from 63°-152°K at 5000 psi 8=34981
- Ne-Xe mixtures, thermal diffusion 8=39239
- Ne + He + CO$_2$ system, thermal diffusion 8=30320
- with NH$_3$, thermal cond., 273-1173°K 8=47962
- Zn 3075. 9 Å, perturbation of resonance line 8=47512

Neon compounds
- NeAr, interatomic potential 8=29749
- Ne-He mixture positive column, region of Pupp current limit 8=34421
- NeI, eigenvectors of configuration (2p)^5(3p) and rel. probabilities of 2s-2p transitions 8=25362
- Ne-N liquid-vapour phase equilib., density and supercritical excess vols., 66-114°K and < 8000 lb in^{-2} 8=30592

Neptunium
- Np^{237}, Mossbauer resonance, 59. 6 keV, isomer shift and hyperfine splittings 8=43955
- Np^{237} resistivity, low-temp., α self-irrad. effects. obs. 8=31322

Neptunium compounds
- NpF$_6$, electron diffr. and molec. struct. 8=38858

Nernst effect. See Magnetothermal effects.

Nernst–Ettingshausen effect. See Magnetothermal effects.

Neumann algebra. See Algebra; Elementary particles; Field theory, quantum.

Neutrettos. See Neutrinos and antineutrinos.

Neutrinos and antineutrinos

See also Nuclear reactions due to/neutrinos.
- antineutrinos from U^{235} fission, energy spectrum calc. 8=42992
- cosmological model with neutrino fluid density dominant over photon and matter densities 8=32392
- e.m. form factor, effect of W-boson assumption 8=33567
- emission of stellar energy, taking account of Pauli principle 8=50308
- e–ν, scatt. rel. to difficulties in weak interaction 8=33566
- experiments of CERN and Brookhaven 8=24712
- experiments at CERN and Brookhaven 8=24713
- high-energy reactions rel. to a test of current-current nature of weak interactions 8=24711
- interactions at polarized target, polarized μ angular yield distrib. 8=29090
- $K^+ \rightarrow e^+ + \nu_e$, branching ratio obs. 8=42574
- Kolar gold fields project 8=37931
- motion and statistics in superdense matter 8=42465
- π prod. and charge-exchange scatt. by N, Lewis-Oppenheime Wouthuysen model 8=42464
- production in lepton-baryon interactions 8=47075
- nature and invariance principles 8=25173
- N* prod. rel. to quark charge-commutation relations 8=29108
- $\bar{\nu}_e$-d interaction, expt. investigation 8=47078
- ν-e scattering, cross-section meas. 8=47079
- ν-e$^\pm$, μ production, exam. using two- and four-component theory 8=29090
- $\nu + H^2 \rightarrow e^- + 2p$, cross section obs. 8=47077
- $\nu + N \rightarrow B + \mu$, polarization correl. calc. 8=29091
- $\nu + N + B^* + \mu \rightarrow B + \pi + \mu$, polarization correl. calc. 8=29091
- ν, ν elastic scatt. by nuclei, cross-sections relation from algebra of charges 8=47076
- production of the W-meson in nuclear field 8=46839
- solar, as evidence for solar structure 8=45861
- solar, from B^8 decay, calc. 8=45888
- solar interior models, flux calc. 8=45860
- stellar, loss rel. to carbon burning phase lifetime of carbon star 8=41507
- sun, spectrum, detect. and rel. to stellar nuclear reactions 8=32585
- third neutrino hypothesis 8=42463
- underground expts., survey 8=33848
- Utah cosmic-ray experiment 8=38147
- B^8 flux limit obs., and rel. to solar spin-down 8=50446
- B^8 solar flux, reduction by core spin-down 8=45887
- in C stars, loss effect on evolution 8=32433

Neutron diffraction
- piezoelectric vibrating resonators 8=35378

Neutron diffraction crystallography

See also Crystal structure, atomic.
- automatic and programmable control for diffractometer 8=48630
- automatic double-diffractometer 8=39764
- atomic scattering factors from structure-factor meas. 8=39736
- bent O-H---O bonds 8=48300
- computer-controlled system 8=26362
- diffraction peak line profiles in determining structures 8=26357

Neutron diffraction crystallography—contd
dynamic interference theory for thermal neutrons, and exptl. results 8=48629
high-pressure apparatus and appls. 8=26361
line broadening effects, separation by means of line-width relations 8=45147
polarized slow n-diffractometer, flipper-chopper operation 8=26360
powder data, computer indexing 8=44188
tapiolite and synthetic trirutile substances 8=48614
time-of-flight method for structure investigations on fast-pulsed reactor IBR 8=26358
time-of-flight powder diffractometry, intensity and resolution calcs. 8=26359
α-Ti and O mixed crystals, hydrogenation 8=35357

Neutron diffraction examination of materials
antiferromagnetics, with easy plane, slow scatt. rel. to magneto-elastic coupling 8=40855
antiferromagnets, critical mag. scatt., theory 8=36096
carbon tetrachloride 8=34761
cynostat, He for use 3°-300°K 8=39763
ferromagnetics, with easy plane, slow scatt. rel. to magneto-elastic coupling 8=40855
ferromagnets, critical mag. scatt., theory 8=36096
γ-oxygen, vapour-condensed, (200) and (210) faces 8=26260
liquids, struct. and transport props., scatt. studies compared with X-ray methods 8=30402
metal sheet texture determ. 8=35261
metals, liquid, structure factor 8=43757
magnetic fluctuations, critical 8=31481
magnetic moments in crystals, local distrib. 8=31643
moment fluctuations, temporal 8=31516
rare-earth oxysulphides, mag. structures 8=40869
scattering, time-of-flight meas. by mag. pulsed beam 8=35314
small angle scatt. on lattice distortions, advantages to X-ray scatt., and techn. 8=26355
solid solns., disordered, monophonon scatt. 8=35379
solutions, liq., x-ray and n diffr. methods 8=34763
$Ba_{0\cdot15}Ca_{0\cdot85}MnO_3$, at. mag. structure 8=40859
Bi, liq., structure factor 8=48062
$Ca_2Fe_2O_5$, magnetic structure 8=31759
$CoCr_2O_4$, mag. structure determ. 8=31721
CoF_2, rel. to mag. excitations near Neel pt. from n. scattering meas. 8=31762
$CoMn_2O_4$, mag. structure, low-temp. determ. 8=31722
Cr, magnetic props., pressure and mag. field dependence n-diffr. exam 8=31766
CrX_3, (X = Br, F), rel. to paramagnetism 8=31521
$CuCr_2Se_3Br$, ferromag. props. from n-diffr. exam. 8=31606
$DyAlO_3$, nuclear and magnetic structure 8=48647
DyC_2, mag. struct. 8=40865
$ErAl_2$, mag. struct. 8=31611
Fe, susceptibility above Curie temp., temp. depend. 8=40812
Fe-Ni alloy, rel. to spin wave dispersion relation 8=31624
Fe_2O_3, spin-wave excitation-energy changes 8=31638
α-FeOOH, crystal and mag. structures, —190 to 120°C 8=30894
H bonding, from n. scattering by protons, double potential well model rel. to solids study 8=35017
H_xWO_3, same crystal structure as $Na_{(0\cdot1)}WO_3$ 8=35336
K_2ICl_5, mag. ordering from n. diffr. exam. 8=40870
K_2ReBr_6, mag. ordering from n. diffr. exam. 8=40870
K_2ReCl_6, mag. ordering from n. diffr. exam. 8=40870
$LiClO_4.3H_2O$, struct. by n diff. exam. 8=35339
$MgCr_2O_4$, mag. structre 8=45063
Mn–Cu null-matrix alloy 8=44195
$MnCr_2O_4$, mag. structure determ. 8=31721
MnO, low-angle, covalency parameters 8=30617
α-MnS, low-angle, covalency parameters 8=30617
$MnSn_2$, antiferromagnetic, rel. to structure transitions 8=31779
NH_4Cl, long range order parameter in order-disorder transitions 8=44242
Nb hydrides (deuterides), structure and phase transitions 8=39725
Ni_3Fe, near order from n. -scatt., 8=39531
NiO, low-angle, covalency parameters 8=30617
Pb, liq., structure factor 8=48062
α-PbN_6 8=30908
Si slices, impurities distrib. 8=40014
Sn liq., structure factor 8=48062
$TbAg_2$, mag. struct. 8=40877
$TiFe_xCo_{1-x}$ alloys, structure and mag. props. 8=30912
Ti_2O_3, rel. to mag. phase 8=31800
Tl, liq., structure factor 8=48062
U_3O_8, antiferromag. struct. study 8=31801
V_2O_3, rel. to mag. phase 8=31800
Zn, liq., structure factor 8=48062

Neutron sources. See Neutrons/production.

Neutron spectra
accelerator stray neutrons, < 0.5 and up to 200 MeV 8=33824
anisotropic, determ. from p recoil tracks 8=47161
d(p, n)2p, Ep = 45.5 MeV obs. 8=43017
from foil activation data, tech. using linear eqns. representing differential flux 8=29209

Neutron spectra—contd
in heavy gas, thermalization, with nonuniform temp. distrib. 8=29556
in multiplying assemblies with pseudo fundamental mode behaviour, puked spectra 8=38563
nucleon-meson cascade, theory appl. to accelerator shielding 8=24964
perturbed thermal, Laguerre expansion coeffs., activation meas. 8=33775
polarized, anal. using time-const mag. fields, expt. checking 8=38069
in polyethylene, thin slabs 8=24968
reactor, "cold" n segregation technique 8=24975
resonance, area, analysis, self-indication corrections 8=24982
resonance, area analysis, self-indication method 8=24981
resonance self-screening technique, epithermal 8=34109
scattering, polarization-dependent, spin-flip chopper meas. 8=47174
slowing down energy spectra of fast n from fission source 8=38584
threshold detector data anal. 8=38070
threshold detectors, "appropriate" solutions 8=24984
Ag thickness transmission meas. 8=24980
Al, results from thres-axis crystal spectrometer 8=33827
Am–Be source 8=24974
Am^{241}–Be^9 sources, p-recoil spectrometry with shaped converter foil, obs. 8=33784
$Be^9(\alpha, n)$ sources, calc. for Am^{241}, Po^{210}, Pu^{239} α-emitters 8=38515
Ca, μ capture, 7.7-52.5 MeV obs. 8=29415
Cf^{252} spontaneous fission fragments 8=25278
D plasma, ion component diagnostics 8=34512
$Er^{164,166,167,168,170}$, n resonance obs. 8=25153
Mo^{94}, isobaric analogue resonances 8=29320
$O^{18}(p, n)F^{18}$, E_p = 5.0 MeV, n time-of-flight spectrometry for O^{18} determ. 8=32149
Po-B source, and γ spectrum, fast-slow n-γ coincidence obs. 8=33783
Po–Be source, and γ spectrum, fast-slow n-γ coincidence obs. 8=33783
PuF_4 source, obs. 8=42650
in $Pu^{238}O_2$ 8=34099
S, μ capture, 7.7-52.5 MeV obs. 8=29415
Si, μ capture, 7.7-52.5 MeV obs. 8=29415
$U^{235,233}$ and Pu^{239}, thermal n fission, comparison for 0.8 to 16 MeV 8=38536

Neutron spectrometers
for accelerator stray n dosimetry, <0.5 and up to 200 MeV 8=33824
calibration and resolution determ., Bragg break meas. method 8=47171
correlation chopper, mechanical, expt. test 8=47170
crystal, three-axis design 8=33827
γ discrimination by scintillation decay time, circuit, $E_n \geqslant 0.2$ MeV 8=33384
improvements for quasi-elastic scatt. 8=24983
monochromator, curved-slit chopper 8=24985
polarized, accuracy with scatt. vectors not ⊥ mag. field 8=47175
p-recoil, organic scintillator, 0.4–18 MeV 8=33823
p-recoil, with shaped converter foil 8=33784
pulse shape discrimination system 8=33818
from recoil tracks, determ. 8=47161
resolution and intensity, Monte Carlo simulation 8=33826
stilbene response to internally generated protons 8=47169
stilbene scintillation with γ discrimination, $E_n \geqslant 0.1$ MeV 8=33821
stilbene scintillation, with γ discrimination, 1–10 MeV 8=33822
scintillation, double-summation with γ discrimination by scintillation decay time 8=47168
time-of-flight, buffer memory design 8=47172
time-of-flight data recording, synchronous drum store 8=47155
time-of-flight, for detecting neutrons in energy region from 10 to 100 MeV 8=47166
time-of-flight, for isochronous cyclotron 8=47167
triple-axis, for reactor inelastic scatt. 8=33828
Ag thickness transmission meas. 8=24980
C^{12} recoil meas. of n scatt. asymmetry 8=29457
$CaCO_3$ monochromator, crystal structure props. 8=42651
He^3 90° instrument 8=47173
He scintillation, with sodium salicylate wavelength converter, 14 MeV 8=33825
Li^6 sandwich semiconductor detector 8=38083
Li^6 semicond. sandwich type, efficiency calc. by Monte Carlo tech. 8=38084

Neutrons and antineutrons
See also Cosmic rays/neutrons; Nucleons and antinucleons.
beam prod., magnetically pulsed for scatt. expts. on crystals 8=35314
cross-section from nd high energy interaction 8=42645
damage flux in critical assemblies, rel. to inpile thermionic reactors 8=28504
decay constant, prompt in critical state of heavily reflected reactor 8=47377
double reflection monochromator 8=24977

Neutrons and antineutrons—contd
electric dipole moment, T nonconservation effect 8=42325
electric dipole moment, upper limit from mag. resonance expt. 8=42644
electric form factor threshold values depend. on d wave function 8=47139
excitation functions in low energy V^{51} (p, n) Cr^{51} reaction 8=33998
flux distributions space-time/energy in infinite homogeneous media 8=42643
flux profiles, fast and thermal, comparison from bucklings in UO_2 assembly 8=43138
flux ratios in tangential channels in reactor 8=34093
form factor, magnetic rel. to quasielastic e-d scatt. 8=24722
half-life, rel. to cosmological He prod. 8=24945
high energy expts. at CERN development 8=33624
liquid, bubbles due to zero-point motion of positronium atoms 8=30388
mechanical high transmissin selector of vels. 8=29201
models, non-relativistic 8=29016
n^3 bound state search 8=43039
neutron-proton mass difference, Cottingham formula 8=42630
n-γ, flux and Kerma distance depend., counter and Na activation obs. 8=33771
noise in reactors with external control loop 8=38589
nonlinear reactor kinetics, stability anal. for equilib. states 8=43134
n, p, single particle states similarity at same mass number 8=42815
in nuclear reactors, importance, thermal and total, theory and meas. 8=43137
optics of slow neutron beams 8=47143
Pauli's hypothesis, interaction, and one- or two-ν problem 8=24646
p-n mass difference 8=38058
population fluctuations in reactors, Monte Carlo anal. compared with one-mode model 8=38553
prompt n time const., reln. with stable reactor period in ANNA assembly 8=34091
pulsed reactivity expts in reflected reactor, interpret with Cohn model 8=43139
radius of distribution of Pb^{208} 8=33937
in reactor, number fluctuations 8=38552
resonance parameter correlations 8=25234
resonances, numerical determ. 8=24971
secondary, from 400—660 MeV proton bombard., on nuclei obs. 8=25219
shielding of fast sources, reduction in weight 8=29206
strange rel. to Cabibbo theory 8=24708
structure, rel. to quasi-elastic e-d scatt. 8=47084
transport, complementary variational principles appls. 8=33328
tri-neutron, non-existence, obs. 8=38383
velocity selector 8=47159
wave propag. along axis of infinite prism, dispersion law 8=38583
Ag nucleus, peripheral n excess, K^- capture obs. 8=34022-3
Br nucleus, peripheral n excess, K^- capture obs. 8=34022-3
absorption
See also Nuclear excitation; Nuclear reactions due to/ neutrons.
Albedo and Milne's problem 8=29550
body dose rel. to counter obs., isotropic fast flux and beam 8=38072
capture cross-section curves, automatic decomposition to Breit-Wigner terms 8=29194
concrete shielding for D-T neutrons 8=29199
cross sections, total, for 14.7 MeV neutrons 8=47148
dose in human phantom, distrib., obs. 8=38074
dose in tissue-equiv. human phantom, $\leq$ 5 MeV 8=38073
dose in tissue-equiv. human phantom, calc., 100 eV-10 MeV 8=38075
fuel rod lattice, reson. absorpt., calc. 8=34086
hydrocarbons, linear energy transfer, 14 MeV 8=43033
local pile oscillator, epithermal, calibration 8=38077
Milne problem, thermal-n in absorbing medium, arbitrary scatt. kernel 8=38574
moderators, wide reson., intermediate reson. integral, exact soln. 8=38571
MUFT programme, inclusion of Doppler broadening 8=43132
properties, use for radiography 8=46769
pulse decay in slabs and spheres 8=47376
in reactor lattices, resonance absorption, Boltzmann integral eqn. 8=29551
resonance absorpt., rapidly convergent iterative soln. 8=24970
resonances in slab lattice, interferences and flux depend. on lethargy and space 8=38582
scattering anisotropy correction, in transport theory 8=29200
in tissue and equivalents, Kerma calc., 0.1-10 MeV 8=33772
by d, thermal, zero-range approximation theory 8=29219
Sb, resonance parameters 8=47331
Sb^{121}, Sb^{123}, thermal capture cross section 8=29478
U^{237} cross-section 8=29481

Neutrons and antineutrons—contd
absorption—contd
U^{238} by 6.7 and 192 eV resons., exact calc. 8=38571
U^{228}-metal fuel rod lattice in H_2O and C, intermediate reson. absorpt. calc. 8=34086
$U^{238}O_2$ fuel rod lattice in H_2O and C, intermediate reson. absorpt. calc. 8=34086
angular distribution
cyclotron meas., accidental coincidence background reduction 8=29005
d(p, n)2p, Ep = 45.5 MeV, obs. 8=43017
4 MeV from nuclei, optical model analysis 8=29451
in reactor, appl. of space angle synthesis by simple approx. 8=38561
$Be^9(\alpha, n)C^{12}$, E_α = 6-10 MeV, obs. 8=43079
C^{12} scatt., E_n=15.85 MeV, obs. 8=29458
Ca, μ capture, asymmetry obs. 8=29416
$Ca^{42}(d, n)Sc^{43}$, E_d=5.15 MeV, obs. 8=34034
Fe reson. scatt., 1-2 MeV 8=29462
He target, E_n = 0.2-7.0 MeV, obs. 8=24957
S, μ capture, asymmetry obs. 8=29416
Si, μ capture, asymmetry obs. 8=29416
t(d, n)He^4, n energy dispersion obs. rel. to accelerators 8=29220
capture. See Nuclear reactions due to/neutrons.
detection, measurement
See also Dosimetry; Neutron spectrometers.
(α, n) sources calibration, continuous, in Mn bath 8=33782
alumophosphate: Li and B slow n dosimeters, personnel 8=33797
Campbell channels, comparison of γ discrimination of averaging and r.m.s. circuits 8=47163
Cauchois γ spectrometer for (n, γ) reactions, precision angle meas. device 8=25236
concentric detector for dose and rate meas. 8=38081
converter in reactor for investigation of scatt. and attenuation 8=29543
detector films from polyvinyl alcohol 8=24978
dosimeters, α-acetylaminoacrylic acid-N-vinylpyrrolidone copolymer-gelatin emulsion for fast-n dosimetry 8=33800
dosimeter, by emulsion scanning, edge effects and track length meas. 8=33804
dosimeters calibration, thermal-20 MeV 8=33806
dosimeter calibration with (α, n) sources, fluence-dose conversion 8=33805
dosimeters, 2, 4-disulphonic acid benzaldehyde polyvinyl acetate-gelatin emulsion for fast-n dosimetry 8=33800
dosimeter, fast and intermediate, personnel reson. film dosimeter with filters 8=33801
dosimeter, fast-n, by Cereknov radiation meas. 8=33798
dosimeter, personnel monitoring, review 8=33808
dosimeter, personnel, thermal and intermediate energy, body backscatt. effects 8=33803
dosimeter, plastic scintillator, tissue dose distrib. 8=33809
dosimeters radiation element, personnel 8=33799
dosimeters, solid state, Al_2O_3 and W 8=47162
dosimetry, body absorpt. rel. to counter obs., isotropic fast flux and beam 8=38072
dosimetry, fast n, use of synthetic polymers in emulsions 8=47152
dosimetry, personnel, by solid-state nuclear track detector 8=46920
exposure meas. with Si radiation damage monitors 8=29207
fast hodoscope, improvement 8=47164
fast n-γ detector for space research 8=47158
fission fragments, emission, indirect method 8=47363
flux determ. by back-to-back fission chamber 8=33814
flux meas. in reactor core, self-powered detector 8=43148
flux-density standards at N.P.L., thermal-19 MeV 8=33816
by foil activation in rad. effects studies, tech. for spectra determ. 8=29209
γ-compensated ionization chamber 8=47156
ionization chamber n detector, transient γ field behaviour 8=47160
ionization chambers, hexane and CCl filled 8=33811
isotope applic. 8=43245
Kodak NTA films, for personal fast n monitoring 8=33812
luminphor composition based on ZnS(Ag) and Li^6F registration of slow neutrons 8=47153
n and γ body doses in criticality accident, meas. 8=33767
organic phosphor efficiency meas. 8=29208
organic scintillator, recoil p distrib. 8=24979
personnel monitoring and high-energy meas., review 8=33810
polarimeter, liq. He, time of flight type 8=47145
p-recoil counter, rein sensitivity energy depend, 0.1-6.3 MeV 8=33807
proton recoils, n-induced, response of NE213 scintillator 8=46881
pulse transformer links in meas. lines for n. detectors 8=47151
reactor, EBR-II, counting-mean-square voltage channel performance 8=47157
rem meas. method for mixed γ-neutron radiation fields 8=46923

Neutrons and antineutrons—contd
- **detection, measurement**—contd
    - scattered on deuterium, 4, 6 MeV, polarization determ. 8=47324
    - scintillation counter, plastic, props. 8=29205
    - source calibration by point detector 8=33786
    - spherical dose equiv. n detector, improvements 8=47165
    - stilbene, use of anisotropy in scintillation response for directional meas. 8=47154
    - streamer chamber, design and performance 8=46978
    - thermal, flux meas. by foil activation 8=24976
    - thermal neutron flux density standard, calibration 8=47149
    - thermal, spectrum determ., appl. of Dy^{164}, Lu^{176} and Pu^{239} 8=29568
    - third moment of count in short time interval 8=38082
    - time-of-flight data recording, synchronous drum store 8=47155
    - Au activation n flux calibration 8=33802
    - BF$_3$, proportional counters, wall effect 8=24508
    - BF$_3$ short counter with spherical moderator for neutrons in γ background 8=33792
    - Gd thermal neutron counter 8=33813
    - He scintillation counter with sodium salicylate wavelength converter, 14 MeV 8=33825
    - He^3(n, p) T method 8=29459
    - Li^6 sandwich semiconductor detector 8=38083
    - LiF and Li$_2$B$_4$O$_7$:Mn, fast-n personnel dosimeter 8=33796
    - Sc^{46} monitor for reactors 8=47330
- **diffusion**
    - approximation, perturb. method, including leakage term 8=33777
    - Boltzmann eqn. for stationary multilayer problems in plane geometry, semianalytical methods 8=25289
    - Boltzmann eqn., two-dimens. linear, biorthogonal angular polynomial expansion 8=32856
    - discrete S$_n$ approx. for flux from pencil of n, accuracy tests 8=38560
    - distributions, reactor kinetics stability 8=25292
    - dual variational principles, for error estimation, in approx. solns. 8=28355
    - few-group eqns., interface conditions 8=33781
    - flux equations in reactor kinetics 8=47385
    - flux synthesis method, extension 8=38568
    - flux synthesis, using Green's function 8=29549
    - flux transients digital analysis, reactivity calibration 8=34078
    - in graphite, effect of Bragg cut-off energy and group coupling 8=47375
    - in graphite of ANNA reactor, parameters $<\Sigma_a V>$ and D 8=34073
    - in graphite, pulse propag. meas. 8=34066
    - in graphite, thermal wave propagation and effect of Bragg continuum 8=47374
    - graphite/H$_2$O and /D$_2$O, waves refl. and refr. at interfaces, theory 8=38071
    - group problems, soln., in finite-difference form 8=29548
    - in heavy gas, thermalization, with nonuniform temp. distrib. 8=29556
    - kinetics of zero power heterogeneous lattices 8=34076
    - Milne problem, thermal-n in absorbing medium, arbitrary scatt. kernel 8=38574
    - Milne's problem with general anisotropic scatt., exact soln. 8=34072
    - monoenergetic transport operator, fundamental mode and decay constant, for spherical assembly 8=24973
    - Monte Carlo deep-penetration calcs., track length distrib. biasing 8=33776
    - multigroup eqns, time-depend., numerical soln. and truncation error 8=38564
    - multigroup, time-depend., in complex geometry, asymptotic theory extension 8=34071
    - multiregion transport problem in plane geometry, boundary-sources method 8=33778
    - in polyethylene, thin slabs 8=24968
    - pulses and space-depend. transfer function, time-dependence synthesis 8=34069
    - reactor, adjoint weighting, anomalous effect on an approx. method 8=38562
    - reactor geometries calc. by extended flux synthesis method 8=38569
    - reactor theory, group eqns. synthesis techniques 8=29545
    - resonance integrals, effect of source distrib. 8=29547
    - scattering kernel, synthetic, with applications in neutron transport theory 8=47372
    - in slab geometry, recursion formulae 8=34067
    - slab, n extrapolation distance 8=25296
    - in slabs or spheres, decay consts and monoenergetic critical parameters 8=38555
    - slowing down in cylindrical bounded medium 8=47146
    - space-angle synthesis appl. to transport problem 8=38561
    - space-angle transport theory, Green functions 8=38570
    - thermal/fast ratio obs. 8=47380
    - thermalization of pulsed neutrons, few-pole expansion method calc. 8=47147
    - three-dimensional eqn. numerical solns. 8=47383

Neutrons and antineutrons—contd
- **diffusion**—contd
    - transfer function meas., higher space modes excitation 8=34070
    - transfer operator, monoenergetic, spectrum 8=33779
    - transport, absorpt. cross sections and region capture integrals fitting 8=34087
    - transport calcs, time depend., use of method of 'expected leakage probability' 8=38581
    - transport, discrete ordinates eqns., ray effect anomalies 8=38572
    - transport eqn. approx. soln. in 2- and 3-dimens. system 8=47381
    - transport eqn., asymptotic P$_N$ approx. 8=29544
    - transport eqn. in spherical geometry Green's functions 8=38579
    - transport eqn, spherical harmonics approx. rel. to critical radius of spherical reactor 8=38580
    - transport in arbitrary finite body employing imbedding eqns. for Green's function 8=28228
    - transport in plane lattice, asymptotic solns. and pulsed-n and n-wave appls. 8=38575
    - transport in plane geometry with isotropic scatt., S$_\infty$ theory 8=34088
    - transport, Monte Carlo deep-penetration calcs., track length distrib. biasing 8=33776
    - transport, Monte Carlo sampling appls. 8=32855
    - transport theory, two-group, eigen function expansion 8=33763
    - two-dimens. four group calc. based on partial buckling 8=38551
    - in water, effect of voids 8=24967
    - in water, energy dependent Milne problem 8=47382
    - in water, thermal wave propag. obs. analysis, one-vel. calc. 8=34065
    - in Be, isotropic, decay const. and diffusion length calcs. in transport and diffusion theories 8=38590
    - Be, n wave propag. and diffusion consts., calc. 8=33774
    - U^{235} 93.15 wt% subcritical cylinders, prompt-n decay consts., obs. 8=38578
- **effects**
    - See also Nuclear reactions due to/neutrons.
    - acoustic cavitation, n-induced, apparatus and results 8=48032
    - armo iron, ferromag. props. 8=36169
    - buckling, in UO$_2$ assembly, comparison fast and thermal flux profiles 8=43138
    - calibration of thermocouples 8=46273
    - ceramics, isothermal irrad. assembly for damage rel. to elec., thermal and mech. props. 8=35597
    - concrete, conventional, radiation damage 8=26730
    - dielectrics, B impurities, rel. to breakdown 8=31417
    - displacement damage rates in differing reactor types 8=47408
    - dose-equivalent outside vector shielding, intermediate n contribution 8=33766
    - electronic components, transient effects 8=31126
    - field effect transistors, junction and bipolar, comparison of rad. tolerance 8=27194
    - glasses, physicochem. props., effect of mixed γ-n radiation 8=44493
    - graphite, dimensional changes, influence of crystallite size 8=35600
    - graphite, grade A reactor, irradiated at 80°K and annealed at temps. up to 300°K, e.s.r. 8=45081
    - graphite, interstitial formation below 200°C, cluster size and temp. dependence 8=44419
    - graphite, irrad. effects 8=43143
    - graphite, on Vickers hardness 8=35666
    - graphite, pyrolytic, on shear compliance (C$_{44}$), by 'pinning' defects 8=35665
    - graphite, radiation damage annealing studies by ESR 8=26729
    - graphite, 'restrained growth', structural changes 8=31149
    - Hastelloy neutron irrad. effects on stress rupture and creep 8=47400
    - hexane ionization chamber rel. to dosimetry 8=37787
    - hydrogeneous liquids, cross section meas., rel. to proton motions 8=48065
    - millisecond isomers, from 14 MeV n, cross sections 8=47220
    - M1040 Vacodur 16 permeability, 6 × 10^{19} n/cm^2, > 1 MeV 8=29553
    - neutron irradiated, dosage-damage correlations and X-ray diffr. studies 8=26733
    - noise neoplasms regression rel. to B^{10} dose, thermal flux and reactor design 8=45926
    - permalloy films, induced uniaxial anisotropy 8=31694
    - perovskites, high-temp. phase transformations, radiation-induced 8=39538
    - quartz, production of crystalline-amorphous phase transform. 8=26146
    - quartz, rel. to structural changes 8=26080
    - quartz, u.s. attenuation 8=39897
    - semiconductors based on GeTe:(Bi, Cu), electrical conductivity, thermoelectricity compressive strength 8=40637

Neutrons and antineutrons—contd
- **effects**—contd
  - semiconds., compound, effects on optical attenuation and absorpt. edge 8=27569
  - semiconductors, disordered region production and effect on carrier recombination 8=40431
  - semiconductors, heavily doped, slow neutron scattering study of lattice dynamics 8=44759
  - Sicral F_1, swelling rel. to fission gas bubbles, 10^{14} n/cm² sec 8=44506
  - Sicral F_2, swelling rel. to fission gas bubbles, 10^{14} n/cm² sec 8=44506
  - steel irrad. embrittlement, sensitivity depend. on N conc. 8=47405
  - in steel, stainless He prod., due to (n, α) reaction 8=47406
  - steel, stainless, irradiation creep. obs. at 100°C 8=26833
  - steel, Cr–Ni/Nb stainless, CO_2 oxidation, 580°–840°C obs. 8=27705
  - steels with f.c.c. lattice of solid soln., rel. to internal friction peak 8=35678
  - superconductors, type II, interaction with polarized neutrons 8=26998
  - tetrachloroethylene, u.s. cavitation using pulsed n source 8=25849
  - transistor current gain prediction, influencing variables 8=31412
  - Ultraperm 10 6 × 10^{19} n/cm², > 1 MeV 8=29553
  - X-ray reflection of Si plane crystals 8=30911
  - Al-base Cu, precipitation 8=48379
  - 16 Al Fe Vacodor 16 permeability, 6 × 10^{19} n/cm², > 1 MeV 8=29553
  - α-Al_2O_3, macroscopic growth and damage 8=26666
  - Al_2O_3, damage and macroscopic props. changes, review 8=44496
  - Al_2O_3, meas. of macroscopic and lattice growth 8=26234
  - Al_2O_3, polycryst., effect on lattice, porosity and thermal resistivity 8=26366
  - Ar, thermal neutron capture, γ-ray emission 8=25242
  - Au single crystal sputtering 8=48911
  - BaF_2, self-trapped hole formation, e.s.r. exam. 8=31854
  - $BeAl_2O_4$, chrysoberyl, irrad., crystal growth obs. 8=31145
  - BeO, damage and macroscopic props. changes, review 8=44496
  - BeO, meas. of macroscopic and lattice growth 8=26234
  - n-$Bi_2(Te, Se)_3$, elec. and thermal parameter changes 8=27136
  - C, dimensional changes, influence of crystallite size 8=35600
  - C, pyrolytic, dimensional changes, model 8=31148
  - CaF_2, irradiated at liq. N_2 temps., induced colour centre obs. 8=26719
  - CaF_2, self-trapped hole formation, e.s.r. exam. 8=31854
  - CaO, colour centre formation 8=31115
  - CaO crysts., Ca^{40} (n, α) Ar^{37}, Ar^{37} diff. 8=39969
  - $CaWO_4$, oxygen vacancies prod. by fast reactor neutrons, direct obs. 8=31047
  - CdS, on dark resistivity and Hall mobility 8=49235
  - n-CdTe, thermal irrad., Cd vacancies, Hall and cond. obs. 8=35533
  - CrO_4K_2, n-irradiated, e.s.r. 8=49605
  - $CrO_4(NH_4)_2$, n-irradiated, e.s.r. 8=49605
  - Cs halides, Xe diffusion 8=39970
  - Cu crystal, defects induced on irradiation at 400°C 8=48804
  - Cu crystals, radiation hardened, critical shear stress temp. and strain rate dependence 8=31196-7
  - Cu, irradiated, cyclic deformation 8=26801
  - Cu, irradiated, rel. to active crystal length in yield region under deform. 8=40054
  - Cu nearly perfect crystals, radiation damage obs. by X-ray diffraction 8=26732
  - Cu, on yield surfaces 8=44564
  - Cu–0.01 wt, % B^{10}, dislocation loop spheres surrounding B particles, obs. 8=35564
  - α-Fe, irradiation effects saturation 8=31151
  - Fe-Ni(50-50) crystals, ordered in mag. fields, magnetization curves 8=36144
  - Ge, defect production and detection by anomalous X-ray transmission, 8=48834
  - Ge, diodes, point-contact, pile-n irrad. effects on switching props. 8=31406
  - Ge, dosage-damage correlations and X-ray diffr. studies 8=26733
  - Ge, two level model for lifetime reduction processes 8=27126
  - Ge(Li) γ detector degradation 8=42453
  - K halides, activation energies for Ar diffusion 8=35498
  - KCl, hardening from critical shear stress analysis 8=49037
  - Li_2SO_4, irradiated, OH radical thermal decay, e.s.r. study 8=27481
  - in LiF negative thread crystal formation 8=26256
  - LiH fission attenuation and γ-ray buildup factors by the Monte Carlo method 8=47401
  - MgO, colour centre prod. 8=35589
  - MgO, effect on luminesc. 8=49809
  - MgO, damage and macroscopic props. changes, review 8=44496

Neutrons and antineutrons—contd
- **effects**—contd
  - MgO, hardening, lattice damage, and colour centre conc. 8=26829
  - MgO, irradiated, defect clusters, very small, study by neutron scattering meas. 8=35525
  - MgO, irradiated, $(OF)^{2-}$ molecular ion as paramag. defect 8=44404
  - MgO, irradiated, phonon-assisted optical absorpt. 8=41049
  - MgO, n-irradiated at 80°K, zero-phonon lines and phonon-coupling 8=27588
  - MgO, negative ion vacancies 8=44412
  - Mo, irradiation creep obs. at 100°C 8=26833
  - Mu metal permeability, 6 × 10^{19} n/cm², > 1 MeV 8=29553
  - NaCl, hardening from critical shear stress analysis 8=49037
  - Nb, supercond., resist. and magnetization, obs. 8=40373
  - Nb, superconducting magnetization, changes on > 1 MeV irrad. 8=40379
  - NbZr superconducting coil performance effect rel. to accelerators 8=33405
  - Ni alloys, irradiation creep obs. at 100°C 8=26833
  - Ni-base alloy, irradiated, dislocation haloes 8=44452
  - Ni, ferromag. props. 8=36169
  - Ni, irradiation creep obs. at 100°C 8=26833
  - Ni, irrad., vacancy and interstitial clusters 8=35538
  - Ni, near Curie point, depolarization meas. of spontaneous magnetization 8=45019
  - Pt, irradiated, hardening 8=35716
  - Rb halides, rare-gas diffusion 8=40079
  - Re, identification of defect clusters 8=40080
  - Re, irradiated, unit cell and dimensional changes 8=26737
  - p-$(Sb, Bi)_2Te_3$, elec. and thermal parameter changes 8=27136
  - Se, hexagonal, irradiations, effect on cond. and photocond. 8=44809
  - Si, carrier lifetime degradation, induced, rel. to dopant impurities 8=31156
  - Si, carrier removal and annealing, influence of impurities 8=27124
  - Si, defect character from anomalously wide images using stereo e-microscopy 8=31025
  - Si, defect production and detection by anomalous X-ray transmission, 8=48834
  - p-Si, disordered region production, dimensions and conductivity 8=35913
  - Si, dosage-damage correlations and X-ray diffr. studies 8=26733
  - Si devices, injection level and temp. depend. of transient annealing 8=27122
  - Si, disordered regions formation from carrier mobility decrease 8=35551
  - Si, divacancy and A-centre production 8=44416
  - n-, p-Si, electrically active defect introduction rates on irradiation 8=39998
  - Si, injection level studies, and carrier lifetime depend. on excess density 8=27125
  - Si, plane crystal, X-ray reflection 8=30911
  - Si solar cells damage, Li effects, obs. 8=24095
  - Si transistors, effects in neutral and space-charge regions, annealing characts. 8=27202
  - Si, two level model for lifetime reduction processes 8=27126
  - β-SiC, porous, changes in growth, elasticity and thermal props. 8=26735
  - Si: Li diode, on diffusion coeffs. of Li 8=39982
  - Te, on elect. cond. of single crystal 8=31393
  - Ti, irradiation creep obs. at 100°C 8=26833
  - U, growth and elec. resistivity changes during burn up at 4.6°K 8=48933
  - α-U, swelling rel. to solid fission prods. segregation 8=44507
  - U-Mo 1, 1 alloy, swelling rel. to fission gas bubbles, 10^{14} n/cm²sec 8=44506
  - U-Mo-Al-Sn, swelling rel. to fission gas bubbles, 10^{14} n/cm² sec 8=44506
  - UO_2, on electronic props. from e.m.f. meas. 8=40290
  - V_2O_5-P_4O_{10} semicond. glasses, effect on elec. cond. 8=27137
  - W, n-irradiated, stage III recovery 8=31157
  - ZnS, colour centres, accumulation during bombardment 8=31125
  - ZrO_2 films, damage and effect on props. 8=35607
- **interactions**
  - charge depend. study and violation of charge symmetry 8=24864
  - $\gamma + n \rightarrow \pi^- + p$, photoproduction of π° meson near $N_{1/2}(1525)$ resonance 8=47108
  - high energy, theoretical survey 8=24710
  - $K^-d \rightarrow \pi^-(\Sigma^+n) \rightarrow \pi^-(\Lambda p)$ 8=38093
  - nd, 14-27 GeV/c, total cross section and Glauber screening protection 8=29196
  - nd, n cross-section, high energy 8=42645
  - $n + d \rightarrow 2n + p$, 14 MeV, ang. distrib. obs., anomaly and rel. to spectator model 8=33768
  - $n + d \rightarrow p + 2n$, 199 MeV, n-p bound scatt., polarization 8=24961
  - n-n, ^1S interact. comp. with pp data, charge asymmetry rel. to energy diff. between H^3 and He^3 8=24950
  - np, 14-27 GeV/c, total cross-section and Glauber screening correction 8=29196

Neutrons and antineutrons—contd
interactions—contd
n-p residual interaction in odd-odd nuclei quasiparticle random-phase-approx. 8=42791
n-p total cross sections 8=24952
nT, at 14.1 MeV, study of outgoing p, d and T 8=42646
n-t resonance energy, $Be^9 + t \rightarrow n + t + Be^8$ obs. 8=29502
neutron-C cross-section meas., erratum 8=42647
neutron-proton cross-section meas., erratum 8=42647
$\pi^- n \rightarrow \{p\pi^-\}\pi^-\pi^\circ$, nucleon isobars, 5 GeV/c 8=33675
$\pi^- n \rightarrow p\pi^-\pi^-\pi^\circ$, $N\pi\pi$ enhancements, 5 GeV/c 8=33676
p-n final state interacts. in d(p, 2p)n and p(d, 2p)n reactions 8=24902
$p + n \rightarrow \Delta^{++} + \Delta^-$, exchange mechanism 8=24917
$p + n \rightarrow W^- \rightarrow e + \bar{\nu}_e$, form factors and polarization 8=42642
$\Sigma^+ n \rightarrow \Lambda p$ obs. in $K^- d \rightarrow \pi^-(\Sigma^+ n) \rightarrow \pi^-(\Lambda p)$ 8=38093
steel, for determ. of B content 8=37100
$D(n, n^2)p$ interact. peak. at 14 MeV, rel. to n-n interact. 8=24951
H^3 at 14.1 MeV, outgoing particles obs. 8=33769
H^3, cross-section angular depend. rel. to H^4 existence, 0.007-5 eV 8=29195
$He^3(n, p)H^3$, resonance parameters from p-T scatt., 300-990 KeV 8=29185
$He^3[n, p(n)]T$, He^3, diff. cross section extrema due to excited state of He^4, Feymann diag. 8=24914
$He^4(n, p)H^4$, H^4 excited levels and bound states, obs. 8=34007
moderation
absorption in wide reson. moderators, intermediate reson., integral, exact soln. 8=38571
Boltzmann eqn., boundary ang. flux approximation 8=28350
decay const., pulse meas., time-of-flight effects 8=33773
fast n from fission source, energy spectrum for slowing down in homogeneous medium 8=38584
in graphite, pulse propag. meas. of thermalization process 8=34066
nonhydrogeneous infinite homogeneous media, formal soln. 8=33780
in nonmultiplying medium, energy correl. 8=34074
paraffin wax havitzers, optimum design, obs. 8=42649
pulsed n theory and expt. 8=24966
rethermalization cross sections, vel. depend. free-gas kernel calc. 8=34089
shielding penetration, Monte Carlo calc., self-optimized exponential biasing 8=34075
slowing down in cylindrical bounded medium 8=47146
thermalization in graphite-water system at large temp. gradients 8=47384
thermalization in heavy gas, with nonuniform temp. distrib. 8=29556
thermalization of pulsed neutrons, few-pole expansion method calc. 8=47147
water, effect of voids 8=24967
by water, heavy, calcs. on coherent scatt. of slow n 8=25237
$Al-H_2O$ plate lattices, slowing down anisotropy, obs. 8=38576
$Al-H_2O$ slab systems, slowing down anisotropy, Monte Carlo calcs. 8=38577
Be, assemblies, transient spectra for pulse 8=29541
Be, n wave propag. and diffusion const., calc. 8=33774
$ThO_2-D_2O-H_2O$ lattices, age meas. 8=29552
U-metal exponential columns, buckling rel. to U^{235} enrichment, 4.3-9.1% 8=34085
polarization
d(p, n)2p, polarization transfer calc., Ep = 30-150 MeV 8=38101
$\gamma + p \rightarrow \pi^+ + n$, n polarization obs. 8=24965
in n-d elastic scatt., rel. to phases at low energy 8=29221
polarimeter, liq.-He, time of flight type 8=47145
scattered on deuterium, 4, 6 MeV, apparatus for meas. 8=47324
spectra anal. using const mag. fields, expt. checking 8=38069
C^{12} scatt., E_n =15.85 MeV, obs. 8=29458
C^{12} stripping obs. 8=25238
He liquid polarimeter, description 8=33819
He liquid polarimeter for fast n, analysing power calc. 8=33820
N-nucleus, optical model analysis 8=29451
$N^{14}(d, n)O^{15}$ 2.9, 3.7 MeV calc. distorted wave theory 8=38509
$N^{15}(d, n)O^{16}$, 3.1-3.8 MeV, obs. 8=43059
production
in atmosphere by cosmic ray nucleons 8=29254
by cosmic ray μ in Pb, Cd, Fe, Al at a depth of 150 m. water equivalent 8=38461
emission reactions, nonscatt., energy-angle correl. neglect 8=24948
$\gamma + p \rightarrow \pi^+ + n$, n polarization obs. 8=24965
gas-filled neutron tube, ionization in accelerating space 8=47141
generator, described with 200 kV supply, vacuum system, ion source and accel. tube 8=29203
generator for undergraduate laboratory 8=38076
generator, target, wear meas. with current integrator 8=47142
generator with self-target using D-T reactions 8=29204
high-yield generator for radiographic TV system 8=37725

Neutrons and antineutrons—contd
production—contd
in nuclear explosions, possible source for energy depend. n-n scatt. expts. 8=24958
(dn) Penning tube with ion source 8=24949
positive-ion beam target for accelerator 8=33398
pulsed source, rate of yield decrease from tritium-Ti targets 8=33785
pulsed source using remodelled electron linear accelerator 8=46986
pulses, from $D(d, n)He^3$ reaction 8=47150
p reactions in C, 24 GeV/c, obs. 8=29439
$t(d, n)\alpha$ reaction, n yield, 14 MeV, α-counting 8=24946
reactor photoeffect, on Be reflector population analysis 8=38454
rotating target system for D^+, T^+ ion beams 8=33396
in soils, due to natural radioact., production rates 8=36681
source calibration by point detector 8=33786
sources, pulsed, and their applications 8=29202
tube, accel. voltage, work parameters, for D containers, and T target parameters 8=29193
windowless gas target for ion beams 8=33395
in Be(d, n) reaction, energy ang. distribs. and yields at 1 and 3 MeV 8=34029
D_2O by U^{235} fission fragment γ-rays, delayed n half-lives, obs. 8=33764
Pu-Be (α, n) sources, n yield increases 8=47428
U^{233} in soln, array of bottles determ. of neutron criticality condition 8=47398
reflection
beam enrichment in total refl. tube 8=38078
graphite/H_2O and /D_2O interfaces, diffusion waves refl. and refr., theory 8=38071
by human body dependence on surface tissue depth and energy 8=41606
scattering
acetic acid, use of atomic substitution techs. in spectroscopy of microscopic transport props. 8=30403
anisotropy, absorpt. correction, in transport theory 8=29200
beryl, l.f. vibrs. of H_2O mols. 8=48704
Bijoveet type generalized eqns. 8=35297
by condensed systems, generalization of 3-D Patterson function to 4-dimens. 8=26356
corrections calculation 8=47144
cross-section evaluation, computer graphics 8=47323
cross section meas., low-energy region 8=38068
cryostat, continuous flow, for scatt. expts. 8=49548
crystal, incoherent approximation 8=26354
on deuterium, 4, 6 MeV, apparatus for meas. polarization 8=47324
deuterium, liq. ortho-para solns. 8=30404
d-n, scintillation counter resolving effects 8=24513
diffuse elastic, from ferromagnetic alloys, second order effects 8=49491
at E_n = 1.01/2.44 MeV, obs. 8=24956
elastic, and nuclear polarizability, for underange mass nos, optical model anal. 8=29451
elastic, at 2.8 MeV, applicability of optical model for description 8=29197
ferromagnetic, critical, incident spectrum broadening by inelastic scatt. 8=40795
gas, molecular, rotational correl. functions 8=43277
by heavy water, coherent, calcs. with acoustic freq. distrib. 8=25237
Heisenberg antiferromagnet with impurities, diffuse elastic n. cross section 8=31752
hydrogeneous liquids, proton motions by cross-section meas. 8=48065
hydrogenous molec. solids, freq. spectrum determ. 8=39875
ice, freq. spectrum determ. 8=39875
ice, inelastic, freq. distrib. determ. 8=26574
in ice, rel. to proton dynamics 8=39303
inelastic, coherent obs. of localized vibrations in Cu-4% Al 8=39872
inelastic, near threshold, γ ang. distrib. 8=34006
inelastic, reactor triple-axis spectrometer 8=33828
inelastic, time-of-flight meas. and data analysis 8=24962
Ising magnet, temp. and freq. depend. 8=31571
$K^\pm n$ real part predicted by dispersion relation 8=24831
from light nuclei four-parameter optical model 8=29450
liquid metals, heating arrangement up to 900°C in experiment 8=34762
liquids, and relaxation phenomena 8=39305
media, inhomogeneous, time correl. function formalism 8=29386
methane, gaseous, rel. to intermolecular interactions 8=38898
methanol, use of atomic substitution techs. in spectroscopy of microscopic transport props. 8=30403
Milne problem, thermal-n in absorbing medium, arbitrary scatt. kernel 8=38574
Milne problem with capture, thermal 8=24969
mixtures of amorphous solids or liquids, data anal. 8=39628
multiple, in slab geometry, recursion formulae 8=34067
from n-dimensional lattice (n = 1, 2, 3) rel. to multiphonon processes 8=31132

Neutrons and antineutrons—contd
  scattering—contd
    neopentane mols. rel. to methyl group librations obs. 8=34345
    n-d, Born approximation with tensor interaction 8=24960
    n-d, elastic, different phases w.r.t. polarization of n, d 8=29221
    n-d, elastic, phase analysis accuracy enhancement 8=29198
    n-n cross-section, energy depend, possible use of nuclear explosion 8=24958
    (n, n), length calc. from (He^3, d) 8=43005
    n-n scatt. length, extraction by comparison anal. of reactions with $^1S_0$ N-N final state interact. 8=24954
    nn scatt. length from $\pi^- d \rightarrow 2n\gamma$; obs. 8=42648
    n-n, Wolfenstein amps at t = 0, rel. to meson exchange and coupling consts. 8=24931
    n-n and n-p scatt. length difference, pion instability effects 8=24883
    nuclei, even-even, exchange interaction 8=43034
    optical model, parameters from 1.5 MeV scatt. data 8=29452
    optical pot. for 6, 7, 8 MeV, Al-Bi evidence for symm. term 8=29449
    π^+ n, 4, 5 π prod. 3.29 GeV/c 8=37983
    pn, pp, Chou-Yang diffraction model, proton and neutron form factors proportionality obs. 8=47140
    polarization-dependent, spin-flip chopper meas. 8=47174
    polarization effects, including nuclear polarization 8=27392
    polyacrylonitrile 8=25686
    polyethylene, normal and deuterated 8=26579
    polymer solns., quasielastic scatt. 8=30419
    rare earth h.c.p. paramagnetic crystal field effects 8=40749
    rare earth nuclei, deformed, level density obs. 8=29328
    rare earths, paramagnetic 8=48890
    in reactor, Br-5, with a convertor 8=29543
    resonance, angular distrib., filter method 8=29462
    skyshine, Monte Carlo calc. 8=36758
    space-angle transport theory, Green functions 8=38570
    spectrometer improvements 8=24983
    s-wave strength function, threshold cusp. 8=42805
    thermal and subthermal, by crystal dislocations 8=24959
    thermal and subthermal, by l.f. sound modes 8=24959
    thermal and subthermal, by solid 8=24959
    time-of-flight measurements, using magnetically pulsed beam 8=35314
    total cross section, new method for s, p, d-wave strength functions determ. 8=25232
    water, ang. distrib. using Debye-Einstein frequency spectrum 8=30405
    from water, light, cross-sections, multiple scatt., rel. to molec. motion 8=39304
    in water, rel. to proton dynamics 8=39303
    Al^{27} inelastic, ang. distrib. of γ obs. 8=38481
    Al^{27}, inelastic to 2.980 and 3002 keV levels 8=43036
    Al^{27}, 1-4 MeV, inelastic, levels 8=29459
    Al, by n-irrad. defects rel. to lattice distortion, subthermal, 20°K 8=44203
    Al, inelasitc, cross-sections, calc. and obs. 8=29460
    Al, natural, elastic and inelastic differential cross sections 5.95 MeV 8=38480
    from Ar liquid, convolution approx. in theory 8=43758
    in Be, isotropic, decay const. and diffusion length calcs. in transport and diffusion theories 8=38590
    Be-U, 8 heavy elements, total cross sections obs. 27 GeV/c 8=43040
    Bi^{209}, 1-4 MeV, inelastic, levels 8=29459
    Bi, inelastic, cross-sections, calc. and obs. 8=29460
    C^{12}, E_n =15.85 MeV, polarization obs. 8=29458
    C^{12} recoil meas. of asymmetry 8=29457
    C, inelastic, cross-sections, calc. and obs. 8=29460
    CH_2I_2 crysts., inelastic, rel. to mol. and lattice vibr., obs. 8=35385
    CH_3I crysts., inelastic, rel. to mol. and lattice vibr., obs. 8=35385
    $Cd^{111}(n, n')Cd^{111m}$, cross section obs. 8=29475
    CeAs, rel. to mag. props. 8=45052
    CeSb, rel. to mag. props. 8=45052
    $Cl^{35}(n, 2n)Cl^{34g,m}$, cross-section obs., compared with statistical model calc. 8=47325
    Co, ferromagnetic, of thermal, rel. to spin correlation function 8=31626
    CoF_2, rel. to mag. excitations near Neel pt. from n. scattering meas. 8=31762
    Cr^{52}, 1-4 MeV, inelastic, levels 8=29459
    Cr, critical, near Neel temp. rel. to itinerant e.-model of mag. props. 8=31764
    CrX_3, (X = Br, F), rel. to paramagnetism 8=31521
    $Cu^{63,65}$ inelastic, ang. distrib. of γ obs. 8=38481
    Dy, total cross-sections, 0.02-1.0 eV 8=38482
    DyAl garnet, critical, rel. to antiferromag. Ising model 8=31769
    Er isotopes, cross-sections, 0.007-1 eV 8=29463
    Er isotopes, slow, cross-section meas., compared with theory 8=38483
    Er, paramagnetic, rel. to mag. interactions 8=31523
    Fe^{56}, inelastic, ang. distrib. of γ obs. 8=38481
    Fe^{56}, 1-4 MeV, inelastic, levels 8=29459
    Fe, by long-wavelength spin waves 8=49520

Neutrons and antineutrons—contd
  scattering—contd
    Fe, ferromagnetic, of thermal, rel. to spin correlation function 8=31626
    Fe, fine struct. rel. to 0.36 MeV intermediate reson. nature, obs. 8=34005
    Fe: impurity atoms, rel. to mag. moment disturbance
    Fe, inelastic, cross-sections, calc. and obs. 8=29460
    Fe, rel. to Fisher's correlation function 8=27412
    Fe, reson., angular distrib., 1-2 MeV 8=29462
    in Fe, unmagnetized, divergence of collimated thermal n beam 8=31642
    FeF_2, rel. to spin-wave dispersion relations 8=31771
    $Fe_xGa_{2-x}O_3$, polarized, rel. to ferrimag. props. 8=31727
    α-Fe_2O_3, by antiferromag. spin-waves, polarization effects. obs. 8=36187
    Fe_2O_3, rel. to spin-wave excitation-energy changes 8=31638
    Fe-(Mn, Er), dilute by virtual magnon states 8=31625
    Ga, liq, energy depend., in wavelength range 1-8Å 8=39301
    H^3, cross-section angular depend. rel. to H^4 existence, 0.007-5 eV 8=29195
    H-bonds 8=24963
    $H_3O.NO_3$ crysts., inelastic, rel. to mol. and lattice vibr., obs. 8=35385
    Ho, paramangetic, rel. to mag. interactions 8=31523
    Ho, total cross-sections, 0.02-1.0 eV 8=38482
    $K^{39}(n, 2n)K^{38g,m}$, cross-section obs., compared with statistical model calc. 8=47325
    $Li_{0.5}Fe_{2.5}O_4$, by ferrimag. spin-waves, polarization effects, obs. 8=36187
    Lu, total cross-sections, 0.02-1.0 eV 8=38482
    MgO, irradiated, rel. to study of small defect clusters 8=35525
    Mn^{55} total cross section, parametric fit, 0.01 eV-50 keV 8=38477
    MnF_2, near critical pt., temp. dependence rel. to mag. behaviour 8=31784
    MnF_2:Co, rel. to localized magnon obs. 8=27380
    MnF_2: Co, rel. to localized magnon obs. 8=31785
    NH_4 salts, phase transitions 8=48393
    Ni by long-wavelength spin waves 8=49520
    Ni, ferromagnetic, of thermal, rel. to spin correlation function 8=31626
    Ni: impurity atoms, rel. to mag. moment disturbance distrib. 8=31637
    Ni, polycrystalline, sub-thermal neutrons at dislocations 8=31084
    $Ni^{58}(n, p) \rightarrow Co^{58g,m}$, cross sections, isomeric ratios and total 8=38489
    P, natural, elastic and inelastic differential cross sections 5.95 MeV 8=38480
    Pb, liquid and solid, Brillouin scatt., rel. to collective particle motion 8=25869
    Pb, liquid, rel. to cooperative modes of motion 8=34725
    Pb, liquid, rel. to cooperative modes of motion, temp. depend 8=34726
    Pt, fast n scatt. obs. 8=29464
    $Pu^{239,241}$, meas. of scatt. resonances, rel. to energy levels 8=43037
    $RbMnF_3$, inelastic n. scattering near Neel pt. rel. to spin fluctuations 8=31796
    Re, fast n scatt. obs. 8=29464
    S, natural, elastic and inelastic differential cross sections 5.95 MeV 8=38480
    S, total cross reactions at 5.36-6.28 MeV 8=34004
    Sb^{121}, Sb^{123}, thermal capture cross section 8=29478
    Sc^{45}, elastic and total cross sections, 14 MeV 8=29461
    Si, natural, elastic and inelastic differential cross sections 5.95 MeV 8=38480
    Si^{29}, E_n = 0.57-2.28 MeV, excitation obs. 8=33906
    $Sr^{87}(n, n')Sr^{87m}$, cross section obs. 8=29475
    Ta, fast n scatt. obs. 8=29464
    Tb, critical, inelasticity above Néel temp. rel. to mag. order 8=31530
    U^{233}, meas. of scatt. resonances, rel. to energy levels 8=43037
    VH_x, inelastic, vibr. spectra in three cryst. phases 8=39878
    V_3Si, paramagnetic, absence of scattering rel. to d electrons in conduction band 8=40754
    W, total cross reactions at 5.36-6.28 MeV 8=34004
    $Y_3Fe_5O_{12}$, by parametrically excited spin-waves 8=36094
  scattering, proton-neutron
    bremsstrahlung at 208 MeV, obs. 8=24953
    in hydrogen bonds, double potential well model rel. to solids study 8=35017
    n-p bound in n + d → p + 2n, 199 MeV obs. 8=24961
    n-p, bremsstrahulng calc. from p-d obs. at 197 MeV 8=29182
    n-p, differential cross sections rel. to residues of π and $\Lambda + \Sigma$ poles 8=38016
    n-p, 199 MeV, cross-section obs. and polarization 8=24961
    n-p π exchange 8=33770
    n-p, 60-100 GeV, from cosmic ray absorpt. in paraffin and graphite 8=38248
    phase-parameter multiple-energy fits for energy range 8 to 340 MeV 8=24934

Neutrons and antineutrons—contd
scattering, proton—neutron—contd
phase shift anal. of data in 140 MeV region 8=24935
polarization and spin-correl. meas., rel. to phase-shift anal. 8=24955
singlet state scatt. length difference with n-n, pion instability effects 8=24883
total cross sections 8=24952
Wolfenstein amps at t = 0, phase shift dual. rel. to meson-nucleon coupling 8=24931
$^1S_0$ phase shift anal. with pp data, rel. to charge splitting 8=24929
Newtonian fluids. See Fluids.
Nickel
absorption, infra-red, at 4.2°K 8=27551
adherence and wettability to sapphire 8=43744
alloying with Mo, Cr, Si and Cu, effect on 3d-electron state 8=35775
anisotropy of energy and magnetization, torque meas. 8=31667
band structure rel. to low-energy optical transitions 8=35774
Barkhausen discontinuities, size distrib. calc. from simple model 8=31669
Barkhausen jumps, ultrasound influence 8=36163
catalyst beds, Q meas. 8=32120
coercivity rel. to dislocation distrib, effects 8=31699
cold-worked, ang. distrib. of scatt. neutrons rel. to defects 8=26355
conducting film formation using electron beam 8=39603
conductivity, thermal, by Jain and Krishnan method 1150-1400°K 8=39949
creep near Curie pt., rel. to stacking fault energy 8=35710
creep, void formation 8=31225-6
crystal, high-purity prep., by e. beam float zone melting 8=48553
crystal. stress-relax. meas., 77-350°K 8=40178
crystals, electro-deposited, structure and orientation in initial crystallization stage 8=30822
deformed, strongly, onset of uniaxial anisotropy after mag. annealing 8=36216
with deposited Ba film, thermionic emission 8=27347
diffusion in Ag 8=34813
diffusion in PbSe, anomalous 8=39981
diffusion of Au, lattice and grain-boundary type, 700–1075°C 8=44391
diffusion of H_2, isotope effects 8=31012
diffusion of H, kinetics 8=31014
diffusion of V, coeffs. 8=35476
diffusion rates, annealing time effects 8=35474
dislocations, e. microscope obs., 8=48859
dislocations magnetostrictive crystalline energy from anisotropy of approach to saturation 8=35571
dispersion-strengthened, mag. props. dispersed effects 8=31620
edge dislocations, vels. rel. to stress, and activation vol. and enthalpy 8=44454
effects on structure of sintered UC 8=26299
electrode contact for ferrites 8=31321
electrodeposited, microstructure, effects of addition agents 8=35277
electrodeposited, process conditions effect on stacking-fault, microstrain and particle size 8=26298
electrodes in vacuo, elect. breakdown 8=47763
electron cold emission in N_2 with elect. field 8=49439
electronic structure of atoms in solid solutions 8=49744
electroplated, mag. anisotropy rel. to vacancies and interstitials formed on H charging 8=49538
epitaxial overgrowth on Cu, reduction in mechanical strength of Cu 8=40146
Fermi-surface from galvanomag. coeffs. and de Haas-van Alphen effect 8=31289
ferrite films, structural properties and ferromag. resonance 8=36192
ferromagnet, elastic limit determ. by Barkhausen effect 8=26838
ferromagnet, hyperfine fields at Cd^{111} and Ru^{99} solutes 8=40992
ferromagnetic and paramagnetic, lattice dynamics 8=35391
ferromagnetic, de Haas-van Alphen effect rel. to electronic structure 8=31698
ferromagnetic, exchange and spin-orbit interactions rel. to mag. break-down and de Haas-van Alphen effect 8=44649
ferromagnetic films, planar Hall effect, thickness (100-1500Å) and temp. (77-293°K) dependence 8=31687
ferromagnetic properties rel. to band structure 8=31632
ferromagnetic reson. of film rel. to internal stresses and magnetization inhomogeneity, obs. 8=31821
ferromagnetic resonance linewidth temp. dependence 8=31815
ferromagnetic, thermal neutrons, critical scattering 8=31626
ferromagnetic, 3d-band, density of states curve 8=40246
ferromag. transition temp. pressure-dependence, itinerant-electron theory 8=27424
film, electrodeposited and charged with H, effect of H on magnetization inversion 8=36170
film on glass, light refl. phase retardation meas. 8=31960

Nickel—contd
film, oscillating hysteresis 8=45021
film, ultrasound from stripe domain resonance 8=31682
films, adsorpt. and interact. of N_2 8=26138
films, chemisorpt. of O_2 and H_2, reconstitution of adsorbate adsorbent interface 8=27737
films, domains and mag. fine structures form., e microscope obs. 8=31640
films, epitaxial, anisotropy constant 8=31631
films, magneto-optical parameter temp. dependence, 20-400°C 8=36398
films, orientation after deposition on NaCl 8=44085
films, p-bombardment effects on mag. props. at 850 keV 8=36168
films, u.v. reflection, near Curie point 8=36399
films, vacuum-condensed, elastic anisotropy rel. to structure 8=44545
films, vacuum-deposited, temp. coeff. of resistance 8=35819
foils, polycrystalline, residual resistivity and Kohler's rule 8=26971
fractional order peaks in diffracted LEED beams, surface asymmetry mech. 8=26100
fuel cell, electrode activation with Pt catalyst 8=46356
grain boundary, large-angle, dislocation form. 8=31105
grain-boundary relax. and damping peaks, rel. to internal friction 8=48872
intergranular structure, angular characts. by small-angle X-ray scattering 8=26297
internal friction, effect of H 8=49041
ions Ni^{++}, polarographic investigation in $LiNO_3$-$NaNO_3$-KNO_3 melt 8=45414
Kerr effect in dielec. permeability tensor freq. dependence determ. 8=31696
lattice dilation by dissolved C 8=44243
liquid, atomic structure from X-ray diffr. exam. 8=25874
in liquid steel, conc. rel. to C activity 8=30458
magnetic disturbances rel. to substitutional impurities 8=36153
magnetic eqn. of state near Curie point 8=40828
magnetic, form factor anisotropy rel. to band structure 8=31600
magnetic hysteresis loss and magnetostriction hysteresis in rotating fields up to 2000 Oe 8=31680
mag. moment disturbance distrib. from dissolved impurity atom, n. scattering obs. 8=31637
magnetic saturation curve anisotropy, edge-dislocation contribution 8=49536
magnetization near Curie pt. 8=31697
magnetization, spontaneous, near Curie pt. by neutron depolarization meas. 8=45019
Magnetocrystalline anisotropy constant, first-order, pressure dependence 8=27407
magnetocrystalline anisotropy temp. dependence from magnetostriction and elastic constants 8=31561
magnetoelastic parametric interaction due to ΔE effect 8=26840
magneto-elastic resonance props. 8=36164
microsegregation in directionally solidified steel 8=39552
Mössbauer spectrum of Fe^{57}, effect of press. 8=43946
neutron bombardment effects on ferromag. props. 8=36169
neutron irradiation creep obs. at 100°C 8=26833
oxidation kinetics 8=27713
oxidation rate-constant determ., low-temp., from discontinuous film resistance changes 8=49883
paramagnetic susceptibility calc. 8=49483
paramagnetic, susceptibility calc., contrib. of intra-atomic exchange enhancement 8=31524
in permanent magnets, effects of extrusion on texture and props. 8=33046
pitting corrosion critical potentials 8=49928
plane Hall effect, temp. depend. and role of scatt. mechanisms 8=40324
plating, electroless, on p-n junctions 8=45396
polycrystalline, dislocations, small angle mag. scattering of sub-thermal neutrons 8=31084
polycrystalline, optical consts. from reflectance ratios 8=45164
positrons, polarized, annihilation 8=49129
powder, superparamag., Mossbauer spectra of Fe^{57}, temp and mag. field effects 8=36161
pure, self-diffusion 8=39979
recovery of mech. props., laws 8=35709
recrystallization during creep, mechanism 8=48552
reversible magnetic susceptibility, dependence on temp. and stress 8=36154
saturation magnetization determs. 8=31618
self-diffusion, 980 to 1400°C 8=48786
solar emission spectrum obs. 8=28615
specific heat at low temp. 8=39919
spin-wave renormalization effects, obs. 8=49520
spin waves 8=31627
spin waves, Stoner modes and critical fluctuations 8=36215
sputtering by Ar^+, [110] and [100] close-packed directions yields, 25-600 eV 8=40078
superplasticity in pure metal 8=31224
surface energy and surface self-diffusion 8=44028

Nickel—contd
surface morphology, rel. to reaction with Br 8=30726
susceptibility, generalized, temp. depend. 8=31665
tensile internal stress during electrodeposition, role of hydrogen 8=31167
thermal cond. var. in mag. field 8=45022
thermal diffusivity meas. by laser flash method 8=39950
thermal expansion coeff. of film, e diffr. meas. 20–420°C 8=35546
thoriated, effect of S impurity on recrystallization 8=44138
vacancy clustering during quenching 8=44413
vacancy concentration during high temp. deformation 8=31038
vacancy and interstitial clusters, neutron-irrad. Ni 8=35538
vacuum-fused, recrystallization diag. 8=39659
x-ray line intensity and lattice consts. rel. to temp. 8=48649
As-plated, electroless, dissolution in acid rel. to Ni_2P phase existence 8=45383
C fibres, recrystallization, Ni stimulated 8=35236
Co, adsorption and oxidation of CO 8=48487
in Co, cathode ray polarographic microdeterm. 8=27776
Cu–Ni system, Cu diffusion on Ni side 8=31013
Fe- and Fe–C alloys, effects on impact properties 8=35693
in GaAs, activation energies 8=40238
H_2 desorpt. obs. 78°-300°K 8=30772
He-Ne laser TEM_{009} modes separation with film, obs. 8=37565
on LiF, films, single-cryst., epitaxial growth 8=35170
on MgO, films, single-cryst., epitaxial growth 8=35170
Na monolayers on (110), one-dimens. incoherent struct., obs. 8=39579
Ni^{61} low levels, h. f. s. and nuclear quadrupole moment 8=38677
Ni, magnetization anisotropy due to screw dislocations, calc. 8=40790
Ni, in thermionic diode, effective work function, comp. with Mo 8=31460
Ni(II) in aq. soln., primary solvation no. determ. by p. m. r. 8=39423
Ni, magnetization anisotropy due to screw dislocations, calc. 8=40790
Ni II, spectra, in excited configs., theory 8=43187
NiXI to XIV, oscillator strengths 8=38668
Ni–Cd flexible thin film batteries 8=33032
$Ni:Mn^{54}$, mag. hyperfine fields and spin-lattice relax., from n.m.r. 8=31891
Ni–Mo, resistivity anomaly rel. to ordering 8=40326
Ni^{2+}, in CaO, uniaxial stress meas. at impurities, strain coeffs. 8=40134
Ni^{2+} in CdF_2 and CaF_2, i. r. absorpt. spectra at room temp. and 4.2°K 8=31967
Ni^{2+} in $KMgF_3$, magnetoelastic coeffs. from acoustic paramag. resonance 8=31817
Ni^{2+} ions in fluorite-type lattices, absorpt. spectra temp. dependences 8=41076
Ni^{2+}: MgO, spin-lattice relaxation by phonon avalanche 8=40941
on n-, o-Si, plated contacts quality 8=44823
ThO_2 dispersed, grain growth and recrystallization rel to cold working 8=48604

Nickel alloys
See also Nickel compounds.
"alni" type, 3-d structure modification 8=35270
alnico, domain structure tracking by magneto-optical Kerr effect 8=36165
alnico, high-coercivity, powder pattern exam. 8=35346
binary, fundamental to Nimonic series, stacking-fault energies 8=35577
creep, relax and tensile data, graphical anal. 8=49042
Curie point and magnetization, change after plastic deform. 8=40823
diffusion rates, annealing time effects 8=35474
with elements of Pd and Pt groups, residual electrical resistivity 8=49168
high-strength, stage I fatigue fracture characts. 8=26839
Hyhro Radio metal, development, props. and appls. 8=27387
Invar, mag. props. rel. to anomalous thermal expansion 8=36162
irradiated, dislocation haloes 8=44452
Mumetal, permeability temp. vars. stabilization and appls. 8=27387
Nimalloy (in Ni-Mn system), high mag. permeability, V additions rel. to props. 8=31685
Nimonic, n irradiation creep obs. at 100°C 8=26833
n.m.r., rel. to dilute impurities of 4d and 5d elements of group VIII 8=49642
oxidation kinetics 8=27713
permalloy, alloying with Mo, Cr, Si and Cu, effect on 3d-electron state 8=35775
permalloy cores, testing at low temperatures 8=49542
Permalloy disc, energy losses on rotating in alternating and direct mag. fields 8=36102
permalloy, elastic limit determ. by Barkhausen effect 8=26838

Nickel alloys—contd
Permalloy films, abnormal Bloch wall motion under hard axis nanosec. pulse drive 8=31668
permalloy, films and coupled double layers with Fe–Ni–Mn, spin-wave resonance 8=31814
Permalloy films anisotropy and blocking fields rel. to r. f. losses, obs. 8=31678
permalloy, film, annealed cylindrical, bimodal magnetization 8=49540
permalloy films, annealing kinetics and increasing S conc. 8=31222
Permalloy films, coercive force and blocking field rel. to substrate temp., obs. 8=31676
Permalloy films, critical switching curves, obs. 8=31671
Permalloy films, domains and coercive force in supercritical transition, obs. 8=31629
permalloy films domain boundary dynamic props. 8=36167
permalloy film, domain boundary energy meas. rel. to thickness 8=40826
Permalloy films domain walls and mag. fine struct. in switching, stroboscopic transmission e microscope obs. 8=31674
permalloy film, domain wall movement, thermally activated 8=45020
Permalloy, films ferromag. reson. and off-reson susceptibility, r.f. 8=31822
Permalloy, film, ferromag. reson. rel. to internal stresses obs. 8=31821
permalloy film in contact with FeNiMn or Gd, spin-wave resonance obs. 8=31681
permalloy films, induced uniaxial anisotropy on n.- and Ar^+ bombardment 8=31694
Permalloy films, internal isotropic stresses and demagnetizing factors ferromag. reson. obs. 8=31223
permalloy films, mag-moment motion in h. f. rotating field 8=36157
Permalloy, films mag. struct. stability in pulsed orthogonal fields, obs. 8=31691
permalloy film memories, keepered and nonkeepered, internal field distrib. 8=40820
Permalloy, films pulse switching, induction and magneto-optical meas. comparison 8=31688
Permalloy films pulse switching rate, –180-250°C 8=31675
permalloy films, spin wave resonances, effect of Au and Ni layers 8=49581
permalloy film, spin-wave resonance 8=27452
Permalloy film spots nucleation, struct. and field rel. to dimensions, obs. 8=31673
permalloy films, supercritical, domain structure, theory 8=31684
Permalloy film thermal expansion coeff., e diffr. meas. 20–420°C 8=35446
permalloy film, 1000Å, Néel wall structure and energy 8=31663
Permalloy films, 360° walls and strong stripe domains 8=45024
Permalloy films uniaxial anisotropy, mag. annealing effects, 20-400°C 8=31677
permalloy films, wall streaming obs. 8=31558
permalloy/Gd/Co-permalloy triple layers, spin-wave resonance temp. dependence, 100–400°K 8=31816
permalloy, mag. anisotropy rel. to vacancies and interstitials formed on H charging 8=49538
permalloy, magnetization axis 8=49543
Permalloy narrow strips, meas. of domain wall energy 8=27420
Permalloy 78 films, demag. rel. to alternating field freq., obs. 8=31692
Permalloy, single-crystal platelets, ferromagnetic domains 8=31664
permalloy stripe-films, domain structure 8=31693
Permalloy thin films, exchange stiffness constant by pulse switching technique 8=31686
permalloy thin film, stationary spin-wave excitation 8=31587
Satmumetal, development, props. and appls. 8=27387
saturation magnetization rel. to conc. fluctuation 8=49537
79HM5, electron reflection, 600 to 1200 keV 8=44197
steel, phase transforms., mag. field effects 8=30702
ticonal, structure formation after thermomagnetic treatment 8=35055
Cu–Ni–Mn system, diffusion rel. to thermodynamic activities, obs. 8=31004
FeNi, film, electrodeposited, mag. switching behaviour 8=27419
on LiF, ferromag. films epitaxial growth 8=35170
on MgO, ferromag. films epitaxial growth 8=35170
Mu metal permeability, n irrad. effects, 6 × 10^{19} n/cm², > 1 MeV 8=29553
Ni–Al cermet, sintering investigations 8=26046
Ni–Al, colour rel. to composition, Fermi surface and Brillouin zones 8=45213
NiAl, cryst. struct. of martensitic phase 8=48668
Ni–Al, γ′ precip. coarsening 8=35120
Ni-11%Al, grain boundary, large-angle, dislocation form. 8=31105
Ni–Al, soft X-ray spectroscopy 8=36419
Ni_3Al–Ni_3Nb system oxide scale X-ray microstructural analysis 8=35276

Nickel alloys—contd
Ni–Au, electrical resistivity, investigation 8=44802
Ni–Au, fibre-reinforced, prep. 8=28208
Ni–Au films, vol. and surface diffusion 8=35486
Ni–Au system interdiffusion rel. to comp., 850–925°C 8=31015
Ni–2.2% Be, ageing, nucleated precip. phase space lattice, obs. 8=35271
Ni-C, metastable extension of C solubility, splat - quenching effects 8=30656
Ni–Co, f.c.c., low temp. sp. ht. 8=48739
NiCo–C, mag. anisotropy rel. to C interstitials 8=49526
Ni-Co-Cr superalloy sulphidation corrosion layers comp. and struct. obs. 8=30806
Ni–Cr, adherence and wettability to sapphire 8=43744
Ni–Cr films, vacuum-deposited, temp. coeff. of resistance 8=35819
Ni–Cr layers, electrical resistances, stability condns. 8=35818
Ni-34.5 at. % Cr, ordering from e. diffr. exam. rel. to elec. resistivity 8=35064
Ni–17%Cr, polycrystalline, alternating micro-deformation 8=35644
Ni—Cr—C—Si system, position of pseudo-eutectic, and reinforcing phase 8=43976
NiCr, ThO_2 dispersed, grain growth and recrystallization rel to cold working 8=48604
Ni-Cu, ferromag. transition temp. pressure-dependence itinerant-electron theory 8=27424
Ni–Cu film, resistivity, temp. (20–600°C) and comp. dependence 8=40325
Ni–2%Cu solid soln., vacancy quenching 8=44410
Ni–Cu, thermal cond. var. in mag. field 8=45022
$Ni_{1-3x}Cu_{2x}Fe_x$, low temp. sp. heat 8=39919
Ni-Fe alloys, sp. ht. 1.2-4.2°K obs. 8=26592
Ni-Fe, e-irradiated, remanence growth during low temp. mag. anneal 8=36156
Ni-Fe ferromagnetic films, planar Hall effect, thickness (100-1500Å) and temp. (77-293°K) dependence 8=31687
Ni-Fe, ferromagnetic thick films, domain-wall width determ. by Lorentz microscopy 8=27422
Ni–Fe films, anisotropy dispersion, temp. depend. 8=40821
Ni–Fe films, columnar grain structure obs., anisotropy existence and origin 8=44169
Ni-Fe films, domain-wall motion and ferromagnetic resonance losses 8=31695
Ni-Fe films, electrolytically prepared, conditions for formation of hexagonal structure 8=26122
48 Ni/52 Fe(111) films, epitaxial, ferromag., flat, of few atomic layers 8=36166
Ni-Fe film, magnon-phonon coupling 8=27421
Ni–Fe films, polycrystalline, susceptibility strain-dependence 8=40824
Ni-Fe, films, s. h. f. susceptibility, < 30 Oe 8=31689
Ni-Fe films single and double, reversible rotation regions, obs. 8=31690
Ni-Fe, films, spin-wave spectra, linewidth and relax. processes for main resonance 8=40887
NiFe films, sputtered, bias appl. during deposition, rel. to reduced sensitivity to gas impurities 8=31679
Ni-Fe film, static reversal of magnetization, rel. to anisotropy dispersion 8=36155
Ni–Fe films, stress, production parameter dependence 8=31192
76%Ni–Fe films, type II stripe domains, obs. 8=40825
Ni81% -Fe 19% film, 180°domain wall energy density rel. to thickness 8=45018
Ni-Fe, high-permeability, classification by props. 8=31662
Ni-Fe, magnetization ripple 8=36159
Ni-Fe, magnetoelastic sensitivity, composition gradient effect 8=36111
Ni-Fe polycrystalline, mag. anisotropy induced during evaporation and annealing 8=36152
Ni-Fe thin films, magnetoresist. and resist studies 8=44695
Ni_3Fe, near order from n. -scatt., 8=39531
Ni-Fe-Al films single and double, reversible rotation regions, obs. 8=31690
NiFe–C, mag. anisotropy rel. to C interstitials 8=49526
Ni-Fe-Co, films, s. h. f. susceptibility, < 30 Oe 8=31689
Ni-Fe-Co films single and double, reversible rotation regions, obs. 8=31690
Ni-Fe-Ni strip, gas emission in vacuum apparatus, rel. to heat and chem. treatment 8=39254
Ni_3Ga with dissolved Fe, giant mag. moments induced by Fe 8=27423
Ni–In, metastable b.c.c. phases formed on quenching 8=48408
NiMn, superlattice struct. due to periodic twinning 8=26712
Ni–18 at. % Mn– 8 at. % Fe, longit. galvanomagnetic effect magnetization dependence rel. to anisotropy 8=40827
Ni_3Mn, thin, antiphase boundaries obs. 8=35279
Ni-Mo, dislocations e. microscope obs., 8=48859
Ni_4Mo, ordered, rel. to tetragonal superstructure, and three classes of interfaces 8=26713
Ni_4Mo-Ni_4W, solid solns., ordering rel. to resistivity 8=39530

Nickel alloys—contd
NiO-MgO solid solns., formation on thermal decomp. of mixed hydroxides 8=39532
Ni–P films, Hall effect obs. 8=26970
Ni-P films, Hall effect structure dependence 8=44696
Ni-Pd, saturation magnetization and g factor meas. 8=31666
Ni-Pt, ferro- and paramag. props., 14-1000°K 8=31683
Ni-Rh, ferro- and paramag. props., 14-1000°K 8=31683
Ni-Rh, nearly ferromagnetic, mag. susceptibility and sp. ht. 8=31660
Ni-Si viscosity temp. dependence rel. to bonding 8=34796
Ni-Sn ferromag. Hall effect 8=27425
Ni-SOCo, cold-rolled, induced mag. anisotropy 8=31661
Ni-Ti, adherence and wettability to sapphire 8=43744
Ni-V, ferro- and paramag. props., 14-1000°K 8=31683
Ni-10 at. %W, local at. arrangements rel. to heat treatment and cold deformation 8=44244
Ni-W metallide phases isolation, investigation 8=39561
Ni-Zn ferrite, ferromag. relax. 8=27491
Ni-Zn, thermodynamic data 8=48726
Ni–Zn, X-ray absorption spectra, K edges 8=41080
Nickel compounds
See also Nickel alloys.
boracites, sector-growth and twinning, exam. by polarized-light microscopy 8=26188
ferrite, Fe^{57} NMR relax. times and amplification of external field 8=36267
ferrites, with high saturation magnetization and improved hystersis 8=31734
ferrites, ultrasonic waves, magnetic hystersis of velocity with Co, Mn and Cu impurities 8=31736
nickelous nitrate–MgO aq. cements, bonding mechanism 8=26010
oxide bicrystals, [001] tilt boundaries, energies and grooving kinetics 8=35278
oxides, thermodynamic props. by e.m.f. meas. 8=48729
oxidized complex with α-benzyldioxime, e.s.r. investigation 8=36248
rare-earth-nickel, R_xNi_y, mag. behaviours 8=31506
Ni complex, bis-(N-ethylsalicylaldiminato)nickel, crystal structure 8=26421
Ni(II) complex, bis(N-isopropyl-3-methylsalicylaldiminato) nickel(II), crystal structure 8=26425
Ni complex, bis(N, N-di-n-propyl-dithiocarbamate)Ni(II), structure 8=26419
Ni complex, bisperchloratotetrakis-(3, 5-dimethylpyridine) nickel (II) crystal structure 8=39817
Ni complex, diaquobisglycinatonickel (II), crystal structure refinement 8=44246
Ni complex, diethylenediamine Ni(II) iodide, Ni $en_2I_2.H_2O$, structure 8=26420
Ni complex, diethylenediamine Ni(II) nitrate, Ni $en_2(NO_2)_2$, structure 8=26420
Ni complex, di-(2-thioimidazolidine)nickel thiocyanate crystal structure 8=26423
Ni complex, hydrazinecarboxylate, crystal structure 8=26427
Ni complex, tetrakis (3, 4-dimethylpyridine) nickel (II) perchlorate crystal structure 8=39818
Ni complex with N-β-diethylamine ethyl-5-chloro-salicylaldimine, crystal structure 8=26424
Ni complex, Ni glyoxime crystal and mol. structure 8=26417
Ni complex, tris-(2-dimethylaminoethyl)amine nickel(II) bromide crystal structure 8=26418
Ni complexes, chloro- and nitro-thiocyanato bis (ethylenediamine) nickel structures 8=26426
Ni complexes, Ni en_2NCSI and Ni $en_2NCSClO_4$ (en=ethylenediamine) structure 8=26422
Ni complexes, thiosemicarbazides, crystal structure 8=26428
Ni ferrite epitaxial growth on MgO (111) and (110) surfaces 8=39594
Ni ferrites, dielectric losses at microwave freq. 8=49346
Ni molybdate hydrates, non-stoichiometric, structures for two phases, and vacancies 8=30916
Ni^{2+} complexes, electron spin density attenuation 8=47593
β^1-NiAl, prismatic dislocation loops 8=44453
$NiAl_2O_4$ cryst, reacts between defects 8=26633
NiAs, order of vacancies 8=35539
$Ni_3B_7O_{13}I$, ferromagnetoelectric props. 8=31670
$Ni_3B_7O_{13}I$, mag. props. 8=49539
$NiBr_2$, ht. of sublimation and dissoc. energy 8=39496
$Ni(CO)_4$, force consts. from vibr. spectra of isotopic species 8=34270
$Ni(CO)_4$, semiempirical MO model 8=47594
$NiCl_2$, aqueous soln., dielec. consts. and loss factors 8=34887
$NiCl_2$, ht. of sublimation and dissoc. energy 8=39496
$NiCl_2$ in alkali halide melts, thermodynamic props. from cell emf's, 8=49946
$NiCl_2$ in alkali halide soln., absorpt. spectra 8=48159
$NiCl_2$, matrix-isolated mols., fluoresc. spectrum 8=29757
$NiCl_2$, specific heat rel. to mag. energy spectrum, 1.8-16°K 8=39918
$NiCl_2.6NH_3$ and $NiCl_2.6ND_3$, dielectric dispersion and proton motional phase transitions 8=40614

Nickel compounds—contd
- $NiCl_4$-$ZnCl_4^{2-}$ mixed crysts., spectra at 4°K 8=27590
- NiCoP films, chem. deposited, mag. props. stability, up to 100°C, 1600 hr exposure 8=45023
- $NiCr_2O_4$, spin-structure determ. from magnetization and resonance 8=31731
- $NiCr_2O_4$, tetragonal to cubic transform., structural parameters, 92-298°K 8=26076
- $NiCr_2S_4$, NiAs-type structure, magnetization, 1.5°K to room temp. 8=45064
- Ni-Fe films, electrochem. deposition rel. to mag. props., obs. 8=31672
- NiFe films, 2-200Å, magnetization anomalies rel. to surface anisotropy 8=36158
- Ni-Fe ferrites with small additions of Co, mag. diffusion after-effect 8=36191
- NiFe, thin coupled films, domain wall behaviour 8=49541
- NiF_2, electron-magnon interaction, effect on absorption band 8=41127
- NiF_6^{-4}, electron delocalization and spectrum 8=25510
- Ni_3Fe, tensile behaviour upon ordering 8=44595
- NiFeCo film, mag. props., effect of Cu layer 8=40822
- $NiFe_2O_4$, effect of tetrahedral site Ni_b^+ ions 8=27455
- $NiFe_2O_4$ films, ferromag. resonance thickness dependence 8=31823
- $NiFe_2O_4$ superparamag. particles, hyperfine splitting in mag. field from Mössbauer spectra of Fe^{57} 8=36160
- $NiFeS_x$ films, electrodeposited rel. to vacuum deposited 8=35177
- NiGa, structure defects constitutional and thermal, 8=48829
- Ni_3Ge, gaseous impurity segregation 8=35673
- $Ni_{1+x}Ge_xFe_{2-2x}O_4$, anisotropy rel. to resonance props., 4.2-393°K 8=36227
- $Ni_{1+x}Ge_xFe_{2-2x}O_4$, internal fields at two sites, Mössbauer determ. 8=36193
- Ni-H system, thermoelec. power rel. to H conc., 77-250°K 8=35998
- $Ni[(H_2O)_6]^{2+}$, O^{17} hyperfine coupling consts., evidence for distortion from octahedral symmetry 8=49652
- Ni–I boracite, paramag. susceptibility temp. dependence 8=31525
- NiI_2, ht. of sublimation 8=39496
- $NiNH_4(PO_3)_3$, rhombohedral form, crystal structure 8=44245
- Ni_3Nb oxide scale X-ray microstructural analysis 8=35276
- Ni-NiO multilayer films, mag. coupling 8=36133
- NiO, antiferromagnetic, magnon dispersion and density states 8=40874
- NiO, conductivity, high freq. 8=31384
- NiO, covalency parameters 8=30617
- NiO, decomposition on photo-absorption 8=36567
- NiO, lattice parameters rel. to pressure 8=48669
- NiO, struct. exam. 8=48592
- NiO whiskers, growth and props. 8=35255
- NiO (100) face, heating effects from e-diffr. exam. 8=39650
- $Ni(OH)_2$ in LiH, anodic oxidation and Li migration in n-semiconducting mat. production 8=45382
- NiO : Li, semiconducting phenomena 8=44803
- NiO-MgO solid soln., struct. and mag. props., 98°-298°K 8=35061
- NiO–MgO solid soln., thermodynamic activities of NiO 8=43979
- Ni_4Mo, order and resulting substructure, electron diffraction and electron microscope study 8=44009
- Ni_2P in Ni, As-plated electroless, electrochem. analysis 8=45383
- NiS, first-order-paramag-antiferromag., metallic-semiconducting transition 8=31788
- NiS_2 pyrite, antiferromag. props. 8=31493
- NiS_2, pyrites struct., growth by Cl_2 transport 8=26249
- Ni Sb_2O_6, neutron and X-ray diffraction studies 8=48614
- $NiSe_3$ pyrite, paramag. props. 8=31493
- $NiSi_8$ crystal, paramag. cross relax. 660Hz-1MHz 8=27486
- Ni_3Sn_2 gaseous impurity segregation 8=35673
- α-$NiSO_4 . 6H_2O$, ht. capacity, mag. moment, 0.4–4.2°K, in mag. field 8=30968
- α $NiSO_4 . 6H_2O$, magnetothermodynamics, theory 8=39920
- $NiTa_2O_6$, neutron and X-ray diffraction studies 8=48614
- Ni–Zn ferrite, ferromag. resonance and non-linear effects 8=31819
- Ni–Zn ferrites, hot-pressed, fine-grained, hf and microwave props. 8=49562
- $Ni_{1-x}Zn_xFe_2O_4$, effective anisotropy, contributing factors 8=31735
- N–NiO films. magnetic after effect of ferro-antiferro magnetic coupling 8=49517
- TiO_2–Sb_2O_3–NiO system, comp., structure and colour 8=26039

Night sky. See Airglow.

Night glow. See Airglow.

Nilsson's model. See Nucleus/models.

Niobium
- b.c.c. lattices, energy of interstition of impurity atoms into octahedral and tetragonal positions 8=35542
- collector of thermionic diode, microhardness rel. to reliability 8=37377
- conductivity, thermal mixed state anisotropy 8=26604
- crystals, shear-stress strain-rate dependence, characterization 8=31220

Niobium—contd
- crystals, slip asymmetry studies 8=26697
- crystals slip and yielding at room temp. 8=26696
- density from X-ray determ. of lattice parameter and hydrostatic meas. 8=48670
- diffusion of V, coeffs. 8=35475
- diffusion in W, electrochem. sectioning tech. to determ conc. profiles 8=48797
- dislocation-Nb velocity, stress dependence, etching meas. 8=31085
- elastic constants, third-order, for mono-and polycrystals 8=40177
- electrode charging with hydrogen to produce pure hydride 8=27755
- electrodes for vacuum gap, breakdown voltage and prebreakdown current on cooling to 4.2°K 8=29909
- electron emission from (110), (100), (111) and (116) faces 8=40689
- electron reflection, 600 to 1200 keV 8=44197
- film deposition by d.c. diode and substrate bias sputtering 8=48455
- films, sputtered cylindrical, flux jumping phenomena 8=49472
- in mixed state, superconducting props., crystalline orientation depend. 8=35852
- oxidation, 450-720°C, kinetics rel. to scale morphology 8=49878
- oxidation mechanism from oxygen diffusion meas. in Nb_2O_5 crystals and scales on Nb 8=48785
- oxidation rate-constant determ., low-temp., from discontinuous film resistance changes 8=49883
- rolled, orientation distrib. of crystallites 8=35275
- single crystal, anisotropic energy gap obs. 8=27023
- sorption of O_2, kinetics 1100-1800°C at 5×10^{-5} and 5×10^{-4} torr 8=49895
- spark-machine notched, dislocation distrib. from etch figures 8=40042
- strain-ageing oxygen dependence 8=26835
- superconducting, a.c. losses near lower critical field 8=44727
- superconducting, anomalous magnetic behaviour 8=27383
- superconducting magnetization, n-irradiation effects ($E > 1$ MeV) 8=40379
- superconducting, microwave surface resistance meas. 8=49195
- superconducting, peak effect rel. to dissolved oxygen clusters 8=49192
- superconducting properties, influence of extended defects 8=49193
- superconducting proximity effect in contact with Cu and Ni 8=27026
- superconducting resistivity and Hall effect meas. 8=44724
- superconducting, resist. and magnetization, n-irrad. effects. obs. 8=43073
- superconducting, tunnelling characteristic detail in high purity single crystal 8=27025
- superconducting, and V in mixed state, nonlinear resistivity and dissipation 8=27027
- superconductivity, K_1 and K_2, theory /expt. discrepancy 8=31342
- surface self-diffusion in strong elec. field, field-emission exam., 8=39978
- u. s. attenuation near H_{c_2} 8=30949
- wetting by Cs and Na, rel. to bare work function 8=35168
- X-ray K-absorpt., fine structure at 300°, 77°, 4.2°K. obs. 8=41124
- Nb^{96}, carrier-free, prep. from Zr^{96}(p, n) 8=47322
- Nb-Al_2O_3 powder between Nb slabs, cermet seal for thermionic diode 8=28499
- Nb + 75% Zr superconducting magnet, for 85 kG 8=41937
- Nb-Zr, type II superconductor, spin-lattice relaxation 8=41005

Niobium compounds
- alloy substrates for non-electrolytic deposition of Ti from fused salts at high temps. 8=44063
- hydride production with high purity by electrolytic charging of Nb with hydrogen 8=27755
- hydrides (deuterides), structure and phase transitions, from n diffr. exam. 8=39725
- niobates, ANb_2O_6 structural comparison with ATa_2O_6 phases 8=48636
- oxidic niobates, cryst. struct. effect on luminesc. 8=45284
- superconducting alloy, instability, source 8=49198
- Nb complex, tetrabromobis (acetonitrile) Nb(IV), struct. and i. r. spectra 8=44241
- Nb oxide, prod. from columbite by ion exchange process with Ta 8=36544
- Nb_3(Al, Ge), β-tungsten phase, high-transition-temp. superconductor, props. 8=40376
- Nb_3(Al, Ge), superconductivity in high mag. field 8=44726
- Nb_3Al-20%Nb_3Ge, sintered, supercond. critical temp. increase by annealing, obs. 8=27019
- NbC, f. c. c. superconducting props., anomalous 8=27022
- NbC-graphite composites, elastic props., 8=49040
- $NbC_{0.64}$, C diffusion coeff. temp. dependence 8=31018
- $(Nb_6Cl_{12})^{n+}$ (n=2, 3, 4), electronic struct. and spectra 8=27595
- NbF_6^-, spin relax. and chem. exchange effects in F^{19} n. m. r. 8=34914

Niobium compounds—contd
Nb-Ga system, superconductivity 8=49197
Nb-Hf alloys, thermoelectric properties 8=49395
Nb-Mo alloys, creep rel. to temp. 8=49038
Nb-Mo alloys, density of states N(O) rel. to thermal cond. depend. on conc. 8=31292
Nb-Mo alloys, lattice dynamics rel. to electronic structures 8=44303
Nb-N, superconducting, peak-effect temp. dependence, 4.2-1.35°K 8=40378
Nb_2N film, deposited by reactive evaporation 8=48454
NbO stability, polarization of solid galvanic cell 8=45374
Nb-O, strain-ageing from resistivity meas. 8=26846
Nb_2O_5 crystals and scales on Nb, oxygen diffusion rel. to Nb oxidation behaviour 8=48785
Nb_2O_5 effect on corundum recrystallization 8=48536
Nb_2O_5 insulating film, refractive index 8=49763
Nb-O-N supersaturated solid solns., oxide and nitride precip. in annealing and hardness, obs. 8=30831
Nb_2O_5-Na_2O-SiO_2 glasses, γ-irrad., e.s.r. of Nb centres 8=40937
$Nb_2O_3 . WO_3$-WO_3 system, structure of stable phases 8=39814
Nb-Sb superconducting alloys, mag. hysteresis, at 4.2°K 8=27024
$NbSe_2$, band model calcs. 8=49105
Nb_2Se_3, crystal structures 8=44240
Nb-Sn superconducting alloy, mag. hysteresis, causes 8=44972
Nb_3Sn-composites, supercond, transition temp. rel. to hot pressing and particle size 8=49190
Nb_3Sn hard supercond. tubes, mag. flux jumps, 4.2°K 8=31341
Nb_3Sn high-Q r.f. coils for 15°K 8=31359
Nb_3Sn, lattice expansion and superconductivity changes on H_2 up-take 8=26414
Nb_3Sn, lattice softening and stiffening at low temps. 8=49039
Nb_3Sn, phase transform. from X-ray diffr. at 300, 15.5 and 10.5°K 8=35118
Nb_3Sn, sintered, supercond. stabilization by liquid He flow through pores, obs. 8=27020
Nb_3Sn strip superconductor, plasma-plates, critical current angular dependence 8=40420
Nb_3Sn superconducting ribbons, vapor-deposition rel. to e.m. performance 8=40418
Nb_3Sn, supercond. transition temp. rel. to hot pressing and particle size 8=49190
Nb_3Sn-Cu-steel composite conductors, e.m. performance and mech. props. 8=40401
Nb_3Sn; ZrO_2 particles, superconducting performance 8=44728
Nb-Ta alloys, Nb rich, superconductivity, K_1 and K_2, theory/expt. discrepancy 8=31342
Nb-Ti alloy, specific ht., temp. depend. at superconducting transition 8=48738
Nb-Ti alloys, thermoelectric properties 8=49395
Nb-45 wt. %Ti and Cu composite conductor for large currents 8=27021
Nb-40%Ti, Cu-clad stabilized superconductors 8=40377
Nb-Ti, superconducting props. 8=35853
Nb-50%Ti superconducting rods, flux jumps 8=49194
Nb-Ti, thermal conductivity rel. to temp. 8=44367
NbTi strips, superconducting, flux flow state stability 8=44725
Nb-Ti-N films, reactively sputtered, superconducting props. rel. to comp. 8=40380
Nb-Ti-Zr alloys, critical mag. fields 8=35851
Nb-W alloys, normal spectral emissivity, temp. and comp. dependence 8=45224
NbZn, μ-phase lattice consts. 8=48392
Nb-Zr alloy, flux jumps at liquid He temp. 8=49189
Nb-Zr alloys, type II superconductors, spin lattice relaxation 8=44744
Nb-1%Zr alloy, mass transfer in Li, temp. effect determ. in convection loop tests 8=35503
Nb-Zr hard supercond. tubes, mag. flux jumps, 4.2°K 8=31341
Nb-25%Zr superconducting solenoid persistent current decay rate, field dependence 8=27039
Nb-25%Zr superconducting tubes, flux jumping rate dependence 8=40375
Nb-Zr25 superconductor, type III, lattice defects, nature, size and distrib. and effect on high-field props. 8=48828
Nb-Zr, type II superconductor, spin-lattice relaxation 8=41005
Nb-25%Zr wire, supercond., meas. of a.c. surface power loss 8=49196
NbZr alloy wire, used in superconducting 85 KG wire 8=46385
NbZr coil superconducting magnets effect of neutron radiation 8=33405
Nb-Zr-N films, reactively sputtered, superconducting props. rel. to comp. 8=43080

Nitrogen
abundance in solar photosphere 8=28171
active, chemiluminesc. reaction and anhydrous Na_2SO_4 8=41255
active, $N_2(A^3\Sigma_u^+)$ 8=38840

Nitrogen—contd
active, u.v. chemiluminescence from reactions with I_2, IBr, ICl and ICN 8=49887
adsorption and desorpt. isotherms for porous mats. rel. to pore struct. anal. 8=30659
adsorption and interact. of N_2 with Ni and Pd films 8=26138
adsorption by ice, isotherms rel. to surface struct. 8=30769
adsorption by W on (110) and (112) planes 8=39621
aerosol with oleic acid particles, sound attenuation and dispersion 8=43889
afterglow, kinetic and spectroscopic constraints 8=29897
afterglow, temp. depend. of chemiluminesc. 8=27712
afterglow, yellow intensity 8=47756
ageing effects on insulators 8=40556
arcs, d.c. wall-stabilized, static and recovery characts. 8=39011
atmospheric, fixation by transition metal hydride complexes 8=25521
atom, fifteen new emission lines in 10 000 to 11 000Å region 8=34144
atom, low-energy e scatt., polarization calc. 8=47527
atomic, in chemiluminescent reactions involving H_2, CH_4, N_2 and Ar 8=41245
atom, metastable (^2D), e.s.r. spectrum 8=25386
atom, photoionization cross-sections 8=39044
atomic, photoionization cross section meas. 8=29949
atoms, Rydberg orbitals calc. 8=29620
band systems, $b'\,^1\Sigma_u^+ \rightarrow X^1\Sigma_g^+$ and $g^1\Sigma_u^+ \rightarrow X^1\Sigma_g^+$, selective enhancement in vacuum u.v. 8=38841
boiling for cooling in X-ray crystallography 8=32992
breakdown, a.c. induced, statistical time lags effect 8=47760
charge transfer from p and H atom, cross-sections 8=38737
in chemiluminescent reactions involving atomic N, and CH_4, H_2 and Ar 8=41245
chemisorption and NH_3 synthesis of Fe purified in ultravacuum 8=41265
chemisorption on metals, expt. and theoretical results for heat of reaction 8=36585
compressibility, ≤ 10 000 atm and 400° C 8=34600
condensation in hypersonic wind tunnel 8=30599
cooling effect in high-vel. streams, on injection into reacting or non-reacting boundary layer 8=32958
diffusion in ZrN, film-thickness determ. 8=44396
discharge, waves of ionization 8=47745
dissociative ionization 8=29976
electron diffusion coeff. rel. to mobility 8=39238
excitation and ionization, simultaneous, by e impact 8=25717
freejet expansion from sonic orifice, rotational relax. and rel. to temp. 8=34629
gas, dilute, thermomagnetic torques, exptl. investigation 8=30287
gas electron transport coeffs. 8=39230
gas: NO_2 and I_2, stimulated thermal Rayleigh scatt., obs. 8=34665
gas, p bombard., Ep=0.56-1.7keV, spectrum obs. 8=43322
gas, viscous flow in strong mag. fields 8=34619
glow discharge, acoustic wave effects on pos. column 8=47747
hydrates, dielec. props. 8=49343
implanted in Si, impurity distrib. determ. 8=27131
interferometric analysis of conc. in gaseous mixtures. 8=49988
interstitial solute trapping in quenched and irrad. Fe 8=44420
ion bombardment of p-Si, donor props. 8=27128
ionization coeffs. 8=39042
ionization and excitation simultaneous, by e impact 8=25717
ionization states of some unidentified lines 8=43223
ions implanted in Si, distrib. 8=49266
ions, low energy, resonance charge exchange 8=47536
ions, N_2^+ excited states rot. and vibr. consts. calc. 8=38792
ions, $N^+ + O^-$ neutralization cross section, obs. 8=34455
isotopes, determ. by recording spectrometer 8=28817
isotope exchange between NO_2^- and NO_3^- 8=27673
isotope exchange between NO and NO_2^- 8=27674
liquid, bubble growth and collapse, rel. to subcooling and decreasing press. 8=34788
liquid, bubble motion study 8=34739
liquid, dielec. permeability meas. at ca. −190°C rel. to liq. air permeability calc. 8=30512
liquid, elec. conduction in diode cell 8=48200
liquid, stimulated Raman scatt., photon distrib. in Stokes components 8=34855
low-energy e stopping cross sections 8=47977
metals, H, O, N joint determ., isotope method 8=27784
molecular beam interaction with stainless steel surface 8=29854
molecule, electronic energy transfer from metastable Xe atom 8=29847
molecule, excitation by 1-12 eV electrons 8=29755
molecule N_2, charge exchange with He^+ and Ne^+, 2-250 eV 8=38758
molecules, N_2 ground state rot. and vibr. consts calc. 8=38792

Nitrogen—contd
molecules, trapped in rare gas matrix, e transitions perturbation 8=39523
multiply-ionized, beam-foil excitation 8=29644
in optical pumping of Cs, enhancement by quenching 8=47514
permeation, diffusion and soln. in W and Mo 8=39987
permeation rates and coeffs. in W, 1800° to 2600°C 8=44394
plasma jet, i.r. emission spectrum 8=30182
plasma jet, temperature determ. by spectroscopic methods 8=30183
plasma laminar jet, mean temp. determ. 8=34469
plasma, non-equilib., emission lines from finite layers, calc. 8=43543
Rayleigh scattering, depolarized, as new probe of intermolecular forces 8=39212
reactions with He^+ and O^+ in afterglow 8=41253
red giants, N^{14} burning before He flash 8=28055
shock-wave ionization, e temp. meas. 8=39221
solid, thermal capacity, 2.6-15°K 8=30967
solubility in Ta; 10^{-8}-10^{-3} torr, 1600-2300 °K, 0.0044-1 atomic %, press.-temp.-conc. ranges 8=49897
solubility of N in cold-deformed α-Fe 8=35543
solubility of water in compressed N_2 8=30302
sorption by Mo 8=49908
spark, laser-prod., expansion mechanism, obs. 8=34432
spectral radiation intensity, shock-tube heated 8=24399
in steel, conc. effect on brittleness, when subject to neutron irrad. 8=47405
thermal cond. and total emission coeffs., high-temp., expt. and theory 8=47955
thermionic emission from conductors, above 600°C 8=36046
vibrational energy relaxation with multiple quantum transitions 8=34640
viscosity, low-temp. 8=39237
CO_2 low conc., mass spectrometric determ. 8=32153
Cd 6^3S_1 level depolarisation in N_2 collisions, cross section, obs. 8=38692
K-N_2 collisions, mixing and quenching cross sections 8=29836
N^{14} data from proton spectra by double irradiation method 8=37537
N^{14} excitation, 8.5-11.5 MeV, by inelastic e scatt. 8=29654
N^{14} ion beams, lifetimes and excited states for multiply charged ions 8=43217
N^{14} ions, 115 MeV, radiation chemical studies 8=41289
N^{14} n.q.r. study of NO_2^- ion in simple nitrites 8=49666
N^{15}, spectrochemical estimation, enhancement by inert gas 8=27791
N^{16}, use in temp. meas. of outlet channel of AGR · 8=47435
$N_2^{28} + N_2^{30} \rightleftarrows 2N_2^{29}$ catalyzed by Mo 8=49908
N^+ ion beam, N_2^{2+} contamination 8=28583
N^+ mobility in dry air, obs. 8=39027
N II $2p^3$-$2p3s$ arrays, line strengths and transition probabilities 8=45915
$N + CH_3CHO \rightarrow HCN + H_2 + HCO$, mass spectrometric study 8=27710
N I, ionization limits 8=43488
N_2, absolute u.v. transition probabilities 8=34230
$N_2(A^3\Sigma^+)$. excitation of Hg 8=34163
$N_2(A^3\Sigma_u^+)$, excitation of NO 8=25494
$N_2(A^3\Sigma_u^+)$ in active N 8=38340
$N_2(A^3\Sigma_u^+)$, reaction with N atoms 8=25493
N_2, collision with He atom, rotational excitation 8=25666
N_2 density and temp. altitude profiles from ground to 300 km, diurnal variation 8=41339
N_2 density and temp. in thermosphere, diurnal 8=36774
N_2 density in lower thermosphere above Sardinia, mass spectrometric determ. 8=27939
N_2, dipole-allowed absorpt. spectrum, absolute f values 8=34264
N_2 discharge, evidence for $^3\Delta_u \rightarrow B^3\Pi_g$ transition 8=47608
N_2, dissociation in shock tube, vac. u.v. absorpt. 8=25651
N_2, effect of O atoms on vibr. relax. 8=47724
N_2, excitation of N_2^+ by vac. u.v. photon impact 8=47609
N_2, first positive system excitation 8=38994
N_2 gas, hot, thermodynamic functions, approx. calcs. 8=47954
N_2 gas, ionization by 0.2-1.8 MeV He^+ ions, effective cross sections 8=39035
N_2, ground and ionized states, potential energy calc. 8=25492
N_2 interaction with Ti, and form. by Ti sorption and diss. of NH_3 8=32103
N_2, $K(b^1\Pi_u) \leftarrow X$ transition, u.v. absorpt. 8=25491
N_2 lasers, high power, parameters affecting power output 8=37572
N_2 mol., Cs-N_2 collisions, cross-section obs. 8=38957
N_2 number densities in thermosphere above Fort Churchill and Sardinia 8=36761
$N_2(1+)$ band system, e transition moment obs. 8=34262
N_2, potential energy curves of ground and ionized states, LCAO calc. 8=43320
N_2 reactions with He^+ in upper atm. 8=27937
N_2, Stark broadening 8=34272
N_2, Vegard-Kaplan bands, intensity obs. 8=34265
N_2 vibr. excitation due to 2-3 eV electron scatt., energy depend. oscills. due to motion of nuclear wave packet 8=43311

Nitrogen—contd
N_2, vibr. relaxation calc. 8=43263
N_2, viscosity, dynamic, meas. to 500°C, and statistical mech. correls. 8=43704
N_2^+, absolute u.v. transition probabilities 8=34230
N_2^+ atm. emission, tropospheric scatt. model 8=41365
N_2^+ aurora zone daytime, rocket spectra 8=45483
N_2^+ band excitation by e-impact (80-1500 eV) 8=25490
$N_2^+(B^2\Sigma_u^+)$, from rot. and vib. energy transfer in N_2 collision with atomic ions 8=39046
N_2^+, fluoresc. spectra from vac. u.v. photon impact 8=47609
$N_2^+ + H_2$ and $N_2^+ + D_2$, low energy ion-mol. reactions 8=27711
N_2^+ ions, excitation by electrons, at near threshold energies 8=47523
$N_2^+(1-)$ ion, first negative bands, e transition, dipole moment, matrix element square determ. 8=29752
N_2^+, Stark-broadened rot. lines, shapes and widths 8=34259
$N_2^* + Ar$ collisions, ionization cross section enhancement, obs. 8=34454
N_2^{-2} state e spectra, obs. 8=34224
N_2^{2+}, charge exchange in N_2, CO_2, and Ar 8=29974
N_3^-, SCF minimal basis set calc. 8=29719
N-He mixture, mass and thermal diffusion coeff. meas. 8=43706
N-I_2 flames, i.r. emission 8=49890
N-N pairs in GaP, energy levels 8=49803
N_2-O_2 diving atmosphere, non-combustion region 8=49884
N_2-O_2, solid-state phase diagram 8=35117
TiNb33, N addition rel. to supercond., microstruct. and workability, obs. 8=44742
TiNb40, N addition rel. to supercond., microstruct. and workability, obs. 8=44742

Nitrogen compounds
charge distribution, molecular spectroscopy by ESCA 8=47604
double nitrates: Pr^{3+}, mag. resonance lineshapes 8=31881
metal thiocyanate molten solns., i.r. spectra 8=25934
nitrite salts, inorganic, luminesc. 8=49810
nitroxide free radical, proton resonance at 310 MHz 8=43415
HNCO, SCF minimal basis set calc. 8=29719
HNO_3-N_2O_4-H_2O solns., phase diagram to −196°C 8=43903
HN_3, SCF minimal basis set calc. 8=29719
N^{14} n.q.r. study of NO_2^- ion in simple nitrites, N^{14} n.q.r. study 8=49666
NCN, singlet and triplet states 8=25495
NCN_3, flash photolysis 8=25495
NCN_3, microwave spectrum 8=25496
NCO^-, SCF minimal basis set calc. 8=29719
NCl_3 in CCl_4, raman spectrum at high resoln., 8=43838
$N^{14,15}ClO_3^{2-}$ anion, i.r. absorpt. spectra 8=29754
ND, $(A^3\pi_i$-$X^3\Sigma^-)$ system, rotational analysis of (2, 2) band 8=38843
N_2D_2, vacuum u.v. absorpt. spectra 8=34267
NF, $b^1\Sigma^+$-$X^3\Sigma^-$ band system 8=25497
N_2F_4, Raman spectrum and struct. 8=38839
NF_3, force field and molec. consts. 8=43319
NF_3, rotation absorpt. spectrum in range 10 to 50 cm^{-1} 8=34260
NH_4 mol., evidence 8=47610-11
NH...H intramolec. H bonds 8=25609
N_2H_2, extended Huckel treatment 8=25509
N_2H_2, i.r. and vacuum u.v. absorpt. spectra 8=34267
N_2H_4, vac.-u.v. photolysis 8=36613
$N_2H_4^+$, e.s.r., temp. depend. 8=47685
NH_2CN, microwave spectrum, N^{14}-quadrupole coupling 8=43297
$NH_4H_2AsO_4$, (ADA) elastic, piezoelectric and dielectric constants 8=27298
$NH_4H_2AsO_4$(ADA) resonator plate, low temp. coeff., props. 8=27299
$NH_4H_2AsO_4$, n.q.r. spectra, rel. to temp. 8=41009
$NH_3OH\ Al\ (SO_4)_2 . 12H_2O$, n.m.r. 8=40983
NO, adsorbed on zeolites, i.r. spectra 8=27553
NO, absolute u.v. transition probabilities 8=34230
NO afterglow discharge, photoionized, e recomb., attachment and ambipolar diffusion obs. 8=47755
NO afterglow, temp. depend. 8=38993
NO, combined Zeeman and Stark effects 8=25498
NO, e beam dissoc., O prod. cross-section obs. 8=47703
NO, effect on muonium, and on polarization of bound muon 8=42482
NO, eqn. of state, 190°-2000°K 8=43676
NO, excitation by $N_2(A^3\Sigma_u^+)$ 8=25494
NO, heterogeneous $(^2\Sigma-^2\Pi)$ interactions 8=34268
NO in H_2O, radiolysis study 8=49975
NO, intensity of fundamental band 8=25499
NO, ionosphere D-layer production 8=32323
NO, ionosphere D region height distribution and recombination coeff. 8=50191
NO, Λ doublets in mag. field 8=29758
NO, linewidth of $J = 1/2 \rightarrow 3/2$ rot. absorpt. 8=47605
NO, luminesc. during u.v. photolysis 8=34266
NO magnetoplasma, electron energy relax. 8=47815
NO, mesosphere upper, vertical motions and distribution 8=45485
NO mols. trapped in rare gas matrix, e transitions perturbation 8=39523

Nitrogen compounds—contd
NO and NO_2^-, exchange and fractionation of N isotopes 8=27674
NO and NO_2, in mesosphere, role in governing electron conc. 8=27880
NO, photoelectron spectrum 8=47606
NO production around 100 km 8=41442
NO, pure rotational spectrum 8=25500
NO, rate consts. for charge exchange with quasithermal ions 8=29975
NO, role in sunrise E-region, from density profiles and NO^+/N_2^+ ion ratios 8=36857
NO, rotating resonance on transitions between Zeeman levels in mag. field rel. to hyperfreq. elec. field meas. 8=38846
NO soln. in H_2O, D_2O; photolysis at 1849Å 8=49958
NO, sorption and mag. susceptibility on Pd 8=44075
NO spectra by double-beam, two-beam interferometry far i.r. 8=28818
NO trapped in NH_3OHCl, X-irradiated, e.s.r., and of radical pairs and V_K centres 8=31878
NO, 2 isotopes, comparison of rotational and spin-orbit coupling consts. 8=43325
NO^{-1} state e spectra, obs. 8=34224
NO^+, absolute u.v. transition probabilities 8=34230
NO^+ + e dissociative-recombination-rate coeff. temp. dependence 8=29958
NO^+ in E-region of ionosphere, effects of metal-ion layers 8=36858
NO^+, electronic states 8=47606
NO–N_2 mixture, diffusion, Senftleben effect 8=30316
NO + O, afterglow mechanism 8=32274
NO_2, absorption in lower stratosphere 8=27877
NO_2, adsorbed on zeolites, i. r. spectra 8=27553
NO_2, adsorbed on ZnO, e.s.r. 8=48499
NO_2, e.s.r. in cryst. N_2O_4 matrix 8=45094-6
NO_2, e.s.r. in frozen solns. 8=45093
NO_2, first ionization potl. and vibr. struct. obs. 8=43487
NO_2 in ionosphere D layer, non polar region, concentration changes after sunset 8=50191
NO_2, luminesc. during u.v. photolysis 8=34266
NO_2, molecular consts. from near i.r. spectrum 8=43326
NO_2, 2491Å electronic transition 8=25503
NO_2^-, charge distrib. in ferroelec. $NaNO_2$ 8=48308
NO_2^-, double-ζ LCAO SCF MO calc. 8=29756
NO_2^- and NO_3^-, exchange and fractionation of N isotopes 8=27673
NO_2^- state e spectra, obs. 8=34224
NO_2, CO, Cl; reactions at 381-473°C. kinetic eqn. setup 8=49857
$2NO_2 \rightleftarrows 2NO + O_2$, thermal separation 8=47986
NO_2 + H, free electron generation 8=49872
NO_3 configuration in $Ba(NO_3)_2$ crystals, from n-diffr. 8=39773
NO_3^- in $NaNO_3$, KNO_3 and $CsNO_3$ near 600°C, i. r. emission spectra 8=38842
NO_3^-, u. v. spectra in molten alkali metal nitrates 8=30489
N_2O absorpt. spectrum rel. to SISAM resolution, 4.5μ 8=28823
N_2O, adsorbed on zeolites, i. r. spectra 8=27553
N_2O band in ammonia, cross-correlation obs. 8=42230
N_2O, chemisorption of both N and O atoms by W, rel. to temp. 8=36586
N_2O, electron attachment, structural resolution 8=39045
N_2O, luminesc. during u.v. photolysis 8=34266
N_2O, N^{14} quadrupole coupling from microwave spectrum 8=25505
N_2O, quadrupole moment, from microwave spectral broadening 8=29729
N_2O, spectral transmission in near i.r. bands, calc. 8=25506
N_2O strength of bands near 4.5μ 8=34263
N_2O^- state e spectra, obs. 8=34224
N_2O^+ and NO excitation, lifetimes and decay cross-sections 8=34261
N_2O_4 gas, P-V-T dependence 8=30280
$N_2O_4 \rightleftharpoons 2NO_2$ system, diffusion of Kr 8=34681
$N_2^{14}O$ and $N_2^{15}O$ for meas. in mixed γ and thermal neutron fields 8=46921
$N^{14}O^{16}$, l.f. satellite band 8=25501
$N^{14}O^{16}O^{17}$, microwave spectrum 8=25504
$N^{15}O^{18}$, vibr. rot. bands 8=25502
$NOIrF_6$ and isotypes, structure from n-diffr. studies 8=25469
$NOPtF_6$ and isotypes, structure from n-diffr. studies 8=25469
$N_4P_4Cl_8$, T form, crystal structure 8=48665
ammonia
adsorbed on Si, vibrations obs., rel. to bonding strength 8=25508
adsorbed on W (100) surface, LEED obs. of electron impact effects 8=26140
adsorption and decomp. on W, field-emission meas. 8=27734
alkali metal-NH_3 solns., internal reflection spectra 8=30490
ammonia-nitrogen viscosity 30°-200°C, below 10cm Hg press: Chapman-Enskog theory 8=43702

Nitrogen compounds—contd
ammonia—contd
collision-induced transitions between rot. levels 8=47612
crystals, lattice vibrs. calc. 8=30926
crystals, stress relaxation 8=35708
ionization energy from NH_4I and $NH_4I(Tl)$ spectra 8=32014
leak detection equipment appl. 8=39258
liquid, solns. of KNH_2, absorpt. spectra 8=39380
maser two-cavity meas. of 3-2 inversion freq. and freq. stability 8=24267
matrix-isolated, i. r. obs. of nuclear-spin-species conversion 8=38830
mixture with methane, laser discharge emission spectral obs. 8=33190
molecular struct., using wavefunction of double minimum potentials 8=25507
oxidation in shock waves 8=41256
photoionization, ion-mol. reactions 8=36612
reaction with hydride ion, MO theory 8=27678
rotational lines, Stark effect observed by far i. r. laser 8=38845
solid, thermal conductivity, 28-114°K 8=35460
sorption of Ti, and dissociation to H_2 and N_2 8=32103
synthesis of Fe purified in ultravacuum and N chemisorption 8=41265
synthesis on Mo catalyst 8=49909
thermal cond., 273-1173°K, also with Ar and Ne 8=47962
thermodynamic props. as ideal gas 8=47960
AgBr, recrystallization and photosensitivity effects 8=30821
Li-NH_3 soln., u. s. vel. obs. and compressibility calc. 8=30468
Na-NH_3 liq. solns., dynamic polarization 8=34925
ND_3, deuteron spin lattice relaxation 8=48217
NH_2^- ion reactions with triatomic mols. 8=29980
NH_3-Pt complexes, far i.r. spectra 8=43330
NH_3-methylamine gas mixtures, heat cond. 8=34644
NH_3 and ND_3, anharmonic consts. and average struct. 8=29753
NH_3-O_2 mixtures, ignition by shock waves 8=27729
$N^{15}H_3$, h. f. s. inversion transition obs. 8=47607
ammonium compounds
and acetonitrile intermol. dipole-dipole interaction, spectral C≡N band shift obs. 8=30487
ammonium, atmosphere, particle size distribution obs. 8=50129
ammonium pentaborate, production of second harmonic of light 8=41167
oxalate, non-linear optical props. 8=36443
phase transitions. neutron scatt. determ. 8=48393
quaternary halides, i. r. spectra, C-N vibrs. 8=38844
salts, phase changes 8=35116
NH_3^+ substituent in π-electron systems, inductive effect 8=25525
NH_3OHCl, X-irradiated, e.s.r. of V_K centres, radical pairs and trapped NO 8=31878
NH_4^+, n. m. r. coupling consts. and isotope shifts 8=29820
$NH_4Ag_4I_5$, ht. of formation 8=48396
$NH_4Al(SO_4)_2 . 12H_2O$, n.m.r. 8=40983
NH_4Br, l. f. vibrs. 8=27596
NH_4Cl, effect of impurities on spin-lattice relax. 8=40955
NH_4Cl, electro-optic effect, linear, electronic contrib. 8=36397
NH_4Cl, l. f. vibrs. 8=27596
NH_4Cl lining of composite coating, rate of decomp. 8=30958
NH_4Cl, long range order parameter by neutron diffraction 8=44242
$NH_4Cl : Mn^{++}$, e.s.r. spectrum, temp. depend. 8=49614
$NH_4Cl : VO^{2+}$, e. p. r. linewidths 8=45103
NH_4ClO_4, sublimation kinetics 8=30609
NH_4ClSnO_3, elastic constants, determ. by optical method 8=26837
$(NH_4)_2CrO_4$ annealing of interstitials formed by Szilard-Chalmers recoil, crystal size effect 8=31049
$(NH_4)_2Cr_2O_7$, absorpt. spectrum at 2°K 8=45212
NH_4F in ice, dielec. relax. time actuation energy 8=44869
NH_4F, phase diagram to 20 kbar 8=34960
NH_4HF_2 in anhydrous HF, electrolysis 8=45391
NH_4HF_2 in HF, electrolysis and subsequent i. r. analysis, cell requirements and construction 8=36606
$NH_4H_2PO_4$, antiferroelec. phase transition, group theory 8=31439
$NH_4H_2PO_4$, antiferroelectric, spontaneous polarization temp. dependence 8=40624
$NH_4H_2PO_4$ crystal, as basis for laser with half-wave Q-factor modulator 8=24323
$NH_4H_2PO_4$, c. w. parametric scatt. with strong absorption in idler band 8=36394
$NH_4H_2PO_4$, electro-optical props., contribution of quadratic effect 8=32015
$NH_4H_2PO_4$, optical parametric scattering 8=45211
$NH_4H_2PO_4$, optical second harmonic generation, effects of He-Ne laser focussing 8=45139
$NH_4H_2PO_4$, paraelec. phase, crystal structure from e. diffr. exam., 8=39816
$(NH_4)H_2PO_4$, precipitates and dislocations exam. by X-ray diffr. microscopy 8=26691
$NH_4H_2 . PO_4$, search for mag. field induced optical second harmonic 8=45140

Nitrogen compounds—contd
- **ammonium compounds**—contd
  - $NH_4H_2PO_4$ spontaneous scatt. of intense light, quantum theory 8=27538
  - NH_4I, cubic and tetragonal magnetization coexistence, proton spin-lattice relaxation determ. 8=40740
  - NH_4I and $NH_4I(Tl)$, absorpt., luminesc. and excitation spectra 8=32014
  - NH_4I polycrystalline, e diff. exam. 8=35343
  - NH_4I-AgI, high-cond. solid systems 8=48396
  - $(NH_4)_2Ir; PtCl_6$, i.r. spectrum and exchange coupling between Ir^{4+} ions 8=32002
  - $(NH_4)_2Mn_2(SO_4)_3$, langbeinite structure, growth and electro-optical props. 8=39678
  - NH_4-NH_4 proton exchange in liq. NH_3 8=27675
  - $NH_4[SC(S)(NH_2)]$ polymorphism 8=48517
  - $(NH_4)_2SO_4$. Cu^{2+}, e.p.r. 8=40940
  - $(NH_4)_2[Sb_2(C_4H_2O_6)_2$. $5H_2O$, crystal structure 8=26416
  - $(NH_4)_3(VO_2F_4)$, space group, unit cell 8=35344
  - $(PO_3)_3CoNH_4$, orthorhombic crystal structure 8=26382

Nobelium
- element 102, methods of discovery 8=43154

Nobelium compounds
- No entries

Noble gases. See Inert gases.

Noctilucent clouds. See Atmosphere/upper; Clouds.

Noise
- dynamical systems, nonlinear, discrete-time, estimation of state variables 8=46009
- emission from open turbulent flames, rel. to changes in struct. 8=32108
- holograms, total internal reflection, improved S/N ratio 8=37716
- nuclear reactor, γ-ray obs. 8=34095
- potential, in K plasma, Q-machine obs. 8=47891
- quantum, obs. in laser oscillator 8=28667
- reflection-type secondary e emission, obs. 8=31475
- statistical props., appl. to graph smoothing 8=32688
- acoustic
  - aerodynamic, depend. on mean shear 8=43671
  - aerodynamic, spoiler generated flow noise 8=32919
  - airliners, air speed and duration effect on subjective rating 8=41847
  - deep-sea, ambient, surface motion effect 8=36697
  - deep-sea, impulsive, resembling whale sounds, analysis 8=50100
  - excitation of linear systems by Gaussian random processes 8=37283
  - flame, natural gas, monopole-type sources 8=28406
  - footstep noise on floors, assessment 8=23967
  - gas freestream, effect on 8=30269
  - impulsive, effect on system reliability 8=37234
  - jet-engine, nacelle treatment for reduction 8=32918
  - measurement and control, book 8=37282
  - monaural hearing, internal correl. effect 8=23984
  - monaural loudness functions rel. to masking 8=46219
  - pitch determ., use of noise bands 8=46198
  - Poisson impulsive excitation of linear systems, response-peak prediction 8=37235
  - sonar transducer blanket dome filtering 8=46180
  - subjective sound intensity analyser 8=46196
  - supersonic jet, visualization 8=46194
  - temporary threshold shift, exposure and recovery models 8=28378
  - rel. to threshold shift in ear 8=46205
  - tones masked by noise, unmasking obs. 8=32929
  - transmission in buildings, indirect paths 8=41848
  - CdSe, and current saturation 8=30942
- **electrical.** See Cosmic radiation, radiofrequency; Fluctuations/electrical; Sun/radiation, radiofrequency.

Noise abatement
- See also Absorption/acoustic waves.
- jet-engine, nacelle treatment for reduction 8=32918

Nomenclature and symbols
- See also Units.
- e.m. theory, SI units 8=24121
- medical tracer kinetics 8=32617
- solar flares, varieties 8=45911

Nomograms
- See also Graphs.
- cemented two-lens objectives design in region of third-order aberrations 8=42163
- radioactivity counting statistics 8=42341
- seismic refraction, multilayer 8=50051
- tangency contact curves replaced by points 8=46006

Non-crystalline state. See Amorphous state; Vitreous state.

Non-Newtonian fluids. See Fluids.

Novae
- See also Stars.
- cosmic ray nuclei in source region and interstellar medium, confinement 8=41494
- Delphini 1967, radio emission, upper limit 8=41518
- Delphini, 1967, spectra and brightness increase 8=45694
- in Galaxy and Andromeda nebula, novae subsystems 8=45737
- Kepler supernovae, γ-ray obs. 8=45795
- light scatt., nonstationary in stellar atms, rel. to theory 8=28039
- N Her 1963, stellar temp., electron density, and electron-density of shell 8=36935

Novae—contd
- Nova Delphini 1967, pre-outburst spectrum 8=28081
- outburst rel. to hydrogen burning model 8=28044
- supernovae, antimatter-matter annihilation theory 8=41492
- supernovae, collapse and anticollapse 8=50327
- supernovae explosions and the origin of cosmic rays 8=38106
- supernova explosions, rapid n-capture 8=32453
- supernovae, heavy nuclei synthesis rel. to explosion hydrodynamics 8=41504
- supernovae light emission, primary and observable luminosity and density of matter, model 8=36953
- supernova, mass ejection theory 8=45678-9
- supernovae, photographic magnitude obs. 8=32457
- supernova 1967 in NGC3389, light and colour curves, obs. 8=28077
- supernovae and remnants, catalogue 8=32452
- Supernovae remnants, interaction with interstellar medium 8=50326
- supernova SN1967h, X-rays, upper limit 8=41517
- Vela-X, supernova remnant, radio emission obs. 8=32505
- Pu^{242} heavy-isobar field in explosion n flux rel. to supernovae reactions, obs. 8=38495
- U^{238} heavy-isobar field in explosion n flux rel. to supernovae reactions, obs. 8=38495

Novoids. See Novae.

Nuclear acoustic resonance. See Absorption/acoustic waves, ultrasonic; Nuclear magnetic resonance and relaxation.

Nuclear alignment. See Nuclear orientation.

Nuclear bombardment targets
- alkaline earth metal stearate, for CERN isotope separator ISOLDE 8=38768
- for bevatron, secondary beam extraction 8=33486
- for boson resonance obs. 8=24841
- gas, windowless for high power beams 8=33395
- liquid, circulating, for isotope on-line separator 8=38605
- manipulator developments 8=33367
- neutron generator target current integrator for wear meas. 8=47142
- optimum design for 14 MeV n yield 8=24946
- polarized p, horizontal cryostat 8=24939
- positive-ion beam target for accelerator 8=33398
- radiative capture obs., thick-target technique 8=33369
- reaction yield increased by accel. projectile between a series of targets 8=29396
- rotating neutron target system 8=33396
- Rutherford scatt. appl. to thickness meas. 8=46850
- thick, effect on p beam monitor reactions 8=25221
- thin rotating, heat transmission calc. 8=37780
- tritium-Ti target, rate of decrease of n yield in accelerators 8=33785
- water cooled for intense ion beams 8=33397
- Al^{27} (p, 3pn) Na^{24}, target thickness rel. to secondary particle prod. affecting p flux monitoring 8=33994
- Au-W thick, bremsstrahlung spectra, meas. 8=33621
- C(α, n) rate obs. in thick targets 8=43141
- H_2 liquid, mechanical refrigeration 8=46849
- Ni foils, thin, proton scattering, 15-90 keV 8=29432
- $La_2Mg_3(NO_3)_{12}$. $24H_2O$ crystal, 660 MeV p elastic scatt. 8=48924

Nuclear decay schemes. See Radioactivity/decay schemes.

Nuclear decay theory
- See also Beta decay theory; Nucleus/theory.
- α-decay, individual shell model 8=25171
- α-decay, microscopic theory and deformed nuclei hindrance factors rel. to struct. 8=29355
- α-emitters, predicted, in A < 200 region 8=38406
- α, for heavy nuclei reassessment of interaction between α and residual nucleus 8=33954
- α-recoil atoms conversion e lines deform. in elec. field 8=29287
- α, rel. to nuclear surface struct., barrier penetrabilities calc. 8=29262
- magic nuclei far from stability, p and n emission, prompt and delayed 8=38328
- μ-capture, "elementary particle" weak-interaction theory 8=33955
- n emission, delayed, systematics 8=38404
- odd-odd deformed nuclei, α decay to vibrational levels 8=47277
- super-heavy nuclei, radiation widths rel. to n capture and nucleosynthesis, mass formula 8=38324
- Z ~ 65 nuclei, high J states dominant α-decay, statistical model 8=38405
- Am^{241} α-decay rel. to Np^{237} levels obs. 8=33946
- As^{74}, matrix calc. by pairing model 8=42946

Nuclear emulsions. See Nuclear track emulsions.

Nuclear excitation
- See also Mössbauer effect; Nucleus/energy levels.
- analog state escape calc. of damping and escape width 8=25135
- collective states, coupling with particle and hole states, perturbation series approximation 8=38356
- compound nuclei, by slow neutrons, level density 8=38333
- deformed nuclei by spin-quadrupole forces, collective states 8=38329
- deformation as a function of Z number in pairing-plus-quadrupole model 8=25055

Nuclear excitation—contd
deformed odd nuclei, single-particle orbits $\Delta N = 2$ mixing 8=29270
dynamic collective theory appl. to photodisintegration of Ni 8=25209
e. m. interaction operators and nucleon-nucleon potentials 8=29278
E2 transitions 8=42823
fissioning symm. nucleus energy calc. using geometric model 8=38526
h. f. interactions caused by e hole formation obs. 8=47271
"heated" nuclei, mean radiative widths 8=29284
by high energy particles 8=33882
intermediate resonance, doorway state model 8=42982
isomers, cross-section depend. d(γ, γ^1) reaction, review of research, (1939-67) 8=33889
level density at 20 MeV 8=42811
light nuclei spectra, rotator model, rotation particle coupling effects 8=25050
multiple Coulomb, quantal effects 8=29281
multiple Coulomb, pulse approximation accuracy 8=29280
negative parity N isobars, rel. to quark model 8=25003
octupole vibrations in deformed heavy nuclei 8=42819
odd-mass nuclei, resonance fluorescence and absorpt. meas. of transition strengths, 0. 8-3. 0 MeV 8=42875
by pulsed-beam techniques, meas. of perturbed angular correlation 8=42810
resonances in $O^{18}(n, \alpha)C^{15}$, 7. 5, 8. 6 MeV 8=47326
by single-N-transfer, multipole sum rules appls. 8=25078
s-wave virtual states and resonances in R- and S-matrix terms, distinction 8=42803
(t, d) reaction at low energies, spectroscopic obs. of low-lying states 8=43050
$Ag^{107,109}$ by 42 MeV α scatt., obs. 8=43077
Al^{26}, spectrum of closely spaced levels, 2. 07 MeV 8=42851
Al^{27} and Al^{28} mean energy level width at high excitation energy 8=47237
Al^{27}, from resonance γ-decay in $Mg^{26}(p, \gamma)$, 9. 991 Me V and 10. 165 MeV levels 8=33903
$Al^{27}(p, \alpha)$ Mg^{24}, excitation function fluctuations 10. 9-19. 7 MeV 8=38473
$B^{10}(N^{14}, N^{13})B^{11}$, neutron tunnelling and nuclear spectroscopic factors extraction 8=43101
Be^7 compound nucleus, resonance parameters determined from cross sections of Li^6 (p; p, $He^4)Li^6$, He^3 8=42832
Be^8 resonance in $Li^7(p, \gamma)Be^8$, 1. 4-2. 5 MeV 8=47320
Bi^{208} from Bi^{209} (d, t), neutron-hole multiplets 8=38398
Bi^{208} from Pb^{207} (He^3, d), proton-particle multiplets 8=38398
Bi^{209} analogue resonances, proton decay of Pb^{208}, γ-ray transitions obs. 8=47264
C^2. nuclei. resonance energies and partial widths of quasimolecular states formed 8=43097
Ca^{40}, giant resonance excited by γ absorpt. 8=47307
$Ca^{40}(N^{14}, N^{13})Ca^{41}$, neutron tunnelling and nuclear spectroscopic factors extraction 8=43101
Ca^{42} from $K^{41}(He^3, d)$ reaction, particle hole states up to 5. 79 MeV obs. 8=47243
Cl^{38} isobaric analog states in Ar^{38} studied by p scatt. from Cl^{37} 8=25118
Cl^{36} isobaric analogues obs. in $Cl^{35}(p, \alpha_n)S^{32}$ 8=25230
Cu^{65}, resonance fluoresc. obs. 8=42883
$Cu^{65}(t, \bar{\alpha})Ni^{64}$, core excitation of 5^- state, 3. 856 keV 8=43066
Fe^{56} rel. to intermediate struct., n total cross section, 0. 5-1. 2 MeV 8=29469
Ge^{69}, hyperfine interactions of excited nuclear states, g factor meas. 8=42810
Hg^{197m} h. f. interaction caused by e hole formation 8=47271
$In^{113,115}$ by 42 MeV α scatt., obs. 8=43077
Ir^{193} core excitation 8=42918
Mg^{24}(p, 2p), spectroscopic analysis, 156 MeV 8=43024
Na^{23}(p, 2p), spectroscopic analysis, 156 MeV 8=43024
Nb^{91} obs. in $Zr^{90}(He^3, d)Nb^{91} \rightarrow Zr^{90}$ 8=25275
Ne^{10}, molecule-like structure from rotational bands study 8=47231
O^{16} from $C^{13}(He^3, \alpha)_{15\cdot1}C^{12}$ $T = 0, 1$ α states in O^{16} obs. 8=42840
O^{16}, giant dipole resonance, structure through obs. of $C^{12}(\alpha; n, p)O^{15}$, N^{15} 8=43084
O^{16}giant resonance levels excited by electron scatt. 8=42843
O^{16*}, molecule-like structure from rotational bands study 8=47231
$Pb^{207, 208}$ analogue resonances due to proton scatt, calc. 8=38466
Pb^{207} h. f. interaction caused by e hole formation 8=47271
Pb^{211} analog resonance obs. in $Pb^{208}(t, p)Pb^{210}$ 8=25158
Pr^{141} isobaric, analog resonance, transition to $2d_{5/2}$ ground state 8=42927
Ru^{100}, excited states study by decay of Rh^{100} 8=29321
Sb, odd mass isotopes, spectral props. calc. using core-particle-coupling 8=42894
$Sb^{121,123}$ by 42 MeV α scatt., obs. 8=43077
$Sc^{46}-Ti^{46}$, isobaric analog states in $Sc^{45}(He^3, d)Ti^{46}$ and $Ti^{47}(He^3, \alpha)Ti^{46}$ 8=25127
Sc^{49}, analog levels, fragmentation calc. comparison with expt. 8=42872
Si^{28}, giant resonance excited by γ absorpt. 8=47307
Si^{28}, nucl. reson. fluoresc. anisotropy meas. 8=30631

Nuclear excitation—contd
Si^{28}(p, 2p), spectroscopic analysis, 156 MeV 8=43024
Si^{29} by p scatt., p spin flip in 2^+ state obs. 30, 40 MeV 8=43009
$Sm^{148, 150, 152, 154}$, by Coulomb excitation with O^{16} 8=38387
$Sn^{112,116,118,120,122,124}$, Coulomb excitation by α at 10 MeV, obs. 8=42890
$Sn^{116,117,118,119,120}$, 34. 4 MeV α scatt., quadrupole and octupole 8=47352
Sn^{124}, Coulomb by N^{3+} rel. to energy levels, 44 and 48 MeV 8=29326
Ta^{181} 482 KeV state by stopping π, evidence 8=42912
$Te^{122,130}$, Coulomb by N^{3+} rel. to energy levels, 44 and 48 MeV 8=29326
$Ti^{48}(p, \gamma)V^{49}$, γ-ray spectra of analogue resonances 1, -1. 4 Mev 8=42806
U^{235}, 22 MeV, n fission products obs. 8=25281
U^{236}, fission fragment mass and charge distrib. 8=43117
U^{238}, p-wave resonance $E_n = 0.200$eV obs. 8=42928
V^{51} rel. to intermediate struct., n total cross section, 0. 5-1. 2 MeV 8=29469
$W^{182,183,184,186}$, Coulomb excitation of lowest states 8=42915
W^{183}, Coulomb excitation by protons and Mossbauer effect 8=47262
Y^{89}, $E_n = 4.2$ MeV, bound levels obs. 8=42886
Y^{89} for analog state in p-Sr^{88} scatt., calc. of damping and escape widths 8=25135
Zr^{90}, isobaric analog resonances in p + Y^{89} scatt. 8=25137
Nuclear explosions. See Explosions/nuclear.
Nuclear field theory. See Field theory, quantum.
Nuclear fission
See also Explosions/nuclear; Nuclear reactors, fission.
acoustic cavitation. fission-induced, apparatus and results 8=48032
binding energy distrib. rel. to fission process 8=38320
blocking in crystals as a method of meas. lifetimes appls. 8=38533
counter, solid state to provide better discrimination between alpha and fission fragments 8=47366
cross-section irregularities rel. to quasistable states of nucleus 8=47358
gas, pressure wave generation, method of characteristics analysis 8=39170
IEEE Region 3 convention, USA (1968) 8=29991
neutron dosimetry appls. 8=38080
n induced and spontaneous models and obs., review 8=29526
nuclides far off stability line prod., rates 8=38442
saddle point calc. including shell effects, asymmetric shapes obs. 8=34050
single-particle energy calculations 8=29528
spontaneous decay of isomers, Dubna heavy-ion research , review 8=38521
spontaneous, mass yield asymmetry rel. to nuclear struct. and spin-orbit coupling 8=34051
spontaneous, of nuclei with $Z \simeq 114$, $N \simeq 184$, island of stability 8=43109
symmetric, geometric model of deformation 8=38526
thermonuclear research related technique 8=34064
$80 \leqslant Z \leqslant 85$ isotopes fission barriers, obs. 8=38527
$Z \sim 126$, $N \sim 184$ nuclei prod. by fusion-fission and cpd. nucleus fission reactions 8=38520
$Am^{241,242,243}$, n capture and fission cross sections and resonance integrals 8=25253
Am^{242m}, cross sections and reson. integrals, 0. 4 eV to 4. 7 MeV 8=34055
Am^{242i}, isomeric cross section ratio 8=25165
Bi nuclei by electrons 8=38534
Bi^{209}, e-induced, cross section 8=29533
Bi^{209}, by $E_n = 1-9$ GeV, cross-section obs. 8=47359
Cf^{252}, spontaneous, light nuclei emission, obs. 8=38527
Cf^{252}, statistical and adiabatic approaches compared 8=38525
Cf^{252}, total energy released per fragment pair, and charge distrib. 8=34054
Cm^{244}, det. of presence from tracks 8=36649
N nonradiative transitions probab. and fission fragments vel., shell model 8=29527
No^{252}, spontaneous, partial period 8=42978
No, spontaneous, review 8=29381
Np^{237}, cross section, 1 keV-10 MeV 8=34057
Np^{237}, n-induced, produced levels 8=29348
Np^{237}, neutron subthreshold cross-section and fission barrier investig. 8=38530
Np^{237}, by $E_n = 1-9$ GeV, cross-section obs. 8=47359
Pb, p induced binary and ternary fission, 3-24 GeV 8=34059
Pu, homogeneous, critical expts., theoretical analysies 8=25293
Pu^{238}, (n, γf) reaction detection 8=43114
Pu^{239} fission cross-section rel. to spin and energy 8=34049
Pu^{239}, n induced rel. to transition state theory 8=29526
$Pu^{239,240,241}$, delayed n precursor yields rel. to n abundance, obs. 8=38546
$Pu^{239,240,241,242}$ cross section, 1 keV-10 MeV 8=34057
$Pu^{239,241}$, I^{135} yield ratios rel. to U^{235} 8=38540
Pu^{239}, by $E_n = 1-9$ GeV, cross-section obs. 8=47359
Pu^{240} subthreshold fission cross section, structure due to intermediate states 8=38528

Nuclear fission—contd
Pu^{242}, nuclear explosion irrad., heavy isobar yield rel. to supernovae reactions, obs. 8=38495
Ra^{226}, by p, asymmetry and excitation function 8=43121
Ra^{226}, by 13MeV p, energetics and n emission 8=43120
Ra^{226}, n fission cross-section 8=25280
Ta^{181}, e-induced, cross section 8=29533
Th^{232}, by 20-85 MeV protons, Xe^{133} isomer yields 8=47362
Th^{232}, cross section, 1 keV-10 MeV 8=34057
Th^{232}, delayed n precursor yields rel. to n abundance, obs. 8=38546
Th^{232} mass and kinetic energy distrib. of fragments 8=38531
U^{233}, I^{135} yield ratios rel. to U^{235} 8=38540
U^{233} + O^{18}, product of 8=42978
U^{235} by thermal n, prompt α-rays angular anisotropy rel. to fragments energy, obs. 8=29537
U^{235}-depleted U^{238}-Np^{237} foil n personnel dosimeter 8=33795
U^{235} epicadmium capture-to-fission ratio, low flux meas. 8=38535
U^{235} Pu^{238,239} fission channels per spin state 8=43114
U^{238} bombarded by Ar^{40}, excitation function and probable kinetic energy relase 8=43107

products
α-particles, from U^{235}, energy distrib. 8=38539
α-particles in ternary fission, emission probab., spectrum and angular correl. 8=29535
angular distrib. irregulatities rel. to quasistable states of nucleus 8=47358
atmosphere, Finland, Dec. 1966 obs. 8=27927
"cold" neutrons, segregation technique 8=24975
decontamination by reaction of U with SF$_6$ 8=43128
deformability of even-even, n-rich fragments 8=38323
deformation fragments and shell effects 8=25284
deformation, shell structure effects 8=38538
delayed n emitters and precursors 8=38404
delayed n precursors, yield calcs. rel. to n abundance obs. 8=38546
n-emission, delayed, by p-induced prods., obs. 8=38463
n energy spectra from U^{235}, U^{233} and Pu^{239}, comparison for range 0.8 to 16 MeV 8=38536
n, fast, energy spectra on slowing down in homogeneous medium 8=38584
fragment n emission, indirect meas. 8=47363
fragment track registration in phosphate glass 8=24538
fragmentation by high energy particles, statistical and non-statistical processes 8=34058
fragments relative vels., shell model 8=29527
from fuel particles, coated, in-pile release, diffusion model 8=38591
in fuels, inert gas bubbles nucleation, irrad. effects 8=31109
γ-ray, X-ray and conversion e emission, obs. 8=38527
in gas conduit, deposition from laminar stream, models 8=34060
gases, short-lived isotopes separation, on-line system 8=38771
inert gases, isotopes decay schemes, on-line separator obs. 8=38545
neutrons, prompt, average number and energy calc. 8=34061
recoil in heterogeneous pyrocarbon structures of varying porosity 8=43127
semiconducting layer structures, fragment tracks 8=44487
separation and yield, ionic and decay props. meas. 8=38543
separation, focusing parabola mass spectrometer 8=43129
separation, mass spectroscopic, and short-lived radiations obs. 8=43130
separation, mass-spectroscopic principles and gas-filled separator 8=38544
in Sicral F$_1$, gas bubbles rel. to irrad. swelling 10^{14} n/cm^2 sec 8=44506
in Sicral F$_2$, gas bubbles rel. to irrad. swelling 10^{14} n/cm^2 sec 8=44506
trapping plant, testing with methyl iodide, experience 8=34111
tritium, diffusional release from BeO, on post.-irrad. annealing 8=25317
yield-mass distrib., ratio circuits 8=47364
n yield var. with fragment mass, semi-empirical curves 8=34063
Ag^{108}, p-induced, evaporated products, characts. calc. 8=25283
As^{83,84,85,87,} half-lives and chem. separation, obs. 8=38419
Be^7 fragments from p-irrad. Ta, Pb, U, obs. 8=43115
Br^{80}, p-induced, evaporated products, characts. calc. 8=25283
Ce^{144} determ. in coated fuel particles 8=47404
Cf^{242,243,244,245,246} production cross sections, from U^{233,234,235,236,238} + C^{12} reaction 8=43106
Cf^{252}, long range α fission props. of neutrons emitted 8=38541
Cf^{252}, long-range fragments yield obs. 8=42976
Cf^{252}, response of double-scintillator detectors 8=37790
Cf^{252}, spontaneous, light nuclei emissions 8=43125

Nuclear fission—contd
products—contd
Cf^{252}, spontaneous, prompt n and γ spectra, and level densities 8=25278
Cs^{137} determ. by β-γ coincidence counting while meas. γ ray spectrum with NaI(TI) analyzer 8=47360
Cs^{137} determ. in coated fuel particles 8=47404
I^{135}, yield ratios from U^{233}, Pu^{239,241} rel. to U^{235} 8=38540
Ir^{191,193}, by 42.2 MeV He^4, cross-section obs. 8=43119
K X-ray meas., bent-crystal spectrometer 8=34062
Kr, gas, mobility and trapping in UO$_2$ and UC fuel elements 8=25318
Kr^{90,91,92,93} from U^{238}O$_2$-stearate source, separation, γ spectra and decay periods, obs. 8=38549
Na^{22,24} fragments from p-irrad. Ta, Pb, U, obs. 8=43115
Na^{24} from p-irrad. noble metal and U targets 8=43116
Ne^{24} from p-irrad. noble metal and U targets 8=43116
Np^{237}, n-induced, fragments kinetic energy obs. 8=47357
Pb^{206} fission by He^4, fragments angular distribs., obs. 8=38527
Pu^{239}(d, pf), ang. correl. obs. 8=43070
Pu^{240}(n, f), subthreshold fission, resonance grouping structure 0.2-8 keV 8-38550
Ra^{226}, angular distrib. of fragments 8=25280
Ra^{226}, photofission, anisotropy of fragments 8=25285
Sr^{90} determ. in coated fuel particles 8=47404
Th^{232}, 1.5-3.3 MeV, n induced n yield obs. 8=38532
U^{233} thermal fission fragments meas. and charge distrib. obs. 8=29534
U^{235}, fission γ-ray spectra, anisotropy obs. 8=47365
U^{235} fission, x- and γ-ray spectra, 30-300 keV 8=38547
U^{235}, identification of 5.3-sec. Ag^{118} 8=43123
U^{235}, 0.4-3.3 MeV, n induced n yield obs. 8=38532
U^{235} photofission, 25 MeV, kinetic energies of pair fragments 8=38537
U^{235}, prompt α-rays angular anisotropy rel. to fragments energy, obs. 8=29537
U^{235} prompt emission, n induced fission, 7-14 MeV 8=29529
U^{235}, thermal-n, Ga^{77} identification and fractional chain yield 8=43113
U^{235}, thermal-n, identification of 5.0-sec. Pd^{117} 8=43124
U^{235}, 22 MeV excitation, obs. 8=25281
U^{235} $\bar{\nu}$ energy spectrum calc. 8=42992
U^{235,233} and Pu^{239}, comparison of n energy spectra 0.8 to 16 MeV 8=38536
U^{236}, by He$^+$, fragment mass and charge distrib. 8=43117
U^{238}, by 6-9 MeV n, mean kinetic energy obs. 8=25282
U^{238}, by 39MeV He^4, ternary fission evidence 8=43118
U^{238}, Ne^{22} ion induced, fragment mass distribution, γ-ray analysis 8=29539
U^{238}, neutrons, evaporation and fission spectra, 800 keV-14 MeV 8=34018
U^{238}, 14 MeV neutrons, cumulative yields 8=47361
U^{238}, proton induced, lifetime meas. using blocking in crystals 8=38533
U^{238}, p induced., n distrib. rel. to fragment mass 8=43122
U^{238}, ternary fission, fragment masses and α angular distrib., obs. 8=29536
93.15 wt%U^{235} subcritical cylinders, reactivity and prompt-n
U migration, decay products in minerals 8=48796
α-U, solid prods. segregation rel. to irrad. swelling 8=44507
in U-Mo 1, 1 alloy, gas bubbles rel. to irrad. swelling 10^{14} n/cm^2 sec 8=44506
in U-Mo-Al-Sn, gas bubbles rel. to irrad. swelling 10^{14} n/cm^2 sec 8=44506
UO$_2$ fuel particles, gas release rate rel. to fission density obs. 8=38592
in UO$_2$ fuel, solid elements anal. after burn-up 8=25286
UO$_2$ particle surface segregation of Mo and Ba 8=29538
in (U$_{0.85}$Pu$_{0.15}$)O$_2$ fuel, irrad., metallic fission-prod. inclusions, obs. 8=29557
Xe from U^{238}O$_2$-stearate source, separation and daughter activities 8=38549
Xe, gas, mobility and trapping in UO$_2$ and UC fuel elements 8=25318
Xe release from sintered UO$_2$ at low temp. 8=26624
Xe^{133} doping of metals 8=48766
Xe^{133} isomeric yield ratios from proton fission 8=47362
Z distrib., fine struct. rel. to closed shells and pairing, obs. 8=38548
Zr^{95} determ. in coated fuel particles 8=47404

uranium
buckling and migration area, sub. crit. meas. 8=38588
decontamination by reaction of U with SF$_6$ 8=43128
growth and elec. resistivity changes during burn up with thermal n.s. at 4.6°K 8=48933
migration, decay products in minerals 8=48796
in minerals, fission fragment tracks made visible by chemical etching 8=32185
neutron dosimeter 8=33794
proton induced binary and ternary fission, 3-24 GeV 8=34059
Cs yield in p-fission, mass spectram 128 $\leqslant$ A $\leqslant$ 144, 150 MeV 8=38542
Rb yield in p-fission, mass spectrom 83 $\leqslant$ A $\leqslant$ 98, 150 MeV 8=38542

Nuclear fission—contd
uranium—contd
U^{232}, n-induced, 5-1900eV, cross section obs. 8=29530
U^{233} aligned nuclei, low-temp, α ang. distrib., low-temp. obs. 8=30634
$U^{233,234,235,236,238}$, cross section, 1 keV-10 MeV 8=34057
$U^{233,235,238}$, delayed n precursor yields rel. to n abundance, obs. 8=38546
$U^{233,235,238}$, by 20-85 MeV protons, Xe^{133} isomer yields 8=47362
U^{235}, α-accompanied ternary, energetics 8=43110
U^{235}, α-accompanied ternary, Q values 8=43111
U^{235}, energy and charge distrib. 8=34054
U^{235}, energy distrib. of emitted α-particles 8=38539
U^{235} fission cross-section rel. to spin and energy 8=34049
U^{235} fission transition nucleus, struct. 8=43112
U^{235}, identification of 5.3-sec. Ag^{118} product 8=43123
U^{235}, n induced, prompt n emission, 7-14 MeV 8=29529
U^{235}, n induced rel. to transition state theory 8=29526
U^{235}, thermal, fragments meas. and charge distrib. obs. 8=29534
U^{235}, thermal-n, Ga^{77} identification and fractional chain yield 8=43113
U^{235}, thermal-n, identification of 5.0-sec. Pd^{117} product 8=43124
U^{235}, thermal, x-rays rel. to fragment mass, obs. 8=38529
U^{235}, 3MeV n-induced, ternary, ang. anisotropy of fragments 8=29531
U^{235}, tripartition, meas. of emitted α particle spectrum, low energy part 8=43126
U^{235}, 22 MeV excitation, fragments obs. 8=25281
U^{235} $\bar{\nu}$ energy spectrum calc. 8=42992
$U^{235,238}$, by $E_p = 1-9$ GeV, cross-section obs. 8=47359
$U^{235,238}$ in 1.03%enriched U - D_2O lattices, obs. 8=38585
$U^{235}O_2F_2$ aqueous soln., minimum critical thickness of water-refl. infinite slab 8=34052
U^{236}, by He^+, fragment mass and charge distrib. 8=43117
U^{236} n capture, resonance integral meas. 8=34056
U^{238}, by 18-21 MeV n, delayed n group yields 8=25279
U^{238}, by n, fission and evaporation n spectra, 800 keV-14 MeV 8=34018
U^{238}, by 6-9 MeV n, fragments mean kinetic energy obs. 8=25282
U^{238}, by 39MeV He^4, ternary fission evidence 8=43118
U^{238}, 14 MeV neutrons, cumulative yields 8=47361
U^{238}, D_2O moderated and diphyl cooled lattices ρ^{28} factor meas. 8=34077
U^{238}, e-induced, cross section 8=29533
U^{238}, nuclear explosion irrad., heavy-isobar yield rel. to supernovae reactions, obs. 8=38495
U^{238} photofission, asymmetry obs. and yields of $Cd^{115,117}$, Ag^{111}, Mo^{99} and $Ba^{139,140}$ 8=29532
U^{238}, ternary fission with α emission, 14 MeV n induced 8=29536
UO_2 fuel element, axial void form rel. to radial temp. gradient 8=43144
UO_2 fuel particles, fission-gas release rate rel. to fission density obs. 8=38592
UO_2 particle surface segregation of Mo and Ba 8=29538
$UO_2(NO_3)_2$-polyethylene mixtures, minimum critical U^{235} enrichment, obs. 8=34053
Nuclear fission reactors. See Nuclear reactors, fission.
Nuclear forces
See also Field theory, quantum/meson field.
binding energy calc. for light nuclei 8=47216
binding energy determined from hole line expansion method 8=47200
binding energy distrib. rel. to fission process 8=38320
binding energy, extended shell model semiempirical mass formula 8=38312
binding energy, far-unstable nuclei, formulae 8=38316
binding energy of ground and excited states with $A \leqslant 61$ 8=42798
binding energy, variational calc. with central Yukawa and vel. depend. 2-body pots. approx. 8=42797
bonding energy, for soft-core pots. with realistic N-N interacts. 8=25069
bound state of two and three nucleons, and wave function 8=38310
deformed nuclei, spin-quadrupole interaction, collective states excitation 8=38329
deformed nucleus potential, and rare-earth, actinide and super-heavy region appls. 8=38325
deuterons, four-parameter optical pot. 8=42826
effective N-N potential for Hartree-Fock calculation 8=33865
eigenpotential problem in the shell model 8=47203
equivalent local potential, new coupled equation 8=42980
fission barrier anomaly rel. to mass shell correction 8=38315
fission threshold and deform. energy, shell corrections 8=38308
Hamada-Johnston soft-core N-N pot. 8=42781
Hartree-Fock calcs. for finite nuclei with nonlocal pots 8=33864
heavy deformed nuclei, surface delta interaction 8=47199
hypertriton n-p tensor interactions from Λ-p scatt. 8=25012

Nuclear forces—contd
isoscalar pairing-force problem, isospin invariation 8=42777
Λ-N interaction from binding energy calcs. on $_\Lambda He^6$ 8=38399
light nuclei, four-body correlations 8=42783
matter, independent pair Fermi model 8=47211
matter, 2-particle correls. without using thermodynamic Green's functions 8=25062
neutron separation energies, systematics 8=25071
n-n interaction, charge depend. study and violation of charge symmetry 8=24864
N-N interaction, density depend. rel. to isotope effect in nuclei 8=42802
rel. to N scatt., optical non-local pot. calc. 8=33985
N-N potential, and boson exchange theory 8=38300
N-N from γ-ray emission following neutron capture 8=33921
N-N interaction and dipole states rel. to photonuclear reactions 8=33861
N-N pairing correlations, interacting through charge independ. forces 8=29266
N-N separable potential 8=42776
odd-odd nuclei, residual n-p interact. in quasi random phase approx. 8=42791
odd spherical nuclei, N-N surface delta interaction, degenerate model 8=29265
potential in nucleus central derived from 2N tensor force 8=38297
potential, optical model, isospin depend. from n cross-sections obs. 8=29267
potential radius, isotope shift calc. 8=25044
potentials, velocity-dependent, for large nuclei 8=25045
proton pairing energies 8=25070
quadrupole in pairing-plus-quadrupole model 8=25054
review 8=38290
role of nonstatic character of N-N interact. in singlet-even states 8=25043
separation and pairing energies, spherical nuclei, semi-empirical calc. 8=38298
Scotti-Wong pot. modified, rel. to N-N scatt., deuteron problem and nuclear matter calcs. 8=24881
single particle parity-nonconserving pot. including OPE forces and 2-body correlations 8=38301
at small distances, combining of large distance meson theory, and phenomenological descripts. at small distances 8=24865
soft core potential for two-nucleon interacts. 8=24882
structure calcs. using realistic two-body interacts. fitting N-N scatt. data 8=25063
tensor used to derive central depend. pot. 8=38297
three-body long range forces shown to be negligible 8=42792
rel. to three-body system 8=33863
2-level system interacting by pairing forces, boson expansion method 8=25046
Volkov's in Hartree-Fock and Hartree-Fock-Bogolyubov calcs. for p shell nuclei 8=33868
C^{14}, tensor component, evidence from β, γ data 8=42835
C^{14}, velocity-dependent interaction calc. 8=25100
Ca^{40}, Hartree-Fock potential scatt. 8=25106
Ca^{40}, optical pot. rel. to N scatt., 10-20 MeV 8=33985
Cl^{38}, potential from residual n-p interaction 8=47239
H^3, binding energy and charge radii 8=33893
He binding energy, variation calc. using two-body central velocity-dependent potential 8=42824
He^3, binding energy and charge radii 8=33893
He^3, Faddeev eqns. and Coulomb effects 8=42829
He^3 spin-orbit pot., spin-flip meas. 8=47228
$_\Lambda He^6$, binding energy calc. rel. to Λ-N interaction 8=38399
K^{40}, potential from residual n-p interaction 8=47239
$_\Lambda Li^6$ binding energy calcs. for p-shell 8=38399
Li^6, model Hamiltonian with harmonic central force and tensor reaction 8=33894
in Li^6, residual two-body N-N interact. rel. to wave function anal. 8=25094
N^{14}, tensor component, evidence from β, γ data 8=42835
N^{14}, velocity-dependence interaction calc. 8=25100
3N system binding energy 8=38319
rel. to $Ni^{58}(p, d)Ni^{57}$ form factors calc., pseudo potential 8=33999
O^{14}, tensor component, evidence from β, γ data 8=42835
O^{16} binding energy, first order 8=33866
O^{16} binding energy per nucleon calc. 8=25102
O^{16}, Hartree-Fock potential scatt. 8=25106
O^{18}, binding energies of spin O states, anomaly 8=25101
O^{18} shell model, exponentially velocity-dependent potential 8=42785
Nuclear fusion
See also Explosions/nuclear; Nuclear reactors, fusion; Thermonuclear reactions.
superheavy nuclei, preferred reactions for formation 8=43131
$Z \sim 126$, $N \sim 184$ nuclei prod. by fusion-fission reactions 8=38520
Nuclear induction. See Nuclear magnetic resonance and relaxation.
Nuclear interactions. See Collision processes; Field theory, quantum/interactions; Elementary particles; Nuclear reactions; Scattering, particles.

Nuclear isomerism
See also Nucleus/energy levels.
excitation possibility by (γ, γ^1) reactions, review of research, (1939-67) 8=33889
isomers with short half-lives obs. in 24 MeV α bombard. of natural targets 8=47221
millisecond isomers, 14 MeV n-induced, cross sections 8=47220
nanosecond states in (particle, xn) reactions, meas. 8=34046
pair prod. in (n, 2n) reactions 8=25248
ratios in (n, γ) obs. 8=38322
short-lived, due to 10 MeV p, obs. 8=47214
Am^{242i} cross section ratio 8=25165
Au^{189}, $Ta^{181}(C^{12}, 4n)$ prod. and half-life, obs. 8=38522
Au^{199} half-life of 55 KeV M2 transition 8=42920
$Ba^{125,127}$, evidence for deformation 8=42900
Bi^{208} j-forbidden transition 8=42924
Cl^{40m}, a new isomer of Cl^{40} 8=25117
Co^{58M}, spectra for transition 8=33966
$Co^{58g,m}$ total cross section and ratios for $Co^{59}(n, 2n)$, $Ni^{58}(n, p)$, $Co^{59}(\gamma, n)$ 8=38489
Eu^{153}, isomer shift of 83.4 keV rot. transition 8=25147
Fe^{53}, discovery of 3.04 MeV isomeric state 8=38465
$Gd^{155,157}$, isomer shifts, ratio obs. 8=33930
Gd^{159}, 26 ns isomeric state at 68 keV, decay obs. 8=29335
Hf^{178m} with $K \geqslant 16$, γ-ray and decay scheme 8=42966
Hf^{179}, decay to ground state 8=47261
$In^{114,116}$, thermal n activation cross sections 8=29477
Ir^{192m}, internal conversion coeffs. for transition 8=33966
Ir^{194m_2} high-spin, by triple neutron capture 8=42917
Ir^{194m}, 32 ms, γ-ray spectrum obs. 8=42919
$Ir^{196g,196m}$, decay obs. 8=42967
La^{128}, $Sn(N^{14}, xn)$ and $Sb^{121}(C^{12}, 5n)$ prod., and half-life, obs. 8=38522
Lu^{172} with $T_{1/2} = 4h$, study of existence 8=47260
Nb isomer, tentative transition 8=25183
Nb^{90m}, decay consts, effect of changes in chem. state, press. and supercond. state 8=42950
Pb^{206}, half-lives of isomeric states, time interval analysis meas. 8=25083
$Po^{197,199,201,203}$ isomenic states and α-decay, obs. 8=38440
Rb^{90} isomer, β decay and γ spectrum obs. 8=29367
Rb^{83}, M2 8=25182
Sb^{120g} and Sb^{120m}, isomeric pairs in $Sb^{121}(n, 2n)$ reaction, isomer ratios and cross sections 8=25250
Se^{81m}, K conversion coeff. obs. for 102.7 keV transition 8=29370
Sn^{119m}, in Pb, In, Cd, Cu, Ag, isomer shifts 8=26015
Te^{133} isomers, radioactive decay to I 8=25186
Tl^{202} isomeric state in (n, 2n) reaction by 14 MeV neutrons 8=38395
Tl^{204}, no evidence for short-lived isomer 8=25194
Tm^{169}, Mössbauer shift rel. to internal conversion 8=29336
U^{235m}, half-life of low energy level meas., environmental effects 8=25164
Nuclear magnetic resonance and relaxation
See also Molecules/nuclear coupling.
$A^{III}B^{V}$ crystals, elastically deformed, rel. to elec. field gradients at nucleus 8=31909
AB-type spectrum, chem. exchange and transient effects 8=37543
acetone/CCl_4 binary mixture, proton mag. relaxation 8=39425
acetonitrile, spin-lattice relax. and molec. reorientation in liq. 8=30539
acid fluoroanhydrides, of F^{19}, variation of chemi-shifts 8=47696
acoustic, Bloch-type equations 8=33150
acoustic, research summary 8=37539
acyclic methine proton chemical shifts, graphic representation 8=25636
L alanine, deuterated, deuteron reson. 8=31894
aliphatic fragment, proton h.f.s. and spin-spin coupling 8=38943
alkali-aromatic radical ion pairs in soln. 8=34919
alkali binary alloys, knight shift 8=43876
alkali halide crystals, chemical shifts of monovalent substitutional ions 8=45113
alkali halide solns., microdyn. model from nucl. mag. relax. 8=25953
alkaline earth halide solns., microdyn. model from nucl. mag. relax. 8=25953
alloys, indirect exchange and pseudo-dipolar interactions by spin-echoes 8=36068
allyl bromide, multiple n. m. r. 8=29813
aluminoalkalisilicate glasses, Al^{27} n.m.r. 8=40971
amino acids in CF_3COOH and CF_3COOD, reson., chem. shifts, 220 MHz 8=39441
p-(anisalamino)-phenyl acetate liq. cryst., elec. field effect 8=34924
anisotropy relaxation in solids 8=49627
anthracene, p n.m.r., anomalies using u.v. and blue light 8=40973
anthraquinone, optically induced Overhauser effect 8=48210
alum single crystals 8=40983
aromatic heterocycles, five-membered, C^{13} 8=47697

Nuclear magnetic resonance and relaxation—contd
benzene derivatives, crystalline polysubstituted 8=49629
benzene, deuterated, deuteron spin lattice relaxation 8=48217
benzene, liquid, proton spin-lattice relaxation 8=39429
benzene, long transversal relax. time, obs. using spin-echo technique 8=48218
benzenes, monosubstituted, p.m.r. 8=43407
benzene, press. depend. of T_1 8=39432
benzene, solid and liq., rel. to rot. barrier heights of intermolec. rots. 8=43963
benzene/NaCl system, proton relax. time 8=45114
p-benzoquinone, oriented in nematic phase 8=34913
1, 2-benzotriazole in acetone solns., p reson., conc-depend., obs. 8=39420
benzone sorbed on silicagel, proton relaxation, temp. depend. 8=49632
benzoyl thiophine, deformation angle determ. 8=34371
bromobenzene, deuterated, deuteron spin lattice relaxation 8=48217
bromobenzene, liquid, proton spin-lattice relaxation 8=39429
1, 3-butadienes 8=38918-20
2-butenes, steric effects 8=47698
cation coordination no. in aq. solns. determ. by p. m.r. 8=39431
m-chlorobenzene, ^1H-^1H coupling constants 8=25641
chlorophyll-ligand interactions 8=29850
collagen, hydrated, d.m.r. 8=49639
coordination cpds, paramag., e. spin density attenuation in ligands 8=47593
F-P coupling const. signs in org. cpds 8=40994
cubic crystals, ultrasonic saturation, dislocation motion, influence 8=36260
dehydro-α-lapacone, double reson. 8=29810
dense gases, spin relax. and collision freq. 8=34669
deuterated compounds 8=49628
diamagnetic susceptibilities determ. 8=34904
diatomic gases, relax., collision theory 8=38913
1, 2 dibromoethane, rot. isomerism study 8=47646
1, 1-dibromo-3-fluorobutadiene-1, 3, energies of conformations, n. m. r. study 8=47631
2, 6-dibromopyridine, oriented mols. 8=43403
1, 2, dichloroethane, rot. isomerism study 8=47646
1, 1-dichloro-3-fluorobutadiene-1, 3, energies of conformations, n. m. r. study 8=47631
diethyl methylphosphanite, hydrolysis, n.m.r. study 8=27727
dihalobenzenes, p.m.r. and C^{13}-H satellite spectra 8=38917
1, 5-dimethylnaphthalene, and bromo-derivatives 8=38926
p-dioxane/CCl_4 binary mixture, proton mag. relaxation 8=39425
diphenyl picryl hydrazyl solns. in org. liqs., dynamic polarization of solvent protons and F nuclei 8=25951
di-tert-butyl-nitroxide liq. free radical. time dependent interactions, p relaxation study 8=48207
double irradiation circuit 8=46526
double, partial-saturation in systems with internal rotation 8=29812
double, periodically pulsed, theory 8=28638
double resonance, line broadening theory, sudden and adiabatic approx. 8=42043
double, systems of two- and three-spin 1/2 nuclei 8=29810
dynamic polarization in conjugated polymers 8=39434
dynamics of centres with S=I=1/2, and double resonance 8=36232
electrolyte diamag. solns., dipolar spin relax. 8=25952
electrolyte diamag. solns., intermolec. proton relax. rate 8=25957
electrolyte solns., form factor of spherical specimen vessels 8=34916
electrolyte solns., paramag. ions effect on Li^7 n. m. r. line 8=34915
electrolyte solns., spin relax., correl. times and viscosity 8=34927
electron dipole dipole interaction, expl. evidence of effect 8=40966
electron spin-echo obs. of E_1^1 centres in crystalline quartz 8=44486
enantiomers in optically active liq. crysts. 8=39422
ethane, liquid, nuclear spin relaxation 8=39428
ether/CCl_4 binary mixture, proton mag. relaxation 8=39425
ethyl derivatives, C^{13} and H^1 chem. shifts 8=29818
ethyl phthalate, molecular rotation restriction rel. to temp. 8=43877
ethyl-alcohol mixtures, proton spin-lattice relax and viscosity 8=43770
ethylene, spin-spin consts. calc. 8=25640
fast reaction rates study 8=49944
ferric complexes in acid solns., p. m. r. 8=43879
ferric complexes with desoxyribonucleotides, p. m. r. 8=43880
ferroelectric phase transitions, study by d.m.r. 8=49358
ferromagnetic alloys, dilute 8=49642
in ferromagnets, theory 8=40964
fluorobenzenes, monohalosubstituted 8=38922
fluoroberyllate complexes in soln. 8=48209
fluorocarbons, dynamic polarization in soln. 8=34911

Nuclear magnetic resonance and relaxation—contd
fluorodurene, crystalline, rel. to molecular reorientation movements 8=27256
fluoroform, gaseous, p spin-lattice relax. density depend., obs. 8=34667
fluoro-organic solns. of free radicals, nuclear-electron interactions and molecular motion 8=39436
2-fluoropyridine solns., solvent and temp. depend. 8=48224
free radical recombination, torsional motion obs. 8=38939
free radical solns. of toluene, nuclear mag. relax. 8=39439
free radicals in crystals, electron resonance and ENDOR spectra 8=40969
frequency decade ND30M in spectroscopy 8=46512
frequency shift in lowest Born approximation 8=46513
gas, spin diff., mag. field effect 8=43698
ginkgolides and derivatives, data 8=48216
glassy thermophosphate, of F^{19} 8=45121
glycerol, mag. relaxation and correlation 8=39430
gramicidine S in soln., structure 8=34332
growth effect rel. to signals in earth's mag. field 8=30529
halomethanes, struct. and electronic effect on C^{13} reson. 8=47700
high resolution spectra, quantum mech. and algebraic anal., computer prog. 8=42046
hydrate of SF_6, dielec. props. and n.m.r. 8=49342
hydrates, crystalline, rel. to H atom position determ. 8=44219
hydration of Al(III) and Ga(III) ions, O^{17} n. m. r. 8=30540
hydrocarbon, saturated, p-p geminal coupling constant, calc. 8=47692
hydrocarbons, planar, long-range trans and cis coupling constants, analysis 8=47691
hydroxyapatite, single crystal 8=40981
hyperfine mag. fields and elect. field gradients caused by mag. impurities in metals 8=40962
ice, hexagonal, proton spin-lattice relax. 8=49644
inhomogeneous broadening and Suhl-Nakamura interaction 8=40956
insulin and A and B chain S-sulphonates, p reson., 220 MHz 8=39441
Knight shift and pseudopotentials 8=45129
line shapes in free precession at high sensibility 8=48213
liquid, alloys, Knight shift comment on WBF theory 8=39421
liquid crysts., effect of sample spinning 8=30530
liquid crystal, rel. to chem. shift anisotropy 8=30411
liquid-crystal solvents, shielding anisotropics of solutes 8=43875
liquids, effects of molec. rot. diffusion on relax. 8=39426
liquids, electron-nucleus interactions in molecules 8=47693
liquids, relax. time, intermol. contribution, hydrodynamic interaction effects 8=34923
liquids, spin-lattice relax., theory 8=39427
in liquids, spin-lattice relax. time rel. to molec. rotation and re-orientation 8=30531
in liquids, study of molecular motion by relax. times 8=30399
luminescence centres, inorganic, ENDOR, rel. to emission, meas. 8=41178
magnus expansion applications 8=40961
medium effects, liqs. consisting of nonpolar, mag. isotropic mols. 8=48208
melting obs. 8=48259
metal single crystals, pulsed n.m.r. 8=40959
metals, Knight shift, review 8=27494
methanol and methanol-d_3 adsorbed on porous glass, proton relaxation times 8=47699
methyl derivatives, C^{13} and H^1 chem. shifts 8=29818
methyl fluoride, gaseous, p spin-lattice relax. density depend., obs. 8=34667
methyl group, narrowing due to coherent zero-point motion 8=25635
methyl groups undergoing tunnelling rotation, line shapes 8=49650
methyl, isolated tunelling group, proton second moment 8=40989
methyl silane, isomeric derivs., rel. to differences in phys. props. 8=43925
methylamines, solid 8=40990
micas, characterisation by p.m.r. 8=40985
minute metallic particles 8=40894
molecular parameters, semiempirical calc. 8=43405
molecular reorientation in liquids 8=39433
molecular reorientational motion in "classical" liquids 8=39292
molecules adsorpt. on SiO_2 gel, n.m.r. signal shift 8=39462
molecules, nonlinear, spin-rot. mag. relax. 8=29808
mol. with p-p interaction, line-shape with approx. equal spins 8=34370
multiple-pulse expts. 8=24263
m-nitrobenzene, ^1H-^1H coupling constants 8=25641
multispin molecules with dissimilar nuclei, relaxation 8=47694
nuclear polarization and relaxation by paramag. porous surfaces 8=48475
nitro azulenes 8=43410
nitroxide free radical, proton resonance at 310 MHz 8=43415

Nuclear magnetic resonance and relaxation—contd
noble metals, solute Knight shifts rel. to rigid band theory 8=45117
non-electrolytes in liq. state, relaxation times T_1 and T_2 obs. 8=48211
optically induced Overhauser effect in soln. 8=48210
organometallic cpds. of groups IV and IIb 8=38925
orientation of molecules adsorbed on solid surfaces, n.m.r. obs. 8=39615
oriented mols., anal. methods 8=43403
oriented mols., effect of sample spinning 8=30530
ortho-hydrogen, solid below T_λ spin-lattice relaxation 8=45124
Overhauser effect, n.m.r. signal profile and width 8=31890
overhauser effect, quantum-statistical theory 8=40968
α-oxalic acid dihydrate, d.m.r. and molec. struct. 8=49638
paraffin, liquid, in rotating mag. field 8=25958
paramagnetic crystals, proton spin-lattice relax. in high fields and low temps. 8=31889
paramagnetic solids, of C^{13} 8=31888
paramagnets, relax. rel. to e-spin pair-correl. 8=36259
pentaerythritol, deuterated, rel. to structural investigations of H bonds 8=43926
pentafluorobenzene 8=34373
phenoxy radicals 8=43411
phenyl and ethinyl derivatives of Ge and Si 8=36268
platelets of Sn particles layered with SiO, supercond., particle size effect 8=44735
poly-β-alanine, rel. to transitions, obs. 8=45112
poly-γ-benzyl-L-glutamate, linewidth rel. to mol. wt. 8=43873
polychlorotrifluoroethylene, low mol. wt., rel. to mol. motion, 77-300°K 8=45118
poly-1, 3-dioxolane, spectra, and dielectric dispersion 8=41003
polyethylene, oligomeric, rel. to conformational struct. in aromatic nonaromatic solvent mixtures obs. 8=43765
polyethylene oxide solns., proton relax. 8=30538
polylentadiene, chlorinated 8=38914
polymers, chemical shift in proton reson. spectra, using rotating sample 8=49626
polymers, oriented, effect of elongation 8=31914
polymethylbenzenes, p mag. relaxation 8=49654
polymethylsorbate 8=40984
polypeptides, molecular weight effect on n. m. r. manifestation of helix-coil transition 8=25637
polypropylene films rel. to mol. motion, CCl_4 effects, 140-373°K 8=48510
(1:1)poly(styrene-co-methyl acrylate) rel. to comp. and microstruct., obs. 8=43773
polytetrafluoroethylene, effect of temp. of post irrad. heat treatment 8=49640
polytetrahydrofuran, spectra, and dielectric dispersion 8=41003
Pound-Watkins type spectrometer, 100 Mc 8=37544
1-propanol, relax. 8=30535
protein solns., proton mag. relaxation, dependence on viscosity and temp. 8=39435
proton accelerator, energy meas. 300-2050 keV 8=33430
proton spin relax. in paramag. ion solns., D isotope effect 8=30536
protons bonded to B^{10}, quadrupole collapse of spin multiplets 8=34372
protons in free radicals, d.n.p., relaxation and paramag. shifts 8=38915
PVC, chlorinated 8=38914
pyrazine, oriented in nematic phase 8=34913
pyridine, anal. of spectrum using different methods 8=29821
pyrrole-dimethyl sulphoxide, H-bonding 8=25644
rapidly-rotating solids 8=40960
rare-earth metals and alloys, ferromagnetic, rel. to hyperfine interactions 8=36280
rare earth metals, ferromag. heavy, indirect spin relax. 8=45132
rare-earth metals, heavy, indirect spin relax. 8=31915
rare-earth-Pt alloys, of Pt^{195} rel. to conduction-electron polarization 8=36279
relaxation in gases and liquids 8=39437
relaxation in 3-spin systems, Overhauser effect of F and C-13 in radical liquid media 8=39424
resolution of chemical shift in solids 8=40963
r.f. resonances, study of nuclear and electron magnetic moments 8=43212
Rochelle salt, deuterated, d.m.r. and dielectric relaxation 8=49651
ruby, Al^{27} dynamic polarization by e reservoir temp. transfer, 1.8°K 8=31892
ruby: Al^{27}, nuclear paramag. acoustic absorption at 4.2°K 8=40914
ruby, Al^{27} structures under dynamic nuclear polarization 8=45111
solids, deuteron resonance and quadrupole interactions 8=49664
solids, extremely narrowed n. m. r. applications 8=27509
solids, linewidth transition and torsional oscillations 8=31940
in solids, magnetization loss on irradiation with r. f. field in single-shot passage 8=27495

Nuclear magnetic resonance and relaxation—contd
in solids, spin dynamics rel. to artificial line narrowing and Zeeman spin-spin relax. 8=27496
solids with two spin types, signals 8=36255
solvent effects on chem. shifts 8=43878
spectra, effect of reorientations about second-order axis 8=46515
spectra, methods of analysis 8=37541
spectrometer permanent magnet with columnar crystal material 8=33152
spectroscopy, pulsed fast recovery probe and receiver 8=36256
spin coupling constants, calc. using σ M.O. theory 8=47690
spin-echo orientation for gaseous diffusion obs. 8=39240
spin exchange between identical configs. of one mol. 8=43404
spin-lattice relax. times by tone-burst modulation meas. 8=36258
spin-lattice relax. times, saturation recovery method 8=33149
spin lattice relaxation by paramagnetic impurities without spin diffusion 8=45108
spin relaxation, anomalous, near mag. transition 8=49582
spin relax. in gases, quantum corrections 8=37187
spin-relax. time in atomic translational-diffusion mechanism studies and order parameter calcs. 8=27498
spin systems, two interacting, in crystal, spectra and line shape 8=27497
starch, modified maize, p spin-lattice relax. time temp. depend., obs. 8=45135
steric factors of H-bonding 8=25639
superconducting compounds, M_3X-type, spin-lattice relax. rel. to energy band structure 8=36257
superconducting solenoid field calibration probe 8=31360
superconductors, Knight shift 8=27494
in superconductors, recent work 8=40957
superconductors, type II 8=40958
1, 2, 3, 4-tetrafluorobenzene 8=47701
tetrafluoroborate salts, ion motion and phase transitions 8=31905
tetrahydrofuran/CCl_4 binary mixture, proton mag. relaxation 8=39425
DL-threonine 8=43398
trans-1, 2-cyclohexylenedinitrilotetracetic acid solns., 5 $\leq$pH$\leq$14, obs. 8=30537
transition metal alloys, local susceptibilities exam. 8=49657
transition metal salts, transferred hyperfine interactions and spin deviations 8=31919
transition metals and alloys, rel. to spin-fluctuation-induced mass renormalization 8=31922
tropylium salts, molec. motion in solid 8=49659
1, 2, 4-trichlorobenzene, oriented mols. 8=43403
1, 3, 5-trideutero-benzene, liquid, proton spin-lattice relaxation 8=39429
trifluoromethylphosphonylchloride, F^{19} reson. 8=34330
3, 3, 3-trifluoropropyne in liq. cryst. solns. 8=34930
trimethylbenzenes, isomeric, between 4°K and m. p. 8=36276
2, 4, 6-trinitrotoluene, isomer determ. 8=30534
two-spin system, complex splitting of spectra 8=36277
DL-valine 8=43398
variable temp. probes, protection against damage by overheating 8=33154
N-vinyl cpds. 8=47671
viscous solns., paramag. relax. determ. 8=30532
water adsorbed on protein, proton relaxation 8=49649
water and D_2O in oriented rayon fibres, broadline 8=27508
water combined in solids 8=45123
water-dioxane mixtures, proton spin-lattice relax. and viscosity 8=43770
water in mesomorphic phases, d.m.r. 8=48220
weak field, applications of transient nuclear demagnetization 8=33148
o-, m-, p-xylene solid, tunneling effect and hindrance pot. 8=31924
Zoelite Linde 13x, temp. depend. of mag. proton and cation reson. 8=49656
Ag solvent, Knight shifts in alloys, origin 8=30528
AgI, of halogen isotope 8=49636
Al^{27}, zero field resonances, in Al containing Zn impurity 8=49631
Al, Knight shift and pseudopotentials 8=45129
Al powder, spin-lattice and spin-spin relax. times rel. to press. 8=45110
Al, powdered: Al^{27}, line narrowing expts. 8=49630
Al III coordination no. in aq. solns. determ. by p.m.r. 8=39431
$AlCl_3$ aqueous solution, rel. to proton transfer between hydration and solvent H_2O 8=34931
$AlCl_3$ in aq. solvent mixtures, p.m.r. coordination number study 8=25954
$Al(NO_3)_3$, aq. soln., hydration no. determ. 8=48215
AlSb, elastically deformed, rel. to elec. field gradients at nucleus 8=31909
AsF_6^- anion in non-aq. solns., spin-lattice relax. 8=34928
Au-V:V^{51}, localized mag. moment 8=27514
BH_3 and trihalide complexes with organic bases, variable temp. 8=38916

Nuclear magnetic resonance and relaxation—contd
B_2O_3, cryst. and vitreous, rel. to structure 8=48634
BaO-B_2O_3 system, B^{11} spectra rel. to struct. 8=27499
Be, Knight shift rel. to Fermi surface 8=27500
Be(II) coordination no. in aq. solns. determ. by p.m.r. 8=39431
C^{13} and N^{14} data from proton spectra by double irradiation method 8=37537
C-liquid adsorption system, H^1 and F^{19} n. m. r. lineshift study 8=30766
$C^{13}H_3NC$, struct. determ. 8=34336
CH_3CN, CH_3CN/CD_3CN solid solns, proton spin-lattice relax., 8=40975
$(CH_3)_2O$ polar molecule, electronic screening effect and relax., perturbed by foreign gases 8=29815
C_6H_6 on silica gel, proton spin relax. 8=29814
$CaAl_2Si_2O_8$: Al^{27}, obs 8=40972
CaF_2: paramag. impurities, of F^{19}, temp. and impurity conc. dependence 8=40974
CaF_2 with Ce impurity, dipolar nucl. relax. 8=45119
CaF_2 : F^{19} longitudinal relaxation, field dependence 8=49634
CaF_2 : Mn^{2+}, F^{19} nuclear spin-lattice relaxation 8=49633
CaF_2:Yb^{3+}, ENDOR meas. rel. to crystal field splitting of Yb^{3+} in cubic sites 8=27501
CaF_2, Yb^{3+} and Tm^{2+} transferred hyperfine interaction, F^{19} ENDOR obs. 8=36266
Cd, Knight shift, temp. depend. 8=41002
$CdCr_2Se_4$, of Cr^{53} and Se^{77}, and magnetization temp. dependence 8=31895
$CdCr_2Se_4$, of Cr^{53} and Se^{77} at 4. 2°K 8=31896
$CeCr_2S_4$, of Cr^{53} at 4. 2°K 8=31896
CeF_4, solid, chemical shift anisotropy 8=40980
of Cl^{35} in solution of paramagnetic ions 8=48214
Co alloys, with impurities of 4d and 5d elements of group VIII, n.m.r. 8=49642
Co films 8=40976
Co, single-domain, relax. rates 8=31897
$CoCl_2 . 6D_2O$, of Cl^-, para- and antiferromagnetic state 8=36261
$CoCl_2 . 2H_2O$, antiferromagnet, 1. 3° to 12°K 8=31898
$CoCl_2 . 6H_2O$, of Cl^-, para- and antiferromagnetic state 8=36261
$CoCr_2O_4$, of Co^{59} rel. to hyperfine field of Co^{2+}in tetrahedral site 8=27502
$CoCr_2S_4$, of Cr^{53}, temp. and d.c. mag. field depend. of reson. freq. 8=36262
Co-Ni alloys, Co^{59} resonance satellite lines rel. to mag. disturbance by solute Ni atoms 8=31899
Co-Rh alloys, relaxation rates, and enhanced susceptibilities 8=31499
Co_3S_4, of Co 8=31901
$CrBe_{12}$, paramagnetic and ferromagnetic state, hyperfine fields meas. 8=45115
Cs form of zeolite 8=27510
Cs, Knight shift and pseudopotentials 8=45129
$CsMnCl_3 . 2H_2O$, rel. to antiferromagnetism 8=36275
$Cs_2MnCl_4 . 2H_2O$, rel. to antiferromagnetism 8=36275
Cu acetate hydrate, proton relax. of methyl group at low temps. 8=45109
Cu alloys, dil., ground-state of mag. impurity problem 8=45116
Cu formate tetrahydrate, antiferroelec. 8=44269
Cu formate tetrahydrate, d. m. r. and molec. struct. 8=49638
Cu liquid solvent, Knight shifts in alloys, origin 8=30528
Cu, spin-lattice relax. time in temp. range 3 × 10^{-3} °K to 2 × 10^{-2} °K 8=31902
Cu(II)2, 2′-dipyridine aq. solns, O^{17} linewidth 8=34926
$CuCl_2 . 2H_2O$, antiferromagnetic, proton relaxation 8=49635
$CuCl_2 . 2H_2O$-d_x, deuteration effects on PMR and antiferromagnetism 8=36264
Cu-Co alloy, of Co^{59} 8=40978
$CuCo_2S_4$, of Co 8=31901
$CuCr_2S_4$, of Cr^{53}, $Cu^{63, 61}$, Cu, temp. and d.c. mag. field depend. of reson. freq. 8=36262
$CuCr_2Se_4$, Cu Knight shifts 8=31901
$CuCr_2Te_4$, Cu Knight shifts 8=31901
$CuCr_2Te_4$, ferromag., of Te^{125} hyperfine field at 1. 4°K 8=27503
$CuCr_2X_4$ (X = Se, Te), Cu Knight shift 8=31901
Cu:Fe, rel. to singlet ground state of Fe 8=31900
CuI(Br), of copper and halogen isotopes 8=49636
$Cu(NH_3)_4SO_4 . H_2O$, PMR rel. to antiferromag. ordering 8=36263
Cu $(NH_3)_4$ $SO_4 . H_2O$, proton double resonance and temp. of electron spins, liq. He temp. 8=40979
$Cu(NO_3)_2 . 3H_2O$, PMR rel. to antiferromag. ordering 8=36263
$CuSO_4 . 5H_2O$ proton spectra down to 0. 3°K antiferromagnetic linear chain 8=49637
$Cu_{1-x}M_xFe_2O_4$, (M = Cu, Zn, Cd), Mossbauer resonance of Fe^{57}, 4. 2°K–1000°K 8=31907
Cu_2S, of copper isotopes 8=49636
$CuSeO_4 . 5H_2O$ proton spectra down to 0. 3°K antiferromagnetic linear chain 8=49637
DF and DCl, calc. D quadrupole coupling consts. 8=38921
D_2O, deuteron spin lattice relaxation 8=48217
D_2O, O^{17} enriched, spin echo O^{17} T_1 and T_2 obs. 8=48212
Dy, of $Dy^{161, 163}$ rel. to relax. mechanisms 8=27504

Nuclear magnetic resonance and relaxation—contd
DyAl garnet, of Al^{27}, quadrupole splitting and paramag. shifts 8=31893
Dy-Gd, of Dy^{163}, rel. to hyperfine interactions 8=36280
EuFe garnet, of Fe^{57}, rel. to sublattice magnetization 8=40839
EuO, of Eu^{115} 8=49641
EuP, of P^{31} rel. to Eu^{3+} spin $\langle S(T) \rangle$ temp. dependence 8=31904
EuS, of Eu^{115} 8=49641
EuSe, of Eu^{115} 8=49641
F^{19} chem-shifts B, P(III), phosphoryl and thiophosphoryl halides 8=43406
F^{19} in NbF_6^-, spin relax. and chem. exchange effects 8=34914
F^{19} in solns., dyn. nucl. polarization expts. 8=34910
F-containing crystals, rel. to electronic structure calcs. 8=27506
F, dynamic polarization of free radicals in fluorocarbon solns. 8=48221
F, in exchanges between tetrabutylammonium hexafluorophosphate and BF_3 or PF_5 in CH_2Cl_2 soln. 8=25960
F^- and HF, aq. solns., F^{19}, effect of Cu^{2+} on relax. 8=48222
Fe alloys, with impurities of 4d and 5d elements of group VIII, n.m.r. 8=49642
Fe, pulsed, rel. to domain-wall dynamics 8=31621
Fe(III)N-methyl-N-phenyldithiocarbamate, and fluorophenyl derivatives 8=27507
Fe–Al alloys, detailed spin-echo spectra rel. to hyperfine interactions 8=31906
$FeCl_2 . 2H_2O$, antiferromagnet, 1.3° to 12°K 8=31898
$Fe(CN)_6{}^{3-}$, aq. soln., position and linewidths of resonances of cations 8=48225
$Fe(CN)_6^{4-}$, aq. solns., position and linewidths of resonances of cations 8=48225
Fe-Co alloys, of Fe^{57} and Co^{57}, rel. to hyperfine field distrib. 8=45120
Fe:Sb^{125}, mag. hyperfine fields and spin-lattice relax. determ. 8=31891
Ga, Knight shift 8=27505
Ga, Knight shift and pseudopotentials 8=45129
Ga(III) coordination no. in aq. solns. determ. by p.m.r. 8=39431
GaAs(Sb), elastically deformed, rel. to elec. field gradients at nucleus 8=31909
$Ga_2(SO_4)_3$, hydrated cryst., evidence of H_3O^+ ions 8=49643
Gd(III) ion in aqueous soln., temp. and freq. depend. of O^{17} signal, rel. to water exchange 8=43882
GdFe garnet, of Fe^{57}, rel. to sublattice magnetization determ. 8=40840
H-bonds, strong, n.m.r. study 8=48301
H-bonding, study by n.m.r., review 8=48219
HBr in DBr, solid solutions, relax. 8=36269
HBr, solid phases 8=49645
HCl aq. solns. of Co(II), O^{17} and Cl^{35} n. m. r. 8=30541
HCl and DCl, solid, and n.q.r. study of molecular motion 8=31903
HCl in DCl, solid solutions, relax 8=36270
HCl, solid, T, δH obs. 8=40965
HCl, solid phases 8=49645
$HClO_4$-$DClO_4$-H_2O-D_2O system, proton reson. 8=34920
$(HCO_3)_2^{2-}$ in $KHCO_3$, structure determ. 8=26032
HD, liquid, double resonance 8=34921
HD, solid and liquid, proton spin-lattice relax. 8=31908
HF, gaseous, F^{19} and H^1 reson. 8=29817
HF in H_2O and D_2O, F^{19} chem. shift 8=43874
HF, nuclear shielding and spin-rot. consts., vibr. corrections 8=38924
HI, solid phases 8=49645
H_3O^+ adsorbed by vermiculite 8=47695
H_2S, three solid phases, pulse and steady state n.m.r. 8=40982
He^3 optically polarized, meas. for pumping time rel. to temp. 8=47689
He^3, spin-lattice relax. time, temp. depend. 8=24055
Hg and alloys, liquid, Knight shift 8=39438
Hg crystal Knight shift at 1.2°K 8=49646
$HgCr_2Se_4$, of Cr^{53} adn Se^{77} at 4.2°K 8=31896
In, cubic phase 8=36271
In(III) coordination no. in aq. solns. determ. by p. m. r. 8=39431
InAs, elastically deformed, rel. to elec. field gradients at nucleus 8=31909
In-Pb alloys, dil., Knight shifts and elec.-quadrupole coupling 8=45125
In-Sn alloys, dil., Knight shifts and elec.-quadrupole coupling 8=45125
K binoxalate, d.m.r. 8=49611
K oxalate hydrate, partly deuterated, isotope effect in d. m. r. 8=45122
K, spin lattice relaxation 8=40926
K_2 malate, double reson. 8=29810
KBr, elec. field gradients at nuclei surrounding different subst. halogen ions, n.m.r. meas. 8=48314
KBr, meas. of distortion effects round substitutional ions. 8=36273
KCl, endor of F-centres 8=36272
KF, impure single crystal, nuclear quadrupole effects by pulsed double resonance 8=41012
KI, elec. field gradients at nuclei surrounding different subst. halogen ions, n.m.r. meas. 8=48314

Nuclear magnetic resonance and relaxation—contd
KI, meas. of distortion effects round substitutional ions. 8=36273
$KMgF_3$, perovskite-type crystals, rel. to electronic structure calcs. 8=27506
$KMgF_3:V^{2+}$, Mn^{2+} hyperfine interactions, transferred through unpaired spin on intervening ions 8=49647
$KMnCl_3 . 2H_2O$, rel. to antiferromagnetism 8=36275
K-Na liquid alloys, Knight shift obs. 8=25955
K–Rb liquid alloys, Knight shift obs. 8=25955
$KTaO_3$, of Ta^{181}, rel. to nuclear spin-acoustic phonon interaction 8=45126
KVO_3, V^{51} quadrupole coupling tensor 8=31923
Kr^{83}, local mag. field shift, obs. and theory 8=39226
LaF_3, of F, temp. depend., rel. to Schottky defects and diffusion of F ions 8=31048
LaF_3, tysonite-type crystals, rel. to electronic structure calcs. 8=27506
$LaF_3:Pr^{3+}(Nd^{3+})$, of F^{19}, relax. times, 150-800°K 8=45127
Li borates, glass and cryst., diffusion of Li^7 8=31007
Li form of zeolite 8=27510
Li, Knight shift and pseudopotentials 8=45129
Li, liquid, self-diffusion meas. 8=48112
LiCl solns., proton relax. 8=30533
$LiD_3(SeO_3)_2$, d.m.r. 8=49648
$LiD_3(SeO_3)_2$, d.m.r. and molec. struct. 8=49638
LiF, F-centres, hyperfine interaction constants, temp. dependence 8=35587
LiF: F^{19} and Li^7 resonance 8=40920
LiF:Fe^{3+}, crystal field distortions obs. 8=48810
$LiH_3(SeO_3)_2$, proton reson. 8=31910
$LiNbO_3$ 8=36274
$LiNbO_3$, ferroelec. 8=40987
$LiNbO_3$, ferroelectric, of Nb^{93}, quadrupole coupling const. 8=45128
$LiNbO_3$, of Li^7 8=40988
$LiTaO_3$, ferroelec. 8=40987
LuFe garnet, of Fe^{57}, rel. to sublattice magnetization determ. 8=40840
Mg^{25} in aq. soln., chemical shift 8=39440
Mg(II) coordination no. in aq. solns. determ. by p.m.r. 8=39431
MgF_2, rutile-type crystals, rel. to electronic structure calcs. 8=27506
MgO: Cr^{53}, ENDOR 8=40977
MnAs, of Mn and As, hydrostatic pressure and temp. dependence 8=31911
$MnCr_2O_4$, ferrimagnetic spiral, of Mn^{55} 8=45130
MnF_2, extremely narrowed, applications 8=27509
α-MnS, paramagnetic, of S^{33}, temp. dependence, 175-300°K 8=45131
MnSb, of Mn and Sb, hydrostatic pressure and temp. dependence 8=31911
$Mn_{2-x} Cr_x Sb$ (x=o, 0.03), spin-reorientation rel. to phase transform, 180-280°K. spin-echo obs. 8=36189
$Mn_2(CO)_{10}$, Mn^{55} spectrum, nuclear quadrupole coupling effects 8=49653
N^{15} formaldoxine, spin-spin interactions 8=43409
N-containing heterocycles, N^{14} quadrupolar relax. and H lineshapes 8=29819
N, N-di-sec-alkyl amides, slow rot. around alkyl-N bond 8=38927
ND_3, deuteron spin lattice relaxation 8=48217
$NH_4{}^+$, signs of coupling consts. and isotope shifts 8=29820
NH_4Cl, effect of impurities on spin-lattice relax. 8=40955
NH_4-NH_4 proton exchange in liq. NH_3 8=27675
Na form of zeolite 8=27510
Na, Knight shift and pseudopotentials 8=45129
Na–alkali alloys, liq. 8=48223
$NaBF_4$, ionic motion 8=31912
$NaD_3(SeO_3)_2$, d.m.r. 8=49648
$(Na_2, Ca)(AlSi_3O_3) . 5H_2O$ and $(Na_2, Ca)(Al_2Si_8O_{16}) . 6H_2O$, complex splitting of spectra 8=36277
NaCl, acoustic, rel. to plastic deformation 8=44320
NaCl, enhancement by e.s.r. 8=35029
$NaD_3(SeO_3)_2$, d.m.r. and molec. struct. 8=49638
$NaH_3(SeO_3)_2$ and seutero-cpd., and ferroelec. props. 8=27511
NaI, of I^{127}, intensity dislocation dependence 8=36278
Na-NH_3 liq. solns., dynamic polarization 8=34925
$NaNO_3$, of Na^{23}, orientation and temp. dependence 8=40991
Nb, type II superconductor, spin-lattice relaxation 8=41005
Nb-Zr, type II superconductor, spin lattice relaxation 8=41005
Ne, double resonance in He-Ne laser operating at 6328 Å π transitions 8=47502
Ni alloys, with impurities of 4d and 5d elements of group VIII, n.m.r. 8=49642
Ni ferrite, of Fe^{57}, relax. times and amplification of external field 8=36267
Ni(II) in aq. soln., primary solvation no. determ. 8=39423
Ni: Cd^{111}, (Ru^{99}), hyperfine fields at solutes from perturbed angular-correlation exam. above and below T_- 8=40992
$Ni[(H_2O)_6]^{2+}$, O^{17} hyperfine coupling consts., evidence for distortion from octahedral symmetry 8=49652
Ni:Mn^{54}, mag. hyperfine fields and spin-lattice relax. determ. 8=31891
O^{17} in aq. electrolyte and nonelectrolyte solns. 8=25956
OH surface groups, effect of adsorbed benzene mols. 8=38923

Nuclear magnetic resonance and relaxation—contd
Os^{189}, Larmor freq. rel. to H^1, and mag. moment 8=27512
P^{31} chem-shifts in P(III), phosphoryl and triphosphoryl halides 8=43406
P^{31} Overhauser effects, and simultaneous obs. of two kinds of nuclei 8=40993
PCl_3, $POCl_3$ and POF_3, liq., spin-lattice relax. and molec. motion 8=34912
Pb-Bi solid soln., indirect nuclear spin-spin interactions in Pb by spin echo 8=40996
Pb-Hg solid soln., indirect nuclear spin-spin interactions in Pb by spin echo 8=40996
Pb-In solid soln., indirect nuclear spin-spin interactions in Pb by spin echo 8=40996
PbTe, Knight shift calcs using augmented-plane-wave method 8=40995
Pd-Ag alloys, 1°-4°K 8=31913
Pd-Fe alloys, spin-lattice relax. time conc. dependence 8=36080
Pd-Pt alloys, susceptibility, correlation effects 8=40997
$PtAs_2$, of As^{75} and Pt^{195} 8=49655
Pt-Co(Fe) alloys, rel. to local moment saturation 8=31527
Pt-Ir alloy, Pt^{195} Knight shift, Ir susceptibility 8=40998
Pt-Mo alloys, Pt-rich, and satellite structure 8=27513
PtP_2, of P^{31} and Pt^{195} 8=49655
Pt-Pd alloys, of Pt^{195}, spin susceptibility 8=40998
$RbCoF_3$, rel. to spin-density space oscills. and hyperfine interaction 8=31917
$Rb_2MnCl_4.2H_2O$, of several nuclei 8=31916
$RbMnF_3$: F^{19}, nuclear acoustic resonance, dispersion mode saturation 8=41000
$RbNiF_3$, and magneto-optical studies 8=32023
$RbNiF_3$, rel. to exchange interaction exam., 8=41001
Rh:Co dilute alloys, Co Knight shift rel. to local exchange enhancement 8=35433
Rh:Co rel. to Rh 5s cond. band exchange polarization, obs. 8=36281
$Sc(Ni_{1-x}Co_x)_2$, line shape for Sc^{45}, rel. to hyperfine interacts. 8=45133
SI_2 type three-spin mol, nucl. spin-lattice relax. 8=47687
Si, dynamic nuclear polarization production using nonresonant Overhauser effect 8=30632
SiC:N, donor conc. dependence rel. to e. delocalization and e. system degeneracy 8=45134
SiH_3 derivatives, spectra 8=34918
SiH_4, liquid, p spin-lattice relax. time, obs. 8=34922
SiH_nD_{4-n}, liquid, p spin-lattice relax. time, obs. 8=34922
SiO_2-Al_2O_3, combined H_2O 8=45123
Sn^{119} crystal, pulsed, obs. 8=31918
Sn, white, Knight shift, temp. depend. 8=41002
SrF_2: paramag. impurities, of F^{19}, temp. and impurity conc. dependence 8=40974
SrF_2: Eu^{++}, F^{19} spin lattice relax. time angular depend., 4.2, 77 and 300°K 8=36265
TbAl garnet, of Al^{27}, quadrupole splitting and paramag. shifts 8=31893
Tb-Dy, of Tb^{159} and Dy^{163}, rel. to hyperfine interactions 8=36280
Tb-Gd, of Tb^{159}, rel. to hyperfine interactions 8=36280
Th carbides, C^{13} Knight shift 8=41004
Ti, in Ti-H systems 8=49658
TiCo alloys, comp. dependence at 295°K and 77°K 8=31920
$TiFe_{1-x}Co_x$:Co^{59}, line profile comp., temp. and stoichiometry dependence 8=31921
TiO^{2+}, ENDOR 8=41007
TiO_2: Mn^{4+}, ENDOR 8=41007
TIO_2: V^{4+}, ENDOR 8=41007
TmFe garnet, of Fe^{57}, rel. to sublattice magnetization determ. 8=40840
U carbides, C^{13} Knight shift 8=41004
UH_3, Knight shift and line width 8=49660
VCx, ($0.75 < x < 0.88$), line shape of V^{51} 8=45133
V_3Sn, type II superconductor, spin-relaxation of V^{51}, temp. depend. obs. 8=40970
VO^{2+} in N, N-dimethylformamide soln., line-broadening 8=39419
Va-Ga alloys, Knight shift of V^{51} and Ga^{71} 8=41006
Xe^{129,131}, local mag. field shift, obs. and theory 8=39226
YBAl garnet, of Al^{27}, quadrupole splitting and paramag. shifts 8=31893
$YH_{1\cdot96}$, absorpt. spectrum, memp. effects 8=31925
$ZnSiF_6.6H_2O$: paramag. impurities, of F^{19}, temp. and impurity conc. dependence 8=40974
$ZrC_{0\cdot32}H_{1\cdot2}$, absorpt. spectrum, temp. effects 8=31925
$Zr_{1-x}Gd_xZn_2$, rel. to localized mag. moments effect in $ZrZn_2$ 8=36180
$ZrH_{1\cdot9}$, absorpt. spectrum, temp. effects 8=31925
$ZrN_{0\cdot47}H_{0\cdot98}$, absorpt. spectrum, temp. effects 8=31925
measurement
analysis, quantitative, based on n.m.r. dispersion 8=49993
applications and present trends 8=42038
broad-line, resonant calibrator 8=24262
broad line spectrometer, improvements 8=46523
direct digital computation of n.m.r. moments from broad-line spectra of varying temps. 8=46524
double, localized saturation effects 8=46514
double resonance, freq. sweep spectrometer 8=33147
double resonance spectroscopy, developments 8=37536

Nuclear magnetic resonance and relaxation—contd
measurement—contd
free precession expts. in terrestrial mag. field 8=46518
gases, apparatus for study 8=39225
historical and theoretical background 8=46527
liquid sample holder for pressure meas. 8=34917
long transversal relax. time, obs. using spin-echo technique 8=48218
multiple reson. techniques 8=29813
p. m. r., tetramethylsilane as internal reference 8=34929
partial-saturation method in double n. m. r. 8=29812
phase transformations, solid-state, high-press technique for n.m.r. study 8=48362
proton freq. to free electron cyclotron freq. ratio. precision meas. 8=46520
pulse technique for weak signal detection 8=37542
r.f. gate with 140dB carrier suppression 8=42044
sensitive nuclear pulse apparatus with digital signal averaging for solids 8=46521
single side-band technique, applic. to proton stabilized F^{19} resonance 8=46522
spectrometer adaptation for heteronuclear double reson. 8=28639
spectrometers, high resolution, freq. swept proton stabilized 8=46525
spectrometer for spin-echo obs. 8=49625
spectrometer marker generator circuit 8=41916
spectrometer sweep synchronization to computer memory scan 8=42047
spectrometer using coaxial components 8=33151
spectrometer, X-band, for paramag. dispersion obs. and ENDOR meas. 8=46511
spectrometry for refined constitution analysis 8=49624
spin relax. in complex systems 8=37540
spin-lattice relax., adiabatic rapid passage timing 8=42048
superconductive spectrometer, high-resolution, Du Pont instrument general performance information 8=46517
terrestrial mag. field range high-resolution n.m.r. 8=46516
transmitter of high-power r.f. pulse 8=33153
water, nuclear mag. susceptibility, prepolarization method 8=25959
water, C^{17} enriched, spin echo O^{17} T_1 and T_2 obs. 8=48212
weak continuous mag. field sensitive n.m.r., expts. 8=46519
KBr, Br nuclei surrounding substitutional Cl ion, field gradient obs. 8=26403
Nuclear matter. See Nucleus/theory; Quantum theory/many-particle systems.
Nuclear orientation
dynamic polarization 8=38349
dynamic polarization and asymmetric e.s.r. in polycrysts. 8=35029
fluorocarbons, dynamic polarization in soln. 8=34911
free radical, dynamic polarization, spin-temp. model 8=25653
free radical solns. of toluene, dynamic nucl. polarization 8=39439
polarized photo absorpt. cross section 8=42987
ruby, polarization, and electron cross relax. 8=40905
ruby, Al^{27} dynamic polarization by e reservoir temp. transfer, 1.8°K 8=31892
semiconductor, polarization on e-heating in cyclotron resonance 8=35806
n. q. r. structures in dynamic polarization with inhomogeneously broadened e. s. r. line 8=27515
CaF_2: Tm^{2+}, 12% using optical pumping 8=30633
F^{19} in solns., dyn. nucl. polarization expts. 8=34910
F, dynamic polarization of free radicals in fluorocarbon solns. 8=48221
He^3, excited level aligning and orientating method 8=42828
He^3, polarization by liq. optical pumping 8=37337
Ho^{165}, rel. to total n cross-section 2-135 MeV 8=25151
Na-NH_3 liq. solns., dynamic polarization 8=34925
Sb^{124}, mag. moment from decay γ anisotropy 8=42891
Sb^{125}, γ-ray anisotropies obs. 8=42892
Si^{29} by optical electronic saturation and optical pumping 8=30632
Nuclear photoeffect. See Gamma-rays/effects; Nuclear reactions due to photons; Photons/interactions.
Nuclear physics
data acquisition counting schemes 8=47194
data acquisition system programming 8=47193
dictionary of nuclear physics and technology, English-German-French-Russian 8=38291
experimental quality monitoring, labelled pulser pulses 8=28966
instrumentation, 1918-1968, review 8=28967
measurement, anal. rel. to sizes of physical objects, space extensions 8=28213
solid angle subtended by one circular disc at another, FORTRAN prog. for calc. 8=32639
transmutations of nuclei, book 8=33950
Nuclear polarization. See Nuclear orientation.
Nuclear power. See Nuclear reactors, fission.
Nuclear quadrupole resonance
ammonium hydrogen monochloroacetate of Cl^{35} 8=49668
chlorobenzenes, effect of D substitution on Cl n. q. r. 8=27517
detection method 8=49661

Nuclear quadrupole resonance—contd
- detector, coaxial bridge with helical line sample holders 8=46529
- n-dichlorobenzene, effect of pressure and temp. 8=49665
- halogen cpds., correl. with average mol. polarizability 8=29811
- metals, indirect nuclear quadrupole-quadrupole interactions through conduction electrons 8=41007
- in molecular crystals, rel. to thermal motions 8=27516
- nitriles, saturated organic, of N^{14}, coupling constants 8=25642
- nitrites, N^{14} study of NO_2^- ion 8=49666
- nuclear polarization, dynamic, with inhomogeneously broadened e. s. r. line, quadrupole structures 8=27515
- organotin dichlorides, coupling, rel. to nature of bonding to tin 8=41013
- pyridines, substituted, pyrimidine and pyridazine, of N^{14}, coupling consts. 8=25643
- pyrrole, cryst. 8=31929
- solids, quadrupole interactions and deuteron resonance 8=49664
- solids, review of quadrupole interactions 8=49662
- spectrometer, high level used for Cl n. q. r. 8=37545
- spectrometer, superregenerative, automatic coherence control 8=24264
- spectrometer using f.e.t. 8=28640
- spin echo, 2-freq., influence of asymmetry parameter 8=37546
- temperature control of spectrometer 8=46528
- 2, 4, 6- trichloroanisol, of Cl 8=41014
- 1, 3, 5-trichlorobenzene, rel. to mol. vibrations 8=27516
- triethylene diamine, pure n.q.r. 8=41015
- Al^{27}, zero field resonances, in Al containing Zn impurity 8=49631
- As_2Se_3 8=31926
- CBr_4 complexes with methyl-substituted benzenes and pyridines 8=36282
- $(CH_3)_3X\text{-}C \equiv C\text{-}Cl(X = C, Si, Ge, Sn)$. bonding props. 8=38912
- $C_2H_5SiCl_3$ mol. crystals, spectra multiplicity and spin lattice relax. time rel. to phase transforms 8=41010
- CsH_2AsO_4, spectra rel. to temp. 8=41009
- Cu_2O, supergenerative spectrometer temp. variations 8=31927
- GaM(M = Sb, As, P), spin-relax. time and chemial shift rel. to cavalence 8=31928
- HCl and DCl, solid, and n.m.r. study of molecular motion 8=31903
- $HGeCl_3$ mol. crystals, spectra multiplicity and spin-lattice relax. time rel. to phase transforms 8=41010
- I^{127}, spin echo, indirect spin-spin interaction beats 77°K 8=41011
- InM, (M = Sb, As, P), spin-relax. time and chemical shift rel. to covalence 8=31928
- KCl: Li^+, Cu^+, shifts of off-centre ions 8=45136
- $KClO_3$: Cl^{35}, resonance freq. temp. variation, use in temp. control of spectrometer 8=46528
- KF, impure single crystal, nuclear quadrupole effects by pulsed double resonance 8=41012
- KH_2AsO_4, As^{75} quadrupole interaction, critical temp. behaviour 8=45137
- KH_2AsO_4, spectra rel. to temp. 8=41009
- $LiNbO_3$, ferroelectric, n. m. r. of Nb^{93}, coupling constant 8=45128
- $Mn_2(CO)_{10}$, quadrupole coupling effects in Mn^{55} n.m.r. spectrum 8=49653
- N^{14} in five-membered heterocyclic compounds 8=25638
- $NH_4H_2AsO_4$, spectra rel. to temp. 8=41009
- $NaNO_2$, charge distrib. determ. of NO_2^- 8=48308
- $Na_2S_2O_6 \cdot 2D_2O$, motion of D2O molecules by n.q.r. 8=49669
- $NaSO_4$, Na^{23} quadrupole coupling 8=49667
- $PrCl_3$, of Cl^{35}, line splitting below 0. 4°K rel. to antiferromagnetic structure 8=36283
- $PtAs_2$, of As^{75} 8=49655
- RbH_2AsO_4, spectra rel. to temp. 8=41009
- Te crystals, I^{127} quadrupole coupling exam. 8=36284

Nuclear reactions
- See also Chemical analysis/by nuclear reactions; Fallout; Nuclear bombardment targets; Nuclear excitation; Nuclear fission; Nuclear fusion; Nuclear spallation; Radioactivity; Thermonuclear reactions.
- analog calc. of damping and escape width 8=25135
- cascades, inverse problem 8=29397
- compound-nucleus interfering resonances 8=42985
- rel. to cosmic rays, galactic, propag., cross sections 8=33852
- cross section distrib., polarization effect, statistical theory 8=33973
- cross-section fluctuation, expt. resolution effect 8=29392
- diffraction theories of collisions, appls. 8=29109
- diffractional, role of unitarity 8=38443
- direct and compound, theories and approximations 8=25200
- direct-capture evidence for $Mn^{55}(n, \gamma)Mn^{56}$ 8=25244
- direct knock-out with polarized beams, theory 8=33976
- direct rearrangement, time-reversal invariance tests 8=29393
- disordered molecular crystals, degree and charact. of disorder meas. 8=26454
- eigenchannel theory, generalization to e scatt. 8=33981

Nuclear reactions—contd
- elementary particle, weak-interaction theory 8=33955
- equivalent local potentials, new coupled equations 8=42980
- exchange effects of particle identity 8=29394
- exchange reactions, high and low energy, peripheral model 8=29384
- Fermi-odd, applic. of Wick theorem 8=42393
- γ-ray spectroscopy rel. to intermediate stages 8=25201
- high energy, models and obs., review 8=29383
- hyperons, review 8=29483
- impulse approx. for 150-180 MeV N scatt. off light nuclei 8=25215
- low-energy collision matrix, unitary model 8=29388
- magic nuclei, charged particle emission effect 8=29473
- Majorana exchange currents in $He^4(\gamma, p)H^3$, $He^4(\gamma, np)D^2$ 8=38452
- molec. wavefunctions calc. check 8=29701
- nanosecond isomeric states meas. 8=34046
- neutron emission, nonscatt., energy-angle correl. neglect 8=24948
- N transfer, finite range effects in DWBA 8=29525
- nucleon, optical pot., energy depend. of real part derived 8=25216
- neutron transfer in heavy-ion direct reactions, finite range effects at low energies 8=43051
- nuclides far off stability line prod., rates 8=38442
- 100-1000 GeV due to mesons and nucleons, intranuclear cascade 8=42530
- optical model analysis of Villar's graphical method 8=42983
- optical model calc. for N-nucleus calc. at 152 MeV 8=42998
- optical pot., amplitudes as sum of direct and compound processes 8=29391
- optical pot., energy depend. of real part derived 8=25216
- optical potential symmetry and its connection with time reversal and reciprocity 8=47204
- particle for production, coherent and incoherent, in nuclei at very high energies, cross section obs. 8=37914
- particle scattering, high energy approx. 8=42984
- particle transfer populating unstable states, extended to include non-resonant contribs. 8=42982
- product extraction, fast e. m. separators 8=38765
- quantum mechanical foundations 8=29395
- R and S-matrix strength functions 8=42804
- R-matrix theory, math. correspondence with e. m. theory of waveguides 8=33972
- radiative capture obs., thick-target technique 8=33369
- radiochemical cross sections for $E\pi^- = 50\text{-}400$ MeV, calc. 8=45400
- rearrangement collisions, coupled channel method 8=25205
- rearrangement collisions in unified theory 8=33975
- with rearrangement, truncated asymptotic method 8=25203
- review 8=38290
- s-resonance diffuse boundary pot. well model 8=29276
- resonance integral and spectra, γ spectrometer for meas. 8=47067
- resonance widths and spacings, collision matrix cals. 8=42986
- scattering at high energy, multiple diffr. theory 8=29385
- scattering, expressions for transmission coeffs. and mean square deviation of amplitude 8=38447
- scattering, inelastic, based on microscopic nuclear descriptions, coupled channel treatment 8=47300
- scattering of spin-½ particles on spinless nuclei with three particle channels 8=38445
- shell model, many-body theory 8=33977
- $\Sigma^- + He^4 \rightarrow \Lambda^\circ + n + t$, impulse-model calc. 8=38094
- in solar flares and atm., particles and radiation prod. 8=37072
- solar material and flare accelerated particles, giving solar neutrons, γ rays 8=41599
- statistical theory rel. to excitation functions for $Fe^{54}(n, 2n)Fe^{53}$, $Cu^{63}(n, 2n)Cu^{62}$, 13. 9-14. 7 MeV 8=38488
- statistics, communication-theory treatment 8=33969-70
- stopping power formulae, K and L shell correction 8=42981
- stripping, (d, p) calc. of p polarization 8=25261
- stripping, form factor in DWBA, influence of 2-body interaction 8=25206
- superheavy nuclei, preferred reactions for formation 8=43131
- s-wave virtual states and resonances in R- and S-matrix terms, distinction 8=42803
- T-matrix element, general form in direct reactions 8=38448
- T-violation and detailed balance in direct reactions 8=33971
- theories of direct and cpd. reactions, critical review 8=25202
- time correl. function formalism 8=29386
- time, velocity of products, using pulsed beam 8=24555
- unified reaction theory, asymptotic channel states and matrix equations 8=42788
- yield increase by accel. projectile between a series of targets 8=29396

Nuclear reactions—contd
Ca isotopes, stripping calc. with amended DWBA form factor 8=25206
O isotopes, stripping calc. with amended DWBA form factor 8=25206
chemical effects
See also Chemical effects of radiations/ionizing radiations.
nucleic-acid bases, irrad., yields of free radicals 8=49891
pyrimidine nucleosides, irrad., yields of free radicals 8=49891
I_2 reactions activated by radiative neutron capture in liq. hydrocarbons 8=41296
Nuclear reactions due to
alpha-rays
isomer prod. by 24 MeV bomard. of natural targets 8=47221
(α, γ) on low and medium 2 nuclei, cross sections and γ-spectra, 59 MeV 8=38462
(α, n), γ-ray angular distribution 8=34037
$(\alpha, 2n\gamma)$ rel. to applicability of statistical model description of ground state level intensities 8=38391
(α, xn) on heavy deformed nuclei, intermediate stages from γ-spectroscopy 8=25201
(p, n), γ-ray angular distribution 8=34037
$Al^{27}(\alpha, n)P^{30}$, obs., 8-25 MeV 8=25273
$Al^{27}(\alpha, 2p)Al^{29}$ obs., 8-25 MeV 8=25273
$Al^{27}(\alpha, p)Si^{30}$, obs., 10-25 MeV 8=25273
in Ar^{36}, α-cluster model 8=25049
$Au^{197}(\alpha, pn)Hg^{199}$, 25 MeV, rel. to conversion electrons 8=29361
$B^{11}(\alpha, Li^7)Be^8$, $E_\alpha = 42$MeV, differential cross-section obs. 8=43081
$Be^9(\alpha, 2\alpha)He^5$ differential cross sections at 28 MeV 8=29510
$Be^9(\alpha, 2\alpha)He^5$, quasi-free scatt., at 37 and 32 MeV 8=34040
Be^9 (α, n) C^{12}, calculated n spectra 8=38515
$Be^9(\alpha, n)C^{12}$, $E_\alpha = 6$-10 MeV, differential cross-section obs. 8=43079
$Be^9(\alpha, n)C^{12}$, 0.34-0.68 MeV, resonances obs. 8=25272
$C(\alpha, n)$ in thick targets 8=43141
$C^{12}(\alpha; n, p)O^{15}, N^{15}$, cross-section obs., 11.3-22.6 MeV 8=43084
$Br^{79}(\alpha, Zn)Rb^{81}$, decay obs. 8=25180
C, effective cross sections of reactions with 90 Mev α-rays 8=29515
C, rel. to effective cross-sections of fragments mass $A \geqslant 6$ 8=25271
$C^{12}(\alpha, 2\alpha)Be^8$, differential cross sections at 28 MeV 8=29510
$C^{12}(\alpha, 2\alpha)Be^8$, quasi-free scatt., at 37 MeV 8=34040
$C^{13}(\alpha, n)O^{16}$, 0.475-0.7 MeV, yield determ. 8=25272
$C^{13}(\alpha, n)O^{16}$, 3.5-6.5 MeV, ang. distrib. meas., set of J^π for O^{17} obtained 8=25103
$Ca^{40}(\alpha, \gamma)Ti^{44}$ levels obs. 8=25126
in Ca^{40}, α-cluster model 8=25049
$Ca^{40}(\alpha, t)$ and (α, He^3), cross sections rel. to DWBA calc., 56 MeV 8=34033
$Ca^{44}(d, p)Sc^{47}$, 760 keV level, mag. moment 8=25122
$Ca(\alpha, \gamma)Ti$, rel. to Ti^{44} first excited states 8=29306
Cd (α, xn), level systematics of Sn isotopes 8=38378
$Cl^{35}(\alpha, n)K^{38}$, rel. to β^+ decay of K^{38} 8=39361
$Co^{59}(\alpha, n)$, $E_\alpha = 8$-25 MeV, cross sections 8=29521
$Cr^{52}(\alpha, d)$, $(1g_{9/2})^2_{8+}$ excited state, $E_\alpha = 50$ MeV 8=38372
$Cu^{63}(\alpha, Zn)Ga^{65}$, decay obs. 8=25178
$D(\alpha, p\alpha)n$, energy spectra, deuteron break-up 8=47337
$Es^{253}(\alpha, p)$, Fm^{256} decay props. obs. 8=42977
$F^{19}(\alpha, Li^{6,7})O^{17,16}$, $E_\alpha = 42$MeV, differential cross-section obs. 8=43081
$F^{19}(\alpha, n\gamma\gamma)Na^{22}$, γ correl. obs. 8=25109
$F^{19}(\alpha, p\gamma)Ne^{22}$, $E_\alpha = 12.55, 13.55$ MeV, ang. correl. and lifetimes 8=29298
$F^{19}(\alpha, p\gamma)Ne^{22}$ at 10.80 MeV α energy, determ. of 5.14 MeV state lifetime in Ne^{22} 8=25108
$Fe^{54,56}(\alpha, d)$, $(1g_{9/2})^2_{8+}$ excited state, $E_\alpha = 50$ MeV 8=38372
$Fe^{54}(\alpha, t)$ and (α, He^3), Fe^{55} and Co^{55} analog states, obs. 8=29311
$Ho^{165}(\alpha, xn)$ $1 \leqslant x \leqslant 5$, total cross sections, 54 MeV 8=29523
$Ho^{165}(\alpha, xn)$ obs 8=29524
$Li^6 + \alpha \rightarrow 2\alpha + d$, 294 MeV α-particles 8=47353
$Li^7 + \alpha \rightarrow 2\alpha + t$ 29.4 MeV α-particles 8=47353
$Mg^{24}(\alpha, p\gamma)Al^{27}$, 3.00 MeV level of Al^{27}, obs. 8=38363
$Mg^{24} + \alpha \rightleftharpoons Al^{27} + p$ time-reversal invariance test 8=43088
N, effective cross sections of reactions with 90 MeV α-rays 8=29515
N, rel. to effective cross-sections of fragments mass $A \geqslant 6$ 8=25271
$N^{15}(\alpha, Li^{6,7})C^{13,12}$, $E_\alpha = 42$MeV, differential cross-section obs. 8=43081
$Na^{23}(\alpha, p\gamma)Mg^{26}$, branching ratios in Mg^{26} obs. 8=25112
$Ne^{20}(\alpha, \alpha'\gamma_{1.63})Ne^{20}$, $E_\alpha = 3.96$-6.08 MeV, γ excitation functions 8=38517
$Ne^{20}(\alpha, p\gamma_{0.44})Na^{23}$, $E_\alpha = 3.96$-6.08 MeV, γ excitation functions 8=38517
$Ni^{58,60,62}(\alpha, d)$, $(1g_{9/2})^2_{8+}$ excited state, $E_\alpha = 50$ MeV 8=38372
$O^{16}(\alpha, 2\alpha)C^{12}$, differential cross sections at 26 MeV 8=29510
$O^{18}(\alpha, \gamma)Ne^{22}$, e.m. deexcitation of Ne^{22} at 11.89 and 12.28 MeV 8=47240

Nuclear reactions due to—contd
alpha rays—contd
$O^{18}(\alpha, n\gamma)$ and (α, γ_0) rel. to Ne^{22} excited levels, $E_\alpha = 2.5$-5 MeV 8=42845
O, effective cross sections of reactions with 90 MeV α-rays 8=29515
$Sm^{150,152,154}(\alpha, Xn)Bd^{150-156}$, reaction mechanism for angular distribution of conversion electrons 8=47258
$Ti^{48}(\alpha, \alpha')$ at 31 MeV, octupole states systematics 8=43089
$Ti^{50}(\alpha, pn)V^{52}$, $Ti^{50}(\alpha, d)V^{52}$, rel. to β^+ decay of V^{52} 8=29361
$Tm^{169}(\alpha, xn)$ obs. 8=29524
$Tm^{169}(\alpha, xn)$ $1 \leqslant x \leqslant 5$, total cross sections, 54 MeV 8=29523
$24 \leqslant Z \leqslant 30$ nuclei, total cross sections rel. to A, 24.7 MeV 8=29518
$U^{235}(He^4)$, Coulomb excitation, 15-19 MeV 8=43105
$Zn^{64,66,68}(\alpha, d)$, $(1g_{9/2})^2_{8+}$ excited state, $E_\alpha = 50$ MeV 8=38372
cosmic rays
See also Cosmic rays/effects and interactions.
Aleph baryons, role 8=42734
elements and compounds, radiation lengths and critical energies 8=29387
with emulsion nuclei, anal. of azimuthal ang. distribs. of secondaries rel. to fireball prod. 8=29390
extremely high energy obs. 8=42733
fireball and jet prod. in photographic emulsions 8=29247
5.10^{10}-10^{12} eV with C and Fe 8=42728
fragmentation parameters of heavy nuclei on 'hydrogen' of nuclear emulsion 8=25031
with low energy transfer into soft component, ang. distrib. and transverse momentum 8=29239
multi-particle prod., calc. using inverse problem 8=42724
nucleon isobar prod. in emulsions, for low multiplicity interacts 8=33855
nucleon-nucleus model 8=42725
n prod. by μ at a depth of 150 m water equivalent in Pb, Cd, Fe, Al 8=38461
100 GeV π and N on C, Pb, cross-section obs. at 2000 m 8=42727
p + C interaction, 10^{10}-10^{12} eV, effective cross-section on 'Proton' satellites 8=25228
radio nuclides produced for tracers of atmospheric precipitation processes 8=50142
200 GeV, asymm. shower prod. 8=42718
200 GeV meas. of energy transfer to neutral pions 8=42730
Ni^{59} produced in meteorites and micrometeorites 8=43003
in O, 150 MeV–19GeV, spallation prod. of $Li^{6,7}$, $Be^{9,10}$, $B^{10,11}$, obs. rel. to these processes between cosmic rays in space 8=38156
deuterons
core excitation amplitude calc. in point d approx. 8=43060
Coulomb stripping on deformed nuclei below barrier 8=47340
(d, n), n generating tube 8=24949
(d, p), J-dependence for strong $l_n = 3$ transitions 8=25072
(d, p) excitation functions, transferred ang. momentum depend. 8=29495
(d, p) finite-range effects in direct reaction at low energies 8=43051
(d, p), isobaric analogues excitation, spectroscopic factors 8=38321
(d, p) stripping, p polarization calc. 8=25261
(d, p) stripping, Pearson and Coz theory 8=34025
(d, p) stripping reaction including charge exchange 8=34027
(d, p) stripping, spectrosopic factors from Butler-Born approximation 8=43049
(d, p) T-matrix element, general form in direct reactions 8=38448
(d, p), Tanifuji–Butler revised model 8=43047
$(d, p\gamma)$ and n capture γ-spectra rel. to mechanisms, 15 keV-15 MeV 8=25235
$(d, p\gamma)$ distinction between direct reactions from ang. correl. 8=34026
excitation of collective nuclear, with d disintegration 8=38499
optical pot. model and distorted-wave method 8=29492
particle transfer, as probes of particle unstable states 8=29496
proton polarization, BHMM theory 8=43048
stripping and pickup, $l = 3$, config. mixing and J dependence 8=43065
stripping, low-energy, sudden approximation 8=47341
stripping, polarized d, apparatus 8=29494
stripping reactions, ang. mom. transfer calc. using polarized d 8=25260
stripping theory, defence of Butler approach 8=43046
stripping theory, error in Butler approach 8=43045
$t(d, n)\alpha$ reaction, n yield, 14 MeV, α-counting 8=24946
triton energy spectrum from $He^3(d, t)2p$ 8=43005
$Al^{27}(d, \alpha)Mg^{25}$, direct and compound cross sections E_d=4 to 20 MeV 8=34032
$Al^{27}(d, He^3)$, 82 MeV 8=29428
$Al^{27}(d, p)Al^{28}$, total cross section and activation depth, 0.6–3.2 MeV 8=43061
$Al^{27}(d, p)$, 82 MeV 8=29428
$Al^{27}(d, p, \alpha)Al^{28}$, Mg^{25} differential absolute cross-sections obs. and compared with Hauser–Feshbach calcs. 8=38505
$Al^{27}(d, t)$, 82 MeV 8=29428
Al^{27}, 710 MeV rel. to optical model 8=38506

Nuclear reactions due to—contd
- **deuterons**—contd
  - $B^{10}(d, \alpha)Be^{8}$, 0.5-2.0 MeV, ang. distrib. of α obs. 8=25266
  - $B^{10}(d, p, \gamma)B^{11}$, 1.6-2.4 MeV p-$\gamma$ ang. correl. obs. 8=34030
  - $B^{11}(d, n)C^{12}$, neutron-gamma angular correlation measurements, 1.6-3.3 MeV 8=38502
  - $B^{11}(d, p\gamma)B^{12}$, 1.6 and 2.4 MeV p-γ correl. parameter, distortion parameter calc. 8=34036
  - Be(d, n), at 1 and 3 MeV, energy, ang. distrib. and yields of fast n 8=34029
  - $Be^{9}(d, p)$, polarized d, total ang. momentum transfer in stripping reaction, E ~ 8 MeV 8=47345
  - $Be^{9}(d, p)Be^{10}$, polarization-vector analysing power, 12 MeV 8=34031
  - $Be^{9}(d, p)Be^{10}$, polarized d, p asymmetry obs. 8=29494
  - $Be^{9}(d, p)Be^{10}$ polarized d induced, p asymmetry rel. to spin-orbit interaction, obs. 8=29503
  - $Be^{10}(d, p)Be^{11}$, polarized d, p asymmetry obs. 8=29494
  - $Bi^{209}(d, t)$, Bi^{208} single proton states obs. 8=38398
  - $C^{12}(d, n)N^{13}$, N polarization calc. 8=38503
  - $C^{12}(d, p)$ polarized d, total ang. momentum transfer in stripping reaction, E ~ 8 MeV 8=47345
  - $C^{12}(d, p)C^{13}$, γ-ray emission, 170 keV, plane polarisation 8=43058
  - $C^{12}(d, p)C^{13}$, j-forbidden reactions stripping 8=47346
  - $C^{12}(d, p)C^{13}$, N polarization calc. 8=38503
  - $C^{12}(d, p)C^{13}$, polarization-vector analysing power, 12 MeV 8=34031
  - $C^{12}(d, p)C^{13*}$-309 MeV state, polarization-vector analysing power, 12 MeV 8=34031
  - $C^{13}(d, t)$, $C^{12}O^{+}$ and 2^{+} spectroscopic factors, 12.1, 13.3 and 14.0 MeV obs. 8=47347
  - Ca^{40}, optical model parameters 8=29497
  - $Ca^{40}(d, p)Ca^{41}$, proton polarization, $E_d = 5$ MeV 8=43063
  - $Ca^{40}(d, p)$, polarized d, total ang. momentum transfer in stripping reaction, E ~ 8 MeV 8=47345
  - $Ca^{42,44}(d, p)Ca^{43,45*}$ with core excitation amplitude calc. in point d approx. 8=43060
  - $Ca^{48}(d, n)Sc^{49}$, ang. distributions obs. 5.5, 6.0 MeV 8=38508
  - $Cr^{50}(d, p)Cr^{51}$, level struct. determ. 8=42874
  - $N^{14}(d, n)O^{15}$, 2.9, 3.7 MeV polarization calc. by distorted wave theory 8=38509
  - $Ca^{40}(d, p)Ca^{41}$, asymmetry of p ang. distrib., with polarized d 8=29507
  - $Ca^{40}(d, p)Ca^{41}$, n strengths for $J = {}^{3}/_{2}{}^{+}$ states 8=33909
  - $Ca^{40}(d, p\gamma)Ca^{41}$, angular correl. of 3.209, 3.623 and 3.740 MeV states 8=29303
  - $Ca^{40}(d, t)$ and (d, He^{3}), cross sections rel. to DWBA calc., 28 MeV 8=34033
  - $Ca^{41,43,45}$ spectroscopic factor calc. 8=33871
  - $Ca^{42}(d, n)Sc^{43}$, E_d=5.15 MeV, obs. 8=34034
  - $Ca^{44}(d, p\gamma)Ca^{45}$, 5 MeV, level structure of Ca^{45} 8=38366
  - $Ca^{48}(d, He^{3})K^{47}$, 34.4 MeV, rel. to levels of K^{47} 8=25268
  - $Cr^{52}(d, He^{3})V^{51}$, 34.4 MeV, rel. to levels of V^{51} 8=25268
  - $Cr^{52}(d, p)$, polarized d, total ang. momentum transfer in stripping reaction, E ~ 8 MeV 8=47345
  - $Cu^{63,65}(d, He^{3})Ni^{62,64}$, spectroscopic factors and transferred angular momenta, E_d=34.2 MeV 8=34035
  - $D(d, n)He^{3}$, in n. pulse production 8=47150
  - $D(d,n)He^{3}$, recoil determ. of phosphor efficiency 8=29208
  - $D(d, n)He^{3}$, recoil particle detection mag. analyser 8=47179
  - $D(d, p)T$, $E_d = 80$ keV, polarized d effects 8=47343
  - $D(d, pd)n$, energy spectra, deuteron 8=47337
  - D, $E_d < 1$ MeV 8=34028
  - $Er^{166,168,170}(d, p)Er^{167,169,171}$ levels obs. 8=25152
  - $Fe^{54}(d, He^{3})Mn^{53}$, 34.4 MeV, rel. to levels of Mn^{53} 8=25268
  - $H^{2}(d, p)H^{3}$ for He^{4} states search, 3-11 MeV 8=38353
  - He^{3} energy spectrum from $t(d, He^{3})2n$ 8=43005
  - $He^{3}(d, t)2p$, p-p final state interactions, 36 MeV 8=43078
  - $Hf^{176,180}(d, p)Hf^{177,181}$, level spectra 8=42911
  - $Hf^{178,180}(d, t)Hf^{177,179}$, level spectra 8=42911
  - $In^{113}(d, 2n)Sn^{113}$, fractional distillation of active Sn^{113} 8=42954
  - $K^{39}(d, \alpha)Ar^{37}$, statistical model analysis, 4.55-5.32 MeV 8=47349
  - $Li^{6}(d, p)Li^{7}$, vector analysing power, j-dependence 8=47344
  - $Li^{7}(d, \alpha, \alpha)n$, rescattering effects, $E_d = 3.0, 3.2$ and 5.9 MeV 8=43057
  - $Mg^{24}(d, p)$, polarized d, total ang. momentum transfer in stripping reaction, E ~ 8 MeV 8=47345
  - $Mg^{24}(d, p)$, j-forbidden stripping reactions 8=47346
  - $Mg^{24,25}(d, n)Al^{25,26}$, 5.5 or 6 MeV, transitions of $Al^{25,26}$ obs. 8=25113
  - $Mg^{25}(d, p)Mg^{26}$ and $Mg^{26}(d, p)Mg^{27}$, mean energy level width of, Al^{27} and Al^{28} 8=47237
  - $Mg^{25}(d, p\gamma)Mg^{26}$, levels of Mg^{26} deduced 8=25112
  - $Mg^{26}(d, \alpha)Na^{24}$ and a new level of Na^{24} 8=38361
  - $Mo^{92}(d, p)Mo^{93}$, excited states obs. 8=25139
  - $N^{15}(d, n)O^{16}$, 3.2-3.8 MeV, n polarization obs. 8=43059
  - $Ne^{20}(d, n\gamma)Na^{21}$, n-$\gamma$ angular correlation 8=47348
  - $Ne^{20}(d, p)Ne^{21}$, p group cross sections 8=29506
  - $Ni^{58,60}(d, n)Cu^{59,61}$, differential cross-sects. 8=29308
  - $O^{16}(d, \alpha)N^{14}$, isospin-allowed differential cross-section obs. 8=29504
  - $O^{16}(d, n)F^{17,17*}$ cross sections, 2-3.5 MeV 8=38504
  - $O^{16}(d, p)$, j-forbidden stripping reactions 8=47346

Nuclear reactions due to—contd
- **deuterons**—contd
  - $O^{16}(d, p)O^{17}$, appl. to oxygen diffusion study in Zr and Zr-Cu alloys 8=31017
  - $O^{16}(d, p)O^{17,17*}$ cross sections, 2-3.5 MeV 8=38504
  - $O^{16}(d, p)O^{17}$, spectroscopic factors 8=29505
  - $O^{18}(d, n)O^{19*}$ with core excitation amplitude calc. in point d approx. 8=43060
  - $P^{31}(d, n)S^{32}$, isobaric analogue states 8=29302
  - $Pb^{206}(d, t)Pb^{205}$, spectroscopic factors, calc. 8=29345
  - $Pb^{207}(d, p)Pb^{208}$, neutron particle-hole structure of Pb^{208} from excitation functions 8=25160
  - $Pb^{208}(d, p)Pb^{209}$, diff. cross-sections, DWA anal. 8=43069
  - $Pb^{208}(d, p)Pb^{209}$, E_d=8 MeV, spectroscopic factors 8=29509
  - $Pu^{239}(d, pf)$, ang. correl. obs. 8=43070
  - $Pu^{242}(d, 2n)Am^{242}$, isomeric cross section calc. 8=25165
  - $Sc^{45}(d, p\gamma)Sc^{46}$, low level transition probabilities 8=25123
  - $Si^{28}(d, He^{3})Al^{27}$, spectra obs. Al compared with nuclear models 8=43062
  - $Si^{28}(d, p)$, 82 MeV 8=29428
  - $Si^{28}(d, p)Si^{29}$, level lifetimes obs. 8=42852
  - $Si^{28}(d, t)$, 82 MeV 8=29428
  - $Si^{28}(d, He^{3})$, 82 MeV 8=29428
  - $Si^{30}(d, p)Si^{31}$, low energy levels obs. 8=42853
  - $Si^{30}(d, p\gamma)$, Si^{31} low-levels e.m. props., 2.95-4.0 MeV 8=38364
  - $Sr^{87}(d, p)Sr^{88}$, $E_d = 7.5$ MeV, n particle-hole states 8=42885
  - $Sr^{88}(d, p)Sr^{89}$ particle-plus-core coupling model interpretation 8=33917
  - $T(d, n)$ at low energies 8=47321
  - $T(d, n)He^{4}$, recoil determ. of phosphor efficiency 8=20208
  - $Te^{126,128,130}(d, He^{3})Sb^{125,127,129}$ energy levels deduced, 34 MeV 8=43068
  - $Ti^{48,50}(d, He^{3})Sc^{47,49}$, 34.4 MeV, rel. to levels of $Sc^{47,49}$ 8=25268
  - $V^{51}(d, He^{3})Ti^{50}$, 34.4 MeV, rel. to levels of Ti^{50} 8=25268
  - $Y^{89}(d, p)Y^{90}$, 12 MeV and the level structure of Y^{90} 8=25136
  - $Yb^{172,174}(d, p)Yb^{173,175}$, angular distribs. rel. to spectroscopic factors, 12 MeV 8=29508
- **electrons**
  - (e, e′p), p ang, distrib. rel. to final state interactions 8=38458
  - (e, e′p), overlap integral calc. using single particle orbitals 8=29263
  - nuclear struct. study by e initiated reactions 8=47209
  - rel. to nucleus structure, T_3 resons excitation 8=33884
  - positron yield calc. evaluation 8=29410
  - positron yield meas. 8=29409
  - W prod. in nuclear Coulomb field 8=42595
  - Ar, capture cross-sections by p, 440 keV to 13.75 MeV 8=42996
  - Be^{9}, yield of charged products 8=25211
  - C, yield of charged products 8=25211
  - $C^{12}(e, e'p)$, p angular and momentum distribs., obs. 8=29413
  - H_2, capture cross-sections by p, 440keV to 2.45 MeV 8=42996
  - He, capture cross-sections by p, 440keV to 5.41 MeV 8=42996
  - N_2, capture cross-sections by p, 440 keV to 13.75 MeV 8=42996
- **gamma-rays.** See Nuclear reactions due to/photons.
- **heavy ions.** See Nuclear reactions due to nuclei of $Z > 2$.
- **helium-3**
  - cluster mechanism contribs. with light nuclei, use of Feynman diagram 8=38516
  - (d, t) on $Ca^{40,42,44,48}$ mixed target, spectroscopic factors, E_d=17 MeV 8=34042
  - $d(He^{3}, t)2p$, p-p final state interactions, 53 MeV 8=43078
  - particle transfer, as probes of particle unstable states 8=29496
  - (p, d) on $Ca^{40,42,44,48}$ mixed target, spectroscopic factors, E_p=19.5 and 20 MeV 8=34042
  - Teflan $(He^{3}, 2n)$, delayed p activity. 33 MeV 8=38415
  - Ar^{33} prod. and delayed-p decay, 32 MeV 8=38414
  - $Ar^{40}(He^{3}, t)K^{40}$, 2-particle 2-hole states 8=42840
  - $B^{10}(He^{3}, \alpha)B^{9}$ Feynman diagram technique applic. 8=38516
  - $B^{11}(\tau, d)C^{12}$, ang. distrib. of d 8=47229
  - $B^{11}(He^{3}, \alpha)B^{10}$, γ decay obs. 8=42834
  - $Be^{9}(He^{3}, \alpha)$, $E_{He^{3}} = 27$ MeV, differential cross section obs. 8=29514
  - $Be^{9}(He^{3}, n)$ at low energies 8=47321
  - $Be^{9}(He^{3}, n)C^{11}$, excitation functions and ang. distrib., 3.49-9.96 MeV 8=43080
  - $Br^{79}(He^{3}, n)Rb^{81}$, obs. 8=25180
  - C^{12}, He^{3} polarization and spin-orbital optical potential 8=38104
  - $C^{12}(He^{3}, \alpha)C^{11}$, $E_{He^{3}} = 13.9$ MeV, obs. 8=43082
  - $C^{12,13}(He^{3}, \alpha)$, $E_{He^{3}} = 19, 27, 37$ MeV, differential cross section obs. 8=29514
  - $C^{13}(He^{3}, \alpha\gamma_{15.1})C^{12}$ $T = 0, 1$ α states in O^{16} obs. 8=42840
  - $C^{13}(He^{3}, Be^{8})Be^{8}$, ground-state Be^{8}, differential cross-sections 8=43083
  - $C^{13}(He^{3}, d)N^{14}$, mechanism rel. to low-levels of N^{14} 8=43085
  - $C^{12}(He^{3}, p)$, N^{14} levels, 20.1 MeV obs. 8=47230
  - $C^{12}(He^{3}, p\gamma)N^{14}$, study of γ rays 8=47354
  - Ca^{37} prod. and delayed-p decay, 32 MeV 8=38414

Nuclear reactions due to—contd
helium-3—contd
$Ca^{40}(He^3, \alpha)Ca^{39}$, anomalous spectroscopic factors, 14-28 MeV 8=34042
$Ca^{40}(He^3, d\gamma)Ca^{39}$, low level struct. 8=25119
$Ca^{40}(He^3, n)Ti^{42}$ energy levels 8.5-10 MeV 8=38371
$Ca^{40}(He^3, p)$, Sc^{42} ang. distrib. and J^π, T assignment 8=42869
$Cl^{37}(He^3, \alpha)Cl^{36}$, S^{36} ground state analogue 8=29516
$Co^{59}(He^3, d\gamma)$, E = 18, 22 MeV, levels obs. 8=25131
$Cu^{65}(He^3, \alpha)$, $E_{He3} = 12$-32 MeV, Cu^{64} ang. distrib. obs. 8=43092
$F^{19}(He^3, Li^6)O^{16}$, relative spectroscopic factor and yield curves, 2.0-6.0 MeV 8=43087
$Fe^{54}(He^3, \alpha)Fe^{53}$, $E_{He^3} = 13.0$ MeV, analysis 8=29520
$Fe^{54}(He^3, p)Co^{56}$, p spectrum and angular distrib. rel. to Co^{56} levels, 18 MeV 8=29519
$Ge^{70}(He^3, d)As^{71}$, energy levels obs. 15 MeV 8=43093
$(He^3,)$ for Sb^{125} and $I^{127,129,131}$ orbital angular-momentum transfers and spectroscopic factors, 25 MeV 8=42893
$He^3(He^3, He^4)2p$, p-p final state interactions, 53 MeV 8=43078
$In^{113,115}(He^3, d)Sn^{114,116}$, p particle-hole pairs excitation, 4 MeV 8=34044
$K^{39}(He^3, d)$, Ca^{40} excited levels γ decay rel. to nature, obs. 8=33910
$K^{41}(He^3, d)Ca^{42}$ particle hole states up to 5.79 MeV obs. 8=47243
$Li^6(He^3, p\text{-}\alpha\alpha)$ below 2MeV 8=29513
$Li^7(He^3, p)Be^9$, n decay branching ratios 8=29358
$Li^7(He^3\{p, \alpha\})\{Be^9, Li^6\}$0.9-12 MeV rel. to unreported levels of Be^9, Li^6 8=25098
$Mg^{24}(He^3, p)Al^{27*}$, γ-ray transition and spin assignments to levels 8=42849
$Mo^{92}(He^3, \alpha)$ rel. to n hole states, 18 MeV 8=29319
Mo^{92} (He^3, d), rel. to p levels, 18 MeV 8=33918
$N^{14}(\tau, d)$, O^{15} levels and ang. distrib., $E_\tau = 11$ MeV 8=33900
Ne^{17} prod. and delayed-p decay, 32 MeV 8=38414
$Ne^{22}(He^3, d\gamma)$, Na^{23} $J^\pi = 1/2^+$ states e.m. decay branching ratio obs. 8=42847
Ni isotopes, (He^3, α) cross sections 8=29522
$Ni^{58}(He^3, d)Cu^{59,61}$, $E_{He} = 16.4$ MeV, level struct. determ. 8=42882
$Ni^{58}(He^3, He^{3\prime})$, optical model analysed, 51.3 MeV 8=43076
$Ni^{58}(He^4, \alpha)$, optical model analysed, 51.3 MeV 8=43076
$O^{16}(He^3, n)Ne^{18}$, double stripping anal., ang. distrib. and transitions 8=43086
$O^{16}(He^3, 2n)$, Ne^{17} delayed p decay, 33 MeV 8=38415
$O^{16}(\tau, \alpha)$, O^{15} levels and ang. distrib., $E_\tau = 11$ MeV 8=33900
$p(He^3, d)2p$, p-p final state interactions, 53 MeV 8=43078
Pb^{207} (He^3, d), Bi^{208} single proton states obs. 8=38398
$Pb^{208}(He^3, d)Bi^{209}$, level struct. obs. 8=42925
$S^{28}(He^3, 2n)$, S^{29} delayed p decay, 33 MeV 8=38415
$S^{32}(He^3, 2n)$, Ar^{33} delayed p decay, 33 MeV 8=38415
$Sc^{45}(He^3, d)Ti^{46}$, ang. distrib. obs. 8=25274
$Sc^{45}(He^3, d)Ti^{46}$, 15 MeV, levels of Ti^{46} 8=25127
Si^{25} prod. and delayed-p decay, 32 MeV 8=38414
$Si^{28}(He^3, p\gamma)P^{30}$, levels below 6 MeV obs. 8=25116
$Sn(He^3, d)$ rel. to Sb odd-odd isotopes levels, ⩽2 MeV 8=34043
$Sr^{88}(He^3, \alpha)$, rel. to n hole states, 18 MeV 8=29319
$Sr^{88}(He^3, d)$, rel. to p levels, 18 MeV 8=33918
Ti^{41} prod. and delayed-p decay, 32 MeV 8=38414
$Ti^{46,47,48,49,50}(He^3, He^4)$ $Ti^{45,46,47,48,49}$ neutron pick up and energy levels obs.: 18.2 MeV 8=43090
$Ti(He^3, H^3)$, "quasi-elastic" data rel. to isobaric-spin-dependent potential strength and shape 8=43091
$Ti(He^3, H^3)$, "quasi-inelastic" transition to excited isobaric
$Ti^{47}(He^3, \alpha)Ti^{46}$, 15 MeV, levels of Ti^{46} 8=25127
$Ti^{47}(He^3, d)V^{48}$, energy levels obs. 8=29517
$Ti^{48}(He^3, t)$, V^{48} levels obs. quasi-inelastic 25 MeV 8=38518
$U^{238}(He^3, \alpha)$, $|743\uparrow|$ Nilsson configuration in U^{237} obs. 8=34045
Zr isotopes, (He^3, α) cross sections 8=29522
Zr^{90} excitation functions and recoil ranges 8=43094
$Zr^{90}(He^3, \alpha)$ rel. to n hole states, 18 MeV 8=29319
Zr^{90} (He^3, d), rel. to p levels, 18 MeV 8=33918
$Zr^{90}(He^3, d)Nb^{91} \to Zr + p$, isobaric analog states of Nb 8=25275
mesons
See also Cosmic rays/effects and interactions.
heavy spallation hypernuclei from K^- 8=25166
K-mesic atoms, review 8=34193
K, review, use as surface probe 8=29483
K^- absorpt. by light nuclei, pair-absorpt. model 8=34019
K^--emulsion nuclei, short range hyperfragments, $p_K = 1.5$ GeV/c 8=33702
K^- on emulsion nuclei, Σπ pair emission obs. 8=33836
K^-, with emulsion nuclei at 10.1 GeV/c, hyperfragment prod. 8=29487
K^- in nuclear emulsions, prod. of He^8 hammer tracks obs. 8=25022
K^- with emulsion nuclei hyperfragment prod. 8=33832
K^- with propane, freon in bubble chamber $\Sigma^\circ\pi^\circ$ prod. which decay to Λ°, γ 8=25254
K^- + C, vector meson decay obs. 8=29491
K^- + Fe, vector meson decay obs. 8=29491

Nuclear reactions due to—contd
mesons—contd
$K^-d \to K^-\pi^+\pi^-d$, $E_K = 12.6$ GeV/c, L, Q-meson prod. 8=29163
K_L° + Pb, Λ and Σ° prod. cross section at E = 150 MeV 8=24989
nuclear emulsion, 16.2 GeV/c π, with d, t prod. 8=38099
nuclear struct. study by pion and kaon initiated reactions 8=47209
π absorption by light nuclei Miyazawas theory 8=42531
π double charge exchange mechanism 8=29484
π, on light nuclei, activation cross section obs., 80-280 MeV 8=25255
π, with photographic emulsion nuclei, energy estimation 8=29486
π radiative capture, pole model of nγ distrib. 8=29485
π^- absorption by C^{12}, nuclear correlation effects 8=25258
π^- + C, vector meson decay obs. 8=29491
π^- + C^{12}, cluster absorption of stopped π^- 8=34021
π^- + Fe, vector meson decay obs. 8=29491
π-nucleus, charge exchange, absorpt. and capture at low energy, review 8=29482
π scatt., optical-model form factor 8=43044
π^-N, 17.2 GeV/c, heavy nuclei surface neutron richness, K, π, prod. 8=42535
π^- + Xe, correl. p pairs prod., 9 GeV 8=34024
π^--Xe interactions at 9 GeV, rel. to π° prod. 8=37973
Ag, K^- capture rel. to surface n excess, obs. 8=34022-3
$Ag(K^-)$ for obs. of Li^8 evaporation, at 10.1 GeV/c 8=29488
$B^{10,11}(\pi^+, \pi^\circ)$ cross sections rel. to single-charge-exchange mechanism 8=38497
Br, K^- capture rel. to surface n excess, obs. 8=34022-3
$Br(K^-)$ for obs. of Li^8 evaporation, at 10.1 GeV/c 8=29488
C, π^- capture, He^8 prod. 8=25257
C^{12}, π absorpt. → Li^8 prod., analysis 8=29490
$C^{12}(\pi^-, nHe^3)Li^8$, absorption of stopped π^- and final particle spectra and angular correlation 8=34021
C^{12}, π^- absorpt., secondary particle obs. 8=29489
$C^{12}(\pi^-, nt)2\alpha$, absorption of stopped π^- and final particle spectra and angular correlation 8=34021
$C^{12}(\pi^+, \pi^\circ)$ cross sections rel. to single-charge-exchange mechanism 8=38497
$C^{12}(\pi^-, \pi^-n)C^{11}$ and $C^{12}(\pi^+, \pi^+n)C^{11}$ cross sections, absolute values compared 8=34020
$C^{12}(\pi^-, \pi^-n)C^{11}$ and $C^{12}(\pi^+, \pi^\circ p)C^{11}$ cross sections, absolute values compared 8=34020
$C^{12}(\pi^-, \pi^-n)C^{11}$, cross-section calc. with pole and triangle calc. 8=25256
$C^{12}(\pi^+, NN)$, $E_\pi = 40$ and 100 MeV, excitation calc. 8=25259
$Li^{6,7}$ pion absorpt. rel. to momentum distrib. of N pairs in ground states 8=25095
$Li^6(\pi^+, pp)$, He^4 T = 1 states, single-pole dominance in transition mechanism, obs. 8=42831
$Li^7(\pi^-, H^3)H^4$ level structure of H^4 8=38351
N, π^- capture, He^8 prod. 8=25257
$N^{14}(\pi^+, NN)$, $E_\pi = 40$ and 100 MeV, excitation calc. 8=25259
$N^{14}(\pi^+, \pi^\circ)$ cross sections rel. to single-charge-exchange mechanism 8=38497
O, π^- capture, He^8 prod. 8=25257
$O^{16}(\pi^+, NN)$, $E_\pi = 40$ and 100 MeV, excitation calc. 8=25259
O^{16} radiative π capture, shell model calc. 8=47334
Ta^{181}, stopping π, 482-KeV state excitation 8=42912
Xe(π), azimuthal symmetry of secondary particle emission 8=47336
Xe, π^- interaction at 9 GeV/c, π^+ prod. 8=47335
muons
capture theory with ground state model and infinite spherical well pot 8=33983
μ-capture, "elementary particle" weak-interaction theory 8=33955
μ^- in emulsion, inelastic, 5 GeV/c 8=25213
rel. to nucleus structure, capture excitation of T_3 resons 8=33884
radiative capture, angular correl. calc. 8=25214
Al, n prod. at a depth of 150 m water equivalent by cosmic rays 8=38461
Ca^{40}, capture rate and g_T, particle-hole wave functions calc. 8=29417
Ca, μ capture, n ang. distrib. asymmetry obs. 8=29416
Ca, μ capture, n spectrum 7.7-52.5 MeV obs. 8=29415
Cd, n prod. at a depth of 150 m water equivalent by cosmic rays 8=38461
Cu, $\mu^\pm$ decay spectra comparison 8=29101
Fe, n prod. at a depth of 150 m water equivalent by cosmic rays 8=38461
He^4, μ^- capture rate obs. 8=38460
Pb, n prod. at a depth of 150 m water equivalent by cosmic rays 8=38461
S, μ capture, n ang. distrib. asymmetry obs. 8=29416
S, μ capture, n spectrum 7.7-52.5 MeV obs. 8=29415
Si^{28}, μ^- capture, charged-particle energy spectrum obs. 8=29414
Si, μ capture, n ang. distrib. asymmetry obs. 8=29416
Si, μ capture, n spectrum 7.7-52.5 MeV obs. 8=29415
Ti^{48}, capture, γ-rays energy, obs. 8=34189

Nuclear reactions due to—contd
neutrinos
rel. to nucleus structure, T_3 resons-excitation 8=33884
$He^3(\bar{\nu}_e, e^+)H^3$, cross-section obs. 8=42992
$He^3(\bar{\nu}_\mu, e^+)H^3$, cross-section obs. 8=42992
neutrons
See also Nuclear fission.
capture and $(n, n'\gamma)$, γ-spectra rel. to mechanisms, 15 keV–15 MeV 8=25235
capture γ-ray rel. to spins and parities of states obs. 8=42808
capture, γ-ray spectra calc. 8=33886
capture, triple, prod. of high-spin isomer Ir^{194m_2} 8=42917
cross-section evaluation, computer graphics 8=47323
curve fitting for cross section computation 8=33789
deuteron n capture, 3-body effects 8=43038
γ-ray prod. cross sections and spectra, formalism 8=29453
heavy nuclei synthesis in supernovae explosions 8=41504
in level density parameter determ. in the mass region 24-28 8=25081
millisecond isomers, from 14 MeV n, cross sections 8=47220
model for very high energy 8=42725
(n, α) in heavy nuclei at thermal energies 8=29454
(n, α) in multilayer target, Xe scintillation detector obs. 8=46873
(n, γ), isomer ratios obs. 8=38322
(n, γ), radiation energy device 8=25236
$(n, 2n)$ excitation functions for various nuclei, 12.6–19.6 MeV obs. 8=43035
$(n, 2n)$, 14 MeV, spin cut-off evaluation 8=38479
from nuclear explosion, underground, radioactive nuclide cross-sections meas. 8=38478
rel. to nuclear optical potential isospin depend., total cross-sections, obs. 8=29267
nuclides far off stability line prod., rates 8=38442
pion formation, charged, 600 MeV 8=37970
PWBAE, He^3-pick-up and diffraction theories in $N^{14}(n, \alpha)B^{11}$ 8=25239
radioisotope production in JRR-3, n irradiation conditions 8=24947
resonance absorpt., rapidly convergent iterative soln. 8=24970
resonance capture. Doppler effect formulation 8=29455
resonance parameter correlations 8=25234
resonance parameters, meas. with slow down time lead spectrometer 8=24972
resonances, numerical determ. 8=24971
resonant capture, internal and channel, radiative transitions 8=25233
sample geometry, optimum, Monte-Carlo calc., 14 MeV 8=43033
stellar nucleosynthesis by captive, abundances rel. to mass laws 8=41503
super-heavy nuclei capture cross-sections, mass formula 8=38324
telescope arrangement for energy determ., particle identification 8=29456
thermal radiative capture cross-sections, Monte Carlo anal. on 87 nuclides 8=38554
2N transfer, vibrational nuclei, quasiparticle Tamm-Dancoff microscopic theories 8=29419
Ag^{107} $(n, 2n)$ cross section obs., 14.8 MeV 8=43043
$Al^{27}(n, \gamma)Al^{28}$, E_n=14 MeV, capture cross section and γ spectrum 8=29466
Al^{28}, capture γ-ray spectrum, calc. 8=33886
$Am^{241,242,243}$, n capture and fission cross sections and resonance integrals 8=25253
Am^{243} multiple capture, $Fm^{257,259}$ and Md^{259} prod. in Cyclamen explosion 8=38496
Ar, thermal neutron capture, γ-ray obs. 8=25242
$As^{75}(n, \gamma)As^{76}$, n separation energy, γ energy and intensity obs. 8=34010
$As^{75}(n, d)Ge^{74}$, transitions angular distrib. rel. to shell model, obs. 8=29468
Au, natural, effective reson. integrals, reactivity obs. 8=34015
Ba isotopes, (n, γ), reactor thermal n cross sections, obs. 8=34012
$Ba^{148}(n^3, n)Ba^{140}$, bound n^3 search En = 14–19 MeV 8=43039
$Be^9(n, 2n)$, Cf^{252} fission spectrum averaged cross sections, obs. 8=34008
BeO compacts, formation and release of He, kinetics 8=25316
Be–U, 8 heavy elements, total cross sections obs. 27 GeV/c 8=43040
$Br^{81}(n, 2n)Br^{80m,g}$, prod. cross-section meas. by activation method 8=25248
C^{12} stripping, polarization obs. 8=25238
$C^{12}(n, \gamma)C^{13}$, 2 γ-rays energy obs. thermal neutrons 8=38484
n–C total and free cross-sections 8=24952
$Ca^{40}(n, \alpha)Ar^{37}$, Ar^{37} diff. in CaO crysts. 8=39969
$Ca^{40}(n, d)K^{39}$, transitions angular distrib. rel. to shell model, obs. 8=29468
$Ca^{40}(n, p)K^{40}$, p spectra and ang. distrib. 8=25243
$Ca^{44}(n, \gamma)$, Ca^{45} levels, Q-value, thermal energies 8=38487
Ca, total cross-sections, at 14 MeV 8=38486

Nuclear reactions due to—contd
neutrons—contd
CaF_2 doped with UO_2, UC or U, neutron irrad. to give inert gases 8=34107
$Cd^{112}(n, 2n)Cd^{111m}$, cross section obs. 8=29475
Cd^{114}, 9.0 MeV γ emission, ang. distrib. asymmetry obs. 8=33921
Cd capture cross-section 8=29476
Ce, total cross-sections for energies 3.2 to 5.2 MeV 8=34009
$Cl^{35}(n, d)S^{34}$, transitions angular distrib. rel. to shell model, obs. 8=29468
Co^{59}, total cross section rel. to intermediate struct., 0.5-1.2 MeV 8=29469
$Co^{59}(n, 2n)Co^{58gm}$ isomeric ratio and total cross section 8=38489
Cr^{52}, total cross section rel. to intermediate struct., 0.5-1.2 MeV 8=29469
Cs^{133}, capture 0.2-3 MeV obs. 8=29472
$Cu^{63,65}(n, \gamma)$, 10-60 keV, γ averaged intensities 8=25247
$Cu^{63}(n, 2n)$ and (n, p) cross-sections, 16.6-17.7 MeV 8=29471
$Cu^{63}(n, 2n)Cu^{62}$, cross section determ. 8=25246
$Cu^{63}(n, 2n)Cu^{62}$ 13.9-14.7 MeV, excitation function obs., rel. to statistical theory 8=38488
Cu, radiative capture, E_n = 200 eV-16.5 keV, obs. 8=38490
$Eu^{151,153}$, n capture, radiative, obs. 8=29479
$Eu^{151}(n, \gamma)Eu^{152}$, conversion e coincidence spectra and low level scheme 8=47255
$F^{19}(n, \alpha)$, spectra and ang. distrib., spectroscopic factors, E_n,= 14.4 MeV 8=47328
$F^{19}(n, d)$, spectra and ang. distrib., spectroscopic factors, E_n = 14.4 MeV 8=47328
$F^{19}(n, d)O^{18}$, E_n=14.1 MeV, compound nucleus and direct effects 8=29465
$F^{19}(n, \gamma)F^{20}$, 73 γ-rays spectral lines obs. thermal neutrons 8=38484
$F^{19}(n, p)$, spectra and ang. distrib., spectroscopic factors, E_n = 14.4 MeV 8=47328
$F^{19}(n, t)$, spectra and ang. distrib., spectroscopic factors, E_n = 14.4 MeV 8=47328
$Fe^{54}(n, 2n)Fe^{53}$, 13.9-17.4 MeV cross-section obtained, compared to statistical theory 8=38488
Fe^{56}, total cross section rel. to intermediate struct., 0.5-1.2 MeV 8=29469
Fe^{57}, capture, rel. to low-energy levels 8=47246
Fe, capture, resonant γ scatt. obs. 8=25245
Ga^{69} $(n, 2n)$ cross section obs., 14.8 MeV 8=43043
$Ga^{70,72}$, slow n capture, γ-spectra rel. to levels, obs. 8=29316
$Gd^{155}(n, \gamma)Gd^{156}$, resonances, intensities of transitions to ground and first excited state 8=38389
$Gd^{157,158}(n, \gamma)$, conversion e detect. in thermal n counter 8=33813
Gd rel. to induced levels spacing, obs. 8=29347
Ge^{74}, capture 0.2-3 MeV obs. 8=29472
$H(n, \gamma)$, tissue autogamma dose calc. from spectrometer obs. 8=38067
$H^3(n, t)$ and $H^3(n, d)$ at 14.1 MeV, outgoing particles obs. 8=33769
Hg isotopes, (n, γ), reactor thermal n cross sections, obs. 8=34012
Ho^{165}, n capture, radiative, obs. 8=29479
$In^{113}(n, \gamma)In^{114}$, thermal n activation cross sections 8=29477
$In^{113}(n, 2n)In^{112g,m}$, cross sections, 14.7 MeV 8=34013
$In^{113}(n, 2n)In^{112m,g}$, prod. cross-section meas. by activation method 8=25248
$In^{115}(n, \alpha)$, 14.4 MeV, direct reaction 8=25249
$In^{115}(n, 2n)In^{114g,m}$, cross sections, 14.7 MeV 8=34013
$P^{27}(n, \gamma)P^{28}$, E_n=14 MeV, capture cross section and γ spectrum 8=29466
$K^{39}(n, 2\alpha)P^{32}$, 14 MeV, prod. cross-section for P^{32} 8=38494
$K^{39}(n, d)Ar^{38}$, transitions angular distrib. rel. to shell model, obs. 8=29468
$K^{39}(n, \gamma)K^{40}$, 29.4 keV γ-ray Mössbauer exam. 8=42859
K, total cross-sections, at 14 MeV 8=38486
$La^{139}(n, \alpha)Cs^{136}$ with polarized neutrons, asymm. of reaction 8=38491
La, total cross-sections for energies 3.2 to 5.2 MeV 8=34009
$Li^6(n, \alpha)H^3$, use of double pulsed ionization chamber 8=24512
$Li^6(n, p)He^6$, He^6 ground state transition dominance, 152 MeV 8=34007
$Li^7(n, n^3)Li^5$, bound n^3 search E_n = 14–19 MeV 8=43039
Lu^{176}, n capture, radiative, obs. 8=29479
Mg^{25}, capture γ-ray spectrum calc. 8=33886
$Mn^{55}(n, \gamma)Mn^{56}$, evidence for direct reaction mechanism 8=25244
Mn^{55} total cross section, parametric fit, 0.01 eV-50 keV 8=38477
Mn^{55}, total cross section rel. to intermediate struct., 0.5-1.2 MeV 8=29469
$Mo^{92}(n, 2n)Mo^{91m,g}$, prod. cross-section meas. by activation method 8=25248
$N^{14}(n, \alpha)B^{11}$ angular distributions obs. 14.9 MeV 8=43042
$N^{14}(n, \alpha)B^{11}$, levels obs., E_n = 14.1 MeV 8=43041
$N^{14}(n, \alpha)B^{11}$, 14.1 MeV, cross-section obs. 8=25239

Nuclear reactions due to—contd

- **neutrons**—contd
  - $N^{14}(n,\gamma)N^{15}$ 9.15 MeV doublet energies from prompt γ-ray spectra 8=42839
  - $Na^{23}(n,d)Ne^{22}$, E_n=14.1 MeV, compound nucleus and direct effects 8=29465
  - $Na^{23}(n,\gamma)$ circular polarization obs. 8=38485
  - Na^{24} in blood activation, calc. from spectrometer obs. 8=38067
  - Na in body activation, emergency dosimetry 8=33765
  - Na, total cross-sections, at 14 MeV 8=38485
  - $Nb^{93}(n,\gamma)Nb^{94}$, levels obs. 8=25138
  - Nb^{93}, (n, 2n) cross-section obs., 14 MeV rel. to magic n number effect 8=29473
  - $Nd^{143}(n,\gamma\alpha)$, thermal, α transition obs. 8=34014
  - $Ne^{20,22}(n,\gamma)Ne^{21,23}$, thermal neutron capture 8=47329
  - $Ni^{58}[(n,d)+(n,np)+(n,pn)]Co^{57}$, cross section obs. 8=29475
  - $Ni^{58}(n,p)Co^{58m+g}$, cross section obs. 8=29475
  - $Ni^{58}(n,p)Co^{58gm}$ isomeric ratio and total cross section 8=38489
  - $Ni^{58}(n,2n)Ni^{57}$, cross section obs. 8=29475
  - $Np^{237}(n,\gamma)Np^{238} \xrightarrow{\beta} Pu^{238}$, yield calc. 8=29480
  - Np isotopes, n capture in thermonuclear explosions 8=25252
  - $O^{16}(n,\alpha_0)C^{13}$, angular distributions obs. 14.9 MeV 8=43042
  - $O^{16}(n,\alpha)C^{13}$, differential cross sections for 15-19 MeV 8=47327
  - $O^{16}(n,\alpha)C^{13}$, 14.1 MeV, cross-sections obs. 8=25240
  - $O^{16}(n,\gamma)N^{16}$ as means of meas. the O content of metals 8=32167
  - $O^{18}(n,\alpha)C^{15}$, 7.5, 8.6 MeV obs. 8=47326
  - O, total cross-sections for energies 3.2 to 5.2 MeV 8=34009
  - Os^{192}, capture 0.2-3 MeV obs. 8=29472
  - $P^{31}(n,\gamma)$ circular polarization obs. 8=38485
  - $P^{31}(n,2n)$ cross sections obs., 14.8 MeV 8=43043
  - $P^{32}(n,p)S^{31}$, fast-n dosimetry by Cerenkov radiation meas. 8=33798
  - Pd^{108}, γ-ray spectrometer 8=47068
  - Pd isotopes, (n,γ), reactor thermal n cross sections, obs. 8=34012
  - Pr, total cross-sections for energies 3.2 to 5.2 MeV 8=34009
  - Pt, capture γ-rays, levels of Pt^{196} 8=38492
  - Pt^{198}, γ-ray spectrometer 8=47068
  - $Pu^{238}(n,\gamma f)$, obs. in neutron-induced fission 8=43114
  - Pu^{242}, nuclear explosion irrad., heavy-isobar yield rel. to supernovae reactions, obs. 8=38495
  - $Rb^{85,87}$, (n, 2n) cross-section obs., 14 MeV rel. to magic n number effect 8=29473
  - Rh, activation foil n personnel dosimeter 8=33795
  - $Rh^{113}(n,\alpha)$, 14.4 MeV statistical and direct reaction 8=25249
  - Ru^{96}, (n, 2n) cross-section obs., 14 MeV rel. to magic n number effect 8=29473
  - $S^{32}(n,p)P^{32}$, fast-n dosimetry by Cerenkov radiation meas. 8=33798
  - $S^{32,34}(n,d)P^{31,33}$, 14 MeV cross-sections and DWBA analysis 8=25241
  - S activation dosimetry and ionization chamber comparison, 3 and 15 MeV 8=38079
  - $Sb^{121}(n,2n)Sb^{120g}$ and Sb^{120m}, isomer ratios and cross sections of isomeric pair product 8=25250
  - $Sc^{45}(n,\gamma)Sc^{46}$, low level struct. 8=25121
  - Sc^{46}, reactor n capture cross-section 8=47330
  - Si^{28}, E_n=21.3 MeV, d, α ang. distrib. obs. 8=29467
  - $Sm^{144}(n,2n)Sm^{143m,g}$, , prod. cross-section meas. by activation method 8=25248
  - $Sm^{149}(n,\gamma)Sm^{150}$, rel. to energy levels 8=29333
  - Sn isotopes, (n,γ), reactor thermal n cross sections, obs. 8=34012
  - $Sr(n,\gamma)$, γ energies and intensities obs. 8=34011
  - Sr^{86}, (n, 2n) cross-section obs., 14 MeV rel. to magic n number effect 8=29473
  - $Sr^{90}(n,\gamma)Sr^{91}$ obs. for reactor n 8=29474
  - $Sr^{90}(n,p)Y^{90}$ obs. for reactor n 8=29474
  - $Tb^{159}(n,\alpha)Eu^{156}$, 14.2 MeV, rel. to evaporation theory 8=25251
  - $Te^{122}(n,\alpha)Sn^{119}$, 14.2 MeV rel. to evaporation theory 8=25251
  - Te, isomeric cross sections E_n = 14.8 MeV 8=47332
  - Th^{232} fission due to neutrons with energies 1.38, 1.51, 1.65, 1.90, 2.37, 2.87, 5.6 MeV 8=38531
  - $Th^{232}(n,\gamma)$, energy depend. of capture cross section, 0.1 to 3.4 eV 8=38493
  - Th^{232}, total cross section and reduced n widths, $\leqslant$ 3 keV 8=29347
  - ThO_2 rods, effective reson. integral temp. depend., obs. 8=34017
  - Ti^{48} n capture, 341 keV transition, multipolarity 8=25125
  - $Ti^{48}(n,\gamma)Ti^{49}$, γ-γ coincidence and angular correl., obs. 8=29470
  - Tl^{202}, (n, 2n), cross-section for production of isomeric state 8=38395
  - $Tm^{169}(n,\alpha)Ho^{166}$, 14.2 MeV, rel. to evaporation theory 8=25251
  - U^{237} absorption cross section 8=29481
  - U^{238}, evaporation and fission n spectra, 800 keV-14 MeV 8=34018
  - U^{238} multiple capture, $Fm^{257,259}$ and Md^{259} prod. in Cyclamen explosion 8=38496
  - β $U^{235}(n,\gamma)U^{236}(n,\gamma)U^{237} \xrightarrow{\beta} Np^{237}(n,\gamma)Np^{238} \xrightarrow{\beta} Pu^{238}$, yield calc. 8=29480
  - U^{238}, nuclear explosion irrad., heavy-isobar yield rel. to supernovae reactions, obs. 8=38495
  - $U^{235,238}$ radiative capture and fission in 1.03% enriched U - D_2O lattices, obs. 8=38585
  - U^{235} slow neutron resonance spins 8=33944
  - U isotopes, n capture in thermonuclear explosions 8=25252
  - V^{51}, total cross section rel. to intermediate struct., 0.5-1.2 MeV 8=29469
  - $V^{51}(n,\gamma)V^{52}$, γ-γ coincidence and angular correl., obs. 8=29470
  - $W^{182,183,184,186}$ and natural, effective reson. integrals, reactivity obs. 8=34015
  - $W^{184,186}$ in natural W, reson. integrals, activation obs. 8=34016
  - Y^{89}, (n, 2n) cross-section obs., 14 MeV rel. to magic n number effect 8=29473
  - $Yb^{168}(n,\gamma)Yb^{169}$ level struct. obs. 8=42909
  - Xe isotopes, (n,γ), reactor thermal n cross sections, obs. 8=34012
  - $Zn^{64}(n,2n)$cross section obs., 14.8 MeV 8=43043
  - Zr^{90}, (n, 2n) cross-section obs., 14 MeV rel. to magic n number effect 8=29473
- **nuclei of Z > 2**
  - See also Ions/scattering.
  - compound nuclei γ-, x-ray and conversion e emission, obs. 8=38527
  - heavy-ion transfer, pot. energy effects 8=25276
  - heavy ions, decay mechanism 8=47355
  - on medium 2 nuclei, short-lived products identification 8=38522
  - N transfer, finite range effects in DWBA 8=29525
  - nuclides far off stability line prod., rates 8=38442
  - proton transfer at energies below Coulomb barrier, DWBA formalism 8=43096
  - for spectroscopy, in-beam 8=38338
  - rel. to transuranic elements, spontaneous fission decay and delayed p emission, Dubna research review 8=38521
  - 2C nuclei, resonance energies and partial widths of quasimolecular states formed 8=43097
  - ultra-n deficient nuclei prod. and identification 8=38424
  - For Z ~ 126, N ~ 184 nuclei prod.. by grazing, n evaporation and Cpd. nucleus fission 8=38520
  - $Ag^{107,109}(N^{14},p)$, (N^{14},d), (N^{14},α), angular and energy distributions obs. 74 MeV 8=43104
  - $Ag^{107}(N^{14},xn)$, $Ag^{102,102m,103}$ decay schemes, obs. 8=38428
  - $Al^{27}(p,\alpha)Mg^{24}$, excitation function fluctuations $Li^{6,7}(Li^6,\alpha)$ ang. distrib. obs. 8=38469
  - $B^{10,11}(Li^7,He^6)C^{11,12}$, ang. distrib. of He^6, 3.0, 3.5, 3.8 MeV 8=43099
  - $B^{10}(N^{14},C^{13})C^{11}$, DWBA formalism applic. 8=43096
  - $B^{10}(N^{14},N^{13})B^{11}$, neutron tunnelling and nuclear spectroscopic factors extraction 8=43101
  - $B^{10,11}(O^{16})$, single- and multi-nucleon transfer reactions 8=47356
  - $Be^9(Li^6,\alpha)$ α ang. distrib. obs. 8=38469
  - $Be^9(Li^6,\alpha)$, sequential 8=43100
  - $Be^9(Li^6,\alpha)$, spectrum and angular distrib. rel. to α- and d-cluster transfer, 26 MeV 8=38524
  - $C^{12}(Li^6,\alpha)$ α ang. distrib. obs. 8=38469
  - $C^{12}(Li^6,\alpha)$, spectrum and angular distrib. rel. to α- and d-cluster transfer, 26 MeV 8=38524
  - $C^{12}(Li^6,\alpha)N^{14}$, cross-section, 20 MeV 8=25277
  - $C^{12}(Li^6,d)O^{16}$, cross-section, 20 MeV 8=25277
  - $C^{12}(Li^6,p)O^{17}$, cross-section, 20 MeV 8=25277
  - $C^{12}(Li^7,t)$, spectrum and angular distrib. rel. to α- and d-cluster transfer, 27.5 MeV 8=38524
  - $C^{12}(Li^7,t)$, t ang. distrib. obs. 8=38469
  - $C^{12}(O^{16},\alpha\gamma)Mg^{24}$, energy levels, spin and parity obs. 8=38362
  - $C^{13}(C^{12},C^{13})C^{12}$ angular distributions and excitation functions obs. 10-30 MeV 8=38523
  - $Ca^{40}(N^{14},N^{13})Ca^{41}$, neutron tunnelling and nuclear spectroscopic factors extraction 8=43101
  - $Cm^{244,246,248}(C^{12,13},xn)No^{251-7}$, excitation functions 8=43108
  - $H^2(Ne^{20},n)$, 13.95 MeV, Na^{21} level lifetime obs. 8=25107
  - $H^2(Ne^{20},p)$, 13.95 MeV, Ne^{21} level lifetime obs. 8=25107
  - $In^{115}(C^{12},4n)$, C^{123} decay scheme, obs. 8=38428
  - $In^{115}(N^{14},xn)$, $Ba^{125,127}$ decay schemes, obs. 8=38428
  - $La^{139}(F^{19},4n)Dy^{154}$, energy levels of Dy^{154} 8=42908
  - $Li^6(C^{12})$, differential cross-section fluctuations 2.4 to 8.5 MeV 8=43102
  - $Li^6(Li^6,\alpha)Be^8$, spectral distortion by final-state Coulomb interactions 8=33888
  - $Li^6(O^{16},d)Nc^{20}$ at 20 MeV, levels ang. distrib. and α widths obs. 8=34048
  - Li^7, $Li^{6,7}$, 2 MeV obs. in accelerator 8=29001
  - $Li^7(Li^7,He^6)Be^8$, ang. distrib. of He^6, 3.0, 3.5, 3.8 MeV 8=43099
  - $Li^{12}(Li^7,t)$, spectrum and angular distrib. rel. to α- and d-cluster transfer, 27.5 MeV 8=38524
  - Li^- ion source 8=24159
  - $Mo^{92}(Ne^{20},3n)$, Te^{109} delayed p emission, obs. 8=38425

Nuclear reactions due to—contd
- **nuclei of Z > 2**—contd
  - $Mo^{92}(Ne^{22}, 3n)$, Te^{111} delayed p emission, obs. 8=38425
  - $Mo^{94}(Ne^{20}, 3n)$, Te^{111} delayed p emission, obs. 8=38425
  - $Mo^{94}(Ne^{20}, 5n)$, Te^{109} delayed p emission, obs. 8=38425
  - $Mo(B^{11}, xn)$, $Ag^{102,102m,103}$ decay schemes, obs. 8=38428
  - $Ne^{20} + Al^{27}$, compound nucleus formation cross sections obs. 8=43103
  - $O^{16} + Al^{27}$, compound nucleus formation cross sections obs. 8=43103
  - $O^{16} + B^{10,11}$, elastic scattering, optical model calcs., energies near appropriate Coulomb barrier 8=34047
  - $O^{16} + Co^{59}$, compound nucleus formation cross sections obs. 8=43103
  - $Pd^{102}(C^{12}, 3n)$, Te^{111} delayed p emission, obs. 8=38425
  - $Pd^{102}(C^{12}3n)Te^{111}$, β^+ p decay coincidence meas. 8=47290
  - $Pu^{139}(O^{18}, 5n)102^{252}$, decay of 102^{252} 8=42978
  - $Sb^{121}(B^{11}, xn)$, $Ba^{125,127}$ decay schemes, obs. 8=38428
  - $Sb^{121}(C^{12}, 5n)$, La^{128} isomer prod., obs. 8=38522
  - $Sn(N^{14}, xn)$, La^{128} isomer prod., obs. 8=38522
  - $Ta^{181}(C^{12}, 4n)$, Au^{189} isomer prod., obs. 8=38522
  - rel. to Th nucleosynthesis in interstellar matter 8=41505
  - rel. to U nucleosynthesis in interstellar matter 8=41505
  - $U^{235}(Ar^{40})$ Coulomb excitation, 182 MeV 8=43105
  - $U^{233,234,235,236,238} + C^{12}$, $Cf^{242,243,244,245,246}$ production cross sections 8=43106
  - $U^{235}(O^{16})$ Coulomb excitation, 60-78 MeV 8=43105
  - $U^{233} + O^{18}$, spontaneous fission of resulting fragments 8=42978
  - U^{238} bombarded by Ar^{40}, production of compound nuclei, atomic number 110 8=43107
  - U^{238} fission, Ne^{22} ion induced, fragment mass distribution 8=29539
  - $U^{238}(Ne^{22}, 5n)102^{255}$, decay of 102^{255} 8=42978
  - Xe compound, formation cross-section from N bombardment of Ag, 74 MeV 8=43104
  - on Z ~ 65 nuclei, spin distribs. rel. to high J states decay, statistical model 8=38405
- **photons**
  - $d(\gamma, n)p$, sum rules, employing Yale and Hamada-Johnston potentials 8=38450
  - (γ, γ^1) excitation possibilities of nuclear isomers, research review (1939-67) 8=33889
  - γ + Al, pair prod. total cross-section, 1.200-4.050 GeV 8=33644
  - γ + C, pair prod. total cross-section, 1.200-4.050 GeV 8=33644
  - γ + Cu, pair prod. total cross-section, 1.200-4.050 GeV 8=33644
  - γ + Pb, pair prod. total cross-section, 1.200-4.050 GeV 8=33644
  - heavy nuclei rel. to dipole states and N-N interaction 8=33861
  - integrated cross-section, appl. of sum rules of quantum mech. 8=33323
  - model for very high energy 8=42725
  - nuclear emulsion, 6.2, 28 GeV/c with d, t prod. 8=38099
  - rel. to nucleus structure, T_3 resons excitation 8=33884
  - photonuclear cross section and nuclei de-excitation 8=38456
  - photoprotons $Li^{6,7}(\gamma, p)$, prod., 100 MeV 8=38453
  - π photoproduction cross-sections, perturbation theory 8=42513
  - $\pi^+\pi^-$ photoprod., 1-2 GeV, obs. 8=29398
  - polarized, absorpt. by oriented nuclei 8=42987
  - 2N transfer, vibrational nuclei, quasiparticle Tamm-Dancoff microscopic theories 8=29419
  - Ag, photoneutron prod. cross-section 8=29406
  - Al bremsstrahlung, secondary photon energy spectra 8=29400
  - Al, (γ, n) cross-section and reson. struct., 13-26 MeV 8=29404
  - Be bremsstrahlung, secondary photon energy spectra 8=29400
  - Be, reactor material, neutron population predictions 8=38454
  - $Bi(\gamma, n)$ cross-section and reson. struct., 8-20 MeV 8=29404
  - $C^{12}(\gamma, \alpha)Be^7$, 300-1000 MeV obs., in agreement with photo-meson model 8=29401
  - $C^{12}(\gamma, n)C^{11}$, 19-19.7 MeV, cross-section investigation using γ-rays from $Li^7(p, \gamma)Be^8$ 8=47306
  - $C^{12}(\gamma, n)C^{11}$, 300-1000 MeV obs., in agreement with photo-meson model 8=29401
  - $C^{12}(\gamma, nHe^3)$, cross section obs. 8=29402
  - $C^{12}(\gamma, p)$ photoproton prod., 100 MeV 8=38453
  - $C^{12}(\gamma, pn)$, cross section obs. 8=29402
  - $C^{12}(\gamma, pt)$, cross section obs. 8=29402
  - $C^{12}(\gamma, n\alpha)$, cross section obs. 8=29402
  - $C^{12}(\gamma, p\alpha)$, cross section obs. 8=29402
  - $C^{12}(\gamma, pn\alpha)$, cross section obs. 8=29402
  - C bremsstrahlung, secondary photon energy spectra 8=29400
  - C, ϕ photoprod. cross section, 1800 MeV 8=38033
  - C, prod. of wide angle electron positron pairs 8=42990
  - $Ca^{40}(\gamma-n)Ca^{39}$, cross-section struct. 8=47308
  - $Ca^{40}(\gamma, p)$ cross section calc. 8=42989
  - Ca^{40}, total absorption cross section in giant resonance region 8=47307

Nuclear reactions due to—contd
- **photons**—contd
  - $Ca^{48}(p, n)Sc^{48}$, $E_p = 4.5, 5.5$ MeV, energy levels obs. 8=42871
  - Cs^{133}, $\gamma\gamma$ cascade at 81 KeV level 8=38384
  - $Cu^{63}(\gamma, \{\alpha n, \alpha 2n, 2n\})$ $\{Co^{58,57}, Cu^{61}\}$, $Co^{57,58}$ half-lives meas. 8=29405
  - Cu bremsstrahlung, secondary photon energy spectra 8=29400
  - $Ga^{69}(\gamma, \gamma)$, E = 1107, 872, 574 keV, resonance fluoresc. 8=25132
  - $He^4(\gamma, np)D^2$ H^3, Majorana exchange currents 8=38452
  - $He^4(\gamma, p)H^3$, Majorana exchange currents 8=38452
  - $He^4(\gamma, p)$ photodisint. cross-section calc. 8=47304
  - He^4, photodisintergration cross section 8=38451
  - He^4, photodisintegration multipole sum rules, shell model wave functions and mean square radius 8=42830
  - $I(\gamma, xn)$, isotope γ-spectra and half-lives, < 900 MeV 8=38456
  - $Li^6(\gamma, np)He^4$(ground), electric dipole approx. 8=47305
  - $Li^6(\gamma, pd)H^3$ obs. 8=33979
  - $Li^6(\gamma, t)$ cross section at $E_\gamma = 24, 35$ MeV 8=42988
  - $Li^6(\gamma, t)He^3$, obs. 8=33979
  - $N^{15}(p, n)O^{15}$, unified Feshbach theory, neutron cross-sections obs. 8=38470
  - Ni isotopes, (t, α) rel. to coupling approach to unified model of Co isotopes 8=25129
  - Ni, photoneutron prod. cross-section 8=29406
  - Ni, photodisintegration, single particle aspects of giant resonance 8=25209
  - $O^{16}(\gamma, p_0)N^{15}$ ang. distrib. obs. 8=29403
  - $O^{16}(\gamma, p)$, N^{15} cross section, photo protons spectra, $\leqslant$ 28 MeV 8=38455
  - $Pb^{208}(\gamma, Tn)$, cross section structure 8=33980
  - $S(\gamma, n)$ cross-section and reson. struct., 13-26 MeV 8=29404
  - $Si^{28}(\gamma, n)Si^{27}$, cross-section struct. 8=47308
  - Si^{28}, total absorption cross section in giant resonance region 8=47307
  - $S^{32}(\gamma, n)S^{31}$, cross-section struct. 8=47308
  - $Ta^{181}(\gamma, n)$ reactions 8=42991
  - $Ta(\gamma, n)$ cross-section and reson. struct., 8-20 MeV 8=29404
  - U^{235} 25 MeV, kinetic energy of pair fragments 8=38537
- **protons**
  - cascade process, 660 MeV, residual nuclei kinematics 8=25220
  - d(p, n)2p, Ep = 45.5 MeV, ang. distrib. obs. 8=43017
  - d(p, n)2p, polarization transfer calc.. Ep = 30-150 MeV 8=38101
  - emulsion nuclei, 5 GeV/c $\bar{p}$, fragment emission, fireball model 8=38065
  - emulsion, secondary diffractional generation, azimuthal ang. distrib. 8=29425
  - hadron-nucleus collisions, semiclassical theory 8=42491
  - heavy nuclei synthesis in supernovae explosions 8=41504
  - isomer prod., study with β-spectrometer and internal conversion electron spectra 8=38346
  - monitor reactions, effect of thick targets 8=25221
  - in photoemulsion nuclei, $E_p = 21$ GeV, secondary shower transversal momentum 8=29424
  - π prod. theory, using 450 MeV p. 8=33987
  - $p + A \rightarrow A + N + n\pi$, mean cross section 8=25218
  - (p, γ) and analogue states in s-d shell, obs. 8=25079
  - $\bar{p}$-nuclei, ^8Be emission cross-section; 5 GeV/c 8=47132
  - p-nuclei, for energetic deuteron momentum spectra calc., 1 GeV 8=42667
  - $p + \text{nucleus} \rightarrow p + \pi^+ + \pi^- + \text{nucleus}$, 20-23 GeV. ang. and momentum distrib. of secondary particles 8=47314
  - (p, n) isobaric analogue state and isospin dependence of optical model, 30 and 50 MeV 8=43001
  - (p, n), neutron energy spectrum, isobaric analogue states obs. 94 MeV 8=42848
  - (p, n), p atomic stopping power for 3.75-5.5 MeV p in Ag, Cd, In and Sn obs. 8=43030
  - (p, pd) at 1 BeV, interpretation 8=29427
  - (p, 2p), 160 MeV to 1 GeV 8=33986
  - (p, 2p) rel. to nuclear matter, re-arrangement energy calc. 8=29273
  - (p, xp), $(p, xpy\alpha)$ on targets A = 11-27 at 156 MeV, Li^9, C^{16}, N^{17} formation cross sections 8=43002
  - polarized, spin-dependence probing 8=47313
  - quasi-three-body, non-local model t-matrix 8=29426
  - radiochemical cross sections for Ep = 50-400 MeV, calc. 8=45400
  - secondary neutron evaporation, 400-660 MeV obs. 8=25219
  - Ag, emulsion nuclei, at 13.8 GeV/c identification of emitted fragments 8=34002
  - Ag, fission-like disintegrations, and model, 25 GeV/c 8=34003
  - $Al^{27}(p, \alpha)Mg^{24}$, excitation function fluctuations 10.9-19.7 MeV 8=38473
  - $Al^{27}(p, \alpha)$ excitation functions, fluctuation analysis 8=29442
  - $Al^{27}(p, \gamma)Si^{28}$, excited state lifetimes and branching ratios 8=42855
  - $Al^{27}(p, \gamma)Si^{28}$ rel. to transition rates for Si^{28} levels 8=29300
  - $Al^{27}(p, \gamma)$, Si^{28} resonance width at $E_x = 12171$ KeV using Doppler shift calc. 8=33995

Nuclear reactions due to—contd
protons—contd
$Al^{27}(p, p\pi^+)Mg^{27}$, E_n=0.6-28 GeV, obs. 8=29443
Al^{27} (p, 3pn) Na^{24}, p flux monitoring, influence of secondary particles 8=33994
$Ar^{36}(p, d)Ar^{35}$ in 2s–1d shell, obs. 8=43023
$Ar^{40}(p, n)K^{40}$, excitation functions 8=43026
Ar^{40}, analogues of Ar^{41} levels 8=43025
As^{75}, (p, 2p) at 156 MeV 8=33993
As^{75}(p, 2p) rel. to energy levels, 156 MeV 8=33914
Au^{197} (p, X), rare earth nuclides prod. cross sections obs. 11.5 GeV 8=38476
Au, 660 MeV, rel. to Ir fraction radiation 8=29342
B^{11} (p, α_0) Be^8, direct reaction analysis of ang. distrib. 8=33990
$Be^9(p, d)Be^8$, evidence for 0^+ excited states in Be^8 8=38354
Be^9(p, n) at low energies 8=47321
Be^9 (p, t) Be^8 to Be^9 (P, d) Be^8 ratio of energy spectra, ang. distrib. and cross sections 8=38467
Be^9, nucleons released at 660 MeV 8=25227
Bi(p, xn), $Po^{197-203}$ prod. and excitation functions, 60-150 MeV 8=38440
Br, emulsion nuclei, at 13.8 GeV/c identification of emitted fragments 8=34002
Br, fission-like disintegrations, and model, 25 GeV/c 8=34003
$C^{12}(p, \gamma)N^{13}$, γ-decay of lowest T=$\frac{3}{2}$ state 8=29440
$C^{12}(p, pn)C^{11}$, energy distrib. of recoil C^{11} atoms, 450 MeV 8=43019
$C^{12}(p, pn)C^{11}$, 660 MeV obs. 8=38468
$C^{12}(p, 3p3n)Be^7$, E_p = 3–12.5 GeV, cross section obs. 8=25229
C^{12} spallation, cross sections obs. review 8=29436
C^{12} stripping, polarization obs. 8=25238
$C^{14}(p, \gamma)N^{15}$, $0.6 < Ep < 2.7$ MeV, obs. 8=43004
$C^{14}(p, p)C^{14}$, $0.6 < Ep < 2.7$ MeV, obs. 8=43004
C^{16} prod. and delayed-n decay, 150 MeV 8=38463
C, $Li^{6,7}$, $Be^{7,10}$ and He^6 prod. cross section, Ep = 125 MeV 8=33991
C, effective cross sections at 125 MeV 8=43018
C fragmentation, Li, Be and B prod., $\leqslant$ 600 MeV 8=29438
C nuclei, 10^{10}-10^{12}eV, effective cross-section on 'Proton' satellites 8=25228
C, 24 GeV/c, energy of n prod. 8=29439
$Ca^{40}(p, d)Ca^{39}$ in 2s–1d shell, obs. 8=43023
$Ca^{40}(p, \gamma_0)Sc^{41}$, inhibited E2 transition 8=29305
$Ca^{40}(p, \gamma)$, Sc^{41} 46 resonances identified, spin assignment 8=42870
$Ca^{40}(p, p')$, excited levels γ decay rel. to nature, obs. 8=33910
$Ca^{42,44}(p, d)Ca^{41,43}$, levels obs., 26.5 MeV 8=38475
$Ca^{48}(p, d)Ca^{47}$, Ep = 18 MeV, obs. 8=43028
Ca^{48} (p, n), n-γ angular correl. rel. to Sc^{48} excited states, obs. 8=33997
$Ca^{48}(p, p')Ca^{48}$, e.m. deexcitation waves at 4.51 MeV 8=47242
$Ca^{48}(p, t)Ca^{46}$, Ep = 18 MeV, obs. 8=43028
Ca(p, t), L = 0, 2n transfer cross-sections 8=43064
$Cl^{35}(p, \alpha_0)S^{32}$, 830-2930 keV, resonances obs., spin and parity assignments 8=25230
Co^{59}(p, 2p 5n)Fe^{53} cross-sections obs. analysis of isomeric ratios 8=38465
$Cr^{50}(p, p'\gamma)$, ang. correl. for low level spin assignment 8=29309
$Cr^{50}(p, p')$, level struct. determ. 8=42874
$Cu^{63,65}$, E_n=9.1 MeV. total reaction cross section 8=29441
Cu, K^- and π^- prod. at 8 GeV/c 8=25231
$F^{19}(p, \alpha\gamma)O^{16}$, effect of proton channeling on γ-ray yield 8=29448
$F^{19}(p, \alpha)O^{16}$ ground-state ang. distrib. analysis 8=38472
$F^{19}(p, n)Ne^{19}$ absolute total cross sections, 4.234–6.010 MeV 8=43021
$F^{19}(p, pn)F^{18}$ 660 MeV ang. distrib. of recoil nuclei obs. 8=38471
Fe^{54} (p, pn) Fe^{53}, Fe^{56} (p, p 3n) Fe^{58} cross-sections obs., analysis of isomeric ratios 8=38465
$Fe^{58}(p, n)Co^{58}$, Co^{58} excited levels and decay, obs. 8=29313
$H^2(p, \gamma)He^3$, 2–12 MeV, cross section obs. 8=47318
He^4, nucleons released at 660 MeV 8=25227
He^8 prod. in cotton fibres, and delayed-n decay, 2 GeV 8=38414
He^4 spallation, cross sections obs. review 8=29436
Ir (p, Na^{21-29}), isotope distrib. obs. 8=34000
$K^{39}(p, \gamma_o)Cu^{40}$ excitation function, 2.9 and 6.0 MeV 8=38474
$La^{137}(p, 3p3n)Co^{134m,j}$, m and j cross sections, 40-155 MeV 8=29447
$Li^6(p, n)Be^6$, ang. distrib. of n, E_n = 8–18 MeV 8=47319
$Li^6(p, 2p)He^5$ and α-d cluster model for Li^6 8=29290
$Li^6(p, He^4)He^3$, Be^7 compound nucleus, resonance parameters determined from cross-sections 8=42832
$Li^7(p, \alpha)He^4$, analysing power for 3-10 MeV p polarization 8=29437
$Li^7(p, \alpha)He^4$, ang. distrib. rel. to p polarization 8=25226
$Li^7(p, \gamma)Be^8$ 1.4–2.5 MeV and levels of Be^8 8=47320
Li^9 prod. and delayed-n decay, 150 MeV 8=38463
$Mg^{24}(p, d)Mg^{23}$ in 2s–1d shell, obs. 8=43023
Mg^{24} (p, γ), Al^{25} resonance width at E_x = 3422 and 4038 KeV, using Doppling shift calc. 8=33995
Mg^{24}, (p, 2p) at 156 MeV 8=33993
Nuclear reactions due to—contd
protons—contd
Mg^{24}(p, 2p), spectroscopic analysis, 156 MeV 8=43024
$Mg^{26}(p, \gamma)Al^{27}$, resonance γ-decay, excitation of 9.991 MeV and 10.165 MeV levels in Al^{27} 8=33903
$Mg^{26}(p, n)Al^{26}$ and lifetimes of levels of Al^{26} 8=33902
Mg, E_n=9.1 MeV, total reaction cross section 8=29441
Mn^{55} (p, 3n) Fe^{53} cross-sections obs., analysis of isomeric ratios 8=38465
$Mo^{96}(p, n)Tc^{96}$, prep. of carrier-free Tc^{96} 8=47322
Mo^{100} (p, Na^{21-29}), isotope distrib. obs. 8=34000
$N^{14}(p, \alpha)$, charged particle yield and ang. distrib., 6-9 MeV 8=43020
$N^{14}(pn)O^{14}$ rel. to O^{14} Fermi decay 8=33958
N^{14} spallation, cross sections obs. review 8=29436
$N^{15}(p, \gamma)O^{16}$, γ decay of O^{16} obs. 8=33899
N^{17} prod. and delayed-n decay, 150 MeV 8=38463
N, effective cross sections at 125 MeV 8=43018
N fragmentation, Li, Be and B prod., $\leqslant$ 600 MeV 8=29438
N, $Li^{6,7}$, $Be^{7,10}$ and He^6 prod. cross section, Ep = 125 MeV 8=33991
Na^{23} (p, α_0) Ne^{20}, Na^{23} (p, α_1) Ne^{20} and Na^{23} (p, p_1) Na^{23}, at E_p = 2.2-4.5 MeV 8=33992
$Na^{23}(p, \gamma)Mg^{24}$, giant dipole resonance in Mg^{24} obs. 4–12.4 MeV obs. 8=43022
$Na^{23}(p, \gamma)Mg^{24}$ rel. to transition rates for Mg^{24} levels 8=29300
Na^{23}, (p, 2p) at 156 MeV 8=33993
Na^{23}(p, 2p), spectroscopic analysis, 156 MeV 8=43024
$Nb^{93}(p, d)Nb^{92}$, analog state excitation 8=33919
$Nb^{93}(p, n)Mo^{93}$, Q-value and Mo^{93} level scheme 8=29320
Ni^{58} (p, d) Ni^{57}, form factors calc. rel. to pseudo pot. 8=33999
$Ni^{58}(p, t)Ni^{56}$, level struct. and spin assignments 8=47247
Ni^{58} (p, 3p3n) Fe^{53} cross-sections obs., analysis of isomeric ratios 8=38465
$Ni^{58,62}(p, \gamma\gamma)Cu^{59,63}$, triple correlations 8=29446
$Ni^{60}(p, p'\gamma)$, E = 13 MeV, levels obs. 8=25131
$Ni^{61}(p, p'n)$, $(p, p'\gamma)$, (p, np'), Weisskopf–Ewing assumption testing 8=43031
Ni(p, t), L = 0, 2n transfer cross-sections 8=43064
O^{16} spallation, cross sections obs. review 8=29436
$O^{18}(p, n)F^{18}$, E_p = 5.0 MeV, O^{18} determ. by n time-of-flight spectrometry 8=32149
O, effective cross sections at 125 MeV 8=43018
O fragmentation, Li, Be and B prod., $\leqslant$ 600 MeV 8=29438
in O, 150MeV–19GeV, spallation prod. of $Li^{6.7}$, $Be^{9.10}$, $B^{10.11}$, obs. rel. to these processes between cosmic rays in space 8=38156
(P, γ) on low and medium 2 nuclei, cross sections and γ-spectra, 16-160 MeV 8=38462
$P^{31}(p, \alpha)Si^{28}$, scatt. cross section, 1.0-3.8 MeV 8=25222
$Pb^{207}(p, t)Pb^{205}$, shell model analyzed 8=38510
Pb^{208}(p, 3p) : Hg^{206} decay properties, spectra obs. 8=42971
$Pb^{208}(p, t)Pb^{206}$ shape and differential cross sections at 40 MeV, expt. and theoretical calc. 8=43032
Pb, fragmentation and fission, 3-24 GeV 8=34059
$Rb^{85.87}(p, n)Sr^{85.87}$, excitation function, 2.3-5.6 MeV 8=25134
$S^{32}(p, d)S^{31}$ in 2s-1d shell, obs. 8=43023
$S^{36}(p, \gamma)$, Cl^{37} resonances obs., spin assignment, 800-1940 KeV 8=42857
$Se^{78,80,82}(p, n)Br^{78,80.82}$, excitation curve obs. 8=42884
$Si^{28}(p, d)Si^{27}$ in 2s–1d shell, obs. 8=43023
Si^{28}, (p, 2p) at 156 MeV 8=33993
Si^{28}(p, 2p), spectroscopic analysis, 156 MeV 8=43024
$Si^{30}(p, \gamma)P^{31}$ resonance levels, spins and decay schemes 8=29444
$Sn^{116,117}(p, p')$, E_p = 55 MeV, levels obs. 8=25144
$Sn^{117,118}$(pd), E_p = 55 MeV, levels obs. 8=25144
Sn^{118}(p, t), E_p = 55 MeV, levels obs. 8=25144
$Sn^{119}(p, d)Sn^{118}$, level structure, 55 MeV 8=38379
$Sn^{119}(p, p'n)$, $(p, p'\gamma)$, (p, np'), Weisskopf–Ewing assumption testing 8=43031
Sn(p, t), spectroscopic factors for two-nuclear transfer reaction, using QTD and QSTD methods calc. 8=42817
$Sr^{89}(p, p')Sr^{88}$ analog meas., particle-plus-core coupling model interpretation calc. 8=33917
T(p, n) at low energies 8=47321
Ta(p, $Cs^{119-130}$), isotope distrib. obs. 8=34001
Ta (p, Na^{21-29}), isotope distrib. obs. 8=34000
Ta(p, Rb^{77-88}), isotope distrib. obs. 8=34001
$Te^{123}(p, \gamma)$, I^{123} prod. for medical diagnostic use 8=45408
Th(p, Rb^{78-96}), isotope distrib. obs. 8=34001
$Ti^{46}(p, d)Ti^{45}$, E_n = 26 MeV, low levels obs. 8=29307
$Ti^{46}(p, p')Ti^{46}$, ang. distrib. obs. 8=25274
$Ti^{48}(p, \gamma)$, V^{49} analogue states and virtual levels, E_n = 1.335-2.290 MeV 8=47245
$Ti^{48}(p, \gamma)V^{49}$, γ-ray spectra of analogue resonance 1, -1.4 Mev 8=42806
$Ti^{48}(p, \gamma)V^{49}$, E_p=1007, 1209, 1362, 1374 keV, γ-transitions and levels obs. 8=29445
Ti, E_n=9.1 MeV, total reaction cross section 8=29441
U^{233} (p, xn), $Np^{230,229}$ production 8=33968
U, fragmentation and fission, 3-24 GeV 8=34059
U(p, $Cs^{120-132}$), isotope distrib. obs. 8=34001
U (p, Na^{21-29}), isotope distrib. obs. 8=34000
U(p, Rb^{78-96}), isotope distrib. obs. 8=34001
U, K^- and π^- prod. at 8 GeV/c 8=25231

Nuclear reactions due to—contd
- **protons**—contd
  - V^{51} (p, n) Cr^{61}, excitation functions of neutrons 8=33998
  - V^{51}(p, n)Cr^{51}, fluctuations of excitation function 8=43029
  - Y^{89}(p, 3p3n)$Rb^{84m,j}$, m and j cross sections, 40-155 MeV 8=29447
  - Zn^{64}(p, 2p), $2p^{3}/_{2}$ and $2s^{3}/_{2}$ shells binding energies, 156 MeV 8=33914
  - Zn^{64}, (p, 2p) at 156 MeV 8=33993
  - Zn^{66}(t, p)Zn^{68} levels energies and spins, below 3 MeV excitation 8=33915
  - Zn^{68}(p, p′), energies and spins of levels below 3 MeV excitation obs. 8=33915
  - Zn^{90}, (p, 2p) at 156 MeV 8=33993
  - $Zr^{90,91,92}$(p, d) $Zr^{89,90,91}$, n hole states 8=42887
  - Zr^{90}(p, 2p), 2p shell binding energy, 156 MeV 8=33914
  - Zr^{96}(p, n)Nb^{96}, prep. of carrier-free Nb^{96} 8=47322
  - Zr, E_n=9.1 MeV, total reaction cross section 8=29441
- **tritons**
  - (t, d) finite-range effects in direct reaction at low energies 8=43051
  - (t, d) reaction at low energies, spectroscopic obs. low-lying states 8=43050
  - (t, p) and pairing potential 8=47339
  - B^{10}(t, α)Be^{9}, energy levels obs., 12.9 MeV 8=42833
  - Be^{9} + t → n + t + Be^{8} rel. to n-t reson. interaction energy, obs. 8=29502
  - Ca(t, p), L = 0, 2n transfer cross-sections 8=43064
  - Ca^{42-50}(t, p), Ca^{48} O^{+} states rel. to shell model, obs. 8=33938
  - Cu^{65}(t, α)Ni^{64}, core excitation of 5^{-} state, 3.856 keV 8=43066
  - (He^{3}, n) and pairing potential 8=47339
  - Ni(t, p), L = 0, 2n transfer cross-sections 8=43064
  - Ni^{58}(t, He^{4})Co^{57}, nucleon interactions 8=29279
  - O^{16} obs. 8=25264
  - O^{16}(t, p)O^{18}, analysis, effective 2-nucleon interaction 8=25267
  - Pb^{208}(t, α), p-hole states rel. to shell model, obs. 8=33938
  - Pb^{208}(t, p)Pb^{210} and analog resonances in Pb^{211} 8=25158
  - $Pb^{207,208}$(T, p)$Pb^{209,210}$ shell model analysed 8=38510
  - $Pb^{207,208}$(t, p), Pb^{209} 2-particle-one-hole, states obs. 8=38511
  - Sm^{144}(t, α), Pm^{113} proton quasi-particle spectrum obs. 8=33928
  - Sn(t, p), spectroscopic factors for two-nuclear transfer reaction, using QTD and QSTD methods calc. 8=42817
  - $Sn^{116,118}$(t, p)$Sn^{118,120}$, 13, 12 MeV, p spectra obs., $Sn^{118,120}$ levels deduced 8=25269
  - $Sn^{116,118}$(t, p) with particular ref. to $J^{\pi} = O^{+}$ channel 8=43067
- **X-rays.** See Nuclear reactions due to/photons.

Nuclear reactors, fission
  - ANNA assembly, reln. between stable period and prompt n time constant 8=34091
  - breeder, Na-cooled, cavitation 8=29560
  - with core of cylindrical elements, press. drop and coolant vel. distrib. 8=39268
  - critical buckling, approx. determ. 8=38559
  - damage flux in critical assemblies, rel. to design of inpile thermionic reactor 8=28504
  - DIDO and PLUTO, hall tritium monitoring system 8=29565
  - EBR-II, n counting-mean-square voltage channel performance 8=47157
  - economics of explosively released energy conversion to electricity 8=25287
  - economies of nuclear power 8=47370
  - fail-safe solid state safety system with dynamic logic circuits 8=25321
  - fuel elements, cooling fin surface geometry 8=24000
  - fuel elements, herringbone cooling fin designs 8=24002
  - gas coolant moisture detection, dewpoint device 8=47932
  - gas cooled, development 8=47391
  - gas cooled, use of N^{16} for outlet channel temp. meas. 8=47435
  - Gewsthacht, n dose-rates, p-recoil, rein and BF_3 counters obs. 8= 33807
  - in-pile calorimeter for simultaneous meas. of n-induced and γ-induced energies 8=25319
  - instrumentation, to 1968, review 8=28967
  - JRR-3 dynamics meas. by pseudo-random binary signals 8=34094
  - kinetics expts. interrelation, theory and obs. 8=38573
  - laminar instability, in gas-cooled passages 8=25809
  - mirror, ion loss by collisions 8=30021
  - moderators, applic. for isotopes 8=43245
  - neutron convertor for investigation of n scatt. and attenuation 8=29543
  - neutron cross section for (n, γ) reactions 8=34012
  - neutron flux detector 8=43148
  - neutron flux meas., γ-compensated ionization chambers 8=47156
  - neutron noise, external control loop. 8=38589
  - neutron number fluctuations 8=38552
  - neutron scatt., triple-axis spectrometer 8=33828
  - neutron spectrometry by transmission meas. 8=24980
  - n transport calcs, use of method of 'expected leakage probability' 8=38581

Nuclear reactors, fission—contd
  - noise, γ-ray obs. 8=34095
  - Orgel-type cluster, internal conversion ratio obs. 8=25305
  - power level monitoring with Cherenkov counter 8=47436
  - power monitoring by plasma microwave diagnosis 8=47432
  - problems for economic power generation 8=47367
  - reflected, pulsed n reactivity meas, interpret. with Cohn model 8=43139
  - radiation heating, adiabatic and steady state calorimeters for meas. 8=47434
  - radioisotope production in JRR-3, n irradiation conditions 8=24947
  - review of nuclear power 8=47369
  - shutdown reactivity, asymmetric n source meas., auxilliary params. 8=38593
  - spherical, critical radius, use of spherical harmonics. approxs to n transport eqn. 8=38580
  - subcritical, modified pulsed source expt, theoretical anal. rel. to reactivities 8=43135
  - subcritical, reactivity calc. by Garelis-Russel formula, spectral correction 8=25298
  - subcritical system, reactivity meas., spatial depend 8=25320
  - tangential channels from lifting of core, ratios of n fluxes 8=34093
  - temperature control of cooling gas in radiation loop 8=29554
  - water-cooled 8=47390
  - ZR-3 critical assembly, rel. to WWM-SM core development 8=34092
  - Na flowmeter, in-core permanent-magnet, calibration and stability 8=48013
  - U^{238}, D_2O moderated and diphyl cooled lattices ρ^{28} factor meas. 8=34077
  - UO_2-H_2O lattices, reactivity pulsed source obs. diffusion theory analysis 8=34065
  - Xe poisoning during shutdown, optimum control using min. energy 8=38587
- **materials**
  - actinide cpds, elec. and thermal props. 8=27233
  - anthracene oil components as coolant 8=49965
  - boiling water loops for irradiation of water-cooled fuel elements 8=47415
  - bubbles growth rate in transient boiling 8=48049
  - buckling and migration area, sub-crit. meas. 8=38588
  - burn-up determ. in zero power expts., by γ-spectrometry 8=25304
  - canning material, high strain fatigue at high temp. 8=35628
  - canning materials for water cooled power reactors 8=43145
  - ceramic fuel elements, design rel. to irrad. damage effects and materials coupling 8=25312
  - ceramics, isothermal irrad. assembly for fast n damage 8=35597
  - ceramics, radiation damage processes and defect cluster growth 8=31129
  - circulation loops for gas-cooled fuel elements 8=47416
  - cluster lattices, enriched UO_2 and PUO_2/UO_2 fuels, obs. of buckling reaction coeffs 8=43142
  - coated-particle fuels, influence of irrad. on stability 8=47425
  - coated particles, system of crack configs., theory 8=29561
  - container of Ta for liquid Pu alloys, corrosion, O, N impurity effects 8=47412
  - coolants, liquid-metal, heat transfer coeffs., effect of variable wall heat flux 8=25309
  - critical mass of reactor fuel in water 8=34101
  - diffusion rates in inorganic materials 8=48772
  - diphenyl, -m-and p-terphenyl, phys. props. for heat transfer calcs. as coolants 8=30422
  - displacement damage rates in differing reactor types 8=47408
  - fission product distribution in coated fuel particles, determination 8=47404
  - fuel, assessment of requirements, conts. heat output, fuel lifetime, toxicity and reprocessing 8=47423
  - fuel, burn up determ., using isotope separator 8=29567
  - fuel element consumption state meas. using γ-ray semiconductor spectrometers 8=47403
  - fuel element shapes compared 8=47419
  - fuel element thermal stress simulation, graphite furnace 8=34112
  - fuel elements, He cooled, heat transfer rel. to surface roughening, in-pile obs. 8=34104
  - fuels, corrosion rate at interface with its can, rel. to extraction 8=29563
  - fuels, inert fission-prod. gas bubbles nucleation, irrad. effects 8=31109
  - fuel inserts for gas-cooled reactors, disintegration with oxidizing acid mixtures 8=47431
  - fuel, irradiated, non-destructive inspection by n radiography 8=46769
  - fuel meltdown, study by fast neutron hodoscope 8=47164
  - fuel particles, coated, fission prod. release, diffusion model 8=38591
  - fuel particles, coated, thermal cond. 8=47410

Nuclear reactors, fission—contd
  materials—contd
    fuel, performance test code 8=34106
    fuel recycle optimization, linear and quadratic programming 8=47397
    fuel reprocessing, Uranyl-hydrogen system, cation exchange equilibria 8=47409
    fuel reprocessing, UO_2 from uranyl nitrate-TBP soln. 8=47413
    fuel spheres, irradiated, swelling meas. by micro-radiography 8=34102
    fuels, thermal diffusion 8=48776
    fracture for thin sheets 8=29558
    gamma-ray absorpt. coeffs. for H, C, H_2O, Al, Ar, Fe, Mo, Pb and U 8=47411
    graphite and neutron wave propagation; effect of Bragg cut-off energy 8=47375
    graphite bricks, unsteady heat conduction 8=28401
    graphite, grade A reactor, n-irrad. at 80°K and annealed at temps up to 300°K, e.s.r. 8=45081
    graphite in ANNA reactor, diffusion parameters $<\Sigma_a V>$ and D 8=34073
    graphite, mech. props meas. before and after n-irrad. 8=26789
    graphite, neutron irrad. obs. 8=43143
    graphite, oxidation anisotropy 8=41239
    graphite, reactor temp. and atm. effects rel. to appls. 8=25312
    graphite, reaction with H at high temp. and press. 8=47422
    Hastelloy, neutron irrad. effects on stress rupture and creep 8=47400
    inert gases, fission gases, release from UO_2 fuel rods 8=34108
    irradiation capsules for coated particles 8=47414
    irradiation, physical effects 8=29564
    liquid metal depth meas. equipment for recovery of spent fuel. 8=38594
    meta-terphenyl, e radiolysis, temp., intensity and post irad. effects, 1.35 MeV 8=36624
    neutron thermal wave propagation and effect of Bragg continuum in graphite 8=47374
    oxides, disintegration effect on power curves in fast reactors 8=47424
    pebble bed reactor, statistical space distrib. of fuel elements calc. program 8=43146
    Sicral F_1, irrad. swelling rel. to fission gas bubbles, 10^{14} n/cm² sec 8=44506
    Sicral F_2, irrad. swelling rel. to fission gas bubbles, 10^{14} n/cm² sec 8=44506
    spherical fuel elements in pebble bed reactor, reson. absorpt. 8=43147
    steel as stainless as reactor material, embrittlement by He prod. in (n, α) reactions 8=47406
    steel, embrittlement sensitivity to n irrad., depend. on uncombined N conc. 8=47405
    superheat fuel elements, seven-rod clusters, micro-parameters 8=25314
    Zircalloy, in-reactor creep rel. to dislocation climb 8=35728
    Zircaloy-2 oxidation in kinetics and mechanism, 350–500°C 8=32106
    Zircalloy-2 pressure tubes, in-reactor creep rel. to n flux, temp. and stress, obs. 8=35733
    Zircalloy-2, uniaxial in-reactor creep rel. to pre-treatment, 200–400°C 8=35729
    Zircalloy-2, ZrH precip. habit planes, obs. 8=44098
    Zircalloy-4, irrad.-enhanced strain relax., 2.4×10^{14} nv > 1 MeV 8=35732
    Zircalloy-4, ZrH precip. habit planes, obs. 8=44098
    Au, natural, effective reson. integrals, reactivity obs. 8=34015
    B compounds in gas cooled reactors, compatibility with graphite 8=29559
    Be moderator, decay const. and diffusion lengths, calcs. by two theories 8=38590
    Be, reactor material, neutron population predictions 8=38454
    BeO compacts, n-irrad., kinetics of escape of He 8=25316
    BeO, diffusional release of tritium on post-irrad. annealing 8=25317
    BeO, thermal diffusion parameters determ. 8=25308
    BeO, thermal diffusion parameters, determ. by pulsed n method 8=25307
    BeO-graphite compatability, 1500°C, Li^6 distribution 8=34100
    BeO_2, reactor conditions and irrad. damage effects rel. to appls. 8=25312
    CaO formation and diffusion of Ar^{37} under neutron bombardment 8=39969
    Co^{60}, props. of encapsulating materials 8=47421
    He loop for irradiation experiments on fuel pins 8=47417
    Hg boiling corrosion of steel boilers, inhibition with Ti and Zr 8=47426
    I and P^{31} concs. in primary water cooling circuit of WWR-S type 8=34105
    Pu^{239} fission cross-section, channel theory 8=34049
    Pu^{239}, mag. moment 8=42930
    $Pu^{239,241}$, meas. of n scatt. resonances 8=43037
    Pu^{240} subthreshold fission cross section, structure due to intermediate states 8=38528

Nuclear reactors, fission—contd
  materials—contd
    $Pu^{238}O_2$ neutron spectrum 8=34099
    Pu alloys, phase diagrams 8=35080
    Pu and cpds as fuel, props. and selection criteria 8=25313
    Pu, difficulties and potentialities 8=25311
    Pu, fuel for thermal reactors 8=47402
    Pu heat content and sp. ht. obs. 8=25306
    Pu, liquid, viscosity, heat of fusion and melting 8=47407
    Pu-Be (α, n) sources, n yield increases 8=47428
    Pu-Co-Ce liquid metal in Ta container determ. of Ta mass transfer 8=47420
    Th and cpds. as fuel, props and selection criteria 8=25313
    ThO_2 microsphere production from alcohol mixtures 8=25310
    ThO_2 rods, effective reson. integral temp. depend., obs. 8=34017
    ThO_2—D_2O—H_2O lattices, age meas. 8=29552
    U^{233}, meas. of n scatt. resonances 8=43037
    U^{235} fission cross-section, channel theory 8=34049
    $U^{235,238}$ isotopic ratio determ. by γ spectrometry 8=47546
    U^{238}, self-shielding factor and its Doppler effect, rel. to Na resonance scatt. 8=25315
    $U^{235}O_2F_2$ aqueous soln., minimum critical thickness of water-refl. infinite slab 8=34052
    U alloys, α-phase grain refinement by B addition, obs. 8=44171
    U and cpds. as fuel, props. and selection criteria 8=25313
    U, growth and elec. resistivity changes during burn up with thermal n.s. at 4.6°K 8=48933
    U, enrichment on commercial basis 8=47399
    U fuel materials in heavy water reactor calc. of k-infinity constant 8=47427
    U rods, undergoing dissolution, criticality 8=25295
    α-U, deform. twinning modes in Bravais lattice, table 8=44090
    α-U, irrad. swelling rel. to solid fission prods. segregation 8=44507
    UC fuel elements, mobility and trapping of fission-prod. Xe and Kr 8=25318
    UC, irrad. at 77°K, density var. during annealing, obs. 8=44605
    UC, prep. by carbothermic reduction of U oxides 8=27720
    $UC_{1-x}O_x$, heat of formation and heat capacity 8=30970
    $UC_{1-x}N_x$, in N_2 gas, change of comp. 8=35063
    U-H_2O subcritical assembly, meas. of buckling by improved 'flux-shape' method 8=34103
    U-Ir system, phase diagram 8=35133
    U-Mo 1,1 alloy, irrad. swelling rel. to fission gas bubbles, 10^{14} n/cm² sec 8=44506
    U-Mo-Al-Sn, irrad. swelling rel. to fission gas bubbles, 10^{14} n/cm² sec 8=44506
    UN, prep. and fabrication techns. 8=27722
    UN, prep. from UCl_4 + Al + N_2, two-step reactions 8=36574
    UN–C system equilib. rel. to UN compacts prep., obs. 8=32083
    UN–UC system liquidus and solidus, obs. 8=32083
    UO_2 assembly, bucklings rel. to comparison of fast and thermal n flux profiles 8=43138
    UO_2, density var. during annealing rel. to fission damage recomb., obs. 8=44605
    UO_2 fuel element, axial void form. rel. to radial temp. gradient 8=43144
    UO_2 fuel elements, mobility and trapping of fission-prods. Xe and Kr 8=25318
    UO_2 fuel, irrad. anal. of solid fission prods. after burn-up 8=25286
    UO_2 fuel particles, fission-gas release rate rel. to fission density, obs. 8=38592
    UO_2, heat content from 1200° to 3100°K 8=35436
    UO_2, limits for equation of state 8=30572
    UO_2, migration of UO_2 bubbles 8=26625
    UO_2 pellets fluorination to UF_6 by Fl, kinetics and chemisorpt. 8=32104
    UO_2 powder, n-irradiated, electronic props. from e.m.f. meas. 8=40290
    UO_2 powders, oxidation in storage rel. to fabrication and irrad. props. 8=45349
    UO_2, thermal cond. rel. to temp. gradient depend., obs. 8=44369
    UO_2-H_2O lattices neutron temperature rel. to activation ratios 8=47418
    UO_2-TaB_2 fuel, heated in steam, reactions 8=27717
    UO_2-WB_2 fuel, heated in steam, reactions 8=27717
    UP, prep. and fabrication techs. 8=27722
    U-Pu monocarbides ceramics, fabrication 8=30664
    U/10% Pu/10% Fz alloy, transform. kinetics 8=30711
    $(U, Pu)O_2$ solid soln. production and Pu distribution 8=2956
    U-Rh system, phase diagram 8=35132
    US, prep. and fabrication techs. 8=27722
    $(U_{0.85}Pu_{0.15})O_2$ fuel, irrad., metallic fission-prod. inclusions, obs. 8=29557
    U_3Si fuel elements, swelling during burnup reduced by provision of central void 8=47429

Nuclear reactors, fission—contd
materials—contd
Va-Ti as reactor fuel jacket, liquid Na corrosion 8=47430
W^{184,186} in natural W, reson. integrals, activation obs. 8=34016
Zr alloys, in-reactor creep rel. to dislocation climb 8=35728
Zr alloys, irrad. creep, yielding creep theory appl. 8=35730
Zr alloys, surface hydrogenation protection with molten $NaNO_3$ 8=32105
Zr, oxidation prevention by Cr coating, ≤650°C 8=32107
Zr–2.5 at.%Nb, creep, in-reactor and unirrad., and mechanism, 300–400°C 8=35731
Zr-2.5 wt.%Nb pressure tubes, in-reactor creep rel. to n flux, temp. and stress obs. 8=35733
Zr–2.5 wt.%Nb, uniaxial in-reactor creep rel. to pre-treatment, 200–400°C 8=35729
Zr-2.5 wt.%Nb–0.5 wt.%Cu, irrad.-enhanced strain relax., 2.4×10^{14} nv > 1 MeV 8=35732
operation
control, digital, on-line 8=43140
coupled cone as time-lag system, stability conditions 8=29555
critical heat flux and heat transfer in transient boiling, expt. 8=47373
effective cross section ratios from fuel burnup data 8=29566
epithermal-neutron spectra meas., resonance self-screening technique 8=34109
n flux monitor, Sc^{46} capture cross-section 8=47330
heat transfer in liquid metal 8=39353
heavy-water, symposium, Vienna (1967) 8=25301
instrumentation and control, state-of-the-art 8=25300
on-line computer programmes and systems 8=47195
neutron population, produced by photoeffect in Be prod., analysis 8=38454
optimal shutdown control, nonlinear programming 8=47395
pile noise anal. by digital meas. of counting rates correl. functions 8=25299
power excursion, SPEX-1 code for calculation 8=47389
radiation accidents and effects, book 8=38586
research reactor, digital computer control 8=47396
shielding, ATTOW two dimensional calc. programme 8=47392
shutdown margin meas. by transfer function 8=47394
SN ratio in Rossi-α experiment 8=47386
subcritical state, pulse response meas. 8=25302
thermometry, resistance, liq. semicond. applicability 8=34110
U rods, criticality control 8=25295
U^{233} in soln, array of bottles determ. of neutron criticality condition 8=47398
1.03 wt % U^{235} metal - D_2O lattices, params., obs. 8=38585
theory
adjoint weighting, anomalous effect on an approx. method 8=38562
albedo criticality eqn. 8=25303
Argonaut-type, coupling-coeff. between two zones, calc-tech 8=38557
circulating fuel, dynamic equations, homogeneous 8=25297
control, digital, of power reactors 8=34096
control, optimal of distributed-parameter reactor 8=34098
core design, thermal, uncertainty analysis, synthesis method 8=34080
coupled-core, cross-spectral density function and reactivity coupling coeff. 8=38556
coupled core, multimode time-synthesis approx. 8=38566
criticality and energy-dependent Boltzmann eqn., slab reactor 8=25294
criticality of heterogeneous arrays undergoing dissolution 8=25295
criticality, iterative determ. of minimal eigenvalue 8=34084
diffusion eqns. time-depend multigroup, numerical soln. and truncation error 8=38564
end point method, generalized, albedo problem 8=47379
fluctuations in n populations, Monte Carlo anal. compared with one-mode stochastic model 8=38553
flux synthesis method, extension 8=38568
gascore, coaxial and vortex flow types, analysis for space-propulsion systems 8=47388
general kinetics eqns. approx. solns for two analytical models 8=43136
geometries calc. by extended flux synthesis method 8=38569
at graphite/H_2O and /D_2O interfaces, n diffusion waves refl. and refr. 8=38071
group diffusion equation, one dimensional, by Laplace transformation 8=47378
group-diffusion problems in finite-difference form 8=29548
hot channels study, in cosine power distrib. reactor 8=25291
kinetic characteristics, meas. of prompt n decay constant 8=47377

Nuclear reactors, fission—contd
theory—contd
kinetics, nonlinear space-depend., stability 8=25292
kinetics, point eqns., generalized formulation 8=34082
kinetics of zero power heterogeneous lattices 8=34076
lattice, heterogeneous, comparison with expt. 8=25290
monoenergetic critical parameters for slab or sphere, and decay consts. 8=38555
multiple scatt. in slab geometry, recursion formulae 8=34067
neutron and precursor populations in time-varying reactor, variances and covariances 8=34081
neutron diffusion eqns., synthesis techniques 8=29545
neutron diffusion, 3-dimens. eqn., numerical solns. 8=47383
neutron distribs. nonlinear kinetics, spatial and temporal behaviour, stability anal. 8=43134
neutron flux equations in reactor kinetics 8=47385
neutron importance, thermal and total, phase space distrib., theory and meas. 8=43137
neutron pulse in slabs and spheres, time decay constants 8=47376
n reson. absorpt. in fuel rod lattice 8=34086
neutron resonance integrals, effect of source distrib. 8=29547
n spectra in multiplying assemblies with pseudo fundamental mode behaviour, pulsed spectra 8=38563
n transport, absorpt. cross sections and region capture integrals fitting 8=34087
n transport, appl. of space angle synthesis by simple approx. 8=38561
neutron transport eqn. approx. soln. in 2- and 3-dimens. system 8=47381
neutron transport eqn., asymptotic P_N approx. 8=29544
neutrons in water, energy dependent Milne problem 8=47382
neutrons, thermal, Albedo and Milne's problem 8=29550
nuclear resonance spacings, synthetic kernels calc. 8=38342
power reactor dynamics, on-line statistical identification 8=34083
power tilting, static, due to manufacturing tolerances, statistical analysis 8=38567
prompt decay const. transform. to static reactivity 8=34090
reactivity calibration, flux transients digital anal. 8=34078
reactivity-coeff. distribs, 3-dimens, appl. of synthesis techs. 8=38558
resonance reactors, intermediate structure 8=47371
rod bundles, parallel-flow, turbulent-flow mixing, model 8=34068
slab, n extrapolation distance 8=25296
SHE critical assembly, meas. of space dependent transfer function of critical assembly 8=47387
stability, homogeneous 8=34079
static reactivity from prompt decay consts. 8=34090
stresses, dynamical, in elements of fast pulse reactor core, numerical calcs. 8=29546
temperature coeff. rel. to parameters 8=43133
thermal, criticality, Monte Carlo calc. 8=38565
thermal/fast neutron ratio, obs. 8=47380
transfer function meas., higher space modes excitation 8=34070
zero-power describing function valid at all freqs. 8=29542
Pu critical expts. analyses 8=25293
U^{238}—graphite lattices, resolved neutron resonance integrals 8=29551
U^{238}-metal fuel rod lattice in H_2O and C, n intermediate reson. absorpt. 8=34086
U^{235}–H_2O, group diffusion eqns., using Green's functions 8=29549
$U^{238}O_2$ fuel rod lattice in H_2O and C, n intermediate reson. absorpt. 8=34086
Nuclear reactors, fusion
fast, review 8=47368
pulsed, plasma confinement expts. 8=25288
stellarator, twisted figure 8 and racetrack, injected plasma confinement 8=30111
Nuclear relaxation. See Nuclear magnetic resonance and relaxation.
Nuclear-solid interactions. See Mössbauer effect; Solids.
Nuclear spallation
cosmic rays, galactic, p-fragmentation rel. to Be/B dating, $6 \leq Z \leq 26$ 8=38176
heavy hypernuclei, from K$^-$ at 800 MeV/c 8=25166
n emission, delayed, precision fragments 8=38404
emulsion nuclei, 5 GeV/c $\bar{p}$, fragment emission, fireball model 8=38065
nuclides far off stability line prod., rates 8=38442
rel. to $Z \leq 5$ elements prod. in universe, p cross sections, obs. 8=32390
Z ≥ fragments prod. at > 0.5 GeV, theory 8=29382
Ag, p-induced fission-like disintegrations, and model, 25 GeV/c 8=34003
rel. to B origin in solar system 8=36990
rel. to Be origin in solar system 8=36990
Br, p-induced fission-like disintegrations, and model, 25 GeV/c 8=34003
C^{12}, p induced, cross sections obs. review 8=29436
C, by p, Li, Be and B prod., ≤ 600 MeV 8=29438
rel. to H^2 origin in solar system 8=36990
He^4, p induced, cross sections obs. review 8=29436

Nuclear spallation—contd
rel. to Li^{6,7} origin in solar system 8=36990
Li^{6,7}, Be^{9,10}, B^{10,11} prod. by p in O, 150MeV-19GeV rel. to cosmic ray reactions in space 8=38156
N, by p, Li, Be and B prod., ≤ 600 MeV 8=29438
N^{14}, p induced, cross sections obs. review 8=29436
O, by p, Li, Be and B prod., ≤ 600 MeV 8=29438
O^{16}, p induced, cross sections obs. review 8=29436
Pb, by p, light Tl and Hg isotopes prod., 3 GeV 8=38394
Pb, p induced, 3-24 GeV 8=34059
Si, by p, Na mass spectrum 20 ≤ A ≤ 25, 150 MeV 8=38542
Nuclear track emulsions
α-acetylaminoacrylic acid-N-vinylpyrrolidone copolymer-gelatin for fast-n dosimetry 8=33800
computer processing of data 8=46985
cosmic ray detector aboard Gemini 8=42705
cosmic ray stars, statistical evaluation of connecting lines 8=38113
2, 4-disulphonic acid benzaldehyde polyvinyl acetal-gelatin for fast-n dosimetry 8=33800
$\bar{p}$ elastic scatt. rel. to nuclear optical model params., 3 GeV/c 8=43000
e.m. cascade energy meas. 8=38135
e.m. cascades, lateral and ang. struct. 8=38137
fast-particle energy estimation from ionization meas. 8=47114
Fowler-Perkins parameter meas. for sensitive determ. of cosmic ray charge and energy spectra 8=42708
heavy-ion track widths meas. 8=44488
inclined track projections 8=37805
p interactions, 6.2 and 28 GeV/c with fast d, t prod. 8=38099
jet and fireball prod., by 10^{12}-10^{13} cosmic ray particles 8=29247
light-element ion paths in NIKFI-YaZ photoemulsion 8=46984
microscope, semiautomatic, for measuring track ionization parameters 8=46983
μ interactions, inelastic, 5 GeV/c 8=25213
neutron dosimetry by scanning edge effects and track length meas. 8=33804
neutron personnel dosimetry, thermal and intermediate energy, body backscatt. effects 8=33803
neutron spectra determ. from recoil tracks 8=47161
photographic films, 17 types sensitivity to ionizing rad. in near earth missions 8=28993
π interactions, 16.2 GeV/c with fast d, t prod. 8=38099
proton recoil scanning, sampling bias 8=24542
proton track meas., photographic scanning 8=46981
resolution of 7-60 keV electron images 8=37722
response to 7-60 keV electrons 8=37721
review 8=33393
with synthetic polymers, for fast n dosimetry 8=47152
Ag nuclei fragmentation by 13.8 GeV/c p, identification of emitted particles 8=34002
Br nuclei fragmentation by 13.8 GeV/c p, identification of emitted particles 8=34002
K^- interactions, prod. of He^8 hammer tracks obs. 8=25022
$\bar{p}$-N interaction, analysis of obs. 8=42641
Nucleation. See Clouds; Crystallization; Freezing.
Nucleic acids. See Macromolecules.
Nucleons and antinucleons
See also Neutrons and antineutrons; Protons and antiprotons.
Core radius investigated in d electrodisintegration 8=33842
double emission after bound pion absorption 8=38299
dynamical status from P_{11} π-N scatt. amplitude 8=42551
e. m. form factors, comp. with π-N and N-N scatt. and 1 and 2π exchange contrib. 8=24879
e. m. radius, new sum rule, rel. to Compton effect 8=37918
electromagnetic struct. 8=33739
enrgy determination of high energy nucleons by absorpt. calorimeter 8=38139
in fission, non radiative transitions probab. 8=29527
form factor, axial-vector, meas. in e + N → e + N + π + π, current algebra and PCAC 8=33738
form factors, e. m., fitting in vector-dominance model 8=42620
form factor, e.m., rel. to vector boson resonances 8=29165
form factor, exponential decrease rel. to equal-time commutator definition ambiguities 8=33652
form factor rel. to extended structure 8=29140
isovector form factor prediction 8=38050
magnetic moment, anomalous from meson field theory 8=29180
magnetic moments, bootstrap model calc. 8=42623
magnetic moment, cross-section sum rules for Compton scatt. 8=42622
mass, sum rule 8=42621
meson field oscills. model rel. to e excitation spectrum, e.m. props. 8=29180
motions in nucleus, literal truth of shell model 8=33869
N and π e. m. radius difference 8=38055
$N\bar{N}$ annihilation at rest, symmetry model tests 8=24894
$N\bar{N}$ charge exchange scatt. model, Regge-pole model 8=24888
N-$\bar{N}$ pot. from single-meson exchange, adaptation of Bryan-Scott pot. 8=24896

Nucleons and antinucleons—contd
N(eé)N* form factors model dependent 8=38056
N*, N sizes compared 8=29216
N* production by neutrinos 8=25004
N* prod. in π(K) + p → π(K) + N*, Regge pole model, N* matrix elements 8=33839
pairs, and literal truth of shell model 8=33870
πN coupling constant determ. 8=33754
p-n mass difference 8=38058
photoprod., meson field model 8=29180
polarization prediction in Regge trajectory interference theory of π^+p scatt. 8=33687
sum rule relating magnetic moment to pion photoproduction amplitude 8=42364
S-matrix calc., many-body theory 8=33977
trinucleon, short-range correls. using spatial part of S-state wave function 8=25013
interactions
air nuclei, models for e.a.s. calc. 8=38217
Compton effect at low energy 8=47129
electroexcitation of baryon resonances, relations between form factors 8=42661
e + N → e + N + π + π, current algebra and PCAC calc. of N axial-vector form factor 8=33738
γ + N → N + V°, cross sections 8=24852
γN → VN, vector-meson prod., conspiracy relations 8=38026
γNN*, form factor rel. to π° electroprod., 0.05-0.4(BeV/c)^2 8=33670
isoscalar pair-force problem, isospin invariance 8=42777
KN, superconvergence relations 8=29115
$\overline{K}$N, superconvergence relations 8=29115
K^-N → Λπ, 1900-2, 215 MeV Y_1^*(1910), $J^P = 5/2^+$ 8=33841
K^- + N → Y + M, amplitude determ. in quark model 8=33703
ΛNN in p-shell hypernuclei, 3-body repulsion rel. to binding energies 8=29350
mesons, pseudoscalar, photoprod., Regge pole model 8=29127
meson-nucleon, very-high-energy polarization theory 8=37963
meson + N → γB for determ. of e. m. couplings of MN resonances 8=37916
$\bar{N}$N, theoretical models, reln. to NN interact. 8=24895
ν + N → B + (π) + μ, polarization correl. between B and μ calc. 8=29091
nuclear emulsion, p-N, π-N, at high energy, d, t prod. 8=38099
with nuclei, 100-1000 GeV, intranuclear cascade 8=42530
photoproduction of ρ, η and ω mesons, and double π 8=33667
πN, 4 GeV/c, in propane bubble chamber 8=47107
π-N inelastic, central and peripheral, 17.2 GeV obs. 8=24783
πN, superconvergence relations 8=29115
π-N transverse momentum at 17.2 GeV 8=24784
π-N vector meson prod., Lorentz pole structure 8=29171
πN → η N* (1236), O(3, 1) symmetry analysis 8=24785
πN → NW, W prod. cross-section, one pion model 8=38022
πN → ππN for calc. of S-wave ππ phase shift 8=29144
π + N → ρ + N*, ang. decay correls. at 8 GeV 8=24781
π + N → ρ + N* → N + 3π, Regge-pole model 8=24780
πN → $\omega_{3/2}$*, (1236), Lorentz pole analysis 8=37974
π^-N, 17.2 GeV/c, heavy nuclei surface neutron richness K, π, prod. 8=42535
π photoproduction cross-sections, perturbation theory 8=42513
pN, Ep = 20 GeV, secondary asymmetric separation obs. 8=29186
p-N in p reactions in C, 24 GeV/c, energy of prod. n obs. 8=29439
$\bar{p}$-N interactions in photo-emulsions, obs. 8=42641
potential, effect of nonstatic character in singlet-even states 8=25043
Y-N, final state, low energy obs. 8=33838
interactions, nucleon—nucleon
above 3 GeV/c range, main theoretical ideas compatible with expt. data 8=24869
binding energy of 3N system 8=38319
Born phase shifts and relativistic terms from three treatments of vector meson field 8=24872
bremsstrahlung prod. rel. to off-energy-shell props. of a potential 8=24871
bremsstrahlung, soft-photon theory 8=42625
charge depend. study and violation of charge symmetry 8=24864
forces at small distances, combining of meson theory and phenomenological descriptions 8=24865
γ N → VN, kinematical singularities and zeros 8=42448
as test of group theory schemes, conservation laws and analyticity struct. of S matrix 8=24866
I = 1, low energy anal. rel. to e.m. effects and phase shifts 8=24867
meson exchange adiabatic local pots. model, consistent with theory and expt. 8=24868
nuclear matter and non-static character 8=42774
in nuclear structure calc, for binding energy and density 8=25063
$N\bar{N}$ annihilation cross sections, isospin dependence 8=24893

Nucleons and antinucleons—contd
  interactions, nucleon-nucleon—contd
    $N\bar{N}$, superconvergence relations 8=29115
    $N\bar{N}$, isospin-one mesons on Regge trajectories 8=24677
    N-$\bar{N}$ pot. from single-meson exchange, adaptation of Bryan-Scott pot. 8=24896
    NN $\rightarrow$ NNW, W prod. cross-section, one pion model 8=38022
    NN $\rightarrow \pi$d, phase-shift analysis 8=38053
    $\bar{N}N \rightarrow \pi\rho$, saturation of superconvergence relations, sum rules and form factors 8=33740
    $\bar{N}N \rightarrow \pi\omega$, saturation of superconvergence relations, sum rules and form factors 8=33740
    $N\bar{N} \rightarrow Y\bar{Y}$, high energy, $O_{3.1}$ symmetry 8=38057
    $N + \bar{N}^* \rightarrow \pi + \pi$, superconvergence sum rules 8=29183
    particle-hole dipole transitions, exchange Majorana pot. 8=24877
    phase shift anal. using single-particle-exchange Feynman diagrams 8=24874
    potential violating parity 8=24876
    one-boson exchange pseudo scalar-vector-scalar meson theory 8=24751
    relation with $\bar{N}N$ interact. theoretical models 8=24895
    $^1S_0$ differences, non-e.m., rel. to charge independence 8=42624
    Schrödinger eqn., soln. with vel.-dependent pot. 8=24461
    separable potential 8=42776
    smooth interactions and meson theory 8=33741
    state of knowledge 1967, overview and conference summary 8=24870
    superconvergence relations 8=29115
    from vector and scalar meson fields having direct and deriv.-type couplings to nucleons 8=29167
    velocity-dependent potential 8=25097
    weak. pot., effect of second class currents on form 8=24875
    He^6, excited bound states, deformed orbits calc. 8=25093
  scattering
    antilepton scatt., polarization dependence calc. 8=42462
    charge exchange scatt., partial wave analysis of ρ Regge amplitude 8=24779
    Compton, finite energy sum rules for Pomeranchuk trajectories 8=24694
    Compton, low-energy theorems 8=33606
    Compton scatt., rel. to calc. of $\pi^\circ \rightarrow 2\gamma, \eta^\circ \rightarrow 2\gamma$ decay rates 8=33663
    coupled eqns., random phase approximation 8=42997
    electron elastic scatt., form factors and vertex amplitudes 8=47086
    e, meson field model for spectrum 8=29180
    Glauber theory tested in π-p, π-d, 0.46-2.67 GeV/c 8=29139
    Hartree-Fock generalized approximation for nucleon one-level nucleus scatt. 8=29418
    impulse approx., 150-180 MeV off light nuclei, polarization-asymm. difference 8=25215
    inelastic, calc. on generalized optical model 8=47312
    kinematic singularities and MacDowell symm. rel. to boson-fermion reactions 8=29047
    knockout exchange contrib. 8=42999
    KN dispersion sum rules, agreement between Regge behaviour and low energy parameters 8=37988
    K-N, finite energy sum rules and crossover problem 8=24832
    KN, finite-energy sum rules, Regge-exchange amplitudes rel. to polarization and K^+n charge exchange 8=33710
    KN finite-energy sum rules rel. to A_2 trajectory no-compensation mechanism 8=42612
    KN low energy with complex singular pot. 8=24829
    $\bar{K}$N low energy with complex singular pot. 8=24829
    KN, Regge trajectories, P and P^1, props. 8=42442
    KN, superconvergent sum rules 8=29157
    KN, s-wave length determ. from obs. of K_s^0-p, 168-343 MeV/c 8=33709
    K^-N, 0.6-2.65 GeV/c, cross-section obs. 8=29159
    Λ-N potential calc. 8=24990
    lepton scatt., polarization dependence calc. 8=42462
    light nuclei, 142-310 MeV, multiple, calc. 8=25047
    meson-nucleon, spin flip effect meas. 8=24764
    N Compton scatt. higher order low energy theorems from helicity amplitudes 8=29078
    np and pp phase shift anal. at 18.2 and 9.9 MeV 8=42627
    in nuclear matter, effect of repulsive core, quantum mechanical problem 8=38309
    in nuclear matter, effect of tensor forces 8=42793
    nucleus, high-energy, geometrical optics, analysis 8=47030
    nucleus, high energy rel. to N-N elastic scatt.
    optical five-parameter model 8=25053
    optical model calc. at 152 MeV 8=42998
    optical model potential 8=25051
    optical potential, non-local, for low energy scatt., calc. 8=33985
    πN amplitude calc. using a field theory 8=24480
    πN amplitudes, backward 180°, applications 8=42548
    πN backward scatt. isospin violation 8=37991
    πN chiral transformations 8=24686
    πN dispersion relations, subtraction by means of canonical commutation relations 8=24798
    πN dispersion sum-rules, agreement between Regge behaviour and low energy parameters 8=37988

Nucleons and antinucleons—contd
  scattering—contd
    πN helicity amplitude relations 8=24658
    πN, Liu-Okobo dispersion relation sensitive test of low energy data 8=29143
    πN, near-backward, finite energy sum rule appl. 8=37989
    πN, phase shifts up to 1600 MeV of C.M.S. from Padé approx. 8=33684
    πN pole branching effect 8=37986
    πN, Regge pole parameters from dispersion relations of superconvergence type 8=42431
    πN Regge trajectories, P and P^1, props. 8=42442
    π-N, rel. to 4π coupling constant 8=29120
    πN, ρ-exchange force method at high energies in many-channel formalism 8=24892
    πN sum rules, new class from dispersion theory 8=33585
    πN, superconvergent sum rules, Regge parameters 8=29138
    πN, s and p partial waves, accounting for short-range effects 8=42552
    πN S_{31} wave analytic expression 8=24664
    πN, s-wave length Adlers consistency relation 8=37992
    πN, unitary impulse approx. method 8=29142
    πN vacuum exchange amplitudes from sum rules 8=33682
    $\pi N \rightarrow \rho N$ regularity of limit $S \rightarrow \infty, t \rightarrow o$ 8=37993
    π rel. to structure analysis 8=29031
    S-matrix calc., R-matrix and eigenchannel methods, comparison 8=42414
    spinless, neutral scalar meson scatt., static limit theory 8=24766
    by weak central potentials, calc. using modified Born approx. 8=24650
    C^{12} impulse approx., 150-180 MeV off light nuclei, polarization-asymm. difference 8=25215
    Ca^{40} impulse approx., 150-180 MeV off light nuclei, polarization-asymm. difference 8=25215
    Ca^{40}, optical pot. calc., 10-20 MeV 8=33985
    He^4, $E < 20$ MeV, optical model 8=29231
    Sn^{118}, inclusion of knockout exchange in amplitude for excitation of 2^+ state 8=42999
  scattering, nucleon—nucleon
    bremsstrahlung at 197 MeV 8=29182
    calc. in Scotti-Wong momentum-depend. pot., for energies 25-350 MeV 8=24881
    coupling consts for one-boson-exchange model 8=24747
    elastic, links between high and low energy 8=29181
    forward elastic, asymptotic behaviour 8=42626
    1 and 2π exchange contribs., comp. with π-N and N-e scatt. 8=24879
    experimental aspects and data on scatt. near 210 MeV, critical review 8=24878
    forward dispersion relations for meson-nucleon coupling consts. 8=24746
    forward scatt., matrix amplitude reconstruction 8=24672
    intermediate energies, at Berkeley, parameter meas. with polarized and unpolarized targets 8=24885
    meson model anal. using 12 adjustable parameters 8=24874
    $N\bar{N}$ backward scatt., superconvergence 8=24889
    $N\bar{N}$, exchange degeneracy and backward superconvergence 8=38051
    $N\bar{N}$ helicity amplitude relations 8=24658
    phase-shift anal. for low energies 8=24884
    phase shift analysis and amplitude determ., energy above π-prod. threshold 8=24886
    phase shift analysis, relativistic of elastic and inelastic 8=38053
    phase shift analysis, 630 MeV, new solutions 8=38054
    phase-shift representations above π-prod. threshold, with inelastic channels open 8=24887
    polarization correlation tensor C_{nnik} 8=42628
    potential, boson exchange theory of nuclear forces 350 MeV 8=38300
    quark model inequality 8=24891
    Regge-pole model, charge-exchange at high energies energies 8=24888
    short-wave repulsion 8=38052
    soft core pots. for elastic scatt. in 0-310 MeV energy region 8=24882
    statistical hypotheses, discrimination method 8=24880
    two-pion exchange effects, calc. 8=24890
    C_{NN} meas. at Harwell, three energies and precision meas. at 100 MeV 8=24918
    rel. to N extended structure, high energies 8=29140
    600-650 MeV, phase-shift anal., and discrimination of sets for determ. of most probable one 8=24873
  scattering, pion—nucleon. See Pions/scattering, pion—nucleon.
  antinucleons
    No entries
Nucleus
    See also Elements/origin; Hypernuclei; Radioactivity; Scattering, particles.
    α, decay rel. to surface structure, barrier penetrabilities calc. 8=29262
    binding energy determined from hole line expansion method 8=47200
    collective motion, microscopic theory 8=38343
    deformation regions, predicted, at $A \simeq 110, 135$ and 190 8=38327

Nucleus—contd
deuteron wave function and G_e, model dependence 8=47139
effective 2-nucleon interaction, from $O^{16}(t, p)O^{18}$ analysis 8=25267
evaporation ang. distrib. and ang. momentum distrib. 8=42812
far off stability line, fission, spallation and reactions prod., rates 8=38442
fissile, quasistable states rel. to cross-section irregularities 8=47358
heavy, d- and α-association 8=25068
heavy, structure and approximations validity 8=29259
hypernuclei expts. rel. to nuclear struct., review 8=29349
local potl. containing hard core, t-matrix calc. 8=42779
magic, super-heavy nuclei, shell model single particle Hamiltonian predictions 8=38304
mass, spherical and deformed nuclei, shell corrections to liquid drop model 8=38308
matter, Brueckner theory 8=29272
μ-capture and photo-, e- and v-excitation of T_3 resons. rel. to struct. 8=33884
rel. to muonic atoms x-ray spectra, heavily deformed nuclei dynamics 8=34192
neutron distrib. 8=33873
odd-odd, residual n-p interact. and quasiparticle random-phase approx. 8=42791
rel. to structure, electrons elastic, inelastic and quasi-elastic scatt. 8=33982
shapes obs. 8=33860
structure and forces, 800 MeV p beam appls. 8=33512
structure, 100-600 MeV, from reactions initiated by particles 8=47209
structure rel. to atomic spectra, electronic and μ- and π-mesic, h. f. s. and isotope shifts 8=29260
structure, research at CERN 8=29261
structure, Schrödinger eqn. validity and high energy expts. appls. 8=29268
surface neutron richness deduced from $\pi \cdot N$ at 17.2 GeV/c 8=42535
velocity-dependent potentials, scatt. props. rel. to IS state 8=24651
velocity-dependent potl., Hamiltonian operator 8=42780
Ag, surface n excess, K^- capture obs. 8=34022-3
Bi^{209}, muonic, hyperfine structure rel. to nuclear magnetism distrib. 8=33940
Br, surface n excess, K^- capture obs. 8=34022-3
Ca^{40} charge distrib., e scatt. obs., 750 MeV 8=29304
$Ca^{40,48}$, charge density distrib., shell model 8=25120
Cd^{114}, 9.0 MeV γ ang. distrib. asymmetry, following polarized n capture 8=33921
$Er^{164,166,167,168,170}$, neutron resonance obs. 8=25153
Eu^{155}, polarization in metallic Sm, from anisotropy of γ-quanta accompanying decay 8=38388
H^3 form factors and interactions 8=42825
He, structure, p-He scatt. angular distrib., 1 GeV 8=33845
In^{115}, possibility of α-clustering on surface 8=25249
Li^6, residual two-body N-N interact. rel. to wave function and harmonic oscillator 8=25094
Li^8 evaporation in 10.1 GeV/c K^- + Ag and K^- + Br nuclei 8=29488
O^{16}, ground state calc. using Hartree-Fock and realistic N-N interacts. 8=25063
Pb^{208}, radius of neutron distrib. calc. method 8=33937
Sn^{119m} Mössbauer source γ quanta correl. props. 8=37923
U^{235}, $K_o + 2$ and $K_o - 2\gamma$ vibrational bands 8=43105
electric moment
See also Molecules/nuclear coupling.
ethylsulphate, e.p.r. obs. for nuclear quadrupole moments of $Tb^{157,158,160}$ 8=42907
first 2^+ states of even nuclei, quadrupole moment calc. 8=25090
hexadecapole interaction, comment on magnitude 8=47224
hexadecapole moment effects in multiple Coulomb excitation 8=42877
hexadecapole-phonon interaction 8=47225
quadrupole, deformed even-even and odd nuclei, $148 \leqslant A \leqslant 192$ 8=29288
quadrupole effective charge, Pauli principle effect 8=33892
quadrupole for 1p shell nuclei, Hartree-Fock and Hartree-Fock-Bogolyubov calcs. 8=33868
quadrupole in pairing-plus-quadrupole model 8=25055
quadrupole, meas. by reorientation effect, correction 8=25091
quadrupole, rotator model, rotation particle coupling effects in light nuclei 8=25050
quadrupole transition rates, seniority four → - two states, comparison with phonon states 8=42822
Ca^{44}, quadrupole, from decay of second 2^+ state 8=38368
$Cd^{110, 112, 114, 116}$ quadrupole of spherical even-even nuclei 8=38376
Co isotopes, treated as p hole coupled to quadrupole vibr. of Ni isotopes 8=25129
Co^{59} low levels, quadrupole moment and h. f. s. 8=38664
Cs^{134} quadrupole moment obs. 8=25145
Dy^{161}, 74.5 keV level, meas. using Mossbauer effect 8=25150
$Eu^{151,153}$, quadrupole Eu II spectrum obs. 8=47495
Gd^{155}, 86.5 and 105.3-KeV states, obs. 8=42906
$Gd^{155,157}$, ratio of quadrupole moments 8=33930

Nucleus—contd
electric moment—contd
He^3, meas. with supercond. mag. shield 8=29000
K^{40}, quadrupole moment from resonance radiation obs. 8=38365
Ni^{61} low levels, quadrupole moment and h. f. s. 8=38677
Np^{37}, quadrupole moments ratio for isomer and ground states 8=33945
O^{17}, quadrupole, for det. of effective change in O^{18} 8=38359
Os^{189} quadrupole moment obs. 8=25155
Pb^{208}, 3-state static quadrupole moment calc. 8=47265
$Pd^{104, 106, 108, 110}$ quadrupole of spherical even-even nuclei 8=38376
$Pt^{194,196,198}$ first 2^+ states static quadrupole moments 8=38393
$Rb^{85,87}$ quadrupole, from optical double resonance obs. 8=34151
$Re^{185,187}$, ratio of quadrupole moments 8=47263
$Ru^{98, 100, 102}$ quadrupole of spherical even-even nuclei 8=38376
Sc^4 γ-γ cascade rel. to quadrupole interaction in $BaTiO_3$ 8=42868
$Tb^{157,158,160}$, quadrupole, from e.p.r. expt. on yttrium ethylsulphate 8=42907
$Te^{122, 124, 126, 128, 130}$ quadrupole of spherical even-even nuclei 8=38376
$W^{182,184,186}$, quadrupole, first excited states obs. 8=42914
energy levels
See also Radioactivity/decay schemes.
A = 11-12, reviews 8=42799
$A \leqslant 61$ binding energy systematics of excited states 8=42798
analogues in s-d shell, M1 transitions obs. 8=25079
closed shell nucleus, validity of random phase approx. for pairing vibrations 8=25104
collective, of even-even spherical nuclei 8=42807
collective states, coupling with particle and hole states, perturbation series approximation 8=38356
compound, excited by slow n, level density 8=38333
$(1g_{9/2})^2_{8+}$ configuration from $Cr^{52}(d, d)$, $E_\alpha = 50$ MeV 8=38372
$(1g_{9/2})^2_{8+}$ configuration from $Fe^{54,56}(\alpha, d)$, $E_\alpha = 50$ MeV 8=38372
$(1g_{9/2})^2_{8+}$ configuration from $Ni^{58,60,62}(\alpha, d)$, $E_\alpha = 50$ MeV 8=38372
$(1g_{9/2})^2_{8+}$ configuration from $Zn^{64,66,68}(\alpha, d)$, $E_\alpha = 50$ MeV 8=38372
Coulomb displacement energies in $1f_{7/2}$ shell 8=38336
deformability, shell and liquid-drop models 8=38318
deformation, shell corrections to liquid drop model 8=38308
deformed even-even nuclei semiempirical mass formula 8=38314
deformed nuclei, spin-quadrupole interaction excited collective states 8=38329
deformed odd nuclei, single-particle orbits $\Delta N = 2$ mixing 8=29270
deformed, pairing model calc. of energy gap and mass differences 8=25060
deformed, reduced distances between levels of some isotopes, isobars and isotones 8=38334
deformed, single-particle states, calcs. accuracy 8=33879
density at excitation energy of 20 MeV 8=42811
density from n and p resonances 8=25075
density of states, effect of Fermi-level occupation 8=47218
density of state function for continuum states 8=25073
density parameter checked in various (n, p), (n, α) and (n, 2n) reactions 8=25081
density, superconductivity effects in Co and In 8=25074
from deuteron scatt. 52 MeV, DWBA with collective model 8=42837
directional correlations perturbed, resonance effects 8=47219
Ejiri plot, comments and criticisms 8=47213
e. m. interaction operators and nucleon-nucleon potentials 8=29278
EO/E2 mixing ratio, odd-mass deformed nuclei beta vibration states transition 8=47217
E2 transitions 8=42823
E2 transitions, $150 < A < 190$, Davydov model 8=25084
excitation by high energy particles 8=33882
excitation by (n, 2n) reaction optical model of absorpt., Fermi gas model of nuclear density 8=43035
g factor and lifetimes meas. by magnetized ferromag. foil 8=38401
first 2^+ states of even nuclei, quadrupole moment calc. 8=25090
fission fragments, even-even n-rich, deformabilities 8=38323
γ-γ directional correl., computer analysis 8=24703
γ-ray angular distrib., isotropic, interpretation for final state of spin 3/2 8=33887
ground state isospin mixing, monopole polarizability and Fermi β-decays 8=25076
Hartree-Fock-Bogoliubov projected spectra 8=42813
Hartree-Fock calc., truncation effects 8=29282
Hartree-Fock state stability condition against four-body correlations 8=38341
heavy-ion research, Dubna, review 8=38521

Nucleus—contd
- **energy levels**—contd
  - intermediate level from Os^{180} decay 8=47298
  - intermediate structure, shell → two channel model calc. 8=38332
  - isobaric analog resonance, fine structure 8=38330
  - isobaric analogue states in (p. n) at 30 and 50 MeV, isospin dependence of optical model 8=43001
  - isobaric analogue states, Coulomb displacement energies 8=29286
  - isobaric analogues, p scatt. and (d, p) excitation, spectroscopic factors 8=38321
  - isobaric analogue resonances in (p, n) or 94 MeV 8=42848
  - isomer shift as a function of pressure for nucleus in solid 8=33925
  - isotope shift calc. using density depend N-N interaction 8=42802
  - isomer shift in muonic atoms, even-even nuclei 8=42809
  - J-dependence for strong $l_n = 3$ transitions in (d, p) reactions 8=25072
  - K- and L-electrons, shell corrections from stopping power formulae 8=42981
  - $K = 2$ states, test to discriminate Bohr-Mottelson and Davydov-Filippov models 8=47226
  - L/K orbital electron capture ratio, theory and expt. compared for $13 \leqslant Z \leqslant 37$ 8=25077
  - lifetime and mixing-ratio of transition, effect on ang. distrib. of photon scatt. 8=33891
  - light nuclei, ang. momentum projection 8=29283
  - low Z s resons., diffuse boundary pot. well model 8=29276
  - magic and spherical nuclei far from stability 8=38328
  - monopole and quadrupole excitations from inelastic e scatt. 8=42993
  - μ-Sm^{152}, 1st rot. transition, energy rel. to isomer shift, obs. 8=29332
  - multiple Coulomb excitation effects 8=29281
  - multipolarity determ. in e pair internal conversion 8=25086
  - 0f-1p shell nuclei, reaction matrix elements 8=38306
  - n, p, single particle states similarity at same mass number 8=42815
  - octupole vibrations in deformed heavy nuclei, energies calc. 8=42819
  - odd A deformed, rel. to collective modes coupling 8=29285
  - odd-mass deformed nuclei N-forbidden β-transitions 8=33956
  - odd-mass nuclei, resonance fluorescence and absorpt. meas. of transition strengths, 0.8-3.0 MeV 8=42875
  - odd-odd deformed, vibrational levels from α decay 8=47277
  - one-phonon states excited by deuteron disintegration reactions 8=38499
  - $18 \leqslant A \leqslant 22$ s-d shell nuclei, and B(E2) values, shell-model calc. 8=33880
  - pairing-force model from self-consistent theory 8=42814
  - particle-hole calcs. applic. to Pb^{208} of new method 8=42922
  - projection method accuracy to obtain ang. momentum states from deformed Hartree-Fock states 8=33881
  - protons, polarized, nuclear interactions 8=47313
  - quadrupole and octupole deformations, $218 \leqslant A \leqslant 232$ 8=38326
  - quadrupole moment, deformed even-even and odd nuclei, $148 \leqslant A \leqslant 192$ 8=29288
  - quasi-particle coupling to pair vibrations 8=33885
  - rare-earth, actinide and super-heavy nuclei deformabilities 8=38325
  - rare earth nuclei E2 transitions conversion electron particle parameters 8=47257
  - rare earths, one-particle protonic states 8=47253
  - rare earths, deformed, level density obs. 8=29328
  - rel. to reactor theory, reson. spacings, synthetic kernels calc. 8=38342
  - resonance, giant, multipole, coupling to surface quadrupole oscills. in hydrodynamic model 8=33876
  - resonance multiplets splitting, perturbation of shell model resonance energies 8=38331
  - from resonant absorpt. and fluorescence exam. 7=47222
  - resonant states inner prod. and shell-model appl. 8=42816
  - review of nuclear spectroscopy 8=46687
  - rot. band, ground state, cranking model for gyromagnetic ratio calc. 8=25088
  - rotational, centrifugal stretching calc. 8=38345
  - shell model, orbital interactions submatrices in irreducible form 8=47215
  - s-d shell nuclei, configuration mixing model 8=33878
  - sd shell, $T = 0$ effective interaction 8=38335
  - single closed shell and closed shell with hole, Ge(Li) detector study 8=47251
  - s, p, d-wave strength functions, determ. from neutron total cross-sections 8=25232
  - spectral distortion by final-state Coulomb interactions 8=33888
  - spectroscopic factors from DWBA and $\langle\gamma^2\rangle$ 8=33874
  - spectroscopy and structure, conference, Khar'kov 1967 8=38294
  - spectroscopy, in-beam, heavy-ion reactions appls. 8=38338
  - shell (ds) model for odd nuclei using U_3 8=25058
  - single-closed-shell nuclei, quasiparticle model applied to 1^+ levels 8=38340

Nucleus—contd
- **energy levels**—contd
  - single-particle orbitals parity-mixing and coeffs. of fractional parentage 8=29263
  - spectral averages in transfer reactions involving targets with single active shell 8=38339
  - spherical nuclei, $90 \leqslant A \leqslant 150$, $186 \leqslant A \leqslant 206$, doubly even, 2^+, 3^- states 8=38337
  - spins and parities rel. to γ spectra formed by n caputre meas. 8=42808
  - super-heavy nuclei, rel. to n capture and nucleosynthesis, mass formula 8=38324
  - s-wave virtual states and resonances in R- and S-matrix terms, distinction 8=42803
  - transition rates, rotator model, rotation particle coupling effects in light nuclei 8=25050
  - 2-level system interaction by pairing forces, boson expansion method 8=25046
  - $20 \leqslant A \leqslant 28$, shell model calc. 8=33877
  - $20 \leqslant Z \leqslant 28$, $N = 30$ nuclei, N-N effective interactions calc. 8=29279
  - $24 \leqslant Z \leqslant 30$, n time-of-flight spectroscopy, obs. 8=29308
  - $T = 1$ effective interaction in s-d shell 8=47212
  - two nucleons plus closed shells, 3-body model 8=29277
  - vibrational, core polarization and quasiparticle theories with realistic N-N forces 8=42818
  - vibrational, multipole sum rules appls. 8=25078
  - vibrational, quasiparticle Tamm-Dancoff microscopic theories for 2N transfer reactions 8=29419
  - vibrational, spectroscopic factors for two-nuclear transfer reaction, using QTD and QSTD methods calc. 8=42817
  - vibrations, octupole, $K = 1, 2, 3$, soln. of Schrodinger eqn. in Bohr-Mottelson hydrodynamic model 8=25082
  - Ag^{109}, from Cd^{109} decay internal conversion spectrum, 88 keV transition obs. 8=38421
  - Ag^{109}, spin and parity and structure 8=47287
  - Ag^{110}, conversion electrons and transition multipolarities 8=33920
  - Al^{25}, $E_x = 4,507$ KeV, unbound state 8=47238
  - Al^{25,26} from Mg^{24,25}(d, n), 5.5 or 6 MeV DWBA analysis, Nilsson model agreement for Al^{26}, but not Al^{25} 8=25113
  - Al^{26}, decay modes of closely spaced levels, spin and parity assigned 2.07 MeV 8=42851
  - Al^{26}, lifetimes and decay props from Mg^{26}(p, n)Al^{26} 8=33902
  - Al^{27} and Al^{28} mean energy level width at high excitation energy 8=47237
  - Al^{27}, branching ratios obs. for bound states 8=42850
  - Al^{27} decay scheme, from Mg^{24}(He^3, p) up to 4 MeV, spin assignments 8=42849
  - Al^{27}, 4509 keV, spin value 8=33904
  - Al^{27}, from Mg^{26}(p, γ), 9.991 MeV and 10.165 MeV widths 8=33903
  - Al^{27}, from n inelastic scatt., 1-4 MeV 8=29459
  - Al^{27}, lifetime obs. 8=25114
  - Al^{27}, n scatt. to 2, 980, 3002 keV levels 8=43036
  - Al^{27} spectroscopic factors, from Si^{28}(d, He^3) 8=43062
  - Al^{27}, 3.00 MeV level, from Mg^{24}(α, pγ)Al^{27} obs. 8=38363
  - Am^{241}, excited levels of Np^{237} 8=33946
  - Ar^{35}, from Ar^{36}(p, d) in 2s–1d shell, obs. 8=43023
  - Ar^{36} in Cl^{35}(p, α_0)S^{32}, 830-2930 keV 8=25230
  - Ar^{37}(from K^{39}(d, α), spin assignments 8=47349
  - Ar^{38} from p-Cl^{37} scatt., 1-18 MeV, analogue states of Cl^{38} 8=25118
  - Ar^{41}, analogues in Ar^{40} p reactions 8=43025
  - As^{71} from Ge^{70}(He^3, d) 15 MeV 8=43093
  - As^{75} from γ-γ e$^-$-γ ang. correl. studies on Se^{75} 8=42949
  - As^{75} from Se^{75} decay, gamma gamma angular correlation 8=33916
  - As^{75}, from (p, 2p) at 156 MeV 8=33993
  - As^{75}, multipolarity mixing ratios determ. 8=25133
  - As^{75}(p, 2p) obs., 156 MeV 8=33914
  - As^{75}, 280 keV, half-life and M1 hindrance factor, obs. 8=29317
  - As^{76} from As^{75}(n, γ) obs. 8=34010
  - As^{76}, odd-odd nuclei excited by radiative capture of neutrons 8=42898
  - As^{77}, from Ge^{77} decay 8=29366
  - At^{215,216}, Fr^{219,220} α-decay spectra obs. 8=33943
  - At^{217}, from Fr^{221} decay study 8=25162
  - Au^{199} half-life of 55 keV M2 transition 8=42920
  - Au^{199,197,195,193} from decay of Pt and Hg isotopes 8=42970
  - B^{10}, from B^{11}(He^3, α), γ decay obs. 8=42834
  - B^{10}, mixing ratio of 2.15 to 0.72 MeV transitions obs. 8=33896
  - B^{11}, from N^{14}(n, α) at 14.1 MeV 8=43041
  - B^{11} spectroscopic factors extraction, from B^{10}(N^{14}, N^{13}) 8=43101
  - B^{11} transitions obs. in N^{14}(n, α)B^{11} 8=25239
  - B^{11}, γ-ray multipole mixing ratio for 6.76, 8.92 MeV states obs. from B^{10}(d, pγ)B^{11} 8=34030
  - B^{11}, 8.92 MeV → 0 transition, multipolarity 8=29291
  - B^{12}, first excited state, 1^+ or 2^+ from B^{11}(d, p)B^{12} 8=34036
  - Ba^{125,127} isomerism and nuclear deformation 8=42900
  - Ba^{132} obs from Cs^{132} decay 8=42899
  - Ba^{134}, even-even nuclei, and spins, comparison with theory 8=42879

- **Nucleus**—contd
  - **energy levels**—contd
    - Ba^{139}, p polarization in Ba^{138}(p, p) 8=42901
    - Be, ground state width calc. from $\alpha-\alpha$ scatt. 8=33748
    - Be^{6} from Li^{6}(p, n), ang. distrib. of n obs. 8=47319
    - Be^{8}, evidence for 0^{+} excited states 8=38354
    - Be^{8} from Li^{7}(p, γ)Be^{8}, 1.4-2.5 MeV 8=47320
    - Be^{8} spectral distortion by final-state Coulomb interactions 8=33888
    - Be^{9} from B^{10}(t, α) at 12.9 MeV 8=42833
    - Be^{9}, from Li^{7}(He^{3}, p), n decay branching ratios 8=29358
    - Be^{9} lowest even and odd parity state projected Hartree-Fock calc. 8=33895
    - Be^{9}, mag. transitions by e scatt. at 180° 8=25096
    - Be^{9} threshold states obs. in p scatt. near threshold for Be^{9}(p, n)B^{9} 8=43014
    - Be^{9}, unreported levels obs. in Li^{6}(He^{3}, p)Be^{9} 8=25098
    - Bi^{208} from Bi^{209} (d, t), neutron-hole multiplets 8=38398
    - Bi^{208} from Pb^{207} (He^{3}, d), proton-particle multiplets 8=38398
    - Bi^{208} isobaric analogue states nucleon widths 8=38373
    - Bi^{209}, from n inelastic scatt., 1-4 MeV 8=29459
    - Bi^{209}, from Pb^{208}(He^{3}, d), level struct. obs. 8=42925
    - Bi^{209} single-particle analogue resonances total width 8=33941
    - Bi^{211} from Pb$^{211}\beta$ decay, γ-ray spectrum obs. 8=47267
    - Bi^{211}, spins and multipole mixing ratios 8=47268
    - Bi^{211} spin and parity, multipolar mixing ratios obs. 8=47266
    - C^{11} from Be^{9}(He^{3}, n) 8=43080
    - C^{11}, 6.49 MeV $\rightarrow$ 0 transition, multipolarity 8=29291
    - C^{12}, elec. levels and transition rates 8=29293
    - C^{12}, from B^{n}(d, n), 1.6-3.3 MeV 8=38502
    - C^{12} giant-dipole state, isospin mixing, energy depend. 8=29292
    - C^{12} giant resonance inelastic electron scatt. cross section 8=47310
    - C^{12}, (Li^{7}, t) and (Li^{6}, α) excited, rel. to α- and d-cluster transfer, 26 MeV 8=38524
    - C^{12}, 1-particle 1-hole model, state calcs. 8=29296
    - C^{12}, spectroscopic factors from B^{11}(τ, d)C^{12} 8=47229
    - C^{12}, O^{+} and 2^{+} states spectroscopic factors from C^{13}(d, t) 8=47347
    - C^{13}, from C^{12}(n, γ), 2 γ-rays obs. 8=38484
    - C^{14}, core deformation in matrix element calc. for O^{18} 8=38359
    - C^{14}, p capture and scatt. effects 8=43004
    - Ca, HF technique applied to calc. energy spacings and e.m. props. 8=25085
    - Ca^{39}, from Ca^{40}(He^{3}, dγ), low level struct. 8=25119
    - Ca^{39}, from Ca^{40}(pd,) in 2s-1d shell, obs. 8=43023
    - Ca^{40}, compared to 1d-2s shells of nonmagic nuclei using Ca^{40}(γ, p) obs. 8=42989
    - Ca^{40} ground states, core excitation components 8=33909
    - Ca^{40} Hartree-Fock potential scatt. 8=25106
    - Ca^{40}, high-precision obs. 8=42861
    - Ca^{40} odd parity states 8=38367
    - Ca^{40} odd-parity states with realistic Tabakin interaction and MSDI 8=42866
    - Ca^{40}, O^{+} state monopole matrix element 8=47234
    - Ca^{40}, (p, p$'$) and K^{39}(He^{3}, d)excited, γ decay rel. to nature, obs. 8=33910
    - Ca^{41} spectroscopic factor at 10 and 12 MeV calc. 8=33871
    - Ca^{41} spectroscopic factors extraction, from Ca^{40} (N^{14}, N^{13}) 8=43101
    - Ca^{41}, 3.209, 3.623 and 3.740 MeV, (d, pγ) angular correl. obs. 8=29303
    - Ca^{41,43}, from Ca^{42,44}(p, d) ground state wave function Ca^{42,44} obs. 26.5 MeV 8=38475
    - Ca^{42}, energy spectrum and transition rates explained 8=42865
    - Ca^{42} from K^{41} (He^{3}, d) reaction, particle hole states up to 5.79 MeV obs. 8=47243
    - Ca$^{42-50}$, (t, p) excited, Ca^{48} O^{+} states rel. to shell model, obs. 8=33938
    - Ca^{43}, forbidden M1 transitions 8=42864
    - Ca^{43}, γ spectra obs. 8=43027
    - Ca^{43,45} spectroscopic factor at 10 MeV calc. 8=33871
    - Ca^{44}, excitation energies and spin assignments 8=47317
    - Ca^{44}, second 2^{+} state, decay obs. 8=38368
    - Ca^{45}, from Ca^{44}(n, γ) thermal energies 8=38487
    - Ca^{45} lifetimes, branching ratios multipole mixing ratio obs. in Ca^{44}(d, pγ)Ca^{45} 8=38366
    - Ca^{48}, from Ca^{48}(p, p$'$), e. m. de-excitation of 4.51 MeV level 8=47242
    - Ca^{50} J$^{\pi}$ = 1^{+} assignment to 1848 KeV level 8=42943
    - Cd^{107} analogue resonances from (p, p) and (p. p$'$) 8=33922
    - Cd^{107} $\rightarrow$ Cd^{106} 2^{+} state analogue resonances from (p, p) and (p, p$'$) 8=33922
    - Cd^{110}, from Ag^{110m} decay 8=47288
    - Cd^{114}, multiple Coulomb excitation, electric hexadecapole moment 8=42877
    - Ce^{138}, decay of 2.2 hr. Pr^{138}, reinvestigation 8=29368
    - Ce^{140} from La^{140} decay, γ energy and intensity obs. 8=33963
    - Ce^{140}, 3^{+} $\rightarrow$ 4^{+} $\rightarrow$ 2^{+} cascade, intermediate state half-life, obs. 8=29329
    - Ce^{141}, p polarization in Ce^{140}(p, p) 8=42901
    - Ce^{142} from Pr^{142} decay obs. 8=38432
    - Cf^{251} high-lying band obs. 8=42974

- **Nucleus**—contd
  - **energy levels**—contd
    - Cl^{36}, from Cl^{37}(He^{3}, α), S^{36} ground state analogue 8=29516
    - Cl^{36}, time reversal invariance of nuclear forces 8=42856
    - Cm^{245} high-lying band obs. 8=42974
    - Co density, superconductivity effects in 8=25074
    - Co isotope as p hole coupled quadrupole vibr. of even-mass Ni nucleus 8=25128
    - Co^{56}, Fe^{54}(He^{3}, p) excited, E$_{He}{}^{3}$ = 18 MeV 8=29519
    - Co^{57}, N-N effective interactions calc. 8=29279
    - Co^{57,59} first excited states, lifetimes and g-factors, obs. 8=29314
    - Co^{58}, and e. m. decay branching ratios, Fe^{58}(p, n) obs. 8=29313
    - Co^{58M}, spectra, conversion electron, γ, X for isomeric transitions 8=33966
    - Cr^{50} low levels, spin assignment from pγ ang. correl. 8=29309
    - Cr^{50,51}, struct. calc. from (p, p$'$)and (d, p) obs. 8=42874
    - Cr^{52}, from n inelastic scatt., 1-4 MeV 8=29459
    - Cr^{52} obs. in p-V^{51} scatt., 4.005-5.515 KeV 8=25224
    - Cr^{56}, shell model calc. 8=25128
    - Cs^{128} from Ba^{128} decay obs. 8=42956
    - Cs^{131}, from Ba ^{131} e capture decay, new-transitions 8=38429
    - Cs^{133}, 81 KeV level, $\gamma\gamma$ ang. correl. 8=38384
    - Cu, HF technique applied to calc. energy spacings and e.m. props. 8=25085
    - Cu^{58,60,62} 1$f_{5/2}$-2p spectra and binding energies, configuration-mixing calc. 8=42880
    - Cu^{59,61}, from Ni^{58,60}(He^{3}, d), level struct. determ. 8=42882
    - Cu^{59,63} from Ni^{58,62}(p, $\gamma\gamma$) reactions 8=29446
    - Cu^{62} from 9.3-h Zn^{62} decay, spin and parity 8=42945
    - Cu^{63,65} γ-ray de-excitation, Cu^{63,65}(p, p$'\gamma$) obs. 8=43012
    - Cu^{64,66}, from Cu^{63,65}(n, γ), thermal-n, low-lying levels structure 8=42881
    - Cu^{65}, from Zn^{65} decay, obs. 8=29365
    - Dy, levels investigated by 12 MeV d scatt., collective vibr. states identified 8=25149
    - Dy^{154} rot. and vibr. bands from β-decay of Ho^{154} and the reaction La^{139}(F^{19}, 4n)Dy^{154} 8=42908
    - Dy^{159} from 115μs Dy^{159m} decay obs. 8=38436
    - Dy^{161}, 74.5 keV, elect., mag. moments using Mossbauer effect obs. 8=25150
    - Er^{165} and cascade factors, Tm^{165} decay scheme obs. 8=29374
    - Er^{166}, energy shift of γ-rays in presence of μ in 1s state 8=42902
    - Er^{167,169,171}, from (d, p) reactions 8=25152
    - Er^{168} spins and parities rel. to γ spectra formed by n capture meas. 8=42808
    - Er^{168} from Tm^{168} decay 8=25191
    - Er^{170}, 79 keV level, pulsed-beam lifetime meas. 8=33927
    - Eu^{152}, from Eu^{151}(n, γ), lower level scheme 8=47255
    - Eu^{153}, isomer shift of 83.4 keV rot. transition 8=25147
    - Eu^{155}, internal conversion and e-γ coincidence, obs. 8=29371
    - Eu^{155} scheme from Sm^{155}(β^{-}) decay 8=47293
    - Eu^{155}, Sm^{155} $\rightarrow$ Eu^{155} β and γ spectra obs. 8=29334
    - for F^{16} from O^{16}(d, d)O^{16}, 1.0 to 2.5 MeV range 8=47235
    - F^{19}, 8.795 MeV state, interpretation as T = $^{3}\!/_{2}$ and 25$^{1}\!/_{2}{}^{+}$ state 8=33901
    - F^{19} low-lying $^{1}\!/_{2}{}^{-}$ state, four-body description 8=42783
    - F^{19}, Mössbauer levels Coulomb excitation in ions deceleration, calc. 8=42878
    - F^{19}, positive parity states rot. particle coupling 8=29297
    - F^{19} 2.79 MeV state mean lifetime using Doppler shift attenuation method 8=42844
    - F^{19,21}, and e. m. props. in Nilsson's model 8=47236
    - F^{20}, from, F^{19}(n, γ) 73 γ spectral lines obs. 8=38484
    - F^{20} scheme from F^{18,19} level energies obs. 8=38335
    - F^{27}, Mössbauer levels Coulomb excitation in ions deceleration, calc. 8=42878
    - Fe^{53}, discovery of 3.04 MeV isomeric state 8=38465
    - Fe^{53}, rel. to N-N effective interactions in 1f$_{7/2}$ shell 8=29312
    - Fe^{55} and Co^{55} analogs., Fe^{54}(α, t) and (α, He^{3}) obs. 8=29311
    - Fe^{56}, from Co^{56} and Mn^{56} decay 8=29364
    - Fe^{56}, from n inelastic scatt., 1-4 MeV 8=29459
    - Fe^{56}, multiple Coulomb excitation, electric hexadecapole moment 8=42877
    - Fe^{56}, obs. from inelastic d scatt. 8=29310
    - Fe^{56}, rel. to intermediate structure, n total cross section, 0.5-1.2 MeV 8=29469
    - Fe^{57}, γ-decay scheme under 2 MeV, from thermal n capture 8=47246
    - Fe^{58}, branching ratio for 2^{+} $\rightarrow$ 2^{+} transition 8=29405
    - Fe^{58}, even-even nuclei, and spins, comparison with theory 8=42879
    - Fe^{58}, shell model calc. 8=25128
    - Fr^{219,220}, Ac^{223,224} α-decay spectra obs. 8=33943
    - Fr^{221}, from Ac^{225} α-disint., mag. spectrography 8=25163
    - Ga^{69} resonance fluorescence, E = 1107, 872, 574 keV 8=25132
    - Ga^{70,72}, low-lying, slow n capture γ-spectra obs. 8=29316
    - Ga^{72} from Zn^{72} decay obs. 8=25177
    - Gd, n induced levels spacing, obs. 8=29347
    - Gd^{152,154} E2 transition conversion electron particle parameters 8=47257
    - Gd^{153} obs. from Tb^{153} electron capture decay 8=42903

Gd^{154}, energy shift of γ-rays in presence of μ in 1s state 8=42902
Gd^{154}, from decay of E^{154}, EO/E2 transitions and electric monopole strengths calc. 8=42904
Gd^{155}, 86.5 and 105.3-KeV states, spins and moments 8=42906
Gd^{155}, intensities of γ-transitions to ground and first excited state in 23 resonances of Gd^{155}(n, γ) 8=38389
Gd^{155,157}, non-rot. states elect. hyperfine interaction determ. by Mossbauer technique 8=33930
Gd^{156} K = 2 state rel. to asymmetric-rotor model 8=47226
Gd^{159}, 26 ns isomeric state at 68 keV, decay obs. 8=29335
Gd^{156}, 289 and 1513 keV, half-lives obs. 8=25148
Gd^{160}, 75 keV level, pulsed-beam lifetime meas. 8=33927
Ge^{71}, 175 keV state, g-factor 8=47248
Ge^{74}, from As^{74} decay 8=42947
H^{4}, widths of two levels evidence for third 8=38351
He^{3}, excited level aligning and orientating method 8=42828
He^{4}, ground state, single-particle model calc. 8=29228
He^{4} states search using H^{2}(d, d) and H^{2}(d, p)H^{3} at 3-11 MeV 8=38353
He^{4} T = 1 states, single-pole dominance in transition mechanism, from Li^{6}(π^+, pp) obs. 8=42831
He^{4}, O^{+} state obs. in 150-400 MeV e scatt. 8=24724
He^{6}, excited bound states, deformed orbits calc. 8=25093
He^{6}, 1.71 MeV (2^{+}) state, three body decay 8=25021
Hf^{177}, 250 KeV level rot. and g factor 8=38390
Hf^{177,179,181}, from (d, p) and d, t), spectroscopy 8=42911
Hf^{178} 2^{+} β-vibrational state E2 + M1 decay 8=33934
Hf^{178}, long-lived isomeric state at ~2.5 MeV 8=42966
Hf^{179}, decay of isomeric state 8=47261
Hf^{181} analogue states, from p + Hf^{180} scatt. obs. 8=33933
Hg$^{192, 194, 196, 198}$, γ-spectra obs. 8=38394
Hg^{199}, L$_{\pi}$ electron-γ correl. giving mixing ratio for 50 keV transition 8=25157
Hg^{200}, from Au^{200} β decay, obs. 8=42969
Hg^{200}, M1 and E2 in 2$_1^+$, mixing ratio 8=42921
Ho^{165}, orientation effect on total n cross section 2-135 MeV 8=25151
I isotopes, lifetimes and g meas. by Xe magnetized ferromag. foil 8=38401
I$^{127, 129, 131}$ from (He^{3}, d), orbital angular-momentum transfer and spectroscopic factors, 25 MeV 8=42893
I^{128}, odd-odd nuclei excited by radiative capture of neutrons 8=42898
I^{133} from decay of Te isomers 8=25186
I^{133}, from Te^{133g,m} β decay, obs. 8=42897
In density, superconductivity effects in 8=25074
In^{111} from decay of 35 min Sn^{111} 8=38423
In^{113}, 393 keV transition, K-conversion coeff. 8=33923
In^{115}, de-excitation γ-spectra rel. to vibr. states, 900-1600 keV 8=29323
In^{117}, from Cd^{117} → In^{117} 8=42889
In^{117}, 748, 659, 587 keV, lifetime obs. 8=25141
Ir^{191}, 129 keV level, magnetic moment obtained from γ-scatt. 8=47303
Ir$^{192\mathrm{M}}{}_{1}$, spectra, conversion electron, γ, X for isomeric transitions 8=33966
Ir^{193} absolute transition probs. and lifetime meas. obs. 8=42916
Ir^{193}, core excitation 8=42918
Ir^{193}, E2-M1 mixing ratio of 73 KeV level, no evidence for T-nonconservation 8=25156
Ir^{193} spin and conversion coeff. 8=38439
Ir^{194} obs. 8=42919
K^{37}, from reactions on Ca and Ar, widths and positions 8=42858
K^{39*} collective core excitation, from K^{39}(d, d$'$) obs. 8=33908
K^{40}, from Ar^{40}(He^{3}, t), 2-particle 2-hole states 8=42860
K^{40} Mossbauer meas. 8=42859
K^{41}, properties of several states near 8.9 MeV 8=47241
K^{47} from Ca^{48}(d, He^{3}), 34.4 MeV 8=25268
Kr^{81}, from Rb^{81} decay obs. 8=25180
La^{140} energy spectrum description in terms of unified model 8=38385
Li^{6} J = B^{+}, T = O from d—He^{4} elastic scatt., Ed = 0.2-10.3 MeV 8=43052
Li^{6}, T = o, generation of lowest as collective band 8=33894
Li^{6,7}, (Li^{7}, t) and (Li^{6}, α)excited, rel. to α- and d-cluster transfer. 26 MeV 8=38524
Li^{6,7}, N pair distrib. in ground state from π absorpt. 8=25095
Li^{7}, resonances obs. in He^{4}-H^{3} 8=24937
Lu^{170}, intrinsic and collective, Hf^{170} e capture decay obs. 8=29340
Lu^{170,172} E1 transitions, Nilsson model 8=42913
Lu^{175}, dipole trans. effects in internal conversion 8=33932
Mg^{23}, from Mg^{24}(p, d) in 2s-1d shell, obs. 8=43023
Mg^{23} J$^{\pi}$ = $\frac{1}{2}^{+}$ states branching ratio of e.m. decay, Ne^{22}(He^{3}, dγ) obs. 8=42847
Mg^{24}, axial and triaxial deformed Hartree-Fock solns. 8=25111
Mg^{24} dipole transitions, isospin selection rule 8=29300
Mg^{24}, excited by 100-260 MeV e, obs. 8=47311

Nucleus—contd
energy levels—contd
Mg^{24}, from C^{12}(O^{16}, $\alpha\gamma$), spin and parity obs. 8=38362
Mg^{24}, from (p, 2p) at 156 MeV 8=33993
Mg^{24} giant dipole resonance, from Na^{23}(p, γ), 4-12.4 MeV 8=43022
Mg^{24,26}, Doppler-shift lifetime meas. 8=25110
Mg^{25} excited states, branching and mixing ratios 8=29301
Mg^{26} branching ratios of transitions obs. after Mg^{25}(d, pγ)Mg^{26}, Na^{23}(α, p)Mg^{26} 8=25112
Mg^{26}, from Al^{26} β-decay, T = 2 component in ground state 8=47282
Mg^{26}, lifetimes from p scatt., rot. bands mixed 8=33902
Mn^{53} from Fe^{54}(d, He^{3}), 34.4 MeV 8=25268
Mn^{55}, total n parametric fit, 0.01 ev-50 keV 8=38477
Mo^{92}, n hole states and configuration mixing, 18 MeV(He^{3}, α) obs. 8=29319
Mo^{92}, p levels, 18 MeV (He^{3}, d) obs. 8=33918
Mo^{93} excited states, obs. 8=25139
Mo^{93}, n decay of isobaric analogue resonances 8=29320
Mo^{94} levels, decay from Tc^{94} isomers 8=38374
Mo^{96} from Nb^{96} decay 8=25183
N^{13}, from C^{12}(p, γ), lowest T=$\frac{3}{2}$ state 8=29440
N^{14}, axially deformed single-nucleon Hartree-Fock orbitals 8=42838
N^{14}, deduced from C^{12}(Li^{6}, α), 20 MeV 8=25277
N^{14} first excited state energy rel. to O^{14} Fermi decay 8=33958
N^{14}, from C^{13}(He^{3}, d), first five states 8=43085
N^{14} from (p, α), spin obs. 8=43020
N^{14}, from O^{16}(d, α), isospin allowed 8=29504
N^{14}, spectroscopic and configuration assignments 8=47230
N^{15}, core polarization effects 8=29294
N^{15} doublet at 9.16 MeV, γ decay branching ratios obs. 8=33898
N^{15} from N^{14} (n, γ), prompt γ-ray spectra obs. 9.15 MeV doublet 8=42839
Na^{21}, first excited state, lifetime obs. 8=25107
Na^{23}, from (p, 2p) at 156 MeV 8=33993
Na^{23} J$^{\pi}$ = $\frac{1}{2}^{+}$ states branching ratio of e.m. decay, Ne^{22}(He^{3}, dγ) obs. 8=42847
Na^{24} at 1.5 MeV, from Mg^{26}(d, α)Na^{24} 8=38361
Na^{24}, 0.563 MeV level, γ polarization obs. 8=38485
Nb^{91} analog states elastic proton decay widths, shell-model calc. 8=47250
Nb^{92} analog state from Nb^{93}(p, d) 8=33919
Nb^{94}, levels and configurations, obs. 8=25138
Nc^{20} from Li^{6}(O^{16}, d), ang. distrib. and α widths obs. 8=34048
Nd^{142} from Pr^{142} decay, 508 KeV γ populating level at 2084 KeV obs. 8=38433
Nd^{142} from Pr^{142} decay obs. 8=38432
Nd^{144}, from Nd^{143}(n, γ α), α transition obs. 8=34014
Nd^{144} isotopes, internal pair formation in electric dipole transitions, 1.49, 2.18 MeV 8=47256
Nd^{150}, energy shift of γ-rays in presence of μ in 1s state 8=42902
Nd^{150}, 131 keV level, pulsed-beam lifetime meas. 8=33927
Ne^{18}, from O^{16}(He^{3}, n), and transitions 8=43086
Ne^{20} ground state, weak-coupling width of 1p holes 8=42846
Ne^{20} scheme from F^{18,19} level energies obs. 8=38335
Ne^{21}, first excited state, lifetime obs. 8=25107
Ne^{21}, from Ne^{20}(d, p), obs. 8=29506
Ne^{21,23}, decay schemes, new parity states from thermal neutron capture 8=47329
Ne^{22}, from F^{19}(α, pγ), ang. correl. and lifetime obs. 8=29298
Ne^{22}, from O^{18}(α, γ), e.m. de-excitation of 11.89 and 12.28 MeV levels 8=47240
Ne^{22}, from O^{18}(α, nγ), α, γ_0) and (α, α), 11.7-13.0 MeV 8=42845
Ne^{22}, lifetime of 5.14 MeV state 8=25108
Ne^{28}, configuration mixing model 8=33878
Ni^{56}, from Ni^{58}(p, t), excitation to 8.5 MeV, obs. 8=47247
Ni^{58}, mean lifetimes of 16 2^{+} states obs. 8=25130
Ni^{58}, 4^{+}, mixing coeffs. of one and two-phonon states 8=38444
Ni^{60}, 13 MeV p scatt. obs. 8=25131
Ni^{61}, and lifetimes, Cu^{61} decay obs. 8=29315
Ni^{62,64} from Cu^{63,65}(d, He^{3}), E$_{d}$=34.2 MeV 8=34035
Ni, Cu, Cr^{52}, Fe^{54}, Ti^{50} comparison from p-scatt. 8=29430
Ni isotopes spectra, quasi-particle configuration mixing calc. 8=33913
Ni, 58 $\leqslant$ A $\leqslant$ 64 8=29344
Ni, HF technique applied to calc. energy spacings and e.m. props 8=25085
Ni rel. to Fe^{54}, from polarized p-scatt. 8=29431
Np^{237}, excited levels by α-decay of Am^{214} 8=33946
Np^{237}, n induced resons., obs. 8=29348
O^{+}-O^{+} vibrational excitation, transition matrix elements from muonic X-rays 8=38344
O^{15}, core polarization effects 8=29294
O^{15}, from N^{14}(τ, d) and O^{16}(τ, α), ang. distrib. E$_{\tau}$ = MeV 8=33900
O^{16}, ave. lifetimes 8=47233
O^{16}, elec. levels and transition rates 8=29293
O^{16}, even parity rot. bands, and elec. quadrupole transition rates 8=42841

Nucleus—contd

energy levels—contd

O^{16} excitation energies in C^{12}-α scatt. 8=25270
O^{16} from C^{13}(He^3, $\alpha\gamma_{15\cdot1}$)C^{12} T = 0.1α states on O^{16} obs. 8=42840
O^{16} γ decay, from N^{15}(p, γ), E_p = 0.4-1.9 MeV 8=33899
O^{16} giant-dipole state, isospin mixing, energy depend. 8=29292
O^{16} Hartree-Fock potential scatt. 8=25106
O^{16}, in vicinity of 13 MeV, obs. 8=29295
O^{16}, one particle level calc., using real N-N interaction 8=42827
O^{16}, 1-particle 1-hole model, state calcs. 8=29296
O^{16} structure at high excitation energy from C^{12}(α, α)C^{12} 8=38357
O^{16}, to 14 MeV, inelastic e scatt. obs. 8=47232
O^{16}, O^{+} state monopole matrix element 8=47234
O^{16,17}, Hauser-Feshbach calc. on Li^6 + C^{12} 8=25277
O^{17}, from O^{16}(d, p), spectroscopic factors 8=29505
O^{17}, set of J$^\pi$ and partial-width values from C^{13} α scatt. and C^{13}(α, n)O^{16} 8=25103
O^{18}, γ transitions, calc. using various shell model wave-functions 8=25105
O^{18}, levels deduced from F^{19}(n, d)O^{18}, 14.4 MeV 8=47328
O^{18}, low-lying, cross-sect. calc., matrix elements 8=38359
O^{18} shell model, exponentially velocity-dependent potential 8=42785
O^{18}, 3.63 MeV $\rightarrow$ 0 transition, multipolarity 8=29291
Os$^{182-192}$ even nuclei rel. to N, and deformation, obs. 8=38383
Os^{186,188}, 1$^-$ $\rightarrow$ 2$^+$ transitions in decay of Re^{186,188} 8=38437
Os^{188} K = 2 state rel. to asymmetric-rotor model 8=47226
P^{30} below 5 MeV, obs. 8=25116
P^{31,33} in S^{32,34}(n, d)S^{31,33}, 14 MeV 8=25241
P^{32}, 1.149 MeV level, γ polarization obs. 8=38485
Pa^{231}, L subshell fluorescence yield obs. 8=43200
Pa^{233}, from Th^{233} decay 8=29380
Pb, from γ-scatt., $\leqslant$ 21 MeV 8=29399
Pb region, residual interaction model 8=38396
Pb, 200 $\leqslant$ A $\leqslant$ 206, A = 210 8=29344
Pb$^{195-205}$ odd A isotopes, S.D.I. calc. 8=29345
Pb^{202,204} first 2$^+$ levels, finite Fermi system theory 8=29325
Pb^{205,207,208} isobaric analog resonances from (p, p), (p, p^1), 10-16 MeV 8=38397
Pb^{205,210} from (t, p) reactions 8=38510
Pb^{206} from Pb^{208}(p, t) at 40 MeV obs. 8=43032
Pb^{206} low levels, 2n-hole config., isobaric analogue meas. 8=42923
Pb^{206,207,208} collective excitations, p scatt. obs., 24.5 MeV 8=29435
Pb^{207} doorway states, single particle strength spreading using particle-core coupling model calc. 8=33939
Pb^{207}, single-n states, mixing of core excitations 8=25161
Pb^{208} and Ca region, isotope shift calc. using density depend N-N interaction 8=42802
Pb^{208} lowest 4$^-$ state configurations 8=33936
Pb^{208}, neutron and particle-hole states γ transitions. from P decay of analogue resonance in Bi^{209} 8=47264
Pb^{208}, neutron particle-hole structure from (d, p) excitation functions 8=25160
Pb^{208} particle-hole calcs., translational invariance violation effect 8=42922
Pb^{208}, (t, α) excited p-hole states rel. to shell model, obs. 8=33938
Pb^{208}, 3- state energy and transition probability calc. 8=47265
Pb^{209}, seven low lying levels, from Pb^{208}(d, p)Pb^{209} reaction 8=43069
Pb^{209} 2-particle-one-hole, from Pb^{207} (t, p) 8=38511
Pb^{211} analog resonance obs. in Pb^{208}(t, p)Pb^{210} 8=25158
Pd^{106}, I$^\pi$ = 2$^+$ two-phonon vibr. state, g-factor obs. 8=29322
Pm^{143}, first excited state, half-life obs. 8=25146
Pm^{143} from Sm^{143} decay 8=25190
Pm^{143} proton quasi-particle spectrum obs. 8=33928
Po^{210}, 50 transitions and 9 K-conversion coeffs. from At^{210} 8=25195
Po^{215}, Rn^{219} deday $\alpha-\gamma$ angular correls., 272 and 401 keV 8=33942
Pr^{141}, from 2f$_{7/2}$ isobaric analogue resonance to 2d$_{5/2}$ ground state 8=42927
Pr^{141,143}, transition multipolarities obs. 8=29330
Pr^{143}, 351 KeV level, $\frac{3}{2}^+$ spin assignment from Ce^{143} $\rightarrow$ Pr^{143} decay obs. 8=38431
Pt, from fast n-scatt. 8=29464
Pt, reson. n capture partial γ width distrib. obs. 8=29343
Pt^{188}, obs. 8=38394
Pt^{192}, from Ir^{192} decay 8=33935
Pt^{193}, from Au^{193} β-decay spectra 8=25193
Pt^{194} from Ir^{194m_2} β decay 8=42917
Pt^{194,196,198} first 2$^+$ states static quadrupole moments 8=38393
Pt^{195}, directional correl. meas. with conversion electrons 8=38392
Pt^{196} from decay of Ir^{196} isomers 8=42967
Pt^{196}, up to 3 MeV from neutron capture γ-rays 8=38492
Pu^{240} subthreshold fission cross section, structure due to intermediate states 8=38528
Ra^{223}, deduced from γ-ray spectrum of Th^{227} decay 8=42973

Nucleus—contd

energy levels—contd

Ra^{223} from Th^{227} decay, scheme obs. 8=25196
Re, from fast n-scatt. 8=29464
Rh^{103}, 538 keV mean lifetime obs. 8=25140
Rn^{219}, γ and conversion spectrometry and α-γ obs. 8=29346
Rn^{219}, Ra^{223} deay $\alpha-\gamma$ angular correl., 270 keV 8=33942
Ru^{98,100,102,104}, O^{16} and He^4 Coulomb excited 8=38375
Ru^{100}, excited states study by decay of Rh^{100} 8=29321
S^{31}, from S^{32}(p, d) in 2s$-$1d shell, obs. 8=43023
S^{32}, from P^{31}(d, n), isobaric analogue states 8=29302
Sb odd-odd isotopes, spectroscopic factors, $\leqslant$2 MeV Sn(He^3, d) obs. 8=34043
Sb odd mass isotopes, low-lying spectral props. calc. 8=42894
Sb^{123}, from Sn^{123} β-decay, level scheme 8=33926
Sb^{125}, β- and γ-spectroscopic studies 8=25185
Sb^{125} decay scheme 8=38382
Sb^{125} from (He^3, d), orbital angular-momentum transfer and spectroscopic factors, 25 MeV 8=42893
Sb^{125} spin assignment 8=42892
Sb^{125,127,129} deduced from Te^{126,128,130}(d, He^3), 34 MeV 8=43068
Sc^{41}, 46 resonances identified, spin assignment, from Ca^{40}(p, γ) 8=42870
Sc^{41}, from Ca^{40}(p, γ_n), inhibited E2 transition 8=29305
Sc^{41} two-particle-one hole states, Ca^{40} + p obs. 8=33905
Sc^{42}, ang. distrib. and J$^\pi$, T assignments, from Ca^{40}(He^3, p) obs. 8=42869
Sc^{43}, even-parity states, shell-model calc. 8=25124
Sc^{43} 472 KeV, mean life 8=42867
Sc^{43}, from Ca^{42}(d, n), spectroscopic factors 8=34034
Sc^{43} $\frac{3}{2}^+$ state, four-body description 8=42783
Sc^{44}γ-γ cascade rel. to quadrupole interaction in BaTiO$_3$ 8=42868
Sc^{45}, excitation energies and spin assignments 8=47317
Sc^{46}, from Sc^{45}(d, pγ), low level transition probabilities 8=25123
Sc^{46}, from Sc^{45}(n, γ), low level struct. 8=25121
Sc^{47}, from Ca^{44}(d, p), 760 keV level mag. moment 8=25122
Sc^{47,49} from Ti^{48,50}(d, He^3), 34.4 MeV 8=25268
Sc^{48}, Ca^{48} (p, n), n-γ angular correl. obs. 8=33997
Sc^{48}, from Ca^{48}(p, n), E_n = 4.5, 5.5 MeV, obs. 8=42871
Sc^{48}(f$^{-}_{7/2}$ f$_{7/2}$)2$^+$ state 8=38369
Sc^{49}, analog, fragmentation calc. comparison with expt. 8=42872
Sc^{49}, Ca^{48}(d, n) determined 5.5, 6.0 MeV 8=38508
Sc^{49}, half-lives of 2.23 and 2.37 MeV states 8=38370
Sc^{50}, calc. from shell model; Ca^{50}, Sc^{50} log ft. for β-decay calc. 8=42863
Sc^{51}, N-N effective interactions calc. 8=29279
Se^{74} from As^{74} decay 8=42947
Se^{76,78,80,82}, isobaric analogue resonance obs. 8=42884
Se^{77}, probability of deformed nucleus 8=29318
Se^{81m}, 102.7 keV transition, K-conversion coeff. obs. 8=29370
Si^{27}, from Si^{28}(p, d) in 2s$-$1d shell, obs. 8=43023
Si^{28} dipole transitions, isospin selection rule 8=29300
Si^{28}, Doppler-shift lifetime meas. 8=25110
Si^{28}, elec. levels and transition rates 8=29293
Si^{28}, excited by 100-260 MeV e, obs. 8=47311
Si^{28}, from Al^{27}(p, γ), lifetimes and branching ratios 8=42855
Si^{28}, from (p, 2p) at 156 MeV 8=33993
Si^{28}, giant dipole resonance by e scatt. 8=25115
Si^{28}, 6.88 MeV $\rightarrow$ 0 transition, multipolarity 8=29291
Si^{29} by p scatt., p spin flip in 2$^+$ state obs. 30, 40 MeV 8=43009
Si^{29}, from Si^{28}(d, p), lifetimes obs. 8=42852
Si^{29}, highly excited, n scatt. 0.57-2.28 MeV obs. 8=33906
Si^{30}, excitation functions obs. 8=25273
Si^{31}, e. m. props. low levels, from Si^{30}(d, pγ), 2.95-4.0 MeV 8=38364
Si^{31}, from Si^{30}(d, p) at 3MeV, obs. 8=42853
Si^{31}, low level struct. strong-coupling model analysis 8=42854
Sm^{144}, 1659 and 2481 KeV levels population (p, p^1) and Eu^{144} decay, obs. 8=38435
Sm^{148} decay α-particle spectra, 3$^-$, 4$^-$ states 8=33929
Sm^{148,150,152,154}, by Coulomb excitation with O^{16} 8=38387
Sm^{150}, branching ratios for E1, E2 transitions obs. in Eu^{150} decay 8=42963
Sm^{150}, (n, γ) excited, e-γ coincidence obs. 8=29333
Sm^{152} E2 transition conversion of electron particle parameters 8=47257
Sm^{152}, multiple Coulomb excitation, electric hexadecapole moment 8=42877
Sm^{152}, 122 keV level, pulsed-beam lifetime meas. 8=33927
Sm^{154}, 82 keV level, pulsed-beam lifetime meas. 8=33927
Sn, even parity states, excitation of quasi-particles, Tamm-Dancoff and second Tamm-Dancoff theories compared 8=38380
Sn isotopes, level systematics studied by Cd (α, xn) 8=38378
Sn, 112 $\leqslant$ A $\leqslant$ 124 8=29344
Sn, reson. n capture partial γ width distrib. obs. 8=29343
Sn^{112,114,116,118,120,122,124} first 2$^+$ levels, finite Fermi system theory 8=29325

Nucleus—contd
energy levels—contd
Sn^{112,116,118,120,122,124}, Coulomb excitation by α at 10 MeV, obs. 8=42890
Sn^{114,116}, p particle-hole pairs excitation rel. to In^{113,115} (He^3, d) struct., 4 MeV 8=34044
Sn^{116}, vibr. states from inelastic e scatt. 8=25143
Sn^{116,117}, structure obs. 8=25144
Sn^{116,118}, pairing vibration model and (t, p) reaction 8=43067
Sn^{116,120,124}, 2$^+$ and 3$^-$ transition probabs. inelastic e scatt., obs. 8=33924
Sn^{117,119,131}, total ang. momenta obs. 8=43015
Sn^{118}, excitation of 2$^+$ state by N scatt., inclusion of knockout exchange amplitude 8=42999
Sn^{118}, from Sn^{119}(p, d), 55 MeV 8=38379
Sn^{118,120} from Sn^{116,118}(t, p)Sn^{118,120} 13, 12 MeV 8=25269
Sn^{119} compared with Sn^{118} levels from (p, p′) isobaric analogue resonances 8.2-12.0 MeV 8=42801
Sn^{119} isomer shift as a function of pressure, obs. in SnMg$_2$, Sn, Pd(12 wgt.%Sn), Sn(SO$_4$)$_2$.2H$_2$O, SnAu 8=33925
Sn^{121,121m} spins obs. 8=38422
Sn^{124}, N^{3+} Coulomb excitation obs. 8=29326
Sr^{86,88}, isobaric analogue states 8=25134
Sr^{88} from γ-decay of Rb^{58} and Y^{88}, nuclear levels 8=47249
Sr^{88}, from Sr^{87}(d, p) at 7.5 MeV, n particle-hole states 8=42885
Sr^{88}, n hole states and configuration mixing, 18 MeV(He^3, α) obs. 8=29319
Sr^{88}, p levels, 18 MeV (He^3, d) obs. 8=33918
Sr^{89}, particle-plus-core coupling model calc. 8=33917
Ta, from fast n-scatt. 8=29464
Ta^{176} E1 transitions, Nilsson model 8=42913
Ta^{177}, W^{177} decay time-to-amplitude coincidence obs. 8=29376
Ta^{181}, 482-KeV state excitation by stopping π, evidence 8=42912
Ta^{181}, 482 keV transition, polarization of γ ray, parity non-conservation in agreement with Cabibbo theory 8=38301
Tb^{159}, from Gd^{159} decay, level scheme 8=29372
Te$^{118-120}$ even A isotopes, 0-3 MeV, γ spectra and N^{3+} Coulomb excitation obs. 8=29326
Te^{119}, from I^{119} decay study 8=25188
Te^{121} from the decay of I^{121} 8=25187
Te^{121,123,125}, low-lying, I^{121,123} decay γ-spectra and Coulomb excitation obs. 8=29327
Te^{123} from I^{123} decay obs. 8=42955
Te^{124}, even-even nuclei, and spins, comparison with theory 8=42879
Te^{124}, 603-keV level lifetime obs. 8=42895
Te^{125}, level scheme 8=38382
Te^{125}, 3-quasiparticle intruder state obs. 8=42896
Te^{125} 321 KeV 9$^-$/2 half-life 8=38381
Th^{232}, intermediate state on fission due to neutrons 8=38531
Th^{232}, reduced n widths, $\leqslant$ 3 keV 8=29347
Ti, HF technique applied to calc. energy spacings and e. m. props. 8=25085
Ti octupole states systematics, from Ti^{48}(α, α') at 31 MeV 8=43089
Ti^{42} from Ca^{40}(He^3, n) 8.5-10 MeV 8=38371
Ti^{44}, first excited states, from obs. of Ca(α, γ)Ti 8=29306
Ti^{44}, from Ca^{40}(α, γ), spin and parity obs. 8=25126
Ti^{44,46,48} 2$^+$ state isospin structure rel. to Ti^{46} 3$_1^-$ γ-decay 8=33912
Ti^{45}, from Ti^{46}(p, d), low levels obs. 8=29307
Ti^{45,46,47,48,49} from Ti^{46,47,48,49,50}(He^3, He^4) 18.2 MeV 8=43090
Ti^{46} excited states obs. 8=25274
Ti^{46}, excitation energies and spin assignments 8=47317
Ti^{46} from Sc^{45}(He^3, d) and Ti^{47}(He^3, α), 15 MeV 8=25127
Ti^{46}, γ-γ correlations 8=47244
Ti^{46} 3$_1^-$ usual γ-decay props. rel. to Ti^{44,46,48} 2$^+$ state isospin structure 8=33912
Ti^{48} 341 keV transition multipolarity rel. to thermal n capture 8=25125
Ti^{49}, 0.34 MeV (M1 + E2) transition, mixing ratio 8=42873
Ti^{50} from V^{51}(d, He^3), 34.4 MeV 8=25268
Tl^{202} isomeric state in (n, 2n) reaction by 14 MeV neutrons 8=38395
Tl^{206} from decay of Hg^{206} from Pb^{208} (p. 3p) 8=42971
Tm^{165} from Yb^{165} decay, scheme and lifetime obs. 8=42965
Tm^{169}, L and M internal conversion of E$_2$ transitions 8=33931
Tm^{169}, rel. to characteristic constants evaluation, obs. 8=29337
Tm^{171} scheme from Er^{171} decay 8=47259
U^{233,235}, ground state rotational bands, study by inelastic d scattering 8=47269
U^{234}, from γ spectra in Pa^{234}(UZ, T$_{1/2}$ = 6.7h) 8=47270
U^{235} slow neutron resonance spins 8=33944
U^{235m}, half-life of low energy level meas., environmental effects 8=25164
U^{237}[743$\uparrow$] Nilsson configuration, from U^{238}(He^3, α) obs. 8=34045
V^{48}, from Ti^{47}(He^3, d), obs. 8=29517
V^{49} analogue states and virtual levels from Ti^{48}(p, γ) E$_p$ = 1.335-2.290 MeV 8=47245
V^{49}, from Ti^{48}(p, γ) reaction, up to 1347 keV 8=29445
V^{51} from Cr^{52}(d, He^3), 34.4 MeV 8=25268
V^{51}, rel. to intermediate structure, n total cross section, 0.5-1.2 MeV 8=29469
W, reson. n capture partial γ width distrib. obs. 8=29343
W^{178,180,182} ground-state rotational transitions, statistical model description of intensities 8=38391
W^{182}, two-quasiparticle state at 1.289 MeV, obs. 8=25154
W^{182,183,184,186}, Coulomb excitation of lowest states 8=42915
W^{182,184,186}, energy shift of γ-rays in presence of μ in 1s state 8=42902
W^{182,184,186}, first excited states, mag. moment and quadrupole ratio obs. 8=42914
Xe$^{122-136}$ even nuclei rel. to N, and deformation, obs. 8=38383
Xe^{128} from Ba^{128} decay obs. 8=42956
Xe^{132} obs from Cs^{132} decay 8=42899
Y^{89} analog states elastic proton decay widths, shell-model calc. 8=47250
Y^{89}, identified in p scatt. 8=25137
Y^{89}, p excitation to 4.2 MeV, bound levels obs. 8=42886
Y^{90} obs. in Y^{89}(d, p), 12 MeV 8=25136
Yb^{168}, from Lu decay period 8=42910
Yb^{168}, Lu^{168m,168} decay obs. rel. to collective model 8=29339
Yb^{169}, from Yb^{168}(n, γ), struct. and γ spectra 8=42909
Yb^{173,175} analogue states, (p, p) and (p, p′) obs. 8=29338
Yb^{173,175}, spectroscopic factors from Yb^{172,174}(d, p), 12 MeV 8=29508
Yb^{176}, from decay of Tm^{176} 8=33964
Zn, HF technique applied to calc. energy spacings and e. m. props. 8=25085
Zn^{64}, from (p, 2p) at 156 MeV 8=33993
Zn^{64}, 2p$^3\!/_2$ and 2s$^1\!/_2$ binding energies, (p, 2p) obs., 156 MeV 8=33914
Zn^{68}, energies and spins from Zn^{66}(t, p) and Zn^{68}(p, p′) and Ga^{68} β decay, below 3 MeV excitation 8=33915
Zr^{89,90,91}, from Zr^{90,91,92}(p, d), n hole states 8=42887
Zr^{90}, from (p, 2p) at 156 MeV 8=33993
Zr^{90} isobaric analogue states nucleon widths 8=38373
Zr^{90}, isobaric-spin analogue resonances, obs. via p scatt. on Y^{89} 8=43013
Zr^{90}, n hole states and configuration mixing, 18 MeV (He^3, α) obs. 8=29319
Zr^{90} obs. in Zr^{90}(He^3, d)Nb^{91} → Zr^{90} 8=25275
Zr^{90}, p levels, 18 MeV (He^3, d) obs. 8=33918
Zr^{90}, 2p binding energy, 156 MeV(p, 2p) obs. 8=33914
excitation. See Nuclear excitation.
magnetic moment
See also Gyromagnetic ratio; Molecules/nuclear coupling; Nuclear magnetic resonance and relaxation.
deformed, finite Fermi system calc. 8=25089
giant fields produced by hole in K shell 8=48315
isobaric multiplet splitting, due to changes 8=29286
of isospin doublets, linear relation for odd nuclei 8=42820
M1 l-forbidden transition 8=42821
sign from atomic level crossing signal line shapes 8=38683
Be^9, velocity-dependent N-N pot. 8=25097
Bi^{209} nuclear magnetism distrib. rel. to hyperfine structure 8=33940
Co isotopes, treated as p hole coupled to quadrupole vibr. of Ni isotopes 8=25129
Cu^{60,62}, atomic-beam magnetic-resonance meas. and configuration-mixing calc. 8=42880
Dy^{161}, 74.5 keV level, meas. using Mossbauer effect 8=25150
Gd^{155}, 86.5 and 105.3-KeV states, obs. 8=42906
Ge^{71}, g-factor of 175 keV state 8=47248
H^3, velocity-dependent N-N pot. 8=25097
Hf^{177}, perturbed ang. correls. and g factor 8=38390
In^{117m}, h. f. s. obs. 8=29324
Ir^{191}, from γ-scatt., of 129 level 8=47303
K^{37} calc. 8=33907
N^{14}, evidence for tensor force 8=42835
Os^{187}, meas. by pulse technique for weak n. m. r. 8=37542
Os^{189} 8=27512
Pd^{106}, I$^\pi$ = 2$^+$ two-phonon vibr. state, g-factor obs. 8=29322
Pu^{239} 8=42930
Sb^{124}, from γ anisotropy of oriented nuclei 8=42891
Sb^{125}, obs. 8=42896
Sc^{47}, from Ca^{44}(d, p), 760 keV level mag. moment 8=25122
Se^{77}, explained by spin polarization 8=29318
Tm^{169}, rel. to characteristic constants evaluation, obs. 8=29337
W^{182}, two-quasiparticle state at 1.289 MeV, obs. 8=25154
W^{182,184,186}, first excited states, obs. 8=42914
models
Akhieser-Pomeranchuk-Blair calcs. of alpha-scatt. from light nuclei 8=25263
α-cluster, α-α interaction in Ar^{36} and Ca^{40} 8=25049
α-particle model for nuclear matter 8=47207
Bohr-Mottelson hydrodynamic and K = 1, 2, 3 octupole vibrations 8=25082
1-boson-exchange potl., for nuclear matter 8=42795
collective for 52 MeV d inelastic scatt. on various nuclei 8=42837

Nucleus—contd
  models—contd
    collective-model analysis of $Mg^{24}(p, p')$ at 49.5 MeV 8=47316
    collective motion, rigid, liquid and related rotations 8=38307
    collective motion, variational principrinciples for self-consistent theory 8=47206
    collective, of even-even spherical nuclei 8=42807
    configuration mixing for s-d shell 8=33878
    core-particle-coupling, Sb odd-mass isotopes, low-energy spectral props. calc. 8=42894
    core-particle coupling, self-consistent, and relation to phenomenological models' 8=47205
    cranking eqns. from Kerman-Klein formalism 8=25048
    cranking for gyromagnetic ratio calc. of ground state rot. band in deformed nuclei 8=25088
    Davydov for E2 transition possibilities 8=25084
    Donner and Greiner, static and dynamic props. 8=38302
    drop model shell correction, mass and deformation 8=38308
    fluctuations, excitation function for $V^{51}(p, n)Cr^{51}$ 8=43029
    heavy deformed nuclei, surface delta interaction model 8=47199
    hydrodynamic, coupling constants between giant multiple resonances and surface quadrupole oscills. 8=33876
    interact. pots., effect of nonstatic character in singlet-even states 8=25043
    liquid drop, for fission deformations rel. to single-particle energy calcs. 8=29528
    mass and binding energy formulae, far-unstable nuclei 8=38316
    mass, deformation and fission threshold 8=38308
    mass, extended shell model semiempirical formula 8=38312
    mass formulae and deformability, shell and liquid-drop models 8=38318
    mass formula, even-even deformed nuclei, semi-empirical 8=38314
    mass, shell correction rel. to anomalies 8=38315
    mass, shell model formula, magic numbers and extrapolation 8=38313
    Nilsson and $Al^{25,26}$ 8=25113
    Nilsson for E1 transitions in $Lu^{170,172}$, Ta^{176} 8=42913
    Nilsson, projected wave function from F^{19} 8=38360
    Nilsson's, rel. to energy levels and e. m. props. of $F^{19,21}$ 8=47236
    non-local, t-matrix in quasi-three-body reaction 8=29426
    optical, ambiguities for Ne^{22} (He^3, He^3) Ne^{22}, 10 MeV 8=38514
    optical, analysis of C^{12}-d scatt., including tensor terms, 5. 25. 6. 10 and 7. 05 MeV obs. 8=38501
    optical analysis of d elastic scatt. from Al^{27}, Si, Ni^{60}, 7-11 MeV 8=25265
    optical, analysis of $Ni^{58}(He^3, He^{3\prime})$ and $Ni^{58}(He^3, \alpha)$ 8=43076
    optical, curve fitting, inadequacy of χ^2 criterion 8=33872
    optical, deformed: neutron s-, p-, d-wave strength functions, doubly even rotor nuclei 8=38303
    optical, for α back-scatt. 8=33974
    optical for complex nuclei, d interactions with Al^{27}, 710 MeV 8=38506
    optical, for He^4-N scatt. < 20 MeV 8=29231
    optical, for N interactions, energy depend. for real part of pot. derived 8=25216
    optical for N scatt. 8=42998
    optical, four-parameter for n scatt. from light nuclei 8=29450
    optical, generalized, inelastic N scatt. calc. 8=47312
    optical, isospin dependence in (p, n) at 30 and 50 MeV, isobaric analogue states obs. 8=43001
    optical, modification with five free parameters 8=25053
    optical, nuclear reaction cross section depend on mass number 8=42983
    optical, parameters deduced from d scatt. off Fe^{54}–Sn^{124} isotopes, 14.5 MeV 8=43054
    optical parameters for 12 MeV d scatt. off Nd isotopes 8=43056
    optical, parameters from 1.5 MeV n scatt. data 8=29452
    optical, params. from $\bar{p}$ elastic scatt. by emulsion nuclei. 3 GeV/c 8=43000
    optical, perturbation theory description of spin-orbit and tensor forces 8=43053
    optical potential, binary, for two-N phase-shift-set discrimination 8=25047
    optical potential calc. for composite particles 8=25052
    optical potential calc. from p. scatt. by Ca^{40}. Ni^{58}. Sn^{120}. Pb^{208}, 40 MeV 8=43011
    optical potential calc. of $O^{16} + B^{10,11}$ scatt., energies near appropriate Coulomb barrier 8=34047
    optical, pot. depth, real part a function of mass number 8=29449
    optical potentials, helion and triton review 8=47338
    optical, potential isospin depend. from n cross-sections obs. 8=29267
    optical potential, non-local, for low energy N scatt. 8=33985
    optical pot., quantum theory of nuclear reactions 8=29395
    optical potential, semi phenomenological form. 8=25051

Nucleus—contd
  models—contd
    optical potential symmetry and its connection with time reversal and reciprocity 8=47204
    optical pot., theory of scatt. and reactions 8=29391
    optical, p-p scatt. partial wave analysis, $E_p = 50\text{-}180$ MeV 8=33750
    optical, real central part potential 8=33988
    optical, reformulated, for p scatt. and nuclear matter radii 8=42790
    pairing energy gap and mass differences calc. 8=25060
    pairing Hamiltonian, single-intermediate-state approx. 8=42789
    pairing, matrix calc. for As^{74} β-decay 8=42946
    pairing potential and two-nucleon transfer reaction 8=47339
    pairing vibration of $Sn^{116,118}$ 8=43067
    pairing-plus-monopole, validity of BCS, RPA approximations 8=42787
    pairing-plus quadrupole deformation as a function of Z number 8=25055
    pairing-plus-quadrupole, nuclear deformations, quadrupole force strength 8=25054
    quark Fermi system 8=24743
    quasiparticle applied to 1^+ levels of single-closed-shell nuclei 8=38340
    quasiparticle gas, for < 40 MeV processes 8=29271
    rel. to rare-earth deformed nuclei β transition rates obs. 8=38411
    rotator, rotation particle coupling effects rel. to light nuclei props. 8=25050
    Schrödinger eqn. validity, high energy expts. appls. 8=29268
    shape and deform., review 8=47197
    shell, accuracy and three-body problem 8=25057
    shell, accuracy of local approx. to non-local pot. 8=25056
    shell, analysis of $Ca^{42,44}(p, p')$ 8=43010
    shell, analysis of $Pb^{207,208}(t, p)Pb^{209,210}$ and $Pb^{207}(p, t)Pb^{205}$ 8=38510
    shell calc. for Cr^{56}, Fe^{58} 8=25128
    shell calc. of B(E2) values in s-d shell nuclei with $18 \leqslant A \leqslant 22$ 8=33880
    shell, Ca^{40} structure 8=33911
    shell, Ca^{41} state spectroscopic factors at 10 and 12 MeV calc. 8=33871
    shell, $Ca^{43,45}$ state spectroscopic factors at 10 MeV calc. 8=33871
    shell, centre-of-mass motion effect avoided 8=42922
    shell, core excited admixture rel. to core-breaking width 8=33867
    shell. eigenparameters for Saxon Wood pot. 8=47203
    shell, expressions for Coulomb energies 8=38305
    shell, for $A = 20 - 28$ calc. 8=33877
    shell for even-parity states of Sc^{43} 8=25124
    shell. for fission deformations rel. to single-particle energy calcs. 8=29528
    shell, for fission fragment relative vel. calc. 8=29527
    shell for O^{16} and neighbouring nuclei 8=38358
    shell, for Y^{89} and Nb^{91} analog states elastic proton decay widths calc. 8=47250
    shell, h. f. calc. for heavy spherical nuclei 8=29274
    shell, individual, α-decay theory 8=25171
    shell, literal truth, nucleon motions 8=33869
    shell, literal truth, nucleon pairs 8=33870
    shell, many-body theory of reactions 8=33977
    shell model potential, reaction matrix theory 8=42786
    shell-model theory of Pb^{206} 8=25159
    shell nuclei Of-1p, reaction matrix elements 8=38306
    shell, of O^{18}, exponentially velocity-dependent potential 8=42785
    shell, 1st order perturbation of resonance energies, splitting of resonance multiplets 8=38331
    shell. 1f, 2p parentage coeffs. 8=33883
    shell, p, Hartree-Fock and Hartree-Fock-Bogolyubov calcs. 8=33868
    shell, particle hole, odd-parity states in A - 6, 14 nuclei calc. 8=42800
    shell, potential rel. to density of matter 8=25061
    shell, rel. to electron scatt. cross section difference 8=25120
    Shell. resonant states inner prod. 8=42816
    shell, sd of odd nuclei, collective motion using U_3 8=25058
    shell, semi-empirical nuclear masses 8=33875
    shell, single particle Hamiltonian rel. to super-heavy magic nuclei prediction 8=38304
    shell → two channel model, intermediate structure 8=38332
    shell 2s-1d, $SU(3) \supset R(3)$ Wigner coeffs. 8=29269
    shell wave functions for O^{18} 8=25105
    single particle potential to account for $\Delta N = 2$ mixing 8=29270
    soluble, parity deform. and pairing 8=25059
    statistical, appl. to describe ground state rotational levels population 8=38391
    statistical appl. to evaporation of compound nucleus 8=42812
    superfluid, dependence of quadrupole, octupole deformations on energy 8=38326
    super-heavy nuclei, mass formula rel. to n capture and nucleosynthesis 8=38324

Nucleus—contd
models—contd
rel. to spectral distribs., basis wave function distrib. among eigenstates 8=25080
three-body of closed shells plus 2 nucleons, energy spectra 8=29277
triton, simple calc. 8=38352
two-level with monopole–monopole interactions, ideal collective coordinate appl. 8=42770
unified, energy spectrum of doubly odd nucleus La^{140} 8=38385
unified reaction theory, asymptotic channel states and matrix equations 8=42788
wave functions for arbitrary number of nucleons 8=47202
Au^{198} rel. to β-γ directional correls. and spectral shape obs. 8=29378
C^{12}(d) at 12.4 MeV, in ang. region 60–100° 8=47342
C^{12} optical pot., phenomenological for p scatt., energy dependence 8=29429
C^{12}, 1-particle 1-hole model, state calcs. 8=29296
C^{12}, three-α, ground-state energy calc. 8=42836
Ca^{40}, deuteron optical parameters 8=29497
Ca^{40} optical pot., phenomenological for p scatt., energy dependence 8=29429
Ca^{40}, shell model with N-N correls. rel. to e elastic scatt., 750 Mev 8=33911
Co isotope as p hole coupled quadrupole vibr. of even-mass Ni nucleus 8=25129
F^{19} shell model Hamiltonian rel. to projected wave function from Nilsson model 8=38360
He^{4}, single-particle, ground state form factor calc. 8=29228
Ho^{165}, orientation effect on total n cross section 2-135 MeV 8=25151
Li^{6}, α-d cluster model rel. to Li^{6}(p, 2p)He^{5} 8=29290
N-nucleus scattering and polarization, optical model analysis 8=29451
Na^{22} struct., γ correl. obs. rel. to rotational model 8=25109
Ni isotope, quadrupole vibr. coupled to p hole as model for Co isotopes 8=25129
Ni^{58} optical pot., phenomenological for p scatt., energy dependence 8=29429
O^{16} and neighbouring nuclei, shell model 8=38358
O^{16}, 1-particle 1-hole model, state calcs. 8=29296
Rb^{86} rel. to β-γ directional correls. and spectral shape obs. 8=29378
Se^{77}, Nilsson versus shell models 8=29318
Si^{31}, strong-coupling, low level struct. analysis 8=42854
Tm^{170} rel. to β-γ directional correls. and spectral shape obs. 8=29378
size
charge distrib. determ. from e scatt. and muonic X-rays 8=25092
effective mass rel. to core polarization 8=29275
in fission, deformations rel. to single-particle energy calcs. 8=29528
$\langle\gamma^2\rangle$ and spectroscopic factors from DWBA 8=33874
Hartree-Fock and Hartree-Fock-Bogolyubov calcs. for 1p shell nuclei 8=33868
implications of Li^{6}(γ, t) cross-section obs. 8=42988
shape and deform., review 8=47197
Ca^{40,48}, radius, shell model 8=25120
H^{3}, binding energy and charge radii 8=33893
He^{3}, binding energy and charge radii 8=33893
He^{4} radius, elec. quadrupole contrib. 8=42830
K^{40}, Mössbauer meas. 8=42859
Nd isotopes charge radii var. from K X-ray isotope shift 8=38386
spin and parity
See also Gyromagnetic ratio; Molecules/nuclear coupling.
A = 6, 14 odd-parity states nuclei calc. photo-absorption studies 8=42800
γ-ray angular distrib., isotropic, interpretation for final state of spin 3/2 8=33887
isospin mixing in ground state, monopole polarizability and Fermi β-decays 8=25076
levels, perturbing effect on ang. distrib. in γ-scatt. 8=33891
metal, spin interaction, indirect, divergences 8=26877
moment of inertia calc. following (n, 2n) reaction 8=43035
moment of inertia in pairing-plus quadrupole model 8=25055
moment of mentia calc. for symm. fission nucleus using geometric model 8=38526
from neutron-capture γ rays meas. 8=42808
single-particle orbitals parity-mixing and coeffs. of fractional parentage 8=29263
solids, nuclear spin energy diffusion 8=48316
spin of short lived states, atomic-beam on-line meas. 8=38347
spin-orbital splitting and spin-wave resonance 8=25087
test with perturbed ang. correl. of two γ-ray 8=33890
Z ~ 65 nuclei in heavy ion reactions, spins rel. to high J states decay, statistical model 8=38405
Ac^{227}, odd ground state parity obs. 8=42926
Ag^{109} levels 8=47287
Al^{25,26} from Mg^{24,25}(d, n)Al^{25,26}, 5.5 or 6 MeV 8=25113
Al^{26}, assigned from decay modes of closely spaced levels obs. 2.07 MeV 8=42851

Nucleus—contd
spin and parity—contd
Al^{27}, 4509 keV level obs. 8=33904
Al^{27}, $J = \frac{9}{2}$ for 3002 keV level 8=43036
Al^{27} levels, γ-ray transitions obs. 8=42849
Ar^{36} in Cl^{35}(p, α_0)S^{32}, 830-2930 keV 8=25230
Ar^{37} levels 8=47349
Au^{199,197,195,193}, by meas. of internal conversion coeffs. 8=42970
B^{10} ground state, spin determ. from Mott scatt. 8=25099
B^{12}, of first excited state from B^{11}(d, p)B^{12} 8=34036
Ba^{134}, even-even, ang. correl. obs. 8=42879
Be^{8}, of 19.05 MeV level from Li^{7}(p, γ)Be^{8}, 1.4–2.5 MeV 8=47320
Bi^{211} levels and multipole mixing ratios 8=47268
Bi^{211}, multipolar mixing ratio obs. 8=47266
C^{12}, of 14.71 MeV level 8=47229
Ca^{42} from K^{41}(He^{3}, d) reaction, particle hole states up to 5.79 MeV obs. 8=47213
Ca^{44} assignment from proton scatt. obs. 8=47173
Ca^{45} 1.43 and 1.9 MeV levels have $J^{\pi} = \frac{3}{2}^{-}$ 8=38366
Ca^{50} $J^{\pi} = 1^{+}$ assignment to 1848 KeV level 8=42943
Cd^{112}, resonant γ scatt. from n capture in Fe, obs. 8=25245
Cd^{115} γ decay, directional correl. obs. 8=38377
Ce^{140} from La^{140} decay 8=33963
Cl^{37} from S^{36}(p, γ) at 800-1940 KeV, > 80 resonances obs., spin assignment 8=42857
Cl^{37} resonances obs. 8=42857
Cl^{38} ground state 8=29359
Co isotopes, treated as p hole coupled to quadrupole vibr. of Ni isotopes 8=25129
Cr^{50} low levels, spin assignment from pγ ang. correl. 8=29309
Cr^{52} 2^{+} level, p spin-flip, 11 MeV 8=33989
Cr^{56}, $J = O^{+}$ state appearing in shell model calc. 8=25128
Cs^{131}, 133.54, 585.1, 620.2 KeV levels assigned 8=38429
Cu, n resonance, E_n = 200 eV-16.5keV, radiative capture obs. 8=38490
Cu^{59,63} from Ni^{58,62}(p, $\gamma\gamma$) reactions 8=29446
Cu^{62}, from 9.3-h Zn^{62} decay 8=42945
Cu^{63,65}, assignment 8=43012
Cu^{64,66} low-lying excited states below 1 MeV 8=42881
Dy, 1300 keV state, $K^{\pi} = 2^{-}$ 8=25149
Er^{168}, from neutron-capture γ-rays meas. 8=42808
Fe^{54} 2^{+} levels, p spin-flip, 11 MeV 8=33989
Fe^{56}, from Co^{56} and Mn^{56} decay 8=29364
Fe^{53}, 19/2^{-} of newly discovered isomeric state 8=38465
Fe^{58}, even-even, ang. correl. obs. 8=42879
Gd^{153} levels obs. 8=42903
Gd^{155}, 86.5 and 105.3-KeV states, obs. 8=42906
Ge^{70} from As^{70} decay, excited states spin assignments 8=42948
He^{3}, spin interaction rel. to thermodynamic props. of magnetized solid 8=41905
He^{3}, spin-orbit pot. from spin-flip meas. 8=47228
In$^{111, 111m}$ from Sn^{111} decay 8=38423
Ir^{193} and conversion coeff. 8=38439
K^{37}, of seven low and three high levels 8=42858
K^{41}, resonance produced in p scatt. on Ar^{40} 8=47241
Li^{6}(d, p)Li^{7}, vector analysing power, j-dependence 8=47344
Mg^{24}, from C^{12}(O^{16}, $\alpha\gamma$), energy levels obs. 8=38362
Mg^{24}, from γ ang. distrib. in Ne^{20}(α, γ) reactions 8=38517
Mg^{25}, 1.614 to 3.400 MeV levels 8=29301
Mo^{93}, from transition probability calc. and n intensity meas. 8=29320
N^{14}, axially deformed single-nucleon Hartree-Fock orbitals used to calc. parity 8=42838
N^{14} levels obs. 8=47230
N^{14} states obs. 8=43020
Na^{24}, from n capture γ circular polarization obs. 8=38485
Ne^{22}, up to 6.68 MeV level 8=29298
Ni^{56}, from Ni^{58}(p, t), spin assignments 8=47247
Ni^{62}, resonant γ scatt. from n capture in Fe, obs. 8=25245
O^{16}, O^{+}, 1^{-}, 3^{-} levels, parameters assigned from α-scatt. 8=25270
O^{17}, set of J^{π} from C^{13}-α scatt. and C^{13}(α, n)O^{16} 8=25103
O^{18}, spin O states, binding energy anomaly 8=25101
P^{32}, from n capture γ circular polarization obs. 8=38485
Pb^{208}, neutron particle-hole states 8=47264
Pb^{208}, resonant γ scatt. from n capture in Fe, obs. 8=25245
Pm^{143} from Sm^{143} decay 8=25190
Pr^{141}, resonant γ scatt. from n capture in Fe, obs. 8=25245
Pr^{144}, first forbidden unique correl., inner bremsstrahlung correction 8=47254
Pr^{143}, 351 KeV level, $\frac{3}{2}^{+}$ spin assignment from Ce^{143} → Pr^{143} decay obs. 8=38431
Pt^{193}, from Au^{193} β-decay spectra 8=25193
Pt^{196} levels obs from Ir^{196} decay 8=42967
Pu^{239}, effect on fission cross-section 8=34049
Pu^{240}, for levels formed by n interact. with resonance levels of Pu^{239} below 80 eV 8=43037
Ru^{100} excited states 8=29321
Sb^{125} obs. 8=42892

Nucleus—contd
  spin and parity—contd
    Sc^{41} states and structure 8=42870
    Sc^{42}, assignment 8=42869
    Sc^{45} assignment from proton scatt. obs. 8=47317
    Sc^{49} 2.23 and 2.37 MeV state, $J^{\pi} = \frac{1}{2}^{+}$ and $\frac{3}{2}^{+}$ assigned 8=38370
    Se^{77}, Nilsson versus shell models 8=29318
    Si^{29}, highly excited, fast n elastic scatt. obs. 8=33906
    $Si^{30}(p,\gamma)P^{31}$, 22 resonances 8=29444
    Sm^{155}, at. beam mag. resonance obs. 8=29331
    Sn even isotopes, quasiparticle second Tamm-Dancoff theory 8=25142
    Sn^{111} obs. 8=38423
    Sr^{83}, obs. 8=25182
    Ta^{181} in Hf, asymmetry of order 10^{-4}, predicted from test with perturbed ang. correl. of two γ-rays 8=33890
    Te^{124}, even-even, ang. correl. obs. 8=42879
    Ti, assignments 8=43089
    Ti^{44}, from $Ca^{40}(\alpha,\gamma)$, energy levels obs. 8=25126
    Ti^{46} assignment from proton scatt. obs. 8=47317
    U^{235}, effect on fission cross-section 8=34049
    U^{235} slow neutron resonance spins 8=33944
    $Yb^{173,175}$ analogue states 8=29338
    Zn^{68} spins of levels below 3 MeV excitation 8=33915
  theory
      See also Nuclear forces.
    α-particle model for matter 8=47207
    antinuclear forces 8=24895
    Bethe-Goldstone eqn. for 2n in O^{18}, degeneracy effect 8=25101
    binding energy distrib. rel. to fission process 8=38320
    binding energy, for soft-core pots with realistic N-N interacts. 8=25069
    bound state solution of three-body problem 8=38295
    Brueckner of nuclear matter, survey 8=29272
    Clebsch-Gordan coeffs. evaluation in SU(n) groups 8=37844
    Clebsch-Gordan coeffs. for ladder representations of U(1, 1) 8=24617
    coherence in nucleus 8=47198
    collective motions, projection-operator treatment 8=42773
    collective motions, random phase approximation, spherical 8=25064
    collective vibrations in terms boson expansions, self-consistent treatment 8=38311
    core polarization and quasiparticle theories with realistic N-N forces 8=42818
    core-polarization effects, Hartree-Fock calc. 8=38348
    correlation energy of many-fermion system 8=42772
    Dirac monopole 8=33513
    double nucleon emission after bound pion absorption 8=38299
    double-π charge exchange mechanism and existence of "isonuclei" 8=33862
    effective mass rel. to core polarization 8=29275
    electric quadrupole transition rates, seniority four → -two states, comparison with phonon states 8=42822
    four-body correlation, Bethe-Faddeev eqn. solved with Day's approx. 8=47201
    G(2) group, Clebsch-Gordan series 8=29264
    $\langle\gamma^2\rangle$ and spectroscopic factors from DWBA 8=33874
    Hartree-Bogoliubov theory with projection method 8=42784
    Hartree-Fock calc. on shell structure of heavy spherical nuclei 8=29274
    Hartree-Fock calc. using effective N-N potentials 8=33865
    Hartree-Fock problem with subsidiary conditions and random phase approx. 8=33859
    Hartree-Fock standard ang. momentum projection calc. 8=33897
    Hartree-Fock state stability condition against four-body correlations 8=38341
    "isonuclei" and double-π charge exchange mechanism 8=33862
    Kerman's band mixing, rel. to isomer shift in Eu^{153} 8=25147
    level density, superconductivity effects in 8=25074
    light nuclei, four-body correlations 8=42783
    magnetic dipole transitions, l-forbidden 8=42821
    masses, shell-model semi-empirical equation 8=33875
    matter calc., hard core in 2-nucleon potential 8=25066
    matter, ground-state props. Λ_{11} approximation 8=25067
    matter, ground state props, method of Green's functions 8=47210
    matter, inelastic e scatt. response function calc. 8=29407
    matter, re-arrangement energy, e scatt. and (p, 2p) obs. calc. 8=29273
    matter, tensor forces effect on nucleon scatt. 8=42793
    matter, 2-particle correls. without using thermodynamic Green's functions 8=25062
    matter, use of 1-boson-exchange potl. model 8=42795
    motion, ideal collective coordinate concept 8=42769
    non-local pots., asymptotic behaviour of phase shifts 8=42782
    non-local potentials, bound states and Levinson's theorem 8=38296
    N-body ground state, upper bound, conditions on two-body potentials 8=42794

Nucleus—contd
  theory—contd
    nucleon–nucleon interaction's non-static character and nuclear matter 8=42774
    N-N potential, and boson exchange theory 8=38300
    nucleon-nucleon separable potential 8=42776
    operators in numerable Hilbert spaces 8=47196
    pair oscillator interaction form factors, elastic for antisymm. states 8=38292
    pairing Hamiltonian, single-intermediate-state approx. 8=42789
    PT invariance, tests for violation 8=38407
    quasiparticle approx., fluctuation-disssipation theorem 8=24596
    quasi-particle coupling to pair vibrations 8=33885
    quasiparticle gas model for < 40 MeV processes 8=29271
    quasiparticle random-phase-approx, residual n–p interaction 8=42791
    reaction matrix elements for closed-shell nuclei using realistic forces 8=33866
    reaction matrix, single-particle potentials 8=42786
    repulsive core effect on N scatt. in nuclear matter 8=38309
    repulsive forces, appl. of Fermi gas pair collision theory 8=32852
    Scotti-Wong pot. modified, rel. to N-N scatt., deuteron problem and nuclear matter calcs. 8=24881
    self-consistent core-particle coupling models, and its relation to phenomenological models 8=47205
    shell model, 1f, 2p, parentage coeffs. 8=33883
    single-particle orbitals parity-mixing and coeffs. of fractional parentage 8=29263
    space theory in free particles observables 8=29022
    spectroscopy and structure, conference, Khar'kov 1967 8=38294
    statistical, energy-density formalism appl. 8=42778
    structure, calcs. using realistic two-body interacts. fitting N-N scatt. data 8=25063
    sum rule, single particle 8=33858
    superfluid nuclear matter, statistical mechanics 8=23886
    symmetry energy of nuclear matter 8=25065
    Tam-Dancoff and second Tamm-Dancoff theories for even parity states of Sn compared 8=38380
    Thomas–Fermi calc. for semi-infinite nuclei, surface properties 8=42771
    three-body potential, pionic, comparable to two-body potential 8=42796
    three nucleon system, tensor forces and Faddeev equations 8=42775
    topology, mappings of type s, and strongly nuclear spaces 8=47208
    triton variational calc. for ground state energy with trial functions 8=47227
    two-N phase-shift-set discrimination, binary optical pot. 8=25047
    two-nucleon interaction as test of group theory schemes 8=24866
    unified reaction theory, asymptotic channel states and matrix equations 8=42788
    variational principles for self-consistent theory of collective motion 8=47206
    wave function, supermultiplet, fractional parentage decomposition 8=38293
    Wigner supermultiplet approximation, allowed β transitions 8=25175
    Ar^{36}, Hartree-Fock standard ang. momentum projection calc. 8=33897
    C^{12}, Hartree-Fock standard ang. momentum projection calc. 8=33897
    C^{12} short-range dynamical correls. from elastic e scatt. 8=38355
    Ca, even isotopes, self-consistent pairing calc. 8=42862
    Eu^{151}, ^{153}, charge distrib. rel. to muonic x-rays obs. 8=34194
    He binding energy, variation calc. using two-body central velocity-dependent potential 8=42824
    Li^{7}, Coulomb form factors 8=29289
    Ne^{20}, Hartree-Fock standard ang. momentum projection calc. 8=33897
    Ne^{20}, projected Hartree-Fock states, two-body pot. 8=29299
    O^{8} broken symmetry and mass relations 8=38317
    O^{16}, continuum struct., eigenchannel reaction theory 8=42842
    O^{18}, eqn. of motion of 2 neutrons 8=25101
    Pb^{206}, shell-model 8=25159
    Si^{28}, projected Hartree-Fock states, two-body pot. 8=29299
    Ti^{44}, Hartree-Fock standard ang. momentum projection calc. 8=33897
    U^{235} fission transition, structure 8=43112

Oceanography
      See also Liquid waves; Seawater.
    acoustic dit., linear array, sector coverage 8=23957
    acoustic propag., horizontal, fluctuation over short depth increments 8=36698
    acoustic ray transmission, pseudorandom bottom structure obs. 8=41329

Oceanography—contd
- acoustic wave propag. at ocean bottom, 2-700 miles, regular var. obs. 8=27863
- acoustic waves in SOFAR layer rel. to Love wave propag. along interface 8=32895
- Aleutian Island arc, mag. anomaly patterns and floor spreading 8=50218
- Arctic basin, ice-field drifts and currents 8=36684
- Atlantic, S., mag. anomalies and floor spreading 8=36897
- Barbados coral, Pb^{231} growth radioactive dating 8=36683
- bottom reverberation from deep explosions 8=50099
- breaking of waves, model integro-differential eqn. 8=30373
- conference, 1967 8=24279
- continental shelf wave propag. 8=32192
- convection, haline, induced by sea water freezing 8=41332
- current mapping by meas. of surface temp. discontinuities from Nimbus II 8=41335
- current rel. to tide, deep obs. off N. Californian coast 8=36690
- deep sea bed acoustic backscatt. at small grazing angles 8=50098
- deep sea bed acoustic transmission rel. to bulk and textural props. sediments 8=36691
- deep sea cores, paleomag. stratigraphy and micropaleontology 8=50102
- deep sea cores, sedimentation rate determ. by γ-ray spectrometry 8=27865
- divers speech during decompression causes of distortion 8=23972
- drogue diffusion, large scale 8=45434
- East Pacific rise, heat flow data, stat. anal. of scatter 8=50112
- explosions at ocean surface 8=28372
- explosions due to pressurized spheres at ocean surface 8=27867
- flow of inhomogeneous fluid at equator, nonlinear model 8=32195
- Great Lakes, wind-driven summer circulation 8=32188
- high-pressure pH sensor 8=45436
- hydrophone arrays, effect of phase errors 8=27862
- hydrophones, simple method of calibrating 8=36695
- Indian Ocean, mag. anomalies and floor spreading 8=36898
- interactions between ocean and atmosphere, model 8=36693
- Kwajelain and Entiwetok, Marshall Islands, sea level regression time series 8=36692
- Laplace tidal eqn. asymptotics, for neg. eigenvalues of equiv. depth 8=32193
- light fields and transfer in sea, survey of mathematical models 8=41333
- magnetic field of underwater mountains 8=45559
- microwave emission, effect of temp., angle of obs., salinity and thin ice 8=50113
- moon-earth system early history from waves in sandstones and calcarenites 8=50115
- navigation using two-component electromag. ship's log 8=27861
- noise, deep-sea, ambient, surface motion effect 8=36697
- noise, impulsive, resembling whale sounds, analysis 8=50100
- Norwegian sea, mag. obs. 8=50208
- oceanic circulation, nonlinear problems 8=36694
- oceanic circulation, wind-driven, overlooked aspect 8=41331
- oceanic currents, theory, exact soln. 8=27869
- oceans as source of ice nuclei 8=41337
- optical props of ocean, new method for study 8=32244
- Pacific beds, magnetic anomalies and floor spreading 8=36896
- planetary equatorial waves 8=50103
- radiance of sea and sky in i.r. window 800-1200 cm^{-1} 8=36689
- radiation field at great depth, calc. from Mie and transfer theory 8=41336
- radiative energy transfer, conference 8=23909
- radiative transfer in sea, expt. methods to meas. props. specified by theory 8=41334
- Ridge, Mid-Atlantic, comparison of earthquakes along median rift and offset fracture zones 8=50050
- ridges, mid-ocean, and geotherm distrib. during mantle convection 8=32172
- ridges, rel. to eustatic changes in sea level 8=41326
- sea-bed conductivity determ. from mag. field due to line source 8=27853
- sea bed quark detection 8=24741
- sea level, surface atmospheric press. and wind components, relation 8=36692
- sediment, deep-sea, velocity, obs. made while reflection profiling 8=32191
- sedimentation patterns of submarine canyons, modern deposits compared with Tertiary age 8=27872
- sedimentation rates of deep sea cores, comparison of paleomag. and ionium methods of determ. 8=50110
- sediments, Bering Sea, elect. resistivity 8=50108
- sediments, deep-sea, velocity from sonobuoy data 8=32190
- seismograph, ocean-bottom 8=50026
- shallow-water c.w. acoustic phase characts. 8=50111
- shipboard gravity meters, La Coste-Romberg performance (1963-1964) 8=36655

Oceanography—contd
- Sofar speed and axis depth contours, Pacific 8=50105
- sound attenuation in marine sediments 8=25961-2
- sound scatt. by ground inhomogeneities of ocean bed 8=50106
- storm generation of waves in earth's crust and atmosphere, meas. limitations 8=36666
- stratified ocean, inertial boundary currents, existence and struct. 8=45435
- submerged structure, rising, wall press. vars. in boundary layer 8=45432
- surface layer of ocean, daily temp. variations 8=27868
- surge and bore, undular, run-up rel. to slope and bottom roughness 8=50116
- thermocline strength fluctuations in coastal waters 8=32194
- tidal motion induced mag. and elec. fields at sea floor and coastal sites 8=45433
- tidal prediction, numerical methods and Thames model 8=27866
- tides in cruciform oceanic basins 8=36699
- tsunamis, gravity-wave system, nature and recent obs. 8=50104
- underwater acoustic pressure calc. 8=50101
- underwater convergence of acoustic waves obs. 8=27864
- underwater sound research before 1939 8=36696
- velocity and press. distributions, spectra relationship 8=27871
- waves, air-sea, excited by volcano Krakatoa, pulse propagation 8=27829
- waves on beach 8=50109
- waves, plane, diffraction by a circular island in rotating basin of const. depth 8=27870
- waves, surface gravity, linear and nonlinear motion (model) 8=39279
- Western Equatorial Pacific, two thermal fronts, obs. 8=41328
- wind-generated wave suppression by surface film, theory 8=48037
- $BaSO_4$ solubility in sea water 8=34783
- I, abundance in deep sea sediments 8=36688

Octet theory. See Elementary particles; Field theory, quantum.

Omegatrons. See Leak detection; Mass spectrometers; Vacuum technique.

Onsager relations. See Statistical mechanics; Thermodynamics.

Optical activity. See Optical rotation.

Optical constants
- See also under individual headings, e.g. Absorption/light; Reflectivity.
- anisotropic mats, from e.-energy loss expts. 8=49672
- film on substrate, reflection-transmission method for determ. 8=36289
- films in vacuo, meas. 8=36288
- glasses, indices of internal strains, glasses in optical glass catalogue 8=41096
- isotropic and uniaxial crystals, u.v., determ. using polarized light refl. power obs. 8=41018
- oxide films, on Ge 8=49721
- polystyrene, in vac. u.v. 8=41174
- reflectometer, double-beam type, for determ. 8=37684
- surface layers, thin, microstructures from ellipsometry 8=48439
- surface ripples, off-crest amplitude meas. 8=34727
- Ag-In alloys, dil., rel. to interband transitions and plasma oscills. 8=49699
- B, amorphous films, 0.6-6.0 eV 8=45174
- $Be_4O(CH_3\text{-}COO)_6$, in 600-1800 cm^{-1} range 8=45239
- Cu, uniaxial and hydrostatic strain dependence rel. to interband transitions 8=49724
- Cu-Au alloys, from transmission and reflection meas. 8=41082
- Cu_2O, and refl. rel. to lattice vibrs., 290°K 8=39873
- Fe-Ni films, and Faraday effect 8=36358
- Ge, nonlinear susceptibilities rel. to band model 8=45219
- nInAs(Sb) nonlinear susceptibilities rel. to band model 8=45219
- K, 0.5-4.0 eV ellipsometric obs. 8=41120
- MgO, from electronic band structure by pseudo-potential calc., 7-28eV 8=27587
- Mo, reflectance meas. 537-5770Å 8=27591
- Na, 0.5-4.9 eV ellipsometric obs. 8=41120
- Pt, from reflectance data 8=45216
- Re, reflectance meas. 537-5770Å 8=27591
- Rh rel. to h.f. polarizability and cryst. e states, 0.4-11μm 8=32026
- Sb_2S_3 films, meas. for diff. thicknesses 8=49748
- Si, nonlinear susceptibilities rel. to band model 8=45219
- Ta, reflectance meas. 537-5770Å 8=27591
- VO_2, 0.25 and 5eV, in semiconducting and metallic states 8=49760
- W, reflectance meas. 537-5770Å 8=27591
- Y_2O_3, in spectral region 0.25 to 9.6μ 8=49762

Optical dispersion. See Dispersion, optical.

Optical fibres. See Optical systems.

Optical films
- See also Filters, optical.
- antireflectant, behaviour, theoretical interpretation 8=42243
- beamsplitters, efficiency, in far i.r. Michelson interferometer 8=28850

Optical films—contd
- deposition of films thicker than 1μ on optical component surfaces 8=44034
- dielectric, as mirrors, windows and filters for laser work 8=49674
- dielectrics, thickness control during vacuum deposition 8=48433
- Fresnel formulae fabrication, props. 8=28847
- multilayers systems least squares method for automatic design 8=46671
- polariser in rotatory dispersion adapter 8=24370
- standard coatings with unchanging radiation props., prep. 8=49673
- B, amorphous, transitions 8=45174
- Ba and absorpt. props. 8=27560
- CuCl, density, refr. index and absorpt. coeff. 8=31982
- ThF_4, dispersion of refractive index and useful range of transparency 8=35184
- α- and β-$TiCl_3$, growing, thickness meas., and absorpt. spectra 8=36417

Optical filters. See Filters, optical.

Optical images
- See also Aberrations, optical; Holography; Resolving power, optics.
- bundles, flexible fibres, image forming, applications 8=46675
- curvature correction in images produced by concentric systems by means of fibre 8=42194
- degraded by diffraction and noise, restoration of resolution 8=28735
- diffraction, algebraic formulation for self imaging 8=46731
- diffraction, of point in focal and out of focus planes 8=42251
- distant source, in lens focus, random displacements due to refractive index vats. 8=24369
- distorted by atmosphere, electronic restoring system 8=42180
- electron, emulsion resolution for 7-60 keV 8=37722
- electrophotographic imaging with cholesteric liquid crystals 8=42279
- distortion, new theory 8=37638
- errors, finite, theory based on diapoint config. 8=46665
- finite sampling, effect in holography 8=28886
- formation and filtering, coherence and incoherence 8=37649
- formation, nonlinear transfer by phase contrast 8=37646
- grid formation using hologram with spatially incoherent illumination 8=42264
- holographic formation, equivalent-lens theory 8=46748
- holographic light flux, effect of photographic characts. 8=44272
- holographic recording props., comp. with photographic method 8=46746
- holographic, transmission by television 8=33293
- illuminance distribution calc. on bases of wave theory 8=42252
- imagery using coherent light, noise minimization 8=37628
- imaging through randomly inhomogeneous medium by wavefront reconstruction 8=28889
- luminance amplification in electro-optical systems 8=42261
- meridiurnal decentering effect on astigmatic ray bundles 8=37647
- photographic relief images 8=28883
- photographs, blurred, sharp-focus restoration by holographic methods 8=24433
- pseudoscopic, formation and inversion 8=28902
- quality assessment for system by comparison with synthesized image 8=37650
- quality in incoherent system, transfer function applic. 8=28736
- quality, theoretical prediction 8=28741
- radiographic, information capacity calc. 8=46770
- reflector, parabolic, source displaced from focus 8=33244
- shape definition, use of coherent optics 8=46669
- simultaneous viewing of image and stop aperture which scans image, six devices 8=42186
- spot diagram of max. sharpness 8=46666
- transfer function rel. to flare and method of meas. 8=28738
- trapezoidal distortion in projected images 8=42168
- two close objects, apparent separation and intensities 8=24368
- visual pattern, charact. features extraction by laser prod. Fraunhofer diffraction 8=33246
- visual, stabilization in vibrating environment, meas. and specifications 8=42172
- from wide angle lenses, asymmetrical, for 35mm photography 8=28910
- wind-tunnel model incidence meas. 8=28733
- CdS self-scanning sensor using high field domains 8=27317

Optical instrument testing
- aberrations, interferometric methods 8=28752
- alignment procedures and flatness testing 8=28746
- Fabry-Perot plates charting, Michelson interferometer meas. 8=28849
- flatness control in optical polishing 8=37652
- flatness, precision meas. 8=28752
- optical flats, contour determ. 8=37686
- refracting telescope, 16-inch, Hartmann results 8=28036

Optical instruments
- Some instruments are listed separately, e.g. Refractometers.
- amplifier, multi-path cell, 15 dB gain, $9\text{-}11\mu$ 8=24374
- angle-doubler for reflectance meas. in vacuum 8=37658
- angle-measuring instrument, specifications 8=41616
- autocollimator, AKF0.5, precision and accuracy of meas. 8=46673
- coelostat for Catania observatory 8=28163
- contact spherometers 8=42184
- converter for vel. meas. in boundary layer of high temp. gas 8=30244
- Corning Glass Works, review 8=37660
- correlator using laser beam diffraction by u.s. waves 8=28751
- crystal orientation goniometer 8=30814
- design for hostile environment 8=28758
- design procedure 8=28753
- design with computers, adaptive automatic correction tech. 8=28748
- diffraction gratings for meas. error in gear hobbing machine table drives 8=24373
- diffractometers, accessory for transferring crystal from one goniometer head to another 8=26345
- dispersion, adapter, rotatory 8=24370
- Fabry-Perot etalon, temp. regulation 8=28747
- Fabry-Perot resonator, with rapid sinusoidal detuning 8=46556
- Fresnel and sine wave zone plates 8=37690
- heliostat, simply-aligned 8=32416
- heterodyne detector, balanced, with oscillator and signal waves perp. polarized 8=42216
- heterodyne expts. with enclosed transmission paths 8=37651
- heterodyne receivers, broadband matching 8=28774
- hypervelocity impact expts. optical lever technique adaption 8=23945
- laser acoustic techniques for variable time compression, expansion and reversal of r.f. signals 8=28721
- laser windows, films and mirrors from dielectric materials 8=49674
- light guide consisting of glass fibres, technology of manufacture 8=28761
- light scatt. meas. in optical materials 8=42181
- loss meas. by He-Ne laser 8=28689
- lucite light pipes coupled to photomultipliers, efficient design 8=24371
- luminescent errors due to "thick" specimens, elimination 8=37657
- machining parts with diamond-tipped tools on metal-cutting lathes 8=45939
- micrometer, contactless, use in thickness meas. technique 8=41615
- modulator, photoelectroplating 8=37631
- open u.v. counter tubes, 900 to 1300Å, obs. 8=28759
- phase-meter 8=28662
- prism line-scanner for high-speed thermography 8=37322
- profile, two-dimensional, Hankel transform appl. 8=41630
- prod. of optical elements, workshop and industrial methods 8=28749
- radii of curvature of test glasses, 0.3 to 6m., meas. apparatus 8=28756
- rangefinder, stadimetric slide rule calculator 8=37661
- range-viewfinder, stereoscopic, photographic 8=42283
- reflectometer techniques, theory 8=37682
- resonator, confocal Fabry-Perot, curvature deviation 8=42215
- simultaneous viewing of image and stop aperture which scans image, six devices 8=42186
- spectrophone for meas. laser beam absorption in gas 8=39218
- spectroscopy, problems enumerated, methods compared 8=28777
- spheres for testing concave mirrors 8=28744
- stopped-flow apparatus for reactions in soln. 8=32084
- stray light 8=46670
- system transfer function meas. 8=42175
- Teflon, high finish polishing 8=37096
- vacuum deposition mask changer registration obs. 8=30338
- window with boundary layer control 8=37655
- windows for i.r. meas. at high pressure 8=33249
- I_2 u.v. photon counter 8=46672
- Si p-n junction u.v. photocells 8=27338

Optical materials
- See also Filters, optical.
- Corning Glass Works, review 8=37660
- corundum, transparent sintered, prep. and props. 8=45940
- crystals for u.v. and i.r. optics, props. 8=42116
- flatness testing of surfaces to 240 mm diam with Fizeau interferom. 8=28859
- flats, contour determ. 8=37686
- fluorite, correcting u.v. objective 2/50 8=37724
- glass, annealing for low residual stress and refractive index homogeneity 8=41141
- glass surfaces, impression by high intensity laser beam 8=33248
- glass, optical, classification according to props., prod. technique 8=31996
- glasses, optical indices of internal strains, glasses in optical glass catalogue 8=41096

Optical materials—contd
  glasses, refractive index determ. 8=37636
  for i.r. optics 8=31954
  light scatt., meas. by new instrument 8=42181
  low expansion, precision thermal expansion meas. 8=39927
  low-temperature obs., glass immersion cryostat 8=41884
  lucite light pipes coupled to photomultipliers, efficient design 8=24371
  nonlinear evaluation by powder technique 8=45142
  nonlinear, for laser communications, search 8=27520
  quartz glass, correcting u.v. objective 2/50 8=37724
  thermal expansion interferometric meas. 8=35439
  transient rad. effects on transmission 8=28742
  u.v. and i.r. transfer of radiation 8=37653
  CdS, light demodulator with u.s. amplification 8=27216
  CsI crystals, mech. behaviour and tensile strength 8=40139
  CuCl crystal prep. process conditions 8=26248
  $KTa_fNb_{1-f}O_3$ (KTN) conc. gradient light beam deflector 8=36382
  $RO\text{-}TiO_2\text{-}SiO_2$ systems (R = Ca, Sr, Ba, Zn, Cd), glass formation 8=44079
  $V_2O_3\text{-}P_2O_5(La_2O_3, Nd_2O_3$ on $CeO_2)$ glasses, i.r. transmission characts. 8=36425
Optical model. See Nucleus/models.
Optical properties of substances
  See also Optical constants; Optical materials.
  absorpt. characteristics using Jogansen's function for meas. integral intensities 8=34865
  alkali-halide crystals, in u.v. 8=27556
  alkali halides, second harmonic generation obs. 8=27555
  alkaline bromides, stability constants of Pb complexes 8=48148
  ammonium oxalate, non-linear props. and double refraction 8=36443
  ammonium pentaborate, nonlinear props., 8=41167
  amplification, nonlinear of propagation pulse 8=46646
  azamerocyanines, polarizability in region of absorpt. band 8=34851
  p-azoxyanisole liquid crystals, optical rot. obs. 8=43826
  beam self-trapping in molecular fluids for saturation of non-linear refractive index 8=30478
  benzene liquid, i.r. stimulated emission at 5μ by phonons obs. 8=43828
  cholesteric, circular polarization 8=48150
  cooling of crystals by transfer of laser radiation into atomic thermal vibrations 8=39900
  colloids, optical nonlinearities 8=34951
  corundum, transparent sintered, prep. and props. 8=45940
  cryptocyanine, alcohol soln., optical width var. during laser giant pulse generation 8=25921
  crystal, laser-illuminated, second harmonic and parametric generation, optimization 8=49671
  crystal, mol., i.r. vibr. line breadth rel. to reorientation 8=36292
  crystal, parametric gain near lattice resonance, theory 8=45141
  crystals, as backward wave light generators 8=24357
  diamond type semiconds and insulators, rel. to band struct. 8=44753
  diamond, Type II, u.v. transparency and abundance 8=49710
  9,10-dimethylanthracene in dimethylformamide: spectra of electrochemiluminescence 8=48177
  dye solns., third-harmonic generation, conc. and dispersion dependences 8=43819
  ferroelectrics, oxygen octahedra, nonlinear tensor coefficients 8=41017
  filament formation due to self-focusing of intense optical beam in liquid 8=43816
  films in vacuo, optical consts. meas. 8=36288
  films, thin granular 8=27521
  fluid, opalescent, spectrum of doubly scatt. light 8=39152
  Franz-Keldysh effect, high-freq. 8=31950
  gas mixtures, scatt. rel. to mol. correls. 8=34663
  gas particle cloud, homogeneous, emittance freq. averages 8=43693
  gases, Rayleigh scatt., finite-size effects 8=39219
  gaseous media, Raman and Brillouin effects stim. in emission and absorption 8=48155
  glass-ceramic, Cer-Vit, transmittance at u.v., visible, i.r. and sub-mm wavelengths 8=45165
  glass-ceramic mirror blanks, transparency under strain 8=41137
  glass, photochromic, produced by Ag^+ exchange 8=41140
  glass second harmonic generation obs. 8=27555
  glass, silicate-alumina, 600°C i.r. emission spectra 8=38842
  gyrotropic crystals, expression for component of reaction forces of Vavilov-Cherenkov radiation 8=31952
  inert gases, third-harmonic coeff. calc. 8=39214
  ionic crystals, lattice vibrs. 8=44287-8
  ionic crystal sphere, vibration modes 8=35374
  Kramers-Kronig relations, molecular spectra, liquids and solns. 8=48153
  leucosapphire effect of γ-radiation 8=41054
  light emission from Si p-n junctions 8=45286
  liquid, anisotropic molecular, in laser resonator 8=42071
  liquid, laser beam irradiated, optical gain 8=30477
  liquid mixtures, scatt. rel. to mol. correls. 8=34663

Optical properties of substances—contd
  liquids, beam self trapping by dielect, waveguide production 8=34843
  liquids, dense, Raman and Brillouin effects stim. in emission and absorption 8=48155
  liquids, emission from hydrodynamic cavitation 8=43813
  liquids, power-depend. distortion of i.r. beam from CO_2 laser 8=25916
  liquids, self-trapping of picosecond pulses in viscous liquids and glass 8=43810
  metal thin films, rel. to e transport 8=26954
  metals, anomalous skin effect for expts. at non-normal angles of incidence 8=49739
  metals, thermodynamic theory 8=27518
  mineral salt, aqueous sol., Kerr effect 8=34844
  modulators, Debye-Sears amorphous-solid wide-band, transfer characts. and freq. response 8=27522
  Mossbauer diffraction in crystals, quantum theory of γ-ray and x-ray optics 8=30636
  naphthalene, deuterated, optical anisotropy of excited state 8=25611
  nonlinear mats., evaluation by powder technique 8=45142
  nonlinear, self-focusing filaments, prod. mechanism 8=42153
  nontrionite, monodisperse sols., electrooptic effects 8=39459
  oil, synthetic immersion, for microscope objectives 8=39363
  opalescence, critical surface 8=25915
  organic crystal solns. generation due to ruby laser pulse 8=30479
  Perspex dosimeters, photosensitivity 8=42347
  phenanthrene crystallites in rigid 3-methylpentane spectroscopic study 8=49429
  photochromic glasses 8=41095
  photoselection, tandem two-photon processes 8=49692
  plane surfaces, evaluation of quality, technique 8=36286
  plasma resonance, review 8=49123
  plasmons in metal spheres, e. bombardment stimulation and radiative decay 8=45145
  polarizability tensor in cubic and hexagonal II-VI cpds. 8=27545
  polycyanacrylates and compositions based on chem. 8=48151
  polymers, electronic theory 8=29867
  polystyrene, filament struct. in laser beam trace 8=49784
  polystyrene films, far u.v. 8=27639
  potassium tartrate, second harmonic generation on ruby laser irrad. 8=45199
  quartz, synthetic, u.v. transmission 8=49751
  Raman effect, stimulated, in gases and liquids 8=43169
  rare earth ions in crystals, energy transfer, temp. depend. 8=45138
  recombination radiation in inorganic solids 8=31953
  rhodamine C solution, optical generation during excitation with pulsed light sources 8=30480
  ruby, effect of γ-radiation 8=41054
  saddle point transitions under crossed elec. and mag. fields 8=27543
  salicylanide, variation in absorpt due to equilibrium between rot. isomers and ionization 8=38903
  sapphire, colourless crystals, optical inhomogeneity 8=41055
  salicylidene aniline, photochromism 8=45302
  second harmonic generation, ang. structure 8=36377
  secondary spectrum of two-element lenses in i.r. 8=45144
  self-excitation of active plane-parallel layer, effect of metal lattices 8=31946
  self-focusing in disperse medium produced in laser 8=36310
  self-focussing of light, electrostriction effect 8=41046
  semiconductor plasma in elec. field, non-linear 8=31930
  solid, isotropic, polarization due to diffraction by u.s. waves 8=36302
  stim. Raman effect in liquids of diff. Kerr coeffs., effect of temp. on threshold 8=48156
  stress-optical meas. by intensity method 8=44510
  spatial synchronism in nonstationary processes of photon-echo type 8=49670
  spherulite, radial, Rayleigh-Gans scatt. 8=36447
  stimulated emission in solutions, use of cuvette 8=46704
  tandem two-photon processes, polarization correl. 8=49692
  trans-4-dimethylamino-4′-nitrostilbene, polarizability in region of absorpt. band 8=34851
  underwater optics, S/N concept 8=37695
  underwater rad. distrib. meas., directional photometer 8=42136
  III-V cpds., second order susceptibility calc. 8=27523
  III-V cpds, second-order susceptibility rel. to Miller coeff. and bond dipole moments 8=36314
  uniaxial absorbing crystals 8=27527
  Vavilov-Cherenkov radiation, integral expression for component of reaction force 8=31952
  water surface, radiation distrib. var. 8=34853
  X-ray interf. at distorted cryst. lattices 8=31951
  X-ray monochromators and resonators from single crystals 8=28928
  zinc-blende type semiconds and insulators, rel. to band struct. 8=44753
  Ag halides particles, bleaching 8=41094

Optical properties of substances—contd
Ag, second-harmonic generation 8=27548
AgBr, AgCland AgI, far i.r. reflection spectra 8=45167
AgCl, 2-21 eV, reflectivity obs. 8=36316
As_2Se_3 film, energy bandgap, reflectance and refractive index 8=31963
$(As_xSb_{1-x})_2Se_3$ film, energy bandgap, reflectance and refractive index 8=31963
$Ba_2NaNb_5O_{15}$, continuous parametric oscillation 8=36328
BeO, phonons, reflection and Raman spectra meas. 8=27561
$Bi_4Te_3O_{12}$ crystals, electrical-optical behaviour 8=27271
CaF_2, photo-effect, influence qf electric field 8=36337
$CaSO_4$, photo-effect, influence of electric field 8=36337
CaV_2O_6 8=30798
$Ca_2V_2O_7$ 8=30798
$Ca_3V_2O_8$ 8=30798
$Ca_5(PO_4)_3F:Nd^{3+}$, spectral and laser characts. 8=37620
Cd, Mg and Sn single crystals, opt. consts. from reflectance ratios 8=45164
CdS, oscillatory exciton emission 8=41077
CdTe, recombination radiation, evidence for superradiance 8=31971
CO_2 spectral transmission functions 8=30300
CO_2-H_2O vapour, optical-acoustic radiation, press. temp. effect 8=30298
CS_2, 4-photon amplification of quartz stimulated M-B scatt. components, obs. 8=43822
Cr black coatings, electrolytically deposited 8=45394
Cr, in the far u.v. 8=31978
Cr, Hf, Ni and Zr, polycrystalline, opt. consts. from reflectance ratios 8=45164
Cs_3CoCl_5, and magnetic and e.p.r. props. 8=31501
Cs_3ZnCl_5: Co^{2+}, and magnetic and e.p.r. props. 8=31501
Cu-isochromat at 10 kV 8=49714
Cu-Au alloys, transmission and reflection meas., 8=41082
CuCl film, density, refr. index and absorpt. coeff. 8=31982
Cu_2O, thin films, rel. to transport props. 8=31983
$Cu_{2-x}S(0 \leq x \leq 0.2)$, and elec. props. 8=49156
D_2O, absorpt. intensities, 4000-1000cm^{-1} obs. 8=34852
Fe films, and elec. props. rel. to absorpt. of bulk Fe 8=41085
GaAs, abs. coeff. at microwave and mm. freqs. 8=27568
GaAs laser diodes, photoelectric props. 8=49305
n-GaAs, modulation of opt. abs. at intrinsic edge by acoustoelectric domains 8=27570
GaP photodiode, strongly compensated p-i-n junction 8=40509
GaP: Cd-O complexes. 8=27648
GaP: Zn-O complexes. 8=27648
GaS semiconducting layer compound 8=44774
p-GaSb, optical modulation by acoustoelect. domains 8=31991
GaSe, semiconducting layer compound 8=44774
Ge, far i.r. modulation, crossed-field, free carrier 8=41093
Ge, optical difference mixing 8=31995
GeSe, and photoelectric props.. in energy range 0.5-1.5eV 8=49727
$GeSe_{0.75}Te_{0.25}$, optical absorption 8=31994
He, liquid, with excess electron, theory 8=34854
He-Ne plasma afterglow rel. to 2s and 2p decay velocities 8=30080
α-HIO_3 crystal, soln. grown, nonlinear obs. and appl. 8=32000
H_2O, absorpt. intensities, 4000-1000cm^{-1} obs. 8=34852
H_2O vapour spectral transmission function 8=30300
In_2O_3, sputtered films, near i.r. 8=40470
InSb, coherent emission from e-hole plasma without mag. field, obs. 8=32001
In_3Te_4 thin layers, rel. to structure and photoconductivity 8=39796
K film, for photons 3.96 to 9.69 eV 8=49731
KBr, F-aggregate bands, optical and thermal stability, half-widths and oscillator strengths 8=49732
KBr optical consts. from energy loss meas. 8=32003
KCl, dependence growth conditions and impurity effects 8=26401
KH_2PO_4, second harmonic generation using a laser 8=41102
$KLiSO_4$, second harmonic generation on ruby laser irrad. 8=45199
LaF_3-SrF_2:Nd^{3+}, induced emission at 300°K 8=27579
LiF, dependence on growth conditions and impurity effects 8=26401
$LiNbO_3$, birefringence and phase-matching temp. as function of melt stoichiometry 8=31433
$LiNbO_3$, melt-grown, second-harmonic generation rel. to comp. 8=41114
$LiNbO_3$, piezo- and thermo-optic behaviour 8=27582
MnTe, antiferromagnetic semiconductor, interpret. using magnon drag. 8=32009
$NaBrO_3$, second-harmonic light generation rel. to natural optical activity 8=45206
NaCl, dependence on impurity effects 8=26401
$NaClO_3$, second-harmonic light generation rel. to natural optical activity 8=45206
Nd self-focusing in disperse medium produced in laser 8=36310
Ni-Al alloys, colour rel. to composition, Fermi surface and Brillouin zones 8=45213
Pb, in the far u.v. 8=31978
$Pb_{1-x}Sn_xSe$, rel. to i.r. rad. generation and detection 8=43980
$Pb_{1-x}Sn_xTe$, rel. to i.r. rad. generation and detection 8=43980
$RbNi_{1-x}Co_xF_3$, Faraday rot. and bulk absorption 8=49555
PbO, and electrical props. 8=26948
PbO-La_2O_3-B_2O_3 glasses 8=45214
$(Pb_xSr_{1-x})TiO_3$ crystals, $x \approx 0.25$ 8=44139
Pd, electronic structure by photoemission and optical studies 8=31293
$PtSb_2$. also preparation and semiconducting props. 8=40479
Rb^{85} vapour, optically pumped, modulation of scattered light beam 8=37629
RbH_2PO_4, detection on laser illumination 8=45203
$Sb_xBi_{1-x}SJ$ and $SbS_xSe_{1-x}J$ 8=40670
Sb_xS_3 film, energy bandgap, reflectance and refractive index 8=31963
Se, trigonal, in polarized vacuum u.v. 8=45217
Se-Cd glass, nonlinear optics 8=32029
SnS, epitaxial film, and structure 8=44060
SnSe, epitaxial film, and structure 8=44060
SnTe epitaxial film, and structure 8=44060
Si, optical difference mixing 8=31995
UO_2^{+2}:Nd^{+3} laser glass, Ce-stabilized 8=28710
W, isochromat at 8kV 8=49761
Xe liquid, −59.0°C-16.5°C, refractive index and Lorentz-Lorenz function obs. 8=43809
Xe vapour, −59.C — 16.5°C, refractive index and Lorentz-Lorentz junction obs. 8=43809
Xe_2 compressed light source for pumping Nd glass laser 8=28709
YVO_4, an i.r. spectral emittance 8=32038
ZnO crystals, laser action under e.-beam pumping 8=49765
ZnO, intrinsic photo effect of dyes, spectral sensibilization mechanism 8=36428
ZnO, low dispersion layer 8=36429
ZnS, coherent fluorescence for excitation by 2 photon absorption 8=32063

Optical pumping
amplifier, quantum, gas mixture 8=24299
atomic system, dynamical eqns., irreducible-tensor-formalism of statistical operators 8=29634
double-pulse, for stimulated emission 8=24265
efficiency calc. by graphical method 8=42067
excited state mixing, collisionally induced 8=29631
h.v. transient pumping technique, prod. of 5-J 200 kW CO_2 laser pulses 8=33180
influence of gas laser on fluoresc. emitted by gas in magnetic field 8=47515
laser, by electrodeless h.f. discharge 8=33178
laser, by tubiular lamps fed by double current pulses 8=46539
laser generator rods, distrib., photographic meas. 8=24324
laser, heating change in active element 8=24325
laser, rel. to rod side surface matting 8=37598
laser resonator with radial gain profile, Gaussian mode 8=37563
lasers, solid, use of spherical reflector 8=46598
lasers with 2 photon pumping, employment in freq. conversion 8=33241
level-crossing meas., effects 8=25342
maser, intensity and freq. effects on Q of material 8=37548
non-uniform, loss in solid laser 8=37600
organic dye laser, flashlamp 8=46629
polymethane dyes, nineteen, stimulated emission over continuous range 710-1060 mμ 8=28713
polymethyl methacrylate rods containing rhodamine dyes, stimulated emission when flashlamp excited 8=28714
power supply for laser pumping source, optimum capacitance 8=42052
pulse generation, mode locked in passively switched lasers 8=28651
Raman effect induction 8=43207
Raman laser pulse generation by focusing ruby output on H_2 cell 8=28684
resonator, measuring Fabry-Perot with rapid sinusoidal detuning 8=46556
resonator with modulated Q, kinetics 8=37559
resonators and waveguides with infinite mirrors, modes 8=33121
resonators with partial polarizers, eigenstates of polarization 8=46559
r.f. resonances, study of nuclear and electron magnetic moments 8=43212
rhodamine dyes in polymethyl methacrylate rods, stimulated emission when flashlamp excited 8=28714
ruby and $CaWO_4$:Nb^{3+} crystals, effect of parameters of pumping light source and discharge regime on output of coherent radiation 8=24330
ruby laser, by Ar ion laser 8=28704
ruby laser giant pulse field development with saturating filter in resonator 8=42100
ruby, photon echoes rel. to irrad. intensity, and echo dephasing model, obs. 8=36321
ruby, population inversion and absorpt. power 8=24331
semiconductor thin-platelets, laser emission 8=46613

Optical pumping—contd
stimulated emission when emission wave beats with second-order scattered wave 8=33173
transformation of flash lamp emission by org. luminophore solns. in laser system 8=28650
two-level system, intense radiation, effect 8=24271
$Ba_2NaNb_5O_{15}$, continuous parametric oscillation 8=36328
CaF_2: Sm^{2+} crystal generation, spectrum-time studies for ruby laser excitation 8=41071
CaF_2: Tm^{2+}, 12% nuclear polarization production 8=30633
Cd(SeS) semiconductor thin-platelets, laser emission 8=46613
Cs in N_2, enhancement by quenching 8=47514
Cs rel. to absorpt. line-width and Ne buffer press., obs. 8=25374
Cs vapour, hyperfine, with mag. filters 8=38693
D atom g_J ratio meas. 8=38734
Eu^{3+} in crystals, elec.-dipole transitions rel. to solid-state i. r. quantum counter-amplifier mechanism 8=42137
GaAs semiconductor thin-platelets, laser emission 8=46613
Ga(AsP) semiconductor thin-platelets, laser emission 8=46613
H atom g_J ratio meas. 8=38734
He, double refraction 8=39216
He^3, liq. nuclear polarization expt. 8=37337
He^3, polarized, n. m. r. meas. for pumping time rel. to temp. 8=47689
He^3, radiooptical resonance 8=47517
Hg^{201}, and pulsating e.m. field effects on dispersion and absorpt. 8=43222
Hg-vapour, rel. to green-band emission 8=29944
K vapour, four wave parametric interaction 8=33177
$LiNbO_3$, pulsed parametric oscilln. and power limiting 8=42078
Na, precision frequency meas. of 0-0 transition 8=47524
Nd glass rod, using compressed Xe_2 light source 8=28709
Nd^{3+} doped calcium fluorophosphate 8=37620
$NH_4H_2PO_4$, by laser, rel. to optical parametric scatt. 8=45211
Rb, in weak mag. field 8=38709
Rb jet atomic clock 8=47525
Rb, $NdCl_3$ D_2 filter for student expts. 8=42196
Rb^{85} vapour, double-quantum resonant, light beam modulation 8=37629
$Rb^{85,87}$ atom g_J ratio meas. 8=38734
Rb^{87}, light shift due to virtual transitions 8=38708
SF_6 gas by CO_2 lasers, photon echoes, obs. 8=34282
Si, dynamic nuclear polarization production 8=30632
Sm^{2+} in crystals, elec.-dipole transitions rel. to solid-state i. r. quantum counter mechanism 8=42137
Optical quantum generators. See Lasers.
Optical rotation
See also Magneto-optical effects; Optical constants; Polarimeters; Polarized light.
p-azoxyanisole, nematic liquid, obs. of two forms 8=43826
cholesteric liq. crystals, rotary power, theory 8=43812
crystal with impurites, nonlinear polarization 8=31948
crystals, cubic, with anisotropic impurity centres, in mag. field 8=45159
dithionic acid salts, dispersion and sp. rotation temp. dependence 8=27602
electron correl. models 8=29706
enantiomers in optically active liq. crysts., n.m.r. 8=39422
Faraday, giant and inverse Faraday effects in systems undergoing self-induced transparency 8=37700
Faraday in gas laser, obs. in He-Ne tubes 8=42094
Hameka's theory 8=37701
ketones, molec. theory 8=38888
liquid crystals, cholesteric, electric-field-induced 8=43811
magneto-optical dispersion, auto-recording type spectrometer for meas. 8=37673
of polarization plane due to weak inhomogeneity 8=46740
poly-L-alanine in soln., u.v. 7=43824
poly-L-serine in soln., u.v. 8=43825
polynucleotides, theory 8=29865
proteins, struct. determ. from dispersion 8=29862
quarter wave plate achromatization and linearization of retardation vs. wavelength 8=41056
quartz, i. r. obs. 1.85-4.00μ 8=36403
quartz, temp. dependence of activity in visible spectrum 8=49755
small birefringence in bovine lens capsule, obs. by opt. rotatory dispersion 8=28881
triglycine sulphate selenate, indicatrix rotation in phase-transition region 8=27638
vinyl polymers, theory 8=38973
$Cd^{111,114}$ polarization of light emitted by optical resonance of 2288Å radiation 8=34158
Cr films, prep. and anisotropy 8=31977
$K_4Fe(CN)_6 \cdot 3H_2O$, birefringence rel. to polytypic transforms., 0 to −100°C 8=31432
Li trihydrogen selenite, indicatrix rotation in phase-transition region 8=27638
$NaBrO_3$, second-harmonic light generation rel. to natural optical activity 8=45206
$NaClO_3$, second-harmonic light generation rel. to natural optical activity 8=45206

Optical rotation—contd
Ni boracites, sector growth and twinning exam by polarized-light microscopy 8=26188
$RbNi_{1-x}Co_xF_3$, Faraday 8=49555
S_2^- centre in alkali halides, under stress rel. to opt. absorpt. bands 8=45173
Optical systems
See also Aberrations, optical; Lenses; Optical images; Optical instruments; Optical materials; Resolving power, optics.
alignment, 2 mile accelerator using large rectangular Fresnel lenses 8=42173
allowable misalignment calc. by transfer coeffs. 8=42179
analysis and synthesis by using dualism of systems 8=28732
angle meas., comparative reflection method 8=32637
anisotropic resonator, theory 8=33270
anisotropic uniaxial, e.m. wave refl., beam displacement 8=24208
aperture, annular, with spherical aberration and coma, irradiance distrib. in diffr. patterns 8=42169
aspherical surfaces insertion, correction of
automatic design, applic. of merit functions 8=28726
Cassegrainian baffle design 8=37642
Cassegrainian mirror-lens isochromatic 8=32408
catadioptric, for cameras 8=46667
classification, for automatic retrieval of available designs 8=42166
coherent optical noise suppression 8=37641
communications, GaAs laser transmitter 8=37611
complex, design 8=42177
computer generated spatial filters for coherent opt. data processing 8=28764
computerized design by refinement in Newton's method 8=42170
contact, vibration-proof, with epoxy resin 8=46674
curvature correction in images produced by concentric systems by means of fibre 8=42194
Czerny-Turner arrangements of 2 spherical mirrors, and spherical mirror and concave grating 8=37644
direct and reversed, numerical comparison of aberrations with Gaussian type lens 8=33245
double lever, light beam intensity comparison 8=42127
double-wedge focusing device in image plasma 8=42164
e. a. s. emission, imaging photomultiplier system 8=38195
electron linear accelerator switchyard beam monitor 8=33077
extreme u.v. mechanical collimator 8=46668
fibre components, struct. anal. and inspection, new method 8=42195
fiber polychromator for separating pulsed plasma emission lines 8=37662
fibers, geometric and waveguide props. 8=28760
flexible fibres, applications for light guides and image forming bundles 8=46675
Fourier transform analogue computer 8=28828
grazing-incidence aplanatic mirror systems 8=46660
hologram transmission bandwidth reduction by elimination of vertical parallex 8=28893
homodyne signal strength rel. to path length 8=42146
image converters and intensifiers, objective design 8=42178
image illuminance distribution, calc. of basis of wave theory 8=42252
image luminance amplification in electro-optical systems 8=42261
image quality assessment by comparison with synthesized one 8=37650
image quality, stray light effect 8=37645
imagery using coherent light, noise minimization 8=37628
information-processing, optimization by transcorrelation-function maximization 8=28740
i. r. optical communication systems 8=33250
i. r. polarizer 8=46738
laser acoustic techniques for variable time compression, expansion and reversal of r. f. signals 8=28721
laser beam expander for divergence correction 8=28743
laser beam scan enhancement through periodic aperture transfer 8=28659
lens, coherent transfer characts. 8=37648
lens, entropy transmission 8=46658
light intensity viewing port for crystal growth 8=42171
magnified interferometry of small displacements 8=41619
using meniscus lens mirrors 8=42149
meridional decentering effect on astigmatic ray bundles 8=37647
modulator, a. m., 3 stage, obs. 8=33240
multicomponent, randomly oriented, alignment to common coordinates 8=42174
multilayer systems, automatic design by least squares method 8=46671
radar system, sidelooking, with coherent optical processor, holographic analysis 8=37524
redirectors and refocusers effect on light transmission through aberrated and misaligned lenses 8=46662
replacement of single-lens components by two-lens components 8=42158
resonator, open, perturbation calc. 8=24366
resonator, open with spherical mirrors, transmission losses 8=24367

Optical systems—contd
resonator, stable and unstable, modes 8=37561
Ritchey–Chretien telescope corrector 8=42188
screen scintillation due to interference 8=46723
separation of variables and principal charact. coeffs. in systems with very thick components 8=42167
short light pulse generation, convenient method 8=24379
solar simulation for 1.5 diam. test objects, using 9 rad. sources and a mosaic mirror 8=28734
solid light funnel for phototube aperture increase 8=41976
sphere for directional reflectance meas. 8=46718
spherical aberrations, correction, optimal conditions, and optimal position of image plane 8=42162
with spherical aberration, quality 8=28739
split-image, division of field of view 8=42165
spot diagram of max. sharpness 8=46666
stereocameras for bubble chamber photographs, adjustment 8=46767
Strehl ratio, depend. on magnitude of variance of wave aberration 8=28731
transfer coefficients 8=42176
transfer function meas. by holography 8=37704
transfer function, meas. instrument 8=42175
transfer function rel. to flare and method of meas. 8=28738
two-component mirror and mirror-lens variable magnification systems 8=42150
viscosity of glass fibres with and without concentric glass casings 8=39631
wave aberration, evaluation of variance, direct approach 8=37640
waveguide, made of tubular gas lenses, beam deformation obs. 8=37639
waveguides, stability of light beam at bends 8=46642

Optics
See also Aberrations, optical; Atmospheric optics; Lenses; Mirrors, etc.; Optical images.
anistropy theory, interacting mixtures of, molecules 8=46635
applied, Corning Glass Works, review 8=37660
coherent, applics. of holography and space freq. filtering 8=46742
in communications, statistical model of Poisson process in current induced from photo-elec. effect 8=41753
corpuscular, punctuation functions in 8=42117
crystal, ciné-films for lectures 8=27519
development in USSR (1917-67) 8=33234
filament formation due to self-focusing of intense optical beam in liquid 8=43816
films, amplitude superposition and boundary condition methods 8=42244
flatness control in optical polishing 8=37652
Fourier transform, fast 8=24407
four-level systems, simultaneous two-freq. generation 8=24353
Gaussian beam fluctuation in random medium, autocorrel. 8=46644
in Germany, basic and applied research, review of current state 8=28716
in hostile environment 8=28758
image distortion, new theory 8=37638
laser acoustic techniques for variable time compression, expansion and reversal of r.f. signals 8=28721
laser freq. doubling by RbH_2PO_4 crystal 8=37557
laser modulation using grating diffraction effects 8=42123
many-particle, dielec. const. and optical dispersion relations 8=37680
monochromatic generation by amplitude modulation 8=24355
nonlinear, and coherent radiation freq. conversion, survey 8=33241
non-linear, coherent freq. conversion in USSR 8=28719
nonlinear, in gyrotropic media 8=24408
nonlinear interactions, review 8=46645
nonlinear media, harmonic prod. and mixing 8=41016
non-linear studies of dense liquids and gaseous media using laser pulses 8=48155
phase state of generation 8=24406
physical-optics theory of planar dielectric waveguides 8=28623
processing of signals, electro-optical coherent 8=46637
quantum, ordering of field operators, normal and antinormal 8=46639
radiation absolute values meas. 8=37632
second harmonic, ang. struct. theory and expt. 8=36377
second harmonic generation by discrete spectra 8=24354
second harmonic generation, effects of laser focussing 8=45139
second harmonic generation in two level systems, rel. to crystals 8=36287
second harmonic, mag. field induced, search using ADP and quartz 8=45140
self-focusing of intense beams 8=24351
statistical, random function model 8=37627
transfer function for image quality 8=28736
transfer function rel. to flare and method of meas. 8=28738
two-frequency generation, material with split metastable levels 8=24356
underwater, S/N concept 8=37695

Optics—contd
wave packet, kinetic behaviour 8=37625
geometrical
aperture, annular, with spherical aberration and coma, irradiance distrib. in diffr. patterns 8=42169
caustics, ratio of amplitudes on and away from smooth curve 8=32908
corner cube reflectors 8=42147
distortion theory 8=37643
double-wedge focusing device in image plane 8=42164
image errors, finite, theory based on diapoint. config. 8=46665
parallel-ray tracing through symmetrically crossed half-prisms in autocollimation 8=42154
ray optics in turbulent atmos., validity 8=32239
reflector, parabolic, source displaced from focus 8=33244
review with ref. to image formation by lenses using matrix methods 8=28725
scattering of strongly interacting composite particles 8=47030
skew rays, vectorial soln. from Fincke's formulae 8=24365

Orbital calculation methods
all-electron calc., approx. methods 8=25578
AMO method, spin degeneracy 8=34314
atom and molecule, superconductivity theory applic., biorbitals 8=34113
atomic, classical motion 8=25346
atomic-orbital bases, choice and definition 8=43265
atomic orbitals for molec. fragments in MO's 8=29785
atomic SCF calcs. correction to exchange pot. giving h.f. energies 8=38615
atomic wave functions, configuration-interaction method 8=25358
atoms, relativistic wave functions, screening constant calc. 8=38630
augmented separated-pair expansion 8=38624-5
biorbitals method 8=47491
bond-orbital, ab initio calc. 8=38891
CNDO calcs. on second-row mols. 8=47573
CNDO method in spectroscopy 8=29767
CNDO/2, ionization potentials calc. 8=47785
conjugate molecules spin props. calc. 8=29707
correlated pair functions in atoms and mols., new method of calc. 8=34114
corresponding orbitals and cofactors 8=47574-5
de Sitter group in molec. quantum mech. 8=25430
distinguishable electron method 8=34118
dyes, photosensitivive, HMO calcs. rel. to work function 8=40687
effective operators and spectrosc. props. 8=34115
electron repulsion integrals one and two centre, for π-electrons in double bonds 8=34218
electron shake-off, SCF wave functions appl. 8=38688
FEMO model, three dimensional, homonuclear diatomic 8=47577
Fermionic-Bosonic approx. in mol. quantum mechanics 8=43264
g-factor of d^3 configuration, covalency and theory 8=43962
ground state calc., orbital exponent 8=25487
Hartree-Fock exchange pot. for electron gas adaptation to atoms and solids 8=38617
Hartree-Fock method, unrestricted, density matrix 8=38797
Hartree-Fock perturbation theory, non-orthogonal formulation 8=25331
Hartree-Fock-Roothaan approx., derivates of energy 8=38799
Hartree-Fock theorem relating upper bounds for ground state energies of $(N+1)$ and N electron systems 8=38618
Hückel theory, self-consistent methods 8=38796
INDO method (immediate neglect of differential overlap) 8=34211
INDO spin unrestricted wavefunctions, spin contamination 8=47508
intermolecular orbital theory 8=27684
iterative extended Hückel theory 8=25432
Koopman's theorem, analysis 8=34116
LCAO–HCO method 8=47571
LCAO–SCF–CO method 8=47572
limited Gaussian basis sets for atoms and mols. 8=29571
localized MO's, method of steepest ascents 8=29700
localized orbitals, σ bonds 8=47578
MO-LCAO crystal field theory, diagram method 8=43931
MOs for large mols., from SCF matrices of related small mols. 8=47570
molec. wavefunctions calc. n.q.r. as check 8=29701
molecules with high period elements, allowance for polarization of atomic shells in MO LCAO calcs. 8=25429
multi-configuration SCF with non-orthogonal orbitals 8=43151
multi-open-shell config., Coulomb operator matrix 8=47440
multi-open-shell config., fractional parentage coeffs. 8=47441
natural orbitals and wavefunctions, perturbation theory calc. 8=38603
nitrovinylbenzoate mol, appl. to structural group interactions 8=34347
Pariser-Parr-Pople calcs for benzo- and naphthothiophenes 8=43355

Orbital calculation methods—contd
perturbation theory of extended Hartree-Fock approx. 8=47469
perturbed Hartree-Fock, force consts. and dipole moment derivatives 8=25425
π-electron computation, general parameters 8=25440
polyatomic mols., improving precision of MO calc. 8=25431
probability loss from arbitrary group of states, upper bound 8=42311
pseudopotential method tested on H atom 8=29595
reduced-density-matrix theory 8=38598
resonance integrals, approximations in semi-empirical calcs. 8=34210
SCF calc., basis sets 8=25622
SCF calcs. without SCF eqns. 8=47444
SCF methods, choice for coupling operators 8=29699
self-consistent field calcs. in zero differential overlap approx., range of applic. extended 8=34357
self-consistent perturbation theory 8=25326
separated-pair approx. and electron correl. 8=38623
Slater-Condon integrals calc. from Hartree-Fock function for atoms from He to Ar 8=34133
Slater-type orbitals, multicentre integrals of γ_{12}^{-1} 8=38600-2
spin-orbital forces and relativistic effect 8=38800
spin-spin contact Hamiltonian, symmetry props. 8=38632
synchrotron lattice, orbit const. computation 8=33438
tetrahedrally localized orbitals, correl. 8=34117
three-body problem solution 8=33315
two-particle density functions for spin-projected Slater determinant 8=47445
uniform localization of AO's and MO's 8=25428
unoccupied natural orbitals of two-electron wavefunctions 8=38599
valence-bond theory of contact nuclear spin-spin coupling 8=47565-6
wave function for Li, Be^+ and B^{++} 8=38672
Be, natural orbital and geminal expansions, from reduced density matrices 8=43182
H_2, numerical single-centre SCF function 8=47601
H_2^+, electronic terms and wave functions for large internuclear separation 8=43310
Li atom, ^2S ground state, Hylleraas wave function 8=38671
Li_2, wave functions and binding energies calc. using quantum defect method 8=25489
Li H, natural orbital and geminal expansions, from reduced density matrices 8=43182
TiO_6^{-n} units, localized, extended Huckel calcs. using set of K parameters 8=45225
ZnO: Cu^{2+}, molecular theory 8=43969
Orbitals. See Molecules/electronic structure.
Order—disorder transformations. See Phase transformations/solid-state.
Ordered structure. See Crystal structure; Solids/structure.
Organic compounds
See also Free radicals; Macromolecules; Plastics; Polymers; Waxes.
acenaphthenequinone, vibrational spectrum 8=43282
acenes, cryst. and in soln., absorpt. spectra in polarized light 8=32042
acetaldehyde absorbed onto silica gel, laser Raman spectra 8=25530
acetaldehyde, ionization and dissoc. by electron impact 8=39056
acetaldehyde reaction with N, mass spectrometric study 8=27710
acetals, depend. of geminal H-H couplings on solent and conc. 8=43831
acetic acid, ionization and dissoc. by electron impact 8=39056
acetic acid, monomer and dimer., vibr. calc. 8=25531
acetic acid, n scatt. spectroscopy of microscopic transport props. 8=30403
acetic acid, vapour phase esterification with ethanol, thermodynamic equilibrium 8=49837
acetone/CCl_4 binary mixture, proton mag. relaxation 8=39425
acetone condensation products, mass spectra 8=29840
acetone-d_6, intermediates in photolysis 8=49951
acetone, electro-osmosis, temp. dependence of rate constants 8=32130
acetone, freezing press. 8=50477
acetone, ionization and dissoc. by electron impact 8=39056
acetone, orthobaric data near crit. pt. 8=34956
acetone, scattering of ruby laser emission, large angle 8=48158
acetone-water mixture, thermometric analysis 8=27771
acetonitrile and NH_4 salts dipole-dipole interaction, spectral C ≡ N band shift obs. 8=30487
acetonitrile, Brownian rotatory motion rel. to dipole-dipole intermol. forces in vibr., 8=43827
acetonitrile: bromine 2:1 complex crystal structure 8=39826
acetonitrile-d_3, γ-irradiated, trapped electron and its reversible reaction, e.s.r. evidence 8=49955
acetonitrile, photoionization 8=47789
acetonitrile, spin-lattice relax. and molec. reorientation in liq. 8=30539

Organic compounds—contd
acetophenone-$SbCl_3$ complexes in CCl_4, i. r. spectra 8=34866
acetophenone in soln at 77°K, medium effects on time-resolved phosphorence spectra 8=45297
para-acetotoluidide crystals, monoclinic modification X-ray study 8=44262
3β-acetoxy-17α-hydroxy-16β-bromo-5α-pregnan-11, 20-dione, crystal and mol. structure 8=26459
acetylacetone, spectra and electronic structure 8=47651
acetyl chloride, gas phase and matrix photolysis 8=43419
acetylcholine and related mols. crystal structure 8=26460
acetylcholine ionic environment in the chemical transmission of nerve impulses 8=28201
acetylene-air flame, intensified by discharge, activation energy of origin of excited radicals OH, CH and C_2 8=45359
acetylene, and acetylene-methane mixtures, ion-mol. reactions 8=49852
acetylene and organic mixing gas in analyzer cell for spectra 8=49986
acetylene, combustion in shock waves, source of schlieren signals 8=49886
acetylene, cryst., i. r. and Raman spectra 8=27618
acetylene, flame, Cu conc., linear absorpt. method 8=27790
acetylene in solution, i. r. absorption band widths 8=34867
acetylene, ionization Frank-Condon factors 8=29982
acetylene. mol., two-centre calcs. 8=47632
acetylene monoderivatives, C ≡ C group oscillation and absorpt. band calc. 8=34300
acetylenes, monosubstituted, C ≡ C bond vibr. freqs. and absorpt. band intensities, calc. 8=34299
acetylene, monosubstituted, solns., C ≡ C group absorpt. band intensity rel. to intermol. H-band form. 8=34301
acetylene, reactions with 0. 5-1200keV positive ions 8=43491
acetylene-t_2, vibr. rot. spectrum 8=25529
acetylene, triplet states, by electron impact 8=34302
acid fluoroanhydrides, F^{19} n. m. r., chemishift variations 8=47696
acid-water-tricresylphosphate systems, liq-liq. equilibrium 8=25883
aconitase substrate, potassium dihydrogen isocitrate crystal structure 8=26462
acridine-biacetyl-benzene solns., triplet acridine form. by triplet biacetyl energy transfer, obs. 8=25925
acridine dyes in 2-chloroethanol, T* ← S bands in absorpt. spectra 8=30494
acridine, photoreduction in alcohols 8=32137
acridine, reactive state in photoreduction in ethanol 8=41284
acridines, cryst. and in soln., absorpt. spectra in polarized light 8=32042
acridizinium cpds., elec. cond. 8=49273
acrolein, photodissoc. 8=32135
acrylamide, γ-irradiated aq. solns, 77°K, e. s. r. 8=30524
acrylic acid, microwave spectra of rotational isomers 8=34303
acrylonitrile-metal complexes, i.r. spectra 8=38865
acryloyl fluoride, microwave spectrum 8=38864
acyclic methine group, n. m. r. proton chem. shifts 8=25636
2-acyl-1, 3-diketones, MO LCAO calcs. of electronic spectra 8=25588
adamantane crystal self-diffusion, n.m.r. and plastic-flow obs. 8=39988
adamantane, solid, phonons, torsons and rotational diffusion 8=35397
adamantane, van der Walls interactions and mol. crystal packing 8=35050
adenosine-3′-phosphate dihydrate, crystal and mol. structure 8=35361
adsorption on Zn electrodes, pot. vars. 8=36601
L alanine, deuterated, deuteron n.m.r. 8=31894
dl-alanine, γ-irradiated, optical annealing investigation by e.s.r. 8=44400
alanine soln., permittivity meas. below 1 MHz 8=28452
alcohol-aliphatic hydrocarbon solns, H bonding entropy and enthalpy, and ratio of molar vols. 8=43799
alcohol, H isotope exchange with mercaptan 8=36545
alcohol, u.s. dispersion of insoluble particles, obs. 8=39442
alcohols, as solvents for Hg 8=48071
alcohols, dielectric dispersion meas. using helix resonator 8=39405
alcohols, hydrogen bonding 8=48059
alcohols, liq. radiolysis, reactions of electrons 8=49964
alcohols, liq., solubility of inert gases, heats of evaporation and enthalpy 8=39319
alcohols, lower aliphatic, photoionization 8=47793
alcohols, n-long chain, monomol. films surface viscosity rel. to phase transitions, 15-30°C 8=30428
n-alcohols, rotary mobility, effect of Li^+ and Cl^- ions 8=34778
aliphatic amines, fundamental vibrs. calc. 8=38866
aliphatic ethers, i. r. and Raman spectra 8=29777
aliphatic ketones, electronic absorpt. spectra 8=32045
aliphatic mononitriles, i. r. spectra 8=38867
n-alkane mixture, adsorption 8=48102

Organic compounds—contd
n-alkanes, cohesive and adhesive energies, calc. 8=43779
alkanes, gaseous, light scattering, depolarization meas. 8=43694
n-alkanes in soln., diffusion coeffs. calc. 8=30452
ortho-alkoxyphenylhydrazones of trimethylene sulphone, dipole moments obs. in solutions 8=38868
alkyl aromatics, radiationless decay 8=32072
alkyl-(aryl)-chlorosilanes, thermal cond. obs. 8=48131
alkyl derivatives of benzene, photoisomerization 8=49949
alkyl-Hg(II) cpds., vibr. spectra 8=43350
alkyl phosphonates, P=O-group valence oscillation calc. 8=30618
alkyl radicals, spin density distrib. calc. 8=43416
alkyl radical, spin density distrib. unrestricted Hartree-Fock calc. 8=43417
alkylbenzenes, symmetrically substituted, dipole moments and dielec. relax. 8=34890
alkylferrocene, e. s. r. spectra 8=47680
alkylphenols, 5-component, i.r. spectroscopic analysis 8=34350
alkylpyridine complexes of transition metal cations, far i. r. spectra 8=29763
allene-h_4 and-d_4, vibr. rot. transitions from i. r. spectra 8=47633
allene, rotational barrier, SCF MO calc. 8=29764
allyl alcohol, microwave spectrum 8=25533
allyl bromide, multiple n. m. r. 8=29813
allyl cyanide, microwave dipole moment obs. 8=34304
alternant hydrocarbons, pairing theorem 8=47650
alternant hydrocarbons, rules 8=25584
amine-BF_3, i.r. absorption spectra of charge transfer complexes 8=25539-40
amine extraction of U^{233} from irrad. ThO_2 8=36634
amino acids, e.s.r. of free radicals in γ-irrad. crysts. 8=40907
amino acids in aq. soln., dielect. dispersion at 350-4000 MHz 8=30513
amino acids in CF_3COOH and CF_3COOD, p mag. reson., 200 MHz 8=39441
amino acids, γ-irradiated, e.s.r. and optical spectral investigation of defects 8=26634
α-amino acids, γ or X irrad., e. s. r. rel. to dissociative electron capture 8=36621
amino acids, mass spectra on photoionization 8=41299
amino acids, non-carboxylic aliphatic, structure determ. by computer-controlled diffractometer 8=35362
aminobenzenes, electronic struct., ground state 8=25534
amino benzene sulphonic acids, isomeric, i. r. spectra 8=29801
aminobenzoic acids, fluorescence quenching by dinitrobenzenes, 8=43846
o-aminobenzoic acid, mol. struct. by phase determ. and X-ray obs. 8=43359
α-aminoethylphosphonic acid, i. r. spectrum 8=47666
1, 2-0-aminoisopropylidene-α-D-glucopyranose, mol. conformations from crystal structure 8=25623
aminomethoxypyridine, u. v. absorpt. spectra 8=34356
aminopyrodines and deuterated analogues, i.r. spectra 8=43391
aminopyridines, fluoresc. 8=48169
p-aminosalicylicacid, epitaxy on quartz 8=48571
ammonium bis-μ-(d-tartrato)-distibate (III) crystal structure 8=39848
ammonium formate, crystal structure rel. to H bonding 8=26528
ammonium hydrogen monochloroacetate. n.q.r. 8=49668
ammonium oxalate, electro-optical effects 8=36442
ammonium oxalate, non-linear optics 8=36443
ammonium pentaborate, second harmonic of light production 8=41167
amphiphile aqueous liq. cryst. solns., structs. for M_1, M_2. V_1 and V_2 phases 8=30408
amphiphiles, lamellar solns., birefringence sign reversal 8=25919
amyl and isoamyl alcohol, refractive index, density and viscosity temp. derivatives 8=34803
amyl-alcohol, scatt. cross-section meas. 8=48065
aniline adsorbed from CCl_4 soln on Cab–O–Sil silica, i.r. spectra 8=48474
aniline, depolarized doublet of light scatt. from thermal shear wave 8=43817
aniline, dielec. relax. 8=43856
aniline, electronic struct., excited singlet states 8=25534
aniline, ht. of mixing in polar solvents 8=34821
aniline, nanosec. pulse radiolysis 8=49978
aniline solns., u.s. velocities, compressibilities 8=30469
anilines, ring-substituted, corrosion inhibition of Fe in H_2O 8=45377-8
p-(anisalamino)-phenyl acetate liq. cryst., elec. field effect on n. m. r. 8=34924
anisole, dielec. relax. 8=43856
anisoles, dielectric absorption and internal rotation in non-polar solvent 8=43859
anisol-nitrobenzene system, complex formation from spectral analysis 8=45347

Organic compounds—contd
anthracene, α-radiation damage studied by etching in benzene. 8=48826
anthracene, band gap from electron photoemission threshold energies 8=44640
anthracene, band structure determ. from e-photoemission of alkali-metals into anthracene 8=31283-4-5
anthracene blue fluorescence from triplet-exciton interaction magnetic field effects 8=41223
anthracene, carrier generation and transport under electron bombard 8=49084
anthracene, charge-transfer exciton and ionic levels 8=27254
anthracene, CH-bond moments 8=34343
anthracene, conduction band structure from photoemission 8=44639
anthracene, cryst growth from vapour with uniform distrib. of tetracene 8=30823
anthracene, crystalline, photo-ionization 8=31267
anthracene, crystalline, triplet exciton phosphorescence 8=27665
anthracene crystals, work hardening 8=26855
anthracene, current carriers mobilities, temp. depend 8=31396
anthracene in cyclohexane, nanosec. pulse radiolysis 8=32141
anthracene, Daydov splittings of intense transitions 8=35048
anthracene derivatives, electrical conductivity and optical absorption 8=49144
9, 10-d_2-anthracene, CH-bond moments 8=34343
anthracene-d_2(9, 10), i. r. vibr. spectrum, 400-3100 cm^{-1} 8=38869
anthracene, dimezo substituted, 1, 2 benzanthracene composite excimers 8=49821
anthracene, dislocations, direct obs. by X-ray topography and Burgers vectors determ. 8=31074
anthracene, dispersion, absorpt. and refl. curves, and exciton phonon interact. 8=41161
anthracene, dye-sensitized photoconduction 8=49427
anthracene, α, e-excited scintillation decay obs. 8=49832
anthracene, excimer emission at v. high press. 8=49823
anthracene, excit. states decay and intersystem crossing, obs. 8=25537
anthracene, 5–100μ thickness meas. from refr. index dispersion 8=32043
anthracene, fluoresc. in host crysts. at high press. 8=49822
anthracene, fluoresc. of doped crysts. at high press. 8=49824
anthracene, fluoresc. polarization quenching data 8=43845
anthracene, hole injection by electrochemical mechanisms 8=45376
anthracene, interaction with biacetyl in visible light 8=36618
anthracene, i.r. cryst. spectra 8=49768
anthracene, low-lying triplet excit. states, 0.4–1.0μ 8=25616
anthracene, low-mobility, electron and hole generation 8=40595
anthracene, luminesc. polarization and impurity mol. orientation 8=36531
anthracene molten, u.s. velocity var. with temp. 8=30470
anthracene oil components, radiochemistry 8=49965
anthracene in n-paraffins, electronic spectra rel. to phase transitions of solvent 8=25938
anthracence-perylene in benzene solns., fluoresc. energy transfer 8=39387
anthracene, phonon freqs. from X-ray scatt. by thermal agitations 8=26577
anthracene, photo-charge carrier generation, exciton–exciton versus exciton–photon interacts. 8=31298
anthracene, photoconductivity, injection-induced long-wavelength 8=27335
anthracene, photoconductivity, mag. field effect 8=27336
anthracene photo-oxide decomp., temp dependence 8=27694
anthracene, p n.m.r., anomalies using u.v. and blue light 8=40973
anthracene, polarization of triplet-triplet absorpt. 8=27621
anthracene $S_0 \rightleftharpoons T_1$ radiative transitions, mag. dipole contribs. calc. 8=25545
anthracene, scintillation pulses excited by α bombard., temp. pressure depend. 8=36526
anthracene, scintillation response to heavy charged particles, directional anisotropy 8=46870
anthracene, singlet exciton-exciton interaction, λ=315-405nm 8=44658
anthracene singlet–triplet transitions, triplet state assignments and spin-orbit coupling 8=25536
anthracene, solid, photo-dimerization by u.v. irradiation 8=41270
anthracene:tetracene, trapping of photo-carriers 8=36030
anthracene, triplet-triplet absorpt. spectrum and extinction coeffs., 3000-8000 Å 8=25926
anthracene triplet-triplet annihilation rate consts., flash photolysis meas., 430-553°K 8=25535
anthracene, two-photon absorpt. in cryst. and molecule 8=45237
anthracene vapours, fluorescence spectrum fine structure 8=47634

Organic compounds—contd
anthracene, Wannier excitons 8=26918
anthracene, X-ray excited, prompt and delayed fluoresc. 8=27666
9-anthraldehyde dimer, crystal structure 8=44263
anthranilic acid, crystal structure by X-ray diffraction 8=26464
9,10-anthraquinone and derivatives, emission spectra 8=43392
9,10-anthraquinone crysts., photoconduction 8=36031
anthraquinone mixed with superconducting metals, crit. temp. increases 8=27005
anthraquinone, optically induced Overhauser effect 8=48210
antifurfuraldoxime, crystal structure 8=26512
aromatic, γ-irrad. radical yield, e.s.r. obs. 8=49967
aromatic, photoelectron spectra and inner ionization pots. 8=34297
aromatics, polycyclic, vapour absorpt. spectra and ionization pots., 1120-3000Å 8=38860
aromatics $S_0 \rightleftharpoons T_1$ radiative transitions, mag. dipole contribs. calc. 8=25545
aromatics, triplet state lifetimes, delayed fluoresc. obs. 8=25610
aromatics, triplet-state lifetimes, effect of partial deuteration 8=34306
aromatic carbonyl cpds., perturbation of singlet-triplet transitions 8=34296
aromatic diterpenes, mass spectrometric studies 8=32152
aromatic free radicals, g-factors, precise meas. and correlation with π-orbital energies 8=47708
aromatic heterocycles, five-membered, C^{13} n.m.r. 8=47697
aromatic hydrocarbon crysts., triplet factor group states 8=27622
aromatic hydrocarbon solns, p-type delayed fluoresc. 8=30498
aromatic hydrocarbons, anharmonic contrib. to radiationless transitions 8=43342
aromatic hydrocarbons, diffusion in H_2O 8=48118
aromatic hydrocarbons, effect of alcoholic solvents on fluoresc. yield 8=48171
aromatic hydrocarbons in glassy soln., e.s.r. line shape rel. to triplet excitation 8=40902
aromatic hydrocarbons in glassy solns., phosphorescent e.s.r. spectra, dynamic effects in line-shapes 8=49596
aromatic hydrocarbons in soln., free carriers from triplet-triplet collisions 8=48201
aromatic hydrocarbons, liqs. in soln, and solid, charge injection 8=30518
aromatic hydrocarbons, localized benzene-like regions 8=47635
aromatic hydrocarbons, luminesc., oxygen quenching 8=48170
aromatic hydrocarbons, mixed crysts., orientation effects 8=27623
aromatic hydrocarbons, phosphoresc. triplet decay, high press. effects 8=49825
aromatic hydrocarbons, radiationless triplet decay and intersystem crossing, Franck-Condon factors 8=25527
aromatic hydrocarbons, solvent Stark effect and spectra shifts 8=39375
aromatic hydrocarbons, triplet state form. efficiencies 8=43832
aromatic mols. phosphoresc., paramag. reson. effects rel. to singlet-triplet admixing 8=27461
aromatic molecules, superconducting-type pair correlations 8=47636
aromatics in soln., delayed luminesc. and triplet quantum yields 8=25941
aryldiazonium cations, electronic structure 8=34363
aryl ketone-iodine complexes, spectra 8=43353
aryl-Hg(II) cpds., vibr. spectra 8=43350
aryl phosphates, P=O-group valence oscillation calc. 8=30618
aryl phosphonates, P=O-group valence oscillation calc. 8=30618
aryl sulphanilides, n-substituted, i.r. spectra 8=34307
azamerocyanines, optical polarizability 8=34851
azanologues of benzenoid hydrocarbons, polarization of electronic transitions 8=25548
azaporphyrin ion structures 8=34308
azaridines and N-deutero derivs., i.r. spectra and structure 8=34309
azines, complexes with Cd, Hg and Zn, prep. and infra-red studies 8=36432
p-azoxyanisole liquid crystals optical rot. identification of two forms 8=43826
p-azoxyanisole liquid crystal, struct. constant elect. fields 8=34771
p-azoxyanisol liquid crystals, structure in permanent and variable elec. fields, X-ray study 8=25881
p-azoxyanisole, liq. crysts., thermal cond. 8=34833
p-azoxyanisole, liq. crystal, X-ray structural in strong mag. field 8=39309
azoxybenzenes, liq. cryst., sound velocity and absorpt. and phase transforms 8=25882
azulene derivatives, anomalous emission spectra 8=43354

Organic compounds—contd
azulene, elec. field broadening of electronic transition 8=45238
azylene, molecular spectrum 8=34310
barium inosine-5′-phosphate, crystal structure 8=44265
1,2 benzanthracene, dimezo substituted-anthracene, composite excimers 8=49821
1,2-benzanthracene, triplet absorpt. and form. yield meas. 8=25401
benzene, adsorpt. on Aerosil, i.r. spectra 8=44076
benzene and deuterobenzenes, new force consts. 8=38871
benzene and its derivatives, spectra obs. 8=48172
benzene-carbon tetrachloride, shock-compressed liquid, brightness temp. measurement and P-T curves 8=48089
benzene, catalytic hydrogenation, effect of intraparticle temp. grads. 8=32121
benzene, CNDO calc. of electronic spectra 8=29767
benzene, condensed-pair and separated-pair models calc. 8=38870
benzene, crystalline, lattice energy in atom-atom approx. 8=35395
benzene, crystalline, quantitative obs. of optical obs. spectra 8=36435
benzene, cryst., $^1B_{2u}$ state, 4th forbidden factor group component 8=40266
benzene, crystal lattice energy and intermolecular potential 8=35396
benzene, cryst., electronic and vibr. exciton struct. 8=49115
benzene, cryst. exciton band, expt. determ. 8=31299
benzene cryst., interaction of two excitons 8=49114
benzene, cryst., Raman spectrum 8=27628
benzene crysts., site group splitting and orientational effects 8=27627
benzene-cyclohexane, electronic spectra of solid solns. 8=27624
benzene-cyclohexane mixtures, surface tension 8=44068
benzene derivatives, crystalline polysubstituted, study by several physical methods 8=49629
benzene derivatives, liq., light scatt. 8=34849
benzene derivatives, Raman spectra at 80°K 8=47637
benzene, deuterated, deuteron spin lattice relaxation 8=48217
benzene dimers, semiempirical MO calc. 8=34313
benzene, disubstituted, intramol. vibrations at l.f.s., calcs. from model 8=34317
benzene, effect of dissolved H_2O on current transport 8=30523
benzene, effect of solvents on u.v. spectra 8=34870
benzene, energy transfer in isotopically mixed crysts. 8=27668
benzene, enthalpy of mixing with CCl_4 8=39348
benzene evaporation rate in vacuum 8=39480
benzene, excited states, AMO calc. 8=34314
benzene, gas phase irrad., formation of fulvene 8=49950
benzene, gaseous, radiationless e relax 8=25546
benzene-halogen complexes, electrostatic contribs. to ground-state props. 8=29768
benzene + n-heptane system, excess isothermal compressibility and molar heat capacity 8=43794
benzene-hexane mixtures, adsorption isotherms 8=30782
benzene-hexane mixtures, adsorption rates 8=30783
benzene, higher excimer states 8=34872
benzene, highly polarized Raman lines, effect of intermolecular interactions on line shapes and depolarization factor 8=34858
benzene, in inert-gas matrix, higher excited states 8=49770
benzene isotopic mixed crysts., phosphorescence, fluorescence and absorpt. spectra 8=49771
benzene isotopic mixed crysts., trap-trap triplet energy transfer 8=36527
benzene, isotopic mixed crysts., triplet-triplet annihilation and delayed fluoresc. 8=41225
benzene, liq. and solid, intermolec. rotation from n.m.r. data 8=43963
benzene, liq., charge carriers, natural, mobility determ 8=43863
benzene liquid, i.r. stimulated emission at 5μ by phonons obs. 8=43828
benzene, liquid, proton spin-lattice relaxation 8=39429
benzene, liq. struct. from x-ray diffrn. 8=34764
benzene, liq. → solid transform., high pressure study 8=26327
benzene, long transversal relax. time, obs. using spin-echo technique 8=48218
benzene, matrix-isolation spectrum, temp. depend. 8=29769
benzene mols. adsorpt. effect on n.m.r. or surface OH groups 8=38923
benzene with Na atoms, absorpt. spectrum at 55-100°K 8=49769
benzene/NaCl system, proton relax. time 8=45114
benzene, nanosec. pulse radiolysis 8=49979
benzene, normal coords. for planar vibrs. 8=29766
benzene, orthobaric data near crit. pt. 8=34956
benzene, oscillator strengths for electronic spectra 8=29780

Organic compounds—contd
benzene, phosphoresc. decay, deuteration effects 8=49826
benzene photochemical oxidation in gas phase, free radical formation 8=41286
benzene, polyalkyl substitutes of, electronic u.v. absorption spectra 8=41162
benzene quinoline and phenol soln., complex form 8=25887
benzene ring substituents, spectroscopic consts. calc. 8=34311
benzene, singlet and triplet π electron states 8=25543
benzene $S_0 \rightleftharpoons T_1$ radiative transitions, mag. dipole contribs. calc. 8=25545
benzene, scattering of ruby laser emission, large angle 8=48158
benzene, SCF-MO-LC(LCGO) calc. 8=47624
benzene, shock wave compressed, refr. index obs. 8=39370
benzene sorbed on silicagel, proton relaxation, temp. depend. 8=49632
benzene, spin-lattice relax., press. depend. 8=39432
benzene, stimulated temp. light scatt., obs. 8=30481
benzene, sublimation energy 8=39495
benzene sulphochlorides, vibrations resonance interaction 8=47639
benzene, supercooled glassy, and polycrystalline states, Mossbauer obs. of mol. motion 8=43751
benzene, theory of cryst. spectra 8=49772
benzene to diacetyl triplet-triplet energy transfer in solns., obs. 8=34316
benzene, vapour fluoresc., press. depend. 8=47640
benzene, vapour fluoresc., yields below 0.1 torr 8=47641
benzene, viscosity, gaseous state 8=25835
benzenes, chlorinated, nonplanar group vibrs. 8=38872
benzenes, F-substituted, ionization potl. calc. 8=43868
benzenes, methyl-substituted, SCF-MO calc. 8=38897
benzenes, monosubstituted, CNDO SCF calcs. 8=25547
benzenes, monosubstituted, correl. of i.r. intensities with chem. reactivity 8=43253
benzenes, mono-substituted, dielec. relax. and enthalpies of activation 8=34889
benzenes, monosubstituted, p.m.r. 8=43407
benzenes, substituent effects on l.f. vibrs. 8=47642
1, 2-benzocoronene, triplet absorpt. and form. yield meas. 8=25401
benzodioxane-1, 4, O-substituted, luminescence spectra 8=48173
benzodioxane-1, 4, solvent effects on absorpt. spectrum 8=39376
benzodioxane-1, 4, 6-substituted, action of substituent structure on electronic spectra 8=47638
benzoic acid, H-bridge complexes, thermodyn. props. from u.v. absorpt. spectra 8=39349
benzol, double light scattering near critical point 8=48147
benzol, heat transfer in boiling rel. to state of heating surfaces 8=35001
benzonitrile-acetonitrile mixture, dielec. relax. 8=43856
benzonitrile, Brownian rotatory motion rel. to dipole-dipole intermol. forces in vibr., 8=43827
benzonitrile-propitrile mixture, dielec. relax. 8=43856
1, 12-benzoperylene at 4°K, line-width obs. in quasiline fluorescence spectrum 8=49827
1, 12-benzoperylene quasiline fluoresc. line-widths temp. depend., 4-175°K 8=36528
benzophenone, assignment of lowest triplet state of C = O group 8=25560
benzo phenone, luminescence at 77°K 8=41224
benzophenone, polarized absorpt. spectra 8=27630
benzophenone singlet–triplet transitions, triplet state assignments and spin-orbit coupling 8=25536
benzophenone + trichloroacetic acid mixture, dielec. props 8=48190
p-benzoquinone and derivatives, emission spectra 8=43392
p-benzoquinone, 2, 5-dihalogen derivs crystal structure 8=26466
p-benzoquinone, effect of solvents on u.v. spectra 8=34870
p-benzoquinone (H_4) and $(D)_4$, electronic spectra of crysts. at 4°K 8=27626
p-benzoquinone, n. m. r. oriented in nematic phase 8=34913
p-benzoquinone, n. m. r. spin coupling constants, calc. using σ M.O. theory 8=47690
n-benzoquinone, on TlI, surface charge-transfer groups form., obs. 8=36028
1, 4-benzoquinone radical in soln., e. s. r. spectral linewidth alterations, 20-80°C 8=47681
benzothiophenes, mol. orbital calcs. 8=43355
1, 2-benzotriazole, in acetone, p mag. reson. conc. depend., obs. 8=39420
4-benzoyl-amino stilbene derivatives, spectra on quasi-atomic chromosphere systems 8=47643
benzoyl thiophine, deformation angle determ. 8=34371
1, 12-benzperylene in crystalline n-paraffin soln., quasi-line spectra, temp. broadening, shift and line profiles 8=45240
benzpyrene in crystalline n-paraffin soln., quasi-line spectra, temp. broadening, shift and line profiles 8=45240
benzyl and substituted benzyltin cpds., i. r. spectra 8=29765
benzyl radical, assignment of excited states by three-step photoselection 8=25542

Organic compounds—contd
benzyl radical, polarization of vibronic transitions 8=25549
benzyl, vibrational frequencies 8=43361
betol, crystallization kinetics rel. to active impurities and centres 8=39667
biacetyl, fluorescence spectrum at 100°C, vibrational analysis 8=43347
bigeranyl tetrahydrochloride, triclinic, crystal and mol. structure 8=39827
binaphthyl, crystal structure and bond distances 8=26470
biphenyl in cyclohexane, nanosec. pulse radiolysis 8=32141
biphenyl, fundamental freqs., normal coords. 8=34349
biphenyl, solid soln. in cyclohexane, delayed fluoresc. 8=36529
biphenyl, vibr. spectrum and molec. config. 8=34348
biphenyl, vibr. symmetry coords. 8=43376
biphenylene, i.r. spectra 8=29770
biphenylene, electron impact and thermal fragmentation 8=39058
biphenylene, electronic spectra 8=27636
biphenylene, positive and negative ions, C^{13} hyperfine splittings 8=47650
bipyridil, α, α' and γ, γ' conjugations in cryst. and liquid states, Raman obs. 8=34355
2, 3-bis-(cis-chloro-1-methylcyclohexyl)-trans-2-butene, crystal and mols. structure 8=39830
bis(dimethylamine) boron chloride, crystal structure 8=39771
4, 4′-bis(dimethylamino)diphenylamine dihydro iodide, unit-cell dimensions and space group 8=26498
4, 4′ and 4, 2′-bis (α, α-diphenyl-β-hydrazyl)-3, 3′, 5, 5′-tetranitro diphenyl sulphones, e.s.r. 8=49595
bispiperidinium $Bi^{III}Br_5$, cryst. struct. 8=26546
bis(tetrahydroindenyl)Fe:tetracyanoethylene, d. c. resistivity rel. to press. and elec. field 8=27078
1, 4-Bis (2, 2, 6, 6-tetramethyl-4-hydroxy-4-piperidyl-1-oxyl) butadiene, stability up to 144°C 8=39417
bis(α-thiopicolinanilido)Cu(II), isotropy of hyperfine struct. from N atoms 8=27463
N, N′-bis(4-tolyl)-p-phenylenediamine iodide, crystal structure 8=26543
bis(trifluoromethyl)-peroxide, i.r. and Raman spectra 8=43366
bitumen and components, crystalline structure 8=48516
boroxine and trialkyl derivatives, aromaticity 8=47644
α-brassylic acid, crystal structure 8=26478
bromobenzaldehydes, i.r. absorpt. spectra 8=43834
bromobenzene, deuterated, deuteron spin lattice relaxation 8=48217
bromobenzene, liquid, proton spin-lattice relaxation 8=39429
p-bromo-benzoyldimethylamine, amido group structure 8=26465
bromocyclobutane, and 3 isotopic species, spectra and structure 8=29771
bromocyclobutane, i.r. and Raman spectra 8=25566
12α-bromo-11β-hydroxyprogesterone, crystal and mol. structure 8=39828
n-bromophenylsulphonyl chloride, i.r. absorption spectra in polarized light 8=41169
trans 1-bromopropylene, microwave spectrum 8=25550
bromostyrenes, liq. isomeric, i.r. absorpt. spectra 8=43841
2-bromo-2-p-tolylethyldimethylammonium bromide, crystal structure 8=26510
1-bromotriptycene $BrC_{20}H_{13}$, crystal and mol. structure 8=44266
5-bromouridine and dimethylsulphoxide 1:1 complex crystal and molecular structure 8=26471
bullvalene, crystal structure 8=39829
1, 3-butadiene, photodissoc. 8=32135
1, 3-butadienes, n.m.r. and conformations 8=38918-20
butane, charge transfer from p and H atom, cross-sections 8=38737
n-butane ionizing collisions and electron mean free paths obs. at 10^{-4} torr 8=34458
butane, reactions with H_3^+ 8=39057
n-butane 10^{-4} due to electron collision, calc. of mean free path 8=34458
t-butanol, gaseous, liquid and solid; absolute scatt. coeffs. of Raman spectral lines 8=43360
1-butanol-water system, nucleate boiling obs. 8=25998
butanone-2-oxime, association in various solvents 8=43763
1-butene, photodissoc. 8=32135
3-butenenitrile, vibr. spectra and rot. isomerism 8=25551
2-butenes, cis-trans isomerization, benzene photosensitization 8=49959
2-butenes, cis and trans, vibr. spectra 8=25552
2-butenes, n. m. r. and steric effects 8=47698
n-butyl alcohol, refractive index, density and viscosity temp. derivatives 8=34803
n-butylamine and N-deutero derivative, i. r. and Raman spectra 8=27620
n-butyl chloride, h.p. viscosity obs. 8=34793
butyl chloride (tertiary), liq. and cryst., far i.r. spectra 8=32044
butyl formate, dipole moment in dil. benzene, comparison with chloroformates, rel. to configs. 8=25555
butyl phthalate oil manometers, correction for variations in room 8=32646

Organic compounds—contd
  calcium dipicolinate trihydrate crystal structure 8=26473
  calcium hexa-antipyrine perchlorate, crystal and mol. structure rel. to other metal salts 8=44268
  carbamide phosphate, crystal structure 8=26475
  carbon tetrachloride, adsorpt. on graphite 8=48473
  carbon tetrachloride, high polarized Raman lines, effect of intermolecular interactions on line shapes and depolarization factor 8=34858
  carbon tetrachloride, i. r. spectrum, difference bands 8=38874
  carbon tetrachloride, liq., charge carriers, natural, mobility determ. 8=43863
  carbon tetrachloride, neutron diffraction 8=34761
  carbon tetrachloride, shock-compressed liquid, brightness temp. measurement and P-T curves 8=48089
  carbon tetrafluoride, octopole moment, from virial coeffs. 8=29849
  carbon tetrafluoride, rotational spectrum, collision-induced 8=47658
  carbonium ions, electronic struct. 8=38876
  carbonyl containing, vapour n ← π* luminescence in vapour 8=34199
  carbonyl group of semicarbazides, semicarbazones and pyrazolecarboxamides, i.r. absorption 8=47645
  carbonyl n → π* transitions, direction of polarization 8=27630
  carborane and derivs. gas e-diff. study 8=25553
  carboxylic acids, H-bonding, i.r. data 8=25554
  Carnauba wax thermoelectret, heterocharge on ionic addition 8=44879
  β-carotene, effect of adsorbed gases on semicond. 8=31397
  carotene films, effect of gas adsorpt. on absorpt. spectra 8=49773
  cellobiose, crystal structure confirmation 8=39838
  cellobiose frozen aqueous solutions, e. s. r. of free radicals 8=47707
  cellulose acetate films, i.r. spectra 8=32048
  cellulose derivatives, e absorpt 8=36436
  cellulose ethers, etherification from i.r. absorpts. obs. 8=27728
  cellulose, $KHCO_3$ contaminated, thermogravimetric and diff. thermal anal. 8=32095
  cellulose nitrate, etchable track formation 8=44492
  cellulose, permittivity and dielectric loss, optical meas with colloidal mass emitter 8=28766
  cellulose propylene phosphite, structure, transformation 8=38966
  α-cellulose, pyrolysis and decomp., reaction kinetics 8=32094
  cellulose sulphoester solns., optical anisotropy and molec. rigidity 8=34850
  cetyl alcohol, negative resistance between metal electrodes 8=40632
  charge-transfer and H-bonded complexes, spectra, internal compression effects in solvents 8=34864
  charge-transfer complexes, crystal structure and solid-state spectra 8=26166
  chars, O^{18}-labelled, i.r. spectra rel. to 1600cm^{-1} band origin 8=43345
  chloralkanes vibr. spectra and C-Cl charact. freqs. rel. to struct., calc. 8=34354
  n-chloranil, on TlI, surface charge-transfer groups form., obs. 8=36028
  chlorinated diphenyls, ion purification 8=45310
  α, β-chlorine naphthalene, vapour and soln. at 77°K, u.v. absorpt. spectra 8=32047
  chloroacetyl DL-alamine, e.s.r. of irrad. crysts. 8=36240
  chloroaniline, o, m and p, in benzene, dielec. props. temp. variation at microwave freqs. 8=48181
  1-chloroaziridine, microwave spectrum and struct. 8=25556
  m-chlorobenzene, ^{1}H-^{1}H coupling constants 8=25641
  chlorobenzene in p-xylene; permittivity. complex: calc. from CWCN maser meas. 8=48179
  chlorobenzene, stimulated Mandel'shtam-Brillouin scatt. threshold, 0.35, 0.69 and 1.06μ 8=32032
  chlorobenzenes, effect of D substitution on Cl n. q. r. 8=27517
  chlorobenzenes in rigid solns., polarization of phosphoresc. 8=27669
  p-chlorobenzonitrile, i.r. absorpt. spectrum 8=43357
  p-chlorobenzonitrile, near-u.v. absorpt. spectrum 8=43357
  chlorobenzotrifluorides, electron absorpt. spectra 8=43358
  3-chloro-5-(3-dimethylaminopropylidene)-5H-dibenzo[a, d]cycloheptane, structure 8=26487
  2-chloroethanol, microwave spectrum 8=25557
  bis-β-chloroethyl-vinyl-phosphonate, γ-induced polymerization, mechanism, obs. 8=49913
  cis-1-chloro-fluoropropene, microwave spectra and molec. consts. 8=34320
  chloroform, orthobaric data near crit. pt. 8=34956
  chloroformates (alkyl and phenyl), dipole moments in dil. benzene, and configs., comparison with butyl formate 8=25555

Organic compounds—contd
  chloromethanes, X-ray emission spectra 8=47653
  o-chlorophenol binary liq. mixtures, excess u.s. absorpt. 8=34842
  chlorophyll, fluoresc. polarization quenching data 8=43845
  chlorophyll-ligand interactions, from n. m. r. 8=29850
  chlorophyll, optical transitions, anisotropy 8=34258
  2-chloropropene-1, 3-d,, internal rot. and vibr. 8=25558
  2-chlorotropene, crystal and mol. structure 8=26476
  cholesteric liq. crystals, optical rotatory power, theory 8=43812
  cholesteric liquid crysts., phase change elec. field induced, 10^5 V/cm 8=34766
  cholesteric liquid crystals, structure distortion by a mag. field 8=30407
  cholesteryl, and derivs., liq. crysts, dielec. props. 8=34893
  cholesterol derivatives, liq. cryst. struct. 8=48069
  cholesterol film, negative resistance between metal electrodes 8=40632
  cholesterol-type liq. cryst., light scattering meas. 8=25882
  cholesteryl 2-(2 ethoxyethoxy) ethyl carbonate Brillouin scatt., 20-60°C 8=48146
  cholesteryl 2-(2-ethoxyethoxy)ethyl carbonate, liq. crystal, refractive index obs. 8=30482
  chromophores, intramolec. energy transfer between triplet states 8=41157/8
  chromophores, u. v. soln. spectra and solvent interactions 8=25927
  chrysene, CH-bond moments 8=34344
  chrysene, delayed luminesc., growth and decay 8=32073
  chrysene, low-lying triplet excit. states, 0.4-1.0μ 8=25616
  chrysophane oxides, N-derivatives, i.r. and u.v. 8=36437
  cinnoline, vapour spectrum 8=25559
  coal, 7 types; magnetic susceptibilities obs. 8=49478
  cobaltocene: tetracyanoethylene, d. c. resistivity rel. to press. and elec. field 8=27078
  complexes, electron donor-acceptor. gas-phase spectra 8=38905
  complexes, monomeric charge-transfer, review of elec. props. 8=26942
  conducting and semiconducting, properties and applic. 8=49271
  copper acetate hydrate, proton relax. of methyl group at low temps. 8=45109
  copper formate tetrahydrate, d.m.r. and molec. struct. 8=49638
  copper formate tetrahydrate, paramag. line width 8=36242
  copper monochloroacetate 2.5 hydrate, unit cell dimensions and density obs. 8=44270
  coronene in cryst. matrices, effect of thermal treatment on spectra 8=45242
  coronene in n-paraffins, elecronic spectra rel. to phase transitions of solvent 8=25938
  corrin analogue, synthetic, spectrum and electronic struct. 8=25561
  corrin skeleton of vit. B_{12}, and its precorrinoid intermediate crystal structure 8=26479
  cosin, luminescent centres, relax. of local time 8=39388
  cryptocyanine, alcohol soln., optical width var. during laser giant pulse generation 8=25921
  cryptocyanine solns., laser-flash spectra 8=48162
  crystal and mol. struct. from triplet states mag. reson. spectra 8=27449
  crystal growth, from vapour phase, technique 8=39662
  crystal growth rate retardation in capillaries 8=26261
  crystal solns., optical excitation by ruby laser pulse 8=30479
  crystal violet films, photocapacitance and photocurrent "memory" 8=36032
  in crystalline phases, i. r. spectroscopy rel. to dielec. constant transitions 8=27617
  crystals, polymorphic transform. process 8=26090
  cumene, h.p. viscosity obs. 8=34793
  cumene, structure determ. by gas e-diffr. rel. to nature of conjugating system 8=25587
  cyanoacetylene, direct l-type doubling transitions 8=34323
  cyanoanthracene solns., vitrous, optical absorpt. temp-dependence 8=43823
  cyanocarbons, electron capture 8=34457
  cyanocobalamin monoacid deriv., n-diffr. study 8=25676
  cyanamide, vibr. spectra 8=48710
  cyanine dye soln., stimulated emission 8=48154
  cyclic alkanes, fragmentation of skeletal bonds in mass spectra 8=29824
  cyclic aromatic hydrocarbon radicals and ions,
  cyclic vicinal dihalogenides, vibr. spectra 8=34324
  trans-1, 3-cyclobutane dicarboxylic acid, crystal structure 8=26484
  cyclobutanol, i.r. and Raman spectra 8=25566
  cyclobutanone-2-t, vibr. excited photodecomp. 8=41288
  cyclobutyl monohalides, conformational behaviour 8=25563
  cyclohexane, liq. and in soln., vac. u. v. photolysis 8=27763
  cyclohexanol, h.f. u.s. wave delay time meas. by phase comparison method 8=44314
  trans-1, 2-cyclohexylenedinitrolotetraacetic and solns., 5≤pH≤14, n. m. r. obs. 8=30537
  cyclononanone, polymorphism study by X-rays, n. m. v. and diffr. thermal anal. 8=30714

Organic compounds—contd
cis, cis, cis, -1, 4, 7-cyclononatriene $AgNO_3$ adduct crystal and mol. structure 8=26485
cyclooctane analogues, crystal structure and ring conformations 8=26483
cyclooctanone, crystalline, crystal and mol. props. of phases rel. to disorder 8=26091
cyclooctanone, polymorphism study by X-rays, n. m. v. and diff. thermal anal. 8=30714
cyclooctatetraenyl radical anion, electronic spectrum 8=25658
cycloparaffin hydrocarbons, diffusion in H_2O 8=48118
cyclopentadienyl anion, SCF-MO-LC(LCGO) calc. 8=47623
cyclopentadienyl iron sulphide, crystal and mol. structure 8=26537
π-cyclopentadienyl molybdenum tricarbonyl chloride, crystal structure 8=26488
cyclopentene, far i. r. spectrum and ring puckering 8=34325
cyclopentene, rot.-vibr. interaction and barrier to ring inversion 8=38878
paracyclophanes, substituted, hindered rot. 8=34326
cyclopropane, SCF-MO-LC(LCGO) calc. 8=47625
cyclopropane-H_6, i.r. spectra 8=43363
cyclopropanecarboxaldehyde, microwave spectrum 8=25562
cyclopropane ring systems, anisotropy of diamag. susceptibility 8=25619
cyclopropanes, symmetry species correl. and group freqs. 8=25564
cyclopropanone, microwave spectrum 8=29774
cyclo-propene, -1, 2-d_2, Raman, vapour and solid phase i.r. spectra obs. 8=43362
cyclotetratriacontane, and mol. structure 8=39831
L-cysteine, crystal and mol. structure 8=44271
cytochrome c, Mössbauer spectra of Fe atom 8=48331
decylhexaoxyethylene glycol monoether + water systems, heat of mixing obs. 25°C 8=48126
dehydro-α-lapacone, double n. m. r. 8=29810
demissidine hydroiodide, $C_{27}H_{46}INO$, crystal structure 8=26489
deoxycholic acid clathrates with naphthalene phenanthrene and benzanthracene structures 8=26491
desoxyribonucleotide complexes with Fe, p. m. r. 8=43880
diacids, saturated aliphatic, crystal structure comparative study 8=26494
diacetyl sensitized luminesc., benzene and toluene triplet-triplet energy transfer, obs. 8=34316
N, N-di-sec-alkyl amides, slow rot. around alkyl-N bond 8=38927
dialkyl disulphides, vibr. spectra 8=43349
dialkyl ketones, protonated, (dialkylhydroxycarbonium ions), proton spectra mag. reson. spectra 8=38907
4, 4′-di-n-alkyloxy azobenzenes, principal molec. polarizabilities 8=48068
dialkyl sulphides, electronic spectra 8=29762
dialkyl-Tl(III) cpds., vibr. spectra 8=43351
diaryl disulphides, vibr. spectra 8=43349
diazines, CNDO calc. of electronic spectra 8=29767
orthodiazines, electronic states and radiationless processes 8=27667
diazonium salts in acid soln., photodecomposition quantum yields 8=45397
diazonium salts, $o\text{-}CH_3OC_6H_4N_2Cl.\ FeCl_3$ and $[(CH_3)_2NC_6H_4N_2Cl]_2.\ ZnCl_2$ structure 8=26492
diazulenium azulene perchlorate, X-ray analysis 8=26495
dibenzothiophene sulphone, crystal structure 8=39832
1, 3-dibenzoylacetone, spectra and electronic structure 8=47651
dibenzoylmethane, spectra and electronic structure 8=47651
paradibromobenzene-paranitrochlorobenzene solid solns., single crystal study 8=26040
1, 1-dibromo-3-fluorobutadiene-1, 3, energies of conformations, n. m. r. study 8=47631
1, 2, dibromoethane, rot. isomerism, n. m. r. study 8=47646
4, 12-di(bromomethyl)[2, 2] metacyclophane, crystal structure 8=26472
1, 4-dibromonaphthalene, electronic Zeeman meas. 8=27629
2, 6-dibromopyridine, n.m.r. of oriented mols. 8=43403
p-di-tert-butylbenzene, π e chord symmetry in crysts., 20°K 8=30648
di-n-butyl diselenide, vibr. spectra 8=43349
di-tert-butyl nitroxide, C^{13} isotopic splitting const. 8=30525
di-tert-butyl-nitroxide liq. free radical, time dependent interactions, e.s.r. and p. relaxation study 8=48207
dicarboxylic acid esters, intramol. mobility and dielec. relax. 8=43340
dicarboxylic acids, $COOH[CH_2]_{2n+1}COOH$ crystal and mol. structure 8=26478
n-dicarboxylic acids, far i.r. spectra 8=27631
n-dichlorobenzene, n.q.r., effect of pressure and temp. 8=49665
dichlorocarbene, i. r. spectrum in solid Ar 8=29775
3, 6-dichloro-2, 5-diaminobenzoquinone-(1, 4), crystal and mol. structure 8=26493
1, 2-dichloroethane, h.p. viscosity obs. 8=34793
1, 2-dichloroethane in various solvents potential barrier 8=43855
cis-dichloroethylene, Raman line intensities and depolarizations, calc. 8=34321

Organic compounds—contd
trans-dichloroethylene, Raman line intensities and depolarizations, calc. 8=34321
1, 2, dichloroethane, rot. isomerism, n. m. r. study 8=47646
1, 2-dichloroethane, vibr. excited, from Hg-photosensitized dichloromethane 8=27761
1, 1-dichloroethylene, Raman line intensities and depolarizations, calc. 8=34321
1, 1-dichloro-3-fluorobutadiene-1, 3, energies of conformations, n. m. r. study 8=47631
dichlorofluoromethane, ice and water clathrates, dielec. props. 8=27255
dichloromethane, Hg-photosensitized, vibr. excited dichloroethane prod. 8=27761
2, 2-dichloro-4, 4, 6, 6, tetraphenylcyclo triphosphazatriene, crystal structure 8=26542
dichlorotoluenes, near-u.v. electronic absorpt. spectra 8=43400
2, 5-dichloro-1, 4-xylene and 4, 5-dichloro-1, 2-xylene crysts., cryst. structure and i.r. vibr. spectra 8=39833
dicyanodiacetylene Σ_g^+ modes, vibr., thermodynamic functions, internal fields and Raman intensities 8=26031
9-dicyanomethylene, -2, 4, 7-trinitrofluorene crystal structure 8=26481
Diels-Alder quinone adducts, charact. i.r. absorpt. bands 8=25924
diethylamine hydrate, $12(C_2H_5)_2NH.104\ H_2O$, crystal structure 8=26505
trans-15, 15-diethyl-15, 15-dihydropyrene, crystal structure at −160°C 8=26552
diethylether, coordination compounds with $MgBr_2$, $ZnCl_2$ and AlX_3=Br, Cl), i.r. spectra 8=25569
diethyl methylphosphanite, hydrolysis, n.m.r. study 8=27727
diethylmethylsulphonium cpds., i. r. spectra 8=29776
NN′-diethylpyrazinium fluoroborate, e.s.r. spectra, line widths and second order structure 8=39414
3, 3′-diethylthiatricarbocyanine laser, time-resolved stimulated emission spectra 8=28712
diferrocenyl and derivs., crystal and mol. structure 8=26497
diffusion pump oil DC-705, δ-η anal. of secondary electron emission 8=48196
difluoroacetone, symmetrical, rotational isomerism 8=29783
difluoro-1-1-chloro-1-ethane, microwave spectrum 8=25575
difluorodiazirine, dipole moment of π^* state 8=25579
2, 2-difluoro-1-methylcyclopropane, microwave spectrum 8=29792
difluorostilbene derivs., crystal and mol. structure 8=26559
diglycine. aq. solns., u. s. absorpt. 8=48142
diglycine nitrate, crystal structure determ. of ferro-and paraelectric phases 8=48685
diglycine soln., permittivity meas. below 1 MHz 8=28452
dihalobenzenes, p.m.r. and C^{13}-H satellite spectra 8=38917
2, 6-dihalogeno-p-benzoquinones, singlet-triplet absorpt. 8=38873
dihydrothymine, cryst. and molec. struct. 8=30918
1, 4-dihydroxyanthraquinone, i. r. and optical spectra 8=3430
2, 5-dihydroxy-para-benzoquinone, i. r. and u. v. absorpt. spectra 8=34318
3β, 17α-dihydroxy-21-bromo-5α-pregnan-11, 20-dione, crystal and mol. structure 8=39834
dihydroxyfumaric acid dihydrate crystal structure 8=39835
p-diiso-propylbenzene, π e chord symmetry in crysts., 20°K 8=30648
beta-diketone negative ions, triplet state e. s. r. 8=47682
2, 5-dimethoxysemiquinone anion radical solvation by protic and aprotic solvants 8=45258
9, 10-dimethylanthracene in dimethylformamide: spectra of electrochemiluminescence 8=48177
dimethylamine, microwave spectrum 8=25599
dimethylamine, microwave spectrum 8=47660
4-dimethylamino-4′-nitrodiphenyl fluoresc. in binary soln., phosphor-impurity group centres props., 77°K 8=36532
dimethylammonium chloride crystal structure rel. to H bonding 8=26525
2, 6-dimethyl-p-benzosemiquinone, e. s. r. in t-pentanol and 1, 2-dimethoxy-ethane, rel. to ionic assoc. 8=34908
8, 8′-dimethyl binaphthyl, crystal structure and bond distances 8=26470
2, 6-dimethyl-4-bromo-N-methyl-anti-benzaldoxime isomer 8=26512
2, 3-dimethylbutadiene, molec. struct. 8=43375
dimethyl cadmium, indirect nucl. spin coupling consts. 8=43408
2, 6-dimethyl-4-chloro-N-methyl-anti-benzaldoxime, crystal structure 8=26511
dimethylcyclohexanes, as solvents for Hg 8=48071
dimethyl (9-fluorenyl) sulphonium bromide, X-irrad., e.s.r. of trapped radicals 8=31883
2, 5-dimethyl furan, vib. spectra 8=43368
1, 3-dimethyl-[1, 7]-heptahydropyrimido[1, 2-a][1, 3, 5] triazine-2-thione-4-one 8=26553
dimethyl NPX_2(X=F, Cl, Br), i.r. and Raman spectra in gas, solid and liq. phases 8=43372

Organic compounds—contd
1, 5-dimethylnaphthalene, and bromo-derivatives, n. m. r. 8=38926
dimethylphenylarsine, vibr. spectra 8=43381
NN′-dimethylpyrazinium fluoroborate e. s. r. spectra, line widths and second order structure 8=39414
1, 3-dimethyl-2-thioxo-4-oxo-1, 2, 3, 4, 6, 7, 8 hepta-hydro-pyrimido [1, 2-a] [1, 3, 5] triazine, crystal and mol. structure 8=48686
dimethyline sulphonyl chloride, $(CH_3)_2NSO_2Cl$, mol. structure 8=25607
2, 2′-dinitrobiphenyl ether and sulphide radical anions, e. s. r. and intramolec. spin exchange 8=34369
N, N′ -dinitroethylenediamine, crystal structure refinement 8=39836
dinitrotetramminecobalt(III) complexes, i. r. spectra 8=45241
p-dioxane/CCl_4 binary mixture, proton mag. relaxation 8=39425
p-dioxane, Raman spectra 80-300°K rel. to phase transform. at 272. 9°K 8=41163
dioxane, rel. to toluene scintillators max. H_2O conc. 8=43844
1, 3-dioxolane, far i. r. spectra 8=25567
diphenyl crystals, void formation process kinetics 8=26709
diphenylamine-nitrobenzene system, complex formation from spectra analysis 8=45347
9, 10-diphenylanthracene, as fluoresc. standard 8=39391
9, 10-diphenylanthracene, laser action 8=46630
diphenyl-α, α' dipyridyl, solid solns., single crystal study 8=26040
diphenyl, heat transfer in boiling rel. to state of heating surfaces 8=35001
1, 6-diphenyl-hexatriene-1. 3. 5. luminesc. polarization and impurity mol. orientation 8=36531
2, 5-diphenyloxazole in benzene, toluene, p-xylene and mesitylene, excimer, fluoresc. solvent-solute energy transfer 8=25940
N, N′-diphenyl-p-phenylenediamine, influence of impurities on electrical conductivity 8=40333
N, N′ -diphenyl-p-phenylenediamine iodide, crystal structure 8=26543
diphenyl picryl hydrazyl solns. in org. liqs., dynamic polarization of solvent protons and F nuclei 8=25951
diphenyl-Tl(III) cpds., vibr. spectra 8=43351
$\alpha\alpha'$ and $\gamma\gamma'$ dipyridol in n-paraffins, structural spectra of phosphorescence 8=36530
disodium inosine-5′-phosphate, crystal structure 8=44265
disordered molecular crystals, X-ray and NQR investigations 8=26454
di(tetramethylammonium)bis(maleonitriledithialato)CuII, X-ray and e. s. r. studies 8=35364
para-dithiane, i.r. absorpt. spectrum at 15°K, fine structure mechanism 8=27632
dithiodiglycolic acid, irrad. at 4. 2°K, ion formation 8=40917
n-dodecanol, adsorpt. on defined rutile surfaces from soln. in p-xylene and n-heptane 8=35196
2-dodecylaminoethanol salts, effect of counterions on micellar props. 8=39289-91
dosimetry, Mrad techniques for p synchrotron 8=46925
DPPH, adsorpt. on catalysts 8=27736
DPPH, conc. solns. in org. solvents, e.p.r. at 3000 MHz as fn. of temp. and dissolved gas 8=48206
duclauxin, structure from monobromo-deriv. crystal and mol. structure exam. 8=44272
durene, photocond. of pure monocrysts. 8=49428
dye, Eastman 9860, electronic transition picosec. lifetime obs. using Nd glass laser 8=43346
dye solns., conc., spectroscopy of intermolecular interactions 8=29841
dye solution laser, cryptocyonine in glycerol and CAP in ethanol, time-resolved spectra 8=33230
dye solutions, optical third-harmonic generation conc. and dispersion dependences 8=43819
dyes, cyanine, sensitizing induced Raman scatt. in nitrobenzene 8=34871
dyes, for Q-switch laser, fluoresc. and bleaching 8=28693
dyes, lasing props. 8=46629
dyes, oriented in glass matrix, polarized absorpt. 8=49767
dyes, quadrupole moments, π-electron theory 8=43268
EDTA, Ba chelate form. study by ultrasonics 8=25914
eperuic acids, config. at C(13) from p-bromophenacyl ester of labdanolic acid structural analysis 8=39840
epoxide ring systems, anisotropy of diamag. susceptibility 8=25619
epoxy resins, thermal expansion, 2°-300°K obs. 8=35443
erbium ethylsulphate, odd-parity cryst.-field parameters 8=48307
erythrosin luminescent centres, relax. of local temp. 8=39388
ethane, ab initio bond-orbital calc. 8=38891
ethane -Ar mixture, ionization coeffs. and sparking voltages 8=25701
ethane-Ar mixtures, u.s. vel. dispersion interferometry 8=47966
ethane, charge transfer from p and H atom, cross-sections 8=38737

Organic compounds—contd
ethane-1, 1, 1-d_3, near-i. r. spectrum 8=25570
ethanes (d_0-d_6), mass spectra 8=47446-7
ethane dissociative ionization 8=29976
ethane, ionization energies 8=34459
ethane, ionizing collisions and electron mean free paths obs. at 10^{-4} torr. 8=34458
ethane, liquid, nuclear spin relaxation 8=39428
ethane, low-temp. virial coeffs. 8=34643
ethane, mobility of electrons, photoelectrically generated 8=39223
ethane dinitrile (cyanogen) condensed in solid N_2 and Ar, luminescence 8=25455
ethanol, adsorpt. on defined rutile surfaces from soln. in p-xylene and n-heptane 8=35196
ethanol-n-decanol mixtures, vapour press. 8=48284
ethanol-ethyl halide mixtures, u.s. relax 8=30471
ethanol, heat transfer in boiling rel. to state of heating surfaces 8=35001
ethanol–H_2O mixture vapour press. isotope effect 8=48283
ether/CCl_4 binary mixture, proton mag. relaxation 8=39425
ether, ketone acid, amine addition products, spectroscopy 8=38880
ethers of aliphatic and aromatic acids, optical parameters of absorpt. band 8=30493
ethionamide hydrobromide, antitubercular cpds. crystal structure 8=26503
ethionamide hydrochloride, antibulercular cpds. crystal structure 8=26502
ethyl acetate, distillation from acetoacetate, liquid/vapour equilib. data 8=25989
ethyl-alcohol mixtures, proton spin-lattice relax and viscosity 8=43770
ethyl alcohol, press. oscills. accompanying heat transfer in tubes 8=34832
ethyl alcohol, shock wave compressed, refr. index, obs. 8=39370
ethyl alcohol, structure and thermodynamic props. from i.r. spectra 8=30401
ethyl alcohol, trans rotamer obs. and rotational consts. meas. 8-34 Gc/sec 8=43364
ethylamine and N-deutero derivative, i. r. and Raman spectra 8=27620
n-ethylaniline, near-u.v. absorpt. spectrum obs. 8=43352
ethyl chloride, HCl and CH_3 hindered-rot. lines, Schottky barrier tunnelling obs. 8=34327
ethyl derivatives, C^{13} and H^1 n. m. r. chem. shifts 8=29818
ethyldimethylsulphonium cpds., i. r. spectra 8=29776
ethyl formate, microwave spectrum and rotational isomerism 8=25572
ethyl free radicals, reactions with SO_2, 28-75°C 8=49848
2-ethyl, 1-hexanol and isoamyl bromide binary solns., complex permittivity 8=48191
ethyliodide, microwave double reson. spectra 8=25634
ethyl iodide mols., spin polarization calc., 300-400 eV 8=34214-5
ethylphenols, electronic absorpt. spectra 8=43385
ethyl phthalate, n.m.r., molecular rotation restriction rel. to temp. 8=43877
ethyl sulphate, Nd^{3+} in lattice, mag. anisotropy and field parametrization 8=43932
ethylvinyl ethers and their S- and N-containing analogues, e.s.r. spectra 8=38909
ethylene and perdeuteroethylene, far u. v. spectra 8=25573
ethylene catalytic hydration on Cr^{3+} and Ti^{3+} doped corundum 8=32122
ethylene, charge transfer from p and H atom, cross-sections 8=38737
ethylene, electrochem. oxidation, oscillatory kinetics 8=49939
ethylene glycol droplets, evaporation rel. to coating of n-dibutylphthalate 8=48272
ethylene, liq., self-diffusion 8=30451
ethylene, n. m. r. spin-spin consts. calc. 8=25640
ethylene, oscillator strengths for electronic spectra 8=29780
ethylene, oxidation by photolysis of NO_2 8=36615
ethylene, photochemistry, spectroscopic basis 8=27760
ethylene, rotational barrier, SCF MO calc. 8=29764
ethylene, SCF-MO-LC(LCGO) calc. 8=47626
ethylene, 6 molecules and 1 ion at 300°K, mean square vibr. amplitudes calc. 8=25571
ethylene, thermal gas phase bromination at room temp., kinetics 8=49863
ethylene, u. v. spectra assignments 8=47667
ethylene-vinyl acetate copolymers heat capacity, —190—250°C 8=24028
ethylenes, methyl-substituted, electronic transitions 8=47647
ethylenebidiguanide silver (III) nitrate, crystal structure 8=26501
ethylenediamine oligomer in soln., dielec. props. —100 to 60°C 8=39404
ethylene glycol aqueous soln., heat transfer in turbulent pipe flow, effect of Prandtl number on temp. profile 8=30367
ethylene glycol-methanol (cellulose membrane) syst., permeation and ultra-filtration 8=25904

Organic compounds—contd
ethylene imine, i. r. absorpt. spectra at 90 and 10°K 8=25568
ethylenimine, reactions to C–C double bonds 8=32097
ethylene oxide, ethylene oxide d_4, spectra vibrational analysis and potential constants 8=38877
ethylene oxide, microwave double reson. spectra 8=25634
eugenol, permittivity and relax. time rel. to pressure 8=39395
evaporation by laser irradiation, obs. 8=39494
ferrihaemoglobin, g factor anisotropy rel. to dynamical Jahn-Teller effect 8=36234
ferrocene, electronic struct. 8=29782
ferrocene, matrix-isolated absorpt. and luminesc. spectra 8=49775
five-membered rings, electronic spectra, CNDO calc. 8=38862
fluoranthene and derivatives, anomalous fluoresc. 8=30500
fluoranthene, CH-bond moments 8=34343
fluoranthene, moment directions of electronic transitions 8=34329
fluorenon, absorpt. bands, elec. field effects 8=34328
fluorescein, aq. soln., pulse radiolysis 8=49969
fluorescein, fluoresc. polarization quenching data 8=43845
fluorescein, luminescent centres, relax. of local time 8=39388
fluorine compounds, bond dissociation energies 8=47702
m-fluoroaniline, liq., i.r. spectrum obs. 8=43833
fluoro-aromatics, phosphoresc. cpds., h.f.s. in $\Delta m=2$ transitions 8=31851
o-fluorobenzene, photoexcit. triplet state yield rel. to vibr., gas-phase obs. 8=25630
fluorobenzenes, monohalosubstituted, n.m.r. 8=38922
fluorocarbons, dynamic polarization in soln. 8=34911
fluorocarbons, high-temp. reaction kinetics 8=41247
fluorocarbons in soln., dynamic polarization of F nuclei 8=48221
fluorochloromethanes, X-ray emission spectra 8=47653
fluorodurene, crystalline, molecular reorientation movements 8=27256
fluoroform, gaseous, p spin-lattice relax. density depend., obs. 8=34667
fluoro-naphthalene, vapour and soln. at 77°K, u.v. absorpt. spectra 8=32047
p-fluorophenol, emission spectrum obs. 8=43384
fluoro-phosphines, n.m.r., signs of F-P coupling consts. 8=40994
2-fluoropyridine solns., n.m.r., solvent and temp. depend. 8=48224
formaldehyde, all-electron calc. 8=25578
formaldehyde derivatives, phosphoresc. lifetimes, 8=25473
formaldehyde, dipole moment of triplet state 8=25580
formaldehyde, elec. field induced spectra 8=25582
formaldehyde, elec.-field-induced spectra 8=38881
formaldehyde, excited states, nonempirical calcs. 8=47648
formaldehyde, molec. g value and susceptibility tensors 8=29784
formaldehyde, normal-coordinate, anal. of singlet excited state 8=43367
formaldehyde, struct., using wavefunctions of double minimum potentials 8=25507
formaldehyde, 3500Å $^1A_2 \leftarrow {}^1A_1$ transition 8=25581
formaldoxime N^{15}, nuclear spin-spin interactions 8=43409
formamide-dioxane liq. system, theromdyn, props. 8=34825
formamide, X-ray diffr. of liq. 8=39306
formate, electrochem. oxidation, oscillatory kinetics 8=49939
formyl fluoride, dipole moment of π^* state 8=25579
freon-12, impurity in Ar, influence on laser-induced breakdown 8=39000
Freon-22-dibutylphthalate soln, heat transfer in boiling on horiz. tube 8=34999
Freon 22, 113 and 142, thermal cond. meas. by regular regime method 8=34824
furan, anomalies in Pariser-Parr-Pople calcs. 8=38882-3
furan, i.r. absorpt. spectra of liq. and crystalline forms 8=43836
furan, methyl-substituted, vibration spectra 8=43368
furan mol. applic. of self-consistent field calc. in differential overlap approx. 8=34357
furfural, photochem., vapour phase 8=32134
gadolinium hexa-antipyrene iodide suppression of spin-lattice relaxation Raman spectra 8=40951
galactose, amorphous, enthalpy and spec. ht., 15-45°C, rel. to mol. structure 8=30966
γ-irradiation, short-life free radical formation and stabilization by nitroso scavengers 8=49980
gaseous, X-ray spectra, carbon emission 8=47652
gelatine gels, elec. cond. and melting 8=34962
gentibiose frozen aqueous solutions, e. s. r. of free radicals 8=47707
ginkgolides and derivatives, n.m.r. data 8=48216
glasses, used as trapping matrices, viscosities 8=49065
gliotoxin, crystal structure at -150°C, 8=26508
glucose, amorphous, enthalpy and sp. ht., 15-45°C, rel. to mol. structure 8=30966
β-D-glucose, crystal structure confirmation 8=39838

Organic compounds—contd
glutaric acid, X-irradiated, polymorphic transforms. rel. to free radical recombination 8=29828
glyceride-water mixture, mesomorphic phase and micelle structure 8=25966
glycerine, scatt. cross-section meas. 8=48065
glycerine, shock wave compressed, refr. index. obs. 8=39370
glycerol, dipole moment 8=34331
glycerol, elastic consts., press. depend. 8=34841
glycerol, mag. relaxation and correlation 8=39430
glycerol, supercooled glassy and polycrystalline states Mossbauer obs. of mol. motion 8=43751
glycerol-water mixture, acoustic absorpt. below 1MHz 8=34840
glycerol, X-ray scatt. rel. to density fluctuations, calc. from compressibility 8=25879
glycine, aq. solns., u. s. absorpt. 8=48142
glycine, γ-irrad., e.s.r. of free radicals formed 8=31844
glycine, irrad. crysts., e.s.r. 8=49610
glycine, partially and completely deuterated, d.m.r. 8=49628
glycine soln., permittivity meas. below 1 MHz 8=28452
glycine sulphate, ferroelectric, temp. depend. of refractive index n_α 8=45243
glycocyanine hydrobromide, 3 dimens. Patterson and heavy atom phased Fourier synthesis 8=44274
gramicidine S in soln., molecular structure from n. m. r. obs. 8=34332
grisan derivatives in monolayers 8=39611
guanidine chromium suplhate hexahydrate, dilution splitting of Cr^{3+} absorpt. lines 8=41164
guanidine, matrix-isolated, i.r. spectrum 8=25583
Hafner's hydrocarbons, substituted, anomalous emission 8=48175
halobenzene photoconductive solns, enhanced conductivity on X-irradiation, 8=43866-7
haloethanes, dielec. relax. in soln. 8=48184
halogenated benzenes, triplet states 8=27625
2-halogenoalkylammonium halides, N-substituted space grouping 8=26510
halomethanes, C^{13} n. m. r., struct. and electronic effects 8=47700
heptaoxyethylene glycol monohexadecyl ether, micellar props. in aq. solns. 8=30559
p-n-heptylhydroxybenzoic acid, liquid crystal, nematic and smectic phases, domain formation 8=34769
heterocycles, five-membered, N^{14} nuclear quadrupole reson. 8=25638
heterocyclic anions, N^{14} hyperfine coupling factors 8=34340
heterocyclic aromatic cpds., molec. fragments, atomic-orbital calc. 8=29785
heterocyclic compounds, i. r. investigations 8=38861
hexabromobenzene singlet–triplet transitions, triplet state assignments and spin-orbit coupling 8=25536
hexachlorocyclohexane, bond mag. anistropies from diamag. meas. 8=31515
hexachloroethane, X-irradiated, polymorphic transforms rel. to free radical recombination 8=29828
n-hexadecane, thermal decomp. 8=45342
hexafluoroacetone-hexafluorobiacetyl mixtures, luminesc. energy transfer 8=48168
hexafluorobenzene, photoexcit. triplet state yield rel. to vibr., gas-phase obs. 8=25630
hexafluoropropylene copolmer, γ-irradiated, photoinduced and thermal radical conversions 8=49953
hexamethylenetetramine aq. solns., differential diffusion coeffs. 8=30446
hexamethylenetetramine-water, solvent-solute interactions 8=41254
n-hexane, dielec. const. rel. to pressure and temp. 8=39396
n-hexane, enthalpy of mixing with CCl_4 8=39348
hexane, in liquid ionization chamber, quality factor 8=37787
n-hexane, light emission, electrically stressed 8=39383
hexane, liquid ionization chamber for dosimetry 8=37786
n-hexane, non-linear dielec. susceptibility obs. 8=34888
hexane, stimulated Brillouin scattering, anti-Stokes components origin 8=25922
hexanes (normal, neo and 3-methyl-pentane), e.s.r. obs. of radicals formed by ionizing radiations 8=25659
hexanitroethane, thermal decomposition in gaseous phase 8=49879
hydrazides, substituted, C–Br bond 8=49780
hydrazidones, substituted, C–Br bond 8=49780
hydrazine, explosive instability, photochem. effect 8=27732
hydrazine, i. r. spectra, vib. anal., and force consts. 8=45244
hydrazine, liq. vapour press, thermal props, surface tension in significant struct. theory 8=43755
hydrazine, photodissoc. 8=32135
hydrocarbon, aromatic, electroluminescence in liquid phase below optical excitation threshold 8=30497
hydrocarbon binary mixtures, adsorpt. at liq.-vapour interface 8=48041
hydrocarbon binary mixtures, correlation of critical props. 8=48250
hydrocarbon fuel/air mixture, ignition in laminar supersonic boundary layer 8=32969

Organic compounds—contd
hydrocarbon fuel cells, electrocatalysts 8=46355
hydrocarbon glasses, electron trapping sites, saturation and removal 8=40082
hydrocarbon glasses, radiation-induced trapped electrons 8=45401
hydrocarbon radicals, spin-extended PPP SCF spin densities 8=47649
hydrocarbon, saturated, p-p geminal coupling constant, calc. 8=47692
hydrocarbon-TCNE complexes, absorpt. spectra, effects of press. 8=36433
hydrocarbons, absorption spectrum similar to dinegative ion 8=38884
hydrocarbons and monochloro derivatives, field-ionization mass spectra 8=47796
hydrocarbons aromatic, quasilinear phosphoresc. spectra 8=36524
hydrocarbons, CNDO calc. of nuclear spin-spin coupling 8=47663
hydrocarbons, conjugated radicals, ground states, MO calc. 8=38885
hydrocarbons, dimers in vapour phase 8=34388
hydrocarbons, electronic states, config. interaction calc. 8=25585
hydrocarbons, F-substituted, n. m. r. spin coupling constants, calc. using σ M.O. theory 8=47690
hydrocarbons, gaseous, photochemical oxidation mechanism, e. s. r. invest. 8=36616
hydrocarbons, I_2 reactions activated by radiative neutron capture 8=41296
hydrocarbons in solvents, vapour-liq. equilib. at low temp. and high press. 8=39481
hydrocarbons, ion impact, charge and proton transfer 8=29984
hydrocarbons, liq. radiolysis, scavenging mechanism 8=27765
hydrocarbons, molecular reactions with electron donating solvents 8=36550
hydrocarbons, molec. struct., floating spherical Gaussian orbital model 8=38886
hydrocarbons, n-irradiated at 14 MeV, linear energy transfer 8=43033
hydrocarbons, planar, long-range trans and cis coupling constants, analysis 8=47691
hydrocarbons, quadrupole moments, π-electron theory 8=43268
hydrocarbons, sat., diff. in coal, meas. 8=48775
hydrocarbons, unsaturated, vibrational spectra 8=47621
hydrocarbons, valence-bond theory for mols., radicals, and ions 8=29786
hydrocarbons, vapour-phase fugacities 8=39481
hydroxy- and methoxybenzaldehydes, dielec. relax in benzene solns. 8=39400
9, 10-hydroxy-borazaro-phenanthrene, crystal structure 8=26540
2-hydroxy-1-phenazine carboxylic acid from pseudomonas aureofaciens, mol. and crystal structure 8=26541
hydroxyurea, crystal structure 8=26511
hydroxyl radical kinetics, deuterium isotope effects 8=27707
imidazole, far-i.r. spectra and H-bond freqs. 8=41165
imidazole, i. r. and Raman spectra 8=29787
indene, substituted, spectroscopic study 8=36440
insulin and A and B chain S-sulphonates, p mag. reson., 220 MHz 8=39441
1-iodofluorenone oxime, e. s. r. in soln. 8=34907
ions in aq. soln., C isotope effect on electrolytic dissoc. 8=29669
n-iso-alkoxybenzal-1-aminonaphthalene-4-azobenzene derivs. mixture liq. crystal formation 8=39308
isoamyl bromide and 2-ethyl 1-hexanol binary solns., complex permittivity 8=48191
isoamyl bromide, dielec-props. of low-temp. liq 8=48188
isobutane, e. s. r. obs. of radicals formed by ionizing radiations 8=25659
isobutylalcohol, dipole moment 8=34331
isobutyric-acid-water system, diffusion coeff. obs. near critical soln. conc. 8=39341
iso-eremolactone, crystal and mol. structure 8=44273
isonitrose-acetyl, derivatives of amines, morphological, optical and X-ray study 8=26533
isoprene, structure determ. by gas e-diffr. rel. to nature of conjugating system 8=25587
isopropylalcohol, dipole moment 8=34331
isopropyl-4-phenol, crystal structure 8=26539
p-isopropyltoluene, π e chord symmetry in crysts., 20°K 8=30648
isoxazole, microwave spectrum 8=25613
ketene, g values and paramag. susceptibility 8=25589
ketones, infrared absorpt., temp. effect 8=34319
ketones, saturated, optical activity, theory 8=38888
ketones, solvent effects in u. v. spectra 8=34876-7
labdanolic acid, config. at C(13) from its p-bromo-phenacylester structural analysis 8=39840
lanthanum ethylsulphate:Er^{3+}, spin-lattice relax. times 8=45089
lead n-butylxanthate, disordered crystal structure 8=39855
lecithins, some structural studies 8=26517

Organic compounds—contd
leucrocristine methiodide dihydrate, mol. structure by anomalous scatt. methods 8=25590
lincomycin hydrochloride, crystal structure 8=26518
liquid crystal mixtures, structural and stability characts., x-ray exam. 8=39310
liquid mixtures, concs., by internal filling counters 8=27817
liquids, apparatus for crystallization, orientation and conservation for routine crystal studies 8=26214
liquids at liq. N temp:Mn atoms stabilized by condensation method e. p. r. spectra 8=30526
low-viscosity insulating oil, formation of partial discharges on points 8=30504
lubricating oils, and component fractions, viscoelastic relax. spectra 8=34698
malachite green films, photocapacitance and photocurrent "memory" 8=36032
malates, cell dimens., from X-ray powder diffr. 8=39841
malonic acid, γ-irrad., e.p.r. separation of overlapping spectra 8=40927
maltose frozen aqueous solutions, e. s. r. of free radicals 8=47707
mannose, amorphous, enthalpy and sp. ht., 15-45°C, rel. to molstructure 8=30966
mass spectra, metastable ion detector 8=43152
matter, radio thermoluminescence, crystalline nature 8=41220
α- and β-mercaptoesters, skeletal rearrangement on electron impact, mass spectra 8=47456
mercapton, H isotope exchange with alcohol 8=36545
mercury di-n-hexyl, liquid: radiolysis to identify composition 8=49976
mercury-organic crystals, R-Hg-X, Hg-X bond regularity rel. to structure 8=30616
mesitylene-benzonitrile liq. mixture, conductance showing charge-transfer interacts. 8=30515
metal complexes, mag. circular dichroism 8=27616
metal complexes, mag. circular dichroism, interpretation 8=27614
metal halide complexes, mag. circular dichroism 8=27615
metal-metal carbonyl derivatives, X-ray study 8=26474
methallyl iodide, rotational isomerism 8=43370
methanal azine, electronic absorpt. spectrum 8=34337
methane, ab initio bond-orbital calc. 8=38891
methane adsorbed on γ-alumina, radiolysis at 77°K 8=41290
methane-air mixture, spectrochem. analysis by three-colour Schlieren system 8=28737
methane-ammonia mixture, laser discharge emission spectral obs. 8=33190
methane, and deuterated, gaseous, collision induced absorpt. in far i. r. 8=47657
methane, and deuterated, rotational spectrum, collision-induced 8=47658
methane-argon mixtures, thermal diffusion rel. to atomic mass distrib. 8=43709
methane-Ar system, solid-liquid equilib. diagram 8=25978
methane, charge transfer from p and H atom, cross-sections 8=38737
methane, in chemiluminescent reactions involving H, atomic N, and H_2, N_2 and Ar 8=41245
methane, compressed, i. r. spectra, rot. correl. functions and intermolecular torque calc. 8=38894
methane, crystalline, creep meas. 8=40190
methane, equilibrium combustion products, thermodynamic props. computer calc. 8=27730
methane, gaseous, scattering of slow neutrons and intermolecular interactions 8=38898
methane I^{129} derivatives, Mössbauer effect 8=48332
methane in solid Ar, nuclear spin conversion and vibr.-rot. spectra 8=27634
methane, ionization energies 8=34459
methane, i.r. spectra of liq. and solid solns. in inert gases 8=25932
methane, laser-excited vibr. fluoresc. and energy transfer 8=25605
methane, liq., self-diffusion 8=30451
methane, low-temp. virial coeffs. 8=34643
methane, mol., intrapair correl. energy 8=38893
methane nuclear r.f. spectrum obs. 8=47588
methane, octopole moment, from virial coeffs. 8=29849
methane, photoionization, mass spectra 8=29986
methane, Raman laser emission, combination freq. generation 8=25598
methane, reaction with hydride ion, MO theory 8=27678
methane, SCF-MO-LC(LCGO) calc. 8=47628
methane, solid, thermal conductivity, 20-80°K 8=30990
methane, solubility of water in compressed CH_4 8=30302
methane theta-pinch discharges, triplet-singlet excitation rate coeff. calc. for C V ions 8=38662
methane-Xe mixtures, charge exchange 8=47792
methanes, halogen-substituted, Raman spectra in gaseous state 8=25591
methanes, substituted, molec. consts. calc. 8=25595
methanes, tetra-substituted anomalous dielec. dispersion in low-temp. phases 8=49326

Organic compounds—contd
methaneselenol, vibr. spectrum 8=25602
methanesulfonanilide, crystal structure 8=39843
methanol-acetaldehyde mixtures, H atom and proton transfer 8=34444
methanol and methanol-d_3, adsorbed on porous glass, proton relaxation times 8=47699
methanol-cyclohexane mixtures, light scatt. near crit. soln. temp. 8=39371
methanol-n-decanol mixtures, vapour press. 8=48284
methanol, effect on stress-corrosion cracking of Ti and Ti–Al–Mo–V 8=40184
methanol ion-mol. reactions, ion cyclotron reson. 8=27709
methanol-d_1, irrad., isotopic comp. of H prod. 8=32136
methanol, mm wave spectrum, torsion-vibr.-rot. interactions 8=47654
methanol, n scatt. spectroscopy of microscopic transport props. 8=30403
methanol-water mixture, thermometric analysis 8=27771
p-methoxy benzylidene-p′-cyanoaniline, X-ray study of nematic cryst. state 8=48067
methoxyl group, detection by i.r. spectroscopy 8=47661
methoxyl group, e.s.r. hyperfine interaction 8=29807
methoxynitropyridine, u.v. absorpt. spectra 8=34356
methoxypyridine, u.v. absorpt. spectra 8=34356
methyl acetate-water mixture, thermometric analysis 8=27771
methylacetylenes C_3D_4, Raman rotational spectra 8=47662
methylacetylenes C_3H_4 Raman rotational spectra 8=47662
methyl alcohol, adsorption on γ-Al_2O_3, privilege ads. of hydroxyl, n.m.r. obs. 8=39615
methyl alcohol, dielec. dispersion 8=43857
methyl alcohol, scatt. cross-section meas. 8=48065
methyl alcohol soln. in heptane, lamination on ions as nuclei 8=37800
methyl alcohol, structure and thermodynamic props. from i.r. spectra 8=30401
methyl alkàli halides, new mol. type, i.r. spectra 8=47656
methylamine-NH_3 gas mixtures, heat cond. 8=34644
methylamines, internal rot. effects in i.r. spectra 8=47655
methylamines, solid, n.m.r. 8=40990
methyl aromatic hydrocarbons, i.r. spectra and conformation of CH_3 group 8=29789
methyl-bearing cpds., proton second moment 8=40989
methyl BF_2, gas-phase i.r. spectra, fine struct. due to int. rotation 8=29793
methylborazines, SCF-MO calc. 8=38897
methyl bromide, photolysis, high-energy CH_3 radicals 8=49961
methyl bromide, vibration-rotation spectra, near 6000 cm^{-1} 8=47659
methylchloride-ethylchloride, thermal cond., 273-1173°K 8=47962
methyl chloride, perturbations in ν_4 band 8=34334
methyl chloride pure and with Ar, ethyl chloride, or Ne, thermal cond., 273-1173°K 8=47962
methylchloride, $2\nu_5$ band near 2880 cm^{-1}, parallel component 8=43374
methyl chloroform, microwave spectra, internal rot. dipole moment and struct. 8=29773
methylcyanide, and solid solns., proton spin-lattice relax., 8=40975
methyl cyanide, direct l-type doubling transitions 8=34323
methylcyclohexane, freezing press. 8=50477
methylcyclopentane, liq. radiolysis 8=45407
methylcyclopropane, microwave spectrum 8=47665
methyl derivatives, C^{13} and H^1 n.m.r. chem. shifts 8=29818
N-methyldiphenylamine, on TlI, surface charge-transfer groups form., obs. 8=36028
methyldiphenylarsine, vibr. spectra 8=43381
methylethyl ketone-water system, nucleate boiling obs. 8=25998
methyl fluoride, gaseous, p spin-lattice relax. density depend., obs. 8=34667
methyl fluoride, i.r. spectra 8=43371
methyl free radicals, reactions with SO_2, 25-164°C 8=49847
2-methyl furan, vib. spectra 8=43368
methyl-α-D-glucopyranoside crystal structure 8=39845
methyl group, electronic rel. to steric effects 8=25593
methyl group, n.m.r. narrowing due to coherent zero-point motion 8=25635
methyl groups undergoing tunnelling rotation, n.m.r. line shapes 8=49650
methyl halides, i.r. absorpt. intensity rel. to electron cloud distrib. 8=43373
methyl halides, linewidths of rot. spectra 8=38889
methyl halides, molec. struct. 8=25596
methyl halides, prebreakdown ionization currents, between parallel electrodes 8=25708
methyl halides, vibr. anharmonicity 8=38895
3-methyl 2, 4-heptanediol, u.s. and dielec. relaxation 8=48189
methyl-heptanols, pressure depend. of assoc. from dielec. props. 8=39394
N-methyl-hydroxylammonium-chloride, crystal structure 8=26511

Organic compounds—contd
methyl iodide, i.r. liq. band shapes 8=39379
methyl iodide, partition coeff. between vapour and H_2O 8=48073
methyl iodide, resonances perturbing ν_5 band 8=25594
methyl iodide, pyrolysis using hot W wire 8=36577
methyl ion, charge transfer dissociative reaction with propylene 8=34445
methyl-3-isopropyl-2-phenol, crystal structure 8=26539
methyl-3-isopropyl-4-phenol, crystal structure 8=26539
p-methyl-2′-methoxybutylbenzene, π e chord symmetry in crysts., 20°K 8=30648
methyl oleate, γ-induced oxidation 8=41293-4
3-methylpentane glass, γ-irrad., e.s.r. of trapped electrons 8=27483
methyl phenanthrene, ionization and dissoc. by electron impact 8=47797
methylphosphonic acid, i.r. spectrum 8=47666
N-methylpyrol, microwave spectrum and mol. props. 8=29798
methylstannane, i.r. spectra 8=43369
methylurea-water, solvent-solute interactions 8=41254
methyl vinyl ether, microwave spectrum 8=29790
methylvinylsulphide, vibr. spectra 8=38899
methylzinc methoxide, crystal structure 8=26529
methylzinc t-butyl sulphide crystal structure 8=26529
methylated dimeric trihalide of aluminium, Coriolis coupling coeffs. 8=43348
methylene, reaction with C_2H_5Cl in gas phase 8=45345
methylene reaction with 2-butane, photochemistry 2-butane photochemistry 8=27759
methylene blue, effect on growth of $Pb(NO_3)_2$ crystals from soln. 8=39679
methylene group, e.s.r. study of hindered roation in $[(C_6H_5)_3P^+ - CH_2]$ radical in crystalline matrix 8=49616
methylene fluoride, molec. g-values and mag. susceptibility 8=34339
micrococcinic acid bis-4′-bromoanilide, crystal and mol. structure 8=26531
molecular complex formation in excited state with short-wave absorbent aromatics 8=47629
molecular complexes emission rel. to charge transfer triplet states, obs. 8=25526
molecules triplet states excit. and low-energy e impact spectrometry 8=25528
molecules triplet states de-excit. in condensed media rel. to mol.-host interactions 8=26029
monobromoduclauxin, crystal and mol. structure rel. to duclauxin structure 8=44272
monochloroethylene, Raman line intensities and depolarizations, calc. 8=34321
monoctadecyl phosphate monolayer desorpt. from air water interface, kinetics 8=30442
mono-deuterobenzene p-derivs., ν(CH) and ν(CD) 8=34315
monoethanolamine, absorpt. of CO_2, optical study of interfacial turbulence 8=32093
monoisopropyldiphenyl, heat transfer in boiling rel. to state of heating surface 8=35001
monomethylammonium perchlorate, crystal structure 8=26522
monoselenoparaldehyde, crystal structure rel. to mol. conformation 8=35365
mylar, S^{32}, Cl^{35}, Br^{79} and P^{27} ion beam stopping powers 8=44508
myristic acid dipole moment in gaseous monolayer at air water interface, obs. 8=30438
myxin, crystal structure at −160°C 8=44277
naphthacene, fluorescence in mag. fields 8=41226
naphthacene in n-paraffins, electronic spectra rel. to phase transitions of solvent 8=25938
naphthalene and d_8-naphthalene mixed crysts., phosphoresc. spectra 8=32074
naphthalene anion in soln., e.p.r., ion pairing effects 8=39416
naphthalene, CH-bond moments 8=34343
naphthalene crystal, band structure, effects of H atoms 8=31291
naphthalene, Davydov splittings of intense transitions 8=35048
naphthalene, delayed luminesc., growth and decay 8=32073
naphthalene, detailed exciton band struct. 8=26919
naphthalene, deuterated, optical anisotropy of excited state 8=25611
naphthalene + 1, 4-dicyanobenzene, triple complex formation 8=48176
naphthalene, effect of solvents on u.v. spectra 8=34870
naphthalene, elastic constant tensor temp. dependence, 20-80°C 8=26856
naphthalene, excimer emission at v. high press. 8=49823
naphthalene, excitation exchange and optical spin polarization in triplet state, e.s.r. study 8=47686
naphthalene, exciton band, expt. determ. 8=31299
naphthalene, fluorescence and absorpt. conc. depend. in n-heptane, cyclohexane 77°K 8=49830
naphthalene, fluoresc. of doped crysts. at high press. 8=49824
naphthalene in soln., monomer and excimer phosphoresc. 8=30501
naphthalene, luminesc. polarization and impurity mol. orientation 8=36531

Organic compounds—contd
naphthalene mixed crysts., phosphoresc. and delayed fluoresc. 8=32075
naphthalene, optical spin polarization in triplet state 8=45298
naphthalene, quenching of triplet state 8=34341
naphthalene, rel. to toluene scintillators max. H_2O conc. 8=43844
naphthalene single crysts., radiation damage 8=40083
naphthalene, singlet and triplet π electron states 8=25543
naphthalene soln. in cyclohexane, $^1B_{3u}$-state, singlet-singlet absorpt. spectrum and intersystem crossing 8=43839
naphthalene, temp. gradient optimization for single crystals 8=44137
naphthalene, theory of cryst. spectra 8=49772
naphthalene, thermal expansion from X-ray meas. and expansion tensor calcs., 78-325°K 8=26596
naphthalene thermo-electret, pure and naphthol-doped, glow peak analysers 8=49378
napthalene, triplet-triplet extinction coeff., 4130 Å 8=25926
naphalene, vapour absorpt. spectrum rel. to e transitions, 30 000-53 000 cm^{-1} 8=38900
naphthalene, vibr. symmetry coords 8=43376
naphthalenes, isotopic, vibr. amplitudes calc. 8=43377
β-naphthol, triplet state, acidity determ. by e. p. r. 8=34342
1, 4-naphthoquinone and derivatives, emission spectra 8=43392
naphthothiophenes, mol. orbital calcs. 8=43355
1, 4-naphthoquinone, vapour absorpt. spectrum 8=43393
N-(α-naphthyl)-carbazole in soln., phosphoresc. 8=43849
natural orbitals, and expansion coeffs., direct calc. 8=29604
natural products, analysis by Raman spectroscopy using laser excitation 8=27793
natural products, crystal structures rel. to stereochemistry 8=26457
neopentane, methyl group librations, n scatt. obs. 8=34345
nitriles, saturated, N^{14} nuclear quadrupole coupling consts. 8=25642
n-nitroaniline, cryst., stimulated Ramn scatt. spectrum fermi reson. splitting, 77°K 8=41160
nitroaniline, in benzene, dielec. props., temp variation at microwave freqs. 8=48181
nitroanilines in ortho, meta and para states, u. s. velocity var. with temp. 8=30470
nitro azulenes, n.m.r. 8=43410
nitrobenzene, depolarized doublet of light scatt. from thermal shear waves 8=43817
nitrobenzene, scattering of ruby laser emission, large angle 8=48158
nitrobenzene, elec. cond. 8=34898
m-nitrobenzene, ^1H-^1H coupling constants 8=25641
nitrobenzene-n-hexane mixtures, u. s. absorpt. near critical region 8=25912
nitrobenzene, induced Raman scatt., sensitizing by cyanine dyes 8=34871
nitrobenzene, liq., X-ray scattering 8=43760
nitrobenzene, Stokes freq. gain on Rayleigh wing, obs. and calc. 8=39364
nitrocellulose powder, ignition by shock wave 8=23950
nitroglycerin powder, ignition by shock wave 8=23950
nitromethane, gas-phase i. r. spectra, fine struct. due to int. rotation 8=29793
5-nitro-6-methyluracil, e.s.r. of γ-irrad. cryst. 8=49615
nitroparaffins, solvent effects in u. v. spectra 8=34876-7
m-nitrotoluene, depolarized doublet of light scatt. from thermal shear waves 8=43817
1-nitro-4-trifluoromethoxybenzene anion radicals, ion pairing 8=39415
nitrovinylbenzoate, structural group interactions, MO calcs. 8=34347
nitrogen derivatives, stereochemistry from gas e-diffr. study 8=25608
nitrogen heterocyclics, ionization potentials 8=39060
nitrotriacetatoaquochelate of Nd(III), crystal structure 8=26415
nitroxide radicals from diethylhydroxylamine, dioctylhydroxylamine and N-hydroxypyrrolidine, e. s. r. obs. 8=25655
n-nonane, sound propag. vel. meas. 8=39361
norbormide, stereochemistry from X-ray investigations 8=26165
nucleic purines, e struct. of first excit. triplet state, calc. 8=25621
nucleic pyrimidines, e struct. of first excit. triplet state, calc. 8=25621
nucleoside derivs, struct. and chem. substitution effects, rotatory and dichroism studies 8=43434
n-octadecanoic acid film on metal oxide, wettability rel. to heat treatment 8=48050
octadecanol monolayers, retention of solvent 8=39613
n-octadecyl alcohol film on metal oxide, wettability rel. to heat treatment 8=48050
n-octadecylamine film on metal oxide, wettability rel. to heat treatment 8=48050
octadecylamine on steel and glass, desorpt. and exchange, obs. 8=30768

Organic compounds—contd
octahydroxycyclobutane, molec. and cryst. struct. 8=44267
n-octanol, adsorpt. on defined rutile surfaces from soln. in p-xylene and n-heptane 8=35196
octanols, pressure depend. of assoc. from dielec. props. 8=39394
octyl alcohols, dielec. props. and intermolec. assoc. 8=30508-
octyl alcohols, isomeric, association, press. depend., dielec determ. 8=48182
octyl alcohols, liq. struct. transform 8=39296
octylbenzoic acid, liq. cryst., ferroelec. behaviour 8=25882
octyl hexaoxyethylene glycol monoether + water systems, heat of mixing obs. 25°C 8=48126
oil, detection on surfaces in vac. systems using ellipsometer 8=39255
oil, synthetic immersion, for microscope objectives 8=39363
olefins, liq., radiolysis 8=27766
olefins, u. v. spectra assignments 8=47667
organo-hectorites, sorption, swelling and intracryst. porosity 8=30779
organometallic cpds. of groups IV and II b, C^{13} n.m.r. 8=38925
organo-montmorillonites, sorption, swelling and intracryst. porosity 8=30779
organophosphorus cpds., C^{13} and P^{31} mag. double resonance obs. 8=43401
organophosphors, photoluminesc. reabsorpt. 8=36525
organotin dichlorides, nuclear quadrupole coupling 8=41013
organotrichlorosilanes, l. f. vibs. 8=47620
Oseksuat oils, narrow-boiling range, temp. depend if thermal cond. 8=30461
oxalic acid dihydrate-d, d.m.r. 8=49628
α-oxalic acid dihydrate, d.m.r. and molec. struct. 8=49638
oxalyl halides, near u. v. absorpt. spectra 8=25612
oxazole, and derivatives, excimer formation 8=29796
oxide layers from reactive cathode sputtering, texture from X-ray obs. 8=39711
palladium-8-mercaptochinolinates, crystal structure 8=39842
palmitic acid dipole moment in gaseous monolayer at air/water interface, obs. 8=30438
paraffin, liquid, n.m.r. in rotating mag. field 8=25958
paraffin, surface charge density meas. and contact electrification 8=49379
paraffin wax n havitzers, optimum design, obs. 8=42649
paraldehyde, laser Raman spectra 8=25530
pentaerythritol, deuterated, structural investigations of H bonds, by n. m. r. 8=43926
pentafluorobenzene, n. m. r. 8=34373
n-pentane, diffusion in polystyrene rel. to second-order transition above glass point 8=44398
n-pentane, H formation in radiolysis 8=41291
n-pentane, radiolysis of liq. 8=49971
pentane, scatt. cross-section meas. 8=48065
pentanes (normal, iso and neo), e. s. r. obs. of radicals formed by ionizing radiations 8=25659
perbromocyclopropane, vibr. spectra 8=25565
perchlorocyclopropane, vibr. spectra 8=25565
perfluorocyclopropane, vibr. spectra 8=25565
perhydrotriphenylene (PHTP) + n-hydrocarbons; + chloroform; + cyclohexane, inclusion cpds. structure 8=30920
peroxidase and derivs., Mössbauer spectroscopy 8=29823
perspex spheres, shock wave propag., reply to comments 8=35734
perylene, CH-bond moments 8=34344
perylene, cryst. spectra at high press. 8=41168
β-perylene, crystal structure and bond distances 8=26470
perylene, in crystalline n-paraffin soln., quasi-line spectra, temp. broadening, shift and line profiles 8=45240
perylene molecular crystal, electronic spectra calc. 8=40249
perylene-N in N-dimethylaniline, fluoresc. quenching via charge transfer 8=34885
phenanthrene-biphenyl mixed crysts., sectra and struct 8=41159
phenanthrene, CH-bond moments 8=34344
phenanthrene, delayed luminesc., growth and decay 8=32073
phenanthrene, excimer emission at v. high press. 8=49823
phenanthrene, excit. states decay and intersystem crossing, obs. 8=25537
phenanthrene, fluoresc. of doped crysts. at high press. 8=49824
phenanthrene in soln., monomer and excimer phosphoresc. 8=30501
phenanthrene, ionization and dissoc. by electron impact 8=47797
phenanthrene, low-lying triplet excit. states, 0.4-1.0μ 8=25616
phenanthrene, matrix isolated crystallites in rigid 3-methylpentane photoelec. props. 8=49429
phenanthrolines, deactivation of excited states 8=43383
phenanthrolines, fluoresc. and phosphoresc. spectra 8=43382
phenazine, singlet–triplet transition in mag. field 8=31296

Organic compounds—contd
phenazine/N-oxyphenazine mixed crystals habit changes 8=48522
phenazine singlet-triplet transitions, triplet state assignments and spin-orbit coupling 8=25536
phenazines, cryst. and in soln., absorpt. spectra in polarized light 8=32042
phenol, fluoresc. polarization quenching data 8=43844
phenol, H-bonding with vinyl derivatives 8=43379
phenol-nitrobenzene system, complex formation from spectral analysis 8=45347
phenol, rot. coeffs., contrib. of internal rot. 8=47668
phenol, struct. in ground and first excited state 8=25614
phenol, 2750Å electronic band system 8=43378
phenolic binary complexes, fluoresc. and hydropholic bonds 8=43850
phenoxy radicals, n.m.r. 8=43411
phenylamines, ⌊C-N⌋ and ⌊N-H⌋ bond valencies 8=47622
1-phenyl-6-benzyl-7, 7-dichlor-3, 5-diaza-bicyclo-1,2,2-hepten-5-on-2, crysts. atomic struct., obs. 8=35363
phenylcyclopropane, structure determ. by gas e-diffr. rel. to nature of conjugating system 8=25587
phenyl derivatives of Ge, As, and Sb, i. r. spectra 8=34352
phenyl and ethinyl derivatives of Ge and Si, proton mag. reson. 8=36268
phenyldichlorophosphine oxide, structure determ. by gas e-diffr. rel. to nature of conjugating system 8=25587
phenylgermane, i. r. and Raman spectra 8=25615
phenyl group IV-A cpds., l.f. vibr. spectra 8=38901
γ-phenyl-pyridene derivatives, u. v. absorpt. spectrum 8=29797
phenyl salicylate, cryst. growth retardation in capillary tube, obs. 8=35247
phenyl salicylate, growth, unit cell dimensions 8=44280
phenyl-2, 1, 3-thio(seleno)diazoles, vibrational spectro 8=43356
o-phenylenebis(dimethylarsine) 8=43381
m-phenylene-bis-phenylmethylene, quintet mol., spectra 8=47669
p-phenylenediamine cations, u. v. spectra, dimerization of radicals 8=25657
p-phenylenediamine-chloranil charge-transfer complex, mag. excitations 8=31880
p-phenylenediamine:tetracyanoethylene, d. c. resistivity rel. to press. and elec. field 8=27078
pheophytin and derivatives for Q-switching of ruby lasers 8=46605
phosphobenzol, crystal structure 8=48687
phosphoenol pyruvate, monocyclohexylammonium salt, crystal structure 8=26544
phospholipids, some structural studies 8=26517
phosphorescence and delayed fluoresc. in solns., kinetics and chem. appls. 8=25936
phosphors structure and luminescence 8=41221
photo iso pyrocalciferyl-m-bromobenzoate, crystal structure 8=26469
phthalazine, n-π* transitions 8=41170
phthalic acid distribs, infrared spectroscopic determ. of isomers 8=34346
phthalimide derivatives, radiationless transitions, activation energy determ. 8=34879
phthalimides, polarisation in fluorescence spectrum, temp. dependence 8=30502
phthalocyanines, polycryst., visible spectra 8=36444
picene, low-lying triplet excit. states, 0.4-1.0μ 8=25616
piperazine hexahydrate, cryst. struct. 8=39846
piperidine, microwave spectrum 8=25617
pivaldehyde, microwave spectrum 8=25618
plastic crystals, similarities of grain growth with metals 8=39657
polarization quenching by excitation transfer 8=43844
polar vapours, thermal cond. obs. 38°-200°C 8=34657
polyenes, oscillator strengths for electronic spectra 8=43386
porphin type cpds., NH oscills. found, problem of internal H bond 8=34353
porphyrin diacids, molec. and cryst. struct. 8=44282
porphyrins, Stark effect 8=43388
porphyrins, Zeeman effect 8=43387
potassium acid maleate, l.f. Raman spectra 8=27633
potassium-chloranil, mag. transition in 210-260°K region 8=31535
potassium dihydrogen isocitrate, aconitase, substrate, crystal structure 8=26462
potassium hydrogen diformate, crystal structure rel. to H bonding 8=39837
potassium hydrogen fumarate, X-ray analysis 8=44275
potassium oxalate monoperhydrate, crystal structure 8=26535
potassium oxalate monoperhydrate, $K_2C_2O_4.H_2O_2$, crystal structure 8=26535
potassium tartrate, second harmonic generation on ruby laser irrad. 8=45199
proflavine, photoreduction in aqueous solution by steady light 8=49962
proline-chloranil complex, formed by interact. in buffered aqueous ethanol 8=36571

Organic compounds—contd
propane, ab initio bond-orbital calc. 8=38891
propane, chemisorption on Pt, effect of pre-adsorbed water 8=27738
propane diffusion flame, C particles size and temp. distrib., i.r. obs. 8=46257
propane ionizing collisions and electron mean free paths obs. at 10^{-4} torr 8=34458
propane, liquid, refr. index, 17.4-65.8°C, 4358, 5461 and 5791Å 8=30483
propane, liq., self-diffusion 8=34812
propane-O_2-Al flame, heat transfer characts. rel. to Al seeding 8=32973
propane-O, K_2CO_3 seeded plasma in m.h.d. duct, pot. distrib., obs. 8=39084
propane-O_2-N_2 detonation products, elec. conductivity at cm. wavelengths 8=27731
propane, reactions with H_3^+ 8=39057
propane, self-inhibited pyrolysis 8=36570
propane, solid, reaction with T atoms 8=27770
n-propanol-benzene-ethylene glycol system, ternary liquid phase equilibrium 8=48079
1-propanol, n. m. r. relax. 8=30535
1-propanol-water mixture, thermometric analysis 8=27771
propargyl alcohol, internal rot. from microwave spectrum 8=43389
propargyl alcohol, microwave spectra for isotopic forms 8=25532
propargyl amine microwave spectra for isotopic forms 8=25532
propene, solid, reaction with T atoms 8=27770
propionic acid, microwave spectrum 8=25620
n-propylamine and N-deutero derivative, i.r. and Raman spectra 8=27620
n-propyl ether, h.p. viscosity obs. 8=34793
propylene, ab initio bond-orbital calc. 8=38891
propylene-Ar system, liq.-vapour phase equilib. and solubility 8=39479
propylene, charge transfer reactions with Ar^+, Kr^+, and CH_4^+ 8=34445
propylene, deuterated, microwave spectrum and internal rot. 8=43390
propylene, ion-mol. reactions 8=43492
propylene-Kr system, liq. -vapour phase equilib., and solubility 8=39479
pyperine, supercooled, dipole polarization activation 8=39403
pyranthrone, crystal structure rel. to that of flavanthone 8=26550
pyrazine, n. m. r. oriented in nematic phase 8=34913
pyrazine, phosphorescence, at 4.2°K 8=36534
pyrazine, SCF calc. 8=25622
pyrazine, SCF wavefunction, all-electron 8=34360
pyrazine, spin-lattice relax. and low temp. phosphoresc. decay 8=36535
pyrazole 3(5) and 4 isomer derivs., u. v. and i. r. absorpt. spectra 8=34361
pyrazolecarboxamides, i. r. abs. of carbonyl group 8=47645
pyrene, carrier photogeneration and luminescence processes 8=40679
pyrene, CH-bond moments 8=34343
pyrene, flash excited absorpt. spectrum 8=43840
pyrene, fluoresc. of monomer in solid soln. 8=45300
pyrene in biphenyl, delayed excimer fluoresc. 8=32076
pyrene in cyclohexane and ethanol, delayed luminesc. and triplet quantum yields, obs. 8=25941
pyrene in n-paraffins, electronic spectra rel. to phase transitions of solvent 8=25938
pyrene-iodine complex, a.c. conductivity rel. to temp. 8=44700
pyrene, low-lying triplet excit. states, 0.4-1.0μ 8=25616
pyrene, luminesc. in soln. and mixed crysts. 8=25942
pyrene molecular crystal, electronic spectra calc. from Davydov decay 8=40248
1, 1-pyrene-pyromellitic dianhydride, structures at 110-300°K 8=26554
pyridazine, e distrib. at N atom by N^{14} quadrupole coupling consts. meas. 8=25643
pyridazine, vibr. spectra 8=25933
pyridine-alcohol solns., light scatt. and intermolec. interacts. 8=34857
pyridine, anal. of n. m. r. spectrum using different methods 8=29821
pyridine-benzonitrile liq. mixture, conductance showing charge-transfer interacts. 8=30515
pyridine, CNDO calc. of electronic spectra 8=29767
pyridine Cu(II) chlorobenzoates, mag. props. 8=36072
pyridine derivs., ν(CH) bands near 3000 cm^{-1}, i. r. absorpt. study 8=29799
pyridine mol. applic. of self-consistent field calc. in differential overlap approx. 8=34357
pyridine-paraffin solns., light scatt. and intermolec. interacts. 8=34857
pyridine, photoexcit. triplet state yield rel. to vibr., gas-phase obs. 8=25630
pyridine, SCF calc. 8=25622
pyridine, SCF wavefunction, all-electron 8=34359

Organic compounds—contd
pyridine-trinitrotoluene liq. mixture, conductance showing charge-transfer interacts. 8=30515
pyridines, substituted, e distrib. at N atom by N^{14} quadrupole coupling consts. meas. 8=25643
pyridinyl diradicals, stable, intramolec. assoc. 8=43424
pyridoxine hydrochloride, crystal structure 8=26551
pyrimidine, e distrib. at N atom by N^{14} quadrupole coupling consts. meas. 8=25643
pyrimidines, polysubstituted, i. r. spectra in 700-200 cm^{-1} range 8=47670
pyrolysis using hot W wire 8=36577
2-pyrone, struct. of electron impact fragments 8=39061
pyrrole-dimethyl sulphoxide, n. m. r. and H-bonding 8=25644
pyrrole mol., applic. of self-consistent field calc. in differential overlap approx. 8=34357
pyrrole, n.q.r. 8=31929
pyrrole, wavefunction, ground-state 8=34358
quaternary ammonium salts displaying anticholinergic activity, crystal structure 8=39847
p-quaterphenyl layers, meas. of space charge limited currents 8=31427
p-quaterphenyl, space charge limited currents 8=49274
quinine bisulphate, as fluoresc. standard 8=39391
quinoline and isoquinoline, at liq. N$_2$ temp., i. r. spectra and interpret. of fund. vibrs. 8=34362
quinoline, depolarized doublet of light scatt. from thermal shear waves 8=43817
quinonediazide cations, electronic structure 8=34363
quinoxaline triplet state excit. and radiative decay paths rel. to mag. interactions 8=25624
radioluminescence rel. to mol. excitation kinetics, obs. 8=39384
rare earth ethyl sulphates, specific heat, mag. contribution 8=44343
rhodamine-B film, photocapacitive effect 8=40680
rhodamine B in ethylene glycol, fluoresc. meas. of photon flux 8=46653
rhodamine C solution, optical generation during excitation with pulsed light sources 8=30480
rhodamine dyes in polymethyl methacrylate rods, stimulated emission when flashlamp excited 8=28714
rhodamine films, photocapacitance and photocurrent "memory" 8=36032
rubidium oxalate monoperhydrate, $Rb_2C_2O_4 . H_2O_2$, crystal structure 8=26535
rubrene, cryst. spectra under press. 8=49779
rubrene, liquid, with luminophor, electroluminescence 8=43848
salicylaldehyde mol. obs. of infrared spectrum 8=43394
salicylanilide, u.v. spectrum 8=38903
salicylic acid and salts, luminescence polarization diagrams 8=32077
N-salicylideneaniline hydrolysis in H_2O-methanol 8=48164
salicylidene aniline, photochromism 8=45302
salol, crystal growth rate retardation in capillaries 8=26261
salutaridine methiodide, cryst. structure 8=44276
Schiff bases, aromatic, lattice parameters and space groups 8=26456
scintillators conference, 1966 8=45250
Seignette salt cryst., surface electroluminescence 8=41228
selenophene, microwave spectrum 8=43395
semicarbazide hydrochloride, e.s.r. of γ-irrad. crysts. 8=49604
semicarbazides, i. r. abs. of carbonyl group 8=47645
semicarbazones, i. r. abs. of carbonyl group 8=47645
semiconductor, photoconductivity meas. in SHF band 8=49406
semiconductors, book review 8=27140
semiconductors, e.s.r. g-shift mechanism due to conjugated π-electrons 8=44747
semiquinones, O^{17} hyperfine components in e.s.r. spectra hyperfine splitting constants and line width variations 8=40942
silacyclobutane, i. r. spectra and ring puckering 8=29800
silicone rubber, C-black filled, elec. cond. rel. to uniaxial stretch ratio 8=26752
soap films, solvation forces 8=27686
sodium salicylate, fluorescent emission band shape interpretation 8=45303
sodium salicylate, luminescence, temp. effects 8=45301
sodium salicylate on MgO, diffusion indicator in far u.v. 8=49778
starch-iodine complex, metallic nature 8=31869-70
stearic acid, monolayer, polarization effects in reflection spectra 8=37683
stearic acid on steel and glass, desorpt. and exchange, obs. 8=30768
stearic acid, reaction with Ca^{2+} ions at air/water interface 8=41264
steroid conformations 8=25626
stilbene, anisotropic, in scintillation response for neutron directional meas. 8=47154
stilbene derivatives, electrical conductivity and optical absorption 8=49145
trans-stilbene, 5–100μ thickness meas. from refr. index dispersion 8=32043

Organic compounds—contd
stilbene powder, Raman line intensities and dispersion effects elimination, obs. 8=36445
stilbene response to internally generated protons 8=47169
stilbene, scintillation γ and n spectrometer, $E_n \geq 0.1$ MeV 8=33821
stilbene, scintillation n counter, 2.5 MeV 8=33817
stilbene, scintillation n counter with γ discrimination 1–10 MeV 8=33822
structure of π-electron chain with bridging struct. at each end, study of elec. cond. mechanism 8=26893
succinonitrile, elastic consts. in plastic phase 8=44611
sucrose growth and habit rel. to adsorbed impurity effect 8=26266
sulpholane/Hg interface, specific adsorpt. rel. to elec. double layer 8=30396
Teflon, high finish polishing 8=37096
terpene alcohols and related cpds. i.r. spectra 8=39381
para-terphenyl crystal structure 8=26560
meta-terphenyl, e radiolysis, temp., intensity and post irrad. effects, 1.35 MeV 8=36624
para-terphenyl, 5–100μ thickness meas. from refr. index dispersion 8=32043
p-terphenyl, space charge limited currents 8=49274
dl-α-terpineol e-transfer oxidation by manganic acetate, 100°C 8=49881
testosterone: mercuric chloride 2:1 complex, crystal structure and absolute config. 8=44283
tetra alkyl metals, total ionization cross section 8=25719
tetrabenznaphthalene, CH-bond moments 8=34344
tetrabenzonaphthalene, MO calcs. 8=34312
1, 2, 3, 4-tetrabromo-1, 2, 3, 4-diphthaloylcyclobutane, cryst. and molec. struct. 8=48688
tetrabutylammonium hexafluorophosphate, F exchange with BF_3 or PF_5 in CH_2Cl_2 soln., n. m. r. obs. 8=25960
tetracene, charge-transfer exciton and ionic levels 8=27254
tetracene, cryst. fluoresc., temp. depend. 8=36536
tetracene, cryst. spectra under press. 8=49779
tetracene, 5–100μ thickness meas. from refr. index dispersion 8=32043
tetracene, fluoresc. in host crysts. at high press. 8=49822
tetrachloroethylene, cavitation bubble dynamics 8=25850
tetrachloroethylene, u.s. cavitation using pulsed n source 8=25849
1, 2, 3, 4-tetrachloro-5-exomercaptobicyclo (2, 2, 1) hept-2-ene. spin coupling consts. of SH proton 8=43412
tetrachlorohydroquinone, structure rel. to H bonding system 8=30619
4, 5, 9, 10-tetrachloro-2, 7, 11, 12-tetrathia, 1, 3, 6, 8, tetrazatricyclo dodeca-3, 8, diene 8=26496
tetracyanocyclobutane, crystal structure 8=39854
tetracyanoethylene, i. r. polarized spectra of charge transfer complexes, rel. to vibr. assignment 8=38879
tetracyanoethylene, on TlI, surface charge-transfer groups form., obs. 8=36028
tetracyanoethylene-Pt complex, cryst. and molec. struct. 8=34322
7, 7, 8, 8-tetracyanoquinodimethan: N, N, N′, N′-tetramethyl-p-phenylenediamine 2:1 complex, crystal structure 8=39852
tetracyanothiophene, crystal structure 8=39850
tetraethylammonium perchlorate, elec. cond. in valeronitrile 8=48197
1, 2, 3, 4-tetrafluorobenzene, n. m. r. 8=47701
tetrafluoroethylene copolymer, γ-irradiated, photoinduced and thermal radical conversions 8=49953
2, 4, 4, 6-tetrahalogenocyclohexa-2, 5-diene-1-one crystal structure 8=26482
tetrahalophthalic anhydride complexes with aza-aromatics, spectra 8=38902
tetrahydrofuran and deutero-substitutes, vibration spectra 8=43397
tatrahydrofuran/CCl_4 binary mixture, proton mag. relaxation 8=39425
tetrahydrofuran, far i. r. spectra 8=25567
tetrahydronaphthalene with acetone, diethylether or ethylbromide, adsorpt. on solids 8=48477
tetrahymanone, crystal structure 8=26562
tetraiodethylene, vibrational spectra and force consts. 8=43396
tetramethyl ammonium chloride in D_2O, polarization effects in reflection spectra 8=37683
tetramethyl ammonium hydroxide pentahydrate, crystal structure 8=26505
tetra methylammonium-uranylchloride, spectra 8=41166
tetramethylbiphosphine-bis(monoborane) crystal and mol. structure 8=39851
N, N, N′, N′-tetramethyl-p-diaminobenzene iodide, crystal and mol. structure 8=26524
tetremethylethylene, intermediates in photolysis 8=49951
N′-tetra methyl-p-phenylenediamine in soln, biphotonic ionization 8=43861
tetra-methyl-n-phenylenediamine, on TlI, surface charge-transfer groups form., obs. 8=36028
2, 2′, 6, 6′-tetramethylpiperidine-4-ol-1-oxy radical, e.s.r. and susceptibility, obs. 8=25661

Organic compounds—contd
2,2′,6,6′-tetramethylpiperidine-4-one-1-oxy radical, e.s.r. and susceptibility obs. 8=25661
2,2,6,6 tetramethyl 4-piperidinol 1-oxyl, sp. ht. 1.3°–74°K 8=30969
(2,2′,5,5′-tetramethylpyrrolidine-3-one-1-oxy) radical, e.s.r. and susceptibility, obs. 8=25661
tetramethylsilane, as internal reference for p.m.r. 8=34929
tetramethyl tin free radical form., e.s.r. detection 8=34382
tetranitromethane, thermal decomposition in gaseous phase 8=49879
tetraphenylbutadienes, effect of intramolec. twisting on fluoresc. 8=39390
tetraphenylphosphonium bis(tetracyanoquinodimethanide), crystal structure 8=39853
tetraphenylporphin and Ag deriv. solid solns., growth and structures 8=26034
s-tetrazine, geom. struct. from 5515Å transition 8=25627
s-tetrazine, visible spectrum 8=25628
thienothiophenes, isomeric; electronic spectra 8=43399
thioacetamide as ion donor for PbS growth in silica gels 8=48555
thioacetamide-S-oxides, crystallography 8=48689
thiobenzophenone anion radical, formed by light excitation in (n, π^*) band 8=29827
thiophene, monoalkyl substitutes, scatter and i.r. absorpt. 8=34364
β-thiophenic acid, disorder from 3D-X-ray exam. 8=26499
thiourea and deuterated deriv., crystal structures by n-diffr. above and below ferroelec. transition 8=44251
thiourea derivatives, X-irrad., e.s.r. 8=31886
thiourea, thermal expansion anisotropy in paraelectric phase 8=26597
DL-threonine, n.m.r. 8=43398
L-threonyl L-phenylalanine p-nitrobenzylester hydrobromide, structures 8=26468
thulium acetylacetonate, Mossbauer effect in structure determ. 8=43959
thulium benzoate, Mossbauer effect in structure determs. 8=43959
thulium oxinate, Mossbauer effect in structure determ. 8=43959
titanium tetramethoxide, crystal and mol. structure 8=44284
titanocene derivs, $(C_5H_5)_2TiCl_2$ and $C_5H_5TiBr_3$, mol. structure by gas e-diffr. 8=25629
tolane-diphenyl mercury solid solns., single crystal study 8=26040
toluene, adsorption on silica, n.m.r. obs. 8=39615
toluene, higher excimer states 8=34872
toluene, nanosec. pulse radiolysis 8=49979
toluene, photoexcit. triplet state yield rel. to vibr., gas-phase obs. 8=25630
toluene, scattering of ruby laser emission, large angle 8=48158
toluene, stimulated Brillouin scattering, anti-Stokes components origin 8=25922
toluene scintillators, max. H_2O conc., dioxane and naphthalene effects 8=43844
toluene, Stokes freq. gain on Rayleigh wing, obs. and calc. 8=39364
toluene to diacetyl triplet-triplet energy transfer in solns., obs. 8=34316
tomatidine hydrobromide and related steroidal sapogenins, crystal structure 8=26563
tosyloxylupinane rearrangement product, structure determ. 8=26564
transition-metal organometallic cpds., mass spectra 8=39053-5
S-triazine, lattice energy calc. 8=26578
s-triazine, low temp. phase transition 8=48411
tribromobenzene singlet–triplet transitions, triplet state assignments and spin-orbit coupling 8=25536
tributylphosphate, association with H_2O 8=34775
trichloroacetic acid + benzophenone mixture, dielec. props 8=48190
2,4,6-trichloroanisol, n.q.r. of Cl 8=41014
1,3,5-trichlorobenzene, mol. vibrations from NQR exam. 8=27516
1,2,4-trichlorobenzene, n.m.r. of oriented mols. 8=43403
trichlorofluoromethane, ice and water clathrates, dielec. props. 8=27255
tricycloquinazoline, and $CuCl_2$ complex crystal structures 8=26486
1,3,5-trideutero-benzene, liquid, proton spin-lattice relaxation 8=39429
triethanolamine, AgBr recrystallization and photosensitivity effects 8=30821
triethylamine-I_2 complexes, dipole moment, dielec. meas. 8=30511
triethylamine in water, hypersound velocity and dispersion near critical stratification point 8=48143
triethylammonium:tetracyanoquinodimethan complex, semicond. electronic cond. 8=27139
triethylsulphonium cpds., i.r. spectra 8=29776
triethylene diamine, pure n.q.r. 8=41015
trifluoromethyl iodide laser, Q switching and mode locking 8=37576
trifluoromethylphosphine, microwave spectrum, molec. struct. 8=25574
trifluoromethylphosphonylchloride, prep. and props. 8=34330
3,3,3-trifluoropropyne, n.m.r. in liq. cryst. solns. 8=34930
triglycine, aq. solns., u.s. absorpt. 8=48142
triglycine fluoberyllate, electrocaloric effect and dielec. constant 8=27291
triglycine selenate ferroelectric props. at high hydrostatic pressures 8=40622
triglycine selenate, optical indicatrix rotation in phase transition region 8=27638
triglycine selenate, spontaneous polarization, permittivity and sp. ht. temp. dependence 8=44890
triglycine sulphate crystals; isomorphous with ferro-electrics, i.r. spectra 8=49774
triglycine sulphate, Cu^{2+} e.p.r. rel. to bonding, obs. 8=36243
tri-glycine sulphate: Cu^{2+}, n.m.r. 8=36241
triglycine sulphate, deuterated, solid soln. prep., ferroelec. props. rel. to conc. 8=49377
triglycine sulphate, domain and defect structs. in ferroelec. and paraelec. phases, obs. 8=31031
triglycine sulphate, domain twins in growth 8=27292
triglycine sulphate, domains, change in width with time 8=31437
triglycine sulphate, elec. resist., effect of atmospheric humidity 8=35985
triglycine sulphate, electro-optical props. near phase transitions 8=27637
triglycine sulphate, ferroelec., anomalous sp. ht. near Curie pt. 8=39923
triglycine sulphate, ferroelectric domains and dislocations interactions 8=27287
triglycine-sulphate ferroelec. group, temp.-induced changes in the 575 cm^{-1} band at phase transition 8=36438
triglycine sulphate, fundamental absorpt. edge temp. dependence, room temp. -62°K 8=41172
triglycine sulphate, γ-irrad., e.s.r. of free radicals formed 8=31844
triglycinesulphate, γ-irradiated, optical annealing investigation by e.s.r. 8=44400
triglycine sulphate, interaction of defect and domain structures in ferro- and paraelectric states 8=40620
triglycine sulphate and isotypes, ferroelec. transition mechanism from i.r. spectra 8=27290
triglycine sulphate and isotypic crystals, solid solns., ferroelectric phase transition 8=27293
triglycine sulphate, optical indicatrix rotation in phase transition region 8=27638
triglycine sulphate, permittivity at 20 kHz obs. 8=44889
triglycine sulphate, polarization in d.c. field and resistivity determ. 8=40618
triglycine sulphate, polarization process, ultrasound effects under static conditions 8=35986
triglycine sulphate, pyroelec. effect for rapid temp. change in Curie pt region 8=31443
triglycine sulphate, second harmonic generation, ferroelectric domain structure influence 8=35977
triglycine sulphate, specific heat in region of Curie temp. 8=35430
triglycine sulphate, surface sparks 8=40623
trilaurin, kinetics of cryst. growth from melt 8=26255
trimethylamino borontrichloride, crystal and mol. structure 8=44264
trimethyl aluminium dimer 8=43348
trimethylammonium chloride, crystal structure rel. to H bonding 8=26526
trimethylbenzenes, isomeric, solid, n.m.r. between 4°K and m.p. 8=36276
trimethylene selenide, ring-puckering vibr. 8=29802
trimethylene sulphide, $(CH_2)_3S$, crystals, i.r. absorpt. and Raman spectra 8=41171
tri-n-alkylsulphonium halides, osmosis 8=30454
trinitrobenzene cryst. complexes, high press. spectra 8=27635
trinitrofluorenone cryst. complexes, high press. spectra 8=27635
trinitrotoluene, equation of state, Debye-Einstein construction method 8=48728
trinitrotoluene, transition conduction zone behind shock wave front, time interval 8=49068
triphenylarsine 8=43381
triphenylarsine, mol. addition compounds with SnX_4 (X=halogen), i.r. spectra, stretching vibs. freq. shifts 8=25631
triphenylphosphine, and complexes, vibr. spectra 8=43380
triphenylphosphine, mol. addition compounds with SnX_4 (X=halogen), i.r. spectra, stretching vibs. freq. shifts 8=25631
triphenylphosphine oxide, and complexes, vibr. spectra 8=43380
triphenylphosphine sulphide-I_2 complex, cryst. struct. 8=44281
1,5,9-d_3-triphenylene, CH-bond moments 8=34344
triphenylene, CH-bond moments 8=34344
triphenylene, delayed luminesc., growth and decay 8=32073

Organic compounds—contd
triphenylene-d_{12}-Rhodamine B solids solns., triplet-singlet energy transfer kinetics, obs. 8=36533
triselenoparaldehyde, crystal structure rel. to mol. conformation 8=35365
tris(α-diimine)Fe(II) complexes, calc. electronic struct. calc. 8=43365
tris-oxalato Cr(III), low temp. emission spectra 8=27670
1, 3, 5-trithiane, crystal structure 8=26565
tropylium salts, molec. motion in solid 8=49659
trypaflavine, photoluminesc. quenching by rhodamine in glycerine solns. 8=48174
tryptamine derivs, preliminary X-ray data 8=39839
tryptophan in mixed polar solvents, photo-induced trapped electron rel. to photobleaching, 77°K 8=36446
tryptophan solns., photo-induced trapped electron behaviour at 77°K 8=25935
$\alpha\beta$-unsaturated ketones, u. v. and i. r. spectra 8=29788
uracil, valence-electron density maps 8=48620
uranine, mol. plus solvation shell vol. in glycerol-ethyl alcohol and glycerol-H_2O solns., obs. 8=34285
uranyl acetate/triphenylphosphine oxide complexes, crystal structure 8=44259
urea and deuterated urea, vibrational spectra, force constants and mean amplitudes of vibrs. 8=38904
urea, as structure breaker for water 8=48085
urea soln., permittivity meas. below 1 MHz 8=28452
urea/thiourea inclusion cpds, gen. structural principle 8=48691
urea-urease mixture, u. s. relax. obs. 8=48144
urethanes, substituted, C–Br bond 8=49780
urotropin and Br, I complexes, vibr. spectra and bond strengths, 4000-350cm^{-1} 8=49781
DL-valine, n.m.r. 8=43398
vanadyl porphyrin complexes, luminesc. 8=45299
vandyl acetylacetonate, effect of co-ord. to sixth posn. on e.s.r. 8=43872
varnish on Fe and Pt anodes, elect. characts. 8=49916
N-vinyl cpds., n. m. r. and i. r. spectra 8=47671
vinyl acetylene, i. r. absorpt. band, electro-optical parameters 8=34365
vinyl bromide, deuterated, i. r. spectra 8=47672
vinyl chloride, passive Q switching of CO_2 laser 8=28679
vinyl diacetylene, i. r. absorpt. band, electro-optical parameters 8=34365
vinyl fluoride, vibr. anal. 8=25632
vinylphosphonic acid dichloride γ-induced polymerization, mechanism, obs. 8=49913
vinylidene fluoride, molec. g values and paramag. susceptibility 8=29803
vit. B_{12}, corrin skeleton and its precorrinoid intermediate crystal structure 8=26479
water dioxane, mixtures, proton spin-lattice relax and viscosity 8=43770
Wurster's blue iodide, crystal and mol. structure 8=26524
xanthene dyes in 2-chloroethanol, $T^* \leftarrow S$ bands in absorpt. spectra 8=30494
X-H bond stretching vibr. intensities in gas to CCl_4 solns. transition, obs. 8=34298
p and m-xylenes, liq. thermodydnamic props, calc. with significant struct. theory 8=43767
o-, m-, p-xylene solid, tunneling effect and hindrance pot. 8=31924
o-xylol, scattering of ruby laser emission, large angle 8=48158
Ag complex, bis(8-hydroxyquinoline)Ag(I) pyridine solvate, cryst. and molec. struct. 8=39765
Ag halide complexes, far i. r. spectra 8=27619
Ba methacrylate dihydrate, polymerization by X-rays 8=27741
BF_3-amine, i.r. absorption spectra of charge transfer complexes 8=25539-40
$BF_3S(CH_3)_2$, Raman and i.r. spectra 8=25541
CBr_4 complexes with methyl-substituted benzenes and pyridines, n. q. r. 8=36282
C–C, C = C and C–H bonds, electron densities 8=26009
CCl_4, with acetonitrile, absorpt. of CN 8=34319
CCl_4, carbonyl C=O and vinyl C-H groups, valence oscills. 8=30493
CCl_4, dielect. const. rel. to pressure and temp. 8=39396
CCl_4, elec. cond. at 65-160 kbar, obs. 8=34903
CCl_4, evaporation and condensation coeffs., maximum values 8=43915
CCl_4, graphite oxidation inhibition 8=27696
CCl_4-Na, K flames, chemiluminesc., C_2 high-press. bands excitation mechanism, obs. 8=38816
CCl_4, non-linear dielec. susceptibility obs. 8=34888
CCl_4, polarization in refl. shock waves 8=43858
CCl_4, rel. to polypropylene mol. motion, 140-373°K 8=48510
CCl_4, Raman intensity in various solvents 8=30488
CCl_4, shock wave compressed, refr. index, anomalies, obs. 8=39370
CCl_4, vibr. relax. and u.s. attenuation 8=39360
$CD_3^+ + CD_4 \rightarrow C_2D_5^+ + D_2$, reaction kinematics 8=38963
$CD_4^+ + CD_4 \rightarrow CD_5^+ + CD_3$, reaction kinematics 8=38962
$(CD_3)_2C{=}O$, torsional vibr. spectra 8=25601
$(CD_3)_2NH$, torsional vibr. spectra 8=25601

Organic compounds — contd
CF_2, unstable mol., microwave spectrum 8=25468
CF_3, struct. calc. 8=47664
$(CF_3)_4As_2$, vibr. spectra and struct. 8=25604
CF_3COOH-$HCOOH$, H-bond, microwave rotation spectra 8=25577
CF_3H, reaction with O atoms, rate const. 8=36568
$(CF_3)_2PF_3$, i. r. spectra and struct. 8=25576
CF_3PF_4, i. r. spectra and struct. 8=25576
CF_3SF_5, vibr. spectra 8=25516
CF_4, far-i. r. absorpt. spectrum 8=29772
CF_4, growth of ionization currents 8=29983
C–H, C–C, C = C bonds, electron densities 8=26009
CH-radicals, h.f.s. null field reson. 8=43418
CH^+, $^1\Delta \rightarrow {}^1\Pi$ and $^3\Sigma \rightarrow {}^3\Pi$ band systems 8=38942
CHF_3, quadrupole moment, from microwave spectral broadening 8=29729
CHO^+, ht. of formation 8=36557
CHO^+ ion-mol. proton transfer reactions 8=49869
CH_2-CDCl, Raman line intensities and depolarizations, calc. 8=34321
CH_2I_2, crysts. n scatt. rel. to mol. and lattice vibr., obs. 8=35385
CH_2X, hybrid orbital force field calcs. 8=29781
CH_3, struct. calc. 8=47664
CH_3Br, reaction with O atoms, rate const. 8=36568
CH_3CCH, linewidths of rot. spectra 8=38889
$CH_3CH{=}CH_2$, far i. r. torsional vibr. spectra 8=25601
CH_3CH_2Br, far i. r. torsional vibr. spectra 8=25601
CH_3CH_2Cl, far i. r. torsional vibr. spectra 8=25601
$(CH_3CD_2)_2O$-AlX_3(X=Cl, Br) coordination compounds 8=25569
CH_3CN, linewidths of rot. spectra 8=38889
CH_3CN. 2HCl, crystal structure by n-diffr. 8=26530
$(CH_3)_3CNCO$, vibr. spectra 8=29732
CH_3Cl, reaction with O atoms, rate const. 8=36568
$C^{13}H_3Cl$, vibr.-rot. bands 8=29794
CH_3D, elec. dipole moment 8=38896
CH_3D, matrix-isolated, i. r. obs. of nuclear-spin-species conversion 8=38830
CH_3I, crysts. n scatt. rel. to mol. and lattice vibr., obs. 8=35385
CH_3I reactive scatt. with Rb atoms, asymmetry 8=47728
$C^{13}H_3NC$, struct. by n. m. r. determ. 8=34336
CH_3NF_2 and CD_3NF_2, i. r. spectra, rot. coupling between vibrs. 8=25597
$4(CH_3)_3N.41H_2O$, cryst. struct. 8=39844
$(CH_3)_2O$ polar molecule, electronic screening effect and relax., perturbed by foreign gases 8=29815
CH_3OPCl_2, vibr. spectra 8=38892
CH_3SiHD_3, i. r. spectrum 8=25603
CH_3SiHD_3, i. r. spectrum 8=34338
$(CH_3)_3X - C \equiv C - Cl$(X = C, Si, Ge, Sn), n.q.r., bonding props. 8=38912
CH_4 and CD_4, fluid, phys. props. 8=30588-9
CH_4 and CD_4, Br^{82} isomeric-transition-induced reactions 8=45410
CO group, assignment of second singlet 8=32045
$COBr_2$, vibr. intensities 8=38875
$COCl_2$, vibr. intensities 8=38875
COF_2, thermodynamic props., 12°K to b. p. 8=30573
COF_2, vibr. intensities 8=38875
C_2Br_2, i. r. spectra and vib. mode assignments 8=45236
C_2Cl_2, i. r. spectra and vib. mode assignments 8=45236
C_2F_6, growth of ionization currents 8=29983
C_2H_4 chemisorpt. on metals, heat of reaction, expt. and theory 8=36585
C_2I_2, i. r. spectra and vib. mode assignments 8=45236
C_2H_5I and CH_3CD_2I, fragment ions from X-irrad. 8=47795
C_2H_5OD–D_2O mixture vapour press. isotope effect 8=48283
C_2H_6, CH_3CD_3, and C_2D_6, i. r. torsional spectra 8=29778-9
C_4F_8, unimolec. decomposition, shock tube-mass spectrometer study 8=45321
$(C_4H_9)_2SnO$, resonance scatt. of γ-quanta, ang. distrib. for component of quadrupole doublet 8=39511
$(C_5H_5)_2TiAl(C_2H_5)_2$, crystal and mol. structure 8=26504
C_6H_4-containing cpds., dielec. relax. 8=30505
$[(C_6H_5)_3FC_4]_2$, isomerization 8=39642
$C_6D_5GeCl_3$, vibr. spectra 8=34351
$C_6H_5GeCl_3$, i. r. and Raman spectra 8=25615
$[(C_6H_5)_3P^+ - CH_2]$ radical in crystalline matrix, hindered rotation of CH_2, e.s.r. study 8=49616
$(C_6H_5)_3Sn. Mn(CO)_5$, cell constants and space group determ. 8=26467
C_6H_6 in silica gel, proton spin relax. 8=29814
C_6H_{12} vapours, u.s. propag. for large freq. /press. 8=43691
C_7H_{12}, mono- and bicyclic isomers, mass spectra 8=39059
$C_{24}H_{10}$, cryst. struct. 8=39856
$C_{26}H_{26}O_2$, cryst. struct. 8=39856
Ca stearate Langmuir films, I-V-temp. characts. and cond. mechanism, obs. 8=44902
Ca tartrate, doped and undoped, gel growth obs. 8=35246
Co acetate tetrahydrate, absorpt. spectrum 8=32046
Co formate, crystal structure 8=26507
Cu acetate monohydrate, anomalous mag. and optical behaviour 8=36434
Cu(II) alkanoates, structure by X-ray analysis 8=26463

Organic compounds — contd
Cu(II) azo complexes in soln., e.p.r. to delocalized mag. electron 8=25950
Cu diethyldithiocarbamate, paramagnetism 8=49485
Cu(II)2, 2′-dipyridine aq. solns., n. m. r. and e. p. r. 8=34926
Cu formate tetrahydrate, antiferroelec., deuteron n. m. r. 8=44269
Cu hexamethylene-dithiocarbamate, struct., X-ray obs. 8=30919
Cu phthalocyanine, α and β forms, crystal structure 8=26545
α-Cu phthalocyanine, e.s.r. 8=49608
Cu phthalocyanine, i.r. emission from cryst. 8=41021
Cu(II) pyridine complexes, e.p.r. in soln, glasses and polycryst. state 8=27469
Cu salicylate hydrate, OD-structure from X-ray investigations 8=26480
Dy elthyl sulphate, paramag. relax. Mossbauer study 8=27472
Eu β-diketone chelates, synthesis, and fluoresc. of cryst. and in soln. 8=32071
Eu chelates, in water-methanol solns., luminesc. spectra 8=30499
Eu chelates, luminesc., D isotope effects 8=30503
Fe oxalate and isotypic cpds, OD-structure from Guinier patterns 8=26534
Fe(III)N-methyl-N-phenyldithiocarbamate, n. m. r. 8=27507
Fe(III) N, N-dialkyldithiocarbamates, Mössbauer effect 8=48329
Gd chelates soln., organic ligand, laser action 8=24349
HCCH, isotopic, force const. displays 8=43302
H^3-labelled, free radical formation by autoradiolysis, e.s.r. study 8=47709
$[HgOSi(CH_3)_4]_2$, crystal structure 8=48683
Ho ethylsulphate, absorpt. and Zeeman effect of $^5I_8 \rightarrow {}^3K_8$ and $^5G_4$ transitions 8=49777
I_2 charge-transfer complexes, far i. r. intensities 8=25586
ICl charge-transfer complexes, far i. r. intensities 8=25586
ICN charge-transfer complexes, Raman intensities 8=48163
K acid phthalate, spherically bent cryst., soft X-ray specroscopy 3 to 30Å 8=32033
K oxalate hydrate, partly deuterated, isotope effect in d. m. r. 8=45122
K phthalocyanine, crystal structure 8=26545
K_2 tetranitroethide, cryst. struct. 8=26561
KH bisphenylacetate, H bonding and crystal structure 8=26514
Li-acetylene, electronic struct. 8=34255
Mg phthalocyanine, films, barrier effect, photoconductivity 8=40678
Mn acetate tetrahydrate, absorpt. spectrum 8=49740
$Mo_3O_4(C_5H_7O_2)(C_2H_5O)_3$, crystal structure 8=26461
N-containing heterocycles, N^{14} quadrupolar relax. and H lineshapes 8=29819
N-phosphorylcreatine hydrate, disodium salt, crystal structure 8=44279
NH. . . H intramolec. H bonds 8=25609
$(NH_4)_2$ dimolybdomalate, crystal structures 8=26521
Na alkyl sulphates, ideal gaseous behaviour at oil/water inteface 8=30395
Na dodecyl sulfonate, adsorpt. on α-Al_2O_3 rel. to heat of immersion 8=49854
Na dodecyl sulphate, equilib. adsorpt. by wool 8=30780
Na hexodecylsulphate, equilib. adsorpt. by wool 8=30781
Ni dimethylglyoxime, spectral shift for high press. meas. 8=50477
Ni glyoximates, origin of colour 8=27535
OD, Zeeman effect in (0, 0) band 8=38848
$OP(OCH_2)_3CCH_3$, cryst. struct. 8=44278
P complexes, P^{31} overhauser effect 8=40993
$Pb(CH_3)_4$, fragment ions from X-irrad. 8=47795
$Rb_2C_2O_4 \cdot H_2O_2$, rubidium oxalate monoperhydrate, crystal structure 8=26535
Rh formate, crystal structure 8=26507
Sc formate, crystal structure 8=26507
$Sn_3(CH_3)_4Fe_4(CO)_{16}$, crystal and mol. structure 8=26537
Tb chelates, luminesc., D isotope effects 8=30503
Ti methoxide, crystal and mol. structure 8=26523
with VB group elements, vib. spectra rel. to freq. changes 8=34294

Orthicons. See Electron tubes.

Oscillations
See also Electromagnetic oscillations; Liquid oscillations; Piezoelectric oscillations; Vibrations.
anharmonic oscillator, perturbations effects, teaching demonstration 8=41803
balance, lever equal-arm, testing and adjusting by oscillation period 8=45953
bar, deflection meas. by microwave interferometry 8=37238
beam-envelope, in orbital accelerators 8=33465
betatron, control by on-line computer 8=33466
chain, composed of two homogeneous parts, small oscills. 8=41647
circular cylinder in elastico-viscous fluid 8=47930
coherent, in synchrotron, damping technique 8=33443
dynamic systems with imperfect boundaries, wave motion and stability 8=23923

Oscillations—contd
elastic isotropic half-space in which transverse velocity is min. at some depth and monotonous in rest 8=46148
electro measuring app. with strings, stability of mobile part 8=33009
ferrites, resonant elastic, excitation at non-linear ferromag. resonance 8=49064
finite radial, of spinning cylinder 8=37244/5
fluid in cavity in rotating solid body 8=46018
fluid, viscous, non-homogeneous 8=47931
forced, conducting, viscous liquid 8=33118
gas masses, adiabatic pulsations and convective unstability 8=50321
gas, nonlinear, resonant tube closed at one end 8=30266
giant, line width rel. to nonlinear de Haas-van Alphen effects 8=31489
high-freq., of thin elastic variable-thickness layer 8=41813
laser, giant pulse tandem using Nd doped glass 8=42075
model suspended in stream, active damping 8=46143
molecular-beam maser, quenching 8=46531
neutron stars, torsional 8=45762
one dimensional oscillator, quasirandom 8=46016
pressure, meas., dynamic charact. of transducers connecting channels 8=45963
quartz, longitudinal and transverse acoustic osc., method of exciting 8=48723
quartz plates, stress depend. of freq. 8=49049
relaxation in avalanche diodes 8=49299
shell, cylindrical, filled with fluid, surrounded by elastic medium 8=41816
sinusoidal, generator for 0.01 to 100 Hz range 8=41912
sphere in elastic solid, rectilinear 8=23928
sphere in elastic solid, torsional 8=23927
sphere in viscoelastic fluid, prod. of secondary flow 8=39155
stars, radial adiabatic pulsation, asymptotic soln. 8=45684
'summed and differential types', in vib. system under parametric excitation 8=32877
synchrotron, Moser transform. appl. 8=33439
3rd order, initial conditions for obs. 8=32866
tori, freely supported, hollow; circumferential axisymmetric oscills 8=32878
torsional of two-layer cylindrical rod, calc. of associated internal friction 8=28362
in two-phase mixture, elec. and mag., damping and dispersion 8=40600
water surface in tank, resonance obs. 8=34724
water surface in tank, resonance theory 8=34723
wave film type, of quantized thickness, propagation 8=46149
CdS photoconductor, l.f., induced by i.r. quenching 8=44934
n-Ge, hot carrier, spatial depend. 8=44786
Sn–SnO–Sn Josephson junction, relax. oscills. 8=40412
Y Fe garnet, standing-spin-wave modulation of reflected microwave power 8=40847

Oscillistor effect. See Semiconductors.

Oscillistors. See Semiconducting devices.

Oscillographs. See Electrical measurement.

Oseen method. See Flow; Hydrodynamics.

Osmium
balls, thermionic emission and vacuum work function 8=31467
Fermi surface anal. from galvanomag. props. 8=43027
Os^{187}, conc., spectrographic determ. of isotopes 8=36635
Os^{189}, Larmor freq. rel. to H^1, and mag. moment 8=27512

Osmium compounds
OsF_6, electron diffr. and molec. struct. 8=38858
Os-Ir alloy with dissolved Fe, solute resistivity temp. dependence 8=40318

Osmosis
electro, temp. dependence of rate constants for acetone and deionized water 8=32130
ethylene glycol-methanol (cellulose membrane) syst., diffusion permeabilities 8=25904
interfacial mass transfer in membrane transport in batch dialyzer 8=48120
ion exchange membranes 8=25901
ion transport, Nernst-Planck eqns. and electroneutrality 8=39345
maleic anhydride-styrene copolymer in tetrahydrofuran, osmolic press. rel. to mol. dimens., obs. 8=43776
membrane systs., ternary, transport processes 8=25903
osmometry with diffusible polymers 8=34819
polyvinylpyrrolidone solns., equilib. at high pressures 8=39347
tri-n-alkysulphonium halides, aq. solns. 8=30454
$Cu_2[Fe(CN)_6]$ membranes, H_2O transport kinetics 8=48121
He isotope solns, pressure and enthalpy 8=28436
He solns, isotropic irreversible osmotic relax. 8=24037

Overhauser effect. See Nuclear magnetic resonance and relaxation.

Oxidation
alloys, linear, comp. changes 8=32092
benzene in gas phase, photochem., and radical formation 8=41286
Chromium molybdenum steels, CO_2 oxidation resistance, effects of chem, comp., mech. treatment and remelting 8=45339
diols by titanous peroxide system, e.s.r. 8=32117

Oxidation—contd

- ethylene, by photolysis of NO_2 8=36615
- ethylene, electrochem., oscillatory kinetics 8=49939
- formate, electrochem., oscillatory kinetics 8=49939
- graphite, anisotropy 8=41239
- graphite, inhibiting effects of Cl and CCl_4 8=27696
- graphite, pyrolytic and isotropic, in atomic O, and O_2, kinetics to 2100°K 8=36556
- graphite, structure after thermal oxidation 8=44167
- hydrocarbons, gaseous, photochemical, mechanism, e.s.r. invest. 8=36616
- magnetite to γ-Fe_2O_3, mechanism rel. to Fe^{2+} diffusion, kinetics 8=27702
- metal dibonde composites, oxidation resistant, synthesis 8=45317
- metals, at high temp., influence of specific area and core dimension changes 8=36551
- metals, growth of thick scale layers, effects of size and shape of specimen 8=36552
- metals, rate-constant determ., low-temp., using discontinuous film resistance changes 8=49883
- methyl oleate, γ-induced 8=41293-4
- molten salts containing CuCl, by gaseous O_2, kinetic data 8=32102
- noble metals and alloys, cathodic reduction kinetics rel. to Tafel slope 8=45380
- silicide films on Nb chromised, titanised and chromo-titanised 8=35176
- steel, austenitic 20% Cr/25% Ni/Nb-stabilized, structure of surface oxides formed in CO_2 at high temp. 8=41238
- steels, austenitic stainless, growth in oxidising gases 8=45338
- steel, Cr-Ni/Nb stainless, by CO_2, n-irrad. 580°-840°C obs. 8=27705
- steel in CO_2, and simultaneous carburisation rel. to transport in porous scales 8=48777
- steels, low alloy, in CO_2, and excrescence form. mechanisms, $\leqslant$ 550°C 8=32098
- steel, stainless, austenitic and ferritic, in CO_2, influence of 0.5%Y alloy addition 8=27704
- steel, transformer, hot-rolled, at 800-1180°C, and structure of oxide films 8=36561
- steel, transformer, hot-rolled, internal oxidation zone structure and props. 8=36562
- stress corrosion cracking, rate controlling step 8=44534
- styrene emulsion polymerization, i.r. spectroscopy 8=32125
- dl-α-terpineol by manganic acetate, e transfer, 100°C - 8=49881
- Zircaloy-2 in O and H_2O vapour, kinetics and mechanism, 350-500°C 8=32106
- Zircaloy-2, of surface layer, white spots rel. to struct. and orientation 8=35187
- Zircaloy-2 in water, 200°-300°C, obs. 8=27726
- in Ag, of dispersed Al, as hardening process 8=35649
- Al alloy, crude; production by reduction of bauxites 8=30956
- Al alloy, crude, production by reduction of Japanese colloidal earth 8=30955
- Al alloys, -vacancy production 8=26640
- $BaTiO_3$ crystals grown from KI flux, hydrogen reduction process 8=27695
- CO adsorbed on Ni 8=48487
- Co, 750° to 1000°C using inert Au spheroidal markers 8=49862
- CrS_x, at 1050°C, weight-gain kinetics 8=36558
- CrS_x-coated-Cr, at 1050°C, weight-gain kinetics 8=36558
- Cs, in flames 8=49877
- in Cu, of dispersed Be or Al, as hardening process 8=35649
- Cu (111) rel. to diffusion in Cu_2O films struct. defects obs. 8=44042
- Fe, film growth in neutral soln. 8=27706
- Fe, passive layer form., presence of H in outer layer 8=35171
- Fe, to form wustite($Fe_{1-y}O$), and composition-oxygen partial pressure diag., thermogravimetric determ. 8=36540
- Fe-18% Cr alloy, complex scale formation 8=45340
- Fe-Cr alloy, oxidized surface film interface 8=44074
- Fe-Cr alloys, study by glancing angle X-ray diffr. technique 8=49868
- Fe-Cr binary alloys 8=36559
- Fe-Cr-O system, low-temp, glancing angle X-ray diffraction film technique 8=27703
- Fe-Mn alloys, internal rate rel. to temp. 8=45336
- α-Fe_2O_3, chemical reduction to Fe_3O_4 and substrate-product topotaxy 8=26072
- α-Fe_2O_3 whiskers and twinned platelet, gaseous oxidation rel. to defect diffusion during growth 8=44150
- GaAs, thermal in range 400-530°C, struct. of layers 8=49870
- HfC, 1790-2000°K 8=45351
- In-Ag alloys, transition from internal to external 8=49874
- Ir, formation of surface "molecular clusters" 8=45343
- K, in flames 8=49877
- NH_3, in shock waves 8=41256
- Na, in flames 8=49877
- Nb, 450°-720°C, kinetics rel. to scale morphology 8=49878
- Nb, mechanism from oxygen diffusion meas. in Nb_2O_5 crystals and scales on Nb 8=48785

Oxidation—contd

- Nb, rate-constant determ., low-temp., using discontinuous film resistance changes 8=49883
- Nb-Ta alloys, kinetics, 550-1050°C 8=36566
- Ni and alloys, kinetics 8=27713
- Ni, oxide layer formation mechanism 8=45346
- Ni, rate-constant determ., low-temp., using discontinuous film resistance changes 8=49883
- Ni_3Al-Ni_3Nb system, scale formation from X-ray microstructural analysis 8=35276
- Ni_3Nb, scale formation from X-ray microstructural analysis 8=35276
- Ni-Y alloys, mechanism rel. to scale formation 8=41257
- Ni-Y, (0.05-5.0 at.% Y), oxidation mechanism 8=41257
- O_2 absorpt. in molten salts containing CuCl 8=32102
- Pd powder 8=41260
- Pt, ellipsometry of O-containing films 8=27754
- Pt surface of Na, K, rel. to thermionic emission of Na^+, K^+ 8=35549
- of Si, in pure O glow discharge, rel. to prod. of uniform and non-porous layers 8=35182
- SiC heater elements, sintered, ageing rel. to elec. ageing 8=49349
- SiC, sintered, heater elements, ageing rel. to elec. resistivity changes 8=31231
- $SiH_4(g) + 2O_2(g) = SiO_2(s) + 2H_2O(g)$, silica film formation 8=44055
- Ti, in boiling dilute H_2SO_4 and HCl, differences in oxide struct. 8=39602
- Ti, kinetics, effect of O_2 press. on growth of diffusion oxygen layer 8=36573
- Ti, rate-constant determ., low-temp., using discontinuous film resistance changes 8=49883
- U intermetallic cpds (with Si, Fe, Mn, Al), kinetics resistance and velocity 8=27721
- U quasitinary cpds, (with Si, Fe, Mn, Al), kinetics, resistance and velocity 8=27721
- UC surface to form UO., film, diffusion mechanism 8=39604
- UN, rel. to deformation, e-microsc. studies 8=27718
- UO_2 powders, in storage rel. to fabrication and irrad. props 8=45349
- US, low temp. behaviour 8=27719
- US-ZrS solid solns, low temp. behaviour 8=27719
- VO_2 in molten $VO_{2.5}$ soln., obs. 8=27724
- W, (112) face, and O_2 adsorpt. 8=26107
- Zr films, 300-500°C, film structure obs. by e. microscope 8=35186
- Zr in CO_2, prevention by Cr coating, $\leqslant$ 650°C 8=32107
- Zr, rate-constant determ., low-temp., using discontinuous film resistance changes 8=49883
- Zr, thin noble metal film effects 8=49882
- ZrC, 1130-2160°K 8=45351

Oxygen

- abundance in NGC7027 obs. 8=45713
- abundance in solar photosphere 8=28171
- absorption in melts containing CuCl, reaction kinetics 8=32102
- acoustic absorpt., effect of H_2, CO_2 or H_2O impurity obs. 8=39211
- adatoms on metal surface, work function and desorpt. energy 8=35193
- adsorption and reactivity with CdS powders, comp. with H,A gases 8=26135
- adsorption by metal surface from CO_2 kinetics 8=27735
- adsorption by Mo and Ti films, effect on resistance and work function 8=40322
- adsorption effect on spectral distrib. fine structure of CdS photocond. 8=44917
- adsorption on Ag films and reaction with co-adsorbed H, 8=39616
- adsorption on Ag(111), surface rearrangement study by LEED 8=26133
- adsorption on Al (100) face, LEED obs. 8=44072
- adsorption on Cu, and resulting surface structs., LEED studies 8=26136
- adsorption on Cu spherical crysts., resulting surface structs. 8=26099
- adsorption on Mo single cryst. face (100) 8=35195
- adsorption by Sb and Bi, rel. to surface reactivity 8=26106
- adsorption on Si, influence of elec. props. 8=27134
- adsorption on (110) and (113) faces of W 8=39622
- adsorption on W, and effects associated with thermal desorpt. 8=39626
- adsorption on W, Cs and Hg coadsorbate interaction with low energy electrons 8=39623
- atmosphere, effective heights and absorption coeffs. at 4.1 mm 8=27909
- atmospheric, abs. 1.3 to 0.23μ, and role of short-living 8=32236
- atmospheric, absorption of solar u.v. radiation 8=50128
- atmospheric emission, red at λ6300Å, rel. to geomag. activity 8=36750
- atmospheric, monitoring using metallized membrane polarographic electrode 8=27775
- atom, and molec., kinetics of attack of graphite, pyrolytic and isotropic 8=36556
- atom, atmospheric, spectral obs., twilight and at night 8=27949
- atom, auto-ionizing e energy spectra 8=39050

Oxygen—contd
atom diffusion through gases 8=49910
atom, fine-struct. level transitions, electron induced, as cooling mech. in ionosphere 8=32298
atom, four-level, resonance line problems and radiative transitions 8=38627
atom reactions with CH_3 radicals 8=49880
atom reactions with CH_3Cl, CH_3Br and CF_3H, rate consts. 8=36568
atom recombination rates, 3000 to 3800°K, direct shock tube meas. 8=29666
atoms, detected during γ-radiolysis of CO gas 8=36623
atoms, radiative combination by inverse dissoc. 8=38932
atoms, Rydberg orbitals calc. 8=29620
atomic, photoionization cross section meas. 8=29949
beam, reflection at Pt surface at different temps. 8=25668
λ Boo, abundance ratio Mg/O calc. from i.r. spectra 8=50286
cathodic reduction in fuel and corrosion cells 8=37374
charge transfer from p and H atom, cross-sections 8=38737
chemisorption and desorption on CdS, effect on surface photoconductivity 8=49413
chemisorption by V, isotherm-isobar kinetics 8=36584
chemisorption on graphon, kinetics, 450-675°C 8=45362
chemisorption on metals, expt. and theoretical results for heat of reaction 8=36585
chemisorption on Ni films, kinetics at adsorbate-adsorbent interface 8=27737
chemisorption states on ZnO and CdS 8=32118
chemisorption on ZnO, effect of d.c. electric field 8=49905
concentration in Si, i.r. spectrophotometric obs. 8=49992
convective diffusion in blood, rel. to membrane-type artificial lungs 8=43793
desorption from W substrate by e. impact 8=49901
diffusion in Nb_2O_5 crystal and scales on Nb rel. to Nb oxidation behaviour 8=48785
diffusion in Zr and Zr-Cu alloys, using $O^{16}(d, p)O^{17}$ reaction 8=31017
diffusivity in P stabilized b.c.c. Fe 8=44387
dilute, use in operation of intermed. temp. fuel cell 8=33030
dipole discharge, self-sustaining 8=38995
dissociated, heat transfer means., with catalytic flat plate 8=25826
dissociative ionization 8=29976
dissolved, effect on stability of Cu_2O surface film on Cu electrode in 3% NaCl aqueous soln. 8=41279
distribution coeff. in Ge, determ. 8=48779
dry graphite burning in stream, temp. meas. by spectrum-line reversal temp. 8=46256
on electron microprobe samples, gas jet decontamination 8=27808
emission line at 6300Å in night airglow, height profiles rel. to position 8=36800
excitation by 0.15-1.0 MeV protons 8=38847
5577 A line and continuum in night airglow 8=41392
γ-oxygen, vapour-condensation and neutronography 8=26260
green line λ 5577 in glow discharge, new emission mechanism 8=29625
HD 161817, high velocity star: abundance calc. from spectra 8=50282
hyperfine contact interaction calc. 8=43199
impurity in metals, determ. by $O^{16}(n,\gamma)N^{16}$ 8=32167
interferometric analysis of conc. in gaseous mixtures 8=49988
Ion IV, V, VI, emission spectra obs. 8=29605
ionic and molecular colision, absorpt. meas. in d.c. discharge 8=47740
ionization of mixture with water vapour, cross sections and mobilities of different species 8=39023
ionosphere D layer, metastable $O_2(^1\Delta)$, ionization by 1027-1118Å 8=32323
ionosphere D region, atoms and ozone associative detachment and dissociative attachment, l.f. obs. 8=32324
isotopes (O^{15}, O^{17} and O^{18}), bibliography of uses, 1963-66 8=34185
isotope exchange on Pt powder 8=41236
isotope meas. of SO_4 ions in water from lakes and rivers 8=50095
isotopic comp. in sulphate ions in Italian thermal springs 8=50093
isotopic composition var. in cave concretion 8=50096
liquid, dielec. permeability meas. at ca. −190°C rel. to liq. air permeability calc. 8=30512
luminescence during u.v. photolysis 8=34266
mass spectrometric analysis 8=36633
in mesosphere, role in governing electron conc. 8=27880
mesosphere, var. during auroral events 8=27938
metals, H, O, N joint determ., isotope method 8=27784
minimum conc. rel. to non-combustion region in diving atmospheres 8=49884
mobility in alkali feldspars, by autodiffusion and alkali atom exchanges 8=35477
mol., r.f. line broadening anomaly obs. at low pressure 8=29759
ordered arrangement in Zr-O interstitial solid soln. 8=35289

Oxygen—contd
π 'Ori', abundance ratio Mg/O calc. from i.r. spectra 8=50286
paramagnetic impurity molecules rel. to positron lifetime 8=29851
penetration into $CaF_2:Sm^{2+}$ 8=44382
α phase, absorption of light rel. to temp. and impurity conc. 8=49745
pressure depend. of min. ignition temp. of metallic mats. 8=36578
radiolysis and photolysis, vibr. excited O_3 8=36620
self diffusion coeffs. in monoclinic ZrO_2 8=35514
solid, at 4°K, absorpt. in range $(15-33) \times 10^3 cm^{-1}$, rel. to simultaneous transitions 8=32019
solubility in b.cc. Fe, and interstitial migration 8=48361
solubility in liquid Ag alloys 8=39313
solubility in liquid Ag 8=39317
sorption in Nb and Ta, kinetics, 1100 ~ 2000°C 8=49895
sound absorpt., effect of applied mag. field 8=39210
spectra, forbidden transitions rel. to O_4 dimer content pressure and temp. dependence 8=34273
thermal cond., mag. field gradient depend., obs. 8=39199
thermal conductivity rel. to mols. collision cross-section reson. in crossed mag. fields, obs. 8=34660
θ Hya, abundance ratio Mg/O calc. from i.r. spectra 8=50286
throughput in Al porous plug, combustion study 8=36580
traces in gases, meas. with solid electrolyte cells 8=41298
vacancies in $CaWO_4$, direct obs. 8=31047
vacuum u.v. absorpt. spectrum 8=34274
vapour press., effect on oxidation kinetics of Ti 8=36573
Venus atmosphere 8=32552
volume diffusion in CoO, meas. by proton activation of O^{18} 8=35483
X-rays, soft, absorpt. cross sections, calc. 8=45727
Zeeman effects for large quantum no.s and freqs. 5-20 MHz 8=47501
Zircaloy-2 oxidation kinetics and mechanism, 350-500°C 8=32106
Al films on Ta(110), interaction 8=35159
CdS {0001} surfaces, adsorption, and structure study, by LEED 8=30719
CO_2 laser-system, sealed-off, effect on gas composition 8=46584
in Fe, liquid, formation factor for alumina inclusions group 8=35651
Fe-3%Si, adsorption, rel. to surface and grain boundary energies 8=26102
in Ne-O laser, 3^3p level population inversion mechanism, obs. 8=28692
Ne-O_2, phase equilib., from 63°-152°K at 5000 psi 8=34981
$O(^1D)$, deactivation by O_2 8=47542
$O(^1D)$ gas-phase reaction with CO_2, rate const. 8=36614
O I lines $\lambda\lambda$ 1302-06, 1152Å, experimental oscillator strengths 8=50319
OI 5577 and 6300Å nightlow intensity, diurnal, seasonal and solar cycle vars. 8=32276
OI, 5577 and 6300 Å, nightglow, S. America photometric obs. 8=45498
[OI] 5577Å emission and continuum at 5300Å in night airglow 8=45499
OI λ 5577 line in night airglow, variations in width 8=27950
O I, improved atomic level values 8=47503
O1 solar forbidden lines wavelengths and equivalent widths, abundance obs. 8=37044
O III $2p^2$-$2p3s$ arrays, line strengths and transition probabilities 8=45915
O VII excitation by electron impact, theoretical rates 8=25378
O VIII solar emission spectrum obs. 8=28165
O-rich Si, Li diffused, annealing of e irradiation induced defect 8=26632
O^{16} ion beams, lifetimes and excited states for multiply charged ions 8=43217
μ-$O^{16,18}$ atoms 2p → 1s transitions and atomic radius, obs 8=34190
$O^{16}O^{18}$-O_2 mixture, diffusion, Senftleben effect 8=30316
O^{17} enriched H_2O and D_2O, spin echo O^{17} T_1 and T_2 obs. 8=48212
O^{17} hyperfine constants in e.s.r. spectra of semiquinones hyperfine splitting constants and linewidth variations 8=40942
O^{17}, n. m. r. in HCl aq. solns. of Co(II) 8=30541
O^-, associative detachment reactions, electron prod. 8=39051
O^- e detachment by e impact, cross-section obs. 8=39036
O^-, laser photodetachment, ang. depend 8=25713
O^-, prod. and extraction from h.f. source 8=46431
O^+ ion beams, abundance of excited ions 8=28582
O^+ ions, reaction with O_2 and N_2, temp. depend of rate coeffs. 8=29977
O^+ mobility in dry air, obs. 8=39027
O^+, photoionization cross-sections 8=39044
O^+, reaction with vibr. excited N_2 8=41253
O_2, ab initio calc. on 62 low-lying states 8=47614
O_2 absorption meas. in lower atmos. 8=36748
O_2, interaction with excited organic mols. 8=38956

Oxygen—contd
O_2, in Ar, effect on muonium, and on polarization of bound muon 8=42482
O_2 in dayglow, altitude profile in i. r. atmos. system 8=36797
O_2, in u.v. afterglow, Herzberg II emission spectra 8=34277
O_2 molecule, charge exchange with He^+ and Ne^+, 2-250 eV 8=38758
O_2 reactions with He^+ in upper atm. 8=27937
O_2, Rydberg absorpt. series and ionization energies 8=47615
O_2, Schumann-Runge bands, isotope effects on Franck-Condon factors 8=34271
O_2, spectral emissivity of Schumann-Runge bands 8=34275
O_2, Stark broadening in Schumann-Runge system 8=34272
O_2, Tanaka-Takamine Rydberg series 8=25512
O_2^-, elastic coupling in KCl 8=48337
O_2^- impurity reorientation in alkali halides 8=48822
O_2^- in NaF, e.s.r. and optical studies 8=45097
O_2^- state e spectra, obs. 8=34224
O_2^-, structure, free and in alkali halide 8=49704
O_2^+, auroral green line excitation by dissociative recombination, rocket expt. 8=41401
O_2^+ band excitation by e-impact (80-1500 eV) 8=25490
O_2^+ in E-region of ionosphere, effects of metal-ion layers 8=36858
O_2^+ ion beams, abundance of excited ions 8=28582
O_2^+, ions, excitation, lifetimes and decay cross-sections 8=34261
O^-_4, stability 8=25718
O-Cu, liquid phase diagrams 8=48074
O + O_2 combination kinetics 8=41258
O^- + N^+, ions, neutralization cross section, obs. 8=34455
O^+ and O^{++} in magnetosphere, concs. 8=50165
O_2 + H_2 mixtures, detonation, influence of molec. mass on limits 8=32115
O_2 and O, density in lower thermosphere above Sardinia, mass spectrometric determ. 8=27939
O_2 and O_1, number densities in thermosphere above Fort Churchill and Sardinia 8=36761
and α-Ti mixed crystals, lattice struct. rel. to hydrogenation, n diffr. obs. 8=35357
TiNb33, N addition rel. to supercond., microstruct. and workability, obs. 8=44742
TiNb40, N addition rel. to supercond., microstruct. and workability, obs. 8=44742
in UO_2, diffusion rel. to oxide films growth on UC, obs. 8=39604
W, adsorption on (110), (211), (111) and (100) planes, field emission study 8=30778
on W (110) and (100), interaction and desorption processes, mass spectrometry 8=35198
in Zr, diffusion inhibition by Cr coating, ≤650°C 8=32107
in Zr, up to 4.2 at. %, effect on tensile deform. 8=44609
in Zr, Mo, Hf, W, anal. by He^3 irrad. 8=27818

Oxygen compounds
oxalyl halides, u. v. absorpt. spectra 8=29795
oxides e microprobe analysis with oxide standards, correction factors 8=27810
oxyhalides, radiation phys. and chem. effects 8=31140
refractory oxide solid solns with fluorite, pyrochlore and perovskite, anionic conduction 8=49920
CO_2, O transfer to metal surface, kinetics 8=27735
OCN^-, ht. of formation 8=29980
OCN^- formation in gas-phase ion-mol. reactions 8=41259
OCS, anisotropy in mag. susceptibility and molec. quadrupole moment 8=25511
OCS, elec. dipole moment 8=47587
OD^- in KCl, ang. correlation function of rotator 8=43968
OF_2, double-ζ LCAO SCF MO calc. 8=29756
OF_2, ht. of formation 8=49864
OH^- and OD, spectra in solid Ne, evidence of rotation 8=32020
OH chemiluminesc. in H_2 + O_2 reaction in shock tube 8=49889
OH emissions in upper atmos., rel. to noctilucent cloud form 8=36794
OH, interstellar, stimulation by phonons 8=28094
OH in KCl, paraelectric resonance characts. 8=49345
OH, matrix-isolated, i.r. spectrum 8=34276
OH mol. doubling transitions obs. and calc. suitable for radioastronomy 8=43328
OH on MgO surface, i.r. spectros. 8=49894
OH, prod. in interstellar shock waves 8=28095
OH^- in KCl, ang. correlation function of rotator 8=43968
OH^+, $^3\Pi_i$ excited state, fine structure 8=29830
O-H_2 and HD solid mixtures, spin-lattice relax. time 8=27493
O_2AsF_6 and isotypes, structure from n-diffr. studies 8=25469
O_2SbF_6 and isotypes, structure from n-diffr. studies 8=25469

Ozone
atmosphere, absorption coefficient, Dobson spectrophotometer obs. 8=45465
atmospheric, absorption of solar u.v. radiation 8=50128
atmospheric content during ring Sun eclipse, 20 May 1966 8=50130
atmospheric content, Jan.-Mar. 1967, obs. 8=50132
atmospheric, 40 years research at Oxford, history 8=36723
atmospheric, mean absorpt. coeffs. rel. to Dobson spectrometer 8=47973

Ozone—contd
density distrib. in mesosphere in Japan, meas. by u. v. photometers 8=36719
distribution on isobaric surfaces from May 3, 4th (1963), rel. to aviation 8=36720
formation, var. across discharge gap 8=25700
fluctuations rel. to upper air perturbations 8=41348
i.r. spectrum 8=34278
ionosphere D-region, and O atoms, associative detachment and dissociative attachment, l.f. obs. 8=32324
in mesosphere, role in governing electron conc. 8=27880
mesosphere, var. during auroral events 8=27938
mesospheric, night meas. by obs. of u. v. airglow 8=36760
planetary distrib., latitude depend., meas. by earth satellites and u. v. spectra 8=36721
on silica gel, adsorpt. rel. to annealing temp., —80°C 8=30786
spectra, line by line calc. rel. to statistical model 8=43327
in stratosphere and mesosphere, quasi-biennial osc. 8=36714
stratospheric, Arctic and Antarctic, seasonal changes 8=45441
stratospheric-tropospheric exchange based on radioactivity, O_3 and potential vorticity 8=45448
transmission meas., appl. of new random model 8=38780
vibrational excitation in radiolysis and photolysis of O_2 8=36620
and zenith radiation depolarization 8=32273

pH. See Electrochemistry.
p—n junctions. See Semiconducting devices/p—n junctions.
P—V—T relations. See Equations of state.
Pair creation. See Electron pairs; and under individual particles, e.g. Mesons.
Palaeomagnetism. See Rock magnetism.

Palladium
atom, first $^3P_1$ state, h. f. s. and lifetime obs. 8=25379
collector in thermionic converter, comparison with Re 8=28487
crystal, anomalous vibr. and electronic sp. ht. 8=26575
degassing with CO or O_2, phase superstructure 8=48395
diffusion in Al, due to near surface effect 8=39964
electrocrystallization 8=41283
electrolytic deposits, internal tension rel. to current density and metal conc. in electrolyte 8=36610
electronic structure by photoemission and optical studies 8=31293
exchange interactions, strain depend. 8=45025
Fermi surface, effective mass 8=40250
films, adsorpt. and interact. of N_2 8=26138
films, orientation after deposition on NaCl 8=44085
$L\beta_2$-emission band rel. to electronic structure 8=41129
magnetic-moment meas. vs field and temp., rel. to exchange enhancement 8=31526
paramagnetic susceptibility calc. 8=49483
powder oxidation 8=41260
resistivity, elec., rel. to s-electron-paramagnon scattering 8=31323-4
sorption of NO, and mag. susceptibility 8=44075
surface annealing changes, effect on CO adsorption 8=48424
surface atoms, mean displacement 8=30935
thermal and elec. cond., e—e and phonon scatt. Lorenz numbers, 4-20°K 8=35462
Pd(100) surface, purity and structure from Auger spectroscopy and LEED 8=27355
Pd-H probe electrode as microreference electrode 8=36605

Palladium compounds
alloys, electronic structure rel. to band structure of pure metals 8=31294
resistance, electrical, at high pressures of gaseous H at room temp. 8=44697
oxidized complex with α-benzyldioxime, e. s. r. investigation 8=36248
Pd(II) complex, bis(N-isopropyl-3-methylsalicylaldiminato) Pd(II) crystal structure 8=26425
Pd—Ag alloys, n.m.r. 8=31913
Pd-Ag alloys with Gd and Nd impurities, resistance anomaly 8=31326
Pd_x—Ag_y: Cd(Nd), resistance anomalies rel. to matrix. comp. 8=31325
Pd-Au alloys, adsorpt. of H, electron-donation model 8=26139
$PdCl_2$ in molten eutectic $MgCl_2$-NaCl-KCl, voltammetry 8=32131
PdCr alloys, thermoelect. power 8=31450
Pd-Cu alloys, thermodynamic props. of formation 8=27714
Pd-D alloys, elec. cond. 4°-300°K obs. 8=40329
Pd-Fe alloys dil, Fe hyperfine fields, 1.3-4.2°K 8=31701
PdFe alloys, exchange interactions, strain depend 8=45025
Pd—Fe alloys, high-field susceptibility 8=40752
Pd-Fe alloys, high field susceptibility and nuclear spin-lattice relax. time conc. dependence 8=36080

Palladium compounds—contd
  Pd-Fe alloys, hyperfine field at Fe, mag. field dependence 8=36081
  Pd-Fe alloys, very dil., low temp. magnetization 8=36079
  Pd-Fe alloys, spin-wave stiffness constant field dependence 8=45026
  Pd-Fe, hyperfine coupling constants from nuclear sp. hts. down to 0.02°K 8=31495
  PdFe, ferromagnetic polarization, distrib. 8=36099
  PdFe, spontaneous magnetization 8=36172
  Pd_3Fe alloy, hyperfine interaction constants from nuclear sp. hts. 0.15-1°K 8=31504
  Pd-H alloys, elec. cond. 4°-300°K obs. 8=40329
  Pd_2MnAl, magnetic and chemical order rel. to order in Heusler alloys 8=31700
  Pd_2MnIn, Pd_2MnSn, Pd_2MnSb(Heuster alloys), order rel. to mag. and chem. order in Pd_2MnAl 8=31700
  Pd-Ni alloys, compressibility in ferro- and paramag. states 8=35715
  Pd-Ni alloys, dynamic susceptibilities 8=31491
  Pd:Ni dilute alloys, e specific heat conc. depend., local exchange enhancement model 8=35433
  Pd:Ni dilute alloys, low-temp. specific heat and ferromag., localized exchange enhancement model 8=35432
  Pd-x at.%Ni, (x⩾O), low temp. resistivity rel. to s-electron-paramagnon scattering 8=31323-4
  PdO-Ln_2O_3, phase relations in air 8=35123
  Pd-Pt alloys. n., susceptibility, correlation effects 8=40997
  $Pd(SO_3)(NH_3)_3$ crystal and mol. structure 8=26431
  PdSb in thin films, electron diff. study 8=30909
  PdSb, superconducting, containing dilute solutions of CrSb and MnSb 8=27029
  $PdSb_2$ in thin films, electron diff. study 8=30909
  $PdSb_3$ in thin films, electron diff. study 8=30909
  Pd_3Sb_5 in thin films, electron diff. study 8=30909
  Pd-20 at.%Si alloy, amorphization on irradiation with U^{235} fission products 8=31154
  Pd-Sn liq. alloys, struct. 8=48082
Paper
  permittivity and dielectric loss, optical meas. with colloidal mass emitter 8=28766
Paramagnetic resonance and relaxation
  See also Lasers; Masers.
  absorption meas. with RE-1301 radiospectrometer at 4.2°K 8=24261
  acetonitrile-d_3, γ-irradiated, rel. to trapped electron and its reversible reaction 8=49955
  acoustic paramag. resonance, 1-200 Mc/s, methods for study 8=49592
  acrylamide, γ-irradiated aq. solns, 77°K, e.s.r. 8=30524
  alkali-arsenate glasses e.s.r. rel. to γ-irrad. 8=45074
  alkali-germanate glasses, e.s.r. rel. to γ-irrad. 8=45074
  in alkali halides, O_2^- centers, electronic structure 8=49703
  alkali-phosphate glasses, e.s.r. rel. to γ-irrad. 8=45074
  alkylferrocene, spectra 8=47680
  alternant hydrocarbons, pairing theorem 8=47650
  alums, Ti^{3+} substituted, explanation from crystal-field origin rel. to structural details 8=43935
  α-amino acids at 77°K, e.s.r. after γ or X irrad. rel. to dissociative electron capture 8=36621
  amino acids, free radicals in γ-irrad. crysts. 8=40907
  amino acids, γ-irradiated, defect investigation 8=26634
  dl-alanine, γ-irradiated, rel. to optical annealing investigation by primary defects 8=44400
  anion radicals, electrolytically prod., study of phys. props and electronic struct. 8=43860
  apatite structure, paramag. centres 8=31848
  apparatus for e.p.r. solid state obs. of radicals formed in gas phase by 5 to 500 eV electrons 8=25652
  aromatic free radicals, g-factors, precise meas. and correlation with π-orbital energies 8=47708
  aromatic hydrocarbons in glassy soln., triplet excitation on transfer rel. to line shape 8=40902
  aromatic mols. and phosphoresc. vars. rel. to singlet-triplet admixing 8=27461
  aromatic phosphorescent hydrocarbons in glassy solns., e.s.r. spectra, dynamic effects in line-shapes 8=49596
  automatic field tracking magnetometer for meas. 8=46370
  barysilite, pyrosilicate and pyrogermanate isomorphs, e.p.r. of Mn^{2+} 8=40931
  1,4-benzoquinone radical in soln., spectral linewidth alterations, 20-80°C 8=47681
  beta-diketone negative ions, triplet state e.s.r. 8=47682
  biphenylene, positive and negative ions, C^{13} hyperfine splittings 8=47650
  4,4′ and 4,2′-bis (α, α-diphenyl-β-hydrazyl)-3,3′,5,5′-tetranitro diphenyl sulphones, e.s.r. 8=49595
  1,4-Bis-(2,2,6,6-tetramethyl-4-hydroxy-4-piperidyl-1-oxyl) butadiene, spectrum stable at room temp. 8=39417
  bis (α-thiopicolinanilido) Cu(II), isotropy of hyperfine struct. from N atoms 8=27463
  Bloch's magnetodynamic eq., two modifications and generalizations 8=47678
  blue proteins: Cu^{2+} 8=49782
  broadening of e.p.r. lines, and dynamic polarization of nuclei 8=40891
  calcite: Mn^{2+}, e.s.r. 8=40932
Paramagnetic resonance and relaxation—contd
  calcite, x-ray irradiated, of CO_3^- 8=49600
  calcite, Y^{3+}-stabilized Co_3^{3-} mol.-ion 8=49620
  cavity-coil config. for ENDOR expts. 8=42042
  cellubiose of free radicals in frozen aqueous solutions 8=47707
  chloroacetyl DL-alanine, irrad. cryst. 8=36240
  closed-shell molecules 8=25439
  colour centres, optical saturation 8=49586
  conduction electron spin relaxation in small particles 8=40896
  conduction electrons 8=40901
  core polarization in $4d^n$ and $5d^n$ configs. from e.s.r. data 8=36087
  crystals, paramag. and ionic energy levels, and internal field coupling coeffs., SO(2) algebra 8=39505
  cupric amine complexes 8=31861
  d^3 and d^8 ions in cubic crystals, strain induced zero-field splitting, e.p.r. study 8=39504
  diamagnet with paramagnetic impurity, spin correlation function 8=40726
  diamond, synthetic, reduction of e.s.r. linewidths 8=31847
  2,6-dimethyl-p-benzosemiquinone, e.s.r. in t-pentanol and 1,2-dimethoxy-ethane, rel. to ionic assoc. 8=34908
  dimethyl (9-fluorenyl) sulphonium bromide, X-irrad., trapped radicals 8=31883
  o, m-dinitro benzenes, alkali-metal derivative, line broadening in e.p.r. spectra 8=47679
  2,2′-dinitrodiphenyl anion, linewidth effects 8=38945
  2,2′-dinitrobiphenyl ether and sulphide radical anions, intramolec. spin exchange effects 8=34369
  diphenyl picryl hydrazyl solns. in org. liqs., dynamic polarization of solvent protons and F nucleu 8=25951
  di-tert-butyl nitroxide, C^{13} isotropic splitting const. 8=30525
  di-tert-butyl-nitroxide liq. free radical, time dependent interactions, e.s.r. and p. relaxation study 8=48207
  di(tetramethylammonium)bis(maleonitriledithialato)CuII, and X-ray studies 8=35364
  di(tetramethyl-2,2,66 piperidinyl-4 oxyl-1)terephthalate strong or weak exchange 8=43423
  dithiodiglycolic acid, irrad. at 4.2°K 8=40917
  DNA, irradiated, obs. 8=34366
  DPPH in rigid matrix, spin-lattice relax. 8=27471
  dynamic polarization and asymmetric e.s.r. in polycrysts. 8=35029
  dynamic polarization of nuclei, and relax. of spin system with paramag. impurities 8=40891
  dynamics of centres with S=I=1/2 8=36232
  effect of light on e.p.r. spectra at liq. He temps, cryostat design 8=24259
  in effective field 8=38908
  effective-spin Hamiltonian for "non-Kramers" doublets 8=45072
  electric field effects, non-linear, theory and appl. to ruby: Cr^{3+} 8=40906
  "electronic" and "ionic" mechanisms, quantitative characts 8=40948
  electrons, free, meas. method using collisions with polarized atoms 8=42040
  e.p.r. near critical point 8=40899
  e.s.r. balanced detector spectrometer 8=33142
  ethylene-silica gel system, γ-ionization-polymerization obs. 8=32127
  ethylvinyl ethers and their S- and N- containing analogues 8=38909
  fast sensitive Smith chart plotter or microwave reflectometer 8=24260
  F-centre g shift values in divalent cpds., theory 8=40057
  felspars, X-irradiated, structure defects, e.p.r. exam. 8=26710
  ferricytochrome c, beef-heart 8=31865
  ferromagnetic metallic film, magnetoelastic waves, boundary-value-problems 8=40797
  ferromagnetic particles in airborne dust 8=36233
  fluoro-aromatics, phosphoresc. cpds., h.f.s. in $\Delta m=2$ transitions 8=31851
  fluoroberyllate glass, of Fe transition group ions 8=40922
  forbidden transitions ($\Delta M=2$) induced by axial crystal field 8=45073
  formamide, irrad., struct. of radical formed 8=32138
  free radical formation by autoradiolysis of radioactive labelled organic compounds, e.s.r. study 8=47709
  free radicals from γ-irrad. organic cpds, stabilized by nitroso scavengers 8=49980
  free radicals in crystals, electron resonance and ENDOR spectra 8=40969
  free radicals in soln., electron-electron double reson 8=38940
  free radical recombination obs. 8=38939
  free-radical solns., h.f.s. in weak fields 8=39418
  free radicals, polyoriented, spectra and interpretation 8=34378
  gentibiose, of free radicals in frozen aqueous solutions 8=47707
  glass borated, lattice defects, study 8=26628
  glass, V-containing, spectra of varadyl ion, hyperfine structure 8=40923

Paramagnetic resonance and relaxation—contd
glasses: Ag atom stabilized by X-rays 8=31114
glycine, γ-irrad., e.s.r. of free radicals formed 8=31844
glycine, irrad. crysts., resolution enhancement 8=49610
graphite, grade A reactor, n-irradiated at 80°K and annealed at temps up to 300°K, 8=45081
graphite, radiation damage annealing studies by ESR 8=26729
graphite, reactor damaged, charge of e.s.r. with annealing 8=36237
hydrocarbon glasses, radiation-induced trapped electrons 8=45401
hydrocarbons (isobutane, pentanes, hexanes), e. s. r. obs. of radicals formed by ionizing radiations 8=25659
hydroxyurea, irrad., struct. of radical formed 8=32138
hyperfine broadening of c. s. r. lines, particle complexes with strong exchange interaction 8=37535
ice and frozen H_2O_2 solns, irrad., l.f. spectra 8=40925
impurities in metals, perturbation method of calc. 8=49591
impurity centres in crystals, effect of applied elec. field 8=45070
impurity, e spin-lattice relax. 8=31842
insulators: rare earth ions, rel. to rare-earth ion interaction study 8=31775
interaction of two spin types, mag. depend. freq. shift 8=40892
1-iodofluorenone oxime radical in soln. 8=34907
isobutene–silia gel system, γ-ionization–polymerization obs. 8=32127
Jahn-Teller effects 8=38910
Jahn–Teller-splitting of absorpt. lines of ions in cubic lattice sites 8=31841
lanthanum ethylsulphate:Er^{3+}, spin-lattice relax. times 8=45089
line form of absorpt. in weak elec. field, calc. for cryst. symmetry Td 8=40898
linewidth near magnetic critical points, and u. s. attenuation 8=30939
liquids, nuclear quadrupole relax. 8=34907
Lorentzian lines, modulation-broadened, intensity determ. 8=43402
luminescence centres, inorganic, rel. to emission, meas. 8=41178
magnetic alloys dilute, line widths, theory 8=27460
magnetically ordered materials, Mossbauer spectra, rel. to atomic spin time fluctuations 8=30642
malonic acid, γ-irrad., separation of overlapping spectra 8=40927
maltose of free radicals in frozen aqueous solutions 8=47707
metal: dilute magnetic-ion system, localized magnetic moments study 8=27459
metals containing nonmag. impurities, temp. depend. of line width 8=49583
methoxyl group, hyperfine interaction 8=29807
methyl and deuteromethyl radicals adsorbed on Si gel, e. s. r. spectra rel. to tumbling 8=25660
methyl radicals, on porous glass surface 8=47684
3-methylpentane glass, γ-irrad., trapped electrons 8=27483
microwave-optical double reson. using circularly polarized light 8=41070
milli sec obs. by single shot sweep 8=46509
minute metallic particles 8=40894
Mössbauer spectra in presence of relax. 8=35030
muonium atom, e. s. r. rates close to splitting freqs., rel. to residual polarization 8=38773
naphthalene anion in soln., ion paring effects 8=39416
naphthalene, e.s.r. emission in phosphoresc. triplet state 8=45298
naphthalene, excitation exchange and optical spin polarization in triplet state, e. s. r. study 8=47686
naphthalene, quenching of triplet state 8=34341
β-naphthol, triplet state, acidity determ. 8=34342
5-nitro-6-methyluracil, γ-irrad. cryst. 8=49615
1-nitro-4-trifluoromethoxybenzene anion radicals, ion pairing 8=39415
nitroxide radicals from diethylhydroxylamine, dioctylhydroxylamine and N-hydroxypyrrolidine 8=25655
NN′-dimethyl and NN′-diethyl pyrazinium fluoroborate e.s.r. spectra, line widths and second order structure 8=39414
noble metal-rare earth, rel. to local moments 8=31882
non-insulating paramagnets, absorpt. and dispersion signal shape during h.f. modulation 8=49588
non-Kramers doublets, electric field induced transitions 8=49584
organic dompounds, γ-irrad., e.s.r. study of radical yield 8=49967
organic free radicals in solution, e.s.r. 8=48205
organic liquids at liquid N temp: Mn atoms stabilized by condensation method 8=30526
organic liquids: Mn atoms stabilized by condensation method 8=30526
organic semiconductors, g-shift mechanism due to conjugated π-electrons 8=44747
oxidation and fragmentation of aromatic radicals in solns. 8=32117

Paramagnetic resonance and relaxation—contd
peroxy radicals, produced by irradiation of tetrafluoroethylene-hexafluoropropylene 8=43422
phase transitions, e.s.r. study 8=49359
phenoxy radicals, C^{13} splittings 8=38947
p-phenylenediamine-chloramil charge-transfer complex. 8=31880
phonon avalanche in paramag. systems 8=23895
phosphate glass, Mo^{3+} doped 8=31879
phosphors: V (II-VI cpds.), rel. to luminesc. 8=45251
poly(α-methylstyrene), photolysis 8=27762
polycaprolactam, γ-irrad., e.p.r. and nature of saturation 8=27464
polyglycols, obs. 8=31868
polymer radicals in aq. soln. 8=34906
polymers, solid, secondary, free radical reactions during mech. damage 8=45361
poly (N-vinyl carbazole)-I complex, e.s. r. rel. to existence of charge-transfer state 8=27462
polystyrene, photolysis 8=27762
pyridinyl diradicals, stable free radicals 8=43424
pyrolytic aromatic polyimide, e.p.r. rel. to elec. cond. and struct. 8=26976
r.f. magnetic field meas. by e.p.r. in effective field 8=46366
radical formation in solutions 8=32117
radical ions of intermediate stability, e.s.r. 8=48204
radicals reaction kinetics, e.p.r. meas. 8=27690
randomly oriented triplets, h.f.s. in $\Delta m=2$ transitions 8=31851
rare gas matrix: Cd^+, Cr^+, Mn^+ by trapping donor and acceptor species and prod. photocurrent 8=40202
resonance lines, inhomogeneously broadened, second-order effects rel. to shape 8=45071
review, and description of new instrument 8=42045
rochelle salt, Cu-doped, electric shifts 8=49617
Rochelle salt: Cu^{2+}, rel. to bonding, obs. 8=36243
ruby: Cr^{3+}, Al^{27} nuclei dynamic polarization by spin–spin reservoir temp. transfer, 1.8°K 8=31892
ruby: Cr^{3+}, electron paramag. acoustic absorption at 4.2°K 8=40914
ruby: Cr^{3+}, non-linear elec.-field effects 8=40906
ruby: Cr^{3+} relaxation time, influence of impurities 8=40915
ruby cryst. with >1% Cr, e.s.r. 8=49598
ruby, electron cross relax. and nuclear polarization 8=40905
ruby, inhomogeneous line broadening 8=49597
ruby, of Cr ion-pairs, exchange-coupled, in excited optical state 8=31859
ruby of Cr^{3+} pairs, elec. field effect 8=40904
ruby, pseudo-Stark components widths rel. to appl. elec. field, ≤1400 kV/cm 8=31850
rutile, Cr-doped, microwave orientation 8=26184
saturation and spectral diffusion 8=49607
S_2^- centre in alkali-halides, paraelastic behaviour 8=45173
semicarbazine hydrochloride, γ-irrad. crysts. 8=49604
in semiconductors, problems 8=40897
semiquinones, O^{17} hyperfine components in e.s.r. spectra hyperfine splitting constants and line width variations 8=40942
silicate glass, irradiated, and thermoluminesc. and electron absorpt. spectra 8=41196
in solids, extreme narrowing techniques, application to e.s.r. 8=27458
solids, rel. to luminescence 8=31840
spectra, interpretation by vibronic mass effect 8=43252
spectrometer for low mag. field spin-lattice relax 8=46507
spectrometer, limiting sensitivity at high power levels 8=46503
spectrometer X-band, for paramag. dispersion obs. and ENDOR meas. 8=46511
spin conc. determ., error analysis 8=49590
spin-flip scatt. of conduction electrons from impurities 8=40893
spin-lattice relax., covalency effect 8=31843
spin-lattice relaxation in solids 8=49594
spin-phonon interactions in paramagnetic ion crystals 8=49593
spin packet width in nonuniformly broadened lines, meas. using double modulation method 8=40900
spin relaxation, anomalous, near mag. transition 8=49582
spin relaxation in magnetically ordered systems rel. to Mössbauer absorpt. spectra 8=43940
spin-spin coupling with n equiv. nuclei, polynomial coeffs. 8=34367
starch, γ-irradiated, e.s.r. of free radicals 8=49618
starch-iodine complex, metallic nature 8=31869-70
static mag. susceptibility meas. 8=46508
strain broadened spin resonance line shapes, broadening by point defects 8=49589
strong spin-lattice coupling, effect on e.p.r. spectra 8=40895
sym-trinitrobenzene anion, effect of Li cation on spin density 8=47714
tert-butyltropenyl radicals, mono- and tri- 8=38944
(2, 2′, 6, 6′-tetramethylpiperidine-4-01-1-oxy) carbonate, obs. 8=25661
2, 2′, 6, 6′-tetramethylpiperidine-4-one-1-oxy radical, obs. 8=25661

Paramagnetic resonance and relaxation—contd

- 2,2′,6,6′-tetramethylpiperidine-4-01-1-oxy radical, obs. 8=25661
- (2,2′,6,6′-tetramethylpiperidine-4-01-1-oxy) suberate radical, obs. 8=25661
- (2,2′,5,5′-tetramethylpyrrolidine-3-one-1-oxy)-3-azine radical, obs. 8=25661
- tetramethyl tin free radical form., e.s.r. detection 8=34382
- thiourea derivatives, X-irrad. 8=31886
- transient free radicals prod. by pulse radiolysis 8=49970
- transition-metal impurity in covalent complexes, rel. to covalency 8=35018
- trifluoromethyl radicals in inert-gas matrices 8=34381
- tri-glycine sulphate: Cu^{2+}, n.m.r. 8=36241
- triglycine sulphate: Cu^{2+}, rel. to bonding, obs. 8=36243
- triglycine sulphate, γ-irrad., e.s.r. of free radicals formed 8=31844
- triglycine sulphate, γ-irradiated, rel. to optical annealing investigation of primary defects 8=44400
- 2,4,6-triphenylpyryl radical 8=29832
- Tutton salts, spin–spin relaxation 8=31845
- two-cavity device as bimodal cavity 8=42041
- vanadyl acetylacetonate in benzene soln, effect of co-ord. to sixth posn. on g-value and hyperfine const. 8=43872
- viscous solns., paramag. relax. determ. by n.m.r. 8=30532
- yttrium ethylsulphate, obs. for nuclear quadrupole moments of $Tb^{157,158,160}$ 8=42907
- Ag, conduction-electron spin resonance obs. 8=31860
- AgCl: Cu^{2+}, Se(S) codopants 8=36235
- AgCl, detection of self-trapped holes 8=45075
- Ag:Mn, spin relax. of localized mag. moments and conduction electrons 8=31875
- AlF_3: Cr^{3+} 8=36236
- Al_2O_3, irradiated, e.s.r. of triplet state trapped hole pairs 8=40903
- α-Al_2O_3:Fe^{3+}, effect of applied elec. field 8=45070
- α-Al_2O_3. V^{2+}, Cr^{3+}, Mn^{4+}, hydrostatic press. effects, rel. to ion interact with lattice 8=45076
- Al_2O_3: V^{3+}, mm. wavelength and in intense field 8=49599
- $Al_2SiO_4F_2$: Fe^{+3} isotropic and dipolar contribs. to shfs tensor 8=36244
- B, zone-melted beta-rhombohedral, with low C content, photo-induced e.p.r. 8=40908
- B–C cpds, conc. dependence 8=31520
- B-C cpds, paramag. centre comp. dependence 8=45077
- BN, F-centres, e.p.r. spectral confirmation 8=35584
- BaF_2, n-irradiated, self-trapped holes 8=31854
- BaF_2:Gd^{3+}, cubic splitting temp. dependence, 77-950°K 8=40909
- $Ba(N_3)_2$, u.v. irrad. cryst. e.s.r. of N_2^- 8=27485
- BaO: Gd^{3+}, at 77, 4 and 2°K 8=45078
- BaO:Mn^{2+}, hyperfine coupling, temp. depend., and vibrational reson. mode 8=45079
- $BaTiO_3$-$BiFeO_3$ solid solns. rel. to dielec. and mag. phase transitions 8=27488
- $BaTiO_3$, of Gd^{3+}, in orthorhombic and rhombohedral phases 8=31852
- $BaTiO_3$, of substituting sites of rare earth ions 8=48818
- $BiFeO_3$, rel. to ferroelec.-antiferromag. props 8=27488
- CH-radicals, h.f.s. null field reson. 8=43418
- C_7H_6D radical, effect of D substituent 8=47706
- $[(C_6H_5)_3P^+ - CH_2]$ radical in crystalline matrix, hindered rotation of CH_2, e.s.r. study 8=49616
- $Cl + H_2 \rightleftarrows HCl + H$ reaction rate, e.s.r. detect. 8=49861
- $CaCO_3$:Gd^{3+}, absorpt. spectrum at 77°K 8=45087
- CaD_2: U^{4+}, u.s. absorption, freq. dependence 8=40946
- CaF_2, charge compensation of Ce^{3+}, Nd^{3+} and Sm^{3+} by interstitial H^- or D^- ions 8=49601
- CaF_2, n-irradiated, self-trapped holes 8=31854
- CaF_2, V_K centre, influence of Y and O on formation, e.s.r. obs. 8=40060
- CaF_2:(Am^{2+}, Cm^{3+}), zero-field splittings 8=30622
- CaF_2: Er^{3+} (Nd^{4+}), spin-lattice relaxation, effect of quasi-local vibrations 8=40910
- CaF_2: Eu^{2+}, hyperfine coupling of S-state ions, temp. depend 8=27465
- CaF_2: Eu^{2+} relaxation time meas. using optical Faraday rotation technique 8=49479
- CaF_2: Gd^{3+}, cubic splitting temp. dependence, 77-950°K 8=40909
- CaF_2: Mn^{2+}, hyperfine coupling temp. depend 8=31876
- CaF_2: Nd^{3+} ions in sites of tetragonal symmetry, direct one-phonon spin-lattice relaxation times 8=40938
- CaF_2: Nd^{3+}, spin-lattice interactions in uniaxially stressed crystal, e.s.r. obs. 8=40939
- CaF_2: Nd^{3+}, (U^{3+}) spin-lattice interactions in uniaxially stressed crystals 8=40912
- CaF_2: U^{3+}, spin-lattice interactions in uniaxially stressed crystal, e.s.r. obs. 8=40939
- CaF_2: U^{3+} ions in sites of tetragonal symmetry, direct one-phonon spin-lattice relaxation times 8=40938
- CaF_2: U^{4+}, ultrasonic, rel. to multiple phonon interactions 8=31853
- (Ca, Mg, Fe) CO_3: Mn^{2+}, e.s.r., allowed and forbidden transitions 8=40933
- CaO: Cu^{2+}, tunneling effect at 1.2°K 8=40916
- $CaWO_3$: Er, $^{3+}$, (Tb^{3+}), spin-lattice relax times, 1.5 to 30°K 8=36238

Paramagnetic resonance and relaxation—contd

- $CaWO_4$, defect sites identification from correlation of e.s.r. and thermoluminesc. meas. 8=31028
- $CaWO_4$, rel. to thermoluminescence meas. 8=49602
- $CaWO_4$: Er, Ce(Mn), electron-spin-echo phase memory limited by lattice relax processes 8=27466
- $CaWO_4$:V, charge compensation 8=31855
- $CaWO_4$:V, e.s.r. rel. to site occupances and charge compensation 8=45082
- $CaWO_4$: Yb^{3+}, microwave-optical double reson. using circularly polarized light 8=41070
- $CaWO_6$: Ce^{3+}, Yb^{3+}, spin-lattice relax., contrib. processes 8=40911
- $CdCl_2$: Ni^{2+}, spectra at 9 and 35 GHz 8=27468
- CdF_2, iron-group ions 8=31857
- CdF_2:Eu, transformation of Eu^{3+} to Eu^{2+} 8=27473
- CdF_2: Gd^{3+}, trigonal spectra obs. 8=49609
- $Cd_xHg_{1-x}Te$: Mn^{2+}, e.p.r. 8=40934
- CdS, e.p.r. of Cu^{2+} ion impurities 8=39779
- CdS, excitation and quenching dependence rel. to trapped electrons 8=27467
- $Cd_2V_2O_7$:Mn^{2+}, spin-Hamiltonian parameters 8=31856
- $CdWO_4$:Cr^{3+}, elec. field effects 8=45084
- $CdWO_4$: Fe^{3+}, lines splitting by elec. field, 320 kv/cm 8=40929
- $CdWO_4$:Gd^{3+}, at 24GHz 8=45083
- $CdWO_4$: Mn^{2+}, lines splitting by elec. field, 320 kv/cm 8=40929
- CeMg nitrate, spin-lattice relax. mag.-field dependence by resonant two-phonon process 8=31858
- CeO_2:Cm^{3+}, at 10 Gc/sec and liq. He temps. 8=27490
- CeO_2: Dy^{3+}, e.s.r. spectra 8=40918
- CF_3OOO radical 8=38941
- $CoCs_2(SO_4)_2 . 6H_2O$, relaxation 8=40913
- CoS_2 powder, above T_c 8=49603
- Cr-Cs alum crystal cross relax. obs. 660Hz-1MHz 8=27486
- $CrOF_5^{2-}$ ions, X- and Q-band spectra, comparison 8=38911
- CrO_4K_2, γ- and n-irradiated, e.s.r. 8=49605
- $CrO_4(NH_4)_2$, γ- and n-irradiated, e.s.r. 8=49605
- Cs_3CoCl_5, and optical and mag. props. 8=31501
- Cs_3ZnBr_5: Co^{2+}, exchange interactions in pairs of coupled Co^{2+} ions 8=49606
- Cs_3ZnCl_5: Co^{2+}, and optical and mag. props. 8=31501
- Cs_3ZnCl_5: Co^{2+}, exchange interactions in pairs of coupled Co^{2+} ions 8=49606
- Cu diethyldithiocarbamate 8=49485
- α-Cu phthalocyamine, org. semicond. 8=49608
- Cu(II) azo complexes, e.p.r. in soln. rel. to delocalized mag. electron 8=25950
- Cu II-Na-chlorophyllin chem. bonding from e.s.r. h.f.s. 8=34368
- Cu(II) pyridine complexes, e.p.r. in soln, glasses and polycryst. state 8=27469
- Cu(II)2,2′-dipyridine aq. solns., Cu linewidth 8=34926
- Cu^{2+} ions in tetrahedral crystal fields, linear elec. field effect 8=49585
- Cu: Mn, meas. of s-d admixture 8=40935
- Cu: T (T = Ti, Mn, Ni), conduction-electron spin relax., interpretation 8=31863
- $CuCs_2(SO_4)_2 . 6H_2O$, spin-lattice ht. transfer in pulsed mag. fields 8=31862
- $Cu(HCOO)_2 . 4H_2O$, line width 8=36242
- $CuSiF_6 . 4H_2O$ at 300°K and 90°K, obs. 8=45085
- $CuSnF_6 . 4H_2O$ at 300° and 90°K, obs. 8=45085
- DPPH, conc. solns. in org. solvents, e.p.r. at 3000 MHz as fn. of temp. and dissolved gas 8=48206
- Dy elthyl sulphate Mossbauer study 8=27472
- $ErAl_3$, Er spin relaxation from Mossbauer effect 8=31864
- Fe^{2+}, high spin, rel. to electronic factors 8=40921
- Fe^{2+}: MgO, spin-lattice relaxation by phenon avalanche 8=40941
- $Fe(CN)_5NO^{3-}$, hyperfine anal. 8=47683
- Fe-Cu, Fe-Ag, Fe-Li associates in II-VI cpds 8=27474
- $FeNH_4(SO_4)_2 . 12H_{20}$, Mossbauer spectrum, rel. to atomic spin time fluctuations 8=30642
- GaAs:Fe, at 77 and 300°K 8=31866
- $Ga_{0.85}Fe_{1.15}O_3$, mag. ordered, external elec. field effects obs. 8=31867
- GdAs, exchange-narrowed lines, 17–1400°K 8=31846
- GdBi, exchange-narrowed lines, 17–400°K 8=31846
- $GdCl_3$, exchange consts. derivation, high freq. meas. 8=40817
- GdP, exchange-narrowed lines, 17–400°K 8=31846
- GdSb, exchange-narrowed lines, 17–400°K 8=31846
- GdX_2(x = Rh, Ir, Mn, Pt, Al), g shift rel. to hyperfine fields 8=27475
- Ge, irradiated 8=27476
- H radical, conc. profile in H_2-O_2 flame, gas phase e.p.r. study 8=49892
- H recomb. rate at room temp., spectroscopic obs. 8=34377
- H_2, solid, radiation damaged, of atoms, at 4.2°K 8=40924
- $2(H_2Ca_2Mg_5(SiO_3)_8)$: Mn^+ at room temp. and 9.2GHz, crystal symn. effects 8=36245
- $HClO_4$, e.s.r. study spatial distrib. of H atoms after γ irrad. 8=49963
- HD, solid, radiation damaged e.p.r. of H atoms 8=40924
- H_2O vapour irrad. with 1 MeV He^+ 8=49968
- H_2SeO_3, γ-irrad. cryst. 8=31884

Paramagnetic resonance and relaxation—contd
n-InSb 8=27477
K, conduction-e.s.r., 0.5 G splitting, theoretical exam. 8=27478
$KBO_3.\frac{1}{2}H_2O$, three types of e.s.r. rel. to RO_2, O_3^- and O_2^- centres 8=45098
KCl, colloidal centre exam. 8=44477
KCl, F-aggregate centres 8=44478
KCl: Cd, uncoloured and coloured. 8=48876
KCl: Cu°, temp. depend. 8=45088
KCl: I, ICl^- V_K centre. 8=48875
$K_3Co(CN)_6$: Cr^{3+}, three-spin cross relaxation processes 8=27479
KBr: Li^+, shift broadening by internal strains on alloying KCl and KI 8=27480
$KMgF_3$: M^{2+}(M=Ni, Fe, Co), acoustic, rel. to magneto-elastic coeffs. of 3d impurity ions 8=31871
$LaCl_3$: Ce^{3+}, rel. to determ. interaction constants in $CeCl_3$ 8=36239
$LaCl_3$: Gd^{3+}, rel. to Gd^{3+} pair-interaction constants determ. 8=31775
$LaFeO_3$, rel. to weak ferromag. 8=27488
$La_2Mg_3(NO_2)_{12}.24H_2O$: Mn^{2+}, e.p.r. 8=40928
$La_2Mg_3(NO_3)_{12}.24H_2O$: Nd, spin lattice relax. rel. to Nd conc. and temp. 8=31872
$LaRu_2$: Gd^{+++}, and mag. susceptibility 8=31502
Li borate glasses and cpds. γ-irrad. 8=49612
Li, conduction-ESR g value meas. 8=27482
$LiAlSiO_4$, X-irradiated, and luminescence 8=40936
LiF, X-irradiated, [111] defect obs. 8=40006
LiF: Fe^{3+} 8=40920
LiF: Fe^{3+}, crystal field distortions obs. 8=48810
$LiNbO_3$: Cr^{3+}, acoustic paramag. reson., 4.2°K 8=44318
$LiNbO_3$: Cr^{3+}, polydomain crystal, hypersound absorpt. by Cr^{3+} 8=31873
$LiNbO_3$: Mn^{2+}, spacing of hyperfine sextet 8=45090
Li_2SO_4, n-irradiated, OH radical thermal decay e.s.r. study 8=27481
$M_2'''M_3''(NO_3)_{12}.24H_2O$: Gd, ($M'''$ = Bi or La; M'' = Zn or Mg), anomalous angular spectra 8=45080
MgO, spin-lattice relax. anisotropies, theory 8=31874
MgO: Cr^{2+}, acoustic 8=45092
MgO: Cr^{3+} (V^{2+}), of excited $^2E(3d^3)$ level 8=27484
MgO: Cr^{3+}, V^{2+}, of excited ^2E level 8=45091
MgO: Cu^{2+}, at 1.2°K, Jahn-Teller effect 8=27470
MgO: Fe^{2+}, spin-relaxation time temp. dependence, 4.2-13°K rel. to Fe^{2+} low-lying energy level 8=45086
MgO: Mn^{2+}, charge transfer at surface, e.s.r. study 8=48422
MgO: Mn^{2+}, e.s.r. at 1.3GHz 8=40930
Mn^{2+} in halide host cpds 8=36246
Mn^{2+} ion, hyperfine interaction depend. on Racah parameter 8=31877
Mo, arsenate complexes, spectrum, superfine structure 8=45099
Mo bronzes 8=40245
Mo cpds., containing dimeric and monomeric oxygen 8=47677
$MoOF_5^{2-}$ ions, X- and Q-band spectra, comparison 8=38911
N, metastable (^2D), spectrum 8=25386
NH_3OHCl, X-irradiated, e.s.r. of V_K centres, radical pairs and trapped NO 8=31878
NH_4 halides, new defect centre, motional effects, e.p.r. study 8=48879
NH_4Cl: Mn^{++}, temp. depend. 8=49614
NH_4Cl: VO^{2+}, linewidths 8=45103
$N_2H_4^+$, temp. depend. 8=47685
$(NH_4)_2SO_4$: Cu^{2+} 8=40940
NO_2, adsorbed on ZnO 8=48499
NO_2, in cryst. N_2O_4 matrix 8=45094-6
NO_2 in frozen solns. 8=45093
Na salt of 2,6-dimethyl-p-benzosemiquinone, e.s.r. in t-pentanol rel. to ion pairs 8=34909
$NaAlSi_3O_8$, X-irradiated, and luminescence 8=40936
$NaBO_3.H_2O$, three types of e.s.r. rel. to RO_2, O_3^- and O_2^- centres 8=45098
Na-Ca silicate glasses 8=30792
NaCl, enhancement of Na^{23} n.m.r. 8=35029
NaCl: Mn^{2+}, impurity distrib. coeff. meas., 8=48823
$NaClO_3$ γ-irrad. crysts., -196°C 8=49613
NaF, of O_2^-, and optical studies 8=45097
Nb centres in irrad. Nb glasses 8=40937
Ne, double resonance in He-Ne laser operating at 6328 Å π transitions 8=47502
Ni and α-benzyldioxime, oxidized complex 8=36248
Ni^{2+}: MgO, spin-lattice relaxation by phenon avalanche 8=40941
$NiSiF_6$ crystal, cross relax. obs. 660Hz-1MHz 8=27486
P in n-Si, strongly doped, hyperfine splitting rel. to compensation, obs. 8=27487
PH_4I, e.p.r. of I_2^- centres 8=31124
Pb halides, γ-irrad., e.s.r. of colour centres of trapped electrons and holes 8=36249
PbF_2: Gd^{3+} rel. to crystal field near Gd^{3+} ion 8=36250
PbF_2: Yb^{3+}, spin-lattice relaxation 8=36253
$Pb(Fe_{0.5}Nb_{0.5})O_3$, rel. to para- to ferroelec. transition 8=27488
$PbMoO_4$: Ce^{3+}, Yb^{3+}, spin-lattice relax., contrib. processes 8=40911

Paramagnetic resonance and relaxation—contd
PbSe: Gd, doping effects 8=44805
Pd, and α-benzyldioxime, oxidized complex 8=36248
Pr^{3+} in double nitrates, lineshapes 8=31881
S, liquid, obs. 190° -320°C 8=30527
Se film, e.p.r. study of distrib. of embedded Hg atoms 8=35179
Si cleavage faces, rel. to surface state 8=40943
n-Si, electron spin-lattice relax., conc.-and compensation dependence 8=27489
Si, of B, rel. to dislocation density 8=45101
Si surfaces, vacuum-crushed, air-crushed or mechanically polished, ht. treatment effects 8=39580
SiC: N, B, and unknown impurity doped, optical charge exchange exam 8=36251
SiF_2 e.s.r. 8=31885
SiO_2-Al_2O_3 catalysts, absorption of DPPH 8=27736
Si: P, broad saturation effect and background line 8=45100
SO_2^- radical ion, e.p.r. investigation 8=38948
$S_2O_6F_2 \rightleftarrows 2SO_3F\cdot$ free radicals in gaseous state 8=47711
SrF_2: Dy^{3+}, in cubic fields 8=36252
SrF_2: Gd^{3+}, cubic splitting temp. dependence, 77-950°K 8=40909
SrF_2: Tb^{3+}, and spin-lattice relax., 8=40944
ThO_2: Cm^{3+}, at 10 Gc/sec and liq. He temps. 8=27490
ThO_2: Dy^{3+}, e.s.r. spectra 8=40918
ThO_2: Er^{3+}, spin-lattice relaxation on cubic sites 8=40919
TiO_2, d^1 config. derived 8=45102
TiO_2: Cr^{3+}, structure determ. by e.s.r. 8=39823
TiO_2: Mo^{5+}, relax. temp. depend. 8=36247
TiO_2: V^{4+}, paramagnetic spin-lattice relaxation 8=40945
VCl_4, Jahn-Teller distortion 8=49619
VO^{2+} in N,N-dimethylformamide soln., line-broadening 8=39419
V_2O_5, of carriers, rel. to localized states 8=40947
V_2O_5-P_2O_5-WO_3 system glasses, rel. to elec. conduction mechanism 8=40291
YAl garnet: Fe^{3+}, pseudo-Stark line-splitting 8=31849
ZnO, effects of additives 8=36254
ZnO: Fe^{3+}, Mn^{2+}, rel. to cubic field parameter 8=45104
ZnS activated with Group IV elements, investigation of luminescence 8=49815
ZnS, CdS: Mn^{2+}, exchange-coupled pairs 8=45105
ZnS: Mn^{2+}, forbidden line obs. at ΔM = Z; ΔM = O, ±1 8=31887
ZnS/ZnSe mixed-crystals, of ^6S-station ions and delocalized electrons 8=26636
ZnSAg monocrystal, rel. to luminesc. 8=36523
ZnSe: Fe^{3+}, spectral lines rel. to Fe^{3+} in cubic and axial fields 8=40949
ZnTe: Pb, rel. to impurity state 8=35738
$ZnWO_4$: Cr^{3+} type crysts, "electronic" and "ionic" mechanisms 8=40948
measurement
autodyne quantum oscillator 8=33143
dispersion meas., as source of information 8=46505
electron-electron double reson. 8=38940
electron-electron double reson., freq. swept 8=40927
Gunn effect, application 8=40890
pulse radiolysis kinetics 8=49942
push-pull field modulation, advantage for minimizing absorption of "empty-cavity" 8=46510
resolution enhancement 8=49610
resonator, cavity, for studying e.p.r. with uniaxial
sample orientation servo 8=27457
single crystal, orientation method 8=49587
spectra, automatic mag. field calibrator 8=37382
spectrometer sensitivity redefinition 8=28637
spectrometer, under irradiation 8=46504
spectrometer with ruby maser preamplifier 8=33146
spectroscopy, rapid scanning of field, appl. to pulse electrolysis 8=33145
spin oscillator, microwave, line width 8=33144
triplet yield determ. 8=29806
Paramagnetism
See also Magnetic properties of substances/paramagnetic.
ferromag. thin films, superparamag. effects 8=36112
impurity in metals, cond. for localized mag. moment formation 8=31519
of ions in solids, axial-field-splitting, covalency effects 8=35046
Ising decorated lattice, 1 phase separated by 2 ferromagnetic phases 8=49493
metals, spin-, effect of electron-lattice interactions 8=36077
Mössbauer absorpt. spectra rel. to spin relax. 8=43940
spin-phonon excitations, kinematic interaction effects 8=36074
Parametric amplifiers. See Amplifiers.
Parent. See Nucleus; Radioactivity.
Parity
See also under individual particles, e.g. Mesons/spin and parity.
conservation laws mirror relations as nondynamical test 8=24685
hyperon nonleptonic decay P-violation, tadpole model 8=33830
nuclear forces, nonconserving 8=38301

Parity—contd
violation, N-N potential 8=24876
CT invariance in $\Sigma^\circ \to \Lambda^\circ + e^+ + e^-$ rel. to Λ° polarization 8=29211
P violation in hyperon decay, model 8=33831
Sb^{119}, polarized, nonconservation by inner bremsstrahlung, obs. 8=33962
Particle accelerators
See also Ion beams.
avalanche multipactoring effect 8=33394
beam bending 90° magnets, field uniformity 8=28997
beam instabilities, throbbing 8=33508
beam pulsing 8=24544
beam separator, r.f., superconducting 8=24543
beam separator, superconducting, r.f. 8=24550
beam shift meas., shape of electrodes 8=46395
cryogenic, aspects of 8=24567
dynamitron, multiloop feedback for voltage stabilization 8=24553
dynamitron, SF$_6$ insulating gas handling system 8=24554
electron beams for use in accelerators 8=33079
electron bunching analysis for accelerator injection 8=33084
electron, high-current cavity, design 8=46997
electron, microwave, medium-energy 8=33401
electron synchrotron radiation in accelerator with megagauss fields 8=46987
electrostatic, low-energy, terminal pulsing 8=24556
e.m. energy absorption rel. to injected plasma density 8=25749
engineering, feasibility and budgeting 8=33407
field without strays within a cylinder, current distrib. soln. 8=33058
injector gun of high-current proton accelerator type, design 8=46401
injector synchrotron and storage ring, use of Al coils 8=33410
injector system for 200 GeV machine 8=33406
klystron, as r.f. energy source 8=24546
liquid H$_2$ target, destructive testing 8=33368
low and medium energy, existing and contemplated, review 8=37807
magnet, alternating gradient, for secondary beam transport 8=28519
magnet coils, hydrodynamic liquid cooling method 8=33048
magnet design 8=28996
magnets for beam transport, focusing props. and params. choice 8=28520
magnetic optics theorems for design appls. 8=28548
magnetometer, turbine driven suitable for magnetic fields in accelerator 8=33043
microtron for two electron beams 8=47002
modular design approach 8=33409
modulator, 70 MW, 250 kV, oil-immersed, compact for driving klystron 8=28994
nanoammeter system for external beam monitoring 8=28998
Nimrod, magnet power supply failure of alternators 8=33411
operation from utility system 8=33408
plasma, h.f., self consistent field and power absorption from electron cyclotron resonance 8=30184
plasma using inhomogenous static mag. and h.f. electromag field 8=30036
positive-ion, high-current target 8=33398
proton, Alvarez-type drift tube 8=24551
proton, residual radiation studies 8=33402
pulsed beam for study of time factor in nuclear reactions 8=24555
quadrupole lenses, new design 8=33104
radiation effects and accidents 8=38586
radiation, ethylene gas-phase dosimetry 8=24524
r.f. amplifier, low distortion using switch tube 8=24548
r.f. buckets, longitudinal effects 8=33097
r.f. system for 200 GeV machine, 2000 amp. diode for ferrite tuning circuit 8=24549
r.f. system, input impedance and response to periodic driving function 8=24552
relativistic e beam guidance 8=33085
resonator on H_{11n} wave, drift tube loaded, study of elec. and mag. field structs. 8=37811
rotating neutron target system 8=33396
shielding, appl. of N-meson cascade n component theory 8=24964
storage ring, electron, 100 MeV 8=29012
storage ring, r.f. system 8=24588
superconducting beam handling, progress since 1966 8=37806
superconducting magnet for beam focusing 8=33404
superconducting magnet for 200 BeV 8=33403
superconducting magnets, for beam handling 8=28995
superconducting magnets, future development 8=33050
superconducting NbZr coil magnet, effects of n irradiation 8=33405
target, gas, windowless for neutron prod. 8=33395
target water cooled for intense ion beams 8 = 33397
techniques rel. to thermonuclear research 8=34064
tubes, sectional, with oblique fields, ALGOL design programme 8=46988
Particle accelerators—contd
vacuum technique, developments 8=34695
Van de Graaff, improved control system 8=24571
Van de Graaf, meas. and reduction of X-radiation from ion sources 8=24545
Van de Graaff, voltage fluctuations due to belt inhomogeneities 8=24570
Cu used in construction, possibility of long-lived activity 8=29405
H$^-$, D$^-$ polarized ion source for injection 8=42352
linear
accelerating field, meas. of perturbations 8=24564
AGS r.f. system for 200 MeV p linac 8=24561
beam dynamics eqns., rigorous derivation 8=33414
beam momentum analyzing magnets 8=33436
beam transport system alignment 8=33427
buncher, third harmonic simulation 8=29002
Cockroft-Walton, modification and arrangement for discharge 8=46992
coupled, construction and performance 8=33433
disc-loaded waveguide beam stability 8=37809
drive signal, r.f. system, design and performance, Stanford two-mile linac 8=24562
double-section, current pulse shortening 8=37814
electron, beam current regulation and meas. 8=46993
electron beam instability due to interaction with accelerator 8=33416
electron, beam monitors optical systems 8=33077
electron beam transport system, e.s., with periodic focussing 8=41965
electron, cryogenic, use of superconductors and superfluid He 8=24567
electron, disc-loaded waveguides, dimensional non-uniformity effects 8=37516
electron, for X-ray radiography, pulse control 8=37818
electron, high-energy, realization 8=37816
electron injection, space charge effects 8=33417
electron, Moscow Atomic Energy Institute accelerator, remodelling as pulsed γ and neutron source 8=46986
electron, operational experience 8=46991
electron, precise control, radiation of required number of pulsed beams 8=42355
electron, 6 MeV, operation characteristics 8=42354
electron, 10 MeV, 3 amp. peak steady-state, design 8=24566
electron, 400 MeV, high duty, high intensity 8=24557
electron, superconducting, optimum slow wave structure determ. 8=24568
electron, travelling wave, design 8=24563
electrostatic, ion sources and accel. systems, review 8=24573
electrostatic, sectional accelerating tubes, with inclined fields, design 8=46990
ion beam current regulator 8=46438
Los Alamos, computer control 8=33428
master control and personnel protection system 8=33418
microwave beam position monitors 8=33421
miniature, laser with grating, proposal 8=37810
multi-section, current pulse shortening 8=37813
positron conversion target 8=33426
as positron source, magneto-optical adaptions 8=42353
proton, calibration, beam current and energy meas. 8=33435
proton, eqn. for calc. of current limit 8=46994
proton, heavily loaded beam, optimum r.f. generator characteristics 8=24560
proton, on H_{11n} wave, 2.5 MeV energy range 8=37812
proton, quadrupole focusing system, space-charge effects 8=33429
proton, quadrupole magnet suitable for drift tubes 8=33105
proton, r.f. amplifier system 8=24558
proton, r.f. amplitude and phase variation improved by multi-drive system 8=24565
proton, space charge effects, computer calc. 8=33431
proton, 200mA injector, design proposals 8=33432
radioactivity products, γ spectra 8=33953
r.f. system, automatic phase and amplitude control 8=24559
SLAC, 2 miles, using large rectangular Fresnel lenses 8=42173
Standford, beam switchyard design and construction 8=33425
Standford, protective ion chamber 8=33420
Stanford, beam dumps, energy slits and collimators 8=33424
Stanford, beam switchyard control computer 8=33423
Stanford, beam switchyard instrumentation 8=33419
Stanford, completion and initial operation 8=33413
Stanford, control system 8=33422
standing-wave tank structures 8=46996
superconducting resonant cavities 8=29000
with superconducting resonators, construction problems 8=46995
tandem, beam tube optics computation 8=37817
tandem folded, with side-by-side accel. tubes 8=46989
tandem, H$_2^+$ beam bunching solid-state system 8=46436
tandem, injection, transmission and acceleration of ion beams 8=24569
transformer-type, possibilities 8=24572

- **Particle accelerators**—contd
  - **linear**—contd
    - 2 MeV, discription 8=29001
    - 200 MeV facility, physical design 8=33434
    - van de Graaff, Brookhaven γ spectroscopy 8=24705
    - van de Graaff, He^{++} source 8=33098
    - van de Graaff, Li$^-$ ion source 8=24159
    - van de Graaff, p energy meas. 300-2050 keV by n.m.r. 8=33430
    - Van der Graaf, use in simulated micrometeoroid impact studies 8=37028
    - variable energy beam, debuncher appl. 8=33415
    - waveguide bunching system, calc. 8=37815
    - H$^-$ ions, 1.5MeV, source and energy stabilization system 8=46434
  - **orbital**
    - AGS conversion, use of folded ferrite loaded cavities 8=24580
    - AGS improved r.f. accelerating system 8=24574
    - AGS, numerical analysis of r.f. field in drift table loaded cavity 8=24579
    - AGS r.f. accelerating cavities, behaviour, rel. to conversion 8=24581
    - beam-envelope oscillations with space charge 8=33465
    - beam instability due to self interaction and interaction with cavity walls 8=33467
    - betatron, efficiency of e extraction 8=29008
    - betatron, mag. field inhomogeneities calc. and correction 8=37823
    - betatron oscillation control by computer 8=33466
    - betatron, output doubling by magnet pulsing 8=24586
    - Bevatron, Cu-tape-wound, edge-cooled solenoid for preinjector 8=33052
    - Bevatron, external p beam facility, expansion 8=33504
    - Bevatron inflection system, digital computer control 8=33495
    - bevatron secondary beam extraction targetry 8=33486
    - CERN storage-ring project 8=33510
    - cybernetic, 1000GeV, design study and 1GeV model 8=33446
    - electron, multi-cycle e$^\pm$ injection 8=33483
    - electron synchrotron, broadband matching of cavities, FFAG 8=33488
    - electron synchrotron, 10 GeV, accelerating system 8=24584
    - electron synchrotron, with amorphous radiator, γ polarization obs. 8=33611
    - electron synchrotrons above 3 GeV 8=33484
    - fixed-field alternating-gradient, slow extraction 8=33464
    - p, LASL, 800 MeV and expt. programme 8=33512
    - microtron, 15 MeV c.w. design 8=33480
    - microtron, four-sector racetrack design 8=33481
    - microtron, high-energy, orbit computation 8=33482
    - microtron, minimum-volume electromagnet 8=33047
    - Nimrod, operation at 1.5 × 10^{12} protons/pulse 8=33503
    - Nimrod resistive wall instability and damping system 8=33502
    - omnitron, prototype gradient magnet 8=33471
    - omnitron, resonator, oscillator and ferrite magnet system 8=24576
    - phase vol. of specified domain, linear theory for small rad. losses 8=29006
    - Princeton-Pennsylvania, beam spill control 8=33494
    - proton beam ejection, meas. and monitoring 8=33489
    - proton beam extraction system 8=33499
    - proton beam, slow extraction from 70 GeV synchrophasotron 8=47004
    - proton synchrotron, ceramic vacuum chamber 8=34696
    - proton synchrotron, charge emission from target 8=33490
    - proton synchrotron, induced radioactivity meas. 8=33506
    - for proton synchrotron magnets, supercond. energy storage system 8=29011
    - proton synchrotron, Mrad dosimetry of organic materials 8=46925
    - proton synchrotron, radiation problems 8=33493
    - proton synchrotrons supercond, pulsed magnets 8=29010
    - proton synchrotrons above 20 GeV 8=33492
    - racetrack system, influence of form and stretch of azimuthal-edge fields 8=33472
    - remote maintenance proposals for 200GeV machine 8=33450
    - resonant slow extraction systems, r.f. stimulation 8=33463
    - resonator broadband f.m. 8=29004
    - review 8=42357
    - Serpukhov 70 GeV p synchrotron 8=33491
    - storage apparatus, convertor for phase-shift meas. 8=47007
    - storage ring, electron, linear theory of motion 8=24589
    - storage ring; low-β insertion design 8=33507
    - storage ring, p beam polarization by strong interactions 8=47008
    - storage ring, 200 MeV e$^+$e$^-$, magnet power supply 8=33511
    - storage rings, CERN intersecting 8=24590
    - storage rings for electrons and positrons 8=33509
    - synchrophasotron, 70 GeV, slow exctraction of proton beam 8=47004
    - synchrotron, AG, laminated magnet 8=33437
    - synchrotron, alternating-gradient, beam loss location and meas. 8=37821

- **Particle accelerators**—contd
  - **orbital**—contd
    - synchrotron, alternating-gradient, damping coherent oscillations 8=33443
    - synchrotron, alternating-gradient, computer control and analysis 8=33447
    - synchrotron, alternating-gradient, conversion to modular construction 8=33459
    - synchrotron, alternating-gradient, injector monitoring 8=33442
    - synchrotron, aperiodic magnetizing coils for f.m. power autogenerators for resonator excitation 8=46998
    - synchrotron, beam extraction techniques 8=24578
    - synchrotron beam-line magnets, thyristor controlled rectifer for power supply 8=47003
    - synchrotron, Braunschweig 140 MeV, rel. to Bremsstrahlung short pulse generation 8=47072
    - synchrotron, Cornell, multiplex control system 8=33485
    - synchrotron, fast-closing valve 8=33456
    - synchrotron, FFAG, orbits 8=33440
    - synchrotron, 50-400 MeV beam behaviour 8=33498
    - synchrotron, interlaced-beam injector, r.f. system 8=33454
    - synchrotron lattice orbit constants, computation 8=33438
    - synchrotron. longit. instabilities, theory and appl. 8=33453
    - synchrotron, magnet employing separated function magnetic lattice 8=33473
    - synchrotron magnet, fault detection in coils 8=33458
    - synchrotron magnet, flat topping 8=33469
    - synchrotron megawatt solid state inverter 8=33487
    - synchrotron oscillation, Moser transform. appl. 8=33439
    - synchrotron proton beam extraction methods 8=33501
    - synchrotron, pulsed ring magnet power supply, protecting and monitoring 8=33457
    - synchrotron, separated function mag. lattice 8=29007
    - synchrotron, 2.5 GeV electron at Bonn 8=24585
    - synchrotron, 200 BeV, parameter selection to minimize cost. 8=33399
    - synchrotron, waveguide, appl. of H-shaped retarding systems 8=42356
    - synchrotron, weak-focusing, resonant extraction 8=37819
    - synchrotron, zero-gradient, beam manipulation equipment 8=33448
    - synchrotron, zero-gradient, energy discharge system for beam-bumper magnet 8=33477
    - synchroton, zero-gradient, external proton beam 8=33497
    - synchrotron, zero-gradient, performance improvements 8=33455
    - synchrotron, zero-gradient, plunging Faraday cup system 8=33444
    - synchrotron, zero-gradient, p beam extraction 8=33496
    - synchrotron, zero-gradient, radiation dose and induced activity obs. (1965-66) 8=33468
    - tune profiles, on-line computer prep. 8=33449
    - 200 GeV, fast kicker magnet 8=33478
    - vacuum behaviour of materials with radiation and heat 8=37822
  - **orbital, cyclotrons**
    - angular correl. meas., accidental coincidence background reduction 8=29005
    - AVF, and nuclear struct. research appls. 8=24583
    - AVF r.f. system, compact 8=24577
    - beam handling, external, solid-state control and logic system 8=33441
    - beam transport system 8=33474
    - central elec. field config., mag. analogue 8=46999
    - compact isochronous, operation and performance 8=33460
    - control setting, computer prog. for pre-calculation 8=42358
    - d.c. regulator for magnet supply 8=47005
    - electron model of 100 MeV p cyclotron, axially symmetric and isochronous 8=29009
    - injection, study with automated electrolytic tank 8=24587
    - isochronous, external beam quality, diagnostic system 8=33445
    - isochronous, fast n time-of-flight spectrometer 8=47167
    - isochronous, magnet poles design and permeability errors effects 8=29003
    - magnet, sector for 10-50 MeV separated orbit cyclotron 8=33476
    - magnetic extraction element effect on field 8=33479
    - Maryland University Sectored Isochronous Cyclotron 8=33452
    - model, conical pendulum stimulated by elect. forces 8=47001
    - proton, beam depolarization calc. 8=37824
    - separated orbit, coaxial cavities 8=24582
    - separated-orbit 4 MeV design 8=33462
    - separated orbit, 4 MeV, magnetic system 8=33475
    - separated orbit, r.f. power system 8=24575
    - synchrocyclotron beam extraction systems 8=47000
    - synchrocyclotron, Harwell, C$_{NN}$ meas. 8=24918
    - synchrocyclotron, Nevis, improvement programme 8=33461

orbital, cyclotrons—contd
synchrocyclotron, phase motion perturbation by space charge 8=37820
synchrocyclotron, 300 MeV extraction system 8=33500
U-120, use in accel. of He^{2+} ions 8=47006
variable-energy, beam meas. 8=33505
variable-energy, design and construction 8=33451
Ge multiply-charged ions 8=46433
He^3 activation analysis machine 8=33470

Particle detectors
See also Bubble chambers; Cloud chambers; Counters; Ionization chambers; Nuclear track emulsions; Particle track visualization.
for aerosol sizing, optical, spurious consts prod. by sub-size particles 8=30560
aluminophosphate on glass, for n dosimetry 8=46920
collimators, focused, digital recording of line-source response 8=24702
computerized, time-of-flight, 1-60 MeV expt. 8=46844
concentric, for thermal n dose and rate meas. 8=38081
LET depend., for mixed radiation dose-equiv. meas. 8=33364
magnetic analyser for $D(d, n)He^3$ recoil 8=47179
magnetosphere satellite meas. suggestions 8=27946
Nuclear Science symposium, Los Angeles, Oct-Nov 1967 8=28968
on-line identification system 8=37778
Penning gauge with quenching circuit 8=37784
polytetrafluoroethylene, by anal. of free radicals prod. 8=28985
position-sensitive, linearity and resoln. 8=24521
semiconductor, current impulses 8=46887
semiconductor detectors in radiation protection and radiation meas., conference, Germany (1967) 8=33377
semiconductor, leakage current monitor 8=37775
semiconductor telescope, for satellite, e and p calibration 8=28025
solid-state, high-voltage supply circuit 8=37364
telescope arrangement for energy determ., particle identification 8=29456
time-constant determ. by selective amplifier 8=33365
Cd cut-off energies for finite filters 8=33366
Ge(Li), pulse height spectral decomp. 8=24533
Ge(Li), surface protective coating 8=46913
Ge(Li), X-ray energy region, charge collection efficiency 8=46915
Li^6 sandwich, for fast n spectrometry 8=38083
Li-Si counters for 4π β-spectrometer 8=24730
Si drifted, β-generated pulse time spread 8=29097
Si: Li, α and p beam response 8=38103
Si(Li), X-ray energy region, charge collection efficiency 8=46915

Particle focusing. See Particle optics.

Particle optics
See also Electron optics; Ion optics.
achromatic helical multipole system 8=33069
beam, cylindrical, space-charge expansion with uniform accel. 8=47038
beam dynamics, matrix representation 8=28547
beam shift meas., shape of electrodes 8=46395
beam tracking by dry photograhic paper 8=46982
beam transport elements, particle trajectories calc. 8=33101
beam transport system for cyclotron 8=33474
beams, curvilinear, design method 8=24128
chromatic aberrations of turnover quadruplet 8=37410
elect. field influence on charged particles in inhomogeneous mag. field 8=24130
electrostatic separation at high energies 8=28999
elliptical beams creating space charge potentials, calc. 8=33072
magnetic lens with period longit. field, equivalence with hexapolar magnet 8=37439
magnetic lenses, quadrupole, mag. centre and axes location 8=28564
magnetic optics theorems for spectrometers and beam transport systems design 8=28548
magnets for beam transport, focusing props. and params. choice 8=28520
mirror, electrostatic, cylindrical-field focusing 8=37411
neutron, beam collimation in total refl. tube 8=38078
non-bunched beam injection in accelerating cavity with circular iris, transient phenomena 8=28551
phase space beam analyser 8=33068
polarized beam, direct nuclear knock-out reactions 8=33976
p accelerator, space charge effects in quadrupole focusing system 8=33429
quadripolar doublet, phase acceptance 8=41951
quadripolar triplet, degeneration 8=28550
quadrupolar helicoidal focusing device 8=24132
quadrupole doublet, stigmatic, coeff. of spherical aberration 8=33070
quadrupole, spherical aberration compensation by octupole 8=33071
r.f. buckets, longitudinal effects 8=33097
stability in short quadrupole lens system 8=37414
synchrotron, weak-focusing, perturbation in resonant extraction 8=37819
symmetrical triplet composed of quadripolar lenses 8=28549

Particle optics—contd
tandem accelerator beam tube, computation 8=37817
trajectories in mag. fields, computation and expt. 8=37413
ultrarelativistic particles, separation in waveguide with EH_{11} hybrid wave 8=33073
wave packets beam, scatt. cross section 8=46400
Yuza-Rozhanskii condenser field, dispersion and focusing rel. to space charge 8=37412

Particle range
absorber, energy straggling distrib. 8=33603
alpha-rays, energy dissipation in finite cavity 8=47350
channeling of fast charged particles through crystals 8=31137
crystal ion trajectories, computer analysis 8=48901
electrons, energy losses in h.v. microscopes rel. to multiple inelastic scatt. 8=37417
electron stopping power, oscillating behaviour 8=48894
electronic stopping cross-section, Z_1 depend. 8=48893
heavy, energy loss correction for multiple scatt. 8=38519
ions, heavy, secondary electron yield 8=37801
ions, light, in heavy substs., computer calc. 8=48898
ions, low-energy, in solids, penetration depth and distrib. 8=31138
projectiles in amorphous solids, calc. 8=48896
proportional counter, multiwire for selecting stoppage in thin gas target 8=46857
proton channeling, angular limit to classical description 8=31134
recoil atoms in stopping materials 8=31136
spin-½ particle beam, depolarization in target 8=35592
universal range—energy relationship, approximation 8=31139
Ag foil with C layer, e energy loss obs. 8=35808
Ag, of 54.4 MeV α, energy loss obs. 8=48919
Al, of D^+, 5-80 keV obs. 8=48912
Au, chem. film technique 8=48920
Au, energy loss of 400keV p and 800 keV He^+ 8=49133
Au, of 54-4 MeV α, energy loss obs. 8=48919
Au, of D^+, 5-80 keV obs. 8=48912
Cu, chem. film technique 8=48920
Cu, e energy loss spectra rel. to plasmon states, 30-350 eV 8=35809
Cu, of 54.4 MeV α, energy loss obs. 8=48919
Cu-Au alloys, stopping power of 0.5 to 3.5 α-particles 8=44497
Ga in Si, anomalous penetration 8=48929
In in Si, anomalous penetration 8=48929
in KBr, fast protons energy loss, orientation dependence 8=35602
Pb^{206} 103 keV recoil, in pure and binary gases 8=29950
Ra^{224} recoil atoms in gases 8=34179
Si crystal, P^{32} ion implantation 8=48928
Si, ion channelling at 100-500 keV, obs. 8=48930
Tb, of 54.4 MeV α, energy loss obs. 8=48919
Tm, of 54.4 MeV α, energy loss obs. 8=48919
W, of ions, temp. dependence 8=48932
W single crystal, of Xe^{133} 40 keV ions 8=48935

Particle size
See also Surface measurement.
in aerosols, and conc., meas. by sound attenuation and dispersion 8=30563
aerosols optical counting, spurious consts prod. by high sub-size particle concs. 8=30560
aerosols, self-preserving 8=39458
Coulter counting, improving resolution by hydrodynamic focusing 8=39445
crystallizers with classified product removal, steady-state distrib. calc. 8=48528
in dispersions, distrib. rel. to heat and mass transfer 8=34936
distribution determ. using Fraunhofer holograms 8=24429
distribution meas. by X-ray scatt., comparison with results from N_2 adsorpt. and electron microscopy 8=26041
Doppler-shifted laser light meas. rel. to Stokes—Einstein relation 8=30552
entrainment of small particles by large sphere 8=34736
grain distrib. rel. to dimensions distrib. on grain section 8=43986
grain size and distrib. meas. 8=44153
grain size depend of linear heating curves for rare gas diffusion systems 8=26617
grain size effect on nature of Portevin-Lechatelier yielding 8=44516
imaged spheres, analyser 8=28218
latexes, by light diffr. 8=48237
maximum in two-phase nozzle flow, influence of liq. surface tension 8=34634
metallic alloys, distrib. in dispersed phases 8=26295
montmorillonite with adsorbed cations, by optical absorption 8=34943
oxides: CdO, CaO, MnO, NiO, rel. to lattice defects 8=48592
polybutadiene-styrene latex, meas. by flow ultramicroscopy 8=30543
in polydisperse suspensions, diameter distrib. determ. by small angle X-ray scattering 8=30553
polystyrene latex, meas. by flow ultramicroscopy 8=30543

Particle size—contd
  polyvinyl toluene latex, meas. by flow ultramicroscopy 8=30543
  powder, analysis by radioactive isotopes 8=43987
  powder grain size determ. from X-ray scatt. intensity 8=30843
  quartz sand, differential thermal analysis 8=26044
  sediment, rel. to compressibility 8=30556
  sedimentation anal., size distrib. 10-2000μ 8=34933
  separation of particles by controlled cycling, apparatus and theory 8=35065
  slurry systems, attrition resistance of solids 8=48233
  sphere dia., meas. by laser beam 8=32638
  unifrom charged, prod. from liq. droplets 8=48045
  ZnS, and morphology, effect of precipitating conditions 8=48565
  Ag colloid in gelatin, effect of shape on spectral absorpt. 8=39460
  α-Al_2O_3 powder, explosively shocked from X-ray line broadening analysis 8=44168
  Au crystals in polyvinyl alcohol films, X-ray obs. 8=30858
  Au, evaporated, multiple-twin struct. and deca- or icosahedron shapes 8=35317
  C in propane diffusion flame, i.r. spectroscopy 8=46257
  CdO, X-ray reflex broadening, rel to lattice distortion 8=48591
  Cr_2O_3 powder, Néel temp. depend. 8=40861
  α-Fe_2O_3 fine particles, spin flip temp. and lattice dilation dependences 8=27414
  FeC_x in carbon steel, coarsening at 720°C and 675°C 8=30691
  Fe-24%Ni-17%Cr-2%Ti, of γ' (Ni_3Ti) phase, effect on creep 8=49002
  β-FeOOH rod crysts. by light scatt. from streaming suspension, obs. 8=30549
  La Mer aerosol generator control 8=34947
  LiF ground powders, crystallite size from X-ray diffr. line-broadening profile analysis 8=48600
  MgO powder, explosively shocked, from X-ray line broadening analysis 8=44168
  Ni, electrodeposited, dependence on process conditions 8=26298
  Ni powder, determ. using variance as measure of line broadening 8=26296
  Sn layered with SiO, supercond., rel. to n.m.r. 8=44735
  Sn, 25Å radius in oxide film, superconductivity obs. 8=40388
  ThO_2, 4-20 μ microspheres from alcohol mixtures 8=25310
  ThO_2 microsphere production from alcohol mixtures 8=25310
  Ti alloys, equiaxed $\alpha + \beta$, determ. of β grain size 8=44170
  UO_2-Al_2O_3, grain growth in presence of liq. phase 8=44014
  in U-Pu mixed monocarbides, distrib. rel. to suitability 8=30664
Particle spectrometers
  See also Alpha-ray spectrometers, etc.
  bent crystal, for K X-ray meas. coincident with fission 8=34062
  correlated and single events, simultaneous analysis by sampling 8=46854
  cylindrical capacitor for relativistic particles 8=28566
  electrostatic analyser, cylindrical plate, charged particle transmission 8=24501
  energy resolution and focusing in inelastic expt. 8=33370
  ferroelectric detector, for differential energy spectrum of pulsed rad. sources 8=28971
  filter, time-dependent, S/N calc. 8=33386
  fluctuations, coeffs of gas mixtures used, minimalization 8=28969
  magnetic, accessory polarimeter 8=24496
  magnetic, appl. of position-sensitive solid-state detector 8=24503
  magnetic, for D(d, n)He^3 recoil detection 8=47179
  magnetic optics theorems for design appls. 8=28548
  magnetic spectrograph, constant-deviation, optimum parameters 8=46853
  magnetic, varying field, characts. 8=28970
  nuclear, pulse shaping by time-dependent filter 8=46339
  nuclear radiation spectra, elimination of pulse pile-up distortion 8=24504
  Nuclear Science symposium, Los Angeles, Oct-Nov 1967 8=28968
  satellite e.s. analyser for 1-100keV particles 8=50241
  scintillation, with multichannel pulse-height analyser, stabilization with light-flash reference peak 8=46852
  semiconductor, ballistic deficit and s/n ratio 8=24502
  semiconductor, timing unit 8=24518
  spark chamber inductive, mag. spectrometer detector 8=37788
  three-crystal-NaI pair spectrometer, efficiency calc. 8=24515
  Ge, calibration by Ra and decay products 8=37781
  Si, Li drifted and surface barrier, p irrad. resist., 2.3 MeV 8=28984
Particle track visualization
  See also Bubble chambers; Cloud chambers; Luminescence chambers; Nuclear track emulsions; Spark chambers.
Particle track visualization—contd
  aluminophosphate on glass, for n dosimetry 8=46920
  beam, dry photographic paper appl. 8=46982
  in binary liq. solns., under critical lamination, by precipitation on ions as nuclei 8=37800
  electrophotographic track determination system, spark chamber 8=46964
  in liquid H_2 chamber, algorithm applic. to computer programme 8=46961
  nuclear emulsion, proton recoil scanning, sampling bias 8=24542
  phosphate glass: Th or U, fission fragment registration 8=24538
Particle tracks
  See also Particle range.
  computer processing of data from nuclear emulsion experiments 8=46985
  coordinate determination with wire spark chamber with ferrite memory 8=46977
  fission tracks in solids, animal tissues, as alternative to autoradiography 8=32622
  light-element ion paths in NIKFI-YzA photo-emulsion 8=46984
  mica. ancient cosmic rays tracks? 8=25036
  mica sheets, thin, fission-fragment tracks, kinetics of healing 8=40055
  streamer chamber, distortions near internal objects 8=46966
Particle velocity analysis
  See also Alpha-ray spectrometers; Beta-ray spectrometers; Ion velocity; Mass spectrometers; Particle range.
  coal, laser heated in source of time-of-flight spectrometer 8=27780
  crossed-field selector for satellite meas. 8=32565
  cylindrical capacitor, relativistic appl. 8=28566
  electrostatic analyser, cylindrical plate, charged particle transmission 8=24501
  in nozzles, entrained by gas flow, investigation 8=43652
  statistical particle acceleration in random fields 8=46396
  time-amplitude converters, calibration 8=24527
  time-of-flight converter for computer display 8=24499
  time-of-flight system, on-line, digital regulation 8=24500
  time-of-flight systems, calibration unit 8=24498
Particles. See Elementary particles; Particle range; Scattering, particles; and under individual particles, e.g. Protons and antiprotons.
Paschen—Back effect. See Spectra.
Patterson diagrams. See X-ray crystallography/calculation methods.
Peierls—Nabarro force. See Crystal imperfections/dislocations; Internal friction.
Peltier effect. See Thermoelectricity.
Pendellösung fringes. See X-ray crystallography.
Pendulums
  air bearing support 8=37122
  conical, as cyclotron model 8=47001
  gravitational constant meas. 8=32780
  quasistatic low-level acceleration prod. 8=41641
Periodic system
  See also Elements.
  Z > 118, electronic config. predictions 8=47458
Permalloy. See Iron alloys; Nickel alloys.
Permeability, magnetic. See Magnetic properties of substances; Magnetization process.
Permeability, mechanical
  See also Diffusion in solids.
  chabazite cryst. plug, hydraulic permeability rel. to ambient salt conc. 8=35473
  ethylene glycol-methanol (cellulose membrane) syst. 8=25904
  granite, Westerly, rel. to press. up to 4 Kb 8=36687
  ice, water migration in transition layer under influence of elec. and temp. grads. 8=30999
  microporous medium, non-Fickian anomalies 8=48769
  porous, mats., relative perms of water, oil and gas in pore spaces, n.m.r. meas. 8=43988
  rubber membranes, elongation dependence 8=44397
  slab γ-penetration, invariant imbedding calc. 8=31131
  soil, moisture migration in freezing, and determ. of stratified texture 8=34969
  thermal transpiration in Knudsen gas 8=25837
  Fe membranes of electrolytic H 8=44389
  α-Fe of S, solubility 8=43974
  Fe-Cr alloys, of hydrogen, temp. dependence rel. to deformation and annealing effects 8=35489
  H, through W and Mo 8=39986
  N, through W and Mo 8=39987
  W, permeation rates and coeffs. of N_2, 1800° to 2600°C 8=44394
Permittivity. See Dielectric properties of substances.
Perturbation theory. See Field theory, quantum; Quantum theory.
Phase-contrast microscopy. See Microscopy.
Phase diagrams. See Phase equilibrium; Phase transformations.
Phase equilibrium
  See also Solubility; Solutions.
  alkali borates, binary, boundaries and microstructures rel. to subliquidus immiscibility 8=43756

Phase equilibrium—contd
alloy, ordered, near antiphase boundary, elastic interaction of atoms 8=35058
carbonized coal-tar pitch, microstruct. of coalesced mesophase 8=30576
chemical potential generation by phase diagram analysis 8=49836
composition equilib. in complex mixtures, generalized free energy method 8=36542
critical gases, anomalous transport 8=47963
critical liquid-vapor point, isochoric thermal capacity meas. 8=48266
decorated lattice model of binary mixture 8=23873
dipenyl-α, α' dipyridyl, rel. tb crystal structure 8=26040
ethyl acetate/acetoacetate liquid/vapour equilib. 8=25989
films, non-equilib. phase origin 8=30736
gas-crystal system with isotopic defects, thermodynamic equilib. 8=48293
hexane-aliphatic ketones solns., vapour-liq. 8=27817
hydrate binary systems, thermal analysis under pressure, $\leqslant$ 500°C 8=28413
hydrocarbons in solvents, vapour-liq. equilib. at low temp. and high press. 8=39481
hydrogen bonded complexes, consts., and heat of formation, calorimetric determ. 8=36543
ice, I and III, equilib. line 8=30696
irreversibility origin from conventional concepts 8=43892
lecithin-water, rel. to polymorphism studies 8=43425
liquid critical state study using gravitational waves 8=48055
liquid mixtures, thermodynamic excess functions 8=39321
liquid-liquid and vapour-liquid equilibria for binary and ternary systems 8=48270
liquid-liquid-gas, high-press., expt. determ. 8=34773
liquid-vapour interface, kinetic condns. 8=43914
liquid-vapour, latticed gas model including thermal expansion 8=34979
liquid/vapour, water, solid interfaces; adsorption from n-alkane mixtures 8=48102
mass spectra deciphering for high temp. thermodynamic reactions 8=38609
mesomorphic states, phase identification, temp. scanning thermal anal. 8=48365
metallic systems, binary diagrams, recognition by using electronic computers 8=48364
multicomponent systems, components concentration. calc. 8=48248
noble metal alloys, α and β, stability 8=26055
ordered phase structures, phenomenological theory 8=30671
paradibromobenzene-paranitrochlorobenzene, rel. to crystal structure 8=26040
polymer-solvent-nonsolvent systems, cluster model calc. 8=43900
polypropylene, isotactic, -organic dilvent systems, obs. 8=43899
polystyrene-solvent-methanol system, rel. to cluster model, obs. 8=43900
n-propanol-benzene-ethylene glycol system, ternary liquid miscibility, obs. 8=48079
propylene-Ar solns, liq-vapour, 100-150°K, and solubility 8=39479
propylene-Kr solns, liq-vapour, 130-200°K, and solubility 8=39479
solid-liquid interface, morphology during melting 8=43897
solid-liquid interface, surface free energy or residual force 8=48106
tolane-diphenyl mercury system, rel. to crystal structure 8=26040
transition metal cpds with S, Se or Te, ordered structs. and non-stoichiometry 8=26164
tricresylphosphate-water-organic acid systems 8=25883
two-phase systems, solid, central scatt. following Porod's law, theory rel. to distrib. of diluted phase 8=26050
vanadate glasses, separation, and structural characterization 8=26152
vapour-liquid calcs. with corresponding states principle, use of molecular shape factors 8=48269
vapour-liquid equilibria in multicomponent mixtures, calculation 8=48271
water-cyclohexane-polyoxyethylene (9.7)nonylphenylether systems, diagrams 8=48249
$Ag_xAu_{51-x}Zn_{49}$ alloys, β-phase stability 8=48368
AgBr cryst/soln. phase, Ag^+ and Br^- energy diagram 8=34958
AgBr cryst. /soln. phase, distrib. equilib. and self defect points 8=34959
Ag-Cu-Zn-Cd alloys, phase constitution 8=48369
Ag-Cu-Zn-20 wt. % Cd partial system, phase diagrams, obs. 8=43896
Ag-Cu-Zn-Cd system, invariant, primary crystallization 8=35083
Ag-Cu-Zn-Cd system, univariant, formation by decomposition 8=30675
$AlBr_3$, liq./vapour coexistence curve 8=43894
Al-Ge alloys, liquid eutectic, atom distribution 8=39298
in Al-U-Zr alloys near region of Al-uAl_2-ZrAl_2 8=35086
in Al-Zn alloys, rel. to Young's mod. temp. depend. 8=48988

Phase equilibrium—contd
Am, phase diagram rel. to pressure 8=39541
Ar-methane system, solid-liquid equilib. diagram 8=25978
β-Au-Cd alloys, structure of martensites 8=26035
Au-Cu-Zn alloy, martensitic θ-struct. 8=48633
Au-Sn system, liquidus 8=48072
BaO-TiO_2 system, new compound 8=48363
$BaSiO_3$-$BaGeO_3$, diagram 8=35092
$(Ba_xSr_yCa_z)MgSi_2O_8$: Eu, subsolidus, rel. to luminescence 8=49789
Bi trihalides, high-press. diagrams 8=39468
Bi-Au system, form. of simple cubic π phases 8=48402
Bi_2Se_3-Bi_2S_3, phase diagram. lattice constants 8=35094
$C_2H_5SiCl_3$ mol. crystals, rel. to n.q.r. multiplicity and spin-lattice relax. times 8=41010
$CaSO_4.H_2O$, chem. and polymorphic, X-ray obs. under hydrostatic press. 8=43901
Ca_2SiO_4, diagram, comments 8=39464-5
in Co molybdate hydrates, non-stoichiometric, structures of two phases 8=30916
in Co-Pb-Te system, (Co-Pb)Te as stable pseudobinary section 8=43995
Cr-Mo-Co steel, R-phase structure and comp. analysis 8=44001
CrO_2-Cr_2O_3 system, up to 35 kbar and 1500°C 8=43996
CsBr-RbBr system, composition of two phases 8=35096
CsCl-RbCl system, composition of two phases 8=35096
Cu-Ag-Zn ternary alloys, Hume-Rothery type, zeta-phase stability 8=30687
$CuAsSe_2$ film, and crystal structure from e. -diffr. exam. 8=39788
$Cu_xAu_{51-x}Zn_{49}$ alloys, β-phase stability 8=48368
CuCl, diag. up to 40 kbar 8=48253
Cu-CuO, liquid, miscibility gap 8=48075
CuBr, diag. up to 40 kbar 8=48253
CuI, diag. up to 40 kbar 8=48253
in Cu-16. 8% In alloy, structure and orientation of equilib. phase, δ-Cu_9In_4 8=39548
Cu-Mn-Sb system, magnetic 8=45056
Cu-O, liquid phase diagrams 8=48074
Cu-Sn system, γ and δ phases, self-diffusion coeff. and energies 8=35484
Dy-Pb system, phase diagram 8=39550
Er-H system 8=39551
Fe alloys containing S, reaction 8=41249
Fe-Al alloys, effect of K-state on mag. props and residual elec. resistance 8=49525
Fe-Mo system, phase identification using diffusion couples 8=48381
Fe-24%Ni-17%Cr-2%Ti, γ' particles of Ni_3Ti phase, size effect on creep 8=49002
Fe-W diagram, 0-45 at % W range 8=30692
Ge-C system at high press., absence of carbide formation 8=48382
$HGeCl_3$ mol. crystals, rel. to n.q.r. multiplicity and spin-lattice relax. time 8=41010
H-He system, press.-temp. co-ords of solid-liq.-vapour locus 8=43893
He^4, solid and liq., diag., below 1.2°K 8=37333
He-H vapour-liq. equilib. to 100 atmos. 8=43913
$HfSb_2$, atomic structure rel. to quasi-homologs 8=35360
Hg_3Te_3-Im_2Te_3 alloy system, phase diagram 8=30697
In-Te system, exam. of phase of comp. between In_2Te_3 and InTe 8=39796
Ir-Fe alloy, with Fe oxide at CO_2-CO atmos. at 1200°C 8=43999
K_2NbO_3F, separation from melts 8=48258
Li(Ag, Au). Li(Tn, Tl, Pb, Sb, Bi) system, Zintl phases, width 8=49102
$Li(Nb_{0.5}Fe_{0.5})O_2F$-$Li(Ta_{0.5}Fe_{0.5})O_2F$ system, and dielec props. 8=31435
$LiNbO_3$-$CdTiO_3$ system, solid solns. of ilmenite structure rel. to ferroelectricity 8=27278
$LiNbO_3$-$LiTaO_3$-$Fe(Mg)TiO_3$ system, X-ray exam. 8=27278
$Li_2O.SiO_2$-$LiO.Al_2O_3.4SiO_2$-SiO_2 system, metastable mixture 8=48386
$LiTaO_3$-$CdTiO_3$ system, solid solns. of ilmenite structure rel. to ferroelectricity 8=27278
Mg-Nd-Mn-Ni system 8=48387
Mo silicides, electron microprobe identification 8=48389
Mo-Mn steel, R-phase structure and comp. analysis 8=44001
NH_4F, 20°-340°C, 1-20 kbar 8=34960
in $Nb_2O_5.WO_3$-WO_3, structural investigations 8=39814
NbZn, μ-phase discovery, unit cell parameters 8=48392
Ne-Kr system, phase separation 8=43675
Ne-N, liquid-vapour, and supercritical excess vols., 66-114°K and < 3190 lb in $^{-2}$ 8=30592
Ne-O_2 from 63°-152°K at 5000 psi 8=34981
in Ni molybdate hydrates, non-stoichiometric, structures of two phases 8=30916
Ni-Cr-C-Si system, rel. to reinforcing phase 8=43976
Ni-In alloys, metastable b.c.c. phases formed on quenching 8=48408
Ni_4Mo, order and resulting substructure, electron diffraction and electron microscope study 8=44009
Ni_4Mo, ordering rel. to tetragonal superstruct. 8=26713

Phase equilibrium—contd
  Ni-W alloys, isolated metallide phases 8=39561
  Pb-Bi, metastable phases 8=30704
  $PbO-B_2O_3-SiO_2$, and liq. immiscibility 8=34749
  Pb-Sb, metastable phases 8=30704
  $Pb_{1-x}Sn_x$ Se alloys, comp.-temp. diag. 8=48594
  $Pb_{1-x}Sn_xTe$ alloys, T — x phase diagrams, and lattice parameter values 8=26077
  $PbTiO_3-PbMn_{2/3}W_{1/3}O_3$ system, solid solns., diag. 8=40616
  Pd, degassing with CO or O_2, phase superstructure 8=48395
  Pu alloys, phase diagrams 8=35080
  $RbNO_3$, diag. in 200-330°C and O-1500 atm. range 8=39469
  Rh–Be system, crystalline phases 8=48397
  Rh–Fe alloy, with Fe oxide at CO_2–CO atmos. at 1200°C 8=43999
  Sb–Au system, form. of simple cubic π phases 8=48402
  Sb–Ni system, form. of simple cubic π phases 8=48402
  Sb–Pd system, form. of simple cubic π phases 8=48402
  Sb–Te system 8=48398
  $SrCl_2-H_2O$, phase boundaries to 40 kbar 8=39467
  Ta-Mo-C alloys, phase diagram through melting range 8=39475
  $Ta_2O_5-TiO_2$ system 8=48403
  Tb-Hg, diag. 8=30706
  Th-ThAs system and lattice params. obs. 8=30577
  in Ti–Ag system, conc.-penetration curves for diffusion processes 8=35509
  Ti-Co system, complete diag., including results of solubility limits study 8=30709
  Ti–Nb–Sb–O system, rutile solid solutions, reaction diagrams 8=48404
  Ti-W-C alloys, phase diagram revision 8=39565
  UC–UN system liquidus and solidus, obs. 8=32083
  UCl_4-PbCl_4 diagram, thermal analysis obs. 8=30584
  U-H system, press.-comp.-temp. diagrams 8=30713
  UN–C system rel. to UN compacts prep., obs. 8=32083
  U-O system, nonstoichiometric oxides 8=48292
  $U-UAl_2-UCo_2$ system, phase diagrams 8=35128
  U-UAs phase boundaries, for thermal, X-ray and microscopic anal. 8=48406
  V-C system, and chem. diffusion above 1900℃ 8=36575
  VC–ZrC(HfC) systems, phase diagrams 8=48409
  V–Ga system, diagram 8=48407
  V–Ni alloys, metastable b.c.c. phases formed on quenching 8=48408
  V_5Sb_4, atomic structure rel. to quasi-hololog 8=35360
  W–C system, in cubic carbide phase 8=48410
  Y-C system, phase diagram 8=39569
  Yb-Hg, diags. 8=30706
  in Zn molybdate hydrates, non-stoichiometric, structures of two phases 8=30916
  Zn-Sn-Cd-Pb alloy, binary liq. phase occurrence 8=34786
  ZrB_2, struct. and orientation of second phase precipitates 8=35136
  $ZrBi_2$, atomic structure rel. to quasi-homologs 8=35360
  $ZrSb_2$, atomic structure rel. to quasi-homologs 8=35360
Phase meters. See Electrical measurement.
Phase transformations
  alkali halides, Born treatment using new van der Waals coeffs. 8=48246
  alloys, contactless thermal analysis, 20-2800℃ 8=28411
  aromatic liq. cryst. forming mats, heats and temps. 8=34772
  benzene, liq. → solid, high pressure studies 8=26327
  binary eutectic alloy system, solidification with time depend surface temp. 8=34967
  carbonized coal-tar pitch, microstruct. of coalesced mesophase 8=30576
  centres in deep supercooling 8=25987
  cholesteric liquid crysts., elec. field induced, 10^5 V/cm 8=34766
  complex solns. at low temp. 8=43903
  correlation functions near crit. point, structure 8=39464
  critical phenomena, review 8=34980
  diffusion eqn., pseudo-similarity solns. 8=23912
  earth's shell, and critical phenomena 8=50077
  entropy, communal, influence on liq. state reappearance 8=25976
  evaporation-condensation, system with 2 interphase surfaces and arbitrary condensation coeffs. 8=34976
  fluctuations, K-depend., above critical point, non-linear effect 8=23904
  hard molecule gas on Bethe lattice 8=28347
  liquid and saturated vapours near critical point, u.s. vel. to curve intersection 8=43802
  liquid crystals, polymesomorphic type 8=34770
  liquid-vapour, free-energy algebraic functions 8=48268
  mesophase, theory 8=39311
  metals, contactless thermal analysis, 20-2800℃ 8=28411
  n-paraffin solvents for anthracene, pyrene, coronene and naphthacene rel. to electronic spectra 8=25938
  nucleation in condensed phases, linked flux analysis 8=30570
  nucleation kinetics, generalized theory 8=48251/2
  particle prod., charged solid, from liq. droplets 8=48045
  plasma, quantum Couloumb, first order transitions, mech. 8=39068
Phase transformations—contd
  polyoctadecene-1, transition temps. and crystallinity 8=39635
  polypeptides, helix-coil transition, comparison of theories 8=43433
  silicate glasses, phase separation and submicroscopic structure 8=30787
  solid-liq., below 500°C, corrected press-temp. trajectories 8=48366
  spheres, local thermal and material transport, rel. to Reynolds numbers, turbulence and polar angle 8=34985
  three-component systems, and crit. pts. 8=48076
  transition metal chalcogenides, order of vacancies and non-stoichiometry 8=26635
  two-phase flow, press. grad. prediction using Reynolds flux concept 8=34984
  two-phase flow, techniques of anal. using Reynolds flux concept 8=34983
  two-phase flow with phase-change, conservation law 8=25789
  upper mantle C-region 8=50076
  water into ice VII by shock compression 8=48262
  water, liq. → solid, high pressure studies 8=26327
  Al, liquid, coordination number transforms, viscosity obs. 8=25866
  Al–Cu alloy, columnar to equiaxed, effect of mech. stirring in melt 8=48372
  Al-Cu, liquid, coordination number transforms, viscosity obs. 8=25866
  Al-Mg, liquid, coordination number transforms., viscosity obs. 8=25866
  Al-Si, liquid, coordination number transforms., viscosity obs. 8=25866
  Ar, coexistence curve shape near critical state from refractive index meas. 8=30590
  Au-Ge-Si alloy, glass-liquid transition 8=39470
  Bi nucleation of liquid, supercooling 8=48257
  CO_2 in crit. region, heat transfer by free convection from Pt wire 8=34823
  C_{16}–OH monomol. films rel. to surface viscosity, 15–30°C 8=30428
  C_{18}–OH monomol. films rel. to surface viscosity, 15–30°C 8=30428
  C_{20}–OH monomol. films rel. to surface viscosity, 15–30°C 8=30428
  C_{22}–OH monomol. films rel. to surface viscosity, 15–30°C 8=30428
  $CeO_{1.75}-La_2O_3$, high mobility due to tri-and tetravalent states of Ce ions
  Cu, ementation with Fe, kinetics and activation enthalpy 8=43898
  Fe nitrides, ϵ and ζ phases, Mŏssbauer effect study in neighbourhood of composition Fe_2N 8=30695
  Fe–Se system 8=48254
  He liquid, fluctuations and λ transition 8=32998
  He^4 near λ transition, Green's functions 8=32997
  in HeII films 8=24043
  HeII, second-order, Landau theory of thermal props. 8=33001
  $Li_2O.SiO_2-Li_2O.Al_2O_3.4SiO_2-SiO_2$ system, liquation isostructure and correl. 8=48255
  NH_4Cl, order-disorder transitions long range parameter by neutron diffraction 8=44242
  Pb liq., nucleated by solid Cu, Fe and Sb, under-cooling 8=43911
  Pb, nucleation of liquid, supercooling 8=48257
  Pb–Ag eutectic elloy, structure during solidification 8=26037
  Xe, specific heat near critical point 8=34977
 solid-state
  acetylene, i. r. and Raman spectra 8=27618
  adamantive structures, ternary, high pressure and temp. decomp. 8=30683
  aging problems in plastics 8=44612
  alloys, degree of order, steep gradient meas. 8=30669
  alloys, ordering, rel. to pressure, including volume depend on degree of long-range order 8=30673
  alloys with several transition pts., ordering structures, theory 8=30672
  Alni alloy, ageing rel. to coercive force and structural changes 8=35090
  Alni alloy, chem. comp. and magnetization ageing dependence, Mössbauer exam. 8=49514
  ammonium salts 8=35116
  amorphous polymers, glass transition region, anomalous cond. 8=26949
  austenite powders, electrolytic, absence of martensitic transforms. 8=35103
  austenitic alloys, hardening without martensitic transform. on ageing with plastic deform. at 600°C 8=35699
  β-brass, B2 superlattice antiphase domain growth kinetics 8=30689
  β-brass, order-disorder critical temp., pressure dependence 8=39547
  β_1-brass, metastable 8=35081
  bulk, hysteresis, inter-phase potential barrier mechanism 8=43990

Phase transformations—contd

solid-state—contd

butadiene-methyl (2-methyl-5-vinyl)-pyridinium iodide copolymers, obs. 8=48508

butadiene-styrene block copolymer 8=40194

cellular reaction, Cahn and Turnbull theories exam. and appl. to Pb-Sn alloys 8=30670

cellulose acetate, amorphous to cryst., i.r. spectra 8=32048

clay minerals, X-ray studies rel. to contact metamorphism 8=39571

cristobalite, polymorphic transform., impurity effects 8=26079

crystal structure, studies using composite reciprical lattice 8=26052

crystals in solid phase, morphology theory 8=26171

cyclooctanone, at −87°C and crystal and mol. studies of phases 8=26091

p-dioxane, at 279.2°K rel. to Raman spectra, 80-300°K 8=41163

disorder problems, theory of X-ray diffraction, correl functions 8=26328

displacement-type, of second kind, theory 8=43991

displacive, at. displacement rel. to Curie temp. and spontaneous polarization 8=44882

eutectoid decomposition theory assuming local equilib. and boundary diffusion 8=26051

faceted/nonfaceted eutectic structures 8=43992

ferrimagnets rel. to spin-reorientation 8=36181

ferroelectrics, soft, spectra-struct. correl. 8=27544

ferromagnetic binary alloys, effect on vapour pressure temp. dependence 8=35014

film deposition, during and after 8=39544-5

film, hysteresis, inter-phase potential barrier mechanism 8=43990

IV-VI cpds, at high pressures 8=35082

glutaric acid, X-irradiated, polymorphic, rel. to free radical recombination 8=29828

graphite, hexagonal to rhombohedral after grinding rel. to mag. props. 8=31497

graphite nitrates, order–disorder transform. around −20°C 8=35827

grinding effects using vibro-grinder, X-ray diffr. and e-microscope exam. 8=26286

hard carbon graphitization with CuO catalyst, kinetic study 8=27740

heat of transition for non-polar transforms., physical significance 8=35075

hexachloroethane, X-irradiated, polymorphic, rel. to free radical recombination 8=29828

ice and D_2O, phase diagrams at high press. 8=48383

ice III-IX, antiferroelec. phase 8=31438

inorganic crystals, under impact pressure 8=26057

intermetallic cpds of β-W structure, lattice instability rel. to supercond. 8=44721

manganic ferrites, rel. to crystal growth techniques 8=26257

martensite ageing in carbon-steels, microcalorimetric exam. 8=35105

martensite decomposition during tempering of quench-hardened steel, C conc. effects 8=35099

martensitic, in ferromag. alloy, mag-fields effects 8=35109

martensite in low carbon-steel, composite nature, crystallographic theory 8=26175

martensite nucleation in Ni-Fe alloys showing disrupture transform. kinetics 8=39555

mesomorphic states, phase identification, temp. scanning thermal anal. 8=48365

methylamines 8=40990

microscopic theory 8=35077

n.m.r. second moment study, high-pressure technique 8=48362

normal-to-supercond., detection for 10μ spheres 8=48367

nylon-6, α-γ phase, by stretching 8=30715

order–disorder effects on supercond. energy gap 8=31331

order-disorder, stabilization energies 8=35529

ordered phase structures, phenomenological theory 8=30671

organic crystals, polymorphic transform process 8=26090

perovskites, in high-temp. phase, on heating and n.-irradiation 8=39538

poly-β-alanine, water soluble and insoluble n.m.r. obs. 8=45112

polyethylene, oriented, rel. to plastic deform. 8=35137

polymethyl mechacrylate, secondary processes and activation energies, −150–75°C 8=44017

polypropylene, isotactic, γ–α transition, obs. 8=44018

polystyrene, atactic, second-order transition above glass point, obs. 8=44398

polystyrene films, glass transitions, i.r. transmission obs., 50-120°C 8=45247

polystyrene-benzophenone mixts., glass transition temps., obs. 8=44146

poly(vinyl acohol) films, glass transitions, i.r. transmission obs., 50-120°C 8=45247

poly(vinyl chloride-co-vinyl acetate) films, glass transitions, i.r. transmission obs., 50-120°C 8=45247

polyvinylidene fluoride, $\alpha \rightleftharpoons \beta$ transform. on stretching in temps., 20-150° and annealing 8=26155

Phase transformations—contd

solid-state—contd

pressure-induced, rel. to crystal radii 8=26054

pressure-temp. corrected trajectories, below 500°C 8=48366

1,1-pyrene-pyromellitic dianhydride, between 170-205°K 8=26554

quartz, anomalous sound absorption near λpt. in $\alpha \rightarrow \beta$ transition 8=26584

quartz, crystalline-amorphous, under fast n-irrad., X-ray diffr. studies 8=26146

quartz high-low inversion, lambda transition, thermodynamics 8=39563

quartz high-low inversion, vol. and compressibility rel. temp. at high press. 8=48401

quartz, structure changes in $\alpha \rightarrow \beta$ transform. and under n-irrad. 8=26080

quartz-glass-coesite system, under high-temp. and pressure 8=48400

rare-earth sesquioxides, metastable structure, formative mechanism 8=26056

second-order, unit cell deform., Landau theory 8=35079

seignettomagnetics, rel. to coupling of ferroelec. and mag. props. 8=27398

solid solns., order-disorder, effect on Mössbauer effect probability 8=35032

spinel ferrite lattice, cubic, to tetragonal, local Jahn-Teller distortions 8=26408

spinels, induced by Jahn-Teller effect 8=35076

spinels, types of order 8=39539

steel austenite lattice parameter changes rel. to intermediate transformation 8=35333

steel, cold-rolled, influence on recrystallization texture 8=39719

steel, directionally solidified, microsegregation of Ni and Cr 8=39552

steel, dynamic strain ageing, Charpy specimen behaviour 8=35686

steel, EI 702, ageing mechanism 8=35100

steel, EI 702, γ' and η' phase precip. or dissoln. on ht. treatment 8=43998

steel E 1702, γ^1-phase precip. mechanism, holding time effects at diff. quenching temps 8=35108

steel, martensitic, magnetic field effect 8=39554

steel, 9%Ni, struct. and growth characts. of bainite 8=44002

steel, quench-hardening, and austenitic grain struct. formation 8=35110

steel, stainless, entropy shock at transform. of first kind in mag. field 8=39553

steels, cast austenitic, on thermal cycling rel. to strength increase and grain size decrease 8=35698

steels, Fe–C and Fe–Ni–C rel. to martensite strength contributing factors 8=26815

steel U8, quenched, during tempering under high hydrostatic pressures 8=35679

succinonitrile, plastic phase 8=44611

talc, structural changes on heating 8=30699

tetracene, effect on fluoresc. 8=36536

tetrafluoroborate salts, n.m.r. 8=31905

thaumasite, $Ca_3H_2(CO_3/SO_4)SiO_4 . 13H_2O$, thermal decomposition, i.r. study 8=26065

ticonal, structure formation after themomagnetic treatment 8=35055

titanomagnetite to titanomaghemite, on cryst. surface 8=35125

transition energies by differential calorimetry, obs. 8=30674

transition metal oxides, centred around Nb_2O_5, non-stoichiometric mechanisms 8=26365

s-triazine, at low temp. 8=48411

X-ray apparatus, low temp. 8=35078

Ag–Al alloys, massive and martensitic, microstructure 8=48370

β-AgCd, ordering crit. temp., temp. dependence, from elec. resistivity meas. 8=30676

Ag-Cu-Zn-Cd system, univariant, equilibria formation by decomposition 8=30675

AgI, to 100 kbar, elec. cond. meas. 8=31311

AgI, rel. to ht. capacity 8=30961

α-AgI, low-temp. 8=43994

β-AgZn, ordering crit. temp., temp. dependence, from elec. resistivity meas. 8=30676

Al, transform. to brass-texture after cold rolling a cast strip 8=35264

in Al alloys with Si, Zn, Cu and Mg, relns reflected in viscosity conc. surves 8=34799

Al-4%Cu, $\theta' \rightarrow \theta$, effect of plastic deform. 8=48371

Al-Cu: MgSi, increase in ageing rate due to two impurity assoc. 8=35089

Al-Cu-Mn alloys, rapidly solidified, supersaturated solid soln. formation comp. and decomposition kinetics 8=35084

Al-Mg-Si alloy, ageing mechanism 8=35088

Al-60-78% Zn alloys, α^1-phase decomposition 8=35091

Al-Zn alloy, decomposition 8=30679/80

Al-25 wt.% Zn alloys, precip., effect of quenching conditions 8=26058

Phase transformations—contd
solid-state—contd
Al-Zn-Mg alloy, ageing 8=35087
Ar, metastable-stable transform. rel. to N_2 soln. 8=39567
$AuAg_3Te_2$, during e microprobe analysis, obs. 8=30857
Au–Cd system, diffusion energetics 8=48373
$AuCu_3$, antiphase-domain growth rel. to antiphase-boundary reactions 8=26060
Au_3Cu ordering after quenching, rel. to energy and resistivity changes 8=26059
BN, dense modifications by high pressures and shear stresses 8=48374
BN, hexagonal, irreversible transformation by shock compression 8=26062
B_2O_3-PbO-Al_2O_3 glass, spinodal decomposition from X-ray diffr. studies 8=26061
$Ba_{1-x}Ca_xMnO_3$, solid solns., structural, rel. to mag. transitions 8=27377
$BaTi_{0.75}Sn_{0.25}O_3$, paraelec-ferroelec. Mossbauer effect and dielec. const., –200 –20°C 8=30639
Bi perovskites, rel. to ferro- and antiferroelec. transitions 8=26063
Bi, under high pressure 8=35093
$BiBr_3$, high-press. 8=39468
$BiFeO_3$-Pb$(Fe_{0.5}Nb_{0.5})O_3$ solid soln. system, X-ray diffr. exam. 8=39543
$BiFeO_3$-$PrFeO_3$ system, rel. to ferroelec. and mag. props. 8=26064
$Bi_{1-x}La_x(Fe_{0.98}Mn_{0.02})O_3$ solid solns., X-ray diffr. exam. 8=39542
Bi-Sn alloy, high pressure changes by n-diffractometry 8=26361
BiI_3, high-press. 8=39468
CO, order-disorder kinetics, molec. theory 8=39546
$CaCO_3$, and decomposition, effect of impurities 8=30682
$Cd_{0.11}Hg_{0.89}Te$, semi-metal → semiconductor transition induced by hydrostatic press. 8=27086
CdI_2, polytypism, interaction energy calc. 8=44012
CdO: Ga_2O_3, mixtures, order-disorder 8=39549
CdS films, epitaxial growth and polymorphic transforms. 8=26113
CdS thin films, amorphous to crystalline 8=43993
$CdTiO_3$, perovskite modification, structure changes over 20-1000°C 8=27242
$Cd_2Zn(PO_4)_2$ 8=35322
Cm_2O_3, up to melting point 8=35425
Co-akermanite system, high-temp. substitution effects 8=35095
$(CrFe)_{23}C_6$, austenization influence on Cr contents and Curie point 8=30684
CrH, hexagonal, to metallic Cr, crystallography and bonding relationships 8=48376
Cr-Ni-Fe solid solns., phase form and dimensions, on prolonged crystallization 8=26246
Cs-graphite lamellar cpds, rel. to Cs vapour press. and temp. 8=35011
CsBr-RbBr system, diagrams, equilib. between two phases 8=35096
CsCl allotropic type crystals, phase transformations 8=48377
CsCl-RbCl system, diagrams, equilib. between two phases 8=35096
$CsCl_2$ 8=26067
Cu-containing perovskites, high temp. X-ray exam. and dielec. meas. 8=27243
Cu formate tetrahydrate, paraelec.-antiferroelec. 8=44269
Cu oxides, phase fields and thermal expansion 8=30686
Cu-Al alloys, β-phase, transform. during continuous cooling 8=26069
Cu_3Au, ordered and disordered, low temp. dislocation mechanisms 8=31076
Cu-2%Be, ageing, nucleated, precip. phase space lattice, obs. 8=35271
Cu–2 wt.%Be alloy, ageing characts. with or without additional elements 8=35674
Cu-Be alloys, ageing rel. to thermodynamic props. 8=35098
in CuCl crystal prep. for optical purposes 8=26248
Cu_5FeS_4, stability of phases 8=35097
Cu-Ga alloy, feathery structure formation in massive transform. 8=30690
Cu-Ga alloy, massive phase, duplex nature and dislocation structure 8=30685
Cu-12.5 wt. %Ge solid soln., f.c.c. → h.c.p. transform. 8=26068
Cu-Ni system, Ferromag. ordering rel. to Debye temp. conc. depend., obs. 8=39913
Cu-S films, kinetics by new e-diffr. procedure 8=26082
Cu_2S–Ag_2S system, rel. to resistivity changes 8=48378
DBr, rel. to crystal struct. 8=26396
DCl, and crystal structure by X-ray and n-diffr. 8=26073
Eu mono-chalcogenides, at high pressures 8=26070
EuS, mag. eqn. of state and sp. ht. near Curie point 8=27405
Fe, α to h.c.p., kinetics study Mössbauer effect 8=43946
Fe, $\alpha \rightleftarrows \gamma$, effect on positive ion emission 8=44955
Fe, in $\alpha \rightleftharpoons \gamma$ region, positive-ion and electron emission 8=27363
Fe, $\alpha \rightleftharpoons \gamma$ transform., internal friction changes 8=40152
Fe, b.c.c., edge disloc.-impurity interaction force-distance curve calc. rel. to hardening model 8=26674
Phase transformations—contd
solid-state—contd
Fe carbides, thermally induced 8=44003
Fe chromites, X-ray and Mössbauer effect study 8=35101
Fe, electrodeposited, natural ageing effects rel. to deposition conditions 8=35104
Fe, high-purity, multiple $\alpha \rightleftharpoons \gamma$ transforms. effect on internal friction 8=35700
Fe, purification by γ-phase zone displacement along α-Fe bar 8=30825
Fe-Al alloys, order-disorder 8=39557
Fe-Al alloys, structure and mechanical props. 8=39720
Fe-C martensite, substructure and yield strength 8=26812
Fe-Co alloys in fine particles, order-disorder 8=39556
Fe–Cr system, athermal martensitic transforms. 8=44000
Fe-8%Cr-1.1%C alloy, bainite, crystallography 8=30693
Fe-Cr-C alloys, bainite, transmission e-microscope exam. 8=30694
FeF_3, cubic–rhombohedral transition, 410°C 8=44005
Fe–Mo alloys, ageing characts., precipitate growth 8=44004
Fe-Ni alloy isothermal compression up to 300 kb 8=49006
Fe-Ni binary martensitic transformation, effect of cyclic heat treatment 8=26071
Fe-Ni-Al-Ti, Laves phase of comp. $(Fe, Ni)_{2-3.5}(Ti, Al)$ 8=35106
Fe–Ni–Ti alloys, $\gamma \rightarrow \alpha$ and $\gamma \rightarrow \alpha \rightarrow \gamma$, texture changes rel. to Young's modulus 8=35701
Fe–Ni–Ti alloys, hardening without martensitic transform. on ageing with plastic deform. at 600°C 8=35699
Fe-0.025% N, enhanced aging due to γ-α transform 8=44577
Fe-Pd alloys, on annealing and plastic deformation rel. to mag. props. 8=35102
α-$Fe_2O_3 \rightarrow Fe_3O_4$, and topotaxial relations between substances 8=26072
Ga, high press. 8=48260
GaAsZn ternary diagram, role in source selection for Zn diffusion in GaAs 8=44390
Ge, amorphous, from cryst. form by Ar ion bombardment 8=39723
Ge, annealed and cleaved surfaces, structure 8=48419
GeO_2, hexagonal to tetragonal, kinetic changes when used in polishing slurry 8=39558
H, normal, 4.2 to 0.91°K, hexagonal close-packed to f.c.c. lattice 8=39795
H_2, f.c.c., oriental transition, nonexistence 8=35112
HCl, and crystal structure by X-ray and n-diffr. 8=26073
HCl, low-temp. phase, phonon freq. distrib. 8=35384
HI, n.m.r. 8=49645
He^3, b.c.c.-h.c.p., volume discontinuity obs. 8=37358
InSb(As, P), produced by Ga 8=48384
K graphite, order-disorder obs. 8=26074
KCN, high press. 8=48385
$KD_3(SeO_3)_2$, growth and dielec. anomaly 8=30698
$K_4Fe(CN)_6 \cdot 3H_2O$, polytypic, rel. to ferroelec. props., 0 to –100°C 8=31432
$K_4Fe(CN)_6 \cdot 3H_2O$, polytypic transition seq. in –45 to –25°C from dielec. meas. 8=40610
KI–AgI, high-cond. systems 8=48396
KO_2, and crystal structures 8=26075
KSCN, high press. 8=48385
La, $\beta \rightarrow \alpha$ transform., model 8=44006
LaC_2, rel. to structure changes 8=26405
LaSb, rel. to lattice rearrangement in 630-720°K range 8=39948
Li_3AlF_6, transition temps. estimation 8=36564
$LiNbO_3$, ferroelec. transitions, 20°-1170°C, X-ray obs. 8=30863
$LiNbO_3$, structural change rel. to ferroelec. transition from x-ray and elec. exam. 8=31435
Li_2SO_4-Na_2SO_4 phase diagram 8=39559
$LiTaO_3$, five transitions, high-temp., X-ray study 8=35978
Mg–Cd alloys, ordering effect on residual resistivity and mag. susceptibility 8=40321
Mg-Cd alloys, ordering from X-ray diff. meas, 50-220°C 8=35113
Mg–Zn alloys, age hardening characts., effects of 1%Au addition 8=26832
MgO-Cr_2O_3-Fe_2O_3 solid solutions at 1300°C in air 8=39529
α-Mn, second-order, Landau-Lifshitz theory, quant. vertification 8=30700
Mn steels, $\gamma \rightleftharpoons \epsilon^1$ and $\gamma \rightleftharpoons \epsilon$, dilatometric and X-ray diffr. exam. 8=35114
Mn-Au alloys, on deform. and ageing rel. to antiferromag props. 8=31776
NH_4 salts, neutron scatt. determ. 8=48393
NH_4Br, l.f. vibr. above and below transition 8=27596
NH_4Cl, l.f. vibr. above and below transition 8=27596
NH_4F, to 20 kbar 8=34960
NH_4I–AgI, high-cond. systems 8=48396
N_2-O_2 phase diagram 8=35117
NaCN, orthorhombic-cubic, high press. 8=30701
NaCl:$Pb(NO_3)_2$, on heat treatment at 300°C 8=26689
$NaNO_3$, sp. ht., thermal diffusivity and conductivity 8=48391
$NaNO_3$, thermodynamics of λ-transition 8=39560
NaO_2, and crystal structures 8=26075
Nb hydrides (deuterides), and structure exam. by n. diffr. exam. 8=39725
Nb, strain-ageing, oxygen dependence 8=26835

Phase transformations—contd
  solid-state—contd
    Nb-O, strain-ageing from resistivity meas. 8=26846
    Nb_3Sn, from X-ray diffr. at 300, 15.5 and 10.5°K 8=35118
    Ni steels, mag. field effects 8=30702
    Ni-2.2%Be, ageing, nucleated, precip. phase space lattice, obs. 8=35271
    $NiCr_2O_4$, tetragonal to cubic, structural parameters, 92-298°K 8=26076
    Ni_3Fe, ordering, rel. to tensile props. 8=44595
    P, yellow–black, polymorphic, h. p. thermal effect 8=30703
    Pb perovskites 8=26063
    Pb rich alloy of Pb-Sn-Sb ternary system, aging 8=26764
    Pb–Bi system, new phases found during annealing 8=35844
    PbI_2, polytypis, interaction energy calc. 8=44012
    $Pb_2(NiW)O_6$ synthesized hnder high pressures 8=35122
    Pb-Sb alloy, (to 2 wt.% Sb), ageing after quenching 8=35121
    Pb-Sn alloys, cell boundary diffusivity calcs from Cahn and Turnbull theories 8=30670
    PbTe, at high pressures 8=35082
    PbTe-SnTe system, diagram rel. to specific alloy composition growth 8=44140
    $PdO-Ln_2O_3$ system in air 8=35123
    RbI–AgI, high-cond. systems 8=48396
    $RbNiF_3$, at high press. to cubic perovskite struct 8=48661
    RbO_2, and crystal structures 8=26075
    Sb, shock-induced polymorphic, dynamic obs. 8=39562
    Sb, structure changes at high pressures, investigation 8=44010
    SbSI, ferroelectric 8=31436
    Se, amorphous → polycrystalline, and monoclinic → hexagonal, kinetics 8=26078
    Si, ion-bombard., amorphous phase form., temp. and channelling effects 8=48931
    SiC, cubic-hexagonal rel. to temp. and pressure 8=48399
    SiC, hexagonal to cubic, under influence of high press. and high temp. 8=35124
    SiC, polytypism, interaction energy calc. 8=44012
    SiO_2, amorphous to cristobalite 8=44011
    SiO_2-glass, α-β quartz transform., effects on Na^{22} diffusion 8=48794
    Sm, mono-chalcogenides, at high pressures 8=26070
    β-Sn, under pressure rel. to Mössbauer line shift 8=43941
    SnRe–SnSe system, diagram 300°, to 900°C 8=44013
    SnTe, at high pressures 8=35082
    SnTe-GeTe system, at high pressures 8=35082
    $SrTiO_3$, 110°K phase transition, soft-phonon at corner of Brillouin zone 8=39564
    $TaN-TiB_2$, hot-pressed, rel. to densification and wear resistance 8=49053
    Ta-O, strain-ageing from resistivity meas. 8=26846
    TeO_2, at high pressures ($p = 60$ kbar) 8=26081
    Ti–Ag system, rel. to diffusion process and conc.-penetration curves 8=35509
    Ti-Co system, solubility limit study by X-ray diffractometry 8=30709
    Ti-6%Mo alloy, quenched, structure study by electron microscopy 8=30869
    Ti-47%Nb, α-phase formation during heating in e-microscope 8=35119
    TiNi crystals, obs. in premartensitic states on cooling 200-0°C 8=30710
    TiNi, second-order, within irreversible critical range rel. to electronic transform 8=30708
    TiNi, shape-memory effect at 90°C after plastic deform. at room temp. rel. to martensitic transform 8=30707
    TiNi transition 8=30899
    Ti–Pd alloys solid solubility 8=35127
    Ti_2O_3, transition, crystallographic study, 390-470°K 8=48678
    Tl amalgams 8=48348
    TlSe films, kinetics by new e-diffr. procedure 8=26082
    Tl–Sn alloy, phase diagram in range 0–20 at.% Sn 8=35126
    Tm_2O_3, up to melting point 8=35425
    α-U at 4.2°K, obs. 8=39567
    U, $\alpha_0 \rightleftharpoons \alpha$ structural change between 35 and 43°K from elastic moduli meas. 8=40185
    U, quenching, and anomalous thermal arrest in β phase, origin rel. to cryst. struct. 8=35129
    U-Ir system 8=35133
    U–Mo(1.5%) alloys, by rapid coolling from γ-phase, form. of pearlitic and martensitic mats. 8=35130
    U_4O_9, cubic-rhombohedral transition at 65°C, order-disorder transform. at 1125°C 8=26083
    UO_{2-x}/UO_{2-x} + U phase boundary, for temp. down to 1210°C 8=30712
    U-Pu alloys, heat evolution obs. 8=25306
    U/10% Pu/10% Fz, changes on annealing 8=30711
    U-Rh system 8=35132
    U-Ru system 8=35131
    U_2Ti, irradiation induced 8=35134
    V carbides formation during $\gamma \rightarrow \alpha$ transform. of austenite in steel 2062 8=35135
    V steel, isothermal, diffraction patterns 8=39791
    V_2Ga_5, structural, thermal and resistivity meas. 200-800°C 8=39566
    VH_x, vibr. spectra in three phases by neutron scatt. 8=39878
    VO, electronic phase transitions 8=26084
    VO_2, electronic phase transitions 8=26084
    V_2O_3, electronic phase transitions 8=26084
    V_3Si, lattice softening 8=31107
    V_3Si, near supercond. temp., X-ray and sp. ht. obs. 8=39567
    V_3Si, sublattice distortion, search 8=26445
    V_3Si, superconducting, martensitic transform., e-transmission microscope study 8=26085
    V_3Si, tetragonal-cubic low-temp. transition rel. to density states effect at Fermi surface 8=39568
    W, C contaminated, (110) face metastable phase, obs. 8=39583
    W-Cr solid soln., decomposition from X-ray diffr. study 8=26086
    Y garnets, synthetic, high pressure decomp. 8=26087
    Yb, mono-chalcogenides, at high pressures 8=26070
    Yb–Zn systeml phase diagram from thermal, X-ray, metallographic and resistivity data 8=44015
    ZnF_2, and phases lattice params., ⩽130 kbar, 25 and 300°C 8=39570
    ZnS, allotropic, induced by mech. pressure 8=44016
    ZnS, polytypism, interaction energy calc. 8=44012
    Zn_2TiO_4, order-disorder transition, influence of non-stoichiometric substitutions 8=26088
    Zr, purification by β-phase zone displacement along α-Zr bar 8=30825
    ZrO_2, $\alpha \rightarrow \beta$, temp. and impurity cation effects 8=26089
    ZrO_2, during heat treatment of $ZrOCl_2.H_2O$ and $Zr(OH)_4$ 8=48357
Phase transitions. See Phase transformations.
Phonographs. See Sound reproduction.
Phonon bottleneck. See Crystals/lattice mechanics.
Phonon drag. See Crystal electron states; Crystals/lattice mechanics.
Phonon–electron interactions. See Crystal electron states; Crystals/lattice mechanics.
Phonons. See Crystals/lattice mechanics.
Phosphorescence. See Luminescence.
Phosphors. See Luminescence; Luminescent devices.
Phosphorus
    abundance in solar photosphere 8=28172
    black, plate crystal growth from vapour phase at h.p. 8=30832
    chemical separation from $SiHCl_3$ and $SiCl_4$. 8=49998
    determination in phospho-silica films on Si substrates 8=49994
    diffusion in n-InAs, coeff. temp. dependence, 650–900°C 8=35496
    diffusion in Si at high-conc., precipitate formation 8=39983
    diffusion in Si, effect on Sn diffusion 8=48791
    diffusion in Si epitaxial layers, effects on defect structure, 4=48833
    diffusion in Si, vacuum method using $POCl_3$ as source 8=48792
    implanted in Si, impurity distrib. determ. 8=27131
    ion bombardment of SiO_2, distrib. and range 8=35604
    ions implanted in Si, distrib. 8=49266
    metastable atoms, from flash photolysis 8=29646
    segregation in steel, determ. by etching 8=30861
    yellow–black polymorphic transition, h. p. thermal effect 8=30703
    P^{31} chem-shifts in P(III), phosphoryl and triphosphoryl halides 8=43406
    P^{31} Overhauser effects, and simultaneous obs. of two kinds of nuclei 8=40993
    P_2, ground state reduced potential curves 8=29717
    in Se, effect on viscoelasticity 8=31230
    Si dopant, Hall effect and elec. cond. obs. 8=49268
    in n-Si, e.p.r. hyperfine splitting rel. to compensation obs. 8=27487
Phosphorus compounds
    diphosphates of heavy metals, i. r. spectra 8=36313
    halides, F^{19} and P^{31} chem. shifts 8=43406
    oxyhalide radicals, electronic emission spectra 8=43414
    polyphosphate, $[Na_3H(PO_3)_4]_x$, crystal structure 8=44239
    phosphate glass, Mo^{3+} doped, e.s.r. and optical absorpt. 8=31879
    phosphoryl cpds., i. r. intensity of PO bands 8=29760
    phosphoryl halides, F^{14} and P^{31} chem. shifts 8=43406
    phospho-silica films on Si substrates, nondestructive determ. of P 8=49994
    phosphosilicate glass film form. on SiO_2, comp. and struct. 8=44048
    thiophosphory halides, F^{14} and P^{31} chem. shifts 8=43406
    HPF_4, microwave spectrum 8=34279
    PBr_3 molecules normal oscillations, dynamic and reduced coeffs. 8=34283
    PBr_7, cryst. struct. and bonding, for Br_3^- ion, compared with $CsBr_3$ 8=44247
    PCl_3, spin-lattice relax., and molec. motion in liq. 8=34912
    PF_3, molecules normal oscillations, dynamic and reduced coeffs. 8=34283
    PF_5, far-i. r. spectrum 8=47617
    PF_5, F exchange with tetrabutylammonium hexafluorophosphate in CH_2Cl_2 soln., n.m.r. obs. 8=25960

Phosphorus compounds—contd
PHF$_2$ and PDF$_2$, microwave spectrum, molec. struct. 8=38849
PH$_4$I, e.p.r. of I_2^- centres 8=31124
PN, dissoc. energy 8=43413
P$_3$N$_5$ vaporization 8=43413
PO radical, analysis of vibr. and rot. structure 8=34280
PO, rotational analysis of u.v. systems 8=34281
PO$_2^-$, SCF matrix elements 8=47616
POCl$_3$, as source in vacuum method for P diffusion in Si 8=48792
POCl$_3$, i.r. spectrum at 77°K 8=49746
POCl$_3$, spin-lattice relax., and molec. motion in liq. 8=34912
POF$_3$, spin-lattice relax., and molec. motion in liq. 8=34912
PSCl$_3$, i.r. spectrum at 77°K 8=49746
PX$_5$, force fields 8=38850
V$_2$O$_5$–P$_2$O$_5$–WO$_3$ system glasses, elec. conduction mechanism from e.p.r. 8=40291

Photochemistry
See also Photographic process.
acetone-d$_6$, intermediates in photolysis 8=49951
acetonitrile-d$_3$, γ-irradiated, trapped electron and its reversible reaction, e.s.r. evidence 8=49955
acetyl chloride gas phase and matrix photolysis 8=43419
acridine, photoreduction in alcohols 8=32137
acridine, reactive state in photoreduction in ethanol 8=41284
acridine-biacetyl-benzene solns., triplet acridine form. by triplet biacetyl energy transfer, obs. 8=25925
acrolein, photodissoc. 8=32135
alkyl derivatives of benzene, photoisomerization 8=49949
alkyl diradicals, formation and rotation about carbon-carbon bonds 8=27759
anthracene, interaction with biacetyl in visible light 8=36618
anthracene triplet-triplet annihilation rate const. flash photolysis meas., 430-553°K 8=25535
benzene, gas phase, formation of fulvene 8=49950
benzene oxidation in gas phase, radical formation 8=41286
benzyl radical, assignment of excited states by three-step photoselection 8=25542
1, 3-butadiene, photodissoc. 8=32135
1-butene, photodissoc. 8=32135
2-butenes, cis-trans isomerization, benzene photosensitization 8=49959
cometary radicals and ions, effects in production 8=50425
cyanogen azide, photolysis and reaction with F 8=29723
cycloadittions, intermolec. orbital theory 8=27685
cyclobutanone-2-t, vibr. excited photodecomp. 8=41288
cyclohexane, liq. and in soln., vac. u. v. photolysis 8=27763
diazonium salts in acid soln., photodecomposition quantum yields 8=45397
dichloromethane, Hg-photosensitized, vibr. excited dichloroethane prod. 8=27761
dithionate ions in soln., photolysis, rel. to optical spectrum of SO$_3^-$ radicals 8=49957
ethylene oxidation by photolysis of NO$_2$ 8=36615
ethylene, spectroscopic basis 8=27760
flash photolysis delay unit 8=41285
flash photolysis, high-intensity pulse light source 8=28771
flash photolysis lamp 8=42206
o-fluorotoluene triplet state yield rel. to vibr., gas-phase obs. 8=25630
furfural, vapour phase 8=32134
gases, luminesc. during u.v. photolysis 8=34266
hexafluorobenzene triplet state yield rel. to vibr., gas-phase obs. 8=25630
hexafluoropropylene copolymer, γ-irradiated, photoinduced and thermal radical conversions 8=49953
hydrazine, photodissoc. 8=32135
hydrazine, vac.-u. v. photolysis 8=36613
hydrocarbon glasses, trapped electrons, optical and e.s,r. spectra 8=45401
hydrocarbons, gaseous, oxidation mechanism, e. s. r. investigations 8=36616
methanal azine, free-radical prod. 8=34337
methyl bromide, photolysis, high-energy CH$_3$ radicals 8=49961
p-methylbenzyl radical formation from p-xylene 8=36617
methylene, formation and rotation about carbon-carbon bonds 8=27759
monofluorobenzene triplet state yield rel. to vibr. gas-phase obs. 8=25630
naphthalene + 1, 4-dicyanobenzene, triple complex formation in excited state 8=48176
photobleaching 8=27756
photobleaching, spectral conformity 8=27757
photolysis, flash, i. r. detection of transient species 8=37672
photoselection, tandem two-photon processes 8=49692
polar solvents, mixed, photo-induced trapped electron rel. to photobleaching study 77°K 8=36446
poly(α-methylstyrene), photolysis, e. s. r. 8=27762
polycaprolactam, stressed, degradation kinetics temp. dependence 8=45399
polyethylene torephthalate, stressed, degradation kinetics temp. dependence 8=45399

Photochemistry—contd
polymer fibres, stressed, degradation kinetics temp. dependence 8=45399
polymers, stressed, photodegradation kinetics 8=36619
polystyrene, photolysis, e. s. r. 8=27762
proflavine, photoreduction in aqueous solution by steady light 8=49962
pyridine triplet state yield rel. to vibr., gas-phase obs. 8=25630
radiation effects on explosive instability 8=27732
rhodamine C solution, optical generation during excitation with pulsed light sources 8=30480
silk, natural, stressed, degradation kinetics temp. dependence 8=45399
tetrafluoroethylene copolymer, γ-irradiated, photoinduced and thermal radical conversions 8=49953
tetramethylethylene, intermediates in photolysis 8=49951
toluene triplet state yield rel. to vibr., gas-phase obs. 8=25630
trifluoromethyl iodide laser, Q switching and mode locking 8=37576
triphenylene-d$_{12}$-Rhodamine B solids solns., triplet-singlet energy transfer kinetics, obs. 8=36533
triple complex formation in excited state 8=48176
tubular-flow reactors for complex nonchain kinetics 8=49954
Ag$_2$S-HgI$_2$, photochromic, bleaching kinetics 8=49952
Al borohydride, flash photolysis 8=25444
As, metastable from flash photolysis 8=29646
AsD$_3$, flash photolysis, AsD$_2$ $^2A_1$–$^2B_1$ band spectra 8=29713
AsH$_3$, flash photolysis, AsH$_2$ $^2A_1$–$^2B_1$ band spectra 8=29713
Ba(N$_3$)$_2$, u.v. irrad. cryst. e.s.r. of N$_2^-$ 8=27485
Br, selective, using ruby laser 8=41287
CF$_3$OOCF$_3$, prod. of CF$_3$OOO radical 8=38941
CN violet emission, shock heated CO$_2$-N$_2$ mixture, chemical model 8=29722
CsBr, additively coloured, optical bleaching and high-temp. transforms. 8=27758
CS$_2$-O$_2$ photolysis, lasing oscill. analysis showing new lines and selective excitation 8=46569
F$_2$O + H$_2$ flash photolysis for HF laser 8=37582
Ge electrodes, surface photoeffect 8=27753
H$_2$, photoionization, ion-mol. and chemi-ionization reactions 8=36611
HClO$_4$, γ-irradiated, spatial distrib. of H atoms 8=49963
HF chem. laser, using UF$_6$ 8=46590
Hg + Cl atom combination 8=49960
KCl, coloured additively, reaction and photocond., at low temp. 8=31457
NCN$_3$, flash photolysis 8=25495
N$_3$CN reaction with F$_2$ in Ar matrix 8=47712
NH$_3$, photoionization, ion-mol. reactions 8=36612
NO soln. in H$_2$O, D$_2$O, photolysis at 1849Å 8=49958
NiO, decomposition on photo-absorption 8=36567
O$_2$, flash photolysis, vibr.-excited O$_3$ 8=36620
O$_2$ + CO + M, vac. u.v. flash photolysis 8=45398
O(^{1}D) gas-phase reaction with CO$_2$, rate const. 8=36614
P, metastable from flash photolysis 8=29646
S$_2$ formation after flash photolysis of CS$_2$, COS, NO in presence of intert gas 8=49956
Sb, metastable from flash photolysis 8=29646
Tl halide photolysis, r.f. mass spectrometry 8=43490

Photoconductivity
anthracene, dye-sensitized 8=49427
anthracene, injection-induced long-wavelength 8=27335
anthracene, mag. field effect 8=27336
anthracene, rel. to charge-transfer exciton and ionic levels 8=27254
anthracene:tetracene, trapping of photo-carriers 8=36030
9, 10-anthraquinone crystals 8=36031
by carriers in nonparabolic band, strong light induced 8=27314
cell for r.f. heating temp. control 8=46276
conductance of semiconducting bar, effect of pulse of photoexcited carriers 8=27312
crystal violet films, photocapacitance and photocurrent "memory" 8=36032
diamond, spectrum 8=44914
diamond with Al acceptors, spectrum, photothermal ionization and photon-induced tunneling 8=44913
durene, pure monocrysts. 8=49428
flying-spot scanner, elect. props. of semiconductors 8=24383
gradual capture rel. to lifetime 8=49408
halobenzene solns, enhanced conductivity on X-irradiation, 8=43866-7
liquid, recombination problem, comparison of β- and photo-ionization 8=49399
'localized' in space charge region, calc. for Si and Ge type semiconds 8=31451
malachite green films, photocapacitance and photocurrent "memory" 8=36032
molecular crysts, recombination problem, comparison of β- and photo-ionization 8=49399
negatively thermally stimulated conductivity, obs. 8=40645
photosensors connected to CdS bulk oscillator, as optical image sensor 8=27317
polystyrene, excitation wavelength depend. 8=49430
pulse response of electro-optic modulators and photocond. detectors at 10.6μ 8=36001
pyrene, spectrum rel. to carrier photogeneration 8=40679

Photoconductivity—contd
- review of work done at Industrial Institute for Electronics Torun Brach 8=40644
- rhodamine films, photocapacitance and photocurrent "memory" 8=36032
- Schottky photodiode, voltage enhanced spectral response 8=31458
- superconducting metals separated by CdS film, tunneling effect 8=35848
- in semiconductor, exciton-exciton collision contrib. 8=36000
- semiconductors, deformed, many —valley (Ge and Si type), kinetics rel. to intervalley transitions 8=36002
- semiconductors, high photovoltages, origin 8=49401
- semiconductor, in presence of, band bendings on surface 8=40646
- semiconductors, light polarization depend., mechanisms 8=49405
- semiconductors, organic, meas. in SHF band 8=49406
- semiconductors, possiblity of negative conductivity in quantizing magnetic fields 8=49403
- semiconductors, spectral response, possibility of observing electron-phonon Umklapp-processes 8=27315
- semiconductors, transient process study using regenerative microwave system 8=49400
- in semiconductor without symmetry centre 8=49404
- steady-state, in presence of traps 8=49402
- tetracene, rel. to charge-transfer exciton and ionic levels 8=27254
- transistor photosensitivity control by light intensity and wavelength changes 8=35941
- $A_VB_{VI}C_{VII}$-type semiconductors, rel. to phase transforms. 8=27077
- AgBr crystals, quenching by constant background illum. method 8=40651
- AgBr, induced by Q-switched ruby laser 8=45255
- AgBr, photoexcited hole diffusion temp. dependence 8=49410
- Al/CdSe(or CdTe)/Au thin-layer structures, voltage-controlled bistable states 8=49303
- AgCl, induced by Q-switched ruby laser 8=45255
- $AgGaTe_2$, spectral characts., forbidden band width 8=40649
- $AgInTe_2$, spectral characts., forbidden band width 8=40649
- Ag_2O, spectra at 77°K 8=40650
- β-Ag_2S film, obs. 8=49152
- Au, thin films 8=36009
- B, zone-melted beta-rhombohedral, with low C content 8=40908
- $Bi_{12}GeO_{20}$, photo-induced carriers, transport processes 8=27318
- BiSCl, and optical absorpt. 8=32028
- CaF_2, synthetic, absorption 8=36338
- CaF_2/Na, synthetic, absorption 8=36338
- Cd chalcogenide epitaxial films, prep. 8=26115
- CdS, behaviour of holes and electrons, revealed by laser excitation 8=36012
- CdS, changes on ht. treatment, 100–600°C rel. to surface topography 8=35268
- CdS crystal, l.f. oscillations induced by i.r. quenching 8=44934
- CdS crystals, local centre formation in presence of free electrons and holes 8=36015
- CdS diodes, thin-film, heat treating in various ambients 8=27176
- CdS, e-beam excited, photocurrent saturation 8=31973
- CdS, e-irradiated, rel. to damage evaluation 8=40654
- CdS films, vapour-deposited, rel. to stoichiometry and impurity conc. 8=26114
- CdS, illuminated, rel. to thermoelectric power 8=35997
- CdS, induced impurity, spectral distrib., effect of i.r. quenching 8=44921
- CdS, intrinsic under unipolar injection conditions, agreement with calc. 8=44919
- CdS layers, chem. deposited, props. 8=44918
- CdS phosphors, microwave meas. 8=49426
- CdS, photocurrent props. under unipolar injection conditions 8=44920
- CdS, optically quenched, electronic fluctuation spectra 8=40659
- CdS, oscillatory depend. on photon energy 8=31452
- CdS, rel. to negative photomechanical effect 8=40137
- CdS, recombination kinetics 8=27645
- CdS, rel. to piezoelectric oscillations 8=27297
- CdS, slow recombination centres, parameters, effect of heat treatment 8=50655
- CdS, sonde characts. 8=49412
- CdS, spectral distrib. fine structure, effect of O adsorption 8=44917
- CdS, surface, effect of self-purification and polarity 8=40658
- CdS, surface, oxygen chemisorption and desorption influence 8=49413
- CdS thick films, chemically deposited 8=39589
- CdS, transient currents 8=40653
- CdS, trapping level disposition 8=49793
- CdS-type devices, temp. depend. 8=27337
- CdS-In contact region, dark current relax. obs. 8=44916
- CdS:P, i.r. quenching band, 2.15 eV 8=40657
- CdS+Te, small inertia photoresistors 8=36014
- CdSe crystal, rel. to 0.93μ luminescence 8=36482

Photoconductivity—contd
- CdSe films, field effect effective mobility freq. and temp. dependence 8=36016
- CdSe films, photocurrent saturation 8=44923
- CdSe influence of doped surface on spectral dependence 8=49417
- CdSe, on X-ray and vis. illumination 8=40656
- CdSe, rel. to i.r. luminescence $(\lambda_m = 1.2\mu)$ mechanism 8=45266
- CdSe, sonde characts. 8=49412
- CdSe(Te), X-ray excited, electron-hole generation energy 8=49418
- CdTe, due to exciton generation 8=36010
- Cs-Sb films, photoelectron attenuation length determ. 8=31455
- Cu phthalocyanine, field effect on carriers 8=36018
- Cu_2O, compensated, non-linear, in recombination centre cross section determ. 8=50660
- Cu_2O thin film 8=31983
- Cu_2O, long duration 8=36017
- CuCl, oscillatory depend. on photon energy 8=31452
- EuS(Se) 8=27320
- GaAs, due to exciton generation 8=36010
- GaAs films, polycrystalline, illumination-current, relax. and spectral characts. 8=27321
- GaAs, photo-excited, current osc. and high field domain vel. meas. 8=31374
- GaAs:Cu, recombination centres, parameters determ. from photoconductivity 8=36020
- $GaP_xAs_{1-x}GaAs$ n-n heterojunctions, photosensitivity spectra 8=36019
- GaP–Cu storage effects 8=49419
- Ge, assoc. with ionization of H-like acceptors 8=44954
- Ge, due to exciton generation 8=36010
- n-Ge, extrinsic surface spectrum 8=40663
- Ge, field electron-emissive photocells 8=40702
- Ge, group III and V impurities photothermal ionization spectroscopy, obs. 8=40662
- Ge, internal photo-elec. effect, quantum efficiency 8=49420
- Ge, irrads, in direct transition region, exciton dissociation 8=40664
- Ge, oscillatory magneto–, rel. to photon energy 8=40661
- Ge, spectra 8=44925
- Ge:In far i.r. photocond., detector, response time 8=32945
- Ge:Zn, Sb, photodielectric effect 8=27322
- In, I-V characts. on X-irradiation and at 6000 V 8=27325
- InAs-GaAs alloys, threshold and impurity levels rel. to comp., obs. 8=27324
- InGaAs:Cr rel. to InAs trap level, obs. 8=27324
- InGaAs:(Cr, Zn) rel. to trap and acceptor levels, obs. 8=27324
- InSb detector in far i.r. 8=40666
- InSb films, surface, and field effect 8=27326
- p-InSb, impurity spectra 8=44926
- p-InSb, surface photoconduction 8=44927
- n-InSb, kinetics, and noise spectrum 8=27327
- InSb, I-V characts. on X-irradiation and at 6000 V 8=27325
- InSb, peaks indicating photon absorpt. and excitation of electronic impurity states 8=40665
- InSb-GaSb alloys, threshold and impurity levels rel. to comp., obs. 8=27324
- In_3Te_4 thin layers, rel. to structure and optical props. 8=39796
- KCl, coloured additively, and photochemical reaction at low temp. 8=31457
- KCl crystals, coloured, deformed, rel. to dislocation–colour centre interaction 8=44928
- KCl:Zr, Z_2 centre 8=44929
- K-Sb-Cs photocathodes 8=36023
- Mg phthalocyanine, films, barrier height, mechanism 8=40678
- MoO_3, cryst. and film, activation energies and decay 8=32013
- PbI_2, spectra rel. to defect energy-level 8=44650
- PbO polycrystalline, rel. to SCL currents and trap distrib. 8=36024
- PbS, effect of temp. 8=44930
- PbS film, monocrystalline, photosensitivity 8=40667
- PbSe films, polycrystalline, meas. at 77°K rel. to mobility changes and heat treatment 8=27328
- Sb, I-V characts. on X-irradiation and at 6000 V 8=27325
- Sb_2S_3, X-ray illuminated, photocurrent distrib. 8=49422
- SbSeI, and optical absorpt. 8=32028
- SbSeI grown from gaseous phase, volatile component vapour pressure effects 8=35989
- SbSi compounds, props 8=49269
- SbSI grown from gaseous phase, volatile component saturation vapour pressure effects 8=36026
- Se crystal, trigonal, transient photoconductivity rel. to carrier behaviour 8=44933
- Se electrophotographic layers, current carrier drift mobilities 8=40671
- Se, hexagonal, and cond., effect of reactor irradiation 8=44809
- Se, hexagonal, internal photoeffect spectral distrib. on X-ray and u.v. irradiation 8=40672
- Se hexagonal, saturation photocurrent, temp. dependence rel. to band structure 8=40673
- Se, trigonal, photocurrent decay rel. to hopping recombination 8=36027

Photoconductivity—contd
- Si, bipolar, lifetime, influence of adsorbed Au, Sb and O_2 8=27134
- Si, field electron-emissive photocells 8=40702
- Si, γ-irrad., recombination lifetimes 8=49424
- p-Si, surface, rel. to illum. intensity and temp. 8=27330
- Si:Au, emission rates of Au acceptor level, photocurrent determ. 8=40674
- α-SiC(6H), high-resistivity, doped accidentally, rel. to a band scheme 8=35779
- p-SiC–n-CdS heterojunctions 8=40517
- SiC: N, B, and unknown impurity doped, optical charge exchange exam. 8=36251
- SnO_2: Zn, chemisorbed oxygen effect on conductivity 8=31391
- $SrTiO_3$, and Hall effect 8=40675
- $SrTiO_3$, anomalous temp. dependence 8=27331
- TlI, adsorbed organic mols. surface charge-transfer groups form., obs. 8=36028
- Te, fast photocond. by CO_2 laser radiation 8=40676
- ZnO crystal, spectral sensitization, electrochem. obs. 8=49425
- ZnO crystal, surface charge discharging on illumination and e. multiplication 8=49354
- ZnO, water vapour in ambient gas conc. dependence 8=27334
- $ZnO:Co^{2+}$, and optical absorpt. 8=36029
- ZnS phosphors, microwave meas. 8=49426
- ZnS:Ag, Ga, donor-acceptor pairs, and optical and photo-excited e.s.r. spectra 8=40677
- ZnSe, photoelectronic props. in p-type-Cu-activated and n-type-self-activated 8=45296
- ZnSe, rel. to intrinsic oscillations 8=27333

Photodisintegration. See Deuterons/photodisintegration; Nuclear reactions due to/photons.

Photodissociation. See Photochemistry.

Photoeffect, nuclear. See Gamma-rays/effects; Nuclear reactions due to/photons; Photons/interactions.

Photoelasticity
- See also Double refraction/mechanical.
- constraints in two-dimensional medium, summation method 8=28265
- for determ. of gravitational stresses using immersion techs. 8=23832
- dielectrics, transparent, failure due to laser rad. 8=40547
- interference fringes of equal thickness; use 8=46741
- epoxy resin, reinforced, internal stresses 8=31243
- gauge for meas. residual stresses, approx. soln. for "shear lag" effect 8=41691
- glass, individual strain-optic coeffs. u.s. determ. 8=41138
- Rayleigh wave propag., photoelastic analysis 8=46152
- rel. to light wave interact. and acoustic wave generation 8=45162
- semi-infinite plate with reinforced notch under uniform tension, stress analysis 8=41653
- strain gauge, Rosette factor dependence on strain, temp. and fringe order 8=26753
- stress-optical meas. by intensity method 8=44510
- transmission-microscope polariscope 8=33283
- CdS, obs. of plastic deformation 8=35670
- CdS, photomechanical effect, negative 8=40137
- Ge, wavelength range causing photomechanical effect 8=36368
- in KBr volume expansion meas., rel. to U → F and U → α transforms 8=26826
- LiF, wavelength range causing photomechanical effect 8=36368
- NaCl, wavelength range causing photomechanical effect 8=36368
- Sb, wavelength range causing photomechanical effect 8=36368
- Si, wavelength range causing photomechanical effect 8=36368

Photoelectrets. See Electrets; Photography.

Photoelectric cells. See Photoconductivity; Photoelectricity; Photovoltaic effects.

Photoelectric effect, atomic. See Atoms.

Photoelectric emission. See Electron emission/photoelectric.

Photoelectricity
- See also Electron emission/photoelectric; Photoconductivity; Photovoltaic effects.
- alkali metal halides, external X-ray effect, quantum yield obs. 8=36005
- avalanche photodiode, working principle and typical design 8=28881
- colorimetry, photoelec., design for clinical laboratories 8=42140
- cross sections in keV range, calcs. 8=44912
- dielectric crystal photocarrier transport meas. 8=35747
- dielectrics, external X-ray effect, quantum yield obs. 8=36005
- devices for photometric meas. on flash tubes and lasers 8=42138
- devices freq. charact. meas. with tunable laser 8=46317
- dust-laden gases, photoelect. enhancement of elect cond. 8=25831
- flowmeter timing system appl. 8=34592
- friction drive for photoelec. star tracking telescope 8=45608
- metal-semiconductor system (photodiode), hot e-scattering from surface on illumination 8=35752/3

Photoelectricity—contd
- metals, external X-ray effect, quantum yield obs. 8=36005
- MOS structure, photoelect. threshold, effect of heating under bias 8=27313
- phenanthrene, matrix isolated crystallites in rigid 3-methylpentane 8=49429
- photocathode formation from alkali-antimonide films, chem. comp. meas. using crystal-quartz microbalance 8=40683
- photodielectric detector using superconducting cavity 8=40681
- photodiode mosaic technology 8=41982
- photodiode, open-circuit voltage, for meas. v. small displacements 8=41618
- photodiodes, multielement, elec. coupling mechanism 8=40682
- photodiodes, thin-base, retarding surface field effects on operation 8=36033
- photoelectric polarization of self-activated phosphors on ZnS and CdS bases 8=36006
- photoelectron spectroscopic system 8=36050
- photoelectron transducers, construction rel. to p-n junctions in CdS 8=49291
- photometer, operation design and circuitry 8=42133
- photoresistors, meas. of u.v. radiation, using org. luminorphors 8=48166
- phototube aperture increase by solid light funnel 8=41976
- polyacrylonitrile films, obs. 8=39605
- pulses, delayed, generation by photoelectric effect in double counter expt. 8=37773
- pyrometer, for W, effective wavelength change calc. 8=32979
- pyrometer for W temp. meas. 8=24021
- rhodamine-B film, photocapacitive effect 8=40680
- semiconductor props. meas. appl. 8=27076
- semiconductors, generation-recombination statistics, two-centred model, rel. to phenomena 8=35872
- semiconductors, piezoelectric, photoelectroacoustic effect and resonance phenomena 8=35871
- single-beam pyrometer for meas. of true flame temp. 8=41875
- solar cell array performance, computer simulation 8=24084
- solar cell flexible deployable array, 500 watt 8=24099
- solar cell irrad. degradation and equiv. 1 MeV e flux, computer calc. 8=24085
- solar cell power systems for satellites, and control 8=24087
- solar cell power systems for satellites, practical problems 8=24096
- solar cells and arrays for lunar surface operations 8=24098
- solar conversion and energy storage systems, for satellites 8=24088
- solar power system of Mariner IV, design and performance 8=24097
- spectropolarimeter, three-channel, appl. 8=36921
- tachometer application 8=28220
- target, junction mosaic, contrast sensitivity variations 8=41979
- thickness meas. by contactless photoelec. technique 8=41615
- windowless photon detector 8=33608
- X-ray defectmeter with Sb_2Se_3 detectors, construction and appls. 8=39989
- Ag, rel. to temp. 8=36008
- AgBr, photoelectron drift, 40 to −100°C 8=36007
- Al, cross sections in 1-150 keV range, calcs. 8=44912
- Al film, photocurrent var. with s and p polarized synchrotron radiation 8=27550
- Al, γ cross-section determ. 50-208 keV 8=36004
- Al-Al_2O_3-Al struct., e energy loss obs. 8=27316
- Au, γ cross-section determ. 50-208 keV 8=36004
- Au, rel. to temp. 8=36008
- n-Au-Si surface barrier photodiode, h.f., technology and props. 8=49432
- CdF_2, props. and carrier mobility 8=36011
- CdS films, photoeffect, electrically induced, props. 8=27319
- CdS layers, photoresistors, prep. and props. 8=49433
- CdS, p-n heterojunctions, props., convertor preparation 8=36013
- CdS, polycrystalline, capacitive changes with optical excitation, temp. effect 8=49414
- CdS, polycrystalline effect of press. on photoelec. props. 8=48539
- CdS solar cells for multikilowatt arrays 8=24100
- CdS solar cells micrometeoroid degradation, simulation obs. 8=24094
- CdS solar cells, performance after micrometeoroid exposure 8=24093
- CdSe crystal photocurrent instability after ion bombard. 8=49415
- CdSe, current noise rel. to light intensity 8=49416
- CdSe evaporated films, photoelectronic props. 8=44922
- CdSe on CdTe sandwiched layers, voltage-controlled bistable states 8=49303
- CdSe or CdTe sandwiched layers, voltage-controlled bistable states 8=49303
- CdS: P, photocurrent excitation spectra 8=31454
- Cu, γ cross-section determ. 50-208 keV 8=36004

Photoelectricity—contd
Cu, rel. to temp. 8=36008
Cs-Sb film in photocathode formation, chem. comp. meas. using crystal-quartz microbalance 8=40683
GaAs layer diodes, props. and emission currents 8=49305
Ge, internal effect, quantum efficiency 8=49420
Ge p-i-n detectors, determination of compensated-region width by light probe 8=46899
Ge:Au photoresistors, surface charge effects in I-V characts. and excess noise 8=36034
GeSe, and optical props., in energy range 0.5-1.5eV 8=49727
He, liquid, photoeffect on negative charges, current wavelength depend. 8=28437
n-InSb, alternating voltage induction by modulated waves, 0.8-10 mm 8=49421
InSb photoresistors, optical heterodyne effect 8=36372
K-Sb film in photocathode formation, chem. comp. meas. using crystal-quartz microbalance 8=40683
Pb, γ cross-section determ. 50-208 keV 8=36004
PbS, chemically deposited, influence of impurities on photosensitivity 8=44931
PbTe films, temp. depend. of photoelec. parameters 8=40668
$Sb_xBi_{1-x}SJ$ and $SbS_xSi_{1-x}J$ properties 8=40670
SbSeI, internal photoeffect, range 83°-293°K 8=44932
SbSI, photodielectric effect 8=40669
Se electrophotographic layers, dark discharge mechanism 8=49423
Si epitaxial layers, meas. of electrical parameters 8=35915
Si photocells, electron bombardment rel. to props. 8=27329
Si photodiodes with demodulation props. independ of wavelength 8=49409
Si p-i-n detectors, study with travelling light probe 8=46888
Si p-n junction u.v. photocells 8=27338
Si solar cells in-flight performance, computer prediction 8=24086
Si solar cells, Li diffused, radiation damage self-healing 8=24091
Si solar cells, p irrad. damage thermal annealing, 4.6 MeV 8=24101
Si solar cells for multikilowatt arrays 8=24100
Si solar cells, n irrad. damage and Li effects, obs. 8=24095
n/p-Si solar cells charged particle irrad. degradation, base resist. effects, 1-25 ohm cm 8=24092
n/p Si solar cells micrometeoroid degradation simulation obs. 8=24094
Si: Li solar cells, efficiency and e irrad. damage annealing, obs. 8=24103
Si: Li solar cells, experience and future of 8=24104
Si: Li solar cells, present status 8=24090
p^+/n-Si: Li solar cells, status 8=24102
p/n-Si: Li and n/p-Si solar cells, comparison 8=24089
Sn, γ cross-section determ. 50-208 keV 8=36004
TlI, adsorbed organic mols. surface charge-transfer groups form., obs. 8=36028
U, cross sections in 80-150 keV range, calcs. 8=44912
W, γ cross-section determ. 50-208 keV 8=36004
ZnS, photodepolarization currents, shallow capture levels rel. to kinetics 8=27332

Photoelectromagnetic effects
contactless meas. method, rel. to lifetime in semiconductors 8=40648
gradual capture rel. to lifetime 8=49408
Dember voltage, ohmic contact effects 8=44911
$AgGaTe_2$, spectral characts. 8=40649
$AgInTe_2$, spectral characts. 8=40649
CdS, influence of surface 8=31453
p-CdTe, obs. rel. to orientation 8=44915
Cu_2O thin film 8=31983
Ge films, spectrum 8=27323
in n-Ge, in pulsed mag. fields 8=36021
n-InSb, photomagnetic effect of hot photoelectrons 8=36022
n-InSb, photomagnetic effect oscills. rel. to e heating 8=31456
$SrTiO_3$, photomagnetoresistance by dc method at 10°K 8=44976

Photofission. See Nuclear fission.

Photographic light sources. See Light sources; Photography.

Photographic materials
See also Nuclear track emulsions.
contrast coeff., vacuum u.v., depend. on incidence 8=24441
emulsions, resolution of 7-60 keV electron images 8=37722
emulsions, thick, verification of Wiener's expts. 8=46766
line photometry and influence of Eberhard effect 8=28795
paper, appl. to particle beam tracking 8=46982
paper, light scatt. rel. to halftone reproduction 8=28905
photographic negative manufacture with parallel lines for spark chamber. 8=33391
plates, background blackening due to ion irrad. 8=28903
solar recording films, modulation transfer functions and 'detectibility threshold' 8=28162
speck size distrib. of exposed photographic emulsion 8=24443
Ag halide emulsions, electron trap distribution and low temp. Herschel effect 8=35744
Ag and Ag halide grains, effect of bleaching 8=33295

Photographic materials—contd
AgBr, photoelectron drift, 40 to −100°C 8=36007
AgBr, recrystallization, effects of NH_3 and triethanolamine 8=30821
Au film, holographic grating prep. 8=33290

sensitivity
emulsion, comparative noise performance in holographic and conventional imagery 8=28901
emulsion, light-sensitivity centres, surface rel. to subsurface 8=37723
emulsions, response to 7-60 keV electrons 8=37721
emulsions, surface and internal sensitivity interaction 8=33296
films, 17 types sensitivity to ionizing rad. in near Earth missions 8=28993
increase in partial vacuum, rel. to holographic appl. 8=42281
orpigment layers, spectral distrib. 8=24442
AgBr dispersion, latent image formation and reduction-plus-sulphur sensitization 8=46765
AgBr, effects of NH_3 and triethanolamine 8=30821

Photographic process
See also Photochemistry.
image-deblurring restoration using "extended source" lensless Fourier-transform holography compensation 8=46763
luminance of hologram reconstructions, effect of photographic gamma 8=24430
negative manufacture with parallel lines for spark chambers. 8=33391
pseudoscopic image formation and inversion 8=28902
stereogram, lenticular, prod. from hologram 8=28904
Ag and Ag halide grains, effect of bleaching 8=33295

development
AgBr dispersion, latent image formation and reduction-plus-sulphur sensitization 8=46765

Photography
See also Cameras; Cinematography; Lenses/photographic; Radiography.
electrophotographic imaging with cholesteric liquid crystals 8=42279
emulsions, thick, verification of Wiener's expts. 8=46766
eruption of solar prominence 8=41601
film transmittance-exposure characts. for 649-F at 6328 Å 8=28907
filters, glass, for daylight simulation in sensitometric exposure 8=42288
focusing method for making integral photographs 8=46761
glass-backed plates, elimination of secondary int. reflections 8=46762
hologram, effect of nonlinear rel. between amplitude transmission and exposure 8=37707
hologram filters for target recognition, simplified method for production 8=28898
hologram information reduction for visual display 8=28900
holographic image, light flux, effect of photographic characts. 8=42272
holographic motion picture film with constant velocity transport 8=33285
holography, biasing for single and multiple exposure 8=42271
line photometry and influence of Eberhard effect 8=28795
long range, oblique, rel. to atmos. optical meas. in central Colorado 8=36746
luminance of hologram reconstructions, effect of photographic gamma 8=24430
moon, earth-based high-resolution 8=28137
moon, light rays struct. anomalies rel. to craters struct. 8=45801
moon topography under oblique illum., grand-based 8=28141
of night airglow, from Gemini spacecraft, rel. to edge-on maximum and layer thickness 8=36802
panoramic aerial photographs, orientation errors and their influence on resolving power of systems 8=42277
photographs, blurred, sharp-focus restoration by holographic methods 8=24433
plate characts., densitometer aperture effects 8=42280
relief images 8=28883
stereoscopic range-viewfinder 8=42283
stroboscopic shutter for linear air track demonstration 8=28253
tone reproduction criterion 8=42278

applications
aerial mapping, camera, specifications 8=42285
air bubbles, bursting, time exposure obs. 8=25856
asteroids, positional obs. (1950-62) 8=45836
borehole direction surveying instruments 8=28906
bubble chamber, photograph analysis by flying image digitizer 8=46960
colour temps. of self luminous objects by high speed motion picture camera with optical compensation 8=46265
comets, positional obs. (1957) 8=45836
condensation kinetics by high-speed photography 8=39483
insultaion failure in rotating equipment 8=40553
laser generator rods, pumping distrib. meas. 8=24324
lunar, techniques and results 8=36994
map matching, contrast correl. meas. 8=42292
nuclear emulsion p track scanning 8=46981

Photography—contd
  applications—contd
    oblique shock wave interaction with supersonic projectile 8=46162
    picosecond pulse of laser light, meas. 8=42290
    planets, minor, obs. 8=32537
    slit lamp section, corneal contour 8=46772
    solar u.v. 2000 Å radiation 8=45869
    spectrum meas., interference method 8=28792
    supernova magnitude obs. 8=32457
    tracking of weak artificial satellites 8=50235
  colour
    No entries
  high-speed
    antiflash reflecting system for ultrabrief exposures 8=46768
    condensation kinetics study 8=39483
    field-ion microscope, recording time reduction 8=28585
    image-tube framing camera, time dispersion effects 8=37433
    materials testing application 8=42291
    motion picture cameras with optical compensation, applic. for meas. of colour temps. of self-luminous objects 8=46265
    Schlieren, subnanosecond, of laser-induced gas breakdown 8=29901
    Ar flash light source 8=28768
Photoionization. See Ionization.
Photolysis. See Photochemistry.
Photomagnetic effects. See Photoelectromagnetic effects.
Photomagnetoelectric effects. See Photoelectromagnetic effects.
Photometers
    See also Spectrophotometers.
  automatic light distribution 8=46650
  Beckman type DK, combined luminesc. and absorpt. meas. 8=33243
  Brice-Pheonix, scatt., sources of error 8=46652
  calibration, for meas. faint luminous effects 8=46678
  calibration of photoelect. polarization meter for directional response var. 8=42126
  detection of feeble luminous flux using photomultiplier 8=46649
  double beam photoelec. filter photometer, for astronomy 8=41497
  interference microphotometer for Fabry-Perot ring photographs analogue reduction 8=28833
  light scatt. by large submicron cylinders, perpendicular and oblique incidence, meas. 8=24361
  recording photoelec., operation design and circuitry 8=42133
  underwater rad. distrib. meas. 8=42136
Photometry
    See also Brightness; Densitometry; Illumination; Spectrophotometry.
  airglow, extreme u.v. detector 8=41393
  astronomical, error analysis, Reiger's theory confirmation 8=41498
  beam intensity comparison, double optical lever system 8=42127
  contrast transfer coeffs. of diffusing screens by MF-4 microphotometer 8=42131
  daylight, internal refl. component, finite-difference split-flux method 8=42132
  detection of feeble luminous flux using photomultiplier 8=46649
  electron microprobes optical signals detect. 8=36461
  flame, design for clinical lab. 8=42134
  interocular brightness matching, pupil diameters and retinal illuminances 8=33297
  line photometry and influence of Eberhard effect 8=28795
  light and optical measurements 8=46651
  lunar surface, in situ meas. 8=36999
  phosphor testing, standard procedures 8=45418
  photoelectric devices for photometric meas. on flash tubes and lasers 8=42138
  photoionization chamber, multichannel 8=29948
  photon counter characts. 8=31471
  photon flux meas. 2500Å-6000Å by rhodamine B fluorescence 8=46653
  photon no. from given area, min. detectable change 8=42125
  Pleiades, faint, UBV obs. 8=36947
  precision, establishing photometric standards and accuracy improvement 8=42130
  primary standard of light, thermodynamic considerations 8=46654
  quantum theory of det., field attenuation 8=29081
  reflection nebulae, star obs. 8=32472
  response of phototube, evaluation 8=37633
  spectral distribution of atomic line from Fabry-Perot ring meas., nonsymm. line 8=25339
  standard source for simulation of air-glow 8=46678
  stars, relative and absolute obs. 8=32434
  stars, UBV and narrow-band uvby obs. 8=32435
  stellar magnitude, electronography 8=28064
  strip-chart reading error analysis 8=42139
  synchronous radiation detectors vs. pulse counting for photomultiplier systems 8=42129
  transmission-to-extinction convertor 8=28723
  X-ray differential for phase modification exam. 8=26323
Photometry—contd
  zodiacal regions in quadrature to Sun 8=45855
  I_2 u.v. counter props. 8=46672
  MgO flame luminance determ. 8=37312
  light sources
    calibration of photoelect. polarization meter for directional response var. 8=42126
Photomultipliers
  blue sensitive, for temp-meas above 800°C of small surface areas 8=24014
  calibration method for nanosecond range 8=37431
  cathode rel. sensitivity distrib., wavelength depend. 8=33094
  cross-field, for nuclear expts. 8=46422
  detection of feeble luminous flux 8=46649
  dosimetry of powerful X-ray pulses 8=46922
  electron multiplier for quadrupole mass spectrometer 8=47449
  electron multiplier pulse-height distribs. 8=37430
  fluctuation errors, validity of conclusions drawn from ratemeter 8=42345
  for fluorescence, nanosecond, decay times meas 8=34884
  gain rel. to count rate at fixed dynode voltage 8=24156
  grid-controlled, methods of suppressing parasitic photoemission 8=24158
  hybrid, use of reverse epitaxial Si diode as multiplying device 8=46424
  imaging system for e.a.s. optical emission 8=38195
  improvements, with total internal reflection sensitivity enhancement 8=37432
  light beams modulated in GHz range, photomultiplier exam. 8=46643
  lucite light pipes coupled to photomultipliers, efficient design 8=24371
  magnetic defocusing with large area semitransparent photocathode, evaluation 8=41977
  measurements using single-electron noise component 8=46426
  miniaturized, capable of withstanding 10,000 g shock accelerations 8=46425
  noise filter for d.c. output 8=28579
  operational mode, controlled, of FEU-33 8=46427
  photocathode response, self-derivative meas. 8=46429
  photon counter, high-speed 8=47042
  pulse-to-analogue convertor 8=33387
  quantum efficiency improvement, practical multiple reflection technique 8=28578
  quantum yield meas. pulsed monochromatic recording 8=24157
  radiometer for plasma r.f. radiation 8=43540
  sensitivity, temp. effect 8=46702
  star tracker tubes, electron induced noise, source 8=28577
  simulated pulses for scintillator decay time meas. 8=46883
  synchronous detectors vs. pulse counters 8=42129
  10μm radiation det. using optical conversion 8=33123
  venetian blind type, new Russian series 8=46428
  X-rays, soft, det. 8=47041
Photons
    See also Cosmic rays/photons; Gamma-rays; Nuclear reactions due to/photons; X-rays.
  absorption in maser molecular spectroscopy 8=38782
  absorpt. processes from radiation field, field-correl. effects 8=28722
  ageing rel. to cosmology theory 8=36914
  beats rel. to spectral composition of light 8=33259
  from broken symmetry in weak interactions 8=33520
  cosmic rays, 10^{13}eV from local radio sources 8=32400
  counter, high-speed 8=47042
  distribution equilib. function in e.m. cascade 8=38207
  distributions versus photocount in laser statistics 8=46532
  emission, from thorax of human male, comparison of predicted and obs. 8=28199
  det., field attenuation, quantum theory 8=29081
  field, unified treatment with vector meson field 8=33716
  i.r., counter-amplifier, solid-state, rel. to elec.-dipole transitions in crystals 8=42137
  Lee-Yang theory of charged spin-one bosons, radiative correction to photon propagation 8=37836
  low-energy, emission in scatt. and decay processes 8=42447
  mass and gauge invariance 8=33605
  mass, formulation of electrodynamics without potentials 8=28539
  mass, new geomagnetic limit 8=42446
  models, non-relativistic 8=29016
  phase, mixed state of excitation of quantum osc., uncertainty of state 8=33604
  2-photon automatic registering spectrophotometer 8=42225
  prod. in lepton pair annihilation, matrix element calc. with anomalous magnetic moment and polarization 8=29089
  prod. in meson + N → γB for determ. of e.m. couplings of MN resonances 8=37916
  punctuation functions in corpuscular optics 8=42117
  radiative correction, limit in e^+, e^--p scatt. 8=42639
  radiative corrections, order-α, to β-decay 8=33630
  radiative corrections to elementary particle scatt., approx. for calc. 8=33569
  radiative corrections to π electroprod. 8=24775

Photons—contd
- rest mass, non-zero if cosmological Einstein const is non-zero 8=37915
- thermal beams, information content 8=41852
- transport in arbitrary finite body employing imbedding eqns. for Green's function 8=28228
- two-photon enhanced emission, strong laser radiation 8=37555
- vector meson eqn. for description 8=47121
- wave function expansion from reduction to irreducible representation of Lorentz group 8=33314
- windowless wide-band detector 8=33608
- CS_2 Lyman-α proportional counter 8=24698
- He-Ne laser radiation, correlation obs. 8=28686
- He-Ne laser, statistics for threshold light with finite counting time 8=24319
- Si single crystals, d. c. photodecay meas. rel. to minority carrier lifetimes 8=40490
- **interactions**
  - absorpt. effect due to intermediate vector-meson state 8=24690
  - atomic cross sections from 1-94 8=47302
  - with cosmic rays in universe 8=33846
  - d disintegration at high energy, covariant form of Austern model 8=25006
  - double-pion photoproduction and isobaric model below 1 GeV 8=33668
  - electron, K-shell, cross section obs., 280-1, 250 KeV 8=43226
  - η prod., Regge-pole model, forward peaking 8=24839
  - $\gamma + d \to \pi^\circ + d$, differential cross-section, around $N_{1/2}^*$ (1525) reson. 8=33665
  - $\gamma + \gamma \to \rho^\circ + \rho^\circ$, high energy 8=47040
  - $\gamma + n \to \pi^\circ + p$, photproduction of π° meson near $N_{1/2}$(1525) resonance 8=47108
  - γN, baryon resonance production of any spin 8=29162
  - $\gamma + N \to N + V^\circ$, cross sections 8=24852
  - $\gamma N \to VN$, kinematical singularities and zeros 8=42448
  - $\gamma N \to VN$, vector-meson prod., conspiracy relations 8=38026
  - $\gamma\pi$, meson resonance production of any spin 8=29162
  - $\gamma\pi \to 2\pi$, for $\pi \to 2\pi$ dissociation study in nuclear field 8=29122
  - γ-3π coupling const. from current algebra 8=42374
  - γp in H, $\mu^+\mu^-$ asymmetric pairs prod. rel. to quantum electrodynamics breakdown, 850 MeV 8=33647
  - γp, multipion prod., η°, $N^{*++}\rho^-$ and ω° resonances 8=33669
  - $\gamma + p \to \eta + p$, 775–850 MeV, ang. distrib. 8=24840
  - $\gamma p \to K^+\Lambda$, polarization of Λ for fine photon energies 8=42658
  - $\gamma p \to K^+ \Lambda^\circ \Sigma^\circ$, via "u channel, high-energy 8=42525
  - $\gamma + p \to n + \pi^+$, 500-800 MeV cross-section obs. 8=24776
  - $\gamma p \to \pi^+ n$, 4, 8 GeV/c, comparison with $\pi^- p \to \rho^0 n$ in Vector dominance model 8=37972
  - $\gamma + p \to \pi^+ + n$, n polarization obs. 8=24965
  - $\gamma + p \to \pi^+ + n$, vector meson dominance analysis 8=24787
  - $\gamma p \to \pi^+ n$ via "channel, high-energy 8=42525
  - $\gamma p \to \pi^- N^{*++}$(1238), failure to obs. asymm. and OPE contrib. 8=37917
  - $\gamma p \to \pi^- N^{*++}$ via "u channel, high-energy 8=42525
  - $\gamma + p \to \pi^\circ + p$, recoil p polarization, $\gamma_E = 240$–420 MeV 8=33756
  - $\gamma p \to p\phi$ and $\gamma p \to p\phi\pi^+\pi^-$, up to 5. 8 GeV 8=33719
  - $\gamma p \to p\rho^\circ, \pi^+\pi^-$, up to 5. 8 GeV 8=33719
  - $\gamma p \to p\rho^\circ$, up to 5. 8 GeV 8=33719
  - $\gamma p \to p\omega$ and $\gamma p \to p\omega\pi^+\pi^-$, up to 5. 8 GeV 8=33719
  - hadron photoprd., rel. to vector meson prod. by meson-nucleon collisions, photon-vector-meson analogy 8=42503
  - K photoprod., conspiracy and evasion 8=42526
  - lepton pair photoprod., Compton diagram 8=33623
  - lepton pair prod. cross section, Compton graph contrib. 8=24709
  - mesons, pseudoscalar, photoprod. on nucleons, Regge pole model 8=29127
  - with nucleons, vector meson production 8=33725
  - pair prod. in condensed medium, effect of multiple scattering 8=24693
  - with phonons, coherent 8=46638
  - photon-photon, electron pair prod., magnetic field effect 8=33643
  - photoproduction, consistency of Regge behaviour 8=24691
  - photoproduction in quark model 8=42495
  - photoprod. of lepton pairs calc. of Bethe-Heitler and Compton diagrams 8=33623
  - photoproduction of π°, η° on protons, 6-17. 8 GeV 8=42523
  - photoprod. on N, meson field model 8=29180
  - photoprod. rel. to N Compton scatt. 8=24694
  - ϕ photoproduction from H_2 differential cross-section obs. 6. 5-17. 8 GeV 8=42602
  - π amplitudes Reggeization, Lorentz invariance 8=42522
  - π photoprod. 8=33770
  - π photoprod. and $\pi N \to VN$ process, γ-V analogy model 8=33666
  - π photoprod., conspiracy and evasion 8=42526
  - π photoprod., conspiracy and residue 8=42517
  - π photoproduction from B^{11}, O^{16}, nuclei treated as elementary 8=42511

Photons—contd
- **interactions**—contd
  - π photoprod., generalized sum rules for A_2 trajectory calc. 8=42519
  - π photoprod, multipole analysis 8=24773
  - π photoprod., ω Regge-pole residue functions 8=37968
  - π° photoprod, below 234MeV multipole analysis 8=24777
  - π^+, high energy photoproduction without conspiracy 8=24778
  - π^+ photoproduction, double conspiracy 8=37969
  - π^+ photoproduction, π and conspirator residues and trajectories from continuous moment sum rules 8=42520
  - π^+ photoprod. on p, cross-section up to 200 MeV 8=42527
  - $\pi^- p \to \Lambda K^\circ \gamma$ rel. to meas. of the magnetic moment of Σ°-Λ transition 8=33835
  - $\pi^- + p \to \pi^+ + \pi^- + n$, N*(1236) prod. ang. distrib. 8=24782
  - quark model sum rule in photoproduction, violation 8=24659
  - ρ° photoproduction from H_2 differential cross-section obs. 6. 5-17. 8 GeV 8=42602
  - ρ^+ photoprod. via Regge-trajectory exchange 8=42611
  - three-photon, CP violation model 8=24692
  - two atom excitation by single photon 8=29633
  - vector dominance in photoproduction 8=38030
  - vector meson photoprod., polarized-photon parity filter 8=42599
  - vector meson photoprod., Regge-pole model 8=42600
  - vector mesons prod., application of optical theorem for quasi-elastic scatt. 8=42601
  - H, ϕ and ρ° prod. cross sections, 15 GeV 8=33724
  - He^3 photodisintegration around first πN resonance obs. 8=29226
  - He^3, photodisintegration, using short-range correls. 8=25013
  - He II ejection of trapped electrons in bubble states 8=41901
- **polarization**
  - Compton γ polarimeter, asymmetry ratio, computer calc. 8=33615
  - Compton γ polarimeter appl. 8=33617
  - Compton γ polarimeter, optimal sensitivity, computer calc. 8=33616
  - Compton scatt., $E_\gamma = 662$ keV, obs. 8=33607
  - in $e^+e^- \to 2\gamma$ at high energies, circular polarization, spin correl. calc. 8=29098
  - γ-rays from e synchrotron with amorphous radiator 8=33611
  - Rayleigh scattering obs. 8=25208
  - vector meson photoprod., polarized-photon parity filter 8=42599
  - Na^{23}, n capture, γ circular polarization obs. 8=38485
  - P^{31}, n capture, γ circular polarization obs. 8=38485
- **scattering**
  - Compton effect, double and triple obs. 8=24697
  - compton, $E_\gamma = 662$ keV, polarization effect obs. 8=33607
  - Compton hadron, kinematic singularity structure of helicity amplitude 8=29079
  - in diffusion in absorbing and scatt. media, number of scatts. 8=29077
  - double, by interacting quadrupolar and octopolar molecules 8=47717
  - by electrons in partially ionized gas 8=43475
  - γ-d, dispersion theory, 0–100 MeV 8=38098
  - laser beam by electrons, relativistic effects 8=42451
  - low-energy form of amplitude given by dispersion-theoretic Born approx. 8=29080
  - nuclear spin, parity mixing-ratio of transition, effect on ang. distrib. 8=33891
  - N, Compton, finite energy sum rules for Pomeranchuk trajectories 8=24694
  - N Compton scatt. higher order low energy theorems from helicity amplitudes 8=29078
  - photon-electron, in refracting medium, inducement of additional photon 8=37937
  - photon-photon, observability, Dirac-Kapitza mechanism 8=42449
  - Rayleigh scatt. of polarized γ 8=37919
  - Regge trajectories, conspiracy test 8=42469
  - resonant, from perturbed two-level system, stochastic theory 8=41755
  - three-dimensional semi-infinite medium, mean number eqns. 8=42450
  - in CdS, photon-photon scatt., obs. with freq. changes 8=49711.
  - Cs^{137} Rayleigh scatt. of 662 keV γ obs. 8=25208
  - Ir^{191}, 129 keV, magnetic moment of 129 keV level obtained 8=47303

Photonuclear reactions. See Nuclear reactions due to/photons.

Photophoresis
- photopheretic, radiometer and thermal forces relationship 8=24011

Photoproduction. See Gamma-rays/effects; Nuclear reactions due to/photons; Photons/interactions.

Photoresistors. See Photoconductivity; Semiconducting devices.

Photosphere. See Sun.

Photovoltaic effects
- photocells with p-n heterotransition, on CdSe films 8=40647

Photovoltaic effects—contd
  p-i-n junction 8=36003
  p-n and p-i-n semiconductor junctions, photo-e.m.f., by probe illumination 8=49407
  Ag_2S., negative effect 8=49411
  CdS-metal barriers from photo-voltage meas. 8=40511
  CdS-Cu_2S film system, rel. to thickness and prep. 8=40652
  CdTe films, gas adsorption effects 8=44924
  Cu_2S-CdS cells, spectral response 8=40684
  Ge intrinsic electrodes, pulse meas. of surface photovoltage 8=27753
  PbS films, polycrystalline, and crystals, photo-e. m. f. force temp. dependence 8=36025
  Si photocells, forward branch of V-I characts 8=49431
  p-Si, solar cell mat., electron damage coeffs. in orbit, calc. 8=27123
  Si solar cells, e irrad, role of Li in degradation and recovery of diffusion length 8=28508
  Si solar cells, surface effects, study with low energy p 8=28506
  Si: P or B p-n junct. solar cells, comparison 8=28507
  ZnS hexagonal crystals, changes rel. to stacking fault introduction 8=31103
  ZnS crystal, 77°-600°K. obs. 8=45291
Physical chemistry
  atomic struct. and valency theory, use of 3-dimens.
  mesosphere, rel. to electron conc. 8=27880
  wustite($Fe_{1\ x}O$), composition-oxygen partial pressure diag., thermogravimetric determ. 8=36540
Physical effects of radiations
    See also under individual radiations, e.g. Neutrons and antineutrons/effects.
  acoustic cavitation, apparatus and results 8=48032
  dl-alanine, γ-irradiated, optical annealing investigation by e.s.r. 8=44400
  alkali azides, mech. and optical effects 8=31140
  alkali carbonates, mech. and optical effects 8=31140
  alkaline earth nitrates, mech. and optical effects 8=31140
  alkali-halide crystals, etch-pit star formation rel. to dislocation mobility 8=26682
  alkali nitrates, mech. and optical effects 8=31140
  anthracene, solid, u.v. irradn., photo-dimerization 8=41270
  atomic movement, computer simulation 8=48887
  austenitic stainless steel, hardening, substructure 8=49015
  "blow-off" phenomena, laser-induced 8=40065
  cellulose nitrate, etchable track formation 8=44492
  ceramic reactor materials and defect cluster growth 8=31129
  ceramics, rel. to physical props. 8=26722
  cleavage surfaces, fission-fragment tracks and dislocation-type defects 8=26693
  concrete, conventional, damage under neutron bombardment 8=26730
  conference, Ashevill, North Carolina, USA, Sept. 1965 8=35593
  crystals, damage, computer studies of dynamics 8=26723
  damage investigation, appl. of anelasticity 8=31127
  damage investigations by liq. He field-ion microscope 8=31128
  dielectrics, etchable track formation 8=44492
  dielectric switch, hardness to transient and steady state ionizing rads. 8=27302
  displacement damage rates in differing reactor types 8=47408
  DNA, effects of binding agents on melting 8=48903
  DNA, e. s. r. obs. 8=34366
  e excitation and luminesc. and cond. induction by atom and ion bombard. 8=26861
  electronic components, transient particle effects 8=31126
  electronic parts, reliability in combined temp., vacuum and nuclear rad. environment 8=27192
  epoxy resins for magnet coil insulation, damage, obs. 8=31159
  ferrites, on ferromag. resonance, due to U^{235} fission fragments 8=36225
  fluorite, irradiated, elec. cond. and optical absorpt. changes 8=26946
  gaseous impurities of air, condensation nuclei production 8=25992
  glass, dielectric breakdown, optimal thickness calc. 8=31417
  halide crystals, ion bombard. damage 8=48888
  ion beam penetration obs., conference, Chalk River (1967) 8=44491
  ionization thermoluminescence, photon counter 8=49785
  insulators, nonlinearities in response 8=35595
  laser, solid, mechanisms of rad. effects of rel. to use in the space environment 8=28694
  Lexan polycarbonate, etchable track formation 8=44492
  mica sheets, thin, fission-fragment tracks, kinetics of healing 8=40055
  metal crystals, ion bombard. damage 8=48888
  metal crystals, laser irradiation, localized damage 8=30716
  metal halides, sulphates, permanganates, mech. and optical effects 8=31140
  metals, porosity formation mechanism 8=35518
  mica, ancient cosmic ray tracks? 8=25036
  mica, etchable track formation 8=44492
Physical effects of radiations—contd
  m. n. o. s. structs., radiation-induced threshold voltage shifts 8=35946
  MOS capacitors, determ. from conductance obs. 8=27204
  MOS, large signal equiv. circuit for predicting behaviour in pulsed rad. 8=27206
  m.o.s. transistor, radiation hard 8=31413
  MOS transistors, sensitivity to space rad. rel. to processing techs. of gate oxide film 8=27209
  MOS-FET's, open geometry p-channel, rad. induced peaking effect 8=27205
  MOS-FET's, operating in common source mode, irrad. damage 8=27208
  muscovite mica, U^{235} fission fragment track annealing anisotropy 8=44505
  naphthalene single crystals, X-ray damage 8=40083
  nuclear accidents, book 8=38586
  optical mats, transmission loss 8=28742
  oxide crystals, ion bombard. damage 8=48888
  oxyhalides, mech. and optical effects 8=31140
  planar devices, surface and bulk effects of nuclear reactor radiation, comp. 8=31400
  plasma production from laser interaction with solid D targets 8=39064
  point defects in non-metallic solids, conference 8=31029
  polyethylene, γ effect on elec. cond. 8=40084
  polymers 8=35608
  polymethyl methacrylate, conductivity, permittivity 8=49597
  polymethylmethacrylate, thermal radiation during damage by laser light 8=30994
  polystyrene, dielectric breakdown, optimal thickness calc. 8=31417
  polystyrene, filamament struct. in laser beam trace 8=49784
  polystyrene, thermal radiation during damage by laser light 8=30994
  porcelain dielectric breakdown, optimal thickness calc. 8=31417
  proton damage of Ge(Li) detectors 8=46910
  quartz, dielectric breakdown, optimal thickness calc. 8=31417
  quartz, fused and cryst., laser prod. damage, 300°K 8=32031
  quartz rel. to density decrease 8=26722
  quartz, resonance frequency modification, various cuts 8=35418
  rel. to reactor materials 8=29564
  s. c. r., switching with ionized rad., model 8=27165
  semiconducting devices, damage, book 8=31399
  semiconducting layer structures, fission fragment tracks 8=44487
  semiconductor junctions, computer prog. for prediction of rad. damage 8=27146
  semiconductors, bandgap depend. and related features of ionization energies 8=27065
  shock wave structure effect 8=37253
  solar cell irrad. degradation and equiv. 1 MeV e flux, computer calc. 8=24085
  swelling of irradiated fuel spheres, meas. by microradiography 8=34102
  sytalls, degree of ordering increase 8=26147
  tetrafluoroethylene-hexafluoropropylene copolymers, prod. of peroxy radicals, e. s. r. 8=43422
  thermionic diode, Xe filled, V-I characts on exposure to nuclear rad. 8=28485
  thermionic diodes, Xe-filled, nuclear-irradiated elec. props., 8=46417
  thin films, hardening during vacuum deposition 8=48965
  transistors, oxide passivated, induced surface recomb. 8=27193
  transistors, response to pulse of ionizing rad., computer prog. 8=27190
  triglycinesulphate, γ-irradiated, optical annealing investigation by e.s.r. 8=44400
  Ag, internal friction after cold drawing and irrad. at low temp. 8=48986
  Al crystal, 50 keV Al^+, Cu^+ bombard., damage obs. 8=48910
  Al, plastically deformed, u.v. prestimulation effect on exoelectron emission 8=44942
  Al_2O_3, n-damage and macroscopic props. changes, review 8=44496
  Al_2O_3 rel. to low-temp. thermal cond. 8=26722
  γ-Al_2O_3, surface defect formation and annealing adsorpt. exam. methods 8=44024
  γ-Al_2O_3, surface defect formation and annealing, exoemission exam. methods 8=44025
  $BeAl_2O_4$, chrysoberyl, n-irrad., growth obs. 8=31145
  BeO, n-damage and macroscopic props. changes, review 8=44496
  BeO rel. to Be diffusion rate 8=26722
  C_4F_2:Mn, thermoluminescent, u. v.-induced second reading 8=45261
  Co, e bombard. at 20°K, point defects, elec. resistivity 8=48914
  GaAs tunnel diode, switching by transient ionizing rad. 8=27187
  Ge etched surfaces, u. v. irradiation, rel. to charge condition 8=35901
  Ge, surface damage rel. to exoelectron emission 8=40694

Physical effects of radiations—contd
- Ge(Li) γ detectors, fast n bombard. degradation 8=42453
- Cu–Co alloys, coherency loss 8=26036
- Fe, pure, reactor irrad. effect on surface struct. and corrosion 8=30720
- H_2 foil laser irradiation, plasma production 8=29995
- H_2, solid damaged, e.p.r. obs. at 4.2°K 8=40924
- HD. solid damaged, e.p.r. obs. at 4.2°K 8=40924
- KCl, radiation-induced macrodefects 8=26711
- LiF, F band, re-irradiation and annealing behaviour between 80°K and 300°K 8=49738
- LiF, radiation-induced macrodefects 8=26711
- MgO, n-damage and macroscopic props. changes, review 8=44496
- Mo, defects, thermal stability 8=40077
- NaCl, electron bombardment at 33.5-44 keV 8=48925
- NaOH ice, γ-irrad. electron traps 8=31153
- Pd–20 at.% Si alloy, amorphization on irradiation with U^{235} fission products 8=31154
- Si detecor, pulse height defects due to nuclear collisions 8=46896
- Si, ion-bombard., amorphous phase form., temp. and channelling effects 8=48931
- n/p-Si solar cells, charged particle degradation, base resist. effects, 1-25 ohm cm 8=24092
- Si, surface damage rel. to exoelectron emission 8=40694
- Si tunnel diode, switching by transient ionizing rad. 8=27187
- Si(Li) detector, response to high-energy particles 8=46898
- SiO_2 rel. to density and colour centres 8=26722
- Te, elect. cond. of single crystal, effect of reactor irradiation 8=31393
- U alloys, n-irradiated, swelling 8=44506
- Zr polycrystals, e-irradiated, low-temp. resistivity recovery 8=31158

Physics
- See also Biographies; Books; Conferences; History; Nuclear physics; Teaching.
- relationship with math. 8=32635
- teaching, reminiscences of a professor 8=37104
- thermodynamics, distinction between "total" and "eddy" heat flux 8=41787

Physics fundamentals
- See also Cosmology; Elementary particles; Field theory, classical; Field theory, quantum; Indeterminacy; Mechanics; Parity; Probability; Quantum theory; Relativity; Thermodynamics; Units.
- analyticity, particularly in elem. particle theories 8=29023
- causality, violation by conformal group 8=32779
- causality, Zeeman theorem, algebraic analogue 8=23857
- e, elementary charge proposed variation with time laboratory test 8=28212
- laws, rel. to cosmology 8=50262
- thermodynamics, impact of Caratheodary ideas 8=41788
- time homogeneity, philosophy 8=32640

Physiology
- See also Biological technique and instruments; Blood; Hearing; Vision.
- echo direction perception 8=46207
- middle ear muscles, acoustic stimulation 8=28377
- muscle filament, structure and packing 8=28200
- rabbit psoas muscle, glycerol-extracted, filament lattice studies 8=26458

Piezoelectric oscillations
- discontinuously plated crystal, forced thickness-shear vibrs. 8=37250
- excitation of elastic waves in piezoelectric slab using electromagnetic waves 8=46157
- excitation of surface waves, optimal crystal cuts and propagation directions, estimation 8=46158
- plate modes, interferometric and Chladni figure determ. 8=41828
- plates, parallel contactless, generation of waves 8=28366
- rectangular ceramic cube, resonant props. 8=32897
- resonator system of electrodes on quartz plate, analysis 8=32896
- spring strip mounts for meas. of linear moments 8=37249
- surface elastic wave excitation by interdigital transducer 8=46155
- transducer, semiconductor of film on delay rod, efficiency 8=23956
- transient analysis in a plate of crystal class 6 mm 8=27295
- in two-phase mixture, damping and dispersion 8=40600
- in CdS, photoconductive 8=27297
- CdS, semiconducting, nonlinear theory of oscillations 8=31372
- CdSe, transient analysis of piezoèlectric oscills. 8=27295
- n-GaAs:Cu, transducer, resonance freq. rel. to diffusion coeff. of impurity (Cu) atoms 8=35491
- ZnO film on delay rod, efficiency for electromechanical conversion 8=23956

Piezoelectricity
- See also Electrostriction; Piezoresistance.
- annular disc, radial deform. rel. to gamma ray heating and appl. elec. voltage 8=31441
- coaxial transducer pin meas. of detonation velocity 8=41836

Piezoelectricity—contd
- crystal, infinite plate, vibr. wave propag. theory 8=46144
- cyclotron resonance freq. shift due to piezoelectric-polaron effect 8=40283
- dielectrics, elastic, electro-mech. interactions vel. to polarization gradient, theory 8=44893
- dielectrics, sound generation rel. to elastic oscills. instability in alternating field 8=30940
- plasma press. direct meas. by piezoelect. probe 8=30096
- probe for mechanical vibrations meas. 8=32868
- quartz, appl. to microwave mixing 8=49382
- quartz, non-linearities and isochronism defect 8=27301
- quartz, phase vel. of u.s. wave propag. 8=48724
- quartz, shock-loaded x-cut, 573°K 8=26844
- quartz shorted-guard-ring stress gauge 8=37110
- α-quartz, constant calc. using Born's theory 8=27300
- readout device for spark chamber 8=33390
- resonator having N electrodes, eqs. governing elec. behaviour 8=49383
- resonators, vibrating, neutron diffraction 8=35378
- II–VI semiconducting cpds., conference 8=31362
- semiconductors, high-elect.-field galvanomag. effects 8=31366
- semiconductors, nonlinear phonon interaction and effect on current saturation 8=31367
- semiconductor, propagating acoustoelec. high-field domain, simple analysis 8=40423
- semiconductors, sound generation rel. to elastic oscills. instability in alternating field 8=30940
- semiconductor, tech. for piezothermal-e.m.f. meas. 8=40426
- semiconductor, transport eqns. for electrons and phonons 8=27061
- semiconductor, u.s. wave amplification and current saturation, non-linear theory 8=44312
- semi-infinite rod in magnetic field longitudinal disturbances 8=40625
- semimetals, piezogalvanomagnetic effects, meas. using stress modulated Alfven waves 8=49147
- stress-pulse-activated element, secondary stresses 8=40107
- strain gauge for surface vibr. meas. 8=41804
- transducer efficiency, effect of intermediate coupling layers 8=44903
- transducers, power limitations of sonic crystals 8=46181
- transducers, thin-film, insertion loss and coupling factors 8=49380-1
- transducer. wideband for seismic modelling 8=50046
- transverse acoustic wave interacts. with cyclotron and helicon waves, in elec. and mag. fields 8=27296
- wave transformation in crystals 8=35987
- CdS film, electromech. coupling coeff. determ. from admittance meas. 8=40626
- CdS, light demodulator with u.s. amplification 8=27216
- $ErCrO_3$, and ferroelectricity, comment 8=27272
- $Ga_{0.85}Fe_{1.15}O_3$, mag. ordered, e.s.r. spectrum, external elec. field effects obs. 8=31867
- GaP, coeff. determ. from electro-optical meas. 8=41092
- $HoCrO_3$, and ferroelectricity, comment 8=27272
- n-$InAs_xSb_{1-x}$ alloys, e scatt. from thermoelec. and Hall coeff. obs. 8=35758
- n-InSb, high mobility, resonant and round trip acoustoelect. gain 8=44797
- KBr, conversion of 10 Mc/s elec. oscills. 8=35988
- KCl, conversion of 10 Mc/s elec. oscills. 8=35988
- KD_2PO_4, dielec. and electromechanical props. near phase transition 8=27275
- $KH_2AsO_4(KD_2AsO_4)$, constants temp. dependence, 20-80°C 8=49368
- $LiNbO_3$, piezoelec. effect on laser illumination 8=45203
- $NH_4H_2AsO_4$, (ADA) constants obs. 8=27298
- NaCl, conversion of 10 Mc/s elec. oscills. 8=35988
- $Pb(Mg_{1/3}Nb_{2/3})O_3$-$PbTiO_3$-$PbZrO_3$ ceramics with Ba or Sr substitutions, props. and phase relations 8=31442
- $PbTiO_3$ ceramics, coupling factors and aging rates 8=49384
- $PbZrO_3$-TiO_3 ceramics, PbO deficiency on vaporization rel to props. 8=35010
- RbH_2PO_4, dielec. and electromechanical props. near phase transition 8=27275
- SbSi compounds, props 8=49269
- ZnO, appl. to microwave mixing 8=49382
- ZnO polar crystals, from point-charge model 8=30630

Piezoresistance
- See also Piezoelectricity.
- semiconductor, meas. by cyclic stress 8=35876
- p-GaSb, dependence on stress causing activation energy change 8=44776
- n-Mg_2Sn, tensor components, 50-300°K rel. to many-valley nature 8=44800
- n-Si stress difference meas. at h.p. 8=45943
- p-Si inversion layers, and mobility anisotropy 8=27133

Piles, nuclear fission. See Nuclear reactors, fission.

Pinch effect. See Discharges, electric; Plasma/confinement; Semiconducting materials.

Pions
- absorption by light nuclei, Miyaxawas theory 8=42531
- absorption, double nucleon emission 8=38299
- charge radius calc. using current algebra, pole dominance and meson coupling constants 8=33526

Pions—contd
- conspiracy in t = o region, dynamical model 8=33661
- cosmic ray nuclear interactions, obs. of energy transfer to neutral pions 8=42730
- coupling constant, πN obtained from π^{+} photoprod. on protons 8=42527
- dose distrib. in water due to 70 MeV π beam 8=37090
- double-π charge exchange mechanism 8=33862
- e.m. mass and form factor calc. 8=42510
- e.m. radius determ. from πHe^{4} scatt. 8=33664
- energy estimation from ionization meas. in nuclear emulsions 8=47114
- exchange in n-p scatt. 8=33770
- F_{π}, constant of PCAC, Kawarabayashi-Suzuki queried 8=24595
- form factor and $\pi\pi$ diffraction cross-section from pp, $p\bar{p}$, πp, $\pi\pi$, diffraction cross sections 8=37964
- form factor calc., ρ control using O(4, 2) dynamical group 8=24768
- form factor data rel. to μ magnetic moment 8=24737
- form factor, e.m., $\pi^{\pm}$ + He scatt. Coulomb distortion obs. 8=29117
- form factor, e.m., $\pi^{\pm} + He^{4} \to \pi^{\pm} + He^{4}$ Coulomb distortion meas. 8=29118
- form factor, electromagnetic, sum rule 8=37965
- form factor from $e^{-}p \to e^{-}n\pi^{+}$ 8=37966
- form factor rel. to extended structure 8=29140
- instability effects in n-n and n-p scatt. lengths 8=24883
- $K\pi\pi$, appearance in eigenchannels with definite quantum numbers 8=24848
- mass difference calc. from Schwinger's chiral dynamics 8=24637
- mass difference calc. using Lagrangian model of $\pi - A_1$ mixing 8=24855
- mass difference, e.m., sum rule modification 8=24772
- mass difference, π^{+}-π^{0}, new form factor contrib. 8=24768
- mass difference, $\pi^{\pm}$-π^{0}, times isovector form factor, finity 8=29123
- mass, rel. to Chiral SU(2) $\otimes$ SU(2) symmetry 8=42378
- multi-partial-wave isotroplet, strong coupling 8=42507
- multipion bound states as η and σ 8=29177
- N and π e.m. radius difference 8=38055
- number in e.a.s., probability distrib. functions 8=38213
- OPE in $\gamma p \to \pi^{-}N^{*++}$ (1238) 8=37917
- OPE model for $N^{*}_{1238} \to p\pi^{+}$ from $pp \to nN^{*}$ 8=38096
- OPE model for $pp \to K^{+}\Sigma^{+}n$, 5 GeV/c 8=24913
- photoproduction amplitudes Reggeization, Lorentz invariance 8=42522
- π exchange in $K^{*\circ}(890)$ prod. in $K^{-}p$ at 10 GeV/c 8=33732
- 4π coupling constant 8=29120
- π^{-} beams, biological effectiveness 8=50464
- π^{-} beams, biological effectiveness on tumor cells 8=50465
- π^{-} by H, mesomolecule capture law 8=47739
- π^{-}, s-orbit, absorpt. by He^{4} 8=24813
- πN coupling constant determ. 8=33754
- π-π resonance, O^{+} isoscalar s-wave, review of evidence 8=24805
- $\pi^{+} - \pi^{0}$ mass difference rel. to Weinberg sum rules 8=24621
- $\pi^{\pm} - \pi^{\circ}$ mass difference, and the decays of A_1, ρ in Schwinger theory 8=24854
- **decay**
  - in baryon-antibaryon model 8=24754
  - electromagnetic, rel. to meson-electromagnetic-Dirac field interactions 8=38015
  - of K° 8=47115
  - leptonic with Weinberg sectral function sum rules 8=42508
  - π°, prod. in K^{-} interaction with complex nuclei in bubble chamber 8=25254
  - $\pi^{\circ} \to 2\gamma$ derived from N Compton scatt. 8=33663
  - $\pi^{\circ} \to 2\gamma$, $\pi \to 2\gamma$ ratio rel. to SU_3 symm. breaking 8=24769
  - π° vector-meson dominance rel. to quark field $U_6 \otimes U_6$ commutation relations 8=33662
  - π^{+} and π^{-} lifetimes, precise comparison rel. to CPT 8=42509
  - π_{l2}, radiative corrections same as for π_{e3} provided π^{0} has vanishing 4-monentum 8=24770
  - $\pi \to e\nu\gamma$, form factor, Schwinger and quasilocal terms 8=47106
  - $\pi \to e\nu\gamma$, ρ and A_1 dominance 8=29176
  - $\pi \to \gamma \to e^{+}e^{-}$ used to meas. K decay parameters 8=33698
  - $\pi \to \gamma + e + \nu$, weak vector current conservation 8=37876
  - $\pi \to l\nu\gamma$, sum rule for use in calc. decay width in $A_2 \to \pi\gamma$ 8=33726
  - $\pi \to l\nu\gamma$ and A_1-ρ-π system 8=42609
  - $\pi \to l + \nu_1 + \gamma$ applic. of Cabibbo theory 8=24753
  - $\pi \to \mu + \nu$, Feynman diagram perturbation theory 8=29121
  - $\pi \to \pi' l\nu\gamma$ subtraction of amplitude in dispersion relation 8=33726
  - radiative corrections, including strong interaction effects 8=37967
  - semi-leptonic, phenomenological model 8=24771
  - as special relativity test 8=32791

Pions—contd
- **interactions**
  - air nuclei, models for e.a.s. calc. 8=38217
  - conspiracy, contributions of evasive, conspiring Regge-pion pole for different reactions 8=37909
  - d disintegration at high energy, covariant form of Austern model 8=25006
  - d disintegration, cavariant theory from threshold to 300 MeV 8=33843
  - $\gamma\pi \to 2\pi$, for $\pi \to 2\pi$ dissociation study in nuclear field 8=29122
  - high energy cosmic ray obs. in emulsion 8=42732
  - $K\pi$, existence of κ resonance 8=24861
  - on nuclei, A_1 prod. by diffraction dissociation 8=42608
  - π^{-}, e pair direct prod. in nuclear emulsion, 16.2 BeV/c 8=33645
  - π^{-} in heavy emulsion nuclei, strange particle prod. $p_{\pi} = 17$ GeV/c 8=33837
  - π-D, absorpt., exact iteration calc. 8=33673
  - π-He^{4} double charge exchange, cross section calc. 8=33674
  - π-nucleus, low energy, review 8=29482
  - $\pi + w \to \pi + \pi$, thin d double spectral function effects 8=24680
  - $\pi^{-}n \to p\pi^{-}\pi^{-}\pi^{\circ}$, $N\pi\pi$ enhancements, 5 GeV/c 8=33676
  - $\pi^{-}n \to \{P\pi^{-}\}\pi^{-}\pi^{\circ}$, nucleon isobars, 5 GeV/c 8=33675
  - π^{-}-Xe, π^{+} production at 9 GeV(c 8=47335
  - $\pi^{+}d$, search for $2\pi^{\circ}$resonance near 730 MeV 8=42532
  - $\pi^{+}d \to pp$, Miyazawas theory of π absorpt. 8=42531
  - Regge pole trajectory for πp, $K\pi$, $\bar{p}p$ interactions with $\Delta(1238)$ prod. 8=29217
- **interactions, pion—nucleon**
  - Bethe–Salpeter amplitudes decomposed into standard covariants and invariant amplitudes 8=37848
  - Bethe-Salpeter eqn., bound-state solns. 8=42534
  - charge exchange, Regge singularities 8=29130
  - inelastic, central and peripheral, 17.2 GeV obs. 8=24783
  - non-invariance, non-compact groups corresponding to SU(4), SU(6) 8=37843
  - non-linear Lagrangian models invariant under generalized chiral groups SL(4, C) and SL(12, C) 8=24752
  - in nuclear emulsion, with d and t prod., 16.2 GeV/c 8=38099
  - π^{-}, three-prong in propane chamber, with 4 GeV/c impulse 8=47107
  - $\pi^{+}d$ at 5.1 GeV/c, dipion system, ϵ° and g quantum number search 8=29128
  - $\pi^{+}d$, search for $2\pi^{\circ}$resonance near 730 MeV 8=42532
  - $\pi^{+}n$ 4, 5, π prod. 3.29 GeV/c 8=37983
  - $\pi^{-}N$, 17.2 GeV/c, heavy nuclei surface neutron richness, K, π, prod. 8=42535
  - $\pi N \to \eta N^{*}$ (1236), O(3, 1) symmetry analysis 8=24785
  - $\pi N \to NW$, W prod. cross-section, one pion model 8=38022
  - $\pi N \to \pi\pi N$, current algebra and coupling consts. 8=42533
  - $\pi N \to \pi\pi N$ for calc. of S-wave $\pi\pi$ phase shift 8=29144
  - $\pi + N \to 2\pi + N'$, theory 8=29129
  - $\pi + N \to \rho + N^{*}$, ang. decay correls. at 8 GeV 8=24781
  - $\pi + N \to \rho + N^{*} \to N + 3\pi$, Regge-pole model 8=24780
  - $\pi N \to \omega N^{*}_{3/2}$, (1236), Lorentz pole analysis 8=37974
  - $\pi N \to VN$ and γ photoprod., γ–V analogy model 8=33666
  - $\pi + N \to V + N$, vector meson prod., conspiracy relations 8=24846
  - $\pi N^{*} \to \rho N$, superconvergent sum rules 8=24786
  - $\pi^{-}N$, nuclear emulsions in magnetic field, 3.85 GeV/c 8=37975
  - $\pi^{-}N$, production of Ξ hyperons at 4.0 GeV/c 8=24999
  - π^{-}-Xe, at 9 GeV, rel. to π° prod. 8=37973
  - resonance prod., differential cross section 8=24843
  - soft-pion calc. of low energy parameters, unitarity correction 8=24796
  - superconvergence relations 8=29115
  - transverse momentum at 17.2 GeV 8=24784
  - vector meson prod. Lorentz pole structure 8=29171
- **interactions, pion—pion**
  - $\pi\pi \to N\bar{N}$ helicity amplitude relations 8=24658
  - vector meson exchange and continuation in ang. momentum 8=29166
  - vector meson prod., Lorentz pole structure 8=29171
- **interactions, pion—proton**
  - and single-π prod. amplitude rel. to current-algebra and PCAC model anomalies removal 8=33691
  - $\Delta(1238)$ prod., π trajectory Regge-pole analysis 8=29217
  - elastic, large-angle, differential cross-section angular var. 8=29191
  - high-momentum transfer collisions, influence of resonance form., Regge model 8=29132
  - multipion prod. 4-11 GeV/c configuration probability of charges rel. to statistical model 8=33672
  - $\pi p \to N(k+1)\pi$, Satz additive quark model for cross section 8=24808
  - $\pi + p \to \pi + N^{*}$, Regge pole model, N^{*} matrix elements 8=33839
  - $\pi p \to \rho N \to \pi\pi N$, ρ shape 8=38037
  - $\pi p \to \rho N^{*}$, energy- and momentum-transfer dependence of cross-sections 8=37981
  - $\pi^{-}p$, E = 11 GeV/c, analysis of 3, 4π systems with mass around 1.7 GeV/c 8=29133
  - $\pi^{-}p$, $A_2(1300)$ region structure, 6 GeV/c 8=38035
  - $\pi^{-}p$, ρ resonance prod. and decay, 2.05-3.22 GeV/c 8=42614
  - $\pi^{-}p$, $\pi\rho$ spectrum at 6.7 GeV/c 8=37979
  - $\pi^{-}p \to \eta n$, polarization and F/D coupling of N_{γ} (2650) 8=24793

Pions—contd

- **interactions, pion—proton**—contd
  - $\pi^- p \to \eta n$, SU(3) symmetry validity 8=37852
  - $\pi^- p \to \eta^\circ n$, 10 GeV/c obs. 8=29160
  - $\pi^- p \to \gamma n$, $N^{*\circ}$ e. m. couplings determ. 8=37916
  - $\pi^- p \to K_1^\circ K_1^\circ n$, 4 and 5 GeV/c obs. 8=42357
  - $\pi^- p \to \Lambda K^\circ \gamma$ rel. to meas. of the magnetic moment of Σ°-Λ transition 8=33835
  - $\pi^- + p \to N^{*-} + \pi^+$ PCAC constraint 8=33678
  - $\pi^- p \to N^{*+}\pi^-$ at 6 GeV/c 8=37980 $\hookrightarrow \pi^- p\pi^+$
  - $\pi^- p \to n$ + missing mass, 2.12 GeV/c particle mass determ. 8=38032
  - $\pi^- p \to p + MM^-$, differential cross section rel. to momentum transfer, 11.5 GeV/c 8=37976
  - $\pi^- p \to \pi^- p\eta^\circ$, A_2^- obs., 5 GeV/c 8=38036
  - $\pi^- p \to \pi^\circ n$, differential cross sections, optical
  - $\pi^- p, \to \pi^\circ n$, $K^+\Sigma^-$, Argand diagrams, bootstrap theories and Regge poles comparison 8=42443
  - $\pi^- p \to \pi^\circ n$, Regge-pole model with absorptive corrections 8=42536
  - $\pi^- p \to \pi^\circ n$, SU(3) symmetry validity 8=37852
  - $\pi^- p \to \pi^\circ n$, 2 to 5 GeV, polarization data interpretation using interf. model 8=24791
  - $\pi^- p \to \pi^\circ\pi^\circ n$, data about s-wave $\pi\pi$ scatt. 8=42541
  - $\pi^- p \to \pi^+\pi^- n$, E = 360, 430 MeV, isobar amplitude determ. 8=29134
  - $\pi^- p \to \pi^+\pi^- n$, 8, 16 GeV/c obs. 8=29131
  - $\pi^- + p \to \pi^+ + \pi^- + n$, N^{*-}(1236) prod. ang. distrib. 8=24782
  - $\pi^- p \to (p\pi^-\pi^-\pi^+)$, $p\pi^0\pi^-\pi^-\pi^+$, $n\pi^+(\pi^-\pi^-\pi^+)$, 5 BeV/c, mass spectrum of $\pi^-\pi^-\pi^+$ 8=37977
  - $\pi^- p \to p\rho^-\rho^\circ$, 8 GeV/c, evidence for new meson resonance in $\rho^-\rho^\circ$, 8 GeV/c 8=38023
  - $\pi^- p \to \rho^- p$, 4 GeV/c, absorpt. model with one-pion-exchange 8=47110
  - $\pi^- p \to \rho^\circ n$, 4 and 8 GeV/c comparison with $\gamma p \to \pi^+ n$, Vector dominance model 8=37972
  - $\pi^- + p \to \rho^\circ + n$, vector meson dominance analysis 8=24787
  - $\pi + p \to \phi + n$ followed by $\phi \to e^+e^-$, partial width obs. 8=33722
  - $\pi^\circ p \to \pi^\circ \Delta^{++}$(1238) Regge-pole model with absorptive corrections 8=42536
  - $\pi^+ p$ at 850 MeV/c, cross section obs. 8=24792
  - $\pi^+ p$, mass dependence of small angle differential cross section, 8 GeV/c 8=42542
  - $\pi^+ p, \rho^+$ and π^+ multipion resons., 1630 and 1720 MeV 8=33729
  - $\pi^+ p$, six prong jets, principal axis analysis rel. to resons., 8 GeV/c 8=33677
  - $\pi^+ p \to K^+\Sigma^+$, parity determ. of $K\Sigma N$ 8=24995
  - $\pi^+ p \to \pi^\circ N^{*++}$ Regge pole model analysis, 2.75-8.0 GeV/c 8=47109
  - $\pi^+ p \to \pi^+\pi^-\pi^0\Delta^{++}$, 3-4 GeV/c obs., H enhancement, kinematic origin 8=37978
  - $\pi^+ + p \to p + 5\pi$, role of baryon variables at 8 GeV/c 8=24790
  - $\pi^+ + p \to p + 6\pi$, role of baryon variables at 8 GeV/c 8=24790
  - $\pi^+ p \to \pi^+\pi^0 p$, spark chamber obs. 8=28990
  - $\pi^+ p \to \pi^+ p\gamma$, isobar Δ^{++} (1236) mag. moment meas. 8=24809
  - $\pi^+ p \to \pi^+ pp\bar{p}$, 8.4 BeV/c, resonance parameters of N isobar 8=24789
  - $\pi^+ + p \to \Sigma^- + K^+$, 1145 MeV/c, Σ^- polarization determ. 8=24996
  - $\pi^\pm p$, multiple particle prod., unitary-symmetrical statistical model, >1 GeV 8=33546
  - $\pi^* p$, at 900 MeV, differential cross-sections, search for zeta meson 8=42539
  - $\pi^* p$, 2.34GeV/c, 20,000 photographs scanned 8=24788
  - $\pi^* p \to \pi^+ p\pi^\circ$, 2.34 GeV/c obs. 8=24788
  - phase shifts, I = O, review of data of evidence for O^+ isoscalar s-wave resonance 8=24805
  - resonance formation influence on basis of infinite Regge recurrencies model 8=29132
  - ten-prong, at 8 GeV/c primary π^+-momentum, ang. correlations between pions 8=42540
  - 2πexchange contrib. to K^+-p potential 8=33708
- **production**
  - charged, collision of 600 MeV neutrons with element nuclei 8=37970
  - charged pair, in γp reaction, momentum spectrum and ang. distrib. 8=42514
  - cosmic ray N induced showers, 10^{12}-10^{14} eV 8=29250
  - by cosmic ray nucleons, 10^{14} ev 8=42690
  - in decay of mesons in baryon-antibaryon model 8=24754
  - double-pion photoproduction and isobaric model below 1 GeV 8=33668
  - double π photoprod. on nucleons, expt. and theory 8=33667
  - electro-, on p, radiative corrections obs. 8=24775
  - $e + p \to e^1 + \rho^\circ + p^1 \to \pi^+ + \pi^-$, analysis for ρ° prod. 8=24859
  - $e^- + p \to e^- + p + \pi^\circ$, differential cross-section near N* (1236) reson., obs. 8=33671
  - $\gamma + N \to N + \gamma$, modified PCAC hypothesis 8=42518
  - γp reactions, multipion with associated resonances 8=33669

Pions—contd

- **production**—contd
  - $\gamma + p \to \pi^+ + n$, n polarization obs. 8=24965
  - K* decay rel. to baryon model for bosons 8=33548
  - from meson which explains double-pole character of A_2^- (1300) 8=24857
  - multipion in $\pi^- p$ interactions, 4-11 GeV/c 8=33672
  - multiple, from $\bar{p}p$ annihilation 8=24943
  - multiple soft-π, PCAC theory 8=42516
  - $p + A \to A + N + n\pi$, in emulsion nuclei 8=25218
  - by p annihilation in emulsion, momentum spectrum and angular distrib., 3 GeV/c 8=42528
  - Photo-, calc. of Δ(1236) partial amplitude 8=33840
  - photo-, general method for deriving ang. correls. 8=24687
  - photoproduction amplitude, sum rule relating to nucleon anomalous magnetic moment 8=42364
  - photoproduction and π exchange in n-p scatt. 8=33770
  - photoprod. and $\pi N \to VN$ process, γ-V analogy model 8=33666
  - photoprod., conspiracy and evasion 8=42562
  - photoproduction, conspiracy and residue 8=42517
  - photoproduction cross-sections, perturbation theory 8=42513
  - photoproduction from B^{11}, O^{16}, nuclei treated as elementary particles 8=42511
  - photoproduction, generalized dispersion sum rules and A_2 trajectory 8=42519
  - photoprod, multipole analysis 8=24773
  - photoprod., ω Regge-pole residue functions 8=37968
  - photoproduction on Λ°, supercovergent sum rule 8=42512
  - photoproduction on nucleons, Regge pole model 8=29127
  - photoprod. on p, 500-1000 MeV 8=29189
  - photoproduction Regge-pole model 8=29124
  - in pN, Ep = 20 GeV 8=29186
  - π photoprod., 6.8-17.8 GeV on protons 8=42523
  - $\pi + N \to 2\pi + N'$, theory 8=29129
  - π^- from $\gamma p \to \pi^- N^{*++}$, k via "u channel," high-energy 8=42525
  - π^-, from Cu and U by 8 GeV/c protons 8=25231
  - π^- photoprod. on H, momentum distrib. rel. to ϕ and ρ° prod., 15 GeV 8=33724
  - π^-N interaction coherent production of $\pi^-\pi^\circ\pi^\circ$, 16 GeV/c 8=42521
  - $\pi^- p \to \pi^\circ n$, 2.4-3.8, 6, 10 GeV/c $N_{3/2}$, $N_{1/2}^*$ obs. 8=29160
  - π° electroprod. rel. to γNN^* form factor, 0.05-0.4$(BeV/c)^2$ 8=33670
  - π°, from $\gamma + d \to \pi^\circ + d$, around $N_{1/2}^*$(1525) reson. 8=33665
  - π°, from 1374 π^--Xe interactions at 9 GeV 8=37973
  - π° in K^- interactions with complex nuclei in bubble chamber 8=25254
  - π°, photo, below 234MeV, multipole analysis 8=24777
  - π^+ by linearly polarized γ, apparatus and method 8=29125
  - π^+, from γ + p, 500-800 MeV cross-section obs. 8=24776
  - π^+ from $\gamma p \to \pi^+ n$, k via "channel, high-energy 8=42525
  - π^+, high energy photoproduction without conspiracy 8=24778
  - π^+, in γ + p interaction, E_γ = 165-230 MeV, differential cross-section obs. 8=29126
  - π^+ in $\gamma p \to \pi^+ n$, 4, 8 GeV/c, comparison with $\pi^- p \to \rho^0 n$ in Vector dominance model 8=37972
  - π^+ in $pp \to pn\pi^+$, 0.5-0.7 GeV, calc. confirming peripheral model 8=33744
  - π^+ photoprod., absorptive correction, 2 ~ 4 GeV 8=37971
  - π^+ photoproduction and divergence conditions 8=24760
  - π^+ photoprod, conspiracy test 8=24774
  - π^+ photoproduction, double conspiracy 8=37969
  - π^+ photoprod. on p, cross-section up to 200 MeV 8=42527
  - π^+ photoproduction, π and conspirator residues and trajectories from continuous moment sum rules 8=4250
  - π^+, slow, in π^--Xe interaction at 9 GeV/c 8=47335
  - π^+ via ρ^+ Regge-trajectory exchange 8=42611
  - $\pi^+\pi^-$ photoprod., 1-2 GeV, obs. 8=29398
  - $p\bar{p}$ annihilation, ang. dist. 8=33761
  - in p-p collisions at 0.97 GeV, 1 π prod. anal. in one-boson-exchange model 8=24920
  - in p-p interacts, and partial-wave p-p absorpts, as function of energy 8=24901
  - p-p scatt., 1 GeV, effect on $^3P_0$, $^3P_1$ absorpt. 8=24933
  - $p\bar{p} \to \pi^+\pi$, 5.7 GeV/c 8=47137
  - $p\bar{p} \to 3\pi^+ 3\pi^- \pi^\circ$, 5.7 GeV/c obs. 8=24940
  - 3π decay, energy distrib. contruction 8=24756
  - in proton nuclear reactions, 450 MeV 8=33987
  - $\Sigma\pi$ pair prod. by K^- on emulsion nuclei 8=33836
  - single-π amplitude rel. to current-algebra and PCAC model π-π scatt. anomalies removal 8=33691
  - soft, from e, ν interact., anal. using current algebra 8=42515
- **scattering**
  - Adler self-consistency condition true if π trajector a member of a conspiracy 8=29136
  - Compton, low-energy theorems 8=33606
  - e, polarization and form factor 8=24767
  - e-π, polarization effects for ultrarelativistic electrons 8=37942
  - $K\pi$ amplitude rel. to K_{l3} decay 8=29149

Pions—contd
- **scattering**—contd
  - $K\pi$, using SU(3) ⊗ SU(3) algebra of currents, π, K pole dominance, κ meson predicted 8=29158
  - lengths from $K^+ \rightarrow \pi^\circ\pi^\circ\pi^+$ and $K_2^\circ \rightarrow \pi^+\pi^-\pi^\circ$ spectra obs. 8=29135
  - light nuclei, activation cross section obs., 80-280 MeV 8=25255
  - low-energy limit dispersion theory 8=42418
  - nucleus, optical-model π form factor 8=43044
  - τ-baryon ($^1\!/_2{}^+$), in formation on Regge exchanges 8=42543
  - π-D, elastic and inelastic, exact iteration calc. 8=33673
  - πd, 0.46-2.67 GeV/c obs., π^- cross-section higher than π^+ 8=29139
  - π-d, 200 MeV, contrib. of Δ_{33} virtual isobar to amplitude 8=42544
  - π-He scatt., Coulomb interference corrections 8=29389
  - π-He^4, impulse model theory 8=33679
  - πHe^4, 129, 140, 150 MeV/c cross-neutron obs., π charge radius calc. 8=33664
  - π-He^4, 139 MeV/c rel. to final state interaction effects in ${}_\Lambda H^4 \rightarrow \pi^- + He^4$ 8=25168
  - πN vacuum exchange amplitudes from sum rules 8=33682
  - $\pi\omega$, bootstrap anal. of ρ, and B mesons 8=42615
  - π-nucleus, low energy, review 8=29482
  - π-particle, antisymm. part of amplitude = universal constant X isotopic spin of particle 8=29136
  - πp, analyticity constraints, soln. by means of resonances and Regge trajectories 8=33680
  - $(\pi\text{-}\overline{Z})_{I=0,1}$ scatt. length 8=37984
  - $\pi^-d \rightarrow 2n\gamma$ for nn scatt. length obs. 8=42648
  - π^--He^4, 8 BeV/c, cross-section 8=29230
  - $\pi^- + p \rightarrow \pi^\circ(\eta^\circ) + n$, differential cross section at high energy 8=24682
  - π^+d, elastic and differential cross sections obs. 3.65 BeV/c 8=37985
  - π^+-He, double charge exchange obs. 8=33681
  - π^+-He^4, elastic, 610 MeV/c obs. 8=24794
  - $\pi^\pm$ + He, Coulomb distortion rel. to e.m. form factor, obs. 8=29117
  - $\pi^\pm$-Pb, inelastic, neutron halo existence, 700 MeV 8=38498
  - $\pi^\pm + He^4 \rightarrow \pi^\pm + He^4$, Coulomb distortion rel. to π e.m. form factor, meas. 8=29118
  - virtual Compton scatt., use of Weinberg sum rules 8=42545
- **scattering, pion–nucleon**
  - amplitude calc. using a field theory 8=24480
  - backward, isospin violation 8=37991
  - Bethe-Salpeter eqn. solns. in ladder approx. with Padé approximants 8=47112
  - charge exchange amplitude, divergence from ρ-dominance model 8=47111
  - charge exchange polarization and Gottfrid-Jackson absorptive corrections 8=33683
  - charge-exchange polarization, $\rho + \rho'$ model 8=42547
  - charge exchange scatt., partial wave analysis of ρ Regge amplitude 8=24779
  - chiral transformations 8=24686
  - coupling const. from spin-flip dispersion relation 8=33685
  - dispersion relations, backward 180°, applications 8=42548
  - dispersion relations, subtraction by means of canonical commutation relations 8=24798
  - dispersion sum rules, agreement between Regge behaviour and low energy parameters 8=37988
  - dispersion sum rules, Cauchy calc. and expt. 8=24797
  - d waves, partial, energy behaviour calc. 8=29141
  - dynamics, rel. to asymmetric fermion Regge trajectories 8=24678
  - 4π coupling constant 8=29120
  - Glauber theory tested in π-p, π-d, 0.46-2.67 GeV/c 8=29139
  - helicity amplitude relations 8=24658
  - kinematic singularities and MacDowell symm. rel. to boson-fermion reactions 8=29047
  - Liu-Okobo dispersion relation sensitive test of low energy data 8=29143
  - near-backward, finite energy sum rule appl. 8=37989
  - nonvanishing asymptotic total cross-sections 8=37990
  - 1 and 2 π exchange contribs. compared with N-e and N-N scatt. and phase shifts 8=24879
  - phase contours below 1.4 GeV and in Regge model 8=24795
  - phase shifts up to 1600 MeV of C.M.S. from Padé approx. 8=33684
  - $\pi N \rightarrow \pi N$ amplitude lower bound, crossed-channel unitarity calc. 8=33686
  - $\pi N \rightarrow \rho N$ regularity of limit $S \rightarrow \infty, t \rightarrow o$ 8=37993
  - P_{11} amplitude, rel. to dynamical status of nucleon 8=42551
  - P_{11}, dynamical model of broken SU(3) 8=42546
  - P_{11} π-N, phase shift analysis and N*(1400) daughter pole hypothesis 8=47113
  - rel. to π and N extended structures, high energies 8=29140
  - pole branching effect 8=37986
  - Regge pole parameters from dispersion relations of superconvergence type 8=42431
  - Regge trajectories, P and P^1, props. 8=42442
  - ρ-exchange force method at high energies in many-channel formalism 8=24892

Pions—contd
- **scattering, pion-nucleon**—contd
  - spin-flip amplitude sum rule 8=42549
  - rel. to structure analysis 8=29031
  - sum rule of superconvergence type and Regge pole model 8=37987
  - sum rules, new class from dispersion theory 8=33585
  - superconvergence and bootstrap, static models 8=24684
  - superconvergence relations, analyticity constraints 8=42406
  - superconvergent sum rules and determ. of Regge trajectories 8=29138
  - s and p partial waves, accounting for short-range effects 8=42552
  - s-wave length Adlers consistency relation 8=37992
  - s-wave scatt. lengths, current algebra and $\rho + \rho'$ dominance 8=24799
  - S_{31} wave analytic expression 8=24664
  - unitary impulse approx. method 8=29142
  - vanishing momentum transfer, SO(4) symmetry 8=42550
- **scattering, pion–pion**
  - amplitude, using current algebra and condition of elastic unitarity 8=29145
  - chiral transformations 8=24686
  - diffraction cross-section and π form factor 8=37964
  - dispersion sum rules, new for testing low-energy phase-shift analysis 8=42417
  - 4π coupling constant 8=29120
  - and $K \rightarrow \pi\pi l \nu_l$ 8=29149
  - lengths, former lower bounds violated 8=42563
  - length through current algebra technique, absence of Mandelstam variables 8=24802
  - low-energy, dominated by ρ in I = 1, J = 1, f° in I = 0, J = 2 8=33692
  - mass-shell current algebra calc., scatt. lengths and effective ranges 8=24804
  - N/D equation, crossing-symmetric, solns. 8=24801
  - phase shift anomaly and $K \rightarrow 2\pi$ 8=24815
  - phase shift calc., dispersion relations 8=24800
  - phase shift information from K_{l4} decay 8=29137
  - $\pi\pi$ bootstrap model, high- and low-energy amplitudes simultaneously calc. 8=37912
  - $\pi\pi \rightarrow \pi\pi$ and $\rightarrow N\overline{N}$ amplitudes lower bounds, crossed-channel unitarity calc. 8=33686
  - $\pi^\circ\pi^\circ$ D wave amplitude below threshold 8=37999
  - π°-π°, S-wave, models based on parametrization of inverse K-matrix element 8=37997
  - p-wave resonance at 308 MeV, self-consistent, bootstrap anal. 8=42615
  - Reggeized short range potential and resonance width 8=47036
  - rel. to π extended structure, high energies 8=29140
  - review 8=33690
  - s-wave, data from $\pi^- p \rightarrow \pi^\circ\pi^\circ n$ 8=42541
  - S-wave, I = 2 amplitude sum rule, I = 0 proved small and negative 8=38000
  - S-wave phase shift determ. from $\pi N \rightarrow \pi\pi N$ 8=29144
  - s-waves, low energy scatt. 8=24803
  - sum rules for partial wave amplitudes on basis of dispersion relations at fixed momentum transfer 8=37998
  - superconvergence relations, analyticity constraints 8=42406
  - Yo(1520) $\rightarrow \Lambda\pi\pi$, scatt. length rel. to triangular diagram contribution 8=38097
- **scattering, pion–proton**
  - differential cross-sections, Regge theory appl. to backward angles other than cos 0*-1 8=42557
  - elementary length, upper limit estimation 8=24601
  - inequalities satisfied by a function of the amplitude 8=33576
  - optical model, back-scatt., E_{π^+} = 2-8 GeV 8=33974
  - p polarization obs. 8=33757
  - P + P′ Regge model, superconvergent dispersion relation 8=37994
  - π^-p, at 180°, 1.6 to 5.3 GeV/c, differential cross section 8=42556
  - π^-p charge exchange, n polarization calc. due to ρ-Regge pole and cut. 8=42427
  - π^-p charge exchange with ρ trajectory 8=37953
  - π^-p obs. at 8, 16 GeV/c, Regge-pole fit 8=37995
  - π^-p polarization parameter, 220 to 390 MeV, 70° to 180° angles 8=42558
  - π^--p, 6 GeV/c, 8 GeV/c obs. 8=42553
  - π^-p, 229-390 MeV, polarization parameter meas. 8=24812
  - $\pi^- p \rightarrow \pi^- p\gamma$, role of $\gamma 3\pi$ interaction 8=24807
  - $\pi^- p \rightarrow \pi^\circ n$, 561-2,106 MeV/c obs. 8=24811
  - $\pi^- p \rightarrow \pi^\circ n$, mean backward differential cross section prediction down to 2 GeV/c 8=42562
  - $\pi^- p \rightarrow \pi^\circ n$, secondary Regge contributions to total cross-section 8=37996
  - $\pi^- + p \rightarrow \pi^+ + \Delta^-$, modified 2π exchange model 8=42408
  - π^+p, dip u ≈ - 0.15 (GeV/c), interference of N_α, N_γ fermion Regge trajectories 8=33687
  - π^+p, 1.7–7.8 GeV/c, cross-section without Regge-pole theory 8=33688
  - $\pi^+ p \rightarrow N^+\rho^\circ$, absence of dip in differential cross section at 8 GeV/c 8=37982
  - $\pi^\pm$-p, backward, data on Regge trajectory functions N_2 and Δ_δ 8=42434

Pions—contd
- **scattering, pion-proton**—contd
  - $\pi^{\pm}p$, backward elastic, possible zero at wrong-signature sense point 8=42555
  - $\pi^{\pm}p$ backward, 1.5-3.0 BeV/c obs. 8=24806
  - $\pi^{\pm}p$, dips in differential cross sections at $t = 3\ (\mathrm{GeV}/c)^2$ at 180° at 2.1 GeV/c 8=42554
  - $\pi^{\pm}p$, elastic, 2.3 to 4.0 BeV/c, cross-sections and backward peaks 8=42560
  - $\pi^{\pm}p$ high energy bakcward scatt., data extrapolation and Reggeized baryon exchange model 8=42562
  - $\pi^{\pm}p$, 0.46-2.67 GeV/c obs. 8=29139
  - $\pi^{\pm}p$, Regge-pole analysis of backward peaks 8=24810
  - $\pi^{\pm}p$, 6-17 GeV/c, structure obs. 8=42561
  - $\pi^{\pm}p$, wide angle, 4 to 10 GeV/c, cross-sections and anal. 8=42559
  - Regge parameters, relation derived, one-parameter fit to cross-section 8=33689
  - 30 GeV. e. m. effects on cross-section 8=37952

Pitch detection. See Acoustical measurement; Hearing.

Plages. See Sun.

Planetary nebulae. See Nebulae; Stars.

Planets
- See also Solar system.
- Asteroid collisions and evolution of mass distribution, Meteoritic flux 8=50411
- asteroid, Icarus, orbit and general relativity 8=41751
- asteroids and meteoroids, mass distrib. theory 8=37007
- asteroids, classification based on Schmidt's law of planetary distances 8=32536
- asteroids, gaps in belt, periodic orbits and restricted 3-body problems 8=32404
- asteroids, growth by accretion, theory 8=28148
- asteroids, Hilda group, long-period effects 8=32541
- asteroids, photographic obs. 8=32542
- asteroids, photographic obs. (1950-62) 8=45836
- atmosphere, internal rad. field for illuminated lower surface 8=37004
- atmosphere, Lorentz absorpt. line in scatt. radiation 8=37006
- atmosphere rad., molec., continuum and line type, expt. and theory study 8=43287
- atmosphere, radiative transfer equation solution using Eddington approx. 8=50409
- atmosphere, Rayleigh scatt. Chandrasekhar's scatt. matrix new formulation 8=50119
- atmosphere, scatt., radiative transfer eigenfunction description 8=50408
- atmosphere, with reflecting bottom surface, diffuse reflection and transmission 8=37005
- atmospheres, absorpt. integral and press. var. 8=41564
- atmospheres, multiple scatt. by large particles, optically thick layers 8=50402
- atmospheres, thermal escape, transition domain in spherical geometry 8=37008
- atmospheres, thin, refractivity profile by radio occultation 8=41563
- atmospheric radiation field, two dimens., Duhamel's principle applied 8=50404
- condensation, overluminous phase of Sun 8=28147
- cores, rel. to low temp. melting of solids under very high press. 8=32535
- distances law and resonant structure of solar system 8=50393
- Earth, halo study, rel. to sunlight scatt. into shadow cone 8=41562
- formation from diffuse rotating cloud of gas and dust, possibility 8=45819
- Fourier transform spectroscopy, advances 8=50273
- Hidalgo, orbital elements 8=32543
- interiors, explicit equations for convection 8=45821
- internal radiation field, functional eqns., time-dependent monodirectional illumination 8=32534
- interplanetary flight, impulse calc. 8=32376
- Jupiter, brightness of great red spot and solar activity correlation 8=41594
- Jupiter, decametric emission rel. to solar wind scatt. 8=41588
- Jupiter, decametric emission, spaced-spectrograph obs. 8=41567
- Jupiter, decametric emission, spectral burst obs. 8=32545
- Jupiter decametric radiation, Finnish obs. 8=32546
- Jupiter, 18 MHz polarization obs. 8=32544
- Jupiter, establishment of orbiting rocket, difficulties 8=28021
- Jupiter, magnetic axis determ. from 21 cm radiations 8=28149
- Jupiter, map of radio emission, at 75 and 21 cm wavelengths obs. 8=45832
- Jupiter, millisecond pulses, spectral characts. 8=45830
- Jupiter, multicolour photoelec. photometry (1963-1965) 8=32533
- Jupiter, polarization of 6cm. radiation 8=41565
- Jupiter radio emission, var. obs. at 620 and 2650 Mc/s 8=45831
- Jupiter, radio rotation period, cyclotron theory 8=41566
- Jupiter radioastronomy, South African obs. 8=28190

Planets—contd
- Jupiter, thermal structure 8=50413
- Jupiter's great red spot and solar activity, correlation 8=45829
- Jupiter's red spot in 1965-1966, fluctuations obs. 8=45833
- Jupiter's satellite, Io, electrodynamic effects 8=37010
- light scatt., anisotropic, in atms. 8=45820
- magnetic fields as test of dynamo theory 8=50405
- mag. fields determ. from meteorite props. 8=37021
- mantles, convection 8=45822
- Mars, atm. CO_2 abundance from 1.05μ spectrometry 8=45828
- Mars, atmos. probe simulation, study of gas-cap rad. intensity 8=41569
- Mars, icecap, possible CO_2-H_2O composition, investigation of freezing and sublimation props. 8=32547
- Mars, lower atm. thermal and dynamical structure 8=41568
- Mars, Mariner 4 occultation expt., uniqueness of results 8=37012
- Mars, multicolour photoelec. photometry (1963-1965) 8=32533
- Mars, radiative equilibrium temp. distribution of atmos. 8=37013
- Mars, survey of long-term observational behaviour 8=5041
- Mars, thermal history, effects of selective melting 8=50403
- Mars, transmission spectra in 2μ region, simplified interpret. 8=37011
- Martian atmospheric entry, CN violet emission model 8=29722
- Mercury, perihelion precession, rel. to equivalence principle validity for Sun 8=50416
- Mercury, phase anomaly 8=45823
- Mercury, phase effect at 3.4 and 19 mm 8=32548
- Mercury, r.f. emission phase depend. rel. to surface layer props., O.8 cm 8=45824
- Mercury, rotational period, from computer anal. of optical obs. 8=28150
- Mercury, sidereal rotation period redetermined, photographic observations 8=50415
- Mercury, two permanent thermal bulges 8=50417
- minor, additions to list (1965) 8=32538
- minor, astrograph obs. results 8=32540
- minor, astrograph obs. technique 8=32539
- minor, photographic obs. 8=32537
- minor, photographic obs., at Sydney, 1966 8=50410
- Pluto, mass determ. 8=32549
- radar aperture synthesis, appl. 8=32616
- radioastronomy, Australian obs. 8=32610
- Saturn, gaps in rings, rel. to periodic orbits of restricted three-body problem 8=32404
- Saturn, mean disc brightness temp. 8=36920
- Saturn, microwave emission 8=50418
- Saturn, multicolour photoelec. photometry (1963-1965) 8=32533
- Saturn, rings, possible ice constituent 8=48289
- Saturnian ring structure, innermost satellite resonance effect theory inadequate 8=45834
- scattering and transmission functions for incoherent scatt. 8=42257
- solar rad. scatt. by atmos. into geometric shadow cone 8=41562
- spectra, Fourier transform digital calc., obs. 8=28788
- spectroscopy, Fourier, 4300-8000 cm^{-1} 8=32413
- USSR radioastronomical apparatus and obs. 8=32523
- Venus, atmos., and phase depend. of light polarization 8=37015
- Venus atmosphere, CO, high resolution interferometric spectra 8=50420
- Venus, brightness temp. in disc centre 8=36920
- Venus, clouds uniformity and photography 8=50423
- Venus, dense model of ionosphere rel. to radio obs. in decimeter and centimeter regions 8=28151
- Venus, elongation in June 1967, calc. from phase and disc obs. 8=50421
- Venus map, a detailed look at the feature β 8=45826
- Venus, multicolour photoelec. photometry (1963-1965) 8=32533
- Venus, new CO_2 i.r. bands 8=28153
- Venus, oxygen in atm. 8=32552
- Venus, photography using different filters 8=50422
- Venus, possibility of an indigenous biology 8=37014
- Venus, revision of Oort's const. B due to diminishing obliquity of equatorial pole 8=50376
- Venus, r.f. backscatt. rel. to surface smoothness, 40 cm 8=45825
- Venus, superadiabatic atmospheric surface layer, calc. Venera 4 obs. 8=28152
- Venus, surface temp. correction to original paper 8=50419
- Venus, thermal history, effects of selective melting 8=5040
- Venus, 3.4mm emission obs. (1965-1967) 8=32551
- Venus, upper atmosphere CO_2 photochemistry rel. to Mariner 5 and Venus 4 obs. 8=41570
- Venus, upper atmospheric temp. and hydrogen, Mariner 5 obs. 8=32550

Plasma
- See also Discharges, electric; Electrons; Ions; Space charge; Thermonuclear reactions.
- absorption of h.f. beam-generated waves 8=47885
- acceleration with e.m. travelling waves 8=30013

Plasma—contd
- accelerator with h. f. field, puffs characteristics, effect of laser preionization 8=30081
- accumulation between mixed field accelerator and pulsed mag. mirror 8=30110
- acoustic pulse propagation, low press. 8=25746
- afterglow, anomalous diffusion obs. 8=38984
- air, radiated power at high temp. 8=34509
- air, shock ionized, cold electrode I-V characts. 8=30029
- alkaline, ionised by l. f. propagation 8=47840
- arc discharge, p beam anomalous deceleration 8=39003
- arc, e beam fluctuation propag. 8=39009
- arc, thermal and elect. cond. calc. 8=29929
- asymmetrical, internal emission coeffs. calc. from externally meas. spectral intensities 8=43500
- beam instability, hydrodynamic nonlinear theory 8=43515
- beam plasma generation by nonvacuum electron beam 8=28556
- binary distrib. function and correl. energy, quantum mechanics 8=25724
- "blow-off", laser-induced, ensuing stress pulses, obs. 8=40065
- breakdown between plasma and electrode at negative potential 8=47762
- Cherenkov electron heating, quasi-linear approx. 8=30010
- classical, density-fluctuation approach 8=34462
- collisionless, co-operative phenomena and shock waves 8=30045
- collisionless, fast randomization phenomenon, exptl. evidence 8=39063
- collisionless, hydrodynamic description 8=30042
- collisionless, one-dimens. free expansion, two methods of soln. 8=43509
- completely ionized, thermodynamic functions, relativistic corrections for e.m. interact 8=39074
- compressible, radiation from annular slot, theory 8=30075
- computer model, 2 dimens., correl. time and r,m.s. E field meas. 8=34466
- conductivity, electrical, at low freqs. 8=30030
- conductivity, high-freq., of partially ionized plasma 8=34478
- conductivity in mag. field of plasma with arbitrary ionization ratio 8=34479
- containing charged cylinder, infinite, particle distribution in proximity 8=34461
- coulomb collisions, energy exchange between components 8=30021
- current carrying slab, overstable modes due to resistivity gradients 8=43521
- current layer, moving, interaction with charged particle 8=29989
- currents, stationary self-compressing, exptl. confirmation of existence 8=47825
- cylindrical discharge, traversed by current, field strength calc. 8=47820
- cylindrical pulse-stimulated emission, decaying ringing 8=25755
- cylindrical symmetry, macroscopic relative equilib. 8=34464
- degenerate, transport coeffs. calc. 8=39079
- density determ. from phase-shift in scattered radiation 8=47855
- diffusion, ambipolar → free, transition microwave meas. 8=39078
- diffusion-controlled, charge carrier distrib. obs. 8=43517
- diffusion decay with recombination, laws for different symmetries 8=30011
- diffusion-recombination equation, asymptotic integral property 8=34473
- discharge, current up to MHz 8=43450
- discharge, acoustic pulse reaction 8=34486
- from discharge, continuous reflex, for interferometric meas. in 8mm band 8=29879
- discharge, high-pressure, excited in diatomic gases, energy exchange 8=47742
- discharge, radial density var., Schottky theory verification 8=43441
- dispersion roots, transition from beam to Landau-type solns. 8=43510
- Doppler effect at electron cyclotron freq., exptl. investigations 8=47823
- double scatt. in bithermal ionosphere 8=45531
- drifting, relativistic magnetoionic theory 8=30068
- electrical cond. by circuit methods, role of capacitance between coil and plasma 8=47822
- elec. and magnetic microfield in relativistic plasma, probability distribution Holtsmarkians 8=34475
- elect. conductivity in induced elect. field, m.h.d. generator model 8=30026
- electric microfield distrib., asymptotic calc. 8=39082
- electrode layer theory in low temp. plasma 8=39081
- electron beam, charge carrier density rel. to volume and wall recombinations 8=47802
- electron clouds in mag. fields, electrostatic equilibrium 8=33074
- electron collision frequency by open plasma resonators 8=47852

Plasma—contd
- electron conc. in turbulent boundary layer calc. for weak ionization 8=30024
- electron density and temp. meas. in He discharge 8=38991
- electron-density, by reflection meas. using microwave bridge 8=39112
- electron density fluctuations in turbulent plasma 8=30172
- electron density meas. interferometers 8=30094
- electron density meas. ion current in Langmuir probe 8=39118
- electron-density profile, microwave meas. appl. to Hg-vapour discharge positive column 8=39113
- electron energies, deviations from Maxwellian distribution 8=39062
- electron momentum and energy relaxation, cyclotron echo meas. 8=47824
- electron, one dimensional, numerical expt. on nonlinear behaviour 8=43495
- electron scatt., multiple, Molière's theory 8=39076
- electron scatt., relativistic, thermodynamic Green's functions 8=34474
- electron temp. and mass flow velocity in axial discharge at high freq. 8=25688
- electron temp. meas. by line reversal method 8=39075
- electron vel. distrib. in relfex discharge, anisotropy obs. by c.w. laser scatt. 8=30012
- electrostatic cylindrical probe in combustion products behaviour 8=39120
- electrostatic wave propag. rel. to absorpt of microwaves near electron cyclotron frequency 8=39020
- emission spectra, growth curves for non-equilib. finite layers, calc. 8=43543
- energetic conditions in plasma of h.f. unipolar discharges 8=47812
- Fermi-Dirac function, tabulated for integer indices, series expansion 8=33329
- flame when gas jet is subject to electric discharge 8=38977
- flow, one dimensional, in m.h.d. energy converter channel 8=30041
- galactic, dynamics 8=50346
- gas inlet valve, electromagnetic, very quick acting, for plasma expts. 8=47935
- gaseous, u.s. wave amplification 8=39111
- gravitational instability, Jean's criterion 8=41528
- guide mode along magnetised column, field distrib. 8=47808
- guiding-centre, linear disturbance propag. and decay 8=30014
- heating, linear turbulent, expt. obs. 8=25727
- heating, turbulent, by mag. field annihilation 8=34467
- high density matter in an intense mag. field, props. 8=45601
- high-temp., in thermodynamic equilib., quantum theory, free energy in 10^6 to 10^8 °K range 8=30020
- homogeneous, electron and ion distribs. 8=47827
- homopolar, azimuthal current excited by equilibrium rot. 8=24170
- hydrogenous, mixed-phase behaviour near ionization temp. 8=39073
- IEEE Region 3 convention, USA (1968) 8=29991
- IEEE, 20th Annual Southwestern conference 8=28645
- immersed antenna, characts. 8=47836
- induced voltage for conducting ring interaction with axially symmetric mag. field 8=47829
- inhomogeneous, in mag. field, kinetic eqn. 8=43502
- interaction with e beam in weak mag. field 8=34477
- interaction with laser rays 8=39110
- ion acoustic wave reflections from negatively biased grid 8=43527
- ion-acoustic waves, ion-atom collision effect on propag. and damping 8=34487
- ion beam extraction 8=37434
- ion energy distribution and heating mechanism 8=25726
- ion heating obs. with magnetic trap in turbulent plasma 8=34561
- ion-level relaxation mechanism 8=34460
- ion-saturation currents in 2-dims. geom. of uniform density, digital computer calcs. 8=47828
- ionization during heating for short-wave radiation amplification 8=47780
- ionization equilib., effect of collisions 8=25722
- ionization rate in shock heated gases, microwave meas. 8=39014
- ionization-recombination equilibrium in a magnetic field 8=29993
- ionized, electron distrib. function in time-depend. elec. and mag. fields 8=43520
- ionized of high density production by shock waves, Mach no. over 30 8=47872
- ionized, partially, Saha eqn. 8=30006
- ionized, slightly, bremsstrahlung calc. 8=30069
- ionized, weakly, convection in nonuniform mag. field 8=34472
- ionized, weakly, electric field, effect of inelastic collisions 8=47821
- ionized, weakly, nonlinear transport props. 8=34471
- ionized weakly, shock wave structure 8=30044
- ionizing atomic, thermodynamic functions 8=25725
- kinetic eqn. for weak turbulence, with collisions 8=43497
- kinetic theory of plasma-wave motion in presence of collisions 8=30155

Plasma — contd
kinetics in uniform elec. field 8=30019
kinetics, sub-relativistic 8=30002/3
Landau pole sites 8=43498
laser beam refraction, interferometry obs. 8=43541
laser prod. for simulation of particle accel. in solar flare 8=29998
laser-produced from solid D targets 8=39064
laser production in air and air/D_2, and high-temp. meas. 8=47799
layers, continuous and stationary, artificially produced, theory 8=30005
leaky-wave beams of multiply layered plasma media 8=30049
Lorentz gas model, a.c. elec-conductivity 8=25735
Lorentzian, inhomogeneous, diffusion and conductivity tensors, non-linear terms calc. 8=30025
magneto-active, relativistic, quasilinear resonant diffusion eqns. 8=47819
magnetoionic medium, lossless, symmetry props. of dyadic Green's function 8=30076
magnetoplasma, compressible electron-ion, wave prop. 8=47842
magnetoplasma, Maxwellian and non-Maxwellian, collision freq. parameters 8=39066
magnetoplasma, radiation of microwaves 8=28600
magnetoplasma, radiation resistance of elect. dipole 8=25758
magnetoplasma, radiation resistance of insulated current filament 8=25757
magnetospheric, density, determ. by use of long-period geomag. micropulsations 8=50167
Maxwellisation by confined electroacoustic waves 8=47847
metal, laser vaporized, electron emission and dispersion 8=44940
microparticle, many-field model 8=29988
model, computer investigation of magnitudes 8=39072
molecular, ions and radials prod. 8=43493
neutralising electrons, sheath 8=43523
nonlinearity of relationship between current density and electric field strength, due to strong electric field 8=46351
non-neutral, Poisson eqn. and soln. 8=34465
optically dense, absorpt. and emission coeffs., radial distribs. 8=30078
parametric excitation from thermal fluctuation at plasma-drift wave frequencies 8=43574
particle interactions, theory 8=30017
particle kinetics, book 8=25721
perturbation, r.f., effect on e density and energy distrib. profiles 8=43519
pinch discharge., parameters for prod. of ionizing radiation 8=29930
plasma-vacuum boundary, radiation pressure 8=39105
plasmons rel. to transverse wave interactions 8=30129
populations of excited states of ions, analysis, and applic. to electron temp. and density obs. 8=30027
positive column, with change in discharge current, non-stationary process 8=25695
primeval fireball recombination theory 8=45596
probe shot noise reduction by collisions 8=43550
production, high temp. and press., using laser 8=29994
production in upper atm. by h.f. discharge feasibility 8=38978
propane-O, K_2CO_3 seeded, in m.h.d. duct, pot. distrib. and electrode voltage drop, obs. 8=39084
properties of high-current discharges 8=43440
quantum Coulomb, first order phase transitions, mech. 8=39068
quantum, pair distrib. function exchange term. 8=47807
quasi-classical, pseudopotential 8=43522
quiescent, with high electron temps., production 8=29992
radial distribution functions at zero particle separation 8=39070
radial distrib. function, quantum mechanical calc. 8=29999
radial distribution of emitters, electronic analogue for Abel inversion 8=30070
radiation and antiradiation conditions 8=47800
radiation from elec. and mag. current density sources 8=34488
radiation transport, atomic plasmas 8=34509
radiative energy transfer, conference 8=23909
radio emission, nonthermal, generation by coherent plasma waves 8=30130
r.f. radiation, photomultiplier radiometer 8=43540
rarefied from broadening of auto-model motions for quasi-neutral plasma 8=39071
ray formation during separation of electric contacts, avoidance 8=29935
reabsorption spectral line shape, multistage approach to calculation 8=30079
reflection of impulse plasma from metallic surface 8=43494
relativistic, of pregeometrical, pretensorial character 8=28327
relaxations, unified theory, physical interpretation 8=28545
resistivity, longit. rel. to enhanced transverse diffusion 8=30028
ring approximation, kinetic eqn. 8=25730
rot. in hollow cathode discharge 8=29885
scalar elec. cond. calc. at low ionized, accuracy 8=34476
scattered energetic particles, distribution function 8=43496
second harmonic generation in current density by nonuniform microwave fields 8=25734
seeded flame, conductivity meas. 8=47853
shear viscosity for Debye-Hückel plasma 8=39080
sheath round wedge excited antenna, effect on admittance 8=42033
shock-produced, electromagnetically driven, electron densities meas. by microwave reflection 8=25720
shock production, wave vel. rel. to initial gas press., drive current and mag. field 8=43529
shock wave front isomagnetic jump at critical Mach number 8=39089
shock-wave generation in rarefied gases by laser impact on Be targets 8=47833
shock wave in Ne-Li, change of sign inside shock transition layer 8=30046
shock wave of Z-pinch discharge, dynamics 8=34410
shock wave, turbulent, effect of ion wave-electron interaction 8=43528
solar-wind, turbulence, viscosity and dissipation obs. 8=45889
spark, effect of cylindrically converging shock wave 8=25745
spectra, Doppler and Stark broadening 8=30092
spectral line broadening, by electron collisions, theory 8=43157
spectral lines profile, emitted by optically thin layer 8=47846
spectral line shift obs. 8=34507
spectral line Stark broadening in strong elec. and mag. fieds 8=25340
spectral separation by fiber polychromator 8=37662
stable, and weakly unstable, kinetic theory 8=25723
Stark broadening, transition from quasi-static to impact electron contrib. 8=43158
stationary nonthermal, population of atom and ion excited levels 8=39069
statistical particle acceleration in random fields 8=46396
statistical thermodynamics 8=30009
streaming along uniform mag. field boundary effects for diffusion 8=30015
streaming in transverse magnetic field, transport and cuto-off 8=30022
streaming, radiation from oscillating mag. dipole 8=30050
stress tensor, in high freq. e.m. field and considering collisions 8=47798
structure, between plane insulating walls for arb. ratio of ion-atom m.f.p. to plasma spacing 8=30001
tail sheet in atmosphere and magnetospheric radiation belt 8=45495
temp. calc. from spectral line quadratic strength distrib. 8=47810
temperature from x-ray emission, meas. 8=30007
temperature, limit attainable, by cyclotron resonance heating in mag. mirror 8=30122
temperature meas. from broadening and shifting of spectral lines of V, Cr, Mn, Fe, Co and Zn 8=47813
temperature rising at discontinuous surface 8=47811
thermal conductivity, effects of electron interactions 8=43505
thermal nonequilib., diffusion and thermodiffusion coeffs. in stationary e.m. field 8=47817
in thermionic converter, ion current density and energy loss rate 8=28496
in thermionic converter, transport eqns rel. to spacing effects, energy losses 8=28494
θ-pinch conical discharge, cond. and temp. 8=43506
Tokamak, flux distribution of emitted fast atoms meas. by charge exchange 8=43501
toroidal weakly ionised magneto-plasma 8=30032/3
transient electron growth due to e.m. wave, intense and suddenly applied 8=43504
transient response and collision data determ. 8=25731
transport processes, eqns. 8=30018
transport processes, 2nd order contributions 8=43513
turbulent, d.c. conductivity 8=30031
turbulent heating by e.m. waves 8=47814
turbulent, transfer coeffs. 8=30023
turbulent (weakly), electron coeff. viscosity in strong mag. field 8=43514
turbulent, weakly, kinetic theory, fundamental eqns. 8=43503
turbulent (weakly), quasilinear theory including microscopic fluctuation fields and coherent waves 8=43512
uhf emission from interaction with e beam 8=30048
Vlasoc eqn. modification, relativistic 8=39065
Vlasov eqn. time reversability, one-way behaviour of Landau's solutions 8=34463
Vlasov, linearized motion and non-trivial constants 8=47816

Plasma—contd
- Vlasov, lowerbound to kinetic energy in terms of mean-density fluctuations 8=30016
- Vlasov, test charge effective potential, inverse 3rd power law 8=43499
- vortices, production of stable system 8=47826
- wave number spectrum analysis 8=47801
- in waveguide, flux deformation due to ponderomotive force 8=30105
- Z-component, correl. function convergence 8=47803
- Al, laser-induced, ion energy and abundances 8=36051
- Ar arc, excitation and ionization rel. to equilib. disturbance 8=29942
- in Ar at. beam from arc source, elec. props. 8=47545
- Ar column, ion temp., charge exchange and coulomb collision 8=39077
- Ar, dense, weakly ionized, kinetic energy exchange 8=47805
- Ar, density decay by three-body electron-ion recombination 8=47882
- Ar, disintegrating in impulse discharge, e-densities 8=43458
- Ar flows, radiating relax. 8=25741
- Ar gases, light emission on laser irradiation 8=29906
- Ar, interferometric meas. in 8mm band 8=38989
- Ar, ionization waves, characteristic pots. rel. to press. and current for three types 8=25742
- Ar, in e.m. shock tube, origin of 2 regions, from shock heating, and driver discharge 8=25714
- Ar plasma-beam discharge stimulated emission, 4545-5145Å 8=28673
- Ar, r.f., local thermodynamic equilib. obs. using emission spectroscopy 8=43508
- Ar, shock tube meas. and theory 8=34485
- ArII spectrum, line shift obs. 8=34507
- Ar-K-plasma, electron temp. meas. by line reversal method 8=39075
- Au, laser-induced, ion energy and abundances 8=36051
- CO_2 laser, influence of Xe 8=33181
- Cs, in thermionic converter, distrib. anal. rel. to electron thermal cond. 8=28495
- Cs, seeded with Ar, ion species present, relative abundance and ion signals 8=29987
- Cs, thermal, e heating in h.f. elec. field, obs. 8=30008
- Cs vapour, light emission on laser irradiation 8=29906
- Cu, laser-induced, ion energy and abundances 8=36051
- H, broadening of spectral lines of excited states 8=34505
- H, conductivities elect. and thermal, and effective current density meas. 8=43518
- H, decaying highly ionized, neutral atom density determ. by photoabsorption 8=43545
- H, dense, spectral and total radiation calc. 8=34508
- H, equations of state 8=47806
- H, formed by neutral injection, Fokker-Planck eqns. for electron and ion distrib. soln. 8=34470
- H, heating by fast large amplitude magnetoacoustic wave, investigation 8=47839
- H, ionized, equation of state determ. by Monte Carlo method 8=30000
- H-like ions in plasma, variable ionization equilib. 8=30004
- H-like ions in plasma, variable ionization equilib. alkali-like 8=30004
- H, non-thermal population densities meas. 8=29996
- H, partially ionised, non-Maxwellian deviation of fast electrons, effects on ionisation equilib. 8=47804
- H, preparation of Ge and Si layers by transport
- H, rad. below 800Å rel. to photo-ionization of H_2 8=34529
- H, radiation from flat isothermal layers, 1-100 atm, 0.6-20 eV, 0.1-100 cm 8=47837
- H, radiative decay spectra, T-tube obs. 8=30057
- H, relax. of occupied levels, considering reabsorpt. of rad. 8=34495
- from H_2 foils, laser-produced 8=29995
- H_2-He isothermal, equilib. spectra, calc. 8=43544
- He^3, disintegrating, in impulse discharge, e-densities 8=43458
- He afterglow, ion-electron recomb. coeff. 8=39038
- He, containing trace of Cs, phys. props. 8=47818
- He discharge, negative glow characts. effect of u.h.f. field 8=43453
- He, electron temp. from spectral line intensities, effects of cascading and metastable atoms 8=34468
- He, highly ionized, decay mechanics 8=43516
- He, laser ionized to 10 atm, afterglow shape, electron density and 6328Å absorption 8=34504
- He, non-equilibrium, optimum seeding with Cs 8=29997
- He, press. build-up 8=29990
- He, rad. below 800Å rel. to photo-ionization of H_2 8=34529
- He, Stark broadening of 3889 and 5016Å, obs. 8=47841
- He-Ne, afterglow, different vel. of 2s and 2p Ne 8=30080
- K, absolute density measurement 8=30093
- K, potential noise study by Q-machine 8=47891
- K-seeded non-eqilibrium, effect of bulk gas on elect. cond. 8=25732
- Li, in arc discharge, exam. from emission spectrum 8=47778
- N_2 laminar jet, mean temp. determ. 8=34469
- NO magneto-, electron energy relax. 8=47815

Plasma—contd
- Ne discharge, 2-32 mm Hg, steady state positive column 8=29899
- Ne, interferometric meas. in 8mm band 8=38989
- Ne, negative conductivity 8=25733
- SF_6 arc, transport props, from temp. meas. 8=39012
- in Xe pulsed arc, radiative and thermal energy transfer, and balance 8=39090
- Zn-Ar, in local thermodynamic equilib., 4000 to 50 000°K, composition 8=47809
- **confinement**
  - accumulation between mixed field accelerator and pulsed mag. mirror 8=30110
  - area waves in theta pinch 8=43584
  - boundary layer between warm, streaming plasma and confined mag. field 8=34520-1
  - compression leading to prod. of intense magnetic field 8=30125
  - current density rel. to mag. trapped particle equilibrium 8=43560
  - cusp injection experiment 8=47867
  - cyclotron resonance heating in mag. mirror, limit of plasma temp. 8=30122
  - discharge, electrodeless, high press., influence of mag. field on plasmoids 8=43444
  - double emitter sheath, density of trapped positive ions 8=34525
  - equilibrium in mag. field 8=25769
  - equilibrium of pinch in toroidal const. mag. field and helical h.f. mag. field 8=43597
  - flute-like mode, favourable mag. curvature, v. low density 8=34544
  - fusion reactors, pulsed, expts. 8=25288
  - galactic, by mag. fields, kinematic theory 8=41527
  - large chamber with 3.5 kGs field, characts. 8=34531
  - lens, magnetoactive, calc. 8=41986
  - magnetic mirror machines, r.f. supplemented, charged particle containment 8=39126
  - magnetic mirror, statistical particle acceleration 8=46396
  - magnetic mirror traps, motion of separate charged particles, exptl. investigations 8=47870
  - magnetic moment for linear multipoles, 1st and 2nd order corrections 8=43559
  - magnetic moment under short-wave electrostatic perturbations, comments 8=30106
  - magnetic moment under short-wave electrostatic perturbations, reply to comments 8=30107
  - magnetic rough walls, end loss reduction 8=30121
  - magnetic shielding of current feeds 8=43566
  - magnetic trap, closed, electron stochastic acceleration in a.c. field elect. 8=43563
  - magnetic trap from spherical multipole 8=47868
  - magnetic well, ion temp. gradient instability 8=34532
  - mag. wells produced by beam current, interchange instability 8=34533
  - magnetized, boundary conditions at plane electrode 8=47865
  - in microwave quasipot. 3-dimens. trap 8=30108
  - by mirror, flute oscs rel. to incoherently precessing ions 8=43565
  - mirror systems, equilibrium relation between press., current density and mag. field 8=30123
  - mirror trap, electron beam-plasma discharge instability 8=43564
  - mirror, turbulent, heating by axially driven current 8=43561
  - negative V^{11} system and its equilibrium 8=47869
  - neutral sheet stability 8=34526
  - quadrupole, linear, nonclassical particle loss, obs. 8=43556
  - rotating-field r.f. pulse generators 8=34523
  - rotating mag. field punch 8=25770
  - self-trapping and redshift of incoherent light in stellar plasma 8=45726
  - sheath, collisionless near electrode, surface effects on structure 8=30112
  - Skornyakov trap, field line trajectories 8=43562
  - snowplough model, 2 dimens. axisymmetric, current sheath dynamics 8=34527
  - stellar, self-trapping effect for line-width of red-shifted light 8=45648
  - stellarator trap, trapping in 8=34524
  - stellarator, twisted figure 8 and racetrack 8=30111
  - stochastic instability of trapped particles 8=39122
  - teaching demonstration, metal tube deform. by pulsed mag. field 8=30116
  - tennis ball seam coil field calc. and design 8=30124
  - thermonuclear fusion, problems for economic power generation 8=47367
  - theta pinch, adiabatic end loss, 8=43554
  - θ-pinch conical discharge, cond. and temp. of plasmas 8=43506-7
  - theta pinch, conical, in mag. guide field, plasmoids in nonlinear Alfven wave 8=43555
  - theta pinch device, high-temp., low mag.-field, diagnostics 8=30117
  - θ-pinch end loss, meas. using He-Ne laser 8=30115
  - theta-pinch, experimental study 8=47866
  - theta pinch field, time of H=O, peaking strip 8=39125
  - theta pinch, generation and motion of plasmoids in mag. field with mirrors 8=43557

Plasma—contd
- **confinement**—contd
  - theta pinch, ion and electron temp. meas. using laser forward scatt. 8=39114
  - theta-pinch, laser diagnostics 8=43552
  - θ-pinch, mag. field meas. by laser beam Faraday rotation 8=37583
  - θ-pinch, Scylla IV, mag. field and density integral product from Faraday rot. 8=34530
  - Θ-pinch, two-step, heating with low-energy capacitor battery 8=39124
  - θ-pinches at temps. in million deg. range, simulation of corona and solar spectra 8=39109
  - toroidal column, thin skin finite beta, hydromag. equilibrium 8=30109
  - toroidal. effect of resist. inertial forces, viscosity, and press. anisotropy on stationary equilibrium 8=30119
  - toroidal high-β plasma, equilibrium 8=30113
  - toroidal octupole, effect of field up to 360 Gauss 8=30118
  - toroidal pinches surrounded by pressureless plasma, equilibrium 8=30114
  - toroidal quadrupole and octopole configs., comparison 8=43558
  - toroidal quadrupole, levitated, fluctuations, azimuthally localized 8=30136
  - trapped particle instability, stabilization by finite orbit effect 8=39123
  - virtual electrodes in cylinder, formation and stability 8=47864
  - Z pinch, non-cylindrical, discharge development 8=43553
  - Ar, sheath, reflection of ion-acoustic waves 8=47876
  - Ba, in Q-machine, self-luminosity 8=34522
  - Cs, lifetime in Q-device 8=47871
  - H ions, high energy, nonadiabatic trapping in mag. mirror machine 8=30120
  - H_2 arc, pulsed high current, pinch effect 8=29943
  - H_2, initial plasma of θ-pinch, photo-ionized by Li filled z-pinch 8=34528
  - H_2, mag. well in coil, obs. 8=30126
  - K, in mirror mag. field, flute oscs. 8=43565
  - K, lifetime in Q-device 8=47871
  - Li filled, z-pinch, for photoionization of H_2 as initial plasma for θ-pinch 8=34528
- **devices**
  - accelerator, h.f., self consistent field and power absorption from electron cyclotron resonance 8=30184
  - accelerator, quasi d.c., with 2 disc electrodes, for injection into mag. field 8=43608
  - accelerator with inductive store 8=34567
  - arc torch, projection system for cathode obs. 8=39144
  - coaxial injector, cond. and e temp. diagnostics 8=39143
  - coaxial injector, operational conditions 8=39142
  - diocotron instability, effect of inductive and capacitive walls 8=41950
  - diode, density distribution rel. electron temp. for ionization equilibrium 8=43606
  - diode, electron-ion collective oscillations at high and low frequency 8=30127
  - diodes, low-voltage arc mode, Monte-Carlo simulation 8=43607
  - duoplasmatron, extraction and emission theory 8=24164
  - duoplasmtron, ion sources 8=46435
  - duoplasmatron source of negative tritium ions 8=46432
  - duoplasmatron source for thin film sputtering 8=48442/3
  - gun, coaxial, acceleration obs. 8=47892
  - homopolar azimuthal current excited by equilibrium rot. 8=24170
  - induction-coupled plasma for high-temp. chem. reactions, design model 8=34568
  - jet, equipped with inexpensive atomizer, improved performance 8=47894
  - jet for discharge gap short-circuit 8=39148
  - jet, interaction with mag. field, current sheet meas., 8=39145
  - jet, scattering spectrum of e.m. wave 8=47895
  - jet temp. and output rel. to current and mass flow 8=43613
  - Langmuir probe obs. of He ion diffusion and conversion 8=43449
  - m.h.d. channels, overflow currents on insulator walls calc. 8=30035
  - m.h.d. generators, plasma parameter meas., review 8=25762
  - m.p.d. thruster, spatial surveys of potential distrib. 8=39121
  - mirror, ion loss by collisions 8=30021
  - molecular ion injection type mirror device (HX), spectra of r.f. radiation 8=30061
  - multipole machine, l.f. instabilities rel. to toroidal mag. field 8=39140
  - plasmatron a.c. arc, dynamic characts. 8=29940
  - plasmatrons, plasma parameter meas., review 8=25762
  - plasmatron, vortex configuration for high current operation 8=30176
  - Q-machine, potential noise in K plasma, obs. 8=47891
  - Q-machine, single-ended with pulsed emitter 8=43611
  - source, coaxial, energy distrib. of H ions, impurity effect 8=30177

Plasma—contd
- **devices**—contd
  - source, conical, electrodynamic acceleration 8=34566
  - source, conical induction, accel. 8=30178
  - source, inductive with reduced impurity content. 8=25784
  - source of molecular ions, multimomentum 650 mA for producing trapped plasma 8=43609
  - source, vacuum apparatus for 8=30180
  - space propulsion concepts, conf. Polo Alto, (1965) 8=41480
  - stellarator, stochastic electron acceleration for low density plasma production 8=43563
  - strong current accelerator with closed electron drift 8=47893
  - theta pinch, high-temp., low mag.-field, diagnostics 8=30117
  - toroidal discharge, current, plasma turbulence due to convective instability 8=30169
  - TP-D machine, oscillations 8=39141
  - Ar h.f. burner, temp. distribution in torch 8=30179
  - Ar jet, atmos. press., test of local thermodynamic equilib 8=39146
  - Ar jet, under expanded, continuum and line rad., rel. to abs., Boltzmann and Saha temp. 8=43612
  - Ar jet, vel. distrib. meas. by BN particles 8=30181
  - Ar, r.f. source for m.h.d. expts, ballistic and spectroscopic study 8=43610
  - Ar torch, electron density in jet nozzle, from Thomson and Rayleigh scatt. 8=34517
  - Ar torch, linewidths, and transition probabilities 8=43181
  - Cs diode, ionic species identification 8=39149
  - Cs diode, seeding with Cd and Hg 8=28475
  - Cs m.h.d. arc jet, operating 4-12 kW at 1000G mag. field strengths 8=39147
  - H_2 source, action of 3cm microwaves 8=34565
  - Hg jet, supersonic, charge exchange of polarized ions 8=39039
  - N jet, temperature determ. by spectroscopic methods 8=30183
  - N_2 jet, i.r. emission spectrum 8=30182
  - Ne diode, low-voltage arc mode, predominant ionization and loss mechanism 8=47779
  - Ti source, nonlinear effects in operation 8=34569
- **electromagnetic wave propagation**
  - absorption in accelerators, with static and h.f. mag. field, rel. to density of injection 8=25749
  - alkali, microwave coherent forward scattering by acoustic waves 8=43536
  - anisotropic, 9 × 9 matrix treatment 8=30058
  - antenna admittance calc. for plasma similar to E-region of ionosphere 8=36903
  - antenna cylindrical in compressible plasma, current distrib. 8=28626
  - antenna, cylindrical monopole, current distribution, frequency effect 8=33139
  - aperture antennas, effects of plasma in near field region 8=24240
  - bounded, influence of temp. 8=47843
  - beam-plasma system, rel. to forbidden zone 8=43537
  - boundary, interaction with parallel external electron beam 8=43539
  - bounded, streaming instability of coupled longit and transverse modes 8=25752
  - bremsstrahlung, free-free, with anisotropic electron vel. distribution 8=30063
  - Brillouin scatt., applic. to ionospheric irregularities 8=41429
  - characteristic waves, interference phenomena 8=39096
  - circularly polarized, dispersion with parallel elect. and mag. fields 8=43532
  - cold homogeneous, rel. to mag. field 8=46473
  - columns, scatt. cross section calc. 8=39107
  - conductivity, r.f., basis of density and collision freq. meas. 8=43546
  - coupled e.m. and e acoustic wave eqns. 8=30053
  - coupled wave eqns for compressible electron-ion magnetoplasma 8=47842
  - current distrib. on cylindrical antenna in plasma column, expt. and theory 8=24249
  - cyclotron, emission and absorpt. in non-equilib. plasma 8=39104
  - cyclotron harmonic waves, nonlinear interactions 8=43575
  - cylinder, non-linear scattering 8=39093
  - cylindrical column, guided waves below gyro frequency 8=39092
  - cylindrical, interaction with plane e.m. waves 8=47845
  - cylindrically inhomogeneous, e.m. wave scattering 8=25753
  - demodulation of a.m. radiowaves at resonance 8=30054
  - diffraction of plane waves on ideally conducting disc in spherically-symmetric plasma 8=25747
  - dipole radiation, numerical solution 8=24248
  - dispersion eqns. for waves parallel and perpendicular to applied field 8=34491
  - electron beam-plasma system in mag. field, and linear amplification 8=39102
  - electron concentration in acoustic waves, microwave obs. 8=43526
  - electron, hot, in mirror field, microwave burst accompanying instability triggering 8=30062

Plasma—contd
electromagnetic wave propagation—contd
electron-photon Compton interactions rel. to radiation distrib. 8=39067
emitter, slotted wedge shaped, in anisotropic plasma, field distrib. 8=30073
em. oscs from interact with density modulated plasma beam 8=39094
Epstein profile across static mag. field 8=39103
excitation of optical and acoustic waves on conducting cylinder 8=47834
far field, due to incidence of supraluminous oscills. on inhomogeneity 8=34502
harmonic components. reflected from free space interface at plasma resonance 8=25750
harmonic generation in ionized slab, effect of collisions 8=43533
hot, attenuation of plane right circularly polarized waves along axial mag. field 8=34503
hot, microwave absorption near electron cyclotron freq. 8=30064
hydromagnetic waves in cold plasma, self-trapping and instability 8=43593
infinite cylindrical antenna, theory 8=37525
inhomogeneous, ion cyclotron instabilities in mag. field 8=43605
input admittance method of plasma diagnostics 8=34515
interaction, nonlinear. in constant mag. field 8=25754
ion effects in ionospheric propagation at v. l. f. (< 1.5 KHz) 8=24255
ion scatt., radial, in H_{11} waveguide 8=39108
layer, r.f. props. 8=43534
l. f. ionization of alkaline plasma 8=47840
light scatter and depolarization 8=30065
long gas discharge, microwave phenomena 8=47774
magnetic current source in plasma with half-space configuration, soln. through similarity principle 8=34498
magnetized, cold, nonlinear interaction 8=43535
magnetized nonuniformly, cyclotron resonance absorption 8=30051
magnetoactive, ellipsoidal antenna reactance 8=28632
magneto-active plane layer, transparency for obliquely incident plane e.m. wave 8=25748
magnetoionic medium, lossless, symmetry props. of dyadic Green's function 8=30076
magnetoplasma, annular slot admittance calc. 8=37523
magnetoplasma pulsed transmission 8=34493
magnetoplasma, vertically stratified, with rad. sources in layered medium 8=42034
magnetosphere, guidance along field aligned stratum 8=32262
microwave cond. in mag. field, particle-orbit theory 8=39083
microwave diagnostics 8=34490
microwave noise emission by gas discharge plasma 8=25756
microwave scattering from plasma column in rectangular waveguide 8=43531
microwaves. refraction. obliquely incident on plasma slab 8=34496
nonequilibrium, radiant energy loss, method for ang. and freq. integrations 8=34489
nonlinear anisotropic time-dependent, transverse wave 8=34500
nonlinear resonance, localized e. s. mode, calc. 8=47838
partially-filled coaxial line, analysis 8=42028
in plasma waveguide, wave amplification rel. to electron beam passage 8=24233
pressure anisotropy effect 8=34492
radiation characts. of pulsed discharge plasma in vacuum 8=29883
radiation from column, pulse stimulated 8=25755
radiation, radial intensity distrib., determ. 8=39095
radiative transfer, rel. to atomic transitions, spectra line shapes and collisional rates 8=39099
r. f. rad. from high-energy molec.-ion injection type mirror device 8=30061
re-entry transmission using modulated electron beam device, simulation 8=36906
reflection and refraction in homogeneous mag. fields 8=43538
reflection and transmission, parallel polarizations 8=34499
reflection from moving layer placed in stationary mag. field 8=30059
reflection, inhomogeneous layers 8=43530
refractive index, effective 8=25751
refractive index eqn., relativistic 8=30068
resonant scatt. by structures and body scatt. in medium 8=37495
scattering by cylindrical irregularity in ionosphere and exosphere 8=45520
scattering by field aligned columns, homogeneous cylindrical 8=30056
scattering by inhomogeneous cylinder 8=47844
scattering by inhomogeneous plasma ellipsoid 8=30072
scattering by warm enclosed cylindrical plasma 8=47835
scattering from inhomogeneous collisionless plasma 8=39100
scattering of plane wave by piece uniform plasma with a zero layer 8=30071

Plasma—contd
electromagnetic wave propagation—contd
self-trapping and self-focusing 8=39098
stability, linearly polarized wave travelling perp. mag. induction 8=34501
stellar, dispersion relation 8=41528
surface wave over thin layer on perfectly conducting ground plane 8=30055
surface waves on column, nonlinear excitation 8=30077
surface waves on columns, anomalous attenuation, explanation 8=39097
symmetric body in cylindrical plasma, radiation pattern 8=24238
synchrotron radiation prod. by electrons, growth rate derived 8=34497
Thomson scatt., continuum theory 8=39091
transformation and scatt. in strong elec. field 8=30060
travelling 10^9Hz, nonlinear interaction with ionic sound waves 10^4Hz 8=30047
turbulent, effective dielec. tensor 8=30074
vacuum u.v. rad. at temps > 20 000°K, spectral anal. rel. to astrophys. 8=39109
Vlasov, relativistic, dispersion relations 8=30066
warm drifting, refractive index for oblique incidence 8=30067
in waveguide, cylindrical, filled with isotropic plasma with slowly varying electron density 8=39106
waveguide excitation of slab, time harmonic analysis 8=28618
in waveguide, gap coupling and appl. to amplifiers 8=42024
waveguide, hollow plasma, characts. 8=24235
waveguide phased array, radiation in anisotropic plasma 8=24239
waveguide refl. coeff. meas. 8=30052
Ar, shock ionized in mag. field, microwave attenuation 8=29960
Ar, shock-prod. skin-depth effect of microwave reflection and transmission 8=25743
Bi, magnetoplasma, u.h.f., propag. vel. 8=49124
$CO_2 : N_2 :$ Ar mixture, meas. of rad. from shock heated stagnation zone, rel. to Martian probes 8=41569
Cs discharge, radiative energy loss 8=34494
H, at 10^5°K, optical emission from α particle and Fe ion slowing down 8=43542
H, dense, spectral and total rad. calc. 8=34508
H, reabsorpt. of rad. rel. to ionization and recomb. 8=34495
H + 10% He, at 5×10^4 K, optical emission from α particle and Fe ion slowing down 8=43542
magnetohydrodynamics
acceleration using inhomogeneous static mag. and h. f. electromag. field 8=30036
adiabatic invariant, nearly periodic Hamiltonian systems 8=28251
axial current, modulated, energy loss calc. 8=34482
behaviour in presence of pulsed or steady magnetic mirrors 8=34481
boundary between stream and dipole mag. field 8=43511
boundary characts. in ducts, influence of flow core boundary conditions 8=30038
channels, overflow currents on insulator walls calc. 8=30035
coaxial flow, 2D, finite conductivity effect 8=30040
cold, hydromagnetic waves, reductive perturbation method 8=43524
collisionless anisotropic, hydromag. wave propag. 8=34484
collisionless anisotropic, jump conditions for finite discontinuities 8=34480
collisionless, hydrodynamic equations, strong mag. field equivalence to m.h.d. equations 8=30042
convection, low press., heated underneath 8=39087
cumulation near zero field line 8=39085
dispersion relation, effect of neglecting Hall term in generalized Ohms. law 8=25739
electric discharge, self-sustained, in supersonic gas flow in transverse mag. field 8=25740
e.m. wave interaction, nonlinear, in constant mag. field 8=25754
energy converter channel, one dimensional flow 8=30041
flow-past profiles, relativistic 8=24183
Friedrich diagram considering Hall effect 8=25736
gyromag. separation constants behaviour 8=25737
gyroradius fluid eqns., finite, guiding centre derivation 8=34483
induced voltage for conducting ring interaction with axially symmetric mag. field 8=47829
inert gases, in generator, prod. of plasma with electron temp. > gas stagnation temp. 8=37448
instability, electrostatic-hydromag. cross stream, propag. perp. to mag. field 8=43601
instability for drift across mag. field 8=30174
instability due to ion temp. gradients 8=30163
magnetospheric, wave instabilities in non-neutral plasma-beam system 8=27942
motion and cavity formed by corpuscular flux incident on a line current 8=25728
m.p.d. thruster, spatial surveys of potential distrib. 8=39121
positive column, diamagnetism 8=34411

Plasma—contd
  magnetohydrodynamics—contd
    power extraction from high speed flow through mag. field 8=24082
    quasi-linear theory of shock-wave thickness 8=30045
    Shafranov-Kruskal instability in discharge, h.f. stabilization 8=39139
    sheet, Alfven speed, infinite diffusion limit of flow 8=30034
    shock wave with conductivity jump 8=33119
    solar wind, magnetized, free molecule flow in lunar vicinity 8=37058
    stability of cyclinder rel. to penetration depth of circular polarization mag. field 8=25782
    tennous flow in mag. field 8=47831
    theory, Maxwell-Boltzmann treatment 8=39086
    waves, non-linear, possibility of driving by transverse secular mag. field 8=39088
    waves in cylindrical column 8=47830
    waves, reductive perturbation method for nonlinear propag. 8=32679
    Ar in generator channel entrance, stabilization time 8=30037
    Ar, linear pinch discharge, acceleration by propag. current sheet 8=34415
    Ar II, arc, e. temp. meas. 8=43525
    BaO$_2$ for ionization enhancement in m.h.d. channel 8=30043
    He, flowing, magnetoacoustic waves 8=25738
    He, in T-tube, flow deceleration in transverse mag. field, obs. 8=47832
  measurement technique
    afterglow, very low e. density meas., microwave diagnostics 8=47848
    antenna input admittance rel. to properties 8=34515
    charge exchange meas. of emitted fast atoms flux distribution 8=43501
    coaxial injector, cond. and e temp. 8=39143
    collision frequency, by analysis of prop. phase constant of T.E.M. wave 8=39116
    correlations determ. by photon counting 8=39115
    correlator, high speed 8=34506
    density and collision freq., from r.f. cond. meas. 8=43546
    density and temp. fluctuations by optical spectroscopy 8=25759
    density fluctuations rel. to diff. coeff. by freq.-swept, one-bit digital correlator 8=47854
    density, spatial distribution from e.m. phase shift 8=43549
    electrical cond. by circuit methods, role of capacitance between coil and plasma 8=47822
    elect., thermal props., momentum, pressure, radiation review 8=30092
    electron-beam probe, influence of secondary electrons 8=30100
    electron collision frequency by open plasma resonators 8=47852
    electron collision freq., effective, spatial distrib. determ. by microwave method 8=25764
    electron densities, using 337 μm CN laser interferometer 8=47856
    electron density, by analysis of prop. phase constant of T.E.M. wave 8=39116
    electron-density, by reflection meas. using microwave bridge 8=39112
    electron density profiles from laser scatt. 8=30082
    electron-density profile, microwave meas. appl. to Hg-vapour discharge positive column 8=39113
    electron density, using gas laser in a homodyne arrangement 8=25761
    electron temp., by He spectral line intensities, effect of plasma conc. 8=30084
    electrostatic probe in combustion products, new technique 8=39119
    harmonically resonating rf, microwave scattering technique 8=39101
    homogeneous, r. f. diagnosis 8=34510
    homopolar, velocity profile of components 8=30086
    interferometer with colour film for electron density meas. 8=30094
    ion and electron temp. meas. in theta pinch using laser forward scatt. 8=39114
    ion-density probe, flat-plate 8=30098
    jet, e density by laser interferometer 8=30085
    jet, pulse, spectroscopic diagnostics 8=34511
    Langmuir probe for electron-density meas. in very low density plasma, ion-current collection mechanism 8=39118
    Langmuir probe, high-impedance with capacitive coupling 8=47858
    Langmuir probe, spherical, charact. of ion collection in drifting Maxwellian distribution 8=25765
    Langmuir probe, transient response at low press. 8=30097
    Langmuir probe, Xe discharge ~ mTorrs 8=30104
    laser diagnostics of theta-pinch plasma 8=43552
    laser, He-Ne, meas. θ-pinch end loss 8=30115
    laser scatt. for meas. of ion temp. 8=39114
    m.h.d. generators and plasmatrons, review 8=25762
    manometer, pulsed, for gas press. in mag. field var. direction and magnitude 8=43548
    microwave beam investigation of turbulent plasma 8=30172

Plasma—contd
  measurement technique—contd
    microwave cavity, freq. shift meas. 8=28604
    microwave diagnostics 8=39117
    microwave diagnostics, from interaction of e. m. waves and plasma 8=34490
    microwave field point meas. method 8=47851
    microwave, for nuclear reactor power monitoring 8=47432
    microwave phasemeters, p. c. m., review 8=30087
    noble gas, high press., temp. and electron density 8=43547
    piezoelectric probe for direct press. meas. 8=30096
    potential determ. by RF probe 8=25766
    probe, cylindrical, free molec., theory rel. to surrounding sheath 8=34519
    probe, electrostatic, characts. 8=47859
    probe, electrostatic, natural vibration freq., elec. field effect 8=47860
    probe, elliptic, resistance in uniform mag. field 8=30102
    probe, hot Langmuir, characts. 8=30103
    probes, inductive loop, elect. 8=30092
    probe, influence of e attachment 8=34518
    probe, spherical, ion collection expt. 8=43551
    probes, three symmetrical, generalization to plasmas with high potential gradients and densities 8=25767
    pulsed discharge simulator 8=34399
    radar interferometric width determ., turbulent column 8=47857
    r.f. impedance probes 8=36854
    refractive methods, interferometry, Schlieren and shadograph photography, Faraday-rotation, review 8=34516
    resonance in harmonic generation process, microwave scattering technique 8=39101
    resonance probe, boundary theories 8=30095
    resonance probes, impedance 8=47861
    Rogovskii loop for current of nsec duration 8=47850
    satellite mass-energy spectrometer for space ions 8=32563
    seeded flame, conductivity meas. 8=47853
    shock tube temperature, by X band rectangular waveguide probe 8=30091
    spectroscopy, multichannel Fabry-Perot with Fresnel lenses 8=30089
    spherical electrostatic probe in stationary weakly ionized plasma, asymptotic theory 8=30101
    Stark and Zeeman transient shifts, Fizeau interferometer meas. 8=30088
    streaming, ion and electron temp. and density using asymmetrical probe techs. 8=47863
    striations, moving, potential var. meas. 8=30083
    temperature from light depolarization 8=30065
    temperature, 5000°-50 000°K, spectral determ. 8=34513
    θ-pinch, mag. field by laser beam Faraday rotation 8=37583
    u. v. emission lines Doppler breadth, multichannel Michelson interferometer 8=30090
    volume recomb. coeffs. from atomic flux emergence 8=47849
    X-band (3cm) interferometer using 90°unbalancing, for electron density decay 8=25763
    Ar, jet, electron density from Thomson and Rayleigh scatt. 8=34517
    Ar jet velocity distrib. use of BN particles 8=30181
    Ar II magnetoplasmadynamics arc, electron-temp. using relative line intensities 8=43525
    Al electromagnet with portholes 8=46384
    Be, created by laser beam, e. density profile by interferometry 8=25760
    Cs. Langmuir probe meas., technique 8=30099
    D ion component from differential n spectrum 8=34512
    D pulse discharge, inverted spectral lines for temp. 8=29895
    D, temp. meas. by escape velocity 8=34514
    H emission energy spectrum 2 keV-1 MeV, meas. and display 8=38646
    HF resonant probes, theory and practice 8=47862
    He, electron temp. from relative line intensities, effects of cascading and metastable atoms 8=34468
    He reflex discharge, e-density and temp. meas. by cw Ar$^+$ laser light scattering 8=38991
    in Hg vapour discharge, Langmuir paradox in electron energy distribs. 8=34419
    Xe discharge, ~ mTorrs, Langmuir probe suitable charge range 8=30104
  oscillations
    acoustic waves, energy density 8=47878
    Alfvén wave prod. due to decay instabilities of helicons 8=40277
    Alfvén waves, compressional, propag. below ion cyclotron freq. 8=30146
    Alfven waves, excitation of red and violet satellites at instability 8=47883
    alkali-vapour arc, at anode 8=43461
    area waves in theta pinch 8=43584
    azimuthally localized fluctuations in levitated toroidal quadrupole 8=30136
    beam-generated waves, absorpt. in inhomogeneous plasma 8=47885
    beam-plasma bounded system with sharp interface between 2 media, small amplitude 8=43590
    bulk wave mode excitation, Fourier soln, inhomogeneous wave eqn. 8=30131

Plasma—contd
- **oscillations**—contd
  - coherent waves excitation and nonthermal r.f. emission prod. 8=30130
  - collisionless, non-isothermal 8=30042
  - cyclotron harmonic waves, nonlinear interactions 8=43575
  - dispersion rels. for longit. and transverse wave propag. perp. h.f. elect. field 8=43571
  - drifting in mag. field, wave propag. 8=30149
  - drift waves in weakly ionized plasma 8=30135
  - echo at upper hybrid resonance, obs. 8=25778
  - echo, collisional damping on free streaming motion 8=25777
  - in electric field, external 8=43567
  - electron beam excited, nonlinear interaction obs. 8=30157
  - electron cyclotron harmonics excitation with anisotropic temp. 8=43589
  - electron cyclotron resonance, anisotropic energy distribution 8=43568
  - electron radial current with varying velocity, instability and amplification 8=43581
  - electron, Vlasov and Poisson eqn. soln. for linear confining potential 8=34548
  - electron, wave amplitudes associated with particle phase mixing, Landau decrement 8=34550
  - electron waves, spatially growing 8=47873
  - electron-ion and electron-hole, in constant elect. and mag. fields 8=43576
  - electron-ion collective, simultaneously at high and low frequency 8=30127
  - electrons, resonant, in large amplitude wave, nonlinear effects 8=43569
  - of electrostatic field, due to electron beam heating 8=43573
  - electrostatic, in cylindrical shell, excited by electron beam with helical trajectory 8=34552
  - electrostatic, linearized theory, integral eq. treatment 8=30142
  - excitation by e current 8=30133
  - first-order orbit theory of rotational discontinuity 8=30137
  - flute instability in presence of elec. field 8=43598
  - flute instability with uncompensated space charge 8=39130
  - flute-like mode, favourable mag. curvature, v. low density 8=34544
  - flute oscs in mirror field, rel. to incoherently precessing ions 8=43565
  - flute perturbations in h. f. e. m. field, stability 8=34558
  - flute, resonance interaction with ion Larmor drift 8=43585
  - gas-discharged plasma, resonance in mag. field 8=39128
  - heated, pierced by monovelocity charged particle flux 8=43580
  - h.f. wave generation by electron beam-plasma instabilities 8=47884
  - hybrid, lower, parametric microwave excitation 8=25772
  - hydromagnetic, excitation by helical p stream 8=39131
  - hydromagnetic stability, book review 8=25780
  - inhomogeneous warm magnetoplasma with uniaxial press., eqns. for waves 8=47880
  - inhomogeneous warm, strongly magnetized, wave theory formulation 8=47877
  - interaction of two waves, coupled mode theory 8=32681
  - interaction with modulated beam in mag. field 8=34542
  - ion-acoustic, propagation and damping 8=47879
  - ion-acoustic, soliton waves 8=30154
  - ion-acoustic waves following sudden applic. of elec. field 8=25729
  - ion acoustic waves, large-amplitude, propag. and damping 8=25771
  - ion acoustic waves near and above ion cyclotron freq., damping 8=30151
  - ion acoustic wave, parametric reson. 8=34545
  - ion-cyclotron, excitation in elect. field, kinetic theory 8=30148
  - ion-wave echoes from reversible nature of collisionless damping obs. 8=25774
  - ion waves, longitudinal, dispersion near and above plasma freq. 8=30152
  - ion wave propagation, harmonics 8=47874
  - ionized, acoustic waves, correl. obs. 8=43570
  - ionized weakly, eqn. for mode amplitudes 8=34471
  - ionized weakly, plasma in constant elect. field 8=30134
  - Landau damping, effect of collisions 8=30138
  - Landau electrostatic space-charge waves, theory and expt. 8=43588
  - linear dispersion, quasi-linear theory 8=43582
  - linear isotropic theory, analogy of classical elasticity 8=34538
  - linear waves, quasi electrostatic, low freq., in mag. field 8=30156
  - longitudinal and transverse in an elect. field 8=30171
  - longitudinal waves excited in inhomogeneous magnetized plasma slab 8=30128
  - longitudinal waves in single component two-stream plasma instability conds. 8=25781
  - l. f., in plasma column, effect of radial elect. fields 8=34539
  - magnetoplasma, boundless, longit. e. oscills., uncoupled theory validity 8=43572
  - microwave, spatial distrib. of intensity, from electron beam interact. with plasma 8=39127
  - moving plasma, surface wave spectra and growth rate calc. 8=34534
  - nonadiabatic behaviour 8=30139
  - non-linear development and settling of initial disturbances 8=39129
  - non-potential, instability effect of current 8=34559
  - non-uniform, turbulence and instability 8=34554
  - non-uniform, with finite pressure 8=25775
  - normal modes of nonuniform plasma 8=30141
  - parametric amplification 8=30144
  - parametric excitation from thermal fluctuation at plasma-drift wave frequencies 8=43574
  - parametric excitation of coupled waves, plasmon-photon interaction 8=43587
  - parametric excitation of ion waves 8=43577
  - periodic struct., helicon propag. theory 8=35793
  - from plasma interact. with density modulated plasma beam 8=39094
  - quasi-longitudinal oscills. and virtual longitudinal wave interacting 8=30150
  - quasi-monochromatic wave inhomogeneous, energy transfer 8=30132
  - radiation-induced nonlinear resonance, calc. 8=47838
  - resonance modes rel. to changes in initial electron distrib. and temp. 8=25773
  - in semiconductors, effect of calc. field and energy dissipation law 8=40276
  - small-amplitude, in bounded beam-plasma systems, inc. collisions 8=34540
  - soliton formation from perturbations 8=34535
  - spectrum of magnetoplasma, effect of neutral impurity levels 8=30140
  - supraluminous, far field e. m. radiation due to incidence on inhomogeneity 8=34502
  - surface wave at interface between 2 plasma media, in presence of charged particle beam 8=34541
  - surface waves of plasma with finite 'longit temp. ' of electrons 8=25776
  - surface waves in uniform collisionless plasma, associated e. m. field 8=34537
  - supraluminous, astrophysical implications 8=41529
  - three-dimensional disturbances in cold plasma 8=43578
  - three-dimensional hydromag. distrubances in cold plasma 8=43579
  - Tonks-Dottner resonances, h. f. and l. f. coupling 8=30147
  - in TP-D machine 8=39141
  - transverse wave-wave interactions in terms of emission of plasmons 8=30129
  - turbulent, scattering of external e. m. waves 8=47881
  - u. h. f. field damping model 8=34536
  - Vlasov, in magnetic field, eigenvalue theory 8=47875
  - Vlasov nonlinear eqn., exact stationary wave soln. 8=34549
  - wave echo 8=34547
  - wave motions, effect of collisions 8=34551
  - waves and mass rotation in gas-fed hollow cathode arc 8=29926
  - waves, electrostatic, analysis using Krook-type collision integral 8=30155
  - waves high frequency, excitation by low frequency waves 8=43586
  - waves in multicomponent beam plasma 8=30159
  - waves in multicomponent Vlasov plasmas 8=30158
  - waves, ion cyclotron harmonic, excitation by perp. injected electron beam 8=34546
  - waves, nonlinear, with arbitrary electron vel. distrib., in mag. field 8=30145
  - waves, non-linear hydromagnetic, propagating along mag. field 8=30153
  - wave transformation into e.m. wave at plasma-dielectric interface 8=43583
  - Ar, damping and reflection of ion-acoustic waves 8=47876
  - Bi, magnetoplasma waves, u.h.f., propag. vel. 8=49124
  - C arc, magnetized, l.f. oscills 8=25779
  - Co, ion acoustic waves amplitude oscills., obs. 8=34543
  - Cs, non-isothermal, ion-sound oscills., in h. f. elec. field, obs. 8=30008
  - K, flute oscs in mirror mag. field 8=43565
  - Xe, damping of ion-acoustic waves 8=47876
- **stability**
  - Alfven waves instability, excitation of red and violet satellites 8=47883
  - anisotropic, transverse instability due to attraction of microscopic current elements 8=43603
  - beam instabilities rel. to particle acceleration, effect of mag. field inhomogeneities 8=43592
  - cold, with relativistic electrons, synchrotron instability, kinetic theory 8=39133
  - collisionless-plasma drift mode in multipoles, theory 8=30162
  - collisionless, thermodynamic rel. to dynamic stability 8=30170
  - cyclinder, rel. to penetration depth of circular polarization mag. field 8=25782
  - cylinder in discharge, h.f. stabilization in longit. mag. field 8=39139
  - in cylindrical wave propag. in collisionless, magnetized, self-gravitating plasma 8=30143

Plasma—contd
stability—contd
decay instability of electron wave into lower and upper hybrid freqs. 8=30160
diffusion, density and temp. fluctuation of neutral meas. by optical spectroscopy 8=25759
discharge, l. p. in transverse mag. field 8=34404
drift-cyclotron instability of plasma in inhomogeneous h. f. field 8=34562
drift-dissipative instabilities, theory 8=47889
electric field effects on weakly ionized plasma 8=30171
electron beam, critical current 8=34557
electron beam-plasma system two stream instabilities control by modulation, obs. 8=43599
electron cyclotron instability, second azimuthal mode 8=34552
electron, hot, in mirror field, microwave burst accompanying triggering 8=30062
electron, loss-cone, effect of temp. 8=43602
equilibrium of pinch in toroidal const. mag. field and helical h.f. mag. field 8=43597
flute instability at confined boundary influence of imperfect boundaries 8=23923
flute oscillations in presence of elec. field 8=43598
flute perturbations in h. f. e. m. field 8=34558
gas lasers, influence of instability in operation 8=46574
general plasma equilibria, formal theory 8=30161
helical instability of hollow column in mag. field with shear 8=30175
helical waves, excitation in positive column 8=34414
h.f. magnetic field effect, on instabilities 8=39132
high-freq. flute-like instabilities in multicomponent plasma 8=30166
hydromagnetic, book review 8=25780
hydromagnetic-electrostatic, cross stream, propag. perp to mag. field 8=43601
hydromagnetic equilibrium of thin skin finite beta toroidal column 8=30109
hydromagnetic waves in cold plasma, self-trapping and instability 8=43593
inhomogeneous, instability induced by thermonuclear reactions products 8=25783
inhomogeneous two-stream instability 8=30165
instabilities, analysis using Krook-type collision integral 8=30155
instability, balloon compensation in toroidal system 8=34560
instabilities due to electron beam interact., form. of h.f. waves 8=47884
instabilities due to two-lumped vel. distrib. across mag. field, computer expt. 8=30173
instability for drift across mag. field 8=30174
interchange instability, low-freq. limit 8=30167
of ion-acoustic waves, if amplitude of solitons exceeds critical value 8=30154
ion beam interacting with rarified gas 8=28580
ion cyclotron, convective and absolute in mirror machines 8=30164
of ion cyclotron modes in mag. field, rel. to inhomogeneity 8=43605
ionized weakly, in nonuniform mag. field, mode amplitude and freq. shift 8=34472
ionospheric, l.f., theoretical discussion 8=45527
with isotropic vel. distrib. function, not Maxwell, unstable to small perturbs. 8=39137
Larmor radius and collisional effects on combined Taylor and Kelvin instabilities in composite medium 8=43596
longitudinal disturbance, theory 8=39135
l. f. interchange instability in "average minimum-B" config. 8=34555
magnetic drift, collisionless, with field curvature and non-uniform temp. 8=43591
in magnetic field, radial, as e cyclotron frequency approaches plasma frequency 8=30022
magnetic mirror trap, electron beam-plasma discharge 8=43564
magnetic moment under short-wave electrostatic perturbations, comments 8=30106
magnetic moment under short-wave electrostatic perturbations, reply to comments 8=30107
mag. trapped particle equilibrium rel. to current density 8=43560
magnetic well, ion temp. gradient instability 8=34532
mag. wells produced by beam current, interchange 8=34533
magnetized, rel. to ion temp. gradients 8=30163
magnetoactive, moving inhomogeneities, lifetime and spreading 8=36840
Maxwellian, second-order perturbation, computer expts. 8=43595
modes, overstable, in current carrying slabs due to resistivity gradients 8=43521
moving plasma, oscillation spectra and growth rate calc. 8=34534
moving striations in positive columns, origin 8=47748
multipole machine, l.f. instabilities rel. to toroidal mag. field 8=39140
neglected, involving bounce resonance 8=47890
non-potential oscillations, effect of current 8=34559
non-uniform, oscillation and turbulence 8=34554

Plasma—contd
stability—contd
occurrence in relatively weak fields 8=47887
plasmoid, ion-cyclotron instability 8=47886
resonant interchange mode, nonlinear evolution 8=30168
sheaths in mag. field 8=34564
soliton formation from perturbations 8=34535
stationary configs, near cylindrical, conds of hydromag. stability 8=39138
strongly inhomogeneous plasma, influence of finite "temp" upon stability 8=34553
synthetic, longitudinal stability 8=34563
theta pinch, generation and motion of plasmoids in mag. field with mirrors 8=43557
toroidal, stationary equilibrium theory including resistivity, inertia and viscosity 8=47888
toroidal, effect of resist. inertial forces, viscosity, and press. anisotropy on stationary equilibrium 8=30119
toroidal high-β plasma, equilibrium 8=30113
toroidal pinches surrounded by pressureless plasma, equilibrium 8=30114
toroidal, resistive instabilities obs., 8=39136
trapped particle instability, stabilization by finite orbit effect 8=39123
turbulence due to electron beam interaction, u. h. f. emission spectrum 8=30048
turbulence in high-current toroidal discharge due to convective instabilities 8=30169
turbulent, amplitude fluctuation of microwave beam 8=30172
turbulent, ion heating investigated with magnetic trap 8=34561
turbulent, weakly, kinetic-theoretical approach to fluctuations 8=39134
two-component columns, drift instabilities 8=43604
two-stream instabilites 8=43600
two-stream instability for longit waves 8=25781
Ar-Co, ionization instability in crossed elec. and mag. fields, obs. 8=34556
Ce, density perturbations, propag., 8=43594
Plasma diagnostics. See Plasma/measurement technique.
Plasma diodes. See Electricity/direct conversion; Electron tubes; Plasma/devices.
Plasma guns. See Plasma/devices.
Plasma in solids. See Crystal electron states/plasma; Electron gas; Semiconductors; Solids.
Plasma jets. See Plasma devices.
Plasma sheath. See Plasma/confinement.
Plasma thermocouples. See Electricity direct conversion; Plasma/devices.
Plasma torches. See Plasma/devices.
Plasma waves. See Plasma/oscillations.
Plasmoids. See Plasma.
Plasmons. See Crystal electron states/plasma.
Plastic deformation
See also Slip.
anelasticity theory due to glide-dislocations motion 8=48943
anti-plane strain, relax. round sharp groove rel. to fracture initiation 8=32766
austenitic alloys, effect in physical props. during ageing 8=35699
beams, indeterminate, elastoplastic analysis under reverse loadings 8=37135
α-brass, effect on absolute thermopower 8=31447
α-brass, single and bi-crystals, rel. to stress corrosion cracking 8=26799
clamped beam with end constraints, permanent deform., anal. as system of one deg. of freedom 8=23838
clamped beams, expt. study of permanent deform. with and without constraints against axial motional ends 8=23839
compression, between parallel plates 8=23852
concrete slabs, reinforced 8=41728
creep theory, contact problems 8=41713
crystals, real, elasto-plastic deform. stages, classification 8=26756
cubic yield condition for compressible bodies 8=48961
clyinders, load limit rel. to geometry 8=28272
cylindrical shell, orthotropic, stability to axial compression, external press. and bending moment 8=32752
cylindrical shells, buckling with increasing load 8=41721
cylindrical shells, dynamic pulse buckling under lateral press., theory 8=32712
damping, correction to critical strain amp. 8=48957
damping recovering, comment on used Granato-Hikata-Lucke eqn. 8=48956
diaphragms, square, bulging and failure under hydrostatic press 8=37155
discs rotating, solid or with central hole, work hardening material 8=26762
elastic-plastic medium, elastic wave propagation 8=23935
extensible circular arch with axial forces, finite deforms 8=41719
f. c. c. crystals, dislocation structures, kinetics 8=31067
fracture, nature in relation to total potential energy 8=26768
front propagation in traction, velocity parameters 8=32768

Plastic deformation—contd

- glass-plastic under plane-problem conditions 8=49023
- graphite, creep strain effects on microstructure at 2500°C 8=44163
- hydrostatic ring test for strain meas. 8=35619
- ice, effect of H disorder 8=35569
- ideal material, plane strain extrusion through concave dies 8=23850
- kapron (nylon), necking and orientation effects 8=31248
- Lüdens front number effect on yield point 8=32767
- metals, max. shears after pear-shaped method of cold-welding 8=37099
- metals, mechanism dependence on strain and temp. 8=26629
- metal polycrystals, rel. to ferromag. resonance 8=31811
- metal, yield-stress curve and working props. 8=40087
- α-Nylon 66, cryst., (010) [100] slip mechanism, obs. 8=40199
- plates, circular, variable thickness, creep bending 8=37153
- polycrystals, ductile-to-brittle transition, effect of solute elements and temp. 8=31177
- polyethylene, molecular mechanism 8=44615
- polyethylene, oriented, texture changes rel. to twinning, slip and phase tranforms 8=35137
- polymers, local strains theory 8=31235
- pulse-loaded rate-sensitive structs., dynamic response 8=41806
- rigid-plastic annular plate under dynamic loads, deflections 8=41811
- rigid-plastic clamped beam, with end constraints, interact. anal. of permanent deform. 8=23837
- shear forming, build-up and diametral growth control 8=48955
- shell cylindrical, of ideal plastic material 8=46062
- shells, long, cylindrical, subject to uniform pressure and ring force 8=41665
- shell, spherical, under large deflections 8=32758
- shock resistance of metals, effect of deformation speed 8=41714
- in soils, soft, volume and shear deform. rel. to shock waves 8=40109
- stamping of plate with rigid stamp, charge limits theory 8=35620
- strain analysis, iterative methods, convergence 8=41730
- superplastic diaphragm, theory and expt. 8=28269
- torsion, of hollow cylinders, length change rel. to texture 8=44523
- transformer steel, change of blast-furnace structure in mag. field 8=40153
- viscoelastic media, eqns. of three-dimens. deform. 8=28275
- viscoplastic cylindrical shell, buckling due to impulsive load 8=32770
- yield point loading criterion, optimum 8=32753
- yielding behaviour of mats and structs., class of one-dimens. models 8=23835
- yielding of V-notched tension bars with circular ccts 8=32762
- AgCl, rel. to strains and dislocations 8=26662
- Al alloy, yield surfaces, prestraining effect, exptl. study 8=40127
- Al crystal, rel. to u.s. propag. 8=31191
- Al, during very high speed cutting 8=44539
- Al macrocrysts., grain boundary props., EPMA-Kossel obs. 8=30856
- Al, oxide coated, rel. to photostimulated exoelectron emission, obs. 8=36039
- Al, rel. to exoelectron emission, photostimulated, temp. effect 8=44943
- Al, rel. to exoelectron emission, pre-stimulated by u.v. or electron bombardment 8=44942
- Al rods and tubes, annealed, waves, exptl. data 8=40126
- Al sheets, local effects on fatigue crack growth rate 8=35652
- Al, stored energy measurement showing recovery stages 8=26784
- Al-4%Cu, by cold rolling, effect on $\theta' \to \theta$ transform. 8=48371
- Al-Mg alloys, yield stress effects on prismatic dislocation loop diam. and density 8=40033
- Al-NbAl$_3$ dispersion phase alloy, 20-450°C 8=44546
- AlSb, rel. to dislocation slip and twinning 8=44443
- Al 78 wt. % Zn alloy, superplastic, and dislocation climb. 8=44538
- Au, quenched, rel. to vacancy clustering 8=31045
- Au$_4$V, ferromagnetic, rel. to mag. disorder 8=27399
- CdS, influence of light 8=35670
- Co, hexagonal, rel. to dislocation arrangement 8=48853
- Cr, effect on Néel temp. 8=45055
- Cu alloys, rel. to Hall constant changes, order and stacking fault energy 8=44689
- Cu crystal, n-irradiated, radiation hardened, critical shear stress temp. and strain rate dependence 8=31196-7
- Cu crystals, macroscopic localization, during alternating torsion 8=44567
- Cu, effect on absolute thermopower 8=31447
- Cu, effect on yield surfaces 8=44564
- Cu, neutron irradiated, cyclic deformation 8=26801
- Cu, n-irradiated, rel. to active crystal length in yield region 8=40054
- Cu-Ni alloys, affected volume and temp. rise in discontinuous slip 8=40147

Plastic deformation—contd

- Cu-Ni alloys, internal stresses rel. to work hardening 8=31194
- Fe, cold, rel. to post-diffusion of C at 350°C 8=35490
- Fe, effects on X-ray diffr. line intensities, with and without annealing 8=35332
- Fe, polycrystals, magnetic after effect rel. to plastic deform. 8=36143
- Fe, rel. to X-ray diffr. line intensity changes 8=44166
- Fe, rolling textures rel. to deformation mechanism and sample orientation 8=26820
- Fe-Cr alloys, cold, rel. to post-diffusion of C at 350°C 8=35490
- Fe-Cr alloys, effect on hydrogen permeability temp. dependence 8=35489
- Fe-Ni-Ti alloys, effect on physical props. during ageing 8=35699
- Fe-Pd alloys, rel. to structural transforms and mag. props. 8=35102
- Fe-Si alloys, cold, rel. to post-diffusion of C at 350°C 8=35490
- Ge, epitaxial, effect on packing defects 8=31099
- Ge, p- and n-doped, rel. to prod. of p-n junctions 8=44835
- n-Ge, rel. to acceptor level position 8=35891
- KBr, effect on F-centre thermal stability 8=35586
- KCl, by dislocation motion, with charge flow 8=35961
- KCl, effect on F-centre thermal stability 8=35586
- KCl, rel. to dislocation structure formation 8=31080
- LiF crystals, and annealing rel. to thermal conductivity 8=30989
- LiF, on pressure sintering rel. to densification 8=35070
- LiF, quenched, translations slipping mechanism 8=26828
- LiF, rel. to dislocation structure formation 8=31080
- LiF, rel. to pt. defect formation 8=44403
- Mg, textured rel. to anisotropy 8=44587
- MgAl$_2$O$_4$ spinel, rel. to stoichiometry, along slip system {110} <110> 8=31216
- MgO, on pressure sintering rel. to densification 8=35070
- NaCl crystal, rel. to u.s. propag. 8=31191
- NaCl, effect on F-centre thermal stability 8=35586
- NaCl, effect on photothermal stability of F-centres 8=35590
- NaCl, on pressure sintering rel. to densification 8=35070
- NaCl, rel. to acoustic n.m.r. 8=44320
- Nb crystals, yielding and slip at room temp. 8=26696
- Nb, rolled, orientation distrib. of crystallites 8=35275
- Ni alloys, effect on Curie point and magnetization 8=40823
- Ni, strongly deformed, onset of uniaxial anisotropy after mag. annealing 8=36216
- Pb cylindrical bars, elastic-plastic deform. pulse propag., 8=44596
- Pt, effect on defect production and recovery 8=39997
- Pt-1at%Co(Fe) alloys, effect in elec. and mag. props. and Mössbauer spectra 8=31327
- Si, by indentation and scratching under light load 8=40180
- Si, rel. to parallel arrays of pure edge dislocations 8=40044
- Ti, mechanism rel. to impurity obstacles 8=44604
- α-Ti, 0-600°K, mechanisms 8=49057
- Ti-8% Al, mechanism rel. to impurity obstacles 8=44604
- TiNi, rel. to shape memory effect at 90°C, and martensitic transform. 8=30707
- in WC-Co alloy fracture, rel. to microstructure 8=26851
- WC-Co alloys, particle dispersed system, recovery processes 8=44606
- Zn crystals, on alternating torsion, macrolocalization characteristics 8=35726
- Zn macrocrysts., grain boundary props., EPMA-Kossel obs. 8=30856
- Zn, rel. to twinning and slip by indentation at 5 kg loads 8=31056

Plastic flow

See also Rheology.

- alkali halide crystals, yield pressure dependence 8=44550
- α-brass, incubation period at start of flow obs. 8=31200
- α-brass, surface hardening, preferential, in early stage II 8=40145
- coagulation structures, solid-like, thixotropically hardened, viscosity 8=40090
- fracture, generalized pyramidal, and yield criteria 8=41712
- h.c.p. polycrystals, ductile-brittle behaviour theory 8=26757
- ice, as mech-for rate of decrease of surface area 8=35073
- at indentation of rigid punch with smooth bases, solution with envelope of slip lines 8=32759
- plane rapid flows, polar-like 8=32760
- plane rapid, with polar-like vel. fields 8=32761
- plastic-viscous conductor, vel. profile of motion through slot in mag. field 8=37446
- steel, age-hardened containing γ' precipitates, tensile yield mechanism 8=49014
- steels, strain-aged, discontinuous yielding grain-size dependence 8=26809
- strip and sheet bending at large deform. exceeding elasticity interval 8=23842
- surface, rel. to crystal symmetry 8=26761
- visco-, circular cylindrical shells 8=28277
- yielding of axially symmetric bars, non-symmetric V-notch 8=32756

Plastic flow—contd
Al, ductile-brittle transition in presence of Hg-3% Zn or Sn-10% Zn liq. 8=35656
Al, ductile-brittle transition temp., in liq. metals, strain-rate depend. 8=35657
Al-Mg alloy, yield point phenomenon 8=40123
Al-Mg-Zn alloy, precip.-free zone effects 8=26785
Be, h.c.p. polycrystals, ductile-brittle behaviour theory 8=26757
Cu, ductile deformation mode, anomalous X-ray transmission exam. 8=26648
Cu, single crystals, flow stress, temp. dependence 8=40142
Cu, surface hardening, preferential, in early stage II 8=40145
Cu whiskers, thickness depend. of behaviour 8=40148
Fe, pressurized, yielding phenomena 8=31206
Fe, stresses, effect of annealing after wet H treatment 8=49018
Fe whiskers, flow, 4-300°K 8=49032
Fe-21%-Cr-0.05%C alloy, ductile fracture mechanism, 20-600°C 8=26819
Fe-3%Si, and critical shear stress and plastic flow 8=44568
$KCl:Ba^{2+}$, yield pt. rel. to Ba^{2+} impurities 8=31079
Mo, creep properties at 650-750°C 8=35707
Pb, polycryst., under simple shear, rel. to grain size and deform. 8=35713
Ta-Re alloy, yielding, rel. to conc. and temp. 8=40182
Th, effect of C content on flow stress 8=44603
Ti circular diaphragm, rel. to anisotropy 8=35720
TiX, (X = Fe, Ni, Co or combinations), relative ductilities 8=26848
Zn circular diaphragm, rel. to anisotropy 8=35720

Plasticity
See also Viscoelasticity.
beam on elastic foundation with moving load, nonlinear effects 8=41652
beams, inderterminate, elastoplastic analysis under reverse loadings 8=37135
beams, perfectly plastic, bending, class of complete solns. 8=41726
diaphragms, rectangular, bursting strength under hydrostatic press. 8=37154
dislocation statistical theory appl. 8=26654
dissipation function in theory of plastic media with strain hardening 8=46059
dissipative function model 8=32754
ductility, workability of metals 8=26758
elastic-plastic problem, analytic method 8=41723
elastic-plastic problems, plastic stress-strain matrix appl. 8=28258
elastic-plastic string, transverse vib. for different plasticity conds. 8=32751
elastoplasticity contact problem 8=37152
equilibrium of revolution in purely coherent heavy medium 8=32765
ethylene-propylene copoymer single cryst. mats. ductility, obs. 8=44616
granular material, moving step load on surface of half-space 8=41711
longitudinal shear crack with infinitely narrow plastic zone 8=46061
Lüdens front number effect on yield point 8=32767
metals, b.c.c. or h.c.p., ductility and fracture rel. to alloying solutes 8=31189
metals, f.c.c., by meas. viscosity of wire samples 8=31169
necking in homogeneous test bar 8=32764
plane flows, polar-like rapid 8=32760
plane rapid flows, with polar-like vel. fields 8=32761
plane states of nonhomogeneous media 8=32757
plates, circular, optimal plastic design 8=37158
plates, fibre-reinforced, under rotationally symmetric conditions, analysis 8=37157
polyethylene, ductility rel. to mol. chain mobility, $\leq$ 40 000 psi 8=44620
polymers, linear amorphous, rel. to fracture theory 8=31249
polymers, linear, high, by meas. viscosity of wire samples 8=31169
polytetrafluoroethylene, ductility rel. to mol. chain mobility, $\leq$ 60 000 psi 8=44620
pressure limit of nozzles, analysis 8=32763
punching inhomogeneous half-plane, kinematic solution 8=41715
radial nozzles in spherical pressure vessels, shakedown loads 8=32750
relaxation around sharp groove in surface of body deforming under anti-plane strain 8=32766
rigid bodies, relations on surface of discontinuities of stress 8=48962
rotating disks, elasto-plastic analysis 8=46044
shell of ideal-plastic, cylindrical, loading 8=46063
shells, thin, classical theory 8=32755
spherical sandwich shells, subjected to hydrostatic press, stress dual 8=41720
steel, austenitic stainless, He injection rel. to ductility loss, 540-760°C 8=31213
steel, e bombard. effects, 2.5 MeV 8=35694

Plasticity—contd
steel, mild, annealed, rimmed, effect of prior cold reduction on ductility 8=26817
step load moving with superseismic velocity on surface of elastic-plastic half-space 8=32749
strain analysis, iterative methods, convergence 8=41730
strain theories for singular loading surfaces 8=41716
stress-strain relations, statistical theory 8=40104
tensile specimen of rate-depend mat., anal. of time variation of strain grads. 8=23851
theory appl. to flow patterns of granular mats. in axisymmetric rotor 8=43884
theory, w.r.t. theory of continuously distributed dislocations 8=46060
viscoelastic-plastic media, nonlinear class of constitutive equations of rate-type 8=32771
viscoplastic cylindrical shell, buckling due to impulsive load 8=32770
viscoplastic fluid stability, analogy with Grad fluid stability 8=47905
viscoplastic plates, rigid, impulse loading 8=41725
viscoplastic rods, impact, strain analysis, nonlinear 8=41724
viscoplastic solid, linearized theory 8=41722
viscoplasticity, flow of circular cylindrical shells 8=28277
viscoplasticity, fundamental problems, bibliography 8=28274
yielding behaviour of mats and structs., class of one-dimens. models 8=23835
yielding of axially symmetric bars, non-symmetric V-notch 8=32756
Zircaloy tubing, tensile type, influence of texture on anisotropy 8=26853
zone due to thermal stress in infinite solid containing penny-shaped crack 8=37156
Al-Al_2O_3, influence of grain size on high-temp. ductility 8=26779
Al-60Zn alloy, superplasticity, struct. depend 8=48990
Be and alloys, microstrain rel. to slip 8=44554
Co, hexagonal, rel. to dislocation arrangement 8=48853
Cr, brittle-ductile transition temp., effects of N conc. and Cr_2N precipitates 8=44561
Cr, deformed under hydrostatic press., rel. to struct., $<$ 18 kbar 8=35562
Mo, deformed under hydrostatic press., rel. to struct., $<$ 18 kbar 8=35562
Mo, hydrostatically-extruded, ductility 8=35706
Mo, hydrostatically extruded, ductility rel. to annealing effects 8=35705
Ni, pure, superplasticity 8=31224
Sn, white, single crysts., rel. to slip instaility, obs. 8=40181
Ti sheet, anisotropy and flow behaviour of circular diaghragm 8=35720
Ti sheet, slip and crystallographic interpret. of anisotropy 8=35721
Zn sheet, anisotropy and flow behaviour of circular diaphragm 8=35720
Zn sheet, slip and crystallographic interpret. of anisotropy 8=35721

Plastics
See also Polymers.
adhesion bond strengths with ice, correl. with phys. and chem. props. 8=31215
aging problems 8=44612
counter, scintillation, appl. for primary cosmic rays 8=47186
electrets, surface charge characts. 8=44892
epoxy resin, reinforced, internal stresses 8=31243
epoxy resins for magnet coil insulation, radiation damage, obs. 8=31159
ferrite-loaded thermoplastic magnets, props. 8=24111
foam, for one shot shock absorption, vibration characts. 8=44514
glass-reinforced, creep in bending 8=31241
glass-reinforced, deformation, stress-strain relations 8=31236
glass-reinforced, long-time strength in oil 8=31239
glass-reinforced, press. distrib. in moulding 8=31240
graphitoplastics, mech. props. 8=31247
increased transparency, for scintillation counters 8=46882
ionomers, physical structure 8=30796
mechanical strength, scale and temp. effects 8=31238
Perspex dosimeters, photosensitivity 8=37792
plastic-oil composite dielectrics 8=40558
plexiglass, creep 8=31250
plexiglass, electron-irradiated sheets, electrical discharges 8=29876
resin reinforcement with alumina fibres, breaking strength and elastic modulus 8=26857
scintillation counter, Kr diffusion 8=35499
scintillator, large area, simulated showers photography 8=38119
scintillator NE 102A, 5-100μ thickness meas. from refr. index dispersion 8=32043
scintillators, mixed 8=49829
scintillator, response to electrons 8=46884
scintillator, transient nonlinear response to electron irradiation 8=46865

Plastics—contd
  solid-plastic dispersion system, fluidity 8=34938
  structures, free vibrations 8=28263
  tape, for detection of shock waves 8=23944
  thermoplastics, torsional creep meas. 8=35624
  track detectors for cosmic rays 8=38117
  vinyl, dispersion and absorption of transverse waves 8=49069
Platinum
  adsorption of CO, i.r. spectrum 8=48488/9
  anode, varnish deposit, elect. characts. 8=49916
  anodic films, ellipsometry 8=27754
  chemisorption of propane, effect of pre-adsorbed water 8=27738
  corrosion in autoclave liners during hydrothermal crystal growth reactions 8=49855
  damage rate meas., by electron irradiation 8=31155
  defect production and recovery, plastic deformation and Au substitution effects 8=39997
  electrical-decoration of Si surface for e.-microscope exam. 8=40496
  electrical and thermal cond. c.f. Ag 8=30987
  electrode, Ag nuclei form. 8=49948
  ellipsometric investigation of anodic films 8=41282
  Fermi surface, effective mass 8=40250
  film, resistance change due to CO adsorption 8=49169
  films on W, structure, work function and adsorpt. of Cs 8=35178
  films, sputtered, oriented growth 8=44049
  films, thermal treatment effect on props 8=44698
  ion microscope tips smoothing by field evaporation, 10 and 78°K 8=39708
  n-irradiated hardening 8=35716
  liquid, interact with transition metal carbides, rel. to their decomposition 8=27715
  magnetic-moment meas. vs field and temp., rel. to exchange enhancement 8=31526
  optical functions deduced from reflectance data 8=45216
  paramagnetic susceptibility calc. 8=49483
  powder, isotopic exchange of O_2 8=41236
  proton beam interactions, K_2^c, γ prod. obs. 8=33709
  quenched, polyhedral voids and prismatic dislocations, e- and field-ion-microscope exam. 8=31086
  radiography using channeled α-particles rel. to defect obs., 8=48830
  surface, appearance of Na, K impurities 20-1100°C 8=35549
  surface ionization of alkaline halide molecules 8=36062
  surface, Na atom ionization coeff. absolute meas. 8=31476
  surface, reflection of molecular beams, at different temps. 8=25668
  temperature meas. using metal ribbon X-ray furnace 8=32978
  thermal cond. and elec. resistivity, 100 to 900°C 8=48763
  thermionic emission of Na^+, K^+, oxide reaction effects 8=35549
  thermometers, resistance, sensitivity 8=28428
  vacancies, divacancies and impurities, thermal quasi-equilib. 8=48813
  wires, thermionic props. 8=36061
  X-rays, ultra-soft, absorption, experimental and theoretical study 8=25364
  Pt^{195} in rare-earth-Pt alloys, n. m. r. rel. to conduction-electron polarization 8=36279
  Pt^{4+}, luminesc. in octahedral complexes 8=36505
  Pt-Ge contact catalysis of germane thermal decomp. 8=32123
  Pt/Pt-10% Rh thermocouple, accuracy of calibration 8=46267
  Si-supported, i. r. absorpt. of adsorbed CO 8=30773
Platinum compounds
  alloys, electronic structure rel. to band structure of pure metals 8=31294
  Magnus' Green salt analogues, semiconductivity 8=40480
  $K_2[Pt(N)_6]$ structure 8=26402
  Pt-ammine complexes, far i.r. spectra 8=43330
  Pt dithizonate in CCl_4, nonlinear abs. of light, positive and negative saturation effects 8=34856
  Pt(II) complex of ethylenediaminedithiocyanate C- and N- substituted, i.r. spectra 8=43329
  $PtAs_2$, n.m.r. of As^{75} and Pt^{195} 8=49655
  PtC, spectrum 8=25513
  PtCo alloys, surface charge distrib. rel. to field ion image formation 8=27366
  Pt-50% Co alloy, uniaxial mag. anisotropy induced by tempering under stress 8=31702
  Pt-Co ordered crystals mag. props. rel to crystallite distrib. (texture) 8=36175
  Pt-1 at% Co(Fe) alloys, elec. and mag. props. plastic deformation effects 8=31327
  Pt-Co(Fe) alloys, local-moment saturation from n.m.r. obs. 8=31527
  Pt-Cu alloys, thermodynamic props. of formation 8=27714
  Pt_3Fe alloy, hyperfine interaction constants from nuclear sp. hts. 0.15-1°K 8=31504
  Pt_3Fe, ordered, mixed antiferromag. ferromag. state 8=31789
  Pt-Ir alloys, n.m.r., meas., susceptibility, Knight shift 8=40998
Platinum compounds—contd
  Pt-Mn alloys, atomic structure and ferromagnetism 8=26432
  Pt-Mo alloys, Pt-rich, n. m. r. of Pt^{195} and satellite structure 8=27513
  PtO_2, synthesis and props. 8=35205
  PtP_2, n.m.r. of P^{31} and Pt^{195} 8=49655
  Pt-Pd alloys, n.m.r. of Pt^{195}, spin susceptibility 8=40998
  PtSb evaporation at 900°C and Sb vapour species determ. 8=30608
  $PtSb_2$, preparation, semiconducting props. 8=40479
Pleochroism
  aliphatic ketones, dichroic ratio 8=32045
  circular dichroism rel. to rotatory dispersion, expt. verification 8=41044
  dichroism, magnetic circular and optical rotatory dispersion meas., applic. 8=33257
  magnetic circular dichroism, meas. apparatus 8=27615
  magnetic circular dichroism, theory 8=27542
  metal complexes, mag. circular dichroism 8=27616
  metal complexes, mag. circular dichroism, interpretation 8=27614
  metal halide complexes, mag. circular dichroism 8=27615
  nucleoside derivs, circular dichroism studies rel. to chem. substitution 8=43434
  poly-L-alanine in soln., u.v. circular dichroism 8=43824
  poly-L-serine in soln., u.v. circular dichroism 8=43825
  polynucleotides, circular dichroism, theory 8=29865
  quartz, smoky, anomalous, rel. to atomic structure 8=27608
  $[(C_6H_5)_3FC_4]_2$ isomers, dichroism 8=39642
  n-Ge, dichroism of microwaves due to hot electrons 8=35903
  $IrBr_6^{2-}$ complexes, mag. circular dichroism 8=49730
  $IrCl_6^{2-}$ complexes, mag. circular dichroism 8=49730
  KCl, mag. circular dichroism rel. to R centre transitions. 8=48874
  Lif, magnetic circular dichoism of R′ centre 8=48878
  $RuBr_6^{3-}$ complexes, mag. circular dichroism 8=49730
  n-Si, dichroism of microwaves due to hot electrons 8=35903
Plexiglas. See Plastics.
Plutonium
  atom, configuration-interaction integrals 8=38679
  cooperative electron transition at 66°K, evidence 8=44632
  fuel for thermal reactors 8=47402
  hemispherical emittance, effect of surface cond. and temp. 8=30993
  Ignition behaviour 8=45353
  microcracks elimination by chill casting and heat treatment 8=31228
  reactor fuel, liquid, viscosity, heat of fusion and melting 8=47407
  α-Pu, microstructs. formed at press. over 30 kbar, by thermal treatmetns 8=35281
  Pu-Be (α, n) sources, n yield increases 8=47428
  Pu^{239} in irrad. samples, non-destructive assay, Pb spectrometer 8=36650
  Pu^{239}, diffusion in α-Al_2O_3, meas. by α-absorpt. method 8=35480
  Pu^{239} fission cross-section rel. to spin and energy 8=34049
  Pu^{240} Auger effect, L_2-subshell yield obs. 8=38715
  $Pu^{3+,4+}$ in CaF_2, optical spectrum 8=31968
Plutonium compounds
  alloys, binary, ignition behaviour 8=45353
  alloys, corrosion of Ta container, O, N impurity effect 8=47412
  alloys, liquid viscosities 8=39330
  alloys, phase diagrams 8=35080
  Pu-α-Be calibrated 4.43 MeV γ source 8=37925
  δ-Pu-Ba alloys, elastic consts. and specific heats below 300°K, temp.-depend. 8=44598
  PuC_2, high temp. sructure by X-ray diffraction 8=44196
  Pu-Co-Ce liquid metal in Ta container determ. of Ta mass transfer 8=47420
  $Pu(C_2O_4)_2 . 3H_2O-Th(C_2O_4)_2 . 2H_2O$, mag. susceptibility 8=36073
  PuF_4 neutron source, spectrum obs. 8=42650
  PuF_6, electron diffr. and molec. struct. 8=38858
  Pu-Fe alloys, electron-probe microanalysis of Fe 8=36647
  Pu-Ga alloys, electron-probe microanalysis of Ga 8=36647
  δ-Pu-Ga alloys, interdiffusion coeff. obs. 350°-517°C 8=35504
  Pu-3.3at.% Ga alloy, growth of large crysts 8=26263
  PuO_2, magnetic susceptibility 8=40753
  $Pu^{238}O_2$ neutron spectrum 8=34099
  PuO_2, thermal conductivity from diffusivity measurements 8=35463
  PuP, thermal conductivity and ht. capacity 8=44368
  PuS, thermal conductivity and ht. capacity 8=44368
  Pu_3Zn_{22}, crystal structure 8=26433
  $(U, Pu)O_2$ solid soln. production and Pu distribution 8=29562
Pockels effect. See Electro-optical effects.
Point defects. See Crystal imperfections.
Point groups. See Crystal structure, atomic.
Poiseuille flow. See Flow; Hydrodynamics.
Poisson ratio. See Elastic constants.
Polar cap absorption. See Electromagnetic wave propagation/ionosphere.
Polar cap glow. See Airglow.

Polarimeters
- automatic electronic, for 350-700 nm, ZEP66 8=46739
- charged-particle, accessory for mag. spectrometer 8=24496
- Compton, appl. to γ polarization meas. 8=33617
- Compton, asymmetry ratio, computer calc. 8=33615
- Compton, optimal sensitivity, computer calc. 8=33616
- high-speed stellar, electronic circuitry 8=50270
- prisms for use with lasers 8=33158
- proton scatt., for isobaric analogue state spin meas. 8=42640
- pulse discharge, light polarization meas. apparatus 8=24425
- spectropolarimeter, astronomical, three-channel photoelec. 8=36921
- transmission-microscope polariscope for photoelasticity 8=33283
- He liquid, for fast n, analysing power calc. 8=33820
- He liquid, for fast neutrons, description 8=33819

Polarized light
- See also Double refraction; Optical rotation; Photoelasticity; Polarimeters.
- analyzer, far u.v., for rocket use 8=41486
- cholesteric material, circular 8=48150
- circular polarizer for Lyman-α flux 8=28880
- correction factors for polarized spectroscopy 8=24426
- crystal orientation goniometer 8=30814
- depolarization rel. to stimulated Raman scatt. intensity 8=29695
- in dielectrics, transparent, study of stresses and failure under laser irrad. 8=40547
- diffracted by u. s. waves in isotropic solids 8=36302
- ellipsometry for modulated reflection studies of surfaces 8=31937
- Fourier spectrometer, field of view and resolution 8=28826
- glass matrix of ordered liq. crysts. 8=49767
- holographic recording of polarization effects 8=28878-9
- interferometer beamsplitters, thin-film far i.r., polarization props. 8=28851
- interferometer, using props. of plane waves in isotropic and anisotropic media 8=28856
- i.r., near, MgF_2 Soleil compensator 8=37699
- i.r. polarizer 8=46738
- laser, anisotropic, Poincaré sphere calc. 8=33170
- laser, single mode, in transverse mag. field 8=37568
- light wave polarization in optically active crystals 8=31947
- microscopes, AMPLIVAL POL-D and AMPLIVAL POL-U, new types 8=42192
- near i. r., polarizing grid efficiency 8=24427
- nebula IC 446 8=45715
- optical activity meas. technique using holography 8=28887
- parallel Wood's anomalies of optical gratings 8=28868
- photoelectric polarization of self-activated phosphors on ZnS and CdS bases 8=36006
- in photoluminescence of solutions 8=39386
- prisms, cutting, rational utilization of geometry of Iceland spar crystals 8=42159
- pulse discharge, polarization meas. apparatus 8=24425
- quarter wave plate achromatization and linearization of retardation us. wavelength 8=41056
- Rayleigh–Cabannes scatt. in dry air 8=30301
- reflection spectra, polarization effects 8=37683
- resonator, eigenstates of polarization 8=46559
- rotation of plane due to weak inhomogeneity of medium 8=46740
- selectively, due to absorption by elongated Ag particles in glass 8=41051
- skylight, effect of conc. turbid layer 8=36743
- skylight neutral points over smooth water 8=50118
- spectrometer, Fourier, Z-cut uniaxial cryst. plate between circular polarizers 8=28802
- spiral galaxies, refl. and absorpt. contributions 8=28116
- tandem two-photon processes, polarization correl. 8=49692
- tetracyanoethylene, i. r. spectra of charge transfer complexes, rel. to vibr. assignment 8=38879
- thickness of transparent film, calc. from ellipsometric obs. 8=30734
- transmission through metal foil, rel. to plasma resonance 8=27531
- variable stars, obs. 8=32455
- CN laser, far i.r., charcts. 8=46582
- $CaWO_4$: Yb^{3+}, microwave-optical double reson. using circularly polarized light 8=41070
- Cd isotope, radiation (2288 Å) emitted by optical reson. 8=25359
- Eu chalcogenides, obs. of ferro- and antiferromag. domains 8=31613
- He, from e impact, obs. 8=29641
- Nd glass laser emission 8=42111
- Pt anodic films, ellipsometry 8=27754

Polarography. See Chemical analysis/electrochemical.

Polarons. See Crystal electron states/polarons.

Polishing. See Surface texture.

Polonium
- Po^{210} α source, neutral excitation of superfluid He 8=24045

Polonium compounds
- No entries

Polyelectrolytes. See Electrochemistry; Polymers; Solutions.

Polymerization
- activation energy, dipolar groups, determ. 8=49912
- anthracene, solid, photo-dimerization by u.v. irradiation 8=41270
- bio-β-chloroethyl-vinyl-phosphonate, γ-induced, mechanism, obs. 8=49913
- butadiene, radiation-induced in emulsion, $RhCl_3$ additive effects 8=44081
- copolymers of methylmethacrylate with methacrylic acid 8=39917
- cyanoanthracene solns., vitrous dimerization rel. to optical absorpt. temp. dependence 8=43823
- ethylene–silica gel system, γ-induced, e.p.r. obs. 8=32127
- ionomers, physical structure 8=30796
- manganic acetylacetonate and related chelates, vinyl polym. initiation 8=32124
- molecular mass distrib. calc. 8=32126
- nonstationary, statistics 8=36588
- polyacetaldehyde, depolymerization of amorphous films in vacuum, 40-80°C 8=45364
- radiation effects at low temp. 8=27742
- styrene emulsion, i.r. spectroscopy, oxidation effect 8=32125
- ternary copolymerization, asymmetric propagation 8=36589
- vinylphosphonic acid dichloride, γ-induced, mechanism, obs. 8=49913
- AlF_3, vapour dimerization 8=30607
- Ba methacrylate dihydrate, by X-rays 8=27741
- by H atoms from elec. discharge 8=32101
- HCN, adsorbed on porous glass 8=48491

Polymers
- See also Plastics.
- α-acetylaminoacrylic acid-N-vinylpyrrolidone copolymer-gelatin emulsion for fast-n dosimetry 8=33800
- acetylene series, luminesc. spectra 8=32079
- activation energy for conduction 8=35831
- addition to non-Newtonian pseudo-plastic liq., effect on mass transfer on circular cylinder 8=30423
- adhesives, for metals, effect of elec. field appl. during bonding on strength 8=31185
- adsorbed layer on TiO_2, thickness determ. 8=39620
- adsorption on TiO_2 8=48494
- aklylacrylates-methacrylic acid copolymers, later particles and films struct., obs. 8=26156
- amorphous linear, fracture theory inc. viscoelastic and plastic props. 8=31249
- amorphous, molec. ordering above glass temp., viscosity obs. 8=39633
- amorphous, strength and hardness, temp.-time charact. 8=31234
- amorphous, tearing strength 8=31237
- amorphous, thermal expansion and compressibility 8=39926
- anomalous cond. in glass transition region of amorphous polymers 8=26949
- atomic parameters of chain, eqn. of repeat angle 8=25685
- bonds, under mechanical stress, i.r. spectroscopy 8=43437
- butadiene acidic and basic copolymers mixtures, H-bonding rel. to elastic props., obs. 8=48506
- butadiene acidic and basic copolymers mixtures, H-bonds mech. lability, obs. 8=48507
- butadiene and isoprene, block- and statistical co-polymers, structural features, radiothermoluminesc. invest. 8=47734
- butadiene copolymer mixtures, ionic bonds, obs. 8=48508
- butadiene copolymers, ionic bonds mech. lability, obs. 8=48509
- butadiene-lithium methylacrylate copolymers, ionic bonds, obs. 8=48508
- butadiene-methacrylic acid copolymers, H-bonding rel. to elastic props., obs. 8=48506
- butadiene-methyl (2-methyl-5-vinyl)-pyridinium iodide copolymer, ionic bonds, obs. 8=48508
- butadiene-styrene block copolymer, viscoelasticity 8=40194
- butadiene-2-methyl-5-vinylpyridine copolymers, H-bonding rel. to elastic props., obs. 8=48506
- calf thymus DNA, elec. cond. 8=40295
- cellulose, Du-Pont K116-207, fracture toughness, obs. 8=44614
- cellulose film, dimens. stability rel. to orientations of phases 8=39634
- cellulose I and II acetylation reactivities, viscosity and X-ray diffr. obs. 8=45325
- cellulose, sorption and diffusion 8=30785
- chain, intrinsic viscosity, excluded volume effect 8=34788
- chain mol. wt., effect on crystallization and melting 8=44108
- chain, translational diffusion 8=48114
- chains, even moments of end-to-end distance 8=47738
- chains, Kerr const. calc. 8=38972
- chains, strain birefringence, theory 8=38971
- chromatography, gel permeation, stochastic model 8=45415
- complexes, charge-transfer, review of elec. props. 8=26942
- conjugated, dynamic polarization 8=39434
- copolymers, graft, i. r. spectra 8=29871
- copolymers of methylmethacrylate with methacrylic acid, thermodynamic props. 8=39917

Polymers—contd
copolymers with F atoms, CH_2 group absorpt. bands 8=34394
crystalline films, optical transmission obs. 8=45245
crystallinity, conference, Arizona, USA, 18 Jan 1966 8=35204
crystallinity, definition rel. to X-ray diffr. obs. 8=44092
crystallinity, thermal meas. 8=44093
crystallization, by chain folding, two-dimens. model 8=39663
crystallization, temp. depend. rel. to nucleation mechanism 8=44109
cyclic polyene with $4n\pi$ electrons, theory of diamag. anisotropy 8=25434
deformation, local strains theory 8=31235
dielectric consts. and losses of polar and non-polar insulators in sheet form, 4.2-300°K 8=27253
diffusible, appl. to high-speed osmometry 8=34819
diffusion in dil. solns., increase in sensitivity of meas. 8=48117
diffusion meas. using Zeiss Schlieren equip. 8=48113
dilute polymer solutions, impact tube meas. 8=48015
dilute solns., flow-time fluctuations in capillary viscometer 8=30431
dilute solns., orifice plate calibration 8=25889
dispersion curves and freq. distrib., single-chain model 8=38975
2,4-disulphonic acid benzaldehyde polyvinyl acetate-gelatin emulsion for fast-n dosimetry 8=33800
electrical cond., carrier mobility theory 8=40593
electrical cond. meas., difficulties 8=40592
electronic cond. theories rel. to eka- and rubi-conjugation 8=26878
epoxide, hardened, electron-microscopy of struct. 8=35292
ethylenelpropylene copolymer, ductility of single crysts. mats. obs. 8=44616
ethylene-methacrylic acid coplymers, i.r. spectra 8=41173
ethylene-silica gel system, γ-polymerization, e.p.r. obs. 8=32127
excluded volume, asymptotic soln. 8=38976
excluded volume problem, variational calc. 8=29870
excluded vol., self-consistent-field calc. 8=34395
fibrillar structures in solutions and in films 8=26153
fillers and pigments, structure forming mechanism 8=35202
film-coated bodies, rolling friction and adhesion 8=31186
films, dielectric breakdown 8=40564
as free-layer damping treatment for vibrating bodies 8=32874
frequency distributions of random polymers 8=47736
gelatin-glycerol system, viscoelast., isochronal temp. conc. diagram 8=44618
geometry of chains 8=25684
glasslike and crosslinked, proliferous growth 8=48505
H-bonded, electrical conductivity 8=40295
helical, spectral effects of electronic interactions 8=29868
helix → coil transition, transitory regimes 8=43432
high linear, plasticity by meas. viscosity of wire samples 8=31169
high-molecular biopolymers, diffusion meas., method and apparatus 8=48116
insulating particles adhering to Se, force rel. to triboelec. and surface charges 8=49045
ionic cond., weak-electrolyte theory 8=40590
isobutene-silica gel system, γ-polymerization, e.p.r . obs. 8=32127
kapron (nylon), deformation, necking and orientation effects 8=31248
light scatt. in binary mixed solvents 8=30472
light scatt., multiple-order, by ringed spherulites 8=45246
linear chains, correl. between excluded vols. and virial coeffs. 8=29864
linear, dilute soln., viscoelastic flow stability 8=25845
liquid silicates, ionic equilibria 8=34787
macromolecular chemistry, Prague, Aug.-Sept. 1965 8=34392
maleic anhydride-styrene copolymer, viscosity and osmolic press. in tetrahydrofuran rel. to mol. dimens. 8=43776
mechanical props at low temp., review 8=26738
melts, kinetics of wetting of surfaces 8=39283
membrane, gas diffusion depend. of time lag on conc. 8=30321
membranes transport processes 8=26049
α-methylstyrene-methyl methacrylate copplymer, dielec. props., stretching effects, 125-150°C 8=49356
molecular mass distrib. calc. 8=32126
molecular wt. determ. by equilib ultracentrifugation 8=38967-8
nylon 4, lattice spacings and morphology, obs. 8=44285
nylon-6, α-γ phase transition by stretching 8=30715
α-Nylon 66, cryst., plastic deform. rel. to (010) [100] slip. obs. 8=40199
Nylon 66, doubly oriented, elec. cond. rel. to direction, 23-150°C 8=27257
nylon 66, elec. cond. 8=42095
nylon 66, spherulite deform. in cold drawing, 20°C 8=44097
nylon, thermal conductivity, 1.2-20°K rel. to ht. transport mechanism 8=44362

Polymers—contd
oriented, effect of elongation on n.m.r. 8=31914
oriented, elasticity, macromol. segmental mobility dependence 8=35735
oriented, intercrystallite layer density from X-ray difr. 8=35290
Perspex dosimeters, photosensitivity 8=42347
phenol sulphonic acid formaldehyde type membranes, electro-osmosis and streaming pots. 8=27745
physical effects of radiations 8=35608
plane polygonal, translational diffusion coeff. 8=34817
plasticity by meas. viscosity of wire samples 8=31169
polarizability, molecular, rel. to rotations 8=34220
polyacenequinones, cond. enhancement by substituting heterocyclic acenes 8=27141
polyacetaldehyde, depolymerization of amorphous films in vacuum, 40-80°C 8=45364
polyacetaldehyde, vibr. assignments from neutron scatt. 8=48712
polyacetylene, linear, elec. cond. Seebeck voltage rel. to O content 8=31398
polyacrylic acid, aqueous solutions, viscometric studies of u.v. irradiation 8=34794
polyacrylonitrile films, deposition, semicond. and photoelec. props., obs. 8=39605
polyacrylonitrile, neutron scatt. 8=25686
polyalkylacrylates later particles and films struct., obs. 8=26156
poly-α-methylstyrene in cyclohexane, and temp. rel. to microtactivity, obs. 8=43750
poly-α-methystyrene in toluene, second virial coeff. rel. to microtactivity, obs. 8=43750
poly(α-methylstyrene), light-scatt. and mol. wt. distrib. 8=48152
poly(α-methylstyrene), photolysis, e. s. r. 8=27762
poly-α-methylstyrene, stress relax. 8=40198
polyamides, elastic consts. in tension and compression 8=31242
poly-benzyl-L-glutamate, conformation of adsorbed layers 8=39612
poly-β-alanine, water soluble and insoluble n. m. r. rel. to transitions, obs. 8=45112
polybutadiene, chlorinated, n.m.r. 8=38914
polybutadiene, radiation-induced in emulsion struct., added $RhCl_3$ effects 8=44081
polybutadiene-styrene latex, particle size meas. by flow ultramicroscopy 8=30543
1,2-polybutadiene, viscoelastic props., 5-50°C 8=44613
polybutene-1, isotactic, crystallization nucleation, obs. 8=44122
polycaprolactam, γ-irrad., e.p.r. and nature of saturation 8=27464
polycaprolactam, melting props. and density rel. to cryst. morphology, obs. 8=43907
polycaprolactum, stressed, photodegradation kinetics temp. dependence 8=45399
polycarpamide, creep of unoriented cryst. film, vel. rel. to stress 8=40196
polychlorotrifluoroethylene copolymer films, crystallization 8=39680
polychlorotrifluoroethylene, low mol. wt., n. m. r. rel. to mol. motion, 77-300°K 8=45118
polycyanacrylates and compositions based on chem., optical props. 8=48151
polydimethylsiloxane blends, viscosity 8=30433
poly (dimethyl siloxane), eqn. of state for elasticity 8=26858
polyester resin based coatings, correl. between internal stresses and thermal props. 8=30759
polyether coatings, structure and props; influence of substratum 8=35188
polyethylene, behaviour of dielectric props. rel. to freq. 8=44875
polyethylene, creep of unoriented cryst. film, vel. rel. to stress 8=40196
polyethylene crystal nucleation, droplet expt. 8=44128
polyethylene, crystallized from diluent mixtures, enthalpy 8=34966
polyethylene, crystallized, lattice defects and crystallite size 8=39990
polyethylene crysts., chain folding, vibr. analysis 8=44305
Polyethylene, dielec. losses at cryogenic temps. 8=49355
polyethylene, dielectric strength subject to polarity reversals 8=35954
polyethylene, e-irradiated, fluorescence by Hg lamp 8=24729
polyethylene enthalpy, —150 —150°C 8= 24028
polyethylene, enthalpy of fusion and crystallinity 8=30578
polyethylene, extended-chain lamellae, origin 8=44094
polyethylene films, stretching processes, X-ray diffr. studies 8=26859
polyethylene, folded-chain crysts., density and ht. of fusion 8=35248
polyethylene, γ-irradiation effect on elec. cond. 8=40084
polyethylene, highly anisotropic, low density, creep 8=40197
polyethylene, lamellar struct. from m. p. and branching determ. 8=44096
polyethylene, linear fractions, mol. dispersed eutectic systems 8=44095

Polymers—contd
polyethylene, mech. props. rel. to mol. chain mobility, $\leq$ 40 000 psi 8=44620
polyethylene, multiple-order light scatt. rel. to spherulite lamellae twisting 8=45246
polyethylene, non-linear viscoelastic behaviour 8=40195
polyethylene, normal and deuterated, neutron scatt. 8=26579
polyethylene, oligomeric, conformational struct. in aromatic nonaromatic solvent mixtures n.m.r. obs. 8=43765
polyethylene oxide solns., proton mag. relax. 8=30538
polyethylene, oriented, plastic deform. and phase transforms 8=35137
polyethylene, plastic deform., molecular mechanism 8=44615
polyethylene, Poisson's ratio incompression 8=31245
polyethylene, structure during orientational stretching 8=35293
polyethylene supermolecular struct., reorientation effects, X-ray obs. 8=26157
polyethylene, surface charge density meas. and contact electrification 8=49379
polyethylene, surface wave propagation 8=35736
polyethylene terephthalate, crystallization behaviour 8=26206
polyethylene terephthalate, dielec. losses at cryogenic temps. 8=49355
poly(ethylene terephthalate) fibres, amorphous orientation and crystallite form., obs. 8=44175
polyethylene terephthalate, oriented, deformation bands 8=31244
polyethylene terephthalate, stressed, photodegradation kinetics temp. dependence 8=45399
polyethylene, thermal conductivity, 1.2–20°K rel. to ht transport mechanism 8=44362
polyethylene, transparency at mm. and sub-mm. wavelengths 8=44876-7
polyethylene, visco-elastic props., at high pressure 8=40189
polyethylene, volume expansion and melting temp. range 8=39472
polyethylene, I-doped, elec. cond. enhancement 8=40596
polyethyleneglycol adipate based, thermal expansion of solid and solns., obs. 8=26595
poly(fluoralkyl acrylates), permittivity and loss meas. 8=40594
polyformaldehyde, antifriction props. 8=31246
poly (4-methyl pentene-1), dielec. losses at cryogenic temps. 8=49355
poly-γ-benzyl-L-glutamate, elec. cond. 8=42095
poly-γ-benzyl-L-glutamate film, planar layered structure obs. 8=26131
poly-γ-benzyl-L-glutamate in soln., conformations 8=48096
poly-γ-benzyl-L-glutamate, proton resonance spectral linewidth rel to mol. wt. 8=43873
polyglycine, vibr. spectra 8=39880
polyglycols, e.p.r. obs. 8=31868
poly-i-butyl methacrylate, bulk and shear relax. processes 8=40193
polyimide films, noncryst., mech props. rel. to mol. struct., obs. 8=44619
polyisobutylene in cyclohexane and benzene, viscosity rel. to conc., obs. 8=30427
polyisobutylene in polybutene oil, intrinsic viscosity gradient depend., obs. 8=43775
polyisobutylene, viscoelasticity of v. dil. solns. 8=39329
poly-L-alanine spherilites, light scattering patterns 8=41175
poly-L-alanine spherulites, morphology 8=35291
poly-L-alanine, u.v. rotation in soln. 8=43824
poly-L-proline II, crystal structure 8=26547
poly-L-serine, u.v. rotation in soln. 8=43825
polymer-solvent-nonsolvent systems phase equilib., cluster model calc. 8=43900
polymethacrylic acid, aqueous and methanol solns., small-angle X-ray scattering 8=25888
polymethane dyes, nineteen, stimulated emission over continuous range 710-1060 mμ 8=28713
poly(methyl acrylate), mol. wt. and dimens. in ethyl acetate, obs. 8=43773
polymethylbenzenes, p mag. relaxation 8=49654
polymethylene, pyrolysis, intramol. radical transfer, obs. 8=45344
polymethyl methacrylate, breakdown, laser-induced 8=40566
polymethylmethacrylate, brittle fracture, study by stress wave propag. and reflection 8=44531
polymethylmethacrylate, const. strain rate failure and creep failure, compared with theory 8=31249
polymethylmethacrylate, crack orientation, laser destruction, stress effect 8=40191
poly(methyl methacrylate), creep compliance and secondary processes activation energies, –150–75°C 8=44017
poly(methyl methacrylate), crystal mounting adhesive 8=31233
polymethyl methacrylate, irradiated, electrical props. 8=40597
polymethyl methacrylate rods containing rhodamine dyes, stimulated emission when flashlamp excited 8=28714
polymethylmethacrylate, stereoregular, internal rot. in side groups 8=38969

Polymers—contd
polymethylmethacrylate, surface wave propagation 8=35736
polymethylmethacrylate, thermal radiation during damage by laser light 8=30994
polymethylmethacrylate, triplet absorpt. and form. yield meas. 8=25401
polymethylsiloxanes, thermal degradation 8=35189
polymethylsorbate, n.m.r. 8=40984
poly-n-butyl methacrylate in chlorinated diphenyl, dilute solns., normal stress effect 8=39333
poly[N, N′-(p, p′-oxydiphenylene) promellitimide], pyrolytic, elec. cond. rel. to struct. and unpaired spin conc. 8=26976
polynucleotides, optical props., theory 8=29865
poly(N-vinyl carbazole)-I complex, e.s.r., Hall effect and transport props. 8=27462
polyoctadecene-1, transition temps. and crystallinity 8=39635
poly-1, 3-dioxolane, n.m.r. and dielectric dispersion 8=41003
poly-2, 2′-octamethylene-5, 5′-dibenzimidozole amorphisation in annealing, obs. 8=26158
polyolefins, Br cpd. effects on thermal degradation at 400℃ 8=36583
polyoxymethylene extended chain crysts., refr. index m.p. and density, X-irrad. effects, $< 4.8 \times 10^7$ R 8=44509
polyoxypropylene, structural transform. under large deform. by uniaxial tension, wide temp. range 8=35203
polypeptide solns., u.s. absorpt. and helix-coil transition 8=48145
polypeptides, helical, optical absorpt., theory 8=25680
poly propylene fibres, structural changes in stretching process 8=49067
polypropylene, isotactic, $\gamma-\alpha$ solid–solid transform., obs. 8=44018
polypropylene, isotactic, -organic diluent systems, phases and thermodyn. interactions, obs. 8=43899
polypropylene lamellae grown from dil. α-chlornaphthalene solns., twinning 8=35218
polypropylene, light scatt. 8=49783
polypropylene melt, elastic behaviour 8=39261
polypropylene, melts rheological props. rel. to mol. wt. distrib. obs. 8=43721
polypropylene, mol. motion, CCl_4 effects, 140-373°K 8=48510
polypropylene, stretching technique for X-ray detector windows 8=50476
polystyrene aq. suspension, angular distribution of scatt. light 8=25964
polystyrene, atactic, heat capacity rel. to annealing, 10–360°K 8=44345
polystyrene, atactic, n-pentane diffusion rel. to second-order transition above glass point 8=44398
polystyrene-benzophenone mixts., glass transition temps., obs. 8=44146
polystyrene, breakdown when subject to ionizing radiations, optimal thickness calc. 8=31417
polystyrene, brittle fracture, study by stress wave propag. and reflection 8=44531
polystyrene, chain dimens. temp. depend. below O point, cyclohexane soln. viscosity obs. 8=43774
polystyrene, crack orientation, laser destruction, stress effect 8=40191
polystyrene, diffusion in polystyrene, effect of mol. wt. 8=30450
polystyrene-diphenylmethane soln., electrolytic cond. rel. to conc., temp and field 8=39412
polystyrene, filament struct. in laser beam trace 8=49784
polystyrene, film-forming solutions 8=44065
polystyrene films, far u.v. optical props. 8=27639
polystyrene, films i.r. transmission rel. to glass transitions, 50-120°C 8=45247
polystyrene in good and theta solvents, viscosity rel. to conc., obs. 8=30427
polystryrene latex, particle size meas. by flow ultramicroscopy 8=30543
polystyrene latex particles in La, Nd and Th nitrates, electrophoretic mobilities 8=49923
polystyrene lattices refr. index, suspension light scatt. meas., 589, 546 and 436 mμ 8=34934
polystyrene, light scatt. 8=49783
polystyrene melt, elastic behaviour 8=39261
polystyrene, optical constants in vac. u.v. 8=41174
polystyrene, photocond., excitation wavelength depend. 8=49430
polystyrene, photolysis, e.s.r. 8=27762
polystyrene, solns. in benzene u.s. absorpt. 8=43807
polystyrene-solvent-methanol system, phase equilib. rel. to cluster model, obs. 8=43900
polystyrene sub-micron particles, electrical mobility 8=43888
polystyrene sulphonic acid, i.r. spectra as function of degree of hydration 8=48165
polystyrene, surface charge density meas. and contact electrification 8=49379
polystyrene, thermal props., low-temp., radiation-induced cross-links effects 8=26606

Polymers—contd
- polystyrene, thermal radiation during damage by laser light 8=30994
- (1:1)poly(styrene-co-methyl acrylate), mol. wt. and dimens. in ethyl acetate, obs. 8=43773
- polystyrenesulfonic acid membranes, dielec. props. rel. to adsorbed H_2O 8=49357
- polystyrenesulphonate membrane forms, optimum ionic electret 8=44878
- polytetrafluoroethylene dielectric props. 8=35952
- polytetrafluoroethylene, mech. props. rel. to mol. chain mobility, ≤ 60 000 psi 8=44620
- polytetrafluoroethylene n.m.r. spectra rel. to temp. of post-irrad. heat treatment 8=49640
- polytetrafluoroethylene oxide crystal packing and molecular configuration 8=35366
- polytetrahydro furan, n.m.r. and dielectric dispersion 8=41003
- poly(tetramethylene oxide), high-mol. wt., crystallization and melting 8=44134
- polythene films, ionization by giant laser pulses 8=40720
- polythene, laminated, dielec. breakdown in voids 8=40591
- polyurethane-cyclohexanone soln. viscosity temp. depend. obs. 8=26595
- polyurethane foams, mech. props, effect of cell membrane 8=48243
- polyurethane, thermal expansion of solid and solns., obs. 8=26595
- polyvinyl acetate latex films, particle packing 8=48471
- polyvinyl alcohol, dehydrated fibre, i. r. spectra 8=34396
- polyvinyl alcohol, electronic absorpt. spectra 8=30492
- polyvinyl-alcohol fibres, structural features characterized by electrokinetic potential 8=26154
- poly (vinyl alcohol), films i. r. transmission rel. to glass transitions, 50-120°C 8=45247
- polyvinyl alcohol, films, Au crystal X-ray sizing 8=30858
- polyvinyl alcohol, water vapour sorpt., crystallinity effect 8=30784
- polyvinyl butyral, critical surface tension with alcohols and hydrocarbons, composition effects 8=30731
- polyvinyl chloride, conformational struct. from vib. anal. 8=43436
- poly (vinyl chloride-co-vinyl acetate), films i. r. transmission rel. to glass transitions, 50-120°C 8=45247
- polyvinyl chloride, dielec. losses at cryogenic temps. 8=49355
- poly(vinylidene fluoride), α- and β-crysts. fundamental modes, i. r. obs. 8=44306
- polyvinylidene fluoride, X-ray studies of crystal structure, orientation and supramol. structure 8=26155
- polyvinylpyrrolidone solns., osmotic equilib. at high pressures 8=39347
- polyvinyltoluene aq. suspension, angular distribution of scatt. light 8=25964
- polyvinyl toluene latex, particle size meas. by flow ultramicroscopy 8=30543
- poly-w-undercanolactum, dielec. losses at cryogenic temps. 8=49355
- porous sphere molec. model, hydrodynamics 8=29866
- proton resonance spectra, obs. of chem. shift using rotating sample 8=49626
- PVC, chlorinated, n.m.r. 8=38914
- PVC, dielec background loss power temp. law polymethylmethacrylate 8=31426
- radicals in aq. soln., e. s. r. 8=34906
- random, vibr. anal. 8=38970
- rigid solutions, molecular orientation of luminophors 8=32078
- rubeanato-Cu co-ord. polymer, cryst., mag. and elec. props., c. f. with amorphous form 8=27385
- semiconductors, band conduction and fluctuations 8=27066
- semidilute solns., quasielastic neutron scatt. 8=30419
- silk, natural, stressed, photodegradation kinetics temp. dependence 8=45399
- solid, secondary free radical reactions during mech. damage 8=45361
- solution, drag on sphere 8=30432
- solution, light scatt. photometry 8=46652
- solution viscosity rel. to concentration 8=48125
- solutions, comblike branched mols., statistical thermodynamics 8=39324
- solutions conc., normal stresses in simple shear flow, molec. theory 8=34699
- solutions, dilute, onset of drag reduction in turbulent flow, molec. approach 8=30368
- solutions, eqns for combined simple and sinusoidal shearing 8=34801
- solutions, flow birefringence and polydispersity 8=39368
- solutions, flow props., kinetic approach 8=39334
- solutions, turbulent drag-reduction 8=30364
- solutions, viscosity, non-Newtonian intrinsic, ellipsoidal model 8=43778
- spectra, i. r., vibr. band intensities and terminal group effects, calc. 8=29857
- spherulite, film, Rayleigh-Gans light scatt. 8=36447
- spherulite growth rate, temp. depend. 8=39681
- starch, modified maize, p spin-lattice relax. time temp. depend., obs. 8=45135

Polymers—contd
- statistical mechanics, integral eqn. for excluded-vol. effect 8=29869
- stressed, photodegradation kinetics 8=36619
- styrene-butadiene copolymers in soln. viscoelastic props. 8=25891
- styrene-methyl methacrylate copolymer in good and theta solvents, viscosity rel. to conc., obs. 8=30427
- styrene-methyl methacrylate random copolymers, dilute soln. props. 8=39323
- sulphurised polymer carbons, form, bonding and behaviour 8=35016
- supramolecular structure, obs. methods 8=30795
- surface tension of molten liquids 8=48105
- tear strength increase 8=49066
- teflon, Poisson's ratio in compression 8=31245
- tetrafluoroethylene-hexafluoropropylene, irradiated, e.s.r. of peroxy radicals 8=43422
- vinyl, mean dimens., effect of side-group interactions 8=29863
- vinyl, optical rotation, theory 8=38973
- viscoelastic, homogeneous submicrocavitation fatigue processes 8=31181
- viscosity, entanglement effects 8=48100
- viscosity, theory with hydrodynamic interaction and excluded vol. 8=47737
- war and friction, effect of C fibre reinforcement 8=40192
- zig-zag chains, randomly folded, vibr. freq. 8=47735
- B cpds., C and H microdeterm. 8=36628
- C fibre reinforced, wear in high vacuum environment 8=35636
- Co(II) di-n-alkylphosphinate polymers, structure and prep. 8=30797
- Na-CMC aqueous soln, 0. 3wt. % Na, viscoelastic props. 8=34700
- Si cpds., C and H microdeterm. 8=36628
- Zn(II) di-n-alkylphosphinate polymers, structure and prep. 8=30797

Polymorphism
- See also Crystal structure.
- cerborate with aragonite isotypes 8=48515
- chlorite, new modification and its possible polytypes, X-ray structural exam. 8=26174
- cyclononanone, study by X-rays, n. m. v. and diff. thermal stability 8=30714
- cyclooctanone, study by X-rays, n. m. v. and diff. thermal stability 8=30714
- elements and simple cpds., temp. and pressure dependence, theory 8=26053
- families, main and subclasses and homeotypes of structure types 8=26162
- glutaric acid, X-irradiated, transforms. rel. to free radical recombination 8=29828
- hexachloroethane, X-irradiated, transforms rel. to free radical recombination 8=29828
- lecithins, from lecithin-water phase analysis 8=43435
- mesomorphic states, phase identification, temp. scanning thermal anal. 8=48365
- polytype structure, stacking sequence determ., calc. method 8=26172
- rare earth borate isotypism 8=48657
- rare-earth sesquioxides, metastable structure, formative mechanism 8=26056
- silicates, layer, some rare polytypes, X-ray exam. 8=26174
- Bi_2Te_3II, high-temp and pressure polymorych, lattice parameters 8=30681
- Cd_3As_2, high-press., retention at atmos. press. and temp. $< 150\,^{\circ}K$ 8=26066
- CdI_2, polytypism as high-order transformation 8=44012
- CdI_2 polytypism, dislocation theory 8=26180
- CdI_2 rhombohedral polytype 12R 8=39644
- Ce-alkali metal tungstates, rel. to hydrothermal crystallization 8=26259
- Ga, identification of metastable forms 8=35111
- KCN, high press. 8=48385
- KSCN, high press. 8=48385
- in $NH_4[SC(S)(NH_2)]$ 8=48517
- NaCN, high press. 8=30701
- NaSCN, high press. 8=30701
- Nd-alkali metal tungstates, rel. to hydrothermal crystallization 8=26259
- PbI_2, polytypism as high-order transformation 8=44012
- Pr-alkali metal tungstates, rel. to hydrothermal crystallization 8=26259
- SiC, conversion of cubic to hexagonal as fn. of temp. and press. 8=48399
- SiC, polytypism as high-order transformation 8=44012
- SiC polytypism, dislocation theory 8=26180
- Ta_2O_5, effect of oxide additions 8=48403
- $VOSO_4 . 5H_2O$ 8=49759
- ZnS, polytype formation rel. to periodic slip processes 8=44461
- ZnS, polytypism as high-order transformation 8=44012

Polynomials. See Algebra; Functions.

Polytypism. See Polymorphism.

Pomeranchuk rule. See Scattering, particles.

Population inversion. See Lasers; Masers; Optical pumping.

Porosity. See Porous materials.
Porous materials
  See also Permeability, mechanical; Surface measurement.
  absorbed moisture, thermodynamic functions 8=44070
  acoustic absorbent, impedance calc. 8=46189
  alumina, plasma-sprayed, porosity changes in reheating 8=48354
  capillary-porous mat., influence of vib. on rate of drying 8=30591
  capillary-type, drying in e. m. field, ht. and mass transfer 8=39487
  ceramics, polycrystalline, creep rate rel. to porosity 8=35625
  clay, colloidal, moisture diffusion coeff. and thermograd. coeff. rel. to moisture content 8=30662
  clays grounds, mass transfer pots. in various meas. scales in region of wet state 8=39282
  convection flow past vertical plate, effect of periodic suction 8=34583
  convective diffusion of salt solns., boundary cond. at inlet of system 8=39959
  cracked, immiscible liq. flow, capillary pressure effect 8=34714
  evaporative cooling, effect of depth of surface 8=41861
  filling particles, form factors meas. rel. to charact. size of each particle 8=39533
  glass, foam, compressive deform., obs. 8=35647
  glass, surface struct. rel. to aq. attack 8=26149
  granularity and porosity meas. by X-ray scatt., comparison with other methods 8=26041
  graphite, synthetic, porosity, access of gases at high temps. 8=48353
  gypsum systems, porosity, hardness, and modulus of elasticity, interrelation 8=40172
  heat transfer, modified Woodside model 8=44359
  hydrophilic clays, porosity coeff. rel. to sorption and water permeability 8=30661
  interaction, elastic and diffusional, of pores with each other and with crystal boundaries 8=30839
  ionizer for alkali surface ionization 8=49449
  liquid saturation meas. using n.m.r. tech., rel. to ion conc. 8=43988
  loams, colloidal, moisture diffusion coeff. and thermograd. coeff. rel. to moisture content 8=30662
  metal plate, meas. of supersonic flow from it after choking 8=34630
  metals, irradiated, porosity formation mechanism 8=35518
  metals, study of liq. evaporation rel. to metal props. and heat flux density 8=30602
  micropores, pore vol. and surface distrib. determ. 8=48350
  microporous, multilayer flow of adsorbed gases 8=48476
  microporous, non-Fickian diffusion anomalies 8=48769
  moisture diffusion eqn. 8=44374
  moisture effect on thermal cond. at temps. above and below 0℃ 8=30985
  moisture extraction 8=45935
  organo-clays, sorption, swelling and intracryst. porosity 8=30779
  pore struct. anal, capillary condensation in N_2 adsorpt. and desorpt. isotherms 8=30659
  pore vol. meas. by gas adsorpt. 8=48352
  porosimeter, Hg l.p. 8=30660
  rubber, axial compression of cylinders in torsion 8=31253
  sand grounds, mass transfer pots. in various meas. scales in region of wet state 8=39282
  saturated with different liq. fillers, heat and mass transfer props. 8=30555
  steel castings, susceptibility to defects due to H 8=30663
  strength, effect of surface energy 8=48969
  subterranean effective porosity, definition 8=34715
  superconductors, synthetic filamentary, magnetization and critical current density rel. to pore size 8=40370
  thermal conductivity, effect of mixing for different gases and mats. 8=30984
  thermal conductivity, exptl. data analysis 8=39941
  transpiration cooled, transient temp. response in forced convection-surroundings 8=35450
  transpiration cooling, heat and mass transfer in evaporation 8=39488
  with transpiration cooling, steady state temp. field 8=28416
  viscoelastic flow through, multiphase 8=39270
  Vycor glass, e. s. r. of methyl radicals on surface 8=47684
  water-oil-gas relative permeabilities in pore spaces, n.m.r. meas. 8=43988
  on Al, anodic oxide films, microstruct. obs. 8=44038
  β-SiC, n-irrad. induced, growth, damage and other changes 8=26735
  Si:P, As, single crystals, porous substruct. 8=30866
  ThO_2, porous and nonporous, adsorpt. of H_2O 8=48492
  U-Pu monocarbides ceramics, fabrication 8=30664
Porterin-LeChatelier effect. See Stress/strain relations.
Positive column. See Discharges, electric.
Positive ray sources. See Ion sources.
Positive rays. See Chemical analysis by mass spectrometry; Ion beams.
Positons. See Positrons.
Positronium
  negative ion, positron annihilation, wave function calc. 8=40287
  molecule, binding energy, var. wave function calc. 8=43430
  particle exchange collision theory appl. 8=29659
  thermalization in inert-gas moderator 8=34177
  triplet annihilation, correl. with struct. of organic liqs. 8=30406
  in Al_2O_3 powder ortho-positronium annihilation and form. rel. to specific area 8=49130
  in Ar, liquid, zero-point motion rel. to bubble formation 8=30388
  in H_2, liquid, zero-point motion rel. to bubble formation 8=30388
  in He, liquid, zero-point motion rel. to bubble formation 8=30388
  in MgO powder ortho-positronium annihilation and form. rel. to specific area 8=49130
  in Ne, liquid, zero-point motion rel. to bubble formation 8=30388
  in SiO_2 powder ortho-positronium annihilation and form. rel. to specific area 8=49130
Positrons
  See also Electron pairs; and Electrons, which include both negative and positive electrons when the differences between them are of no special significance.
  annihilation, by O_2 molecules as paramag. impurity, rel. to long lifetime 8=29851
  annihilation, from positronium negative ion, wave function calc. 8=40287
  annihilation in In and Sb, rel. to ang. distrib. of annihilative γ-quanta 8=49128
  annihilation in α, β Sn 8=49131
  beam production in electron linear accelerator 8=33426
  cosmic ray p-e^+ flux ratio calc. 8=42685
  crystal, single, scatt. rel. to lattice struct. 8=48889
  distribution equilib. function in e. m. cascade 8=38207
  electron-positron g-factor comparison, crossed-field prod. 8=33628
  $e^-e^+ \rightarrow A\bar{B}$ processes with polarised beams 8=33646
  e^+-p, e-p scatt., ratio obs. equal to unity up to $(5\ GeV/c)^2$ 8=42639
  $K^+ \rightarrow e^+ + \nu_e$, branching ratio 8=42574
  lifetime meas. in solids, time-amplitude converter 8=24526
  in metal hydrides, lifetimes 8=40286
  ν-$e^\pm$ interaction, μ production, exam. using two- and four-component theory 8=29090
  polarized, annihilation in Ni and Fe 8=49129
  production in electron bombardment of tungsten 8=33642
  slow, annihilation in He, theory 8=38740
  in solids, single-particle wave functions, assumption-independent, appl. to annihilation angular distribs. 8=44669
  source, linear accelerator, magneto-optical adaptions 8=42353
  storage rings, development and prospects 8=33509
  in Al single-particle wave functions, assumption-independent, appl. to annihilation angular distribs. 8=44669
  H-positron scatt. resonance mechanism 8=38722
  I^{123}, upper limit to positron decay 8=42955
  PbF_2 crystal Cherenkov shower detector 8=33613
  in Si, single-particle wave functions, assumption-independent, appl. to annihilation angular distribs. 8=44669
Potassium
  abundance in solar photosphere 8=28172
  abundance, with U and Th, in peridotite inclusions in basalts 8=50012
  active ionic transport through biological membrane, opposite to Na ions 8=50461
  atom, autoionizing states, metastable, identified 8=43244
  atom-electron scatt., elastic spin-exchange, expt. and close-coupling calc. 8=47538
  atom reactions with Cl, in crossed beams 8=49875
  atom, spin-exchange cross-sections for K^{39} atoms 8=43239
  atomic beam, crossed with Cs atomic beam, spin change collisions 8=47534
  atomic beam, electron scatt., oscill. strength and absolute differential cross-sections 8=43242
  atomic beam, scatt. on CO_2 molec. beam, time-of-flight anal. 8=38952
  atomic beam source for 0.2-45eV 8=43240
  conduction-ESR, 0.5Gsplitting, theoretical exam 8=27478
  content determination in fuel rich air-H_2 flames 8=49990
  crystal lattice freq. distrib. function and sp. ht. calc. 8=44300
  deposition on W emitters in field emission microscope, flicker noise and surface migration 8=44936
  diffusion from soda-potash-baria glass into refractories 8=48780
  electron scatt., energy loss spectra, quantitative comparison with dielectric theory 8=26727
  equation of state, theory, and calc. of thermal parameters 8=30973
  films, LEED exam 8=48453

Potassium—contd
- films, optical props. for photons 3.96 to 9.69 eV 8=49731
- fluorescence, quenching cross-sections, determ. by flame tech. 8=29617
- Hall coeff., field-dependent, rel. to Fermi surface 8=26969
- helicon-wave resonances in Hall coeff. determ. rel. to surface-mode loss 8=44682
- internal friction and relax. peaks in oxygen contaminated samples 8=49029
- ion adsorpt. on Mo, 960-1200°K 8=30770
- ion channelling in NaCl and KCl lattice, computer analysis 8=40075
- magnetoresistance, rel. to band structure 8=44691
- magnetoresistance, strain-dependent 8=49166
- melting curve up to 80 kb 8=34961
- mixtures with N_2, H_2, HD and D_2, mixing and quenching 8=29836
- nuclear spin lattice relaxation 8=40926
- optical constants, ellipsometric obs. 8=41120
- oxidation in flames 8=49877
- pair interaction, phase change 8=35027
- plasma confinement lifetime in Q-device 8=47871
- plasma, K-seeded non-equilibrium, effect of bulk gas on elect cond. 8=25720
- plasma, potential noise obs. by Q-machine 8=47891
- resistance, electrical 8=49167
- r.f. size effect rel. to Fermi surface meas., 8=44645
- solar, profiles photometric obs. 8=37024
- spin waves 8=31659
- structure in liquid state 8=39307
- superconductivity predictions from phonon spectrum and e.-phonon interactions 8=44719
- thermoreflectance spectrum in visible and near u.v. region 8=41101
- u.s. attenuation, 2.5-77°K rel. to dislocation motion effects 8=39894
- vapour charge exchange source of polarized H^- 8=33099
- vapour condensation in presence of Ar or He, effect on heat transfer 8=25993
- vapour, laser pumping four wave parametric interaction 8=33177
- vapour, photoionization absorpt. continua 8=29973
- vapour, proton charge exchange, $E_p = 2.5$-22 KeV 8=38761
- vapour, rel. to disruption of glassy C 8=49888
- vapour, thermal cond., 550-820°C, 0.005 to 1.3 atm., meas. by coaxial cylinder method 8=47965
- vapour, thermal cond. 841 to 1241°K, 0.022 to 0.94 kg/cm² 8=47964
- in Ar plasma, plasma with K, electron temp. meas. by line reversal method 8=39075
- K^+, diff. in $LiSO_4$, 590-820°C 8=39977
- K^+, ionization to K^{2+} by electron impact 8=39047
- K^+, scatt. by Mo, ang. depend. of energy spectra of secondary ions 8=40719
- K_2, pseudopotential theory calc. 8=38838
- KNb_3O_8, mica like, dielect. props. 8=40568
- K-Sb-Cs photocathodes 8=36023

Potassium compounds
- absorption, far i.r., due to U-centres and F-centres 8=44480
- apophyllite crysts., growth mech. study by surface microstructs. 8=26211
- diffusion, reciprocal and self-, along dislocations 8=26620
- graphites, formation and structure 8=30904
- halide crystals, phonon scatt. by U centres, thermal conductivity meas. and theory 8=44301
- impurity anions effects on elec. conductivity 8=40570
- muscovite dehydration, mechanism 8=49876
- muscovite heated in vacuum, superstructure phase, electron microscopy study 8=26190
- muscovites, harmonic, epitaxic power temp. dependence 8=26279
- K binoxalate, d.m.r. 8=49611
- K graphite, order-disorder transformation obs. 8=26074
- K oxalate hydrate, partly deuterated, isotope effect in d.m.r. 8=45122
- in K persulphate soln., corrosion inhibition of Cu 8=45332
- K solutions, unsaturated, in melted KCl, thermodynamics 8=48060
- K_2 malate, double n.m.r. 8=29810
- KAg_4I_5, ht. of formation 8=48396
- $KAl(SO_4)_2$ $12H_2O$ crystal growth and dissolution rates 8=48537
- $KAl(SO_4)_2 . 12H_2O$, n.m.r. 8=40983
- $KBO_3 . {}^1/_2H_2O$, e.s.r., rel. to RO_2, O_3^- and O_2^- centres 8=45098
- KCN, hindered rotation of CN^-, above 168°K 8=26030
- KCN, melting and polymorphism to 44 kbar 8=48385
- KCNO, bonding and stability 8=26006
- $KCOF_3$, i.r. transmission spectra 8=27600
- K_2CO_3, aq. soln., applic. for admission of ionizing into duct of MHD generator 8=46360
- K_2CO_3 soln., acid differentiation, rel. to hydrothermal crystal growth 8=26213
- $K_3CO(CN)_6:Cr^{3+}$, ${}^2E \leftrightarrow {}^4A_2$ transition 8=31979
- $KClO_3 : Cl^{35}$, n.q.r., use in temp. control of spectrometer 8=46528
- K_2CoF_4, absorpt. spectrum, compared to $KCoF_3$ 8=45197

Potassium compounds—contd
- $K_2Cr_2O_7$, spectral line structure at 2°K 8=34253
- $K_2Cr_2O_7$, triclinic, cryst. struct. 8=35337
- $K_2CuCl_4 . 2H_2O$, hyperfine parallel resonance 8=27454
- $K_3[Cu(NO_2)_5]$, crystal structure from i.r. and vis. absorpt. spectra 8=30901
- KD_2PO_2, automatic thermostatic control 8=31431
- KD_2PO_4, Curie temp. shift on hydrostatic pressure, theoretical explanation 8=40818
- KD_2PO_4, dielec. and electromechanical props. near phase transition 8=27275
- KD_2PO_4, specific heat, temp. dependence 8=44338
- KF, impure single crystal, nuclear quadrupole effects by pulsed double resonance 8=41012
- KF, neutron-irrad., diffusion and release of Ar gas 8=35498
- KF, u.v. reflectivity spectra 8=36374
- $K_3Fe(CN)_6$, Mossbauer h.f.s. and internal mag. field, 0.025-0.04°K 8=37330
- $K_4Fe(CN)_6$, Mössbauer radiation scattering by nucl. resonance, diffr. and interference effects 8=26025
- $K_4Fe(CN)_6 . 3H_2O$, dielec. constant and birefringence rel. to polytypic transforms, 0 to −100°C 8=31432
- $K_4Fe(CN)_6 . 3H_2O$, phase transition sequence in −45 to −25°C from permittivity and polarization meas. 8=40610
- KH, pseudopotential theory calc. 8=38838
- $KH_2Al_2(SiO_4)_3$, (muscovite), isomorphic substitution distribution 8=35338
- KH_2AsO_4, critical temp. behaviour of As^{75} quadrupole interaction 8=45137
- KH_2AsO_4, i.r. absorpt. by H-bonds in cryst. 8=27598
- KH_2AsO_4, n.q.r. spectra, rel. to temp. 8=41009
- $KH_2AsO_4(KD_2AsO_4)$, electro-optic and dielec. constants 8=49369
- $KH_2AsO_4(KD_2AsO_4)$, piezoelec. and elastic constants 8=49368
- $KHCO_3$, structure of $(HCO_3)_2^{2-}$ ion 8=26032
- KH_2PO_2, automatic thermostatic control 8=31431
- KH_2PO_4, Curie temp. shift on hydrostatic pressure, theoretical explanation 8=40818
- KH_2PO_4, electroluminescence 8=49804
- KH_2PO_4, electro-optical props. near phase transitions 8=27637
- KH_2PO_4, ferroelec. mode temp. depend., Raman scatt. obs. 8=36376
- KH_2PO_4 ferroelec., vibrational mode disappearance from n. time-of-flight spectra 8=44299
- KH_2PO_4, generation of second harmonic oscills. using a laser 8=41102
- KH_2PO_4, i.r. absorpt. by H-bonds in cryst. 8=27598
- KH_2PO_4, long-range ferroelec. domain interactions, optical obs., 8=49367
- KH_2PO_4-model, modified to include external field 8=27262
- KH_2PO_4, (100) and (101), faces growth rate dependence on Al ions and pH of soln. 8=48547
- KH_2PO_4 parametric light generator, electro-optical tuning, obs. 8=41103
- KH_2PO_4, precipitates and dislocations exam. by X-ray diffr. microscopy 8=26691
- KH_2PO_4, specific heat, temp. dependence 8=44338
- KH_2PO_4, spontaneous scatt. of intense light, quantum theory 8=27538
- KH_4PO_4, ferroelec., l.f. oscills. from Raman spectra study 8=36378
- KH_2PO_4 and KD_2PO_4, ferroelec. Curie temp. pressure-dependence 8=27274
- K_2HPO_3 acqueous solns., lattice energy from ultrasonic velocity 8=25880
- KI, breakdown, laser-induced 8=40566
- KI, Bremstrahlung passage, energy losses rel. to beam collimation and crystal thickness 8=31310
- KI crystal, colour centre form. by e beam pulse 8=44475
- KI, doped, far i.r. absorption 8=49734
- KI, electric field grad. at nuclei near substitutional ion, n.m.v. meas. 8=36273
- KI electric field gradients at nuclei surrounding different subst. halogen ions, n.m.r. meas. 8=48314
- KI, electrical conduction in impure crystals rel. to vacancy migrations 8=40576
- KI, F-centre form. by u.v. irrad. 8=44479
- KI, V band preferential bleaching 8=44476
- KI film, reflection and absorpt. spectra in u.v. 8=32025
- KI, luminscence of α-centre, polarization 8=27654
- KI, neutron-irrad., diffusion and release of Ar gas 8=35498
- KI, optical transmittance curves, room temp., 0.2 to 3.0μ 8=45187
- KI, paraelastic behaviour of S_2^- 8=48336
- KI, reciprocal and self-diffusion along dislocations 8=26620
- KI, Schottky defect formation energy, from dissolution of impurity containing precipitates 8=35536
- KI soln., oxidation by ultrasonic cavitation 8=37278
- KI, ultrasoft X-ray spectra of iodine rel. to band structure 8=41105
- KI:Ag Greek absorp. bands 8=36323
- KI:Ag^+, far i.r. props. of lattice resonant modes rel. to isotope shifts 8=36393
- KI–AgI, high-cond. solid systems 8=48396

Potassium compounds—contd

- $KI:Cl^-$, (Br^-), i. r. lattice vibration absorpt. by gap and resonance modes, theory 8=27576
- KI: Cu, phosphor, complex activation centres 8=45277
- KI: In, Zeeman effect of A absorption bands 8=45200
- K_2IrCl_6, mag. ordering from n. diffr. exam. 8=40870
- KI: NO_2^-, Raman spectra, impurity induced 8=41106
- KIO_4, metaperiodate, thermal expansion 8=35444
- KI–Tl crystals, thallous ion centers 8=41108
- KI: Tl, luminescence, host sensitized 8=27653
- KI: Tl, recomb. luminesc. and F scintillations 8=36493
- $KLiSO_4$, second harmonic generation on ruby laser irrad. 8=45199
- $KMgF_3$, crystal growth, perovskite struct. 8=30830
- $KMgF_3$, i. r. transmission spectra 8=27600
- $KMgF_3$, perovskite type crystals, NMR and electronic structure 8=27506
- $KMgF_3:M^{2+}$(M=Ni, Fe, Co), acoustic paramagnetic resonance rel. to magnetoelastic coeffs. of 3d impurity ions 8=31817
- $KMgF_3$: V^{2+}, Mn^{2+}, hyperfine interactions, transferred, through unpaired spin on intervening ions 8=49647
- $K_2Mn(C_2O_4)_2 . 2H_2O$, crystal chemistry data 8=48512
- $KMnCl_4 . 2H_2O$, NMR and antiferromag. props. 8=36275
- $KMnF_3$, absorpt. spectra of Mn^{2+} 8=41109
- $KMnF_3$, anomalous elasticity at 184°K 8=26827
- $KMnF_3$, crystal growth, perovskite struct. 8=30830
- $KMnF_3$, heat capacity rel. to magnetic spin 8=44340
- $KMnF_3$, i. r. transmission spectra 8=27600
- $KMnF_3$, paramagnetic susceptibility, semi-empirical expression by Padé approximant 8=27386
- $KMnF_3$: Eu^{3+}, luminescence spectra, spin-wave sideline 8=27655
- K_2MnF, heat capacity rel. to magnetic spin 8=44340
- K_2MnF_4, zero-point spin reduction 8=27445
- $K_2Mn_2(SO_4)_3$, langbeinite structure, growth and electro-optical props. 8=39678
- K_xMoO_3, electronic struct. 8=40245
- $K_2MoO_2F_4$ struct., e diffr. obs. 8=30903
- KNH_2, in liq. NH_3, absorption spectra 8=39380
- KNO_2, phase boundaries below 500°C 8=48366
- KNO_3, behaviour at high-temp. 8=49370
- KNO_3, heat capacity, enthalpy and entropy 8=44339
- KNO_3, molten, vib. freqs. by i. r. emission spectroscopy near 600°C 8=38842
- KNO_3, I-II phases, i. r. absorpt. spectra rel. to internal interaction 8=27597
- KNO_3, phase-III, stable and metastable, ferroelec. props., pressure dependence 8=27273
- K–Na liquid alloys, Knight shift obs. 8=25955
- $K_xNa_{1-x}Fe_7O_{11}$, ion mobility 8=48782
- $KNbO_3$, atomic displacements rel. to real structure determ. 8=30887
- $KNbO_3$, e-microdiffr. exam. 8=26430
- $KNbO_3$, spontaneous polarization, elec. field and field gradient calcs. 8=27269
- KNb_3O_8, mica like, dielect. props. 8=40568
- K_2NbOF_5, crystal structure by e-diffr. 8=26404
- K_2NbO_3F, separation from melts 8=48258
- $K_2[Ni(C_2O_4)_2] . 6H_2O$, i. r. spectrum 8=36380
- $KNiF_3$, i. r. transmission spectra 8=27600
- $KNiF_3$, lattice vibration rel. to magnetic ordering 8=48706
- $KNiF_3$ and K_2NiF_4, electron-magnon interaction, effect on absorption band 8=41127
- K_2NiF_4, electronic absorption spectrum 8=41110
- $K_{0.23}NiO_{1.8}$ struct., e diffr. obs. 8=30902
- $K_2Ni_2(SO_4)_3$, langbeinite structure, growth and electro-optical props. 8=39678
- KO, K_2O_2 as impurities on Pt, at 20-1100°C, W, 20-700°C 8=35549
- KO_2, phase transforms and crystal structures 8=26075
- $K_2O-B_2O_3-Al_2O_3$ system glasses, structural units 8=35201
- KOH, solubility of ZnO and electrolytes elec. cond. and vapour press., 10-145°C 8=45373
- KOH, and KOH-ZnO electrolytes, conductivity, 36 to -66°C 8=45372
- K_2O-SiO_2 glasses, comp. vars. in e microanalysis rel. to surface damage, obs. 8=30865
- K_2PtBr_6, luminesc. 8=36505
- K_2PtCl_6, luminesc. 8=36505
- $K_2[Pt(N)_6]$ structure 8=26402
- K-Rb alloys, Zener relaxation 8=49030
- K–Rb liquid alloys, Knight shift obs. 8=25955
- K_2 Rb_2, photon interactions, 3,000-1,100Å spectral range, u.v. cross sections obs. 8=43315
- K_2ReBr_6, mag. ordering from n. diffr. exam. 8=40870
- K_2ReCl_6, mag. ordering from n. diffr. exam. 8=40870
- KSCN, crystal structure refinement from redetermined data 8=44222
- KSCN, melting and polymorphism to 44 kbar 8=48385
- K_2SnCl_6:Pt, luminesc. 8=36505
- $KSnF_3 . \frac{1}{2}H_2O$ crystal structure 8=39798
- $KSr_2Nb_5O_{15}-LaNb_3O_5$ system, ferroelectric props. 8=40611
- $KTa_{0.65}Nb_{0.35}O_3$, lamellae origin 8=48519
- $KTaO_3$, absorpt. edge, elect. field depend 8=32004
- $KTaO_3$, ferroelectric phase transitions, lattice-dynamical theory, elastic and dielectric anomalies 8=27284
- $KTaO_3$, i. r. and Raman spectra 8=27599
- $KTaO_3$, nuclear spin-acoustic phonon interaction 8=45126
- $KTaO_3$, thermal conductivity temp. and field dependence rel. to Cochran modes 8=26605
- KVO_3, V^{51} quardupole coupling tensor 8=31923
- $KY(MoO_4)_2$, structure from growth forms and x-ray diffraction 8=48655
- $KY(WO_4)_2$, crystal structure 8=39797
- $KZnF_3$, i. r. transmission spectra 8=27600

potassium bromide

- breakdown, laser-induced 8=40566
- Bremstrahlung passage, energy losses rel. to beam collimation and crystal thickness 8=31310
- conductivity, elec., ionic, in pure and doped mats. 8=27248
- crystals in organic liquids, interfacial energy calcs. rel. to abrasive wear and adhesion 8=30724
- diffusion of Br, rel. to dislocations and grain boundaries, by isotopic exchange 8=35497
- dislocation motion, velocity temp. and shear-stress dependence 8=26681
- dislocation multiplication 8=26686
- dislocation pinning by lattice defects 8=26680
- electric field grad. at nuclei near substitutional ion, n.m.r. meas. 8=36273
- electric field gradients at nuclei surrounding different subst. halogen ions, n.m.r. meas. 8=48314
- electrical conduction in impure crystals rel. to vacancy migrations 8=40576
- electrolytic colouration, influence of dislocations 8=44469
- electron avalanche, breakdown obs. 8=31421
- electron avalanche, mobility and lifetime obs. 8=31269
- energy loss spectrum, excitons 8=44659
- excitons, longit and transverse, optical absorpt. 8=41107
- F-aggregate bands, optical and thermal stability, half-widths and oscillator strengths 8=49732
- luminescence M-centre 8=41199
- mean inner potential calc. method 8=30629
- mean inner pot. meas. by electron diffr. 8=30628
- neutron-irrad., diffusion and release of Ar gas 8=35498
- optical consts. from energy loss meas. 8=32003
- orientation dependence of fast protons energy loss 8=35602
- plastically deformed, F-centre thermal stability rel. to dislocation density 8=35586
- refractive index and transmittance from asymmetric interferograms, 20-400 cm^{-1} 8=28844
- Schottky defect formation energy, from dissolution of impurity containing precipitates 8=35536
- thermoluminescence, photostimulated, 50-250°K 240-700 mμ 8=27652
- ultrasonic vibrations, generation and reception 8=35988
- volume exansion by $U \rightarrow F$ and $U \rightarrow \alpha$ transforms., photoelastic meas. 8=26826
- X-irradiated, Frenkel defect formation at 8°K 8=40005
- X-ray thermal diffuse scattering by transverse lattice waves 8=44221
- Br nuclei surrounding substitutional Cl ion, field gradient obs. by n. m. r. 8=26403
- KBr:Ag, Greek absorpt. bands 8=36323
- KBr(I), F-centre form. by u.v. irrad. 8=44479
- KBr: In, Zeeman effect of A absorption bands 8=45200
- KBr-KCl solid solutions, luminesc., intrinsic, induced by X-ray 8=41198
- KBr:Li^+, far i. r. props. of lattice resonant modes rel. to isotope shifts 8=36393
- KBr: Li, resonance shift broadening by internal strains on alloying KCl and KI 8=27480
- KBr:Li^+, u.s. velocity and attenuation, temp. and stress dependence, 1.6–77°K 8=35417
- KBr:OH^-, OD^-, dielectric relaxation 8=49344
- KBr:$SrCl_2$, polarisation effects by thermal depolarisation method 8=27245
- KBr: Tl, recomb. luminesc. and F scintillations 8=36493
- KBr:Tl, (In), mono- and di-molecular recombination in luminescence, elec. field 8=45276
- KCl-KBr solid solns., p-irradiated, F-centre generation comp. dependence 8=31117
- KI:Tl, (In), mono- and di-molecular recombination in luminescence, elec. field 8=45276
- KOD doped, dielec. relax. 8=27247
- KOH doped, dielec. relax. 8=27247

potassium chloride

- acoustic emission, rel. to microscopic deform. model 8=26582
- angular correlation functions for OH^- and OD^- 8=43968
- breakdown, laser-induced 8=40566
- Bremstrahlung passage, energy losses rel. to beam collimation and crystal thickness 8=31310
- cationic vacancy displacement during coloration on divalent impurity addition, from conductivity meas. 8=35535
- charge flow during plastic deform., rel. to motion of dislocations 8=35961
- colloidal centres, optical, e.s.r. and elec. exam. 8=44477
- colourability, deformation effects, room temp. 8=31119
- coloured additively, photochemical reaction and photoconductivity, at low temp. 8=31457
- coloured, deformed, photoconduction rel. to dislocation–colour centre interaction 8=44928

Potassium compounds—contd
potassium chloride—contd
compressibility isothermal, meas. by capacitance method 8=49031
conductivity, elec., ionic, in pure and doped mats. 8=27248
crystal growth technique for 10^{-9} mol/mol purity 8=39665
crystals in organic liquids, interfacial energy calcs. rel. to abrasive wear and adhesion 8=30724
crystal polarization by voltage pulses, 100°–350°C 8=40580
crystal structure and mech. and optical props. growth conditions and impurity effects 8=26401
crystallization from acqueous solution, calorimetric study 8=44132
defect interactions in cryst. 8=26633
density changes on γ-irradiation 8=40129
deposition of Au and Ag films, crystal orientation 8=44085
diffusion of Bi ions in cryst. 8=48781
dipped-cathode arc light source for spectroscopy 8=28840
diffusion of protons in aq. soln. 8=48115
dislocation mobility and microhardness dependence on F-centre density 8=26690
dislocation motion, velocity temp. and shear-stress dependence 8=26681
dislocation multiplication 8=26686
dislocation pinning by lattice defects 8=26680
dislocation structure formation by plastic deformation 8=31080
doped crystals, reaction, with H_2 rel. to dislocation decoration mechanism 8=31081
elastic coupling of O_2 centre 8=48337
elect. cond. Teltow 4-defect theory examined 8=27225
electrical conduction in impure crystals rel. to vacancy migrations 8=40576
electron emission due to bombardment with inert gas ions 8=40686
electronic spectra 8=26909
excitons, electronic structure 8=40264
excitons, longit and transverse, optical absorpt. 8=41107
exoelectron emission, photostimulated, external elec. field effects, obs. 8=36041
F-aggregate centres, optical, e.s.r. and elec. exam. 8=44478
F-centres, endor of 8=36272
F centres, simultaneous production and bleaching 8=26720
F_R colour centre 8=26717
film, reflection and absorpt. spectra in u.v. 8=32025
fracture surface as function of crystallographic direction and treatment method 8=44593
grain boundary mobility, meas. technique 8=40052
hardening by F_A centres 8=44583
hardening by n- and γ-irradiation from critical shear stress analysis 8=49037
impure crystals, refractive index and electro-optical effect 8=32005
inert gas depth distrib., sputtering obs. 8=48923
i. r. spectra, temp. dependence, ionic conductivity 8=36381
L bands, absorpt. cross-section for transition from F-center ground state 8=48877
luminescence, M-centre 8=41199
luminescence, X-irradiated crystals under mehcanical impact 8=36491
melted, with unsaturated K solns. thermodynamics 8=48060
neutron-irrad., diffusion and release of Ar gas 8=35498
photostimulated electron exoemission on excitation by electron irradiation 8=40708
plastically deformed, F-centre thermal stability rel. to dislocation density 8=35586
polarisation effects by thermal depolarisation method 8=27245
proton energy loss crystal orientation dependence rel. to lattice effects 8=35598
R-centre transitions from mag. circular dichroism 8=48874
radiation-induced macrodefects 8=26711
r.f. spectra by elec-resonance method, rel. to struct of mol. 8=43316
refractive index and absorpt., far u. v. obs. 8=27592
Schottky defect formation energy, from dissolution of impurity containing precipitates 8=35536
secondary electron emission from porous layers, influence of applied fields 8=36057
solutions in H_2O-alcohol, elec. cond. at high press. 8=39407
spiral patterns and closed loops on etched cleavage faces 8=48525
thermal annealing, Frenkel defect recombination 8=40166
ultrasonic vibrations, generation and reception 8=35988
water evolution on heating in vacuum 8=41263
whiskers, X-irradiated, F-centre accumulation 8=35585
X-irradiated, Frenkel defect formation at 8°K 8=40005
X-irradiated, i.r. absorpt. spectra 8=41104
X-ray scatt. rel. to dislocation density and distrib. 8=45198
CN^- doped, u. s. vel. and absorpt. 8=44316
Cl^- channeling, computer analysis 8=40075
Eu^{2+} doped, optical absorption 8=36379
K^+ channeling, computer analysis 8=40075
KCl: Ag^+, transitions, electronic, of impurities, symm. assignment by two-photon-induced emission 8=36494
KCl: Ba^{2+}, dislocation velocity stress-dependence and yield pt. rel. to Ba^{2+} impurity effect 8=31079
KCl: Cd, uncoloured and coloured, optical, elec. and e.s.r. exam., 8=48876
KCl: $Cu^°$, e.p.r. spectrum, temp. depend. 8=45088
KCl: Cu^+, Ag^+, impurity ion distrib. coeff. on crystallization from melt 8=39674
KCl: Eu, vacancies and dislocations rel. to dopant conc. 8=40001
KCl: H^- interstitial ion, electron-excess colour centre polaron model appl. to U, centre 8=40061
KCl : HF_2^-, broadening of i.r. peak 8=49733
KCl(I), F-centre form. and ICl^- V_K centre due to u.v . irrad. 8=44479
KCl: I, ICl^- V_K centre, optical and e.s.r. exam., 8=48875
KCl: I, luminescence from ICl^-V_K-centre-electron recombination and localized exciton decay 8=27651
KCl: In, F-scintillations, luminesc. kinetics 8=36492
KCl: In, Zeeman effect of A absorption bands 8=45200
KCl-KBr solid solns., p-irradiated, F-centre generation comp. dependence 8=31117
KCl–KBr with Pb admixture, absorption spectra and fluorescence 8=49735
KCl-KI solid solns., decomposition effects on spectral characts. 8=36395
KCl–KI solid solutions, optical absorption 8=49736
KCl: Li, impurity-phonon interactions exam. by sp. ht. meas., rel. to tunneling phenomena 8=44628
KCl: Li, u. s. velocity and attenuation, temp. and stress dependence, 1.6–77°K 8=35417
KCl: LiCl, paraelectric resonance 8=40548
KCl-LiCl, KCl-NaCl, and KCl-KBr, fused mixtures, elect. conductivity and ion conduction activation energy 8=3051
KCl: Li^+, Cu^+, n. q. r. shifts of off-centre ions 8=45136
KCl/NaCl aq. soln., heat of mixing 8=32989
KCl: OH, acoustical paraelec. resonance 8=27246
KCl: OH, dipole interaction through phonon field 8=40577
KCl: Pb, light scattering temp. dependence, 128–298°K 8=45207
KCl: Pb(Ca), impurity ion effect on crystal structure 8=26642
KCl: Pb, F-scintillations, luminesc. kinetics 8=36492
KCl and RbCl, mixed, coloured, L_1 band forbidden transition 8=31118
KCl-RbCl mixed cryst., diff. coeffs. 8=39975
KCl:RbCl, L_1 absorpt. band, new Mollwo-Ivey law 8=36375
KCl: Tl, recomb. luminesc. and F scintillations 8=36493
KCl: Tl, two-e correlation in impurity centres in model pot. approx. 8=32049
KCl : Sr, Z_2 centre, photocond. 8=44929
Li^+ doped, u. s. vel. and absorpt. 8=44316
Na^+ channeling. computer analysis 8=40075
NaCl-KCl, solid solns., decomposition effects on spectral characts. 8=36395
O_2^- and OH^- centres, appl. of point defect theory 8=48800
OH doped, paraelectric resonance characts. 8=49345
Potential energy, gaseous molecules. See Molecules/intermolecular mechanics.
Potential energy, single molecules. See Molecules/internal mechanics; Molecules/vibration.
Potentiometers. See Electrical measurement.
Powder diffraction cameras. See X-ray crystallography/apparatus.
Powder metallurgy. See Metallurgy; Sintering.
Powders
See also Granular structure; Particle size; Sintering; Surface measurement.
in aqueous soln., grain enlargement rel. to crystal production 8=39655
austenite, electrolytic, absence of martensitic transforms. 8=35103
corundum bed, fluidized by vibs. or gas flow, comparison of heat transfer coeffs. 8=39448
dielectric behaviour and struct. of boundaries in highly compressed crystalline powders 8=49325
diffusion parameters in mixture model 8=35472
ferric oxide, influence on ferrite synthesis 8=45035
ferromagnetic, susceptibility calcs. in weak field, model 8=40800
filling particles, form factors meas. rel. to charact. size of each particle 8=39533
fluidized beds, radiative heat transfer with immersed body 8=39456
glass, compression under 10-65 kbar pressure, rel. to optical and mechanical props. 8=40164
grading rel. to dispersion and compactness by means of diffracted intensity 8=43985
grain size determ. from X-ray scatt. intensity 8=30843
of ice spheres, rate of decrease of surface area, rel. to plastic flow 8=35073
i.r. transmission spectroscopy samples, prep. 8=42239
luminescent, deposition by electrophoresis 8=45388
metal compacts, pressure distrib. meas. 8=48950
metallic, echo phenomenon 8=27448
mischmetal-Co alloy, coercivity milling dependence 8=31597
mixture, analysis by photosensitive transformer bridge 8=43984

Powders—contd
mixtures, diffuse reflectance spectrophotometric analysis 8=36636
permittivity calc. for determ. of dielec. constant of crystallites in powder 8=49324
quartz sand, differential thermal analysis, particle size effects 8=26044
radio activity meas. when insoluble in liquid scintillator counter 8=47278
Raman effect, stimulated, observations 8=49684
Raman spectra, laser 8=49685
reactor bed of coated fuel particles, thermal cond. 8=47410
reflectivity meas., Perkin-Elmer attachment 8=28824
Reststrahlen filter, low temp. props. in far i.r. region 8=42197
shear strength, split-ring annular cell meas. 8=35611
sieve, micromesh, u.s. appl. 8=35066
spectrochemical anal., d. c. arc fusion method 8=32154
steel, 18/8 stainless, corrosion and powder formation 8=43983
stilbene, Raman line intensities and dispersion effects elimination, obs. 8=36445
ultramicrotomed, X-ray peak profiles rel. to deformation structures 8=48585
X-ray fluoresc. anal. 8= 32163
X-ray fluoresc. anal., grain size effect 8=45419
Al, nuclear spin-lattice relax. times rel. to press. 8=45110
Al_2O_3, ortho-positronium form. and annihilation 8=49130
B, non-cryst., atomic radial distrib. function, from X-ray diff. studies 8=26043
C, elec. discharge sintering and graphitization 8=30667
Cr_2O_3, Néel temp. depend. on particle size 8=40861
Fe-Co alloy, mag. permeability meas. at 400-40 000 Mc 8=40810
Fe_2O_3, compacts, shrinkage in range 800-1000°C, effect of additives 8=35067
LiF, ground, microstrain and crystallite size determ. from X-ray diffr. line-broadening profile analysis 8=48600
MgO, ortho-positronium form. and annihilation 8=49130
Pd, oxidation 8=41260
SiO_2, ortho-positronium form. and annihilation 8=49130
WC and WC-Co mixed, sintering, effect of 15-45 kbar pressure 8=39536
ZnO, thermoluminesc. spectrum 8=32065
ZnS phosphor, electroluminescence enhancement using resin binders 8=41217
ZnS-type, a.c. electroluminesc 8=36521

Praseodymium
monochalcogenides, antiferromag props., 4-1300°K 8=31761
Pr V, ionization energy calc. and 12 lines, 840-2250 Å obs. 8=47504
Pr^{3+}, absorpt. spectrum and energy levels in hydrated crysts. 8=45215
Pr^{3+} in double nitrates, mag. resonance line shapes 8=31881
Pr^{3+}: $LaCl_3$, i. r. quantum counters, improved sensitivity 8=32940
Pr^{3+} in LaF_3, spontaneous emission probabilities for excited states 8=49805

Praseodymium compounds
Pr-alkali metal tungstates, hydrothermal synthesis and morphology 8=26259
$PrCl_3$, Cl^{35} NQR line splitting below 0. 4°K rel. to anti-ferromagnetic structure 8=36283
$PrFeO_3$-$BiFeO_3$ system, structural transitions rel. to ferroelec. and mag. props. 8=26064
$Pr_2W_2O_9$, structure and hydrothermal synthesis, obs. 8=39636
$PrWO_4Cl$, hydrothermal synthesis and struct., obs. 8=39815

Precipitation
See also Atmosphere/precipitation.
ageing stress- and strain-, terminology 8=31162
in alloys, shape changes by diffusion in dislocation stress field 8=26649
cellular, boundary diffusion limited, anal. of kinetics 8=48533
coherency loss of growing precipitates by prismatic punching of dislocation loops 8=26651
hailstones, artificial, external and internal struct. 8=35228
hardening by coherent particles, review 8=48980
hardening, diffusion in stress field dislocation 8=39537
mangesioferrite, from MgO:Fe solid soln., and coarsening 8=44007
nucleation in condensed phases, linked flux analysis 8=30570
powder-grain enlargement in aqueous soln. 8=39655
semi-coherent precipitates, interfacial structure, electron microscope investigation 8=26656
steel E 1702, of γ^1-phase, mechanism rel. to holding time effects at diff. quenching temps. 8=35108
steel, EI 702, η-phase, mechanism 8=44008
steels, Fe-C and Fe-Ni-C, in hardening rel. to martensite strength 8=26815
thoria, arc-melted, e-microscope obs. 8=30867
vacancies assoc. with pre-precips. 8=31033-4
Al-base Cu, neutron irrad. 8=48379

Precipitation—contd
Al-25 wt. % Zn alloy, effect of quenching conditions 8=26058
Al-Ag alloys, continuous, influence on growth kinetics of cellular reaction 8=39540
Al-Cu alloy, grain boundary precip. 8=26708
Al-Cu-Cd alloys, θ'-precip., vacancy cluster mechanism 8=35085
AlF_3 layer formation on quartz: Al impurity during 3½ yrs. ageing after HF treatment 8=49900
Al-Fe alloy of Fe, Mossbauer study 8=30678
in Al-Fe alloys, morphology and kinetics 8=30677
rel. to Al-0. 04 wt % Fe recryst. and recovery, Fe precip., obs. 8=39664
in Al-Fe-Si alloys, morphology and kinetics 8=30677
in Al:(Fe, Si) sheet, influence on texture formation during final anneal 8=35267
Al-Ge solid solns., and stacking faults 8=31096
Al-Zn-Mg alloy 8=35087
$CaCl_2$ in NaCl 8=48390
CdS : Au, after annealing 8=48375
CdS : Cu, after annealing 8=48375
in Cr, of Cr_2N, effects on brittle-ductile transition temp. 8=44561
Cr-Mo-Co steel, of R-phase, structure and comp. anslysis 8=44001
of Cu in Si, kinetics, near room temp. 8=30705
Cu 1. 79 wt. % Be, discontinuous of γ-phase, orientation 8=43997
Fe, commercial, mechanism, and nature of decomposition products in age hardening 8=40155
FeC_x in carbon steel, particle coarsening at 720°C and 675°C 8=30691
$Fe(OH)_3$, adsorpt. and coprecipitation of Ag 8=48478
KH_2PO_4, precipitates and dislocations exam. by X-ray diffr. microscopy 8=26691
Li, in Si, nucleation and growth 8=44105
in Mo-Fe(8wt. %) alloy, of Mo_6Fe_7 lamellae, and Fe-rich soln at lower temp. 8=35115
Mo-Mn steel, of R-phase, structure and comp. analysis 8=44001
$(NH_4)H_2PO_4$, precipitates and dislocations exam. by X-ray diffr. microscopy 8=26691
Nb-O-N supersaturated solid solns., of oxides and nitrides in annealing, obs. 8=30831
Ni-Al alloys, γ' precip. coarsening 8=35120
Ni 25%-Cr 20%-Nb 0. 7% stainless steel, precips. comp., obs. 8=30805
Si crystals with oxygen and carbon impurities, of SiO_2 and SiC on ht. treatment 8=39702
Si, of B after max. solubility determ. 8=48345
Si-O solid soln, rel. to periodicity changes and anomalous X-ray transmission 8=36409
SiO_2 into $H_2Si_2O_5$ for chem. analysis of glass 8=45413
SiP, on high-conc. P diffusion in Si 8=39983
SnSb in Pb rich alloy of Pb-Sn-Sb ternary system, rel. to aging 8=26764
δ-Su_9In_4, equilib. phase inCu-16. 8% In alloy formed on precip. 8=39548
Ti-22 at. % Nb/Cu composite conductors, of ω particles rel. to critical current densities 8=40419
UO_2-Al_2O_3, grain growth in presence of liq. phase 8=44014
in US crystals, e-microscope exam. 8=35286
V carbides, during $\gamma \rightarrow \alpha$ transform. of austenite in steel 2062 8=35135
ZnS, effect of conditions on particle size and morphology 8=48565
ZrB_2, of second phase particles, struct. and orientation 8=35136
ZrH in Zircalloy-2 and -4, habit planes, obs. 8=44098

Pressure
See also Atmospheric pressure and density; High-pressure phenomena and effects; Radiation pressure; Vapour pressure.
alloys spin density wave to antiferromagnetic transitions pressure effect 8=31767
distribution on cone-cylinders in hypersonic flow 8=34631
drop, in viscous liquid, by sphere setting, Reynold's no. 0. 2 to 21, 000 8=39263
gas, fissioning, pressure wave generation, method of characteristics analysis 8=39170
gas fluidized beds, fluctuations 8=48230
gases, meas. with Mcleod gauge 8=39248
mechanical, rel. to production of imperfections 8=26658
residual gases, partial press. for various means of pumping 8=39242
In N, liq., decreasing effect on bubble growth 8=34738

Pressure measurement
See also Manometers; Vacuum gauges; Vapour pressure measurement.
α-ray gauge for high altitude balloons 8=45964
ballastless diaphragm differential gauge 8=45966
Bayard-Alpert vacuum gauge modification 8=39252
control device for high-vacuum apparatus 8=48004
differential, strain-gauge transducer 8=32642
dual-range mercury/oil manometer 8=28224
dynamic, in gas reaction 8=45319

Pressure measurement—contd
- fluids, at solid boundary, instrument 8=30197
- gas discharge, spectral methods 8=38980
- gas, strain-gauge transducer, control unit 8=28223
- gases, condensible and non condensible with Mcleod gauge 8=39248
- high press., by spectral shift of Ni dimethylglyoxime 8=50477
- high-press., capacitance and resist. piezometers 8=39401
- improvement and development in U. S. S. R. 8=45962
- indicator, differential, calibration technique 8=32645
- ionization gauge, readout system 8=43712
- liquid metals, by automatic manometer 8=48011
- liquid sample holder for n. m. r. 8=34917
- metal powder compacts, distrib. meas. 8=48950
- ocean submerged structure, rising, wall press. vars. in boundary layer 8=45432
- oscillations, dynamic charact. of transducers connecting channels 8=45963
- piezoelectric gauge, miniature, for time dependence of shock waves 8=46174
- of plasma, by piezoelect. probe 8=30096
- plasma, neutral gas, in mag. field var. direction and magnitude, manometer 8=43548
- rapidly changing, method 8=45965
- sealed electrochem. cells, internal press. 8=33035
- thermocouple manometric transducers, thermal rating 8=45961
- transducer for liquid (gas) 8=48012
- transducer for turbulence hydrodynamics 8=28226
- turbulence, wall pressure, orifice hot-wire probe 8=28225
- ultra-high vacuum prod. and meas. 8=39256
- He liquid, transducer for vel. meas. 8=32995
- He^3, expt. thermomolecular press. ratio down to 0.3°K 8=28438
- He^4, var. with temp. 8=37354

Prisms, optical
- coplanar mirror prisms, wedge error and zero error, approx. formulae 8=42151
- dove and right angle, making and testing 8=42235
- Iceland spar 8=42160
- laser, solid, with Kerr cell shutter, appl. 8=24285
- line-scanner for high-speed thermography 8=37322
- polarimeters for use with lasers 8=33158
- polarizing, cutting, rational utilization of geometry of Iceland spar crystals 8=42159
- reflecting, tetrahedral, wedge error and deflection error 8=24362
- ruby laser, speed of Q-switching 8=24332
- for spectra-Fabry-Perot, linear transformation, viewer 8=28834
- spectrometers, calibration with echelle grating 8=33267
- symmetrically crossed half-prisms in autocollimation, parallel-ray tracing 8=42154
- transfer coeffs. in prism system 8=42176

Probability
- See also Random processes; Statistical analysis.
- C*-algebra, rel. to theory, and Mackey's axioms 8=32830
- correlation function, high-speed computation 8=34506
- daily rainfall occurrence, second and higher order stationary Markov chain models 8=32217
- generalized theory, quantum mechanically based, independence, Hilbert space 8=46811
- light-absorpt., steady-state, calc. 8=24409
- non-commutative using Borel structure of C* algebra 8=32655

Procopiu effect. See Films/solid; Magnetoelectric effects; Magnetomechanical effects.

Programming. See Calculating apparatus/digital computer programmes.

Projectiles. See Ballistics.

Projectors, optical
- 8mm. movie, useful light fluxes 8=42282
- near projection screens, theoretical analysis 8=37659
- source enlargement 8=37667
- trapezoidal distortion in projected images 8=42168

Promethium
- Pm I. fundamental energy levels calc. from spectra and Zeeman effect obs. 8=47505
- Pm 147, pure, ion exchange preparation 8=49838

Promethium compounds
- No entries

Prominences, solar. See Sun/prominences.

Propagation. See Acoustic wave propagation; Electromagnetic wave propagation.

Propagators. See Field theory, quantum; Quantum electrodynamics.

Proportional counters. See Counters/proportional.

Prospecting. See Geophysical prospecting.

Protactinium
- diffusion, lattice and grain-boundary, in ThO$_2$ and ThO$_2$–UO$_2$ solid soln. 8=35508
- Pa^{231}, L subshell fluorescence obs. 8=43200
- PaII, magnetic-interaction integrals 8=34147
- U^{233} resistivity, low-temp., α self-irrad. effects, obs. 8=31322

Protactinium compounds
- bromides, crystal struct. obs. 8=26429

Proteins
- actin structure by X-ray scattering and diffr. 8=25674
- aqueous solutions, proton mag. relaxation, dependence on viscosity and temp. 8=39435
- carboxypeptidase A, structure by low resolution technique 8=25675
- chloroplasts, phosphorylation, e. flow and p.-translocation 8=49860
- α-chymotrypsin, crystal structure 8=26477
- collagen and bone, transmission and attenuated total, refl. i.r. spectra 8=32041
- collagen, h. f. dielec. const. 8=30510
- collagen-like, X-ray exam. 8=25682-3
- crystallography, heavy atom location method 8=26548
- DNA additive in water, drag reduction and effect on vel. profiles 8=39265
- DNA, effects of binding agents on X-irrad. 8=48903
- DNA, energy transfer and excited states, from luminescence in soln. of DNA, nucleosides and nucleotides 8=25939
- DNA of phage T2, mol. configs. and lattice structures rel. to glucoside residue effect 8=26490
- DNA rel. to RNA and DNA-RNA hybrids and synthetic analogs 8=26556
- DNA solns, background noise between 300 Hz and 50 kHz 8=30520
- erythrocruorin, crystal structure analysis at 5.5 A resolution 8=48684
- erythrocruorin heavy-atom derivatives structural analysis 8=26500
- ferricytochrome c, beef-heart, e.s.r. 8=31865
- ferritin, crystal and mol. structure 8=26506
- gelatin, regidity and bond energy 7=25972
- gelatine, vitrification temp. 8=48256
- gramicidine S in soln., molecular structure from n. m. r. obs. 8=34332
- gramicidin S, mol. and crystal structures from study of derivatives 8=26509
- haemoglobin crystallization, procedures for human and horse types 8=26210
- helix coil transition in heterogeneous chains 8=47733
- hemoproteins, fine structure of Fe ions 8=35044
- isotypism, statistical tests preliminary to structure determ. 8=26549
- α-keratin, matrix-microfibril texture, by X-ray diffraction and electron microscopy 8=39729
- lactic dehydrogenase from dog-fish muscle structure 8=26515
- β-lactoglobulin, Fourier maps from 2 different crystals 8=26516
- lecithins, polymorphism from lecithin-water phase analysis 8=43435
- lysozyme crystal forms, structural relationships 8=26520
- lysozyme crystals, X-ray exam. of cross-linking at –50°C 8=26519
- lysozyme, proton relaxation of adsorbed H$_2$O 8=49649
- 1-methyl-5-bromouracil: 9-methyladenine, crystal and mol. structure 8=26566
- muscle filament, structure and packing 8=28200
- myoglobins, seal and whale, comparison using rotation-function programme 8=26312
- papain, crystal structure 8=26536
- pepsin, crystal structure 8=26538
- pepsin, isomorphous derivative prep. for x-ray exam 8=30833
- β-poly-γ-methyl-L-glutamate, disordered structural characteristics 8=25677
- polypeptide chains, conformational analysis 8=25673
- polypeptides, energy band structures 8=35777
- polypeptides, molecular weight effect on n. m. r. manifestation of helix-coil transition 8=25637
- polytripeptides with (glycine-iminoacid-iminoacid) sequence, synthesis and X-ray exam. 8=25682-3
- proton relaxation of adsorbed H$_2$O 8=49649
- rabbit psoas muscle, glycerol-extracted, filament lattice studies 8=26458
- rhodopsin extracts in 20°digitonin, luminescence 575-600 mμ 8=49828
- ribonuclease, bovine pancreatic, tertiary structure investigations 8=26557
- ribonuclease, e-density maps obtained using multiple isomorphous replacement 8=26558
- RNA, crystal and mol. structure of double helix 8=26555
- RNA, rel. to DNA and DNA-RNA hybrids and synthetic analogs 8=26556
- s-RNA in water, regularized arrangements and conformational studies 8=25885
- t-RNA, X-ray diffr. study 8=25875
- seal myoglobin, crystal structure determ. at low resolution 8=26532
- secondary structure small deformation model 8=25678
- structure and conformational changes, rotary dispersion 8=29862
- structure determ. by X-ray diffraction 8=32624
- structure refinement 8=25679
- tobacco mosaic virus, binding of Xe 8=25974
- trypsin and DIP deriv., conformation from X-ray scattering of mols. in soln. 8=25681
- virus, crystallization 8=26262
- wool, equilib. adsorpt. of Na dodecyl sulphate 8=30780

Proteins—contd
Cu^{2+} ion in blue proteins 8=49782
Fe(III) porphyrin cpds., zero-field splitting 8=30623
Zn insulin, X-ray study and prep techniques 8=26513
Proton magnetic resonance. See Nuclear magnetic resonance and relaxation.
Proton spectra
(d, p) stripping reactions, Butler–Born approximation approximation 8=43049
Ar^{33} delayed protons, $S^{32}(He^3, 2n)$ obs. 8=38415
$Be^9(d, p)Be^{10}$, asymmetry rel. to spin-orbit interaction, obs. 8=29503
Na^{19} delayed protons, $F^{19}(He^3, 3n)$ obs. 8=38415
Ne^{17} delayed protons, $O^{16}(He^3, 2n)$ obs. 8=38415
S^{29} delayed protons, $Si^{28}(He^3, 2n)$ obs. 8=38415 5
Si^{28}, after μ^- capture 8=29414
$Sn^{116,118}(t, p)Sn^{118,120}$ 13, 12 MeV 8=25269
Te^{111}, β^+ p coincidence meas. 8=47290
Protonium. See Protons and antiprotons.
Protonosphere. See Atmosphere/upper.
Protons and antiprotons
See also Cosmic rays/protons; Nuclear reactions due to/protons; Nucleons and antinucleons.
beams, anomalous deceleration in arc plasma 8=39006
beams on polarized p targets, for direct testing of CPT invariances 8=24909
channeling in single-crystal Au films 8=31286
channelling in ionic crystals, energy losses 8=44672
diffusion of H^+ in aq. salt solns. 8=48115
elastic, isobaric analog resonances, fine structure props. 8=38330
e.m. transitions in three-triplet model 8=38095
extragalactic, mag. cut-off in galactic disc 8=45739
form factors 8=33742
form factor, e.m., depression in charge density 8=47130
form factor, e.m. Hofstader-Wilson formula, theoretical foundation 8=42629
form factors, e.m., three-pole formula 8=24897
form factor in timelike region calc. 8=29184
gyrofrequency band emission in upper atmosphere 8=36821
halo existence rel. to antibound state in p-wave of two-pion system 8=47131
mass difference with n 8=38058
polarized beam source, in $2S_{1/2}$ metastable state 8=38763
n, p, single particle states similarity at same mass number 8=42815
p motions in hydrogeneous liquids by n scatt. cross-section meas. 8=48065
proton-neutron mass difference. Cottingham formula 8=42630
$p\bar{p}$ annihilation, ang. distrib. of π pair prod. 8=33761
p-$\bar{p}$, optical model, Gaussian pot. 8=33747
$p\bar{p} \to \pi^+\pi^-\pi^\circ$ obs., $\rho\pi$, 3π, final states 8=33762
$p\bar{p} \to 3\pi^+3\pi^-\pi^\circ$, 5.7 GeV/c, ρ, A_1, A_2, ω obs. 8=24940
$\bar{p}p \to \bar{n}n$, 50-180 MeV, ang. distrib. obs. for 215 events 8=24942
quark model rel. to discrepancy in h.f.s. of H 8=33743
radio sources, compact, synchrotron emission 8=45756
spectator p study in $\pi^+d \to \pi^+\pi^-\pi^\circ pp$ at 3.65 BeV/c 8=42529
absorption
quality factor in water phantom, depth distrib. 8=33758
angular distribution
asymmetry from reaction $Ca^{40}(d, p)Ca^{41}$ with polarized d 8=29507
cyclotron meas., accidental coincidence background reduction 8=29005
organic scintillator for fast n detect. 8=24979
$C^{12}(e, e'p)$ rel. to p momentum distrib., obs. 8=29413
$Ca^{40}(d, p\gamma)Ca^{41}$, angular correl. 8=29303
$Ca^{40}(n, p)K^{40}$, spectra obs. 8=25243
$O^{16}(\gamma, p_0)N^{15}$, giant resonance obs. 8=29403
$Pu^{239}(d, pf)$, ang. correl. obs. 8=43070
detection, measurement
accelerator, energy meas. 300-2050 keV by n.m.r. 8=33430
aurora, moderate storm, >50 keV rocket obs. 8=32283
delayed protons, counter telescope and transmission detector 8=38414
energy estimation from ionization meas. in nuclear emulsions 8=47114
monitor reactions, effect of thick targets 8=25221
nuclear emulsion track meas., photographic scanning 8=46981
$\bar{p}$ beam purity meas. using δ-ray spectrum 8=47138
range-energy spectrometer for 6-100MeV p 8=50245
satellite spectrometers for 100keV-6MeV p 8=50244
semiconductor detector telescope for satellite, calibration 8=28025
from stripping reactions 8=29494
telescope, meas. from fast n-reaction 8=29456
rel. to ultra-n deficient nuclei identification 8=38424
Al^{27} (p, 3pn) Na^{24}, p flux monitoring, influence of secondary particles 8=33994
CsI(Tl) scintillator for low energy 8=46877
Ge(Li) detector, with side entry geometry 8=46910
Si diode dosimetry 8=38064
Si: Li detector response 8=38103

Protons and antiprotons—contd
effects
alloys, strained, on work function 8=44938
channeling, angular limit to classical description 8=31134
channelled, as probe to generate charact. X-rays rel. to impurity atoms location in cryst. matrix 8=40009
channelling through crystals 8=31137
diamond bombardment, chem. reactions 8=45406
d(p, n)2p, polarization transfer calc., Ep = 30–150 MeV 8=38101
energy loss in KBr, orientation dependence 8=35602
fast, (6.3 MeV), penetration in solid, theory 8=31133
metal foils, rel. to diffusion-out of rare earth impurities on heating in vacuum, 1500-2800°C 8=40081
secondary particles, ang. and momentum distrib., in reactions $p + \text{nucleus} \to p + \pi^+ + \pi^- + \text{nucleus}$, 20–23 GeV 8=47314
structure determs. by protonography 8=26363
10 MeV, on natural targets, 12 isomers obs. 8=47214
Ag films, on resistance, –13 to –158°C 8=40302
Ag, stopping power for 3.75–5.5 MeV p, using (p, n) obs. 8=43030
Al, blistering on 10-200 KeV irradiation 8=40070
Be^7 fragments from irrad. Ta, Pb, U, obs. 8=43115
Cd, stopping power, for 3.75–5.5 MeV, p, using (p, n) obs. 8=43030
Cu, strained, on work function 8=44938
$F^{19}(p, \alpha\gamma)O^{16}$ reaction, proton channelling rel. to γ-ray yield 8=29448
He, e ejectron cross sections calc. 8=34452
He–CO_2 mixture, energy loss freq. distrib. of 43.7 MeV protons 8=29663
In, stoppping power, for 3.75–5.5 MeV p, using (p. n) obs. 8=43030
K vapour, charge exchange, E_0 =2.5-22 keV 8=38761
KBr, fast protons energy loss, orientation dependence 8=35602
in KCl, energy loss orientation dependence rel. to lattice effects 8=35598
KCl-KBr solid solns., F-centre generation rel. to comp. dependence 8=31117
N_2 bombard, Ep=0.56-1.7 keV, spectrum obs. 8=43322
$Na^{22,24}$ fragments from irrad. Ta, Pb, U, obs. 8=43115
Na^{24} from irrad. noble metal and U targets 8=43116
in NaCl, energy loss orientation dependence rel. to lattice effects 8=35598
NaF crystals, R_N and N centre formation at liq. N_2 temp. 8=48883
Ne^{24} from irrad. noble metal and U targets 8=43116
Ni films, at 850 keV on mag. props. 8=36168
Pt, 1.5 in., K_α° and γ prod. 8=33709
Si solar cell damage thermal annealing, 4.6 MeV 8=24101
Si spectrometers, Li drifted and surface barrier, 2.3 MeV 8=28984
Si surface barrier detector damage 8=46897
Si surface-barrier detectors, effects of damage by 0.8-5.0 MeV protons 8=46918
Sn, stopping power for 3.75–5.5 MeV p, using (p. n) obs. 8=43030
interactions
See also Nuclear reactions due to/protons.
annihilation, multineutral state production 8=24944
emulsion nuclei, 5 GeV/c $\bar{p}$, fragment emission, fireball model 8=38065
$e + p \to e^1 + \rho^\circ + p^1 \to \pi^+ + \pi^-$, analysis for ρ° prod. 8=24859
$e^- p \to e^- n\pi^+$, pion form factor evaluation 8=37966
γp in H, ϕ and ρ° prod. cross sections, 15 GeV 8=33724
γp, multipion prod., η°, N^{*++} ρ^- and ω° resonances 8=33669
$\gamma + p \to n + \pi^+$, 500-800 MeV cross section obs. 8=24776
$\gamma + p \to \pi^\circ + p$, recoil p polarization, γ_E = 240–420 MeV 8=33756
$\gamma + p \to \pi^+ + n$, vector meson dominance analysis 8=24787
$\gamma + p \to \pi^+ + n$, E_γ = 165-230 MeV, differential cross-section obs. 8=29126
$\gamma + p \to \pi^+ + n$, n polarization obs. 8=24965
$\gamma p \to \pi\rho n$, 4, 8 GeV/c, comparison with $\pi^- p \to \rho^0 n$ in Vector dominance models 8=37972
Kp with Δ(1238) prod., π trajectory Regge pole analysis 8=29217
K^-, Λ° production, 6 GeV/c 8=38087
K^- p, K*(890)(1420), prod. obs. comparison with Regge pole model 8=33732
K^-p, Λ prod. cross-section, 10 GeV/c 8=33834
K^- p at 1.33 GeV/c, 2-body final states 8=42588
K^-p, 1.7-2.7 BeV/c, Ξ^-, Ξ^* prod., spin and decay parameters 8=24997
K^-p, 5.5 GeV/c, Ω^- prod. obs. 8=29213
K^- p, 6 GeV/c, cross-sections obs., density-matrix elements estimate 8=33705
$K^- p \to \gamma\Lambda$, rel. to isospin props. of e. m. interactions, predictions of quark model 8=37916
$K^- p \to \bar{K}N\pi$, 1.33 GeV/c, $\bar{K}^*(890)N$, $N^*(1236)\bar{K}$ and $Y_0^*(1520)\pi$ prod. 8=33706
K^+ p, 5.5 GeV/c, K(13)) prod. 8=38024
K^+ p at 9 BeV/c, hyperon prod. 8=24991
K^+ p, S = 2 boson resonance in mass region 1.0-3.1 GeV search 8=38045

Protons and antiprotons—contd
interactions—contd
$K^+p \rightarrow K^+\pi^+n$, double peripheral model 8=29156
Λ-p, low energy obs. 8=33838
meson-proton coherent prod. and deck effect best with deuterium 8=24911
np, 14-27 GeV/c, total cross-section and Glauber screening protection 8=29196
in nuclear emulsion, with d and t prod., 6.2 and 28 GeV/c 8=38099
photoproduction of η, theoretical cross section 8=24838
photoproduction of K, π, Regge-pole model 8=29124
photoprod. of π°, 500-1000 MeV, p polarization obs. 8=29189
photoprod. of π° on p, 500-1000 MeV, p polarization obs. 8=29189
photoproduction of π°, η°, 6-17.8 GeV 8=42523
photoproduction of π^+, absorptive correction, 2 ~ 4 GeV 8=37971
photoproduction of π^+, conspiracy test 8=24774
Photoprod of π, calc. of Δ(1236) partial-wave amplitude 8=33840
photoproduction of π on Λ , superconvergent sum rule 8=42512
π electroprod, radiative corrections obs. 8=24775
$\bar{p}$-nuclei, ^{8}Be emission cross-section; 5 GeV/c 8=47132
p-n final state interacts. in d(p, 2p)n and p(d, 2p)n reactions 8=24902
$p + n \rightarrow \Delta^{++} + \Delta^-$, exchange mechanism 8=24917
$\bar{p} + n \rightarrow W^- \rightarrow e + \bar{\nu}_e$, form factors and polarization 8=42642
pN, Ep = 20 GeV, secondary asymmetric separation obs. 8=29186
$\bar{p}$N annihilation, multiple particle prod., unitary-symmetrical statistical model 8=33546
$\bar{p}$-N interactions in photo-emulsions, obs. 8=42641
polarized, as nuclear probes 8=47313
πp, multipion prod., 4-11 GeV/c statistical model 8=33672
πp with Δ(1238) prod., π trajectory Regge-pole analysis 8=29217
$\pi p \rightarrow \rho N^*$, energy- and momentum-transfer dependence of cross-sections 8=37981
$\pi^- p$, A_2(1300) region structure, 6 GeV/c 8=38035
$\pi^- p \rightarrow \eta n$, polarization and F/D coupling of N_ν
$\pi^- p \rightarrow \eta^\circ n$, 10 GeV/c obs. 8=29160
$\pi^- p \rightarrow \gamma n$, $N^{*\circ}$ e.m. couplings determ. 8=37916
$\pi^- p \rightarrow K_1^\circ K_1^\circ n$, 4 and 5 GeV/c obs. 8=42537
$\pi^- p \rightarrow n$ + missing mass, 2.12 GeV/c particle mass determ. 8=38032
$\pi^- + p \rightarrow N^* + \pi^+$ PCAC constraint 8=33678
$\pi^- p \rightarrow \pi^- p\eta^\circ, A_2^-$ obs., 5 GeV/c 8=38036
$\pi^- p, \rightarrow \pi^\circ K^+ \Sigma^-$, Argand diagrams bootstrap theories and Regge poles comparison 8=42443
$\pi^- p \rightarrow \pi^\circ n$, 2 to 5 GeV, polarization data interpretation using interf. model 8=24791
$\pi^- p \rightarrow \pi^\circ n$, Regge-pole model with absorptive corrections 8=42536
$\pi^- p \rightarrow \pi^\circ \pi^\circ n$, data about s-wave ππ scatt. 8=42541
$\pi^- p \rightarrow \pi^+\pi^- n$, E = 360, 430 MeV, isobar amplitude determ. 8=29134
$\pi^- + p \rightarrow \phi + n$ followed by $\phi \rightarrow e^+e^-$, partial width obs. 8=33722
$\pi^- p \rightarrow p(\pi^-\pi^-\pi^+), p\pi^\circ(\pi^-\pi^-\pi^+), n\pi^+(\pi^-\pi^-\pi^+)$, 5 BeV/c, mass spectrum of $\pi^-\pi^-\pi^+$ 8=37977
$\pi^- p \rightarrow p + MM^-$, differential cross section rel. to momentum transfer, 11.5 GeV/c 8=37976
$\pi^- p \rightarrow p\rho^-\rho^\circ$, 8 GeV/c, evidence for new meson resonance in $\rho^-\rho^\circ$ enhancement 8=38023
$\pi p \rightarrow \rho^- p$, 4 GeV/c, absorpt. model with one-pion-exchange 8=47110
$\pi^- p \rightarrow \rho^\circ n$, 4 and 8 GeV/c comparison with $\gamma p \rightarrow \pi^+ n$, Vector dominance model 8=37972
$\pi^- + p \rightarrow \rho^\circ + n$, vector meson dominance analysis 8=24787
π° photoprod. below 234MeV multipole analysis 8=24777
$\pi^\circ p \rightarrow \pi^\circ \Delta^{++}$(1238) Regge-pole model with absorptive corrections 8=42536
$\pi^+ p$ at 850 MeV/c, cross section obs. 8=24792
$\pi^+ p \rightarrow K^+ \Sigma^+$, parity determ. of KΣN 8=24995
$\pi^- p \rightarrow \pi^+\pi^-\pi^0\Delta^{++}$, 3-4 GeV/c obs., H enhancement, kinematic origin 8=37978
$\pi^+ p \rightarrow \pi^+ pp\bar{p}$, 8.4 BeV/c, resonance parameters of N isobar 8=24789
$\pi^+ + p \rightarrow \Sigma^- + K^+$ 1145 MeV/c, Σ^- polarization determ. 8=24996
production of ρ^0, ang. distrib. obs. 8=37914
p-T, review, spin-orbit effect negligible 8=29222
secondary particles, ang. and momentum distrib., in reactions $p + \text{nucleus} \rightarrow p + \pi^+ + \pi^- + \text{nucleus}$, 20-23 GeV 8=47314
T[p, p(γ)(n)]T, He^4, He^3, diff. cross section extrema due to excited state of He^4, Feymann diag. 8=24914
$\Sigma^- p$ capture $\Sigma^\circ n/\Lambda^\circ n$ ratio and $\Sigma^- - \Lambda^\circ$ mass difference 8=38092
Σ^--p, low energy obs. 8=33838
Σ^+-p, low energy obs. 8=33838
He^3 photodisint., two-body, calc. 8=25018
O_2, excitation by 0.15-1.0 MeV p 8=38847

Protons and antiprotons—contd
interactions, proton—proton
bremsstrahlung cross-sections using separable nuclear interact. 8=24899
bremsstrahlung emitted at 61.8 MeV 8=24898
bremsstrahlung prod. at energies between 1 and 10 MeV, rel. to $^1S_0$ state 8=24908
bremsstrahlung prod., calc. using pot. model and initial and final scatt. wave functions 8=24900
bremsstrahlung at 10.5 MeV, obs. 8=24906
bremsstrahlung at 20 MeV, 35°, obs. 8=24903
bremsstrahlung at 20 MeV, 35°, theory 8=24904
bremsstrahlung obs. at 52.3 MeV 8=42633
bremsstrahlung, 61.7 MeV, obs. 8=24905
charge asymmetry comp. with n-n data, rel. to energy difference between He^3 and H^3 8=24950
collision, Regge-pole model for ρ°, ω° prod. 8=24858
collisions, 1-32 GeV/c, data compilation 8=24863
deuteron prod., differential cross-sections, 1.5 to 3 GeV 8=42668
K^+ prod., 2.85, 2.4 BeV obs. 8=29188
nucleon isobar prod. at 3-7 GeV/c 8=42634
one π prod. anal. in one-boson-exchange model 8=24920
π-production amplitudes and partial-wave p-p absorpt. below 1.5 GeV 8=24901
polarized targets and p and $\bar{p}$ beams, for direct testing of CPT invariances 8=24909
$p\bar{p}$ annihilation, meson prod., quark model 8=29103
$\bar{p}p$ annihilation, multiple particle prod., unitary-symmetrical statistical model 8=33546
$\bar{p}p$ rel. to total cross-section 1.3 GeV/c struct., 1.2-1.6 GeV/c 8=33760
$\bar{p}p$ with Δ(1238) prod., π trajectory Regge-pole analysis 8=29217
$p + p \rightarrow d + \pi^+$, differential cross sections calc. 8=33745
$pp \rightarrow \Delta^{++}p\pi^-$, 6.6 GeV/c double Regge-pole analysis 8=24912
$\bar{p}p \rightarrow KK3(4)\pi$, analysis of results with prod. of various mesons, 1.2 GeV/c 8=33759
$\bar{p}p \rightarrow \bar{n}n$, branching in the j-plane 8=38063
$pp \rightarrow nN^*_{1238}$ rel. to $N^*_{1238} \rightarrow p\pi^+$ decay 2.8-10 GeV/c 8=38096
$pp \rightarrow NNk\pi$, Satz additive quark model for cross section 8=24808
$p\bar{p} \rightarrow \pi^+\pi$, 5.7 GeV/c 8=47137
$pp \rightarrow \pi^+\pi^-\pi^\circ$, at rest 8=38042
$n\bar{n} \rightarrow \pi^+\pi^-\pi^\circ$ obs. ρπ. 3π final states 8=33762
$p\bar{p} \rightarrow 3\pi^+3\pi^-\pi^\circ$, 5.7 GeV/c, ρ, A_1, A_2, ω obs. 8=24940
$pp \rightarrow pn\pi^+$, 0.5-0.7 GeV, calc. confirming peripheral model 8=33744
$pp \rightarrow pp\pi^+\pi^-$ at 8.1 GeV/c, cross section obs. 8=24915
$pp \rightarrow \Sigma^+K^\circ p$, cross-section calc. 8=24913
$pp \rightarrow \Sigma^+K^+n$, 5 GeV/c cross-section obs. 8=24913
s-wave shape-dependent parameter P, Q of effective range expansion, 0-10 MeV 8=42631
seconcary spectra, non resonant, at 30 BeV/c, resulting from central and peripheral interacts. 8=24910
6 GeV/c, (Nπ), (Nππ) isobar contrib. obs. 8=29187
6.92 BeV/c, YN resonances not obs., $N^*_{3/2}$ (1236), Y_1^* (1385) obs. 8=24916
total cross section compared with n-p 8=29196
magnetic moment
No entries
polarization
accessory polarimeter for (d, p) reaction spectrometry 8=24496
beam in storage ring, strong-interaction methods 8=47008
cyclotron accelerator beam depolarization calc. 8=37824
from (d, p) reactions, BHMM theory 8=43048
in (d, p) stripping, Mott-Schwinger interaction calc. 8=25261
in p-d elastic scatt. between 22-46.3 MeV 8=38464
elastic scatt. by complex nuclei 8=29421
elastic scattering by C 8=47136
e-p scatt. 900 MeV, obs. 8=29189
from $\pi^- p$ scatt., various angles, 229 to 390 MeV 8=42558
horizontal cryostat for targets 8=24939
$K^- p$ elastic scatt., 1.4-2.4 GeV/c 8=38017
Lamb-shift source, enhancement by static field methods 8=37436
phasotron accelerator beam depolarization calc. 8=37824
πp elastic scatt. at 550-1025 MeV 8=33757
π photoprod, of recoil p 8=24773
π° photoprod. 500-1000 MeV obs. 8=29189
$\pi^+ p$, 2-4 GeV/c, different from prediction from adding resonant and Regge exchange amplitudes 8=33688
polarimeter for isobaric analogue state spin meas. 8=42640
(p, p) asymmetry, 20 MeV obs. 8=24938
in pp elastic scatt. with fixed momentum transfer 8=47133
in p-p elastic scatt. with fixed momentum transfer 8=47133
in pp scatt. expts. at 150 and 600 MeV by Orsay group, survey of results 8=24923
recoil form $\gamma + p \rightarrow \pi^\circ + p$ 8=33756
sources 8=24161
from Ba^{138}(p, p) at 9.6-12.0 MeV 8=42901
and C_{nn} meas. using polarized target, at energies between 0.5 and 1.2 GeV 8=24923
C^{12} stripping obs. 8=25238
from $Ca^{40}(d, p)Ca^{41}$, E_d = 5 MeV 8=43063
from Ce^{140}(p, p) at 9.6-12.0 MeV 8=42901

- **Protons and antiprotons**—contd
  - **polarization**—contd
    - He^3 elastic scatt., Ep = 30 MeV, obs. 8=29192
    - He^4, 10 MeV scatt., obs. 8=43006
    - Li^7(p, α)He^4, rel. to ang. distrib. 8=25226
    - Li^7(p, α)He^4, E_p = 3-10 MeV, analysing power 8=29437
    - from Sn^{116,118,120}(p, p), 6.7–9.5 MeV 8=43015
  - **production**
    - beam extraction, slow, from 70 sychrophasotron 8=47004
    - π^- + Xe interactions, correl. p pairs prod., 9 GeV 8=34024
    - polarized, sources 8=24161
  - **scattering**
    - analogue state excitation in heavy nuclei, microscopic calc. 8=38466
    - beam penetrating cold electrons, rel. to Akasofu's hypothesis 8=41409
    - elastic, by complex nuclei, polarization 8=29421
    - elastic, optical model calc., 18.6 MeV 8=29420
    - e-p, 5 BeV, inelastic, search for heavy e 8=24714
    - e-p, 900 MeV, p polarization obs. 8=29189
    - e-p, inelastic, obs. of first πN resonance 8=37938
    - e-p, polarization effects for ultrarelativistic electrons 8=37942
    - e-p, e$^+$-p ratio obs. equal to unity up to (5 GeV/c)^2 8=42639
    - ep $\rightarrow$ eN*, quark model, form factors 8=33631
    - $e^- + p \rightarrow e^- + p + \pi^\circ$, differential cross-section near N* (1236) reson., obs. 8=33671
    - excitation of He 8=38698
    - γP Compton scatt., < 150 MeV, expt. and calc. 8=24696
    - inelastic, 30 MeV, theoretical analysis 8=29422
    - inequalities satisfied by a function of the amplitude 8=33576
    - isobaric analogue resonances, closed n shells 8=29423
    - isobaric analogues excitation, spectroscopic factors 8=38321
    - $K + p \rightarrow K + \pi + p'$, cuts in complex l-plane 8=24834
    - K$^-$-p, 6 GeV/c obs. 8=42553
    - $K^-p \rightarrow \Lambda\eta$ in modified exchange model 8=33707
    - K$^+$p, forward scatt. amplitude, prediction of ΛKN and ΣKN coupling constants 8=24833
    - K$^\pm$p forward, dispersion relations calc. 8=24830
    - K$^\pm$p real part predicted by dispersion relation 8=24831
    - K$^+$-p, rel. to diffraction amplitude, ρ and hyperon exchanges, elastic at 3.5 and 5 GeV/c 8=38018
    - K$^\pm$ + p, 0.6-2.65 GeV/c obs., Y_1*, Y_0* resonances obs. 8=29159
    - K_2°-p, 168-343 MeV/c meas. for determ. of $\overline{K}$N s-wave scatt. length 8=33709
    - $K_2^\circ + p \rightarrow K_1^\circ + p$, domination by ω exchange 8=42587
    - Λ-p rel. to n-p tensor interaction in $_\Lambda H^3$ 8=25012
    - n-p bound in $n + d \rightarrow p + 2n$, 199 MeV obs. 8=24961
    - n-p bremsstrahlung deduced from p-d 8=29182
    - n-p, 199 MeV, cross-section obs. and polarization 8=24961
    - n-p, 60-100 GeV, from cosmic ray absorpt. in paraffin and graphite 8=38248
    - nuclear, 19.3 BeV/c, Cabibbo-Horwitz-Ne'eman treatment 8=25217
    - nucleus, reformulated optical model 8=42790
    - optical potential, real central part 8=33988
    - phosphorus 8=25222
    - polarimeter for isobaric analogue state spin meas. 8=42640
    - πN, soft-pion calc. of low energy parameters, unitarity correction 8=24796
    - πp, obs. of p polarization 8=33757
    - πp, Regge parameters, relation derived, one-parameter fit to cross-section 8=33689
    - π^-p obs. at 8, 16 GeV/c, Regge-pole fit 8=37995
    - π^-p, 229-390 MeV, polarization parameter meas. 8=24812
    - π^--p, 6 GeV/c, 8 GeV/c obs. 8=42553
    - $\pi^-p \rightarrow \pi^-p\gamma$, role of $\gamma 3\pi$ interaction 8=24807
    - $\pi^-p \rightarrow \pi^\circ n$, secondary Regge contributions to total cross-section 8=37996
    - $\pi^-p \rightarrow \pi^\circ n$, 561-2, 106 MeV/c obs. 8=24811
    - $\pi^-p \rightarrow \pi^\circ n$, 2.4-3.8, 6, 10 GeV/c $N_{\delta\Lambda}$, $N_{1\Lambda}$* obs. 8=29160
    - π^+p, dip u ≈ - 0.15 (GeV/c), interference of N_α, N_γ fermion Regge trajectories 8=33687
    - π^+p, 1.7–7.8 GeV/c, cross-section without Regge-pole theory 8=33688
    - $\pi^\pm$-p, backward, data on Regge trajectory functions N_2 and Δ_δ 8=42434
    - $\pi^\pm$p, dips in differential cross sections at t = 3 (GeV/c)^2 at 180° at 2.1 GeV/c 8=42554
    - $\pi^\pm$p, Regge-pole analysis of backward peaks 8=24810
    - $\pi^\pm$p, 0.46-2.67 GeV/c obs. 8=29139
    - $\pi^\pm$-p, 6-17 GeV/c, structure obs. 8=42561
    - $\pi^+p \rightarrow N^+\rho^\circ$, absence of dip in differential cross section at 8 GeV/c 8=37982
    - $\pi^+p \rightarrow \pi^+p\gamma$, isobar Δ^{++} (1236) mag. moment meas. 8=24809
    - $\overline{p}$, elastic, by emulsion nuclei rel. to optical model params., 3GeV/c 8=43000
    - pn, charge exchange, branching in j-plane 8=38063
    - p-n, polarization and spin-correl. meas., rel. to phase-shift anal. 8=24955
    - pn, pp, Chou-Yang diffraction model, proton and neutron form factors proportionality obs. 8=47140
    - p-T obs. 300-990 KeV 8=29185
    - from quartz, Rutherford, orientation depend. 8=44504

- **Protons and antiprotons**—contd
  - **scattering**—contd
    - Rutherford scatt. by He, Ne and Ar 8=38754
    - t-p, 147-530 MeV obs., possible resonance 8=25007
    - 30 GeV, e.m. effects on cross-section 8=37952
    - Al^{27}, 6.4 MeV, excitation functions, fluctuation analysis 8=29442
    - Ar^{40}, resonances near 1.1 MeV 8=47241
    - B^{11}(p, p), (p, p$'$), cross-sections and polarizations obs. 155 MeV 8=43007
    - Ba^{138}(p, p), polarization, E = 9.6-12.0 MeV 8=42901
    - Be^9(p, p)Be^9 near the threshold for Be^9(p, n)B^9, 2.21 MeV, structure obs. 8=43014
    - C, polarization obs. 8=47136
    - C^{12}, E_p = 152 MeV, inelastic, impulse-approximation calc. 8=47315
    - C^{12}, elastic and inelastic at 1 GeV, WKB calc. 8=25223
    - C^{12} optical model calc. at 152 MeV 8=42998
    - C^{12} optical-model pot., phenomenological, energy dependence 8=29429
    - C^{14}, elastic scatt., 12.54 MeV level obs. 8=43004
    - C^{14}, Ep = 1–2.7 MeV, differential cross section obs. 8=43008
    - Ca^{40}, control and spin-orbit optical potential calc. 40 MeV 8=43011
    - Ca^{40}, inelastic, Sc^{41} two particle-one hole states, obs. 8=33905
    - Ca^{40}, microscopic description 8=29422
    - Ca^{40} optical-model pot., phenomenological, energy dependence 8=29429
    - Ca^{40} (p, p^1), polarization and cross section DWBA calc. of 3$^-$ level, exchange terms effect 8=33996
    - Ca^{40}, E_n = 155 MeV, optical-model analysis 8=29428
    - Ca^{42,44}(p, p$'$), shell-model form factors, analysis, 22.9 MeV 8=43010
    - Ca^{43}(p, p$'\gamma$)Ca^{43}, γ spectra obs., 2.550, 3.235, 3.605 MeV 8=43027
    - Ca^{44}, elastic and inelastic at 17.5 MeV, levels obs. 8=47317
    - Ce^{140}(p, p), polarization, E = 9.6–12.0 MeV 8=42901
    - Cl^{37} 1-18 MeV, isobaric analog states of Cl^{38} 8=25118
    - Cr^{52} (p, p$'\gamma$), p spin-flip in 2$^+$ level, 11 MeV 8=33989
    - Cr^{52}, polarized p elastic and inelastic scatt., asymmetry, 18.6 MeV 8=29430
    - Cu^{63}, polarized p elastic and inelastic scatt., asymmetry, 18.6 MeV 8=29430
    - Cu^{63,65}, excitation functions, search for p-n channel coupling near threshold for (p, n) reaction 8=25225
    - Cu^{63,65}(p, p$'\gamma$)Cu^{63,65}, γ-ray de-excitation obs. 6.5 MeV 8=43012
    - Cu surface, E_n = 40-120 keV, obs. 8=47135
    - Fe^{54}, polarized inelastic scatt. asymmetry, calc. 8=29431
    - Fe^{54} (p, p$'\gamma$), p spin-flip in 2$^+$ levels, 11 MeV 8=33989
    - Fe^{56}, excitation functions, search for p-n channel coupling near threshold for (p, n) reaction 8=25225
    - H atom, Sturmian coupled-state calc. 8=38736
    - H-bonds, neutron scatt. 8=24963
    - p-H with variable effective charge, cross sections calc. 25 keV 8=38752
    - H^3–p, 3–11 MeV, no sharp structure 8=24937
    - p-He nuclei, angular distrib. rel. to nucleus struct., 1 GeV 8=33845
    - He^3, Ep = 30 MeV, polarization obs. 8=29192
    - He^4, elastic scatt. rel. to diffr. approx., 600 MeV 8=33746
    - He^4, optical model calc. at 152 MeV 8=42998
    - He^4, 10 MeV, polarization obs. 8=43006
    - p-He^4, nucleons released at 660 MeV 8=25227
    - p-He^4, 1.7 BeV/c, cross-section calc. 8=29230
    - p-He^4, spin dependence, and test for existence of Regge cuts 8=42635
    - Hf^{180}, Hf^{181} analogue states and structure obs. 8=33933
    - $La_2Mg_3(NO_3)_{12} \cdot 24H_2O$ crystal, E_p = 660 MeV, obs. 8=48924
    - Li^6(p, p), Be^7 compound nucleus, resonance parameters determined from cross-sections 8=42832
    - Li^{6,7}(p, p), (p, p$'$), cross-sections and polarizations obs. 155 MeV 8=43007
    - Mg^{24}, E_p = 155 MeV, optical-model analysis 8=29428
    - Mg^{24} optical model calc. at 152 MeV 8=42998
    - Mg^{24}(p, p$'$), collective-model analysis, 49.5 MeV 8=47316
    - Mg^{26}, level lifetimes and mixed nature of rot. bands 8=33902
    - Mn^{55}, excitation functions, search for p-n channel coupling near threshold for (p, n) reaction 8=25225
    - N^{14}(p, p), (p, p$'$), cross-sections and polarizations obs. 155 MeV 8=43007
    - Nb^{91} analog states elastic proton decay widths, shell-model calc. 8=47250
    - Ni foils, thin, 15-90 keV energies 8=29432
    - Ni, polarized inelastic scatt. asymmetry, calc. 8=29431
    - Ni^{58}, central and spin-orbit optical potential calc. 40 MeV 8=43011
    - Ni^{58} optical-model pot., phenomenological, energy dependence 8=29429
    - Ni^{58,62,64}, polarized p elastic and inelastic scatt., asymmetry, 18.6 MeV 8=29430
    - O^{16}, elastic and inelastic at 1 GeV, WKB calc. 8=25223
    - Pb^{204,206,207} (p, p), (p, p^1), isobaric analog resonances, 10-16 MeV 8=38397
    - Pb^{206,207,208} rel. to collective excitations, 24.5 MeV 8=29435
    - Pb^{207,208}, excitation of anologue states, calc. 8=38466

Protons and antiprotons—contd
scattering—contd
Pb^{208}, central and spin-orbit optical potential calc. 40 MeV 8=43011
Pb^{208} (p, p^{I}), polarization and cross section DWBA calc. of 3$^-$ level, exchange terms effect 8=33996
Pb^{208}(p, p')Pb^{208}, 4$^-$ lowest state configurations 8=33936
Pb^{208}(p, p')Pb^{208}, Bi^{209} single-particle analogue resonances total width 8=33941
S^{32}, E$_p$ = 155 MeV, optical-model analysis 8=29428
Sc^{45}, elastic and inelastic at 17.5 MeV, levels obs. 8=47317
Sc^{78,80,82}(p, n) Br^{78,80,82}, excitation curve obs. 8=42884
Si^{28}, E$_p$ = 155 MeV, optical-model analysis 8=29428
Si^{28} optical model calc. at 152 MeV 8=42998
Si^{29} inelastically, proton spin flip in 2$^+$ state excitation, 30, 40 MeV 8=43009
Sm^{148}, elastic and inelastic rel. to spectroscopy appls., obs. 8=29434
Sm^{148,152} to 10-12 MeV, excitation of 2$^+$ levels, spin-flip probabilities 8=43016
Sm^{154}, elastic and inelastic rel. to spectroscopy appls., obs. 8=29434
Sn^{116,118,120}(p, p), energy levels obs., 6.7-9.5 MeV 8=43015
Sn^{118}(p, p')and Sn^{119}, cold nucleus, isobaric analogue resonances E = 8.2-12.0 Mev 8=42801
Sn^{120}, central and spin-orbit optical potential calc. 40 MeV 8=43011
Sr^{88}, Y^{89} analog levels, calc. of damping and escape widths 8=25135
Ti^{46}, elastic and inelastic at 17.5 MeV, levels obs. 8=47317
V^{51}, 4.005-5.515 and levels of Cr^{52} 8=25224
W^{183}, Coulomb excitation and Mossbauer effect 8=47262
Y^{89} analog states elastic proton decay widths, shell-model calc. 8=47250
Y^{89}, isobaric analog resonances of Zr^{90} 8=25137
Y^{89}(p, p)Y^{89*}, rel. to isobaric-spin analogue resonances in Zr^{90} 8=43013
Yb^{173,175} (p, p) and (p, p') rel. to analogue states, obs. 8=29338
Yb^{174}, elastic and inelastic rel. to spectroscopy appls., obs. 8=29434
Zr^{90,92,94}(p, p'), E$_p$ = 12.7 MeV. obs. 8=29433
scattering, proton—deuteron
amplitude, real part obs. at 1 GeV 8=24928
bremsstrahlung obs. at 197 MeV protons 8=29182
differential cross-sections, proton polarization, elastic between 22-46.3 MeV 8=38464
spin dependence, and test for existence of Regge cuts 8=42635
scattering, proton-neutron. See Neutrons and antineutrons/ scattering, proton–neutron.
scattering, proton–proton
bremsstrahlung, coplanar and non-coplanar, potential model calc. 8=24907
bremsstrahlung cross-section in terms of quasi phases of pp off shell matrix 8=24930
differential cross-section meas. at 50 MeV 8=24918
differential cross section, polarization in p-p scatt., 98 MeV 8=38059
differential cross-sections and phase-shift anal., normalized at 50 MeV 8=24926
diffraction-like structure, large momentum transfer, 7 and 12 GeV/c 8=33749
diffraction model for asymptotic limit of cross section 8=24936
Elastic, differential cross section, 1 GeV 8=33845
elastic, high-energy, cross-section kinks 8=29190
elastic, large-angle, differential cross-section angular var. 8=29191
elastic, Pearson and Coz theory 8=34025
elastic $^1S_0$, velocity-dependent pot. parametrization 8=42637
e.m. effects on cross-section at high energies 8=37952
forward amplitude, spin independent, real part, 1.29, 1.39 and 1.54 GeV/c 8=33752
high energy fixed momentum transfer, polarization 8=47133
meson bremsstrahlungs model taking phase space into account 8=24758
Morse pot. of offshell $^1S_0$ 8=47134
narrow dips at large $|t|$, high-energy 8=33751
and np, phase shift anal. at 18.2 and 9.9 MeV 8=42627
partial wave amps, empirical, rel. to coupling consts of scalar and vector mesons 8=24748
phase-parameter multiple-energy fits for energy range 8 to 340 MeV 8=24934
phase-shift anal. and elastic scatt. matrix 8=24927
phase-shift anal. of data in 140 and 50 MeV region 8=24935
phase shift anal. in inelastic region, 400 MeV to few GeV, new scheme 8=29421
$^3P_0$, $^3P_1$ absorpt. violation of unitarity, 1 GeV 8=24933
polarization, depolarization and correl. meas. at 150 MeV and 600 MeV by Orsay group 8=24922
polarization, Wolfenstein parameters meas., 430 MeV 8=33753
(p, p) and (p, p'), Cd^{107} analogue resonances obs. 8=33922
$\bar{p}$p elastic 63-175 MeV, cross-section obs. 8=24941
$\bar{p}$-p, elastic scatt. cross section and angular distribution obs. 6.9 GeV/c 8=38060

Protons and antiprotons—contd
scattering, proton—proton—contd
p$\bar{p}$, high energy fixed momentum transfer, polarization 8=47133
(p, p), length calc. from (He^3, d) 8=43005
p-p, optical model, Gaussian pot. 8=33747
p-$\bar{p}$, optical model, Gaussian pot. 8=33747
$\bar{p}$-p scatt., partial-wave analysis and optical model, E$_p$ = 50-180 MeV 8=33750
$\bar{p}$p with Δ(1238) prod., π trajectory Regge-pole analysis 8=29217
p$\bar{p}$, 5.7 GeV/c, elastic 8=47137
p-p, 6 GeV/c obs. 8=42553
$\bar{p}$p → $\bar{n}$n, 50-180 MeV, ang. distrib. obs. for 215 events 8=24942
Regge-pole fit 8=38061
$^1S_0$ phase shift anal. with np data rel. to charge splitting 8=24929
$^1S_0$-wave, approx. analytical soln. 8=24932
S-wave scatt., vacuum polarization effects 8=33748
Serber's model at high energy transfer, anal. with Bakamjian-Thomas theory 8=42636
off shell scatt. in $^1S_0$ channel, computed cross-sections for energies around 5 MeV 8=24919
spin-correlation parameter meas. and comparison with phase-shift models 8=24925
spin-spin correl. C$_{NN}$, 305-415 MeV obs. 8=42638
Wolfenstein amps at t = 0, phase shift dual. rel. to meson-nucleon coupling 8=24931
1-400 MeV phase-shift energy depend. 8=33754
9-330 MeV twelve models 8=38062
350-750 MeV, scatt. matrix determ. up to 450 MeV 8=33755
600-650 MeV, phase-shift anal. and determ. of most probable set 8=24873
at 0.97 GeV, anal. in one-boson-exchange model 8=24920
C$_{NN}$ meas. at 5 energies, 305 to 415 MeV, comp. with theory 8=24924
C$_{NN}$ parameter and polarization meas. using polarized target, 0.5 to 1.2 GeV 8=24923
antiprotons
annihilation, four-prong, 1.2 GeV/c 8=38066
annihilation in liquid hydrogen, multineutral state production 8=24944
beam purity meas. using δ-ray spectrum 8=47138
cosmic ray $\bar{p}$-e$^+$ flux ratio calc. 8=42685
by emulsion nuclei, elastic scatt. rel. to optical model params., 3GeV/c 8=43000
$\bar{p}$N annihilation, multiple particle prod., unitary-symmetrical statistical model 8=33546
$\bar{p}$-N interactions in photo-emulsions, obs. 8=42641
$\bar{p}$p annihilation cross sections, multi-π prod. 8=24943
$\bar{p}$p annihilation, multiple particle prod., unitary-symmetrical statistical model 8=33546
$\bar{p}$-p, elastic scatt. cross section and angular distribution obs. 6.9 GeV/c 8=38060
$\bar{p}$p elastic scatt., 63-175 MeV, cross-section obs. 8=24941
$\bar{p}$p interactions rel. to total cross-section 1.3 GeV/c struct., 1.2-1.6 GeV/c 8=33760
$\bar{p}$-p scatt., partial-wave analysis and optical model, E$_p$ = 50-180 MeV 8=33750
$\bar{p}$-p-scatt., 6 GeV/c obs. 8=42553
$\bar{p}$p → $\pi^+\pi^-\pi^\circ$, at rest 8=38042
Pulse generators. See Circuits.
Pulse-height analysers. See Counting circuits.
Pumps
See also Vacuum pumps.
aqueous electrolyte circulation 8=32128
e.m. based on pinch effect with constant metal flow 8=24178
ion drag, prod. of uniform droplets 8=43742
Purkinje effect. See Vision.
Pyroelectricity
ceramic detector for at. beams 8=47544
coeff. calc. from laser anharmonic oscillator model 8=28657
film, dielectric const. meas. in low elec. field, method and app. 8=40599
i.r. detector for meas. Q-switched CO$_2$ laser pulses 8=46581
triglycine sulphate as pyroelectric radiation detector 8=28383
triglycine sulphate, in Curie pt region with rapid temp. changes 8=31443
ultra-sensitive miniature temp. sensor with pyroelec. mat. on m.o.s.t. gate 8=46259
BaTiO$_3$ transducer for hypersonic wind-tunnel heat transfer 8=47953
LiTaO$_3$ ferroelec., coeff.; temp. dependence, 25-700°C 8=44888
SbSeI grown from gaseous phase, volatile component vapour pressure effects 8=35989
ZnO polar crystals, from point-charge model 8=30630
ZnS properties rel. to u.v. radiation dosimetry 8=46924
Pyrolysis. See Chemical reactions.
Pyrometers
ferroelectric crystal, operating near Curie point 8=28383
i.r., meas. limits 8=46258
light filters appln. to high temp. meas. 8=46266

Pyrometers—contd
  micro-, with optical-electronic transducer 8=46275
  moving objects, temp. meas., 60-180°C 8=24019
  optical automatic 8=37323
  photoelectric, for W, effective wavelength change calc. 8=32979
  photoelectric, for W temp., principle and error analysis 8=24021
  single-beam photoelec., true flame temp. meas. 8=41875
  for Al extrusion temp. meas. using BACO radiation pyrometer 8=32982

Quadrupole moments, molecular. See Molecules/moments.
Quadrupole moments, nuclear. See Nucleus/electric moment.
Quanticule theory (of chemical binding). See Bonds.
Quantization. See Field theory, quantum/quantization; Quantum theory/quantization.
Quantum chemistry
  density functional representation 8=47569
  Morse oscillator dynamics 8=33333
  perturbation calc. without H^0 or H^1 8=45308
  second-order unimolec. rate const., rapid calc. 8=32089
  spin-free concept 8=27672
Quantum counters. See Photons; Radiation detectors.
Quantum electrodynamics
  See also Electrodynamics; Electromagnetism.
  Bloch electron motion in external elec. and mag. fields 8=26875
  charge in uniform mag. field, quantum mechanics 8=42328
  charge renormalization, finite impossibility in sixth order 8=37766
  and cosmology, reln. 8=45588
  coulomb poles motion in J-plane 8=37765
  Dirac condition $A^\mu A_\mu = m_0^2/\epsilon^2$ 8=37933
  Dirac current for leptons, two possible tests 8=46833
  Dirac, e. m. and meson fields interacting 8=38015
  Dirac eqn., homogeneous solns. 8=29093
  Dirac equation, perturbation theory 8=24488
  Dirac theory reformolation in O(4, 2) rel. to antiparticles 8=33627
  dispersion approach, improved Lagrangian formalism 8=46832
  divergence-free, relativistic, gauge-invariant, macrocausal formulation 8=33356
  divergences in perturbation theory, impossibility of cancellation to sixth order 8=37766
  e-He^4 scatt. applic. 8=24723
  electrical transport in mag. field rel. to corresponding Boltzmann transport eqn., 8=44674
  elementary length, upper limit 8=24601
  exchanged photon, emission and absorption time correl. 8=46834
  exclusion of divergences, Lagrangian method 8=24489
  extended adiabatic invariance, proof 8=46835
  external current and potential 8=28960
  fermions of non-zero mass, in terms of 2-component helicity spinors 8=37767
  field interaction vacuum correction theory 8=28962
  four-potentials and four-momentum operator, in Landau gauge 8=33357
  free electron in closed metal container 8=28542
  Gupta-Bleuler subsidiary condition, inadequacy 8=42327
  heavy e search, unsuccessful search in 5 BeV e-p scatt. 8=24714
  Hestenes and Dirac theories 8=42467
  high-momentum vertex function for spinors 8=42326
  of higher spin fields, structural inconsistency 8=42330
  in Landau gauge, four-momentum operator formulation, unitary equiv. to Feynman gauge 8=33357
  Lorentz-invariant, paradox of energy conservation 8=37769
  mass and charge renormalization consts. in zero bare mass theory 8=28961
  momentum, velocity, acceleration and spin, relations 8=42313
  motion in field of two Coulomb centres, elementary solns. 8=37749
  Mossbauer diffraction in crystals, γ-ray and x-ray optics 8=30636
  $\mu^+\mu^-$ asymmetric pairs photoprod. on H rel. to propagator modification, 850 MeV 8=33647
  muon anomalous magnetic moment as test 8=29099
  new Lagrangian formulation, results 8=37768
  N-molecule-radiation-field Hamiltonian exact solution 8=39191
  pair prod. symm., radiative corrections 8=29075
  photon propagators, and Landau gauge representation 8=42331
  Pugh's eqn. for S-matrix, calc. of third order vertex term 8=24486
  quantization proceedure, canonical in covariant guages 8=28950
  relativistic, symmetry rel. to Coulomb problem double degeneracy 8=37840
  S-matrix vs. perturbation calc., comparison 8=24487
  spin-1 particle, stationary, gyrating, nonrelativistic in classical e.m. field, expectation value eqns. 8=33563
Quantum electrodynamics—contd
  tested in polarization det. for $e^+e^- \to 2\gamma$, $e^+e^- \to \mu^+\mu^-$ 8=37941
  total photon propagator, logarithmic asymptotic behaviour from 8=42329
  two-point functions from classical field eqns., perturbation calc. 8=33067
  vacuum polarization effects on S-wave p-p and $\alpha-\alpha$ scatt. 8=33748
  vacuum polarization in Lee-Yang theory of charged spin-one bosons 8=37836
  vertex function, unrenormalized Schwinger-Dyson equation for 8=33358
Quantum electronics. See Lasers; Masers; Optics; Photons.
Quantum field theory. See Field theory, quantum.
Quantum generators. See Masers.
Quantum mechanics. See Quantum theory.
Quantum statistics. See Statistical mechanics.
Quantum theory
  See also Electron theory; Field theory, quantum; Elementary particles.
  advanced quantum mechanics, book 8=33312
  alternative interpretation, criticism 8=37734
  alternative interpretation, criticism 8=37736
  alternative interpretation, rebuttal of criticism 8=37735
  alternative interpretation, rebuttal of criticism 8=37737
  in America between the wars 8=28934
  anharmonic oscillator calc. 8=33334
  anharmonic oscillator, field theoretic functional calculus. 8=28942
  anharmonic oscill., functional calculus 8=46819
  anharmonic oscills., 2 simple systems with two degrees of freedom, semi-infinite square well oscill. 8=33332
  atom ionization by e impact 8=43470
  Banach space techniques in perturbation theory of self-adjoint operators with continuous spectra 8=46812
  bounds on density matrices 8=42311
  bounds on polarizabilities 8=25324
  Bra-ket formalism for free relativistic particles 8=24462
  C*-algebra rel. to quantum mechanics, and Mackey's axioms 8=32830
  canonical Bogoliubov-Valatin transform., classification 8=41764
  cononical Bogolubov-Valatin transform., classification 8=41764
  Casimir operators, eigenvalues 8=24591
  classical and quantum theory, fundamentals 8=46013
  Clebsch-Gordan coefficients, an operator method 8=33307
  Clebsch-Gordan coeffs., quasi-binomial representations 8=32298
  of collisions, employing imbedding eqns. for Green's function 8=28228
  correspondence principle, weak, between classical theory and quantum generators 8=28948
  Coulomb-Dirac multipole radial matrix elements, analytic props. 8=28941
  Coulomb functions, phases and amplitudes 8=37751
  density matrix, 'regular' form of Sudarshan-Glauber representation 8=46806
  density of state function for continuum states 8=25073
  diamagnetic molecules, magnetic birefringences 8=47567
  Dirac Hamiltonian as member of hierarchy of matrices 8=46807
  dynamics in phase space 8=37745
  for electrical engineers, review 8=46789
  e. m. wave scatt. by free electrons, freq. shift 8=42020
  energy eigenvalue spectroscopy 8=46800
  equivalence, weak, in quantum mechanics 8=33308
  equivalent local potential, new coupled equation 8=42980
  expectation values as phase-space averages with Wigner density function, use of Weyl transforms. 8=33305
  experimental tests to distinguish hidden variable explanations 8=24455
  extremal norm-determining measures for Hilbert spaces of entire functions 8=46810
  Fermi-dirac function, tabulated for integer indices, series expansion 8=33329
  Fermionic-Bosonic approx. in mol. quantum mechanics 8=43264
  of gravitation, Hamilton-Jacobi theory applied by correspondence principle 8=32777
  Green's function, spectral analysis 8=46801
  Hamilton-Jacobi partial diff. eqn., complete integration 8=32662
  harmonic oscillation phase operators 8=37748
  harmonic oscillator, nonisotropic, not of dynamic symm. SU_n 8=24467
  Heisenberg eqns, graphical representation 8=24465
  helicity and energy as members of hierachy of eigenvalues 8=46808
  Hilbert space bilinear forms properties, rel. to stability of partial differential operators 8=46809
  Hilbert space, construction of fixed points of nonlinear mappings 8=45967
  Hilbert space, remarks on critical point theory 8=45989
  integral-differential eqns. system, numerical soln. 8=46798

Quantum theory—contd

- integral virial therem and generalized differential Hellmann-Feynman formula 8=25323
- intermolecular thermodynamics, correspondence principle 8=25663
- Josephson tunnelling, quantum-mechanical derivation 8=27051
- kinetic eqn., differential operator form 8=42299
- Klein-Gordan eqn., integral transform. 8=24453
- lasers, internally phase-modulated 8=28660
- Lie algebras, Poisson bracket realization by analytic functions of generators 8=28231
- liquids, rotating, statistical mechanics 8=23879
- magnetodynamic effect, rel. to effects of Dirac electron spin 8=33629
- matrices, reduced density, n-representability 8=28940
- mechanics, algebraic struct., reformulation of axiomatic basis 8=33324
- mechanics, axiomatic, systems of observables 8=28935
- mechanics, non-Hermitian Hamiltonians spectral 8=28936
- mechanics, phase and angle variables 8=24460
- mechanics, phase function method, review 8=28937
- mechanics, sum rules generalization and application 8=33323
- in molecular spectroscopy 8=38775
- molecular symmetry groups, Altmann's Schrödinger supergroup, criticism 8=34212
- Morse oscillator 8=33333
- motion in field of two Coulomb centres, elementary solns. 8=37749
- numbers in Poincaré subgroups 8=24457
- nonlinear optical phenomena, anharmonic oscillator model 8=28657
- one electron, with Dirac condition $A^{\mu}A_{\mu} = m_0^2/\epsilon^2$ 8=37933
- operators, classical counterparts 8=32673
- optics, normal and antinormal ordering of field operators 8=46639
- orbital ang. momentum and group respresentations 8=33309
- oscillator system symmetries 8=46817
- parametric scattering, spontaneous, of intense light 8=27538
- plasma, radial distrib. function calc. 8=29999
- perturbation theory in quantum mech., complementary upper and lower bounds 8=28354
- phase shifts calc. for spherically symmetric potentials 8=37753
- photoelectric detection, shot noise calc. rel. to photon bunching effects 8=46418
- photon det., field attenuation theory 8=29081
- pot., singular, attractive, leading to nonself-adjoint Hamiltonians 8=33335
- probability densities providing unique restoration of wave functions 8=46793
- probability theory, generalized, existence of sums of bounded variables 8=46811
- pseudo-potentials, analytic props. 8=46788
- quantum fluids, h.f. elasticity moduli 8=41772
- quantum mech. anal. of n. m. r. spectra, computer tech. 8=42046
- quantum mechanics, action and formulation 8=33310
- quantum mech. operators in general coords. 8=28933
- relativistic, Feynman diagram model, Fubini identities and the algebra of currents 8=24610
- scattering and bound-state roblem, distortion operator 8=42314
- Schrödinger equation, solution for linear potential inside one-dimen. infinite 8=24454
- Schrodinger eqn. soln., test of α-decay shell model theory. 8=47276
- semiclassical analysis of weakly coupled reson. systems, validity rel. to zero-point oscills. 8=32674
- spinors, nonlinear, baryon mass eigenvalue 8=24862
- stable states of particles in their own gravitational fields 8=28296
- $SU(3) \supset R(3)$ Wigner coeffs. in 2s-1d shell 8=29269
- three-level system; resonance interaction with three e.m. waves 8=37750
- transport theory in strong magnetic fields 8=41794
- two-centre Kepler problem, constant of motion 8=46791
- 2-photon absorpt. from radiation field, field-correl. effects 8=28722
- unitary representation of Lorentz group function with spin 8=24456
- variational bounds for dynamic polarizability 8=47580
- vector methods, motion problems of classical mechanics 8=46787
- vibrational transition probabilities, WKB evaluation 8=47442
- virial theorem, variational principle, and nonlinear parameter 8=46802
- wavefunctions and correll. energies for 2-, 3-, and 4-electron atoms 8=25333
- wavefunction, relativistic, reduction to representation of inhomogeneous Lorentz group 8=33314
- wave function normalizable before 2-particle interaction is finite after it 8=33556
- waves in fluctuating medium, statistical mechanics 8=23880
- Wigner inequalities for strong and weak causality conds. 8=33560

Quantum theory—contd

- WKB method for symmetric pot. function, first approx. 8=46816
- of X-ray incoherent scattering, rel. to exchange contribs. for assoc. Compton band 8=43278
- Z = O conds. for bound sate with small binding energy, rel. to perturbation theory 8=33311
- Rb atom, free precession of spin states 8=38710

application methods

- anharmonic oscillators, WKB method 8=46818
- atom, bound states, Green's function phase-integral approx. in momentum space 8=29586
- collision of oscillator with particle, vibr. energy transfer 8=47721
- correct operator for spin-forbidden electronic transition probabilities 8=25327
- crystal anharmonic vibrations, quantum-dissipation theory 8=48695
- de Sitter group in molec. calcs. 8=25430
- degenerate perturbation theory of intermolec. potentials 8=38955
- e. m. field operators, calc. of correl. functions 8=33062
- energy bands, pseudopotential method for calc. ultra-localized functions 8=40231
- expectation value of arbitrary operator, least squares, method 8=42301
- harmonic oscillator appl. to atoms and mols. 8=38597
- harmonic oscillator thermal functions, finite orthogonal polynomials 8=29702
- Hartree-Fock approx. applied to harmonic oscillator 8=25329
- Hartree product wavefunctions, projected 8=29572
- inelastic collisions 8=37743-4
- integral Hellmann-Feynman method, local energies 8=25325
- intramolecular regroupings, quantum theory 8=45320
- iteration procedure to generate scatt. wave function 8=28947
- Kondo system, Green's function perturbation theory of Suhl's eqn. 8=37756
- Landau, Fermi quantum liquids, book 8=30397
- magnetism theory, kinematic interactions 8=49456
- many-electron systems, GF wavefunctions 8=47439
- molecule rotator strengths, f-sum rule 8=29688
- natural orbitals and wavefunctions, perturbation theory calc. 8=38603
- nuclear reactions, scatt., using Green's functions and integral operators 8=29395
- oscillator, algebraic generalizations of symm. 8=33523
- oscillators, interacting driven, P-distrib. time development for systems 8=37747
- perturbation technique, Green's function for Kondo system 8=37755
- perturbation theory extension in describing composite particle as field 8=42372
- point rotor dynamic groups and the H atom 8=34128
- position meas. thought expt. 8=33313
- relativistic related operators at resonance 8=38616
- self-consistent perturbation theory 8=25326
- spin systems, two interacting, in crystal, NMR spectra and line shape calcs. 8=27497
- spin wave in ferromagnet, wave mechanics 8=40778
- time correl. functions formation for interaction of particles with a complex system 8=29386
- transient processes with three-magnon non-linear transitions, quantum mechanical treatment 8=49497
- two coupled harmonic oscillators, semiclassical approx. restrictions 8=42312
- variational approach to Fadeev eqns. 8=29056
- variational, complementary principles and n transport appls. 8=33328
- variational principle for intensity of forbidden transitions 8=47443
- H atom, algebraic generalizations of symm. 8=33523

many-particle systems

See also Bosons; Fermions; Helium/liquid; Statistical mechanics; Superconductivity; Superfluidity.

- Bogoliubov's functional ansatz. 8=28328
- Bose-Einstein condensation of ideal gas 8=32846
- Bose fluids, degenerate, cluster expansion at finite temp. 8=37209
- bose system, cricical current of foreign particles, calc. 8=37208
- boson avalanche, spontaneous development of coherent states 8=23895
- boson systems, Bogoliubov approx., asymptotic exactness 8=23894
- bosons system density-density correlation and one-particle Green's function connection, 0°K 8=46098
- classical, with long-range interactions, correlation at large distances 8=37204
- correlation functions in ring-diagram approximation 8=46114
- critical phenomena 8=28310
- damped non-Markovian, interaction with thermal bath 8=37194
- dense dispersed system, number of particles in any vol., fluctuations 8=37203
- density field, rel. to two-body interact. 8=33331

- **Quantum theory**—contd
  - **many-particle systems**—contd
    - diffusion eqn. for density matrix, in strong external field 8=37202
    - dissipative processes, quantum states, and entropy 8=23878
    - electron gas, dielec. const. in Hartree-Fock approximation 8=23900
    - entropy, Gibbs theorem counterpart 8=23884
    - Fermi and Bose integral evaluation 8=28333
    - fermion system, correlation energy 8=42772
    - Feynman technique applic. 8=37771
    - free systems, structure of algebras 8=32853
    - Gaussian statistics, finite sample correlations 8=37195
    - general theorem 8=37200
    - Green's functions, appl. 8=24452
    - Hamiltonian perturbation method, statistical generalization 8=32834
    - hard core gas at high temps. 8=41785
    - hard molecule gas on Bethe lattice, phase transition 8=28347
    - hard spheres, pair correl. function at low density 8=28345
    - hard spheres, two cluster integrals in fifth virial coeffs. 8=41786
    - ideal gas, pressure calc. 8=37185
    - Ising problem, with arbitrary interacts., asymptotic soln. at low temp. 8=37181
    - Ising problem with arbitrary particle interaction, high-temp. asymptotic solutions 8=28311
    - kinetic eqns. for scatt. events 8=23882
    - kinetic operators properties 8=46109
    - Kronig-Penny model, gaps in electronic energy spectrum 8=32844
    - lattice dynamics, collective fluctuation approx. 8=26568
    - lattice space, Heisenberg theory 8=46119
    - liquid-like one-dimensional, energy spectrum gaps 8=32844
    - low-concentration particles interact. with phonons, in Bose system 8=37207
    - luminescence, solid-state, theory 8=36458
    - many-electron system, periodic field, perturb. theory and random phase approx. 8=34123
    - measuring process, model 8=34097
    - metals, soft X-ray emission, quantum-mechanical treatment 8=27541
    - multispecies fluid, ground state, var. method 8=37199
    - N-body ground state, upper bound, conditions on two-body potentials 8=42794
    - N-body systems, lower bound to ground-state energy and conditions for existence of bound states 8=37201
    - N-particle system in radiation field, dipole coupling 8=39191
    - noise spectrum and admittance of a system relation 8=28326
    - non-Markovian damped systems 8=46105
    - non-maximally degenerate, group theory soln. 8=33306
    - nuclear matter, Green's functions approach 8=47210
    - nucleus, 3-body model of closed shells plus 2 nucleons 8=29277
    - one dimens., integral eqn. soln. 8=41775
    - ortholattices and Baer*-semigroups, quantum logic 8=32823
    - overlap function 8=37880
    - Piron's axioms, modification 8=28319
    - plasma, pair distrib. function exchange term. 8=47807
    - plasma, radial distrib. functions at zero separation 8=39070
    - plasma, 2-component, correl. function 8=47803
    - polyelectronic config. interact. wave functions, theory of reduced density matrices 8=43182
    - quasi-particle interacts, damping and freq. shifts 8=35019
    - quasi-particles, kinetic equations with non-conservation 8=46103
    - reduced density matrices, natural expansion of wave function in terms of eigenvalues 8=42302
    - relativistic mechanics for action-at-a-distance, conomical formulation 8=23890
    - response to external perturbation and time-depend. correls. 8=23889
    - Schroedinger equation solution 8=33317
    - self-consistent polarization waves and dispersion forces in crystals 8=30921
    - spin system of interacting particles 8=32843
    - statistical mechanics of quantum spin system 8=46104
    - statistics, generalized, non-equivalnce of formulations in quantum and field theories 8=42318
    - superfluid nuclear matter, statistical mechanics 8=23886
    - three-body forces in dense system 8=37198
    - three-body problem bound state solution 8=38295
    - three-level system; resonance interaction with three e.m. waves 8=37750
    - transition amplitudes in continuous spectrum 8=28325
    - 2-matrix, angular symmetry props. 8=46113
    - W* algebras with dispersion-free normal states, struct. theorem 8=28318
    - wave function closure property 8=33517
    - weak-coupling model, failure in real gas transport theory 8=39234
    - He^4 pair distrib. function, 3-particle density matrix 8=41759

- **Quantum theory**—contd
  - **many-particle systems**—contd
    - Rb^{85} vapour undergoing double-quantum resonance in ground state, scattering light, modulation effect 8=37629
  - **quantization**
    - See also Field theory, quantum/quantization.
    - canonical, differential geometric techniques 8=37746
    - of electrodynamics in covariant guages 8=28950
    - particles with an spin and internal symmetry, second quantization process 8=42363
    - space-time, rel. to Mössbauer effect 8=24689
  - **wave equations**
    - in angular momentum plane, interpolation formulae 8=28938
    - asymptotic props. at singular points of potential function 8=33318
    - atomic orbitals and classical motion 8=25346
    - broken U(3, 1) symmetry, soln. 8=42307
    - covariant form on hyperplane 8=42308
    - density of states in sphere and cylinder 8=37738
    - Dirac equation exact solns. 8=29092
    - Dirac equation, perturbation theory 8=24488
    - Dirac eqn., symmetry algebra calc. 8=46803
    - Dirac-Pauli eqn. dequantization to obtain eqns. of motion of classical analogue 8=33555
    - double solution theory verification 8=33326
    - eigenvalue theory of Vlasov plasma oscillations in magnetic field 8=47875
    - electron in e.m. wave, Volkov soln. for scatt. 8=33633
    - energy levels of electrons in e.m. waves 8=28598
    - error bounds for energy and overlap of approx. wave-functions 8=46792
    - expansion of time-dependent wavefunction 8=37740
    - extended Hartree-Fock wavefunctions 8=25330
    - Galilei invariant, for study of non-relativistic particles 8=33320
    - group properties for zero mass particles 8=47014
    - higherspin theory consistent when interacts are included 8=33515
    - infinite-component, spacelike solns. 8=42303
    - kinetic energy as a perturbation Schrödinger equation 8=46804
    - Klein-Gordon for particles in their own gravitational fields 8=28296
    - light propag. in laser-active medium 8=37626
    - lower bounds to expectation values 8=33321
    - many centre problem, exact formal soln. 8=46795
    - many-particle, closure property 8=33517
    - momentum transfer rel. to Schroedinger eqn. in crystals 8=35609
    - natural expansion of wave function rel. to reduced density matrixes 8=42302
    - non-linear additional term 8=42306
    - non-orthogonal wavefunctions, linked cluster theorem 8=33325
    - nuclear wave functions for arbitrary number of nucleons 8=47202
    - Padé approximant pole location 8=46796
    - pair eqns., numerical soln. 8=47438
    - perturbation theory, energy uniqueness 8=33322
    - photon-spinor CP-odd interactions, vertex function 8=29076
    - reduced wave equation in infinite components 8=37764
    - reflection coeff. of inhomogeneous layer, determ. 8=46015
    - relativistic for states of H atom 8=29594
    - relativistic spin equation 8=37763
    - remainder theorem, general 8=46797
    - restrictions on particle position operators 8=42387
    - S-limit Schrodinger eqn., numerical soln. 8=29596
    - scattering from separable non-local potential, rel. to phase shift, elastic 8=33337
    - Schrodinger, construction of solvable potentials 8=33319
    - Schrödinger eqn. for three-electron atoms, Euler-angle reduction 8=47461
    - Schrödinger equation, kinetic energy as a perturbation 8=46805
    - Schrödinger eqn., study by phase eqns of bounds and props of functionals 8=46799
    - Schrödinger eqn. with α/r central pot., factorization by finding ladder operators 8=34129
    - Schrodinger eqn. with singular pots., props. of wave function 8=28946
    - Schrödinger, exact soln. for pot. scatt. compared with Born approx. 8=33587
    - Schrodinger, for interactions with exchanges 8=37742
    - Schrödinger, for Li atom, numerical soln. 8=29579
    - Schrodinger like for 2 fermion system applied to $q\bar{q}$ 8=29104
    - Schrodinger, low-energy expansion of S(k) matrix for spherically symp. pot. 8=28939
    - Schrodinger, many-particle systems 8=33317
    - Schrodinger operator in exterior domain, scattering 8=33336
    - Schrodinger operator, spectral functional, asymptotic behaviour 8=33316
    - Schrodinger, solutions and eigenvalues 8=37741
    - Schrödinger, soln. with vel.-dependent pot. 8=24461
    - Schrodinger theory, potential producing phase shift below 11/2 8=33327
    - Schrödinger, time-independent, bound states rel. to solitons 8=24464

Quantum theory—contd
wave equations—contd
Schrödinger, two-dimens. analogue to H atom 8=34131
spacelike and timelike at infinite momentum, coupling 8=42309
spin-$\frac{1}{2}$ particle polarization calc. 8=37739
spin-1, field, satisfied by e.m. current coordinates 8=47010
spinor currents and baryon-meson symmetry 8=42483
spinor, finite charge renormalization 8=24485
spinor sign change under Zπ rot., observability 8=42300
teaching, wave function, meaning and matter waves reality 8=42305
thought expt. for position meas. 8=33313
three-body problem solution 8=33315
two-electron wave function expansion coefficients, perturbation theory 8=46794
two-electron wavefunctions, unoccupied natural orbitals 8=38599
two types of meas. theory 8=33326
variational calculations "best" lower bound 8=24463
waveguide, appl. of theory of double soln. 8=42025
WKB method, generalized, second approx. 8=42310
B^{++} new type of wave function 8=38672
Be^{+} ion, new type of wave function 8=38672
Li atom, new type of wave function 8=38672
Li atom, ^2S ground state, Hylleraas function calc. 8=38671
Quarks. See Elementary particles.
atmospheric, cyclic reflection mechanism 8=24741
baryon-antibaryon interactions, strangeness-exchange, quark model 8=33659
baryon model, quarks-on-springs 8=33733
baryon model with d-wave forces, energy spectrum for baryons and their resonances 8=38046
baryon resonances D-wave decays, SU(6) × O(3) quark model 8=29215
baryons, higher, SU(6)XO(3) model of decay 8=33735
β-decay, α-order corrections proved finite 8=33630
rel. to bootstrapping and local current 8=29073
charge-commutation relations, saturation of covariant sum rules 8=29108
cosmic ray production, estimate 8=24636
cosmic rays at sea level, large area proportional detectors 8=38126
current divergence and equal-time commutation, quark model 8=33529
detection in solids, limits of possibility 8=47099
Dirac and anti-Dirac particles, bound state problem 8=42359
elastic scatt. model with factorizability assumption 8=29112
$ep \rightarrow eN^*$, quark model, form factors 8=33631
$\eta \rightarrow 2\gamma$ model 8=24835
factorization model, large momentum transfer scattering 8=37945
form factor model with energy depend. mixing angle 8=29039
and group theory 8=37847
hadron dynamics in $U(6) \otimes U(6)$ 8=33648
hadron-hadron scattering model at high energy, sum rule 8=33653
hadron resonance decay model 8=42494
hadron struct. and interactions, quark models 8=29103
K resonance decay model 8=33731
loss from quasars, reinterpretation of spectrum 8=45781
mass and Fermi gas nuclear model 8=24743
meson-baryon interactions, strangeness-exchange, quark model 8=33659
meson prod., neutral vector and pseudoscalar in meson-baryon interactions 8=37957
model, $A_1 \rightarrow \rho\pi$ decay 8=29175
model and relation between differential cross-sections 8=42492
model calc. of hadron decay rates, mesons annihilating into vacuum 8=42497
model calcs. of meson-baryon scatt. 8=24765
model for high energy elastic scatt. 8=37947
model for magnetic moments of baryons calc. 8=38048
model for N-N scatt., inequality 8=24891
model for resonance decay 8=42493
model for soft-pion meson decay 8=24755
model, leptonic decays and exchange current of baryons 8=47126
model, negative parity N isobar excitation 8=25003
model of interaction of elementary particles, and additional reson prod. at hadron scattering 8=47101
model, rel. to cross-sections of prod. of hadrons, and spin correls. 8=37951
model, semirelativistic for mesons 8=42360
model sum rule in photoproduction, violation 8=24659
models tested in $\pi^- p \rightarrow \gamma n$, $K^- p \rightarrow \gamma\Lambda$ 8=37916
octet state, assignment of Roper resonance 8=47124
p model, rel. to discrepancy in h.f.s. of H 8=33743
particle symmetry interpretation 8=47015
photoproduction model 8=42495
$q\bar{q}$ system solved by means of Schrodinger-like relativistic eqn. for 2 fermions 8=29104
refractice index and transmittance from asymmetric interferograms, 20-400 cm^{-1} 8=28844
Quarks—contd
relativistic two-particle Hamiltonian, bound states 8=47039
sakaton rearrangement interactions and high energy hadron-hadron scatt., model agreement 8=47103
Satz additive model, for high multiplicity processes 8=24808
search, unsuccessful, for fractionally charges particle in cosmic rays 8=42490
in solid, $< 10^{-17}$ per nucleaon expt. deduction 8=24742
superconvergence relations, saturation with qq states 8=24669
s-wave model for baryons and their resonances 8=25000
tachyons, faster than light, exptl. search 8=42388
terrestrial, mag. levitation electrometer search 8=29013
two in bound system, Bargmann-Wigner eqns. 8=37946
U_6 composite model for baryons and resonances 8=47100
$U_6 \otimes U_6$ field commutation relations rel. to vector-meson dominance in π° decay 8=33662
unsuccessful search for $^2/_3$e charged particle in cosmic rays 8=42489
Quartz
acoustic wave generation by electrostrictive mixing of light waves 8=45162
α-quartz crystal, refractivity interpret. 8=49756
α-quartz, elastic coeffs. and moduli, polarizing tensor 8=49048
α-quartz, extraordinary optical phonons, directional dispersion 8=45221
α-quartz, piezoelectric constant calc. using Born's theory 8=27300
α-quartz, Raman spectrum excitation by Hg discharge 8=49753
amorphous, density fluctuations rel. to X-ray scatt. 8=25879
amorphous substrates, moving mask growth of single-crystal Si films 8=26126
breakdown when subject to ionizing radiations, optimal thickness calc. 8=31417
brittle crystals, microhardness rel. to dislocation mobility 8=26796
coloured varieties synthesis and pigment distribution 8=26264
to correct u.v. wavelength 8=37724
crystal microbalance, direct gravimetric calibration 8=23793
crystalline, n.m.r. electron spin-echo obs. of E_1^1 centres 8=44486
crystalline, stimulated Mandel'shtam-Brillouin scatt. threshold, 0.35, 0.69 and 1.06μ 8=32032
crystals, artificial, overgrowth of holes 8=39700
density, radiation damage effects 8=26722
diffusion of H_2 in irrad. quartz 8=48790
dispersion in vac. u.v. from interference in thin parallal plate 8=32034
elastic constants of α-modification, calc. from model 8=44599
elastic moduli, third-order, pulse-echo interferometric obs. 8=49050
electron diffr. exam. 8=35355
epitaxy of p-amino salicylicacid 8=48571
ϵ-colour centre formation mechanism and kinetics 8=48885
fused, and $Gd_3Fe_5O_{12}$, chem. interaction 8=41251
fused, far i.r. absorpt. rel. to inherent disorder 8=49681
fused, reflectance in vac. u.v., obs. 8=27558
glass, X-ray exam. of structure 8=39629
heat-pulse propag. in α-modification, phonon dispersion effects on pulse-shape 8=48753
high-low inversion, volume and compressibility rel. temp. at high press. 8=48401
hydrothermal crystallization kinetics 8=26230
interstellar grains, extinction curves 8=28096
inversion, high-low, lambda transition, thermodynamics 8=39563
i.r. rotation obs. 1.85-4.00μ 8=36403
knick-band indexing using the X-ray universal stage 8=26714
laser-illuminated, interferometric analysis and separation of three Brillouin scattering components 8=36408
laser irrad. damage and stimulated Mandel'shtam-Brillouin scatt., 300°K 8=32031
laser-stimulated, hypersound parametric amplification Brillouin effects 8=26583
microbalance for oil diffusion pump backstreaming meas. 8=39243
microwave phonons, second-harmonic generation 8=30950
natural and synthetic, fault-surfaces from X-ray exam. 8=26707
non-linearities, and isochronism defect 8=27301
optical activity, temp. dependence in visible spectrum 8=49755
optical second harmonic generation, mag. field induced, search 8=45140
phonons, 10 GHz, method of excitation 8=48723
piezoelectric appl. to microwave mixing 8=49382
plano-convex plates, meas. of vibration modes 8=46141
Pockels effect, meas. at 9GHz 8=41144

Quartz—contd
- quartz-glass-coesite, phase transforms. under high-temp. and pressure 8=48400
- quartz, in stimulated Mandel'shtam-Brillovin scatt., elastic nonlinearity effects 8=41036
- quartz production of crystalline-amorphous phase transform, X-ray diffr. exam. 8=26146
- resonance frequency modification, various cuts, particle irrad. 8=35418
- resonator, electrode optimum sizes and shapes 8=37246
- Rutherford scattering of protons, orientation depend. 8=44504
- sand, differential thermal analysis, particle size effects 8=26044
- shock-loaded x-cut, mech. and piezoelectric props. 8=26844
- smoky, anomalous pleochrism rel. to atomic structure 8=27608
- sound absorption near λ pt. in $\alpha \rightarrow \beta$ transition 8=26584
- specific heat and enthalpies of change of phase; meas. 8=46286
- spherically bent cryst., soft X-ray spectroscopy 3 to 30Å 8=32033
- stress dependence of freq. of oscillator plates 8=49049
- stress gauge, shorted guard-ring development 8=37110
- structure changes in $\alpha \rightarrow \beta$ transform. and under n-irrad. 8=26080
- structural defects, delineation by selective etching 8=44428
- surface and bond-forming props., applic. in processing technique 8=48427
- synthetic, Al impurity capture during crystal growth, effect of supersaturation and temp. 8=44424
- synthetic, birefringence, 1500 to 3000 Å 8=41056
- synthetic crystals, homogeneity of refractive index 8=35207
- synthetic, etch patterns on habit and fracture prism faces 8=35224
- synthetic, with high u.v. transmission 8=49751
- thermoluminescence, rel. to defects due to γ-irrad. 8=49812
- thermometer with digital readout, —40 - +230°C 8=24023
- thin film capacitor by r.f sputtering on Al and counter-electroding, props. 8=44059
- toroidal sectioning machine 8=41607
- u.s. attenuation, unirrad., and neutron irrad., 8=39897
- u.s. vibration, X-ray topography 8=48722
- u.s. wave, propag., phase vels 8=48724
- welding with CO$_2$ laser 8=33179
- Z-cut, phonon lifetime meas. by two successive light pulses 8=44323
- AlF$_3$ layer formation during 3½ yrs. ageing after HF treatment 8=49900
- Co-doping during synthesis, and opt. props. 8=48556
- α-SiO$_2$, changes in electric field 8=44600

Quartz resonators. See Acoustic transducers; Piezoelectric oscillations; Resonators.

Quasars. See Cosmic radiations, radiofrequency; Cosmology; Galaxies; Stars.
- absorption-line spectra obs. TON 1530, PKS 0237-23, PHL 938 8=50387
- absorption lines, systematic identification 8=45791
- angular size variation with red-shift 8=50389
- collapse and anticollapse 8=50327
- Compton effect inverse, stimulated term rel. to distance of quasars 8=28134
- cosmic ray source, interaction with photons 8=42714
- cosmological model test in obs. from opposite directions 8=28030
- detection, by reflecting telescope at Herstmonceux, Sussex 8=50267
- diameters of some at wavelength of 66.9 cm 8=36988
- directed emission model 8=36987
- distance rel. to compact n star studded galaxies redshifts 8=28112
- ejected, assocs. and parent galaxies struct. obs. 8=45772
- energy of relativistic particles and mag. fields, ratio of full to minimal 8=32511
- evolutionary properties, luminosity-volume test 8=36985
- forbidden line excitation 8=45790
- formation, rel. to non-linear eqs. of spherical collapse 8=50258
- Japanese obs. 8=32615
- matter-antimatter model, prediction and obs. of γ-ray flux 8=45789
- M87, γ-ray obs. 8=45789
- optical continuum, physical processes responsible for radiation, possible obs. tests 8=45787
- optical spectrum due to inverse Compton process 8=45780
- Parkes 2134 + 004, unusual radio spectrum 8=50388
- PHL 938 absorption-line spectra obs. 8=50387
- PHL 938, photoelec. line intensity obs. 8=45786
- PKS 0237-23, absorption-line spectra obs. 8=50387
- PKS 0237-23, absorpt. spectrum obs. 8=45792
- PKS2251 + 11, line intensity obs. 8=45786
- polarization, circular, observed limits at radio freq. 8=28133
- proton synchrotron emission 8=45756
- quasi-stellar objects with absorption lines 8=28132
- radio emission, flux densities at λ 5.2 cm 8=41552

Quasars—contd
- radio galaxies in an early stage 8=32521
- radio sources opposite, cosmological test 8=50378
- red-shift-law, and for radio galaxies 8=45793
- with redshifts larger than 2.2, predicted colour-indices, U–B and B–V values 8=28131
- relativity theory, multitemporal, appl. 8=46076
- Sagittarius A, 1415, 2695 MHz obs. 8=45785
- Seyfert and N-type galaxies and quasars, common source 8=45778
- spectral red-shift, gravitational interpretation 8=45788
- stellar head-on collision theory 8=45619
- 3C249-1, photoelec. line intensity obs. 8=45786
- 3C 273, optical luminosity fluctuations 8=32522
- 3C 273, optical luminosity fluctuations, randomness 8=36986
- 3C273, spectrum anomaly, 1.6μ 8=45783
- 3C273B, γ-ray obs. 8=45789
- 3C345, optical brightness and polarization var. 8=32519
- spectra optical, absorption features 8=45784
- spectrum, reinterpretation with quark losses 8=45781
- TON 1530 absorption-line spectra obs. 8=50387
- variable, intensity rel. to wavelength 8=32520

Quasi-particles. See Excitons, Magnons, Phonons, Polarons, etc.

Quenching, optical. See Luminescence.

Quenching, thermal. See Heat treatment.

RS coupling. See Atoms; Spectra/atoms.

Racah coefficients. See Quantum theory.

Radiation

See also Acoustic radiators; Bremsstrahlung; Cherenkov radiation; Electromagnetic waves; Electrons/radiation; Emissivity; Radiative transfer; Stars/radiation; Sun/radiation; Sunlight.
- in air, rel. to coupling of normal chem. nonequilib. shock wave 8=39182
- from annular slot in compressible plasma, theory 8=30075
- from black body, weakly heated, meas. of atmos. absorption 8=32228
- coherence, partial, calculus for space-coherent e.m. radiation 8=37449
- compressible grey gas, flow near plate impulsively set in motion, finite Mach number 8=43686
- diffraction field of nearby source, h.f. 8=23810
- emissive and absorptive power of trapezoidal grooves 8=23987
- flame radiant props meas. by radiometer without condensing agents 8=28408
- gas behind shock front, maximum of nonequilibrium emission 8=30299
- gas layer, cond.-rad. interact., appl, of nongray gas model 8=34659
- gravitational, metric logarithmic terms from radiative corrections 8=28299
- gravitational, outgoing/incoming mixture, mass transfer from source 8=32804
- light on solid surface, plasma reson. emission 8=35802
- microwave, from magneto-plasma 8=28600
- in multi fluid system, effects of shock wave struct. 8=39016
- in nongray gas, coupled with conduction and convection, effects on entrance region flow 8=25827
- nonstationary field, Duhamel's principle 8=33233
- optical, absolute values meas. 8=37632
- particles, charged, in waveguides with gyrotropic filling 8=41939
- in plasma, cylindrical, radial intensity distrib., determ. 8=39095
- plasma, harmonic generation from e beam interaction 8=30048
- point source in strongly focussing medium, modal solution 8=23808
- proton gyrofrequency band emissions obs. from OGO2 8=36821
- pulsed ionizing, ruby fluoresc. dosimeter 8=45258
- radiative correction to photon propagator in Lee-Yang theory 8=37836
- spectral emissivity of materials with low thermal conductivity 8=23988
- synchrotron calc. of electron density for laser action 8=33636
- synchrotron, due to electrons in plasma, growth rate 8=34497
- 10μm, photomultiplier det. using optical conversion in proustite 8=33123
- transport in atomic plasmas 8=34509
- u.v., meas. with photoresistors, using org. luminophors 8=48166
- water surface, distrib. var. 8=34853
- He, weakly ionized, and collision mechanisms 8=29969
- Mo, thermal emittance of small cavities in surface, rel. to temp. 8=26611
- W, thermal emittance of small cavities in surface, rel. to temp. 8=26611

heat
- Absorbing and scattering slab heating 8=46228

- **Radiation**—contd
  - **heat**—contd
    - by air, in hypervelocity Couette and boundary-layer flow 8=39207
    - angular and spectral depend., rel. to emissivity calcs by simple model 8=28390
    - arrays of plates and cubes in vacuum, transient temps. 8=24017
    - Auer-Welsbach grids in flames, thermal peculiarities 8=26609
    - black-body laws, correction for a real body 8=32935
    - with conduction in steady-state heat transfer, soln. of matrix eqn. 8=32953
    - to cylinder, rotating w.r.t. source, anal. of temp. distrib. 8=32980
    - emissivity of diffuse spherical cavity 8=46222
    - emissivity of isothermal spherical cavity with gray Lambertian walls 8=46623
    - gas, emitting and absorbing, spectral heat flux distrib. for temp-depend. absorpt 8=39197
    - in gas supersonic flow, two-dimens., parabolic eqns. of flow 8=39185
    - gases, non-isothermal, in superposed vibr.-rot. bands 8=43680
    - in gases, smoothing mech. of shock waves to prod. cont. temp. profile 8=39200
    - i.r. interf. filters, props. 8=32937
    - i.r. modulation by air driven chopping wheel 8=28379
    - i.r., nature and detection 8=28381
    - i.r. optical communication systems 8=33250
    - i.r. optics, materials 8=31954
    - i.r. radiometer, obs. meas. 8=32943
    - i.r. sources, comparison 8=41851
    - from isothermal dispersions with isotropic scatt., for plane-parallel geometry 8=23990
    - parallelepipeds filled with grey fluid, form factors for surfaces 8=28391
    - polymethylmethacrylate, transparent dielec., during damage by laser light 8=30994
    - polystyrene, transparent dielec., during damage by laser light 8=30994
    - radiometer for environmental studies 8=28384
    - radiometer, photophoretic and thermal forces relationship 8=24011
    - radiometer spectral responsivity determ. 8=42232
    - through screens with holes, reduction of flux, and similarity to grey gas 8=37297
    - semi-infinite slab, two-dimens. absorbing-scatt. medium, directional emissivity 8=23991
    - spectral density form 8=23989
    - spheres, at bounding surface, rel. to transient heating and cooling 8=41859
    - taut-wire temp. meas. transducer 8=24016
    - temp. determ. in thermal analysis 8=28412
    - thermal force on spherical particle, 13-moment theory comments 8=23992
    - thermal force on spherical particle, 13-moment theory reply to comments 8=23993
    - CO, Planck and Rosseland mean absorpt. coeffs., calc. 8=25822
    - CO$_2$, Planck and Rosseland mean absorpt. coeffs, calc. 8=25822
    - H$_2$O vapour, non-isothermal, in 2.7μ region 8=43680
    - H$_2$O vapour, Planck and Rosseland mean absorpt. coeffs., calc. 8=25822
    - Pu, hemispherical emittance, effect of surface cond. and temp. 8=30993
    - W, Cs-covered, spectral distrib. during thermionic electron emission 8=31465
- **Radiation belts**. See Atmosphere/radiation belts.
- **Radiation chemistry**. See Chemical effects of radiations/ionizing radiations; Radiochemistry.
- **Radiation damage**. See Physical effects of radiations.
- **Radiation detectors**
  - See also Bolometers; Photometry; Radioactivity measurement.
  - bolometer operating points for max. sensitivity 8=37300
  - Cherenkov, for e.a.s. obs. at 5200m altitude 8=38259
  - circular foil thermoelec. radiometer, dynamic functioning 8=28382
  - diodes, p.i.n., for astrophotometry 8=42135
  - information content in thermal beams 8=41852
  - i.r., and appl. 8=28381
  - infrared, avalanche, thermal noise behaviour 8=46227
  - i.r. balloon borne coronagraph 8=45609
  - i.r., cooling techniques 8=32947
  - i.r., detection by up-conversion to visible in HgS crystal 8=46552
  - i.r., far, Josephson-effect device 8=46225
  - i.r., far, point-contact supercond. junction 8=31357
  - i.r., Joule-Thomson coders 8=32944
  - i.r. modulation by air driven chopping wheel 8=28379
  - i.r. multi-element, for high information rate systs. 8=32942
  - i.r., new solid-state detectors 8=32941
  - i.r. quantum counter-amplifier, solid-state rel. to elec.-dipole transitions in crystals 8=42137
  - infrared quantum counters, rare-earth trichloride crystals, improved sensitivity 8=32940
- **Radiation detectors**—contd
  - i.r. radiometer, obs. meas. 8=32943
  - i.r. radiometers, spectral responsivity determ. 8=42232
  - i.r., use of pyroelectric detector to meas. Q-switched pulses 8=46581
  - i.r. windows for h.p. optical meas. 8=33249
  - lead slow down time spectrometer for meas. of n resonance parameters 8=24972
  - luminescent dosimeter for hard radiation 8=45930
  - nonlinear, sensitivity 8=42128
  - phosphors for detection of vac. u.v. radiation 8=41179
  - photoelectric, shot noise, photon bunching effects 8=46418
  - photomultiplier for feeble luminous flux 8=46649
  - photomultiplier for plasma r.f. radiation 8=43540
  - photon no. from given area, min. detectable change 8=42125
  - radiometer without condensing agents, for meas. radiant props of flame 8=28408
  - synchronous vs. pulse counting for photomultiplier systems 8=42129
  - thermal viewer, 100 line 8=32948
  - u.v., extreme, for airglow photometry 8=41393
  - u.v., using filters, Zn$_2$SiO$_4$ phosphors on glass base and photoresistors 8=24372
  - X-ray counters and detectors, review 8=46842
  - Ge, i.r., photoconductivity-type 8=41854
  - Ge, Cu doped, i.r. detector 8=46226
  - Ge, Cu doped, i.r. detector, low freq. noise 8=32946
  - Ge : In far i.r. photocond. detector, response time 8=32945
  - InSb, for far i.r. spectroscopy 8=32939
  - InSb i.r., low-noise f.e.t. amplifier 8=41856
  - InSb, photoconductive, infrared 8=40666
  - InSb RPY51 in i.r. microscope for temp. distribution small areas 8=28380
- **Radiation effects**. See Biological effects of radiations; Chemical effects of radiations; Physical effects of radiations.
- **Radiation monitoring**
  - See also Dosimetry.
  - Cherenkov counter for meas. of reactor power level 8=47436
  - counting and sampling, statistical criteria 8=24494
  - deadtime losses, automatic compensation 8=24525
  - γ-rays, reflected by concrete, lead from Co^{60}, Cs^{137}, Ir^{192} point sources; dose rates 8=47393
  - in-core γ flux, fast-response thermometer 8=47050
  - in-pile calorimeter for simultaneous meas. of n-induced and γ-induced energies 8=25319
  - luminescent dosimeter for hard radiation 8=45930
  - particle size distribution of radioactive aerosols in selected areas at AERE 8=50159
  - personal fast n monitoring, with Kodak NTA films 8=33812
  - proton accelerator, medium range 8=33402
  - reactor neutrons, Sc^{46} capture cross-section 8=47330
  - small animals, linear scanning 8=50467
  - synchrotron, alternating-gradient, beam loss location and meas. 8=37821
  - Thoron meas. devices, calibration method 8=47433
  - tritium monitoring system for DIDO and PLUTO reactor halls 8=29565
  - Ge(Li) detector paralleling for large samples 8=46912
  - by Si damage, appl. to n exposure meas. 8=29207
- **Radiation pressure**
  - See also Acoustic streaming.
  - piston, vel. and accel. due to e.m. waves 8=33129
  - radiometer, photophoretic and thermal forces relationship 8=24011
  - solar corona composition, recalc. 8=45922
  - space vehicles, black and white, oscills. 8=32374
  - thermal force on spherical particle, 13-moment theory, comments 8=23992
  - thermal force on spherical particle, 13-moment theory, reply to comments 8=23993
- **Radiation protection**
  - See also Radiation monitoring.
  - concrete, for D-T neutrons 8=29199
  - depth dose distrib. prop. by electron irrad., energy losses and ionization 8=31143
  - γ from Co^{60}, vertical steel slab, barrier and geometry attenuation 8=37922
  - γ-rays, governing of transfer and scattering 8=33609
  - γ-rays, two-layer slabs penetration and composite slabs buildup factor calc. 8=37921
  - γ shielding, ang. distrib. for complex calc. 8=24700
  - hexane ionization chamber, quality factor 8=37787
  - irradiation capsules for coated particles 8=47414
  - neutron activation analysis, thermal flux var. with irradiation and shielding systems, 14 MeV 8=47380
  - neutron reflection by human body dependence on surface tissue depth and energy 8=41606
  - neutron sources, fast, reducing the weight of shielding 8=29206
  - nuclear accident and effects, book 8=38586
  - polyethylene slabs, back scatt. spectra rel. to thickness for γ ray 8=25207
  - shielding, applic for isotopes 8=43245
  - shielding ATTOW two dimensional calc. programme 8=47392
  - shielding penetration, Monte Carlo calc., self-optimized exponential biasing 8=34075

Radiation protection—contd
- space vehicle shielding, calcs., straightahead approx. validity 8=36901
- X-ray shield for texture goniometer 8=39705
- Al cylindrical satellites, shielding against energetic electrons, lab. study 8=32384
- Al slabs, back scatt. spectra rel. to thickness for γ-ray 8=25207
- C(α, N) yield rate from targets rel. to shielding design 8=43141
- Co^{60} heat source, encapsulation 8=47421
- Cs-137 in humans, meas. in 1958-67 8=41605
- Fe, fast n shielding and collimation props. 8=33793
- NaI(Tl) crystal, cosmic-ray Cherenkov shield 8=28981
- Pb, fast n shielding and collimation props. 8=33793
- Pb shield, γ-ray leakage through slit 8=38595
- Pb slabs, back scatt. spectra rel. to thickness for γ-ray 8=25207
- RaA, inhalation hazard dependence on diffusion coeff. rel. to humidity 8=32257

Radiative transfer
- air, in hypervelocity Couette and boundar-layer flow 8=39207
- albedo of striated medium of isotropically scatt. particles 8=45462
- angular and spectral depend., rel. to calcs by simple transfer model 8=28390
- atmosphere scatt. eigenfunction description 8=50408
- atoms, multilevel, transfer of line rad., effects of coupling mechanisms 8=38628
- auxiliary eqn., computation of resolvent 8=41799
- between two dielectrics, effect of small spacings 8=26607
- to cylinder, rotating w.r.t. distant source, rel. to temp. distrib. 8=32980
- density-independent partition functions 8=41798
- diffuse reflection and transmission by inhomogeneous infinite cylindrical region 8=37233
- diffusion in anisotropically scatt. plane layer 8=46131
- diffusion in presence elongated dispersion indicatrix 8=50246
- diffusion in spherical envelope surrounding point source 8=41801
- dispersive media, from photon distrib. function 8=46132
- dissipation functions of anisotropically scatt. invariant imbedding eqns. 8=28843
- Duhamel's principle in two-dimens. radiation field 8=50404
- during superorbital re-entry, effects of non-grey self-absorpt. and energy loss 8=41488
- Eddington approximation 8=50409
- emissivity relations, role in calcs. 8=41800
- equation, numerical soln. 8=37230
- external radiation-field measurements, source distribution, numerical estimation 8=32858
- fibre-glass spacer mats, influence on transfer below 300°K 8=39955
- in finite slab, integral eqn. soln., resolvent kernel in terms of X- and Y-functions 8=37228
- in flow over symmetric bodies, with absorpt., zeroth order and rad.-convection coupled fields 8=37298
- fluidized bed, heat flux between immersed body 8=39456
- flux from illuminated slab 8=23917
- in gas boundary layer flow, effect of viscous dissipation and mass addition 8=39180
- in gas flow, supersonic, two-dimens., effects on eqns. of motion 8=39185
- gas, in viscous flow, emitting and absorbing, method of soln. 8=39204
- gas, thermal radiating, effect of wall temp. sudden change 8=30288
- gases, i. r. rad., calc. of Planck and Rosseland mean absorpt. coeffs. 8=25822
- gases, i. r. radiating, integral eqn. for radiative equilib. 8=34649
- gases, Planck mean absorpt. coeff., and rad. props., appl. to fluid mech. 8=39198
- in glass, hot, rel. to melting and forming ops., i.r. asborpt. temp. changes and thickness 8=44371
- grey absorpt. coeffs. 8=32862
- grey medium between concentric spheres and cylinders 8=32859
- high-temperature solar devices, calorimetric investig. 8=41864
- in hot stars, models to test validity of assumption of black body distrib. 8=41513
- hydrologic optics, light fields, mathematical models 8=41333
- incoherent, scatt. and transmission functions, calc. 8=42257
- internal radiation field, functional eqns., time-dependent monodirectional illumination 8=32534
- from isothermal dispersions with isotropic scatt., for plane-parallel geometry 8=23990
- laser radiation to atomic thermal vibrations in solids 8=39900
- in liquids, rad. field at depth, for known size distrib. of particles and variable absorpt. 8=41336
- in medium with strong anisotropy phase function 8=41362
- modification by scatt. processes in medium with absorpt. and emission 8=37227
- non-homogeneous media, use of spectral band models 8=23918
- nonlinear system, convolution integral and Volterra kernels 8=37229
- non-planar systems, modified moment method 8=32861
- Monte Carlo sampling appls. 8=32855
- parallelepiped filled with grey fluid, surface form factors 8=28391
- planetary atmosphere, diffuse reflection and transmission 8=41561
- planetary cloud layers rel. to i. r. optical props. of water and ice spheres 8=50140
- radiant thermal cond. coeff., in presence of molecular spectum 8=46242
- radiative energy transfer, conference 8=23909
- resonance-line scatt., Monte Carlo technique 8=29585
- from rocket exhaust, to vehicle base, i. r. heating 8=41482
- with scattering, eqn. 8=32860
- in sea, expt. methods and app. to meas. props. specified by theory 8=41334
- in slab of anisotropically scatt. media, effect of Fresnel reflection at interfaces 8=32936
- softening of radiation by multiple Compton scatt. 8=37231
- spectral line formation by noncoherent scatt. 8=37232
- starlight, direct and scatt., model 8=28092
- stellar atmosphere, radiation field and atomic states distrib. 8=41511
- in stellar wind region, rel. to thermal diffusion and ionization processes 8=41512
- theory, historical summary, appl. to planetary atmos. 8=41363
- through shields of screens with holes, similarity to grey gas 8=37297
- X- and Y-functions, time-dependent, for diffuse reflection and transmission of rays 8=41560
- FeI, lifetimes of energy levels calc. from transition probabilities of spectra 8=47496

Radiators. See Acoustic transducers; Electromagnetic waves/radiators.

Radicals. See Free radicals.

Radioactive dating
- deep sea cores, sedimentation rate determ. by γ-ray spectrometry 8=27865
- firn samples from Antarctica, dating and accumulation meas. 8=27855
- igneous rocks from Iceland, Pb isotope studies 8=50085
- meteorites, hypersthene achondrites 8=37023
- meteorites, olivine from 6 pallasites 8=37023
- muscovite samples, etchable length of fission tracks rel. to age 8=27854
- oldest exposed lavas in Iceland, K/Ar ages 8=50083
- xenolithic rocks, extremely high Ar^{40}/K ratios 8=50084
- Zoetlief volcanics in S. Africa, from Pb isotopic data 8=50082
- Fe meteorites, K/Ar age determ., improved neutron activation tech. 8=50434
- K-Ar ages of recent rhyolites of Mono and Inyo craters, California 8=27857
- Pa^{231} growth, Barbados coral 8=36683
- Rb-Sr age of Vanda porphyry dikes, Wright Valley, Antartica 8=27859
- Th^{230} ages of volcanic rock from Mono and Inyo Craters 8=27860
- from U^{238}/Pb^{204} ratio in concordia plots 8=27856

Radioactive tracers
- medical, nomenclature 8=32617
- scintillomicroscope for detection in biological specimens 8=32623
- for self-diffusion coeffs., by capillary method 8=25899
- small animals, linear scanning 8=50467
- in Al electro-refining process, study of effectiveness 8=36607
- C^{14}, scintillation counting with Triton X-100 8=46880
- Cr^{51}, labelling sand 8=50092
- Hg solubility determ. in various liqs. 8=30416
- KCl-RbCl mixed cryst., tracer diff. rel. to chem. diff. 8=39975
- Kr^{85}, for flow meas. of condensable gases 8=34621
- Kr^{85} monitoring of atmospheric diffusion 8=36729
- O^{15}, bibliography of uses, 1963-66 8=34185

Radioactivity
- See also Alpha-, Beta-, Gamma-rays; Atmosphere/Radioactivity; Beta-decay theory; Chemical analysis, radioactive; Chemical effects of radiations/ionizing radiations; Fallout; Geophysical prospecting; Nuclear decay theory; Nuclear bombardment targets; Nuclear excitation; Nuclear reactions; Radiochemistry.
- α-decay, individual shell model 8=25171
- α-decay shell model theory, validity of exponential law 8=47276
- α-decay of 11 isotopes of heavy elements obs. 8=38412
- α decay, unified theory 8=42935
- α-emitters, predicted, in $A < 200$ region 8=38406
- α, rel. to nuclear surface struct., barrier penetrabilities calc. 8=29262

Radioactivity — contd
β-decay, forbidden, internal bremsstrahlung 8=42938
β emitters, identification using scintillation counter 8=33951
decay mechanism of fissile nuclei 8=47355
element 102, synthesis and props., review 8=29381
fission and spallation prods. delayed n emission 8=38404
fission products, p-induced, delayed-n decay, obs. 8=38463
L_1/K orbital electron capture ratio for allowed transitions Hartree-Fock calc., low-z elements 8=38408
meteorite, Leighton, Kr and Xe isotopic abundances in dark sphase 8=37022
mineral, pulse-height spectrum analysis 8=46939
N-forbidden β transitions in odd-mass deformed nuclei 8=33956
neutrons in soils, due to natural radioact., production rates 8=36681
nuclides emitting γ-rays on lunar surface 8=32531
pipetter, remotely operated for liquid samples 8=41295
products of linear accelerator, γ spectra 8=33953
proton emission, delayed, Dubna heavy-ion expts. review 8=38521
rare-earth deformed nuclei, Gamow-Teller and fast transition rates rel. to models 8=38411
stopping cross-section meas. in C using recoil ions from radioactive decay 8=29658
synchrotron, zero-gradient, radiation dose and induced activity obs. (1965-66) 8=33468
transmutations of nuclei, book 8=33950
2-forbidden β transitions, spectrum calc. 8=25172
Wigner supermultiplet approximation, allowed β transitions 8=25175
$Ac^{224} \xrightarrow{\alpha} Fr^{220}$ 8=47299
Ac^{225} α-disintegration, Fr^{221} levels mag. spectrography obs. 8=25163
$Ag^{105} \rightarrow Pd^{105}$, multipolarity of some transitions 8=33961
Al^{26} β-decay, $T = 2$ component in Mg^{26} ground state 8=47282
Al^{26} in terrestrial rock, induced by cosmic-ray muons search 8=41324
$Al^{28,29}$, from p reaction on Si, excitation functions 8=42942
Am^{241} α-disintegration obs. 8=25198
Am^{243} α-decay obs. 8=42975
Ar^{37}, trace amounts, apparatus for meas. 8=47283
As^{74}, β-decay, nuclear matrix pairing-model calc. 8=42946
As^{74}, ϵ/β^+ ratio 8=42941
Au^{193}, using internal conversion obs. 8=25193
Au^{199} half-life of 55 KeV M2 transition 8=42920
Au^{200} decay, γ obs. attributable to Hg^{200} 8=42969
$B^8 \rightarrow e^+ \nu Be^8$, calc. of ν spectrum rel. to solar neutrinos 8=45888
$Ba^{128} \rightarrow Cs^{128} \rightarrow Xe^{128}$, γ-ray spectrum obs. 8=42956
Ba^{133} decay energy, redeterm. 8=25189
Ba^{133} decay, KX-γ directional correl. 8=42957
Ba^{133} KX-ray γ-ray directional correl., zero anisotropy obs. 8=38417
Be^7, from p reaction on Si, excitation functions 8=42942
Bi^{207}, conversion ratio for 570 and 1064 KeV transition obs. 8=33967
Bi^{210}, β^- decay, autoionization 8=29373
$C^{12} + C^{13}$, angular distributions and excitation junctions obs. 10-30 MeV 8=38523
C^{16}, delayed-n decay, obs. 8=38463
Ca^{44}, second 2^+ state, decay obs. 8=38368
Ca^{47} β decay from $Ca^{46}(n, \gamma)$ 8=38416
$Cd^{109} \rightarrow Ag^{109}$ decay, internal conversion 8=38421
Ce^{146}, γ spectrum and β decay theory 8=42959
Cf^{252}, long-range fragments yield obs. 8=42976
Cl^{38}, β, γ-transitions obs. 8=29359
Cl^{38} decay, first forbidden β transitions, $\beta-\gamma$ ang. correl. 8=29360
Co^{60}, β end-point energy obs. 8=29363
Cr^{51}, β-decay, internal bremsstrahlung 8=29362
Cs-137 in humans, meas. in 1958-67 8=41605
Cs^{137}, β end-point energy obs. 8=29363
Cs^{137}, doubly forbidden β-spectra 8=47292
Er^{169}, β^- decay, auto-ionization 8=29373
F^{18}, from p reaction on Si, excitation functions 8=42942
Ga^{68} β-decay rel. to Zn^{68} levels spins and energies 8=33915
Ge^{69}, from $Ga^{69}(d, 2n)$, γ-spectrum obs. 8=25132
He^8, delayed-n, β and γ emission obs. 8=38414
$Hf^{178}2^+$ β-vibrational state E2 + M1 decay 8=33934
In^{113} γ-decay, 393 keV transition, K-conversion coeff. 8=33923
Ir^{194m}, 32 ms, γ-ray spectrum obs. 8=42919
K^{42} decay, first forbidden β transitions, $\beta-\gamma$ ang. correl. 8=29360
$La^{134,136}$ decay obs. and γ spectra 8=42958
Li^9, delayed-n decay, obs. 8=38463
Mg^{27}, from p reaction on Si, excitation functions 8=42942
N^{15} decay 8=29294
N^{17}, delayed-n decay, obs. 8=38463
Na^{22}, electron capture ratio to positron emission 8=47281
Na^{22}, ϵ/β^+ ratio 8=42941
$Na^{22,24}$, from p reaction on Si, excitation functions 8=42942
Nb^{90m}, decay consts, effect of changes in chem. state, press. and supercond. state 8=42950

Radioactivity—contd
$Nd^{141g,m}$, γ spectra obs. 8=42960
$Ni^{57,65}$, β-γ (CP) correlation measurements, deduced Coulomb matrix elements 8=42944
$Np^{230,229}$ production from $U^{233}(p, xn)$ 8=33968
$Np^{238} \xrightarrow{\beta^-} Pu^{238}$ 8=29480
$O^{14} \xrightarrow{\beta^+} N^{14*}$ Fermi decay ft value calc. 8=33958
O^{15} decay 8=29294
P^{32}, β helicity meas. method 8=24718
P^{32} prod. in $K^{39}(n, 2\alpha)P^{32}$, 14 MeV identified by its β-decay 8=38494
Pa^{231}, new α-decay lines with energies, 5631, 5027, 5009 KeV 8=38412
$Pb^{211} \rightarrow Bi^{211}$, γ spectrum obs. 8=47266
$Pr^{142} \rightarrow Ce^{142}$, γ rays obs. 8=38432
$Pr^{142} \rightarrow Nd^{142}$, γ rays obs. 8=38432
$Pr^{142} \rightarrow Nd^{142}$, 508 KeV γ populating level at 2084 KeV 8=38433
Pr^{144}, first forbidden unique correl., inner bremsstrahlung correction 8=47254
$Pr^{144} \xrightarrow{\beta^-} Nd^{144}$, γ rays energies precision meas. 8=38434
Ra^{224} recoil atoms in gases, ranges 8=34179
Rb and Sr isotopes in granite, post-crystallization movement rel. to feldspar alteration 8=50081
Rb^{88} decay, first forbidden β transitions, $\beta-\gamma$ ang. correl. 8=29360
Rb^{91} β and γ spectra obs. 8=25181
$Re^{186,188} \rightarrow Os^{186,188}$ $K = 2$ states, asymmetric-rotor model disfavoured 8=47226
Rn decay products, diffusion coeffs. and mean free paths in air 8=38441
Se^{75}, γ-γ angular correlation 8=33916
Si^{28} nuclear resonance fluorescence in Al single crystals 8=30631
Sn^{113} KX-ray γ-ray directional correl., zero anisotropy obs. 8=38417
Sn^{113} source, from $In^{113}(d, 2n)$, fractional distillation 8=42954
Sr and Pb, isotopes evolution model with crustal material recycling through mantle 8=36682
Sr^{85} KX-ray γ-ray correl., zero anisotropy obs. 8=38417
Tc^{94} isomers, decay to Mo^{94} levels 8=38374
$Te^{107,108,109,110}$, α-and delayed p-decay, obs. 8=38424
Te^{111}, β^+ p coincidence meas. 8=47290
Te^{127} β decay, excitation of I^{127} in Te crystal, rel. to quadrupole coupling 8=36284
Te^{130} double beta decay, half life obs. 8=38426
$Te^{133g,m}$ β-decay and I^{133} level struct. obs. 8=42897
$Th^{233} \rightarrow Pa^{233}$ internal conversion electron spectrum 8=42979
Th^{227} α-decay, Ra^{223} recoil atoms charge, obs. 8=29379
Tl^{204}, β end-point energy obs. 8=29363
U, new γ log for direct determ. in ores 8=32184
U^{233}, amine extraction from irrad. ThO_2 8=36634
$U^{237} \xrightarrow{\beta} Np^{237}(n, \gamma)Np^{238} \xrightarrow{\beta} Pu^{238}$ yield obs. 8=29480
Xe^{127}, hyperfine interaction, pressure effect 8=47291
Zn^{62} 9.3-h, Cu^{62} levels obs. 8=42945
Zn^{65} KX-ray γ-ray directional correl., zero anisotropy obs. 8=38417
Zn^{69m} β-decay, conversion coeff. and K-fluoresc. yield obs. 8=38418
dating. See Radioactive dating.
decay periods
α-emitters, $Z > 50$ and $N < 126$, tables 8=38413
fission fragments, primary, meas. 8=38543
measurement and 13 isotopes obs. 8=42940
nuclei embedded in magnetized ferromag. foil, meas. 8=38401
36 nuclides, obs. 8=33957
Ag^{118} product of U^{235} fission, obs. 8=43123
Al^{26m}, precision meas. 8=42939
Ar^{33}, delayed p decay and spectrum, $S^{32}(He^3, 2n)$ obs. 8=38415
Ar^{89}, $BaTiO_3$ internal electric field effect 8=33960
As^{75}, 280 keV level 8=29317
$As^{83,84,85,87}$, and chem. separation, obs. 8=38419
Au^{189} isomer, $Ta^{181}(C^{12}, 4n)$ prod., obs. 8=38522
Ca^{50} log ft for β-decay; Sc^{50} energy levels calc. 8=42863
Ce^{140} cascade, intermediate states 8=29329
Ce^{147}, chromatographically separated, obs. 8=38430
$Co^{144} \rightarrow Ba^{144} \rightarrow La^{144}$, obs. 8=29367
Eu^{150} isomer half-life obs. 8=42963
F^{19} 2.79 MeV state mean lifetime using Doppler shift attenuation method 8=42844
Fm^{256}, from $Es^{253}(\alpha, p)$, α-decay rate 8=42977
Fm^{259}, predictions rel. to thermonuclear explosion abundance obs. 8=38496
Gd^{156} 289 and 1513 levels obs. 8=25148
Hg^{206} from Pb^{208} (p, 3p), spectra obs. 8=42971
Ho^{163} e capture obs. 8=42964
I isotopes, (γ, xn) prod., $E_\gamma < 900$ MeV 8=38456
I isotopes, meas. by Xe nuclei magnetized ferromag. foil 8=38401
I^{129}/xenon, for achondritic meteorites rel. to early solar system synthesis 8=45845
In^{117}, 748, 659, 587 keV, lifetime obs. 8=25141
$Ir^{196g,196m}$ obs. 8=42967

Radioactivity—contd
  decay periods—contd
    K^{38} and β^+ spectrum obs. 8=29361
    K^{38m} and β^+ spectrum, obs. 8=29361
    $Kr^{90,91,92,93}$ from $U^{238}O_2$-stearate fission source, obs. 8=38549
    La^{128} isomer, $Sn(N^{14}, xn)$ and $Sb^{121}(C^{12}, 5n)$ prod., obs. 8=38522
    Lu, rel. to Yb^{168} energy levels 8=42910
    Md^{259}, predictions rel. to thermonuclear explosion abundance obs. 8=38496
    Mg^{23}, precision meas. 8=42939
    $Mg^{24,26}$ levels, Doppler-shift lifetime meas. 8=25110
    Mg^{25}, 3.400 MeV level 8=29301
    Mn^{54}, obs. 8=33959
    Na^{19}, delayed p decay, $F^{19}(He^3, 3n)$ obs. 8=38415
    Ne^{17}, delayed p decay and spectrum, $O^{16}(He^3, 2n)$ obs. 8=38415
    Ne^{19}, precision meas. 8=42939
    Ne^{22}, 3.35 to 6.35 MeV levels 8=29298
    Ne^{22} 5.14 MeV state 8=25108
    Ni^{58} 2^+ states, mean lifetime obs. 8=25130
    Ni^{61}, 283 keV level 8=29315
    No^{256}, α-energy and half-life obs. 8=25199
    O^{16} obs. 8=47233
    Os^{180} intermediate level half-life 8=47298
    Pb^{206} isomeric state, time interval analysis meas. 8=25083
    $Pb^{208}(p, 3p)$, spectra obs. 8=42971
    Pd^{117} product of U^{235} thermal-n fission, obs. 8=43124
    Pm^{143} first excited state obs. 8=25146
    Pr^{138}, 2.2 hour, reinvestigation 8=29368
    Pu^{244}/xenon, for achondritic meteorites rel. to early solar system synthesis 8=45845
    Rb^{90-96} and β-decay derivatives, and Rb^{90} isomer, obs. 8=29367
    Rh^{105} 538 keV state mean lifetime obs. 8=25140
    S^{29}, delayed p decay and spectrum, $O^{16}(He^3, 2n)$ $Si^{28}(He^3, 2n)$ obs. 8=38415
    Sc^{43} 472 KeV excited state 8=42867
    Sc^{50}, log ft for β-decay; Sc^{50} energy levels calc. 8=42863
    Se^{77}, Nilsson versus shell models 8=29318
    Si^{27}, precision meas. 8=42939
    Si^{28} levels, Doppler-shift lifetime meas. 8=25110
    Si^{31} 8=29474
    Sn^{121} level spin obs. 8=38422
    Tb^{149} from $Au^{197}(p, X)$ 8=38476
    Te^{109}, delayed p emission, $Mo^{92}(Ne^{20}, 3n)$ and $Mo^{94}(Ne^{20}, 5n)$ obs. 8=38425
    Te^{111}, delayed p emission, heavy-ion reactions, obs. 8=38425
    Te^{125} 321 KeV $9^-/2$ state 8=38381
    Te^{130} double beta decay 8=38426
    Tl^{204}, 9.4 years obs., no evidence for short lived isomer 8=25194
    U^{235m}, effect of environment 8=25164
    V^{52} and β^- spectrum, obs. 8=29361
    Xe^{127m} and 125 and 175 keV γ transitions assignments, obs. 8=38427
    Yb^{165}, Tm^{165} levels obs. 8=42965
    Zn^{63}, precision meas. 8=42939
  decay schemes
    α-emitters, $Z > 50$ and $N < 126$, tables 8=38413
    fission fragments, primary, meas. 8=38543
    odd-odd deformed nuclei, α decay to vibrational levels 8=47277
    $102^{252,255}$ α-decay props. obs. 8=42978
    $Ag^{102,102m,103}$, $Ag^{107}(N^{14}, xn)$ and $Mo(B^{11}, xn)$ obs. 8=38428
    $Ag^{108}(T_{1/2} \geqslant 5$ years) γ spectrum 8=42953
    $Ag^{110m} \rightarrow Cd^{110}$ γ intensities 8=47288
    Al^{26}, closely spaced levels, 2.07 MeV 8=42851
    Al^{27} levels, spin assignments 8=42849
    Am^{241} in Th lattice, α-decay and Np^{237} Mössbauer spectrum 8=42929
    Ar^{33}, delayed-p decay, obs. 8=38414
    As^{70} to Ge^{70}, γ-ray spectrum obs. 8=42948
    $As^{74} \rightarrow Ge^{74}$, Se^{74} obs., additional γ-ray 8=42947
    $At^{210} \rightarrow Po^{210}$, e capture decay 8=25195
    $Au^{195} \rightarrow Pt^{195}$ conversion electrons need to study levels of Pt^{195} 8=38392
    $Ba^{125,127}$, $In^{115}(N^{14}, xn)$ and $Sb^{121}(B^{11}, xn)$ obs. 8=38428
    $Ba^{131} \rightarrow Cs^{131}$, γ-ray spectrum, new transitions obs. 8=38429
    Bi^{208} 2.5 ms isomeric state, j-forbidden transition 8=42924
    $Bk^{243-249}$, rel. to energy level diagrams of daughter nuclei 8=42974
    Ca^{37}, delayed-p decay, obs. 8=38414
    Ca^{50}, β-decay to 1848 KeV level, resolution of discrepancy 8=42943
    $Cd^{115m} \rightarrow In^{115}$, γ spectra obs. 8=25184
    $Cd^{117} \rightarrow In^{117}$, rel. to In^{117} energy level determ. 8=42889
    $Ce^{143} \rightarrow Pr^{43}$, β-γ ang. correl. obs. 8=38431
    $Ce^{145,146}$ and total β-decay energy, obs. 8=38430
    Cf^{249}, rel. to energy level diagrams of daughter nuclei 8=42974
    Co^{56}, γ-γ coincidence obs. 8=29364
    $Co^{57,58}$ prod. in photo-reaction on Cu^{63} 8=29405
    Co^{58}, excited levels branching ratios, $Fe^{58}(p, n)$ obs. 8=29313

Radioactivity—contd
  decay schemes—contd
    Co^{123}, $In^{115}(C^{12}, 4n)$ obs. 8=38428
    $Cs^{132} \rightarrow Ba^{132}$, Xe^{132} obs. 8=42899
    $Cu^{61} \rightarrow Ni^{61}$ 8=29315
    Dy^{159m} 115μs obs. 8=38436
    Dy^{165}, β-decay, new γ transitions 8=47296
    $Dy^{165,165m}$ 8=47295
    E^{154} to Gd^{154}, EO/E2 transition probability ratios calc. 8=42904
    Er^{171}, Tm^{171} level scheme, γ-ray spectrum obs. 8=47259
    Eu^{144}, rel. to Sm^{144} 1659 and 2481 KeV levels population in (p, p^1), obs. 8=38435
    $Eu^{150} \rightarrow Sm^{150}$, γ-spectrum obs. 8=42963
    $Eu^{154} \rightarrow Sm^{154}$, Gd^{154}, γ spectra obs. 8=42962
    $Eu^{155} \rightarrow Gd^{155}$, rel. to Gd^{155} internal conversion coeff. at 86.5 KeV 8=42905
    Fm^{255}, rel. to energy level diagrams of daughter nuclei 8=42974
    Ga^{65} to Zn^{65}, obs. 8=25178
    Gd^{159}, 68 keV 26 nsec isomeric state 8=29335
    $Gd^{159} \rightarrow Tb^{159}$, γ energy obs. and Tb^{159} level scheme 8=29372
    $Ge^{77} \rightarrow As^{77}$ decay, γ spectroscopic obs. 8=29366
    $Hf^{170} \rightarrow Lu^{170}$ 8=29340
    Hf^{178} isomeric state with $K \geqslant 16$ 8=42966
    Hf^{180m}, studies 8=29341
    $Hg^{192,194,196,198}$, γ-spectra obs. 8=38394
    $Ho^{154} \rightarrow Dy^{154}$ by β-decay 8=42908
    Ho^{163}, by e capture from M and higher shells 8=42964
    $I^{119} \xrightarrow{\beta^+} Te^{119}$ and e capture, energy levels obs. 8=25188
    $I^{121} \rightarrow Te^{121}$, 58 transitions 8=25187
    $I^{123} \rightarrow Te^{123}$ obs. 8=42955
    In isotopes, γ-ray spectra 8=47251
    $In^{116m}1(5^+$, 54 min) 8=47286
    In^{192M_1}, L-X-ray and gamma conversion electron spectra 8=33966
    $Ir^{192} \rightarrow Pt^{192}$ 8=33935
    $Ir^{196g,196m} \rightarrow Pt^{196}$ γ transitions obs. 8=42967
    K^{43} obs. 8=43027
    $La^{140} \rightarrow Ce^{140}$, spin and parity of Ce^{140} levels obs. 8=33963
    Lu^{177}, Nilsson model rel. to 386 keV β-113 keV γ directional correl. obs. 8=29375
    $Lu^{168,168m} \rightarrow Yb^{168}$ 8=29339
    Mn^{56}, γ-γ coincidence obs. 8=29364
    Mo^{94}, n-decay, isobaric analogue resonances 8=29320
    $Nb^{94} \rightarrow Mo^{94}$, twice forbidden β-decay, matrix element calc. 8=42951
    Nb^{96}, negaton and conversion electron spectra 8=2518
    $Nd^{147} \rightarrow Pm^{147}$, β-γ and γ-γ coincidence obs. 8=29369
    Ne^{17}, delayed-p decay, obs. 8=38414
    $Ni^{57,65}$, β-γ (CP) correlation measurements, deduced Coulomb matrix elements 8=42944
    Os^{180} 8=47298
    $Os^{180,181}$, internal conversion coeffs. obs. 8=38438
    Os^{193}, beta decay populates excited states of Os^{193} 8=38439
    $Os^{193} \rightarrow Ir^{193}$, obs. 8=42916
    Pb^{211} β decay, γ-ray spectrum of Bi^{211} levels obs. 8=47267
    Pd^{109}, Ag^{109} energy levels using Ge(Li)-Ge(Li) coincidence obs. 8=47287
    Pm^{148}, directional β-γ correl. obs. 8=42961
    $Pr^{138} \rightarrow Ce^{138}$ 8=29368
    Pr^{139}, γ-ray spectra 8=47251
    Pt^{188}, obs. 8=38394
    Pt^{188} obs, resolution of ambiguities 8=42968
    Pu^{239}, rel. to energy level diagrams of daughter nuclei 8=42974
    Rb^{81}, from $Br^{79}(\alpha, Zn)$ and $Br^{79}(He^3, n)$, obs. 8=25180
    Re^{178} decay, conversion coeffs. obs., transition multipolarities calc. 8=38438
    Re^{186}, high energy γ-spectrum 8=29377
    Re^{188} to Os^{188}, γ-ray spectrum obs. 8=25192
    $Rh^{104m}(5^+$, 4.4min) 8=47286
    $Rh^{105g}(1^+$, 42 sec) 8=47286
    Rn^{222} in atmosphere, equilib. with daughters, obs. by α-pulse spectroscopy 8=32255
    Ru^{95}, and β- and γ- spectra, obs. 8=42952
    Ru^{100}, excited states study from Rh^{100} 8=29321
    Sb^{124}, disintegration scheme 8=47289
    Sb^{125} 8=38382
    Sb^{125}, β- and γ-spectroscopic studies 8=25185
    Sc^{43}, log ft obs. 8=43027
    Sc^{46}, β-branching ratio 8=47330
    $Se^{75} \rightarrow As^{75}$, energy and intensity of conversion electrons, obs. 8=25179
    $Se^{75} \rightarrow As^{75}$, γ-γ, e^--γ ang. correl. obs. 8=42949
    Se^{81m}, K conversion coeff. obs. for 102.7 keV transition 8=29370
    Se^{83m}(69 sec), branching ratios, β- and γ-spectra obs. 8=38420
    Si^{25}, delayed-p decay, obs. 8=38414
    $Si^{30}(p, \gamma)P^{31}$, 22 resonances 8=29444
    Sm^{143}, γ-ray spectra 8=47251
    $Sm^{143} \rightarrow Pm^{143}$, obs. 8=25190
    Sm^{148}, highly excited states, α-spectra 8=33929
    $Sm^{155} \rightarrow Eu^{155}$ 8=29334
    $Sm^{155}(\beta^-)Eu^{155}$, conversion electron spectrum 8=47293
    Sn isotopes, γ-ray spectra 8=47251
    Sn^{111}, 35 min, to levels of In^{111} 8=38423

Radioactivity—contd
decay schemes—contd
$Sn^{121,121m}$ level and spins 8=38422
Sn^{123}, β-decay, Sb^{123} level scheme 8=33926
Ta^{182m}(16.3min) 8=47286
Te^{108} α-and p-decay, obs. 8=38424
Te^{111}, delayed p emission, heavy-ion reactions obs. 8=38425
$Te^{133g,133m}$, to levels of I^{133} 8=25186
Te^{164}, max. energy, half-life 8=47294
Th^{233} β, Pa^{233}, γ-ray spectra obs. 8=29380
$Th^{227} \rightarrow Ra^{223}$, level scheme obs. 8=25196
Th^{227}, γ-ray spectrum, Ra^{223} energy levels deduced 8=42973
Ti^{41}, delayed-p decay, obs. 8=38414
$Tl^{192, 194, 196, 198}$ γ-spectra obs. 8=38394
$Tm^{165} \rightarrow Er^{165}$, conversion e coincidence obs. 8=29374
Tm^{168}, transitions obs., internal conversion coeffs. 8=25191
Tm^{174}, from γ and β meas. 8=33965
Tm^{176}, rel. to energy levels of Yb^{176} 8=33964
U^{233}, rel. to energy level diagrams of daughter nuclei 8=42974
$W^{177} \rightarrow Ta^{177}$ 8=29376
Xe^{127m}, 125 and 175 keV γ transitions assignments, obs. 8=38427
Yb^{165}, Tm^{165} levels obs. 8=42965
Yb^{175}, Nilsson model rel. to 352 keV β-114 keV γ directional correl. obs. 8=29375
$Zn^{65} \rightarrow Cu^{65}$, obs. 8=29365
Zn^{72}, γ-transitions obs. 8=25177
electron capture
hole formation in atom, h.f. interaction with nucleus obs. 8=47271
K-capture, internal bremsstrahlung probability calc. 8=29354
L/K orbital electron capture ratio, theory and expt. compared for $13 \leqslant Z \leqslant 37$ 8=25077
theory and expt., 1963/1967, review 8=25176
$At^{210} \rightarrow Po^{210}$ 8=25195
$Ba^{131} \rightarrow Cs^{131}$, γ-ray spectrum new transitions obs. 8=38429
Ba^{133} decay energy, redeterm. 8=25189
Co^{57} K-capture fraction obs. 8=42876
Cr^{51}, internal bremsstrahlung assoc. with ground-to-ground transition 8=29362
Hf^{170} rel. to Lu^{170} intrinsic and collective levels, obs. 8=29340
Ho^{163}, half-life obs. 8=42964
Pt^{188} obs, K-to-total E.C. ratio 8=42968
$Rm^{165} \rightarrow Er^{165}$ decay scheme, conversion e coincidence obs. 8=29374
Sb^{119}, polarized inner bremsstrahlung parity nonconservation, obs. 8=33962
Sr^{83}, rel. to M2 isomerism in Rb^{83} 8=25182
Tb^{153}, levels of Gd^{153} obs. 8=42903
Zr^{65} decay, Cu fluoresc. yield and $\overline{P}_K \omega_K$ obs. 8=47284
protection. See Radiation protection.
Radioactivity measurement
See also Dosimetry; Radiation monitoring; and the specific radiation, e.g. Gamma rays.
absolute method selection for standards labs. 8=42933
biological material, γ spectrometer 8=47065
correlation counting appl. to absolute disint. rate determ. 8=25170
counting and sampling, statistical criteria 8=24494
counting errors, times and instrum. settings optimization, nomogram 8=42341
counting results, statistical examination 8=46845
deadtime losses, automatic compensation 8=24525
decay periods, and 13 isotopes obs. 8=42940
energy absorpt.-radiation dose conversion operator 8=24495
gamma spectra analysis 8=47043
γ spectroscopy fallout from 7th Chinese nuclear explosion 8=50162
geometry factor for source-detector separation 8=47274
liquid scintillation counting, phase separation detect., double ratio technique 8=42340
neutrons, delayed, from short-lived p-induced emitters 8=38463
nuclear level lifetimes and g factor by embedding in magnetized ferromag. foil 8=38401
prediction analysis applied to meas. of half-lives 8=47275
proton synchrotron, induced activity 8=33506
short-lived activities, using constant pause intervals 8=47272
spectrometry, peaks statistical fluctuations rel. to background, obs. 8=42456
standards, appl. of liq. scintillation counters 8=28977
statistical error in technique, computation bases 8=47273
tritium solns., using sealed standard 8=49999
water in tolvene scintillators, dioxane and naphthalene effects 8=43844
C^{14} counting in liq. scintillators, by u.s. dispension 8=33372
C^{14}-labelled powders, insoluble in liquid scintillator counter 8=47278
C^{14}, natural β, scintillation counter obs. 8=47279
I, biological samples prep. 8=42339

Radioactivity measurement—contd
Pu^{241}, average β energy, calorimetry 8=25197
T, aq., scintillation counting efficiencies 8=28979
apparatus
See also Particle detectors.
beta-ray spectrometer for fallout meas. 8=46851
collimators, focused, drg. recording of line-source response 8=24702
in mammalian tissue, solid-state detector, geometrical efficiency 8=32621
nuclides far off stability total decay energy, isotope separator accessory 8=38402
reservoir water contamination detector 8=38403
scintillomicroscope for radioactive tracer detection in biological specimens 8=32623
Ar^{37}, trace amounts 8=47283
$C^{14}O_2$ from large animals, metabolism chamber 8=45928
Cs^{137} in human infants, 4π plastic scintillation counter 8=42934
Ge(Li) detectors, coaxial, current and charge pulses 8=46911
K^{40} in human infants, 4π plastic scintillation counter 8=42934
Radioastronomy
See also Cosmic radiations, radiofrequency; Sun/radiation, radiofrequency.
antenna, 20m. parabolic, of Bochun observatory 8=50460
Argentina, observatories and equipment 8=32613
Australia, new equipment and observations 8=32610
Belgium, obs. and theoretical studies 8=28188
British equipment and galactic obs. 1963-66 8=32608
Canada, satellite and telescope obs. 8=32609
conference, 1967 8=24279
Czechoslovak solar and meteor obs. 8=32611
extension of number flux density relation to small flux densities 8=41541
French observatories and results 8=28191
German instruments and equipment 8=32612
Indian radiotelescope project 8=37063
interferometry, earth tides effect on baseline 8=45423
Italian observatory equipment and results 8=28195
Japanese instruments and obs. 8=32615
Jodrell Bank Mark III telescope 8=28198
Jupiter, map of radio emission, at 75 and 21 cm wavelengths obs. 8=45832
lunar emissions, mm and sub-mm range 8=45804
lunar radar astronomy, brightness distrib. calc. by two-dimens. aperture synthesis 8=32524
maser, travelling wave, amplification at 36 GHz, rel. to use as r.f. preamplifier 8=28641
multi-element arrays of telesocpe UTR-1, impedance and radiator matching 8=28197
multilobe antenna for 169 MHz solar imaging 8=28167
Netherlands, 1963-66, review 8=28194
NGC 2024, electron temps. of H II regions 8=50338
NGC 2024, electron temp. radio recombination lines obst. 8=50339
Orion nebula, electron temp. radio recombination lines obs. 8=50339
Orion nebulae electron temps. of H II regions 8=50338
Parkes 2134 + 004 quasar, unusual spectrum 8=50388
Peruvian obs. 8=28193
Polish research report 8=28192
pulsating source, accurate position 8=28127
pulsating source CP1919, detection at 13 cm wavelength 8=28125
pulsating source 8=28124
pulsating source 8=28126
pulsating source linear polarization 8=28123
pulsating source, obs. 8=28122
pulsating source meas. on period at 1919 + 21 8=28121
pulsating source, rapid 8=28119
pulsating source, rapid, possible models 8=28120
pulsed radio source fields, time resolved photometry 8=41535
radar, aperture synthesis and appl. to lunar and planetary studies 8=32616
sattellites, artificial; obs. 8=50238
Saturn, microwave emission 8=50418
Scorpio X-1 radio emission detection 8=41551
solar radiation, 35 GHz, atmospheric absorption meas. 8=27902
source, pulsating, obs. at 81.5 MHz 8=28118
sources, $5C_2$ survey 8=41540
South African equipment and programmes 8=28190
spaced-spectrograph obs. of Jupiter decametric emission 8=41567
Swedish radiotelescope and galactic obs. 8=28189
Swiss equipment and obs. 8=32614
USSR apparatus and obs. 8=32523
wideband arrays 8=28196
X-radiation spectrum relation with optical spectrum for Cas A and Vir A 8=45775
OH mol. doubling transitions obs. and calc. suitable for radioastronomy 8=43328
Radiocarbon dating. See Radioactive dating.
Radiochemistry
See also Chemical analysis/radioactive; Chemical effects of radiations/ionizing radiations; Radioactive tracers.

Radiochemistry—contd
- aliphatic alcohol glasses, γ irrad. at 77 °K 8=49966
- alkali metal bromates, n-irrad. crysts., Br^{82g} recoils 8=27769
- alkali metals, separation on org. ion exchangers, effect of temp. 8=32145
- alloys, radioactive, C, O, N, H determ. 8=36629
- of anthracene oil components 8=49965
- element 104, props., obs. 8=38521
- energy distrib. of energetic atoms in gas 8=36626
- fallout, α-emitting radionuclides analysis 8=27928
- isotope separation of gases, solids and solns., rapid methods review 8=38767
- mercury di-n-hexyl, liquid: radiolysis to identify composition 8=49976
- organic compounds, γ irrad., e.s.r. study of radical yield 8=49967
- pipetter, remotely operated, for highly radioactive liquid samples 8=41295
- sorption in chromatographic columns, steady-state conc. distrib. 8=32144
- tetramethyl tin free radical form. by γ-radiolysis at 77°K 8=34382
- tritium-recoil reactions in solid phase 8=45411
- As^{83,84,85,87,} separation from U^{235} fission source and half-lives obs. 8=38419
- Br^{82} isomeric-transition-induced reactions with CH_4 8=45410
- HCl, gaseous, gamma-radiolysis, effect of applied elec. field 8=36622
- $HClO_4$, γ irrad., spatial distrib. of H atoms 8=49963
- $HgCl_2$ as γ-ray dosimeter, radiolytic and photolytic consts. 8=45409
- I_2 reactions activated by radiative neutron capture in liq. hydrocarbons 8=41296
- I^{123} for medical diagnostic use, prep. 8=45408
- I^{129} chlorides, β-decay giving Xe^{129} Mossbauer effect in Xe chlorides 8=30645
- NO in H_2O, radiolysis study 8=49975
- Sn^{113} source, from In^{113}(d, 2n), fractional distillation 8=42954
- T-atom reactions with solid propene and propane 8=27770

Radiography
- See also Luminescent devices; X-ray tubes.
- flash X-ray actuated switch 8=33300
- images produced by extended sources, degredation compensation by optical filtering 8=28911
- low energy radiation from thorax of human male, comparison of predicted and obs. 8=28199
- microradiograph for small specimens 8=32619
- microwave devices, interference of e.m. waves in space between probes 8=24216
- neutron therapy of noise neoplasms, B^{10} dose effects 8=45926
- neutron, use 8=46769
- radiation effects and accidents 8=38586
- thermal neutron, TV system with high-yield generator 8=37725
- X-ray diagnosis, ferrites as contrast mats. 8=37093
- X-ray image intensifier, electron-optical, development 8=46781
- X-ray, images, information capacity calc. 8=46770
- X-ray reflections, Weissenberg goniometer attachment for recording 8=39756

Radiolysis. See Chemical effects of radiations/ionizing radiations.

Radiometer gauges. See Vacuum gauges.

Radiosondes. See Meteorological instruments.

Radiosources. See Cosmic radiations, radiofrequency.

Radiostars. See Cosmic radiations, radiofrequency; Stars.

Radiotelescopes. See Radioastronomy.

Radiowave propagation. See Electromagnetic wave propagation.

Radiowave spectra. See Nuclear magnetic resonance and relaxation; Paramagnetic resonance and relaxation; Spectra.

Radium
- calibration of Ge particle spectrometers 8=37781
- RaA, inhalation hazard dependence on diffusion coeff. rel. to humidity 8=32257

Radium compounds
- No entries

Radium emanation. See Radon.

Radon
- diurnal variations of exhalation and conc. in atmos. 8=50160
- atmospheric conc., urban and rural Washington D.C. obs. 8=27881

Rain
- See also Condensation; Snow.
- daily occurrence, second and higher order stationary Markov chain models 8=32217
- hailstones, artificial, rough, rate of melting and heat transfer 8=34963
- radar anal. of warm showers 8=41358
- SW monsoon in India, meteorology and vorticity considerations 8=36708
- H_2O, optical back scatt. from single droplets 8=27916

Raman spectra
- See also Luminescence.
- antiferromagnet, spin-wave stimulated second-order scattering 8=31944

Raman spectra—contd
- asymmetry of scatt. tensor for electronic transitions 8=41030
- benzyl compounds, vibrational frequencies 8=43361
- complex octahedral anions in crystals, cation effects 8=49683
- crystal with impurity centre, density matrix method considerations 8=45249
- experiment for senior laboratory 8=29696
- gases, review (1950-1966) 8=29694
- image intensifier tube for studying rapidly changing molecular structures 8=38781
- intensity in immediate neighbourhood of resonance 8=29693
- laser excited rotation-vibration Raman scatt. in ultra-small gas samples 8=29683
- laser-excited, under very high pressure 8=41031
- laser, of crystal powders 8=49685
- laser-Raman spectroscopy, current progress 8=25397
- laser stimulated, in gases and liquids 8=43169
- linewidths for stimulated threshold and gain calcs. 8=39372
- liquids, use of laser beam rel. to analysis of natural products 8=27793
- liquids and solids, resolution improvement by He-Ne laser 8=24398
- maser application 8=38782
- mixtures, forced scatt., line intensity 8=29678
- molecules, in vapour and liq. state, comparison rel. to refractive index and intermolec. interact 8=34207
- monomolecular chain linewidth calcs., and appl. to molecular crystal 8=36300
- nonlinear susceptibility theory, diagrammatic approach 8=48297
- photoelectric recording, adaptor for three-prism spectrograph 8=46709
- powdered crystal, stimulated 8=49684
- rare earth ions, Rayleigh and electronic Raman scatt. 8=27546
- resonance factor determ. 8=43835
- scattering, antisymmetric tensor, obs. 8=25398
- scattering by polaritons 8=41032
- stimulated in emission and absorption in dense liquids and gaseous media 8=48155
- stimulated, relativistic theory 8=24278
- stimulated scatt., intensity rel. to depolarization 8=29695
- stimulated threshold, effect of temp. for liquids with diff. Kerr coeffs. 8=48156
- stimulated transitions in gases, competition 8=25399
- stimulated, two-photon absorpt. as quenching mech. 8=24337
- Stokes mode freq. shift, theory 8=41029
- symmetric tops, computer anal. 8=25412
- theory of Raman effect 8=47552
- trimethylene sulphide, $(CH_2)_3S$, crystals, and i.r. absorp., 8=41171
- vibrational, depolarization ratio of overtone and combination bands 8=43248
- wing intensity in liquids due to time depend. mol. reorientation 8=43830
- α-Al_2O_3, Raman active lattice modes, temp. dependence 8=39868
- CCl_4, teaching demonstration 8=29696
- CS_2-acetone mixtures, angular distribution of anti-Stokes emission 8=46631
- CS_2, teaching demonstration 8=29696
- H_2 gas, simultaneous fundamental and second harmonic laser radiation 8=46592
- **inorganic substances**
  - alkali metal nitrate aq. solns. 8=34869
  - bismuthyl halides, rel. to vibr. modes 8=38812
  - parahydrogen, solid, freq. analysis 8=43967
  - α quartz, excitation by mercury discharge 8=49753
  - siloxanes, solvent effect, freq. spectroscopic investigation 8=25884
  - solution, aq., for ion obs. 8=34863
  - AgN_3, rel. to crystal growth method 8=48535
  - $BaTiO_3$ resonant interference between one and two phonon states 8=41066
  - $BaTiO_3$, tetragonal, rel. to long-wavelength phonons 8=27559
  - C_3N_{12} 8=25456
  - C_3N_{12} 8=31976
  - CS_2 8=43835
  - $CaCO_3$ cryst., stimulated scatt., additional anti-Stokes components, obs. 8=41073
  - $CaMoO_4$, laser induced 8=31969
  - $CaWO_4$, laser induced 8=31969
  - CdS crystalline powders, light scatt. cross section at 273°K 8=45189
  - Ce^{3+} in hexagonal cryst. field, electronic scatt. tensor 8=31975
  - $ClSi(NCO)_3$ 8=29732
  - Cl_3SiNCO 8=29732
  - Cl_3SiNCS 8=29732
  - $Co(CO)_3NO$, laser-excited 8=48161
  - CsF, second-order, rel. to lattice dynamics 8=31980
  - GaP crystalline powders, light scatt. cross section temp. dependence, 103-723°K 8=45189
  - H_2, combination freq. generation emission 8=25598
  - H_2, stimulated; Q [1] vibr. line shift depend. on press. temp. 8=43306

Raman spectra—contd
- **inorganic substances**—contd
  - Hg-CN-SCN complex in aqueous soln, study of mixed ligands 8=43842
  - ICN charge-transfer complexes 8=48163
  - I_2, in liq. mixtures, freq. shift 8=34875
  - I_2Cl_6, solid 8=45195
  - KH_4PO_4, ferroelec., l. f. oscills. 8=36378
  - $KI:NO_2^-$, impurity induced 8=41106
  - $KTaO_3$ 8=27599
  - $LaCl_3$, first-order scattering depolarization 8=27578
  - LiF single-crystal scatt. centres 8=49737
  - $LiNbO_3$, and Rayleigh scattering temp. dependence, 90-1100°K, rel. to ferroelectric props. 8=27585
  - $LiNbO_3$, near forward scattering, dispersion characts. 8=27584
  - $LiTaO_3$, and Rayleigh scattering temp. dependence, 90-1100°K, rel. to ferroelectric props. 8=27585
  - MgF_2 crystal, rel. to vibr. freq. determ. by n. scatt. 8=44302
  - Mg(II) oxalate complex, conc. soln, rel. to co-ord. and coupling 8=43843
  - MgO, second order scattering 8=36386
  - $Mo(CN)_8^{4-}$ 8=41118
  - N, liquid, stimulated Raman scatt., photon distrib. in Stokes components 8=34855
  - NCl_3 in CCl_4, high resoln., 8=43838
  - NH_4Br, above and below transition 8=27596
  - NH_4Cl, above and below transition 8=27596
  - N_2F_4 8=38839
  - NaCl single-crystal scatt. centres 8=49737
  - $Ni(CO)_4$, 8=34270
  - $PbMoO_4$, laser induced 8=31969
  - $PbWO_4$, laser induced 8=31969
  - SF_5Cl 8=25516
  - SO_4^{2-} in cryst. $M_2^IM^{II}(SO_4)_2.6H_2O$ 8=27601
  - $SPClF_2$ 8=25517
  - $SPCl_2F$ 8=25517
  - $SrTiO_3$ down to 25°K 8=32035
  - $SrTiO_3$, 110°K phase transition, soft-phonon at corner of Brillouin zone 8=39564
  - TaF_8^{3-} 8=41118
  - $ThCl_6^{2-}$ complexes 8=47619
  - UCl_6^{2-} complexes 8=47619
  - $W(CN)_8^{4-}$ 8=41118
  - YGa garnet:Eu, electronic transitions 8=27612
  - YGa garnet:Nd, electronic transitions 8=27612
  - YVO_4, rel. to lattice vibrations 8=36424
  - Zn(II) oxalate complexes, conc. soln, rel. to co-ord. and coupling 8=43843
  - Zn-CN-NH_3 complex in aqueous soln, study of mixed ligands 8=43842
  - ZnS blende, second order 8=36427
  - ZnS, wurtzite- and zinc-blende-types 8=45234
- **organic substances**
  - acetaldehyde absorbed onto silica gel 8=25530
  - acetylene, cryst. phases 8=27618
  - aliphatic ethers 8=29777
  - alkyl-Hg(II) cpds 8=43350
  - aryl-Hg(II) cpds 8=43350
  - benzene cryst. 8=27628
  - benzene derivatives, at 80°K 8=47637
  - benzene, highly polarized lines, effect of intermolecular interactions on line shapes and depolarization factors 8=34858
  - benzene, non sym. molc. vibr. due to time depend. reorientation 8=43830
  - benzene, raman spectra asymm., due to time depend. mol. reorientatation 8=43830
  - biphenyl, re-analysis 8=34348
  - bis(trifluoromethyl)-peroxide 8=43366
  - γ, γ'-bipyridil rel. to conjugation in cryst. and liq. states, obs. 8=34355
  - α, α'-bipyridil rel. to conjugation in cryst. and liq. states, obs. 8=34355
  - bromocyclobutane 8=25566
  - t-butanol, gaseous, liquid and solid; absolute scatt. coeffs. of Raman lines 8=43360
  - 3-butenenitrile, rotational isomerism 8=25551
  - 2-butenes, cis and trans 8=25552
  - n-butylamine and N-deutero derivatives, H and D bridge bonds 8=27620
  - carbon tetrachloride, highly polarized lines, effect of intermolecular interactions on line shapes and depolarization factors 8=34858
  - chlorobenzenes, effect of D substitution 8=27517
  - cyanamide 8=48710
  - cyclobutanol 8=25566
  - dialkyl disulphides 8=43349
  - dialkyl-Tl(III) cpds 8=43351
  - 1,1-dichloroethylene, line intensities and depolarizations, calc. 8=34321
  - trans-dichloroethylene, line intensities and depolarizations, calc. 8=34321
  - cis-dichloroethylene, line intensities and depolarizations, calc. 8=34321
  - dimethylphenylarsine 8=43381
  - di-n-butyl diselenide 8=43349
  - p-dioxane, 80-300°K rel. to phase transform. at 272.9°K 8=41163

Raman spectra—contd
- **organic substances**—contd
  - diphenyl-Tl(III) cpds 8=43351
  - ethylamine and N-deutero derivatives, H and D bridge bonds 8=27620
  - imidazole 8=29787
  - methane, combination freq. generation emission 8=25598
  - methanes, halogen-substituted, gaseous 8=25591
  - methaneselenol 8=25602
  - methylacetylenes, C_3H_4, C_3D_4, rotational 8=47662
  - methyldiphenylarsine 8=43381
  - methylvinylsuphide 8=38899
  - mixtures, scatt. power rel. to conc. 8=34862
  - monochloroethylene, line intensities and depolarizations, calc. 8=34321
  - organotrichlorosilanes, l.f. vibrations 8=47620
  - perbromocyclopropane 8=25565
  - perchlorocyclopropane 8=25565
  - perfluorocyclopropane 8=25565
  - o-phenylenebis(dimethylarsine) 8=43381
  - phenylgermane 8=25615
  - n-propylamine and N-deutero derivatives, H and D bridge bonds 8=27620
  - pyridazine, and deuterium analogues 8=25933
  - rare-earth ions in crysts., theory of electronic transitions 8=41030
  - stilbene powder, line intensities and dispersion effects elimination, obs. 8=36445
  - triphenylarsine 8=43381
  - triphenylphosphine 8=43380
  - $BF_3S(CH_3)_2$ 8=25541
  - CCl_4, intensity in various solvents 8=30488
  - CCl_4 non system mole. vibr. due to time depend. reorientation 8=43830
  - $C_6D_5GeCl_3$ 8=25615
  - $C_6D_5GeCl_3$ 8=34351
  - CF_3SF_5 8=25516
  - CH_2-CDCl, line intensities and depolarizations, calc. 8=34321
  - $(CH_3)_3CNCO$ 8=29732
  - CH_3OPCl_2 and CD_3OPCl_2 8=38892
  - $Ge(C{\equiv}H)_4$ 8=25625
  - $KH(CHOO)_2$, l.f. 8=27633
  - $NaNO_3$ cryst. 8=41122
  - $Si(C{\equiv}H)_4$ 8=25625
  - SiC, first-order, on laser excitation 8=41139
  - $Sn(C{\equiv}H)_4$ 8=25625

Ramsauer effect. See Electron beams; Electrons/absorption; Particle range.

Random functions. See Random processes.

Random processes
- See also Brownian movement; Fluctuations; Statistical analysis.
- aperiodic systems coarse-grained quantities 8=37178
- asymptotic distribution of eigenvalues of random matrices 8=45971
- derandomization, adequacy of scaling circuit 8=33380
- derandomization, inadequacy of scaling circuit 8=33379
- energy fluxes prod. by regular source and system of random ones. distrib. 8=37196
- Gaussian excitation of linear systems 8=37283
- generalized stochastic eqns. 8=37176
- interacting systems, kinetic eqns., uniform derivation 8=23871
- isolated ion pair, theory of neutralization 8=29957
- laser light 8=46538
- molecular systems, time-correl. functions of random motions 8=34386
- noise, 1/f, statistics 8=37371
- photon scattering, resonant, from perturbed two-level system, stochastic theory 8=41755
- plasma, collionless, fast randomization phenomenon, exptl. evidence 8=39063
- pulse sequence, optimum processing for amplitude analysis 8=24531
- vector random field spectral representation 8=46091
- walk model, colmatage 8=32822

Range of particles. See Particle range.

Rare earth metals
- See also the individual metals.
- additions in low C steel castings, effect on mechanical properties 8=49009
- cathodoluminescence analysis 8=36643
- crystal and mag. structural relns. 8=35350
- crystals, mag.-ordering temp., pressure dependence 8=31652
- diffusion out of p-irradiated metal foils in vacuum, at 1500-2800°C 8=40081
- electric multipole interactions 8=31255
- energy transfer between ions in crystals, temp. depend. 8=45138
- Fermi surface topology thermal deform. rel. to anomalous e props. 8=31280
- ferromagnetic, heavy, indirect nuclear spin relax. 8=45132
- generalized susceptibilities and mag. ordering 8=44973
- glass, oxide, luminesc. of Er^{3+}, sensitization 8=36486
- h.c.p., entropy associated with mag. transitions 8=49453

Rare earth metals—contd
  h. c. p. paramagnetic crystal field effects from neutron scattering 8=40749
  heat capacities, low temp. containg two or more contributions, analysis 8=35434
  heavy, nuclear spin relax., indirect 8=31915
  hyperfine interactions from n. m. r. 8=36280
  interactions, exchange, enhanced effective, due to localized spins 8=31594
  ion interactions in insulators 8=31775
  ions in CaF_2 lattice, field splitting 8=35025
  ions in cryst. field, Zeeman effect theory 8=36357
  ions in crysts., theory of electronic Raman transitions 8=41030
  ions in soln., p relax. time and cluster asymmetry obs. 8=43870
  ions in Y_2O_3, radiative and multiphonon relaxation 8=45289
  ions, magnetoelastic coupling constants, from optical spectroscopic data 8=31229
  ions, Rayleigh and electronic Raman scatt. 8=27546
  ions, trivalent, in Y_2O_3, cathodoluminescence 8=49814
  impurity doping in Th, Ce and Hf oxides, melt-grown 8=26645
  lanthanide complexes, octahdral, free and in crystals, vibronic level Zeeman splitting 8=43964
  lanthanides, compressed polymorphs, crystal structure sequence rel. to 4f contrib. to bonding 8=26178
  lanthanides, first ionization potentials 8=31477
  magnetic anisotropies 8=31505
  in noble metals, local moments from e.p.r. and susceptibility 8=31882
  in noble metals, mag. effects on electron transport of dil. alloy 8=31316
  spin waves and magnetic reson., thermal, applied field, and magnetoelastic effects 8=31703
  substituting sites in $BaTiO_3$, e.s.r. and F-centre obs. 8=48818
  superconducting magnet pole-pieces for field enhancement 8=28530
  trivalent, in inorganic phosphors 8=32052
  X-ray M spectra, sample self absorpt. effects 8=36355
  in $LaRu_2$, magnetic susceptibility and e.p.r. study 8=31502
  in CaF_2, charge compensation by interstitial H^- or D^- ions 8=49601
  Pm I, fundamental energy levels calc. from spectra and Zeeman effect obs. 8=47505
Rare earth compounds
    See also the compounds of the individual metals; Ferrites.
  alloys, crystal structures 8=48671
  alloys, hyperfine interactions from n. m. r. 8=36280
  alloys with 4f e. conc = 10, 11; magnetization 8=31654
  alpha-alaninates of rare-earth elements, stability constants 8=36539
  borate isotypism 8=48657
  borates of dolomite structure, prep. and cryst. characts. 8=44249
  chlorides, hydrated crysts., absorpt. spectrum of Pr^{3+} 8=45215
  crystal-field spectra, low-lying 8=36296
  crystalline complexes, luminescence tests on structural forms 8=36467
  dicarbides, vol. variation rel. to electron structure 8=48340
  double oxides of type $LaTO_3$, (T = rare earth), crystallography and mag. props. 8=48656
  electrical and magnetic props. 8=49348
  electron moment, itinerant, in cubic Laves-phase, rare-earth-transition-metal compounds 8=49473
  electronic shielding from Mossbauer effect 8=39508
  ferrite garnets, para-process near Curie temp. 8=45040
  ferroelectric props., magnetic structure 8=40619
  ferromagnets, mag. viscosity 8=45029
  fluoride complexes, A_2NaTF_6 (A = Rb, Cs; T = rare earth metal), crystal structure 8=44250
  halide-terpyridyl complexes, i.r. spectra 8=41131
  hydroxides, mag. props. 8=31507
  iron garnets: Eu^{153} Mossbauer determ. of exchange interactions 8=36194
  iron garnets, Faraday effect in far i.r. 8=41133
  iron garnets, mag. moment at 0°K substitution dependence, mol.-field model 8=45027
  lanthanide oxidecarbides, cryst. struct. 8=39802
  lanthanide sulphates, ultrasonic absorption 8=48141
  lanthanides, intra-alloys, crystal structure sequence rel. to 4f contrib. to binding 8=26178
  magnetic and elec. meas. rel. to mag. ordering 8=27234
  magnetic ordering and collective excitations rel. to singlet crystal-field ground state 8=44964
  magneto-optical expts. status rel. to ordering 8=36401
  metal oxides, forbidden zone, width 8=35740
  monochalcogenides, antiferromag. props., 4-1300°K 8=31761
  orthochromites, ferroelectricity studies 8=27282
  orthoferrites, antiferromag. resonance in spin reorientation region 8=27456
  orthoferrites, antiferromagnets with weak ferromagnetism, anisotropy pressure dependence 8=40857
Rare earth compounds—contd
  orthoferrites, hydrothermal growth 8=35249
  orthoferrites, ordering in anisotropy change region 8=31793
  orthoferrites, simple preparation technique 8=49865
  oxide mixtures, Eu_2O_3 determ. by u. v. spectrophotometry 8=27786
  oxides, hemispherical spectral emittance 8=35466
  oxides in H_2SO_4, chemiluminesc. in visible and u. v. ranges 8=30495
  oxysulphides, mag. props. and structures 8=40869
  paramagnetic neutron scattering 8=48890
  perovskites, specific heat and magnetic ordering between 1.2° and 5°K 8=39921
  phosphate-based phosphors, spectral props. 8=49747
  phosphate based phosphors with fast decay times 8=45285
  phosphors, suitability as radiation detectors 8=46874
  rare-earth antimonides, mag. anisotropies 8=31791
  Re-rare-earth alloys, work function obs. 8=40690
  sesquioxides, metastable structure, formative mechanism 8=26056
  silicates, trivalent, synthesis of single crystals, Verneuil's method 8=35350
  sodium molybdates, $R_{1/2}$ $Na_{1/2}MnO_4$, axial mag. anisotropy 8=31528
  sulphates, i.r. spectra 8=41130
  sulphates, structural study 8=26434
  trace analysis methods 8=49983
  Al alloys, mag. props. 8=36176
  Co intermetallics, R_xCo_y, mag. behaviours 8=31506
  Ni intermetallics, R_xNi_y, mag. behaviours 8=31506
  -Pt alloys, conduction-electron polarization from n. m. r. 8=36279
  $RCrO_3$, magnetostatic props. 8=31790
  $RMnO_3$, magnetostatoc props. 8=31790
  Th alloys, f.c.c., Th effect on mag. ordering 8=36218
Rare gases. See Inert gases.
Rayleigh scattering. See Scattering/light.
Rayleigh waves. See Elastic waves; Seismic waves.
Reaction kinetics
    See also Catalysis; Chemical reactions; Exchanges, chemical; Explosions.
  activated radicals, vibr. energy transfer from homologous series 8=49846
  adsorbed gases 8=41268
  air afterglow 8=32274
  α-cellusose, pyrolysis and decomp., X-ray photographic obs. 8=32094
  anthracene photo-oxide decomp., temp dependence 8=27694
  aryl ketone-iodine complexes, equilib. consts. 8=43353
  association, gaseous, effects of dead space 8=49841
  bio-β-chloroethyl-vinyl-phosphonate, γ-induced polymerization, obs. 8=49913
  biochemical systems, differential microcalorimeter 8=27687
  chain reactions, $A + B \rightarrow C, C + D \rightarrow E$ syst. 8=49843
  Chapman-Enskog method 8=49849
  chemiluminescence, preannihilative 8=27692/3
  clays sintering, thermal analysis meas. 8=30665
  coagulation of compounds 8=48238
  combustion, nonpremixed systems near equilibrium 8=36579
  complex nonchain, tubular flow photoreactors 8=49954
  complex systems cont. irreversible steps, structure and anal. 8=32085
  conjugated systems, intermolec. orbital theory 8=27684
  cycloadditions, intermolec. orbital theory 8=27684-5
  diffusion and heterogeneous reaction 8=49910
  diffusion-controlled reactions, statistical anal. 8=34882
  direct meas. time range 10^{-6} to 10^{-8} sec. 8=49850
  dissipative systems, symmetry breaking instabilities 8=32836
  dissociation, Kossel model modification 8=25646
  dl-α-terpineol e-transfer oxidation by manganic acetate, 100°C 8=49881
  energetic atoms, collision density 8=41242
  energy distrib. of energetic atoms in gas 8=36626
  equilibrium point, stability and uniqueness 8=41233
  ethylene, electrochem. oxidation, oscillatory. 8=49939
  ethylene, thermal gas phase bromination at room temp. 8=49863
  fast reaction rates, n.m.r. study 8=49944
  fluorocarbon reactions, high temp. 8=41247
  formate, electrochem. oxidation, oscillatory 8=49939
  free-radical recomb., nonequilib. effects 8=27679
  graphite, pyrolytic and isotropic, attack by O-atom or O_2, to 2100°K 8=36556
  graphon chemisorpt. of O_2, 450-675°C 8=45362
  hard carbon graphitization with CuO catalyst, kinetic study 8=27740
  heterogeneous surface reactions, diffusion 8=41244
  n-hexadecane, thermal decomp. 8=45342
  hydride ion reaction with HF and H_2, MO theory 8=27676
  hydride ion reaction with NH_3 and CH_4 8=27678
  hydride ion reaction with H_2O, MO theory 8=27677
  hydroxyl radicals, deuterium isotope effects 8=27707

Reaction kinetics—contd
intramolecular regroupings, quantum theory 8=45320
iodination of 8 metals, effects of Co^{60} γ-irrad. 8=36555
ion-molecule reactions, energy partition 8=45323
ion-molecule reactions, nonequilib. effects 8=27679
light scatt. from chem. reactive fluid 8=32090
linearization of expt. curves, application 8=27680
magnetite oxidation to γ-Fe_2O_3, mechanism rel. to Fe^{2+} diffusion kinetics 8=27702
metal oxidation at high temp., rel. to specific area and core dimensions 8=36551
metal oxidation rate-constant determ., low-temp., from discontinuous film resistance changes 8=49883
methanol ion-mol. reactions, ion cyclotron reson. 8=27709
minerals sintering, thermal analysis meas. 8=30665
mixer for obs. in soln. 8=32086
molecular beams, use in 8=27683
multi-ionic reaction rates, strength independ. 8=49845
oxide-containing graphite arc electrodes 8=34436
in organic single cysts. mag. reson. meas. 8=27449
quantum dynamics of Morse oscillator 8=33333
R-matrix theory appl. in molec. scatt. cases 8=43427
radicals in flow capillaries, e.p.r. meas. 8=27690
rare-earth orthoferrites, calcination preparation technique 8=49865
reactivity correl. with i.r. intensities 8=43253
reactor, continuous flow stirred tank, limit cycle behaviour analysis 8=32081
relaxation effects on dielec. dispersion 8=48187
stearic acid and Ca^{2+} ions at air/water inferface, using surface viscometry 8=41264
substitution reactions in octahedral complexes, ligand field theory 8=45318
thermal unimolec., collisional energy transfer 8=27682
thermobalance for h.p. studies 8=45316
thermobalance, 0.1 mg sensitivity, $\leqslant$ 1,150°C 8=23792
unimolec. rate const., second-order, rapid calc. 8=32089
unimolecular breakdown, Lindemann-Hinshelwood mechanism 8=49842
unimolecular rate theory, adiabatic rotations 8=41243
unimolecular reaction rates, Monte Carlo calc. 8=25645
vapour phase esterification of acetic acid with ethanol, thermodynamic equilibrium 8=49837
vinylphosphonic acid dichloride, γ-induced polymerization, obs. 8=49913
Zircaloy-2 oxidation in O and H_2O vapour 350-500°C 8=32106
zirconium nitriding 8=44396
Ag_2S form. on AgBr cryst. 8=49853
Al on SiO_2, moisture effects, obs. 8=45328
$Ar^+ + D_2$ and $Ar^+ + H_2$ 8=45323
B, particulate, gas-phase chem. kinetics for burning in dry air 8=36581
CaF_2 hydrolysis, 1000-1120°C 8=49859
C-H-N-O explosives, detonation velocity prediction 8=41262
CHO^+ ion-mol. proton transfer 8=49869
CH_3I reactive scatt. with Rb atoms, asymmetry 8=47728
$Cl + H_2 \rightleftarrows HCl + H$, using e.s.r. detect. 8=49861
CN, e absorpt spectroscopy 8=27700
CN, excitation in active N_2 8=27699
CO, chemiluminesc. from flames 8=27698
Cs–O system, heats of formations 8=32096
CuF^+ complex, lifetime 8=48222
$F_2SO_3 + SO_3$, thermal reaction 8=45333
Fe oxide film growth in neutral soln. 8=27706
Fe_2S, thermal decomposition in fluidized bed 8=41250
H atom recombination, homogeneous rate 8=36563
H isotope exchange between alcohol and mercaptan 8=36545
H radical, conc. profile in H_2-O_2 flame, gas phase e.p.r. study 8=49892
H with graphite at high temp. and press. 8=47422
H-atom transfers, activation energies 8=27708
$H + D_2$, energetic atom reaction 8=41242
$H + NO_2$, free electron generation 8=49872
HF, dissociation in shock waves 8=25650
H_2–O_2 combustion in shock waves 8=32109
$H_2 + O_2$, luminous emission and combustion peninsula 8=45354
He^+, $He(2^3S)$, with vibr. excited N_2 8=41253
HgCl, dimerization 8=49960
Hg + Cl atom combination 8=49960
K, Rb and Cs reactions with Cl_2 in crossed beams 8=49875
$MgSO_4$, decomposition kinetics rel. to sample mass and processing press. 8=36565
N, active 8=38840
N-salicylideneaniline hydrolysis in H_2O-methanol 8=48164
$N + CH_3CHO \rightarrow HCN + H_2 + HCO$ rate constant 8=27710
NH_2^- ion reactions with triatomic mols. 8=29980
NO afterglow, chemiluminesc. rate consts. 8=38993
N_2 afterglow, temp. depend. of chemiluminesc. 8=27712
$N_2(A^3\Sigma_u^+)$, excitation of NO 8=25494
$N_2(A^3\Sigma_u^+)$, reaction with N atoms 8=25493
$N_2(A^3\Sigma_u^+)$ + Hg 8=34163

Reaction kinetics—contd
$N_2^+ + H_2$ and $N_2^+ + D_2$, low-energy ion-mol. reactions 8=27711
Nb oxidation, 450°-720°C, rel. to scale morphology 8=49878
Nb oxidation rate-constant determ., low-temp., from discontinuous film resistance changes 8=49883
Nb-Ta alloys, oxidation, 550-1050°C 8=36566
$Ne^+ \rightarrow Ne_2^+$ association rate obs. 300°K 8=39049
Ni and alloys oxidation 8=27713
Ni oxidation rate-constant determ., low-temp., from discontinuous film resistance changes 8=49883
O atoms with CH_3 radicals 8=49880
O atoms with CH_3Cl, CH_3Br and CF_3H, rate consts. 8=36568
O transfer from CO_2 to metal surface 8=27735
$O(^1D)$ gas-phase reaction with CO_2, rate const. 8=36614
$O + O_2$ combination 8=41258
O^-, associative detachment reactions, electron prod. 8=39051
O^+, with vibr. excited N_2 8=41253
O_2, interaction with excited organic mols. 8=38956
O_2 + CO + M, vac. u.v. flash photolysis 8=45398
$PbS + CdO \rightarrow PbO + CdS$, solid state 8=49839-40
S^- ion reactions with triatomic mols. 8=29979
Ti oxidation rate-constant determ., low-temp., from discontinuous film resistance changes 8=49883
UO_2 pellets fluorination by Fl to UF_6, 300–540°C 8=32104
V, engassing by O, and chemisorpt. 8=36584
VO_2 oxidation in molten $VO_{2\cdot5}$ soln., obs. 8=27724
$VO_{2\cdot5}$, molten, thermal dissoc., obs. 8=27724
$W(CO_6)$, thermal decomposition kinetics 8=45350
Zn^{65} drop extraction, between liq. metals and fused salts 8=27725
Zr oxidation rate-constant determ., low-temp., from discontinuous film resistance changes 8=49883
Reactors. See Nuclear reactors, fission; Nuclear reactors, fusion.
Re(h)binder effect. See Mechanical strength; Surface phenomena.
Recombination. See Ions, recombination; Semiconductors.
Recombination radiation. See Luminescence.
Recording
See also Sound recording.
all-glass membrane 10-760 torr manometer 8=41625
bubble chamber, photographs analysis by flying image digitizer 8=46960
cinematographic, of holographic interferrogram for time-dependent deform. 8=46760
corona discharge, peak-reading instruments 8=24062
digital, for mass spectra, system design theory 8=38604
digital system for Fourier-transform spectrometry 8=37677
dilatometer for –150° to +1500°C 8=28216
electron trajectories with analogue computer 8=46406
ferromagnet coercive force and magnetization, apparatus 8=49505
flowmeter for 1 ml/min. 8=30363
gas flowmeter, continuous automatic 8=43647
information storage system, energetic model 8=46390
internal mag. field of ellipsoidal specimen 8=46372
i. r. spectrometer, digital 8=24401
laser pulse, Q-modulated, memory tube appl. 8=46535
liquid surface temp., thermistor apparatus 8=37318
magnetic system, effective gap length estimation 8=28534
mass spectrometer ion current ratios, servo-amplifier 8=38610
pen drive, buffer power amplifier 8=41908
photographic, data transfer to computer-compatible mag. tape 8=42351
photomultiplier, pulsed monochromatic light, quantum yield meas. 8=24157
shock waves, detector and gated interval timer 8=41831
synchronous drum for n time-of-flight data 8=47155
two-channel data logger 8=37359
X-ray reflections, Weissenberg goniometer attachment 8=39756
Rectifiers
See also Electron tubes; Semiconducting devices.
inverter, single phase bridge, commutation 8=28461
metal-aluminium oxide contact, rectification at high temps. 8=40630
polar double membranes, I-V and I-time meas. 8=27748
polar double membranes, static effects 8=27747
power supply, s.c.r. preregulator 8=24068
s.c.r., model for prediction of switching with ionizing rad. 8=27165
thyristors, caused of instability and self-switching of p-n-p-n devices 8=27151
Si, impurities effect on reverse current charac. 8=49304
Te-Se-Cd struct., using Se single-crystal film 8=35930
Recrystallization (metals). See Heat treatment.
Red giants. See Stars.
Red shifts. See Astronomical spectra; Cosmology; Relativity/general.
Reflectance. See Reflectivity.
Reflection
See also Neutrons/reflection; X-ray reflection.
dielectric coating on opaque substrate, refl. of monodirect. flux. 8=31935
double Machian, of strong shock wave 8=23947
of electrons from standing light meas. 8=47089

Reflection—contd
flexural waves from intermediate rod of variable thickness 8=41826
Fresnel, at boundary of slab cont. scatterers, effect of radiative transfer 8=32936
plasma, impulse moving, from metallic surface 8=43494
semimetals, of electrons, specular, rel. to Sondheimer effect 8=26957
InAs solid solutions with $A^{II}B^{VI}$ type cpds., spectra 8=41099
Si, of electron pulses (20-1000 eV) 8=35605
acoustic waves
See also Echo; Reverberation.
absorbents, impedence calc. 8=46189
acoustic target, moving as equivalent of filter 8=32910
cardioid microphone meas. method 8=46190
phase determ. from underwater sediment 8=37266
moving fluid layer, theory and reflectivity calc. 8=37267
piston array, reception and refl. calc. 8=46182
plane plastic waves in presence of boundary plane 8=41832
pressure-release surface, expt. 8=46191
pulses, by plane interface 8=23963
transition-zone, theory 8=46184
acoustic waves, ultrasonic
birefringence in deformed isotropic elastic materials 8=46187
harmonics generated by finite-amplitude waves 8=48713
liquid-solid boundary, goniometry 8=48134
time distributions by visualization of airborne waves, effect of hall shape 8=23970
Cu single crystal, low index surface reflectivity 8=30944
electromagnetic waves
beam displacement at anisotropic optical system 8=24208
bianisotropic medium, at interface 8=28616
coefficient meas. for waveguide plasma parameters 8=30052
coefficient of inhomogeneous layer, determ. 8=46015
diffuse, from nonequilibrium medium 8=42012
electro-optical effects at medium-free space interface, static elec. field 8=28607
energy dissipated in absorbing plane parallel plate 8=33131
ferrites, imaginary index 8=46473
films, thin, after excitation of plasmons by e.m. waves 8=40272
freezing clouds, radiometric obs. 8=32224
impedance cylinder of arbitrary shape, asymptotic laws 8=46476
ionosphere, anisotropic and sharply bounded 8=50183
ionosphere, l.f. and v.l.f., coeff. calc. 8=42035
ionosphere, lower, l.f. and v.l.f. calc. 8=50185
lateral wave effect total internal 8=37477
layer radiation, effect of double metallic lattice with equal periods and diff. slots 8=33130
layered media reflecting rays between distant antennas, modified coeff. 8=28615
microwave reflectometer fast sensitive Smith chart plotter 8=24260
microwaves, by shock produced Ar plasma, skin depth effect 8=25743
at moving interface separating two media of different relative permittivities 8=24210
at moving interface separating two media of different relative permittivities 8=24210
at moving interfaces, of e.m. power 8=37476
multiple, in Michelson interferometry, velocity meas. correction 8=42017
piston, vel. and accel. due to e.m. waves 8=33129
at plane boundary of two homogeneous isotropic dielectrics, graphs of describing quantities 8=37479
plane, from perfectly conducting triaxial ellipsoid 8=46475
from plane stratified medium 8=28614
plane wave, incident on sandwiched dielectric reinforced by metal elements with complex shapes 8=24211
plasma, effective index 8=25751
plasma free space interface, harmonic components 8=25750
by plasma inhomogeneous layers 8=43530
on plasma in homogeneous mag. field 8=43538
plasma, shock-produced, electromagnetically driven, electron densities by microwave meas. 8=25720
radio, v.h.f. from star, by visible aurora 8=50170
radio waves, MF-HF band, by method glacier surface 8=24209
radiosignals, from complex shapes, statistical model 8=37478
semiconductors, in mm. range 8=31934
strip, h.f. condition 8=46477
surface, multimode, excitation 8=24212
surface X-ray reflection, anomalous, rel. to surface perfection dependence 8=27529
waveguide with losses and large number of discontinuities resultant refl. coeff. 8=24231
light
See also Mirrors; Optical films.
anthracene, rel. to exciton-phonon interact. and band struct. 8=41161
antireflectant films, theoretical interpretation of behaviour 8=42243
beam at plane interface 8=28845
beam self-trapping in molecular fluids for saturation of non-linear refractive index 8=30478

Reflection—contd
light—contd
B, β-rhombohedral, coeff. anistropy 8=41064
by cloud and dust layers, appl. of probability distrib. of photon optical paths 8=41362
clouds, rel. to particle size distribution 8=41367
coeff. determ., from inhomgeneous layer 8=46015
corner cube reflectors, optics 8=42147
crystal, anisotropic and isotropic medium, refl. laws at boundary 8=27525
diffuse nonequilibrium, in nonhomogeneous plane-parallel layer 8=28873
directional reflection meas. in integrating sphere 8=46718
electrodes in cylindrical spark chamber 8=37804
ellipsometry for modulated reflection studies of surfaces 8=31937
focon reflecting system 8=42124
glare impression, influence of luminance and geometry 8=33298
glass-backed photographic plates, secondary int. reflection, elimination 8=46762
graphite, electronic structure, optical study 8=31279
holograms, copying 8=33292
insulators, surface finish effect 8=27528
internal, total, 2 layer phase compensation 8=46716
intra-cavity reflector for gas laser Q control 8=28670
laser, by plasma, interferometry obs. 8=43541
laser material antireflection coating, single layer, mismatch 8=42060
lattice excited by ultrasonic waves, analytical calc. 8=36290
light source control system for electroreflectance studies on semiconductors 8=27062
metal rough surface, i.r. 8=31932
metals, single crystal and polycrystalline, optical const. determ. 8=45164
multiple internal, spectroscopy of adsorbed layer conformation in polybenzyl-L-glutamate 8=39612
phase-shift transform. props. 8=46719
by planetary atmos. with reflecting bottom surface 8=37005
polarization effects in reflection spectra 8=37683
powder, Perkin-Elmer spectrophotometer attachment 8=28824
prism, tetrahedral reflecting, wedge error and deflection error 8=24362
projector source enlargement 8=37667
quartz, fused, reflectance in vac. u.v., obs. 8=27558
reflectometer determ. principal angle of incidence and azimuth, theory 8=37682
reflector, parabolic, source displaced from focus 8=33244
reflecting surfaces, highly polished, comparison by holographic interferometry 8=31936
reflection echelon, effect of sinusoidal polish errors 8=24414
Rochelle salt crystals, vacuum u.v. spectra 8=36441
from scattering medium 8=42242
solids, double refr. meas. of anisotropy 8=30938
spectral, from wing of butterfly Morpho 8=46656
specular, from a rough surface, var. with incident angle 8=46717
specular reflection at ground, effect on light scatt. from Rayleigh atmos. 8=32242
spiral galaxies, polarization obs. 8=28116
transparent electrodes, internal reflect. spectra 8=41280
uniaxial absorbing crystals, reflectance 8=27527
u.v., rough and smooth surfaces, 1216Å 8=37698
water reflectance obs. rel. to refractive index and dielectric constant calc. 8=43752
$A^{III}B^{V}$ crystals, in determ. orientation 8=39645
Al film on glass, phase retardation meas. 8=31960
Al thin film, of synchrotron radiation 8=27549
Al, thin films, plasma resonance in reflection spectrum 8=30746
Ag film on glass, phase retardation meas. 8=31960
As_2Se_3 and $(As_xSb_{1-x})_2Se_3$ and Sb_xS_3 films 8=31963
Au, reflectance in vac. u.v., obs. 8=27558
[C-N] and [N-H] bonds, valencies in phenylamines 8=47622
CaO, i.r. dielectric response rel. to lattice vibrations 8=41075
CdS, photoreflectance spectra at fundamental absorption edge 8=45183
CdSe:Cu, rel. to fundamental absorpt. edge impurity conc. dependence 8=36349
Cu film on glass, phase retardation meas. 8=31960
Fe film on glass, phase retardation meas. 8=31960
Fe layers, thick evaporated, meas. rel. to gyroelectric and gyromag. consts. 8=36141
GaSb, i.r. spectra, band structure 8=41089
GeSi alloys, spectra in energy region 1.13 eV 8=36366
InAs crystals, in determ. orientation 8=39645
n-InAs, spectra rel. to conduction band structure determ. 8=35771
n-InSe, and absorpt. spectra, optical transitions 8=45196
LiF, improved Kramers-Kronig dispersion analysis of i.r. reflectance data 8=27580
Ni film on glass, phase retardation meas. 8=31960
Ni films, u.v., near Curie point 8=36399
Pt, ellipsometric investigation of anodic films 8=41282
Se films, thin, absorption and reflecting power, in fundamenetal absorpt. region 8=27605

Reflection—contd
light—contd
SnO_2, restrahl spectrum in static dielec. constant, determ., 8=49353
SrO, i.r. dielectric response rel. to lattice vibrations 8=41075
TlSe, spectrum beyond fundamental absorpt. edge 8=36423
VO_2 crystal, spectra in 1.4-6.0eV at 25, 59 and 62°C rel. to semiconductor-metal transition 8=41150
ZnS with one dimensional stacking faults, internal 8=45230
ZnSe, i.r. lattice vibrations 8=49764
ZnTe, i.r. lattice vibrations 8=49764
Reflectivity
See also Diffusion/light; Optical constants; Optical films.
ablation chars, visible and near i.r., from 2200 to 3500°K 8=36334
acoustic, of moving fluid layer, calc. 8=37267
bidirectional reflectance meas. for satellite calibration target in visible and near i.r. 8=41489
clouds of dust and smoke, plane-parallel, reflectance 8=39447
coefficient of inhomgeneous layer, determ. 8=46019
dielectric thin films as mirrors for laser work 8=49674
duralumin changes during laser pulse 8=45169
gas laser mirror, meas. 8=24297
graphite, visible and near i.r., from 2200 to 3500°K 8=36334
inert gases, liq., far u.v., cell meas. 8=34846
measurement using attachment to spectrophotometer 8=46691
metals, pure and alloyed, i.r. reflectances at low temp. 8=27526
photoreflectance effect mechanism 8=49676
powder, Perkin-Elmer spectrophotometer attachment 8=28824
reflectometer, double-beam type, for optical consts. determ. 8=37684
Scotchlite sheeting, in liq. H_2, obs. 8=36312
semiconductor layers, i.v., rel. to meas. of surface concs. and junction depths 8=49265
spatial total reflectivity, for determ. of radiation characts. as fn. of λ and temp. 8=49677
steel, changes during laser pulse 8=45169
transition metals, in vacuum u.v. rel. to dielec. constants and loss calcs. 8=41147
vacuum system meas., angle-doubler 8=37658
Ag film, absorbent and anisotropic, and transmissivity of light 8=49707
Ag, liquid, from thermal emissivity meas. 8=43821
Ag, Al, changes during laser pulse 8=45169
AgCl, 2-21 eV energy range 8=36316
Al_2O_3, reflectance, absorption and transmittance 8=41057
Al_2O_3, spectral reflectance 8=41128
As, infrared, magneto- rel. to interband transitions 8=26900
Au film, absorbent and anisotropic, and transmissivity of light 8=49707
BaF_2, spectra from (111)-cleavage plane, 78°K 8=45175
BaF_2, u.v. spectra 8=36374
$BaTiO_3$:1 at% La, semicond., polaron model and 0.7-7.4 μ 8=35878
Be, far u.v., rel. to 1/ϵ resonance 8=49709
C, visible and near i.r., from 2200 to 3500°K 8=36334
CaF_2, u.v. spectra 8=36374
$Cd_xCa_{1-x}O$, optical, and elec. props. 8=49137
$CdGeAs_2$, amorphous and polycryst., in 0.6-5.5 eV region 8=49712
$Cd_xSr_{1-x}O$, optical, and elec. props. 8=49137
CdTe, pure and In doped, free carrier effect 8=31974
CeO_2, spectral reflectance 8=41128
Cs, thermoreflectance spectrum in visible and near u.v. region 8=41101
CsBr in rock salt structure, reflectivity 8=45184
CsI in rock salt structure, reflectivity 8=45184
Cu, changes during laser pulse 8=45169
Cu_2O rel. to lattice fundamental vibrs., 290°K 8=39873
GaAs, change with excitation by laser radiation 8=36367
GaAs, electroreflectance rel to interband transitions 8=49728
GaAs, electroreflectance stress dependence rel. to electronic structure 8=49725
p-GaAs, rel. to hole masses, light and heavy 8=35886
GaAs, rel. to plasma reson. on non-equilib. carriers, 10.6μ 8=40454
(Ga, In)As, electroreflectance rel to interband transitions 8=49728
p-GaSb, rel. to hole masses, light and heavy 8=35886
Ge, change with excitation by laser radiation 8=36367
Ge, electroreflectance stress dependence rel. to electronic structure 8=49725
Ge, rel. to plasma reson. on non-equilib. carriers, 10.6μ 8=40454
InAs, electroreflectance rel to interband transitions 8=49728
K, thermoreflectance spectrum in visible and near u.v. region 8=41101
KF, u.v. spectra 8=36374
LiF crystals, far u.v. props., effect of polishing 8=41112
MgO, spectral and i.r. dispersion 8=41022

Reflectivity—contd
Pt, optical functions deduced from reflectance data 8=45216
Rb, thermoreflectance spectrum in visible and near u.v. region 8=41101
Se, trigonal, spectrum in vacuum u.v. 8=27606
Si, electroreflectance stress dependence rel. to electronic structure 8=49725
Si, rel. to plasma reson. on non-equilib. carriers, 10.6μ 8=40454
SiO_2, glassy, curve rel. to absorpt. 8=49754
SiP_2 and $SiAs_2$, reflectance meas. 8=40484
$SrTiO_3$, electrorefl. oscills. rel. to h.f. free-carrier mass 8=36415
$SrTiO_3$, near absorpt. edge 8=27609
TiO_2, spectral reflectance 8=41128
VO_2, in semiconducting and metallic states 8=49760
Y_2O_3, spectral reflectance 8=41128
Zn, basal-plane vacuum u.v. reflectance meas. 8=45233
$Zn_xHg_{1-x}Te$ solid solutions, fundamental spectrum 8=45232
ZnO, spectral reflectance 8=41128
Refraction
Michelson interferometer, for refractometry, and for absorpt. and spectroscopy 8=33272
random media, wave propag. 8=42005
acoustic waves
See also Dispersion/acoustic.
underwater horizontal propag., fluctuation, due to refraction 8=36698
acoustic waves, ultrasonic
No entries
electromagnetic waves
See also Electromagnetic wave propagation.
bianisotropic medium, at interface 8=28616
cylindrically stratified media 8=42013
electro-optical effects at medium-free space interface, static elec. field 8=28607
microwaves, obliquely incident on plasma slab 8=34496
new methods and results 8=37480
at plane boundary of two homogeneous isotropic dielectrics, graph of describing quantities 8=37479
refractive index, surface of magnetized medium 8=24214
rel. to earth satellite path meas., r.f. refr. in inhomogeneous medium 8=28635
screen with random inhomgeneities, field structure behind 8=37481
troposphere, fine scale struct. and refr. index meas. 8=32201
troposphere, psychrometer radiosonde 8=28601
troposphere, superrefractive with nontrapping surface layer 8=32252
light
See also Double refraction.
beam at plane interface 8=28845
birefringent media, Brillouin scattering 8=27537
n-butyl alcohol, temp. derivatives 8=34803
crystal, anisotropic, and isotropic medium, refraction laws at boundary 8=27525
glasses, refractometer determ. refr. index 8=37636
heat-transfer interferometry, error evaluation 8=28395
nonlinear media, self-focusing filaments, prod. mechanism 8=42153
plane surfaces, spectrum meas. 8=28846
by-pyrex vacuum coated surface, obs. 8=36319
rough surface obs. 8=36319
scalar wave in random medium, statistical props. calc. 8=42240
self-focusing pulses freq. spectrum broadening 8=28842
triglycine sulphate single crystal, rel. to temp. 8=36439
uniaxial absorbing crystals, reflectance 8=27527
by Al vacuum coated surface, obs. 8=36319
As_2Se_3 and $(As_xSb_{1-x})_2Se_3$ and Sb_xS_x films 8=31963
CdS active oscillator, focusing of laser beam 8=28882
Refractive index
α-quartz crystal, refractivity interpret. 8=49756
atmosphere, r.f. difference spectra 8=50153
glycine sulphate, ferroelec., temp. depend. 8=45243
plasma, for e.m. waves at oblique incidence, calc. 8=30067
of polarizable particle system, calc 8=24215
profiles in spherically stratified isotropic media 8=33128
radio, troposphere, variations, relation with meteorological conditions 8=50154
radio, troposphere, variations, spectral charact. 8=50155
$BaTiO_3$, temp. dependence 8=49708
Be atom, Hartree-Fock calc. 8=47485
He atom, Hartree-Fock calc. 8=47485
Ne atom, Hartree-Fock calc. 8=47485
$SrTiO_3$, temp. dependence 8=49708
Xe liquid and vapour, —59.0°C — 16.5°C, and Lorentz-Lorentz junction 8=43809
light
See also Dispersion, optical; Double refraction; Optical constants.
α- and β-$TiCl_3$, and absorpt. spectra 8=36417
amyl and isoamyl alcohol, temp. derivatives 8=34803
anthracene, 5–100μ thickness meas. from refr. index dispersion 8=32043
benzene, shock wave compressed, obs. 8=39370

Refractive index—contd
light—contd
benzodioxane-1, 4 soln., of solvent rel. to absorpt. spectrum of soln. 8=39376
cholesteryl 2-(2-ethoxyethoxy)ethyl carbonate, liq. crystal, obs. 8=30482
complex, in theory of hyperchromism 8= 39365
crystalline lens (rabbit), distribution model 8=46779
determ. with sample in form of sphere 8=28744
Duc de Chaulnes' method for determination 8=28729
electrostriction effect in solids rel. to self-focussing 8=41046
ethyl alcohol, shock wave compressed, obs. 8=39370
europium chalcogenides, meas. rel. to dispersion theory 8=49716
films, thin luminesc., rel. to porosity 8=36454
gases, having non-resonant absorpt. in microwave region, rel. to molecular polarizability, 8=47972
glass, fine annealing for homogeneity 8=41141
glass, mean reference for F and C achromatism, simplified expression 8=42161
glass powder, compression under 10-65 kbar effects 8=40164
glass, variation in strong field of ruby laser 8=41098
glasses, effect of mixed γ-n radiation 8=44493
glasses, reference index proposal 8=36410
glasses, rel. to composition 8=31996
glycerine, shock wave compressed, obs. 8=39370
group index for air 8=47967
interference filters, rel. to bandwidth 8=24376
interferometer for direct recording 8=28861
ionic crystals rel. to polarizabilities 8=36390
leucosapphire, grown from tungstate melts 8=39648
liquids, nonlinear, rel. to molecular light scatt. 8=43815
liquids, ruby laser-induced variation absolute meas., 8=43818
liquids, variation in strong field of ruby laser 8=41098
lithium niobate, melt-grown, rel. to comp. 8=41114
many-particle system, dielec. const. theory 8=37680
minerals, absorbing anisotropic, and absorpt. coeff. 8=41061
in optical density determ., correction factor 8=37681
optical glasses, meas. 8=37636
para-terphenyl, 5–100μ thickness meas. from refr. index dispersion 8=32043
plane surfaces, differential meas. 8=28846
plastic scintillator NE 102A, 5–100μ thickness meas. from refr. index dispersion 8=32043
polymers in binary mixed solvents 8=30472
polyoxymethylene extended chain crysts., X-irrad. effects, $< 4.8 \times 10^7$ R 8=44509
polystyrene lattices, suspension light scatt. meas., 589, 546 and 436 mμ 8=34934
polystyrene solns., , depene. on conc. and temp. 8=44065
propane, liquid, 17.4-65.8°C, 4358, 5461 and 5791 Å 8=30483
quartz, from asymmetric interferograms, 20-400 cm^{-1} 8=28844
quartz, ordinary and extraordinary, in vac. u.v., from interference in thin parallel plate 8=32034
quasi-monochromatic wave through dispersive medium, meas. 8=46713
random heterogeneities, rel. to dispersion laser emission, 8=37566
ruby, grown from tungstate melts 8=39648
seawater, Copenhagen, spec. refraction and dilutions, chlorinity, wavelength and temp. dependences 8=50114
secondary spectrum of two-element lenses in i.r. 8=45144
silicon polymer, glow-discharge deposited 8=49763
tetracene, 5–100μ thickness meas. from refr. index dispersion 8=32043
theoretical formulae from correlation functions 8=28876
thin films, and thickness obs. by ellipsometry 8=31931
trans-stilbene, 5–100μ thickness meas. from refr. index dispersion 8=32043
uniaxial absorbing crystals, reflectance 8=27527
water, calc. from reflectance obs. 8=43752
AgBr, colloidal, complex refr. index, near-u.v. 8=43891
Ar, gas, liq. and crit. state 8=47967
Ar, rel. to gas-liquid coexistence curve shape near critical state 8=30590
CaF_2-Tb_2O_3($Tb(OF)_3$)(TbF_3) solid solns., rel. to crystal chemistry 8=39640
CCl_4, shock wave compressed, anomalies, obs. 8=39370
CdS single crystals, rel. to temp. 8=45182
CO_2 cryodeposits on 77°K surface, from Bragg interference meas. 8=41068
CuCl film, obs. 8=31982
GaP, meas. between 0.545 and 0.70μ 8=41092
GaSb near energy gap, from diode laser modes temp. depend., 80°K 8=41088
K film, for photons 3.96 to 9.69 eV 8=49731
KBr, from asymmetric interferograms, 20-400 cm^{-1} 8=28844
KCl, far u.v. obs. 8=27592
KCl, impure crystals 8=32005
$K_2Mn_2(SO_4)_3$, langbeinite structure, rel. to electro-optical props. 8=39678
$K_2Ni_2(SO_4)_3$, langbeinite structure, rel. to electro-optical props. 8=39678

Refractive index—contd
light—contd
$LiNbO_3$, ordinary and extraordinary, variation with hydroatatic press. 8=27582
$LiTaO_3$, ferroelectric, 20-800°C, 468-644 mμ 8=41113
$LiTaO_3$, refr. indices, 20-800°C, 468-644 mμ 8=41113
NaCl, far u.v. obs. 8=27592
Nb_2O_5, insulating films 8=49763
$(NH_4)_2Mn_2(SO_4)_3$, langbeinite structure, rel. to electro-optical props. 8=39678
RO-TiO_2-SiO_2 systems (R = Ca, Sr, Ba, Zn, Cd), $\mu = 1.58-2.11$ 8=44079
$Rb_2Mn_2(SO_4)_3$, langbeinite structure, rel. to electro-optical props.. 8=39678
SiC, 6H polytype, 2.43-0.336μ 8=36407
Si_3N_4, insulating films 8=49763
$SnSe_2$, and absorpt. coeff. 8=45220
Ta_2O_5, insulating films 8=49763
ThF_4 films, dispersion 8=35184
$Tl_2Mn_2(SO_4)_3$, langbeinite structure, rel. to electro-optical props. 8=39678
ZnO, meas. room to liq. He temps. in region near absorpt. edge for $E \perp C$ and $E \parallel C$. 8=41154
ZnO, using interference technique 8=49763
ZnS, using interference technqiue 8=49763
Refractive index measurement
gas, dispersion, microwave dual-mode cavity 8=47969
glass and liquids, by precision refractometer 8=42190
i.r. interferrometric arrangement 8=42246
small changes, with interferometer 8=46722
troposphere, for e.m. waves, psychrometer radiosonde meas. 8=28601
Refractometers
for liquids and gases, automatic with digital or analog readout 8=28750
precision meas. 8=28752
PR2-PULFRICH type, universal precision instrument for glass and liquids 8=42190
Refractories. See High-temperature production and effects.
Refrigerators. See Low-temperature production.
Regge poles. See Scattering, particles.
Relativity
Boltzmann transport eqn., Cauchy problem 8=23911
de Sitter model for elementary particles in non static frame 8=29024
dynamical system with geodesic trajectory in Riemannian spaces, conservation laws 8=32694
Einstein-Maxwell axially-symmetric field construction 8=32783
gauge fields with noninvariant interactions 8=32776
geodesic clock, Marzke-Wheeler method depend. on atomic constitution of matter 8=23866
Kepler problem, radiationless, classical soln. in strong coupling limit 8=28250
Lorentz spaces, 4 dim and symmetric, metrics 8=41739
Maxwell-Einstein eqns., singularity-free soln. 8=33061
multitemporal theory and appl. to quasars and elementary particles 8=46076
multitemporal theory and Dicke effect 8=46073
multitemporal theory, and masses of elementary particle 8=47019
Noether eqns. and conservation laws 8=32782
Poincaré group modification rel. to combination of relativity and internal symm. 8=37847
principle and application, book 8=28286
Riemann space and elementary particles 8=28284
Riemann space and physical reality 8=28283
Riemannian spaces, systems with geodesic trajectories, conservation laws 8=32694
space-time causal automorphisms, proof of continuity 8=23859
space-time, flat, time like helices 8=46074
temporal reversal, by special conformal transformations, examples presented 8=32779
trajectory transformation under special conformal transformations 8=32779
verification by supercond. gyroscope 8=29000
$G_{\mu\nu} = O$, Kasmer's proof that no soln. can be embedded in a flat five-space 8=28285
general
See also Cosmology; Gravitation.
Bianchi identities, breakdown rel. to anomalous gravitational interaction of Dirac particle 8=46081
Brans-Dicke coupling constant, necessarily positive 8=45589
Brans-Dicke theory, equiv. of gravitational and inertial mass 8=32818
Cantan problem 8=32794
charged dust distribs in rigid rotation, stationary cylindrically symmetric solns. 8=32810
charged dust static distrib., relation between g_{00} and electrostatic pot. 8=32815
circular motion in relativistic Kepler problem stability 8=37123
conformally invariant geometrical objects and tensors, functions of metric tensor 8=32811
with cosmological consts., and elementary particle theory, vacuum props. 8=28292
cosmological red-shift, and gravitational waves, theory 8=41744

Relativity—contd
  general—contd
    Curzon metric, structure 8=37172
    cylinder, infinite with multipole moments, exterior metric 8=28295
    dust and e. m. fields, stationary distrib. 8=32803
    dust metrics new solns. of Einstein's field eqns. 8=28289
    Einstein eqns., soln. in Gaussian co-ords., with only one singularity, solution 8=37167
    Einstein field equations with ideal fluidity 8=37174
    Einstein theory, equiv. of gravitational and inertial mass 8=32818
    Einstein's empty-space field eqns, axi-symmetric stationary solns. 8=32814
    energy radiation from arbitrary axially symmetric system 8=41746
    e. m. fields and dust, stationary distrib. 8=32803
    e.m. wave propag. between planets, calc. up to third order in v/c 8=37163
    event horizons in static electrovac space-times 8=32807
    field energy, in 3-space, chronometrically invariant definition 8=32799
    field of constant-mass-density sphere 8=32800
    5D space, dynamic transformation, motion of particle with var. rest mass. 8=28300
    fluid spheres, solns. of eqns. for $e^{-\lambda}$ 8=41740
    fourth test, preliminary results 8=37175
    force on particle moving in isotropic rad. field 8=41741
    Friedmann space on plane, generalised, conformal representation 8=41747
    galaxies, origin, oscillating world model 8=50370
    gravitation, scalar theories with variable velocity of light 8=46086
    gravitational collapse rel. to Schwarzschild singularity 8=32812
    gravitational energy, sign 8=28297
    gravitational field, cylindrical non stationary solution 8=28301
    gravitational field nature and metric principle validity 8=28290
    gravitational field, timelike energy-momentum 8=32802
    rel. to gravitational field quantization, modified theory 8=32819
    gravitational/inertial mass ratio of earth, meas. by lunar laser ranging 8=41748
    gravitational motions of collapse or of expansion 8=50250
    gravitational radiation from uniformly accelerated particles 8=23868
    gravitational radiation mixture, mass transfer from source 8=32804
    gravitational waves, detection by electromag. radiation 8=23864
    gravitational waves, plane, without polarization, Klein-Gordon eq. sol. 8=32813
    graviton mass and light deflection 8=46079
    Hamilton-Jacobi eqns. isomorphic to mappings of solns. of Einstein's field eqns. 8=32777
    hypersurface, changed, motion under spherical symm. with gravit. effect of e.m. field 8=28291
    Jordan's gravitational theory rel. to cosmic microwave radiation at 3°K 8=32795-6
    junction conditions, tetrad formulation 8=23865
    Klein-Gordon eq., sol. for plane gravitational waves without polarization 8=32813
    Lagrangian functions in X_4 space, classification of real one component fields 8=46084
    Mach's principle 8=32797-8
    Mach's principle and Green's function in expanding universe 8=45587
    matter distrib. models for fluid spheres 8=46080
    metric forms with removable singularities, and the causality principle 8=37171
    Minkowski formulation of Einstein's gravitational theory by a Rosen method 8=46083
    Newtonian orbit in pulsating Universe 8=46082
    Noether identities in covariant field theory 8=37169
    photons, ageing effect as test of theory 8=36914
    pulsars, effect on observed freqs. if pulsars are orbiting 8=41534
    pulsating radio sources, rel. to new test 8=41536
    radiation damping in conformally flat spaces 8=32809
    radiation damping, vierbein formalism 8=32808
    rotating massive stars structure and stability 8=50281
    Schwarzschild metric, transforms. eliminating singularities on gravitational radius 8=37170
    Schwarzschild space and expanding universe, book 8=28286
    shells, charged, and their gravitational collapse 8=46088
    solution for spherical symmetrical bodies 8=41495
    space and time models in elementary physics 8=46075
    space-times, relativistic, with corresponding geodesics 8=37173
    space-times, spherically symmetric, theory 8=46087
    spheroidal bodies, rotation 8=28294
    stationary fields, multipole expansions and source moments in Newtonian field 8=23869
    stellar dynamics, applicability 8=45606

Relativity—contd
  general—contd
    synthesis of expt. to meas. precesion of spinning test mass orbiting in 3-dimens space 8=41745
    teaching bibliography resource letter 8=32805
    tested in obs. on the orbit of Icarus 8=41751
    uniqueness, derivation from gravitational field eqns. 8=37162
    white dwarfs, Hamada-Salpeter, effect on oscillations 8=50325
  special
    attenuated waves, relativistic Doppler eqns. and drag effect 8=46470
    case against 8=32787
    Einstein's theory and its implications 8=46077
    e. m. field transformation using test charge at rest 8=32788
    experimental verification reviewed 8=23860
    force-free space experimental validation unavailable 8=23861
    Heaviside formulae connection with relativity 8=46347
    Lorentz contraction for rod passing through slit 8=32790
    Lorentz, covariant field eqns., sets of solns. for infinite no. of field components 8=33352
    Lorentz invariant distribs and scale transforms., spectral representations 8=32792
    Lorentz or Galileo invariant electrodynamics, energy conservation paradox 8=37769
    Lorentz transformation, derivation without use of light 8=32784
    Lorentz transformation, representation using vector of rapidity 8=32785
    Lorentz transformations, spinorial representations 8=32789
    Lorentz-Fitzgerald contraction explanation 8=33065
    Maxwell's eqns., use in derivation 8=41997
    mechanics, Lorentz-invariant eqns. with accel. as function of position and rel. 8=23888
    mechanics, relativistic, for action-at-a-distance, conomical formulation 8=23890
    Michelson-Monley modification, used to test ageing of photons 8=36914
    in Minkowski space-time, solns. to Bel-Lapiedra-Montserrat eqns. 8=28535
    motions in relativistic spaces 8=46011
    "preferred clock" misunderstanding 8=28287
    relativistic xtv space, geometrical model 8=37161
    Runge-Lenz vector, physical interpret. 8=38649
    shape, apparent, of rapidly moving objects 8=23863
    singularities of theory 8=46078
    small distances, possibility of testing in π decay 8=32791
    space and time models in elementary physics 8=46075
    temperature and entropy invariance 8=28288
    time dilation formula 8=32786
  unified field theories
    axially symm. gravitational problem, new formulation 8=28303
    charged particle, energy, Møller's tetrad calc. 8=23870
    galaxies, spiral and radio 8=50371
    geometrodynamics, non-null field 8=28305
    gravitational field, quantum field theory 8=32820
    Riemannian space of class one, conformally flat, curvature restrictions 8=28304
    symm. tensor-antisymm. tensor theory from a quaternion representation 8=28302

Relaxation
    See also Acoustic wave propagation; Dielectric phenomena; Elastic relaxation; Ferroelectric phenomena; Ferromagnetic relaxation; Molecules/relaxation; Nuclear magnetic resonance and relaxation; Paramagnetic resonance and relaxation.
    alkali halides, reorientation time of O_2^- impurities 8=48822
    alkaline vapour mixture, spin exchange relax. in collisions, obs. 8=38749
    alumina, l.f. grain boundary 8=44549
    aniline, dielec. relax. 8=43856
    anisole, dielec. relax. 8=43856
    benzonitrile-acetonitrile mixture, dielec. relax. 8=43856
    benzonitrile-propionitrile mixture, dielec. relax 8=43856
    binary mixtures of polar liqs., r.f. relaxation spectra 8=48185
    Boltzmann equation, validity 8=32857
    cavitation, ultrasonic, applications 8=37278
    chemical, timing by pressure shock technique 8=45360
    critical point phenomena 8=28317
    dielectric, of polar viscous soln., microwave obs. and theory 8=43852
    distribution of relaxation times, numerical evaluation 8=46349
    electrolyte, laser temp.-jump apparatus 8=36595
    electron energy, in NO magnetoplasma 8=47815
    gas described by Boltzmann kinetic equation 8=47948
    gas mixtures, polyatomic, and transfer phenomena 8=43699
    generation peaks, double-kink, strength 8=31062
    hydrodynamics, characteristic manifolds 8=47902
    ice crystals, understanding of relax. phenomena 8=49366
    liquid, non-Newtonian, rot. viscometer meas. evaluation 8=34800

Relaxation—contd
organic liquids at 1 GHz 8=25910
orthodeuterium-inert gas mixtures, rotation 8=30295
parahydrogen-inert gas mixtures, rotation 8=30294
phenomena due to interstitial impurities 8=44421
processes, rel. to time depend. of strength of adhesive joints 8=48967
solids, of polarization time in shock wave 8=40563
superfluid rotating He, hydrodynamics 8=37347
3-methyl 2, 4-heptanediol, u.s. and dielec. relaxation 8=48189
time meas. from polarizability plot for nearly spherical mols. 8=43267
urea-urease mixture, u. s., obs. 8=48144
Au, cold drawn, peaks 8=48997
B_2O_3, viscous relaxation and non-Arrhenius behaviour 8=34802
Cs vapour, hyperfine, rel. to diffusion coeff. and cross section meas. 8=47537
n-Ge surface states, obs. 8=44788
H isotope-inert gas mixtures, rot., theory and obs. 8=30296
He solns, isotropic irreversible osmotic 8=24037
Hg^{198} atoms, collision with inert gases, temp. effect 20°-600°C 8=29664
KBr:OH$^-$, OD$^-$, dielectric 8=49344
K-Rb alloys, Zener relax. 8=49030
in N_2 freejet expansion from sonic orifice, rotational relax. rel. to temp. 8=34629
N_2 up to 7000°K, vibrational with multiple quantum transitions 8=34640
Ni crystals, of stress, meas. 77-350°K 8=40178
Rb^{87} maser theory 8=24266
Zn twinned crystals, of stress at twin boundaries rel. to internal friction 8=35727
Remanence. See Magnetization state.
Renner effect. See Molecules.
Replica techniques. See Electron microscopy.
Reproduction. See Sound reproduction.
Resistance, electrical
See also Conduction, electrical; Conductivity, electrical; Contact resistance; Magnetoresistance; Piezoresistance.
alloys, dilute, Kondo effect, Takano-Ogawa theory exam. and mag. susceptibility calc. 8=44956
crystal, magnetic-ion multiplicity effects 8=31254
electron tube parameter meas., standardization 8=37426
heater circuits for calorimetry, stabilization 8=28423
insulators, partial discharge testing 8=24060
Kondo effect, physical perspective 8=26867
measurement method without contacts 8=49136
metals, Kondo problem rel. to mag. impurities 8=35816
noble-metal-rare-earth alloys, dilute, Kondo effect rel. to impurity mag. effects 8=31316
sheet, test apparatus 8=28457
theorem, curvilinear squares proof 8=24077
thick-film, trimming by abrasive jet machining 8=29033
thin films, contactless meas. 8=49134
zero-temp. impurity resistivity, breakdown of conc. expansion 8=31306
Am, rel. to pressure 8=39541
Cu with magnetic impurity solute, concentration depend. 8=26966
Cu-10. 5 at. % Ge, recovery after quenching 8=49160
Fe-Ni alloys, deformed, return with saturation magnetization 8=31639
n-Ge, neg. differential res., by electron transfer from (111) minima to <100> minima 8=27105
MgO at high temp., impurity effects 8=26950
MgO based insulating materials 8=31445
Mo, thin-film resistors for integrated circuits 8=44693
$NH_4H_2AsO_4$(ADA), obs. 8=27298
Si-Cr film resistors, temp. coeff., struct. and stability at 200°C 8=44818
Si_3N_4 based insulating materials 8=31445
Te, molten 8=34965
Resistance thermometers. See Thermometers/resistance.
Resistivity. See Conductivity, electrical.
Resolving power, optics
See also Optical instrument testing.
electron lens, spherical correction in two-sections 8=24144
electron-optical systems, limitations imposed by individual elements 8=41978
emulsions, imaging of 7-60 keV images 8=37722
image quality, theoretical prediction 8=28741
photographic systems, influence of orientation errors in panoramic aerial photographs 8=42277
Raman spectra, improvement by He-Ne laser light source 8=24398
restoration of detail to optical image degraded by diffraction and noise 8=28735
slow n spectrometer, Bragg break meas. method 8=47171
uniformly broadened spectral line 8=33261
Resonance, elementary particles. See Hyperons/resonances; Mesons/resonances.
Resonance, magnetic. See Magnetic resonance and relaxation.
Resonance spectra. See Spectra.
Resonators
cavity-coil config. for ENDOR expts. 8=42042
Resonators—contd
cavity, field eqns. for coupled systems 8=37456
cavity, for e.p.r. meas., with uniaxial pressure on sample 8=46506
cavity microwave, temp. stability 1.25 in 10^8/°C 8=37455
cavity, Q determ. method 8=37454
dielectric X-band in rectangular waveguide 8=28625
electrometer needle, parametric resonance obs. 8=37360
e. m. system with total internal reflection 8=42022
Fabry-Perot, for laser with self-resonant feedback 8=24270
Fabry-Perot, in short-mm. region 8=42003
Fabry-Pérot, meas. of sphere scatt. cross-section 8=33282
Fabry-Perot meas. with rapid sinusoidal detuning 8=46556
Fabry-Perot, r. f., field strength perturbation meas., theory 8=37453
ferrite, new method of liquid cooling 8=33048
laser, gaseous, single-freq., parameter optimixation 8=33188
laser, mirror, angular oscillatory modes 8=28664
laser, molecular, stability and selectivity 8=46557
laser multicavity adjustment for freq. modulation of single mode 8=24295
laser, Q-modulation, use of opto-mechanical shutter 8=42077
laser, rod between parallel plates which act as mirrors, frequency of axial modes 8=24291
laser, ruby, with filter, loss calc. 8=37603
laser, switching rate rel. to radiation characts. 8=24286
laser, two-dimensional 8=24290
microwave cavity, freq. shift meas. 8=28604
mode system for radial wavebeams 8=37457
modes, equations for amplitudes 8=46563
molecular liquid, anisotropic in laser, mode locking and ultrashort pulses 8=42071
optical, and waveguides, modes with infinite mirrors 8=33121
optical anisotropic, theory 8=33270
optical appl. meas. freq. laser and passive resonators 8=24292
optical cavity, X-band microwave exptl. scaling 8=41998
optical, modulated Q, kinetics 8=37559
optical, open, perturbation calc. 8=24366
optical, open two-mirror astigmatic 8=33174
optical, open with spherical mirrors, transmission losses 8=24367
optical, scalar theory 8=28668
optical, solid state, laser modes rel. to deform. by pumping pulse 8=42068-9
optical, stable and unstable, modes 8=37561
optical, with partial polarizers, eigenstates of polarization 8=46559
orbital accelerator, broadband f.m. 8=29004
piezoelectric ceramic cube, analysis 8=32897
piezoelectric, system of electrodes on quartz plate, analysis 8=32896
quartz, electrode optimum sizes and shapes 8=37246
single crystal 8=28928
spherical cavity with concentric shell system. e. m. field calc. 8=37452
standing-wave tank structures for linac 8=46996
stimulated combinational scattering 8=46564
superconducting cavity for linear accelerator 8=29000
superconducting, for linac, construction 8=46995
thick discs and rods, resonant freq. corrections 8=37243
X-ray, planar using Bragg reflectors 8=46786
CO_2 laser with near confocal optical resonator, obs. 8=42076
$LiNbO_3$ crystal in optical cavity pumped by laser, parametric oscilln. 8=42072
$NH_4H_2AsO_4$, (ADA), low temp. coeff., props. 8=27299
Nd glass laser, nonlinearity rel. to radiation flux 8=33227
Nd laser, plane mirrors, spectral effects 8=24287
Nd laser, selective, spectral effects 8=24289
Nd:YAG laser intracavity tuning, polarization and Q switching 8=28707
acoustic. See Acoustic resonators.
electromagnetic. See Electromagnetic oscillations.
Reverberation
See also Architectural acoustics; Echo.
limited sonar, beamwidth and multiple transmission effects 8=37270
ocean bottom, from deep explosions 8=50099
portable device with coiled springs 8=41846
statistical props. of reverberant sound field 8=37256
Reviews
alkali halides, dielectric constant measurements 8=40567
anisotropic crystals, band structure 8=35766
applied optics at Corning glass 8=37660
astronomical techniques, general 8=32417
atomic absorption spectroscopy, applic. of graphite cuvette 8=38619
atomic absorption spectroscopy with high temp. flames 8=46686
atomic nucleus, shape 8=47197
atmosphere, upper, structure 8=45481
atmospherics, sub-ionospheric source and propag. phenom. 8=32250
aurora, characts. rel. to excitation by electrons, protons or m.h.d. p waves 8=32288

Reviews—contd
auroral rocket obs. 8=45500
auroral substorms, theoretical 8=36807
baryon interactions, data compilation 8=24863
bond properties of molecules 8=38803
Brueckner theory of nuclear matter 8=29272
canning materials for water cooled power reactors 8=43145
ceramics, point defects, study and interpret. 8=35519
Cherenkov radiation in cosmic ray physics 8=33847
coherence, optical with special reference to interferometry 8=28718
cosmic ray origin in supernovae explosions 8=38106
cosmic ray showers, composition, development, obs. 8=29244
counters, semiconductor 8=28982
critical phenomena in equilibrium systems 8=28310
critical phenomena, in liquid vapour systems, He liquid and magnetism 8=34980
detonation, physical approach 8=46175
diamond, atomic vibration spectrum, exptl. evidence 8=43922
diffuse nebulae, obs. and theory 8=28089
dislocation dynamics 8=44434
electrets, phenomenological theories 8=46344
electrical props. of monomeric and polymeric charge-transfer complexes 8=26942
e.m. wave propag. in troposphere, Soviet contrib., 1957-67 8=27922
e.m. wave scattering and diffraction, two-dimensional 8=46464
electron capture, 1963/1967, theory and expt. 8=25176
electron microscopy, new developments 8=46411-12
electron synchrotrons above 3 GeV 8=33484
electrostatic accelerators and ion sources 8=24573
element 102, synthesis and study 8=29381
elements origin, teaching aids and literature 8=45585
η decay obs. rel. to C nonconservation 8=33711
fast-acting e. m. isotope separators 8=38765
field theoretical methods in physics 8=24479
fluids, theory and structure 8=30190
free radicals, mass spectrometry 8=29829
fuel cells 8=46358
gas lasers, investigations and applications 8=42080
geometrical optic, matrix theory 8=28725
glasses, thermal props. at low temp., rel. to vib. density of states 8=35455
group theory in particle physics 8=29014
heat transfer in liquid metal 8=39353
heat transfer, of 1965, 66 literature 8=28388
helion and triton optical potentials 8=47338
high-speed spectrometry 8=42227
hydrologic optics, expt. methods and app. to meas. radiative transfer 8=41334
hydrologic optics, mathematical models of light fields 8=41333
hypernuclei expts. and nuclear struct. appls. 8=29349
infrared analysis of macromolecular systems 8=34393
infrared spectra of H-bonded systems 8=38887
interfacial cohesion, practical implications of breakdown 8=39499
interferometric techniques, pre-laser advances 8=28855
interplanetary magnetic field 8=32566
ionic crystals, luminescence, Russian research 8=36455
ionosphere electron and ion temp. profiles at temperate latits. 8=27985
ionosphere electron density, by ground-based obs. of radio signals from cosmic vehicles 8=41415
ionosphere, F-region, large-scale behaviour 8=32334
ionosphere, lower, as region of active development of disturbances, in meteorological sense 8=32316
ionosphere and magnetosphere e, ion and neutral particle temps., rocket and satellite obs. review 8=32297
ionospheric radio propag., 20th century U.S.S.R. work 8=36836
isotope applications 8=43245
isotope separation on-line systems 8=38770
isotope separation, radiochem., rapid methods 8=38767
isotopes, stable, separation 8=34187
K-mesic atoms 8=34193
laser operation and applic. 8=28653
laser output energy meas. 8=42059
lasers, principles, operating characts. and appl. 8=33165
liquid thermal conductivity research at Moscow 8=30462
light sources 8=28769
luminescence of molecular crystals, 1930-67 8=36452
luminescence of molecules in gaseous, Russian work to 1967 8=38776
lunar photography, techniques and results 8=36994
magnetic ceramics, structure rel. to ferrimagnetism 8=49554
magnetic recording, theory and expt. 8=33053
magnetic, thin film, switching models 8=36115
magneto-optical diffusion in matrix density formalism 8=41935
magneto-optical effects 8=49695
magneto-optical rotatory dispersion and magnetic circular dichroism applied to spectroscopy 8=33257

Reviews—contd
magnetospheric v. l. f. phenom., satellite obs. 8=32263
magnetostriction, since 1961 8=31480
maser molecular spectroscopy 8=38782
masers, theory and expt. in USSR 8=28644
masers, USSR 8=33157
mass spectrometers, ironless time-of-flight 8=34121
mechanical props of mats at low temp. 8=26738
membranology 8=26048
metallic alloys, thermionic emission props. 8=36047
micropolar and dipolar fluids rel. to Poiseuille flow in circular channel 8=47907
microwave molecular spectroscopy 8=33140
Mössbauer effect in materials science 8=43938
Mössbauer effect, study of nuclear hyperfine interactions in solids 8=48317
muon, e. m. props. 8=29099
muon physics, theoretical 8=24735
neutron personnel dosimetry 8=33808
neutron personnel monitoring 8=33810
nonlinear, and coherent radiation freq. conversion 8=33241
nonlinear optics 8=46645
nuclear fission 8=29526
nuclear isomers, gamma-ray excitation, research (1939-67) 8=33889
nuclear power 8=47369
nuclear quadrupole interactions in solids 8=49662
nuclear reactions due to heavy-ions, Dubna 8=38521
nuclear reaction theories 8=25202
nuclear reactions due to strange particles 8=29483
nuclear reactions, high energy, models and obs. 8=29383
nuclear structure at medium energies 8=47209
nuclear structure, force and reactions 8=38290
nuclear track emulsions 8=33393
nuclei energy levels, A = 11-12 8=42799
nucleons, electromag. struct. 8=33739
of N-N interacts, expts. at Dubna rel. to phase-shift anal. 8=24873
nucleon-nucleon scatt. near 210 MeV, expt. aspects and data 8=24878
optical plasma resonance in solids 8=49123
optical props. of thin films 8=28847
optics in Germany, basic and applied research, education 8=28716
orbital accelerators 8=42357
orbital theory of spin props. of conjugated molecules 8=29707
particle accelerators, low and medium energy, existing and contemplated 8=37807
particle counters, semiconductor 8=24519
permanent magnetism 8=46381
phasemeters, p. c. m. microwave for plasma diagnostics 8=30087
physics of liq. metals, links between solid state and liq. state physics 8=30398
π-nucleus scatt. and interactions, low energy 8=29482
π-π phase shift in $K^+ \to \pi^+ + \pi^- + e^+ + \nu$ 8=24805
π-π scatt. 8=33690
plasma parameter meas., m.h.d. generators and plasmatrons 8=25762
plasma, particle interactions 8=30017
plasma thermodynamics 8=30009
plasma, transport processes, eqns. 8=30018
plasma, refractive methods in diagnostics 8=34516
polymers, local strains theory 8=31235
precipitation hardening by coherent particles 8=48980
p-T interactions above T(p, n)He^3 threshold 8=29222
quantum mechanics, phase function method 8=28937
radio propag., troposphere, mm to sub-mm, waves, USSR work 8=36756
Raman effect in gases (1950-1966) 8=29694
radiowave propag. in ionosphere study in USSR during last 50 years 8=27974
reactors, fast 8=47368
reactors, gas-cooled 8=47391
reactors, water-cooled 8=47390
recombination emission in inorganic solids 8=31953
relativity, special, apparent shape of rapidly moving objects 8=23863
rheology, historical 8=46064
rocket technology for space research 8=32380
satellite meteorological study 8=45438
semiconds, III-V compound, electron-hole radiative recomb. 8=45248
semiconductor donor-acceptor pairs rel. to radiative recombination 8=27055
semiconductor electronic transitions, USSR work over 20 years 8=35869
semiconductor junction development in USSR during last 20 years 8=27150
semiconductor-metal contacts, potential barriers 8=35924
semiconductor surfaces 8=44761
solar energy conversion to electricity, thermionic method 8=41934
spark chambers 8=28992
special theory of relativity, experimental verification 8=23860
spectroscopies of particles, atoms or mols., and atomic nuclei 8=46687

- **Reviews**—contd
  - stratosphere and mesosphere, quasi-biennial osc. and struct. 8=36714
  - superconducting a.c. loss mechanism 8=40336
  - superconducting magnet materials and fabrication 8=37386
  - superconducting magnets 8=28526
  - superconducting magnets for high-energy physics 8=37385
  - superconducting materials and devices 8=27003
  - superconducting mats. and devices, high-field and commercial 8=49187
  - superconductive pair-breaking mechanisms 8=40336
  - superconductive tunnelling, device appls. 8=40398
  - superconductivity 8=40339
  - superconductivity 8=49172
  - surface chemistry, by Mössbauer effect. 8=49902
  - teaching films, 16 mm. 8=41611
  - temperature meas., for past 40 years 8=46263
  - thermoelectricity and power generation 8=49390
  - transistors, field effect 8=35940
  - travelling ionospheric disturbances 8=27981
  - underwater sound research before 1939 8=36696
  - upper atmosphere characts, comparison with CIRA (1965) data and new research 8=36762
  - van der Waals interactions, calc. 8=29852
  - weak interactions and neutrons 8=24710
  - X-ray Compton effect 8=26283
  - Al_2O_3, n-induced damage obs. 8=44496
  - BeO, n-induced damage obs. 8=44496
  - C^{12} p-spallation cross sections obs. 8=29436
  - Fe-Ni-Co ferromag. films, anisotropy 8=36148
  - Ge γ-ray spectrometers 8=47070
  - H-bonding, n.m.r. study 8=48219
  - He^4 p-spallation cross sections obs. 8=29436
  - MgO, n-induced damage obs. 8=44496
  - N^{14} p-spallation cross sections obs. 8=29436
  - O^{16} p-spallation cross sections obs. 8=29436
  - Pu, liquid reactor fuel, physical props. 8=47407
  - Si m.i.s. devs, polarization effects in insulating SiO_2 film 8=44854
  - UO_2 powders storage behaviour 8=45349
- **Reynolds number.** See Flow; Hydrodynamics.
- **Rhenium**
  - cathode with Mo substrate, in thermionic converter, post test anal. 8=28501
  - collector in thermionic converter, comparison with Pd 8=28487
  - emitter for thermionic converter, interdiffusion with Ta substrate 8=28502
  - irradiated, unit cell and dimensional changes 8=26737
  - neutron irrad., identification of defect clusters 8=40080
  - optical consts., reflectance meas. 537-5770Å 8=27591
  - surface migration, from field-emission studies 8=27343
  - surface structs., He field-ion microscopy, comparison with Ru 8=26105
  - thermal conductivity below 1°K, rel. to supercond. energy gap 8=30988
  - wetting by Cs and Na, rel. to bare work function 8=35168
  - work function and desorpt. energies of O_2, thermionic meas. 8=31469
  - work function determ. and surface characts. 8=31468
- **Rhenium compounds**
  - Re complexes, $[Re(en)_2OOH][ClO_4]_2$, $[Re_2O_2H(CO)_8]^-$, $ReCl_2(acac)(PPh_3)_2$, crystal structures 8=26435
  - Re-rare-earth alloys, work function obs. 8=40690
  - $ReCl_5$, crystal structure 8=39819
  - α-ReO_2, distorted rutile, metal-metal bonding 8=48305
  - $ReTe_2$, formation in sealed evacuated fused silica tubes, between 450° and 935°C 8=39726
- **Rheology**
  - See also Plasticity; Viscoelasticity.
  - Bingham plastic in tube flow, heat transfer by forced convection 8=39266
  - Bingham plastic surface flow, analysis in canal type viscometer 8=30343
  - cement-water mixture, rheological behaviour as function of conc. 8=30545
  - creeping flow of power law fluid over Newtonian fluid sphere 8=39163
  - deformation props. of viscoelastic materials. mathematical description 8=41731
  - elastico-viscous liquids, linear, theory 8=25841
  - emulsions. determ. of Van der Waals const 8=48241
  - emulsions, dilute 8=39461
  - flow, turbulent Rayleigh shear 8=30219
  - historical review 8=46064
  - laminated medium, stability eqns. applied to edge buckling 8=41732
  - liquid gap btw. rot. coaxial cylinders, skin friction and heat transfer 8=30463
  - liquid transfer in two-phase dispersed annular flow 8=34707/8
  - non-Newtonian fluids, laminar incompressible boundary layer flow 8=34585
  - non-Newtonian liquid in rotational viscometer, relaxation meas. evaluation 8=34800
  - oligoethylene glycols crosslinked with hiphenylimethane triisocyanate, rel. to struct. obs. 8=44617
  - plasticity theory, w.r.t. dynamic theory of continuously distributed dislocations 8=46060
- **Rheology**—contd
  - polymer solns., kinetic approach 8=39334
  - polypropylene melts, rel. to mol. wt. distrib. obs. 8=43721
  - porous rubber, axial compression of cylinders in torsion 8=31253
  - power law dimensional problem 8=28273
  - power law, three non-dimensional constants 8=30353
  - rheometer, audio-frequency 8=34797
  - sand-water mixture, behaviour as function of conc. 8=30545
  - torsional vibration of two-layer rod, model 8=28362
  - viscoelastic and elastic parameters meas. rel. to rational geometry 8=32774
  - viscoelastic fluids, elasticity determ. from tangential stress meas. 8=48099
  - viscoelastic thin-walled tube with temp. depend. props, thermal stresses 8=23855
  - viscoplastic analysis of circular cylindrical shells 8=28277
  - visco-plastic medium, rectilinear steady motion 8=34706
  - viscous flow between eccentric rotating cylinders, stability 8=30216
  - viscous flow, h.f. oscillatory 8=30217
  - Weissenberg effect, mechanical model 8=28276
- **Rhodium**
  - chemisorbed H_2 and D_2, i.r. spectra 8=25470
  - electrolytic deposits, internal tension rel. to current density and metal conc. in electrolyte 8=36610
  - Fermi surface, effective mass. 8=40250
  - induced-β detector for thermal n dose meas. 8=38081
  - neutron dosimetry, personnel by foil activation 8=33795
  - optical props. rel. to cryst. e states, 0.4-11.0μm 8=32026
  - surface migration, from field-emission studies 8=27343
  - thermal expansion from X-ray powder diffr. exam. 8=44347
- **Rhodium compounds**
  - Co-Rh alloys, enhanced susceptibilities and n.m.r. relax. rates 8=31499
  - Rh-acetate complexes, crystal structure 8=26437
  - Rh complex, triacetylacetonatorpodium(III), crystal structure 8=26436
  - Rh-Be system, crystalline phases 8=48397
  - RhC, spectrum 8=25513
  - $RhCl_3$, effect on radiation-induced polybutadiene struct. 8=44081
  - Rh:Co dilute alloys, Co knight shift rel. to local exchange enhancement 8=35433
  - Rh:Co, Rh 5s cond. band exchange polarization, n.m.r. obs. 8=36281
  - Rh-Fe, magnetic impurity, ordinary scattering rel. to exchange scattering 8=26863
  - RhO_2, synthesis and props. 8=35205
  - Rh-Pd-Ag alloys, band struct. and density of states 8=35778
- **Riemann-Cristoffel tensors.** See Relativity; Tensors.
- **Righi-Leduc effect.** See Magnetothermal effects.
- **Ring currents.** See Atmosphere; Ionosphere.
- **Riometers.** See Ionosphere measuring apparatus.
- **Rochelle salt**
  - crystals, vacuum u.v. reflection spectra 8=36441
  - deuterated. d.m.r. and dielec. relax. 8=49651
  - deuterated, ferroelectric props., rel. to pressure and temp. 8=40621
  - dielectric constant relax., −50 to 45°C 8=27289
  - electro-optical props. near ferroelec. phase transitions 8=27577
  - polarization non-linearities in strong elec. fields, −35 to +35°C 8=35982
  - relaxation sound absorpt. near phase transition 8=39899
  - Cu-doped. e.p.r. electric shifts 8=49617
  - Cu^{2+} e.p.r. rel. to bonding, obs. 8=36243
- **Rock magnetism**
  - African data and discussion 8=36894
  - Aleutian Island arc, anomaly patterns and sea floor spreading 8=50218
  - Atlantic, S., mag. anomalies and floor spreading 8=36897
  - anomalies assoc. with mid-oceanic rises, rel. to crustal spreading theory 8=50089
  - basalt, North Mountain, of Nova Scotia 8=32368
  - basalt samples from Bavaria 8=50232
  - Bulgarian andesites, stability and petrology 8=28013
  - deep sea cores, paleomag. stratigraphy and micro-paleontology 8=50102
  - Dotswood red beds, (Queensland), magnetization 8=28014
  - igneous rocks, remagnetization problems 8=50229
  - Indian Ocean, anomalies and floor spreading 8=36898
  - Juan de Fuca ridge and linear inverse problem soln. 8=28019
  - Keweenawan partial self-reversal, magnetization of Portage Lake lavas 8=32369
  - Keweenawan, partial self-reversal, magnetization of upper lavas and sediments and lower dikes 8=32370
  - late mesozoic dolerites from Spitsbergen, anomalous poles 8=50224
  - magnetic bed, residual magnetization change occasioned by explosion 8=50220
  - magnetite, at margins of crystallites. domain struct. behaviour 8=50225
  - magnetite, single domain, in pyroxene grains, rel. to total thermoremanence 8=50230

Rock magnetism—contd
  magnetometers, spinner, static charge elimination 8=50231
  marine anomalies, reversals, floor and continent movements 8=36899
  Maringouin formation, New Brunswick, diagenitic remanent magnetization of samples 8=32373
  mid-Atlantic Ridge crest anomalies form., dyke injections scatter 8=28016
  mineral, anomalously magnetic, in mag. props. 8=31595
  Monteregian Hills, paleomagnetism, new results 8=36895
  Pacific, anomalies and sea floor spreading 8=36896
  paleomagnetic field intensity, outline from 25 × 10^{-9} yr to present 8=28017
  paleomagnetism, book 8=45574
  palaeomagnetism, palaeozoic 8=45572
  Palaeozoic palaeomag. poles for Europe, synthesis and reliability of data 8=28015
  Pliocene basalts from S.W. U.S.A. 8=32371
  pyrrhotite samples, mag. phases 8=50222
  ridge, mid-oceanic, simulation of linear anomalies by dyke injection 8=36900
  suggested rotation of New Guinea 8=32372
  surveys spectral analysis and Carlsberg Ridge anomalies 8=28018
  Talchir series in central Indra, mean magnetization dirn 8=50219
  thermally activated mag. viscosity in multidomain particles of ferromag. subst., theory 8=50226
  volcanic rocks, tertiary, remanent magnetization rel. to paleo-intensities of geomag. field 8=45573
  volcanics of Reunion Island, palesmag. obs. 8=50221
Rockets
  Ablestar, orbital period increases (1966) 8=41483
  data handling system for solar X-ray meas. 8=50445
  E-region electron temp., rocket obs. 8=41444
  exhaust, drag coeff. small spherical particles 8=30569
  exhausts, i. r. radiant heat transfer from H_2O, CO_2, CO and C mixtures 8=41482
  high altitude obs. of electron density profiles in magnetosphere 8=50166
  in ionosphere D-region, meas. of height distrib. of electron density 8=32327
  laser beam attenuation and polarization rotation meas. through rocket plumes 8=50234
  motor chambers and exhaust plumes, meas. of gas and particle temps. 8=32977
  Nike Apache, D-layer sunrise electron obs. 8=27988
  orbiting Jupiter, difficulties 8=28021
  polarization analyzer, far u.v., for rocket use 8=41486
  Saturn auxiliary solid fuel motor exhaust, spectral radiance obs. 8=38815
  scale model exhaust, spectral radiance props. 8=38815
  space-propulsion systems, analysis of gascore reactors 8=47388
  for space research, review of technology 8=32380
  v.l.f. Doppler expt. for rocket obs. of ionosphere 8=45537
  [OI] 5577 Å emission and continuum at 5300 Å in night airglow, rocket obs. 8=45499
Rotating bodies
    See also Angular velocity measurement; Centrifuges; Earth/rotation; Gyroscopes.
  discs solid or with central hole, plastic deformation for work hardening materials 8=26762
  paraboloidal mirrors made by rotation method, surface shape investig. 8=46659
  precession types in rotary motion of rigid body 8=23817
  rigid, geometrical vector representation 8=32700
  satellite, magnetized equatorial, motion about own centre of mass 8=45579
  satellite, symmetric, in elliptic orbit, altitude instability 8=28022
  δ Scuti variable star, pulsation limitation 8=45687
  solid with fluid field cavity 8=46018
  sphere, deformation soln. 8=32698
  wheel, elastic, lateral force property in presence of thrust, exptl. study 8=41644
Rotation, molecular. See Molecules/rotation.
Rotatory power, dispersion. See Optical rotation.
Rubber
  chloroprene-vulcanizate blocks, crystalline structures 8=26145
  compression of cylinders by end loads, stability 8=44610
  crystallization in extension, kinetics 8=39683
  crystallization, stress-induced, light scattering obs. 8=39682
  dielectric props. and molec. struct 8=31425
  elasticity, eqn. of state 8=26858
  elastomers, fatigue fracture rel. to loading history 8=31178
  equilibrium compression, stress/strain relations 8=31251
  friction, effect of load on temp. and velocity depend. 8=31252
  gasket sizing and shaping technique 8=45932
  latexes, light diffr. 8=48237
  magnets, ferrite-loaded, props. 8=24111
  membrane permeability, elongation dependence 8=44397
  porous, axial compression of cylinders in torsion 8=31253
Rubber—contd
  vulcanizates, natural, filled with carbon black creep behaviour 8=26860
Rubidium
  atoms in flames, quenching of excited 5^2P atoms 8=34150
  atom reactions with Cl_2 in crossed beams 8=49875
  atom scatt. on Kr, total scattering cross sections 8=34178
  atom, time dependence of quantum-state amplitudes 8=38710
  atomic beams, reactive scatt. with oriented CH_3I 8=47728
  atomic clock as frequency standard 8=45958
  distribution between potassium feldspar and plagioclase simultaneously crystallized at 600°C 8=36627
  equation of state, theory, and calc. of thermal parameters 8=30973
  films, LEED exam 8=48453
  films, vacuum-condensed, photoelec. props. 8=44944
  fluorescence, quenching cross-sections, determ. by flame tech. 8=29617
  inert-gas collision excitation transfer cross-section calc. 8=47543
  isotope distrib. in p-reactions on U, Th, Ta 8=34001
  jet atomic clock, optical pumping 8=47525
  liquid near melting point, meas. 8=30421
  melting curve up to 80 kb 8=34961
  metal, indirect nuclear interactions, theory 8=43937
  optical pumping in weak mag. field 8=38709
  resonance radiation, quenching by gases 8=29626
  solar photosphere, abundance obs. 8=45894
  thermoreflectance spectrum in visible and near u.v. region 8=41101
  vapour, photoionization absorpt. continua 8=29973
  Rb^{85} vapour, double-quantum resonant, light beam modulation 8=37629
  $Rb^{85,87}$ atom g_J ratio meas. by optical pumping 8=38734
  $Rb^{85,87}$ atom, $8^2P_{3/2}$ state hyperfine structure and lifetime 8=34149
  $Rb^{85,87}$ hyperfine structure and lifetime of $7\,^2P_{3/2}$ state 8=34151
  Rb^{87} atom, light shift following optical pumping 8=38708
  Rb^{87} maser, theory rel. to relax. times 8=24266
  Rb^+, diff. in $LiSO_4$, 590-820°C 8=39977
Rubidium compounds
  halides, neutron irrad., rare-gas diffusion 8=40079
  K_2Rb_2 photon interactions, 3000-1100Å, spectral range, u.v. cross section obs. 8=43315
  $RbAg_4I_5$, ht. of formation 8=48396
  $RbAg_4I_5$, Ag diffusion rel. to high-conductivity in solid electrolyte 8=48787
  $RbBiF_3$ mag. props. meas. in strong pulsed fields at 4.2 and 77°K 8=40844
  RbBr-CsBr system, phase diagrams and comp. of phases 8=35096
  RbCl beam, state selection and focusing 8=38964
  RbCl crystal, phonon scatt. by U centres, thermal conductivity meas. and theory 8=44301
  RbCl, K-absorption, stress-induced effects 8=41132
  RbCl-CsCl system, phase diagrams and comp. of phases 8=35096
  $RbClO_4$ in dioxane-water mixtures, conductance meas. at 25°C 8=41274
  $RbCoF_3$, spin-density space oscills. and hyperfine interaction, from n.m.r. 8=31917
  RbF, electron irrad., colour centres. obs. with oven cryostat. 8=48880
  $Rb^{85}F^{19}$, h.f.s., Stark and Zeeman effects 8=25514
  $RbFeF_3$, Fe^{57} hyperfine structure from Mossbauer effect 8=31795
  $RbFeF_3$, : Fe^{2+} octahedral, magnetically induced elec. field gradients Mossbauer determ. 8=31794
  RbH_2AsO_4, crystal lattice parameters, temp. depend. and thermal expansion anisotropy 8=44348
  RbH_2AsO_4, n.q.r. spectra, rel. to temp. 8=41009
  RbH_2PO_4 crystal for laser freq. doubler 8=37557
  RbH_2PO_4, crystal growing, static method, optimal conditions 8=44142
  RbH_2PO_4, dielec. and electromechanical props. near phase transition 8=27275
  RbH_2PO_4, dielec. props. near phase transition pt. at u.h.f. 8=40617
  RbH_2PO_4, optical detection on laser illumination 8=45203
  RbI, crystal dislocations, selective etchant 8=31087
  RbI, dislocation pinning by lattice defects 8=26680
  RbI, F-centre form. by u.v. irrad. 8=44479
  RbI film, reflection and absorpt. spectra in u.v. 8=32025
  RbI, Schottky defect formation energy, from dissolution of impurity containing precipitates 8=35536
  RbI-AgI, high-cond. solid systems 8=48396
  RbI: Tl, exciton induced luminesc. in activator centre 8=26506
  $Rb_2MnCl_4 . 2H_2O$, nuclear spin-lattice relax. of several nuclei 8=31916
  $RbMnF_3$, absorpt. spectra of Mn^{2+} 8=41109
  $RbMnF_3$, broad-band fluorescence rel. to temp. 8=49811
  $RbMnF_3$ dielec. props. 8=40584
  $RbMnF_3$, fine structure in $^6A_1 \rightarrow {}^4T_1(^4G)$ obs.
  $RbMnF_3$, inelastic n. scattering near Neel pt. rel. to spin fluctuations 8=31796
  $RbMnF_3$, i. r. transmission spectra 8=27600

Rubidium compounds—contd
  - $RbMnF_3$, magnon-magnon interactions evidence 8=40875
  - $RbMnF_3$, nucl. and electronic spinwave excitation by parallel pumping 8=31835
  - $RbMnF_3$, spin correlations in paramag. state 8=49484
  - $RbMnF_3$: F^{19}, nuclear acoustic resonance, dispersion mode saturation 8=41000
  - $RbMnF_3$:Nd^{3+}, luminesc. anomalies near antiferromag. ordering temp. 8=32057
  - $Rb_2Mn_2(SO_4)_3$, langbeinite structure, growth and electro-optical props. 8=39678
  - $RbNO_3$ molten, optical determ of thermal cond. 8=39255
  - $RbNO_3$, phase diag. in 200-330°C and 0-1500 atm. range 8=39469
  - Rb_2NaTF_6, (T = Yb, Er, Ho, Y, Tb and Sm), crystal structure 8=44250
  - $RbNi_{1-x}Co_xF_3$, mag. and optical props. 8=49555
  - $RbNiF_3$, electron-magnon interaction, effect on absorption band 8=41127
  - $RbNiF_3$, high press. phase transform. and mag. susceptibility 8=48661
  - $RbNiF_3$, mag. structure 8=31737
  - $RbNiF_3$, magneto-optical and n.m.r. studies 8=32023
  - $RbNiF_3$, n.m.r. rel. to exchange interaction exam. 8=41001
  - $RbNiF_3$. spin-ordering on Ni ion substitution 8=31738
  - RbO_2, phase transforms and crystal structures 8=26075
  - Rb_2PtCl_6, luminesc. 8=36505

Ruby
  - coherent radiation from crystal, effect of parameters of pumping light source and discharge regime on output 8=24330
  - conductivity, electrical 8=49338
  - electrical conductivity, 20-850°C 8=27236
  - e.p.r. line broadening, inhomogeneous 8=49597
  - e.p.r. of Cr ion-paris, exchange-coupled, in excited optical state 8=31859
  - e.p.r., pseudo-Stark components widths rel. to appl. elec. field, ≤1400 kV/cm 8=31850
  - ferromagnetic interactions 8=49580
  - fluorescence dosimeter for pulsed ionizing radiation 8=45258
  - fluorescence, spatial distribution. R-line quantum efficiency 8=42101
  - frequency shifts, time-dependent, in pulsed laser spectroscopy 8=42054
  - growth from tungstate melts, morphology and optical props. 8=39648
  - laser, and Nd, beam superposition in freq. mixing 8=24333
  - laser at 78°K, generation threshold and axial mode distrib. 8=37601
  - laser, axial mode discrimination calc. 8=33197
  - laser, axial mode separation, generation kinetics and emission spectrum 8=24334
  - laser. coherence function determ. from diffraction 8=37607
  - laser crystal thermal deform. 8=24335
  - laser damage associated with liq. Raman freq. changer 8=42108
  - laser, defects, influence on radiation characts. 8=42105
  - laser, energy of giant pulse, dependence on crystal temp. 8=24329
  - laser excited, photon echoes irrad. intensity depend. and echo dephasing model, obs. 8=36321
  - laser, giant pulse production 8=42102
  - laser, giant pulsing, new method 8=37606
  - laser, in constant resonator Q mode, generation energy and threshold, engineering evaluation 8=42107
  - laser, internal scanning rel. to time charact. improvement 8=46611
  - laser light scattering exam., 8=41058
  - laser light, second-harmonic generation in Ag 8=27548
  - laser, limitation by adiabatic crystal heating 8=37602
  - laser loss meas. 8=28703
  - laser μsec pulse production 8=42114
  - laser, nanosec. pulse production 8=42106
  - laser, oscillation characts. by interaction between two lasers 8=42103
  - laser, passive Q-switched, rooftop prism cavity, single mode beam 8=46606
  - laser pulse, excitation of organic crystal solns. 8=30479
  - laser, pulsed passive optical shutter for reducing fluorescent output 8=24328
  - laser, pumped by Ar ion laser 8=28704
  - laser, Q-modulated, actuated by external signal, time characts. investigation 8=46609
  - laser, Q-switched, periodic pulse generation and diffraction limited osc. 8=28702
  - laser, Q-switching by natural chlorophyll and effect of solvents 8=33199
  - laser, Q-switching speeded by rotary prism 8=24332
  - laser, radial temp. distribution during pumping 8=39909
  - laser, relation between total energy and Q-switching time 8=24338
  - laser resonator filter, loss calc. 8=37603
  - laser, ring, for ultrashort pulses 8=33200
  - laser, self-Q-switching 8=37604
  - laser, single mode generation 8=33196
  - laser, single-mode giant-pulse 8=46607
  - laser, single pulse spectrum 8=42104

Ruby—contd
  - laser, time depend. of spectrum of modes 8=46610
  - laser, undamped regular spiking, in misaligned cavity 8=37605
  - laser with external tilted mirrors, field genesis and structure 8=37608
  - laser, with spatially homogeneous inverse population, generation kinetics, radiation spectrum and direction 8=46608
  - lasers, Q-switching by pheophytin and its derivatives 8=46605
  - light scatt. for quality evaluation 8=45170
  - maser preamplifier for e.p.r. spectrometer 8=33146
  - optical cooling by transfer of energy into atomic vibration 8=39900
  - optical props., effect of γ-radiation 8=41054
  - paramagnetic resonance of Cr^{3+}, non-linear elec. -field effects 8=40906
  - piezospectroscopic studies of exchange-coupled Cr^{3+} pion pairs 8=27646
  - population inversion and pumping absorpt. power 8=24331
  - R-line quantum efficiency and spatial fluorescence distribution 8=42101
  - spin-lattice relaxation and effect of Cr distribution on spin-lattice interaction 8=49621
  - synthetic, Cr nonuniform distribution, causes 8=40011
  - vapour scintillation, emission spectrum time scanning 8=34231
  - Al^{27} n. m. r. structures under dynamic nuclear polarization 8=45111
  - Al^{27} nuclei dynamic polarization by e reservoir temp. transfer, 1. 8°K 8=31892
  - with Cr > 1%, e.s.r. 8=49598
  - Cr^{3+} pair, mag. resonance, elec. field effects 8=40904
  - Cr^{3+} relaxation time, influence of impurities 8=40915
  - Cr^{3+} and Al^{27} in ruby, electron and nuclear paramag. acoustic absorption at 4. 2°K 8=40914
  - TiO_2 doping, reduction of laser prod. damage 8=33198

Russell-Saunders coupling. See Atoms; Spectra/atoms.

Ruthenium
  - electrolytic deposits, internal tension rel. to current density and metal conc. in electrolyte 8=36610
  - filter to select $AgK\alpha_2$ rad., appl. to topography 8=35306
  - surface structs., He field-ion microscopy, comparison with Re 8=26105
  - on $Fe(OH)_2$, ions and colloids sorption, obs. 8=44073
  - Ru^{99} in Ni, hyperfine fields at solute 8=40992

Ruthenium compounds
  - nitrosylrothenium, sorption on $Fe(OH)_2$ of ions and colloids, obs. 8=44073
  - Ru complex, tetraphenyl arsonium tetrachloro cis-diaquo ruthanate monohydrate structure 8=35351
  - Ru diethyldithiocarbamate and nitrosyl salt crystal and mol. structure 8=26375
  - Ru(II) complexes, absorpt. and luminesc. spectra 8=32027
  - Ru-Rh-Pd-Ag: Fe, resistivity, 1. 5-40°K 8=31328
  - $RuBr_6^{3-}$ complexes, mag. circular dichroism 8=49730
  - $[RuBr_2(CO)_3]_2$ crystal and mol. structure 8=26438
  - $RuNO(OH)(NO_2)_2(NH_3)_2$, crystal structure 8=26439
  - RuO_2, rutile structure, de Haas-van Alphen effect meas. 8=27382

Rutile. See Titanium compounds.

SC (sudden commencement). See Magnetic storms.

S-matrix theory
  - See also Dispersion relations.
  - analytic props. from causality conditions in interactions 8=29046
  - approximate formulation using direct mathematic methods 8=46840
  - bubble diagrams, singularity props. rel. to scatt. amplitudes 8=24491
  - causality groups, Zeeman and complex 8=33584
  - classical and quantum, in Born-Infeld two-dim. field model 8=46826
  - crossing-symmetric eqns., solns. proved by fixed-point theorem 8=42415
  - cluster decomp. in time separated non-relativistic scatt. expts. 8=28944
  - in 8-dimensional space by combining isotopic and Minkowskian space-time 8=47025
  - elements, determinantal method generalized to continuous eqns. 8=29063
  - forward scatt. amplitude reconstruction 8=24672
  - functional formulation, quasilocal terms 8=37757
  - functional, generalization for vector field with mass 8=37758
  - general analyticity struct., test using two-nucleon interact. 8=24866
  - high energy behaviour of scatt. amplitudes 8=33590
  - highly absorptive resonant wave, applic. to π-N 8=24664
  - invariant in generalized free field and Zachariasen model 8=28957
  - multichannel analytical properties on impulse complex plane 8=47032

S-matrix theory—contd
N-body problem, equal mass with δ-function interaction 8=29061
nucleon scatt., many-body theoretical calc. 8=33977
nucleon scatt., R-matrix and eigenchannel calc., comparison 8=42414
parametrization in nonorthogonal basis 8=29064
partial harmonics construction for central interact. 8=29062
perturbation expansion, elmination for Klein–Gordon double terms 8=37767
physical, connection between singularities with non-relativistic quantum field matrix elements 8=37759
poles, correspondence to unstable particles 8=33552
potential many-channel scatt., construction 8=29057
potential scattering, rel. to calculations based on Calogero's equation, unitarity 8=33339
production amplitude theorem for scatt. with isotopic spin 8=24665
Pugh eqns. derived 8=24486
quantum electrodynamics, comparison with perturbation calc. 8=24487
Regge pole discussion of S-matrix element behaviour 8=37906
relativistic in terms of wave functions 8=47031
scatt., non-relativistic, single-channel, Mandelstam symm. 8=24663
semi-classical approx. rel. to tree approx. 8=24492
singularities, sheet struct. and multiparticle amplitudes 8=24668
of strong interactions 8=37872
transformation and maximum props. rel. to structure and dynamical group of strongly interaction particles 8=37845
unitarity, in diffractional reactions 8=38443
Cu-Mn(Cr) alloy, magnetoresist. calc. using s-d model 8=26965
SU$_3$ group theory. See Elementary particles; Field theory, quantum/interactions, strong; Group theory.
Safety precautions. See Radiation protection.
Sakata model. See Elementary particles.
Samarium
antiferromagnetic props. from mag. moment meas. at 4.2°K 8=31706
ground level h.f.s. Stark effect obs. 8=29602
monochalcogenides, high pressure phase transformations 8=26070
spectrochem. and nephelauxetic parameters 8=43927
trivalent, in oxide glasses, absorpt. and luminesc. 8=36412
Samarium compounds
SmFe garnets, mag. props. from Mossbauer effect, 85-600°K 8=36196
$SmFe_2$, hyperfine field at Fe from Mössbauer effect 8=36146
$SmFeO_3$, mag. reorientation temp., hydrogen ht. treatment effects 8=40876
$Sm_{1-x}Tm_xFeO_3$, antiferromag. props. 78°-500°K 8=31797
Sampling. See Statistical analysis.
Sand
labelling with Cr^{51} 8=50092
quartz, differential thermal analysis, particle size effects 8=26044
-water mixture, rheological behaviour as function of conc. 8=30545
Satellites, artificial
Ariel III, description, orbit parameters, and characts. 8=41438
Aerial III, equipment for terrestrial radio noise survey 8=28026
Ariel III, spin axis direction from glints of solar reflections 8=36902
atmospheric 4.5μ meas., error sources 8=36747
atmospheric surface press. meas. using laser beam 8=45439
calibration target in visible and near i.r., bidirectional reflectance obs. 8=41489
communications in UHF band, scintillation fading out effects 8=45581
cylindrical, internal rad. environment, lab. study 8=32384
Discoverer 36, scintillation of 20 Mc/s radio signals rel. to spread-F 8=32354
dynamics, effect of elasticity 8=41640
earth, r.f. path meas., refraction errors calc. 8=28635
earth, stabilization, mag. and gravit. fields effects 8=32381
for earth's external gravity field determ. 8=27819
by earth's magnetic field, passive stabilization 8=32383
elastic, dynamics 8=45578
electrostatic analyser for 1-100keV particles 8=50241
Explorer 17 Langmuir probe, end effect 8=32320
free fall structure design 8=23818
FR-1, instrumentation 8=45582
geomagnetic field meas., suggestions 8=28004
gravity meter meas., comparison with satellite obs. results 8=50008
grid-sphere, orbital behaviour 8=28024
interference and noise, influence on design of receiving systems at < 50 MHz 8=50240
Satellites, artificial—contd
ionosphere, electron density, by ground-based obs. of radio signals from cosmic vehicles, review 8=41415
ionosphere, F region, electron-ion collision effect on wake structure 8=34443
ionospheric investigation using signals 8=50189
ionospheric, spherical, electrostatic pot-fields and wake 8=41414
at low perigee, for meas. of density variations 8=36767
magnetic analyser for 100keV-1MeV e 8=50242
magnetosphere expts., suggestions 8=32260
magnetospheric radio noise obs. from satellite 8=45496
meteorological, review 8=45438
meteorology, observing techniques 8=36704
movement study by intermediate orbit method 8=50237
motion about own centre of mass, magnetized equatorial 8=45579
motion, rel. to determ. of sectorial harmonics in geopotential 8=28003
Nimbus II, obs. of cloud systems in 7 spectral bands and 4 size scales 8=41338
Nimbus II, obs of sea surface temps. and ocean currents 8=41335
observation methods; visual, radio, radar and optical 8=50238
orbits, circular, stability in planet's gravitational and dipole magnetic fields 8=50236
orbit disturbances due to gravity anomalies anal. integration 8=45580
orbit, near-circular, contraction under air drag, rel. to day-to-night density variation 8=28023
orbits, plane, invariant curves 8=32385
Orbiting Astronomical Observatory, alignment of multi-component optical system to common coordinates 8=42174
OV3-3, electrostatic and e.m. wave detection 8=41490
perturbation methods appl. to resonance 8=32387
perturbation rel. to aerodynamic resistance 8=32386
photographic tracking 8=50235
range-energy spectrometer for 6-100MeV p
rotating, elastically connected rigid bodies, dynamics 8=41487
rotation in elliptical orbit 8=32382
satellite particle detector systems for cosmic rays 8=47183
scintillation spectrometer for relativistic e 8=50243
spectrometers for 100keV-6MeV p 8=50244
spinning, symmetric, in elliptic orbit, altitude instability 8=28022
Sun, crossed by unidentified object August 1966 8=45575
torque in non-inverse square gravitational field 8=32388
tracking, Minitrack system, effect of satellite interference 8=50239
for unknown parts of earth's gravity field from successive passages 8=41315
v.l.f. receiver parameters 8=32264
Scalers. See Circuits; Counting circuits.
Scandium
lattice params. and thermal expansion rel. to para-antiferromag. transition, 20-660°C 8=44253
Sc III spectra, principle series, transition probabilities in doublets 8=47506
Scandium compounds
halides subgroup, molecular vibrational freqs. calc. 8=29761
$(Sc, Er)VO_4$, lattice parameters and Miller indices, using computer programmes 8=44252
ScF_3, vapour press., enthalpies and entropies in range 1050°-1200°C 8=35015
$Sc(Ni_{1-x}Co_x)_2$, n.m.r. line shape of Sc^{45} rel. to impurities and vacancies 8=45133
ScO, red system, rot anal. 8=25518
Sc_2O_3, cryst. struct. 8=48673
Sc_2O_3:Nd^{3+} spectra, Stark splitting scheme and $^4F_{3/2}$ lifetime, 4.2–293°K 8=32017
$ScVO_4$, lattice parameters and Miller indices, using computer programmes 8=44252
$ScVO_4$: Eu^{3+}, luminescence rel. to Hamiltonians at Eu^{3+} site 8=41208
Scattering
alkali-inert gas interatomic pot. from scatt. data 8=47541
atoms, impact parameter treatment 8=38741
atoms in collisions, rel. to cross-section for electronic excitation 8=25387
central scatt. by two-phase systems, theory rel. to distrib. of diluted phase 8=26050
Coulomb functions, phases and amplitudes 8=37751
diffraction of nuclear particles on atomic nuclei, state mixing effect on cross-section 8=38444
diffuse, in crystal, periodic bond chain theory rel. to thermal vibrations 8=26005
Dirichlet, l.f. scalar, by general ellipsoid 8=41636
disortion-operator perturbation theory 8=42314
effect on radiative transfer in medium with absorpt. and emission 8=37227
elastic, from separable non-local potential, rel. to phase shift 8=33337
energetic atoms in gas, energy distrib. 8=36626

Scattering—contd
impact parameter representation, applic. to pot. scatt. and protons on H 8=46821
inelastic, based on microscopic nuclear descriptions, coupled channel treatment 8=47300
inelastic, semiclassical theory 8=46822
inverse, interpolation formulae in angular momentum plane 8=28938
iteration procedure to generate approx. 8=28947
Kondo system, Green's function perturbation technique 8=37755
metals with magnetic impurity, ordinary rel. to exchange 8=26863
molecular cross sections, exptl. determ. 8=29846
Mott, of electrons on Hg atom, obs. rel. to Lin theory 8=34171
multiple coherent, theory verification from Ne excitation expts 8=43224
multiple scatt. on plane layer of matter anal. including slowing down processes 8=40064
multiple turning-point, semiclassical calc. 8=28945
multiple wave theory, soln. of eqns. by smooth perturbation method 8=46001
non-local pots. asymptotic behaviour of phase shifts 8=42782
nuclear, Coulomb interference corrections 8=29389
one-dimensional, in configuration and momentum space, teaching film 8=37754
optical theorem in theory of multiple wave scatt. 8=37119
phase shifts calc. for spherically symmetric potentials 8=37753
polarization waves in liquids, exciton theory 8=34754
potential, angular momentum continuation of radial s-wave function 8=24468
potential many channel, construction of V, S matrices 8=29057
pot. nonrelativistic, Regge-pole analysis 8=28943
potential, nuclear Hartree-Fock spectra 8=25106
pot., singular, attractive, leading to nonself-adjoint Hamiltonians 8=33335
pot., values at origin in terms of S-wave phase shift and bound-state parameters 8=33330
pressure broadening of rot. and vibr.-rot. transitions 8=47558
quantum mechanical foundations 8=29395
radiant heating of an absorbing and scattering slab 8=46228
radiation, multiple, equivalence of isotropic and mono-directional source problems 8=36744
in radiative transfer, eqn. 8=32860
Raman, by polaritons 8=41032
Regge-type representations for Yukawa pot., partial-wave amplitudes 8=33595
resistivity anomaly due to mag. impurities, effect 8=44673
S matrices, classical and quantum in Born-Infeld field theory 8=46826
S matrix cluster decomp. in time separated non-relativistic scatt. expts. 8=28944
S-matrix, functional, generalization for vector field with mass 8=37758
S-matrix theory, functional formulation, quasilocal terms 8=37757
scalar massless waves on Schwarzschild singularity 8=36929
Schrodinger eqn. with singular pot. 8=28946
for Schrodinger operator in exterior domain, scattering 8=33336
time delay, collision lifetime matrix 8=41947
time correl. function formalism 8=29386
two-body collisions, method of moments 8=46820
2-body, non-local factorizable potential, with and without Coulomb repulsion 8=37752
yakawa potential, relation between scatt. amplitude for imaginary ang. mom. and pot 8=33571
II-VI crystals, of polaritons by phonons, rel. to absorption of light waves 8=27533
Rh-Fe, magnetic impurity, ordinary rel. to exchange 8=26863
acoustic waves
Brillouin, sound absorpt. effect on hypersonic vel. meas. 8=32912
cylinder containing one fluid and surrounded by another, creeping-wave analysis 8=32911
deep sea bed, backscatt. at small grazing angles 8=50098
by ground inhomogeneities of ocean bed 8=50106
moving elastic nonlinearity, Doppler effect 8=46192
shadow zone below isothermal layer 8=46193
by spheroid penetrable, exact soln. 8=23962
underwater explosion, reverberation meas. 8=50099
acoustic waves, ultrasonic
grains in polycrystalline aggregate, var. with elastic wave velocity 8=30936
Al cylinder, solid, circumferential waves 8=37268
electromagnetic waves
by atoms rel. to reson. radiation transfer 8=29635
backscatter ionospheric sounding, field strength 8=50190
backscattered by finitely cond. curved surface, depolarization 8=24228
backscattering, ionospheric, role of land and sea 8=27977

Scattering—contd
electromagnetic waves—contd
bistatic microwave probing of refractively perturbed clear atmos. 8=32254
Brillouin, in plasmas, applic. to ionospheric irregularities 8=41429
conductor, arbitrarily shaped, moving rel. to source 8=46487
conformal mapping application 8=37488
correlated signals from uncorrelated scatterers 8=37502
dielectric objects inhomogeneous along radius and angular coordinates, back scatter. cross sections 8=42021
electron wave eqn., Volkov soln. appl. 8=33633
in ferromagnetics, by sound, rel. to magneto-elastic coupling 8=40796
by free electron, effect of constant uniform mag. field 8=24726
by free electrons, freq. shift, quantum theory 8=42020
h.f., by impenetrable sphere 8=37501
in irregular media, multiple, statistical calc. 8=46485
Moon, radio scattering cross section, models in optical range 8=45803
non-linear, by plasma cylinder 8=39093
non-uniform e.m. field on any object 8=33133
particle, moving, theory 8=37496
plane monochromatic, by rough surface, statistical props. 8=24230
plasma, alkali, acoustic wave coherent forward scatt. microwaves 8=43536
plasma columns, field calc. 8=39107
plasma cylinder, inhomogeneous 8=25753
from plasma cylinder, inhomogeneous collisionless 8=39100
plasma cylindrical columns, field aligned homogeneous 8=30056
plasma ellipsoid, inhomogeneous 8=30072
plasma, inhomogeneous cylinder 8=47844
by plasma jet 8=47895
plasma, piece uniform with zero layer 8=30071
plasma, Thomson scatt., continuum theory 8=39091
on plasma turbulent oscillations 8=47881
plasma, warm enclosed cylindrical, calc. 8=47835
radio waves, MF-HF band, by method glacier surface 8=24209
reduction to potential theory 8=37499
ring laser, field spatial distribution rel. scatt. mechanism 8=42073
rough boundary between dielec. media 8=37498
from rough surface, freq. and spatial correl. 8=24227
slots on a sphere, scattered field 8=46486
by sphere, anomalous diffraction approx., range of validity 8=28617
by spheres, two perfectly conducting, h.f. method appl. for $r \geqslant \lambda/2$ 8=24229
spherical conducting shell with conical hole 8=37500
stratified bodies, invariant imbedding calc. 8=37497
troposphere, wind produced Doppler shifts 8=27921
two-dimensional, theory, advances 8=46464
Venus, backscatt. rel. to surface smoothness, 40 cm 8=45825
VHF propag. in Himalayan region, terrain scatt. 8=24250
v.l.f. radiowave scatt. in curved earth-ionosphere waveguide 8=27975
light
See also Diffusion, light; Raman spectra.
acetone, ruby laser emission, large-angle 8=48158
aerosols, backward scattering of laser radiation optical thickness dependence 8=34949
alkanes, gaseous depolarization meas., 8=43694
amplitude, exact near field, and evanescent waves 8=37696
aniline, thermal shear waves, depolarized doublet obs. 8=43817
antiferromagnet, spin-wave stimulated second-order Raman scattering 8=31944
atmosphere, at small angle distances from sun, spectral studies 8=50152
atmosphere, (semi-infinite) new formulation of Chandrasekhar's scatt. matrix 8=50119
in atmospheric surface layer, phase function 8=32241
benzene derivatives, liq., spectrum of depolarized light 8=34849
benzene, ruby laser emission, large-angle 8=48158
benzene, stimulated temp. scatt., obs. 8=30481
benzol, double, near critical point 8=48147
in binary mixtures, by fluctuations of conc., inelastic rel. to photon beating 8=25918
in birefringent media, Brillouin 8=27537
Brillouin, in maser molecular spectroscopy 8=38782
Brillouin, measurement of damping of hypersonic waves in solids, laser source 8=49686
Brillouin, stimulated, large and small angle, threshold condition 8=34661
Brillouin, stimulated thermal, obs. 8=28649
carbon black, struct. determ. 8=43885
chemically reactive fluid 8=32090
cholesteryl 2-(2 ethoxyethoxy) ethyl carbonate liquid crystal, Brillouin scatt., 20-60°C 8=48146
chlorobenzene, stimulated Mandel'shtam-Brillouin scatt. threshold, 0.35, 0.69 and 1.06μ 8=32032

Scattering—contd
- light—contd
  - cholesterol-type liq. cryst. 8=25882
  - Christiansen filter shape and bandwidth calc. 8=37665
  - from clouds, Monte Carlo calcs. 8=36741
  - from clouds, radiant intensity 8=32226
  - clouds, reflected and transmitted light, effect of particle size distribution 8=41367
  - coherent multiple scatt., effect on spectral line shapes 8=25403
  - colloidal electrolytes 8=43890
  - in coronograph objective, laboratory meas. 8=45921
  - critical opalescence in elec. field, relax times 8=30473
  - critical opalescence of dipolar mixtures, elec.-field effect 8=39312
  - crystal with impurity centre, Raman, density matrix method considerations 8=45249
  - crystals, ionic, thermal, rel. to defects 8=41034
  - diffuse galactic radiation, by interstellar dust 8=28092
  - diffuse, of laser radiation, rel. to space freq. spectrum of granulation 8=42256
  - diffuse, reln. with particles of subst. 8=46737
  - 2-dodecylaminoethanol salts, effect of counterions on micellar props. 8=39290
  - elastic second harmonic scatt., spectral widths 8=25917
  - by electron in refracting medium, inducement of additional photon 8=37937
  - by eye protection filters, meas. and characts 8=28922
  - ferroelectric ceramic, coarse-grained, Rayleigh scatt., polarization dependence 8=45151
  - films, thin luminesc., prep. and props. 8=36454
  - fluid, opalescent, double-scatt. spectrum 8=39152
  - gases, molecular collision-induced 8=30474
  - gases, monatomic, kinetic theory 8=25829
  - glass, K-8 silicate, stimulated Mandel'shtam–Brillouin scatt. threshold, 0.35, 0.69 and 1.06μ 8=32032
  - helical macromols. in soln., size and shape determ. 8=30420
  - hexane, stimulated Brillouin scattering, anti-Stokes components origin 8=25922
  - holographic imaging through scatterers 8=24435
  - hyperchromism, two-band model 8=39365
  - incoherent, scatt. and transmission functions, calc. 8=42257
  - incoherent scatt. by atomic e, spectral line form., parametrized models 8=43168
  - inert gases, Rayleigh light press-induced depolarisation 8=39217
  - instrument for meas. 8=42181
  - intensity vs. angle curves, corrections 8=37697
  - interaction of self-trapped laser beams 8=28877
  - interstellar dust, rel. to diffuse galactic light 8=45730
  - isobutyric-acid-water system, diffusion coeff. obs. near critical soln. conc. 8=39341
  - isotopic dielectric crystal, Rayleigh 8=41033
  - by large submicron cylinders, perpendicular and oblique incidence, meas. by photometer 8=24361
  - laser beam, by bound electrons into their natural frequency 8=42259
  - laser, Doppler shift meas. of turbulent velocities 8=39272
  - laser, higher-order elastic scatt. in dense isotropic media 8=34223
  - laser radiation, backward, from smokes and fogs, optical thickness dependence 8=34949
  - latex hydrosols, coherent and incoherent light 8=34932
  - from lenses and mirrors, limitation imposed on daytime astrometry 8=50271
  - liquid and gas mixtures rel. to mol. correls. 8=34663
  - liquid and gaseous media, Brillouin and Raman effects stimulated in emission and absorpt. 8=48155
  - liquids, combination meas. using standard, line intensity determ. 8=43808
  - liquid crystal, Brillouin scatt., 20-60°C 8=48146
  - liquid films, by spontaneous thickness fluctuations 8=48051
  - liquids, fluctuation theory 8=30475-6
  - liquid mixtures, above and below crit. soln. temp. 8=39371
  - liquids, molecular collision-induced gases 8=30474
  - liquids, molecular, rel. to nonlinear refractive index 8=43815
  - liquids, Rayleigh wings and Brillouin stimulated scatt. obs. 8=39364
  - liquids, spectrum of depolarized light 8=34849
  - liquids, stimulated scatt. transverse to laser beam 8=39366
  - liquids, thermal shear waves, depolarized doublet obs. 8=43817
  - liquids, vertical diffusion meas. 8=43791
  - magnetic crystals, theories 8=36297
  - magnetic dielectrics near phase transition of second kind 8=36301
  - methanol-cyclohexane mixtures, above and below crit. soln. temp. 8=39371
  - microstructure of media particles 8=46736
  - mixtures, forced Raman scatt., line intensity 8=29678
  - molecules, double quantum scatt. 8=25400
  - monodisperse rigid rods, spectral distrib. 8=39362
  - multiple, coherent radiation by nonabsorbing aerosol, lab. meas. 8=42258

Scattering—contd
- light—contd
  - multiple, equivalence of isotropic and monodirectional source problems 8=36744
  - multiple, theory 8=24422
  - narrow beams, single scattering theoretical formulae validity from expts. with disperse systems 8=28874
  - n-nitroaniline, cryst., Fermi reson. in stimulated Raman scatt. spectrum, 77°K 8=41160
  - nitrobenzene, ruby laser emission, large-angle 8=48158
  - nitrobenzene, thermal shear waves, depolarized doublet obs. 8=43817
  - m-nitrotoluene, thermal shear waves, depolarized doublet obs. 8=43817
  - non-coherent, by dust particles in astronomical spectra effect of continuous absorption on spectral line formation 8=50337
  - nonionic detergent in aq. soln., micellar props. 8=30559
  - opalescence, critical surface 8=25915
  - paper, rel. to halftone reproduction 8=28905
  - parametric, spontaneous, quantum theory 8=27538
  - in planetary atms., anisotropic scatt. 8=45820
  - plant canopy, lab. rel. expt. rel. to theory 8=46735
  - plasma, coherent, for e density profile 8=30082
  - from plasma in solid, effect of band nonparabolicity 8=45152
  - poly-L-alanine spherilites, patterns 8=41175
  - polyethylene, multiple-order scatt. rel. to spherulite lamellae twisting 8=45246
  - polymer films, by ringed spherulites, multiple-order scatt. 8=45246
  - polymers in binary mixed solvents 8=30472
  - poly(methyl acrylate)in ethyl acetate rel. to mol. wt. and dimens., obs. 8=43773
  - poly(α-methylstyrene), effect of mol. wt. heterogeneity on 2nd virial coeff. 8=48152
  - polypropylene, cryst. 8=49783
  - polystyrene, aq. suspension, angular distribution 8=25964
  - polystyrene, cryst. 8=49783
  - polystyrene latex suspensions rel. to particles refr. index, 589, 546 and 436 mμ 8=34934
  - (1:1)poly(styrene-co-methyl acrylate in ethyl acetate rel. to mol. wt. and dimens.. obs. 8=43773
  - polyvinyltoluene aq. suspension, angular distibution 8=25964
  - in pyridine-alcohol solns., rel. to intermolec. interacts. 8=34857
  - in pyridine-paraffin solns., rel. to intermolec. interacts. 8=34857
  - quartz, cryst., stimulated Mandel'shtam–Brillouin scatt. threshold, 0.35, 0.69 and 1.06μ 8=32032
  - quartz, fused and cryst., stimulated Mandel'shtam–Brillouin scatt. and laser prod. damage, 300°K 8=32031
  - quartz, stimulated Mandel'shtam-Brillouin, elastic nonlinearity effects 8=41036
  - quinoline, thermal shear waves, depolarized doublet obs. 8=43817
  - Raman effect induced by optical pumping 8=43207
  - Raman, laser-excited rotation-vibration, in ultra-small gas samples 8=29683
  - Raman spectra, antisymmetric tensor, obs. 8=25398
  - Raman, spontaneous, partial coherence possibility 8=38778
  - from Rayleigh atmos., effect of specular reflection at ground 8=32242
  - Rayleigh, correlation theory 8=24423
  - Rayleigh, finite-size effects, obs. 8=39219
  - Rayleigh, in maser molecular spectroscopy 8=38782
  - Rayleigh scatt. from real chain mols. 8=47732
  - Rayleigh-Cabannes, in dry air, depolarization meas. 8=30301
  - reflection from scatt. medium 8=42242
  - rubber, rel. to stress-induced crystallization 8=39682
  - ruby crystals, of laser light 8=41058
  - ruby, quality evaluation 8=45170
  - second harmonic, in dense isotropic media rel. to mols. moments and cowels 8=34222
  - semiconductors, by charged centres 8=36361
  - single scattering theory, with and without secondary scatt. considerations 8=28875
  - spectral line formation by noncoherent scatt. 8=37232
  - sphere cross-section meas. by Fabry-Pérot resonator 8=33282
  - spheres, m≃1, obs. 8=24420
  - by spherical liq. droplets using computer-synthesized holograms 8=34848
  - in spherical nebulae, modeling with digital computer 8=36962
  - spherulite, radial, Rayleigh-Gans scatt. 8=36447
  - spurious obs. in u.v. instruments 8=28807
  - in stellar atms. and rel. to novae theory, nonstationary scatt. 8=28039
  - stimulated combinational in resonators 8=46564
  - stimulated Mandel'shtam-Brillouin elastic nonlinearity effects 8=41036
  - stimulated temperature (entropy), theory 8=24424
  - styrene-methyl methacrylate random copolymers, dilute solns. 8=39323
  - submicroscopic particle, obs. 8=39446

Scattering—contd
  light—contd
    Thomson, toroidal discharge conductivity meas. 8=29878
    time delay, collision lifetime matrix 8=41947
    toluene, ruby laser emission, large-angle 8=48158
    toluene, stimulated Brillouin scattering, anti-Stokes components origin 8=25922
    transient signals in turbid medium 8=30558
    trimethylene sulphide, $(CH_2)_3S$, crystals, Raman, and i.r. absorpt. spectra 8=41171
    tropospheric, of twilight N_2^+ emission, model 8=41365
    turbid medium illuminated by narrow beam, field 8=24421
    underwater optics, S/N concept 8=37695
    u.v., rough and smooth surfaces, 1216Å 8=37698
    water droplet evaporation rate determ. 8=39484
    water, fluctuation theory 8=30476
    water, optical back scatt. from single droplets 8=27916
    water, ruby laser emission, large-angle 8=48158
    water, stimulated Mandel'shtam-Brillouin scatt. threshold, 0.35, 0.69 and 1.06μ 8=32032
    o-xylol, ruby laser emission, large-angle 8=48158
    by Ar plasma jet, Thomson and Rayleigh, rel. to electron density determ. 8=34517
    Ar, Rayleigh light depolarisation, 15-1500 bar 8=39217
    $BaTiO_3$, Raman, resonant interference between one
    Bi-Ga, liq., critical opalescence, temp. depend. 8=48149
    Bi-Zn, liq., critical opalescence, temp. depend. 8=48149
    CO_2, Rayleigh depolarized, as new probe of intermolecular forces 8=39212
    CO_2, solid, Brillouin linewidths near critical point 8=41069
    CO_2:NO_2 and I_2, gaseous, stimulated thermal Rayleigh scatt., obs. 8=34665
    CS_2, by fluctuations of anisotropy 8=25920
    CS_2, stimulated Brillouin scattering, anti-Stokes components origin 8=25922
    CS_2, stimulated Raman scatt. of quartz M-B scatt. components, 4-photon amplification, obs. 8=43822
    $CaCO_3$ cryst., stimulated Raman scatt., additional anti-Stokes components, obs. 8=41073
    CdS amplifying, Brillouin scatt. meas. showing acoustic freq. spectrum time and field dependences 8=48718
    in CdS, by light, obs. with freq. changes 8=49711
    CdS crystalline powders, Raman, cross section at 293°K 8=45189
    CdTe by screened single-particle e excitations, obs. 8=36363
    FeF_2 rutile antiferromagnet, by spin waves 8=36387
    β-FeOOH rod crysts. suspension, streaming, rel. to particle size, obs. 8=30549
    GaAs, by charged centres 8=36361
    GaAs by screened single-particle e excitations, obs. 8=36363
    GaP crystalline powders, Raman, cross section temp. dependence, 103-723°K 8=45189
    n-GaP, mechanisms, by i.r. absorpt. 8=41090
    Ge, stimulated Brillouin, and intensity limiting 8=45191
    H gas, stimulated, at low press. 8=47971
    H_2, Rayleigh depolarized, as new probe of intermolecular forces 8=39212
    He atom, Rayleigh scatt. and e. m. susceptibility 8=25375
    InAs, from plasma, effect of band nonparabolicity 8=45152
    InP by screened single-particle e excitations, obs. 8=36363
    InSb, from plasma, effect of band nonparabolicity 8=45152
    KCl: Fb, temp. dependence, 128-298°K 8=45207
    KH_2PO_4 rel. to ferroelec. mode temp. depend., Raman scatt., obs. 8=36376
    KH_2PO_4, spontaneous scatt. of intense light, quantum theory 8=27538
    LiF single-crystal centres, Raman spectra 8=49737
    $LiNbO_3$, Raman and Rayleigh, temp. dependence, 90-1100°K rel. to ferroelec. props. 8=27585
    $LiNbO_3$, spontaneous scatt. of intense light, quantum theory 8=27538
    $LiTaO_3$, Raman and Rayleigh, temp. dependence, 90-1100°K rel. to ferroelec. props. 8=27585
    MnF_2 rutile antiferromagnet, by spin waves 8=36387
    N, liquid, stimulated Raman scatt., photon distrib. in Stokes components 8=34855
    N_2, Rayleigh depolarized, as new probe of intermolecular forces 8=39212
    $NH_4H_2PO_4$, c. w. parametric scatt. with strong absorption in idler band 8=36394
    $NH_4H_2PO_4$, parametric scatt., on laser pumping 8=45211
    $NH_4H_2PO_4$, spontaneous scatt. of intense light, quantum theory 8=27538
    N:NO_2 and I_2, gaseous, stimulated thermal Rayleigh scatt., obs. 8=34665
    NaCl single-crystal centres, Raman spectra 8=49737
    NaCl, temp. dependence, 128-298°K 8=45207
    NaCl:Ca, flux temp. dependence, −140 to 150°C 8=32016
    Ne atom, Rayleigh scatt. and e. m. susceptibility 8=25375
    Pb-Ga, liq., critical opalescence, temp. depend. 8=48149
    Rb vapour optically pumped modulation of light beam 8=37629
    SiC, Raman first-order, on laser excitation 8=41139

Scattering—contd
  light—contd
    Xe atom, Rayleigh scatt. and e. m. susceptibility 8=25375
    Xe, depolarization meas., 8=43694
    ZnO, Brillouin, from shear waves in crysts. under high elec. fields 8=44325
  X-rays. See X-ray scattering.
Scattering, particles
    See also Collision processes; Elementary particles; Field theory, quantum/interactions; Nuclear forces; Nuclear reactions; Particle range; Particle tracks; S-matrix theory; and under individual particles, e.g. Alpha-rays.
    absorption model for K* prod. in K^- p, 10 GeV/c 8=33732
    algebra of factorized Regge residues, meson and baryon scale factors 8=42440
    amplitude forward obeys a dispersion relation 8=33576
    amplitude, "little group" decomposition using covariant variables 8=29052
    amplitude, non-oscillation, rel. to sum rules and Regge cuts. 8=33588
    amplitude, relativistic quasipotential type equation 8=37886
    amplitude singularities derived from unitarity rel. to bubble diagrams 8=24491
    analyticity in momentum transfer in pot. theory 8=37832
    by atoms, extended polarization pot. 8=25390
    Bethe-Salpeter eqn. Wick transformation modification with limited detours into complex energy plane 8=29053
    bootstrap hypothesis, Lagragian field theory 8=42444
    bootstrap of vector and tensor trajectories from superconvergence 8=33602
    bootstrap Reggeized, based on finite-energy sum rules and unitarity 8=37912
    bootstrap theories, Regge poles and Argand diagrams 8=42443
    bootstrapping, quark and local current 8=29073
    Born approx., disadvantages of first 8=33587
    causality conditions, analytical props. of S-matrix 8=29046
    charged, in thin monocryst, rel. to spatial regrouping of particle stream 8=40066
    classical, mechanics, relativistically invariant Hamiltonian 8=28249
    collision matrix, unitary pole resonance form 8=24667
    composite, influence of breakup channels 8=43095
    composite particle, generalized Lovelace equation in relativistic Faddeev formalism 8=37890
    composite, strongly interacting, geometrical optics 8=47030
    "Compton", theory of Reggeon Feynman diagrams 8=28964
    conspiracy of singularities in j plane 8=37888
    conspiracy problem, group-theoretical solns. 8=47047
    coupling consts., approximate bounds from analyticity 8=42400
    cross-section relations, systematics from quark model 8=42492
    cross sections and density matrices rel. to kinematical singularities 8=33570
    daughter trajectories, parallel, generation from superconvergence and Regge asymptotics 8=42435
    direct-channel amplitudes, Regge pole contribution 8=33597
    dispersion sum rules for forward scatt., new class 8=42417
    dispersion sum rules for non-decreasing amplitudes 8=24671
    double charge exchange, modified 2π exchange model 8=42408
    elastic, criterion of weak perturbing systems 8=24657
    elastic diffr., real nuclear and Coulomb phases 8=25204
    elastic, large momentum transfer, recurring minima 8=24661
    elastic, lower bound at fixed momentum transfer 8=47026
    elastic, two-particle, centre-of-mass calc. 8=42452
    elastic, unitary resonance form of collision matrix 8=42985
    elastic, upper limit and relation between total cross sections and s-amplitude 8=29055
    emitted by plane δ-source, spatial distrib. Fourier integral evaluation 8=32657
    e.m. polarization expressions 8=24662
    end point method, generalized, albedo problem 8=47379
    energetic, by plasma, distribution function 8=43496
    external, Regge trajectory determ. 8=42438
    Faddeev eqn. for 3-particles identical, with Yukawa pot. 8=33581
    Faddeev equation reduction to multichannel 2-particle Lippmann-Schwinger eqns. 8=29054
    Faddeev eqns., variational approach for three-body problem 8=29056
    fermion Regge poles and ratios between cross-sections of large angle scatt. 8=42441
    finite energy sum rules, misuses 8=37896
    forward matrix amplitude reconstruction 8=24672
    generalized unitarity and low energy theorems 8=37891
    Green's function having multiple poles and Bethe-Salpeter amplitude lightlike limit 8=37887

Scattering, particles—contd
Gribov-Pomeranchuk singularities at values of J with wrong signature 8=24676
Haag's theorem, generalization 8=24654
hadrons, high-energy currents model 8=29105
Hamiltonian, separable iterative method of construction 8=24653
heavy, energy loss correction for multiple scatt. 8=38519
helicity amp., applic. to dispersion relations and Regge-pole models 8=37961
helicity amplitudes kinematical singularities, definition of regularized 8=24658
helicity amps. removal of kinematic singularities and Reggeization 8=42426
helion and triton optical potentials 8=47338
high energy bounds, in Kinoshita-Loeffel-Martin method. 8=33577
high-energy collision theory 8=24656
high energy two-body and quasi-two-body, SU(3) symmetry validity 8=37852
inelastic, expt. energy resoln. and focusing 8=33370
inelastic processes, unitarity for matrix elements 8=37881
inelastic, rel. to incident spectrum broadening 8=40795
inelastic, space-time correls. in intensity, rel. to scatterer 8=43215
inelastic with secondary particle prod. at high energy. model 8=37889
inverse problem soln., 8=33572
with isotopic spin, proof of neccessity of prod. amplitudes 8=24665
kinetic eqns., quantum, many-particle theory 8=23882
Kohn variational method singularities 8=42403
large-angle elastic, perturbation calc. 8=29569
Lee model with Coulomb interaction 8=47029
Lorentz poles in equal-mass scatt. from analyticity and factorization 8=42416
low-energy, by long-range singular potentials 8=37882
low-energy, dispersion relations for high energy limits 8=37894
Low eqn. in Lee model, N/D solns. 8=47034
Mandelstam cuts, props. deduced from Feynman integrals 8=42424
many-body, analytical continuation under rot. from real to complex 8=29058
Marchenko formalism rel. to N/D eqns. 8=24670
massless, 2-body, analytical props. of helicity amplitudes 8=37910
matrix, in case of arbitrary number of channels, analytical props. 8=47032
Moliere theory improvements for 7°–20°, second approx. 8=47301
multiple, in Gaussian approx., small-angle treatment, systematic, improvement 8=26724
multiple of limited beam on plane layer 8=38446
multiple prod. processes, creation on peripheral trajectories 8=42394
multi-Regge-exchange model, elastic scatt. shadow 8=37883
multi-Reggeon model and Pomeranchuk exchange 8=42437
N-body problem, equal mass with δ-function interaction 8=29061
N-particle production amplitudes, necessity due to S-matrix theory 8=42410
N/D eqns. rel. to Gribov-Pomeranchuk singularity 8=24679
N/D eqns. singular, with vector boson exchange inelasticity, soln. 8=24673
N/D eqns. solved with Born approx. and compared with exact soln. of Schrödinger eqn. 8=33587
N/D in potential scatt. 8=33586
nonanalyticity at u = o in scatt. amplitude 8=33575
non-Regge singularities in helicity amplitudes 8=24676
by nuclei, at high energy, multiple diffr. theory 8=29385
on nuclei, high energy approx. 8=42984
one-channel N/D method, inelastic contributions 8=42421
one-particle-exchange model for low energy, many-channel case. 8=24763
overlap function, many-body theory 8=37880
partial-wave amplitudes, parameter-independent threshold corrections 8=42419
partial-wave unitarity integral evaluation and N/D method appls. 8=29065
phase contours and resonance poles and zeros consistency 8=24795
phase contours rel. to crossing symmetry 8=42402
phase contours rel. to zeros and high-energy behaviour 8=42401
phase shifts with cut-off parameter, approximation 8=47027
planet atmospheres, optically thick layers 8=50402
plasma in bithermal ionosphere, double scatt. 8=45531
pomeranchons, SU(3) assignment 8=24683
Pomeranchuk intercept, shift due to electromagnetism 8=29071
Pomeranchuk theory generalization at high energy 8=33590
Pomeranchuk trajectory built from nonresonating background at low energies 8=37903

Scattering, particles—contd
potential and S-wave scatt. amplitude calc. S-wave scatt. left hand cut 8=33583
potential; new approach, development concerning unitarity 8=33339
potential scatt., O_3 group space formulation 8=29049
potential strength, analyticity 8=24475
quasi-potential approach and expansion in relativistic spherical functions 8=33573
quasi-potential equations, relativistic, particles with spin 8=33574
radiative corrections, approx. for calc. 8=33569
real phase shift, channel coupling effect, using pole approx. to N/D method 8=47033
with rearrangement, truncated asymptotic method 8=25203
recoil atoms, range in stopping materials 8=31136
Regge amplitude for backward unequal mass, analyticity requirement 8=33596
Regge asymptotic behaviour, difficulties of use of finite energy sum rules 8=37896
Regge asymptotic behaviour, unitarity and analyticity 8=42399
Regge asymptotics and superconvergence generation of parallel daughter 8=42435
Regge boundary conditions on boots trapping 8=33600
Regge contributions, secondary in $\pi^- p \rightarrow \pi^\circ n$ 8=37996
Regge-cut effects estimation 8=37907
Regge daughter trajectories for Bethe-Salpeter eqn. 8=37911
Regge daughter trajectory in field theory model 8=42428
Regge exchange, modified and πN charge exchange polarization 8=33683
Regge exchanges, data from pion-baryon (spin $\frac{1}{2}^+$) scatt. 8=42543
Regge families in Wick-Cutkosky model 8=47035
Regge fermion trajectories N_α and N_γ interference to explain dip in $\pi^+ p$ cross-section 8=33687
Regge framework from π°, η°photoprod. on p, dominance of B° 8=42523
Regge model, double, and density matrix for single-particle prod. 8=37901
Regge-model for n-particle prod. cross-section 8=24681
Regge parameters, dispersion relations 8=33599
Regge pole discussion of S-matrix element behaviour 8=37906
Regge-pole fit, p-p scatt. 8=38061
Regge pole fit to $\pi^- p$ scatt., 8.16 GeV/c 8=37995
Regge pole mode and sum rule of superconvergence type 8=37987
Regge pole model for calc. of proton e. m. form factor 8=42629
Regge pole model for K* prod. in $K^- p$, 10 GeV/c 8=33732
Regge-pole model for particles whose mass goes to zero 8=29069
Regge pole model for $\pi^+ p \rightarrow \pi^\circ N^{*\circ\circ}$. 2.75–8.0GeV/c 8=47109
Regge pole parameters for πN scatt., from dispersion relations of superconvergence type 8=42431
Regge-pole pole, helicity amp. applic. 8=37961
Regge-pole residue, ω, in π photoprod. 8=37968
Regge-pole theory extrapolation to 50-1000 GeV/c range 8=33589
Regge pole theory forward and near forward limits 8=37993
Regge pole theory of composite states 8=33594
Regge poles, argand diagram and inelastic resonances 8=33593
Regge poles at high energy and SU(3) symmetry 8=24682
Regge poles for spinless particle in backward scatt. 8=42430
Regge poles, mixing with moving cuts 8=33591
Regge poles, the analytic S-matrix and nuclear democracy 8=37872
Regge recurrence generation, algebraical 8=33523
Regge residues, natural zeros 8=42429
Regge theory, anomaly in p polarization meas. for $\pi^+ p$ scatt., 2–4 GeV/c 8=33688
Regge theory, group theoretical approach to complex ang. mom. and signature 8=24674
Regge trajectories, conspiracy test for e and massive γ 8=42469
Regge trajectories in πp scatt. 8=33680
Regge trajectories, 3 high-lying vacuum proposed rel. to existence of 2^+ meson resonance 8=33714
Regge trajectories, nucleon and delta, applications of mass formula in broken $SL_{2,}$ 8=37904
Regge trajectories of non-strange mesons, contrib. to cross-sections 8=42432
Regge trajectories of resonances not yielding asymptotic behaviour 8=42433
Regge trajectories P and P^1, props. from πN, KN scatt. 8=42442
Regge trajectories threshold cusps 8=33598
Regge trajectory conspiracies for $\gamma N \rightarrow VN$ 8=38026
Regge trajectory coupling to integer spin particles, Feynman diagram model 8=29068
Regge trajectory families at nonvanishing energy 8=33592

Scattering, particles—contd
Regge-trajectory, line extrapolation of baryon exchange through mass spectra 8=42434
Regge trajectory model containing daughters 8=37899
Reggeization of U(6) ⊗ U(6) 8=42439
Reggeon diagram method for inelastic processes with arbitrary number of particles 8=37898
Reggeon graphs for inelastic processes 8=29072
relativistic 3-particle, contour-distortion method, extension 8=42412
resonance phenomena, partial wave amplitude related to threshold conditions 8=24655
ρ-π superconvergence, approximate saturation 8=38044
Rutherford elastic scattering experiment 8=25009
S- and P-wave, off mass shell extrapolation method 8=42376
S-matrix crossing-symmetric eqns., solns. proved by fixed-point theorem 8=42415
S-matrix elements in terms of Fredholm determinant generalized to continuous channels 8=29063
S-matrix of highly absorptive resonant waves 8=24664
S-matrix in nonorthogonal basis, parametrization 8=29064
S-matrix singularities, sheet struct. and multiparticle amplitudes 8=24668
S-matrix treatment, Mandelstam symm. 8=24663
S-reaction, complex ang. momentum plane, study of singularities 8=42425
scattering matrix parametrization, props. of diffraction cross-section 8=37878
singularities, kinematic of 2-body helicity amplitudes 8=33578
spin processes, $0 + \frac{1}{2} \rightarrow 1 + \frac{3}{2}$, O_3, symmetry 8=37900
spinless, ladder series convergence and Bethe-Salpeter equation 8=37884
spinless, study by collision lifetime matrix method 8=29051
for structure analysis 8=29031
superconvergence conditions for forward amplitudes, general method obtaining 8=33579
superconvergence relations, analyticity constraints 8=42406
superconvergent amplitude, diffractionlike possibility 8=37892
t channel threshold singularities eliminated from differential cross sections 8=37905
3-body Amado model, Faddeev perturbation 8=42413
3-body, amplitude calc. for Coulomb pot. 8=42411
3-body effects in deuteron n capture 8=43038
three-body problem, partial wave function method 8=29060
three-body, use of Faddeev eqns. 8=29056
three-particle K-matrix 8=29059
3-particle, momentum transfer dispersion relations 8=33582
three particle system with Coulombs interact., amplitudes 8=33580
2-body amplitude, crossing-symmetric var. principles 8=42409
two-body, breaking of generalized seniority 8=24641
2-body, low-energy photon emission 8=42447
2-body relativistic, kinematic broadening 8=47028
2-hadron elastic high-energy model 8=42407
unitary impulse approx. method for 3-particle 8=29142
by velocity-depend. pots, rel. to maintaining a ^1S state bound near zero energy 8=24651
W boson, Bjarken's asymptotic formula validity in perturbation theory 8=29050
wave packets beam, scatt. cross section 8=46400
by weak central potentials, calc. using modified Born approx. 8=24650
zero-angle amplitudes, high-energy behaviour 8=29070
$C^{12} + C^{13}$, angular distributions and excitation functions obs. 10-30 MeV 8=38523
$He^4(He^3, He^3)Be^7$ compound nucleus, resonance parameters determined from cross-sections 8=42832
$Ni^{58,60,61,64}$, He^3 scatt. obs. 8=29512
$O^{16} + O^{16}$ scatt. nuclear molecular potentials cross sections, angular distribution obs 8-30 MeV 8=43098
$O^{16} + Sm^{148, 150, 152, 154}$, Coulomb excited states obs. 8=38387
$Ru^{98,100,102,104} + O^{16}$ Coulomb excited states obs. 8=38375
Zr^{90}, t inelastic scatt. at 20 MeV, obs. 8=43055
$Zr^{90,91,92,94}$, He^3 scatt. obs. 8=29512

Schizons. See Elementary particles; Field theory, quantum/interactions, weak.

Schlieren systems
acetylene combustion in shock waves 8=49886
oblique shock wave interaction with supersonic projectile 8=46162
photography, subnanosecond, of laser-induced gas breakdown 8=29901
three-colour, for methane-air spectrochem. analysis 8=28737

Schottky defects. See Crystal imperfections/vacancies.

Schottky effect (noise). See Electron tubes; Fluctuations/electrical; Semiconducting devices.

Schrödinger equation. See Quantum theory/wave equations.

Schwarzschild space. See Cosmology; Gravitation; Relativity/general.

Scintillation. See Luminescence.

Scintillation chambers. See Luminescence chambers.

Scintillation counters. See Counters/scintillation.

Seals, glass-metal. See Glass-metal seals.

Seawater
acoustic backscatt. from bed at small grazing angles 8=50098
coastal waters, thermocline strength fluctuations 8=32194
conductivity, effect of freq. 8=48202
Copenhagen, spec. refraction and dilutions, chlorinity, wave length and temp. dependences 8=50114
microwave emission, effect of temp., angle of obs., salinity and thin ice 8=50113
over-saturation with $CaCO_3$, causes 8=50097
shallow, c.w. acoustic phase characts. 8=50111
surface layer of ocean, daily temp. variations 8=27868
surface temp. obs. by radiowave emission 8=50107
surface temp. meas. from Nimbus II, and posns. of ocean currents 8=41335
temperature inhomogeneities, 3-D characts. 8=32187
tidal displacement, rel. to geomagnetic field var. 8=28012
under Arctic ice, CO_2 content 8=41327
underwater acoustic pressure calc. 8=50101
wave 'set-down' and set-up 8=32189
waves on beach of uneven bottom 8=50109

Second sound. See Helium/liquid, sound propagation.

Secondary electron emission. See Electron emission/secondary.

Sedimentation
electrolytic flocculation, sediment compress. rel. to particle size 8=30556
floc formation, geometrical model using Smoluchocoski's rate eqn. 8=30566
helical macromols. in soln., size and shape determ. 8=30420
Hudson river, seismic refraction and borehole obs. 8=50045
kaolin, settle ability rel. to adsorpt. of surfactant 8=44071
in moving suspension, determ. of solid-phase conc. distrib. in boundary layer 8=34952
nonconducting solid spherical particles 8=39449
particle size distrib. determ. 8=34933
particles diffusing in stationary fluid between parallel plane surfaces 8=48236
power metallurgy, radioactivity isotope analysis 8=43987
spheres falling in viscous fluid, spatial distrib. 8=30546
underwater, acoustic reflection phase determ. 8=37266

Seebeck effect. See Thermoelectricity.

Seidel theory. See Aberrations, optical.

Seignette salt. See Rochelle salt.

Seignettoelectric materials. See Ferroelectric materials.

Seismic waves
See also Seismology.
attenuation rel. to dynamic viscosity, transient creep and ϕ calc. 8=27830
attenuation, with lens shaped molten inclusion or melt surrounding solid grains 8=36659
compressional pulse propag. in liquid sphere, wave theory 8=28364
compressional, vel. and rock density, correl. 8=27822
compressional vel. changes across stressed region, rel. to stress accumulation meas. 8=36673
earthquake source mechanisms in California-Nevada region from surface wave analysis 8=50020
rel. to earth's mantle inhomogeneities, vel. profiles obs. 8=27824
fields, three-dimens., due to Volterra dislocation imbedded in layered half-space 8=50060
high-resolution seismic uphole surveys at Lawrence Radiation Laboratory 8=50023
in layered medium, amplitude-distance curves, freq. depend. calc. 8=23933
long-period surface waves obs., rel. to structure of earth's mantle 8=41322
longitudinal wave amplitude rel. to focal depth 8=50027
Love waves propag. along homogeneous and heterogeneous media interface 8=32895
marine storm produced, limitation on determ. of wave vector 8=36666
optimal algorithms for discriminating interfering waves 8=50059
P attenuation and mantle Q structure 8=36669
P, diffr. and attenuation rel. to core-mantle boundary struct. 8=27842
P, short-period teleseismic, amplitude-distance curve 8=27827
P times from Greeley nuclear explosion 8=50049
P wave spectrum rel. to crustal thickness in central USA and Bolivia 8=50071
point-sources in layered media, theoretical seismograms 8=32176
Rayleigh wave propag. in elastic half-space, inhomogeneous in x and z co-ords 8=23936
Rayleigh wave propag. past step change in elevation, transmission and refl. coeffs. 8=46152
reflection detection, automatic 8=50053
reflections, average velocity calc. 8=41318
reflections, deep crustal at near vertical incidence 8=50054
reflected and refracted at boundary between transversely isotropic media, distribution 8=41825

Seismic waves—contd
  response calcs for composite structs, static and dynamic characts 8=32885
  SH, diffraction by earth's spheroidal core 8=27844
  shear waves multiply refl. from earth's core, rel. to rigidity and viscosity of core 8=36664
  signal generated noise, Eskdolemuir array, site dependence of records 8=46133
  surface motion, theoretical, from pulse transmission through layered elastic structs 8=32888
  surface wave particle-motion patterns rel. to freq., computer discrimination process 8=50033
  SV-wave rad. patterns, effect of elastically restrained boundary 8=50031
  travel time curve derivative dependence on epicentral distance, $dT/d\Delta$ 8=27826
  from travel-time curves, vel. cross-section soln. existence 8=27834
  velocity determ. in upper mantle, curvature corrections 8=27841
  viscoelastic medium, disturbances produced by impulsive torsional body forces 8=46150
Seismology
  See also Geophysical prospecting; Seismic waves.
  accelerogram, interpret, error effects on calc. vel., displacement and shock spectra 8=36663
  air-sea waves excited by volcano Krakatoa, pulse propagation 8=27829
  Alaskan earthquake, 1964, rel. to long period geomag. fluctuations 8=28009
  anisotropic layer of finite thickness, dispersion curves of phase vels. of nat. vibs. 8=23925
  array, large aperture and short period signal processing 8=50055
  attenuation, with lens shaped molten inclusion or melt surrounding solid grains 8=36659
  California-Nevada region earthquakes, moment, stress and source dimensions 8=50020
  common data point, effect of vel. layering and steep dip 8=50052
  compressional wave vel. and rock density, correl. 8=27822
  cross-sections calc. from obs. 8=27832
  crustal structure 3D model, middle Atlantic states, by time term technique 8=36674
  deep refraction expt., NH_4NO_3-fuel oil explosive as energy source 8=50047
  deep-sea sediment velocity, obs. made while reflection profiling 8=32191
  deep-sea sediments, velocity from sonobuoy data 8=32190
  dynamic correlation analysis 8=50043
  earthquake epicentres and strain release in Canada 8=50035
  earthquake magnitude estimation, comments 8=50042
  earthquake P phases penetrating core, travel time model cont. two vel. discontinuities 8=36662
  earthquake risk in California, map from model and $\geq$ magnitude 4.0 obs. 8=27839
  earthquakes, effect of Hyderabad magnetographs 8=32365
  earthquakes in N. Iran, historical compared with recent activity 8=50030
  earthquakes, solar activity as triggering mechanism 8=27846
  earth strain observatory, signal processing system design 8=36671
  earth's strain, use of Michelson interferom. as sensor 8=27848
  earth tides, effect on long-baseline radio interferometry 8=45423
  earth upper mantle model from seismologic data 8=36672
  rel. to earth's upper mantle boundaries nature, deep-focus earthquakes hodographs 8=27833
  elastic sphere surface motion due to radial impulsive force and explosive point-source 8=36667
  fault-length and rupture velocity in small-magnitude earthquakes 8=50063
  faulting, shallow focus strike slip, rel. between stress drop, fault friction and crustal strength 8=36668
  geometrical, stability of inverse problems 8=50034
  ground waves, propag., study 8=37528
  high-resolution seismic uphole surveys at Lawrence Radiation Laboratory 8=50023
  Icelandic geysers, charact. activity patterns 8=50048
  Juan de Fuca ridge, refraction profiles 8=36658
  Lake Superior crustal struct., 1963 seismic expt., reinterpretation 8=32178
  layered sphere, model study of elastic wave propag. 8=32887
  longitudinal wave amplitude rel. to focal depth 8=50027
  magneto telluric soundings 8=36660
  in mantle, compress. and shear energies attenuation 8=27843
  mean-square criterion for calc. of arrays in seismic exploration 8=50028
  microseisms in 1 c/s range, struct., method of analysis 8=50024
  microseisms in 1 c/s range, struct., results of obs. 8=50025
  Mid-Atlantic Ridge, earthquakes along median rift and offset fracture zones 8=50050
Seismology—contd
  minimum microquake recording times to determ. short-term seismicity 8=50040
  model, interface problem 8=50056
  modelling, wideband piezoelect. transducer 8=50046
  ocean-bottom seismograph 8=50026
  1 km laser interferometer for earth strains 8=50061
  P and S wave study of discontinuities in upper mantle to West of Lake Superior 8=50065
  P wave attenuation and mantle Q structure 8=36669
  P-wave records, short period, computer synthesis from distant explosion sources 8=50038
  P wave signals, linear mode filtering from Rayleigh wave type noise 8=45424
  P wave spectrum rel. to crustal thickness in central USA and Bolivia 8=50071
  Parkfield earthquake, June 26, 1966, magnitude and source mechanism 8=50036
  Peru earthquake, Oct 17th, 1966, epicentre, maps, correl. between intensity and geol. factors 8=50039
  PKP in range $115° \leq \Delta \leq 140°$, travel times 8=50022
  point-sources in layered media, theoretical seismograms 8=32176
  point-sources in layered media, theoretical seismograms, numerical calc. 8=50021
  pulse propag. in elastic half-spaces, numerical soln. 8=27828
  reflection detection, automatic 8=50053
  reflections, deep crustal at near vertical incidence 8=50054
  refraction determ. water table and alluvium depth 8=50057
  refraction nomogram, multilayer 8=50051
  S waves, long-period, travel-time curves rel. to upper mantle struct. 8=36661
  sediments in Hudson river, refraction and borehole obs. 8=50045
  seismic equation of state and earth density models 8=27823
  seismicity calc. and seismic activity math. formulation 8=27835
  seismicity in vicinity of Ramapo fault near New York New Jersey border 8=50037
  seismicity, new determ. 8=45425
  seismograms of homogeneous, coreless, gravit. earth 8=27838
  seismograms, synthetic, basic eqns. using z transform 8=50058
  shallow earthquake in Himalayan foothills, P wave study rel. to crustal struct. 8=50068
  shock free oscills. spectrum, aftershock sequence effects 8=27831
  SH and SV, diffracted 8=45426
  sialic low-vel. channel in S. German Triangle, seismic refr. obs. 8=27836
  signal generated noise, Eskdolemuir array, site dependence of records 8=46133
  standing waves in layered fluid half-space, theory 8=32889
  strong tectonic earthquake, percursor 8=36665
  T phase source in Caribbean, Oct 24, 1965, comments 8=50041
  tectonic deformation and atmospheric press. waves, 28 March 1964 Alaskan earthquake 8=41317
  teleseismic microseismic noise, correl. function for vertical coup. of Earth motion 8=50032
  teleseismic response of array above non-uniform crust and equalization 8=27837
  teleseismic signals analysis and mantle struct. obs. 8=27845
  tide-generating forces and distrib. of intermediate and deep-foci earthquakes 8=41319
  transform fault concept, spherical surface, and verification with Africa-S. America data 8=36670
  turbidity of real media and investigation 8=50064
  underground explosions and earthquakes, diagnosing 8=27825
  upper mantle refraction surveys, curvative corrections 8=27841
  upper mantle structure in Canada, from seismic obs. using chem. explosions 8=32179
Selenium
  adhesion of insulating polymer particles, force rel. to triboelec. charge 8=49045
  amorphous, thin layers, voltage-current limits of spatial load 8=40482
  crystal growth 8=39685
  crystal growth by seeding under high-pressure 8=44143
  crystal, trigonal, transient photoconductivity rel. to carrier behaviour 8=44933
  electronic spectrum of trigonal 8=32030
  electrophotographic layers, current carrier drift mobilities 8=40671
  epitaxial deposition on Te, effects of evap. cond. on struct. 8=48457
  evaporation, vapour mol. comp. and Se_{1-8} appearance pots., obs. 8=43916
  film, single-crystal, in rectifying Te-Se-Cd structures 8=35930
  film, thin, vacuum-deposition illumination 8=30757

Selenium—contd
film, with embedded Hg atoms, distrib. study by e. p. r. 8=35179
films, amorphous, prep. by vacuum evap., crystn. by electron irradn. 8=39691
films, thin, absorption and reflecting power in fundamental absorpt. region 8=27605
granular, optical absorpt., phenomenological quant. descript. rel. to permittivity of bulk mat., 8=41135
hexagonal, conductivity and photocond., effect of reactor irradiation 8=44809
hexagonal, internal photoeffect spectral distrib. on X-ray and u.v. irradiation 8=40672
hexagonal saturation photocurrent temp. dependence rel. to band structure 8=40673
layers, specific resistance across normal section, local distrib. studies 8=49259
phase transformation kinetics for amorphous → polycrystalline, and monoclinic → hexagonal 8=26078
thermal expansion of thin layers, linear coeff. meas. and Ag impurity dependence 8=48746
trigonal, electronic spectrum 8=32030
trigonal, electro-optical effects at 1.15μ 8=36402
trigonal, morphology of spherulites and single-crystals rel. to crystallization process 8=44100
trigonal, optical absorpt. edge 8=27604
trigonal, optical props. in polarized vacuum u.v. 8=45217
trigonal, photocurrent decay rel. to hopping recombination 8=36027
trigonal, reflectivity spectrum in vacuum u.v. 8=27606
vaporization of cryst. and amorphous states, laser induced study of species in vapour 8=35006
vaporization, partial press of Se_2(g) 8=48285
viscoelasticity, P admixture effect 8=31230
vitreous, atomic arrangements by X-ray diffr. at 25 and −196°C 8=30793
Se electrophotographic layers, dark discharge mechanism 8=49423
Se-polypropylene glycol suspensions, thermal cond. meas. 8=43883
Se_2, dissoc. energy 8=38936
Se : Ag hexagonal evaporated films, struct. and props. 8=48458
Selenium compounds
CH_3SeH, indirect spin coupling 8=29822
H_2SeO_3, e.p.r. of γ-irrad. cryst. 8=31884
Se−Cd glass, nonlinear optics 8=32029
$Se(CH_3)_2$, indirect spin coupling 8=29822
SeF_6, i.r. spectra and force fields 8=25519
SeH_2, indirect spin coupling 8=29822
SeO, force consts. correl. with SO 8=38854
$SeOCl_2$:Nd^{3+}, absorption cross section for Nd^{+3} laser transition 8=46624
$SeOCl_2$:Nd^{3+} liquid laser, improvements 8=37624
$SeOCl_2$-Nd^{3+} liquid laser, Q-switched, 20°C 8=37623
$SeOCl_2$:Nd^{3+} liq. laser, stimulated emission in $^4F_{3/2} \rightarrow {}^4I_{13/2}$ transition 8=46628
Se-Te alloy, crystal growth 8=39685
$Se_xTe_{1-x}Hg$ solid soln., crystal growth and structure 8=26269
Self-diffusion. See Diffusion in gases, in liquids, in solids.
Semiconducting devices
See also Counters/semiconductors; Lasers; Masers.
analytical representations, effects of impurity concentrations 8=35925
bulk negative mobility, effect of field dependence of diff const. on small signal behav. 8=44827
capacitance, dynamic, direct meas. method 8=28451
capacitor, m. n. s., memory behaviour 8=40629
contacts, ohmic, for Gunn elements 8=49282
current flow, two-dimensional 8=49285
electroluminescence, review 8=36464
film, integrated monolithic, comprising conductor and insulator films, basic technology 8=44852
flying-spot scanner, electrical props. study 8=24383
Gunn device as broadband neg. resistance, v. h. f. and u. h. f. oscillators 8=27144
Gunn oscillator, GaAs, high efficiency 8=49283
Gunn oscillator, GaAs, wide range variable freqs. 8=40546
Gunn oscillators, X band, freq. modulation noise 8=27143
heterojunctions, abrupt n-n, computer soln. of depletion and accumulation layers and anal. 8=44841
heterojunction, semiconductor-dielectric, volt-ampere characts. 8=49287
infrared detector, avalanche, thermal noise behaviour 8=46227
i. r. detectors, Cu doped Ge 8=46226
i.r. detector, Ge:Cu, low freq. noise 8=32946
isotype heterojunction, Poisson equation soln. under zero-current condition 8=31401
junctions, metal-semiconductor tunnel, resistance anomalies 8=35918
junctions, prediction of transient and permanent rad. damage, computer program 8=27146
laser amplifier 8=33219
lasers, variable wavelength, as spectroscopy light sources, 1-20μ 8=28838
layer structures, fission fragment tracks 8=44487

Semiconducting devices—contd
liquid resistance thermometer for nuclear reactors 8=34110
'long'Gunn effect dev., osc. characts. rel. to internal inhomogenities 8=49278
microwave generators 8=27142
m.i.s. and m.i.o.s. types fromSi_3N_4-SiO_2 films on Si, characts. 8=49319
m.i.s., polarization effects in SiO_2 films on Si, review 8=44854
m. n. o. s. structs., radiation effects and elec. stability 8=35946
m. n. s. capacitor, memory behaviour 8=40629
MOS capacitors, radiation effects, determ. from conductance obs. 8=27204
MOS structure, photoelect. threshold, effect of heating under bias 8=27313
m. o. s. structures with Si containing metal surface impurities, elec. props. 8=35944
m.o.s. transducers with digital measurement capability 8=28909
m.o.s., use of sputtered SiO_2 for multilayer, interconnects 8=44855
motion due to self-heating, holographic detection 8=49279
parallel diodes, or thyristors with current sharing transformers, current distribution calc. 8=31405
particle spectrometers, ballistic deficit and signal/noise ratio 8=24502
physics, and circuits of application, book 8=49284
p-i junctions, penetration of energetic ions 8=44490
p−i−n detector for pulse shape discrimination 8=46951
p-i-n-n^+ junction waveguides, use for phase-matching in optical second harmonic generation 8=33136
planar, surface and bulk effects of nuclear reactor radiation, comp. 8=31400
radiation damage, book 8=31399
radiation detector, electron avalanche and using Goods theorem for branching 8=33376
thermistor hygrometer, soil moisture free energy meas. 8=50090
thermistor with negative temp. coeffs. in Mn_2O_3-NiO-Cu_2O system 8=49280
thermocouple, Peltier coeff. determ. from initial steepness of V-I characts. 8=40635
thermoelectric, performance at constant heat flux 8=49397
thickness meas. of thin films 8=44029
thin-film active devices, use of CdS and CdSe films 8=48444
III-V compounds, appl. to integrated circuits and arrays 8=44856
thyristor triggering by displacement and leakage currents 8=40521
transducers, electromechanical conversion efficiency, thin film on delay rod 8=23956
trigger circuit, s.c.r., for ignition discharge 8=49277
tunnel junction, quantum size effect 8=35935
two-layer struct. impedance expressions, anal. of spiral-shaped curves 8=35917
varactor, as microwave generator, design and performance 8=27142
wafer in magnetic field, resistance calculation 8=44829
Au-Ag bonds, ultrasonically joined, purple-plague formation 8=48771
Au−n−Si, contact, potential barrier 8=35924
CdS, light demodulator with u. s. amplification 8=27216
CdS-metal barriers from photo-voltage meas. 8=40511
Cds solar cells for multikilowatt arrays 8=24100
CdS solar cells micrometeoroid degradation, simulation obs. 8=24094
CdS−SiO_2−Al structure, field-effect conductance temp dependence 8=40544
GaAs bulk oscillators, LSA mode, multiple frequency operation 8=40501
GaAs, bulk subcritically doped, series-connected, microwave amplifiers and oscillators 8=49281
GaAs injection laser, multilayer 8=33210
GaAs injection laser, phase locking and external cavity coupling 8=33211
GaAs junction lasers, compensation effects of Zn and Te impurities 8=46616
GaAs laser bulk field-ionized, stimulated emission 8=33207
GaAs laser, electron-beam pumped, nonradiative surface recombination 8=49226
GaAs laser injection, optimum stimulation 8=33218
GaAs laser, internal Q switching 8=33212
GaAs laser junction, transverse modes 8=33206
GaAs, laser, n-type at 77°K, threshold current, power output and quantum efficiency 8=33216
GaAs, planar bulk, Sn-Au contact prep. and device characts. 8=27157
GaAs planar Gunn oscillator, for microwave integrated circuits 8=44857
GaAs with ohmic contacts, prep. using hot H_2 and HCl gases 8=27156
$GaAs_{1-x}P_x$ injection laser, delay and memory effects 8=33209
$GaAs_{1-x}P_x$ injection laser diode, pulsed, temporal-line shift 8=49307
$GaAs_{1-x}P_x$ injection lasers 8=46617

Semiconducting devices—contd
- $GaAs_xP_{1-x}$ laser, applic. to phase-modulated optical ranging system 8=42110
- GaP photodiode, strongly compensated p–i–n junction, elec. and optical props. 8=40509
- GaP_xAs_{1-x}-GaAs n-n heterojunctions, photosensitivity spectra 8=36019
- Ge, i.r. detector 8=41854
- Ge p-i-n detectors, determination of compensated-region width by light probe 8=46899
- Ge, prep. of tetragonal GeO_2 for passivation 8=40502
- Ge:In far i.r. photocond. detector, response time 8=32945
- Ge(Li) detector surface protective coating 8=46913
- Ge, Li drifted, counter, ionization energy determ. 8=24522
- Ge–Si n–n heterojunction, interlace layer, X-ray anal. 8=40516
- Ge-Si(GaAs) abrupt heterojunctions, fabrication by solution growth 8=49293
- n-Ge-W point contact, oscillatory back-current induced by sonic vibrations after d.c. pulse 8=40503
- InSb i.r. detector, low-noise amplifier 8=41856
- n-InSb magnetoresistance probe for mag. fields at liquid He temp. 8=46371
- Li-drifted Si detectors in β-ray spectrometer for fallout meas. 8=46851
- Li^6 sandwich detector for n spectrometry 8=38083
- SCRs planar, on-characts. rel. to use in monolithic circuits 8=27215
- Si, injection level and temp. depend. of transient annealing in n-irrad. devices 8=27122
- Si junctions, formed by B, N and P ion implantation 8=49263
- Si, ohmic contacts by rubbing with Au 8=49286
- Si p-i-n detectors, study with travelling light probe 8=46888
- Si position-sensitive detector, linearity and resolution 8=24521
- Si solar cells for multikilowatt arrays 8=24100
- Si solar cells in-flight performance, computer prediction 8=24086
- Si solar cells, Li diffused, radiation damage self-healing 8=24091
- Si solar cells, n irrad. damage and Li effects, obs. 8=24095
- n/p-Si solar cells charged particle irrad. degradation, base resist. effects, 1-25 ohm cm 8=24092
- n/p Si solar cells micrometeoroid degradation simulation obs. 8=24094
- Si solar cells, p irrad. damage thermal annealing, 4.6 MeV 8=24101
- Si, stress effects in masking films 8=49047
- n-Si surface barrier detectors for X-ray spectroscopy 8=47071
- Si: Au m.o.s. structures, minority carrier lifetime meas. 8=49315
- SiC varistor with voltage nonlinearity, effect of the content in particles 8=31404
- Si–Cr film resistors, struct., stability at 200°C and resistivity 8=44818
- Si, Li drifted, counter, ionization energy determ. 8=24522
- p/n-Si: Li and n/p-Si solar cells, comparison 8=24089
- Si: Li solar cells, efficiency and e irrad. damage annealing, obs. 8=24103
- Si: Li solar cells, experience and future of 8=24104
- Si: Li solar cells, present status 8=24090
- p^+/n-Si: Li solar cells, status 8=24102
- Si-SiO_2 fast interface state meas. from MOS-C(V) curves at 77°K 8=49320
- Si-SiO_2 in m.o.s. structure, Au-doping effect on admittance and surface-state density 8=49317
- Si–SiO_2 solid–solid interface system 8=40504
- Si-SiO_x system, surface damages in Si after thermal treatment 8=49276
- Si-SiO_2-Al, MIS structure, e-irradiated, capacitance and parallel conductance 8=27211
- SiO_2–Si m.i.s. capacitors, elec. propsl 8=44055
- VO_2 on alumina substrates, rel. to device fabrication 8=30758
- ZnO-Cu_2O heterojunctions, electroluminescence 8=36516
- ZnSe epitaxial layers, on p-Ge, growth and elec. characts. 8=44834
- ZnS electroluminesc. resistor meas. 8=27145

diodes
- avalanche and Gunn, microwave generators, operation, construction and props. 8=35929
- avalanche and transferred electron, as microwave generator, design and performance 8=27142
- avalanche, p-n junction, dispersion relationship 8=35931
- avalanche, relaxation oscillations 8=49299
- avalanche, space-charge-induced negative resistance, analysis 8=44840
- avalanching pin, current filaments 8=27166
- base minority carrier density distrib. of diode turned on with forward current pulse 8=27171
- carrier excitation mechanisms rel. to recombination radiation 8=31953
- channelling of p-i junctions, ion beam penetration 8=44490
- curve tracer, resistance-compensating 8=35926
- diffusion comp. of current pulses, shape under X-ray irrad., theory 8=27164
- electronic processes, method of similarity 8=35928

Semiconducting devices—contd
diodes—contd
- Gunn, high-field domain annihilation rel. to parameters 8=49301
- Gunn, l.f. oscills., dynamics 8=49298
- IMPATT diode oscillators, transmission efficiency, theory 8=40526
- junctions, in avalanche, noise meas. in r.f. and ultra-r.f. region 8=40544
- laser, band tail spreading energy rel. to temp. 8=28698
- laser, temp. dependence of linewidth of spontaneous emission 8=42099
- magnetodiode effect, injection of current carriers 8=49300
- metal-semiconductor system (photodiode), hot e-scattering from surface on illumination 8=35752/3
- metal-Si contacts, surface effects from I–V characts. in gate-controlled Schottky-barrier structure 8=40536
- in parametric amplifiers with self-polarized junction, I-V charact. effect on amplifier parameters 8=28460
- p–i–n, induction of l.f. oscillations by anomalous avalanche negative resistance 8=40524
- p-n-n^+, current-voltage characts., allowing for carrier lifetime variations in base 8=27170
- p-n-n^+, frequency characteristics, with steady-state carrier-distrib. minimum in base 8=27169
- p–n–n^+, small-signed impedance at high forward current densities, theory 8=40527
- p-ν-p, noise at room. temp. 8=44839
- photodetectors, p. i. n. for astrophotometry 8=42135
- photodiodes, thin-base, retarding surface field effects on operation 8=36033
- photodiodes, multielement, elec. coupling mechanism 8=40682
- point, recovery phenomena 8=27173
- Schottky barrier, peripheral electric gield counteraction at contacts 8=28871
- schottky barriers, use as source and drain contacts for insulated-gate FET 8=49318
- Schottky photodiode, voltage enhanced spectral response 8=31458
- SCL, h.f. noise source 8=27172
- surface-barrier, for e position sensing 8=47094
- switching, constant reverse current phase duration 8=27167
- transitional processes for inhomogeneous base on instantaneous disconnection 8=44842
- 2000 amp. for ferrite tuning circuit in 200 GeV accelerator 8=24549
- u.h.f. diode processes, modelling using variable delay eqns. 8=27175
- Al-CdS-Au thin film, prep. and elec. props. 8=27174
- Al/CdSe(or CdTe)/Au thin-layer structures, voltage-controlled bistable states 8=49303
- Al–Si_3N_4–Si MNS, C–V curves and prop., obs. 8=40545
- Au–As alloy-Si Schottky, barrier height rel. to Au content 8=40522
- n–Au–Si surface barrier photodiode, h.f., technology and props. 8=49432
- Au-Si_3N_4-ZnSe, visible electroluminesc. 8=41230
- Bi-Te alloyed diode, spectra at 78 and 300°K, I-V characts. at 300° C 8=36538
- Bi-Te alloyed luminescent, spectra at 78 and 300°K, I-V characts. at 300°K 8=36538
- CdS, MOS, electroluminescence at low-voltage, high-current and 77° K 8=27644
- CdS space-charge-limited, noise, limiting 8=27177
- CdS, thin-film, effect of heat treatment 8=27176
- CdS:rare earth heterojunction, injection luminesc. 8=45265
- CdS-CdTe thin film heterojunction 8=49306
- CdTe, electroluminesc., temp. depend. 8=49790
- GaAs and Si alloyed diodes, V–I characts. and electroluminesc. 8=32058
- GaAs bulk oscillators, random one-dimensional doping fluctuations effect, computer study 8=49308
- GaAs diffused-junction varacter diodes 8=35927
- n-GaAs, electron-hole generation and switching mechanism 8=27180
- GaAs, electroluminesc., external efficiency rel. to junction depth and doping 8=45268
- GaAs epitaxial, electrical and spectral characts. 8=27147
- GaAs Gunn diode, l.f. current fluctuations 8=49302
- GaAs injection laser, phase locking and external cavity coupling 8=33211
- GaAs i. r. pulse generator 8=28770
- GaAs lasers, near-field pattern, effect of material inhomogeneities 8=42109
- GaAs laser, optical losses and efficiency 8=33213
- GaAs laser, short wavelength radiation emission spectrum 8=37613
- GaAs, lasers, temp. depend. of delay time between current pulse and laser emission 8=24339
- GaAs laser, transient temp. distribution and o/p pulse duration 8=33217
- GaAs layer, emission currents, optical and photoelectric props. 8=49305
- GaAs, luminescence mode, current noise spectra 8=46614
- GaAs Schottky barrier, effect of surface treatments on $C^{-2}V$ characts. 8=27178
- GaAs surface barrier, trapping analysis 8=27092

Semiconducting devices—contd
diodes—contd
GaAs$_{1-x}$P$_x$, electroluminesc., external efficiency rel. to junction depth and doping 8=45268
GaAs$_{1-x}$P$_x$ injection laser, pulsed, temporal-line shift 8=49307
GaAs-W junction grown from vapour phase, elec. props. 8=49296
GaP, depend. of radiative efficiency on heat treatment 8=27179
GaP electroluminescent, prep. from p-on-n liquid-phase epitaxial layers 8=41229
GaP, luminescence, 300-900°K 8=45188
GaP p-n junctions grown by liq-phase epitaxy, green electroluminescence 8=41231
GaP, reverse-biased for h.f. light modulation 8=40528
GaP, solution-grown, effect of donor conc. on optical efficiency 8=44843
GaSb, laser modes temp. depend. rel. to optical consts. near energy gap, 80°K 8=41088
Ge-magnetodiodes, V-A characts. in liq. He. 8=31407
Ge, minority carrier lifetime, anisotropic pressure dependence 8=27168
Ge, point-contact, switching time, rel. to pile-neutron irrad. 8=31406
Ge p–i–p, multiple negative resist. rel. to filamentary current paths 8=40529
Ge p–i–p, negative resist. mag. field depend., 770K 8=40530
Ge:Au photoresistors, surface charge effects on I-V characts. and excess noise 8=36034
Ge-GaAs system, V-I characts. and spectral distribution of photosensitivity 8=35174
Ge(Li), surface treatment 8=49309
InAs, alloyed, capacitance depend. on reverse voltage 8=27181
InAs, alloyed, I–V characts. at 4.2°K 8=40532
InAs, stimulated recombinational emission from p-n junction 8=44838
InAs, stimulated recombinational emission from p-n junction 8=49297
In–CdS··SiO$_x$–Al heterojunctions, SCL currents at saw-tooth voltage pulses 8=40523
InSb p$^+$–p–n$^+$, negative-resistance I-V characts. 8=40531
Si and GaAs alloyed diodes, V–I characts. and electroluminesc. 8=32058
Si, avalanche discharge, noise 8=35933
Si, avalanche discharge, self-sustaining, noise meas. at microwave freqs. 8=40537
Si avalanche, high-power, high-efficiency, at u.h.f. 8=49310
Si fast-neutron dosimeter, <1–15,000 rads. 8=33788
Si, Frenkel effect due to X-ray irradiation 8=40533
Si IMPATT type, osc. modes, current depend of freq. 8=49312
Si-intermetallic cpds.-SiC light diodes, V-I depend. of recomb. rad. intensity 8=27184
Si, p beam dosimetry 8=38064
Si, p-i-n avalanche type, effects of applied mag. field on osc. 8=27185
Si p–i–n, instability in avalanche region 8=40535
Si p$^+$-i-n$^+$, avalanching negative resistance and filamentary currents 8=49313
Si p$^+$-n-n$^+$ junctions, V-I characts. rel. to carrier injection 8=27184
Si photodiodes with demodulation props. independent of wavelength 8=49409
Si, point contact, neg. resistance without osc. 8=49311
Si, reverse epitaxial for photomultiplier tube 8=46424
Si, Schottby barrier for 5-6 mm region, fabrication 8=31408
Si Schottky barrier, with near-ideal I–V characts. 8=40525
Si, space charge limited triode, noise parameters 8=31409
Si:Au, computer simulation of charge distrib., space charge and recomb. rate 8=27182
SiC, with carrier injection into heavily doped regions and of V-I characts. 8=27183
Si: Li, diffusion coeffs. of Li on exposure to electron and neutron irrad. 8=39982
TiO$_2$ rectifying barriers, capacitance and resistance meas. 8=27186
Zn–Al–n-Si:P alloy, hole capture by Zn^{2-} in Si, effective cross section 8=40520
p–n junctions
abrupt asymmetrical, spatial variation of electrostatic potential, analysis 8=44830
avalanche-transit effects 8=40507
breakdown localization, effect of mag. field 8=27153
contact potential across junction 8=44832
depth meas. by spherical contouring 8=44833
displaced directly, noise at l.f. 8=40510
doped, heavily, thermally activated current and radiation 8=27147
doping profile, neighbouring evaluation from capacitance meas. 8=27072
electron beam active dev., dynamic response anal. 8=44831
electron thermodynamic nonequilibrium 8=35919

Semiconducting devices—contd
p–n junctions—contd
excess current associated with surface states 8=44828
forward-biased, l.f. noise due to charge fluctuations in depletion layer 8=40519
laser, carrier lifetime meas. by direct modulation 8=33191
laser c. w. operation noncatastrophic degradation 8=33205
laser diode, minority carrier lifetime rel. to impedance 8=33195
laser, internal parameters, determ. 8=28701
l. f. noise, surface-state related 8=35920
metal-Si contacts, surface effects from I–V characts. in gate-controlled Schottky-barrier structure 8=40536
noise calc. using fluctuation-dissipation theorem 8=37370
photoelectromotive force, by probe illumination, and p-i-n junctions 8=49407
p-i-n, carrier lifetime meas. method 8=27149
p-i-n junction, photovoltaic effect 8=36003
p-n-p-n structure, establishing stationary state for turning on 8=27154
p-n-p-n struct., switch-off process under influence of reverse anode voltage, time const. 8=27152
p-n-p-n symmetrical struct., switching process anal. inc. amplification factors on current 8=27148
planar, deep diffused, capacitance 8=27155
production by plastic deform. of p- and n-doped Ge 8=44835
in radiation detectors, applic. in nuclear instrument making 8=46886
review of development in USSR during last 20 years 8=27150
step p$^+$-n, with traps, reverse-biased capacitance 8=40508
symmetrically doped steady-state, closed form soln., 8=49289
temperature sensitive output, appl. to thermometry 8=31402
Au-Si, surface barrier rectification characteristics 8=49294
CdS, high conductivity, light emission under forward bias 8=40444
CdS, props., and construction of photoelectron transducers 8=49291
CdSe film, as base for photocells with p-n hetero-transition 8=40647
CdTe, electroluminescence 8=36521
n-CdTe, production by As$^+$ implantation 8=35882
CdTe p-n counters for γ-ray spectrometry 8=33618
CdTe-ZnTe alloys, electroluminescence 8=36521
GaAs, elec. imperfections rel. to crystal defect location 8=49292
GaAs, electroluminescence 8=36509
GaAs epitaxial compensated, recombination rel. to temp., and band tailing 8=33225
GaAs laser, applic. to phase-modulated optical ranging system 8=42110
GaAs laser diode soln. grown, gain and loss rel. to orientation 8=33214
GaAs laser diode, transient temp. distribution and o/p pulse duration 8=33217
GaAs laser injection, self damage 8=33208
GaAs laser, output light spikes at room temp. 8=33204
GaAs lasers near room temp., delay characts. 8=33222
GaAs laser structures, thermal impedance meas. 8=33223
in GaAs polycryst. films, tunnel junctions, characts. rel. to carrier density, operating temp. etc. 8=27188
GaAs stimulated emission delays rel. to temp., trapping model 8=33221
GaAsP, Zn-diffused, geom. irregularities dislocation structure dependence 8=40512
GaAs$_{1-x}$P$_x$, threshold and emission efficiency temp. dependence 8=33224
GaAs-W junction grown from vapour phase, elec. props. 8=49296
GaP, alloyed, capacitance voltage dependence, 80–300°C 8=40513
GaP, electroluminescence 8=36509
GaP, electroluminescence, 77-420°K 8=45273
GaP, electroluminescent, synthesis and epitaxial growth by fused salt electrolysis 8=48573
GaP, forward-biasing, edge luminescence spectra 8=36490
GaP, grown by liq. phase epitazy, green electroluminescence 8=41231
GaP, I-V charact., effect of simultaneous illumination and mech. stress 8=49288
GaP, I-V charact., stress effects 8=31403
GaP p-n, electroluminescent, synthesis and epitaxial growth by fused salt electrolysis 8=48573
GaP, red-emitting, prep. by soln. growth of p-type thick layers on n-type substrates 8=41232
GaP$_x$As$_{1-x}$-based injection lasers, production and props. 8=36360
GaP: Zn-O, (Te), red emission time-delay characts. 8=45272
n-GaSb(Te), formation on Cd diffusion 8=31005
Ge, breakdown in microwave elec. field, exptl. investigation 8=27158
Ge diffused, low-breakdown-voltage, reverse V-I characts. obs. 8=44836

Semiconducting devices—contd
p-n junctions—contd
Ge, electroluminescence 8=36509
Ge, high-pressure effects rel. to Δ_1 conduction-band minimum 8=44783
Ge mosaic for image tube, epitaxial growth 8=44844
Ge, tunnel breakdown, microwave oscillations generation 8=40506
Ge:Cu, reverse bias capacitance in breakdown region 8=40515
InAs diodes, stimulated recombinational emission 8=44838
InAs diodes, stimulated recombinational emission 8=49297
InAs radiative recombination mechanism 8=36489
InGa, alloyed, tunnelling electrons scatt. by impurity vibrs.. 1-10°K 8=35938
InP, diffused, I-V characts., 77-590°K 8=35921
InP, radiative recomb. mechanism 8=27159
InP, radiative recombination mechanisms 8=41197
InSb, at liq. He temp., V-I characts. 8=27160
Li, in Si, electron mirror microscopic obs. 8=35922
$Pb_{1-x}Sn_xTe$ laser, i. r. up to 28μ, props. at 12° and 77°K 8=37621
PbTe:In, tunnelling electrons scatt. by impurity vibrs. 1-10°K 8=35938
Si, abrupt and linearly graded, temp. coeff. of breakdown voltage 8=27162
Si, avalanche current temp. dependence 8=49290
Si breakdown development 8=40518
Si, breakdown voltage, effects of multiply-charged Au impurity 8=27161
in Si diode, electron beam active, dynamic response anal. 8=44831
Si, effective carrier ionization coeff. at breakdown 8=27163
Si, electroluminescence 8=36509
Si fast-n dosimeters 8=33790
Si, forward-biased, l.f. noise due to charge fluctuations in depletion layer 8=40519
Si, forward biased, interband recombination model for
Si, shallow ion-implanted, electron beam induced elec. response rel. to surface structs. 8=27129
Si, shallow prepared by ion bombardment 8=40505
Si step, spatial variation of charged Au concentration 8=49295
Si, surface charge inhomogeneity and surface breakdown 8=35923
Si, tunnel breakdown, microwave oscillations generation 8=40506
Si u. v. photocells 8=27338
Si : Au, capacitance meas. 8=44837
Si: Au diodes, minority carrier lifetime meas. 8=49315
SiC, electroluminescence 8=36509
n-SiC (6H): B diffusion counters, for strongly ionizing particles, elec. props. 8=33378
p-SiC-n-CdS heterojunctions, optical and electrical props. 8=40517
Si:P or B solar cells, comparison 8=28507
ZnTe-ZnSe alloys, electroluminescence 8=36521
transistors
alloy junction, diffusion of minority carriers in base region, in mag. field 8=27196
common base, resonance effect in input impedance 8=35939
current gain in n-irrad., prediction, accuracy, influencing variables 8=31412
FET's, insulated gate, carrier mobilities in inversion layers, effect of e irrad. 8=27191
FET, insulated-gate, using Schottky barrier contacts for source and frain 8=49318
FET traveling-wave type, analysis of operation 8=40541
field effect, review 8=35940
field-effect, theory and applications 8=27195
field effect type, junction and bipolar, comparison of n rad. tolerance 8=27194
four-layer structure with deep impurity levels, I–V characts. 8=40539
linear effects on surface props., inverse current and current amplification obs. 8=44787
m.i.s., surface states anal. 8=31415
MOS, e-irradiated selectively, transient and steady-state changes 8=27212
MOS, large signal equiv. circuit for predicting behaviour in pulsed rad. 8=27206
m. o. s., l. f. noise, surface-state related 8=35920
MOS, impedance dispersion mechanisms 8=27210
m.o.s. radiation-hard, good thermal stability, using state-of-the art fabrication techs. 8=31413
MOS, sensitivity to space rad. rel. to processing techs. of gate oxide film 8=27209
MOS, silicon, temperature dependence of threshold voltage, cryogenic range 8=44853
m.o.s. f.e.t. amplification at 4.2°K, test circuit 8=27207
MOSFETs, e-irradiated, thermal annealing characts. 8=27213
MOS-FET's, open geometry p-channel, rad. induced peaking effect 8=27205
MOS-FET's operating in common source mode, irrad. damage 8=27208
metal nitride-oxide-silicon f.e.t. 's, with self-aligned gates 8=44851

Semiconducting devices—contd
transistors—contd
microwave avalanche oscillator with on-off control of oscillation 8=40540
as microwave generator, design and performance 8=27142
optical, noise figure 8=44849
oxide passivated, surface recomb., rad. induced 8=27193
photosensitivity control by light intensity and wavelength changes 8=35941
p-n-p-n devices, spontaneous switching rel. to instability in thyristors 8=27151
reliability in combined environments of temp., vacuum and nuclear rad. 8=27192
response to pulse of ionizing rad., computer prog. 8=27190
step recovery, theory of switching operation, fabrication and characteristics 8=49314
storage-time dimination by Schottky-barrier collector 8=40542
temp. distrib. with i. r. microscope 8=28380
ultra-fast, parameter meas. using a simulator 8=27197
ultra-sensitive miniature temp. sensor with pyroelec. mat. on m.o.s.t. gate 8=46259
voltage stabilizing, efficiency increase 8=33022
CdS thin film, if spray-deposited in air or N_2 8=31414
CdSe, thin film, electron Hall mobility in space-charge layer 8=27199
CdSe thin film, if vapour deposited in vacuum 8=31414
CdSe thin film, instability and stabilization techniques 8=44848
CdSe-SiO_2 t. f. t. s., effects of instability on l. f. characts. 8=27198
GaAs optical, noise figure 8=44849
Ge, alloyed, surface recombination in base 8=27200
Ge, bridge circuit for temp. meas. 8=32984
Ge, emitter injection efficiency meas. 8=44849
Ge f. e. t., low-temp. characts. obs. to 1°K 8=35942
Mo-gate m.o.s.f.e.t., self-registered 8=49316
Si, m.o.s., carrier motion in surface band, $1/f$ noise 8=40213
Si, n-irrad., annealing characts rel. to neutral and space-charge regions 8=27202
Si, noise at v.l.f., .05-.0001Hz obs. 8=40543
Si-on-sapphire, epitaxial bipolar, prep. and props. 8=27214
SiN insulated gate FET's, effect of electron irrad. 8=27201
Si-SiO_2 fast interface state meas. from MOS-C(V) curves at 77°K 8=49320
tunnel diodes
barrier capacitance and built-in voltage 8=44845
binary scaler isolated-diode appl. 8=46933
esaki, current hydrostatic pressure dependence 8=40538
excess and diffusion currents, effect of pressure 8=35934
m. o. s., lineshape of d^2I/dV^2, tunnelling electrons interaction 8=35943
oscillator in freq. transducer for liq. conductivity meas. 8=30521
with parmagnetic impurities in oxide layer, anomalous tunneling theory 8=31410
switching mode, step response and periodic square functions 8=35936
Al barrier decrease on oxidation, cancellation by n-type zone narrowing 8=31459
p-GaAs, degenerate in prep. by closed-space growth using $ZnCl_2$ transport agent 8=44846
GaAs epitaxial layers on Ge 8=30752
GaAs polycryst. films, p-n junctions, characts. rel. to carrier density, fabrication and temp. 8=27188
GaAs, switching by transient ionizing rad. 8=27187
p-$Ga(As_xP_{1-x})$, degenerate in prep. by closed-space growth using $ZnCl_2$ transport agent 8=44846
p-GaP, degenerate in prep. by closed-space growth using $ZnCl_2$ transport agent 8=44846
GaSb, I–V characts. in band structure determ. 8=35764
GaSb, tunneling in crossed elec. and mag. fields 8=35937
Ge films, amorphous, electron tunnelling conductance well 8=31411
Ge, oscillatory behaviour of reverse current, in longit. mag. field 8=27189
Ge, phonon-assisted current components, separation 8=44847
Ge–Au and Ge–In, tunneling theory 8=35932
InGa junctions, tunnelling electrons scatt. by impurity vibrs., 1-10°K 8=35938
PbTe: In p-n junctions, tunnelling electrons scatt. by impurity vibrs., 1-10°K 8=35938
Si, switching by transient ionizing rad. 8=27187
Semiconducting materials
See also Magnetoelectric effects; Photoconductivity; Photovoltaic effects.
$A^{III}B^{V}$ compounds, dissociation by light pulses from laser 8=40437
$A_VB_{VI}C_{VII}$-type, phase transitions rel. to elec. and optical props. 8=27077
alkali halides, electron emission, thermostimulated 8=40697
anthracene, charge-transfer exciton and ionic levels 8=27254
anthracene, current carriers mobilities, temp. depend. 8=31396

Semiconducting materials—contd
- anthracene, hole injection by electrochemical mechanisms 8=45376
- anthracene, singlet exciton-exciton interaction, λ=315-405nm 8=44658
- β-carotene, effect of adsorbed gases 8=31397
- conference, American Ceramic Society 70th annual meeting, Chicago (USA), 1968 8=40085
- crystals, pure, electroluminescence polarization mechanism 8=41180
- diamond, total single-particle energy calcs. 8=40228
- diamond with Al acceptors, photoconductivity spectrum, photothermal ionization and photon-induced tunneling 8=44913
- with dislocations, magnetoconductivity and low-field magnetoresist., n-type 8=35890
- electron-hole plasma l. f. drift instability, appl. of theory 8=40430
- electron irrad., negative resistance due to impact ionization 8=49244
- ethyl chloride, Schottky barrier tunnelling spectroscopy of HCl and CH_3 hindered-rot. lines 8=34327
- extrinsic surface photoconductivity spectrum n-type 8=40663
- film production techniques 8=26120
- films, e.m. power-transmission coeffs., 8=49698
- flying-spot scanner, electrical props. study 8=24383
- glass, and props. in comparison with ordered lattice 8=44806
- heat treatment during prep. rel. to dislocation distrib. 8=26679
- impurity distrib. anisotropy in growing crystals 8=26207
- injection, 2 carrier, current filaments at room temp. 8=40447
- Magnus' Green salt analogues 8=40480
- microcrystal growth from melt on foreign substrate, thermal conditions mathematically analysed 8=26275
- n-type, epitaxial, magnetophonon oscillations in magnetoresistance 8=40448
- n-type, negative resistance appearance, new mechanism 8=40458
- organic, book review 8=27140
- organic, e.s.r. g-shift mechanism due to conjugated π-electrons 8=44747
- organic, properties and applic. 8=49271
- organic, properties and uses 8=49272
- piezoelectric, diffusion coeff. of impurity atoms determ. 8=35491
- piezoelectric, sound amplification wave amplitude dependence 8=44315
- polyacenequinones, specific resistivities, thermal activation energies and energy intervals 8=27141
- polyacetylene, linear, cond. rel. to O content 8=31398
- polyacrylonitrile films, resistivity and photoelec. props., obs. 8=39605
- properties, photoelec. meas. 8=27076
- p-type, electrical conductivity, X-ray induced changes 8=40471
- pyrdytic graphite, Esaki effect at liquid N_2 temp., 8=44764
- p-quaterphenyl, space charge limited currents 8=49274
- rectangular ferrite, minimum switching time calc. 8=27430
- in resistor, thin film, characts., 8=44675
- secondary emission, characteristics meas. 8=49442
- surface phenomena, optical investigation 8=40435
- synthesis and crystallization, universal apparatus 8=48527
- p-terphenyl, space charge limited currents 8=49274
- tetracene, charge-transfer exciton and ionic levels 8=27254
- thin, single-crystal layers, production and props. 8=40436
- triethylammonium:tetracyanoquinodimethan complex, theory for energy gap 8=27139
- II-VI cpds., conference 8=31362
- AgI films, polycrystalline dye-sensitized, thermally stimulated conductivity 8=35994
- $Al_xGa_{1-x}P$, preparation and photoluminescence 8=26233
- AlSb, Se-doped, sharp-line donor-acceptor pair spectra 8=36471
- AnSb, thermoelectric power anisotropy 8=44910
- As_2Se_3, electron emission, thermostimulated 8=40697
- As_2Se_3, thermal cond., Ge and Ag impurities effect 8=44360
- Au-Se_1-Se_2 Au, specific resistance acroes normal section, local distrib. studies 8=49259
- B amorphous layers, switching and negative resistance 8=27079
- $BaTiO_3$ ceramic, I-V characts. rel. to current channeling model 8=40438
- $BaTiO_3$, ionic-relax. polarization 8=35974
- $BaTiO_3$ plates with c-domains, thermodynamic equilib. 8=27081
- $BaTiO_3$:Al_2O_3(SiO_2, TiO_2), conduction promotion by additions 8=49228
- $BaTiO_3$:1 at. %La, cond., thermo-e. m. f. and i. r. refl., polaron model and −198-300℃ 8=35878
- $BaTiO_3$:La, oxide impurity effect on resistivity 8=49229
- $BaTiO_3$:La, resistivity dependence on oxide impurities 8=27080

Semiconducting materials—contd
- $BaTiO_3$: Sm(La), baked electrophoretic films, and dielec. props. 8=44885
- Bi, thin film, thickness depend. of resistivity, Hall const. and magnetoresistance 8=27082
- Bi thin films, transition to semiconducting state 8=27083
- n and p-Bi_2Te_3, conductivity, Hall coeff., carrier lifetime 8=40439
- n-Bi_2Te_3, specific ht. from 1. 3 to 90°K 8=39910
- Bi-Te-Se, scatt. mechanism 8=40440
- Bi-Te-Se (Sb) system, γ-irriad. effects on conductivity 8=44763
- n-$Bi_2(Te, Se)_3$, n-irradiated, thermo-emf, elec. and thermal conductivity 8=27136
- CaO-(B_2O_3, P_2O_3)-V_2O_5 glasses, role of network former in elec. props. 8=27085
- Cd_3As_2, evaporated Hall elements, props. 8=27088
- Cd_3As_2 films, high mobility, prep-by evap. method 8=48447
- $CdCr_2Se_4$, growth and properties 8=48541
- $CdGeP_2$, electrical props. rel. to conc. 8=49791
- $Cd_{0.23}Hg_{0.77}Te$ alloy, quantum yield of internal photoelectric effect 8=35879
- $Cd_{0.11}Hg_{0.89}Te$, semi-metal → semiconductor transition induced by hydrostatic press. 8=27086
- $Cd_xHg_{1-x}Te:Mn^{2+}$, e.p.r. 8=40934
- CdS, acoustic amplification with space- and time-varying parameters 8=30941
- CdS, acoustoelectric interaction nonlinearity 8=35409
- CdS, current-oscillating microwave transmission meas. 8=27087
- CdS, domains, stationary anode-adjacent high-field electron density depend. 8=44769
- n-CdS, elect. cond., 1. 8 to 294°K 8=31369
- CdS evaporated thin film, conductivity rel. to thickness 8=49233
- CdS films, vapour-deposited elec. props. rel. to stoichiometry and impurity conc. 8=26114
- CdS, high field domains used in self-scanning image sensor 8=27317
- CdS, implanted with high energy P^+, change to p type conductivity on implanted surface 8=40443
- CdS, microwave cond. rel. to relax. of excess phonons 8=49234
- CdS monocrystals with blocking cathode, current flow characts. and mechanism 8=49231
- CdS, n-irradiated, dark resistivity and Hall mobility 8=49235
- CdS, oscillatory photocond. 8=31452
- CdS, p type high conductivity, Hall effect and carrier lifetime 8=40444
- CdS, phonon-assisted free exciton recombination 8=44760
- CdS, piezoelectric, current oscillation, nonlinear theory 8=31372
- CdS, piezoelectric, sound amplification wave amplitude dependence 8=44315
- CdS, polycrystalline, capacitive changes with optical excitation, temp. effect 8=49414
- CdS, sound wave coupling mode, at crit. elec. field of current saturation 8=35413
- CdS, stationary high-field domains in neg. differential conductivity range 8=44770
- CdS_xSe_{1-x} crystals, electron effective mass 8=35768
- p-CdSb, negative magnetoresistance, rel. to impurity band conduction 8=35880
- CdSb, p- and n-type, electroconductivity, anisotropy, 5-500°K 8=35881
- CdSb, Ag doped, resistivity and Hall-effect at low-temp. 8=44773
- CdSb: In(Cu), elec. conductivity, Hall effect and thermoelectric power rel. to temp. 8=44768
- CdSe, current noise measurement in relation to light intensity 8=49416
- CdSe, domain formation due to Joule heating 8=44767
- CdSe films, photocurrent saturation 8=44923
- CdSe films, resistance 8=44772
- CdSe lasers, two-photon absorpt. anisotropy in the optical excitation 8=36341
- CdSe, optical props., effect of uniaxial stress 8=36342
- n-CdSe, prepared under N pressure, elec. props. 8=49230
- CdSe, surface enhancement by SiO_2 8=49232
- n-$CdSnAs_2$, elec. props. rel. to temp. and impurity concs. 8=31370
- n-CdTe, electric instability 8=40445
- CdTe, growth process rel. to stoichiometry and electrophysical props. 8=26243
- CdTe, photoeffect due to exciton generation 8=36010
- CdTe, transient currents charact. of deep traps 8=40441
- CdTe, transport phenomena at low temps. 8=44771
- n-CdTe, type conversion and p-n junctions produced by As^+ implantation 8=35882
- $CrTe_{1-x}Sb_x$ alloys, resistivity and Hall effect comp.and temp. dependence 8=35883
- α-Cu phthalocyanine, e.s.r. 8=49608
- $CuAsSe_2$ film, phases and crystal structure from e. diffr. exam. 8=39788
- CuCl, oscillatory photocond 8=31452
- Eu chalcogenides: $(\text{rare-earth})^{3+}$, resistivity anomaly 8=35884
- $FeCr_2S_4$-$CuCr_2S_4$ spinels, elec. transport props. 8=31373
- β-$FeSi_2$:Co, Al, electrical conduction mechanism 8=35885

Semiconducting materials—contd
$GaAs_{1-x}P_x$, effect of Te and S donor levels on direct-indirect transition 8=27093
$GaAs_{1-x}P_x$ injection laser diode, pulsed, temporal-line shift 8=49307
$GaAs_xP_{1-x}$ p-n junction laser, applic. to phase-modulated optical ranging system 8=42110
GaP, band gap from absorpt. meas., 0-900°K 8=45188
GaP, electroluminescent p-n junction obs. 8=36509
GaP, Franz-Keldysh effect 8=36362
GaP, i.r. donor-acceptor pair spectra involving deep oxygen donor 8=36488
GaP, photoluminescence excitation spectra above interband absorpt. threshold and capture cross-sections 8=27647
n-GaP, photoluminescence, influence of Si 8=36496
GaP p-on-n liq.-phase-epitaxial layers in prep. of electroluminescent diodes 8=41229
GaP, synthesis and epitaxial growth by fused salt electrolysis 8=48573
GaP:Te of improved homogeneity, Hall meas. 8=27096
GaP : Zn(Cd), epitaxial growth by $GaCl_2$ vapour transport 8=48544
GaP, (Zn, Te), elec. props 8=48543
GaS layer compound, band structure near Fermi level 8=44774
GaSb band structure from I-V characts. of tunnel diodes 8=35764
GaSb, undoped, electron irrad. effects on elec. props. and recovery 8=27091
n-GaSb, carrier conc. temp. dependence and conduction-band minima 8=49241
n-GaSb, epitaxial growth on p-type substrate 8=44044
n-GaSb, oscillations of longitudinal magnetic resistance in degenerate electron gas 8=40466
p-GaSb, activation energy change due to piezoresistance dependence on stress 8=44776
p: GaSb, elec. conductivity, Hall effect and magnetoresistance rel. to impurity conc. 8=44780
p-GaSb, hole masses, light and heavy, reflectivity meas. 8=35886
p-GaSb, optical modulation by acoustoelect. domains 8=31991
n-GaSb:S, (Se), (Te), conduction-band structure, from resistivity-pressure dependence to 50 kbar 8=49236
GaSe layer compound, band structure near Fermi level 8=44774
$Ge_{1-x}Mn_xTe$, $0.01 < x < 0.1$, Hall const. and s-d scatt. resist., 4.2-400°K 8=40456
$GeSe_{0.75}Te_{0.25}$, optical absorption 8=31994
p-Ge-Si alloys, Hall meas. 8=31377
Ge-Si alloys: Au, electrical conductivity, Hall coeff., donor level 8=40460
Ge-Si alloys, hot-pressed, resistivity and Hall coeff. meas. 8=35893
GeTe, optical and elec. meas. rel. to band structure determ. 8=49726
β-HgS films, conductivity temp. dependence 8=44792
HgS_xSe_{1-x}, $0 \leqslant x \leqslant 0.4$, cond. and Hall effect, 25-300°K 8=40319
n-Hg Te, magnetic susceptibility singularity 8=44981
Hg Te, magnetoplasma reflection rel. to temp. 8=49247
Hg_3Te_3-In_2Te_3 alloys, elec. props. 8=40464
I_2, anisotropic elec. cond., a. c. and d. c., meas. and by thermally generated noise 8=27107
In, photoeffect, I-V characts. on X-irradiation and at 6000 V 8=27325
InAs diode, stimulated recombinational emission from p-n junction 8=44838
InAs diode, stimulated recombinational emission from p-n junction 8=49297
InAs, energy band parameters at 20, 80 and 298°K 8=40240
InAs, films, annealed, elec. props. 8=44794
InAs, magnetoresist., anomalous, in two dim. transport below 4.2°K 8=35905
InAs, non-ohmic transport, non-parabolicity effects 8=27115
InAs p-n junction, radiative recombination mechanism 8=36489
n-InAs, conduction band structure from reflection spectra 8=35771
n-InAs, diffusion of P, coeff. temp. dependence, 650-900°C 8=35496
n-InAs, magnetophonon oscillations in longitudinal thermoelec. power 8=27308
n-InAs, optical susceptibilities, nonlinear, rel. to band structure 8=45219
p-InAs, electrical props. 8=27114
InAs:Cu, elec. props. rel. to effect of Cu and decomp. of solid soln. 8=40473
n-$InAs_xSb_{1-x}$ alloys, e scatt. from thermoelec. and Hall coeff. obs. 8=35758
n-$InAs_xSb_{1-x}$ alloys, Hall coeff., elec. cond. and thermoelec. power obs. 8=40475
In_2O_3, sputtered films, electrical props., intrinsic absorption 8=40469
In_2O_3, sputtered films, near i. r. optical props. 8=40470
n-InSb, photomagnetic effect of hot photoelectrons 8=36022
n-InSe, absorpt. and reflection spectra, optical transitions 8=45196

Semiconducting materials—contd
InP, p-n junction radiative recomb. mechanism 8=27159
n-Mg_2Sn, piezoresistance tensor components, 50-300°K rel. to many-valley processes 8=44800
n-Mg_2Sn, thermal conductivity from 4.2 to 300°K 8=26603
$Mn(Mn_xV^{4+}_xV^{3+}_{2-2x})O_4$, $x < 0.68$, resistivity, thermoelectric power and structure 8=35340
MnO, Hall mobility of electrons and holes at 943°C 8=27118
MnO, thermoelectric force versus resistivity 8=40477
MnO : Li, electrical conduction 8=44801
MnO_2, characts. rel. to contact mats and way of coating 8=31383
NiO, conductivity at h.f. 8=31384
NiO : Li, elec. and mag. props 8=44803
NiS, metallic-semiconducting transition 8=31788
n-PbS, conduction band nonparabolicity 8=35776
PbS films, polycrystalline, polarization currents rel. to oxygen diffusion 8=35909
n-PbSe, conduction band nonparabolicity 8=35776
PbSe:Gd, doping rel. to elec. props. 8=44805
$Pb_{1-x}Sn_xTe$ laser, i. r. up to 28μ, props. at 12° and 77°K 8=37621
PbTe, localized energy levels in forbidden gap, PbTe-Al_2O_3 junction tunnelling obs. 8=35910
p-PbTe-CdTe alloy, magnetoresistance at 77°K 8=49257
PbTe:Na, drift mobility of light-mass holes 8=49258
PbTe:Sb, electrical cond. and Hall effect 8=40478
$PbTe_xSe_{1-x}$ solid solns., forbidden band width temp. dependence 8=40247
PbTe(Se) (S), lattice and electronic thermal conductivities rel. to carrier scattering 8=39951
PbTe-SnTe, general elec. props. rel. to composition 8=44140
PbTe-SnTe-PbS system, current carrier scattering mechanism 8=31385
$PtSb_2$, mobilities of electrons and tides, band gap, carrier conc. 8=40479
Sb, photoeffect, I-V characts. on X-irradiation and at 6000 V 8=27325
p-$(Sb, Bi)_2Te_3$, n-irradiated, thermo-emf, elec. and thermal conductivity 8=27136
p-Sb_2S_3, trap depths from thermally stimulated and dark conductivities 8=44807
Sb_2Se_3 melts, doping effects on conductivity and thermopower temp. dependence, 1300-1400°K 8=34899
SbSi cpds, elec. and photoelec. props. 8=49269
$Sb_2Te_{3-x}Se_x$ syst., struct 8=48677
Se, amorphous, thin layered, voltage-current limits of spatial load 8=40482
Se, electrical conductivity, temp. dependence, thermoelectric power in phase transition region 8=40481
Se, hexagonal, cond. and photocond., effect of reactor irradiation 8=44809
Se layers, specific resistance across normal section, local distrib. studies 8=49259
p-Se, trigonal, electron injection 8=35866
SiC, electroluminescent p-n junction obs. 8=36509
SiC, sintered, heater elements, oxidation ageing rel. to elec. resistivity changes 8=31231
SiO_2, effect on surface of CdSe 8=49232
SiP_2 and $SiAs_2$, preparation and properties 8=40484
Si : Te, resistivity, carrier density and mobility distributions 8=44817
n-SnO_2:Sb, e.-mobility and optical energy gap 8=27135
n-SnO_2:Sb, e.-mobility rel. to opt mode lattice and impurity scatt., 8=49270
SnO_2: Zn, chemisorbed oxygen effect on conductivity 8=31391
SnTe, optical and elec. meas. rel. to band structure determ. 8=49726
p-SnTe, valence band structure 8=44652
$SrTiO_3$, a.c. Hall obs., depend. of Hall mobility on charge-carrier density 8=31392
Te, anisotropy of galvanomagnetic effects, statistical interpret. 8=31394
Te, elect. cond. of single crystal, effect of reactor irradiation 8=31393
Te, magnetoelectric effect, down to 0.05°K 8=35916
$Te_{70}Cu_{25}Au_5$ alloy, amorphous, resistance and thermopower meas., 80-300°K 8=40497
Te-Se-Cd rectifying struct., using Se single-crystal film 8=35930
TiO_2-containing-glasses, small polaron as charge carrier 8=40499
TiO_2, small polaron conductivity 8=40498
TlI, adsorbed organic mols. surface charge-transfer groups form., obs. 8=36028
Tl_2Se film, substrate temp. effect on semicond. props. 8=31395
Tl-Te alloys, liquid, n-type, elect. props. 8=34897
Tl_2Te film, substrate temp. effect on semicond. props. 8=31395
α-U_3O_8, props. from thermoelec. power meas. 8=35999
V_2O_5-containing-glasses, small polarons as charge carrier 8=40499
V_2O_5-P_4O_{10} glasses, elec. cond. rel. to n and γ irrad. 8=27137
VO_2 crystal, semiconductor-metal transition rel. to reflection spectra 8=41150

Semiconducting materials—contd
  VO_2 sputtered films, transport props. 8=27138
  WSe_2, band model calcs. 8=49105
  $Zn_xCd_{1-x}S$ graded-band-bap crystals, growth and elec. props. 8=39696
  $ZnNi_xMn_{2-x}O_4$, conduction mechanism comp. dependence 8=40745
  ZnO, acousto-electrically excited, microwave transmission 8=42011
  ZnO, Brillouin scattering from shear waves in cryst. under high elec. field 8=44325
  ZnO films, polycrystalline dye-sensitized, thermally stimulated conductivity 8=35994
  ZnO, phonon-assisted free exciton recombination 8=44760
  ZnS, drift mobilities of electrons and holes 8=40500
  ZnS electroluminesc. resistor props. 8=27145
 gallium arsenide
  bulk, two circuits using GaAs to generate subnanosec. pulses 8=27094
  conductivity, Hall effect, current instability 8=44779
  current carrier lifetime, effect of heat treatment 8=40449
  defects, rel. to cryst. and epitaxial growth, sawing and polishing, routine handling 8=44427
  depletion layers, large signal a.c. field effect 8=35867
  dielec. constant meas. method 8=44775
  electroluminescent p-n junction obs. 8=36509
  electron concs. and conc.-profiles from Faraday effect obs. 8=40239
  electron distribution function, velocity-field relationship 8=40450
  electro-optical effect, mobile domains 8=44777
  electroreflectance stress dependence rel. to electronic structure 8=49725
  epitaxial films, effect of substrate orientation on electron mobility 8=39592
  epitaxial, for high-efficiency Gunn oscillators, process and device evaluation rel. to doping 8=49283
  epitaxial, surface features and twins 8=35241
  film formation by flash evaporation 8=48450
  film, 2-source vacuum evaporation 8=44045
  Gunn diode, l.f. current fluctuations 8=49302
  Gunn effect, simple transient and non-linear analysis of high-field domain 8=49243
  Gunn oscillator, wide range variable freq. 8=40546
  Hall mobility, microwave, of hot electrons 8=49239
  high field domain vel. meas. and current oscs. in photo-excited sample 8=31374
  high mobility layers, obtained by liq. phase epitaxy 8=30753
  hole masses, light and heavy, reflectivity meas., p-type 8=35886
  insulating region, excitonic, possible existence 8=40514
  interface properties with SiO_2, m.o.s. characts. 8=40446
  i.r. light pulse generator appl. 8=28770
  joule heating in liq. N_2 8=40459
  laser diode critical temp. for excited carriers in exponential of band tail 8=35749
  laser diode, oblique angles betw. resonator mirrors and p-n junction 8=46603
  laser diodes, optical losses and efficiency 8=33213
  laser diode spectrograph, temp. tunable 8=46589
  laser, effect of multiple Zn diffusions on threshold and c.w. output power 8=46615
  laser, electron-beam pumped, nonradiative surface recombination 8=49226
  laser, injection diode, internal mode excitation 8=24341
  laser, injection, optimum stimulation 8=33218
  laser junction, continuous microwave oscills. 8=33220
  laser junction, epitaxial compensated, recombination rel. to temp., and band tailing 8=33225
  laser, liq. N_2 temp., spectral characts. 8=24336
  lasers near room temp., delay characts. 8=33222
  laser structures, thermal impedance meas. 8=33223
  light scattering by charged centres 8=36361
  localized vib. mode of impurities, i.r. active 8=44298
  modulation of opt. abs. at intrinsic edge by acousto-electric domains 8=27570
  n-type, Cu diffusion rel. to transducer prep. 8=35491
  n-type, current saturation 8=49238
  n-type, differential neg. cond. due to intervalley transfer of hot electrons, microwave meas. 8=31375
  n-type, epitaxial, impact ionization breakdown at liq. He temps. 8=27098
  n-type, field effect meas. 150 to 298°K, mobility, relax. and hysteresis 8=35887
  n-type, self-activated luminescence, rel. to Ga vacancy-donor centres 8=36495
  n-type, with high donor conc., diffusion of Zn at 900°C 8=31006
  n-type, UHF emission rel. to acoustoelectric domain 8=27095
  optical attenuation and absorpt. edge after n-irrad., model 8=27569
  photoeffect due to exciton generation 8=36010
  photo-excited, current osc. and high field domain vel. meas. 8=31374
  planar Gunn oscillator for microwave integrated circuits 8=44857
  plasma mode, variation with field 8=40451

Semiconducting materials—contd
 gallium arsenide—contd
  plasma reson. on non-equilib. carriers, refl. obs., 10.6μ 8=40454
  p-n junction laser, applic. to phase-modulated optical ranging system 8=42110
  polaron mass change, conduction band nonparabolicity effect 8=31302
  p-type, Ag-Mn evaporated ohmic contacts 8=49237
  reflective props., change with excitation by laser radiation 8=36367
  resistivity, mobility, impurity levels 8=40452
  space-charge accumulation, limited, effect of doping fluctuations, n-type 8=49242
  stimulated emission delays rel. to temp., trapping model 8=33221
  stimulation, laser structure and applications 8=44778
  surface cleanliness meas. by ellipsometry 8=49240
  surface props, trap density, effects of SiO_2 deposition 8=35144
  surface, {111}, potential temp. dependence 8=44766
  transient temp. distribution and o/p pulse duration 8=33217
  transport, high-field, n-type 8=27097
  trapping analysis 8=27092
  ultrasonic absorpt. prediction 8=35402
  unipolar electroluminesc., by tunnel injection of minority carriers 8=36497
  with Cu atoms as substitutional impurity, charact. recomb. times 8=27089
  GaAs lattice, microwave dielect. const. rel. to temp. 8=27090
  GaAs-InAs solid solns., epitaxial films, crystallization kinetics and structure 8=26119
  GaAs-W junction grown from vapour phase, elec. props. 8=49296
  Si-doped, grown by liquid-phase epitaxy, luminescence 8=27650
  Zn diffusion, reproducible, roles of phase diagram, diffusion and solubility anals. 8=44390
 germanium
  amorphous films, electron tunnelling conductance well 8=31411
  amorphous, resistivity hall effect and photocond. rel. to band struct. 8=44791
  Auger-recombination, indirect band to band 8=35892
  bolometer, cooled, depend, of parameters on conc. of Sb and Ga impurities 8=41855
  breakdown, electrical, low-temp., effect of uniaxial stress on critical field 8=27104
  breakdown at 10°K in extra-pure mat. 8=35894
  carrier momentum relax time and effective mass determ. from microwave magneto-Kerr effect 8=49261
  with compensating impurities, recombination wave excitation conditions 8=35897
  conductivity, accepted e mobility on dislocation lines, obs. 8=35900
  conductivity anisotropy due to warm holes in p-type, elect. field effect 8=35914
  current oscillations in n-type, effect of hydrostatic press. 8=35902
  cyclotron resonance of hot carriers, line width angular dependence 8=35898
  cyclotron resonance of hot holes 8=35807
  cyclotron resonance obs. at 4°K and 70GHz from d.c. thermoelectric current obs. 8=27099
  Δ_1 conduction-band minimum from high pressure effects on p-n junctions 8=44783
  dislocation acceptor level position, n-type 8=35891
  elastic modulus temp. and illumination dependence rel. to carrier generation 8=35702
  electrode-electrolyte interface, surface states and radicals, reln. 8=36599
  electron emission, thermostimulated 8=40697
  electroreflectance at oblique incidence 8=49722
  electroreflectance stress dependence rel. to electronic structure 8=49725
  energy gap rel. to high uniaxial press. along main axes 8=27102
  epitaxially grown layer, sheet resistivity 8=40465
  etched surfaces, low energy electron and u.v. irradiations, rel. to charge condition 8=35901
  f.e.t. low-temp. characts. obs. to 1°K 8=35942
  films, photomagnetic effect spectrum 8=27323
  film, thickness meas., laser i.r. absorpt. 8=35173
  galvanomagnetic effects and negative resistance of hot electrons in bulk specimens 8=31379
  galvanomagnetic recombination effect 8=40461
  galvanomagnetic recombination effect, with unequal Lorentz forces 8=40462
  Hall factor and conductivity, complex, from microwave magneto-Kerr effect 8=27127
  hot electrons, transverse negative differential mobilities, and domain formation 8=40453
  impurity distrib., nonuniform, meas. by anomalous X-ray transmission 8=31376
  impurity doped, epitaxial films, crystallization kinetics and structure 8=26119
  impurity hop conduction in n-type, mag. induced spin-reversal transitions 8=31380

Semiconducting materials—contd
- **germanium**—contd
  - interimpurity radiative recombination, thermal quenching 8=36364
  - internal photo-elec. effect, quantum efficiency 8=49420
  - intrinsic electrodes, pulse meas. of surface photovoltage 8=27753
  - ion bombard., damage and chem. impurity obs. 8=48922
  - i.r. detector, Cu doped, low freq. noise 8=32946
  - joule heating in liq. N_2 8=40459
  - layers, preparation by chem. H plasma transport 8=44781
  - lifetime reduction and recomb. processes on n-irrad., two level model 8=27126
  - linear effects on surface props., obs. 8=44787
  - magnetodiodes, V-A characts. in liq. He. 8=31407
  - mechanical stress effect on diffusion path length of minority carriers 8=35889
  - microwave second-harmonic generation 8=40463
  - minority carrier lifetime, anisotropic pressure dependence 8=27168
  - mosaic for infrared analyzer tube 8=41980
  - n, neg. differential resistance, by electron transfer from (111) minima to <100> minima 8=27105
  - n-type, current oscillations, effect of hydrostatic press. 8=35902
  - n-type, deformed, magnetoresistance and Hall mobility 8=44784
  - n-type, dispersion and absorption in Q-band 8=27572
  - n-type, e.m. rad. absorpt by hopping at low temp. 8=49723
  - n-type, helical surface waves and oscillator effect in electron-hole-plasma 8=27103
  - n-type, hot carrier phenomena rel. to thickness, surface effects. 8=44785
  - n-type, hot carriers, thermoelectric force 8=40641
  - n-type, hot electrons, birefringence and dichroism of microwaves 8=35903
  - n-type, irradiated, conductivity change recovery stages rel. to e. energy 8=44789
  - n-type, magnetically induced spin-reversal transitions in impurity hop conduction 8=31380
  - n-type, phonon-induced electron transitions 8=27100
  - n-type, piezothermo e.m.f., stresses 0-5 × 10^9 dn ′cm^2, 20-140°C 8=40426
  - n-type, Sb-doped, e-irradiated, microhardness and carrier-density, e-flux dependence 8=27101
  - n-type, Sb doped, longit. and transverse, magnetoresistance, elastic deformation effects 8=35899
  - n-type, surface states relax. time obs. 8=44788
  - (111) face, deformations, rel. to Jahn-Teller effect, LEED obs. 8=26917
  - optical susceptibilities, non-linear, rel. to band structure 8=45219
  - oscillations, hot carrier, spatial depend. in n-type 8=44786
  - oscillator effect 8=49245
  - oscillatory magneto-photoconductivity effect rel. to photon energy 8=40661
  - passivation by Ge_3N_4 film growth on stained surfaces 8=48451
  - photoconductivity, absorption, in direct transition region 8=40664
  - photoconductivity, group III and V impurities photothermal ionization spectroscopy, obs. 8=40662
  - photoconductivity in space charge region, calc. 8=31451
  - photoconductivity spectra 8=44925
  - photoeffect due to exciton generation 8=36010
  - plasma oscs., effect of elec. field and energy dissipation law 8=40276
  - plasma reson. on non-equilib. carriers, refl. obs., 10.6μ 8=40454
  - plastic deform of p- and n-doped, rel. to prod. of p-n junctions 8=44835
  - p-n junction, diffused, low-breakdown-voltage, reverse V-I characts. obs. 8=44836
  - p-type, Ga-doped, e-irradiated, microhardness and carrier-density, e-flux dependence 8=27101
  - p-type, impurity a.c. cond. and phonon-induced hopping, calc., 10^2-10^5 cps 8=35888
  - p-type, noise of hot current carriers 8=40457
  - p-type powder, mechanism of H_2O chemisorption 8=35192
  - p-type, transverse magnetoresistance and Hall effect field and temp. dependence 8=44790
  - radiation defects, reduction of rate of formation by heat treatment 8=31152
  - reflective props., change with excitation by laser radiation 8=36367
  - resistivity, mobility, impurity levels 8=40452
  - resistivity, temp. coeff. near room temp. 8=44820
  - shallow impurity surface states 8=44810
  - strained n-type, intervalley transfer and microwave current, oscills. 8=26881
  - surface conductivity of cleaved surfaces 8=40455
  - surface conductivity rel. to clean surfaces and O_2 adsorpt. 8=48421
  - surface, electronic states, effect of metal impurities 8=40257
  - surface exam. by total internal reflection spectroscopy 8=35895-6
  - surface structures, computer calcs. 8=30721
  - target in photodiode 8=41982

Semiconducting materials—contd
- **germanium**—contd
  - thermoelec. eddy current expt. in n type 8=40642
  - thin, single-crystal layers, production and props. 8=40436
  - transistor bridge circuit for temp. meas. 8=32984
  - transport properties, crystal symmetry rel. to theory, p-type 8=26907
  - tunnelling diode, current oscillatory behaviour, in longit. mag. field 8=27189
  - Au$^=$ centres, dynamics of slow domains, shape depend. 8=49215
  - n-Ge:Au, size and shape of electrical domains 8=44782
  - Ge:In far i.r. photocond., detector, response time 8=32945
  - Ge(Li) detector surface protective coating 8=46913
  - Ge(Li), effects of fast n bombard. in γ detectors 8=42453
  - Ge(Li) planar detectors, low rising pulse obs. 8=37791
  - Ge(Li) radiation detectors, coaxial, current and charge pulses 8=46911
  - n-Ge:Mn, Sb compensated, current oscills. rel. to recomb. waves, obs. 8=31378
  - Ge-Si solid solutions, electronic props 8=49225
  - Ge-Si(GaAs) abrupt heterojunctions, fabrication by solution growth 8=49293
  - Ge:Zn, Sb, photodielectric effect 8=27322
  - Li driftability 8=49246
  - Sb-doped, electron mobility at high temperatures 8=49086
  - with ZnSe epitaxial layers, growth and elec. characts. 8=44834
- **indium antimonide**
  - acoustoelectric phenomena, by acoustic wave packets injected from CdS 8=27112
  - avalanche plasma, instabilities 8=49227
  - avalanche plasma prod. by impact ionization, instabilities 8=35794
  - band structure, including spin-orbit effects 8=44825
  - carrier waves, growth obs. 8=35908
  - conduction band carrier density, theoretical investigation under carrier multiplication condns. 8=44793
  - cyclotron resonance lines resolved rel. to intraband transitions 8=44796
  - electrical props., effect of dislocations 8=49254
  - electron effective mass, pressure effect 8=35772
  - electron mobility investigation 8=31381
  - electron spin resonance, n-type 8=27477
  - film microminiature Hall probe 8=28509
  - films, surface photoconductivity and field effect 8=27326
  - impact ionization rates and instabilities, effect of mag. fields 8=31303
  - impurity states, mag. field depend., n-type 8=49250
  - intrinsic, conductivity in high electric fields 8=49253
  - i.r. detector amplifier 8=41856
  - l.f. plasma instability in weak mag. fields 8=49126
  - magnetoresistance rel. to method of preparation of crystals 8=44798
  - microwave conductivity in hot e. region, small signal anisotropy 8=44795
  - microwave emission from nonequilib. plasmas in mag. fields 8=40476
  - microwave emission spectrum 8=31382
  - microwave emission stimulated by acoustic wave amplification 8=49249
  - microwave instabilities in plasma, theory 8=26930
  - Nernst-Ettingshausen effect, magnetophonon oscs., n-type 8=27113
  - non-ohmic transport, non-parabolicity effects 8=27115
  - n, Hall angle at 77°K, rel. to angle between current and mag. field 8=27109
  - n-type, acoustic amplification of 9GHZ waves due to application of elect. field 8=39892
  - n-type acousto-electric domains, helicon diagnostics 8=49256
  - n-type, compensated, l.f. oscillation generation 8=40474
  - n-type, e-effective mass pressure dependence from magnetophonon resonance meas. 8=27110
  - n-type films, dendritic, microwave magnetoresistance 8=27111
  - n-type, galvanomag. props. at 77°K 8=27117
  - n type, high mobility, resonant and round trip acousto-elect. gain 8=44797
  - n-type, impurity conc. determ. from I-V characts. 8=35906
  - n-type magnetoresistive magn. field sensor for He temps 8=46367
  - n-type, microwave conductivity in high elec. field 8=49251
  - n-type, photoconductivity kinetics and noise spectrum 8=27327
  - optical susceptibilities, non-linear, rel. to band structure 8=45219
  - p-n junctions, V-I characts. at liq. He temp. 8=27160
  - p-type, longit. magnetoresistance magnetophonon oscills. 8=35904
  - p-type single crystals, magnetoresistance and Hall effect 8=49248
  - photoconduction, surface, in p-type 8=44927
  - photoconductive detectors in the far i.r. 8=40666
  - photoeffect, I-V characts. on X-irradiation and at 6000 V 8=27325
  - photoelectricity, alternating voltage induction by modulated waves, n-type, 0.8-10 mm 8=49421

Semiconducting materials—contd
  indium antimonide—contd
    piezoelectric interact. of u.h.f. acoustic waves with drifting electrons 8=27116
    plasma effects, electron-hole prod., instabilities and decay 8=27108
    plasma, nonequilibrium, magnetoconductance 8=44667
    resistance, negative, current-controlled, and instabilities 8=35907
    S-doped films, electron mobility 8=49255
    surface, electronic configuration 8=26916
    thin plate in waveguide, field distrib. 8=49385
    transverse breakdown, Hall voltage caused by instability 8=40468
    ultrasonic absorpt. prediction 8=35402
    InSb-InAs alloys, Hall coeff. and conductivity meas., 300-700°K 8=40472
    InSb: Mn, temp-dependence of Hall effect, electrical conductivity and mobility 8=44799
  silicon
    annealed surfaces, nature 8=30727
    anodized surface potential 8=44816
    avalanche discharge, noise 8=35933
    Brillouin zone, wave function expansion 8=26910
    carrier density rel. to conductivity after ion irradiation 8=44814
    carrier lifetime depend. on excess density for n-irrad. 8=27125
    carrier mobility of epitaxial films on spinels 8=35181
    carrier momentum relax time and effective mass determ. from microwave magneto-Kerr effect 8=49261
    carrier removal and annealing on n-irrad., influence of impurities 8=27124
    clean surface, influence of adsorbed Au, Sb or O_2 on elec. props. 8=27134
    conductivity anisotropy due to warm holes in p-type, elect. field effect 8=35914
    crystal (100) face, inversion layer, magnetoresistance at 77°K 8=27130
    cyclotron reson. of holes in p-type 8=44819
    d.c. photodecay meas. rel. to minority carrier lifetimes 8=40490
    deep impurities, lifetime and capture cross-sections 8=35911
    defects, electrically active, introduction rates in n- and p-type mat. on e.- and n.-irradiation 8=39998
    diffused layers, meas. of surface concs and junction depths 8=49265
    diode p beam dosimetry 8=38064
    donor properties of N_2, p-type 8=27128
    doping by Al ion implantation 8=40485
    double injection currents, exptl. investigation, p-type 8=40493
    drift vel. of hot carriers, exptl. results, and assoc. anisotropic effects 8=44821
    electroluminescent p-n junction obs. 8=36509
    electron emission, thermostimulated 8=40697
    electron scatt. at 50-625 keV, obs. 8=33638
    electronic structure of surface, influence of thermal treatment 8=40487
    electroreflectance stress dependence rel. to electronic structure 8=49725
    energy gap rel. to high uniaxial press. along main axes 8=27102
    epitaxial film doping on deposition of $SiCl_4$ with gaseous impurity, deposition conditions effect 8=44811
    epitaxial films on sapphire, prep. and props. 8=40491
    epitaxial layer, impurity conc., non-destructive determ. using metal-silicon Schottky barrier 8=44815
    epitaxial layers, photoelectric meas. of electrical parameters 8=35915
    epitaxial layers, by sublimation in vacuum 8=35256
    film deposition on sapphire, by electron beam evap. 8=44056
    film, on quartz substrate, deposition, struct. and elec. props. 8=35180
    film on sapphire, vacuum deposition 8=44057
    films, epitaxial, autodopant transfer from n-type substrate 8=44812
    films, 1-2μ thick, epitaxially grown on sapphire, carrier transport 8=40489
    Hall factor and conductivity, complex, from microwave magneto-Kerr effect 8=27127
    impurity distribs. resulting from B^{11}, N^{14}, P^{31} and As^{75} implants 8=27131
    injection level and temp. depend. of transient annealing in n-irrad. devices 8=27122
    interband Faraday rotation and ellipticity at absorpt. edge 8=36404
    ion-implanted, impurity distrib. 8=49266
    ion implanted layers, Hall meas. 8=44822
    ion injection, profiles and channelling dose depend., obs. 8=44813
    junction form by B, N and P ion implantation 8=49263
    Landau levels in surface quantization capacitance obs., p-type 8=40492
    layers, preparation by chem. H plasma transport 8=44781
    LCAO energy bands, empirical third neighbour 8=49106

Semiconducting materials—contd
  silicon—contd
    lifetime reduction and recomb. processes on n-irrad., two level model 8=27126
    lineshapes for deform.-potential coupling to optical phonons 8=35943
    masking films, stress effects rel. to devices 8=49047
    with metallic impurities, gettering effect 8=40494
    with metal surface impurities, effect on elec. props. of m.o.s. structures 8=35944
    n-type, Au-doped, noise temp. and light-illumination dependence 8=44824
    n-type, electron spin-lattice relax., conc- and compensation-dependence 8=27489
    n-type, e.m. rad. absorpt. by hopping at low temp. 8=49723
    n-type, hot electrons, absorption by surface 8=49260
    n-type, hot electrons, birefringence and dichroism of microwaves 8=35903
    n-type, oxide layer effect on surface recombination velocities 8=40486
    n-type, phonon-induced electron transitions 8=27100
    n-type, semiconductor to metal transition 8=40252
    neutron irradiated, disordered regions formation from carrier mobility decrease 8=35551
    nuclear dynamic polarization by optical electronic saturation and optical pumping 8=30632
    ohmic contacts by rubbing with Au 8=49286
    (111) face, deformations, rel. to Jahn-Teller effect, LEED obs. 8=26917
    optical susceptibilities, non-linear, rel. to band structure 8=45219
    oxidized, surface props. rel. to device technology 8=49267
    passivation props of $Si_xO_yN_z$ films 8=49351
    photoconductive spectral response, possibility of observing electron-phonon Umklapp-processes 8=27315
    photoconductivity in space charge region, calc. 8=31451
    photoconductivity, surface, rel. to illum. intensity and temp. 8=27330
    piezoresistance meas. of stress difference 8=45943
    plasma oscs., effect of elec. field and energy dissipation law 8=40276
    plasma reson. on non-equilib. carriers, refl. obs., 10.6μ 8= 40454
    p-n-junction avalanche current temp. dependence 8=49290
    p-n junction reverse current meas. rel. to gettering processes 8=44077
    polarization effects in SiO_2 insulating film 8=44854
    proton damage effects in surface-barrier detectors 8=46918
    p-type crystal, ohmic contact with Al wire 8=40483
    p-type, elec. fluctuations due to hot electrons, room temp. and liq. N_2 temp. meas. 8=35759
    p-type inversion layers, mobility anisotropy and piezoresistance 8=27133
    p-type, n-irradiated, dimensions and conductivity of disordered regions temp. dependence 8=35913
    p-type, solar cell mat., electron damage coeffs in orbit, calc. 8=27123
    p-type, thermomag. effects, 100-400°K rel. to phonon drag 8=35912
    recombination rates, surface and bulk, effects of Co^{60} γ-irrad. 8=27120
    reflection of electromagnetic energy in mm. range 8=31934
    resistivity by four probes method 8=49252
    resistivity, mobility, impurity levels 8=40452
    resistivity, temp. coeff. near room temp. 8=44820
    saturation drift vels. of carriers, determ. from I-V characts. in space charge limited region 8=31387
    shallow impurity surface states 8=44810
    single-particle energy calcs. 8=40228
    solar cells, e irrad, role of Li in degradation and recovery of diffusion length 8=28508
    solar cells in-flight performance, computer prediction 8=24086
    solar cells, p-irrad., characts. during thermal annealing 8=24105
    solar cells, surface effects, study with low energy p 8=28506
    spin-lattice relax., concentration depend., n-type 8=45107
    surface conductivity rel. to clean surfaces and O_2 adsorpt. 8=48421
    surface damages after thermal treatment of Si-SiO_x system 8=49276
    surface Fermi level and work function from photoelec. emission, n-, p-type and caesiated, 80-290°K 8=40495
    surface micro p-n junctions, electrically-decorated by Pt 8=40496
    surface structures, computer calcs. 8=30721
    thermally oxidized, majority carrier surface mobilities 8=31390
    thermal treatment, surface imperfections 8=30728
    transport props. of electrons in inverted surfaces 8=31388
    web crystal, resistivity homogeneity 8=31389
    web-dendrites, dislocation origin and reactions 8=26692
    Au and Cu impurity and dopant distribs. on pulling crystals in floating-zone technique 8=40015
    B-doped, Hall effect and elec. cond. obs. 8=49268

Semiconducting materials—contd
  silicon—contd
    B redistribution in Si with SiO_x coating 8=48793
    n-GaP, rel. to photoluminescence 8=36496
    In and Tl ion implanted, diffusion from subst. to interstitial sites 8=40007
    Li-doped, Hall effect and elec. cond. obs. 8=49268
    Li doped, majority carrier removal rates for e irrad. 8=27121
    Ni contacts, plated, on n- and p-type, quality 8=44823
    P diffusion, vacuum method using $POCl_3$ as source 8=48792
    P-doped, Hall effect and elec. cond. obs 8=49268
    P^+ bombard., struct. defect conc. rel. to temp. 8=48831
    Si:Au, emission rates of Au acceptor level, photocurrent determ. 8=40674
    Si-B phase surface layer after exposure to diborane, tech appls. 8=49264
    p-SiC–n-CdS heterojunctions, optical and electrical props. 8=40517
    p-Si:Cu, resist. and Hall consts. 8=49262
Semiconductors
    See also Crystal electron states; Magnetoelectric effects; Photoconductivity; Photovoltaic effects.
  $A^{III}B^{V}$ crystal orientation determ. by light refl. 8=39645
  $A^{III}B^{V}$, mobility, distribution function, temp. dependence 8=35860
  absorption in electron-optical-phonon system at zero temp. 8=27532
  acoustic domains and I-V charact. under acoustic instability condns. 8=27053
  in alternating elec. field, reaction of system with moving elec. domains 8=35863
  amplification and absorption of hypersound Mott excitons 8=39888
  amplification of ultrasound 8=39887
  antiferromagnetic, conductivity electron state, autolocalized, new 8=40429
  antiferromagnetic, coupled spin, plasmic and e.m. waves in const. fields 8=40771
  bandgap dependence and related features of radiation ionization energies 8=27065
  blende-type structure, anomalous X-ray scatt. rel. to polarity determ. 8=45153
  bulk, dynamics of high-field propagating domains 8=49221
  bulk, surface transport props. 8=27063
  carrier recombination of disordered regions, statistics 8=40431
  catalysts, combined action with metal 8=49906
  cathodoluminescence, obs. 8=41187
  with chalcopyrite structure, band structure 8=26887
  charged impurities, dielec. response model 8=49222
  charged prod. determ. method 8=49224
  chemisorbed molecules, electronic processes, reactivity in semiconductor 8=41267
  complex, magnetic resonance 8=40889
  conductivity, changes with elect. field, expt. using stationary high-field domain analysis 8=31368
  coupled lattice, plasmic and e.m. waves 8=31304
  current noise, double injection 8=44748
  cyclotron resonance from static conductivity changes 8=26934
  cyclotron resonance of hot electrons, theory 8=44749
  deformed, many-valley (Ge and Si type), photoconductivity kinetics rel. to intervalley transitions 8=36002
  degenerate, generalized Einstein relation, alternative formulation 8=49218
  degenerate, strong quantum damping of helicons 8=49121
  degenerate, superconductivity 8=49188
  Dember voltage, ohmic contact effects 8=44911
  diamond and zinc-blende type, band struct. and optical props. 8=44753
  diffusion instabilities 8=26616
  diffused layers, meas. of surface concs. and junction depths 8=49265
  diffusion processes, sequential, interactions 8=48770
  diffusion, simultaneous and consecutive, of impurities rel. to internal elec. field 8=30997
  dimensions effect on Alfvén and helicon waves in plasma 8=40278
  domains, steadily travelling, velocity and current determination, and recombination instability 8=49215
  donor-acceptor pairs rel. to radiative recombination, review 8=27055
  doping during ion implantation, substitutional 8=27070
  doping profile evaluation near p-n junction from capacitance meas. 8=27072
  drift temperature waves stability 8=44756
  effective mass of carriers, microwave methods of meas. 8=26898
  electrical cond. calc. in strong elec. field 8=27075
  electrical domains instability 8=49212
  electro-absorption, excitonic effects 8=31297
  electron excitation nonlinear, in strong a.c. elec. field 8=49209
  electron-hole plasma, l.f. drift instability 8=40430
  electron injection into p-type 8=35866
  electron mechanism for superconductivity 8=40338
  electron-phonon inelastic scatt. in many-valley semicond. dissipative effects loss 8=31264
Semiconductors—contd
  electron transitions, USSR work over 20 years, development survey 8=35869
  electroluminescence, review 8=36464
  electro-optical anisotropy 8=35859
  electro-optical effects, Green's function calc., general formalism and interband transitions 8=35861
  electroreflectance studies, light source control system 8=27062
  e.m. wave amplification, carrier diffusion effects for neg. I–V charact. 8=26923
  evaporation by laser irradiation, obs. 8=39494
  exciton interacts., scatt. props., ground state energy and Bose condensation 8=40263
  exciton theory in crystals with complex band structure 8=49112
  ferromagnetic, coupled spin, plasmic and e. m. waves in const. fields 8=40771
  ferromagnetic temp. range 8=49509
  films, surface capacitance rel. to thickness 8=35873
  film, thin, field ionization 8=31463
  Franz-Keldysh effect, high-freq. 8=31950
  free carrier autooscillations recombination 8=49077
  generation-recombination statistics, two-centred model 8=35872
  glass, and props. in comparison with ordered lattice 8=44806
  gradient instability of currents 8=44754-5
  growing surface waves in presence of transverse mag. field 8=35868
  Gunn effect, application in e. s. r. meas. 8=40890
  Gunn effect, intervalley transfer, plasma freq. test 8=44758
  Gunn effect oscillator, theory for dynamic behaviour and efficiency in l. s. a. operation 8=27203
  Gunn effect, theoretical model 8=49210
  Gunn instability, soft plasma mode 8=31365
  Hall effect and conductivity, high-resistivity, single electrometer method of meas. 8=27060
  Hall effect and conductivity, remote meas. apparatus 8=49220
  Hall effect and conductivity, single electrometer method of meas. 8=27060
  Hall effect constant meas., thin films 8=40424
  heavily doped, possible use of slow neutron scattering study 8=44759
  heterogeneous systems dielec. losses 8=44757
  high photovoltages, origin 8=49401
  homogeneous, microwave mixing by hot electrons 8=27056
  hot electron kinetics, using non-equilib. density matrix 8=27067
  impact ionization of impurity atoms, in strong elec. fields 8=35864
  impurity conc. meas. by simplified MIS method 8=27073
  impurity profiles from ion implants, statistical model 8=27132
  inhomogeneously doped, mobility gradient effects on minority carrier lifetimes 8=40432
  inhomogeneous, non-linear second harmonic generation at low temp. 8=49211
  interband transitions in mag. field and strong e.m. wave 8=31261
  intrinsic, current instability in Ohm's law region 8=35862
  intrinsic, laser emission by direct band-band transitions 8=36291
  ion-beam interactions, regularities 8=48892
  ion bombard. induced conductivity 8=26861
  ion implantation sources, description rel. to types of metals used 8=27068
  ionic, nonlinear thermoelectric phenomena, theoretical study 8=35992
  isotropic, total single-particle energy calc. 8=40228
  laser, electron-beam-pumped, effect of inhomogeneous minority carrier distributions 8=28696
  laser generation efficiency, increase using amplification of a resonator 8=28695
  laser, thermal operating conditions, continuous generation region 8=37599
  lifetime meas., by contactless photomagneto-electric effect method 8=40648
  light absorpt. and form. of electron-hole complexes 8=31941
  light absorption, nonlinear negative, in inhomogeneously inverted semicond. 8=31943
  light scattering by charged centres 8=36361
  liquid, applicability to nuclear reactor thermometry 8=34110
  magnetic, indirect exchange interactions, intervalley transitions effect 8=40768
  magnetic, spin-disorder scattering of carriers 8=27058
  magnetic, thermal and mag. induced optical absorpt. edge shifts rel. to strain 8=36299
  magnetoabsorption, multiphonon, theory 8=45156
  magnetooptic interband absorpt., effect of spatial dispersion of optical phonons 8=45160
  magneto-optical absorption spectrum in exciton region, elec. field effects 8=36305
  magnetoresistance at low temp., rel. to impurity 8=27069

Semiconductors—contd
- many-valley dissipative effects disappearance 8=40427
- many-valley, indirect exchange interactions 8=36085
- metal contacts, potential barriers 8=35924
- metal-insulator transition for donors in random array of centres 8=40206
- model for elec. cond. in alkali metal vapour 8=43696
- m. o. s. capacitance at v. l. f., meas. 8=35945
- narrow-gap, displacive vibronic phase transitions 8=49075
- negative conductivity with equilib. electrons in quantizing mag. field 8=49403
- with non-constant mobility, waves 8=49219
- nonlinearity of relationship between current density and electric field strength, due to strong electric field 8=46351
- nuclei polarization on e-heating in cyclotron resonance 8=35806
- optical mixing by mobile carriers 8=44750
- optical phonons interaction with electrons in impurity states 8=44629
- organic cpds, donor-acceptor type, polarization energy calc. 8=29947
- organic, dark cond., energy gap and pre-exponential factor 8=26891
- organic, kinetic transport coeffs. 8=40425
- organic materials, properties and uses 8=49272
- organic, mechanisms 8=28742
- organic, photoconductivity meas. in SHF band 8=49406
- organic, with π-electron chains, elec. cond. mechanism 8=26893
- organic, with short-range order, carrier generation and transport 8=26879
- panel, spot excitation 8=49214
- paramagnetic resonance, problems 8=40897
- permittivity of free electrons, quantum theory 8=35761
- phonon excitation by elec. field 8=27059
- photoconductivity due to localized excitation 8=27312
- photoconductivity, exciton-exciton collision contrib. 8=36000
- photoconductivity, light polarization depend., mechanisms 8=49405
- photoconductivity in presence of band bendings on surface 8=40646
- photoconductivity spectral response, possibility of observing electron-phonon Umklapp-processes 8=27315
- photoconductivity, transient process study using regenerative microwave system 8=49400
- photocurrent in semiconductor without symmetry centre 8=49404
- photoemission, calculation methods 8=49441
- photothermal effect in sinusoidal state 8=30981
- physics and electronics, English-German; German-English dictionary 8=41609
- with piezoelectric and deformational electron-phonon interactions, attenuation of hypersound by excitons 8=44311
- piezoelectric, high-elect.-field galvanomag. effects 8=31366
- piezoelectric, nonlinear phonon interaction and effect on current saturation 8=31367
- piezoelectric, non-ohmic conduction, transport eqns. for e and phonons 8=27061
- piezoelectric, photoelectroacoustic effect and resonance phenomena 8=35871
- piezoelectric-polaron effect on cyclotron resonance, calcs. in quantum limit 8=40283
- piezoelectric, propagating acoustoelec. high-field domain, simple analysis 8=40423
- piezoelectric, sound generation in alternating field rel. to elastic oscills. instability 8=30940
- piezoelectric, u. s. wave amplification and current saturation, non-linear theory 8=44312
- piezoelectric, with traps, sound amplification theory 8=35404
- piezoresistance meas. by cyclic stress 8=35876
- plaquettes, Hall fields 8=44752
- plasma eqns. soln. 8=35745
- plasma, overheating instability in crossed elec. and mag. fields 8=40421
- polarisation at high voltages, conditions 8=27064
- polar, warm electron temp. and mobility 8=40214-5
- polymeric, band conduction and fluctuations 8=27066
- population inversion at lasing threshold, rel. to impurities 8=46601
- with rare earth additives, thermal rad. during thermionic emission 8=31465
- recombination of electrons and holes, inter-impurity statistics 8=31363
- recombination waves at long wavelengths, nonlinear theory 8=27054
- reflection of electromagnetic energy in mm. range 8=31934
- removal of thin layers from surfaces, ion bombardment-enhanced solubility 8=40068
- resistivity distrib. meas. from β cond. response 8=35877
- resistivity ratio, automatic meas. apparatus 8=33013
- rotation of polarization of e.m. waves, in strong elec. field 8=31364

Semiconductors —contd
- sandwich, mid-region, small signal bulk minority carrier lifetime determ. 8=49216
- saturation drift vels. of carriers, determ. from I-V characts. in space charge limited region 8=31387
- Schottky barrier meas., light source control 8=35875
- scintillation phosphors, CdS:Te and ZnTe:O for particle detection 8=46864
- space-charge layers, accumulation and inversion approximations 8=44762
- space-charge layer, minority carriers distrib. 8=40433
- space-charge-limited currents in presence of donors 8=35870
- specific conductivity meas., thin films 8=40424
- spectral intensity of current fluctuations in strong electric fields 8=40428
- with spheroidal conduction band, optical absorpt. due to donor electrons 8=36293
- spin-e-phonon coupling const., magnetooptic interband absorpt. meas. 8=27074
- structure, protonographic exam. 8=26363
- superconducting, acoustic dispersion theory 8=35403
- superconducting and insulating mechanisms 8=26886
- surface band bendings, rel. to photomag. determ. of surface recombination vel. 8=40434
- surface-barrier stability 8=49223
- surface electron states calcs. using pseudopotential method 8=35783
- surface layers, transverse impedance and field-effect theory, rel. to nonequilib. carrier generation 8=26915
- surface phenomena, optical investigation 8=40435
- surface props., chem. control, two- and one-equiv. additives 8=35874
- surfaces, review 8=44761
- surface states, intrinsic, model 8=35785
- theory 8=49213
- thermal conductivity meas. by bridge method 8=39942
- thermal conductivity, 100-400°K 8=44357
- thermoelectric power meas. 77°-600°K 8=31446
- thermogalvanomagnetic phenomena at high mag. fields 8=44751
- thermopower calc. in quantizing mag. field allowing for phonon drag 8=35993
- thin films, temp. variation using thin film thermocouples, props. rel. to thickness 8=40638
- III-V and II to VI compounds, chem. bonding and structure 8=30614
- III-V compounds, appl. to integrated circuits and arrays 8=44856
- III-V compounds, electron-hole radiative recomb., review 8=45248
- transient radiation effects on electronic components 8=31126
- transport coeff. calc. for constant-energy surfaces with cubic symmetry 8=35865
- transverse electrical conductivity, spherical energy band 8=49217
- trap parameters, determ. by thermally stimulated capacitor discharge method 8=27052
- trapping centre parameter investigation by thermo-stimulated capacitor discharge 8=27071
- u.s. amplification, theory rel. to high dielec. const. 8=35405
- vitreous, recombination radiation 8=36453
- wave motion, energy-depend. mobility in small-signal anal. 8=26924
- wide gap, large signal a. c. field effect in depletion layers 8=35867
- wurtzite type, mag. levels of holes in upper valence bands 8=49094
- X-band Gunn oscillators, freq. modulation noise 8=27143
- zero-gap, frequency dependent dielectric function at low temp. 8=40422
- zero-gap, static dielectric function, behaviour 8=27057
- CdS implanted with high energy P^+, change to p type conductivity on implanted surface 8=40443
- GaAs Gunn diode, l.f. current fluctuations 8=49302
- GaP, synthesis and epitaxial growth by fused salt electrolysis 8=48573
- InSb type, electron scattering 8=40217
- InSb type, transport phenomena, inelastic carrier scattering 8=40467

Semi-insulating materials (high-resistivity semiconductors). See Semiconducting materials.

Semimetals. See Metals; Semiconductors.

Series
- Fourier integrals representations 8=45975
- Padé approximation, generalization 8=45969
- Stieltjes with nonzero radius of convergence, bounds and Padé approximants 8=32652

Sferics. See Atmospherics.

Shadow universe. See Cosmology; Elementary particles.

Shear strength. See Mechanical strength/shear.

Shell model. See Nucleus/models.

Shielding. See Radiation protection.

Shock tubes
- diaphragm clamp, gas-operated 8=46160
- diaphragm cutter, fast acting 8=32630

Shock tubes—contd
diaphragm-type, for high speed shocks 8=37252
coupled to molec. beam mass spectrometer, to obs. gas phase chem. reactions 8=45321
electric, with diaphragm, use in study of luminous flow region ahead of cylinder 8=47943
entrance region flow, coupling bet. inviscid flow and compressible boundary layer 8=25803
flow round models, inside use of interferometer with diffraction grating for investigation 8=39172
heat transfer, end-wall, secular change obs. 8=34653
high-vacuum valve 8=32900
ionizing waves, vel. rel. to initial gas press., drive current and mag. field 8=43529
low-density, resistance film gauge 8=32899
m.h.d. generator, unsteady flow 8=28594
pinch, current sheet dynamic obs. 8=34448
plasma temp. meas. by X band rectangular waveguide probe 8=30091
pulse delay time interval multiplying circuit 8=46338
test times, effect of boundary layer growth 8=46159
vapour condensation, electrostatic effects 8=23943
Ar plasma, azimuthal current and Hall e. m. f. in radial mag. field, obs. 8=34485
Ar–O, dissoc., flow heat transfer meas., with catalytic flat plate 8=25826
Cl at. spectrum, spectroscopic investigation 8=29610
T-type em. tube, for temps 720,000°K, spectral anal. of vacuum u.v. rad. 8=39109

Shock waves
See also Detonation; Explosions; Supersonic flow.
in air, chemical nonequilib. radiating normal wave 8=39182
air, non-equilibrium ionization by front of shock wave at 5-10 km/sec velocity 8=29959
air, spark, laser-induced, theory 8=28369
arrival timing by Al pressure switches 8=32904
atmosphere, effects of earth's rotation 8=36724
in atmosphere, from strong explosion, propag. upward 8=28371
binary gas mixture, structure of normal waves 8=30261
blast, intermediate strength, trajectory and overpress. eqns. 8=46171
boundary layer following shock over semi-infinite plate in tube, heat transfer and shear stress 8=28386
of bullets, acoustic characteristics, survey 8=46163
compression, at low pressure, calc. method 8=39183
convergent, under Chapman–Jonguet conditions 8=41835
data, for minerals, phase implication in lower mantle 8=41321
detection, with plastic tapes 8=23944
detonation, propagation, asymptotic laws 8=46172
detonation velocity meas. by piezoelec. coaxial transducer pins 8=41836
differencing methods for flow, comparison rel. to coding, resolution and execution time 8=34632
earth's bow, plasma wave emission 8=41389
in elastic rod, anal. 8=46166
electromagnetic, steady-state solution, laser pulse propagation in Kerr liquid 8=46549
e.m. tube, ionizing, coincident and reflected structure 8=43472
e.m. waves in nonlinear active lines, similar to detonation wave in gas 8=46168
electron-fluid-dynamical waves, nature 8=28546
explosions at ocean surface 8=28372
explosions due to pressurized spheres at ocean surface 8=27867
front structure in e. m. non-linear transmission-line 8=42027
gas and dust clouds, collision 8=45725
in gas binary mixtures, struct. rel. to eqns of state of gas 8=43668
gas detonation velocity fluctuation, origin 8=45356
gas, ionized, wave coupling theory 8=46165
in gas of infinite cond., fading in transverse mag. field 8=33106
in gases, radiation smoothing to prod. continuous temp. profile 8=39200
generation in rarefied gases by laser impact on Be targets 8=47833
gradient of acoustic line in axisymmetric flow 8=30208
hypervelocity impact expts, optical lever technique adaption 8=23945
interactions, pressure fluctuation obs. and theory 8=32903
interstellar, OH production 8=28095
ionized gases in e. m. field 8=47945
ionizing, vel. rel. to initial gas press., drive current and mag. field 8=43599
on laminar boundary layer, interaction 8=47946
in lattice, non-ideal, rel to collision of two semi-infinite crystals 8=48700
from lightning discharge 8=41369
lightning, pressure pulse from triggered lab. stroke 8=36752
in liquid explosives, triple, propag. and configuration 8=30341
lunar bow wave and wake, hypothesis for absence 8=36997
at Mach number interface, irregular refraction 8=30260
magnetodynamic, device for studying effect of transverse magnetic fields 8=23942

Shock waves—contd
magnetogasdynamic with conductivity jump 8=33119
Mandel'shtam-Brillouin scatt. in quartz 8=41036
m. h. d., decay 8=33108
metal plate, classical detonation wave structure for condensed explosives 8=44515
MGD unsteady, curvature and torsion of mag. lines behind wave 8=46167
modelling of detonation waves in gas using nonlinear active lines 8=46169
N-shaped, radiation from finite line source (spark), directional depend. 8=32901
in nonequilibrium flows, onset 8=41833
nonlinear dissipative materials, deformation gradient and stress 8=46151
nonlinear, possibility of driving by transverse secular mag. fields 8=39088
nonuniform, subjected to oblique mag. field, family of solns. for flow 8=39184
in nozzle, flow of gas-particle mixture downstream 8=43688
oblique, conditions of detachment 8=37251
oblique, on supersonic projectile, interaction meas. 8=46162
in perspex spheres, reply to comments on propag. 8=35734
plasma, collisionless, and co-operative phenomena 8=30045
in plasma, front isomagnetic jump at critical Mach number 8=39089
plasma, ion-acoustic, ion-atom collision effect on propag. and damping 8=34487
plasma, ion-acoustic, propagation and damping 8=47879
plasma, ion acoustic reflections from negatively biased grid 8=43527
plasma, ion acoustic waves near and above ion cyclotron freq., damping 8=30151
plasma, jump conditions for finite discontinuities 8=34480
plasma, weakly ionized 8=30044
plastic, plane, reflection and refraction in presence of boundary plane 8=41832
in plexiglass, polarization relax. time, meas. 8=40563
pressure driven, associated precursor 8=34623
pressure-time meas. using miniature piezoelectric gauge 8=46174
propagation, spherically symmetric exponential atmosphere 8=43670
radiative effect on structure 8=37253
radiative energy transfer, conference 8=23909
reflected from adiabatic or isothermal wall, unsteady viscous struct. 8=41829
in relativistic m.h.d., and compressibility hypotheses 8=28587
remote recording detector and gated interval timer 8=41831
resonating radiation scattering in front of shock wave in tube 8=28368
self-similar, strong, in medium with exponentially varying density 8=28367
sliding over liq. surface, interact 8=23949
soils, soft, rel. to plastic volume and shear deform. 8=40109
in solids, polarization relax. time, meas. 8=40563
sonic boom meas., instrumentation requirements 8=32902
Sonic boom, N waves, frequency spectrum with finite rise time 8=23946
sonic boom, rattling of windows 8=46164
sonic boom, underwater sound pressure 8=46161
spherical and plane, propagation and attenuation, effects of solid strength 8=26751
steel, shock wave technique for cladding with refractory metals 8=28206
steel, stainless, explosive shock-loaded thermal recovery 8=49004
stellar collision, 2-dimensional theory 8=45619
in stellar envelopes, propag. Brinkley-Kirkwood theory 8=45637
step-function, propag. through constricted ducts 8=23948
strong, double Machian reflection 8=23947
structure descript. with non-equilib. rad. and ionization 8=39016
strong, struct. accounting for continuum subsonic flow downstream, and hypersonic flow upstream 8=43667
thermal shock on lateral surface of sphere 8=32898
underwater exploding wires, scaling using miniature piezoelectric guage 8=46174
velocity in crossed e.m. fields 8=41830
in viscous rarified gases, kinetic theory 8=34602
water, explosion pressure pulse phase shift 8=48034
water, isothermal at max. density 8=34728
water, pulse phase shift at caustic 8=48035
Z-pinch discharge wave, dynamics 8=34410
in Ar, front propag. for e. m. excitation 8=34635
Ar plasma, ionization, characteristic pots. rel. to press. and current for three types 8=25742
Ar, precursor radiation in explosive-driven shock tube 8=25830
Ar and He gas mixture, structure of normal waves 8=30261
Bi, front, diffusion of charged carriers 8=35826

Shock waves—contd
D_2/O_2 mixture detonation, dual regime 8=45355
H_2O_2 mixture detonation, dual regime 8=45355
in He, front propag. for e. m. excitation 8=34635
Sb, plastic waves in shock-induced polymorphic phase transforms., dynamic obs. 8=39562
effects
acetylene combustion, source of schlieren signals 8=49886
air, ionization e temp. meas. 8=39221
atomic spectral peak of non-equilib. gas behind wave front 8=29632
benzene, refr. index rel. to compression. obs. 8=39370
boundary layer growth, effect on shock tube test times 8=46159
electrostatic turbulent, effect of ion wave-electron interaction 8=43528
ethyl alcohol, refr. index rel. to compression obs. 8=39370
experimental studies of forces on model structures by wind and blast waves, bibliography 8=46170
explosive claddings, microhardness and metallographic props 8=48945
explosive liq. films, sensitivity, and detonation initiation 8=34748
explosives, impact sensitivity testing 8=32907
ferroelectrics, on resistivity, estimates 8=44880
gas behind shock front, maximum of nonequilibrium radiation 8=30299
gas, fast chem. reactions study technique 8=45315
gas flow, two dimensional, transonic 8=47938
gas motion behind expanding deformation wave 8=41834
gas oscills., nonlinear, resonant tube closed at one end 8=30266
gas, shock heated, Cr spectral emissions 8=29611
glycerine, refr. index rel. to compression, obs. 8=39370
hypersonic layer, radiative heat loss effect on subsonic region 8=34636
inorganic crystals, phase transforms. under impact pressure 8=26057
ionization of gases, simple model 8=47781
ionization rate meas. in shock heated gases, microwave method 8=39014
ionizing, transverse elect. field ahead (Alfven Mach > 2) 8=34440
liquid compression, elec. cond. meas. 8=34903
m.h.d. blast, cylindrical with uniform axial mag. field, obs. 8=28595
magnetite bed, residual magnetization change occasioned by explosion 8=50220
metals, resistance of metals, effect of deformation speed 8=41714
monatomic gas. singly ionized, effect of line rad. on precursor ionization 8=39015
nitrocellulose powder, shock ignition 8=23950
nitroglycerin powder, shock ignition 8=23950
non-eqilibrium ionization of air by front of 5-10 km/sec velocity, shock wave 8=29959
pinch tube, current sheet dynamics, obs. 8=34448
plasma, He-Cs, Ne-Li, elect. field intensity determ. 8=30046
plasma ionic sound 10^4Hz, nonlinear interaction with travelling wave 10^9Hz 8=30047
plasma production, Mach no. over 30 for fully ionized high density plasmas 8=47872
plasma, shock-produced, electromagnetically driven, electron densities meas. by microwave reflection 8=25720
plate, with finite Mach number, impulsive motion effect on flow of radiating gas 8=43686
rigid sphere motion in ideal compressed fluid, hydrodynamic force analysis 8=39264
solids, compression, crystallographic analysis 8=26745
sonic boom, comments and reply on Farfeld spectrum 8=25817-18
spark plasma, cylindrically converging wave 8=25745
strings and membranes, travelling forces 8=37241
trinitrotoluene, transition conduction zone behind front, time interval 8=49068
water into ice VII phase transform; by compression 8=48262
water, viscosity under shock load 8=48094
wire thermally shocked into longitudinal vibration by current pulse 8=40088
α-Al_2O_3 powder, explosive shock treatment effects from X-ray line-braodening analysis 8=44168
Ar-air mixtures, equilib. props. behind incident and refl. waves 8=34625
Ar, in e.m. shock tube, origin of plasma , 8=25744
Ar, ionization e temp. meas. 8=39221
Ar, ionization in mag. field and microwave signal attenuation 8=29960
Ar plasma flow, relaxation phenomena 8=25741
Ar, plasma prod. and skin-depth effect of microwave refl. and transmission 8=25743
BN, hexagonal, irreversible transformation 8=26062
CCl_4 liquid, shock-compressed, brightness temp. meas. and P-T curves 8=48089
CCl_4, polarization in refl. shock waves 8=43858
CCl_4, refr. index. rel. to compression, anomalies, obs. 8=39370

Shock waves—contd
effects—contd
CCl_4-C_6H_6 soln., shock-compressed, brightness temp. meas. and P-T curves 8=48089
CsBr, luminescence after shock compression 8=49806
D_2, decomp. and recomb. rate 8=25649
HCl, dissociation 8=38931
HF, dissociation 8=25650
H_2–O_2 mixtures, combustion kinetics 8=32109
Hg, viscosity under shock load 8=48094
LiF, luminescence after shock compression 8=49806
MgO powder, explosive shock treatment effects from X-ray line-broadening analysis 8=44168
N_2, dissociation in shock tube 8=25651
N_2, effect of O atoms on vibr. relax. 8=47724
N_2, ionization e temp. meas. 8=39221
N_2, temp. depend. of afterglow in glow discharge shock tube 8=27712
NH_3, oxidation 8=41256
NH_3-O_2 mixtures, ignition 8=27729
NO, intensity determ. of fundamental band 8=25499
NaCl, luminescence after shock compression 8=49806
O atoms recomb. rates, direct meas. 8=29666
O_2, radiative combination of O atoms 8=38932
OH chemiluminesc. in $H_2 + O_2$ reaction in shock tube 8=49889
Pt, evaporation of submicron particles in shock tube 8=39493
on Ti Br_4-Ar mixture, TiI, II absolute gf-values determ. 8=43489
Xe, compression rel. to conversion to metal-like state 8=43851
YFe garnet, rel. to demagnetization 8=31744
Shot noise. See Fluctuations/electrical.
Showers. See Cosmic rays/showers and bursts.
Shubnikov–de Haas effect. See Magnetoresistance.
Silicon
See also Semiconducting devices; Semiconducting materials/silicon.
absorption spectrum, one-electron, high-resolution exam. 8=45218
abundance in solar photosphere 8=28173
activation anal. to determine trace element impurities 8=50000
activity in molten Ag-Si alloys by e.m.f. meas. 8=48078
addition to Fe-Cr alloys, influence on anodic passivation 8=36602
amorphous phase form. by ion bombard., temp. and channelling effects 8=48931
atomic planes, [111], imaging 8=44218
auger electron emission, chemical effect 8=43227
avalanche diodes, high-power, high-efficiency, at u.h.f. 8=49310
carrier lifetime degradation, n-induced, rel. to dopant impurities 8=31156
crystals, Bragg refl. effect on electron scatt. 8=35354
crystals, impurity atom effects on lattice defects, X-ray studies 8=26644
crystal, (220) reflection, effects of fast neutrons 8=30911
crystals with oxygen and carbon impurities, precip. of SiO_2 and SiC on heat treatment 8=39702
crystallization from Al-Si melts by zone-melting with temp. gradient, mechanism 8=39686
defect formation by epitaxial deposition of Mg-Al 8=48832
defects causing anomalous etching and X-ray double images, origin and struct. 8=48835
defects, interaction of Li with O 8=26632
diffusion in Mo, phase identification 8=48784
diffusion of P. at high-conc., precipitate formation 8=39983
diffusion of P from oxide film, rel. to model 8=44375
diffusion of Sn, effects of P and B codoping 8=48791
diffusion of T 8=48346
diode junction, avalanche noise meas. in r.f. and ultra-r.f. region 8=40534
dislocation distribs. from Laue-case diffr. expts. 8=48860
dislocation-free crystals, e. p. r. of B 8=45101
dislocations, pure edge, parallel arrays, obs. on plastic deformation 8=40044
e.p.r. from clean single-crystal cleavage faces rel. to surface states 8=40943
electron-hole-plasma of p-type, helical density waves and oscillistor-effect 8=49127
electron microscopy at high voltages 8=41971
electron pulse reflection (20–1000 eV) 8=35605
electron radiation damage rate rel. to depth 8=26736
electron scattering, inelastic, and incoherent X-ray scattering 8=44155
epitaxial deposition conditions at low-temps 8=48461
epitaxial deposition on sapphire, substrate prep. 8=39699
epitaxial film growth 8=39597
epitaxial films, impurity penetration in growing process 8=26128
epitaxial films on quartz 8=48465
epitaxial films on spinels, growth twins and carrier mobility 8=35181
epitaxial growth on {311} planes, surface characts. 8=39582

silicon—contd
  - epitaxial layers, crystal perfection, effect of substrate surfaces 8=39596
  - epitaxial layers, P diffusion effects on defect structure, 4=48833
  - epitaxial layers, stacking-fault defect nature 8=40050
  - epitaxial layers, stacking fault disappearance 8=40049
  - epitaxial (111) and (100), shallow surface depressions stability, obs. 8=44145
  - epitaxial, shear and twin-type stacking faults 8=31100
  - excitonic molecule binding energy 8=40262
  - exoelectron emission after irradiation and mech. treatment rel. to surface defects 8=40694
  - exoemission rel. to surface treatment 8=40693
  - field electron-emissive photocell 8=40702
  - films, chemically grown epitaxial, nucleation study using molecular beam techniques 8=44144
  - films, deposited by sputtering through moving mask, low-temp. orientation 8=26127
  - film deposition on sapphire, struct. correls. with substrate 8=44056
  - films on α-quartz substrates, deposition, struct. and elec. props. 8=35180
  - film on sapphire, crystallog. orientation relations 8=44058
  - film on sapphire, vacuum deposition 8=44057
  - film, perfect single cryst., on sapphire, by vacuum evaporation 8=39595
  - films, single crystal, moving mask growth on amorphous quartz substrates 8=26126
  - gamma-irradiated, recombination lifetimes 8=49424
  - gettered, study of lattice disorders rel. to process 8=44077
  - imperfection near oxide film edge rel. to localized diffusion, X-ray micrographic obs. 8=35552
  - impurity striations, reasons for appearance in single cryst. grown by Czochralski method 8=48824
  - ion bombardment damage 8=44503
  - ion channelling at 100-500 keV, obs. 8=48930
  - ion implantation analysis by 1 MeV He$^+$ scatt. 8=48927
  - ions, oscillator strengths for resonance lines present in solar spectrum 8=29647
  - lattice parameter C conc. dependence 8=48674
  - lattice vibrations, microscopic dielectric model 8=44304
  - luminescence and growth techniques 8=36475
  - neutron dosimeter, surface barrier, 2-5 MeV 8=33787
  - neutron-irradiated, defect character from anomalously wide images using stereo e-microscopy 8=31025
  - neutron-irradiated, defect detection using anomalous X-ray transmission 8=48834
  - neutron-irradiated, divacancy and A-centre production 8=44416
  - neutron irradiated, dosage-damage correlations and X-ray diffr. studies 8=26733
  - for neutrons, fast, diode, dosimeter, <1-15,000 rads. 8=33788
  - for neutrons, fast, p-n junction dosimeter 8=33790
  - optical difference mixing 8=31995
  - oxidation in cathode fall area of pure O glow discharge 8=35182
  - oxide films on crystal, i.r. spectroscopic study 8=39598
  - Pendellösung fringes in crystal free of dislocations 8=48675
  - phonon conductivity and acoustic attenuation 8=44324
  - photocells, electron bombardment rel. to props. 8=27329
  - photocells, study of forward branch of V-I characts 8=49431
  - photodiodes with demodulation props. independ of wavelength 8=49409
  - photomechanical effect, wavelength dependence 8=36368
  - planar chem. polishing 8=48425
  - plastic deformation by indentation and scatching under light load 8=40180
  - p-n junctions, forward biased, interband recombination model for light emission 8=45286
  - positron annihilation angular distribs. rel. to single-particle positron wavefunctions 8=44669
  - precipitation kinetics of Cu near room temp. 8=30705
  - radiation detector, pulse height defects due to nuclear collisions 8=46896
  - radiation detector, response to high-energy particles 8=46898
  - recombination radiation at high excitation levels 8=41209
  - in rocks, neutron activation analysis 8=50062
  - Schottky barrier diode, with near-ideal I-V characts. 8=40525
  - secondary dislocations formed after diffusion of B and P 8=35572
  - secondary electron emission angular dependence in primary e. range, 100-2000 eV 8=44952
  - secondary emission angular dependence for 1000 eV primary beam 8=40714
  - single crystals, d. c. photodecay meas. rel. to minority carrier lifetimes 8=40490
  - single crystal slices, analysis by neutron activation 8=40014
  - Sirius, abundance clac. from Si II lines 8=50285
  - solar, abundance rel. to Fe 8=37084
  - solar cells, p irrad. damage thermal annealing, 4. 6 MeV 8=24101
  - soldered contact prep., metal hydride flux 8=45931

Silicon—contd
  - solubility, max., of B, and precipitation kinetics 8=48345
  - solubility of T 8=48346
  - spectrum, Si$_2$O 9μ vibr. states rel. to isotope effects and c-o stretching vibr., 1104 cm^{-1} 8=27607
  - stresses, thermally-induced, rel. to X-ray diffr. and birefringence obs. 8=49051
  - substrate, epitaxial growth of ZnS by vac. evaporation 8=30740
  - surface barrier detector, p damage 8=46897
  - surface cleaning by high field and heating, field emission characts. 8=35148
  - surface dislocation sources 8=26694
  - surface facets formed by HCl selective vapour etching 8=48523
  - surface imperfections during thermal treatment 8=30728
  - surfaces (100), (110) and (111), Berg-Barret skew reflection tables for Kα X-rays 8=35347
  - surfaces, vacuum-crushed, air-crushed and mechanically polished, ht. treatment effects on e.p.r. spectra 8=39580
  - thermal expansion coeff. temp. depend., theory and obs. 8=26594
  - thermal radiation on laser beam irrad. 8=35467
  - twinning in web dendrites, scanning e microscopy obs. 8=44089
  - n-type, electron spin-lattice relax., conc- and compensation-dependence 8=27489
  - p-type inversion layers, mobility anisotropy and piezoresistance 8=27133
  - ultrasonic attenuation in single crystals, frequency dependance 8=48725
  - ultrasound, velocity of propagation variation rel. to temp. 8=39896
  - vacancies at diffusion induced dislocations, and dislocation-enhanced diffusion in (001) crystals 8=26622
  - vibration spectra, freq. along asymmetric dims. 8=30934
  - web-dendrites, semiconducting quality, dislocation origin and reactions 8=26692
  - work function temp. dependence up to 1000°K 8=49436
  - Au and Cu impurity and dopant distribs. on pulling crystals in floating-zone technique 8=40015
  - Ga and In implanted, anomalous penetration 8=48929
  - Li diffused solar cells, efficiency and e irrad. damage annealing, obs. 8=24103
  - Li doped solar cells, experience and future of 8=24104
  - Li doped solar cells, p$^+$/n, status 8=24102
  - Li precipitates, nucleation and growth 8=44105
  - NH$_3$ adsorbed on, vibrations obs., rel. to bonding strength 8=25508
  - Ni electroless plating on p-n junctions 8=45396
  - O analysis, by i.r. spectrophotometer 8=49992
  - P^{32} ion implantation profiles 8=48928
  - P diffused, obs. of induced dislocation by X-ray and etching techs. 8=48861
  - P e.p.r. in n-Si, hyperfine splitting rel. to compensation, obs. 8=27487
  - P, As-doped, single crystals, porous substruct. 8=30866
  - Sb-doped, structural defects rel. to doping conc. 8=40018
  - Si1 absolute oscillator strengths 8=34134
  - Si1 solar abosrption lines, 2935-25578Å, equivalent width calc. 8=37048
  - Si II/III, e impact line broadening calc. 8=47507
  - SiII, IV, spectra, doublets oscillator strength ratios, Fermi calc. and obs. 8=34152
  - Si: Au m.o.s. structures, minority carrier lifetime meas. 8=49315
  - Si: Li detectors of α and p beams 8=38103
  - Si: P, broad saturation effect and background e.p.r. line 8=45100
  - Si: P diffusion junctions, intense interjunction strain 8=49046
  - Si-SiO$_2$ fast interface state meas. from MOS-C(V) curves at 77°K 8=49320
  - Si-SiO$_2$ solid-solid interface system 8=40504

Silicon compounds
  - See also Quartz.
  - Aerosil, adsorpt. of benzene, i. r. spectra 8=44076
  - amethyst, Fe colour centres 8=31116
  - chlorite, new polymorph and possible polytypes, crystal structure 8=26174
  - cristobalite, polymorphic transform., impurity effects 8=26079
  - cristobalite, stacking fault conc. calc. from X-ray diffr. line profiles 8=26703
  - ion exchangers, isotope exchange rate investigation 8=45313
  - methyl silane, isomeric mono-subs. derivs., differences in phys. props. 8=43925
  - methylsilanes, far u. v. spectra 8=25592
  - opals, gem, crystal structure determ., by light diffr. 8=44254
  - polymeric, C and H microdeterm. 8=36628
  - silica and feldspar mixtures, structural characteristics, thermodynamic props. 8=39297
  - silica, fused, ion diffusion from molten salts 8=48789
  - silica, fused, microcrystal orientation in ordered isotopic structure 8=26150
  - silica gels, "adsorbed, adsorbent" interactions 8=34954

Silicon compounds—contd
- silica gel, AgI single crystal growth 8=26227
- silica gel, brittle, structural evolutions during ageing 8=26150
- silica gel, complete pore struct. anal., surface areas of micropores 8=48351
- in silica gel, growth of crystals, using a co-solute 8=35243
- silica gel, O_3 adsorpt. rel. to annealing temp., —80°C 8=30786
- silica gel, pore surface accessible to N_2 8=48350
- silica-gel spheres, wet, drying by moisture transfer to dry particles in mixing 8=34978
- silica glass, densified at very high press., quasi-crystalline atomic arrangements 8=48504
- silica, molten, speed of ultrasound and adiabatic compressibility 8=48140
- silica monodisperse spheres, controlled growth 8=48235
- silica, vitreous random-network model 8=26151
- silica, vitreous, vibational spectra 8=35392
- silicates e microprobe analysis with oxide standards, correction factors 8=27810
- silicate glasses, strengthening by ion exchange 8=26845
- silicates, layer, some rare polytypes, X-ray exam. 8=26174
- silicates, layer-lattice, thermal studies using adapted Unicam high-temp. camera 8=26326
- silicate-mineral inclusions, orientation in natural diamond 8=26179
- silicide films, on Nb chromised, titanised and chromo-titanised, structure and props. 8=35176
- silicides of transition metals, auxiliary metal bath procedure for synthesis 8=49835
- silicon polymer, glow-discharge deposited, refractive index 8=49763
- siloxanes, solvent effect, freq. spectroscopic investigation 8=25884
- Zeolite Linde 13x, temp. depend. of mag. proton and cation reson. 8=49656
- Al chlorite, dioctahedral, structure 8=26174
- $C_2H_5SiCl_3$ mol. crystals, n.q.r. multiplicity and spin-lattice relax times rel. to phase transforms 8=41010
- CaO–Fe O–Fe_2O_3–SiO_2 melts, ion and electron cond. 8=25946
- GeO_2-SiO_2 glasses, binary, non-ideal mixing 8=44080
- Si carbides, formation by chemical vapour deposition, discussion 8=45348
- Si–B phase formed during deposition, removal 8=48463
- SiC abrasive grains, frictional coeffs. with metals 8=31184
- α-SiC, absorption spectra of exciton-impurity complexes 8=36406
- n-SiC, Be diffusion, 1700–2250°C, mechanisms and anisotropy 8=35506
- SiC, C X-rays absorption, extended Philibert's correction 8=27798
- SiC compacted bodies, elec. props, compared with sintered oxes 8=49142
- SiC, conversion of cubic to hexagonal as fn. of temp. and press. 8=48399
- SiC, crysts. growth from soln., theory 8=35232
- SiC, effect of N_2 and P impurities in crystallization 8=26208
- SiC, elastic properties 8=35717
- SiC, electroluminescent p-n junction obs. 8=36509
- SiC film, dielec., breakdown mechanism 8=27249
- SiC films, noncrystalline, prep. and elec. props 8=48467
- SiC heater elements, sintered elec. ageing rel. to oxidation ageing 8=49349
- SiC, higher absorpt. edges 8=49752
- SiC, luminesc. and growth techniques 8=36475
- SiC, luminescence energy levels and capture centres 8=41210
- SiC, luminescence on irradiation with electrons, H and D ions of 20 keV 8=36510
- SiC particles in varistor with voltage nonlinearity, effect of Al content 8=31404
- SiC, polytypis, as high-order transformation 8=44012
- SiC polytypism, dislocation theory 8=26180
- β-SiC, porous, n-irrad. induced changes in growth, elasticity and thermal props. 8=26735
- β-SiC, radiation recombination on fast electron bombardment effects 8=36508
- SiC, Raman spectra on laser excitation 8=41139
- SiC, sintered, heater elements, oxidation ageing rel. to elec. resistivity changes 8=31231
- α-SiC (6H), high-resistivity, doped accidentally, band scheme 8=35779
- α-SiC (6H), photoluminesc. of single crystals 8=36511
- SiC, 6H polytype, low-freq. dielectric constant and refractive index 8=36407
- n-SiC (6H): B diffusion counters, for strongly ionizing particles, elec. props. 8=33378
- β-SiC, soln.-grown, stacking faults, partial dislocations and twinning 8=31101
- SiC, transition from hexagonal to cubic phase, effect of high press. and high temp. 8=35124
- SiC, ultrasoft X-ray emission spectra rel. to energy structures 8=41136
- SiC vapour scintillation, emission spectrum time scanning 8=34231

Silicon compounds—contd
- $Si(C \equiv CH)_4$ i.r. and Raman spectra 8=25625
- SiC:N, n.m.r. donor conc. dependence rel. to e. delocalization and e. system degeneracy 8=45134
- SiC: N, B, and unknown impurity doped, optical charge exchange exam by e.s.r. and photoconductivity 8=36251
- α-SiC: Ni and Al complexes, luminescence 8=36507
- $SiCl_4$, neutron activation analysis of trace impurities 8=49998
- $SiCl_4$, vibr. relax. and u.s. attenuation 8=39360
- Si–Cr films, annealed, resistivity, struct. and stability at 200°C 8=44818
- SiF, rot. anal. of γ bands 8=38855
- SiF_2, absorpt. spectrum 8=25520
- SiF_2, e.s.r. 8=31885
- SiF_4, rate of ionizaion by electron attachment, three-body process 8=43471
- Si-Fe crystals, coercivity rel. to domain structure 8=31704
- Si-Fe crystals, domain structure, tensile elastic strain effects 8=36173
- Si-Fe crystals, domain structure temp. dependence up to 650°C 8=50829
- Si-Fe, dislocation density during low cycle fatigue 8=39963
- Si-Fe single crystals, effect of dislocations on magnetization process 8=26677
- Si-Ge alloys, pressure sintered, props. rel. to microstructure 8=30668
- Si(Ge)-ZnO films, I-V characts., conductivity change 8=40488
- SiH_3 derivatives n.m.r. spectra 8=34918
- SiH_4, liquid, p spin-lattice relax. time, obs. 8=34922
- SiH_4, nuclear r.f. spectrum obs. 8=47588
- $SiHClO_3$, neutron activation analysis of trace impurities 8=49998
- SiH_nD_{4-n}, liquid, p spin-lattice relax. time, obs. 8=34922
- SiI_4, Mossbauer effect 8=39520
- SiN film on Si, from $SiCl_2$–NH_3–H_2 system, anomalous etching rate 8=48464
- SiN, ground state reduced potential curves 8=29717
- SiN insulated gate FET's, effect of electron irrad. 8=27201
- Si_3N_4 based insulating materials, phase composition and electrophysical props. 8=31445
- Si_3N_4 films deposition on Si and MNS diodes props., obs. 8=40545
- Si_3N_4 films, diffusion of Al substrate, coeff. and activation energy temp. dependence 8=31001
- Si_3N_4 films, etching 8=39652
- Si_3N_4 films on Si, vapour deposited, elec. props. 8=49350
- Si_3N_4 films, prep. from $SiCl_4$ + NH_3 and elec. props. 8=44051
- Si_3N_4 films, pyrolytic, conduction props. 8=49352
- Si_3N_4 films, structure and Na migration 8=48605
- Si_3N_4 insulating film, refractive index 8=49763
- Si_3N_4, prep. by r.f. discharge reaction of silane and N_2 8=35183
- Si_3N_4, ultrasoft X-ray emission spectra rel. to energy structures 8=41136
- Si_3N_4-SiO_2 films, amorphous on Si, struct, optical and elec. props. 8=49319
- Si–Ni, alloy diffusion phenomena omnidirectional pressure effects 8=35488
- SiO amorphous films, formation and structure 8=44052
- SiO film, pulse breakdown obs. 8=40586
- SiO, from graphite cloth 8=35005
- SiO, optical absorpt. 8=41145
- SiO, rot. spectrum, 42 373-43 424 MHz 8=38856
- Si-O solid soln, anomalous X-ray transmission, rel. to periodicity changes on decomposition 8=36409
- SiO($A^1\Pi$-$X^1\Sigma^+$) band system, oscillator strength meas. 8=43334
- SiO_2, addition to $BaTiO_3$ to promote conduction 8=49228
- on SiO_2, Al reactivity, moisture effects, obs. 8=45328
- SiO_2, amorphous, crystallization 8=44011
- SiO_2 coating for protection of aluminized mirrors operating in u.v. 8=42148
- SiO_2 density and colour centres rel. to radiation damage 8=26722
- SiO_2 diffusion masks obtained by evaporation, use 8=48459
- SiO_2 dispersions, scatt. and absorpt. rel. to reflectance of clouds 8=39447
- SiO_2, distrib. and range of B and P ions on bombardment 8=35604
- SiO_2 films, amorphous, elec. strength temp. dependence, —196 to + 50°C 8=40561
- SiO_2, film, amorphous, on Si, prod. by oxidation of silane 8=44055
- SiO_2 film, chemically vapour-plated, environmental effects 8=48466
- SiO_2 films, diffusion of Au 8=39984
- SiO_2 films, e diff. and microscope investigation 8=30910
- SiO_2 films on GaAs, S diffusion through film into GaAs 8=35493
- SiO_2 films on Si, thickness meas. by i.r. techs 8=48460
- SiO_2 films on Si, vapour deposited, elec. props. 8=49350
- SiO_2 films, ordered structure and ion mgration 8=44054
- SiO_2 film, oxide layer thickness and nature from i.r. props. 8=26125

Silicon compounds—contd
- SiO_2 films pyrolytic deposition under vacuum 8=44050
- SiO_2 films on Si wafers, prod. by SiH_4 oxidation 8=44053
- SiO_2 in glass, precip. into $H_2Si_2O_5$ for chem. analysis 8=45413
- SiO_2, form. of phospholsilicate glass film 8=44048
- SiO_2, fused, effect of rad. on optical transmission 8=28742
- SiO_2 fused, modified with thermal expansion coeff. $\sim10^{-7}$/°C, physical props. 8=39930
- SiO_2 gel, adsorpt. of binary, org., liq. mixtures 8=48477
- SiO_2 gel, adsorpt. of mols., n.m.r. signal shifts 8=39462
- SiO_2 gel, proton spin relax. of adsorbed C_6H_6 8=29814
- SiO_2-glass, diffusion of Na^{22}, α-β quartz transformation effects 8=48794
- SiO_2 glass, synthetic, mobility of Na ions 8=48795
- SiO_2, glassy, i.r. reflectivity, absorpt. and transmission 8=49754
- SiO_2 in marine sediments, by nondestructive determ. by 14 MeV neutron activation 8=41314
- SiO_2 insulating film on Si, polarization effects 8=44854
- SiO_2 layers, prod. in cathode fall area of pure O glow discharge 8=35182
- SiO_2 powder from pyrolytic decomp. of silicone, crystallization by annelaing 8=35251
- SiO_2 powder, positronium diffusion constant and annihilation spectra mean length 8=44378
- SiO_2 slip refractory for melting optical glasses 8=45936
- SiO_2, solubility equation, in H_2O, valid up to critical density range 8=48070
- SiO_2, sputtered, for multilayer interconnects in MOS dev. 8=44855
- SiO_2 structural changes in fusion 8=48264
- SiO_2, thermal photoresists adherence rel. to surface constitution, obs. 8=44601
- SiO_2, vitreous, density fluctuations rel. to X-ray scatt. 8=25879
- SiO_2, vitreous, vib. density of states and thermal cond. 8=35455
- SiO_2, wetting by water obs. 8=35140
- SiO_2 with W inclusions network, 2000°C 8=48092
- SiO_x coating on Si, B redistribution 8=48793
- Si_2O in Si, vibr. states rel. to isotope effects, 9μ 8=27607
- Si_2O_3 glass, struct. determ. by X-ray diffr. 8=48503
- Si_3O_{10} group in ardennite crystal structure 8=39808
- $[Si_2O_5]$-layer silicates, crystal chemistry 8=39641
- SiO_2-Al_2O_3 catalysts, adsorption of DPPH 8=27736
- SiO_2-Al_2O_3, n. m. r. of combined H_2O 8=45123
- SiO/Cr mixed films, structural and elec. props. 8=48448
- $SiO_{2-x}N_x$ films on Si, prep. by chem. vapour deposition and stress-comp. dependence 8=48462
- $Si_xO_yN_z$ films on Si, elec. and passivation props. 8=49351
- SiP precipitation on high-conc. P diffusion in Si 8=39983
- SiP_2 and $SiAs_2$, preparation and properties 8=40484
- SiS, ground state reduced potential curves 8=29717

Silver
- absorption in 50-340Å range, calc. of partial oscillator sums 8=31981
- absorption of light by surface plasmon excitation 8=49700
- additions to aged Al alloys, influence on struct. and props. 8=48590
- adsorption and coprecipitation on $Fe(OH)_3$ 8=48478
- α-ray absorpt. at 54.4 MeV, obs. 8=48919
- cohesive energy and isotropic band effective mass 8=48303
- colloid in gelatin, effect of particle shape on spectral absopt. 8=39460
- conduction-electron spin resonance obs. 8=31860
- conducting film formation using electron beam 8=39603
- corrosion in autoclave liners during hydrothermal crystal growth reactions 8=49855
- creep rate at low pressure rel. to annealing in air effect 8=26803
- creep, void formation 8=31225-6
- crystal surface, scatt. of inert gases 8=39575
- crystallization in thin films 8=30741
- crystal growth through 2-dimen. nucleus formation and mono-atomic layer spread on dislocation-free surfaces 8=44113
- crystals, electro-deposited, structure and orientation in initial crystallization stage 8=30822
- depth dose distrib. prop. by electron irrad., energy losses and ionization 8=31143
- determination by atomic fluoresc. spectroscopy 8=36641
- diffusion of Ag^{110m} in Li, 67°-160°C 8=31008
- diffusion in Al, due to near surface effect 8=39964
- diffusion of Ni 8=34813
- diffusion in $RbAg_4I_5$, rel. to high-conductivity in solid electrolyte 8=48787
- diffusion in TiO_2-based dielec. 8=31016
- electrical and thermal cond. c.f. Pt 8=30987
- electrocrystallization 8=41283
- electron beam energy loss distrib. obs. 8=31142
- electrotransfer in liq. Ga, temp. depend. 8=36597
- energy bands, self-consistent, by augmented-plane wave method 8=49097
- evaporation from crystal due to e bombard., deposition 8=40712

Silver—contd
- Fermi surface, effect of lattice parameters change 8=40237
- film, absorbent and anisotropic, optical props., theoretical study 8=49707
- film, epitaxial growth on NaCl crystal 8=30745
- film on glass, light refl. phase retardation meas. 8=31960
- film on mica, growth in ultra-high vacuum 8=44037
- film, polycrystalline thin, photoelec. emissivity obs. 8=27353
- films, abnormal optical absorpt. in vacuum and Ar atmos. 8=45168
- films, adsorpt. of O_2 and substrate for H_2 and O_2 8=39616
- films, electrical resistivity, 4.2 to 295°K 8=26944
- films, excitation of surface plasma oscillations 8=35804
- films on CaF_2 and NaCl, X-ray structure investigations 8=44158
- films, orientation after deposition on NaCl and KCl 8=44085
- films, p-bombardment effects on resistance, —13 to —158°C 8=40302
- films, stacking faults, thermal behaviour 8=40047
- films, thin, optical transmission near plasma freq. 8=27547
- films, vacuum-condensed, elastic anisotropy rel. to structure 8=44545
- films, vacuum deposited, internal friction temp. dependence rel. to prep. 8=35650
- films, vacuum-deposited, structural formation rel. to elec. resistance behaviour 8=26110
- films, vacuum-deposited, temp. coeff. of resistance 8=35819
- foil, with C layer, e energy loss spectra obs. 8=35808
- foil, plasma resonance peak obs. 8=26927
- in glasses, atom impurity stabilization and atomic centre production by X-rays 8=31114
- impurity electrotransfer in liquid tin 8=39408
- impurity in liq. Pb-Sn alloys, self-diffusion 8=34806
- ion orbitals, reduced basis set expansions 8=43176
- liquid, interband transitions 8=43821
- liquid, solubility of O_2 8=39317
- liquid, vapour press., 1450° to 1600°C 8=43918
- magnetothermal oscs. meas., rel. to Fermi surface 8=44686
- nuclei form. on Pt electrode 8=49948
- particles in glass, elongated, selective light polarization by absorption 8=41051
- pastes hardened at 20-150°C 8=35820
- photoelectric effect rel. to temp. 8=36008
- photographic grains, effect of bleaching 8=33295
- radioactive, electrochem. props. 8=36594
- reflectivity changes during laser pulse 8=45169
- solidifying, bubble formation 8=30587
- solvent, Knight shifts in alloys, origin 8=30528
- spectra, absorpt. after x-radiation of frozen solns. of salts 8=47488
- specific ht. and ht. of melting 8=35424
- specific heat in pure samples below 3°K 8=39912
- stacking fault energies 8=31097
- stopping power for 3.75-5.5 MeV proton, using (p, n) obs. 8=43030
- surface structure from electron diffraction 8=35153
- thermal diffusion in Bi_2Te_3 and ht. of transport calc. 8=39968
- thermal expansion and fusion 8=39928
- thermal expansion coeff. of film, e diffr. meas., 20-420°C 8=35446
- thin film, resistivity, ion-bombardment induced changes 8=49151
- thin films, mean free path of conduction electrons rel. to optical absorption 8=36315
- ultramicrotome-cut foils, deformation 8=48850
- vapour pressure, over Cu-Ag-Au liq. ternary alloy rel. to electron cell model 8=26002
- visible radiation produced by electron bombardment 8=36317
- Ag^{110} diffusion in Al, 450-630°C 8=44381
- Ag alloys, solubility of O_2 8=39313
- Ag, internal friction after cold drawing and irrad. at low temp. 8=48986
- Ag-molten $BiCl_3$ solns., elec. cond. rel. to study of metal-molten salts reaction 8=39409
- Ag(I) electrode in $NaNO_3$-KNO_3 eutectic, linear sweep voltammetry 8=27750
- Ag(111) surface rearrangement on O_2 adsorpt., study by LEED 8=26133
- Ag: Mn, spin relax. of localised mag. moments and conduction electrons 8=31875
- Ag-Si molten alloys, Si activity by e. m. f. meas. 8=48078
- Ag^+, diff. in $LiSO_4$, 590-820°C 8=39977
- and Au, dechannelling of 40 kV Au ions at planar defects 8=35599
- Kr bombard., thermal desorption obs. 8=48483
- Sn^{119m} isomer shift 8=26015
- in Sn/Pb solder, X-ray spectrometric analysis 8=27816
- Xe bombard., thermal desorption obs. 8=48483

Silver compounds
- dental alloys, X-ray fluoresc. anal. 8=32165
- halide particles in glass, optical and thermal bleaching 8=41094

Silver compounds—contd
halides, diffusion of Mn^{2+}, 8=39962
halides, electroluminescence at low temps. 8=45256
halides, emulsions, electron trap distribution and low temp. Herschel effect 8=35744
halides, photographic grains, effect of bleaching 8=33295
halides, photoluminesc. rel. to lattice structure 8=36470
halides, single crystal growth from silica gel 8=26229
halogens, optical absorption and ionic conductivity of Cr and Ti ions 8=41052
magnetic alloys, dil., solute Knight shifts rel. to rigid band theory 8=45117
Ag complex, bis(8-hydroxyquinoline)Ag(I) pyridine solvate, cryst. and molec. struct. 8=39765
Ag–Al alloy, dispersion hardening by internal oxidation 8=35649
Ag–Al films, diffusion 8=31000
Ag–Al system, cell growth, calc. of limiting boundary diffusivities 8=48533
Ag_2Al, lattice parameters rel. to temp. 8=44201
Ag_3AsS_3, proustite, crystal growth from melt 8=26228
Ag_3AsS_3(proustite), electro-optic effect 8=45166
Ag-Au alloys, short range order kinetics, rel. to diffusion 8=35059
$Ag_xAu_{51-x}Zn_{49}$ alloys, β-phase stability, low temp. 8=48368
AgBr, absorpt. spectra pressure dependence up to 50 kbar 8=41053
AgBr, colloidal, complex refr. index, near-u.v. 8=43891
AgBr containing iodide, mirror-like absorpt. and luminesc. 8=41050
AgBr cryst, reacts between defects 8=26633
AgBr cryst/soln. phase, Ag^+ and Br^- energy diagram 8=34958
AgBr cryst. /soln. phase, distrib. equilib. and self defect points 8=34959
AgBr crystals, photoconductivity quenching by constant background illum. method 8=40651
AgBr, diffusion of photoexcited holes rel to temp. 8=49410
AgBr dispersion, latent image formation and reduction-plus-sulphur sensitization 8=46765
AgBr, e distribs. from X-ray structural analysis 8=48302
AgBr, luminesc. and photocond. induced by Q-switched laser 8=45255
AgBr, luminescence, behaviour in temp. extinction range 8=41181
AgBr, recrystallization and photosensitivity, effects of NH_3 and triethanolamine 8=30821
AgBr, photoelectron drift, 40 to −100°C 8=36007
AgBr, X-ray diffraction, study of crystallization 8=44114
AgBr, AgCl and AgI epitaxial films vacuum deposition 8=44036
AgBr, AgCl, and AgI far i.r. reflection spectra 8=45167
$AgBr:I^-$, absorption spectra, multiphonon structures 8=31956
β-AgCd, ordering crit. temp., temp. dependence, from elec. resistivity meas. 8=30676
AgCl, absorpt. spectra pressure dependence up to 50kbar 8=41053
AgCl, intrinsic defect conc., effect of defect interactions 8=40003
AgCl, luminesc. and photocond. induced by Q-switched laser 8=45255
AgCl, luminescence, behaviour in temp. extinction range 8=41181
AgCl, luminescence excited by u.v. laser 8=36469
AgCl, opt. props., by reflectivity obs. 8=36316
AgCl, phonon scattering by point-defect aggregates from thermal conductivity meas. 8=30986
AgCl, plastically deformed, strain and dislocation exam. methods 8=26662
AgCl, self-trapped holes, e.s.r. detection 8=45075
AgCl sheet as supporting matrix for micro i.r. spectrophotometry 8=24403
AgCl, structural defects in slip-lines during fatigue 8=48827
AgCl: Cu^{2+}, Se(S) codopants, e.s.r. 8=36235
AgCl, Fe impurity ions, Mossbauer effect study 8=39510
$AgCl:Fe^{n+}$, valency state determ. of Fe impurities 8=35550
$AgCl:I^-$, absorption spectra, multiphonon structures 8=31956
AgCl:V, optical absorpt. and ionic cond. meas. on V ions 8=35523
AgCNO, bonding and stability 8=26006
Ag_2CrO_4, phase boundaries below 500°C 8=48366
$AgCrS(Se)_2$, crystal structure and mag. props., 8=39810
Ag–Cu–Zn–Cd alloys, phase constitution 8=48369
Ag-Cu-Zn-20 wt. % Cd partial system, phase diagrams, obs. 8=43896
Ag-Cu-Zn-Cd system, equilibria and primary crystallization 8=35083
Ag-Cu-Zn-Cd system, univariant, equilibria formation by decomposition 8=30675
AgCu alloy film, vapour-quenched, structure from X-ray scatt. 8=44159

Silver compounds—contd
$AgGaTe_2$, photomagnetoelectric effect, photoconductivity 8=40649
AgI, cryst. struct. at 3 kbar 8=35316
AgI, elec. cond. to 100 kbar 8=31311
AgI films, polycrystalline dye-sensitized, thermally stimulated conductivity 8=35994
AgI, ht. capacity 50°-400°C 8=30961
AgI, ice nucleation, nature of nucleating site 8=32216
α-AgI, low temp., phase transforms. 8=43994
AgI, molten, electrical conductivity 8=35810
AgI, powdered, phosphorescent excitation spectra recording 8=36484
AgI, H_2O vapour to ice conversion 8=45458
AgI, ht. capacity, theory 8=48733
Ag I, nuclear resonance 8=49636
AgI, I^- centre, excited state structure 8=45257
Ag-In alloys, dil., optical constants rel. to interband transitions and plasma oscills. 8=49699
Ag–In solid solns., Zener relax. activation energies 8=31190
AgIn molecule, system B of u.v. absorpt. bands 8=25443
$AgInTe_2$, photomagnetoelectric effect, photoconductivity 8=40649
Ag_3Mg, long range order, quenching temp. dependence 8=44200
Ag-Mn alloy, evaporated ohmic contacts to p-GaAs 8=49237
Ag–Mn alloy, transmission spin resonance of conduction-electron-local-moment obs. 8=31860
AgMn films prod. by simultaneous condensation, magnetic props., conc. depend. 8=40802
$AgMnO_4$, crystal structure redetermination 8=44199
$AgNO_3$, molten electrolyte, cell pot. gravit. component obs. 8=45367
$AgNO_3$-AgCl, molten electrolyte, cell pot. gravit. component, obs. 8=45367
AgN_3, crystal growth method for i.r. and Raman spectral exam. 8=48535
Ag-Ni thin film thermocouples, temp. variation across thin semiconductors 8=40638
Ag_2O, photoconductivity spectra at 77°K 8=40650
Ag-41.8 wt. % Pt alloy, resistivity recovery stages and mechanisms 8=40303-4
Ag_2S form. on AgBr cryst., kinetics 8=49853
Ag_2S, negative photovoltaic effect 8=49411
β Ag_2S, thin films, conductivity and photoconductivity 8=49152
Ag_2S–Cu_2S system phase transformations rel. to elec. resistivity changes 8=48378
Ag_2S-HgI_2, photochromism 8=49952
Ag_2SO_4, i.r. spectrum 8=31955
Ag_2SO_4, phase boundaries below 500°C 8=48366
ζ-AgSb stacking fault probab., X-ray obs. 8=26704
Ag–Sb solid solns., Zener relax. activation energies 8=31190
Ag_3SbS_3, pryargyrite, crystal growth from melt 8=26228
Ag_2SeO_4, phase boundaries below 500°C 8=48366
Ag-Sn amalgam, corrosion studies 8=45326
Ag–Sn solid solutions, extended dislocation modes, effect of annealing 8=35561
Ag–Zn solid solns., vacancy-controlled atomic mobility, Zener-relax. studies 8=31040-1
Ag–Sn solid solns., Zener relax. activation energies 8=31190
β-AgZn, ordering crit. temp., temp. dependence, from elec. resistivity meas. 8=30676
NaCl-AgCl, solid soln., structural changes followed by conductivity and loss tangent meas. 8=35060

Sinanoğlu's theory. See Atoms/structure.

Sintering
alumina ceramic, densification rel. to grinding and abrasion resistance 8=48987
ceramic dielectrics, in reducing atmos. for high quality capacitor production 8=27220
clays, kinetics, thermal analysis meas. 8=30665
ceramic dielectric, in reducing atmos., prep., constitution and elec. props., 8=49332
conference, American Ceramic Society 70th annual meeting, Chicago (USA), 1968 8=40085
corundum, transparent, prep. and props. 8=45940
ferrites, to fine-grain structure with h.f. and microwave props. 8=27435
films, thin, review of results 8=26954
graphitic mats. hot-worked with dispersed liq. carbide rel. to thermal and elec. conductivities 8=44361
ice, spheres in powder, rate of decrease of surface area, due to plastic flow 8=35073
kinetics based on geometric models 8=35069
minerals, kinetics, thermal analysis meas. 8=30665
C amorphous powders, by elec. discharge 8=30667
C composite materials containing excess silica, temp. depend. of elec. resistivity 8=44687
CdS, kinetics, 780°-820°C 8=39534
Cr_2O_3/C compacts, shrinkage and cavitation 8=35072
in Cu with grain boundary cavities on annealing 8=26802
Fe_2O_3 compacts, shrinkage in range 800-1000°C 8=35067
Li-Zn ferrites, to fine-grain structure with h.f. and microwave props. 8=27435

Sintering—contd
- MgO, isostatically hot-pressed, fabrication and characterization 8=26045
- Mn-Zn ferrite, conditions effect on mag. props. 8=27432
- Mn-Zn ferrite, effect on mag. props. 8=49561
- NaCl, and LiF and MgO, pressure densification data rel. to plastic deform 8=35070
- Ni-Al cermet alloys, effect of porosity, temp. and Al content 8=26046
- Ni-Zn ferrites, to fine-grain structure with h.f. and microwave props. 8=27435
- Pb ferrites, oxide additives effect rel. to mag. props. 8=40842
- $PbZrO_3$-$PbTiO_3$ ceramics, by hot-pressing, and elec. props. 8=39535
- Si-Ge alloys, pressure sintered, props. rel. to microstructure 8=30668
- SiO_2 slip refractory for melting optical glasses 8=45936
- TaC, grain growth during hot-pressing 8=35283
- TaN-TiB_2, hot-pressed, densification and wear resistance 8=49053
- UC, with Ar, effects of Ni on structure 8=26299
- UO_2, Dorn method in study of initial phase 8=35068
- UO_2, high temp. thermal cond. 8=44370
- UO_2 with dispersed Gd_2O_3, behaviour at high temp. 8=35074
- W, nucleation of brittle fracture at low temp. 8=44608
- WC powder and WC-Co mixed powder, effect of 15-45 kbar pressure 8=39536
- ZrO_2, grain growth and phase transition 8=48357

Skin effect
- anomalous, confirmed by line shape theory of radio frequency size effect 8=44638
- common-wall directional coupler for waveguides 8=37519
- detector for clear-sky 8=50146
- at high frequencies 8=44678
- impedance in pulsed LCR ccts., anal. of transients 8=41927
- in metal opt. props. theory for specular e. scattering 8=49739
- metals, surface impedance, theory of low-field oscillations 8=36311
- spectral distrib. at Delhi, solar eclipse (1961) obs. 8=41364
- in superconductors 8=49177
- K, radio-freq. size effect rel. to Fermi surface meas. 8=44645

Sky brightness
- See also Airglow; Twilight.
- Musalla in Bulgaria, sky radiation and polarization 8=36798
- sky components due to clear blue sky for vertical rectangular aperture, precise values 8=50151
- stratosphere, diffuse as function of height, rel. to aerosol layer in stratosphere 8=36716
- three-channel photoelec. spectropolarimeter obs. 8=36921
- u.v. dayglow meas. with x-15 aircraft 8=36791
- zenith, and colour, during total solar eclipse, 12-11-66, Bolivia 8=36742

Sliderules
- No entries

Slip
- alloys containing hard particles, rel. to dislocation and work hardening 8=35640
- b.c.c. and h.c.p. structures, cross slip energy, activation volume rel. to stress 8=48963
- b.c.c. crystals, asymmetry, rel. to stacking faults and dislocations 8=44458
- component parallel to longit. marker line, determ. using Moire effect 8=40046
- dislocation incorporation in crystal twins 8=44088
- gas near solid surface, thermal, velocity, gas-kinetic analysis 8=39175
- grain boundary sliding, role in creep of polycryst. mats. 8=35621
- lines, rel. to indentation of rigid punch with smooth base 8=32759
- α-Nylon 66, cryst., (010) [100] slip rel. to plastic deform., obs. 8=40199
- slip-line fields, geometric props. for compression and extrusion 8=40112
- slip velocity, thermal, near solid surface, gas-kinetic analysis 8=39175
- steel, austenitic stainless, of grain boundaries rel. to He embrittlement 8=31213
- step height meas., replica technique 8=31069
- translational, rel. to crystal symmetry 8=26761
- Al, band continuity across grain boundaries 8=31090
- Be and alloys, rel. to temp., transmission electron microscopy 8=44555
- Be and alloys, surface traces above 200°C 8=44554
- Be-Cu alloy, basal and prismatic slip rel. to hardness anisotropy, obs. 8=44552
- Co single crysts. rel. to dislocation struct. and impurities, 78-573°K 8=40138
- Cu, distrib. rel. to initial dislocation substruct. 8=44459
- in Ge-GaAs epitaxial combinations 8=31077
- Ge-GaAs epitaxial combinations, linear defects interpretation as misfit dislocations 8=31078

Slip—contd
- Cu, n-irradiated, strengthening mechanism after mild annealing 8=31198
- Cu single crystals, persistent bands, fatigued at low stress amplitude 8=40140
- Cu-Ni alloys, discontinuous, temp. transients and affected volume 8=40147
- Fe-3% Si, critical shear stress and plastic flow 8=44568
- LiF, quenched, translational slipping mechanism 8=26828
- Mg and alloy MA-8, contrib. to fast deform. mechanism 8=40169
- $MgAl_2O_4$ spinel, and plastic deform. rel. to stoichiometry 8=31216
- Mo crystals, deformed in tension, line pattern and active systems 8=31091
- Nb crystal, slip asymmetry studies 8=26697
- Nb crystals, and yielding at room temp. 8=26696
- Si, rel. to parallel arrays of pure edge dislocations 8=40044
- Sn, white, single crysts., instability rel. to plasticity, obs. 8=40181
- Ti sheet, rel. to yield stresses, strain-ratios and plastic anisotropy 8=35721
- US, behaviour from e-microscope exam. 8=35285
- W crystals, deformed in tension, line pattern and active systems 8=31091
- Zn, by indentation at 5 kg loads 8=31056
- Zn sheet, rel. to yield stresses, strain-ratios and plastic anisotropy 8=35721
- ZnS, periodic processes rel. to polytype formation 8=44461

Smectic phase. See Liquid crystals.

Smokes. See Aerosols.

Snoek effect. See Crystal imperfections/interstitials; Elastic relaxation.

Snow
- firn samples from Antarctica, dating by meas. of natural and artificial radioactivity 8=27855
- heat transfer, model 8=32219

Sodium
- abundance in solar photosphere 8=28172
- active ionic transport through biological membrane, opposite to K ions 8=50461
- atom, D_1 line, profile and equivalent width 8=25361
- atom Na^{23}, h.f.s. in $3^2P_{3/2}$ state, level crossing investigation 8=34145
- atom scatt. on Ar, total scattering cross sections 8=34178
- atom, three-level, resonance problems and radiative transitions for D lines 8=38627
- atom, $3\ ^2P_{3/2}$ hyperfine structure resolution of level-crossing curves 8=43197
- atomic abs. cross sections, 500-600 Å 8=29622
- atomic lifetimes, direct obs. 8=29612
- atoms collisions in Na-Hg system, meas. 8=29665
- atoms in arc discharge with Cu, Ca, Zn atoms, effect on spectral line breadth 8=34437
- atoms in benzene, absorpt. spectrum at 55-100°K 8=49769
- atoms, quadrupolar birefringence in excited states 8=43271
- content determination in fuel rich air-H_2 flames 8=49990
- crystal lattice freq. distrib. function and sp. ht. calc. 8=44300
- diffusion in Li obs. btw. 50-176°C 8=31009
- diffusion in Si_3N_4 films 8=48605
- electron momenta from X-ray meas. 8=44647
- emission spectra, L_{23}, rel. to Al X-ray band spectra interpret. 8=45172
- equation of state, theory based on lattice free energy concepts in quasi-harmonic approx. 8=35021
- film condensation of pure vapour, intensity of heat transfer 8=48132
- friction, internal, in nominally pure samples 8=49029
- helicon-wave resonances in Hall coeff. determ. rel. to surface-mode loss 8=44682
- ion channeling in NaCl and KCl lattices, computer analysis 8=40075
- incipient pool boiling 8=48279
- ion mobility in synthetic SiO_2 glass 8=48795
- isotope distrib. in p-reactions on Mo^{100}, Ta, Ir, U 8=34000
- Knight shift and pseudopotentials 8=45129
- K-type stars, abundance by photometric meas. 8=45633
- liquid, C photon activation analysis 8=32148
- liquid, Faraday station of Alfvén waves 8=46445
- liquid, in breeder reactor cooling system, cavitation 8=29560
- liquid, in-core permanent-magnet flowmeter, calibration and stability 8=48013
- liquid, dynamic three-dimensional structure 8=25867
- liquid, heat transfer rates from moving spheres 8=34839
- liquid, properties, and order in liquid phase 8=48084
- liquid, solubility of Pb 8=43762
- melting curve up to 80 kb 8=34961
- optical constants, ellipsometric obs. 8=41120
- optically pumped, precision frequency meas. of 0-0 transition 8=47524
- oxidation in flames 8=49877
- pair interaction, phase change 8=35027
- photoelectric two-quantum volume effect 8=44948
- reaction with Va-Ti alloys as reactor fuel jacket 8=47430
- resistance, electrical 8=49167
- solid, equation of state 8=26588
- spin waves 8=31659

Sodium—contd
- superconductivity predictions from phonon spectrum and e. -phonon interactions 8=44719
- vapour, electrical conductivity above 10 torr, effect of molecular association 8=39220
- vapour, fluoresc. and energy transfer in collisions with inert gases 8=34182
- vapour lamp, thermal insulation and pressure effects 8=42208
- vapour, thermal cond. 886 to 1264°K, 0.034 to 0.69 kg/cm² 8=47964
- vapour, thermal cond., 670-900°C, 0.008 to 0.82 atm., meas. by coaxial cylinder method 8=47965
- velocity fields in Iyeka-Seki coment 8=45841
- wetting of Re, W, Mo, Ta and Nb rel. to bare work function of metal 8=35168
- Na^{22} diffusion in SiO_2 glass, α-β quartz transformation effects 8=48794
- $Na^{22,23}$ ions, electromigration in molten nitrates 8=43782
- Na^{23} in $NaSO_4$, nuclear quadruple coupling 8=49667
- Na^+, diff. in $LiSO_4$, 590-820°C 8=39977
- Na^+, ionization to Na^+ by electron impact 8=39047
- Na-NH_3 liq. solns., dynamic polarization 8=34925
- NaI 58900-96Å nightglow intensity, diurnal, seasonal and solar cycle vars. 8=32276
- NaI stellar D lines equivalent widths 8=41525
- Na_2, pseudopotential theory calc. 8=38838
- on Ni(110), monolayers one-dimens. incoherent struct., obs. 8=39579
- Pt surface ionization coeff. absolute meas. 8=31476
- V-10wt. % Ti alloy corrosion, influence of Ca content 8=27723
- W surface ionization coeff. absolute meas. 8=31476

Sodium compounds
- halides, ads. of Br_2 and I_2, refl. spectroscopy 8=48480
- halides, photoabsorpt. obs. 30-75 eV using synchrotron radiation 8=41123
- kröhnkite, $Na_2Cu(SO_4)_2.2H_2O$, cryst. struct. and n.m.r. 8=48660
- silicate glasses, high-temp. internal friction and transport mechanisms 8=40176
- sodium arsenoaluminate, hydrated, crystal growth 8=26411
- sodium halides, 30-75eV near Na $L_{2,3}$ edge, obs. using synchrotron radiation 8=41123
- solubility equation, in H_2O, valid up to critical density range 8=48070
- Na-alkali alloys, liq., n.m.r. 8=48223
- Na complex, sodium-N-diethyldithiocarbamate 8=26368
- Na disilicate glass, with diffusion zones of Fe, mag. susceptibility meas. 8=27381
- Na salt of 2, 6-dimethyl-p-benzosemiquinone, e. s. r. in t-pentanol, rel. to ion pairs 8=34909
- Na_3AlF_6 (cryolite) films, dielectric, l.f. polarization effects 8=44870
- Na_3AlF_6 effect on corundum recrystallization 8=48536
- Na_3AlF_6: Eu^{3+} luminescence obs. 8=36502
- $NaAlSi_3O_8$, X-irradiated, e.p.r. and luminescence 8=40936
- $Na_2B_4O_7.10D_2O$ (borax), d.m.r. 8=49628
- $NaBF_4$, n.m.r and ionic motion 8=31912
- $NaBO_3.H_2O$, e.s.r., rel. to RO_2, O_3^- and O_2^- centres 8=45098
- $NaBeF_3$-$NaPO_3$ system, i. r. spectroscopy for Be phosphate glass struct. 8=30791
- $Na_{0.5}Bi_{4.5}Ti_4O_{15}$, cation ordering 8=26413
- NaBr aq. solns., elec. cond. 0°-800°C and to 4000 bars 8=48195
- NaBr surface distortions, electrostatic potential contribution to LEED intensities 8=48423
- $NaBrO_3$, second-harmonic light generation rel. to natural optical activity 8=45206
- NaCN, polymorphism and melting to 40 kbar 8=30701
- NaCNO, bonding and stability 8=26006
- Na-Ca silicate glass, thermoluminesc., e. s. r. and e absorpt. spectra 8=30792
- $(Na_2, Ca)(AlSiO_3).5H_2O$ and $(Na_2, Ca)(Al_2Si_6O_{16}).6H_2O$, complex splitting of n. m. r. spectra 8=36277
- NaCl crystals F-colouring dependence, at room temp., on quenching, 300-710 °C 8=48882
- NaCl, 33.5-44 keV directional breakdown 8=48925
- NaCl:$CdCl_2$, colour centres induced by X-rays, absorpt. bands 8=31113
- NaCl-NaBr fused mixture, elect. conductivity and ion conduction activation energy 8=30519
- NaCl-Tl, -Ag. phosphors: recombination lum. efficiency after photothermal destruction of F centres 8=48881
- $NaClO_4$ aq. soln., diff. of protons 8=48115
- $NaClO_3$, e.s.r. of γ-irrad. cryst. 8=49613
- $NaClO_3$, phase boundaries below 500°C 8=48366
- $NaClO_3$, second-harmonic light generation rel. to natural optical activity 8=45206
- $NaClO_3$, i. r. reflectance bands, dispersion anal. 8=27593
- $NaClO_3$-$NaNO_3$ molten system, density, viscosity, surface tension 8=48086
- $NaClO_3$-$NaNO_3$ molten system, elec. cond. 8=48088
- $NaClO_3$-$NaNO_3$ system, sp. ht. liq., solid 8=48087
- $NaCrS(Se)_2$, crystal structure and mag. props., 8=39810
- Na_2CrO_4, phase boundaries below 500°C 8=48366
- $Na_2Cr_2O_7$, absorpt. spectrum at 2°K 8=45212
- $NaD_3(SeO_3)_2$, d.m.r. 8=49648

Sodium compounds — contd
- $NaD_3(SeO_3)_2$, d.m.r. and molec. struct. 8=49638
- NaF crystals, R_N and N centres, thermal annealing after p.-irrad. at liq. N_2 temp. 8=48883
- NaF, density changes on γ-irradiation 8=40129
- NaF, electron irrad., colour centres, obs. with oven cryostat 8=48880
- NaF, e.s.r. and optical studies of O_2^- 8=45097
- NaF, lattice vibrations in thin film, electron diffraction obs. 8=35387
- NaF, luminescence, delayed of M centre in F-to M conversion 8=41203
- NaF, r. f. spectra by elec-resonance method, rel. to struct of mol. 8=43316
- NaF, sp. ht. temp. dependence, 0.05-15°K 8=26591
- NaF, thermal vibr. and Debye-Waller factor obs. 8=30905
- NaF, X-ray scattering by phonons 8=44286
- NaF : Co^{2+}, absorpt. spectrum 8=49743
- NaF, F_3^+ centre, linear Stark effect 8=31120
- NaF, MO calc. of molec. props. 8=34269
- NaF:OH^-, u. v. and i. r. absorpt 8=45208
- Na_3FeF_6, x-ray diffraction powder data 8=48666
- $Na_xFe_xTi_{2-x}O_4$, $0.90 > x > 0.75$, crystal structure 8=39813
- $Na_2Ge_4O_9$, X-ray powder data 8=26412
- NaH, pseudopotential theory calc. 8=38838
- $NaHCO_3$, aqueous soln, (plus glucose or isopropanol), γ-radiolysis 8=36625
- $Na(H_xD_{1-x})_3(SeO_3)_2$, permittivity and spontaneous polarisation temp. and field strength dependence 8=40581
- $[Na_3H(PO_3)_4]_x$ polyphosphate, crystal structure 8=44239
- $NaH_3(SeO_3)_2$ and deutero-cpd., NMR and ferroelectric props. 8=27511
- $NaH_3(SeO_3)_2$, thermal, hysteresis in both phase transitions 8=44873
- $Na_2(H_2SiO_4).4H_2O$, structure in soln. and solid-state 8=48081
- NaI, surface distortions, electrostatic potential contribution to LEED intensities 8=48423
- NaI, I^{127} n. m. r. intensity dislocation dependence 8=36278
- $NaIO_4$, lattice thermal expansion 8=39929
- NaI: Tl, luminescence temp. and conc. dependence rel. to Tl^+ dimer centre characts. 8=27658
- NaI: Tl^+, luminescence temp. and conc. dependence rel. to energy transfer 8=27659
- NaI(Tl), contribution to total lineswidth of scintillation counter, monte-carlo calculation 8=46879
- NaI(Tl), long-lived phosphoresc. components in cryst. 8=27657
- NaI(Tl) monocrystals, vibration- and thermo-stable characts. 8=24514
- NaI(Tl), pulse shape rel. to Tl conc. and temp. 8=46876
- NaI(Tl) response to ions, $Z > 5$, 1-10 MeV/amu 8=44501
- NaI(Tl) scintillation characteristics, vacuum deposited 8=46875
- NaI(Tl), scintillators, emission bands, excited by X-irradiation, 5-80°K 8=46856
- NaI(Tl) single-crystal γ spectrometer 8=47066
- NaK eutectic, temp. profiles in turbulent flow, effect of superimposed free convection 8=34836
- $(Na_{0.7}K_{0.3})NbO_3$, antiferroelec., electro-optical effects 8=27294
- $NaLn_{1-x}Eu_xTiO_4$, Eu^{3+} fluoresc. 8=41191
- $NaMF_3$, $(M=Mg^{2+}, Co^{2+}, Ni^{2+}, Zn^{2+})$, chem. synthesis and structural data 8=26258
- $NaMgF_3$ crystal growth, perovskite struct. 8=30830
- $Na_4Mn_4Ti_5O_{18}$, crystal structure 8=44234
- Na_xMoO_3, electronic struct. 8=40245
- NaN_3, thermal decomposition, crystal size effects, topochemistry and gas analysis 8=39701
- $NaNO_2$, birefringence, dispersion and temp. depend. determ. 8=27594
- $NaNO_2$, charge distrib. of NO_2^- 8=48308
- $NaNO_2$, dielectric relax. mechanism 8=40613
- $NaNO_2$, dielectric relaxation, exptl. study 8=40612
- $NaNO_2$, phase boundaries below 500°C 8=48366
- $NaNO_3$, dislocations visualization by etching 8=48858
- $NaNO_3$, elec. cond. anisotropy rel. to interstitial defects 8=35964
- $NaNO_3$, far i.r. absorpt., solid and fused 8=49742
- $NaNO_3$, molten, surface treatment of Zr alloys 8=32105
- $NaNO_3$, molten, vib. freqs. by i. r. emission spectroscopy near 600°C 8=38842
- $NaNO_3$, n. m. r. of Na^{23}, orientation and temp. dependence 8=40991
- $NaNO_3$, Raman spectrum 8=41122
- Na NO_3, sp. ht., thermal diffusivity and conductivity in phase transition 8=48391
- $NaNO_3$, thermodynamics of λ-transition 8=39560
- $NaNb_3O_8$—$Nb_2W_3O_4$ solid solutions, existence and crystallographic study 8=43978
- $NaNiF_3$, orthorhombic weak ferromagnet, AFMR rel. to canting 8=31839
- NaO_2, phase transforms. and crystal structures 8=26075
- Na_2O activities in melts of Na_2SO_4 and Na silicate 8=34826
- $Na_2O.2MnO.2SiO_2$, absorpt. spectra, rel. to Mn^{2+} bands changes on temp. decrease 8=41119
- 25 Na_2O. 75 SiO_2 (mole %) glass fibre, thermal-elastic relax. 8=44513
- NaOBr, γ-radiolysis, radical yields 8=27767

Sodium compounds—contd
- NaOH ice, γ-irrad. electron traps 8=31153
- NaO_2-FeO-SiO_2 glasses, comp. vars. in e microanalysis rel. to surface damage, obs. 8=30865
- NaO, Na_2O_2 as impurities on Pt, at 20-1100°C, W, 20-700°C 8=35549
- $Na_2O.2SiO_2$; Fe system, kinetics of surface reaction and diffusion processes 8=26621
- $Na_3PMo_{12}O_{40}$, corrosion inhibition for steel in H_2O 8=45370
- $NaPO_3$, glassy and cryst., thermoluminesc., −180 to +20°C 8=41204
- $NaPO_3$, vitreous, crystallization on metallic condensation-nuclei with cubic lattice 8=44136
- Na_5Pb, cryst. struct. 8=43762
- (Na-Rb)NO_3 molten, elec. cond. 8=43865
- NaSCN, polymorphism and melting to 40kbar 8=30701
- $Na_2S_2O_6.2D_2O$, motion of D_2O molecules by n.q.r. 8=49669
- Na_2SO_4 aq. solns., viscosity and molal vol. 8=48098
- $NaSO_3$, oxidation in packed bubble column, 8=25858
- Na_2SO_4, phase boundaries below 500°C 8=48366
- Na_2SO_4, solubility equation, in H_2O, valid up to critical density range 8=48070
- Na_2SO_4, X-irradiated, single crystal absorpt. peaks obs. 8=44483
- Na_2SO_4-Li_2SO_4 phase diagram 8=39559
- $NaSO_4$, Na^{23} nuclear quadrupole coupling 8=49667
- β-$Na_2Si_2O_5$ crystal structure refinement from redetermined data 8=44237
- Na_2SiO_3, surface structure after etching, i.r. spectroscopy 8=39578
- $NaSmSiO_4$, crystal structure 8=39811
- Na-Sr-Cd niobates, dielectric props. and phase transitions 8=35979
- $Na_4Ti_4[Si_2O_6]_2[Si_4O_{10}]O_4.nH_2O$, crystal structure 8=48667
- $Na_6V_{10}O_{28}.18H_2O$, cryst. struct. 8=44238
- $Na_2W_4O_{13}$, crystallographic data 8=44235
- Na_2ZnGeO_4, electroluminescence in constant elec. field 8=45283
- $Na_2Zn_2[Si_2O_7]$, crystal structure 8=39812
- Na_2ZrSiO_5 phosphor, zone scheme for luminescence 8=41219
- **sodium chloride**
  - aggregation of Ca^{2+} ions, determ. by ionic cond., dielec. absorpt. and bulk density 8=35965
  - atomic charges, effective, X-ray determ. 8=26169
  - band structure, dielectric function pseudopotential calc. 8=41121
  - benzene/NaCl system, proton relax. time 8=45114
  - breakdown, laser-induced 8=40566
  - carrier mobility temp. dependence, 7.7-200°K, theory 8=44872
  - charged dislocations, effect of impurities 8=40041
  - cleavage faces, thermal etching in vacuum 8=35221
  - cleavage surface, decoration, through amorphous C layer 8=26200
  - conductivity, dielectric constant and refractive index spectra 8=45205
  - conductivity, elec., ionic, in pure, doped and irradiated mats. 8=27248
  - crystal, colour centre form. by e beam pulse 8=44475
  - crystal dielec. and mech. relaxation 8=30995
  - crystal growth containing ⟨110⟩ oriented Na dendrites, mechanism 8=30836
  - crystal growth micromechanism in vacuum-condensation process rel. to dislocation distrib. 8=48551
  - crystal growth technique for 4×10^{-8} mol/mol purity 8=39665
  - crystal polarization by voltage pulses, 100°–350°C 8=40580
  - crystal in organic liquids, interfacial energy calcs. rel. to abrasive wear and adhesion 8=30724
  - crysts., additively discoloured, effect of laser irrad. 8=44485
  - crystals containing cavities, work of fracture 8=26834
  - deformed and aged, temp-depend of Mn vacancy pairs 8=48811
  - deposition of Au, Ag, Ni, Pd and Al films, crystal orientation 8=44085
  - density changes on γ-irradiation 8=40129
  - dielectric, unipolar conduction mechanism from solid-state electrolysis 8=40579
  - diffusion of Pb^{2+} 8=31011
  - diffusion of protons in aq. soln. 8=48115
  - diffusion, reciprocal and self-, along dislocations and break surfaces 8=26620
  - dislocation mobility and microhardness dependence on F-centre density 8=26690
  - dislocation multiplication 8=26686
  - dislocation pinning by lattice defects 8=26680
  - dislocations, single edge, penetration through slip lines 8=26687
  - dissolution kinetics at dislocation sites, rel. to solvent and poisons 8=26685
  - doping with OH^- and CO_3 8=48550
  - elastic constants and tensile strength 8=49036
  - electrical conductance, high temp. 8=40323
  - electron emission due to bombardment with inert gas ions 8=40686

Sodium compounds—contd
- **sodium chloride**—contd
  - electron exoemission, X-ray excited, obs. and model 8=36053
  - electronic spectra 8=26909
  - energy bands, plane wave calc. 8=40224
  - with epitaxial Au layer, electrostatic field effect on initial orientation 8=26111
  - evaporation struct. of crystals doped with divalent cations 8=48603
  - exoelectron emission, photostimulated, external elec. field effects, obs. 8=36041
  - F-centres, optical absorption 8=35591
  - F-colour centres, photothermal stability, effect of plastic deformation 8=35590
  - fracture surface as function of crystallographic direction and treatment method 8=44593
  - glycerol soln., dielec. relaxation 8=48192
  - grain boundary energies, rigid lattice approx. 8=40053
  - hardening by n- and γ-irradiation from critical shear stress analysis 8=49037
  - interfacial polarisation, electrode performance effects 8=40582
  - light scattering temp. dependence, 128-298°K 8=45207
  - luminescence after shock compression 8=49806
  - mean inner potential calc. method 8=30629
  - mean inner pot. meas. by electron diffr. 8=30628
  - mechanical props. rel. to impurity effects 8=26401
  - n. m. r., acoustic, rel. to plastic deformation 8=44320
  - photomechanical effect, wavelength dependence 8=36368
  - photostimulated electron exoemission on excitation by electron irradiation 8=40708
  - plastically deformed, F-centre thermal stability rel. to dislocation density 8=35586
  - precipitation and association of $CaCl_2$ 8=48390
  - pressure sintering, densification data rel. to plastic deform. 8=35070
  - proton energy loss crystal orientation dependence rel. to lattice effects 8=35598
  - pure, ionic cond., motion of cation vacancy and form. of Schottky pair 8=35537
  - refractive index and absorpt., far u.v. obs. 8=27592
  - rocksalt films, breakdown strength, anode surface and mats. effects 8=40578
  - Schottky defect formation energy, from dissolution of impurty containing precipitates 8=35536
  - single-crystal scatt. centres, Raman spectra 8=49737
  - single crystal, u.s. propag. rel. to plastic deform. 8=31191
  - solutions, homogeneous nucleation 8=34973
  - specific heat and enthalpies of change of phase; meas. 8=46286
  - strength, theoretical, along body and face diagonals 8=44594
  - surface distortions, electrostatic potential contribution to LEED intensities 8=48423
  - transverse acoustic [OhO] phonon dispersion curve from X-ray thermal diffuse scatt. 8=39876
  - thermal diffusivity at high press. and temp. 8=48762
  - thermal vibr. and Debye-Waller factor obs. 8=30905
  - thermoluminescence, activation energy for glow peaks, by initial rise method 8=32056
  - tribo-photostimulated exoemission of electrons and triboluminesc. 8=40709
  - type crystals, LEED obs. of (11) beam from (100) surfaces 8=44236
  - ultrasonic vibrations, generation and reception 8=35988
  - ultrasonically irradiated, dislocation behaviour 8=26688
  - ultraviolet spectrum and band structure 8=41121
  - u.s. wave delay time meas. at h.f. by phase comparison method 8=44314
  - vaporization effect of dislocations on rate 8=35008
  - water evolution on heating in vacuum 8=41263
  - X-ray scatt. rel. to dislocation density and distrib. 8=45198
  - X-ray study under high pressures 8=35303
  - Ag film, epitaxial growth 8=30745
  - AgCl-doped single crystal, far i. r. absorpt. spectra 8=36391
  - Ag-NaCl layers, e exoemission, X-ray excited, obs. and model 8=36053
  - Al film, epitaxial growth 8=30745
  - Au nucleation rel. to surface F-centre formation in γ-irrad. 8=44152
  - Cl^- channeling, computer analysis 8=40075
  - Co^{60} γ-irradiated crystals, chemical method for the determ. of F-centres 8=48884
  - Cu film, epitaxial growth 8=30745
  - CuCl-doped single crystal, far i.r. absorpt. spectra 8=36391
  - Fe impurity ions, Mossbauer effect study 8=39510
  - K^+ channeling, computer analysis 8=40075
  - M centre, lifetime of first excited state 8=40063
  - Mn-doped, ionic cond., motion of cation vacancy and form. of Schottky pair 8=35537
  - Na^+ channeling, computer analysis 8=40075
  - $NaCl^{35,37}$, isotope-induced acoustic band far i. r. absorpt., 7°K 8=36396
  - NaCl, divalent impurity elec. behaviour 8=44423
  - NaCl, F-centre thermal destruction rel. to dielec. losses 8=44484
  - NaCl-type ionic crystal, energy loss of electron beam due to surface optical mode 8=44871

Sodium compounds—contd
  sodium chloride—contd
    NaCl: Ag, luminescence excited with extreme u.v. radiation 8=36501
    NaCl-Ag phosphors, F centers decomposition, thermal and photothermal 8=31123
    NaCl-AgCl, solid soln., structural changes followed by conductivity and loss tangent meas. 8=35060
    NaCl:Ca, luminous flux scattering temp. dependence, 140 to 150°C 8=32016
    NaCl:Cu$^+$, far i. r. props. of lattice resonant modes rel. to isotope shifts 8=36393
    NaCl: Cu$^+$, resonant bandmode, stress dependent freq. shift 8=48708
    NaCl: Cu$^+$, Ag$^+$, impurity ion distrib. coeff. on crystallization from melt 8=39674
    NaCl: Cu conc., absorpt. and fluoresc. after period of storage 8=49741
    NaCl/KCl aq. soln., heat of mixing 8=32989
    NaCl-KCl solid solns., decomposition effects on spectral characts. 8=36395
    NaCl:Mn, impurity distrib. coeff. from e.p.r., 8=48823
    NaCl:Mn, yield strength 8=40175
    NaCl: Pb(Ca), impurity ion effect on crystal structure 8=26642
    NaCl: Pb(NO$_3$)$_2$, structural changes on heat treatment at 300°C 8=26689
    UCl$_3$ soln., partial v.p. obs. 8=30456
Sofar. See Sound ranging.
Sogicons. See Semiconducting devices.
Soil
    density meas. with γ back-scatter guage, restricted angle 8=41325
    freezing, calc. of moisture migration, and determ. of stratified texture 8=34969
    lunar, particle size distrib. 8=32530
    magnetic susceptibility, direct-reading bridge 8=37380
    moisture, free energy meas. using thermistor hygrometer 8=50090
    neutron production due to natural radioact., rates 8=36681
    soft, plastic volume and shear deformation rel. to shock waves 8=40109
Solar activity. See Sun; Sunspots.
Solar batteries. See Electricity/direct conversion.
Solar cells. See Electricity/direct conversion; Semiconducting devices.
Solar constant. See Sunlight.
Solar corona. See Sun/corona.
Solar corpuscular streams. See Sun/radiation, corpuscular.
Solar eclipses. See Sun/eclipses.
Solar flares. See Sun/flares.
Solar furnaces. See Heating; High-temperature production and effects.
Solar noise. See Sun/radiation, radiofrequency.
Solar prominences. See Sun/prominences.
Solar system
    See also Planets, etc.
    asteroid belt, scatt. of bodies 8=45835
    Asteroid collisions and evolution of mass distribution, meteoritic flux 8=50411
    asteroids, classification based on Schmidt's law of planetary distances 8=32536
    British radioastronomical obs. 1963-66 8=32608
    obliquity of ecliptic secular change and Oorts' const. B, var. with earth's rotation 8=50392
    origin, ionization mechanisms, rel. to Alfven's critical vel. hypothesis 8=36989
    resonant structure and planetary distances law 8=50393
    B origin, big bang and solar spallation theory 8=36990
    Be origin, big bang and solar spallation theory 8=36990
    Fe fractionation, influence of ferromagnetism 8=28135
    H^2 origin, big bang and solar spallation theory 8=36990
    P^{29} in nucleosynthesis process 8=45845
    Li^{6,7} origin, big bang and solar spallation theory 8=36990
    Pu^{244} in nucleosynthesis process 8=45845
Solar wind. See Sun/radiation, corpuscular.
Solid solutions
    See also Alloys; and under compounds of the individual elements. Solid solutions such as Au—Cu, Au—Cu—Zn are indexed under compounds of the first named element, i.e. "Gold compounds" in these examples.
    biphenyl, in cyclohexane, delayed fluoresc. 8=36529
    composition, X-ray diffr. and fluoresc. spectrometry 8=27814
    diffusion, effect of deviations from Vegard rule under multilateral pressure conditions 8=48765
    diphenyl-α, α' dipyridyl, single crystal study rel. to phase diag. 8=26040
    ferrite-spinels, two-component, vacancy formation and behaviour 8=26638
    ferroxplane, dielectric props. 8=49321
    hardening in conc. solns., stress analysis 8=48964
    with impurities, slow neutron scatt. cross-sections 8=35379
    lattice vibrs. and order in substitutional solns. 8=30923
    metal-oxygen, kinetics of oxygen uptake 8=30651
    mixed crysts., deformed AB-type, surface e states, calc. 8=35784
Solid solutions—contd
    Mössbauer effect probability rel. to order-disorder transforms. effects 8=35032
    noble metal-rare earth, e.p.r. and susceptibility meas. rel. to local moments 8=31882
    organic, phosphoresc. and delayed fluoresc., kinetics and chem. appls. 8=25936
    oscillation absorption bands, Davydov's splitting 8=35547
    paradibromobenzene-paranitrochlorobenzene, single crystal study rel. to phase diag. 8=26040
    perovskite-type, ferroelec. transitions, phase fluctuations 8=35970
    photoluminescence, quenching energy transfer model 8=36459
    short-range order, rel. to deformation, annealing and quenching 8=26033
    short-range ordering rel. to diffuse scattering in e.-diffr. patterns 8=39758
    single crystal production, rel. to component segregation on crystallization 8=39654
    spinels, activity computation of cations 8=35045
    steels, Fe–C and Fe–Ni–C, in hardening rel. to martensite strength 8=26815
    sulpho spinels, binary, miscibility from x-ray diffr, and mag. props. 8=30653
    supersaturated, periodic conc. distrib. 8=30654
    superstructures, concentration inhomogeneites in ordered soln. 8=35057
    ternary f.c.c. substitution, hardening action of short range order 8=26806
    tetraphenylporphin and Ag deriv., intermediate comps. growth and structures 8=26034
    tolane-dipherylmercury single crystal study rel. to phase diag. 8=26040
    in triglycine sulphate and isotypic crystal system, ferroelec. phase transition 8=27293
    triglycine sulphate, dueterated, prep., conc. depend. of ferroelec. props. 8=49377
    triphenylene-d$_{12}$-Rhodamine B, triplet-singlet energy transfer kinetics, obs. 8=36533
    yield stress of binary crystals, depend. on temp. and alloy conc. 8=26763
    Ag–M, (M = In, Sn, Sb), activation energies for Zener relax. 8=31190
    Ag–Sn, extended dislocation modes, effect of annealing 8=35561
    Ag–Zn, vacancy-controlled atomic mobility, Zener-relax. studies 8=31040-1
    in Al-Cu-Mn alloys, rapidly solidifed, supersaturated comp. and decomposition kinetics 8=35084
    Al--Ge, stacking faults in precip. particles and elastic stresses 8=31096
    Au-V dilute, V^{51} n. m. r. 8=27514
    Ba$_{1-x}$Ca$_x$MnO$_3$, structure and mag. phase transitions 8=27377
    BaTi$_{0.75}$Sn$_{0.25}$O$_3$, Mössbauer effect and dielec. const., —200 –20°C 8=30639
    BaTiO$_3$-KF system on BaTiO$_3$ growth from KF flux 8=26163
    BaTiO$_3$-La$_{2/3}$TiO$_3$, -Sm$_{2/3}$TiO$_3$, and -Ba$_{1/2}$NbO$_3$, relax. polarization due to vacancies 8=35975
    (1-x)BiFeO$_3$-xSr(Sn$_{1/2}$Mn$_{2/3}$)O$_3$, transitions from Mossbauer studies 8=27442
    C—Cr—Ni—Si system, position of pseudo-eutectic rel. to reinforcing phase 8=43976
    CaF$_2$-Tb$_2$O$_3$(Tb(OF)$_3$)(TbF$_3$) crystal chemistry 8=39640
    CeO$_{1.75}$-La$_2$O$_3$, tri-and tetra-valency of Ce ions from X-ray absorpt. spectra. 8=39638
    Co with P, magnetic moment rel. to P content 8=45006
    Co-C, metastable extension of C solubility, splat-quenching effects 8=30656
    Co$_x$Ni$_{1-x}$S$_2$, pyrite, prep. and lattice parameters 8=48342
    Cr–Ni–Fe, prolonged, crystallization, rel. to lattice parameters and phase dimensions 8=26246
    Cu alloy, dilute thermally activated dislocation depinning 8=26670
    Cu-Al, stacking fault energy, annealing and irrad. effects 8=26702
    Cu-Au alloys, friction, wear and surface hardness in abrasion 8=40149
    Cu-12.5 wt. %Ge, f. c. c. → h. c. p. transform. 8=26068
    Cu$_x$Ni$_{1-x}$S$_2$, pyrite, prep. and lattice parameters 8=48342
    Cu-Zn-Sn, ternary diffusion 8=39972
    Fe base alloys, interstitial, thermodynamic props. 8=44328
    α-Fe, cold-deformed, with stacking faults of C and N 8=35543
    α-Fe, internal friction of C, effect of osc. modes on quantitative anal. 8=35695
    Fe–rich alloys with non-transition elements, saturation magnetization 8=49519
    Fe-Be alloy, ageing, 3-D modulation of struct 8=30650
    Fe$_x$Co$_{1-x}$S$_2$, pyrite, prep. and lattice parameters 8=48342
    Fe-N single crystals, strengthening 8=49013
    Fe-N, solid solns, resistivity mag. field dependence at 4.2°K 8=31319
    Fe-Ni-C martensites, hardening and thermally activated deformation 8=26816
    GaAs-InAs, epitaxial films, crystallization kinetics and structure 8=26119
    GaP-GaAs epitaxially grown, departures from homogeneity 8=30838

Solid solutions—contd
  Ge-Si electronic props 8=49225
  HBr in DBr, n.m.r. 8=36269
  HCl in DCl, n.m.r. 8=36270
  Hg_3Te_3-Im_2Te_3 alloy system, phase diagram 8=30697
  InAs with $A^{III}B^{V}$ type cpds., reflection spectra 8=41099
  InAs:Cu, formation and decomposition effects on elec. props. 8=40473
  In–Cd, densities 8=43977
  In–Ce, superconductivity, low-temp. resistivity and thermoelec. power rel. to localized moments 8=31339
  $In_{1-x}Ga_xSb$, thermal conductivity temp. dependence 8=44363
  KBr-KCl, luminesc., intrinsic, induced by X-ray 8=41198
  KCl-KBr, p-irradiated, F-centre generation comp. dependence 8=31117
  KCl-KI, decomposition effects on spectral characts. 8=36395
  KCl–KI, optical absorption spectra 8=49736
  $Li(Nb_{0.5}Fe_{0.5})O_2F$–$Li(Ta_{0.5}Fe_{0.5})O_2F$ system, phase diag. and dielec props. 8=31435
  Li_2O-LiF, oxide and hydroxide activity determ. 8=36593
  MgO-Cr_2O_3-Fe_2O_3 at 1300°C in air, phase relations 8=39529
  MgO–MnO, and with LiO_2, struct. and mag. props. 8=48662
  Mg_2SnO_4-$MgFe_2O_4$, magnetic props., crystal structure 8=40738
  $MnAs_x Sb_{1-x}$, paramagnetic susceptibility and structure 8=49482
  $Mn_{1-x}Fe_xP$, magnetic props. rel. to props. of FeP 8=27378
  MnP–MnAs magnetic and structural study 8=48388
  Mo, of S, Se and Te, effect on lattice consts. expansion and densities 8=48664
  NaCl-AgCl, structural changes followed by conductivity and loss tangent meas. 8=35060
  NaCl-KCl, decomposition effects on spectral characts. 8=36395
  $NaNb_3O_8$–Nb_2WWO_4, existence and crystallographic study 8=43978
  Na-Sr-Cd niobates, dielectric props. and phase transitions 8=35979
  Nb-O-N, supersaturated, oxide and nitride precip. in annealing and hardness, obs. 8=30831
  Ni-C metastable extension of C solubility, splat-quenching effects 8=30656
  Ni_4Mo-Ni_4W, ordering rel. to resistivity 8=39530
  NiO-MgO, formation on thermal decomp. of mixed hydroxides 8=39532
  NiO–MgO, thermodynamic activites of NiO 8=43979
  NiO-MgO, struct. and mag. props., 98°-298°K 8=35061
  Pb-Bi, indirect nuclear spin-spin interactions in Pb by spin echo 8=40996
  Pb-Hg, indirect nuclear spin-spin interactions in Pb by spin echo 8=40996
  Pb-In, indirect nuclear spin-spin interactions in Pb by spin echo 8=40996
  $PbTe_xSe_{1-x}$, rel. to forbidden band width temp. dependence 8=40247
  PbTe-SnTe-PbS system, current carrier scattering mechanism 8=31385
  $PbTiO_3$–$PbMn_{2/3}W_{1/3}I_3$ system, structures and permittivities 8=40616
  Pt-1 at.% Co(Fe), elec. and mag. props., plastic deformation effects 8=31327
  Sb_2S_3–Bi_2Te_3 solid solns., morphotropy 8=48672
  $Se_xTe_{1-x}Hg$, crystal growth and structure 8=26269
  Si-O, anomalous X-ray transmission, rel. to periodicity changes on decomposition 8=36409
  Sn-Ce, superconductivity, low-temp. resistivity and thermoelec. power rel. to localized moments 8=31339
  $(Sr_{0.4}Bi_xLa_{0.6-x})MnO_3$, structure, mag. and dielec. props. 8=26038
  $Sr_{1-y}Bi_y)MnO_3$, structure, mag. and dielec. props. 8=26038
  Ti, separation of α- and β-, conditions 8=48347
  Ti–Ni–Sb–O system, rutile formation 8=48405
  Ti–Ni–Sb–O system, rutile, reaction diagrams 8=48404
  TiO_2-Sb_2O_3-NiO system, comp., structure and colour 8=26039
  Tl, superconducting transition temp., effect of impurities 8=49201
  $UC_{1-x}N_x$, in N_2 gas, change of comp. 8=35063
  UP-ThP and UP_2-ThP_2, antiferromagnetic 8=45067
  $(U, Pu)O_2$, production and Pu distrib. 8=29562
  WC-Co hard metal foils, microstructure 8=35287
  W-Cr, decomposition from X-ray diffr. study 8=26086
  $91Y_2O_3 + 9ThO_2$, elastic moduli, temp. depend. from 25°C to 1100°C 8=35724
  $Zn_{0.1}Cd_{0.9}Sb$ crystals, thermoelectric power anisotropy 8=27311
  $Zn_xHg_{1-x}Te$, crystal growth and structure 8=26269
  $Zn_xHg_{1-x}Te$, fundamental reflectivity spectrum 8=45232
  $Zn_xHg_{1-x}Te$, thermal conductivity 8=44372
  ZnSe–SnTe, growth in Te_2 atmosphere 8=48564
  ZnTe–CdTe, absorption spectra, energy structure 8=40253
  Zr–O interstitial, ordered arrangement of O 8=35289
  Zr-O, microprobe and e microscope obs. 8=30658
  ZrO_2, hydrated amorphous, nature and thermal behaviour 8=43982
Solidification. See Freezing.

Solids
    See also Crystals; Films/solid; Metals; Plastics; Powders; Semiconductors; Vitreous state.
  anisotropy detect. by sound meas. 8=30038
  filling particles, form factors meas. rel. to charact. size of each particle 8=39533
  graphite, anisotropy in energy calcs. 8=48299
  metal iodides with layer structures, optical absorpt. spectra 8=45176
  non-metallic, indentation deform, effects of adsorption 8=44524
  optical absorption bands of impurities, method of moments 8=41028
  surfaces, rough, contact area 8=35139
  thermal and subthermal n scatt. 8=24959
  Van der Waals forces between two ferrodielecs, separated by narrow gap 8=40602
 structure
    See also Crystal structure; Electron diffraction examination of materials; Electron microscope examination of materials; Granular structure; Neutron diffraction examination of materials; X-ray examination of materials.
  bulk semiconductors, dynamics of high-field propagating domains 8=49221
  coating with variable Al contents, hot galvanized 8=39704
  disordered, thermal conductivity 8=35449
  glass, silicates, substructure 8=30794
  glass, solid and melt, similarities 8=30790
  Hartree-Fock exchange potential for electrons 8=38617
  interstratified, formed by acid treatments on pre-heated mica 8=36572
  models, ball-drilling methods 8=32631
  molecular systems organized by deposition of successive thin layers 8=43921
  n.m.r. resolution of chemical shift in solids 8=40963
  ordered phase structures, phenomenological theory 8=30671
  paracrystalline state theory 8=30799
  polymers, molec. ordering above glass temp. 8=39633
  polymers, supramolec. struct., obs. methods 8=30795
  Rayleigh functions, localized, for analysis 8=37129
  rel. to bremsstrahlung coincidence spectrum 8=41037
  spinel solid solution, activity computation of cations 8=35045
  tungstates, binary, new group 8=39526
  vanadate glasses, characterization, and phase separation 8=26152
  B, non-cryst., atomic radial distrib. function, from X-ray diff. studies 8=26043
  Cu foil, texture parameters 8=49663
  Fe glazes, FeO content rel. to shade 8=49717
  Fe(III) coordination no. in organic complexes, Mossbauer determ. 8=39516
  Fe-Be alloy, ageing 3-D modulation of struct 8=30650
  NH_4 salts, barriers to rot. of NH_4 ions 8=48393
  Pb alloys with 0.5% Sb, Te, Cu, effect of dopant rel. to alloy life fatigue 8=26841
  Si_2O_3 glass, struct. determ. by X-ray diffr. 8=48503
 theory
  alloys, binary, spherical model and Clapp-Moss eqns. rel. to Ising model 8=39527
  anisotropy relaxation in solids 8=49627
  antisymmetric exchange interaction between electrons on different ions 8=39522
  atomic translational-diffusion mechanism from NMR spin-relax. time exam. and order parameter calcs. 8=27498
  electron-phonon interaction and phonon dispersion relations using augmented-plane-wave method 8=31260
  energy spectra computation methods 8=35762
  e excitation and luminesc. and cond. induction by atom and ion bombard. 8=26861
  rel. to galvanomagnetic effects, transport in strong mag. field, semiclassical theory 8=35755
  internal field coupling coeffs. and ionic and paramag. energy levels, SO(2) algebra 8=39505
  ionic crysts., quantum-statistical ab initio calcs. 8=48338
  ion-lattice interaction, and motion of neighbouring ions 8=48339
  local, magnetic moment formation at impurity site, resistivity exhibits Kondo-like behaviour 8=40299
  luminescence, models 8=36458
  magneto-conductivity in a.c. elec. field, nonlinear Boltzmann eqn. soln. 8=35748
  nuclear spin energy diffusion 8=48316
  optical absorpt. and emission rel. to molecular Einstein coeffs. 8=39367
  parahydrogen, rot. and vibr. excitation 8=43967
  periodic bond chain, rel. to thermal vibrations in a crystal 8=26005
  pseudo-potentials, analytic props. 8=46788
  quasi-particle interacts, damping and freq. shifts 8=35019
  rigid spheres near close packing tunnel model and partition function 8=23903
  semiconductor, bulk, surface transport props. 8=27063
  transition metals, atomic mag. moment rel. to localized d electrons 8=35047
  van der Waal's forces atomistic derivation 8=43234

Solids—contd
  theory—contd
    Ar, pair and non-pair potential 8=43924
    GaAs, electronic charge transfer 8=31266
    H. bonded. dielec. absorption study 8=49330
Solions. See Acoustic transducers.
Sols
    See also Colloids; Sedimentation.
    molecular containing CH_3 groups, motion and phase changes 8=36276
    $CaCO_3$, stable conc. oil sols form., rel. to adsorpt. of Ca sulphonate on $CaCO_3$ 8=30767
    Pt, for electrical-decoration of Si surface for e.-microscope exam. 8=40496
Solubility
    See also Phase equilibrium.
    alcohols, liq., of inert gases, CH_4 and CF_4 8=39319
    austenite, solubility of Cu, effect of Cr 8=30655
    crystals for u.v. and i.r. optics 8=42116
    2-dodecylaminoethanol salts, study of micellar props., effect of counterions 8=39291
    dye solubilization by polymer-surfactant complex 8=34777
    hydrocarbons in H_2O, structural theory 8=48085
    inert gases in fused $AgNO_3$ 8=25949
    inert gases in H_2O 8=48077
    in isomorphous impurity diffusion process in crystals 8=26612
    liquid-liquid-gas equilib., high-press., expt. determ. 8=34773
    methyl iodide, partition coeff. between vapour and H_2O 8=48073
    in propylene-Ar system, 100-150°K 8=39479
    in propylene-Kr system, 130-200°K 8=39479
    solid matter, in liquid phases, equation valid up to critical density ranges 8=48070
    water-cyclohexane, polyoxyethylene (9.7) nonylphenylether system, mutual, temp. effect 8=48249
    Ag alloys, of O_2 8=39313
    $BaO-Li_2O-SiO_2$ system, metastable ummiscibility 8=30413
    $BaO-SiO_2$ system, liquid-liquid immiscibility, phase separation 8=39318
    $BaSO_4$ in sea water 8=34783
    Co, of C, metastable extension, splat-quenching effects 8=30656
    Cu-CuO, liquid, miscibility gap 8=48075
    Fe, b.c.c., of O 8=48361
    α-Fe, cold-deformed, with stacking faults of C and N 8=35543
    α-Fe of S, permeability 8=43974
    H_2O in compressed N_2, Ar, and CH_4 8=30302
    Hg, in dimethylcyclohexanes and alcohols 8=48071
    Hg, in various liqs., free-vol. theory 8=30417
    Hg, in various liqs., tracer determ. 8=30416
    Hg, temp-depend, entropy, solute-solvent interact 8=43789
    InAs, of Cu, effect on elec. props. 8=40473
    KOH-ZnO solns., 10-55°C 8=45373
    Li soaps in water miscible alcohols 8=39316
    Mo, of IV A-group metal carbides in solid-state 8=48344
    N, in W and Mo 8=39987
    Ni, of C, metastable extension, splat-quenching effects 8=30656
    of O_2 in liquid Ag 8=39317
    Pb in liquid Na 8=43762
    $PbO-B_2O_3-PbF_2$ melts, of trivalent oxides, temp. dependence, 1000-1500°C 8=39320
    $Pb_{1-x}Sn_xSe$, mutual solid solubility 8=43980
    $Pb_{1-x}Sn_xTe$, mutual solid solubitity 8=43980
    Si, activity in molten Ag-Si alloys by e.m.f. meas. 8=48078
    Si, of B, max. 8=48345
    SiP_2 and $SiAs_2$, continuous solid solubility 8=40484
    in SnTe-SnSe system, rel. to phase diagram, 300° to 900°C 8=44013
    T in Si 8=48346
    Ti-Pd alloys phase diagrams 8=35127
    U, of Ir, solid 8=35133
    U, of Ru, solid 8=35131
    U, of Rh, solid 8=35132
    U in UO_2, phase boundary for temps. down to 1210°C 8=30712
    UO_2 in HNO_3 rel. to cryst. orientation, 1-37 molal 8=30818
    Zn-Sn-Cd-Pb alloy, binary liq. phase occurrence 8=34786
Solution energy. See Heat of solution.
Solutions
    See also Heat of solution; Liquids; Solid solutions.
    acqueous, activation energy of conduction in capillaries 8=34895
    adsorption on free liq. surface and on solid 8=44068
    alcohol-hydrocarbon, molec. model, excess Gibbs energy and enthalpy 8=43797
    alcohol-inert solvent, H bonding entropy and enthalpy and ratio of molar vols. 8=43799
    alcohols in p-xylene or n-heptane, adsorpt. on rutile defined surfaces 8=35196
    n-alcohols, with LiCl solute, relaxation time of molecular reorientation 8=34778
    alkali-chlorozirconate cpds. in alkali-chloride melts, activities 8=34780

Solutions—contd
    alkali halides, microdyn. model from nucl. mag. relax. 8=25953
    alkali metal nitrates, interactions in aq. solns. 8=34869
    alkali metals in fused alkali metal salts, spectra 8=39374
    alkaline earth halides, microdyn. model from nucl. mag. relax. 8=25953
    amphiphiles, lamellar liq. crystalline solns., birefringence sign reversal 8=25919
    aniline solns., free volumes 8=30469
    aqueous, at infinite dilution, ion-water interact. energies and thermodynamic props. 8=43754
    aqueous electrolyte solns., surface potentials 8=30516
    aqueous, metastable structures as crystallization centres 8=34776
    aqueous solns., γ-radiolysis at high press., reaction of hydrated electron 8=32143
    aromatic hydrocarbons, triplet state form. efficiencies 8=43832
    benzene, quinoline and phenol, complex form. 8=25887
    binary, critical phases, negative partial molar volume of solvent 8=34774
    binary, under critical lamination, precipitation on ions as nuclei, in supersaturated state 8=37800
    biological material, for I radioactivity meas., prep. 8=42339
    brines, total Br determ., X-ray fluorescence obs. 8=27815
    cations in aq. soln., coordination numbers 8=34779
    chemical reaction obs., stopped-flow apparatus 8=32084
    chemical reactions, diffusion-controlled, statistical anal. 8=34882
    chromophore-solvent interactions 8=25927
    concentrated electrolytes, ion-pair theory 8=41272-3
    containing molecules, reversible orientation, mech. 8=39322
    critical mixtures, anomalous viscosities 8=48097
    critical opalescence in elec. field, relax times 8=30473
    critical opalescence of dipolar mixtures, elec.-field effect 8=39312
    decorated lattice model of binary mixture 8=23873
    dilute polymer, orifice plate calibration 8=25889
    dispersion forces of solvents, effect on u.v. spectra 8=34870
    dissolution of calcined ferric oxides rel. to calcining temp. 8=45337
    dyes, Q-switch, for Nd lasers 8=42112
    electrolyte diamag. solns., intermolec. proton relax. rate 8=25957
    electrolyte, isothermal equilib., independ. of changes in dielec. const. 8=43761
    electrolyte, nuclear spin relax. and viscosity 8=34927
    electrolyte solns., diffusion potential decay 8=30448
    electrolytes, aq., Hall effect meas. 8=48199
    electrolytes, diamag., dipolar spin relax. and self-diffusion 8=25952
    enantiomers in optically active liq. crysts., n.m.r. 8=39422
    ethanol-ethyl halide mixtures, u.s. relax 8=30471
    gases in non-polar solvents, entropy of vol. expansion 8=39288
    gas-liquid, filtration, residual water effects 8=39233
    fluorescence quenching kinetics 8=39385
    hexamethylenetetramine aq. solns., differential diffusion coeffs. 8=30446
    hexamethylenetetramine-water, solvent-solute interactions 8=41254
    hyperchromism, two-band model 8=39365
    inert gases in H_2O, struct. theory 8=48077
    intramolecular barrier in solns., dielec. meas. 8=48186
    ion hydration in aq. solns., i.r. spectra 8=39373
    ion-solvent interaction, preferential solvation in mixed solvents 8=39314
    ionic, equilib. props., computation methods 8=34782
    ionic, magneto-optical rot. meas. by sample exchange 8=34847
    ionic, thermodynamic instability consts. of complexes, calc. by Debye-Huckel type eqns. 8=25905
    ionic, very dilute, ionic distrib. and freezing pots 8=34971
    isobutyric-acid-water system, diffusion coeff. obs. near critical soln. conc. 8=39341
    liquid mixtures, light scatt. above and below crit. soln. temp. 8=39371
    liquid binary mixtures, thermodynamic props. determ. 8=43814
    liquid mixtures, surface props., statistical-mech. calc. 8=48107-8
    liquid mixtures, thermodynamic excess functions 8=39321
    lyophilic, stability and mech. of coagulation by electrolytes 8=25970
    lyophobic, stability and mech. of coagulation by electrolytes 8=25970
    macromolecular, normal stress difference meas. 8=25893
    macromolecules, i.r. spectra and molec. interactions 8=30485
    of macromolecules, theory of diffuse small-angle X-ray scattering 8=25870
    metal thiocyanate molten solns., i.r. spectra 8=25934
    methylurea-water, solvent-solute interactions 8=41254

Solutions—contd
  mixture at vertical point, anomalous increase rel. to damping of hypersonic waves 8=30465
  molecules in aq. soln., dipole moment determ. 8=34213
  molecules, polar, in non-polar solvents, dipole moments formulae 8=34216
  molten salts, conformal soln. theory 8=34784
  monodisperse rigid rods, spectral distrib. 8=39362
  nitrobenzene-n-hexane mixtures, u.s. absorpt. near critical region 8=25912
  nonionic detergent in aq. soln. micellar props. 8=30559
  nonradiative energy transfer in systems with frozen rot. Brownian motion 8=34883
  polar viscous, dielec. relax., microwave obs. and theory 8=43852
  polyisobutylene, v. dil., viscoelasticity 8=39329
  polymer, boson representation of gyration radius 8=38974
  polymer, comblike branched mols., statistical thermodynamics 8=39324
  polymer, flow birefringence and polydispersity 8=39368
  polymer, flow-time fluctuations in capillary viscometer 8=30431
  polymer, mol. wt. determ. by ultracentrifugation 8=38967-8
  polymer, semidilute, quasielestic neutron scatt. 8=30419
  polymers, conc., normal stresses in simple shear flow, molec. theory 8=34699
  of polymers, fibrillar structures 8=26153
  polymers in binary mixed solvents, light scatt. 8=30472
  polymers, linear, dilute flow, friction factor characts. 8=25845
  polymethacrylic acid, aqueous and methanol solns., small-angle X-ray scattering 8=25888
  poly-n-butyl methacrylate in chlorinated diphenyl, normal stress effect 8=39333
  polystyrene, film-forming 8=44065
  s-RNA in water, regularized arrangements from X-ray scattering studies 8=25885
  salts, convective diffusion in porous mats., boundary cond. at inlet of system 8=39959
  siloxanes, solvent effect, freq. spectroscopic investigation 8=25884
  small molecules in solvents, rotation-like motion, spectral evidence 8=25928
  solute concentration, effect on macromolecular adsorpt. 8=39614
  solute-solute interactions in aq. solns. 8=25886
  solutes, diffusivity in rel. to heat of vaporization 8=25900
  solvated electron in polar liqs., oriented dipole model 8=34785
  solvent effects in u.v. spectra 8=34876-7
  solvent-solute interactions, effect on macromolecular adsorpt. 8=39614
  solvent Stark effects and spectral shifts 8=39375
  spectra, charge-transfer absorpt. band shape and polarization, calc. 8=34200
  structure in above-critical region, theory 8=25995
  structure rel. to morphology of hydrothermally grown crystals 8=26223
  styrene-methyl methacrylate random copolymers, dilute soln. props. 8=39323
  ternary liq. systems, decorated lattice model 8=34781
  ternary, thermodynamics, quasi-chem. approx. 8=48083
  thermal conductivity, calc. rel. to molecular component sizes reln. 8=39354
  three-component, phase transitions and crit. pts. 8=48076
  transfer of electronic excitation energy, effect of diffusion 8=34881-2
  trypin and DIP deriv., in water and salt solns., X-ray scattering study 8=25681
  Tschitschibabin carbohydrates in benzolic soln., mol. states 8=48064
  uranine in glycerol-ethyl alcohol and glycerol-H_2O, mol. plus solvation shell vol., obs. 8=34285
  water-oil system solubilized with Aerosol OT, dielec. props., 5-60°C 8=39406
  AgBr cryst/soln. phase, distrib. equilib. 8=34959
  AsF_6^- anion in non-aq. solns., spin-lattice relax. 8=34928
  Ag-Si molten alloys, Si activity by e.m.f. meas. 8=48078
  Ar-N_2 liq. mixtures, surface tension statistical-mech. calc. 8=48107-8
  Bi-Bi Br_3, molten, thermoelec. power 8=25947
  Cd-$CdCl_2$ liq. system, vol. change on mixing 8=30414
  Co(II) Br, in water, methanol and ethanol, bonding, interact and ion form 8=43764
  CO(II) Cl, in water, methanol and ethanol, bonding, interact and ion form 8=43764
  Fe(III)-Cl in methanol, bonding and interacts. 8=43764
  Ga-In liq. alloys, activities 8=39315
  H_2, vibr. solvent shifts in induced i.r. spectra 8=43837
  HSO_3Cl solns. of simple bases, elec. cond. 8=48194
  He^3 in He^4, Fermi-liq. transport coeffs. 8=37340
  KCl/NaCl aq., heat of mixing, calorimeter 8=32989
  KCl in H_2O-alcohol, elec. cond. at high press. 8=39407
  KI in formamide, X-ray diffr. 8=39306
  Li soaps in alcohols, physical props. 8=39316
  NO in H_2O, radiolysis study 8=49975
  NO in H_2O, D_2O photolysis at 1849 Å 8=49958
  Na, liquid, properties, and order in liquid phase 8=48084
  NaCl/KCl aq., heat of mixing, calorimeter 8=32989

Solutions—contd
  $Na_2(H_2SiO_4).4H_2O$, structure in soln. and solid-state 8=48081
  Na-NH_3, dynamic polarization 8=34925
  Ni(II) in aq. soln., primary solvation no. determ. by p.m.r. 8=39423
  O^{17}-n.m.r. study of aq. electrolyte and nonelectrolyte solns. 8=25956
Sonar. See Sound ranging.
Sonic boom. See Aerodynamics; Shock waves/effects.
Sonoluminescence. See Luminescence/liquids and solutions.
Soret effect. See Diffusion in liquids, thermal.
Sorption
    See also Adsorption.
  benzene sorbed on silicagel, proton relaxation, temp. depend. 8=49632
  cellulose, of water, and diffusion 8=30785
  chemisorbed atoms, long-range forces 8=47533
  chemisorption, heat of, calc. using H-MO approx. 8=36585
  chemisorption in mol. separator, deactivation 8=32150
  chemisorption, negative temp. coefficients for surface diffusion 8=49898
  chemisorption of diphite molecules on AC and Mg 8=49899
  chemisorption of N and NH_3 synthesis of Fe purified in ultra vacuum 8=41265
  chemisorption of gases on solid surfaces, molec. thermodynamic treatment 8=44069
  chemisorption of O_2 on electro-graphite 8=41266
  chemisorption of O_2 on ZnO, effect of d.c. electric field 8=49905
  chemisorption states of ionic lattices 8=32118
  chemisorption systems, interpret of LEED data rel. to interact with adatoms 8=27733
  desorbed atoms from specular surfaces, ang. distrib. 8=39574
  desorption by emerging high-energy electrons, kinematics 8=39607
  desorption of thin films on solid surfaces, interpretation of kinetic results 8=39610
  electrical field effect 8=39606
  glass, octadecylamine and stearic acid desorpt. and exchange, obs. 8=30768
  graphon, of O_2, kinetics, 450-675°C 8=45362
  hydrophilic clays, H_2O permeability, porosity and effective specific surface of filling 8=30661
  ionic pump, leak detection appl. 8=39260
  ionic pump, residual gas analysis in ultra-high vacuum system 8=36630
  ionic pumps for Ar 8=39245
  liquid in wetted-wall columns, of gases, acceleration by corona discharge 8=32119
  metal surfaces, gas interact. in field ion microscope 8=35143
  in metallic lattices, atomic capture coeff. and desorpt. rate at very low temps. 8=30762
  metals, H^+ implantation rel. to sputtering 8=30764
  moisture by porous bodies, thermodynamic functions 8=44070
  monooctadecyl phosphate monolayer desorpt. from air/water interface, kinetics 8=30442
  organo-clays, isotherms rel. to swelling and intra-cryst. porosity 8=30779
  oxygen desorption from W substrate by e. impact. 8=49901
  polyvinyl alcohol, of water, crystallinity effect 8=30784
  pump, fast, for 10-150 mtorr 8=30327
  of radioactive substances in chromatographic columns, steady-state conc. distrib. 8=32144
  residual gas on metal surfaces, rel. to secondary electron emission 8=49445
  sample holder for simultaneous gas sorpt. and X-ray obs. 8=33301
  sepiolite, vapour sorption 8=26137
  steel, octadecylamine and stearic acid desorpt. and exchange, obs. 8=30768
  surface scanning with electron probe and ion desorption exam. by mass spectrometer 8=30760
  zeolites, synthesis 8=36541
  Ag, Kr, Xe bombard., thermal desorption obs. 8=48483
  Al_2O_3, chemisorption effects on electronic props. 8=44866
  Au, Kr, Xe bombard., thermal desorption obs. 8=48483
  C membranes, time-lag and blind pore behaviour 8=26134
  CO_2, mixed-gas adsorption and vacuum desorption on mol. sieve, thermodynamic and rate behaviour 8=48481
  CO_2 on MgO, i.r. study 8=47974
  CdS, chemisorption states of oxygen 8=32118
  CdS, influence of oxygen chemisorption and desorption on surface photoconductivity 8=49413
  Cr, chemisorpt. of alcohols, aldehydes, ketones, i.r. of spectra formed 8=45363
  Cu crystal, Xe^+ thermal desorption obs. 8=48482
  Cu, Kr, Xe bombard., thermal desorption obs. 8=48483
  $Fe(OH)_2$, of Ru and nitrosylrothenium, ionic and colloidal, obs. 8=44073
  H atoms, chemisorbed, long-range forces 8=47533
  H on W chemisorption 8=49904
  H-metal system, theory 8=49896

Sorption—contd
H_2O on MgO, i.r. study 8=47974
KCl, water evolution on heating in vacuum 8=41263
MgO, chemisorption of H_2 and surface OH, i.r. spectros. 8=49894
Mn, chemosprt. of alcohols, aldehydes, ketones, i.r. of spectra formed 8=45363
Mo, of N_2 8=49908
Mo films, desorption of N_2 8=30771
N in Ta; 10^{-8}-10^{-3} torr, 1600-2300 °K, 0.0044-1 atomic %, press.-temp.-conc. ranges 8=49897
NaCl, water evolution on heating in vaccum 8=41263
Nb, of O_2, kinetics, 1100-1800 °C at 5×10^{-5} and 5×10^{-4} torr 8=49895
Ne desorption from glass, temp. depend. 8=48485
Ni films, chemisorpt. of O_2 and H_2, reconstitution of adsorbate adsorbent interface 8=27737
Ni, H_2 desorpt., obs. 78°-300°K 8=30772
O transfer from CO_2 to metal surface, kinetics 8=27735
Pd, of NO, and mag. susceptibility 8=44075
Pt, of propane chemisorption, effect of pre-adsorbed water 8=27738
Pt powder, isotopic exchange of O_2 8=41236
Rh, i.r. spectra of chemisorbed H_2 and D_2 8=25470
SnO_2: Zn, chemisorbed oxygen effect on elec. conductivity 8=31391
Ta, of O_2, kinetics, 1100-2000 °C at 5×10^{-4} torr 8=49895
TaC, chemisorption of CO 8=49903
Te films, desorption of CO_2 on e-bombardment rel. to resistivity increase 8=35829
Ti films, desorption of N_2 8=30771
Ti, sorption of NH_3 with dissociation to H_2 and N_2 8=32103
Ti, H_2 desorpt., obs. 78°-390°K 8=30772
TiO_2, chemisorption of O rel. to work function and elec. cond. changes 8=40691
UO_2, Fl chemisorpt. in pellets fluorination, 300-540°C 8=32104
V, chemosprt. of alcohols, aldehydes, ketones, i.r. spectra of species formed 8=45363
V, kinetics of O chemisorpt. and engassing 8=36584
W, binding and field desorpt. of individual atoms 8=30775
W, chemisorbed gases effects on adhesion and friction 8=49061
W, chemisorption of N_2O rel. to temp. 8=36586
W, inert gas bombard., thermal desorption obs. 8=48497
W, of Cs, Hg and O, desorption on coadsorbate interaction with low energy electrons 8=39623
W, desorption, thermal, of O_2, associated effects 8=39626
W (110) and (100), oxide formation and desorpt. processes, mass-spectrometry 8=35198
W, surface chemisorption of water, investigation 8=27739
Zn, effect of chemisorbed O_2 on Kr physisorption 8=48500
ZnO, chemisorption states of oxygen 8=32118
Sound. See Acoustics.
Sound field. See Acoustic radiators; Acoustics; Intensity measurement/acoustics.
Sound ranging
auditory, dual rôle of freq. spectrum 8=46214
auditory soud range perception expt. 8=46217
echolocation by sea lion 8=37295/6
elemental transducer system 8=46178
reverberation-limited, beamwidth and multiple transmission effects 8=37270
transducer blanket dome noise filtering 8=46180
transducer radiation impedance at air-water interface, effect of compliant-tube arrays 8=37271
underwater sonar, pressure and displacement sensors used simultaneously 8=41330
Sound recording
No entries
Sound reproduction
See also Acoustic radiators; Acoustic transducers; Sound recording.
acoustic field, twelve-channel sampled-space system 8=37255
stereophonic, stability of amplification systems 8=41841
Space charge
accelerator, orbital, beam-envelope 8=33465
compensation, ion beam interaction with rarified gas 8=28580
current, interface-charge-limited, unipolar 8=26871
defocusing of bunched ion beams 8=33103
electron beam accelerated in gun, abnormal energy distribution 8=24140
electron bunching analysis for accelerator injection 8=33084
electron gas oscills., Vlasov and Poisson eqns., soln. for linear confining potential 8=34548
insulating films, negative space-charge effect on Schottky current 8=44901
layers, in semiconductors, accumulation and inversion approximations 8=44762
limited transient currents at saw-tooth voltage pulses in thin film heterojunction diodes 8=40523
linear e accelerator, injection system, effects 8=33417
longitudinal effects in r.f. buckets 8=33097
Space charge—contd
plasma, flute oscillations 8=39130
potentials due to elliptical beams, calc. 8=33072
proton linear accelerators, computer assessment 8=33431
liquid dielec., transient space-charge-limited conduction 8=39392
neutralisation in ion beam by injection of thermionic electrons 8=46441
oil-paper insulation breakdown 8=40559
particle beam, cylindrical, expansion with uniform accel. 8=47038
proton linear accelerator, stability effects 8=33432
quadrupole focusing system, proton linear accelerator 8=33429
p-quaterphenyl, limited currents existence 8=49274
region in electrode layer of low temp. plasma 8=39081
semiconductor, p-type, electron injection 8=35866
synchrocyclotron phase motion perturbation 8=37820
p-terphenyl, limited currents existence 8=49274
Vlasov eqn., linearized, soln. for space-time dependent distribution function 8=29954
waves, solid, interaction with charged carrier streams, effects of collision 8=26873
Yuza-Rozhanskii condenser field, particle dispersion and focusing effects 8=37412
GaAs bulk oscillators, LSA mode, multiple frequency operation 8=40501
n-GaAs, limited, effect of doping fluctuations on accumulation 8=49242
Se electrophotographic layers, dark discharge mechanism 8=49423
p-Se, trigonal, electron injection 8=35866
Space groups. See Crystal structure, atomic.
Space research
See also Atmosphere.
auroral rocket obs., review 8=45500
conference, London (1967) 8=28020
dosimetry, proportional counter appl. 8=46858
electrostatic and e.m. wave detection, OV3-3 system 8=41490
fast n-γ detector 8=47158
free fall structure design 8=23818
Gemini XI S4 blood experiment 8=50466
interference and noise, influence on design of satellite-borne receiving systems at < 50 MHz 8=50240
lunar surface material size distribution, Surveyor I data interpretation 8=36995
lunar surface samples, contamination by lunar module exhaust 8=37000
magnetosphere, proposals for satellite expts. 8=32260
nightglow photography from Gemini spacecraft 8=36802
radiative energy transfer, conference 8=23909
rocket technology review 8=32380
solar simulator for 3m space environment chamber 8=28734
spectrometers, Los Angeles Conference, Oct-Nov 1967 8=28968
tracking, laser, of Saturn V launch vehicle, with automatic reaquisition 8=45577
vehicle cooling loop, heat carrier choice 8=32389
Venus 4 and Mariner 5 data and CO_2 photochemistry Venusian atmosphere 8=41570
weightless liquids outside earth's gravitational field 8=48104
Space vehicles
See also Rockets; Satellites, artificial.
cooling loop, heat carrier choice 8=32389
dust collection in vicinity of earth, rel. to influx of microparticles 8=41371
free fall structure design 8=23818
interplanetary and interorbital flight, impulse calc. 8=32376
lunar orbiter probes, monitoring of micrometeorites, radiation near moon 8=45576
magnetic shields, analog simulation and meas. of forbidden volume 8=41481
magnetometers, fluxgate, magnetodynamically induced ambiguities 8=36904-5
mean surface and satellite orbits to earth, return trajectories 8=32375
motion optimization rel. to linear dynamic systems control 8=32378
propulsion concepts, conf. Polo Alto, (1965) 8=41480
radiation pressure stabilized black and white bodies oscills. 8=32374
radiation shielding calcs., straightahead approx. validity 8=36901
re-entry into Earth's atmos., optimium parameters of trajectories 8=50233
re-entry models, spherical and conical, time resolved spectra from lab. simulation 8=41485
reentry problems, temp. of wakes, determ. using i.r. radiation 8=41484
re-entry shock layer, radiative loss effect on subsonic region 8=34636
in superorbital re-entry, effects of non-grey self-absorpt. and energy loss on heating 8=41488
thermal-control coatings, effects of interplanetary space 8=32562

- **Space vehicles**—contd
  - thermal scale modelling 8=32379
  - trajectory params., nonlinear continuous estimation from obs. 8=32377
  - Al cylindrical type, lab. study of shielding against energetic electrons 8=32384
  - Pu and cpds. as nuclear rocket fuels, props. and selection criteria 8=25313
  - Th and cpds. as nuclear rocket fuels, props. and selection criteria 8=25313
  - U and cpds as nuclear rocket fuels, props. and selection criteria 8=25313
  - **instrumentation**
    - antenna admittance calc. for plasma similar to E-region of ionosphere 8=36903
    - antenna in cylindrical plasma, radiation pattern calc. 8=24238
    - bidirectional reflectance meas. for satellite calibration target in visible and near i.r. 8=41489
    - crossed-field particle velocity selector 8=32565
    - data handling system for solar X-ray meas. 8=50445
    - earth satellite maser, freq. stability obs. 8=28643
    - Gemini S-10 and S-12, equipment, techs. and exposure conds. for micrometeorite expts. 8=41578
    - lunar photography, techniques and results 8=36994
    - Mariner IV power system, design and performance 8=24097
    - microphone sensors of cosmic dust, appl. of hypervel. impact studies to data anal. 8=41577
    - plasma data processing computer 8=32564
    - photomultiplier, capable of withstanding 10,000 g 8=46425
    - 'Proton' type satellites, spectrometer for high energy primary cosmic rays 8=25024
    - pulse-height analyser for γ spectra 8=47064
    - re-entry transmission using modulated electron beam device, simulation 8=36906
    - rocket probe for ionospheric e density and temp. meas. 8=36847
    - satellite β scintillation spectrometer 8=50243
    - satellite e.s. analyser for 1-100keV particles 8=50241
    - satellite FR-1, meas. instruments 8=45582
    - satellite mag. analyser for 100keV-1MeV e 8=50242
    - satellite particle detector systems for cosmic rays 8=47183
    - satellite plasma ion mass-energy spectrometer 8=32563
    - satellite range-energy spectrometer for 6-100MeV p 8=50245
    - satellite spectrometers for 100keV-6MeV p 8=50244
    - semiconductor detector telescope, calibration 8=28025
    - solar cell power systems for satellites, and control 8=24087
    - solar conversion and energy storage systems, for near-earth satellites 8=24088
    - solar cell power systems for satellites, practical problems 8=24096
    - v.l.f. receiver parameters 8=32264
- **Spallation.** See Nuclear spallation.
- **Spark chambers**
  - acoustic, microphones for multiple particle detection 8=46963
  - air admixture effects on performance 8=42350
  - air shower core fine struct. obs. at 5200m altitude 8=38227
  - calibration with pulsed light source 8=46962
  - characteristics, 36-gap with rubber seals 8=46968
  - control with light pulse 8=46970
  - cosmic-ray e flux and east-west asymmetry meas. 8=33849
  - cylindrical, high-Z construction 8=28990
  - cylindrical, with light-reflecting electrodes 8=37804
  - digital transmission line type 8=46976
  - digitized readout, nonmagnetic 8=46972
  - discharge switch ion controlled by small-amplitude pulse 8=46967
  - electrophotographic track determination system 8=46965
  - fine structure of air shower cores, obs. 8=38226
  - magnetostrictive, delay-line multiplexing for data storage 8=46979
  - magnetostrictive, digitizing spectra 8=46974
  - magnetostrictive readout in mag. field 8=37803
  - monogal, isotropic, optimum elec. pulses to obtain tracks 8=33389
  - particle coordinate determination, with ferrite memory 8=46977
  - photographic negative manufacture with parallel lines 8=33391
  - plate, appl. of polyurethane foam 8=24540
  - range chamber with electronic readout 8=28991
  - register, direct readout 8=46964
  - review of principles of operation, and construction 8=28992
  - sparkostrictive, with piezoelec. readout 8=33390
  - streamer chamber, proportional counter controlled, for slow-meson stops 8=47105
  - streamer, for neutral beams, design and performance 8=46978
  - streamer, track distortions near internal objects 8=46966
  - vidicon, balloon mounted, search for γ-ray balloon sources 8=45796
  - vidicon for γ det. aboard balloons and satellites 8=45610
  - wide-gap, breakdown along particle trajectories 8=24541
  - wire, capacitor-f.e.t. readout device 8=33392
- **Spark chambers**—contd
  - wire, design and performance 8=46975
  - wire, readout, useful in string magnetic fields 8=46971
  - $Ar-C_2H_2$ filled, registration efficiency, two-particle 8=46969
  - He discharge condensation 8=46973
- **Spark counters.** See Counters/spark.
- **Sparks, electric**
  - See also Breakdown, electric; Lightning.
  - air, at atmos. press., superradiant laser action obs. 8=24301
  - air, influence of water vapour on impulse flashover 8=34428
  - air, laser-induced in mag. field emission, 210 kG 8=29925
  - air, laser-induced, shock wave theory 8=28369
  - air, laser-prod., expansion mechanism, obs. 8=34432
  - condensing, in vacuum, prod. 8=29921
  - continuum radiation source 8=28841
  - detonation mechanism and switching power of spark gap with auxiliary spark in cathode 8=29917-8-9
  - diamond erosion shaping method 8=35662
  - electrode material consumption obs. 8=29922
  - erosion of electrode subs, calc. of charact. props 8=29915
  - gas, subnanosec. discharge generation 8=47771
  - high-current, as intense u.v.-light source 8=47770
  - laser-induced, light source for wide band-gap drift mobility mes. 8=42205
  - laser travelling spark, ignition below breakdown threshold intensity 8=42061
  - laser-triggered spark gap 8=34431
  - light source for shock tube densitometry 8=33254
  - light source with plane boundaries 8=28767
  - lightning, pressure pulse from triggered lab. stroke 8=36752
  - plasma diagnostics 8=30092
  - pulsed discharge in air, fast electrons and X-radiation during intial growth 8=39002
  - for sintering and graphitization of amorphous C powders 8=30667
  - temperature determ. in air from spectrum 8=39004
  - on triglycine sulphate crystal surfaces 8=40623
  - underwater, characts. study 8=29916
  - in vacuum gaps $<$ 1mm, current growth in impulse breakdown 8=34429
  - vacuum, study of x-rays produced 8=39005
  - vacuum, X-ray emission theory and expt. 8=37732
  - voltage drop during pulse discharge in nsec. time range 8=29920
  - Ar, laser-prod., expansion mechanism, obs. 8=34432
  - Ar and $Ar-C_2H_6$ mixture, ionization coeffs. and sparkling voltages 8=25701
  - Fe line intensity rel. to gas pressure reduction 8=34433
  - GaP, erosion and dislocation formation 8=40037
  - He, turbulent eddies in high press. μ sec channels 8=29924
  - N, laser-prod. expansion mechanism, obs. 8=34432
  - Ne, laser-prod., expansion mechanism, obs. 8=34432
  - O_3 formation, var. across gap 8=25700
- **Specific heat**
  - See also Thermodynamic properties.
  - C_v discontinuity across liquid-vapour coexistence curve near critical point 8=25988
  - constant-volume, thermodynamic upper bounds 8=37225
  - crystals, axial, Grüneisen functions 8=26598
  - ethylene-vinyl acetate copolymers heat capacity, -190-250°C 8=24028
  - Fermi liquid, low-temp. expansion 8=37216
  - Ising model, 3-dim., below T_c 8=48731
  - K crystal lattice, calc. 8=44300
  - liquid-vapour systems 8=34980
  - polystyrene, heat capacity, radiation-induced cross-links at low temp., effects 8=26606
  - reference materials for high-temperature measurements 8=46224
  - thermal capacity, isochoric, meas. near critical liquid-vapour point 8=48266
  - thermodynamic compatibility relation with Grüneison ratio 8=39907
  - triglycine sulphate, temp. dependence near ferroelec. Curie pt. 8=44890
  - BaF_2, Grüneisen parameter, low-temp. limit, calc. on Axe's shell model 8=48748
  - CaF_2, Grüneisen parameter, low-temp. limit, calc. on Axe's shell model 8=48748
  - α-Ce, heat capacity at 11 kbar pressure between 0.3 and 6°K 8=39911
  - COF_2, molar ht. capacity, from 12°K to b.p. 8=30573
  - EuS, mag., near Curie point 8=27405
  - EuS, mag., in non-zero field 8=27406
  - He^3, b.c.c., obs. 8=37356
  - $He^{3,4}$ monolayer films on Cu at 4°K 8=24056
  - Na crystal lattice, calc. 8=44300
  - SrF_2, Grüneisen parameter, low-temp. limit, calc. on Axe's shell model 8=48748
  - Xe, near critical point 8=34977
  - Zr–Hf alloy, 1.1–4.2°K 8=35437
  - Zr–Sc alloy, 1.1–4.2°K 8=35437
  - Zr–Ti, 1.1–4.2°K rel. to superconducting transition temp. 8=35437

Specific heat—contd
gases
heat capacities meas. with electronic calorimeter 8=37327
liquids
Ar, ratio γ at high press. 8=48138
Ga, in stable and undercooled states 611-245°K 8=30459
$NaClO_3$-$NaNO_3$ molten system 8=48087
Sn, in stable and undercooled states, 632-425°K 8=30459
solids
Anderson-Gruneisen parameter for general interatomic potential 8=48939
b.c.c. metals, zero-point energy and Θ_c^∞ 8=30932
brass, Debye temp. determ. by one-temp. X-ray method 8=48736
cerium magnesium nitrate, used in low temp. thermometry 8=30962
cobalt borides, electronic, meas. 8=35426
copolymers of methylmethacrylate with methacrylic acid 8=39917
critical temp. region, smoothness due to random impurities 8=44987
diamond, thermal energy evaluation rel. to at. vibration spectrum, review 8=43922
with electron-gas, almost-degenerate, corrections for Grüneisen coeff. and sp. ht., 8=39908
ferromagnets, and linear expansion coeff. at Curie pt., critical fluctuations and anomalous behavour 8=30959
galactose, amorphous, and enthalpy, 15-45℃, rel. to mol. structure 8=30966
glass, Corning 7560, between 4.5° and 20°K 8=26589
glucose, amorphous, and enthalpy, 15-45℃, rel. to mol. structure 8=30966
gold-transition metal alloy, below 3°K 8=39912
Grüneisen coeff. evaluation 8=44352
heat capacities, low temp. containing two or more contributions, analyses 8=35434
Heisenberg antiferromagnet, free surface effects 8=45048
Heisenberg ferromagnet, and high temp. susceptibility, for general spin 8=40780
Heisenberg ferromagnets, impure, calcs. 8=35422
ice, sp. heat near ferroelectric transition temp. 8=48737
Ising lattice with impurities, behaviour near critical point 8=40773
magnetic systems with long-range interactions, shape dependence 8=35423
mannose, amorphous, and enthalpy, 15-45℃, rel. to mol. structure 8=30966
metals, modified modulation method 8=48732
metals, weakly ferromagnetic, spin-fluctuation contrib. 8=30960
methyl-ammonium alum, low-temp. anomalies meas. by continuous heating calrimetry 8=46299
moist mats., simultaneous determ. of thermophys. characts. for any values of Fourier no. 8=37315
particle of dispersed mat, transient heating without temp. grad. 8=30957
polystyrene, atactic, heat capacity rel. to annealing, 10-360°K 8=44345
quartz, from eddy current heated microcalorimeter 8=46286
rare-earth ethyl sulphates, mag. contribution 8=44343
rare-earth metals, low temp. ht. capacities containing two or more contrib., analyses 8=35434
rare-earth ortho-aluminates, antiferromag., near Neel point 8=35435
rare earth perovskites, between 1.2° and 5°K 8=39921
steel, stainless and Polish, at low temp. 8=48730
subliming type, heat capacity meas. with electronic calorimeter 8=37327
2, 2, 6, 6 tetramethyl 4-piperidinol 1-oxyl, 1.3°-74°K 8=30969
transition metals and alloys, low temp. electronic enhancement by spin fluctuations in electron gas near mag. instability 8=31922
transition metals, nearly ferromag., spin fluctuations effect on low temp. electronic coeff. 8=44992
triglycine sulphate, ferroelec. anomaly near Curie pt. 8=39923
triglycine sulphate, near Curie temp., meas. of transtion energy and entropy change 8=35430
two-layer composite samples, ht. capacity meas. by flash method 8=48751
Ag 8=35424
Ag, pure, below 3°K 8=39912
AgI, ht. capacity 50°-400℃ 8=30961
AgI, ht. capacity, theory 8=48733
Al-Ng alloy, superconducting, and energy gap anisotropy 8=48734
Al_2O_3, from eddy current heated microcalorimeter 8=46286
Au 8=35424
Au, pure, below 3°K 8=39912
Au-Fe alloys, rel. to hyperfine coupling constant determ. 8=31495
Au-Ge-Si alloy, at glass-liq. transition 8=39470
$BaCl_2$, heat content meas. in range 298 to 1700°K 8=44339
BaI_2, heat content meas. in range 298 to 1700°K 8=44339

Specific heat—contd
solids—contd
BaO glasses, heat capacity as function of composition and temp. 8=44333
n-Bi_2Te_3, from 1.3 to 90°K 8=39910
CN^- in KCN, rotation ht. cpaacity above 168°K 8=26030
$CeCl_3.7H_2O$, between 1.1 and 3.3°K 8=30963
Cr-Mn alloys, antiferromagnetic 8=48735
Cs halides, lattice dynamics calc. 8=39871
Cu 8=35424
Cu, Debye temp. determ. by one-temp. X-ray method 8=48736
Cu, pure, below 3°K 8=39912
Cu, Cryostat obs. 1°-30°K 8=24033
Cu, 40-920℃ 8=30964
Cu-Fe Kondo alloy obs. down to $2 \times 10^{-3} T_K$ 8=44334
Cu-La double nitrate, heat capacity below 1°K 8=44336
Cu-Ni: system, Debye temp. conc. depend. rel. to ferromag. ordering, obs. 8=39913
Cu-Zn, electronic 8=44335
$Cu(NO_3)_2.2.5H_2O$, ht. capacity, 0.5-4.2°K, rel. to antiferromagnetic props. 8=35428
$CuSO_4.5H_2O$, ht. capacity at 0.4°-4.2°K in mag. fields 8=39915
$CuSO_4.5H_2O$, ht. capacity below 4°K in mag. fields 8=39914
Cu_3Au, below 3°K, effect of ordering 8=35427
$DyFeO_3$, 1.2-80°K rel. to mag. ordering 8=35429
EuS:Gd, magnetic 8=44337
Fe^{57} in cubic lattices, Gruneisen's formula rel. to recoil-free fractions for γ-rays 8=44498
Fe_xB, $(x = 1, 2)$, electron terms 8=30965
Fe_xO, comp-dependence 8=39916
GaP, Debye temp. calc. from u.s. phase-comparison meas. of elastic constants 8=49021
$GdCl_3$, magnetic, high freq. susceptibility exp. 8=40817
GeO_2, heat content meas. in range 298 to 1700°K 8=44339
In-7.05 wt.% Pb alloy, type II superconducting, rel. to irreversibility effects on Maki's parameters 8=44342
Ir alloys, electronic, and mag. susceptibility rel. to rigid band model 8=31532
K, Debye temp. calcs. from Mossbauer meas. with K^{40} 8=42859
KH_2PO_4, temp. dependence 8=44338
$KMnF_3$, heat capacity rel. to magnetic spin 8=44340
KNO_3, heat content meas. in range 298 to 1700°K 8=44339
K_2MnF. heat capacity rel. to magnetic spin 8=44340
Kr, solid, meas. rel. to thermodynamic props. 8=48745
La-Cu double nitrate, heat capacity below 1°K 8=44336
$LiNbO_3$, 77-500°K 8=44341
$LiTaO_3$ ferroelec., temp. dependence, 25-700°C 8=44888
N_2, thermal capacity, 2.6-15°K 8=30967
NaCl, from eddy current heated microcalorimeter 8=46286
$NaClO_3$-$NaNO_3$ system 8=48087
NaF, temp. dependence, 0.05-15°K 8=26591
$NaNO_3$, in phase transition 8=48391
Nb-Ti alloy, temp. depend. at superconducting transition 8=48738
Ni, low temp., 8=39919
Ni-Co alloys, f.c.c., low temp., rel. to band model determ. 8=48739
Ni-Fe alloys, 1.2-4.2°K obs. 8=26592
Ni-Rh alloy, nearly ferromagnetic, and mag. susceptibility 8=31660
$NiCl_2$, rel. to mag. energy spectrum, 1.8-16°K 8=39918
$Ni_{1-3x}Cu_{2x}Fe_x$, low temp., 8=39919
α-$NiSO_4.6H_2O$, ht. capacity, 0.4-4.2°K in mag. field 8=30968
α $NiSO_4.6H_2O$, in mag. fields, theory 8=39920
PbTe, Debye temp. calc. at 0°K from elastic constants and thermal expansion meas., 8=49044
Pd alloys, rel. to band structure and exchange-enhancement effects 8=31294
Pd, electronic 8=26575
Pd-Fe alloys, rel. to hyperfine coupling constant determ. 8=31495
Pd_3Fe alloy, 0.15-1°K, rel. to hyperfine interaction constants determ. 8=31504
Pd:Ni dilute alloys, e heat conc. depend., local exchange enhancement model 8=35433
Pd:Ni dilute alloys, low-temp., localized exchange enhancement model 8=35432
Pt alloys, rel. to band structure and exchange-enhancement effects 8=31294
Pt_3Fe alloy, 0.15-1°K, rel. to hyperfine interaction constants determ. 8=31504
Pu fast reactor fuels, obs. 8=25306
δ-Pu-Ga alloys, temp. depend. below 300°K 8=44598
PuP, cold-pressed, sintered, ht. capacity up to 650°C 8=44368
PuS, cold-pressed, sintered, ht. capacity up to 650°C 8=44368
SnTe, Debye temp. determ. using Mossbauer effect in Sn^{119} and Te^{125} 8=44344
SrF_2, heat content meas. in range 298 to 1700K 8=44339
Ti-Mo alloys, low temp., 8=39922
$UC_{1-x}O_x$, and heat of formation 8=30970
UO_2, heat content from 1200° to 3100°K 8=35436
W, electronic parameter rel. to low temp. CMN scale 8=37331

Specific heat—contd
  solids—contd
    W, Nernst-Lindemann eqn. in range 24°-1800°C, validity 8=26590
    W, specific heat, 1300-3000°K, modified modulation method 8=48732
    YAg, 1.3-5°K, rel. to density of states at Fermi level 8=48740
    YCu, 1.3-5°K, rel. to density of states at Fermi level 8=48740
    Zn, Debye temp. evaluation rel. to mean square at displacements thermal variation 8=44395
    ZnO, from eddy current heated microcalorimeter 8=46286
Spectra
    See also Absorption/light; Astronomical spectra; Atmospheric spectra; Colour; Mass spectra; Raman spectra; Spectrochemical analysis; Spectroscopy; Stark effect; X-ray spectra; Zeeman effect.
  absorpt. characteristics using Jogansen's function for meas. integral intensities 8=34865
  absorption band, apparent bandwidth parameters, obs. 8=24388
  absorption, excitons, low temp., theory 8=40258
  absorption line form. in mag. field, anomalous dispersion 8=29570
  adiabatic inversion with light pulses 8=47437
  auroral, 1050-1550Å region 8=36812
  axially symmetric mols., elec. field induced 8=29676
  chemiluminescent reaction of active N_2 with anhydrous Na_2SO_4 8=41255
  complex, decomp., digital computer programme 8=28245
  complex octahedral anions in crystals, i.r., rel. to cation effects 8=49683
  cyclotron double resonance for spectroscopic study of ion-molecule reaction mechanisms 8=47554
  difference band systems, temp. depend. of total intensity 8=25463
  discrete, generation of second harmonic 8=24354
  dispersed, any wavelength region, real time multiplexing 8=42221
  Doppler shift of spectral line, meas. with optical wedge 8=47471
  effective operators and spectrosc. props. 8=34115
  Elasser band model, Doppler analog 8=34198
  electronic band structure, solvent depend. 8=47583
  emission coeffs. internal calc. from externally meas. spectral intensity for asymmetrical plasma 8=43500
  ethers, vinyl, absorpt. band characteristics 8=30493
  exhaust of scale model rocket, radiative props. 8=38815
  fluid, opalescent, double scattering 8=39152
  forbidden transitions, variational principle for intensity 8=47443
  Franck-Condon factors, isotope effects 8=34271
  Franck-Condon principle, expt. test 8=29966
  gas analysis, selectivity of optical-acoustic method 8=49986
  gas discharge rel. to excitation freq., obs. 8=29880
  gas behind shock front, maximum of nonequilibrium emission 8=30299
  gases, elec. field induced 8=25582
  gases, radiant heat flux distrib. in cylinder with black interior 8=39197
  H-bonded systems, i.r., theory 8=38787
  imaginary-dielec.-index bands, Cauchy analysis 8=25408
  i.r. emission from molec. crysts. 8=41021
  i.r., H-bonds, strong 8=48301
  laser, single-pulse operation 8=24268
  line formation by noncoherent scatt. 8=37232
  line form. in homogeneous mag. field, theory 8=43250
  line intensities, effects of coherent multiple scatt. 8=25403
  Lorentz line, equivalent width, accuracy of simple approx. 8=34126
  luminescent solids, absorption and excitation 8=36449
  magnon-sidebands in antiferromagnetic insulators 8=36298
  matrix-isolated mols., rotation-translation coupling 8=27536
  meteors, ion 8=41571
  molecular crysts., moment theorems for vibronic exciton spectra 8=41023
  molecular ions, r.f. transitions between energy levels, bolometric technique 8=38659
  molecular, microwave review of developments at Duke 8=37534
  molecular optical anisotropy dispersion, by appl. of laser waves and certain harmonics 8=38774
  molecular, very high resolution study using Fabry-Perot spectrometer and hollow cathode lamps 8=29675
  molecules, charge-transfer absorpt. band shape and polarization in solns., calc. 8=34200
  molecules Einstein coeffs. rel. to condensed media optical props. 8=39367
  molecules, in absorbing medium, effects of conversion to non-wave zone heat 8=38629
  molecules, periodic, i.r. vibr. band intensities and terminal group effects, calc. 8=29857
  molecules, secondary emission of light 8=34195
  molecules, ternary symmetry, hyperfine structure of rotation levels, vibr. effects 8=29698
  optical and e.p.r., interpretation by vibronic mass effect 8=43252
  phosphorescent T-S band decay rate meas., effect of absorpt. T*←T bands 8=38777
  photon scattering, resonant, from perturbed two-level system, stochastic theory 8=41755
  plasma flame prod. when elect. field is applied to gas jet 8=38977
  plasma, non-equilib. finite layers, emission lines growth curves, calc. 8=43543
  polar liquid films, i.r. absorpt., rel. to orientation by cell surface elec. fields 8=39302
  polar mols. in inert solvents, far i.r. absorpt. 8=48157
  polishing compounds, i.r. spectra 8=31933
  polyatomic mols., anomalies in intensity distrib. of rot.-vibr. lines 8=43257
  polymers, i.r. vibr. band intensities and terminal group effects, calc. 8=29857
  reflection, polarization effects 8=37683
  ruby laser, time depend. 8=46610
  salicylanide, variation in absorpt. due to equilibrium between rot. isomers and ionization 8=38903
  from shock cap and wake of re-entry models, lab. simulated 8=41485
  solid solutions, Davydov's splitting of oscillation bands 8=35547
  solids, energy spectra computation methods 8=35762
  solvent Stark effects and spectral shifts 8=39375
  thermal radiation density, form 8=23989
  transitions between degenerate levels 8=49682
  two-phonon spectroscopy in solids, theory 8=41025
  Voigt profile, empirical approx. 8=43170
  BaF_2, reflectivity from (111)-cleavage plane, 78°K 8=45175
  C_3 cometary emission, synthetic profile computed, 4050Å 8=50424
  He-Ne gas, effect of one laser beam on the transmission of another 8=46576
  He-Ne laser 8=42081
  He-Xe laser 8=42081
  Ne laser 8=42081
  atoms
      See also Atoms/excitation; Atoms/structure.
    absorpt. band, estimation of position of intensity maximum 8=43150
    absorpt. spectroscopy, lamp 8=36638
    absorption, graphite cuvette meas., interferences calc. 8=25348
    absorption-line profiles, parametrization 8=38684
    absorption using laser discharge to produce vapour 8=34122
    adiabatic inversion with light pulses 8=47437
    alkali, in colls. with N_2, H_2, HD, D_2, sensitized fluorescence and quenching 8=29836
    alkali-like, oscillator strength calc. 8=34136
    alkali, meas. of elec. dipole moment 8=29614
    alkali metal oscillator strengths 8=47500
    alkali metals, absorpt. oscillator strengths and photoionization continua 8=29603
    alkali metals, theory of satellite bands prod. by foreign gases 8=47532
    arc and hollow cathode discharge tube, sensitivity analysis 8=29578
    atmospheric and inert gases, vac. u.v. region, abs. spectra 8=43196
    digital computer theoretical calc. 8=38631
    distribution of non-symm. line from Fabry-Perot ring meas., using Fourier transform. 8=25339
    electronic spectra, theory including electron correl. 8=25347
    Feynman diagrams of 1st and 2nd orders of some states 8=47472
    fine structure transitions of photons and collision cross-sections 8=47476
    fluorescence, sensitized, conservation of r.f. coherence 8=38733
    gas mixtures, excitation, analysis 8=34159
    graphite cuvette applic. 8=38619
    hydrogen-like, 2s state two-photon decay, analytic soln. 8=38647
    hyperfine-struct. matrices in at. config., checks 8=29581
    integrated absorptance for simple spectral lines and lines with hyperfine struct. and isotope shifts, asymptotic expansions 8=29590
    ionized, microwave absorpt. lines from dielectronic recombination 8=47479
    ions, electron-impact linewidths, formulae 8=38718
    ions, r.f. transitions between energy levels, bolometric technique 8=38659
    iron group elements, ionic states, theory 8=43202
    Lamb shift, source of polarized H^- 8=37435
    level-crossing spectroscopy, improved resolution using excited atoms which have survived longer than the average 8=43197
    level non-exponential decay 8=25370
    line broadening, combined Doppler and collision 8=43235
    line formation with scatt. by e, parametrized models 8=43168

Spectra—contd
- **atoms**—contd
  - line-narrowing effects, freq. spectrum, laser induced 8=29589
  - line radiation transfer in multilevel atoms, effect of various coupling mechanisms 8=38628
  - molecules, in absorbing medium, effects of conversion to non-wave zone heat 8=38629
  - multilevel, resonance line problems and radiative transitions 8=38627
  - natural line-breadth, theory 8=47465
  - rel. to nucleus structure, electronic, μ- and π-mesic atoms h. f. s. and isotope shifts 8=29260
  - null coefficients and f shell mag. spin-spin interaction selection roles 8=29580
  - oscillator strengths, spectral distrib. 8=43166
  - oxygen 5577 Å line and continuum in night airglow 8=41392
  - Paschen-Back effect, 3rd-order corrections 8=25341
  - peak, nonequilibrium gas behind shock wave front 8=29632
  - π-mesic, $4 \leqslant Z \leqslant 28$, 2p → 1s and 3d → 2p transitions, obs. 8=34190
  - radio-optical resonance, coherence transfer at nutation frequency 8=38614
  - resonance-line scatt., Monte Carlo technique 8=29585
  - resonance radiation spectrometry 8=46699
  - r. f. emission in optical resonance 8=38689
  - review of nuclear spectroscopy 8=46687
  - satellite X-ray lines due to transitions involving double ionization of inner shells 8=43228
  - Stark effect, quadratic h. f. s., theory 8=29601
  - stepwise excitation, cross-section estimation, choice of method 8=25344
  - transitions coupled through upper excited state 8=25337
  - two-electron spectra line strength 8=38639
  - two-photon bound state-bound state transitions in Coulomb field 8=29648
  - vacuum u.v. emission, bibliography 8=24384
  - virtual transitions, effect in optical and r.f. spectroscopy 8=47473
  - Ag, absorpt. after x-radiation of frozen solns. of salts 8=47488
  - Al, in u.v., relative instensities of selected lines, photoelec. compared with photographic meas. 8=42219
  - Al sequence to Fe^{+13}, config. mixing for transitions from ground state 8=34137
  - Ar, absorption, 1070-1135 Å region 8=25355
  - Ar, emission on laser irradiation of gas 8=29906
  - Ar, hot compressed, with graphite powder trace, absorpt. and emission of impurity lines 8=34138
  - Ar isoelectronic sequence, classification 8=38668
  - Ar, jet excitation for u. v. source 8=38660
  - in Ar plasma jet, continuum and line rad., rel. to temp. 8=43612
  - Ar, u. v. absorpt. cross sections, bandwidth depend. 8=25356
  - Ar, widths and transition probabilities, in plasma torch 8=43181
  - Ar I, $3p^m$-$3p^{m\ 1}3d$ transitions 8=43178
  - Ar I, transition probabilities and relative level populations calc. 8=47490
  - Ar II, line profiles, obs. in plasma torch jet 8=43180
  - ArII, line shift in dense plasma, obs. in pulsed arc 8=34507
  - Ar II multiplets, Stark broadening temp. depend 8=39028
  - Ar II transition probabilities and continuous spectra meas. Ar, Ne 8=43179
  - Ar, Ar II transition probabilities and continuous spectra meas. 8=43179
  - As(4^2D), cross-sections for deactivation 8=34160
  - Au I resonance doublets, absolute line strengths, quantum-mechanical calcs. 8=43216
  - B in B_2O_3, X-ray emission band, valency e structure 8=29716
  - $Ba^{135,137}$, h. f. s. of $6s6p\,^3P_1$ level, obs. 8=34139
  - Ba, lowest $^1P_1$ and $^3P_1$ states, g_J factor obs. 8=38691
  - Ba, metastable 6s5d levels and g_J obs. 8=34140
  - Be III, IV emission spectra obs. 8=29605
  - Be III, IV, vacuum u.v., high energy satellites 8=47492
  - Bi^{209} hyperfine structure in $6p^2(^3P_0)7s\,^4P_{1/2}$ state 8=43183
  - Bi^{209}, muonic, hyperfine interactions obs. 8=38772
  - Bi, obs. on each side of resonance line 8=29600
  - C high-pressure bands, in CO discharge, isotope shift obs. 8=34161
  - CI, $2p^2$-2p3s arrays, strengths and transition probabilities 8=45915
  - CI, II, III, IV emission spectra obs. 8=29605
  - CI, vac. u. v. 8=33264
  - C IV hydrogenic transition rel. to excitation temp. of Wolf-Rayet stars 8=45661
  - Ca, autoionization broadening fitted to Shore parameters 8=43185
  - Ca, in arc discharge, impurity Na effect on line breadth 8=34437
  - Ca, oscillator strengths and matrix elements, calc. 8=29607
  - Ca II solar line, centre-limb var. of $K_{2,3}$ components calc. 8=45878

Spectra—contd
- **atoms**—contd
  - Ca XV and XVI ions, laser prod. plasma, 120-240 Å 8=29608
  - $Cd^{111,114}$ polarization of light emitted by optical resonance of 2288Å radiation 8=34158
  - Cd in discharge tube with high voltage pulses 8=29630
  - Cd isotopes, optical, polarization of radiation (2288 Å) emitted 8=25359
  - Cd 3261A line collision broadening by Ar gas, pressure and temp. dependence 8=38750
  - Cd 5^3P_1 level, double resonance excited by modulated light 8=38685
  - Cd–Ar(Ne) low pressure discharges, 2288Å and 3261Å radiation intensities 8=38990
  - Cl I, $3p^m$-$3p^{m-1}3d$ transitions 8=43178
  - ClI and II, vac. u. v. 8=33264
  - Cl, absorpt. series 8=38663
  - Cl, affinity continuum 8=29610
  - Cl isoelectronic sequence, classification 8=38668
  - Cl I-lines in u.v., absorpt. oscill. strengths meas. 8=29609
  - Co^{59} low levels, h. f. s. and nuclear quadrupole moment 8=38664
  - Cr I, gf for 41 lines, shock heated gas emission obs. 8=29611
  - Co I, in excited configs., theory 8=43187
  - Cr II, gf for 2 lines, shock heated gas emission obs. 8=29611
  - Cs absorpt. line-width rel. to optical pumping and Ne buffer press., obs. 8=25374
  - Cs, atomic lifetimes, direct obs. 8=29612
  - Cs, emission on laser irradiation of vapour 8=29906
  - Cs, emission, satellite bands 8=25360
  - Cs, ground state, differential polarizability of Zeeman substates, atomic-beam resonance obs. 8=38667
  - Cs meas. of elec. dipole moment 8=29614
  - Cs, spectra profile of r.f. modulated light beam in optical pumping expt. 8=29613
  - Cs, standard line obs. 8=28210
  - Cu, in arc discharge, impurity Na effect on line breadth 8=34437
  - Cu III, in excited configs., theory 8=43187
  - CV triplet to singlet excitation, relative intensities 8=38662
  - D, 6 Balmer lines obs. and Rydberg constant calc. 8=47494
  - Dy, isotopic shift 8=47493
  - Dy, isotope shifts and nuclear deform. 8=43188
  - Er 1, Zeeman effect, 3000-5000Å in 26 kOe field, obs. 8=29637
  - Er, L-emission, dipole transitions 8=34141
  - Es^{253} emission, hyperfine structure 8=43189
  - F, KLL Auger in 3 fluoride salts 8=34166
  - FI, vac. u. v. 8=33264
  - Fe group, interactions between d electrons in 2nd spectra 8=43190
  - Fe-period elements, far vac. u. v., classification 8=38668
  - Fe IX to XIV, oscillator strengths 8=38668
  - Fe XV in solar corona, lines relative intensities 8=37082
  - FeI, neutral; radiative lifetimes of energy levels calc. 8=47496
  - Ga vapour, absorpt. 250-150 nm region S^2p-Sp^2 transition cross sections obs. 8=47486
  - H, correction of exptl. Lamb shift 8=25351
  - H, excited, in plasma, line broadening for $n \rightarrow n^1$ transition 8=34505
  - H, Faraday effect 8=29639
  - H, h.f.s. discrepancy, A meson contrib. to Feynmann diagram, quark model of proton 8=33743
  - H, plasma decay, T-tube obs. 8=30057
  - H_α profile, strong-collision effects 8=38645
  - H_β profile in spectrum, meas. absorpt. and emission lines in Zodiac light 8=41353
  - H_β radiation in night sky spectrum 8=41354
  - H, Sommerfeld fine-structure constant measurement 8=38648
  - H Stark effect intensity distrib. 8=47480
  - H(2S) in weak electric fields, Lyman-α radiation polarization 8=25349
  - H, 2s state two-photon decay, analytic soln. 8=38647
  - H, H_2, Lyman-α emission in collisions with He^+ 8=38755
  - He, e impact light, polarization obs. 8=29641
  - He, excited by e bombard. 8=29651
  - He, lifetime of 2^1P state obs., oscillator strength for 2^1P-2^1S transition 8=38654
  - HeI, combined Zeeman and Stark effects on hydrogenic lines 8=38653
  - He I λ 584 resonance line, oscillator strength 8=43173
  - He II, enhancement of λ4686 by mag. field 8=34132
  - He 2^1S, 3^1S states, Born cross sections for electron impact excitation 8=38695
  - He 3^3D fine structure 8=29598
  - He^- free-free absorpt. coefficient 8=47484
  - He^+, Lamb shift of $n = 4$ level, meas. by r.f. spectroscopy 8=43172
  - Hg, coeffs. for internal conversion for K, L and M shell e. m. transitions 8=38670
  - Hg $\lambda = 1850$ Å line, isotope shift and hyperfine structure 8=43192

Spectra—contd
atoms—contd
Hg, in preionized flow, intensity relax. of certain lines in flow dirn. 8=47753
Hg, r.f. discharge afterglow 8=29616
Hg, 15.295 Å line h.f.s., Fourier spectroscopy 8=28830
Hg, 2537 Å line broadening and shift by H_2 inpact 8=43194
Hg^{119}, hyperfine structure constants in 6 $^1P_1$ level, and hyperfine structure of line 6 ^1P,-8 $^1S_0$ 8=43195
Ho^{67}, s, t doublet in L-spectrum 8=47499
μ-Ho^{165}, x-ray, rel. to dynamic quadrupole interaction, obs. 8=34191
Ho, X-ray L emission spectrum 8=45193
I, absorpt. series 8=38663
In vapour, absorpt. 250-150 nm region S^{2}p-Sp^2 transition cross section obs. 8=47486
K^{40} resonance radiation, nuclear quadrupole calc. 8=38365
K vapour, 4000Å violet, laser pumping four wave parametric interaction 8=33177
Kr, visible afterglow emission 8=47754
Kr, 4p^5, 5s level excited in Ne-Kr mixtures 8=29882
Kr^{86} line profiles from complex visibility Fourier transform, obs. 8=29619
La III, principle series, transition probabilities in doublets 8=47506
Li, emission spectrum study of plasma in arc discharge 8=47778
Li, identification of unassigned lines 8=43243
Li in sunspot, abundance calc. 8=50452
Li^{7+} ion, ^{1}D, ^{3}D, ^{1}F and ^{3}F states, mag. h. f. s. calc. 8=38673
Mg, weak line transition probability calc. 8=29621
Mg1, f-values calc. 8=34135
N, ionization states of some unidentified lines 8=43223
N, metastable (^{2}D), e. s. r. 8=25386
N, multiply ionized, beam-foil excitation 8=29644
N, new emission lines in 10 000 to 11 000A region 8=34144
N plasma, non-equilib., emission lines from finite layers calc. 8=43543
NII, 2p^2-2p3s arrays, line strengths and transition probabilities 8=45915
Na^{23}, h. f. s. in $3^2P_{3/2}$ state, level crossing investigation 8=34145
Na^{23}, hyperfine coupling constant meas. 8=43197
Na, at. -abs. cross sections, 500-600 Å 8=29622
Na, atomic lifetimes, direct obs. 8=29612
Na, optically pumped, frequency measurements of 0-0 transition 8=47524
Na-D_1-line, profile and equivalent width as function of temp. and mag. induction 8=25361
NaI 5900-96Å nocturnal internsity vars. 8=32276
Nd in complexes, fund. level splitting 8=29623
Ne, Ar II transition probabilities and continuous spectra meas. 8=43179
Ne, double resonance in He-Ne laser operating at 6328Å π transitions 8=47502
Ne, radiative transition probabilities 8=34146
Ne, $^2P_4$ fluoresc. under laser reson. illum., 6328A 8=38675
Ne($2p_4 \rightarrow 1s_4$) spontaneous emission along axis of He-Ne laser 8=25363
Ne, 2p^6, 2p^{5}3s, 2p^{5}3p, 2p^{5}4s states, wave functions 8=29624
NeI, eigenvectors of configuration (2p)^5(3p) and rel. probabilities of 2s-2p transitions 8=25362
NeI, relative transition probabilities determ. by Faraday effect 8=38676
NeIX, 2-photon continuum emission 8=29599
Ni II, in excited configs., theory 8=43187
Ni XI to XIV, oscillator strengths 8=38668
Ni^{61} low levels, h. f. s. and nuclear quadrupole moment 8=38677
O I, establishment of terms and improved level values 8=47503
OI 5577 and 6300Å noctural intensity vars. 8=32276
O III, 2p^2-2p3s arrays, line strengths and transition probabilities 8=45915
O IV, V, VI emission spectra obs. 8=29605
O green line λ 5577 in glow discharge, new emission mechanism 8=29625
μ-O^{16,18}, 2p → 1s transitions and atomic radius, obs. 8=34190
O I' lines λλ 1302-06, 1152Å, experimental oscillator strengths 8=50319
PaII, magnetic-interaction integrals 8=34147
Pa^{231}, L subshell fluorescence obs. 8=43200
Pb$^{206-8}$, muonic, hyperfine interactions obs. 8=38772
Pb, arc spectrum 8=38678
PbI 7229 A line and solar abundance 8=45866
Pm I, fundamental energy levels calc. and Zeeman effect obs. 8=47505
Pr V, ionization energy calc. and 12 lines, 840-2250 Å obs. 8=47504
Rb, in flames, quenching of excited 5^{2}P atoms 8=34150
Rb^{85,87} $8^2P_{3/2}$ state hyperfine structure and life-time 8=34149
Rb^{87}, light shift following optical pumping 8=38708
Rb, resonance, quenching by gases 8=29626
Rb1 resonance lines, solar, rel. to abundance obs. 8=45894
S, forbidden lines, wavelengths and A-coeffs. 8=25365
S ions, oscillator strengths for resonance lines present in solar spectrum 8=29647

Spectra—contd
atoms—contd
S isoelectronic sequence, classification 8=38668
S, satellite X-ray lines due to transitions involving double ionization of inner shells 8=43228
Sc III, principle series, transition probabilities in doublets 8=47506
Sc XIII to Cu XXI fluorine isoelectronic sequence 8=29628
Si ions, oscillator strengths for resonance lines present in solar spectrum 8=29647
Si1 absolute oscillator strengths 8=34134
Si1 solar absorption lines, 2935-25578Å, equivalent width calc. 8=37048
SiII, IV, doublets oscillator strength ratios, Fermi calc. and obs. 8=34152
Sn^{117} and Sn^{119}, level crossing investigation of hyperfine struct. 8=29629
Sn, weak line transition probability calc. 8=29621
Tb^{65}, L-spectrum, new lines 8=47487
μ-Tb^{159}, x-ray, rel. to dynamic quadrupole interaction, obs. 8=34191
Tb 1, additional levels obs. 8=25366
Tb I, relative oscillator strengths 8=43201
Tc I, II, 2000-9000 Å arc and spark sources 8=47508
Te (I), g values of 5p^4 configuration 8=25380
Th I, Ritz standards from energy level obs. 8=47509
Ti lines press. broadening in Ar atm. 8=34153
Ti, press, broadening and shift of lines by Ar 8=43203
TiI, II absolute gf-value, shock tube obs. 8=43489
Ti II, in excited configurations, theory 8=43203
Ti V, 3p^6-3p^{5}4d transitions 8=43178
μ-Ti^{48}, X-ray Lyman and Balmer line energies, obs. 8=34189
Tl, coeffs. for internal conversion for K, L and M shell e. m. transitions 8=38670
Tl in TlI vapour, superradiance of green line 8=34154
Tl^{205} as frequency standard, superior to Cs 8=28211
Tm^{69}, new diagram lines in L emission spectrum, β-γ region 8=38681
Tm^{69}, new diagram lines in L emission spectrum, γ region 8=38680
V III, in excited configurations, theory 8=43203
X_2O_7-type ions, vibration and chemical structure 8=47475
Xe, arc, high press., in stationary and flashed modes, spectral emission and abs. obs. 8=29945
Xe, attenuation cross section near resonance line 1469.6Å 8=43205
Xe, cross-sections for line excitation by electron collisions 8=34165
Xe high pressure lamps, energy distrib. meas. 8=47510
Xe, isotopic shifts of 13 i. r. laser lines, meas. 8=25367
Xe, photo-attenuation cross section, 1050-1550Å 8=43206
in Xe pulsed arc, radial distrib. of radiance in u.v. rel. to temp. distrib. 8=39090
Y III, principle series, transition probabilities in doublets 8=47506
Yb II, energy levels calc., Zeeman effect obs. 8=47511
YbII, 4f^{13}5d^2 configuration 8=34155
Zn, in arc discharge, impurity Na effect on line breadth 8=34437
Zn in discharge tube with high voltage pulses 8=29630
Zn II, IV, spark spectrum extension 8=34156
Zn III spark spectra and energy levels 8=38682
Zn 3075.9 Å, resonance line perturbed by He, A, Ne, Kr and Xe 8=47512
inorganic molecules
See also Molecules.
absorpt. band, estimation of position of intensity maximum 8=43150
absorption, rel. to reactivity 8=34225
atmospheric gases, absorption in vac. u.v. region 8=43196
basalt vapour scintillation, time scanning 8=34231
composite, bonded, triplet enhancement with small singlet effect 8=38779
electron-impact spectra at 33-100 eV energies 8=47585
furan, i.r. absorpt. 8=43836
gases, highly reactive, high-temp. i.r. cell. 8=41302
inert gas mixture, collision-induced translational absorpt. theory 8=34384
line by line calc. rel. to statistical model 8=43327
maser application 8=38782
microwave, review of techniques 8=33140
oxygen, forbidden transitions rel. to O_4 dimer content pressure and temp. dependence 8=34273
pressure-induced, i. r., intercollisional interf. effects 8=34385
radiant thermal conduction, effect on 8=46242
radiative lifetimes of u. v. transitions 8=25442
ruby vapour scintillation, time scanning 8=34231
steel vapour scintillation, time scanning 8=34231
u. v., absolute transition probabilities 8=34230
vibration-rotation energy-level density calc. 8=29685
As_2, bands in D → X system, high-resoln. analysis 8=43284
BiF, rotational structure of 2650-2850 Å system 8=38813
CO pulse radiolysis products 8=45405
CO_2-N_2 mixture, meas. of molec, line and continuum rad. at 7,000-16000°K 8=43287
CS_2 alkali-metal vapours, u.v. cross-sections 3,000-1,100Å 8=43315

Spectra—contd
  inorganic molecules—contd
    H_2-He plasmas, isothermal, calc. 8=43544
    Hg_- band emission in r.f. discharge 8=29616
    K, alkali-metal vapours, u.v. cross-sections, 3,000-1,100 Å 8=43315
    Rb alkali-metal vapours, u.v. cross-sections 8=43315
    SiC vapour scintillation, time scanning 8=34231
    SrH Franck-Cordon factors and r-centroids for bands of $D^2\Sigma^+ \leftrightarrow X^2\Sigma^+$ 8=43337
    X_2O_7-type, vibration and chemical structure 8=47475
    Xe pulse discharge in presence of 2n, 240-300 nm 8=34292
  inorganic molecules, diatomic
    alkali halides, molec. beam elec. reson. 8=25670
    computer analysis, separation of branches 8=29681
    computer analysis, wavelength calc. 8=29680
    halogen acids, photoelectron spectra and ionized states 8=34229
    hydrides, first-row, rel. to electronic structure 8=34256
    hydrides, second-row, rel. to electronic structure 8=34257
    inert-gas couples, translation band, transition probability at l.f. 8=29711
    rotational and vibr. consts. calc. 8=38792
    rotational constants, computer calc. 8=38790
    $^1\Sigma$-state, expectation values as functions of internuclear separation 8=29689
    vibration-rotation, computer analysis, line rot. quantum numbers 8=29684
    vibrational transitions, most favourable orientation 8=43254
    AgIn, system B of u.v. absorpt. bands 8=25443
    AlH, absorpt. 8=25444
    BBr, radiative lifetimes 8=38807
    BS, blue-green systems 8=25448
    BeBr, emission obs. 8=25452
    Be Br excited in presence of argon, emission spectrum 8=38810
    Br_2 ads. on oxides, refl. spectra 8=48479
    BrCl, visible absorption 8=29718
    BrO, γ-absorpt. from oxybromine cpd. radiolysis 8=27768
    C_2, dissoc. through rot. 8=29826
    C_2, higher rot. levels 8=29724
    C_2 mol., new $c'\,^1\Pi_g$-$b^1\Pi_u$ band syst. 8=29725
    C_2, Swan band emission in flames 8=29727
    CN, $B^2\Sigma \rightarrow A^2\Pi i$ bands 8=29721
    CN, extension of red and violet bands 8=29726
    CN, stimulated emission, optical detection at 20 cm wavelength 8=38819
    CN violet emission, shock heated CO_2-N_2 mixture, chemical model 8=29722
    CO, absorpt. in extreme u.v. 8=25458
    CO, adsorbed on Pt, i.r. 8=48488/9
    CO, adsorbed on Si-supported Pt, i.r. absorpt. 8=30773
    CO, Asundi bands, in gas discharge 8=38994
    CO, high resolution by double-beam, two-beam interferometry far i.r. 8=28818
    CO, i.r., absorpt. coeffs. 8=34236
    CO, line absorpt. in late-type stellar atm. 8=45666
    CO, radiance from scale model rocket exhaust 8=38815
    CO trapped in rare gas matrix, e transitions perturbation 8=39523
    CO, 2-0 band line-strengths 8=42218
    CO_2, 4.3 μband, use to determ. temp. of wake behind hypersonic sphere 8=41484
    Ca_2, orange bands, $^1\Sigma$-$^1\Sigma$ system, rotary quantum analysis 8=43296
    CaBr, discharge-excited, u.v. emission bands 8=43295
    CaH and CaD, u.v. absorpt. 8=38820
    CaO, i.r. bands 8=34237
    CrH, CrD, $^6\Sigma^+$-$^6\Sigma^+$ infrared obs. 8=47595
    Cs_2, 6250Å band system 8=29733
    $Cs^{133}F^{19}$, hyperfine struct. of J=1 rot. state 8=43298
    D_2, chemisorbed on Rh, i.r. spectra 8=25470
    D_2, selective enhancement in Ar discharge 8=25471
    DCl, high resolution by double-beam, two-beam interferometry far i.r. 8=28818
    F_2, absorpt. band spectrum 8=34376
    F_2, emission spectrum 8=29735
    GeO, u.v. absorpt. bands 8=43301
    H_2, chemisorbed on Rh, i.r. spectra 8=25470
    H_2 dissolved in solid Ar, induced i.r. fund. band obs. 8=36326
    H_2, ground state rot. and vibr. consts. calc. 8=38792
    H_2 in cryst. Ar, i.r. absorpt. 8=27573
    H_2, in H_2-Kr mixture, pressure-induced, i.r. absorpt. 8=38833
    H_2, in H_2-Ne mixture, pressure-induced i.r. absorpt. 8=38833
    H_2, large vibr.-rot. interaction effects in Franck-Condon factors 8=43304
    H_2, Lyman bands, isotope effects on Franck-Condon factors 8=34271
    H_2, Lyman bands, oscillator strengths 8=43309
    H_2, spectroscopy 850 to 792 Å 8=43303
    H_2, vacuum u.v. emission from p and H-atom impact 8=38834
    H_2, HD, D_2 electronic isotope shifts in Lyman bands 8=34244

Spectra—contd
  inorganic molecules, diatomic—contd
    HBr, line broadening rel. to Debye forces of dispersion and induction 8=25407
    HCl, first rotational linewidths determ. 8=38825
    HCl, line broadening rel. to Debye forces of dispersion and induction 8=25407
    HD, rot. and elec. dipole moment obs. 8=34242
    HD, selective enhancement in Ar discharge 8=25471
    HF, line broadening rel. to Debye forces of dispersion and induction 8=25407
    HF, 1-0 and 2-0 bands 8=25476
    HF, pure rotation 8=29734
    HI, line broadening rel. to Debye forces of dispersion and induction 8=25407
    He_2 ($a^3\Sigma\,u$ (6 = O) at 77°K, metal stability 8=34227
    HgD, hyperfine struct. 8=43314
    HgT, hyperfine struct. 8=43314
    I_2 ads. on oxides, refl. spectra 8=48479
    I_2, time-resolved emission from $B^3\Pi_{o,u+}$ state 8=34251
    ICl, Stark effects in $A^3\Pi_1$-$X^1\Sigma^+$ transition 8=25488
    LaO, very high resolution study using hollow cathode lamp and Fabry-Perot spectrometer 8=29675
    LiCl-KCl eutectic at 550°C, i.r. emission 8=38842
    $N_2(A^2\Sigma_u{}^+)$ in active N 8=38840
    $N_2(A^3\Sigma_u{}^+)$, reaction with N atoms 8=25493
    N_2 afterglow, spectroscopic constraints 8=29897
    N_2, band systems, $b'\,^1\Sigma^+_u \rightarrow X^1\Sigma^+_g$ and $g^1\Sigma^+_u \rightarrow X^1\Sigma^+_g$, selective enhancement in vacuum u.v. 8=38841
    N_2, dipole-allowed absorpt., absolute f values 8=34264
    N_2 discharge, evidence for $^3\Delta_u \rightarrow B^3\Pi_g$ transition 8=47608
    N_2, first positive system, in gas discharge 8=38994
    N_2, ground state rot. and vibr. consts. calc. 8=38792
    N_2, $K(b^1\Pi_u) \leftarrow X$ transition, u.v. absorpt. 8=25491
    N_2 plasma jet, i.r. emission 8=30182
    N_2, p-bombard., Ep=0.56-1.7 keV, obs. 8=43322
    N_2, Stark broadening 8=34272
    N_2 trapped in rare gas matrix, e transitions perturbation 8=39523
    N_2, Vegard-Kaplan bands, intensity obs. 8=34265
    N_2^+, excited by vac. u.v. photon impact 8=47609
    N_2^+, excited states rot. and vibr. consts. calc. 8=38792
    $N_2{}^+(1-)$ ion, first negative bands, e transition, dipole moment, matrix element square determ. 8=29752
    $N_2{}^+$, rot. lines, Stark-broadened, shapes and
    NF, $b^1\Sigma^+$-$X^3\Sigma^-$ band system 8=25497
    N-I_2 flames, i.r. emission 8=49890
    NO afterglow 8=38993
    NO, heterogeneous ($^2\Sigma$-$^2\Pi$) interactions 8=34268
    NO, high resolution by double-beam, two-beam interferometry far i.r. 8=28818
    NO, i.r., adsorbed on zeolites 8=27553
    NO, i.r. bands used to follow rise in temp. behind shock waves 8=41484
    NO, intensity of fundamental band 8=25499
    NO, photoelectron spectrum 8=47606
    NO trapped in rare gas matrix, e transitions perturbation 8=39523
    NO, 2 isotopes, comparison of rotational and spin-orbit coupling consts. 8=43325
    $N^{14}O^{16}$, l.f. satellite band 8=25501
    $N^{15}O^{18}$, i.r. vibr. rot. bands 8=25502
    O_2, absorpt. in vacuum u.v., obs. 8=34274
    O_2, emission induced by 0.15-1.0 MeV protons 8=38847
    O_2, in u.v. afterglow, Herzberg II emission 8=34277
    O_2, radiative combination of O atoms 8=38932
    O_2, Rydberg absorpt. series 8=47615
    O_2, Schumann-Runge bands, isotope effects on Franck-Condon factors 8=34271
    O_2, spectral emissivity of Schumann-Runge bands 8=34275
    O_2, Stark broadening in Schumann-Runge system 8=34272
    O_2, Tanaka-Takamine Rydberg series 8=25512
    OD, Zeeman effect in (0,0) band 8=38848
    OH and OD, in solid Ne 8=32020
    OH, matrix-isolated, i.r. 8=34276
    OH^+, $^3\Pi_i$ excited state, fine structure 8=29830
    PbI, Zeeman effect and intensity anomalies 8=34148
    PtC 8=25513
    $Rb^{85}F^{19}$, h.f.s., Stark and Zeeman effects 8=25514
    RhC 8=25513
    S_2, $^1\Delta^u$-$^1\Delta_-$ transitions 8=38851
    S_2, rare gas matrix effect 8=47618
    SO $B^3\,\Sigma^-$-$X^3\,\Sigma^-$ system Morse Franck-Condon factors, r-centroids for 8=43336
    SO, b $^1\Sigma^+$—$X^3\Sigma^-$ band system obs. 8=38852
    ScO, red system, rot anal. 8=25518
    SiF, γ bands, rot. anal. 8=38855
    SiO ($A^1\Pi$ - $X^1\Sigma^+$) band system, oscillator strength meas. 8=43334
    SnBr, u.v. absorpt. after flash photolysis of $SnBr_4$, $B^2\Sigma$-$X^2\pi$ transition 8=34284
    SnI, u.v. absorpt. after flash photolysis of SnI_4, $B^2\Sigma$-$X^2\pi$ transition 8=34284
    SrD, new u.v. absorpt. bands 8=43338
    SrH, new u.v. absorpt. bands 8=43338
    SrO, i.r. bands 8=34237
    Xe_2, attenuation cross section near resonance line 1469.6Å 8=43205
    Xe_2, photo-attenuation cross section, 1050-1550Å 8=43206

Spectra—contd
inorganic molecules, diatomic, radiofrequency
See also Nuclear magnetic resonance and relaxation; Paramagnetic resonance and relaxation.
alkali halides, molec. beam elec. reson. 8=25670
H_2^+ radio-frequency spectrum, interstellar abundance 8=45722
KCl, by elec.-resonance method, rel. to molec. struct. 8=43316
LiF, by elec.-resonance method, rel. to molec. struct. 8=43316
NO, pure rotational 8=25500
NaF, by elec.-resonance method, rel. to molec. struct. 8=43316
O, at low pressure, anomalous line-broadening obs. 8=29759
OH, doubling transitions obs. and calc. suitable for radioastronomy 8=43328
SiO, rot. spectrum, 42 373-43 424 MHz 8=38856
inorganic molecules, polyatomic
alkali-AlH_4, i.r., obs. 8=31959
alkaline bromides, stability constants of Pb complexes 8=48148
amide ion and ion aggregates, in solns. of KNH_2 in liq. NH_3, absorption 8=39380
bismuthyl halides, i.r. absorpt., rel. to vibr. modes 8=38812
metallochlorins, anistropy of optical transitions 8=34258
oxalyl halides, u.v. absorpt. 8=29795
phosphorus oxyhalide radicals, electronic emission 8=43414
phosphoryl cpds., i.r. intensity of PO bands 8=29760
symmetric tops, computer anal. 8=25412
uranyl cpds., fluorescence and oscillator model 8=34286
uranyl cpds., i.r., U-O bond distance calc. 8=34287
zeolites, synthetic, containing transition metal ions, rel. to coordination states 8=41143
AsD_2, flash photolysis, $^2A_1$-$^2B_1$ band system 8=29713
AsH_2, flash photolysis, $^2A_1$-$^2B_1$ band system 8=29713
AsH_3, K-type doubling in ν_3 band 8=25445
BBr_3, electron-beam excited, u.v. emission 8=38807
BF_3-dimethyl selenide and sulphide complexes, i.r. 8=38806
BF_3, ν_2 band 8=29715
BF_3, $2\nu_3$ bands, ζ_{33} determ. 8=34233
BO_4 group complexes, i.r. spectra rel. to asymmetric stretching vibrations 8=29714
B_2O_3, X-ray emission band of B, valency electron structure 8=29716
BeI_2, i.r. 8=25449
$BeBr_2$, i.r. 8=25449
$BeCl_2$, i.r. 8=25449
BrO_2, γ-absorpt. from oxybromine cpd. radiolysis 8=27768
CF_2, absorpt. 8=25453
CF_2, matrix-isolated, i.r. 8=29723
CF_3, matrix-isolated, i.r. 8=29723
C_2N_2 (cyanogen) condensed in solid N_2 and Ar, luminescence 8=25455
CO_2, absorpt. band Q-branch transmission calc. 8=43294
CO_2, absorpt. in artificial atmos. 8=27907
CO_2, bands at 4.3μ 8=29730
CO_2, band and total emissivities at press. where rot. hyperfine struct. removed 8=43280
CO_2, 4.3μ transient laser oscill. 8=28680
CO_2, i.r. abs., 1-1.25μ 8=29728
CO_2, integrated intensity meas., 2.0-, 1.6- and 1.43-μ regions 8=34235
CO_2, intensities of 12-18 μ bands 8=25462
CO_2, intensity of 1.6μ bands 8=34234
CO_2 line parameters using CO_2-N_2-He laser 8=29720
CO_2, new i.r. bands in Venus spectra 8=28153
CO_2, 9.4 and 10.4μ bands, strengths and widths 8=43289
CO_2, radiance, from scale model rocket exhaust 8=38815
CO_2, 667 cm^{-1} band strength determ. 8=25461
CO_2, 10 μ band, temp. depend. of total intensity 8=25463
CO_2, transmittance, 4590-5346 cm^{-1}, eqns. 8=43293
CO_3, i.r. 8=25464
CO_4 group complexes, i.r. spectra rel. to asymmetric stretching vibrations 8=29714
C_3O_2, vac. u.v. absorpt. 8=25467
$(ClO)_2$, i.r. 8=29731
$ClSi(NCO)_3$, i.r. 8=29732
Cl_3SiNCO, i.r. 8=29732
Cl_3SiNCS, i.r. 8=29732
D_2, sensitized fluorescence in alkali atom collisions 8=29836
D_2S_2, i.r., mol. force field evaluation 8=43331
D_2S, ν_2 fundamental vibr. 8=25484
F_2CN, matrix-isolated, i.r. 8=38946
FNCN, i.r., matrix-isolated 8=47712
GeH_4, deuterosubstituted, i.r. band intensities calc. 8=29737
H_2, sensitized fluorescence in alkali atom collisions 8=29836
H_2Ar, i.r. absorpt. 8=25472
HBr dimer bands in solid matrices 8=27575
HCl dimer bands in solid matrices 8=27575

Spectra—contd
inorganic molecules, polyatomic—contd
HCN dimer, matrix-isolated 8=29740
HCN lines from CH_4-NH_3 laser discharge 8=33190
HD, sensitized fluorescence in alkali atom collisions 8=29836
HF, trimer and dimer, i.r. 8=29747
H_2Kr, i.r. absorpt. 8=25472
$HNCLO_3^-$ ion, i.r. absorpt. obs. and structure 8=34247
HOF, i.r. 8=43299
H_2O, band and total emissivities at press. where rot. hyperfine struct. removed 8=43280
H_2O far i.r. calc. for vapour laser 8=42089
H_2O, high resolution by double-beam, two-beam interferometry far i.r. 8=28818
H_2O, radiance exhaust of scale model rocket 8=38815
H_2O vapour, abs. lines in ν_2 band, product of strength and self-broadened half-widths 8=34239
H_2O vapour, absorpt. coeff. 600-1000 cm^{-1} obs. 8=43312
H_2O vapour, band absorpt. meas. 8=27908
H_2O vapour laser line identification 8=29748
H_2O vapour laser line identification 8=29745
H_2O vapour laser, transitions in $2\nu_2$, ν_3 and ν_1 states 8=29741
H_2O vapour, line strengths in $\nu_{1,3}$ bands 8=25480
H_2O vapour, radiation at nonequilibrium temps. 8=47597
H_2O vapour, spectral emissivity, theory allowing for line struct. 8=25481
H_2O vapour, 2.7μ band, statistical model rel. to line by line calc. 8=43327
H_2O, CO_2, CO and C mixtures in rocket exhausts, i.r. radiant transfer 8=41482
H_2O-CO_2 mixture, band and total emissivities at press. where rot. hyperfine struct. removed 8=43280
H_2O^{16} and H_2O^{18}, high-resolution i.r. 8=25478
HOCl, i.r. 8=25475
H_2S_2, i.r., mol. force field evaluation 8=43331
H_2Xe, i.r. absorpt. 8=25472
$K_2Cr_2O_7$, line structure at 2°K 8=34253
Mo complex halides, electron spectra 8=38857
Mo_6Cl_{12}-2,5-dithiahexane complex, i.r. 8=43318
N_2, sensitized fluorescence in alkali atom collisions 8=29836
NCN, in flash photolysis of NCN_3 8=25495
$N^{14,15}ClO_3^{2-}$ anion, i.r. absorpt. 8=29754
N_2D_2, vacuum u.v. absorpt. obs. 8=34267
NF_3, rot. absorpt. in range 10 to 50 cm^{-1} 8=34260
NF_2CN, i.r., matrix-isolated 8=47712
NH_3 adsorbed on Si, vibrational, rel. to bonding strength 8=25508
NH_4 quaternary halides, i.r. 8=38844
N_2H_2, i.r. absorpt. 3.1μ obs. 8=34267
N_2H_2, vacuum u.v. absorpt. obs. 8=34267
NO_2, i.r., adsorbed on zeolites 8=27553
NO_2, molecular consts. from near i.r. spectrum 8=43326
NO_2, 2491 Å electronic transition 8=25503
NO_3^- in $NaNO_3$, KNO_3, and $CsNO_3$ near 600°C, i.r. obs. 8=38842
N_2O absorpt. rel. to SISAM resolution, 4.5μ 8=28823
N_2O bond in ammonia, cross-correlation obs. 8=42230
N_2O, i.r., adsorbed on zeolites 8=27553
N_2O, strength of bands near 4.5μ 8=34263
N_2O, transmission in near i.r. bands, calc. 8=25506
$(Ni(CO)_4)$, i.r. spectra of isotopic species 8=34270
O_3, i.r. bands 8=34278
O_3, 9.6μ band, statistical model rel. to line by line calc. 8=43327
PF_5, far-i.r. 8=47617
Pt-ammine complexes, far i.r. 8=43330
Pt(II) complex of ethylenediaminedithio-cyanate C- and N- substituted, i.r. 8=43329
SF_5Cl, i.r. 8=25516
SF_5Cl rotation spectrum at 8mm. 8=25515
$SOCl_2$, rotation, 8000-18000 MHz 8=43335
$SPCl_3$, far i.r. 8=25517
$SPClF_2$, i.r. 8=25517
$SPCl_2F$, i.r. 8=25517
SeF_6 8=25519
SiF_2, u.v. absorpt. 8=25520
$ThCl_6^{2-}$ complexes, i.r. 8=47619
UCl_6^{2-} complexes, i.r. 8=47619
W complex halides, electron spectra 8=38857
WF_6 8=25519
inorganic molecules, polyatomic, radiofrequency
apatite structure, e.p.r. 8=31848
CsOH, unstable mol. 8=25468
$Fe(CN)_5NO^{3-}$, e.p.r., hyperfine anal. 8=47683
HPF_4 8=34279
H_2S, elec. reson. 8=25483
H_2S, mm.h.f.s., elec. resonance spectroscopy 8=38826
H_2S_2, mm-wave rotational 8=25485
Li^6F^{19}, elec. reson. 8=25483
NH_3, collision-induced transitions between rot. levels 8=47612
NH_2CN, N^{14}-quadrupole coupling 8=43297
NO, linewidth of $J = \frac{1}{2} \rightarrow \frac{3}{2}$ rot. absorpt. 8=47605
N_2O, high resolution, N^{14} quadrupole coupling 8=25505
$N^{14}O^{16}O^{17}$ 8=25504
NCN_3 8=25496

Spectra—contd
- **inorganic molecules, polyatomic, radiofrequency**—contd
  - OCS, Zeeman effect 8=25511
  - PHF_2 and PDF_2 8=38849
  - SiH_4, nuclear spectrum obs. 8=47588
  - $XeOF_4$ 8=43339
- **inorganic liquids and solutions**
  - alkali ions in soln., i. r. bands due to motion 8=25931
  - alkali metals in fused alkali metal salts 8=39374
  - alkali metal-amine solns., origin of 660 mμ band 8=34868
  - alkalimetal-NH_3 solns., internal reflection 8=30490
  - alkali metal nitrate aq. solns., i. r. 8=34869
  - alkali metal nitrate melts, i.r. 8=39378
  - anisol-nitrobenzene system, complex formation 8=45347
  - diphenylamine-nitrobenzene system, complex formation 8=45347
  - furan, i.r. absorpt. 8=43836
  - glass, alumina-silicate, at 600°C, i. r. emission 8=38842
  - ions in aq. solns. i.r., hydration effects 8=39373
  - ion obs., Raman spectra 8=34863
  - metal thiocyanate molten solns., i.r. 8=25934
  - phenol-nitrobenzene system, complex formation 8=45347
  - siloxanes, solvent effect, freq. spectroscopic investigation 8=25884
  - solutions in liquified gases, apparatus for study of abs. spectra 8=30486
  - uranyl cpds., classification of e states 8=34880
  - water, i.r., effect of solutes and temp. 8=39295
  - water i. r. optical properties; application to radiative transfer in planetary cloud layers 8=50140
  - C_3N_{12}, in CCl_4 soln., i. r. 8=31976
  - $Co(CO)_3NO$ 8=48161
  - $CoCl_2$ and $CoBr_2$ in alkali halide soln., absorpt. spectra 8=48159
  - $CsNO_3$, fused, far i.r. absorpt. 8=49742
  - D_2O, hyperfine structure by beam maser microscopy 8=25923
  - H_2 and solns., translation-vibrational branches, theory 8=34860
  - H_2, vibr. solvent shifts in induced i.r. spectra 8=43837
  - HCl, second harmonic vibation-rotation band at 300°K 8=25929
  - HCl in solvents, rotation-like motion 8=25928
  - HDO, hyperfine structure by beam maser microscopy 8=25923
  - H_2O in dichloroethane, self-association 8=34874
  - H_2O, HDO and D_2O in non-aq. solvents, i.r. intensities 8=39377
  - He, laser light transmission 8=32993
  - I ions, u.v. absorption 8=34820
  - $K_3[Cu(NO_2)_5]$, aq. soln., vis. and i. r. absorpt. rel. to crystal structure 8=30901
  - KNH_2 in liq. NH_3, absorption 8=39380
  - LiCl-KCl eutectic at 550°C, i. r. emission 8=38842
  - $Mo(CN)_8^{4-}$ in aq. soln. 8=41118
  - NO_3^- in molten alkali metal nitrates, u. v. 8=30489
  - $NaNO_3$, fused, far i.r. absorpt. 8=49742
  - $NiCl_2$ in alkali halide soln., absorpt. spectra 8=48159
  - Pb-$BiCl_3$ molten mixtures, absorpt. rel. to interacts. 8=34878
  - SO_2 aq. soln., absorpt. spectra, 25°C and up to 6 kbar 8=48160
  - $SPClF_2$, i.r. 8=25517
  - $SPCl_2F$, i.r. 8=25517
  - $SbCl_3$-acetophenone complexes in CCl_4, i. r. 8=34866
  - UO_2^{2+} in perchlorate media, resolution of u. v. bands 8=39382
  - $W(CN)_8^{4-}$ in aq. soln. 8=41118
  - WCl_6, mols. vibr. modes assignments. obs. 8=38859
- **inorganic solids**
  - alkali-AlH_4, i. r. spectra, obs. 8=31959
  - alkali halides, O_2^- centers, electronic structure 8=49703
  - alkali-metal chlorosulphates, i.r. 8=49705
  - alkaline-earth carbonates, C-isotope effects 8=31966
  - alkaline-earth metal chlorosulphates, i.r. 8=49705
  - beryl, l.f. vibrs. of H_2O mols. 8=48704
  - broadening and shifting of lines of V, Cr, Mn, Fe, Co and Zn, rel. to plasma temp. meas. 8=47813
  - corundum, exchange-coupled Cr ion pairs 8=36322
  - corundum group crystals correlation between optical spectra and struct. 8=35024
  - cupric amine complexes 8=31861
  - diamond, i. r., rel. to at. vibration spectrum, review 8=43922
  - diamond, natural, luminesc. excitation 8=36473
  - ferroelectrics, soft, spectra-struct. correl. 8=27544
  - fluorite crystals, magneto-optical rotation of Ce impurity centres 8=49718
  - galolinium ferrite, spontaneous radiation temp. dependence 8=45190
  - glass powder, compression under 10-65 kbar effects 8=40164
  - glass, ternary silicate, struct. rel. to chem. elements 8=36411
  - heavy-metal diphosphates, anhydrous, i. r. 8=36313
  - Heisenberg antiferromagnet, free surface effects 8=45048
  - ice, far i. r., rel. to long range forces 8=31997
  - ice, orientationally-disordered, far i. r. 8=27574
  - i.r., oxide films on Si crystal 8=39598
  - ions in cryst. fields, config.-interaction effects 8=34115
  - kaolin-dimethylsulphoxide complexes, i. r. 8=27554
  - metal iodides with layer structures, optical absorpt. 8=45176

Spectra—contd
- **inorganic solids**—contd
  - metals, rough surface, i.r. reflection 8=31932
  - mineral apatites, i.v. spectra 8=41047
  - minerals, i.r. as basis for crystal-chemical classifi cation 8=39637
  - molecular crysts. of tetrahedral or pyramidal mols., far i.r. 8=45223
  - molecular sieve, type A linde, containing Ni^{2+} ions, rel. to coordination states 8=41143
  - noble, metals, rel. to band structure 8=32036
  - parahydrogen, i.r., freq. analysis 8=43967
  - perovskite fluorides, i. r. transmission 8=27600
  - photoluminophors, conversion efficiency investigation 8=36466
  - α-quartz, optical phonons, extraordinary, directional dispersion 8=45221
  - quartz: Co-doped, absorpt., and changes on X-ray exposure 8=48556
  - rare earth cpds, low-lying crystal-field 8=36296
  - rare earth phosphates rel. to phosphor basis 8=49747
  - rare-earth sulphates, hydrates and anhydrous, i.r. 8=41130
  - ruby, emission rel. to laser axial mode separation 8=24334
  - ruby, exchange-coupled Cr^{3+} ion pairs, piezo spectroscopic studies 8=27646
  - ruby laser, single pulse spectrum 8=42104
  - silicate glasses, containing As, Sb oxides, vibr. and struct. 8=31964
  - thaumasite, $Ca_3H_2(CO_3/SO_4)SiO_4.13H_2O$, thermal decomposition, i. r. study 8=26065
  - torsional ocsillations and n.m.r. linewidth transition 8=31940
  - transition metals, rel. to band structure 8=32036
  - uranyl cpds., electron vibration, analysis and interpretation 8=49758
  - vibronic, of e transitions at probe ion, for lattice mechanics obs. 8=39859
  - X-ray spectroscopy, conference USSR, July 1966 8=45163
  - zeolites, i. r., rel. to chem. struct. 8=27552
  - zeolites, synthetic, containing transition metal ions, $d^9(d^1)$ and $d^8(d^2)$ configs in D_{3h} symmetry 8=41142
  - zeolite, synthetic, surface state evolution from r. f. spectrometry during dehydration 8=39581
  - AgBr, absorpt., pressure dependence up to 50kbar 8=41053
  - AgBr, AgCl and AgI, reflection in far i. r. 8=45167
  - AgCl, absorpt. pressure dependence up to 50kbar 8=41053
  - AgCNO, i.r., bond nature determ. 8=26006
  - AgN_3, i.r., rel. to crystal growth method 8=48535
  - Ag_2SO_4, i. r. 8=31955
  - α-Al_2O_3:V^{2+}(Cr^{3+}), (Mn^{4+}), trigonal splitting, stress dependence 8=43929
  - Al-Si catalysate, water-induced p centres obs. 8=36318
  - Ar, induced i. r. fundamental band of dissolved H_2 8=36326
  - AsI_3, far i. r. 8=45223
  - BH_4^- in alkali halides, i. r. 8=36327
  - Ba tetraoxometalates, i. r. 8=31965
  - BaF_2: Co^{2+}, temp. dependences 8=41076
  - $BaTiO_3$, absorpt. edge, rel. to props. of TiO_6^{-n} unit 8=45225
  - Be, i. r. absorpt. obs. 8=36330
  - BeO, exciton line splitting, phonon induction, obs. 8=36331
  - $BeSO_4$, $4H_2O$ and $BeSO_4.4D_2O$, i.r. refl. spectra 8=35381
  - Bi, hyperfine structure 8=27562
  - $BiCl_3$, far i. r. 8=45223
  - C_3N_{12}, i.r. 8=25456
  - C_3N_{12}, i. r. 8=31976
  - CaF_2 crystal, emissivity, infrared 8=32006
  - CaF_2:Ce^{3+} line splitting in electric field 8=36308
  - CaF_2:Ce^{3+}, rel. to 4f ↔ 5d transitions 8=45263
  - CaF_2: Co^{2+}(Ni^{2+}), temp. dependences 8=41076
  - CaF_2:Eu^{2+}, rel. to Zeeman effect 8=45177
  - CaF_2: H interstitial atoms, i.r. absorpt. rel. to localized vibrations of H 8=41072
  - CaF_2:Ni^{2+}, vis. and near i. r. absorpt., at room temp. and 4.2°K 8=31967
  - CaF_2:$Pu^{3+,4+}$ 8=31968
  - CaF_2: Sm^{2+} crystal generation, spectrum-time studies for ruby laser excitation 8=41071
  - $CaMoO_4$ 8=45179
  - CaO, i.r. dielectric response rel. to lattice vibrations 8=41075
  - $Ca(OH)_2$ and $Ca(OD)_2$, i. r. vibr. 8=31970
  - $Ca(OH)_2$, i. r. 8=27563
  - $CaSO_4.2H_2O$, i.r. combination vibr. spectrum, 10,000-1,200 cm^{-1} 8=41074
  - $CaWO_4$ 8=45179
  - $CaWO_4$:Gd^{3+}, ^6P Stark levels and line polarization 8=31993
  - $CaWO_4$: Yb^{3+}, microwave-optical double reson. using circularly polarized light 8=41070
  - $CdCr_2Se_4$, ferromagnetic, i. r. absorption 8=41078
  - CdF_2: Co^{2+}, (Ni^{2+}), temp. dependences 8=41076
  - CdF_2:Ni^{2+}, vis. and near i. r. absorpt., at toom temp. and 4.2°K 8=31967
  - CdS, absorpt., two-photon, anisotropy 8=45181
  - CdS, anticrossing of dispersive curves 8=36346
  - CdS, exciton lines split by stress, e-hole spin interaction 8=26920
  - CdS, phonon-assisted free exciton recombination 8=44760

Spectra—contd
  inorganic solids—contd
    CdS, photoreflectance at fundamental absorption edge 8=45183
    CdS:Co^{2+}, Co^{2+} absorpt. and emission rel. to ion centre levels, 3500 cm^{-1} 8=27613
    CdSe, anticrossing of dispersive curves 8=36346
    CdSe, coherent radiation of free excitons 8=36343
    CdSe, exciton lines split by stress, e–hole spin interaction 8=26920
    CdSe$_x$(CdTe)$_{1-x}$ alloys, forbidden band width comp. dependence 8=36344
    CdSe:Cu, fundamental absorpt. edge impurity conc. dependence 8=36349
    CdSe:Cu, i. r. absorpt. rel. to Cu impurity conc. 8=36345
    CdTe, pure and In doped, reflection 20 to 200μ, and Reststrahlen band 8=31974
    Cr glasses, high-press. effect 8=39632
    Cr surface species from chemisorpt. of molec. subs., i.r. study 8=45363
    CsNO$_3$, far i.r. absorpt. 8=49742
    Cu, in plasma jet, pulsation of intensity 8=36353
    Cu–Au alloys, absorption, electron transition mechanisms 8=41082
    CuCl, Zeeman effect, 4. 2°K 8=36351
    Cu–Zn, X-ray absorption, K edges 8=41080
    CoCl$_4^{2-}$-ZnCl$_4^{2-}$ mixed crysts. at 4°K 8=27590
    Cs$_2$SO$_4$, i.r. refl. spectra 8=35382
    Cu$_2$O, absorpt., rel. to annealing prod. stoichiometric defects, obs. 8=41083
    Cu$_2$O crystal defects, energy spectra 8=31055
    Cu$_2$O, electroreflectance spectrum 8=49159
    Cu$_2$O, stressed, exciton lines, polarization effect 8=45185
    D, para-, obs. 8=45192
    DyAlO$_3$, absorpt. rel. to mag. props. 8=36356
    DyFeO$_3$, absorpt. rel. to mag. props. 8=36356
    Eu^{2+} in alkaline-earth fluorides, absorpt., multiplet structure 8=31986
    Fe metal, X-ray K-absorpt. spectrum 8=45186
    FeF$_2$, i.r., rel. to mag. susceptibility 8=36210
    FeNi$_3$ alloy, X-ray K-absorpt. spectrum 8=45186
    FeS$_2$, pyrites, X-ray K-absorpt. spectrum 8=45186
    GdVO$_4$:Eu^{3+}, crystal field Hamiltonian, determ. of phenomenological parameters of 8=31992
    Ge, i. r. absorption of Co^{60} γ rel. to annealing 8=36365
    Ge periodate, i.r. absorpt. spectrum 8=43300
    Ge, photoconductivity 8=44925
    Ge surface exam. by total internal reflection spectroscopy 8=35895-6
    H, ortho-, obs. 8=45192
    H$_2$ in cryst. Ar, i. r. absorpt. 8=27573
    HBr, trapped in matrices, far i. r. dimer bands 8=27575
    HCN, adsorbed on porous glass 8=48491
    HCN, matrix-isolated dimer 8=29740
    HCl, cubic and orthorhombic phases, second harmonic vibration-rotation band 8=25929
    HCl, trapped in matrices, far i. r. dimer bands 8=27575
    H$_2$O in matrices, i. r., nuclear-spin-species conversion 8=38830
    H$_2$O, D$_2$O, and HDO, i.r. intensities of stretching and vibrational bands 8=36369
    Hg(CNO)$_2$, i.r., bond nature determ. 8=26006
    Ho, X-ray L emission spectrum 8=45193
    HoFeO$_3$, absorpt. rel. to mag. props. 8=36356
    n-InAs, reflection, rel. to conduction band structure determ. 8=35771
    InAs solid solns. with $A^{II}B^{VI}$ type cpds., reflection 8=41099
    InSb, magneto-optical interband transition linear-$\vec{k}$ valence-band splitting, obs 8=36373
    InSb, microwave emission from nonequilib. plasmas in mag. fields 8=40476
    n-InSe, absorpt. and reflection, optical transitions 8=45196
    n-InSe, fundamental absorpt. and optical transitions 8=41100
    KBr:Li$^+$, far i. r., of lattice resonant modes rel. to isotope shifts 8=36393
    KCl, absorpt. cross-section for transition from F-center ground state to L bands 8=48877
    KCl complexes, i. r., temp. dependence 8=36381
    KCl film, reflection and absorpt., in u.v. 8=32025
    KCl, X-irradiated, i.r. absorpt. 8=41104
    KCl: HF$_2^-$, broadening of i.r. peak 8=49733
    KCl–KBr with Pb admixture, absorption spectra and fluorescence 8=49735
    KCl–KI solid solns, decomposition effects 8=36395
    KCNO, i.r., bond nature determ. 8=26006
    K$_3$CO(CN)$_6$:Cr^{3+}, $^2E \leftrightarrow {}^4A_2$ transition 8=31979
    KCOF$_3$, i. r. transmission 8=27600
    K$_2$CoF$_4$, absorpt., compared to KCoF$_3$ 8=45197
    K$_3$[Cu(NO$_2$)$_5$], vis. and i. r. absorpt. rel. to crystal structure 8=30901
    KH$_2$AsO$_4$, i. r. absorpt. by H-bonds 8=27598
    KH$_2$PO$_4$, i. r. absorpt. by H-bonds 8=27598
    KI film, reflection and absorpt., in u.v. 8=32025
    KI:Ag$^+$, far i. r., of lattice resonant modes rel. to isotope shifts 8=36393
    KI-Tl crystals, absorpt., excitation and emission, 10° to 300°K, rel. to thallous ion centres 8=41108
    KMgF$_3$, i. r. transmission 8=27600
    KMnF$_3$, absorpt., of Mn^{2+} 8=41109

Spectra—contd
  inorganic solids—contd
    KMnF$_3$, i. r. transmission 8=27600
    KNO$_3$, I-II phases, i. r. absorpt. rel. to internal interaction 8=27597
    K$_2$[Ni(C$_2$O$_4$)$_2$]. 6H$_2$O, i. r. 8=36380
    KNiF$_3$, i. r. transmission 8=27600
    KTaO$_3$, i. r. reflection 8=27599
    KZnF$_3$, i. r. transmission 8=27600
    La tetrahydrate perrhenate, i. r. absorpt. obs. 8=36384
    LaF$_3$:Dy^{3+} 8=31985
    Li^{6,7}F, far i. r., isotope-induced acoustic band absorpt., 7°K 8=36396
    LiF colour centres absorpt., linear Stark effect on zero-phonon lines, obs. 8=27581
    LiF crystal, emissivity, infrared 8=32006
    LiNbO$_3$, spontaneous parametric emission power and bandwidth 8=27586
    LiNbO$_3$:Cr^{3+}, polydomain crystal, elec. paramag. resonance of Cr^{3+} 8=27277
    MgAl$_2$O$_4$:Cr, emission and absorpt., visible and u.v. 8=45210
    MgAl$_2$O$_4$:Cr^{3+}, optical absorpt. and fluorescence 8=49715
    MgO, exciton line splitting, phonon induction, obs. 8=36331
    MgO:Fe^{2+}, far i. r. absorpt. at low temps. 8=27589
    MgSO$_4$. 7H$_2$O and MgSO$_4$. 7D$_2$O, i.r. refl. spectra 8=35382
    Mn, Kβ_5-emission and K-absorpt. edge, rel. to band structure 8=41115
    Mn surface species from chemisorpt. of molec. subs. i.r. study 8=45363
    MnCO$_3$, absorpt., at 4. 2°K rel. to magnon side-bands 8=32010
    MnCO$_3$, vis. and u.v. absorpt. 8=32008
    MnCl$_2$, new absorpt. band 8=32012
    Mn$_3$Cl$_2$(NO$_3$)$_{12}$. 24H$_2$O, Zeeman splitting of blue lines, theory and obs. 8=41117
    MnCl$_4^{2-}$-ZnCl$_4^{2-}$ mixed crysts. at 4°K 8=27590
    MnF$_2$, octahedral field, i.r. absorpt. of Co^{2+} ions 8=32011
    MnF$_2$, spin-wave sidebands 8=36388
    Mo bronzes 8=40245
    Mo, 8 kV isochromat obs. 8=45227
    Mo, i. r. meas. rel. to Fermi surface and correlation effects 8=36392
    Mo(CN)$_8^{4-}$, i. r. 8=41118
    MoO$_3$, film and cryst., temp. depend. of absorpt. edge 8=32013
    NH$_3$ in matrices, i. r., nuclear-spin-species conversion 8=38830
    NH$_4$Br, i. r., above and below transition 8=27596
    NH$_4$Cl, i. r., above and below transition 8=27596
    (NH$_4$)$_2$Cr$_2$O$_7$, absorpt., at 2°K 8=45212
    NH$_4$I and NH$_4$I(Tl), absorpt., luminesc. and excitation spectra 8=32014
    (NH$_4$)$_2$Ir; PtCl$_6$, i.r., exchange coupling between Ir^{4+} ions 8=32002
    Na aluminosilicate glass, i. r., rel. to ion-exchange hardening 8=30864
    NaBeF$_3$-NaPO$_3$ system, i. r. spectroscopy for Be phosphate glass struct. 8=30791
    NaCl, conductivity, dielectric constant and refractive index 8=45205
    NaCl, ultraviolet and band structure 8=41121
    NaCl^{35,37}, far i. r., isotope-induced acoustic band absorpt., 7°K 8=36396
    NaCl:AgCl single crystal, far i. r. absorpt. obs. 8=36391
    NaCl:Cu$^+$, far i. r., of lattice resonant modes rel. to isotope shifts 8=36393
    NaCl:CuCl single crystal, far i. r. absorpt. obs. 8=36391
    NaCl-KCl solid solns, decomposition effects 8=36395
    NaClO$_3$, i. r. reflectance bands, dispersion anal. 8=27593
    NaCNO, i.r. bond nature determ. 8=26006
    Na$_2$Cr$_2$O$_7$, absorpt., at 2°K 8=45212
    NaF : Co^{2+}, absorpt. 8=49743
    NaNO$_3$, far i.r. absorpt. 8=49742
    Na$_2$O. 2MnO. 2SiO$_2$, absorpt. rel. to Mn^{2+} bands changes on temp. decrease 8=41119
    Na$_2$SiO$_3$, i.r., surface structure after etching 8=39578
    Nb complex, tetrabromobis (acetonitrile) Nb(IV), i. r. 8=44241
    (Nb$_6$Cl$_{12}$)$^{n+}$ (n=2, 3, 4) 8=27595
    Ni, low-energy transitions rel. to band structure 8=35774
    NiCl$_4^{2-}$-ZnCl$_4^{2-}$ mixed crysts. at 4°K 8=27590
    Ni–Zn, X-ray absorption, K edges 8=41080
    O, at 4°K, simultaneous transition rel. to absorpt. in range (15-33) × 10^3cm^{-1} 8=32019
    OH, matrix-isolated, i.r. 8=34276
    OH and OD in solid Ne, evidence of rotation 8=32020
    POCl$_3$, i.r., at 77°K 8=49746
    PSCl$_3$, i.r., at 77°K 8=49746
    PbF$_2$: Gd^{3+}, rel. to excited levels of Gd^{3+} at 77°K 8=36250
    PbMoO$_4$ 8=45179
    PbO, yellow, forbidden band width, determ. 8=32022
    PbO–SiO$_2$ silicates, crystalline and vitreous, obs. 8=32021
    PbWO$_4$ 8=45179
    Pd, Lβ_2-emission band rel. to electronic structure 8=41129
    RbI film, reflection and absorpt., in u.v. 8=32025
    RbMnF$_3$, absorpt. of Mn^{2+} 8=41109

Spectra—contd
inorganic solids—contd
$RbMnF_3$, fine structure in $^6A_1 \rightarrow {}^4T_1(^4G)$ obs. transition 8=32024
$RbMnF_3$, i. r. transmission 8=27600
Pr^{3+} in rare-earth chloride hydrated crysts. 8=45215
Ru(II) complexes in rigid glasses 8=32027
S_2^- centre in alkali halides, absorpt. bands rel. to para-elastic behaviour 8=45173
SO_4^{2-} in $M_2^IM^{II}(SO_4)_2 . 6H_2O$, i. r. 8=27601
$SPClF_2$, i.r. 8=25517
$SPCl_2F$, i.r. 8=25517
Sb_2S_3 reflection in photon energy range 1. 5-3. 0eV 8=49749
SbSi, ferroelectric, far i.r. spectra 8=41134
Sc_2O_3:Nd^{3+} absorpt. rel. to Stark splitting scheme and $^4F_{3/2}$ lifetime, 4. 2-293°K 8=32017
Se, trigonal, electronic spectrum 8=32030
Si, absorpt., one-electron, high-resolution exam. 8=45218
Si, Si_2O 9μ vibr. states rel. to isotope effects and c-o stretching vibr., 1104 cm^{-1} 8=27607
α-SiC, absorption of exciton-impurity complexes 8=36406
SiO_2, oxide layer thickness and nature from i. r. props. 8=26125
Sn salts with mixed anions, i. r. absorpt. 8=36413
SnI_4, far i. r. 8=45223
SnO_2 crystal, i. r. absorpt. rel. to optical lattice-vibration modes 8=45222
SnO_2, restrahl reflection, in static dielec. constant determ., 8=49353
$Sr_2(Cu_xZn_{1-x}Me)O_6$, ($Me = W^{6+}, Te^{6+}$) Jahn-Teller effect of Cu^{2+} 8=41081
SrF_2 : Co^{2+}, temp. dependences 8=41076
SrO, i.r. dielectric response rel. to lattice vibrations 8=41075
Ta, 8 kV isochromat obs. 8=45227
TaF_8^{3-}, i. r. 8=41118
Tb, quadrupole transition $LMv(\beta_9)$obs. 8=41146
$TbAlO_3$, absorpt. rel. to mag. interactions 8=45066
$TeBr_4$, far i. r. 8=45223
$TeCl_4$, far i. r. 8=45223
Ti cpds., i. r. absorpt. 8=36421
TiO_2, absorpt. edge, rel. to props. of TiO_6^{-n} unit 8=45225
TlCNO, i.r., bond nature determ. 8=26006
TlI-42% TlBr single crystals, i.r. transmission, impurity effects 8=36422
Tl_2SO_4, i. r. 8=31955
TlSe, reflection spectrum beyond fundamental absorpt. edge 8=36423
$TmFeO_3$, coalescing of resonant peaks by rot. of applied field 8=45226
V surface species from chemisorpt of molec. subs., i.r. study 8=45363
VMn_2 alloy, $K\beta_5$-emission and K-absorpt. edge, rel. to band structure 8=41115
VO_2 crystal, reflection, in 1. 4-6. 0eV at 25, 59 and 62°C rel. to semiconductor-metal transition 8=41150
$VOSO_4 . 5H_2O$, cryst. polymorphs, polarized absorpt. 8=49759
W, 8 kV isochromat obs. 8=45227
WCl_3 8=38357
$W(CN)_8^{4-}$, i. r. 8=41118
W-Mo alloys, normal emissivity 8=45228
Y tetrahydrate perrhenate, i. r. absorpt. obs. 8=36384
Y_2O_3:Nd^{3+} absorpt., rel. to Stark splitting scheme and $^4F_{3/2}$ lifetime, 4. 2-293°K 8=32017
YFe garnet rods, axially magnetized, abs. 8=36426
YVO_4: Eu^{3+}, absorpt. and fluoresc., $(4f)^6$ level splittings rel. to internal field, obs. 8=41152
YVO_4, i.r., rel. to lattice vibrations 8=36424
YVO_4, i.r. spectral emittance and opt. props. 8=32038
$ZnAl_2O_4$:Cr^{3+}, optical absorpt. and fluorescence 8=49715
ZnO, exciton lines split by stress, e-hole spin interaction 8=26920
ZnO, phonon-assisted free exciton recombination 8=44760
ZnS and similar lattices, absorpt. rel. to luminescence props. 8=36522
Zns, exciton complexes, absorption and emission 8=36430
ZnS, exciton, rel. to stacking fault probability 8=49766
ZnS: Ag, Ga, absorpt., photoconductivity and photoexcited e. s. r., rel. to donor-acceptor pairs 8=40677
(ZnS-CdS):Co^{2+}, Co^{2+} absorpt. and emission rel. to ion centre levels, 3500 cm^{-1} 8=27613
ZnS:Co^{2+}, Co^{2+} absorpt. and emission rel. to ion centre levels, 3500 cm^{-1} 8=27613
ZnS: Cu, Al(Ag, Al), i.r. absorpt. due to donor states 8=41156
ZnS: La, (La = lanthanides), rel. to crystal field effects 8=26646
Zn(S:Se):Mn phosphors, emission and excitation 8=45235
ZnSe, i.r. lattice vibrations 8=49764
ZnSe:Co^{2+}, Co^{2+} absorpt. and emission rel. to ion centre levels, 3500 cm^{-1} 8=27613
$ZnSnAs_2$, edge absorption spectrum 8=45231
ZnTe, i.r. lattice vibrations 8=49764
α-$Zn_3(VO_4)_2$: Ni^{2+}, optical spectra rel. to crystal field theory 8=48310
$ZnWO_4$, octahedral field, i.r. absorpt. of Co^{2+} ions 8=32011
$ZrCl_4$, i.r. 8=32040
$Zr(NO_3)_4$, i.r. 8=32040

inorganic solids, radiofrequency
See also Nuclear magnetic resonance and relaxation; Paramagnetic resonance and relaxation.
ferro-spinels, Mössbauer quadrupole splitting 8=43942
n-InSb microwave emission rel. to instabilities in avalanche plasma 8=49227
InSb 10 MHz-10 GHz, elect. and magnetic field effects 8=36371

organic molecules and substances
See also Molecules.
absorpt. band, estimation of position of intensity maximum 8=43150
absorption, rel. to reactivity 8=34225
acenes, cryst. and in soln., absorpt., with polarized light orientation 8=32042
acetals, depend. of geminal H-H couplings on solvent and conc. 8=43831
acetonite, Brownian rotatory motion rel. to dipole-dipole intermol. forces in vibr., 8=43827
acetonitrile in NH_4 salts solns., C≡N band shift rel. to dipole-dipole interaction 8=30487
acetylacetone 8=47651
acetylene, Frank-Condon factors rel. to ionization 8=29982
acetylene, low-energy electron impact, triplet states 8=34302
acetylene monoderivatives, C≡C group oscillation and absorpt. band calc. 8=34300
acetylenes, monosubstituted, C≡C bond vibr. freqs. and absorpt. band intensities, calc. 8=34299
acridine dyes in 2-chloroethanol, $T^* \leftarrow S$ bands in absorpt. 8=30494
acridines, cryst. and in soln., absorpt., with polarized light orientation 8=32042
2-acyl-1, 3-diketones, MO LCAO calcs. of electronic spectra 8=25588
aliphatic ketones, assignment of second singlet in CO group 8=32045
αβ-unsaturated ketones, u. v. absorpt. 8=29788
aminomethoxypyridine, u. v. absorpt. 8=34356
anthracene, Davydov splittings of intense transitions 8=35048
anthracene delayed fluoresc. rel. to excit. states decay and intersystem crossing, obs. 8=25537
anthracene, low-lying triplet excit. states absorpt., 0. 4-1. 0μ 8=25616
anthracene in n-paraffin solvents, electronic spectra rel. to phase transitions of solvent 8=25938
anthracene triplet-triplet annihilation rate const., flash photolysis meas., 430-553°K 8=25535
anthracene, two-photon absorpt. 8=45237
anthracene, polarization of triplet-triplet absorpt. 8=27621
anthracene singlet-triplet transitions, triplet state assignments and spin-orbit coupling 8=25536
anthracene, soln., triplet-triplet absorpt. and extinction coeffs., 3000-8000 Å 8=25926
anthracene vapours, fluorescence fine structure 8=47634
anthracene, Wannier exciton levels 8=26918
9, 10-anthraquinone and derivatives, emission obs. 8=43392
aromatic carbonyl cpds., perturbation of singlet-triplet transitions 8=34296
aromatic compounds, photoelectron spectra and inner ionization pots. 8=34297
aromatic hydrocarbons, anharmonic contrib. to radiationless transitions 8=43342
aromatic hydrocarbons in soln., triplet state form. efficiencies 8=43832
aromatic hydrocarbons, mixed crysts., orientation effects 8=27623
aromatic hydrocarbons, solvent Stark effect and spectral shifts 8=39375
aromatics, polycyclic, vapour phase absorpt., 1550-3000Å 8=38860
aromatics, triplet state lifetimes, delayed fluoresc. obs. 8=25610
aryl ketone-iodine complexes 8=43353
azaporphyrin ion structures 8=34308
azulene derivatives, anomalous emission 8=43354
azulene, elec. field broadening of electronic transition 8=45238
azylene 8=34310
benzene and derivatives, excitation by electron impact 8=48172
benzene ⇌ biacetyl energy transfer and triplet benzene lifetime, vapour phosphoresc. obs. 8=25544
benzene, CNDO calc. of electronic spectra 8=29767
benzene cryst., theory 8=49772
benzene, crystalline, quantitative obs. of optical obs. spectra 8=36435
benzene crysts., site group splitting and orientational effects 8=27627
benzene-cyclohexane, solid solns. at 77°C 8=27624
benzene, effect of solvents on near u. v. absorpt. 8=34870
benzene, in inert-gas matrix, higher excited states 8=49770
benzene isotopic mixed crysts., absorpt. spectra, static cryst. effects 8=49771
benzene, matrix-isolated, temp. depend. 8=29769

Spectra—contd
- **organic molecules and substances**—contd
  - benzene, polyalkyl substitutes of, electronic u.v. absorption 8=41162
  - benzene sulphochlorides, vibrations resonance interaction 8=47639
  - benzodioxane-1, 4, solvent effects on absorpt. band B position 8=39376
  - benzodioxane-1, 4, 6-substituted, action of substituent structure 8=47638
  - 4-benzoyl-aminostilbene derivatives, quasiatomic chromosphere systems 8=47643
  - 1, 12-benzperylene in crystalline n-paraffin solns., quasi-line temp. broadening, shift and line profile 8=45240
  - benzoic acid, H-bridge complexes, thermodyn. props. from u.v. absorpt. spectra 8=39349
  - benzonitrile, Brownian rotatory motion rel. to dipole-dipole intermol. forces in vibr., 8=43827
  - 1, 12-benzoperylene at 4°K, line-width obs. in quasiline fluorescence spectrum 8=49827
  - benzophenone, assignment of lowest triplet state of C = O group 8=25560
  - benzophenone, polarized absorpt. 8=27630
  - benzophenone singlet-triplet transitions, triplet state assignments and spin-orbit coupling 8=25536
  - p-benzoquinone and derivatives, emission obs. 8=43392
  - benzpyrene in crystalline n-paraffin solns., quasi-line temp. broadening, shift and line profile 8=45240
  - benzyl, free radical 8=43420
  - bromostyrenes, liq. isomeric, absorpt. obs. 8=43841
  - p-benzoquinone, effect of solvents on near u. v. absorpt. 8=34870
  - p-benzoquinone (H_4) and $(D)_4$ crysts. at 4°K 8=27626
  - biphenylene, electronic 8=27636
  - carbonyl $n \rightarrow \pi^*$ transitions, direction of polarization 8=27630
  - carotene films, effect of gas adsorpt. 8=49773
  - cellulose derivatives, e absorpt 8=36436
  - cellulose propylene phosphite, transformation, structure 8=38966
  - charge-transfer and H-bonded complexes, internal compression effects in solvents 8=34864
  - charge-transfer complexes, solid-state, and crystal structure 8=26166
  - chloralkanes, normal vibrs. and C-Cl charact. freqs. rel. to struct., calc. 8=34354
  - chlorobenzotrifluorides, electronic absorpt. bands obs. 8=43358
  - α,β-chlorine naphthalene, u.v. absorpt. at 77°K for vapour and soln. 8=32047
  - p-chlorobenzonitrile, near-u.v. absorpt. obs. 8=43357
  - chlorophyll, anisotropy of optical transitions 8=34258
  - chromophores, intramolec. energy transfer between triplet states 8=41157/8
  - chromophores, u. v. soln. spectra 8=25927
  - chrysene, low-lying triplet excit. states absorpt., 0. 4-1. 0μ 8=25616
  - chrysophane oxides, N-derivatives, i.r. and u.v. 8=36437
  - cinnoline, vapour, u.v. and visible 8=25559
  - collagen and bone transmission and attenuated total, refl. i.r. spectra 8=32041
  - complexes, electron donor-acceptor, gas phase 8=38905
  - composite, bonded, triplet enhancement with small singlet effect 8=38779
  - compounds with VB group elements, vib. spectra rel. to freq. changes 8=34294
  - copolymers with F atoms, CH_2 group absorpt. bands 8=34394
  - coronene, in cryst. matrices, effect of thermal treatment 8=45242
  - coronene in n-paraffin solvents, electronic spectra rel. to phase transitions of solvent 8=25938
  - corrin analogue, synthetic 8=25561
  - cryptocyanine, laser flash 8=48162
  - cyanine dye soln., stimulated emission 8=48154
  - cyclooctatetraenyl radical anion 8=25658
  - p-di-tert-butylbenzene crysts. rel. to mol. π e chord symmetry, 20°K 8=30648
  - dialkyl sulphides, electronic 8=29762
  - diazines, CNDO calc. of electronic spectra 8=29767
  - 1, 3-dibenzoylacetone 8=47651
  - dibenzoylmethane 8=47651
  - 1, 4-dibromonaphthalene, electronic Zeeman meas. 8=27629
  - dichlorotoluenes, electronic absorpt., near-u.v. obs. 8=43400
  - 3, 3′-diethylthiatricarbocyanine laser, time-resolved stimulated emission spectra 8=28712
  - difluorodiazirine, Stark effect 8=25579
  - 2, 6-dihalogeno-p-benzoquinones, singlet-triplet absorpt. 8=38873
  - 1, 4-dihydroxyanthraquinone, optical emission and absorption 8=34305
  - p-diiso-propylbenzene crysts. rel. to mol. π e chord symmetry, 20°K 8=30648
  - dyes oriented in glass matrix, polarized absorpt. 8=49767
  - $\alpha\alpha'$ and $\gamma\gamma'$ dipyridol in n-paraffins, structural spectra of phosphorescence 8=36530
  - electron-impact spectra at 33-100 eV energies 8=47585
  - ether, ketone acid, amine addition products 8=38880

Spectra—contd
- **organic molecules and substances**—contd
  - ethyl alcohol, trans rotamer obs. and rotational consts. meas. 8-34 Gc/sec 8=43364
  - n-ethylaniline, near-u.v. absorpt. obs. 8=43352
  - ethyl chloride, HCl and CH_3 hindered-rot. lines, Schottky barrier tunnelling obs. 8=34327
  - ethylene oxide, ethylene oxide d_4, potential constants and vibrational analysis 8=38877
  - ethylene, 6 molecules and 1 ion at 300°K, mean square vibr. amplitudes calc. 8=25571
  - ethylene and perdeuteroethylene, far u. v. 8=25573
  - ethylene, u. v. assignments 8=47667
  - ethylphenols, electronic absorpt. bands obs. 8=43385
  - ferrocene, matrix-isolated 8=49775
  - ferroelectrics, soft, spectra-struct. correl. 8=27544
  - five-membered rings, CNDO calc. 8=38862
  - fluoranthene, electronic 8=34329
  - fluorenon, absorpt. bands, elec. field effects 8=34328
  - p-fluorophenol, emission obs. 8=43384
  - fluoro-naphthalene, u.v. absorpt. at 77°K for vapour and soln. 8=32047
  - formaldehyde, elec. field induced 8=25582
  - formaldehyde, elec. field-induced 8=38881
  - formaldehyde, 3500Å $^1A_2 \leftarrow {}^1A_1$ transition 8=25581
  - formyl fluoride, Stark effect 8=25579
  - halogenated benzenes, singlet-triplet absorpt. 8=27625
  - helical polymers, effects of electronic interactions 8=29868
  - hexabromobenzene singlet-triplet transitions, triplet state assignments and spin-orbit coupling 8=25536
  - n-hexane, light emission, electrically stressed 8=39383
  - hydrazides, substituted, C-Br bond 8=49780
  - hydrocarbon glasses, radiation-induced trapped electrons 8=45401
  - hydrocarbon TCNE complexes, effects of press. on charge transfer absorpt. 8=36433
  - hydrocarbons, absorption spectrum similar to dinegative ion 8=38884
  - hydrocarbons aromatic, quasilinear phosphoresc. spectra 8=36524
  - hydrocarbons, unsaturated, vibrational spectra 8=47621
  - indene, substituted, spectroscopic study 8=36440
  - p-isopropyltoluene crysts. rel. to mol. π e chord symmetry, 20°K 8=30648
  - ketones, solvent effects in u. v. 8=34876-7
  - laser flash spectroscopy 8=43341
  - liquid, radiationless transitions, direct meas. 8=43829
  - liquids and solutions, Kramers-Kronig relations 8=48153
  - methanal azine, electronic absorpt. 8=34337
  - methane, nuclear r.f. spectrum obs. 8=47588
  - methylchloride, $2\nu_5$ band near 2880cm^{-1}, parallel component 8=43374
  - p-methyl-2′-methoxybutylbenzene crysts. rel. to mol. π e chord symmetry, 20°K 8=30648
  - methoxynitropyridine, u. v. absorpt. 8=34356
  - methoxypyridine, u. v. absorpt. 8=34356
  - methylcyclopropane, microwave spectra 8=47665
  - methyl iodide, resonances perturbing ν_5 band 8=25594
  - methyleniminyl free radical, electronic absorpt. 8=34337
  - methylsilanes, far u. v. 8=25592
  - mixed crystals 8=41159
  - molecular crysts., absorpt. and vibronic spectra, dynamic theory 8=39860
  - molecules, triplet state props. and spin-orbit and spin-spin interactions 8=25409
  - naphthacene in n-paraffin solvents, electronic spectra rel. to phase transitions of solvent 8=25938
  - naphthalene cryst., theory 8=49772
  - naphthalene, Davydov splittings of intense transitions 8=35048
  - naphthalene, effect of solvents on near u. v. absorpt. 8=34870
  - naphthalene, fluorescence and absorpt. conc. depend. in n-heptane, cyclohexane 77°K 8=49830
  - naphthalene soln. in cyclohexane, $^1B_{3u-}$ state, intersystem crossing 8=43839
  - 1, 4-naphthoquinone, absorpt. obs. 8=43393
  - 1, 4-naphthoquinone and derivatives, emission obs. 8=43392
  - napthalene, Davydov splittings of intense transitions 8=35048
  - napthalene soln., triplet-triplet extinction coeff., 4130 Å 8=25926
  - n-nitroaniline, cryst., stimulated Raman scatt., fermi reson. splitting, 77°K 8=41160
  - nitrobenzene, induced Raman scatt., sensitizing by cyanine dyes 8=34871
  - nitroparaffins, solvent effects in u. v. 8=34876-7
  - olefins, u.v. assignments 8=47667
  - orthodiazines, electronic states and radiationless processes 8=27667
  - oxalyl halides, near u. v. absorpt. 8=25612
  - perdeuteronaphthalene, triplet-triplet absorpt. 4500-3800Å, h. p. obs. 8=30491
  - perylene, α-and β-type crysts., high press. 8=41168
  - perylene in crystalline n-paraffin solns., quasi-line temp. broadening, shift and line profile 8=45240
  - phenanthrene-biphenyl mixed crysts. 8=41150
  - phenanthrene delayed fluoresc. rel. to excit. states decay and intersystem crossing, obs. 8=25537
  - phenanthrene, low-lying triplet excit. states absorpt., 0. 4-1. 0μ 8=25616

Spectra—contd
organic molecules and substances—contd
phenanthrolines, fluoresc. and phosphoresc. spectra 8=43382
phenazine singlet-triplet transitions, triplet state assignments and spin-orbit coupling 8=25536
phenazines, cryst. and in soln., absorpt. with polarized light orientation 8=32042
phenoxyl, free radical 8=43420
phenol, 2750 Å electronic band system 8=43378
m-phenylene-bis-phenylmethylene, quintet mol. 8=47669
p-phenylenediamine cations, dimerization of radicals in solns. and solids 8=25657
γ-phenyl-pyridine derivatives, u. v. absorpt., due to position of saturated substitutes 8=29797
phthalazine, n-π^* transitions 8=41170
phthalimide derivatives, radiationless transitions, activation energy determ. 8=34879
phthalocyanines, polycryst., visible region 8=36444
picene, low-lying triplet excit. states absorpt., 0.4-1.0μ 8=25616
polyvinyl alcohol, electronic absorpt. 8=30492
porphin type cpds., NH oscills. found, problem of internal H bond 8=34353
porphyrins, Stark effect 8=43388
porphyrins, Zeeman effect 8=43387
pyrazole 3(5) and 4 isomer derivs., u. v. and i. r. absorpt. 8=34361
pyrene, flash excited absorpt. 8=43840
pyrene, low-lying triplet excit. states absorpt., 0.4-1.0μ 8=25616
pyrene in n-paraffin solvents, electronic spectra rel. to phase transitions of solvent 8=25938
pyridine, CNDO calc. of electronic spectra 8=29767
radiant thermal conduction effect on 8=46242
Rochelle salt crystals, vacuum u.v. spectra 8=36441
rubrene, crysts. under press. 8=49779
salicylanide, u.v. 8=38903
substituent consts. calc. 8=34311
tetra methylammonium-uranylchloride, luminescent, polarization 8=41166
tetracene, cryst. under press. 8=49779
tetrahalophthalic anhydride complexes with aza-aromatics 8=38902
tetraidoethylene, vibrational spectra and force 8=43396
tetraphenylbutadienes, effect of intramolec. twisting 8=39390
s-tetrazine, gaseous, 5515Å electronic transition 8=25627
s-tetrazine, visible bands 8=25628
thienothiophenes, isomeric, electronic spectra 8=43399
thiophene, monoalkyl substitutes, scatter and i. r. absorpt. 8=34364
tributylphosphate, association with H_2O in organic solvent 8=34775
triglycine sulphate and isotypes, i.r. reflection, rel. to ferroelectric transition mechanism 8=27290
triglycine sulphate group's ferroelectric crystals 8=49776
trimethylene selenide 8=29802
trimethylene sulphide, $(CH_2)_3S$, crystals i.r. absorpt. and Raman scatt., 8=41171
trinitrobenzene crystal, complexes, high press. 8=27635
triplet-triplet transitions, extinction coeffs. 8=34293
triromobenzene singlet-triplet transitions, triplet state assignments and spin-orbit coupling 8=25536
trinitrofluorenone cryst. complexes, high presss. 8=27635
urethanes, substituted, C–Br bond 8=49780
xanthene dyes in 2-chloroethanol, $T^* \leftarrow S$ bands in absorpt. 8=30494
CH^+, $^1\Delta \rightarrow {}^1\Pi$ and $^3\Sigma \rightarrow {}^3\Pi$ band systems 8=38942
Ce^{3+} organic liq. complexes, absorpt. 8=34873
Co acetate tetrahydrate, absorpt. obs. 8=32046
Cu acetate monohydrate, rel. to anomalous mag. behaviour 8=36434
Ho ethylsulphate, absorpt. and Zeeman effect of $^5I_8 \rightarrow {}^3K_8$ and $^5G_4$ transitions 8=49777
Mn acetate tetrahydrate, absorpt. 8=49740
N-salicylideneaniline in H_2O-methanol, hydrolysis 8=48164
NH_3^+ substituent in π-electron systems, inductive effect 8=25525
Ni dimethylglyoxime, spectral shift for high press. meas. 8=50477
X-H bond stretching vibr. intensities in gas to CCl_4 solns. transition, obs. 8=34298
organic molecules and substances, infrared
acenaphthenequinone, vibrational spectrum 8=43282
acetophenone-$SbCl_3$ complexes in CCl_4 8=34866
acetyl radical, rel. to force fields and bond orders 8=43419
acetylene, cryst. phases 8=27618
acetylene, monosubstituted, solns., $C \equiv C$ group absorpt. band intensity rel. to intermol. H-band form. 8=34301
acetylene-t_2 8=25529
acrylonitrile-metal complexes 8=38865
aliphatic ethers 8=29777
aliphatic mononitriles 8=38867
alkali ions in tetrahydrofuran soln. 8=25931
alkyl-Hg(II) cpds 8=43350
alkylphenols, 5-component, analysis 8=34350

Spectra—contd
organic molecules and substances, infrared—contd
alkylpyridine complexes of transition metal cations 8=29763
allene-h_4 and-d_4, vibr. rot. transitions 8=47633
$\alpha\beta$-unsaturated ketones 8=29788
amine–BF_3, absorption of charge transfer complexes 8=25539-40
amino benzene sulphonic acids, isomeric 8=29801
α-aminoethylphosphonic acid 8=47666
aminopyridines and deuterated analogues, obs. 8=43391
aniline adsorbed from CCl_4 soln on Cab–O–Sil silica 8=48474
anthracene crysts. 8=49768
anthracene-d_2(9, 10), vibr. spectrum, 400-3100 cm^{-1} 8=38869
aromatic non-planar hydrocarbons, absorpt. intensities of CH-stretching vibrs. 8=34344
aromatic planar hydrocarbons, absorpt. intensities of CH-stretching vibrs. 8=34343
aryl-Hg(II) cpds 8=43350
aryl sulphanilides, n-substituted 8=34307
aziridines and N-deutero derivs., rel. to structure 8=34309
benzene, adsorbed on Aerosil 8=44076
benzene-2, 1, 3-thio(seleno) diazoles, vibrational spectra 8=43356
benzenes, monosubstituted, correl. of i. r. intensities with chem. reactivity 8=43253
benzenes, substituent effects on l. f. vibrs. 8=47642
benzyl and substituted benzyltin cpds 8=29765
benzyl compounds, vibrational frequencies 8=43361
biphenyl, re-analysis 8=34348
biphenylene, vapour, soln. and cryst. 8=29770
bis(trifluoromethyl)-peroxide 8=43366
bromobenzaldehydes, liq., vibr. obs. 8=43834
p-bromobenzaldehyde, solid, vibr. obs. 8=43834
bromocyclobutane 8=25566
bromocyclobutane, and 3 isotopic species, liq. and vapour, rel. to structure 8=29771
n-bromo phenylsulphonylchloride, absorption, in polarized light 8=41169
butanone-2-oxime in solvents, association determ. 8=43763
3-butenenitrile, rotational isomerism 8=25551
2-butenes, cis and trans 8=25552
butyl chloride (tertiary), liq. and cryst. 8=32044
n-butylamine and N-deutero derivatives, H and D bridge bonds 8=27620
carbon tetrachloride, difference bands 8=38874
carbon tetrafluoride, collision-induced rotational, theory 8=47658
carbonyl group of semicarbazides, semicarbazones and pyrazolecarboxamides, i. r. abs. 8=47645
carboxylic acids, H-bonding 8=25554
cellulose acetate films 8=32048
chars, O^{18}-labelled, rel. to 1600cm^{-1} band origin 8=43345
p-chlorobenzonitrile, absorpt. obs. 8=43357
copolymers, graft, obs. 8=29871
cyanamide, far i.r. 8=48710
cyclobutanol, and Raman spectra 8=25566
cyclopentene, far i. r. and ring-puckering 8=34325
cyclo-propene, -1, 2-d_2, Raman, vapour and solid phase i.r. spectra obs. 8=43362
cyclopropane-H_6 8=43363
dialkyl disulphides 8=43349
dialkyl-Tl(III) cpds 8=43351
diaryl disulphides 8=43349
n-dicarboxylic acids, crysts., far i.r. 8=27631
2, 5-dichloro-1, 4-xylene and 4, 5 dichloro-1, 2-xylene crysts., and cryst. structure 8=39833
dichlorocarbene in solid Ar 8=29775
dichlorocarbene in solid Ar 8=29775
dicyanodiacetylene Σ_g^+ modes, absolute Raman intensities 8=26031
1, 2-dichloroethane in various solvents, rel. to potential barrier 8=43855
diethylmethylsulphonium cpds 8=29776
diethylether, coordination compounds with $MgBr_2$, $ZnCl_2$ and AlX_3(X=Br, Cl) 8=25569
difluoroacetone, symmetrical, rotational isomerism 8=29783
2, 5-dihydroxy-para-benzoquinone, absorpt., and u. v. 8=34318
1, 4-dihydroxyanthraquinone, rel. to hydrogen bonding 8=34305
dimethyl NPX_2(X=F, Cl, Br), gas, liq. and solid, vib. anal. 8=43372
dimethylphenylarsine 8=43381
di-n-butyl diselenide 8=43349
dinitrotetramminecobalt(III) complexes 8=45241
1, 3-dioxolane, far i. r. 8=25567
diphenyl-Tl(III) cpds 8=43351
ethane-1, 1, 1-d_3, near-i. r. 8=25570
ethyl alcohol, rel. to struct. and thermodynamic props. 8=30401
ethylamine and N-deutero derivatives, H and D bridge bonds 8=27620
ethyldimethylsulphonium cpds 8=29776
ethylene imine, absorption, at 90 and 10°K 8=25568
ethylene-methacrylic acid copolymers 8=41173
m-fluoroaniline, liq., obs. 8=43833

Spectra—contd
organic molecules and substances, infrared—contd
furan, methyl-substituted, vibration spectra 8=43368
guanidine, matrix-isolated 8=25583
H-bonded systems, solid and liquid, review 8=38887
H-bonded systems, theory 8=38787
heterocyclic compounds, CH valency oscills. 8=38861
hydrazine, cryst., normal co-ord anal., force consts. and 8=45244
imidazole 8=29787
imidazole, far i.r. 8=41165
ketones, absorpt. band, temp. depend. 8=34319
liquid, effect of local intermol. field 8=34861
macromolecular systems analysis, review 8=34393
maser application 8=38782
methallyl iodide 8=43370
methane, and deuterated, collision induced absorpt. 8=47657
methane, and deuterated, collision-induced rotational, theory 8=47658
methane, compressed, rot. correl. functions and intermolecular torque calc. 8=38894
methane in solid Ar 8=27634
methane, liq. and solid solns. in inert gases 8=25932
methaneselenol 8=25602
methoxyl group detection 8=47661
methyl alcohol, rel. to struct. and thermodynamic props. 8=30401
methyl alkali halides, matrix-isolated 8=47656
methyl aromatic hydrocarbons, conformation of CH$_3$ group 8=29789
methyl BF$_2$, gas, fine struct. due to internal rotation 8=29793
methyl bromide, vibration-rotation, near 6000 cm^{-1} 8=47659
methyl chloride, perturbations in ν_4 band 8=34334
methyl fluoride 8=43371
methyl halides, absorpt. intensity rel. to C-H bond electron cloud distrib. 8=43373
methyl iodide, liq., band shapes 8=39379
methylamines, internal rot. effects 8=47655
methyldiboranes, characteristic i. r. freqs. 8=34335
methyldiphenylarsine 8=43381
methylphosphonic acid 8=47666
methylstannane 8=43369
methylvinylsuphide 8=38899
naphalene vapour, absorpt. rel. to e transitions, 30 000-53 000 cm^{-1} 8=38900
nitriles, absorpt. band, temp. depend. 8=34319
nitromethane, gas, fine struct. due to internal rotation 8=29793
organotrichlorosilanes, l. f. vibrations 8=47620
para-dithiane, fine structure mechanisms, at 15°K 8=27632
perbromocyclopropane 8=25565
perchlorocyclopropane 8=25565
perfluorocyclopropane 8=25565
phenol, H-bonded with vinyl derivatives 8=43379
o-phenylenebis (dimethylarsine) 8=43381
phenyl group IV-A cpds. 8=38901
polar cpds in crystalline phases, rel. to dielec. constant transitions 8=27617
poly-2, 2′-octamethylene-5, 5′-dibenzimidozole rel. to amorphisation in annealing, obs. 8=26158
phenol, struct. in ground and first excited state 8=25614
phenyl derivatives of Ge, As, and Sb 8=34352
phenylgermane 8=25615
phthalic acid distribs., infrared spectroscopic determ. of isomers 8=34346
polymers, freq. distribs., 8=47736
polyvinyl alcohol, dehydrated fibre, i. r. obs. 8=34396
poly(vinylidene fluoride), α- and β-crysts., rel. to fundamental modes, obs. 8=44306
n-proplylamine and N-deutero derivatives, H and D bridge bonds 8=27620
polystyrene sulphonic acid, effect of hydration 8=48165
pyrazolecarboxamides, i. r. abs. of carbonyl group 8=47645
pyridazine, and deuterium analogues 8=25933
pyridine derivs., rel. to ν(CH) bands near 3000 cm^{-1} 8=29799
pyrimidines, polysubstituted, 700-200 cm^{-1} 8=47670
quinoline and isoquinoline, at liq. N$_2$ temp., and interpret. of fund. vibrs. 8=34362
quinone adducts and derivs., Diels-Alder, correl. for carbonyl and C-C double bonds 8=25924
salicylaldehyde obs. 8=43394
semicarbazides, i. r. abs. of carbonyl group 8=47645
semicarbazones, i. r. abs. of carbonyl group 8=47645
silacyclobutane 8=29800
steric factors of H-bonding 8=25639
symmetric tops, computer anal. 8=25412
terpene alcohols, and related cpds, rel. to correl. of struct. and i.r. absorpt 8=39381
tetracyanoethylene charge transfer complexes, polarized spectra, vibr. assignment 8=38879
tetrahydrofuran and deutero-substitutes, vibration spectra 8=43397
tetrahydrofuran, far i. r. 8=25567
trichloromethyl radical in solid Ar 8=29831
triethylsulphonium cpds 8=29776
trifluoromethylphosphonylchloride 8=34330
triglycine sulphate crystals; isomorphous with ferroelectrics 8=49774

Spectra—contd
organic molecules and substances, infrared—contd
triphenylarsine 8=43381
triphenylarsine, mol. addition compounds with SnX$_4$ (X=halogen), stretching vibs. freq. shifts 8=25631
triphenylphosphine, and complexes 8=43380
triphenylphosphine, mol. addition compounds with SnX$_4$ (X=halogen), stretching vibs. freq. shifts 8=25631
triphenylphosphine oxide, and complexes 8=43380
urotropin and Br, I complexes, vibr. analysis and bond strengths, 4000-350 cm^{-1} 8=49781
vinyl acetylene, absorpt., electro-optical parameters 8=34365
vinyl bromide, deuterated 8=47672
vinyl diacetylene, absorpt., electro-optical parameters 8=34365
Ag halide complexes, far i. r. 8=27619
BF$_3$-amine, absorption of charge transfer complexes 8=25539-40
BF$_3$S(CH$_3$)$_2$ 8=25541
C$_2$Br$_2$, absorpt. band assignments to normal modes of vib. 8=45236
C$_2$Cl$_2$, absorpt. band assignments to normal modes of vib. 8=45236
(CD$_3$)$_2$C=O, torsional vibr. 8=25601
(CD$_3$)$_2$NH, torsional vibr. 8=25601
C$_6$D$_5$GeCl$_3$ 8=25615
C$_6$D$_5$GeCl$_3$ 8=34351
(CF$_3$)$_4$As$_2$ 8=25604
(CF$_3$)$_2$PF$_3$ 8=25576
CF$_3$PF$_4$ 8=25576
CF$_3$SF$_5$ 8=25516
CF$_4$, collision induced absorpt. 8=29772
(CH$_3$CD$_2$)$_2$O-AlX$_3$(X=Cl, Br) coordination compounds 8=25569
CH$_3$CH$_2$Br, torsional vibr. 8=25601
C$_2$H$_6$, CH$_3$CD$_3$, and C$_2$D$_6$, torsional vibr. 8=29778-9
CH$_3$CH=CH$_2$, torsional vibr. 8=25601
CH$_3$CH$_2$Cl, torsional vibr. 8=25601
(CH$_3$)$_3$CNCO 8=29732
CH$_3$D, in matrices, nuclear-spin-species conversion 8=38830
C^{13}H$_3$Cl, vibr.-rot. bands 8=29794
CH$_3$NF$_2$ and CD$_3$NF$_2$ 8=25597
CH$_3$OPCl$_2$ and CD$_3$OPCl$_2$ 8=38892
CH$_3$SiHD$_2$ 8=25603
CH$_3$SiHD$_2$ 8=34338
CN, absorpt., effect of acetonitrile conc. in CCl$_4$ 8=34319
C$_2$I$_2$ absorpt. band assignments to normal modes of vib. 8=45236
Cd halide complex with azines 8=36432
Cu phthalocyanine, cryst. emission 8=41021
Ge(C≡CH)$_4$ 8=25625
H$_2$O, absolute intensity meas. of dipole moments 8=38837
Hg halide complex with azines 8=36432
I$_2$ charge-transfer complexes, far i. r. intensities 8=25586
ICl charge-transfer complexes, far i. r. intensities 8=25586
N-vinyl cpds. 8=47671
Si(C≡CH)$_4$ 8=25625
Sn(C≡H)$_4$ 8=25625
Zn halide complex with azines 8=36432
organic molecules and substances, radiofrequency
See also Nuclear magnetic resonance and relaxation; Paramagnetic resonance and relaxation.
acrylic acid, rotational isomers, microwave freq. 8=34303
acryloyl fluoride 8=38864
allyl alcohol 8=25533
allyl cyanide, microwave obs. 8-26 GHz 8=34304
cis-1-chloro-2-fluoropropene 8=34320
1-chloroaziridine 8=25556
2-chloroethanol, microwave 8=25557
cyclopropanecarboxaldehyde 8=25562
cyclopropanone 8=29774
difluoro-1-1-chloro-1-ethane, microwave 8=25575
2, 2-difluoro-1-methylcyclopropane 8=29792
dimethylamine 8=25599
dimethylamine 8=47660
ethyl formate, rotational isomers 8=25572
ethylene oxide, microwave double reson. 8=25634
ethyliodide, microwave double reson. 8=25634
heterocycles, five-membered, N^{14} nuclear quadrupole reson. 8=25638
isoxazole, microwave 8=25613
methanol, mm wave 8=47654
methyl chloroform, internal rot. 8=29773
methyl vinyl ether 8=29790
methylene fluoride, Zeeman effect 8=34339
1-methylpentaborane 8=25600
1-methylpentaborane(9) 8=29791
microwave, review of techniques 8=33140
nitriles, saturated, quadrupole resonance 8=25642
piperidine, non-rigid rotor transitions 8=25617
pivaldehyde, microwave 8=25618
propargyl alcohol 8=43389
propargyl alcohol, rot. isomerisms rel. to COH, CNH$_2$ groups 8=25532
propargyl amine, rot. isomerisms rel. to COH, CNH$_2$ groups 8=25532
propionic acid, microwave 8=25620
propylene, deuterated 8=43390

Spectra—contd
  organic molecules and substances, radiofrequency—contd
    pyridazine, N^{14} quadrupole resonance 8=25643
    pyridines, substituted, N^{14} quadrupole resonance 8=25643
    pyridinyl diradicals, stable, intramolec. assoc. by e.p.r. study 8=43424
    pyrimidine, N^{14} quadrupole resonance 8=25643
    selenophene 8=43395
    trans 1-bromopropylene 8=25550
    trifluoromethylphosphine 8=25574
    CF_2, unstable mol. 8=25468
    CH_3D, elec. reson. 8=38896
    N-methylpyrol, hindrance pot. of internal rot. 8=29798
    N-vinyl cpds., n. m. r. 8=47671
Spectral line breadth
    See also Doppler effect; Stark effect; Zeeman effect.
  absorption band, apparent bandwidth parameters, obs. 8=24388
  absorpt. band, estimation of position of intensity maximum 8=43150
  anthracene, fluoresc. in host crysts. at high press. 8=49822
  azulene, elec. field broadening of electronic transitions 8=45238
  broadening and shifting of V, Cr, Mn, Fe, Co and Zn, rel. to plasma temp. meas. 8=47813
  broadening, combined Doppler and collision 8=43235
  broadening, non-uniform, of operating transition line, effect on dynamics of processes in media 8=43247
  broadening of H stretching peak on H bonding 8=49733
  effects of coherent multiple scatt. and beam convergence 8=25403
  collision broadening, distorted-wave approx. 8=47556
  crystal, mol., reorientation rel. to vibr. i. r. absorpt. 8=36292
  diatomic molecules, rel. to Debye forces of dispersion and induction 8=25407
  distorted-wave approx. for rot. and vibr.-rot. linewidths 8=47556
  Doppler and collision broadened profiles, isolated lines 8=43165
  Doppler and collision, combined, broadened profiles, equiv. widths of isolated lines 8=43161
  Doppler narrowing in standing light wave 8=47970
  electron collision broadening, theory 8=43157
  of electron spin resonance oscillator 8=33144
  e.p.r. meas. of mag. susceptibility 8=46508
  equivalent, growth curve construction by computer 8=28776
  Fabry-Perot high-resolution spectrometer meas. 8=28806
  formation by noncoherent scatt. 8=37232
  impurity states in crystals, by resonant phonon interactions 8=41027
  instrumental broadening, correction for Littrow mount grating spectrometer 8=42223
  ion linewidths, formulae for predicting 8=38718
  ions, e collision excitation cross-section theory 8=43210
  laser diode, spontaneous emission effect of band-tailing 8=46602
  laser, gas, inhomogeneous broadening, optimum output coupling 8=37567
  laser-induced narrowing, freq. spectrum, theory 8=29589
  laser, solid, rel. to non-linear mode interaction 8=33193
  Lorentz half-width in atomic spectroscopy, graphite cuvette applic. 8=38619
  Lorentz line, equivalent width, accuracy of simple approx. 8=34126
  Lorentzian e.p.r., modulation-broadened, intensity determ. 8=43402
  methyl halides, rot. lines 8=38889
  modulation broadening of unsaturated mag. resonance line shapes 8=47674
  natural line-breadth, theory 8=47465
  plasma, optically thin layer, emission 8=47846
  plasma spectrum 8=30092
  plasma, Stark broadening in strong mag. and elec. fields 8=25340
  Raman linewidths for stimulated threshold and gain calcs. 8=39372
  resolution method, uniformly broadened 8=33261
  ruby, e.p.r. inhomogeneous broadening 8=49597
  scattering theory of press. broadening of rot. and vibr.-rot. transitions 8=47558
  sensitivity of recording spectral lines limitation 8=24386
  Stark broadening, transition from quasi-static to impact electron contrib. 8=43158
  stars, blue horizontal-branch, obs. 8=32479
  strain broadened spin resonance line shapes, broadening by point defects 8=49589
  symmetric-top mols., rot. lines 8=38889
  tetracene, fluoresc. in host crysts. at high press. 8=49822
  2-body relativistic collisions, kinematic broadening 8=47028
  van Vleck-Weisskopf line shape 8=34197
  velocity-dependent broadening, line absorpt. coeff. profiles 8=43164
  Ar, in plasma torch 8=43181
  Ar II multiplets, Stark broadening temp. depend 8=39028
  C, broadening of lines due to pressure increase 8=45652

Spectral line breadth—contd
  C resonance lamp, band identification 8=43288
  C II, e impact broadening calc. 8=47507
  CH_3CCH, rot. lines 8=38889
  CH_3CN, rot. lines 8=38889
  CHF_3, microwave, quadrupole moment determ. 8=29729
  CO_2 in crit. region, Rayleigh scatt. for thermal diffusivity calc. 8=39241
  CO_2 in Martian atm., 1.05μ spectrometry 8=45828
  CO_2, 9.4 and 10.4μ bands 8=43289
  Ca atom, effect of Na impurity in arc discharge 8=34437
  Cd, 3261Å collision broadening by Ar gas, pressure and temp. dependence 8=38750
  Cs absorption line, influence on optical pumping 8=25374
  Cu atom, effect of Na impurity in arc discharge 8=34437
  H, excited, in plasma, broadening mechanism 8=34505
  HCl, first rotational, determ. 8=38825
  HR 9080 variable star, Hβ, γ, δ obs. 8=28083
  He, 3889, 5016 Å lines, Stark broadening 8=47841
  Hg, 2537 Å line broadening and shift by H_2 impact 8=43194
  Hg 2537 Å line broadening in presence of Cd, Zn and Mg vapour 8=43193
  Hg atom, double-resonance broadening, 6^3P_1 state 8=38732
  Li, emission line width study of plasma in arc discharge 8=47778
  Mg II, e impact broadening calc. 8=47507
  N, broadening of lines due to pressure increase 8=45652
  NO, J = $\frac{1}{2} \to \frac{3}{2}$ rot. absorpt. 8=47605
  N_2, Stark broadening 8=34272
  N_2^+, Stark broadened rot. lines, shapes and widths 8=34259
  N_2O, microwave, quadrupole moment determ. 8=29729
  Na-D_1-line, profile and equivalent width as function of temp. and mag. induction 8=25361
  O, at low pressure, anomalous line-broadening obs. 8=29759
  O, broadening of lines due to pressure increase 8=45652
  O_2, Stark broadening in Schumann-Runge system 8=34272
  OCS, microwave, quadrupole moment determ. 8=29729
  S II/III, e impact broadening calc. 8=47507
  Si II/III, e impact broadening calc. 8=47507
  Ti, press. broadening and shift of lines by Ar 8=43204
  Zn atom, effect of Na impurity in arc discharge 8=34437
Spectrochemical analysis
    See also Chemical analysis by mass spectrometry; Spectroscopy.
  absorption spectroscopy, slot burner 8=36637
  atomic absorpt., a. c. scanning method 8=36640
  atomic absorpt. and flame emission simultaneous 8=46700
  atomic absorption filtering meter, twin, with extended scale 8=36639
  atomic absorption, lamp 8=36638
  atomic absorption spectrochem. using hot-tube flame, chamber 8=46684
  atomic emission of acetylene-nitrous oxide flame 8=49985
  cellulose ethers, etherification from i.r. absorpt. obs. 8=27728
  discharge, h. f. at atm. pressure, appl. 8=29889
  electrodeless discharge lamps for atomic fluoresc. 8=41301
  flame optics for atomic absorpt. 8=42238
  flame spectroscopy, Ca, Mg interferences 8=29606
  gas mixtures, isotopically labelled, i. r. method 8=32160
  gases, highly reactive, i.r. exam., high temp. cell 8=41302
  glow-discharge lamp 8=42237
  hollow cathode, simple demountable, for atomic abs. spectroscopy 8=49989
  impurities, gaseous, simultaneous determ. by isotope dilution 8=27783
  i. r. cell for corrosive, volatile mats. 8=36606
  insulating materials, using ionoluminescence 8=40555
  light source, use of Ulbricht sphere 8=42236
  logic algebra applic. 8=41303
  metals, H, O, N joint determ., isotope method 8=27784
  methane-air mixture, three-colour Schlieren system 8=28737
  microspark emission spectroscopy, technique 8=49991
  moisture, spectrophotometric determ. 8=27785
  molecular correlation spectrometry 8=32159
  natural products, use of lasers in Raman spectroscopy 8=27793
  oxide-containing graphite electrodes, thermochem. mechanism 8=34436
  phosphor, photometric standard procedures 8=45418
  photolysis, flash, i. r. detection of transient species 8=3767
  powder mixtures, diffuse reflectance spectrophotometry 8=36636
  powders, d. c. arc fusion method 8=32154
  quantitative, based on n.m.r. dispersion 8=49993
  rare earths, cathodoluminesc. technique 8=36643
  selectivity of optical-acoustic method, acetylene and organic mixing gas in analyzer cell for spectra 8=4998
  specimen-changing device for i.r. spectrophotometer 8=46698
  spectro-analytical function, approximation methods 8=2778
  spectrograph, instrum. function, exptl. determ. 8=24397
  spectrophotofluorometer for absorpt. and transmission 8=46694

Spectrochemical analysis—contd
- standard preparation 8=36644
- steel, emission anal., decomp. and inter-element effects 8=32156
- steel, of C, using vacuum spectrometer interference of Al 8=32155
- substance utilization, improvement by laser 8 =36645
- sun, Ga abundance from sunspot obs. 8=32573
- thermochemistry of samples in carbon arc 8=41237
- u.v. and visible absorption spectrometry 8=46695
- use of universal arc-pulse generator UBI 1 8=43464
- weak lines on continuous background, extraction method 8=27782
- Ag, atomic fluoresc. using hollow cathode lamp 8=36641
- Al in white cast iron, hollow-cathode discharge determ. 8=36642
- Al, prep. of powder briquets 8=32158
- Au(I) in cyanide solns., at. absorpt. spectrometry 8=32162
- B in white cast iron, hollow-cathode discharge determ. 8= 36642
- Bi in white cast iron, hollow-cathode discharge determ. 8=36642
- Br in brines, X-ray fluorescence obs. 8=27815
- Ca and Mg in Ta 8=45416
- Co, nanogram amounts in blood, Cu-spark method 8=49987
- Cs, specialized flame photometer 8=28825
- Cu in acetylene flame, linear absorpt. method 8=27790
- DC-arc emission spectrography, Li cpd buffers 8=27792
- Eu_2O_3 in rare-earth oxide mixtures, u. v. spectrophotometry 8=27786
- F^- determ. by atomic absorption 8=27788
- Fe^{3+}/Fe^{2+} ratios in phosphate and oxide mixtures, Mössbauer quantitative anal. 8=27778
- K and Na determination in fuel rich air-H_2 flames 8=49990
- K content of new tissue growth 8=27787
- Mg alloyed cast iron with C electrode and lasers 8=32157
- Mg in blood plasma, using improved plasma jet equipped with inexpensive atomizer 8=47894
- N^{15} emission spectrometry, enhancement by inert gas 8=27791
- NH_4HF_2-HF electrolytic products, i. r. cell 8=36606
- Os^{187} d. c. arc spectrum method 8=36635
- Pb, in lead crystal, determ. by atomic absorpt. spectrometry 8=27789
- Sb species in vapour from PtSb at 900°C by atomic absorpt. 8=30608
- Si, O analysis, by i.r. spectrophotometer 8=49992
- Sr, atomic absorpt. 8=45417
- U oxide impurities, mixed carrier 8=32161
- Y_2O_3, determ. of trace amounts of rare-earth impurities 8=27794

Spectrometers
- See also Mass spectrometers; Monochromators; Particle spectrometers; Spectrophotometers; X-ray spectrometers.
- astronomical Fourier, 4300-8000 cm^{-1} 8=32413
- astronomical, telescope mounted Mock interferometer, visible and near i.r. 8=32412
- atomic absorption and flame emission simultaneous analysis, multichannel 8=46700
- auto-recording type, for magneto-optical rotatory dispersion 8=37673
- continuously scanning, recording error 8=42233
- conversion from photographic to automatic recording 8=28817
- cross-correlating for vibration-rotation bands 8=42230
- Czerny-Turner, 4m asymmetric, optimization of configuration 8=42231
- Czerny-Turner, lens correction of astigmatism 8=46664
- Czerny-Turner spectrograph, coma compensation 8=28730
- Dobson, mean absorpt. coeffs. for atm. ozone 8=47973
- electron-impact, electrostatic lens 8=47585
- Fabry-Perot, astronomical, for rocket appls., 1700-5500Å 8=32411
- Fabry-Perot astronomical interferometer 8=32415
- Fabry-Perot, double, press. scanned and digital recording 8=28796
- Fabry-Perot, double, scanning synchronization and plates parallel spacing, servocontrols 8=28821
- Fabry-Perot, high-resolution 8=28806
- Fabry-Perot interferometer with electromechanical scanning system 8=46696
- Fabry-Perot, plate spacing automatic control 8=28819
- Fabry-Perot polyetalon, importance of high contrast 8=42220
- focal isolation, amplitude modulated using lens chromatic aberration 8=28797
- Fourier, high resolution, path difference 0-180 cm 8=28830
- Fourier, interferometers and computer system for far i.r. 8=28799
- Fourier lamellar interferameter with saw-tooth drive, far i.r. 8=28812
- Fourier, Michelson interferometer for balloon-borne solar meas., 10-100μ 8=32571
- Fourier transform, i.r., use of two-beam interferometer with 1m path difference 8=28815
- Fourier, Z-cut uniaxial cryst. plate between circular polarizers 8=28802

Spectrometers—contd
- for galactic emission regions meas., multi-lens Perot-Fabry assembly 8=32414
- γ-ray, Ge(Li), total absorption, for improved peak-to-continuum ratios 8=47053
- grating, Girard coding, with photographic plate 8=28822
- grating, multiplex 16-channel, for near i. r. 8=28798
- high resolution, allowable nonparallelism in beams incident on plane diffraction gratings 8=42228
- high-speed, review 8=42227
- i. r., far, double-beam, high resolution 8=28809
- i. r., high-resolution, improvements 8=24404
- i. r., precision calibration and digital recording 8=24401
- infrared, prism, calibration with echelle grating 8=33267
- i.r. radiometer spectral responsivity determ. 8=42232
- i. r., small, description 8=24396
- i.r., synchronized high speed scanning 8=24399
- instrument functions for wide angle Michelson interferom. type 8=28811
- interferometer, lamellar grating far i.r., double-beam differencing 8=28818
- Littrow mount grating, correction of instrumental broadening 8=42223
- mechanical for analysis of energy distrib. of Cu or Au sputtered atoms 8=48915
- optical, laser calibration for colour blind spectroscopists 8=37675
- PEPSIOS three Fabry-Perot, high resolution scanning spectrometer 8=37674
- photoelectric multi-channel, Fabry-Perot etalon and axicon mapping 8=28804
- photoelectron, rel. to photo-ion kinetic energy anal. 8=47784
- for photoelectrons, parallel-plate 8=31470
- plane-grating, heterochromatic fringe prod. 8=46693
- for plasma meas., multichannel Fabry-Perot with Fresnel lenses 8=30089
- plasma transient Stark and Zeeman shifts, Fizeau interferometer meas. 8=30088
- polarization Fourier, field of view and resolution 8=28826
- Raman, resolution improvement by He-Ne laser light source 8=24398
- rapid-response, for i.r. 0. 8-3μ 8=24392
- recording, for derivative spectroscopy 8=24391
- scanning spectroradiometer 8=37676
- SIMAC, Fabry-Perot spectrometer with scanning multi-receiver grating spectrograph 8=28801
- SISAM, resolution 0-03 cm^{-1}, 4-5μ 8=28823
- SISAM, resolutions 200 mK and 27 mK, 0. 8-2. 5μ 8=28800
- slit width, temp. effect 8=46702
- solar spectra meas. in 1-3. 5 μ range at altitudes below 18 km 8=45873
- specimen-changing device, automatic 8=46698
- spectrofluorimeter, fully compensated 8=33263
- spectrograph design (1918-68) 8=33268
- spectrograph, high resolution, 3 prism 8=46697
- spectrograph, instrum. function, exptl. determ. 8=24397
- spectrograph shutter for 10 μsec. exposures 8=33262
- stray light meas. with n filters 8=46701
- tuned laser differential spectrometry, observation of saturation peaks 8=42091
- for twilight and zodiacal light, press. scanned Fabry-Perot 8=32568
- two-crystal, in X-ray spectroscopy, utilization of X-ray beam divergence 8=49690
- u.v. and visible absorption spectrometry 8=46695
- for upper atmosphere, Fabry-Perot, appls. 8=32271
- wide angle Michelson interferom. type, instrument function 8=28811
- GaAs laser diode spectrograph, temp. tunable 8=46589
- **accessories**
  - adaptor for photoelectric recording of Raman spectra with three-prism spectrograph 8=46709
  - cuvette for stimulated emission in solutions 8=46704
  - cuvette, high-temp. for i. r. absorpt. obs. 8=37679
  - delay unit for flash photolysis 8=41285
  - discharge tubes microwave-excited electrodeless for atomic spect. 8=46707
  - explosive high-speed shutter 8=28835
  - Fabry-Perot photoelec., h.f.s. digital calc., programme 8=28829
  - for Fabry-Perot spectra linear transformation, optical prism viewers 8=28834
  - flow burner laminar with i.r. heated spray chamber and condenser 8=46706
  - Fourier inverter for multiplex spectrometer, Simoramic analyser appls. 8=28831
  - Fourier transform analogue computer IFTAC 8=28827
  - Fourier transform analogue computer, optical 8=28828
  - Fourier-transform, digital recording system 8=37677
  - Fourier transform real time synthesizer 8=28832
  - furnace cell with "rectangular" temp. field 8=46708
  - Fuwa tubes, heated, for at. absorpt. spectroscopy 8=46690
  - heated chamber burner for atomic absorpt. spect. 8=46703
  - hot tube for at. absorpt. spectrochemistry 8=46684
  - image splitters, application in spectroscopy 8=28836
  - integrator for 15-2 spectrogram 8=46328

Spectrometers—contd
  accessories—contd
    interference microphotometer for Fabry-Perot ring photographs analogue reduction 8=28833
    micro-cuvette attachment for VSU 2 type spectrophotometer 8=42226
    n. m. r., spin-lattice relax. timing by adiabatic rapid passage 8=42048
    predispenser to avoid superpositioning 8=46710
    prisms, right angle, and dove, making and testing 8=42235
    PTFE cell for corrosive media in 0.22-7 μ range 8=46705
    spectropolarimeter, astronomical, three-channel photoelec. 8=36921
    stellar spectrograph, high speed, design concept 8=36946
    u.s. nebulizer for at. absorpt. spectroscopy 8=46689
    C resistance far i. r. bolometer 8=32939
    Ge doped far i. r. bolometer 8=32939
    InSb far i.r. detector 8=32939
Spectrometers, radiofrequency
    See also Nuclear magnetic resonance and relaxation/measurement; Paramagnetic resonance and relaxation/measurement.
    broad line, improvements 8=46523
    double resonance, freq. sweep, field-freq. stabilized 8=33147
    8-mm, pulse for magn. resonances 8=46502
    e.p.r., for low mag. field spin-lattice relax. 8=46507
    e.p.r., limiting sensitivity at high power levels 8=46503
    e. p. r., new French instrument 8=42045
    e.p.r., push-pull field modulation, advantage for minimizing absorption of "empty-cavity" 8=46510
    e.p.r., sensitivity redefinition 8=28637
    e.p.r., under irradiation 8=46504
    e. p. r., X-band, with ruby maser preamplifier 8=33146
    e. s. r. balanced detector 8=33142
    free precession, expts. in terrestrial mag. field 8=46518
    high level, autodyne used in Cl n. q. r. 8=37545
    microwave noise spectrometer, sensitive,
    n. m. r. freq. sweep synchronization to computer memory scan 8=42047
    n.m.r., high resolution, freq. swept proton stabilized 8=46525
    n. m. r., marker generator circuit 8=41916
    n. m. r., using coaxial components 8=33151
    n. m. r., permanent magnet 8=33152
    n.q.r. detector, coaxial bridge with helical line sample holders 8=46529
    n.q.r., superregenerative n.q.r. of $Cu^{63,65}$ in Cu_2O, meas., temp. variations 8=31927
    nuclear quadrupole resonance, f. e. t. appl. 8=28640
    n.q.r., temp. control 8=46528
    propagation of e.m. wave on shorted helix of microwave spectrometer 8=46488
    sensitive nuclear pulse apparatus with digital signal averaging for solids 8=46521
    for spin-echo obs., 180-250 MHz 8=49625
    square-wave generator, bidirectional, for mag. resonance 8=33141
    superconductive, high-resolution, Du Pont instrument general performance information 8=46517
    superregenerative n.q.r., automatic coherence control 8=24264
    whole-body n. m. r. spectrometer 8=32618
    X-band, for paramag. dispersion obs. and ENDOR meas. 8=46511
Spectrophotometers
    astronomical, Fabry-Perot use with telescope, non-uniform illum. effects 8=32410
    atomic absorpt. spectroscopy, lamps 8=36638
    attachment for meas. of reflection coeff. 8=46691
    Beckman DK-2 recording type, accurate temp. control 8=24402
    derivative, self-modulating, and characts. 8=33269
    double beam vacuum, for far u.v. 8=24395
    double-beam vibrating mirror flying spot scanning-integrating microspectrophotometer 8=24394
    Fabry-Perot, for isotopic abundances meas. 8=28803
    Fabry-Perot, photoelec., press. scanned for low intensities 8=28820
    i.r., recording time decrease by automatic control of scanning speed 8=42224
    linearity testing by supplementary light methods 8=42229
    micro-cuvette attachment for VSU 2 type 8=42226
    Perkin-Elmer, reflectance attachment for powder obs. 8=28824
    PTFE cell for corrosive media in 0.22-7 μ range 8=46705
    in rotatory dispersion adapter 8=24370
    sample furnace for 50°-1000°C 8=33266
    for solar and daylow meas., photoelec. Fabry-Perot, magnetostriction scanned 8=32272
    SPECORD-UV-VIS type, specifications 8=42222
    spectrophotofluorometer for absorpt. and transmission 8=46694
    system specialized for Cs 8=28825
    2-photon automatic registration 8=42225
    vacuum u. v., double beam, rotating cell 8=33265
Spectrophotometry
    See also Colorimetry.
    atomic absorption analysis, critical review 8=46692
    atomic absorption flame, design of heated spray chamber 8=46706
Spectrophotometry—contd
    atomic absorpt., with u. v. filters 8=28805
    atomic resonance lines, isolation and detection 8=46699
    diffuse reflectance, powder mixture spectrochem. analysis 8=36636
    dispersed spectra in any wavelength region, real time multiplexing 8=42221
    flame photometry, design for clinical lab. 8=42134
    galaxies, five-colour intermediate-band 8=41508
    HR9080 variable star, Balmer line breadth 8=28083
    line photometry and influence of Eberhard effect 8=28795
    linearity testing by supplementary light method 8=42229
    moisture determ. appl. 8=27785
    molecular correlation spectrometry 8=32159
    Raman spectrography using image intensifer tube 8=38781
    spatial frequency, new method 8=28793
    starclusters, five-colour intermediate-band 8=41508
    stars, five-colour intermediate-band 8=41508
    Eu_2O_3 in rare-earth oxide mixtures, u. v. determ. 8=27786
    F^- in aq. soln., determ. by atomic absorpt. 8=27788
    Hβ, of F dwarf stars, for temp. determ. 8=45649
    W lamp for standard source, astron. appl. 8=45667
Spectroscopy
    See also Spectra; Spectrometers; Spectrophotometry.
    absorption calc., net interval requirement 8=28794
    arc and hollow cathode discharge tube, sensitivity analysis 8=29578
    atom-absorpt. analysis, discharge electrode pulse heating 8=29877
    atomic absorption, aerosol production 8=48239
    atomic absorption spectrochem. using hot-tube flame, chamber 8=46684
    atomic absorption, use of high temp. flames, review 8=46686
    atomic absorption, use of ultrasonic nebulization 8=46689
    atomic, applications of microwave-excited electrodeless discharge tubes 8=46707
    atomic emission of acetylene-nitrous oxide flame 8=49985
    Coudé, use of cascade intensifier 8=28773
    convolution rel. to resolution and signal:noise ratio 8=28785
    Czerny-Turner spectrograph, 4m asymmetric, optimization of configuration 8=42231
    derivative, with recording spectrometers 8=24391
    development in USSR (1917-67) 8=33234
    dispersed, spectra in any wavelength region, real time multiplexing 8=42221
    electric-field-induced spectra 8=38881
    electron impact, low-energy 8=25384
    electron-impact spectra at 33-100 eV energies 8=47585
    emission spectra, absorpt. method for determination 8=24385
    epitaxial layers of wafers, i. r. depth determ. 8=26108
    Fabry-Pérot polyetalon spectrometer, importance of high contrast 8=42220
    Faraday rotation meas. in megagauss fields 8=46683
    fiber, optic polychromator for separating pulsed plasma emission lines 8=37662
    flame, applic. of separated flames 8=46685
    flash, monochromatic, with Hg reson. radiation 8=24389
    Fourier, by transmission grating resons. scanning 8=28787
    Fourier, intensity error from finite series approx. 8=28781
    Fourier, interferograms modulation by source noise 8=28780
    Fourier, rapid repetitive scanning for faint sources 8=28791
    Fourier, resolution and noise 8=28779
    Fourier transform, asymmetric, pseudo-coherence effect 8=24390
    Fourier transform digital calc. 8=28788
    Fourier transform., for astrophysical line profiles obs. 8=42217
    Fourier transforms digital calc. 8=28789
    Fourier, use of Mobius band tilt compensated interferometer 8=28814
    Fourier, use of rapid scanning Michelson interferometer with cats eye reflectors 8=28813
    gases, highly reactive, high-temp. i.r. cell. 8=41302
    giant pulse laser, ruby time-dependent freq. shifts 8=42054
    holography, white-light reflection, appls. 8=28896
    Holstein problem, 8=46688
    illumination value, balanced system for determ. 8=37678
    image splitters, application in spectroscopy 8=28836
    i. r. absorpt. band intensity eval. from meas. above room temp. 8=30484
    infra-red and Raman 8=24405
    infrared detection of transient species from flash photolysis 8=37672
    infrared, logico-formal integration according to charact. freqs. 8=24387
    i. r. of micro quantities, tech. using AgCl sheet as supporting matrix 8=24403
    instrumental methods, review 8=28777
    integrated absorptance for simple spectral lines and lines with hyperfine struct. and isotope shifts, asymptotic expansions 8=29590
    interference photographic meas. method 8=28792

Spectroscopy—contd
  interferogram phases rel. to spectra analysis 8=28782
  interferograms zero-order correction and extrapolation 8=28783
  laser isotope shifts, i.r., variable length cavity meas. 8=28652
  laser-Raman, current progress 8=25397
  light, spectral composition rel. to photon beats 8=33259
  limiting sensitivity of recording spectral lines 8=24386
  line recording, sensitivity as function of instrument, source and radiation detector 8=28778
  line shapes by magnetic scanning 8=28784
  line-strengths meas. at low press. 8=42218
  low noise solar and laboratory, PbI 7229 Å line and solar Pb abundance 8=45866
  magnetic circular dichroism applic. 8=33257
  magnetic materials, far-i. r., techniques, mag. ion spectra and magnon absorpt. in antiferromagnets 8=36294
  magneto-optical rotatory dispersion applic. 8=33257
  Michelson interferometer, and for absorption and refractometry 8=33272
  microwave molecular, review of developments at Duke 8=37534
  molecular and quantum chemistry 8=47553
  molecular beam elec. reson., at Berkeley 8=25405
  molecular, review of maser applic. 8=38782
  Mössbauer, using high-field superconducting magnets 8=37387
  multiple internal relfection, appl. to adsorbed layer conformation 8=39612
  multiplex, theory, instrums. and appls. 8=28786
  n.m.r. pulsed, fast recovery probe and receiver 8=36256
  nuclear, pulse shaping by time-dependent filter 8=46339
  optical amplifier, linear, wide-band, by stagger tuning 8=28654
  optical and r.f., effect of virtual transitions 8=47473
  organic mols., laser flash spectroscopy 8=43341
  of particles, atoms or mols., and atomic nuclei 8=46687
  plasma density and temp. fluctuations meas. 8=25759
  polarized, correction factors 8=24426
  pulse plasma jet diagnostics 8=34511
  pulsed laser, use of defocused Fabry-Pérot interferometer 8=42250
  rare earth ions, magnetoelastic coupling constants, from optical data 8=31229
  reabsorption method using Fabry-Pérot etalon 8=33260
  reflection nebulae, star obs. 8=32472
  Ritz standards from Th I energy levels obs. 8=47509
  scanning and averaging spectra of nanosec. pulsed light sources 8=42234
  scattering substs., weakly absorbent, plane sample method 8=33258
  slit-less by selective modulation, and appls. 8=28790
  solutions in liquified gases, apparatus for study of abs. spectra 8=30486
  spectroanalytic problem, general method of finding optimal soln. 8=33256
  spectrograph design (1918-68) 8=33268
  spectrophone meas. laser beam absorption in gas 8=39218
  spectroradiometer, spectral distribution of daylight, data collection 8=27900
  superpositioning avoided with predispenser 8=46710
  thermal diffusion, application 8=30322
  transmission i.r. prep. of powder samples 8=42239
  transparent electrodes, internal reflec. 8=41280
  ultrasonic of material defects 8=23964
  u.v. and visible absorption spectrometry 8=46695
  u. v. instruments, spurious obs. of scatt. light 8=28807
  in u.v., relative intensities of selected lines, photoelec. compared with photographic meas. 8=42219
  uniformly broadened line, resolution method 8=33261
  vacuum u.v., instrumentation, bibliography 8=24384
  Ca flame, at. fluoresc. interferences 8=29606
  Mg flame, at. fluoresc. interferences 8=29606
  N plasma jet, tel. to temp. determ. 8=30183
  PbI 7229 Å line and solar abundance low noise solar spectroscopy 8=45866
 light sources
  delay unit for flash photolysis 8=41285
  dipped-cathode arc 8=28840
  electrodeless discharge lamps for atomic fluoresc. anal. 8=41301
  flames, high temp. for atomic absorpt. spect., review 8=46686
  flame optics for atomic absorpt. 8=42238
  flames, separated 8=46685
  gas discharges, electrodeless, microwave excitation 8=29873
  gas laser, applic. 8=42080
  glow-discharge lamp for spectrochem. anal. 8=42237
  hollow cathode lamp for atomic fluoresc. 8=36641
  hollow cathode lamps for very high resolution mol. spectroscopy using Fabry-Perot spectrometer 8=29675
  hollow cathode, simple demountable, for atomic abs. spectroscopy 8=49989
  incandescent, calibration and standardization 8=42211
  i. r., far, sources, comparison of radiance 8=28837

Spectroscopy—contd
 light sources—contd
  i.r. sources, comparison 8=41851
  laser discharge for absorpt. spectra 8=34122
  lasers, semicond. variable wavelength, 1-20 μ 8=28838
  Raman, helium lamp 8=46711
  sliding-spark continuum radiation 8=28841
  slot burner for absorpt. spectroscopy 8=36637
  sparks, high-current, as intense u.v. source 8=47770
  Ulbricht sphere, use in spectrochem. anal. 8=42236
  C arc as standard source, electrode temp. determ. 8=29927
  C resonance lamp, line width and band obs. 8=43288
  Th lamps and interferometrically measured Th wavelengths 8=28839
  W lamp, astron. spectrophotometric standard 8=45667
Spectroscopy, radiofrequency
   See also Nuclear magnetic resonance and relaxation; Paramagnetic resonance and relaxation; Spectrometers, radiofrequency.
  electric reson., mm and sub-mm 8=25483
  e. p. r., rapid scanning of mag. field, appl. to pulse electrolysis 8=33145
  e. p. r. spectra, automatic mag. field calibrator 8=37382
  gas-phase rotational transitions, radiation power and field change 8=25422
  high temp. mm and sub-mm at Duke 8=24257
  ions, r. f. transitions between energy levels, bolometric technique 8=38659
  microwave double reson., by use of high power 8=25634
  microwave, molecular, review 8=33140
  new technique for studying metastable autoionizing states of atoms 8=43244
  n.m.r. decade ND30M 8=46512
  n. m. r. high-power transmitter 8=33153
  quantitative data determ., improved meas. method 8=24258
  stored ions, exchange-collision technique 8=38596
  terrestrial mag. field range high-resolution n.m.r. 8=46516
  time-résolved, sampling tech. for meas. Lamb shift in He^+ 8=43172
  virtual transitions, effects 8=47473
  weak continuous mag. field sensitive n.m.r., expts. 8=46519
  H-bonds, strong, n.m.r. study 8=48301
Speech
   See also Hearing
  auditory feedback delay effects 8=23975
  consonants, English, short-term memory confusion 8=46201
  distortion due to helium, correction 8=32924
  divers during decompression, causes of distortion 8=23972
  evaluation, isopreference method 8=46199
  fundamental frequency meas. using higher harmonics 8=23974
  intelligibility, semi-automatic measurements 8=46199
  Italian, minimal elements for synthesis 8=37284
  phenemic symbols, computer transcription standard 8=46202
  sex identification from isolated, voiceless fricatives 8=32927
  speech synthesizer, digital formant 8=23971
  subglobal and esophageal pressure obs. and compared 8=32922
  u.s. sound 8=41849
  vocal fold motion meas. with u. s. Doppler vel. monitor 8=32923
  Vocoder filter design 8=23973
  whispered, air consumption per syllable, obs. 8=37285
Spherical aberration. See Aberrations, optical.
Spicules. See Sun, prominences.
Spin. See Elementary particles; Hyperons/spin and parity; Mesons/spin and parity; Nucleus/spin and parity; Rotating bodies.
Spin echo. See Nuclear magnetic resonance and relaxation.
Spin—lattice relaxation. See Crystals/lattice mechanics; Magnetic resonance and relaxation.
Spin waves. See Ferromagnetism/spin-wave theory.
Spinors. See Quantum theory, wave equations.
Spions (pions with spin). See Pions.
Spirality. See Elementary particles; Field theory, quantum.
Sporadic-E. See Ionosphere/E-region.
Sprays
   See also Aerosols; Drops; Jets.
  evaporation in air 8=48273
Spurions. See Elementary particles.
Sputtering
  amorphous substs., efficiency calc. 8=48895
  computer simulation in mechanism investigation 8=48902
  crystal, and ion-electron emission coeffs. anisotropy rel. to lattice thermal vibrations 8=40685
  efficient, in cold-cathode discharges with magnetron geometry 8=25694
  film, duoplasmatron ion source 8=48442/3
  focusing collisions, model 8=48900
  focusing collisions, role 8=31135
  metal polycrystals, ratio rel. to ion incidence 8=48899
  metals, porous 8=35594

Sputtering—contd
metals, rel. to H$^+$ implantation coeff. 8=30764
metals, with low-energy inert gas ions, rel. to trapped gas 8=26726
pattern distortions on plane and cylindrical collectors 8=48906
quartz, on Aland counter-electroding, props. of capacitor 8=44059
quartz, r.f. sputtered on Al, props. of capacitor rel. to film thickness 8=44059
radio frequency, ion energy distrib. calc. 8=25687
spectrometer, mechanical, for analysis of energy distrib. of Cu or Au atoms 8=48915
systems, r.f., choice between single-ended and balanced 8=39586
rel. to vacuum technology 8=30323
Al, ang. distrib. of Mg, Kr, Gd ions, obs. 8=48909
Al, by 1 to 5 keV Ar$^+$ 8=40069
Al oxide films, in plasma anodization 8=39587
Al pattern, deposit structure between 100 and 560°K 8=48906
Al, with Bi atoms, D$^+$ range obs. 8=48912
Al_2O_3, inert gas depth distrib. obs. 8=48923
Au atoms, energy distrib. analysis by mechanical spectrometer 8=48915
Au, by 1 to 5 keV Ar$^+$ 8=40069
Au, energy spectrum of ejected atoms 8=48916
Au films, by low-energy H ions, transmission method, low energy 8=40072
Au films, by transmission of H and D ions 8=44495
Au single crystal by fast neutrons 8=48911
$BaTiO_3$ films, ferroelec., prep. 8=35161
Cd, by 1- to 5 keV Ar$^+$, rel. to orientation dependence 8=40076
CdS, rel. to long range oriented crystallization 8=30809
Cu atoms, energy distrib. analysis by mechanical spectrometer 8=48915
Cu, by 1 to 5 keV Ar$^+$ 8=40069
Cu, energy spectrum of ejected atoms 8=48917
Cu, intensity in directions of dense packing rel. to incidence angle of ions 8=26731
Cu, of Ar$^+$, channelling obs. 8=48921
Cu, of Cs-ions, 77°K 8=31150
He-Ne laser tube, cathode particles 8=24317
Hg$^+$, yield and ang. distrib. rel. to random and preferential ejection correlation 8=44499
In_2O_3 films, electrical props., intrinsic absorption 8=40469
In_2O_3, films, near i. r. optical props. 8=40470
K cathode, atomic beam source for 0.2-45eV 8=43240
KCl, inert gas depth distrib. obs. 8=48923
Mg, by 1- to 5-keV Ar$^+$, rel. to orientation dependence 8=40076
Mo, ang. distrib. of Mg, Kr ions, obs. 8=48909
Mo, by Ar$^+$, mechanism 8=35606
Nb film deposition by d.c. diode and substrate bias sputtering 8=48455
Nb films, sputtered cylindrical, flux jumping phenomena 8=49472
Ni by Ar$^+$, [110] and [100] close-packed directions yields, 25-600 eV 8=40078
Pt films, oriented growth 8=44049
Si films, deposited through moving mask, low-temp. orientation 8=27127
Si in O_2, SiO_2 coatings for protection of aluminized mirrors for u. v. 8=42148
SiO_2, to form multilayer interconnects in MOS devices 8=44855
SnO_2 film, prep. and props. by reactive cathode sputtering 8=44062
Ta, ang. distrib. of Mg, Kr, Gd ions, obs. 8=48909
TiO_2, inert gas depth distrib. obs. 8=48923
VO_2 films, rel. to transport props. 8=27138
W, by Ar$^+$, mechanism 8=35605
W-Mo alloy, by Ar$^+$, mechanism 8=35606
Zn, by 1- to 5-keV Ar$^+$, rel. to orientation dependence 8=40076
Zr, by 1- to 5-keV Ar$^+$, rel. to orientation dependence 8=40076
Zr carbide, by Ar$^+$, mechanism 8=35606
Zr polycrystals, by Ar$^+$, mechanism 8=35606

Stacking faults. See Crystal imperfections.

Standards
See also Constants; Units.
atomic units and scales of time 8=45957
colour meas., standardization 8=46657
electrical units and transfer of their dimensions to meas. and instruments 8=46315
electron tube resistance meas. methods 8=37426
fluorescence, quinine bisulphate and 9,10-diphenylanthracene 8=39391
fluorescent glass 8=45945
frequency, atomic Cs 8=28210
frequency, Tl^{205} spectrum 8=28211
frequency, vapour rubidium atomic clocks 8=45958
high-temperature ref. mats., 8=46224
length, unit, reference interference equipment for reproducing unit of length 8=45949
light, thermodynamic consideration 8=46654
liquid scintillation counter, efficiency determ. 8=33375

Standards—contd
low-luminance source 8=28772
mass, precise and reproducible standard definition 8=45946
measurement, historical review (1918-1968) 8=28209
metal oxide e probe microanalysis 8=41307
1-metre line-standard interferometer 8=45951
molecular freq., for mm. waves 8=45959
near-zone mag. field of antenna, reference for calibrating field-strength meters 8=46493
optical isotope applic. 8=43245
phonemic symbols, computer transcription 8=46202
photometric, using precision work 8=42130
radioactivity, absolute meas. 8=42933
radioactivity, appl. of liq. scintillation counters 8=28977
for spectrochem. analysis, prep. 8=36644
temperature meas., reference standards 8=46260
temperature, Sb freezing-point, apparatus 8=30585
temperature, Sb freezing-point, measurements 8=30586
thermal neutron flux density, calibration 8=47149
Kr^{86}, wavelength standard, reproducibility, discussion 8=23789
Pt, as thermal cond. standard reference material 8=48763
W lamp for astron. spectrophotometry 8=45667

Stark effect
air molecules, broadening 8=34272
allyl cyanide, microwave dipole moment obs. 8=34304
in colour centres of alkali halides 8=31112
crystal, local centre spectra, linear effect calc. 8=36308
electron collision broadening, theory 8=43157
F_A centres, electro-optically aligned 8=44471
formaldehyde, dipole moment of triplet state 8=25580
linear broadening, transition from quasi-static to impact electron contrib. 8=43158
plasma spectral line broadening in strong mag. and elec. fields 8=25340
plasma spectrum 8=30092
plasma transient shifts, Fizeau interferometer meas. 8=30088
porphyrins 8=43388
quadratic constants, for 13 elements 8=47467
quadratic h. f. s., theory 8=29601
Al, ground level h.f.s., obs. 8=29602
Ar II lines, Stark shifts 8=25354
ArII multiplets, temp. depend. 8=39028
$CaWO_4$:Gd^{3+}, ^6P Stark levels and line polarization 8=31993
CdS, exciton levels 8=36348
D source, colorimetry tables 8=46655
Eu, ground level h.f.s., obs. 8=29602
He, 3889, 5016 Å line broadening, obs. 8=47841
HeI, combined Zeeman and Stark effects 8=38653
He II, 3203Å line broadening 8=43225
LiF, linear effect on colour centres, zero-phonon lines. obs. 8=27581
LiF, F_3^+ centre 8=31120
N_2^+, broadening of rot. lines, shapes and widths 8=34259
NH_3, rotational lines observed by far i. r. laser 8=38845
NO molecule, and Zeeman effect, combined 8=25498
NaF, F_3^+ centre 8=31120
Sm, ground level h.f.s., obs. 8=29602
YAl garnet:Fe^{3+}, e.p.r. and pseudo-stark line-splitting 8=31849

Stars
See also Nebulae; Novae; Sun.
A-type, microturbulent velocity parameters 8=50276
A-type within 20pc of Sun, moving pairs obs. 8=50278
AG Peg, brightness oscs. with period of near 800 days 8=32438
angular diameter meas. with stellar interferometer at Narrabi, procedure 8=28073
angular diameters of 15 stars, and obs. monochromatic flux at surface 8=28074
AR Andromedae nature, obs. 8=28078
atmosphere models, influence of turbulence, anal. with corrective element 8=36934
atmosphere, non-LTE, calc. of line spectrum, influence of ordered macroscopic vel. 8=41514
BD + 34°1051 binary, orbital elements, from photoelec. obs. 8=36957
binary, colours and magnitudes in UBV system calc. from photoelectric obs. 8=50332
binary, distances corrected statistically 8=50333
binary eclipsing stars, darkening at limb, interpretation 8=36955
binary ϵ Coronae Australis, eclipsing, blue and yellow filter obs. 8=32471
binary, possibility of many single star systems being resolved 8=45700
binary, spectroscopic, masses obs. 8=45699
binaries, spectroscopic, galactic distrib. 8=41520
binaries, 12 new pairs, orbital parameters tabulated 8=3247
BV342 binary, orbital elements from photoelec. obs. 8=36956
carbon, thermal stability rel. to ν losses, models 8=45636
Cas A, X-ray spectrum rel. to optical 8=45775
cepheids, classical, period-radius relation 8=45681
cluster, gravitational microfield, stellar density gradient effect 8=36959

Stars—contd
clusters, open, statistics and mutual independ. for neighbours 8=32474
collisional relaxation calc. 8=50275
Coma Cluster, distribution of galaxies near centre 8=50363
contracting, model convective envelopes 8=32428
CP1919, Parkes period confirm. 8=45753
declinations, absolute meas. with instrums. without precise graduated circles 8=45613
δ Lyrae cluster, photometric evidence 8=28087
δ Scuti variable, pulsation limited by axial rot. 8=45687
density in galactic halo SA 57, RGU photometry determ. 8=41531
dimensions, rel. to Jeans's criterium 8=50280
double, interferometer obs. 8=32466
double, table of micrometer obs. 8=32465 -7-8
doubles in Melbourne Astrographic Catalogue, 635, search and count results 8=32469
dwarf, white, effects of accretion 8=36928
dwarfs, Sculptor-type, distrib. in near galactic clusters 8=28109
dynamics, collective effects, one-dimensional model 8=50287
dynamics, tensor virial-equation 8=45621
eclipsing binaries, obs. 8=28086
53 Arietis, period calc. from light variation, photoelectric study 8=50274
formation of single and multiple stars effect of rotation and magnetic fields 8=50294
4 C Vn, as δ Scuti variable for radial velocity var. explanation 8=50320
fundamental, proper motions and radial vels. 8=32499
Galactic, near sun, kinematic models 8=36970
in galaxies, absolute proper motions, 14000 obs. 8=45740
in Galaxy, vel. relax. rel. to interstellar gas gravit. condensation 8=45733
γ-Pegasi, atmos. from equiv. widths and depths and H and He lines 8=32422
Giades cluster, structure, density distrib. curves, radius 8=32459
globular clusters in Andromeda Nebula, forming ellipsoidal subsystem 8=32477
groups of uniform spectral type, having same systematic motions (expansions) as OB = associations 8=28085
Hamada-Salpeter model of white dwarfs 8=41502
HD 191566, duplicity, obs. 8=45705
head-on collision, 2-dimensional theory 8=45619
Hevel's object, X Orionis, 1667 8=45612
horizontal-branch, at high galactic latitudes ten new stars 8=50283
hot main-sequence, models of out layers 8=45629
Hyades cluster, distance from earth meas. 8=50330
Hyades cluster, mass-luminosity and He content 8=45697
Hyades cluster star stream 8=45695
Jean's type gravitation instability of finite isothermal gas spheres 8=45618
lagrangian systems, self-adjointness 8=50277
late type, atms. convective instabilities, mag. field effects, calc. 8=50289
light scatt., nonstationary, in atms. and rel. to novae theory 8=28039
magnitudes, determ. with integrating photometers 8=36974
mass-luminosity relationship and He content of Hyades cluster, young stars 8=45697
massive and supermassive, mass and energy balance 8=50288
massive, gravit. modes, stable and unstable, asymptotic solns. 8=45635
meridian circulation velocities in radiative envelope, Cowling model 8=45617
middle-aged, densities 8=28051
models, theory of similarity, rel. to rad. press. and convective cores 8=32426
motion in Galactic plane, perturbations by gravitation irregularities 8=45620
Neugebauer-Martz-Leighton objects 8=50385
neutron, mass infall as source of X and cosmic rays 8=45676
neutron, possible optical identification from pulsating radio source 8=36949
neutron, radio obs., position in HR diagram 8=32451
neutron, radius and struct. 8=28076
neutron rotating, as origin of pulsating radio sources 8=41539
neutron, torsional oscills. and crystallization 8=45762
NGC2360 cluster, photoelectric obs. 8=28088
NGC6397 cluster, blue horizontal-branch obs. 8=32461
OB associations, grains, accretion of solid H mantles 8=41519
OB, distances corrected statistically 8=50333
occultations, tables for 1966 at Sydney Observatory 8=50398
old moving groups, past galactic orbits, numerical computations 8=32478
orbits, rel. to spiral structure stability 8=50364
P Cygni, proper motion and obs. magnitude 8=32420
photographic images, coma tolerances 8=36941
plasma gravitational instability 8=41528
polarimetry, new technique 8=36945

Stars—contd
pulsars, obs. at 11 cm. 8=45765
pulsars, preliminary obs. 8=45745
pulsars, proper motion search 8=50379
pulsating, damping in emission of gravitational waves 8=41516
pulsating, one-zone model vibr. stability 8=45688
pulsating, path length of mixing, theory rel. to estimate of upper boundary 8=36954
pulsation, non-radial and non adiabatic: one zone approximation, p-, g modes stability 8=50322
pulsations, adiabatic and convective unstability 8=50321
pulsational instability in pre-main sequence phase 8=36950
II Puppis and delta cepheid-var. AQ Pupis, assoc. 8=32419
R Z Scuti, close binary system, mass, radius and luminosity calc. 8=50331
radial velocities, from Coude' spectrograms, southern 8=36930
radiation characts. rel. to nebulae radio emission 8=32484
radio, visibility fades in Alaska near solar minimum 8=41437
radio, visibility fades, phase variance and autocorrelation obs. 8=41436
radio, v.h.f. refraction by visible aurora 8=50170
relative magnitudes, determ. with differential astrophotometer 8=36933
rotating neutron with dipole magnetic field 8=45677
rotation, implications of vorticity expulsion by turbulence 8=45622
Schwarzschild singularity, at $r = 2m$ scatt. of massless scalar waves 8=36929
secular stability of chemically, inhomogeneous layers against nonspherical perturbs. 8=28050
self-gravitating stellar system with uniform rotation, stability of density waves 8=28037
shock propag. through hot and giant star envelopes, Brinkley-Kirkwood theory 8=45637
space-velocity vectors, bulletin (1962), criticism 8=45615-6
starlight, scintillation as detector of gravitational waves 8=37164
stellar wind, effects on radiative transfer, rel. to diffusion and ionization processes 8=41512
system stability rel. to velocity distribs. 8=50279
thermodynamic conditions in deep interior 8=32418
T Tauri, props. rel. to pre-main sequence stellar evolution 8=45639
Tr. 15, galactic cluster 8=32473
Tr22 and Ho17 open clusters, photographic magnitudes 8=50329
U Oph and R CMa binaries, eclipsing minima times 8=32470
UV Ceti type, flares nature, spectroscopy obs. 8=32441
u.v. object in Sagittarius, nature 8=45614
variable flare, new, of U Geminorum type, spectrum and periodicity 8=45693
variable, period-density calc., oscill. in phase space 8=45686
variables, eclipsing, epochs of photoelec. minima 8=36951
variables, long-period, 23, relative proper motions, from Leiden plates 8=36952
Vir A, X-ray spectrum rel. to optical 8=45775
white dwarf Hamada-Salpeter models, stability and radial vibr. periods rel. to pulsating radio sources 8=41545
white dwarfs, Hamada-Salpeter, oscillations including general relativistic effects 8=50325
white dwarfs, radial oscillation periods 8=41502
white dwarfs, rotating, pulsation periods 8=50324
Wolf-Rayet, excitation temp. calc. from C IV hydrogenic transitions 8=45661
Wolf-Rayet, wavelength dependent interstellar observation rel. to dust props. 8=36943
W Virginis, halo characts. 8=28038
Be, radial vel. rel. to galactic rot. 8=45735
He content and mass-luminosity relation of Hyades cluster, young stars 8=45697
He, H shells thermal instability 8=45624
composition
See also Elements/origin.
AO Cas, binary, atm. physics 8=32462
BD + 10°2179 He star, C content 8=28066
l Carinae atmosphere, H line profiles 8=50323
clusters, globular, heavy-element abundances 8=32480
early A, model atm. anomalies 8=32421
η Leo, supergiant, atmosphere 8=32427
γ Capricorni, abundance anal. with curve of growth tech. appl. to Conde mat. 8=32424
graphite grain form. by condensation 8=45645
HD 161817, high velocity star, oxygen abundance calc. from spectra 8=50282
HR774, BaII abundance and metal-iron ratios 8=45638
λ Boo, abundance ratio Mg/O calc. from i.r. spectra 8=50286
material exchange in atmospheres of contact binaries 8=50291
π 'Ori', abundance ratio Mg/O calc. from i.r. spectra 8=50286
Population II, He determ., test for gravitation theories 8=23858
red giants, Tc^{97} synthesis 8=45644

Stars—contd
  composition—contd
    RU Cam atmosphere in recent quiescent phase 8=28046
    Sagittarius, X-ray sources celestial positions 8=50390/1
    Sirius, iron group elements abundances and effective temp. calc. 8=50285
    sub-dwarfs, population II, H–R diagram position and He content 8=28047
    surface convective zones and acceleration mechanisms, Li, Be formation cross-sects. 8=32390
    T Tauri, atm. Li content rel. to He^6 β decay, calc. 8=36926
    τ Bootis, metal abundances 8=45626
    θ Hya, abundance ratio Mg/O calc. from i.r. spectra 8=50286
    T Tauri, Li formation, 8=50297
    Be^9 abundance, obs. 8=36927
    H^2 abundance, obs. 8=36927
    He^3 abundance, obs. 8=36927
    K-type giants, Na, Mg, Ca abundances photometric meas. 8=45633
    Li^{6,7} abundance obs. 8=36927
    Tc^{97} synthesis in red giants 8=45644
  evolution
    binary systems, close 8=50334
    blue supergiants, pulsational stability 8=28084
    cluster formation, rel. to non-linear eqs. of spherical collapse 8=50258
    clusters formed by delayed evolution, 8=50305
    clusters, spherical, initial collapse and dynamical mixing, 8=50335
    compression and nuclear explosion after stability loss, $M > 6 \times 10^4\ M_\odot$ 8=32429
    contact binaries, exchange of material in their atmospheres 8=50291
    dense systems, 8=50304
    few-body problems, 8=50298
    fragmentation and angular momentum in theories 8=50302
    gas cloud, collapsing, stability against fragmentation 8=50301
    graphite grain form by condensation 8=45645
    gravitational instability prod. system, stability rel. to density 8=28052
    hydrogen burning model, rel. to nova outburst 8=28044
    isothermal sphere, dynamical collapse 8=32432
    $0.1\ M_\odot$ stars, model calc., and electrostatic interact. modifications 8=45643
    magnetic field configuration in galactic spiral arms 8=50366
    massive, early main-sequence phase 8=50306
    matter outflow rel. to atm. opacity, model 8=45623
    neutron, crystallization and torsional oscills. 8=45762
    rel. to nucleosynthesis of heavy nuclei 8=41504
    numerical studies rel. to formation 8=50299
    Orion association, Ia Ori subgroup, internal motions and expansion rate 8=50296
    Orion association, interstellar extinction 8=50295
    Population II, age and initial He abundance 8=45641
    pre-main sequence, rel. to props. of T Tauri stars 8=45639
    protostar in free-fall collapse 8=45640
    protostar, quasi-hydrostatic equilibrium onset stage, one solar mass 8=41506
    protostars, hydrodynamic calc. method 8=45646
    protostellar bodies, massive superdense, models rel. to stability 8=28053
    red giant, of S solar masses, influence of mass loss 8=45642
    red giant with mass loss 8=45647
    red giants Li content in photosphere and core, and mass dependence 8=50292
    red giants, N^{14} burning before He flash 8=28055
    rel. to gravitational instability in interstellar matter 8=50348
    in rotating mag. clouds, 8=50300
    runaway, from cluster gravit. collapse 8=36960
    secular stability against meridional motions in radiative zones of stationary rotating stars 8=32425
    small system and double stars, 8=50303
    supermassive, nucleosynthesis in little bangs 8=36911
    variable FG Sagittae, obs. (1960-7) 8=45692
    vector bosons, charged intermediate, consequences 8=29161
    white dwarfs, luminosity function and space density 8=28059
    young, early-type, with gaseous envelope of similar mass, from study of rotating gas cloud 8=32431
    C, carbon burning phase lifetime rel. to neutrino loss 8=41507
    C-O in gravitational contraction, computer study 8=32433
    HI cloud, structural changes on condensation of interstellar gas 8=50293
    He-burning supergiants, models 8=28054
    Li destruction and rotational braking 8=32430
    Li in young (T Tauri) stars, formation process, 8=50297
  magnetism
    See also Sun/magnetism.
    No entries
  radiation
    See also Cosmic radiations, radiofrequency; Sun/radiation.

Stars—contd
  radiation—contd
    AB Cyg, light, intrinsic polarization vars. rel. to brightness and wavelength 8=45672
    absorption lines, effect of rapid rotation 8=45664
    AK Peg, light, intrinsic polarization vars. rel. to brightness and wavelength 8=45672
    Be stars, theoretical Balmer decrement, and rad. field 8=32445
    binary, visual, absolute magnitude obs. 8=45704
    BL Lac, identified as radio source 8=41547
    in Caosiopeia, starlight polarization rel. to interstellar clouds, obs. 8=50355
    Cepheus IV association, additional members 8=45660
    cluster NGC 5897, colour-magnitude diagram data 8=45670
    cluster NGC 6823, photometric obs. 8=36972
    clusters and O associations, anomalous reddening 8=32448
    clusters, five-colour intermediate-band photometry 8=41508
    convective model envelope and mixing length theory, density gradient calc. 8=50309
    CP 0950, impulsive emission 8=50314
    Cygnus X-2, population type 8=28061
    disc cepheid κ Pavonis, temp., metal-abundance and mass obs. 8=45689
    field in resonance lines, using concept of "thermalization length" 8=41511
    five-colour intermediate-band photometry 8=41508
    flare, u.v. photoelec. obs. 8=45685
    flares, far i.r., quiet electron mechanism 8=45691
    flux obs. at centres of H, K lines 8=45657
    galactic light, diffuse, rel. to interstellar dust scattering props. 8=45730
    HD6870, rapid rotation, spectrophotometric obs. 8=28072
    HD 116994, photoelec. photometry 8=32454
    hot, atmos. models to test validity of black body assumption and gravity effect on flux 8=41513
    interstellar absorption bands, diffuse, origin 8=28062
    luminosity function new determ. from proper motion survey 8=45673
    magnetic braking by stellar wind 8=36932
    magnitude, electronographic determ. 8=28064
    Milky Way, u.v. obs. from Venera-4 8=28101
    neutrino emission, taking account of Pauli principle 8=50308
    occultation by moon, effect of gravit. deflection of light 8=32801
    photometry, relative and absolute obs. 8=32434
    photon escape from infinite cylinder 8=41509
    pulsar CP 1919, meas. between 85 and 2,700 MHz 8=45759
    pulsar Io effect 8=45764
    pulsars, submillisecond radio intensity variations 8=45758
    pulses, interpretation based on plasma oscills. in magnetosphere of neutron star 8=45763
    reflection nebulae, photometric obs. 8=32472
    RU Cam, mass and magnitude in quiescent phase 8=28046
    RX Boo, light, intrinsic polarization vars. rel. to brightness and wavelength 8=45672
    scintillations and spread-F in auroral zone 8=32355
    73 Draconis, short-period variations 8=45682
    short-period blue variable, photoelec. obs. 8=45683
    in stellar wind region, rel. to thermal diffusion and ionization processes 8=41512
    subluminous late-type white dwarfs, obs. 8=45659
    SX Cas eclipsing binary, photoelec. obs. 8=32464
    UBV and narrow-band uv by photometry 8=32435
    V544 Cygni eclipsing Wolf-Rayet variable 8=28079
    variable, polarization obs. 8=32455
    variables continuous emission rel. to inverse Compton effect 8=32458
    white dwarf. pulsar condition, 8=50317
    white dwarfs, luminosity function and space density 8=28059
    white dwarfs, pulsating, pulse profiles 8=50380
    YZ CMi variable, photoelec. obs. 8=32456
    W lamps for spectrophotometric standards 8=45667
  spectra
    absorption lines, effect of rapid rotation 8=45664
    absorption lines, effects of axial rot. on equiv. widths 8=50313
    accelerated particles, mean spectrum from Li^{6,7}, Be^9 obs. 8=45665
    AD Leonis rel. to flares nature, obs. 8=32441
    AG Pegasi rel. to structure, (1965) 8=32447
    α Ori asymmetric Hα, rel. to circumstellar envelope changes, obs. 8=45650
    atomic collisions and local thermodynamic equilib., obs. and theory 8=36939
    B, effective temp, Balmer discontinuities obs. 8=50312
    β Lyrae, changes in polarization 8=45653
    binary, eclipsing, classification and surface gravity calc. 8=45696
    blue, horizontal-branch, obs. 8=32479
    CaII H- and K-lines, Wilson-Bappu effect 8=28070
    carbon and M stars, spectrograms 8=28067
    carbon, U Hya and Y CVn, λ4380-λ6900 and λ4380-λ6300 obs. 8=36938
    Cas A obs. of γ-rays 8=45799
    Cepheid RU Camelopardalis 8=36944
    cepheids, H envelope CaII emission, model 8=45680

Stars—contd
  spectra—contd
    cool stars, u.v. spectrum prediction rel. to existence and struct. of chromospheres 8=41515
    χ Cygni, Al H emission lines near minimum light 8=45662
    Cyg A, obs. of γ-rays 8=45799
    diffuse interstellar absorpt. bands, origin 8=28099
    early A, rocket u.v. 2000-3000 Å computation 8=45655
    effective temp., Balmer discontinuities obs. 8=50312
    extinction curves rel. to reddening for various Milky Way regions 8=32443
    far u.v. filter obs., analysis 8=45669
    F dwarfs, Hβ photometry for temp. determ. 8=45649
    Feige blue, quantitative analysis 8=32436
    flux in 2100, 2500, 2800 A bands, obs. 8=45668
    Fourier transform spectroscopy for line profiles obs. 8=42217
    Fraunhofer lines calc. by wt. function theory 8=36908
    Fraunhofer lines saturation explanation 8=50442
    F-type main-sequence, Strömgren indices, microturbulence and metal abundance effects 8=32444
    γ-Pegasi, H and He lines rel. to atmos. and electron density 8=32422
    HD116994 delta Scuti, period and amplitude obs. 8=36942
    HD 161817, high velocity star, oxygen abundance calc. 8=50282
    HD30353, anal. rel. to abundances of metals 8=36937
    HD33579 Magellanic Cloud, element abundance obs. 8=36940
    HD 98088 mag. binary, variation rel. to orbit, calc. 8=45698
    HR234 variable, periodic obs 8=28080
    HR9080 variable, Balmer-line photometry 8=28083
    HR1105, Zr isotope ratios 8=28069
    interferometer at Narrabi Observatory 8=41510
    interstellar absorption bands, unidentified, at 4890Å and 4760Å at diff. Galactic longit., profiles 8=36948
    interstellar absorpt., rel. to spectral absorpt. of excited mols. in Fe aerosols 8=34950
    i.r. region, energy distrib. in continuous spectrum 8=32437
    K, narrow band photometry in near i.r. 8=45674
    λ Boo, abundance ratio Mg/O calc. from i.r. spectra 8=50286
    late-type, Hα luminosity criterion 8=28065
    line emission, in non-LTE atmos. with differential Doppler shift 8=41514
    M, narrow band photometry in near i.r. 8=45674
    M67, blue 'horizontal-branch' stars, mass and spectra determ. 8=50311
    microturbulence effect, rel. to anisotropy and depth depend. 8=28058
    Milne problem rel. line form. 8=45671
    NGC 6475, Hγ and Hδ equivalent widths 8=45675
    non-coherent scatt., Milne-Eddington growth curves 8=28068
    Nova Delphini 1967, pre-outburst obs. 82=8081
    O Γ lines λλ 1302-06, 1152Å, experimental oscillator strengths 8=50319
    1 Carinae atmosphere, H line profiles 8=50323
    Orion, far u.v. 8=36936
    o Her, obs. 8=32446
    π 'Ori', abundance ratio Mg/O calc. from i.r. spectra 8=50286
    plasma, line-width of redshifted light by self-trapping effect 8=45648
    Pleiades, faint, UBV photometry 8=36947
    Procyon, oscillator strengths calc. 8=32449
    pulsating object, spectral shift of light rays 8=28033
    reflection nebulae, obs. 8=32472
    RZ Cassiopeiae limb darkening 8=41521
    R Z Scuti, close binary system: mass, radius and luminosity calc. 8=50331
    Scorpio-Centaurus association, types and rot. velocities of 82 members 8=28075
    16 Piscium, binary 13 spectra obtained, chemical content determ. 8=50328
    SCO X-1, narrow-band and UBV photometry 8=45656
    spectrograph, high speed, for gratings to ruled depth of 128 mm and dispersions 80 to 20Å/mm 8=36946
    SSCyg, Z Gam and RU Peg, autocorrelation and spectral analysis of light curves 8=45651
    statistical spectroscopy appl. to 4000-40000°K 8=45663
    stellar position, atmospheric refraction effect 8=28063
    subdwarfs, changes on metal line removal 8=45658
    subdwarfs, energy curves 8=32440
    subdwarfs, strong line profile analysis 8=32439
    surface of eclipsing binary stars, calc. 8=45696
    Taurus A near occultation by Sun, search for 21 cm line frequency shift 8=50318
    Taurus, i.r. object: light variation and period obs. 8=50316
    three-channel photoelec. spectropolarimeter obs. 8=36921
    θ Hya, abundance ratio Mg/O calc. from i.r. spectra 8=50286
    UBV system, colours and magnitudes of binaries, photoelectric obs. 8=50332
    Upsilon Sagi Harii, Hα displaced absorption line explained by mass flow mechanism 8=50307

Stars—contd
  spectra—contd
    UV Ceti rel. to flares nature, obs. 8=32441
    V568 Cyg, obs. 8=32446
    variable FG Sagittae, obs. (1960-7) 8=45692
    variable HDE 310376, obs. 8=45690
    variables, eclipsing, epochs of photoelec. minima 8=36951
    velocity-dependent broadening, line absorpt. coeff. profiles 8=43164
    Wolf-Rayet, C, N and O broadening of lines due to pressure increase 8=45652
    Wolf-Rayet, spectral classification system and new catalogue 8=50315
    Wolf-Rayet V 444 Cyg (HD193576), eclipsing binary, He II emission lines λ4686 and 5411, spectrophotometric obs. 8=45654
    W Velorum variable, objective-prism obs. 8=28082
    X-ray, Sco XR-1, calc. 8=45727
    Zeeman triplets, shape of line profile and line intensity compared 8=50310
    ζ Oph, optical interstellar line spectrum 8=32442
    Be stars, theoretical Balmer decrement, and rad. field 8=32445
    CO molecular line absorpt. in late-type atm., theory 8=45666
    Ca II H and K lines equivalent widths 8=41525
    Hβ–Hζ equivalent widths, energy distribs. and dispersions, photoelec. obs. 8=28057
    Hγ profiles and temp. calc. 8=28056
    H, K line central flux obs. 8=45657
    He line λ10830Å obs. 8=28071
    M, TiO molecular bands obs. 8=28060
    Na I D lines equivalent widths 8=41525
    O, high galactic latit., analysis 8=32450
  structure
    AG Pegasi from 1965 spectra 8=32447
    atmosphere statistical-equilib. models, comparison with obs. 8=45632
    AX Mon, binary with envelope 8=32463
    B, main-sequence, surface-gravity determ. 8=50284
    Be, envelope support, hypothesis 8=28041
    binary, in astrographic zones +32°/34°, obs. 8=45701
    binary, 1164 examples, micrometry 8=32475
    binary, viscous tides, dynamics 8=32460
    binary, visual, absolute magnitude obs. 8=45704
    B4V atmosphere, line blanketing, model 8=28042
    BOV atmosphere, line blanketing, model 8=28043
    central condensation, models 8=32423
    continuum deviations from local thermodynamic equilib. 8=45627
    convective model envelope and mixing length theory, density gradient calc. 8=50309
    convective outer zone and energy transport 8=45631
    dwarfs FO to BO, coefficient of limb-darkening 8=50290
    dwarfs, massive white, in differential rotation 8=28049
    Eddington approximation, 3Do form 8=28045
    equilibrium, with rot. comparable to gavitational energy, determination 8=28048
    gaseous, convective instability 8=45628
    gravo-thermal catastrophe and red-giant structure for stellar system 8=36958
    HD 23631, short-period binary 8=45702
    HD 98088 mag. binary, mass and inclination calc. 8=45698
    limb-darkening eqn., inversion by Prony algorithm 8=28040
    N Her 1963, stellar temp., electron density, and electron-density of shell 8=36935
    neutrinos, motion and statistics 8=42465
    neutron, rel. to radius 8=28076
    non-spherical, new pertubation method 8=45630
    O5V atmosphere, line blanketing, model 8=28043
    0.1 M_O and 0.05 M_O, with electrostatic interact. modifying thermodyn. props. 8=45643
    polytrope with purely toroidal mag. field 8=41501
    polytropes, rapid rotation, equilib. struct. 8=45625
    pulsations, radial adiabatic, asymptotic soln. 8=45684
    radial oscillations, dependence of Q on stellar model 8=36931
    rotating massive stars, and stability, rel. to general relativity 8=50281
    Σ 2398 visual binary, parallax, proper and orbital motion 8=45703
    T Tauri, props. rel. to pre-main sequence stellar evolution 8=45639
    variable R Coronae Borealis, model atm. 8=45634
Stars (nuclear). See Particle track visualization.
Statistical analysis
    See also Measurement/errors; Probability; Random processes.
  classical, operator relations in kinetic theory 8=46115
  data fitting by least-squares method 8=28241
  dense dispersed system, number of particles in any vol. at any time 8=37203
  energy fluxes prod. by regular source and system of random ones, distrib. 8=37196
  Fermi integrals evaluation 8=41779
  Hamiltonian formulation, time-depend, general laws 8=41752
  hypotheses at close values of χ^2, discrimination 8=24880

Statistical analysis—contd
    isolines of principal stress, holography as aid to determ. 8=24432
    laser light 8=46538
    lightning discharge, noise from predischarge part 8=45470
    many-body problem, interpolation method 8=24606
    Markov-chains of high order, approx. by Markov-chains of low order 8=23874
    modified normal distribs., generalized theory 8=45947
    Monte Carlo expt. on diurnal variation difference between filtered and unfiltered data 8=42749
    Monte-Carlo method algorithms appl. to narrow light beam propag. theory 8=46714
    Monte Carlo sampling, and radiation transport appls. 8=32855
    Morse Code signals and rhythmic patterns, structural theory for perception and confusability 8=41754
    nomogram applic. 8=46006
    prediction analysis applied to meas. of half-lives 8=47275
    spectral analysis and its applications 8=45977
    stochastic processes in spin systems 8=29804
    time-reversible difference procedures 8=32687
    time series, geophysical, filtering 8=41637
    Yang-Lee distribution zeros for classical one-dimensional system 8=23902
    H atom 8=29595
  applications
      See also Counters/statistical analysis.
    camera, dielectric tape, S/N rel. to scanning rate 8=42287
    chemical reactions, diffusion-controlled 8=34882
    classical ideal gas, correlation of density fluctuations 8=23883
    closure problem in system of random waves 8=36656
    coherent radiation 8=46640
    copolymerization, ternary 8=36589
    counting results of radiation measurements 8=46845
    critical behaviour in lattice statistics from series expansions 8=41757
    daily rainfall occurrence, second and higher order stationary Markov chain models 8=32217
    elasticity, moments formulation of problems 8=46040
    electro measuring app. with strings, stability of mobile part 8=33009
    electron probe microanalysis obs. 8=30850
    electronic contribution to energy and press. of elements and mixture, high temp. 8=23901
    ferroelectric lattice problem, combinatorial approach 8=44883
    fluctuation distribution of Gaussian beam propagating through random medium 8=33235
    fluctuations in gas lasers 8=37573
    fluid and fluid mixture properties 8=34573
    form factors of filling particles 8=39533
    galaxies, superclusters, statistical characts. 8=45741
    gases, energy transition probabilities in molecular collisions 8=34642
    Gaussian beam fluctuation in random medium, autocorrel. 8=46644
    image, quality, theoretical prediction 8=28741
    ion velocity distributions in partially ionized plasma 8=29955
    ionosphere f_0F2 and M(3000)F2, model for monthly distributions 8=28000
    Ising problem with arbitrary particle interaction, high-temp. asymptotic solutions 8=28311
    laser design formulas 8=42107
    local equilib. distrib., information theory 8=23876
    Markov chain model of molecules 8=25672
    meteorological variates, probabilities of moving time averages 8=50123
    mixture of charged and neutral particles, equilibrium 8=28330
    neutron cross section evaluation, curve fitting technique 8=33789
    noise, appl. to graph smoothing 8=32688
    nonlinear systems, Volterra kernels, and convolution integral 8=37229
    nuclear radiation meas. technique, computation bases for statistical error 8=47273
    nuclear reactions, communication theory 8=33969-70
    nuclear reactors, n and precursor populations, variances and covariances 8=34081
    one-dimensional hard-rod system, total distrib., function time evolution 8=41774
    particle transport, Monte Carlo deep-penetration calcs., track length distrib. biasing 8=33776
    Pc stable pulsations, dependence of amplitude on phase of moon 8=45565
    Poisson process due to optical rad., model rel. to optical communications 8=41753
    polymerization, nonstationary 8=36588
    quantum noise, multitime correspondence between quantum and classical stochastic processes 8=42055
    quantum noise, six-classical variable description 8=42056
    random temp. field in plate under conditions of turbulent heat transfer, statistical characts. 8=46230
    reactor static power tilting due to manufacturing tolerances 8=38567
    relative conformity method, appl. to heat and mass transfer problems 8=23998

Statistical analysis—contd
  applications—contd
    relaxation time distribution, numerical evaluation 8=46349
    reverberant acoustic field props. 8=37256
    scaler-ratemeter combination 8=46932
    scalar wave in random medium, statistical props. calc. 8=42240
    selective rejection of exptl. data 8=28214
    semiconductor laser junction, noise 8=33194
    shielding penetration, Monte Carlo calc., self-optimized exponential biasing 8=34075
    solar radiation reflection from clouds, angular distrib., TIROS IV radiometer obs. 8=32229
    steel, mild, stress-strain curve 8=35692
    stochastic model for low field resonance and relaxation 8=47673
    temperature inhomogeneities in sea, 3-D characts. 8=32187
    thermal photon beam, superposition of two 8=41852
    thermionic converter data, correl. method using 'figure of merit for electrode mats' 8=28498
    thermodynamics, asymptotic problem for real system 8=23885
    time-of-flight system, on-line, digital regulation 8=24500
    time-to-breakdown curves for insulators under action of partial discharge 8=44861
    unimolecular reaction rates, Monte Carlo calc. 8=25645
    wave propag., random refractive index media 8=42005
Statistical mechanics
      See also Bosons; Fermions; Quantum theory/many-particle systems.
    aperiodic systems coarse-grained quantities 8=37178
    approximate radial distrib. function 8=47897
    array of dumbbells, 1D, occupation statistics 8=28309
    atom model, Gaussian approximation for quantum corrections 8=41766
    BBGKY expansions, compatibility requirements 8=28320
    BBGKY hierarchy of eqns., decoupling 8=37183
    book 8=28324
    Boltzmann distrib., development of partition function, summation of leading diagrams 8=41769
    Boltzmann distrib., development of partition function, T-chains and W-rings 8=41768
    Boltzmann eqn. for dilute quantum-mechanical, slightly inhomogeneous gas 8=37226
    Boltzmann eqn., spherical harmonic and power series expansion appl. to electrons in weakly ionized gas 8=34442
    Born-Green-Yvon and Kirkwood hierarchies in equilib. 8=47898
    Bose-Einstein condensation of ideal gas 8=32846
    Bose fluids, degenerate, cluster expansion at finite temp. 8=37209
    Brachman relations in statistical atom model 8=38642
    canonical Bogolubov-Valatin transform., classification 8=41764
    chemical potential, upper bounds, var. principle 8=37184
    classical and quantum, of non-equilib. systems, generating functional and functional eqns. of motion 8=41770
    classical, correlation and distrib. functions, asymptotics, Bogolyubov cond. for weakening 8=32831
    classical electron gas pair distribution function asymptotic behaviour 8=41782
    classical fluid of hard spheres, distrib. function 8=37221
    classical, generalized adiabatic invariants using quantum-mech. technique 8=32829
    classical ideal, correlation of density fluctuations 8=23883
    classical particle systems, short and long range interactions 8=46107
    classical statistics in functional formalism 8=46089
    classical using Σ* algebra approach to quantum mechanics 8=32830
    classical two-body distrib. function 8=23875
    and combinatory topology 8=46106
    composite particles, generalized master eqn. 8=28316
    concentrated electrolytes, ion-pair theory 8=41272-3
    correlation functions as hydrodynamic Green's functions 8=46101
    Coulomb gas, dense, Bogolyubov equations 8=23881
    critical exponent values at λ-transitions 8=28308
    critical fluctuations, dynamics 8=37179
    damped non-Markovian system, quantum dynamics 8=37194
    decorated lattice model of binary mixture 8=23873
    defect motion in solids, rate formula including quantum effects 8=35516
    dimer problem soln by transfer matrix method 8=28312
    dissipative processes, quantum states, and entropy 8=23878
    dissipative systems, symmetry breaking instabilities 8=32836
    dynamical systems, noisy discrete-time nonlinear, state variables estimation 8=46009
    electrical transport in mag. field, quantum theory rel. to corresponding Boltzmann transport eqn., 8=44674
    electrostriction in gases 8=39224
    elliptic boundary value problems, asymptotic distribution of eigen values and eigen functions 8=46110

Statistical mechanics—contd
  e. m. phenomena, thermodynamics 8=32839
  energy-momentum laws, macroscopic 8=32837-41
  energy-momentum tensor, literature discussion 8=32841
  energy-momentum tensor, material, macroscopic 8=32838
  energy-momentum tensor, with and without external fields 8=32840
  entropy Boltzmann equilib. distrib. retention conditions 8=32835
  Fermi system phase transitions, quantum field theory 8=46823
  fermions, odd number, N-representability problem 8=37215
  fibrous structures with steric constraints 8=30400
  finite Ising lattice with periodic boundary conds., correls. 8=37180
  friction-constant formalism 8=39150-1
  gas under action of nonconservative forces, kinetic equations 8=34641
  Gaussian, quantized, finite sample correlations 8=37195
  general theorem for interacting many-particle systems 8=37200
  generalized Bel-Robinson tensor as generator 8=32821
  Green function theory of ferromagnetism 8=49488
  H-function convexity 8=41761
  Hamiltonian perturbation method, statistical generalization 8=32834
  hard disks, mixture of different sizes, excess free energy 8=28343
  hard molecule gas on Bethe lattice, phase transition 8=28347
  hard-particle systems 8=37219
  hard rod gas, 1D, pair distrib. function 8=32842
  hard-sphere gas, N-particle, exact pseudopotential derived 8=28346
  hard-sphere gas, struct. of H function 8=37220
  hard spheres, quantum-mech. pair-correl. function 8=28348
  harmonic lattice, "non-statistical" Boltzmann statistics 8=41773
  Hartree-Bogolyubov antilinear operators 8=41765
  heavy particle in finite cryst., momentum autocorrel. function 8=46102
  Heisenberg chain, anisotropic, Bethe hypothesis considerations 8=22869
  Heisenberg magnet, rotational invariance constraints on Green functions 8=27393
  homogeneous nucleation, thermodynamics 8=30594
  hydromechanics with random force action 8=46100
  infinite systems of classical particles 8=28238
  interactions, transition point 8=41756
  ionic crysts., quantum-statistical ab initio calcs. 8=48338
  irreversibility, comments 8=46111
  irreversible condensation, translation-rotation paradox 8=30597
  Ising lattice, square, with first and second neighbour interactions, transition point 8=41756
  Ising lattices, impurities and defects 8=41758
  Ising lattices, plane, cluster correlations 8=46093
  Ising model finite, thermodynamics 8=46092
  Ising models, critical phenomena 8=28310
  Ising problem, with arbitrary interact. between particles, asymptotic soln. at low temp. 8=37181
  kinetic eqns. derivations 8=37189/90/91
  kinetic operators, props. 8=46109
  Lagrange multipliers for system with constraints, geometrical view 8=23887
  lattice congruence of lattices, characterizations 8=32824
  lattice of dimers, quadratic 8=28315
  lattice system, integral eqn. for infinite volume correlation function 8=46095
  lattices, one-dimens., equilib. props. and thermal cond., numerical study 8=32825
  linear chain, monatomic, with impurity vibr. with long-range interaction 8=23872
  linear chain with free ends, energy flow 8=41760
  magnetism, theory, quantum methods 8=24106
  many body eqns. of motion, linearization method 8=37193
  many boson systems, Bogoliubov approx., asymptotic exactness 8=23894
  Markov-chains of high order, approx, by Markov-chains of low order 8=23874
  Maxwell gas, principle of maximum uniformity, distrib. of internal forces 8=37121
  Maxwell-Boltzmann distrib., grand-canonical partition function, quantum formulation 8=32832
  Maxwell-Boltzmann distrib., modification by intermolecular interactions-quasi-ideal approx. 8=41767
  Maxwell-Boltzmann distrib., quantum mech. partition function, diagram notation 8=32833
  Maxwell molecule gas, 2 temp. uniform mixture, equilibration 8=34639
  Maxwell relations in statistical atom model 8=38643
  mean-value and most-probable-value methods, equivalence 8=37186
  molecular systems, time-correl. functions of random motions 8=34386
  molecules, nonspherical, free energy of assembly with hard core 8=41771

Statistical mechanics—contd
  multiphoton absorption theory, limits of applicability of iteration method 8=24350
  multiple correlation function, form in Ornstein-Zernike approx. 8=37192
  natural expansion of wave function in terms of eigenvalues of reduced density matrices 8=42302
  nonequilibrium, applic. to stellar dynamics 8=32405
  non-equilibrium thermodynamics, foundation 8=46099
  non-equilibrium dense fluid, Prigogine theory 8=43618
  non-simultaneous method for correlation functions 8=28307
  nucleus, energy-density formalism appl. 8=42778
  one-dimens. gas with square-well potential 8=41784
  Onsager reaction field, mol. field theory and spherical model 8=32826
  ordering theorems generalized space distribs. 8=23877
  pair-correlation functions of ⩾ 3 particles systems, necessary restriction 8=28321
  particles in box, pair distrib. function 8=46112
  perturbation theory of thermal accommodation coeff. 8=44066
  phenomenological theory near critical points 8=44989
  plasma, high-temp. in thermodynamic equilib., quantum theory, free energy in 10^6 to 10^8 °K range 8=30020
  plasma, relativistic, of pregeometrical, pretensorial character 8=28327
  plasma in uniform elec. field 8=30019
  polymer chain, asymptotic soln. of excluded vol. 8=38976
  polymer chains, Kerr const. calc. 8=38972
  polymer crystallization, two-dimens. chain-folding model 8=39663
  polymer solns., thermodynamics 8=39324
  polymers, integral eqn. for excluded-vol. effect 8=29869
  polypeptides, helix-coil transition theories 8=43433
  potential-correlation function duality 8=28322
  quantum crystal, cluster expansions for cohesive energy 8=26007
  quantum fluids, multispecies, ground state, var. method 8=37199
  quantum liquids, rotation 8=23879
  quantum, Piron's axioms, modification 8=28319
  quantum spin system 8=46104
  random matrices in physics 8=46090
  relativistic kinetic eqns. including radiation effects 8=39065
  relativistic, Lorentz-invariant eqns. with accel. as function of position and rel. 8=23888
  rigid spheres near close packing, tunnel model and partition function 8=23903
  self-consistent field theory and Kirkwood variation method 8=28306
  spatial distrib. function, temp. -depend., integral-differential eqn. 8=41762
  square-well fluid, binary-collision expansion of classical N-body propagator 8=37197
  status of irreversibility 8=28323
  superfluid nuclear matter 8=23886
  systems of non-conservative interactions, application to kinetic problems 8=46108
  ternary alloys, disordered, linear approx. 8=30652
  thermal transport coeffs. in simple liquids, local equilib. model 8=25908
  thermodynamic functions on Thomas-Fermi-Dirac theories 8=38641
  three-body forces in dense system 8=37198
  3-particle correlation function in a many particle system 8=28329
  time correl. functions, quantum corrections 8=37187
  2-matrix, angular symmetry props., 8=46113
  van der Waals forces between macroscopic bodies 8=30610
  of violent relaxation, rel. to galaxy formation 8=50374
  viscosity of binary liq. systems 8=34795
  von Neumann lattices, decompositions 8=46094
  W* algebras with dispersion-free normal states, struct. theorem 8=28318
  waves in fluctuating medium, quantum theory 8=23880
  XY model of quantum lattice fluid, critical props. 8=37177
  MnF_2, antiferromagnet, uniaxial, first- and second-neighbour exchanges 8=31782
Statistical thermodynamics. See Statistical mechanics.
Steady-state theory. See Cosmology.
Steam
  charge transfer from proton and H atom, cross-sections 8=38737
  condensation, dropwise. on Cu, heat transfer rel. to presence of non-condensable gases 8=34993
  dielectric const. in supercrit. region 8=48183
  internal energy, adiabatic calorimeter 8=28424
  virial coeffs. 150°-450°C 8=39195
Steel
  age-hardened containing ordered γ' precipitates tensile yield mechanism 8=49014
  ageing mechanism, EI 702 8=35100
  analysis of C using vacuum spectrometer, interference of Al 8=32155
  austenite lattice parameter changes rel. to intermediate transformation 8=35333

Steel—contd
  austenite powders, electrolytic, absence of martensitic transforms. 8=35103
  austenite, solubility of Cu, effect of Cr 8=30655
  austenitic stainless electrodes, brittleness at bonded part of welded joint with ferritic steel 8=31210
  austenitic stainless, irrad. hardening, substructure 8=49015
  austenitic stainless, growth in oxidising gases 8=45338
  austenitic stainless, growth of M_{23} C_6 carbide 8=39668
  austenitic stainless, stress corrosion cracking study by internal friction meas. 8=40159
  austenitic stainless weld metal solidification 8=48265
  austenitic, temp. cond. at 0° to 1000°C 8=39944
  austenitic 20% Cr/25% Ni/Nb-stabilised, structure of surface oxides formed in CO_2 at high temps. 8=41238
  ball bearing, fatigue crack propag. rel. to crack growth, electron microfractographical studies 8=35696
  carbon, hyper eutectoid, Cr diffusion coating 8=39973
  carbon, particle coarsening of FeC_x, 720°C and 675°C 8=30691
  carbon, u. s. attenuation, 20-800°C 8=30945
  cast austenitic, strength increase and grain size decrease by phase transform. on thermal cycling 8=35698
  cementite, dislocations 8=31075
  chromic, modulus of elasticity change at tempering 8=49003
  cladding with refractory metals, shock wave technique 8=28206
  cold-rolled, recrystallization texture, influence of phase transformations 8=39719
  corrosion by H_2S 8=35691
  corrosion in H_2SO_4, inhibition by $Na_3PMO_{12}O_{40}$, mechanism 8=45370
  corrosion in nitrate soln., stress effects 8=45335
  corrosion resistance of austenitic stainless steels in nitric environment, influence of Mo 8=49867
  crack initiation and propagation, influence of notches 8=35689
  creep at room temperature 8=40160
  deep drawn 1 mm sheet, bonded simple and constrained layers, acoustic damping characts. 8=35612
  deformation, discontinuous, grain size and C content effects 8=35682
  diaphragm, square, plastic deform. and failure 8=37155
  directionally solidified, microsegregation of Ni and Cr 8=39552
  ductility of mild annealed rimmed steel, effect of prior cold reduction 8=26817
  dynamic strain ageing, Charpy specimen behaviour 8=35686
  E 1702, γ'-phase precip. mechanism, holding time effects at diff. quenching temps. 8=35108
  EI 702, ageing mechanism 8=35100
  EI 702, η-phase, precip. mechanism 8=44008
  EI 702, γ' and η' phase precip. or dissoln. on ht. treatment 8=43998
  EI 702, segregation kinetics 8=35054
  electron probe microanalysis of particles, 2.8-30μ 8=30557
  embrittlement sensitivity to n irrad., depend. on uncombined N conc. 8=47405
  etching to determ. P segregation, comp. with autoradiography 8=30861
  exoelectronic emission during friction 8=44939
  fatigue crack propagation and fracture analysis rel. to environment 8=49008
  fatigue props., notch effect, specimen design and loading 8=35690
  fatigue tests of sharply notched mild specimens 8=26821
  with f.c.c. lattice of solid soln., internal friction peak 8=35678
  ferritic, brittleness at bonded part of welded joint with austenitic stainless steel electrodes 8=31210
  field-ion microscopy study 8=48596
  frames, in stability in elasto-plastic range 8=40156
  40KhN5S, properties, effect of programmed loading 8=49005
  high-carbon, martensite defect structure from e. microscope exam. 8=35272
  high-carbon type, heat transfer between liq. and solid crust on Cu wall cooled by water 8=30974
  high-strength cast steels, props 8=49016
  high-strength, fracture toughness dependence on thickness, work-hardening exponent effect 8=26766
  high tensile, stress-corrosion cracking 8=31212
  hot-rolled, properties and process control 8=48598
  ignition temp., min, rel. to O_2 press. and surface deform. 8=36578
  inclusion behaviour, non-metallic in 0.2%carbon steel during hot rolling 8=49020
  inclusions, their thermal expansion and reln. to tessellated stresses 8=44350
  liquid, C activity rel. to Co, Mo, Ni, V, W conc. 8=30458
  low C castings, effect of rare-earth additions on mechanical properties 8=49009
  low carbon, composite martensite, crystallographic theory 8=26175
  low-carbon, deformation and recrystallization textures, rolling temp. dependence 8=26818
  low C, strain age-hardening, time law 8=40158
  Luders front exam. by transmission electron microscopy 8=44449

Steel—contd
  magnetic properties ht. treatment dependence 8=45014
  martensite ageing in carbon-steels, microcalorimetric exam. 8=35105
  martensite crystals of high-C Cr steel, domains from e-microscope exam. 8=40805
  martensite strength, contributing factors 8=26815
  martensitic, tempered, optimum C content 8=35684
  martensite transformation, magnetic field effect 8=39554
  mass spectrographic analysis, using ion beam chopper 8=27779
  microplastic strain energy criterion appl. to fatigue 8=35688
  mild and high strength, fatigue crack propag. behaviour 8=35697
  mild, in chromate solutions, kinetics of film growth, effect of surface prep. 8=44039
  mild, corrosion in NaCl, transient charge fluctuations, obs. 8=45368
  mild, stress-strain curve, statistical examination 8=35692
  oblique impact of Cu–Ni specimens, meas. of temp. developed 8=32981
  octadecylamine desorpt. and exchange, obs. 8=30768
  particle size distrib. in dispersed phases 8=26295
  pearlite and spheroidite, dislocation velocity exponent from strain-rate change tests 8=35557
  pipe with water flow, corrosion, effect of velocity, mass transfer model 8=36560
  plasticity and mech. strength, e bombard. effects, 2.5 MeV 8=35694
  porous castings, behaviour of H rel. to defects, compared with wrought steel 8=30663
  powder formation of 18/8 stainless 8=43983
  quench-hardened, austenitic grain struct. formation 8=35110
  quench-hardened, tempering rel. to martensite decomp. C conc. effects 8=35099
  rectangular diaphragm, ultimate strength 8=37154
  reflectivity changes during laser pulse 8=45169
  reversible temper brittleness development rel. to C content changes in grain boundary regions 8=35683
  ridging formation in 17%Cr stainless 8=26810
  rosette, star, tensile fracture 8=35687
  segregation study by X-ray fluorescence technique 8=30860
  Snoek effect, orientation dependence 8=26747
  sonic and ultrasonic pulses during crack propagation 8=35415
  spectral emission anal., decomp. and inter-element effects 8=32156
  split, layered, cup and cone tensile fracture 8=35685
  stainless, austenitic, deformation, annealing, stacking faults, compositional effects 8=40157
  stainless austenitic, He embrittlement, 540–760°C 8=31213
  stainless, austenitic, mag. field effect on phase transforms, and entropy shock 8=39553
  stainless, craters and penetration holes after exposure to micrometeorites 8=41579
  stainless, dislocations in surface layers in cyclic deform., obs. 8=40035
  stainless, electrolytic and thermal corrosion, effect of Si content 8=45334
  stainless, electron microscopy at high voltages 8=41971
  stainless, explosive shock-loaded, thermal recovery 8=49004
  stainless-fracture micro-mechanisms 8=49012
  stainless, heat-resistant, thermal conductivity 8=39943
  stainless, n irradiation creep obs. at 100°C 8=26833
  stainless, oxide X-ray fluorescence analysis 8=41304
  stainless, pitting corrosion critical potentials 8=49928
  stainless, Polish, low temp. specific heat 8=48730
  stainless, reactor material, embrittlement due to He prod. in (n, α) reaction 8=47406
  stainless, u. s. attenuation, 20-800°C 8=30945
  stearic acid desorpt. and exchange, obs. 8=30768
  strain-aged, discontinuous yielding grain-size dependence 8=26809
  strain rate sensitivity and yield point behaviour 8=44571
  stress-corrosion cracking and grain boundary corrosion, effect of structure 8=44569
  stress-corrosion cracking in high-tensile steel 8=31212
  temperature meas. from heat prod. softening, Templugs, 70-850°C 8=24024
  tempering, e-diffr. exam. 8=35680
  thermal recovery of explosive shock-loaded stainless 8=49004
  three-phase core of cold rolled sheet, flux density distrib. in mag. knot. 8=46377
  transformer, annealing effects at high-temp and vacuum 8=35107
  transformer, change of blast-furnace structure in mag. field 8=40153
  transformer, hot-rolled, internal oxidation zone structure and props. 8=36562
  transformer, hot-rolled, oxidation at 800-1180°C, and structure of oxide films 8=36561
  transformer, mag. props. cubic texture perfection dependence 8=36140

Steel—contd
- 2062, vanadium carbides formation during austenite $\gamma \rightarrow \alpha$ transform. 8=35135
- U8, quenched, tempering under high hydrostatic pressures 8=35679
- ultra-high strength, fracture toughness, effects of microstructure 8=49010
- vanadium, diffraction pattern, isothermal transformation 8=39791
- vapour scintillation, emission spectrum time scanning 8=34231
- Youngs mod. of hardened steel, effect of austenite decomp. 8=31208
- Al-killed, low C, recrystallization and texture development 8=44129
- B content determ. from neutron flux depression 8=37100
- C, internal friction and fatigue mechanisms 8=26813
- C–Mn steel, creep under cyclic stress and temp. conds. 8=26822
- in CO$_2$, corrosion and excrescence form. mechanisms, low alloy steels, $\leqslant$ 550°C 8=32098
- in CO$_2$, simultaneous oxidation and carburisation rel. to transport in porous scales 8=48777
- 17%Cr stainless, ridging formation mechanism 8=26810
- 15%Cr–4%Al ferritic, effect of 0.5%Y on oxidation in CO$_2$ 8=27704
- Cr-Mo, CO$_2$ oxidation resistance, effects of chem. comp., mech. treatment and remelting 8=45339
- Cr–Mo–Co, R-phase precip., structure and comp. analysis 8=44001
- 12%Cr-Mo-V-Nb creep resisting, creep and creep-rupture data rel. to microstructure 8=44576
- 20%Cr–25%Ni–Nb stainless, effect of 0.5%Y on oxidation in CO$_2$ 8=27704
- 27%Cr, annealed, Guinier-preston zones rel. to brittleness 475°C 8=35273
- Cr-Ni/Nb stainless, CO$_2$ oxidation n-irrad. 580°-840°C obs. 8=27705
- Fe–Mn–C, c/a ratio variation during martensitic transformation, –196 to 20°C 8=35334
- Fe-24%Ni-17%Cr-2%Ti, creep, rel. to γ' (Ni$_3$Ti) particle size 8=49002
- Mn effect on corrosion 8=49866
- Mn effects on impact properties 8=35693
- Mn, $\gamma \rightleftharpoons \epsilon^1$ and $\gamma \rightleftharpoons \epsilon$ transforms. dilatometric and X-ray diffr. exam. 8=35114
- Mo–Mn, R-phase precip., structure and comp. analysis 8=44001
- Ni effects on impact properties 8=35693
- Ni, phase transforms., mag. field effects 8=30702
- 9%Ni, struct. and growth characts. of bainite 8=44002
- 18 Ni-9 Co-5 Mo maraging heat treatment in 520-700°C temp. range 8=44572
- NiCoMo, mechanical properties 8=49016
- Ni 25%-Cr 20%-Nb 0.7% stainless, precipitates comp., obs. 8=30805
- O content determ. by O^{16}(n, γ)N^{16} 8=32167
- Si steel, deformed crystals, coercive forces temp. dependence 8=36174
- Si-Mn, fatigue crack initiation and propag., previous austenitic grain size effects 8=44575

Stellar atmospheres. See Stars.
Stellar clusters. See Stars.
Stellar composition. See Stars/composition.
Stellar motion. See Celestial mechanics; Stars.
Stellar structure. See Stars/structure.
Stellarator. See Plasma/devices.
Stereoisomerism. See Isomerism.
Stereophonic sound. See Acoustics.
Stereoscopy
- photographic range-viewfinder 8=42283

Stimulated emission. See Lasers; Luminescence; Masers.
Stimulated Raman scattering. See Lasers; Raman spectra; Scattering/light.
Stochastic processes. See Probability; Random processes; Statistical analysis.
Stokes flow. See Flow; Hydrodynamics.
Stokes law, fluids. See Flow; Viscosity.
Stokes law, optical. See Luminescence.
Stokes lines. See Luminescence; Raman spectra; Spectra.
Stopping power. See Particle range.
Storms. See Atmosphere/movements; Magnetic storms; Thunderstorms.
Strain effects. See Deformation; Elastic deformation; Plastic deformation.
Strain gauges
- capacitive, for solid He^3 compressibility meas. 8=37358
- hand-held, for surface vibration meas. 8=41804
- high-temp. fatigue, diametral extensometer 8=35630
- magnetostrictive load cell for use under high hydrostatic pressures 8=40103
- photoelastic, Rosette factor rel. to strain, temp. and fringe order 8=26753
- plastic strain meas., hydrostatic ring 8=35619
- quartz, shorted guard-ring development 8=37110
- surface displacement, hologram interferometry 8=37713
- transducers effect of adhesives on sensitivity 8=48981
- transducer for pressure difference meas. 8=32642

Strain hardening. See Work hardening.
Strange particles
- decays, survey 8=24827
- $\Delta S = -\Delta Q$ selection rule, decay rates of K$^\circ$, $\bar{K}^\circ$, K$^+$, Σ^+, Ξ° 8=33696
- $\Delta S = 2$ leptonic decays rel. to $\Delta S = -\Delta Q$ decay rates 8=33696
- leptons, in currents for weak interactions 8=24708
- meson exchange, effect on cross-section for Λ prod. in K$^-$p at 10 GeV/c 8=33834
- neutrinos, Cabibbo theory 8=24708
- nuclear reactions, review 8=29483
- production 8=25004
- production from 17 GeV/c π^- in heavy emulsion nuclei 8=33837
- p-p collisions, 6.92 BeV/c, YN resonances not obs., $N^*_{3/2}$ (1236), Y^*_1 (1385) obs. 8=24916
- tachyons, faster than light, fractionally charged, exptl. search 8=42388

Strangeness. See Elementary particles; Field theory, quantum.
Stratosphere. See Atmosphere.
Streamers. See Discharges, electric.
Strength. See Electric strength; Mechanical strength.
Stress analysis
- See also Bending; Photoelasticity; Strain gauges; Torsion.
- axi-symmetric elastic solids with cavities inside, under loading or torsion 8=41666
- beam subject to bending, stress distribution round hole in web 8=23826
- biharmonic, numerical, and applications 8=37131
- body deforming under anti-plane strain, plastic relax. and spread from sharp groove 8=32766
- boundary layer following shock wave over semi-infinite plate in tube 8=28386
- buckling of plates and beams by Lagrangian multipliers method, incorrect results 8=41661
- cast iron with spherical graphite, notch impact and inpact bend strength, testing 8=49017
- circular hole in infinite plate, micropolar elasticity 8=32738
- composite material reinforced with discontinuous fibres, stress, strain and displacement fields 8=46049
- concrete, of creep characts. 8=44536
- in contact of rigid cylinder on elastic layer connected to rigid base 8=37139
- continuum, assoc. between stress and strain tensors 8=46047
- cosserat plate, stress singularities around crack 8=41698
- cosserat surfaces and shells, elastic, linear theory 8=41700
- couple-stresses, effects on singularities due to discontinuous loading 8=32733
- cubic yield condition for incompressible bodies 8=48961
- in cylinder, thermal stresses due to heating or cooling in medium with variable heat transfer 8=37321
- diaphragms, rectangular, ultimate strength under hydrostatic press. 8=37154
- dielectric rectangle reinforced with inextensible cords, flexure and deform. 8=23843
- disc, infinite, with elliptic hole, induced state by temp. decrease 8=32736
- dynamic elasticity, difference method 8=23849
- elastic body with couple-stresses, two-dimensional problem of equilib. 8=41686
- elastic circular cylinder, homogeneous, general soln. 8=41696
- elastic sheets, overlapping, bonded 8=41689
- elastic sphere in solid, uniformly stressed at infinity, contact stresses 8=23831
- elasticae, plane, extensible, general solns. 8=46043
- elliptic die press. on elastic half-space 8=32711
- fading memory of material, weak principle formulation 8=32707
- with grating, f.m. amplitude 8=35616
- Griffith cracks, two coplanar, in infinite elastic medium 8=46042
- hollow cylinder with axisymmetric end loads 8=28264
- kinetic stress function determination in elastodynamics 8=46037
- laminated medium, edge buckling 8=41732
- line-loaded cylindrical shell 8=46034
- metal films, cubic, thermally induced strains 8=40122
- metal samples at 1.3°K, micromachine 8=48959
- metal working, microphotoplasticity techniques using laser systems 8=48954
- magnetostrictive composite rotating cylinder 8=28261
- mirror, parabolic, 4 m diam, elastic deformations by dynamic relaxation technique 8=41663
- mixture of two elastic solids, plane strain, linearized theory 8=32744
- noncircular rings under shear load 8=32720
- orthotropic circular plate, large deflection under concentrated load 8=32721
- plane stress theories for stretched plates 8=23848
- plane, upper bounds for breaking loads 8=23824
- plastic spherical sandwich shells subjected to hydrostatic press 8=41720
- plastic strain, iterative methods, convergence 8=41730
- plates and shells, use of hypergeometric functions 8=46038

Stress analysis—contd
  plate stability problem solution without preliminary determination of initial stress state 8=46031
  photoelastic, transmission-microscope polariscope 8=33283
  plate bending, triangular equilib. model 8=41660
  plates, circular, of hardening material, bending anal. 8=41727
  plate, thick stress state 8=46033
  in plate, with harmonic oscs. of temp. medium, calc. of thermal stresses 8=37160
  polystyrene melt, elastic behaviour 8=39261
  quartz plates, freq., stress depend. 8=49049
  radial nozzles in spherical pressure vessels, shakedown loads 8=32750
  in rate-dependent mats., anal. of time variation of strain grads. 8=23851
  Rayleigh functions, localized 8=37129
  rectangular plates, with cambered cross-sections, bending instability 8=37138
  rigid-plastic annular plate under dynamic loads, deflections 8=41811
  rods, general theory 8=37127
  sandwich plates, thermoelastic stability and thermally induced vibrations 8=46072
  sandwich tie/beam, optimum design 8=41659
  semi-infinite plate containing reinforced notch under uniform tension 8=41653
  in semilinear viscoelastic mats, of wave propag. after impact 8=32886
  rel. to shear modulus meas. in vibr. expts. 8=41810
  shells, helicoidal, axial extension and tension to rotationally symm. states 8=32734
  shells, linear theory, multivaluedness of stress functions 8=32718
  in shells of revolution, with symmetry about a curve 8=32713
  shells, shallow, multivaluedness of solns. 8=32719
  solenoid, bonded plain helical, elasticity 8=31166
  in solidification of infinite plate, tensile and compressive stress laws 8=39478
  solid-solution hardening in conc. solns., 8=48964
  solids, elastic, direct numerical determ., as shown by torsion problem 8=41702
  spherical caps buckled under conc. load 8=41697
  step load moving with superseismic velocity on surface of elastic-plastic half-space 8=32749
  stress-equilibrium and compatability eqns. body forces and arbitrary temp. fields effect 8=46023
  stress fields, solenoidal, general expressions 8=41681
  in thermoelasticity, stress function completeness 8=32775
  thick plate with cylindrical hole, thermoelastic eqns. 8=28279
  thin elastic layer, stress state properties 8=46029
  torsion, elastic-plastic, as problem in non-linear programming 8=41710
  twins, dynamic, rel. to deformation behaviour 8=48825
  two-dimensional frameworks, flexural, field solns. 8=32745
  viscoelastic materials, in rapid deformation 8=30376
  wave propagation in half-plane with boundary loading 8=37130
  window, rattling by sonic boom 8=46164
  X-ray analysers, portable, use in Boeing Co. 8=26754
  Cu-Cr alloys, stress rupture curves, 50-140°C, rel. to cavity formation, 8=48871
  KCl, critical shear, rel. to n- and γ-irrad. hardening 8=49037
  LiF ground powders, microstrains from X-ray diffr. line-broadening profiles 8=48600
  NaCl, critical shear, rel. to n- and γ-irrad hardening 8=49037
  Pb cylinders, compressive strain-time, strain-rate and dynamic force-time characts. 8=35711
  Si, thermally-induced, rel. to X-ray diffr. and birefringence obs. 8=49041
Stress effects
  ageing and strain ageing, terminology rel. to precip. phenomena 8=31162
  alkali metals, strained, phonon spectra 8=44296
  alloys, heat resistant, creep and fracture in creep, physical parameters, high temp. 8=26760
  alloys, strain excitation from exo-emission meas. rel. to defect props. 8=44938
  basalt and granite, strength, rel. to stress rate and temp. 8=48985
  b.c.c. and h.c.p. structures, activation volume relationship, cross slip energy 8=48963
  brass–NH_3 system, stress-corrosion cracking mechanism 8=35675
  α-brass, single and bi-crystals, rel. to corrosion cracking 8=26799
  brass, stress-corrosion cracking, mechanism 8=26798
  calcite, twin layer expansion, twinning and dislocation growth 8=31104
  central boss loading of rot. symmetric shells, limit anal. by numerical method 8=23840
  circular cylindrical shells, parametric instability, on in-plane longit. inertia loading 8=23821
  circular ring, radially constrained, instability due to thermal stress rel. to initial imperfections 8=23823
Stress effects—contd
  clamped plastic beam, anal. of permanent deform. considered as system of one deg. of freedom 8=23838
  corrosion cracking, rate controlling step 8=44534
  crack, elastic brittle, propagating, distrib. on extension surface 8=35634
  cracked plates, fracture 8=46025
  crystal point defect ordering, rel. to anelasticity 8=31027
  crystal of rock-salt structure, cyclic stressing 8=44518
  cylindrical elastic bars, suddenly loaded, stress and strain distribs. 8=23833
  cylindrical shell, orthotropic, stability to axial compression, bending moment and ext. press. 8=32752
  cylindrical shells, stability under axial compression due moving loads, soln. by Liapunov method 8=23822
  cylindrical shells, under lateral transient press., theory of dynamic pulse buckling 8=32712
  diffused structures, planar, strain effects, 8=48844
  dislocations, mobile, density and velocity, stress dependence from Lüders band front propag. velocity 8=31057
  dislocation movement through solid with dislocation pileups 8=40021
  dislocation segment bending and Franck–Read sources 8=44437
  elastic-plastic distrib. and fracture strength of notched bars 8=46058
  elastic waves in plates, prod. by impulse load on portion of edge 8=23834
  f. c. c. metals, fatigue mechanisms rel. to stress magnitude, ductility and texture 8=26772
  ferromagnetic films, uniaxially anisotropic, magnetization axis rotation under external stress 8=36131
  fibres, broken, in composite materials, load transfer 8=48975
  fracture in solids, invariant criterion, qualitatively correct 8=26770
  frame, two-member, non-linear buckling and snap-over 8=41655
  gas bubbles in solids, obs. 8=31108
  glass, residual, in heat treatment 8=26824
  gravitational stresses determ. using immersion analogy of Biot, generalization 8=23832
  Hastelloy, reactor material, stress-rupture due to neutron irrad. 8=47400
  h. c. p. metals, elastically strained, inner-displacement tensor 8=26406
  hollow dielectric, effects of polarization under extension, inflation and torsion 8=35947
  impact on finite elastoplastic bar, rel. to compression wave propag. 8=23934
  inclusion, circular, in infinite compressible medium, 2nd order elastic effects 8=23841
  mag. permeability induced by stress variations, instability study 8=49552
  metallic mats, localized peak stresses, meas. with thermo elastic effect 8=44517
  α-methylstyrene-methyl methacrylate copolymer, stretching effects, 125-150°C 8=49356
  microstrain and cyclic loading, surface effects 8=31170
  muscovites, shearing force anisotropy rel. to surface condition 8=44602
  polycaprolactam, photodegradation kinetics temp. dependence 8=45399
  polyethylene terephthalate, oriented, deformation bands 8=31244
  polyethylene terephthalate, photodegradation kinetics temp. dependence 8=45399
  polymer bonds, i.r. spectroscopy 8=43437
  polymer fibres, photodegradation kinetics temp. dependence 8=45399
  polymers, rel. to photodegradation kinetics 8=36619
  polymethylmethacrylate, laser destruction crack orientation 8=40191
  poly-n-butyl methacrylate in chlorinated diphenyl dilute solns. 8=39333
  polystyrene, laser destruction crack orientation 8=40191
  rigid-plastic bodies, surface of discontinuities of stress, relns. 8=48962
  rubber, crystallization, light scattering obs. 8=39682
  rubber, stretched, crystallization kinetics 8=39683
  in ruby piezospectroscopic studies of exchange-coupled Cr^{3+} pion pairs 8=27646
  rupture characts. of metals on basis of short-term creep data 8=44526
  silk, natural, photodegradation kinetics temp. dependence 8=45399
  steel, austenitic stainless corrosion cracking by internal friction meas. 8=40159
  Steel, corrosion in nitrate 8=45335
  steel, low C, strain age-hardening, time law 8=40158
  steel, mild, sharply notched, random and block-loading fatigue tests 8=26821
  steel, mild, stress-corrosion cracking and grain boundary corrosion effect of structure 8=44569
  steel, stainless, dislocation arrays under certain types of loading 8=40035
  superconductors, rel. to micromagnetic equations, derivation 8=35836

Stress effects—contd
- superconductors, type II, theory 8=40357
- tensor of finite length dislocation 8=48836
- turbulence, distortion of irrotational plane strain 8=39169
- understressing effects on fatigue strength, explanation 8=40114
- vicalloy strip, thermomechanical treatment effects in mag. props. 8=36135
- vicalloy in various structural states strained in tension, domain structure 8=40804
- Al alloy, 2024-T3, broad and narrow band random loading fatigue 8=44547
- Al alloy, yield surfaces, prestraining effect, exptl. study 8=40127
- Al, second-order strain accumulation, reverse cyclic torsion, temps. 8=40125
- Al, strain rate, during reversed loading 8=40128
- Al-Mg single crystals, flow stress 8=40123
- Al-Zn-Mg alloy, fatigue-crack propag. rel. to cycle freq. 8=44542
- BN, shear, and high pressure production of dense modifications 8=48374
- $BaTiO_3$, relaxation processes on subjecting to unidirectional mech. pressure pulses 8=35976
- BeO ceramics, extruded, residual, and grain deform. 8=44556
- C-Mn steel, creep under cyclic stress and temp. conds. 8=26822
- $CaF_2:Ho^{2+}$, g-factor stress dependence 8=31510
- CaF_2: Nd^{3+}, (U^{3+}) spin-lattice interactions in uniaxially stressed crystals 8=40912
- CdS, exciton splitting due to interactions between spins of e and hole 8=26920
- CdSe, exciton splitting due to interactions between spins of e and hole 8=26920
- CdSe, uniaxial, rel. to optical props. 8=36342
- Co crystals, tensile elastic strain effects on domain structure 8=36173
- Cu, crystal, n-irradiated, radiation hardened, critical shear stress temp. and strain rate dependence 8=31196-7
- Cu, cyclic stressing, shear modulus rel. to resistivity 8=40317
- Cu deformed crystals, flow stress gradient between surface and centre 8=26804
- Cu, heated in Zn vapour, weight increase due to Zn diffusion 8=35485
- Cu, on pore formation during creep 8=35524
- Cu, optical constants, uniaxial and hydrostatic strain dependence rel. to interband transitions 8=49724
- Cu, strain excitation from exo-emission meas. rel. to defect props. 8=44938
- Cu whiskers, plastic behaviour, thickness depend. 8=40148
- Cu-Al alloys, stacking faults 8=48868
- Cu_2O, absorpt. exciton lines, polarization effect 8=45185
- Cu_2O, uniaxial deform., change of bond energy of excitons 8=35790
- Fe, local stress relax. rel. to strain rate 8=35676
- Fe-0.025% N, enhanced aging due to γ-α transform 8=44577
- GaAs, electroreflectance, rel. to electronic structure 8=49725
- in GaP p-n junction I-V charact. 8=31403
- GaP p-n junction, on I-V charact., and simultaneous illumination effect 8=49288
- p-GaSb, piezoresistance dependence causing activation energy change 8=44776
- n-Ge, breakdown, elec. low-temp., uniaxial rel. to critical field 8=27104
- Ge, electroreflectance, rel. to electronic structure 8=49725
- Ge energy gap rel. to high uniaxial press. along main axes 8=27102
- Ge, mechanical, on diffusion path length of minority carriers 8=35889
- K, strain-dependent magnetoresistance 8=49166
- LiF, programme-hardened dislocation mobility 8=44450
- Mg-6 wt.% Zn-0.5 wt.% Zr alloy, diffusional creep with low strain rate sensitivity 8=26830
- $NaCl:Cu^+$, resonant bandmode freq. shift 8=48708
- Nb, rel. to dislocation-velocity, etching meas. 8=31085
- Ni crystals, stress-relax. meas., 77-350°K 8=40178
- Pb, creep at high temp., stress depend. of secondary stages 8=49043
- Pb, simple shear, flow rel. to grain size and boundaries 8=35713
- Pb, slip bands, orientation distrib. under pure shear 8=48864
- Pt-50% Co alloy, uniaxial mag. anisotropy induced by tempering under stress 8=31702
- RbCl, induction, effect on K-absorption 8=41132
- S_2^- centre in alkali halides, paraelastic behaviour rel. to opt. absorpt. bands 8=45173
- Si, electroreflectance, rel. to electronic structure 8=49725
- Si energy gap rel. to high uniaxial press. along main axes 8=27102
- Si masking films rel. to devices 8=49047
- Si-Fe crystals, tensile elastic strain effects on domain structure 8=36173
- Ta, on surface superconductivity 8=44739

Stress effects—contd
- Th, flow stress, effect of C content, 0.008 to 2.83 at % 8=44603
- $ThO_2:Yb^{3+}$, g-factor stress dependence 8=31510
- Ti alloys, corrosion cracking 8=27716
- Zn, rel. to twinning and slip by indentation at 5 kg loads 8=31056
- Zn, shear, mobility of edge dislocations 8=44457
- Zn, stress state required for pyramidal dislocation movement 8=40045
- ZnO, exciton splitting due to interactions between spins of e and hole 8=26920

Stress measurement. See Strain gauges.

Stress/strain relations
- See also Elastic constants.
- adiabatic strain-cycling and temp. rise model, dispersion relations appl. 8=40102
- ageing stress- and strain-, terminology rel. to precip. phenomena 8=31162
- alloys, calc. of critical resolved shear stress due to particles 8=40106
- alloys, critical resolved shear stress calc. 8=40105
- bars, thick straight, theory of bending 8=41664
- bonded joint adhesives, capacitive meas. 8=35639
- Burgers media, thermodynamic derivation 8=28260
- circular ring, radially constrained, stability when subjected to thermal stress 8=23823
- composite material reinforced with discontinuous fibres, stress, strain and displacement fields 8=46049
- crystals of rock-salt structure, cyclic stressing 8=44518
- in cylindrical shells under lateral transient press., rel. to dynamic pulse buckling 8=32712
- displacements and strains, finite element method 8=41677
- distributions in suddenly loaded cylindrical elastic bars 8=23833
- ferromagnetic solid with lattice imperfections, stress equation props. 8=48937
- glass-reinforced plastics, nonlinear deformation 8=31236
- hysteresis in microstrain regions, rel. to dislocation substructure and friction stress 8=26744
- iron and some alloys strain-rate sensitivity and temp. dependence of flow stress 8=44573
- Lüdens front number effect on yield point 8=32767
- mechanical deform. of elec. cond. mats, theories 8=26752
- membrane displacements and strains, finite element method 8=41677
- metals, f.c.c., internal friction rel. to strain amplitude 8=26742
- metal films, cubic, thermally induced strains 8=40122
- metal, strain ratio meas. method 8=35641
- metal, test behaviour and working props. 8=40087
- nonlinear, for isotropic, homogeneous material 8=41658
- nuclear canning material, tension-compression tests at elevated temp. 8=35628
- pavement, dynamic testing, mobile unit 8=32633
- plastic, matrix method 8=28258
- plasticity, statistical theory 8=40104
- polymers, local stress strains theory 8=31235
- Portevin-Lechatelier yielding, effect of grain size 8=44516
- rubber, in equilib. compression 8=31251
- steel, mild, logarithmic depend. for strains up to 5% 8=44571
- steel, mild, stress-strain curve, statistical examination 8=35692
- Torpin's strain-gradient theory, boundary conditions 8=41684
- in torsion of elastic cylinder welded to elastic half space 8=23827
- two-dimensional frameworks, flexural, field solns. 8=32745
- viscoelastic media, three-dimens. deform. 8=28275
- viscoelastic solid sphere, axisymmetric loaded, linear wave propag. 8=26750
- viscoplastic rods under impact 8=41724
- Zircaloy tubing, strain behaviour effect of texture on ansiotropy 8=26853
- Zircaloy-2, rel. to corrosion behaviour 8=26852
- Al, strain-rate depend. of ductile-brittle transition temp., in liq. metals 8=35657
- Al, third harmonic generation of sinusoidal stress wave, rel. to dislocations 8=44442
- Al-Cu alloys, aged, orientation effect on crit. shear stress 8=48991
- CaO, Fe group impurities, uniaxial stress meas., strain coeffs. 8=40134
- Co single crysts. rel. to slip and dislocation struct., 78-573°K 8=40138
- Cu, commercially pure, tension and torsion creep recovery 8=26805
- Cu crystal, n-irradiated, radiation hardened, critical shear stress temp. and strain rate dependence 8=31196-7
- Cu deformed crystals, flow stress gradient between surface and centre 8=26804
- Cu, initial dislocation substruct. influence on curves 8=44459
- Cu–58% Zn alloy, polycrystalline, in alternating microdeformation 8=35644
- LiF crystal, dislocation distrib. rel. to loading 8=31082
- Mg, textured, deform. rel. to plastic anisotropy 8=44587

Stress/strain relations—contd
Nb crystals, shear-stress strain-rate dependence, characterization 8=31220
Ni-17%Cr alloy, polycrystalline, in alternating microdeformation 8=35644
α-SiO$_2$ moduli changes in electric field 8=44600
Sn, stress and temperature, rel. to strain-rate 8=31232
Ta–Mo alloys, effect of Mo content 8=35718
Ta–Nb alloys, effect of Nb content 8=35718
Ti sheet, anal. of plastic anisotropy by crystallographic tech. 8=35721
W, rel. to dislocation substructures 8=44455
W–Re alloys, rel. to dislocation substructures 8=44455
W–3%Ta, rel. to dislocation substructures 8=44455
Zn sheet, anal. of plastic anisotropy by crystallographic tech. 8=35721
Zn–Al alloys, flow rate behaviour rel. to structure 8=40187
Zr, rel. to corrosion behaviour 8=26852
Stresses, internal
alumina (96%) rods, thermally conditioned, residual, and flexural strength 8=35659
ammonia crystals, relaxation 8=35708
α-brass, relax., 78–295°K rel. to dislocation behaviour 8=31193
α-brass, stretcher strains and discontinuous yielding rel. to grain size, obs. 8=40141
"blow-off" phenomena, laser-induced, ensuing stress pulses, obs. 8=40065
concentrated forces rel. to edge dislocations 8=48838
concentrations, dynamical, in elastic plate, effect of non-propagating wave 8=41694
cosserat plate, singularities around crack 8=41698
in crystal growing, theoretical investigation 8=26224
crystal plate, thermal, and plane temp. field 8=44355
crystalline solid, conc. at step on surface 8=48951
in deformation transmission through crystal by dislocation pile-up break-through mechanism 8=26661
dielectrics, transparent, constraints developed by luminous wave 8=27524
diffused structures, planar, strain effects 8=48844
rel. to dislocation linear array pile-up 8=31073
due to dislocation random distrib. 8=31165
in elastic anisotropic medium, field round elliptical crack 8=41706
elastic plates, dynamic concentrations 8=37150
elasticity, plane, depend on Poisson's ratio 8=41683
epitaxial films on mica and NaCl substrates, causing film curling 8=35157
epoxy resin, reinforced 8=31243
films, condensed, macrostresses form and classification 8=31164
films, vacuum deposited, residual stresses, X-ray diffr. obs. 8=44537
h.c.p. crystals, anisotropic, fields around edge multipole and multipole arrays 8=26795
inclusions in steels, their thermal expansion and reln. to tessellated stresses 8=44350
isotopes evolution model with crustal material recycling through mantle 8=36682
in magnetomechanical damping, distrib. effects 8=31568
in medium with microstructure, extension of dislocation continuum theory 8=44519
metal films 8=48953
metals, electrodeposited, effect of hydrogen 8=31167
optical indices, glasses in optical glass catalogue 8=41096
Permalloy film, rel. to ferromag. reson., obs. 8=31821
Permalloy films, ferromag. reson. obs. 8=31223
piezoelectric element, stress-pulse-activated, secondary stresses 8=40107
in plates, thin, flexure 8=37137
point and line defect movement in continuum theory 8=48952
rel. to Poisson's ratio anomalies after deform. and annealing, $\mu < 0.5$ 8=40095
polymer coatings, correl. with thermal props. 8=30759
residual, meas. using photoelastic gauge, approx. soln. for shear lag effect 8=41691
in reversing sliding, effect of surface-active lubricants 8=35617
semiconductors, mag., rel. to thermal and mag. induced optical absorpt. edge shifts 8=36299
shear-stress field of simple dislocation cell 8=44433
shells, shallow spherical, membrane and bending stresses 8=37141
solenoid, bonded plain helical, elasticity 8=31166
solids, ultrasonic meas. 8=31163
strain deformation, near crack tip in power-law hardening material 8=41717-8
strain field, X-ray determ. 8=26786
tetrahedral lattice, h.p. stress difference meas. 8=45943
thermal, in viscoelastic tube with temp. depend. props. 8=23855
Zircaloy-2, rel. to corrosion behaviour 8=26852
Zircalloy-4, irrad.-enhanced strain relax., 2.4×10^{14} nv > 1 MeV 8=35732
AgCl, plastically deformed, strain and dislocation exam. methods 8=26662
Stresses, internal—contd
Al films, grown by evaporation, rel. to elec. props. 8=44040
Al, rel. to stored energy at low temp. deformation 8=49000
Al-8.7 at.%Zn alloy, strain field, X-ray determ. 8=26786
Al–Ge solid solns., rel. to stacking faults in precip. 8=31096
BeO polycrystals, grains, subgrains and stress analyses 8=26291
Co electroless films, microstrain, obs. 8=44165
Co–Ni–Fe films, production parameter dependence 8=31192
Cu, rel. to stored energy at low temp. deformation 8=49000
Cu-2%Be alloy, diffuse striations obs. at 200°C rel. to strain-contrast effect 8=30859
Cu–Ni alloys, post-deformational, rel. to work hardening 8=31194
Cu–Si–Mn, relax. anomalies, 200-400°C 8=35668
Fe, degree of heterogeneity of local stresses from relax. meas. 8=35676
Fe films, condensed, macrostresses form. rel. to substrate temp., obs. 8=31164
Fe, residual strain distrib. 8=31214
LiF ground powders, microstrains from X-ray diffr. line-broadening profiles 8=48600
LiF, relax. during thermal processing 8=40167
Mo, dislocation velocity stress dependence at 77 and 300°K 8=26684
Ni, electrodeposited, process conditions rel. to microstrain formation 8=26298
Ni film, rel. to ferromag. reson., obs. 8=31821
Ni–Fe films, production parameter dependence 8=31192
Si, thermally-induced, rel. to X-ray diffr. and birefringence obs. 8=49051
SiO$_{2-x}$N$_x$ films on Si, comp. dependence rel. to chem. vapour deposition 8=48462
Si:P diffusion junctions, intense interjunction strain 8=49046
Si:P planar diffused structure, propag. through strain effects 8=48844
SrCl$_2$, coeffs from lattice constants meas. 26-294°C 8=39931
Zn, effect on basal dislocation mobility 8=44456
Zn twinned crystals, relax. at twin boundaries rel. to internal friction 8=35727
Zr, rel. to corrosion behaviour 8=26852
Zr–2.5 wt.%Nb–0.5 wt.%Cu, irrad.-enhanced strain relax., 2.4×10^{14} nv > 1 MeV 8=35732
Striations. See Discharges, electric.
Stripping reactions. See Nuclear reactions.
Stroboscopes
electron microscopy, stroboscopic scanning 8=33008
u.s., for acoustic vel. meas. 8=28373
u.s., for dispersion meas. 8=46197
vibration analysis by stroboscopic holography 8=23919
Strong interactions. See Field theory, quantum/interactions, strong.
Strontium
determination, by atomic absorpt. 8=45417
distribution between potassium feldspar and plagioclase simultaneously crystallized at 600°C 8=36627
isotope ratios in volcanic rocks of three island arc areas 8=32186
Sr^{90} as fission product on coated fuel particles, determination 8=47404
Strontium compounds
(Sr$_{0.4}$Bi$_x$La$_{0.6-x}$)MnO$_3$, structure, mag. and dielc. props. 8=26038
(Sr$_{1-y}$Bi$_y$)MnO$_3$, structure, mag. and dielec. props. 8=26038
(Sr$_y$Ca$_z$Ba$_x$)MgSi$_2$O$_8$, equilibria in subsolidus phases rel. to luminescence 8=49789
SrC^{14}O$_3$ powder, radioactivity meas. when insoluble in liquid scintillator counter 8=47278
SrCl$_2$, lattice thermal expansion, 26-294°C 8=39931
SrCl$_2$-H$_2$O, phase boundaries below 500°C 8=48366
SrCl$_2$-H$_2$O, phase boundaries to 40 kbar 8=39467
SrD, new u.v. absorpt. bands 8=43338
SrF$_2$, exoelectron emission, X-ray and thermo-stimulated, obs. 8=36040
SrF$_2$, formation energies of anion and cation point defects Born-model calc. 8=35540
SrF$_2$, Grüneisen parameter, low-temp. limit, calc. on Axe's shell model 8=48748
SrF$_2$, heat capacity, enthalpy and entropy 8=44339
SrF$_2$: paramagnetic impurities, n.m.r. of F^{19}, temp. and impurity conc. dependence 8=40974
SrF$_2$: Co^{2+}, absorpt. spectra temp. dependences 8=41076
SrF$_2$: Dy^{3+}, e.s.r. in cubic fields 8=36252
SrF$_2$: Eu^{++}, F^{19} spin lattice relax. time angular depend., 4.2, 77 and 300°K 8=36265
SrF$_2$: Gd^{3+}, e.p.r. spectral cubic splitting temp. dependence, 77-950°K 8=40909
SrF$_2$: Tb^{3+}, e.p.r. and spin-lattice relax., 8=40944
SrF$_2$: Y, X-irradiated, polarized luminescence and structure of luminescence centres 8=36478
Sr$_2$(FeMo)O$_6$, mag. ordering from n-diffr. studies 8=27436
Sr$_2$(FeMo)O$_6$, ordered perovskite, mag. and elec. props. 8=36195
SrH, new u.v. absorpt. bands 8=43338
SrHAsO$_4$. H$_2$O, haidingerites, cry. struct. 8=48641
SrNO$_3$, vibration freq. uniaxial pressure-dependence 8=39877

Strontium compounds—contd
  SrO, emission props. in BaO stream 8=27349
  SrO, i.r. bands 8=34237
  SrO, i.r. dielectric response rel. to lattice vibrations 8=41075
  SrO, x-irrad., thermoluminescence 8=41184
  SrO-TiO_2-SiO_2 systems, glass formation 8=44079
  SrO. $4Fe_2O_3$. $2Al_2O_3$ single crystal, magnetization process and reversal 8=31741
  $Sr_3(PO_4)_2$, phosphor for detection of vac. u.v. radiation 8=41179
  $Sr_3(PO_4)_2$: Tb, bluish-white emitting cathode-ray phosphor with long decay time 8=49813
  $SrRuO_3$, ferromagnetic props. 8=36177
  SrS, lattice thermal expansion, 30-273°C 8=39931
  $SrTi_{1-x}Fe_xO_{3-x/2}\phi_{x/2}$, prep., struct., and elec. props. for varying x 8=35252
  $SrTiO_3$, a.c. Hall obs., depend. of Hall mobility on charge-carrier density 8=31392
  $SrTiO_3$, acoustic wave generation by electrostrictive mixing of light waves 8=45162
  $SrTiO_3$, annealed, elec. double hysteresis 8=49376
  $SrTiO_3$ crystals, electro-optical effect, 23 to —183°C 8=36416
  $SrTiO_3$, electro-optical effect, temp. dependence 8=36414
  $SrTiO_3$, electrorefl. oscills. rel. to h. f. free-carrier mass 8=36415
  $SrTiO_3$, ferroelectric phase transitions, lattice-dynamical theory, elastic and dielectric anomalies 8=27284
  $SrTiO_3$ ferroelec. props. rel. to similarity transformations 8=49360
  $SrTiO_3$, ferroelectrically active vibration mode, 77 to —173°C 8=35984
  $SrTiO_3$, growth from molten salts 8=48559
  $SrTiO_3$, optical lattice vibrs. 8=44287-8
  $SrTiO_3$, optical props. near absorpt. edge 8=27609
  $SrTiO_3$, photoconductivity and Hall effect 8=40675
  $SrTiO_3$, photoconductivity, anomalous temp. dependence 8=27331
  $SrTiO_3$, photomagnetoresistance by dc method at 10°K 8=44976
  $SrTiO_3$, polarons, in anisotropic energy bands 8=49118
  $SrTiO_3$, press. depend. of dielec. consts. at low temp. 8=27283
  $SrTiO_3$, Raman spectrum down to 25°K 8=32035
  $SrTiO_3$, refractive index, temp. depend. 8=49708
  $SrTiO_3$, solid solutions, dielectric relaxation 8=49375
  $SrTiO_3$, superconductivity 8=27034
  $SrTiO_3$, thermal conductivity temp. and field dependence rel. to Cochran modes 8=26605
  $SrTiO_3$, 110°K phase transition, soft-phonon at corner of Brillouin zone 8=39564
  $SrTiO_3$:Fe^{57}, Mossbauer study rel. to iron sites in lattice and oxygen vacancies 8=43958
  $Sr_3Yb_2Ge_3O_{12}$, synthesis by precipitation in IM NaOH 8=48557
  $Sr_3(Yb, Lu)_2(OH)_{12}$, synthesis by precipitation in IM NaOH 8=48557
Structure factors. See Crystal structure, atomic; X-ray crystallography.
Structure of matter. See Crystal structure; Liquids/structure; Solids/structure.
Sublimation
  See also Heat of sublimation; Vaporization.
  benzene, energy, molec. calc. 8=39495
  metal absorbing laser radiation 8=26003
  from walls of duct, mass transfer coupled with heat transfer from gas flow 8=35013
  BeO-BeF_2 system at high temp. 8=35012
  CdO crystal growth 8=26244
  CO_2-H_2O mixture, 80-230°K obs. rel. to composition of Martian icecaps 8=32547
  Cs_2CO_3, evaporation products, mass-spectrometer obs. 8=48294
  NH_4ClO_4, kinetics 8=30609
  MnSe, Knudsen meas. 8=39498
  Si epitaxial layers, obtained in vacuum 8=35256
  ZnSe(Cu, I. Cl) layers, prod. and electroluminesc. obs. 8=41211
Sudden commencement. See Magnetic storms.
Suhl effect. See Hall effect; Semiconductors.
Sulphur
  abundance in solar photosphere 8=28172
  adsorption layers on Cu, structure and formation conditions 8=48490
  atom, nonempirical SCF calc. 8=47596
  atom, satellite X-ray lines due to transitions involving double ionization of inner shells 8=43228
  atomic, forbidden lines, wavelengths and A-coeffs. 8=25365
  Auger electron emission, chemical effect 8=43227
  diffusion in Cr_2O_3 at 1000°C 8=44384
  diffusion in Mo, 2220–2470°K 8=35502
  diffusion into GaAs through SiO_2 films 8=35493
  direct recovery from white metal 8=41281
  impurity in thoriated Ni, effect on recrystallization 8=44138
  inner-electron binding energy and chem. bonding 8=29627
Sulphur—contd
  ions, oscillator strengths for resonance lines present in solar spectrum 8=29647
  liquid, e. p. r. obs. 190°-320°C 8=30527
  in liquid Fe alloys, phase equilibrium 8=41249
  orthorhombic, electron, electron drift, temporal variations 8=31386
  potential energy calc. of orthorhombic crystal as a function of unit cell parameters 8=39502
  sulphur dioxide-hydrogen viscosity, 30°-200°C, below 10 cm Hg press: Chapman-Enskog theory 8=43702
  S^{32} ion beams in mylar, stopping powers 8=44508
  S^{35} amino acid and synthesis, high-temp. attempt. 8=41261
  S^- ion reactions with triatomic mols. 8=29979
  S_2, ${}^1\Delta^u$-${}^1\Delta_-$ transitions 8=38851
  S_2, dissoc. energy 8=38935
  S_2 formation after flash photolysis of CS_2, COS, NO in presence of inert gas 8=49956
  S_2, molecular spectrum, rare gas matrix effect 8=47618
  S_2^- centre in alkali-halides, paraelastic behaviour 8=45173
  S_2^-, paraelastic behaviour in KI 8=48336
  S II/III, e impact line broadening calc. 8=47507
  S_6, force and torsional consts. comparison with S_8 values 8=43332
  S_n, high-temp. vapours, photoionization 8=47791
Sulphur compounds
  bisthiourea $Cd(NO_3)_2$ atomic crystal structure 8=35324
  dithionic acid salts, rotatory dispersion and sp. rotation temp. dependence 8=27602
  metal thiocyanate molten solns., i.r. spectra 8=25934
  sulphate, atmosphere, particle size distribution obs. 8=50129
  sulphide polycrystalline ores, annealing effect on grain boundary movement 8=26843
  sulphospinels, binary, miscibility studies from x-ray diffr. and mag. props 8=30653
  D_2S_2, force field from i.r. spectra 8=43331
  HSO_3Cl solns. of simple bases, elec. cond. 8=48194
  H_2S and H_2S-Ar, thermal cond., 273-1173°K 8=47962
  H_2S, nonempirical SCF calc. 8=47596
  H_2S_2, force field from i.r. spectra 8=43331
  H_2SO, nonempirical SCF calc. 8=47596
  H_2SO_4. H_2O, H bonding rel. to crystal structure 8=26400
  SCN^-, ht. of formation 8=29980
  $S(CN)_2$ mol. force field and Coriolis coupling coeffs. Calc. 8=43333
  SF_5Cl, rotation spectrum at 8 mm 8=25515
  SF_5Cl, vibr. spectra 8=25516
  SF_6 arc plasma, transport props. from temp. meas. 8=39012
  SF_6, electron detachment in swarm conds 8=29978
  SF_6 hydrate, dielec. props. and n.m.r. 8=49342
  SF_6 injection into ionized Ar flow at high temps. 8=43478
  SF_6, mols. coherent excitation by lasers, photon echoes obs. 8=34282
  SF_6, rate of ionization by electron attachment, two-body process 8=43471
  SI, Fraunhofer solar spectrum, forbidden line $3p^4\ {}^3P_2$-$3p^4\ {}^1D_2$ obs. 8=50444
  SO molecule, $b\,{}^1\Sigma^+$—$X^3\Sigma^-$ band spectrum obs. 8=38852
  SO $B^3\Sigma^-$ - $X^3\Sigma^-$ system Morse Franck-Condon factors, r-centroids for 8=43336
  $SOCl_2$, rotation spectrum, 8=43335
  SO_2 and SO_2-Ar, thermal cond., 273-1173°K 8=47962
  SO_2 aq. soln., absorpt. spectra, 25°C and up to 6 kbar 8=48160
  SO_2, lifetime of lowest triplet state 8=38853
  SO_2, reactions with free ethyl radicals; 28-75°C 8=49848
  SO_2^- radical ion, e.p.r. investigation 8=38948
  SO_2, reactions with free methyl radicals, 25-164°C 8=49847
  SO_3+F_2SO_3, reaction kinetics 8=45333
  SO_3^- free radicals optical spectrum from photolysis of dithionate ions in soln. 8=49957
  SO_4 ions in water from lakes and rivers, O isotope meas. 8=50095
  SO_4^{2-}, vibr. spectra in cryst. $M_2^IM^{II}(SO_4)_2$. $6H_2O$ 8=27601
  $S_2O_6F_2 \rightleftarrows 2SO_3F\cdot$ free radical equilib. in gaseous state, e.s.r. 8=47711
  $SPClF_2$ vibr. spectra 8=25517
  $SPCl_2F$, vibr. spectra 8=25517
  $SPCl_3$, vibr. spectra 8=25517
Sun
  See also Sunspots.
  active regions, struct. and development, symposium, Budapest (1967) 8=45900
  activity and brightness of Jupiter's great red spot, correlation 8=45829
  activity as triggering mechanism for earthquakes 8=27846
  activity and geomagnetic storms, 1966 8=28176
  activity max., rel. to variations of ionization rate in F2 layer at high latitudes 8=45550
  activity, prediction, possible method 8=50451
  activity, rel. to E-2 layer appearance 8=50193
  activity, rel. to mag. disturbance in Arctic 8=45571
  activity rel. to tidal force induced by planets 8=37064
  activity, strong surge, Sep. 2 1966, obs. at Alma-Ata 8=45897
  atmosphere, convective instability rel. to mag. field 8=45913
  atmosphere, H^- forbidden continuum effect 8=50440

Sun—contd
atmosphere, nuclear reactions, high energy 8=37072
atmosphere, turbulent vels, changes rel. to height 8=32606
auroele, 4′–66′ from limb, intensity rel. to weather conds. 8=37041
blast wave, dynamics and interact. with standing magnetopheric shock wave 8=41391
brightness-temp. meas. modification of chromospheric models 8=50455
chromosphere-corona interface, magnetic fields and temp. structure modification 8=45920
chromosphere, high resolution photography 8=45917
chromosphere, low, temp. gradient from limb intensity var. obs. 8=37089
chromosphere, lower, Ti^+, Y^+ and Fe^+ emission regions and H conc. 8=45914
chromospheric filament, field of Lα-emission 8=32605
coelostat for Catania observatory 8=28163
cosmic ray modulation 8=32500
differential rotation, rel. to energy transport from samller modes, and eddy dissipation 8=45859
disc centre growth curve, obs. 8=45891
equivalence principle validity from perihelion precession of Mercury 8=50416
Fabry–Perot etalon use for monochromatic imaging 8=45857
facolae and photosphere turbulent vels., obs. 8=45892
granulation, rel. to excitation of azimuthal current in rot. fluid 8=24170
gravitational field, internal, rel. to light waves bending, metric theory 8=32569
gravitational field quadrupole moment from Icarus' orbit 8=41751
interior, models and neutrino flux calc. 8=45860
ionosphere spread-F influence 8=32358
m. h. d. processes, laboratory simulation 8=33109
modulation of cosmic ray, α to electron ratio as test 8=42691
object, unidentified, crossing the Sun August 1966 8=45575
overluminous phase, condensation of planets 8=28147
photographic recording films, modulation transfer functions and 'detectibility threshold' 8=28162
photosphere, abundance of Rb 8=45894
photosphere, C, N_2 and O_2 abundances 8=28171
photosphere, curve of growth, effect of parity terms 8=32595
photosphere, Fe abundances 8=28174
photosphere in convective motion and gravitational red shift, rel. to Fraunhofer line absolute wavelength 8=37062
photosphere, lower, vertical oscs. of Δ 300 sec, rel. to underlying convection zone 8=45893
photosphere, Na, Al, P, S and K, abundances 8=28172
photosphere, oscillations and vel. fields, props. 8=28170
photosphere, Si abundance 8=28173
photosphere, turbulent motion, theory of random walk of magnetic lines 8=41526
photosphere, vel. fields, spatio-temporal Fourier analysis obs. 8=50449
photospheric granulation, high spatial resolution cinematography 8=32578
photospheric vel. meas., fluctuations rel. to scanning effect of atmos. seeing 8=41591
rotation, effect on solar wind plasma 8=32591
solar modulation effect 8=32500
solar plasma, interaction with geomag. field, importance to theory of generalized Riemann problem 8=45482
structure, evidence from neutrino flux 8=45861
structure of quiet photosphere and low chromosphere, conference, Arnhem, Holland 1967 8=32592
temperature reversal, radiation-driven waves 8=45858
Ca flocculi, 1965, obs. 8=50450
Fe absorpt., for photospheric abundances 8=28174
Li content, comparison with earth's composition 8=50292
Y abundance from Hartree-Fock self-consistent wave functions 8=50441

corona
chromosphere-corona interface, magnetic fields and temp. structure modification 8=45920
composition, radiation pressure recalc. 8=45922
dynamical theory 8=41586
emission intensity, 5303Å, obs. (July-Sept. 1967) 8=32570
green, autocorrelations of obs. 8=50459
green line photoelectric meas. of eclipse, November 12, 1966 8=45864
hydromagnetic disturbances propag., Moreton's wave phenomenon obs. 8=37086
inhomogeneities rel. to spicules 8=37079
ionization equilib., effect of collisions 8=25722
isophote study from eclipse of Nov. 12, 1966, ellipticity and brightness grads 8=37087-8
jets, photographed from stratospheric balloons 8=45912
Lyot-coronagraph with 53cm objective, description 8=28187
magnetohydrostatic eqn. soln. predict temp. electron density, var. with height 8=50456
microwave absorpt. lines from dielectronic recombination of highly ionized atoms 8=47479
photometric data from 1962 Feb. eclipse 8=37083
small-scale inhomogeneities of mag. field 8=45848
streamer of active region obs. at 1962 New Guinea eclipse 8=50458

Sun—contd
corona—contd
structures, helmeted, general props. 8=37081
temperature rel. to Fe^{+m}, ($8 \leq m \leq 15$), ionization cross-sections 8=37085
temperature, revaluation from new ionization obs. 8=45923
u. v. heliograms for struct. and intensity 8=37080
Fe and Si relative abundance obs. 8=37084
Fe XV lines relative intensities 8=37082
Si and Fe relative abundance obs. 8=37084
T Coronae Borealis outbursts obs. 8=50457

eclipses
ionosphere, f_0F2 (20 May 1966) 8=50200
line profile charges rel. to distance from centre, comparison with non-eclipse obs. 8=32572
1961 Feb. 15, sky radiance spectra distrib. at Delhi, obs. 8=41364
1962 Feb., rel. to solar corona photometric data 8=37083
1962, February 5, chromospheric spectrum 8=45919
1962, New Guinea; active region streamer of solar corona obs. 8=50458
1963, July 20, eastern region occultation, obs. at Ann Arbor at 4 cm, wavelength 8=28164
1966 Nov., rel. to S-component of radiation obs. 8=37055
1966, Nov. 12, at Bajé, study of coronal isophotes 8=37087-8
1966 Nov. 12, ionospheric absorption var. obs. 8=27978
1966, November 12, photoelectric meas. of green coronal line 8=45864
1966 November 12, total eclipse 8=45863
20 May 1966, ring eclipse, O_3 content in atmos. 8=50130
zenith sky brightness and colour during total eclipse of 12-11-66, Bolivia 8=36742

flares
accompanied by type IV bursts 8=32602
association in time with radiobursts and surges 8=37056
astronaut radiation damage rel. to shielding 8=41595
blast wave induction, interact. with standing magnetospheric shockwave 8=41391
rel. to cosmic-ray var. characteristics and interplanetary space 8=42762
chromospheric, intensity analysis after cosmic rays generation 8=38153
in corona, photographed from stratospheric balloons 8=45912
cosmic ray composition effect of nuclei obs. 8=29236
cosmic ray increase of January 28, 1967 8=41598
cosmic ray rel. to sunspot mag. fields 8=32599
development, and acceleration of solar cosmic rays 8=45904
effects on v.l.f. radiowave propag. in lower ionosphere 8=32325
electron events in solar-flares obs. correlations with radio, X-ray emission from sun 8=41596
electrons, energetic, obs. 8=37076
electrons, fast, production 8=37078
11-year var. rel. to cosmic ray rigidity 8=42763
rel. to filaments, type IV bursts and loop prominences 8=45905
and force-free mag. fields 8=37074
ionospheric effects, theory 8=41413
magnetic field annihilation, Petschek model, neutral-point anomaly 8=32600
modulation of cosmic electron and helium 8=42687
neutron and γ rays produced by nuclear interactions 8=41599
noise storm sources rel. to optical features 8=32603
nuclear reactions, high energy, particles and radiation prod. 8=37072
observations (July-Sept. 1967) 8=32570
1942, March 7, cosmic ray flare 8=37073
1966 March 24, 10 to 100 MeV, proton obs. 8=28181
1966 September 2, composition and characteristics 8=41597
particle accel. by mag-field, simulation by laser prod. plasma 8=29998
positions rel. to photospheric mag. fields, and neutral line of longit. component 8=28183
production of two anomalous X-ray emissions, effects of superposition in middle ionosphere 8=45516
proton and e propag. event (7 July 1966) 8=45907
proton, international project, symposium, Budapest (1967) 8=45900
proton, long-term forecasts, 174 flares obs. during 1956-1965 8=37075
proton (7 July 1966), sector boundary crossing effects 8=45908
proton, August 28, 1966 from 2 plages 8=45910
proton, var. rel. to solar cycle 8=32604
proton, X-ray ionospheric disturbances 8=36838
r. f. and X-radiation 8=32601
sector boundary crossing effects, generality 8=45909
strong surge of activity Sep. 2 1966, obs. at Alma-Ata 8=45897
varieties, identification and nomenclature 8=45911
white-light 23 May 1967, obs. 8=28186
X-radiation, temporal var. obs. 8=32577
X-ray bursts, energetic, onset, intensity and duration comp. with r. f. emission 8=28182

Sun—contd
- **magnetism**
  - activity centres, symposium, Budapest (1967) 8=45900
  - rel. to atmosphere convective instability 8=45913
  - chromosphere-corona interface, magnetic fields and temp. structure modification 8=45920
  - cosmic ray flares rel. to sunspot mag. fields 8=32599
  - fields in quiescent prominences 8=45906
  - field interaction with solar wind 8=50438
  - instrument for field meas. using atomic beam method 8=37040
  - magnetograph, Locarno photoelec., errors 8=50439
  - photosphere, magnetograph obs. method 8=45890
  - photospheric mag. field, flare positions relative to neutral line of longit. component 8=28183
  - solar magnetograph using a subtracting double-dispersion optical system 8=41581
  - sunspot and pore field meas. 8=32598
- **prominences**
  - eruption, 80MHz photography 8=41601
  - eruption of solar prominence, high angular resolution 8=41602
  - formation 8=41600
  - rel. to flares, type IV bursts and filaments, loop prominences 8=45905
  - observations (July-Sept. 1967) 8=32570
  - 1967 March 25 activation description giving timing 8=28180
  - quiescent, excitation of He IIλ 4686 line 8=28179
  - quiescent, motions and mag. fields 8=45906
  - surge, twisted, Nov. 10, 1967 8=37077
  - surges, assoc. in time with radio bursts and flares 8=37056
  - Hα, activity, obs. at Catania Observatory, (1967) 8=37071
- **radiation**
  - See also Sunlight.
  - constant, new value 8=27905
  - cycle variation effect on f_0F2 layer 8=36867
  - energy emitted by disc centre, absolute meas., 4477-8638 A 8=45874
  - EUV, heating effect on upper atmos. 8=27934
  - faculae, chromo- and photospheric, relationship 8=45918
  - flare, X-ray temporal var. obs. 8=32577
  - i.r. coronagraph, balloon borne 8=45609
  - Lα-emission in chromospheric filament, diffusion and field 8=32605
  - on Pacific, total flux obs. 8=27904
  - photosphere, continuum source function determ. 8=32594
  - photosphere, 2000A-100μ, intensity data 8=50448
  - reflected from clouds, angular distrib. TIROS IV radiometer obs. 8=32229
  - tropospheric absorption effect at 7 GHz and apparent sky temp. 8=45877
  - ultraviolet, high-resolution 2000 Å photographs 8=45869
  - u.v., transfer through earths molec. atmos. 8=41360
  - wave, rel. to polar mag. substorms in conjugate areas 8=41462
  - X-ray bursts and cosmic ray $Z \geqslant 15$ nuclei increase, 23-24 Feb., (1964) 8=32586
  - X-ray emission obs. and source model 8=28166
  - X-ray events August, 1966, obs. 8=32576
  - X-ray events, energetic, rel. to solar flares and radio bursts 8=28182
  - X-ray, rocket-borne data handling system 8=50445
  - X-ray spectrum of active region 8=28165
  - X-rays, advances in knowledge 8=37050
  - X-rays effects on pc 3 pulsations in ionosphere 8=41472
  - X-rays, 200-500 km above earth, $\leqslant$ 1038Å and $\leqslant$ 44Å 8=20234
- **radiation, corpuscular**
  - cosmic ray accel. at solar wind boundary by magnetic field 8=47182
  - cosmic ray photons, diurnal time variation near sea level 8=29258
  - cosmic rays inducted isotopic changes in cosmic dust 8=28168
  - cosmic rays, $Z \geqslant 15$ nuclei increase and X-ray bursts, 23-24 Feb., (1964) 8=32586
  - diffusion of particles through interplanetary space 8=38152
  - diurnal vars., dynamic phenomena 8=25042
  - electron production rate in ionosphere of bolar cap due to solar cosmic rays 8=50177
  - electrons, fast, production in flares 8=37078
  - electrons interplanetary and solar, 3-12 MeV 8=41590
  - electrons, terrestrial energetic, upstream beyond bow shock 8=32587
  - energetic particle propag. and structure of interplanetary space 8=41589
  - flare of September 2, 1966 composition and characteristics 8=41597
  - ion temp. meas., satellite mass-energy spectrometer 8=32563
  - lunar bow wave and wake, hypothesis for absence 8=36997
  - lunar magnetospheric interaction with wind, models 8=41558
  - magnetized wind in lunar vicinity, free molecule flow 8=37058

Sun—contd
- **radiation, corpuscular**—contd
  - neutrinos, from B^8 decay, calc. 8=45888
  - neutrons, flux at earth in 1962, meas. by BF_3 counters on OSO-1 8=32588
  - neutrons of high energy, measurement of flux 8=41585
  - ν, spectrum, detect. and rel. to stellar nuclear reactions 8=32585
  - plasma turbulence, viscosity and dissipation 8=45889
  - proton and electron intensities near moon, meas. from Luna II 8=37060
  - protons associated with activity centres, propag. in mag. field corot. sun 8=41587
  - protons, 10 to 100 MeV, from flare of March 24, 1966 8=28181
  - radio bursts, four-frequency characteristics identification 8=50447
  - shock fronts in interplanetary space, acceleration of energetic particle fluxes, $>$ 7.5 MeV 8=38283
  - solar p, α differential energy spectrum meas. 8=47184
  - solar wind, acousto-ionic wave instability 8=45885
  - solar wind, confining effect on earth's magnetic field 8=36822/3
  - solar wind, energy flux 8=45886
  - solar wind plasma, effect of suns rotation 8=32591
  - speed rel. to magnetospheric elect. field 8=36786
  - solar wind rel. to dynamics of the corona 8=41586
  - tangential discontinuities, mag. field re-connection 8=45854
  - wind and F-2 layer ionization 8=41452
  - wind and solar mag. field interaction rel. to interplanetary mag. field 8=50438
  - wind, initial interact. with large obstacle, and particle trajectories 8=28169
  - wind, modulation of cosmic ray intensity 8=42675
  - wind, multicomponent, ion cyclotron whistlers growth and damping 8=41584
  - wind, origin, impact on earth's magnetic field 8=32584
  - wind, Parker's, plasma flow with 3D heat source 8=37061
  - wind, rel. to jovian decametric radio emission 8=41588
  - wind stability 8=37059
  - B^8 neutrinos flux not obs., and rel. to solar spin-down 8=50446
  - B^8 ν flux reduction by core spin-down 8=45887
  - $Be^{7,9}$ in cosmic rays, flux, calc. 8=37057
  - Cl^{37} neutrino search, exptl. results 8=32589
  - Cl^{37} neutrino search, theoretical predictions 8=32590
  - $Co^{56,59}$ in cosmic rays, flux, calc. 8=37057
- **radiation, radiofrequency**
  - activity centres, heliographic longit. distrib. 8=32582
  - Australian obs. 8=32610
  - burst, model for early stage 8=45883
  - burst, 23 May 1967, flux-density spectrum 8=45884
  - bursts at 8mm, characts. 8=32583
  - bursts at 186 MHz in 1958, assoc. in time with optical flares and surges 8=37056
  - bursts, types II and III, polarization rel. to output and propag. conds. 8=32580
  - bursts, type V, origin rel. to electron capture in mag. trap 8=32579
  - bursts, type IV, rel. to flares, filaments and loop prominences 8=45905
  - Canadian radioastronomical obs. 8=32609
  - cosmic rays, activity increase 1966-7 8=38108
  - cyclotron whistlers, ionic, growth and damping 8=41584
  - Czechoslovak obs. 8=32611
  - flares, e deceleration 8=32601
  - German meas. and evaluation 8=32612
  - images, instataneous, obtained by multilobe array at 169 MHz 8=28167
  - Japanese instruments and obs. 8=32615
  - local sources at 4.5 cm, assoc. with sunspot groups sizes 8=32581
  - microwave emission obs. and source model 8=28166
  - multichannel radiospectrographic obs. 8=45882
  - observations (July-Sept. 1967) 8=32570
  - 10cm, obs. affected by terrestrial atm. absorpt. 8=37054
  - quiet sun, Indian 49cm. obs. 8=37063
  - *S* -component characteristic identified on Nov. 1966 eclipse at 4.28 cm wavelength 8=37055
  - slowly varying, rel. to cyclotron and bremsstrahlung mechanisms 8=45881
  - synchrotron emission of intermediate energy electrons, influence of ionized medium 8=37052
  - USSR apparatus and obs. 8=32523
- **spectra**
  - See also Sun/corona; Sun/flares; Sun/prominences.
  - activity centres, spectroscopy, symposium, Budapest (1967) 8=45900
  - atomic and mol., analysis, for C, N_2 and O_2 abundances 8=28171
  - chromosphere. of eclipse, February 5, 1962 8=45919
  - chromosphere XUV region, line strengths of $2p^2$-2p3s arrays of CI, N II, O III 8=45915
  - continuous spectrum energy distrib. and centre-to-limb var., 5000Å–1500Å 8=37045
  - corona emission and atm. D meas., photoelec. Fabry–Perot magnetostriction scanned 8=32272
  - coronal green line photoelectric meas. of eclipse, November 12, 1966 8=45864

Sun—contd
spectra—contd
extreme u.v. heliograms of corona rel. to structure and intensity 8=37080
far vac. u.v., laboratory identification 8=38668
fine structure transitions of photons and collision cross-sections 8=47476
Fraunhofer lines calc. by wt. function theory 8=36908
Fraunhofer lines obs. for calc. solar atmosphere intensity and velocity fluctuations 8=45879
Fraunhofer lines of NaI and CaII collisional damping by H atoms and electrons 8=37049
Fraunhofer lines saturation explanation 8=50442
γ-ray obs. from quiet sun 8=45796
γ-ray, spacecraft obs. 8=45794
gyro-synchrotron emission, spectrum time var. 8=37053
image or spectrum scanning technique 8=37047
interferometer, Fabry-Perot, for rocket appls., 1700-2400Å 8=32411
interferometer, Michelson, balloon-borne for Fourier meas., 10-100μ 8=32571
limb intensity var. rel. to temp. gradient in low chromosphere 8=37089
line profiles, λ 4281-4302Å, rel. to distance from disc centre 8=32572
Lyman-α emission line, solar chromospheric fine structure 8=45916
magnetic field fine structure, velocity, intensity 8=45902
measurement in 1-3.5 μ range at altitudes below 18 km 8=45873
moustaches, metallic emission lines 8=32574
photosphere, lower, hydrodynamics obs. 8=32593
photospheric, around 6708Å, and Li abundance 8=45865
photospheric intensity, velocity and magnetic fields relationship 8=45903
radio burst, 23 May 1967, flux density obs. 8=45884
red shift, Compton effect interpret., predict of variation with position 8=41582
sight-line vel. signal variations from photosphere rel. to atmos. seeing 8=41591
simulation by θ-pinches in million deg. range 8=39109
soft X-ray, 33-110Å obs. 8=32575
spectrogram, granulation 8=37043
stigmatic, between 1800 and 2800Å 8=37046
synthesis for determ. of element abundances 8=45872
two-colour surface inhomogeneity differences 8=45868
velocity fields, short period oscs., possibly caused by local seeing conds. 8=41583
X-ray, below 25Å, rel. to solar activity 8=37051
X-ray, soft, and XUV 8=45880
CN red system vibr. band oscill. strengths, and equiv. widths meas. 8=45867
CO fourth positive system in u.v., obs. 8=45870
C_2, centre-limb vars. rel. to polyatomic mols. form., calc. 8=45875
Ca II in sunspots, K_3 absorpt. line rel. to origin of K-line emission 8=28178
Ca II, K-line in sunspots 8=50453
Ca II solar line, centre-limb var. of $K_{2,3}$ components calc. 8=45878
Cr I and II gf laboratory values, appl. computed solar abundances 8=29611
Ga abundance from sunspot obs. 8=32573
Hα-line, rel. to velocity field round sunspots, at chromospheric heights 8=28184
H emission spectrum, computation 8=45876
HNO_3 and NO_2, absorption in lower stratosphere 8=27877
H profiles photometric obs. 8=37042
He II λ 4686 line in quiescent prominences, excitation 8=28179
K profiles photometric obs. 8=37042
Na, Al, P, S and K, absorpt. lines 8=28172
Ne I and Ar I isoelectronic sequences, resonance line strengths 8=45871
Ne IV-VIII, emission lines obs. and abundance determ. 8=50443
O i.r. triplet, depth of origin in facolae and photosphere obs. 8=45892
O1 forbidden lines wavelengths and equivalent widths, O abundance obs. 8=37044
PbI 7229 Å line and solar abundance 8=45866
S ions, oscillator strengths for resonance lines 8=29647
SI Fraunhofer forbidden line $3p^4\ ^3P_2$-$3p^4\ ^1D_2$ obs. 8=50444
Si ions, oscillator strengths for resonance lines 8=29647
Si I lines, for abundance determ. 8=28173
Si1 absorption lines, 2935-25578Å, equivalent width calc. 8=37048

Sunlight
See also Sky brightness.
outgoing radiances from earth-atmos. system inverted rel. to cloud amounts 8=41361
polarization of skylight, effect of conc. turbid layer 8=36743
radiation intensity var. in sun's vertical for different vapour stratifications 8=27901
reflection and transmission by clouds, depend. on single scatt. albedo 8=32230
scattering into planetary shadow cones, effect on appearance 8=41562
solar constant of radiation, new value 8=27905

Sunlight—contd
surface diffusive radiation flux under cloudy conditions 8=27903
O_3 absorption coefficient, Dobson spectrophotometer obs. 8=45465

Sunspots
activity and brightness of Jupiter's great red spot, correlation 8=41594
activity and geomagnetic storms, 1966 8=28176
activity, increase, early effects on earth's atmosphere at 1000 km 8=41386
complex group, Evershed vel. and mag. field 8=32596
cycle rel. to quasi-biennial stratospheric oscillation 8=27884
effect on F-region drift speed 8=28175
electrical conductivity 8=37066
Evershed motion 8=45901
Evershed motion origin, and growth rate of mag. config. 8=41593
frequency, min. and maxima, secularly smoothed data 8=28185
geomag. Sq semi-annual amplitude vars. rel. to spot number 8=28010
groups, sizes of local sources of radioemission at 4.5 cm 8=32581
magnetic field fine structure, velocity, intensity 8=45902
mag. fields rel. to cosmic ray flares 8=32599
magnetic field, spectrogram meas. 8=32598
max. and min. effects on density scale height 8=27933
new, longit. distrib. at start of 11 year cycles 8=45898
number, relation with charged particle density in upper ionosphere 8=32293
observations (July-Sept. 1967) 8=32570
penumbra m.h.d., horiz. radial field and mag. amplification 8=41592
penumbral material motion, and Evershed effect 8=45899
photospheric intensity, velocity and magnetic fields relationship 8=45903
and S_D mag. vars. at Yakutsk 8=36892
solar activity and brightness of Jupiters great red spot, correlation 8=45829
spectra, high dispersion, Li abundance calc. 8=50452
structure, Wilson effect obs. 8=37068
surfaces, time autocorrelation 8=50454
Umbra convective instability and overstability 8=37067
umbra, model for narrow range of electron press. at spot surface 8=28177
umbra, normal triplet, π component saturation effect 8=45895
umbral dots, lifetime and intensity obs. 8=45896
velocity field at appearance stage 8=32597
velocity field at atmospheric heights, from obs. of Hα line spectra 8=28184
Zeeman triplet appl., magneto-sonic wave effect 8=37070
Zeeman triplets, shape of line profile and line intensity compared 8=50310
zonal activity duration 8=37069
Ca II, K-line 8=50453
Ca II K-line, K_3 line rel. to double reversal and origin of emission 8=28178
Ga abundance from spectra 8=32573
Li abundance calc. from high dispersion spectra 8=50452
TiO lines equivalent widths calc. 8=37065

Superconducting materials and devices
See also Magnets.
alloys, dil. mag., behaviour in applied mag. field 8=27004
alloys, dilute, with paramagnetic impurity, formulation and appl. 8=40366
amplifier, parametric, for d.c. voltage meas. 8=31347
applied superconductivity, conference 8=31338
beam handling and accelerator structures, progress since 1966 8=37806
carbides, anomalous props. 8=49191
characterization parameters 8=40363
coaxial line, frequency and domain analysis using two-fluid model 8=40409
composite strip conductors for large magnets in Argonne and Brookhaven bubble chamhers 8=42349
conductors, stabilized for superconducting bending magnet 8=27001
conductor-substrate systems stability params. and heat transfer, obs. 8=27002
cryoelectric arrays, dynamic fault tolerance 8=40408
cryoelectric content-addressable memories using flux-shuttling non-destructive readout 8=40403
cryoelectric storage element: anisotropic structured cell 8=40405
cryogenic storage cell, multi-aperture 8=40404
current leads, determ. of heat flux along leads to cryostat with liq. He 8=31361
current loops, magnetic levitation 8=28522
domain struct. config. 8=48577
double Josephson junction, phase-sensitive detection of small d.c. voltage 8=46321
echo phenomena in superconductors and normal metals 8=40364
filamentary, synthetic, magnetization and critical current density temp. and field dependence 8=40370
film, modulated flux flow 8=27043

Superconducting materials and devices—contd
  films for radiant-energy detection, microwave-near i.r. 8=37299
  films, superposed, superconductor-superconductor, metal-superconductor, critical magnetic field 8=35846
  films, thin, field effects 8=27007
  films, thin, superconducting and ferromagnetic, proximity effect 8=27008
  films, thin, superconducting and normal, zero-field proximity effect 8=27006
  films, ultrathin, enhanced transition temp. phenomena 8=40400
  flux pumps and transformers for d.c. current storage 8=41931
  flux quantization ammeters 8=40410
  generators, homopolar d.c., high-efficiency 8=37372
  gravimeter 8=31352
  gravimeter 8=50013
  gyroscope, drift data and mathematical model 8=23820
  gyroscope for relativity verification 8=29000
  high-field, and commercial alloys, review 8=49187
  high-temperature superconductors 8=40376
  inductor, modulation by mag. field, appl. 8=31348
  interference, quantum, in resistive state 8=49203
  Josephson barrrers, prep. using glow discharge technique and performance of arrays 8=40414
  Josephson-effect far i.r. detector 8=46225
  Josephson junction, a.c. interaction with surface plasmons 8=27048
  Josephson junction, millimetre-wave mixing 8=27047
  Josephson junction, switching appl. 8=27040
  Josephson junctions, fluctuation phenomena, quantum-field theory 8=27050
  Josephson junctions, quantization and thermodynamic fluctuations 8=27041
  Josephson junctions in series, supercurrent tunnelling studies 8=27049
  Josephson junctions, I–V characts. 8=40395
  Josphson junctions, weak multiply connected, freq. conversion 8=40416
  Josephson tunnel effect in anisotropic superconductors with non-magnetic impurities 8=27046
  Josephson tunnel junctions, current fluctuations 8=27042
  Josephson tunnel junctions, plasma reson., obs. 8=35858
  Josephson tunnelling and quantized phase effect 8=27051
  junctions, weak-link, d.c. I–V characts., a.c. impedance effect 8=40397
  magnet, apparatus for high-field low-temp. magneto-thermodynamic props. 8=41882
  magnet coil, high-homogeneity tape-wound 8=37397
  magnet coils, meas. techniques 8=37396
  magnet fabrication from many mats. 8=37386
  magnet, field meas. by magnetoresistor 8=41938
  magnet for ANL 12-ft hydrogen bubble chamber 8=37802
  magnet for focusing accelerator beam 8=33404
  magnet for polarized π-p scatt., and semi-stabilized cable props., 400 kJ 8=28529
  magnet, high-current-density, high-field, stabilization 8=37389
  magnet, high-field (up to 20 kG) 8=37393
  magnet, peak return field, optimal winding 8=28524
  magnet rings, stabilized, levitated 8=37395
  magnet system, 88-kG, 20-in-bore 8=37391
  magnet system in pulsed MHD generator 8=37376
  magnet systems, nonaxisymmetrical 8=37388
  magnet, using Nb Zr alloy wire, 85KG 8=46385
  magnets, construction, state-of-the-art 8=46387
  magnets, degradation effects, method for reduction 8=46386
  magnets, coil, future development 8=33050
  magnets, degradation and stabilization 8=28527
  magnets for beam handling and accelerators 8=28995
  magnets for high-energy physics 8=24113
  magnets for high-energy physics 8=37385
  magnets, high-field, for use in Mössbauer spectroscopy 8=37387
  magnets, permanent and solenoids, with ferromag. pole pieces, optimum design 8=28525
  magnets, pulsed, for p synchrotrons 8=29010
  magnets, review of behaviour 8=28526
  for magnetic flux change enlarging 8=44745
  magnetic structs., high-res. magneto-optical obs. 8=31336
  magnetizing coil optimum shape 8=28531
  magnetometer, supercond. loop 8=28511
  meander lines 8=40411
  metal, conductivity increase near critical temp. 8=35843
  metal-superconductor superimposed films, transition temp., numerical soln. of eqn. 8=27011
  microwave cavity appl. 8=31350
  microwave mixer with weak coupling 8=31351
  nitrides, anomalous props. 8=49191
  n.m.r. spectrometer, high-resolution, Du Pont instrument general performance information 8=46517
  with nonmagnetic impurities and overlapping bands two-band model 8=44720
  oscillator, microwave monotron with superconducting cavity, freq. stability 8=27012
  oscillator with u.l.f. stability using superconducting cavity 8=46466

Superconducting materials and devices—contd
  persistent current magnetometer 8=31355
  phonon spectrum and e.-phenon interactions in calc. props of simple metals 8=44719
  photodielectric detector using superconducting cavity 8=40681
  point-contact junction i.r. detector 8=31357
  point-contact junction detector for r.f. oscillations 8=31356
  power sensor, high-sensitivity 8=40415
  pressure contacts 8=40417
  for proton synchrotron magnets, supercond. energy storage system 8=29011
  quantum interference, for strong mag. field meas., shielding 8=31349
  rare-earth magnet pole-pieces for field enhancement 8=28530
  resistance of current-carrying filament, no mag. field 8=27045
  resonant cavities in linear accelerator 8=29000
  resonant circuits in oscillators and filters 8=40413
  resonator-solenoid 8=49208
  resonators for linac, construction 8=46995
  review 8=27003
  semiconductors, acoustic dispersion theory 8=35403
  shielding, mag. for He^3 nucleus elec. moment meas. 8=29000
  solenoid, composite, partially stable 90 kG 8=37394
  solenoid, field calibration, n.m.r. probe 8=31360
  solenoid, flux linkage and self-inductance, rel. to self-excitation 8=31354
  solenoid for meas. of magnetostriction at low temps. 8=45000
  solenoid, for meas. of magnetostriction at low temp. 8=49507
  solenoid, 88-kG, 51-cm-bore diam. 8=37390
  solenoids with high homogeneity mag. fields 8=28528
  stabilized compound conductors, flux flow and thermal stability 8=40402
  stabilized, theoretical and expt. I-V characts. in transition region 8=40377
  strip delay line, 50nsec delay 8=49206
  strip transmission lines with periodic load, characts. 8=49205
  structures, self and mutual inductances 8=27009
  superconductor-metal-superconductor junction, phase dependent current density 8=49204
  superconductor-normal metal sandwich (Cooper pair), reduction in spin flip breaking 8=49502
  switches, automatic 8=37363
  thermodynamic and electronic props. of supercond. with nonmag. impurity 3=39901
  thermometer, manufacture 8=46272
  tunnel junction for 1m° thermometry 8=31358
  tunnel junctions, excess currents rel. to multiparticle and subharmonic tunneling 8=44746
  tunnel junctions in circuitry of electronic grey matter 8=40407
  tunnel, radiated freq. band width rel. to quantum fluctuations 8=31346
  tunneling junctions, application as negative resistance devices above 4.2°K 8=49207
  tunnelling cryotron flip-flop 8=40406
  tunnelling, device appls. 8=40398
  tunnelling Ti-doped, magnetic field splitting of conductance peaks 8=40396
  voltmeter using Josephson junction props. 8=31353
  volume expansion for very low mag. field 8=28513
  weak-link and tunnelling phenomena rel. to potential device appls. 8=40399
  wires as exciting coil in magnetic lenses of electron microscope 8=24146
  Al amorphous film, tunnelling obs. 8=40368
  Al, energy gap temp. variation, from thermal cond. meas. below 1°K 8=30988
  Al films, diffusion of impaired electrons obs. 8=40212
  Al films, granular, prep. and enhanced T_c value 8=27013
  Al, props. calc. from phonon spectrum and e.-phonon interactions 8=44719
  Al, quasiparticle recomb. time, temp. depend. obs. 8=35847
  Al, thin film, unique energy gap obs. 8=35845
  Al, u.s. absorpt. rel. to min. energy gap 8=40367
  Al-Ng alloy, energy gap anisotropy and sp. ht. 8=48734
  Bi amorphous film, tunnelling obs. 8=40368
  Bi eutectic alloys, metastable 8=44722
  CdS film sandwiched between superconductors, photosensitive tunneling 8=35848
  Cu layer on Pb, proximity effects, microwave study 8=27015
  Cu–Nb_3Sn-stainless steeel, non-symmetric composite conductors mech. and elec. props., obs. 8=27014
  Cu-Pb alloys, magnetization meas. rel. to microstructure 8=44723
  Ga amorphous film, tunnelling obs. 8=40368
  Ga, β and amorphous phases, energy gap 8=40369
  HfN, f.c.c., transition temp. stoichiometry and lattice parameter dependence 8=27022
  (Hf, Zr)N solid soln., f.c.c., transition temp. stoichiometry and lattice parameter dependence 8=27022
  In films, props. rel. to degree of crystal lattice distortion 8=35849

Superconducting materials and devices—contd
In, non-Londonean resistance jump 8=40371
In thin films, critical mag. field rel. to structural disorder and defects 8=40382
InAl films, Tomash oscillations in density of states 8=40358
InBi film, Mn layers on each side, proximity effect obs. via thermal conductivity 8=40372
In-Ce solid solns., T_c impurity (Ce) conc. dependence rel. to localized moments 8=31339
In-7.05 wt.% Pb alloy, type II, sp. ht. rel. to irreversibility effects on Maki's parameters 8=44342
In-Pb alloy, upper crit. field, temp. and mean free path depend. 8=31340
In-Pb alloys, type II, comparison with Caroli-Cyrot theory 8=39946
In-Pb films, Tomash oscillations in density of states 8=40358
K, props. calc. from phonon spectrum and e.-phonon interactions 8=44719
La, thermal expansion and magnetostriction, 1.5-40°K, rel. to transition temp. pressure dependence 8=35438
La, tunneling density structure of states 8=35850
La_3Se_4, transition temp. rel. to lattice and electronic props. 8=27017
MoC, upper critical field at 4.2°K 8=27018
Mo_2C, upper critical field at 4.2°K 8=27018
M_3X-type, spin-lattice relax. rel. to energy band structure 8=36257
Na, props. calc. from phonon spectrum and e.-phonon interactions 8=44719
Nb, a.c. losses near lower critical field 8=44727
Nb alloy, instability, source 8=49198
Nb alloys, critical current rel. to mag. field and temp. 8=49199
Nb, anomalous magnetic behaviour 8=27383
Nb, extended defects, influence 8=49193
Nb, microwave surface resistance meas. 8=49195
Nb in mixed state, rel. to crystalline orientation 8=35852
Nb, Nernst effect rel. to magnetic field 8=40374
Nb, n-irradiation effects ($E > 1$ MeV) 8=40379
Nb, peak effect rel. to dissolved oxygen clusters 8=49192
Nb, proximity effect in contact with Cu and Ni 8=27026
Nb, resist. and magnetization, n-irrad. effects, obs. 8=40373
Nb, resistive elec. field and Hall effect meas., 8=44724
Nb single crystal, anisotropic energy gap obs. 8=27023
Nb, tunnelling characteristic detail in high purity single crystal 8=27025
Nb, type II, spin-lattice relaxation 8=41005
$Nb_3(Al, Ge)$, β-tungsten phase, high-transition-temp., props. 8=40376
$Nb_3(Al, Ge)$, high mag. field characts. 8=44726
Nb_3Al-20% Nb_3Ge, sintered, critical temp. increase by annealing obs. 8=27019
NbC, f.c.c., transition temp. stoichiometry and lattice parameter dependence 8=27022
Nb-Ga system 8=49197
Nb, K_1 and K_2, theory/expt. discrepancy 8=31342
Nb-N, peak-effect temp. dependence, 4.2-1.35°K 8=40378
Nb-Sb alloys, mag. hysteresis at 4.2°K 8=27024
$NbSe_2$, band model calcs. 8=49105
Nb-Sn alloy, mag. hysteresis, causes 8=44972
Nb_3Sn composite ribbon magnets, transient stabilization 8=37392
Nb_3Sn-composites transition temp. rel. to hot pressing, particle size and admixtures 8=49190
Nb_3Sn, hard tubes, mag. flux jumps, 4.2°K 8=31341
Nb_3Sn high-Q r.f. coils for 15°K 8=31359
Nb_3Sn ribbons, vapor-deposition rel. to e.m. performance 8=40418
Nb_3Sn, sintered, flux jumping control by liquid He flow through pores, obs. 8=27020
Nb_3Sn strip conductor, plasma-plated, critical current angular dependence 8=40420
Nb_3Sn, superconductivity changes on H_2 up-take 8=26414
Nb_3Sn, transition temp. rel. to hot pressing, particle size and admixtures 8=49190
Nb_3Sn-Cu-steel composite conductors, e.m. performance and mech. props. 8=40401
Nb_3Sn; ZrO_2 particles, performance rel. to microstructure 8=44728
Nb-Ta alloys, Nb rich, K_1 and K_2, theory/expt. discrepancy 8=31342
Nb-Ti alloy, at transition temp., temp. depend. of specific heat 8=48738
Nb-Ti alloy, critical temp. and current density 8=35853
Nb-50%Ti rods, flux jumps 8=49194
NbTi strips, flux flow state stability 8=44725
Nb-40% Ti, Cu-clad, stabilization, I-V characts. rel. to theory 8=40377
Nb-45 wt.% Ti and Cu composite conductor for large currents 8=27021
Nb-Ti-N films, reactively sputtered, props. rel. to comp. 8=40380
Nb-Ti-Zr alloys, critical mag. fields 8=35851
Nb and V in mixed state, nonlinear resistivity and dissipation 8=27027
Nb-Zr alloy, flux jumps at liquid He temp. 8=49189

Superconducting materials and devices—contd
Nb-Zr alloys, type II, spin lattice relaxation times 8=44744
NbZr coil magnet, effect of neutron radiation 8=33405
Nb-Zr, hard tubes, mag. flux jumps, 4.2°K 8=31341
Nb-Zr25, type III, lattice defects, nature, size and distrib. and effect on high-field props. 8=48828
Nb-25% Zr solenoid, persistent current decay rate, field dependence 8=27039
Nb-25% Zr tubes, flux jumping rate dependence 8=40375
Nb + 75% Zr magnet for 85 kG 8=41937
Nb-Zr, type II, spin-lattice relaxation 8=41005
Nb-Zr-N films, reactively sputtered, props. rel. to comp. 8=40380
Nb-25%Zr wire, meas. of a.c. surface power loss 8=49196
Pb-base alloys transition temps. 8=44729
Pb, complex elec. cond., strong-coupling calc. 8=35854
Pb, dislocation attenuation mech. rel. to amplitude-independent u.s. attenuation in normal-state 8=44321
Pb, dislocation attenuation mechanism rel. to amplitude-independent u.s. attenuation 8=44322
Pb films and foils, parallel and perpendicular mag. transitions, 1-4.2°K 8=40741
Pb, props. calc. from phonon spectrum and e.-interactions 8=44719
Pb shell, zero mag. field attainment 8=27044
Pb, surface resistance meas. at 2.868 GHz 8=40383
Pb thin films, critical mag. field rel. to structural disorder and defects 8=40382
Pb, tunnel effect under pressures up to 15kbar at 1.3°K 8=44737
Pb thin films, transition, critical fields 8=27028
Pb-Bi alloys, mag. field spatial distrib. and crit. current density 8=40381
Pb-Bi alloys, pinning of flux vortices 8=49200
Pb-Bi system, transition temp. of amorphous phase 8=35844
Pb-In alloy, intermediate state structures, transition from flux lattice 8=44731
Pb-6.3 at.% In foils, type II, flux line arrangement 8=40384
$Pb_{85}In_{15}$ resistive and mag. props., demonstration 8=35855
Pb-Tl alloys, critical currents 8=40385
Pb-Tl alloys, transition temp. comp. dependence 8=44730
in PdSb, dilute solutions of CrSb and MnSb 8=27029
Re, energy gap temp. variation, from thermal cond. meas. below 1°K 8=30988
Sn, coherent coupling of two Josephson junctions 8=44733
Sn, complex elec. cond., strong-coupling calc. 8=35854
Sn film, electron tunnelling, current influence 8=31343
Sn film, tunneling expts in mag. field 8=44732
Sn films and foils, parallel and perpendicular mag. transitions, 1°K-T_c 8=40741
Sn films, clean and dirty, critical mag. field 8=44734
Sn films, energy gap mag. field and film thickness dependence by e-tunnelling 8=27033
Sn films, microwave transmission meas. 8=40386
Sn, helicon-like oscillations 8=44736
Sn, magnetoresistance at liq. He temps. and over large range of mag. fields 8=27031
Sn, particles in oxide film, obs. down to 25Ǎ radius 8=40388
with Sn particles, layered with SiO, size effects in n.m.r. 8=44735
Sn ring, current fluctuations and critical currents as a function of temp. 8=40387
Sn, thin films, hyperfreq. nonlinearities 8=27030
Sn II, modification, critical field plots 8=35856
Sn with Al admixtures 8=40389
Sn-Ce solid solns., T_c impurity (Ce) conc. dependence rel. to localized moments 8=31339
Sn-In alloy films, tunneling expts. in mag. field 8=44732
Sn-In films, mag. props. 8=44974
Sn-Sn tunnel junctions, anomalous behaviour at superconducting transition 8=44738
Sn-SnO-Sn Josephson junction, relax. oscills. 8=40412
Sn-SnOx-Pb junction, electron tunnelling, current influence 8=31343
SnTe, interactions 8=27032
$SrTiO_3$, behaviour of $T_c(n)$ 8=27034
Ta, energy gap temp. variation, from thermal cond. meas. below 1°K 8=30988
Ta, surface prop., strain and impurity effects 8=44739
TaC, f.c.c., transition temp. stoichiometry and lattice parameter dependence 8=27022
Ta-Nb alloys, $K_1(t)$ and $K_2(t)$ meas. rel. to temp. 8=44740
Tc, $\partial T_c/\partial P$, sign rel. to other transition metals 8=31344
Th, gapless, critical-field curves 8=44741
Th-Gd alloys, critical-field curves 8=44741
Ti-16at.% Mo alloys, type II, mixed-state Hall effect 8=27035
Ti-47% Nb, α-phase formation during heating in e-microscope 8=35119
Ti-22 at.% Nb/Cu composite conductors, critical current densities rel. to omega precip. 8=40419
TiNb33:N, O and metals, transition temp. and critical field 8=44742
TiNb40:N, O and metals, transition temp. and critical field 8=44742
TiO, dependence on lattice vacancy conc. 8=31345
Tl, density of states and phonon spectrum by electron tunnelling 8=44743

Superconducting materials and devices—contd
- Tl, transition temp., effect of impurities 8=49201
- Tl_5Te_3, γ-phase in Tl–Te system, transition temp., 2.19°K 8=40390
- Ti-V alloys, critical current densities rel. to ht. treatment 8=40391
- α-U, filamentary, impurity effects 8=49202
- U_6M, (M = Mn, Fe, Co, Ni) and alloys rel. to ferromagnetism 8=27036
- V, anomalous magnetic behaviour 8=27383
- V, type II, Hall effect 8=40392
- V_3Si, martensitic phase transform., e-microscope study 8=26085
- V_3Si, superconductivity dependence on lattice instability 8=27037
- V_3Si, β-tungsten phase, high-transition-temp., props. 8=40376
- V_3Si, type II, lattice softening rel. to phase transformations 8=31107
- V_3Sn, type II superconductor, spin relaxation of V^{51}, temp. depend. obs. 8=40970
- V-Ti alloys, type II, spin lattice relaxation times 8=44744
- V-Ti, type II, spin-lattice relaxation 8=41005
- W, evaporated films 8=40393
- W, evaporated films 8=40394
- W, magnetic field curve rel. to low temp. CMN scale 8=37331
- Zr-Nb alloys, critical current density rel. to dispersed precips. 8=35857
- Zr-Ti, sp. ht., 1.1–4.2°K 8=35437

Superconductivity
- See also Quantum theory/many-particle systems.
- accelerator beam separator r.f. 8=24543
- a.c. loss mechanism, review 8=40335
- alloys with paramag. impurities, effect of concentration non-uniformity on props 8=44705
- alloys, with paramag. impurities, nonstationary generalization of Ginzburg-Landau theory 8=40341
- anisotropic upper critical field of weakly coupled linear chains at temps. above T_c 8=40430
- atom and molecule systems, method of biorbitals 8=34113
- Bernoulli pot. var. with elec. field depends on band structure 8=40348
- composite conductors, stability, effect of nucleate to film boiling transition 8=44706
- continuous cooling between 1° and 293°K 8=37328
- correlation function method, elec. current density calc. 8=35840
- crystal magnetic-ion multiplicity effects 8=31254
- current attenuation in ring in alternating mag. field, obs. 8=44704
- degenerate BCS model, exact thermal Greens-function rel. to Bogolyubov–Haag method 8=35842
- destruction by a current 8=40343
- dilute alloys, nonmagnetic localized impurity states 8=26984
- dislocations effect 8=40342
- DNA, double-stranded, pairon condensation 8=32620
- electron linac, optimum slow wave structure determ. 8=24568
- electron mechanism in semiconductors 8=40338
- and electron-phonon interaction, magnitude 8=35838
- electron scatt. by paramag. impurities and transition temp. calc. 8=40211
- energy gap, depend. on phonon spectrum and order-disorder effects 8=31331
- explanation of occurence 8=31330
- field emission characts. 8=49175
- film sandwiches, cond.-dielec., and filaments, high critical temp. 8=35839
- films, thin mixed state condition from crit. field temp. and angular dependences 8=44713
- films, tomash oscillations in density of states 8=40358
- films, ultrathin, enhanced transition temp. phenomena 8=40400
- flux distribution, effect of metallurgical factors 8=40365
- flux jumps in hard superconds., rel. to temp. variations during magnetization 8=26979
- Ginzburg-Landau equations, cylindrically symmetric solutions 8=26985
- Ginzberg–Landau eqns., existence and bifurcation theorems 8=31337
- Gorkou's eqns., for type II, transformation into Luders transport eqn. 8=40361
- granular, transition temp. enhancement mechanisms 8=40353
- Hall effect, gravitation-induced, in type I superconductor 8=31333
- hard wires, macrovortex structure formation 8=40354
- h.f. sound attenuation 8=44309
- horizontal wires heated in liq. He II, limiting heat removal rates 8=28442
- impure superconds., theory 8=40351
- impurity scattering effects on free energy 8=40346
- induced transient fluxoid echoes 8=27010
- interaction current losses 8=49178
- intermediate state current-carrying supercond., macroscopic theory 8=26982
- intermediate state, quadratic response to transverse alt. mag. field 8=35835

Superconductivity—contd
- intermediate state, thermal cond. 8=44354
- intermetallic cpds of β-W structure, rel. to lattice instability 8=44721
- Josephson current, max., self field limited 8=49176
- Josephson direct current, microscopic calc. 8=40334
- Josephson effect in superconductor-normal metal-superconductor junction 8=44701
- Josephson tunnel current in sound field 8=44708
- kinetic eqn. for impure anisotropic superconductor 8=35841
- with mag. impurity, appearance of local bound states 8=44710
- magnet for 200 BeV accelerator 8=33403
- in magnetic alloys, dilute, below Kondo temp., Nagaoka's model 8=26988
- magnetic alloys, dilute, order parameter spatial variations 8=31332
- magnetic field penetration depth temp. dependence in overlapping zone type 8=35833
- magnetic resonance in superconductors, recent work 8=40957
- magnetization curve measurement by electronic integration 8=49458
- Meissner state stability limits and spontaneous vortex nucleation mechanism 8=40359
- metals with incomplete inner shells 8=35837
- micromagnetic equations, derivation 8=35836
- model of superconductor with anisotropic energy gap 8=44709
- Nernst effect in Nb rel. to magnetic field 8=40374
- normal-to-supercond. transition, 10μ spheres, detection 8=48367
- nuclear level density theory applic. 8=25074
- nucleation above H_{c3} for systems with special geometry 8=40345
- one-band, with paramag. impurities, persistent currents 8=49174
- order parameter, critical fluctuation with near transition temp. 8=49185
- order parameter relaxation in type I 8=26986
- ordinary and gapless, infinite conductivity due to current-electron-phonon interaction 8=49180
- organic macromols., near room temp., hypothesis and reasons 8=27038
- with P-pairing, electrodynamics and collective excitations 8=44703
- pair-breaking mechanisms 8=40336
- pair splitting interaction of magnetic field 8=49179
- pair theory of superconductor 8=40350
- phenomena in one-dimensional systems, effect of impurities 8=40344
- piperine, dipole polarization activation, enthalpy and entropy 8=39403
- and quasi one-dimensional (thread-like) structures 8=44702
- quasiparticle approx., fluctuation-dissipation theorem 8=24596
- resistive transition rounding of phenomenlogical theory 8=44707
- review 8=40339
- review 8=49172
- r.f. losses in penetration depth due to flux-trapping 8=40352
- of semiconductors and semimetals, and insulating mechanisms 8=26886
- in semiconductors, degenerate 8=49188
- skin effect in superconductors 8=49177
- stability of supercond. cylinder, Lange's criterion 8=26977
- stabilized wires, calc. methods for predicting performance 8=26987
- strong-coupling, longit. u. s. attenuation 8=44310
- strong-coupling theory 8=26862
- superheating of Meissner and giant vortex states of finite cylinder 8=26989
- surface, Ginzburg-Landau theory rel. to mag. hysteresis 8=44718
- surface, magnetic levels 8=44958
- surface nucleation fields, influence of planar defects 8=35834
- surface sheath collective fluctuations of order parameter, e. m. response to microwave 8=40347
- temperature depend. of upper crit. fields 8=27000
- theory of long-range fermion interaction 8=26983
- theory, phenomenological and microscopic, book 8=26981
- thermodynamics in mag. fields 8=49181
- transition metals, nearly ferromag., effect of spin fluctuations on transition temp. 8=44992
- transition temp. calc. 8=26990
- transitions meas. in very small mean-free-path films 8=26980
- tunnelling, microwave assisted 8=49173
- two-band superconductors, critical temp. 8=26978
- two-band superconductors, localized mag. states 8=49455
- two-zone superconductors with nonmag. impurities, tunnel current impurity conc. dependence, theory 8=35832
- two-zone type II, longitudinal acoustic wave absorpt. near T_c 8=35400
- type I, elec. field obs. in presence of quasistatic magnetic field 8=26991

Superconductivity—contd
type I, Hall effect, gravitation-induced 8=31333
type-I hollow cylinders, diamagnetic and field-retaining props. rel. to surface strains 8=44711
type-II alloy, step structure in resistive transition 8=40356
type II, collective modes of vortex lattices 8=25785
type II, complex r.f. impedance 8=44716
type II current-carrying superconductor, magnetic induction distribution 8=40360
type II, elasticit y effects 8=40357
type II, flux-flow resistance temp. dependence near H_{c2} 8=44715
type II, flux-flow viscosity rel. to local temp. gradient 8=26997
type II, flux-line arrangement obs. by decoration method 8=49182
type II, flux vortices, forces in an arbitrary configuration 8=44717
type II foils, flux-flow resistivity and critical current density orientation dependence 8=26999
tyep-II gapless clear, ee.m. transport coeff. 8=40362
type II, hysteresis loss calc. 8=31335
type II, interaction of vortex filaments with elastic deform. field 8=49186
type II, interaction with polarized neutrons 8=26998
type II, Landau-Ginzburg eqns. 8=26993
type II, n.m.r. 8=40958
type II, peak effect occurrence 8=49184
type II, pinning freq. 8=49183
type II, pinning of flux vortices 8=49200
type-II, pinning potential and h.f. studies 8=40355
type-II, pure, excitations 8=26992
type II, resistive states 8=26995
type II, stress depend. of free energy 8=26996
type II, V–I charact., linearity 8=31334
type II with oriented pins, critical current density 8=44714
type II, zero bias tunnelling cond. 8=26994
very low temp. production 8=37329
voltage-current charact., linearity, in type-II 8=31334
vortex flow, obs., mechanisms and appls., review 8=40337
wires, driven from current sources intrinsic resistive transition 8=44712
M_3X type, with two overlapping energy bands, n.m.r. study 8=40349
Pb—Tl alloys, critical currents 8=40385
Sn II, modification, critical field plots 8=35856
Ti-Mo alloys, electronic sp. heat, BCS theory 8=39922

Supercooling
aqueous solns., free growth rate of ice crysts. rel. to ice-soln. interface 8=35242
austenitic stainless weld metal solidification 8=48265
benzene, Mossbauer scatt. obs. of mol. motion 8=43751
deep, transformation centres and crystal growth 8=25987
during solidification, constitutional, thermal diffusion effects 8=34974
ethylenediamine oligomer in supercooled state, dielec. props., —100 to 60°C 8=39404
fluids, non-or weakly polar, crystal form. on ions and ion complexes 8=39656
glycerol, Mossbauer scatt. obs. of mol. motion 8=43751
ice crystals growing in supercooled water morphology 8=26176
isoamyl bromide, dielec. props. of low-temp. liq 8=48188
liquids, viscoelastic behaviour rel. to viscosity and rigidity modulus 8=30430
water droplets falling in air and other gases 8=25984
water drops, supercooled, crystallization processes 8=25985
water-ice interface, precrystallization theory applied to surface-free energy 8=34957
water, rel. to basal-plane solidification, effects of impurities 8=25982
water, rel. to nucleation on freezing by cavitation 8=25981
Bi, liq., u.s. vibs effect on nucleation 8=48261
Bi nucleation behaviour 8=48257
Pb liq., nucleated by solid Cu, Fe and Sb, under-cooling 8=43911
Pb, nucleation behaviour 8=48257

Superexchange. See Antiferromagnetism.

Superfluidity
See also Helium/liquid; Quantum theory/many-particle systems.
Bose system, 2-dimensional, coherent phonon states 8=46116
boson system model, eqn. of motion of condensate wave function, excitation spectrum gap 8=37212
nuclear system, statistical mechanics 8=23886
persistent currents decay, log. time dependent 8=41894
phenomenological theory, "three parameter" form 8=46311
semimetals, possibility at dielec. transition 8=44627
theory of long-range fermion interaction 8=26983
He ion mobility discontinuities, inadequacy of Huang-Olinto theory 8=41897
He, liq., persistent flow and pot. motion 8=33002
He liquid, electron bubble vibration, freq. estimate 8=37346
He liquid, vortex ring annihilation at surface with electron ejection 8=37344
He, liquid, vortex-ring interaction cross section 8=41895

Superfluidity—contd
He, neutral excitation with Po^{210} α source 8=24045
He, λ point shift in rotating angular gap, obs. 8=37348
He, rotating, hydrodynamic theory of relaxation 8=37347
He, superfluid eddy emergence on free surface 8=37352
He II, bubble model, validity from obs. of photoejection of trapped electrons 8=41901
He II, capillary wave modes 8=37350
He II, heat torques and circulation 8=37345
He II in capillaries, connecting points at different temps, heat conduction 8=28443
He II, injection of electrons from immersed tungsten filament up to 2500°K 8=37351
He II, particle motion and heat exchange 8=37349
He II, quantized circulation round vib. wire 8=41903
He II, vortex wheels 8=41900
He II, vorticity, in flow 8=43731
He^3 soln. in He^4, first viscosity calc. from phonon Boltzmann eqn. 8=41898
He^3-He^4 solutions, mobility of positive ions, 1.4 to 2.15°K 8=46312
He^4 transition, gravit. field effect 8=41899
He^4, vortex ring prod. by negative ions, effect of He^3 impurities 8=37339

Superlattice structure. See alloys; Crystal structure, atomic; Solid solutions.

Supernovae. See Novae.

Superparamagnetism. See Ferromagnetism.

Supersonic flow
See also Shock waves.
air, couette and boundary layer, with radiative transfer 8=39207
air, rarefied, visual picture using wedge shaped Fabry-Perot interferom. 8=30243
boundary-layer transition on cone, effects of roughness with cooling 8=39189
gas, at leading edge of plate, behaviour of mass, impulse and energy fluxes 8=34609
gas round convex profile, with detached shock wave 8=34604
gas, viscous, near wall with corner 8=34606
gases, transonic, two dimensional, in presence of normal shock waves 8=47938
heat transfer in hypersonic wind tunnels, pyroelectric transducer abs. 8=47953
of hot gases, anal. of two-dimens. flow, allowing for heat transfer 8=39185
hydrocarbon fuel/air mixture, in boundary layer of plate, ignition regime 8=32969
hypersonic shock layer, radiative heat loss effect on subsonic region 8=34636
Lavalle nozzle, transonic gas flow 8=39173
past cone-cylinders, calc. of pressure distrib. 8=34631
from porous metal plate, rel. to disordered flow after choking 8=34630
rarefied, density disturbance ahead of sphere 8=43672
reactive, one dimens., steady state analysis 8=34617
sphere wakes, convection vel. meas., comparison of decay curves 8=39188
two-phase nozzle flow, max. particle size, effect of liq. surface tension 8=34634
wake turbulence regimes for flows behind hypersonic bodies 8=34633
Ar beam, low-temp. viscosity cross-sections 8=30311
N_2, low-density, rotational relax. anal. rel. to rot. temp. 8=34629

Supersonics. See Ultrasonics.

Surface diffusion. See Diffusion in liquids; Diffusion in solids; Surface phenomena.

Surface energy
alkali halide/organic liquid interphase, rel. to crystal abrasive wear props. 8=30724
n-alkanes, cohesive and adhesive, calc. 8=43779
crystals, thermodynamics 8=48414
density, effective, in solids dependence on rate of crack growth, strain history etc. 8=44533
of graphite and diamond interfaces with liq. metals 8=30718
ice, rel. to contact angle with water for rapidly freezing interface 8=35146
ionic crystal/organic liquid interphase, rel. to crystal abrasive wear props. 8=30724
of liquid metal interfaces with graphite and diamond 8=30718
mixed crysts., deformed, surface states 8=35784
particles, spherical, radii less than 500Å 8=26000
polycaprolactam, rel. to cryst. morphology, obs. 8=43907
polyvinyl butyral, rel. to composition 8=30731
porous solid, effect on strength 8=48969
solid-liquid interface, or residual force 8=48106
water-ice interface, precrystallization theory application 8=34957
Au, heated in air, and impurity adsorption 8=26095
Co f.c.c., grain boundary and twin boundary 8=44026
Fe-3% Si, and grain boundary energy in presence of O_2 8=26102
Fe-3% Si (100) and (110) surfaces, by surface relax. meas. 8=26101
Ge, semiconducting, computer calcs. using H model for surface structure 8=30721

Surface energy—contd
- Ni, of (100) and (110) surfaces, from self-diffusion coeffs. 8=44028
- Si, semiconducting, computer calcs. using H model for surface structure 8=30721
- UC, rel. to grain boundary grooving 8=30871
- W, binding energy of individual atoms 8=30775
- ZnO crystal, charge and e. multiplication 8=49354

Surface ionization. See Ionization, surface.

Surface measurement

See also Area measurement.
- aerosol, laser technique 8=34948
- colloid deposit on planar inorg. substrate, conc. determ. rel. to removal 8=30568
- ellipsometry, LEED and FEM, combined in one instrument 8=26092
- dispersed materials, neg. adsorpt. and other methods 8=48228
- displacement, hologram interferometry 8=37713
- graphite, by energy anal. of back-scattered electrons 8=30730
- ice, power of spheres, rate of decrease of area due to plastic flow 8=35073
- microscopic differences in height by reflection electron microscopy 8=44023
- non-optical, topography by projected fringes 8=26093
- optical flat, to 240 mm dram., Fizeau interferom. for testing 8=28859
- porous solid, by gas adsorpt. 8=48352
- secondary electron detector with flexibility of mech. motion 8=31474
- silicate minerals, by Xe adsorpt. 8=48426
- temperature above 800°C, with blue sensitive photomultiplier 8=24014
- by third-order gas-solid interactions 8=48472
- u. h. vacuum reflection electron diffraction camera, for energies (10-50 kV) 8=26353
- use of surface plasma oscs. and inelastic electron scatt. 8=26926
- zeolites, by adsorpt. and X-ray crystallog. 8=48432
- $BaTiO_3$, strain, by using semiconductor thin films 8=49364
- Cu, by energy anal. of back-scattered electrons 8=30730
- W, by energy anal. of back-scattered electrons 8=30730

Surface phenomena

See also Adsorption; Capillarity; Catalysis; Electron emission; Films; Ionization, surface; Liquid waves/surface. Sorption.
- accomodation effect on momentum and temp.-slip coeffs. 8=47940
- adsorption on patchwise heterogeneous; math. anal. of step-function approximation to local isotherm 8=30761
- alkali halides, elec. field gradient at (100) surface 8=30717
- alkali halides, surface distortion calc. 8=30725
- alumina ceramics, resistivity, cleaning and humidity effects 8=49337
- alumina ceramics, surface resistivity dependence on ambient humidity and cleanness 8=27237
- aqueous electrolyte solns., surface potentials 8=30516
- atoms scatt. from specular surfaces, ang. distrib. 8=39574
- Bingham plastic surface flow anal. in canal viscometer 8=30343
- α-brass, preferential hardening in early stage II 8=40145
- bubble "microtome" for sampling liq. surface 8=30380
- charges due to electron beam incident on metallic surface, temp. effect 8=27364
- chemistry, by Mössbauer effect, review. 8=49902
- colloid-surface interacts, method for determ. small cones of colloids on planar inorg. subs 8=30568
- contact angle of water on ice, for rapidly freezing interface 8=35146
- contact pot. difference induced by gravit. field 8=44679
- crack propagation in continuous media 8=44533
- crystalline solid, stress conc. at step. 8=48951
- crystallites migration theory 8=44021
- crystallites on cleavage planes, Brownian movement 8=44022
- crystals, anisotropic, elastic wave propag., forbidden directions 8=48946
- desorption of thin films 8=39609
- diffusion, activation energy, elec. field dependence (10^7–10^8V/cm), theory 8=35512
- elastic waves, isotropic medium, impedance effect 8=28365
- electrets, plastic, surface charge characts. 8=44892
- e. m. boundary wave propagation 8=37469
- ellipsometric, surface tension and contact potential using a controlled atmosphere Langmuir trough 8=34805
- f.c.c. crystals, surface force-constant changes rel. to atomic square displacements 8=26567
- film surface pressure recording system 8=39573
- free surfaces in Hamiltonian hydrodynamics 8=34702
- gas adsorption, mass spectrometer scanning 8=30760
- glass surfaces, impression by high intensity laser beam 8=33248
- Heisenberg antiferromagnet, free surface effects 8=45048
- heterogeneity effect on adsorpt. isotherm for gases 8=44069

Surface phenomena—contd
- ice, features obs. during thermal etching 8=35147
- ice, liq.-like transition layer, survey 8=34975
- ice, mass transfer along surface, neck growth and particle migration 8=30723
- ice on silicate surfaces, existence of liq. like, unfrozen interfacial water layer 8=35142
- ice-solution interface, model, rel. to 'freezing potential effect' 8=34970
- ice, surface diffusion at ice-air interface rel. to step propag. across basal plane 8=35145
- ice, type of struct. from N_2 adsorpt. isotherms 8=30769
- impurity formation on narrow e-beam irradiation rel. to adsorbant diffusion 8=40010
- interfacial cohesion, practical implications of breakdown, review 8=39499
- ionic crysts., thermoelec. power, theory 8=49389
- leaf, artificial, exchange of momentum, mass and heat with airflow in wind tunnel 8=34608
- liquid-vapour interface, kinetic condns. 8=43914
- magnetic levels in prescence of superconductivity 8=44958
- metal, f. c. c., purity by Auger electron spectroscopy 8=27355
- metal, friction and abrasion rel. to contact area 8=26775
- metals, molec. orbital model, and gas interact. in field ion microscope 8=35143
- metals, rough, i.r. reflection spectra 8=31932
- metals, secondary electron emission and contamination 8=49445
- in microstrain and cyclic loading 8=31170
- microwave surface impedance, reason for oscillations 8=36311
- migration during K deposition on W emitters in field emission microscope 8=44936
- monolayer liquid films on aqueous substrates at low surface pressures, circulation 8=34746
- moving plasma, oscillation spectra and growth rate calc. 8=34534
- myristic acid dipole moment in gaseous monolayer at air/water interface, obs. 8=30438
- nuclear polarization and relaxation by paramag. porous surfaces 8=48475
- opalescence, critical surface 8=25915
- pair splitting interaction of magnetic field in surface superconduction 8=49179
- palmitic acid dipole moment in gaseous monolayer at air/water interface, obs. 8=30438
- plasma reflection from metal 8=43494
- porous Vycor glass, e. s. r. of methyl radicals on surface 8=47684
- quartz, surface and bond-forming props. 8=48427
- quartz: Al impurity, AlF_3 formation during ageing (3½ yrs) after HF treatment. 8=49900
- reconstructed surface uncertainty, comments 8=35141
- refraction of light from rough surfaces obs. 8=36319
- sapphire, interface growth morphology of czochralski crystals 8=44117
- sapphire, thermal resistance of contacts 8=48749
- selective coatings for solar energy receivers 8=44020
- semiconductors, additives to control surface Fermi level 8=35874
- semiconductor, bulk, transport props. 8=27063
- semiconductor, optical investigation 8=40435
- semiconductors, review 8=44761
- silicates, surface and bond-forming props. 8=48427
- sliding discharge at solid dielec., in vacuum 8=27224
- solids, desorption of thin films 8=39610
- solids, rough contact area 8=35139
- solids, thin films, physicochemical relations between 8=39608
- solid-liquid interface, morphology during melting 8=43897
- solid-liquid interface stability during solidification 8=43910
- structure defects, active centres and long-range effects rel. to epitaxy 8=26274
- surface state calc., model of crystal potential 8=40255
- transient deforms of opaque bodies, obs. by birefringent strips 8=44521
- transport meas. using sinusoidal grating diffraction phenomena 8=41019
- transport meas. using sinusoidal grating diffr. phenomena 8=41020
- triglycine sulphate, sparking phenomena 8=40623
- u.v. scatt. from rough and smooth surfaces 8=37698
- vibration modes, obs. by stroboscopic hologram interferometry 8=32883
- waves in joined elastic materials 8=46050
- wettability of high energy rough surfaces 8=35140
- zeolite, synthetic, r. f. spectrometry during dehydration 8=39581
- Ag, scatt. of inert gases 8=39575
- Al, oxide film effect on dislocation-surface interacts. 8=26094
- γ-Al_2O_3, radiational defects, adsorpt. exam. methods 8=44024
- γ-Al_2O_3, radiational defects, exo-emission exam. methods 8=44025
- Au crystallites on KCl cleavage planes, Brownian movement 8=44022

Surface phenomena—contd
- CdS, influence on photomag. effects 8=31453
- CdS, photoconductivity, effect of self-purification and polarity 8=40658
- CdS, photoconductivity, influence of oxygen desorpt. and chemisorp. 8=49413
- CdS {0001}, potential temp. dependence 8=44766
- Cr, cleavage cracks due to spark machining 8=39577
- Cu and Ar atom collisions 8=29661,
- Cu, preferential hardening in early stage II 8=40145
- Cu, origin of fractional order peaks in diffracted LEED beams 8=26100
- Cu, p scatt., $E_p = 40\text{-}120$ keV, obs. 8=47135
- Cu, spherical crysts., LEED spot patterns, behaviour during voltage and cryst. position changes 8=26098
- Cu–Au, films, surface and vol. diffusion 8=35486
- Fe, pure, influence of reactor irrad. on surface struct. and corrosion 8=30720
- n-GaAs, barrier, trap density, mobility, and effect of SiO_2 layer 8=35144
- GaAs {111}, potential temp. dependence 8=44766
- GaAs, swing and polishing effects on defects 8=44427
- GaAs-SiO_2 interface props., m. o. s. characts. 8=40446
- Ge, clean surface prep., adsorpt. characts. and surface conductivities 8=48421
- Ge crystals, smooth surface defects, effect on breaking strength at 300°K and 4.2°K 8=40161
- Ge, effect of adsorption-desorption mechanism on electrophysical parameters 8=48484
- Ge etched, charge condition under low energy electron and u.v. irrads. 8=35901
- Ge, semiconducting, structures, computer calcs. 8=30721
- n-Ge, surface states relax. time obs. 8=44788
- Ge, total internal reflection spectroscopy 8=35895-6
- Hg-Tl eutectic, interfacial reactions with metals, dielectrics and polymers 8=49873
- p-InSb, photoconduction 8=44927
- Ir, migration, from field-emission studies 8=27343
- Ir oxidation, formation of "molecular clusters" 8=45343
- MgO : Mn^{2+}, charge transfer at surface, e.s.r. study 8=48422
- Mo, activation energy elec. field dependence (10^7–10^8V/cm) 1300–1800°K 8=35512
- NaCl-type crystals, LEED obs. of (11) beam from (100) surfaces 8=44236
- NaCl(Br, I), distorted, electrostatic potential contribution to LEED intensities 8=48423
- Nb, self-diffusion in strong elec. field, field-emission exam., 8=39978
- Ni, morphology, effects of reaction with Br 8=30726
- Ni, origin of fractional order peaks in diffracted LEED beams 8=26100
- Ni–Au films, surface and vol. diffusion 8=35486
- Pb, crysts., mean displacement of surface atoms 8=30935
- Pd crysts., mean displacement of surface atoms 8=30935
- Pt, appearance of Na, K oxide impurities at 20-1100°C 8=35549
- Re, migration, from field-emission studies 8=27343
- Rh, migration, from field-emission studies 8=27343
- n-Si, absorption of hot electrons 8=49260
- Si, clean surface prep., adsorpt. characts. and surface conductivities 8=48421
- Si crystal inversion layer, magnetoresistance at 77°K 8=27130
- Si, dislocation sources 8=26694
- Si, electronic structure, influence of thermal treatment 8=40487
- Si film on sapphire, orientation relns. at interface 8=44058
- Si, oxidized, rel. to device technology 8=49267
- Si, semiconducting, structures, computer calcs. 8=30721
- Si {311} planes, epitaxial growth 8=39582
- Ti_2O_3 protective layer on cemented carbide cutting tools 8=48428
- UO_2, diffusivity of U ions, 1544°–1915°C obs. 8=35511
- W appearance of Na, K oxide impurities at 20-700°C 8=35549
- W, C contaminated, (110) face metastable phase, obs. 8=39583
- W, chemisorption of water 8=27739
- W, diffusion, activation energy elec. field dependence (10^7–10^8V/cm), 1200–2100°K 8=35512
- W, field evaporation rel. to surface atoms cohesive energy, obs. 8=39503
- W, migration, from field-emission studies 8=27343
- W, O_2-covered, thermal rearrangement 8=31464
- W, origin of fractional order peaks in diffracted LEED beams 8=26100
- W-Mo-Re alloys, comp. changes on ht. treatment and effect on work function 8=39727
- Zr alloys, hydrogenation, protection with molten $NaNO_3$ 8=32105

Surface tension
- See also Capillarity.
- alkali metals, liquid, ultra high vac. obs. 8=25897
- n-alkane mixture, liquid/vapour, water, solid interfaces 8=48102
- n-alkanes, and interface tension calc. 8=43779
- benzene-cyclohexane binary mixturs 8=44068
- of binary hydrocarbon liq. mixtures, at liq.-vapour interface 8=48041

Surface tension—contd
- crystals, thermodynamics 8=48414
- discontinuity, optical obs. 8=25896
- 2-dodecylaminoethanol salts, study of micellar props., effect of counterions 8=39289
- droplets from vapour, rel. to radius 8=43781
- liquid, effect on max. particle size in two-phase nozzle flow 8=34634
- liquid film breaking on vert. surface, contact angles meas. under heat transfer condns. 8=25895
- liquid jet leaving Poisseuille tube, effect 8=48039
- liquid sessile drops, rel. to shape analysis 8=25857
- liquids and liq. mixtures, statistical-mech. calc. 8=48107-8
- liquid/liquid interface, approach of rigid sphere 8=34744
- liquid-vapour interface, importance for weightless liquids 8=48104
- menisci, advancing, deformation 8=48103
- nematic liq. crysts. interfacial effects on thermal cond. 8=34833
- polymer liquids 8=48105
- polyvinyl butyral, critical, in alcohols and hydrocarbons, effect of composition 8=30731
- quasi-brittle, crack propagation in continuous media 8=44533
- solids, crack propagation in continuous media 8=44533
- surfactant solns. capillary nipple damping and films Gibbs elasticity 8=30445
- transition metals, and cohesion, by tight binding method 8=43928
- Ar, rel. to mol.-statistical theory, 87-140°K 8=25898
- Ar-N_2 liq. mixtures, statistical-mech. calc. 8=48107-8
- $CdCl_2$-alkali chloride liquid systems 8=30439
- Cs amalgam, conc., and electron work function 8=49435
- Ga boundary with non-polar org. liqs., interphase 8=39338
- H normal solns. in Ne, 24.59 to 29°K 8=43780
- H_2-Ar solns., temp. and conc. depend. rel. to mol.-statistical theory, 87-120°K 8=25898
- H_2O, contact angle on Au 8=48418
- Hg monolayer obs. 8=48061
- In(Liq.) on Al 8=39336
- Li soaps in water miscible alcohols 8=39316
- $NaClO_3$-$NaNO_3$ molten system 8=48086
- UO_2, critical, for complete melting by liq., comp. in oxidizing and reducing atmos. 8=30729
- $UO_2(NO_3)_2$ in diluent + TBPP/ImHNO$_3$, interfacial tension and partition coeff. 8=34804

Surface tension measurement
- automatic recording for liquids 8=30443
- by bubble profile dimens. 8=39337
- controlled atmosphere Langmuir trough 8=34805
- drop-weight-volume method, correction factors 8=30441
- interfacial, by pendent drop method, eqns for 1/H vs S values 8=48042
- interfacial tension, visual cell, high-press, high-temp. 8=30444
- sodium alkylbenzene sulfonates, free energy change in adsorption 8=39339
- solid, elastic, kink-capillary oscills. 8=26748
- surfactant aqueous solns. by du Nov̌y tensiometer rel. to reproducibility 8=30440

Surface texture
- apophyllite crysts., microstruct. study rel. to growth mech. 8=26211
- cathode spots in high-current vacuum arc, theory 8 =25704
- damage of film coatings on Cu single crystals rel. to strengthening effects 8=40150
- dislocation etch pits shape at intersection with crystal surface 8=48837
- electron diffraction exam., anomalous ring patterns due to secondary e. emission 8=48587
- fracture study, comparison of transmission and scanning electron microscopy 8=48415
- glass fracture, mist zone microstructure 8=30722
- glass, inorg., mech. condition rel. to fracture strength 8=31176
- glass, porosity rel. to aq. attack 8=26149
- glass, structure after etching, i.r. spectroscopy 8=39578
- goniometer, X-ray shield 8=39705
- graphite microtopography using gold decorant, rel. to gold epitaxial growth 8=44099
- laser rod, matting, effect on optical pumping 8=37598
- metal crystals, laser irradiation, localized damage 8=30716
- metal, industrial vacuum technology aspects 8=39572
- metallurgical, scanning e.-microscope exam. 8=50472
- microscopic differences in height by reflection electron microscopy 8=44023
- molybdenite cleavage surface, LEED study 8=48524
- muscovites, rel. to shearing force anisotropy 8=44602
- nitrocellulose films, craters and penetration holes after exposure to micrometeorites 8=41579
- polishing, disproving previous hypotheses 8=50468
- polishing glass, temp. rise from GeO_2 hexagonal-tetragonal transition 8=39558
- porous, transpiration cooled, transient temp. response in forced convection surroundings 8=35450
- profilometry, relocation technique 8=44019

Surface texture—contd
- reconstructed surface uncertainty, comments 8=35141
- rough, optical reflection, var. with angle of incidence 8=46717
- roughness, effect on contact resistance of rough flat surfaces 8=48412
- roughness, effect on contact resistance of tarnished contacts 8=48413
- roughness effect on u.s. velocity calc. 8=37277
- roughness effects on diffusion 8=39956
- roughness measurement techniques, development in U.S.S.R. 8=48416
- roughness of cone, with cooling, rel. to boundary-layer transition at supersonic speeds 8=39189
- roughness of wing elements, effects on heat transfer intensities 8=39208
- scanning electron microscope exam. 8=41968
- seal faces, mean surface profile meas. 8=35138
- selective coatings for solar energy receivers 8=44020
- stainless steel, craters and penetration holes after exposure to micrometeorites 8=41579
- steel, mild, rel. to film growth kinetics in chromate solns. 8=44039
- rel. to X-ray reflection, anomalous 8=27529
- Zircaloy-2, effect on corrosion in water and steam 8=45352
- Al, blistering on p-irradiation, 10-200 KeV 8=40070
- Al, fatigue damage from Au nucleation exam. rel. to fatiguing environments 8=26778
- Al, structure appearance during brightening and anodizing 8=48417
- Au, anomalous structures, as prop. of clean metal surface 8=26097
- Au, interpret. of complex LEED patterns rel. to coincident site lattices, and phase and spacing modulation 8=26096
- Au(100) surface, purity and structure from Auger spectroscopy and LEED 8=27355
- $BaTiO_3$, domain structure and topography from e.-mirror photomicrographs 8=39576
- Be, effect on mod. of rupture 8=26788
- Bi, {001}, {01$\bar{1}$2}, {11$\bar{2}$0}, structure study by LEED 8=26106
- CdS {0001}, structure study and O_2 adsorption by LEED 8=30719
- Cr black coatings, electrolytically deposited 8=45394
- Cu crystal, dislocation distrib. after tensile deform. 8=48856
- Cu spherical crysts., struct. after O_2 adsorpt. 8=26099
- Cu(100) surface, purity and structure from Auger spectroscopy and LEED 8=27355
- Cu-Au alloy, roughening during electolytic dissolution 8=49938
- Cu_2O film on Cu electrode in 3% NaCl aqueous soln., effect of dissolved O on stability 8=41279
- Fe and Fe alloys, electropolishing, "Universal" technique applications 8=44027
- Fe-Cr alloy-oxide interface, e microscopy 8=26103
- GaAs, automatic jet thinning 8=33088
- n-GaAs, cleanliness meas. by ellipsometry 8=49240
- GaAs, epitaxial surface features and twins 8=35241
- Ge, annealed and cleaved, structure transformations 8=48419
- Ge, preparation, stabilization and chemical treatment 8=48420
- LiF crystals, reflectance props. in far u.v. effect of polishing 8=41112
- Mo, (001) and (110), damage due to bombard. by Ne^+, Ar^+, Kr^+ or Xe^+ LEED study 8=26104
- Na_2SiO_3, structure after etching, i.r. spectroscopy 8=39578
- Pd, annealing changes, effect on CO adsorption 8=48424
- Pd(100) surface, purity and structure from Auger spectroscopy and LEED 8=27355
- Pu, effect on total hemispherical emittance 8=30993
- Pt, ion microscope tips smoothing by field evaporation, 10 and 78°K 8=39708
- Re, h. c. p., He field-ion microscopy, comparison with Ru 8=26105
- Re, vapour deposited, rel. to thermionic emission 8=31468
- Ru, h. c. p., He field-ion microscopy, comparison with Re 8=26105
- Sb, {0001}, {01$\bar{1}$2}, {11$\bar{2}$0}, structure study by LEED 8=26106
- Si annealed, nature 8=30727
- Si, damages after thermal treatment of $Si-SiO_x$ system 8=49276
- Si, effect on electron exoemission 8=40693
- Si, imperfections during thermal treatment 8=30728
- Si, micro-relief exam. after elec.-decoration by Pt 8=40496
- Si, planar chemical polishing 8=48425
- Si, struct. and field emission, cleaning by heating 8=35148
- Si, thermal behaviour of vacuum-crushed, air-crushed and mechanically polished surfaces, e.p.r. exam. 8=39580
- UO_2, low-energy electron diffr. 8=48430
- UO_2, steps, LEED 8=48429
- W emitter in thermionic converter, effect of etching to 110 planes on characts 8=28476

Surface texture—contd
- W, (110), damage due to bombard. by Ne^+, Ar^+, Kr^+ or Xe^+ LEED study 8=26104
- W, (110), LEED study 8=48431
- W, (112) face, initial oxidation structs. 8=26107

Surveys. See Reviews

Suspensions
- See also Aerosols; Sedimentation; Sols.
- bentonite-water system, opacity rel. to extinction coeff. 8=30547
- carbon black, chain struct. by light scatt. 8=43885
- carbon black in nonpolar media, electrokinetic pot. and stability, H_2O effects, obs. 8=30550
- Christiansen filter shape and bandwidth by multiple scattering calc. 8=37665
- chrysotile asbestos, colloidal, stability due to surface charge enhancement 8=48242
- clay, aqueous, classification by Newton's cooling coeffs. 8=25963
- Coulter counting, improving resolution by hydrodynamic focusing 8=39445
- crystal size distribution, effect of suspension density 8=48532
- diffusion through porous medium, mathematical representation by random walking particle 8=32822
- double hydrosilicates of Ca and Na aqueous, dispersion structures 8=34937
- fluid containing small particles, viscosity 8=39443
- gas-solid flow, heat and mass transfer 8=43650
- gas/solid, heat transfer theory for turbulent flows, small particle conc. 8=39457
- gas/solid particles, sound vel. and damping, from distrib. of disturbances 8=39455
- halloysite, flow behaviour, rheological model 8=39444
- latex hydrosols, coherent and incoherent light scatt. 8=34932
- layers containing coarse particles, light transmission 8=30554
- liquid/solid, heat transfer theory for turbulent flows, small particle conc. 8=39457
- monodispersed system, stationary flow of particles in rectilinear channel 8=30544
- montmorillonite, tactoid rearrangement and optical density 8=39450
- mosaic virus, southern bean, interparticle interactions, small-angle X-ray scattering studies 8=25967
- particles diffusive and settling in stationary fluid, distrib. and deposition 8=48236
- particle size and residence time distribs, rel. to coupled heat and mass transfer 8=34936
- polydisperse, electrophoretic mobilities, effect of double layer overlap 8=34942
- polydisperse, particle-diameter distrib. determ. by small-angle X-ray scattering 8=30553
- polystyrene, aq. suspension, angular distribution of scatt. light 8=25964
- polystyrene lattices, particles refr. index by light scatt. 589, 546 and 436 mμ 8=34934
- polyvinyltoluene, aq. suspension, angular distribution of scatt. light 8=25964
- of rigid spheres, reductions in vol. conc. on flow through narrow tubes 8=48229
- sheared Couette flow, streamlines round cylinders and spheres 8=48227
- silica spheres, uniform size, controlled growth 8=48235
- slurry systems, attrition resistance of solids 8=48233
- solid-liquid, heat transfer in agitated vessel 8=48232
- solid-phase conc. distrib. in moving medium, rel. to sedimentation 8=34952
- sound attenuation 8=25961-2
- spherical solid particles, adhesion 8=39451-4
- sprays of pure liquid drops, evaporation rates 8=48278
- thermal conductivity of liq.-solid systems, digital simulation compared with expt. 8=43883
- turbid, transient light scatt. 8=30558
- viscosity, effect of particle motion in shear and elec. fields 8=48231
- $BaSO_4$ in nonpolar media, electrokinetic pot. and stability, H_2O effects, obs. 8=30550
- β-FeOOH rod crysts., streaming, particle size by light scatt., obs. 8=30549

Suzuki atmospheres. See Crystal imperfections/dislocations.

Switching time, ferroelectric. See Ferroelectric materials; Ferroelectric phenomena.

Switching time, ferromagnetic. See Ferromagnetism; Magnetic properties of substances/ferromagnetic.

Symbols. See Nomenclature and symbols.

Symposia. See Conferences.

Synchrocyclotrons. See Particle accelerators/orbital, cyclotrons.

Synchrotron radiation. See Electrons/radiation.

Synchrotrons. See Particle accelerators/orbital.

Szilard–Chalmers reactions. See Radiochemistry.

Tables, mathematical
- binary systems, viscous tidal lag 8=32460
- constant field parameters, computation tables for least squares estimation 8=48122

Tables, mathematical—contd
- $SU(3) \supset R(3)$ Wigner coeffs. in 2s-1d shell model for nucleus 8=29269
- torsional vibrations calc. 8=46138

Tables, physical. See Collections of physical data.

Tachometers. See Angular velocity measurement.

Tandel. See Dielectric devices.

Tantalum
- anodic film, activation energies of conduction 8=49924
- b.c.c. lattices, energy of interstition of impurity atoms into octahedral and tetragonal positions 8=35542
- bellows for thermionic diode, microhardness and bonding rel. to reliability 8=37377
- capsule for Pu-Co-Ce melt in reactor Ta mass transfer determ. 8=47420
- conducting film formation using electron beam 8=39603
- container for liquid Pu, O, N impurity effects on corrosion 8=47412
- crystals, zone-refined, orientation, purity and structural perfection rel. to growth condition effects 8=35231
- 8 kV isochromat obs. 8=45227
- electron emission, laser-induced, using ruby and Ar lasers 8=40710
- electron reflection, 600 to 1200 keV 8=44197
- optical consts., reflectance meas. 537-5770Å 8=27591
- oxide plate formation, crystallographic analysis 8=39690
- oxide plate formation, growth and morphology 8=39689
- oxidised film electroluminescence 8=45287
- polycrystal, secondary ionization by 40keV Ar^+, mass spectrum 8=49448
- positron annihilation, single-quantum, cross sections 8=44670
- sintered, recrystallization rel. to deformation and temp. 8=48560
- solubility of N; 10^{-8}-10^{-3} torr, 1600-2300 °K, 0.0044-1 atomic %, press.-temp.-conc. ranges 8=49897
- Sorption of O_2, kinetics, 1100-2000 °C at 5×10^{-4} torr 8=49895
- substrate for Re emitter, interdiffusion 8=28502
- surface superconductivity, strain and impurity effects 8=44739
- thermal conductivity below 1°K, rel. to supercond. energy gap 8=30988
- wetting by Cs and Na, rel. to bare work function 8=35168
- work function and desorpt. energies of O_2, thermionic meas. 8=31469
- Al films grown on (110), interaction of O_2 and CO 8=35159
- Ca and Mg impurities, spectrochem. detect. 8=45416
- Gd ion sputtering, ang. distrib. obs. 8=48999
- Kr ion sputtering, ang. distrib. obs. 8=48909
- Mg ion sputtering, ang. distrib. obs. 8=48909
- Ta wire, loaded with N rel. to Snoek damping 8=48468
- W-Ta thermocouple, potentials 0°-420°C 8=28418
- X-rays, ultra-soft, absorption, experimental and theoretical study 8=25364

Tantalum compounds
- tantalates, ATa_2O_6, structural comparison with AnB_2O_6 phases 8=48636
- oxidic tantalates, cryst. struct. effect on luminesc. 8=45284
- TaB_2 in Cs vapour, e- and ion-emission rel. to other refractory metal cpds 8=27350
- TaC, C diffusivity rel. to comp., 2100-2650°C 8=44392
- TaC, chemisorption of CO 8=49903
- TaC, f.c.c. superconducting props., anomalous 8=27022
- TaC, field ion microscopy 8=26289
- TaC grain growth during hot-pressing 8=35283
- $TaC_{0.66}$, C diffusion coeff. temp. dependence 8=31018
- TaC_x, Hall coeff. comp. and temp. dependence 8=26972
- Ta_2C, C diffusivity, 2100-2650°C 8=44392
- TaF_5, molec-stability 8=38938
- $TaF_8{}^{3-}$, spectra and struct. 8=41118
- TaFe lamellas in TaFe-$TaFe_2$ position and melting point 8=35220
- Ta-Mo alloys, effect of Mo conc. on yield stress and work hardening 8=35718
- Ta-Mo-C alloys, phase diagram, melting point 8=39474
- Ta_2N film, deposited by reactive evaporation 8=48454
- TaN-TiB_2, hot-pressed, densification and wear resistance 8=49053
- Ta-Nb alloys, effect of Nb conc. on yield stress and work hardening 8=35718
- Ta-Nb alloys, $K_1(t)$ and $K_2(t)$ meas. rel. to temp. 8=44740
- Ta-O, strain-ageing from resistivity meas. 8=26846
- Ta-O system, γ-phase, annealed, crystal structure, e. diffr. exam. 8=39822
- Ta_2O_5, ion exchange separation from Nb in columbite 8=36544
- Ta_2O_5 insulating film, refractive index 8=49763
- Ta_2O_5, polymorphism, effect of oxide additions 8=48403
- Ta_2O_5 thin films, electron microscope obs. of superstruct. 8=26129
- $TaOF_3$, molec-stability 8=38938
- Ta-Re alloy, yielding, work hardening, cleavage 8=40182
- Ta_2Se_3, crystal structures 8=44240
- $TaSi_2$ in Cs vapour, e- and ion-emission rel. to other refractory metal cpds 8=27350
- Ta/Ta_2O_5 structures, annealed, exponential vacancy distrib. origin 8=44417

Tantalum compounds—contd
- Ta-W alloys, normal spectral emissivity, temp. and comp. dependence 8=45224
- Ta-W alloys, resistivity, 300 to 2400°K 8=26973

Targets. See Nuclear bombardment targets.

Teaching
- atomic struct., chem. bonding and valency theory, effect of using 3-dimens. molec. models 8=45309
- electrostatics, imaging methods, computer-animated film 8=37366
- elements origin, literature and teaching aids review 8=45585
- Films, 1020 16 mm., for physics students, list 8=41611
- Green's function method, ferromag. of 2-spin system 8=40769
- mechanics, thought-provoking problems for students 8=37103
- optical filter transmission characts., educational expt. 8=37666
- physics, reminiscences of a professor 8=37104
- relativity, general, resource letter 8=32805
- vacuum apparatus for student practical work 8=30324
- wave function meaning and matter waves reality 8=42305
- **demonstrations**
  - conservation of momentum 8=28255
  - crystal growth, cine-films 8=26202
  - crystal optics, ciné-films for lectures 8=27519
  - crystallography, apparatus and techniques 8=26330
  - cyclotron, conical pendulum, elect. stimulated as model 8=47001
  - electric field plotting expt., modification 8=37367
  - Faraday's law of induction 8=24122
  - ferromagnetic films domains, hysteresis and magneto-optical effects 8=27397
  - γ-rays particle nature 8=29082
  - heat conduction and loss in bar 8=32956
  - holography with double-focus lens, simple lecture demonstration 8=46758
  - interference fringes, lower-order multiray 8=28854
  - linear air track, strobe photography, demonstration 8=28253
  - linear air track to demonstrate electron atom collision 8=29652
  - neutron generator for undergraduate laboratory 8=38076
  - one-dimensional scatt. film 8=37754
  - perturbations, diosectable anharmonic oscillator 8=41803
  - plasma confinement, metal tube deform. by pulsed mag. field 8=30116
  - projectile motion, wooden shell and moving net target 8=41646
  - Raman spectroscopy experiment for the senior laboratory 8=29696
  - Rutherford elastic scattering experiment 8=25009
  - Rutherford scatt., annular target expts. 8=42669
  - sophomores, instrum. familiarisation programme and projects 8=41612
  - thermal expansion 8=46253
  - viscosity of liquids, falling-ball viscometer for undergraduates, < 2 k bar 8=43769
  - Bi hyperfine structure, using plane grating spectrograph 8=27562
  - HeII second sound propagation 8=33003
  - X-ray diffraction, analogies in interference patterns 8=30879
  - Y-T recorder for linear air track 8=28256
  - $Pb_{85}In_{15}$ superconductor, resistive and mag. props. 8=35855

Technetium
- in stars, red giant, Tc^{97} synthesis 8=45644
- superconductivity, $\partial T_c/\partial P$, sign rel. to other transition metals 8=31344
- Tc^{96}, carrier-free, prep. from $Mo^{96}(p, n)$ 8=47322
- Tc I, II, spectra, 2000-9000 Å from arc and spark sources 8=47508

Technetium compounds
- No entries

Tektites. See Meteorites.

Telescopes
- design, principles 8=28753
- focus testing with spheres 8=28744
- inbalance in rotating parts, obs. 8=42185
- large, recent advances in optics 8=42187
- mirror type with free aperture of 3.5m, optical design 8=36919
- Ritchey-Chretien, corrector system 8=42188
- **astronomical**
  - See also Radioastronomy.
  - Cassegrain, for obs. of Lyman-α emission line, solar chromospheric fine structures 8=45916
  - Cassegrain type with parafocal plates, third order errors 8=41496
  - Cassegrainian mirror-lens isochromatic systems 8=32408
  - Cassegrain type, reflecting, corrector systems for first and secondary focus 8=32409
  - Cerro Tololo Inter-American Observatory, facilities 8=32407
  - coma tolerance in photographic star images 8=36941
  - high resolution photography of solar chromosphere 8=45917
  - Kitt Peak National Observatory, facilities 8=32407
  - mirrors, large aperture Al alloys 8=46677

Telescopes—contd
  astronomical—contd
    multi-element arrays, impedance and radiator matching 8=28197
    photoelectric star tracking, friction drive 8=45608
    Queen Elizabeth II 8=28035
    reflecting, at Herstmonceux, Sussex, capable of detecting quasars 8=50267
    refractor, 16-inch, Hartmann test results 8=28036
    Richey—Chrétien, and extended field systems 8=50268
    3.5 m free aperture, mirror type, optical design 8=36919
Tellurium
    atom coordinates in lattice, temp. depend. 8=44256
    crystals, I^{127} quadrupole coupling exam. 8=36284
    crystals, pulse-heated, anomalous Hall reversal at 515°K rel. to vacancy behaviour 8=31329
    dielectric constant, contribution of free carriers 8=40587
    elastic constants temp. dependence, 270–700°K from ultrasound velocity meas. 8=35719
    electron microscope investtgation 8=35356
    films, e-irradiated, resistance increase due to CO_2 desorpt. 8=35829
    galvanomagnetic effects, anisotropy, statistical interpret. 8=31394
    galvanomagnetic props., down to 0.05°K 8=35916
    Hall effect meas. in mag. fields up to 150kg 8=49171
    isotope fractionation 8=41234
    liquid, resistivity, Hall effect, and comp. 8=34965
    photoconductivity, fast, by CO_2 laser radiation 8=40676
    Shubnikov-de Haas effect, and struct. of isoenergetic surface 8=40331
    $Sb_2Te_{3-x}Se_x$ syst., struct. 8=48677
    Te_2, dissoc. energy 8=38937
    Te (I), g values of $5p^4$ configuration 8=25380
    Te II pulsed laser transition 8=46596
    Te-Se-Cd rectifying struct., using Se single-crystal film 8=35930
Tellurium compounds
    isostructural oxide, crystal structure 8=48676
    $Re(CH_3)_2$, indirect spin coupling 8=29822
    $TeBr_4$, far i.r. cryst. spectra 8=45223
    $TeCl_4$, far i.r. cryst. spectra 8=45223
    $Te_{70}Cu_{25}Au_5$ alloy, amorphous, resistance and thermopower meas., 80-300°K 8=40497
    TeO_2, phase transform. at high pressures ($p = 60$ kbar) 8=26081
Temperature control. See Cryostats; thermostats.
Temperature
      See also High-temperature production and effects; Low-temperature production.
    arbitrary upstream changes, used maximum store method for anal. 8=34574
    Bayard-Alpert gauge, influence 8=39251
    control for epitaxial growth, solid-state linear ramp generator 8=41919
    control, for n.q.r. spectrometer 8=46528
    developed during oblique impact of two bodies 8=32981
    flat disc in transversal air flow, boundary layer stability and heat transfer 8=37314
    galvanometer control, modulation systems 8=32985
    gas stream temp. control device for range –195° to 250°C 8=28421
    generated by non-stationary frictional contact, analog simulation 8=37319
    invariance in special relativity 8=28288
    nonequilibrium, definition 8=23876
    plasma jet, output rel. to current and mass flow 8=43613
    in plate of finite thicknesses, harmonic oscs. of medium and temp. stresses 8=37160
    potentials in laser medium 8=24273
    rarefied u.s. flow, excitation and gas temps. 8=30257
    standard definition, precise and reproducible 8=45946
    stars, calc. from Hγ profiles 8=28056
    in turbulence wake of sphere in water, fluctuations 8=34701
    transient temps of arrays of radiating plates and cubes 8=24017
    transition at fluid-vapour interface in bubble boiling 8=39490
    variations on surface of strip-heated flat plate 8=24018
    He-Ne laser, effect on output power 8=33186
    Pu, surface, rel. to hemispherical emittance 8=30993
    Sb freezing-point standard, apparatus 8=30585
    Sb freezing-point standard, measurements 8=30586
Temperature distribution
    in air jet, field meas. and osc. intensity and temp. 8=39190
    in bars, solidifying, rel. to location and shape of solid-liq. interface 8=43908
    in boundary layer of liq. flow along permeable plate 8=39267
    in burning zone of bed, rel. to difference in temp. between gas and mat. 8=37313
    calorimetry, guard-heater automatic control 8=32988
    convection flow stability of fluids heated from below in gravitational field 8=46251
    crystal plate, plane field, unsteady, generalized 8=44355
    in cylinder, cooled or heated in liq., for variable heat transfer 8=37321
    in cylinder with temp. depend. conductance in const. longit. elec. field 8=41946
Temperature distribution—contd
    in cylinders, rotating, and heated by rad. from distant source 8=32980
    diffusion equation, solution using continuous method of approx. 8=32934
    electric arc cathode, temp. field 8=43462
    field in solids with variable heat-transfer coeffs, approx. calc. 8=28415
    field under conditions of monotonic heating 8=37316
    in flow in annular duct, allowing for mech. energy dissipation 8=39356
    in fluid flow with variable physical characts., numerical integration of ht. of propagation eqn., 8=39196
    fuel element, current heated with temp. dependent parameters, nonstationary field calc. 8=30976
    in gases, high-temp., by meas. of rad. from seeded emitters at two seeding rates 8=34650
    in hollow cylinder, two rapidly convergent solns. for numerical computation 8=32959
    in linear shear flow past flat plate, rel. to heat transfer coeff. 8=34651
    moist mats., simultaneous determ. of thermophys. characts. for any values of Fourier no. 8=37315
    in plate, infinite, field for changing heat transfer coeff. and temp. of ext. medium 8=37320
    in porous body under transpiration cooling 8=28416
    power fluid, non-Fourier, on plate of variable temp. in thermal boundary layer 8=39357
    profiles for convection near cooled disk rotating with its environment 8=32967
    profiles for turbulent natural convection in air 8=34648
    along rectangular fin with vapour condensation 8=34991
    ruby laser, radial distrib. during pumping 8=39909
    streamlines, closed, in laminar flow at high Péclet number 8=34710
    thermal regime, regular, boundary conditions 8=41873
    thermography, high-speed, use of prism line-scanner 8=37322
    transient, analytical solution, in slab absorbing and scattering radiant energy 8=46228
    transient in thin films, estimation rel. to electron beam heating 8=30733
    transistors and integrated circuits with i.r. microscope 8=28380
    in turbulent natural convection boundary layer of vertical plate 8=32965
    wall temp prediction in post burnout region 8=46229
    CO_2, temp. field in volume of gas 8=47959
    Ge melt temp. field in growing crystals by the Czochralski method 8=30829
    Ge single crystals grown by Czochralskii method 8=30827/8
    Hg, liq., temp. profiles in turbulent flow, effect of superimposed free convection 8=34836
    InI_3 discharge lamp 8=43454
    N plasma jet, determ. by spectroscopic methods 8=30183
    NaK eutectic, temp. profiles in turbulent flow, effect of superimposed free convection 8=34836
Temperature measurement
      See also Pyrometers; Thermocouples; Thermometers.
    in anisotropic crystals, based on birefringence changes 8=35420
    apparatus for thermal analysis, 1000-3000°C 8=28414
    black body laws, violation for real bodies 8=32935
    cerium magnesium nitrate scale, evidence from critical magnetic field curve of superconducting W 8=37331
    cerium magnesium nitrate thermometry, use in liquid He 8=37332
    Cerous magnesium nitrate, high field magnetization anomaly obs. 8=44968
    colour coordinates of thermosensitive prints, obs. 8=24015
    combined conductivity-temperature probe for use up to 3000°K 8=46271
    devices, survey for past 40 years 8=46263
    differential, by Pt resistance thermometers, calc. 8=37317
    flame temp. meas. by single-beam photoelec. pyrometer 8=41875
    gas, acoustic and Pt resistance scales compared, 20°-20°K 8=46262
    heat exchanger, surface temp., accurate meas. 8=46237
    i.r. pyrometry, limits 8=46258
    laser temp. determ. of working substance by dilatometric method 8=28661
    liquid surface, thermistor sensor and recorder 8=37318
    low, specific heat of cerium magnesium nitrate 8=30962
    metal, thin films, during vapour dposition 8=44035
    micropyrometer with optical-electronic transducer 8=46275
    microscope, i.r., for temp. distribution over transistor and integrated circuit surfaces 8=28380
    moving objects, by pyrometer, 60-180°C 8=24019
    moving surfaces, by stationary contact thermocouple 8=37324
    optical pyrometer, automatic 8=37323
    outlet channel of AGR, use of N^{16} 8=47435
    plasma, from light depolarization 8=30065
    p-n function as ultralinear calculable thermometer 8=31402

Temperature measurement—contd
- radiation taut-wire transducer 8=24016
- radiometer for environmental studies 8=28384
- reactor, nuclear, liq. semicond. applicability 8=34110
- reference standards above 0°C 8=46260
- sea surface, by radiowave emission 8=50107
- of small surface areas above 800°C, using blue sensitive photomultiplier 8=24014
- solid in liq. N_2 bath during adsorpt. meas. 8=48352
- steam-to-surface temp. difference in dropwise condensation, effects of local venting 8=34986
- stratopause, diurnal var. estimation from horizon radiance satellite obs. 8=36709
- thermocouples, free end temp., automatic correction 8=24026
- thermography, high-speed, use of prism line-scanner 8=37322
- transducer for instantaneous temp. meas. in shock tunnels 8=46264
- transient, resistance thermometer design 8=46269
- tunnel junction, supercond., for 1m° meas. 8=31358
- ultra-high-temperature thermocouples 8=46268
- ultra-sensitive miniature temp. sensor 8=46259
- in wakes of vehicles on reentry, use of i.r. radiation 8=41484
- D plasma, by escape velocity 8=34514
- Ge single crystals grown by Czochralskii method of, field distrib. 8=30828
- Ge transistor bridge sensor 8=32984
- Ge–Ga–Zn, appl. to low temp. thermometry 8=41874
- Mo, by emittance of small cones and cylinders, in surface 8=26611
- Pt ribbon high-temp. X-ray furnace 8=32978
- W, by emittance of small cones and cylinders, in surface 8=26611
- **spectral methods**
  - discharge, h. f. induction, stationary 8=29900
  - discharge, hollow-cathode, gas thermometry 8=34402
  - gas and particle cloud in flames, by comparison method 8=32977
  - graphite surface burning in stream of dry oxygen, temp. profile 8=46256
  - high, appln. of pyrometric light filters, theory 8=46266
  - plasma, 5000°-50 000°K determ. 8=34513
  - propane diffusion flame, spectroscopy 8=46257
  - self-luminous objects, using high speed photography 8=46265
  - of spark in air 8=39004
  - spectral line reversal with objective methods of recording 8=46255
  - C electrode, rel. to arc as standard spectroscopic source 8=29927
  - D pulse discharge plasma, inverted lines 8=29895
  - F dwarf stars, Hβ photometry 8=45649
  - Mg flame by MgO electron vibr. obs. 8=24013
  - W, photoelec. pyrometer principle and error analysis 8=24021

Tensile strength. See Mechanical strength/tensile.

Tensors
- asymmetry in mag. second-rank tensor quantities 8=49575
- Bel-Robinson, generalized, as generator 8=32821
- conformal, function of metric tensor, and diff. concomitant of object K^a_{bc} 8=32811
- dielectric, for waves in random anisotropic medium 8=30074
- differential operators used in meteorology, theory 8=50124
- in e. m. field theory rel. to coherence 8=37401
- energy-momentum, literature discussion 8=32841
- energy-momentum, material, macroscopic 8=32838
- energy-momentum, with and without external fields 8=32840
- operators in unitary groups, pattern calculus 8=32669
- pretensors, applic. to relativistic plasma 8=28327
- Raman scatt., antisymmetric, obs. 8=25398
- representations 8=45979
- Ricci, for complex scalar field 8=24476
- stress and displacement tensor fields, random, boundary valve problem formulation in elasticity 8=46040
- stress-energy, generalized, rel. to 2^+ meson mass formulae 8=24757
- stress, for plasma in high freq. e. m. field and considering collisions 8=47798
- trace extraction, symmetrized 8=32649
- virial-equation for stellar dynamics 8=45621

Terbium
- activator in industrial fluorescent lamps 8=42212
- α-ray absorpt. at 54.4 MeV, obs. 8=48919
- electronic sructure from positron annihilation studies 8=26906
- ferromagnetic anisotropy constant temp. dependence 8=31651
- ferromagnetic, mag. viscosity 8=45029
- magnetic damping 8=49475
- magnetic exchange interactions from n. -scattering 8=31709
- magnetic-ordering temp., pressure dependence 8=31652
- magnetic ordering temps. at high pressures 8=40730
- magnetic props. from mag. moment meas. at 4.2°K and high fields 8=31705
- magnetic properties hydrostatic pressure dependence 8=36082
- magnetization anisotropy and magnetostriction meas. in pulsed fields up to 150 kOe 8=40743
- magnetostriction, anisotropic single-ion props. 8=44977
- magnetostriction, exchange props. 8=44978
- magnon energies and exchange interactions 8=45030
- neutron scattering, critical, inelasticity above Néel temp. 8=31530
- nuclear spin relaxation, indirect 8=31915
- in perovskites, mag. ordering 8=31799
- quadrupole transition $L_I M_V(\beta_q)$, obs. 8=41146
- spin-wave spectrum and exchange interactions 8=31707
- spin waves and mag. resons: thermal applied field, and magnetoelastic effects 8=31703
- thermal expansion and forced magnetostriction 8=35447
- Tb^{65}, L-spectrum, new lines 8=47487
- μ-Tb^{159} atoms dynamic quadrupole interaction, K and L x-rays obs. 8=34191
- Tb1, additional levels obs. 8=25366
- Tb I, relative oscillator strengths of 250 lines 8=43201
- Tb^{3+} in SrF_2, e.p.r. and spin-lattice relax., 8=40944
- Tb^{3+} in YFe garnet, energy levels, wavefunctions and relax. times rel. to FMR linewidths 8=31824
- Tb–Au alloys, resistivity meas., 1.3–20°K 8=40311
- Tb-Y alloys, helicoidal mag. struct., effect of replacing Tb by Y 8=40742
- $TbAlO_3$, mag. interactions from optical spectroscopy 8=45066

Terbium compounds
- alloys, ferromagnetic, mag. viscosity 8=45029
- aluminates, antiferromag., thermal props. 8=35435
- chelates, luminesc., D isotope effects 8=30503
- Tb complex, ethylenediaminetetra acetic Tb (III), cryst. struct. 8=44223
- $TbAg_2$, mag. struct. by neutron diffr. 8=40877
- TbAl garnet, n.m.r. of Al^{27}, quadrupole splitting and paramag. shifts 8=31893
- TbAl, magnetic structure, neutron diffraction study 8=27447
- Tb_3Al_2, metamagnetic props. 8=49544
- $TbAlO_3$, metamagnetic transitions at 1.5°K 8=31798
- $TbAu_2$, mag. structus. 8=27426
- TbFe garnet, Faraday rotation, 100°-450°K 8=32039
- $TbFe_2$, hyperfine field at Fe from Mössbauer effect 8=36146
- TbFeG, Faraday effect in i.r. 8=32037
- Tb-Hg system, phase diag. 8=30706
- Tb-10% Ho, magnetic exchange interactions from n. -scattering 8=31709
- $Tb(NO_3)_3 \cdot 6H_2O$ luminesc. aromatic ketones sensitized energy transfer mechanism, obs. 8=36487
- Tb-Th slloys, f.c.c., antiferromag. ordering stabilization by Th 8=36218
- Tb-Y alloy, ferromag. props, mol. field soln. 8=31708

Terrestrial electricity. See Earth/electricity.

Terrestrial heat. See Earth/heat.

Terrestrial magnetism. See Earth/magnetic field; Magnetic storms.

Tetraneutrons. See Neutrons.

Thallium
- atom fluoresc. quenching cross-sections, determ. by flame tech. 8=29618
- atom, superradiance of green line in TlI vapour 8=34154
- atom, Tl^{205}, spectrum as frequency standard 8=28211
- atomic, photoionization cross section meas. 8=29949
- ion-implanted in Si, diffusion from subst. to interstitial sites 8=40007
- ions Tl^+, polarographic investigation in $LiNO_3$-$NaNO_3$-KNO_3 melt 8=45414
- liquid, sturcture factor 8=48062
- liquid, structure temp. dependence by X-ray diffr. exam. 8=25873
- resonance radiation, electrodeless h. f. source 8=24380
- superconducting, density of states and phonon spectrum by electron tunnelling 8=44743
- superconducting transition temp., effect of impurities 8=49201
- thallous dimer centre characts in NaI from luminescence study 8=27658
- Tl^4, diff. in $LiSO_4$, 590-820°C 8=39977

Thallium compounds
- Tl amalgams, densities and mag. susceptibilities 8=48348
- Tl halides, ion recomb. rates after photo-ionization rel. to press and inert gases 8=43490
- TlCNO, bonding and stability 8=26006
- Tl-Cd liquid alloy, thermodynamic props. 8=30455
- TlI, adsorbed organic mols. surface charge-transfer groups form., obs. 8=36028
- TlI, ionic recomb. rates for weak ionization 8=43476
- TlI-42% TlBr single crystals, i.r. transmission, spectra 8=36422
- Tl $MeSO_4$ (Me=alkali metal), elec. cond. and density, 700-1150°C 8=39411
- (Tl-Rb) NO_3 molten, elec. cond. 8=43865
- Tl–Sn alloy, phase diagram in range 0-20 at.%Sn 8=35126
- Tl-Te alloys, liquid, n-type, elect. props. 8=34897

Thallium compounds—contd
- $TlNO_3$, molten, elec. cond., viscosity, density 8=39331
- TlSe, films, phase transform kinetics by new c.-diffr. procedure 8=26082
- $Tl_2Mn_2(SO_4)_3$, langbeinite structure, growth and electro-optical props. 8=39678
- Tl_2Se film, substrate temp. effect on semicond. props. 8=31395
- TlSe, reflection spectrum beyond fundamental absorpt. edge 8=36423
- Tl_2Se, thermoelectric power temp. dependence, 100-540°K, rel. to carrier props. 8=49396
- Tl_2SO_4, elec. cond. and density, 700-1150°C 8=39411
- Tl_2SO_4, i. r. spectrum 8=31955
- Tl_2Te film, substrate temp. effect on semicond. props. 8=31395
- Tl_2Te_3, crystal growth from melt rel. to segregation of Se, S, Tl and Fe 8=26242
- Tl_5Te_3, γ-phase in Tl–Te system, conductivity and superconductivity 8=40390

Thermal conductivity. See Conductivity, thermal.

Thermal decomposition. See Chemical reactions.

Thermal diffusion. See Diffusion in gases/thermal; Diffusion in liquids/thermal.

Thermal diffusion columns. See Diffusion in gases/thermal; Isotope separation.

Thermal diffusivity. See Conductivity, thermal; Heat conduction.

Thermal expansion
- alkali halides, calc. for validity test of box model 8=35315
- apparatus for X-ray determination at high-temps 8=26593
- crystals, axial, Grüneisen functions 8=26598
- crystals for u. v. and i. r. optics 8=42116
- cubiform crysts., coeff. temp. depend., theory 8=26594
- deflection, thermal, of non-homogeneous rectangular plate 8=41872
- demonstration 8=46253
- in dielectrics with high permittivity, elec. field effects, theory 8=40560
- epoxy resins, 2°-300°K apparatus and obs. 8=35443
- explosions, thermal, theory, stability of steady-state solutions 8=46173
- ferromagnets, and sp. ht. at Curie pt., critical fluctuations and anomalous behaviour 8=30959
- filament dilatometer 8=48742
- films, effect on temp. coeff. of resistance 8=31315
- gases used in spectrophone to detect laser light absorption 8=39218
- γ-Ce, slow-cooled, temp. dependence, 300-100°K 8=30891
- glass-ceramic mirror blanks $0 \pm 0.3 \times 10^{-7}$/°C from 5 to 50°C 8=41137
- glass, fused silica modified with coeff. ~10^{-7}/°C 8=39930
- glass, rel. to oxide dilution 8=44579
- glass, shrinkage, compression under 10-65 kbar effects 8=40164
- glasses, effect of mixed γ-n radiation 8=44493
- graphite, polycryst., rel. to orientation, averaging techs. 8=35663
- Grüneisen coeff. evaluation 8=44352
- Grüneisen ratio and sp. ht., thermodynamic compatibility reln., 8=39907
- Grüneisen solid, h.p., thermodynamic calc. 8=30972
- high-temp. strain fatigue, diametral extensometer 8=35630
- inclusions in steels, and reln. to tessellated stresses 8=44350
- Invar alloys, rel. to mag. props. 8=36162
- ionic crystals. coeff. and Grüneisen constant calc., semiempirical formulae 8=39924
- metals, cubic, Grüneisen parameters rel. to temp. 8=48743
- metals, linear, comparison of plated and unplated samples 8=35815
- naphthalene, from X-ray meas. and expansion tensor calcs, 78-325°K 8=26596
- optical materials, low coeffs., interferrometric precision obs. 8=39927
- optical materials, small samples, interferometry 8=35439
- periodic bond chain theory rel. to thermal vibrations in a crystal 8=26005
- piezoelectric annular disc, radial deform., rel. to gamma ray heating and appl. elec. voltage 8=31441
- polyethylene, volume coeff. rel. to melting temp. range 8=39472
- polymers, amorphous, and compressibility 8=39926
- polymers, polyethyleneglycol adipate based, solid and solns., obs. 8=26595
- polyurethanes, solid and solns., obs. 8=26595
- pyrocarbons compressed at high temps., anisotropy 8=45941
- recording dilatometer for −150° to +1500°C 8=28216
- reference materials for high-temperature measurements 8=46224
- ruby laser crystal deform. 8=24335
- sintered optical glass fibres 8=39925
- solid, microinhomogeneous, macroscopic coeff., eqn. 8=48741
- solids, book 8=35441
- thiourea, anisotropy in paraelec. phase 8=26597

Thermal expansion—contd
- wire heated by current pulse, longitudinal vibration 8=40088
- Ag film, e diffr. meas., 20-420°C 8=35446
- Ag, small crystals, and fusion 8=39928
- Al film, e diffr. meas., 20-420°C 8=35446
- $2Al_2O_3.5WO_3$, linear 8=35448
- Ar, liquid, meas. and computation 8=28219
- BaF_2, Grüneisen parameter, low-temp. limit, calc. on Axe's shell model 8=48748
- C, pyrolytic, coeff., relation with preferred orientation 8=30971
- C, pyrolytic, dimensional changes during n-irrad., model 8=31148
- CaF_2, Grüneisen parameter, low-temp. limit, calc. on Axe's shell model 8=48748
- $CoCl_2.6H_2O$ crystals, coeffs., 1.5°-4.2°K 8=35442
- Cr_2WO_6, linear 8=35448
- Cs, volumetric, and Grúneisen constant calcs. from eq. of state 8=30973
- $CsCl_2$, rel. to phase transform 8=26067
- Cu alloys, X-ray determ. at high temps 8=26593
- Cu, coeff. temp. depend., theory 8=26594
- Cu oxides, and phase fields 8=30686
- $Cu(HCO_2)_2.4H_2O$, in antiferroelectric transition region −170°C to 30°C 8=44346
- Ge, coeff. temp. depend., theory and obs. 8=26594
- Ge, lattice parameter temp. dependence from X-ray powder diffr. exam. 8=44347
- He^3, solid, obs. 8=37358
- He-Ne laser meas. of small coeffs. 8=35440
- HgTe, lattice dilation rel. to temp. 8=48744
- Ir, lattice parameter temp. dependence from X-ray powder diffr. exam. 8=44347
- K, volumetric, and Gruneisen constant calcs. from eq. of state 8=30973
- KIO_4, metaperiodate 8=35444
- Kr, solid, meas. rel. to thermodynamic props. 8=48745
- La, 1.5-40°K, rel. to superconducting transition temp. pressure dependence 8=35438
- LaF_3, temp. depend., rel. to Schottky defects and diffusion of F ions 8=31048
- LaSb, lattice constant temp. dependence rel. to semi-metal charact., 8=39948
- $LiNbO_3$, linear coeffs., 77-500°K, anisotropy 8=44341
- Mn, linear coeff. rel. to para-antiferromag. transition, −180-950°C 8=44253
- $MnCl_2.4H_2O$, anomaly near Neel pt. due to antiferromag. ordering 8=35445
- Mo, coefficient between 15° and 65°C 8=44233
- Mo, effect of S, Se and Te in soln 8=48664
- $NaIO_4$, coeffs from lattice parameters 8=39929
- Ni film, e diffr. meas., 20-420°C 8=35446
- PbTe and elastic constants, 4.2-303°K 8=49044
- Rb, volumetric, and Grüneisen constant calcs. from eqn. of state 8=30973
- RbH_2AsO_4 crystal, anisotropy from lattice parameter obs. 8=44348
- Rh, lattice parameter temp. dependence from X-ray powder diffr. exam. 8=44347
- Sc, linear coeff. rel. to para-antiferromag. transition, 20-660°C 8=44253
- Se thin layers, linear coeff. meas. and Ag impurity dependence 8=48746
- Si, coeff. temp. depend., theory and obs. 8=26594
- SrF_2, Grüneisen parameter, low-temp. limit, calc. on Axe's shell model 8=48748
- SrS, coeffs. from lattice constants meas. 30-273°C 8=39931
- Tb, and forced magnetostriction 8=35447
- Ti, linear coeff. rel. to para-antiferromag. transition, −180-1500°C 8=44253
- Ti, 2° to 30°K 8=44349
- α-U, behaviour at low temp. 8=48747
- α-U, below 10°K 8=39932
- V, linear coeff. rel. to para-antiferromag. transition, −180-1500°C 8=44253
- Y, lattice constants meas., 77-300°K, by X-ray diffr. 8=39935
- ZnO, coeffs from lattice constants meas., 27-619°C 8=39934
- ZnO polar crystals, from point-charge model 8=30630
- ZnS, anisotropy 8=44351
- ZnTe, 0-460°C 8=39933
- Zr, 2° to 30°K 8=44349
- ZrW_2O_8, linear 8=35448

Thermal measurement

See also Calorimeters; Calorimetry; Conductivity, thermal/measurement; Temperature measurement; Vapour pressure measurement. Entries describing measurement methods for specific thermal quantities and effects may also be found listed under the various headings for the subjects concerned.
- analysis, adiabatic calorimeter 8=24028
- analysis, contactless, 20-2800°C 8=28411
- analysis by hot-stage microscopy, ≤ 2000°C 8=28409
- apparatus for thermal analysis, 1000-3000°C 8=28414
- boiler, coal-fired, radial disk fluxmeter 8=32955
- hydrate binary systems, analysis under pressure 8=28413
- i. r. detectors and appl. 8=28381

Thermal measurement—contd
i.r. image scanning system 8=42213
polymers, crystallinity determ. 8=44093
refractories, differential thermal analysis apparatus, ≤ 2000°C 8=28410
regular regime, boundary conditions 8=41873
sensors, with varying medium temp. and transfer coeff. 8=28385
temp. determ. using thermal radiation meas. 8=28412
thermal effectiveness determ. 8=46254
thermocouple manometric transducers, rating 8=45961
MgO:Fe, microsec. heat pulses in large mag. field 8=44366
Thermal radiation. See Radiation/heat.
Thermal spikes. See Crystal imperfections; Physical effects of radiations.
Thermal transformations. See Boiling; Condensation; Freezing; Heat of transformation; Melting; Phase transformations; Sublimation; Vaporization.
Thermionic emission. See Electron emission/thermionic; Ion emission/thermionic; Ionization, surface.
Thermionic generators. See Electricity/direct conversion; Electron tubes.
Thermionic tubes. See Electron tubes.
Thermistors. See Semiconducting devices.
Thermochemistry. See Heat of reaction, etc.
Thermocouples
conductivity-temperature probe for use up to 3000°K 8=46271
equilibrium concepts of irreversibility 8=43892
free ends, automatic temp. correction 8=24026
for gas stream velocity fluctuations meas., 8=39177
heat exchanger, surface temp. meas. by steel tube/Ni coating thermocouple 8=46237
high-temperature hermetic lead 8=46270
neutron radiation effect on calibration 8=46273
non-equilibrium, foundation 8=46099
parallel, theory 8=24022
probe for meas. of thermal conductivity of insulating materials 8=30983
response in liq. medium, timing and calc. 8=28419
semiconductor, Peltier coeff. determ. 8=40635
stationary contact, for temp. meas. of moving surfaces 8=37324
for ultra-high-temperature range meas. 8=46268
Ag-Ni, thin film, temp. variation across thin semiconductors, thermoelectric props. rel. to thickness 8=40638
Au-Fe wire, props. 8=35995
Au-Ni, thin film, for temp. variation across thin semiconductors, thermoelectric props. rel. to thickness 8=40638
Cu-Ni film, for mag. film substrates meas. 8=31676
Pt/Pt-10% Rh, accuracy of calibration 8=46267
W-Ta, thermoelec. potentials 0°-420°C 8=28418
Thermodynamic properties
See also Critical constants, thermal; Entropy; Heat of reaction; Latent heat.
agents, surface-active non-ionic, + water systems; heat of mixing obs. 25°C 8=48126
air, up to 1000° C and 1000 bars 8=34654
alcohol-hydrocarbon solns, model and excess Gibbs energy and enthalpy 8=43797
alcohol-inert solvent solns, H bonding entropy and enthalpy and ratio of molar vols. 8=43799
alcohols, with dissolved gases, excess molar free enthalpy 8=39319
alkali halides, NaCl-type, Anderson-Grüneison parameter for Born-Mayer potential 8=39906
alkaline earth metals, vapour pressure calc. 8=40699
antiferromagnetic Heisenberg linear chains, alternating and eigenvalue spectrum 8=31751
austenitic Fe base alloys, statistical thermodynamics of C 8=39903
bauxites, rel. to production of crude Al alloys by reduction of aluminous ores 8=30956
benzene + n-heptane system, excess isothermal compressibility and molar heat capacity 8=43794
benzenes, mono-substituted, enthalpies of activation 8=34889
benzoic acid, H-bridge complexes, from u.v. absorpt. spectra 8=39349
binary hydrocarbon liq.-vapour interface, adsorpt isotherms 8=48041
bismuth titanate, rel. to ferroelectricity 8=44887
by calorimetry, stored energy spectra 8=24029
cell theory, equilibrium and thermodynamical functions 8=48057
chemical potential generation by phase diagram analysis 8=49836
classical non-uniform gas, moderately strong coupled, entropy balance eq. 8=30292
complexes in solns. cont. $NaClO_4$, instability consts. calc. via Debye-Huckel type eqn. 8=25905
crystal, anharmonic, molec. field theory, classical and quantum, book 8=30954
crystal, bravais, anharmonic freq. shift and free energy, analysis of cubic contribs 8=30952
crystal cooling by transfer of laser radiation energy into heat energy of atomic vibrations 8=39900
enthalpies of thermochem. reactions, by matrix formulation of Hess's law 8=36546
equibilrium, stability conditions 8=37223
ethanol-n-decanol mixtures, molar excess props. 8=48284

Thermodynamic properties—contd
ethyl alcohol, i.r. study rel. to simple model of liq. 8=30401
feldspar and silica mixtures 8=39297
ferromagnet, magnetocrystalline anisotropy free energy, temp. dependence 8=44996
films, fluctuations 8=35421
fluid mixtures, effects of molec. sizes 8=47896
fluids, confined, thermal stability, Hilbert spaces analysis 8=25786
fluids, equilibrium configurational properties, appln. of statistical mechanics 8=34573
formamide-dioxane liq. system 8=34825
free energy in type II supercond., stress depend. 8=26996
galactose, amorphous, enthalpy and sp. ht., 15-45°C, rel. to mol. structure 8=30966
gas and crystal system with isotopic defects, equilib. 8=48293
gas mixtures, chem. reacting, equilib. comp. etc. 8=32088
gases, hot, approx. calcs. 8=47954
gases, of resonant atoms, effect of dipole-dipole interact 8=39194
glucose, amorphous, enthalpy and sp. ht., 15-45°C, rel. to mol. structure 8=30966
h.c.p. crystals, rel. to non-control force model 8=30621
Heisenberg antiferromagnet, free surface effects 8=45048
Heisenberg ferromagnet, and spin-wave distrib. function 8=44983
Heisenberg ferromagnet with arbitrary spin 8=49490
of homogeneous gaseous, liq. or equilib. systems with components undergoing reaction 8=27681
inert gases, analytical potential models 8=30272
ionic solns, computation of equilib. props. 8=34782
Japanese colloidal earth, rel. to production of crude Al alloys from aluminous ores 8=30955
laser, periodically pulsed, thermal conditions in active material 8=46599
lattice vibr., calc. from continued fractions 8=44291
light-producing devices, limits 8=24382
liquid mixtures, determ. from light scatt. 8=43814
liquid mixtures, excess functions 8=39321
liquid mixtures, nonpolar, molec. model and excess Gibbs energy, enthalpy and vol. 8=43797
liquids, laminar flow and viscosity, thermodyn. state 8=25848
magnetic systems, shape dependence 8=44326
magnetic systems with dipole interactions, shape-dependence 8=44329
magnetothermodynamic, high-field, low-temp., use of supercond. magnet 8=41882
mannose, amorphous, enthalpy and sp. ht., 15-45°C, rel. to mol. structure 8=30966
metal, influence of band structure 8=39904
methane equilibrium combustion products, computer calc. 8=27730
methanol-n-decanol mixtures, molar excess props. 8=48284
methyl alcohol, i.r. study, rel. to simple model of liq. 8=30401
moisture absorbed in porous bodies 8=44070
p and m-xylenes, calc. using significant struct. theory 8=43767
permalloy film, thermally activated domain wall movement 8=45020
phonon mode distrib. rel. to absorpt. of ultrasonic waves in insulators 8=35402
plasma, collisionless, stability 8=30170
plasma, completely ionized, relativistic corrections for e.m. interact. 8=39074
plasma, partially ionized, Saha eqn. 8=30006
polyethylene, crystallized from diluent mixtures, enthalpy of fusion 8=34966
polyethylene enthalpy, −150-+150°C 8=24028
polyethylene, linear fractions, mol. dispersed eutectic systems 8=44095
polypropylene, isotactic, in θ solvents, interaction params., obs. 8=43899
quartz high-low inversion 8=48401
quartz, high-low inversion, of lambda transition 8=39563
sphere in stream of small Reynolds number, heat transfer 8=30457
stars' interiors 8=32418
steel, liq., C activity rel. to Co, Mo, Ni, V, W conc. 8=30458
steel, stainless, explosive shock-loaded recovery 8=49004
superconductor with nonmag. impurity and energy bands overlap 8=39901
superconductors, impurity scattering effects 8=40346
superconductors in mag. fields 8=49181
supercooled liqs, enthalpy and entropy of dipole polarization activation 8=39403
ternary systems, quasi-chem. approx. 8=48083
thin turbulent liq. boundary layer with blowing 8=43728
transition metal carbides, nitrides and oxides, rel. to M-M interaction 8=26441
trifluoromethylphosphonylchloride 8=34330
vanadyl acetylacetonate, enthalpy changes for reaction in nitrobenzene soln. 8=43872

Thermodynamic properties—contd
- viscoelastic media, and waves 8=41734
- water, light and heavy, calc. using significant struct theory 8=43767
- water, with ions at infinite dilution, for hydration numbers 8=43754
- Ar-air, 50° to 3500° K 8=25838
- Ar, liq., calc. from Lennard-Jones parameters by Monte-Carlo method 8=25907
- Ar plasma jet, atmos. press., test of local equilib. 8=39146
- AsH_3, liq., crit. props. and entropy, rel. to significant struct. theory 8=43755
- $BaCl_2$, enthalpy and entropy, and heat capacity rel. to temp. 8=44339
- BaI_2, enthalpy and entropy, and heat capacity rel. to temp. 8=44339
- $BaTiO_3$, enthalpy changes at Curie point 8=35972
- C in austenite, electrochemical study 8=44327
- CF_3 radical 8=29723
- CO_2-air, 50° to 3500° K 8=25838
- COF_2, from 12°K to b. p. 8=30573
- Cu, cementation with Fe, activation enthalpy 8=43898
- Cu oxides, by e.m.f. meas. 8=48729
- Cu-Be alloys, rel. to ageing 8=35098
- $CuSO_4.5H_2O$, below 4°K in mag. fields 8=39914
- Er-D system 8=44330
- Fe base alloys, interstitial solutions 8=44328
- Fe oxides, by e.m.f. meas. 8=48729
- FeP, and magnetic props. 8=27378
- Ga-In liq. alloys, activities 8=39315
- GeO_2, enthalpy and entropy, and heat capacity rel. to temp. 8=44339
- H_2O, i.r. study, rel. to simple model of the liq. 8=30401
- He-air, 50° to 3500° K 8=25838
- He isotope solns, enthalpy and osmotic pressure 8=28436
- He^3, b. c. c., obs. 8=37356
- He^3, solid magnetized, rel. to nuclear spin interaction 8=41905
- HeII, Landau theory of phase transitions 8=33001
- He II, potential function near T_λ 8=24052
- Hg solubility in 17 solvents, temp. depend. and entropies 8=43798
- K solutions, unsaturated, in melted KCl. 8=48060
- KBr, F-aggregate bands, thermal and optical stability, half-widths and oscillator strengths 8=49732
- KD_2PO_4, entropy of phase transition 8=44338
- KH_2PO_4, entropy of phase transition 8=44338
- KNO_3, enthalpy and entropy, and heat capacity rel. to temp. 8=44339
- Kr, solid, from thermal expansion, sp. ht., compressibility and vacancy equilib. conc. meas. 8=48745
- LaF_3, entropy and enthalpy in range 1050°-1200°C 8=35015
- LiF solid, oxide doped, oxide and hydroxide activity determ. 8=36593
- Mn oxides, by e.m.f. meas. 8=48729
- N_2 gas, hot, approx. calcs. 8=47954
- NF_3, molec. calc., 200° to 2000°K 8=43319
- NH_3, as ideal gas 8=47960
- Na_2SO_4, molten, rel. to props. of Na silicate, and N_2O activities 8=34826
- Na_2SO_4, molten, thermodynamic activity rel. to props. of Na silicate 8=34826
- Ni oxides, by e.m.f. meas. 8=48729
- $NiCl_2$ in alkali halide melts, thermodynamic props from cells emf's, 8=49946
- NiO in NiO-MgO solid soln. 8=43979
- Ni-Zn alloys, data 8=48726
- PH_3, liq., crit. props. and entropy, rel. to significant struct. theory 8=43755
- Pb oxides, by e.m.f. meas. 8=48729
- Pd-Cu alloys, of formation 8=27714
- Pt-Cu alloys, of formation 8=27714
- ScF_3, entropy and enthralpy in range 1050-1200°C 8=35015
- SnH_3CH_3 and $SnCl_3CH_3$ mols. 8=38890
- SrF_2, enthalpy and entropy, and heat capacity rel. to temp. 8=44339
- Tl-Cd liquid soln. 8=30455
- UCl_3 soln. in molten NaCl, partial v.p. obs. 8=30456
- UO_2, enthalpy as function of temp. to 3100°K 8=35436
- UO_2, high temp. enthalpy and heat of fusion 8=39902
- YF_3, entropy and enthalpy in range 1050°-1200°C 8=35015
- Zn in liq. Zn-Au, activity by e. m. f. meas. 8=25906
- Zn-Sn-Cd-Pb liq. solns, rel. to calc. of Zn activity coeffs. 8=43795
- ZrO_2, hydrated amorphous, behaviour, and nature 8=43982

Thermodynamics

See also Atmosphere/thermodynamics; Entropy; Equations of state; Statistical mechanics.
- Arrhenius plots, curved, analysis 8=30953
- book 8=37222
- classical and quantum spatial distrib. functions, temp.-depend., integral-differential eqn. 8=41762
- critical phenomena in equilibrium systems reviewed 8=28310
- critical point relaxation phenomena 8=28317
- critical region, multiple correlation function 8=37192
- discontinuity surface in finitely deformed medium 8=37142
- of earth's heat 8=32171

Thermodynamics—contd
- entropy existence principle 8=41791
- entropy and temp. invariance in special relativity 8=28288
- evolution in the method of local pot., variational formulation 8=37188
- Fermi liq. entropy, shielded pot. approximation 8=28338
- fundamental, impact of Caratheodory ideas 8=41788
- hard disks, mixture of different sizes, excess free energy 8=28343
- heat flux, "total" and "eddy", distinction 8=41787
- irreversible processes, entropy changes, theory 8=32854
- of irreversible processes, steady-state, algorithm for stationary Markovian systems 8=28349
- irreversible, reciprocity principle 8=41763
- Ising model finite 8=46092
- maximum work in isolated system of continuous cycles 8=46123
- metals, theory of optical effects 8=27518
- Onsager relns. for interphase heat and mass transfer in flow systems 8=34828
- particles in box, pair distrib. function 8=46112
- radial distribution function 8=30192
- rotational viscosity, irreversible statistical thermodynamics 8=47917
- second law applied to extensive functionals 8=46122
- second law, classical concepts as basis 8=41790
- 2nd law of thermodynamics and necessity of irreversible processes 8=41789
- statistical asymptotic problem for real system 8=23885
- statistical, of e. m. phenomena 8=32839
- strict meaning of heat concept should be generalized 8=23986
- three-body forces in dense system 8=37198
- useful energy theorem appl. to Brownian movement 8=28314
- water layer formed by melting ice from below, convection onset 8=34827
- XY model of quantum lattice fluid, critical props. 8=37177
- applications
  - Burgers media, stress/strain relations 8=28260
  - constant-volume heat capacity and adiabatic compressibility, upper bounds 8=37225
  - continuous systems, fluctuations and irreversible processes 8=37224
  - crystal point defects, anelasticity and internal friction 8=31027
  - dicyanodiacetylene Σ_g^+ modes, thermodynamic functions 8=26031
  - dissipative systems, symmetry breaking instabilities 8=32836
  - electronic contribution to energy and press. of elements and mixture, high temp. 8=23901
  - energy converter staging, thermoelectric-thermomagnetic 8=46238
  - gas, dissociating, nonequilibrium past convex corner, entropy gradients 8=43655
  - Gruneisen solid, h.p. thermal expansion and bulk modulus 8=20972
  - irreversible, appl. to heat and mass transfer 8=46127
  - irreversible, appln. to internal heat and mass transfer 8=46128
  - irreversible, appl. to molec. transfer eqns. 8=41792
  - luminescence, solid-state, theory 8=36458
  - mass and energy transfer, generalized laws 8=41793
  - metals migration of vacancies 8=35528
  - primary standard of light 8=46654
  - statistical, Coulomb plasma interactions 8=30009
  - transport eqns. from least-dissipation principle 8=23906

Thermoelasticity
- circular ring, radially constrained, instability rel. to initial imperfections on thermal stressing 8=23823
- crystal plate, thermal stresses, and plane temp. field 8=44355
- dynamic coupled problem, for half-space 8=46068
- glass fibres, internal friction as function of freq. for transverse vibs. relax 8=44513
- heat transfer at metal interface 8=41738
- layered solids, linear wave motions, soln. of potential eqns. 8=23829
- linear couples; inhomogeneous anisotropic continuum, variational principles 8=46070
- linear creep problems, use in solution 8=41737
- magnetoelasticity and magneto-thermoelasticity 8=28278
- metallic mats, meas. of localized peak stresses via adiabatic deform 8=44517
- micropolar, coupled, theory 8=28280
- micropolar, linear theory 8=46069
- sandwich plates, thermoelastic stability and thermally induced vibrations 8=46072
- solids, elastic and temp. wave interact, temp. depend. 8=39882
- stress function completeness 8=32775
- temperature stresses in plate, with harmonic oscs. of temp. medium 8=37160
- thick plate with cylindrical hole, eqns. 8=28279
- thin-wall tube, viscoelastic with temp. depend. props, thermal stresses 8=23855
- MgF_2, and elastic behaviour 8=44590

Thermoelasticity—contd
  MnF_2, and elastic behaviour 8=44590
Thermoelectric conversion. See Electricity/direct conversion.
Thermoelectricity
  See also Thermocouples.
  actinide cpds, power meas. 8=27234
  actinide cpds, Seebeck coeff. 8=27233
  actinide cpds, Seebeck coeff. 8=49336
  actinide cpds, thermo-power at low temps. 8=49348
  alkali metals, thermopower, e-diff. contrib. 8=44631
  alloy, binary ordered, thermo-e.m.f., effect of phonon drag 8=35817
  alloys of alkalis in alkalis, power 8=27305
  α-brass, absolute thermopower, effect of plastic deform. 8=31447
  devices, semicond., performance at constant heat flux 8=49397
  diffusion thermoelec. power, appl. of integral over Fermi surface 8=40220
  energy converter staging, thermoelectric-thermomagnetic 8=46238
  ferroelectric crystals, thermocurrents existence 8=40634
  graphite nitrates, rel. to order–disorder transform. near –20°C 8=35827
  ionic crysts., theory 8=49389
  iron semi-borides, power 8=40640
  metals, thermodynamic and free electron gas theories 8=40636
  parallel thermocouple, thermoelectric power 8=24022
  Peltier coeff. of semicond. thermocouples, determ. from steepness of V-I characts. 8=40635
  Peltier effect, use in gas lenses 8=42155
  power generation, review 8=49390
  radiometer, circular foil, anal. of dynamic functioning 8=28382
  rare earth cpds, power meas. 8=27234
  rare earth cpds, thermo-power at low temps. 8=49348
  ruby crystals, Seebeck coeff. 500-850°C 8=49338
  ruby, Seebeck coeff. 500-850°C and conductivity, 20-850°C 8=27236
  sapphire crystals, Seebeck coeff. 500-850°C 8=49338
  semiconductors based on GeTe: (Bi, Cu), effect of n and γ irrad. 8=40637
  semiconductors, ionic, nonlinear phenomena, theoretical study 8=35992
  semiconductor, meas. tech. for piezothermo e. m. f., $0\text{-}5 \times 19^9$ dn/cm² 8=40426
  semiconductors, power meas. 77°-600°K 8=31446
  semiconductor thermo-couple, Peltier coeff. determ. from dynamic V-I characts. 8=40635
  semiconductor, thermopower calc. in quantizing mag. field allowing for phonon drag 8=35993
  thermoelement bonding in devices 8=49398
  thermo-elements, non-stationary regime of cooling 8=37378
  AgI films, polycrystalline dye-sensitized 8=35994
  Al alloys, dil. thermopower phonon-drag and e. diff. components 8=44904
  Al, thermopower phonon-drag and e.-diff. components 8=44904
  Au-Fe thermocouple wire, props. 8=35995
  B, melts and sintered mats., thermopower, 50-1000°C 8=35824
  B, thermopower temp. depend., 300-1500°K 8=35823
  (BaSrCa)O, electrical cond., thermoelectric power and work function, effect of Ba vapour 8=26945
  $BaTiO_3$ crystal, thermocurrents rel. to ferroelec. transition 8=27306
  $BaTiO_3$: 1 at. % La, semicond., polaron model and 0.7-7.4μ 8=35878
  Bi, Umkehr effect at 80°K 8=27307
  Bi + $BiBr_3$ solutions, thermoelect. power 8=25947
  Bi–Sb alloys, extrinsic, magneto-seebeck effect 8=44905
  n-$Bi_2Se_{0.45}Te_{3+x}$, growth conditions and Te phase effects 8=49392
  Bi-Sn-Te alloys, thermoelec. and magnetothermoelec. props. 8=35996
  Bi-Te, in arbitrary mag. fields 8=31312
  p-$Bi_{0.5}Te_{3+x}$, growth conditions and Te phase effects 8=49392
  n-Bi_2Te_{3+x}, growth conditions and Te phase effects 8=49392
  Bi_2Te_3 + 20 mol% Bi_2Se_3, power rel. to supercooling conditions 8=44906
  Bi_2Te_3-Sb_2Te_3-Sb_2Se_3 pseudoternary alloy, growth-rate dependence rel. to p- and n-types 8=44907
  n-$Bi_2(Te, Se)_3$, n-irradiated, thermo-emf, elec. and thermal conductivity 8=27136
  Bi-Te-Se(Sb) system, γ-irrad. effects on thermoelec. force 8=44763
  $Cd_xCa_{1-x}O$, thermopower, and elec. and optical props. 8=49137
  CdS crystals, rel. to local centre formation in presence of free electrons and holes 8=36015
  CdS, illuminated, power 8=35997
  CdSb, thermopower anisotropy in intrinsic conduction region 8=40639
  CdSb: In(Cu), power rel. to temp. 8=44768
  $Cd_xSr_{1-x}O$, thermopower, and elec. and optical props. 8=49137

Thermoelectricity—contd
  Cr-Mo alloys, absolute power between 100 and 600°K 8=49393
  Cu, absolute thermopower, effect of plastic deform. 8=31447
  Cu, power due to electron phonon interaction 8=49394
  Cu ternary chalcogenides, Seebeck coeff. at room temp. 8=31448
  CuAu alloy, power and electrical resist. 8=26967
  Cu-Co alloy, dilute, thermoelect. power in mag. field 8=31449
  Cu-Ni alloys, dilute, thermoelect. power in mag. field 8=31449
  β-$FeSi_2$:Co, Al, power, mechanism 8=35885
  Ge, d. c. current meas. rel. to cyclotron resonance obs. 8=27099
  n-Ge, eddy current expt. 8=40642
  n-Ge, force, hot carriers 8=40641
  Ge, second-harmonic thermoelec. voltage 8=40463
  Hf diborides, rel. to conduction e-parameter calcs. based on single zone model 8=53830
  β-HgS films, e, m.f. temp. dependence 8=44792
  HgTe, power, 100° at 300°K 8=40242
  n-InAs, magnetophonon oscillations in longitudinal thermoelec. power 8=27308
  n-$InAs_xSb_{1-x}$ alloys, obs. and e scatt. calc. 8=35758
  n-$InAs_xSb_{1-x}$ alloys, high-temp. obs. 8=40475
  In-Ce solid solns., power (Ce) conc.-dependence rel. to localized moments 8=31339
  LaSb, power temp. dependence, 80-500°K 8=27309
  LaSb, thermopower temp. dependence rel. to semi-metal charact., 8=39948
  $Mn(Mn_xV^{4+}_xV^{3+}_{2-2x})O_4$, $x < 0.68$, thermoelectric power and structure 8=35340
  MnO, thermoelectric force, 1100°C 8=40477
  MnO: Li, power, rel. to conduction 8=44801
  MnTe, antiferromagnetic semiconductor, power, interpret. using magnon drag. 8=32009
  p-MnTe: Ag, fig. of merit obs. 300°-1000°K 8=44908
  Nb–Hf alloys, thermoelectric properties 8=49395
  Nb–Ti alloys, thermoelectric properties 8=49395
  Ni-H system, power rel. to H conc., 77-250°K 8=35998
  n-PbS, thermoelectric power rel. to conduction band structure, 77-300°K 8=27119
  $PbTe_xSe_{1-x}$ thermopower meas. rel. to forbidden band width temp. dependence 8=40247
  PbTe-SnTe-PbS system, meas. rel. to current carrier scattering mechanism 8=31385
  PdCr alloys, thermoelect. power 8=31450
  Sb, solid-liquid boundary, Peltier coeff. meas. rel. to impurity 8=44909
  Sb, thermopower, 5-300°K, rel. to phonon drag effects 8=40219
  p-$(Sb, Bi)_2Te_3$, n-irradiated, thermo-emf, elec. and thermal conductivity 8=27136
  p-Sb_2S_3, trap depths from thermally stimulated and dark conductivities 8=44807
  SbSI grown from gaseous phase, volatile component saturation vapour pressure effects 8=36026
  Sb_2Se_3, energy spectrum of traps from thermally stimulated depolarization meas. 8=40251
  Sb_2Se_3 melts, doping effects on thermopower temp. dependence, 1300-1400°K 8=34899
  SbSeI grown from gaseous phase, volatile component vapour pressure effects 8=35989
  Sb_2Te_3, thermopower rel. to complex valence band structure 8=44808
  Se, power in phase transition region, conductivity rel. to temp. 8=40481
  p-Si, thermopower and magnetothermal effects 8=35912
  α-SiC (6H), high-resistivity, doped accidentally, rel. to band scheme 8=35779
  Sn quantum oscills. in e. m. f. at 1.3°K 8=40643
  Sn-Ce solid solns., power (Ce) conc.-dependence rel. to localized moments 8=31339
  $Te_{70}Cu_{25}Au_5$ alloy, amorphous, resistance and thermopower meas., 80-300°K 8=40497
  Ti diborides, rel. to conduction e-parameter calcs. based on single zone model 8=35830
  TiC, power and elec. conductivity, 20-2000°C 8=2 7310
  TiO_2 (rutile) thermally stimulated currents 8=36513
  Tl_2Se, thermopower temp dependence, 100-540°K rel. to carrier props. 8=49396
  Tl-Te alloys, liquid, n-type, Seebeck coeff. 8=34897
  α-U_3O_8, power meas. rel. to semicond props. 8=35999
  US, power near Curie temp., and elec. cond. 8=44677
  VO_2 sputtered films, power rel. to transport props. 8=27138
  W-Ta thermocouple, potentials 0°-420°C 8=28418
  Y-Ce dilute alloys, mag. susceptibility and thermopower due to s-f anomaly 8=27384
  $Zn_{0.1}Cd_{0.9}Sb$ solid solution crystals, thermoelectric power anisotropy 8=27311
  ZnO films, polycrystalline dye-sensitized 8=35994
  ZnSb, power anisotropy, 200°-300°K 8=44910
  Zr diborides, rel. to conduction e-parameter calcs. based on single zone model 8=35830
  ZrC, power and elec. conductivity, 20-2000°C 8=27310
  $(ZrO_2)_{0.85}(CaO)_{0.15}$ electrolytic thermocell, Seebeck coeff. 8=45392

Thermoluminescence
concretion, and formation 8=50004
crystal, ionic, photon counter 8=49785
devices for low and high temperatures 8=49831
diamonds, synthetic u.v. and X-ray irradiated, 20-400°C rel. to impurity and crystallization effects 8=36474
felspars, X-irradiated, rel. to structure defect exam. 8=26710
fluorites, dosimetric parameters, from Bulgarian ore deposits 8=49799
glasses, industrial, rel. to heat treatment 8=36460
organic matter, radiothermoluminescence 8=41220
quartz, rel. to γ-irrad. effects 8=49812
silicate glass, irradiated, and e.p.r. and electron absorpt. spectra 8=41196
with spectral dispersion, lab. apparatus for exam. 8=45252
II-VI semiconducting cpds., conference 8=31362
vitreous state, rel. to struct. and phys. props. 8=36465
BaO, x-irrad., 8=41184
Ca halide phosphates, obs. 8=36480
CaF_2, γ-irradiated at 77°K, activation energies and emission spectra 8=36477
CaF_2, synthetic γ-irradiated, spectra and transition kinetics 8=45262
CaF_2:Ce^{3+}, rel. to 4f ↔ 5d transitions 8=45263
CaF_2:Mn, read-out, u.v. induced luminesc. rel. to irrad. dose, obs. 8=45261
CaF_2 : Mn, rel. to doping and dosimetric props. 8=49807
CaO, x-irrad., 8=41184
CaS: Ce phosphor, obs. rel. to decay 8=45305
CaS: Zr phosphor, peak shift and trap depth obs. 8=45306
$CaWO_4$, defect sites identification from correlation of e.s.r. and thermoluminesc. meas. 8=31028
$CaWO_4$, rel. to e.p.r. meas. 8=49602
He II, heated by small wires 8=24044
KBr, photostimulated, 50-250°K, 240-700 mμ 8=27652
KCl:I, rel. to ICl^- V_k centre, 8=48875
LiF, spectral emission of intense peaks rel. to heating and irrad. 8=36498
LiF, stimulation by excitation of a centre 8=41200
LiF/CaF_2:Mn dosimeters in tandem, for effective energy of X- or γ-ray fields 8=25169
LiF : Cu, Ag, rel. to doping and dosimetric props. 8=49807
LiF: Mg, effects of pre-irrad. isothermal annealing 8=45280
MgO, V^1 centre thermal decay temp. dependence, 18°-50°C 8=31121
Na-Ca silicate glasses 8=30792
NaCl, activation energy for glow peaks, by initial rise method 8=32056
$NaPO_3$, glassy and cryst., —180 to +20°C 8=41204
SrO, x-irrad., 8=41184
ZnO powder spectrum 8=32065
ZnS, doped, after u.v. irrad. correl. with thermally stimulated elec. cond. 8=49817
ZnS: Cu, Cl, and thermally stimulated dielectric effect 8=36518
Thermomagnetic effects. See Magnetothermal effects.
Thermometers
See also Pyrometers; Thermocouples.
Allen-Bradley carbon type, magnetoresistance 8=24020
cerium magnesium nitrate thermometer, props. 8=30962
digital, multi-purpose 8=46261
γ flux in reactor core, fast-response instruments 8=47050
manometer type linear over 100 to 1000°C, using eutectic alloy 8=24025
quartz, resonator with digital readout, —40 - +230°C 8=24023
small globe instruments 8=41876
steel Templugs, heat prod. softening as temp. meas., 70-850°C 8=24024
superconducting, manufacture 8=46272
Ge transistor bridge sensor 8=32984
resistance
air temp. indicator for enclosures 8=28417
as film gauge for low density shock tubes 8=32899
calibration deviation from calibration tables, calc. 8=46274
semiconductor, liq., applicability to nuclear reactors 8=34110
thin-film, film thickness meas. by optical interference method 8=39585
transient temperature meas., design 8=46269
C, self-supporting, for low temps. 8=32983
Pt, comparison with gas and acoustic in range 2-20°K 8=46262
Pt, differential temp. calculation 8=37317
Pt, 2-10°K, sensitivity 8=28428
Thermonuclear devices. See Plasma/devices.
Thermonuclear reactions
See also Elements/origin; Nuclear fusion.
explosions, n capture by heavy isotopes 8=25252
high energy nuclear reactions in astrophysics, Pennsylvania University, Jan. 1967 8=28029
nucleosynthesis by captive, abundances rel. to mass laws 8=41503
nucleosynthesis in interstellar matter 8=41505
nucleosynthesis of heavy nuclei 8=41504
plasma, induced instability 8=25783
Thermonuclear reactions—contd
stellar, $C^{13}(\alpha, n)O^{16}$, $Be^9(\alpha, n)C^{12}$ 8=25272
stellar nucleosynthesis, information on n prod. rate in $C^{13}(\alpha, n)$ 8=43141
supernova explosion, n capture models 8=32453
techniques rel. to particle accelerators 8=34064
C stars, neutrino loss effect on core temp. 8=32433
Li depletion in stars, rel. to rotational braking 8=32430
$2\ Si^{28} \rightarrow Fe^{54} + 2p$, statistical equilib., erratum 8=29540
Thermopiles. See Thermocouples.
Thermostats
See also Cryostats.
accurate control for Beckman DK-2 recording spectrophotometer 8=24402
astatic follower system for stabilizing block temp in range 10-150°K 8=24027
control of Fabry-Perot etalon temp. 8=28747
double-feedback regulator 8=46279
galvanometer-controlled, modulation systems 8=32985
gas stream temp. control device for range —195° to 250°C 8=28421
internal temp. control in h.p. apparatus 8=28422
LEED expt., temp. controller 8=46277
for magnetic balances of Sucksmiths' type, for temps. to 1100°C 8=46278
multilayer jackets for keeping adiabatic conditions 8=46281
photoconductive cell for r.f. heating temp. control 8=46276
precise, with long term stability 8=46280
proportional heat regulation circuit 8=28420
vapour, for back-refl. X-ray camera 8=33301
KD_2PO_2, automatic thermostatic control 8=31431
KH_2PO_2, automatic thermostatic control 8=31431
Theta pinch. See Plasma/confinement.
Thickness measurement
See also Particle size.
anthracene, 5—100μ thickness meas. from refr. index dispersion 8=32043
coatings, by beta backscatter 8=48436
contactless photoelec. technique 8=41615
epitaxial layers, infrared beam meas. 8=26108
films, interference microscope 8=35149
film, liq., mag. reluctance technique 8=39287
films, effect of numerical aperture of microscope objectives 8=39584
film in thin-film resistance thermometer, by optical method 8=39585
foil target, Rutherford scatt. appl. 8=46850
junction depth, by spherical contouring 8=44833
metal film, by fast e.-backscatt. 8=48434
para-terphenyl, 5—100μ thickness meas. from refr. index dispersion 8=32043
plastic scintillator NE 102A, 5—100μ thickness meas. from refr. index dispersion 8=32043
polymer layer adsorbed on TiO_2 8=39620
tetracene, 5—100μ thickness meas. from refr. index dispersion 8=32043
thin films, and refractive index obs. by ellipsometry 8=31931
thin films using semiconductor detector 8=44029
transparent film, calc. from ellipsometric obs. 8=30734
trans-stilbene, 5—100μ thickness meas. from refr. index dispersion 8=32043
by X-ray defectmeter with Sb_2Se_3 detectors 8=39989
Al films, use of anodisation 8=35158
CdS thick films, chemically deposited 8=39589
Ge film, laser i.r. absorpt. method 8=35173
SiO_2 films on Si, by i.r. tech. 8=48460
ZrN films, rel. to diffusion coeff. of N_2 determ. 8=44396
Thirring model. See Elementary particles; Field theory, quantum.
Thixotropy
bentonite-water system, properties rel. to extinction coeff. 8=30547
coagulation structures, solid-like, thixotropically hardened, elasticity and plastic flow 8=40090
hysteresis-loop determ. of props. 8=25965
Thomas—Fermi method. See Atoms/structure.
Thomson effect. See Thermoelectricity.
Thorium
abundance, with U and K, in peridotite inclusions in basalts 8=50012
epitaxially grown on Ta (100), LEED obs. 8=48469
lamps and interferometrically measured Th wavelengths 8=28839
in rare-earth alloys, f.c.c., effect on mag. ordering 8=36218
in river sediments, conc. and Th/U isotope ratio 8=50094
stacking fault probability plastically deformed 8=35579
strength and flow stress, effect of C content, 0.008 to 2.83 at % 8=44603
strength, effect of C solid solution 8=40183
superconductor, gapless, critical-field curves 8=44741
Thoron meas. devices, calibration method 8=47433
Th I energy levels 8=47509
in ThO_2, cations self-diffusion, α-spectrometry obs. 8=35510
ThO_2: Er^{3+}, spin-lattice relaxation on cubic sites 8=40919
in $ZrSiO_4$, e microprobe meas. 8=27811

- **Thorium compounds**
  - carbides, C^{13} Knight shift 8=41004
  - carbides, mag. susceptibility 8=31531
  - carbonitrides, mag. susceptibility 8=31531
  - nitrides, mag. susceptibility 8=31531
  - thoria, arc-melted, precip. e-microscope obs. 8=30867
  - thoria gel, crystallite sizes, equivalence of X-ray and electron microscopy 8=35284
  - Th nitrate soln, electrophoretic behaviour of monodisperse polystyrene latex particles 8=49923
  - Th-Gd alloys, superconductor, gapless, critical-field curves 8=44741
  - ThC_2, crystal structures of cubic phase above 1480°C, tetragonal, 1430-1480°C and C_k-type monoclinic 8=44257
  - $ThCl_6^{2-}$, vibr. spectra 8=47619
  - ThF_4 films, prod., refractive index, transparency and dielec. const. 8=35184
  - ThO_2, adsorpt. of H_2O rel. to specific surface area 8=48493
  - ThO_2 crystal, dielec. and mech. relaxation 8=30995
  - ThO_2 inclusions in W, e microscopy 8=44173
  - ThO_2, lattice and grain-boundary diffusion of Pa 8=35508
  - ThO_2 microsphere production from alcohol mixtures 8=25310
  - ThO_2, porous and nonporous, adsorpt. of H_2O 8=48492
  - ThO_2, rare-earth impurity ion doping in melt-grown crystals 8=26645
  - ThO_2:Cm^{3+}, e. s. r. at 10 Gc/sec and liq. He temps. 8=27490
  - ThO_2: Dy^{3+}, e.s.r. spectra 8=40918
  - ThO_2, Th^{230} cations self-diffusion, α-spectrometry obs. 8=35510
  - ThO_2, U lattice and grain-boundary diffusion, obs. 8=35507
  - ThO_2–UO_2 solid soln., lattice and grain-boundary diffusion of Pa 8=35508
  - ThO_2-UO_2 solid soln., U lattice and grain boundary diffusion, obs. 8=35507
  - ThO_2: Yb^{3+}, g-factor stress dependence 8=31510
  - Th-ThAs system phase diagram and lattice params., obs. 8=30577
- **Thulium**
  - α-ray absorpt. at 54.4 MeV, obs. 8=48919
  - ferromagnetic props. from mag. moment meas. at 4.2°K 8=31706
  - Mössbauer hyperfine structure below Neel temp., analysis 8=30644
  - salts, hyperfine nuclear interaction and electronic shielding from Mössbauer effect 8=39508
  - Tm^{2+} in CaF_2, transferred hyperfine interactions, F^{19} ENDOR obs. 8=36266
  - Tm^{2+} in CaF_2, 12% nuclear polarization using optical pumping 8=30633
  - Tm^{69} L emission spectrum in β-γ region, new diagram lines 8=38681
  - Tm^{69} L emission spectrum in γ region, new diagram lines 8=38680
  - Tm^{169} implanted in Fe, time-dependent hyperfine interaction 8=39524
- **Thulium compounds**
  - orthoferrites, antiferromag. resonance in spin reorientation region 8=27456
  - orthoferrites, microwave mag. loss meas. near spin-reorientation temps. 8=36224
  - ThFe garnet, sublattice magnetization 8=40840
  - $TmAl_3$, cryst. stark splitting 8=48309
  - $TmCl_3$, Mossbauer effect in structure determs. 8=43959
  - TmF_3, Mossbauer effect in structure determs. 8=43959
  - $TmFeO_3$, microwave absorpt. spectrum, effect of rot. of applied field 8=45226
  - TmGa garnet, susceptibility rel. to low-lying energy levels 8=31742
  - Tm_2O_3, high temp. stability rel. to Tm^{170} use as isotopic heat source 8=35425
  - TmSb, magnetization anisotropy 8=31512
- **Thunderstorms**
  - See also Lightning.
  - Arabian Sea summer monsoon, air-mass dynamics or subsidence processes? 8=45446
  - associated background cosmic count increase 8=38263
  - atmospheric press. variations, obs. Saskatoon, Canada (1962-63) 8=27894
  - cloud and ground lightning, comparison of discharge processes 8=27919
  - conditions for occurrence of severe storms 8=41355
  - effects of Hyderabad magnetographs 8=32365
  - high speed updraft 8=32214
  - lightning flash counter calibration using elect. field changes 8=36755
  - lightning, single stroke, peak power and dissipation 8=36751
  - split into anticyclonic and cyclonic storms, motion from numerical model expts. 8=45452
- **Thyratrons.** See Gas-discharge tubes.
- **Tides.** See Atmosphere/movements; Ionosphere; Oceanography.
- **Time interval measurement**
  - delay unit for flash photolysis spectroscopy 8=41285
  - digital instrument 8=45956
  - flowmeter, photoelec. system 8=34592
- **Time interval measurement**—contd
  - spark timer, transistorized 8=28221
  - standards, historical review (1918-1968) 8=28209
  - time-amplitude converters, calibration 8=24527
  - time-of-flight systems, calibration unit 8=24498
  - time-to-amplitude converters appl. 8=23794
  - timing unit for semicond. spectrometer 8=24518
  - transistorized time amplitude convertor 8=45954
  - Ge(Li) detector pulses, constant-fraction discriminator 8=37796
- **Time measurement**
  - astronomical time scales 8=45955
  - atomic clock, vapour rubidium, as freq. standard 8=45958
  - atomic clocks, Cs beam, systems analysis 8=41621
  - atomic units and scales of time 8=45957
  - fluorescence decay, instrum. response correction 8=32051
  - frequency synthesiser, digital control circuit 8=33014
  - geodesic clock, Marzke-Wheeler method depend. on atomic constitution of matter 8=23866
  - microwave cavity, freq. shift meas. 8=28604
  - precise and reproducible standard definition 8=45946
  - relativistic time-dilation formula 8=32786
  - thermocouple response in liq. medium 8=28419
- **Tin**
  - absorption in 50-340Å range, calc. of partial oscillator sums 8=31981
  - atom, inelastic e scatt., E_e=200, 400 keV, cross-section 8=38719
  - β-Sn, Mössbauer line shift during phase transform under pressure 8=43941
  - Bormann effect obs. 8=49750
  - diffusion in Al, due to near surface effect 8=39964
  - diffusion in Si, effects of P and B codoping 8=48791
  - electrodes, measured conductance rel. to measured capacitance and Faradaic current 8=49929
  - electrodes, polycryst., double layer in aqueous soln. capacitance obs. 8=45384
  - film, supercond., clean and dirty, critical mag. field 8=44734
  - films and foils, parallel and perpendicular mag. transitions, 1°K-T_c 8=40741
  - films, elec. resistance rel. to impurity conc. 8=35828
  - films, thin, supercond., hyperfreq. nonlinearities 8=27030
  - fractionation trends in plagioclases, comp. with Ca 8=50074
  - γ-ray backscatt. from slab rel. to thickness 8=41035
  - gray, Sb-doped, Γ_8^+ conduction band non-parabolocity 8=26911
  - gray, Γ_8^+ conduction band anisotropy 8=26912
  - lifetime and oscillator strength of $^3P_1^0$ state 8=38707
  - liquid, density 8=39325
  - liquid, electrotransfer of Ag impurities 8=39408
  - liquid, 226-1140°C, at. distrib. curve 8=39299
  - liquid, structure factor 8=48062
  - magnetoresistance at liq. He temps. and over large range of mag. fields 8=27031
  - magnetoresistance, quantum oscillations, obs. 8=44975
  - optical consts. of single crystal from reflectance ratios 8=45164
  - particle layered with SiO, supercond., size effect on n.m.r. 8=44735
  - photoelectric γ cross-section determ. 50-208 keV 8=36004
  - plasticity and slip instability in white Sn single crysts., obs. 8=40181
  - positron annihilation 8=49131
  - positron annihilation, single-quantum, cross sections 8=44670
  - sheet, bound by Araldite or Cemendine 3000, hardness 8=40121
  - stopping power for 3.75–5.5 MeV proton, using (p, n) obs. 8=43030
  - stress and temperature, rel. to strain-rate 8=31232
  - superconducting, complex elec. cond., strong-coupling calc. 8=35854
  - superconducting films, energy gap mag. field and film thickness dependence by e-tunnelling 8=27033
  - superconducting films, microwave transmission meas. 8=40386
  - superconducting, helicon-like oscillations 8=44736
  - superconductivity of particles embedded in oxide film 8=40388
  - superconducting props. rel. to Al admixture 8=40389
  - superconducting ring, current fluctuations and critical currents obs., temp. depend. 8=40387
  - superconductor film, clean and dirty, critical mag. field 8=44734
  - superconductor, film, tunneling expts in mag. field 8=44732
  - superconductor, quantum phase coherence in two coupled, Josephson junctions 8=44733
  - tempered, as ohmic contacts for Gunn elements 8=49282
  - thermoelectric e. m. f. variations, rel. to magnetic breakdown 8=40643
  - weak line transition probability calc. 8=29621
  - whiskers, electrolytic growth conditions 8=30837
  - white, anomalous Shubnikov-de Haas amplitudes 8=49474
  - white, helicon propagation, mag. breakdown effects 8=62932
  - white, thermal lattice vibration spectrum determ. 8=35393
  - white, Knight shift, temp. depend. 8=41002
  - X-rays, anomalous transition 8=49757

Tin—contd
- zone-refined, solute-induced hardening near grain boundaries 8=26842
- Sn^{2+} for activation of $Zn(SCN)_2$, luminesc. 8=36520
- Sn^{117} and Sn^{119}, level crossing investigation of hyperfine struct. 8=29629
- Sn^{119} crystal, pulsed n.m.r. obs. 8=31918
- Sn^{119}, diffraction of resonance γ-rays, on nuclei and electrons 8=39821
- Sn^{119} impurity in metallic matrices, Mössbauer absorpt. spectra, interpret. of isomer (chem.) shift 8=48318
- Sn^{119}, resonant radiation, diffraction on electrons and nuclei, obs. 8=48334
- α-Sn, band structure, including spin-orbit effects 8=44825
- Sn(IV), isomer shifts in ice, conc. depend. 8=43957
- Sn-Sn tunnel junction, anomalous behaviour at superconducting transition 8=44738

Tin compounds
- chalcogenides, epitaxial deposition on NaCl/KBr substrates at 293-873°K 8=39599
- Mossbauer effect, isomer shifts and nuclear radius change 8=26026
- salts with mixed anions, i. r. absorpt. spectra 8=36413
- tetrahalides, mol. addition compounds with triphenyl (phosphine and arsine), i. r. spectra, stretching vibs. freq. shifts 8=25631
- tetramethyl tin free radical form., e. s. r. detection 8=34382
- tin(II) hydroxide, structure 8=44255
- Sn chalcogenides, thin films, struct. and props. 8=39600
- Sn complex, diacetate tetramethyl distannoxane 8=26368
- Sn-Bi alloy substance entering in He and air arc discharges 8=47777
- SnBr, $B^2\Sigma$-$X^2\pi$ system, u. v. absorpt. after flash photolysis of $SnBr_4$ 8=34284
- Sn-Ce solid solns., superconductivity, resistivity and thermoelec. power rel. to localized moments 8=31339
- $Sn(C\equiv H)_4$, i. r. and Raman spectra 8=25625
- $Sn_3(CH_3)_4Fe(CO)_{16}$, crystal and mol. structure 8=26537
- $SnCl_4$, Coriolis coupling consts. and force fields 8=38822
- $SnCl_4$, vibr. relax. and u.s. attenuation 8=39360
- Sn-Co, ferromagnetism in liq. state, and elec. resist 8=43871
- SnF, dissoc. energy 8=38933
- SnF_2, mass spectra of vapour 8=38933
- SnH_3CH_3 and $SnCl_3CH_3$, force consts. and thermodyn. props. 8=38890
- SnI, $B^2\Sigma$-$X^2\pi$ system, u. v. absorpt. after flash photolysis of SnI_4 8=34284
- SnI_4, far i. r. cryst. spectra 8=45223
- Sn-In alloy film, supercond. tunneling expts in mag. field field 8=44732
- Sn–In films, superconducting, mag. props. 8=44974
- Sn-Ni, ferromagnetism in liq. state, and elec. resist 8=43871
- Sn/Pb solder, determ. of Au, Ag and Cu by X-ray spectrometry 8=27816
- SnO, transparent and elec. conducting film, deposition on glass 8=44061
- SnO_2-coated glass analogue system for electrochem. system 8=32129
- SnO_2 colloidal soln. in glycerine-alcohol mixture, γ-rays reson. absorpt. 8=24701
- SnO_2 crystals, i. r. absorpt. spectra rel. to optical lattice-vibration modes 8=45222
- SnO_2 films, prep. and props. by reactive cathode sputtering 8=44062
- SnO_2, static dielec. constant 8=49353
- n-SnO_2:Sb, elec. and optical props. 8=27135
- n-SnO_2:Sb, elec. and opt. props 8=49270
- SnO_2: Zn, chemisorbed oxygen effect on elect. conductivity 8=31391
- Sn-Pb alloys, liquid, density 8=39325
- SnS, epitaxial film, structure and optical props. 8=44060
- SnS, thermal conductivity from experimental parameters 8=48764
- SnSb precipitation from Pb rich alloy of Pb-Sn-Sb ternary system, rel. to aging 8=26764
- Sn-Sb, second-phase deformations after cold rolling 8=49001
- SnSe, epitaxial film, structure and optical props. 8=44060
- $SnSe_2$, photoelectric emission 8=36055
- $SnSe_2$, refractive index and absorpt. coeff. 8=45220
- Sn–SnO–Sn Josephson junction, relax. oscills. 8=40412
- SnTe, Debye temp. determ. using Mössbauer effect in Sn^{119} and Te^{125} 8=44344
- SnTe epitaxial film, structure and optical props. 8=44060
- SnTe, high pressure phase transformations 8=35082
- SnTe, optical and elec. meas. rel. to band structure determ. 8=49726
- SnTe, superconducting interactions 8=27032
- SnTe, thermal conductivity investigation, 100-450°K 8=30992
- p-SnTe, valence band structure 8=44652
- SnTe-GeTe, high pressure phase transformations 8=35082
- SnTe–PbTe, solid solns., heats of formation, hardening, and lattice characts. 8=43981
- SnTe–SnSe system, phase diagram 300° to 900°C 8=44013
- SnX_4, (X = Cl, Br, I, H, Li, Na), Sn^{119} isomeric shift dependence on at. radius of X 8=30637

Tin compounds —contd
- Sn-Zn alloys, electrotransport at 500°C 8=34901
- Sn-Zn alloys, liq., heat conductance 8=39351
- Sn–10% Zn liquid, rel. to ductile-brittle transition in Al 8=35656
- Sn–10% Zn liquid, rel. to ductile-brittle transition temp. of Al, strain rate depend. 8=35657

Titanium
- additions, rel. to props. of Malcolloy (Co–Al), magnetic alloy 8=40803
- α- and β-solid solutions, separation conditions 8=48347
- atom, internal conversion coeff. for e. m. transition between shells 8=38670
- deformation mechanisms, rel. to impurity obstacles 8=44604
- desorption from W in strong electric field 8=35197
- diffusion of H in h.c.p. and b.c.c. types, 610° to 900°C 8=44393
- diffusion processes in weld joints under transient pressure 8=44373
- elastic constants, temp. dependence, 4. 2-36°K 8=49054
- electrodes, measured conductance rel. to measured capacitance and Faradaic current 8=49929
- electron reflection, 500 to 1200 keV 8=44197
- films on Nb alloys, non-electrolytic deposition from fused slats at high temps. 8=44063
- films, resistance and work function rel. to adsorpt. of Ba, O_2 and BaO 8=40322
- films, sticking probabilities of N_2 8=30771
- foil, self-supporting, vacuum deposition method 8=39601
- h. c. p., angular relns. between plane normals and crystallog. directions 8=44087
- interaction of NH_3, H_2 and N_2 8=32103
- ions, Ti^{3+} doped corundum, catalytic C_2H_5 hydration 8=32122
- lattice params. and thermal expansion rel. to para-antiferromag. transition, —180-1500°C 8=44253
- neutron irradiation creep obs. at 100°C 8=26833
- n.m.r. in Ti-H systems 8=49658
- optical absorption and ionic conductivity in silver halogens 8=41052
- oxidation kinetics and growth of diffusion layer, effect of O_2 press. 8=36573
- oxidation rate-constant determ., low-temp., from discontinuous film resistance changes 8=49883
- oxide film form. in boiling dilute H_2SO_4 and HCl, differences in struct. 8=39602
- plasma source, nonlinear effects in operation 8=34569
- press broadening and shift of lines by Ar 8=43204
- reorientation mechanism during recrystallization 8=44086
- sheet, crystallographic anal. of plastic anisotropy 8=35721
- sheet, plastic anisotropy and plastic flow of circular diaphragm 8=35720
- in solar chromosphere, lower, Ti^+ emission regions 8=45914
- stacking fault probab. of cold-worked, X-ray obs. 8=26704
- stress-corrosion cracking in methanol vapour 8=40184
- thermal expansion, 2° to 30°K 8=44349
- thin film, resistivity, ion-bombardment induced changes 8=49151
- weight determination in alnico alloys and ferro-titanium 8=49984
- X-ray K_α, emission, depth distrib. and absorpt. in anti-cathode, 17-29 kV 8=36420
- in Al melts, u. s. dispersion, 740-800°C 8=39442
- H_2 desorpt. obs. 78°-300°K 8=30772
- Hg boiling corrosion of steel inhibited by Ti impurity 8=47426
- Ti^{48}, μ-mesic x-ray Lyman and Balmer lines and μ-capture x-rays, obs. 8=34189
- α-Ti and O mixed crystals, lattice struct. rel. to hydrogenation, n diffr. obs. 8=35357
- α-Ti, plastic flow mechanisms, 0-600°K 8=49057
- Ti II, spectra in excited configurations, theory 8=43203
- Ti V, $3p^6$-$3p^54d$ transitions 8=43178
- Ti^{3+} ion in $BaTiO_3$, electronic transition theory 8=49362
- Ti^{3+} substituted alums, crystal-field origin 8=43935
- Ti : Fe^{57}, f number isomer shift pressure dependence 8=48321

Titanium compounds
- alloy, equiaxed $\alpha + \beta$ type, determ. of β grain zize 8=44170
- alloys, high-strength, fracture toughness dependence on thickness, work-hardening exponent effect 8=26766
- alloys, stress corrosion cracking 8=27716
- atom. spectra line press. broadening in Ar atm. 8=34153
- diborides, conduction e-parameters calc. based on single zone method 8=35830
- infrared absorpt. spectra 8=36421
- oxides, vaporization from liq. phase 8=30603
- oxidic titanates, cryst. struct. effect on luminesc. 8=45284
- rutile, h.f. conductivity, dielectric const. 8=49331
- rutile, Cr-doped, microwave orientation 8=26184
- rutile (TiO_2) crystals, doped, optical absorpt. by polarons 8=36418
- titanomagnetite transform. to titanomaghemite on cryst. margin 8=35125
- Ti alloys, fracture toughness parameters 8=49058
- Ti carbides, formation by chemical vapour deposition, discussion 8=45348

Titanium compounds—contd
Ti methoxide, crystal and mol. structure 8=26523
Ti-Ag system, phase diagram in reln. to diffusion process 8=35509
Ti-6Al-4V alloy, addition of Co, properties 8=49055
Ti-8% Al alloy deform. mechs. rel. to impurity obstacles 8=44604
Ti-9 A-Mo-V, stress-corrosion cracking in methanol vapour 8=40184
Ti-Co system, solubility limit study by X-ray diffractometry 8=30709
Ti-H systems, n.m.r. of Ti 8=48658
Ti-Mo alloys, low temp-electronic sp. heat, BCS theory 8=39922
Ti-16 at.%Mo alloys, type II superconductor, mixed state Hall effect 8=27035
Ti-6%Mo alloy, quenched, structure study by electron microscopy 8=30869
Ti-47% Nb, α-phase formation during heating in e-microscope 8=35119
Ti-22 at.%Nb/Cu composite conductors, ω precip. rel. to critical current densities 8=40419
Ti-Ni, soft X-ray spectroscopy 8=36419
Ti-Ni-Sb-O system, rutile solid solution and reaction diagrams 8=48404
Ti-Ni-Sb-O system, rutile solid solution formation 8=48405
Ti-Pd alloys, phase diagrams, solubility 8=35127
Ti-V alloys, self-diffusion comp. -temp. dependence 8=26623
Ti-V alloys, superconducting critical current densities rel. to ht. treatment 8=40391
Ti-W-C alloys, phase diagram revision 8=39565
Ti-Zr-O alloys, creep rel. to polymorphic substitution temp. 8=49059
$TiBe_{12}$, hexagonal, OD-structure 8=26442
on $TiBr_4$-Ar mixture, TiI, II absolute gf-values determ. 8=43489
TiC, field ion microscopy 8=26289
TiC, self-diffusion coeff. of C^{14}, comp.-dependence, 1450-2280°C 8=39985
TiC, thermoelec. power and elec. conductivity, 20-2000°C 8=27310
TiC-TiO solid solution with outer layer of TiO_2 with intermediate Ti_2O_3 as cutting tool protection layer 8=48428
α- and β-$TiCl_3$, optical props. 8=36417
$TiCl_4$, vibr. relax. and u.s. attenuation 8=39360
TiCo alloys, n.m.r. and mag. susceptibility at 295 and 77°K 8=31920
$TiCr_2S_4$, cryst. and mag. struct., comparison with $TiCr_2Se_4$ 8=35358
$TiCr_2Se_4$ cryst. and struct. mag., comparison with $TiCr_2S_4$ 8=35358
TiFe alloys, 3d-electron redistrib. from X-ray spectra 8=35780
$TiFe_{1-x}Co_x$, n.m.r. and Mossbauer effect line profile comp. temp. and stoichiometry dependence 8=31921
$TiFe_xCo_{1-x}$ alloys, structure and mag. props. from n-diffr. exam. 8=30912
TiH_2, positron lifetime 8=40286
TiH_x, $(x < 2)$, H orbital expansion effects on d-electron exchange rel. to mag. props. 8=49480
TiN inclusions in steel, thermal expansion and reln. to tessellated stresses 8=44350
TiN, Ti Kα band in X-ray emission spectra rel. to electronic structure 8=41148
TiNb33:N, O and metals, supercond., microstruct. and workability, obs. 8=44742
TiNb40:N, O and metals, supercond., microstruct. and workability, obs. 8=44742
TiNi and associated cpds., conf. 8=30868
TiNi, creep obs., 700-1000°C 8=26849
TiNi crystals, obs. in premartensitic states on cooling 200-0°C 8=30710
TiNi, internal friction and elastic constants temp. dependence, −170 to 800°C 8=26847
TiNi, phase transform. within irreversible critical range rel. to electronic transform 8=30708
TiNi, shape-memory effect at 90°C after plastic deform. at room temp. rel. to martensitic transform 8=30707
TiO, molecular bands in M star spectra 8=28060
TiO solar lines equivalent widths calc. 8=37065
TiO, vacancies and supercond. 8=31345
TiO_2, acoustic wave generation by electrostrictive mixing of light waves 8=45162
TiO_2, addition to $BaTiO_3$ to promote conduction 8=49228
TiO_2, adsorbed polymer layer thickness 8=39620
TiO_2, adsorption of surface-active substances and polymers 8=48494
TiO_2-based dielec., Ag diffusion 8=31016
TiO_2-containing-glasses, small polaron as charge carrier 8=40499
TiO_2, e.s.r. spectrum, d^1 config. 8=45102
TiO_2 films, amorphous, prep. by vacuum evap., crystn. by electron irradn. 8=39691
TiO_2 for ruby and sapphire doping, reduction of laser prod. damage 8=33198

Titanium compounds—contd
TiO_2 in BaO-TiO_2-SiO_2 glasses, structural states 8=44078
TiO_2, inert gas depth distrib., sputtering obs. 8=48923
TiO_{2-x}, resist. rel. to stoichiometric defects, 20-1000°C 8=39999
TiO_2, rutile, defined surfaces, adsorpt. of ethanol, n-octanol and n-dodecanol 8=35196
TiO_2 (rutile), thermally stimulated currents and luminescence 8=36513
TiO_2 single crystals, time-dependent elect. conduction 8=27250
TiO_2, small polaron conductivity, i.r. absorption 8=40498
TiO_2, spectral reflectance 8=41128
TiO_2, thin film deposition from thermal decomp. of tetraisopropyl titanate 8=35185
TiO_2 outer layer on TiC-TiO solid solution with intermediate Ti_2O_3 layer as cutting tool protection 8=48428
TiO_2, Voigt-Reuss-Hill approx. rel. to meas. of elastic moduli 8=40188
TiO_2, work function and elec. cond., changes in response to chemisorpt. of O 8=40691
TiO_2: Co^{2+}, ENDOR 8=41007
TiO_2 : M^{4+}, ENDOR 8=41007
TiO_2:Cr^{3+}, structure determ. by e.s.r. 8=39823
TiO_2, MO calcs on TiO_6^{-n} unit, rel. to energy levels and absorpt. spectra 8=45225
TiO_2: Mo^{5+}, paramag. relax., temp. depend. 8=36247
TiO_2, Ti $\mathbf{K}_\alpha$ line shift rel. to e microprobe analysis, obs. 8=27804
TiO_2-Sb_2O_3-NiO system, comp., structure and colour 8=26039
TiO_2-SnO_2 system, spinodal decomposition 8=39703
TiO_2: V^{4+}, ENDOR 8=41007
TiO_2: V^{4+}, paramagnetic spin-lattice relaxation 8=40945
TiO_2-WO_2 system, melting relation 8=39476
TiO_n, Ti Kα band in X-ray emission spectra rel. to electronic structure. 8=41148
TiO_6^{-n} localized units, extended Huckel MO calcs. rel. to absorpt. spectra and energy levels 8=45225
$TiTa_2O_7$, cryst. struct. 8=48403
TiX, (X=Fe, Ni, Co or combinations), relative ductilities 8=26848
Ti_2O_3, crystallographic studies of transition 8=48678
Ti_2O_3, neutron-diffraction data, rel. to mag. phase 8=31800
Ti_2O_3, protective oxide layer in cemented WC-TiC cutting tools 8=48428
Ti_2O_3, resistivity and mag. order 8=31313
Ti_5O_9, magnetic properties, anomalous, 77°-160° 8=31511
Ti_8Te_8 phase, unit cell parameters and ordering of vacancies 8=35359
Torquemeters. See Mechanical measurement.
Torsion
See also Elastic constants; Stress analysis.
balance for low-temp. mag. anisotropy meas. 8=31723
elastic cylinders in contact 8=32717
elastic-plastic, as problem in non-linear programming 8=41710
magnetostrictive circular bar, permeated by longit. mag. field, problem 8=33039
microbalance, elec. for mag. torque meas. 8=37381
plastic, of hollow cylinders, length change rel. to texture 8=44523
solids, elastic, rel. to direct numerical determ. of stresses 8=41702
thermoplastics, torsional creep meas. 8=35624
torque meas. at low temps., clarification 8=41624
tube, compressible elastic and reinforced, calc. 8=41667
vibration of moving band 8=23931
Al tubes, cyclic creep rel. to second-order strain increments amplification obs. 8=44541
Cu whiskers, deformation, rel. to structural features 8=35254
Cu_x crystals, under alternating, plastic deform., macroscopic localization 8=44567
Zn crystal, alternating effects on plastic deformation, macrolocalization characts. 8=35726
Total cross-sections. See under individual particles, no sub-heading.
Townsend coefficient. See Ionization/gases.
Tracers
See also Radioactive tracers; Radiochemistry.
isotope labelling of cpds., for probing chemistry underlying mass spectra 8=25393
radioactive decay effects, soln. of vector eqn. 8=32166
tritium, for mass return flow of air and H_2O vapour to stratosphere 8=36725
Transducers. See Acoustic transducers.
Transformations. See Phase transformations.
Transformations, mathematical
fast Fourier, effectiveness 8=24407
Foldy-Wouthuysen, appl. to relativistic-symmetric Hamiltonian 8=24634
generation by Bel-Robinson generalized tensor 8=32821
of hydrodynamic eqns, for conservation in curvilinear co-ord. systems 8=34578
invariant, rel. to Newman-Penrose constants 8=24474

Transformations, mathematical—contd
- Klein-Gordan, eqn., integral transform. 8=24453
- Laplace, disturbances in semi-infinite visco-elastic bar in mag. field 8=23854
- Laplace, inverse-transformable soln. calc. for right-angled dielectric wedge 8=46482
- Laplace transform space, transient elastodynamics 8=46054
- linear, of field operators 8=28950
- Lorentz, geometrical and tensorial 8=28327
- Moser, theory of synchrotron oscillations 8=33439
- parabolic systems 8=32647
- space-momentum commutations, general relation 8=28234
- static reactivity from prompt decay consts. 8=34090
- unitary of Foldy-Wouthyusen Hamiltonian to laboratory system 8=29025
- Weyl transforms., applic. in classical limit of quantum mechanics 8=33305

Transistors. See Semiconducting devices/transistors.

Transition metals
- atoms mag. moment, ferro- and antiferromag., rel. to localized d electrons 8=35047
- band structure of energy spectra by various techniques 8=26913
- band structure, theory 8=35781
- d bands structure dependence 8=44653
- b.c.c., elastic consts. temp. depend. rel. to entropy of diffusion 8=48984
- body-centred cubic, dislocation relax. 8=31088
- bond between surface and adsorbed Co 8=48298
- dielectric, constants and loss calcs. from vacuum u.v. reflectivity data 8=41147
- electron–electron scatt., Baber's model 8=40209
- ferromagnetic, e.-magnon interaction 8=36178
- ferromagnetic properties rel. to band structure 8=31632
- impurity in covalent complexes, covalency 8=35018
- impurity states, magnetic 8=35741
- ions in synthetic zeolites, spectra, theory 8=41142
- localized impurity in noble metals, d state splitting 8=26868
- mass renormalization, spin-fluctuation-induced, rel. to n.m.r. 8=31922
- optical spectra rel. to band structure 8=32036
- paramagnetic, magnetostriction 8=31533
- reflectivity, vacuum u.v. rel. to dielec. constants and loss calcs. 8=41147
- secondary ion emission from first series metals rel. to ionization process 8=40717
- spin fluctuations, nearly ferromag., effect on supercond., specific heat and susceptibility 8=44992
- stacking fault energies on {111} planes in b.c.c. lattice 8=48870
- structure 8=44258
- surface tension and cohesion, by tight binding method 8=43928
- susceptibility, orbital, calc. from band structure 8=31529
- in Cu, conduction-electron spin relax., interpretation 8=31863

Transition metal compounds
- alkylpyridine complexes, far i.r. spectra 8=29763
- alloys, dilute, ferro-and paramag., rel. to impurity states 8=45005
- alloys, dilute, intra-atomic Coulomb interactions and local exchange-enhancement 8=35433
- alloys, dilute, mag. moments 8=45031
- alloys, dynamic susceptibilities 8=31491
- alloys, energy spectra by various techniques 8=26913
- alloys, local magnetic moments, statements from macroscopic meas. 8=31509
- alloys mass renormalization, spin-fluctuation-induced, rel. to n.m.r. 8=31922
- alloys, n.m.r. for local susceptibilities exam. 8=49657
- alloys, paramagnetic, magnetostriction 8=31533
- alloys, strongly paramagnetic, exchange enhancement of spin susceptibility, breakdown of rigid-band model 8=31532
- arsenides, mag. and elec. props. 8=41079
- antiferromagnetic salts, transferred hyperfine interactions and spin deviations 8=31919
- carbides, elastic props. directional variations 8=49056
- boracites, mag. properties between 1, 8°and 300°K 8=45065
- carbides, interact with liq. Pt rel. to their decomposition 8=27715
- carbides, structure and thermodynamic props. rel. to M-M interaction 8=26441
- chalcogenides, order of vacancies and non-stoichiometry 8=26635
- dialkylamido-transition metal cpds., metal-N$_2$ i.r. stretching frequencies 8=29712
- hydride complexes, chemistry and applications 8=25521
- iron-group containing crystals, colour dependence on structure 8=27534
- lubrication at high temp. by H$_2$S gas forming surface metal sulphide film 8=31219
- magnetic moments, localized, and Pauling valence 8=49528
- metal-metal carbonyl derivatives, X-ray study 8=26474

Transition metal compounds—contd
- neutron scatt., use of continuous flow cryostat in expts. 8=49548
- niobates, cryst. growth and transport reactions 8=26209
- nitrides, structure and thermodynamic props. rel. to M-M interaction 8=26441
- organometallic cpds., mass spectra 8=39053-5
- oxides centred around Nb$_2$O$_5$ in comp., non-stoichiometric mechs and suitable diffusion paths 8=26365
- oxides, structure and thermodynamic props. rel. to M-M interaction 8=26441
- polynuclear complexes, bonding 8=27595
- selenides, binary systems, crystal chem., ordered structs. and non-stoichiometry 8=26164
- spin-orbit coupling effects 8=45028
- sulphides, binary systems, crystal chem., ordered structs. and non-stoichiometry 8=26164
- tellurides, binary systems, crystal chem., ordered structs. and non-stoichiometry 8=26164
- transport props. dependence on e-no 8=26872
- V alloys, elec. cond. anomalies 8=44699

Transmission
- e.m. waves and pulses into the earth 8=46471
- entropy, by lens system 8=46658
- glass-ceramic, Cer-Vit, at u.v., visible, i.r. and sub-mm wavelengths 8=45165
- metal films, e.m. power-transmission coeffs. 8=49698
- microwave surface impedance, reason for oscillations 8=36311
- semiconducting films, e.m. power-transmission coeffs., 8=49698
- X-ray diffraction cameras treated as transmission systems 8=48625
- X-ray interf. at distorted cryst. lattices 8=31951
- Si-O solid soln, anomalous X-ray, rel. to periodicity changes on decomposition 8=36409
- Sn, X-rays, anomalous 8=49757
- **acoustic waves**
  - See also Acoustic wave propagation.
  - cylindrical shell, finite, closed 8=23958/9
  - doors and windows, sound transmission loss 8=23966
  - moving fluid layer, theory and coeff. calc. 8=37267
  - multiple, effect on reverberation-limited sonar 8=37270
  - noise in buildings, indirect path effects 8=41848
  - sea bed, deep, rel. to bulk and textural props. sediments 8=36691
  - solids, meas. for anisotropy detect. 8=30938
  - transition zone, theory 8=46184
  - underwater sound research before 1939 8=36696
- **acoustic waves, ultrasonic**
  - gas mixture with molecular masses largely different 8=43690
  - mica, rel. to freq. 8=30947
  - C$_6$H$_{12}$ vapours, for large freq./press. 8=43691
  - Cu, n-irradiated, third-order elastic constants from u.s. meas. of non-linearity parameters 8=26800
- **electromagnetic waves.** See Electromagnetic wave propagation.
- light
  - See also Absorption/light; Filters, optical.
  - aberrated and misaligned, light transmission, effect of redirectors refocusers and mode filters 8=46662
  - atmospheric, 92 km air to surface path 8=50150
  - bentonite-water suspension, rel. to extinction coeff. 8=30547
  - Christiansen filter shape and bandwidth by multiple scattering calc. 8=37665
  - by cloud and dust layers, appl. of probability distrib. of photon optical paths 8=41362
  - clouds, rel. to particle size distribution 8=41367
  - dielectric mats, for electro- and elasto-optic, and u.s. device appls. 8=27229
  - dielectric narrow-band interference filter with passbands exactly matching specification 8=42202
  - dielectrics, transparent, constraints developed by luminous wave 8=27524
  - Fabry-Perot interferometer, method for increasing intensity 8=46728
  - far i.r. from asymmetric Michelson interferograms pseudo-coherence effect 8=28844
  - films of crystalline polymers, obs. 8=45245
  - foil, metal, plasma resonance absorpt. calc. 8=27531
  - gaseous, rel. to average absorpt., strong-line region and intermed. between strong and weak 8=34666
  - glass, transient and permanent loss due to rad. 8=28742
  - glasses, rel. to composition 8=31996
  - Kubelka-Munk coeffs. from transmittance 8=33271
  - laser output mirror, determination of optimum coefficient 8=46566
  - layers containing coarse particles 8=30554
  - lenses, aberrated and misaligned, effect of redirectors, refocusers and mode filters 8=46662
  - polystyrene films, rel. to glass transitions detect., i.r., 50-120°C 8=45247
  - poly (vinyl alcohol) films, rel. to glass transitions detect., i.r., 50-120°C 8=45247
  - polyvinyl chloride-co-vinyl acetate films, rel. to glass transitions detect., i.r., 50-120°C 8=45247
  - quartz, from asymmetric interferograms, 20-400 cm^{-1} 8=28844

- **Transmission**—contd
  - **light**—contd
    - quartz, transient and permanent loss due to rad. 8=28742
    - quasi-monochromatic wave through dispersive medium meas. 8=46713
    - radiation field perturbation by local inhomogeneity, calcs. 8=45146
    - resonator, open with spherical mirrors, losses 8=24367
    - saturation of irradiance fluctuations due to turbulent atmos. 8=32240
    - spectrophotofluorometer 8=46694
    - transmission-to-extinction convertor for photometry 8=28723
    - underwater optics, S/N concept 8=37695
    - u.v. in synthetic quartz 8=49751
    - Ag film, absorbent and anisotropic, and reflectivity 8=49707
    - Ag thin films, near plasma freq., obs. 8=27547
    - Al thin film, of synchrotron radiation 8=27549
    - Al_2O_3, transmittance, reflectance and absorption 8=41057
    - Au gilm, absorbent and anisotropic, and reflectivity 8=49707
    - CaO, i.r. dielectric response rel. to lattice vibrations 8=41075
    - CdSe:Cu, rel. to fundamental absorpt. edge impurity conc. dependence 8=36349
    - GaAs, n-irrad., model for optical attenuation 8=27569
    - GaAs, GaSb, room temp. curves from 0.2 to 3.0μ 8=45187
    - KBr, from asymmetric interferograms, 20-400 cm^{-1} 8=28844
    - KI, room temp. curves from 0.2 to 3.0μ 8=45187
    - LiF rel. to second harmonic generation 8=27555
    - $LiTaO_3$, variations 8=36385
    - RbBr, RbCl and RbI, room temp. curves from 0.2 to 3.0μ 8=45187
    - RbH_2PO_4 crystals grown by static method 8=44142
    - SrO, i.r. dielectric response rel. to lattice vibrations 8=41075
    - VO_2, in semiconducting and metallic states 8=49760
    - V_2O_5-P_2O_5-(La_2O_3, Nd_2O_3 or CeO_2) glasses, i. r. characts 8=36425
    - ZnSe, i.r. lattice vibrations 8=49764
    - ZnTe, i.r. lattice vibrations 8=49764
- **Transmission lines, r.f.** See Electromagnetic wave propagation/ guided waves.
- **Transparency**
  - See also Optical constants; Transmission/light.
  - acoustic, of moving fluid layer, calc. 8=37267
  - corundum, sintered, prep. and props. 8=45940
  - glass-ceramic, Cer-Vit, at u.v., visible, i. r. and sub-mm wavelengths 8=45165
  - plastic with increased transparency for scintillation counters 8=46882
  - self-induced, in systems undergoing giant Faraday rotation 8=37700
  - Al films, thickness depend. oscills. rel. to e quantization, 4.2°K 8=31957
  - LiF crystals, investigation of influence factors 8=32007
  - ThF_4 films, useful range 8=35184
- **Transport processes**
  - See also Diffusion; Kinetic theory; Liquids/theory; Radiative transfer; Solids/theory; Statistical mechanics.
  - acetic acid, microscopic props., scatt. spectroscopy, use of atomic substitution techs. 8=30403
  - Boltzmann eqn., approximation in cylindrical geometry 8=28351
  - Boltzmann eqn., boundary ang. flux approximation 8=28350
  - Boltzmann eqn., energy-dependent, for slab reactor criticality 8=25294
  - Boltzmann equation, for neutron resonance absorpt., in reactor lattices 8=29551
  - Boltzmann equation, linear and stationary, solution 8=28352
  - Boltzmann eqn. for polyat. gases 8=30309
  - Boltzmann eqn., two-dimens. linear, biorthogonal angular polynomial expansion 8=32856
  - Boltzmann equation, linearized, functional-analytic discussion 8=46124
  - Boltzmann eqns. for dilute quantum-mechanical, slightly inhomogeneous gas 8=37226
  - Boltzmann kinetic equation dependent on particle velocity 8=46125
  - Boltzmann relaxation eqn., validity 8=32857
  - Boltzmann relativistic eqn., Cauchy problem 8=23911
  - Boltzmann's H function, proof that successive derivatives alternate in sign 8=30278
  - in boundary layer of reacting gas over porous plate 8=30308
  - capillary-porous mats., mass transfer on drying in e. m. field 8=39487
  - Chapman-Enskog method in chem. kinetics 8=49849
  - coefficients rel. to thermal equilibr. correlation functions 8=23907
  - collision integrals for globular mols. 8=29848
  - composite mats, coeff. 8=26939
  - convective mass transfer on cylinder in flow of non-Newtonian liq., effect of polymer additions 8=30423
  - crystal symmetry rel. to theory 8=26907
  - crystallization on constant temp. surface, heat and mass transfer effect 8=48529
- **Transport processes**—contd
  - cylinders, coaxial multipole, inductive energy transfer (general relativity) 8=28295
  - degenerate plasma, calc. 8=39079
  - density discontinuity evolution, governed by Boltzmann collision integral 8=41795
  - diatomic gas, coeffs. calc. 8=30307
  - dielectric crystal photocarriers, meas. apparatus 8=35747
  - diphenyl, terphenyl and mixtures, phys. props. rel. to heat transfer calcs. 8=30422
  - in dispersions, coupled heat and mass transfer, rel. to particle size and residence time distribs. 8=34936
  - electrons in solids rel. to microprobe calibration calc. 8=28560
  - electrical transport in mag. field, quantum theory rel. to corresponding Boltzmann eqn. 8=44674
  - energy, inductive transfer between coaxial multipole cylinders, (general relativity) 8=28295
  - Enskog eqns., temp. depend. of rigid-sphere dia. 8=30185
  - error bounds, via P_N approximations 8=23915
  - Fermi liquid calc. 8=41778
  - Fermi liquid, low-temp. expansion 8=37216
  - Fermi-systems, many-component, fit of generalized Boltzmann eqns. 8=32851
  - in flow systems, interphase heat and mass transfer, and Onsager relns. 8=34828
  - fluid, compressible, velocity potl. eqn. 8=43700
  - fluid, numerically calc. heat flux rel. to supercritical transition 8=32951
  - Fokker-Planck equation, properties 8=23908
  - friction-constant formalism 8=39150-1
  - galvanomagnetic effects, high-elect.-field, in piezoelectric semiconductors 8=31366
  - rel. to galvanomagnetic effects in strong mag. field, semiclassical theory 8=35755
  - gas, Boltzmann, dense, divergence free kinetic equation 8=23910
  - gas critical region 8=39229
  - gas, dense real, failure of weak-coupling model 8=39234
  - gas, dense, space-time correl. functions for Enskog theory 8=43674
  - gas density fluctuations, spectrum from soln. linearized Boltzmann eqn. 8=30285
  - gas, dilute, of polar molecules; Senfrieben-Beenakker effects in electric field. 8=47980
  - gas-discharge tube, collision-induced pumping force 8=38986
  - gas, e drift velocity, new theory 8=39222
  - gas, e drift vel. rel. to resonance scatt. 8=47979
  - in gas flow in duct, heat transfer and sublimation mass transfer at walls 8=35013
  - gas, in radiation boundary-layer flow, effect of viscous dissipation and mass addition 8=39180
  - in gas jets, mixing of two plane non-uniform jets 8=30241
  - gas, mass transfer between concentric spheres at low press 8=39235
  - gas mixtures, polyatomic, transfer and relax. phenomena 8=43699
  - gas mixtures, press. depend. of thermal conc. shift 8=47982
  - gas, monatomic, unsteady cylindrically symmetric expansion into vacuum, Boltzmann eqn. soln. 8=30276
  - gas, nongrey, radiative transfer near equilibrium differential approximation 8=30289
  - gas, partially ionized, modified Chapman-Enskog treatment 8=43473
  - gas phase, turbulent, mass transfer at ordinary rates, rate of concentration of nondiffusing species 8=47978
  - gas, spin diff., mag. field effect 8=43698
  - gas-liquid solns., filtration, residual water effects 8=39233
  - gas-solid suspension flow, heat and mass 8=43650
  - gases, collective-effect approach 8=25833
  - gases, dilute, transport prop. tables, validity range for real gases 8=34672
  - gases, moderately dense, Landau's eqn appl. 8=25832
  - gases, polyatomic, odd terms in ang. momentum 8=30304
  - gases, rigid sphere perturbation calc. 8=30303
  - heat and mass, in evaporative cooling 8=41861
  - ice, mass transfer along surface, neck growth and particle migration 8=30723
  - inert gases, analytical potential models 8=30272
  - interfacial mass transfer in membrane transport in batch dialyzer 8=48120
  - interference effects 8=49080
  - internal heat and mass, irreversible thermodynamics 8=46128
  - intramembrane transport 8=39346
  - ions across membrane, Nernst-Planck eqns. 8=39345
  - kinetic eqn. for impure anisotropic superconductor 8=35841
  - laminar mass transfer in plane m. h. d. flow, in oriented mag. field 8=33112
  - liquid films, falling, mass transfer at low Reynolds numbers 8=34745
  - liquid, momentum auto-correl. function 8=30424
  - liquids, radiation scatt. studies, comparison of X-rays and neutrons 8=30402
  - low-melting salts 8=39331
  - magneto-conductivity in a.c. elec. field, nonlinear Boltzmann eqn. soln. 8=35748

Transport processes—contd
- in m.h.d. field-aligned flow past plate, mass transfer 8=33111
- in many particle systems 8=23889
- mass and energy, in multicomponent medium 8=41763
- mass and energy, thermodynamic laws 8=41793
- mass and heat, irreversible thermodynamics 8=46127
- mass, to spherical drops or bubbles at high Reynolds no. 8=30387
- mass transfer across liq. interfaces agitated by large bubbles 8=43743
- mass transfer across mobile interfaces 8=48123
- mass transfer and slip at laminar boundary surface 8=3458
- mass transfer coeffs., effect of pulsation, ionic mass transfer 8=49940
- mass transfer in aqueous systems, enhanced rates due to turbulence promoters 8=34792
- mass transfer in cylinder, kinetic theory 8=48109
- mass transfer in flow in porous channel, soln for large suction at walls 8=30214
- mass transfer in system of plane turbulent layers in presence of diffusion combustion 8=43666
- mass transfer rate through long tube connecting two reservoirs, with oscillatory flow 8=34811
- mass transfer pots., defined by contact with ret. body, and capillary pot., interconnection 8=39282
- mass transfer problems, appl. of method of relative conformity 8=23998
- mass transfer through liq. films in wavy motion 8=39327
- mass transport under oscillatory fluid flow conds. 8=30351
- membrane ternary systs. 8=25903
- membranes, and performance in tubular and flat plate equipment 8=48124
- metal alloys, dilute, impurity transport meas. using e-micoprobe 8=44380
- methanol, microscopic props., scatt. spectrocopy, use of atomic substitution techs. 8=30403
- Milne's problem with general anisotropic scatt., exact soln. 8=34072
- molecular flow in tubes with particle adsorpt. 8=47983
- molecular, irreversible thermodynamics 8=41792
- monoethanolamine, absorpt. of CO_2, study of mass transfer and interfacial turbulence 8=32093
- neutron, approx. soln. to eqns. in 2- and 3-dimens. system 8=47381
- neutron pulse in slabs and spheres, time decay constants 8=47376
- neutrons in plane lattice, asymptotic solns. and pulsed-n and n wave appl. 8=38576
- neutrons in water, thermal, energy dependent Milne problem 8=47382
- nonspherical mols., kinetic theory 8=39153
- one-dimensional, criticality characterization 8=46126
- one-speed multiregion, in plane geometry, boundary-sources method 8=33778
- organic semiconductors 8=40425
- plasma, equations 8=30018
- plasma, 2nd order contributions 8=43513
- plasma, streaming, e penetration of transverse mag. field 8=30022
- plasma, turbulent, transfer ooeffs. 8=30023
- plasma, weakly turbulent, electron coeff. viscosity in strong mag. field 8=43514
- p-n junctions, generalized field theory applied to forward conduction 8=35919
- polar gas mixtures 8=34644
- polystyrene sub-micron particles, electrical mobility 8=43888
- quantum corrections to time correl. functions 8=37187
- quantum theory, in strong magnetic fields 8=41794
- radiation and charged particles, Monte Carlo sampling appls. 8=32855
- separating tubes, initial transport determ. 8=43701
- silica-gel spheres, wet, drying by moisture transfer to dry particles in mixing 8=34978
- simulation by M.H.D. effects in electrolyte 8=41989
- single spheres and packed beds, heat and mass transfer with turbulent gas flow 8=30951
- from spheres, local thermal and mass. transport, rel. to turbulence and Reynold number 8=34985
- stagnation point, axisymmetric, boundary layer containing 4 inert species 8=43654
- in surface catalysis, rel. to characts of laminar boundary layers 8=36587
- thermal transport coeffs. in simple liquids, local equilib. model 8=25908
- thermodynamic, eqns. from least-dissipation principle 8=23906
- turbulent energy and scalar quantities, large wave numbers 8=34598
- turbulent scalar fields, diffusion approx. for spectral component transfer 8=47925
- two-group transport theory, eigen function expansion 8=33763
- van der Waals gas in critical region 8=30305
- Vlasov equation, validity for one-dimensional self-gravitating gas 8=50251

Transport processes—contd
- water/n-alkane interface, ideal gaseous behaviour of Na alkyl sulphates 8=30395
- withdrawal equations, direct evaluation 8=48090
- zero-temp. impurity resistivity, breakdown of conc. expansion 8=31306
- Ar-air props., 50° to 3500° K 8=25838
- Ar arc, energy balance with axial gas flow 8=43466
- Ar, electron mobility from laser interferometry of transient arc 8=39231
- Ar, mass transfer cooling effect in boundary layers of high vel. streams 8=32958
- Be, isotropic, neutron decay const. and diffusion length 8=38590
- $Bi_{12}GeO_{20}$, rel. to photo-induced carriers 8=27318
- CO_2 absorpt. into turbulent jets of water 8=30425
- CO_2-air props., 50° to 3500° K 8=25838
- Cs vapour, coeffs. calc. 8=30306
- $Cu_2|Fe(CN)_6|$ membranes, H_2O transport kinetics 8=48121
- Ga, liq., electrotransfer of Ag, temp. depend. 8=36597
- n-GaAs, high-field 8=27097
- p-Ge, crystal symmetry rel. to theory 8=26907
- H, electron mobility and diffusion 8=39238
- H, mass transfer cooling effect in boundary layers of high vel. streats 8=32958
- H_2 absorpt. into turbulent jets of water 8=30425
- He-air props., 50° to 3500° K 8=25838
- He, e back-scatt. in crossed elec. and mag. fields, obs. 8=39232
- He, mass transfer cooling effect in boundary layers of high vel. streams 8=32958
- He, partially ionized, at several press and temp to 35000°K 8=29968
- He^3 in liquid He^4, dilute mixture, transport coeffs. for degenerate Fermi system 8=41781
- He^3 soln. in He^4, Fermi-liq. coeffs. 8=37340
- He^3 soln. in superfluid He^4, phonon Boltzmann eqn. 8=41898
- He^3 and He^4, gaseous, at low temps., mutual consistency rel. to quantum effects 8=34671
- N, electron mobility and diffusion 8=39238
- N, mass transfer cooling effect in boundary layers of high vel. steams 8=32958
- Pb, liquid, mass-current fluctuations 8=25890
- $ZnBr_2$ molten, external transport numbers 8=34791

Trapped free radicals. See Free radicals.

Traps. See Crystal electron states; Crystal imperfections; Semiconductors.

Travelling wave tubes. See Electron tubes.

Triboelectric emission. See Electron emission.

Triboelectricity
- organic insulators and alkali halides, charge transfer by friction 8=27223
- Se surface, meas. of force of adhesion of insulating polymer particles 8=49045

Triboluminescence. See Luminescence.

Trions (He^3, H^3). See Alpha-particles and helium nuclei; Tritons.

Triple point. See Critical constants, thermal.

Tritium
- aqueous samples, scintillation counting efficiencies 8=28979
- assay of solns. using sealed standard 8=49999
- atmosphere, isotopic content in H_2, 1958 to 1963 obs. 8=27882
- atom reactions with solid propene and propane 8=27770
- counting, background rates, effects of vial, tests on glass and polythene 8=25014
- diffusion in Si 8=48346
- duoplasmatron negative ion source 8=46432
- fallout, from 1961/2 nuclear tests 8=32256
- in meteorites, cosmic ray produced 8=50428
- molecules first excited ${}^1\Sigma^+_g$ state rot. and vibr. levels calc. 8=38823
- monitoring system for DIDO and PLUTO reactor halls 8=29565
- organic compounds, H^3-labelled, free radical formation by autoradiolysis, e.s.r. study 8=47709
- problem, role of three-particle forces 8=25010
- recoil reactions in solid phase 8=45411
- scintillation detector 8=29224
- tracer for study of mass return flow of air to stratosphere 8=36725
- in water, ethane gas counting meas. and counter shielding 8=42474
- in water, toluene-Triton-water emulsion scintillator optimum comp. 8=42473
- in water vapour filled counter 8=42475
- in CH_4, atmospheric 8=27883

Tritium compounds. See Hydrogen compounds.

Tritons
  See also Nuclear reactions due to/tritons.
- binding energy calc. 8=25013
- bound state of three-nucleon system 8=33844
- $d + t \rightarrow \alpha + n$, single-level resonance formula 8=25007
- energy spectrum from $He^3(d, t)2p$ 8=43005
- form factors and interactions 8=42825
- hypertriton n-p tensor interactions from Λ-p scatt. 8=25012
- interaction with 14.4 MeV, study of outgoing p, d and T 8=42646

Tritons—contd
- n-t resonance interaction energy, $Be^9 + t \rightarrow n + t + Be^8$ obs. 8=29502
- optical potentials review 8=47338
- polarization meas. from t-He^4 scatt. 8=38102
- production in nuclear emulsion by high energy p and π beams 8=38099
- p-T interaction, review, spin-orbit effect negligible 8=29222
- p-T scatt., obs. 300-990 KeV 8=29185
- role in nuclear forces determ. 8=33863
- scattering, elastic, by O^{16} 8=25264
- simple model, calculations 8=38352
- t-d scatt., 76-660 MeV obs. 8=25007
- t-p scatt., 147-530 MeV obs., possible resonance 8=25007
- three-body photodisintegration 8=29223
- three-particle forces role in tritium problem 8=25010
- 3N system binding energy 8=38319
- tri-neutron, non-existence, obs. 8=38383
- variational calc. for ground state energy with trial functions 8=47227
- $C^{12}(Li^7, t)$ spectrum and angular distrib. rel. to α- and d-cluster transfer, 27.5 MeV 8=38524
- H^3 and He^3 e.m. and binding energy difference, rel. to charge asymmetry in n-n and p-p interacts. 8=24950
- H^3, binding energy and charge radii 8=33893
- H^3 n cross-sections angular depend. rel. to H^4 existence, 0.007-5 eV 8=29195
- H^3, velocity-dependent N-N pot. 8=25097
- $_{\Lambda}H^3$, lifetime determ. 8=38400
- $_{\Lambda}H^3$ lifetime obs. 8=25011
- $_{\Lambda}H^3 \rightarrow e^- + \bar{\nu} + He^3$, all e^- β-decay rate calc. 8=29351
- α-H^3 scatt., resonances obs. rel. to levels of Li^7 8=24937
- d-H^3 scatt., cross-section obs. 8=24937
- $d + H^3 \rightarrow \alpha + n$, cross-section obs. 8=24937
- p-H^3 scatt., no sharp structure 8=24937
- He^3-H^3 scatt., cross-section obs. 8=24937
- t-He^4 scatt., polarization meas. on He^4 8=38102
- $t(d, n)He^4$, n energy dispersion obs. rel. to accelerators 8=29220
- $Li^6(Li^7, t)$ spectrum and angular distrib. rel. to α- and d-cluster transfer, 27.5 MeV 8=38524
- $T(^3He, np)^4He$, final-state interactions 8=25020
- $T[p, p(\gamma)(n)]T, He^4, He^3$, diff. cross section extrema due to excited state of He^4, Feymann diag. 8=24914
- Zr^{90}, $E_t = 20$ MeV, inelastic scatt. obs. 8=43055

Troposphere. See Atmosphere.

Tungsten
- adhesion and friction, chemisorbed gases effects 8=49061
- adsorption of alkaline atoms, heat, bonds and ionization probab., quantum calc. 8=35199
- adsorption of Ba, search for substrate rearrangement 8=30777
- adsorption of CO on (110) plane 8=39627
- adsorption of CsF 8=48498
- adsorption of N_2 on (110) and (112) planes 8=39621
- adsorption of O_2, and effects associated with thermal desorpt. 8=39626
- adsorption of O_2 on (110) and (113) faces 8=39622
- adsorption of O_2 on (110), (211), (111) and (100) planes, field emission study 8=30778
- with adsorbed NH_3 on (100) surface, LEED obs. of electron impact effects 8=26140
- analysis of O content by He^3 irrad. 8=27818
- binding and field desorpt. of individual atoms 8=30775
- cathode with Mo substrate, in thermionic converter, post test anal. 8=28501
- chemisorption of N_2O, of both N and O atoms, rel. to temp. 8=36586
- cohesive energy of surface atoms, field evaporation, obs. 8=39503
- crystals, deformed in tension, slip line pattern and active systems 8=31091
- crystal, isothermal magnetocaloric oscills. 8=31514
- crystal (110) and (100) faces, oxide formation and desorpt. processes, mass-spectrometry 8=35198
- deformation mode, anomalous X-ray transmission exam. 8=26648
- deposition and chemisorption of H beams 8=49904
- desorption of adsorbed oxygen by e. impact 8=49901
- desorption of CO 8=48496
- desorption of CO by electron bombard. 8=48495
- desorption of Cs, Hg and O on coadsorbate interaction with low energy electrons 8=39623
- desorption of Ti in strong electric field 8=35197
- diffusion of C, mobility determ. from low temp. internal friction peaks 8=35513
- diffusion of Nb, electrochem. sectioning tech. to determ conc. profiles 8=48797
- electron emission, laser-induced, using ruby and Ar lasers 8=40710
- electron field emission rel. to thickness of Al_2O_3 film coating 8=27341
- electron irradiation and recovery 8=48934
- electron work function with various impurities 8=31461
- emitters in field emission microscope, K deposition, flicker noise and surface migration 8=44936
- emitter in thermionic converter, effect of etching to expose 110 planes on characts 8=28476

Tungsten—contd
- emitter, UO_2 fuelled in cylindrical thermionic converter, post test anal. 8=28500
- film on glass, ultrahigh-vacuum-evaporated, elec. conductance 8=40332
- flow stress, in presence of non-equilib. conc. of kinks 8=26850
- fractional order peaks in diffracted LEED beams, surface asymmetry mech. 8=26100
- grain boundaries, step structs. and heights 8=39728
- hardness and microhardness anisotropy of doped and undoped W 8=44607
- hot, dissociative chemisorption of CO 8=49893
- hot filament, mol. beam interact. rel. to pyrolysis 8=36577
- inert gas bombard., thermal desorption obs. 8=48497
- isochromat at 8kV 8=49761
- isochromat obs. at 8 kV 8=45227
- lamp astron. spectrophotometric standard 8=45667
- in liquid steel, conc. rel. to C activity 8=30458
- Nernst-Lindemann eqn. in range 24°-1800° C, validity 8=26590
- n-irradiated, stage III recovery 8=31157
- (110) face, struct. and work function of Li-O double film 8=39593
- (110) surface, damage due to Ne^+, Ar^+, Kr^+ or Xe^+ bombard., study by LEED 8=26104
- (110) surface, LEED exam. 8=48431
- (112) face, adsorpt. of O_2 and oxidation structs. 8=26107
- optical consts., reflectance meas. 537-5770Å 8=27591
- orientation when deposited from WF_6, rel. to temp. and annealing 8=35154
- permeation, diffusion and soln. of N 8=39987
- permeation of H 8=39986
- permeation rates and coeffs. of N_2, 1800° to 2600°C 8=44394
- photoelectric γ cross-section determ. 50-208 keV 8=36004
- powder, absolute atomic scattering factors 8=48681
- pyrometry, photoelec., effective wavelength change calc. 8=32979
- residual resistivity, varying C content 8=26974
- screw dislocation, field-ion microscope exam. 8=31089
- secondary electron emission, variation depend. on electron absorpt. 8=40715
- secondary emission, shot noise fluctuations 8=44949
- shear modulus freq. and temp. dependence (0.0004-20 cps, 1400-2000°K) 8=35723
- single crystal, ion max, range, temp. dependence 8=48932
- sintered, brittle fracture nucleation at low temp. 8=44608
- specific heat, 1300-3000°K, modified modulation method 8=48732
- sputtering by Ar^+ ions, mechanism 8=35606
- stacking faults, ion microscope investigation 8=35580
- stress-strain curves, and dislocation structures 8=44455
- substrate for Pt films, work function and adsorp. of Cs 8=35178
- superconducting magnetic field curve rel. to low temp. CMN scale 8=37331
- surface, appearance of Na, K impurities, 20-700°C 8=35549
- surface, chemisorption of water 8=27739
- surface diffusion, activation energy elec. field dependence, (10^7-10^8V/cm), 1200-2100°K 8=35512
- surfaces, energy anal. of back-scattered electrons rel. to structs. 8=30730
- surface migration, from field-emission studies 8=27343
- surface, Na atom ionization coeff. absolute meas. 8=31476
- temperature meas. by photoelec. pyrometer 8=24021
- thermal emittance of small cavities in surface, rel. to temp. 8=26611
- thermal rearrangement of O_2-covered surface 8=31464
- thermionic emission in Ba and Cs atom flux 8=36048
- thin film, resistivity, ion-bombardment induced changes 8=49151
- vapour-deposited emitter with (110) preferred orientation, bare and caesiated work function 8=28477
- wetting by Cs and Na, rel. to bare work function 8=35168
- whisker-formation on W by chloromethane adsorption using field-emission micro. 8=26272
- wires, exploding in vacuum, undegassed and degassed, X-ray emission and discharge currents 8=40294
- work function and desorpt. energies of O_2, thermionic meas. 8=31469
- C contaminated, (110) face metastable struct., obs. 8=39583
- CO adsorpt. on (100) and (211) faces, work function 8=35200
- CO adsorption, electron bombard. effect 8=30776
- Cs adsorpt. and work function, theory comp. with expt. 8=31466
- Cs coated, work function 8=36038
- Cs-covered, thermal rad. during thermionic electron emission 8=31465
- Cs^+ emission from 50-75μ dia. hole in (110) face 8=49446
- NH_3 adsorption and decomp; field-emission meas. 8=27734
- ThO_2 inclusions, e microscopy 8=44173
- U on substrate work function, effect of H contamination 8=49437
- W^{183}, Mossbauer effect following Coulomb excitation with protons 8=47262

Tungsten—contd
W neutron dosimeters 8=47162
W-Ta thermocouple, potentials 0°-420°C 8=28418
αW–βW–WO$_2$ mixture, quantititive X-ray anal., calibration problems 8=35288
Xe^{133} ions, 40 keV, depth distrib. 8=48935
Zr adsorption and nucleation, α and β phases, obs. 8=39625
Tungsten compounds
binary tungstates, new group 8=39526
carbonyl complex, (CO)$_5$WCO. CH$_3$. C$_6$H$_5$, crystal structure 8=26446
lubrication at high temp. by exposure to H$_2$S and film form. 8=31219
oxidic tungstates, cryst. struct. effect on luminesc. 8=45284
K$_4$W(CN)$_8$. 2H$_2$O, mol. struct. 8=43317
V$_2$O$_5$–P$_2$O$_5$–WO$_3$ system glasses, elec. conduction mechanism from e.p.r. 8=40291
W complex halides, electron spectra 8=38857
WC cemented cutting tools, surface protection by Ti$_2$O$_3$ 8=48428
WC powder and WC-Co mixed powder, sintering effect of 15-45 kbar pressure 8=39536
WC and W$_2$C, indexing of field-ion micrograph using computer 8=44174
W–C system, phase equilibrium in cubic carbide phase 8=48410
WC-Co alloys, fracture rel. to plastic deformation and microstructure 8=26851
WC-Co alloys, particle deformation under load, cracks and recovery processes 8=44606
WC-Co alloys, transverse-rupture strength increase on porosity strenth 8=49062
WC-Co hard metals, electropolish thinning for transmission e microscopy 8=36608
WC–Co hard metals, thin foils, microstructure 8=35287
W-C-Co system alloys, cracks around Vickers hardness indentation, lapping time effects 8=49063
W(CN)$_8^{4-}$, spectra and struct. 8=41118
W(CO)$_6$, thermal decomposition kinetics 8=45350
WC-TiC-TaC-10%Co, properties rel. to C content 8=30657
WCl$_6$, mols. vibr. modes assignment, obs. 8=38859
WCl$_6$, solid state spectrum 8=38857
W-Cr solid soln., decomposition from X-ray diffr. study 8=26086
WF$_6$, electron diffr. and molec. struct. 8=38858
WF$_6$, i.r. spectra and force fields 8=25519
W-Mo alloys, secondary electron emission 8=27360
W-Mo alloys, spectral emissivity 8=45228
W-Mo alloy, sputtering by Ar$^+$ ions, mechanism 8=35606
W-Mo-Re alloys, structural and surface props. from field emission and ion microscopy 8=39727
WO$_2$, distorted rutile, metal-metal bonding 8=48305
W–Re alloys, dislocation structs. rel. to stress-strain curves 8=44455
WS$_2$, irrad. in nuclear reactor, electrical props. 8=49143
WSe$_2$, band model calcs. 8=49105
W-3% Ta alloy, dislocation structs. rel. to stress-strain curves 8=44455
W-Ta alloys, secondary electron emission 8=27360
Tuning forks. See Vibrating bodies.
Tunnel diodes. See Semiconducting devices/tunnel diodes.
Turbidimetry. See Chemical analysis.
Turbidity. See Scattering/light; Suspensions.
Turbulence
See also Cavitation; Flow; Vortices.
acoustic boundary layer, response of flush-mounted transducers 8=37261
in air flow in pipe, effect of Prandtl number on temp. profiles for heat transfer 8=30367
in air flow through annuli with small cores, rel. to heat transfer 8=34647
air flow, wall pressure, orifice hot-wire probe 8=28225
air mixture motion in pipes 8=39176
in atmosphere below turbopause, stratification of processes 8=36839
atmosphere, clear air, optical remote sensing 8=50121
atmosphere, rel. to optical propagation 8=27912
atmospheric, island wake, energy dissipation obs. 8=36730
axisymmetric wake slender body, Mach 3 obs. 8=30254
boundary layer development in compressible flow, prediction 8=30220
boundary layers, external region universal properties 8=34599
boundary layer on plate in incompressible liquid with mass injection 8=39271
boundary-layer pressure fluctuations, nondimensional form 8=39273
boundary-layer separation 8=30227
boundary transition, sharp cones at hypersonic speeds, obs. 8=30221
condensation of moving vapour stream on fluid jet 8=30598
conducting sub-layer, flow near smooth wall 8=43642
convected scalar field, straining of small-spatial-scale amplitude vars. 8=30232
in convection from vertical plate, mean. temp. distribs. and mean vel. in boundary layer 8=32965
convective heat transfer during turbulent flow of elec. cond liq. in channel, alt. mag. field effect 8=41994
Turbulence—contd
cylinder in flow, steady laminar forced convection at low Reynolds numbers 8=30231
distortion by irrotational plane strain 8=39169
effect on local transport, mass and thermal, from spheres 8=34985
energy and scalar quantities, transfer, large wave numbers 8=34598
equations, fluid flow 8=47923
ethyleneglycol aqueous soln., effect of Prandtl number on temp. profiles for heat transfer 8=30367
flow between parallel planes 8=34597
flow in concentric annuli 8=39178
flow in concentric annuli, heat transfer and boundary layer at entrance 8=34834
flow in pipes, velocity distribution expression and eddy diffusivity profile 8=47927
flow, mathematical model for deposition from 8=34586
flow, mol. transport processes accel. 8=34719
flow, Rayleigh shear 8=30219
in flow through concentric annuli, anal. of heat transfer 8=34595
in flow through concentric annuli, comments and reply 8=25810-11
w. r. t. fluctuations in light wave propag., for meas. of temp. field inhomogeneities 8=35710
fluid boundary layer, incompressible with mass addition, press. fluctuations 8=30230
fluid, circular flow in annular channels between rot. coax. cylinders, turbulence 8=30225
fluid curved mixing layer, energy budgets, spectral const. and Reynolds number 8=34596
fluid, numerically calc. heat flux rel. to supercritical transition 8=32951
fluid pipe Poiseuille flow, linear azimuthally periodic disturbances 8=43627
fluid with time depend. temp. profile, convection onset rel. to boundary conditions 8=34593
free flows, equilib. state of finite disturbance 8=39161
free surface dispersion coefficients by particle simulation method 8=39165
gas agitation of liquids 8=48029
gas density fluctuations, wake of hypersonic sphere 8=30264
in gas flow in entrance region, heat transfer and wall friction for varying props. 8=39201
gas freestream boundary layer transition 8=30269
gas flow in nozzles, effects of flow-acceleration on heat transfer 8=25808
gases, in channel of circular cross-section, obs. 8=34607
gas, isotropic, spectrum 8=43665
gas, mass transfer rel. to conc. of nondiffusing species 8=47978
heat and mass transfer in system of plane turbulent layers in presence of diffusion combustion 8=43666
heat exchange, nonstationary, in tube when heat flux and gas flow rate change 8=47961
heat transfer in drag reducing fluids 8=46233
homogeneous, isotropic, turbulent flow, probability dist. of velocity difference at two distinct points 8=47924
hydraulic resist. coeffs. calc., channels of non-circular cross-section 8=25800
incompressible, fine-grained, viscoelastic props. 8=43643
initial in fluid flow, effects on optimal suction from boundary layer onto porous plate 8=30256
jet axis, shape in unbounded horizontal cross flows 8=39167
laminar-turbulent transitions 8=47922
laser beam phase fluctuations, effect upon 8=42058
limiting dynamic and thermal layers, determ. of conditions 8=25798
limiting layers with temperature gradient at wall 8=25793
liquid flow, boundary layer momentum equation, solutions, analysis. 8=48030
liquid, flow in annular plane channels 8=30365
liquid flow in channel of rectangular section, velocity field calc. 8=48028
liquid with constant density, field probability distributions 8=48031
mass transfer in flat duct, effect of diffusion on surface reaction rate 8=36548
magnetospheric particle flux 8=36784
MHD boundary with longitudinal press. gradient 8=24193
MHD flow in channel, velocity profile 8=46461
m. h. d., numerical expt. with incompressible eqns. 8=33116
mean flow irrotational far from boundaries, vorticity expulsion 8=45622
in monoethanolamine absorpt. of CO$_2$, interfacial turbulence 8=32093
motion of separation, numerical experiment 8=47928
neat transfer by free convection from vertical plate 8=41869
non-homogeneous, theory 8=25799
non-Newtonian fluids, stability of parallel flows 8=48009
in pipe, rel. to aerodynamic sound generation 8=39186
in pipes, damping by longit. and transverse mag. fields 8=24194
plasma boundary layer, electron conc. calc. 8=30024

Turbulence—contd
- plasma, heating by mag. field annihilation 8=34467
- plasma, mirror confined, heating by axially driven current 8=43561
- plasma, non-uniform, instability 8=34554
- plasma, quasilinear theory including microscopic fluctuation fields and coherent waves 8=43512
- plasma, transfer coeffs. 8=30023
- in polymer solns., dilute, flow, onset of drag reduction, molec. approach 8=30368
- reactor rod bundles, parallel-flow-turbulent-flow mixing, model 8=34068
- relativistic, of incompressible fluids, mean flow equations 8=34594
- Reynolds stress meas., single hot wire anemometer 8=47926
- satellite in F region, electron-ion collision effect on wake structure 8=34443
- scalar fields, diffusion approx. for transfer of spectral components 8=47925
- scale distrib. in channels formed by closely packed rods, for liq. flow 8=34720
- shear-flow, drag reduction 8=30364
- solar-wind plasma, Mariner 2 obs. 8=45889
- in sphere wake, initially heated, vel. and temp. fluctuations 8=34701
- stagnation point forward of circular cylinder, wake induced effects 8=43717
- Stoke's fluids, linear and non-linear, differences, and characts in plane-parallel channel 8=30228
- stratosphere over Minicoy Island, obs. 8=45445
- strongly turbulent Lorentz gas in mag. field, mobility tensor 8=30039
- in submerged jets, initial rel. to averaged vel. and vel. fluctuations 8=30223
- thermal instability of water near 4°C 8=48010
- thin liq. boundary layer with blowing, thermal state 8=43728
- transducer for pressure meas. 8=28226
- velocity meas. from Doppler shift in laser scatt. 8=39272
- of viscous plastic fluids with small plastic additives, reduction of viscosity 8=30436
- in wake regimes for flow behind hypersonic bodies 8=34633
- wall-pressure fluctuations on body of revolution 8=39274
- in water pipe flow, near wall, rel. to fluctuations in heat transfer rates 8=34830
- water, swirling, in vertical and inclined tubes 8=30366
- Wiener–Hermite expansion use for nearly normal turbulence 8=30226
- wind interaction with severely convective clouds 8=27893
- Hg, liq, temp. profiles effect of superimposed free convection 8=34836
- NaK eutectic, temp. profiles effect of superimposed free convection 8=34836
- Pr number of gas stream rel. to friction and heat transfer coeffs for immersed plate 8=30255

Turbulent flow. See Flow.

Twilight
- See also Atmospheric spectra; Zodiacal light.
- spectrometry, press. scanned Fabry-Perot 8=32568
- N_2^+ atm. emission, tropospheric scatt. model. 8=41365
- O atomic spectrum obs., atmospheric 8=27949

Twinning. See Crystals, twinning.

Twistors. See Calculating apparatus; Magnetic devices.

Ultracentrifuges. See Centrifuges.

Ultrasonics
- See also separate headings, e.g. Absorption.
- acoustic imaging by holography 8=37273
- acoustical holograms, ultrasound camera system for viewing 8=37276
- amplifier using ZnO cryst. as amp. medium, construction and relative gain 8=26586
- cavitation cell for liquids 8=34722
- cavitation, relaxation phenomena appl. 8=37278
- devices, study of suitable dielec. mats rel. to low-loss optical transmission 8=27229
- Doppler vel. monitor for meas. of vocal fold motion 8=32923
- flowmeter, dual-frequency 8=47911
- glass, strain-optic coeffs. determ. 8=41138
- high-temp. meas. of elastic moduli, buffer-rod technique 8=40096
- holographic image convertor for image visualisation in opaque media 8=28374
- hypersonic waves in solids, measurement of damping by Brillouin scattering 8=49686
- interferometry of thin film growth 8=44031
- internal stress meas. in solids 8=31163
- laser beam diffraction use in optical correlator 8=28751
- laser emissive power meas. with ultrasonic device 8=46534
- light beam, Gaussian, theory of diffraction by ultrasonic waves 8=24417
- light diffraction and polarization in solids 8=36302
- light diffraction by short acoustic pulses 8=24418
- light diffraction, gas, approx. formula 8=34662

Ultrasonics—contd
- liquid, h.p. absorpt., meas. method and error analysis 8=48137
- low-noise u.h.f. preamplifier for ultrasonics 8=41909
- phase transition in liquid crystals of polymesomorphic type. 8=34770
- powders, u.s. micromesh sifting 8=35066
- probes using shear wave crystals, principles 8=46195
- pulse-echo apparatus, tests 8=37281
- pulse-echo instrumentation, 0.2-2.0 GHz 8=32914
- radiation field, finite amp, of focusing spherical source in water 8=43804
- rarefied flow, excitation and gas temps. 8=30257
- shear waves in molten glass, high-temp. interferometry 8=39280
- solidification profiles with ultrasonic pulses 8=39477
- spectroscopy of defective materials 8=23964
- speech sound 8=41849
- 10 GHz phonons, method of excitation in quartz 8=48723
- transducers, power limitations of sonic cyrstals 8=46181
- u.s. field effect on heat transfer in flash boiling system 8=25994
- u.v. source, gas jet with e beam excitation 8=38660
- vibrations in supercooled liq., effect on dynamic nucleation 8=48261
- wave modulation of Gaussian light beam, Fourier series 8=37630
- wax dielec. props., effects 8=27258
- CdS, light demodulator with u.s. amplification 8=27216
- Cu, grain growth, enhancement 8=26247
- Ni film, ultrasound from stripe domain resonance 8=31682
- Ni, influence on Barkhausen jumps 8=36163

Ultraviolet detectors. See Radiation detectors.

Ultraviolet sources. See Light sources

Umklapp process. See Crystals/lattice mechanics.

Uncertainty. See Indeterminacy; Probability.

Undor. See Electron theory; Field theory, quantum.

Unified field theory. See Relativity/unified field theories.

Unimolecular layers. See Adsorbed layers.

Units
- See also Constants; Dimensions; Nomenclature and symbols.
- angular velocity, fallacious definition of hertz 8=37107
- e.m. theory conventions and nomenclature 8=24121
- frequency and angular velocity, relationships 8=37108
- Gauss and international system, relationship 8=37105
- relationship, misuse of dimensional method 8=37106

Upper atmosphere. See Atmosphere/upper; Ionosphere.

Uranium
- See also Nuclear fission/uranium.
- abundance, with K and Th, in peridotite inclusions in basalts 8=50012
- anomalous thermal arrest within β phase, origin rel. to cryst. struct. 8=35129
- deformation twinning in α-phase Bravais lattice, modes table 8=44090
- doped CaF_2, diffusion of Ar, Kr and Xe 8=26618
- doped CaF_2, inert gas diffusion mechanism 8=26619
- elastic moduli and phase transition at $T < 43^\circ K$ 8=40185
- enrichment on commercial basis 8=47399
- fallout particles, in rainwater and soil, activity 8=41373
- fuel materials in heavy water reactor calc. of k-infinity coeff. 8=47427
- growth and elec. resistivity changes by thermal n-irrad. at 4.6°K 8=48933
- migration, decay products in minerals 8=48796
- in minerals, fission fragment tracks made visible by chemical etching 8=32185
- ore, direct determ. by natural γ logging, new log 8=32184
- photoelectric cross sections in 80-150 keV range, calcs. 8=44912
- positron annihilation, single-quantum, cross sections 8=44670
- in river sediments, conc. and Th/U isotope ratio 8=50094
- solubility in UO_2, phase boundary for temps. down to 1210°C 8=30712
- thermal diffusivity, 20° to 850°C laser pulse method 8=39952
- Al-coated, parametric study rel. to max. corrosion protection 8=49844
- with SF_6, fission product decontamination 8=43128
- in ThO_2, diffusion, lattice and grain-boundary, obs. 8=35507
- in ThO_2-UO_2 solid soln., diffusion, lattice and grain-boundary, obs. 8=35507
- U^{233}, amine extraction from irrad. ThO_2 8=36634
- U^{233} in soln, array of bottles determ. of neutron criticality condition 8=47398
- U^{233} resistivity, low-temp., α self-irrad. effects, obs. 8=31322
- $U^{234,236}$ Auger effect, L_2-subshell yield obs. 8=38715
- U^{235} in irrad. samples, non-destructive assay, Pb spectrometer 8=36650
- $U^{235,238}$ in natural U, Fabry-Perot spectrometer, meas. 8=28803
- $U^{235/238}$ isotopic ratio determ. by γ spectrometry 8=47546
- U^{253}-depleted U^{238}-Np^{237} fission foil n personnel by dosimeter 8=33795

Uranium—contd
- U-mica foil neutron dosimeter 8=33794
- U^{3+} in CaF_2, ions in sites of tetragonal symmetry direct one-phonon spin-lattice relaxation times 8=40938
- U^{3+} in CaF_2, spin-lattice interactions in uniaxially stressed crystal, e.s.r. obs. 8=40939
- U^{4+}, in CaF_2, u.s. paramag. resonance rel. to multiple phonon interactions 8=31853
- α-U, filamentary superconductivity, impurity effects 8=49202
- α-U, irrad. swelling rel. to solid fission prods. segregation 8=44507
- α-U, phase transition at 4.2°K, obs. 8=39567
- α-U, stacking faults and extended dislocations in (110) and (001) planes, theory 8=31102
- α-U, thermal expansion behaviour at low temp. 8=48747
- α-U, thermal expansion below 10°K 8=39932
- 1.03 wt % U^{235} - D_2O lattices, reactor physics params., obs. 8=38585
- U-H_2O subcritical assembly, meas. of buckling by improved 'flux-shape' method 8=34103
- U-UAs phase diagram 8=48406
- in UO_{2+x}, cations self-diffusion, α-spectrometry obs. 8=35510
- U/UO_2 system, melting point, meas. of solidus and liquidus temp. 8=30581
- on W. work function, effect of H contamination 8=49437
- in $ZrSiO_4$, e microprobe meas. 8=27811

Uranium compounds
- alloy, electrodes, measured conductance rel. to measured capacitance and Faradaic current 8=49929
- alloys, dilute, α-phase grain refinement by B addition, obs. 8=44171
- chalcogenides, ferromag. props. explanatory model 8=36179
- carbides, C^{13} Knight shift 8=41004
- with V elements, antiferromag. props. explanatory model 8=36179
- fluorescence of U-activated cpds with rocksalt lattice and codopant quenching 8=49808
- intermetallic (with Si, Fe, Mn, Al) oxidation kinetics, resistance and rate 8=27721
- oxides, hyperstoichiometric, Young's modulus and internal friction, at room temp. 8=35722
- oxides, phase limits 8=48292
- Sicral F_1, irrad. swelling rel. to fission gas bubbles, 10^{14} n/cm^2 sec 8=44506
- Sicral F_2, irrad. swelling rel. to fission gas bubbles, 10^{14} n/cm^2 sec 8=44506
- uranyl cpds., classification of e states by absorpt. spectra 8=34880
- uranyl cpds., electron vibration analysis and interpretation 8=49758
- uranyl cpds., fluorescence and oscillator model 8=34286
- uranyl cpds., U-O bond distance calc. from i.r. spectra 8=34287
- uranyl nitrates, complexed, luminesc. spectrum struct. rel. to anion and cation vibrs., 77°K 8=36514
- uranyl salts, fluoresc. decay rel. to temp., obs. 8=45288
- CaF_2 doped with UO_2, UC or U, inert gas diffusion 8=34107
- with SF_6, fission product decontamination 8=43128
- U-1.5%Mo, phase transform. by rapid cooling from γ-phase, mechanism 8=35130
- UAs, antiferromag., magnetic ordering from n. diffr. study 8=40878
- UC, Ar-sintered, effects of Ni on structure 8=26299
- UC, grain boundary grooving rel. to surface energy 8=30871
- UC, irrad. at 77°K, density var. during annealing, obs. 8=44605
- UC, prep. by carbothermic reduction of U oxides 8=27720
- UC, UO_2 films growth rel. to O diffusion, 60-160°C 8=39604
- $UC_{1-x}N_x$, in N_2 gas, change of comp. 8=35063
- $UC_{1-x}O_x$, heat of formation and heat capacity 8=30970
- UC_xO_y, C- and O-deficient, lattice parameter obs. 8=35541
- $U_{20}C_3Si_{16}$, structural refinement 8=44261
- UC-UN system liquidus and solidus, obs. 8=32083
- UCl_3 soln. in molten NaCl, partial v.p. obs. 8=30456
- UCl_6^{2-}, vibr. spectra 8=47619
- UCl_4-$PbCl_4$ phase diagram, thermal analysis obs. 8=30584
- UF_4, 2.5H_2O, rhombic, and dehydration products, X-ray diffr. obs. 8=30870
- UF_6, electron diffr. and molec. struct. 8=38858
- UF_6 gas chromatography, −10°C-40°C 8=49981
- UF_6, in HF chem. laser 8=46590
- $UFeO_4$, crystal structure from neutron diffraction 8=26443
- U-H system, pressure-composition-temp. diagrams 8=30713
- UH_3, n.m.r. 8=49660
- U-Ir system, phase diagram 8=35133
- U_6M, (M = Mn, Fe, Co, Ni) and alloys, superconductivity rel. to ferromagnetism 8=27036
- U-Mo 1.1 alloy, irrad. swelling rel. to fission gas bubbles, 10^{14} n/cm^2 sec 8=44506
- U-Mo-Al-Sn, irrad. swelling rel. to fission gas bubbles, 10^{14} n/cm^2 sec 8=44506
- UN, oxidation and deformation studies by e-micros. 8=27718
- UN, prep. and fabrication, rel. to nuclear fuels 8=27722

Uranium compounds—contd
- UN, prep. from UCl_4 + Al + N_2, two-step reactions 8=36574
- UN-C system equilib. rel. to UN compacts prep., obs. 8=32083
- U(NH)Cl, crys. structure 8=48680
- UO_2, antiferromagnetic, structure 8=49574
- UO_2, columnar grain growth under steep thermal grads 8=26301
- UO_2, critical surface tension in oxidizing and reducing atmos., comparison and theory 8=30729
- UO_2, density var. during annealing rel. to fission damage recomb., obs. 8=44605
- UO_2, distillation from uranyl nitrate-TBP soln. 8=47413
- UO_2, enthalpy as function of temp. to 3100°K 8=35436
- UO_2, equiaxed grain growth, influencing factors 8=26300
- UO_2 etching by HNO_3 rel. to cryst. orientation, 1-37 molar 8=30818
- UO_2, films growth on UC rel. to O diffusion, 60-160°C 8=39604
- UO_2 fuel element, axial void form. rel. to radial temp. gradient 8=43144
- UO_2 fuel rods, release of fission gases 8=34108
- UO_2 fuelled W emitter in thermionic converter, post test anal. 8=28500
- UO_2, high temp. enthalpy and heat of fusion 8=39902
- UO_2, LEED from surface steps 8=48429
- UO_2, limits for equation of state 8=30572
- UO_2, magnetic exchange interactions, orbital effects 8=31544
- UO_2, mag. excitations temp. dependence 8=31802
- UO_2, migration of Kr bubbles, before and after annealing 8=26625
- UO_2, n-irradiated, crystal struct. using X-ray counter diffractometer 8=44260
- UO_2 pellets fluorination to UF_6 by Fl, kinetics and chemisorpt. 8=32104
- UO_2 powder, n-irradiated, electronic props. from e.m.f. meas. 8=40290
- UO_2, powders oxidation in storage rel. to fabrication and irrad. props. 8=45349
- UO_2, relax. peaks in internal friction spectrum, rel. to O interstitial reorient 8=35545
- UO_2, sintered, diffusion and release of Xe, from 400°~800°C 8=26624
- UO_2, sintered, high temp. thermal cond. 8=44370
- UO_2 sintering, Dorn method in study of initial phase 8=35068
- UO_2, solubility of U and phase boundary for temps. down to 1210°C 8=30712
- UO_2, surface diffusivity of U ions, 1544°-1915°C obs. 8=35511
- UO_2 surfaces, low-energy electron diffr. 8=48430
- UO_2, thermal cond. rel. to temp. gradient depend., obs. 8=44369
- UO_2 u.s. attenuation and elastic constants, 4.2-300°K 8=49898
- UO_2, with Gd_2O_3 dispersions, behaviour at high temp. 8=35074
- UO_{2+x}, U^{233} cations self-diffusion, α-spectrometry obs. 8=35510
- UO_2^{2+} excitation in β-diketone + N-containing organic bases triple complexes by intramol. energy transfer, obs. 8=34288
- UO_2^{2+}, photo-induced absorpt. in glass, solns., and in spinel 8=27610
- UO_2^{2+}, spectrum in aq. perchlorate resolution of u.v. bands 8=39382
- UO_2-Al_2O_3, grain growth in presence of liq. phase 8=44014
- UO_2-CeO_2, thermal diffusion 8=48776
- UO_2-H_2O lattice n temp. rel. to activation ratios 8=47418
- $UO_2(NO_3)_2$ in diluent + TBPP/ImHNO$_3$, interfacial tension and partition coeff. 8=34804
- $UO_2(NO_3)_2$ water solns. in presence of $Na_4P_4O_{12}$ photoluminescence 8=25943
- UO_2^{+2}:Nd^{+3} laser glass, Ce-stabilized 8=28710
- $UO_2(OAc)_2$. 2Ph_3AsO and $[UO(OAc)_2.Ph_3AsO]_3$; (Ac = acetate, Ph = phenyl), crystal structure 8=44259
- UO_2-TaB_2 fuel, heated in steam, reactions 8=27717
- UO_2/U system, melting point, meas. of solidus and liquidus temp. 8=30581
- UO_2-WB_2 fuel, heated in steam, reactions 8=27717
- U_3O_8, antiferromag. struct. study of neutron diffraction 8=31801
- U_3O_8 layers, prep. by h. v. electrophoresis 8=26130
- α-U_3O_8, thermoelec. power meas. rel. to semicond. props. 8=35999
- U_4O_9, structural changes rel. to temp. 8=26083
- $U^{235}O_2F_2$ aqueous soln., minimum critical thickness of water-refl. infinite slab 8=34052
- $UO_2(NO_3)_2$-polyethylene mixtures, minimum critical U^{235} enrichment, obs. 8=34053
- UP, prep. and fabrication, rel. to nuclear fuels 8=27722
- UP-ThP and UP_2-ThP_2 solid solns, antiferromagnetic 8=45067
- U-Pu monocarbides ceramics, fabrication 8=30664
- U/10% Pu/10% Fz, annealing rel. to changes in structure, hardness and elastic modulus 8=30711

Uranium compounds—contd
$(U, Pu)O_2$ solid soln. production and Pu distribution 8=29562
$(U, Pu)O_{2-x}$, thermal cond. and diffusivity rel. to comp., 50–2000°C 8=35464
U-Rh system, phase diagram 8=35132
U-Ru system, phase diagram 8=35131
U_2Si fuel elements, swelling during burnup reduced by provision of central void 8=47429
US crystals, precip. from e-microscope exam. 8=35286
US, electrical conductivity and thermoelec. power
US, low-temp. oxidation, comp. with US-ZrS solid soln. 8=27719
US, prep. and fabrication, rel. to nueclear fuels 8=27722
US, slip behaviour from e-microscope exam. 8=35285
US–ThS system, mag. props. 8=49545
US-ZrS, low-temp. oxidation, comp. with US 8=27719
$(U_{1-x}Th_x)O_2$, susceptibility temp. dependence and transitions 8=31803
U_2Ti, phase transformations, irradiation induced 8=35134
$U–UAl_2–UCo_2$ system, phase diagrams 8=35128
U-UAs phase diagram 8=48406
Urey–Bradley forces. See Molecules/internal machines.

V-centres. See Colour centres.
V-particles. See Hyperons; Mesons.
Vacancies. See Crystal imperfections/vacancies.
Vacancy breakdown. See Diffusion in solids.
Vacuum apparatus
See also Glass–metal seals
ball-and-socket valve, compact version 8=43711
cement for high-temp. substrate bonding 8=48005
ceramic-to-metal seals, graded, fabrication by isostatic gas, bonding 8=34692
cermet seal with high strength and thermal cond., of $Nb-Al_2O_3$ powder between Nb slabs 8=28499
charcoal adsorbent cooled with liquid N_2 8=43710
connector, elastic for use in cryogenics 8=48003
cryogenic chamber, parameters calc. by Monte Carlo method 8=30340
feedthrough for rotational and translational motion 8=30339
high-vacuum metrology, achievements 8=48000
isolation valve 8=48007
insulators, residual gas heat transfer at low temp. 8=25823
ion trap coupled to rotating pump 8=39246
joints, high-temperature, with vacuum cement 8=48002
lead-through for 1 μtorr systems 8=43714
mask changer for thin film deposition 8=30338
metrology, apparatus and methods 8=39253
micromanipulator for simultaneous feeding of gas and electricity 8=48006
motor with airflow cooling 8=34690
for plasma source, consisting of ion source, neutralizing chamber 8=30180
pressure control device 8=48004
residual gas analysis, methods and equipment 8=41297
sample holder, high-temp. for Kratky camera 8=34688
for student practical work 8=30324
systems for ultra-high vacuum work. 8=47989
ultra-high vacuum prod. and meas. 8=39256
valve for cryostat appl. 8=34689
valve for shock tube 8=32900
X-ray spectrometer for fine struct. and chem. analysis 8=41305
Ni-Fe-Ni strip, gas emission rel. to thermal and chem. treatment 8=39254
Sb distillation, with graphite lining 8=28204
Vacuum gauges
Bayard-Alpert, ambient temp. influence 8=39251
Bayard-Alpert modification, short collector 8=39252
Bayard-Alpert modulated, comparison with extractor 8=25839
Bayard-Alpert, X-radiation residual current 8=34685
calibration and related problems 8=30328
calibration, design of precision system 8=30330
calibration by McLeod gauge method 8=30329
calibration by pulsed gas flow technique 8=30331
calibration, mobile apparatus 8=43713
calibration of vacuum gauges and related problems, conference, Teddington, England (1967) 8=30336
calibration vessel, variation of molecular impact rate 8=30333
combined leak detector and high sensitivity vac. gauge 8=30337
interferrometric differential manometer 8=39249
ionization, calibration and collation apparatus 8=47998
ionization, pressure readout system 8=43712
ionization, radio-isotope, 10^{-5} — 760 torr 8=47997
JG ionization gauge, increased sensitivity due to e oscills. 8=30335
McLeod, capillary depression obs. 8=25840
Mcleod for condensible and non-condensible gas pressure meas. 8=39248
Vacuum gauges —contd
McLeod, Hg-vapour pumping errors 8=30332
McLeod, standardization 8=39250
metrology, apparatus and methods 8=39253
orbitron gauge with stable ion current charact. 8=34686
Penning, response to neutral He, N_2 and Ar pulses 8=30334
Philips ionization gauge, discharge mech. 8=38979
radiometer, photophoretic and thermal forces relationship 8=24011
ultra-high vacuum prod. and meas. 8=39256
vacuum chamber, extension of Greening's theory 8=47999
Vacuum polarization. See Quantum electrodynamics.
Vacuum pumps
adsorptive, for low temp. serial mass spectrometer evacuation 8=38608
cryopump for u. h. v., description 8=30326
cryopump system, fast, for ultra-high vac. 8=47992
cryopumping, theory 8=39247
diffusion pumping theory. 8=47993
French development, mechanical and diffusion pumps pumps 8=39244
ionic sorption, leak detection appl. 8=39260
ionic sorption, residual gas analysis in ultra-high vacuum system 8=36630
oil diffusion, backstreaming meas. by cooled quartz crystal microbalance 8=39243
oil-free, for e microscope 8=34684
Penning discharge getter-ion, improvement 8=34683
rotating, with ion trap 8=39246
sorption, fast, for 10-150 mtorr 8=30327
sputter-ion, economical powering 8=34682
triode ion, for deuterium, voltage reduction for thermal stability 8=30325
ultra-high vacuum prod. and meas. 8=39256
vapour pumping using cooled condensers 8=47994
Ar pumping, ionic sorption 8=39245
H and D, condensation pumping on to liq-He -cooled surface 8=30593
Vacuum technique
adsorption of air with activated charcoal, ultimate attainable vacuum 8=47988
alkali metals, liquid, surface tension obs. 8=25897
alumina ceramic chambers for e accelerator 8=34693
ceramic chamber for p synchrotron 8=34696
chamber for high radiation environment 8=34694
coaxial h.v. bakeable seal 8=48008
colloquium; Warsaw, June 1966 8=47991
condensing spark production 8=29921
cryopumping, theory 8=39247
emission e microscope 8=28570
flange joint, remotely welded and removable 8=34697
gas analysis, equipment and limitations 8=43715
glass dielectrics for microcircuits, deposition of 8=44895
high-temperature vacuum-tight joints using vacuum cement 8=48002
high-vacuum metrology, achievements 8=48000
leak detection apparatus 8=39258
leak detector analysis cells 8=39259
materials, radiation and thermal behaviour rel. to synchrotron application 8=37822
metal seal gasket 8=48001
metal surface cleanness, industrial aspects 8=39572
metrology, apparatus and methods 8=39253
micromanipulator for gas-fed apparatus 8=48006
oil or Hg detection on surfaces in vac. systems using ellipsometer 8=39255
partial press. of residual gases, for various means of pumping out 8=39242
particle accelerators and storage rings, developments 8=34695
pressure 10^{-8} torr., physical principles 8=30323
production and meas. for tube manufacture 8=39257
quartz-metal tube jointing 8=34687
ultra-high vacua, below 10^{-9} torr. 8=47989
ultra-high vacuum prod. and meas. 8=39256
valve, greaseless, for mercury reservoir 8=34691
GaAs thin film prep. 8=27354
H_2 gas jet trapping 8=43645
Kr^{85} leak test for tubes 8=47990
P diffusion in Si, method using $POCl_3$ as source 8=48792
Sb, distillation 8=28204
Si single-crystal films, moving mask growth on amorphous quartz substrates 8=26126
Ti foils, self-supporting, evaporation method 8=39601
Vacuum tubes. See Electron tubes
Valence bands. See Crystal electron states.
Valency
translawrencium elements, SCF calcs. 8=47513
B_2O_3, X-ray emission band of B, valency electron structure 8=29716
C-H valence oscills. in vinyl ether 8=30493
C=O valence oscills. in vinyl ether 8=30493
Ce ions in oxide solid solns., from X-ray absorpt. spectra 8=39638
Valves, thermionic. See Electron tubes.
Vanadium
b.c.c. lattices, energy of interstition of impurity atoms into octahedral and tetragonal positions 8=35542

Vanadium—contd
  chemisorption of alcohols, aldehydes, ketones and oxides surface species formed, i.r. spectra 8=45363
  corrosion, influence of Ca content in Na 8=27723
  Compton scattering 8=41149
  diffusion in Al and Ni, coeffs. 8=35476
  diffusion in Nb, Zr and V, coeffs. 8=35475
  diffusion of V, coeffs. 8=35475
  e.p.r. in $CaWO_4$ 8=31855
  Hall effect, type II superconductor 8=40392
  lattice params. and thermal expansion rel. to para-antiferromag. transition, −180-1500°C 8=44253
  lattice vib. curves and phonon spectra 8=26576
  in liquid steel, conc. rel. to C activity 8=30458
  sorption and chemisorpt. of O, isotherm-isobar kinetics 8=36584
  superconducting, anomalous magnetic behaviour 8=27383
  superconducting, and Nb in mixed state, nonlinear resistivity and dissipation 8=27027
  in AgCl, optical absorpt. and ionic cond. meas. on V ions 8=35523
  in Au_4V, moment from Mössbauer effect meas. 8=26016
  V II, spectra in excited configurations, theory 8=43203
  V^{51} in V_3Sn, nuclear spin relaxation, temp. depend. obs. 8=40970
  V^{51}, quadrupole coupling in KVO_3 8=31923
  V^{2+} in α-Al_2O_3, trigonal splittings stress dependence 8=43929
  V^{2+}, in CaO, uniaxial stress meas. at impurities, strain coeffs. 8=40134
  V^{3+} in Al_2O_3, Jahn–Teller effect in $^3T_{2g}$ state, Zeeman study 8=43965
  V^{3+} in Al_2O_3, resonance at mm. wavelength and in intense field 8=49599
  V^{4+} in TiO_2, ENDOR 8=41007
  V : Fe^{57}, f number and isomer shift pressure dependence 8=48321
Vanadium compounds
  carbides formation during $\gamma \rightarrow \alpha$ transform. of austenite in steel 2062 8=35135
  hydride, β-phase, p.m.r. 8=40986
  steel, diffraction pattern, isothermal transformation 8=39791
  transition-metal alloys, elec. cond. anomalies 8=44699
  vicalloy, domain structure in various structural states strained in tension 8=40804
  vicalloy strip, mag. props., thermomechanical treatment effects 8=36135
  CaV_2O_6, microscopic props. 8=30798
  $Ca_2V_2O_7$, microscopic props. 8=30798
  $Ca_3V_2O_8$, microscopic props. 8=30798
  $M_xV_2O_5$ bronzes, homogeneity range rel. to charge and ionic radius of inserted element 8=26444
  Ti-V alloys, self-diffusion comp.-temp. dependence 8=26623
  VAu_4, mag. props. effect of at. environment, correction to paper 8=31513
  V-C system, chem. diffusion and phase equilibria above 1900°C 8=36575
  $VC_x (0.75 < x < 0.88)$, n.m.r. line shape of V^{51} 8=45133
  VC_{1-x} with non-stoichiometric vacancies lattice structure determ. 8=30913
  V_6C_5, ordered cpd., structure 8=44172
  VC–ZrC(HfC) systems, phase diagrams 8=48409
  VCl_4, e.s.r., Jahn-Teller distortion 8=49619
  VFe alloys, 3d-electron redistrib. from X-ray spectra 8=35780
  V-Ga alloys, Knight shift of V^{51} and Ga^{71} 8=41006
  V–Ga system, phase diagram 8=48407
  V_2Ga_5, phase transforms. from structural, thermal and resistivity meas. 200-800°C 8=39566
  $V_{17}Ge_{31}$, crystal structure 8=39782
  VH_x, vibr. spectra in three cryst. phases by neutron scatt. 8=39878
  VMn alloy, spectra, rel. to band structure 8=41115
  V–Ni alloys, metastable b.c.c. phases formed on quenching 8=48408
  VO, electronic phase transitions 8=26084
  VO ground state nuclear hyperfine interactions 8=25522
  VO thin film single crystals, epitaxial growth, electrical resistivity 8=48470
  VO^{2+}, e.p.r. linewidths in NH_4Cl cryst. 8=45103
  VO^{2+} in soln., n.m.r. and e.p.r. line-broadening 8=39419
  VO_2 crystal, reflection spectra rel. to semiconductor metal transition 8=41150
  VO_2 crystal, resistivity anisotropy 8=40292
  VO_2, electrical and mag. props. 8=40293
  VO_2, electronic phase transitions 8=26084
  VO_2 on alumina substrates, rel. to device fabrication 8=30758
  VO_2, opt. props. between 0.25 and 5eV in semiconducting and metallic states 8=49760
  VO_2 oxidation in molten $VO_{2.5}$ soln., obs. 8=27724
  VO_2 sputtered films, transport props. 8=27138
  $VO_{2.5}$, molten, thermal dissoc., obs. 8=27724
  V_2O_3, electronic phase transitions 8=26084
  V_2O_3, mag. susceptibilities 8=31534
  V_2O_3, neutron-diffraction data, rel. to mag. phase 8=31800
Vanadium compounds—contd
  V_2O_4 anodic films growth in acetic acid-$Na_2B_4O_7$ solns., obs. 8=45375
  V_2O_5, carrier e.s.r. spectrum rel. to localized states 8=40947
  V_2O_5-containing-glasses, small polaron as charge carrier 8=40499
  V_2O_5 magnetic susceptibility meas. and calcs. 8=36083
  V_2O_5-P_4O_{10} semicond. glasses, effect of n and γ irrad. on elec. cond. 8=27137
  V_2O_5-P_2O_5-(La_2O_3, Nd_2O_3 or CeO_2) glasses, i.r. transmission 8=36425
  V_2O_5–P_2O_5–WO_3 system glasses, elec. conduction mechanism from e.p.r. 8=40291
  $VOSO_4 \cdot 5H_2O$, polarized absorpt. spectra of polymorphs 8=49759
  V_5Sb_4, at. structure rel. to quasi-homologs 8=35360
  V_3Si, β-tungsten phase, high-transition-temp. superconductor, props. 8=40376
  V_3Si, lattice softening, rel. to phase transformations 8=31107
  V_3Si, paramagnetic, absence of n. scattering rel. to d electrons in conduction band 8=40754
  V_3Si, phase transition near supercond. temp., obs. 8=39567
  V_3Si, sublattice distortion, search 8=26445
  V_3Si, superconducting, martensitic phase transform., e-microscope study 8=26085
  V_3Si, superconductivity dependence on lattice instability 8=27037
  V_3Si, tetragonal-cubic low-temp. transition rel. to density states effect at Fermi surface 8=39568
  V_3Sn, type II superconductor, spin-relaxation of V^{51}, temp. depend. obs 8=40970
  V-10wt.% Ti alloy, corrosion, influence of Ca content in Na 8=27723
  V-Ti alloys, type II superconductors, spin lattice relaxation 8=44744
  V-Ti, type II superconductor, spin-lattice relaxation 8=41005
  Va-Ti alloys as reactor fuel jackets, corrosion by flowing Na 8=47430
Van Allen radiation. See Atmosphere/radiation belts.
Van de Graaff generators. See High voltage production; Particle accelerators/linear.
van der Waals forces. See Atoms; Kinetic theory; Molecules/intermolecular mechanics; Solids.
Vaporization
    See also Boiling; Condensation; Distillation; Evaporation; Heat of vaporization; Vapour pressure.
  C_v discontinuity across liquid-vapour coexistence curve near critical point 8=25988
  gas of known conc. in air, dynamic prod. 8=34994
  laser radiation action 8=48288
  radiation-heated vapours steady state motion 8=48291
  sample vaporization system for mass spectrometer 8=47451
  spectrochemical samples in carbon arc 8=41237
  water aerosol in optical radiation field 8=30564
  As 8=39497
  BaO, vapour species 8=30606
  BeO-BeF_2 system at high temp., mass spectra 8=35012
  Bi-Se system, cryst. and amorphous, ionic and neutral species in vapour 8=35007
  Cm_2O_3, high temp. stability 8=35425
  Cs-O system products, mass spectrometric obs. 8=32096
  LaS 8=48287
  NaCl single crystals, effect of dislocations on rate 8=35008
  P_3N_5 8=43413
  PbF_2, mass spectra 8=38933
  $PbZrO_3$-TiO_3 ceramics, PbO deficiency rel. to piezoelectric props. 8=35010
  $Pb(Zr_{0.65}Ti_{0.35})O_3$, cold-pressed, thermogravimetric determ. in vacuo, 690-1130°C 8=35009
  $Pb(Zr_{0.65}Ti_{0.35})O_3$, hot pressed pellets of near theoretical density 8=43919
  Se, cryst. and amorphous, laser induced, study of ionic and neutral species 8=35006
  Se, partial press. of $Se_2(g)$ 8=48285
  SnF_2, mass spectra 8=38933
  Ti oxides, from liq. phase 8=30603
  Tm_2O_3, high temp. stability 8=35425
  YbC_2 8=43920
Vapour density. See Density/gases.
Vapour pressure
    See also Humidity; Vaporization.
  acetone, near crit. pt. 8=34956
  alkaline earth metals, thermodynamic parameters 8=40699
  benzene, near crit. pt. 8=34956
  chloroform, near crit. pt. 8=34956
  dry air, 34°-64°K 8=35004
  ethanol-n-decanol mixtures 8=48284
  ferromagnetic binary alloy, temp. dependence rel. to mag. and structural transitions 8=35014
  ice, isotope effects 8=39491
  liquids, isotopic differences, appl. of significant struct. theory 8=43755

Vapour pressure—contd
- methanol-n-decanol mixtures 8=48284
- trifluoromethylphosphonylchloride 8=34330
- void fraction in subcooled boiling 8=35000
- water, isotope effects 8=39491
- Ag, liquid, 1450° to 1600°C 8=43918
- Ag, over Cu-Ag-Au liq. ternary alloy rel. to electron cell model 8=26002
- $AlBr_3$, molten, to crit. pt. 8=43895
- AlF_3, by entrainment method 8=30607
- BaO 8=30606
- CH_4 and CD_4 8=30588-9
- COF_2 8=30573
- Ca_3N_2 8=48295
- of Cs, above Cs-graphite lamella cpds, rel. to compound transitions 8=35011
- Cs saturated, obs. 8=30604
- D_2O-C_2H_5OD mixture, isotope effect 8=48283
- He-3, in mag. field, press. increase, 3°K and 40-80 kOe 8=28433
- He^3, thermomolec. press. between ambient temp. and region 1-0.32°K 8=28438
- H_2O-C_2H_5OH mixture, isotope effect 8=48283
- KOH-ZnO electrolytes, 100-140°C 8=45373
- LaF_3, and entropies and enthalpies in range 1050°-1200°C 8=35015
- $NiCl_2$, $NiBr_2$ and NiI_2, anhydrous solids 8=39496
- SbSI grown from gaseous phase, of volatile components, effect on elec. props. 8=36026
- SbSeI grown from gaseous phase, of volatile components, effect on elec. props. 8=35989
- ScF_3, and entropies and enthalpies in range 1050°-1200°C 8=35015
- XeF_2 and XeF_4 8=39492
- YF_3, and entropies and enthalpies in range 1050°-1200°C 8=35015

Vapour pressure measurement
- solid-vapour, entrainment method 8=30607

Variable stars. See Stars.

Variational calculus. See Mathematics.

Variational method. See Quantum theory/application methods.

Vavilov–Cherenkov radiation. See Cherenkov radiation.

Vectons(vector mesons). See Mesons.

Vectors
- Poynting e.m., calculation 8=41943
- rotation of rigid body, geometrical representation 8=32700

Velocity
- electrodynamics, non-linear, ray diagram 8=46397
- gas near solid surface, thermal slip, gas-kinetic analysis 8=39175
- simple waves, for nonlinear eqn., upper boundary 8=37236
- **acoustic waves**
  - See also Dispersion, acoustic; Helium/liquid, sound propagation; Shock waves.
  - azoxybenzenes, liq. cryst. 8=25882
  - faster than light in ultradense matter 8=45598
  - in ferromagnetic dielectric, change due to magnon-phonon interaction 8=30937
  - in gas/solid particle suspension, from distrib. of small disturbances 8=39455
  - lattice vibration, rel. to isotopic mass 8=35375
  - liquid metal, calc. 8=43803
  - in liquids, modification of diffusivity eqn. 8=25900
  - in metals, liquid 8=25911
  - n-nonane, meas. by saturation line 8=39361
  - poly(ethylene terephthalate) fibres, rel. to amorphous orientation and crystallinity, obs. 8=44175
  - Sofar, Pacific contours 8=50105
  - solids, meas. for anisotropy detect. 8=30938
  - triethylamine in water, hypersound, dispersion near critical stratification point 8=48143
  - in water, distilled, temp. dependence 8=43805
  - CdS, rel. to drift field intensity, obs. 8=39889
  - Ne liquid, 24.6 to 27°K, Debye-Sears meas. 8=25913
- **acoustic waves, ultrasonic**
  - See also Dispersion, acoustic/ultrasonic.
  - adepic acid and carbazole, molten, var. with temp. 8=30470
  - aniline solns. 8=30469
  - anthracene, molten, var. with temp. 8=30470
  - in binary liquid mixtures 8=25998
  - chloroacetic acid and chloral hydrate, molten, var. with temp. 8=30470
  - cyclohexanol, delay time meas. by phase comparison method 8=44314
  - EDTA, Ba chelate form. study 8=25914
  - ethane-Ar mixtures, vel. dispersion interferometry 8=47966
  - gas mixture, with molecular masses largely different 8=43690
  - gases, "rot. relax." time, origin of temp. depend 8=39209
  - glycerol, press. depend. 8=34841
  - by interferometer of constant length, freq. dependence of corrections 8=41843
  - liquid and saturated vapours near critical point, intersection of surves 8=43802
  - nitroanilines in ortho, meta and para states, molten, var. with temp. 8=30470
  - nitrobenzene-n-hexane mixtures near critical region 8=25912

Velocity—contd
- **acoustic waves, ultrasonic**—contd
  - quartz, phase vel., rel. to piezoelectricity 8=48724
  - silica, molten, and adiabatic compressibility 8=48140
  - succinonitrile, in plastic phase 8=44611
  - surface roughness effect on calc. 8=37277
    - Ar, liq., high press. 8=48138
  - Ar, temp. and pressure dependence 8=25828
  - CdS, delay time meas. by phase comparison method 8=44314
  - CoO, rel. to elastic and mag. props., 8=44560
  - Cu single crystal, low index surface phase vels. 8=30944
  - GaP, calc. from u.s. phase-comparison meas., of elastic constants 8=49021
  - He^3, liquid, h.f. sound vel., X-ray scatt. obs. 8=32999
  - KBr:Li^+, and attenuation, temp. and stress dependence, 1.6–77°K 8=35417
  - KCl, effect of Li^+ and CN^- doping 8=44316
  - KCl:Li^+, and attenuation, temp. and stress dependence, 1.6–77°K 8=35417
  - K_2HPO_3 aqueous soln., rel. to lattice energy 8=25880
  - Li salt solns. at 1 MHz, obs. 8=43806
  - Li-NH_3 soln., adiabatic compressibility calc. 8=30468
  - NaCl, delay time meas. by phase comparison method 8=44314
  - $PbCl_2$, meas., rel. to elastic consts. calc. 8=35712
  - Te crystal, rel. to elastic constants determ. 8=35719
- **light**
  - extinction/re-emission analysis rel. to Fizeau expt. 8=33242
  - slower than sound in ultradense matter 8=45598
  - variable, scalar gravitation theories 8=46086

Velocity analysis, particles. See Particle velocity analysis.

Velocity measurement
- See also Angular velocity measurement; Stroboscopes.
- fluid, tracer-particle laser application 8=41623
- gas stream fluctuations, thermoelec. method 8=39177
- heat transfer methods 8=34591
- ions in air, time-of-flight method 8=43474
- laser Doppler velocimeter 8=37553
- Mössbauer spectrometer, calibration, interferometric method 8=37927
- plasma components, in homopolar, profile 8=30086
- projectile, impacted, optical Doppler method 8=41622
- transducer, e.m. with air suspension 8=28222
- turbulence, from Doppler shift in laser scatt. 8=39272
- water flow, low vel. meter 8=34717
- Y-T recorder for linear air track 8=28256
- **acoustic waves**
  - detonation, piezoelec. coaxial transducer pin method 8=41836
  - by u.s. stroboscope, and dispersion in liqs. 8=28373
- **acoustic waves, ultrasonic**
  - ethane-Ar mixtures, vel. dispersion interferometry 8=47966
  - pulse transmission time methods 8=37279
- **light**
  - Michelson microwave interferometry, multiple-refl. correction 8=42017

Venus. See Planets.

Verdet constant. See Magneto-optical effects.

Verneuil process. See Crystals/growth.

Vertex functions. See Elementary particles; Field theory, quantum; Functions.

Vibrating bodies
- See also Crystals/lattice mechanics; Elastic waves; Pendulums; Piezoelectric oscillations.
- anisotropic layer of finite thickness, dispersion curves of phase vels 8=23925
- bandsaw blades, lateral vibr. parametric excitation 8=23924
- beam, compressed, oscillation freq. calc. 8=45140
- beams, extremal fundamental freqs. 8=41812
- beams, nonlinear vibrs., with various boundary conditions 8=23844
- bridge, cantilever, natural freq. parameter calc. 8=32880
- cantilevered bars, instability modes, induced by fluid flow through attached pipe 8=37239
- circular plates, stiffened, flexural vibs. rel. to rotatory inertia 8=41808
- clamped cylindrical shells, natural freqs for various mode shapes 8=32869
- composite structs. with shear walls, nat. freqs, mode shapes and response quantities 8=32885
- conical and cylindrical shells, parameters for impedance analysis 8=23922
- crystal, piezoelec., discontinuously plated, forced thickness-shear vibrs. 8=37250
- cylinder, hollow, bonded to thin shell, axial shear vibrations 8=32876
- cylinder, hollow, bonded to thin shell, elastic vibrations 8=32875
- cylindrical, far field rel. to radiation impedance 8=37257
- cylindrical shell, ring-stiffened, vibrational analysis 8=32873
- damped system chatter minimization 8=23929
- dynamic response of one-degree-of-freedom system, effects of hysteretic damping 8=32870
- elastic circular rings, internal constraints calc. 8=23930

Vibrating bodies—contd
electrode for quartz resonator, optimum size and shape 8=37246
Fitzgerald resonances, rel. to particle-wave theory 8=46176
flight vehicle components, static/dynamic load interactions 8=32872
free-layer damping, effectiveness of polymer blend 8=32874
mass acting on vib. surface, frictional viscosity effect 8=32695
membrane, circular, variable density, calc. 8=28358
moving band, torsion 8=23931
one-zone model for non-radial pulsation of stars 8=45688
piston in nonrigid baffle, radiation impedance 8=23921
plastic structures, free vibrations 8=28263
plate, circular with parabolic thickness var., axisymmetric vibr. 8=46139
plate, dyn. response to transverse force 8=46142
plate, elastic, stability rel. to surface tension 8=26748
plate, rectangular finite elements for analysis 8=32879
plate stiffening, acoustic excitation expts. 8=32871
pulley belts, bandsaw blades, lateral vibr. parametric excitation 8=23924
quartz plates, plano-convex, modes 8=46141
response of system to displacement excitation at a support 8=23926
rigid-plastic annular plate under dynamic loads, deflections 8=41811
rotatory vibration of a composite orthotropic circular cylinder 8=41807
shear modulus meas., analysis 8=41810
shells, sandwich cylindrical, non-symmetric inextensional vibs. 8=46137
spinning cylinder, finite radial oscillations 8=37244/5
spinning disc, stationary waves 8=23937
surfaces during rubbing, normal and tangential vibrations 8=32884
structural member, flexural-torsional freq. spectrum 8=28359
thick discs and rods, resonant freq. corrections 8=37243
$NH_4H_2AsO_4$(ADA) resonator plate, low temp. coeff., props. 8=27299

Vibration, molecular. See Molecules/vibration.

Vibrations
See also Acoustics; Damping; Oscillations; Vibrating bodies; Waves.
anisotropic layer of finite thickness, natural vibs. dispersion curves of phase vels. 8=23925
annular plate, free lateral vibs. rel. to initial static torque 8=41809
beam, elastic, closed form soln. for transverse vibrations 8=41678
of beams, nonlinear, with various boundary conditions 8=23844
building, earthquake-resistant design, elastic analyses 8=28361
in capillary-porous mats., influence on rate of drying 8=30591
circular membrane, composite, transverse 8=32881
circular plate of concentric rings of different materials, forced vibration 8=41805
circular plate with attached mass, spring and dashpot 8=32882
in clamped cylindrical shells, natural freqs for various mode shapes 8=32869
continuous systems with point discontinuities, solution 8=32867
corundum particle bed, rel. to fluidizing and heat transfer 8=39448
cylindrical shells with orthogonal discrete element stiffeners 8=23920
crystal, infinite piezoelec. plate, wave propag. theory 8=46144
earth, spheroidal vibs., elementary theory 8=50091
of elastic half-space, torsional damped due to radial stress distrib. 8=28262
electron bubble in liq. He, freq. estimate 8=37346
flexural, of stiffened circular plates, rel. to rotatory inertia 8=41808
fluid coupling, vibration damping, quantitative analysis 8=25788
foam plastics, characts. 8=44514
linear chain, monatomic containing impurity, long-range interactions 8=23872
linear damped system with periodically varying rigidity 8=32865
metal thin sheet, simple and constrained acoustic damping layers, loss factor obs. 8=35612
in micropolar elastic solids, with radial and axial symmetries 8=32893
non-linear, systems with many degrees of freedom 8=28356
non symmetric inextensional, in sandwich cylindrical shells 8=46137
plastic rate-sensitive structs., pulse-loaded 8=41806
plate, analysis using rectangular finite elements 8=32879
in plate, effect on heat transfer to air by free convection 8=34646

Vibrations—contd
quartz crystal, u.s. X-ray topography 8=48722
radial, of cylindrical inhomogeneous annulus of aeolotropic materials 8=32716
random, of coupled system, power flow and energy distrib. 8=37242
residuals treatment 8=32863
shell, cylindrical, forced axi-symmetric motions 8=32715
steady-state, in non-linear systems, stability investig. 8=41802
string, influence of imperfect boundaries 8=23923
subharmonic oscillations, 3rd order, initial conditions for obs. 8=32866
surface modes, obs. by stroboscopic hologram interferometry 8=32883
at surfaces during rubbing, normal and tangential components 8=32884
system in impulsive-noise environment, reliability prediction 8=37234
thermally induced, in sandwich plates 8=46072
torsional and flexural systems, receptances due to displacement excitation at a support 8=23926
torsional, use of calculating tables 8=46138
under parametric excitation, oscs of 'summed and differential types', characts 8=32877
Cu and Ge, resonant, dislocation line 8=35563

excitation
bandsaw blades, lateral parametric, theory 8=23924
coupled systems subjected to determinate and random input 8=37240
gas, nonlinear in resonant tube, press. amplitude 8=30266
linear systems, by impulsive noise, response-peak prediction 8=37235
pulley belts, lateral parametric, theory 8=23924
road vehicle, response to profile 8=28360
self-excited, in axially symmetric shell of finite length subjected to internal supersonic flow 8=32864
wire, longitudinal, due to thermal shock by current pulse 8=40088
$LiNbO_3$, elastic, 20-2000 Mc/s 8=44584

measurement
See also Seismology.
amplitude-phase characteristics, contactless meas. 8=46135
bar, deflection microwave interferometry 8=37238
basic vibrometric methods and means 8=46134
displacement rel. to light wavelength, interferometry 8=28357
mechanical, piezoelectric probe 8=32868
Moire-band method for high-amplitude vibrations 8=46136
plastic model, dynamic response, comparison with prototype 8=37237
stroboscopic holographic analysis 8=23919
surface, hand-held dynamic strain gauge 8=41804

Vibronic states. See Molecules/electronic structure; Molecules/vibration

Vidicons. See Electron tubes.

Virial coefficients. See Equations of state.

Virtuons (virtual phonons). See Crystals/lattice mechanics.

Viscoelasticity
See also Plasticity.
anisotropic linear solids, restrictions on relax moduli 8=41719
behaviour, non-linear integral representation 8=41735
biological soft tissues, discrete models 8=45924
butadiene-styrene block copolymer 8=40194
coagulation structures, solid-like, thixotropically hardened, viscosity 8=40090
composite medium, wedge-like waves 8=37159
concrete, response in creep characts. stress anal. 8=44536
creep and relaxation very early-time props. 8=32773
deformation properties of material, mathematical description 8=41731
dissipation function for thermomech. processes in viscoelastic bodies 8=46066
disturbance in visco-elastic slab due to transient torsional forces 8=32769
disturbances produced in viscoelastic medium by impulsive torsional body forces 8=46150
drag reduction in turbulent flow, viscoelastic model and its appln. 8=48093
film, liquid, flowing down inclined plane, stability 8=43745
flow in multiply connected regions 8=32772
flow through porous media, multiphase 8=39270
flows, dimensional considerations 8=47915
fluid, elastico-viscous, static stability 8=43616
fluid, plane parallel Couette flow, linear instability 8=47909
fluid, secondary flow due to rot. oscills. of sphere 8=39155
fluids, stability against shear waves of steady flows 8=43635
gelatin-glycerol system, isochronal temp. -conc. diagram 8=44618
glass-plastic body, deformation under plane-problem conditions 8=49023
half-space, linear, impact of rigid sphere, numerical soln. and comparison with expt. 8=41736

Viscoelasticity—contd
- linear mats., crack initiation rel. to loading history 8=31178
- linear media, eqns. of three-dimens. deform. 8=28275
- linear theory 8=46067
- liquids, elastico-viscous linear, elastic props. and viscosity, theory 8=25841
- liquid, magnetostrictive meas. 20-100 kHz 8=30429
- liquids, stability in parallel flows, used hereditary stress/strain law 8=43720
- lubricating oils, and component fractions, relax. spectra 8=34698
- media, thermodynamics and waves 8=41734
- medium, sound absorpt. effect on Brillouin scatt. 8=32912
- micropolar materials, hereditary, linear theory 8=41708
- nonlinear class of constitutive equations of rate-type 8=32771
- nonlinear, short-time approx. 8=41733
- poly-α-methylstyrene, stress relax. 8=40198
- 1, 2-polybutadiene, rel. to rubber and synthetic elastomers, 5-50°C 8=44613
- polyethylene at high pressure 8=40189
- polyethylene, non-linear behaviour 8=40195
- polyisobutylene, v. dil. solns. 8=39329
- polymer solns., rel. to inter- and intra-molec. interacts. 8=34700
- polymers, homogeneous submicrocavitation fatigue processes 8=31181
- polymers, linear amorphous, rel. to fracture theory 8=31249
- properties of fine-grained incompressible turbulence 8=43643
- relaxation in supercooled liqs. 8=30430
- rheological behaviour, elasticity determ. from tangential stress meas. 8=48099
- semi-infinite visco-elastic bar, disturbances in mag. field 8=23854
- semilinear mats in bar form., wave propag. after longit. impact 8=32886
- solid sphere, axisymmetric wave propag. 8=26750
- stability of initially imperfect, nonlinearly viscoelastic column 8=41729
- styrene-butadiene copolymers in soln. 8=25891
- tensile stresses in rapidly deforming materials 8=30376
- thin plate, impact of rigid sphere, resulting eqns. of motion 8=23853
- thin-walled tube with temp. depend. props, thermal stresses 8=23855
- three dimensional linear mechanical model 8=46065
- tube, flexible, containing viscous liq., acoustic wave propag. 8=48136
- viscoplastic fluid stability, analogy with Grad fluid stability 8=47905
- viscoplastic rod, impact on rigid obstacle, heat conduction equation 8=46241
- waves, non-homogeneous bars, propagation 8=28363
- Weissenberg effect, mechanical model 8=28276
- 0.3 wt % Na-CMC aqueous soln., rel. to inter- and intra-molec. interacts. 8=34700
- in Se, P admixture effect 8=31230

Viscometers
- air turbine, concentric-cylinder apparatus 8=43777
- canal type, anal. for Bingham plastic surface flow 8=30343
- Couette-type, air bearing description 8=30313
- Couette-type, magnetically anisotropic rotor driven by rotating mag. field 8=30435
- falling cylinder, effect of eccentricity 8=39335
- gas, absolute, low-temp. h. p. design 8=34674
- jet orifices, liq. Poiseuille flow rel. to geometrical shape determ. 8=30362
- magnetostrictive, for liq. viscoelasticity 20-100 kHz 8=30429
- oscillating-disc, for gases to temp. of 500°C, atmos. press. 8=43706
- parallel-disc, inertia effects for second-order fluid, anal. and interpret. of results 8=25842
- remote-control, for compressed electrolytes 8=34793
- rheometer, audio-frequency 8=34797
- rotational, relax. meas. on non-Newtonian liq. 8=34800
- skin friction meas. with thin film gauges 8=39236

Viscoplasticity. See Plasticity.

Viscosity
- adsorbed layer of polymer, thickness determ. 8=39620
- amorphous polymers, molec. ordering obs. 8=39633
- dissipation in Poiseuille flow, effects on steady conjugated heat transfer 8=30253
- 2-dodecylaminoethanol salts, study of micellar props. effect of counterions 8=39290
- drag on motion of magnetically anisotropic crystal in rotating mag. field 8=30435
- falling cylinder viscosimeter, verification of eccentricity effects on terminal velocity 8=48091
- Fermi liquid, calc. 8=41778
- fluid containing small particles 8=39443
- fluid, non-homogeneous, rel. oscillations 8=47931
- fluids, dissipative function model 8=32754
- fluids, non-Newtonian viscous, radial flow between discs 8=39160

Viscosity—contd
- fluids, vertical motion of spherical particles 8=47921
- flux-flow in type II supercond. rel. to local temp. gradient 8=26997
- glass fibres with and without concentric glass casings 8=39631
- macromolecular solns., normal stress difference meas. 8=25893
- nonlinear singular boundary value problem in viscous fluid theory, analytical solution 8=47918
- organic glasses used as trapping matrices 8=49065
- plasma, Debye-Hückel, shear viscosity 8=39080
- plasma, toroidal, rel. to stationary equilibrium 8=30119
- plasma, weakly turbulent, electron coefficient in strong mag. field 8=43514
- polyisobutylene in cyclohexane and benzene, conc. effects, obs. 8=30427
- polymer chain, viscosity, excluded volume effect 8=34788
- polymer mols., theory with hydrodynamic interaction and excluded vol. 8=47737
- polystyrene in good and theta solvents, conc. effects, obs. 8=30427
- rotational, irreversible statistical thermodynamics 8=47917
- from seismic wave attenuation obs., dynamic viscosity calc. 8=27830
- solar-wind plasma, Mariner 2 obs. 8=45889
- styrene-methyl methacrylate copolymer in good and theta solvents, conc. effects, obs. 8=30427
- surface, stearic acid reaction with Ca^{2+} ions at air/water interface 8=41264
- volume viscosity of simple fluids, relax. times 8=30194
- B_2O_3, viscous relaxation and non-Arrhenious behaviour 8=34802
- C_{16}-OH monomol. films surface viscosity rel. to phase transitions, 15-30°C 8=30428
- C_{18}-OH monomol. films surface viscosity rel. to phase transitions, 15-30°C 8=30428
- C_{20}-OH monomol. films surface viscosity rel. to phase transitions, 15-30°C 8=30428
- C_{22}-OH monomol. films surface viscosity rel. to phase transitions, 15-30°C 8=30428
- Fe, molten, by oscillating crucible method 8=34798
- Ni-Si alloys, temp. dependence rel. to bonding 8=34796

gases
- acetylene 8=25835
- air, dynamic viscosity, meas, statistical-mech. correls. 8=43704
- ammonia-nitrogen 30°-200°C below 10cm Hg press: Chapman-Enskog theory 8=43702
- atmosphere, variable, rel. to vertical sound propag. 8=32258
- benzene 8=25835
- free fall in a rarified atmosphere 8=28257
- friction at plate immersed in gas stream, influence of turbulent Pr number 8=30255
- inert gases, dynamic viscosity meas, statistical-mech correls. 8=43704
- kinetic theory, shock wave structure, ultrasonic propag. 8=34602
- mixtures, rarefied nonreacting, temp. dependence 8=30286
- monatomic gas, represented by relaxation theory 8=30297
- nonpolar mixtures, calc. at ordinary pressures 8=47981
- polar-nonpolar gas mixtures, 30°-200°C, below 10cm Hg press: Chapman-Enskog theory 8=43702
- quadrupolar gases and vapours 8=25835
- radiation coupled viscous flow, soln. for stagnation region and flat plate 8=39204
- resistance to spherical particle 8=34673
- shear, near critical point, anomalous due to large density fluctuation 8=30291
- shearing flow past flat plate, heat transfer coeffs. 8=34651
- sulphur dioxide-hydrogen 30°-200°C below 10cm Hg press: Chapman-Enskog theory 8=43702
- ternary mixtures, constancy of dynamic viscosities 8=25836
- turbulent boundary layers, with arbitrary press. gradients 8=25834
- viscometer, absolute, low-temp. h. p. design 8=34674
- Ar, 114°-374°K 8=39237
- Ar, supersonic beam, low-temp. cross-sections 8=30311
- CO_2 8=25835
- CO_2, dynamic viscosity, meas. statistical-mech. correls. 8=43704
- CS_2 8=25835
- Cs, partial ionization effect in temp. range 1000° to 2400°K 8=30310
- Cs vapour, 1000 to 10 000°K and 10^{-5} to 10 atm 8=30312
- H with const. density, 16.6-300°K 8=43703
- He^3 and He^4, rel. to low temp. transport props. mutual consistency 8=34671
- Kr, 114°-374°K 8=39237
- N_2, dynamic viscosity meas, statistical-mech. correls. 8=43704
- N_2, low-temp. 8=39237
- Xe, 114°-374°K 8=39237

liquids
- See also Lubrication; Superfluidity.
- amyl and isoamyl alcohol, temp. derivatives 8=34803

Viscosity—contd
  liquids—contd
    with Arrhenium temp. depend., influence of molec. rotation 8=30426
    batch mixing of viscous liqs.with rotating agitators, model studies 8=30437
    binary mixtures, comp. depend 8=34795
    n-butyl alcohol, temp. derivatives 8=34803
    cellulose solns. rel. to -I and -II acetylation, obs. 8=45325
    cellulose sulphoester solns., molec. rigidity 8=34850
    changes in flow past rotating disc, rel. to heat transfer 8=39358
    critical mixtures, anomalous 8=48097
    drag on sphere at low Reynolds numbers, expt. determ. 8=48095
    drag reduction, viscoelastic model and its appln. 8=48093
    droplets of various liqs. falling through air, drag coeffs. rel. to Reynolds number 8=30384
    elastic liqs. superposed simple and sinusoidal shearing eqns. 8=34801
    elastico-viscous liquids, linear, non-Newtonian viscosity and elastic props, theory 8=25841
    elastoviscous, oscillating thermal convection 8=43771
    electrolyte solns., nuclear spin relax. correl. 8=34927
    emulsifying agents adsorbing at oil-water interfaces 8=48101
    ethyl-alcohol mixtures, and proton spin-lattice relax 8=43770
    in flow reaction vessels, effect on transient response 8=32087
    generalized liqs., Euclidean geometry and flow 8=25894
    glycerol, press. depend. 8=34841
    helical macromols. in soln., size and shape determ. 8=30420
    inertia forces, soln. of two examples 8=39328
    rel. to liquid drop shape as it approaches a flat plate through a viscous liq. 8=30385
    local equilib. model 8=25908
    maleic anhydride-styrene copolymer in tetrahydrofuran rel. to mo-. dimens. obs. 8=43776
    mixture at vertical point, anomalous increase rel. to damping of hypersonic waves 8=30465
    moment method approximation 8=39332
    n-alcohols, with LiCl solute, viscous flow and relax. time of reorientation 8=34778
    nonionic detergent in aq. soln. micellar props. 8=30559
    polyacrylic acid, aqueous solutions, viscometic studies of u.v. irradiation 8=34794
    polydimethylsiloxane blends 8=30433
    poly-γ-benzyl-L-glutamate in soln., conformations 8=48096
    polyisobutylene in polybutene oil, gradient depend. of intrinsic viscosity obs. 8=43775
    polymer melts, entanglement effects 8=48100
    polymer solns, conc., molec. theory of shear depend stress props. 8=34699
    polymer solns., dilute, onset of drag reduction in turbulent flow, molec. approach 8=30368
    polymer solns., drag on sphere 8=30432
    polymer solns., flow-time fluctuations in capillary viscometer 8=30431
    polymer solns., kinetic approach 8=39334
    polymer solns., non-Newtonian intrinsic, ellipsoidal model 8=43778
    polymer solns., porous sphere molec. model 8=29866
    polymers, dynamic, a.f. 8=34797
    polymers, rel. to concentration 8=48125
    poly(methyl acrylate) in ethyl acetate rel. to mol. wt. and dimens., obs. 8=43773
    poly-n-butyl methacrylate in chlorinated diphenyl, dilute solns., normal stress effect 8=39333
    polypropylene, rel. to mol. wt. distribs. obs. 8=43721
    (1:1) poly(styrene-co-methyl acrylate) in ethyl acetate rel. to mol. wt. and dimens., obs. 8=43773
    polystyrene-cyclohexane, rel. to mol. chain dimensions below O temp., obs. 8=43774
    polystyrene solns., depend. on conc. and temp. 8=44065
    polyurethane-cyclohexanone soln., temp. depend. obs. 8=26595
    rigid sphere, approach to deformable liquid/liquid interface 8=34744
    sphere moving perpendicular to wall, hydrodynamic force for small gap widths, inc. inertial effects 8=43718
    styrene-methyl methacrylate random copolymers, dilute solns. 8=39323
    supercooled liqs., viscoelastic relax. 8=30430
    suspensions, effect of particle motion in shear and elec. fields 8=48231
    thermodynamic state of laminar flow 8=25848
    viscometer, falling-ball, for undergraduate expts. < 2kbar 8=43769
    viscous plastic fluids, with additives, reduction of turbulent viscosity 8=30436
    viscous solns., paramag. relax. determ. by n. m. r. 8=30532
    water-dioxane mixtures, and proton spin-lattice relax. 8=43770
    water, drag reduction by DNA additive, from vel. profiles 8=39265
    water, under shock load 8=48094

Viscosity—contd
  liquids—contd
    wormlike chains in soln. 8=30434
    Al alloys with Si, Zn, Cu and Mg, visc. - conc. curves rel. to solid state phase relns. 8=34799
    Al, coordination number transforms. obs. 8=25866
    Al-Cu, coordination number transforms. obs. 8=25866
    Al-Mg, coordination number transforms. obs. 8=25866
    Al-Si, coordination number transforms. obs. 8=25866
    Au-Ge-Si alloy, at glass-liq. transition 8=39470
    BeF_2, molten, temp. depend. 8=25892
    Bi-Bi halide molten solns. 8=43772
    D_2O, bulk viscosity calc. 8=43768
    H with const. density, 16. 6-300°K 8=43703
    He II, fluid and superfluid contrib. to damping of cylinder oscs. 8=41902
    He^3 soln. in superfluid He^4, calc. from phonon Boltzmann eqn. 8=41898
    Hg, under shock load 8=48094
    Li soaps in water miscible alcohols 8=39316
    $NaClO_3$-$NaNO_3$ molten system 8=48086
    Na_2SO_4 aq. solns., and molal vol. 8=48098
    Pu alloys 8=39330
    Pu, reactor fuel 8=47407
    SiO_2 with W inclusions network, 2000°C 8=48092
    $TlNO_3$, molten 8=39331
Visibility. See Atmospheric optics.
Vision
    See also Colour vision; Eye; Stereoscopy.
    accommodation of eye, lens astigmatism 8=37726
    cats, recovery time following high luminance stimulation 8=28916
    critical duration, differential luminance threshold, critical flicker freq., and visual adaption, theory 8=28919
    disinhibition, binocular and interocular presentations 8=24446
    eye, human, smooth pursuit movements, direct evidence against intermittency or sampling 8=24445
    eye protection filters, meas. and characts of scatt. light 8=28922
    fine detail vision and Stiles-Crawford effect, applic. of analysis of images 8=42295
    glare impression, influence of luminance and geometry 8=33298
    haze, subjective, overlying cockpit details at high altitude 8=42297
    human, movement direction and contour orientation mechanisms, selectivities 8=46774
    increment and decrement visual thresholds 8=28921
    interocular brightness matching, pupil diameters and retinal illuminances 8=33297
    luminance discrimination and flicker detection, model 8=46776
    optical illusions, anal. by model based on lateral inhibition 8=28920
    perception rel. to fixation during inspection of Muller-Lyer figures 8=37729
    perception rel. to fixation during inspection of Muller-Lyer figures 8=37730
    perspective and rotating trapezoid 8=28918
    photopic mechanisms of early dark adaption 8=28923
    pupil light reflex, optimizing use of criterion response 8=28915
    rabbit lens (crystalline), refractive index distribution model 8=46779
    retinal illumination distrib. using gradual correction lens 8=46661
    retinal image given by correcting glass of progressive power 8=46775
    retinal image motion, effect on critical flicker-fusion obs. 8=37727
    rods, excitation modes 8=37728
    strip-chart astrophotometric reading, error analysis 8=42139
    subjective light patters caused by lateral inhibition of cones in human retina 8=42294
    suppression during passive eye movement 8=46773
    suppression prior to onset of a voluntary saccadic eue movement 8=42296
    time course of visual inhibition during voluntary saccades 8=28917
    time-varying light signals detection, as meas. by pupillary response 8=28914
    triple-function ocular monitor 8=28913
Vitreous state
    See also Glass.
    aromatic phosphorescent hydrocarbons in glassy solns., e.s.r. spectra, dynamic effects in line-shapes 8=49596
    hydrocarbon glasses, electron trapping sites, saturation and removal 8=40082
    luminescence rel. to struct. and phys. props. 8=36465
    silica, fused, microcrystal orientation in ordered isotopic structure 8=26150
    silica gel, brittle, structural evolutions during ageing 8=26150
    silica, random-network model 8=26151
    silicate glasses, phase separation and submicroscopic structure 8=30787

Vitreous state—contd
- structural units, permitted and forbidden 8=48502
- Au-Ge-Si alloy, glass-liq. transition 8=39470
- BeF$_2$, atomic radial distrib. from X-ray diffr. meas. 8=26148
- B$_2$O$_3$, n.m.r. and struct. 8=48634
- C, internal friction and elastic modulus, 4-570°K 8=44557
- NaPO$_3$, crystallization on metallic condensation-nuclei with cubic lattice 8=44136
- PbO-SiO$_2$ silicates, spectra 8=32021
- Se, atomic arrangements by X-ray diffr. at 25 and −196°C 8=30793

Vlasov equation. See Plasma.

Vocoders. See Speech.

Voigt effect. See Magneto-optical effects.

Volta effect. See Contact potential.

Volume measurement
- CaF$_2$:GDF$_3$, changes due to pt. defects 8=44559
- Fe, high-purity, plastically deformed, on heating to 600°C 8=35677
- in KBr expansion by $U \rightarrow F$ and $U \rightarrow \alpha$ transforms, photoelastic meas. 8=26826
- Si, activity in molten Ag-Si alloys by e.m.f. meas. 8=48078

Vortices

See also Cavitation; Turbulence.
- eddies, embedded in swirling stream, struct. 8=48033
- expulsion by turbulence rel. to stellar rotation 8=45622
- inducing cavitation at smooth flat well 8=30369
- initiation by horiz. mixing of angular momentum on external stirring 8=47929
- kinetic eqns. in vortex field 8=39275
- MHD confined flow for elect. conduct., viscous, incompressible fluid 8=41996
- plasma. production of stable system 8=47826
- ring creation by fluid sphere abrupt acceleration 8=30233
- stretching, effect on drag-reducing additives 8=34721
- Vortex lattices in fluids, collective anodes 8=25785
- vortex tube, Ranque effect at low temp. 8=43648
- wake, axisymmetric, stability 8=30229
- wake of three cylinders, low Reynolds, number, smoke obs. 8=30371
- He, liquid, ion-vortex-ring transition obs. 8=24047
- He, liquid resonance theory 8=24046
- He II, distrib. in rotating cylinder 8=24050
- He II, rotating, vortex density from computer calcs. 8=24051
- He II, superfluid, vorticity in flow 8=43731

WKB method. See Quantum theory.

Water

See also Ice; Seawater; Steam.
- acoustic 150 kHz wave, finite-amplitude distortion 8=48139
- adsorbed on protein, proton relaxation 8=49649
- adsorbed on zeolite, translational diffusion, model 8=39619
- adsorption on MgO, i.r. study 8=47974
- adsorption on porous and nonporous ThO. 8=48492
- aerosol, evaporation kinetics in optical radiation field 8=30564
- in atmosphere, content meas. by radiowave absorpt. near $\lambda = 1.35$ cm 8=32205
- atmosphere, effective heights and absorption coeffs. at 4.1 mm 8=27909
- atmospheric, rel. astronomical obs., absorpt., 50 μ-1 mm 8=41499
- bubble growth rel. to Jakob. number 8=34996
- in capillaries, shift in temp. of max. density 8=34790
- rel. to carbon black suspension stability and electrokinetic pot. in nonpolar media, obs. 8=30550
- cavitation bubbles u.s. induced, models and damaging mechanism 8=43733
- chemisorption on W surface, investigation 8=27739
- Compton scattering profile 8=48066
- rel. to clouds electrifications by selective ion-capture, drops charging in ion stream, obs. 8=30517
- collisions, vibr. transition probabilities 8=34389
- combined in solids, n.m.r. 8=45123
- condensation in cloud chamber 8=30595
- corrosivity to Al, eqn. 8=41240
- of crystallization, H atom postiion determ. by NRM 8=44219
- deionized, electro-osmosis, temp. dependence of rate constants 8=32130
- desportion of CO$_2$ in packed bubble column 8=25858
- dielectric constant calc. from reflectance 8=43752
- dielectric props., changes during adsorption by solids below 0°C 8=39402
- dielectric relaxation, l. f., and viscous flow, mechanism 8=39398
- diffusion vel. through Ge oxide film on Ge 8=48778
- discharge, elect., computer soln. 8=30522
- dissociative ionization 8=29976
- distilled, sound velocity temp. dependence 8=43805
- with DNA additive, vel. profiles and drag reduction 8=39265
- drop photographed pulsed motion 8=43741
- droplet evaporation rate meas. by optical scatter 8=39484
- droplet, time change of radius in evaporation processes, asymptotic soln. 8=30600

Water—contd
- droplets, evaporation rates rel. to coating of n-decanol film 8=48272
- droplets, falling in air and other gases, supercooling and freezing 8=25984
- droplets, nucleation from vapour, surface tension rel. to radius 8=43781
- drops on metal plate, cooling rate and freezing temp. interdependence 8=48263
- drops, photomultiplier investigations 8=48043
- drops, supercooled, crystallization processes 8=25985
- equipment cooling, protection 8=32986
- evaporation and condensation coeffs., maximum values 8=43915
- evaporation rate in vacuum 8=39480
- exciton and interband transitions 8=43752
- explosion pressure pulse phase shift, interpretation 8=48C34
- far i.r. absorpt rel. to rotational transitions 8=49681
- film breaking on vert. surface, ht. transfer condns., contact angles meas. 8=25895
- flow, low velocity meter 8=34717
- flow through steel pipe, vel. effect on corrosion, mass transfer model 8=36560
- free convection at 4°C, heat transfer coeffs. to immersed plate 8=34838
- free convection below 277°K, minimum effect for pos. temp. differences $< 16°$ 8=34837
- freely falling drops, structure of ventilation coeff. 8=25854
- on glass, porous Vycor, adsorption of vapour, surface conduction current variation 8=27252
- glyceride-water mixture, mesomorphic phase and micelle structure 8=25966
- Great Lakes, wind-driven summer circulation 8=32188
- groundwater, steady radial flow towards circular well 8=43725
- HDO mol. deform. vibrs. characterization by vectors nonperpendicular to bonds 8=29679
- heavy, neutron scatt. including intermolecular interference 8=30405
- homogeneous nucleation and condensation 8=30596
- hydrated electron, structural model 8=34752
- hydration of Al(III) and Ga(III) ions, O^{17} n. m. r. 8=30540
- ice crystals growing in supercooled water, morphology 8=26176
- -ice interface, precrystallisation theory applied to surface-free energy 8=34957
- interfacial layer between ice and silicate surface 8=35142
- internal energy, adiabatic calorimeter 8=28424
- with ions at infinite dilution, ion-water interact. and thermodynamic props. 8=43754
- i.r. determ. of non-H-bonded OH-groups, and thermodynamic props. rel. to struct. 8=30401
- i. r. optical properties; application to radiative transfer in planetary cloud layers 8=50140
- Lagrangian one-dimensional wave motion meas. 8=34729
- laminar flow over heated and cooled plates, stability rel. to heat transfer 8=34709
- laser, pulsed vapour, gain characts. 8=24310
- laser, vapour molecular, far i. r. spectrum calc. 8=42089
- layer formed by melting ice from below, convection onset 8=34827
- light, neutron scatt. cross-sections, comp. with models of molec. motion 8=39304
- light scatt., fluctuation theory 8=30476
- liquid, absorption spectra, vacuum u. v. 8=31998
- liquid-solid transform, high pressure study 8=26327
- in mesomorphic phases, d. m. r. 8=48220
- mixture, glycerol-water acoustic absorpt. below 1 MHz 8=34840
- moisture diffusion coeff. in colloidal capillary-porous mats. rel. to moisture content 8=30662
- molecule, dipole moment from i. r. absolute intensity meas. 8=38837
- molecule, mesonic formed with K$^+$, π^+ or Σ 8=29872
- molecule, Rydberg terms calc. 8=25479
- molecules deform. vibrs. characterization by vectors nonperpendicular to bonds 8=29679
- neutron scatt., slow 8=30405
- nuclear mag. susceptibility meas., prepolariation method 8=25959
- nucleate boiling in systems with methyl ethyl ketone and 1-butanol 8=25998
- oil-water interface, viscosity of adsorbing emulsifying agents 8=48101
- oscs., small, in moving rigid circular and elliptic cylindrical containers 8=43735
- permeability, relative, with oil and gas in porous mats. 8=43988
- phase jumps on surface 8=39278
- phase transform. into ice VII by shock compression 8=48262
- pipe flow, heat transfer rate, turbulence induced fluctuations near wall 8=34830
- pre-adsorbed on Pt, effect on propane chemisorption 8=27738
- proton affinity 8=32110
- proton dynamics from slow n. inelastic scatt., at. 273.4°K 8=39303

Water—contd
- radiation distrib. var. at surface 8=34853
- radiolysis, reactions of electrons 8=49964
- in rayon fibres, broadline n. m. r. 8=27508
- refractive index calc. from reflectance 8=43752
- reservoir, detector of radioactive contamination 8=38403
- resonant oscillations in tank, obs. 8=34724
- resonant oscillations in tank, theory 8=34723
- reaction with hydride ion, MO theory 8=27677
- salt, flow through porous medium 8=43726
- scattering of ruby laser emission, large angle 8=48158
- self-association in dichloroethane 8=34874
- shallow, wave generation by unsteady flow 8=30374
- shock wave, isothermal at max. density 8=34728
- silicate K-8, stimulated Mandel'shtam-Brillouin scatt. threshold, 0.35, 0.69 and 1.06μ 8=32032
- single droplets, optical back scatt. 8=27916
- solubility in compressed N_2, Ar, and CH_4 8=30302
- solvent power for hydrocarbons, structural theory 8=48085
- sonoluminescence, temp. depend. 8=39389
- structure, effect of solutes and temp. 8=39295
- subcooled boiling, average vapour voids, predict, compared with theory 8=35000
- in sun-earth's atm. space, mols. density, obs. 8=29234
- supercooled, basal-plane solidification effects of impurities 8=25982
- supercooled, nucleation on freezing by cavitation 8=25981
- supercritical, high electrical conductivity at high temps. and pressures 8=43862
- supersaturated vapour, molec. association 8=25477
- supply, rel. to pitting corrosion of Cu, mechanism 8=45331
- suspended drops, freezing and fragmentation influence of environmental parameters 8=25853
- swirling in vertical and inclined tubes 8=30366
- thermal springs in Italy, O isotopic comp. of sulphate ions 8=50093
- in tolvene scintillators, max. conc., dioxane and naphthalene effects 8=43844
- and toughness of MgO cryst., reln. 8=40173
- transition boiling, meas. of heat-flux vs surface-temp. reaction 8=35002
- turbulent jets, absorpt. of CO_2 and H_2 8=30425
- underwater rad. distrib. meas., directional photometer 8=42136
- u.s. dispersion of insoluble particles, obs. 8=39442
- u.s. rad. field from focusing spherical source, at finite amps. 8=43804
- vapour, abs. lines in ν_2 band, product of strength and self-broadened half-widths 8=34239
- vapour, absorpt. coeff. 600-1000 cm^{-1} obs. 8=43312
- vapour, atmos. density, space averages by dispersion for refractive correction of e. m. range meas. 8=36722
- vapour, atmosphere attentuation of mm. waves 8=45473
- vapour, CO_2-H_2O mixture, optical-acoustic radiative power, absorpt., press. temp. effects 8=30298
- vapour distribution in stratosphere and high troposphere 8=32202
- vapour impurity in O_2, effect on acoustic absorpt. 8=39211
- vapour in atm., luminesc. under laser irradiation 8=38824
- vapour, i. r. spectrum, line strengths in $\nu_{1\ 3}$ bands 8=25480
- vapour, irrad. with 1 MeV He^+, e.s.r. 8=49968
- vapour laser line identification 8=29745
- vapour laser spectrum, transitions in $2\nu_2$, ν_3 and ν_1 states 8=29741
- vapour mass in atmos. column., meas. by total vertical absorpt. at $\lambda = 1.3$ cm 8=32204
- vapour, meas. of spectral absorpt. in bands 8=27908
- vapour mixture with oxygen, ionization cross-sections and mobilities of different species 8=39023
- vapour, molecular level parameters rel. to laser line identification 8=29748
- vapour, non-isothermal radiation in 2.7μ region 8=43680
- vapour pressure, isotope effects 8=39491
- vapour, radiation at nonequilibrium temps. 8=47597
- vapour, selective radiation obs. near 2.7μ 8=36749
- vapour, spectra by double-beam, two-beam interferometry, far i. r. 8=28818
- vapour spectra, line by line calc. rel. to statistical model 8=43327
- vapour, spectral emissivity, theory allowing for line struct. 8=25481
- vapour spectral transmission function 8=30300
- vapour to ice conversion by AgI 8=45458
- vapour traces in gases, meas. with solid electrolyte cells 8=41298
- vapour, wet bulb depression meas. in mass transfer boundary layer 8=25996
- vertical jets to free water surface, expt. and vel. distribs. 8=34732
- viscosity under press. between 40 and 440 kbars 8=48094
- water-air horiz. annular flow, heat transfer and pressure drop 8=43653
- water-cyclohexane, nonionic surfactant system, phase equilib. and types of dispersions 8=48249
- water/n-alkane interface, ideal gaseous behaviour of Na alkyl sulphates 8=30395
- water-oil system solubilized with Aerosol OT, dielect. props. 5-60°C 8=39406
- wetting of Au 8=48418

Water—contd
- X-ray scatt. from free surface in equilib. with vapour, rel. to struct. and distrib. functions 8=25872
- Zircaloy-2 oxidation in vapour, kinetics and mechanism, 350-500°C 8=32106
- $AlCl_3$ aqueous solution, proton transfer between hydration and solvent H_2O, n. m. r. studies 8=34931
- rel. to $BaSO_4$ suspension stability and electrokinetic pot. in nonpolar media, obs. 8=30550
- $Cu_2[Fe(CN)_6]$ membranes, H_2O transport kinetics 8=48121
- D_2O, absorpt. intensities, 4000-1000cm^{-1} obs. 8=34852
- D_2O. bulk viscosity calc. 8=43768
- D_2O, deuteron spin lattice relaxation 8=48217
- D_2O, max. density temp., and dielec. consts, using significant struct theory 8=43767
- D_2O mol. deform. vibrs. characterization by vectors nonperpendicular to bonds 8=29679
- D_2O molecules, motion in $Na_2S_2O_6 . D_2O$, study by n.q.r. 8=49669
- D_2O-C_2H_5OD mixture vapour press. isotope effect 8=48283
- D_2O, O^{17} enriched, spin echo O^{17} T_1 and T_2 obs. 8=48212
- D_2O, X-irrad., primary radical yields 8=49972
- H bonding, mol. orbital treatment 8=43313
- HCl mass transfer in cylinder with pulsed flow 8=34811
- H^3 content, ethane gas counting meas. and counter shielding 8=42474
- H^3 content, water vapour filled counter 8=42475
- H^3 meas., toluene-Triton-water emulsion scintillator optimum comp. 8=42473
- H_2O, absorpt. intensities, 4000-1000cm^{-1} obs. 8=34852
- H_2O, max. density temp., and dielec. consts, using significant struct. theory 8=43767
- H_2O-C_2H_5OH mixture vapour press. isotope effect 8=48283
- $H_2O + H_2$ laser, sub-mm. sealed-off 8=37581
- H_2O, HDO and D_2O in non-aq. solvents, i.r. intensities 8=39377
- H_3O^+ adsorbed by vermiculite, n. m. r. 8=47695
- O^{17} enriched, spin echo O^{17} T_1 and T_2 obs. 8=48212
- on SiO_2, wetting obs. 8=35140
- rel. to ZnS-MgF_2 layer Fabry-Perot filters max. transmission wavelength shift, obs. 8=28763

Wave equations, quantum theory. See Quantum theory/wave equations.

Wave functions. See Quantum theory/wave equations.

Wave mechanics. See Quantum theory.

Wavefront-reconstruction imaging. See Diffraction/light; Optical images.

Waveguides. See Electromagnetic wave propagation/guided waves.

Waves
- See also Acoustic waves; Elastic waves; Electromagnetic waves; Liquid waves; Magnetohydrodynamics; Seismic waves; Shock waves.
- acceleration, in isotropic, elastic materials, growth 8=32678
- air-sea, excited by volcano Krakatoa, pulse propagation 8=27829
- atmosphere, gravity internal in hydrostatic compressible fluid with vertical wind shear 8=50137
- in boundary layer, three-dimensional packets, development 8=30236
- coupled, parametric excitation, general formulation 8=32680
- diffraction reduction on non-closed, infinitely thin screens 8=46000
- dispersive medium, weak nonlinear interactions and time closures 8=45995
- dynamic systems with imperfect boundaries, wave motion and stability 8=23923
- equation, solution with point singularities 8=23809
- equations with variable coefficients, unique continuation theorem for solutions 8=32677
- gravity, weakly interacting random, closure problem 8=36656
- h.f. and l.f., interaction, in nonlinear dispersive media 8=45999
- hydromag. propag. under action of Coriolis force 8=28596
- interaction of two waves, coupled mode theory 8=32681
- Korteweg-de Vries eq., asymptotic relations for soln. 8=28239
- lee-wave amps and wave drag for thin barrier in stratified flow 8=43659
- linear propagation, matrix transform. 8=37118
- magnetostatic waves at singular turning points, effect of finite linewidth 8=27372
- mechanical, e.m., and De Broglie, reflection coeff. of inhomogeneous layer, determ. 8=46015
- method for solution of problems over regions with time-dependant shape 8=46240
- multiple scattering theory, soln. of eqns. by smooth perturbation method 8=46001
- non-linear, dissipation and dispersion, model 8=41635
- nonlinear propagation, reductive perturbation method 8=32679
- oceanic and atmospheric, equatorial planetary 8=50103
- oscillations, wave film type, of quantized thickness propagation 8=46149

- **Waves**—contd
  - perturbation problems, singular 8=45996-7
  - plane dilational pulse. transient diffraction at fluid-solid interface 8=23940
  - planetary atmospheric, geostrophic scale analysis 8=50136
  - planetary atmospheric, structure and motion 8=50134
  - in plasma, surface 8=34537
  - plate, non-propagating, effects on dynamical stress concentrations 8=41694
  - polyethylene, surface propagation 8=35736
  - polymethylmethacrylate, surface propagation 8=35736
  - propag. of 1D waves from a source in random motion 8=32675
  - radiation-driven, solar temp. reversal 8=45858
  - reduced equation, "interior" solns. in platelike region 8=32676
  - resonant interaction of neutral disturbances in two inviscid shear flows 8=30235
  - scalar Dirichlet diffr. by elliptic disc 8=23811
  - shear, stability of steady flows of non-linear viscoelastic fluids 8=43635
  - simple settled, vel. of propag., upper boundary for non-linear eqn. 8=37236
  - standing waves in layered fluid half-space, prod. by plane harmonic waves from below 8=32889
  - troposphere, mesoscale, seasonal propagation into stratosphere 8=27885
  - tropospheric mesometeorological solitary 8=27891
  - ultralong, behaviour in atmosphere 8=50148
  - viscoelastic media, and thermodynamics 8=41734
  - wavetrain in inhomogeneous media, intrinsic freq. and wave energy conservation 8=23807
  - Zilch of plane undamped waves 8=28240
  - Al rods and tubes, annealed, plastic deform., exptl. data 8=40126
  - SH, diffraction by half-plane 8=45998
- **Waxes**
  - dielectric, u.s. field effects 8=27258
  - melting point, technique for determ. 8=43906
- **Weak interactions.** See Field theory, quantum/interactions, weak.
- **Wear**
  - alkali halide crystals in org. liquids, rel. to interfacial energy calcs. 8=30724
  - effect on friction and stick/slip performance 8=35638
  - graphite, rate changes on condensable vapour intercalation rel. to lattice expansion 8=44208
  - grinding process dynamics, theoretical anal. 8=40120
  - polymers, and friction, effect of C fibre reinforcement 8=40192
  - polymers, C fibre reinforced, in high vacuum environment 8=35636
  - Cu-Au solid solution alloys, and friction and surface hardness, in abrasion 8=40149
  - Cu-Zn alloys, abraded, rel. to surface and subsurface structure 8=26294
  - Fe-based sintered metals, self-lubricating, sliding wear characts. 8=31187
  - TaN-TiB$_2$, hot-pressed, resistance 8=49053
- **Weather**. See Meteorology.
- **Weighing**. See Balances; Mechanical measurement.
- **Weissenberg cameras.** See Cameras; X-ray crystallography/apparatus.
- **Wentzel–Kramers–Brillouin method.** See Quantum theory.
- **Wertheim effect.** See Magnetomechanical effects.
- **Wetting**
  - See also Capillarity.
  - n-octadecanoic acid film on metal oxide, rel. to heat treatment 8=48050
  - n-octadecyl alcohol film on metal oxide, rel. to heat treatment 8=48050
  - n-octadecylamine film on metal oxide, rel. to heat treatment 8=48050
  - by polymer melts, kinetics 8=39283
  - sapphire, by Ni, Ni-Cr and Ni-Ti alloys 8=437444
  - transition metal carbides, weltability by liq. Pt. 8=27715
  - water on SiO$_2$ film obs. 8=35140
  - Al, by liq. In 8=39336
  - Au, by H$_2$O 8=48418
  - Mo, by Cs and Na, rel. to bare work function of substrate 8=35168
  - Nb, by Cs and Na, rel. to bare work function of substrate 8=35168
  - Re, by Cs and Na, rel. to bare work function of substrate 8=35168
  - Ta, by Cs and Na, rel. to bare work function of substrate 8=35168
  - UO$_2$, complete, critical surface tension in oxidizing and reducing atmos. 8=30729
  - W, by Cs and Na, rel. to bare work function of substrate 8=35168
- **Whiskers**. See Crystals/whiskers.
- **Whistlers**. See Atmospherics; Ionosphere.
- **White dwarfs**. See Stars.
- **Wiedemann effect.** See Magnetomechanical effects; Magnetostriction.
- **Wiedemann–Franz Law.** See Conductivity, electrical/solids; Conductivity, thermal/solids.
- **Wien effect**. See Conductivity, electrical/liquids, electrolytic.
- **Wigner coefficients**. See Quantum theory.
- **Wigner effect.** See Physical effects of radiations.
- **Wilson cloud chambers**. See Cloud chambers.
- **Wind**
  - ambient, effects on initiation and development of cumulus clouds over mountains 8=45457
  - biennial oscillation, propagation 8=45451
  - boundary layer adjustment as initial value problem 8=32210
  - breeze in stable stratified atmos., non-stationary nonlinear soln. 8=32206
  - components, and sea level, atmospheric surface press., relation 8=36692
  - eddy cond. to eddy viscosity ratio in lapse conditions 8=41340
  - in 80-100 km region, wind shear determ. from meteor drifts 8=36779
  - in 80-110 km range, components of different period, study by meteoritic radar 8=36780
  - front ogenesis, quasi-geostropic equation solution 8=32209
  - high speed updraft, key to severe thunderstorm 8=32214
  - hurricane, lab. model, incorporating analogue to release of latent heat 8=32208
  - hurricane vortex, evidence of existence of Rossby-like waves 8=36734
  - information entropy, monthly, for horiz. wind-vectors, Potsdam, 1951 8=50138
  - interaction with severely convectice clouds 8=27893
  - ionosphere, meridional and zonal components, anal. rel. to flucutation patterns 8=36842
  - ionospheric, over Yuma, Arizona, obs. by gun-launched projectiles 8=36843
  - ionospheric, short period oscillations, exptl. demonstration 8=27983
  - island wake eddies, energy dissipation obs. 8=36730
  - line squalls in the Cameroon 8=45453
  - lunar tidal, semi-diurnal surface, American obs. 8=50139
  - measurement, shadow effect, wind tunnel expt. with scale model launch tower 8=36732
  - mountain, velocity fluctuations 8=45450
  - profile definition in lower atmosphere 8=27874
  - quasi-biennial oscillation, diagnostic numerical model 8=32212
  - to 60 km, meas. by rocket-grenade method from Indonesia 8=36712
  - spring transition in mesophere, rel. to abundance of noctilucent clouds 8=41356
  - stratosphere and mesosphere, southern hemisphere, obs. 8=50135
  - summer circulation in Great Lakes, wind-driven 8=32188
  - in stratosphere and mesosphere, quasi-biennial osc. 8=36714
  - in 30 to 100 km region, variations, review of results, comparison with CIRA (1965) 8=36731
  - in upper atmos. equatorial, zonal and meridianal comps., variations 8=36778
  - in upper atmos., evidence for strong nonlinearity of horiz. flow 8=27941
  - zonal, excitation and propagation in atmos. with Newtonian cooling 8=32213
  - zonal oscillation, 26-month, in lower stratosphere of southern hemisphere 8=32211
  - S-N components below 60 km, diurnal variations 8=36733
- **Wolfram**. See Tungsten.
- **Wood**
  - fibres, small- and wide-angle X-ray diffr. patterns 8=26047
- **Work function**
  - See also Electron emission.
  - alloys, strained, irradiation dependence 8=44938
  - apparent, of thermionic emitters having multiple cavities 8=28480
  - contact pot. difference induced by gravit. field 8=44679
  - dyes, photosensitive, from polarograms, electronic spectra and HMO calcs. 8=40687
  - films, monoatomic, impurities, maximum and optimal cones 8=35150
  - metal films, thickness, shape and size factors 8=36037
  - metals, caesiated, rel. to vapour press. temp. ion energy and coverage 8=31466
  - metals with halogen or O adsorbate 8=35193
  - oxide cathodes, well-activated, temp. range 500 to 1100°K 8=27346
  - Al crystal face dependence in external photoelec. effect exam. 8=40704
  - Al$_2$O$_3$-metal electrode, rel. to electroluminescent brightness waves 8=45260
  - (BaSrCa)O and electrical cond. and thermoelectric power, effect of Ba vapour 8=26945
  - Cs amalgam, conc., and surface tension 8=49435
  - Cs layers on refractory metals 8=39624
  - Cu, strained, irradiation dependence 8=44938
  - GaAs, cesiated, obs. of giant temp. depend. 8=40688
  - Li-O-W (110) surface 8=39593
  - Mo, adsorbed O$_2$ and N effects, obs. 8=41269
  - Mo, bare, rel. to wetting by Cs and Na 8=35168
  - Mo, clean and gas-covered 8=34422

Work function—contd
Mo, effective, as collector in thermionic diode, comp. with Ni 8=31460
Mo, effective, rel. to O_2 press. and filament temp. 8=31469
Mo, film, effect of Ba, O_2 and BaO adsorpt. 8=40322
Nb, bare, rel. to wetting by Cs and Na 8=35168
Ni, effective, as collector in thermionic diode comp. with Mo 8=31460
Os balls, in vacuum, and Richardson consts. 8=31467
Pt films on W, rel. to structure 8=35178
Re, bare, rel. to wetting by Cs and Na 8=35168
Re, effective, rel. to O_2 press. and filament temp. 8=31469
Re-rare-earth alloys, obs. 8=40690
Re, vapour deposited, effective and Richardson 8=31468
Si, n-, p-type and caesiated, from photoelec. emission, 80 and 290°K 8=40495
Si, temp. dependence up to 1000°K 8=49436
Ta, bare, rel. to wetting by Cs and Na 8=35168
Ta, contact pot. for O and O-Cs atmos. 8=31469
Ti, film, effect of Ba, O_2 and BaO adsorpt. 8=40322
TiO_2, and elec. cond., changes in response to chemisorpt. of O 8=40691
U on W, effect of H contamination 8=49437
W, adsorpt. of CO on (100) and (211) faces 8=35200
W, bare, rel. to wetting by Cs and Na 8=35168
W, covering by adsorpt. of NH_3 8=27734
W, dependence on surface conc. of adsorbed O., 8=39622
W, effective, rel. to O_2 press. and filament temp. 8=31469
W, rel. to O_2 coverage 8=39626
W single crystal, (110) and (112) planes, effect of N_2 adsorpt. 8=39621
W, vapour-deposited (110) oriented thermionic, emitter, X-ray and vacuum 8=28477
W with coadsorbates, desorpt. cross section determ. 8=39623
W, Cs coated 8=36038
W-Mo-Re alloys, trace impurity effects 8=39727

Work hardening
See also Cold working; Surface texture.
alloys, rel. to superdislocations with thresholds in the LI_2 superstructure, braking 8=26655
alloys containing hard particles, model 8=35640
anthracene crystals 8=26855
axisymmetric propag. in solid viscoelastic sphere 8=26750
barrier, dispersed, temp. depend. 8=26631
high-strength mats., exponent effect on fracture toughness dependence on thickness 8=26766
metals, face-centred, theories rel. to dislocation density and flow stress 8=35558
plastic deformation of rot. disc by strain incremental theory 8=26762
plastic square bar, numerical anal. of combined bending and torsion 8=23836
plates, circular, of hardening material, bending anal. 8=41727
rel. to fatigue failure 8=31171
solid solution hardening of metal crystals 8=26763
steel, high-strength, exponent effect on fracture toughness dependence on thickness 8=26766
superstructures, model 8=44527
Al, high strength, exponent effect on fracture toughness dependence on thickness 8=26766
Al sheet, secondary softening rel. to previous cold work 8=44543
Cu, by strain, rel. to slip distrib. and initial dislocation substruct. 8=44459
Cu crystal, n-irradiated, radiation hardened, critical shear stress temp. and strain rate dependence 8=31196-7
Cu-Ni alloy, rel. to internal strains from plastic deformation 8=31194
Ge, curve under deform., dislocation structure at various stages 8=35565
Pb cylinders, strain-time, strain-rate and dynamic force-time characts. 8=35711
Ta-Mo alloys, effect of Mo content 8=35718
Ta-Re alloy, rel. to conc. and temp. 8=40182
Ta-Nb alloys, effect of Nb content 8=35718
Ti alloys, high-strength, exponent effect on fracture toughness dependence on thickness 8=26766

X-ray absorption
See also X-ray spectra/absorption.
angular dip. of abs. X-ray lines by cylindrical and spherical specimens 8=35296
electron microprobe analysis, target absorpt. correction 8=27799
electron microprobe correction factors, calc. methods evaluation 8=27801
electron probe microanalysis correction functions, evaluation 8=27797
electron probe microanalysis, corrections rel. to target Z 8=27796
extended fine structure of crystals, k-absorption spectra 8=39748
in interstellar gas, soft X-ray cross sections, calc. 8=45727

X-ray absorption—contd
in light elements, Philibert's correction extension 8=27798
mass absorpts. coeffs. meas. for various substances 8=41048
radiation shield for texture goniometer 8=39705
rare earths M spectra, sample self absorpt. effects 8=36355
scintillators, noble-gas, for X-rays, quantum efficiency meas. 8=37928
silicate minerals rel. to quantitative microprobe analysis, obs. 8=27809
Ar, of K_α, double e photoejection 8=38714
Cu L spectrum, sample self absorpt. effects 8=36355
Ne, of K_α, double e photoejection 8=38714
Pb L_α, emission in anticathode, 17-29 kV 8=36420
in SiC of C radiation, extended Philibert's correction 8=27798
Ti K_α, emission in anticathode, 17-29 kV 8=36420

X-ray analysis. See Chemical analysis/X-ray; Crystal structure, atomic; X-ray crystallography.

X-ray astronomy. See Astronomy and astrophysics.

X-ray characteristic temperature. See Specific heat.

X-ray crystallography
For results of structure analysis see Crystal structure, atomic.
alkali halides, Debye-Waller factors temp. dependence, calcs. 0-900°K 8=39869
angular dep. of abs. X-ray lines by cylindrical and spherical specimens 8=35296
Bijoveet type generalized eqns. 8=35297
crystals, perfect, unstrained and lightly strained 8=35295
Debye-Waller factor and low temp. anharmonicity 8=35372
Debye-Waller factor in single crystal absorbers, Mossbauer effect obs. 8=39745
diffraction, divergent beam, errors 8=30880
diffraction, introduction through analogies in interference patterns 8=30879
diffraction, simultaneous, n-beam case dynamics 8=35301
diffraction, simultaneous, 3-beam case dynamics 8=35302
diffractometry, liquid He cryostat 8=48622
impurity atoms, location in cryst. matrix. 8=40009
librating atom temp. factor, expression for analysis corrections 8=44184
non-cubic cell parameters, depend. of accuracy on reflection indices 8=35298
Pendellösung, X-ray interferences, experimental results 8=39749
refraction modified back-reflection diffractometry 8=48615
thermal scatt. component, integral, exptl. determ. 8=48612
two-line Fourier analysis, influence of cut-off 8=35299
volume determ., interf. point counting 8=35259
zeolites, surface area determ. 8=48432
AgBr, e.-distribs. 8=48302
Fe in Cu and Au, Debye-Waller factor, anharmonic contribution 8=39874
Ge, divergent beam tech. for precise lattice consts 8=48653
LiCl, Debye-Waller factors from diffr. meas., 298 and 78°K 8=44224
Si, Pendellösung fringes in crystal free of dislocations 8=48675
Sn, anomalous transition 8=49757
apparatus
See also X-ray monochromators; X-ray spectrometers.
Automatic Precision X-ray Goniometer for diffr. angle meas. 8=26342
automatic single-crystal diffractometer system PAILRED, principles 8=44189
back-reflection camera for single crystal areas 8=30842
balanced filter device, automatic, for diffr. expt. 8=44191
camera, far X-ray diffraction topography 8=26331
camera, point-focusing, for single-crystal diffr. 8=44192
computer-controlled diffractometer, programme variety 8=26339
computer-controlled low angle diffractometer 8=26340
computer, controlled single-crystal diffractometer 8=26337
counter diffractometer for crystal struct. investigations on n-irradiated materials 8=44260
diffraction cameras treated as transmission systems 8=48625
diffraction spectrometers, elastic quasi-mosaic effect after diffraction from deformed crystals 8=39706
electronic programmer for automatic scanning of small-angle scatt. curves 8=48626
high-pressure-high temp. diffractometer 8=26335
interplanar distance determ. 8=39754
diffractometers, automatic: Pailred and General Electric Datex; a comparison 8=26341
film goniometer, principle and appl. 8=30816
filter for $K\alpha_2$ radiation 8=35306
goniostat, crystal orientation aid 8=35211
high-pressure single-crystal cell for use with precession camera 8=26327
image intensifier for diffraction patterns 8=26344
Kossel pattern generator with single e. m. lens 8=30883
low-temperature diffraction apparatus for meas. room temp. to −180°C 8=26333

X-ray crystallography—contd
- **apparatus**—contd
  - microdensitometer, c.r.t. with computer control 8=35304
  - multichannel diffractometer for quantitative phase analysis 8=26329
  - phase transformations, low temp. 8=35078
  - polaroid adapter for alignment of single-crystals in Weissenberg goniometer 8=44190
  - pulse height spectrum display 8=26284
  - Siemens horizontal diffractometer modifications for surface reflexion topography 8=26325
  - specimen-holder, thermoelec. annealing 8=39755
  - for teaching elementary crystallography 8=26330
  - for thermal expansion determ. at high temps. 8=26593
  - for transferring crystal from one goniometer head to another 8=26345
  - Unicam high-temp. camera, adaption for thermal studies of layer-lattice silicates 8=26326
  - Weissenberg camera, shutter for photographic alignment 8=35305
  - Weissenberg goniometer attachment for equivalent recording of all reflections 8=39756
- **calculating apparatus**
  - automatic single-crystal diffractometer system PAILRED. principles 8=44189
  - computer-controlled diffractometers-the OLDMAN system 8=26338
- **calculation methods**
  - absorption correction method from intensity meas. 8=39740
  - absorption correction, semi-empirical method 8=39737
  - absorption corrections appl. to high-pressure single-crystal studies 8=44177
  - atom deformation in diffr. data, model calc. exam. 8=39742
  - atomic scattering factors from structure-factor meas. 8=39736
  - Compton line intensity distrib. calc. using Thomas-Fermi models 8=39739
  - computer formulae of structure analysis, representation in parametrical form 8=26310
  - cylindrical lattice, faulted, (chrysotile), diffr. profile calc. and meas. 8=39805-6
  - Debye-Waller factor without Debye distrib. 8=44185
  - diffraction profile interpret. by central scattering and Fourier analysis 8=30874
  - distorted crystal, line shape, dynamical calc. 8=26306
  - elastic constants determ., correction for second-order diffuse scattering 8=40093
  - electron density maps, errors, and use of integrated densities in charge density distrib. exam. 8=39751
  - four-axis hexagonal lattice construction in reciprocal space 8=30873
  - h.c.p., indices and directions 8=30873
  - integrated Bragg intensities, correction of measured values for first order thermal diffuse scatt. 8=44179
  - Kikuchi line interpret. rel. to 2 dimensional lattice 8=44202
  - least-squares refinement, applied results 8=26314
  - least-squares refinement method for isomorphous replacement 8=44186
  - lattice energy minimum search 8=26316
  - least-squares determ. of positional parameters, sinple approx. matrix. 8=39743
  - least squares refinement computer programme 8=39753
  - least-squares refinement, convergence-criteria 8=39752
  - least-squares refinement, filter technique 8=39750
  - least squares refinement in crystals with constraints, approx. matrix method 8=26313
  - least-squares refinement using anisotropic temp. factors from lattice dynamical calcs. 8=26569
  - line-profile parameters, statistical variance 8=26307
  - minimization method for solving structure, analysis problems 8=26317
  - molecular crystals, calc. method for densest distrib. of plane mols. in layers 8=30878
  - MONITO computer programmes 8=39744
  - non-cubic crysts. lattice params. from Kossel lines 8=30881
  - non-cubic crysts., lattice params. and symmetry from Kossel lines 8=30882
  - optimal algorithm, principles, consequences and applications 8=23783
  - optical-diffractometer masks for interpreting X-ray diffr. patterns, prep. techniques 8=26319
  - orientation distribs. in fibres and sheets 8=44178
  - Patterson diags. for orthorhombic diatomic groups 8=26305
  - phase determ. using correlation-eqn. method 8=48611
  - phases of structure factors, direct determ. using non-perfect model of electron density 8=30875
  - pole figure plotting from intensity, computer direction 8=48584
  - pole figure recording and analysis by computer 8=48580
  - pole figures, computer plotting using terminal printer as output device 8=48583
  - potential distribs. in atoms, Z=1-18, integral characts. 8=39731
  - powder pattern indexing, reliability criterion 8=44176

X-ray crystallography—contd
- **calculation methods**—contd
  - powder patterns of unknown structures, indexing by computer 8=26311
  - protein crystals, heavy atom location method 8=26548
  - quantitative analysis with calculated X-ray powder patterns 8=48621
  - random-layer line profile, Fourier-transform methods 8=26308
  - refinement of parameter of atoms in special positions, general procedure 8=26315
  - refinement using aspherical at. scattering factors 8=26309
  - rotation-function high-speed programme and appl. 8=26312
  - scattering factors, relativistic Hartree-Fock 8=39741
  - spinel structure, line profiles, effect of substitutional disorder 8=44225
  - stereographic projections, computer constructions 8=48623
  - structure refinement from powder data 8=48673
  - texture representation, complex, by biaxial pole figures, analysis 8=48576
  - valence struct. from coherent scatt., Fourier difference synthesis 8=48620
  - variance as measure of line broadening rel. to particle size determ. in Ni powder 8=26296
  - Weissenberg photograph analytical indexing, computer-aided 8=26318
  - OD groupoid-family, intensities sum rel. to single layer structure, and appl. 8=26480
  - W, absolute atomic scattering factors 8=48681
- **structures**. See Crystal structure, atomic.
- **technique**
  - alignment of single-crystals with polaroid adapter for Weissenberg goniometer 8=44190
  - anomalous dispersion in structure analysis 8=26321
  - Berg-Barret, for obs. dislocations 8=44430
  - Berg-Barrett topography using Siemens horizontal diffractometer 8=26325
  - crystal cooling by N_2 boiling 8=32992
  - differential diffractometric, for lattice parameter change determ. 8=39757
  - differential photometric, for phase modification analysis 8=26323
  - diffraction angle meas. of very high precision 8=26342
  - divergent beam, for anisotropic distortion exam 8=48619
  - double-crystal diffr. topography with small set of reference crystals 8=26332
  - filter difference method in combination with film method 8=44187
  - for high-temperature exam. of graphite 8=39792
  - Kossel line, in back reflection region, for precision determ. of lattice constants 8=39738
  - lattice-parameter determ. at liq. He temps. by double-scanning diffractometry 8=26334
  - Laue photography, glancing-angle, determ. of crystal orientation 8=26182
  - microscopy for selected-area diffr. patterns and magnified Lane-diffr. images 8=48586
  - mounting, methacrylate adhesive 8=31233
  - oscillation photography for routine structure analysis 8=26346
  - phase determ. using anomalous dispersion and directly measurable parameters 8=39733
  - phase shift determ. 8=48617
  - polarized X-ray photography for extinction and absolute intensity meas. 8=26343
  - powder, peak intensity errors rel. to grain size and crystalline structure 8=26285
  - protein crystals, heavy atom location method 8=26548
  - pulse height spectrum display and appl. 8=26284
  - Siemens diffractometry for precision lattice parameter determ. 8=26324
  - Siemens microphotometer for single-crystal photographs 8=26320
  - structure determ. based on intensity meas. with automatic Nonius diffractometer 8=26336
  - substructure in single-crystal, quantitative determ. by Laue patterns of high resolution 8=26322
  - in teaching elementary crystallography 8=26330
  - topographs, contrast caused by imperf. 8=48618

X-ray diffraction
- See also X-ray crystallography; X-ray scattering.
- absorption corrections appl. to high-pressure single-crystal strudies 8=44177
- angle meas. of very high precision 8=26342
- anomalous transmission, multiple, theory and expt. using Ge 8=35335
- apparatus, at very low temp. 8=35212
- atom deformation from data, model calc. exam. 8=39742
- automatic single-crystall difractometer system PAILRED, principles 8=44189
- back-reflection camera for single crystal areas 8=30842
- balanced filter device, automatic 8=44191
- cellulose I and II rel. to acetylation, obs. 8=45325
- coconut fibre, spiral orientation and cell dimensions 8=48358
- collimator slits, principal limit of meas. 8=28931

X-ray diffraction—contd
cristobalite, stacking fault conc. calc. from line profiles 8=26703
crystal monochromated X-rays, polarization 8=41039
crystalline, effect of X-ray coherence 8=48613
by crystalline medium, diffuse scatt. rel. to electron density 8=26347
crystallography, divergent beam, errors 8=30880
cylindrical lattice, faulted, (chrysotile), profile calc. and meas. 8=39805-6
data averaging, continuous, with multichannel analyser 8=28242
diamonds, natural and synthetic, comparison 8=30889
differential photometric technique, for phase modification analysis 8=26323
diffractometer DRD-1, remote controlled 8=48624
diffractometer, sample holder for spinning device 8=28932
diffractometry, single-crystal, low-temp. system 8=30884
in diffusion coeff. determ. 8=35469
in disordered crysts. with nearly perfect unit cells, correl. functions and theory 8=26328
double-crystal topography with small set of reference crystals 8=26332
dynamical, spherical-wave theory, for absorbing perfect crystals, crystal wave fields 8=30876
dynamical, spherical-wave theory, for absorbing perfect crystals, integrated reflection power 8=30877
elastically deformed crystals, elastic quasi-mosaic effect 8=39706
electret exam., dipole orientation rel. to polarizing field 8=44891
extinction and Borrmann effect in CaF$_2$ spheres 8=44183
extinction and Borrmann effect in mosaic crystals 8=44182
goniometer for single-crystal alignment 8=35210
grating, ruling engine design and construction 8=33303
gratings, 1Å dispersion 8=28929
holography, and appls. 8=24436
image intensifier for patterns 8=46233
imaging furnace, evaluation as heat source 8=33304
introduction through analogies in interference patterns 8=30879
line broadening effects, separation by means of line-width relations 8=45147
liquid He cryostat 8=48622
polymer crystallinity obs., definition 8=44092
powder data from rystals, computer indexing 8=44188
rabbit psoas muscle, glycerol-extracted, filament lattice studies 8=26458
refraction modified diffr. law for back reflection 8=48615
selected-area patterns and magnified Lane-diffr. images from microscopy 8=48586
simultaneous, n-beam case dynamics 8=35301
simultaneous, 3-beam case dynamics 8=35302
solid solns., chemical comp. determ. 8=27814
spinal structure, line profiles, effect of substitutional disorder 8=44225
spinel structure, line profiles, effect of substitutional disorder in MgFe$_2$O$_4$ and Mg(Cr, Al)O$_4$ 8=44226
stationary crystal and film topography, slit system 8=33302
tapiolite and synthetic trirutile substances 8=48614
tobacco mosaic virus with imbedded Xe, binding props. of Xe 8=25974
AgBr, crystallization 8=44114
Au films, lattice parameter thickness dependence, meas. 8=30748
BaTiO$_3$, fine-grained, line shifts 8=39716
CaSO$_4$. H$_2$O, chem. and phase equilibria under hydrostatic press. 8=43901
CdS, microstructure, calc. 8=39779
Cu crystals, deformed, dislocation density determ. 8=26673
for Cu crystals, fast neutron radiation damage obs. 8=26732
CuAuII long period ordered alloy, rel. to lattice modulation 8=30893
Fe, line intensity changes on plastic deform. 8=44166
Fe-Cr alloys, oxidation study by glancing angle technique 8=49868
Fe-Si crystals, contrast at ferromagnetic domain walls 8=27409
In, liquid structure temp. dependence exam. 8=25873
KH$_2$Al$_2$(SiO$_4$)$_3$, isomorphic substitution distribution 8=35338
LiF powder, Debye-Scherrer obs. with Fe^{55} source 8=28930
Mg (Cr, Al)O$_4$, disorder, study 8=44226
MgFe$_2$O$_4$, disorder, study 8=44226
Pt ribbon diffractometer attachment, temp. meas 8=32978
Si, dislocation distribs. from Laue-case diffr. expts., 8=48860
Si-O solid soln, anomalous transmission rel. to periodicity changes on decomposition 8=36409
Sn, Borrmann effect 8=49750
Sn^{119}, resonance γ-rays, on nuclei and electrons 8=39821
Tl, liquid structure temp. dependence exam. 8=25873
UF$_4$, 2. 5H$_2$O, rhombic, and dehydration product obs. 8=30870

X-ray diffractometers. See X-ray crystallography/apparatus.
X-ray examination of materials
See also Chemical analysis/X-ray; Radiography.
alnico, high-coercivity, powder pattern exam. 8=35346
anthracene, dislocations, direct topographical obs. 8=31074
apparatus for high pressure study 8=35303
banana fibres, normal and treated 8=48359
borate glasses, dissociated regions 8=39630
clay minerals, rel. to contact metamorphism 8=39571
collagen-like polymers 8=25682-3
crystallite vol. determ., interf. point counting 8=35259
crystals, Compton effect, review of recent articles rel. to appls. 8=26283
crystals, perfect, unstrained and lightly strained 8=35295
crystals, thin, contrast in topographs 8=48618
defectmeter with Sb$_2$Se$_3$ detectors, construction and appls. 8=39989
deoxycholic acid fibres, 8=26491
di(tetramethylammonium)bis(maleonitriledithialato)CuII, and e. s. r. studies 8=35364
diamond, dynamic reflection, rel. to at. vibration spectrum, review 8=43922
films, from interference fringes 8=48435
fission fragment K, bent-crystal spectrometer 8=34062
goniometer, texture, X-ray shield 8=39705
graphite at > 2000°C, techniques 8=39792
graphite, line intensity on X-ray diagrams 8=35319
for high-pressure studies 8=35303
liquid crystals in mag. fields 8=30410
lysozyme crystals at -50°C rel. to cross-linking 8=26519
microanalyzer, neutralizing insulating targets by low-energy electrons 8=45421
microradiograph for small specimens 8=32619
microscope, MIR-1, shadow 8=48581
minerals, powder diag. peak intensity errors rel. to grain size and crystalline structure 8=26285
photographic emulsion, speck size distrib. determ. 8=24443
planar defect, dynamical contracts 8=31094
point-projection microscopy, technique and limitations 8=48582
polydisperse suspensions, diameter distrib. determ. by small-angle scattering 8=30553
polyethylene, crystallized, crystallite size and lattice defects 8=39990
polymer crystallinity, definition rel. to X-ray diffr. obs. 8=44092
polytripeptides with (glycine-iminoacid-iminoacid) sequence, and synthesis 8=25682-3
powders, grading rel. to dispersion and compactness using diffracted intensity 8=43985
powders, ultramicrotomed, peak profiles rel. to deformation structure 8=48585
protein and nucleic acid structure determ. 8=32624
quartz crystal, u.s. vibrations, topographical obs. 8=48722
quartz glass, structural exam. 8=39629
rabbit psoas muscle, glycerol-extracted, filament lattice studies 8=26458
silicates, layer-lattice, thermal studies using adapted Unicam high-temp. camera 8=26326
sisal fibres, normal and treated 8=48359
stacking fault energy determ. from diffr. analysis, temp. effects 8=31093
stacking fault, image contrast on topographs 8=35574
steel, stainless, oxide fluorescence analysis 8=41304
stress analysis, portable equip. used by Boeing Co. 8=26754
substructure of single crystals by high resolution Laue diagrams 8=35300
Suzuki atmosphere 8=40029
thoria gel, crystallite sizes, equivalence with electron microscopy 8=35284
topography, using Kα_2 rad. monochromated by Ru filter 8=35306
vapour thermostat for back-refl. camera 8=33301
Au films, lattice parameter thickness dependence, diffr. meas. 8=30748
Al-8.7 at. % Zn alloy, internal strain field determ. 8=26786
Al, qualification by fluorescent spectrum line shift 8=41059
Al surface, Kikuchi line interpret. rel. to 2 dimensional lattice 8=44202
Al-Ag alloy, Ag conc. from Guinier-Preston zone exam., 8=49996
AlNi alloy, structural changes on ageing rel. to mag. props. 8=35090
Al(OH)$_3$ gel, struct. 8=25971
Au-Cd alloys, hexagonal, stacking faults 8=26701
BeF$_2$, glassy, atomic radial distrib. from diffr. meas. 8=26148
CdSe crystal, defect structure from topography 8=39994
Cr-Mo-Co steel R-phase precip., structure and comp. analysis 8=44001
Cs$_3$Sb films on MnO 8=39591
Cu alloys, thermal expansion at high temps. 8=26593
Cu crystals, deformed, dislocation density determ. from diffr. profiles 8=26673
Cu, ductile deformation mode, by anomalous transmission 8=26648

X-ray examination of materials—contd
    Cu foils for use in nuclear resonance obs., texture parameters 8=49663
    Cu hexamethylene-dithiocarbamate, struct. obs. 8=30919
    Cu, nearly perfect crystals, vacancy clusters, topograph exam. 8=35534
    Cu whiskers, structural features rel. to deformation by torsion 8=35254
    Fe, deformed, diffraction line intesity changes on annealing 8=35332
    Fe, diffr. line intensity changes on plastic deform. 8=44166
    Fe, high-purity plastically deformed, on heating to 600°C 8=35677
    Fe-Be alloy, ageing 3-D modulation of struct 8=30650
    Fe-Cr-O system, low-temp. oxidation, glancing angle diffractometry 8=27703
    Fe-Si crystals, diffr. contrast at ferromag. domain walls 8=27409
    $FeAl_2O_4$, cation distrib., diffraction and Mössbauer study 8=35331
    Ga, liq. x-ray scatt. 8=34765
    GaAs, liq. x-ray scatt. 8=34765
    Ge, brittle deformation mode, by anomalous transmission 8=26648
    Ge, impurity distrib., non-uniform, meas. by anomalous transmission 8=31376
    Ge, n-irradiated, damage studies by diffr. 8=26733
    Ge, n-irradiated, defect detection using anomalous transmission 8=48834
    Ge, thermal expansion from powder diffr. meas. 8=44347
    H_xWO_3, same crystal structure as $Na_{(0\cdot1)}WO_3$ 8=35336
    Ir, thermal expansion from powder diffr. meas. 8=44347
    KH_2PO_4, dislocations and precipitates exam. by diffr. microscopy 8=26691
    $LiF:Ni^{2+}$, impurity ion clustering from small-angle exam. 8=44422
    MgO, effective atomic charge-determ. 8=26169
    Mo-Mn steel R-phase precip., structure and comp. analysis 8=44001
    $Na_{0.5}Bi_{4.5}Ti_4O_{15}$, cation ordering 8=26413
    $Na_8Ba_2Ti_4O_4(B_4Si_{20}O_{56})$, leucospherite, at. struct. obs. 8=30907
    NaCl, effective atomic charge-determ. 8=26169
    NaCl, under high pressure 8=35303
    Nb_3Sn, phase transform. from diffr. at 300, 15.5 and 10.5°K 8=35118
    $(NH_4)H_2PO_4$, dislocations and precipitates exam. by diffr. microscopy 8=26691
    PbS, deformation state, investigation by harmonic analysis of form of interference lines 8=31227
    Rh, thermal expansion from powder diffr. meas. 8=44347
    Sb, liq. x-ray scatt. 8=34765
    Se, vitreous, atomic arrangements from diffr. data at 25 and −196°C 8=30793
    Si, and inelastic electron scattering 8=44155
    Si, n-irradiated, damage studies by diffr. 8=26733
    Si, n-irradiated, defect detection using anomalous transmission 4=48834
    Si, Pendellösung fringes in crystal free of dislocations 8=48675
    W, deformation mode, by anomalous transmission 8=26648
    $\alpha W-\beta W-WO_2$ mixture, quantitative anal., calibration problems 8=35288
  liquids
    p-azoxyanisol, liq.-crystal, in strong mag. field 8=39309
    benzene, structure 8=34764
    DNA, conformation in soln., by small-angle scatt. 8=29860
    formamide 8=39306
    liquid crystal mixtures, structural and stability characts., x-ray exam. 8=39310
    p-methoxybenzylidene-p′-cyanoaniline, nematic struct. study 8=48067
    molecular, thermal agitation coeff. determ. for diffr. studies 8=25878
    nitrobenzene, liq., X-ray scattering 8=43760
    t-RNA, mol. behaviour at different conc. and ionic strengths 8=25875
    scattering techs., reln. between X-ray and neutron methods for structure 8=30402
    solutions, x-ray and n diffr. methods 8=34763
    structure determ. 8=25876
    transition metals, liquid structure 8=25874
    water, struct. and distrib. functions from scatt. by free surface in equilib. with vapour 8=25872
    Ar, diffraction rel. to determ. of intermolec. pot. and correl. functions 8=25877
    In, liquid structure temp. dependence 8=25873
    Tl, liquid structure temp. dependence 8=25873
  microstructure
      See also Crystal structure/microstructure.
    alloy, ticonal-type, oriented modulated structure 8=35056
    β-brass, quenching effects 8=48595
    electron microprobe, camera for stereo projection micrographs 8=30844
    grain size determ. of coarse crystals 8=30841
    α-keratin, matrix-microfibril texture 8=39729
    muscle filament, structure and packing 8=28200
    pole figure recording and analysis by computer 8=48580

X-ray examination of materials—contd
  microstructure—contd
    polyethylene, during orientational stretching 8=35293
    polyethylene films, rel. to stretching processes, diffr. studies 8=26859
    polyethylene terephthalate, crystallization behaviour 8=26206
    scans integration, photographic, optical and electronic, evaluation 8=30840
    wood fibres, small- and wide-angle diffr. patterns 8=26047
    α-Al_2O_3 powder, explosive shock treatment effects from line-broadening analysis 8=44168
    Au crystals in polyvinyl alcohol films, sizing 8=30858
    CdO, X-ray reflex broadening, lattice distortion and particle size 8=48591
    Fe chromites, phase transformation study 8=35101
    LiF ground powders, microstrain and crystallite size determ. by line-broadening profile analysis 8=48600
    $LiNbO_3$, ferroelec. phase transitions, 20° – 1170 °C obs. 8=30863
    MgO powder, explosive shock treatment effects from line-broadening analysis 8=44168
    Mo, X-ray topographic investigation 8=35274
    Si, diffr. patterns rel. to thermally induced stresses 8=49051
    Si(100), (110) and (111) surfaces, Berg-Barret skew tables for Kα 8=35347
    Si: P, As, single crystals, porous substruct. 8=30866
    SiO_2, amorphous → cristobalite transformation 8=44011
    Y-C system, phase diagram proposal 8=39569
  molecular structure
    actin 8=25674
    o-aminobenzoic acid, H-bonding dimer obs. 8=43359
    high polymers, degree of crystallinity 8=48690
    pepsin, isomorphous derivative prep. 8=30833
    polyvinylidene fluoride, supramol. structure and $\alpha \rightleftharpoons \beta$ phase transformations 8=26155
    H_2O, Compton scattering profile 8=48066
    $In_2(MoO_4)_3$, monoclinic, rel. to $Fe_2(MoO_4)_3$ model 8=30900
X-ray fluorescence. See Luminescence; X-ray spectra/emission.
X-ray measurement
      See also Dosimetry.
    astronomical, optimum drilled scintillation collimators 8=50269
    cosmic, thin-window proportional counter 8=47187
    counter, proportional, cosmic background reduction 8=33620
    diffraction at collimator slits, limit 8=28931
    polypropylene window, stretching technique 8=50476
    pulses, powerful, dosimetry using photomultiplier 8=46922
    soft, detectors, employing channel electron multipliers 8=47041
    solar, rocket-borne data handling system 8=50445
    Z-crystal interferometer, construction and operation 8=37733
    $FeSO_4$ Fricke-Miller dosimeter, $G(Fe^{3+})$ yield, 62 keV 8=42457
X-ray microscopes. See Microscopes.
X-ray monochromators
    crystal monochromated X-rays, harmonic radiation elimination 8=41040
    crystal monochromated X-rays, polarization 8=41039
    crystal, polarization factor determ. 8=46785
    high-aperture evacuated, with fixed receiver station 8=46780
    for $K\alpha_2$ rad., appl. to topographical and powder photographs 8=35306
    sing crystal 8=28928
X-ray photoeffect. See Electron emission/photoelectric.
X-ray reflection
    curve shape, effect of insufficiently monochromatic and insufficiently parallel beam 8=49689
    diamond, synthetic, anomalous refl. obs. 8=30889
    integral thermal scatt. component, exptl. determ. 8=48612
    non-cubic cell parameter, depend. of accuracy on reflection indices 8=35298
    paraffin mirrors for $\lambda > 20Å$ 8=24449
    polarized, onto periodic pile of dielectric layers 8=49675
    resonator, planar using Bragg reflectors 8=46786
    vapour thermostat for back-refl. camera 8=33301
    Al film on BK7 glass, obs. 8=31961
    Si(100), (110) and (111) surfaces, Berg-Barret skew tables for Kα 8=35347
    Si, plane crystal, (220) reflection, effects of fast neutrons 8=30911
X-ray scattering
      See also Compton effect; X-ray diffraction.
    anthracene, by thermal agitations, rel. to phonon freqs. 8=26577
    Bijoveet type generalized eqns. 8=35297
    Compton effect in crysts., review of recent articles rel. to appls. 8=26283
    crystal monochromated X-rays, polarization 8=41039
    by crystalline medium, diffuse scatt. rel. to electron density 8=26347
    from crystallite models of amorphous mats., calc. of upper bounds 8=26142

X-ray scattering—contd
- diamond, random defect distribution, neutron irrad. 8=40016
- distorted crystal, line shape, dynamical calc. 8=26306
- ferrite, diffuse, from doublet defects 8=39996
- by homogeneous substances, limit for zero angle of intensity rel. to mean fluctuation of density 8=25879
- liquids, struct. determ. 8=25876
- by macromolecules in soln., theory of diffuse small-angle scattering 8=25870
- martensite, diffuse, from doublet defects 8=39996
- mixtures of amorphous solids or liquids, data anal. 8=39628
- by mosaic virus, southern bean, interparticle interactions 8=25967
- nitrobenzene, liq. 8=43760
- polydisperse suspensions, small-angle, diameter distrib. determ. 8=30553
- polymethacrylic acid, aqueous and methanol solns., rel. to conformational changes 8=25888
- powder grain size determ. from scatt. intensity 8=30843
- regular crystals, resonance Bragg scattering of γ-quanta 8=39746
- semiconductors of blende-type structure, anomalous, rel. to polarity determ. 8=45153
- thermal diffuse, dynamical treatment 8=45154
- thermal diffuse, harmonic radiation elimination 8=41040
- thermal diffuse, integrated first and second-order evaluation 8=27540
- thermal diffuse, rel. to generalized theory of X-ray phonon cross-sections 8=27539
- by two-phase systems, for determ. of particle size distrib. 8=26041
- two-phonon, in diatomic crystals, intensity calc. 8=35369
- vacuum sample holder for Kratky camera 8=34688
- valence struct. from coherent scatt., Fourier difference synthesis 8=48620
- weighting functions for collimation corrections 8=46782
- Al polycrystals, thermal diffuse, temp. dependence 8=48632
- Ar gas for determ. of intermol. pot. 8=30274
- $BaTiO_3$, anomalous 8=36329
- BeO, random defect distribution, neutron irrad. 8=40016
- Cu-16. 7% Pd alloy, diffuse, rel. to elec. resistivity and short-range-order 8=36354
- Cu polycrystals, thermal diffuse, temp. dependence 8=48632
- CuNi, small angle scatt. obs. of clustering 8=30892
- Fe, Compton profile 8=31989
- Ga, liq., intensity curves 8=34765
- GaAs, liq. intensity curves 8=34765
- Ge, thermal, accompanying Bragg reflection, direction dependence of intensity 8=44217
- He^3, liquid, rel. to h.f. sound vel., and zero-point scatt., obs. 8=32999
- KBr, thermal diffuse by transverse lattice waves 8=44221
- KCl, rel. to dislocation density and distrib. 8=45198
- LiF, rel. to dislocation density and distrib. 8=45198
- NaCl, rel. to dislocation density and distrib. 8=45198
- NaCl, thermal diffuse, rel. to transverse acoustic [OhO] phonon dispersion curve 8=39876
- NaF, by phonons 8=44286
- Sb, liq., intensity curves 8=34765
- Si, incoherent, and inelastic electron scattering 8=44155

X-ray spectra
- See also Atmospheric spectra; Chemical analysis/X-ray.
- beam divergence utilization in two-crystal spectrometer 8=49690
- crystal band structure interpret. from BN calcs. and obs.. 8=41041
- film emission, surface ionization function rel. to over-voltage and substrate Z, obs. 8=31945
- gypsum, spherically bent cryst., 3 to 30Å: comparative meas. 8=32033
- iron oxides, Fe Kβ lines rel. to valency energy bands 8=41084
- K and L lines, relative intensities 8=49691
- metals and alloys, soft-ray spectrometry rel. to electron theory 8=49687
- mica, spherically bent cryst., 3 to 30Å, comparitive meas. 8=32033
- muonic, different phys. and chem. targets, intensity obs. 8=25396
- production efficiencies, K, L and M shell meas. 8=25345
- quartz, spherically bent cryst., 3 to 30Å, comparative meas. 8=32033
- scattering, thermal diffuse, dynamical treatment 8=45154
- sun, and XUV spectra 8=45880
- sun, 33-110Å obs. 8=32575
- vacuum spark emitted x-rays 8=39005
- wavelength criteria, effect of statistical counting errors 8=46784
- Al emission from gas-ion tube, long-wavelength 8=43286
- Al_2O_3, K- and L-, zone structure 8=49702
- As_2Se_3, amorphous, band structure from ultrasoft spectroscopy 8=26901
- B emission from gas-ion tube, long-wavelength 8=43286
- BN, hexagonal and cubic, investigation 8=41063
- BN, rel. to crystal band structure interpretation 8=41041
- BP, ultrasoft, rel. to energy band structure 8=41062
- Be emission from gas-ion tube, long-wavelength 8=43286
- Co^{58M}, isomeric transition 8=33966
- Co-V alloys outer energetic band electron distribution 8=49713
- Cr_2O_3, K- and L-, zone structure 8=49702
- Cu, band structure calc. 8=36352
- Eu^{151}, ^{153}, muonic x-rays spectra rel. to nuclear charge distrib., obs. 8=34194
- Fe in ferrites and oxides with spinel struct, Kβ-group of lines 8=31988
- μ-Ho^{165} atoms rel. to dynamic quadrupole interaction, K and L emission, obs., 8=34191
- I in KI, ultrasoft emission and absorpt. rel. to KI band structure 8=41105
- Ir^{192M}, L-X-rays in isomeric transition 8=33966
- K acid phthalate, spherically bent cryst., 3 to 30Å comparative meas. 8=32033
- KCl-KI solid solns, decomposition effects 8=36395
- Mn in ferrites and oxides with spinel struct, Kβ-group of lines 8=31988
- Mn, Kβ_5-emission and K-absorpt. edge, rel. to band structure 8=41115
- Mn-V alloys, outer energetic band electron distribution 8=49713
- MoS_2, spherically bent cryst., 3 to 30Å, comparative meas. 8=32033
- NaCl-KCl solid solns, decomposition effects 8=36395
- Ni-Al alloy, soft- 8=36419
- Sc, Ti, Y, Zr, Lu, Hf, La, Ce, isochromats rel. to width of conduction band 8=36405
- μ-Tb^{159} atoms rel. to dynamic quadrupole interaction, K and L emission, obs., 8=34191
- μ-Ti^{48} atoms, Lyman and Balmer line energies, obs. 8=34189
- Ti^{48}, μ-capture x-rays, obs. 8=34189
- TiNi, soft- 8=36419
- VMn_2 alloy, Kβ_5-emission and K-absorpt. edge, rel. to band structure 8=41115
- **absorption**
  - crystal mechanically processed to cylinder or sphere 8=41038
  - mass absorpt. coeffs., computer fit 8=31938
  - Ca metallic, K edge 8=27565
  - Ca^{++} in $CaSO_4$ and hydrides, K edge fine structure 8=27564
  - $Ce_{1.75}$-La_2O_3, identification of di and trivalent ions 8=39638
  - Cu, fine structure of K-absorpt., 3oo°, 77°, 4. 2°K obs. 8=42224
  - Cu K edge, optimized spectroscopy procedures for glossy mats 8=27567
  - Cu-Zn, K edges 8=41080
  - $CuMn_2O_4$ spinel, rel. to valence states of Cu determ. 8=30801
  - CuO 8=27567
  - Fe metal, K-absorpt. spectrum 8=45186
  - $FeNi_3$ alloy, K-absorpt. spectrum 8=45186
  - FeS_2, pyrites, K-absorpt. spectrum 8=45186
  - Ga, and cpds, K-absorpt-edge, shifts rel. to chem. effects 8=31990
  - Nb, fine structure of K-absorpt., 33°, 77°, 4. 2°K obs. 8=41124
  - Ni in solid solutions, electronic structure of atoms 8=49744
  - Ni-Zn, K edges 8=41080
  - Pt, ultra-soft X-rays, experimental and theoretical study 8=25364
  - S, chem. shift, and inner-electron binding energy 8=29627
  - Sb_2S_3, rel. to photocurrent distribution 8=49422
  - Ta, ultra-soft X-rays, experimental and theoretical study 8=25364
  - Y in Y cpds., K-absorpt. edge 8=41151
- **emission**
  - chlorinated methanes and fluorochloromethanes 8=47653
  - electron microprobe analysis, fluoresc. corrections errors 8=27800
  - electron microprobe, fluorescence correction factors 8=27801
  - gases, carbon spectra 8=47652
  - Ge, L-series 8=49719
  - intensity, effect of excitation 8=49688
  - metals, soft X-rays, quantum-mechanical many-body treatment 8=27541
  - rare earths M spectra, sample self absorpt. effects 8=36355
  - satellite occurrence 8=41042
  - secondary fluorescence effects rel. to absorpt. correction 8=32050
  - soft, plasmon on satellite 8=41043
  - solar active region obs. 8=2 8165
  - solar events August, 1966 obs. 8=32576
  - solid solns., chemical comp-determ. 8=27814
  - vacuum spark, theory and expt. 8=3 7732
  - Al, band, intensity distrib., interpretation 8=45171
  - Al, band spectra interpret. from effective potentials determ. 8=45172
  - AlN, energy structure exam. by ultrasoft spectroscopy 8=36320

Al_2O_3, energy structure exam. by ultrasoft spectroscopy 8=36320
Al_2O_3, Al, K_α line shift rel. to e microprobe analysis, obs. 8=27804
Br in brines meas. 8=27815
CoO, Co K_α line shift rel. to e microprobe analysis, obs. 8=27804
CrFe alloys, rel. to 3d-electron redistrib. 8=35780
Cu, depth distrib. in anticathode, 17-35 kV 8=36420
Cu L spectrum, sample self absorpt. effects 8=36355
Fe_2O_3, Fe K_α line shift rel. to e microprobe analysis, obs. 8=27804
Ho^{67}, $L_I N_{IV,V}$ and $L_I O_I$ transitions, obs. 8=31999
La, K-ionized, L-K ang. correl.,obs. 8=41111
Mg, rel. to Al band spectra interpret., effective potentials determ. 8=45172
Na, rel. to Al band spectra interpret., effective potentials determ. 8=45172
Pb Lα, depth distrib. in anticathode, 29 and 33 kV 8=36420
SCO X-1, narrow-band and UBV photometry 8=45656
SiC, ultrasoft, rel. to energy structures 8=41136
Si_3N_4, ultrasoft, rel. to energy structures 8=41136
Ti Kα, depth distrib. in anticathode, 17-29 kV 8=36420
TiFe alloys, rel. to 3d-electron redistrib. 8=35780
TiN, Kα band of Ti rel. to electronic structure 8=41148
TiO_2, Ti, K_α line shift rel. to e microprobe analysis, obs. 8=27804
TiO_n, Kα band of Ti rel. to electronic structure 8=41148
U^{235} fission prods., 30-300 keV 8=38547
VFe alloys, rel. to 3d-electron redistrib. 8=35780

X-ray spectrometers
See also Gamma-ray spectrometers; X-ray crystallography/apparatus.
bent-crystal, for fission fragment K meas. 8=34062
concave grating, mounting 8=24450
diffraction grating, abnormal behaviour 8=46734
for electron microscope Phillips EM-200 8=24451
for fission prods. meas. bent crystal spectrometer, 30-300 keV 8=38547
focusing, use with e microprobe 8=28573
vacuum, for fine struct. and chem. analysis 8=41305

X-ray spectroscopy
See also X-ray crystallography; X-ray diffraction.
effect of excitation on emisssion intensities 8=49688
for electron probe, scanning single channel pulse height analyser, and lines identification tables 8=24530
flash, time-resolved discharge obs. 8=34409
micrometeorites, e microscope appl. 8=28156
semiconductor detectors for anal. 8=46783
solid solns., chemical comp. determ. 8=27814
wavelength standard selection and line shifts, 10-100 keV 8=29084
n-Si surface barrier detectors 8=47071

X-ray tubes
effect of excitation on emission intensities 8=49688
gas-ion, Be, B, Al emission, long-wavelength spectra 8=43286
image intensifier, electron-optical, development 8=46781
weighting functions for collimation corrections in X-ray scatt. 8=46782

X-rays
See also Gamma-rays.
above atmosphere, and u. v. background, rel. to intergalactic gas density, obs. 8=32490
astronomy meas., instrumental background effects 8=45611
auroral, interrupted by sudden geomag. impulse, persisting 24 sec. periodicity 8=45504
auroral microburst obs. 8=32279-80
auroral microburst rel. to electrons, obs. 8=32280-81
bremsstrahlung spectra during auroral absorpt. events 8=36808
coherence, effect on crystalline diffraction 8=48613
cosmic background, galactic and non-galactic components 8=32398
emission from exploding W wires, undegassed and degassed 8=40294
ion sources in Van de Graaf accelerators, reduction 8=24545
rel. to microanalysis, prod. and e scatt. in specimen, transport eqn. calc. 8=28560
primary diffuse flux, isotropy between 20 and 80 keV 8=38175
production from metal surfaces by 90 keV Ar^+ ion bombardment 8=31130
solar bursts and cosmic ray Z $\geqslant$ 15 nuclei increase, 23-24 Feb., (1964) 8=32586
solar emission obs. and source model 8=28166
space, outer, diffuse background, 1–1.5 keV 8=32399
spark discharge, pulsed, in air, during initial growth 8=39002
in upper atmos., correl. with density variations 8=36766
U^{235} thermal fission radiation rel. to fragment mass, obs. 8=38529

effects
See also Nuclear reactions due to/photons.
alkali halides, irradiated, lattice disorder at room temp. 8=44198
anthracene, prompt and delayed fluoresc. 8=27666
Bayard-Alpert manometer, residual current 8=34685

X-rays—contd
effects—contd
calcite, CO_3^- paramag. resonance 8=49600
concrete, attenuation 8=48891
DNA, diamine bound 8=48903
elastic quasi-mosaic effect after diffraction from elastically deformed crystals 8=39706
electron emission in vacuo, secondary emission mechanism 8=49444
felspars, structure defect production, e.p.r. and thermoluminescence exam. 8=26710
flash radiographic trigger switch actuation 8=33300
glasses, Ag atom impurity stabilization and atomic centres production 8=31114
halobenzene photoconductive solns, conductivity enhancement 8=43866-7
naphthalene single crysts., radiation damage 8=40083
neon-like, ions, X-ray satellite intensities 8=25372
polyoxymethylene extended chain crysts. rel. to m. p., refr. index and density, < 4.8 × 10^7 R 8=44509
quartz : Co-doped, on absorpt. spectrum 8=48556
semiconductor diodes, theoretical shape of diffusion comp. of current pulses 8=27164
Ba methacrylate dihydrate, polymerization 8=27741
CaF_2, F-centre vacancies, formation and bleaching 8=40059
CaF_2:Y, irradiated, polarized luminesc. and structure of luminesc. centres 8=36478
CdSe photocurrent on X-ray illumination 8=40656
C_2H_5I and CH_3CD_2I, fragment ions from X-irrad. 8=47795
In, photoelectron emission on excitation, energy distrib. 8=40707
p-InSb, changes in electrical conductivity 8=40471
InSb, photoelectron emission on excitation, energy distrib. 8=40707
KBr, irradiated, low-temp., Frenkel defect formation at 8°K 8=40005
KBr-KCl solid solutions, induced intrinsic luminesc. 8=41198
KCl, i.r. absorpt. spectra 8=41104
KCl, irradiated, low-temp., Frenkel defect formation at 8°K 8=40005
KCl whiskers, F-centre accumulation 8=35585
KCl-KI solid so'ns, decomposition rel. to effect on spectral characts. 8=36395
KCl, X-irrad., thermal annealing Frenkel defect recombination 8=40166
LiF, change in lattice constant, concentration of F-centres, electrical conductivity 8=35603
NaCl—KCl solid solns, decomposition rel. to effect on spectral characts. 8=36395
NH_4 halides, new defect centre, motional effects 8=48879
NH_3OHCl, irradiated, e.s.r. of V_K centres, radical pairs and trapped NO 8=31878
NaCl:$CdCl_2$, F-centres, associated absorpt. bands 8=31113
$Pb(CH_3)_4$, fragment ions from X-irrad. 8=47795
Sb, photoelectron emission on excitation, energy distrib. 8=40707
Se, hexagonal, internal photoeffect spectral distrib. on X-ray and u. v. irradiation 8=40672
Si diode, Frenkel effect due to irradiation 8=40533
SrF_2: Y, irradiated, polarized luminesc. and structure of luminesc. centres 8=36478
U_2Ti, induced phase changes 8=35134
protection. See Radiation protection.

Xenon
in achondrites, U and Ca-rich, two types of fission Xe 8=28160
adsorption on pyrex 8=30774
arc, high press., in stationary and flashed modes, spectral emission and abs. obs. 8=29945
arc lamp, simple power supply system for stable operation 8=24073
atom, electron scattering, elastic 8=47529
atom, interaction with H^+, H° and H^-, charge state changes, investigation by coincidence method 8=43238
atoms, photo-attenuation cross section, 1050-1550Å 8=43206
compressed, light source for pumping Nd glass laser 8=28709
crystalline, kinematic resonances in optical absorpt. spectrum 8=27611
diatomic, attenuation cross section near resonance line 1469.6Å 8=43205
diffusion and release from sintered UO_2 at low temps. 8=26624
diffusion in CaF_2 and U doped CaF_2 8=26618
diffusion in neutron irrad. Cs halides 8=39970
diffusion in UO_2, UC and U doped CaF_2 8=34107
discharge, h. f. induction stationary, temp. 8=29900
discharge, ~ mTorrs, charge range suitable for Langmuir probe 8=30104
electron-atom scattering, mobility mx. 8=43229
equation of state 8=39193
flash tube with delay line 8=42209
gas prop. scintill. counters 8=46878
high pressure lamps, spectral energy distrib. meas. 8=47510
in inclusions of Fe meteorites, conc. and isotopic comp. rel. to age 8=50436

Xenon—contd
- ionic, ground state, alignment by e impact ionization 8=39052
- isotopic shifts of 13 i.r. laser lines, meas. 8=25367
- laser discharges, time varying, perturbations of microwave cavity fields 8=24294
- laser, isotope shifts on i.r. lines, obs. 8=28652
- light scattering, depolarization meas., 8=43694
- liquid and vapour, −59.0°C — 16.5°C, refractive index and Lorentz-Lorentz junction obs. 8=43809
- liquid, luminescence in electric field, induced by α-particle 8=25937
- liquid, radial distrib. and distrib. functions, X-ray atudy 8=43759
- metastable atom, electronic energy transfer to N_2 mol. 8=29847
- monatomic, attenuation cross section near resonance line 1469.6Å 8=43205
- near-critical isotherms, interferometric determ. 8=25977
- photoionization cross sections of M shell 8=29981
- plasma, damping of ion-acoustic waves 8=47876
- pulsed arc, radiative plasma, study of energy transport and balance 8=39090
- Rayleigh scatt. and atomic e.m. susceptibility 8=25375
- scintillation counter for (n, α) reactions in multilayer counter 8=46873
- shock compression rel. to conversion to metal-like state 8=43851
- solid, adsorpt. of noble gases on (100) face, Van der Waals interactions 8=39617
- solid, adsorpt. of noble gases on (111) face, Van der Waals interactions 8=39618
- solid and liquid, charge transport 8=26943
- solid, band struct., deformation pots and effective masses 8=44646
- solid, model potentials 8=35389
- solid, pair pot. calc. 8=30615
- specific heat near critical point 8=34977
- spectral line excitation by electron-atom collisions 8=34165
- thermal cond., Langmuir calc. for incandescent lamps 8=42210
- in thermionic converter, effect on V-I characts 8=28481
- in thermionic diode, V-I characts on exposure to nuclear rad. 8=28485
- in tobacco mosaic virus, binding 8=25974
- viscosity, low-temp. 8=39237
- Ag thermal desorption obs. 8=48483
- Au thermal desorption obs. 8=48483
- CO_2 laser plasmas, influence of Xe 8=33181
- Cd-Xe atom collision cross section calc. 8=34180
- Cu crystal bombard., thermal desorption obs. 8=48482
- Cu thermal desorption obs. 8=48483
- $Xe^{129,131}$ n.m.r., local mag. field shift, obs. and theory 8=39226
- Xe^{133} diff. in metals, rel. to mech. props. 8=48766
- $Xe^{134,136}$ abundance ratio, mass spectrometer meas. 8=47452
- Xe-methane mixtures, charge exchange 8=47792
- Xe pulse discharge in presence of Zn, spectrum, 240-300 nm 8=34292
- Xe_2, photo-attenuation cross section, 1050-1550Å 8=43206
- Xe−CO_2, mixtures, thermal diffusion 8=34679
- Xe-He laser, c.w. with diffuse mirror non-reson. feedback, freq. characts., 3.50μ 8=37592
- in Zn presence, pulse discharge spectrum, 240-300 nm 8=34292
- Zn 3075.9Å, perturbation of resonance line 8=47512

Xenon compounds
- chlorides, Xe^{129} Mossbauer studies 8=30645
- H_2Xe, bound states, i.r. absorpt. 8=25472
- XeF_2, vapour press. and m.p. 8=39492
- XeF_4, semiempirical MO energy levels 8=25524
- XeF_4, vapour press. and m.p. 8=39492
- XeF_6, molec. struct. from gas-phase electron diffr. 8=34290-1
- XeF_6, struct. and inversion, electron diffr. 8=25523
- XeO_4, root-mean-square amplitudes 8=34289
- $XeOF_4$, microwave spectrum molec. consts. 8=43339

Xerography. See Photography.

Y-particles. See Hyperons/resonances.

Yield. See Elastic limit; Plastic deformation; Plastic flow.

Young's modulus. See Elastic constants.

Ytterbium
- ion in silicate glass, stimulated emission 8=36512
- magnetoresistance, Fermi surface 8=40744
- monochalcogenides, high pressure phase transformations 8=26070
- paramagnetic susceptibility from mag. moment meas. at 4.2 ~ 300°K 8=31706
- spectrochem. and nephelauxetic parameters 8=43927
- CaF_2:Yb^{3+}, ENDOR meas. rel. to crystal field splitting of Yb^{3+} in cubic sites 8=27501
- YbII, $4f^{13}5d^2$ configuration 8=34155
- Yb II, spectra and Zeeman effect obs., energy levels calc. 8=47511

Ytterbium—contd
- Yb^{3+}, spin lattice relaxation in CeO_2 8=36222
- Yb^{3+} in CaF_2, transferred hyperfine interactions, F^{19} ENDOR obs. 8=36266
- Yb^{3+} in $CaWO_4$, microwave-optical double reson. 8=41070
- Yb^{3+} in ThO_2, g-factor stress dependence 8=31510

Ytterbium compounds
- Yb-Hg system, phase diag. 8=30706
- Yb−Zn system, phase diagram from thermal, X-ray, metallographic and resistivity data 8=44015
- YbAl garnet, n.m.r. of Al^{27}, quadrupole splitting and paramag. shifts 8=31893
- YbC_2, vaporization 8=43920
- $Yb(ReO_4)_3$ crystal struct., high-temp. modification, X-ray obs. 8=30914
- Yb_3S_4, unit cell and cryst. structure 8=26449

Yttrium
- electronic structure from positron annihilation studies 8=26906
- electrotransfer of impurities 8=36596
- Hall effect meas. 8°-320°K, mag. fields to 7.8kOe 8=44690
- Hall effect, temp. depend. 8=26975
- lattice constants meas., 77-300°K, by X-ray diffr. 8=39935
- secondary e emission coeff. and energy spectrum obs. 8=40716
- solar abundance 8=50441
- in solar chromosphere, lower, Y^+ emission regions 8=45914
- in steels, stainless, austenitic and ferritic, effect on oxidation in CO_2 8=27704
- structural study 8=26434
- Y III spectra, principle series, transition probabilities in doublets 8=47506
- Y^{3+} in Y cpds., K-absorpt. edge 8=41151
- Y^{3+}-stabilized CO_3^{3-} mol.-ion, e.s.r. in calcite 8=49620

Yttrium compounds
- garnet, dispersion of magnetoelastic waves 8=40186
- garnets, magnetoacoustic resonance in 3-cm wavelength range, obs. using transverse pumping 8=35419
- garnets, Si-substituted, permeability and coercive force, spectral dependence 8=40845
- garnets, synthetic, high-pressure decomp. 8=26087
- K-absorption edge 8=41151
- manganites, ferroelectric props., magnetic structure 8=40619
- Fe garnet: Yb, ion-ion interaction via magnon field 8=40830
- Y tetrahydrate perrhenate, i.r. absorpt. obs. 8=36384
- YAg, sp. ht. 1.3-5°K, rel. to density of states at Fermi level 8=48740
- YFe garnet, e.m. conversion to exchange spin wave energy, coherent i.r. diffraction determ. 8=40848
- YFe garnet, Faraday rotation, 100°−450°K 8=32039
- YAl garnet, morphology rel. to growth on seed by flux technique 8=26198
- YAl garnet, planar defects from e.microscope exam. 8=44249
- YAl garnet:Fe^{3+}, e.p.r. and pseudo-Stark line-splitting 8=31849
- YFe garnet, Ho, giant-anisotropy ferromag. resonance linewidth, crystallographic angle and temp. dependence 8=31832
- YAl garnet:Nd laser, continuous 0.532μ solid-state source using $Ba_2NaNb_5O_{15}$ in cavity 8=33253
- YAl garnet:Nd^{3+} laser pumping efficiency of Kr and Xe flash tubes 8=46550
- in $Y_3Al_5O_{12}$, energy transfer between rare earth ions, temp. depend. 8=45138
- $Y_3Al_5O_{12}$, Faraday rotation for Er^{3+}, wavelength dependence 8=44982
- Y-C system, phase diagram 8=39569
- $Y_{3-2x}Ca_{2x}Fe_{5-x-y}V_xIn_yO_{12}$, ($x \leq 1.5, y \leq 0.5$), linewidth reduction 8=31833
- $Y_{2.1}Ca_{0.9}O_{12}$, effective mag. fields at Fe^{57} and Sn^{119} nuclei, rel. to nonmag. Sn^{4+} conc. 8=36197
- YCd_2, crystal structure and refinement 8=26448
- Y−Ce alloys, bound state, magnetoresistance at low temp. 8=49476
- Y-Ce dilute alloys, magnetic susceptibility and thermopower due to s-f anomaly 8=27384
- YCu, sp. ht. 1.3-5°K, rel. to density of states at Fermi level 8=48740
- YF_3, vapour press., enthalpies and entropies in range 1050°-1200°C 8=35015
- YFe garnet, delay of microwave signals 8=49564
- YFe garnet, demagnetization, shock-induced 8=31744
- YFe garnet, Fe^{3+} anisotropy 8=31743
- YFe garnet, freq. and amp. of spin waves in subsidiary absorpt. region 8=49563
- YFe garnet, hydrothermal and flux-grown, OH groups and Fe valence 8=35206
- YFe garnet in two-port magnetoelastic delay lines 8=40850
- Y Fe garnet, magnetic domains, X-ray topographic and optical obs. 8=45044
- YFe garnet, mag. domain-wall propag. vel., effect of Er doping 8=49565
- YFe garnets, mag. props. from Mossbauer effect, 85-600°K 8=36196
- YFe garnet, magnetoelastic pulse excitation and propag. in non-uniform field, loss meas. 8=45043

Yttrium compounds—contd
YFe garnet, magnetoelastic waves, rel. to nondispersive variable delay in two-port device 8=31745
YFe garnet microwave mixer, energy balance 8=41999
YFe garnet, microwave phonon attenuation 8=26585
YFe garnet, nonlinear ferromag. resonance, self-modulation anisotropy 8=45069
YFe garnet, para process in h.f. mag. field near Curie point 8=49566
YFe garnet polycrystals, linewidth and off-resonance loss at microwave freq. 8=31834
YFe garnet rods, axially magnetized, abs. spectra 8=36426
YFe garnet rods, axially magnetized, containing turning pt., magnetostatic mode propagation 8=40846
YFe garnet, sound wave attenuation due to magnon-phonon interaction 8=35401
Y Fe garnet, spin wave excitation time in first- and second-order nonlinear processes 8=45041
Y Fe garnet, standing-spin-wave modulation of reflected microwave power 8=40847
YFe garnets:Fe^{4+}, linewidth temp. dependence, 4.2°-300°K at 10 and 25 kMc/sec 8=31827
YFe garnet: Si, domain wall mobility 8=31746
YFe garnet:Si, ferromag. resonance temp. dependence, 4.2-400°K at 10 and 30 GHz 8=31825
YFe garnet: Tb^{3+}, FMR linewidth rel. to energy levels, wave functions and relax. times 8=31824
$Y_3Fe_{5-x}In_xO_{12}$, two-sublattice cpd., first magneto-crystalline anisotropy constant temp. dependence 8=45042
$Y_3Fe_5O_{12}$, ferromag. res., effects of defects from U^{235} fission fragments 8=36225
$Y_3Fe_5O_{12}$, n-scattering by parametrically excited spin-waves 8=36094
YGa garnet:Eu, electronic Raman transitions 8=27612
YGa garnet: Eu^{3+}, mag. susceptibilities 8=49468
YGa garnet: Nd, crysts. growth and laser oscills., obs. 8=39694
YGa garnet:Nd, electronic Raman transitions 8=27612
in $Y_3Ga_5O_{12}$, energy transfer between rare earth ions, temp. depend. 8=45138
YGdAl garnet:Nd^{3+} growth and laser characts. 8=39692
$YH_{1.96}$, n.m.r. absorpt. spectrum, temp. effects 8=31925
Y_6Mn_{23}, ferrimag. coupling, polarized n obs. 8=40849
$Y_y(Mn_xFe_{1-x})_z$, (y = 1, 6: z = 2.23), magnetisation and susceptibility 8=31710
$YMnO_3$, antiferromag. and ferroelec. props. 8=27285
$YNbO_4$: Nd^{3+} luminescence obs. 8=36515
Y_2O_3, determ. of trace amounts of rare-earth impurities 8=27794
Y_2O_3, optical consts in spectral region 0.25 to 9.6μ 8=49762
Y_2O_3, retention of additives 8=39693
Y_2O_3, spectral reflectance 8=41128
Y_2O_3:Ln^{3+}, (Ln = Pr, Nd, Eu, Er, Tm), radiative and multiphonon relax. of Ln^{3+} 8=45289
Y_2O_3: Nd^{3+} spectra, Stark splitting scheme and $^4F_{3/2}$ lifetime, 4.2-293°K 8=32017
Y_2O_3: R^{3+}, (R = rare earths), cathodoluminescence 8=49814
91Y_2O_3 + 9ThO_2 in solid solution, elastic moduli, temp. depend. from 25° to 1100°C 8=35724
Y-Sn alloys, Mössbauer effect 8=35043
$YTaO_4$, M^1 phase structure, bond angle correction 8=26447
$YTaO_4$: Nd^{3+} luminescence obs. 8=36515
YVO_4, high temp. absorpt. and brightness under 3650 Å excitation 8=45229
YVO_4, i.r. spectral emittance and opt. props. 8=32038
YVO_4, lattice vibrations rel. to Raman and i.r. spectra 8=36424
YVO_4 tetragonal crystals containing Nd^{3+}, induced emission at 300°K 8=33229
YVO_4:Eu, high temp. absorpt. and brightness under 3650 Å excitation 8=45229
YVO_4: Eu^{3+}, absorpt. and fluorcoc., $(4f)^6$ level splittings rel. to cryst. field, obs. 8=41152
Yukawa potential. See Field theory, quantum/meson field; Nuclear forces; Scattering.

Zeeman effect
actinide complexes, octahedral, free and in crystals, vibronic level splitting 8=43964
alkali atoms, meas. of elec. dipole moment 8=29614
anthracene singlet-triplet transitions rel. to spin-orbit coupling 8=25536
asymmetric rotors, quadratic effect 8=47555
benzophenone singlet-triplet transitions rel. to spin-orbit coupling 8=25536
1,4-dibromonaphthalene, electronic Zeeman meas. 8=27629
hexabromobenzene singlet-triplet transitions rel. to spin-orbit coupling 8=25536
lanthanide complexes, octahedral, free and in crystals, vibronic level splitting 8=43964
level-crossing meas., effects of uneven population distrib. among sublevels 8=25342
luminescence centres, inorganic, rel. to emission, meas. 8=41178

Zeeman effect—contd
phenazine singlet-triplet transitions rel. to spin-orbit coupling 8=25536
plasma transient shifts, Fizeau interferometer meas. 8=30088
porphyrins 8=43387
rare-earth ions in cryst. field with C_{3h} symmetry 8=36357
tribromobenzene single-triplet transitions rel. to spin-orbit coupling 8=25536
Al_2O_3:V^{3+}, rel. to Jahn-Teller effect in $^3T_{2g}$ state 8=4396
CS, from millimeter inferometry 8=38814
CaF_2 with Ce impurity, Zeeman relax. 8=45119
CaF_2:Eu^{2+}, rel. to emission spectra 8=45177
CuCl, 4.2°K 8=36351
Er^{3+} in ethylsulphate crysts. 8=36357
Er ferrite garnet, temp. dependence, 4.2-20.4 °K 8=36185
Er 1, 3000-5000Å in 26 kOe field, obs. 8=29637
H, for large quantum no.s and freqs. 5-20 MHz 8=47501
H maser freq. shifts, due to coherently excited $\Delta m_F = \pm 1$ transitions between F = 1 levels of ground state 8=25350
HeI, combined Zeeman and Stark effects 8=38653
Hg, decay constant of metastable 6^3P_2 state, investigated by pulse technique 8=34142
Ho ehtylsulphate, $^5I_8 \rightarrow {}^3K_8$ and $^5G_8$ transitions 8=49777
K, magnetically oriented 4^2p atoms, collisional depolarization 8=47520
KBr:In, A absorption bands 8=45200
KCl:In, A absorption bands 8=45200
KI:In, A absorption bands 8=45200
$LaCl_3$:Ce^{3+}, i.r., at 77 and 27°K 8=36383
$Mn_3Cl_2(NO_3)_{12}\cdot 24H_2O$, blue lines splitting, theory and obs. 8=41117
NO molecule, and Stark effect, combined 8=25498
Na-D_1-line, profile and equivalent width as function of temp. and mag. induction 8=25361
Ne, for large quantum no.s and freqs. 5-20 MHz 8=47501
O, for large quantum no.s and freqs. 5-20 MHz 8=47501
OD, (0, 0) band 8=38848
PbI, and intensity anomalies 8=34148
Yb II, spectra and Zeeman effect obs., energy levels calc. 8=47511
Zener diodes. See Semiconducting devices/diodes.
Zener effect. See Metals; Semiconducting materials; Semiconductors.
Zeta-potential. See Electrokinetic effects.
Zinc
adsorption of Kr, effect of chemisorbed O_2 8=48500
in α-brass, rel. to activation energy of vacancy formation 8=48808
anodic behaviour in KOH solns., 8=45385
atomic displacements, mean square, thermal variations rel. to Debye temp. evaluation 8=44395
atomic spectrum obs. in discharge tube with high voltage pulses 8=29630
bicrystals, grain boundary sliding anisotropy rel. to dislocation climb-glide mechanism 8=31106
clustering in Al-Zn 10% alloy, assisted by defects 8=48802
compressive internal stress during electrodeposition, role of hydrogen 8=31167
conducting film formation using electron beam 8=39603
corrosion in NaCl, transient charge fluctuations obs. 8=45368
crystal growth forms, microscopic obs. 8=48562
crystals, dislocation motion, velocity shear-stress dependence 8=26695
crystals, melt-grown, substructure dependence on impurities 8=26268
crystals, single, {0001} plane decoration with metal chlorides 8=48520
diffusion in Cu crystals and whiskers, mechanism 8=35487
diffusion in Cu, rel. to Cu weight increase, effects of thickness and orientation 8=35485
diffusion in GaAs 8=39974
diffusion in GaAs 8=48774
diffusion in GaAs, roles of phase diagram, diffusion and solubility anals. rel. to sources 8=44390
diffusion in n-GaAs with high donor conc., at 900°C 8=31006
dislocation density and rate effects in twinning 8=26189
dislocations, basal mobility and internal stress effects 8=44456
edge dislocations in basal slip system, vels. rel. to applied shear stress 8=44457
electrodes, adsorpt. of org. materials, pot. vars. 8=36601
electrodes, measured conductance rel. to measured capacitance and Faradaic current 8=49929
films, cold-rolled, from Hall effect and magnetoresistance anisotropy obs. 8=30810
hexagonal, quasidipoles in basal plane 8=48862
impurity in Al, Al^{27} zero field resonances 8=49631
ions, electrochem. in fused $AlCl_3$-NaCl-KCl 8=49917
ions Zn^{++}, polarographic investigation in $LiNO_3$-$NaNO_3$-KNO_3 melt 8=45414
liquid, structure factor 8=48062
magneto resistance and quantum oscs anisotropy at low temp. press-depend. 8=24034
magnetothermal oscillations 8=49477

Zinc—contd
- multiple diffusions, effect on threshold and c.w. output power of GaAs laser 8=46615
- plastic deformation on alternating torsion, macro-localization characteristics 8=35726
- plastic deform. of macrocrysts., grain boundary props., EPMA-Kossel obs. 8=30856
- preferred orientation during recrystallization 8=35213
- radioactive, electrochem. props. 8=36594
- reflectance meas., basal-plane vacuum u.v. 8=45233
- sheet, crystallographic anal. of plastic anisotropy 8=35721
- sheet, plastic anisotropy and plastic flow of circular diaphragm 8=35720
- spectral line breadth with Na as impurity in arc discharge 8=34437
- stacking faults on prism planes of first kind, obs. 8=44466
- stress state required for pyramidal dislocation movement 8=40045
- sputtering by 1- to 5 keV Ar$^+$, rel. to orientation dependence 8=40076
- twinned crystals, internal friction peak at 265°K due to stress relax. at twin boundaries 8=35727
- twinning and slip by indentation at 5 kg loads 8=31056
- vacancy dislocation loops, multilayer 8=40002
- zone-refined, solute-induced hardening near grain boundaries 8=26842
- K-absorption edge in Zn-Al alloys, fine structure investigation 8=41155
- Zn 3075.9 Å, resonance line perturbed by He, A, Ne, Kr and Xe 8=47512
- Zn II, IV, spark spectrum extension 8=34156
- Zn III spark spectra and energy levels 8=38682
- Zn^{65} drop extraction, between liq. metals and fused salts 8=27725
- Zn-Ar plasma, in local thermodynamic equilib., 4000 to 50 000°K, composition 8=47809

Zinc compounds
- chalcogenide films, mono- and multilayer, epitaxially grown structure 8=26115
- chalcogenides, hexagonal or cubic phases formation rel. to stoichiometry effects 8=44082
- chalcogenides, synthesis and growth in Ga and In melts 8=48563
- electroluminescence of polycrystalline ZnTe 8=32064
- phonon-assisted free exciton recombination 8=44760
- specific heat and enthalpies of change of phase; meas. 8=46286
- u.v. radiation dosimetry by use of pyroelectric properties 8=46924
- wurtzite, dielec. model for electronegativity 8=27251
- zincblende, dielec. model for electronegativity 8=27251
- zinkite, hydrothermal crystallization kinetics 8=26230
- Zn complex, bis(acetylacetonato)zinc(II), crystal and mol. structure 8=39824
- Zn complex, di-thiourea-zinc acetate, crystal structure 8=26451
- Zn complex tris(thiourea) zinc (II) sulphate, crystal and mol. structure 8=39825
- Zn complex, zinc-N-N-diethyldithiocarbamate 8=26368
- Zn halide complex with azines, prep. and infra-red study 8=36432
- Zn in liq. Zn-Au, thermodyn. props. by e.m.f. meas. 8=25906
- Zn molybdate hydrates, non-stoichiometric, structures for two phases, and vacancies 8=30916
- Zn(II) di-n-alkylphosphinates, single crystal studies and polymeric structures 8=30797
- Zn(II) oxalate complexes, conc. solns, raman spectra rel. to co-ord. and coupling 8=43843
- Zn-Al alloys, fine structure of Zn K-absorpt. edge 8=41155
- Zn-Al alloys, flow stress-strain rate behaviour rel. to structure 8=40187
- Zn-Al, superplastic alloy, microstructure 8=30872
- Zn-Al-n-Si:P alloyed diode, hole capture by Zn^{2-} in Si, effective cross section 8=40520
- $ZnAl_2O_4:Cr^{3+}$, optical spectra 8=49715
- $ZnBr_2$ molten, external transport numbers 8=34791
- Zn-Cd-Ag-Cu system, univarient equilibria formation by decomposition 8=30675
- (Zn, Cd)O, luminescence 8=45292
- $Zn_xCd_{1-x}S$ graded-band-gap crystals, growth and elec. props. 8=39696
- (Zn, Cd)(S, Se): Cu phosphors, photo- and electroluminesc., obs. 8=45293
- $Zn_{0.1}Cd_{0.9}Sb$ solid solution crystals, thermoelectric power anisotropy 8=27311
- Zn-CN-NH_3 complex in aqueous soln, raman spectra rel. to mixed ligands 8=43842
- $ZnCl_2$-diethylether coordination compound, i.r. spectrum 8=25569
- $ZnCl_2$ molten, self-diffusion 8=34815
- $ZnCr_2O_4$, spin-structure determ. from magnetization and resonance 8=31731
- $ZnCr_2S(Se)_4$ insulating spiral, antiferromag. resonance freq. and temp. dependence 8=31831
- $ZnCr_2Se_4$, distant-neighbour interaction analysis 8=31596
- $ZnCr_2Se_4$, spin magnetism 8=36136

Zinc compounds—contd
- ZnF_2 phase transforms, and lattice params., ≤130 kbar, 25 and 300°C 8=39570
- $Zn_xHg_{1\ x}Te$, growth from soln., with temp. distrib. adjustment 8=44147
- $Zn_xHg_{1-x}Te$ solid soln. crystal growth and structure 8=26269
- $Zn_xHg_{1-x}Te$ solid solutions, fundamental reflectivity spectrum 8=45232
- $Zn_xHg_{1-x}Te$ solid solutions, thermal cond. 8=44372
- ZnI series, intercombinational transition probabilities 8=38711
- $(Zn_{0.65}Mg_{0.35})_2SiO_4$, high-temp. mech. props. 8=35725
- Zn-Mn ferrites, permeabilities rel. to micro- and chemical structures 8=27431
- Zn-Mn ferrite, sintering conditions effect on mag. props. 8=27432
- $ZnNi_xMn_{2-x}O_4$, elec. and mag. props. 8=40745
- ZnO, acousto-electrically excited, transmission of 35 GHz microwaves 8=42011
- ZnO, Brillouin scattering from shear waves in crysts. under high elec. fields 8=44325
- ZnO, chemisorption of O_2, effect of d.c. electric field 8=49905
- ZnO, chemisorption states of oxygen 8=32118
- ZnO crystal, photocurrent sensitization, electrochem. obs. 8=49425
- ZnO crystal, recomb. radiation of bound excitons, 4.2°–90°K 8=31301
- ZnO crystals, e multiplication and surface charge 8=49354
- n-ZnO, current flow on dissolution in acid, 8=49918
- ZnO, edge luminescence, exciton contribution 8=27660
- ZnO, e.s.r. effects of additives 8=36254
- ZnO, e.s.r. of adsorbed NO_2 8=48499
- ZnO film on delay, efficiency as acoustic transducer 8=23956
- ZnO films, polycrystalline dye-sensitized, thermally stimulated conductivity 8=35994
- ZnO, hydrothermally crystallized, effect of Li on facet effect and dendritic growth 8=26201
- ZnO, intrinsic photo effect by dyes, spectral sensibilization, mechanism 8=36428
- ZnO laser, electron pumped, far field patterns 8=33202
- ZnO lattice, crystal field changes by collective distortion rel. to Cu_2^+ ions 8=48311
- ZnO, lattice thermal expansion, 27-619°C, X-ray meas. 8=39934
- ZnO, low dispersion layer, optical props. 8=36429
- ZnO, luminescence 8=45292
- ZnO luminophor, pulse-excited, decay rel. to temp. 8=45290
- ZnO, photoconductivity dependence on water vapour conc. in ambient gas 8=27334
- ZnO, piezoelectric, appl. to microwave mixing 8=49382
- ZnO, polar crystals, model for thermal eqn. of state 8=30630
- ZnO powder, thermoluminescence 8=32065
- ZnO, refractive index 8=49763
- ZnO, refractive index meas., room to liq. He temps. 8=41154
- ZnO, shallow donor ground states 8=31278
- ZnO single crysts., electroluminesc. 8=32059
- ZnO, solubility in KOH and electrolytes elec. cond. and vapour press., 10-145°C 8=45373
- ZnO, spectral reflectance 8=41128
- ZnO, stress induced splitting of exciton lines 8=26920
- ZnO, u.v. luminescent spectrum, 4.2°-77°K 8=41216
- ZnO, valence band symmetry and deform. potentials 8=35782
- ZnO, vapour-phase grown, in ultrasonic amplifier 8=26586
- ZnO, Voigt-Reuss-Hill approx. rel. to meas. of elastic moduli 8=40188
- ZnO, wurtzite-type crysts., optically active lattice vibrs. 8=35394
- $ZnO:Co^{2+}$, optical absorpt. and photocond. 8=36029
- ZnO-Cu_2O heterojunctions, electroluminescence 8=36516
- ZnO, Cu^{2+}, molecular orbital theory 8=43969
- $ZnO:Fe^{3+}$, Mn^{2+}, cubic field parameter by e.s.r. investigations 8=45104
- ZnO:Ga scintillation due to α, obs. 8=37789
- ZnO: Li, high-resistivity, electronic drift mobilities and SCL currents 8=40588
- ZnO-TiO_2-SiO_2 systems, glass formation 8=44079
- $ZnRh_2O_4$, single crystals, growth from PbO flux 8=39695
- ZnS: Cl luminophor, pulse-excited, decay rel. to temp. 8=45290
- ZnS activated with Group IVB elements, e.p.r. investigation of luminescence 8=49815
- ZnS blende, second order Raman spectra 8=36427
- ZnS, coherent fluorescence for excitation by 2 photon absorption 8=32063
- ZnS, colour centres, accumulation during bombardment with fast neutrons 8=31125
- ZnS, energy bands, spin-orbit splittings 8=44826
- ZnS luminophors, preparation, effect of halide addition 8=49819
- ZnS, photodepolarization currents, shallow capture levels rel. to kinetics 8=27332

Zinc compounds—contd
- ZnS, thermal expansion anisotropy 8=44351
- ZnSAg monocrystal, luminesc. rel. to e.s.r. 8=36523
- ZnS(Ag) and Li^6F registration of slow neutrons for luminphor 8=47153
- ZnS:Al(Ga), luminescence, self-activated, polarization 8=32067
- ZnS:Cu^{2+}, molecular theory 8=43969
- $Zn(SCN)_2$, Pb^{2+} or Sn^{2+} activated, luminesc. 8=36520
- Zn(S:Se):Mn phosphors, emission and excitation spectra 8=45235
- Zn(S: Se) phosphors, activator free luminescence 8=36517
- ZnSe, absorption, photo-induced i.r. 8=41153
- ZnSe, codoped, of Er^{3+} 8=30646
- ZnSe, codoped, Zeeman effect of Er^{3+} 8=30646
- ZnSe, energy bands, spin-orbit splittings 8=44826
- ZnSe epitaxial layers on p-Ge, growth and elec. characts. 8=44834
- ZnSe, intrinsic oscillations in photoconductivity 8=27333
- ZnSe, i.r. lattice vibrations 8=49764
- ZnSe, photoelectronic props. in p-type-Cu-activated and n-type-self-activated 8=45296
- ZnSe, photoluminescent props. of activated emissions 8=49816
- ZnSe, semiconducting, growth and morphology 8=48561
- ZnSe-type phosphors, electroluminescent props. 8=49820
- ZnSe:Co^{2+}, Co^{2+} absorpt. and emission rel. to ion centre levels, 3500 cm^{-1} 8=27613
- p-ZnSe: Cu, radiative pair transitions 8=45294
- ZnSe(Cu, I, Cl) sublimated layers, electroluminesc. obs 8=41211
- ZnSe:Fe^{3+}, cubic field splitting for S-state ions 8=43934
- ZnSe : Fe^{3+}, e.p.r. rel. to Fe^{3+} in cubic and axial fields 8=40949
- ZnSe: Tm^{3+} (Er^{3+})(Ho^{3+}), with Li or Cu codopants, luminescence 8=27664
- $ZnSeO_3 . 3H_2O$, crystal structure 8=26450
- $ZnSiF_6 . 6H_2O$: paramagnetic impurities, n.m.r. of F^{19}, temp. and impurity conc. dependence 8=40974
- $ZnSnAs_2$, edge absorption spectrum 8=45231
- Zn-Sn-Cd-Pb alloy, binary liq. phase occurrence 8=34786
- Zn-Sn-Cd-Pb liq. solns, thermodynamic props rel. to activity coeffs. 8=43795
- $ZnSnP_2$ platelets, prep. and props. 8=26267
- $ZnSnP_2$, radiative recombination, photoluminescence spectra 8=41213
- ZnTe, crysts. growth from melt in Zn atm., gradient freeze method 8=35253
- ZnTe, crysts. growth from soln., theory 8=35232
- ZnTe, energy bands, spin-orbit splittings 8=44826
- ZnTe, growth by temp. gradient soln. zoning 8=44148
- ZnTe, hole-traps, Ge- and Pb-associated 8=26884
- ZnTe, i.r. lattice vibrations 8=49764
- ZnTe, polycrystalline, electroluminescence 8=32064
- ZnTe, thermal expansion, 0-460°C 8=39933
- ZnTe–CdTe solid solutions, energy struct. 8=40253
- ZnTe:Fe^{3+}, cubic field splitting for S-state ions 8=43934
- ZnTe:O as scintillation counter material 8=46864
- ZnTe:Pb, impurity state, e.p.r. meas. 8=35738
- $ZnTe_{1-x}Se_x$, growth by temp. gradient soln. zoning 8=44148
- ZnTe-ZnSe alloys, p-n junction, electroluminesc. 8=36521
- Zn_2TiO_4, order-disorder transition, influence of non-stoichiometric substitutions 8=26088
- α-$Zn_3(VO_4)_2$: Ni^{2+}, optical spectra rel. to crystal field theory 8=48310
- $ZnWO_4$, octahedral symmetry, i.r. absorpt. spectra of Co^{2+} ions 8=32011
- $ZnWO_4$, pseudo-rhombic crystal struct. obs. 8=30915
- $ZnWO_4$: Cr^{3+} type crysts, paramag. res., "electronic" and "ionic" mechanisms 8=40948
- Zn_2Y, hexagonal ferrite, two-magnon ferrimag. reson. linewidth 8=36228
- ZnY($Ba_2Zn_2Fe_{12}O_{22}$, Mossbauer spectroscopy 8=36198
- Zr hydride, thermal diffusion of H 8=26627
- **zinc sulphide**
  - allotropic transformation induced by mech. pressure 8=44016
  - brittle crystals, microhardness rel. to dislocation mobility 8=26796
  - crystal growth and morphology in semiconducting mat. 8=48561
  - crystal structure when melt-grown under pressure 8=44084
  - crystals, hexagonal, stacking fault introduction rel. to photovoltaic effect changes 8=31103
  - cubic, growth from molten $PbCl_2$ 8=44149
  - drift mobilities of electrons and holes 8=40500
  - electroluminescence, influence of structure 8=41215
  - electroluminescence in sublimated layers 8=32061
  - electroluminescence rad., reabsorpt. and form. of stimulated state 8=32062
  - electroluminescent semicond. resistor props. 8=27145
  - epitaxial growth on Si, by vac. evaporation 8=30740
  - exciton complexes spectrum 8=36430
  - exciton spectrum rel. to stacking fault probability rel. to exciton spectrum 8=49766
  - film, epitaxial growth on CdS and ZnS platelets, dislocations and cryst. orientation 8=35165
  - impurity ion diffusion mechanism 8=26626

Zinc compounds—contd
- **zinc sulphide**—contd
  - lanthanide impurity doped, crystal field effects rel. to structures 8=26646
  - lattice luminesc. props. 8=36522
  - luminescence excitation at low temp. 8=27661
  - particle size and morphology, effect of precipitating conditions 8=48565
  - platelets, growth, structural properties 8=40034
  - phosphor, trace metal determ. by n. activation 8=50001
  - phosphors, green-Cu luminescence band, temp. shift 8=32068
  - photoconductivity, microwave meas. 8=49426
  - polytypism as high-order transformation 8=44012
  - powders, a.c. electroluminesc 8=36521
  - Raman spectra of wurtzite- and zinc-blende-types 8=45234
  - refractive index 8=49763
  - silicates activated by Mn, Cr, Hf and rare-earth's elements, luminescence props. 8=41219
  - slip, periodic processes rel. to polytype formation 8=44461
  - with stacking faults, one dimensional, internal optical reflection 8=45230
  - stimulated cond. and electroluminesc. of sublimated layers 8=32060
  - thermoluminescence correl. with thermally stimulated elec. cond. 8=49817
  - twist boudaries, effect on electroluminescence 8=41214
  - würtzite classification 8=35209
  - wurtzite, electro-optical effect 8=36431
  - Cu-activated luminophor, two-band emission 8=45307
  - ZnS phosphor, electroluminescence enhancement using
  - ZnS(Ag) based crystals, scintillation output rel. to α-radiation of surface 8=27662
  - ZnS: Ag, Ga, donor-acceptor pairs, photoconductivity, optical and photoescited e. s. r. spectra 8=40677
  - ZnS_x-CdS_{1-x} mixed crysts, luminesc. 8=41212
  - ZnS/CdS mixture, e. p. r. of Mn^{2+} exchange-coupled pairs 8=45105
  - (ZnS-CdS):Co^{2+}, Co^{2+} absorpt. and emission rel. to ion centre levels, 3500 cm^{-1} 8=27613
  - ZnS–CdSe alloy systems 8=32066
  - ZnS:Co^{2+}, Co^{2+} absorpt. and emission rel. to ion centre levels, 3500 cm^{-1} 8=27613
  - ZnS:Cu, electroluminescence rel. to Cl, Br, I co-activators effect 8=32069
  - ZnS: Cu electroluminescence spectrum dependence on heating processes 8=36519
  - ZnS; Cu phosphors freq. dependence of electro luminescence 8=41218
  - ZnS: Cu^{2+}, molecular orbital theory 8=43969
  - ZnS: Cu, Al(Ag, Al), i.r. absorpt. due to donor states 8=41156
  - ZnS: Cu, Cl, thermoluminescence and thermally stimulated dielectric effecy 8=36518
  - ZnS:Fe^{3+}, cubic field splitting for S-state ions 8=43934
  - ZnS-MgF_2 layer Fabry-Perot filters, max. transmission wavelength, H_2O vapour effects 8=28763
  - ZnS:Mn Cu phosphor sublimate, electroluminescence annealing effect 8=27663
  - ZnS : Mn, Cu, Cl films, electroluminesc. in gap and sandwich cells 8=49818
  - ZnS:Mn^{2+}, e.p.r. forbidden line obs. at $\Delta M = Z$; $\Delta m = O, \pm 1$ 8=31887
  - ZnS/ZnSe mixed-crystals, associate defects of ^6S-state ions obs. by e.s.r. 8=26636
  - ZnTe, semiconducting, growth and morphology 8=48561
  - ZnV_2O_4–LiV_2O_4 system, V–V separation, i.r. spectra, electronic props., connection 8=35739

Zirconium
- analysis of O content by He^3 irrad. 8=27818
- deformed single crystals, texture formation by twinning 8=44091
- diffusion of V, coeffs. 8=35475
- corrosion behaviour rel. to internal stresses and deformation 8=26852
- corrosion breakaway region, inelastic behaviour of metal and oxide 8=36576
- films, oxidised 300-500°C, structure obs. by e. microscope 8=35186
- HR1105 star, isotope ratios 8=28069
- monoclinic, stereographic projection 8=35214
- oxidation rate-constant determ., low-temp., from discontinuous film resistance changes 8=49883
- oxidation, thin noble metal film effects 8=49882
- oxygen diffusion study using $O^{16}(d, p)O^{17}$ reaction 8=31017
- paramagnetic susceptibility anisotropy temp. dependence 8=40755
- polycrystalline, optical consts. from reflectance ratios 8=45164
- polycrystalline, sputtering by Ar^+ ions, mechanism 8=35606
- polycrystals, e-irradiated, low-temp. resistivity recovery 8=31158
- purification by β-phase zone displacement along bar of α-Zr 8=30825
- sputtering by 1- to 5-keV Ar^+, rel. to orientation dependence 8=40076
- stacking fault probab. of cold-worked, X-ray obs. 8=26704

Zirconium—contd
- tensile deform., effect of up to 4.2 at. % O 8=44609
- thermal expansion, 2° to 30°K 8=44349
- CaS:Zr phosphors, mag. susceptibility rel. to Zr conc. 8=44967
- in CO_2, oxidation prevention and O diffusion inhibition by Cr coating $\leq$ 650°C 8=32107
- Hf/Zr ratio, metamorphic rocks from Ontario 8=50067
- Hg boiling corrosion of steel inhibited by Zr impurity 8=47426
- in Mg–Zr alloys, rel. to fine grain effect 8=48343
- on W, adsorption and nucleation of α and β phases, obs. 8=39625
- ZrO_2, structure analysis using method of coordination no. determ. without density meas. 8=26141

Zirconium compounds
- alloys, anti-hydrogenation treatment with molten $NaNO_3$ 8=32105
- alloys, irradiation creep, yielding creep theory appl. 8=35730
- carbides, sputtering by Ar^+ ions, mechanism 8=35606
- crystal photolum., electrolum. and photovoltaic effects, 77°-600°K. obs. 8=45291
- diborides, conduction e-paraeters calc. based on single zone method 8=35830
- with Laves structure, magnetism and crystal structure 8=31711
- luminophor emission spectra 8=45295
- Zircalloy-4, irrad.-enhanced strain relax., 2.4×10^{14} nv > 1 MeV 8=35732
- Zircalloy-4, ZrH precip. habit planes, obs. 8=44098
- Zircalloy, in-reactor creep rel. to dislocation climb 8=35728
- Zircalloy-2, fatigue-crack initiation 8=26854
- Zircalloy-2 pressure tubes, in-reactor creep rel. to n flux, temp. and stress, obs. 8=53733
- Zircaloy tubing, strain behaviour, effect of texture on anisotropy 8=26853
- Zircaloy-2 corrosion behaviour rel. to internal stresses and deformation 8=26852
- Zircaloy-2, corrosion in water and steam, effect of surface prep. and fluorine contamination 8=45352
- Zircaloy-2 oxidation in O and H_2O vapour, kinetics and mechanism, , 350–500°C 8=32106
- Zircaloy-2, oxidation in water, 200°-300°C, obs. 8=27726
- Zircaloy-2, white spotting in oxide films rel. to struct. and orientation 8=35187
- Zircalloy-2, ZrH precip. habit planes, obs. 8=44098
- Zr^{95} as fission product in coated fuel particles, determination 8=47404
- Zr alloys, in-reactor creep rel. to dislocation climb 8=35728
- Zr phosphate membranes for intermed. temp. fuel cells 8=46354
- Zr, sample porous material for fracture tests 8=48974
- Zr–Cu alloys, oxygen diffusion study using $O^{16}(d, p)O^{17}$ reaction 8=31017
- $Zr_{1-x}Gd_xZn_2$, mag. props. and NMR rel. to localized mag. moments effect in $ZrZn_2$ 8=36180
- Zr–Hf alloy, sp. ht. 1.1–4.2°K 8=35437
- Zr-Nb alloys, critical current density rel. to dispersed precips. 8=35857
- Zr-2.5 wt.%Nb pressure tubes, in-reactor creep rel. to n flux, temp. and stress, obs. 8=35733
- Zr-2.5 wt.%Nb–0.5 wt.%Cu, irrad.-enhanced strain relax., 2.4×10^{14} nv > 1 MeV 8=35732
- Zr-2.7 w/o Nb oxide film, structure and morphology exam., 300-500°C 8=44064
- Zr–O solid solution, interstitial, ordered arrangement of O 8=35289
- Zr-O solid solns., microprobe and e microscope obs. 8=30658
- Zr–Sc alloy, sp. ht. 1.1–4.2°K 8=35437
- Zr–Ti alloys, sp. ht., 1.1–4.2°K rel. to superconducting transition temp. 8=35437
- ZrB_2, struct. and orientation of second phase precipitates 8=35136
- $ZrBi_2$, atomic structure rel. to quasi-homologs 8=33560

Zirconium compounds—contd
- $ZrC_{0.56}$, diffusion coeff. temp. dependence 8=31018
- ZrC, oxidation 1130-2160°K 8=45351
- ZrC, thermoelec. power and elec. conductivity, 20-2000°C 8=27310
- ZrC in Cs vapour, e- and ion-emission rel. to other refractory metal cpds 8=27350
- $ZrC_{0.32}H_{1.2}$, n.m.r. absorpt. spectrum, temp. efects 8=31925
- $ZrCl_4$ and $HfCl_4$ vapours, thermal diffusion constant 8=34676
- $ZrCl_4$, vibrational spectra 8=32040
- $Zr_4Co_4Ge_7$, crystal structure 8=48682
- $(ZrCo_2)_x(ZrFe_2)_{1-x}$ alloys, hyperfine field distrib. from Mossbauer spectra 8=31712
- ZrH_2, central force lattice dynamical model 8=39879
- $ZrH_{1.9}$, n.m.r. absorpt. spectrum, temp. efects 8=31925
- ZrH_2, positron lifetime 8=40286
- $(Zr_{1-x}Hf_x)Zn_2$ system, ferromagnetism 8=40831
- $Zr_{1-x}M_xZn_2$, where M = Ti, Y, Nb or Hf, magnetic props. 8=49546
- ZrN, diffusion of N_2, film-thickness determ. 8=44396
- $ZrN_{0.47}H_{0.98}$ n.m.r. absorpt. spectrum, temp. effects 8=31925
- $Zr(NO_3)_4$, vibrational spectra 8=32040
- ZrO_2, $\alpha \rightarrow \beta$ phase transform., temp. and impurity cation effects 8=26089
- ZrO_2 effect on corundum recrystallization 8=48536
- ZrO_2, films, gamma, neutron and neon damage 8=35607
- ZrO_2, grain growth and phase transition 8=48357
- ZrO_2, hemispherical spectral emittance 8=35466
- ZrO_2, hydrated amorphous, nature and thermal behaviour 8=43982
- ZrO_2, monoclinic, O self-diffusion coeffs. 8=35514
- ZrO_2, permittivity, effective and intrinsic 8=40589
- $(ZrO_2)_{0.85}(CaO)_{0.15}$ electrolytic thermocell, Seebeck coeff. 8=45392
- ZrO_2:Ce, baddeleyite, impurity positions 8=30917
- $ZrOCl_2.8H_2O$, heat treatment, ZrO_2 grain growth and phase transition 8=48357
- $Zr(OH)_4$, heat treatment, ZrO_2 grain growth and phase transition 8=48357
- $ZrSb_2$, atomic structure rel. to quasi-homologs 8=35360
- Zr_2Se, crystal structure and refinement, rel. to isostructures 8=26452
- $ZrSiO_4$, Pb, U and Th traces, e microprobe meas. 8=27811
- $ZrZn_2$, ferromagnetism, very weak itinerant 8=31547
- ZrW_2O_8, linear thermal expansion 8=35448

Zodiacal light
- brightness and polarization, and interplanetary dist. 8=45856
- dust cloud, cosmic light search 8=50272
- geocentric contribution, evidence against 8=37039
- polarization, negative, search 8=32567
- regions in quadrature to Sun, photometry 8=45855
- spectrometry, press. scanned Fabry-Perot 8=32568
- H_β profile in spectrum, meas. absorpt. and emission lines 8=41353

Zonal heating. See Atmosphere/thermodynamics.

Zone melting and refining
- advances 8=39653
- in alkali-halide crystals growing with high-purity 8=39665
- floating-zone, induction-heated, control system 8=45937
- Al, impurities behaviour, effect of third component 8=35235
- Fe, purification by γ-phase zone displacement along α-Fe bar 8=30825
- in KCl crystal growing with 10^{-9} mol/mol purity 8=39665
- in NaCl crystal growing with 4×10^{-6} mol/mol purity 8=39665
- Ni, high-purity prep., by e. beam float zone melting 8=48553
- Ta crystals, growth conditions rel. to orientation, purity and structural perfection 8=35231
- Zr, purification by β-phase zone displacement along α-Zr bar 8=30825

Zone plates. See Diffraction/light.

Zoology
- bottlenose dolphin, sonic burst count matching 8=37258

Great activity in silicon-iron

Intense research activity into silicon-iron is brought to light in this new IEE publication which reviews the whole ambit of magnetic materials and their applications throughout the world.

The book contains 53 papers, presented at a conference held in London in September 1967 and sponsored by the IEE, IPPS and IEEE, which are grouped as follows:

Orientation and domain structure
Measurements on silicon-iron
Permanent magnets
Magnetostriction in silicon-iron
Transformer noise
Losses in silicon-iron
Nickel-iron and aluminium-iron
Garnets and ferrites
Microwave properties of ferrites
Thin films.

IEE Conference Publication 33: Magnetic materials and their applications.

266 pp. photolitho. A4. soft covers. 1967.

Price £3 15s. (members £2 10s. if ordered through sponsoring society)

Orders, with remittances, should be sent to:
Publications Department, IEE, Savoy Place, London WC2

MAGNETIC MATERIALS AND THEIR APPLICATIONS
26th–28th SEPTEMBER 1967
CONFERENCE PUBLICATION No. 33
IEE

Magnetic materials and their applications

LONG RADIO WAVES

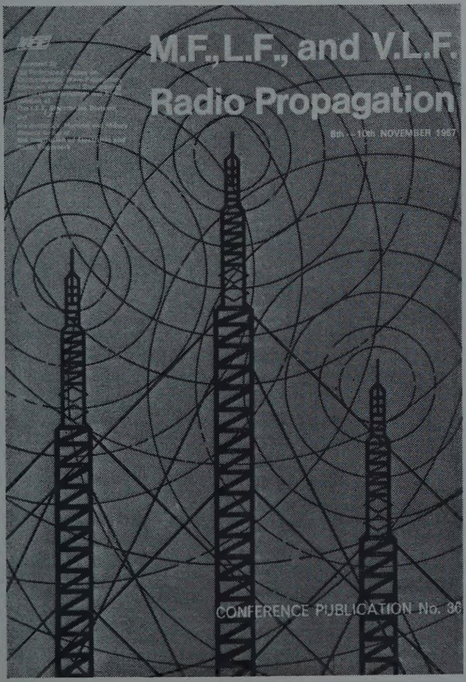
IEE
M.F., L.F., and V.L.F. Radio Propagation
8th–10th NOVEMBER 1967
CONFERENCE PUBLICATION No. 36

The future of long-range aviation depends on artificial satellites. For the present, however, reliance must be placed on radio-navigational aids based on those radio waves in the m.f., l.f. and v.l.f. bands which are well known to propagate over long distances. Propagation of these waves has many technical applications as well as being of interest to the pure scientist studying the ionosphere.
This new book contains 43 papers, presented at a conference held in London in November 1967 and sponsored by the IEE and the IERE, which are grouped as follows:

The ionosphere
Waveguide mode and ray theories
Terrestrial propagation over great distances
Atmospherics
Magnetosphere
Subsurface propagation.

IEE Conference Publication 36: 'M.F., l.f. and v.l.f. radio propagation'. 354 pp. photolitho. A4 size. soft covers. 1967. price £5 (members £3 6s. if ordered through sponsoring society)

Orders, with remittances, should be sent to:
Publications Department, IEE, Savoy Place, London WC2

IEE PERIODICALS 1969

Copies and information can be obtained from the

Publications Department

IEE, Savoy Place, London WC2

Proceedings IEE, published monthly, contains papers of industrial and technological interest from engineers and scientists the world over. Each issue comprises three self-contained groups of papers on Electronics; Power; and Control and Electrical Science, and these can be ordered as separate publications—*Electronics Record, Power Record, and Control & Science Record.*

Subscriptions to *Proceedings IEE:*

£21 p.a. *IEE Associates and Associate Members under 28 and IEE Students: £2 10s. Other IEE members: £5*

Separate copies of individual papers are available when they have been published in the *Proceedings. Price 2s. each.*

Electronics Record is published every two months, the papers being taken from the two previous issues of *Proceedings IEE.*

£10 p.a. *IEE Associates and Associate Members under 28 and IEE Students: 25s. Other IEE members: £2 10s.*

Power Record, quarterly, takes its material from the three preceding issues of *Proceedings IEE.*

£6 p.a. *IEE Associates and Associate Members under 28 and IEE Students: 15s. Other IEE members: 30s.*

Control & Science Record, quarterly, includes papers on control and automation and electrical science taken from the three previous issues of *Proceedings IEE.*

£6 p.a. *IEE Associates and Associate Members under 28 and IEE Students: 15s. Other IEE members: 30s.*

Electronics Letters, published fortnightly, is an international journal offering speedy dissemination of research and development results in electronics, control and allied subjects, in the form of communications up to about 1200 words in length. Publication is within two to six weeks of receipt, giving the engineer an immediate picture of the latest developments in the field.

£10 p.a. *IEE members: £3*

Electronics & Power, published monthly, is a wide-ranging magazine covering the complete field of interest of electrical, electronics, and control technology by means of articles, product reviews, correspondence, editorial comment and book reviews.

Electronics & Power: £8 p.a.

IEE members: free

IEE News is a twice-monthly tabloid newspaper for the professional electrical, electronics and control systems engineer.

IEE News: £2
IEE members: free

Students' Quarterly Journal is received free of further subscription by all IEE Students, Associates and Associate Members under the age of 30. It caters particularly for the younger member, and specialises in concise, topical articles on the latest advances in electrical, electronics and control engineering.

20s. p.a. *Senior members: 10s. p.a.*

SCIENCE ABSTRACTS PUBLICATIONS

Physics Abstracts (PA), published fortnightly, will provide 65 000 abstracts in 1969. In addition to covering the established periodical literature as in the past, PA will in 1969 give increasing coverage to the report and patent literature. Alphabetical author and subject indexes will be given twice in the year.

£80 p.a.

Electrical & Electronics Abstracts (EEA) is the comprehensive literature-retrieval service for electrical and electronics engineers. Published monthly, it will in 1969 include 34 000 abstracts and be computer typeset. The usual indexes will be provided.

£65 p.a.

Computer & Control Abstracts (CCA) begins in January 1969 as a development of **Control Abstracts,** whose coverage is being much enlarged to embrace computer science and technology, hardware, software and applications. Published monthly, it will provide 16 000 abstracts in 1969, as well as the usual indexes.

£35 p.a.

Cumulative Indexes

Physics Abstracts—subject index for the five years 1955–59 inclusive, bound in one volume, stiff covers and buckram cloth, 800 pp.

£20

Physics Abstracts—author index for the five years 1960–64 inclusive, bound in four parts, stiff covers and buckram cloth, 2300 pp.

£17 set *Members: £10 set*

Physics Abstracts—subject index for the five years 1960–64 inclusive, bound in two parts, stiff covers and buckram cloth.

£40 set

Electrical Engineering Abstracts—subject index for the five years 1955–59 inclusive, bound in one volume, stiff covers and buckram cloth, 320 pp.

£15 *Members: £9*

Electrical Engineering Abstracts—author index for the five years 1960–64 inclusive, bound in two volumes, stiff covers and buckram cloth, 970 pp.

£12 10s. set *Members: £7 10s. set*

Electrical Engineering Abstracts—subject index for the five years 1960–64 inclusive, bound in one volume, stiff covers and buckram cloth, 950 pp.

£20 *Members: £12*

Current Papers in Electrical & Electronics Engineering (CPE) will in 1969 be a monthly 'current awareness' publication in A4 size (210×297 mm) providing the full bibliographic reference of every abstract published in EEA. Each issue will list an average of 2800 titles and references from the world's literature on electrical and electronic engineering, including patents and reports.

£7 10s. p.a. *IEE members: £3 15s.*

Current Papers in Physics (CPP) will in 1969 be an A4-sized publication providing the full bibliographic reference of every abstract published in PA. An average of 2500 titles and references will be published in each fortnightly issue, using the same classification as in PA.

£4 p.a.

Current Papers on Computers & Control (CPC) will in 1969 provide the full bibliographic reference of every abstract published in CCA. It will be published monthly in A4 size and will be computer typeset.

£5 p.a. *IEE members: £2 10s.*

PUBLISHED BY THE INSTITUTION OF ELECTRICAL ENGINEERS. PRINTED BY UNWIN BROTHERS LIMITED, WOKING AND LONDON (U 3161)